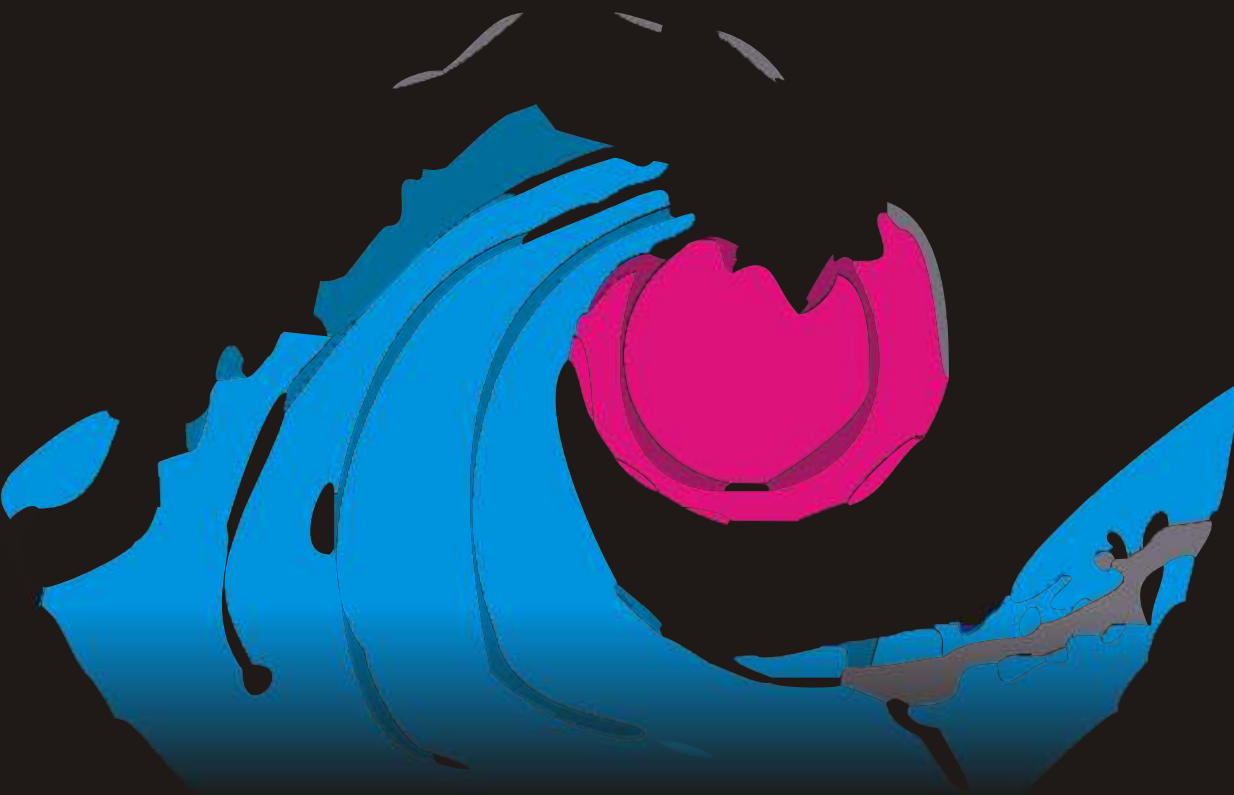


MICHAL LEBL  
RICHARD A. HOUGHTEN

# Peptides

THE WAVE OF THE FUTURE



© COPYRIGHT 2001  
AMERICAN PEPTIDE SOCIETY  
ALL RIGHTS RESERVED

# Peptides

**The Wave of the Future**

## Peptides: The Wave of the Future

# Peptides

## **The Wave of the Future**

Proceedings of the Second International  
and the Seventeenth American  
Peptide Symposium

Edited by

**Michal Lebl**

and

**Richard A. Houghten**

**American Peptide Society**



# Peptides: The Wave of the Future

Proceedings of the Second International and the  
Seventeenth American Peptide Symposium  
June 9–14, 2001, San Diego, California, U.S.A.

Edited by

**Michal Lebl**

*Spyder Instruments, Inc. and Illumina, Inc.*  
9885 Towne Centre Drive  
San Diego, CA 92121  
*michal@5z.com*

and

**Richard A. Houghten**

*Torrey Pines Institute for Molecular Studies*  
*Mixture Sciences, Inc.*  
3550 General Atomics Court  
San Diego, CA 92121  
*rhoughten@tpims.org*

**American Peptide Society**  
**San Diego**

A C.I.P. Catalogue record for this book is available from the Library of Congress.

ISBN 0-9715560-0-8 (American Peptide Society)

ISBN 1-4020-0473-7 (Kluwer)

---

Published by American Peptide Society,  
c/o Torrey Pines Institute of Molecular Studies  
3550 General Atomics Court  
San Diego, CA 92121, U.S.A.

Sold and distributed by American Peptide Society  
c/o Torrey Pines Institute of Molecular Studies  
3550 General Atomics Court  
San Diego, CA 92121, U.S.A.

and by Kluwer Academic Publishers  
101 Philip Drive, Norwell, MA 02061, U.S.A.  
(in North, Central and South America)  
P.O. Box 322, 3300 AH Dordrecht,  
The Netherlands  
(in all other countries)

Copyright ©2001 by American Peptide Society

All Rights Reserved. No part of the material protected by this copyright notice may be reproduced or utilized in any form or by any means, electronic or mechanical, including photocopying, recording or by any information storage and retrieval system, without written permission from the copyright owner.

Printed in the Czech Republic

*Dedicated to Bruce Merrifield on the occasion of his 80th birthday*



## Preface

The Second International Peptide Symposium continued the tradition of international meetings of peptide scientists started by Josef Rudinger in 1958 in Prague, Czech Republic. It was held under the auspices of the Seventeenth American Peptide Symposium at the Town and Country Resort in San Diego, California from June 9 to June 15. In addition to the main Symposium, we were honored to have the Merrifield Satellite Symposium, honoring Bruce Merrifield's accomplishments on his 80th birthday.

Over 1,250 participants from around the world attended the lectures, posters and exhibits. Reflecting the international nature of the Symposium, there were participants from 37 countries in attendance (Table 1, Figure 1). In addition to the 75 plenary lectures, there were over 575 poster presentations, and 70 commercial exhibits as well as booths from the American, Australian, Chinese, European, and Japanese Peptide Societies.

In order to afford an opportunity for the younger members of our field to present their work to the attendees, there were 15 lectures in the Young Investigator's Mini-Symposium, organized by Carrie Haskell-Luevano. The quality of the lectures in this section is proven by the fact that these papers are published in this proceedings volume in the middle of papers submitted by more senior scientists, and there is no way to find out who was the young investigator and who was not.

As is true for the Chairs of any scientific meeting, our intent was to have the best possible science presented, while also being able to relax and thoroughly enjoy the so-

*Table 1. IPS/APS Country Representation.*

USA	708	Taiwan	6
Japan	69	India	6
Canada	58	Spain	4
Germany	57	Poland	3
Switzerland	34	Norway	3
Italy	32	Latvia	3
Denmark	32	England	3
Korea	29	Czech Republic	3
France	28	Scotland	2
UK	26	Portugal	2
China	20	Argentina	2
Sweden	19	Slovenia	1
Australia	19	Singapore	1
Hungary	15	Saudi Arabia	1
Israel	14	Ireland	1
Netherlands	13	Greece	1
Russia	12	Finland	1
Belgium	11	Croatia	1
Brazil	8		

## Preface

cial and local attractions. In the beautifully cooperative San Diego sun, the attendees were able to enjoy both.

The scientific program covered almost every aspect of our ever-broadening field. Topics covered during the week encompassed synthetic methods, combinatorial approaches, delivery methodologies, therapeutics, modeling and design, solid phase approaches, receptor specific interactions, biomaterials, immunology, as well as genomics and bio-infomatics. The “Biologically active peptides” category was chosen as the First Preference by almost 15% of all submitting authors. Two of the many high points in the week’s scientific program were Garland Marshall’s Merrifield award lecture entitled “From Merrifield to MetaPhore: A Random Walk with Serendipity” and the plenary lecture by Craig Venter of Celera entitled “Genomics: From Microbes to Man.”

This was the first American Peptide Symposium in which abstracts, manuscripts, and galley proofs were submitted and communicated exclusively electronically. Even though it was obviously the first contact with the computer submission for several peptide scientists, the manuscripts were successfully submitted after an average of 1.3 attempts. The major problem was the compatibility of the versions of text processors and Internet browsers. We would like to express our thanks to the authors who followed instructions for the preparation of the manuscript. We thank the rest of the authors as well, even though they made our life a little more complicated. It was very amusing to find out how many scientists named their manuscript file 17thaps.doc, in a firm belief that their name is so unique that it would stand out in the middle of hundreds of files named, as we suggested, for example SmithAB.doc. We would have never guessed that we would get back the files containing the unchanged text of the template (“...text text text text...”) under the different file name. Amusing were also the attempts to squeeze four pages of text on the two pages of the template by very creative shrinking of the font size and figures. However, we believe that our (authors’ and editors’) pains in preparation of this proceedings volume were good for learning how to produce the next proceedings in the future. Our goal was to publish the book in the year of the symposium. We have shown not only that it is achievable, but also that it is theoretically possible to have the proceedings book ready in two months after the symposium. The only requirement is the willingness of the authors to cooperate in this effort. We would like to express our thanks to people who helped us most in editing the book, Jutta Eichler, Jon Appel, and Eileen Weiler. And, last but not least, it was

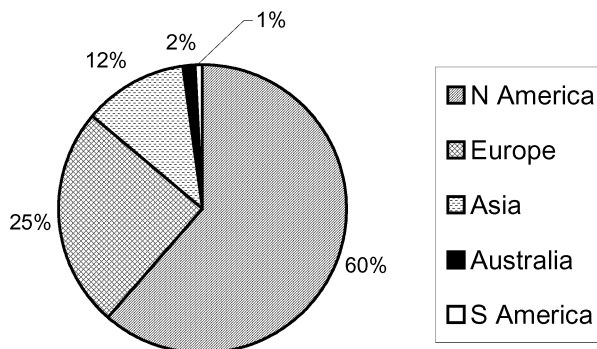


Fig. 1. Participants by Continent – TOTAL: 1,248.

## *Preface*

the effort of Bohumir Valter, in the Prague office, which made the publication of this book in the year 2001 possible.

This is also the first symposium in which the proceedings are being published by the American Peptide Society. The significance and benefits of the APS becoming its own scientific publisher will become evident in the coming years. In addition, this is the first proceedings to be available electronically, as well as in hard copy. The symposium home page is now and will be available in the coming years ([www.5z.com/aps](http://www.5z.com/aps)). You will always be able to come back to the abstract book, addresses of participants, pictures from the symposium, collection of Merrifield resin bead memorials (see for example Figure 2), and the electronic version of proceedings book.

Another first in this symposium was the award for the best joke delivered in the scientific lecture. The success of the joke delivery was evaluated by the “joke committee” (the members of the committee do not wish to be named here) and by the intensity of the audience response, evaluated by the audio-visual crew of AudioVisual Reality, Inc., led by Kurt Dommers (thanks for the excellent AV support). The award was given to Sandor Lovas, for his beer mug illustration of protein folding.

The Symposium Chairs tried to set precedence and minimize the length of “official talks” at the opening and closing the symposium. Introductory talks took 13.5 minutes and the closing ceremony was over in 42 minutes, maximizing thus the time for scientific lectures in the first case and the dance party in the second case.

To the members of the Program Committee who assisted in organizing the scientific program, your timely hard work was greatly appreciated. We are all grateful to the Session Chair Pairs who kept the speakers to their allotted times and prompted stimulating discussions. Very special thanks to Donna Freher-Lyons, Symposium Coordinator, for her brilliant coordination efforts and Santa M. Pecoraro, Database Management, for her skillful assistance regarding the abstract and manuscript submissions.

The 18th American Peptide Society Symposium will be held on July 19–23, 2003 at the Boston Marriott Copley Place in Boston, Massachusetts and will be chaired by Dr. Tomi Sawyer. For more information, contact PCMI at (858) 565-9921.

*Michal Lebl  
Richard A. Houghten*



*Fig. 2. “Merrifield resin bead memorial” on Prospect Street in San Diego. (If you happen to have a similar picture, you are invited to submit it to the collection available on symposium web site, [www.5z.com/aps](http://www.5z.com/aps).)*

## **2nd INTERNATIONAL PEPTIDE SYMPOSIUM/ 17th AMERICAN PEPTIDE SYMPOSIUM**

June 9–14, 2001  
San Diego, California

### **Co-Chairs**

**Richard A. Houghten**

Torrey Pines Institute for Molecular Studies  
Mixture Sciences, Inc.  
3550 General Atomics Court  
San Diego, CA 92121  
rhoughten@tpims.org

**Michal Lebl**

Spyder Instruments, Inc.  
Illumina, Inc.  
9885 Towne Centre Drive  
San Diego, CA 92121  
michal@5z.com

### **Program Committee**

**Gordon L. Amidon**

University of Michigan, USA

**Ettore Benedetti**

University of Naples, Italy

**Yu-cang Du**

Shanghai Inst. of Biochemistry, China

**Ben M. Dunn**

University of Florida, USA

**Mati Fridkin**

Weizmann Inst. of Science, Israel

**Lila M. Gierasch**

Univ. of Massachusetts, USA

**Helene Gras-Masse**

Lille Institute of Biology, France

**Milton T. W. Hearn**

Monash University, Australia

**Robert S. Hodges**

University of Colorado, USA

**Jeffery W. Kelly**

Scripps Research Inst., USA

**Terutoshi Kimura**

Peptide Institute Inc., Japan

**Garland R. Marshall**

Washington University, USA

**Jean Martinez**

University of Montpellier, France

**Yasuyuki Shimohigashi**

Kyushu University, Japan

**Takayuki Shioiri**

Nagoya City University, Japan

### **Planning Committee**

Richard A. Houghten

Michal Lebl

Donna M. Freher-Lyons

Peggy Totzke

Santa M. Pecoraro

Karen Garitta

Jon Appel

Joseph Taulane

Murray Goodman

Co-Chair

Co-Chair, Symposium Webmaster

Symposium Coordinator

Fiscal Officer

Abstract Database Management

Artwork & Logistics Coordinator

Exhibitor/Sponsor Coordinator

Lab Reunion Coordinator, Volunteer Activities

Merrifield Award Committee

Charlotte Hoffman  
Patti Bennett  
Rodney Arnayro

Volunteer Activities  
Volunteer Activities  
Merrifield Satellite Symposium  
Liaison

## **Volunteer Staff**

Aaron Jones  
Achyut Acharya  
Agnes Vidal  
America Mauher  
Amy Schink  
Ana Sandoval  
Antonia De Capua  
Aric Mabini  
Audrey Kelleman  
Brett Ellman  
Cassandra Christolos  
Cattram Thai  
Cesar Boggiano  
Chiara Perazzolo  
Chris Santos  
Christa Hamashin  
Christine Burger  
Christoph Zapf  
Churl Seong  
Clemencia Pinilla  
Colette Dooley  
Cornelia Hoesl  
David Heiner  
Dean Kirby  
Debbie Johns

Dorene Wood  
Edward Brehm  
Eileen Weiler  
Eva Borrás  
Garth Kinberger  
George Lebl  
Georges Ibrahim  
Gina Allicotti  
Hai Tran  
Hernan Mateo  
James Thomas  
Jess Freher-Lyons  
John Ostresh  
Jon Appel  
Jozsef Gulyas  
Juan Del Valle  
Judit Erchehyi  
Juliann Kwak  
Jutta Eichler  
Keiko Osawa  
Lisa Spindler  
Long Troung  
Marcello Giulianotti  
Marie Cronk  
Mark Nibbe

Marketa Rinnova  
Martin Lebl  
Michael Hsu  
Mika Tomioka  
Nhi Ong  
Nicole Smith  
Rachel Blake  
Richard Mimna  
Roseann Story  
Rosita Moya-Castro  
Sandra Moore  
Shan Madasamy  
Shannon Russell  
Somkit Rattan  
Sophie Perrin-Ninkovic  
Thu Thai  
Todd Williams  
Travis Cook  
Tyler Sylvester  
Weibo Cai  
Yongping Yu  
Yosup Rew  
Zuzana Leblova

## **Student Affairs Committee**

Carrie Haskell-Luevano, Co-Chair  
Richard Agnes  
Bret Beyer  
Balvinder Vig

DeAnna Long, Co-Chair  
Carol Fowler  
Ryan Holder

## **Travel Awards Committee**

Ben M. Dunn, Chair  
Sylvie Blondelle  
John D. Wade

Claudio Toniolo  
Yuji Kobayashi

## Symposium Sponsors and Exhibitors

The 2nd International Peptide Symposium/17th American Peptide Symposium gratefully acknowledges the following sponsors and exhibitors:

### Sponsors

Advanced ChemTech  
Akzo Nobel  
Applied Biosystems  
Bachem  
Cambridge Research Biochemicals  
CSPS (CoshiSoft/PeptiSearch)  
Eka Chemicals  
Eli Lilly and Company  
Flamma s.p.a.  
Midwest Biotech, Inc.  
Mixture Sciences, Inc.  
Multiple Peptide Systems, Inc.  
New England Peptide, Inc.  
PepTech Corp  
Peptides International, Inc.  
Polypeptide Laboratories  
Primm Labs, Inc.  
Senn Chemicals  
Synthetech, Inc.

### Exhibitors

Advanced ChemTech  
Agilent Technologies  
Akzo Nobel  
American Peptide Company  
AnaSpec  
Applied Biosystems  
Australian Peptide Association  
Bachem  
Biosource International  
Bio-Synthesis, Inc.  
C S Bio Inc.  
Calbiochem-Novabiochem Corp  
Cambridge Research Biochemicals  
CAT GmbH & Co  
Charybdis Technologies  
CHEMI S.p.A  
Chem-Impex International, Inc.  
Chemspeed, Inc.  
CSPS (CoshiSoft/PeptiSearch)  
EKA Chemicals  
European Peptide Society

FASEB  
Flamma Spa  
Genzyme Corporation  
GL Biochem (Shanghai) Ltd.  
Hyundai Pharm. Ind. Co., Ltd.  
ISOCHEM, GROUPE SNPE  
Japanese Peptide Society  
Jupiter Bioscience Limited  
Magellan Laboratories  
Micromass, Inc.  
Mimotopes  
Multiple Peptide Systems, Inc., GROUPE SNPE  
Neosystem, GROUPE SNPE  
New England Peptide, Inc.  
NOVASEP  
ORPEGEN Pharma GmbH  
Penta Biotech, Inc.  
PepTech Corp  
Peptides International  
Peptisyntha et Cie SNC  
PharmaCore, Inc.  
Polymer Laboratories, Inc.  
Polypeptide Laboratories  
Protein Technologies, Inc.  
Rapp Polymere GmbH  
Reanal Finechemical Co.  
RSP Amino Acid Analogues, Inc.  
Senn Chemicals  
Sigma-Genosys  
Syn Pep Corporation  
Synthetech, Inc.  
Thieme Publishers  
Tianjin Hecheng Science & Technology Development Co.  
UCB Bioproducts  
Vydac  
W. L. Gore & Associates, Inc.  
World Courier, Inc.

## **The American Peptide Society**

The American Peptide Society (APS), a nonprofit scientific and educational organization founded in 1990, provides a forum for advancing and promoting knowledge of the chemistry and biology of peptides. The approximately one thousand members of the Society come from North America and from more than thirty other countries throughout the world. Establishment of the American Peptide Society was a result of the rapid worldwide growth that has occurred in peptide-related research, and of the increasing interaction of peptide scientists with virtually all fields of science.

A major function of the Society is the biennial American Peptide Symposium. The Society also sponsors the Journal of Peptide Research and Biopolymers (Peptide Science), recommends awards to outstanding peptide scientists, works to foster the professional development of its student members, interacts and coordinates activities with other national and international scientific societies, sponsors travel awards to the American Peptide Symposium, and maintains a website at [www.chem.umn.edu/orgs/ampepsoc](http://www.chem.umn.edu/orgs/ampepsoc).

The American Peptide Society is administered by Officers and Councilors who are nominated and elected by members of the Society. The Officers are: Tomi K. Sawyer, President (ARIAD Pharmaceuticals); Murray Goodman, President-Elect (University of California-San Diego); Arno F. Spatola, Secretary (University of Louisville); and Richard A. Houghten, Treasurer (Torrey Pines Institute for Molecular Studies). The Councilors are: Fernando Albericio (University of Barcelona); Jean Chmielewski (Purdue University); Charles M. Deber (Hospital for Sick Children, University of Toronto); Gregg B. Fields (Florida Atlantic University); Victor J. Hruby (University of Arizona); Barbara Imperiali (Massachusetts Institute of Technology); Teresa M. Kubiak (Pharmacia & Upjohn, Inc.); Thomas Lobl (Newbiotics, Inc.); Robin Offord (GeneProt, Inc. and University of Geneva); Daniel H. Rich (University of Wisconsin-Madison); Arno F. Spatola (University of Louisville); and James P. Tam (Vanderbilt University).

Membership in the American Peptide Society is open to scientists throughout the world who are engaged or interested in the chemistry or biology of peptides and small proteins. Categories of membership include Active Member, Associate Member, Student Member, Emeritus Member and Honorary Member. For application forms or further information on the American Peptide Society, please visit the Society web site at [www.chem.umn.edu/orgs/ampepsoc](http://www.chem.umn.edu/orgs/ampepsoc) or contact Donna M. Freher-Lyons, APS Membership Coordinator, Torrey Pines Institute for Molecular Studies, 3550 General Atomics Ct., San Diego, CA 92121 USA.; tel (858)455-4752; fax (858) 455-2545; e-mail "APS\_Member@tpims.org".

## **International Liaison Committee of Peptide Societies**

This year we were very pleased that the 2nd International Peptide Symposium was held in conjunction with the 17th American Peptide Symposium. International Peptide Symposia are held every 3 or 4 years together with an American, Australian, European, or Japanese Peptide Symposium, as agreed upon by the International Liason Committee of Peptide Societies. The First International Peptide Symposium was held in Kyoto, Japan in 1997. The Third International Peptide Symposium will be held in Israel in 2004.

## American Peptide Symposia

<b>Symposium</b>	<b>Year</b>	<b>Chair(s)</b>	<b>Location</b>
First	1968	Saul Lande <i>Yale University</i> Boris Weinstein <i>University of Washington-Seattle</i>	Yale University New Haven, CT
Second	1970	F. Merlin Bumpus <i>Cleveland Clinic</i>	Cleveland Clinic Cleveland, OH
Third	1972	Johannes Meienhofer <i>Harvard Medical School</i>	Children's Cancer Research Foundation Boston, MA
Fourth	1975	Roderich Walter <i>University of Illinois</i> <i>Medical Center-Chicago</i>	The Rockefeller University and Barbizon Plaza Hotel New York, NY
Fifth	1977	Murray Goodman <i>University of California-San Diego</i>	University of California-San Diego San Diego, CA
Sixth	1979	Erhard Gross <i>National Institutes of Health</i>	Georgetown University Washington, DC
Seventh	1981	Daniel H. Rich <i>University of Wisconsin-Madison</i>	University of Wisconsin-Madison Madison, WI
Eighth	1983	Victor J. Hruby <i>University of Arizona</i>	University of Arizona Tucson, AZ
Ninth	1985	Kenneth D. Kopple <i>Illinois Institute of Technology</i> Charles M. Deber <i>University of Toronto</i>	University of Toronto Toronto, Ontario, Canada
10th	1987	Garland R. Marshall <i>Washington University</i> <i>School of Medicine, St. Louis</i>	Washington University St. Louis, MO
11th	1989	Jean E. Rivier <i>The Salk Institute for Biological</i> <i>Studies, La Jolla</i>	University of California-San Diego San Diego, CA
12th	1991	John A. Smith <i>Massachusetts General Hospital</i>	Massachusetts Institute of Technology, Cambridge, MA
13th	1993	Robert S. Hodges <i>University of Alberta-Edmonton</i>	Edmonton Convention Center Edmonton, Alberta, Canada
14th	1995	Pravin T.P. Kaumaya <i>The Ohio State University</i>	The Ohio State University Columbus, OH
15th	1997	James P. Tam <i>Vanderbilt University</i>	Nashville Convention Center Nashville, TN
16th	1999	George Barany <i>University of Minnesota</i> Gregg B. Fields <i>Florida Atalantic University</i>	Minneapolis Convention Center Minneapolis, MN
17th	2001	Richard A. Houghten <i>Torrey Pines Institute for Molecular</i> <i>Studies</i> Michal Lebl <i>Spyder Instruments and Illumina, Inc.</i>	Town and Country Resort Hotel San Diego, CA
18th	2003	Tomi K. Sawyer <i>ARIAD Pharmaceuticals</i>	Massachusetts

## International Peptide Symposia

Symposium	Year	Chair(s)	Location
First	1997	Yasutsugu Shimonishi <i>Osaka University</i>	Kyoto Kaikan Hall & Kyoto International Exhibition Hall Kyoto, Japan
Second	2001	Richard A. Houghten <i>Torrey Pines Institute for Molecular Studies</i> Michal Lebl <i>Spyder Instruments and Illumina, Inc.</i>	Town and Country Resort Hotel San Diego, CA, USA

## **The Merrifield Award**

**(previously the Alan E. Pierce Award)**

Endowed by Rao Makineni (1997)

Sponsored by the Pierce Chemical Company (1977–1995)

### **Garland R. Marshall**



The Bruce Merrifield Award for outstanding career achievements in peptide research was presented by the American Peptide Society to Garland R Marshall.

Garland R. Marshall is currently Professor of Biochemistry and Molecular Biophysics and of Biomedical Engineering and a member of the Center for Computational Biology at Washington University Medical School in St. Louis, Missouri. He was born in San Angelo, Texas in 1940; graduated from Rusk High School (Rusk, Texas) in 1958; and the California Institute of Technology with a B.S. in biology in 1962. He received his Ph.D. in 1966 from the Rockefeller University and was immediately re-

cruited to a faculty position at Washington University Medical School where he has remained, rising to Professorial rank in 1976.

Prof. Marshall has been a significant factor in the development of two important technologies that have revolutionized the practice of biological sciences. First was the development of solid-phase synthesis starting as the first graduate student in the laboratory of R. Bruce Merrifield, Nobel Laureate, during the initial development of peptide synthesis using a polymeric support. His second scientific area of significant impact was the development of molecular modeling and associated computer graphics approaches to three-dimensional structure-activity studies and the design of novel therapeutics. Starting in 1967 at Washington University, Marshall and his colleagues developed algorithms that allowed analysis of three-dimensional structures of sets of molecules active at the same receptor. From these analyses, predictive models were obtained which could be used to guide the synthesis of novel compounds as potential new drugs. In 1979, Marshall founded a company, Tripos (Nasdaq, TRPS), that further developed and marketed software in this area.

His scientific contributions to specific areas have also been significant. Marshall first described a peptide inhibitor of the angiotensin II, a hormone involved in hypertension. He has led the exploration of peptidomimetics and the use of chimeric amino acids in determining the receptor-bound conformation of peptides. Marshall pioneered the development of HIV protease inhibitors for the treatment of AIDS; the first crystal structure of HIV protease complexed with an inhibitor utilized the inhibitor MVT-101 from the Marshall lab. He has also shown through molecular simulations the dynamically nature of the helical conformation of peptides. Most recently, Marshall has experimentally determined the conformation of a peptide ligand when bound to a G-protein coupled receptor. Exploration of the molecular interaction between rhodopsin and its G-protein, transducin, and the mechanism of signal transduction is a current

focus of his research. In the last few years, modeling of metals in biological systems has also become a research objective. To compliment this interest, Prof. Marshall founded a second company, MetaPhore Pharmaceuticals, in 1995 to develop novel ligands for metals through combinatorial chemistry for therapeutic applications. An enzyme mimetic of superoxide dismutase developed by MetaPhore entered clinical trials the first quarter of 2001.

**2001 Garland R. Marshall, Washington University Medical School**

- 1999 Daniel H. Rich, University of Wisconsin-Madison
- 1997 Shumpei Sakakibara, Peptide Institute, Inc.
- 1995 John M. Stewart, University of Colorado-Denver
- 1993 Victor J. Hruby, University of Arizona
- 1991 Daniel F. Veber, Merck Sharp & Dohme
- 1989 Murray Goodman, University of California-San Diego
- 1987 Choh Hao Li, University of California-San Francisco
- 1985 Robert Schwyzer, Swiss Federal Institute of Technology
- 1983 Ralph F. Hirschmann, Merck Sharp & Dohme
- 1981 Klaus Hofmann, University of Pittsburgh, School of Medicine
- 1979 Bruce Merrifield, The Rockefeller University
- 1977 Miklos Bodanszky, Case Western Reserve University

## Peptide Society Travel Grants

<b>Name</b>	<b>Institution</b>	<b>Mentor</b>
Richard S. Agnes	University of Arizona, Tucson	Victor J. Hruby
Shawn I. Ahmed	Creighton University, Omaha	Sandor Lovas
Isabel M.D. Alves	University of Arizona, Tucson	Victor J. Hruby
Enrique Arevalo	College of Staten Island, New York	Fred Naider
Christopher J. Armishaw	Institute for Molecular Bioscience, Australia	Paul Alewood
Dorit Avrahami	Weizmann Institute of Science, Israel	Yechiel Shai
Marco A. Bennett	University of Maryland, Baltimore	Jane V. Aldrich
Alberto Bianco	Institut de Biologie Moléculaire Cellulaire, France	Jean-Paul Briand
Zsolt Bozsó	Creighton University, Omaha	Sandor Lovas
Matthias Brewer	University of Wisconsin, Madison	Daniel H. Rich
Maria Portia P. Briones	Kyushu Institute of Technology, Japan	Kouji Okamoto
Alexandre Brkovic	INRS - Institut Armand-Frappier, Canada	Alain Fournier
Florence M. Brunel	University of Louisville	Arno F. Spatola
Matthew G. Bursavich	University of Wisconsin, Madison	Daniel H. Rich
Gabriel H.H. Chan	The Chinese University of Hong Kong	Ronald R. Fiscus
Yuxin Chen	University of Alberta, Canada	Robert S. Hodges
Alexey N. Chulin	Shemyakin-Ovchinnikov Institute of Bioorganic Chemistry, Russia	Igor Rodionov
Predrag Cudic	University of Pennsylvania, Philadelphia	Dewey McCafferty
Naveen K. Dakappagari	The Ohio State University, Columbus	Pravin T.P. Kaumaya
Armida Difenza	Universita' di Salerno, Italy	Paolo Rovero
Fa-Xiang Ding	College of Staten Island, New York	Fred Naider
Khee Dong Eom	Vanderbilt University, Nashville	James P. Tam
Angels Estiarte	University of Wisconsin, Madison	Daniel H. Rich
Michelle J. Farquhar	University of Wolverhampton, UK	John Howl
Marcos Antonio Fázio	Universidade Federal de Sao Paulo, Brazil	Antonio Miranda
Gil Fridkin	The Hebrew University of Jerusalem, Israel	Chaim Gilon
Yanwen Fu	Louisiana State University, Baton Rouge	Robert P. Hammer
Juliana A. Gill	University of Delaware, Newark	Joel P. Schneider
José Giraldeś	Louisiana State University, Baton Rouge	Mark L. McLaughlin
Jennifer L. Gironlund	University of Pennsylvania, Philadelphia	Dewey McCafferty
Xuyuan Gu	University of Arizona, Tucson	Victor J. Hruby
Tatiana Gudasheva	Institute of Pharmacology RAMS, Russia	
Sibylle Gurner	Institute of Organic Chemistry and Biochemistry TUM, Germany	Horst Kessler
Lars G.J. Hammarstrom	Louisiana State University, Baton Rouge	Mark L. McLaughlin
Elana Hariton-Gasal	The Hebrew University of Jerusalem, Israel	Chaim Gilon
Bengt Erik Haug	University of Tromso, Norway	John S. Svendsen
Shu He	University of Pennsylvania, Philadelphia	Dewey McCafferty
Roseanne M. Hofmann	Rockefeller University, New York	Tom Muir
Koen Iterbeke	Free University of Brussels, Belgium	D. Tourwé
Malcolm J. Kavarana	University of Arizona, Tucson	Victor J. Hruby
Sanjay K. Khare	College of Staten Island, New York	Fred Naider
Ekaterina F. Kolessanova	Institute of Biomedical Chemistry RAMS, Russia	

Goran Kragol Zoltan Kupihar Darin L. Lee Inta Liepina	The Wistar Institute, Philadelphia University of Szeged, Hungary University of Colorado, Denver Latvian Institute of Organic Synthesis, Latvia	Laszlo Otvos Botond Penke Robert S. Hodges
Rong-Quiang Liu Elsa Locardi	University of Minnesota, Minneapolis Institute of Organic Chemistry and Biochemistry TUM, Germany	George Barany Horst Kessler
Leo Solomon Lucas Jan Mařík	Eastern Michigan University, Ypsilanti Academy of Sciences of the Czech Republic	Deborah L. Heyl-Clegg Jan Hlaváček
Marc N. Mathieu Alessandro Moretto Umut Oguz Michael M. Palian Anthony W. Partridge Kshitij A. Patkar Jan A. Piron Chadler T. Pool Christopher W. Reid Maja Roščič Katri Rosenthal-Aizman Barbara Saccà	Howard Florey Institute, Australia University of Padova, Italy Louisiana State University, Baton Rouge University of Arizona, Tucson University of Toronto, Canada University of Maryland, Baltimore Free University of Brussels, Belgium Vanderbilt University, Nashville University of Waterloo, Canada Ruder Bošković Institute, Croatia Stockholm University, Sweden Max-Planck-Institute of Biochemistry, Germany	Geoffrey W. Tregear Claudio Toniolo Mark L. McLaughlin Robin L. Polt Charles M. Deber Jane V. Aldrich D. Tourwé James P. Tam Gilles Lajoie Štefica Horvat Anders Undén Luis Moroder
Kristen E. Sadler Christy A. Sasiela Martin J. Sellers Simon K. Shannon Ying Sun Hiroaki Taguchi Yan-Chun Tang Xuejun Tang Alex G. Therian Georgina G. Tonarelli	Vanderbilt University, Nashville University of Maryland, Baltimore UMIST, United Kingdom University of Minnesota, Minneapolis Peking Union Medical College, China University of Texas, Houston University of Toronto, Canada University of Arizona, Tucson University of Toronto, Canada Universidad Nacional Del Litoral Argentina	James P. Tam Jane V. Aldrich P.J. Heggs George Barany Guishen Lu Sudhir Paul Charles M. Deber Victor J. Hruby Charles M. Deber
Judit Tulla David M. Vogel Ilze Vosekalna	University of Minnesota, Minneapolis University of Louisville Latvian Institute of Organic Synthesis Latvia	George Barany Arno F. Spatola
Wei Wang Andrzej M. Wilczynski Chiyi Xiong Quingchai Xu Christine R. Xu Dror Yahalom Natalya I. Zaitseva Zhanna V. Zhilina	University of Arizona, Tucson University of Florida, Gainesville University of Arizona, Tucson University of Missouri - Kansas City University of Kansas, Lawrence Harvard Medical School, Boston Institute of Pharmacology RAMS, Russia University of Arizona, Tucson	Victor J. Hruby Carrie Haskell-Luevano Victor J. Hruby William Gutheil Teruna J. Siahaan Michael Chorev Tatiana A. Gudasheva Victor J. Hruby

## **The Bruce W. Erickson Young Investigator's Awards**

The Bruce W. Erickson Young Investigator's Awards were supported by the American Peptide Society.

### **First Place**

**Anja Johansson**, Uppsala University

### **Second Place**

**Mathias Brewer**, University of Wisconsin  
**Wei Wang**, University of Arizona

### **Third Place**

**Jung Mo Ahn**, University of Arizona  
**Matthew Bursavich**, University of Wisconsin  
**M. Angels Estiarte**, University of Wisconsin  
**Alex Therien**, University of Toronto

### **Honorable Mention**

**Jasper Brask**, Technical University of Denmark  
**Bret Beyer**, University of Florida  
**Naveen Dakappagari**, Ohio State University  
**Carol Fowler**, University of Michigan  
**Roman Melnyk**, Hospital for Sick Children, Toronto  
**Chiyi Xiong**, University of Arizona



## Abbreviations

2-Nal	3-(2-naphthyl)alanine	AMCA	7-amino-4-methyl-
3-Pal	3-(3-pyridinyl)alanine		coumarin-3-acetic acid
Abc	4'-aminomethyl-2,2'-	Amn	8-(aminomethyl)naphth-
	bipyridine-4-carboxylic		2-oic acid
	acid	AMPA	<i>o</i> -aminomethylphenyl-
Abh	azabicyclo[2.2.1]heptane-		acetic acid
	2-carboxylic acid	ANS	8-anilino-1-naphthalene-
Abl	Abelson kinase		sulfonic acid
Abu	$\alpha$ -aminobutyric acid	Aoc	8-aminooctanoic acid
Abu	$\alpha$ -amino-n-butyric acid	APB	(4-amino)phenylazo-
Abz	2-amino-benzoic acid		benzoic acid
Abz	2-aminobenzoyl	APC	antigen presenting cell
AC	adenyl cyclase	Apn	5-aminopentanoic acid
Aca	adamantanecarboxyl	Arg-al	argininal
ACHPA	4-amino-5-cyclohexyl-	Arg-ol	argininol
	3-hydroxypentanoic	ATP	adenosine triphosphate
	acid	AUC	area under the curve
Acm	acetamidomethyl	Aun	11-aminoundecanoic
Adc	10-aminodecanoic acid		acid
Ado	12-aminododecanoic acid	Ava	5-aminovaleric acid
AEDANS	5-[(2-aminoethyl)amino]-	AVP	Arg8-vasopressin
	naphthalene-1-sulfonic	BAL	backbone amide linker
	acid	BAPG	<i>N,N</i> -bis(3-aminopropyl)-
			glycine
AEDI	aminoethyldithio-2-		
	isobutyric acid	BBB	blood-brain barrier
AFM	atomic force microscopy	Bes	<i>N,N</i> -bis[2-hydroxyethyl]-
Ahd	2-aminohexadecanoic		2-aminoethanesulfonic
	acid		acid
Ahp	2-aminoheptanoic acid	BHA	benzhydramine
AHPPA	4-amino-3-hydroxy-5-	Bhoc	benzhydrioxycarbonyl
	phenylpentanoic acid	Bicine	<i>N,N</i> -bis[2-hydroxyethyl]-
Ahx	6-aminohexanoic acid		glycine
Aib	$\alpha$ -aminoisobutyric acid	Bip	biphenylalanine,
AIBN	2,2'-azobisisobutyro-		4-phenyl-phenylalanine
	nitrile	BK	bradykinin
AII	angiotensin II	BMAP	bovine myeloid
Al	allyl		antimicrobial peptide
Alloc	allyloxycarbonyl	BME	$\beta$ -mercaptoethanol
AM	alveolar macrophage	Bn	benzyl
Amb	4-(aminomethyl)benzoic	Boc	<i>tert</i> -butyloxycarbonyl
	acid	Boc, <i>t</i> Boc	<i>t</i> -butyloxycarbonyl
AMBER	assisted model building	BOC <sub>2</sub> O	di- <i>tert</i> -butyl dicarbonate
	and energy refinement	Boc-ON	2- <i>tert</i> -butyloxy-carbonyl-
AMC	aminomethylcoumaride		amino-2-phenylaceto-
Amc	4-(aminomethyl)cyclo-		nitrile
	hexanecarboxylic acid	Bom	benzyloxymethyl

## Abbreviations

BOP	(benzotriazol-1-yloxy)- tris(dimethylamino)- phosphonium hexafluoro- phosphate	Dde	1-(4,4-dimethyl-2,6-dioxo- cyclohexylidene)ethyl
BOP-Cl	N,N'-bis(2-oxo-3-oxa- zolidinyl)phosphonic chloride	DDQ	2,3-dichloro-5,6-dicyano- 1,4-benzoquinone
Bpa	<i>p</i> -benzoylphenylalanine	Ddz	2-(3,5-dimethoxyphenyl)- propyl[2]oxycarbonyl
BPTI	bovine pancreatic trypsin inhibitor	DEA	diethylamine
Bpy	2,2'-bipyridine	Deg	diethylglycine
But, <i>t</i> Bu	<i>t</i> -butyl	DHFR	dihydrofolate reductase
Bz	benzoyl	DHP	3,4-dihydro-2 <i>H</i> -pyran
Bzl	benzyl	DIAD	diisopropyl azodi- carboxylate
CAMM	computer assisted molecu- lar modeling	Dibal-H	diisobutylaluminium hydride
Cba	2-amino-4-cyanobutanoic acid	DIC	diisopropylcarbodiimide
Cbz, Z	benzyloxycarbonyl	DIEA	<i>N,N</i> -diisopropylethyl- amine
CCK	cholecystokinin	DIPCDI	<i>N,N'</i> -diisopropylcarbo- diimide
CD	circular dichroism	DMA	<i>N,N</i> -dimethylacetamide
CDI	<i>N,N'</i> -carbonyldiimidazole	DMAP	4-(dimethylamino)- pyridine
CF	5(6)-carboxyfluorescein	DME	dimethoxyethane, glyme
CFU	colony forming units	DMER-Plot	difference minimum energy Ramachandran plot
Cha	cyclohexylalanine	DMF	<i>N,N</i> -dimethylformamide
CHA	cyclohexylamine	Dmob	2,4-dimethoxybenzyl
CHAPS	3-[(3-cholamidopropyl)- dimethyl-ammonio]-1- propanesulfonate	DMS	dimethyl sulfide
cHex	cyclohexyl	DMSO	dimethyl sulfoxide
Chg	cyclohexylglycine	Dnp	2,4-dinitrophenyl
Clt	2-chlorotriyl	DOPC	dioleoyl-DL-3-phospha- tidylcholine
Cl-Z	2-chlorobenzyloxy- carbonyl	DPDPB	[(1,4-di-[3'-(2'-pyridyl- dithio)propionamido]- butane
Cpa	4-chlorophenylalanine	Dpg	di- <i>n</i> -propylglycine
Cpg	cyclopentylglycine	Dpm	diphenylmethyl
CRF	corticotropin releasing factor	DPPA	diphenylphosphoryl azide
CTL	cytotoxic T-lymphocyte	DTT	dithiothreitol
Dab	2,4-diaminobutyric acid	DVB	divinylbenzene
Dap	2,3-diaminopropionic acid	EAE	experimental allergic encephalomyelitis
DBU	1,8-diazabicyclo[5.4.0]- undec-7-ene	EBP	erythropoietin binding protein
Dbu	2,4-diaminobutyric acid	EBV	Epstein-Barr-virus
DCC	<i>N,N</i> -dicyclohexylcarbo- dimide	ECD	extracellular domain
DCHA	dicyclohexylamine	ED <sub>50</sub>	median effective dose
DCM	dichloromethane		

## Abbreviations

EDC	1-(3-dimethylamino-propyl)-3-ethyl carbodiimide hydrochloride	GS	gramicidin S
EDT	1,2-ethanedithiol	GSH	reduced glutathione
EDTA	ethylenediaminetetraacetic acid	GSSG	oxidized glutathione
EEDQ	2-ethoxy-1-ethoxycarbonyl-1,2-dihydroquinoline	GST	glutathione S-transferase
EGF	epidermal growth factor	HATU	<i>N</i> -[(dimethylamino)-1 <i>H</i> -1,2,3-triazolo[4,5- <i>bi</i> -pyridin-1-yl-methylene] <i>N</i> -methylmethanaminium hexafluorophosphate <i>N</i> -oxide
EGFR	EGF receptor	HBTU	2-(1 <i>H</i> -benzotriazol-1-yl)-1,1,3,3-tetramethyluronium hexafluorophosphate
EGS	ethylene glycol	HBV	hepatitis B virus
ELISA	enzyme-linked immunosorbent assay	HCV	hepatitis C virus
EMP	erythropoietin mimetic protein	HDV	hepatitis delta virus
EPO	erythropoietin	Heppso	<i>N</i> -[2-hydroxyethyl]-piperazine- <i>N'</i> -[2-hydroxypropane]sulfonic acid
ES-MS	electrospray mass spectrometry	HFIP	hexafluoroisopropanol
ESR	electron spin resonance	HG	human gastrin
Et <sub>2</sub> O	diethyl ether	HIMBA	4-hydroxymethylbenzoic acid
ET-I	endothelin-I	HIMPA	4-hydroxymethylphenoxyacetic acid
FAB-MS	fast atom bombardment mass spectrometry	HIV	human immunodeficiency virus
FACS	fluorescence-activated cell sorting	HLA	human leukocyte antigen
FcεRI	IgE-receptor	HMBA	4-hydroxymethylbenzoic acid
FITC	fluorescein isothiocyanate	HMPA	hexamethylphosphoramide
Fm	9-fluorenylmethyl	HMPB	4-(4-hydroxy-3-methoxyphenoxy)-butanoic acid
fMLP	formyl-Met-Leu-Phe	HOAt	1-hydroxy-7-azabenzotriazole
Fmoc	9-fluorenylmethoxycarbonyl	HOBt	1-hydroxybenzotriazole
For	formyl	HONp	<i>p</i> -nitrophenol
FTIR	Fourier transform infrared	HOSu	<i>N</i> -hydroxysuccinimide
GdnHCl	guanidinium hydrochloride	HPLC	high performance liquid chromatography
GFC	gel filtration chromatography	HPV	human papilloma virus
Gla	γ-carboxyglutamic acid	Hse	homoserine
GlcNAc	<i>N</i> -acetylglactosamine	HTLV	human T cell leukemia virus
GMO	glycerol monooleate	Htyr	homotyrosine
GPCR	G-protein-coupled receptor	Hyp	hydroxyproline
GpIIb/IIIa	glycoprotein IIb/IIIa	i.v.	intravenous
Grb2	growth factor receptor-bound protein 2		
GRF	growth hormone releasing factor		

## Abbreviations

IAPP	islet amyloid polypeptide	MIF	macrophage migration inhibitory factor
IC <sub>50</sub>	50% inhibition concentration	MMA	<i>N</i> -methylmercapto-acetamide
IFN	interferon	MMP	matrix metalloproteinase
iNOS	inducible nitric oxide synthetase	Mmt	4-methoxytrityl
Inp	isonipecotic acid	MS	mass spectrometry
IP3	inositol trisphosphate	MsCl	methanesulfonyl chloride
IPE	isopropyl ether	MSH	melanocyte stimulating hormone (melanotropin)
ITC	isothermal titration calorimetry	MSNT	2,4,6-mesitylene-sulfonyl-3-nitro-1,2,4-triazolide
KHMDS	potassium hexamethyldisilazane	Mtr	2,3,6-trimethyl-4-methoxy-benzenesulfonyl
LAH	lithium aluminum hydride	Mts	mesitylene-2-sulfonyl
LDA	lithium diisopropylamide	Mtt	4-methyltrityl
LDL	low density lipoprotein	NADPH	nicotinamide adenine dinucleotide phosphate, reduced form
LHR	lutropin receptor	NECA	5'- <i>N</i> -ethylcarboxamido-adenosine
LiHMDS	lithium bis(trimethylsilyl)-amide/lithium hexamethyl disilazide	NEM	<i>N</i> -ethylmorpholine; <i>N</i> -ethylmaleimide
LNC	lymph node cells	Nic	nicotinyl
LPS	lipopolysaccharide	Nip	nipecotic acid
LUV	large unilamellar vesicle	NIR-FT	near-infrared Fourier-transform
mAb	monoclonal antibody	NK-1	neurokinin-1 receptor (substance P receptor)
MALDI	matrix-assisted laser desorption/ionization	NKA	neurokinin A
MALDI-TOF	MALDI time-of-flight	NKB	neurokinin B
MAP	multiple antigenic peptide	NMM	<i>N</i> -methylmorpholine
Mbc	4'-methyl-2,2'-bipyridine-4-carboxylic acid	NMMO	<i>N</i> -methylmorpholine- <i>N</i> -oxide
MBHA	<i>p</i> -methylbenzhydryl-amine	NMP	<i>N</i> -methylpyrrolidone
MBP	myelin basic protein	NMR	nuclear magnetic resonance
MbzI	4-methoxybenzyl	NO	nitric oxide
mCPBA	3-chloroperbenzoic acid	nOct	<i>n</i> -octanoyl
MCR	melanocortin receptor	NOE	nuclear Overhauser effect
MD	molecular dynamics	NOESY	nuclear Overhauser enhanced spectroscopy
MDP	muramyl dipeptide	Nps	2-nitrophenylsulfonyl
MeCN	acetonitrile	NPY	neuropeptide Y
MeIm	methylimidazole	Npys	5-nitro-2-pyridinesulfonyl
MeOBzl	<i>p</i> -methoxybenzyl	NSG	<i>N</i> -substituted glycine
MeOSuc	methoxysuccinyl	NTA	nitrilo-triacetic acid
Mes	2-[ <i>N</i> -morpholino]ethane-sulfonic acid	Nva	norvaline
MHC	major histocompatibility complex		
MIC	minimum inhibitory concentration		

## Abbreviations

O	defined sequence position in peptide libraries	PI	phosphatidylinositol
OChx	cyclohexyl ester	Pip	pipecolic acid
OHA	octahydroacridine	PLC	phospholipase C
OHx	hexyl ester	PLN	phospholamban
Oic	octahydroindolyl-2- carboxylic acid	PLP	proteolipid protein
ONp	4-nitrophenyl ester	PM	plasma membranes
OPCP	pentachlorophenyl ester	Pmc	2,2,5,7,8-pentamethyl- chroman-6-sulfonyl
Opfp	pentafluorophenyl ester	pMeBzl	<i>p</i> -methylbenzyl
OPhe	phenyl ester	Pmp	4-phosphonomethyl- phenylalanine
OPT	oligopeptide transport	pNA	<i>p</i> -nitroaniline
Orn	ornithine	PPCE	post-proline cleaving enzyme
Osu	<i>N</i> -hydroxysuccinimide ester	PS	polystyrene
PAC	peptide acid linker, <i>p</i> -alkoxybenzyl ester; phenacyl	PS-SCL	positional scanning SCL
Pac	phenylacetyl	PTH	parathyroid hormone
PAL	peptide amide linker, 5-(4-Fmoc aminomethyl- 3,5-dimethoxyphenoxy)- valeric acid	PTHrP	parathyroid hormone related protein
Pam	palmitoyl	PTK	protein tyrosine kinase
PAM	phenylacetamidomethyl	PTP	protein tyrosine phosphatase
PBMC	peripheral blood mononuclear cells	PTR	peptide transport
PBS	phosphate-buffered saline	pTyr	phosphotyrosine
PC	phosphatidylcholine	PyAOP	(7-azabenzotriazol-1- yloxy)tris(pyrrolidino)- phosphonium
PCC	pyridinium chlorochromate	PyBOP	hexafluorophosphate (benzotriazol-1-yloxy)- tris(pyrrolidino)phospho- nium hexafluoro- phosphate
PCR	polymerase chain reaction	QSAR	quantitative structure- activity relationships
Pd/C	palladium on carbon	RGD	Arg-Gly-Asp
PDC	pyridinium dichromate	RMSD	root mean square deviation
PDI	protein disulfide isomerase	RNA	ribonucleic acid
PEG	polyethylene glycol	RP-HPLC	reversed-phase HPLC
PEGA	polyethylene glycol acrylamide copolymer	rt/RT/r.t.	room temperature
PEG-PS	polyethylene glycol- polystyrene graft polymer	Sar	sarcosine
Pen	penicillamine	SAR	structure activity relationships
Pfb	2,2,4,6,7-pentamethyl- dihydrobenzofuran-5- sulfonyl	SCLC	small cell lung cancer
Pfp	pentafluorophenyl	SCLs	synthetic combinatorial libraries
pGlu	pyroglutarnic acid	SD	standard deviation
Phg	phenylglycine	SP	substance P

## Abbreviations

SPPS	solid-phase peptide synthesis	Tic	1,2,3,4-tetrahydroisoquinoline-3-carboxylic acid
SPR	surface plasmon resonance	TIS	triisopropyl silane
Sta	statine, 2-amino-3-hydroxy-6-methyl-heptanoic acid	TLC	thin layer chromatography
StBu	<i>t</i> -butylthio	Tle	<i>tert</i> -leucine/ <i>C-tert</i> -butyl glycine
Suc	succinyl	TMH	transmembrane helix
SUV	small unilamellar vesicle	Tmob	2,4,6-trimethoxybenzyl
TASP	template-assembled synthetic protein(s)	TMP	2,4,6-trimethylpyridine
TBA	<i>t</i> -butylammonium salt	TMS-Cl	trimethylsilyl chloride
TBAF	tetra- <i>n</i> -butylammonium fluoride	TMSOTf	trimethylsilyloxytrifluoromethanesulfonate
TBDMS	<i>tert</i> -butyldimethylsilyl	TOAC	2,2,6,6-tetramethylpiperidine-1-oxyl-4-amino-4-carboxylic acid
TBTU	2-(1 <i>H</i> -benzotriazol-yl)-1,1,3,3-tetramethyluronium tetrafluoroborate	TOCSY	total correlation spectroscopy
TCEP	tris-(2-carboxyethyl)-phosphine	Tos	4-toluenesulfonyl
TEA	triethylamine	TRH	thyrotropin-releasing hormone
TEMP	2,3,5,6-tetramethylpyridine	Tris	tris(hydroxymethyl)-aminomethane
TEOF	triethylorthoformate	Trt	trityl (triphenylmethyl)
TES	triethylsilane	TsOH	<i>p</i> -toluenesulfonic acid
TFA	trifluoroacetic acid	TSTU	<i>O</i> -( <i>N</i> -succinimidyl)-1,1,3,3-tetramethyluronium tetrafluoroborate
TFE	2,2,2-trifluoroethanol		
TFFH	tetramethylfluoroformamidinium hexafluorophosphate	Tyr(NO <sub>2</sub> )	3-nitrotyrosine
TFMSA	trifluoromethanesulfonic acid	X	randomized sequence position in peptide libraries
THF	tetrahydrofuran	XAL	5-(9-aminoxanthen-2-oxy)valeric acid
Thi	3-(2-thienyl)alanine	Xan	9 <i>H</i> -xanthen-9-yl
THP	triple-helical peptide	Xan	xanthyl
Thz	thiazolidine-4-carboxylic acid, thioproline	Z, Cbz	benzyloxycarbonyl
		β-CD	β-cyclodextrin

## Contents

Preface	<a href="#">ix</a>
People Behind the Symposium	<a href="#">xii</a>
Symposium Sponsors and Exhibitors	<a href="#">xiv</a>
American Peptide Society	<a href="#">xvi</a>
International Liaison Committee of Peptide Societies	<a href="#">xvi</a>
American and International Peptide Symposia	<a href="#">xvii</a>
The 2001 Merrifield Award Winner: Garland R. Marshall	<a href="#">xix</a>
The Merrifield Award Recipients	<a href="#">xx</a>
Peptide Society Travel Grants	<a href="#">xxi</a>
The Bruce W. Erickson Young Investigator's Awards	<a href="#">xxiii</a>
Abbreviations	<a href="#">xxv</a>

### **The 2001 Merrifield Award/Rao Makineni Lecture**

From Merrifield to MetaPhore: A Random Walk with Serendipity <i>Garland R. Marshall</i>	<a href="#">3</a>
Genomics: From Microbes to Man <i>J. Craig Venter</i>	<a href="#">13</a>

### **Synthetic Methodologies, Solid Phase Synthesis, Solid Phase Organic Synthesis, Combinatorial Techniques**

Fluorous Methods for Synthesis and Separation of Organic Molecules: From Separating Mixtures to Making Mixtures <i>Dennis P. Curran</i>	<a href="#">17</a>
Synthesis of $\beta$ and $\gamma$ -Substituted Prolines for Conformation-Activity Relationship Studies of the $\alpha$ -MSH Analogue MT-II <i>Chaozhong Cai, Wei Wang, Chiyi Xiong, Vadim A. Soloshonok, Minying Cai and Victor J. Hruby</i>	<a href="#">20</a>
The General Asymmetric Synthesis of <i>Syn</i> - and <i>Anti</i> - $\beta$ -substituted Cysteine and Serine Derivatives <i>Chiyi Xiong, Wei Wang and Victor J. Hruby</i>	<a href="#">22</a>
The Novel Asymmetric Synthesis of $\beta$ -Functionalized Phenylalanine Derivatives <i>Chiyi Xiong, Wei Wang, Chaozhong Cai and Victor J. Hruby</i>	<a href="#">24</a>
An Efficient Method for Large-Scale Synthesis of Stereochemically Defined and Conformationally Constrained $\beta$ -Substituted or $\alpha,\beta$ -Disubstituted Amino Acids <i>Xuejun Tang, Vadim A. Soloshonok and Victor J. Hruby</i>	<a href="#">26</a>

## Contents

Synthesis of Amino Acids with Novel Biophysical Properties <i>Zhanna Zhilina, Isabel Alves, Scott Cowell, Xuejun Tang, Malcolm Kavarana and Victor J. Hruby</i>	<a href="#">28</a>
Two Novel and Efficient Approaches to Synthesis of Enantiopure Dipeptide $\beta$ -Turn Mimetics: Indolizidinone Amino Acids <i>Wei Wang, Chiyi Xiong, Jiangqian Yang and Victor J. Hruby</i>	<a href="#">30</a>
Enantioselective Synthesis of $\beta^2$ -Homotryptophan for a Somatostatin Mimetic <i>Peter Micuch and Dieter Seebach</i>	<a href="#">32</a>
Ethyl Nitroacetate as a Useful Synthon for the Synthesis of Orthogonally Protected, Poly-Functional $C^{\alpha,\alpha}$ -Disubstituted Amino Acids <i>Yanwen Fu, Lars G. J. Hammarström, Tod J. Miller, Mark L. McLaughlin and Robert P. Hammer</i>	<a href="#">34</a>
Synthesis of $\beta$ -Benzo[b]thiophene Dehydroamino Acids by Suzuki Palladium Catalyzed Cross Coupling <i>Paula M. T. Ferreira, Hernâni L. S. Maia, Luís S. Monteiro, Maria-João R. P. Queiroz and Natália Silva</i>	<a href="#">36</a>
Efficient Diastereoselective Synthesis of a Hydroxyethylene Dipeptide Isostere <i>Satendra Singh, Pius Baur and Michael W. Pennington</i>	<a href="#">38</a>
One-Pot Conversion of Azides to Protected Guanidines <i>via</i> the Staudinger Reduction; Synthesis and Utilization of the Phe-Arg Hydroxyethylene Dipeptide Isostere <i>Matthias Brewer and Daniel H. Rich</i>	<a href="#">40</a>
The Synthesis of Tyrosine Mimetics <i>via</i> a Novel N(1)-C(4) Beta-Lactam Cleavage Reaction <i>Larry A. Cabell, David R. Coleman, IV and John S. McMurray</i>	<a href="#">42</a>
Michael Additions to Dehydroalanine Derivatives <i>Luís S. Monteiro, Paula M.T. Ferreira, Hernâni L.S. Maia and Joana Sacramento</i>	<a href="#">44</a>
Facile Synthesis of a Constrained Dipeptide Unit (DPU) for Use as a $\beta$ -Sheet Promoter <i>Umut Oğuz, Ted J. Gauthier and Mark L. McLaughlin</i>	<a href="#">46</a>
Synthesis of $N^{\alpha}$ -(Fluoren-9-ylmethoxycarbonyl)- $N^{\epsilon}$ -[(7-methoxycoumarin-4-yl)- acetyl]-L-lysine for Use in Solid-Phase Synthesis of Fluorogenic Substrates <i>Navdeep Malkar and Gregg B. Fields</i>	<a href="#">48</a>
Preparation of $\beta$ -Amino- $\alpha$ -mercapto Acids and Amides: Stereocontrolled Syntheses of 2'-Sulfur Analogues of the Taxol C-13 Side Chain, Both <i>syn</i> and <i>anti</i> S-Acetyl-N-benzoyl-3-phenylisocysteine <i>Sang-Hyeup Lee, Juyoung Yoon, Kensuke Nakamura and Yoon-Sik Lee</i>	<a href="#">50</a>
New Approach for Preparation of C-Glycoamino Acid Building Blocks <i>Istvan Jablonkai</i>	<a href="#">52</a>
New Quencher Derivatives for Fluorescence Quenching Peptide Assays <i>T. A. Walton, D. J. Dick, D. Hudson, M. K. Johansson, M. H. Lyttle, M. F. Songster and R.M. Cook</i>	<a href="#">54</a>

## Contents

Preparation of (2 <i>S</i> )-2-Amino-3-(2-(2,2,5,7,8-pentamethylchroman-6-sulfonyl)-1 <i>H</i> -indol-3-yl)-propionic acid and Its Incorporation into Antibacterial Lactoferricin Peptides <i>Bengt Erik Haug and John S. Svendsen</i>	56
UniChemo Protection (UCP) <i>Les Miranda and Morten Meldal</i>	58
An Improved Synthesis of Fmoc-Asp(O-3-methylpent-3-yl)-OH, an Aspartate Derivative That Resists Base Induced Aspartimide Formation <i>James G. Boyd and Wen Lin</i>	61
Systematic Investigation of the Aspartimide Problem <i>M. Mergler, F. Dick, B. Sax, P. Weiler and T. Vorherr</i>	63
Ninhydrin as a Reversible Protecting Group of N-Terminal Cysteine <i>Chadler T. Pool, James G. Boyd and James P. Tam</i>	65
Novel Synthesis and Application of a Protected Bicyclic $\alpha$ -Helix-Initiating Heptapeptide Suitable for Segment Condensation Syntheses: Utility of Pentaaminecobalt(III) for Carboxyl Protection <i>John W. Taylor, Prasanna Reddy, Ketel Patel, Tom Dineen and Sumreen Naqvi</i>	67
N <sup>in</sup> -4-Nitrobenzenesulfonyl Tryptophan: A Convenient Preparation of N <sup><math>\alpha</math></sup> -Boc and N <sup><math>\alpha</math></sup> -Fmoc Derivatives <i>Aydar Sabirov and Anita Hong</i>	69
Syntheses of Difficult Hydrophobic Sequences Using 2-(4-Nitrophenyl)sulfonyl-ethoxycarbonyl(Nsc)-N <sup><math>\alpha</math></sup> -(2-hydroxy-4-methoxybenzyl)Ala-OH: (Ala) <sub>10</sub> -Valine, (Ala) <sub>15</sub> -Valine <i>Hyun Jin Lee, Weonu Chweh, Young-Deug Kim, Sang-Sun Lee and Hack-Joo Kim</i>	71
A Highly Efficient Method for Synthesis of Fmoc-Lysine(Mmt)-OH <i>Xiao-He Tong and Anita Hong</i>	73
A New Practical Approach to the Synthesis of Fmoc-L-Cysteine <i>Ming Zhao</i>	75
A Novel Protocol of Solid Phase Peptide Synthesis with 2-(4-Nitrophenyl)sulfonyl-ethoxycarbonyl(Nsc)-Amino Acids <i>Hack-Joo Kim, Chan-Young Ko, Jeong Su Jang and Young-Deug Kim</i>	77
S-Xanthenyl Protected 1-Thiosugars as Building Blocks for Glycopeptide Assembly <i>Robert A. Falconer</i>	79
Late Deprotection Difficulties During SPPS Depend on the Preceding Sequence <i>Phillip W. Banda</i>	81
Towards a Selective Boc Deprotection on Acid Cleavable Resin <i>Florine Cavalier, Valérie Lejeune and Jean Martinez</i>	83
By-Product Formation During SPPS of Linear, Cyclic, and Novel Bicyclic Peptides as AChE Inhibitors <i>Peteris Romanovskis, Terrone L. Rosenberry, Bernadette Cusack and Arno F. Spatola</i>	85

## Contents

Acidic Cleavage of the Side Chain Protecting Groups of Peptides Attached to a Modified Polystyrene Carrier: Synthesis of Peptide Generics <i>Luděk Lepša, Anna Ammerová and Martin Flegel</i>	<a href="#">87</a>
The Use of a Novel Safety Catch Linker for BOC-Based Assembly of Cyclic Peptide Libraries <i>Simon W. Golding, Gregory T. Bourne, Wim D. F. Meutermans, Alun Jones and Mark L. Smythe</i>	<a href="#">89</a>
Diurethanyl 1 <i>H</i> -Benzotriazole-1-carboxamidines as Guanidinyllating Reagents <i>Hans-Jürgen Musiol and Luis Moroder</i>	<a href="#">91</a>
Amino Acid Bromides: A Convenient Choice for Very Difficult Couplings <i>Alma DalPozzo, Roberto Bergonzi, Minghong Ni and Paola Cossettini</i>	<a href="#">93</a>
Synthesis of the Two Isomeric Benzo Derivatives of 1-Hydroxy-7-azabenzotriazole and Preliminary Studies of Their Effectiveness as Coupling Reagents <i>Fernando J. Ferrer and Louis A. Carpino</i>	<a href="#">95</a>
Optimization of Coupling Methods for the Introduction of Mono-Benzyl Phosphate Esters of Fmoc Protected Phosphoamino Acids <i>Peter White</i>	<a href="#">97</a>
HATU-HOAt-CuCl <sub>2</sub> : A Reliable Racemization-Free Segment Coupling System <i>Yasuhiro Nishiyama, Sou Ishizuka and Keisuke Kurita</i>	<a href="#">99</a>
Search for a Safe, Inexpensive and Convenient Amidation Process for Protected Amino Acids and/or Peptides <i>Kripa Srivastava</i>	<a href="#">101</a>
Extending Synthetic Access to Proteins <i>John L. Offer and Philip E. Dawson</i>	<a href="#">103</a>
A New Scaffold for Amide Ligation <i>Chiara Marini, John Offer and Philip E. Dawson</i>	<a href="#">105</a>
Chemical Ligation of Multiple Peptide Fragments Using a New Protection Strategy <i>Matteo Villain, Jean Vizzavona and Hubert Gaertner</i>	<a href="#">107</a>
Synthesis of Oligodeoxynucleotide-Peptide Conjugates Using Hydrazone Chemical Ligation <i>Oleg Melnyk, Nathalie Ollivier, Christophe Olivier, Catherine Gouyette, Tam Huynh-Dinh and Hélène Gras-Masse</i>	<a href="#">109</a>
The Use of a Free Peptide for Preparation of a C-Terminal Building Block for Polypeptide Synthesis in Combination with a Peptide Thioester <i>Saburo Aimoto, Kenta Teruya, Koki Hasegawa, Kenichi Akaji and Toru Kawakami</i>	<a href="#">111</a>
Synthesis of N to C Terminal Cyclic Analogues of $\alpha$ -Conotoxin ImI by Chemoselective Ligation of Unprotected Linear Precursors <i>Christopher J. Armishaw, Julie Dutton, Ron C. Hogg, David J. Adams, David J. Craik and Paul F. Alewood</i>	<a href="#">113</a>
Total Chemical Synthesis of $\kappa$ -Casein Using Native Ligation Methodology <i>Paramjit S. Bansal and Paul F. Alewood</i>	<a href="#">115</a>

## Contents

Fmoc Chemistry Compatible Methods for Thio-Ligation Assembly of Proteins <i>S. Biancalana, D. Hudson, M. F. Songster and S. A. Thompson</i>	<a href="#">117</a>
Simultaneous Lipidation of a Multi-Epitope Peptide Cocktail by Chemoselective Hydrazone Formation <i>Line Bourel-Bonnet, Oleg Melnyk, Frédéric Malingue, Pascal Joly, Dominique Bonnet and Hélène Gras-Masse</i>	<a href="#">119</a>
Privilege Structures: New Strategies for the Synthesis of Cyclic Tetrapeptides <i>Wim D. F. Meutermans, Simon W. Golding, Marc R. Campitelli, Douglas A. Horton, Gregory T. Bourne and Mark L. Smythe</i>	<a href="#">122</a>
Incorporation of a cis-Amide Bond Isostere in the Synthesis of Cyclic Tetrapeptides <i>Gregory T. Bourne, Peter J. Cassidy, Wim D. F. Meutermans, Marc R. Campitelli and Mark L. Smythe</i>	<a href="#">125</a>
Covalent Control of Shape and Folding in Peptides by Ring-Closing Metathesis <i>Rob M. J. Liskamp, John F. Reichwein, Bas Wels, John A.W. Kruijtzter and Cees Versluis</i>	<a href="#">127</a>
New Synthetic Routes to N <sup>Et</sup> Xaa <sup>4</sup> -Cyclosporin Derivatives as Potential Anti-HIV Drugs <i>T. Muamba, F. Hubler, J.-F. Guichou, L. Patiny, T. Rückle, L. Brunner, R. Wenger and M. Mutter</i>	<a href="#">130</a>
Transition Metal Complexes of Linear and Cyclic Pseudopeptides <i>Siegmund Reissmann, Sebastian Künzel, Regina Reissmann, Susanne Nolden, Georg Greiner, Inge Agricola, Dietmar Strehlow, Wolfgang Poppitz, Raiker Witter and Ulrich Sternberg</i>	<a href="#">132</a>
An Efficient Synthesis of Integrin Antagonists cyclo(-RGDfK-), cyclo(-GRGDfK-) and Their Conjugates with MAG3 Chelate <i>Vladimir V. Samukov, Pavel I. Pozdnyakov, Aydar N. Sabirov, Irina M. Bushueva, Paul O. Zamora and Prantika Som</i>	<a href="#">134</a>
Design and Synthesis of Cyclic Peptide Antagonists Intended to Block Coactivator Binding to Steroid Nuclear Receptors <i>Anne-Marie Leduc, Kelli S. Bramlett, Thomas P. Burris and Arno F. Spatola</i>	<a href="#">136</a>
A Novel Design and Synthesis of Bicyclic Peptide Library <i>Ying Sun, Guishen Lu and James P. Tam</i>	<a href="#">138</a>
Strategies for the Synthesis of Cyclic Peptides <i>Ashok Khatri, Nicholas P. Ambulos, Steven A. Kates, Katalin F. Medzihradzsky, George Ösapay, Henriette Remmer and Arpad Somogyi</i>	<a href="#">140</a>
Vinyl Sulfide Cyclized Analogues of Angiotensin II with High Affinity to the AT <sub>1</sub> -Receptor <i>Petra Johannesson, Gunnar Lindeberg, Gregory V. Nikiforovich, Anja Johansson, Adolf Gogoll, Anders Karlén and Anders Hallberg</i>	<a href="#">142</a>
Strategies for the Synthesis of Novel Head-to-Side Chain Cyclic Peptides: Application to Dynorphin A Analogs <i>Balvinder S. Vig and Jane V. Aldrich</i>	<a href="#">144</a>

## Contents

Study on the Influence of Different Metal Ions on Cyclization of Linear Pentapeptides and Heptapeptide <i>Yun-hua Ye, Mian Liu, Yan-chun Tang and Xiao-hui Jiang</i>	<a href="#">146</a>
Disulfide Bond Formation of a Hydrophobic Peptide by Dimethyl Sulfoxide <i>Jingming Zhang and Lili Guo</i>	<a href="#">148</a>
Stereoselective Synthesis of Transition State Analog Inhibitors of DPP-IV Using 2-Substituted Thiazoles <i>J. Piron and D. Tourwé</i>	<a href="#">150</a>
Original and General Strategy of Dimerization of Bioactive Molecules <i>Florine Cavelier, Matthieu Giraud, Nicole Bernad and Jean Martinez</i>	<a href="#">152</a>
An Efficient Approach for the Synthesis of Salmon Calcitonin Using Oxazolidine Dipeptides <i>Weonu Chweh, Hyun Jin Lee, Young-Deug Kim, Sang Sun Lee and Hack-Joo Kim</i>	<a href="#">155</a>
A Combined Solid-Phase and Solution Strategy for Chemical Synthesis of Human Leptin <i>Yuji Nishiuchi, Tatsuya Inui, Hideki Nishio and Terutoshi Kimura</i>	<a href="#">157</a>
Synthesis of Phosphorylated Polypeptide by the Thioester Method Using a Recombinant Protein <i>Toru Kawakami, Koki Hasegawa, Kenta Teruya, Kenichi Akaji, Masataka Horiuchi, Fuyuhiko Inagaki, Yasuyuki Kurihara, Seiichi Uesugi and Saburo Aimoto</i>	<a href="#">160</a>
The Synthesis of the K-Ras-Derived Peptide <i>Xiao-He Tong, Xiaowei Zhang, Lei Liu and Anita Hong</i>	<a href="#">162</a>
Synthesis of Phosphopeptides on Solid Phase Using <i>tert</i> -Butyl- <i>H</i> -phosphonate Salts <i>Gábor K. Tóth, András Molnár and Zoltán Kupihár</i>	<a href="#">164</a>
Solid Phase Synthesis of Seleno-Methionine Peptides by tBoc/Bzl and Fmoc/tBu Protection Strategy Suitable for the Crystallographic Phase Determination by <i>Multi-Wavelength Anomalous Diffraction</i> (MAD) <i>Stefan R. K. Hoffmann, Christine A. Deillon and Bernd Gutte</i>	<a href="#">166</a>
Synthesis of a C-Terminal Fluorescein-Labeled 36-mer Peptide <i>Reagan J. Greene, Jonathan M. White, Catherine J. Mader, Ralph A. Picking, J. William Lackey, Joel B. Erickson and Dennis M. Lambert</i>	<a href="#">168</a>
Expanding Diversity: Modification of Linear and Cyclic Peptides by C-Glycosylation and N-Methylation <i>Florence Brunel, Anne-Marie Leduc, Sujana Singh, Xiaoping Tang, David M. Vogel, K. Grant Taylor and Arno F. Spatola</i>	<a href="#">170</a>
One-Dimensional Spatial Encoding: Split/Mix Synthetic Parallelism with Tag-Free Identification and Assays at the Speed of Light <i>Alan W. Schwabacher and Peter Geissinger</i>	<a href="#">172</a>
Spatial Screening of Lectin Ligands. Cyclic Peptides as Scaffolds for Multivalent Presentation of Carbohydrates <i>Valentin Wittmann and Sonja Seeberger</i>	<a href="#">174</a>

## Contents

Combinatorial Syntheses of Polyhydroxamate Siderophores: Desferrioxamine, Exochelin, Mycobactin, and Aerobactin Libraries <i>Urszula Slomczynska, P. Amruta Reddy, Otto F. Schall, Todd Osiek, Arati Naik, W. Barry Edwards, James Wheatley and Garland R. Marshall</i>	<a href="#">177</a>
Identification of Peptide Ligands for $\alpha 4\beta 1$ Integrin Receptor as Potential Targeting Agents for Non-Hodgkin's Lymphoma <i>Steven I. Park, Renil Manat, Brian Vikstrom, Nail Amro and Kit S. Lam</i>	<a href="#">180</a>
Development of Peptidomimetic Substrates and Inhibitors that Bind to the Peptide Binding Pocket of the Catalytic Site of p60 <sup>c-src</sup> Protein Tyrosine Kinase <i>Jayesh R. Kamath, Ruiwu Liu, Amanda M. Enstrom, Gang Liu and Kit S. Lam</i>	<a href="#">183</a>
Pseudoproline Libraries for Tuning Inhibitors of SH3 Domain Mediated Protein-Protein Interactions <i>Jimena Fernandez-Carneado, Patricia Durieux, Luc Patiny, Yoshiro Tatsu, Daniel Grell, Christian Kardinal, Stephan Feller and Gabriele Tuchscherer</i>	<a href="#">185</a>
Towards a Set of Peptides with Orthogonal HIV Seroreactivity Using Adaptively Coded Peptide Libraries: Decoding by Mass Spectrometry and Immunofluorescent Screening <i>Christian Hoffmann, Dierk Blechschmidt, Ralf Krüger, Michael Karas, Christoph Königs, Ursula Dietrich and Christian Griesinger</i>	<a href="#">187</a>
Mapping of Discontinuous Epitopes on FSH <i>Jerry W. Slootstra, Wouter C. Puijk, Rob H. Meloen and Wim M. M. Schaaper</i>	<a href="#">189</a>
Development of Highly Specific, Membrane Permeable Peptide Blockers of cGMP-Dependent Protein Kinase Utilizing Affinity Selection from Peptide Libraries <i>Werner Tegge, Ronald Frank, Mark S. Taylor, Joseph E. Brayden, Christian K. Nickl and Wolfgang R.G. Dostmann</i>	<a href="#">191</a>
The Integration of Positional Scanning Libraries with Bioinformatics and Proteomics <i>Clemencia Pinilla, Eva Borràs, Roland Martin, Yingdong Zhao and Richard Simon</i>	<a href="#">194</a>
Screening and Synthesis of a Positional Scanning Library Based on the Bowman-Birk Reactive Site Loop <i>Emma M. Watson, Jeffrey D. McBride and Robin J Leatherbarrow</i>	<a href="#">196</a>
A Bicyclic Peptide Template Useful for Solution-Phase Combinatorial Synthesis <i>Qingchai Xu and Frans Borremans</i>	<a href="#">198</a>
Synthesis of Combinatorial Libraries Associated with Constrained $\beta$ -Turn Mimetics <i>James Dattilo, Chris Lum, Stephanie Beigle-Orme, Burt Goodman, Vince Huber, Jeff Keilman, Cheryl Schwenk, Gangadhar Nagula, Nataly Hawthorn, Jennifer Young and Tomáš Vaisar</i>	<a href="#">200</a>

## Contents

Screening and Design of Hybrid Peptide That Binds with Glucose Oxidase <i>Kenji Yokoyama, Toshifumi Sakai, Hideo Ishikawa, Yasutaka Morita and Eiichi Tamiya</i>	<a href="#">202</a>
Combinatorial Synthesis, Screening and Testing of Peptidic RNA-Ligands <i>Michael Baumann, Delf Schmid, Hilmar Bischoff, Christoph Königs, Ursula Dietrich and Christian Griesinger</i>	<a href="#">204</a>
High Throughput Peptide Syntheses Generate Ligands for Proteomic Database <i>Lin Chen, Brian Korenstein, Michael James, Leonid Kvecher and J. Mark Carter</i>	<a href="#">206</a>
MHC Ligand Motifs from Peptide Libraries: The Software EPIPREDICT <i>B. Fleckenstein, G. Jung, K.H. Wiesmueller, F. von der Muelbe, D. Niethammer and J. T. Wessels</i>	<a href="#">208</a>
High-Density Compound Arrays of Combinatorial Chemical Libraries by a New Pen-Directed and Computer-Navigated Plotter Device <i>Stefan R. K. Hoffmann</i>	<a href="#">210</a>
Combining SPOT Synthesis and Native Chemical Ligation to Generate Large Arrays of Small Protein Domains <i>Florian Toepert, Tobias Knaute, Stefan Guffler and Jens Schneider-Mergener</i>	<a href="#">212</a>
Peptides as Drugs: Is There a Market? <i>Albert Loffet</i>	<a href="#">214</a>
Solid-Phase Total Syntheses of Trunkamide A and Kahalalide F, Cyclic Peptides from Marine Origin <i>Fernando Albericio, Josep M. Caba, Àngel López-Macià, Jose C. Jiménez, Marta Carrascal, Laia Solé, Ignacio Rodriguez, Ignacio Manzanares, Miriam Royo and Ernest Giralt</i>	<a href="#">217</a>
Solid Phase Synthesis of Large Cyclic Peptides <i>Katri Rosenthal-Aizman and Anders Undén</i>	<a href="#">220</a>
Solid-Phase Synthesis of Consolidated Ligands Containing an Intramolecular Lactam Bridge: Comparison of Strategies and Tactics <i>Jaya T. Varkey, David Cowburn, Hong Ji and George Barany</i>	<a href="#">222</a>
Backbone Amide Linker (BAL)/Fmoc Synthesis of Peptide Thioester Intermediates Required for Native Chemical Ligation <i>Dominique Lelièvre and George Barany</i>	<a href="#">224</a>
Ampullosporin Analogs: Solid Phase Synthesis, Conformational Studies, and Biological Activities <i>Hoai Huong Nguyen, Diana Imhof, Brigitte Schlegel, Albert Härtl, Matthias Kronen, Udo Gräfe and Siegmund Reissmann</i>	<a href="#">226</a>
Synthesis of Lanthionine-Containing Peptides on Solid Phase via an Orthogonal Protecting Group Strategy <i>M. F. Mohd Mustapa, A. B. Tabor, N. A. L. Chubb and D. Schulz</i>	<a href="#">228</a>
Systematic Solid Phase Synthesis of Linear Pseudooligolysines Containing Multiple Adjacent CH <sub>2</sub> NH Amide Bond Surrogates: Potential Agents for Gene Delivery <i>Gil Fridkin, Tamar Gilon, Abrahm Loyter and Chaim Gilon</i>	<a href="#">230</a>

## Contents

Peptide Transformation and Synthesis of Oligopeptidomimetics <i>Rob M. J. Liskamp, John A. W. Kruijtzer, Lovina J. F. Hofmeyer, Astrid Boeijen, Arwin J. Brouwer and Menno C. F. Monnee</i>	<a href="#">232</a>
A New Strategy for Inverse Solid-Phase Peptide Synthesis <i>Qingchai Xu and William G. Gutheil</i>	<a href="#">234</a>
Optimization of the Chemical Synthesis of Human Ghrelin <i>David B. Flora, Min Liu, Julia A. Drane, Patrick J. Edwards and John P. Mayer</i>	<a href="#">236</a>
Rational Design and Synthesis of a Potent Amide-Linked Cyclic Analogue of MBP87-99 Based on 2D-NMR Studies and Molecular Dynamics <i>Ioanna Daliani, Theodore Tselios, Lesley Probert, Spyros Deraos, Thomas Mavromoustakos and John Matsoukas</i>	<a href="#">238</a>
Solid-Phase Synthesis Utilizing Azido- $\alpha$ -Amino Acids: Reduction of Azido-Protected Proline <i>Parissa Heshmati, James Whitehurst and Garland R. Marshall</i>	<a href="#">240</a>
Improved Fmoc-Solid Phase Synthesis of $\beta$ -Amyloid Peptides Using DBU as $N^\alpha$ -Deprotection Reagent <i>Anna K. Tickler, Colin J. Barrow and John D. Wade</i>	<a href="#">242</a>
Triphosgene as Peptide Coupling Reagent: Highly Efficient Total Synthesis of Cyclosporin O <i>Bernd Thern, Joachim Rudolph and Günther Jung</i>	<a href="#">244</a>
Synthesis of Ferrocene Linkers for Solid-Phase Synthesis of Peptides <i>José Giraldeś and Mark L. McLaughlin</i>	<a href="#">246</a>
Efficient HF Conditions for Suppressing Trp Modification Associated with Use of the $N^{\text{in}}$ -Cyclohexyloxycarbonyl (Hoc) Group <i>Hideki Nishio, Yuji Nishiuchi, Tatsuya Inui, Makoto Nakata, Kumiko Yoshizawa-Kumagaye and Terutoshi Kimura</i>	<a href="#">248</a>
Structural Characterization of a Dibenzylated-CGRP(8-37), a Byproduct from $N$ - $\alpha$ -Benzylation of CGRP(8-37) <i>D. David Smith, Martin Hulce, David J. J. Waugh and Peter W. Abel</i>	<a href="#">250</a>
Polyamines as Intermediates for the Synthesis of Heterocyclic Compounds and Oligomeric Heterocyclic Compounds from Resin-Bound Polyamides <i>Adel Nefzi and Richard A. Houghten</i>	<a href="#">252</a>
Solid-Phase Synthesis of Substituted Dihydroimidazoles and Their Bis Analogs <i>Achyuta N. Acharya, John M. Ostresh, Adel Nefzi and Richard A. Houghten</i>	<a href="#">255</a>
Solid Phase Synthesis of 1,2,5-Substituted Derivatives of 4-Imidazolidinone <i>Markéta Rinnová, Agnès Vidal, Adel Nefzi and Richard A. Houghten</i>	<a href="#">257</a>
Solid Phase Synthesis of 1,2,4-Triazinan-3-ones <i>Yongping Yu, John M. Ostresh and Richard A. Houghten</i>	<a href="#">259</a>
Solid-Phase Synthesis of $\alpha$ -Difluoro- $\beta$ -amino Acids by a Reformatsky Reaction <i>Agnès Vidal, Adel Nefzi and Richard A. Houghten</i>	<a href="#">261</a>

## Contents

Peptidotriazoles: Copper(I)-Catalyzed 1,3-Dipolar Cycloadditions on Solid-Phase <i>Christian W. Tornøe and Morten Meldal</i>	<a href="#">263</a>
Solid-Phase Synthesis of Lidocaine Analogues Using Backbone Amide Linker (BAL) Anchoring <i>Simon K. Shannon, Steven A. Kates and George Barany</i>	<a href="#">265</a>
Solid-Supported Triazenes as Alkylating Polymers Employed for the Versatile Derivatization of Peptides <i>Joachim Smerdka, Tobias Seyberth, Dietmar G. Schmid, Günther Jung and Jörg Rademann</i>	<a href="#">267</a>
Oxidation of Threonine and Serine Residues on Solid-Phase: Pyrazine Formation by Dess-Martin Periodinane Oxidation <i>Caspar Christensen and Morten Meldal</i>	<a href="#">269</a>
A Novel Solid Phase Approach to Thioether Cyclized Peptides: Discovery of Mouse Melanocortin-1 Receptor Agonists <i>Jon Bondebjerg, Morten Meldal, Rayna M. Bauzo and Carrie Haskell-Luevano</i>	<a href="#">271</a>
Bifurcated Dipeptide Schiff Bases as Ligands for Enantioselective Catalysis: Micro-Metalloenzymes <i>Robin Polt, Brian Dangel, Bhaskar Tadikonda and Brian Kelly</i>	<a href="#">273</a>
Recent Advances in the Solid-Phase Synthesis of Long-Chain $\beta$ -Peptides <i>Jens Frackenhohl, Jürg V. Schreiber, Per I. Arvidsson and Dieter Seebach</i>	<a href="#">275</a>
Fully Automated Parallel Oligonucleotide Synthesizer <i>Michal Lebl, Christine Burger, Brett Ellman, David Heiner, Georges Ibrahim, Aaron Jones, Mark Nibbe, Jaylynn Pires, Petr Mudra, Vít Pokorný, Pavel Poncar and Karel Ženíšek</i>	<a href="#">277</a>
N to C Solid Phase Organic Synthesis of Peptidic and Peptidomimetic Derivatives Using 9-Fluorenylmethyl Esters <i>Sandrine A. M. Mérette, Christopher A. Goodwin, Michael F. Scully and John J. Deadman</i>	<a href="#">279</a>

## Analytical and Biophysical Methods, Peptides and Proteins Folding, De Novo Design of Peptides and Proteins

A New Method to Quantify the Swelling Properties of Polymer Beads Used in Solid Phase Peptide Synthesis (SPPS) <i>Martin J. Sellers and Peter J. Heggs</i>	<a href="#">283</a>
A Novel High Throughput Analysis of Total Nitrogen Content by a Colorimetric Method <i>Kiyoshi Nokihara and Tadashi Yasuhara</i>	<a href="#">285</a>
Conformational Studies of Cyclotetrapeptides [Xaa-D-Ala] <sub>2</sub> by NMR, CD and Molecular Modeling <i>Maria Ngu-Schwemlein, Toni Bowie, Rebecca Eden and Frank Zhou</i>	<a href="#">287</a>

## Contents

Conformation of $\beta^3$ -Residues-Containing Cyclic Pentapeptide Analogues of the Antitumoral Astin Family <i>Filomena Rossi, Antonia De Capua, Giancarlo Zanotti, Teodorico Tancredi, Pietro Amodeo, Gabriella Saviano, Michele Saviano, Rosa Iacovino and Ettore Benedetti</i>	<a href="#">289</a>
Structure-Activity Relationship of Antimicrobial Peptide, Gaegurin 4, Isolated from Korean Frog <i>Sang-Ho Park and Bong-Jin Lee</i>	<a href="#">291</a>
Tethering of the Proximal Region of the Angiotensin II Receptor ( $AT_{1A}$ ) C-Terminus to the Cell Membrane <i>Henriette Mozsolits, Sharon Unabia, Walter G. Thomas and Marie-Isabel Aguilar</i>	<a href="#">293</a>
Amide I Frequency as a Probe of Tertiary Structure: FTIR Studies of Helix Bundle Peptides <i>Karen Monteiro, Wendy Barber-Armstrong and Sean M. Decatur</i>	<a href="#">295</a>
Coupled Plasmon Waveguide Resonance Studies of Agonist/Antagonist Binding to the Human $\delta$ -Opioid Receptor Provide New Structural Insights Into the Three-State Model for Receptor-Ligand Interactions <i>Z. Salamon, I. Alves, S. Cowell, V. J. Hruby and G. Tollin</i>	<a href="#">297</a>
Structure Elucidation of Peptides with Unnatural Amino Acids Using an Automated Protein Sequencer <i>Ruiwu Liu and Kit S. Lam</i>	<a href="#">299</a>
Structural Study of the Pro-Sequence of Protegrin-3 <i>Jean-Frédéric Sanchez, Yin-Shan Yang, François Hoh, Marie-Paule Strub, Christian Dumas, Jean-Marc Strub, Alain Van Dorsselaer, Robert Lehrer, Tomas Ganz, Alain Chavanieu, Bernard Calas and André Aumelas</i>	<a href="#">301</a>
$\alpha$ -Helix Stabilizing Aromatic-Backbone Interactions <i>Gergely Tóth, Katalin E. Kövér, Jonathan Hirst, Richard F. Murphy and Sándor Lovas</i>	<a href="#">303</a>
Solution Structure of Oligopeptides-Copper(II) Complexes <i>Ilze Vosekalna, Bela Gyurcsik and Erik Larsen</i>	<a href="#">306</a>
Development of Antibodies Against Conjugated Benzophenone, as a Tool in Photoaffinity Crosslinking Studies <i>Dror Yahalom, Michael Rosenblatt and Michael Chorev</i>	<a href="#">308</a>
Monitoring Peptide-Induced Liposome Breakdown with Fluorescence Correlation Spectroscopy <i>Susanne Gangl, M. Knapp, S. Kuepcue, G. Koehler and Jack Blazyk</i>	<a href="#">310</a>
NMR Structural Investigation of a $\beta^3$ -Dodecapeptide with Proteinogenic Side Chains in MeOH and Water <i>Touraj Etezady-Esfarjani, Christian Hilty, Kurt Wüthrich, Magnus Rueping and Dieter Seebach</i>	<a href="#">312</a>
Conformational Studies on a Synthetic Peptide with Prolactin-Releasing Activity in a Membrane Mimetic Environment <i>A. Di Fenza, S. Albrizio, A. D'Ursi, D. Picone and P. Rovero</i>	<a href="#">314</a>

## Contents

Analysis and Characterization of Combinatorial Mixtures of Mucin-2 Antigen Peptides <i>Emöke Windberg, Ferenc Hudecz, Andreas Marquardt, Szilvia Bösze, Ferenc Sebestyén, Hedvig Medzihradszky-Schweiger and Michael Przybylski</i>	<a href="#">316</a>
High Throughput Validation and Quantitation of Synthetic Peptides via LC-MS <i>Lin Chen, Michael James, Brian Korenstein, Brian Miller and J. Mark Carter</i>	<a href="#">318</a>
Synthesis and Solution Three-Dimensional Structure of the Immunodominant Region of Protein G of Human RSV <i>A. Beck, M. Sugawara, J. Czaplicki, C. Klinguer-Hamour, J.-F. Haeuw, T. Nguyen, A. Van Dorsselaer, J.-Y. Bonnefoy and A. Milon</i>	<a href="#">320</a>
Role of Residues in Position 2 and 7 on the Conformation of the N-Terminal Apamin Loop <i>André Aumelas, Léo Barry, Marie France Martin-Eauclaire and Dung Le-Nguyen</i>	<a href="#">322</a>
Conformational Study of [desHis <sup>1</sup> , desPhe <sup>6</sup> , Glu <sup>9</sup> ]glucagon-NH <sub>2</sub> by 2D-NMR Spectroscopy in the Presence of Perdeuterated Dodecylphosphocholine <i>Jung-Mo Ahn, Neil E. Jacobsen, Michael F. Brown and Victor J. Hruby</i>	<a href="#">324</a>
Molecular Modeling Study of the $\beta$ -Turn-Type Reversals Involved in 3D Structure of IFABP <i>Gregory V. Nikiforovich and Carl Frieden</i>	<a href="#">326</a>
Structural Features of Short, Linear Peptides in Solution by Fluorescence and Molecular Mechanics Studies <i>Basilio Pispisa, Claudia Mazzuca, Lorenzo Stella, Mariano Venanzi, Antonio Palleschi, Fernando Formaggio, Claudio Toniolo and Quirinus B. Broxterman</i>	<a href="#">328</a>
Influence of Stereochemistry of the Preceding Acyl Residue on the <i>cis/trans</i> Ratio of the Proline Peptide Bond <i>Matej Breznik, Simona Golič Grdadolnik, Gerald Giester, Ivan Leban and Danijel Kikelj</i>	<a href="#">330</a>
The Influence of the Surrounding Media on the Structural Propensities of Amino Acid Residues in Proteins <i>Alex Rubinstein and Simon Sherman</i>	<a href="#">332</a>
CD Evidence of the Conformational Transitions in rMOG[1-125] in the Presence of Membrane Mimicking Detergents <i>Maria Ngu-Schwemlein, Michelle Corzette, Rod Balhorn and Monique Cosman</i>	<a href="#">334</a>
Coacervation and CD and FT-IR Spectroscopic Studies of Elastin-Derived Polypentapeptide and Its Analogs <i>Kouji Okamoto, Yoshiteru Fukumoto, Iori Maeda, Elemer Vass, Zsuzsanna Majer Gabor Dibo and Miklos Hollosi</i>	<a href="#">336</a>

## Contents

Conformational Analysis of Human Calcitonin in Aqueous Solution and Comparison with a Highly Potent Lactam-Bridged Analogue <i>C. M. McIntosh, K. S. Rotondi, M. Dhanasekaran, K. Gunasekaran, A. Kazantzis, A. Kapurniotu and L. M. Gierasch</i>	<a href="#">338</a>
Conformational Studies of a Glycopeptide Recognized with High Affinity by Autoantibodies in Multiple Sclerosis <i>Alfonso Carotenuto, Armida Di Fenza, Elena Nardi, Anna M. Papini and Paolo Rovero</i>	<a href="#">340</a>
Human Relaxin Chain Combination and Folding <i>Jian-Guo Tang, Geoffrey W. Tregear and John D. Wade</i>	<a href="#">342</a>
Effects of Human Leptin Fragments in Hypothalamic Nucleus C-Fos Expression <i>Vani X. Oliveira Jr., M. Terêsa M. Miranda, Jackson C. Bittencourt, Carol F. Elias and Antonio Miranda</i>	<a href="#">344</a>
Introduction of Temperature-Sensitive Elastin-Based Switches to Stabilize Globular Proteins <i>Bin Li, Darwin O. V. Alonso and Valerie Daggett</i>	<a href="#">346</a>
A Short-Range Interaction of the <i>cis-trans</i> Urea Motif in Ureapeptides <i>Michel Marraud, Christine Hemmerlin, Claude Didierjean, André Aubry, Vincent Semetey, Arnaud-Pierre Schaffner, Jean-Paul Briand and Gilles Guichard</i>	<a href="#">348</a>
A New N-Terminal Helix Capping Box <i>Toshimasa Yamazaki, Etsuko Katoh, Tomohisa Hatta, Teruhisa Tomari, Sakurako Tashiro, Heisaburo Shindo and Takeshi Mizuno</i>	<a href="#">350</a>
The Determination of Helix Stability Coefficients Using D-Amino Acid Substitutions in the non-Polar Face of an Amphipathic $\alpha$ -Helical Model Peptide <i>Yuxin Chen, Colin T. Mant and Robert S. Hodges</i>	<a href="#">353</a>
NMR-Based Studies of a Collagenous Substrate of Collagenase <i>Stella Fiori and Luis Moroder</i>	<a href="#">355</a>
Conformational Analysis of Model Polypeptides Having Repetitive Xaa-Pro Sequences <i>Yoshiaki Hirano, Masashi Shimoda, Masahiro Hattori, Masahito Oka and Toshio Hayashi</i>	<a href="#">357</a>
The Role of Unstructured Highly Charged Regions on the Stability and Specificity of Dimerization of Two-Stranded $\alpha$ -Helical Coiled-Coils: Neck Region of Kinesin-Like Motor Protein Kif3A <i>Mundeep S. Chana, Brian P. Tripet and Robert S. Hodges</i>	<a href="#">359</a>
A Leu-Thr-Trp-Lys "Lock" Stabilizes the N-Terminus of the Kinesin Neck Coiled-Coil <i>Brian Tripet and Robert S. Hodges</i>	<a href="#">361</a>
Template-Assisted Stabilization of a Short HIV-1 gp41 Inner-Core Coiled-Coil Peptide <i>Edelmira Cabezas and Arnold C. Satterthwait</i>	<a href="#">363</a>

## Contents

STABLECOIL: An Algorithm Designed to Predict the Location and Relative Stability of Coiled-Coils in Native Protein Sequences <i>Brian Tripet and Robert S. Hodges</i>	<a href="#">365</a>
Stabilization of Helical Conformation in Model Peptides by 2,2,2-Trifluoro-ethanol: An FTIR Study <i>Wendy Barber-Armstrong, Mohini Sridharan and Sean M. Decatur</i>	<a href="#">367</a>
Peptides Based on Daf, the First Rigid, Transition-Metal Receptor: C <sup>α,α</sup> -Disubstituted Glycine <i>Marco Crisma, Cristina Peggion, Fernando Formaggio, Claudio Toniolo, Karen Wright, Michel Wakselman and Jean-Paul Mazaleyrat</i>	<a href="#">369</a>
Allyl-Based, C <sup>α</sup> -Methylated α-Amino Acids in the Side-Chain to Side-Chain Ring-Closing Metathesis Reaction of β-Turn/3 <sub>10</sub> -Helical Peptides <i>Claudio Toniolo, Marco Crisma, Fernando Formaggio, Cristina Peggion, Quirinus B. Broxterman, Bernard Kaptein, Hans E. Schoemaker, Floris P.J.T. Rutjes, Johan J.N. Veerman, Rosa Maria Vitale, Ettore Benedetti and Michele Saviano</i>	<a href="#">371</a>
Synthesis and Conformational Analysis of Polypeptides Having Repetitive Xaa-Pro-Pro Sequences <i>Masahito Oka, Masahiro Wakahara, Tatsuya Nakamura, Yuichi Onoda, Toshio Hayashi and Yoshiaki Hirano</i>	<a href="#">373</a>
Biophysical Studies of a Proline-Rich Peptide from the Coral Bleach Pathogen <i>Vibrio shiloi</i> <i>Sanjay K. Khare, Boris Arshava, Ehud Banin, Eugene Rosenberg and Fred Naider</i>	<a href="#">375</a>
Lactam-Bridged and Disulfide-Bridged Peptide Mimic of a Stable α-Helical Folded Protein <i>Stanley C. Kwok, Colin T. Mant and Robert S. Hodges</i>	<a href="#">377</a>
Stabilization of the Triple Helix of Collagen Peptides Using Fluoroproline and/or Triacid Scaffolds <i>Erik T. Rump, Dirk T. S. Rijkers, Philip G. de Groot and Rob M. J. Liskamp</i>	<a href="#">379</a>
Conformational Studies of O-Glycosylated 15-Residue Peptide from the Human Mucin (MUC1) Protein Core <i>Simon Sherman, Leo Kinarsky and Alex Rubinstein</i>	<a href="#">381</a>
Folding of β- and γ-Peptides - the Influence of Substitution Patterns on the Formation of Secondary Structures <i>Magnus Rueping, Bernhard Jaun and Dieter Seebach</i>	<a href="#">383</a>
The β-Methyne of Ile3 in the Propeptide Region of Prouroguanylin is Crucial for Chaperone Function in the Folding of the Mature Peptide, Uroguanylin <i>Yuji Hidaka, Chisei Shimono and Yasutsugu Shimonishi</i>	<a href="#">385</a>
Solution Structure of the Macrocyclic Squash Trypsin Inhibitor MCoTI-II, the First Member of a New Family of Cyclic Knottins <i>Annie Heitz, Jean-François Hernandez, Jean Gagnon, Thai Trinh Hong, Châu T.T. Pham, Tuyet M. Nguyen, Dung Le-Nguyen and Laurent Chiche</i>	<a href="#">387</a>

## Contents

Delineation of Structural Constraints Imposed by a Dimerizer Peptide When Grafted Onto the Terminal Ends of a Test Peptide <i>Tarikere L. Gururaja, Gowda A. Naganagowda, Donald G. Payan and Dave Anderson</i>	<a href="#">389</a>
Local and Long-Range Sequence Contributions to the Folding of a Predominantly $\beta$ -Sheet Protein <i>Lila M. Gierasch, Kenneth S. Rotondi, Kannan Gunasekaran, Jennifer A. Habink and Arnold T. Hagler</i>	<a href="#">391</a>
3D Models for Conformational States of the V3 and V1/V2 Loops in gp120/CD4/Antibody Complex <i>Stan Galaktionov, Gregory V. Nikiforovich and Garland R. Marshall</i>	<a href="#">394</a>
Structure and Dynamics of Ribosome Recycling Factor <i>Takuya Yoshida, Susumu Uchiyama, Hiroaki Nakano and Yuji Kobayashi</i>	<a href="#">396</a>
Peptide Models for Studying Autonomous Folding of Subdomain Sections of Protein Molecules <i>Gerardo Byk, Dikla Engel, Vardah Ittah and Elisha Haas</i>	<a href="#">398</a>
Towards New Designed Proteins: Oxime Ligation of Core Modules <i>Natalia Carulla, Clare Woodward and George Barany</i>	<a href="#">400</a>
Do Bioactive Peptides Display Native-Like Conformations When Bound to a Solid Support? <i>Alberto Bianco, Julien Furrer, Martial Piotto, Maryse Bourdonneau, David Limal, Gilles Guichard, Karim Elbayed, Jésus Raya and Jean-Paul Briand</i>	<a href="#">402</a>
Direct Observation of Backbone Hydrogen Bonding in the Folding Transition of Chymotrypsin Inhibitor 2 (CI2) <i>Gangamani S. Beligere, Radha Plachikkat and Philip E. Dawson</i>	<a href="#">404</a>
Optimizing Aqueous Fold Stability for Short Polypeptides: 20 Residue Miniprotein Constructs That Melt as High as at 61 °C <i>Niels H. Andersen, Bipasha Barua, R. Matthew Fesinmeyer and Jonathan Neidigh</i>	<a href="#">406</a>
Synthetic Approach to Study the Effects of $\beta$ -Turn Residues on the Structure and Folding of Bovine Pancreatic Trypsin Inhibitor (BPTI) <i>Judit Tulla, Clare Woodward and George Barany</i>	<a href="#">409</a>
NMR Solution Structure of B-Motif, a Signature Motif of Type-B Response Regulators for His-to-Asp Phosphorelay Signal Transduction System, and Its Interactions with DNA <i>Kazuo Hosoda, Etsuko Katoh, Tomohisa Hatta, Takeshi Mizuno and Toshimasa Yamazaki</i>	<a href="#">411</a>
Synthesis and Characterization of the Pain-Killing Peptide <i>Grammostola spatulata</i> Analgesic Factor (GsAF-1) Containing Three Disulfide Bonds <i>Rong-qiang Liu, Robert T. Jacobs, Russell C. Spreen and George Barany</i>	<a href="#">413</a>

## Contents

Molecular Modeling: Indispensable Tool at the Interface Between Structural Analysis and Molecular Design <i>Christian Lehmann</i>	<a href="#">415</a>
Molecular Modeling and Binding Energy Calculations for Drug Resistant Mutations in HIV-1 Protease-Inhibitor Complexes <i>Mark D. Shenderovich, Vladimir Tseitin, Cindy L. Fisher and Kalyanaraman Ramnarayan</i>	<a href="#">418</a>
Electrostatic and Hydrophobic Nature of the Binding of Gelsolin 135-142 and Gelsolin 150-169 Fragments to the PIP2-Containing Lipid Bilayer <i>Inta Liepina, Cezary Czaplewski, Paul Janmey and Adam Liwo</i>	<a href="#">420</a>
Prediction of Antibody Complexes with Rationally-Designed and Library-Derived Cyclic Peptides: A Computer Modeling Study <i>Tobias Knaute, Livia Otte and Rudolf Volkmer-Engert</i>	<a href="#">422</a>
Ligand-Receptor Interactions Regulating Cell Trafficking and Signaling of the Human PTH1Rc: An <i>in Silica</i> Examination <i>Luca Monticelli, Stefano Mammi, Evaristo Peggion, Serge Ferrari, Michael Rosenblatt, Michael Chorev, Alessandro Bisello and Dale F. Mierke</i>	<a href="#">424</a>
Theoretical Design of $\alpha$ -Hairpin Structures <i>Masahito Oka and Toshio Hayashi</i>	<a href="#">426</a>
Application of a Detailed Energy Surface to Homology Modeling of the $\omega$ -Conotoxin Family <i>Michael J. Dudek and K. Ramnarayan</i>	<a href="#">428</a>
DARWINIZER® - a Computer Based Method for Peptide and Peptidomimetics Design <i>Matthias Filter and Paul Wrede</i>	<a href="#">430</a>
Proline: A Key Building Block in “de novo” Designed Peptide Molecules <i>Ernest Giralt, Miriam Royo, Marcelo Kogan, Laia Crespo, Glòria Sanclimens, Josep Farrera, Miquel Pons and Fernando Albericio</i>	<a href="#">432</a>
Complementary Assembly of Heterogeneous Multiple Peptides into Amyloid Fibrils with $\alpha$ - $\beta$ Structural Transitions <i>Yuta Takahashi, Akihiko Ueno and Hisakazu Mihara</i>	<a href="#">435</a>
Conformational Uniqueness via Designed Ion Pairs <i>Juliana K. Gill and Joel P. Schneider</i>	<a href="#">438</a>
Design, Synthesis and Incorporation in Peptides of a $\beta$ -Turn Mimetic <i>Selvasekaran Janardhanam, Devan Balachari and Krishnan P. Nambiar</i>	<a href="#">440</a>
Evaluating PERMs as Protein Mimics <i>Arno F. Spatola, Anne-Marie Leduc, James L. Wittliff and K. Grant Taylor</i>	<a href="#">442</a>
Amphipathic Stabilization of the $3_{10}$ -/ $\alpha$ -Helix Equilibrium in Synthetic Peptides Rich in C $^{\alpha}$ , C $^{\alpha}$ -Disubstituted Glycines <i>Lars G. J. Hammarström, Ted J. Gauthier and Mark L. McLaughlin</i>	<a href="#">444</a>

## Contents

Design, Synthesis and Characterization of Novel Scaffold-Assembled Collagen Mimetics <i>Garth A. Kinberger and Murray Goodman</i>	<a href="#">446</a>
Design and Synthesis of a Mini-Prorelaxin Model <i>Marc Mathieu, Nicola F. Dawson, John D. Wade and Geoffrey W. Tregear</i>	<a href="#">448</a>
Site Specificity Metal Binding Affinity in C-Terminal of Calmodulin <i>Yiming Ye and Jenny J. Yang</i>	<a href="#">450</a>
A Cassette Ribonuclease: Site Selective Cleavage of RNA by a Ribonuclease S-Bearing RNA-Recognition Segment <i>Shiroh Futaki, Michihiro Araki, Tatsuto Kiwada, Ikuhiko Nakase and Yukio Sugiura</i>	<a href="#">452</a>
Protein Models on Carbohydrate Templates: Effect of the Template <i>Jesper Brask, Jan M. Dideriksen and Knud J. Jensen</i>	<a href="#">454</a>
New Foldamers: Rigid Peptides with an Alternating <i>cis-trans</i> Amide Sequence <i>Marco Crisma, Alessandro Moretto, Claudio Toniolo, Krzysztof Kaczmarek and Janusz Zabrocki</i>	<a href="#">456</a>
Design, Synthesis, and Conformational Studies of Short Peptides Containing C <sup>αα</sup> -Dipropylglycine and Dibenzylglycine <i>Yanwen Fu, Zhe Zhou, W. Dale Treleaven, Jorge Escobedo and Robert P. Hammer</i>	<a href="#">458</a>
Bromo Tryptophan Based Antisickling Peptides: Design, Synthesis and Evaluation <i>M. Prabhakaran, Seetharama A. Acharya, Shabbir A. Khan and K. Ramnarayan</i>	<a href="#">460</a>
Synthesis, Redox and Structural Properties of Cystine-Cyclopeptides Containing the Active-Site of the Thioredoxin Superfamily <i>Chiara Cabrele, Stella Fiori, Stefano Pegoraro and Luis Moroder</i>	<a href="#">462</a>
Probing Backbone Flexibility Within the Active Site of Glutaredoxin 3 <i>John W. Blankenship and Philip E. Dawson</i>	<a href="#">464</a>
Homostranded and Heterostranded $\alpha$ -Helical Templates for Combinatorial Library Display: Differences in Stability and Solubility <i>Stephen M. Lu, Jennifer R. Litowski, Brian Tripet and Robert S. Hodges</i>	<a href="#">466</a>
Synthesis and Solution Structures of Cyclic Hexapeptides Cyclo(Pro-Leu-Xxx) <sub>2</sub> <i>Satoshi Osada, Ryo Hayashi, Taichi Yamashita, Masahiro Yoshiki, Yuki Okamoto, Toshihisa Ueda, Hiroaki Kodama and Michio Kondo</i>	<a href="#">468</a>
Functional and Structural Comparisons of Linear and Dendritic Arrays of Polypeptides <i>Yi-An Lu, Jin-Long Yang and James P. Tam</i>	<a href="#">470</a>

## Contents

### **Biologically Active Peptides, Enzyme Inhibitors, Peptide Neurotoxins and Antibiotics, Peptidomimetics, Peptide and Peptidomimetic Therapeutics and Delivery**

Synthetic Studies on the Antimicrobial Activity of Pleurocidin <i>Lenore M. Martin, Khaled A. Elsaid, Tarquin Dorrington and Marta Gómez-Chiarri</i>	<a href="#">475</a>
Disruption of the $\beta$ -Sheet Structure of Cyclic Peptides by Single Amino Acid Substitution: Influence on Prokaryotic and Eukaryotic Cell Viability <i>Darin L. Lee, Susan W. Farmer, Karin Pflegerl, Robert E. W. Hancock, Michael L. Vasil and Robert S. Hodges</i>	<a href="#">477</a>
Relationship Between Amphipathic Secondary Structure and Activity in Model Linear Cationic Antimicrobial Peptides <i>Jack Blazyk, Janet Hammer, Yi Jin, Yu Zhang and Fang Zhu</i>	<a href="#">479</a>
Shedding Light on the Aglycon Formation of Glycopeptide Antibiotics <i>Daniel Bischoff, Bojan Bister, Stefan Weist, Stefan Pelzer, Alexandra Hölzel, Graeme Nicholson, Sigrid Stockert, Wolfgang Wohlleben, Günther Jung and Roderich D. Süssmuth</i>	<a href="#">481</a>
Synthesis of $\lambda$ -Conotoxins, a New Family of Conotoxins with Unique Disulfide Pattern <i>Kazuki Sato, Yuko Sugahara, R. Ashok Balaji and P. Gopalakrishnakone</i>	<a href="#">483</a>
Solution Conformation of an $\alpha$ -Conotoxin GI with a D-Tyr at Position 11 <i>Do-Hyung Kim, Kyu-Hwan Park and Kyou-Hoon Han</i>	<a href="#">485</a>
Antimicrobial and Chemotactic Activities of $\omega$ -Conotoxin Cyclic Analogues <i>Jin-Long Yang, Yi-An Lu, Chengwei Wu and James P. Tam</i>	<a href="#">487</a>
Synthesis of Parallel and Antiparallel Magainin 2 Dimers and Their Interaction with Lipid and Cell Membrane <i>Takuro Niidome, Yuko Matsushita, Tomomitsu Hatakeyama and Haruhiko Aoyagi</i>	<a href="#">489</a>
Interaction of the Antimicrobial Peptide PGLa and Its Ala-Substitution Analog with Membrane-Mimetic Systems <i>Sylvie E. Blondelle and Karl Lohner</i>	<a href="#">491</a>
Antibacterial Activity Spectrum of Designed Pyrrhocoricin Analogs <i>Mare Cudic, Philippe Bulet, Goran Kragol and Laszlo Otvos, Jr.</i>	<a href="#">493</a>
Importance of the Intramolecular Disulfide Bridges in the Biological Activity of Gomesin <i>Marcos A. Fázio, Sirlei Daffre, M. Terêsa M. Miranda, Philippe Bulet and Antonio Miranda</i>	<a href="#">495</a>
Variation in Ring Size of Cyclic Antimicrobial Peptides Results in Diversity and Selectivity of Biological Activity <i>Masood Jelokhani-Niaraki, Leslie H. Kondejewski, Cyril M. Kay and Robert S. Hodges</i>	<a href="#">497</a>

## Contents

$\alpha$ -Helical Glycopeptide Analgesics: $\beta$ -Endorphin Mimics with Good <i>in vivo</i> Potency	<a href="#">499</a>
<i>Michael M. Palian, Nura Elmagbari, Peg Davis, Hong-Bing Wei, Richard Egleton, Frank Porecca, Henry I. Yamamura, Victor J. Hruby, Edward J. Bilsky and Robin Polt</i>	
Efforts to Investigate the Conformational Changes of the Prion Protein by N-Glycosylation	<a href="#">502</a>
<i>Kristina Münnich, Stefan Becker and Christian Griesinger</i>	
Glycation of Leucine-Enkephalin: Imidazolidinones and Amadori Compounds	<a href="#">504</a>
<i>Maja Roscic and Stefica Horvat</i>	
Solid-Phase Synthesis of Thio-Linked C-Terminal Glycopeptides via a Mitsunobu Reaction	<a href="#">506</a>
<i>John P. Malkinson and Robert A. Falconer</i>	
Synthesis of the Extracellular Ig Domain I (34-94) of Emmpirin Carrying a Chitobiose Unit	<a href="#">508</a>
<i>Hironobu Hojo, Jun Watabe, Yoshiaki Nakahara, Yuko Nakahara, Yukishige Ito, Kazuki Nabeshima and Bryan P. Toole</i>	
Synthesis of Peptide- and Glycopeptide-Conjugates for Specific Drug Targeting	<a href="#">510</a>
<i>Shui-Tein Chen</i>	
Complexation of Peptidoglycan Intermediates by the Lipoglycopeptide Antibiotic Ramoplanin: Structural Requirements for Intermolecular Complexation and Fibril Formation	<a href="#">512</a>
<i>Predrag Cudic, James Kranz, Douglas C. Behenna, Ryan G. Kruger, A. Joshua Wand and Dewey G. McCafferty</i>	
Short Analogues of the Lipopeptaibol Trichogin GA IV	<a href="#">514</a>
<i>Marco Crisma, Cristina Peggion, Fernando Formaggio and Claudio Toniolo</i>	
Dinuclear Zinc(II) Complexes of Linear and Cyclic Peptides Containing Two Bis(2-pyridylmethyl)amino Groups as Catalysts for Hydrolysis of RNA Model Substrate	<a href="#">516</a>
<i>Masao Kawai, Hatsuo Yamamura, Nobuko Izuhara, Tomotsugu Kawaguchi, Ryoji Tanaka, Ryougo Akasaka, Yu-ichi Takahashi, Keiichi Yamada and Shuki Araki</i>	
Construction of RNA-Binding Proteins Having Nucleobase Amino Acids Based on HIV-1 Nucleocapsid Protein	<a href="#">518</a>
<i>Tsuyoshi Takahashi, Akihiko Ueno and Hisakazu Mihara</i>	
Screening of Peptides that Control Interaction Between Nucleobases from Peptide Libraries Based on Loop Structures	<a href="#">520</a>
<i>Mizuki Takahashi, Akihiko Ueno and Hisakazu Mihara</i>	
Preparation of a Site-Specifically Labeled Fluorescent Chemokine by Chemical Synthesis	<a href="#">522</a>
<i>Andrew E. Strong and Antonio S. Verdini</i>	

## Contents

Synthesis, Characterization, and Calorimetric Studies of a Series of Novel Bioconjugates for Selective Targeting of Microbubbles to GPIIb/IIIa Receptors on Vascular Thrombi	<a href="#">524</a>
<i>Patricia A. Schumann, Rachel M. Quigley, Varadarajan Ramaswami, Evan C. Unger and Terry O. Matsunaga</i>	
Energy and Electron Transfer Systems Built in Dendritic Poly(L-lysine)s	<a href="#">526</a>
<i>Louis A. Watanabe, Motonori Uchiyama, Yusuke Oniki, Tamaki Kato, Toru Arai and Norikazu Nishino</i>	
Design of Analogs of Trapoxin, Cyl-1, and Chlamydocin for MHC Class-I Molecule Up-Regulation	<a href="#">528</a>
<i>Norikazu Nishino, Tamaki Kato, Yasuhiko Komatsu and Minoru Yoshida</i>	
Backbone Assignment of Gyrase-B P24 Fragment and Its Interactions with the Inhibitor GR122222	<a href="#">530</a>
<i>Massimo Bellanda, Stefano Mammi, Evaristo Peggion, Gottfried Otting, Johan Weigelt, Elisabetta Perdonà, Enrico Domenici and Carla Marchioro</i>	
Synthetic Progress Towards a TMC-95 Analogue as a Potential Proteasome Inhibitor	<a href="#">532</a>
<i>M. Angels Estiarte, Amy M. Elder and Daniel H. Rich</i>	
Prime Site Binding Inhibitors of the Hepatitis C Virus NS3/4A Serine Protease	<a href="#">534</a>
<i>Elisabetta Bianchi, Paolo Ingallinella, Daniela Fattori, Sergio Altamura, Christian Steinkühler, Daniel Cicero, Renzo Bazzo, Riccardo Cortese and Antonello Pessi</i>	
Solution and Solid Phase Synthesis of Non-Peptide Peptidomimetic Aspartic Peptidase Inhibitors	<a href="#">537</a>
<i>Matthew G. Bursavich and Daniel H. Rich</i>	
Design and Synthesis of Novel Matrix Metalloproteinase Inhibitors	<a href="#">539</a>
<i>Jiaxi Xu, Ding Wang and Qihan Zhang</i>	
A Novel Continuous Assay for the Mechanistic Characterization of Histone Deacetylases and Homologues Using a Small Molecule Fluorescent Substrate	<a href="#">541</a>
<i>Jennifer L. Gronlund, Michael K. Yu, A. Melissa Concepcion, Shu He, Ravi Venkataramani, Ronen Marmorstein and Dewey G. McCafferty</i>	
Peptide Inhibitors of $\alpha$ -Amylase Based on Tendamistat: Synthesis and Kinetic Studies	<a href="#">543</a>
<i>Deborah Heyl, Leo Lucas, Rebecca Himm, Jennifer Kappler, Jason Groom, Jeffrey Asbill, Jon Nzoma, Janice Lima and Mary Gillispie</i>	
Structural Studies of the Complex Between Decapeptide Inhibitors and the Serine Protease NS3/4A of Hepatitis C Virus	<a href="#">545</a>
<i>Paolo Ingallinella, Piero Pucci, Fabrizio Dal Piaz, Antonello Pessi and Elisabetta Bianchi</i>	
Synthesis and Activity of a Small Cyclic Protease Inhibitor from Sunflower Seeds, SFTI-1	<a href="#">547</a>
<i>Agnès M. Jaulent, Jeffrey D. McBride and Robin J. Leatherbarrow</i>	

## Contents

Different Types of P1 Residues in Peptide-Based Inhibitors of Hepatitis C Virus Full-Length NS3 Protease <i>Anja Johansson, Eva Åkerblom, Gunnar Lindeberg, Anton Poliakov, U. Helena Danielsson and Anders Hallberg</i>	<a href="#">549</a>
Development and Characterization of Potent Peptide Inhibitors of p60 <sup>c-src</sup> PTK Using Pseudosubstrate-Based Inhibitor Design Approach <i>Jayesh R. Kamath, Ruiwu Liu, Amanda M. Enstrom, Gang Liu, Qiang Lou and Kit S. Lam</i>	<a href="#">551</a>
Use of $\beta$ -Amino Acids in the Design of Substrate-Based Peptidase Inhibitors <i>R. A. Lew, E. Boulos, K. M. Stewart, P. Perlmutter, M. F. Harte, S. Bond, S. B. Reeve, M. U. Norman, M. J. Lew, M.-I. Aguilar and A. I. Smith</i>	<a href="#">553</a>
Bivalent Inhibition of Human $\beta$ -Trypsin: Probing the Distance Between Neighbouring Subunits by Dibasic Inhibitors <i>Norbert Schaschke, Andreas Dominik, Gabriele Matschiner and Christian P. Sommerhoff</i>	<a href="#">555</a>
A Highly Selective Cell Permeable Peptide Inhibitor of Proprotein Convertase 1: Design, Synthesis and Biological Evaluation in Cellular PC1-Mediated Proteolysis <i>Ajoy Basak, Peter Koch, Marcel Dupelle, Francine Sirois, Michel Chrétien, Nabil G. Seidah and Majambu Mbikay</i>	<a href="#">558</a>
Bicyclic Peptide Inhibitors of an Epithelial Cell-Derived Transmembrane Protease, Matriptase <i>Peter P. Roller, Ya-Qiu Long, Peng Li, Sheau-Ling Lee, Chen-Yong Lin, Istvan Enyedy, Shaomeng Wang and Robert B. Dickson</i>	<a href="#">561</a>
Probing the Substrate Specificity of Hepatitis C Virus Nonstructural 3 Protein Serine Protease by Intramolecularly Quenched Fluorogenic Peptide Substrates <i>Addy Po, Morgan Martin, Martin Richer, Maria A. Juliano, Luiz Juliano and François Jean</i>	<a href="#">563</a>
Characterization of the <i>Staphylococcus aureus</i> Sortase Transpeptidase: A Novel Target for the Development of Chemotherapeutics Against Gram-Positive Bacteria <i>Ryan Kruger, Scott Pesiridis and Dewey G. McCafferty</i>	<a href="#">565</a>
Cyclic Octapeptide Inhibitors of the Acetylcholinesterase Peripheral Site: Implications for Inhibition of Nerve Toxins <i>Peteris Romanovskis, Terrone L. Rosenberry, Bernadette Cusack and Arno F. Spatola</i>	<a href="#">567</a>
Homologs of Amino Acids and Explorations into the Worlds of $\beta$ - and $\gamma$ -Peptides <i>Dieter Seebach</i>	<a href="#">569</a>
Designed Amino Acids That Induce $\beta$ -Sheet Folding and $\beta$ -Sheet Interactions in Peptides <i>James S. Nowick, Kit S. Lam, Chris M. Gothard, Jeffrey K. Huon, William E. Kemnitzer, Tatyana Khasanova, Hong Woo Kim, Ruiwu Liu, Santanu Maitra, Hao T. Mee and Kimberly D. Stigers</i>	<a href="#">572</a>

## Contents

Triply-Templated Artificial $\beta$ -Sheets <i>James S. Nowick, Jennifer M. Cary, James H. Tsai and Wade A. Russu</i>	<a href="#">575</a>
Stepwise Peptide-Peptoid Transformation via SPOT Synthesis <i>Ulrich Reineke, Berit Hoffmann, Thomas Ast, Thomas Polakowski, Jens Schneider-Mergener and Rudolf Volkmer-Engert</i>	<a href="#">577</a>
SPOT Synthesis of 1,3,5-Trisubstituted Hydantoins on Cellulose Membranes <i>Niklas Heine, Jens Schneider-Mergener and Holger Wenschuh</i>	<a href="#">579</a>
Synthesis and CD Spectra of $\beta^2$ -(3-Aza-peptides) <i>Gérald Lelais and Dieter Seebach</i>	<a href="#">581</a>
Preferred Conformations of Azaamino Acids <i>Dong-Kyu Shin, Ho-Jin Lee, Kang-Bong Lee, Young-Sang Choi, Chang-Ju Yoon and Seonggu Ro</i>	<a href="#">583</a>
Higher Anti-HIV-1 Activity of Peptides Derived from gp41 Carboxyl-Terminal Coiled Coil Structure of HIV-1 89.6 Strain <i>Myung Kyu Lee, Jeong Kon Seo, Hee Kyung Kim, Ju Hyun Cho and Kil Lyong Kim</i>	<a href="#">585</a>
Synthetic Approach to Dipeptide Mimetics Based on Aminoacyl Incorporation Reaction <i>Alexey N. Chulin, Igor L. Rodionov and Vadim T. Ivanov</i>	<a href="#">587</a>
Convenient Conversion of Amino Acids to Their <i>N</i> -Hydroxylated Derivatives on a Solid Support: Synthesis of Hydroxamate-Based Pseudo-Peptides <i>Yunpeng Ye and Garland R. Marshall</i>	<a href="#">589</a>
Peptide Bond Modification for Metal Coordination: 1. Metal-Binding Properties of Hydroxamate-Based Pseudo-Peptides <i>Yunpeng Ye and Garland R. Marshall</i>	<a href="#">591</a>
Peptide Bond Modification for Metal Coordination: 2. Metal-Binding Properties of Peptide-Derived Pentaaza-Macrocyclic Templates <i>Yunpeng Ye and Garland R. Marshall, Ron Smith, Craig Durmstorff and Urszula Slomczynska</i>	<a href="#">593</a>
Peptide Bond Modification for Metal Coordination: 3. Metal-Binding Properties of Phosphorus-Based Pseudo-Peptides <i>Yunpeng Ye, Garland R. Marshall</i>	<a href="#">595</a>
Mimicry of the Backbone and Side-Chain Geometry of Peptide Turns: Synthesis of Novel 4-Substituted Indolizidin-9-one Amino Acids <i>Jérôme Cluzeau and William D. Lubell</i>	<a href="#">597</a>
Employing the Steric Interactions of 5- <i>tert</i> -Butylproline to Control Peptide Folding and Biology <i>Liliane Halab, Laurent Bélec and William D. Lubell</i>	<a href="#">599</a>
Synthesis of $\beta$ -Turn Mimetics: [5,5]-Fused Bicyclic $\gamma$ -Lactam Dipeptide Analogues <i>Xuyuan Gu, Wei Qiu, Jinfa Ying, John M. Ndungu and Victor J. Hruby</i>	<a href="#">602</a>

## Contents

Pyridine as a Tripeptidomimetic Scaffold <i>Stina Saitton, Jan Kihlberg and Kristina Luthman</i>	<a href="#">604</a>
Synthesis of Fluoroalkene Dipeptide Isosteres Utilizing Organometallic Reagents <i>Akira Otake, Hideaki Watanabe, Junko Watanabe, Hirokazu Tamamura and Nobutaka Fujii</i>	<a href="#">606</a>
Synthesis of Peptide Mimetics and Amino Acid Mimetics Bearing Aminoxy Instead of Amino Group <i>Toratane Munegumi, Tokanori Yoshii, Masahide Nakamura and Kunie Sakurai</i>	<a href="#">608</a>
Design and Synthesis of Amide Isosteres of Phe-Gly: Potential Peptidomimetic Ligands for the Intestinal Oligopeptide Transporter PepT1 <i>Jon Våbenø, Magnus Brisander, Weiqing Chen, Ronald T. Borchardt and Kristina Luthman</i>	<a href="#">610</a>
$\beta$ -D-Mannose Based Peptidomimetics in the Design of $\alpha_4\beta_1$ and $\alpha_4\beta_7$ Antagonists <i>Jürgen Boer, Elsa Locardi, Anja Schuster, Bernhard Holzmann and Horst Kessler</i>	<a href="#">612</a>
Design, Synthesis and Modulation of Angiogenesis by Thrombin Receptor Non-Peptide Antagonists <i>Kostas A. Alexopoulos, Michael Maragoudakis and John M. Matsoukas</i>	<a href="#">614</a>
Development of Endomorphin Derivatives with Dual Functions and Studies on Their Three-Dimensional Structure <i>Yoshio Fujita, Motohiro Takahashi, Toshio Yokoi, Yuko Tsuda, Lawrence H. Lazarus, Sharon D. Bryant, Akihiro Anbo, Yusuke Sasaki and Yoshio Okada</i>	<a href="#">616</a>
Stereoselective Synthesis of Tyr $\psi$ [CH <sub>2</sub> O]Phe and Tyr $\psi$ [CH <sub>2</sub> O]Ile, Methylene-oxy Analogs of Oxytocin and [8-Arginine]Vasopressin <i>Jan Mařík, Jan Hlaváček, Miloš Buděšínský and Jiřina Slaninová</i>	<a href="#">618</a>
Exploration of the DTrp-NMeLys Motif in the Search for Potent Somatostatin Antagonists <i>W. G. Rajeswaran, William A. Murphy, John E. Taylor and David H. Coy</i>	<a href="#">620</a>
Synthesis and Biological Evaluation of Mixed $\beta^2/\beta^3$ -Dipeptides as Somatostatin Analogs <i>T. Kimmerlin, D. Hoyer and D. Seebach</i>	<a href="#">622</a>
Cyclic Peptides Related to Somatostatin Containing a Novel Imidazole Derived <i>cis</i> -Amide Mimetic <i>Tom Gordon, John Eynon, John Taylor, Michael Culler and Barry Morgan</i>	<a href="#">624</a>
Human Somatostatin Receptor Specificity of Backbone-Cyclic Analogs Containing Novel Sulfur Building Units <i>Sharon Gazal, Gary Gellerman, Ofer Ziv, Olga Karpov, Pninit Litman, Moshe Bracha, Michel Afargan and Chaim Gilon</i>	<a href="#">626</a>

## Contents

Linear and Cyclic Thr6-Bradykinin Analogues Containing <i>N</i> -Benzylglycine as a Replacement for Residues Phe <sup>5</sup> and Phe <sup>8</sup> <i>Marina Gobbo, Laura Biondi, Fernando Filira, Barbara Scolaro, Raniero Rocchi and Tom Piek</i>	<a href="#">628</a>
Design, Synthesis and Conformational Analysis of Human Urotensin II (U-II) Analogues with Lactam Bridge <i>Paolo Grieco, Riccardo Patacchini, Alfonso Carotenuto, Carlo A. Maggi, Ettore Novellino and Paolo Rovero</i>	<a href="#">630</a>
PACAP27 Analogues Incorporating Type II/II' $\beta$ -Turn Mimetics <i>Rosario González-Muñiz, Mercedes Martín-Martínez, Cesare Granata, Eliandre de Oliveira, Clara M. Santiveri, Carlos González, Diana Frechilla, Rosario Herranz, M. Teresa García-López, Joaquín Del Río, M. Angeles Jiménez and David Andreu</i>	<a href="#">632</a>
Bicyclic $\beta$ -Strand Templates: Epimerization and Biological Activity of Non-Electrophilic Serine Protease Inhibitors <i>Jan Urban, Hiroshi Nakanishi, Cyprian O. Ogbu, Geoffrey Kozu, Kenneth Farber, Polina Kazavchinskaya and Min S. Lee</i>	<a href="#">634</a>
Design, Synthesis and Biological Evaluation of Pilicides: Inhibitors of Pilus Assembly in Pathogenic Bacteria <i>Andreas Larsson, Hans Emtenäs, Anette Svensson, Jerome S. Pinkner, Scott J. Hultgren, Fredrik Almqvist and Jan Kihlberg</i>	<a href="#">636</a>
Phenylahistin, a Small Dipeptidic Colchicine-Like Anti-Microtubule Agent: Total Synthesis and SAR Study of the Derivatives <i>Yoshio Hayashi, Sumie Orikasa, Koji Tanaka, Kaneo Kanoh and Yoshiaki Kiso</i>	<a href="#">638</a>
New Antiproliferative Agents from a Peptidomimetic Library <i>László Őrfi, Györgyi Bökönyi, Anikó Horváth, Richard A. Houghten, John M. Ostresh, István Teplán and György Kéri</i>	<a href="#">640</a>
Development of New Analogs of the Highly Potent Anti-Cancer Compound BKM-570 <i>Lajos Gera, Daniel C. Chan, Barbara Helfrich, Paul A. Bunn, Jr., Eunice J. York and John M. Stewart</i>	<a href="#">642</a>
Design and Synthesis of a Selective PSA Cleavable Peptide- Doxorubicin Prodrug Which Targets PSA Positive Tumor Cells <i>Victor M. Garsky, Patricia K. Lumma, Dong-Mei Feng, Jenny Wai, Mohinder K. Sardana, Harri Ramjit, Bradley K. Wong, Allen Oliff, Raymond E. Jones, Deborah DeFeo-Jones and Roger M. Freidinger</i>	<a href="#">644</a>
Peptidic Inhibitors for Protein-Protein Interactions at Cell Surfaces <i>Horst Kessler, Jürgen Boer, Dirk Gottschling, Niko Schmiedeberg, Christian Rölz, Vincent Truffault, Bernhard Holzmann, Anja Schuster, Markus Bürgle, Olaf Wilhelm, Viktor Magdolen and Manfred Schmitt</i>	<a href="#">647</a>
Prodrug Forms of Peptidomimetic HIV Protease Inhibitors Using Intramolecular Cyclization Reaction <i>Yoshiaki Kiso, Hikaru Matsumoto, Tomonori Hamawaki, Youhei Sohma, Tooru Kimura and Yoshio Hayashi</i>	<a href="#">650</a>

## Contents

Effect of Poly[L-Lysine] Based Polymer Polypeptides on Chemotaxis and Phagocytosis of the Unicellular <i>Tetrahymena pyriformis</i> GL <i>Rita Szabó, Éva Pállinger, Gábor Mezö, László Köhidai and Ferenc Hudecz</i>	<a href="#">652</a>
Costimulatory Blockade by CD28 Peptide Mimics: Suppression of Experimental Autoimmune Encephalomyelitis <i>Mythily Srinivasan, Ingrid E. Gienapp, Connie J. Rogers, Caroline C. Whitacre and Pravin T. P. Kaumaya</i>	<a href="#">654</a>
Design and Synthesis of an Amide-Linked Angiotensin II Analogue with 3,5 Side Chain Bridge: Structural Resemblance of Ring Cluster Conformation with AT <sub>1</sub> Non-Peptide Antagonists <i>Panagiota Roumelioti, Ludmila Polevaya, Nektarios Giatas, Anastasia Zoga, Ilze Mutule, Tatjana Keivish, Thomas Mavromoustakos, Panagiotis Zoumpoulakis, Demetrios Vlahakos and John Matsoukas</i>	<a href="#">656</a>
Sustained Delivery of an ApolipoproteinE Peptidomimetic Lowers Serum Cholesterol Levels in Dyslipidemic Mice <i>Mysore P. Ramprasad, Arjang Amini, Nandini Katre, David Garber, Manjula Chadda and G. M. Anantharamaiah</i>	<a href="#">658</a>
Design, Synthesis and Biological Evaluation of Novel Non-Peptide Opioid Ligands for Human Pain <i>Xuejun Tang, Xuyuan Gu, Jinfa Ying, Vadim A. Soloshonok and Victor J. Hruby</i>	<a href="#">660</a>
Design and Synthesis of Novel Pure Motilin Antagonists <i>Masayuki Haramura, Akira Okamachi, Kouichi Tsuzuki, Kenji Yogo, Makoto Ikuta, Toshiro Kozono, Hisanori Takanashi and Eigoro Murayama</i>	<a href="#">662</a>
Active Somatostatin Analogues Containing Sugar Amino Acids <i>Sibylle A. W. Gruner, Horst Kessler, Gyorgy Kéri and Aniko Venetianer</i>	<a href="#">664</a>
A Potent Non-Peptide Inhibitor of Anthrax Lethal Factor <i>Venkatachalapathi V. Yalamoori, M. G. de Luna, D. H. Rideout, M. D. Shenderovich, J. H. Zheng, N. Duesberry, S. H. Leppla, C. S. Niemeyer, J. Sun and K. Ramnarayan</i>	<a href="#">666</a>
Highly Potent Analogs of Human Parathyroid Hormone and Human Parathyroid Hormone-Related Protein <i>Jesse Z. Dong, Yeelana Shen, Michael Culler, John E. Taylor, Chee-Wai Woon, Jean-Jacques Legrand, Barry Morgan, Michael Chorev, Michael Rosenblatt, Chizu Nakamoto and Jacques-Pierre Moreau</i>	<a href="#">668</a>
Glucagon-Like Peptide-1 Analogs with Significantly Improved <i>in vivo</i> Activity <i>Jesse Z. Dong, Yeelana Shen, John E. Taylor, Michael Culler, Chee-Wai Woon, Barry Morgan, Steve Skinner and Jacques-Pierre Moreau</i>	<a href="#">670</a>

## Contents

Neuropeptide Y (NPY) Y1 Receptor Antagonists <i>V.C. Dhawan, D.E. Mullins, W.T. Chance, S. Sheriff, M. Guzzi, E.M. Parker and A. Balasubramaniam</i>	<a href="#">672</a>
Template-Directed Ligation of Peptides with Nucleobase Amino Acids <i>Sachiko Matsumura, Akihiko Ueno and Hisakazu Mihara</i>	<a href="#">674</a>
A General New Concept for the Development of Opioid Peptide Derived $\mu$ -, $\delta$ - and $\kappa$ -Antagonists <i>Peter W. Schiller, Yixin Lu, Grazyna Weltrowska, Irena Berezowska, Brian C. Wilkes, Thi M.-D. Nguyen, Nga N. Chung and Carole Lemieux</i>	<a href="#">676</a>
Synthesis and Pharmacological Activity of Dmt-Tic Analogs with Highly Potent Agonist and Antagonist/Agonist Opioid Activity <i>Remo Guerrini, Gianfranco Balboni, Daniela Rizzi, Girolamo Calo, Sharon D. Bryant, Lawrence H. Lazarus and Severo Salvadori</i>	<a href="#">679</a>
A Novel Cyclic Opioid Peptide Antagonist Containing a Hydroxy Group in Place of the N-Terminal Amino Function <i>Grazyna Weltrowska, Carole Lemieux, Nga N. Chung and Peter W. Schiller</i>	<a href="#">681</a>
Modifications of the Tic Residue in TIPP-Peptides <i>D. Tourwé, S. Van Cauwenberghe, K. Vanommeslaeghe, E. Mannekens, P. Geerlings, G. Toth, A. Péter and J. Csombos</i>	<a href="#">683</a>
Structure-Activity Relationships of Linear and Cyclic Nociceptin Analogs and Conformational Analysis by CD and NMR Spectroscopy <i>Ralf Schmidt, Ibtihal Fadhil, Katharine Carpenter, Joanne Butterworth and Kemal Payza</i>	<a href="#">685</a>
Design and Synthesis of Dynorphin A-(1-11) Analogs with C-Terminal Modifications and Evaluation of their Opioid Activity <i>Kshitij A. Patkar, Thomas F. Murray and Jane V. Aldrich</i>	<a href="#">687</a>
C-Terminal Structure-Activity Relationships for the Novel Opioid Peptide JVA-901 (Venorphin) <i>Christy A. Sasiela, Marco A. Bennett, Thomas F. Murray and Jane V. Aldrich</i>	<a href="#">689</a>
Design and Synthesis of Bifunctional Peptides: Antagonists at CCKA/CCKB Receptors and Agonists at $\mu/\delta$ Opioid Receptors <i>Richard S. Agnes, Yeon Sun Lee, Peg Davis, Shou-Wu Ma, Josephine Lai, Frank Porreca and Victor J. Hruby</i>	<a href="#">691</a>
Role of the C-Terminal and Central Region of Gastrin for Recognition by the Human CCK <sub>2</sub> Receptor <i>Shawn I. Ahmed, Felice Wibowo, Dmitry S. Gembitsky, Richard F. Murphy and Sándor Lovas</i>	<a href="#">693</a>
Structure and Peptide Binding Specificity of the SH3 and SH2 Domain from a Self-Regulated Protein Tyrosine Kinase - BTK <i>Jya-Wei Cheng, Shiou-Ru Tzeng and Ming-Tao Pai</i>	<a href="#">695</a>
Pseudoprolines for Studying Bioactive <i>cis</i> -Prolyl Conformations <i>Angela Wittelsberger, Luc Patiny, Jiřina Slaninová and Manfred Mutter</i>	<a href="#">697</a>

## Contents

Design of Oxytocin Antagonists Which Are More Selective than Atosiban in Rat Bioassays and in Human Receptor Assays <i>Stoytcho Stoev, Ling Ling Cheng, Maurice Manning, N. C. Wo, W. Y. Chan, Thierry Durroux and Claude Barberis</i>	<a href="#">699</a>
Highly Selective Cyclic Peptides for Human Melanocortin-4 Receptor (MC-4 R): Design, Synthesis, Bioactive Conformation, and Pharmacological Evaluation as an Anti-Obesity Agent <i>Waleed Danho, Joseph Swistok, Adrian Cheung, Xin-Jie Chu, Yao Wang, Li Chen, David Bartkovitz, Vijay Gore, Lida Qi, David Fry, David Greeley, Hongmao Sun, Jeanmarie Guenot, Lucia Franco, Grazyna Kurylko, Leonid Rumennik and Keith Yagaloff</i>	<a href="#">701</a>
SAR of Melanin-concentration Hormone (MCH), an Important Regulatory Hormone in Feeding Behavior <i>Waleed Danho, Joseph Swistok, Wajiha Khan, Theresa Truitt, Anthony Aglione, Ralph Garippa, Kui Xu, Yingsi Chen, Qing Xiang, Jarema Kochan and Fiorenza Falcioni</i>	<a href="#">704</a>
Structure-Activity Relationship Studies (SAR) of Melanocortin Agonists Central His-Phe-Arg-Trp Sequence <i>Jerry Ryan Holder, Rayna M. Bauzo, Zhimin Xiang and Carrie Haskell-Luevano</i>	<a href="#">706</a>
The Development of a Novel Highly Selective and Potent Agonist for Human Melanocortin 4 Receptor <i>Malcolm Kavarana, M. Cai, D. Trivedi, G. Han and Victor J. Hruby</i>	<a href="#">708</a>
Synthesis and NMR Characterization of Melanin-Concentrating Hormone <i>Rosa Maria Vitale, Laura Zaccaro, Benedetto Di Blasio, Roberto Fattorusso, Carla Isernia, Pietro Amodeo, Ettore Benedetti, Michele Saviano and Carlo Pedone</i>	<a href="#">710</a>
Synergism Between Agouti Protein Fragment 91-131 and Melanin Concentrating Hormone <i>Alex N. Eberle, Jozsef Bódi, György Orosz, Helga Süli-Vargha, Verena Jäggin and Urs Zumsteg</i>	<a href="#">712</a>
Development of a Human Growth Hormone Peptide Analogue AOD9604 into an Anti-Obesity Drug <i>Woei-Jia Jiang, Robert Gianello, Mark Heffernan, Esra Ogru, Roksan Libinaki and Frank Ng</i>	<a href="#">714</a>
Rational Approach to Stable, Universal Somatostatin Analogues with Superior Therapeutic Potential <i>Ian Lewis, Wilfried Bauer, Rainer Albert, Nagarajan Chandramouli, Janos Pless, Günter Engel, Gisbert Weckbecker and Christian Bruns</i>	<a href="#">716</a>
N-Methyl Scan of a sst1-Selective Somatostatin (SRIF) Analog <i>Judit Erchegyi, Carl Hoeger, Sandra Wenger, Beatrice Waser, Jean-Claude Schaer, Jean Claude Reubi and Jean E. Rivier</i>	<a href="#">719</a>
Exploring the “Double-Ring” Motif in Bradykinin Antagonists <i>Eunice J. York, Daniel C. Chan, Barbara Helfrich, Paul A. Bunn, Jr., Lajos Gera and John M. Stewart</i>	<a href="#">721</a>

## Contents

Conformational Studies of Angiotensin II Cyclic Analogues <i>Vani X. Oliveira, Jr., Shirley Schreier, Fabio Casallanovo, Therezinha B. Paiva, Antonio C. M. Paiva and Antonio Miranda</i>	<a href="#">723</a>
Identification of Key-Residues of Urotensin II, a Potent Mammalian Vasoconstrictor <i>A. Brkovic, P. Lampron, M. Létourneau and A. Fournier</i>	<a href="#">725</a>
Structure-Activity Studies on the Corticotropin Releasing Factor Antagonist Astressin, Minimal Sequence Necessary for Antagonistic Activity: Implications for a New Pharmacophoric Model <i>Dirk T. S. Rijkers, Jack A. J. den Hartog and Rob M. J. Liskamp</i>	<a href="#">727</a>
Solid-Phase Synthesis and Radiolabeling of a Bombesin Peptide Analog for Diagnostic Imaging of Tumors: A Preliminary Report <i>Subhani M. Okarvi</i>	<a href="#">729</a>
Investigation on the Structural Requirements for Binding Integrin $\alpha_{IIb}\beta_3$ <i>Silke Schabbert, Elsa Locardi, Ralph-Heiko Mattern, Michael D. Pierschbacher, Shaokai Jiang and Murray Goodman</i>	<a href="#">731</a>
Linear and Cyclic Peptides for Integrin $\alpha_v\beta_6$ Inhibition <i>Gunther Zischinsky, Ulrich Groth, Beate Diefenbach and Alfred Jonczyk</i>	<a href="#">733</a>
The Synthesis of Collagen Peptides and Characterization of Their Inhibitory Effects on the Collagen Binding Activities of Integrins $\alpha_1\beta_1$ and $\alpha_2\beta_1$ <i>Sivashankarappa Gurusiddappa, Yi Xu, Rebecca L. Rich, Rick T. Owens, Douglas R. Keene, Richard Mayne, Agneta Höök and Magnus Höök</i>	<a href="#">735</a>
Probing the Importance of the N-Terminal Helix of Parathyroid Hormone: Introduction of Cyclohexylalanine to Tether to the Membrane <i>Maria Pellegrini, Andrea Piserchio, Dale F. Mierke and Jesse Dong</i>	<a href="#">737</a>
Structure-Function Relationship Studies on Parathyroid Hormone (PTH) 1-34 Analogues Containing $\beta$ -Amino Acid Residues in Positions 11, 12, and 13 <i>Evaristo Peggion, Stefano Mammi, Elisabetta Schievano, Laura Silvestri, Lukas Scheibler, Martina Corich, Alessandro Bisello, Michael Rosenblatt and Michael Chorev</i>	<a href="#">739</a>
Local Conformation Around Position 12 of the (1-34) Fragment of Parathyroid Hormone Probed by Substitution with Aib Residues <i>Evaristo Peggion, Stefano Mammi, Elisabetta Schievano, Laura Silvestri, Lukas Scheibler, Martina Corich, Alessandro Bisello, Michael Rosenblatt and Michael Chorev</i>	<a href="#">742</a>
Positional Cyclization Scanning: A New Method to Evaluate the Bioactive Conformation of Glucagon <i>Jung-Mo Ahn, Dev Trivedi, Peter M. Gitu, Matthew Medeiros, Jennifer R. Swift and Victor J. Hruby</i>	<a href="#">744</a>
Age-Related Decreases of Calcitonin Gene-Related Peptide (CGRP)-Induced Hypotension <i>in vivo</i> and Vasorelaxant Responses <i>in vitro</i> in Rats <i>Gabriel H. H. Chan and Ronald R. Fiscus</i>	<a href="#">746</a>

## Contents

A Novel Series of Growth Hormone Secretagogues <i>Vincent Guerlavais, Damien Boeglin, Jean-Alain Fehrentz, Romano Deghenghi, Vittorio Locatelli, Giampiero Muccioli and Jean Martinez</i>	<a href="#">748</a>
Chimeric Mastoparans: Biological Probes and Designer Secretagogues <i>Michelle Farquhar, Ursel Soomets, Ashley Martin, Ülo Langel and John Howl</i>	<a href="#">750</a>
Design of Cyclic $\alpha$ -Defensin Dimers as Channel Forming Building Blocks <i>Qitao Yu, Jin-Long Yang and James P. Tam</i>	<a href="#">752</a>
The Effect of Multiple Substitution of Aliphatic Amino Acids on the Structure, Function and Mode of Action of Lytic Peptides <i>Dorit Avrahami, Ziv Oren and Yechiel Shai</i>	<a href="#">754</a>
Three-Dimensional Structure of Big Defensin, a Novel Antimicrobial Peptide Isolated from Horseshoe Crab <i>Naoki Fujitani, Shun-ichiro Kawabata, Tsukasa Osaki, Makoto Demura, Katsutoshi Nitta and Keiichi Kawano</i>	<a href="#">756</a>
Selective Bioactivity of Synthetic Amphipathic Peptides Against Murine Macrophages Infected with <i>Brucella abortus</i> <i>Lars G. J. Hammarström, Ted J. Gauthier and Mark L. McLaughlin</i>	<a href="#">758</a>
Antibacterial Peptides Derived from the C-Terminal Domain of the Hemolytic Lectin, CEL-III <i>Tomomitsu Hatakeyama, Tomoko Suenaga, Takuro Niidome and Haruhiko Aoyagi</i>	<a href="#">760</a>
Low Molecular Weight $\psi$ [CH <sub>2</sub> NH] Pseudopeptides Yield Potent Antimicrobial Agents <i>David M. Vogel, Sylvie Blondelle and Arno F. Spatola</i>	<a href="#">762</a>
Synthesis and Study of the Antimicrobial Action of Cecropin A-Melittin Hybrids with Aib Substitution <i>Padmaja Juvvadi, Satyanarayana Vunnam, Barney Yoo and Bruce Merrifield</i>	<a href="#">764</a>
Structure-Function Relationship of Gramicidin-Alamethicin Hybrid Analogs <i>Hiroaki Kodama, Mitsukuni Shibue, Kimiko Hashimoto, Hiroshi Yamaguchi, Toshiaki Hara, Masood Jelokhani-Niaraki and Michio Kondo</i>	<a href="#">766</a>
Biaryl-Bridged Lipopeptides from <i>Streptomyces</i> sp. T $\ddot{U}$ 6075 <i>Dietmar G. Schmid, Alexandra Hölzel, Graeme J. Nicholson, Stefan Stevanovic, Judith Schimana, Klaus Gebhardt, Johannes Müller, Hans-Peter Fiedler and Günther Jung</i>	<a href="#">768</a>
Generation of Bioactive Peptides Derived from Caseins Using a <i>Lactobacillus helveticus</i> Strain <i>Marie-Claude Robert, Anne Donnet-Hughes and Marcel-Alexandre Juillerat</i>	<a href="#">770</a>
Bioactive Peptides Produced by a Strain of <i>Lactobacillus plantarum</i> : Characterization and Partial Purification <i>Diana M. Müller, Marta S. Carrasco, Arturo Simonetta and Georgina G. Tonarelli</i>	<a href="#">772</a>

## Contents

Stilboflavins, a Natural Peptaibol Library from the Mold <i>Stilbella flavipes</i> <i>Hans Brückner and Andreas Jaworski</i>	<a href="#">774</a>
Cyclic Analogues of the Insect Antimicrobial Peptides Drosocin and Apidaecin <i>Marina Gobbo, Monica Benincasa, Laura Biondi, Fernando Filira, Renato Gennaro and Raniero Rocchi</i>	<a href="#">776</a>
Interaction of Antithrombin III-Binding Domain in Heparins with Novel Heparin Binding Peptides <i>Satomi Onoue, Yoshitaka Nemoto, Takahiro Mizumoto, Sunao Harada, Takehiko Yajima and Kazuhisa Kashimoto</i>	<a href="#">778</a>
Antithrombin III-Derived Novel Heparin Binding Peptides Have an Antagonistic Effect on Heparins <i>Satomi Onoue, Sunao Harada, Yoshitaka Nemoto, Takehiko Yajima and Kazuhisa Kashimoto</i>	<a href="#">780</a>
The Octapeptide (Fragment of Differentiation Factor HLDF) Exhibits Nuclease Activity and Induces Apoptosis <i>Valery M. Lipkin, Svetlana M. Dranitsina, Igor I. Babichenko, Igor L. Rodionov, Ludmila K. Baidakova and Irina A. Kostanyan</i>	<a href="#">782</a>
<i>In vivo</i> Proteolytic Hemoglobin Products as Tissue Growth Promoters <i>Olga V. Sazonova, Elena Yu. Blishchenko, Sergei V. Khaidukov, Andrei A. Karelin and Vadim T. Ivanov</i>	<a href="#">785</a>
Synthesis and Pharmacological Activity of Superagonists of the ORL1 Receptor <i>Severo Salvadori, Remo Guerrini, Roberto Tomatis, Girolamo Calo, Raffaella Bigoni, Anna Rizzi, Daniela Rizzi and Domenico Regoli</i>	<a href="#">787</a>
Rational Designing of CXCR-4 Agonists and Antagonists: Synthesis of Novel Cyclam Derivatives of Stromal Cell-Derived Factor (SDF-1) <i>A. Merzouk, C. Tudan, L. Arab, S. Chahal, G. E. Willick and H. Salari</i>	<a href="#">789</a>
A Computational Study of Conformational Properties for N-Methylated Azapeptide Models <i>Ho-Jin Lee, Dong-Kyu Shin, Young-Sang Choi, Chang-Ju Yoon, Kang-Bong Lee and Seonggu Ro</i>	<a href="#">791</a>
Structural Requirements of Non-Mammalian Vasodilatory Peptide Maxadilan, an Excellent Agonist of PACAP Type 1 Receptors <i>Kiyoshi Nokihara, Yoshihiro Nakata, Ethan Lerner, Tadashi Yasuhara and Victor Wray</i>	<a href="#">793</a>
Effect of Deficiency of Cytochrome C Oxidase Assembly Peptide Cox17p on Mitochondrial Functions and Respiratory-Chain in Mice <i>Yoshinori Takahashi, Koichiro Kako, Hidenori Arai, Akio Takehara and Eisuke Munekata</i>	<a href="#">795</a>
Circadian Rhythm Pacemaker Neuropeptide “PDF” in Nocturnal Insect Cricket <i>Gryllus bimaculatus</i> : cDNA Cloning, mRNA Expression, and Nuclear Localization <i>Yoshiro Chuman, Ayami Matsushima, Yasuyuki Shimohigashi and Miki Shimohigashi</i>	<a href="#">797</a>

## Contents

Design and Synthesis of the Hydroxamic Acid Variants Antitumorigenic and Antimetastatic Hydroxamate Based Ac-PHSXX'-NH <sub>2</sub> Sequences <i>Yingchuan Sun and Arno F. Spatola</i>	<a href="#">799</a>
Design, Synthesis and Evaluation of Growth Regulating SDF-1 Peptides on Breast Carcinoma Cells <i>Megan K. Condon, Christy A. Sasiela, Angela H. Brodie and Sandra C. Vigil-Cruz</i>	<a href="#">801</a>
Components of Tissue-Specific Peptide Pools as Negative Regulators of Cell Growth <i>Elena Yu. Blischenko, Olga V. Sazonova, Sergei V. Khaidukov, Yury A. Sheikine, Dmitry I. Sokolov, Irina S. Freidlin, Marina M. Philippova, Andrei A. Karelin and Vadim T. Ivanov</i>	<a href="#">803</a>
HPLC Analysis, Modeling, and Biological Studies of Antiproliferative Heterocyclic Carboxamides <i>János Seprődi, Ferenc Hollósy, Dániel Erős, László Örfi, István Teplán, György Kéri and Miklós Idei</i>	<a href="#">805</a>
Macrophage Chemotactic Response to Elastin-Derived VGVAPG and VGVPG Permutations: A Structure-Activity Relationship and Receptor Binding Assay <i>Maria Portia P. Briones, Satsuki Kamisato, Iori Maeda, Noboru Takami and Kouji Okamoto</i>	<a href="#">807</a>
 <b>Peptide Conjugates, Glycopeptides and Lipopeptides, Transmembrane Peptides and Proteins, Receptors and Receptor Interactions, Signal Transduction</b>	
Analysis and Evaluation of Rational Designed Calcium Binding Sites in CD2 <i>Wei Yang, Hsiau-wei Lee and Jenny J. Yang</i>	<a href="#">811</a>
Structural Basis for Selective Binding of Integrins to Extracellular Matrix <i>Barbara Saccà, Eva Schmidt, Johannes A. Eble and Luis Moroder</i>	<a href="#">814</a>
Regulation of the Promoter Binding Activity of a Bacterial Sigma Factor Explored Using Segmental Isotopic Labeling and NMR Spectroscopy <i>Julio A. Camarero, Alex Shekhtman, Elizabeth Campbell, Seth Darst, David Cowburn and Tom W. Muir</i>	<a href="#">816</a>
Chemically Engineering the Prion Protein Using Stepwise SPPS and Expressed Protein Ligation <i>Haydn L. Ball, Giuseppe Legname, Nicole Bradon, Guan Zhengyu, David S. King, Michael A. Baldwin and Stanley B. Prusiner</i>	<a href="#">818</a>
Covalent and Non-Covalent Oligomerization of the Transmembrane $\alpha$ -Helix 4 from the Cystic Fibrosis Conductance Regulator <i>Anthony W. Partridge, Roman A. Melnyk and Charles M. Deber</i>	<a href="#">820</a>
CtrAe13, a Calcitonin Receptor Isoform Lacking 14 Amino Acids in Transmembrane Helix 7: Structure and Topology <i>Maria Pellegrini, Veronique Grignoux, William C. Horne, Roland Baron and Dale F. Mierke</i>	<a href="#">822</a>

## Contents

Transmembrane Segment Peptides of the Ff Phage Major Coat Protein Form Parallel Homodimers <i>Roman A. Melnyk, Anthony W. Partridge and Charles M. Deber</i>	<a href="#">824</a>
Refined 3D Model of hMC4R and Docking Study for hMC4R with $\alpha$ -Melanocyte Stimulating Hormone Analogue Ligands <i>Jee-Young Lee, Dong-Il Kang, Seung-Gull Kim and Chang-Ju Yoon</i>	<a href="#">826</a>
Effect of Detergents on Intramolecular Helix-Helix Packing in a Membrane-Based Peptide Derived from CFTR <i>Alex G. Therien and Charles M. Deber</i>	<a href="#">828</a>
Primary Amphipathic Shuttle Peptides: Structural Requirements and Interactions with Model Membranes <i>Frédéric Heitz, Christian Le Grimellec, Jean Méry, Gilles Divita and Nicole Van Mau</i>	<a href="#">830</a>
Synthesis, Purification, and Analysis of the Transmembrane Domain of Phospholamban <i>Patrick S. Wesdock, Phillip W. Banda, Steven C. Hall, Sally U and Gary Lorigan</i>	<a href="#">832</a>
Verification of a $\mu$ Opioid Receptor Model by Site-Directed Mutagenesis <i>Carol Fowler, Irina Pogozeva and Henry I. Mosberg</i>	<a href="#">834</a>
Solid-Phase Synthesis and Chemical Ligation of Transmembrane Segments of Rhodopsin <i>Wei-Jun Zhang, Parissa Heshmati, Yunpeng Ye and Garland R. Marshall</i>	<a href="#">836</a>
Ion Gating and Selectivity in Gramicidin A <i>W.L. Duax, V. Pletnev, B.M. Burkhardt and M. Glowka</i>	<a href="#">838</a>
Docking of Transmembrane Helices Into Four Helix Bundles in the High Affinity IgE Receptor <i>Mire Zloh, Diego Esposito and William A. Gibbons</i>	<a href="#">841</a>
Helical Net Plots and Surface Lipophilicity Mapping of Transmembrane Helices of Integral Membrane Proteins: Aids to 3D Structure Determination of Integral Membrane Proteins <i>Mire Zloh, Diego Esposito and William A. Gibbons</i>	<a href="#">843</a>
Studies on the Involvement of a His Residue of mt1 GPCR TM Helix V in the Interaction with Melatonin <i>Andrea Calderan, Paolo Ruzza, Donata Favretto, Barbara Biondi, Barbara Scolaro and Gianfranco Borin</i>	<a href="#">845</a>
Biosynthesis and Biophysical Studies of Domains of sTE2P, a Yeast G Protein-Coupled Receptor <i>Enrique Arevalo, David Schreiber, Jennifer Madeo, Boris Arshava, Jeffrey M. Becker, Mark Dumont and Fred Naider</i>	<a href="#">847</a>
Transmembrane Segment Mimic Peptides Containing Peptoid Residues <i>Yan-Chun Tang, Mitsuko Maeda and Charles M. Deber</i>	<a href="#">849</a>

## Contents

Computational Chemistry and Opioidmimetics: Receptor-Ligand Interactions of Dmt-Tic Peptides	<a href="#"><u>851</u></a>
<i>Sharon D. Bryant, Severo Salvadori, Remo Guerrini, Gianfranco Balboni, Yoshio Okada, Yoshio Fujita and Lawrence H. Lazarus</i>	
Conformational Model of Signal Transduction in the Transmembrane Region of the AT-1 Receptor	<a href="#"><u>853</u></a>
<i>Gregory V. Nikiforovich and Garland R. Marshall</i>	
Role of the Water Medium in the Process of Signal Transmission from Peptides to Cellular Receptors	<a href="#"><u>855</u></a>
<i>Evgueny I. Grigoriev, Vladimir Kh. Khavinson, Igor N. Kochnev and Alexey E. Grigoriev</i>	
Structure-Based Design, Synthesis, and Surface Plasmon Resonance (SPR) Detection of Antagonists of the Grb2 SH2 Domain	<a href="#"><u>857</u></a>
<i>Feng-Di T. Lung, Jia-Yin Tsai, Shu-Yie Wei, Peter P. Roller and Jya-Wei Cheng</i>	
Global Conformational Constraint in the Design of a Grb2 SH2 Domain Inhibitor	<a href="#"><u>859</u></a>
<i>Yang Gao, Chang-Qing Wei, Johannes Voigt, Jane Wu, Dajun Yang and Terrence R. Burke, Jr.</i>	
Local Conformational Constraint in the Design of a Grb2 SH2 Domain Inhibitor	<a href="#"><u>862</u></a>
<i>Ding-Guo Liu, Yang Gao, Johannes Voigt, Jane Wu, Dajun Yang and Terrence R. Burke, Jr.</i>	
Further Studies of the Signaling Mechanisms of the Antitumor Somatostatin Analogue TT-232	<a href="#"><u>864</u></a>
<i>Attila Steták, Tibor Vántus, Gyöngyi Bökönyi, Péter Csermely, Jackie Vandenheede, Axel Ullrich, János Seprődi, István Teplán and György Kéri</i>	
Generation of Cellulose Membrane-Bound Peptides with Free C-Termini: A Useful Approach for PDZ Binding Studies	<a href="#"><u>866</u></a>
<i>Liyang Dong, Prisca Boisguérin, Jens Schneider-Mergener and Rudolf Volkmer-Engert</i>	
A Focused Library Approach to PTP Inhibitor Discovery Predicated on the X-ray Structure of a PTP1B-Bound Lead Compound	<a href="#"><u>868</u></a>
<i>Terrence R. Burke, Jr., Ding-Guo Liu, Johannes Voigt, Li Wu, Zhong-Yin Zhang and Yang Gao</i>	
Synthesis of the Ras-RBD Protein Pair	<a href="#"><u>870</u></a>
<i>Christian F.W. Becker, Christie L. Hunter, Ralf P. Seidel, Stephen B.H. Kent, Roger S. Goody and Martin Engelhard</i>	
The Proline-Rich Antibacterial Peptide Family Inhibits Chaperone-Assisted Protein Folding	<a href="#"><u>873</u></a>
<i>Laszlo Otvos, Jr., Goran Kragol, Gyorgyi Varadi, Barry A. Condie and Sandor Lovas</i>	

## Contents

Probing the Binding Site of a Heptahelical Peptide Pheromone Receptor Using Photoaffinity Labelling, Site-Directed Mutagenesis and Spectroscopic Approaches <i>Fred Naider, B. K. Lee, L. Keith Henry, Faxiang Ding, S. K. Khare and Jeffrey M. Becker</i>	<a href="#">876</a>
The Naturally Occurring Melanocortin Antagonist Agouti-Related Protein (AGRP) Possesses Similar and Distinct Interactions at the MC4 Receptor Compared with Melanocortin Agonist <i>Carrie Haskell-Luevano, Eileen K. Monck and Y.-P. Wan</i>	<a href="#">879</a>
Identification of Regions of the Epidermal Growth Factor Receptor Involved in Ligand Binding Specificity Using a High Affinity Form of the Ectodomain <i>E. Nice, J. Rothacker, R. Jorissen, M. Nerrie, T. Domagala, T. Adams, J. Lewis, N. McKern, G. Lovrecz, T. Elleman, P. Hoyne, T. Garrett, K. Richards, G. Howlett, A. Burgess and C. Ward</i>	<a href="#">881</a>
Thrombin Receptor Aromatic Residues for Edge-to-Face CH/ $\pi$ Interaction with Ligand Phe-2-phenyl Group <i>Tsugumi Fujita, Yoshiro Chuman, Daniela Riitano, Takeru Nose, Tommaso Costa and Yasuyuki Shimohigashi</i>	<a href="#">884</a>
Regions of G-Protein-Coupled Receptors Identified by Multiple Sequence Alignment <i>Laerte Oliveira, Gerrit Vriend and Antonio C. M. Paiva</i>	<a href="#">886</a>
Tools for the Identification of Receptor Dimmers: Synthesis and Biological Evaluation of On-Resin Dimerized, Photosensitive Analogues of Angiotensin II <i>Kimberley A. Therrien, Maud Deraët, Anick Dubois, Lenka Rihakova, Eric A. Kitas, Walter Meister, Robert Speth and Emanuel Escher</i>	<a href="#">888</a>
Minimization of Parathyroid Hormone Using Simultaneous Multiple Peptide Synthesis: Implications for Structure Based Drug Design <i>Ashok Khatri, Xiang-Chen Huang, Brian D. Petroni and Thomas J. Gardella</i>	<a href="#">890</a>
Structure-Activity Relationship Studies of New Cyclic MSH Analogues Using Cloned-Human Melanocortin Receptors Lead to Greater Selectivity and Inverse Agonists <i>Minying Cai, Paolo Grieco, Jonathan Wiens, Dev Trivedi and Victor J. Hruby</i>	<a href="#">892</a>
Structure-Activity Relationships of Arodyn, a Novel Dynorphin A-(1-11) Analogue <i>Marco A. Bennett, Thomas F. Murray and Jane V. Aldrich</i>	<a href="#">894</a>
Neurohypophyseal Receptors-Ligands: Where We Are After the Landmark Rhodopsin Structure Determination <i>Jerzy Ciarkowski, Piotr Drabik, Artur Giełdoń, Rajmund Kaźmierkiewicz and Rafał Ślusarz</i>	<a href="#">896</a>
Synthesis, Bioactivity and Receptor Binding of Fluorescent NBD Labeled Analogs of the Tridecapeptide Mating Pheromone of <i>Saccharomyces cerevisiae</i> <i>Fa-Xiang Ding, B.K. Lee, Jeffrey M. Becker and Fred Naider</i>	<a href="#">898</a>

## Contents

Molecular Model of the BNP-NPR-A Receptor Complex <i>Brian C. Wilkes, André De Léan, Katharine A. Carpenter and Peter W. Schiller</i>	<a href="#">900</a>
Characterizing the Interactions Between Cholecystokinin and the G-Protein Coupled Receptors CCK <sub>1</sub> and CCK <sub>2</sub> : An NMR-Based Study <i>Craig Giragossian, Maria Pellegrini and Dale F. Mierke</i>	<a href="#">902</a>
Human Colon Cancers Recognize N-Carboxymethyl Gastrin by a Non-CCK <sub>1</sub> , Non-CCK <sub>2</sub> Receptor <i>Felicitas I. Wibowo, Shawn Ahmed, Dmitry S. Gembitsky, Sándor Lovas and Richard F. Murphy</i>	<a href="#">905</a>
Functional Characterization of Two <i>Drosophila melanogaster</i> Type A Allatostatin Receptors Expressed in CHO Cells <i>Teresa M. Kubiak, Martha J. Larsen, Katherine J. Burton, Marjorie R. Zantello, Erich W. Zinser, Valdin G. Smith and David E. Lowery</i>	<a href="#">907</a>
Receptor-Bound Conformation of $\alpha$ -Peptide of Transducin (G <sub>t</sub> ) is not Stabilized by a “ $\pi$ -Cation” Interaction but by Constrained Lactam Bridges Between Residues 341 and 350 <i>Wei Sha, Rieko Arimoto and Garland R. Marshall</i>	<a href="#">909</a>
Solution and Membrane-Bound Conformational Properties of a Peptide from the First Extracellular Loop of the Angiotensin II AT <sub>1</sub> Receptor <i>Shirley Schreier, Roberto K. Salinas, Cláudio S. Shida, Thelma A. Pertinhez, Alberto Spisni, Clovis R. Nakaie and Antonio C. M. Paiva</i>	<a href="#">911</a>
Synthesis of a Biotinylated Chemotactic Peptide Analog as a Probe for Formylpeptide-Receptor Interaction <i>Masaya Miyazaki, Mitsukuni Shibue, Masahiro Yoshiki, Ichiro Fujita, Hideaki Maeda, Seiji Yasuda, Yuhei Hamasaki, Hiroaki Kodama and Michio Kondo</i>	<a href="#">913</a>
Specific Activation of the Insulin Receptor by the Transmembrane Domain Peptides <i>Masaya Miyazaki, Jongsoon Lee, Mitsukuni Shibue, Takashi Fujiura, Hideaki Maeda and Steven E. Shoelson</i>	<a href="#">915</a>
Cyclopentapeptides as Rigidified Templates for Probing Interactions with the AT-1 Receptors <i>Gregory V. Nikiforovich, Gunnar Lindeberg, Katalin E. Kövér, Yunpeng Ye, Per-Anders Frändberg, Fred Nyberg, Anders Karlén, Anders Hallberg and Garland R. Marshall</i>	<a href="#">917</a>
Receptor Binding Site of Arg-Lys Triple Repeat in Nociceptin Superagonist <i>Kazushi Okada, Yoshiro Chuman, Tsugumi Fujita, Takeru Nose, Tommaso Costa and Yasuyuki Shimohigashi</i>	<a href="#">919</a>
Identification of Novel Ligands for Vasopressin V <sub>2</sub> Receptor from Positional Scanning Libraries <i>Colette T. Dooley, Aric Mabini, Tyler Sylvester, Jon R. Appel and Richard A. Houghten</i>	<a href="#">921</a>

## Contents

- Diversity Generation and Guest-Templated Self-Sorting in Dynamic Combinatorial Libraries [923](#)  
*Peter Timmerman and David N. Reinhoudt*

- NMR Studies of the Interaction of  $\alpha$ -Bungarotoxin with a Mimotope of the Nicotinic Acetylcholine Receptor [925](#)  
*Ottavia Spiga, Maria Scarselli, Arianna Ciutti, Luisa Bracci, Barbara Lelli, Luisa Lozzi, Samuel Klein, Duccio Calamandrei, Andrea Bernini, Daniela Di Maro and Neri Niccolai*

- Selection of Antagonists of Fibroblast Growth Factor from a Phage-Display Peptide Library [927](#)  
*Hongkuan Fan, Hui Zhou, Wei Li, Roger W. Roeske and Lili Guo*

## Peptides in Immunology, Synthetic Vaccines, Molecular Mechanisms of Diseases, Peptides in Diagnostics, Pharmacology and Biotechnology, Peptide Delivery Approaches

- Peptide Carrier for Efficient Drug Transport Into Living Cells [931](#)  
*R. Pipkorn, K. Braun, W. Waldeck, M. Koch, I. Braun and J. Debus*

- Design of Novel Cell Penetrating Peptides [933](#)  
*Kristen Sadler, Khee Dong Eom and James P. Tam*

- Synthesis and Targeting with Novel Multi-Mannosylated Glycopeptide Modules [935](#)  
*Goran Kragol, David C. Jackson, Walter Gerhard, Michael Chatergoon, Luis Montaner and Laszlo Otvos, Jr.*

- Liposaccharides: Utilisation for Peptide Delivery and for Enhancing Synthetic Peptide Immunogenicity [937](#)  
*Istvan Toth, Ross McGeary, Joanne Blanchfield, Handoo Rhee, Paul Alewood, David Adams and Michael Good*

- Down-Regulation of HIV-1 Long Terminal Repeat Controlled Viral Transcription by DNA-Binding, Arginine-Rich Fusion Proteins Derived from HIV-1 TAT for the Direct Delivery into the Nucleus [940](#)  
*Stefan R. K. Hoffmann*

- New Insights Into the Membrane Translocating Process of the Tat Peptide Used for Cellular Delivery of Various Biological Molecules [942](#)  
*Eric Vivès, Michelle Silhol and Bernard Lebleu*

- DUROS(r) Osmotic Implant for the Delivery of Peptides and Proteins [944](#)  
*Jeremy Wright, James Matsuura, Stephen Berry and Catherine Lucas*

- Utilization of ICAM-1 Peptide Conjugates for Drug Targeting to T-Cells [946](#)  
*Christine R. Xu, Meagan E. Anderson, Tatyana V. Yakovleva and Teruna J. Siahaan*

- Regulation of Cadherin-Cadherin Interaction: Secondary Structure of the HAV and ADT Peptides Derived from Human E-Cadherin Sequence [948](#)  
*Christine R. Xu, Ernawati Sinaga, Irwan T. Makagiansar and Teruna J. Siahaan*

## Contents

Translocation of Various Arginine-Rich Peptides and the Potential of These Peptides as Carriers for Intracellular Protein Delivery <i>Shiroh Futaki, Tomoki Suzuki, Wakana Ohashi, Takeshi Yagami, Seigo Tanaka, Kunihiro Ueda, and Yukio Sugiura</i>	950
Reversible PEGylation: Thiolytic Regeneration of Active Protein from Its Polymer Conjugates <i>Samuel Zalipsky, Radwan Kiwan and Nasreen Mullah</i>	953
Lipoamino Acid and Liposaccharide Conjugated Peptides: Enhancement of Bioavailability <i>Yiu-Ngok Chan, Allan K. Wong and Istvan Toth</i>	955
Regulation and Multiplicity of Peptide Transporters in Model Systems <i>Jeffrey M. Becker, V. Narita, A. Wiles, M. Hauser, S. Koh, G. Stacey and F. Naider</i>	957
A Novel Class of Cell Permeable “Karyophilic” Peptides: NLS-Mediated Nuclear Import of Dermaseptin Derived Peptides in Intact Cells <i>Elana Hariton-Gazal, Chaim Gilon, Amram Mor and Abraham Loyter</i>	959
Characterization of Translocation Behavior of Arginine-Rich Membrane-Permeable Peptides <i>Tomoki Suzuki, Wakana Ohashi, Ikuhiko Nakase, Seigo Tanaka, Kunihiro Ueda, Shiroh Futaki and Yukio Sugiura</i>	961
Structure and Activity of the N-Terminal Peptides of HIV-1 Glycoprotein 41 Types M (Major) and O (Outlier) <i>Patrick W. Mobley, Alan J. Waring and Larry M. Gordon</i>	963
Specific Cleavage at Lys-147/Gly-148 in the Serine Protease Domain of Human Factor IXa $\beta$ by Plasmin: Effect on Catalytic Efficiency and Factor VIIIa Binding <i>Amy E. Schmidt and S. Paul Bajaj</i>	965
Stability and Peptide Binding Specificity of BTK SH2 Domain: Molecular Basis for X-Linked Agammaglobulinemia <i>Shiou-Ru Tzeng, Ming-Tao Pai, Feng-Di T. Lung, Peter P. Roller, Benfang Lei, Shiao-Chun Tu, Shi-Han Chen, Wen-Jue Soong and Jya-Wei Cheng</i>	967
Designing Peptide Drugs/Ligands for Pathological States. A New Paradigm for Design of Bioactive Peptide Hormones and Neurotransmitters <i>Victor J. Hruby, Richard S. Agnes, Yeon-Sun Lee, Peg Davis, Shou-Wu Ma, Josephine Lai and Frank Porreca</i>	969
Alternate Aggregation Pathways of Alzheimer $\beta$ -Amyloid Peptides <i>Paul Gorman, Christopher M. Yip, Paul E. Fraser and Avijit Chakrabartty</i>	971
Diabetes mellitus (DM) Causes Severe Impairment of Hypotensive Responses <i>in vivo</i> and Vasorelaxant Responses <i>in vitro</i> to the Neuropeptide CGRP <i>Ronald R. Fiscus, Gabriel H. H. Chan and Arisina C. Y. Ma</i>	973
Triple-Helical Peptide Analysis of Collagenolytic Protease Activity <i>Gregg B. Fields, Janelle L. Lauer-Fields, Thilaka Sritharan and Hideaki Nagase</i>	975

## Contents

Design of More Potent, Radioiodinatable and Fluorescent Vasopressin Hypotensive Peptide Agonists <i>L. L. Cheng, S. Stoev, M. Manning, N. C. Wo and W. Y. Chan</i>	<a href="#">978</a>
Antagonism of the Neurochemical Effect of Thyrotropin-Releasing Hormone by Its Peptide Analog <i>Laszlo Prokai, Alevtina Zharikova, Vien Nguyen and Xiaoxu Li</i>	<a href="#">980</a>
Synthesis of Selective Substrates for Syk PTK <i>Paolo Ruzza, Andrea Calderan, Arianna Donella-Deana, Luca Cesaro, Stefano Elardo, Lorenzo A. Pinna and Gianfranco Borin</i>	<a href="#">982</a>
Synthesis of Potent and Enzymatically Stable 4- <sup>18</sup> F-Benzoyl-NT(8-13) Analogs for Tumour Diagnosis Using PET <i>K. Ierbeke, R. Bergmann, B. Johanssen, G. Török, G. Laus and D. Tourwe</i>	<a href="#">984</a>
<i>In vivo</i> Imaging of Protease Activity and Drug Screening <i>Ching-Hsuan Tung, Christoph Bremer and Ralph Weissleder</i>	<a href="#">986</a>
Passive Repression of HIV-1 Long Terminal Repeat Enhancer Controlled Viral Transcription in HIV-1 Infected Cells by Cationic DNA-Binding Fusion Proteins <i>S. R. K. Hoffmann, L. Bisset, J. Schüpbach and B. Gutte</i>	<a href="#">988</a>
Passive Repression of HIV-1 Long Terminal Repeat Controlled Viral Transcription by Site-Directed Combinatorial Design of Artificial DNA-Binding Proteins Screened from Combinatorial Chemical Libraries <i>Stefan R. K. Hoffmann</i>	<a href="#">990</a>
Fluorescent Biosensor for CrkII Phosphorylation by the Abl Tyrosine Kinase <i>Roseanne M. Hofmann, Graham J. Cotton, William Bornman, Emmanuel Chang and Tom W. Muir</i>	<a href="#">992</a>
Antibodies to Distinct Protein Epitopes from a Single Polyclonal Serum <i>Ella A. Yurkina, Vyacheslav I. Ofitserov, Vladimir V. Samukov, Aydar N. Sabirov and Georgy A. Mizenko</i>	<a href="#">994</a>
Epitope Mapping of Anti-Type I Collagen Crosslinked N-Telopeptide Antibody with Synthetic Peptides <i>Huey-Yi Chen, Yen-Meng Liou, Chiu-Heng Chen, Shing-Tzu Lin and Feng-Di T. Lung</i>	<a href="#">996</a>
The Use of a Synthetic Biotinylated Peptide Probe for the Isolation of Adenomatous Polyposis Coli (APC) Tumor Suppressor Protein Complexes <i>Bruno Catimel, John D Wade, M. Faux, Anthony Burgess, Laszlo Otvos, Jr. and Edouard Nice</i>	<a href="#">998</a>
Folding and Peptide Binding of TPR Motifs from SGT <i>Ming-Tao Pai, Chih-Sheng Yang, Shiou-Ru Tzeng, Chung Wang and Jya-Wei Cheng</i>	<a href="#">1000</a>
CCT mRNA and CREB Phosphorylation Up Regulated by Peptide ZNC(C)PR in Rat Hippocampus <i>Yu-cang Du, Kan-yan Xu, Ying Xiong, Ming Dong and Xiu-Fang Chen</i>	<a href="#">1002</a>

## Contents

A Combination of HER-2 Peptide Epitope Vaccines Mediate Superior Biological Effects <i>Pravin T.P. Kaumaya, John Pyles and Naveen Dakappagari</i>	<a href="#">1004</a>
Multivalent Vaccine Studies for HTLV-1 Associated Diseases <i>Roshni Sundaram and Pravin T. P. Kaumaya</i>	<a href="#">1006</a>
Evaluation of HTLV-1 Cytotoxic T-Cell Epitopes in HLA-A2.1 Transgenic Mice <i>Roshni Sundaram, Christopher M. Walker and Pravin T. P. Kaumaya</i>	<a href="#">1008</a>
New Branched Polypeptide Based Epitope-Conjugates: Synthesis and Immunorecognition <i>Ferenc Hudecz, Gábor Mezö, Nikolett Mihala, Balázs Dalmadi, Szilvia Bösze, David Andreu, Sytske Welling-Wester, Eva Rajnavölgyi and Gjalt Welling</i>	<a href="#">1010</a>
Evaluation of Synergistic Interaction Between Cytokines and Peptide Epitope Vaccines in Protection Against HER-2 Expressing Lung Metastases <i>Naveen Dakappagari, Robin Parihar, John Pyles, William E. Carson and Pravin T. P. Kaumaya</i>	<a href="#">1012</a>
Novel Classes of Neutrophil-Activating Peptides: Isolation and Their Physiological Significance <i>Hidehito Mukai, Yoshinori Hokari, Tetsuo Seki, Hiroko Nakano, Toshifumi Takao, Yasutsugu Shimonishi, Yoshisuke Nishi and Eisuke Munekata</i>	<a href="#">1014</a>
Affinity of the HIV-1-Neutralizing Monoclonal Antibody 2F5 for gp41 ELDKWA Peptide Analogues <i>Yu Tian, Chintala V. Ramesh, Xuejun Ma, Tanaz Patel, Myles Tiscione, Teodorica Cenizal, John W. Taylor, Gail Ferstandig Arnold and Edward Arnold</i>	<a href="#">1016</a>
A Discontinuous Antigenic Site Is Functionally Reproduced by Synthetic Peptide Constructions <i>Judit Villén, Eva Borràs, Mercedes Dávila, Esteban Domingo, Wim M. M. Schaaper, Rob H. Melen, Ernest Giralt and David Andreu</i>	<a href="#">1018</a>
Four-Segment Tandem Ligation of Proteins with Unusual Branched Architecture <i>K. D. Eom, Z. Miao and J. P. Tam</i>	<a href="#">1021</a>
Identification and Optimization of HIV-Specific CTL Antigens for Vaccine Design <i>César Boggiano, Clemencia Pinilla, Bruce D. Walker and Sylvie E. Blondelle</i>	<a href="#">1023</a>
The Natural T-Helper Cell Epitope Repertoire is Unlikely to Contain Glycopeptides with Extended Carbohydrate Side-Chains <i>Laszlo Orvos, Jr., Hildegund C. J. Ertl and Mare Cudic</i>	<a href="#">1025</a>

## Contents

Peptide Analogues of a Subdominant Epitope Expressed in EBV-Associated Tumors: Synthesis and Activity <i>Mauro Marastoni, Martina Bazzaro, Fabiola Micheletti, Riccardo Gavioli and Roberto Tomatis</i>	<a href="#">1027</a>
Synthetic Epitopes from Equine Infectious Anemia Virus (EIAV) Surface and Core Proteins <i>Adriana Soutullo, María Santi, Juan C. Perin, Javier Lottersberger, Leila Beltramini and Georgina Tonarelli</i>	<a href="#">1029</a>
B-Cell Linear Epitopes in the Conservative Regions of Hepatitis C Virus Envelope Glycoproteins <i>Ekaterina F. Kolesanova, Ludmila V. Olenina, Boris N. Sobolev, Ludmila I. Nikolaeva and Alexander I. Archakov</i>	<a href="#">1031</a>
Synthesis of a Covalently Reactive Antigen Analog Derived from a Conserved Sequence of HIV-1 gp120 <i>Hiroaki Taguchi, Yasuhiro Nishiyama, Gary S. Burr, Sangeeta A. Karle and Sudhir Paul</i>	<a href="#">1033</a>
Isolation, cDNA Cloning, and Chemical Synthesis of <i>Oryctes rhinoceros</i> Defensin <i>Jun Ishibashi, Hisako Saido-Sakanaka and Minoru Yamakawa</i>	<a href="#">1035</a>
Deamidation within a $\gamma$ -Gliadin-Derived Peptide Enhances Its Recognition by Serum Antibodies of CD Patients <i>Florian v.d. Muelbe, Thomas Mothes, Holm Uhlig, A. A. Osman, Toni Weinschenk, Dietmar G. Schmid, Günther Jung and Burkhard Fleckenstein</i>	<a href="#">1037</a>
Identification of Conserved HIV-1-Derived Helper T Lymphocyte Epitopes Using Synthetic Peptides and High Throughput Binding Assays <i>Yuichiro Higashimoto, Cara C. Wilson, Brent Palmer, Scott Southwood, John Sidney, Ettore Appella, Robert Chesnut, Alessandro Sette and Brian D. Livingston</i>	<a href="#">1039</a>
Determining the Fate of Glycopeptides During Antigen Processing in Antigen Presenting Cells <i>Rodney Gagné, Shiro Komba, Teis Jensen, Monika Gad, Ole Werdelin and Morten Meldal</i>	<a href="#">1041</a>
Evaluation of Immune Response Elicited by Peptide Libraries Against Foot-and-Mouth Disease Virus <i>Eliandre de Oliveira, Miguel Ángel Jimenez-Clavero, José Ignacio Núñez, Francisco Sobrino, Ernest Giralt and David Andreu</i>	<a href="#">1043</a>
Peptoid-Peptide Hybrids: Design, Synthesis and MHC Binding <i>Ellen C. de Haan, Marca H. M. Wauben, Mayken C. Grosfeld-Stulemeyer, John A. W. Kruijtzter, Rob M. J. Liskamp and Ed E. Moret</i>	<a href="#">1045</a>
Synthetic Glycopeptide Models of MUC1 Core Protein <i>Mare Cudic, David J. Craik and Laszlo Otvos, Jr.</i>	<a href="#">1047</a>

## Contents

Cathepsin D Produces the Potent Antimicrobial Peptide Parasin I from Histone H2A in Scaleless Fish Skin <i>Ju Hyun Cho, In Yup Park and Sun Chang Kim</i>	<a href="#">1049</a>
Characterization of Highly Stimulatory T Cell Ligands Identified Using Positional Scanning Libraries <i>Eva Borràs, Bruno Gran, Roland Martin and Clemencia Pinilla</i>	<a href="#">1051</a>
Proteomics Approach for Identifying Interacting Partners of a C-Terminal Functional Peptide Derived from the Tumor Suppressor, p21 <sup>cip/waf1</sup> <i>Tarikere L. Gururaja, Weiqun Li, Tong Lin, Donald G. Payan and D. C. Anderson</i>	<a href="#">1053</a>
Cuvette-Based Biosensors as Micropreparative Affinity Surfaces <i>Bruno Catimel, Julie Rothacker and Ed Nice</i>	<a href="#">1055</a>
A Comprehensive Database of Protein-Protein Interactions <i>J. Mark Carter, Michael James, Brian Korenstein, Juan Herrero, Brian Miller, Hai Hu, Ruslana Zhitnitsky, Christine Luczak and Lin Chen</i>	<a href="#">1057</a>
Cell Attachment and Neurite Outgrowth Activities of Laminin Peptide-Conjugated Chitosan Membrane <i>Motoyoshi Nomizu, Mayumi Mochizuki, Kozue Kato, Ikuko Okazaki, Yoko Wakabayashi, Taku Sato, Satoshi Rikimaru, Yuichi Kadoya, Nobuo Sakairi and Norio Nishi</i>	<a href="#">1060</a>
Peptide-Amphiphile Induction of $\alpha$ -Helical Molecular Architecture and Interaction with Biomaterial Surfaces <i>Navdeep Malkar, Neal Niemczyk and Gregg B. Fields</i>	<a href="#">1063</a>
TOAC Peptides as Catalysts of Enantioselective Oxidations <i>Claudio Toniolo, Marco Crisma, Fernando Formaggio, Marcella Bonchio, Quirinus B. Broxterman, Bernard Kaptein, Rosa Maria Vitale, Ettore Benedetti and Michele Saviano</i>	<a href="#">1065</a>
Synthesis of Arg-Gly-Asp-Ser Containing Oligopeptides and Evaluation of Their Cell-Attachment Activity <i>Tadashi Iuchi, Mitsutaka Kayahara, Keiko Sato, Yoshiaki Hirano, Masahito Oka and Toshio Hayashi</i>	<a href="#">1067</a>
Author Index	<a href="#">1071</a>
Index of E-mail Addresses	<a href="#">1090</a>
Subject Index	<a href="#">1097</a>

**Merrifield Award Lecture**  
**Professor Garland R. Marshall**



## **From Merrifield to MetaPhore: A Random Walk with Serendipity**

**Garland R. Marshall**

*Department of Biochemistry and Molecular Biophysics, Washington University, St. Louis,  
MO 63110, USA*

### **Introduction**

It is the highpoint of my career to receive this award, named in honor of my Ph.D. mentor, Bruce Merrifield. There is little that I can add to what we all know regarding the impact that Bruce has had on peptide research. Certainly, he has had a more significant impact on my scientific development than any other individual. I do need, however, to acknowledge from the start that I have made a habit of associating myself with outstanding individuals, such as Bruce, who have made me look good. My mother always advised, "You are known by your friends" and I took those words to heart. I also need to acknowledge the support of my wife Suzanne, our four children and their spouses for their sacrifices and encouragement over the many years. Suzanne and I are in the middle of our 42nd year of marriage. She received a Ph.T. (put husband through) degree from Caltech when I graduated in 1962, and has never wavered in her support. So my thanks to my family, students, postdocs and collaborators for allowing me to be associated with their lives; this award belongs to you collectively.

What I would like to share with you is an intellectual journey, a quest that has dominated my scientific career. The problem of molecular recognition manifests itself in many contexts; I will focus on one of its manifestations, G-protein coupled receptor (GPCR) activation. I would also like to emphasize those colleagues who have dominated my intellectual development and impacted my branch-point decisions. As you will discover, my career has been stochastic; unanticipated opportunities have been discovered and exploited, new paradigms and software have been developed, some of which has even turned out useful.

### **The Quest**

The quest began, some 40 years ago, in 1961 as an undergraduate at Caltech where I was trying my hand at research with a neurophysiologist, Prof. Anton van Harreveld. Somehow the idea of isolating the acetylcholine receptor from denervated skeletal muscle seemed like a good project, and I began my quest to understand how a small molecule can interact with a transmembrane receptor and transmit a signal to the interior of the cell. I will describe our hypothesis for GPCRs at the end of this lecture. The Caltech research project was a dismal failure, but I was determined to continue the quest and went to Rockefeller University to further my education in neurophysiology. In my stochastic way, I started my research in immunology with Prof. Henry Kunkel who suggested using peptide hormones as haptens for developing immunoassays. Berson and Yalow had just reported the immunoassay for insulin for which they later received the Nobel Prize. The project required attaching the octapeptide angiotensin II to a protein carrier before injecting it into a rabbit. Henry suggested I go ask Bruce Merrifield the best way to conjugate AII, and the rest is history. We picked a protocol and I injected the rabbits, got some AII-antibody titre, but needed a larger supply of AII. I'm embarrassed to admit today that my thesis consisted only of the solid-phase synthesis of an octapeptide, AII, and an investigation of the potential side reaction, aspartyl  $\alpha$ - $\beta$  rearrangement [1]. But those times were different; first you had to make all your protected Boc amino acids from scratch, amino acid analysis was a 24-h col-

## Marshall

umn with manual colorimetric analysis, no HPLCs, if you can imagine it, *etc.* Definitely not the good old days!

But there were compensations, Lyman Craig, the inventor of counter-current distribution that we used for purification, was one floor up; Stanford Moore and William Stein, the protein chemists who invented the amino acid analyzer and later shared the Noble Prize, were two floors up. These were golden days as I was Bruce's apprentice, overnight trouble shooter for the first automated synthesizer, and a goad to generalize the approach beyond peptide chemistry (in fact, I prepared dTT, a dinucleotide on a



Fig. 1. A graduate student's view of R. Bruce Merrifield (1962–1966).

polymer in Bruce's lab in 1965, but abandoned the project as premature considering the limited development of nucleotide chemistry at that point). This perspective that was shared with a few synthetic chemists such as Leznoff [2] is somewhat ironic considering the recent explosion in combinatorial chemistry and the delay for the synthetic organic community to discover the advantages of a filterable protecting group. Many of the major figures of science of that day came to do homage. I remember the Nobel Laureate in Chemistry, Sir Robert Robinson, pulling me aside during a visit and telling me how lucky I was to be working with Prof. Merrifield whom he intended to nominate for a Nobel Prize. That was 1964; it only took 20 years for that nomination to be confirmed.

Certainly, the association with Bruce impacted my career. I gave a talk at the Federation meeting in 1965 on the synthesis of AII by SPS and was recruited to Washington University Medical School as a result. I gave up a postdoc that Stanford Moore had arranged for me with Per Edman in Australia to develop solid-phase Edman degradation, and accepted a position in the Department of Physiology & Biophysics to teach endocrine physiology starting in 1966, with a joint appointment in Biological Chemistry headed by Prof. P. Roy Vagelos. I wrote my first successful NIH grant prior to my Ph.D. thesis, and spent the summer of 1966 as a guest in Prof. Geoffrey Young's lab at Oxford to experience the classic solution approach to peptide chemistry.

*Molecular Modeling.* My last year at Rockefeller was very influential. I had naively assumed that the ability to change the chemical structure of a peptide hormone would readily allow a rapid understanding of its recognition requirements. While it was relatively easy to identify those residues (Tyr4, His6 and Phe8 in angiotensin II, for example) that were crucial for recognition, their three-dimensional arrangement, the

receptor-bound conformation, required for activation of the receptor proved problematic due to the inherent flexibility of small peptides. A young assistant professor, George Nemethy, had just been recruited from Cornell from the group of Prof. Harold Scheraga. I convinced him that I needed to understand the computational approach to protein conformation that was just emerging [3] and he agreed to tutor me. This exposure became the basis for much that followed.

Upon my arrival in St. Louis, I began the construction of the second automated solid-phase synthesizer adapting the design of the original to include a subroutine implemented with relays to save spaces on the rotary drum programmer. My colleague, Charles Molnar from across the hall, worked on auditory physiology and used to come watch me and listen to my explanations, occasionally breaking into a grin. As a graduate student, he had helped design and construct the LINC, the first laboratory computer [4] at MIT, and the predecessor to the PDP8 and Digital Equipment Company. He knew, as I was later to discover, why the only serious attempt to use relays in computers was abandoned; they chatter and generate multiple signals. But this became the basis of a lifelong friendship and my collaboration with computer scientists and engineers in molecular modeling. Within a year, we had a prototypical molecular modeling system, CHEMAST, running in a LINC with two thousand words of 12-bit memory and an oscilloscope output [5]. We recruited Dr. C. David Barry, a British physicist, from the Levinthal group at MIT (Project Mac and the first molecular graphics) and Robert Ellis, a computer scientist at Washington University, to help with software and hardware development in molecular modeling.

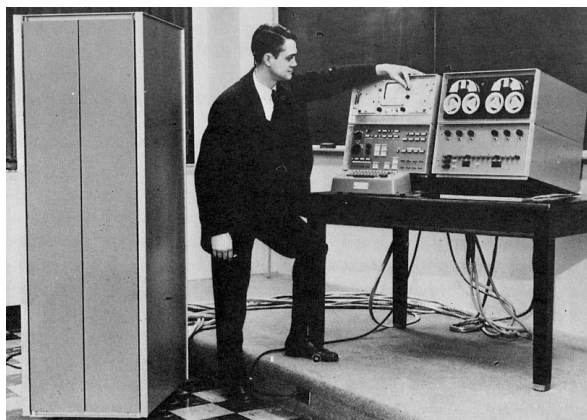


*Fig. 2. Prof. Wesley Clark with LINC computer. A molecular modeling system CHEMAST utilized this primitive computer with an oscilloscope for graphical output.*

*$\alpha$ -Alkyl Amino Acids.* By 1969, we were sufficiently advanced to run a workshop on molecular modeling in St. Louis with Prof. Robert Schwyzler, a former winner of this award, of the ETH sending one of his graduate students. Heinz Bosshard returned as a postdoc and colleague, a productive association that lasted for over 10 years. Heinz and I applied our software to generate Ramachandran plots of the effects of methyl for proton substitution on the peptide backbone [6]. Much to our surprise at the time, the impact of replacing the  $\alpha$ -proton of a peptide with a methyl group imposed a dramatic constraint on the local backbone conformation, favoring the right- or

## Marshall

left-handed  $\alpha$ -helix. This observation has been verified and extended by numerous colleagues over the years, but especially by the groups of Leplawy, Balaram, Toniolo, and Karle. This initiated a program to synthesize, resolve and incorporate  $\alpha$ -methyl amino acids into bioactive peptides to limit their conformations and probe receptor selectivity. We studied angiotensin, bradykinin, TRH, glutathione, opioids, *etc.* and were pleased when several of our analogs retained significant biological activity suggesting reverse-turn conformations for the backbone at the substituted amino acids with receptor recognition of the side chains as they were arrayed in three dimensions on the different turn motifs.

*Improvements in SPS.* We were, of course, simultaneously attempting to improve the general solid-phase approach to peptide synthesis. I wandered off into the oxidation chemistry of indoles and scavengers in my efforts to include tryptophan in SPS. My first postdoc, Pier-Giorgio Pietta, came from the Weygand group and helped develop the benzhydryl resin for synthesis of peptides with C-terminal amides [7], a common feature of biologically active peptides such as oxytocin, vasopressin, TRH, LHRH, *etc.* The issue of truncation in SPS arose as well when we attempted to synthesize [8] acyl carrier protein (ACP), a key component of fatty acid synthesis and the scientific focus of the Vagelos research group. The C-terminal sequence of ACP became a standard test for various protocols attempting to deal with aggregation of the growing peptide chain on the polymer. I have been amazed that the phenomenon has turned out to be so reproducible in different labs with different batches of polymers. Bill Hancock and David Prescott utilized  $^{36}\text{Cl}$  to demonstrate [9] in our lab that parts of the polymer matrix became inaccessible to solvent as a function of peptide length and then became reactive again once the truncation segment was passed. Steve Kent later spent considerable effort exploring this problem and suggested that aggregation of the growing peptide chain within the polymeric matrix was the underlying cause of changes in accessibility of the growing peptide chain.

We successfully prepared a 74-residue synthetic acyl carrier protein that the Vagelos lab could not distinguish by either enzymatic or analytical biochemistry from the naturally isolated protein [8]. I was invited to the European Peptide Symposium in 1971 in Vienna and presented our ACP synthesis. I had never been flayed in public or private as efficiently before or since; the classic solution giants of peptide chemistry, Klaus Hoffman, Eric Wunsch and several others considered my presentation an affront as I had not isolated and characterized each intermediate during the synthesis. Ralph Hirshmann saw the impact of their criticism and invited me to have a drink with him where he put things into perspective. That was the beginning of a long friendship with this gentle giant of medicinal chemistry, another former winner of this award. This meeting also gave me a chance to enhance my friendship with Josef Rudinger, the Czech peptide chemist and polyglot. Joe Rudinger had more insight and diplomatic skill in sharing his insight into science and its practitioners without causing offense that anyone I have ever met. He was an inspiration through his writings on peptide-receptor interactions, and would have been my mentor on a sabbatical had the Czech regime not been suppressed. I did take the sabbatical in 1975 at Massey University in New Zealand with Bill Hancock, a former Vagelos postdoc who had worked on ACP. This sabbatical solidified the decision to focus my efforts on computer-aided drug design upon my return to Washington University, and leave the optimization of solid-phase peptide chemistry to Bruce Merrifield, Steve Kent, Jimmy Tam, and others with more expertise in synthetic chemistry.

*Enzyme Inhibitors.* Because of our exposure to the biology of the renin-angiotensin system, we set out, as did many others, to develop an inhibitor of renin. We had been successful with the development of the first competitive inhibitor of the interaction of AII with its receptor [10] with Phil Needleman, a long-time collaborator, and pharmacologist of considerable repute due to his discovery of cyclooxygenase II and the development of the drug Celebrex. But we reasoned that blocking the AI-AII cascade at the renin level would be more efficient and started to synthesize pepstatin, the natural product inhibitor of aspartyl proteases isolated by Umezawa, as a precursor to analogs targeted at renin. Fortunately, I met Dan Rich at a Gordon Conference and discovered that he was not only ahead in the pepstatin synthesis, but was clearly not someone that I wanted as a competitor. Once again, you are known by your associates, and I decided to withdraw from the renin arena and collaborate with Dan whenever the chance arose as it did later on HIV protease inhibitors [11]. I had followed the development of angiotensin converting enzyme (ACE, the enzyme responsible for the conversion of AI to AII) inhibitors by both the Ondetti group at Squibb [12] and later the Patchett group [13] at Merck, but was reluctant to involve my group in such a competitive arena. In many ways, the therapeutic success of these compounds in treating hypertension in man curtailed much enthusiasm at the time for development of renin inhibitors, or AII-receptor blockers.

In 1987, I terminated my involvement with Tripos Associates, the molecular modeling company I had started in 1979, to devote myself totally to academic science. I was concerned with the emergence of AIDS and discovered a paper in which the aspartyl protease motif DTG was discovered in a gene of HIV based on the RNA sequence [14]. It was suggested that an aspartyl protease might be responsible for proteolysis of one of the polyproteins encoded by the virus. As the cleavage sites were known by the sequence of the products including HIV protease that contained the DTG motif, we decided to test the hypothesis by developing a transition-state inhibitor of the proposed enzyme. The obvious strategy was to use reductive amination of the reaction of amino acid aldehydes on the polymeric support to generate reduced amide analogs of short substrate sequences. This strategy was successful and we developed a high-throughput fluorescent assay based on fluorescent quenching in order to characterize the inhibitors [15]. We had contacted the protein expression group at Monsanto to collaborate on the production of expressed HIV protease for this project, but they were experiencing difficulties. We had started the SPS of the 99-residue protein ourselves when I became aware that Steve Kent was ahead in this effort. A call to Steve and synthetic HIV protease was the basis for our inhibitor work for two years [16] until reconstitution of expressed HIV protease from inclusion bodies was developed by our Monsanto neighbors. The reduced amide analogs were useful in exploring sequence specificity of the protease and provided the first crystal structure of an HIV protease complexed with an inhibitor, MVT-101, that demonstrated (Figure 3) the dramatic conformation change of the “flaps” on inhibitor binding for the first time [17]. Nevertheless, it was common knowledge that more potent inhibitors could be obtained by other transition state analogs containing a hydroxyl attached to a tetrahedral carbon in the active site. Because of the experience that Dan Rich had with aspartyl proteases, he was quickly recruited as a collaborator on HIV protease inhibitors. All of us assumed that we would have some window of time before the pharmaceutical giants focused their attention on HIV protease, but we were wrong. Roche, Abbott and Merck among others had initiated HIV protease programs, and I withdrew my postdocs from

### Marshall

the competition, and focused our effort on trying to understand the basis of molecular recognition by the enzyme and how to utilize that knowledge in the design of inhibitors that were less likely to develop resistant-strains of virus.

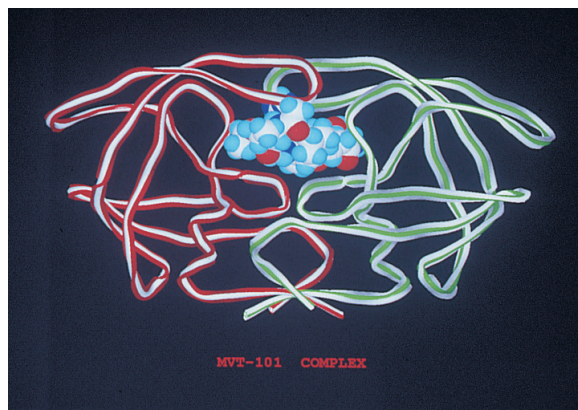
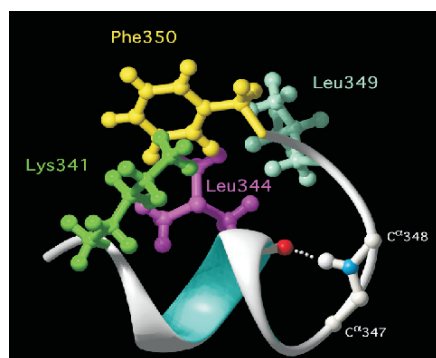


Fig. 3. MVT-101 (space-filling) complexed with HIV-1 protease homodimer (green and red ribbons) [17]. The structure was entirely synthetic, both enzyme and inhibitor.

*Affinity Prediction.* We had been using modern statistical approaches to correlate structure with affinity based on a concept of Dr. Richard Cramer that I encouraged at Tripos. Comparative Molecular Field Analysis (CoMFA) was based on the premise that one molecule could be adequately represented in its recognition properties by its potential field [18]. When the values of the potential field were sampled on a grid and those values correlated with a training set of molecules by sophisticated statistical techniques, a predictive model of activity usually resulted. We demonstrated this approach with ACE inhibitors [19] as well as HIV protease inhibitors [20]. Since the physical basis of molecular interaction is the same regardless of the complexes studied, we decided to extend this approach to complexes in general resulting in VALIDATE [21], where the enthalpy of binding is estimated through molecular mechanics, and the entropy of binding essentially interpolated from a heuristic model.

*Dream Realized.* The prototypical G-protein coupled receptor (GPCR) is rhodopsin as it is readily available in quantity (0.5 mg purified rhodopsin per eye) from bovine eyes in dramatic contrast to other GPCRs that interact with peptide hormones. From the perspective of a peptide chemist, however, it was of no interest since the SAR of a photon is simply a spectrum. Much to my surprise, Oleg Kisselev appeared at my door and asked for help in determining the rhodopsin-bound conformation of a peptide. He had determined that the C-terminal segment of the  $\gamma$ -subunit of transducin bound and stabilized the photoactivated state of rhodopsin. He introduced me to the work of Hamm that showed that the C-terminal of the  $\alpha$ -subunit also showed the same phenomenon. In fact, Dratz and Hamm had attempted to experimentally determine the R\*-bound conformation of the  $\alpha$ -peptide by transfer NOE NMR. We decided to repeat their experiment as a control before we attempted a similar study with the  $\gamma$ -peptide that was potentially complicated by a lipid modification on the C-terminal cysteine. In the case of the studies by Dratz *et al.* [22], the peptide used was an analog (IRENLKDCGLF) of the native sequence with higher affinity for R\*. This higher affinity with an exchange rate far from the optimum for the TrNOE experiment resulted

in suboptimal spectra leading to a misassignment of resonances and a wrong conclusion concerning the R\*-bound structure [23]. The native sequence has the exchange characteristics appropriate for obtaining optimal TrNOE spectra and the resulting structure was unambiguous. When a higher-affinity analog (VLEDLKSCGLF) was subjected to the same experimental conditions, little useful information was obtained. In summary of the results we obtained [24], the Gt $\alpha$  (340-350) binds to photoactivated rhodopsin to form a continuous helix terminated by a reverse glycine C-cap turn with a distinctive hydrophobic cluster of the side chains of two leucines, a lysine and a phenylalanine (Figure 4). Based on the conservation of these residues in most subclasses of G-proteins, this motif may be of significance in GPCR/G-protein interactions, at least for the rhodopsin family of GPCRs.



*Fig. 4. Receptor-bound conformation of a peptide complexed with a GPCR [24] – the end of one quest and beginning of another.*

As the structure of rhodopsin was not known, we could not include it in our structural determination, and there was, therefore, some concern of artifact due to spin diffusion with receptor protons in the active site. We, therefore, took a page from our peptidomimetic approach and designed a set of analogs constrained to help stabilize the deduced conformation. The majority of the peptides showed enhanced activity as would be expected if we had preorganized their conformations similarly to that when bound, providing indirect evidence that our structure was correct [25]. The crystal structure of dark-adapted rhodopsin has recently been solved, but rhodopsin does not bind transducin or the peptide fragments in this state. By moving helix 6 in accord with biophysical studies, however, a binding site is exposed. In order to test its relevance, the experimental affinities of the constrained analogs were compared with their affinities when bound as estimated by VALIDATE giving a  $R^2 = 0.90$  [26]. Thus, movement of helix 6 in response to the photoisomerization of retinal seems to be a necessary and sufficient change in rhodopsin to provide a binding site for the C-terminus of the  $\alpha$ -subunit that initiates transduction. A plausible model of photo-transduction can be derived simply from juxtaposition of experimental data, and testing of that model is underway.

*Entrepreneur Activities.* Despite any interest in ever being involved in a business after my termination of the Tripos affiliation, time has an interesting way of modifying memory. In 1995 I started a second company MetaPhore Pharmaceuticals to focus on metals in medicine bringing the latest in combinatorial chemistry and high-throughput screening to bioinorganic therapeutics. In December of 1998, the

## Marshall

company outlicensed a highly developed technology based on bioinorganic chemistry from Monsanto/Searle. The development [27] of a synthetic superoxide dismutase based on pentaazacrown complexes of manganese that had all the properties of a drug (catalytically efficient, less than 500 molecular weight, bioavailability, metabolic stability, *etc.*) that was curative in a number of animal models of disease is a reality due to my latest set of incredible associates (Drs. Denis Forster, Dennis Riley, Daniela Salvemini and Ursula Slomczynska at MetaPhore). Phase I clinical studies of the first of these compounds has been successfully completed and M40403 will enter Phase II clinical trials in combination with interleukin-2 for melanoma and renal carcinoma this fall.

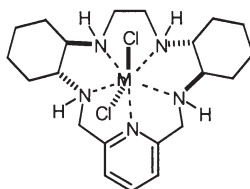


Fig. 5. M40403, a SOD mimetic, demonstrated in numerous preclinical studies as a potential therapeutic.

Perhaps of more interest, however, is my realization that the chemistry developed for pentaazacrown macrocycles as SOD mimetics can readily be applied to peptidomimetics to generate diverse defined 3D arrangements of side chains to probe peptide receptors. Simple reduction of the amide bonds of cyclic peptides gives chiral azacrowns [28], and complexation with different metals allows variation in the orientation of side chains.

## Summary

My career is ample demonstration that serendipity is still king and that the mind is often not prepared, but that data will eventually penetrate even my most closed of minds. My career is also ample testimony to the magnificent discipline that we practice; every day we have a new world; every day a colleague has published new results and new insights into the location of our holy grail. If there was ever a better time to be a scientist, I'm afraid I can't identify it. I have been particularly lucky to have interests bridging molecular biology and microelectronics, the engines that lead our technology revolution. But my real source of inspiration has been those with whom I have shared this journey, the credit is yours. I look forward to further unanticipated adventures in your company.

## Acknowledgments

While I have tried to cite many of my colleagues in the text who have had significant impact on my career, the vast majority are student and postdocs cited in my references. In particular, I want to acknowledge my current and long-term colleagues, Stan Galaktionov and Gregory Nikiforovich, who were unable to attend this meeting due to Stan's stroke. Prof. Wei-Jun Zhang from Shanghai is a key figure in our synthetic efforts, and Dr. C. M. W. Ho carries the burden of computational support. It is a real pleasure to have friends who share your scientific interests. Naturally, NIH support has played an essential role in our efforts and we thank you for your tax support. Most

of all, it is the tolerance of my family who have indulged my intellectual adventures who deserve my thanks.

## References

1. Marshall, G.R., Merrifield, R.B. *Biochemistry* **4**, 2394–2401, 1965.
2. Leznoff, C. *Acc. Chem. Res.* **11**, 327–333, 1978.
3. Nemethy, G., Scheraga, H.A. *Biopolymers* **3**, 155–184, 1965.
4. Clark, W.A., Molnar, C.E. *MD Computing* **11**, 311–317, 1994.
5. Barry, C.D., Graesser, S., Marshall, G.R., In Faiman, M., Nievergelt, J. (Eds.) *Pertinent Concepts in Computer Graphics*, University of Illinois Press, Chicago, 1969.
6. Marshall, G.R., Bosshard, H.E. *Circulation Res.* **31** (Suppl. 2), II-143-II-150, 1972.
7. Pietta, P.G., Marshall, G.R. *Chem. Commun.* 650–651, 1970.
8. Hancock, W.S., Marshall, G.R., Vagelos, P.R. *J. Biol. Chem.* **248**, 2424–2434, 1973.
9. Hancock, W.S., Prescott, D.J., Vagelos, P.R., Marshall, G.R. *J. Org. Chem.* **38**, 774–781, 1973.
10. Marshall, G.R., Vine, W., Needleman, P. *Proc. Natl. Acad. Sci. U.S.A.* **67**, 1624–1630, 1970.
11. Rich, D.H., Sun, C.-Q., Prasad, J.V.N.V., Pathiasseril, A., Toth, M.V., Marshall, G.R., Clare, M., Mueller, R.A., Houseman, K. *J. Med. Chem.* **34**, 1222–1225, 1991.
12. Ondetti, M.A., Cushman, D.W. *Ann. Rev. Biochem.* **51**, 283–308, 1982.
13. Wyvratt, M.J., Patchett, A.A. *Med. Res. Rev.* **5**, 483–531, 1985.
14. Toh, H., Ono, M., Saigo, K., Miyata, T. *Nature* **315**, 691, 1985.
15. Toth, M.V., Marshall, G.R. *Int. J. Pept. Protein Res.* **36**, 544–550, 1990.
16. Toth, M.V., Chiu, F., Glover, G., Kent, S.B.H., Ratner, L., Heyden, N.V., Green, J., Rich, D.H., Marshall, G.R., In *Peptides: Chemistry, Structure, and Biology (Proceedings of the 11th American Symposium)*, ESCOM, Leiden, 1990.
17. Miller, M., Sathyanarayana, B.K., Wlodawer, A., Toth, M.V., Marshall, G.R., Clawson, L., Selk, L., Schneider, J., Kent, S.B.H. *Science* **246**, 1149–1152, 1989.
18. Marshall, G.R., Cramer III, R.D. *Trends Pharmacol. Sci.* **9**, 285–289, 1988.
19. DePriest, S.A., Mayer, D., Naylor, C.B., Marshall, G.R. *J. Am. Chem. Soc.* **115**, 5372–5384, 1993.
20. Waller, C.L., Oprea, T.I., Giolitti, A., Marshall, G.R. *J. Med. Chem.* **36**, 4152–4160, 1993.
21. Head, R.D., Smythe, M.L., Oprea, T.I., Waller, C.L., Green, S.M., Marshall, G.R. *J. Am. Chem. Soc.* **118**, 3959–3969, 1996.
22. Dratz, E.A., Furstenau, J.E., Lambert, C.G., Thireault, D.L., Rarick, H., Schepers, T., Pakhlevaniants, S., Hamm, H.E. *Nature* **363**, 276–281, 1993.
23. Dratz, E.A., Furstenau, L.E., Lambert, C.G., Thireault, D.L., Rarick, H., Schepers, T., Pakhlevaniants, S., Hamm, H.E. *Nature* **390**, 424, 1997.
24. Kisselev, O.G., Kao, J., Ponder, J.W., Fann, Y.C., Gautam, N., Marshall, G.R. *Proc. Natl. Acad. Sci. U.S.A.* **95**, 4270–4275, 1998.
25. Marshall, G.R., Ragno, R., Makara, G.M., Arimoto, R., Kisselev, O. *Lett. Peptide Sci.* **6**, 283–288, 1999.
26. Arimoto, R., Kisselev, O.G., Makara, G.M., Marshall, G.R. *Biophys. J.* (2001), submitted.
27. Riley, D.P. *Adv. Supramol. Chem.* **6**, 217–244, 2000.
28. Aston, K.W., Henke, S.L., Modak, A.S., Riley, D.P., Sample, K.R., Weiss, R.H., Neumann, W.L. *Tetrahedron Lett.* **35**, 3687–3690, 1994.



## **Genomics: From Microbes to Man**

**J. Craig Venter**

*Celera Genomics, Rockville, MD 20850, USA*

J. Craig Venter, Ph.D. is the President and Chief Scientific Officer of Celera Genomics Corporation and the Founder, Chairman of the Board and former President of The Institute for Genomic Research (TIGR), a not-for-profit genomics research institution.

Between 1984 and the formation of TIGR in 1992, Dr. Venter was a Section Chief, and a Lab Chief, in the National Institute of Neurological Disorders and Stroke at the National Institutes of Health (NIH). In 1990, he developed expressed sequence tags (ESTs), a new strategy for gene discovery that has revolutionized the biological sciences. Over 72% of all accessions in the public database GenBank are ESTs from a wide range of species including human, plants and microbes. Out of new algorithms developed to deal with 100,000's of sequences TIGR developed the whole genome shotgun method that led to TIGR completing the first 3 genomes in history and a total of 21 to date.

In May of 1998, Dr. Venter and Perkin-Elmer (now known as Applera) announced the formation of Celera Genomics. Celera's goal is to become the definitive source of genomic and medical information thereby facilitating a new generation of advances in molecular medicine. Celera is building the expertise and information that will enable scientists to transform the way in which human and health problems are diagnosed and treated. On June 26, 2000, Celera announced that it had completed the first assembly of the human genome, which has revealed a total of 3.12 billion base pairs in the human genome. On February 16, 2001, Celera's manuscript on the sequencing of the human genome was published in *Science* Magazine.

Dr. Venter has published more than 160 research articles and is one of the most cited scientists in biology and medicine. He has been the recipient of numerous awards, including the 2000 King Faisal Award in Science and was recently selected as a runner up for TIME Magazine's Man of the Year and was selected as Man of the Year for the Financial Times. In addition to receiving honorary degrees for his pioneering work, he has been elected a Fellow of several societies including the American Association for the Advancement of Science and the American Academy of Microbiology. He received his Ph.D. in Physiology and Pharmacology from the University of California, San Diego.

### **Scientific papers published include:**

1. Complementary DNA Sequencing: "Expressed Sequence Tags" and the Human Genome Project. *Science* **252**, 1651–1656 (1991).
2. Potential Virulence Determinants in Terminal Regions of Variola Smallpox Virus Genome. *Nature* **366**, 748–751 (1993).
3. Whole-Genome Random Sequencing and Assembly of *Haemophilus influenzae* Rd. *Science* **269**, 496–512 (1995)
4. Initial Assessment of Human Gene Diversity and Expression Patterns Based Upon 52 Million Basepairs of cDNA Sequence. *Nature* **377** suppl., 3–174 (1995).
5. The Minimal Gene Complement of *Mycoplasma genitalium*. *Science* **270**, 397–403 (1995).
6. Complete Genome Sequence of the Methanogenic Archeon, *Methanococcus jannaschii*. *Science* **273**, 1058–1073 (1996).

## ***Venter***

7. The Complete Genome Sequence of the Gastric Pathogen *Helicobacter pylori*. *Nature* **388**, 539–547 (1997).
8. The Complete Genome Sequence of the Hyperthermophilic, Sulphate-Reducing Archaeon *Archaeoglobus fulgidus*. *Nature* **390**, 364–370 (1997).
9. Genome Sequence of the Lyme Disease Spirochaete, *Borrelia burgdorferi*. *Nature* **390**, 580–586 (1997).
10. Shotgun Sequencing of the Human Genome. *Science* **280**, 1540–1542 (1998).
11. Complete Genome Sequence of *Treponema pallidum*, the Syphilis Spirochete. *Science* **281**, 375–388 (1998).
12. Chromosome 2 sequence of the human parasite *Plasmodium falciparum*: Plasticity of a eukaryotic chromosome. *Science* **282**, 1126–1132 (1998).
13. Global Transposon Mutagenesis and a Minimal Mycoplasma Genome. *Science* **286**, 2165–2169 (1999).
14. Sequence and Analysis of Chromosome 2 of *Arabidopsis thaliana*. *Nature* **402**, 761–767 (1999).
15. Complete Genome Sequencing of the Radioresistant Bacterium, *Deinococcus radiodurans* R1. *Science* **286**, 1571–1577 (1999).
16. The Genome Sequence of *Drosophila melanogaster*. *Science* **287**, 2185–2204 (2000).
17. Sequencing of the Human Genome. *Science* **291**, 1304–1351 (2001).

**Synthetic Methodologies,  
Solid Phase Synthesis,  
Solid Phase Organic Synthesis,  
Combinatorial Techniques**



## **Fluorous Methods for Synthesis and Separation of Organic Molecules: From Separating Mixtures to Making Mixtures**

**Dennis P. Curran**

*Department of Chemistry, University of Pittsburgh, Pittsburgh, PA 15260, USA,*

Fluorous molecules partition out of an organic phase and into a fluorous (highly fluorinated) phase in a liquid-liquid extraction. New fluorous techniques allow simple yet substantive separations of organic reaction mixtures based on the presence or absence of a fluorous tag. Fluorous-tagged molecules can also be separated from non-tagged molecules by solid phase extraction over fluorous reverse phase silica gel. This technique is ideal for solution phase parallel synthesis because it allows simple yet substantive separations of organic reaction mixtures.

Fluorous techniques are rapidly developing as a solution phase alternative to solid phase synthesis. Like solid phase techniques, a reaction component (reactant, reagent, catalyst) is tagged with a functionality for the purpose of strategic separation. However, the tag is not a polymer but a small or moderately sized fluorinated piece or domain. Reactions of fluorous molecules can be conducted in solution, and fluorous products can be purified and characterized by using standard small molecule spectroscopic and chromatographic techniques.

Fluorous molecules can be separated by unique fluorous techniques including liquid-liquid extraction, solid-liquid extraction and fluorous chromatography. Liquid-liquid extraction and solid liquid extraction are typically used to separate molecules bearing fluorous tags from untagged (organic or inorganic) molecules. Fluorous chromatography is used to separate fluorous molecules from each other based on fluorine content. Both fluorous solid phase extraction and fluorous chromatography typically employ silica gel with a fluorocarbon bonded phase ("fluorous reverse phase silica gel").

Table 1 summarizes the four main fluorous methods outlined in this lecture and compares and contrasts them. Each technique is briefly summarized, and then selected references [1–20] are provided.

*Fluorous Biphasic Catalysis:* In this first fluorous technique, a catalyst containing one or more highly fluorinated ligands promotes a reaction of an organic substrate in a mixture of organic and fluorous solvents. Depending on solvents and reaction condi-

*Table 1.*

Technique	Fluorine Content	Rxn Solvent	Separation	Uses
Fluorous Biphasic Catalysis	high	fluorous and organic	single liquid-liquid separation	green chemical processes
Fluorous Reagents	low-medium	organic or hybrid	liquid-liquid or solid-liquid extraction	universal
Fluorous Substrates	low	organic	solid-liquid extraction	chemical discovery, intermediate synthesis
Fluorous Mixture Synthesis	low, variable	organic	fluorous chromatography	leveraged chemical discovery

## Curran

tions, the reaction may be mono- or multiphasic. In either case, two liquid phases are generated at the end of the reaction, and simple separation gives the product from the organic phase and the catalyst from the fluorous phase.

**Fluorous Reagents:** Here a reagent, catalyst or scavenger bearing a low-medium number of fluorines is used to convert an organic substrate to a product in a traditional organic solvent, sometimes with a lightly fluorinated cosolvent. Fluorous solvents are not used. The fluorous products are removed from the organic product by liquid-liquid or solid-liquid extraction, depending on the fluorine content.

**Fluorous Substrates:** In this conceptual equivalent of “solid phase synthesis”, organic substrates are tagged with fluorous groups (protecting groups, traceless tags, *etc.*) and then carried through a series of steps. Solid-phase extraction is used to separate the desired tagged products from all untagged reaction components. The tag is finally removed followed by a final spe (or chromatography) to give the target organic product.

**Fluorous Mixture Synthesis:** In this variant, a series of fluorous substrates are given tags differing in fluorine content. The tagged substrates are then mixed and taken through several steps. Finally, the mixture is resolved into its individual pure components (demixed) by fluorous chromatography, and each product is detagged. The technique harvests the efficiency advantage of mixture synthesis without the usual purification and identification detractions.

**Commercialization:** Fluorous Technologies, Inc. intends to commercialize reagents, silica gel and other components needed for fluorous synthesis techniques. Information can be found at [www.fluorous.com](http://www.fluorous.com).

## Acknowledgments

I warmly thank an enthusiastic group of co-workers for their intellectual and experimental contributions to this project. I also thank the National Science Foundation, the National Institutes of Health, Warner-Lambert, CombiChem, and Merck for funding our work in this area.

## References

### Reviews:

1. D.P. Curran, “Combinatorial organic synthesis and phase separation: Back to the future”, *Chemtracts-Org. Chem.* **9**, 75–87 (1996).
2. D.P. Curran, “Strategy-level separations in organic synthesis: From planning to practice”, *Angew. Chem., Int. Ed. Engl.* **37**, 1175–1196 (1998).
3. J.J. Maul, P.J. Ostrowski, G.A. Ublacker, B. Linclau, D.P. Curran “Benzotrifluoride and related solvents in organic synthesis”, In P. Knochel (Ed.), *Topics in Current Chemistry, Modern Solvents in Organic Synthesis*. Vol. 206, Springer-Verlag, Berlin, 1999, pp. 80–104.
4. D.P. Curran, “Parallel synthesis with fluorous reagents and reactants”, *Med. Res. Rev.* **19**, 432–438 (1999).
5. D.P. Curran, “Fluorous techniques for the synthesis of organic molecules: A unified strategy for reaction and separation”, In *Stimulating Concepts in Chemistry*, F. Stoddart, D. Reinhoudt, M. Shibasaki, (Eds.), Wiley-VCH, 2000, pp. 25–37.
6. D.P. Curran, “Fluorous methods for synthesis and separation of organic molecules” *Pure Appl. Chem.* **72**, 1649–1653 (2000).
7. Curran, D.P., Hadida, S., Studer, A., He, M., Kim, S.-Y., Luo, Z., Larhed, M., Hallberg, M., Linclau, B. “Experimental techniques in fluorous synthesis: A user’s guide” In H.

Fenniri (Ed.) *Combinatorial Chemistry: A Practical Approach*; Vol. 2; Oxford Univ Press, Oxford, 2000, pp. 327–352.

*Issued Patents:*

8. Curran, D.P., Hadida, S., Hoshino, M., Studer, A. "Fluorous Reaction Systems", US 5777121, 1998; Curran, D.P., Hadida, S., Hoshino, M., Studer, A., Kim, S.-Y., Wipf, P., Jäger, P. "Fluorous Reaction and Separation Systems", US 5859247, 1999; Curran, D.P., Hadida, S., Hoshino, M., Studer, A., Kim, S.-Y., Wipf, P., Jäger, P. "Fluorous Reaction and Separation Systems", US 6156896, 2000.

*Fluorous Biphasic Catalysis:*

9. I.T. Horvath, J. Rabai "Facile catalyst separation without water: Fluorous biphasic hydroformylation of olefins", *Science* **266**, 72–75 (1994).
10. I.T. Horvath "Fluorous biphasic chemistry", *Acc. Chem. Res.* **31**, 641–650 (1998).
11. Dinh, L.V., Gladysz, J.A. *Tetrahedron Lett.* **40**, 8995 (1999).
12. Y. Nakamura, S. Takeuchi, Y. Ohgo, D.P. Curran, "Asymmetric alkylation of aromatic aldehydes with diethylzinc catalyzed by a fluorous BINOL-Ti complex in an organic and fluorous biphasic system", *Tetrahedron Lett.* **41**, 57–60 (2000).
13. Y. Nakamura, S. Takeuchi, Y. Ohgo, D.P. Curran, "Preparation of a fluorous chiral BINOL derivative and application to an asymmetric protonation reaction" *Tetrahedron* **56**, 351–356 (2000).

*Fluorous Reagents:*

14. D.P. Curran, S. Hadida, "Tris(2-(perfluorohexyl)ethyl)tin hydride: A new fluorous reagent for use in traditional organic synthesis and liquid phase combinatorial synthesis", *J. Am. Chem. Soc.* **118**, 2531–2532 (1996).
15. D.P. Curran, S. Hadida, S.Y. Kim, Z.Y. Luo, "Fluorous tin hydrides: A new family of reagents for use and reuse in radical reactions", *J. Am. Chem. Soc.* **121**, 6607–6615 (1999).
16. B. Bucher, D.P. Curran, "Selective sulfonylation of 1,2-diols and derivatives catalyzed by a recoverable fluorous tin oxide" *Tetrahedron Lett.* **41**, 9617–9621 (2000).
17. Q. Zhang, Z.Y. Luo, D.P. Curran, "Separation of 'light fluorous' reagents and catalysts by fluorous solid-phase extraction: Synthesis and study of a family of triarylphosphines bearing linear and branched fluorous tags" *J. Org. Chem.* **65**, 8866–8873 (2000).

*Fluorous Synthesis:*

18. A. Studer, S. Hadida, R. Ferritto, S.Y. Kim, P. Jeger, P. Wipf, D.P. Curran, "Fluorous synthesis: A fluorous-phase strategy for improving separation efficiency in organic synthesis", *Science* **275**, 823–826 (1997).
19. D.P. Curran, Z.Y. Luo, "Fluorous synthesis with fewer fluorines (Light fluorous synthesis): separation of tagged from untagged products by solid-phase extraction with fluorous reverse-phase silica gel", *J. Am. Chem. Soc.* **121**, 9069–9072 (1999).

*Fluorous Mixture Synthesis:*

20. Z. Luo, D.P. Curran, Y. Oderaotoshi, Q. Zhang, "Fluorous mixture synthesis: A fluorous-tagging strategy for synthesis and separation of mixtures of organic compounds", *Science* **291**, 1766–1769 (2001).

## Synthesis of $\beta$ and $\gamma$ -Substituted Prolines for Conformation-Activity Relationship Studies of the $\alpha$ -MSH Analogue MT-II

Chaozhong Cai, Wei Wang, Chiyi Xiong, Vadim A. Soloshonok,  
 Mingying Cai and Victor J. Hruby

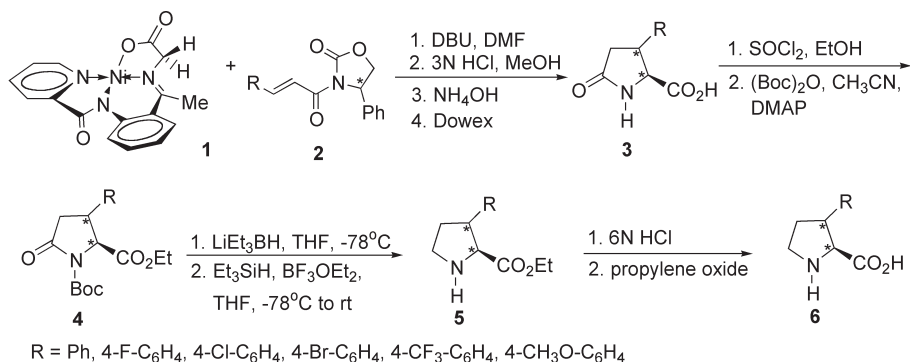
Department of Chemistry, University of Arizona, Tucson, AZ 85721, USA

### Introduction

Substituted prolines have limited rotational freedom about  $\chi_1$  and  $\chi_2$ , and therefore can be used as unique probes for conformation-activity studies by incorporating them into biologically important peptides [1]. For example, substitution of Pro for His6 in the  $\alpha$ -MSH analogue MT-II led to analogues with high agonist potency and selectivity for agonist activity at the human MC5R [2]. To explore this function, we have synthesized a series of novel, topographically constrained  $\beta$  and  $\gamma$ -substituted prolines and incorporated these optically pure substituted prolines into MT-II at positions 6 and 7.

### Results and Discussion

Synthesis of  $\beta$ -substituted prolines is shown in Scheme 1. Highly diastereoselective Michael addition reactions between the Ni(II) complex of glycine Schiff base **1** and (*S*) or (*R*)-3-(*E*-enoyl)-4-phenyl-1,3-oxazolidin-2-ones **2**, followed by decomposition and neutralization, gave optically pure  $\beta$ -substituted pyroglutamic acids **3** in good yields (>80%) [3,4]. The resulting  $\beta$ -substituted pyroglutamic acids were converted to their esters and protected with Boc groups to give ethyl *N* $\alpha$ -Boc- $\beta$ -substituted pyroglutamates **4** in 86–92% yields. By using Pedregal's protocol [5], selective reduction of the amide carbonyl group in **4** was accomplished to afford the corresponding proline esters **5** in high chemical yields (82–95%), which were hydrolyzed to quantitatively give optically pure  $\beta$ -substituted prolines **6**. No stereoisomers were found from  $^1\text{H}$  NMR.

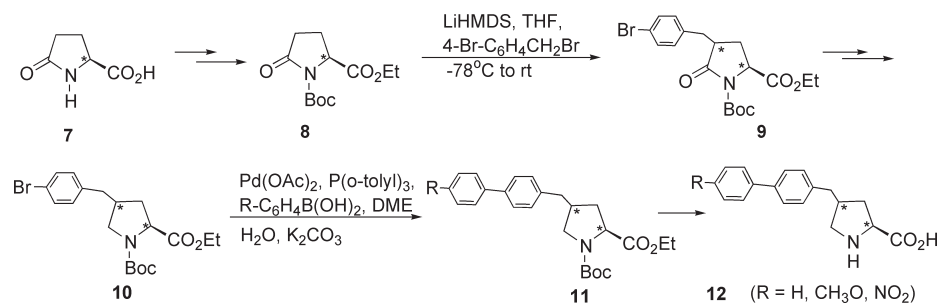


Scheme 1. Synthesis of novel  $\beta$ -substituted prolines.

Highly constrained  $\gamma$ -substituted prolines were synthesized by using pyroglutamic acid **7** as a building block (Scheme 2). Ethyl *N* $\alpha$ -Boc-pyroglutamate **8** was prepared from **7** in 91% yield. Alkylation of lithium enolate derived from **8** with benzylic bromides afforded benzylated pyroglutamates **9** in good yield (84%) and excellent diastereoselectivity (>98%). After selective reduction and protection, the resulting

## Synthetic Methods

$N\alpha$ -Boc- $\gamma$ -substituted prolinates **10** were coupled with  $p$ -substituted phenyl borates to lead more constrained  $N\alpha$ -Boc- $\gamma$ -substituted prolinates **11** (95–96%), which quantitatively afforded the corresponding  $\gamma$ -substituted prolines **12** after acidic hydrolysis.



Scheme 2. Synthesis of novel  $\gamma$ -substituted prolines.

Both novel  $\beta$  and  $\gamma$ -substituted prolines were incorporated into MT-II at positions 6 and 7 by solid phase synthesis [6]. A series of highly topographically constrained MT-II analogues were obtained and their conformation-biological activity studies are in process.

## Acknowledgments

This research was supported by grants from the U.S. Public Health Service and the National Institute of Drug Abuse (DA 06284, DA 13449 and DK 17420).

## References

1. Hruby, V.J., Balse, P.M. *Curr. Med. Chem.* **7**, 945 (2000).
2. Grieco, P., Gantz, I., Hruby, V.J. *J. Med. Chem.* submitted.
3. Soloshonok, V.A., Cai, C.; Hruby, V.J. *Org. Lett.* **2**, 747 (2000).
4. Soloshonok, V.A., Cai, C.; Hruby, V.J. *Angew. Chem., Int. Ed. Engl.* **39**, 2172 (2000).
5. Pedregal, C., Ezruerra, J., Escribano, A., Carreno, M.C., Garcia Ruano, J.L. *Tetrahedron Lett.* **35**, 2053 (1994).
6. Hruby, V.J., Wilke, S., Al-Obeidi, F., Jiao, D., Lin, Y. *Reactive Polymers* **22**, 231 (1994).

## The General Asymmetric Synthesis of *Syn*- and *Anti*- $\beta$ -substituted Cysteine and Serine Derivatives

Chiyi Xiong, Wei Wang and Victor J. Hruby

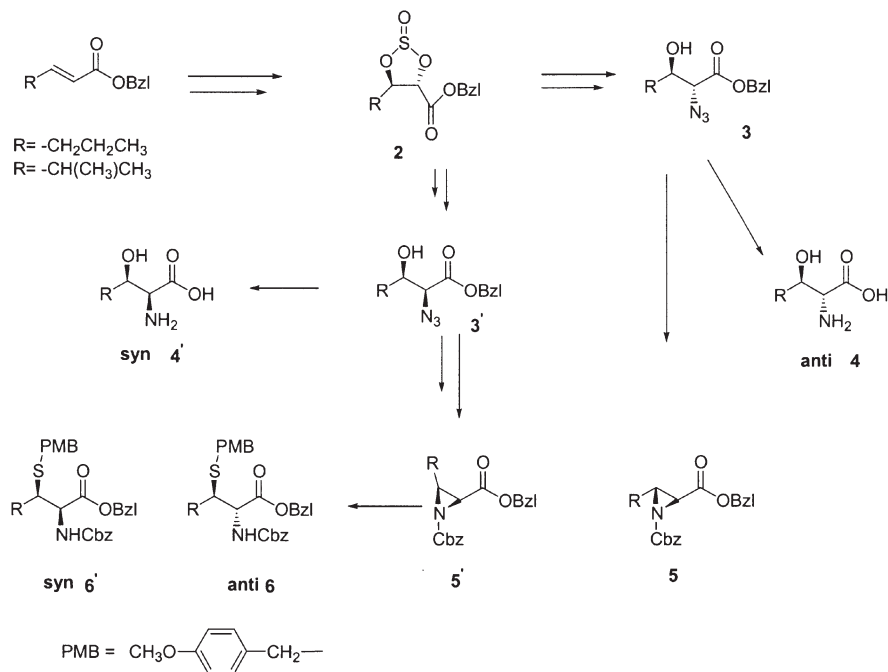
Department of Chemistry, University of Arizona, Tucson, AZ 85721, USA

### Introduction

Complete understanding of the stereochemical requirements of side chain groups important in peptide ligand-receptor/acceptor interactions plays a crucial role in the rational design of bioactive peptides and nonpeptide mimetics. This approach can be realized by incorporation of conformationally constrained novel amino acids into a peptide or nonpeptide template. Among the novel amino acids,  $\beta$ -substituted cysteines and  $\beta$ -substituted serines play a unique function in peptide conformational constraints.  $\beta$ -Substituted cysteines when introduced into the peptide chain can not only constrain the backbone conformation through the formation of a disulfide bridge, but also preserve side chains which are very important for molecular recognition [1].  $\beta$ -Substituted cysteines and serines also can be used as building blocks for dipeptide  $\beta$ -turn mimetics [2].

### Results and Discussion

The synthesis of  $\beta$ -alkylsubstituted serine analogues (Scheme 1) begins with the Sharpless asymmetric dihydroxylation [3] of benzyl  $\alpha,\beta$ -unsaturated esters **1** in the presence of (DHQD)<sub>2</sub>PHAL (AD-mix  $\alpha$ ) and methanesulfonamide. The reaction proceeded smoothly to yield the (2*R*,3*S*)-diols **2** with excellent optical purity (>95% ee).



Scheme 1. Stereodivergent synthesis of *anti*- and *syn*-cysteines and serines.

### Synthetic Methods

The diols were converted to their 2, 3-cyclic sulfites with thionyl chloride and oxidized to the cyclic sulfates **2** in a one-pot reaction. Nucleophilic substitution by NaN<sub>3</sub> gave  $\alpha$ -azido esters **3**, and subsequent hydrogenation provided the  $\beta$ -alkylsubstituted serines **4**. Diastereomers **3'** of **3** can be obtained using NH<sub>4</sub>Br to ring open the sulfates **2** followed by a second nucleophilic displacement with NaN<sub>3</sub> to obtain the desired stereochemistry at the  $\alpha$ -position [4]. The result of this double-inversion procedure is a net retention of configuration, and the products **3'** is diastereomers of compounds **3** generated from direct azide displacement of the sulfates **2**.

The first general asymmetric synthesis of  $\beta$ -substituted cysteines started with the azido esters **3** and **3'** which can be converted to aziridine-2-carboxylic esters **5** and **5'** under Staudinger reaction conditions with high enantiomeric purity. In the presence of a Lewis-acid catalyst, the activated *N*-(benzyloxycarbonyl) aziridine-2-carboxylic esters **5** and **5'** reacted with 4-methoxybenzylthiol to provide the desired protected *syn*- and *anti*- $\beta$ -alkylsubstituted cysteines **6** and **6'**.

### Acknowledgments

This work was supported by grants from US Public Health Service (DK 17420) and the National Institute of Drug Abuse (DA 13449).

### References

1. Hruby, V.J. *Life Sci.* **31**, 189–199 (1982).
2. (a) Nagai, U., Sato, K. *Tetrahedron Lett.* **26**, 647–650 (1985). (b) Estiarte, M.A., Rubiralta, M., Diez, A. *J. Org. Chem.* **65**, 6992–6999 (2000).
3. Berrisford, D. J., Bolm, C., Sharpless, K.B. *Angew. Chem., Int. Ed. Engl.* **34**, 1059–1070 (1995).
4. Shao, H., Rueter, J.K., Goodman, M. *J. Org. Chem.* **63**, 5240–5244 (1998).

## The Novel Asymmetric Synthesis of $\beta$ -Functionalized Phenylalanine Derivatives

Chiyi Xiong, Wei Wang, Chaozhong Cai and Victor J. Hruby

Department of Chemistry, University of Arizona, 85721, USA

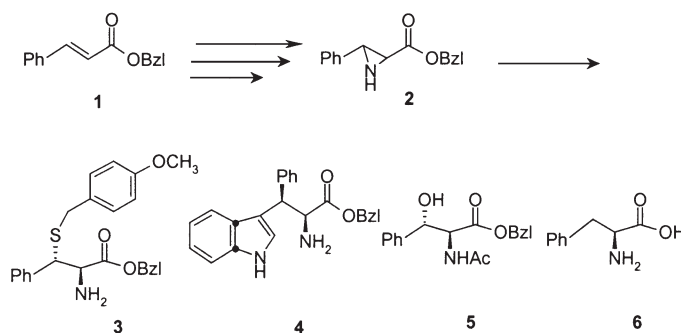
### Introduction

As part of a continuing effort in our laboratory to obtain either backbone and/or side chain conformationally constrained, novel amino acids, we have designed and synthesized new types of  $\beta$ -functionalized amino acids, namely  $\beta$ -substituted cysteines,  $\beta$ -substituted serines and  $\beta$ -substituted tryptophanes.  $\beta$ -Substituted cysteines when introduced into the peptide chain can not only constrain backbone conformation through the formation of a disulfide bridge, but also preserve the respective side chains, which is important for the molecular recognition [1].  $\beta$ -Substituted cysteines and  $\beta$ -substituted serines are also building blocks for so-called "rigid dipeptide  $\beta$ -turn mimetics" [2].  $\beta$ -Phenylsubstituted tryptophans are chimeric amino acids containing two bulky side chain groups, a indole and a phenyl group. The interaction between these two bulky side chain groups can produce strong constraints simultaneously for both  $\chi^1$  and  $\chi^2$  side chain torsional angles [3].

### Results and Discussion

Commercially available benzyl cinnamate was the starting point of our synthesis. Cinnamate **1** was subjected to the Sharpless asymmetric dihydroxylation in the presence of (DHQD)<sub>2</sub>PHAL (AD-mix- $\alpha$ ) and methanesulfonamide (Scheme 1). The reaction proceeded smoothly to yield (2*R*,3*S*)-diol in high yield and excellent optical purity (98% ee) [4]. The vicinal diol was first converted to the cyclic sulfite, and then the cyclic sulfite was further oxidized to cyclic sulfate with RuO<sub>4</sub> (NaIO<sub>4</sub>/cat, RuCl<sub>3</sub>). Ring opening reaction of the cyclic sulfate in an S<sub>N</sub>2 fashion with N<sub>3</sub> provided azido alcohols as regioisomers in 6 : 1 ratio ( $\beta/\alpha = 6 : 1$ ). In the following so-called Staudinger reaction [5], the aziridine **2** was formed stereospecifically.

Treatment of aziridine **2** with 3 equivalents of 4-methoxybenzylthiol in dichloromethane in the presence of 1.5 equivalents of boron-trifluoride etherate followed by amino group protection resulted in the (3*S*,3'*S*)- $\beta$ -phenyl-cysteine derivative **3**. The reaction is stereospecific with nucleophile attacking in an S<sub>N</sub>2 fashion at the benzylic C3



Scheme 1. Synthesis of novel amino acids via aziridines.

position. The regiochemistry of the product was unequivocally established from the mass spectrum which exhibits the fragment  $[\text{C}_5\text{H}_5\text{CHSCH}_2\text{C}_6\text{H}_4\text{OCH}_3]^+$  ( $m/z$ : 231). The exclusive, stereospecific attack of the carbon nucleophile at C3 position also was observed upon reaction with indole in the presence of boron trifluoride etherate. The regiochemistry of the reaction could be deduced from the mass spectrum and  $^1\text{H}$  NMR characteristics of the (2*S*,3*R*)-product **4**. When substrate **2** was stirred at 70 °C with acetic acid for 2 h, acidolysis of the aziridine occurred. The ring opening proceeded with complete inversion of configuration at C3 position, probably via the initial ring opening by attack of acetate anion at C3, and following acyl migration from oxygen to nitrogen gave the (2*S*,3*S*)-product **5** in high yield [6]. Substrate **2** also underwent smooth reductive opening reaction *via* hydrogenation at the aziridine benzylic position to stereospecifically provide (*S*)-phenylalanine **6**.

In conclusion, an efficient procedure for making chiral phenylsubstituted aziridines is described. The stereospecific and regioselective ring-opening reaction of aziridine intermediates with various nucleophiles, could provide us many novel amino acids.

#### Acknowledgments

This work was supported by grants from US Public Health Service (DK 17420) and the National Institute of Drug Abuse (DA 13449 and DA 06284).

#### References

1. Hruby, V.J. *Life Sci.* **31**, 189–199 (1982).
2. (a) Nagai, U., Sato, K. *Tetrahedron Lett.* **26**, 647–650 (1985). (b) Estiarte, M.A., Rubiralta, M., Diez, A. *J. Org. Chem.* **65**, 6992–6999 (2000).
3. For reviews see: Gibson, S.E., Guillo, N., Tozer, M.J. *Tetrahedron* **55**, 585–615 (1999).
4. Berrisford, D.J., Bolm, C., Sharpless, K.B. *Angew. Chem., Int. Ed. Engl.* **34**, 1059–1070 (1995).
5. Gololobov, Y.G., Zhmurova, I.N., Kasukhin, L.F. *Tetrahedron* **37**, 437–472 (1981).
6. Legters, J., Thijs, L., Zwanenburg, B. *Recl Trav. Chim. Pays-Bas* **111**, 16–21 (1992).

## An Efficient Method for Large-Scale Synthesis of Stereochemically Defined and Conformationally Constrained $\beta$ -Substituted or $\alpha,\beta$ -Disubstituted Amino Acids

Xuejun Tang, Vadim A. Soloshonok and Victor J. Hruby

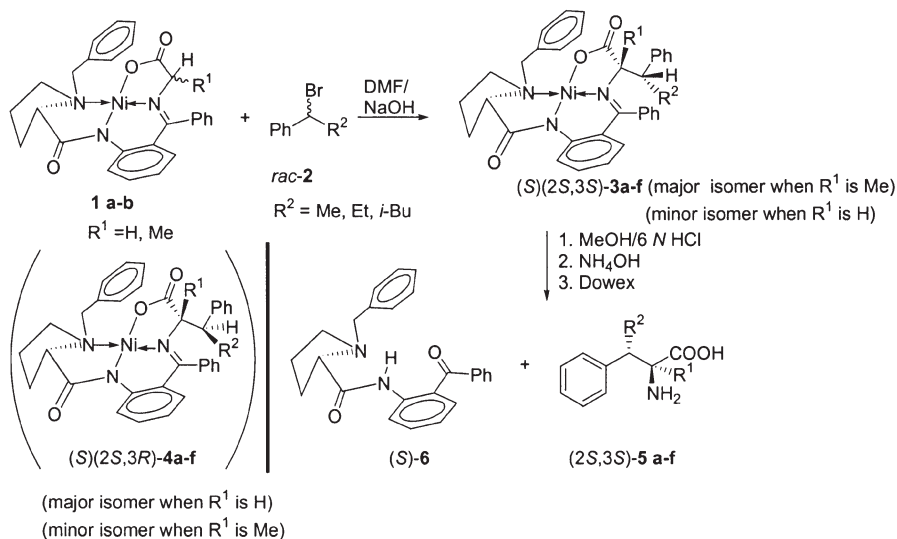
Department of Chemistry, University of Arizona, Tucson, AZ 85721, USA

### Introduction

In our continuing efforts to design and synthesize conformationally constrained peptides to understand the interactions between receptors and ligands, a wide range of sterically constrained amino acids are needed [1]. As a part of our efforts in this area, we have developed a systematic practical method for preparation of conformationally constrained novel amino acids in gram quantities. Starting from chiral nickel (II) complexes containing a glycine or alanine moiety, which were prepared from commercially available materials, alkylations with the corresponding alkyl halides followed by routine work-up, provide the target amino acids in good overall yields and excellent optical purity [2–7].

### Results and Discussion

Aiming to develop a versatile method to synthesize  $\beta$ -substituted, or  $\alpha,\beta$ -disubstituted amino acids **5** (**a**: R<sup>1</sup> = H, R<sup>2</sup> = Me; **b**: R<sup>1</sup> = H, R<sup>2</sup> = Et; **c**: R<sup>1</sup> = H, R<sup>2</sup> = *i*-Bu; **d**: R<sup>1</sup> = Me, R<sup>2</sup> = Me; **e**: R<sup>1</sup> = Me, R<sup>2</sup> = Et; **f**: R<sup>1</sup> = Et, R<sup>2</sup> = *i*-Bu), we have investigated the direct alkylation of pre-formed Ni(II) glycine (**a**: R<sup>1</sup> = H) and alanine (**b**: R<sup>1</sup> = Me) complexes **1** with  $\alpha$ -alkylbenzyl bromides. After the treatment of complex **1** with regular bases such as NaOH and KOH in DMF under argon atmosphere, the bromide **2** was added and the reaction progress was monitored by TLC with 1 : 1 acetone/hexanes as eluent. It was found that with the increase of the size of R<sup>2</sup> (from Me to *i*-Bu) the reaction time increases. Also alkylation of the glycine complex (R<sup>1</sup> = H) is much faster than of the alanine complex (R<sup>1</sup> = Me). Alkylation of either complex (R<sup>1</sup> = H, or R<sup>1</sup> = Me) gives the  $\alpha$ -(*S*) isomers as the predominant major products.



With R1 as H, only small amounts of the  $\alpha$ -(R) isomers were detected after alkylation in the case of R2 as Me or Et, and the amount of  $\alpha$ -(R) isomers can be significantly decreased under elevated reaction temperatures or longer reaction times. The ratio of  $\alpha$ -(S) to  $\alpha$ -(R) was greater than 30 : 1. With R2 as i-Bu, no  $\alpha$ -(R) isomers were detected. With R1 as H, the major  $\alpha$ -(S) products have a configuration of (2S,3R) **4a–c** (**a**: R1 = H, R2 = Me; **b**: R1 = H, R2 = Et; **c**: R1 = H, R2 = i-Bu ) and the minor  $\alpha$ -(S) products have (2S,3S) configuration (**3a–c**, **a**: R1 = H, R2 = Me; **b**: R1 = H, R2 = Et; **c**: R1 = H, R2 = i-Bu).

In case of R1 as Me, no  $\alpha$ -(R) isomers were detected after alkylation. But the (2S,3S) isomers **3d–f** (**d**: R1 = Me, R2 = Me; **e**: R1 = Me, R2 = Et; **f**: R1 = Et, R2 = i-Bu) were the major products and (2S,3R) were assigned as the minor products (**4d–f**) (**d**: R1 = Me, R2 = Me; **e**: R1 = Me, R2 = Et; **f**: R1 = Et, R2 = i-Bu) based on the X-ray crystal structure.

After column purification the enantiopure and diastereopure alkylated Ni (II) complexes were decomposed with 3 M HCl in MeOH to release the amino acids. Upon treatment with ammonium hydroxide, free amino acids can be obtained in multi-gram quantities. The ligand can be recycled.

#### Acknowledgments

The work was supported by grants from U.S. Public health Service and the National Institute of Drug Abuse Grants DK 17420 and DA 13449. The views expressed are those of the authors and not necessarily of the USPHHS.

#### References

1. Gante, J. *Angew. Chem., Int. Ed. Engl.* **33**, 1699 (1994).
2. Hruby, V.J. *Med. Res. Rev.* **9**, 343 (1989).
3. Hruby, V.J. *Drug Discovery Today* **2**, 165 (1997).
4. Soloshonok, V.A., Tang, X., Hruby, V.J. *Org. Lett.* **3**, 341 (2001).
5. Soloshonok, V.A., Tang, X., Hruby, V.J. *Tetrahedron*, in press (2001).
6. Tang, X., Soloshonok, V.A., Hruby, V.J. *Tetrahedron: Asymmetry* **11**, 2917 (2000).
7. Qiu, W., Soloshonok, V.A., Cai, C., Tang, X., Hruby, V.J. *Tetrahedron* **56**, 2577 (2000).

## Synthesis of Amino Acids with Novel Biophysical Properties

**Zhanna Zhilina, Isabel Alves, Scott Cowell, Xuejun Tang,  
Malcolm Kavarana and Victor J. Hruby**

*Department of Chemistry, University of Arizona, Tucson, AZ 85721, USA*

### Introduction

Amino acids with unique physical properties have been used to study the conformational interactions of peptides and proteins. Two such molecules are pyrenylalanine and ferrocenylalkyl derivatives of amino acids. Pyrenylalanine has unique spectroscopic properties that can be exploited to understand conformations of peptides [1]. Ferrocenylalkyl derivatives of amino acids combine the properties of ferrocene and amino acids to offer compounds that will intercalate with DNA and can be targeted towards cancerous cells [2]. This paper describes the synthesis of these compounds and presents preliminary data concerning the intercalation of the ferrocenylalkyl amino acids towards DNA.

### Results and Discussion

Pyrenylalanine (Figure 1) was prepared using Belokon's Ni-complex (Arcos) [3] in three steps starting with pyrenemethanol. Proton NMR shows the *S* configuration at a 19 : 1 ratio to the *R* configuration. The enantiomers were easily separated by column chromatography. The decomposition of the complex gave the desired compound in quantitative yield. The resulting pyrenylalanine was fully characterized including optical rotation. This compound can be placed in peptide ligands to study energy transfer between the pyrenylalanine and tyrosines that may be present in the system.

Ferrocenylalkyl derivatives of amino acids (Table 1) were synthesized by using standard procedures [4]. We proposed that ferrocenylalkyl containing amino acids could interact covalently and noncovalently with DNA. Experiments show that these compounds act as alkylating agents toward the DNA fragment adenine and also intercalate by a flat aromatic cyclopentadienyl ring between two adjacent bases of DNA. These results let us consider ferrocenylalkyl containing amino acids as possible potent antitumor agents. Experiments on tumor cells are in progress.

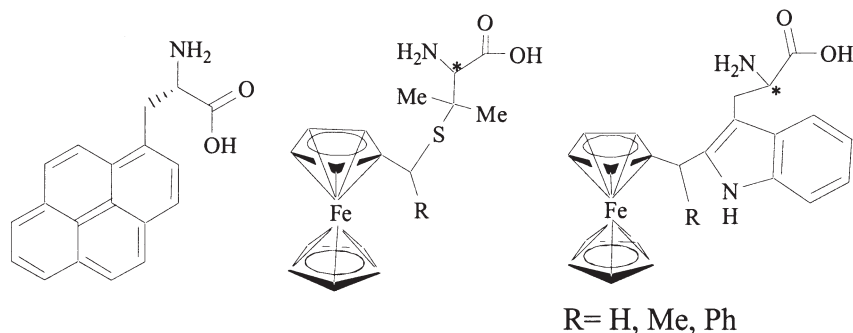


*Fig 1. Structures of pyrenylalanine and ferrocenylalkyl derivatives.*

Table 1. Yields and optical rotation of synthesized molecules.

Product	Characteristics	
	$[\alpha]_D^{25}$ (c 0.5)	% Yield
<i>N</i> -Ferrocenylmethyl-L-histidine	+25 <sup>a</sup>	55
<i>S</i> -Ferrocenylmethyl-L-cysteine	+16 <sup>b</sup>	96
<i>S</i> -Ferrocenylethyl-L-cysteine		92
<i>N</i> -Ferrocenylmethyl-L-tryptophan		15
<i>S</i> -Ferrocenylmethyl-D-penicillamine	−38 <sup>a</sup>	93
<i>S</i> -Ferrocenylethyl-D-penicillamine		87
Ferrocenylmethyl-L-tryptophan		70
<i>N</i> - $\alpha$ -Fmoc- <i>N</i> -in- <i>t</i> -Boc-Ferrocenylmethyl-L-tryptophan	−16.5 <sup>c</sup>	80
Bromomethyl Pyrene	n/a	70
Ni-complexed Pyrene	n/a	90
Pyrenylalanine	+64.8 <sup>c,d</sup>	quant

<sup>a</sup> MeOH + 1%TFA. <sup>b</sup> MeOH. <sup>c</sup> DMSO. <sup>d</sup> 9.865 gm/100 mL.

### Acknowledgments

We thank Dr. Polt for use of his UV spectrometer and Dr. McGrath for use of his polarimeter. Supported by grant from NIH-NIDA, DK 17420 and DA 06284.

### References

1. Sisido, M., Imanishi, Y., Egusa, S. *Chem. Lett.* 1307–1310 (1983).
2. Snegur, L.V., Nekrasov, Yu.S., Gumenyk, V.V., Zhilina, Zh.V., Morozova, N.B., Sviridova, I.K., Rodina, I.A., Sergeeva, N.S., Shchitkov, K.G., Babin, V.N. *Russ. Khim. Zh.* **42**, 178–183 (1998).
3. Soloshonok, V., Cai, C., Hruby, V. *Tetrahedron* **55**, 12045–12058 (1999).
4. Stewart, A., Drey, Ch. *J. Chem. Soc., Perkin Trans. 1* **6**, 1753–1756 (1990).

## Two Novel and Efficient Approaches to Synthesis of Enantiopure Dipeptide $\beta$ -Turn Mimetics: Indolizidinone Amino Acids

Wei Wang, Chiyi Xiong, Jiangqian Yang and Victor J. Hruby

Department of Chemistry, University of Arizona, Tucson, AZ 85721, USA

### Introduction

Indolizidinone amino acids **1** (Figure 1) have been proposed to mimic or induce  $\beta$ -turn secondary structural features for peptides and proteins [1,2]. It has been demonstrated that incorporation of some of these scaffolds into biologically active peptides has led to peptide mimetic ligands with enhanced activities and metabolic stabilities [1,2]. However, the lack of efficient methods for the asymmetric synthesis of these compounds is one of the major bottlenecks in the field. Recently we have developed two novel approaches for the synthesis of such compounds in high stereoselectivity.

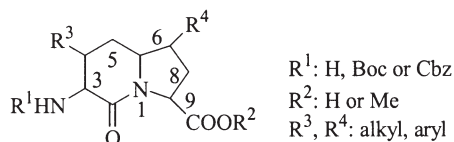
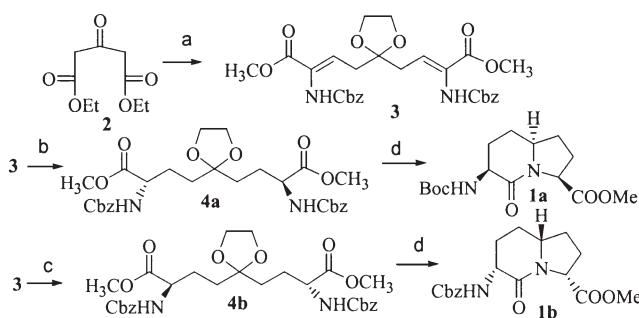


Fig. 1. Indolizidinone amino acids **1**.

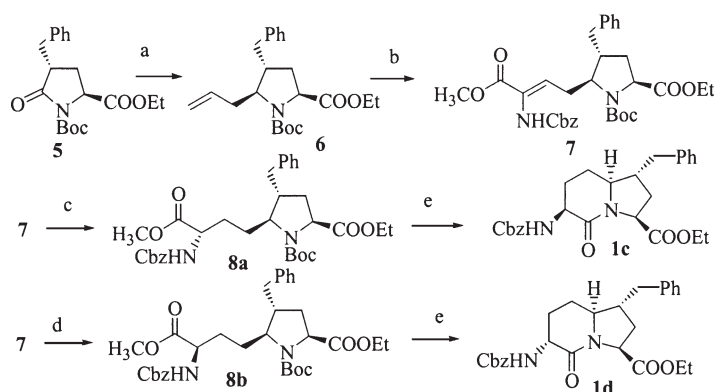
### Results and Discussion

In our initial effort, we have developed an efficient method for the preparation of the scaffolds of the indolizidinone amino acids **1a,b** from commercially available diethyl 1,3-acetonedicarboxylate (**2**) in 5 steps (Scheme 1) [3]. The protection of ketone as a ketal, then reduction of the diester to dialdehyde following by the Horner–Emmons reaction gave the dehydroamino ester **3**. The asymmetric hydrogenations of **3** using (*S,S*) or (*R,R*) Et-DUPHOS, Rh(I)-based catalysts generated the key intermediates **4a** and **4b** with *S* and *R* configurations, respectively, in high stereoselectivity (>96% ee) [4]. Compounds **4a,b** were subjected to one-pot reaction to afford final products **1**.



(a) (i)  $\text{HO}(\text{CH}_2)_2\text{OH}$ ,  $\text{BF}_3 \cdot \text{OEt}_2$ , benzene, reflux, 24 h, 76%; (ii) DIBAL,  $-78^\circ\text{C}$ , toluene, 70 min, ca. 70%; (iii)  $(\text{MeO})_2\text{P}(\text{O})\text{CH}(\text{NHCbz})\text{COOCH}_3$ , DBU,  $\text{CH}_2\text{Cl}_2$ , RT, 4 h, 72%; (b) Rh(I) (COD) (*S,S*) Et-DUPHOS,  $\text{H}_2$  (70 psi), 24 h, MeOH, 97%; (c) Rh(I) (COD) (*R,R*) Et-DUPHOS,  $\text{H}_2$  (70 psi), 24 h, MeOH, 95%; (d) (i) 10% Pd/C,  $\text{H}_2$  (70 psi), MeOH/con. HCl (1/4), 24 h, (ii)  $\text{NaHCO}_3$ , 1,4-dioxane,  $\text{H}_2\text{O}$ , 3–4 h, then  $(\text{Boc})_2\text{O}$  or Cbz-Cl, 3 h, 71–74%.

Scheme 1. Synthesis of the scaffolds of indolizidinone amino acids **1**.



(a) (i)  $\text{LiBEt}_3\text{H}$ , then PPTS, MeOH, 100%; (ii)  $\text{CH}_2=\text{CHCH}_2\text{Si}(\text{CH}_3)_3$ ,  $\text{BF}_3\cdot\text{OEt}_2$ ,  $-78^\circ\text{C}$ , 82%;  
 (b) (i)  $\text{O}_3/\text{Me}_2\text{S}$ , 65%; (ii)  $(\text{MeO})_2\text{P}(\text{O})\text{CH}(\text{NHCBz})\text{COOCH}_3$ , DBU,  $\text{CH}_2\text{Cl}_2$ , RT, 4.5 h, 96%; (c) Rh(I) (COD) (*S,S*) Et-DUPHOS,  $\text{H}_2$  (80 psi), 24 h, MeOH, 93%; (d) Rh(I) (COD) (*R,R*) Et-DUPHOS,  $\text{H}_2$  (80 psi), 24 h, MeOH, 95%;  
 (e) 30% TFA, then TEA,  $\text{CH}_2\text{Cl}_2$ , 74–83%.

Scheme 2. Synthesis of 7-benzyl indolizidinone amino acids **1c,d**.

Since the side chains of peptides play very important roles in molecular recognitions, we have developed an approach to the synthesis of 7 substituted amino acids **1c,d**, (Scheme 2). The key intermediates **8a,b** were synthesized from  $\gamma$ -benzyl pyroglutamic acid ester **5**. The allyl group in **6** was introduced by the reduction of amide group in **5**, then treatment with  $\text{Me}_3\text{SiCH}=\text{CHCH}_3$  with an exclusively *trans* product related to  $\gamma$ -benzyl group. Ozonolysis of the double bond of **6** afforded an aldehyde, which reacted with  $(\text{MeO})_2\text{P}(\text{O})\text{CH}(\text{NHCBz})\text{COOMe}$  to give the dehydroamino ester **7**. Compound **7** underwent asymmetric hydrogenations using the same procedures we used earlier to generate **8a,b**. The final products **1a,b** were obtained by deprotection of Boc in **8a,b** and cyclizations. These new methods provide new avenues for the synthesis of a variety of  $\beta$ -turn mimetics in a highly stereo controlled manner. The synthesis of other isomers and the incorporation of the  $\beta$ -turn mimetics into biologically active peptides are under investigation.

### Acknowledgments

This work was supported by grants from US Public Health Service (DK 17420) and the National Institute of Drug Abuse (DA 13449).

### References

- Halab, L., Gosselin, F., Lubell, W.D. *Biopolymers (Peptide Science)* **55**, 101 (2000).
- Hanessian, S., McNaughton-Smith, G., Lombart, H.-G., Lubell, W.D. *Tetrahedron* **53**, 12789 (1997).
- Wang, W., Xiong, C.-Y., Hruby, V.J. *Tetrahedron Lett.* **42**, 3159 (2001).
- Burk, M.J., Feaster, J.E., Nugent, W.A., Harlow, R.L. *J. Am. Chem. Soc.* **115**, 10125 (1993).

## Enantioselective Synthesis of $\beta^2$ -Homotryptophan for a Somatostatin Mimetic

Peter Micuch and Dieter Seebach

*Laboratorium für Organische Chemie der Eidgenössischen Technischen Hochschule Zürich,  
 Universitätstrasse 16, CH-8092 Zürich, Switzerland*

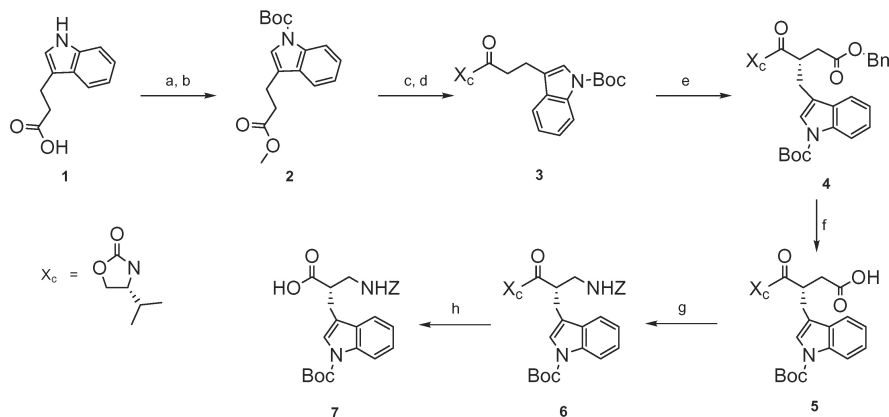
### Introduction

There is no general method available for preparation of enantiomerically pure  $\beta^2$ -amino acids. They can be prepared by stereoselective alkylation of chiral enolates which are synthetic equivalents of "β-alanine" (= H-β-HGly-OH) [1]. In another approach, the amino acid side chain is first attached to the auxiliary, followed by aminomethylation with synthetic equivalents of the  $[H_2NCH_2]^+$  cation [2]. Similarly, using bromoacetates as electrophiles, with reagents, which are synthetically equivalent to chiral enolates, followed by Curtius rearrangement also leads to the net attachment of the protected aminomethyl group [2a,3]. To the present day only  $\beta^2$ -HAla [1b,4],  $\beta^2$ -HVal [4],  $\beta^2$ -HLeu [1b,4],  $\beta^2$ -HPhe [1b,2a,4],  $\beta^2$ -HThr [5],  $\beta^2$ -HLys [6] and  $\beta^2$ -HAsp [7] have been prepared. Also, syntheses of the precursors of  $\beta^2$ -HTyr,  $\beta^2$ -HSer and  $\beta^2$ -HGlut have been published [2b], and  $\beta^2$ -HPro (piperidine-3-carboxylic acid) is known from 1951 [8]. To the best of our knowledge, the preparation of other  $\beta^2$ -homologs of proteinogenic amino acids has not been published yet.

The fact that β-peptides fold into well-defined secondary structures, which are stable to peptidases, makes them suitable candidates for Somatostatin mimetics. It has been shown that even a small open-chain β-tetrapeptide with a central  $\beta^3$ -HTrp- $\beta^2$ -HLys segment exhibits high affinity for a Somatostatin receptor [6].

### Results and Discussion

In order to find non-α-peptidic mimetics for Somatostatin we intend to prepare β-dipeptides with a proposed  $\beta^2$ -HTrp- $\beta^3$ -HLys 10-membered H-bonded turn which is

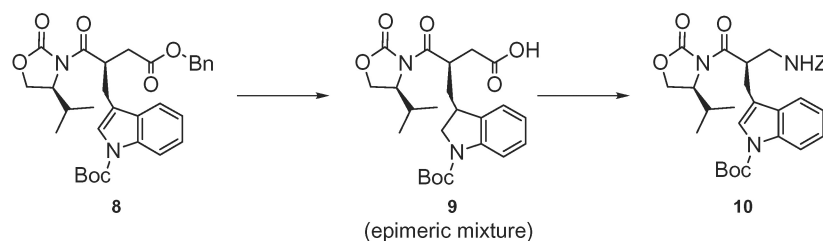


(a)  $CH_2N_2$ ,  $Et_2O$ , 100%; (b)  $Boc_2O$ , DMAP,  $CH_3CN$ , 92%; (c)  $LiOH \cdot H_2O$ ,  $THF/H_2O$ , 94%; (d) 1.  $Et_3N$ ,  $t-BuCOCl$ ; 2. (R)-4-isopropyl-2-oxazolidinone,  $LiCl$ , 83%; (e) 1.  $NaHMDS$ ,  $THF$ ; 2.  $BrCH_2CO_2Bn$ , 76%; (f)  $H_2$  (1 atm.), 10%  $Pd/C$ ,  $THF$ ; (g) 1.  $(PhO)_2P(O)N_3$ ,  $Et_3N$ ,  $BnOH$ ,  $Tol$ ; 2. reflux, 74% over two steps; (h)  $LiOH \cdot H_2O$ , 30%  $H_2O_2$ ,  $THF/H_2O$ , 54%.

comparable to a “ $\beta$ -turn” in  $\alpha$ -peptides. For that purpose we needed to develop a suitable synthesis of both enantiomers of  $\beta^2$ -homotryptophan.

Direct alkylation of Z- $\beta$ -HGly-OH attached to the auxiliary [2b] was not successful. Also aminomethylation of Z-protected 3-(3-indolyl)propionic acid attached to the auxiliary [2b] has not led to desired product. Finally, the route outlined in the accompanying scheme has led to the desired  $\beta^2$ -homotryptophan.

First, the indole nitrogen of 3-(3-indolyl)propionic acid (**1**) was protected with the Boc group and the Evans auxiliary was attached in four steps in an overall yield of 72%. Sodium hexamethyldisilazane gave a chiral enolate which was trapped by benzyl bromoacetate in 76% yield. Excellent selectivity was observed: only diastereoisomer **4** was detected in the reaction mixture. Using LDA as a base was less satisfactory, although selectivity was also excellent, the yield was only 36% and laborious separation from unreacted starting material **3** was required. The benzyl group was cleaved by hydrogenolysis in dry THF with Pd/C as the catalyst. From the corresponding acid **5** an acyl azide was prepared *in situ* and decomposed with Curtius rearrangement in the presence of benzyl alcohol. Subsequently, the Evans auxiliary was removed by treatment with LiOH/H<sub>2</sub>O<sub>2</sub>, leading to Z- $\beta^2$ -HTrp(Boc)-OH in an overall yield of 22% over eight steps.



It has to be noted, that hydrogenolysis of the benzyl ester **8** in a mixture of methanol/THF (1 : 1) causes partial hydrogenation of the indole ring producing an epimeric mixture of indoline derivatives **9**; although these can be used for Curtius rearrangement, followed by re-oxidation with DDQ, the yield is smaller as compared to that obtained as described above.

## References

1. (a) Seebach, D., Boog, A., Schweizer, W.B. *Eur. J. Org. Chem.* **335** (1999). (b) Ponsinet, R., Chassaing, G., Vaissermann, J., Lavielle, S. *Eur. J. Org. Chem.* **83** (2000).
2. (a) Arvanitis, E., Ernst, H., Ludwig, A.A., Robinson, A.J., Wyatt, P.B. *J. Chem. Soc., Perkin Trans. 1* 521 (1998). (b) Hintermann, T., Seebach, D. *Helv. Chim. Acta* **81**, 2093 (1998).
3. Sibi, M.P., Deshpande, P. K. *J. Chem. Soc., Perkin Trans. 1* 1461 (2000).
4. Seebach, D., Abele, S., Gademann, K., Guichard, G., Hintermann, T., Juan, B., Matthews, J.L., Schreiber, J.V., Oberer, L., Hommel, U., Widmer, H. *Helv. Chim. Acta* **81**, 932 (1998).
5. Seki, M., Furutani, T., Miyake, T., Yamanaka, T., Ohmizu, H. *Tetrahedron: Asymmetry* **7**, 1241 (1996).
6. Gademann, K., Kimmerlin, T., Hoyer, D., Seebach, D. *J. Med. Chem.* **44**, 2460 (2001).
7. Arvanitis, E., Motevalli, M., Wyatt, P.B. *Tetrahedron Lett.* **37**, 4277 (1996).
8. (a) Akkerman, et al. *Rec. Trav. Chim. Pays-Bas* **70**, 899 (1951). (b) Abele, S., Voegtli, K., Seebach, D. *Helv. Chim. Acta* **82**, 1539 (1999).

## Ethyl Nitroacetate as a Useful Synthon for the Synthesis of Orthogonally Protected, Poly-Functional C<sup>α,α</sup>-Disubstituted Amino Acids

Yanwen Fu, Lars G. J. Hammarström, Tod J. Miller,  
 Mark L. McLaughlin and Robert P. Hammer

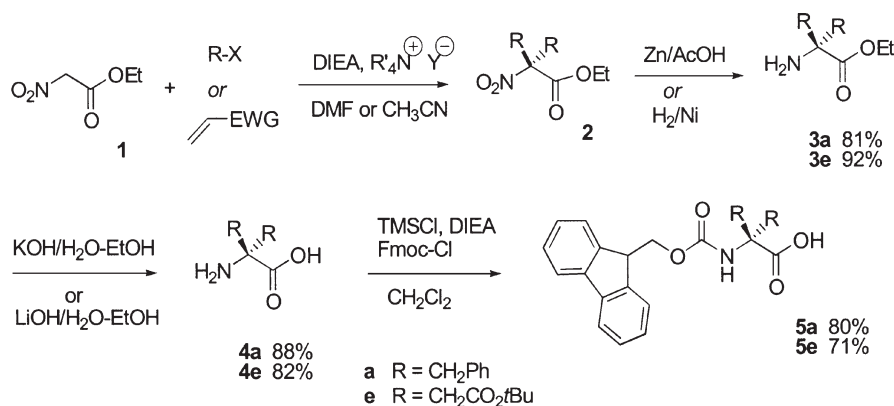
Department of Chemistry, Louisiana State University, Baton Rouge, LA 70803, USA

### Introduction

The discovery of C<sup>α,α</sup>-disubstituted amino acids (ααAAs) and their propensity to induce secondary structure even into short peptides has resulted in an increased interest in novel methods for their synthesis [1,2]. Herein ethyl nitroacetate, a useful synthetic intermediate for a variety of biologically significant compounds [3], has been employed for the preparation of sterically hindered and polyfunctional ααAAs which are suitable for incorporation into peptides.

### Results and Discussion

We have found that treatment of ethyl nitroacetate with two equivalents of DIEA in the presence of catalytic amounts of tetraalkylammonium salts followed by the addition of an activated alkyl halide or Michael acceptor, provided the disubstituted nitroacetate ester in good yields (Scheme 1, Table 1). DIEA was employed based on the evidence, which suggested that ethyl nitroacetate anion exhibits high nucleophilic reactivity in the presence of a quaternary ammonium cation that does not tend to form a strong ion pair [4]. Reduction of nitro ester **2a** under Zn/AcOH conditions and hydrogenation of nitro ester **2e** over Raney nickel afforded the amino ester **3a** and **3e** in 81 and 92% yield, respectively. Saponification of the resulting amino esters gave free ααAA **4a** and **4e** which were N<sup>α</sup>-protected with fluorenylmethyloxycarbonyl (Fmoc) group to provide the C<sup>α,α</sup>-disubstituted phenylalanine analog, dibenzylglycine (Fmoc-Dbg-OH) **5a** and the orthogonally protected, tetra-functional aspartic acid analog, 2,2-bis(*tert*-butylcarboxymethyl)glycine (Fmoc-Bcmg(O*t*-Bu)<sub>2</sub>) **5e** in good yields.



Scheme 1. Synthesis of N<sup>α</sup>-Fmoc-protected ααAAs.

Table 1. Alkylation of ethyl nitroacetate to  $C^{\alpha,\alpha}$ -dialkylated nitroacetates **2**.

Entry	Electrophile	Time (h)	Temp. (°C)	Prod #	Yield (%)
1	PhCH <sub>2</sub> Br	1	25–60	<b>2a</b>	63
2	<i>p</i> -O <sub>2</sub> NPhCH <sub>2</sub> Br	2	0–25	<b>2b</b>	75
3	<i>p</i> -NCPhCH <sub>2</sub> Br	2	0–25	<b>2c</b>	82
4	<i>p</i> -CH <sub>3</sub> O <sub>2</sub> CPhCH <sub>2</sub> Br	2	0–25	<b>2d</b>	72
5	(CH <sub>3</sub> ) <sub>3</sub> CO <sub>2</sub> CCH <sub>2</sub> Br	24	50	<b>2e</b>	79
6	CH <sub>2</sub> =CHCH <sub>2</sub> Br	24	60	<b>2f</b>	trace
7	CH <sub>2</sub> =CHCH <sub>2</sub> I	24	60	<b>2f</b>	45
8	CH <sub>2</sub> =CHSO <sub>2</sub> Ph	30	25	<b>2g</b>	70
9	CH <sub>2</sub> =CHCO <sub>2</sub> <i>t</i> -Bu	48	25	<b>2h</b>	89
10	CH <sub>2</sub> =CHCN	48	25	<b>2i</b>	87

As an example of their utility for peptide synthesis, sterically hindered Dbg was incorporated into peptide using SPPS. In our studies, coupling of Fmoc-Lys(Boc)-OH onto the N-terminus of Dbg on PAL resin using PyAOP, PyAOP/HOAt or HATU were ineffective, however the acylation of Dbg with pre-formed Fmoc-Lys(Boc)-symmetrical anhydride in DCE/DMF (v/v, 9 : 1) in the absence of base gave an almost quantitative coupling yield. The enhanced reactivity of the symmetrical anhydride may be due to the anchimeric assistance provided by H-bonding (Figure 1), which was more pronounced in the aprotic non-polar solvent. When the acylation was carried out in a more polar solvent, the coupling efficiency decreased (81% coupling yield in 1 : 1 DCE/DMF; 52% coupling yield in pure DMF). The fact that the non-polar solvent swells the PAL resin efficiently may also attribute to the successful coupling.

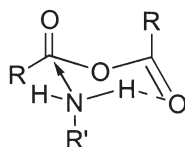


Fig. 1. Anchimeric assistance from H-bonding when coupling to symmetrical anhydrides.

## References

1. Nagaraj, R., Balaram, P. *Chem. Res.* **14**, 356–362 (1981).
2. Yokum, T.S., Gauthier, T.J., Hammer, R.P., McLaughlin, M.L. *J. Am. Chem. Soc.* **119**, 1167–1168 (1997).
3. Shipchandler, M.T. *Synthesis* 666–686 (1979).
4. Niyazymbetov, M.E., Evans, D.H. *J. Org. Chem.* **58**, 779–783 (1993).

## Synthesis of $\beta$ -Benzo[*b*]thiophene Dehydroamino Acids by Suzuki Palladium Catalyzed Cross Coupling

Paula M. T. Ferreira, Hernâni L. S. Maia, Luís S. Monteiro,  
 Maria-João R. P. Queiroz and Natália Silva

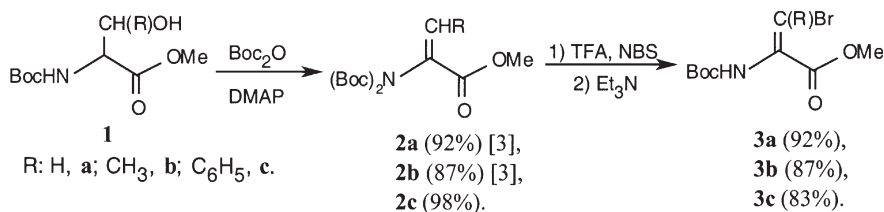
Department of Chemistry, University of Minho, Gualtar, 4700-320 Braga, Portugal

### Introduction

$\alpha,\beta$ -Dehydroamino acids are an important class of non-proteinogenic compounds. Some of them are found in natural biologically active peptides, and, when inserted in peptide chains, cause conformational constraints [1]. In addition, they are valuable synthons for chemical synthesis of new amino acids [2]. Recently, we developed an efficient method for the dehydration of  $\beta$ -hydroxyamino acids to obtain C-protected *N*-acyl-*N*-Boc-dehydroamino acids [3]. We now report the use of these compounds as precursors for palladium-catalyzed Suzuki cross-couplings [4] to give  $\beta$ -benzo[*b*]thiophene dehydroamino acids.

### Results and Discussion

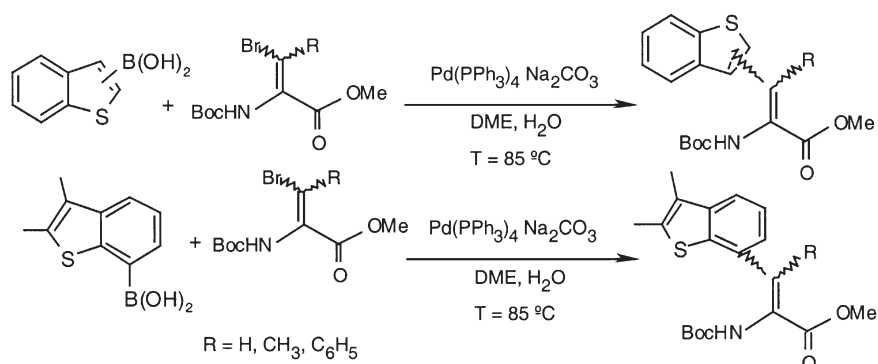
The *Z*-isomer of *N,N*-diacyl dehydroamino acid derivatives was stereoselectively synthesised from the respective *N*-Boc- $\beta$ -hydroxyamino acids by a previously described method [3]. In a one-pot procedure, the methyl ester of *N*-*tert*-butoxy-carbonyl- $\beta$ -bromo-dehydroamino acids [Boc- $\Delta$ aa( $\beta$ -Br)-OMe] was obtained by selective cleavage of one of the Boc groups of the methyl ester of the corresponding *N,N*-Boc<sub>2</sub>-dehydroamino acids with trifluoroacetic acid, followed by bromination with *N*-bromosuccinimide. In the case of Boc- $\Delta$ Abu( $\beta$ -Br)-OMe and Boc- $\Delta$ Phe( $\beta$ -Br)-OMe the reaction yielded the *Z*-isomer predominantly.



Scheme 1.

Benzo[*b*]thiophenes were functionalized by boronation, either on the thiophene ring (position 2 or 3), or on the benzene ring (position 7). This was achieved by halogen lithium exchange of the corresponding bromo benzo[*b*]thiophenes, followed by boron transmetalation and acid treatment. The obtained boronic benzo[*b*]thiophene acids were reacted with the above  $\beta$ -bromine-dehydroamino acid derivatives under the Suzuki cross-coupling conditions, in which the stereochemistry is generally maintained [4] (Scheme 2). After chromatographic purification, the yields of  $\beta$ -benzo[*b*]thiophene-dehydroamino acid methyl esters were within the range of 72 to 82%, except for Boc- $\Delta$ Ala( $\beta$ -2,3-dimethylbenzo[*b*]thien-7-yl)-OMe (Table 1). These compounds were fully characterized by spectroscopic methods and elemental analysis.

These results show that the Suzuki reaction offers a valuable method for the synthesis of the target compounds. Some of the obtained coupling products might be useful for peptide mimetics, as they are sulfur analogues of dehydrotryptophan.



Scheme 2.

Table 1. Yields and elemental analysis of the  $\beta$ -benzo[b]thiophene derivatives.

Compound	Yield	Elemental analysis found (calculated)
Boc- $\Delta$ Ala( $\beta$ -benzo[b]thien-2-yl)-OMe	81	C, 61.00; H, 5.74; N, 4.07; S, 9.31 (C, 61.24; H, 5.74; N, 4.20; S, 9.62)
Boc- $\Delta$ Ala( $\beta$ -benzo[b]thien-3-yl)-OMe	72	C, 61.12; H, 5.77; N, 4.23; S, 9.52 (C, 61.24; H, 5.74; N, 4.20; S, 9.62)
Boc- $\Delta$ Ala( $\beta$ -2,3-dimethylbenzo[b]thien-7-yl)-OMe	40	C, 63.39; H, 6.57; N, 3.88; S, 8.68 (C, 63.14; H, 6.41; N, 3.88; S, 8.87)
Boc- $\Delta$ Abu( $\beta$ -benzo[b]thien-2-yl)-OMe	77	C, 62.29; H, 6.10; N, 4.00; S, 8.99 (C, 62.32; H, 6.09; N, 4.03; S, 9.23)
Boc- $\Delta$ Phe( $\beta$ -benzo[b]thien-3-yl)-OMe	820	C, 67.17; H, 5.92; N, 3.46; S, 7.54 (C, 67.46; H, 5.66; N, 3.42; S, 7.83)

### Acknowledgments

Thanks are due to Fundação para a Ciência e a Tecnologia for financial support. (Project POCTI/1999/QUI/32639).

### References

- Schmidt, U., Lieberknecht, A., Wild, J. *Synthesis* 159–171 (1988).
- Hoerrner, R.S., Askin, D., Volante, R.P., Reider, P.J. *Tetrahedron Lett.* **39**, 3455–2458 (1998).
- Ferreira, P.M.T., Maia, H.L.S., Monteiro, L.S., Sacramento, J. *J. Chem. Soc., Perkin Trans. 1* 3697–3703 (1999).
- Suzuki, A., Miyaura, N. *Chem. Rev.* **95**, 2457–2483 (1995).

## Efficient Diastereoselective Synthesis of a Hydroxyethylene Dipeptide Isostere

Satendra Singh, Pius Baur and Michael W. Pennington

BACHEM Bioscience Inc., King of Prussia, PA 19406, USA

### Introduction

Many inhibitors of enzymes have been designed by replacing the scissile amide bond in a substrate with a hydrolytically stable functionality, such as hydroxyethylene [1]. The hydroxyethylene (HET) dipeptide isostere serves as a “transition state” inhibitor and mimics the tetrahedral intermediate formed during hydrolysis (Figure 1) [2].

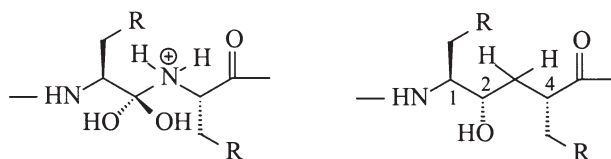
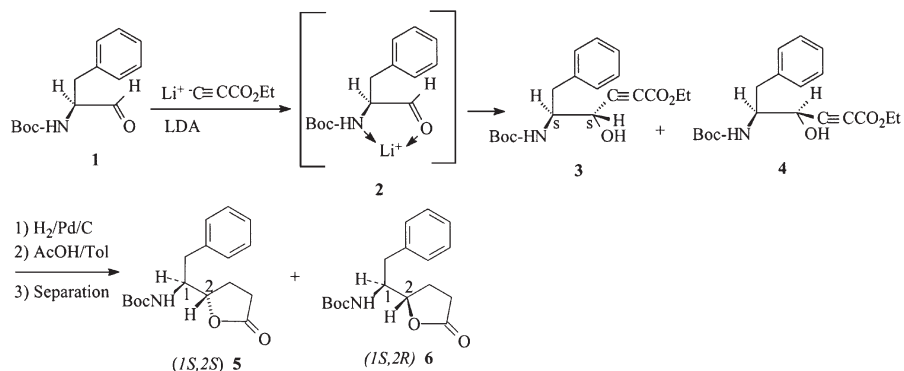


Fig. 1. Structure of isosteric replacement.

The HET isostere contains three asymmetric carbons. An appropriate stereochemistry at each chiral carbon is of utmost importance for biological activity. For example,  $\beta$ -secretase inhibitor, OM99-2 has Leu-Ala HET isostere in the 1*S*,2*S*,4*R* configuration [3]. However,  $\gamma$ -secretase inhibitor, L-685458 has Phe-Phe HET isostere in the 1*S*,2*R*,4*R* configuration [4]. This work presents an efficient methodology to prepare all the four possible stereoisomers of HET starting from an aldehyde.

### Results and Discussion

The first step in the synthesis was nucleophilic addition of lithium ethylpropiolate anion to L-Boc-Phe-H (**1**) [5]. The reaction proceeds *via* a chelated five-membered transition state (**2**), which is formed by coordination of lithium anion with carbonyl oxygen and amine simultaneously [6]. This mechanistic insight suggested that addition of a transmetalation agent would enhance Cram-selectivity (*threo*) (**3**) and addition of a cation-complexing agent would enhance *anti*-Cram-selectivity (*erythro*) (**4**)

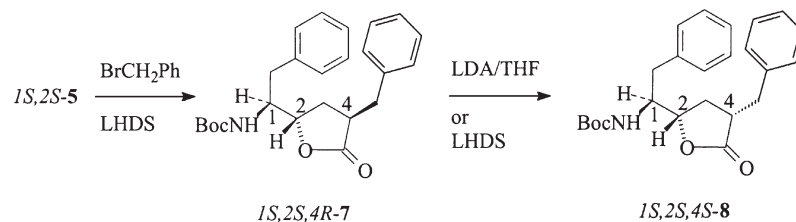


Scheme 1.

## Synthetic Methods

[7]. Thus addition of  $\text{ZnBr}_2$  to the reaction mixture significantly improved Cram-selectivity to afford *threo* product (**3**), which was hydrogenated and cyclized in 2.5%  $\text{AcOH}$ /toluene to afford lactones (Scheme 1) (**5** : **6** = 9 : 1). In the absence of  $\text{ZnBr}_2$ , the ratio of **5** : **6** was 7 : 3. Surprisingly, addition of a complexing agent, HMPT or TMEDA did not improve *anti*-Cram-selectivity (**5** : **6** = 7 : 3). Furthermore, it was expected that changing the reaction solvent from THF to ether would enhance Cram-selectivity ( $\epsilon$  of ether and THF 4.3 vs 7.6, respectively), but the ratio of *threo* to *erythro* remained approximately same (**5** : **6** = 7 : 3).

After chromatographic separation, lactone **5** was alkylated in a kinetically-controlled fashion with benzyl bromide at  $-78^\circ\text{C}$  in the presence of LHDS base to afford *S,S,R*-lactone (**7**) [8]. *S,S,S*-Lactone **8** was obtained from **5** by epimerization in the presence of LDA at reflux or LHDS at  $0^\circ\text{C}$  (Scheme 2). *S,R,S*- and *S,R,R*-lactones were obtained in the similar fashion starting from lactone *1S,2R*-**6**.



Scheme 2.

The lactone **7** or **8** could be opened with 1 N  $\text{NaOH}$ /acetone to a hydroxy acid and the hydroxyl group is selectively protected as TBS prior to incorporating in the synthesis.

## References

1. Gante, J. *Angew. Chem., Int. Ed. Engl.* **33**, 1699–1720 (1994).
2. Ripka, A.S., Rich, D.H. *Curr. Opin. Chem. Biol.* **2**, 441–452 (1998).
3. Hong, L., Koelsch, G., Lin, X., Wu, S., Terzyan, S., et al. *Science* **290**, 150–153 (2000).
4. Shearman, M.S., Beher, D., Clarke, E.E., et al. *Biochemistry* **39**, 8698–8704 (2000).
5. Fray, A.H., Kaye, R.L., Kleinman, E.F. *J. Org. Chem.* **51**, 4828–4833 (1986).
6. Still, W.C., Schneider, J.A. *Tetrahedron Lett.* **21**, 1035–1038 (1980).
7. Herold, P. *Helv. Chim. Acta* **71**, 354–362 (1988).
8. Takano, S., Uchida, W., Hatakeyama, S., Ogasawara, K. *Chem. Lett.* 733–736 (1982).

## One-Pot Conversion of Azides to Protected Guanidines via the Staudinger Reduction; Synthesis and Utilization of the Phe-Arg Hydroxyethylene Dipeptide Isostere

Matthias Brewer<sup>1</sup> and Daniel H. Rich<sup>1,2</sup>

<sup>1</sup>Department of Chemistry, University of Wisconsin-Madison, Madison, WI 53706, USA

<sup>2</sup>School of Pharmacy, University of Wisconsin-Madison, Madison, WI 53706, USA

### Introduction

During the course of the synthesis of the Phe-Arg hydroxyethylene dipeptide isostere [1] as a potential inhibitor of botulinum neurotoxin A we developed a simple one-pot reduction/guanylation procedure for the conversion of alkyl azides to *N,N'*-bis(*tert*-butoxycarbonyl)guanidines. Herein we describe this procedure and discuss progress made towards incorporating this isostere into a 17-mer peptide chain.

### Results and Discussion

Reduction of azide **1** (Figure 1) via catalytic hydrogenation or tin(II) chloride consistently gave only complex reaction mixtures and low yields of the desired amine, presumably due to an intramolecular (or intermolecular) attack of the newly formed amine on the lactone carbonyl. In order to minimize these possible side reactions, a one step reduction/guanylation procedure was envisioned which would eliminate the need to isolate the free amine. The Staudinger reduction is a mild conversion of azides to primary amines [2,3]. Preliminary studies indicated that known guanylation reagent **2** [4] was stable to these reduction conditions, and these conditions were chosen for the desired overall transformation.

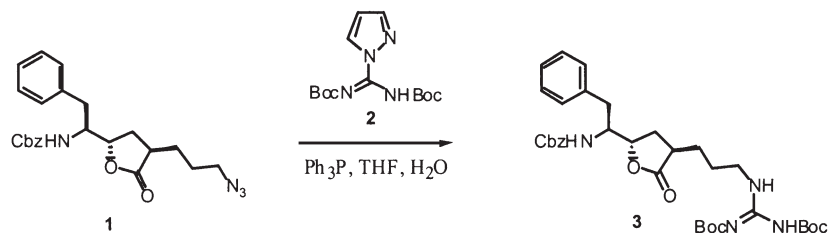


Fig. 1. Staudinger based guanylation.

In the event, triphenylphosphine was added to a room temperature mixture of **1**, **2** and H<sub>2</sub>O in THF (Figure 1). Evolution of nitrogen commenced immediately and the reaction was allowed to stir overnight at room temperature. The mixture was concentrated *in vacuo* and the residue purified by flash column chromatography to yield 71% of the desired product **3**.

Surprisingly, when azide **4** was treated according to the conditions in Figure 2, none of the desired guanidine **5** was obtained. Instead, the major product was identified as the stable betaine in which the phosphazene nitrogen has deprotonated the carboxylic acid. By altering the reaction conditions to 1 M LiOH, azide **4** is converted to guanidine **5** in 62% yield after purification by flash column chromatography and crystallization. Removal of the Cbz group from **5** via hydrogenolysis, followed by protection as the Fmoc derivative, occurred uneventfully to produce the desired dipeptide isostere **6** as a tripeptide derivative in a form amendable to solid phase peptide synthesis.

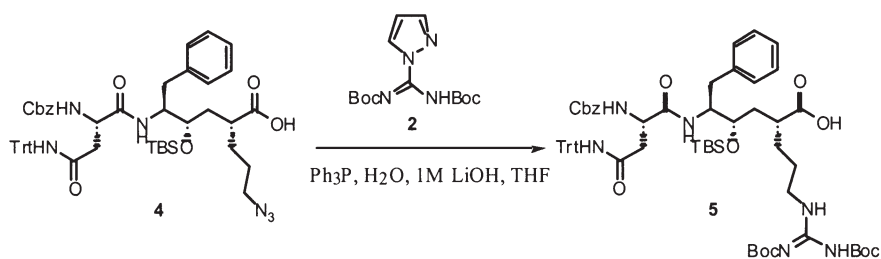


Fig. 2. Guanylation in presence of acid functionality.

Initial attempts to couple isostere **6** to resin bound 5-mer **7** (Figure 3) using DIPCDI and HOBt as coupling reagents were unfruitful. The major product isolated from the reaction washings was determined to result from intramolecular cyclization to form the  $\delta$ -lactam. In an attempt to avoid this competing reaction, DPPA was used as the coupling reagent [5]. While  $\delta$ -lactam formation was indeed slowed, the coupling to 5-mer **7** failed. Success was obtained by pre-forming the pentafluorophenyl ester of **6** in  $\text{CH}_2\text{Cl}_2$  at  $0^\circ\text{C}$ . Addition of 5-mer **7** in  $0^\circ\text{C}$  DMF to this mixture afforded the desired resin bound isostere **8** after repeated couplings. Work is currently in progress to elongate this chain to the complete 17-mer.

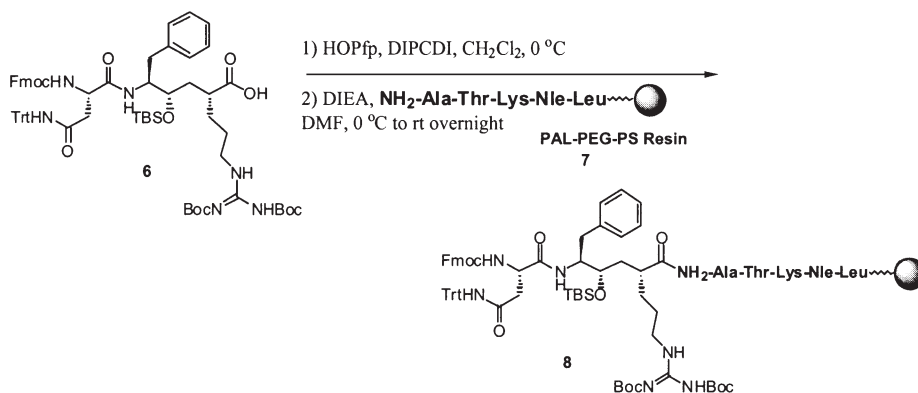


Fig. 3. Coupling of isostere **6** to 5-mer **8**.

### Acknowledgments

Supported by grant NIHGMS (GM 59 956).

### References

1. Brewer, M., Rich, D.H. *Org. Lett.* **3**, 945 (2001).
2. (a) Gololobov, Y.G., Zhmurova, I.N., Kasukhin, L.F. *Tetrahedron* **37**, 437 (1981). (b) Barluenga, J., Palacios, F. *Org. Prep. Proced. Int.* **23**, 3 (1991).
3. Knouzi, N., Vaultier, M., Carrie, R. *Bull. Soc. Chim. Fr.* 1985, 815.
4. (a) Bernatowicz, M.S., Wu, Y., Matsueda, G.R. *Tetrahedron Lett.* **34**, 3389 (1993). (b) Drake, B., Patek, M., Lebl, M. *Synthesis* 1994, 579.
5. Cezari, M.H.S., Juliano, L. *Pept. Res.* **9**, 88 (1996).

## The Synthesis of Tyrosine Mimetics via a Novel N(1)–C(4) Beta-Lactam Cleavage Reaction

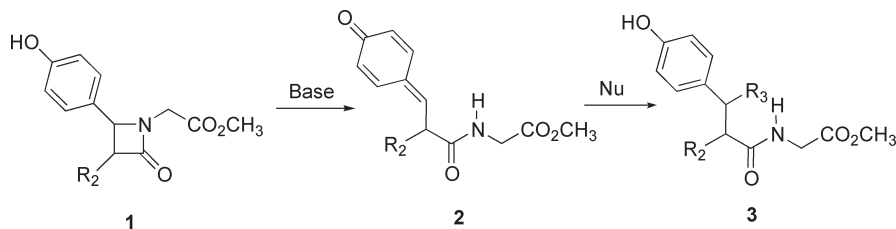
Larry A. Cabell, David R. Coleman, IV and John S. McMurray

Department of Neuro-Oncology, University of Texas M. D. Anderson Cancer Center, Houston, TX 77030, USA

### Introduction

Phosphorylation and dephosphorylation of tyrosine are important mechanisms of signal transduction in the cell. These processes are mediated by tyrosine kinases, tyrosine phosphatases, SH2 domains, and phosphotyrosine binding domains. In several disease states, such as cancer and diabetes, various signaling pathways have gone awry. Thus tyrosine-based peptidomimetics are important for the development of inhibitors of signal transduction proteins.

We have developed a reaction in which 4-(4'-hydroxyphenyl)  $\beta$ -lactams (**1**), under basic conditions, undergo a unique cleavage of the C(4)–N(1) bond with concomitant quinone methide formation (**2**) (Scheme 1). Addition of nucleophiles to the quinone methide produces tyrosine-like molecules (**3**) that have potential use in the development of inhibitors of the signal transduction proteins above. Due to the inherent ring strain,



Scheme 1. Synthesis of tyrosine mimetics.

$\beta$ -lactams are subject to ring opening reactions. The most common is cleavage of the amide bond, *i.e.* 1,2 cleavage. This reaction is the basis of the activity of the penicillin and cephalosporin antibiotics [1], as well as the mechanism-based inhibitors of human leukocyte elastase [2] and the cytomegalovirus protease [3]. 1,2-Cleavage reactions have also been employed in the synthesis of a variety of compounds such as macrocyclic alkaloids [4] and  $\beta$ -amino acids [5]. Thus our 1,4-cleavage reaction is a unique mechanism in the field of  $\beta$ -lactam chemistry.

### Results and Discussion

Starting with 4-(4'-hydroxyphenyl)-3-methyl-1-carbomethoxymethyl-azetidine-2-one, a series of tyrosyl-glycine mimetics were synthesized (**3**). Nucleophiles used were anions derived from methanol, nitromethane, benzylamine, malononitrile, methyl acetoacetate, and *tert*-butyl methylmalonate. Bases employed were NaOMe or DBU. In the reaction with NaOMe in MeOH, two products were formed in a 3 : 2 ratio, no doubt due to addition of methoxide on either face of the quinone methide intermediate. This suggested asymmetric induction. A series of analogues of **1** were synthesized in which R<sub>2</sub> was methyl, ethyl, isopropyl, benzyl and cyclohexylmethyl. As the size increased from methyl to isopropyl, the diastereomeric excess increased from 20 to 66%. Cyclohexylmethyl also produced a large d.e., 55%, but surprisingly the benzyl substituent

resulted in a very low d.e. A similar trend occurred when the nucleophile was nitromethane.

When R<sub>2</sub> of **1** (Figure 1) was phenoxy or acetamido, 1,6 conjugate addition to the quinone methide did not occur. Instead, elimination to the corresponding cinnamidylglycine was observed (**4**). Protection of the phenolic oxygen of the  $\beta$ -lactam as a benzyl ether lead to recovery of only starting material. Thus the observed elimination was actually a rearrangement of the quinone methide intermediate.

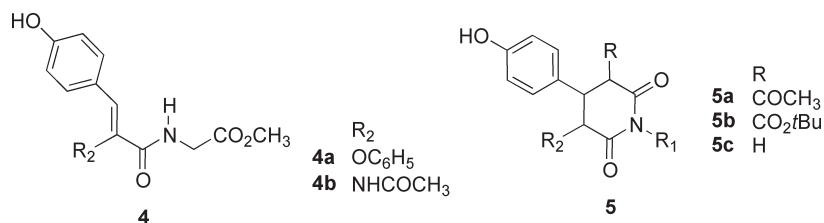


Fig. 1. Tyrosine mimetics.

1,6-Conjugate addition of methyl acetoacetate or *tert*-butyl methylmalonate anions to **2** lead to further reaction. The glycyl nitrogen atom attacked the carbonyl carbon of the methyl ester in an intramolecular aminolysis reaction to give the corresponding piperidine 2,6-diones (**5**). These compounds are of interest because they represent highly constrained tyrosine mimetics that have " $\chi^1$ " angles similar to those found in peptide substrates of insulin receptor kinase [6] and SH2 domains [7], *ca*  $-60^\circ$ .

In conclusion, we have developed a novel method to synthesize tyrosine mimetics. We will be applying these mimetics as inhibitors of the Src kinase and SH2 domains in the future.

### Acknowledgments

This work was supported by the Texas Higher Education Coordinating Board, 003657-0073, and the National Cancer Institute, CA53617 and CA16672 (NMR and mass spectrometry facilities at the M. D. Anderson Cancer Center).

### References

- Tipper, D.J. In Queener, R.B., Webber, J.A., Queener, S.W. (Eds.) *Beta-Lactam Antibiotics for Clinical Use*, Marcel Dekker, New York, 1986, pp. 17–48.
- Shah K.S., Dorn, C.P., Finke, P.E., Hale, J.J., Hagmann, W.K., Brause, K.A., Chandler, G.O., Kissinger, A.L., Ashe, B.M., Weston, H., Knight, W.B., Maycock, A.L., Dellea, P.S., Fletcher, D.S., Hand, K.M., Mimford, R.A., Underwood, D.J., Doherty, J.B. *J. Med. Chem.* **35**, 3745–3754 (1992).
- Yoakim, C., Ogilvie, W.W., Cameron, D.R., Chabot, C., Guse, I., Hache, B., Naud, J., O'Meara, J.A., Plante, R., Deziel, R. *J. Med. Chem.* **41**, 2882–2891 (1998).
- Wasserman, H.H., Matsuyama, H. *J. Am. Chem. Soc.* **103**, 462–464 (1981).
- Boge, T.C., Georg, G., In Juaristi, E. (Ed.) *Enantioselective Synthesis of  $\beta$ -Amino Acids*, Wiley-VCH, New York, 1997, pp. 1–44.
- Hubbard, S.R. *EMBO J.* **16**, 5572–5581 (1997).
- Waksman, G., Kominos, D., Robertson, S.C., Pant, N., Baltimore, D., Birge, D., Hanafusa, H., Mayer, B.J., Overduin, M., Resh, M.D., Rios, C.B., Silverman, L., Kuriyan, J. *Nature* **358**, 646–653 (1992).

## Michael Additions to Dehydroalanine Derivatives

Luís S. Monteiro, Paula M.T. Ferreira, Hernâni L.S. Maia  
 and Joana Sacramento

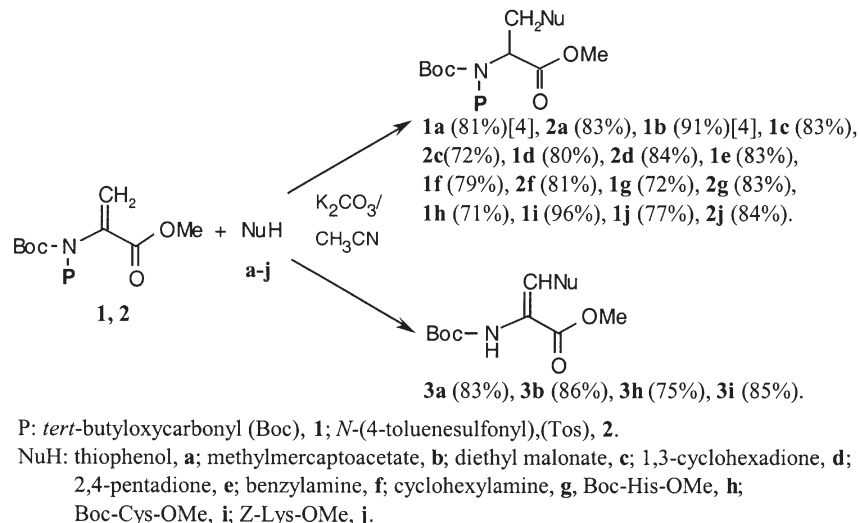
*Department of Chemistry, University of Minho, Gualtar, 4700-320 Braga, Portugal*

### Introduction

The Michael addition is one of the most important and generic synthetic tools for producing quaternary carbon atoms. However, there are few reports on the use of this conjugate addition of nucleophiles to  $\alpha,\beta$ -dehydroamino acids [1–3]. The limited use of dehydroamino acids in these reactions can be assigned mainly to the fact that these compounds are poor Michael acceptors. However, we found that double acylation of the amino group of  $\alpha,\beta$ -dehydroalanine derivatives greatly enhances the reactivity of these compounds towards nucleophilic addition. Thus, by addition of nitrogen and sulfur nucleophiles to these double acylated dehydroalanine derivatives, with potassium carbonate as base and acetonitrile as solvent, we were able to carry out high-yield syntheses of several  $\beta$ -substituted alanines [4]. The same method gave the corresponding  $\beta$ -substituted dehydroalanine derivatives when 4-toluenesulfonyl was substituted for one of the amine acyl groups [5]. In view of these results, we decided to expand the scope of this reaction to other nucleophiles.

### Results and Discussion

Addition of thiols, carbon nucleophiles and amines to *N,N*-diacyl dehydroalanine methyl esters was carried out in acetonitrile in the presence of  $K_2CO_3$  (Scheme 1).



Scheme 1.

Reaction of the nucleophiles with compound 1 gave the corresponding  $\beta$ -substituted alanine derivatives in high yields. Addition of amine and carbon nucleophiles to compound 2 gave similar results, but the sulfur nucleophiles behaved in a way similar to that found for heterocyclic nitrogen nucleophiles [5], the product of addition under-

going elimination of tosyl to give the corresponding  $\alpha,\beta$ -unsaturated product. With thiophenol it was possible to isolate the  $\beta$ -substituted alanine intermediate derivative, leading to the respective *N*-Boc- $\beta$ -substituted dehydroalanine methyl ester when the reaction was extended for 3 days. However, isolation of the addition product could not be achieved with methylmercaptoacetate, since it rapidly evolved to the  $\beta$ -substituted dehydroalanine derivative. The reaction of thiols with dehydroalanine derivatives was much faster than that with carbon nucleophiles or amines, making it possible to add 4-aminothiophenol to compound **1** selectively to give Boc-Ala(*N*-Boc, $\beta$ -4-amino-phenylthio)-OMe in 87% yield. Addition of these nucleophiles to a dehydroalanine dipeptide was also carried out successfully. Thus, reaction of thiophenol, methylmercaptoacetate, 1,3-cyclohexadione and benzylamine with Tos-Gly(*N*-Boc)- $\Delta$ Ala(*N*-Boc)-OMe yielded the respective  $\beta$ -substituted alanine dipeptides in yields of 87, 90, 60 and 53%, respectively.

These results led us to investigate the possibility of linking amino acids containing imidazole, thiol and amine functions on their side chains to Boc- $\Delta$ Ala(*N*-Boc)-OMe. The reaction of Boc-His-OMe, Boc-Cys-OMe and Z-Lys-OMe with **1** afforded the corresponding cross-linked amino acids in yields of 71, 96 and 77%, respectively. These cross-linked amino acids can be found in food after food processing, and some have biological activity [6]. The product of addition of Boc-Cys-OMe to **1** is a lanthionine derivative; lanthionine is a component of a class of natural peptides known as lanthibiotics (nisin, subtilin and others) and is also found in other natural products with immunostimulant and antitumoral activities [7]. Reaction of Z-Lys-OMe with **2** afforded the expected cross-linked  $\beta$ -substituted alanine derivative in an 84% yield, but Boc-His-OMe and Boc-Cys-OMe afforded the corresponding dehydroalanine derivatives, Boc- $\Delta$ Ala( $\beta$ -Boc-His-OMe)-OMe and Boc- $\Delta$ Ala( $\beta$ -Boc-Cys-OMe)-OMe, in yields of 75 and 85%, respectively. These novel cross-linked  $\beta$ -substituted  $\alpha,\beta$ -dehydro-amino acid derivatives are unique in that their double bond introduces an additional rigidity into the molecule, which might be of importance for application in peptide mimetics.

### Acknowledgments

Thanks are due to Fundação para a Ciência e a Tecnologia for financial support (Project POCTI/1999/QUI/32639).

### References

1. Belokon, Y.N., Sagyan, A.S., Djamgaryan, S.M., Bakhmutov, N.T., Belikov, V.M. *Tetrahedron* **44**, 5507–5514 (1988).
2. Probert, J.M., Rennex, D., Bradley, M. *Tetrahedron Lett.* **37**, 1101–1104 (1996).
3. Rolland-Fulcrand, V., Roumestant, M.L., Viallefont, P., Martinez, J. *Tetrahedron: Asymmetry* **11**, 4719–4724 (2000).
4. Ferreira, P.M.T., Maia, H.L.S., Monteiro, L.S., Sacramento, J., Sebastião, J. *J. Chem. Soc., Perkin Trans. 1* 3317–3324 (2000).
5. Ferreira, P.M.T., Maia, H.L.S., Monteiro, L.S., Sacramento, J. *Tetrahedron Lett.* **41**, 7437–7441 (2000).
6. Friedman, M. *J. Agric. Food Chem.* **47**, 1295–1349 (1999).
7. Jung, G. *Angew. Chem., Int. Ed. Engl.* **30**, 1051–1058 (1991).

## Facile Synthesis of a Constrained Dipeptide Unit (DPU) for Use as a $\beta$ -Sheet Promoter

Umut Oguz, Ted J. Gauthier and Mark L. McLaughlin

Louisiana State University, Department of Chemistry, Baton Rouge, LA 70803, USA

### Introduction

Previously described syntheses of lactam-constrained dipeptide amino acids involve lengthy and expensive procedures to obtain an aldehyde intermediate **4** [1]. We report a general route from D-glutamic acid to lactam-dipeptide units. The target lactam-constrained amino acid has a six-membered ring back-bone and isopropyl and isobutyl side-chains (Figure 1). The overall synthesis is shown in Figure 2.

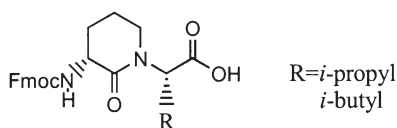


Fig. 1. Target lactam-constrained amino acid.

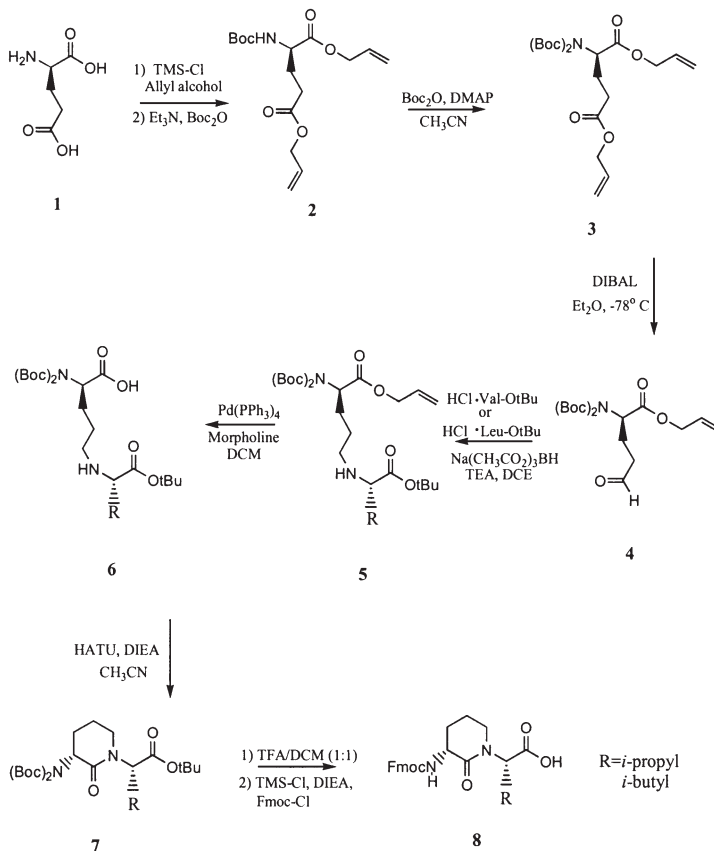


Fig. 2. Overall synthesis of DPUs.

## Results and Discussion

The key to the synthesis of DPU is the synthesis of the  $\alpha$ -amino acid semialdehyde **4**. The first two steps involve the protection of the carboxylic acid units and amine nitrogen with allyl alcohol and di-*t*-butyl dicarbonate, respectively. Diallyl diester **3** reduction is extremely selective, where reduction of only the side-chain ester over the  $\alpha$ -ester is needed. Martin *et al.* achieved the selective reduction to the semialdehyde by the use of methyl ester [2]. Using the methyl ester, the reaction conditions were highly sensitive to the reaction temperature and the reaction time. Over-reduction of both ester functions is observed and in addition reduction takes place to the corresponding alcohols as side reactions. We eliminated these side reactions by using allyl ester instead of methyl ester and achieved high selectivity and a 99.6% yield. Temperature changes and extended reaction time have no effect on the selectivity or yields. We believe that the additional steric bulk of allyl ester in addition to the Boc- groups on the nitrogen results in exclusive DIBAL-H reduction of the side-chain allyl ester. Reduction product was verified by FAB-MS (372,  $M+H^+$ ) and by the disappearance of one allyl group according to  $^1H$  and  $^{13}C$  NMR, and the appearance of the characteristic aldehyde proton. Compound **6** can be cyclized to the constrained dipeptide amino acid **7** by an intramolecular amide bond formation. X-Ray crystal structure of the product having the isopropyl side-chain is shown in Figure 3. Subsequent transformation yields the desired dipeptide unit **8** in 51% overall yield from the eight step synthesis. DPU products were verified by FAB-MS (437,  $M+H^+$ ) and (451,  $M+H^+$ ) for R = isopropyl and R = isobutyl, respectively.

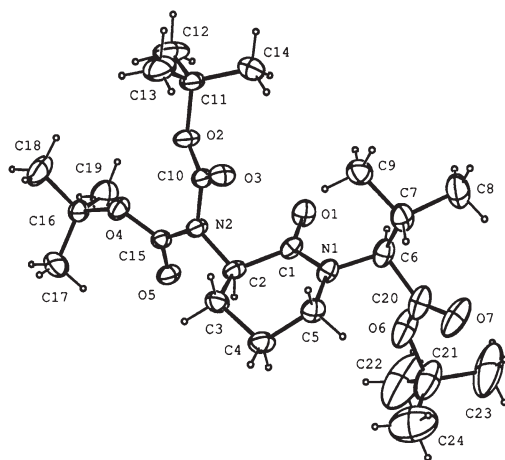


Fig. 3. X-Ray crystal structure of DPU (R = isopropyl).

## Acknowledgments

This work has been supported by NIH AI-17981 and AI-17983.

## References

1. Moss, N., Beaulieu, P., Duceppe, J.-S., Ferland, J.-M., Gauthier, J., Ghiri, E., Goulet, S., Guse, I., Llinas-Bruntet, M., Plante, R., Plamondon, L., Wernic, D., Deziel, R. *J. Med. Chem.* **39**, 2178 (1996).
2. Padron, J.M., Kokotos, G., Martin, T., Markidis, T., Gibbons, W.A., Martin, V.S. *Tetrahedron: Asymmetry* **9**, 3381–3394 (1998).

## Synthesis of $N^\alpha$ -(Fluoren-9-ylmethoxycarbonyl)- $N^\epsilon$ -[(7-methoxycoumarin-4-yl)-acetyl]-L-lysine for Use in Solid-Phase Synthesis of Fluorogenic Substrates

Navdeep Malkar and Gregg B. Fields

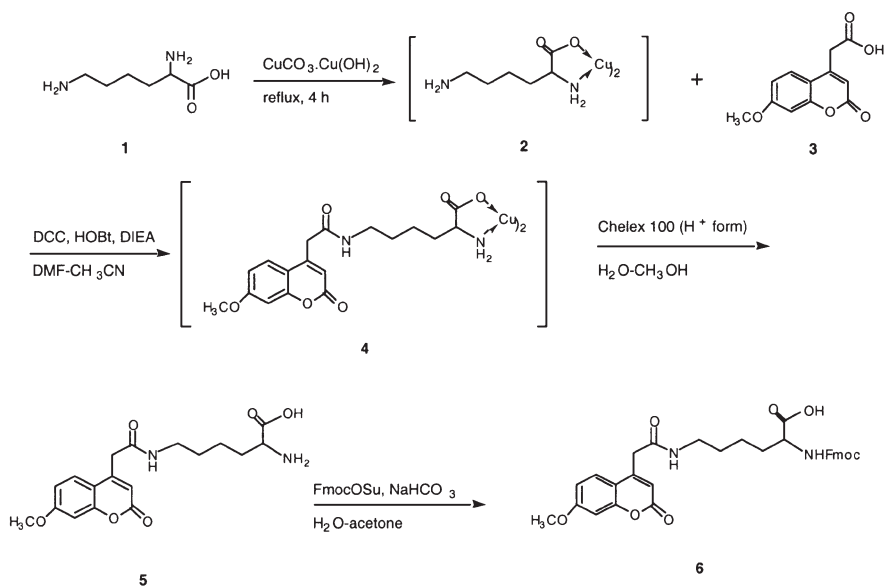
Department of Chemistry & Biochemistry, Florida Atlantic University, Boca Raton,  
 FL 33431-0991, USA

### Introduction

Quenched fluorescent peptides contain a fluorescent group separated by a short peptide sequence from another moiety which quenches fluorescence by resonance energy transfer. Fluorogenic substrates provide a particularly convenient enzyme assay method, as they can be monitored continuously and utilized at reasonably low concentration ranges. Peptides labeled at the  $N^\alpha$ -terminus with 7-methoxycoumarin-4-acetic acid and quenched by the 2,4-dinitrophenyl group at the  $N^\epsilon$ -position of lysine or L-2,3-diaminopropionic acid have been used in the design of fluorogenic substrates for matrix metalloproteinases [1,2]. However, we presently wish to incorporate 7-methoxycoumarin-4-acetic acid within the sequence Gly-Pro-Lys[(7-methoxycoumarin-4-yl)acetyl]-Gly-Pro-Gln-Gly-Leu-Arg-Gly-Gln-Lys(Dnp). In order to achieve this goal, we explored the direct synthesis of Fmoc-Lys(Mca). If Fmoc-Lys(Mca) could be prepared easily, it could then be incorporated efficiently into a desired sequence by Fmoc-based solid-phase peptide synthesis.

### Results and Discussion

The preparation of Fmoc-Lys(Mca) was considered by several routes. Initially, we examined the use of commercially available Fmoc-L-Lys to prepare the desired derivative. Fmoc-Lys could be dissolved in DMF and reacted with the preformed HOBt ester



Scheme 1.

## Synthetic Methods

of 7-methoxycoumarin-4-acetic acid. However, separation of Fmoc-Lys(Mca) from unreacted 7-methoxycoumarin-4-acetic acid proved to be difficult. We were recently successful in preparing a glycosylated derivative of 4-hydroxy-L-lysine using a copper-complexed intermediate [3], and thus decided to use an analogous approach to prepare Fmoc-Lys(Mca) (Scheme 1).

Fmoc-Lys(Mca) (**6**) was recovered by crystallization from hexane in good yield (51%). The integrity of the Fmoc-Lys(Mca) derivative was confirmed by ESMS and  $^1\text{H}$  NMR spectroscopy. Fmoc-Lys(Mca) exhibited an excitation maximum at  $\lambda = 330$  nm and an emission maximum at  $\lambda = 390$  nm. These properties are consistent with those previously reported for peptides containing an  $N^\alpha$ -amino Mca group or Amp [1,2]. Fmoc-Lys(Mca) is being used for the solid-phase synthesis of the triple-helical fluorogenic substrate (Gly-Pro-Hyp) $_5$ -Gly-Pro-Lys(Mca)-Gly-Pro-Gln-Gly~Leu-Arg-Gly-Gln-Lys(Dnp)-Gly-Val-Arg-(Gly-Pro-Hyp) $_5$ -NH $_2$  (fTHP-4; Figure 1). This substrate is used to study matrix metalloproteinase triple-helical peptidase activity [4]. fTHP-4 will be assembled on a PE-Biosystems 433A Peptide Synthesizer using Fmoc-Lys(Mca) in conjunction with Fmoc-based chemistry.

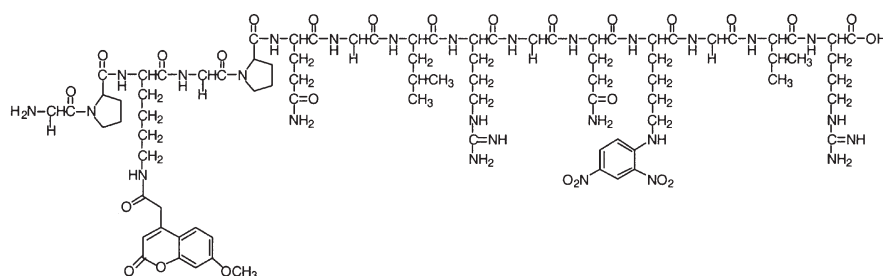


Fig. 1. Structure of fTHP-4.

## Acknowledgments

We thank Dr. W. Craig Byrdwell for providing ESMS data and gratefully acknowledge support from the NIH (CA 77402).

## References

1. Knight, C.G., Willenbrock, F., Murphy, G. *FEBS Lett.* **296**, 263 (1992).
2. Nagase, H., Fields, C.G., Fields, G.B. *J. Biol. Chem.* **269**, 20952–20957 (1994).
3. Malkar, N.B., Lauer-Fields, J.L., Fields, G.B. *Tetrahedron Lett.* **41**, 1137–1140 (2000).
4. Lauer-Fields, J.L., Broder, T., Sritharan, T., Chung, L., Nagase, H., Fields, G.B. *Biochemistry* **40**, 5795–5803 (2001).

# Preparation of $\beta$ -Amino- $\alpha$ -mercapto Acids and Amides: Stereocontrolled Syntheses of 2'-Sulfur Analogues of the Taxol C-13 Side Chain, Both *syn* and *anti* *S*-Acetyl-*N*-benzoyl-3-phenylisocysteine

Sang-Hyeup Lee<sup>1</sup>, Juyoung Yoon<sup>2</sup>, Kensuke Nakamura<sup>3</sup>  
 and Yoon-Sik Lee<sup>1</sup>

<sup>1</sup>School of Chemical Engineering, Seoul National University, Seoul 151-742, Korea

<sup>2</sup>Department of New Materials Chemistry, Silla University, Pusan 617-736, Korea

<sup>3</sup>Institute of Medicinal Molecular Design, Bunkyo-ku, Tokyo, 113-0033 Japan

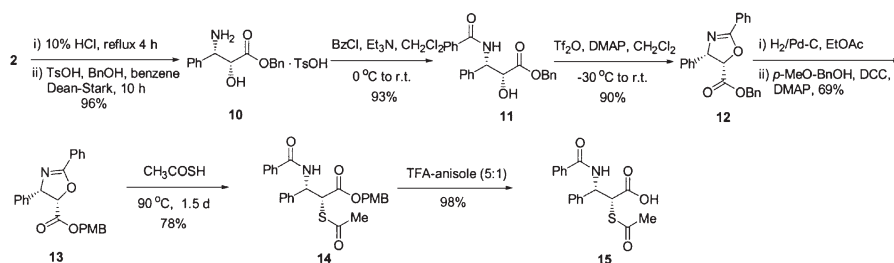
## Introduction

Paclitaxel (taxol), one of the most promising anticancer agents, bears the (2*R*,3*S*)-*N*-benzoyl-3-phenylisoserine unit in its C-13 side chain. Recent studies have shown that the 2'-hydroxyl functionality is crucial for microtubule binding, perhaps acting as a hydrogen bond donor [1]. In light of this postulate, the synthesis of analogues containing the 2'-thiol functionality would be of considerable interest to understand the features of the paclitaxel-binding site on microtubules and to develop more desirable compound than paclitaxel. In addition, peptidomimetics bearing a thiol moiety as a zinc-chelating group are of great interest in the development of potent inhibitors for numerous zinc-metalloproteases.

## Results and Discussion

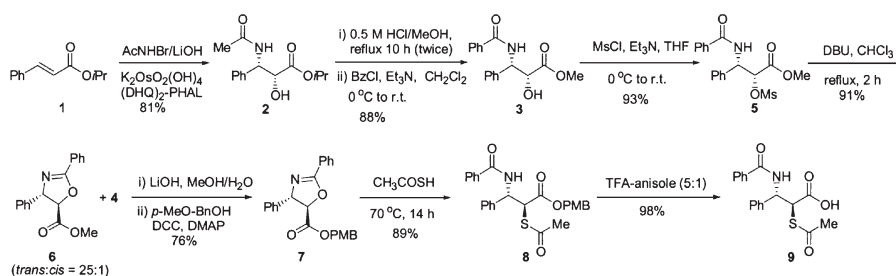
In the previous paper, we demonstrated the potential utility of oxazoline-5-carboxylates as the synthetic equivalents of an  $\alpha$ -cation for the preparation of  $\alpha$ -substituted- $\beta$ -amino esters [2]. In this presentation, we report stereoselective synthesis of both *anti* and *syn* *S*-acetyl-*N*-benzoyl-3-phenylisocysteine, coupling-ready reagents for the synthesis of 2'-sulfur analogues of taxol C-13 side chain. The synthesis of *anti* isomer **9** was relatively straightforward (Scheme 1). On the other hand, the preparation of *syn* isomer **15** was rather complex and the choice of protecting group was essential throughout the synthesis (Scheme 2).

To prepare dipeptides containing the  $\beta$ -amino- $\alpha$ -mercapto acid, we examined the ring-opening reaction of oxazoline-5-carboxamides with thiolacetic acid (Scheme 3). Treatment of *trans*-**18** with thiolacetic acid led to the *anti* acetylthio amide **19**. Removal of the acetyl group using lithium hydroxide gave the *anti* thiol amide **20**. On the other hand, *cis*-**17** was not ring-opened with thiolacetic acid even at higher reaction

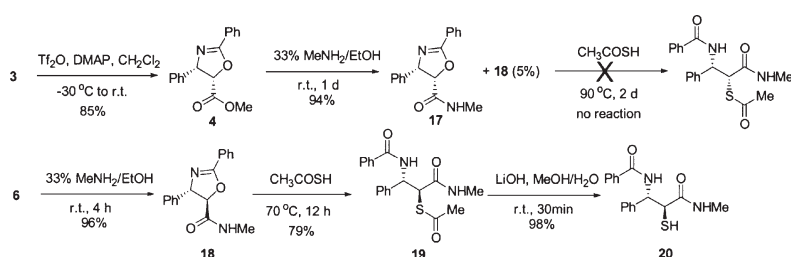


Scheme 1. Preparation of *anti*  $\beta$ -amino- $\alpha$ -mercapto acid.

## Synthetic Methods

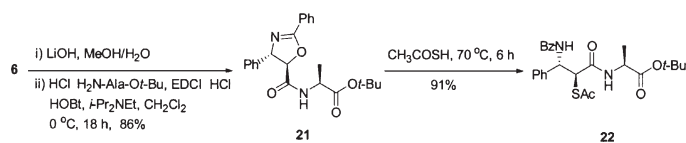


Scheme 2. Preparation of *syn* β-amino-α-mercapto acid.



Scheme 3. Ring-opening reaction of oxazoline-5-carboxamide.

temperature and longer reaction time. As explained in the previous paper [2], the lower reactivity of the *cis*-oxazoline rings is due to the severe steric repulsion between the phenyl group and the ester or amide groups at the transition state. To demonstrate the possible utility of this method, the model dipeptide **22** was synthesized from **6** in excellent yield (Scheme 4).



Scheme 4. Preparation of *anti* β-amino-α-mercapto acid containing dipeptide.

## Acknowledgments

Financial supports from Korean Research Foundation (2000-042-D00044) and Brain Korea 21 program are gratefully acknowledged.

## References

- Williams, H.J., Moyna, G., Scott, A.I. *J. Med. Chem.* **39**, 1555 (1996).
- Lee, S.-H., Yoon, J., Nakamura, K., Lee, Y.-S. *Org. Lett.* **2**, 1243 (2000).

## New Approach for Preparation of C-Glycoamino Acid Building Blocks

Istvan Jablonkai

*Institute of Chemistry, Chemical Research Center, Hungarian Academy of Sciences,  
 H-1525 Budapest, Hungary*

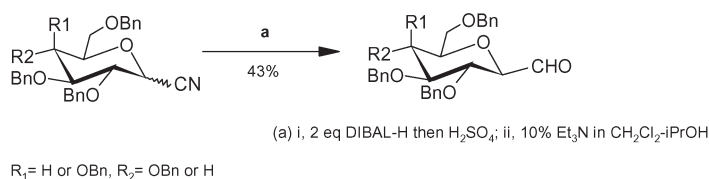
### Introduction

Oxygen-linked glycopeptides are vital constituents of biological membranes and their carbohydrate moieties play key role in molecular recognition processes [1]. However, *O*-glycosidic bonds in these molecules are sensitive to both chemical and enzymatic deglycosylation. Preparation of the hydrolytically more stable *C*-glycosylated analogs has attracted much attention recently. The objectives of this study were to prepare  $\alpha$ - and  $\beta$ -amino acids  $\beta$ -linked to the carbohydrate moiety as building blocks in combinatorial approaches to generate glycopeptide mimetics by solid phase peptide synthesis methods.

### Results and Discussion

The key intermediates for synthesis of *C*-glycoamino acids were formyl *C*-glycosides prepared from either  $\alpha/\beta$ -perbenzylated gluco-/galactopyranosyl cyanides (Figure 1a) or sugar lactones (Figure 1b). The  $\beta$ -glycosyl cyanides were obtained from the corresponding sugar bromides with  $\text{Hg}(\text{CN})_2$  [2]. The  $\alpha$ -anomeric forms were obtained from either  $\beta$ -*S*-ethyl thioglycosides [3] or  $\alpha$ -trichloroacetimidate [4] with trimethylsilylcyanide (TMSCN). The reaction of 1-*O*-acetyl sugar derivatives with TMSCN in the presence of boron trifluoride resulted in anomeric mixture of the cyanides ( $\alpha : \beta \approx 1 : 1$ ) [5]. The sugar lactones were prepared by oxidation of the corresponding hemiacetal [6]. Reductive hydrolysis of the cyanides by diisobutylaluminium hydride (DIBAL-H) [7] and epimerization under mild basic conditions [8] afforded the more stable  $\exists$ -form of the respective aldehyde. An efficient method by Dondoni [6] for the

#### a. from glycosyl cyanides[7]:



#### b. from sugar lactones [6]:

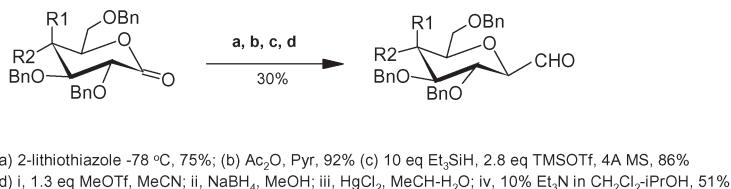
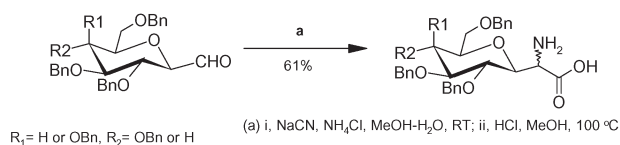


Fig. 1. Preparation of formyl *C*-glycosides from (a) glycosyl cyanides and (b) sugar lactones.

introduction of a formyl group at the anomeric position of sugars provided also the very important aldehyde intermediates for the preparation of C-glycoamino acids.

The Strecker synthesis of  $\beta$ -linked  $\alpha$ -glycoamino acids of glucose and galactose was carried out by reacting the respective sugar aldehyde with sodium cyanide and  $\text{NH}_4\text{Cl}$  in methanol-water solvent. The resulting  $\beta$ -linked  $\alpha$ -amino nitriles were hydrolyzed to the corresponding racemic amino acids (Figure 2a). Reformatsky reaction of the starting  $\beta$ -formyl sugar with 2-bromoacetic acid ester and zinc provided the  $\beta$ -linked  $\beta$ -hydroxy acids from which functional group manipulation yielded the  $\beta$ -linked target molecules as racemic mixtures (Figure 2b).

**a.  $\alpha$ -glycoamino acids by Strecker synthesis:**



**b.  $\beta$ -glycoamino acids by Reformatsky reaction:**

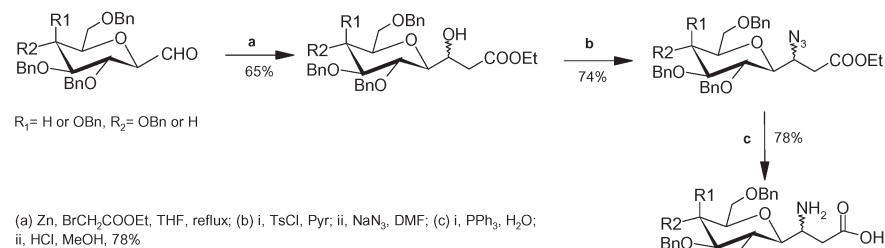


Fig. 2. Preparation of C-glycoamino acids by Strecker and Reformatsky methods.

**References**

1. Allen, H.J., Kisaiulis, E.C. (Eds) *Glycoconjugates*, Marcel Dekker, New York, 1997.
2. Myers, R.W., Lee, Y.C. *Carbohydr. Res.* **132**, 61–82 (1984).
3. Igarashi, Y., Shiozawa, T., Ichikawa, Y. *Biorg. Med. Chem. Lett.* **7**, 613–616 (1997).
4. Hoffmann, M.G., Schmidt, R.R. *Liebigs Ann. Chem.* 2403–2419 (1985).
5. Lai, W., Martin, O.R. *Carbohydr. Res.* **250**, 185–193 (1993).
6. Dondoni, A., Scherrmann, M.-C. *J. Org. Chem.* **59**, 6404–6412 (1994).
7. Gallagher, T.F., Adams, J.L. *J. Org. Chem.* **57**, 3347–3353 (1992).
8. Kobertz, W.R., Bertozzi, C.R., Bednarski, M.D. *Tetrahedron Lett.* **33**, 737–740 (1992).

## New Quencher Derivatives for Fluorescence Quenching Peptide Assays

T. A. Walton, D. J. Dick, D. Hudson, M. K. Johansson, M. H. Lyttle,  
M. F. Songster and R.M. Cook

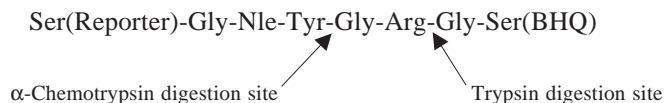
Biosearch Technologies, Inc., Novato, CA 94949, USA

### Introduction

Doubly dye labeled peptides that utilize FRET quenching have many applications. A new class of efficient quencher molecules, termed Black Hole Quenchers™, have been introduced into peptides *via* phosphoramidite derivatives coupled to the hydroxylic functions of serine, tyrosine, or hydroxyproline residues. The spectral characteristics for the entire family (BHQ-1, BHQ-2, *etc.*) are matched to sets of fluorophores, providing high sensitivity and low background detection in a variety of fluorogenic assays.

### Results and Discussion

The following peptide was synthesized using Fmoc synthesis chemistry:



The quenchers were coupled to the hydroxyl groups on serine, tyrosine, and hydroxyproline on NovaGel resins using phosphoramidite chemistry. The solvent was CH<sub>3</sub>CN and the activator used was ethyl thiotetrazole (32 mg/mL). Couplings were done at 100 mg/ml for 0.5 h followed by 1 min oxidation. The reporter was coupled to the N-terminus in the same manner. Capping was not used in this synthesis. Four different peptides were synthesized with the following dye/quencher combinations: TAMRA/BHQ-1 (1), ROX/BHQ-1 (2), TAMRA/BHQ-2 (3), and ROX/BHQ-2 (4). Final products were HPLC purified on a Hamilton PRP-1 column (10 × 250 mm, 7 μm) using a linear gradient of 95 : 5 to 0 : 100 A : B over 20 min [A = 0.1% TFA (aq), B = 0.1% TFA in CH<sub>3</sub>CN].

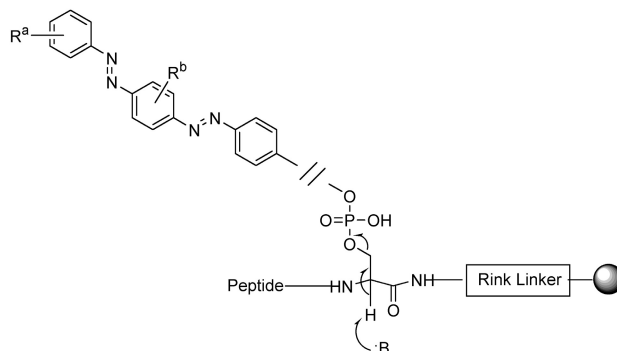


Fig. 1. Schematic representation of the loss of quencher moiety through a proposed  $\beta$ -elimination mechanism.

### Synthetic Methods

The lyophilized fractions from the HPLC purification were suspended in 1 : 2.5 CH<sub>3</sub>CN/H<sub>2</sub>O. This solution was diluted 1 : 40 in  $\alpha$ -chymotrypsin digestion buffer (0.1 M NH<sub>4</sub>HCO<sub>3</sub>) and 5  $\mu$ L ( $\approx$ 0.5 U) of  $\alpha$ -chymotrypsin solution (2 mg in 1 mL buffer) was added and allowed to react for 10 min before 2 $\times$  serial dilutions were made out to 1 : 320 of the original solution. Fluorescence measurements were then taken for these solutions using a Molecular Devices SpectraMax Gemini fluorescence plate reader providing signal to noise ratios of 34 for peptide **1** and 100 for peptide **3**.

During the Fmoc deprotection step of the peptide synthesis, BHQ's attached to the hydroxyl functionalized resin were removed by  $\beta$ -elimination (Figure 1), the extent of this side reaction is shown in Figure 2.

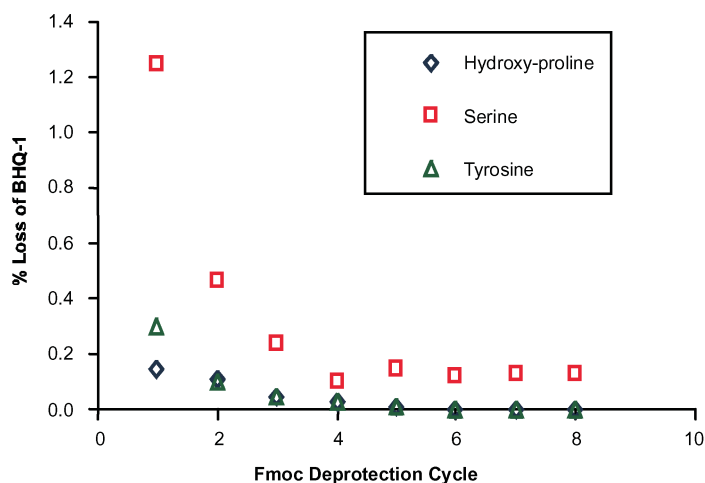


Fig. 2. Extent of elimination from BHQ resins during synthesis.

In conclusion, fluorophore/BHQ FRET peptides provide a sensitive detection method for enzyme cleavage assays; Hydroxyproline residues provide the most stable attachment of BHQ's *via* phosphoramidite chemistry. A new attachment method under development involves the use of H-Lys(BHQ)-OH, which is expected to simplify the procedure.

## Preparation of (2*S*)-2-Amino-3-(2-(2,2,5,7,8-pentamethyl-chroman-6-sulfonyl)-1*H*-indol-3-yl)-propionic acid and Its Incorporation into Antibacterial Lactoferricin Peptides

Bengt Erik Haug and John S. Svendsen

Department of Chemistry, Faculty of Science, University of Tromsø N-9037 Tromsø, Norway

### Introduction

The transfer of the Pmc protecting group from arginine to tryptophan during deprotection of peptides is a well-known side reaction in solid phase peptide synthesis [1,2]. We have found that derivatives of bovine lactoferricin containing the Pmc moiety have a higher antibacterial activity than unmodified peptides [3]. This has led to the development of a strategy for synthesizing the Pmc-modified tryptophan residue **1** (Tpc), and incorporation of Tpc into the bovine lactoferricin model peptide FKCRRWQWRMKKLGA (LFB) [4–6].

### Results and Discussion

By employing trifluoroacetamide-protected tryptophan, the Pmc-modified tryptophan **1** (Tpc) was prepared as described in Figure 1. Instead of using Pmc-protected arginine as the source of Pmc, an analogue **2** was prepared and used to synthesize Tpc. In order to elucidate the effect of Tpc on LFB, the two tryptophan residues were replaced by Tpc and the resulting peptides were tested for antibacterial activity against *Escherichia coli* and *Staphylococcus aureus* (Table 1).

LFB is believed to be antibacterial by a membrane disrupting mechanism, in which the tryptophan residues are inserted into the bacterial cell membrane. The larger side chain of Tpc can possibly position itself deeper into the cell membrane of the bacteria,

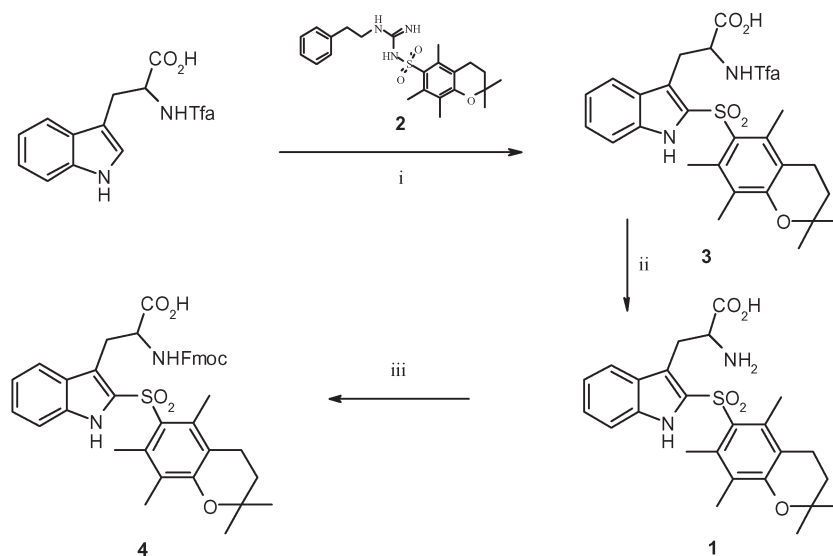


Fig. 1. Preparation of Tpc. Reagents and conditions: i) TFA, r.t., 1 h, 45–55%; ii) LiOH, THF/MeOH/H<sub>2</sub>O, 12 h, 95%; iii) Fmoc-OSu, DIPEA, CH<sub>2</sub>Cl<sub>2</sub>, 12 h, 65%.

Table 1. Antibacterial activity of LFB peptides containing Tpc.

Peptide <sup>a</sup>	MIC <sup>b</sup> <i>E. coli</i>		MIC <sup>b</sup> <i>S. aureus</i>	
LFB	50	(24)	100	(48)
LFB Tpc 6	7.5	(3.2)	10	(4.3)
LFB Tpc 8	15	(6.4)	7.5	(3.2)
LFB Tpc 6,8	25	(9.6)	7.5	(2.9)

<sup>a</sup> Sequence of LFB: FKRRW<sup>6</sup>QW<sup>8</sup>RMKKLGA. <sup>b</sup> Minimal inhibitory concentration in µg/ml and (µM).

and thereby disturb the packing of the phospholipids more effectively than tryptophan itself. This results in a higher antibacterial activity of the Tpc containing peptides.

### Acknowledgments

We thank the Norwegian Research Council and Alpharma for providing financial support for this work. We thank Gerd Berge for skilful peptide synthesis and Ørjan Samuelsen at the University Hospital of Tromsø for performing the MIC analyses.

### References

1. Riniker, B., Hartmann, A., In Rivier, J.E. and Marshall, G.R. (Eds.) *Peptides: Chemistry, Structure and Biology (Proceedings of the 11th American Peptide Symposium)*, ESCOM, Leiden, 1990, p. 950.
2. Stierandová, A., Sepetov, N.F., Nikiforovich, G.V., Lebl, M. *Int. J. Pept. Protein Res.* **43**, 31–38 (1994).
3. Rekdal, Ø., Andersen, J., Vorland, H.J., Svendsen, J.S. *J. Peptide Sci.* **5**, 32–45 (1999).
4. Andersen, J., unpublished results.
5. Strom, M.B., Rekdal, Ø., Svendsen, J.S. *J. Peptide Res.* **56**, 265–274 (2000).
6. Haug, B.E., Svendsen, J.S. *J. Peptide Sci.* **7**, 190–196 (2001).

## UniChemo Protection (UCP)

Les Miranda and Morten Meldal

*Department of Chemistry, Carlsberg Laboratory, DK-2500, Copenhagen, Denmark*

### Introduction

The applicability of chemical synthesis to peptides, oligosaccharides and other organic molecules is limited and inherently complicated by existing functional group protecting strategies. Protecting group strategies are used to render otherwise reactive functional groups inert to a particular chemical reaction by appending a protecting group that can later be removed without damage to the product [1]. In this arena, the number and type of protecting groups influences the length, efficiency and complexity of a given synthesis, and is often responsible for its success or failure. The differential protection of functional groups of similar reactivity in chemical synthesis is a major challenge with conventional protecting group strategies, namely orthogonal protection and graduated lability. In particular, the development of effective protective schemes for polyfunctional molecules is not a trivial exercise.

### Results and Discussion

To circumvent these restrictions, a novel protection strategy that greatly simplifies and increases the ability to construct polyfunctional molecules is introduced. This new concept, termed UniChemo Protection (UCP), is illustrated in Figure 1.

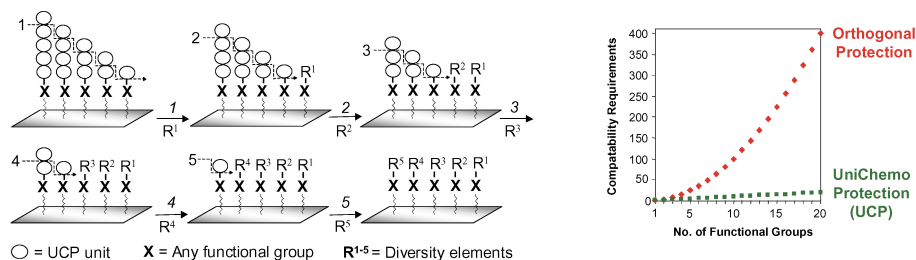


*Fig. 1. A. (left) The principle of unichemo protection (UCP). B. (right) Comparison of the minimal number of chemical compatibility requirements for the synthesis of polyfunctional molecules with existing orthogonal protection strategies and unichemo protection (UCP).*

In contrast to existing approaches, this strategy only requires a single chemical process for all deprotection reactions, and is not dependent on a multitude of finely tuned and different compatible chemistries. The UCP groups are derived from a repetitive module that permits their controlled and efficient step-wise removal. Functional site selectivity is easily engineered by varying the degree of oligomerization at each site. After each removal cycle, only the newly-liberated functional site is available for derivatization. In principle, the UCP strategy does not impose a restriction to the possible number of selectively protected sites in a molecule.

The effectiveness and power of UCP chemistry was demonstrated by the controlled derivatization of a pentyllysine-based amino functionalized scaffold on the solid-support. With conventional protection strategies, the controlled derivatization of five or more otherwise identical amino groups (or hydroxyl groups) on the solid-support is a very difficult or near impossible challenge in practice, requiring at least

## Synthetic Methods

7-dimensions of orthogonality. To solve this problem, a *N*-*sec*-butylglycyl-based protecting group unit for the protection of amine functionality was devised. More specifically, the UCP concept in the form of *N*<sup>ε</sup>-oligo(*N*-*sec*-butylglycyl) protected lysine building blocks for the assembly of scaffold **1** has been successfully demonstrated.

In this system, the UCP concept takes advantage of large reactivity differences between primary amino functional groups and the otherwise similar protecting group units (Figure 2). High yields of oligomeric *N*-*sec*-butylglycyl protecting groups are readily obtained using strong activation during amide-bond formation, *i.e.* PyBroP [1], on the solid-support. Importantly, the UCP groups were completely inert to less activated ONp and OSu esters derivatives. The inert character of the UCP secondary amine protecting groups under mild acylation conditions thus allows for the chemoselective derivatization of newly liberated primary amino group with nitrophenyl or succinimide esters.

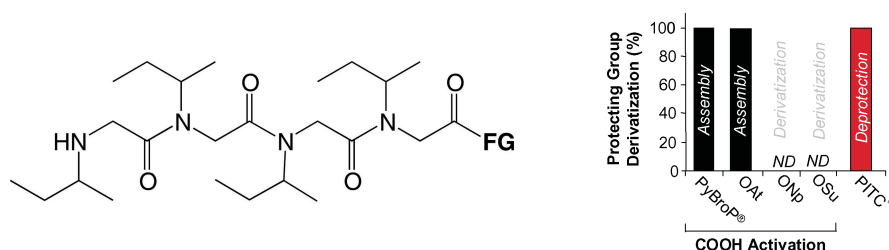


Fig. 2. A. (left) Prototype UCP group: oligo *N*-*sec*-butylglycines. B. (right) Engineered properties of oligo *N*-*sec*-butylglycines group: For the assembly of the oligomeric UCP groups, strong coupling chemistry (*i.e.* PyBroP) efficiently acylated the hindered secondary amine in DMF at rt in 1 h. Importantly, for the derivatization of liberated primary amines, the protecting group secondary amine was resistant to acylation by less activated esters, such as 0.1 M Boc-Ala-ONp in DMF. For deprotection, phenylisothiocyanate (PITC) reacted in high yield to form the key phenylthiocarbamyl intermediate before elimination.

For deprotection cycles, efficient step-wise removal of terminal protecting group units was facilitated by a simple and reliable two-step procedure originally developed by Edman for protein sequencing [2]. In the first step, PITC reacted quantitatively at pH 8 with the terminal unit of the oligomeric protecting group (Figure 3). In the second step, a quantitative cyclization and elimination reaction occurred at acidic pH, to give the shortened protecting group *via* the expulsion of a phenylthiohydantoin derivative.

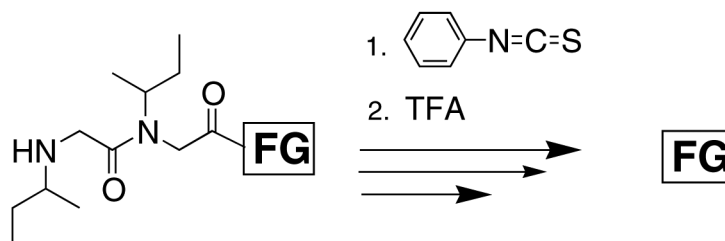


Fig. 3. UCP deprotection procedure for the removal *N*-*sec*-butylglycyl modules.

**Miranda et al.**

Accordingly, after the assembly of scaffold **1**, each of the five primary amino groups on the scaffold were successively liberated with PITC/TFA deprotection cycles (Figure 4). Each newly liberated amino functional site was then readily acylated with a given ONp ester derivative. After five deprotection-derivatization cycles, cleavage from the solid-support afforded the desired molecule, **2**, in good purity and yield.

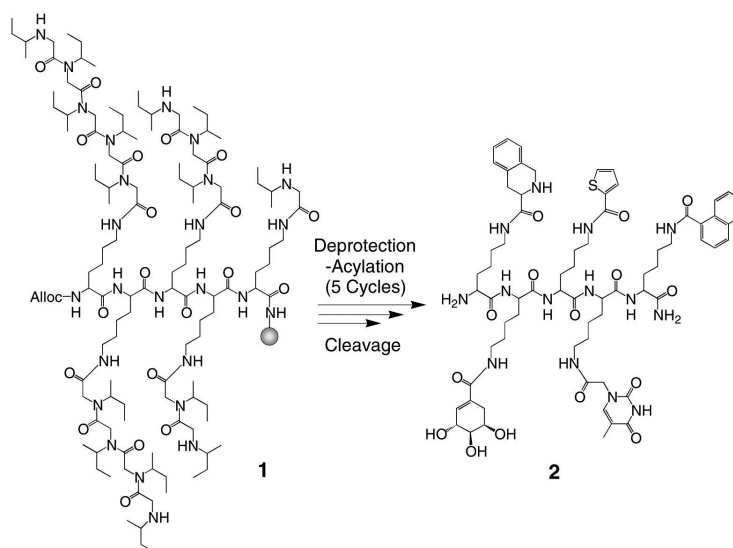


Fig. 4. Protection and controlled derivatization of a polyamino scaffold with UCP.

Although elegant and widely applicable, the *N*-sec-butylglycyl-based protecting group reported here should be considered as a preliminary first generation system to demonstrate the UCP concept. Forthcoming innovations and refinements of UCP protecting group modules should produce more robust, practical and broadly applicable protection chemistries.

It is envisaged that this simple yet powerful generic strategy will open up many new possibilities in areas including the combinatorial synthesis of highly substituted scaffolds, peptides, template-assisted synthetic proteins (TASP), multiple antigen peptides (MAP), oligosaccharide synthesis, and the general goal of automated organic synthesis.

#### Acknowledgments

We acknowledge Rodney Gagné for helpful discussions. Supported by the Danish National Research Council.

#### References

- 1Greene, T.W., Wuts, P.G.M. *Protective Groups in Organic Synthesis*, 3rd ed., John Wiley & Sons, New York, 1999.
2. Edman, P. *Acta Chem. Scand.* **4**, 283–293 (1950).
3. Coste, J., Frérot, E., Jouin, P. *Tetrahedron Lett.* **32**, 1967–1970 (1991).

## **An Improved Synthesis of Fmoc-Asp(O-3-methylpent-3-yl)-OH, an Aspartate Derivative That Resists Base Induced Aspartimide Formation**

**James G. Boyd and Wen Lin**

*Exploratory Medicinal Sciences, Pfizer Global Research and Development, Groton, CT 06340, USA*

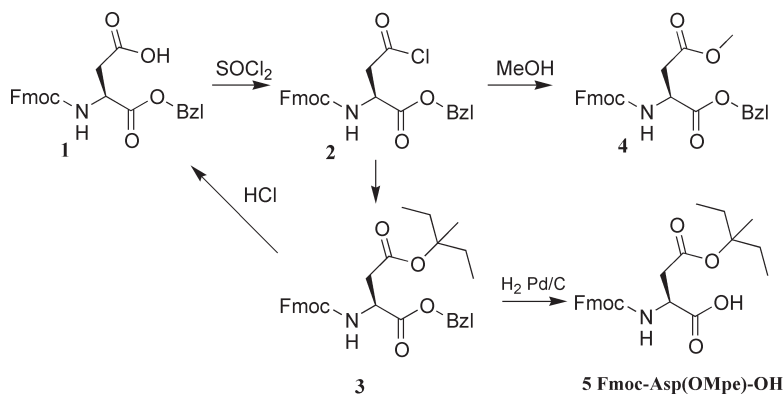
### **Introduction**

The problem of aspartimide formation at Asp(OtBu) during Fmoc based solid phase synthesis is well documented [1]. In 1996 Karlstrom and Unden demonstrated that the more hindered 3-methylpent-3-yl (Mpe)  $\beta$ -ester of aspartate is remarkably resistant to piperidine induced aspartimide formation, and its use results in significantly cleaner crude products [2]. In our hands, the critical Mpe esterification step (*via* acid chloride **2**) has been troublesome, with yields typically in the range of 15–25%. We describe significant yield enhancements and crystallization conditions for Fmoc-Asp(OMpe)-OH (**5**).

### **Results and Discussion**

In order to assess various synthetic routes, a simple HPLC assay was developed. Intermediate **2** can be conveniently monitored as methyl ester **4**, which forms quantitatively upon dissolution of **2** in neat MeOH. Conversion of **2** to diester **3** or back to starting material **1** (Fmoc-Asp(OH)-OBzl, purchased from Bachem) was used to optimize reaction conditions. In multiple experiments it was noted that the concentration ratio of product ester to starting acid [**3**]/[**1**] decreases with time. We suspected that *in situ* generation of HCl at 60 °C was creating equilibrium deprotection conditions within the reaction vessel. To minimize the accumulation of HCl, two equivalents thionyl chloride in DCM were used to form the acid chloride. The solvent was evaporated after 10 min and residual volatiles removed under high vacuum for 1 h. Alumina (activated at 450 °C overnight) [3] was added to **2** followed by dry DCM and a large excess of dry distilled 3-methylpentan-3-ol. The vessel was immersed in an oil bath, DCM was evaporated under stream of nitrogen, and the syrup/alumina mixture stirred at 55 °C for 1 h. This procedure routinely results in 70–90% crude yield of **3**. Recrystallization of **3** from hot ethanol/water provided a pure product.

With careful monitoring by TLC or HPLC, benzyl ester **3** can be quantitatively removed by catalytic hydrogenation without loss of the Fmoc group, although on several



**Boyd et al.**

occasions significant loss of Fmoc was detected by the appearance of 9-methylfluorene.

While crude product **5** was >95% pure by HPLC and HNMR, it resisted many attempts to crystallize. An unorthodox but reproducible procedure was developed. Crude **5** was dissolved in of 10% ether/hexane and hexane added until cloudy. After most of the solute settled as an oily precipitate, the supernatant was decanted to a clean beaker. More hexane was added to the cloud point and after settling, the clear supernatant was decanted again to third beaker. Passive evaporation of the ether at room temperature was accompanied by formation of seed crystals, which were collected for recrystallization. The above precipitates/oils were pooled and dissolved in a minimum of warm 10% ether/hexane. Slow cooling to 23 °C with seeding gave air stable crystals (m.p. = 86–86.5 °C). Attempts to improve recoveries by cooling resulted in the formation of oil or oily crystals.

**References**

1. Doelling, R., Beyermann, M., Haenel, J., Kernchen, F., Krause, E., Franke, P., Brudel, M., Bienert, M. *J. Chem. Soc., Chem. Commun.* 853–854 (1994).
2. Karlstrom, A., Unden, A. *Tetrahedron Lett.* **37**, 4243–4246 (1996).
3. Nagasawa, K., Yoshitake, S., Amiya, T., Ito, K. *Synth. Commun.* **20**, 2033–2040 (1990).

## Systematic Investigation of the Aspartimide Problem

M. Mergler, F. Dick, B. Sax, P. Weiler and T. Vorherr

BACHEM AG, CH-4416 Bubendorf, Switzerland

### Introduction

Aspartimide formation is one of the best-documented side reactions in peptide synthesis. Even bulky side-chain protecting groups such as OtBu do not prevent this undesired reaction. In Fmoc/tBu-based SPPS, the repetitive piperidine treatments needed for Fmoc removal lead to aspartimide formation and further by-products. Since the combination Asp-Gly represents the worst-case scenario, the hexapeptide Val-Lys-Asp-Gly-Tyr-Ile (**I**) [1] was used in the present work to investigate parameters influencing aspartimide formation (Fmoc-cleavage conditions, nature of Asp side chain protection). Based on the idea of backbone-protection [2], Fmoc-Asp(OtBu)-(Hmb)-Gly-OH was also synthesised and included in this study.

### Results and Discussion

For Asp side chain protection, the following groups were applied for synthesis of **I** as their Fmoc-derivatives: OtBu,  $\beta$ -3-methylpent-3-yl ester (OMpe) [3], 4-pyridyldiphenyl-methyl ester (OPyBzh) [4], the bicyclic ortho-ester 4-methyl-2,6,7-trioxabicyclo-[2,2,2]-octane (OBO) [4] and, as already mentioned, the combination OtBu side chain protection plus Hmb-backbone protection. In the first step, several potential by-products, VKdGYI, VKd(GYI), VKD(GYI), VKD(piperidide)GYI and VKD(GYI)-piperidide, resulting from the opening of the aspartimide cycle, were independently synthesized. Furthermore, RP-HPLC-optimization of these potential contaminants was carried out to properly resolve and quantify the different side products.

The OPyBzh-protecting group had ideal TFA lability. Unfortunately, high levels of aspartimide and piperidides were detected following synthesis of **I**. Another new derivative, the orthoester protected Asp derivative (OBO-protection), was designed to completely suppress nucleophilic attack at the  $\beta$ -carboxy group. Surprisingly,  $\alpha$ -piperidide was generated during synthesis and, in addition, large quantities of aspartimide were observed during the second stage of OBO removal, which consists of the saponification under basic conditions. Therefore, the disappointing results obtained on OPyBzh- and OBO-protection were not included in Table 1.

Table 1. HPLC-analysis of crude products (Bakerbond C18 300 Å, phosphate buffer pH 2.3, CH<sub>3</sub>CN as modifier).

Protection	Base <sup>a</sup>	Product (%)	D/L-Aspartimide (%)	L- $\alpha$ -Piperidide (%)	L- $\beta$ -Piperidide (%)
OtBu	Pip.	89.1	3.0	1.5	<0.3 <sup>b</sup>
OMpe	Pip.	93.9	0.7	<0.3 <sup>b</sup>	<0.3 <sup>b</sup>
OtBu/Hmb	Pip.	94.0	<0.3 <sup>b</sup>	<0.3 <sup>b</sup>	<0.3 <sup>b</sup>
OtBu	DBU	52.1	21.8	9.4	0.6
OMpe	DBU	83.0	7.8	1.9	<0.3 <sup>b</sup>
OtBu/Hmb	DBU	94.1	<0.3 <sup>b</sup>	<0.3 <sup>b</sup>	<0.3 <sup>b</sup>

<sup>a</sup> Pip.: Piperidine/DMF 1 : 4, DBU: DBU/Piperidine/DMF 1 : 20 : 79; <sup>b</sup> below detection limit.

Two Fmoc-cleavage procedures, the standard protocol piperidine/DMF (1 : 4) and 1% DBU in piperidine/DMF (1 : 4), and different protecting groups for the Asp residue in model peptide **I** (see Table 1) were employed to study aspartimide formation. Peptide **I**, synthesized according to the various strategies indicated above, was obtained after TFA assisted cleavage, and the crude products were subsequently analysed by HPLC.

In fact, Fmoc-removal in the presence of DBU worsened the effects already observed in the case of the standard piperidine treatment. However, no significant amounts of  $\beta$ -peptide were detected. In the case of OtBu-protection, upon DBU treatment an as yet undefined component (5.8%) was observed in addition to the known compounds. The OMpe-protecting group showed a significant improvement with respect to aspartimide formation when compared to regular OtBu-protection. Most interestingly, if the Hmb-backbone protection approach was followed, neither under standard conditions nor in the presence of DBU, aspartimide or related side product was observed (detection limit 0.3%).

### Conclusions

This systematic investigation clearly showed that in our test system, no detectable amounts of aspartimide were formed if Hmb-backbone protection was applied in addition to standard OtBu-protection of the Asp side chain. However, the synthesis of all different Hmb protected amino acid derivatives followed by their incorporation into dipeptides would be quite labourious. Therefore, taking into account the markedly improved properties of Mpe-protection compared to the standard OtBu-group, this recently described variant should be considered for sequences prone to aspartimide formation.

### References

1. Nicolás, E., Pedroso, E., Giralt, E. *Tetrahedron Lett.* **30**, 497 (1989).
2. Offer, J., Quibell, M., Johnson, T. *J. Chem. Soc., Perkin Trans. 1* 175 (1996).
3. Karlström, A., Undén, A. *Tetrahedron Lett.* **37**, 4243 (1996).
4. Unpublished derivatives.

## Ninhydrin as a Reversible Protecting Group of N-Terminal Cysteine

Chadler T. Pool<sup>1</sup>, James G. Boyd<sup>2</sup> and James P. Tam<sup>1</sup>

<sup>1</sup>Vanderbilt University Department of Microbiology/Immunology, Nashville, TN 37232, USA

<sup>2</sup>Pfizer, Inc., Groton, CT 06340, USA

### Introduction

The proximity of the  $\alpha$ -amino group and thiol group of N-terminal cysteine residues imparts unique chemical properties that have been utilized to cyclize unprotected peptides obtained through both synthetic and biological means [1–3]. A protecting group orthogonal to other protection strategies and reversible under mild conditions would be useful in simplifying the synthesis, cleavage, purification and handling of such peptides. It could also be useful for the sequential ligation of peptides.

To this end, we have found that the thiazolidine structure formed by the reaction of cysteine with ninhydrin protects both the amino and thiol groups of cysteine (see Figure 1) during synthesis and cleavage, yet can be easily removed.

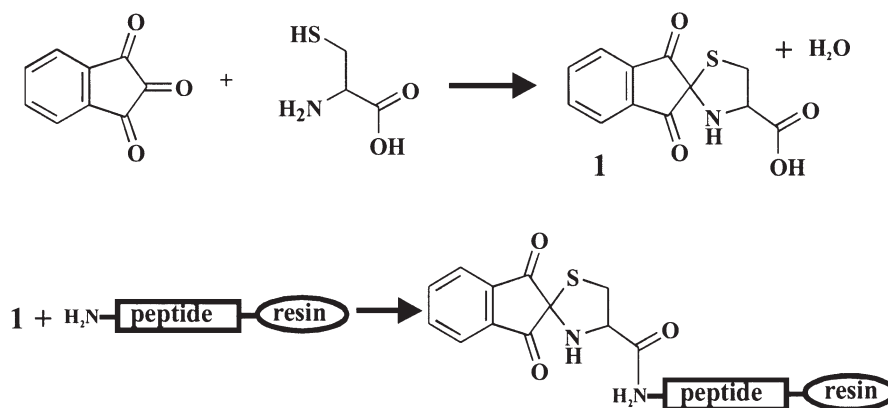


Fig. 1. The reaction of ninhydrin with cysteine and the structure of the resulting product (top). The general scheme of coupling Nin-Cys-OH to a peptide resin (bottom).

### Results and Discussion

Two approaches were explored for Nin-Cys containing peptides. First, Nin-Cys was performed as described by Protta and Ponsiglione [4]. In their studies, the authors show that the product formed under these conditions was the spiro form **1**. Nin-Cys-OH was coupled to several model peptides. In all cases, the Nin-Cys-OH coupled efficiently to the peptide resins without acylation at the secondary amine of the thiazolidine ring under our experimental conditions using HBTU activation. Coupling efficiencies to bulky residues, such as Met and Ile, appeared to be similar to those observed with glycine.

Second, Nin-Cys containing peptides were synthesized *in situ*. Considering the much higher nucleophilicity of thiol groups compared to amino groups and other functional groups found on unprotected peptides at acidic pH, we postulated that it might be possible to protect or label unprotected peptides with ninhydrin specifically at

**Pool et al.**

N-terminal cysteine residues. As predicted, we found that N-terminal cysteine-containing peptides were readily modified at pH 2 to 5 and ninhydrin concentrations of 0.5 to 10 mM forming a thiazolidine structure in under 2 h. No reaction with any other residues, other than internal cysteines, was observed and the derivatives formed with the internal cysteines were not stable.

Removal of the ninhydrin group was accomplished using reducing conditions involving thiols such as cysteine or 3-mercapto-1-propanesulfonic acid (MPS) in combination with tris[2-carboxyethyl]phosphine (TCEP), or using 10% trifluoroacetic acid (TFA) in combination with zinc. Using these conditions, we found that the ninhydrin moiety can be readily removed from model peptides in under 1 h.

Nin-Cys was stable to both treatment by TFA and HF cleavage conditions which allows the use of Nin-Cys to reduce side reactions in peptide synthesis. For example, thiazolidine formation of N-terminal cysteine residues during cleavage of peptides containing benzyloxymethyl-protected histidine, His(Bom), has been well documented [5] and poses significant problems in both cleaving and synthesizing histidine-containing peptides. Our results show that despite the use of His(Bom) during synthesis, the ninhydrin completely protects N-terminal cysteine residues from thiazolidine formation in the absence of appropriate scavengers during cleavage.

To broaden the applicability of Nin-Cys as a protecting group, we attached Nin-Cys-OH to a 40 residue, thioester-containing peptide synthesized using standard Boc chemistries. End-to-end cyclization of this peptide *via* thioester ligation was achieved through the addition of MPS which deprotected the Nin-Cys group and subsequently regenerated the thioester [6]. Cyclization of this 40 residue peptide was complete in under 2 h.

**References**

1. Tam, J.P., Lu, Y.A. *Protein Sci.* **7**, 1583–1592 (1998).
2. Ayers, B., Blaschke, U.K., Camarero, J.A., Cotton, G.J., Holford, M., Muir, T.W. *Biopolymers* **51**, 343–354 (2000).
3. Botti, P., Pallin, T.D., Tam, J.P. *J. Am. Chem. Soc.* **118**, 10018–10024 (1996).
4. Prota, G., Ponsiglione, E. *Tetrahedron* **29**, 4271–4274 (1973).
5. Kumagaye, K.Y., Inui, T., Nakajima, K., Kimura, T., Sakakibara, S. *Peptide Res.* **4**, 84–87 (1991).
6. Zhang, L., Tam, J.P. *J. Am. Chem. Soc.* **119**, 2363–2370 (1997).

## **Novel Synthesis and Application of a Protected Bicyclic $\alpha$ -Helix-Initiating Heptapeptide Suitable for Segment Condensation Syntheses: Utility of Pentaaminecobalt(III) for Carboxyl Protection**

**John W. Taylor, Prasanna Reddy, Ketel Patel, Tom Dineen and Sumreen Naqvi**

*Department of Chemistry and Chemical Biology, Rutgers University, Piscataway, NJ 08854, USA*

### **Introduction**

We have previously demonstrated that incorporation of side-chain lactam linkages between two pairs of lysine and aspartic acid residues placed in the *i* and *i*+4 and the *i*+1 and *i*+5 positions in a peptide chain generates a fully  $\alpha$ -helical structure that is highly resistant to heat denaturation, and is capable of propagating the  $\alpha$ -helical conformation in both the N- and C-terminal directions [1]. The synthesis of such helix-initiated peptides is desirable in order to probe the propagation and thermodynamic stability of  $\alpha$  helices as a function of their amino-acid sequences. However, the use of solid-phase chemistry to incorporate just one such bicyclic structure into a peptide is highly unreliable, due to the interchain reactions that occur at each attempted intrachain cyclization step. Therefore, we have undertaken the development of a synthetic route to bicyclic helix-initiated peptides that involves the solution-phase preparation of a protected bicyclic peptide segment, **1** (Figure 1), that is suitable for incorporation into a standard Fmoc-based solid-phase synthesis by segment-condensation. This synthetic approach has been demonstrated through the synthesis of an N-terminal helix-initiated analogue of the epitope on the HIV-1 surface glyco-protein gp41 that is recognized by 2F5, an HIV-1 neutralizing monoclonal antibody.

#### *A: Protected peptides*

Fmoc-(*cyclo* 1-5, 2-6)-Lys-Lys-Ala-Ala-Asp-Asp-Ala-OH (**1**)  
Fmoc-Lys(Mtt)-Lys(Boc)-Ala-Ala-Asp(OPip)-Asp(OBu<sup>t</sup>)-OH (**2**)  
Fmoc-Lys(Mtt)-Lys(Boc)-Ala-Ala-Asp(OPip)-Asp(OBu<sup>t</sup>)-Ala-O-Co(NH<sub>3</sub>)<sub>5</sub>-Cl<sub>2</sub> (**3**)  
Fmoc-(*cyclo* 1-5)-Lys-Lys(Boc)-Ala-Ala-Asp-Asp(OBu<sup>t</sup>)-Ala-O-Co(NH<sub>3</sub>)<sub>5</sub>-Cl<sub>2</sub> (**4**)  
Fmoc-(*cyclo* 1-5, 2-6)-Lys-Lys-Ala-Ala-Asp-Asp-Ala-O-Co(NH<sub>3</sub>)<sub>5</sub>-Cl<sub>2</sub> (**5**)

#### *B: Unprotected peptides*

Ac-Nle-Nle-Ala-Ala-Asn-Asn-Ala-Leu-Glu-Leu-Asp-Lys-Trp-Ala-Ser-Leu-NH<sub>2</sub> (**6**)  
Ac-[*cyclo* 1-5, 2-6]-Lys-Lys-Ala-Ala-Asp-Asp-Ala-Leu-Glu-Leu-Asp-Lys-Trp-Ala-Ser-Leu-NH<sub>2</sub> (**7**)

*Fig. 1. Structures of synthetic peptides.*

### **Results and Discussion**

Protected hexapeptide **2** was assembled on the Rink acid resin (1.0 g), then cleaved from the solid support using 10% (v/v) acetic acid in dichloromethane without loss of the acid-sensitive 4-methyltrityl (Mtt) and 2-phenylpropyl ester (OPip) protecting groups. This peptide was then coupled to H-Ala-O-Co<sup>III</sup>(NH<sub>3</sub>)<sub>5</sub>·(BF<sub>4</sub>)<sub>3</sub> [2] in DMF, using DCC and HOBt, to give heptapeptide **3** (56%). Side-chain deprotection at Lys<sup>1</sup> and Asp<sup>5</sup> with 1% TFA in DCM, followed by cyclization with PyBOP, HOBt and DIEA of the dilute peptide in DMF gave the protected monocyclic peptide **4** (58%).

**Taylor et al.**

Side-chain deprotection in 100% TFA followed by a second cyclization in DMF yielded 100  $\mu\text{mol}$  of pure bicyclic peptide Fmoc-cyclo(1-5, 2-6)-[Lys-Lys-Ala-Ala-Asp-Asp-Ala]-O-Co<sup>III</sup>(NH<sub>3</sub>)<sub>5</sub>, **5** (74%).

By using exchange-inert cobalt(III) protection of the  $\alpha$ -carboxyl group [2], full orthogonality to the base-labile Fmoc group and the acid-labile side-chain protecting groups was achieved. In addition, all of the peptide intermediates were solubilized in both DMF and also in aqueous solvent mixtures, such as water–acetonitrile, or water–DMF. This allowed facile, low-resolution, low-pressure ion-exchange and reversed-phase chromatographies to be used in combination after each solution-phase coupling (peptide **3**) or cyclization (peptides **4** and **5**). Deprotection of **5** was achieved by mild reduction to the exchange-labile cobalt(II) form, using DTT and DIEA in water-acetonitrile. After acidification, low-pressure, reversed-phase chromatography then gave the Fmoc-protected bicyclic peptide **1** in quantitative yield from **5**, and in an HPLC-pure form.

The use of bicyclic heptapeptide **1** in segment-condensation syntheses was then demonstrated by coupling this peptide with PyBOP, HOBt and DIEA to the protected peptide NH<sub>2</sub>-Leu-Glu(OBu<sup>t</sup>)-Leu-Asp(OBu<sup>t</sup>)-Lys(Boc)-Trp(Boc)-Ala-Ser(Bu<sup>t</sup>)-Leu assembled on the Rink amide MBHA resin (Novabiochem Corp.). Quantitative analysis by HPLC of the cleaved, deprotected peptides indicated a 60% yield for this coupling reaction. Circular dichroism spectropolarimetry of the purified bicyclic peptide **7** in 10 mM NaH<sub>2</sub>PO<sub>4</sub>–NaOH buffer, pH 7.0, at 25 °C indicated that it had a significantly higher  $\alpha$ -helix content ( $[\theta]_{222} = -18,800 \text{ deg cm}^2/\text{dmol}$ ) than the corresponding isosteric, linear, control peptide, **6** ( $[\theta]_{222} = -4,800 \text{ deg cm}^2/\text{dmol}$ ).

**Acknowledgments**

This research was supported by PHS grant R21 AI45316 (J. W. T.).

**References**

1. Zhang, M., Wu, B., Baum, J., Taylor, J.W. *J. Peptide Res.* **55**, 398–408 (2000).
2. Isied, S.S., Vassilian, A., Lyon, J.M. *J. Am. Chem. Soc.* **104**, 3910–3916 (1982).

## **N<sup>in</sup>-4-Nitrobenzenesulfonyl Tryptophan: A Convenient Preparation of N<sup>α</sup>-Boc and N<sup>α</sup>-Fmoc Derivatives**

**Aydar Sabirov and Anita Hong**

*AnaSpec Inc., San Jose, CA 95131, USA*

### **Introduction**

Protection of the indole moiety of tryptophan is often required because it is susceptible to oxidative degradation and to alkylation, when acidic conditions are used for removal of protecting groups in peptide synthesis [1]. Recently Nbs-group has been proposed for side protection of tryptophan [2]. Laborious synthesis of such protected derivatives, however, limits its application in SPPS and prompted us to develop convenient method of introducing Nbs-protection to the indole moiety of tryptophan.

### **Results and Discussion**

1-(4-Nitrobenzenesulfonyl)-1,2,4-triazolide (**1**) can be prepared in good yield by treatment of 1,2,4-triazole by 4-nitrobenzenesulfonyl chloride in the presence of TEA. We found, that the indole moiety of tryptophan can be sulfonylated by **1** in presence of DBU. Boc-Trp(Nbs)-OMe (**2**) was synthesized from Boc-Trp-OMe (**3**) by sulfonylation with **1** at room temperature in anhydrous dioxane using DBU as a base. Crystallization from methanol gave an 85% yield of **2**. Subsequent saponification of Boc-Trp(Nbs)-OMe (**2**) with 2.5 eq NaOH in aqueous dioxane led to Boc-Trp(Nbs)-OH (**4**). TFA treatment of **4** followed by Fmoc introduction resulted in the final Fmoc protected product **6** (Figure 1 and Table 1). The method is applicable for large scale synthesis of Fmoc-Trp(Nbs)-OH (**6**) and Boc-Trp(Nbs)-OH (**4**).

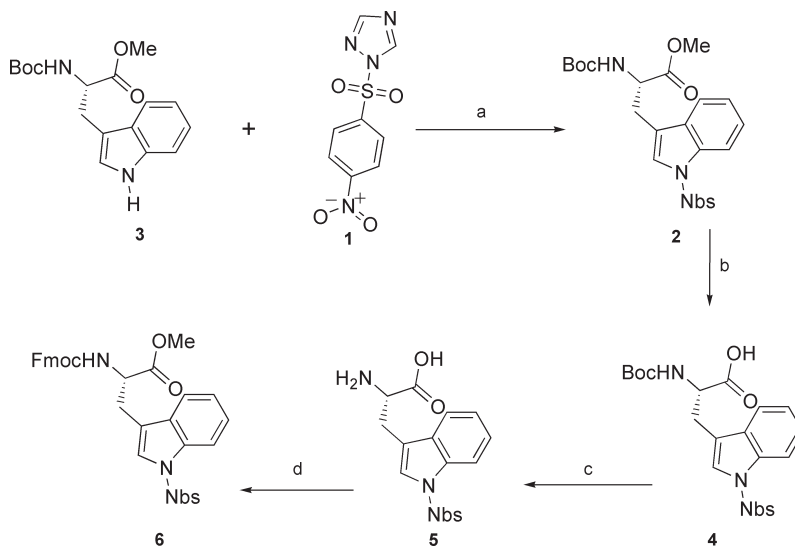


**Fig. 1.** Synthesis of Boc-Trp(Nbs)-OH and Fmoc-Trp(Nbs)-OH. Reagents and conditions: (a) DBU/dioxane, 40 min, 85%; (b) NaOH/H<sub>2</sub>O/dioxane, 20 min, 95%; (c) TFA/CH<sub>2</sub>Cl<sub>2</sub>, 15 min, 100%; (d) Fmoc-OSu/H<sub>2</sub>O/MeCN/K<sub>2</sub>CO<sub>3</sub>, 240 min, 90%.

*Table 1. Physical properties of the synthesized compounds.*

Compound	Melting point, °C	Rotation $[\alpha]_{\text{D}}^{25}$ (cl, DMF), °
1-(4-Nitrobenzenesulfonyl)-1,2,4-triazolide	153–154	–
Boc-Trp(Nbs)-OMe	164–165	–30.7
Boc-Trp(Nbs)-OH	153–155	–23.0
Fmoc-Trp(Nbs)-OH	125–128	–17.1

## References

1. Field, G.B., Noble, R.L. *Int. J. Peptide Protein Res.* **35**, 161 (1990).
2. Sabirov, A.N., Samukov, V.V., Pozdnyakov, P.I., Kim, H.J., In Fields, G.B., Tam, J.P. and Barany, G. (Eds.) *Peptides for the New Millenium (Proceedings of the 16th American Peptide Symposium)*, Kluwer, Dordrecht, 1999, p. 60.

## Syntheses of Difficult Hydrophobic Sequences Using 2-(4-Nitrophenyl)sulfonylethoxycarbonyl(Nsc)-*N*<sup>α</sup>-(2-hydroxy-4-methoxybenzyl)Ala-OH: (Ala)<sub>10</sub>-Valine, (Ala)<sub>15</sub>-Valine

Hyun Jin Lee, Weonu Chweh, Young-Deug Kim, Sang-Sun Lee  
and Hack-Joo Kim

A&PEP Inc., 213, Sosabon-1-dong, Bucheon, 422-231, Korea

### Introduction

Aggregation due to hydrogen-bonded interchain association, through the secondary amide bonds of the peptide backbone (*i.e.*,  $\beta$ -sheet formation), is thought to be the cause of difficult sequences in solid-phase peptide synthesis. The Hmb protection strategy was designed to circumvent this problem by removing the potential of backbone hydrogen bond formation and resulted in inhibited aggregation [1–3]. Especially, the hydrophobic alanine polymer showed a strong tendency to aggregate on the addition of more alanine residues [4]. Therefore, we focused on the automatic peptide syntheses of two hydrophobic difficult sequences ((Ala)<sub>10</sub>-Valine and (Ala)<sub>15</sub>-Valine), which were performed using Nsc-*N*<sup>α</sup>-(Hmb)Ala-OH [5,6].

### Results and Discussion

The 2-hydroxy-4-methoxybenzyl group has always been introduced through *N,O*-bis Fmoc-*N*-(2-hydroxy-4-methoxybenzyl)Ala until now. We have synthesized *N*-mono Nsc-*N*-(2-hydroxy-4-methoxybenzyl)Ala in two steps (Figure 1): reductive amination of the amino function of alanine with 2-hydroxy-4-methoxybenzylaldehyde yielding *N*-(Hmb)Ala, followed by introduction of Nsc group to the secondary amino group of Hmb group using Nsc-Cl under basic media. The yield of the second step is low in general. However, we obtained *mono* Nsc-(Hmb)Ala in high yield (>75%).

Using *mono* Nsc-(Hmb)Ala, we attempted to synthesize hydrophobic alanine polymer. (Ala)<sub>10</sub>-Valine was synthesized successfully by using Nsc-(Hmb)Ala-OH in the Ala5 site, while it was impossible to synthesize it using only Nsc-Ala-OH and Nsc-Val-OH without Nsc-(Hmb)Ala-OH (Figure 2).

In conclusion, new *mono* Nsc-(Hmb)Ala-OH could be obtained in high purity and yield using Nsc amino protection group. (Ala)<sub>10</sub>-Valine was synthesized in high yield by using Hmb backbone protection in this difficult hydrophobic sequence. In case of (Ala)<sub>15</sub>-Valine, there was no difference between Hmb introduction in Ala5 and Ala5 and 11 sites. (Ala)<sub>15</sub>-Valine could be synthesized successfully by introducing Hmb in Ala5 position only. Nsc-(Hmb)amino acids may be applied to the syntheses of difficult sequences, especially hydrophobic repeated sequences of peptides.

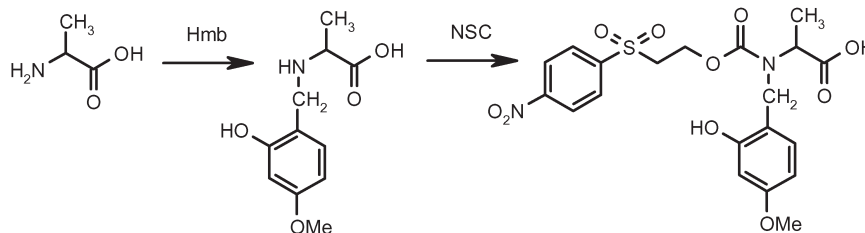


Fig. 1. Synthesis of the Nsc-*N*<sup>α</sup>-(2-hydroxy-4-methoxybenzyl)Ala-OH.

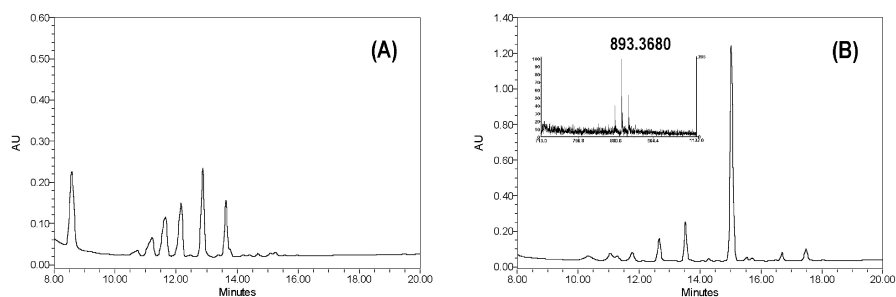


Fig. 2. HPLC Profiles of crude (Ala)<sub>10</sub>-Valine; (A) (Ala)<sub>10</sub>-Valine using Nsc-Ala-OH and Nsc-Val-OH (0%) (B) (Ala)<sub>10</sub>-Valine using Nsc-(Hmb)Ala-OH in the Ala5 site (71%), Synthesis: PerSeptive Pioneer Automatic Synthesizer, Coupling: 4 eq Nsc a.a.s, 4 eq BOP/4 eq HOBt, 8 eq DIEA in DMF, 40 °C, 1 h (Ala5,6 position: double coupling for 2 h), Deprotection: 1% DBU/20% Piperidine in DMF, Cleavage: TFA/TIS/H<sub>2</sub>O (9.5/0.25/0.25), 2 h, Analysis: A-0.1% TFA/H<sub>2</sub>O, B-0.1% TFA/AcCN; 1 mL/min, 0–100% B for 50 min; Mass Analysis: PerSeptive Voyager<sup>TM</sup> DE-STR Maldi-Tof Mass spectrometer.

## References

- Hyde, C., Johnson, T., Owen, D., Quibell, M., Sheppard, R.C. *Int. J. Pept. Protein Res.* **43**, 431 (1994).
- Quibell, M., Turnell, W.G., Johnson, T. *J. Chem. Soc., Perkin Trans. 1* 2019 (1995).
- Zeng, W., Regamey, P.O., Rose, K., Wangl, Y., Bayer, E. *Int. J. Pept. Res.* **49**, 273 (1997).
- Krchnak, V., Flegelova, Z., Vagner, J. *Int. J. Pept. Protein Res.* **42**, 450 (1993).
- Sabirov, A.N., Kim, Y.D., Kim, H.J., Samukov, V.V. *Protein Pept. Lett.* **5**, 57 (1998).
- Lee, Y.S., Lee, H.J., Pozdnyakov, P.I., Samukov, V.V., Kim, H.J. *J. Peptide Res.* **54**, 328 (1999).

## A Highly Efficient Method for Synthesis of Fmoc-Lysine(Mmt)-OH

Xiao-He Tong and Anita Hong

AnaSpec Inc., San Jose, CA 95131, USA

### Introduction

*N*<sup>α</sup>-9-Fluorenylmethoxycarbonyl-*N*<sup>ε</sup>-4-methoxytrityl-lysine [Fmoc-Lys(Mmt)-OH], an extremely acid labile derivative of lysine, was previously reported by Matyslak [1]. Because the *N*<sup>ε</sup>-Mmt moiety of lysine is extremely acid labile, the first attempt to synthesize it failed [2]. Compared to Mtt group, the Mmt moiety of lysine can be effectively cleaved by DCM/TFE/AcOH (7 : 2 : 1), even if the compound is coupled to hydrophilic Tentagel and PEG resins. For the preparation of branched and cyclic peptides or the modification of peptides with dye labels, biotin, or many particular functional groups, Fmoc-Lys(Mmt)-OH is a useful building block. In this report, we describe a highly efficient method for synthesis of Fmoc-Lys(Mmt)-OH.

### Results and Discussion

The Fmoc-Lys-OH was treated with *N,O*-bis(trimethylsilyl)acetamide (BSA, 1.6 eq) in dry DCM at ambient temperature for 20 min, then 4-methoxytrityl chloride (Mmt-Cl, 1 eq) and DIEA (1.3 eq) were added. The reaction was complete after 2–3 h at room temperature. The mixture was evaporated to oil (Figure 1).

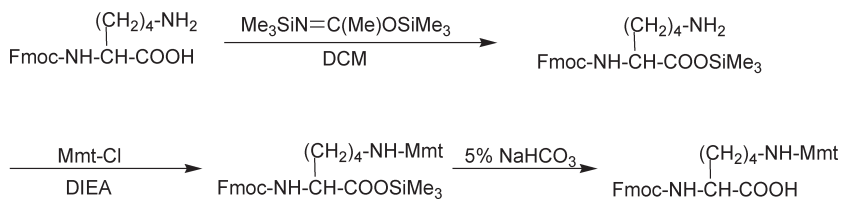


Fig. 1. Synthesis of Fmoc-Lys(Mmt)-OH.

The oil was diluted with ethyl acetate, washed with 5% NaHCO<sub>3</sub>, followed by another wash with saturated NaCl. The organic layer was dried with anhydrous Na<sub>2</sub>SO<sub>4</sub> and concentrated. Ether/hexane was added under stirring to precipitate the product. The product collected as an amorphous powder in 80% yield with >95% purity (Figure 2).

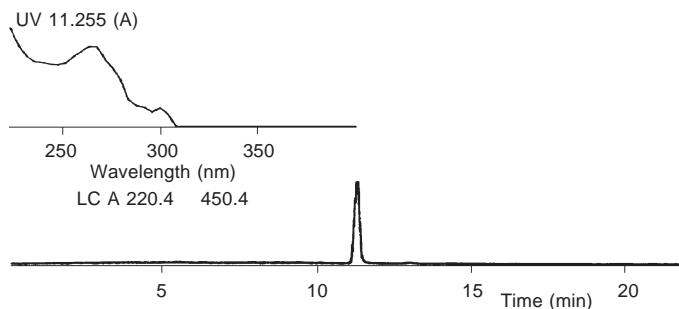


Fig. 2. RP-HPLC of Fmoc-Lys(Mmt)-OH, eluent A: CH<sub>3</sub>COONH<sub>4</sub>, 50 mM, pH 6.5, eluent B: MeCN, Linear gradient 20–100% B in 20 min, flow 1 ml/min.

***Tong et al.***

BSA is a commonly used silylating agent for several kinds of groups. Treatment of Fmoc-Lys-OH with BSA results in silylation of the carboxyl of lysine to obtain Fmoc-Lys-OSiMe<sub>3</sub>, which is very soluble in DCM. Using DCM as solvent, the N<sup>ε</sup>-amino group is easily reacted with Mmt-Cl in mild conditions. Therefore, it is possible to use a simple work up procedure (no chromatography) to obtain the final product with good yield and high purity.

**References**

1. Matyslak, S., Boldicke, T., Tegge, W., Frank, R. *Tetrahedron Lett.* **39**, 1733–1734 (1998).
2. Aletras, A., Barlos, K., Gatos, D., Koutsogianni, S., Mamos, P. *Int. J. Peptide Protein Res.* **45**, 488–496 (1995).

## A New Practical Approach to the Synthesis of Fmoc-L-Cysteine

Ming Zhao

Glycopep Chemicals, Inc., Chicago, IL 60612, USA

### Introduction

Recent increasing awareness of the importance of glycoproteins in biological processes has resulted in a great interest in the synthesis of glycopeptides and their derivatives [1]. Due to their high chemical and enzymatic stability, thioglycosides have become attractive synthetic targets in biomedical research and pharmaceutical development. *N*<sup>α</sup>-(9-Fluorenylmethyloxycarbonyl)-L-cysteine (Fmoc-L-cysteine **1**) is a useful intermediate for the preparation of *S*-substituted Fmoc-L-cysteine derivatives.

Fmoc-L-cysteine **1** can be usually prepared by two methods: 1) reduction of bis-(Fmoc)-L-cystine (**2**) and 2) cleavage of *S*-protecting groups of commercially available Fmoc-cysteine derivatives [2]. Reductive cleavage of the disulfide bridge of bis-(Fmoc)-L-cystine with triethylphosphine or Zn/TFA gives Fmoc-L-cysteine in good yields. However, the poor solubility of bis(Fmoc)-L-cystine and high cost of phosphine reagents limits the usefulness of this method. Of the *S*-protecting groups compatible with the Fmoc chemistry, triphenylmethyl (Trt) and acetamidomethyl (Acm) are the most commonly used. Removal of the Trt group using appropriate silanes often results in incomplete cleavage while using TFA with thiol scavengers complicates the subsequent purification. Oxidative cleavage of the Acm group using iodine (I<sub>2</sub>), mercury acetate [Hg(OAc)<sub>2</sub>] or thallium tris(trifluoroacetate) [Tl(tfa)<sub>3</sub>] affords the cystine products. We report here a simple and practical method for the synthesis of Fmoc-L-cysteine **1**.

### Results and Discussion

When cysteine is treated with an acylating reagent such as *t*-butyl chloroformate, both the thiol and amino groups are protected, forming a thiocarbonate and a carbamate, respectively [3]. Similar results are obtained when L-cysteine reacts with Fmoc-OSu and four major products **1**, **2**, **3** and **4** formed (Figure 1). The desired product **1** was less than 50%. Under the basic reaction conditions, Fmoc-L-cysteine **1** could be oxidized to form **2**. Therefore, the key elements to improve the reaction yield rely on inhibiting the formation of **2**, and converting **3** and **4** to the desired compound **1**.

It has been demonstrated in native peptide chemical ligation that an N-terminal cysteine residue of a peptide can interact with the second α-thioester peptide through

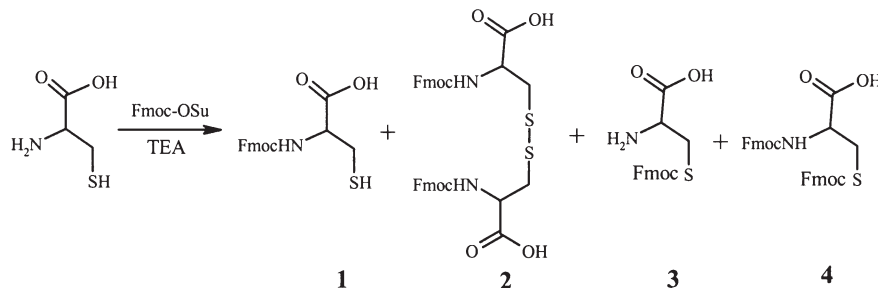


Fig. 1. Reaction of L-cysteine with Fmoc-OSu in aqueous acetonitrile solution.

## Zhao

intermolecular transthioesterification. The resulting thioester intermediate undergoes an S  $\rightarrow$  N acyl rearrangement to yield the final amide-linked product [4]. A thiol reagent is needed in native peptide chemical ligation in order to enhance reaction activity of the  $\alpha$ -thioester moiety and prevent disulfide formation between the cysteine residues [5]. We hypothesized that the use of thiophenol in the synthesis of Fmoc-L-cysteine should prevent the formation of compounds **2** and, moreover, convert **3** and **4** to Fmoc-L-cysteine **1** (Figure 2). In the presence of thiophenol, the reaction yield of Fmoc-L-cysteine **1** was indeed increased significantly from <50% to >80% and the product **1** was easy to purify.

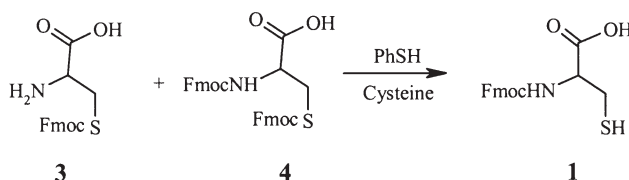


Fig. 2. Conversion of by-products **3** and **4** to Fmoc-L-cysteine in the presence of thiophenol.

In conclusion, the present new synthetic method provides a cost-effective and practical way to prepare Fmoc-L-cysteine since it is a simple one-pot reaction with a good yield.

## References

1. Arsequell, G., Valencia, G. *Tetrahedron: Asymmetry* **10**, 3045 (1999).
2. Han, Y., Barany, G. *J. Org. Chem.* **62**, 3841 (1997).
3. (a) Muraki, M., Mizoguchi, T. *Chem. Pharm. Bull.* **19**, 1708 (1971). (b) Gibson, F.S., Bergmeier, S.C., Rapoport, H. *J. Org. Chem.* **59**, 3216 (1994).
4. Dawson, P.E., Muir, T.W., Clark-Lewis, I., Kent, S.B.H. *Science* **266**, 229 (1995).
5. Dawson, P.E., Churchill, M.J., Ghadiri, M.R., Kent, S.B.H.A. *J. Am. Chem. Soc.* **119**, 4325 (1997).

## A Novel Protocol of Solid Phase Peptide Synthesis with 2-(4-Nitrophenyl)sulfonylethoxycarbonyl(Nsc)-Amino Acids

Hack-Joo Kim, Chan-Young Ko, Jeong Su Jang and Young-Deug Kim

A&PEP Inc., Sosabon-1-dong, Bucheon, 422-231, Korea

### Introduction

Although the use of Fmoc-based SPPS has increased enormously in recent years as the method of choice for the peptide synthesis, the main drawbacks of Fmoc-amino acids are low solubility, low coupling yield in the difficult sequences and poor stability in the solvents commonly used in SPPS during automation process. The Nsc-amino acids may become the possible candidates to overcome the intrinsic drawbacks of Fmoc-amino acids, and were extensively studied by our group [1]. Our previous results have shown that the Nsc-amino acids have peculiar characteristics such as polarity and solubility in solvents commonly used in peptide synthesis. As a next step, we extended our study to peptides with difficult sequences such as tyrosine polymer and long chain amino acids. Here, we show improved methodology on SPPS, so-called high temperature-short time (HTST) coupling reaction in a new solvent system using Nsc-amino acids.

### Results and Discussion

Previously, we have shown that Nsc-amino acids are more stable in various organic media at elevated temperature than Fmoc-amino acids [2]. To demonstrate the diverse application of Nsc-amino acids in SPPS compared with Fmoc-amino acids, we synthesized tyrosine 12mer (Y12) using HTST coupling reaction as a function of temperature and coupling solvent. Figure 1 (left) shows the coupling kinetics of Tyr polymer (Y8 to Y9) in several conditions using Nsc- and Fmoc-Tyr(tBu)-OH. As shown in Figure 1 (left), Nsc-Tyr showed improved coupling yields in dichloromethane (MC) at 40 °C compared to Fmoc-Tyr.

When the resultant Y12 was analyzed by HPLC, the Nsc-amino acids showed single major peak (87%) compared with five peaks (23%) of Fmoc-amino acids (Figure 1, right). These results indicate that the peptide synthesis yield can be increased using Nsc-amino acids through combined use of HTST coupling reaction and MC.

To show the effectiveness of general HTST coupling reaction using Nsc-amino acids in peptide synthesis, we synthesized salmon calcitonin (32aas) under the HTST

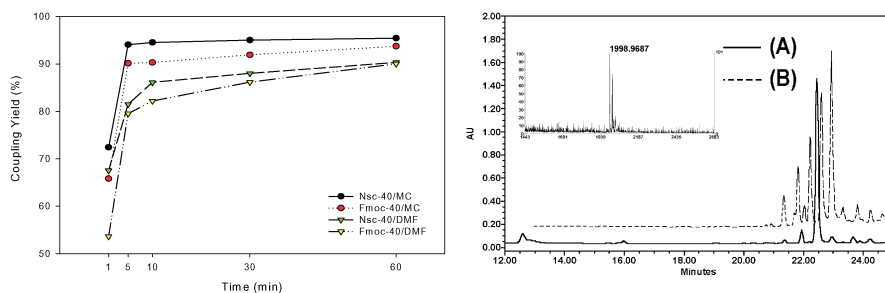
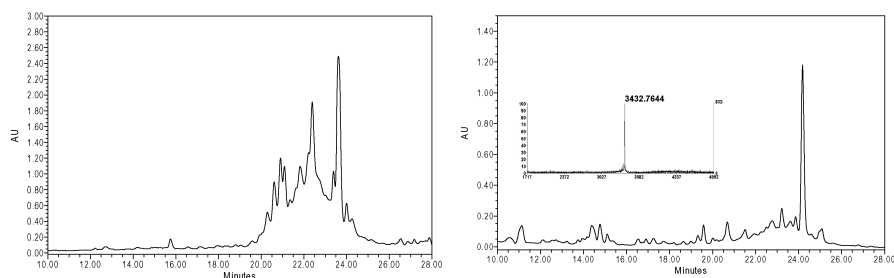


Fig. 1. Kinetic study of tyrosine oligomer (Y8 to Y9) in several conditions (left). HPLC profile of tyrosine 12mer (right) with Nsc-Tyr(tBu)-OH synthesized by using HTST protocol (A) and with Fmoc-Tyr(tBu)-OH in DMF at 25 °C, 1 h (B); 0–100% TFA/MeCN in 50 min; 1 mL/min.

**Kim et al.**

condition (Figure 2). The salmon calcitonin synthesized using Fmoc-amino acids was used as a control. As shown in Figure 2, the Nsc-amino acids showed better results (Figure 2B) than Fmoc-amino acids (Figure 2A). This result implies that the Nsc-amino acids under present reaction condition in MC, could be the desirable choice to overcome the intrinsic drawbacks of Fmoc-amino acids.



**Fig. 2.** HPLC profile of salmon calcitonin (32 aas) with Fmoc-amino acid synthesized in DMF at 25 °C, 1 h (A) and with NSC-amino acid synthesized in MC by using HTST protocol (B); 0–100% TFA/MeCN in 50 min; 1 mL/min.

Results from the present studies, we suggest that the new HTST coupling reactions using Nsc-amino acids under MC solvent system may be another superior choice in the field of SPPS.

## References

1. Sabirov, A.N., Kim, Y.D., Kim, H.J., Samukov, V.V. *Protein Pept. Lett.* **5**, 57–63, (1998).
2. Ramage R., Jiang L., Kim Y.D., Shaw K., Park J.I., Kim H.J. *J. Peptide Sci.* **5**, 195–200 (1999).
3. Kim, Y.D., Cho, B.K., Park, J.I., Lee, S.H., Kim, H.J. *5th Innovation and Perspectives in Solid Phase Synthesis & Combinatorial Libraries*, London, 1997.
4. Carreno, C., Mendez, M.E., Kim, Y.D., Kim, H.J., Kates, S.A., Andreu, D., Albericio, F. *J. Peptide Res.* **56**, 63–69 (2000).

## **S-Xanthenyl Protected 1-Thiosugars as Building Blocks for Glycopeptide Assembly**

**Robert A. Falconer**

*Department of Pharmaceutical and Biological Chemistry, The School of Pharmacy,  
University of London, London WC1N 1AX, UK*

### **Introduction**

Thioglycosides are key intermediates for oligosaccharide assembly and are of importance in biological systems due to their increased enzymatic stability. They are more stable to the action of glycosidases than their *O*-linked isosteres, making them potential enzyme inhibitors and a potential means by which to facilitate the delivery of therapeutic peptides.

The assembly of *S*-linked glycopeptides on a solid support is complicated by the need to anchor a sugar moiety to the resin, and by the requirement for a selectively removable thiol protecting group that is compatible with standard Fmoc solid phase synthesis. Potential protecting groups include triphenylmethyl (Trt) and 9-fluorenylmethyl (Fm). However, each presented problems both with introduction (low yields) and removal.

### **Results and Discussion**

The recently reported 9*H*-xanthen-9-yl (Xan) protecting group [1], used as a temporary cysteine *S*-protecting group in the synthesis of  $\alpha$ -conotoxin [2], has been successfully utilized here as a temporary thio-protection compatible with other carbohydrate protecting groups. 1-Thiosugars of glucose **2a**, galactose **2b** and mannose **2c** were synthesized from their respective bromosugars **1a–1c** by reaction with thiourea, followed by basic hydrolysis. The xanthenyl protecting group was introduced in quantitative yield by reaction of the 1-thiosugar **2** with 9-hydroxyxanthene in the presence of TFA (Figure 1).

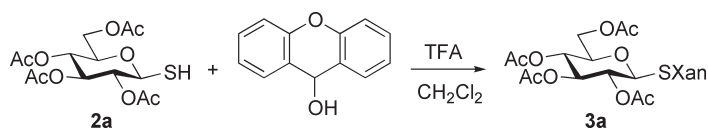


*Fig. 1. Introduction of xanthenyl protection.*

Following de-*O*-acetylation of the Xan-protected thiosugar, *e.g.* **3c**, a silyl (TBDMS) protecting group was selectively introduced to the 6-OH group. After re-*O*-acetylation, the TBDMS group could be selectively cleaved with tetrabutylammonium fluoride (TBAF) to give **7c** (Figure 2).

*S*-Xan is completely stable to the conditions required to introduce and remove both acetate and silyl protecting groups, commonly used in carbohydrate synthesis. Glycoside **7** is a convenient building block suitable for loading onto a solid support. In addition, the Xan-protected sugar was anchored *via* a succinate linker.

Once on the resin, the Xan-protection was removed in a facile manner, and a peptide chain extended *via* a Mitsunobu reaction [3]. The xanthenyl group was also stable to the conditions required for the introduction of both benzyl ether and benzylidene

**Falconer**

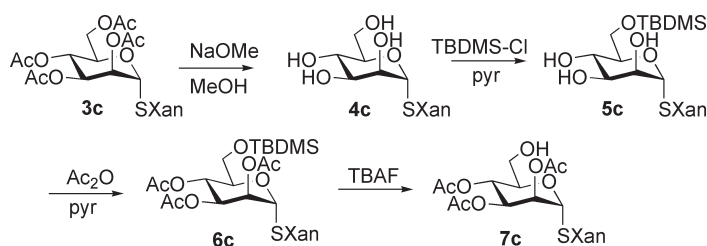


Fig. 2. Preparation of building block.

acetal protecting groups and was not cleaved by either acetic or formic acid. Benzyl groups were selectively removed by catalytic hydrogenation.

The *S*-Xan protection was removed in solution using 1% TFA to allow the synthesis of conjugates **8** and **9** via a Mitsunobu reaction [3,4] (Figure 3).

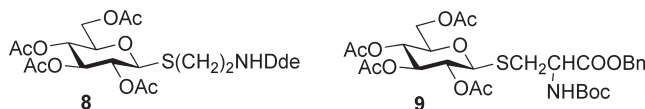


Fig. 3. Thio-linked glycosides.

In summary, the xanthenyl protecting group was used as an effective temporary thio-protecting group, and found to be stable to a wide range of conditions commonly encountered in carbohydrate synthesis. *S*-Protected glycosyl donors suitable for attachment solid phase attachment were prepared. In addition, the *S*-Xan group was easily removed to allow synthesis of thio-linked conjugates bearing protected amines.

**Acknowledgments**

This work was supported by a School of Pharmacy Research & Teaching Fellowship.

**References**

1. Han, Y., Barany, G. *J. Org. Chem.* **62**, 3841–3848 (1997).
2. Hargittai, B., Barany, G. *J. Peptide Res.* **54**, 468–479 (1999).
3. Mitsunobu, O. *Synthesis* 1–28 (1981).
4. Falconer, R.A., Jablonkai, I., Toth, I. *Tetrahedron Lett.* **40**, 8663–8666 (1999).

## Late Deprotection Difficulties During SPPS Depend on the Preceding Sequence

Phillip W. Banda

Applied Biosystems, Foster City, CA 94404, USA

### Introduction

Via UV monitoring on the 433A, the early onset of Fmoc-deprotection difficulty arises 7 to 15 residues after SPPS begins at the C-terminus of a peptide sequence [1]. Secondary structure takes shape and inhibits access of the growing chain-end to both deprotection and coupling reagents. The difficult deprotections of interest to us arise long after the SPPS process has begun, *i.e.* after 30 or 50 or more residues have been coupled, and they are likely signaling a different process within the peptide-resin environment, namely, tertiary structure [2].

We have been studying MCP-1 as a C-terminal 40-mer, and Rantes as the corresponding C-terminal 34-mer, to examine the late deprotection differences between the two beta-chemokines. Both have similar free solution structures [3,4] but each displays a distinctly different pattern of Fmoc-deprotections during SPPS. MCP-1 displays “easy” deprotections from the C-terminus to residue 33, and then runs into a largely hydrophobic sequence of several “difficult” deprotections, Figure 1a. Rantes displays “easy” deprotections for its corresponding hydrophobic sequence, Figure 1b.

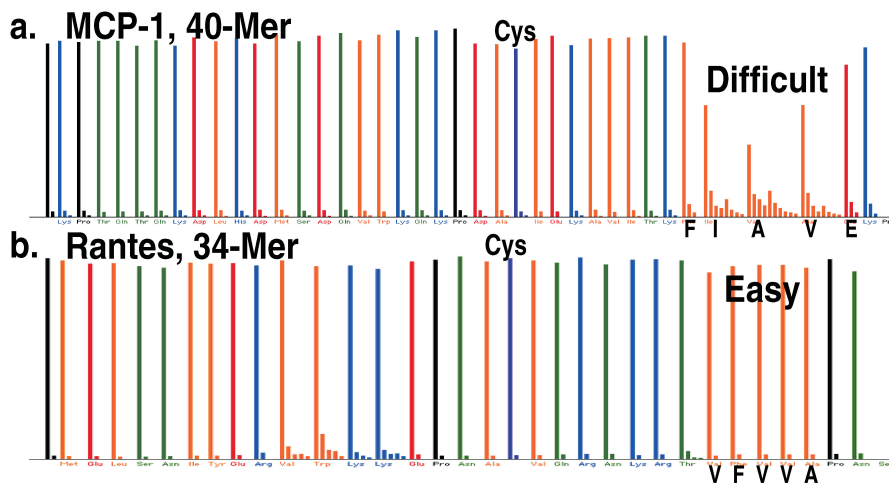


Figure 1. C-Terminal UV deprotection profiles: a) MCP-1 40-Mer; b) Rantes 34-Mer.

### Results and Discussion

a) *MCP-1 into Rantes*. If the “difficult” residues 34-39 in MCP-1 are, indeed, an inherently “difficult” string, then they should display extended deprotections anywhere in a sequence (except at the very C-terminus). If, on the other hand, the deprotection problems in MCP-1 are not inherent in the particular string of residues but are dependent on the previous sequence, then the extended deprotections should change when the problem residues are substituted into another sequence. Figure 2a shows just such an experiment, namely, placing the “difficult” residues 33-39 of MCP-1 into their corresponding position in Rantes: the deprotections become “easy”.

## Banda

b) *Rantes into MCP-1*. Similarly, if the hydrophobic sequence from Rantes 27-31 is inherently “easy” to deprotect, then these residues should remain “easy” wherever they appear. If, however, “easy/difficult” depends on the previous sequence, then the deprotections of these hydrophobic residues should change when they are placed into another sequence. In fact, when these residues from Rantes are placed into MCP-1, the deprotection trace becomes “very difficult”, Figure 2b.

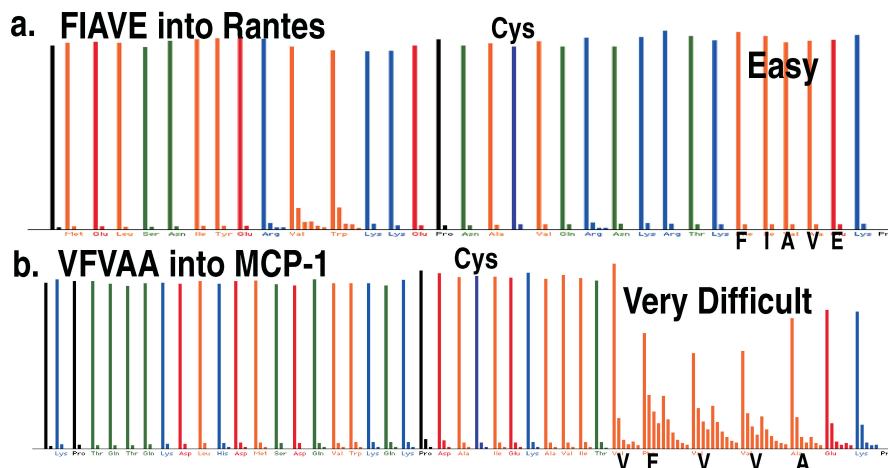


Figure 2. Substituting strings: a) MCP-1 into Rantes; b) Rantes into MCP-1.

The beta-chemokine substitution experiments demonstrate that the “easy/difficult” deprotections of an amino acid string - positioned long after the start of a synthesis – is not an inherent property of the particular sequence but clearly depends on the earlier residues, *i.e.* on the overall structure of the peptide. The 433A *via* UV monitoring of Fmoc-deprotections is providing structural information about peptide-resins.

## References

1. Otteson, K.M., Nobel, R.L., Banda, P.W., Sanchez, A., Smith, A.J., In Kaumaya, P.T.P. (Ed.) *Proceedings of the 14th American Peptide Symposium*, 1995, P051.
2. Banda, P.W., Leopold, M.F., In J. Martinez and J-A. Fehrentz (Eds.) *Peptides 2000 (Proceedings of the 26th European Peptide Symposium)*, EDK, Paris, 2001, p. 191.
3. Handel, T.M., Domaille, P.J. *Biochemistry* **35**, 6569-6584 (1996).
4. Skelton, N.J., Aspiras, F., Ogez, J., Schall, T.J. *Biochemistry* **34**, 5329-5342 (1995).

## Towards a Selective Boc Deprotection on Acid Cleavable Resin

Florine Cavelier, Valérie Lejeune and Jean Martinez

Laboratoire des Aminoacides, Peptides et Protéines, UMR-CNRS 5810,  
 Universités Montpellier I et II, 34095 Montpellier cedex 05 – France

### Introduction

The Wang resin is one of the most commonly used solid polymers in SPPS. An Fmoc strategy for the lengthening of the peptide chain is compatible with the final acid cleavage of the peptide–resin bond. To increase tactic possibilities, it would be interesting to be able to use the Boc group on this resin type. Classical acid conditions (TFA 30 to 90% in DCM) for Boc removal cleave the peptide from the Wang resin simultaneously. Therefore, we investigated new conditions for deprotecting the Boc group which would preserve the peptide–resin bond.

### Results and Discussion

We screened numerous conditions on a model substrate, Fmoc-Lys(Boc) attached to the Wang resin. The Fmoc group was left unaffected and allowed us to evaluate the amount of cleaved and supported amino acids, respectively, by HPLC.

We first used acidic conditions, like *in situ* generated HCl with alcohol and chlorosilane [1] (entries 1 and 2) or diluted TFA (entry 3) without any success. A method for removal of N-Boc groups on Rink's amide resin was described by treatment of the peptide resin with a combination of TMSOTf and 2,6-lutidine [2]. However, in our hands these conditions led to a high percentage of peptide cleavage (entry 4). We then tried pyridine with TMSOTf and found that we could remove the Boc group without any cleavage of the peptide from the resin, although the yield was not satisfactory (entry 5). We therefore kept these reagents and varied reaction time, solvent and concentration in TMSOTf (entries 6 to 12). We also tested TEA as base in several conditions (entries 13 to 18).

Kinetic studies of the reaction showed that a short reaction time is preferable, DCE is a better solvent than DCM, and TEA is eligible. Conditions 18 were defined to be the most satisfactory (Figure 1). We extended our study from Wang resin to SynPhase™ lanterns (Figure 2).

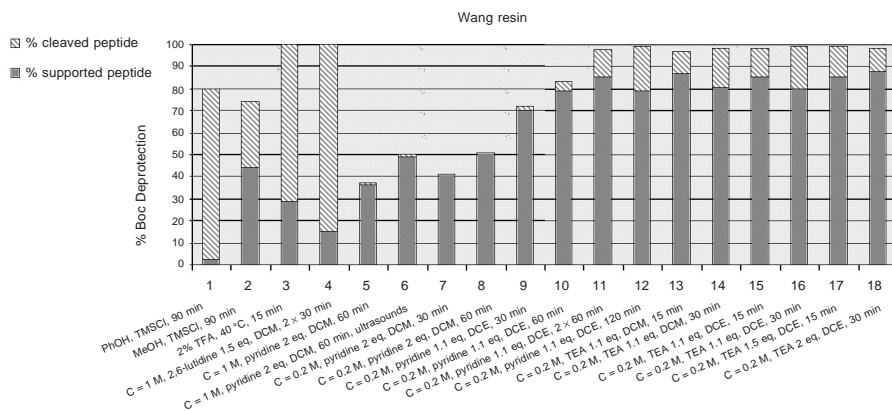


Fig. 1. Boc cleavage conditions on Wang resin.

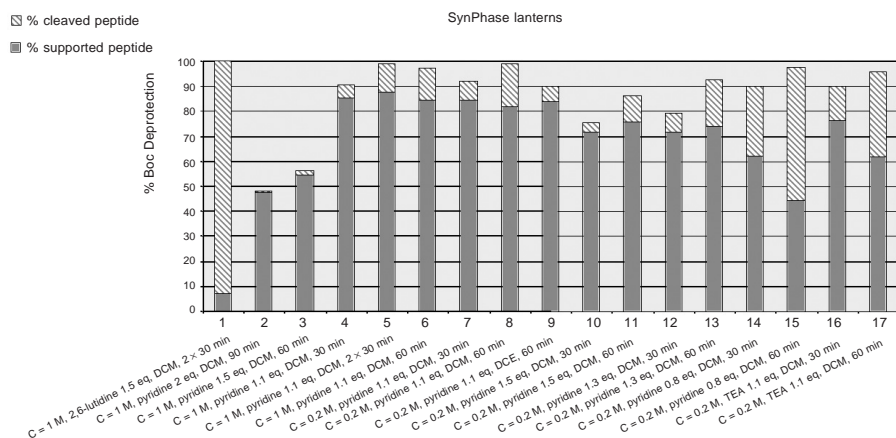


Fig. 2. Boc cleavage conditions on SynPhase lanterns.

In conclusion, we found that avoiding acidic conditions by using a trimethylsilyl transitory protection allowed Boc removal on the resin in a good yield with only a small percentage of peptide cleavage from the support.

## References

1. Kaiser Sr., E., Tam, J.P., Kubiak, T.M., Merrifield, R.B. *Tetrahedron Lett.* **29**, 303–306 (1988).
2. Zhang, A.J., Russell, D.H., Zhu J., Burgess, K. *Tetrahedron Lett.* **39**, 7439–7442 (1998).

## **By-Product Formation During SPPS of Linear, Cyclic, and Novel Bicyclic Peptides as AChE Inhibitors**

**Peteris Romanovskis<sup>1</sup>, Terrone L. Rosenberry<sup>2</sup>, Bernadette Cusack<sup>2</sup>  
and Arno F. Spatola<sup>1</sup>**

<sup>1</sup>*Department of Chemistry and the Institute for Molecular Diversity and Drug Design  
University of Louisville, Louisville, KY 40292, USA*

<sup>2</sup>*Department of Neuroscience at Mayo Clinic, Jacksonville, FL 32224, USA*

### **Introduction**

We have been interested in the synthesis of loop II of the AChE inhibitor of the fasciculin (a “three-finger” snake venom polypeptide neurotoxin from green mambas (genus *Dendroaspis*)) [1]. Our parent sequence involves amino acids 27-34 or -Arg-Ala-His-Pro-Pro-Lys-Met-Gln- as the base peptide from which cyclic and bicyclic analogues have been prepared. These may serve as chemical probes to study peripheral site acetylcholinesterase (AChE) inhibition.

For that goal we used SPPS methods, with orthogonalities based on Boc/Bzl/OFm, Boc- or Fmoc/Bzl/ONB and Fmoc/Bzl/OtBu strategies, using a side chain attachment approach [2]. Next, peptide chain elongation and subsequent on-resin head-to-tail cyclization was followed by deprotection and cleavage from the resin by liquid HF; this allowed us to compare the advantages and drawbacks of the three strategies.

### **Results and Discussion**

Although we have synthesized more than 50 cyclic analogues of the fasciculin loop II fragment and some of their linear precursors, this work describes the synthesis of a mixed heterodetic bicyclic peptide c(Arg-Ala-Cys-His-Pro-Pro-Lys-Cys-Nal-Gln), with Mmt- and Mob-groups for Cys S-protection. A synthesis (with Cys S-Mmt protection) led first to disulfide bond formation on the resin using DMSO, with subsequent amide bond formation by HATU also on the resin. However, the on-resin amide bond cyclization, after the intramolecular disulfide bond had been formed, turned out to be extremely slow. In a second approach (with Cys S-Mob), the amide bond cyclization was first accomplished on-resin, after which the peptide-resin was HF treated and the disulfide bond created in solution by hydrogen peroxide. Although the yields of the desired product were low in both cases (<5–10%), the second procedure proved more effective in providing the desired compound.

During routine MS analysis we again noted the advantage of running a combination of parallel synthesis of closely related compounds, not only for confirmation of the desired products, but also for identifying the contaminants/side products originating in steps associated with on-resin cyclization and following cleavage/deprotection. Thus, along with the described N-terminal tetramethylguanidino derivatives  $[M + H] + 116$  Da [3], we also observed  $[M + H] + 45$  Da that could be attributed to C-terminal dimethylamides. Previously we were able to correlate the additional mass signal  $[M + H] - 48$  Da with the presence of Met in the original molecule [4]: we suspected the alkylation of the Met side chain turned it into the corresponding sulfonium derivative with subsequent transformation, probably into the Freidinger lactam [5], by losing the methylthio group as a result of unspecific interaction with nucleophiles. This Met *S-tert*-butylsulfonium salt reactivity pathway has been confirmed also by formation of the corresponding C-terminal homoserine lactone when Met is the C-terminal amino

acid in a peptide [6]. Combination of both the latter two modifications in one molecule  $[M + H] - 48 + 45$  Da also pointed towards the origin of the MS signal  $[M + H] - 3$  Da as resulting from a peptide with a C-terminal dimethylamide whose Met had suffered the above-mentioned modification.

In the case of MALDI-TOF-MS analysis of the bicyclic peptide (calculated MW = 1215; found  $[M + H]^+ = 1216$ ) both in the crude product and in its RP-HPLC purification fractions we saw additional MS signals  $[M + H + 124]^+ = 1340$ . Similar MS fragments were observed in the -S-S- containing monocyclic precursor (calculated MW = 1233; found  $[M + H]^+ = 1234$ ;  $[M + H + 124]^+ = 1358$  and  $[M + H + 248]^+ = 1482$ . These results agree with and confirm the previously reported findings [4] that HF deprotection of peptides containing *N*-ε-2-chloro-Z-protected Lys is accompanied by Friedel-Crafts alkylation of aromatic side chains (in this case Nal) by 2-chlorobenzyl carbocation that is reflected by the increase of the mass signal of the alkylated product by 124 Da or its multiples over its precursor.

### Acknowledgments

Funded by US Army/Mayo Clinic Grant, DAMD17-2-8019. Mass spectral data are from a MALDI-TOF-MS in Chemistry (State of Kentucky funds). Biological activities of the compounds will be reported elsewhere.

### References

1. Rosenberry, T.L., Mallender, W.D., Cusac, B., Szegletes, T., Romanovskis, P., Spatola, A.F. *Medical Defense Review, Proceedings of the USARMC Bioscience* **2000**, in press.
2. Spatola, A.F., Romanovskis, P. *The Amide Linkage: Selected Structural Aspects in Chemistry, Biochemistry and Material Science*, Greenberg, A., Breneman, C.M., Liebman, J.F., John Wiley, New York, 2000, pp. 519–564.
3. Story, S.C., Aldrich, J.V. *Int. J. Pept. Protein Res.* **43**, 292–296 (1994).
4. Romanovskis, P., Smith, N., Pierce, W.E., Spatola, A.F., In Martinez, J., Fehrentz, J.-A. (Eds.) *Peptides 2000*, EDK, Paris, France, 2001, pp. 1009–1010.
5. Freidinger, R.M., Schwenk Perlow, D., Veber, D.F. *J. Org. Chem.* **47**, 104–109 (1982).
6. Gairi, M., Loyd-Williams, P., Albericio, F., Giralt, E. *Tetrahedron Lett.* **35**, 175–178 (1994).

## Acidic Cleavage of the Side Chain Protecting Groups of Peptides Attached to a Modified Polystyrene Carrier: Synthesis of Peptide Generics

**Luděk Lepša, Anna Ammerová and Martin Flegel**

*PolyPeptide Laboratories, Radiova 1, 102 28 Prague 10, Czech Republic*

### Introduction

High or good yield is essential for peptide production. The side chain protecting groups are cleaved usually in solution, after peptide detachment from the solid carrier. This can, however, be accompanied by the loss of material and the decrease in yield. Such problems can be circumvented when the side chain deprotection steps are carried out on the peptide still bound to resin. Just before purification, the final product can be detached from resin. Analogues of Vasopressin and LH-RH were synthesized on hydroxyalkylated aminopolystyrene. Stability of polymeric like alkyl ester towards hard acid (TFMSA, HF) makes possible the assembling of peptides protected with Benzyl and Tosyl groups. All cleavage steps were carried out on the peptide bound to resin. In this way salts and scavengers can also be washed away prior to detachment of peptide from the resin. Ammonolysis in gas [1] or ethylaminolysis was employed as the detachment step. The crude peptide amides were obtained in the high yield and purity. Conditions for the complete cleavage of Tos group were developed. Moreover, the resin could be used again for the new peptide synthesis.

### Results and Discussion

Aminomethyl-resin opened the cycle of butyrolacton (Figure 1) and hydroxypropyl-amido-resin was formed (70 °C, 24 h). The C-terminal amino acid of the synthesized peptides was either Boc-Pro or Boc-Gly, therefore the danger of racemisation was eliminated.



*Fig. 1. Modification of the polymeric carrier by butyrolacton.*

Boc-Pro (3 eq.) or Boc-Gly were coupled to resin (1 mmol/g) overnight, by addition of DIC, HOBt and DIEA (3 eq. each) in DCM : DMF 4 : 1, (Boc-Gly, Boc-Pro: 0.89, 0.96 mmol/g). Lecirelin, Desmopressin and Fertirelin were chosen for testing the synthetic method. Boc-group was the temporary and Bzl-/Tos-/For were the side chain protecting groups during the peptide synthesis. Boc-AA were preactivated with 1.5–2 eq., DCC, HOBt in DCM/DMF mixture, Boc group was cleaved in HCl/DCM solution, or 50% TFA/DCM. 10% DIEA/DCM was used for neutralization. Protected precursors of Lecirelin(I), Desmopressin(II) and Fertirelin (III) were prepared on the modified resin.

*p*Glu-His-Trp(For)-Ser(Bzl)-Tyr(Bzl)-D-*tert*Leu-Leu-Arg(Tos)-Pro-O-(CH<sub>2</sub>)<sub>3</sub>-CO-NH-P (I)  
 Mpa(Acm)-Tyr-Phe-Gln-Asn-Cys(Acm)-Pro-D-Arg(Tos)-Gly-O-(CH<sub>2</sub>)<sub>3</sub>-CO-NH-P (II)  
*p*Glu-His-Trp(For)-Ser(Bzl)-Tyr(Bzl)-Gly-Leu-Arg(Tos)-Pro-O-(CH<sub>2</sub>)<sub>3</sub>-CO-NH-P (III)

Stability of the ester bond was checked with the mixture containing 40% TFMSA (TFMSA : TFA : TGA, 4 : 4 : 2). The bond between the peptide and polymeric carrier survived, even when the reaction was extended overnight (RT). Benzyl and Tosyl groups could be removed in the optimized cocktail containing TFMSA : TFA : thioanisol : phenol, 17.5 : 62 : 17.5 : 3 (v/v/v/w). AcM group on Desmopressin remained stable. After washing and resin drying, the peptide was ready for detachment. It was carried out during 24 h by ammonolysis in gaseous ammonia [1] or by aminolysis in ethylamine. The Formyl group was removed in this step as well. Lecirelin and Fertirelin were isolated and purified (IEC, HPLC). In Desmopressin AcM groups had to be removed and disulfide bridge formed in solution. Diastereomers, particularly [D-His<sup>2</sup>]-Lecirelin, [D-His<sup>2</sup>]-Fertirelin and [D-Asn<sup>5</sup>]-Desmopressin were identified. Position 2 in LH-RH molecule and asparagine-5 in the group of neurohypophyseal hormone analogues is known as the sensitive site for racemization [2,3].

Table 1. The yields of peptides.

Peptide	Peptide-resin [g] %	Crude peptide [g] %	A.P.I. peptide [g] PhEu quality	Yield total (%)
Lecirelin	136 (98)	59 (97)	32 (54)	51
Fertirelin	1250 (98)	586 (98)	325 (54)	52
Desmopressin	5 (99)	2.3 (87)bis-AcMDP	1.0 (49)	42

TFMSA containing mixtures [4] can be the good cleavage alternative in the large-scale peptide synthesis. The Tos group was fully removable under the optimized conditions. Modification of polystyrene resin exhibited excellent stability during the deprotections and peptides were than easily detached in ammonolytic or aminolytic procedures. Polymeric alkyl ester resin can be used for the synthesis of peptides multiple times.

## References

1. Flegel, M., et al., In Kaumaya, P.T.P. and Hodges, R.S. (Eds.) *Peptides: Chemistry, Structure and Biology* (Proc. 14th Am. Pept. Symp.), Mayflower, 1996, p. 119.
2. Pánek, Z., Pavlík, M. Flegel, M., In Epton, R. (Ed.) *Solid phase synthesis & combinatorial libraries*, Mayflower Scientific Ltd, 1998, p. 365.
3. Buserelin, In *European Pharmacopoeia* 1997, p. 500
4. Bergot, J., Noble, R.F., Geiser, T., In Theodoropoulos, D. (Ed.) *Peptides 1986 (Proceeding of the 19th European Peptide Symposium)*, Walter de Gruyter, 1987, p. 97.

## The Use of a Novel Safety Catch Linker for BOC-Based Assembly of Cyclic Peptide Libraries

Simon W. Golding, Gregory T. Bourne, Wim D. F. Meutermans,  
Alun Jones and Mark L. Smythe

*Institute for Molecular Bioscience, The University of Queensland, Brisbane, 4072, Australia*

### Introduction

Cyclization of peptides is an important method for identifying active molecules, stabilizing and elucidating receptor-bound conformations, and ultimately developing lead compounds. As such, we have been interested in the rapid synthesis of discrete cyclic peptide libraries using a novel "safety catch" linker **1** [1]. This linker allows BOC solid-phase peptide assembly and on completion is unmasked using deprotection conditions commonly employed within peptide chemistries (HF or strong acid). The resulting linking group permits cyclization of the linear peptide, with concomitant cleavage upon neutralization of the N-terminal amine.

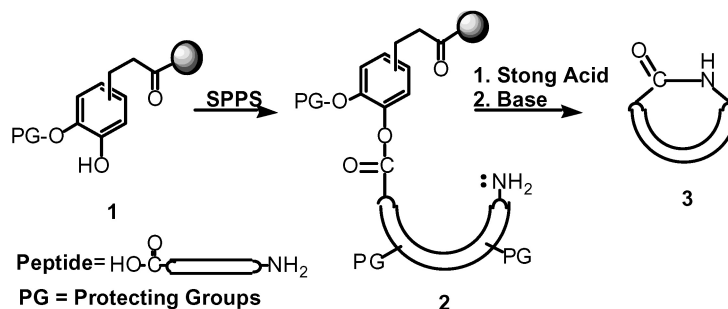


Fig. 1. Synthesis of cyclic peptides using the safety catch linker.

To exemplify this strategy, several cyclic peptides have previously been synthesized and reported [1]. From this initial study and to show the strength of the method, we are now able to report the synthesis of a cyclic peptide library containing over 400 members.

### Discussion

The safety-catch linker is conceptually ideal for the parallel synthesis of cyclic peptide libraries since it utilizes on-resin side-chain deprotection which, after neutralization and cyclization, gives the desired cyclic peptides in solution. Although previous synthesized examples prove this concept [1], an alternative deprotection strategy had to be found since no HF apparatus is commercially available for handling the large numbers of compounds encountered in parallel synthesis.

The first choice was HBr/TFA; early experiments suggested that it gave similar results to HF, although with small amounts of partially protected products. When we synthesized small libraries, however, we found HBr/TFA to be unreliable, and often repeated treatments were required to remove all the protecting groups.

An alternative deprotection strategy that is commonly employed in BOC-based peptide synthesis is TFMSA/TFA; in comparison with HF we found that it provided similar on-resin deprotection. However, some compromise is required concerning protecting groups. For example, Mts or tosyl on arginine are quite resistant and require

longer reaction times at room temperature. We found that 10% TFMSA with up to 5 h reaction time at 0° C, or 1 h at room temperature, was required for complete deprotection. The use of thiol scavengers such as thiocresol or thioanisole were equally as effective as *p*-cresol. Other alternative side-chain deprotection strategies such as TMSOF/TFA and TMSBr/TFA were also tried, but were not as effective as TFMSA/TFA.

Based on these results, a library comprised of 432 cyclic peptides was synthesized using TFMSA/TFA for activation/deprotection. The sequences were either cyclic hexa- or pentapeptides containing various natural and unnatural amino acids, including: Gly, Ala, Ile, Phe, Tyr, Arg, Ser, Thr, Trp, His, Pro, D-Pro,  $\beta$ -Ala, 3-Amb and 6-aminohexanoic acid. At least four of the amino acids in the sequence corresponded to the natural amino acids. After synthesis and workup, all samples were analyzed by RP-HPLC and MS, and by LCMS. The peak purity of the major peak was then ranked on a scale of 1-4 (1->75%, 2-75-50%, 3-50-25%, 4-<25%); results for the library are shown in Figure 2. The high variability of these results suggests that the cyclization of these small cyclic peptides is highly sequence dependent and, hence, difficult in some cases.

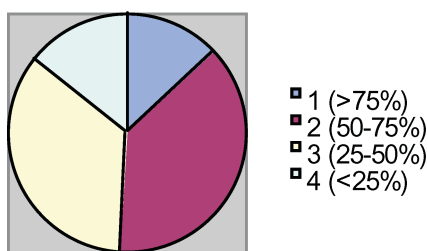


*Fig. 2. Library HPLC purity.*

In conclusion, this safety catch linker technology provides a new solid-phase avenue to access large arrays of cyclic peptides. We are now currently synthesizing in excess of 3,000 discrete cyclic peptides.

## References

1. Bourne, G.T., McGeary, R.P., Golding, S.W., Meutermans, W.D.F., Smythe, M.L. In Fields G.B., Tam, J.P., and Barany, G. (Eds) *Peptides, Biology and Chemistry (Proceedings of the 16th American Peptide Symposium)*, Kluwer Dordrecht, 2000, p. 98-99.

## Diurethanyl 1*H*-Benzotriazole-1-carboxamidines as Guanidinylation Reagents

Hans-Jürgen Musiol and Luis Moroder

Max-Planck-Institute of Biochemistry, D-82152 Martinsried, Germany

### Introduction

There is a growing interest in efficient arginine mimetics for the design of enzyme inhibitors and receptor antagonists. Since highly reactive guanidinylation reagents are required for their synthesis, recent developments were focused on *N,N'*-diurethanyl carboxamidines to enhance the electrophilicity of the amidino carbon, thus increasing its reactivity toward amines [1], but also to facilitate subsequent synthetic steps in the presence of protected  $\omega$ -guanidine groups. Among the proposed reagents, the most reactive ones are the compounds **1** [1] and **2a** [2] and, particularly, the traceless resin-bound reagent **2b** [3] (see Figure 1).

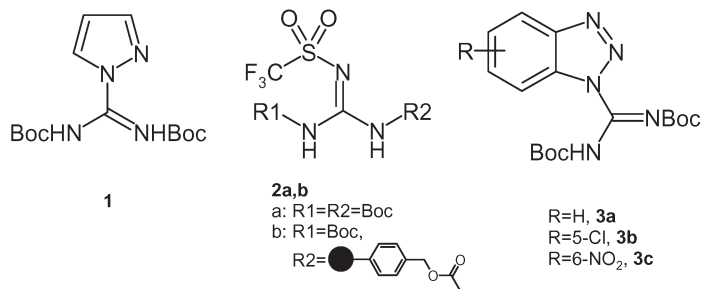


Fig. 1. Guanidinylation reagents.

### Results and Discussion

In order to exploit the good leaving group character of benzotriazole [4], *N,N'*-di-(*tert*-butoxycarbonyl)-1*H*-benzotriazole-1-carboxamidine (**3a**) was synthesized by reacting benzotriazole with the commercially available diurethane-protected *S*-methylisothiourea derivative in the presence of mercuric chloride. In a similar manner, the di-protected 5-chloro- (**3b**) and 6-nitro-1*H*-benzotriazole-1-carboxamidine (**3c**) were prepared to further enhance the reactivity of the benzotriazole derivatives. All three benzotriazole reagents were found to be superior to compounds **1** and **2a** in guanidinylation of aniline at 20 °C, with the 6-nitro derivative **3c** being the most reactive. The results obtained with diisopropylamine as sterically hindered amine in solution are reported in Figure 2A. While the resin-bound reagent **2b** is more reactive than the unsubstituted benzotriazole derivative **3a**, because of its stronger activation *via* the benzyl-type urethane group [3], reagent **3c** is again the most potent, despite the *N,N'*-protection as *tert*-butoxycarbonyl derivative.

As shown in Figure 2B, for guanidinylation of (4-amino)phenylalanine on resin all the benzotriazole derivatives were found to be superior to the reagents analyzed in comparison and, again, the 6-nitro derivative **3c** proved to be the most potent, resulting in quantitative conversion of the amine into the guanidine group after 2 h reaction time both in CH<sub>2</sub>Cl<sub>2</sub> and DMF.

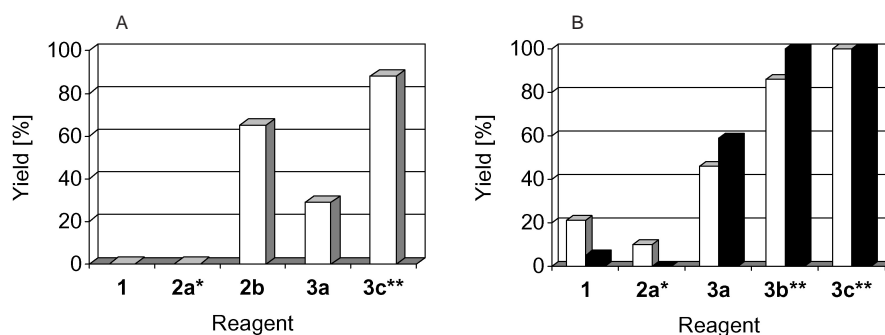


Fig. 2. A) Yields of product isolated upon reacting diisopropylamine with reagents **1**, **2a**, **2b**, **3a** and **3c** [1 equiv. of a 0.2 M solution of reagent **3a** or **3c** in CH<sub>2</sub>Cl<sub>2</sub> and 1.2 equiv. diisopropylamine at 20 °C for 12 h; \*) with 1 equiv Et<sub>3</sub>N and \*\*) with 1 equiv. DIEA]; with reagent **1** or **2a** in CH<sub>2</sub>Cl<sub>2</sub> or CHCl<sub>3</sub> no reaction has been reported [1,2], while with reagent **2b** a yield of 65% has been obtained after 24 h reaction time [3]). B) Yields of product upon reacting Boc-Phe(4-NH<sub>2</sub>)-Gly-trityl resin with **1**, **2a**, **3a**, **3b** and **3c** in CH<sub>2</sub>Cl<sub>2</sub> (open bars) or DMF (filled bars) [1 equiv. Boc-Phe(4-NH<sub>2</sub>)-Gly-trityl resin and 2.5 equiv. reagent at 20 °C for 2 h; \*) with 2.5 equiv. Et<sub>3</sub>N; \*\*) with 2.5 equiv. DIEA]; yields were determined by HPLC after product cleavage from the resin with CH<sub>2</sub>Cl<sub>2</sub>/TFE/AcOH, 8 : 1 : 1, for 1 h.

## References

1. Drake, B., Patek, M., Lebl, M. *Synthesis* 579–582 (1994).
2. Feichtinger, K., Zapf, C., Sings, H.L., Goodman, M. *J. Org. Chem.* **63**, 8432–8439 (1998).
3. Zapf, C.W., Creighton, C.J., Tomioka, M., Goodman, M. *Org. Lett.* **3**, 1133–1136 (2001).
4. Katritzky, A.R., Parris, R.L., Allin, S.M., Steel, P. *J. Synth. Commun.* **25**, 1173–1186 (1995).

## Amino Acid Bromides: A Convenient Choice for Very Difficult Couplings

Alma DalPozzo, Roberto Bergonzi, Minghong Ni  
 and Paola Cossettini

*Istituto di Ricerche Chimiche e Biochimiche G.Ronzoni, 20133 Milano, Italy*

### Introduction

During the synthesis of pseudopeptides, many difficulties can be encountered for introduction of very hindered pseudoamino acids into a peptide chain. In the case of  $\alpha$ -trifluoromethyl or difluoromethyl amino acids ( $\alpha$ -Tfm or Dfm-AA), all methods known in modern peptide chemistry fail to afford peptides in significant yields. In fact, besides the steric hindrance, the polarizing effect of fluorine renders the amino function totally unreactive. We and others have obtained some peptides containing the least bulky  $\alpha$ -Tfm-alanine, although the yields were low [1]. Moreover, it was possible to prepare peptides bearing an  $\alpha$ -Tfm-amino acid at the N-terminal position [2], but the problem of chain elongation by derivatization of the amino group was not yet resolved until recently. We have successfully synthesized peptides containing different extremely hindered amino acids *via* amino acid bromides, prepared from N-protected amino acids and 1-bromo-N,N-2-trimethyl-1-propenylamine, a reagent proposed in the literature for the synthesis of some simple acylbromides. The resulting bromides were used *in situ* for the coupling reactions, affording a number of di- or tripeptides containing fluoroalkyl residues, in very high yields and without racemization [3]. We then extended the series of N-protected amino acid bromides, with the purpose to verify the general applicability of our method.

### Results and Discussion

So far, we have obtained: Pht-Phe-Br, Pht-Val-Br, Pht-Leu-Br, Pht-Allyl-Gly-Br, Cbz-Pro-Br, Fmoc-Pro-Br, which were successfully employed in the acylation of very hindered amino groups, but we failed to obtain Pht-Asp(OtBu)-Br, because the molecule underwent fast cyclization to phthaloylamino-succinic anhydride.

A major difficulty encountered with amino acid bromides is to find alternative N-protecting groups other than phthaloyl, which is not always compatible with the total synthesis of a peptide, due to the need of hydrazinolysis for deprotection. In fact, with the common Boc, Cbz or Fmoc protecting groups, AA bromides mostly undergo spon-

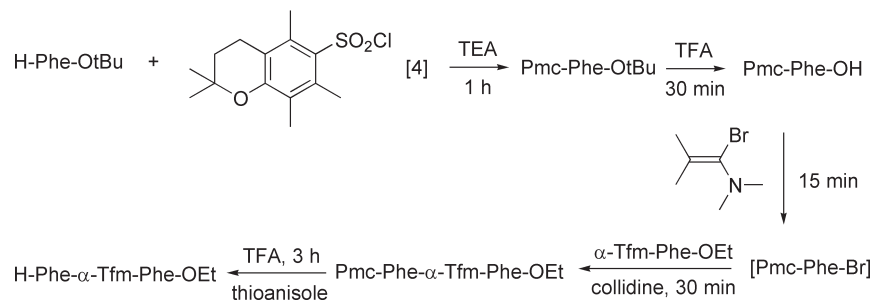


Fig. 1. Synthesis of dipeptide using Pmc-Phe-Br.

taneous decomposition to the corresponding Leuch's anhydrides; this happened in every case, except for proline bromides. The prerequisite for these overactivated amino acid halides to survive their own preparation is to be N-protected as diacylamines or with groups unable to give intramolecular reactions.

To overcome these limitations, we tried  $\alpha$ -Tosyl- or Pmc-sulphonamides protections and the corresponding bromides were stable enough to afford formation of the amide bond; the latter protection can be easily removed by TFA/thioanisole for 3 h, as shown in Figure 1.

The search for new N-protected AA bromides generally applicable for solution and solid phase peptide synthesis continues in our laboratories. Apart from the above described inherent difficulties, amino acid bromides can become a precious tool for particularly hard coupling reactions.

### References

1. Koksche, B., Sewald, N., Hoffmann, H., Burger, K., Jakubke, H.D. *J. Peptide Sci.* **3**, 157–167 (1997).
2. DalPozzo, A., Muzi, L., Moroni, M., Rondanin, R., de Castiglione, R., Bravo, P., Zanda, M. *Tetrahedron* **54**, 6019–6028 (1998).
3. DalPozzo, A., Bergonzi, R., Minghong Ni. *Tetrahedron Lett.* **42** (2001) in press.
4. Fujino, M., Wakimasu, M., Kitada, C. *Chem. Pharm. Bull.* **29**, 2825–2831 (1981).

## Synthesis of the Two Isomeric Benzo Derivatives of 1-Hydroxy-7-azabenzotriazole and Preliminary Studies of Their Effectiveness as Coupling Reagents

Fernando J. Ferrer and Louis A. Carpino

Department of Chemistry, University of Massachusetts, Amherst, MA 01003, USA

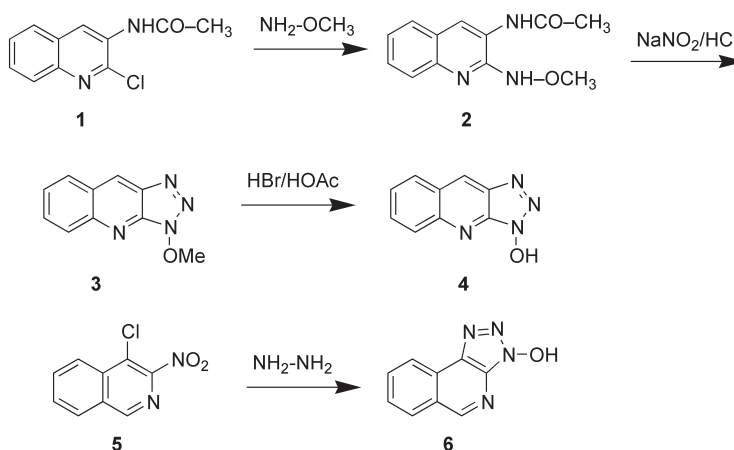
### Introduction

Coupling reactions involving carbodiimides involve two or more consecutive reactions, each of which is concentration dependent. It is often useful to add an additive, sometimes referred to as an auxiliary nucleophile, which reacts with these highly reactive intermediates, *e.g.* the *O*-acylisourea, symmetric anhydride or oxazolone to give an active ester which itself can take part in peptide bond formation thus reducing the lifetime of such intermediates with consequent reduction in by-product formation. The best results reported to date have been achieved with 1-hydroxybenzotriazole (HOBt) *N*-hydroxysuccinimide (HOSu), 3-hydroxy-3,4-dihydro-1,2,3-benzotriazine-4-one (HODhbt) and particularly 1-hydroxy-7-azabenzotriazole (HOAt) [1].

### Results and Discussion

The synthesis of 1-H-1-Hydroxy-1-azanaphtho[2,3-*d*]triazole (1-HOANt) **4** was accomplished by treatment of the acetylated derivative of 2-chloro-3-aminoquinoline **1** with methoxyamine to give 2-methoxyamino-3-acetylaminoquinoline **2**. The acetyl group was removed by hydrolysis and the hydrochloride was treated with sodium nitrite to give *via* the diazonium salt the methoxy derivate **3**. Deblocking of the methyl group by means of HBr in acetic acid gave 1-HOANt **4** (Scheme 1). The synthesis of 1-H-1-Hydroxy-2-azanaphtho[3,4-*d*]triazole (2-HOANt) **6** was carried out by reaction of 4-chloro-3-nitroisoquinoline **5** with a large excess hydrazine in ethanol (Scheme 1).

A comparison of the effect of HOAt, 1-HOANt (**4**) and 2-HOANt (**6**) as additives on loss of configuration during the formation of tripeptides Z-Phe-Val-Pro-NH<sub>2</sub> (peptide **7**) formed by reaction of Z-Phe-ValOH and H-Pro-NH<sub>2</sub>, and Z-Gly-Phe-Pro-NH<sub>2</sub> (peptide **8**) formed by reaction of Z-Gly-Phe-OH and H-Pro-NH<sub>2</sub> was established *via*



Scheme 1. Synthesis of 1-HOANt and 2-HOANt.

**Ferrer et al.**

[2+1] segment condensation using DIC. In the same manner a third comparison was established by [3+3] segment condensation for the formation of Z-Gly-Gly-Val-Ala-Gly-Gly-OMe (peptide **9**). All model peptides have been reported previously [2]. The results show that 2-HOANt is more efficient than 1-HOANt, but less efficient than HOAt (Table 1).

*Table 1. Comparison of the effect of 2-HOANt, 1-HOANt, and HOAt on loss of configuration during formation of tripeptides **7** and **8** via [2+1] segment condensation and during formation of hexapeptide **9** via [3+3] segment condensation in DMF.*

Peptide	Coupling reagent	% D,L	Yield, %
<b>7</b>	DIC/2-HOANt	3.3	72.2
<b>7</b>	DIC/1-HOANt	4.7	65.0
<b>7</b>	DIC/HOAt	2.4	63.2
<b>8</b>	DIC/2-HOANt	0.6	86.4
<b>8</b>	DIC/HOAt	0.2	43.6
<b>9</b> <sup>a</sup>	DIC/2-HOANt	5.7	90.0
<b>9</b>	DIC/HOAt	4.6	85.0

<sup>a</sup> 1 eq. of TMP was used.

The uronium/guanidinium salt derived from 2-HOANt by treatment with tetramethylchloroformamidinium hexafluorophosphate was shown to be more reactive than the analogous HATU for the conversion of Z-Aib-OH to the active ester ( $t_{1/2} \approx 1$  min vs 6 min). The effectiveness of the new uronium/guanidinium salt derived from **6** was tested for assembly of the ACP decapeptide [3]. Under “normal” conditions (4 equivalents of the protected amino acid and 30 min coupling) there was very little difference between HATU and the salt derived from 2-HOANt. However under “forcing” conditions (1.5 equivalents of the amino acid and 1.5 min coupling time) the new salt was more effective (81.8% of purity vs 73.6%). The synthesis of longer peptides by this technique is under study.

**References**

1. Carpino, L.A. *J. Am. Chem. Soc.* **115**, 4397 (1993).
2. Carpino, L.A., Ionescu, D., El-Faham, A., Albericio, F. *J. Org. Chem.* **60**, 405 (1995).
3. Carpino, L.A., El-Faham, A., Minor, C.A., Albericio, F. *J. Chem. Soc., Chem. Commun.* 201 (1994).

## **Optimization of Coupling Methods for the Introduction of Mono-Benzyl Phosphate Esters of Fmoc Protected Phosphoamino Acids**

**Peter White**

*Novabiochem, CN Biosciences UK, Beeston, Nottingham, NG9 2JR, UK*

### **Introduction**

Mono-benzyl phosphate esters of Fmoc protected phosphoamino acids, Fmoc-Aaa(PO(OBzl)OH)-OH (Aaa = Ser, Thr, Tyr), are extremely valuable tools for the synthesis of phosphopeptides by Fmoc SPPS methods [1]. However, a recent report [2] has indicated that the use of standard activation methods with these derivatives can lead to poor yields. In this poster, the development of an optimized coupling protocol and its application in the synthesis of multiphosphorylated peptides is described.

### **Results and Discussion**

Of the methods tested by Perich, *et al.*, which included PyBrOP, BOP and carbo-diimide activation, the use of uronium salts in conjunction with HOBt/HATU and DIPEA was found to be the most effective. This approach was, therefore, taken as the starting point in our evaluation. For a test system, the acylation of the resin-bound Val by Fmoc-Thr(PO(OBzl)OH)-OH **1** was chosen, since phosphothreonine (pThr) was found to be the most problematic phosphoamino acid to couple by Perich, *et al.* and the coupling together of  $\beta$ -branched amino acids is known to be particularly sterically challenging.

The reactions were performed on a NovaSyn Crystal peptide synthesizer, which, by virtue of its UV monitoring system, provided the capability to semi-quantitatively assess of the efficiency of coupling reactions by monitoring of the subsequent deprotection reactions. The accuracy of the system is approximately 5% (effects due to resin swelling notwithstanding) which was deemed sufficient to make the initial differentiation between poor and good coupling methods. A 5-fold excess of **1** was coupled to H-Val-NovaSyn® TGR resin using TBTU/HOBt/DIPEA (1 : 1 : 2) for 2 h, followed by addition of Fmoc-Gly-OH under the same conditions. A comparison of the deprotection peak area of the pThr with that of the previous Val and subsequent Gly residue indicated a coupling efficiency of between 70–80%. These results appear to confirm the findings of Perich, *et al.* regarding the difficulty in coupling Fmoc-Thr(PO(OBzl)OH)-OH and also validate the choice of model peptide as a taxing example.

Following consideration of the stoichiometry of the reaction, it was concluded that one possible reason for the observed sluggish coupling might be that the quantity of base used is insufficient for efficient activation, as 1 eq. of base will be neutralized by the acidic partially protected phosphate group. Therefore, the model coupling reaction was repeated using 3 eq. of DIPEA. In this case, deprotection monitoring indicated an incorporation of Thr(PO(OBzl)OH) of somewhere between 90 and 100% based on the comparison of the Thr(PO(OBzl)OH) deprotection peak areas against those obtained for Val and Gly, respectively.

Encouraged by these results, it was decided to test these optimized conditions in the synthesis of the following peptides containing pThr and pSer residues:

H-Gly-Phe-Glu-Thr(PO<sub>3</sub>H<sub>2</sub>)-Val-Pro-Glu-Thr(PO<sub>3</sub>H<sub>2</sub>)-Gly-NH<sub>2</sub> **2**

H-Ala-Asp-Phe-Glu-Ser(PO<sub>3</sub>H<sub>2</sub>)-Ile-Pro-Ser(PO<sub>3</sub>H<sub>2</sub>)-Glu-Ser(PO<sub>3</sub>H<sub>2</sub>)-Leu-NH<sub>2</sub> **3**

## White

Cleavage and side-chain deprotection of both peptides was effected by treating with TFA/water/TIPS (95 : 2.5 : 2.5) for 3 h. The HPLC elution profiles of the total crude products are shown in Figures 1 and 2. Detailed LC/ES-MS analysis of crude peptides revealed the major by-products to be the des-Val peptide and the desired sequence retaining a benzyl group for peptide **2** and the des-Ile peptide for **3**. In both examples there was no evidence to suggest the presence of any impurities arising from incomplete incorporation of either phosphoresidues.

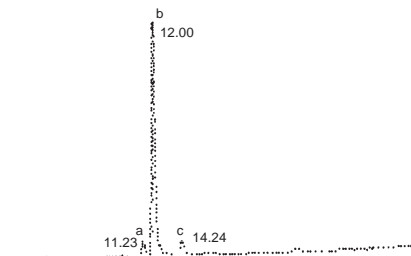


Fig. 1. HPLC elution profile of total crude **2**. Conditions: 2 min at 5% B to 100% B over 35 min; solvent A, 0.1% TFA in water; solvent B, acetonitrile/water/TFA (90 : 10 : 0.1); column, Vydac C18; detection, 220 nm. Peak a: des-Val-**2** [expected M+1 996.3, found M+1 996.3]; peak b: **2** [expected M+1 1095.4, found 1095.3]; peak c: **2** + benzyl [expected M+1 1185.4, found M+1 1185.4].

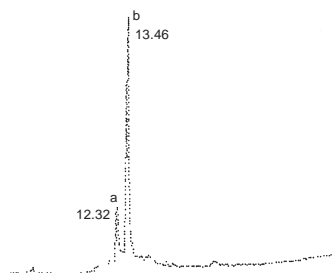


Fig. 2. HPLC elution profile of total crude **3**. Conditions: 2 min at 5% B, 5% to 100% B over 35 min; solvent A, 0.1% TFA in water; solvent B, acetonitrile/water/TFA (90 : 10 : 0.1); column, Vydac C18; detection, 220 nm. Peak a: des-Ile-**3** [expected M+1 1320.4, found M+1 1320.3]; peak b: **3** [expected M+1 1433.5, found 1433.4].

## References

1. Wakamiya, T., Saruta, K., Yasuoka, J., Kusumoto, S. *Chem. Lett.* 1099 (1994); White, P., Beythien, J., In Epton, R. (Ed.) *Innovations & Perspectives in Solid Phase Synthesis & Combinatorial Libraries*, 4th International Symposium, Mayflower Scientific Ltd., Birmingham, 1996, p. 557.
2. Perich, J., Ede, N., Eagle, S., Bray, A. *Lett. Peptide Sci.* **6**, 91 (1999).
3. Pascal, R., Schmit, P.-O., Mendre, C., Dufour, M.-N., Guillon, G., In Martinez, J. and Fehrentz, J.-A. (Eds) *Peptides 2000, Proc. 26th European Peptide Symposium*, Éditions EDK, Paris, 2001, p. 263.

## HATU-HOAt-CuCl<sub>2</sub>: A Reliable Racemization-Free Segment Coupling System

Yasuhiro Nishiyama<sup>1</sup>, Sou Ishizuka<sup>2</sup> and Keisuke Kurita<sup>2</sup>

<sup>1</sup>Department of Pathology & Laboratory Medicine, University of Texas-Houston Medical School, Houston, TX 77030, USA

<sup>2</sup>Department of Industrial Chemistry, Faculty of Engineering, Seikei University, Musashino-shi, Tokyo 180-8611, Japan

### Introduction

Phosphonium/uronium coupling reagents are commonly used in peptide synthesis because of their advantages over classical coupling reagents. This class of reagents, however, gives rise to considerable racemization of the carboxy-terminal residue of the activated peptide segment.

CuCl<sub>2</sub> was reported to reduce the racemization effectively not only in the carbodiimide-mediated segment coupling [1], but also in mixed anhydride-, EEDQ, and BOP-Cl-mediated coupling [2]. Furthermore, CuCl<sub>2</sub> eliminates the racemization in segment condensation of a peptide having a carboxy-terminal *N*-methylamino acid, which is highly prone to racemization, by means of a carbodiimide and *O*-(*N*-succinimidyl)-1,1,3,3-tetramethyluronium tetrafluoroborate [3,4]. These results have prompted us to utilize an effective racemization suppressant, CuCl<sub>2</sub>, in combination with the efficient HATU-HOAt coupling system [5]. This report deals with a novel reagent system for racemization-free segment condensation, HATU-HOAt-CuCl<sub>2</sub>.

### Results and Discussion

Boc-Phe-Val-OH + H-Val-OBn was employed as a model reaction. After storage of each reaction mixture at room temperature for >24 h, a portion was subjected to HPLC analysis. % L-D-L isomer and % yield of the desired L-L-L product were determined as (peak area of L-D-L isomer) × 100/[(peak area of L-D-L isomer) + (peak area of L-L-L isomer)] and (peak area of L-L-L isomer) × 100/(expected peak area calculated from peak area of standard solution of authentic L-L-L isomer), respectively.

The results are compiled in Table 1. A considerable level of racemization was detected in the coupling with EDC-HOBt, a most common racemization-free segment condensation method. The EDC-HOAt and EDC-HOBt-CuCl<sub>2</sub> methods also gave significant amounts of the L-D-L product, although the values were much lower than that of the ECC-HOBt coupling. These results indicate that the model reaction employed in this study is a highly sensitive system for the racemization test. The HATU-HOAt (*in situ*) coupling gave a very low level of racemization, whereas HBTU-HOBt (*in situ*) gave a considerable amount of L-D-L isomer. The preactivation coupling with HATU-HOAt, however, gave a much higher amount of the L-D-L product than *in situ* coupling. This result indicates that the HATU-HOAt method is not compatible with the preactivation procedure and that a considerable level of racemization would occur even in the *in situ* coupling when the coupling reaction is very slow. The HATU-HOAt-CuCl<sub>2</sub> (*in situ*) method gave an almost negligible level of racemization with a satisfactory yield, whereas HBTU-HOBt-CuCl<sub>2</sub> gave a significant level. Furthermore, the HATU-HOAt-CuCl<sub>2</sub> afforded an almost negligible level of racemization also in preactivation coupling. These results indicate that the HATU-HOAt-CuCl<sub>2</sub> method is suitable for both *in situ* and preactivation procedures and is highly reliable even for very slow segment coupling reactions. HATU-HOAt-CuCl<sub>2</sub> was confirmed to

give the undetectable level of racemization also in a different system, Boc-Phe-Ala-OH + H-Phe-OBn (86% yield).

Table 1. Extent of epimerization during the coupling of Boc-Phe-Val-OH and H-Val-OBn.

Coupling method <sup>a</sup>		% L-D-L <sup>b</sup>	% Yield <sup>b</sup>
EDC-HOBt	<i>in situ</i>	9.8	81
EDC-HOAt	<i>in situ</i>	1.6	89
EDC-HOBt-CuCl <sub>2</sub>	<i>in situ</i>	0.9	62
	preactivation	1.2	64
HBTU-HOBt	<i>in situ</i>	8.2	83
	preactivation	15.1	76
HATU-HOAt	<i>in situ</i>	0.8	84
	preactivation	6.9	81
HBTU-HOBt-CuCl <sub>2</sub>	<i>in situ</i>	1.2	62
	preactivation	1.4	60
HATU-HOAt-CuCl <sub>2</sub>	<i>in situ</i>	0.4	76
	preactivation	0.2	70

<sup>a</sup> All reactions were carried out in DMF. Two eq. DIEA for HBTU/HATU coupling. *In situ*: reaction components are combined at ice-bath temp, and allowed to react at RT for >24 h; preactivation: at an ice-bath temp for 30 min. <sup>b</sup> Means of 2–4 replications.

Consequently, it can be concluded that HATU-HOAt-CuCl<sub>2</sub> is an efficient racemization-free segment coupling method. The segment condensation between large protected peptides as employed in the practical peptide synthesis is occasionally much slower process than model reactions using small peptides and is more susceptible to racemization. The data from preactivation experiments, which simulate such slow reactions, suggest high reliability on this new method.

## References

1. (a) Miyazawa, T., Otomatsu, T., Yamada, T., Kuwata, S. *Tetrahedron Lett.* **25**, 771 (1984). (b) Miyazawa, T., Otomatsu, T., Fukui, Y., Yamada, T., Kuwata, S. *J. Chem. Soc., Chem. Commun.* 419 (1988). (c) Miyazawa, T., Otomatsu, T., Fukui, Y., Yamada, T., Kuwata, S. *Int. J. Peptide Protein Res.* **39**, 237 (1992). (d) Miyazawa, T., Otomatsu, T., Fukui, Y., Yamada, T., Kuwata, S. *Int. J. Peptide Protein Res.* **39**, 308 (1992).
2. (a) Miyazawa, T., Donkai, T., Yamada, T., Kuwata, S. *Chem. Lett.* 2125 (1989). (b) Miyazawa, T., Donkai, T., Yamada, T., Kuwata, S. *Int. J. Peptide Protein Res.* **40**, 49 (1992).
3. Nishiyama, Y., Tanaka, M., Saito, S., Ishizuka, S., Mori, T., Kurita, K. *Chem. Pharm. Bull.* **47**, 576 (1999).
4. Nishiyama, Y., Ishizuka, S., Mori, T., Kurita, K. *Chem. Pharm. Bull.* **48**, 442 (2000).
5. Carpino, L.A., El-Faham, A., Albericio, F. *Tetrahedron Lett.* **35**, 2279 (1994).

## **Search for a Safe, Inexpensive and Convenient Amidation Process for Protected Amino Acids and/or Peptides**

**Kripa Srivastava**

*Pharmaceuticals Division of Mallinckrodt, Tyco Healthcare, St. Louis, MO 63147, USA*

### **Introduction**

A large class of peptide hormones contain C-terminal amides, and, as a consequence, the importance of carboxamides in biologically active peptides encouraged us to search for an efficient, inexpensive, safe and a suitable method for the amidation of protected amino acids (peptides). The general approach for the carboxamide formation involves the reaction of the amines with an activated intermediate of the corresponding acid formed by its treatment with an activating reagent. Unfortunately, not all methods involved in the conversion of acids to amides may be suitable for the synthesis of the protected amino acids (peptides) amides, possibly due to certain disadvantages associated with the use of certain activating reagents which may impair the peptide backbone. Considering these facts, and after a careful comparative study of several existing methods [1–9], a suitable amidation process for amino acids was selected and was improved for its scale-up.

### **Results and Discussion**

The investigation was focused on the amidation of the protected amino acids by known methods, with an intention to develop an efficient, inexpensive, and scalable synthesis process for primary carboxamides. Hence, ease of work, yields, safety, and cost were compared with respect to the feasibility of large-scale synthesis technology. Our primary consideration in the selection of the synthesis method for amino acids amides was the preservation of their chiral integrity, since the stereochemical control is a pre-requisite for the successful synthesis of peptides. Although changes in configuration most frequently occur during the combination of two residues, it may also take place during the derivitization of the amino acids. Therefore Boc-Phe and Boc-Cys(Trt) amino acids were selected for the examination of amidation reaction, as these amino acids are known to be prone to racemization.

The conventional routes for the preparation of carboxamides, *i.e.* condensation of carboxylic acids chlorides and alkyl esters with ammonia were not considered because they require corrosive/toxic reagents and long reaction time, and also generated the racemized derivative, as well as self-condensed diketopiperazine (DKP) byproducts. A much milder route involving the transamidation reaction of the acid active esters or acid anhydrides with amines has been utilized for the preparation of a variety of amino acid (peptide) amides, but such traditional coupling regimes yielded comparatively low yields and impure product.

Therefore, we examined the reaction of protected amino acids *via* their active esters and mixed anhydride intermediates with easily available and inexpensive ammonium bicarbonate and ammonium hydroxide as the amine source. The activated acid intermediate, generated by treating the protected amino acid (1 mole equivalent) solution in 50% ACN–DMF with an activating agent (1.1–1.3 mole equivalent), either in presence or in absence of an additive (1.1–1.3 mole equivalent) at or below 0 °C, was reacted with an amine (1.2–2 mole equivalent). The reaction mixture was then agitated for several hours while being allowed to warm to room temperature. Completion of the reaction was monitored by HPLC and the product formed was isolated either by

### Srivastava

water precipitation, or by ethyl acetate extraction. The purity of the product was determined by HPLC analysis. The yields of Boc-Phe-amide prepared by DCC–NHS and by mixed anhydride methods using ammonium hydroxide and ammonium bicarbonate; by DCC method using  $\text{NH}_4\text{OH}\cdot\text{NHS}$ ; by triazine method using ammonium bicarbonate; by di-*t*-butyl dicarbonate/pyridine method using ammonium bicarbonate were 31, 38.5, 77, 85.6, 79.5, 12, and 92.4% respectively. All the experiments were carried out on a 10-mmol scale except DCC–NHS method (0.5-mmol scale) under similar conditions. The prepared Boc-Phe-amide by different methods were indistinguishable from the standard Boc-Phe-amide, prepared by the reaction of di-*t*-butyl dicarbonate with Phe-amide (85% yield, 10-mmol scale). On the other hand, Boc-Cys (Trt)-amide prepared by mixed anhydride method (10-mmol scale) using ammonium hydroxide and ammonium bicarbonate gave 95.8 and 98.8% yield respectively. The yields of carboxamides obtained by the use of ammonium bicarbonate were generally higher except in triazine method, which gave a very complex mixture as judged by HPLC analysis. In addition, the use of ammonium bicarbonate was also found to be advantageous as it allowed better control of the stoichiometry of the reaction and of the pH.

In conclusion, the application of an inexpensive and safe di-*t*-butyl dicarbonate, and ammonium bicarbonate as a source of activation and amine respectively under a mild condition resulted in a simple, scalable, and an efficient synthesis process for the protected amino acids (peptides) amide.

### Acknowledgments

We thank John Dykes and Tom Gordon for their assistance for the analytical analysis of the reaction mixtures and the isolated products.

### References

1. Gustus, E.L. *J. Org. Chem.* **32**, 3425–3430 (1967).
2. Kenner, G.W., et al. *J. Chem. Soc. C* 761–764 (1968).
3. Pozdnev, F. *Tetrahedron Lett.* **36**, 7115–7118 (1995).
4. Bodanszky, M., et al. *J. Am. Chem. Soc.* **89**, 685–689 (1967).
5. Chen, S.T., et al. *Synthesis* 285–287 (1992).
6. Rosangela, M., et al. *Int. J. Pept. Protein Res.* **42**, 53–57 (1993).
7. Somlai, Cs., et al. *Synthesis* 285–287 (1992).
8. Froyen, P. *Synth. Commun.* **25**, 959–968 (1995).
9. Rayle, H.L., et al. *Org. Proc. Res. Dev.* **3**, 172–176 (1999).

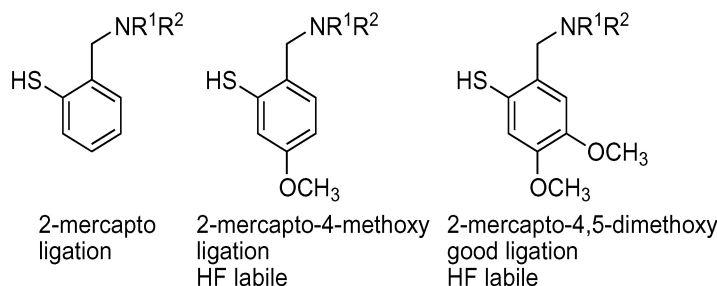
## Extending Synthetic Access to Proteins

John L. Offer and Philip E. Dawson

*The Scripps Research Institute, Departments of Cell Biology and Chemistry  
and The Skaggs Institute for Chemical Biology, La Jolla, CA 92037, USA*

### Introduction

The ligation of an unprotected peptide thioester and an N-terminal cysteine in denaturing aqueous buffer to give an unmodified amide bond at the ligation junction, has given rapid synthetic access to proteins [1]. A general amide bond ligation can be modeled after native chemical ligation by attaching a removable cysteine mimic to the N-terminus of a peptide, combining thioester exchange with efficient intramolecular acyl transfer. Auxiliary assisted intramolecular acyl transfer has been used to synthesize peptides [2] and to introduce backbone protection into peptides [3]. The cysteine mimic must satisfy several requirements; easy introduction to the peptide, ligation comparable to cysteine and it must leave a native amide bond.



### Results and Discussion

Auxiliaries based on ethylmercaptan tethered to the N-terminus of a peptide [4] behaved poorly in our hands and could not be translated to ligation of the larger peptides required for protein synthesis in all but the most favourable cases (Gly-Gly, His-Gly, Cys-Gly). Practical application was further complicated by the presence of a stereogenic center [5]. In contrast, ligations with 2-mercaptobenzyl tethered to the N-terminus of model peptides had promising rates and suggested wider generality of ligation sites [6].

The behaviour of substituted benzyl on the peptide bond is familiar from peptide bond protection and backbone linkers. One useful property is that benzylamines are stable to strong acid conditions, but the corresponding suitably substituted benzylamide, for example after ligation, is acid labile [6,7]. This provides a simple strategy for the introduction of several auxiliaries to the N-terminus of peptides for screening of their ligation and removal properties. The scaffolds were coupled to the N-terminus of a peptide on-resin using the submonomer approach [4,5].

The 2-mercapto-4-methoxybenzyl auxiliary was synthesized by acylation of 2-hydroxy-4-methoxybenzyl with dimethylcarbamyldichloride and thermal rearrangement. The 2-mercapto-4,5-dimethoxybenzyl [8] (Acros) had improved ligation properties presumably because the methoxy group para to the 2-mercapto group increased its nucleophilicity and consequently improved thioester exchange. A C-terminal lysine thioester to glycine ligation site was chosen as the corresponding lysine to cysteine ligation is representative for the majority of amino acids for native chemical ligation [9]

Offer et al.

(Figure 1). A more sterically challenging C-terminal glycine thioester to N-terminal alanine ligation was also successful at low mM peptide concentration, suggesting applicability of this ligation to sites with glycine either side of the ligation junction.

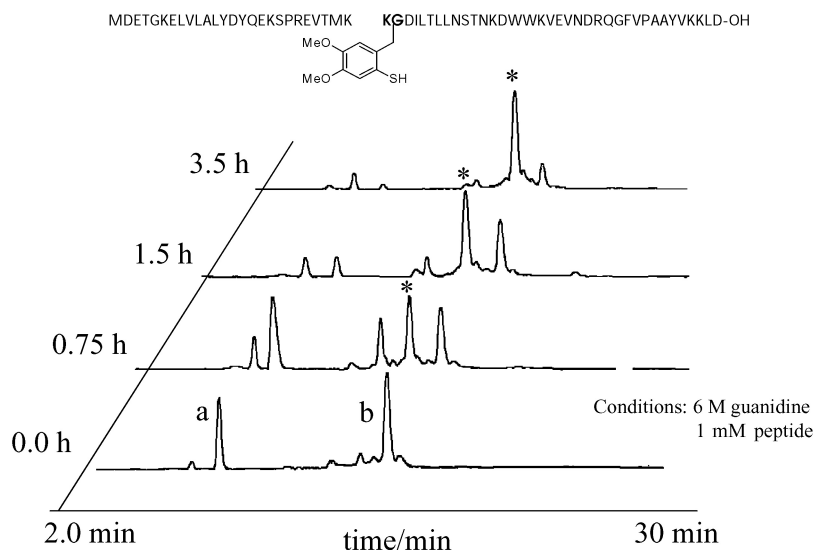


Fig. 1. Analytical HPLC for time course of ligation of two pieces of the SH3 domain of  $\alpha$ -spectrin; a 1-27 Lys thiophenol thioester and b 2-mercapto-4,5-dimethoxybenzyl 28-62.

## References

1. Dawson, P.E., Kent, S.B.H.T. *Annu. Rev. Biochem.* **69** (2000).
2. Coltart, D.M. *Tetrahedron* 3449–3491 (2000).
3. Quibell, M., Johnson, T., In Chan, W.C. and White, P.D. (Ed.) *Fmoc Solid Phase Peptide Synthesis a Practical Approach*, OUP, pp. 115–135.
4. Canne, L.E., Bark, S.J., Kent, S.B.H. *J. Am. Chem. Soc.* **119**, 4325–4329 (1997).
5. Marinzi, C., Bark, S.J., Offer, J., Dawson, P.E. *Bioorg. Med. Chem.* (2001), in press.
6. Offer, J., Dawson, P.E. *Org. Lett.* **2**, 23–26 (2000).
7. Tolborg, J.F., Jensen, K.J. *Chem. Commun.* **2**, 147–148 (2000).
8. Ligation has been shown at a Gly-Gly site with this auxiliary and an ingenious method for its introduction Kawakami, T., Akaji, K., Aimoto, S. *Org. Lett.* **3**, 1403–1405 (2001).
9. Hackeng, T.M., Griffin, J.H., Dawson, P.E. *Proc. Natl. Acad. Sci. U.S.A.* **96**, 10068–10073 (1999).

## A New Scaffold for Amide Ligation

Chiara Marinzi<sup>1</sup>, John Offer<sup>2</sup> and Philip E. Dawson<sup>2</sup>

<sup>1</sup>IBRM, CNR, Milan, 20132, Italy

<sup>2</sup>The Scripps Research Institute, La Jolla, CA 92037, USA

### Introduction

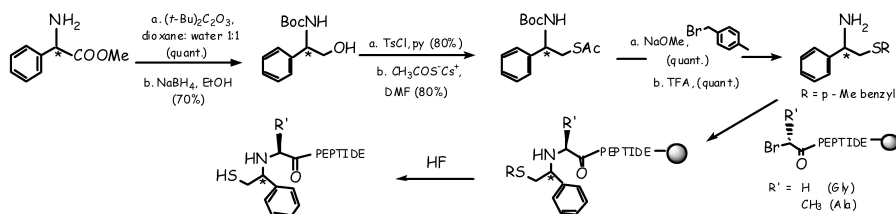
The chemoselective ligation of unprotected peptides has proven to be a valuable alternative to biological expression for protein synthesis [1]. The ligation of an unprotected peptide thioester to an unprotected peptide possessing an N-terminal Cys to give an amide bond at the ligation junction in neutral aqueous solution has been termed native chemical ligation [2]. Extension of this approach to even a single non-Cys site would give greater flexibility to the synthesis of proteins and expand the scope of native chemical ligation to embrace more protein targets or other unhindered bioconjugates.

An irreversible  $N^\alpha$ -ethanethiol modification of the N-terminus showed promising ligation properties in unhindered model systems [3]. In principle, the addition of a phenyl ring to the  $N^\alpha$ -ethanethiol modification can be used to introduce post ligation lability: a methoxybenzyl group is acid labile when substituted at an amide bond but acid stable as a benzylamine on the peptide terminus [4,5]. After ligation, the scaffold could be cleaved from the backbone amide.

The  $N^\alpha$ -2-phenylethanethiol (Pet) scaffold, is ideal for determining the suitability of this auxiliary for ligation, although the unsubstituted benzylamide cannot be removed after formation of the amide bond.

### Results and Discussion

The proposed auxiliary group possesses a stereogenic center that was anticipated to affect the *S*- to *N*-acyl transfer [6,7]. An unambiguous synthetic route to the two enantiomers was required in order to compare ligation rates. The scaffolds were synthesized and incorporated onto the N-terminus of a polypeptide by the submonomer approach (Scheme 1).  $N^\alpha$ -Phenylethanethiol-Gly peptide undergoes efficient ligation with both Ala and Gly and remarkably, the ligation rate is independent of the stereochemistry of the scaffold (Table 1). In contrast, neither scaffold was competent for ligation when attached to a more sterically challenging N-terminal Ala peptide: the thioester exchange proceeded efficiently but no rearrangement was observed. The detection of substantial quantities of unrearranged thioester intermediate suggests that rearrangement is rate determining in the case of  $N^\alpha$ -phenylethanethiol mediated ligation. This is consistent with the observation that added thiophenol, commonly used to activate the thioester in the native ligation reaction had no effect on the rate of ligation.



Scheme 1. Synthesis of the auxiliary and introduction onto the peptide sequence.

**Marinzi et al.**

*Table 1. Ligations between peptide thioesters and the N<sup>α</sup>-phenylethanethiol (Pet)-peptides. Ligation conditions: 100 mM phosphate buffer, pH 7.5, in the presence of 35 mM tris(2-carboxyethyl) phosphine hydrochloride. Peptide concentration: 8 mM each.*

	t <sub>1/2</sub> (min)			
	R-(Pet) GLLRPFFRK	S-(Pet) GLLRPFFRK	R-(Pet) ALLRPFFRK	S-(Pet) ALLRPFFRK
LWAPYRAG-thioester	40	30	n.p. <sup>a</sup>	n.p. <sup>a</sup>
LWAPYRAA-thioester	140	120	n.p. <sup>a</sup>	n.p. <sup>a</sup>

<sup>a</sup> No rearranged product was detected after 48 h of reaction.

Although the stereogenic center did not affect the ligation rate, the generation of a mixture of diastereomeric compounds can complicate the purification of crude peptides possessing the N<sup>α</sup> modification. An acid labile analogue of this auxiliary has recently been described [8] and other modifications such as photolabile analogues could also be introduced.

**Acknowledgments**

Supported by The Skaggs Institute for Chemical Biology, The Sloan Foundation and NIH MH62261.

**References**

1. Fields, G. *TIBITECH* **18**, 6, 243–251 (2000).
2. Dawson, P.E., Muir, T.W., Clark-Lewis, I., Kent, S.B.H. *Science* **266**, 776–779 (1994).
3. Canne, L.E., Bark, S.J., Kent, S.B.H. *J. Am. Chem. Soc.* **118**, 5891–5896 (1996).
4. Johnson, T., Quibell, M., Sheppard, R.C. *J. Pept. Sci.* **1**, 11–25 (1995).
5. Tolborg, J.F., Jensen, K.L. *Chem. Commun.* **2**, 147–148 (2000).
6. Kemp, D.S., Buckler, D.R. *Tetrahedron Lett.* **32**, 3009–3012 (1991).
7. Miao, Z., Tam, J.P. *J. Am. Chem. Soc.* **18**, 4254–4260 (2000).
8. Botti, P., Carrasco, M.R., Kent, S.B.H. *Tetrahedron Lett.* **42**, 1831–1833 (2001).

## Chemical Ligation of Multiple Peptide Fragments Using a New Protection Strategy

Matteo Villain<sup>1</sup>, Jean Vizzavona<sup>2</sup> and Hubert Gaertner<sup>1</sup>

<sup>1</sup>GeneProt Inc., Swiss Branch, Pré de-la-Fontaine, CH-1217 Meyrin, Switzerland

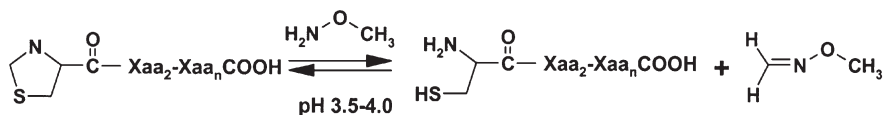
<sup>2</sup>Medical Biochemistry Department, University of Geneva, Switzerland

### Introduction

Synthesis of large polypeptides requires the assembly by chemical ligation [1] of three or more unprotected peptide segments of thirty or more amino acids. In the synthesis in the C-to-N direction, a key issue is the potential reactivity of the middle segments, which would bear both an N-terminal Cys and C-terminal thioester. Up until now, an Ac<sup>m</sup> [2] or Msc [3] group has usually been employed to temporarily protect either the S<sup>β</sup> or N<sup>α</sup> of the N-terminal Cys residue, to prevent self condensation and other side reactions. In order to overcome the limitations of these two approaches, we investigated the use of a thiazolidine derivative, thioproline, as a precursor of the N-terminal Cys in the synthesis of the middle peptide segments.

### Results and Discussion

Thiazolidine derivatives are readily accessible by cyclization of Cys with aldehydes or ketones and stability is highly dependent on modifications introduced in the C-2 position of the ring system [4]. The ring can be easily reopened in the presence of methoxamine under acidic conditions (Scheme 1). Even though aminooxy and aldehyde functionalities have already been used in chemoselective modification of proteins using oxime linkage [5] or capture [6], we investigated the compatibility of this type of reversible protection with our chemistry and the occurrence of any side reaction through the ligations.



Scheme 1.

Opening of the thiazolidine ring at different pH and different *O*-methylhydroxylamine ( $\text{NH}_2\text{-O-CH}_3$ ) concentrations was studied on a model peptide Spr-YAKYAKL (Spr corresponding to thioproline), as shown in Figure 1.

These deprotection conditions were applied to the synthesis of a protein from four peptide segments obtained by SPPS using standard *in situ* neutralisation/HBTU activation procedure for Boc-chemistry [7]. The two “middle” fragments were synthesized on a thioester generating resin and the N-terminal Cys was replaced by thioproline. After completion of the ligation reaction, 20% 2-mercaptoethanol was added to the reaction mixture, the pH adjusted to 9.0 for 1 h to remove the formyl group of Trp and hydrolyze any unreacted thioester. The reaction mixture was then acidified to pH 3.5 and  $\text{NH}_2\text{-O-CH}_3$  was added to a 0.5 M final concentration and incubated for 2 h at 37 °C for complete opening of the N-terminal thiazolidine ring. The reaction mixture was further treated with 10-fold excess of TCEP (2-carboxyethylphosphine) for 15 min before HPLC purification. After work-up of the reaction medium, EIMS analysis of the major peak showed a mass loss of 39.4 Da, consistent with the loss of the formyl

group from Trp and thioproline ring opening (−40 amu). In the same way, deprotection of the second ligation product, resulted in a loss of 12 amu, in agreement with N-terminal thioproline ring opening.

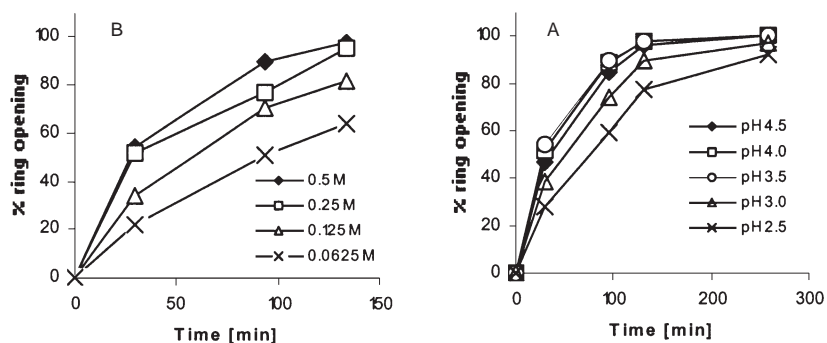


Fig. 1. Extent of N-terminal ring opening at room temperature as a function of time, pH (A) and O-methylhydroxylamine concentration (B).

Thioproline represents a convenient temporary protection of the N-terminal Cys for peptide segments with a C-terminal thioester and the one pot deprotection procedure proposed here permits a considerable reduction in losses related to multistep purifications associated with solution syntheses.

## References

1. Dawson, P.E., Muir, T.W., Clark-Lewis, I., Kent, S.B.H. *Science* **266**, 776–779 (1994).
2. Canne, L.Y., Botti, P., Simon, R.J., Chen, Y., Dennis, E.A., Kent, S.B.H. *J. Am. Chem. Soc.* **121**, 8720–8727 (1999).
3. Brik, A., Keinan, E., Dawson, P.E. *J. Org. Chem.* **65**, 3829–3835 (2000).
4. Wöhr, T., Rohwedder, B., Wahl, F., Mutter, M. *J. Am. Chem. Soc.* **118**, 9218–9224 (1994).
5. Offord, R.E., Gaertner, H.F., Wells, T.N.C., Proudfoot, A.E.I. *Methods Enzymol.* **287**, 348–369 (1997).
6. Villain, M., Vizzavona, J., Rose, K., *Chem. Biol.* **8**, 673–679 (2001).
7. Schnölzer, M., Alewood, P., Jones, A., Alewood, D., Kent, S.B.H. *Int. J. Pept. Protein Res.* **40**, 180–193 (1992).

## Synthesis of Oligodeoxynucleotide-Peptide Conjugates Using Hydrazone Chemical Ligation

Oleg Melnyk<sup>1</sup>, Nathalie Ollivier<sup>1</sup>, Christophe Olivier<sup>1</sup>,  
Catherine Gouyette<sup>1</sup>, Tam Huynh-Dinh<sup>2</sup> and Hélène Gras-Masse<sup>1</sup>

<sup>1</sup>Biological Institute of Lille, 59021 Lille, France

<sup>2</sup>Pasteur Institute, 75000 Paris, France

### Introduction

Oligonucleotides constitute a class of potential therapeutic agents. Improvement of certain properties, such as cell-specific delivery, cellular uptake efficiency, intracellular distribution, and target specificity can be accomplished by covalent association to peptides [1]. Rather than forming ionic oligonucleotide-peptide complexes, covalent association results in more consistent products, in which the desired properties can be controlled by structural variations. We present in this paper a novel methodology for the site-specific ligation of oligonucleotides to peptides through a hydrazone link (Figure 1) [2].

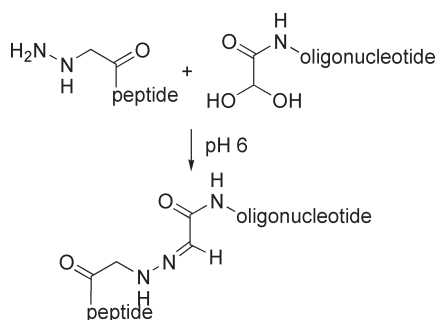
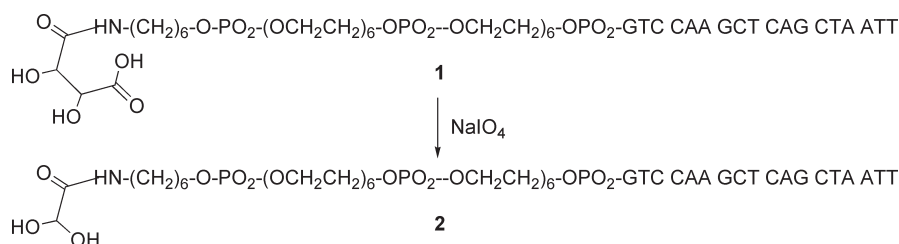


Fig. 1. Site-specific hydrazone ligation between an  $\alpha$ -hydrazinoacetyl peptide and a glyoxylyl oligonucleotide.

### Results and Discussion

Oligonucleotide 2 functionalized at the 5' end by a glyoxylyl group was synthesized as shown in Scheme 1. Compound **1** was assembled on CPG using solid phase phosphoramidite chemistry. The amino link was protected by a MMT group. The tartaryl moiety was easily incorporated using (+)-diacetyl-L-tartaric anhydride/2,6-lutidine in THF, immediately following removal of the MMT group of the amino link with trichloroacetic acid in dichloromethane. The tartaramide bond was found to be fully stable during the aminolysis step, and the purity of crude oligonucleotide **1** was found to be high (ES-MS M calculated 6458.48, found 6454.5). Periodic oxidation was cleanly performed using 2 eq of  $\text{NaIO}_4$  at pH 6.6 100 mM phosphate buffer to give glyoxylyl oligonucleotide **2** in 63% yield after purification by RP-HPLC and lyophilization.  $(n\text{-Bu})_3\text{P}$  was added to the pure RP-HPLC fractions prior to the lyophilization step to avoid partial oxidation of the  $\alpha$ -oxo-aldehyde group by traces of peroxides. Importantly, compound **2** was found to be stable for months when stored at  $-20^\circ\text{C}$ . No imine formation (intramolecular or intermolecular) could be detected either by RP-HPLC, ES-MS or MALDI-TOF.



In conclusion, glyoxylyl oligonucleotides were found to be useful derivatives for the convergent synthesis of peptide-oligonucleotide conjugates using hydrazone chemical ligation.

We thank CNRS, Université de Lille 2, Institut Pasteur de Lille and Institut Pasteur for financial support.

1. Tung, C.-H. *Bioconjug. Chem.* **11**, 605–618 (2000).
2. This ligation strategy was found to be very efficient in the context of one-pot double ligation reactions (synthesis of antigen-bearing glycodendrimers), for the elaboration of peptide-peptide constructs or for the synthesis of lipopeptides. (a) Grandjean, C., Rommens, C., Gras-Masse, H., Melnyk, O. *Angew. Chem., Int. Ed.* **39**, 1068–1071. (b) Bonnet, D., Bourel, L., Gras-Masse, H., Melnyk, O. *Tetrahedron Lett.* **41**, 10003–10007 (2000). (c) Melnyk, O., Fruchart, J.-S., Grandjean, C., Gras-Masse, H. *J. Org. Chem.*, in press (2001).
3. Wender, P.A., Mitchell, D.J., Pattabiraman, K., Pelkey, E.T., Steinman, L., Rothbard, J.B. *Proc. Natl. Acad. Sci. USA* **97**, 13003–13008 (2000).
4. Bonnet, D., Ollivier, N., Gras-Masse, H., Melnyk, O. *J. Org. Chem.* **66**, 443–449 (2001).

## **The Use of a Free Peptide for Preparation of a C-Terminal Building Block for Polypeptide Synthesis in Combination with a Peptide Thioester**

**Saburo Aimoto, Kenta Teruya, Koki Hasegawa, Kenichi Akaji and Toru Kawakami**

*Institute for Protein Research, Osaka University, Osaka 565-0871, Japan*

### **Introduction**

We report herein a new strategy for the synthesis of polypeptides using recombinant proteins (non-protected peptides) in combination with *S*-alkyl peptide thioesters (peptide thioesters) [1,2] for the use as building blocks.

Semisynthesis using biologically prepared peptides has been investigated *via* chemical ligation methods [3]. For example, Gaertner *et al.* reported on hydrazone bond formation as the result of the reaction of peptide hydrazide and  $N^\alpha$ -glyoxyloyl peptides [4]. Although these reactions proceed chemoselectively, they do not give rise to a native peptide bond. Dawson *et al.* reported on a chemoselective reaction of peptide thioesters and peptides, which have a cysteine residue at the N-terminus, to result in the formation of a native peptide bond [5]. This peptide bond formation *via* an S-N acyl shift had been previously reported by Wieland *et al.* [6]. Thiol containing linkers, such as 2-mercaptoethoxy [7], 2-mercaptobenzyl [8], and 1-phenyl-2-mercaptoethyl [9] groups on the terminal amino group can be used to replace the cysteine residue. These methods are quite convenient, because protecting groups are not required and the reaction can be carried out in neutral aqueous solutions. Furthermore, biologically prepared peptides have been used as building blocks in the native chemical ligation method [10,11]. An expressed peptide was also used as a C-terminal building block, in which a partially protected peptide segment was condensed with a peptide thioester in the presence of silver ions [12]. Here we present an alternative method for the use of expressed peptides in the peptide bond formation at X-Gly sequences.

### **Results and Discussion**

C-Terminal peptide building blocks would be prepared from recombinant proteins (free peptides), which have a serine or threonine residue at the N-terminus, by the following steps [13]: first, the N-terminal amino alcohol moiety is oxidized with periodate to an  $N^\alpha$ -glyoxyloyl peptide [14], then 4,5-dimethoxy-2-(triphenylmethylthio)-benzylamine (**1**) is introduced to obtain an  $N^\alpha$ -4,5-dimethoxy-2-mercaptobenzyl (Dmmb)-glycyl peptide, which would undergo condensation with a peptide thioester.

A model sequence, Gly-Ser-Arg-Ala-His-Ser-His-Leu-Lys, was examined as a C-terminal segment. The  $N^\alpha$ -glyoxyloyl peptide, CHOCO-Ser-Arg-Ala-His-Ser-Ser-His-Leu-Lys-NH<sub>2</sub>, was obtained by the periodate oxidation of Ser-Ser-Arg-Ala-His-Ser-Ser-His-Leu-Lys-NH<sub>2</sub>. This peptide was treated with amine **1** and sodium cyanoborohydride in DMF containing acetic acid, followed by trifluoroacetic acid (TFA) containing triisopropylsilane to give the  $N^\alpha$ -Dmmb-glycyl peptide. This peptide was condensed with a peptide thioester, Lys-Asp-Ala-Gln-Ala-Gly-Lys-Glu-Pro-Gly-SCH<sub>2</sub>CH<sub>2</sub>CO-Leu, in neutral phosphate buffer containing 0.20 M thiophenol [15]. After stirring for 24 h, dithiothreitol was added, and the product, Lys-Asp-Ala-Gln-Ala-Gly-Lys-Glu-Pro-Gly-(Dmmb)Gly-Ser-Arg-Ala-His-Ser-Ser-His-Leu-Lys-NH<sub>2</sub>, was purified by RP-HPLC. The Dmmb group was removed by treatment with

*Aimoto et al.*

trifluoromethanesulfonic acid (TFMSA) in TFA to give Lys-Asp-Ala-Gln-Ala-Gly-Lys-Glu-Pro-Gly-Gly-Ser-Arg-Ala-His-Ser-Ser-His-Leu-Lys-NH<sub>2</sub>.

In conclusion, we reported the successful preparation of a thiol linker-attached peptide, for condensation with the peptide thioesters, from a non-protected peptide *via* periodate oxidation of the N-terminal serine residue, and reductive amination with the Dmmb amine. Transamination reaction of N-terminal amino groups can also be used instead of the periodate oxidation of the serine or threonine residue, in principle, though the stereochemistry, formed in the reductive amination, should be controlled.

### Acknowledgments

This research was supported, in part, by a Grant-in-Aid for Scientific Research Nos. 10179103 and 12780440 from the Ministry of Education, Science, Sports and Culture, Japan.

### References

1. Aimoto, S. *Biopolymers (Peptide Sci.)* **51**, 247–265 (1999).
2. (a) Hojo, H., Aimoto, S. *Bull. Chem. Soc. Jpn.* **64**, 111–117 (1991). (b) Mizuno, M., Haneda, K., Iguchi, R., Muramoto, I., Kawakami, T., Aimoto, S., Yamamoto, K., Inazu, T. *J. Am. Chem. Soc.* **121**, 284–290 (1999). (c) Kawakami, T., Hasegawa, K., Aimoto, S. *Bull. Chem. Soc. Jpn.* **73**, 197–203 (2000).
3. In Wallace, C.J.A. (Ed.) *Protein Engineering by Semisynthesis*, CRC Press, Boca Raton, 2000.
4. Gaertner, H.F., Rose, K., Cotton, R., Timms, D., Camble, R., Offerd, R.E. *Bioconjugate Chem.* **3**, 262–268 (1992).
5. Dawson, P.E., Muir, T.M., Clark-Lewis, I., Kent, S.B.H. *Science* **266**, 776–779 (1994).
6. Wieland, T., Bokelmann, E., Bauer, L., Lang, H.U., Lau, H. *Liebigs Ann. Chem.* **583**, 129–149 (1953).
7. Canne, L.E., Bark, S.J., Kent, S.B.H. *J. Am. Chem. Soc.* **118**, 5891–5896 (1996).
8. Offer, J., Dawson, P.E. *Org. Lett.* **2**, 23–26 (2000).
9. Botti, P., Carrasco, M.R., Kent, S.B.H. *Tetrahedron Lett.* **42**, 1831–1833 (2001).
10. Muir, T.W., Sondhi, D., Cole, P.A. *Proc. Natl. Acad. Sci. U.S.A.* **95**, 6705–6710 (1998).
11. Evans, Jr., T.C., Benner, J., Xu, M.-Q. *Protein Sci.* **7**, 2256–2264 (1998).
12. Kawakami, T., Hasegawa, K., Teruya, K., Akaji, K., Horiuchi, M., Inagaki, F., Kurihara, Y., Uesugi, S., Aimoto, S. *Tetrahedron Lett.* **41**, 2625–2628 (2000).
13. Kawakami, T., Akaji, K., Aimoto, S. *Org. Lett.* **3**, 1403–1405 (2001).
14. Dixon, H.B.F. *J. Protein Chem.* **3**, 99–108 (1984).
15. Dawson, P.E., Churchill, M.J., Ghadiri, M.R., Kent, S.B.H. *J. Am. Chem. Soc.* **119**, 4325–4329 (1997).

## Synthesis of N to C Terminal Cyclic Analogues of $\alpha$ -Conotoxin ImI by Chemoselective Ligation of Unprotected Linear Precursors

Christopher J. Armishaw<sup>1</sup>, Julie Dutton<sup>1</sup>, Ron C. Hogg<sup>2</sup>, David J. Adams<sup>2</sup>,  
David J. Craik<sup>1</sup> and Paul F. Alewood<sup>1</sup>

<sup>1</sup>*Institute for Molecular Bioscience and* <sup>2</sup>*Department of Physiology & Pharmacology,*  
*The University of Queensland, Brisbane, Queensland 4072, Australia*

### Introduction

$\alpha$ -Conotoxin ImI [GCCSDPRCAWRC-NH<sub>2</sub>, S-S connectivity: 1-3; 2-4] is isolated from the worm hunting cone snail *Conus imperialis* and is a potent and specific antagonist for the neuronal  $\alpha 7$  nicotinic acetylcholine receptor (nAChR). Previous <sup>1</sup>H NMR structural studies in our laboratory showed that the N and C termini are in close proximity. Furthermore, residues which have previously been found to be crucial for binding [2] are well separated from the termini and appear on one face of the molecule.

We hypothesised that N to C terminal cyclization of ImI with insertion of a single amino acid or dipeptide spacer (or equivalent chemical moiety) would further enhance its stability and potentially its bioavailability with minimal disruption to the native ImI structure. We describe here our initial experiments with two cyclic ImI analogues, cImI-A (Ala spacer) and cImI-AG (Ala-Gly spacer)

### Results and Discussion

The two acyclic conopeptides were synthesized using a one-pot native chemical ligation strategy as the target molecules contain a convenient Gly-Cys ligation site [1]. Furthermore, conditions used to effect cyclization using this strategy also induce disulfide bond formation. The thioester linker was prepared using a simple three step procedure on a Boc-Phe-OCH<sub>2</sub> PAM resin [3] and the peptides were assembled using *in situ* neutralization in Boc chemistry [4]. Simultaneous cleavage and removal of side chain protecting groups were effected using HF/*p*-cresol/*p*-thiocresol (9 : 0.8 : 0.2).

Following purification, a series of trial cyclizations were attempted under various conditions. For both analogues 0.1 M Tris + 2 M Gn-HCl, pH 8.4 were most effective. cImI-AG displayed a mixture of disulfide isomers in approximately 1 : 4 : 1 ratio whereas cImI-A displayed one major isomer. The major product of each experiment was isolated and further characterised.

The disulfide bond connectivity of the two analogues were elucidated using a directed disulfide bond synthesis with orthogonal cysteine protection (fluorenylmethyl and *p*-methylbenzyl) and subsequent cyclization with BOP. Co-injection of the directed synthetic material with the major products of the native chemical ligation synthesis showed that the major product of cImIAG corresponded to the 1-3, 2-4 isomer and cImIA corresponded to the 1-4, 2-3 isomer.

Samples for NMR experiments contained ~3 mM peptide in either 100% D<sub>2</sub>O or 10% D<sub>2</sub>O/90% H<sub>2</sub>O at pH 3.5. Experiments were carried out on Bruker 500 and 750 MHz NMR spectrometers. Spectra were routinely acquired at 280, 285 and 290 K. Structures were calculated using XPLOR and the pictures generated in MolMol. Ribbon depictions of the NMR structures of the cyclic analogues show that the arrangement of residues in the first loop including Asp5, Pro6 and Arg7 is conserved, however Trp10 in the second loop is significantly displaced, and may be unable to interact (Figure 1) with its receptor.

Preliminary binding assays to parasympathetic neurons from neonatal rat intracardia ganglia show that the analogues bind to the  $\alpha 7$  subunit of nAChR's with approximately 30-fold decrease in activity which is consistent with previous mutagenesis studies of Trp10 [2]. A full dose response study is yet to be performed.

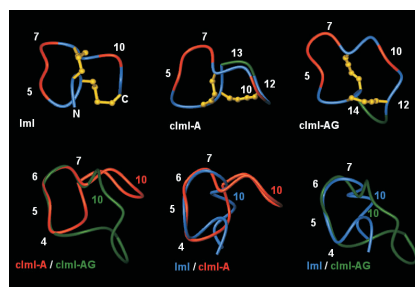


*Fig. 1. (Top) Ribbon depictions of lml, clml-A and clml-AG (Bottom) Overlays of ribbon depictions showing that residues in the first loop fit with the native lml structure whereas the second loop is displaced.*

### Acknowledgments

CJA acknowledges a U of Queensland Graduate School Award for financial support and the American Peptide Society for providing a travel grant to attend this conference.

### References

1. Gehrmann, J., Daly, N.L., Alewood, P.F., Craik, D.J. *J. Med. Chem.* **42**, 2364–2372 (1999).
2. Quiram, P.A., Sine, S.N. *J. Biol. Chem.* **273**, 11007–11011 (1998).
3. Camarero, J.A., Cotton, G.J., Adeva, A., Muir, T.W. *J. Peptide Res.* **51**, 303–316 (1998).
4. Schnolzer, M., Alewood, P.F., Jones, A., Alewood, D., Kent, S.B.H. *Int. J. Peptide Protein Res.* **40**, 180–193 (1992).

## **Total Chemical Synthesis of $\kappa$ -Casein Using Native Ligation Methodology**

**Paramjit S. Bansal and Paul F. Alewood**

*Institute for Molecular Bioscience, The University of Queensland, Brisbane, 4072, Australia*

### **Introduction**

Casein milk proteins ( $\alpha_{s1}$ ,  $\alpha_{s2}$ ,  $\beta$ , and  $\kappa$ ) together with calcium phosphate form heavily hydrated loose colloidal particles known as milk micelles [1]. Whereas the primary structures of the caseins are well known there are no reports in the literature on their tertiary structures. This may be attributed to the difficulties experienced in obtaining homogeneous proteins from milk due to the abundance of genetic variations and post-translational modifications (PTMs).  $\kappa$ -Casein which contains 169 residues plays an important role in the stability and size of milk micelles. In our first efforts in a wider “chemical synthesis of caseins” program we decided to synthesise  $\kappa$ -casein without its common PTMs and investigate its properties. Here we report the synthesis of  $\kappa$ -casein using native ligation methodology.

### **Results and Discussion**

$\kappa$ -Casein consists of 169 amino acids with a hydrophobic N-terminal and a hydrophilic C-terminal [1]. For synthetic convenience the protein sequence was divided into the following four segments each tailored to facilitate native chemical ligation:

<sup>1</sup>EEQNQEPIRCEKDERFFSDKIAKYIPIQYVLSRYPSYGLNYYA<sup>44</sup>  
<sup>45</sup>CKPVALINNQLPYPYAKPAAVRSPAQILQWQVLSNTVPAKA<sup>87</sup>  
<sup>88</sup>CQAQPTTMARHPHPLHSFMAIPPKKNQDKTEIPTINTIASG<sup>128</sup>  
<sup>129</sup>CPTSTPTTEAVESTVATLEDSPEVIESPPEINTVQVTSTAV<sup>169</sup>

The peptide segments were synthesised in high yield manually using *t*-BocAla(Gly)-S-mercaptopropionyl-alanyl-Pam resin and rapid *t*-Boc amino acid/HBTU/DPIEA *in situ* neutralization chemistry [2]. Cysteine residues were protected by AcM with other side chain protection described elsewhere [3]. Each peptide segment was isolated in high purity after HF cleavage and RP-HPLC purification. Mass spectrometry was used to characterise various peptide segments.

The  $\kappa$ -casein was then assembled using “native ligation” chemistry [4]. Segments 88-128 and 129-169 were ligated in phosphate buffer (pH 6) within 2 h (HPLC) using thiophenol as an activating catalyst (Figure 1). The ligated peptide (88-169) was purified (HPLC), and the free cysteine capped with iodoacetic acid. Following removal of AcM from the N-terminal cysteine 88 (mercuric acetate, pH 4)  $\kappa$ -casein (88-169) was ligated with the next segment (45-87) under the same reaction conditions. Similarly, following the same sequence of steps the fourth segment (1-44) was ligated to obtain  $\kappa$ -casein [Q44A, Q45C, S87X, E129X, X = Cys(CH<sub>2</sub>COOH)]. In conclusion, this is the first report on the total chemical synthesis of  $\kappa$ -casein using rapid SPPS and “native ligation” methodology.

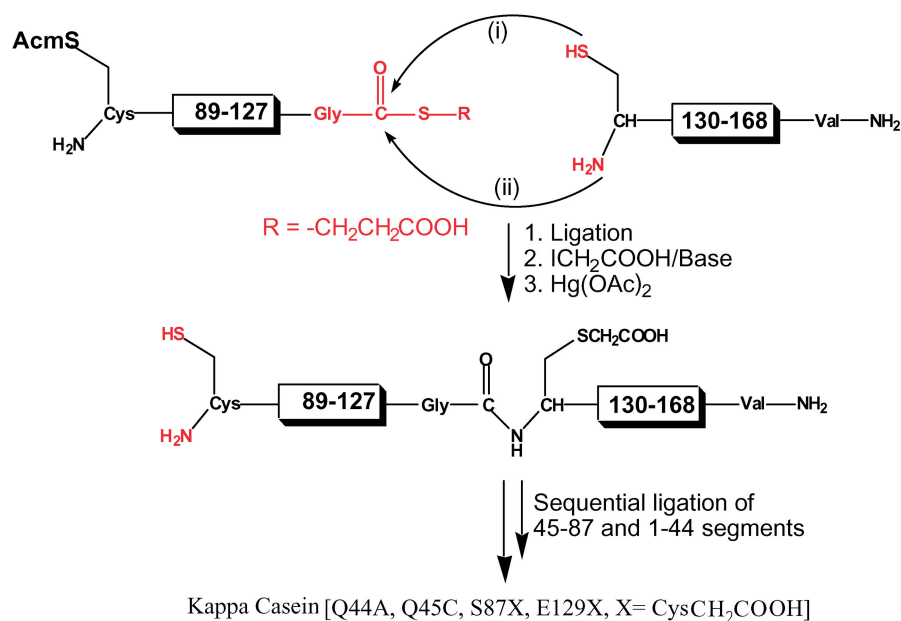


Fig. 1. Synthesis of  $\kappa$ -casein via native ligation of protein segment.

#### Acknowledgments

The authors thank Dairy Research and Development Corporation, Australia for financial assistance and Mr. Alun Jones for mass spectrometry support.

#### References

1. Swaisgood, H.E., In Fox, P.F. (Ed.) *Advanced Dairy Chemistry, Proteins*, Vol. 1, pp. 63–110, and Rollema, H.S., pp. 111–140, Elsevier, UK, 1992.
2. Schnolzer, M., Alewood, P., Alewood, D., Jones, A., Kent, S.B.H. *Int. J. Peptide Res.* **40**, 180–193 (1992).
3. Kent, S.B.H., Alewood, D., Alewood, P., Baca, M., Jones, A., Schnollzer, M., In Epton, R. (Ed.) *Innovation and Perspectives in Solid Phase Synthesis*, Intercept Limited, Andover, 1992, pp. 1–22.
4. Wilson, J., Kent, S.B.H. *Curr. Opin. Biotechnol.* **9**, 412–426 (1998).

## Fmoc Chemistry Compatible Methods for Thio-Ligation Assembly of Proteins

S. Biancalana<sup>2</sup>, D. Hudson<sup>1</sup>, M. F. Songster<sup>1</sup> and S. A. Thompson<sup>2,3</sup>

<sup>1</sup>Biosearch Technologies, Inc., Novato, CA 94949, USA

<sup>2</sup>Berlex Biosciences, Richmond, CA 94804, USA

<sup>3</sup>Inhale Therapeutics, San Carlos, CA 94070, USA

### Introduction

Two methods are compared for the synthesis of peptide thioester fragments by Fmoc chemistry-mediated solid phase synthesis. The first, which utilizes isothiuronium salts [1], allows formation of thiophenyl esters directly from partially protected peptides, either in solution or on resin. The chloride salt, named CTTU, reacts far more rapidly than does the variant bearing a non-nucleophilic counterion, TTTU. This observation suggests active participation of the chloride ion during thiophenyl ester formation (Figure 1), and that use of CTTU may give rise to significant levels of racemization. Solution and on resin derivatization have been shown to be satisfactory and equivalent methods in the synthesis of SDF-1 $\beta$  47-64 (Figure 2).

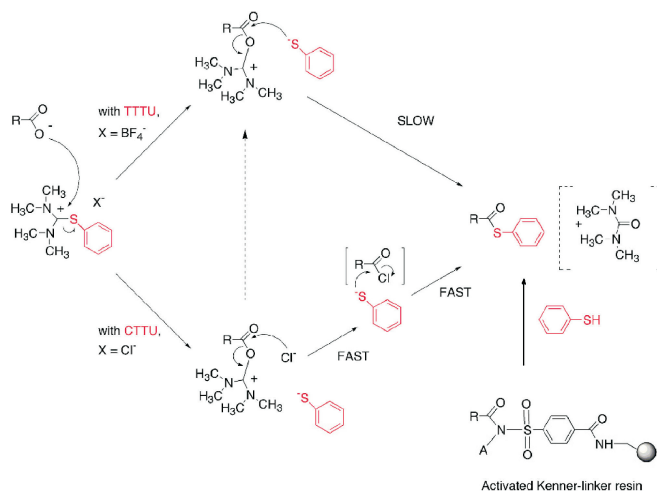


Fig. 1. Schematic representation of the formation of thiophenyl esters via the use of isothiuronium salts (suggested mechanism), and using an activated Kenner sulfonamide resin; **R** represents a protected peptide chain, and **A** either a methyl or cyanomethyl group.

### Results and Discussion

Recent publications [2,3] have demonstrated straightforward application of the Backes/Ellman safety-catch method to ligation assembly of several complex peptides. Our initial studies with this procedure gave very low to no yield of target peptides. Rather than continue with the SDF sequence, our evaluations switched to a variant of a difficult test sequence, tBoc-Gly-Tyr(tBu)-Leu-Phe-Glu(OtBu)-Val-Asn(Trt), which still maintained a C-terminal Asn(Trt).

Application of the simultaneous comparative approach yielded the following results: (1) Activation by methylation is effective, iodoacetonitrile is not; (2) Thiolytic cleavage only occurs in the presence of sodium thiophenoxide; (3) Thiolytic cleavage

with mercaptopropionic acid ethyl ester is safest, a significant side-reaction occurs with benzylmercaptan and thiophenol due to thioester migration during base treatment (the byproducts from all side reactions have been identified); (4) The Kenner safety catch linker is as effective as the sulfamoylbutyryl linker of Backes/Ellman; (5) PS and NovaGel supports are equally effective.

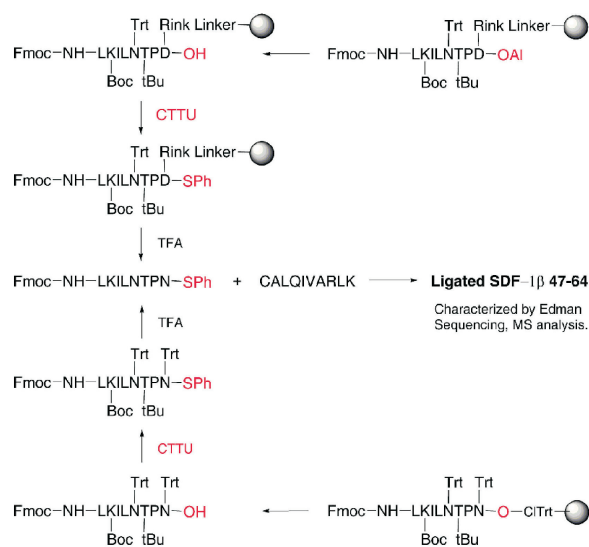


Fig. 2. Schematic representation of the synthesis of SDF-Iβ 47-64 via on resin (top path) and in solution (bottom path) formation of thioester fragments.

In conclusion, CTTU is an effective, readily prepared and non-noxious reagent, which can form thiophenyl esters on resin or in solution, although its use may result in significant levels of racemization. Additionally, safety catch approaches are subject to steric effects at the C-terminus, and may require catalysis with sodium thiophenoxide. Lastly, it was found that thiolysis is best performed with mercaptopropionic acid ethyl ester, the use of which avoids a thioester migration side-reaction.

### Acknowledgments

Support by the SBIR program of the NIGMS division of the NIH (grant 1R43 GM58947 to D. H.) is gratefully acknowledged.

### References

1. Hudson, D., Thompson, S.A., US Patent allowed 2001.
2. Ingenito, R., Bianchi, E., Fattori, D., Pessi, A. *J. Am. Chem. Soc.* **121**, 11369 (1999).
3. Shin, Y., Winans, K.A., Backes, B.J., Kent, S.B.H., Ellman, J.A., Bertozzi, C.R. *J. Am. Chem. Soc.* **121**, 11684 (1999).

## **Simultaneous Lipidation of a Multi-Epitope Peptide Cocktail by Chemoselective Hydrazone Formation**

**Line Bourel-Bonnet<sup>1</sup>, Oleg Melnyk<sup>1</sup>, Frédéric Malingue<sup>2</sup>, Pascal Joly<sup>1</sup>,  
Dominique Bonnet<sup>1</sup> and Hélène Gras-Masse<sup>1</sup>**

<sup>1</sup>UMR 8525 CNRS and

<sup>2</sup>Sedac-Therapeutics, Institut de Biologie de Lille, BP 447, F-59021 Lille, France

### **Introduction**

Several experiments have revealed that multiple cellular responses can be induced fairly efficiently by immunisation with several peptide antigens possessing an N-ε palmitoylated lysylamide at C-terminus. The tolerance and immunogenicity of a cocktail composed of 6 HIV-1-derived multi-epitopic lipopeptides used in the ANRS-VAC04 phase I clinical trial, confirmed that such synthetic formulations represent a promising alternative approach to conventional and recombinant vaccines [1]. With the aim of producing a vaccine that could, ideally, induce in each individual a polyclonal T-cell response, in order to prevent the selection of escape mutants, thus increasing the diversity of the immunising cocktail, now represents one of the most attractive optimisation strategies.

Lipopeptides tend to aggregate in aqueous media. Therefore, the major difficulty encountered during their production is associated with preparative RP-HPLC steps. As efficient chromatographic separation of lipopeptides can be achieved only with a limited column loading, a considerable part of the labour cost is spent on the repetition of chromatography runs.

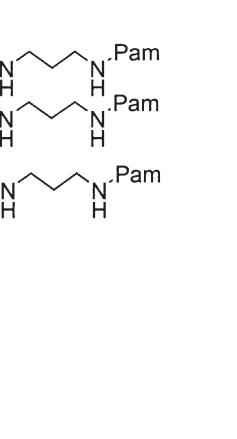
In order to circumvent the difficulty encountered during the preparative RP-HPLC of lipopeptides, we envisioned a strategy of lipidation by chemoselective hydrazone formation between a lipophilic glyoxaldehyde vector and prepurified hydrazino-peptides.

We have recently described the rapid and almost quantitative lipidation of a 38-mer hydrazinopeptide in quasi-stoichiometric amounts (1.1 eq.) of the lipophilic vector **1**. The ligation was performed under salt-free conditions, using a 95 : 5 mixture of 2-methyl-propan-2-ol/water [2]. We now demonstrate that this method can be adapted for the lipidation of several fully purified hydrazino acetyl peptides **2a**, **b**, ...**n** with only 1.2 equivalent of the lipophilic glyoxaldehyde **1**, with simultaneous production of the corresponding hydrazone lipopeptides **3a**, **b**, ...**n** (Scheme 1).

### **Results and Discussion**

The lipophilic glyoxaldehyde **1**, composed of a palmitoyl and glyoxylyl group linked by a 1,3-diaminopropane moiety, was obtained by solid-phase synthesis, using our recently described isopropylidene tartrate (IPT) linker on an amino PEGA resin [3]. The palmitic acid was introduced using BOP activation. Unmasking the 1,2-diol was followed by solid-phase periodic oxidation in a 2-methyl-propan-2-ol/H<sub>2</sub>O/AcOH mixture (3/2/1), which resulted in both the formation of the α-oxo-aldehyde moiety, and the cleavage of the product from the solid support.

In view of the preparation of lipopeptide antigens which could be compared to our previously described C-terminal palmitoyl-peptides, and in order to validate our approach with diverse sequence models incorporating any amino acid (including cysteine), we selected seven hydrazinopeptides **2a–g** deriving from proteins of the Simian Immunodeficiency Virus (SIV) [4].



hydrazone lipopeptides.  
5, RT.

hydroacetate salts by a peptide strategy. Our  $\alpha$ -COOH was used for selectively deprotected

ed by combining pre-  
tening the lyophilized  
ethyl-propan-2-ol (1.2  
ored by RP-HPLC us-  
d cleanly and rapidly  
yields were obtained  
vered at the end of the  
ptides **3a–g** (Table 1).

ention time determined

$[H]^+$ c.	$[M+H]^+$ found	$r_t$ [min]
3.9	3608	19.43
3.3	3318	20.72
3.5	3462	25.17
3.5	3538	23.41
3.7	3802	19.57
2.9	3851.5	23.12
3.5	5155	21.21

## Synthetic Methods

According to the ICH Q3C Guideline of the European Agency for the Evaluation of Medicinal products, trifluoroacetic acid is an ICH class 4 solvent, for which no adequate toxicological information is available. We therefore performed a trifluoroacetate-acetate salt exchange (over 95% yield by RP-HPLC), followed by 0.22  $\mu\text{m}$  sterilising filtration, distribution of the solution into sterile glass vials, and final lyophilization.

In another experiment, the direct lipidation of acetate salts of the hydrazino acetyl precursors was attempted using the same conditions. However, the formation of ill-defined aggregates was observed, indicating that the efficiency of the reaction was dependent upon the nature of the counter-ion.

A major advantage of this approach is the absence of any resolutive purification step after introduction of the lipid tail. The collective treatment of the peptide antigens for several consecutive steps (lipidation, ion-exchange and sterilizing filtration) with excellent overall yields permits a considerable reduction of the production cost of complex lipopeptide cocktails.

The immunogenicity of our new hydrazone lipopeptide cocktail is now under investigation in the laboratory of J.-G. Guillet (INSERM U445, Paris).

## Acknowledgments

This work was financially supported by the CNRS, the Pasteur Institute of Lille, the University of Lille 2 and the ANRS. D. B. holded a CNRS/Région Nord Pas-de-Calais fellowship.

## References

1. Pialoux, G., Gahéry-Ségard, H., Sermet, S., Poncelet, H., Fournier, S., Gérard, L., Tartar, A., Gras-Masse, H., Levy, J.-P., Guillet, J.-G. *The ANRS VAC04 trial. AIDS*, in press (2001).
2. Bonnet, D., Bourel, L., Gras-Masse, H., Melnyk, O. *Tetrahedron Lett.* **41**, 10003–10007 (2000).
3. Melnyk, O., Fruchart, J.-S., Grandjean, C., Gras-Masse, H. *J. Org. Chem.*, in press (2001).
4. Bourgault-Villada, I., Mortara, L., Aubertin, A.-M., Gras-Masse, H., Lévy, J.-P., Guillet, J.-G. *FEMS Immunol. Med. Microbiol.* **19**, 81–87 (1997).
5. Mortara, L., Gras-Masse, H., Rommens, C., Venet, A., Guillet, J.-G., Bourgault-Villada, I. *J. Virol.* **73**, 4447–4451 (1999).
6. Bonnet, D., Ollivier, N., Gras-Masse, H., Melnyk, O. *J. Org. Chem.* **66**, 443–446 (2001).

## Privilege Structures: New Strategies for the Synthesis of Cyclic Tetrapeptides

Wim D. F. Meutermans, Simon W. Golding, Marc R. Campitelli,  
Douglas A. Horton, Gregory T. Bourne and Mark L. Smythe

*Institute for Molecular Bioscience, The University of Queensland, Brisbane, 4072, Australia*

### Introduction

The term privilege structure has been coined [1] to describe classes of molecules that are capable of binding to multiple, unrelated receptors. For example, various cyclic tetrapeptides have been isolated from bioactive fractionation and have wide-ranging biological activities, including anti-cancer, anti-parasitic, opiate agonist, tyrosinase inhibitors and potential selective herbicides. No synthetic routes have been described that enable access to this “difficult” class of compounds in a versatile fashion. In this work, we have developed a strategy that makes use of two types of auxiliaries, one that enables a ring closure/ring contraction process, and a second one which performs the role of promoting cis-amide bond conformations at selected positions in the backbone.

### Discussion

Our reported strategy [2–4] on the synthesis of difficult cyclic peptides is outlined in Figure 1, Route A. Briefly, the synthesis of the linear peptide **Ia** followed by the initial ring closure generates a more accessible larger ring **IIa**, whereby the N- and C-termini are preorganised for cyclisation. Subsequent *O*- to *N*-acyl transfer leads to the desired macrocycle **IIIa** and removal of the auxiliary gives the desired cyclic peptide **IV**. Currently, using this strategy, we have been able to synthesise 6 cyclic tetrapeptides with the general formula cyclo-[AA<sub>1</sub>-AA<sub>2</sub>-AA<sub>3</sub>-Gly] (Table 1).

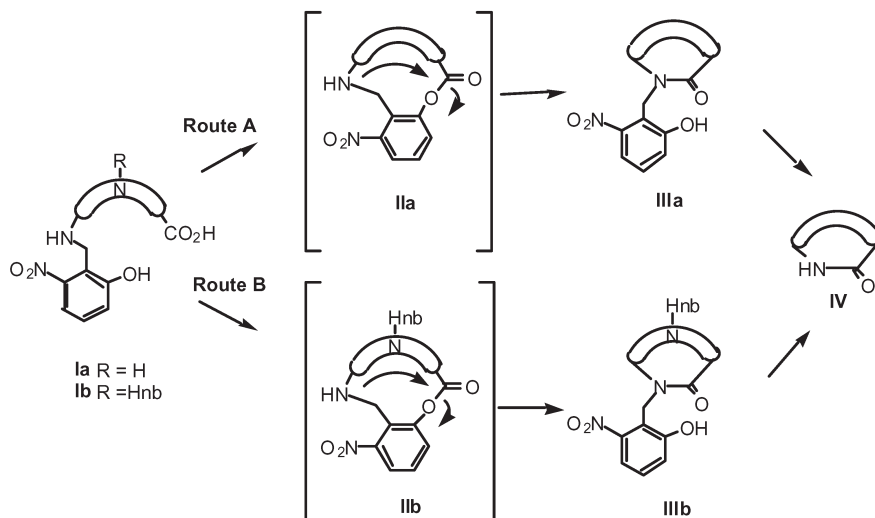


Fig. 1. Synthesis of cyclic peptides using the ring contraction strategy.

Table 1. Synthesis of cyclic tetrapeptides via ring contraction (Route A).

Entry	Peptide <b>Ia</b>	% Yield <b>IIIa</b> (by HPLC)	% Yield <b>IIIa</b>	% Yield <b>IV</b>
a	[Hnb]Tyr-Arg-Phe-Gly-OH	85	62	49
b	[Hnb]Asn-His-Phe-Gly-OH	70	32	26
c	[Hnb]Asn-Arg-Phe-Gly-OH	75	57	30
d	[Hnb]Asn-Ser-Trp-Gly-OH	25	26	49
e	[Hnb]Arg-His-Asn-Gly-OH	60	51	52
f	[Hnb]Arg-Ile-His-Gly-OH	55	32	10

Following this success, we set out to evaluate the strategy using all-L-amino acid functionalised tetrapeptides. To our knowledge, the only reported examples contain glycine, proline or N-substituted residues in the sequence. The standard ring closure/ring contraction conditions, when applied to a model tetrapeptide Tyr-Arg-Phe-Ala, failed to generate the cyclic tetrapeptide. Through careful examination of the product mixture it became apparent that the ring closure to the intermediate nitrophenyl ester proceeded rapidly, but ring contraction failed at room temperature. We therefore examined if ring contraction could be enhanced by the introduction of a backbone substituents in the sequence (Figure 1, Route B). It has previously been shown that backbone substitution lowers the energy barrier for cis-amide bond formation, thereby increasing the propensity for cyclisation.

Synthesis of [Hnb]Tyr-Arg-[Hnb]Phe-Ala-OH proceeded *via* similar chemistry as reported previously [1–3]. Cyclisation followed by ring contraction afforded two monocyclic peptides in a combined yield of 59%. The first eluting product (33%) was characterised as the all-L cyclic peptide, while the second eluting monocyclic product (26%) contained D-alanine.

Subsequent removal of the auxiliaries by photolysis from the all-L cyclic peptide lead to a reverse *N*-to-*O*-acyl shift, which results in ring opening side reactions and complete loss of the cyclic products (Figure 2). It was found that Hnb removal can be effectively achieved by diazomethane induced methylation of the Hnb groups, followed by photolysis of the crude product (Figure 3). Following this route, the all-L cyclic tetrapeptide, cyclo-[Tyr-Arg-Phe-Ala] was successfully synthesized. It is expected that this route will provide, for the first time, a versatile approach to cyclic tetrapeptides.

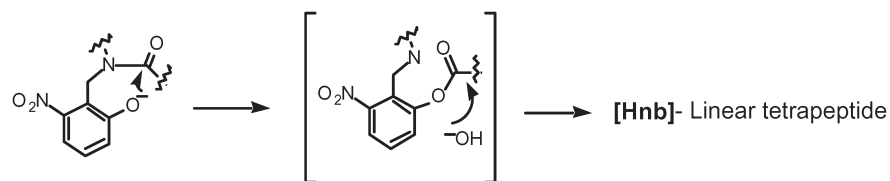


Fig. 2. Proposed hydrolysis of the cyclic [Hnb]-tetrapeptide.

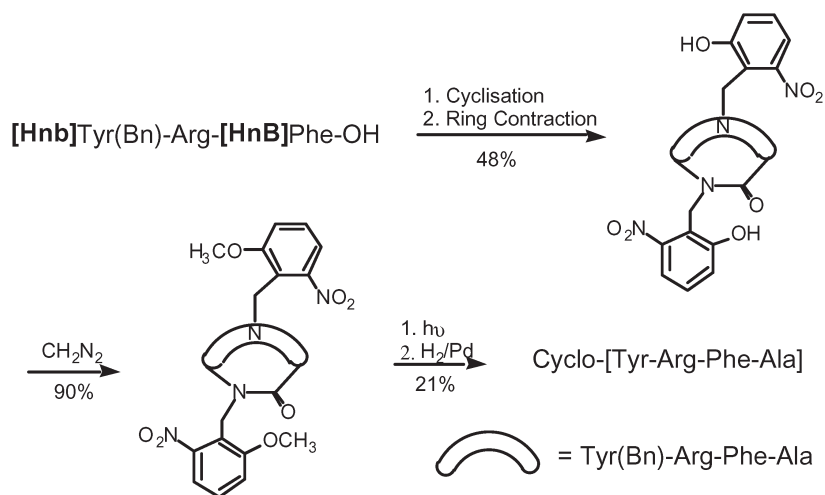


Fig. 3. Alternative route for the synthesis of cyclo-[Tyr-Arg-Phe-Ala].

### Acknowledgments

We thank the ARC, Glaxo Wellcome, Australia and Glaxo Wellcome, UK for the financial support and Dr. M. Hann for useful discussions.

### References

1. Evans, B.E., et al. *J. Med. Chem.* **31**, 2235–2246 (1998).
2. Meutermans W.D.F., Golding, S.W., Bourne, G.T., Miranda L.P., Dooley, M.J., Alewood, P.F., Smythe, M.L. *J. Am. Chem. Soc.* **121**, 9790–9796 (1999).
3. Meutermans, W.D.F., Golding, S.W., Bourne, G.T., Miranda, L.P., Dooley, M.J., Alewood, P.F., Smythe, M. L. In Fields G.B., Tam, J.P. and Barany, G. (Eds) *Peptides, Biology and Chemistry (Proceedings of the 16th American Peptide Symposium)*, Kluwer, Dordrecht, 2000, p. 183–186.
4. Miranda, L.P., Meutermans, W.D.F. Smythe, M.L., Alewood, P.F. *J. Org. Chem.* **65**, 5460–5468 (2000).
5. Bourne, G.T., Meutermans, W.D.F., Alewood, P.F., McGear, R.P., Scanlon, M., Watson, A.A., Smythe, M.L. *J. Org. Chem.* **64**, 3095–3101 (1999).

## Incorporation of a cis-Amide Bond Isostere in the Synthesis of Cyclic Tetrapeptides

Gregory T. Bourne, Peter J. Cassidy, Wim D. F. Meutermans,  
Marc R. Campitelli and Mark L. Smythe

*Institute for Molecular Bioscience, The University of Queensland, Brisbane, 4072, Australia*

### Introduction

Cyclic tetrapeptides are an exciting class of molecules showing a wide range of biological activities. They are very difficult to synthesize due to the inherent strain of the 12 membered ring. Our initial experiments on the inclusion of backbone substituents to increase the propensity for cis conformations of the amide bond [1] resulted in significant improvements in yields for cyclizing these linear precursors. To support the hypothesis on the role of cis amide bonds in reducing ring strain within cyclic tetrapeptides, and to provide a simple synthetic method in accessing these molecules we have been evaluating cis-amide bond surrogates. We initially decided on the synthesis of a pyrrole as a conformational isostere and to incorporate this into a cyclic motif to examine its effect on cyclization. Herein, we report on a simple preparation of an unprotected H-Gly-Tyr-OH dipeptide surrogate which contains a 1,2-pyrrole  $\Psi[C_4H_3N]$  moiety designed to mimic a cis amide bond (Figure 1).

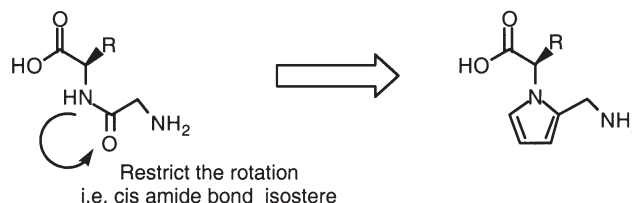


Fig. 1. A cis-amide bond isostere.

### Results and Discussion

We initially decided to incorporate the cis-amide bond isostere into a model cyclic peptide cyclo-[Arg-Phe-Gly-Tyr]. We found that this sequence was a suitable model since: i) in our hands the linear precursor, H-Arg(Pmc)-Phe-Gly-Tyr-OH affords only cyclic oligomers with no detection of the cyclic monomer under standard cyclization conditions and ii) the synthesis of a similar pyrroles to **2** had previously been reported in the literature [2] starting from the tetrahydrofuran **1**.

The synthesis of the modified cyclic tetrapeptide proceeded through formation of the aldehyde from **1** (Figure 2). Hydrolysis, imine formation followed by hydrogenation removed the benzyl protecting group and reduced the corresponding hydroxy-imine to give the desired amino acid **2**. Due to the lack of acid stability the amino acid **2** was reacted immediately with the activated ester of Fmoc-Phe-OH. Removal of the fluorenylmethyl protecting group, subsequent addition of the final residue Fmoc-Arg(Pmc)-OH followed by Fmoc removal afforded the wanted linear tetrapeptide **4**. Cyclization of the linear peptide **4** at 0.1 mM,  $-10^\circ\text{C}$ , resulted in the formation of the desired monocyclic products **5a** (11%) and the diastereomer cyclo-[Arg-Phe-Gly $\Psi(C_4H_3N)(D)$ Tyr] **5b** (10%, confirmed by NMR). Also isolated was the cyclic dimer in 20% yield. Separation and treatment of **5a** with 95% TFA removed the Pmc

group to give the cyclic material **6a** in 32% yield. However, under these conditions substantial racemization occurred at the C- $\alpha$  of tyrosine site to afford 23% of the diastereomer **6b**. This was initially confirmed by NMR and later by the treatment of **5b** with strong acid to afford **6b** as the only product.

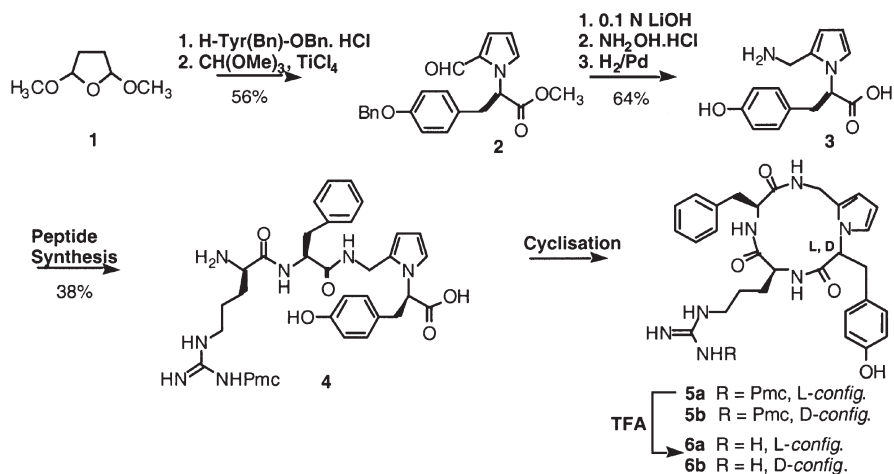


Fig. 2. Synthesis of a cyclic tetrapeptide containing a cis-amide bond isostere.

Interestingly, racemization only occurred upon Pmc deprotection of the all L cyclic tetrapeptide and not the D containing diastereomer. This is presumably related to ring strain.

In conclusion, the stabilization of a cis-amide bond with a pyrrole moiety allowed the synthesis of cyclic tetrapeptide derivative which was not accessible from the non-pyrrole containing sequence. Shortcomings of the approach includes pyrrole stability and racemization. Other isosteric replacements are now being investigated in conjunction with the use of the HnB auxiliary.

## References

1. Meutermans W.D. F., Golding, S.W., Bourne, G.T., Miranda L.P., Dooley, M.J., Alewood, P.F., Smythe, M.L. *J. Am. Chem. Soc.* **121**, 9790–9796 (1999).
2. Abell, A.D., Houlst, D.A., Jamieson, E.J. *Tetrahedron Lett.* **33**, 5831–5832 (1992).

## Covalent Control of Shape and Folding in Peptides by Ring-Closing Metathesis

Rob M. J. Liskamp<sup>1</sup>, John F. Reichwein<sup>1</sup>, Bas Wels<sup>1</sup>,  
 John A.W. Kruijtz<sup>1</sup> and Cees Versluis<sup>2</sup>

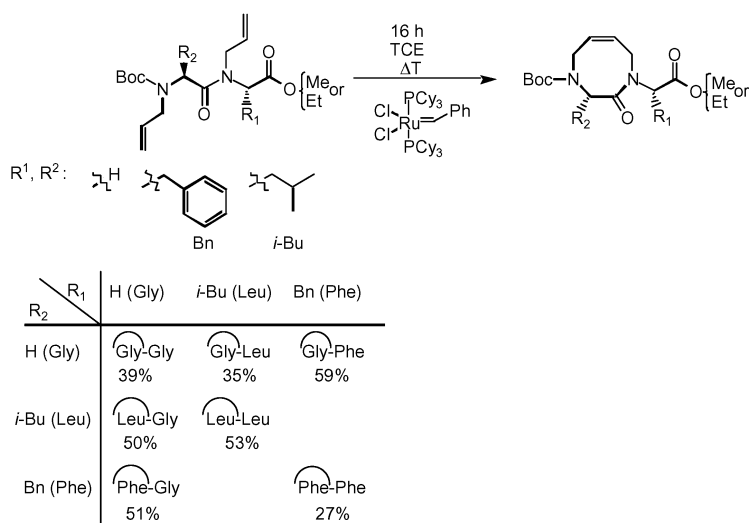
<sup>1</sup>Department of Medicinal Chemistry and

<sup>2</sup>Department of Biomolecular Mass Spectrometry, Faculty of Pharmacy, Utrecht Institute  
 for Pharmaceutical Sciences, Utrecht University, 3508 TB Utrecht, The Netherlands

### Introduction

Nature has found many intriguing and elegant ways to reduce the flexibility of peptides and proteins in order to control their folding and shape. Apart from the size of a peptide or protein, reduction of the flexibility by disulfide bridges is probably the most well-known way to control shape. One of the most sophisticated ways is probably “multiple-side chain knotting”, in which a number of side chains are tied together in such a way that almost absolute control is gained over the shape of a molecule. Outstanding examples in this respect are the glycopeptide antibiotics of which vancomycin is an important representative.

As part of a program towards finding new and general approaches for covalent control of shape and folding in peptide and peptide-derived compounds we aim at cyclizations without using the side chains of amino acids, the so-called *amide to amide* cyclizations as well as cyclizations in which the amino acid side chains are involved. Clearly, the former approach will allow the preservation of side chain interactions if they are involved in the interaction of the biologically active conformation. It might be possible to probe the biologically active conformation or even create alternative bio-active conformations. Both approaches are directed towards covalent control of folding and shape and should therefore lead to an increased affinity and selectivity by limiting the unfavorable entropy loss. The second approach is explicitly



Scheme 1. Ring closing metathesis of bis-(*N*-allyl) dipeptides [2].

directed towards finding alternatives for lactam and disulfide bridges. For the realization of both aims ring-closing metathesis (RCM) of peptides containing substituents with double bonds was considered as a very attractive possibility.

## Results and Discussion

In the first approach our recently developed method for site-specific alkylation of amide nitrogens in peptides was used [1]. This enabled the introduction by Mitsunobu reaction of *e.g.* allyl substituents. The preparation of bis-(*N*-allyl)dipeptides using among others this method furnished the starting materials for RCM leading to 8-membered ring containing cyclic peptides (Scheme 1) [2]. The synthesis can be carried out in an array-like format opening up possibilities for combinatorial approaches.

For the preparation of larger cyclized peptides a general solid phase procedure was developed for preparation of the cyclization precursors [3]. Unfortunately, it was not possible to apply RCM to bis-(*N*-allyl)oligopeptides. Depending on the number of amino acid residues and therefore the number of peptide amide bonds involved in the cyclization reaction the substituents on the amide nitrogens had to be elongated for the RCM to take place. This led to a set of rules which have to be taken into account when bis-(*N*-alkenyl)oligopeptides are subjected to RCM (Figure 1) [4].

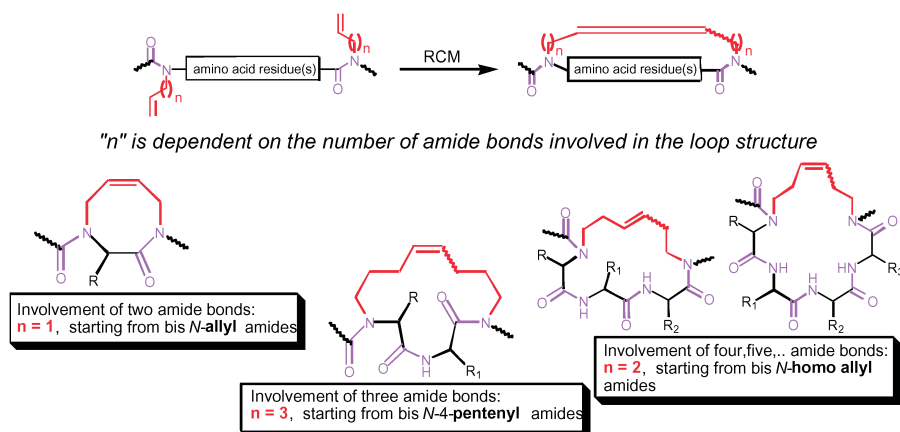
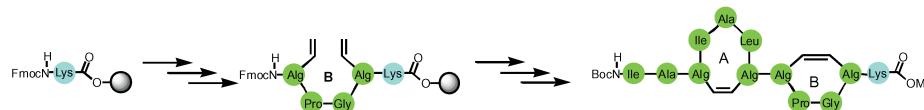


Fig. 1. "Rules" for cyclization of bis-*N*-alkylated peptides by RCM [4].

Obeying these rules a "rolling loop scan" of Leu-enkephalin was carried out. All possible loops of Leu-enkephalin were prepared by RCM of the appropriate bis-(*N*-alkylated) amides (Figure 2) [3].

In the second approach, we want to use the ethene or ethylene (after reduction) moiety as a replacement of the lactam, disulfide or even sulfide moiety. The latter is present in nisin antibiotics. Therefore we recently synthesized a nisin AB mimic by "tandem" ring-closing metathesis (Scheme 2). In this mimic the sulfide moieties are



Scheme 2. Synthesis of the nisin AB mimic by tandem ring closing metathesis.

replaced by ethene moieties. Furthermore, RCM is being extended to “double” RCM for covalent control of shape by preparation of mimics of “multiple-side chain knot-  
 tied” peptide derived compounds of which vancomycin is an outstanding example. This may lead to entirely new peptidic molecules, in this case vanco-mimics possibly possessing cavity or shell-like structures, which might resemble the crucial parts of the glycopeptide antibiotics.

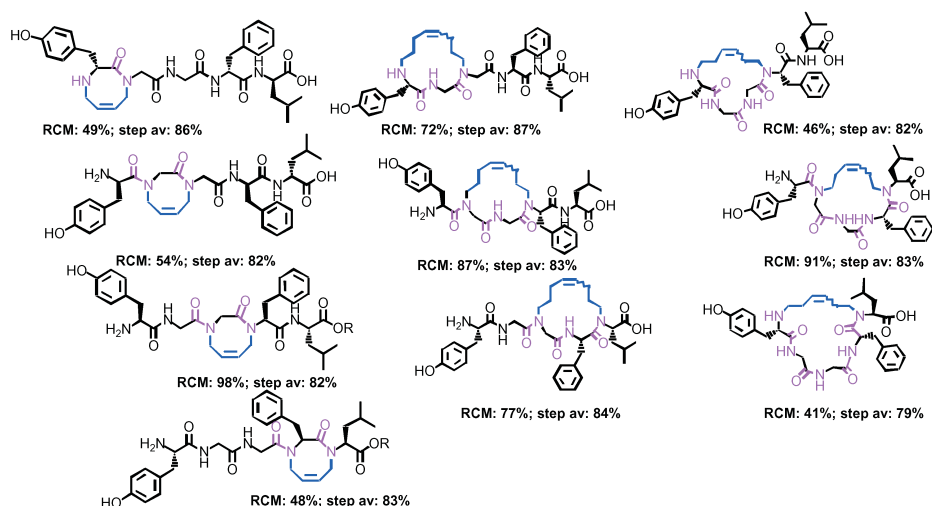


Fig. 2. All possible loop-containing Leu-enkephalin derivatives obtained by RCM [3].

### Acknowledgments

These investigations were supported by the Council for Chemical Sciences of the Netherlands Organization for Scientific Research (CW-NWO) with financial aid from The Netherlands Technology foundation.

### References

1. Reichwein, J.F., Liskamp, R.M.J. *Tetrahedron Lett.* **39**, 1243–1246 (1998).
2. Reichwein, J.F., Liskamp, R.M.J. *Eur. J. Org. Chem.* 2335–2344 (2000).
3. Reichwein, J.F., Wels, B., Kruijtzter, J.A.W., Versluis, C., Liskamp, R.M.J. *Angew. Chem., Int. Ed.* **38**, 3684–3687 (1999).
4. Reichwein, J.F., Versluis, C., Liskamp, R.M.J. *J. Org. Chem.* **65**, 6187–6195 (2000).

## New Synthetic Routes to NEtXaa<sup>4</sup>-Cyclosporin Derivatives as Potential Anti-HIV Drugs

T. Muamba, F. Hubler, J.-F. Guichou, L. Patiny, T. Rückle, L. Brunner,  
 R. Wenger and M. Mutter

*Institute of Organic Chemistry, University of Lausanne, CH-1015 Lausanne, Switzerland*

### Introduction

Since the discovery of the immunosuppressive activity of Cyclosporin A (CsA), considerable work has been devoted to the chemical synthesis of analogues. More recently, the finding of potential anti-HIV I activity of CsA evoked interest for the design of more selective cyclosporins active against HIV I but devoid of immunosuppressive activity. Based on previous observations that a *N*-methyl group at residue 4 is involved in one of the main metabolic degradation pathways [1], the synthesis of CsA analogues disposing various *N*-ethyl substituted residues at position 4 appeared particularly appealing for developing potential anti-HIV drugs [2]. Here we present the synthesis of new NEtXaa<sup>4</sup>CsA derivatives and their biological activities.

### Results and Discussion

Peptide 1 (Figure 1) was synthesized from CsA using described procedures [2]. The reactive site of **1** was inverted to **2** by Boc-protection of the N-terminal group (step i) and saponification at the C-terminus (ii). Subsequent activation (HATU) of **2** and coupling to the C-protected *N*-ethyl amino acid [3] (iii), resulted after N- and C-terminal deprotection (iv) in the linear precursor **3**. Cyclization (1 h) applying TFFH as coupling agent in the presence of a weak base (v) proceeded in good yields without observable epimerisation. Finally, methanolysis of the acetate protecting group (vi) gave the corresponding CsA analogues **4a–g** (Table 1) in overall yields of 15 to 46%.

*In vitro* activities of cyclosporin derivatives **4a–g** were evaluated applying the IL-2 reporter gene assay (measuring immunosuppressive activity in detecting substances interfering with IL-2 gene activation along the T cell signalling pathway [4]) and the binding affinity to CypA using the improved spectrophotometric assay described by Kofron *et al.* [5]. The results (Table 1) indicate that the synthetic cyclosporin *N*-ethyl<sup>4</sup> derivatives **4a–g** show comparable binding affinities but strongly reduced immunosuppressive activities compared to CsA. In particular, compound **4b**, **4f** and **4g**

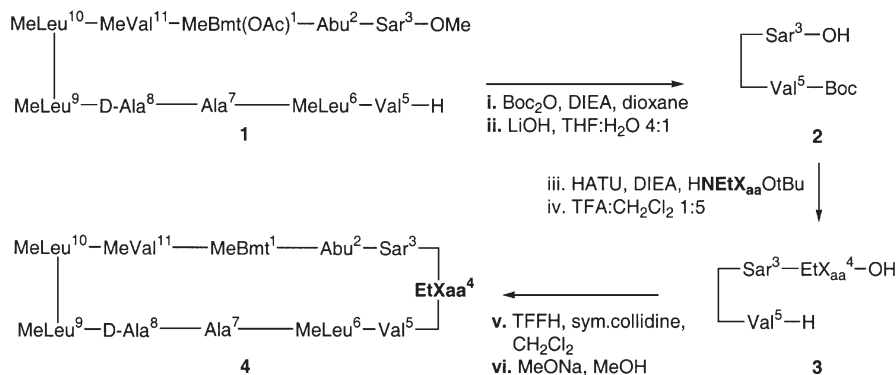


Fig. 1. Reaction scheme for the synthesis of NEtXaa<sup>4</sup>-CsA.

Table 1. Characterisation and biological activities of CsA analogues.

Product <b>4</b>	Yield %	HPLC t <sub>R</sub> min	Mass m/z [M+H] <sup>+</sup> (theor.)	CyP-A IC <sub>50</sub> /IC <sub>50</sub> CsA	IL2-RGA IC <sub>50</sub> /IC <sub>50</sub> CsA
(a) NEtLeu <sup>4</sup> CsA	32	25.8	1217.2 (1215.9)	1.2	1.6
(b) NEtVal <sup>4</sup> CsA	46	23.1	1203.3 (1201.8)	0.67	>1200
(c) NEtIle <sup>4</sup> CsA	30	25.1	1217.2 (1215.9)	0.83	~300
(d) NEtPhe <sup>4</sup> CsA	33	23.8	1251.6 (1249.8)	1.30	28
(e) NEtCmp <sup>4</sup> CsA	15	22.5	1308.9 (1307.8)	n.d.	>2500
(f) NEtCmp(Me) <sup>4</sup> CsA	17	29.1	1323.9 (1321.9)	0.6	>2500
(g) NEtPmp(Me) <sup>4</sup> CsA	31	23.2	1373.1 (1371.8)	0.37	>2500

*Cmp*: *p*-carboxymethyl-*L*-phenylalanine; *Cmp(Me)*: *p*-carbomethoxymethylphenylalanine; *Pmp(Me)*<sub>2</sub>: 4-[(*O,O'*-dimethyl)phenylmethyl]phenylalanine.

may serve as lead for the design of non-immunosuppressive cyclosporins with potential anti-HIV activity.

### Acknowledgments

This work was supported by the Swiss National Science Foundation.

### References

1. Wenger, R., Martin, K., Timbers, C., Tromelin, A. *Chimia* **46**, 314 (1992).
2. Hubler, F., Rückle, T., Patiny, L., Muamba, T., Guichou, J.-F., Mutter, M., Wenger, R. *Tetrahedron Lett.* **41**, 7193 (2000).
3. Rückle, T., Dubray, B., Hubler, F., Mutter, M. *J. Peptide Sci.* **5**, 56 (1999).
4. (a) Baumann, G., Zenke, G., Wenger, R., Hiestand, P., Quesniaux, V., Andersen, E., Schreier, M. *J. Autoimmun.* **5**, 67 (1992). (b) Mattila, P.S., Ullman, K.S., Fiering, S., Emmel, E.A., McCutcheon, M., Crabtree, G.R., Herzenberg, L.A. *EMBO J.* **9**, 4425 (1990).
5. (a) Kofron, J.L., Kuzmic, P., Kishore, V., Colon-Bonilla, E., Rich, D.H. *Biochemistry* **30**, 6127 (1991). (b) Kofron, J.L., Kuzmic, P., Kishore, V., Gemmecker, G., Fesik, S.W., Rich, D.H. *J. Am. Chem. Soc.* **114**, 2670 (1992).

## Transition Metal Complexes of Linear and Cyclic Pseudopeptides

Siegmund Reissmann<sup>1</sup>, Sebastian Künzel<sup>1</sup>, Regina Reissmann<sup>1</sup>,  
Susanne Nolden<sup>1</sup>, Georg Greiner<sup>1</sup>, Inge Agricola<sup>1</sup>, Dietmar Strehlow<sup>1</sup>,  
Wolfgang Poppitz<sup>2</sup>, Raiker Witter<sup>3</sup> and Ulrich Sternberg<sup>3</sup>

<sup>1</sup>*Institute of Biochemistry and Biophysics*

<sup>2</sup>*Institute of Inorganic and Analytical Chemistry*

<sup>3</sup>*Institute of Optics and Quantum Electronics, Friedrich-Schiller-University Jena,  
D-07743 Jena, Germany*

### Introduction

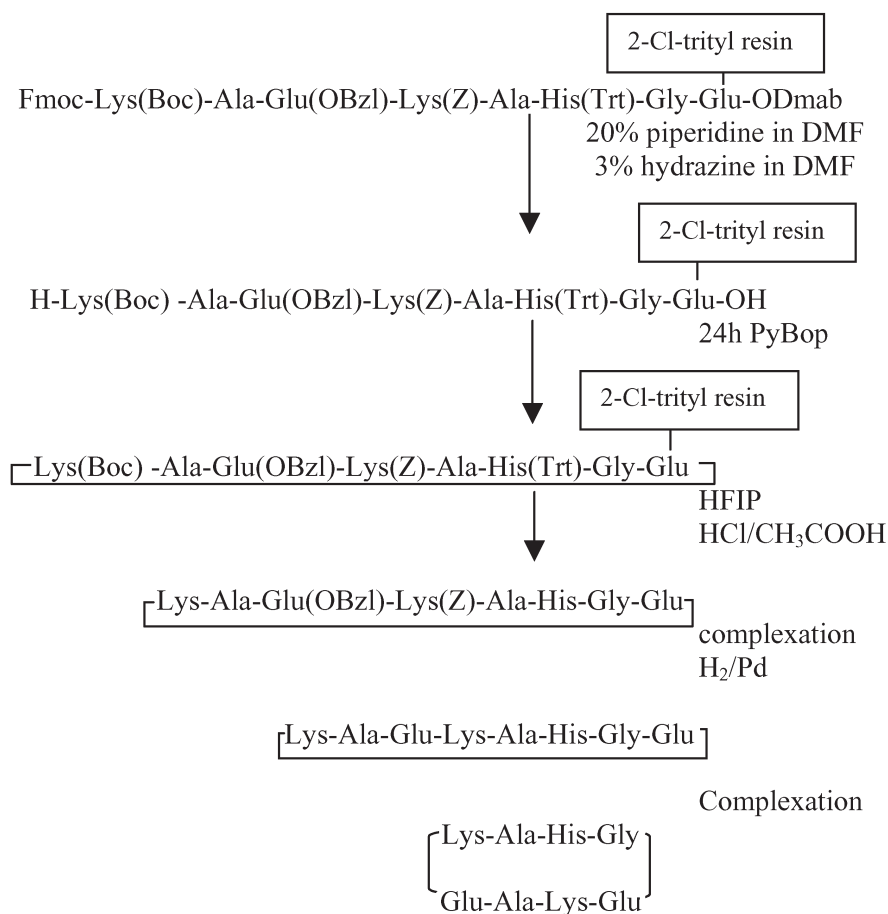
Many enzymes require metal ions for substrate binding and product formation. In order to study the complexation of transition metal ions and the possible catalytic activities of the formed complexes, we synthesized linear and cyclic pseudopeptides and peptides with different sequences and sizes. We are interested in testing and improving the modeling program COSMOS<sup>TM</sup>. Therefore, all synthesized structures are in advance conformationally designed for complexation of certain metals. Some metalloenzymes contain two or more metal ions. Therefore an octapeptide with two different chelating centers was designed for complexation of Ni<sup>++</sup> and Co<sup>++</sup>. We were interested in developing a synthetic strategy for the assembly of homo and hetero dinuclear metal complexes of this cyclic peptide. Complexation of metal ions and subsequent polarization of the complex bound water are assumed to be prerequisites for catalytic hydrolysis of carbonic or phosphoric acid esters.

### Results and Discussion

The pseudotripeptide Bz-His-N(CH<sub>2</sub>-CH<sub>2</sub>-NH<sub>2</sub>)Gly-His-NH<sub>2</sub> (**1**), the pseudohexapeptide cyclo[His-Lys-N(CH<sub>2</sub>-CH<sub>2</sub>-NH<sub>2</sub>)Gly-βAla-N(CH<sub>2</sub>-CH<sub>2</sub>-NH<sub>2</sub>)Gly-Gly] (**2**) and the cyclic octapeptide cyclo[Lys-Ala-His-Gly-Glu-Lys-Ala-Glu] (**3**) were assembled on solid support. *N*-Aminoalkyl peptide bonds were synthesized on the resin according to Zuckerman [3] or preformed in solution as dipeptide building units [4]. Cyclization on the resin provided better yield and purity than in solution. The developed synthetic strategy for the cyclic octapeptide **3** (Scheme 1) might allow the selective and consecutive deprotection of both chelating centers and by this way the formation of homo- and heterodinuclear complexes. The linear pseudotripeptide **1** forms complexes with Zn<sup>++</sup>, Cu<sup>++</sup>, Ni<sup>++</sup>, Co<sup>++</sup> and Mn<sup>++</sup> as estimated by ESI-MS [1]. Semiquantitative estimation of complex stabilities by ESI-MS gave the same rank order as more generally reported by Irving and Williams for other chelate complexes of bivalent transition metal ions [2]. The linear as well as the cyclic pseudohexapeptide **2** are able to form complexes with certain bivalent transition metal ions, but the cyclic peptide forms complexes more selectively and shows a stronger preference for Ni<sup>++</sup>. This finding agrees well with the ion preference designed by the program COSMOS<sup>TM</sup> [5]. Complexation can be characterized quantitatively by potentiometric titration and by CD-measurements. The different shapes of the CD curves depend significantly on the metal ligand interaction. It could be shown that the affinity of ligand **1** to Zn<sup>++</sup>, Co<sup>++</sup> and Cu<sup>++</sup> is much higher than to Ni<sup>++</sup>. Depending on the metal ions, the complexes hydrolyze *p*-nitrophenyl acetate, bis[*p*-nitrophenyl phosphate], and DNA. The found "catalytic" activities can be correlated neither to complex formation tendency nor to the acidity of the complex bound water. Some of our complexes are more active than

## Synthetic Methods

the corresponding cyclen analogs [6]. Generally, the phosphate esters were hydrolyzed with lower activity than carbonic acid esters.



Scheme 1. Synthesis of a dinuclear cyclic octapeptide complex.

## Acknowledgments

Financial support by the Deutsche Forschungsgemeinschaft (Collaborative Research Center 436, Jena, Germany) is gratefully acknowledged.

## References

1. Greiner, G., Seyfarth, L., Poppitz, W., Witter, R., Sternberg, U. *LIPS* **7**, 133 (2000).
2. Seyfahrt, L., Greiner, G., Poppitz, W., Keutel, H. *LIPS*, submitted.
3. Zuckerman, R.N., Kerr, J.M., Kent, S., Moss, W.H. *J. Am. Chem. Soc.* **114**, 10646 (1992).
4. Müller, B., Besser, D., Kleinwächter, P., Arad, O., Reissmann, S. *J. Peptide Res.* **54**, 383 (1999).
5. Sternberg, U., Koch, F.T., Möllhof, M.J. *J. Comput. Chem.* **15**, 542 (1994).
6. Kimura, E., Hashimoto, H., Koike, T. *J. Am. Chem. Soc.* **118**, 10963 (1996).

## **An Efficient Synthesis of Integrin Antagonists *cyclo(-RGDfK-)*, *cyclo(-GRGDfK-)* and Their Conjugates with MAG3 Chelate**

**Vladimir V. Samukov<sup>1</sup>, Pavel I. Pozdnyakov<sup>1</sup>, Aydar N. Sabirov<sup>1</sup>,  
Irina M. Bushueva<sup>1</sup>, Paul O. Zamora<sup>2</sup> and Prantika Som<sup>2</sup>**

<sup>1</sup>*SRC VB Vector, Koltsovo, Novosibirsk reg. 630559, Russia*

<sup>2</sup>*Medical Department of Brookhaven National Laboratory, Upton, NY 11973, USA*

### **Introduction**

Cyclic RGD-containing peptides are selective antagonists of integrins, proteins that play important roles in cell-cell and cell-matrix interactions. In a suitably labeled form, these peptides may serve as useful tools for diagnostic imaging and peptide targeted therapy of some types of cancer. Cyclo(-RGDfK-) developed by Kessler *et al.* [1] is a very promising compound for this purpose, because it exhibits highly selective and potent binding to  $\alpha_v\beta_3$  integrin receptors and at the same time contains a free amino group, which can be employed safely for appending labels of various nature. This cyclopeptide receives considerable attention, and several solid phase synthetic schemes for its preparation have been developed very recently [2,3].

### **Results and Discussion**

We have elaborated a liquid phase synthetic approach to cyclo(-RGDfK-), to its six-membered analog cyclo(-GRGDfK-), and to their conjugates with mercaptoacetyl-triglycine (MAG3), a chelating arm capable of binding Re and Tc isotopes. Our scheme is based on the use of H-Arg-Gly-Asp(OBzl)-OPse, a tripeptide containing the differentially protected C-terminal Asp residue as a common intermediate for preparing linear penta- and hexapeptide precursors by the elongation from the free N-terminus. Orange colored  $\alpha$ -[2-(4-phenylazo)benzylsulfonyl]ethyl (Pse) ester can be selectively cleaved in the presence of  $\beta$ -Bzl ester by 30% piperidine or 2 eq. DBU in DMF [4], thus releasing an  $\alpha$ -carboxyl group for subsequent cyclization.

The key tripeptide has been prepared by coupling H-Asp(OBzl)-OPse with Boc-Arg-Gly-OH followed by removal of the Boc-group. Protected penta- and hexapeptides have been synthesized by a step-wise method; selective removal of Pse-group with DBU/DMF and subsequent elimination of Boc-protection have led to linear precursors with free  $\alpha$ -amino and carboxyl groups, H-D-Phe-Lys(Z)-Arg-Gly-Asp(OBzl)-OH and H-D-Phe-Lys(Z)-Gly-Arg-Gly-Asp(OBzl)-OH. The linear peptides have been cyclized with BOP/HOBt in diluted DMF solution, then subjected to low pressure reversed-phase preparative chromatography, giving protected cyclic peptides in 70–80% isolated yields. Hydrogenolysis on Pd/C has led to pure target cyclo(-RGDfK-) and cyclo(-GRGDfK-), which have been further coupled with S-Trt-MAG3 hydroxysuccinimide ester through the only available  $\epsilon$ -amino group of Lys residue. Cleavage of S-Trt group with TFA/triisopropylsilane provides the desired peptide-chelate conjugates in a stable water-soluble form suitable for immediate isotope labeling (Figure 1). The developed synthetic scheme allows for the simple preparation of gram amounts of pure cyclopeptides and conjugates. The evaluation of the metal-loaded peptide-chelate conjugates in scintigraphic imaging is now in progress.

In conclusion, the designed tripeptide intermediate may be conveniently employed for synthesizing not only the cyclopeptides described above but also a wide variety of other cyclic RGD-peptides.

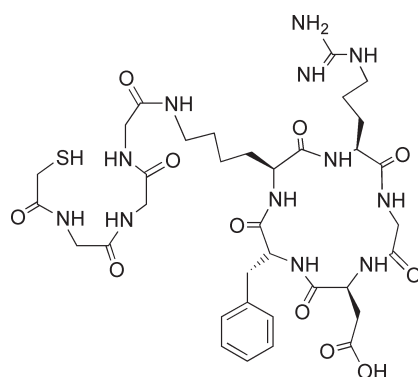


Fig. 1. Structure of cyclo(-RGDfK-)-MAG3 conjugate.

### Acknowledgments

This work is supported by IPP Grant # BNL-T1-0031-RU.

### References

1. Haubner, R., Gratias, R., Diefenbach, B., Goodman, S.L., Jonczyk, A., Kessler, H. *J. Amer. Chem. Soc.* **118**, 7461–7472 (1996).
2. Dai, X., Su, Z., Liu, J.O. *Tetrahedron Lett.* **41**, 6295–6298 (2000).
3. Boturn, D., Dumy, P. *Tetrahedron Lett.* **42**, 2787–2790 (2001).
4. Samukov, V., Kalashnikov, V., Ofitserov, V., Shevalier, A. *Zh. Obshch. Khimii (Rus)* **59**, 703–711 (1989).

## **Design and Synthesis of Cyclic Peptide Antagonists Intended to Block Coactivator Binding to Steroid Nuclear Receptors**

**Anne-Marie Leduc<sup>1</sup>, Kelli S. Bramlett<sup>2</sup>, Thomas P. Burris<sup>2</sup>  
and Arno F. Spatola<sup>1</sup>**

<sup>1</sup>*Department of Chemistry and of Biochemistry and Molecular Biology and the Institute for Molecular Diversity and Drug Design, University of Louisville, Louisville, KY 40292, USA*

<sup>2</sup>*Lilly Research Laboratories, Indianapolis, IN 46285, USA*

### **Introduction**

Estrogen Receptor (ER), a member of the nuclear receptor superfamily, is involved in various diseases, including breast cancer. A widely used estrogen antagonist, tamoxifen, binds to ER in the steroid-binding pocket in place of estrogen. It induces a conformational change within the receptor, such that coactivators can no longer bind to ER, thereby potentially blocking transcription.

In contrast normal ligand binding causes a displacement of ER helix 12, exposing a region on ER that can bind a consensus LXXLL pentapeptide sequence [1]. This motif, known as the NR box, is found on approximately 20 coactivators isolated to date [2]. Following the discovery of the NR box, genetic experiments, phage display libraries, and X-ray studies have revealed further insights into the mechanism of LXXLL binding and suggest a new approach for drug design by targeting the coactivator/ER interaction directly [3].

### **Results and Discussion**

To mimic the coactivator structure, the NR box peptides have to be  $\alpha$ -helical, and short peptides generally are not. To increase their  $\alpha$ -helicity, we considered using either disulfide constraints [4] between the side chain of two cysteines at the *i* and *i*+3 positions, or lactam bridges [5] between *i* and *i*+4 residues. Next, molecular dynamics was performed using MacroModel [6] version 7.0 on an SGI workstation in order to evaluate the ability of the peptides to mimic the coactivator structure. The calculations were carried out at 300 K, with the AMBER\* Force Field and the GB/SA solvation model. Each structure was superimposed with a truncated version of the coactivator [7]. The best fit came from one of the disulfide bridged peptides.

The peptides that provided the more compelling computer fits were synthesized by Boc-based solid phase synthesis, using Boc-D- and L-Cys(MeB) for the disulfide analog. The peptide was deprotected and cleaved from the resin by HF and the ring formed *via* DMSO oxidation in solution [8]. For the lactam bridge, the Lys(Fmoc) and Asp(OFm) residues were removed by piperidine treatment, and side chain to side chain cyclization was effected with BOP/HOBt. Circular dichroism of the peptides suggested a partial  $\alpha$ -helical behavior for the disulfide derivatives in 7 and 20% TFE, but none of the peptides appeared to be helical in water. Table 1 contains a partial listing of constrained peptides prepared as novel ER antagonists. Using a time resolved fluorescence competition assay *vs* a linear 14-mer [9], the cyclic peptides show a significant improvement with IC<sub>50</sub> values <50 nM over their linear counterparts.

This is the first step in the design of a class of drugs that would interfere with ER/coactivator interactions, and that have potential applications in a variety of disease states including breast cancer and prostate tumors.

Table 1. LXXLL Analogs and  $IC_{50}$  values in an  $ER_{\alpha}$  competition binding assay.

Structure	$IC_{50}$ ( $\mu$ M)	MW
H-Lys-Lys-Ile-Leu-His-Arg-Leu-Leu-Gln-NH <sub>2</sub>	0.30	1147.7
H-Leu-Glu-Gln-Leu-Leu-OH	499	614.3
H-Lys-His-Lys-Ile-Leu-His-Arg-Leu-Leu-Gln-Asp-Ser-Ser-OH	0.41	1573.9
H-Lys-Glu-Ile-Leu-Arg-Lys-Leu-Leu-Gln-NH <sub>2</sub> <div style="margin-left: 40px;"> <math>\begin{array}{c}   \qquad \qquad   \\ \text{CO-NH} \end{array}</math> </div>	0.38	1120.6
H-Lys-D-Cys-Ile-Leu-Cys-Arg-Leu-Leu-Gln-NH <sub>2</sub> <div style="margin-left: 40px;"> <math>\begin{array}{c}   \qquad \qquad   \\ \text{S} \text{ ————— } \text{S} \end{array}</math> </div>	0.035	1085.9
Ac-Lys-D-Cys-Ile-Leu-Cys-Arg-Leu-Leu-Gln-NH <sub>2</sub> <div style="margin-left: 40px;"> <math>\begin{array}{c}   \qquad \qquad   \\ \text{S} \text{ ————— } \text{S} \end{array}</math> </div>	0.15	1127.9
H-Aib-Lys-D-Cys-Ile-Leu-Cys-Arg-Leu-Leu-Gln-NH <sub>2</sub> <div style="margin-left: 40px;"> <math>\begin{array}{c}   \qquad \qquad   \\ \text{S} \text{ ————— } \text{S} \end{array}</math> </div>	0.32	1170.9
Guanidyl-Lys-D-Cys-Ile-Leu-Cys-Arg-Leu-Leu-Gln-NH <sub>2</sub> <div style="margin-left: 40px;"> <math>\begin{array}{c}   \qquad \qquad   \\ \text{S} \text{ ————— } \text{S} \end{array}</math> </div>	0.29	1183.9

## References

1. Heery, D.M., Kalkhoven, E., Hoare, S., Parker, M.G. *Nature* **387**, 733–736 (1997).
2. Klinge, C.M. *Steroids* **65**, 227–251 (2000).
3. Norris, J.D., Paige, L.A., Christensen, D.J., Chang, C.-Y., Huacani, D.F., Hamilton, P.T., Fowlkes, D.M., McDonnell, D.P. *Science* **285**, 744–746 (1999).
4. Jackson, D.Y., King, D.S., Chmielewski, J., Singh, S., Schultz, P.G. *J. Am. Chem. Soc.* **113**, 9391–9392 (1991).
5. Campbell, R.M., Bongers, J., Felix, A.M. *Biopolymers* **37**, 67–88 (1995).
6. Mohamadi, F., Richards, N.G.J., Guida, W.C., Liskamp, M., Caufield, C., Chang, G., Hendrickson, T., Still, W.C. *J. Comput. Chem.* **11**, 440–467 (1990).
7. Shiau, A.K., Barstad, D., Loria, P.M., Cheng, L., Kushner, P.J., Agard, D.A., Greene, G.L. *Cell* **95**, 927–937 (1998).
8. Tam, J.P., Wu, C.-R., Liu, W., Zhang, J.-W. *J. Am. Chem. Soc.* **113**, 6657–6662 (1991).
9. Bramlett, K.S., Wu, Y., Burris, T.P. *Mol. Endocrinol.* **15**, 909–922 (2001).

## A Novel Design and Synthesis of Bicyclic Peptide Library

Ying Sun<sup>1</sup>, Guishen Lu<sup>1</sup> and James P. Tam<sup>2</sup>

<sup>1</sup>*Institute of Materia Medica, Chinese Academy of Medical Sciences and Peking Union Medical College, Beijing 100050, China*

<sup>2</sup>*Department of Microbiology and Immunology, Vanderbilt University, Nashville, TN 37232-2363, USA*

### Introduction

A significant aspect of combinatorial chemistry is its ability to generate a peptide library for studying specific interactions such as antibody-antigen, enzyme-substrate/inhibitor as well as receptor-ligand. Generally, the diversity of a peptide library is achieved by altering the building blocks of a parent peptide or template [1]. This method aims at creating a collection of building-block-based diversity with the same scaffold. However, methods to create collections of structure-based diversity with a large number of different scaffolds remain a challenge. Cyclic peptides due to their end-to-end constraints are increasingly used in drug discovery to achieve enhanced receptor-binding affinity and selectivity, improved bioavailability and metabolic stability [2]. Here we report a strategy to increase a multi-level structure-based diversity of cyclic peptide library by a thioester cyclization method [3].

### Results and Discussion

To demonstrate our strategy, a series of cyclic peptide libraries containing two cysteines at different positions were designed based on a TNF $\alpha$  antagonist [4]. This strategy can efficiently increase the diversity of the library in three levels (Figure 1). The first-level library of end-to-end cyclic peptides with free thiol side chains can be obtained by a previously described intramolecular thioester ligation of the linear peptide precursors containing an N-terminal cysteine and a C-terminal thioester [3,5,6]. The second-level library of side-chain modified cyclic peptides is achieved directly by

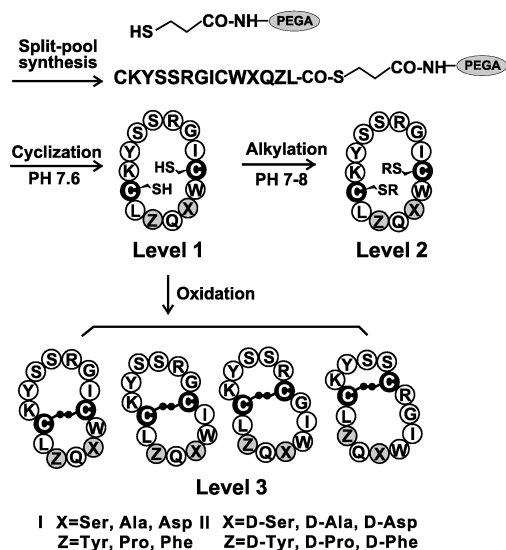


Fig. 1. Design and synthesis of bicyclic peptide libraries.

alkylation of the free thiols of the first-level library. The third-level library can be achieved by the DMSO-mediated oxidation of free thiols of the first-level library to form an intramolecular disulfide bond and a bicyclic structure.

By varying substitutions with three different amino acids in two positions (I: X = Ser, Ala, Asp, Z = Tyr, Pro, Phe; II: X = D-Ser, D-Ala, D-Asp, Z = D-Tyr, D-Pro, D-Phe), the first-level library containing nine different end-to-end cyclic peptides was obtained. Previously, we have optimized both off-resin and on-resin thioester cyclization to afford quantitatively monocyclic peptides. Further, we demonstrated that no dimer or oligomer was observed [7]. Thus, the efficient thioester cyclization was used for our on-resin synthesis of cyclic peptide library. The peptide synthesis was performed by a split-pool method on PEGA resin using Boc/Bzl chemistry. After deprotection of side chain with HF, the subsequent on-resin thioester cyclization was carried out in a 6 M guanidine-HCl solution buffered with 0.2 M Tris-HCl at pH 7.6. The cyclic peptides were simultaneously cleaved from the resin and released into the solution. Nine compounds of each library were identified by HPLC and MALDI-MS after desalting the guanidine-HCl.

The second-level library of side-chain-modified peptides was obtained by thiol alkylation of the first-level library. The modification of thiol groups of the first-level library with CH<sub>3</sub>I was successfully obtained in high yield based on the thioalkylation of single peptides performed in a 6 M guanidine-HCl solution at pH 7 to 8. Similar condition was then used for the thioalkylation of a library using CH<sub>3</sub>I, ICH<sub>2</sub>CO<sub>2</sub>H, ICH<sub>2</sub>CONH<sub>2</sub> and ICH<sub>2</sub>CN as alkylation agents, respectively. The side-chain modified library was characterized by HPLC and MALDI-MS.

The third-level library of bicyclic peptides was obtained by oxidation of the thiol groups of the first-level library. The oxidation was carried out in 20% DMSO aqueous buffers at pH 5 to 6 [7]. The intramolecular disulfide bond in each bicyclic peptide provides an additional conformational constraint. Furthermore, altering the positions of the disulfide bonds resulted in various shaped bicyclic peptides.

In conclusion, a strategy that efficiently increases the diversity of cyclic peptide libraries in multiple levels has been developed based on the synthetic efficiency of the thioester cyclization, alkylation and oxidation to generate three levels of cyclic peptides with high chemoselective control. The structure-based cyclic peptide library is useful to explore the structure-activity relationship in drug discovery. Moreover, this methodology developed for the shaped bicyclic peptide libraries with different spatial structures can be used directly for screening by various bioassays to distinguish different receptor binding affinity and selectivity.

### Acknowledgments

This work was supported in part by U.S. Public Health Service Grants CA36544 and AI46164.

### References

1. Lam, K.S., Lebl, M., Krchňák, V. *Chem. Rev.* **97**, 411–448 (1997).
2. Shan, D., Nicolaou, M.G., Borchardt, R.T., Wang, B. *J. Pharm. Sci.* **86**, 765–768 (1997).
3. Zhang, L.S., Tam, J.P. *J. Am. Chem. Soc.* **119**, 2363–2370 (1997).
4. Takasaki, W., Kajino, Y., Kajino, K., Murali, R., Greene, M.I. *Nat. Biotechnol.* **15**, 1266–1270 (1997).
5. Tam, J.P., Lu, Y.-A. *Protein Sci.* **7**, 1583–1592 (1998).
6. Zhang, L.S., Tam, J.P. *J. Am. Chem. Soc.* **121**, 3311–3320 (1999).
7. Sun, Y., Lu, G.S., Tam, J.P. *Org. Lett.* **3**, 1681–1684 (2001).

## Strategies for the Synthesis of Cyclic Peptides

Ashok Khatri<sup>1</sup>, Nicholas P. Ambulos<sup>2</sup>, Steven A. Kates<sup>3</sup>,  
Katalin F. Medzihradzsky<sup>4</sup>, George Ösapay<sup>5</sup>, Henriette Remmer<sup>6</sup>  
and Arpad Somogyi<sup>7</sup>

<sup>1</sup>Massachusetts General Hospital, Boston, MA 02114, USA

<sup>2</sup>University of Maryland at Baltimore, Baltimore, MD 21201, USA

<sup>3</sup>Consensus Pharmaceuticals, Inc., Medford, MA 02155, USA

<sup>4</sup>University of California, San Francisco, CA 94143, USA

<sup>5</sup>University of California, Irvine, CA 92697, USA

<sup>6</sup>University of Illinois, Urbana, IL 61801, USA

<sup>7</sup>University of Arizona, Tucson, AZ 85721, USA

### Introduction

The Peptide Synthesis Research Group (PSRG) of the Association of Biomolecular Research Facilities (ABRF) conducts annual studies to help member laboratories evaluate their synthesis abilities as well as introduce new methods. This year's study focuses on the construction of a "head-to-tail" cyclic peptide in which an amide bond is formed between the amino and carboxyl termini of a linear precursor. Cyclic peptides may exhibit improved metabolic stability, increased potency, better receptor selectivity and more controlled bioavailability as a variety of biological studies have suggested.

In an effort to introduce member laboratories to this technique, the PSRG prepared and characterized a peptide sequence derived from the autophosphorylation site of the tyrosine kinase, pp<sup>60c-src</sup> [1]:

*cyclo*(Tyr-Glu-Ala-Ala-Arg-DPhe-Pro-Glu-Asp-Asn)

*cyclo*(YEAARfPEDN) may be prepared completely *via* solid-phase techniques [2] by the following protocol: a) side-chain anchoring of a trifunctional residue [Glu,Asp,Asn] to a solid support in which the  $\alpha$ -carboxylic acid incorporates an *orthogonal* semi-permanent protecting group [allyl,Dmab]; b) standard chain elongation; c)  $\alpha$ -carboxylic acid protecting group removal at the C-terminus; d)  $N^\alpha$ -protecting group removal; e) cyclization; f) cleavage. Member laboratories were requested to assemble this peptide by a method of their choice and submit the crude product without purification.

In order to obtain the peptide standard, the PSRG synthesized the model peptide commencing with side-chain anchoring Fmoc-Asp(OH)-ODmab [3] to Fmoc-PAL-PEG-PS resin. After linear assembly of the sequence and  $N^\alpha$ -Fmoc deprotection, the removal of Dmab protecting group was accomplished by hydrazine-DMF (1 : 49, v/v) treatment for 5 min. Complete on resin cyclization was achieved with two consecutive treatments with PyBOP/HOBt/DIEA (1 : 1 : 2, 5 equiv.) in DMF for 6 and 18 h and HATU/HOAt/DIEA (1 : 1 : 1.5, 4 equiv.) in DMF for additional 24 h as judged by ninhydrin test. Release of the product from the solid support with concomitant side-chain protecting group removal was accomplished with TFA-H<sub>2</sub>O (9.5 : 0.5) for 2 h at 25 °C followed by precipitation with *tert*-butyl methyl ether.

## Results and Discussion

The member laboratories submitted sixteen samples. The PSRG evaluated each sample by amino acid analysis, capillary electrophoresis, RP-HPLC, MALDI-TOF/MS, and ESI/MS, as described previously [4]. Below is a summary of the results.

1. Most samples contained the desired product. One participant modified the sequence intentionally and substituted Asn<sup>10</sup> with Gln.

2. The purity range was 6–98% and 9–93% by HPLC and capillary electrophoresis analysis, respectively.

3. The peptide content by amino acid analysis varied between 60–94%.

4. The method used by eleven laboratories was similar to that described by the PSRG. Three of these samples contained less than 25% of the desired peptide.

5. Two laboratories used a strategy of side-chain anchoring Fmoc-Asp(OH)-OAl to PAL-PEG-PS resin as the initial support. The quality of these peptides was excellent.

6. One laboratory used a Boc/Bzl/Fm strategy and prepared the peptide in high purity.

7. Cyclization times were between 2–48 h.

8. A variety of coupling reagents was used for ring closure. Many of the laboratories that incorporated uronium-based coupling reagents (HATU, HBTU, TBTU) partially capped the amino terminus to form the tetramethylguanidine derivative [5].

9. Side products associated with removal of the Dmab group were observed. Elimination of the 4,4-dimethyl-2,6-dioxocyclohexylidene moiety occurred during the construction of the peptide to afford the 4-aminobenzyl ester of the C-terminal amino acid. The amino function was further converted to the corresponding tetramethylguanidine derivative upon exposure to uronium-based coupling reagents. Low energy CID analysis of these peptides clearly established where the modifications occurred, while the high accuracy mass measurements unambiguously confirmed the structures of these modifications [Medzihradszky, K.F., *et al.* manuscript submitted to *Lett. Peptide Sci.*].

*General conclusions.* (1) The participants synthesized the correct peptide albeit in a wide range of purity. Most of the laboratories selected a Fmoc/tBu/Dmab protecting group scheme; two participants incorporated a Fmoc/tBu/Allyl. Only one member used a Boc/Bzl/Fm strategy (HF final cleavage). (2) Phosphonium reagents (PyAOP, PyBOP, BOP) proved high efficiency in slow coupling reactions. (3) High resolution ESI/MS/MS was an extremely useful tool for the identification of novel side products in the submitted peptides.

## References

1. McMurray, J.S. *Tetrahedron Lett.* **32**, 7669 (1991).
2. Blackburn, C., Kates, S.A. *Methods Enzymol.* **289**, 175 (1997).
3. Chan, W.C., Bycroft, B.W., Evans, D.J. White, P.D. *J. Chem. Soc. Chem. Commun.* 2209 (1995).
4. Bonewald, L.F., Bibbs, L., Kates, S.A., Khatri, A., Medzihradszky, K.F., McMurray, J.S., Weintraub, S.T. *J. Peptide Res.* **53**, 161 (1999).
5. Story, S.C., Aldrich, J.V. *Int. J. Pept. Protein Res.* **43**, 292 (1994).

## Vinyl Sulfide Cyclized Analogues of Angiotensin II with High Affinity to the AT<sub>1</sub>-Receptor

Petra Johannesson<sup>1</sup>, Gunnar Lindeberg<sup>1</sup>, Gregory V. Nikiforovich<sup>2</sup>,  
 Anja Johansson<sup>1</sup>, Adolf Gogoll<sup>3</sup>, Anders Karlén<sup>1</sup> and Anders Hallberg<sup>1</sup>

<sup>1</sup>Department of Medicinal Chemistry, Uppsala University, SE-751 23 Uppsala, Sweden

<sup>2</sup>Department of Biochemistry and Molecular Biophysics, Washington University,  
 St Louis, MO 63110, USA

<sup>3</sup>Department of Organic Chemistry, Uppsala University, SE-751 21 Uppsala, Sweden

### Introduction

We have an interest in developing alternative methods for cyclization of peptides. The use of aldehyde precursors as building blocks for the synthesis of bicyclic Ang II analogues was previously reported by us [1,2]. We herein present the aldehyde precursor **1** and its use in a novel cyclization method, creating the vinyl sulfide bridged Ang II analogues **3** and **4** (Figure 1).

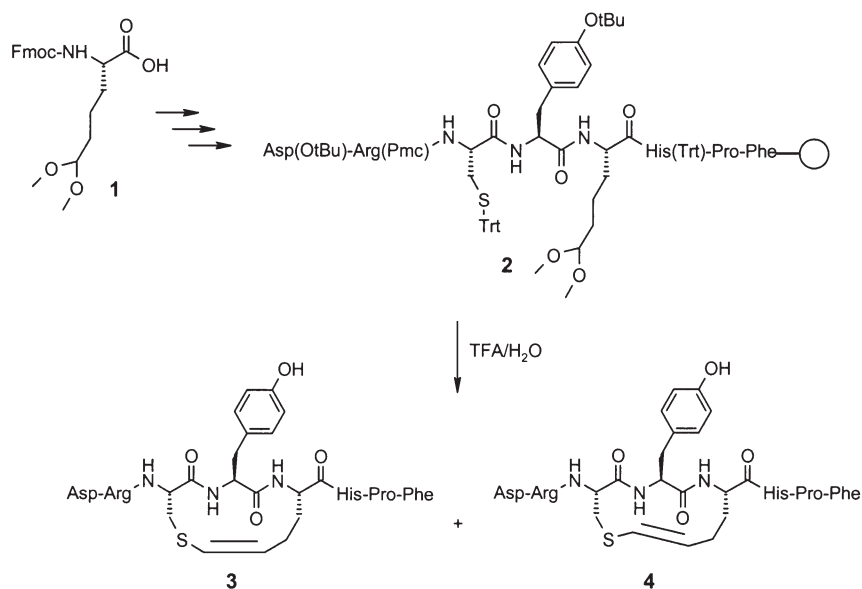


Fig. 1. A novel cyclization method, creating the vinyl sulfide bridged Ang II analogues **3** and **4**.

### Results and Discussion

The aldehyde precursor **1** was synthesized from 2-aminoadipic acid (Aad) and incorporated into precursor peptide **2** by standard solid phase peptide synthesis using Fmoc/*tert*-butyl protection. Cyclization of **2** was achieved by treatment with 95% TFA. The *cis*- (**3**) and *trans*- (**4**) analogues were formed in a ratio of 4 : 6 and in a total yield of 15%.

Ang II analogues **3** and **4** were both found to bind with high affinities to the AT<sub>1</sub>-receptor (Table 1).

*Table 1. In vitro AT<sub>1</sub>-receptor binding affinities (rat liver membranes). c[Hcy<sup>3,5</sup>]Ang II [3] was used as reference substance.*

Compound	K <sub>i</sub> (nM) ± SEM
Ang II	0.31 ± 0.08
c[Hcy <sup>3,5</sup> ]Ang II	0.23 ± 0.14
<b>3</b>	1.7 ± 0.26
<b>4</b>	1.7 ± 0.32

Conformational analysis showed that Ang II analogues **3** and **4** both possess low energy conformers compatible with suggested 3D models of Ang II in its bioactive conformation [4].

### Acknowledgments

We thank the Swedish Foundation for Strategic Research (SSF) for financial support.

### References

1. Johannesson, P., Lindeberg, G., Tong, W., Gogoll, A., Karlén, A., Hallberg, A. *J. Med. Chem.* **42**, 601–608 (1999).
2. Johannesson, P., Lindeberg, G., Tong, W., Gogoll, A., Synnergren, B., Nyberg, F., Karlén, A., Hallberg, A. *J. Med. Chem.* **42**, 4524–4537 (1999).
3. Spear, K.L., Brown, M.S., Reinhard, E.J., McMahon, E.G., Olins, G.M., Palomo, M.A., Patton, D.R. *J. Med. Chem.* **33**, 1935–1940 (1990).
4. See structure II, Table 2 in: Nikiforovich, G.V., Marshall, G.R. *Biochem. Biophys. Res. Commun.* **195**, 222–228 (1993).

## Strategies for the Synthesis of Novel Head-to-Side Chain Cyclic Peptides: Application to Dynorphin A Analogs

Balvinder S. Vig and Jane V. Aldrich

*Department of Pharmaceutical Sciences, School of Pharmacy, University of Maryland,  
 Baltimore, MD 21201, USA*

### Introduction

Although dynorphin A (Dyn A) is thought to be an endogenous ligand for kappa opioid receptors, it also exhibits high affinity for mu and delta opioid receptors [1]. The flexibility of Dyn A may be responsible for its lack of selectivity. A large number of side chain-to-side chain cyclic analogs of Dyn A have been synthesized in order to reduce its flexibility and increase its affinity and selectivity for  $\kappa$  receptors [see ref. 2 for a review]. Tyr<sup>1</sup> is one of the key pharmacophoric groups in Dyn A [3], but none of the cyclic analogs of Dyn A synthesized to date restrict the conformation of this important residue. Here we describe the synthesis of novel head-to-side chain cyclic analogs of Dyn A that constrain this important residue and retain a basic N-terminal amine (Figure 1).

The strategy described here provides a general methodology to synthesize novel head-to-side chain cyclic peptides.

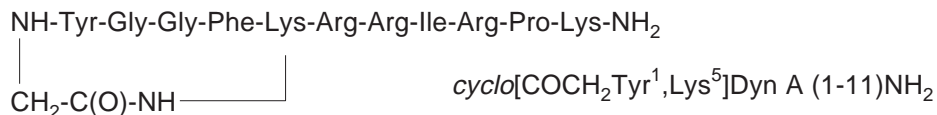


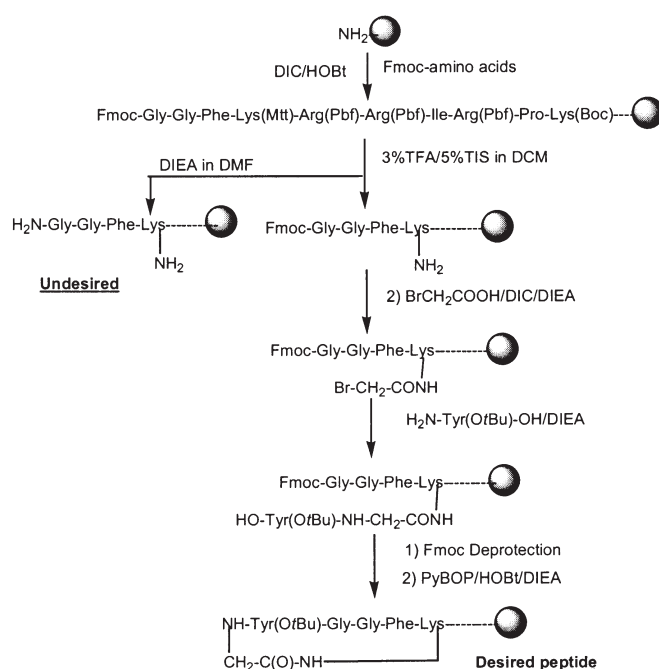
Fig. 1. A head-to-side chain cyclic analog of Dyn A.

### Results and Discussion

The peptide chain was assembled on a PAL-PEG-PS resin using Fmoc-protected amino acids. In the initial attempted syntheses of the novel cyclic peptide, the full-length protected linear peptide was assembled on the resin. Two variations of this synthetic strategy were evaluated. In the first approach, the side chain protecting group was first removed from Lys<sup>5</sup> and bromoacetic acid was coupled to the free N<sup>ε</sup>-amine. The next step involved deprotection of the N-terminal Fmoc group, followed by intramolecular alkylation of the N-terminal amine by the bromoacetyl group to yield the desired cyclic peptide. However, the deprotection of the N-terminal Fmoc group resulting in nucleophilic displacement of the bromine, yielding a piperidine derivative. Alternatively, the N-terminal amine could be deprotected first, followed by alkylation with bromoacetic acid. Subsequent deprotection of the side chain protecting group of Lys<sup>5</sup> yielded a free amine, and on resin cyclization was performed in an attempt to obtain the desired cyclic peptide. HPLC and MS analysis of final product, however, showed the presence of multiple peaks including the desired monosubstituted peptide, plus the dialkylated peptide and a cyclic imide side product. These side products presumably were formed during alkylation of the N-terminal amine by bromoacetic acid.

The successful strategy involved the synthesis of the protected linear peptide up through Gly<sup>2</sup> and functionalization through the N<sup>ε</sup>-amine of lysine (Scheme 1). Following deprotection of the lysine side chain protecting group (Mtt), neutralization with DIEA resulted in premature loss of the N-terminal Fmoc group, presumably due

to deprotection of the Fmoc group by the resulting deprotonated amine. This side reaction is very rapid, with 50% loss within 10 min of neutralization and complete loss of the Fmoc group on longer exposure. This is the first report of this side reaction during the selective deprotection of the Mtt protecting group. This side reaction can be very serious when selective deprotection of the N<sup>ε</sup>-amine protecting group of lysine is required in the presence of an N<sup>α</sup>-Fmoc group. To avoid this side reaction the base wash following Mtt deprotection was eliminated and in situ neutralization [4] was performed during the coupling of bromoacetic acid to the N<sup>ε</sup>-amine of lysine. The next step in the synthesis involved nucleophilic substitution of bromine by the free N<sup>α</sup>-amine of tyrosine. Subsequent Fmoc deprotection and on resin cyclization resulted in the desired cyclic peptide in high purity (>85% for the crude peptide). This scheme has been successfully utilized to synthesize various head-to-side chain analogs of Dyn A.



Scheme 1. Successful strategy for the synthesis of head-to-side chain cyclic Dyn A analogs.

The scheme described above can be used generally for the synthesis of a new class of head-to-side chain cyclic peptides that retain the basicity of the N-terminus.

#### Acknowledgments

This research was supported by NIDA grant DA05195.

#### References

1. Chavkin, C., Goldstein, A. *Proc. Natl. Acad. Sci. U.S.A.* **78**, 6543–6547 (1981).
2. Naqvi, T., Haq, W., Mathur, K.B. *Peptides* **19**, 1277–1292 (1998).
3. Turcotte, A., Lalonde, J., St-Pierre, S., Lemaire, S. *Int. J. Pept. Protein Res.* **23**, 361–367 (1984).
4. Schnolzer, M., Alewood, P., Jones, A., Alewood, D., Kent, S.B.H. *Int. J. Pept. Protein Res.* **40**, 180–193 (1992).

## Study on the Influence of Different Metal Ions on Cyclization of Linear Pentapeptides and Heptapeptide

Yun-hua Ye<sup>1</sup>, Mian Liu<sup>1</sup>, Yan-chun Tang<sup>1</sup> and Xiao-hui Jiang<sup>2</sup>

<sup>1</sup>Department of Chemistry, Peking University, Beijing, 100871, China

<sup>2</sup>Molecular Simulation Inc., San Diego, CA 92121, USA

### Introduction

A cyclopentapeptide, c(Gly-Pro-Tyr-Leu-Ala) (**I**) and a cycloheptapeptide c(Gly-Tyr-Gly-Gly-Pro-Phe-Pro) (**II**) were isolated and identified from a Chinese herb, *Stellaria yunnanensis* Franch (M). These two cyclic peptides have been synthesized successfully by an organophosphorus reagent, 3-(diethoxyphosphoryloxy)-1,2,3-benzotriazin-4(3H)-one (DEPBT) [1–3]. In order to improve yields of the cyclization, they were chosen as model cyclopeptides to study the influences of different metal ions on the ring closure. Three of their linear peptide precursors, H-Tyr-Leu-Ala-Gly-Pro-OH (**I-1**), H-Ala-Gly-Pro-Tyr-Leu-OH (**I-2**) and H-Gly-Tyr-Gly-Gly-Pro-Phe-Pro-OH (**II-1**) were selected for cyclization. Preliminary study of the molecular modeling was discussed.

**I-1**, **I-2** and **II-1** were cyclized in DMF using DEPBT as the coupling reagent. The concentration of **I-1** and **I-2** was 1 mM and **II-1** was 2 mM. Two groups of nine (Li<sup>+</sup>, Na<sup>+</sup>, K<sup>+</sup>, Cs<sup>+</sup>, Mg<sup>2+</sup>, Ca<sup>2+</sup>, Ba<sup>2+</sup>, Zn<sup>2+</sup>, Cr<sup>3+</sup>) and eleven (Li<sup>+</sup>, Na<sup>+</sup>, K<sup>+</sup>, Cs<sup>+</sup>, Mg<sup>2+</sup>, Ca<sup>2+</sup>, Ba<sup>2+</sup>, Zn<sup>2+</sup>, Fe<sup>2+</sup>, Ni<sup>2+</sup>, Cr<sup>3+</sup>) metal ions were used to study the cyclization of the linear pentapeptides and linear heptapeptide respectively. All the cyclization reactions were monitored by HPLC.

### Results and Discussion

The results of our experiments are shown in Table 1 and Table 2. It is shown that all univalent metal ions can enhance not only the cyclization yields, but also the cyclization rates. The cyclization yields of **I-1** and **I-2** were increased from 22 to 39% and 67 to 80%, respectively, in the presence of Na<sup>+</sup>, and yield of **II-1** was increased

Table 1. Cyclization yields (%) of **I-1** and **I-2** induced by different metal ions.

Metal ions	Reaction time (h)		
	2	4	24
Li <sup>+</sup>	7.8	16.7	37
Na <sup>+</sup>	9.6	19.7	39 (80) <sup>a</sup>
K <sup>+</sup>	12	19	38 (69) <sup>a</sup>
Cs <sup>+</sup>	12.1	20.7	36 (68.6) <sup>a</sup>
Mg <sup>2+</sup>	6	8.3	22.4
Ca <sup>2+</sup>	8.8	14.2	26.7
Ba <sup>2+</sup>	9.8	10.5	31.2
Zn <sup>2+</sup>	—	—	—
Cr <sup>3+</sup>	—	—	—
none	5.4	8.6	22 (66.8) <sup>a</sup>

<sup>a</sup> Cyclization yields of **I-2**; “—” cyclopentapeptide (**I**) was not found.

Table 2. Cyclization yields (%) of **II-1** induced by different metal ions.

Metal ions	Reaction time (h)			
	1	3	5	24
Li <sup>+</sup>	21.0	38.7	51.7	68.1
Na <sup>+</sup>	36.4	56.8	57.6	71.3
K <sup>+</sup>	34.4	55.1	66.2	70.7
Cs <sup>+</sup>	38.8	65.5	72.8	77.7
Mg <sup>2+</sup>	2.1	10.4	11.5	29.0
Ca <sup>2+</sup>	5.9	12.4	21.1	40.6
Ba <sup>2+</sup>	21.8	37.5	50.7	63.7
Zn <sup>2+</sup>	–	–	1.7	4.1
Ni <sup>2+</sup>	–	2.0	2.4	11.8
Fe <sup>2+</sup>	–	–	–	–
Cr <sup>3+</sup>	–	–	–	–
none	19.6	38.3	48.6	60.0

“–” Cycloheptapeptide (**II**) was not found.

from 60 to 78% by Cs<sup>+</sup>. The metal ions may act as a promoter to coordinate with the linear peptides during cyclization. Influences of different concentration of Na<sup>+</sup> and Cs<sup>+</sup> were also studied. Five equivalents of Na<sup>+</sup> or Cs<sup>+</sup> were required for the optimum yield.

Molecular modeling studies were carried out to estimate the ring size of the cyclic penta- and heptapeptides. The backbone of the cyclopentapeptide is a circle with a diameter of  $6.0 \pm 0.5$  Å (standard deviation) while the cyclic heptapeptide is a rectangle or ellipse with the dimensions of  $6.3 \pm 0.5$  Å and  $9.0 \pm 0.3$  Å. The diameter of Na<sup>+</sup> is 1.96 Å while the diameter of Cs<sup>+</sup> is 3.30 Å. The results are consistent with the above coordination hypothesis.

### Acknowledgments

The authors thank the National Natural Science Foundation of China for the financial support (No. 2977200).

### References

1. Fan, C.X., Hao, X.L., Ye, Y.H. *Synth. Commun.* **26**, 1455–1460 (1996).
2. Xie, H.B., Tian, G.L., Ye, Y.H. *Synth. Commun.* **30**, 4233–4240 (2000).
3. Tang, Y.C., Gao, X.M., Tian, G.L., Ye, Y.H. *Chem. Lett.* 826–827 (2000).

## Disulfide Bond Formation of a Hydrophobic Peptide by Dimethyl Sulfoxide

Jingming Zhang and Lili Guo

*Department of Biochemistry and Molecular Biology, Indiana University School of Medicine,  
Indianapolis, IN 46202, USA*

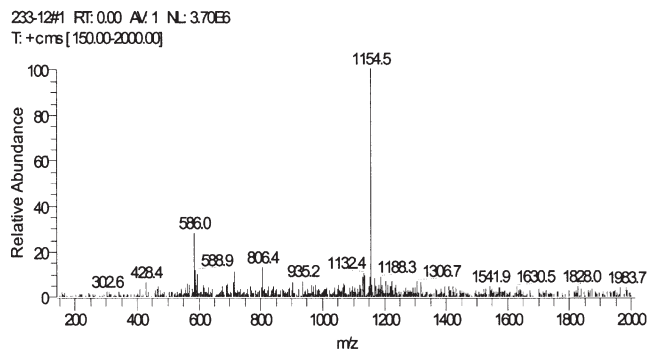
### Introduction

Although air oxidation in aqueous medium is the most common method for the formation of disulfide bonds, the formation of disulfide bonds of hydrophobic peptides is limited by poor solubility. Addition of dimethyl sulfoxide (DMSO) has been successful for promoting oxidation of free thiols to disulfides in several cases [1–3]. Because DMSO is miscible with water, up to 20% DMSO in water solution has been used to complete the formation of the disulfide bond over an extended pH range (pH 3–8). In our synthesis of the following peptide, the disulfide bond was readily formed by extension of the DMSO mediated oxidation method.



### Results and Discussion

The peptide was synthesized on an ABI 431 peptide synthesizer using Fmoc/OtBu chemistry and Fmoc-Amide-Resin. The 42 mg of crude peptide was dissolved in 80% DMSO solution containing 0.1 M NH<sub>4</sub>OAc pH 7.0 up to 1 mg/ml. The peptide didn't dissolve in a lower DMSO concentration. The disulfide formation was finished in six hours as monitored by HPLC and the Ellman test. The ESI-MS of the sample before and after oxidation is shown in Figure 1. The reaction mixture was directly loaded onto a preparative C18 RP-HPLC column (Vydac 218TP101550 5 × 25 cm). Because the high concentration of DMSO would cause the peptide to be eluted with the solvent front, the lower amount B solution (5% B, B is 70% CH<sub>3</sub>CN in H<sub>2</sub>O containing 0.09% TFA) and lower flow rate (10 ml/min) was used to load the reaction mixture to the column. 27 mg of purified peptide (60% yield) was characterized by ESI-MS. There is no evidence of the oxidation of the methionine residue. For comparison, air oxidation of the peptide in 0.01 M PB, pH 8 with 80% MeOH as co-solvent had several disadvantages of a) long duration (72 h), b) evaporation of the solvent during the long process, c) poor yield (42%).



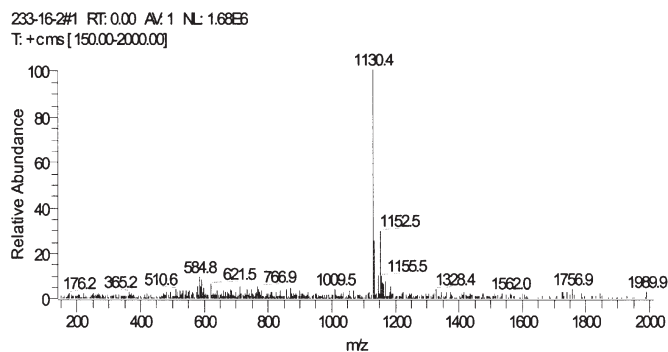


Fig. 1. ESI-MS of the crude peptide before (previous page) and after (this page) the DMSO mediated oxidation.

In summary, a very hydrophobic peptide was converted to the disulfide in 80% DMSO solution.

#### References

1. Tam, J.P., Wu, C-R., Liu, W., Zhang, J-W. *J. Am. Chem. Soc.* **113**, 6657–6662 (1991).
2. Wallace, T.J. *J. Am. Chem. Soc.* **86**, 2018–2021 (1964).
3. Barany, G., Angell, Y.M., Annis, I., Chen, L., Gross, C.M., Hargittai B., In R. Epton (Ed.) *Proceedings of the Fifth International Symposium on Solid-Phase Synthesis and Combinatorial Chemical Libraries*, Mayflower Scientific Ltd., UK, 1998, pp. 85–88.

## Stereoselective Synthesis of Transition State Analog Inhibitors of DPP-IV Using 2-Substituted Thiazoles

J. Piron and D. Tourwé

*Vrije Universiteit Brussel, Department of Organic Chemistry, B-1050 Brussels, Belgium*

### Introduction

Dipeptidylpeptidase IV or DPP-IV belongs to the class of serine proteases and catalyzes the cleavage of dipeptides at the amino terminus of peptides. Natural substrates of DPP-IV are peptides such as substance P,  $\beta$ -casomorphin, monomeric fibrin, pro-melittin and hGHRH. Two high affinity inhibitors for DPP-IV are the tripeptides Diprotin A (Ile-Pro-Ile) and Diprotin B (Val-Pro-Leu) [1]. The most effective is Diprotin A with an  $IC_{50}$  value in the  $\mu M$  range, but it suffers from rapid enzymatic degradation. In order to prepare more stable analogues and to test the influence on the inhibitory properties, we used a convergent synthetic method to prepare several Pro-Ile isosteres (Figure 1).

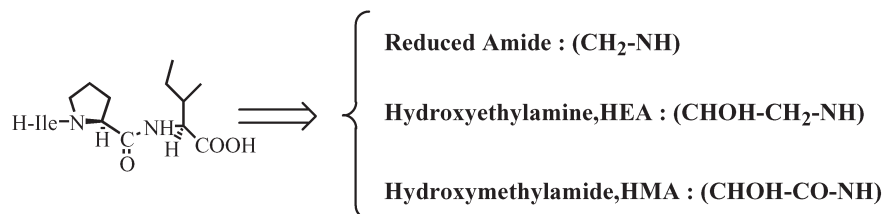


Fig. 1. Isosteric replacements in Diprotin A.

### Results and Discussion

**Building block synthesis:** Boc-L-Pro-aldehyde was prepared by reduction of the hydroxamate [2]. During the thiazole group addition a second stereocenter is formed according to the Felkin-Ahn non-chelate model for asymmetric induction. This delivers the thiazole adducts in an 85 : 15 (*S,S*) : (*S,R*) ratio. The (*S,S*)-adduct is obtained pure by crystallization in hexanes. The (*S,R*)-adduct is obtained pure after silica gel column chromatography performed on the mother liquor. The thiazole group is subsequently unmasked to the aldehyde on both epimers separately following a three step procedure developed by Dondoni *et al.* [3] (Figure 2).

For the synthesis of the  $\alpha$ -hydroxyacid, a TBDMS hydroxyl protecting group was used, since the free alcohol interfered during the oxidation process to the acid which led to cleavage of the molecule between the aldehyde and the alcohol. The thiazole

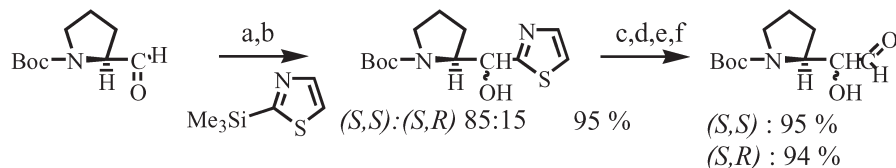


Fig. 2. Synthesis of key structures for HEA-isostere; a)  $CH_2Cl_2$ , r.t., 17 h; b) TBAF; c) crystallization: 71%, mother liquor (20% (*S,S*), 80% (*S,R*)) separated on silica; d)  $CH_3$ -triflate,  $CH_3CN$ , 15 min, r.t.; e)  $NaBH_4$ ,  $CH_3OH$ ; f)  $Hg_2Cl_2$ ,  $CH_3CN/H_2O$  (4/1).

was unmasked as before, although the extra steric hindrance resulted in lower yields especially for the (*S,R*) adduct. The (*S,S*)-hydroxy acid was obtained after  $\text{KMnO}_4$  oxidation of the aldehyde and subsequent cleavage of the TBDMS group (Figure 3).

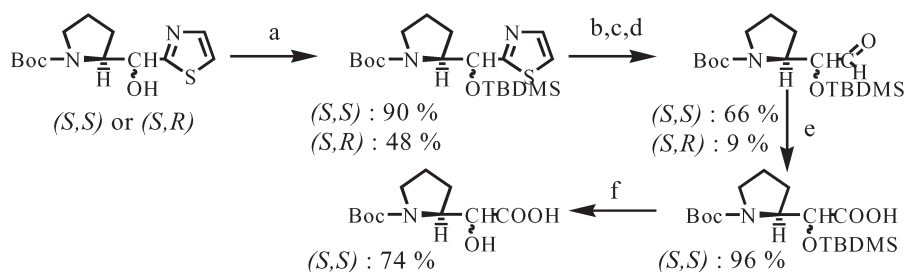


Fig. 3. Synthesis of the key structure for the HMA-isostere; a) TBDMS-Cl, imidazole, 3 days, 35 °C; b)  $\text{CH}_3\text{-triflate}$ ,  $\text{CH}_3\text{CN}$ , 15 min, r.t.; c)  $\text{NaBH}_4$ ,  $\text{CH}_3\text{OH}$ , 30 min, r.t.; d)  $\text{Hg}_2\text{Cl}_2$ ,  $\text{CH}_3\text{CN}/\text{H}_2\text{O}$  (4/1), 15 min, r.t.; e)  $\text{KMnO}_4$ , overnight, r.t., pH 7; f) TBAF, 48 h, r.t.

**Peptide synthesis:** The peptides Ile-ProΨIle were synthesized on solid phase using a Merrifield resin. Coupling was performed with 2 eq. of DIC and 2 eq. of HOBt as coupling reagents and 2 eq. of protected amino acid for 3 up to 16 h depending on the completion of the reaction. For the (*S,S*)-hydroxy acid coupling BOP was used as a coupling reagent followed by HATU, but a complete coupling was never observed. Reductive amination was performed with 2.5 eq. excess of the aldehydes and 2.5 eq. excess of  $\text{NaCNBH}_3$  [4]. Reaction took place overnight.

The resulting pseudotripeptides have been tested as competitive inhibitors of DPP-IV. None of the new analogs shows a higher potency than Diprotin A (Table 1).

Table 1. Yields and biological results.

Pseudotripeptide: Ile-ProΨIle	Yield (%)	IC <sub>50</sub> (mM)
Boc-L-prolinal ⇒ reduced amide	55	>5
Boc-( <i>S,S</i> )-Pro-α-hydroxyaldehyde ⇒ ( <i>R</i> )-HEA-isostere	63	1.2
Boc-( <i>S,R</i> )-Pro-α-hydroxyaldehyde ⇒ ( <i>S</i> )-HEA-isostere	46	0.85
Boc-( <i>S,S</i> )-Pro-α-hydroxyacid ⇒ ( <i>S</i> )-HMA-isostere	14	5.1
Diprotin A: H-Ile-Pro-Ile-OH	ND	0.033

### Acknowledgments

The authors thank the Instituut voor de Aanmoediging van Innovatie door Wetenschap en Technologie in Vlaanderen (IWT) for a research grant. Prof. S. Scharpé from the Medical Biochemistry Department at the UA is thanked for the biological results.

### References

1. Rahfeld, J., et al. *Biochim. Biophys. Acta* **1076**, 314–316 (1991).
2. Fehrentz, J.-A., Castro, B. *Synthesis* 676–678 (1983).
3. Dondoni, A. In Scheffold, R. (Ed.) *Modern Synthetic Methods*, Verlag Helvetica Chimica Acta, Basel, 1992, pp. 377–437.
4. Tourwé, D., et al. *Tetrahedron Lett.* **34**, 5499–5502 (1993).

## Original and General Strategy of Dimerization of Bioactive Molecules

Florine Cavelier, Matthieu Giraud, Nicole Bernad and Jean Martinez

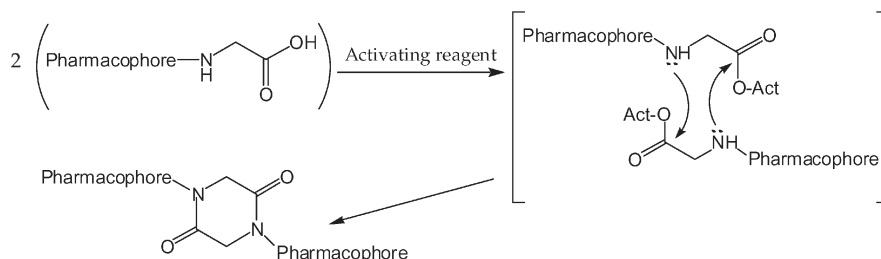
*Laboratoire des Aminoacides, Peptides et Protéines, UMR-CNRS 5810,  
Universités Montpellier I et II, UMII, CC19, 34095 Montpellier Cédex 05, France*

### Introduction

Dimerization of an active compound often results in enhanced binding and improved pharmacological properties. This potency is attributed to a higher concentration of pharmacophores in the proximity of recognition sites. This bivalent ligand approach is generally presumed to use a symmetrical bifunctional linker X to anchor two substrates P, giving rise to the general structure P-X-P [1].

Diketopiperazines (2,5-piperazinediones, DKPs), which are the smallest cyclic peptides, are common motifs in several natural products with therapeutic properties [2–5]. Furthermore, DKPs have been shown to be useful scaffolds for the rational design of several drugs [6]. Whereas the intramolecular diketopiperazine cyclization is well documented as a side reaction in peptide synthesis [7,8], the intermolecular formation has not yet been explored.

In this study, we show that it is possible to build a different dimeric structure, involving a Gly-Gly diketopiperazine scaffold, by activating the C-terminal glycine monomer [9] (Scheme 1).



*Scheme 1. General strategy of dimerization.*

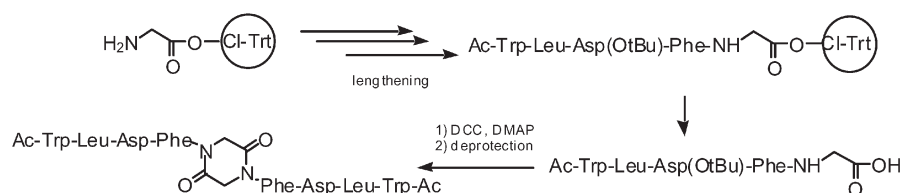
### Results and Discussion

Our strategy started by introducing a C-terminal glycine moiety on a pharmacophore, followed by an activation step to provide the diketopiperazine bearing the two substrates. We studied the activation step on a dipeptide (Boc-Leu-Gly-OH). Several activating reagents (BOP, HBTU, DCC...) were used and all produced high yields of diketopiperazine when combined with DMAP. The couple DCC/DMAP, which presents a good stability in basic pH solution (required for the cyclisation step), gave good results despite the well-known problem of *N*-acylurea formation. Indeed, it was possible to limit formation of this side product by using a high concentration of the starting monomer.

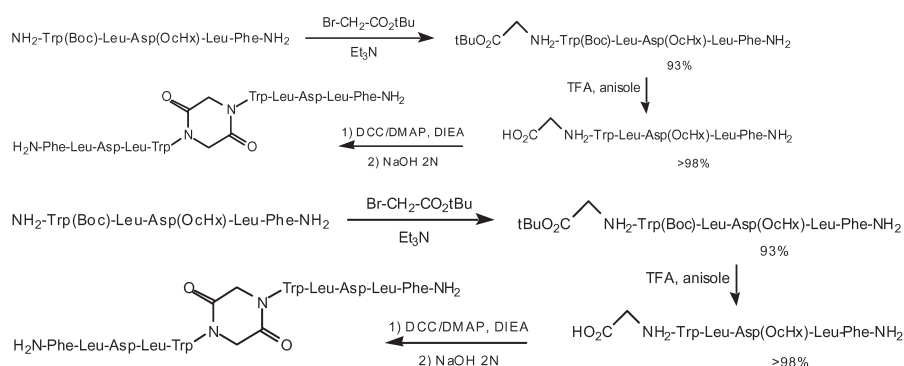
In these reaction conditions, various dipeptides were dimerized in high yields (82 to 99%). However, epimerization of the carbon in the alpha position involved in diketopiperazine formation was observed when the C-terminal Gly was replaced by chiral amino acids.

## Synthetic Methods

In the first application, we synthesized several N-terminal (Scheme 3) and C-terminal (Scheme 2) cholecystokinin tetrapeptide (CCK-4) dimers. In the case of the N-terminal dimer, the Gly moiety was introduced *via* a Williamson reaction of the N-terminal peptide on the *t*-butylbromoacetate, and the *tert*-butyl group was cleaved by acid treatment.



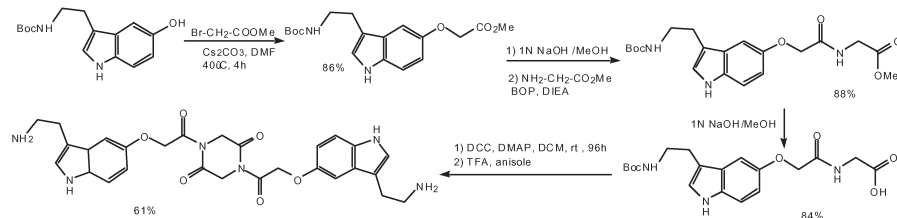
Scheme 2. C-terminal dimerization of CCK-4.



Scheme 3. N-terminal dimerization of CCK-4.

To illustrate this straightforward strategy of dimerization with an example of an active organic molecule, we dimerized serotonin through its hydroxyl group (Scheme 4).

In a second part, exploratory experiments were conducted to use *c*-(Gly-Gly) diketopiperazine as a bifunctional synthon in combinatorial chemistry. The idea was to acylate diketopiperazine using haloacetyl halides and subsequently displace the halogen substituent in the derived intermediate by nucleophiles. However, the imide bond to the DKP proved to be too labile. This situation was overcome by reacting DKP with acryloyl chloride followed by Michael addition of nucleophiles. At present,



Scheme 4. Dimerization of serotonin.

*Cavelier et al.*

this strategy has been validated only for the reaction with benzylamine as the nucleophile.

### Conclusion

In this study we have described a new method for the dimerization of various active molecules using a diketopiperazine scaffold, resulting from an additional glycine moiety. This strategy does not need a bifunctional linker and the reaction is easy to carry out. It is worth pointing out that this dimerization reaction can be a side reaction during activation of peptides on their C-terminal in peptide synthesis. The development of this innovative concept as a means to generate dimers of bioactive molecules can, in principle, be exploited in a combinatorial approach to the creation of compound libraries.

### References

1. Erez, M., Tkemori, A.E., Portoghese, P.S. *J. Med. Chem.* **25**, 847–849 (1982).
2. Cui, C-B., Kakeya, H., Osada, H. *Tetrahedron* **52**, 12651–12666 (1996).
3. Charlton, P.A., Faint, R.W., Bent, F., Bryans, J., Chicarelli-Robinson, I., Mackie, I., Machin, S., Bevan, P. *Thromb. Haemostasis* **75**, 808–815 (1996).
4. Funabashi, Y., Horigushi, T., Iinuma, S., Tanida, S., Harada, S. *J. Antibiot.* **47**, 1202–1218 (1994).
5. Barrow, C.J., Musza, L.L., Cooper, R. *Bioorg. Med. Chem. Lett.* **5**, 377–380 (1995).
6. Weng, J.H., Bado, A., Garbay, C., Roques, B.P. *Regul. Pept.* **65**, 3–9 (1996).
7. Goodman, M., Stueben, K.C. *J. Am. Chem. Soc.* **84**, 1279–1283 (1962).
8. Gisin, B.F.; Merrifield, R.B. *J. Am. Chem. Soc.* **94**, 3102–3131 (1972).
9. Giraud, M., Bernad, N., Martinez, J., Cavelier, F. *Tetrahedron Lett.* **42**, 1895–1897 (2001).

## An Efficient Approach for the Synthesis of Salmon Calcitonin Using Oxazolidine Dipeptides

Weonu Chweh, Hyun Jin Lee, Young-Deug Kim, Sang Sun Lee  
 and Hack-Joo Kim

A&PEP Inc., 213, Sosabon-1-Dong, Bucheon, 422-231, Korea

### Introduction

Salmon calcitonin (sCT) is a calcium regulating hormone, inhibiting bone resorption of  $\text{Ca}^{2+}$  with accompanying hypocalcemia and hypophosphatemia and decreased urinary  $\text{Ca}^{2+}$  concentrations. Although many ways to synthesize sCT have been reported, efficient syntheses of sCT is still an attractive goal for chemists. In an attempt to synthesize sCT, we selected a full protecting strategy using 2-(4-nitrophenyl)sulfonyl-ethoxycarbonyl (Nsc)/*t*-Bu without any breakage on solid support [1]. To improve purity and yield, Nsc-protected oxazolidine dipeptides were inserted in appropriate sites of sCT. We expected sCT having 5 threonines, 3 serines, and 2 cysteines would be a good model to investigate  $\Psi$ -proline effect. Incorporation of  $\Psi$ -proline residues into difficult sequence peptides was reported to improve assembling yields and synthetic purities [2]. In this report, we illustrate a synthetic method of Nsc-protected oxazolidine dipeptides, its insertion effect on the assembling sCT, and the structural influence of N-terminal cysteine in oxidation reaction.

### Results and Discussion

Nsc-protected oxazolidine dipeptide **4**, Nsc-Leu-Ser( $\Psi^{\text{Me,Me}}\text{Pro}$ )-OH was synthesized as shown in Figure 1. Nsc-Leu-OH **1** was activated *via* pfp esters, then L-Ser was added in basic aqueous MeCN and yielded Nsc-Leu-Ser-OH **3**. While refluxing **3** in THF with 2,2-dimethoxypropane and pyridinium 4-toluenesulfonate, serine of dipeptide **3** was cyclized to Nsc-protected oxazolidine dipeptide **4**.

Salmon calcitonin is a single chain C-terminally amidated 32 amino acid peptide hormone containing a single disulfide bridge. To synthesize sCT effectively, we have divided synthetic pathway into 2 steps, such as a chain assembly step and an oxidation

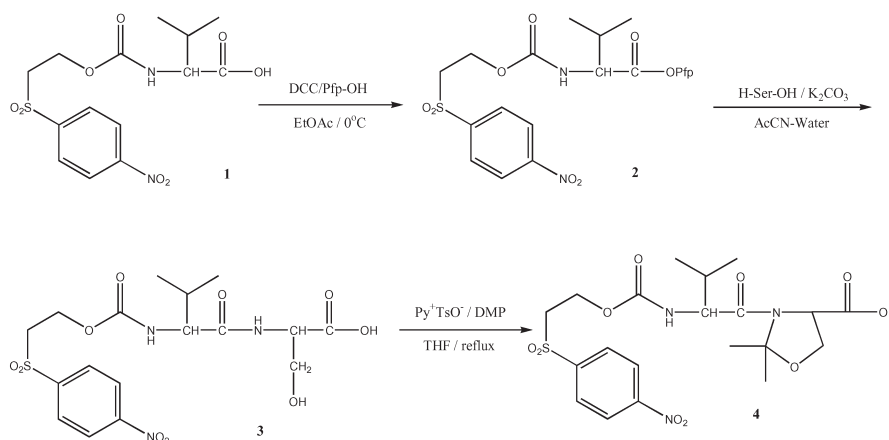


Fig. 1. Synthesis of Nsc-Leu-Ser( $\Psi^{\text{Me,Me}}\text{Pro}$ )-OH.

process. When assembling an sCT chain using standard SPPS protocols, aggregations were detected at Leu<sup>4</sup>, Val<sup>8</sup>, Leu<sup>9</sup>, and Gln<sup>20</sup> so that this synthesis was very difficult.

Inserting the oxazolidine dipeptide derivative **4** at 13th position, aggregation was decreased remarkably and a very pure crude product obtained (Figure 2). An additional insertion of an oxazolidine at 5th position did not provide obvious improvements in this synthesis.

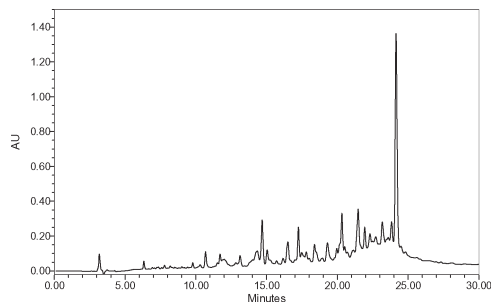


Fig. 2. HPLC profile of sCT (oxidation, Nsc-deprotection and TFA based cleavage of I-Nsc-di-Cys<sup>1,7</sup>(Acm)-Ser<sup>13</sup>( $\Psi^{MeMe}Pro$ )-fully protected sCT; 0–100% MeCN in water for 50 min).

The effect of N-terminal environment on the oxidation of sCT was studied. The oxidation was proceeded with fully protected sCT on the resin using iodine-ascorbic acid. The oxidation of Nsc protected sCT proceeded well without any purity loss. When Nsc was replaced with Boc, the oxidation yield decreased no more than 50%. Using N-terminal free amine, oxidized peptide was scrambled with complex impurities. On the effect of  $\Psi$ -proline in oxidation step: 13th  $\Psi$ -proline sCT proceeded well with a good HPLC purity, however 5th  $\Psi$ -proline contributed negatively in oxidation step.

## References

1. Sabirov, A.N., Kim, Y.D., Kim, H.J., Samukov, V.V. *Protein Pept. Lett.* **5**, 57 (1998).
2. Wohr, T., Wahl, F., Nefzi, A., Rohwedder, B., Sato, T., Sun, X., Mutter, M. *J. Am. Chem. Soc.* **118**, 9218 (1996).

## **A Combined Solid-Phase and Solution Strategy for Chemical Synthesis of Human Leptin**

**Yuji Nishiuchi, Tatsuya Inui, Hideki Nishio and Terutoshi Kimura**

*Peptide Institute Inc., Protein Research Foundation, Minoh-shi, Osaka 562-8686, Japan*

### **Introduction**

The segment condensation strategy performed using either a solution or solid phase is one of the most advantageous procedures for synthesizing large peptides or proteins. We have recently demonstrated the utility of a combined solid-phase and solution approach for rapid protein synthesis by synthesizing muscarinic toxin 1 (66 AAs) [1] and green fluorescent protein (238 AAs) [2]. The procedure involves performing the segment condensation reaction in solution employing a maximum protection strategy with Boc chemistry, followed by final deprotection using HF. Each segment used in the subsequent segment condensation is prepared by solid-phase assembly on an *N*-[9-(hydroxymethyl)-2-fluorenyl] succinamic acid (HMFS) linker [3], which is designed to be cleaved by nucleophiles such as morpholine to produce fully protected segments with a free  $\alpha$ -carboxyl group. To establish the present strategy for general protein synthesis, we had to resolve the following issues encountered during preparation of the protected segments on the resin as well as the subsequent segment condensation in solution and HF treatment: 1) development of base-resistant side-chain protecting groups for Trp and Tyr, 2) completion of amino acid-coupling in a mixture of chloroform (CHL) and trifluoroethanol (TFE) on the resin, 3) exclusion of deletion products generated at the N-terminus of His(Bom), 4) development of a solvent system for segment condensation of sparingly soluble protected peptides, and 5) suppression of the Trp modification associated with use of an *N*<sup>in</sup>-carbamate-type protecting group in HF. In order to further demonstrate the usefulness of our strategy, we tried to synthesize human leptin by resolving these issues.

### **Results and Discussion**

To prepare highly homogenous protected segments using the HMFS resin, there must be a high compatibility between the anchoring group and the side-chain protecting groups on the segment. Among the commonly used side-chain protecting groups in Boc chemistry, the For group for Trp and the BrZ group for Tyr are partially or completely cleaved during detachment of the segments from the HMFS resin by treatment with 20% morpholine/DMF for 30 min, which are the optimal conditions for avoiding the aspartimide formation arising from the sequence susceptible to base, such as Asp-Asn or Asp-Gly. In the present study, we employed the cyclohexyloxycarbonyl (Hoc) group for Trp [4] and the 3-pentyl (Pen) group for Tyr [5] as base-resistant side-chain protecting groups cleavable by HF. However, we recently identified the modification of Trp associated with use of the Hoc group when treating Trp(Hoc)-containing peptide with HF in the presence of *p*-cresol or anisole as a scavenger [6]. In practical peptide synthesis, use of thiol (*e.g.* 1,4-butanedithiol) as an additive during the HF reaction was found to significantly reduce the extent of the side reaction with Trp(Hoc), although the Hoc group can be removed without resorting to the use of thiols.

Each segment was designed for the size range of 10–15 amino acid-peptides, which was expected to facilitate the purification by recrystallization, reprecipitation and/or silica gel chromatography. For this purpose we needed to find the procedure to prevent

contamination by the deletion products generated during the chain-assembly on the HMFS resin, which would make difficult purification of the segment. The failure of Boc deprotection or amino acid-coupling reaction causes contamination of the terminated products as well as the deletion products lacking one or more amino acid residues. Incomplete amino acid-coupling reaction often occurs in the case of segments related to a “difficult sequence”, even with use of the optimized protocol, *i.e.* the *in situ* neutralization protocol [7]. In order to avoid this problem, we altered segment structures and/or performed the amino acid-coupling reaction mediated with EDC/HOObt in a  $\beta$ -sheet disrupting solvent, a mixture of CHL and TFE (3 : 1). As previously reported by Li *et al.* [8], the coupling efficiency was improved by the use of CHL/TFE swelling the peptide-resin to approximately 1.5–2-fold the volume of that in DCM or NMP. On the other hand, amino acid deletion products generated at the N-terminus of His(Bom) resulted more or less from incomplete deprotection of the Boc group even with high concentrations of TFA. By reviewing the removability of the Boc group on amino acid derivatives, the Boc group on His(Bom) was found to be much more resistant under the deprotecting conditions than we had expected. This finding enabled us to complete Boc deprotection from His(Bom) by prolonging the duration of TFA treatment and/or increasing TFA concentration.

#### *Synthesis of Human Leptin*

In order to demonstrate the utility of the combined solid-phase and solution approach, our present strategy was applied to the synthesis of human leptin, a protein consisting of 146 amino acids, which is secreted from adipocytes and influences body weight homeostasis. The molecular structure was designed for assembly from 14 segments (Figure 1) using the following side chain protecting groups: Tos for Arg, Bom for His, ClZ for Lys, cHex for Asp and Glu, Pen for Tyr, Hoc for Trp, Xan for Asn and Gln, Bzl for Ser and Thr, and MeBzl for Cys. Each protected segment was detached from the HMFS resin by treatment with 20% morpholine/DMF for 30 min without any side reactions as described above. This detachment procedure could be effectively performed even in the case of insoluble segments in DMF, *e.g.* segment 1, 2, 3, 6 and 7, which could be quantitatively extracted with hexafluoroisopropanol (HFIP). The homogeneity of each segment was determined by amino acid analysis, TLC, RP-HPLC and ESI MS and was found to be more than 95% pure.

The segment condensation reaction was carried out by using EDC in the presence of HOObt or HOObt in appropriate solvent as indicated in Figure 1. In the course of assembling the molecule, some of the intermediates were insoluble in routinely used solvents including CHL/TFE mixed solvent. Therefore, we needed to use CHL/phenol mixed solvent (5 : 1 or 9 : 1) possessing much higher solubilizing potential than CHL/TFE. In CHL/phenol, the segment condensation reaction proceeded smoothly without danger of epimerization or significant ester formation with C-terminal amino acid residue when EDC was employed in the presence of HOObt [9]. After completion of the synthesis of two big segments, Boc-(1-69)-OPac and Boc-(70-146)-OBzl, the terminal phenacyl (Pac) group was removed using zinc dust in 20% acetic acid in HFIP, and the homogeneity of each segment was confirmed by HPLC after deprotection in HF. Next, these segments were coupled in CHL/phenol to the fully protected leptin molecule. The protected peptide thus obtained was treated with HF in the presence of 1,4-butanedithiol and *p*-cresol at  $-5^{\circ}\text{C}$  for 1 h. After purification by RP-HPLC, the product containing two free Cys was oxidized using hydrogen peroxide procedure in 0.1 M Tris buffer (pH 8.2) containing 6 M guanidine. The product was

## Synthetic Methods

further purified by RP-HPLC. Amino acid analysis of the purified peptide gave values which agreed well with the theoretical ones. The molecular weight measured by MALDI-TOF mass spectroscopy was 16,025.7 ( $[M + H]^+$ ), which agreed well with the theoretical value (16,025.4:  $[M + H]^+$ ).

VPIQKVQDDT KTLIKTIVTR INDISHTQSV SSKQKVTGLD FIPGLHPILT  
LSKMDQTLAV YQQILTSMPs RNVIQISNDL ENLRDLLHVL AFSKSchLPW  
ASGLETLDSL GGVLEASGYS TEVVALSRLQ GSLQDMLWQL DLSPGC

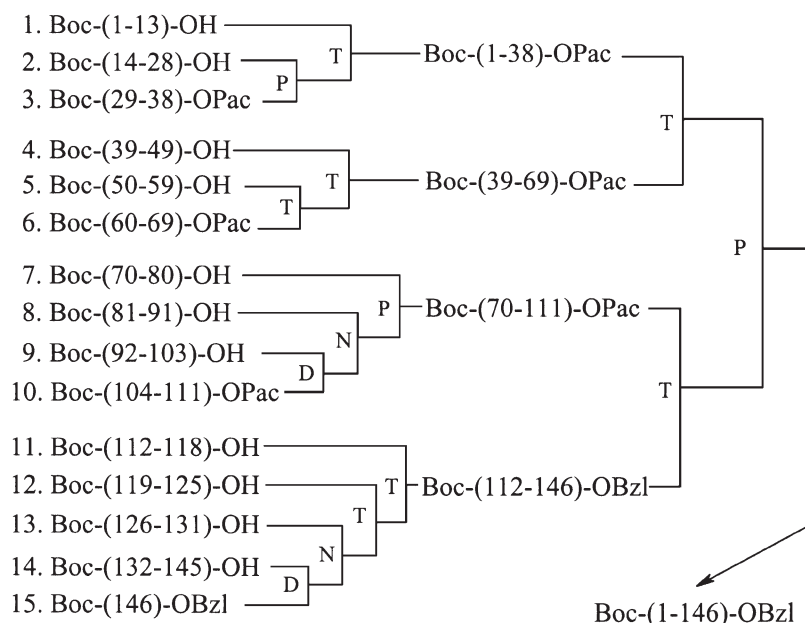


Fig. 1. Synthesis of protected human leptin. D: DMF, N: NMP, P: CHL-phenol, T: CHL-TFE.

In conclusion, the combination of a solid-phase and a solution approach can be used for the rapid synthesis of proteins of sufficiently good quality. In particular, the segment condensation reaction performed in a  $\beta$ -sheet disrupting solvent, CHL/TFE and/or CHL/phenol, proved to be one of the most advantageous methods for protein synthesis.

## References

1. Nishiuchi, Y., Nishio, H., Inui, T., Kimura, T. *J. Peptide Sci.* **6**, 84–93 (2000).
2. Nishiuchi, Y., et al. *Proc. Natl. Acad. Sci. USA* **95**, 13549–13554 (1998).
3. Rabanal, F., Giralt, E., Albericio, F. *Tetrahedron* **51**, 1449–1458 (1995).
4. Nishiuchi, Y., et al. *Tetrahedron Lett.* **37**, 7529–7532 (1996).
5. Bódi, J., et al. *Tetrahedron Lett.* **39**, 7117–7120 (1998).
6. Nishio, H., et al. *Tetrahedron Lett.* **41**, 6839–6832 (2000).
7. Schnölzer, M., et al. *Int. J. Peptide Protein Res.* **40**, 180–193 (1992).
8. Yamashiro, D., Blake, J., Li, C.H. *Tetrahedron Lett.* 1469–1472 (1976).
9. Inui, T., Nishio, H., Bódi, J., Nishiuchi, Y., Kimura, T., In Fields, G.B., Tam, J.P. and Barany, G. (Eds.) *Peptides for the New Millennium (Proceedings of the 16th American Peptide Symposium)*, Kluwer, Dordrecht, 2000, pp. 715–716.

## Synthesis of Phosphorylated Polypeptide by the Thioester Method Using a Recombinant Protein

Toru Kawakami<sup>1</sup>, Koki Hasegawa<sup>1</sup>, Kenta Teruya<sup>1</sup>, Kenichi Akaji<sup>1</sup>,  
Masataka Horiuchi<sup>2,3</sup>, Fuyuhiko Inagaki<sup>2,3</sup>, Yasuyuki Kurihara<sup>4</sup>,  
Seiichi Uesugi<sup>4</sup> and Saburo Aimoto<sup>1</sup>

<sup>1</sup>*Institute for Protein Research, Osaka University, Osaka 565-0871, Japan*

<sup>2</sup>*Graduate School of Pharmaceutical Sciences, Hokkaido University,  
Hokkaido 060-0812, Japan*

<sup>3</sup>*CREST, JST, Tokyo 170-0013, Japan*

<sup>4</sup>*Faculty of Engineering, Yokohama National University, Kanagawa 240-8051, Japan*

### Introduction

The availability of site-specifically modified peptides is of importance for biochemical and biophysical studies. Although biological methods, such as expression using bacteria, are useful, they are not always applied to the synthesis of peptides with site-specific modifications. Chemical methods constitute viable alternatives to those biological approaches. Furthermore, combinations of peptides, obtained by chemical and biological means, for use as building blocks offer great potential as a route to the synthesis of a wide variety of polypeptides.

We have been developing a thioester method for polypeptide synthesis using *S*-alkyl peptide thioesters (peptide thioesters) as building blocks [1–3]. Several ligation methods using the peptide thioesters as building blocks have been also developed [4,5], including the so-called native chemical ligation [6]. Recently expressed peptides were used for peptide synthesis. Protein splicing elements, which produce the thioester intermediates, were used in combination with the native chemical ligation method [7,8]. In those, however, a Cys residue is required at the coupling site. In contrast, the thioester method does not restrict the residues at the condensation sites in principle. This is of great advantage to the synthesis of any desired sequences by the use of expressed peptides as building blocks.

In this paper we describe a method for the preparation of a partially protected peptide segment as a building block, for the thioester method, from an expressed peptide. Its condensation with a peptide thioester, which contained *O*-phosphoserine residues, was achieved. A synthesis of a partial sequence of phosphorylated p21Max protein [9] is described as a model [10]. Max protein is known to bind specifically to duplex DNA by forming homo- and hetero-complexes with the Myc family of proteins, and its binding activity is reduced by phosphorylation. The success of this synthesis would greatly contribute to our understanding of the structural basis of the regulation mechanism of Max protein, as the result of phosphorylation.

### Results and Discussion

p21Max(13-101) (**1**) was prepared by expression using *E. coli* [11], which was converted to CH<sub>3</sub>COCO-p21Max(14-101) (**3**) by the reaction with glyoxylic acid in the presence of nickel(II) sulfate in sodium acetate buffer [12]. After introduction of Boc groups, the pyruvoyl group was removed by the reaction with *o*-phenylenediamine [12], to give [Lys(Boc)<sup>15,25,31,48,57,68,80,95</sup>]-Max(14-101) (**3**) in 34% yield based on peptide **1**. The transamination of peptide **1** using copper(II) sulfate also gave the desired product **2**, which gradually degraded under the reaction conditions. The reaction can be controlled easily by using nickel ions rather than copper ions. Removal of

$\alpha$ -oxoacyl group was carried out in the presence of *N,N*-dimethylformamide (DMF) as a co-solvent because of the low solubility of a Boc-protected peptide in an aqueous-only buffer.

On the other hand, a peptide thioester, Boc-[Ser(PO<sub>3</sub>H<sub>2</sub>)<sup>2,11</sup>]-p21Max(1-13)-SCH<sub>2</sub>CH<sub>2</sub>CO-Leu-OH (**4**) was synthesized *via* a Boc solid-phase method in 11% yield. These peptides **3** and **4** were condensed in the presence of silver chloride, 3,4-dihydro-3-hydroxy-4-oxo-1,2,3-benzotriazine, and *N,N*-diisopropylethylamine to give Boc-[Lys(Boc)<sup>15,25,31,48,57,68,80,95</sup>,Ser(PO<sub>3</sub>H<sub>2</sub>)<sup>2,11</sup>]-p21Max(1-101) (**5**), which was treated with trifluoroacetic acid to afford [Ser(PO<sub>3</sub>H<sub>2</sub>)<sup>2,11</sup>]-p21Max(1-101) (**6**). In this synthesis, DMF was used as a solvent for the condensation reaction, and peptide **6** was obtained in 31% yield based on peptide **3**. Epimerization of the Ala13 residue was less than 5%. It was also possible to prepare the non-phosphorylated p21Max(1-101) in about the same yield as for the phosphorylated sample with less than 3% epimerization.

The above data clearly show that an expressed peptide can be used as a building block for the thioester method, *via* transamination of the N-terminal amino acid residue. Although some difficulty in the preparation of phosphorylated peptide thioesters, which contains multiple Asp residues, remains, once those can be prepared, it should be possible to perform segment condensation by the thioester method without any problems. Furthermore, epimerization at the condensation site can be suppressed by using DMF as a solvent, and this greatly simplifies the synthesis of proteins from recombinant proteins, because any condensation sites can be selected. This methodology will, in the future, be applied to the synthesis of a wide variety of polypeptides including segmentally isotope-labeled proteins.

### Acknowledgments

This research was supported, in part, by Grants-in-Aid for Scientific Research Nos. 10179103 and 12780440 from the Ministry of Education, Science, Sports and Culture of Japan.

### References

1. Aimoto, S. *Biopolymers (Peptide Sci.)* **51**, 247–256 (1999).
2. Hojo, H., Aimoto, S. *Bull. Chem. Soc. Jpn.* **64**, 111–117 (1991).
3. Kawakami, T., Hasegawa, K., Aimoto, S. *Bull. Chem. Soc. Jpn.* **73**, 197–203 (2000).
4. Muir, T.M., Dawson, P.E., Kent, S.B.H. *Methods Enzymol.* **289**, 266–298 (1997).
5. Tam, J.A., Yu, Q., Miao, Z. *Biopolymers (Peptide Sci.)* **51**, 311–332 (1999).
6. Dawson, P.E., Muir, T.M., Clark-Lewis, I., Kent, S.B.H. *Science* **266**, 776–779 (1994).
7. Muir, T.W., Sondhi, D., Cole, P.A. *Proc. Natl. Acad. Sci. USA* **95**, 6705–6710 (1998).
8. Evans, T.C., Jr., Benner, J., Xu, M.Q. *Protein Sci.* **7**, 2256–2264 (1998).
9. Blackwood, E.M., Eisenman, R.N. *Science* **251**, 1211–1217 (1991).
10. Kawakami, T., Hasegawa, K., Teruya, K., Akaji, K., Horiuchi, M., Inagaki, F., Kurihara, Y., Uesugi, S., Aimoto, S. *Tetrahedron Lett.* **41**, 2625–2628 (2000).
11. Horiuchi, M., Kurihara, Y., Katahira, M., Maeda, T., Saito, T., Uesugi, S. *J. Biochem.* **122**, 711–716 (1997).
12. Dixon, H.B.F. *J. Protein Chem.* **3**, 99–108 (1984).

## The Synthesis of the K-Ras-Derived Peptide

Xiao-He Tong, Xiaowei Zhang, Lei Liu and Anita Hong

AnaSpec Inc., San Jose, CA 95131, USA

### Introduction

A farnesylated 9-aa peptide, H-Lys-Ser-Lys-Thr-Lys-Cys(farnesyl)-Val-Ile-Met-OH, comes from the C-terminus of K-Ras, which is the most frequently mutated member in human tumours. The hRCE1 protease cleaved H-Lys-Ser-Lys-Thr-Lys-Cys(farnesyl)-Val-Ile-Met-OH between the Cys(farnesyl) and Val positions, generating H-Lys-Ser-Lys-Thr-Lys-Cys(farnesyl)-OH and H-Val-Ile-Met-OH as products. For developing a useful direct fluorogenic assay for both cloned hRCE1 analysis and inhibitor discovery, we synthesized twenty K-Ras-derived peptides for screening [1]. Some peptides (Table 1) were modified with either (7-Methyloxy-coumarin-4-yl)acetyl (Mca) or 2-Aminobenzoyl (Abz) fluorescent chromophores at the N-terminus, and quenching-group-containing amino acids at the amino acid position of H-Val-Ile-Met-OH. The quenching-group-containing amino acids used were either  $N^{\beta}$ -2,4-dinitrophenyl-L-di-aminopropionic acid [Dap(Dnp)] or  $N^{\epsilon}$ -2,4-dinitrophenyl-L-lysine [Lys(Dnp)].

Table 1. K-Ras-derived peptide sequence.

1.	H-Lys-Ser-Lys-Thr-Lys-Cys(farnesyl)-Val-Ile-Met-OH
2.	H-Lys-Ser-Lys-Thr-Lys-Cys(farnesyl)-OH
3.	Mca-Lys-Ser-Lys-Thr-Lys-Cys(farnesyl)-Val-Ile-Met-OH
4.	Mca-Lys-Ser-Lys-Thr-Lys-Cys(farnesyl)-OH
5.	Mca-Lys-Ser-Lys-Thr-Lys-Cys(farnesyl)-Lys(Dnp)-Ile-Met-OH
6.	Mca-Lys-Ser-Lys-Thr-Lys-Cys(farnesyl)-Val-Lys(Dnp)-Met-OH
7.	Mca-Lys-Ser-Lys-Thr-Lys-Cys(farnesyl)-Val-Ile-Lys(Dnp)-OH
8.	Mca-Lys-Ser-Lys-Thr-Lys-Cys(farnesyl)-Dap(Dnp)-Ile-Met-OH
9.	Mca-Lys-Ser-Lys-Thr-Lys-Cys(farnesyl)-Val-Dap(Dnp)-Met-OH
10.	Mca-Lys-Ser-Lys-Thr-Lys-Cys(farnesyl)-Val-Ile-Dap(Dnp)-OH
11.	Abz-Lys-Ser-Lys-Thr-Lys-Cys(farnesyl)-Val-Ile-Met-OH
12.	Abz-Lys-Ser-Lys-Thr-Lys-Cys(farnesyl)-Val-Ile-OH
13.	Abz-Lys-Ser-Lys-Thr-Lys-Cys(farnesyl)-Val-OH
14.	Abz-Lys-Ser-Lys-Thr-Lys-Cys(farnesyl)-OH
15.	Abz-Lys-Ser-Lys-Thr-Lys-Cys(farnesyl)-Lys(Dnp)-Ile-Met-OH
16.	Abz-Lys-Ser-Lys-Thr-Lys-Cys(farnesyl)-Val-Lys(Dnp)-Met-OH
17.	Abz-Lys-Ser-Lys-Thr-Lys-Cys(farnesyl)-Val-Ile-Lys(Dnp)-OH
18.	Abz-Lys-Ser-Lys-Thr-Lys-Cys(farnesyl)-Dap(Dnp)-Ile-Met-OH
19.	Abz-Lys-Ser-Lys-Thr-Lys-Cys(farnesyl)-Val-Dap(Dnp)-Met-OH
20.	Abz-Lys-Ser-Lys-Thr-Lys-Cys(farnesyl)-Val-Ile-Dap(Dnp)-OH

### **Results and Discussion**

Nonfarnesylated peptides were synthesized by the solid phase method using Fmoc chemistry and HMP-MBHA resin. All couplings, including Fmoc-Dap(Dnp)-OH and Fmoc-Lys(Dnp)-OH, were performed using fourfold excess of activated amino acid. The amino acids were activated using HBTU : HOBt : DIEA (1 : 1 : 2) or DIC : HOBt (1 : 1). Peptide resins were cleaved and deprotected by treatment with a mixture of TFA : thioanisole : DTT : water : phenol (82.5 : 5 : 2.5 : 5 : 5) for 3 h. The non-farnesylated peptides were purified by RP HPLC with a 0.1% TFA/CH<sub>3</sub>CN gradient system. Peptides containing Dnp group are best synthesized using DIC : HOBt coupling.

The farnesyl peptide derivatives were synthesized by our improved procedure, based on the method of Yang [2]. Nonfarnesylated peptides were dissolved in the mixed solvent DMSO/DMF/ACN (3 : 2 : 1) at a concentration of 10 mM at 0 °C under nitrogen atmosphere, and treated with 1.2 eq. of farnesyl bromide and 8 eq. of DIEA for 0.5–1 h. On this condition, farnesyl bromide reacts exclusively with the sulfhydryl anion of the unprotected peptide. Use of greater amounts of farnesyl bromide (>3 eq.) often generate multifarnesylated peptides. After the reaction was completed, the reaction mixture was quenched with acetic acid, and then purified by RP-HPLC. Using this condition, we can obtain the desired mono-farnesylated peptides with good yield.

### **References**

1. Hollander, I., Frommer, E., Mallon, R. *Anal. Biochem.* **286**, 129–137 (2000).
2. Yang, C., Marlowe, C., Kania, R. *J. Am. Chem. Soc.* **113**, 3177–3178 (1991).

## Synthesis of Phosphopeptides on Solid Phase Using *tert*-Butyl-*H*-phosphonate Salts

Gábor K. Tóth, András Molnár and Zoltán Kupihár

Department of Medical Chemistry, University of Szeged, Szeged H-6720, Hungary

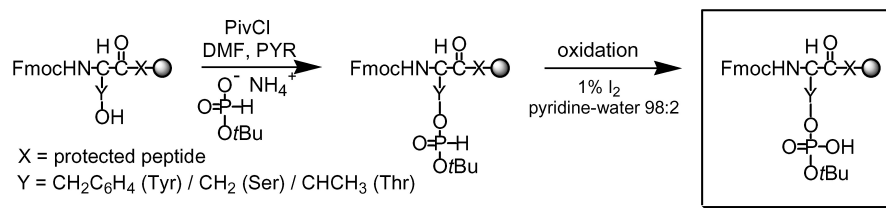
### Introduction

The phosphorylation of proteins is probably the most important reversible element of the cell regulation. The involvement of tyrosine residue in this process is well known, and a similar controlling mechanism concerning serine/threonine containing proteins was recently discovered [1]. The isolation of phosphorylated peptides from biological sources for functional or conformational studies is usually not feasible, therefore there is a need for efficient chemical phosphorylation methods. Although many papers on phosphopeptide synthesis were published in the past, a universal method, which can be applied with high efficiency in all cases does not exist. In several cases, after incorporation of the phosphate moiety, the molecule can undergo different side-reactions [2]. To overcome these problems, one of the most widely used and favorable methods makes use of monoprotected phosphate-containing building blocks of Tyr, Ser and Thr [3]. Another alternative is the use of an asymmetrically protected amidite reagent [4,5] or the use of *H*-phosphonates (phosphonic acid monoesters) that have been applied successfully in oligonucleotide synthesis.

### Results and Discussion

There are several possible solutions to avoid the phosphate loss by  $\beta$ -elimination: 1) incorporation of a monoprotected phosphate because it contains a negative charge during piperidine treatment and it can prevent the  $\beta$ -elimination [3], 2) employment of asymmetrically protected phosphoramidite reagents [4,5], 3) and application of *H*-phosphonates as phosphorylating agents [6,7].

We wanted to examine whether the latter is universally suitable for phosphorylation of peptides and whether there are side-reactions during the oxidation step. The scheme of the synthesis is shown in Scheme 1.

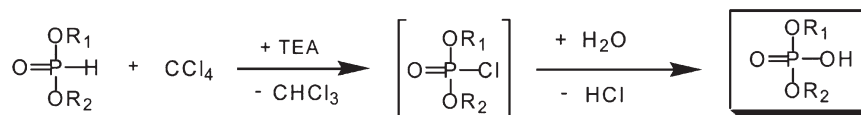


Scheme 1.

Subsequent oxidation after phosphorylation of a free hydroxyl function with the corresponding *H*-phosphonate yields the desired monoprotected peptide phosphate. Being P(III) compounds, *H*-phosphonates exhibit the same reactivity as phosphoramidites, but are much less sensitive to oxidation and moisture. The above method have been applied successfully for the synthesis of the following phosphopeptide sequences: H-RKKRIS(P)ALPG-OH, H-IQEANY(P)VPMTGP-NH<sub>2</sub> [7], H-WISHRST(P)VASCMHRQETVDC-OH. In these cases, the oxidation of the *H*-phosphonate derivatives was carried out by 1% iodine in pyridine–water mixture.

## Synthetic Methods

There are no significant side-reactions during the oxidation step even in the presence of methionine. In addition to the iodine oxidation, carbon tetrachloride can be used to the P(III)→P(V) transformation (Scheme 2).



Scheme 2.

The HPLC profile of the crude H-RKKRIS(P)ALPG-OH peptide after CCl<sub>4</sub>-oxidation is shown in Figure 1. This method has several advantages of both the global and synthon procedures and seems to be applicable for preparation of multiphosphorylated peptides without the need of selective protection of the amino acids.

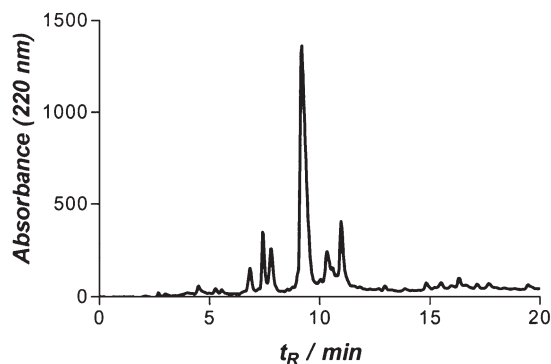


Fig. 1. The HPLC profile of the crude H-RKKRIS(P)ALPG-OH peptide after CCl<sub>4</sub>-oxidation.

## Acknowledgments

Supported by grant 34912 (OTKA) and the Foundation for the Hungarian Peptide and Protein Research.

## References

1. Hunter, T. *Cell* **7**, 113–127 (2000).
2. Lacombe, J.M., Andriamanampisoa, F., Pavia, A.A. *Int. J. Pept. Protein Res.* **36**, 275–280 (1990).
3. Wakamiya, T., Saruta, K., Yasuoka, J., Kusumoto, S. *Chem. Lett.* 1099–1102 (1994).
4. Kupihár, Z., Váradi, G., Monostori, É., Tóth, G.K., In Martinez, J. and Fehrentz, J.A. (Eds.) *Peptides: 2000 (Proceedings of the 26th European Peptide Symposium)*, EDK Paris, 2001, p. 239.
5. Kupihár, Z., Váradi, G., Monostori, É., Tóth, G.K. *Tetrahedron Lett.* **41**, 4457–4461 (2000).
6. Larsson, E., Lüning, B. *Tetrahedron Lett.* **35**, 2737–2738 (1994).
7. Kupihár, Z., Kele, Z., Tóth, G.K. *Org. Lett.* **3**, 1033–1035 (2001).
8. Atherton, F.R., Todd, A.R. *J. Chem. Soc.* 674–677 (1947).
9. Steinberg, G.M. *J. Org. Chem.* **15**, 637–647 (1950).

**Solid Phase Synthesis of Seleno-Methionine Peptides by tBoc/Bzl  
and Fmoc/tBu Protection Strategy Suitable  
for the Crystallographic Phase Determination  
by *Multi-Wavelength Anomalous Diffraction* (MAD)**

**Stefan R. K. Hoffmann, Christine A. Deillon and Bernd Gutte**

*Department of Biochemistry, University of Zurich, 8057 Zurich, Switzerland*

**Introduction**

The phase determination is one of the central problems for the determination of the electron density map during the X-ray crystallographic analysis of biomolecules. Thus several methods have been developed, which include isomorphous replacement [1], molecular replacement [2] and *multi-wavelength anomalous diffraction* (MAD) [3,4]. The last method uses the preparation of seleno-methionine derivatives of the protein structure. While molecular biology techniques unspecifically insert the seleno-methionine in the protein structure, chemistry allows in general the rapid position-selective chemical synthesis. We report here a solid phase synthesis strategy for seleno-methionine derivatives of synthetic peptide and protein structures, which is tightly fitted into the overall Fmoc/tBu or tBoc/Bzl protection scheme.

**Results and Discussion**

Both the Fmoc and the tBoc protected derivatives of selenomethionine were synthesized in high yield. While the preparation of the Boc-L-Met[Se]-OH proceeded by standard procedures using di-*tert*-butylpyrocarbonate, the preparation of the Fmoc protected derivative only yields a homogeneous compound when using 1.1eq. fluorenylmethylchloroformate in tetrahydrofuran/10.0% Na<sub>2</sub>CO<sub>3</sub> in water (3 : 1; v/v). Several eight to eleven amino acid residue peptides were synthesized on solid support using the standard chemistries. The incorporation of the selenomethionine derivatives was nearly quantitative and gave in homogeneous peptides. The formation of the cystine bridge proceeded cleanly in solution following the release from solid phase even in the presence of selenomethionine.

In our endeavour to determine the first X-ray structure of a retro-peptide [5,6], which was derived from the homodimerized and CGG extended retro-sequence of the leucine-zipper of the yeast transcription factor GCN4, and the X-ray structure of an artificial DDT binding peptide [7], the synthesis of the selenomethionine derivatives of these peptides was started. While all three possible selenomethionine mutants of the DDT binding peptide and the retro-leucine zipper were synthesized and released from solid phase in high purity without oxidation of selenomethionine, the direct cystine-mediated homodimerization of the retro-leucine zipper proceeded in an unreproducible manner and with low yield. All attempts to dimerize this sequence using the standard techniques were not successful due to several side reactions. Surprisingly, the dimerization rate of the leucine zipper was much higher when compared to that of the retro sequence, which we explained by folding-assisted cysteine oxidation.

The novel convergent fragment condensation strategy outlined in Figure 1 was developed both for the C-terminal carboxylate and the carboxamide of the dimerized and seleno-methionine derived retro-leucine zipper, which in general allows the direct preparation of cystine bridged homo- and heterodimers. Therefore the retro-leucine zipper (2-38) was synthesized on solid phase using the standard Fmoc chemistry.

## Synthetic Methods

*N,N'*-Bis-boc-L-cystine was activated by dicyclohexylcarbodiimide in dichloromethane at 0 °C to form the symmetric anhydride **2**. Reaction with the retro-leucine zipper (2-38) yields in the intermediate **3**, which was activated on the solid support with DIPC/HOBt followed by the condensation with the protected retro-leucine zipper (2-38) fragment to form the dimer **4**. The release by standard acidolytic TFA cleavage directly yielded in the seleno-methionine derived and dimerized retro-leucine zipper in high yield. All inter-mediate and products were completely characterized by HPLC and MS.

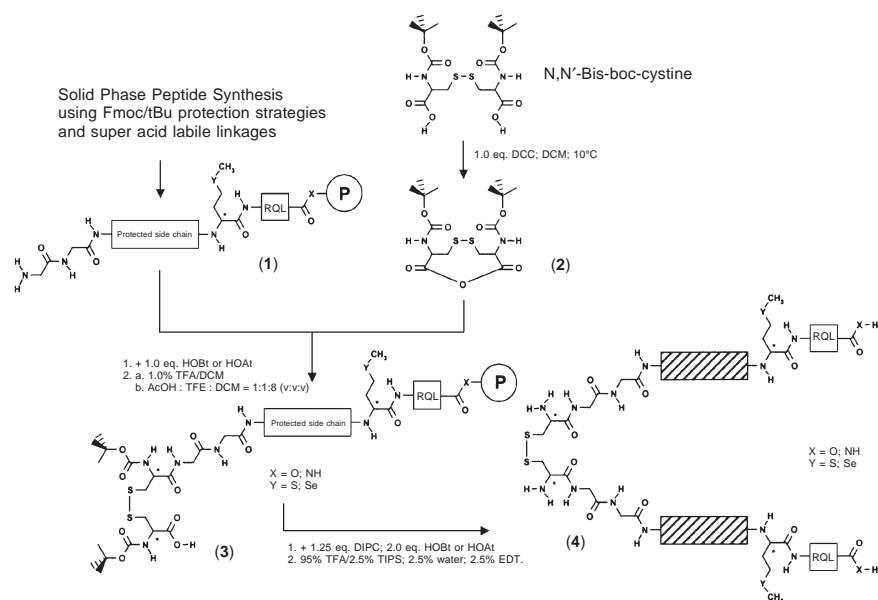


Fig. 1. The convergent fragment condensation strategy for the preparation of the seleno-methionine-derived and cystine-bridged retro-leucine zipper (CGGREGVLKKLRAVENEHNY KSELLVKDELQKM[Se]RQL).

## References

1. Ke, H.M. *Methods Enzymol.* **276**, 448–461 (1997).
2. Brunger, A.T. *Annu. Rev. Phys. Chem.* **42**, 197–223 (1991).
3. Ealick, S.E. *Curr. Opin. Chem. Biol.* **4**, 495–499 (2000).
4. Fourme, R., Shepard, W., Kahn, R. *Prog. Biophys. Mol. Biol.* **62**, 167–199 (1995).
5. Deillon, C.A., Sargent, D., Gutte, B., In Bajusz, S., Hudecz, F. (Eds.) *Peptides 1998*, Budapest, 1999, p. 412.
6. Mittl, P.R.E., Deillon, C.A., Sargent, D., Liu, N., Klauser, S., Thomas, R.M., Gutte, B., Grütter, M.G. *PNAS* **97**, 2562–2566 (2000).
7. Moser, R., Thomas, R.M., Gutte, B. *FEBS Lett.* **157**, 246–251 (1983).

## Synthesis of a C-Terminal Fluorescein-Labeled 36-mer Peptide

Reagan J. Greene, Jonathan M. White, Catherine J. Mader,  
Ralph A. Picking, J. William Lackey, Joel B. Erickson  
and Dennis M. Lambert

Trimeris, Inc., Durham, NC 27707, USA

### Introduction

Biomedical researchers routinely incorporate fluorescently labeled peptides into assays to enhance detection sensitivity and/or to study receptor binding mechanisms associated with cellular physiology. While there are many methods available that allow a researcher to fluorescently label a peptide at the N-terminus, or on a lysine residue, there are no strategies for C-terminal labeling with fluorescein derivatives that utilize the carboxylic acid of amino acids [1,2].

Here we report a synthetic strategy to incorporate one moiety of fluorescein isothiocyanate (FITC) onto the C-terminus of T-20, Ac-YTSLIHSLIEESQNQQEKN-EQELLELDKWASLWNWF-NH<sub>2</sub>. T-20 is the first peptide in a new class of anti-retroviral agents called fusion inhibitors [3], and a new anti-HIV drug candidate. Fluorescence polarization binding studies suggest that the presence of a fluorescein label on either the amino or carboxy terminus does not alter T-20's ability to bind to its target in gp41.

### Results and Discussion

The C-terminal amino acid (phenylalanine) of the T-20 sequence was modified to produce a "fluorescent" phenylalanine analog as illustrated in Figure 1.

Three protected fragments (Figure 2) were synthesized on acid sensitive 2-chlorotrityl chloride resin using Fmoc chemistry. Cleavage from the resin with 1% trifluoroacetic acid (TFA) in methylene chloride resulted in fully protected peptide fragments with >80% purity.

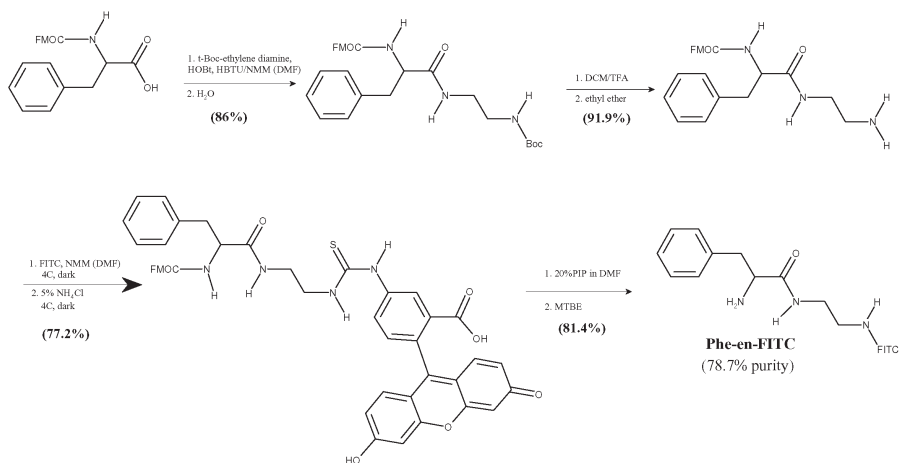


Fig. 1. Synthesis of "fluorescent" phenylalanine precursor.

Peptide Fragment 1:  
 Ac-Tyr(tBu)-Thr(tBu)-Ser(tBu)-Leu-Ile-His(Trt)-Ser(tBu)-Leu-Ile-Glu(OtBu)-Glu(OtBu)-Ser(tBu)-Gln(Trt)-Asn(Trt)-Gln(Trt)-Gln-OH

Peptide Fragment 2:  
 Fmoc-Glu(OtBu)-Lys(Boc)-Asn(Trt)-Glu(OtBu)-Gln(Trt)-Glu(OtBu)-Leu-Leu-Glu(OtBu)-Leu-OH

Peptide Fragment 3:  
 Fmoc-Asp(OtBu)-Lys(Boc)-Trp(Boc)-Ala-Ser(tBu)-Leu-Trp(Boc)-Asn(Trt)-Trp(Boc)-OH

Fig. 2. Protected peptide fragments from T-20 sequence.

The C-terminally fluoresceinated T-20 peptide was synthesized using fragment condensation [4], utilizing the “fluorescent” phenylalanine precursor as the C-terminal amino acid. Side-chain deprotection with TFA/H<sub>2</sub>O/DTT (90 : 5 : 5) and precipitation in ethyl ether yielded the C-terminally fluoresceinated T-20 peptide, Ac-YTSLIHSLIEE-SQNQQEKNEQELLELDKWASLWNWF-en-FITC. The crude peptide (30.45% by area) was purified by RP-HPLC to 91% purity, and Ion-Trap MS confirmed the accurate molecular weight of 4923.65 g/mol.

Fluorescence polarization binding studies were utilized to confirm that amino-terminal and carboxy-terminal fluorescein-labeled T-20 analogues bind to the same region in gp41 as native T-20. Figure 3 depicts the ability of native T-20 to compete with amino-terminal or carboxy-terminal fluorescein-labeled T-20 peptides for binding to the M41Δ614 protein construct (containing the HR1 binding region of gp41).

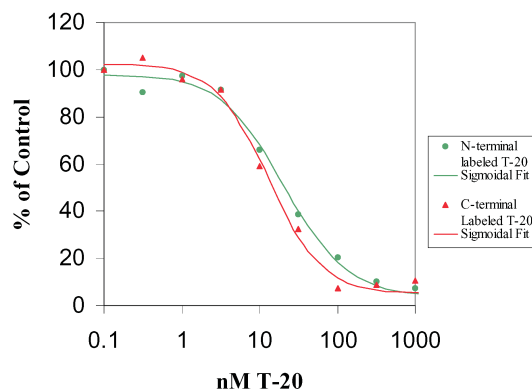


Fig. 3. Fluorescence polarization study of amino-terminal and carboxy-terminal fluorescein-labeled T-20 analogues (0.25 nM). Reactions carried out in TBST (Tris-buffered saline: 50 mM Tris, 138 mM NaCl, 2.7 mM KCl, with 0.01% Tween 20; pH 7.5). [ $\lambda_{ex}$  = 485 nm;  $\lambda_{em}$  = 530 nm; measured with LJL Analyst fluorometer (Molecular Devices Corp.) in FP mode.]

## References

1. Consalvo, A.P., Tamburini, P.P., Stern, W., Young, S.D. *Tetrahedron Lett.* **30**, 39–42 (1989).
2. Pennington, M.W., Baur, P. *Lett. Peptide Sci.* **1** 143–148 (1994).
3. Wild, C.T., Shugars, D.C., Greenwell, T.K., McDanal, C.B., Matthews, T.J. *Proc. Natl. Acad. Sci. U.S.A.* **91**, 9770–9774 (1994).
4. Kang, M., Bray, B., Lichty, M., Mader, C., Merutka U.S. Patent 6 015 881, 2000.

## Expanding Diversity: Modification of Linear and Cyclic Peptides by C-Glycosylation and N-Methylation

Florence Brunel, Anne-Marie Leduc, Sujan Singh, Xiaoping Tang,  
David M. Vogel, K. Grant Taylor and Arno F. Spatola

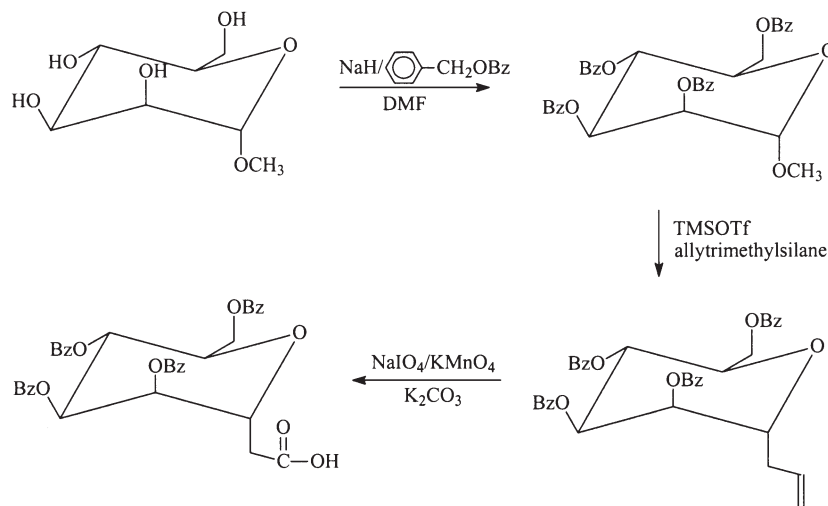
Department of Chemistry and The Institute for Molecular Diversity and Drug Design,  
University of Louisville, Louisville, KY 40292, USA

### Introduction

The stereochemical versatility of carbohydrates provides much structural diversity and has made them useful also as peptidomimetic scaffolds [1]. Just as peptides can be rendered more stable by backbone modifications including N-methylation and amide bond replacements [2], carbohydrates can likewise be stabilized by replacement of their vulnerable hemiacetal linkages. C-sugars are derivatives of carbohydrates in which the anomeric carbon is replaced by a methylene unit [3,4]. Carbohydrates are known to be involved in numerous biological processes such as cell-cell recognition [5]. Some glycoconjugate vaccines are being tested for prostate cancer [6]. C-sugars appear as very attractive substrates because of their increased stability especially against hydrolysis, but at the same time their structural and chemical properties are similar to O-glycosides [3,4]. This explains the increase of interest for C-glycosides [7]. Accordingly, we have initiated the synthesis of different pseudoglycopeptides.

### Results and Discussion

As shown in Scheme 1, after benzyl protection of the pyranoside, allylation is performed with allyltrimethylsilane and trimethylsilyl triflate as a Lewis acid catalyst. The acid is then obtained by treatment with sodium periodate and potassium permanganate. An alternative method used was the formation of the aldehyde by osmylation and subsequent oxidation with sodium periodate. The first method was preferred because it avoids using the poisonous osmium. These C-sugars are thus in the form of



Scheme 1. Synthesis of a protected  $\alpha$ -D-mannosyl acetic acid C-sugar.

## Synthetic Methods

O-protected acids and therefore can be easily introduced to the N-terminal or amine side chains of different peptides. We have previously reported the synthesis of solubility-enhanced N-methylated diketopiperazines and pseudodiketopiperazines [8]. We have suggested that these structures might represent an attractive template for drug discovery, particularly when combined with known structural motifs and transport enhancing glyconjugates. To this end we are preparing the first example of a heterocycle conjugate in which a stabilized C-sugar is linked to a functionalized diketopiperazine through an amide function.

We have also introduced a C-sugar moiety to a short version of a linear NR box pentapeptide as well as a  $\Psi[\text{CH}_2\text{NH}]$  pseudopeptide counterpart (Table 1). These C-sugar linkages tend to make these compounds slightly less hydrophilic, as seen in their corresponding RP-HPLC retention times.

Table 1. Mass and HPLC retention times of two peptides and their C-glycoside derivatives.

Structure	MW Calculated	MW found	RP-HPLC <sup>a</sup> retention time (min) <sup>b</sup>
Mannosylacetyl-Leu-Gln-Leu-Leu-OH	818.3	841.6 [M+Na]	17.1
H-Leu-Gln-Leu-Leu-OH	614.3	615.8 [M+1]	15.78
Mannosylacetyl-Leu-2Na $\Psi[\text{CH}_2\text{NH}]$ Gln-Leu-Leu-OH	872.7	873.6 [M+1]	21.15
H-Leu-2Na $\Psi[\text{CH}_2\text{NH}]$ Gln-Leu-Leu-OH	668.5	669.4 [M+1]	20.4

<sup>a</sup> Analytical RP-HPLC was performed on a Vydac 218TP54  $C_{18}$  column ( $4.6 \times 250$  mm) on a Hitachi 655A system equipped with an L-5000 controller and D-2000 integrator; <sup>b</sup> HPLC analysis was performed using the following gradient system: 5–90%  $\text{CH}_3\text{CN}/0.05\%$  TFA (B) in 30 min, flow 1.0 ml/min.

## Conclusion

N-methylation and the introduction of C-carbohydrate moieties allow us to synthesize a range of different pseudoglycopeptides. These compounds are being tested in a variety of assays and the initial platform can be optimized by structure activity relationship studies for delivery to the preferred target.

## References

1. Hirschmann, R. et al. *J. Am. Chem. Soc.* **115**, 12550–12568 (1993).
2. Spatola, A.F., In Weinstein, B. (Ed.) *Chemistry and Biochemistry of Amino Acids, Peptides and Proteins*, Vol VII, 1983, p. 257–347.
3. Levy, D.E., Tang, C. *The Chemistry of C-Glycosides*, Pergamon, BPC, Exeter, 1995.
4. Postema, M.H.D. *C-glycoside Synthesis*, CRC Press, Boca Raton, 1995.
5. Feizi, T. *Curr. Opin. Struct. Biol.* **3**, 701–710 (1993).
6. Kobertz, W.R., Bertozzi, C.R., Bednarski, M.D. *Tetrahedron Lett.* **33**, 737–740 (1992).
7. Kuduk, S.D. et al. *J. Am. Chem. Soc.* **120**, 12474–12485 (1998).
8. Brunel, F.M., Sing, L., Wittliff, J.L., Spatola, A.F. *Peptides 2000, Proceedings of the 26th EPS, EDK, Paris, 2001*, p. 611–612.

## One-Dimensional Spatial Encoding: Split/Mix Synthetic Parallelism with Tag-Free Identification and Assays at the Speed of Light

Alan W. Schwabacher and Peter Geissinger

Department of Chemistry, University of Wisconsin-Milwaukee, Milwaukee, WI 53211, USA

### Introduction

We have recently developed a method for combinatorial chemistry that allows fully parallel synthesis, while retaining information on the identity of each library member. In this context, we use the term “fully parallel” in a *very* restrictive sense, *i.e.*, to specify not only that a given synthetic step is carried out simultaneously for the entire library, but also that each reagent used in a given step need be handled only once. The key to spatially encoded synthesis with such parallelism is to use a linear organization of the library, and a solid support of linear morphology [1].

One significant application of arrays of substances prepared in a combinatorial manner is as a sensor array. We envisioned the preparation of large arrays of fluorescent chemosensors to be quite useful for the selective detection of a variety of analytes. Synthesis of the chemosensor compounds may be carried out by a variety of techniques. Fabrication of arrays of such substances in a useful configuration is a separate problem that is frequently addressed by preparation of a 2-dimensional array by spotting individual substances upon an appropriate surface substrate. Readout of such arrays requires some kind of imaging or spatially discriminating detection. We considered the question of whether the linear arrays we can prepare with such efficiency are compatible with rapid sensor readout simpler than imaging.

We demonstrate here that virtually instantaneous readout of the entire array is possible if the linear array is distributed along an optical fiber. No imaging is required: the entire array output is obtained as a single time-varying signal [2].

### Results and Discussion

The challenge in spatially encoded synthesis is to subdivide the support for one reaction, and then to re-subdivide it in a mathematically orthogonal manner for the next reaction, without loss of information. Our solution is quite simple, as shown in Figure 1. A. The linear support (thread or fiber) is wrapped around a cylinder of precisely determined circumference in a single spiral layer. Division of the cylinder lengthwise into regions allows treatment of the space between a pair of divisions as a reaction vessel. B. After carrying out a separate reaction in each region (placing each reagent in *one* region) the linear support may be removed from the cylinder. C. It now bears a set of repeating domains, the position of each specifying compound identity. D. In order to

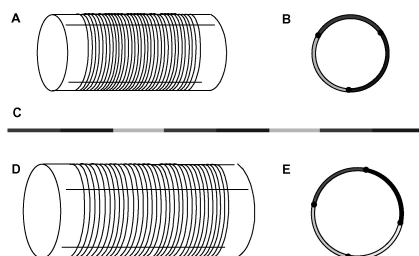


Fig. 1. 1-Dimensional combinatorial synthesis.

re-subdivide in an orthogonal manner such that all combinations will be formed in the next step, the linear solid support is wrapped around another cylinder of a different well-defined circumference. Because the cylinder is of a different appropriate size, adjacent regions bear unrelated substances, and regions bearing like substances are distributed around the cylinder. E. A second set of reagents is applied, one to a region. F. This second set of reagents, after removal of support from the cylinder, is seen to have formed a repeating pattern along the linear support. Since the period of the repeat is distinct from that of the first step, all combinations are formed. This process can be repeated with an arbitrary number of steps.

Given that one could prepare an array of sensors in this manner, the question remains as to its readout. If each sensor region were distributed along an optical fiber, light propagating within the fiber core could excite a fluorosensor by an evanescent mechanism, which would minimize interference from solution. Discrimination of the output of each sensor is possible by various approaches. If a short (*ca* 0.5 ns) pulse is sent down the fiber, each region is excited at a slightly different time. By detecting the emission that is captured by the fiber (a second evanescent process) and propagates back toward the front of the fiber, regions can be distinguished by the arrival time. This technique is limited by the fluorescence lifetimes; while individual regions can be localized with high precision, output from closely-spaced regions can overlap.

We have overcome this limitation by introducing a two-fiber scheme (Figure 2) [2]. On one fiber, the sensor regions may be spaced closer than the limit imposed by the fluorescence lifetimes. A laser pulse propagating through this fiber may excite fluorophores in these regions essentially simultaneously. A fraction of the emitted light is now coupled evanescently into the second fiber, which periodically contacts each region. The distance between adjacent sensor regions along the second fiber is large enough to delay the light pulses with respect to each other on their way to the detector. The two-fiber scheme allows for separation of the optical delay from the synthesis support, and separate optimization for each fiber's distinct role.

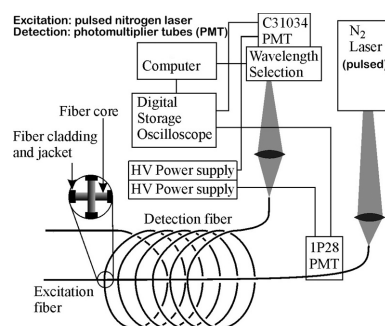


Fig. 2. Two-fiber detection scheme.

### Acknowledgments

This material is based upon work supported by the National Science Foundation under Grants CHE-9874241 (A. W. S.) and CHE-0078895 (P. G.). We gratefully acknowledge our coworkers Dr. Barry Prince, Christopher Johnson, and Yixing Shen.

### References

1. Schwabacher, A.W., Shen, Y., Johnson, C.W. *J. Am. Chem. Soc.* **121**, 8669–8670 (1999).
2. Prince, B.J., Schwabacher, A.W., Geissinger, P. *Anal. Chem.* **73**, 1007–1015 (2001).

## Spatial Screening of Lectin Ligands. Cyclic Peptides as Scaffolds for Multivalent Presentation of Carbohydrates

Valentin Wittmann and Sonja Seeberger

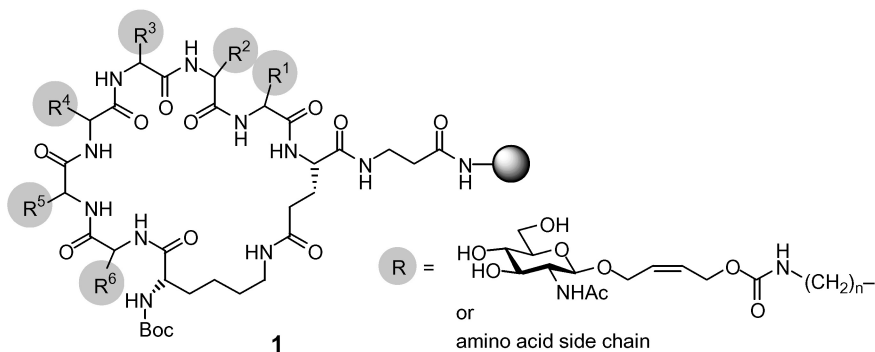
*Institut für Organische Chemie, Johann Wolfgang Goethe-Universität, 60439 Frankfurt, Germany*

### Introduction

Carbohydrate-lectin interactions are the basis of numerous biologically important recognition processes [1]. Examples include the initiation of the inflammatory response, bacterial and viral pathogenesis, fertilization, and even protein folding. High-affinity lectin ligands are of considerable medicinal interest in the diagnosis, therapy, and prevention of conditions associated with these processes. One approach to arrive at such ligands is the design of small oligovalent carbohydrate derivatives (mini clusters) which can simultaneously bind to several binding sites of a single (oligomeric) lectin proximate in space and may be tailored to lectins with known 3D-structure [2] ("directed" multivalency). However, if the structure of the targeted lectin and thus the required orientation of the sugar epitopes of the mini clusters are unknown, an efficient procedure for the generation and screening of libraries of spatially diverse mini clusters is desirable. Here we present a new strategy for finding multivalent lectin ligands by spatial screening using libraries of cyclic peptides as scaffolds for multivalent presentation of carbohydrate epitopes [3,4].

### Results and Discussion

Our strategy comprises four steps: a) split-mix synthesis of a library of scaffold molecules with side chain amino groups in varying amounts and spatial orientation, b) attachment of several copies of a carbohydrate ligand to the amino groups, c) on-bead screening of the library for lectin-binding properties, and d) identification of potent ligands by single-bead analysis.



As scaffolds for the multivalent presentation of carbohydrate ligands, we have chosen cyclic peptides of general type **1**. At the combinatorially varied positions indicated by gray circles, D- and L-amino acids without a side chain functionality as well as D- and L-diamino acids such as lysine, diaminobutyric acid, or diaminopropionic acid are incorporated. The latter represent the points of attachment of the carbohydrates. This library design allows for generation of spatial diversity in two dimensions. Positional diversity generates different carbohydrate patterns displayed on the scaffolds. Varying

the stereochemistry of the amino acids increases spatial diversity by generating different backbone folds [5].

Application of this screening approach is demonstrated using wheat germ agglutinin (WGA) as an example. WGA, a 36 kDa lectin composed of two glycine- and cysteine-rich subunits, contains several carbohydrate binding sites for *N*-acetylglucosamine (GlcNAc) and oligomers thereof, thus being a promising candidate for a multivalent interaction. Using a synthetic approach developed earlier in our laboratory [3], a neoglycopeptide library of 19440 compounds was synthesized on aminofunctionalized TentaGel without employing a linker following the “split and combine” synthesis method (Figure 1). GlcNAc residues were attached to side chain amino groups *via* an Aloc derived urethane. The carbohydrate content of the library members ranges from 0 (2.6% of all compounds) over 1 (14.5%), 2 (30.3%), 3 (30.9%), 4 (16.6%), 5 (4.5%) up to 6 (0.5%).

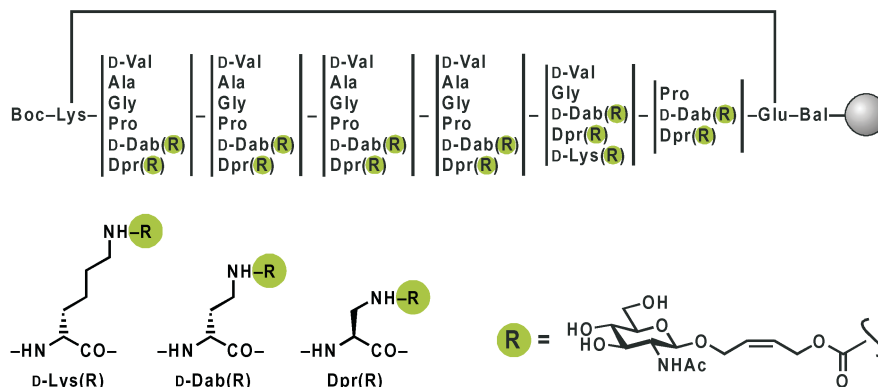


Fig. 1. Library of 19440 cyclic neoglycopeptides. Bal = β-alanine.

In order to screen the library for lectin binding properties, we developed an on-bead assay (Figure 2). Briefly, the resin-bound neoglycopeptides were incubated with biotinylated WGA followed by addition of an anti-biotin alkaline-phosphatase conjugate. Beads with bound lectin were detected by an alkaline phosphatase catalyzed color reaction. When the assay was carried out in the presence of competing monovalent ligand (GlcNAc), a small part (approx. 0.1%) of the beads stained very darkly. These beads were manually selected under a microscope and treated with

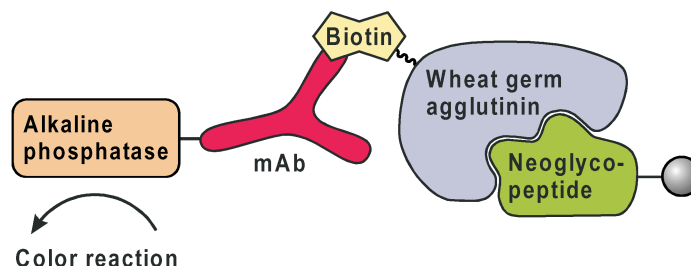
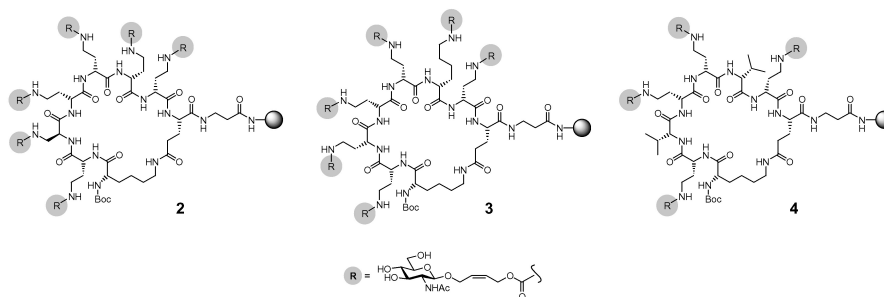


Fig. 2. Immunosorbent lectin binding assay.

Wittmann et al.

[Pd(PPh<sub>3</sub>)<sub>4</sub>]/morpholine in order to remove the carbohydrates. After cleavage of the *N*-terminal Boc protecting group, “hit” structures were identified by automated single-bead Edman degradation. Due to the side chain cyclization, a negative answer is expected during the first degradation step, as long as cyclization has occurred completely (cyclization control).

So far, three WGA ligands could be identified, the hexavalent compounds **2** and **3** and, interestingly, tetravalent **4**. Its four D-Dab(R) residues in positions 2, 4, 5, and 7 are conserved among all three ligands. Except for position 3 in compound **2** (Dpr(R)), we found exclusively D-amino acids at the combinatorially varied positions 2–7. Further sequencing results are necessary to confirm the observed consensus sequence and preference for D-amino acids.



Since the corresponding non-glycosylated cyclopeptide library (Figure 1, R = Ac) does not contain any WGA ligands, we assume the spatial presentation of the GlcNAc residues on the cyclopeptide scaffolds to be responsible for different binding affinities to WGA.

### Acknowledgments

This work was kindly supported by the Deutsche Forschungsgemeinschaft (grants WI 1479/2-1 and 2-2) and the Adolf Messer-Stiftung (Adolf Messer-Stiftungspreis 2000 for interdisciplinary research to V. W.).

### References

1. Varki, A., Cummings, R., Esko, J., Freeze, H., Hart, G., Marth, J. (Eds.) *Essentials of Glycobiology*, Cold Spring Harbor Laboratory Press, Cold Spring Harbor, 1999.
2. a) Kitov, P.I., et al. *Nature* **403**, 669–672 (2000); b) Fan, E., et al. *J. Am. Chem. Soc.* **122**, 2663–2664 (2000); c) Mammen, M., et al. *Angew. Chem., Int. Ed.* **37**, 2754–2794 (1998).
3. Wittmann, V., Seeberger, S. *Angew. Chem., Int. Ed.* **39**, 4348–4352 (2000).
4. On the use of cyclic peptides as scaffolds see: a) Franzyk, H., et al. *Bioorg. Med. Chem.* **5**, 21–40 (1997); b) Sprengard, U., et al. *Angew. Chem., Int. Ed. Engl.* **35**, 321–324 (1996); c) Tuchscherer, G., Mutter, M. *Pure Appl. Chem.* **68**, 2153–2162 (1996).
5. Haubner, R., Finsinger, D., Kessler, H. *Angew. Chem., Int. Ed. Engl.* **36**, 1374–1389 (1997).

## Combinatorial Syntheses of Polyhydroxamate Siderophores: Desferrioxamine, Exochelin, Mycobactin, and Aerobactin Libraries

Urszula Slomczynska<sup>1</sup>, P. Amruta Reddy<sup>1</sup>, Otto F. Schall<sup>1</sup>, Todd Osiek<sup>1</sup>,  
 Arati Naik<sup>1</sup>, W. Barry Edwards<sup>1</sup>, James Wheatley<sup>1</sup> and  
 Garland R. Marshall<sup>2</sup>

<sup>1</sup>MetaPhore Pharmaceuticals, Inc., St. Louis, MO 63114, USA

<sup>2</sup>Department of Biochemistry and Molecular Biophysics, Washington University, St. Louis,  
 MO 63110, USA

### Introduction

Siderophores are natural products, often containing amino acid derivatives, that are produced by microorganisms to chelate ferric ion as part of an iron-uptake system essential for survival. In order to explore several therapeutic opportunities, we have developed a combinatorial synthetic strategy to prepare libraries of analogs of a number of different siderophores, including desferrioxamine (DFO), for potential treatment of iron overload [1]; and exochelin, mycobactin and aerobactin for potential antibiotic applications. These siderophores all contain hydroxamate groups as primary coordination sites for the ferric ion (Figure 1). Their typical stability constants ( $K_s$ ) for ferric ion are from  $10^{23}$  to  $10^{32}$ .

### Results and Discussion

To facilitate synthesis of various analogs of the parent siderophore, we have developed novel synthetic approaches in which the hydroxamate groups were constructed *in*

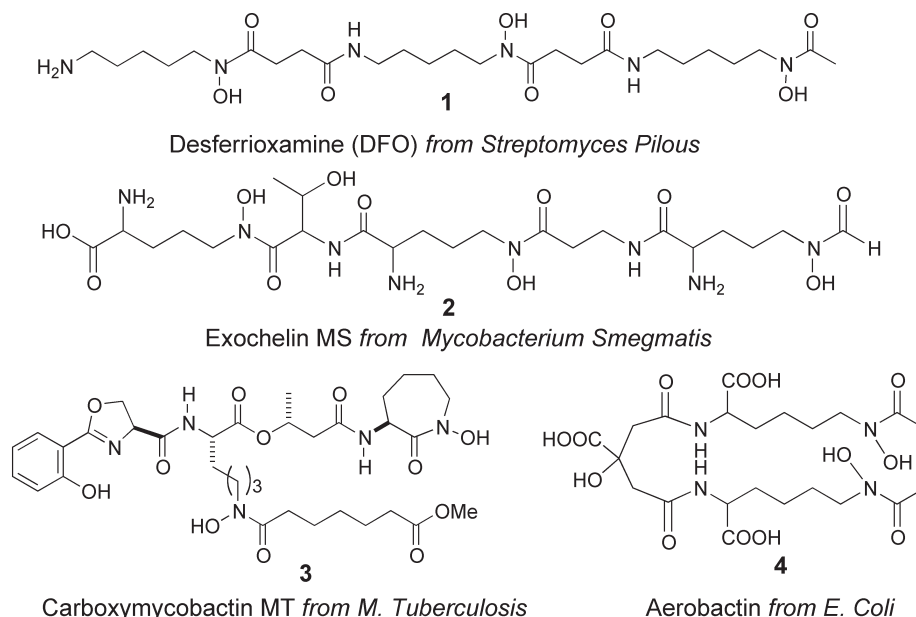
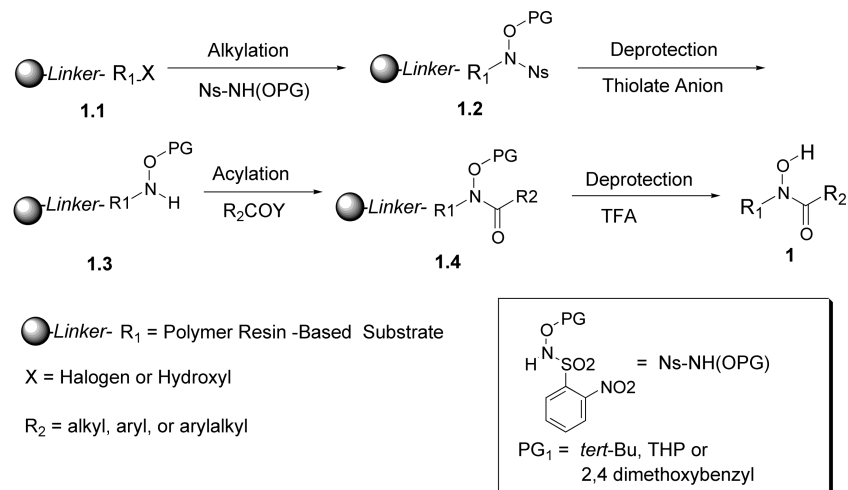


Fig. 1. Polyhydroxamate siderophores.

*situ* during the solid-phase procedure (Scheme 1). The key to this approach was choice of *N*-nosyl (2-nitrophenylsulfonyl = Ns) protection [2] of the hydroxylamine group and an appropriate protecting group PG. The presence of the temporary *N*-protecting 2-nosyl group activates the nitrogen for alkylation with alkyl halides by conventional methods or alcohols under Mitsunobu reaction conditions to give **1.2**. Selective removal of the nosyl group with thiolate anion then leads to **1.3** that facilitates further elaboration of the molecule by *N*-acylation to afford the intermediate **1.4**. The choice



Scheme 1. Solid-phase synthesis of hydroxamate.

of acid-labile *O*-protecting groups (*e.g.* *tert*-Bu, THP, 2,4-dimethoxybenzyl) for the hydroxylamine moiety makes our automated high-throughput synthesis a robust process, as the protecting group is also removed during the final cleavage from the solid support. Also, some of these protecting groups (*e.g.* THP) offer the convenience of on-resin deprotection leading to libraries on solid support for further evaluation. Removal of the permanent *O*-protecting group (PG) leads to the desired hydroxamate **1**. When this approach is combined with an orthogonal protecting scheme for other building blocks (*e.g.* acid-sensitive groups for permanent protection and base, thiolate or mild acid-sensitive groups for temporary protection) such as amino acids, amino alcohols or carboxylic acids, the strategy is very versatile and suitable for generation of a large number of polyhydroxamate analogs. Another advantage of this approach is the ease of synthesis through the use of readily available, simple building blocks. A wide variety of structurally diverse analogs of DFO [3], aerobactin, carboxymycobactin, and exochelin (more than 200 compounds) were prepared via solid-phase combinatorial synthesis to explore metabolism, bioavailability, metal affinity and selectivity, and iron transport.

High-throughput screening to determine metal binding was developed based on competitive colorimetric and mass spectrometric assays. The spectrophotometric methods have proven to be more suitable for high-throughput screening, with sulfoxine (8-hydroxyquinoline 5-sulfonic acid) being the most robust. The measurement reflects relative affinities of ligands, expressed as a percentage of iron stripped

from sulfoxine-Fe complex, and was correlated with information about  $K_{\text{eff}}$  by using ligands with known affinities (*e.g.* 67% for DFO with  $\log K_{\text{eff}} = 24.26$  vs 14% for EDTA with  $\log K_{\text{eff}} = 21.90$ ).

Thirty-five DFO analogs with  $\log K_{\text{eff}}$  ranging from 22 to 24 were selected as promising candidates for screening for iron removal from animal models of iron overload diseases. The iron-mobilization efficacy of novel chelators was evaluated in rats with hepatocytes labeled with Fe-59-ferritin as described by Pippard *et al.* [4] and compared to DFO (Desferal<sup>®</sup>, in clinical use for the treatment of iron-overload, s.c. infusion, orally not active). The chelators were first administrated i.p. to identify candidates for oral screening. Among fifteen DFO library analogs tested, seven compounds were as effective or better than DFO. Screening of selected candidates for oral activity is underway. So far, one DFO analog was identified with oral activity and comparable efficacy to L<sub>1</sub> (Deferiprone<sup>®</sup> – a bidentate oral drug conditionally approved in Europe and India for the treatment of iron-overload). The combinatorial strategy for synthesis and screening of polyhydroxamate analogs proved useful in identification of novel iron-binding ligands with improved therapeutic properties.

#### **Acknowledgments**

Supported in part by NIH SBIR grants DK54157, AI43730, and AI44584.

#### **References**

1. Bergeron, R.J., Brittenham G.M. (Eds.) *The Development of Iron Chelators for Clinical Use*, CRC Press, Boca Raton (FL), 1994.
2. Fukuyama, T.J., Cheung, M. *Tetrahedron Lett.* **36**, 6373–6374 (1995).
3. Published in part: Slomczynska, U., Reddy, P.A., Schall, O.F., Rosik, L., Wheatley, J.R., Marshall, G.R. *Transfusion Sci.* **23**, 265–266 (2000).
4. Pippard, M.J., Johnson, D.K., Finch, C.A. *Blood* **58**, 685–692 (1981).

## Identification of Peptide Ligands for $\alpha 4\beta 1$ Integrin Receptor as Potential Targeting Agents for Non-Hodgkin's Lymphoma

Steven I. Park, Renil Manat, Brian Vikstrom, Nail Amro and Kit S. Lam

*Division of Hematology and Oncology, Department of Internal Medicine, UC Davis Cancer Center, University of California Davis, Sacramento, CA 95817, USA*

### Introduction

$\alpha 4\beta 1$  integrin is widely expressed on both T- and B-lymphocytes. It is involved in cell migration into tissue during inflammatory responses and normal lymphocyte trafficking and plays an important role in inflammation and autoimmune diseases [1]. Over the past few years, a number of investigators have developed peptide or peptidomimetic inhibitors/ligands for  $\alpha 4\beta 1$  based on the known peptide sequence ILDV in fibronectin [2]. Most of these studies have been directed to the treatment of a number of inflammatory and autoimmune diseases. In this study, we used a whole cell binding assay to screen a random "one-bead one-compound" combinatorial peptide-bead library [3] with a human T-lymphoma line (Jurkat) and discovered a number of lymphoid tumor cell line specific peptides that contain pLDI motif.

### Results and Discussion

To discover lymphoid tumor cell line-specific peptide ligands, two " $\beta$ -turn" peptide libraries XXXpXXX and xXXXpXXX (wherein "X"= all 19 eukaryotic amino acids except cysteine, "x"= the corresponding 19 D-amino acids, and "p"= D-proline) were used. From screening these peptide libraries with live Jurkat cells, a number of beads bound by a monolayer of cells were retrieved. The beads were then recycled and tested against a human myeloid leukemia cell line (K562). The beads, which were specific to Jurkat cell line, were isolated for microsequencing (Table 1). Most ligands contained LDI or LDF motifs. This data corroborate well with the previous study that Jurkat cell line has high level of  $\alpha 4\beta 1$  integrin on the cell surface [4], and that -LDV- is a known natural  $\alpha 4\beta 1$  integrin binding motif in fibronectin. We have selected LTGpLDI as the parent peptide for SAR studies (Table 2). We tested each of the deletion and substitution analogues against Jurkat, OCILY8 (human B-cell immunoblastic lymphoma), K562, HL-60 (human myeloid leukemia) cell lines as well as mononuclear cells obtained from peripheral blood of normal volunteers. The binding profiles of LTGpLDI, TGpLDI, and GpLDI were essentially identical, indicating that the two N-terminal residues LT are not critical. These peptides bound preferentially to hu-

Table 1. Jurkat cell specific peptide ligands isolated from primary screen.

Library	XXXpXXX	xXXXpXXX	
Ligand sequences	LTGpLDI	gVSHpLDI	nLDFpFFN
	WDGpLDI	eGWQpLDI	fLDFpDPM
	HQMpLDI	eFAFpLDF	nLDHpHNL
	DIQpLDI	fMWFpLDF	wADFpHET
	YVGpLDF	gYWYpLDY	
	HHWpLDF		
	IWHpLDV		

## Synthetic Methods

man T and B lymphoma lines, and weakly to a myeloid leukemia line (K562) and did not interact with another human myeloid leukemia line (HL-60) or mononuclear cells derived from the peripheral blood of normal volunteers. pLDI was found to be the minimal sequence necessary for cell binding as further deletion of D-pro totally eliminated cell binding. Further SAR studies with substitution analogues showed that replacement of D-pro (residue 4) with L-pro greatly decreased the binding affinity. Replacement of Leu (residue 5) or Asp (residue 6) with Ala rendered the peptide completely inactive. However, significant binding to Jurkat cells (T-lymphoma) remained when Ile (residue 7) was replaced by Ala. Interestingly, this latter peptide (LTGpLDA) no longer bound to the B-lymphoma cell line.

Table 2. Binding specificity of LTGpLDI peptide analogues to different cancer cell lines and mononuclear cells derived from normal volunteers.

	Jurkat	OCILY8	K562	HL-60	Peripheral mononuclear cells
(A) Deletion Analogues					
LTGpLDI	3+	3+	1+	–	–
TGpLDI	3+	3+	1+	–	–
GpLDI	3+	3+	1+	–	–
pLDI	2+	2+	–	–	–
LDI	–	–	–	–	–
(B) Substitution Analogues					
LTGPLDI	1+	–	–	–	–
LTGaLDI	1+	–	–	–	–
LTGpADI	–	–	–	–	–
LTGpLAI	–	–	–	–	–
LTGpLDA	2+	–	–	–	–

Semi-quantitative whole cell binding assay: “–” average number of less than 5 cells bound per bead, “1+” 5 to 20 cells per bead, “2+” 20 to 40 cells per bead, and “3+” > 40 cells per bead.

The peptide ligands identified from one-bead binding were synthesized in solution phase and evaluated for their binding activities. One  $\mu\text{M}$  of biotinylated peptides in solution phase were immobilized on 96-well plate precoated with Neutralite-Avidin, and Jurkat cells were added to the well in the presence or absence of different antibodies (Figure 1). Jurkat cells without any antibody treatment showed good binding affinity. A similar pattern was noted in Jurkat cells pretreated with integrin-activating anti- $\beta 1$  TS2/16 antibody or anti- $\alpha 5$  antibody. In contrast, treatment of anti- $\alpha 4$  HP2/1 antibody prevented Jurkat cells from adhering to the peptide with an  $\text{IC}_{50}$  value of  $0.1 \mu\text{g/ml}$ , suggesting that the peptide interacts with  $\alpha 4$  integrin on the surface of the cell.

Using the “one-bead one-compound” combinatorial peptide-bead library method, we discovered lymphoid tumor cell line specific peptides containing pLDI motif. The ligands were specific to both T- and B-lymphoid tumor cell lines (Jurkat and OCILY8

**Park et al.**

cell lines respectively) and did not bind to myeloid tumor cell lines (K562 or HL-60) or to normal human peripheral lymphocytes. These findings may have important implications in targeted-therapy and imaging of both T- and B-cell lymphoid malignancies.

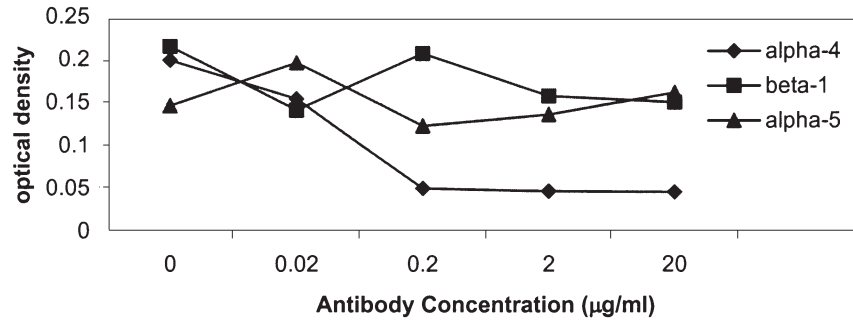


*Fig. 1. Jurkat cell adhesion to WDGpLDI in the presence of anti-integrin antibodies.*

#### **Acknowledgments**

This work is supported by grants from NCI (CA89706) and California Cancer Research Program (764V-20133).

#### **References**

1. Lobb, R.R., Hemler, M.E. *J. Clin. Invest.* **94**, 1722–1728 (1994).
2. McIntyre, B.W., Woodside, D.G., Caruso, D.A., Wooten, D.K., Simon, S.I., Neelamegham, S., Reville, J.K., Vanderslice, P. *J. Immunol.* **158**, 4180–4186 (1997).
3. Pennington, M.E., Lam, K.S., Cress, A.E. *Mol. Diversity* **2**, 19–28 (1996).
4. Moyano, J.V., Carnemolla, B., Dominguez-Jimenez, C., Garcia-Gila, M., Albar, J.P., Sanchez-Aparicio, P., Leprini, A., Querze, G., Zardi, L., Garcia-Pardo, A. *J. Biol. Chem.* **272**, 24832–24836 (1997).

## Development of Peptidomimetic Substrates and Inhibitors that Bind to the Peptide Binding Pocket of the Catalytic Site of p60<sup>c-src</sup> Protein Tyrosine Kinase

Jayesh R. Kamath, Ruiwu Liu, Amanda M. Enstrom, Gang Liu  
and Kit S. Lam

*Division of Hematology and Oncology, Department of Internal Medicine, UC Davis Cancer  
Center, University of California Davis, Sacramento, CA 95817, USA*

### Introduction

Src family protein tyrosine kinases (PTKs) are excellent targets for anti-cancer drug discovery due to their association with cell transformation and carcinogenesis. In the past few years, we have developed a pseudosubstrate-based inhibitor strategy to target the active site of p60<sup>c-src</sup> PTK. This strategy has led to the identification of highly selective and potent peptide inhibitors of p60<sup>c-src</sup> PTK [1,2] that bind to the peptide substrate binding pocket and not the ATP binding pocket. Despite their high inhibitory activity against p60<sup>c-src</sup> PTK in a cell free protein kinase assay, the peptide inhibitors did not show any significant biological effect on intact v-src transfected 3T3 cells. This was probably due to their inability to penetrate the cell membrane and their susceptibility to proteolysis. Previous work in our laboratory on peptide substrates [3,4] and inhibitors [1,2] led us to believe that the dipeptide motif, -Ile-Tyr- (-I-Y-), is critical for binding to the active site of p60<sup>c-src</sup> PTK. In this study, we describe the development of cell permeable peptidomimetic substrates and inhibitors of p60<sup>c-src</sup> PTK using -Ile-Tyr- as a core structure.

### Results and Discussion

Our approach to identify peptidomimetic substrates is to use the on-bead functional screening method [4] with [ $\gamma$ -<sup>32</sup>P] ATP and p60<sup>c-src</sup> PTK. These substrates are then used as templates to develop potent inhibitors that bind to the protein substrate binding pocket. We first synthesized a biased “one-bead one-compound” peptidomimetic library (R-I-Y-X) with a “split synthesis” method (wherein R represents 96 alkyl groups and X stands for 38 amino acids that include both the L- and D-isomers of all 20 eukaryotic amino acids except cysteine). By the end of the synthesis, each of the sub-libraries remained separate in each well of the 96-well plate. We then screened each of the sub-libraries with an on-bead functional <sup>32</sup>P-phosphorylation assay.

The positive [<sup>32</sup>P]-labeled beads were detected with autoradiography. The first library screening led to the identification of peptidomimetic sub-libraries, with specific R groups, which are excellent substrates for p60<sup>c-src</sup> PTK (Figure 1). In the second step, we synthesized and screened all the individual compounds of the active sub-libraries. This screening enables us to identify individual peptidomimetic substrates of p60<sup>c-src</sup> PTK. A few of these substrates, when modified and tested as inhibitors in our cell free protein kinase assay [5], showed moderate potency with IC<sub>50</sub>

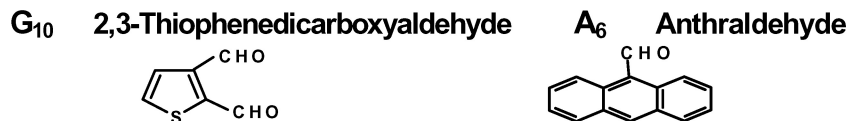


Fig. 1. Chemical structure of R groups that cap the active sub-libraries (R-I-Y-X).

values in the range of 5 to 20  $\mu\text{M}$ . Unlike our peptide inhibitors, some of the peptidomimetics also showed significant growth inhibitory or morphological effects on various cancer cell lines including v-src transfected 3T3 cells, colon, bladder and prostate carcinoma (Table 1). This was probably due to their peptidomimetic nature, small size and their resistance to proteases. However not all the peptidomimetic compounds active in the enzyme assay exert biological effects on intact cells. Work is currently underway in our laboratory to further optimize these peptidomimetic compounds for more potent and selective anti-tumor activities.

Table 1. Biological effects of the peptidomimetic p60<sup>c-src</sup> PTK inhibitors.

Peptidomimetics	Protein kinase inhibition IC <sub>50</sub> $\mu\text{M}$ <sup>a</sup>	Cytotoxicity IC <sub>50</sub> $\mu\text{M}$ <sup>b</sup>	Morphological changes <sup>c</sup>
G <sub>10</sub> -I-Y-K	18 $\pm$ 2.0	None	Yes
G <sub>10</sub> -( $\beta$ -Phe)-K	12 $\pm$ 2.1	None	Yes
A <sub>6</sub> -I-Y-K	14 $\pm$ 2.0	None	Yes
A <sub>6</sub> -( $\beta$ -Phe)-Dpr	13 $\pm$ 2.8	90 $\pm$ 17	Cell death
H <sub>4</sub> -(nal-2)-Dpr	6.3 $\pm$ 1.0	6.8 $\pm$ 1.0 <sup>d</sup>	Cell death

$\beta$ -Phe, L- $\beta$ -phenylalanine; Dpr, L-diaminopropionic acid; nal-2, D-3-(2-naphthyl)alanine.

<sup>a</sup> The substrate used in these experiments was YIYGSFK at 55  $\mu\text{M}$  (its  $K_m$  value). <sup>b</sup> Based on proliferation of v-src-3T3 cells (assessed by MTT proliferation assays). <sup>c</sup> "Yes" indicates changes in cell morphology and restoration of contact inhibition. <sup>d</sup> Tested on HT-29, a human colon carcinoma cell line with overexpression of p60<sup>c-src</sup>.

### Acknowledgments

We thank Dr. Kung's laboratory at the UCD Cancer Center for technical assistance with the cellular assays. This work is supported by NSF grant MCB9728399.

### References

1. Lou, Q., Leftwich, M., et al. *Cancer Res.* **57**, 1877–1888 (1997).
2. Alfaro-Lopez, J., Wei, Y., et al. *J. Med. Chem.* **41**, 2252–2260 (1998).
3. Lam, K. S., Wu, J. S., Lou, Q. *Int. J. Pept. Protein Res.* **45**, 587–592 (1995).
4. Lou, Q., Leftwich, M. E., Lam, K. S. *Bioorg. Med. Chem.* **4**, 677–682 (1996).
5. Lou, Q., Wu, J., Lam, K. S. *Anal. Biochem.* **235**, 107–109 (1996).

## Pseudoproline Libraries for Tuning Inhibitors of SH3 Domain Mediated Protein–Protein Interactions

Jimena Fernandez-Carneado<sup>1</sup>, Patricia Durieux<sup>1</sup>, Luc Patiny<sup>1</sup>, Yoshiro Tatsu<sup>1</sup>, Daniel Grell<sup>1</sup>, Christian Kardinal<sup>2</sup>, Stephan Feller<sup>2</sup> and Gabriele Tuchscherer<sup>1</sup>

<sup>1</sup>*Institute of Organic Chemistry, BCH, University of Lausanne, CH-1015 Lausanne, Switzerland*

<sup>2</sup>*Laboratory of Molecular Oncology, MSZ-Institute for Medical Radiation and Cell Research, D-97078 Würzburg, Germany*

### Introduction

Specific protein–protein interactions are essential facets in cellular communication and the formation and specific assembly of multicomponent protein complexes often is regulated by binding to proline (Pro)-rich peptide sequences. Pro-rich ligands adopt a left-handed polyproline II helical conformation (PPII, all trans amide bonds) and bind to a highly conserved patch of aromatic amino acids of *e.g.* Src homology (SH3) domains [1]. The essential feature of SH3 binding ligands is the consensus sequence Pro-Xaa-Xaa-Pro (Xaa representing variable amino acids). In the search for novel inhibitors, recently introduced pseudoprolines ( $\Psi$ Pro), *i.e.* Ser, Thr, Cys derived proline-ring structures with enhanced inherent properties of L-Pro, were used to study ligand receptor interactions of Pro-rich peptides [2]. Binding affinities in the order typically found for SH3-mediated interactions and most notably, enhanced binding specificity as well as inhibition of Grb2 SH3 (N)-SoS complex formation (Figure 1) illustrate that  $\Psi$ Pro building blocks exert a dual functionality, *i.e.* i) increase and optimization of van der Waals contacts and hydrogen bonding to the receptor molecule, and ii) enhancement of the relevant PPII conformation [3]. To further optimize ligand-receptor interactions in the search of potent SH3 ligands, 2C-substituted  $\Psi$ Pro libraries applying post-insertion strategies have been generated allowing for rapid screening of ligands that optimally complement the SH3 topography.

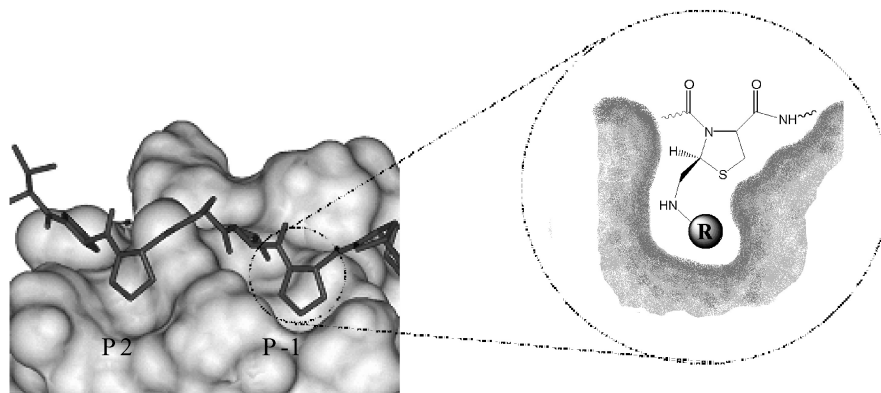


Fig. 1. The consensus sequence of a proline-rich sequence bound to Grb2 (N) SH3 domain (left); close-up (right): a 2C-functionalized  $\Psi$ Pro library replacing Pro at P-1 allows to rapidly screen for the best binding ligand.

## Results and Discussion

To exploit the principle of the dual role of functional pseudoprolines further, a Pro was replaced by a  $\Psi$ Pro-moiety at position P-1 in the SoS related sequence Val-Pro-Pro-Pro-Val-Cys( $\Psi$ pro<sup>H,CH<sub>2</sub>NH<sub>2</sub></sup>)-Pro-Lys-Lys-Lys [4] and in a non natural high affinity Pro-rich ligand Tyr-Pro-Pro-Pro-Ala-Leu-Cys( $\Psi$ pro<sup>H,CH<sub>2</sub>NH<sub>2</sub></sup>)-Pro-Lys-Arg-Arg-Arg [5]. Cyclocondensation of Cys with Boc-protected glycinal results in an NH<sub>2</sub>-group at 2C of the  $\Psi$ Pro moiety accessible for the covalent ligation of a broad palette of various substituents either on solid phase or in solution. To this end, the Cys( $\Psi$ pro<sup>H,CH<sub>2</sub>NHBoc</sup>) building block was reacted with Fmoc-Val-F and Fmoc-Leu-F, respectively, to yield the corresponding dipeptides used in Fmoc-based solid-phase peptide synthesis. After removal of Boc and simultaneous cleavage from the resin, different residues, *e.g.* R = -CO-C<sub>6</sub>H<sub>5</sub>; -CO-(CH<sub>2</sub>)<sub>4</sub>CH<sub>3</sub>; -CO-CH<sub>3</sub>; -SO<sub>2</sub>-CH<sub>3</sub>; -D-galacturonic acid) were covalently attached in solution *via* amide bond formation. Interestingly, as shown by 2-D NMR the unprotected thiazolidine dipeptides adopt a *cis* conformation, whereas the corresponding  $\Psi$ Pro-containing peptides exhibit all *trans* conformation as prerequisite for the required PPII helical conformation.

In conclusion, the generation of  $\Psi$ Pro-libraries exhibiting enhanced Pro properties allows for rapid screening of a large number of Pro-rich peptides in the search of potent inhibitors of SH3-mediated interactions.

## Acknowledgments

This work is supported by the Swiss National Science Foundation.

## References

1. Kuriyan, J., Cowburn, D. *Ann. Rev. Biophys. Biomol. Struct.* **26**, 259–288 (1997).
2. Wöhr, T., Wahl, F., Nefzi, A., Rohwedder, B., Sato, T., Sun, X., Mutter, M. *J. Am. Chem. Soc.* **118**, 9218–9227 (1996) and references therein.
3. Tuchscherer, G., Grell, D., Tatsu, Y., Durieux, P., Fernandez-Carneado, J., Hengst, B., Kardinal, C., Feller, S.M. *Angew. Chem., Int. Ed.*, in press.
4. Chardin, P., Camonis, J.H., Gale, N.W., Van Aelst, L., Schlessinger, J., Wigler, M.H., Bar-Sagi, D. *Science* **60**, 1338–1343 (1993).
5. Posern, G., Zheng, J., Knudsen, B., Feller, S.M., et al. *Oncogene* **16**, 1903–1912 (1998).

## Towards a Set of Peptides with Orthogonal HIV Seroreactivity Using Adaptively Coded Peptide Libraries: Decoding by Mass Spectrometry and Immunofluorescent Screening

Christian Hoffmann<sup>1</sup>, Dierk Blechschmidt<sup>1</sup>, Ralf Krüger<sup>2</sup>, Michael Karas<sup>2</sup>, Christoph Königs<sup>3</sup>, Ursula Dietrich<sup>3</sup> and Christian Griesinger<sup>1,4</sup>

<sup>1</sup>*Institute of Organic Chemistry, 60439 Frankfurt, Germany*

<sup>2</sup>*Division of Instrumental Analytical Chemistry, 60590 Frankfurt, Germany*

<sup>3</sup>*Georg-Speyer-Haus, 60596 Frankfurt, Germany*

<sup>4</sup>*Max-Planck-Institute for Biophysical Chemistry, 37077 Göttingen, Germany*

### Introduction

The V3-loop is an immunodominant region within the envelope protein of HIV-1. Peptides of this region are used to classify HIV-1 into subtypes based on the seroreactivity of patients' sera. However, correlation between genetically determined subtypes and their seroreactivity is not yet fully established. Therefore, new approaches have been pursued [1]. We evaluated the immunological reactivity of polyclonal human anti-HIV antibodies from patient sera against a solid phase decapeptide library derived from HIV-1 V3 sequence data in order to achieve a minimal set of peptides with orthogonal seroreactivities against different subtypes. This approach serves as a basis to establish an immunofluorescence based assay for subtyping HIV-1.

### Results and Discussion

Our process for the identification of reactive peptides from combinatorial libraries is visualized in Figure 1. For the quick and reliable identification, we encode the peptide sequences during combinatorial library synthesis by 5% capping and subsequent MALDI MS analysis [4]. The capping is computer-optimized to achieve a minimum of capping steps for the specific library; synthesis is carried out using mixtures of the Fmoc-protected amino acid and its N-terminally blocked derivative during split and mix synthesis [3]. Thus the peptide sequence can be decoded from a single bead. For example, the library we considered contains 432 000 members. The computer algo-

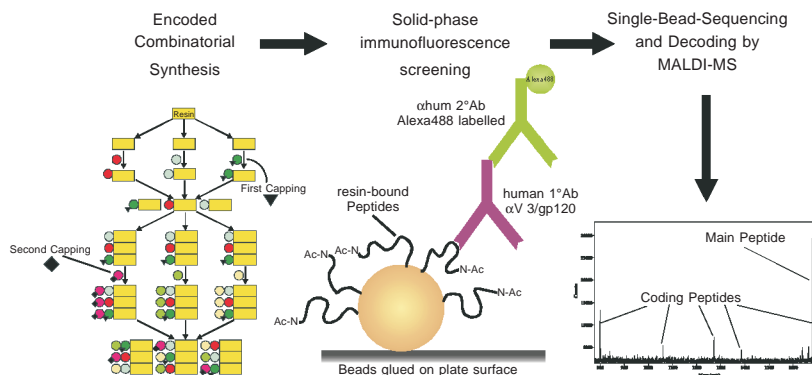


Fig. 1. Immunofluorescence and MS based identification of reactive peptides.

rithm *Biblio* [2] we developed calculated five necessary capping steps, providing a unique capping pattern for any given peptide of the library. Therefore, the MALDI mass spectrum reveals six signals, five coding peptides and the main peptide, as shown in Figure 2 (right).

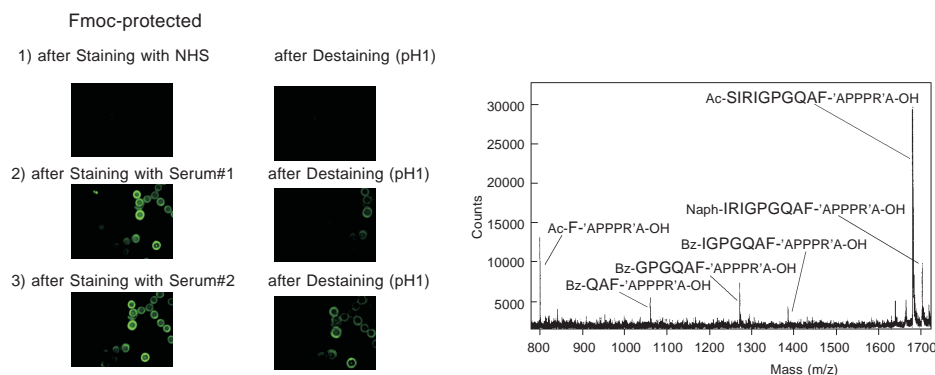


Fig. 2. Immunofluorescent staining and MS decoding of the model peptide Ac-SIRIGPGQAF.

For the identification of a minimal set of peptides with orthogonal cross reactivities between HIV-positive sera, we developed a method to screen the resin beads carrying the peptides iteratively. The coded peptide beads are glued to the petri dish with an epoxy adhesive, enabling to wash off the immune complex at low pH. Thus, any reactive bead can be recognized positionally due to a background grid pattern on the petri dish.

Resin-bound peptides found to be most reactive throughout all staining series can be selected, sequenced by recording a single mass spectrum and decoded by *Biblio*, as demonstrated with a coded model peptide from our library [2] screened with two HIV positive sera and normal human serum (NHS) as negative control in Figure 2.

### Acknowledgments

We thank the DFG, the MPG and the FCI for financial support.

### References

1. Zolla-Pazner, S., Gorny, M.W., Nyambi, P.N., VanCott, T.C., Nádas, A. *J. Virol.* **73**, 4042–4051 (1999).
2. Hoffmann, C., Blechschmidt, D., Karas, M., Griesinger, C. In J. Martinez and J.-A. Fehrentz (Eds.) *Peptides 2000 (Proceedings of the 26th European Peptide Symposium)*, Éditions EDK, Paris, 2001, p. 963.
3. Furka, Á., Sebestyén, F., Asgedom, M., Dibo, G. *Int. J. Pept. Protein Res.* **37**, 487–493 (1991).
4. Bahr, U., Karas, M., Hillenkamp, F. In Kellner, R., Lottspeich, F. and Meyer, E. (Eds.) *Microcharacterization of Proteins*, VCH Weinheim, 1994, p. 149.

## Mapping of Discontinuous Epitopes on FSH

Jerry W. Slootstra, Wouter C. Puijk, Rob H. Melen  
and Wim M. M. Schaaper

PEPSCAN Systems, NL-8219 PH Lelystad, The Netherlands

### Introduction

The majority of protein-interaction sites are discontinuous, this means that various loops form the three-dimensional binding pocket. For proteins with unknown sequence and structure random libraries can be used to define the interaction site [1]. Proteins with a defined sequence and/or structure can be scanned with overlapping peptides against, for instance, monoclonal antibodies. However, testing monoclonal antibodies in ELISA against all overlapping 12- to 15-mer peptides from these proteins is not always successful. Scanning against 25- to 30-mer peptides [2] reveals more information, since these peptides cover a larger area of the protein surface. However, to discover complete discontinuous interaction sites that contain different parts of the epitope – which are (far) apart in the primary sequence, but are brought close spatially in the protein – we developed the matrix scan. The method consists of making all possible peptides that comprise two or more different regions from a protein. The scan includes also branched combinations. Screening of these peptides provides clear insight into the nature and composition of the discontinuous epitopes as demonstrated for FSH (Follicle Stimulating Hormone).

### Results and Discussion

We tested 20 different monoclonal antibodies in ELISA against different sets of overlapping peptides spanning the entire sequence of FSH. The antibodies were raised against native FSH and directed against the  $\beta$ -subunit of FSH. Three types of pepscans were synthesized: a) all overlapping 12- and 15-mers, b) all overlapping 24- and 30-mers, and c) a complete matrix scan with construct 30-mers. For the matrix scan

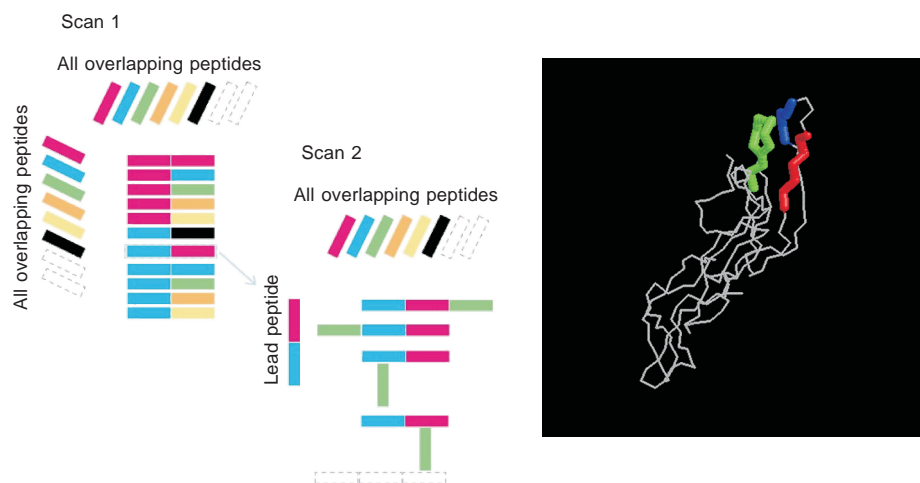


Fig. 1. Schematic presentation of the matrix scan (left) and the reactive segments found, using this matrix scan, projected in the model of the  $\beta$ -subunit of FSH (right).

about 120,000 construct peptides, including both the  $\alpha$ - and the  $\beta$ -subunit, were tested. For the synthesis we followed the scheme shown in Figure 1.

All overlapping 12-, 15-, 24-, and 30-mer peptides from FSH were synthesized in small wells in credit card format mini-cards (455 peptides per card) using standard Fmoc chemistry. The cards were functionalized with amino groups as described previously [1]. All overlapping 24- and 30-mer peptides were synthesized from two 12-, respectively 15-mer peptides. The N-terminal peptides were synthesized in mini-cards using a cleavable linker, and after synthesis and cleavage linked to the C-terminal sequence in other mini-cards using ligation chemistry.

Only one of the 20 monoclonal antibodies reacted with the linear 12- and 15-mers, this was only a small peak. About 5 of the 20 monoclonal antibodies clearly reacted with the 24- and 30-mer peptides. These were high peaks which covered one of the loops from the  $\beta$ -subunit. In contrast, all of the 20 monoclonal antibodies reacted in the matrix-scan of the 30-mer construct peptides. The identified peaks included the loop found earlier using the 24-mer peptides, but added two sequences in the same area that were located far apart in the primary sequence (Figure 1, right).

We conclude that scanning of protein sequences with monoclonal antibodies, using up to 30-mer peptides, allows the definition of parts of discontinuous sites. However, scanning of protein sequences with monoclonal antibodies, using the matrix scan makes it possible to define accurately complete discontinuous sites.

## References

1. Slootstra, J.W., Puijk, W.C., Ligtoet, G.J., Langeveld, J.P.M., Meloen, R.H. *Mol. Divers.* **1**, 87–96 (1995).
2. Slootstra, J.W., Puijk, W.C., Borràs, E., Villén, J., Giralt, E., Andreu, D., Meloen, R.H., Schaaper, W.M.M., In Martinez, J. and Fehrentz, J.A. (Eds.) *Peptides 2000*, EDK, Paris, 2001, pp. 899–900.

## Development of Highly Specific, Membrane Permeable Peptide Blockers of cGMP-Dependent Protein Kinase Utilizing Affinity Selection from Peptide Libraries

Werner Tegge<sup>1</sup>, Ronald Frank<sup>1</sup>, Mark S. Taylor<sup>2</sup>, Joseph E. Brayden<sup>2</sup>,  
Christian K. Nickl<sup>2</sup> and Wolfgang R.G. Dostmann<sup>2</sup>

<sup>1</sup>German Research Centre for Biotechnology (GBF), AG Molecular Recognition,  
D-38124 Braunschweig, Germany

<sup>2</sup>Departments of Pharmacology and Molecular Physiology, University of Vermont,  
College of Medicine, Burlington, VT, USA

### Introduction

The cGMP-dependent protein kinases type I $\alpha$  and I $\beta$  (cGPK) act directly downstream in the nitric oxide (NO) mediated signaling pathway in the control of a variety of cellular responses, ranging from smooth muscle cell relaxation to neuronal synaptic plasticity [1,2]. The structural similarity of cGPK and its closest relative, the cAMP-dependent protein kinase (cAPK), has made it difficult to study cGPK pathways independent of those mediated by cAPK, primarily due to the lack of potent and selective cGPK inhibitors. Here we report a novel peptide library screen specifically designed to select for tight binding peptides that identified selective inhibitors of the kinases. The most potent sequences were made cell permeable by the addition of membrane translocation sequences from *HIV* and *Drosophila* and physiological effects of the constructs were studied *in vivo* and *in vitro*.

### Results and Discussion

Peptide libraries without Ser and Thr were constructed and the binding of <sup>32</sup>P autophosphorylated cGPK I $\alpha$  was investigated. The octameric library array XXX12XXX revealed strong binding to the kinase with the amino acid combinations RR, KR and RK at positions 1 and 2. The RK motif gave the strongest signal. The second-generation library with the structure XXXRK12X identified unambiguously the combination KK as the strongest binding motif. In the third library XRKKK12X, again KK was favored, although other lysine containing combinations (AK, WK, KF) were also selected by cGPK. In the fourth library 1RKKKKK2, cGPK strongly selected Leu at position 1 and His at position 2 (Figure 1). C- and N-terminal extended libraries identified more hydrophobic residues surrounding the cluster of positive residues (data not shown), with the dodecamer FLLRKKKKKHHK as the longest peptide included in our search. The octamer LRK<sub>5</sub>H (W45) derived from the fourth generation library was a potent and selective competitive inhibitor of cGPK (Table 1). N- and C-terminal extensions in 5th and 6th generation libraries did not improve the K<sub>i</sub> values.

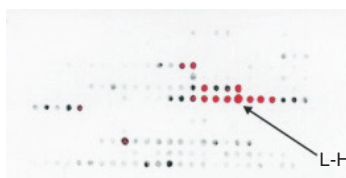


Fig. 1. Binding of autophosphorylated cGPK to the array 1RKKKKK2.

To allow internalization of the highly charged peptide W45 into live cells, we employed two membrane translocation sequences, one from the *HIV-1* Tat protein (47-59) and the other from the *Drosophila* Antennapedia homeo-domain (43-58). N-terminal fusion of either of these sequences to W45 resulted in a potentiating effect with respect to the inhibitory potency, with  $K_i$  values 40–80-fold lower than W45 (Table 1). Interestingly, the fusion peptides alone had significant cGPK inhibitory activity. The internalization of DT-2 and DT-3 into living cells was monitored by peptide derivatives furnished with an additional N-terminal Cys to which a fluorescein label was attached, spaced by a  $\beta$ -Ala (Fluo-DT-2/3). The labeled peptide analogs of DT-2 and DT-3 were rapidly internalized and distributed through the cytosol and nuclei in a time dependent manner, while Fluo-W45 did not noticeably penetrate through the plasma membrane.

To demonstrate that DT-2 and DT-3 are both capable of inhibiting cGPK under conditions where the cAPK selective inhibitor PKI<sup>(5-24)</sup> and/or cAPK are present, we established an *in vitro* reconstitution assay (Figure 2). In this assay cyclic nucleotide concentrations of 1  $\mu$ M were used, conditions under which cAMP will activate only cAPK and cGMP will activate only cGPK. Figure 2 shows that cGPK and cAPK are stimulated only by their specific agonists and inhibited only by their specific inhibitors (DT-2/3 or PKI). The result could be verified with a mixture of both enzymes.

To further evaluate the physiological effects of DT-2 and DT-3 as selective cGPK inhibitors in smooth muscle, we studied their effects on nitric oxide-induced

Table 1. Kinetics of inhibitory peptides.

Designation	Sequence	$K_i$ cGPK ( $\mu$ M)	$K_i$ cAPK ( $\mu$ M)	Specificity index
W45	LRKKKKKH	0.8	559	680
DT-2	YGRKKRRQRRRPPLRKKKKKH	0.012	17	1 375
DT-3	RQIKIWFQNRRMKWKKLRKKKKKH	0.025	493	19 720
HIV-1 Tat (47-59)	YGRKKRRQRRRP	1.1	26	24
Dros. Antp. (43-58)	RQIKIWFQNRRMKWKK	0.97	107	110

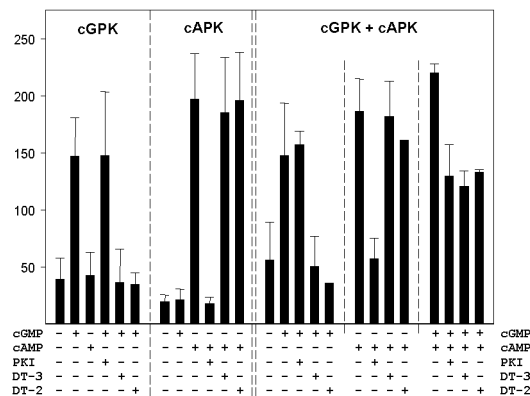


Fig. 2. *In vitro* inhibition of cGPK and cAPK.

vasodilation in intact arteries. The nitric oxide donor NONOate elicited a concentration-dependent dilation of pressurized rat cerebral arteries. Pretreatment of arteries with cGPK inhibitors DT-2 or DT-3 for 20 min substantially impaired NO mediated vasodilation: DT-2 (1  $\mu$ M) significantly increased the EC<sub>50</sub> for NONOate compared to untreated vessels or vessels treated with the HIV tat carrier sequence alone. Similarly, DT-3 (0.1  $\mu$ M) significantly increased the NONOate EC<sub>50</sub> compared to untreated vessels or vessels treated with the Antennapedia carrier sequence alone. Nitric oxide responses in arteries treated with the carrier sequences were not significantly different from those in untreated arteries. In all cases, the fusion peptides or carrier peptides alone caused slight to moderate increases (<10%) in vascular tone.

Collectively, these data indicate that the combination peptides DT-2 and DT-3 translocate into smooth muscle cells in intact arteries and effectively inhibit NO-induced vasodilation, presumably by inhibiting cGPK.

#### **Acknowledgments**

We thank B. Kornak and S. Daenicke for excellent technical assistance. Supported by grants from the Deutsche Forschungsgemeinschaft (Do329/3-3, Do329/4-1), the Lake Champlain Cancer Research Organization and by NIH grants HL44455 and HL58231.

#### **References**

1. Lincoln, T.M., Komalavilas, P., Boerth, N.J., Mac-Millan-Crow, L.A., Cornwell, T.L. *Adv. Pharmacol.* **34**, 305–322 (1995).
2. Pfeifer, A., Ruth, P., Dostmann, W., Sausbier, M., Klatt, P., Hofmann, F. *Rev. Physiol. Biochem. Pharmacol.* **135**, 105–149 (1999).
3. Part of this work has been published elsewhere: Dostmann, W.R.G., Taylor, M.S., Nickl, C.K., Brayden, J.E., Frank, R., Tegge, W. *Proc. Natl. Acad. Sci. U.S.A.* **97**, 14772–14777 (2000).

## **The Integration of Positional Scanning Libraries with Bioinformatics and Proteomics**

**Clemencia Pinilla<sup>1,2</sup>, Eva Borràs<sup>1</sup>, Roland Martin<sup>3</sup>, Yingdong Zhao<sup>4</sup>  
and Richard Simon<sup>4</sup>**

<sup>1</sup>*Torrey Pines Institute for Molecular Studies and*

<sup>2</sup>*Mixture Sciences, Inc., San Diego, CA 92121, USA*

<sup>3</sup>*Neuroimmunology Branch, NINDS, NIH, Bethesda, MD 20892, USA*

<sup>4</sup>*Molecular Statistics and Bioinformatics Section, Biometric Research Branch, NCI, NIH,  
Bethesda, MD 20892, USA*

### **Introduction**

The efficacy of using positional scanning synthetic combinatorial libraries (PS-SCL) for the identification of T cell ligands has been demonstrated in a number of studies carried out by us and others [1]. The studies with PS-SCL for clones of known specificity when compared with the results from single substitution analogs [2] clearly demonstrated that each amino acid within a peptide contributes to recognition almost independently and in an additive fashion. Thus, the overall stimulatory value of a peptide results from the combination of positive or negative effects of each of the amino acids. This assumption has allowed the development of a new search algorithm, which provides a predicted stimulatory score for a given peptide. This score is the sum of position specific scores of the component amino acids in a given PS-SCL screening data set.

### **Results and Discussion**

We have recently reported a new strategy that integrates the data acquisition from PS-SCL and protein sequence databases using a biometrical analysis in order to identify peptide ligands from proteins in databases for T cell clones of known [3] and unknown specificity [4]. Peptides can be identified from database searches with unprecedented efficiency and ranked according to a score that is predictive of their stimulatory potency. The experimental data from the screening of a PS-SCL provides information to generate a matrix. In the matrix the columns represent the position of the peptide sequence, and the rows represent the 20 amino acids used in the PS-SCL. The matrix entry for a particular amino acid in a specific position is based on the stimulation index value for the mixture from the PS-SCL corresponding to that amino acid defined in that position. The biometrical analysis then uses this matrix to score all the peptides of the same length of the tested PS-SCL in all the proteins in the Genpept database by moving a scoring window across the known protein sequences in one amino acid increments. A predicted stimulatory score is calculated for all peptides. The example shown in Figure 1 represents the scoring distribution for more than 23 million peptides of the viral database that were scored based on the screening of T cell clone GP5F11. It can be seen that a relative small number of peptides have the highest scores, and the native epitope (Influenza virus hemagglutinin peptide, HA 309-318) recognized by T cell clone GP5F11 is among them and ranked number 9. The database analysis results in a list of peptide sequences, with their score and rank, and the protein identifier and its name. At this step, selected peptides are synthesized and their activities are determined.

The predictive power of this novel strategy has been demonstrated for both CD4<sup>+</sup> and CD8<sup>+</sup> T cell clones as well as G protein-coupled receptors for which the ligand is

known. Also, the specificity of a cerebrospinal fluid derived T cell clone from a patient suffering from Lyme disease was elucidated, and a number of peptides representing both *B. burgdorferi* and human protein sequences were identified [4].

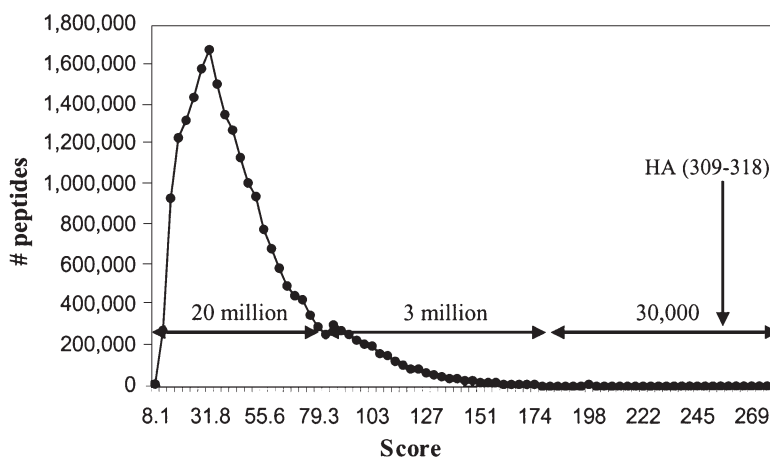


Fig. 1. Scoring distribution for the decapeptides in the viral database for T cell clone GP5F11.

It is important to note that this approach can be used to identify ligands within proteins in databases for any molecular interaction that has been or can be studied with PS-SCL composed of L-amino acids. Thus, the integration of data derived from PS-SCL screening with proteomics and the biometrical analysis can be applied to biological targets having peptides as natural ligands, such as T cells, proteolytic enzymes and cloned orphan G protein-coupled receptors.

## References

1. Pinilla, C., Martin, R., Gran, B., Appel, J.R., Boggiano, C., Wilson, D.B., Houghten, R.A. *Curr. Opin. Immunol.* **11**, 193–202 (1999).
2. Hemmer, B., Pinilla, C., Gran, B., Vergelli, M., Ling, N., Conlon, P., McFarland, H.F., Houghten, R.A., Martin, R. *J. Immunol.* **164**, 861–871 (2000).
3. Zhao, Y., Gran, B., Pinilla, C., Markovic-Plese, S., Hemmer, B., Tzou, A., Whitney, L.W., Biddison, W.E., Martin, R., Simon, R. *J. Immunol.* **167**, 2130–2141 (2001).
4. Hemmer, B., Gran, B., Zhao, Y., Marques, A., Pascal, J., Tzou, A., Kondo, T., Cortese, I., Bielekova, B., Straus, S., McFarland, H.F., Houghten, R.A., Simon, R., Pinilla, C., Martin, R. *Nature Med.* **5**, 1375–1382 (1999).

## **Screening and Synthesis of a Positional Scanning Library Based on the Bowman–Birk Reactive Site Loop**

**Emma M. Watson, Jeffrey D. McBride and Robin J Leatherbarrow**

*Department of Chemistry, Imperial College of Science, Technology and Medicine,  
South Kensington, London, SW7 2AY, UK*

### **Introduction**

Proteinases are essential components of a wide variety of biological processes [1] such as the digestion of food, the cascade systems of blood clotting and complement, activation of hormones, and the degradation of endogenous proteins. The regulation of proteinase activity is, therefore, of great importance both *in vivo*, and for therapeutic reasons. The gross physiological function of proteinase inhibitors is the prevention of unwanted proteolysis. Inhibitors are associated with the prevention and treatment of a wide range of disorders such as lung disease emphysema, liver disease septicaemia, renal disease, arthritis and HIV prevention.

Bowman–Birk Inhibitors are small serine protease inhibitors found in seeds of legumes and in many other plants. Their sequence consists of two tandem homology regions on opposite ends of the same polypeptide chain. Each loop is linked by a disulphide bridge and exhibits the consensus sequence CTP<sub>1</sub>SXPPQC (X being any amino acid residue) [2]. (P<sub>1</sub> following the notation of Schetcher and Berger [3]). It is these “canonical” loops that interact with the proteinase. It is possible to reproduce the loop region of this protein by short peptide sequences incorporating a minimal disulphide-linked nonapeptide [4,5].

We have previously reported the synthesis of “one-bead one-peptide” cyclic peptide libraries based on the sequence of the reactive site loop of the Bowman–Birk inhibitor [6]. This constrained loop was retained throughout the library whilst randomising positions of the sequence considered to be important for inhibitory specificity. We now report the synthesis and screening of a positional scanning solution phase library [7] based on the same template and randomising the four positions P<sub>4</sub>, P<sub>2</sub>, P<sub>1</sub> and P<sub>2</sub>′.

### **Results and Discussion**

The positional scanning soluble library consists of four sub-libraries: OCXXSXPPQCY “P4-lib”; XCOXSXPPQCY “P2-lib”; XCXOSXPPQCY “P1-lib”; XCXXSOPPQCY “P2′-lib”; where X represents a mixture of 24 amino acids, whereas O represents positions occupied by individual amino acids. The four sub-libraries only differ in the position of the defined residue. Each of these groups consists of 24 peptide mixtures representing a total of 331776 individual peptides. The amino acids used for the randomisations were the common amino acids (except for Cys, but including Abu, βAla, Nva, Nle, Orn). The library was synthesised semi-automatically using an ABI 431A peptide synthesiser for the unrandomised amino acids of the sequence and the Shimadzu PSSM-8 for positions of randomisation (X and O) within the sequence. The synthesis was carried out using Fmoc synthesis, with HBTU/HOBt activation at a 4-fold excess. Randomisation was achieved using the split-mix method.

P4-lib, P2-lib and P1-lib were successfully synthesised and screened against chymotrypsin, trypsin, subtilisin, porcine pancreatic elastase and human leukocyte elastase.

Results of the screening of the three sublibraries are listed in the table below.

## Synthetic Methods

From Table 1, it can be seen that specificity away from the P1-S1 subsite (at P4) has been identified. Reassuringly the P1 results conform to known specificity of these enzymes. Synthesis of P2-lib will enable the full sequences to be identified. Individual peptides will then be synthesised and assayed against the enzymes.

*Table 1. Summary of active residues at positions P4, P2, and P1 identified from the three sublibraries.*

	P4	P2	P1
Chymotrypsin	I	T	F, Y
Trypsin	H	K, N, D, T	R, K
Subtilisin	F	Nva	T, M
Porcine Elastase	P, I, V, L	T	Nva
Human Elastase	Nle	Abu	A, V, Nva, T

## Acknowledgments

This work is sponsored by the EPSRC.

## References

1. Neurath, H. *Trends Biochem. Sci.* **14**, 268–271 (1989).
2. Ikenaka, T., S. Norioka, B. Salvesen, (Ed). *Elsevier Science* 361–374 (1986).
3. Schechter, I., Berger, A. *Biochem. Biophys. Res. Commun.* **27**, 157–162 (1967).
4. Maeder, D.L., et al. *Int. J. Pept. Protein Res.* **40**, 97–102 (1992).
5. Domingo, G.L., et al. *Int. J. Pept. Protein Res.* **46**, 79–87 (1995).
6. McBride, J.D., et al. *J. Mol. Biol.* **259**, 819–827 (1996).
7. Pinilla, C., et al. *Biotechniques* **13**, 901 (1992).

## A Bicyclic Peptide Template Useful for Solution-Phase Combinatorial Synthesis

Qingchai Xu and Frans Borremans

Department of Organic Chemistry, Ghent University, Ghent, B-9000, Belgium

### Introduction

The use of a topological structure as a template for the construction of combinatorial libraries is one of the recent advances in combinatorial chemistry [1,2]. Here we report a (quasi)orthogonally protected template **1** [bicyclo-(K(Fmoc)CK(Dde)PGK(Boc)-CK(Aloc)PG)] that appears to be very useful in solution-phase combinatorial synthesis (Figure 1). This template has been synthesized in our laboratory in gram-scale [3]. The importance of this peptide lies in: (1) the rigidity of backbone-conformation [3] and (2) the (quasi)orthogonal protection (Fmoc, Boc, Aloc and Dde). Its conformational feature provides a molecular scaffold for constructing the library with a specific three-dimensional molecular surface. The orthogonal protection allows site-selective assembly of building blocks.

### Results and Discussion

The idea of the application of template **1** to solution-phase synthesis of libraries was inspired by our observation that these bicyclic peptides appear to readily give quantitative precipitation in diethyl ether. Starting with 47  $\mu\text{mol}$  of **1**, we performed a solution (split) synthesis of a model library **2** containing 81 compounds. Assembly of the selected building blocks (Table 1) followed such order: first at the B-site after the selective deprotection of Boc, then at the F-site after the removal of Fmoc, the A-site after removal of Aloc and finally on the D-site after Dde-deprotection.

In each growth site, three different amino acids were introduced by three parallel HBTU-mediated couplings. After incorporation of the three building blocks at the last amine-moiety, the resulting three portions were separately subjected to deprotection, acetylation and total cleavage reactions. The synthesis yielded three sub-libraries, each having a defined residue (Nal, Pro or Glu) at the last coupling-step (D-site), hereafter referred to as the Nal-, Pro- and Glu-sub-libraries, respectively. All reactions were controlled by RP-HPLC. After each reaction, excessive reactants and byproducts formed can be removed simply by multi-precipitation with diethyl ether [4]. Using this method, (15 reaction steps), the Nal-, Pro- and Glu-sub-libraries were obtained in

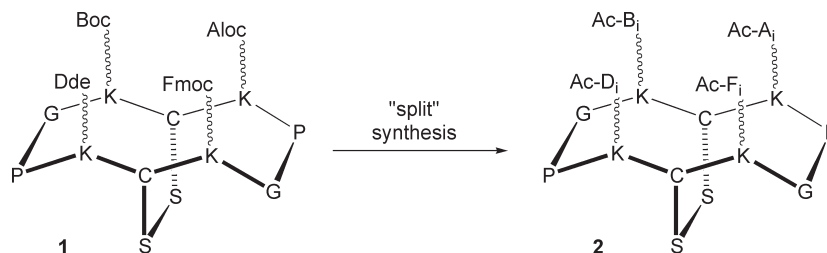


Fig. 1. Schematic representation of template (**1**)-based combinatorial synthesis of a tetrapodal library (**2**). B<sub>i</sub>: Phe, Ala or Asp; F<sub>i</sub>: Tyr, Ile or Glu; A<sub>i</sub>: (D)-4-Cpa, Ser or (D)-Asp, with Cpa = chlorophenylalanine; D<sub>i</sub>: Nal, Pro or Glu, with Nal = (L)-3-(2-naphthyl)alanine).

## Synthetic Methods

crude yields (by weight) of 73%, 75%, and 80%, respectively. As shown in Figure 2, RP-HPLC traces of these three mixtures indicate the presence of a reasonable number of peaks in roughly equimolar ratio.

Table 1. The selected building blocks to be assembled on the four sites (A,B, D and F) of **1**.

i	A-site	B-site	D-site	F-site
1	Fmoc-D-4-Cpa	Ac-Phe	Fmoc-Nal	Fmoc-Tyr(OtBu)
2	Fmoc-Ser(tBu)	Ac-Ala	Fmoc-Pro	Fmoc-Ile
3	Fmoc-D-Asp(OtBu)	Ac-Asp(OtBu)	Fmoc-Glu(OtBu)	Fmoc-Glu(OtBu)

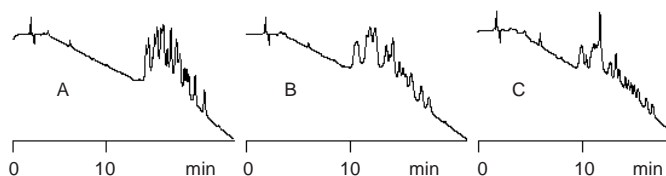


Fig. 2. HPLC analysis of three sub-mixtures. **A**: Nal-sublibrary, **B**: Pro-sublibrary, **C**: Glu-sublibrary.

The three sub-libraries have been evaluated using MALDI-TOF MS and LC/ES-MS. Using these techniques, the theoretically expected  $27 \times 3$  library compounds were all detected and appeared as major components [5]. These analytical results validate the three synthetic mixtures, and also show that the solution approach to combinatorial synthesis with template **1** is reliable and very useful.

## Acknowledgments

The authors are indebted to the GOA (GOA96009) program for financial support. Q. Xu. thanks Christian and Frank Becu, Dr. Bart Devreese and Dr. Franky Fant for technical assistance.

## References

1. Hirschmann, R., Sprengeler, P.A., Kawasaki, T., Leahy, J.W., Shakespeare, W.C., Smith, A.B. *J. Am. Chem. Soc.* **114**, 9699–9701 (1992).
2. Barry, J.F., Davis, A. P., Pérez-Payan, M.N. *Tetrahedron Lett.* **40**, 2849–2852 (1999).
3. Xu, Q.C. *Synthesis and Application of Bicyclic Decapeptide Template for Combinatorial Libraries*, Ph.D. Thesis (Ghent University). Ghent, Belgium, 2000.
4. An extractive washing with DCM/water is needed after every HBTU-mediated coupling.
5. Expected compounds were found in 33 mass spectra as major signals. Only a few signals related to side products were observed and assigned as minor components.

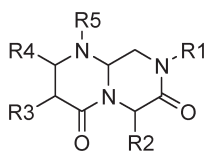
## Synthesis of Combinatorial Libraries Associated with Constrained $\beta$ -Turn Mimetics

**James Dattilo, Chris Lum, Stephanie Beigle-Orme, Burt Goodman,  
Vince Huber, Jeff Keilman, Cheryl Schwenk, Gangadhar Nagula,  
Nataly Hawthorn, Jennifer Young and Tomáš Vaisar**

*Molecumetics, Ltd., Bellevue, WA 98005, USA*

### Introduction

For several years we have investigated the preparation of compounds which mimic  $\beta$ -turn secondary structures that are intrinsic to certain protein–protein interactions and that are therefore able to effect antigen-antibody and ligand-receptor relationships. We have shown in our third and fourth generation  $\beta$ -turn mimetics that they express activity in targets such as opioid receptors and in GPCRs [1–3]. Based on the fourth generation template, we have applied similar procedures used in the production of our  $\beta$ -sheet libraries [4] to generate libraries based on the template shown below.



### Results and Discussion

After the derivatization of hydroxymethyl resin with bromoacetaldehyde diethyl acetal to give the corresponding bromoacetaldehyde resin, it is converted to various secondary amine resins, which represent the first point of diversity (R1). The second diversity point (R2) is represented by an Fmoc amino acid coupled to the secondary amine. After deblocking of the Fmoc group, an Fmoc- $\beta$ -amino acid, which can represent multiple diversity points (R3 + R4), is coupled and deblocked. At this point the final point of diversity (R5), represented by various reactions with the amine of the  $\beta$ -amino acid, is generated, completing thus the synthesis. The design of the library can be initiated using the Afferent™ software, which permits the editing and importing diversity elements into reaction schemes. With the completion of the design, it can be exported to the IRORI™ Synthman synthesis system [5] for implementation. The porous capsules (Kans™) are sorted on the IRORI™ 10-X auto sorter to establish an association with the radio frequency tag and the amine resin. The Kans™ are then sorted for each reaction step and the cleavage.

The N- $\alpha$ -Fmoc amino acid derivatives are commercially available but there are a limited number of Fmoc- $\beta$ -amino acids that can be purchased and some are cost prohibitive. We have taken three approaches in the synthesis of this key intermediate. The first process creates diversity at the R3 position and utilizes the conversion of an N- $\alpha$ -Fmoc amino acid to the acid chloride, then to diazoketone and finally to the Fmoc- $\beta$ -amino acid with silver benzoate and triethylamine [6]. The second approach exploits diversity at the R4 position. The reaction sequence as described by Nagula *et al.* [7] involves direct alkylation of pseudoephedrine  $\beta$ -alaninimide followed by hydrolysis. The third methodology also involves R3 and requires the use of N- $\alpha$ -Alloc-N- $\beta$ -Fmoc diaminopropionic acid [8]. The  $\beta$ -amine is deblocked and reac-

tions are conducted. The Alloc protected  $\alpha$ -amine is then deblocked using  $\text{Pd}(\text{PPh}_3)_4/\text{PhSiH}_3$  and similar reaction scenarios are performed. After the synthetic steps are completed, the Kans<sup>TM</sup> are sorted for cleavage into 48-well Bohdan mini-blocks. The cleavages and cyclizations are accomplished simultaneously by treatment with formic acid. The products are formatted into 96-well blocks and analytically evaluated by mass spectroscopy to determine acceptability. The analysis is performed by LCMS equipped with OpenLynx<sup>TM</sup> for retrieval of the data associated with the compounds contained in the bar-coded blocks. The data is reviewed to reformat the successful candidates and eliminate the failed compounds. The block is then ready for the formation of daughter plates and/or the appropriate bioscreening.

### Conclusions

The fourth generation  $\beta$ -turn bicyclic template has been incorporated into the IRORI method of one compound per well combinatorial library production. As with its  $\beta$ -strand predecessor, it was necessary to alter the reaction parameters to assure completion of each step of the process. In addition to the analytical evaluations of intermediates, it also contains the same validation efforts in terms of test synthesis of the amine resins, Fmoc- $\alpha$ -amino acids, Fmoc- $\beta$ -amino acids and other key intermediates. With the use of N- $\alpha$ -Alloc-N- $\beta$ -Fmoc diaminopropionic acid, the ability to conduct reactions on the amine off of the R3 position gave us the potential for greater diversity overall. By having these five points of variation on this template, it is easily possible to create libraries ranging from 5000–10,000 compounds with a theoretical yield of 30  $\mu$ moles per well. The success rate is typically 75–85% based on a purity level of >80%.

### References

1. Gardner, B., Nakanishi, H., Kahn, M. *Tetrahedron Symposia in Print* **17**, 3433 (1993).
2. Saragovi, H.U., Fitzpatrick, D., Raktabutr, A., Nakanishi, H., Kahn, M., Greene, M.I. *Science* **253**, 792 (1991).
3. Eguchi, M., Lee, M.S., Nakanishi, H., Stasiak, M., Lovell, S., Kahn, M. *J. Am. Chem. Soc.* **121**, 12202–12208 (1999).
4. Dattilo, J., Goodman, B., Lum, C., Elliott, C., Deiparine, M., Beigel-Orme, S., Cunningham, D., Young, J. *Proceedings of the 16th American Peptide Symposium* **1999**, 194–195.
5. Czarnik, A.W., *Proc. Int. Sym. Lab. Automation and Robotics* **1997**, 166–173.
6. Whittaker *The Chemistry of Diazoium and Diazo Compounds*, Wiley, New York, 1978, pp. 593–644.
7. Nagula, G., Huber, V., Lum, C., Goodman, B. *Org. Lett.* **2**, 3527–3529 (2001).
8. Radhakrishna, A.S., Parham, M.E., Riggs, R.M., Loudon, G.M. *J. Org. Chem.* **44**, 1746–1747 (1979).

## Screening and Design of Hybrid Peptide That Binds with Glucose Oxidase

**Kenji Yokoyama, Toshifumi Sakai, Hideo Ishikawa, Yasutaka Morita  
and Eiichi Tamiya**

*School of Materials Science, Japan Advanced Institute of Science and Technology,  
Tatsunokuchi, Ishikawa 923-1292, Japan*

### Introduction

Phage display peptide library is based on a combinatorial library of random peptide fused to a minor coat protein of the filamentous M13 phage [1,2]. Phage display creates a physical linkage between a displayed selectable function and the DNA encoding that function. This allows rapid identification of peptide ligands for a variety of target molecules by an *in vitro* selection process. In this study, we screened the peptides, which specifically bind with glucose oxidase (GOx), using phage display random peptide library. In addition, in order to increase the affinity with GOx, a hybrid peptide with two different binding sites was designed.

### Results and Discussion

We screened the peptides that bind with the specific site of GOx using a phage display random peptide library. Amino acid sequence (52-58 GSYESDR) that is located near the active site of GOx was selected as a target. Biopanning was carried out directly on a bead at which the 7mer peptide was synthesized using Fmoc chemistry. Six groups of the peptides were screened after the fourth panning selection.

Affinity of the selected peptides to GOx was investigated using SPR detector (Biacore 3000). GOx, and galactose oxidase or bovine serum albumin (BSA) as a control were immobilized on the sensor chip (Biacore, CM5) with a standard method using carbodiimide and *N*-hydroxysuccinimide. A HBS-EP buffer (Biacore; 10 mM HEPES, 150 mM NaCl, 3 mM EDTA, 0.005% Tween 20, pH 7.4) containing the screened 12mer peptides was delivered into the flow cell. The resulting SPR signal showed that affinity of the selected peptide to GOx was observed. On the other hand, affinity to galactose oxidase and BSA was over 100 times lower than GOx. The dissociation constant values  $K_D$  were determined by variation of the peptide concentration, as shown in Table 1. These peptides demonstrated the affinity with GOx at  $K_D$  value of around  $10^{-4}$  M.

Peptides that bind with the other site (197-203 GVPTKKD) of GOx were also screened. Five plaques and 5 different sequences were obtained. Similarly, affinity of

*Table 1.  $K_D$  value resulting from targeting 52-58 GSYESDR.*

No.	Sequence	$K_D$ (M)
A	HPPMDFHKAMTR	$5.4 \cdot 10^{-4}$
B	APWSPATHYLKD	$1.3 \cdot 10^{-4}$
C	HPNMHRHGYY	$1.7 \cdot 10^{-4}$
D	DPPTVLPKLAYR	$2.4 \cdot 10^{-3}$
E	QIPLMKPGGYMY	$2.1 \cdot 10^{-4}$
F	YPHYSQPLYWRQ	$6.5 \cdot 10^{-4}$
G	APAQAGQTQWPL	$3.7 \cdot 10^{-3}$
H	SVSVGMKPSRP	$8.7 \cdot 10^{-4}$

the screened peptides was investigated. Table 2 shows the  $K_D$  values, and the peptide with the highest affinity showed  $K_D$  at around  $10^{-5}$  M.

Table 2.  $K_D$  value resulting from targeting 197-203 GVPTKKD.

No.	Sequence	$K_D$ (M)
1	SLASSDIGWIGK	$2.1 \cdot 10^{-2}$
2	CHPQPLKSRNPL	$2.4 \cdot 10^{-5}$
3	ACLITPQKGS	$1.3 \cdot 10^{-4}$
4	NMLKSYSDMQPS	$6.3 \cdot 10^{-3}$
5	LLRNRSKLPEPH	$3.6 \cdot 10^{-5}$

In order to increase the affinity with GOx, a hybrid peptide with two different binding sites was designed. A peptide binding with 53-58 and a peptide binding with 197-203 were conjugated with a peptide linker. Hybrid peptides with various linker lengths were synthesized and the affinity with GOx was investigated. Hybrid peptides with 14 or 15 amino acid linker were synthesized. These peptides indicated  $K_D$  value to be around  $10^{-5}$  M, which was the same level of Peptide2 only. This is due to too long and flexible linker, and hence, Peptide A with smaller binding constant cannot bind with GOx. Subsequently, hybrid peptides with a short linker were designed. Table 3 shows  $K_D$  values of hybrid peptides with a short linker against GOx. The increase in the affinity between synthetic peptide and GOx was observed. The hybrid with a 3mer linker showed the highest. In conclusion, we clarified that peptide hybrid can enhance the binding affinity to the target.

Table 3.  $K_D$  value of hybrid peptide.

No.	Sequence	$K_D$ (M)	Linker length
1	Peptide2 <sup>a</sup> -GGG-PeptideB	$1.5 \cdot 10^{-4}$	3
2	Peptide2-G-PeptideA	$2.0 \cdot 10^{-4}$	1
3	Peptide2-GG-PeptideA	$7.3 \cdot 10^{-5}$	2
4	Peptide2-GGG-PeptideA	$4.7 \cdot 10^{-6}$	3
5	Peptide2-HFH-PeptideA	$2.8 \cdot 10^{-6}$	3
6	(Peptide2-HFH-PeptideA) <sup>a</sup>	$4.2 \cdot 10^{-6}$	3
7	Peptide2-FLF-PeptideA	$6.3 \cdot 10^{-6}$	3
8	Peptide2-GGGG-PeptideA	$5.2 \cdot 10^{-5}$	4
9	Peptide2-EFHFE-PeptideA	$2.5 \cdot 10^{-5}$	5
10	Peptide2-GGGGGG-PeptideA	$9.8 \cdot 10^{-4}$	6
11	Peptide2-GGG-PeptideB	$3.2 \cdot 10^{-4}$	3
12	Peptide2-GPG-Peptide2 <sup>a</sup>	$2.9 \cdot 10^{-5}$	3
13	Peptide2-HFH	$1.8 \cdot 10^{-5}$	—

<sup>a</sup> Reverse sequence.

### Acknowledgments

This work was financially supported by the Research for the Future Program from JSPS and the Grant-in-Aid for Scientific Research (No. 10145216, 11132220, 11167239, 12019223) from the Ministry of Education, Sports, Science and Technology.

### References

1. Parmley, S.F., Smith, G.P. *Gene* **73**, 305–318 (1988).
2. Scott, K., Smith, G.P. *Science* **249**, 386–390 (1990).

## Combinatorial Synthesis, Screening and Testing of Peptidic RNA-Ligands

Michael Baumann<sup>1,4</sup>, Delf Schmid<sup>2</sup>, Hilmar Bischoff<sup>2</sup>, Christoph Königs<sup>3</sup>,  
Ursula Dietrich<sup>3</sup> and Christian Griesinger<sup>4,5</sup>

<sup>1</sup>Massachusetts Institute of Technology, Department of Chemistry, Cambridge MA, 02139, USA

<sup>2</sup>Bayer AG, Wuppertal, 42096, Germany

<sup>3</sup>Georg-Speyer-Haus, Frankfurt, 60596, Germany

<sup>4</sup>Johann Wolfgang Goethe-Universität Frankfurt, Frankfurt, 60439, Germany

<sup>5</sup>Max Planck Institute for Biophysical Chemistry, Göttingen, 37077, Germany

### Introduction

RNA, as one of the biomolecules with the most structural and functional diversity, is an attractive therapeutic target [1]. Employing combinatorial chemistry methods, small peptide ligands were found, which bind to a short RNA with important biological functions. A 23nt RNA-oligonucleotide from the Cholesterol Ester Transfer Protein mRNA (CETP-RNA) was chosen as the molecular target [2]. Tetrapeptide libraries, composed of the amino acids Lys, Tyr, Leu, Ile and Arg were synthesized by a combination of combinatorial and divergent solid phase synthesis. Gel-shift affinity screening was used to extract the peptides with the best RNA binding properties. The peptide Lys-Tyr-Lys-Leu-Tyr-Lys-Cys-NH<sub>2</sub> **1** showing micromolar affinity to its RNA-target was characterized with Circular Dichroism (CD)-, Ultra Violet (UV)-measurement and <sup>1</sup>H-NMR-spectroscopy and tested for its physiological activity.

### Results and Discussion

We screened the (polyethyleneglycole)-PEG derivatized peptides (Figure 1) for high affinity to this target molecule by non-denaturing gel-electrophoresis. Each library contains 625 different peptides. The libraries were synthesized as 25 mixtures of 25 different peptides and cleaved from the resin. They were then attached to a PEG-Linker *via* a Cys [3]. The PEG-derivation was necessary to obtain a larger gel-retardation of the RNA-oligonucleotides that were used for selection of the strongest binders. At first, 25 mixtures of 25 peptides (25 × 25 = 625 peptides) were run in 25 lanes of a non-denaturing polyacrylamide gel with the target RNA. Afterwards, the mixture containing individual peptides exhibiting the largest gel-shift and the highest content of hydrophobic amino acid residues were synthesized individually and run through the gel shift assay to obtain the best binding sequences. The peptide sequence Lys-Tyr-Lys-Leu-Tyr-Lys-Cys-NH<sub>2</sub> **1**, found by that procedure, has the same or better affinities as full basic peptides, the hydrophobic side chains of Leu and Tyr enhance the sequence specificity.

Peptide ligand **1** has a strong binding affinity to the 23nt CETP-RNA, whereas an affinity to the 28nt ΔTAR-RNA [4] cannot be detected in the gel shift assay with equal concentrations (data not shown). To prove the binding specificity to the CETP-RNA by CD, UV and NMR experiments [5], as well as for the physiological tests, **1** was synthesized again without PEG derivatization.

A lower CETP activity was detected by a reduced cholesterol ester transfer. Groups of three mice were injected (i. v.) with **1** (100 mg/kg) or 0.9% NaCl (control group) and a blood sample was taken (Table 1). Because it was possible to take blood only once, for each time point a different group of mice was used. Each value corresponds to the median of three mice. In case of a stronger lowering of the cholesterol ester

## Synthetic Methods

transfer, as in the control group, the CETP-activity should be lowered. The stronger reduction of the CETP-activity as in the control group after 15 min is unclear. Only 2 mice were used for this experiment. After 90 min the mice treated with **1** show a clear reduction of the cholesterol ester transfer.

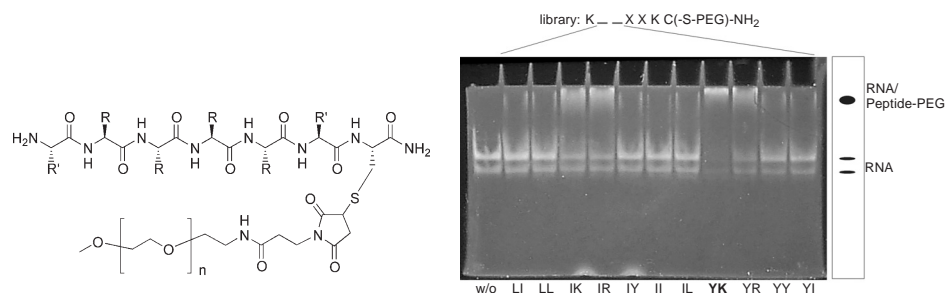


Fig. 1. Polyethyleneglycol ( $n \sim 100$ ) derivatized peptide library ( $R$  = side chains of Ile, Lys, Tyr, Arg, Lys;  $R'$  = side chain of Lys) screened by non-denaturing gel-electrophoresis.

To check the stability of the peptide **1** under physiological conditions, **1** was incubated with mouse serum (10%) for 24 h and analyzed by HPLC. After 24 h, more than 90% of the peptide was still unchanged.

Table 1. Averaged rate of cholesterol ester transfer between HDL and VLDL in pmol/h in mice measured after the given time after injection of physiological salt solution and 100 mg/kg of **1**.

	0 min	15 min	0 min	30 min	0 min	60 min	0 min	90 min
0.9% NaCl	75.83	128.67	85.02	15.13	115.87	108.9	105.8	91.33
100 mg/kg <b>1</b>	85.4	98.05 <sup>a</sup>	107.83	15.53	122.77	120.73	161.7	64.3

<sup>a</sup> Only two mice.

## Acknowledgments

This work was supported by the Fonds der Chemischen Industrie, the Deutsche Forschungsgemeinschaft, and the Max-Planck-Gesellschaft. All NMR measurements were done at the Large Scale Facility for Biomolecular NMR at the Johann Wolfgang Goethe-Universität Frankfurt.

## References

1. Pearson, N.D., Prescott, C.D. *Chem. Biol.* **4** (6), 409–414 (1997).
2. Richter, C. NMR-spektroskopische Untersuchungen zur Strukturaufklärung von RNA. Diploma-Thesis, University of Frankfurt, Germany, 1996.
3. Wang, J., Huang, S.Y., Choudhury, I., Leibowitz, M.J., Stein, S. *Anal. Biochem.* **232**, 238–242 (1995).
4. Long, K.S.; Crothers, D. M. *Biochemistry* **34**, 8885–8895 (1995).
5. Baumann, M., Koenigs, C., Dietrich, U., Griesinger, C. *Proceedings of the 16th American Peptide Symposium: Peptides for the New Millennium*, Kluwer, Dordrecht, 1999, p. 171.

## High Throughput Peptide Syntheses Generate Ligands for Proteomic Database

Lin Chen, Brian Korenstein, Michael James, Leonid Kvecher and  
J. Mark Carter

AxCell Biosciences, Newtown, PA 18940-1721, USA

### Introduction

In order to comprehensively chart protein-protein interactions for the human proteome, our group generates approximately 1000 peptides per month. Highly parallel peptide synthesis by Fmoc chemistry is achieved using Mimotopes' SynPhase™ solid phase support [1] in 96 well microtiter plates. Accuracy in this manual assembly method is facilitated by a PinPal™ Amino Acid Indexer [2]. Common steps (*e.g.*, deprotection and washing) are performed batchwise on the synthesis crowns, in order to optimize economy, and throughput. Even after trifluoroacetic acid (TFA) cleavage, samples continue to be handled in parallel during ether precipitation, washes, re-dissolving, and lyophilization.

### Results and Discussion

The peptides (shown in Figure 1) we generated for this study ranged from 12-15 amino acids and include ligands used for binding with WW, SH2, SH3, PDZ, and EH protein domains. All peptides contained a Lys-Lys-Lys-Gly spacer that is necessary for our affinity binding assay, and also serves to improve the solubility of peptides. A dansyl group served as a chromophore (330 nm) to facilitate peptide quantitation and was attached to the side chain of the last spacer lysine. The N-terminus biotin served as a "handle" for quantitation of peptide binding in AxCell's high throughput screening assay.

As a solid phase support we use Mimotopes' (Clayton, Victoria, Australia) SynPhase™ acrylic-grafted polypropylene crowns with a preloaded linker. The crowns were arranged in 12 X 8 format and there were 10 X 96 crowns in each synthesis. In order to optimize throughput and economy, Fmoc deprotection was carried out in a polypropylene tub containing 20% piperidine, and all crowns were immersed in the bath for 1 h. Washing steps were performed similarly in tubs containing DMF or methanol. By doing these common steps batchwise, we increased the throughput. By reusing the piperidine baths through the entire synthesis, we achieved economy.

The couplings were performed in ten deep well microplates. The key step is to deliver the amino acid solutions (250  $\mu$ L, 0.2 M) to the appropriate wells. This was performed with the aid of the PinPal™ Amino Acid Indexer (see Figure 2). The PinPal™ contains 10 LED boards in 96 well format. It is driven by proprietary software that first processes the peptide sequences for synthesis, and then lights up LEDs under the individual wells of 10 deep-well microplates, indicating the appropriate amino acid to be delivered for each peptide in each coupling cycle. After dispensing amino acid solutions, the activating solution of HOBt/HBTU/DIEA (250  $\mu$ L/well, 0.2/0.2/0.4 M)



Fig. 1. Peptide ligands. X = OH, peptide acid; NH<sub>2</sub>, peptide amide.

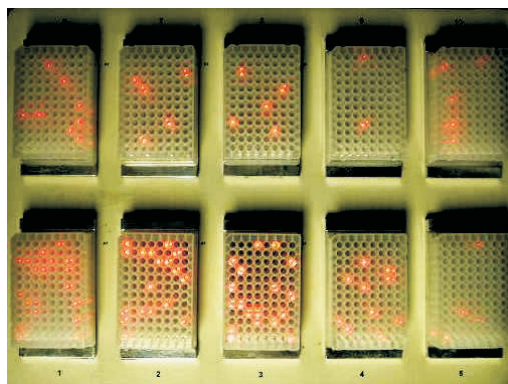


Fig. 2. PinPal™ Amino Acid Indexer.

was dispensed to all wells. Finally the crowns were immersed in the amino acid coupling solution in the plates for a minimum of 2 h.

When assembly was completed, the peptides were cleaved off the solid support by immersing the crowns into wells of microplate containing 0.5 mL/well Reagent R for 2 h. Then the crowns were removed, and the resulting cleavage solutions were concentrated under vacuum to approximately 0.2 mL/well using the GeneVac. The concentrated cleaved peptide solutions were transferred into a Robbins (Sunnyvale, CA) FlexChem™ block containing cold methyl *t*-butyl ether (MTBE) (1 mL/well). The block was then sealed, shaken and flipped. After they precipitated out, the crude peptides were filtered using a vacuum manifold and washed twice with MTBE (1 mL/well). The peptides were dissolved in 1 mL/well of water/acetic acid/acetonitrile (80 : 10 : 10) and lyophilized by GeneVac (Valley Cottage, NY) prior to characterization. High throughput liquid handling was facilitated by HYDRA™ 96 (Robbins), which contains 96 glass and Teflon syringes for parallel handling. It helped: (1) dispense cocktail to microplates; (2) aspirate concentrated cleaved peptide solutions from microplates and dispense them into new microplates; (3) dispense MTBE to microplates to precipitate out or wash peptides; and (4) dispense solution to microplates for dissolving peptides while preventing cross-contamination.

In summary, we have developed a high throughput method to generate peptides by using parallel synthesis. The PinPal™ Amino Acid Indexer, (combined with operating software developed in house) and HYDRA™ 96, are very important for us to achieve rapid and accurate peptide synthesis. With them we are able to generate about 1000 peptides (12–25mers)/month with only one chemist.

## References

1. Maeji, N.J., Valerio, R.M., Bray, A.M., Campbell, R.A., Geysen, H.M. *React. Polym.* **22**, 203–212 (1994).
2. Carter J.M., VanAlbert, S., Lee, J., Lyon, J., Deal, C. *Biotechnology*, **10**, 509–513 (1992).

## MHC Ligand Motifs from Peptide Libraries: The Software EPIPREDICT

**B. Fleckenstein<sup>1</sup>, G. Jung<sup>1</sup>, K.H. Wiesmueller<sup>2</sup>, F. von der Muelbe<sup>1</sup>,  
 D. Niethammer<sup>3</sup> and J. T. Wessels<sup>3</sup>**

<sup>1</sup>Universität Tübingen, Institut für Organische Chemie, 72076 Tübingen, Germany

<sup>2</sup>EMC Microcollections GmbH, 72070 Tübingen, Germany

<sup>3</sup>Universitätsklinik für Kinderheilkunde und Jugendmedizin, 72076 Tübingen, Germany

### Introduction

Synthetic peptide libraries have been shown to represent tools in elucidating molecular interactions in T cell mediated immune response [1,2]. New reliable synthetic concepts and bioassays were developed to describe peptide-MHC interactions in a quantitative way [3]. Two-dimensional databases, describing perfectly the allele-specific peptide binding to many MHC class I and II alleles, have been generated using purified MHC molecules. The databases are used for the design and synthesis of so-called directed peptide and nonpeptide libraries, which are applied to study antigen recognition of T cells from patients with autoimmune diseases. The knowledge about interactions within the trimolecular complex (MHC-peptide-TCR, Figure 1) is used for our new algorithm EPIPREDICT predicting MHC class II self and foreign ligands T cell epitopes.

### Results and Discussion

Two valuable Internet programs predict MHC restricted potential T cell epitopes. The first program is based on sequence motifs from isolated natural peptide libraries and experimentally determined natural T cell epitopes [4]. The second recently developed prediction program is based on complete allele specific HLA class II ligand-binding motifs determined from synthetic peptide libraries [5].

The binding contribution of every amino acid side chain in a class II-ligand is described by allele-specific two-dimensional data bases (Binding Patterns) which are now generated for a growing list of HLA DR and DQ alleles. Furthermore, with this combinatorial approach the relative contribution of all residues within peptide

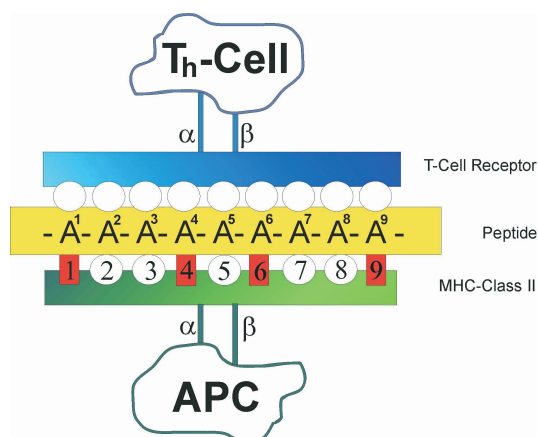


Fig. 1. Interactions within the trimolecular complex.

## Synthetic Methods

epitopes to T cell activation can be quantified and specific Recognition Patterns are deduced [1,3]. These quantitative matrices – describing the interactions within the trimolecular complex – represent optimal data bases for the prediction of HLA class II-ligands and class II-restricted T cell epitopes (Figure 2). Compared to other methods, the accuracy of epitope prediction *via* EPIPREDICT is clearly improved as shown by prediction studies for already known T cell epitopes. Moreover, new T cell epitopes for IgA-protease of *Neisseria* were successfully identified. An epitope prediction for any desired protein antigen (up to 3000 amino acids) from common protein data bases is possible as demonstrated in the search for novel autoantigens in juvenile arthritis and coeliac disease [6,7]. Suggested peptide sequences are ranked according to the predicted epitope probability and thresholds can be introduced freely by the user. EPIPREDICT together with the HLA class II allele-specific matrices is accessible for scientific use in the Internet, allowing a permanent upgrading of its prediction possibilities [6,7].

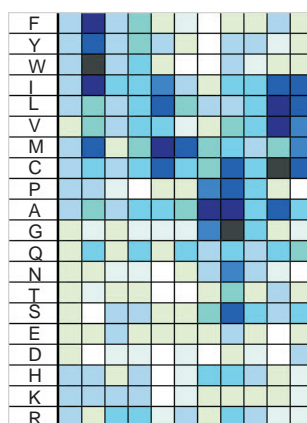


Fig. 2. Two-dimensional HLA class II allele-specific matrix for DRB1\*0101. The darker the colour, the better is the binding to the shown amino acid on this position.

## Acknowledgments

Supported by the DFG/Sonderforschungsbereich 510 (projects D4 and E3.2).

## References

1. Fleckenstein, B., Jung, G., Wiesmüller, K.H., In Jung, G. (Ed.) *Combinatorial Chemistry – Synthesis, Analysis, Screening*, Wiley-VCH, Weinheim, 1999, p. 355.
2. Jung, G., *Combinatorial Peptide and Nonpeptide Libraries*, Wiley-VCH, Weinheim, 1996.
3. Fleckenstein, B., Jung, G., Wiesmüller, K.H. *Semin. Immunol.* **11**, 405–416 (1999).
4. <http://www.syfpeithi.de>, internet data base by Rammensee, et al.
5. <http://www.epipredict.de>, internet data base by Wessels J.T., Fleckenstein B., et al.
6. Wessels, J.T., Fleckenstein, B., et al. *Immunobiology* **203**, 61 (2000).
7. Fleckenstein, B., Wessels, J.T., et al. *Blood* **96**, 239a (2000).

## High-Density Compound Arrays of Combinatorial Chemical Libraries by a New Pen-Directed and Computer-Navigated Plotter Device

Stefan R. K. Hoffmann

Department of Biochemistry, University of Zurich, 8057 Zurich, Switzerland

### Introduction

The search for new drugs and synthetic vaccines by screening the vast diversity of chemical structures is one of the most challenging goals of modern synthetic chemistry and molecular biology. While nature uses the three-dimensional structures of linear sequences of amino acids in peptides and proteins in nearly all the life processes, chemistry makes in principle accessible the whole structural space of chemical compounds and artificial protein architectures. But the de novo design of artificial architectures with predefined structure–function relationship is still a challenging problem, due to the unknown theoretical concepts in which nature rules a linear sequence to fold and to interact with a molecular ligand. In contrast, combinatorial chemistry allows the search for new structures with predefined function by screening the diversity of synthetic libraries. While the synthesis and screening of chemical libraries is quite routine both as bead- [1] and array-type libraries [2] since their introduction a decade ago, the development of new devices for their preparation can greatly simplify and boost their application for the search towards new drug-like compounds.

### Results and Discussion

For the search for passive repressors of HIV-1 *long terminal repeat* enhancer controlled transcription, we have screened the sequence space of artificial peptide structures derived from the DNA-binding domain of the bacteriophage 434 repressor with combinatorial chemical libraries. Both “one bead-one compound” libraries and high-density compound arrays were employed. While bead-type libraries were established by conventional “split-mix” technology [1], the preparation of high-density compound arrays on porous membranes using the SPOT technology [2] needed a precise and high-throughput pipetting system for the delivery of chemical compound solutions due to the enormous number of compounds established in these libraries. For example, the manual preparation of compound arrays on porous membranes exploiting the conventional SPOT technology in a microtiter format of  $8 \times 12 = 96$  compound positions on an operational space of  $129 \text{ mm} \times 87 \text{ mm}$  needs the finest available manual pipette (*e.g.* Eppendorf Research 2.5  $\mu\text{l}$ ) and the delivery of a 0.2 to 0.7  $\mu\text{l}$  fluid volume. A complete combinatorial chemical library derived from a peptide sequence, which is randomized in 3 or 4 positions with the 20 natural amino acids, consists of 8,000 and 160,000 compounds, respectively. By using the manual SPOT synthesis 84 and 1667 membranes in a microtiter format are needed. This means a total operational space of  $0.94 \text{ m}^2$  ( $1.0 \text{ m} \times 1.0 \text{ m}$ ) and  $18.70 \text{ m}^2$  ( $4.3 \text{ m} \times 4.3 \text{ m}$ ), and, in conclusion, an enormous amount of chemicals both for the synthesis and screening procedures.

We report here the development of a new pen-directed, semi-automated and computer-navigated plotter device for the synthesis of combinatorial chemical libraries as membrane-type spatially adressable high-density compound arrays (Figure 1). It allows the synthesis of up to 10,000 preparations of distinct compounds or mixtures in distinct sublibraries on a microtiter operational space ( $129 \times 87 \text{ mm}$ ) or up to 55,000

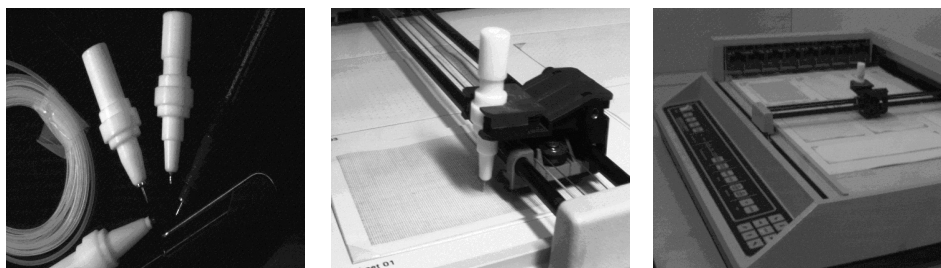


Fig. 1. Images of the flat-screen computer-plotter device for the preparation of high-density microarrays of combinatorial chemical libraries on porous membranes.

distinct preparations on an A4 operational space ( $297 \times 210$  mm). Both permanently fixed compounds for the direct screening on solid support and compounds ready for the elution by aqueous buffers for the screening in solution can be prepared. While the porous membrane is used as a solid support, a teflon-made conventional plotter pen with solutions of chemicals is used for the distribution to the positionally addressable array. The contact time between the pen and membrane determines the distributed fluid quantity and the spot size. Using this technology ligand-DNA interactions with the goal to find new repressors of HIV-1 LTR enhancer controlled transcription were screened. This technology is now further developed towards an automated synthesis device using the Mitsubishi RV-M1 Movemaster EX robotic platform.

#### Acknowledgments

This research was supported by the German Research Foundation (DFG) and the Hartmann-Müller Foundation for Medical Research.

#### References

1. (a) Furka, A., Sebestyen, F., Asgedom, M., Dibo, G. *Int. J. Pept. Protein Res.* **37**, 487–493 (1991). (b) Houghten, R.A., Pinilla, C., Blondelle, S.E., Appel, J.R., Dooley, C.T., Cuervo, J.H. *Nature* **354**, 84–86 (1991). (c) Lam, K.S., Salmon, S.E., Hersh, E.M., Hruby, V.J., Kazmierski, W.M., Knapp, R.J. *Nature* **354**, 82–84 (1991).
2. Frank, R. *Tetrahedron* **48**, 9217–9232 (1992).

## Combining SPOT Synthesis and Native Chemical Ligation to Generate Large Arrays of Small Protein Domains

Florian Toepert<sup>1</sup>, Tobias Knaute<sup>1</sup>, Stefan Guffler<sup>2</sup> and  
Jens Schneider-Mergener<sup>1,2</sup>

<sup>1</sup>Institute of Medical Immunology, Charité, Humboldt-University, 10098 Berlin, Germany

<sup>2</sup>Jerini AG, 12489 Berlin, Germany

### Introduction

We present a novel approach for the construction of large arrays of synthetic protein domains. A combination of SPOT synthesis [1] and native chemical ligation [2] was applied to generate 6859 variants of the hYAP WW protein domain [3,4] consisting of 38 amino acids. Leucine 30, histidine 32 and glutamine 35 were substituted by all other L-amino acids (excluding cysteine) resulting in  $19 \times 19 \times 19 = 6859$  variants. The C-terminal parts of the protein domains were prepared by SPOT synthesis creating 6859 C-terminal peptides comprising 24 residues with variations in the positions described above and an N-terminal cysteine. Full length protein domains were assembled upon ligation of a thioester-peptide comprising the remaining 14 residues. The ligation site (originally a serine) had been identified in previous studies [5].

### Results and Discussion

The combination of SPOT synthesis and native chemical ligation allows the construction of full length cellulose bound peptides. In a quantitative monitoring experiment of the ligation of a model peptide with this strategy we found that the reaction was completed after 2 h (data not shown).

Employing this combination of techniques we were able to synthesize an array of functional variants of the hYAP WW protein domain. The wildtype (wt) domain was detected by HPLC-MS analysis of the wt spots in the array (data not shown).

The array of WW domains was screened with the natural ligand. 3D representation of the spot signal data (see Figure 1) reveals details of the molecular interaction be-

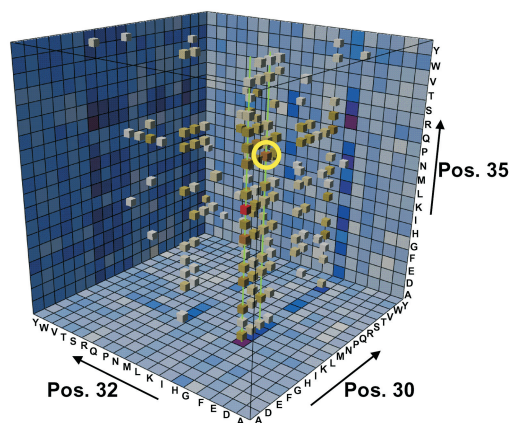


Fig. 1. 3D representation of spot signal data obtained by binding studies with an array of synthetic WW variants and a dye-labeled peptide ligand (GTPPPPYTVG). The intensity of a spot is depicted by the color of the corresponding cubicle (dark = strong signal). WW domain wt = L30, H32, Q35 (circle).

tween ligand and WW domain: Two lines mark a plane of cubicles that represent WW variants with His in position 32. The clustering of cubicles in this plane indicates a strong substitutional preference for His in position 32. Similarly, clustering of cubicles along Ile 30 suggests a substitutional preference for Ile in position 30, which is particularly remarkable because it differs from the wildtype residue (Leu) in this position. In addition a number of cubicles can be identified representing WW variants that differ from the wildtype WW domain in all three sequence positions that were varied in this study.

## **References**

1. Frank, R. *Tetrahedron* **48**, 9217 (1992).
2. Dawson, P.E., Kent, S.B. *Annu. Rev. Biochem.* **69**, 923 (2000).
3. Sudol, M., Chen, H.I., Bougeret, C., Einbond, A., Bork, P. *FEBS Lett.* **369**, 67 (1995).
4. Bedford, M.T., Sarbassova, D., Xu, J., Leder, P., Yaffe, M.B. *J. Biol. Chem.* **275**, 10359 (2000).
5. Toepert, F., Pires, J.R., Landgraf, C., Oschkinat, H., Schneider-Mergener, J. *Angew. Chem., Int. Ed. Engl.* **40**, 897 (2001).

## Peptides as Drugs: Is There a Market?

Albert Loffet

*Senn Chemicals, Gentilly, 94250, France*

### Introduction

What is the value of the ethical pharmaceutical market? What is the share of the peptides and proteins market within it? Is it worthwhile to invest in research in that field with the hope of finding new drugs? Do we, as scientists, have a future when starting our career in the isolation, synthesis or production of peptides and proteins?

### Results and Discussion

With \$265 billion worldwide the ethical pharmaceutical market has increased by over 10% in 2000 *versus* 1999. All “peptide” products (synthetic peptides; peptidomimetics, proteins including antibodies but excluding vaccines) are worth \$28 billion; this total value can be split into 3 sub-groups of products:

Recombinant proteins: \$14 billion

Monoclonal antibodies: \$4 billion

Synthetic products: \$10 billion

Advantages and disadvantages of peptides are well known; they are summarized in Table 1.

*Table 1. Advantages and disadvantages of peptides*

Advantages	Disadvantages
High activity	Low oral bioavailability
High specificity	Usually injected
No accumulation in the organs	Cost of synthesis
Low toxicity	

The method of administration, and the low bioavailability, implies that peptides should be used mainly for treatment of acute diseases and should be less valued for chronic treatments, at least when no specific formulation can be used. The exception to this is insulin, which has not yet been replaced, even if multi injections have to be made daily. Peptides are used in a variety of indications as shown in Table 2.

*Table 2. Uses of peptides.*

Allergy/Asthma	Analgesia	Antivirals
Arthritis	Baldness	Calcium metabolism
Cancer	Cardiovascular	C N S
Diabetes	Epilepsy	Gastro-intestinal
Growth	Gynecology	Haemostasis
Immunity	Impotency	Incontinence
Infection	Inflammation	Obesity
Ophthalmology	Vaccines	Diagnostic

## Synthetic Methods

Table 3 shows the composition and an indication of the “pipeline” of the 3 sub-classes.

*Table 3. Composition and an indication of the “pipeline” of the 3 sub-classes.*

Recombinant proteins	Monoclonal antibodies	Synthetic peptides
Marketed > 50 products	Marketed > 20 products	Marketed > 40 products
Pre-registration and Phase III > 40 products	Pre-registration and Phase III > 20 products	Pre-registration and Phase III > 20 products
Phase II > 60 products	Phase II > 45 products	Phase II > 60 products

What are the new registered products and the ones just waiting for approval? Table 4 shows recently registered products and their indication, whereas Table 5 shows products in Phase III.

*Table 4. Recently registered products.*

Integrilin	Cardiovascular
Bivalirudin	Cardiovascular
Atosiban	Gynecology
VIP	Impotency
Techtide P 289	Diagnostic
Groliberin	Diagnostic

*Table 5. Products in phase III.*

Pramlintide	Diabetes
SPC 3	HIV
Pentafuside (T-20)	HIV
Abarelix	Cancer
Ambamustine	Cancer
Ziconotide	Analgesia
Protegrin	Infection
SF-250	Infection

What are the arguments that make us more optimistic than a decade ago about the future of peptides? First of all, the arrival on the market of many proteins with invaluable activities, which in any case will have to be injected. All major pharmaceutical companies now have recombinant proteins or monoclonal antibodies in their portfolio. Why should these companies accept to market a protein of 300 amino acids and not a peptide of 40, both being injectable? Biotech companies have helped a lot in this change of attitude and we should be grateful to them!

Secondly, the development of formulations which are much less stressful for the patient than injections, is booming; from the classical biodegradable polymers which

### ***Loffet***

slowly liberate the drug, to the non-degradable implants incorporating membranes, which make them work as osmotic pumps; from transdermal powder injection to sophisticated tools allowing for custom tailored particles to be inhaled directly into the lungs. There are over 50 companies specializing in this field.

Thirdly, the costs have to be addressed. The production of amino-acid derivatives and of peptides has never been an industrial market because all quantities needed have always been too small to obtain real economies of scale.

Even now, because of the diversity of the products and the strategies used it is still a “niche market”, but this is changing as the cost of reagents have reduced tremendously in the last three years. Would Bruce Merrifield have believed it 30 years ago if someone had told him that solid-phase synthesis would be performed in reactors of a few hundred liters? The development of chromatography technologies (equipment and phases) has also helped in reducing the costs of purification, which finally allows peptides to be produced at a cost/efficacy ratio fully comparable with other complex API's.

Finally, the success of the Human Genome Project with as a consequence the development of proteomics and the unbelievable number of sequences which will have to be synthesized will undoubtedly give more peptide leads from which we strongly believe that some blockbuster drug will emerge.

Will these products be manufactured by recombinant technologies and fermentation or will they be strictly synthetic is just a question of cost...

### **Acknowledgments**

In 40 years of career, the list of acknowledgments could be very long. I nevertheless would like to thank Jean Close who allowed me to start solid-phase synthesis in 1965 at UCB, Joe Rudinger who was really my mentor, even if I never worked in his laboratory and Guido Senn who allowed me to finish my career within a wonderful team.

## Solid-Phase Total Syntheses of Trunkamide A and Kahalalide F, Cyclic Peptides from Marine Origin

Fernando Albericio<sup>1</sup>, Josep M. Caba<sup>1</sup>, Àngel López-Macià<sup>1</sup>, Jose C. Jiménez<sup>1</sup>, Marta Carrascal<sup>1</sup>, Laia Solé<sup>1</sup>, Ignacio Rodríguez<sup>2</sup>, Ignacio Manzanares<sup>2</sup>, Miriam Royo<sup>1</sup> and Ernest Giralt<sup>1</sup>

<sup>1</sup>Department of Organic Chemistry, University of Barcelona, Barcelona, E-08028, Spain

<sup>2</sup>Phama Mar Inc., 28760-Tres Cantos, Spain

### Introduction

The sea is a great source of biodiversity, because life conditions there create unique mechanisms of chemical defense. Herein, the solid-phase total synthesis of Trunkamide A [1] and Kahalalide F [2] (Figure 1), two cyclic peptides from marine origin which are currently in preclinical and clinical phase I trials respectively, are discussed. Trunkamide A contains a thiazoline heterocycle and Ser and Thr with the hydroxy function modified as reverse prenyl (rPr). Kahalalide F contains: (i) an ester bond between two sterically hindered amino acids (Val and D-allo-Thr); (ii) the didehydro-amino butyric acid (Dhb); and (iii) a rather hydrophobic sequences with two fragments containing several  $\beta$ -branched amino acids in a row, one of them terminated with an aliphatic acid. Common features of both syntheses are: (i) solid-phase peptide chain elongation using a quasi orthogonal protecting scheme with allyl, *t*-butyl, fluorenyl based groups, on a chlorotrityl resin; (ii) concourse of HOAt based coupling reagents; and (iii) cyclizations in solution.

### Results and Discussion

#### Trunkamide A

The reverse-prenylated derivatives were prepared from Fmoc-Ser/Thr(*t*Bu)-OH according the following pathway: (i) orthogonal protection of the carboxyl group in form of its trichloroethyl ester by reaction with the appropriate alcohol, DCC, and DMAP; (ii) removal of the *t*-butyl groups with TFA/H<sub>2</sub>O (19 : 1); (iii) formation of the 1,1-dimethylpropionyl ether by reaction with the corresponding trichloroacetimidate; (iv) partial reduction of the triple bond to the double bond by catalytic hydrogenation in the presence of Pd/C and quinoline; and (v) removal of the trichloroethyl ester with

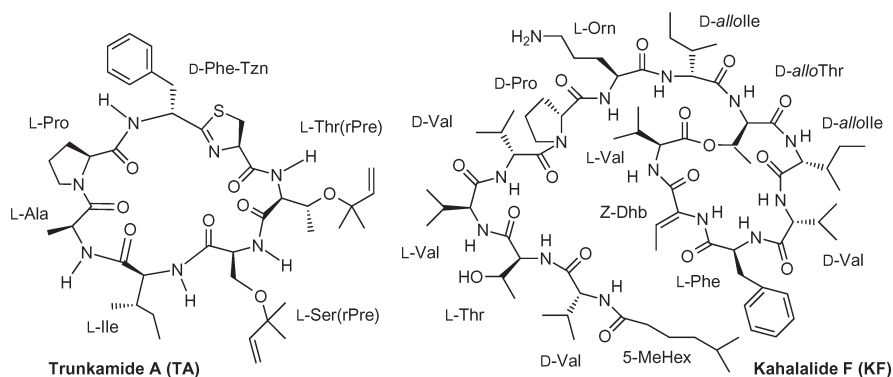


Fig. 1. Structures of Trunkamide A and Kahalalide F.

Zn and  $\text{NH}_4\text{OAc}$ . For the activation of the thioacid, the 1-(*N*-Fmoc-D-thionophenylalaninyl)-6-nitrobenzotriazole [Fmoc-D-Phe(S)-NBt] derivative was used.

The linear sequence was synthesized on the ClTrt-Cl-resin. The partial incorporation of Fmoc-Pro-OH (0.5 equiv) was performed in the presence of DIEA (2 equiv). The incorporation of the first six protected amino acids was carried out using DIPCDI as the coupling reagent. The reverse-prenylated derivatives were incorporated with an excess of 1.7 equiv. The last Ser unit was incorporated with an unprotected hydroxy side chain. Finally, the Fmoc-D-Phe(S)-NBt coupled very smoothly to give a negative ninhydrin test after 90 min. Cleavage of the reverse-prenylated peptide was carried out very smoothly with HFIP/ $\text{CH}_2\text{Cl}_2$  (1 : 4). The macrocyclization was carried out with PyAOP/DIEA. The formation of the thiazoline ring was performed in a single step by exposure of the  $\beta$ -hydroxy thiopeptide to DAST (Figure 2).

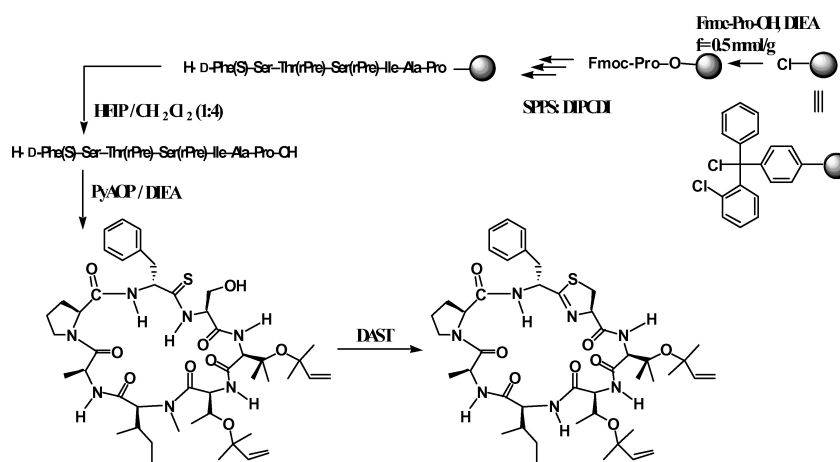


Fig. 2. Synthetic strategy for Trunkamide A.

#### Kahalalide F

The linear sequence was also synthesized on a ClTrt-Cl-resin. The limited incorporation of Fmoc-D-Val-OH (0.2 equiv) was performed in the presence of DIEA (2 equiv). The elongation of the peptide chain was carried out using the Fmoc/*t*Bu strategy. The *D*-allo-Thr and the Thr precursor of the *Z*-Dhb were both introduced without protection of the hydroxyl function. HATU-DIEA was used for all the amide formation.

The esterification with Alloc-Val-OH took place quantitatively with DIPCDI-DMAP. Removal of the Alloc group was carried out with  $\text{Pd}(\text{PPh}_3)_4$  (0.1 equiv) in the presence of  $\text{PhSiH}_3$  (10 equiv) under an atmosphere of Ar. The double bond of the didehydroamino acid was formed on the solid-phase through a  $\beta$ -elimination reaction (left strategy), using a method developed recently in our laboratory, which uses EDC (100 equiv) as activating reagent of the hydroxyl function in the presence of CuCl (60 equiv) in DMF- $\text{CH}_2\text{Cl}_2$  (5 : 1) for 6 days. Alternatively, the dipeptide Alloc-Phe-(*Z*)-Dhb-OH (5 equiv), which was prepared in solution from Alloc-Phe-OH and H-Thr-*O**t*Bu with EDC, and subsequent dehydration with EDC (6.5 equiv) in the presence of CuCl (2.7 equiv) and treatment with TFA, was coupled with HATU-DIEA (5 : 10) for 16 h with a further recoupling for 3 h. Before the

## Synthetic Methods

cleavage of the protected peptide from the resin [TFA-CH<sub>2</sub>Cl<sub>2</sub> (1 : 99), 5 × 0.5 min], the Alloc group was removed as described above. The cyclization step was performed with PyBOP-DIEA in DMF for 1 h. Final deprotection was carried out with TFA-H<sub>2</sub>O (95 : 5) for 1 h (Figure 3).

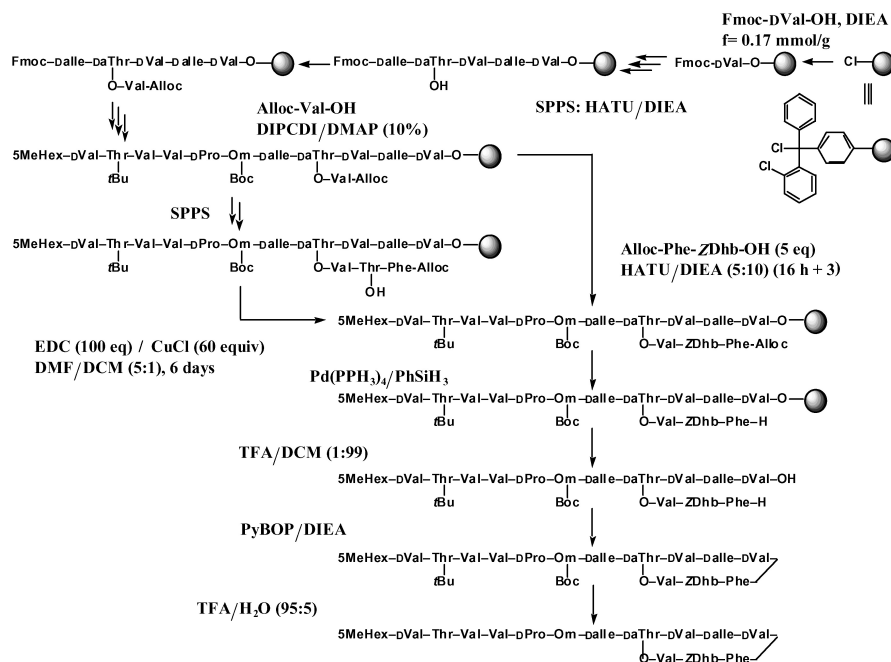


Fig. 3. Synthetic strategy for Kahalalide F.

## Acknowledgments

This work was supported by DGICYT (BQU2000-0235) and Generalitat de Catalunya [Grups Consolidats (SGR 0042) and Centre de Referència en Biotecnologia].

## References

1. Carroll, A.R., Coll, J.C., Bourne, D.J., McLeod, J.K., Zabriskie, T.M., Ireland, C.M., Bowden, B.F. *Aust. J. Chem.* **49**, 659–667 (1996).
2. Hamann, M.T., Scheuer, P.J. *J. Am. Chem. Soc.* **115**, 5825–5826 (1993).

## Solid Phase Synthesis of Large Cyclic Peptides

Katri Rosenthal-Aizman and Anders Undén

Department of Neurochemistry and Neurotoxicology, Stockholm University,  
Stockholm, S-106 91, Sweden

### Introduction

Cyclic peptides with alternating D- and L-amino acids can oligomerize to tubular structures where the peptide backbone adopt a flat disc like conformation. Such structures, usually called nanotubes can be formed by polymerisation of octameric cyclic peptides and has been found to have interesting properties such as pore formation in phospholipid membranes. These structures have been investigated in a number of studies by Ghadiri's group [1].

As we were interested in the structural requirements for nanotube formation, in particular the properties of large cyclic peptides with alternating D- and L-amino acids, we initiated a study to investigate the reaction conditions for the solid phase synthesis and cyclization of this class of peptides.

### Results and Discussion

Solid phase peptide synthesis was carried out with the Boc/benzyl strategy. Anchoring of the first amino acid was first carried out by coupling of Boc-Glu-Oallyl to a MBHA resin (1.27 mmol/g), but in the end of the synthesis it proved difficult to remove the allyl protective group completely, probably largely as a result of aggregation of the peptide.

We therefore carried out the synthesis with Boc-Glu-OBzl as the first amino acid as the benzyl ester can be cleaved by low TFMSA [2], reaction conditions under which the linkage of the peptide to the resin is stable. Solid phase peptide synthesis proceeded without problems up to the coupling of the 6th amino acid when a dramatic ( $\approx 30\%$ ) shrinkage of the resin was observed. Coupling of this residue was far from complete as shown by a strongly positive Kaiser test, even after two couplings with TBTU/HOBt. However, remaining amino groups could be acylated after 30 min with TFFH [3].

These problems suggest the formation of  $\beta$ -sheet like structures and all the following couplings were therefore performed by the *in situ* neutralization method developed by Kent [4].

Cyclizations were carried out with a seven different procedures (Table 1). Reactions were carried out for 20 h. The best yields were obtained by BOP/DIEA in DMF. For all other procedures different side products could be observed. Based on results from mass spectrometry we suggest that carbodiimide gives rise to *N*-acylurea.

Synthesis of the linear form of 16-residue peptide proceeded without problems and the HPLC elution profile is shown in Figure 1. Cyclization proved to be more problematic though, and the results after 40 h activation/cyclization with BOP/DIEA in DMF is shown in Figure 1. Mass spectrometry indicated apart from unreacted linear peptide, the presence of the desired cyclic hexadecapeptide but also products that probably correspond to linear and cyclic dimers.

We conclude from this, and similar studies that we performed on other peptides, that peptides with alternating D- and L-amino acids are prone to aggregation during the synthesis after 6 to 8 residues and that the synthesis is best performed with Boc chemistry where *in situ* neutralization method can be used. The success of the

Table 1. Cyclization of DL-octapeptide:  
*H-DVal-Lys(Fmoc)-DVal-Lys(Dnp)-DVal-Lys(Fmoc)-DVal-Glu(MBHA)-OH*.

Cyclization procedure	Yield (%) <sup>a</sup>		
	cyclic	linear	side products
BOP 3 eq, DIEA 6 eq, DMF	33	54	13
BOP 3 eq, DIEA 6 eq, DCM	20	69	11
TFFH 3 eq, TMP 6 eq, DCM	13	67	20
TFFH 3 eq, HOAt 1 eq, TMP 3 eq, DCM/DMF	14	65	21
HATU 2 eq, HOAt 2 eq, TMP 4 eq, DCM/DMF	20	70	10
DIPCDI 2 eq, HOBt 2 eq, DCM/DMF	9	71	20
DIPCDI 3 eq, HOAt 3 eq, DCM/DMF	11	70	19

<sup>a</sup> As determined by RP-HPLC (analytical  $C_{18}$ , 420 nm) and MALDI-TOF MS.

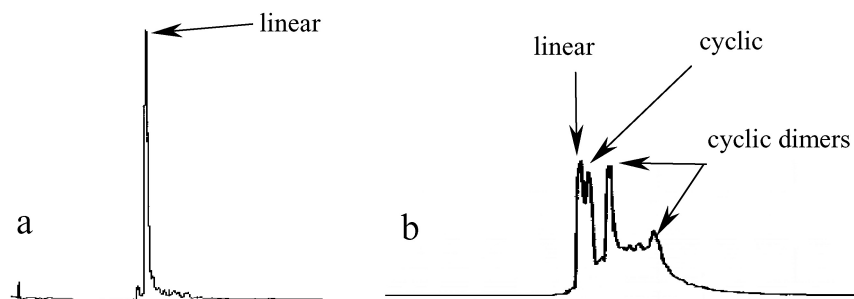


Fig. 1. Analytical RP-HPLC ( $C_{18}$ , 420 nm) profiles of crude hexadecapeptide: a linear form, b BOP 3 eq, DIEA 6 eq in DMF, cyclization 40 h.

cyclization step is very dependent on the sequence of the peptide but, as in the case reported in this presentation, the rates of cyclization can be very slow.

#### Acknowledgments

Supported by Magnus Bergwall stiftelse and Swedish Natural Science Research council.

#### References

1. Ghadiri, M.R., Granja, J.R., Milligan, R.A., McRee, D.E., Khasanovich, N. *Nature* **366**, 324 (1993).
2. Tam, J.P., Heath, W.F., Merrifield R.B. *J. Am. Chem. Soc.* **108**, 5242 (1986).
3. Carpino, L.A., El-Faham, Ayman *J. Am. Chem. Soc.* **117**, 19 (1995).
4. Schnölzer, M., Alewood, P., Jones, A., Alewood, D., Kent, S.B.H. *Int. J. Pept. Protein Res.* **40**, 180 (1992).

## Solid-Phase Synthesis of Consolidated Ligands Containing an Intramolecular Lactam Bridge: Comparison of Strategies and Tactics

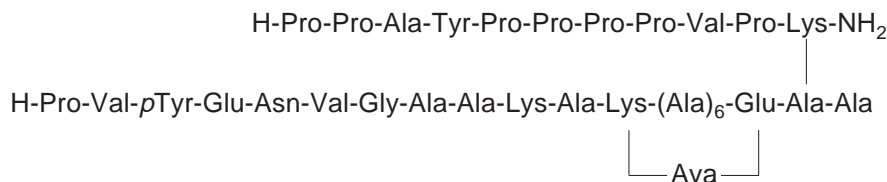
Jaya T. Varkey<sup>1</sup>, David Cowburn<sup>2</sup>, Hong Ji<sup>2</sup> and George Barany<sup>1</sup>

<sup>1</sup>Department of Chemistry, University of Minnesota, Minneapolis, MN 55455, USA

<sup>2</sup>The Rockefeller University, New York, NY 10021, USA

### Introduction

Src homology (SH) domains are building blocks involved in intracellular signal transduction [1]. Previous work has defined and demonstrated *consolidated ligands*, which combine in the same molecule peptide sequences recognized by SH2 and SH3 domains (*i.e.*, Pro-Val-*p*Tyr-Glu-Asn-Val and Pro-Pro-Ala-Tyr-Pro-Pro-Pro-Val-Pro, respectively), and exhibit enhanced affinities and specificities towards dual SH(32) Abelson kinase [2,3]. For first-generation consolidated ligands, binding sequences were connected by a flexible linker, *e.g.*, Gly<sub>n</sub>. With the goal to further improve their efficacies, several second-generation consolidated ligands with a more rigid linker, *e.g.*, Ala<sub>n</sub>, and optionally including an intramolecular lactam bridge “lock”, were designed and synthesized [4]. The present report focuses on the 32-residue structure shown below, which contains an *i* to *i*+7 lactam bridge to connect the side-chains of Glu and Lys, with an intervening 5-aminovaleric acid (Ava) as a spacer. Two different solid-phase synthetic strategies were evaluated.



### Results and Discussion

The first strategy began with Fmoc-Lys(Dde)-PAL-PEG-PS and used Fmoc chemistry to build both branches essentially as described previously [2–4]. Couplings were mediated by HBTU/HOBt/DIEA (4 eq each) in DMF, 1 h. The starting protected derivatives leading to the ultimate lactam were Fmoc-Glu(OAl)-OH and Fmoc-Lys(Dde)-OH. However, Fmoc-Lys(Boc)-OH and Fmoc-Glu(O*t*Bu)-OH were used when the parent residues were elsewhere in the sequence. Asparagine was introduced as Fmoc-Asn(Tmob)-OH and the phosphotyrosine moiety was incorporated as Fmoc-Tyr(PO<sub>3</sub>H<sub>2</sub>)-OH. After chain assemblies were complete, the Dde group was removed from the Lys side-chain by 2% anhydrous NH<sub>2</sub>NH<sub>2</sub> in DMF, then Fmoc-Ava-OH was coupled, then the OAl ester was cleaved off Glu by treatment with Pd(P(Ph)<sub>3</sub>)<sub>4</sub>, and then the Fmoc group was removed from Ava. Cyclization to form the lactam bridge was achieved by addition of PyBOP/HOBt/DIEA (10 eq each) in DMF, 2 × 1 h. After cleavage from the support with reagent K, a complex product mixture was observed. Careful fractionation through three semipreparative reversed-phase HPLC runs allowed isolation of the pure peptide in ~3% yield. The expected molecular weight of the peptide was confirmed by its MALDI-TOF mass spectrum.

In the second strategy, synthesis began with Mtt-Lys(Fmoc)-PAL-PEG-PS and used Fmoc stepwise procedures to add onto the Lys side-chain the 10 residues which eventually comprise the lactam-bridged linker. For somewhat better coupling efficiencies, HATU/HOAt/DIEA (4 eq each) in DMF, 1 h, was now used. The starting protected derivatives leading to the lactam were Fmoc-Glu(OAl)-OH and Dde-Lys(Fmoc)-OH. After incorporation of the aforementioned Lys derivative, the standard Fmoc removal step exposed the Lys side-chain; from this point on, the already described lactamization strategy was followed [*i.e.*, couple Fmoc-Ava, remove OAl from Glu, remove Fmoc, cyclize] with the exception that PyAOP/HOAt/DIEA (10 eq each) in DMF,  $2 \times 1$  h, was now used to close the ring. Next, the peptide chain was extended by first removing Mtt from Lys, continuing with 9 cycles of Fmoc chemistry, and final incorporation of Boc-Pro as the *N*-terminal residue of the Pro-rich branch. After that, Dde was removed from Lys, and Fmoc chemistry introduced all remaining residues of the second, *p*Tyr-containing branch. Cleavage of the completed peptide showed a considerably better analytical profile, and a single semipreparative purification gave the desired peptide in an isolated yield of ~20%. As before, mass spectrometric characterization agreed with expectation.

The title lactam-bridged consolidated ligand was bound by Abl SH(32) with a  $K_d$  of  $380 \pm 17$  nM, comparable to related linear and cyclic molecules evaluated in this research.

### Conclusion

Two different strategies were compared for the synthesis of consolidated ligands with an intramolecular lactam bridge. In the first strategy, on-resin steps to establish the lactam were carried out after all 32 amino acids had been incorporated. However, better results were obtained with the second strategy, when the decapeptide grown off the Lys side-chain was subjected to cyclization *prior* to further chain elongation.

### Acknowledgments

Supported by National Institute of Health grants GM 42722 and 55429.

### References

1. Pawson, T. *Nature* **373**, 573–580 (1995).
2. Cowburn, D., Zheng, J., Xu, Q., Barany, G. *J. Biol. Chem.* **270**, 26738–26741 (1995).
3. Xu, Q., Cowburn, D., Zheng, J., Barany, G. *Lett. Peptide Sci.* **3**, 31–36 (1996).
4. Chen, L., Xu, Q., Cowburn, D., Barany, G., In Fields, G.B., Tam, J.P. and Barany, G. (Eds.) *Peptides for the New Millennium (Proceedings of the 16th American Peptide Symposium)*, Minneapolis, MN, (1999), p. 579.

## Backbone Amide Linker (BAL)/Fmoc Synthesis of Peptide Thioester Intermediates Required for Native Chemical Ligation

Dominique Lelièvre<sup>1,2</sup> and George Barany<sup>1</sup>

<sup>1</sup>Department of Chemistry, University of Minnesota, Minneapolis, MN 55455, USA

<sup>2</sup>Centre de Biophysique Moléculaire (CNRS), 45071 Orléans Cedex 2, France

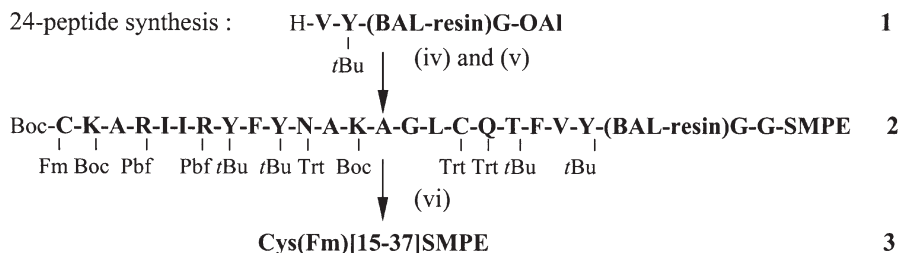
### Introduction

Medium-size peptide thioesters, which are key intermediates for solution or solid-phase native chemical ligation [1], have until recently been accessible only by Boc/Bzl solid-phase strategies with appropriate linkers and supports. The Backbone Amide Linker (BAL) approach introduced by our laboratory [2] provides a way to prepare peptide thioesters [3] in concert with Fmoc/*t*Bu chemistry, and may be contrasted to several other methods reported within the past three years [4].

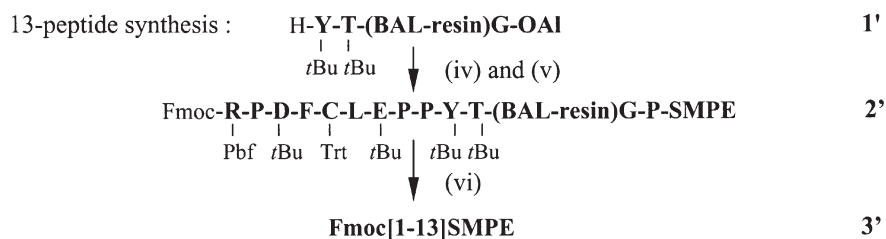
Here, we describe the synthesis, using BAL/Fmoc methodology, of two peptide thioesters, with the eventual goal to prepare BPTI, a protein of 58 amino acid residues, by solid-phase chemical ligation. These peptides correspond to the 14-37 and 1-13 sequences of natural BPTI and will be used as middle and *N*-terminal fragments respectively.

### Results and Discussion

The strategy comprises: (i) anchoring the penultimate residue, AA<sub>n-1</sub>-OAl, onto a *o,p*-PALdehyde-Ile-PEG-PS resin *via* a reductive amination reaction; (ii) coupling of Ddz-AA<sub>n-2</sub> and acetylation; (iii) Ddz removal followed by *in situ* neutralization/coupling with Fmoc-AA<sub>n-3</sub>; (iv) peptide elongation with standard Fmoc/*t*Bu chemistry; (v) selective OAl removal and coupling with AA<sub>n</sub>-SMPE (H-SMPE: ethyl 3-mercaptopropionate); (vi) final cleavage/deprotection with TFA/scavengers to release the free peptide. The thiol side-chain of the *N*-terminal cysteine of the 24-residue peptide was protected with an Fm group to prevent cyclization or polymerization, while the 13-residue peptide was synthesized with an *N*-Fmoc terminal protecting group. Both the *S*-Fm and *N*-Fmoc groups have the added advantage of providing a chromophoric handle which should be easily removed by piperidine treatment after chemical ligation.



“Intermediate” yields, based on the loadings of the tripeptide-resin starting materials **1** and **1'**, were respectively 75% and 88% for the crude 24- and 13-peptides **3** and **3'**. Purification of **3** was achieved using a C4 column with a recovery yield of 21%. Purification of **3'** was achieved using a C8 column with a recovery yield of 63%. The identity of each product was confirmed by MALDI-TOF mass spectroscopy.



These results show how the BAL methodology can be extended for Fmoc SPS of medium-size peptide thioesters. Thus, key intermediates for solution, as well as solid-phase native chemical ligation should be readily available. No significant loss of chains was observed during elongation by Fmoc chemistry. Final cleavage yields were high. The crude quality of Cys(Fm)[15-37]SMPE, a well-known difficult sequence to synthesize, could probably be improved after characterization of secondary peaks. Importantly, peptide thioesters were found to be stable to cleavage cocktails that are commonly used in Fmoc chemistry.

## Acknowledgments

Supported by the National Institutes of Health Grants GM 42722 and 51628.

## References

1. Dawson, P.E., Kent, S.B.H. *Annu. Rev. Biochem.* **69**, 923–960 (2000).
2. Jensen, K.J., Alsina, J., Songster, M.F., Vágner, J., Albericio, F., Barany, G. *J. Am. Chem. Soc.* **120**, 5441–5452 (1998).
3. Alsina, J., Yokum, T.S., Albericio, F., Barany, G. *J. Org. Chem.* **64**, 8761–8769 (1999).
4. (a) Li, X., Kawakami, T., Aimoto, S. *Tetrahedron Lett.* **39**, 8669–8672 (1998). (b) Ingenito, R., Bianchi, E., Fattori, D., Pessi, A. *J. Am. Chem. Soc.* **121**, 11369–11374 (1999). (c) Shin, Y., Winans, K.A., Backes, B.J., Kent, S.B.H., Ellman, J.A., Bertozzi, C.R. *J. Am. Chem. Soc.* **121**, 11684–11689 (1999). (d) Clippingdale, A.B., Barrow, C.J., Wade, J.D. *J. Peptide Sci.* **6**, 225–234 (2000). (e) Swinnen, D., Hilvert, D. *Org. Lett.* **2**, 2439–2442 (2000).

## Ampullosporin Analogs: Solid Phase Synthesis, Conformational Studies, and Biological Activities

Hoai Huong Nguyen<sup>1</sup>, Diana Imhof<sup>1</sup>, Brigitte Schlegel<sup>2</sup>, Albert Härtl<sup>2</sup>,  
 Matthias Kronen<sup>2</sup>, Udo Gräfe<sup>2</sup> and Siegmund Reissmann<sup>1</sup>

<sup>1</sup>*Institute of Biochemistry and Biophysics, Friedrich-Schiller-University Jena,  
 D-07743, Germany*

<sup>2</sup>*Hans-Knöll-Institute, Jena, D-07745, Germany*

### Introduction

Ampullosporin A (Amp A) Ac-Trp-Ala-Aib-Aib-Leu-Aib-Gln-Aib-Aib-Aib-Gln-Leu-Aib-Gln-Leuol, extracted from fungus *Sepedonium ampullosporum* surface culture belongs to the class of peptaibols rich in Aib, with an acetylated N-terminus and an alcohol at C-terminus [1]. Besides antimicrobial effects, Amp A induces the formation of black pigment on fungus *Phoma destructiva*, as do cyclosporin A, chrysospermin, and also neuroleptic drugs, including haloperidol, chlorpromazine, clozapine, and sertindol. Moreover, Amp A was found to cause the hypothermia in mice suggesting a neuroleptic activity [1]. Recently, peptides containing adjacent sterically hindered Aib-residues have been synthesized without difficulties *via* Fmoc amino acid fluorides, which can be generated *in situ* by using tetramethylfluoroformamidium hexafluorophosphate (TFFH) as coupling reagent [2].

In this work, we synthesize native Amp A and 16 of its analogs using TFFH as coupling reagent for the N-terminal nonapeptide sequence and study the relationship between their conformation and biological activities, namely the pigment induction on *Phoma destructiva* and hypothermic effect in mice.

### Results and Discussion

Ampullosporin analogs have been obtained by modification of C-, N-terminus and substitution of Aib-residues at different sequence positions by Ala, Ile, and 1-amino-1-cyclohexane carboxylic acid (Ac<sub>6</sub>c) (Table 1). Depending on C-terminus, an appropriate resin was used, 2-Cl-Trt for Leu<sup>15</sup>ol analogs, Wang for carboxylic acids and Rink amide MBHA for amide. A double coupling protocol using 4 eq. Fmoc amino acids in DMF, 8 eq. DIEA as a base, and 4 eq. HBTU/HOBt as coupling reagent for first five amino acid residues and 4 eq. TFFH for the remaining residues was adopted (Scheme 1). After the N-terminus has been acetylated, Leu<sup>15</sup>ol analogs were cleaved from the 2-Cl-Trt resin with 20% HFIP/DCM, and subsequently cleaved from the side chain protecting groups with 50% TFA/DCM, 5% water, and 2% triisopropylsilane, while analogs containing Leu or Leu-NH<sub>2</sub> at C-terminus were cleaved with TFA, 2.5% water, and 2.5% EDT. After purification, analogs were used for conformational study and biological tests.



*Scheme 1. Coupling reagents in the synthesis of Amp A and analogs.*

CD spectra of all analogs were recorded in water, water/TFE = 1/1, and pure TFE to find the differences in their conformational shapes and flexibility. Substitution of Aib-residues by chiral amino acids Ala and Ile increased the helicity (CD-band inten-

## Synthetic Methods

sities at 208 and 222 nm), but reduced biological activities, while replacement of Aib-residue with Ac<sub>6</sub>c did not affect the conformational shape, but reduced the pigment induction. Analogs charged at N- or C-terminus (A6 and A7) displayed strong effect on *Phoma destructiva* and no or only weak hypothermic effect. The modified C-terminus analog A8 (Leu<sup>15</sup>-NH<sub>2</sub>), in similarity to native Amp A, exhibited pronounced pigment induction as well as strong hypothermic effect. However, no effect was observed for analogs containing less than 15 amino acids or without aromatic residues.

Table 1. Ampullosporin analogs.

Peptide	Ret. time RP-HPLC	M.W. (ESI-MS)	Pigment induction <sup>a</sup>	Hypothermic effect <sup>b</sup>
Amp A (native)	42.0	1622	++	+++
A8 (Leu <sup>15</sup> -ol→Leu <sup>15</sup> -NH <sub>2</sub> )	40.9	1635	++	+++
A7 (Leu <sup>15</sup> -ol→Leu <sup>15</sup> )	41.8	1636	++	+
A9 (Leu <sup>15</sup> -ol removed)	32.5	1522	0	0
A6 (Amp A deacetylated)	30.3	1580	++	0
A12 (Amp A deacetylated, Trp <sup>1</sup> removed)	27.7	1394	0	0
A13 (A12 acetylated)	35.0	1436	0	0
A14 (Trp <sup>1</sup> →D-Trp <sup>1</sup> )	42.0	1622	++	+
A15 (Trp <sup>1</sup> →Tic <sup>1</sup> )	44.5	1595	++	+
A16 (Trp <sup>1</sup> →Oic <sup>1</sup> )	45.7	1587	0	0
A17 (Trp <sup>1</sup> →2-Nal <sup>1</sup> )	46.6	1633	+	+
A18 (Trp <sup>1</sup> →Igl <sup>1</sup> )	46.3	1609	+	+
A19 (Trp <sup>1</sup> →Nig <sup>1</sup> )	46.7	1609	+	+++
Natural analog Amp C (Aib <sup>9</sup> →Ala <sup>9</sup> )	40.8	1608	+	++
A10 ((Aib) <sub>7</sub> →(Ala) <sub>7</sub> )	31.7	1524	0	0
A11 ((Aib) <sub>7</sub> →(Ile) <sub>7</sub> )	–	1818	0	0
A20 (Aib <sup>4</sup> →Ac <sub>6</sub> c <sup>4</sup> )	47.3	1662	+	+++

<sup>a</sup> Evaluated based on the *Phoma destructiva* halo colour induced by ampullosporin analogs.

<sup>b</sup> Mice rectal body temperature after intraperitoneal application of 20 mg/kg b.w. analogs.

## Acknowledgments

The work was supported by Deutsche Forschungsgemeinschaft (Re 853/7-1).

## References

1. Ritzau, M., et al. *J. Antibiotics* **50**, 722–728 (1997).
2. Carpino, L., et al. *Acc. Chem. Res.* **29**, 268–274 (1996).

## Synthesis of Lanthionine-Containing Peptides on Solid Phase via an Orthogonal Protecting Group Strategy

M. F. Mohd Mustapa<sup>1</sup>, A. B. Tabor<sup>1</sup>, N. A. L. Chubb<sup>2</sup> and D. Schulz<sup>2</sup>

<sup>1</sup>Department of Chemistry, University College London, 20 Gordon Street,  
 London WC1 8AJ, UK

<sup>2</sup>Pfizer Ltd. UK, Ramsgate Road, Sandwich, Kent CT13 9NJ, UK

### Introduction

*meso*-Lanthionine (Figure 1) is a monosulfide analogue of cystine that occurs in a family of polycyclic peptides with antibiotic properties called lantibiotics. So far only nisin has been made synthetically [1]. With their high specificity against Gram-positive bacteria [2], biological studies of these peptides are of interest, especially in the search for new groups of antibiotics. The aim of this project is to develop the foundation of the total solid phase synthesis of lantibiotics and their analogues by investigating the possibility of a rapid and high yielding method for synthesizing smaller lanthionine-containing peptides, solely on solid phase.

We therefore would like to report on the synthesis of the thioether-bridged cyclic peptide (Figure 1) containing the naturally-occurring amino acid lanthionine.

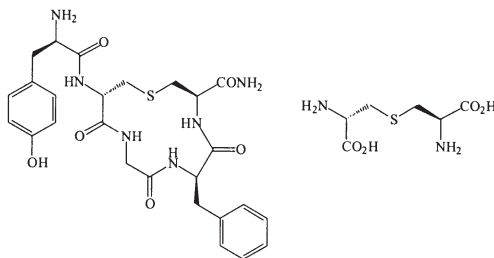


Fig. 1. Lanthionine analogue of an opioid enkephalin peptide and *meso*-lanthionine.

### Results and Discussion

The synthesis of the appropriately protected lanthionine residue was firstly carried out (Figure 2), following the methods described by Dugave and Menez [3].

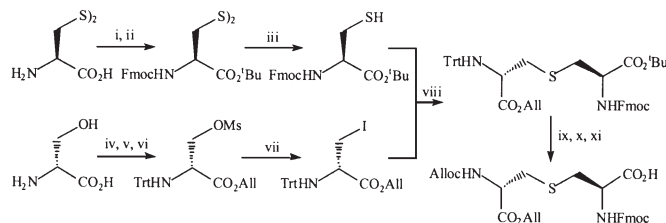


Fig. 2. Synthesis of the lanthionine derivative for solid phase peptide synthesis; i) *t*BuOAc,  $\text{HClO}_4$ , ii) *Fmoc*-Cl, *NMM*, *THF*, iii)  $\text{PBU}_3$ , *THF*/ $\text{H}_2\text{O}$ , iv) *TMS*-Cl, *MeOH*, *Trt*-Cl, *TEA*, *DCM*, v)  $\text{Cs}_2\text{CO}_3$ , *MeOH*, *Allyl* bromide, *DMF*, vi) *Ms*-Cl, *TEA*, *THF*, vii) *NaI*, *acetone*, viii)  $\text{Cs}_2\text{CO}_3$ , *DMF*, ix) *TFA*, *DCM*, x) *Alloc*-Cl,  $\text{NaHCO}_3$ , *Dioxane*/ $\text{H}_2\text{O}$ , xi) *TFA*, *DCM*.

## Synthetic Methods

The *N*-trityl-3-iodoalanine allyl ester exists in two conformationally-locked forms due to the bulkiness of the iodo and trityl groups, and the two rotamers can also be observed at the lanthionine stage. The methodology of synthesising the lanthionine derivative proved to be high-yielding and reproducible.

The lanthionine analogue of the opioid enkephalin peptide [4,5] was synthesised on solid phase (NovaSyn™ TG Sieber resin) as described in Figure 3. HPLC, mass spectrometry and NMR were used to identify the peptide. However the yield of the synthesis was low and investigation is under way to determine the cause of the problem.

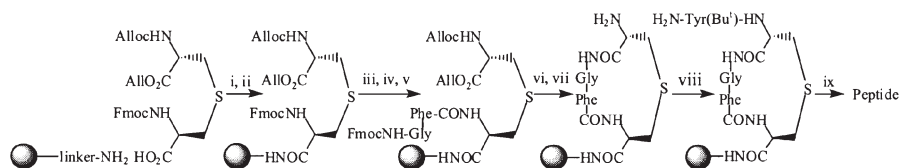


Fig. 3. Methodology for the synthesis of the target peptide in Figure 1; i) HOBt/DMF, DIC/dioxane, ii) 1-Acetylimidazole, DMF, iii) Piperidine, DMF, iv) Fmoc-Phe-OH, i, ii, iii, v) Fmoc-Gly-OH, i, ii, vi) Pd(PPh<sub>3</sub>)<sub>4</sub>, CHCl<sub>3</sub>/AcOH, NMM, iii, vii) PyAOP, HOAt, DIEA, DMF, vii) Fmoc-Tyr(tBu)-OH, i, ii, iii, ix) TFA, H<sub>2</sub>O, Et<sub>3</sub>SiH.

We are also currently working on the ivDde/Dmab-protected lanthionine (in place of the allylic groups) in a bid to synthesise the lanthionine analogue of the overlapping bicyclic rings D and E of nisin (Figure 4).

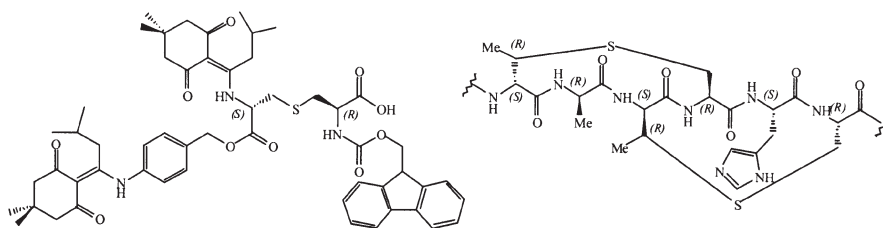


Fig. 4. ivDde/Dmab protected lanthionine and rings D and E of nisin.

## Acknowledgments

Dr. Jessica Mould, UCL Graduate School, Overseas Research Students' Award Scheme and Pfizer Ltd. UK.

## References

1. Fukase, K., Kitazawa, M., Sano, A., Shimbo, K., Horimoto, S., Fujita, H., Wakamiya, T., Shiba, T. *Tetrahedron Lett.* **29**, 795 (1988).
2. Jung, G. *Angew. Chem., Int. Ed. Engl.* **30**, 1051 (1991).
3. Dugave, C., Menez, A. *Tetrahedron: Asymmetry* **8**, 1453 (1997).
4. Osapay, G., Goodman, M. *J. Chem. Soc., Chem. Commun.* 1599 (1993).
5. Mayer, J.P., Zhang, J., Groeger, S., Liu, C.F., Jarosinski, M.A. *J. Peptide Res.* **51**, 432 (1998).

## **Systematic Solid Phase Synthesis of Linear Pseudooligolysines Containing Multiple Adjacent CH<sub>2</sub>NH Amide Bond Surrogates: Potential Agents for Gene Delivery**

**Gil Fridkin<sup>1</sup>, Tamar Gilon<sup>2</sup>, Abrahm Loyter<sup>2</sup> and Chaim Gilon<sup>1</sup>**

<sup>1</sup>Department of Organic Chemistry and <sup>2</sup>Department of Biological Chemistry,  
Hebrew University, Jerusalem, 91904, Israel

### **Introduction**

Positively charged peptides have been extensively used as vehicles to deliver functional DNA molecules into cultured cells [1,2]. Indeed polypeptides such as polylysine and polyarginine have been shown to efficiently complex negatively charged DNA molecules and to introduce the complexed DNA into the nuclei of recipient cultured cells. However being composed of amino acids, peptidic carriers should be digested by proteolytic enzymes present within the circulation and within cells and hence their action *in vivo* is limited. It is well known that chemical reduction of peptide bonds render them unsusceptible to proteolytic digestion. Indeed it has been shown that replacement of a CO–NH peptide bond by the CH<sub>2</sub>NH isostere, *i.e.* a reduced peptide bond, results in increased resistance of the peptide towards enzymatic degradation [3]. In addition, such modification increases the number of the positively charged moieties within the peptide and enlarges the flexibility of the backbone [3].

Another aspect that should be considered when developing a gene carrier for *in vivo* use is that it should carry its cargo, namely its complexed DNA molecules, into the nuclei of nondividing cells. It has been clearly demonstrated that a major obstacle for the use of viral and nonviral vectors for gene therapy is their failure to efficiently transfer the foreign gene through the Nuclear Pore Complex into the nuclei of transfected cells. Recently this was partially solved by the introduction of Nuclear Localization Signals into such vectors. In this regard it should be mentioned that most of the known and used Nuclear Localization Signals are characterized by the presence of four or more positively charged amino acids especially lysine and arginine. Taking the above into consideration, an oligolysine in which all the peptide bonds have been replaced by CH<sub>2</sub>NH moieties (pseudooligolysine) may potentially possess the appropriate properties required from efficient nonviral gene carrier for *in vivo* use.

### **Results and Discussion**

A series of five linear, fully reduced oligolysines (abbreviated herein as PLs, Table1) in which all the peptide bonds have been “replaced” by CH<sub>2</sub>NH moieties were synthesized by solid phase Fmoc chemistry. The reduced peptide bonds were introduced by the reductive alkylation reaction between Fmoc-Lys-(Boc)-al and a free  $\alpha$ -amine moiety on the pseudopeptidyl resin, using sodium cyanoborohydride in an acidified mixture of NMP : CH<sub>3</sub>OH (1 : 1, v/v). Since the reduced peptide bonds do not absorb in the UV range, the monitoring of fully reduced pseudopeptides during HPLC analysis is impossible. For this purpose the terminal Fmoc group was left attached to the pseudopeptides, allowing efficient HPLC monitoring of the PLs. The susceptibility of one of the PLs namely of PL3, as a representative of the PLs synthesized, to hydrolysis by trypsin was studied and compared to that of Fmoc-trilysine. PL3 was found to be highly resistant to tryptic digestion; only about 30–40% of it was hydrolyzed within 1–3 h of incubation, as was inferred from the reduction in its peak area as determined by HPLC. It is our assumption that this decrease reflects the spontaneous removal of

the Fmoc protecting group by the free amines (primary and secondary) present within these molecules during the relatively long period of incubation at pH 7.8 and not due to digestion by trypsin. On the other hand, the Fmoc-trilysine was completely hydrolyzed under the same conditions within 1 h of incubation.

Table 1. Physical and analytical characterizations of the various PLs.

Name	Pseudopeptide	% Purity by HPLC	Calculated M.W.	Observed M.W.
PL1	Fmoc-Lysψ[CH <sub>2</sub> NH <sub>2</sub> ]	96	353.4	354.2
PL2	Fmoc-Lysψ[CH <sub>2</sub> NH]Lysψ[CH <sub>2</sub> NH <sub>2</sub> ]	98	467.6	468.3
PL3	Fmoc-Lysψ[CH <sub>2</sub> NH]Lysψ[CH <sub>2</sub> NH]Lysψ[CH <sub>2</sub> NH <sub>2</sub> ]	91	581.8	582.4
PL4	Fmoc-Lysψ[CH <sub>2</sub> NH]Lysψ[CH <sub>2</sub> NH]Lysψ[CH <sub>2</sub> NH] Lysψ[CH <sub>2</sub> NH <sub>2</sub> ]	85	696.0	697.1
PL5	Fmoc-Lysψ[CH <sub>2</sub> NH]Lysψ[CH <sub>2</sub> NH]Lysψ[CH <sub>2</sub> NH] Lysψ[CH <sub>2</sub> NH]Lysψ[CH <sub>2</sub> NH <sub>2</sub> ]	79	810.2	811.1

The ability of PLs to complex DNA molecules was examined using gel shift as an experimental assay system. Plasmid DNA was incubated with increasing concentrations of the various PLs resulting in mixtures bearing increasing ratios of positive/negative charges. The mobility of the DNA towards the cathode was then monitored. A decrease in the mobility of the plasmid DNA, present within the various mixtures, as compared to the mobility of a free plasmid suggests masking of the plasmid negative charges due to the formation of PLs-DNA complexes. All five PLs obtained (PL1-5) were analyzed over a wide range of positive/negative charge ratios (1 : 1 +/- to 100 : 1 +/-). PL3 and PL4 were found to be the most efficient complexing oligomers. Already at a relatively low charge ratio of 2 : 1 +/- these oligomers effectively retarded the migration of the plasmid DNA and completely inhibited it at a charge ratio of 4 : 1 +/- . The ability of the PLs to tightly complex the DNA was also studied by monitoring the susceptibility of the DNA molecules within the PLs-DNA mixtures to digestion by DNaseI. This was studied by analyzing the DNA pattern obtained in gel electrophoresis following incubation of these mixtures with DNaseI. Incubation of the plasmid DNA with PL4, and PL5 resulted in partial inhibition of the plasmid degradation, indicating a complex was formed. These DNA binding activities and the increased resistance to hydrolysis by trypsin make these molecules potential candidates for future use as DNA carriers in gene delivery.

## References

1. Cotten, M., Wagner, E. *Curr. Opin. Biotechnol.* **4**, 705–710 (1993).
2. Murphy, J.E., Uno, T., Hamer, J.D., Cohen, F.E., Dwarki, V., Zuckermann, R.N. *Proc. Natl. Acad. Sci. U.S.A.* **95**, 1517-1522 (1998).
3. Spatola, A.F., In Weinstein, B. (Ed.) *Chemistry and Biochemistry of Amino Acids Peptides and Proteins*, Marcel Dekker, Basel, 1983, p. 267.

## Peptide Transformation and Synthesis of Oligopeptidomimetics

**Rob M. J. Liskamp, John A. W. Kruijtz, Lovina J. F. Hofmeyer,  
 Astrid Boeijen, Arwin J. Brouwer and Menno C. F. Monnee**

*Department of Medicinal Chemistry, Utrecht Institute for Pharmaceutical Sciences,  
 Utrecht University, Utrecht, 3508 TB Utrecht, The Netherlands*

### Introduction

Peptides can be transformed to peptide-peptidomimetic hybrids in which one or several amino acid residues are replaced by amino acid “transforms”. If all amino acid residues are replaced, the peptide is transformed to an oligopeptidomimetic or foldamer (Figure 1). One goal of peptide transformation is to obtain peptidomimetics *e.g.* with an improved stability towards degradation by proteases. Other goals include studies of the effects of transformation on biological activity and structure. We are interested in peptide transformation in which peptoid, amino sulfonic acid or urea building blocks (transforms) are introduced.

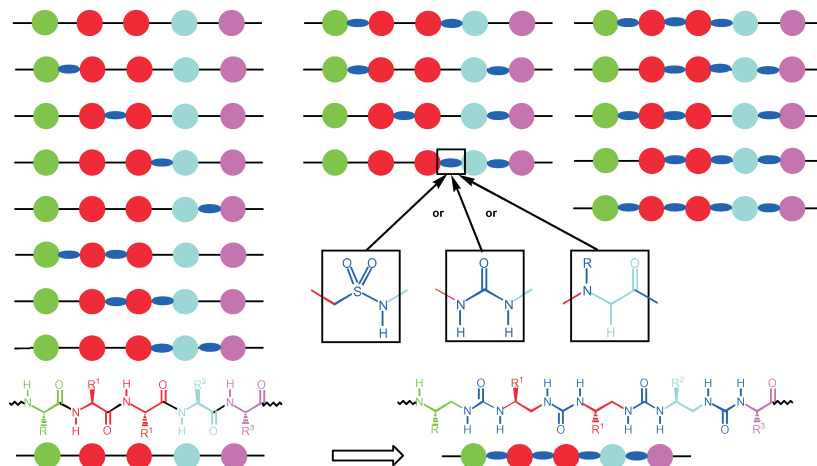
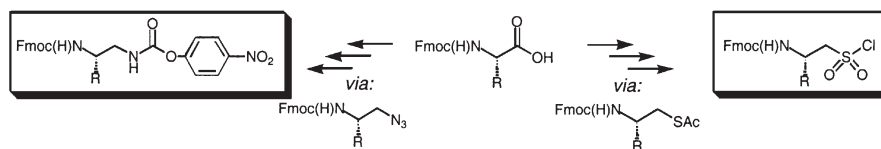


*Fig. 1. Peptide transformation: combinatorial synthesis of peptide-peptidomimetic hybrids. Complete transformation leads to an oligopeptidomimetic or foldamer. Transformation to an oligoureia peptidomimetic is shown [1].*

### Results and Discussion

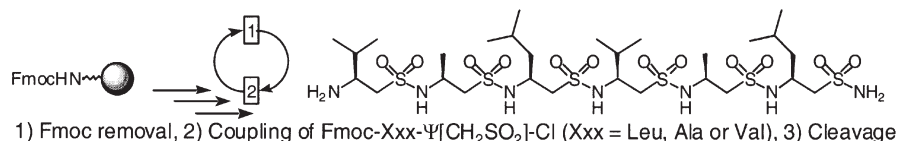
The synthesis of Fmoc-protected peptoid monomers as well as their use in the solid phase synthesis of peptoids was recently described [2]. Starting from Fmoc-protected amino acids, an efficient synthesis of *N*-protected  $\beta$ -aminoethane sulfonyl chlorides was developed [3]. These sulfonyl chlorides are versatile building blocks for the synthesis of oligopeptidosulfonamide foldamers [4] (Scheme 2). Boc-protected amino acids [1], but more recently Fmoc-protected amino acids [5] were also suitable starting materials for the preparation of building blocks for oligoureia peptidomimetics (Scheme 1).

These building blocks have been employed in peptide transformation in which sets of peptide-peptidomimetic hybrids were prepared. These peptide transforms showed *e.g.* an improved stability against degradation by proteases. The construction of partially or completely “transformed” peptides *e.g.* oligopeptidosulfonamide foldamers



Scheme 1. Representation of the preparation from Fmoc-protected amino acid of the urea peptidomimetic building blocks (left) as well as aminoethane sulfonylchloride building blocks (right).

can be used to dissect the structural requirements for biological activity and might even lead to the construction of larger oligomeric structures such as proteinaceous sulfonamides.



Scheme 2. Solid phase synthesis of oligopeptidosulfonamide foldamers.

### Acknowledgments

Support from the Council for Chemical Sciences of the Netherlands Organization for Scientific Research (CW-NWO) with financial aid from The Netherlands Technology foundation is gratefully acknowledged as well financial support by the strategic alliance between Solvay Pharmaceuticals, the Ministry of Economic Affairs and Utrecht University, The Netherlands.

### References

1. Boeijen, A., Liskamp, R.M.J. *Eur. J. Org. Chem.* 2127–2135 (1999).
2. Kruijtzter, J.A.W., Hofmeyer, L.J.F., Heerma, W., Versluis, C., Liskamp, R.M.J. *Chem. Eur. J.* **4**, 1570–1580 (1998).
3. Brouwer, A.J., Monnee, C.F., Liskamp, R.M.J. *Synthesis* 1579–1584 (2000).
4. Monnee, C.F., Marijne, M.F., Brouwer, A.J., Liskamp, R.M.J. *Tetrahedron Lett.* **41**, 7991–7995 (2000).
5. Boeijen, A., Van Ameijde, J., Liskamp, R.M.J. *J. Org. Chem.* (2001), in press.

## A New Strategy for Inverse Solid-Phase Peptide Synthesis

Qingchai Xu and William G. Gutheil

Division of Pharmaceutical Sciences, School of Pharmacy, University  
of Missouri-Kansas City, Kansas City, MO 64110, USA

### Introduction

Solid-phase peptide synthesis (SPPS) in the N-to-C direction (inverse SPPS [1–4]) provides the synthetically versatile peptide C-terminal carboxyl group for further modification, which is particularly useful in synthesis of C-terminally modified peptide mimetics. As part of our ongoing program to find peptide mimetic protease and penicillin-binding protein inhibitors, a strategy for inverse SPPS based on amino acid *t*-butyl esters has been developed. A principle advantage of this approach is the commercial availability of suitably side chain protected amino acid *t*-butyl esters. Based on this strategy, peptide trifluoromethyl ketones and peptide aldehydes have also been prepared, as well as several peptide aldehyde derivatives. These results demonstrate the feasibility and utility of this approach for peptide mimetic synthesis.

### Results and Discussion

The strategy of the amino acid *t*-butyl ester based inverse SPPS synthesis is exemplified by the synthesis of the model peptide Suc-Ala-Leu-Pro-Phe as shown in Figure 1.

The same model peptide was separately synthesized *via* DCC/HOBt, HBTU/DIEA, and HATU/TMP coupling methods. HPLC and HPLC/MS were used to evaluate the products. The peptide prepared *via* the DCC/HOBt method contained 60% of target peptide and 20% each of two deletion peptides (Suc-Ala-Leu-Pro and Suc-Ala-Pro-Phe). However, syntheses with the HBTU/DIEA and HATU/TMP methods both yielded the target peptide in high purity (>80%) by HPLC. The degree of racemization on the peptides synthesized by the HBTU/DIEA and HATU/TMP methods were determined by Marfey's method [5]. The results are shown in Table 1. Significant racemization of the first residue (Ala) occurred with both methods. This phenomenon is possibly due to the succinate linker, which may favor the formation of an oxazolone of the first (Ala) residue. To overcome this problem, Z-Glu-OtBu was tested as a linker. Z-Glu-OtBu was coupled to Pam or MBHA resin, followed by removal of the OtBu group, giving Pam- $\gamma$ -(N $^{\alpha}$ -Z)-Glu or MBHA- $\gamma$ -(N $^{\alpha}$ -Z)-Glu. With such derivatized resins, several peptides (1–7, in Table 2) were synthesized in reasonably high purity *via* HATU/TMP method. The resulting peptides from Pam or MBHA resins contain either a Glu or a Gln at the N-terminus.

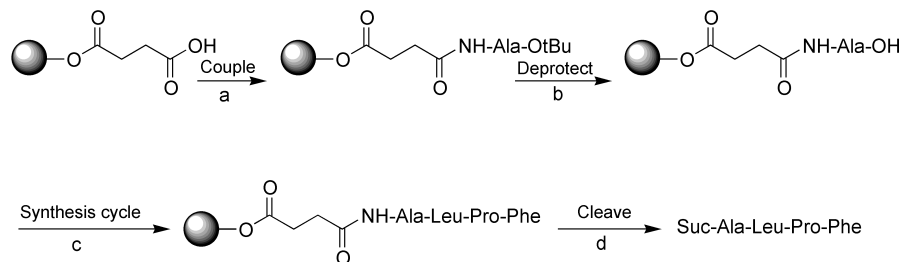


Fig. 1. Strategy for amino acid *t*-butyl ester based inverse SPPS on succinylated Pam resin. a. coupling reagent b. 25–50% TFA/DCM; c. repeat a and b; d. TFMSA/TFA or HF.

## Synthetic Methods

Table 1. Percentage of D-isomers after Marfey's derivatization (determined by HPLC) of the amino acids in the model peptide samples synthesized according to the indicated method.

Method	D-Ala	D-Leu	D-Pro	D-Phe
HBTU/DIEA	26.8%	22.8%	1.8%	1.6%
HATU/TMP	37.6%	5.4%	1.1%	1.4%

Table 2. Peptides and peptide mimetics prepared via amino acid *t*-butyl ester based inverse SPPS. **1** prepared on the Pam-(N<sup>α</sup>-Z)-Glu; **2–7** and **10–14** prepared on the MBHA-(N<sup>α</sup>-Z)-Glu; **8** and **9** prepared on the succinylated Pam resin.

(1) Glu-Ala-Phe	(8) Suc-Ala-Leu-Pro-Phe-NHCH(CH <sub>3</sub> )COCF <sub>3</sub>
(2) Gln-Phe-Lys	(9) Suc-Phe-Lys-NHCH(CH <sub>3</sub> )COCF <sub>3</sub>
(3) Gln-Ala-γ-Glu(α-OMe)-Lys	(10) Gln-Ala-γ-Glu(α-OMe)-Lys-NHCH(CH <sub>3</sub> )COCF <sub>3</sub>
(4) Gln-Val-Gln-Orn	(11) Gln-Phe-Lys-NHCH(CH <sub>3</sub> )CHO
(5) Gln-Leu-Trp-Phe	(12) Gln-Phe-Lys-NHCH(CH <sub>3</sub> )CH(OCH <sub>2</sub> ) <sub>2</sub>
(6) Gln-Pro-Phe-Asn	(13) Gln-Phe-Lys-NHCH(CH <sub>3</sub> )CH(SCH <sub>2</sub> ) <sub>2</sub>
(7) Gln-Thr-Arg-Tyr	(14) Gln-Phe-Lys-NHCH(CH <sub>3</sub> )CH(OH)CH(CH <sub>3</sub> )NO <sub>2</sub>

The synthetic peptides **1**, **2**, **4** and **6** were selected for the determination of the degree of racemization. Less than 6% racemization was detected for each amino acid in any of these peptides. These results indicate that a combination of Z-Glu-OtBu derivatized Pam or MBHA resin and the HATU/TMP method is applicable to inverse SPPS with amino acid *t*-butyl esters.

Peptide trifluoromethylketones (**8–10**) were obtained in good purity through oxidation of peptidyl-trifluoromethylaminoalcohols using DCC/DMSO/toluene/ dichloroacetic acid [6–8]. Oxidation of a peptide-alcohol using the same oxidation procedure gave the peptide aldehyde **11** in low yield after TFMSA cleavage from the resin due to degradation of aldehyde. The resin-bound peptide aldehyde could be protected by treatment with ethylene glycol/TFA to give the acetal **12**, or with 1,2-ethanedithiol/TFA to give the dithiane **13**, both in good yield and purity. Treatment of the resin-bound aldehyde with nitroethane/TEA yielded aldehyde derivative **14** also in good yield and purity. These results demonstrate the potential of the amino acid *t*-butyl ester inverse SPPS strategy for the preparation of peptide mimetics.

## Acknowledgments

This work was supported by Grant GM60149 from the NIH.

## References

1. Letsinger, R.L., Kornet, M.J. *J. Am. Chem. Soc.* **85**, 3045–3046 (1963).
2. Felix, A.M., Merifield, R.B. *J. Am. Chem. Soc.* **92**, 1385–1391 (1970).
3. Henkel, B., Zhang, L., Bayer, E. *Liebigs Ann./Recueil* 2161–2168 (1997).
4. Johansson, A., Akerblom, E., Ersmark, K., Lindeberg, G., Hallberg, A. *J. Comb. Chem.* **2**, 496–507 (2000).
5. Marfey, P. *Carlsberg Res. Commun.* **49**, 591–596 (1984).
6. Imperiali, B., Abeles, R.H. *Tetrahedron Lett.* **27**, 135–138 (1986).
7. Pfitzner, K.E., Moffat, J.G. *J. Am. Chem. Soc.* **87**, 5661–5670 (1965).
8. Fearon, K., Spaltenstein, A., Hopkins, P.B., Gelb, M.H. *J. Med. Chem.* **30**, 1617–1622 (1987).

## Optimization of the Chemical Synthesis of Human Ghrelin

David B. Flora, Min Liu, Julia A. Drane, Patrick J. Edwards and  
John P. Mayer

Discovery Chemistry, Lilly Research Laboratories, Eli Lilly and Co., Indianapolis,  
IN 46285, USA

### Introduction

Since its initial discovery and characterization as the native growth hormone secretagogue [1], ghrelin GSS(n-octanoyl)FLSPEHQRVQQRKESKKPPAKLQPR has stimulated extensive studies directed toward clarifying its role in feeding, energy balance and growth hormone release [2–5]. A flexible and efficient synthetic procedure was required to produce sufficient quantities of human ghrelin in order to conduct structure-activity studies related to the native peptide. To this end we carried out four separate solid-phase Fmoc/tBu based synthetic protocols which differed with respect to the method of incorporation of the Ser<sup>3</sup>-octanoyl moiety. The methods were evaluated for yield and purity of final product. In addition, we optimized a procedure for the esterification of the Ser<sup>3</sup> side chain with respect to stoichiometry and time course.

**Method 1.** A previously published [6] automated Fmoc/tBu based synthesis utilizing HBTU coupling with incorporation of Fmoc-Ser(Trt)OH at position 3, followed by de-tritylation (1% TFA/DCM, r.t., 45 min) and global serine side chain esterification (Figure 1).

**Method 2.** Automated Fmoc/tBu based assembly of the primary sequence utilizing HBTU chemistry, incorporation of Fmoc-Ser (side chain unprotected) at position 3, followed by global esterification.

**Method 3.** Identical to Method 2 but utilizing DCC/HOBt chemistry.

**Method 4.** Automated Fmoc/tBu based assembly utilizing HBTU chemistry to Phe<sup>4</sup>, manual coupling with DIC/HOBt of Fmoc-Ser (side chain unprotected), followed by esterification of the serine side chain and automated incorporation of the remaining residues.

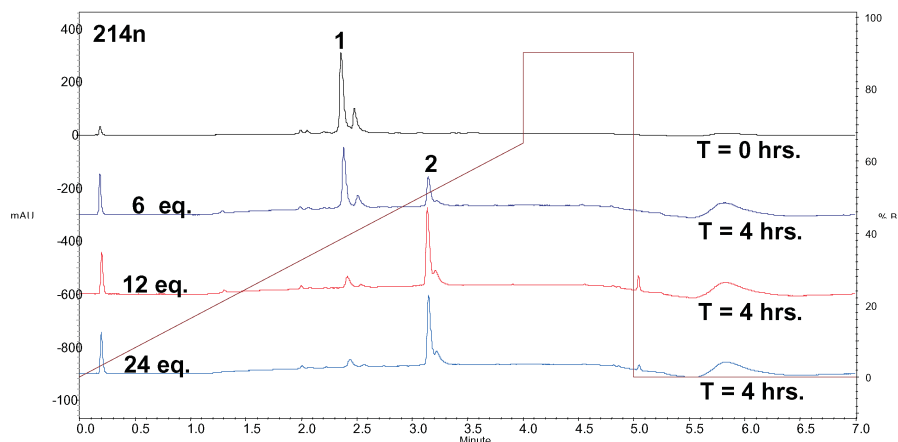


Fig. 1. Effect of varying octanoic acid and DIC concentration on O-acylation efficiency. Synthesis Method 1: Peak 1: des-octanoyl ghrelin, Peak 2: ghrelin.

## Results and Discussion

The optimal conditions of the esterification of the Ser<sup>3</sup> residue were found to be 12 equivalents (relative to resin substitution) each of octanoic acid and DIC in the presence of 0.3 equivalents of DMAP in NMP (5 ml NMP/mg resin). The esterification appeared complete after 4.0 h under these conditions, which were worked out in the context of Method 1 and were subsequently extended to Methods 2, 3 and 4.

With the exception of Method 2 all of the protocols generated product. The best results were obtained with Method 1 and 4, which produced consistently superior results. Of the two protocols, Method 4 gave a slightly higher yield of crude peptide (62.2 vs 59.8% by weight), but after normalizing data for HPLC purity, Method 1 provides a slightly better yield (0.141 vs 0.120 mg product/mg resin).

In summary, both Methods 1 and 4 were found to be optimal for the synthesis of native ghrelin. The advantages of Method 1 lie in its direct synthesis of the peptide sequence and the purity of the crude octanoylated ghrelin. Its disadvantage is the loss of peptide during the de-tritylation of Ser<sup>3</sup> (9% loss by fulvene assay at 301 nm). In contrast, the advantage of Method 4 lies in the ability to acylate the Ser<sup>3</sup> side-chain without de-tritylation. Its disadvantages are that the synthesis is interrupted, and the purity of the crude octanoylated ghrelin is lower with respect to Method 1. In view of the current data, Method 1 is the preferred approach because the synthesis is not interrupted and its crude purity (54.8% Method 1 vs 44.6% Method 4) compensates the loss of peptide during Ser<sup>3</sup> de-tritylation.

## References

1. Kojima, M., Hosoda, H., Date, Y., Nakazato, M., Matsuo, H., Kangawa, K. *Nature* **402**, 656–660 (1999).
2. Nakazato, M., Murakami, N., Date, Y., Kojima, M., Matsuo, H., Kangawa, K., Matsukura, S. *Nature* **409**, 194–198 (2001).
3. Tschop, M., Smiley, D.L., Heiman, M.L. *Nature* **407**, 908–913 (2000).
4. Tschop, M., Weyer, C., Tataranni, P.A., Devanarayan, V., Ravussin, E., Heiman, M.L. *Diabetes* **50**, 707–709 (2001).
5. Wren, A.M., Small, C.J., Ward, H.L., Murphy, K.G., Dakin, C.L., Taheri, S., Kennedy, A.R., Roberts, G.H., Morgan, D.G.A., Ghatei, M.A., Bloom, S.R. *Endocrinology* **141**, 4325–4328 (2000).
6. Bednarek, M.A., Feighner, S.D., Pong, S., McKee, K.K., Hreniuk, D.L., Silva, M.V., Warren, V.A., Howard, A.D., Van der Ploeg, L.H.Y., Heck, J.V. *J. Med. Chem.* **43**, 4370–4376 (2000).

## **Rational Design and Synthesis of a Potent Amide-Linked Cyclic Analogue of MBP<sub>87-99</sub> Based on 2D-NMR Studies and Molecular Dynamics**

**Ioanna Daliani<sup>1,2</sup>, Theodore Tselios<sup>3</sup>, Lesley Probert<sup>2</sup>, Spyros Deraos<sup>3</sup>,  
Thomas Mavromoustakos<sup>1</sup> and John Matsoukas<sup>3</sup>**

<sup>1</sup>*National Hellenic Research Foundation, Institute of Organic and Pharmaceutical Chemistry,  
11635 Athens, Greece*

<sup>2</sup>*Department of Molecular Genetics, Hellenic Pasteur Institute, 11521 Athens, Greece*

<sup>3</sup>*Department of Chemistry, University of Patras, 26500 Patras, Greece*

### **Introduction**

We have designed and synthesized altered peptide ligands based on the human myelin basic protein epitope MBP<sub>87-99</sub> in order to examine whether or not these molecules can treat Experimental Allergic Encephalomyelitis (EAE) in Lewis rats. We synthesized an amide-linked cyclic analogue (cyclo(87-99)[Arg<sup>91</sup>,Ala<sup>96</sup>]MBP<sub>87-99</sub>), by connecting the N- and C-terminus, and a linear analogue [Arg<sup>91</sup>,Ala<sup>96</sup>]MBP<sub>87-99</sub> in which Lys<sup>91</sup> and Pro<sup>96</sup> were replaced by Arg and Ala, respectively [1]. The cyclo(87-99)[Arg<sup>91</sup>,Ala<sup>96</sup>]MBP<sub>87-99</sub> was synthesized using the Fmoc/tBu methodology and the cyclization was achieved using *O*-Benzotriazol-1-yl-*N,N,N'*-tetramethyluronium tetrafluoroborate (TBTU), 1-Hydroxy-7-azabenzotriazol and 2,4,6-collidine as cyclization reagents [2]. Both altered peptides were found to be strong inhibitors of EAE when administered to Lewis rats together with the unrelated encephalitogenic Guinea Pig peptide MBP<sub>72-85</sub>. The cyclic peptide was synthesized after nuclear magnetic resonance (NMR) studies revealed pseudocyclic conformation. Cyclization is known to restrict the number of possible conformations, increasing stability, potency, receptor selectivity and bioavailability. All of them reflect a better pharmacological profile for use in the treatment of multiple sclerosis.

### **Results and Discussion**

The synthesis of the cyclic peptide analogue cyclo(87-99)[Arg<sup>91</sup>,Ala<sup>96</sup>]MBP<sub>87-99</sub>, was carried out by the Fmoc/tBu methodology, utilizing the 2-chlorotriptyl chloride resin. The cyclic peptide analogue was designed based on the preferred cyclic conformation of the linear analogue [2,3]. These peptides were tested for their ability to induce EAE in Lewis rats. Guinea Pig Myelin Basic Protein peptide 74-85 induces severe monophasic EAE when injected subcutaneously in Lewis rats. In contrast immunization with the [Arg<sup>91</sup>,Ala<sup>96</sup>]MBP<sub>87-99</sub>, or cyclo(87-99)[Arg<sup>91</sup>,Ala<sup>96</sup>]MBP<sub>87-99</sub> did not result in the induction of EAE. However, these peptide analogues when co-injected with guinea-pig MBP<sub>74-85</sub> were found to completely block the development of EAE [3].

2D-NMR experiments were performed using a Bruker 600 MHz NMR spectrometer. Long range assignments were made through NOESY experiment. The NOE connectivities observed for analogue [Arg<sup>91</sup>,Ala<sup>96</sup>]MBP<sub>87-99</sub> define a cyclic conformation for this molecule, and are:  $\alpha\text{Phe}^{89}\text{-}\delta_2\text{Pro}^{97}$ ,  $\alpha\text{Val}^{87}\text{-}\beta\text{Thr}^{98}$ ,  $\alpha\text{Val}^{87}\text{-}\gamma\text{Thr}^{98}$  (Figure 1).

To extend the observation made using NMR, a theoretical modeling approach was used. Theoretical calculations were performed using Silicon Graphics O2 workstation and Quanta software of MSI. The structures were first minimized using a combination of steepest descent and conjugate gradient algorithms. To adopt NOEs, distance con-

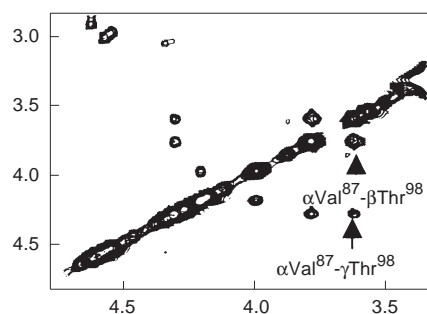


Fig. 1. Homonuclear 2D-NOESY spectrum of  $[Arg^{91},Ala^{96}]MBP_{87-99}$ .

straints were applied. To further explore the low energy conformers of the compounds, molecular dynamics and Boltzman jump methods were applied (Figure 2).



Fig. 2. Low energy conformation of a)  $[Arg^{91},Ala^{96}]MBP_{87-99}$  and b)  $(cyclo(87-99)[Arg^{91},Ala^{96}]MBP_{87-99})$ .

### Acknowledgments

This work was supported by the European Social Fund and the Ministry of Development (GSRT, PENED 99, ED-349, EPET II, 115).

### References

1. Vergelli, M., Hemmer, B., Utz, U., Vogt, A., Kalbus, M., Tranquill, L., Conlon, P., Ling, N., Steinman, L., McFarland, H., Martin, R. *Eur. J. Immunol.* **26**, 2624 (1996).
2. Tselios, T., Probert, L., Daliani, I., Matsoukas, E., Troganis, A., Gerothanassis, P., Mavromoustakos, T., Moore, G., Matsoukas, J. *J. Med. Chem.* **42**, 1170 (1999).
3. Tselios, T., Daliani, I., Probert, L., Deraos, S., Matsoukas, E., Roy, S., Pires, J., Moore, G., Matsoukas, J. *Bioorg. Med. Chem.* **8**, 1903–1909 (2000).

## Solid-Phase Synthesis Utilizing Azido- $\alpha$ -Amino Acids: Reduction of Azido-Protected Proline

Parissa Heshmati, James Whitehurst and Garland R. Marshall

*Department of Biochemistry and Molecular Biophysics, School of Medicine,  
Washington University, St. Louis, MO 63110, USA*

### Introduction

During an evaluation of azido- $\alpha$ -amino acids and their utility in solid-phase peptide chemistry, the octapeptide angiotensin II and a tripeptide thyrotropin-releasing hormone (TRH) analog have been prepared using Meldal's procedure [1]. A necessary novel step was the reduction of the azido moiety of L-proline, a secondary amine constrained by a ring, to the corresponding free amine for coupling and peptide elongation. In this step a solution of tin(II)chloride ( $\text{SnCl}_2$ ), thiophenol ( $\text{PhSH}$ ) and triethylamine (TEA) [2] in dimethylformamide (DMF) was added at ambient temperature to the azido-L-proline-peptide-resin to afford the desired free amino group (Figure 1) and make the use of azido- $\alpha$ -amino acids more general for solid-phase peptide synthesis.

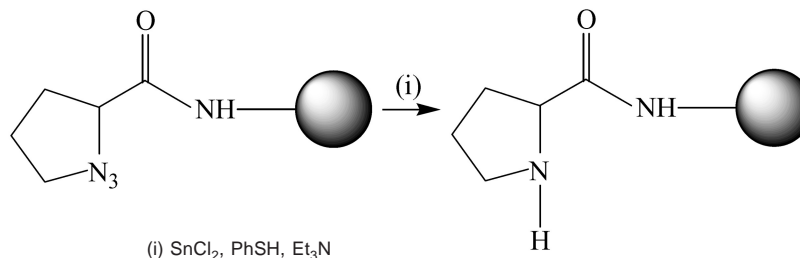


Fig. 1. Reduction of azido-protected proline.

### Results and Discussion

Our motivation to explore this chemistry was the use of the azido group in the synthesis of chiral amino acids that could be utilized directly in SPPS, and the reported higher reactivity by use of the acid chloride for coupling combined with the reduced steric bulk of the azido protecting group [1]. The synthesis of the two peptides, a thyrotropin-releasing hormone analog [ $\text{Phe}^2$ ]-TRH and the octapeptide angiotensin II was performed by solid-phase synthesis using the acid chlorides of azido- $\alpha$ -amino acids to evaluate this approach. TRH is responsible for pituitary simulation of TSH release from the thyroid whereas angiotensin II is a potent vasopressor agent involved in blood pressure homeostasis.

The major problem encountered during the synthesis of angiotensin II was the reduction of the azido-L-prolyl-L-phenylalanyl-resin. During these syntheses, it was discovered that the use of 2 M dithiothreitol (DTT) and 1 M diisopropylethylamine (DIEPA), in DMF at reflux temperature [1], in the reduction of the azido-proline-peptide-resin to the corresponding amino group, was not effective. This azido-reductive method [2] had not been previously applied to SPPS, and hence, it was necessary to optimize its application. The use of  $\text{SnCl}_2$ ,  $\text{PhSH}$  and TEA [2] solution in DMF led to the formation of the free amino group of azido-proline. This was sup-

ported by the mass spectroscopy analysis of the cleaved dipeptide (Pro-Phe-OH) resulting in the required molecular ion (MW = 261).

Wong's Cu(II) catalyzed diazo-transfer method [3] was used to generate the azido- $\alpha$ -amino acids that were converted to the acid chlorides with thionyl chloride for coupling. The main byproduct in the preparation of azido- $\alpha$ -amino acids is trifluoromethanesulfonic amide [4], which interferes with purification, analysis and synthesis, but can be completely removed by washing. While it is not necessary to use acid chlorides to activate the carboxylates, they have greater reactivity and increase the rate of reaction, a useful attribute in difficult sequences. The choice of protecting group is crucial; while forming the acid chlorides of the azido-amino acids, acid-labile protecting groups can be cleaved releasing reactive side chains or  $\alpha$ -amino groups leading to further side reactions. We chose to use the following side-chain protection during the synthesis of the two peptides: Arg(Tos), Arg(Mtr), Asp(OBut), His(Bom), Pro-OMe·HCl, Pro-OBzl·HCl, Tyr(But), Tyr(2-Br-Z). [Phe<sup>2</sup>]-TRH was obtained in 65% yield and 58% purity on cleavage from the support. Angiotensin II was obtained in 75% yield and 63% purity on cleavage from the support.

#### **Acknowledgments**

The authors acknowledge the support for this research from NIH Grant GM53630. The assistance of Mr. James Carlton at the Health Science Center Core Laboratories at LSU for mass spectra is greatly appreciated.

#### **References**

1. Meldal, M., Juliano, M.A., Jansson, A.M. *Tetrahedron Lett.* **38**, 2531–2534 (1997).
2. Bartra, M., Romea, P., Urpi, F., Vilarrasa, J. *Tetrahedron* **46**, 587–594 (1990).
3. Alper, P.B., Hung, S-C., Wong, C-H. *Tetrahedron Lett.* **37**, 6029–6032 (1996).
4. Lundquist, J.T., Pelletier, J.C. *Org. Lett.* **3**, 781–783 (2001).

## Improved Fmoc-Solid Phase Synthesis of $\beta$ -Amyloid Peptides Using DBU as $N^\alpha$ -Deprotection Reagent

Anna K. Tickler<sup>1,2</sup>, Colin J. Barrow<sup>2</sup> and John D. Wade<sup>1</sup>

<sup>1</sup>Howard Florey Institute of Experimental Physiology and Medicine and <sup>2</sup>School of Chemistry,  
University of Melbourne, Victoria 3010, Australia

### Introduction

Alzheimer's Disease (AD) is the most common form of dementia affecting society today. It is a neurodegenerative disease, the histopathological features of which include extracellular deposition of amyloid  $\beta$  peptide ( $A\beta$ )-loaded senile plaques in the brain parenchyma and blood vessels.

$A\beta$ , a 39 to 42 residue peptide (Figure 1), is excised from the Amyloid Precursor Protein (APP) by the sequential action of secretases, resulting in a peptide fragment that spans the extracellular and transmembrane regions of APP.  $A\beta$ 1-40 is the major species found in biological fluids whereas  $A\beta$ 1-42 is enriched in senile plaques [1]. With the recent finding that immunization against  $A\beta$  leads to amelioration of AD [2], there is renewed interest in the large-scale preparation of such peptides for further physicochemical study. However, as a so-called "difficult" sequence due to the high hydrophobicity of the C-terminal segment and resulting on-resin aggregation, the peptide remains a considerable challenge for the synthetic chemist. In an attempt to overcome this difficulty, we have examined the effect of simple replacement of  $N^\alpha$ -deprotection base with the strong tertiary amidine, DBU, in the Fmoc-solid phase synthesis (SPS) of  $A\beta$ .



Fig. 1. Primary structure of  $A\beta$  1-42. Bold residues show  $A\beta$  29-42 sequence used in model SPS experiments.

### Results and Discussion

A preliminary synthesis of  $A\beta$  29-40 using standard Fmoc-continuous flow methodology throughout together with 20% piperidine/DMF solution to effect  $N^\alpha$ -deprotection, yielded a product that was shown by MALDITOF MS to contain several deletion peptides. Incomplete deprotection of Val, a residue that has a known propensity for slow  $N^\alpha$ -Fmoc deprotection, was identified as a primary cause of byproduct formation. Consequently, a repeat assembly was undertaken using a solution of 2% DBU/DMF for  $N^\alpha$ -Fmoc deprotection [3], a base that has been previously used in successful "difficult" peptide synthesis [4]. A substantially improved crude product was obtained that suggested that, at least for this peptide, incomplete Fmoc group removal may be a more significant problem in Fmoc-SPS than incomplete acylation. This base was then used during the synthesis of both  $A\beta$ 1-40 and  $A\beta$ 1-42, up to and including Ser<sup>8</sup>, from which point 20% piperidine in DMF was utilised so as to avoid potential aspartimide formation at Asp<sup>7</sup>. By this means, the deprotection efficiency through the difficult C-terminal portion of the sequence was much improved and resulted in acquisition of high quality crude products (for example, Figure 2). This simple strategy that obviates

### Synthetic Methods

the need for special conditions significantly improved crude peptide quality and allowed considerable facilitation of subsequent purification. Overall recovery of purified synthetic A $\beta$ 1-40 and 1-42 was 24 and 17%, respectively.

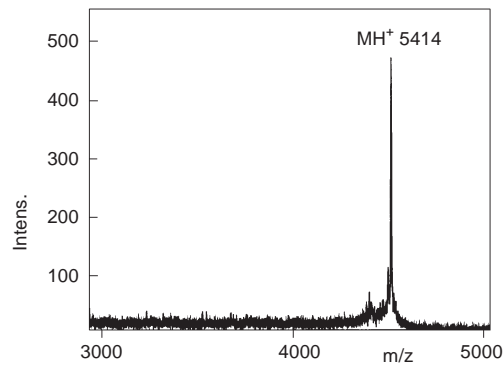


Fig. 2. MALDITOF mass spectrum of crude synthetic A $\beta$  1-40. Theoretical MH<sup>+</sup> value: 5415.

### Acknowledgments

The work carried out at the Howard Florey Institute was supported by an Institute block grant (reg. key #983001) from the NHMRC.

### References

1. Wilson, C.A., Doms, R.W., Lee, V.M.-Y. *J. Neuropath. Exp. Neurol.* **58**, 787–794 (1999).
2. Janus, C., Pearson, J., McLaurin, J., Mathews, P.M., Jiang, Y., Schmidt, S.D., Chishti, M.A., Horne, P., Heslin, D., French, J., Mount, H.T.J., Nixon, R.A., Bergson, C., Fraser, P.E., St George-Hyslop, P., Westaway, D. *Nature* **408**, 979–982 (2000).
3. Wade, J.D., Bedford, J., Sheppard, R.C., Tregear, G.W. *Peptide Res.* **4**, 194–199 (1991).
4. Wade, J.D., Mathieu, M.N., Macris, M., Tregear, G.W. *Lett. Peptide Sci.* **7**, 107–112 (2000).

## Triphosgene as Peptide Coupling Reagent: Highly Efficient Total Synthesis of Cyclosporin O

Bernd Thern<sup>1</sup>, Joachim Rudolph<sup>2</sup> and Günther Jung<sup>1</sup>

<sup>1</sup>University of Tübingen, Institute of Organic Chemistry, 72076 Tübingen, Germany

<sup>2</sup>Bayer AG, Central Research, Life Science, 51368 Leverkusen, Germany

### Introduction

Cyclosporins are immunosuppressive cyclic peptides from *Cylindrocarpum lucidum* Booth and *Tolypocladium inflatum* Gams. Cyclosporin A (CsA, Sandimmune) is a widely used drug for preventing the rejection of transplanted organs and for therapy of autoimmune diseases. The synthesis of cyclosporins is problematic due to their high content of *N*-methylated amino acids. We developed a highly efficient, racemization free solid phase synthesis of Cyclosporin O (CsO) using a combination of HOAt/DIC couplings and a novel, modified form of a recently described triphosgene coupling [1]. The latter was adapted for the synthesis of peptides with free carboxy terminus on highly acid labile TCP resin (trityl chloride polystyrene resin) using a specific combination of bases for activation and coupling at room temperature.

### Results and Discussion

Our optimized and reproducible synthesis protocol enabled us to use triphosgene as coupling reagent on highly acid labile TCP resin, thus circumventing the diketopiperazine formation and premature cleavage we encountered using the original method of Falb [2]. This was accomplished by using collidine for activation of the amino acid and DIEA for the coupling reaction.

With <sup>13</sup>C NMR, the main component in the activation mixture was identified as symmetric anhydride of the Fmoc-*N*-methyl amino acid. In accordance with a previous publication describing triphosgene as a reagent for the preparation for symmetric anhydrides [3], we propose the following mechanism for its formation (Figure 1).

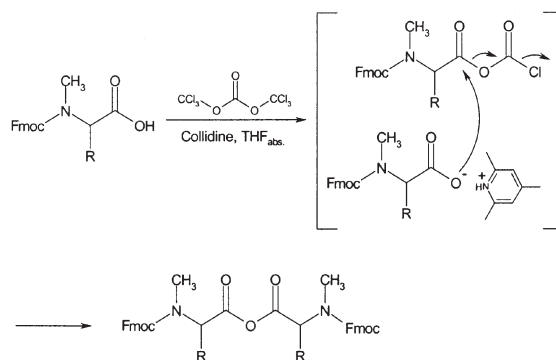


Fig. 1. Proposed action of triphosgene activation. The symmetric anhydride is formed via a chloroformate.

The synthesis of Cyclosporin O (CsO) was started with residue 1 (MeLeu) attached to trityl chloride polystyrene resin (Figure 2). The tetrapeptide 9-1 (Fmoc-MeLeu-MeLeu-MeVal-MeLeu-OH), which comprises the most difficult sequence as it is composed exclusively of *N*-methyl amino acids, was synthesized in >99% purity as shown

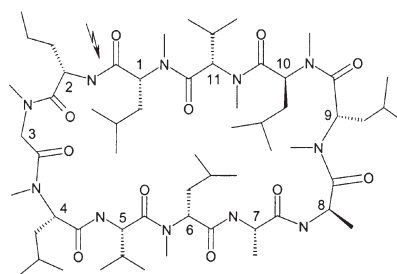


Fig. 2. The first residue attached to the resin was MeLeu (1). The cyclization site is indicated by an arrow.

by HPLC. Only the first coupling had to be repeated. After triphosgene coupling of the fifth residue, Fmoc-D-Ala-OH, however, HPLC showed only about 10% conversion. However, the coupling was driven to completion with an additional single HOAt/DIC coupling (16 h). Using a combination of triphosgene and HOAt/DIC couplings, the linear, unprotected undeca-peptide cyclosporin precursor was obtained in a HPLC-purity of 90% (Figure 3; crude product; 214 nm). Only 4 of the 10 coupling reactions had to be done twice. The whole synthesis took only a few days, and the use of triphosgene minimizes the costs for chemicals. Due to the fact that hexafluoroisopropanol could be used for the cleavage of the linear peptide, the crude peptide could be cyclized after lyophilization without further workup. Cyclization was done in DCM with HOAt, EDCI and DIEA (16 h) and proceeded with a crude yield of about 75–80%.

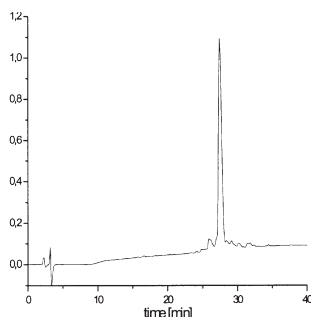


Fig. 3. HPLC of crude linear undeca-peptide.

After preparative HPLC, an overall yield of 15% with respect to the first resin loading was calculated. This yield is within the range of most of the liquid phase syntheses reported for various cyclosporin analogs.  $^1\text{H}$  NMR proved the identity of the synthetic Cyclosporin O with the natural product, and no diastereomers were detected.

### Acknowledgments

Parts of this work were supported by the “Graduiertenkolleg Analytische Chemie” of the Deutsche Forschungsgemeinschaft (DFG).

### References

1. Falb, F., Yechezkel, T., Salitra, Y., Gilon, C. *J. Peptide Res.* **53**, 507–551 (1999).
2. Jung, G., Thern, B., Rudolph, J., Patent Application Pending, Bayer AG.
3. Kocz, R., Roestamadji, J., Mobashery, S. *J. Org. Chem.* **59**, 2913–2914 (1994).

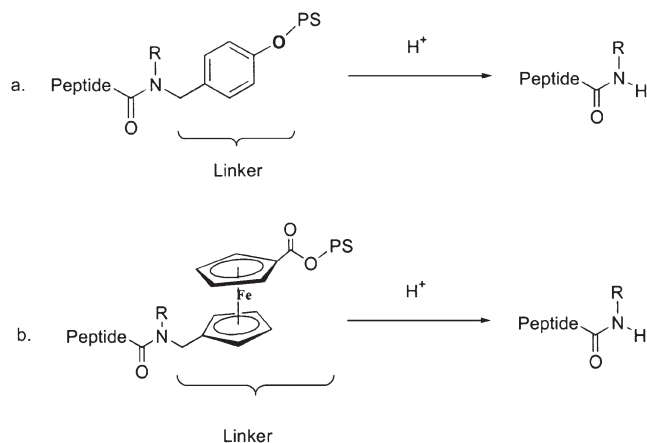
## Synthesis of Ferrocene Linkers for Solid-Phase Synthesis of Peptides

José Giraldez and Mark L. McLaughlin

Louisiana State University, Department of Chemistry, Baton Rouge, LA 70803, USA

### Introduction

Peptides can be cleaved from the resin easier if they are attached to the resin through a selectively labile linker. The most common strategies used to date for the release of amides from insoluble supports are: (a) cleavage of a benzylic C–N bond of resin-bound *N*-alkyl-*N*-benzyl amides, (b) nucleophilic cleavage of resin bound acylating agents with amines and (c) acylation/debenzylation of resin-bound *N,N*-dibenzylamines [1]. However, no effort has been taken to explore the possible application of the C–N bond cleavage of resin bound ferrocenyl amides. The typical backbone amide linker (BAL) consists of a benzylic C–N bond which is cleaved with acid to yield the peptide amide (Scheme 1). Benzylamine linkers require the introduction of electron donating groups onto the benzene ring to make C–N bond cleavage more efficient.



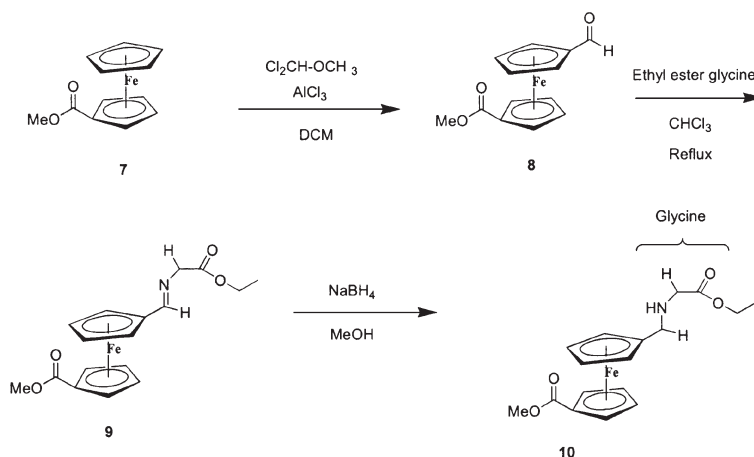
Scheme 1. Benzylamide [2]-based (a) and ferrocenylamide-based linkers (b).

Introducing electron-donating groups complicates the preparation of benzylamide linkers. The ferrocenyl cation is much more stable than the benzylic cation [3], which is expected to make the cleavage of the peptide from the ferrocenyl linker more efficient. Herein we report the synthesis of a new ferrocenylamide-based linker.

### Results and Discussion

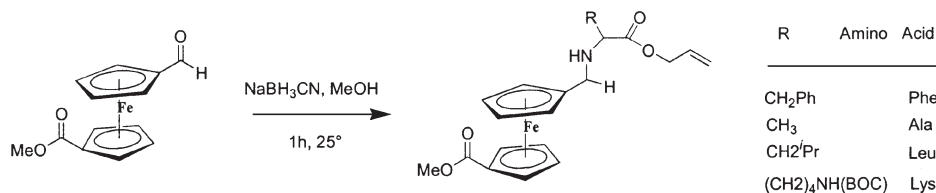
We report synthesis of a ferroceneamide-based linker for the synthesis and cleavage of peptide. The synthesis was accomplished in a four-step procedure. Friedel–Crafts acylation, Schiff base formation of the ferrocenealdehyde [4] and reduction of the Schiff base with sodium borohydride yields the ferrocenylamine linker (Scheme 2) [5]. This new linker should find widespread use throughout solid phase peptide synthesis (SPPS) and other applications.

## Synthetic Methods



Scheme 2. Ferrocenyl amine synthesis.

Another route to the ferrocenyl amine was explored. In this route the formation of the ferrocenyl amine is accomplished in one step (yields 85–100%). Different allyl ester protected amino acids were used (Scheme 3). These allyl ester protected amino acids are key intermediates in BAL solid phase peptide synthesis.



Scheme 3. Reductive amination with allyl ester amino acids.

## Acknowledgments

This work was supported by NIH GM 56835.

## References

1. Bui, C.T. *Tetrahedron Lett.* **39**, 9279–9282 (1998).
2. Jensen, J., et al. *J. Am. Chem. Soc.* **120**, 5441–5452 (1998).
3. Watts, W.E. *J. Organomet. Chem. Libr.* **7**, 399 (1979).
4. Chensheng, Li, et al. *Supramol. Chem.* **6**, 79–85 (1995).
5. Hess, A., et al. *Inorg. Chem.* **39**, 5437–5443 (2000).

## Efficient HF Conditions for Suppressing Trp Modification Associated with Use of the $N^{\text{in}}$ -Cyclohexyloxycarbonyl (Hoc) Group

Hideki Nishio, Yuji Nishiuchi, Tatsuya Inui, Makoto Nakata,  
Kumiko Yoshizawa-Kumagaye and Terutoshi Kimura

Peptide Institute Inc., Protein Research Foundation, Minoh-shi, Osaka 562-8686, Japan

### Introduction

We have recently demonstrated the utility of a combined solid-phase and solution approach for protein synthesis [1]. The procedure consists of the preparation of protected segments by solid-phase with Boc chemistry and subsequent segment condensation in solution, followed by final deprotection using HF. Each fully protected segment with a free  $\alpha$ -carboxyl group is detached from an  $N$ -[9-(hydroxymethyl)-2-fluorenyl] succinamic acid (HMFS) linker [2] by treatment with 20% morpholine/DMF. When employing a base-labile linker such as HMFS, the side-chain protecting groups must be completely stable under the basic conditions used to detach the segments from the resin. For this purpose, the cyclohexyloxycarbonyl (Hoc) group was developed as a base-resistant side-chain protecting group for the Trp residue suited to our synthetic strategy. However, side products of MW 108 higher than that of the desired product were observed, when the Hoc group was exposed to HF in the presence of *p*-cresol, and these side products were identified as two steric *trans*-isomers of 2-[2'-(*p*-cresol)]-2,3-dihydrotryptophan (Figure 1) [3]. The side reaction arising from modification of the Trp residue is inherent to the carbamate-type  $N^{\text{in}}$ -protecting groups when performing HF treatment in the presence a scavenger. In the present study, we investigated the HF conditions applicable to the practical peptide synthesis for suppressing the modification of the Trp residue. Furthermore, application of this side reaction was examined to develop a facile procedure for introducing aromatic ring systems at the 2-position of the indole moiety.

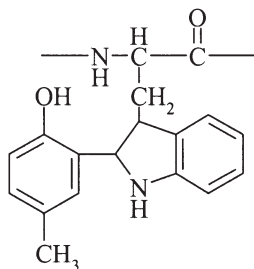


Fig. 1. Structure of 2-[2'-(*p*-cresol)]-*trans*-2,3-dihydrotryptophan.

### Results and Discussion

To establish the HF conditions for suppressing this side reaction applicable to the practical peptide synthesis, we carried out a model experiment using the segment for green fluorescent protein [GFP(52-58): K(ClZ)LPVPW(Hoc)P]. Even if a commonly used scavenger, such as anisole, *m*-cresol or thiocresol, is employed in place of *p*-cresol, the same side reaction occurred to produce the respective *trans*-adducts corresponding to *p*-cresol adducts (Table 1). The use of thiol [*e.g.* 1,4-butanedithiol

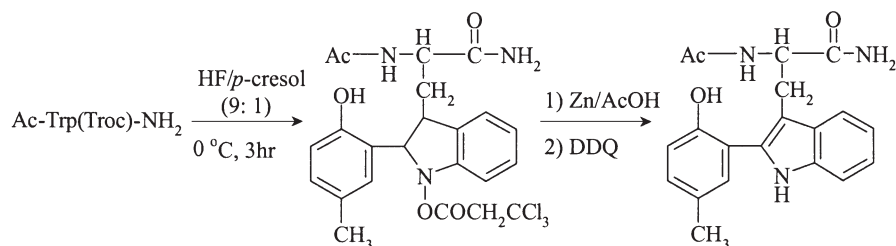
(BDT)] during the HF reaction was found to almost completely eliminate this Trp modification. However, BDT causes the handling problems such as unpleasant odor and could be replaced if an efficient scavenger which does not participate in Trp modification were available. As alternative scavengers, Fmoc-amino acid (Fmoc-Leu or Fmoc-Met) were examined, because the Fmoc group is known to be capable of capturing cations generated from the side-chain protected groups by HF [4]. The results indicated that this side reaction could be completely suppressed by performing the HF reaction in the presence of a scavenger, Fmoc-Leu or Fmoc-Met, to quantitatively yield the desired product. Furthermore, such Fmoc amino acids can be easily removed by washing with ether after HF treatment.

Table 1. Products obtained after treatment of *K(ClZ)LPVPW(Hoc)P* with HF.

Conditions <sup>b</sup>	Yield (%) <sup>a</sup>	
	KLPVPWP	Trans-adducts
HF/ <i>p</i> -cresol (8 : 2)	92.5	7.5
HF/anisole (8 : 2)	90.2	9.8
HF/BDT/ <i>p</i> -cresol (8 : 15 : 5)	99.3	0.7
HF + Fmoc-Leu (10 eq)	100	–

<sup>a</sup> Determined by CZE (200 nm). <sup>b</sup> The reactions were carried out at  $-5^{\circ}\text{C}$  for 1 h.

When treating Ac-Trp(Troc)-NH<sub>2</sub> (Troc: 2,2,2-trichloroethoxycarbonyl) with HF in the presence of *p*-cresol, the *p*-cresol adducts gave a quantitative yield (Scheme 1). Furthermore, removal of the Troc group followed by oxidation of the indoline ring could convert the side products to the Trp derivative in which *p*-cresol was substituted at the 2-position of the indole moiety. Thus, this side reaction offers a facile procedure for introducing aromatic ring systems at the 2-position of the indole moiety of the Trp residue, as had been reported previously for selective introduction of the mercaptoethanol moiety at position 2 or 7 [5].



Scheme 1. Introduction of aromatic ring systems at the 2-position of the indole moiety of Trp.

## References

1. Nishiuchi, Y., Nishio, H., Inui, T., Bódi, J., Kimura, T. *J. Peptide Sci.* **6**, 84–93 (2000).
2. Rabanal, F., Giralt, E., Albericio, F. *Tetrahedron* **51**, 1449–1458 (1995).
3. Nishio, H., Nishiuchi, Y., Inui, T., Yoshizawa-Kumagaye, K., Kimura, T. *Tetrahedron Lett.* **41**, 6839–6842 (2000).
4. Grode, S.H., Strother, D.S., Runge, T.A. Dobrowolski, P.L. *Int. J. Peptide Protein Res.* **40**, 538–545 (1992).
5. Nishio, H., Kimura, T., Sakakibara, S. *Tetrahedron Lett.* **35**, 1239–1242 (1994).

## Structural Characterization of a Dibenzylated-CGRP(8-37), a Byproduct from *N*- $\alpha$ -Benzylation of CGRP(8-37)

D. David Smith<sup>1</sup>, Martin Hulce<sup>2</sup>, David J. J. Waugh<sup>3</sup> and Peter W. Abel<sup>3</sup>

<sup>1</sup>Department of Biomedical Sciences, <sup>2</sup>Department of Chemistry and <sup>3</sup>Department  
of Pharmacology, Creighton University, Omaha, NE 68178, USA

### Introduction

Calcitonin gene-related peptide (CGRP) is a 37-residue peptide with a C-terminal amide group and disulfide bridge between positions 2 and 7 (Figure 1). CGRP is a potent vasodilator that is distributed throughout the peripheral and central nervous systems. The N-truncated fragment CGRP(8-37), which lacks the disulfide bridge, is a competitive antagonist. Recently, we reported that blocking the N-terminus of CGRP(8-37) resulted in a series of antagonists that have higher affinity for CGRP receptors than CGRP(8-37) [1]. During solid phase synthesis of *N*- $\alpha$ -benzyl-CGRP(8-37) a dibenzylated CGRP(8-37) analogue was isolated as a minor byproduct that also possessed high affinity for CGRP receptors. We report here the structural characterization of this analogue.

### Results and Discussion

Benzylating the N-terminal free amino group of the resin-bound protected peptide of h- $\alpha$ -CGRP(8-37) with excess benzyl bromide and DIEA produced N- $\alpha$ -benzyl-h- $\alpha$ -CGRP(8-37). RP-HPLC analysis of the crude product after cleavage of the peptide from the resin revealed the presence of a more hydrophobic byproduct that was purified by preparative RP-HPLC. The mass of the byproduct was 3305.6 by ESI-MS, which is consistent with the byproduct being a dibenzylated analogue of h- $\alpha$ -CGRP(8-37) (theoretical mass 3305.5). Amino acid analysis revealed that the byproduct does not contain His in contrast to the amino acid composition of the monobenzylated peptide. Hence, benzylation of the N-terminal  $\alpha$ -amino group of h- $\alpha$ -CGRP(8-37) is accompanied to a lesser extent by benzylation of the histidyl residue in position 10.

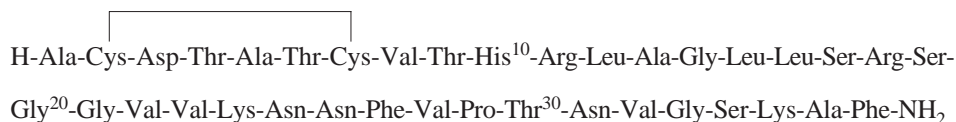


Fig. 1. Primary structure of human- $\alpha$ -Calcitonin Gene-Related Peptide.

N-Terminal tetrapeptides spanning positions 8 to 11 of h- $\alpha$ -CGRP(8-37) and dibenzyl-h- $\alpha$ -CGRP(8-37) were subjected to intense NMR analysis to determine the site of secondary benzylation within the His<sup>10</sup> residue. The tetrapeptides were generated by digestion of h- $\alpha$ -CGRP(8-37) and dibenzyl-h- $\alpha$ -CGRP(8-37) with trypsin and purified by RP-HPLC using our previously published methods [2]. <sup>1</sup>H NMR spectroscopy of h- $\alpha$ -CGRP(8-11) in D<sub>2</sub>O unambiguously located the His imidazole ring hydrogens H2 and H4 at 8.52 ppm (doublet, *J* = 1.20 Hz) and 7.23 ppm (singlet), respectively [3]. When the complementary experiment was performed using dibenzyl-h- $\alpha$ -CGRP(8-11), the presence of two benzyl groups in the tetrapeptide was confirmed by observation of 10 new aromatic hydrogens in the region 7.48–7.26 ppm, a doubly benzylic methylene

group at 7.35–7.26 ppm, and by a new *N*-benzyl methylene group at 5.31 ppm. The His imidazole ring hydrogen H2 was retained at 8.64 ppm (triplet,  $J = 1.69$  Hz), whereas the H4 resonance no longer was apparent.

Benzylation of His<sup>10</sup> therefore occurred through alkylation of the benzyloxymethyl (BOM) protected imidazole ring at carbon C4, presumably by an electrophilic mechanism (Figure 2). Long-range coupling of H2 to the doubly benzylic methylene group at 7.35–7.26 ppm confirmed the site of benzylation to be at C4 of the His imidazole ring. To our knowledge this is the first report of the susceptibility of a protected imidazole ring of His to benzylation. The C4 regiochemistry of this benzylation is striking: N1-protected imidazoles exhibit nearly exclusive reaction at C2 during base-promoted electrophilic substitutions [4].

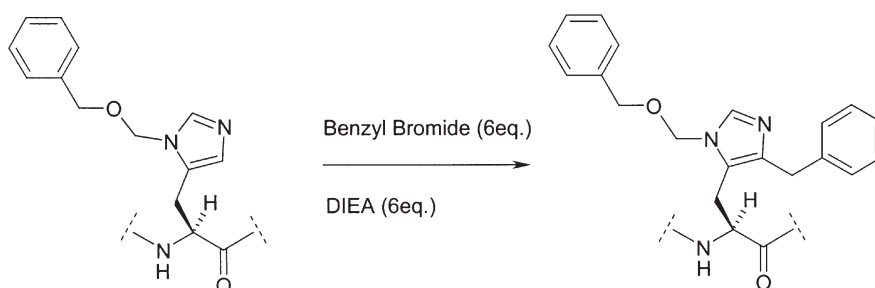


Fig. 2. Benzylation of the BOM-protected imidazole group on the histidyl side chain.

### Acknowledgments

The authors gratefully acknowledge the State of Nebraska, Cancer and Smoking Related Disease Program and the U. S. Public Health Service, HL51131 for funding this work and the National Science Foundation, CHE-9512267 for an instrument grant.

### References

1. Smith, D.D., Saha, S., Waugh, D.J.J., Abel, P.W., In Martinez, J. and Fehrentz, J.-A. (Eds.) *Peptides 2000 (Proceedings of the 26th European Peptide Symposium)*, EDK, Paris, France, 2001, p. 741.
2. Smith, D.D., Li, J., Wang, Q., Murphy, R.F., Adrian, T.E., Elias, Y., Bockman, C.S., Abel, P.W. *J. Med. Chem.* **36**, 2536–2541 (1993).
3. Matthews, H.R., Rapoport, H. *J. Am. Chem. Soc.* **95**, 2297–2303 (1973).
4. e.g. Macco, A.A., Godefroi, E.F., Drouen, J.J.M. *J. Org. Chem.* **40**, 252–255 (1975).

## Polyamines as Intermediates for the Synthesis of Heterocyclic Compounds and Oligomeric Heterocyclic Compounds from Resin-Bound Polyamides

Adel Nefzi and Richard A. Houghten

Torrey Pines Institute for Molecular Studies, San Diego, CA 92121, USA

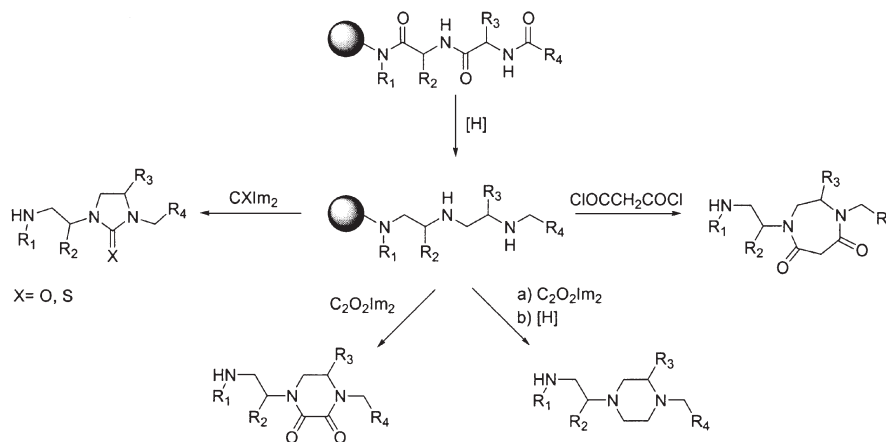
### Introduction

Due to the well-understood chemistry, and excellent synthetic purity and yields obtained during the solid-phase synthesis of peptides, our focus has been directed toward the synthesis and design of acyclic organic and heterocyclic compounds using modified peptides and peptidomimetics as starting materials [1]. Thus, over the past five years, this strategy was successfully used to design and generate a range of novel solid phase chemistries. Specifically, we used our approach of the exhaustive reduction of resin-bound amides to generate resin-bound polyamines for the solid-phase synthesis of highly diverse heterocyclic libraries [2].

### Results and Discussion

Different disubstituted heterocyclic compounds were prepared from resin-bound *N*-acylated amino acids. Thus, following exhaustive reduction of the two amides, the resulting two secondary amines were treated with different commercially available bifunctional reagents such as carbonyldiimidazole, thiocarbonyldiimidazole, oxalyl-diimidazole, and malonyl chloride to form the corresponding disubstituted heterocyclic compounds: cyclic ureas, cyclic thioureas, diketopiperazines, piperazines, and diazepinediones, respectively. The piperazine compounds were generated following reduction on the solid support of the oxamide moiety in the presence of borane.

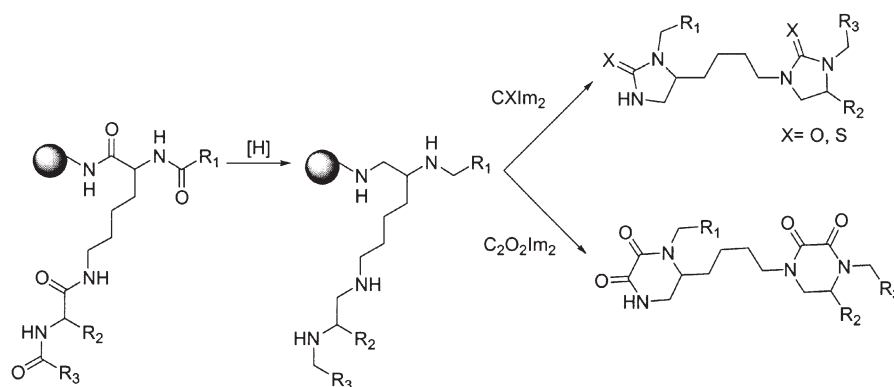
In order to increase the diversity of each heterocyclic pharmacophore, we extended our approach to the combinatorial synthesis of the trisubstituted heterocyclic analogs following a selective *N*-alkylation and exhaustive reduction of resin-bound *N*-acylated dipeptide (Scheme 1).



Scheme 1. Solid-phase synthesis of trisubstituted heterocyclic compounds from resin-bound reduced acylated dipeptides.

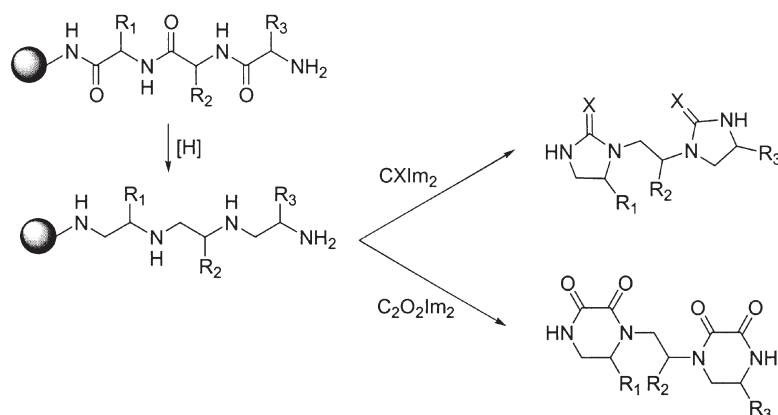
## Synthetic Methods

Along similar lines, an efficient method for the solid phase synthesis of bis-heterocyclic compounds from resin-bound orthogonally protected lysine was developed. The initial reaction step involved the exhaustive reduction of resin-bound tetraamides using borane-THF, followed by cyclization of the resulting tetra-amine with either carbonyldiimidazole, thiocarbonyldiimidazole, or oxalyldiimidazole to generate resin-bound bis-cyclic ureas, bis-cyclic thioureas and bis-diketopiperazines, respectively (Scheme 2). Cleavage from the solid support with hydrogen fluoride, followed by extraction and lyophilization, yielded the desired bis-heterocyclic compounds in excellent yield and high purity.



Scheme 2. Solid-phase synthesis of bis-heterocyclic compounds from resin-bound orthogonally protected lysine.

Extending the above mentioned approaches to larger polyamines, tripeptide amides were synthesized using the conventional Boc/Bzl chemistry. Following coupling of the third amino acid and Boc deprotection, the resin-bound tripeptide was exhaustively reduced with borane in THF to yield resin-bound tetra-amines containing three secondary amines and one terminal primary amine. The resin-bound tetra-amine was then treated with the above-mentioned bifunctional reagents to afford, following HF cleavage, the corresponding bis-heterocyclic compounds (Scheme 3). Kinetically,



Scheme 3. Solid-phase synthesis of bis-heterocyclic compounds from resin-bound reduced tripeptides.

*Nefzi et al.*

the primary amine reacts first with diimidazole reagent, which favors intermolecular cyclization with the adjacent secondary amine to yield the first cyclization through formation of the energetically favorable five or six member ring. The two remaining secondary amines then further react with the diimidazole reagent to yield the second heterocycle. Following optimization using different concentrations of the reagents, we observed that working at lower concentrations with small excesses of the reagent led to the desired bis-heterocyclic compounds with purities greater than 80%. In support of our kinetic hypothesis, we found that the treatment of a resin-bound polyamine containing four secondary amines led to the formation of multiple products.

#### **Acknowledgments**

This work was supported by National Cancer Institute (Grant No. CA78040) and Mixture Sciences.

#### **References**

1. Houghten, R.A., Pinilla, C., Appel, J.R., Blondelle, S.E., Dooley, C.T., Eichler, J., Nefzi, A., Ostresh, J.M. *J. Med. Chem.* **42**, 3743–3778 (1999).
2. (a) Nefzi, A., Ostresh, J.M., Giulianotti, M.A., Houghten, R.A. *J. Com. Chem.* **1**, 195–198 (1999). (b) Ostresh, J.M., Schoner, C.C., Hamashin, V.T., Nefzi, A., Meyer, J-P., Houghten, R.A. *J. Org. Chem.* **63**, 8622–8623 (1998). (c) Nefzi, A., Ostresh, J.M., Houghten, R.A. *Tetrahedron* **55**, 335–344 (1999).

## Solid-Phase Synthesis of Substituted Dihydroimidazoles and Their Bis Analogs

Achyuta N. Acharya, John M. Ostresh, Adel Nefzi and  
 Richard A. Houghten

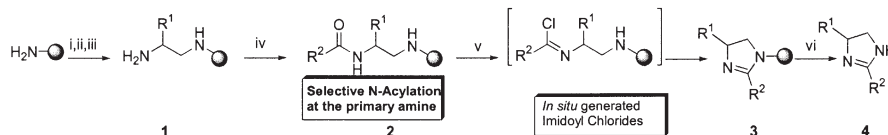
Torrey Pines Institute for Molecular Studies, San Diego, CA 92121, USA

### Introduction

Dihydroimidazoles (imidazolines) are known to exhibit a wide range of pharmacological activities [1,2]. A 2-imidazoline derivative has previously been incorporated into a very active antihypertensive agent, clonidine [1]. We report here a novel approach for the synthesis of substituted imidazolines and bis-imidazolines from resin-bound amino acids *via* cyclization using POCl<sub>3</sub> [3].

### Results and Discussion

(i) *2,4-Disubstituted imidazolines*. An individual Boc-amino acid was coupled to MBHA resin (Scheme 1), the Boc group deprotected, and exhaustively reduced [4] to generate diamine **1**. The resin-bound diamine **1** was treated with a carboxylic acid in the presence of HBTU and DIEA to yield amide **2** by selective *N*-acylation at the primary amine. Treatment of amide **2** with phosphorous oxychloride (POCl<sub>3</sub>) in dioxane led to cyclodehydration [3] of the *in situ* formed imidoyl chloride intermediate generating the resin-bound imidazoline **3**. Cleavage using anhydrous HF gave dihydroimidazole **4**. Coupling of Boc-protected amino acids, deprotection of the Boc group, cleavage from the solid-support, extraction, purification, and characterization (by



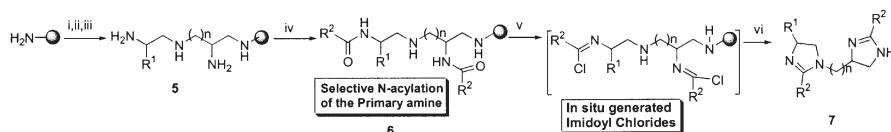
Scheme 1. (i) Boc-aa (6×, 0.1 M in DMF), DIC (6×), HOBt (6×), 2 h, rt; (ii) 55% TFA in DCM, 30 min, rt; (iii) BH<sub>3</sub>-THF, 65 °C, 4 days; Piperidine, 65 °C, 20 h; (iv) R<sup>2</sup>COOH (3×, 0.06 M in DMF), HBTU (3×), DIEA (6×), 3.5 h, rt; (v) POCl<sub>3</sub> (10×, 0.09 M in dioxane), 110 °C, 2.5 h; (vi) HF, anisole, 7 h.

HRMS, <sup>1</sup>H NMR, and <sup>13</sup>C NMR) of the compounds has been described previously [5]. Incomplete cyclization occurred for several carboxylic acids. Most likely, this was due to the formation of more strongly basic imidoyl chloride intermediates that slowly transformed to their quaternary *N*-methylated imidoyl chloride derivatives thus hindering the cyclization [3]. In all other cases, complete cyclization was observed by LC-MS. The lower than expected yield was attributed to the premature cleavage of the compounds from the resin during cyclodehydration due to the formation of HCl as a byproduct [6].

(ii) *Trisubstituted Bis-imidazolines*. N<sup>α</sup>-Fmoc-N<sup>ε</sup>-Boc-lysine was coupled to MBHA resin (Scheme 2), the Boc group deprotected, a Boc-amino acid coupled at the resulting primary amine, the Boc group deprotected [5], and exhaustively reduced [4] to generate tetraamine **5**. Selective *N*-acylation of the two primary amines of tetraamine **5** using a carboxylic acid in the presence of HBTU and DIEA generated diamide **6**. Treatment of **6** with POCl<sub>3</sub> in dioxane resulted in the resin-bound bis-imidazoline *via*

Acharya et al.

cyclization of the imidoyl chloride intermediate [3]. Cleavage from the solid-support gave bis-imidazoline **7**. Starting materials and/or undesirable impurities were obtained for *p*-toluic acid, 1-adamantanecarboxylic acid, and isobutyric acid as described above. In all other cases, complete cyclization was observed by LC-MS and HPLC.



Scheme 2. (i) *N*<sup>α</sup>-Fmoc-*N*<sup>ε</sup>-Boc-lysine (2.5×, 0.05 M in DMF), rt, overnight; 55% TFA in DCM, 30 min, rt; (ii) Boc-aa (6×, 0.1 M in DMF), DIC (6×), HOBt (6×), 2 h, rt; 55% TFA in DCM, 30 min, rt; (iii) BH<sub>3</sub>-THF, 65 °C, 4 days; Piperidine, 65 °C, 20 h; (iv) R<sup>2</sup>COOH (5×, 0.1 M in DMF), HBTU (5×), DIEA (10×), 3.5 h, rt; (v) POCl<sub>3</sub> (10×, 0.09 M in dioxane), 110 °C, 2.5 h; (vi) Cyclization followed by HF, anisole, 7 h. *n* = 4 (denotes the carbon tether length).

In conclusion, we have developed an efficient strategy for the solid-phase synthesis of imidazolines and their respective bis-analogs *via* direct linkage of the resin to the imidazoline moiety. This approach utilizes cyclization of the *in situ* generated imidoyl chloride intermediates in the key step and allows independent variation of the substituents on the imidazoline core. The compounds were obtained in moderate yield (>60%) and high purity. This approach can be employed to prepare large number of individual substituted imidazolines and bis-imidazolines as well as mixture-based synthetic combinatorial libraries.

### Acknowledgments

A.N.A. thanks the Department of Science and Technology, Govt. of India for the award of a BOYSCAST fellowship and Department of Industries, Govt. of Orissa, India for sanction of study leave. This work was funded by National Cancer Institute Grant 78040 (Houghten).

### References

1. Gilman, A.G., Goodman, L.S., In *The Pharmacological Basis of Therapeutics*, 6th ed., Macmillan & Co., New York, 1980, p 710.
2. Bihan, G.L. et al. *J. Med. Chem.* **42**, 1587 (1999); Katritzky, A.R., et. al. *B. J. Org. Chem.* **65**, 3683 (2000); Matsumoto, H., et al. *J. Med. Chem.* **42**, 1661 (2001).
3. Whaley, W.M., Govindachari, T.R. *Org. React.* **6**, 74 (1951).
4. Ostresh, J.M., et. al. *J. Org. Chem.* **63**, 8622 (1998).
5. Acharya, A.N., et. al. *J. Comb. Chem.* **3**, 189 (2001).
6. Huheey, J.E., In *Inorganic Chemistry*, 3rd ed., Harper and Row, New York, 1983, p. 289.

## Solid Phase Synthesis of 1,2,5-Substituted Derivatives of 4-Imidazolidinone

Markéta Rinnová, Agnès Vidal, Adel Nefzi and Richard A. Houghten

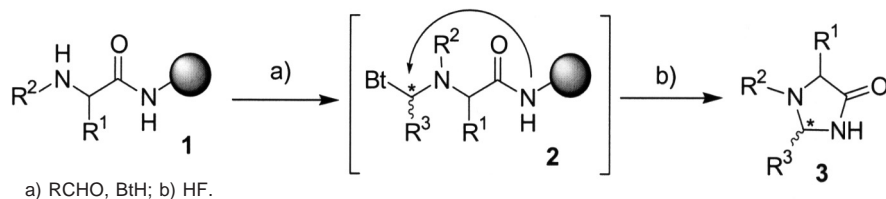
Torrey Pines Institute for Molecular Studies, San Diego, CA 92 121, USA

### Introduction

Solid phase synthetic approaches enable the preparation of large numbers of new biologically interesting compounds. Small molecule libraries of heterocycles have proven effective for the identification of various bioactive compounds [1]. 4-Imidazolidinones belong to a group of biologically interesting and less-explored heterocyclic compounds. This type of molecule was identified as a product of a spontaneous cyclization of N-terminal amino groups of peptides or proteins, with formaldehyde, acetone or acetaldehyde in aqueous solutions [2]. N-terminal 4-imidazolidinones derivatives of proteins or peptides were also identified in the human liver during chronic ethanol oxidation [3]. The same type of modification was used to form enzymatically stable prodrugs based on peptides [4].

### Results and Discussion

There are several methods for the solution synthesis of 2,5-substituted 4-imidazolidinones involving either Beckman rearrangement of 1-alkoxycarbonyl azetidin-3-one based intermediate [5], or cyclization of  $\alpha$ -aminocarboxamides with aldehydes in the presence of a catalyst or acid [6,7]. The oldest method is based on dehydration and intramolecular cyclization of acylated dipeptides [8]. However, none of these methods is compatible with a solid phase or combinatorial approach. Katritzky *et al.* [9] developed a general reaction of benzotriazole (BtH) with aldehydes and amines for the formation of *N*-benzotriazol-1-yl adduct that can be readily displaced with nucleophiles. We used this method for the solid phase synthesis of trisubstituted 4-imidazolidinones (Scheme 1). The initial step is based on the reductive alkylation of a primary amino group of a MeBHA-resin bound amino acid [10] to form intermediate **1**. For optimization, we alkylated Ala and Phe bound to the resin with benzaldehyde, 4-nitrobenzaldehyde and 4-fluorobenzaldehyde.



Scheme 1. Synthesis of trisubstituted 4-imidazolidinones.

The second step involves reaction of the generated secondary amine with aldehyde and BtH (intermediate **2**) and subsequent intramolecular ring closure *via* nucleophilic substitution of Bt group by the amidic nitrogen. The non-stereospecific reaction was accomplished with 10 molar excess of an aldehyde (butyraldehyde, benzaldehyde, 4-nitrobenzaldehyde and anisaldehyde) and BtH in solution of anhydrous benzene under reflux with a Dean–Stark trap (8–36 h). Products **3** (24 individual compounds with two diastereoisomers each) were obtained following HF treatment, extraction and

lyophilization as white or yellowish solids in satisfactory purity and nearly quantitative yields. Obtained compounds were analyzed and characterized by LC-MS,  $^1\text{H}$  and/or  $^{13}\text{C}$  NMR. We have observed significant differences in the capability of ring closure for various substituents. All the combinations of three aromatic rings on the imidazolidinone skeleton required significant prolongation of reaction time compared to those with aliphatic substituents ( $-\text{CH}_3$  of Ala,  $-\text{CH}(\text{CH}_2)_2\text{CH}_3$  from butyraldehyde). The cyclization step using butyraldehyde provided better results in shorter time and all alanine-based imidazolidinones had a superior purity than those based on phenylalanine. The effect of 4-fluoro-, 4-methoxy- or 4-nitrophenyl groups were found to be more complex and is under further investigation. This synthesis protocol can be used to generate a variety of individual compounds or complex mixtures that will prove important in the design of new drugs having a variety of different biological activities.

#### **Acknowledgments**

This work was supported by National Cancer Institute Grant No. CA78040 (R. A. Houghten).

#### **References**

1. (a) Nefzi, A., Dooley, C., Ostresh, J.M., Houghten, R.A. *Bioorg. Med. Chem. Lett.* **8**, 2273–2278 (1998). (b) Franzen, R.G. *J. Comb. Chem.* **2**, 195–214 (2000).
2. Heck, A.J., Bonnici, P.J., Morris, D., Wills, M. *Chemistry* **7**, 910–916 (2001).
3. Fowles, L.F., Beck, E., Worrall, S., Shanley, B.C., de Jersey, J. *Biochem. Pharmacol.* **17**, 1259–1267 (1996).
4. Bak, A., Fich, M., Larsen, B.D., Frokjaer, S., Friis, G.J. *Eur. J. Pharm. Sci.* **7**, 317–323 (1999).
5. Nitta, Y., Yamaguchi, T., Tanaka, T. *Heterocycles* **24**, 25–28 (1986).
6. (a) Blank, S., Seebach, D. *Angew. Chem., Int. Ed. Engl.* **32**, 1765–1766 (1993). (b) Khalaj, A., Bazaz, R.D., Shekarchi, M. *Monatsh. Chem.* **128**, 395–398 (1997).
7. Nooshabadi, M.A., Aghapoor, K., Bolourtchian, M., Heravi, M.M. *J. Chem. Res. (S)* 498–499 (1999).
8. Gränacher, C., Mahler, M. *Chem. Ber.* **10**, 246–262 (1927).
9. Katritzky, A.R., Rachwal, S., Rachwal, B. *J. Chem. Soc., Perkin Trans. 1* 799 (1987).
10. Nefzi, A., Ostresh, J.M., Houghten, R.A. *Tetrahedron* **55**, 335–344 (1999).

## Solid Phase Synthesis of 1,2,4-Triazinan-3-ones

Yongping Yu, John M. Ostresh and Richard A. Houghten

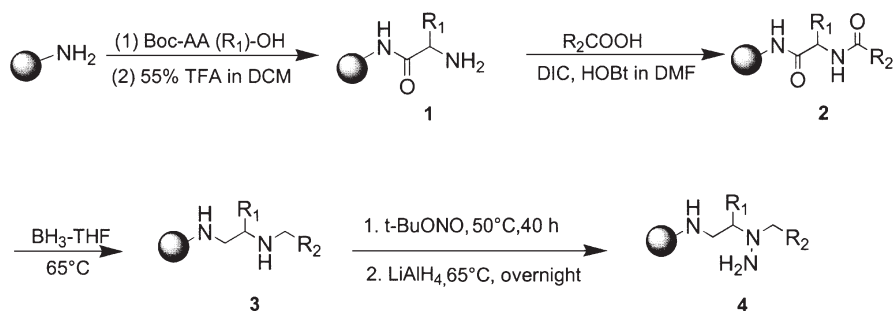
Torrey Pines Institute for Molecular Studies, San Diego, CA 92121, USA

### Introduction

Solid-phase parallel synthesis is used worldwide to generate libraries of small organic compounds in order to accelerate the drug discovery process [1]. The focus of this field of research, which initially involved the synthesis of peptides and oligonucleotides, is now on the synthesis of small organic molecules on the solid-phase. Heterocycles, such as benzodiazepines, hydantoin, pyrrolidines, and bicyclic guanidines, have received special attention in combinatorial synthesis due to their biologically interesting properties [2]. This strategy has permitted the synthesis of large numbers of heterocycles in a short time frame, enabling their use in high-throughput screening. Compounds containing the 1,2,4-triazine moiety are in use as pharmaceuticals, pesticides, herbicides *etc.* [3]. As part of our ongoing efforts directed toward the solid phase synthesis of small molecule and heterocyclic compounds and the generation of their combinatorial libraries [4], we report here an efficient method for the synthesis of 1,2,4-triazinan-3-ones from resin-bound acylated amino acid amides.

### Results and Discussion

The solid phase synthesis of 1,2,4-triazinan-3-ones is illustrated in Scheme 1. Starting from *p*-methylbenzhydrylamine (MBHA) resin-bound *N*-*tert*-butoxycarbonyl (Boc) amino acid (Boc-AA(R<sub>1</sub>)-OH) **1**, the Boc group was removed using 55% trifluoroacetic acid (TFA) in dichloromethane (DCM). The resulting free amine was *N*-acylated with a carboxylic acid (R<sup>3</sup>CO<sub>2</sub>H) in DMF using diisopropylcarbodiimide (DIC) and hydroxybenzotriazole (HOBt) as coupling reagents to give acylated peptides **2**. The exhaustive reduction of amide bonds of **2** on the solid support was performed in the presence of borane in tetrahydrofuran to generate secondary amines **3**. The resin-bound hydrazine **4** was obtained by treatment of **3** with a 20-fold excess of *t*-BuONO in THF at 50 °C for 50 h followed by reduction with lithium aluminum hydride in THF at 65 °C overnight. Treatment of the resin-bound hydrazine with carbonyldiimidazole resulted in the formation of resin-bound 1,2,4-triazinan-3-ones. The desired products **5** were readily obtained in moderate yield (25–45%) after cleavage using HF/anisole (95/5). The lower than expected yield was caused by cleavage



Scheme 1. Solid phase synthesis of 1,2,4-triazinan-3-ones.

**Yu et al.**

during the reduction of the nitrosamine with lithium aluminum hydride. The products were characterized by electrospray LC-MS under APCI conditions and  $^1\text{H}$  NMR.

In summary, we have demonstrated the feasibility of the synthesis of 1,2,4-triazinan-3-ones from acylated dipeptides on the solid phase. As in earlier studies, the described chemistries will be used to generate both individual compounds and mixture-based combinatorial libraries [4].

#### **Acknowledgments**

This work was supported by National Cancer Institute Grant No. CA78040 (RAH).

#### **References**

1. (a) Geysen, H.M., Meloen, R.H., Barteling, S.J. *Proc. Natl. Acad. Sci. U.S.A.* **81**, 3998 (1984). (b) Houghten, R.A. *Proc. Natl. Acad. Sci. U.S.A.* **82**, 5131 (1985). (c) Houghten, R.A., Pinilla, C., Blondelle, S.E., Appel, J.R., Dooley, C.T., Cuervo, J.H. *Nature* **345**, 8486 (1991).
2. Robert, G.F. *J. Comb. Chem.* **2**, 195 (2000).
3. Ashry, E.S.H.EL., Rached, N., Taha, M., Ramadan, E. *Adv. Heterocycl. Chem.* **59**, 41 (1994).
4. Houghten, R.A., Pinilla, C., Appel, J.R., Blondelle, S.E., Dooley, C.T., Eichler, J., Nefzi, A., Ostresh, J.M. *J. Med. Chem.* **42**, 3743 (1999).

## Solid-Phase Synthesis of $\alpha$ -Difluoro- $\beta$ -amino Acids by a Reformatsky Reaction

Agnès Vidal, Adel Nefzi and Richard A. Houghten

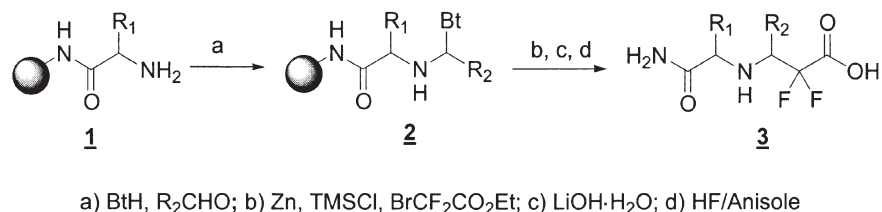
Torrey Pines Institute For Molecular Studies, San Diego, California, 92121, USA

### Introduction

Fluorine substitution is a highly effective approach for altering the chemical properties of compounds that affect the biological activity and pharmacological distribution of numerous drugs, including anti-depressants, anti-inflammatory agents, anti-psychotics, steroids, antivirals and anesthetics [1]. Given the importance of small molecule combinatorial libraries in the process of drug design, we decided to explore the synthesis of fluorinated compounds using solid-phase chemistry. The Reformatsky reaction with ethyl bromodifluoroacetate is commonly used for the incorporation of the  $-\text{CF}_2\text{CO}-$  group [2]. Katrizky *et al.* [3] successfully developed the Reformatsky reaction of bromodifluoroacetates with *N*-( $\alpha$ -aminoalkyl)benzotriazole in solution, and showed its utility in the synthesis of difluoro- $\beta$ -amino esters. Herein, we describe the solid-phase Reformatsky reaction of ethyl bromodifluoroacetate and a polymer-supported imine for the parallel synthesis of  $\alpha$ -difluoro- $\beta$ -amino acids.

### Results and Discussion

The syntheses were carried out on MBHA resin using the tea-bag technology [4]. *N*-( $\alpha$ -aminoalkyl)benzotriazole **2** was prepared from the amine **1**, an aldehyde and benzotriazole in refluxing benzene using a Dean–Stark trap [5]. The  $\alpha$ -difluorinated- $\beta$ -amino esters **3** were obtained *via* a high yielding Reformatsky reaction with ethyl bromodifluoroacetate, zinc and trimethylsilyl chloride in refluxing tetrahydrofuran (Scheme 1).



Scheme 1.

The use of a large excess of  $\text{BrZnCF}_2\text{CO}_2\text{Et}$  (12 eq) allowed the complete conversion of the benzotriazole derivatives to their difluorocarbonyl analogs. However, it also led to products of double condensation and their decarboxylated derivatives. This problem of overaddition has been described with lithium enolates from *tert*-butyl difluoroacetate and their reaction with electrophiles [6]. Using 24 equivalents of Reformatsky reagent with repeated condensations, we observed a triple addition product. Using a secondary amine (*N*-alkylated amino acid or proline) as starting material, the aldehyde/benzotriazole treatment led to the formation of imidazolidinones as exclusive products before cleavage with HF. No Reformatsky product was detected. These cyclic compounds were also obtained from primary amines upon HF treatment of the benzotriazole derivatives **2**. We examined the feasibility of the reaction de-

scribed in Scheme 1 using five L-amino acids (Phe, Val, Ala, Gly, Leu) and six aldehydes (benzaldehyde, 2-nitrobenzaldehyde, 2-fluorobenzaldehyde, *p*-methoxy-benzaldehyde, 2,5-dimethylbenzaldehyde and 3-furaldehyde). All compounds were characterized by LC-MS. Six selected compounds have been purified and fully characterized by NMR ( $^1\text{H}$ ,  $^{13}\text{C}$ , 2D-COSY, HMBC and HMQC). In all cases, two diastereoisomers were obtained, except for the glycine derivative that gave non-separable enantiomers. The absolute configurations of the diastereoisomers were determined by NOE difference spectroscopy. The (*R,S*) diastereoisomers were always the more polar. The reactivities of aryl- and alkylaldehydes were shown to be similar. This procedure was also applied directly to the MBHA resin, leading to the corresponding primary  $\alpha$ -difluoro- $\beta$ -amino acids.

In summary, we have explored a solid-phase method for the conversion of primary amines to  $\alpha$ -difluoro- $\beta$ -amino acids by condensation of an amine, an aldehyde, benzotriazole and a Reformatsky reagent prepared *in situ* from ethyl bromodifluoroacetate, trimethylsilyl chloride and zinc. These derivatives represent a useful tool for the generation of large libraries of fluorinated peptide analogs. Furthermore, the presence of the carboxyl group permits a wide range of possible transformations.

#### Acknowledgments

This work was supported by National Cancer Institute Grant No. CA78040 (RAH).

#### References

1. Park, B.K., Kitteringham, N.R., O'Neill, P.M. *Annu. Rev. Pharmacol. Toxicol.* **41**, 443–470 (2001).
2. Hallinan, E.A., Fried, J. *Tetrahedron Lett.* **25**, 2301–2302 (1984).
3. Katritzky, A.R., Nichols, D.A., Qi, M. *Tetrahedron Lett.* **39**, 7063–7066 (1998).
4. Houghten, R.A. *Proc. Natl. Acad. Sci. U.S.A.* **82**, 5131–5135 (1985).
5. Katritzky, A.R., Lan, X., Yang, J.Z., Denisko, O.V. *Chem. Rev.* **98**, 409–548 (1998).
6. Taguchi T., Kitagawa O., Morikawa T., Nishiwaki T., Uehara H., Endo H., Kobayashi Y. *Tetrahedron Lett.* **27**, 6103–6106 (1986).

## Peptidotriazoles: Copper(I)-Catalyzed 1,3-Dipolar Cycloadditions on Solid-Phase

Christian W. Tornøe and Morten Meldal

Center for Solid Phase Organic Combinatorial Chemistry, Department of Chemistry,  
 Carlsberg Laboratory, DK-2500 Valby, Denmark

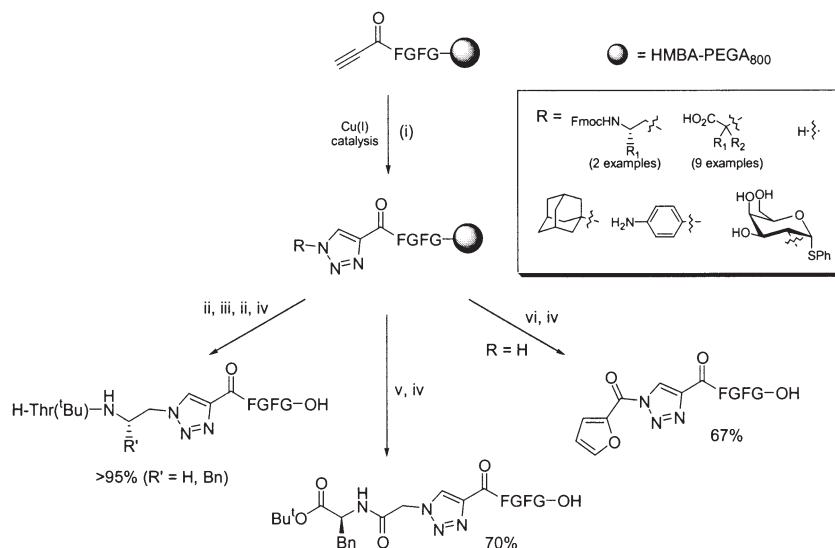
### Introduction

[1,2,3]-Triazoles are important pharmacophores in medicinal chemistry and it is therefore important to develop synthetic methods for triazoles that are both mild, high yielding and applicable to combinatorial synthesis. [1,2,3]-Triazoles are typically prepared by refluxing an alkyne and an azide in toluene (110 °C), but the 1,3-dipolar cycloaddition has also been performed at lower temperatures by using sodium acetylide [1], lithium and magnesium acetylide [2,3] with varying success. The present work describes the preparation of [1,2,3]-triazoles at 25 °C on solid-phase with high yields (80–95%), and is compatible with Fmoc chemistry.

### Results and Discussion

A very mild and efficient method for preparing [1,2,3]-triazoles on solid-phase is presented using Cu(I) to catalyze the 1,3-dipolar cycloaddition giving only one regioisomer, the 1,4-substituted [1,2,3]-triazole. The catalytic mechanism has not been determined, but it is known that Cu(I) readily coordinates terminal alkynes in the presence of base [4]. Cu(I) presumably polarizes the triple bond and thereby catalyzes the cycloaddition.

Fifteen different azides including  $\alpha$ -azido acids, aryl, alkyl and sugar substituted azides have been used in the Cu(I)-catalyzed 1,3-dipolar cycloaddition, with

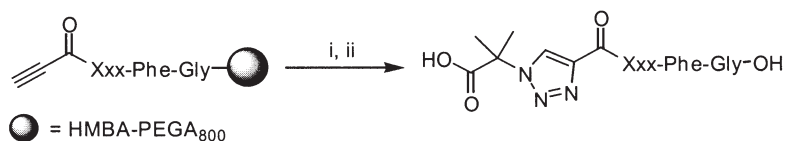


*Scheme 1.* (i)  $R\text{-N}_3$ , Cu(I), DIPEA, THF, 25 °C; (ii) 20% piperidine/DMF; (iii) Fmoc-Thr(<sup>t</sup>Bu)-OPfp, DMF; (iv) 0.1 M NaOH; (v) H-Phe-O<sup>t</sup>Bu, PyAOP, HOAt, DIPEA, DMF; (vi) 2-Furoyl chloride, DIPEA, DCM.

**Tornøe et al.**

resin-bound propargylic acid displaying high conversion and purities determined by RP-HPLC (conversion >95% and purity ranging from 84–95%).

Several triazoles have been further functionalized as illustrated in Scheme 1 giving a diverse set of products. The stability of important protecting groups in Fmoc chemistry (<sup>t</sup>Bu, Trt, Boc and Pmc) was examined as well as the compatibility of the Cu(I)-catalyzed 1,3-dipolar cycloaddition with SPPS (see Scheme 2 and Table 1). All



Scheme 2. (i)  $N_3C(CH_3)_2CO_2H$ , Cu(I), DIPEA, THF, 25 °C; (ii) 0.1 M NaOH.

Table 1. Results from the 1,3-dipolar cycloaddition in Scheme 2.

	Xxx	Conversion (purity)	Ret. time min	ES-MS found (MNa <sup>+</sup> )	MNa+ calc.
17	Ala	>95% (>95%)	10.5	497.0	497.2
18	Pro	>95% (>95%)	11.3	523.0	523.2
19	Thr( <sup>t</sup> Bu)	>95% (>95%)	14.2	583.0	583.3
20	Tyr( <sup>t</sup> Bu)	>95% (>95%)	14.9	645.1	645.3
21	Asp( <sup>t</sup> Bu)	>95% (>95%)	13.3	597.1	597.2
22	Asn(Trt)	>95% (90%)	16.7	782.4	782.3
23	His(Trt)	>95% (80%)	15.7	783.4 <sup>a</sup>	783.3 <sup>a</sup>
24	Cys(Trt)	>95% (81%)	18.4		771.3
25	Met	>95% (85%)	12.0	557.6	557.2
26	Lys(Boc)	>95% (>95%)	13.7	654.1	654.3
27	Trp(Boc)	>95% (>95%)	16.8	712.0	712.3
28	Arg(Pmc)	>95% (88%)	16.2	848.2	848.4

<sup>a</sup> MH<sup>+</sup>.

the protecting groups used were stable to the reaction conditions, so the regiospecific copper(I)-catalyzed cycloaddition is compatible with Fmoc-based SPPS. In conclusion, a mild and efficient method for preparing [1,2,3]-triazoles on solid-phase has been presented and a diverse set of 1,4-substituted [1,2,3]-triazoles have been synthesized.

## Acknowledgments

This work was supported by the Danish National Research Foundation.

## References

1. Boyer, J.H., Mack, C.H., Goebel, N., Morgan, Jr., L.R. *J. Org. Chem.* **23**, 1051–1053 (1958).
2. Akimova, G.S., Chistokletov, V.N., Petrov, A.A. *Chem. Abstr.* **67**, 100071a (1967).
3. Akimova, G.S., Chistokletov, V.N., Petrov, A.A. *Chem. Abstr.* **68**, 105100q (1968).
4. Hopkinson, A.C., In Patai, S. (Ed.) *The Chemistry of the Carbon-Carbon Triple Bond*, Interscience Publishers, London, 1978, pp. 75–136.

## Solid-Phase Synthesis of Lidocaine Analogues Using Backbone Amide Linker (BAL) Anchoring

Simon K. Shannon<sup>1</sup>, Steven A. Kates<sup>2</sup> and George Barany<sup>1</sup>

<sup>1</sup>University of Minnesota, Minneapolis, MN, 55414, USA

<sup>2</sup>Consensus Pharmaceuticals, Inc., Medford, MA 02155, USA

### Introduction

Previous studies from our laboratory reported on Backbone Amide Linker (BAL) anchoring approaches for solid-phase syntheses of C-terminal modified and cyclic peptides [1], diketopiperazines [2], peptide aldehydes [3], unprotected peptide *p*-nitroanilides and thioesters [4], and peptides containing prolyl, *N*-alkylaminoacyl, and histidyl groups at the C-terminus [5]. The BAL methodology [6] and variations have been extended to the solid-phase syntheses of non-peptidic small organic molecules such as benzodiazepines, hydroxamic acids, 2,9-substituted purines, modified amino sugars, 1,3-bis(acylamino)-2-butanones, benzimidazoles, hapalosin mimetics, quinoxalinones, heterocyclic ethylenediamine-derivatized libraries, *N,N'*-disubstituted ureas, and perhydroimidazo[1,5-*a*]pyrazines. As an addition to the types of compounds accessible *via* BAL anchoring, we describe herein an attractive solid-phase synthesis of lidocaine, a common antiarrhythmic drug, and several analogues.

### Results and Discussion

The general strategy (Figure 1) involves four key steps: (i) attachment of an aromatic or primary aliphatic amine to the solid support *via* reductive amination; (ii) acylation using bromoacetic acid to give a halogen substituted adduct; (iii) *N*-alkyl substitution by displacement of the halogen with a secondary amine; and (iv) trifluoroacetic acid (TFA) mediated cleavage from the solid support.

A manual 4 × 7 parallel synthesis was carried out. Reductive aminations (Figure 1, step b) were performed using the following primary aromatic and aliphatic amines: 2,6-dimethylaniline, aniline, benzylamine, *n*-butylamine, tetrahydrofurfurylamine,

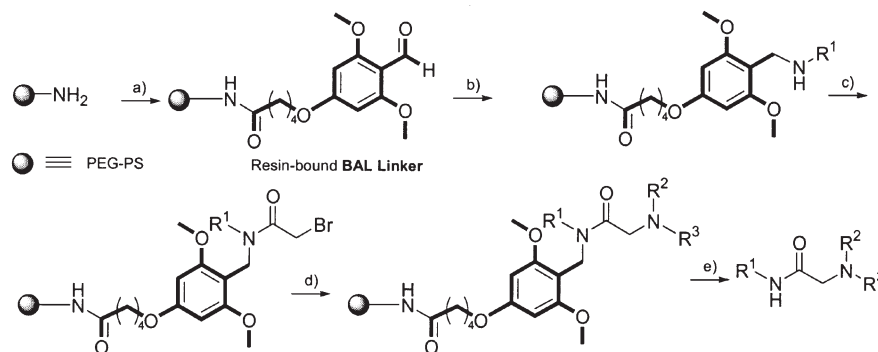


Fig. 1. BAL strategy for the synthesis of lidocaine analogues. Reagents and conditions: (a) BAL Linker, HATU, DIEA, in DMF, 24 h; (b)  $R^1$ -NH<sub>2</sub>, NaCNBH<sub>3</sub>, in MeOH or  $R^1$ -NH<sub>2</sub>, Na(OAc)<sub>3</sub>BH, in 1,2-dichloroethane, 24 h; (c) bromoacetic acid, DIPCDI, in DMF, 2 × 0.5 h; (d) HNR<sup>2</sup>R<sup>3</sup>, in DMF, 4 h, 75 °C; (e) TFA-H<sub>2</sub>O (19 : 1), 5 h. Temperatures 25 °C unless indicated otherwise.

cyclohexylamine, and *n*-propylamine. Reactivities were excellent for most amines when using sodium cyanoborohydride as the reducing agent, but transformations of anilines required the use of sodium triacetoxyborohydride in the presence of catalytic amounts of acetic acid [7].

Acylation with bromoacetic acid proceeded smoothly (Figure 1, step c). Four secondary amines (diethylamine, dipropylamine, *N*-ethylmethylaniline and piperidine) were used for R<sup>2</sup> and R<sup>3</sup> diversity. *N*-alkyl substitution (Figure 1, step d) proceeded to completion when the resin was heated at 75 °C for 4 h and the secondary amine was used in large excess [co-solvent with DMF (amine–DMF, 1 : 1)]. TFA-mediated cleavages (Figure 1, step d) produced the substituted amides in yields ranging from 40–88% and crude purities as high as 97%. Initial purity appears to be dependent on the success of the reductive amination step, which involves the attachment of R<sup>1</sup> to the resin-bound BAL linker.

#### Acknowledgments

We thank Christopher Gross, T. Scott Yokum, and Jordi Alsina for helpful discussions. Research at Minnesota was supported by the National Institutes of Health (GM 42722).

#### References

1. Jensen, K.J., Alsina, J., Songster, M.F., Vagner, J., Albericio, F., Barany, G. *J. Am. Chem. Soc.* **120**, 5441–5452 (1998).
2. Fresno, M., Alsina, J., Royo, M., Barany, G., Albericio, F. *Tetrahedron Lett.* **39**, 2639–2642 (1998).
3. Guillaumie, F., Kappel, J.C., Kelly, N.M., Barany, G., Jensen, K.J. *Tetrahedron Lett.* **41**, 6131–6135 (2000).
4. Alsina, J., Yokum, T.S., Albericio, F., Barany, G. *J. Org. Chem.* **64**, 8761–8769 (1999).
5. Alsina, J., Yokum, T.S., Albericio, F., Barany, G. *Tetrahedron Lett.* **41**, 7277–7280 (2000).
6. For a review, see Alsina, J., Jensen, K.J., Albericio, F., Barany, G. *Chem. Eur. J.* **5**, 2787–2795 (1999).
7. Abdel-Magid, A.F., Carson, K.G., Harris, B.D., Maryanoff, C.A., Shah, R.D. *J. Org. Chem.* **61**, 3849–3862 (1996).

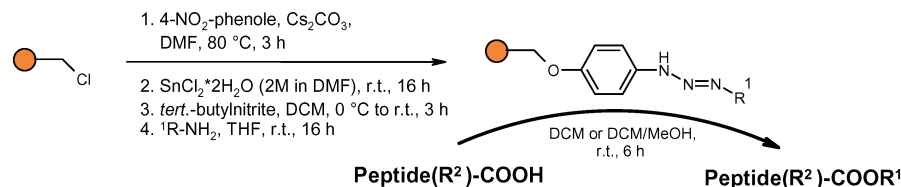
## Solid-Supported Triazenes as Alkylating Polymers Employed for the Versatile Derivatization of Peptides

Joachim Smerdka, Tobias Seyberth, Dietmar G. Schmid, Günther Jung and Jörg Rademann

University of Tübingen, Institute of Organic Chemistry, 72076 Tübingen, Germany

### Introduction

Recently, we have shown polymer-bound 1-aryl-3-alkyl-triazenes to be versatile tools for the smooth esterification of various carboxylic acids [1], including peptides and products of combinatorial synthesis [2]. The triazenes are prepared in a 4-step synthesis on Merrifield resin. They react with carboxylic acids under loss of nitrogen and release of highly reactive carbenium ions forming the corresponding esters (Scheme 1).



Scheme 1. Alkylation of carboxylic acids by polymer-bound triazenes.

The reaction is best performed in DCM containing up to 50 vol.% MeOH. Common alkylating reagents (*e.g.* diazoalkanes, alkyl halides or dialkylsulfonates) are often toxic or even explosive. Activation of carboxy groups of peptides for esterification also shows significant disadvantages (hydroxy groups need to be protected, long reaction times and racemization). For this reason we developed a novel esterification procedure for complex cyclic- and polypeptides allowing the selective transfer of protective groups (methyl, benzyl, allyl) as well as the introduction of additional functionality and structural diversity.

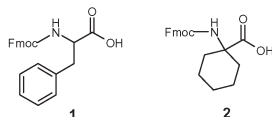
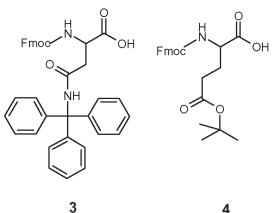
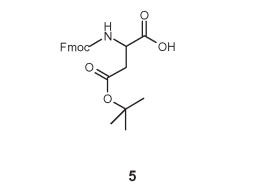
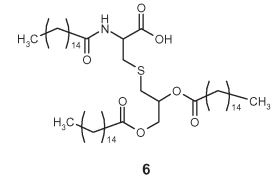
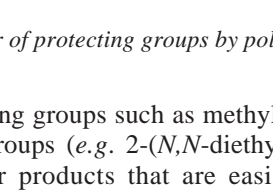
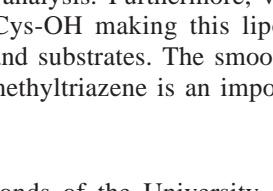
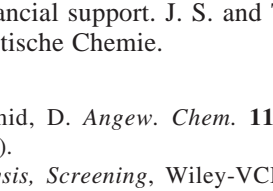

### Results and Discussion

Polymer-bound triazenes carrying various alkyl moieties have been reacted with several selected carboxylic acids bearing a broad range of functionality [1].

Due to the excellent purities of the resulting esters, the method is particularly suitable for parallel combinatorial synthesis.

Next we investigated the use of the polymeric reagent for the modification of peptidic structures. Several polymer bound triazenes were synthesized from various amines differing in polarity and basicity. These triazenes were then reacted with various peptides, amino acids, and amino acid derivatives such as Pam<sub>3</sub>Cys-OH. Thus we were able to introduce protecting groups such as methyl, allyl, and benzyl to amino acids and a fully protected pentadecapeptide as well as a fluoresceine-labelled nonapeptide. The lipophilic amino acid derivative Pam<sub>3</sub>Cys-OH was converted into the corresponding methyl ester, and even the derivatization with 13-amino-4,7,10-trioxa-tridecan-1-yl (amino-PEG-200) was successful. All products were obtained in good to excellent purities. The results are shown in Scheme 2.

In summary, we present the use of polymer-bound alkyl triazenes for the fast and efficient conversion of amino acids and peptides into their C-terminally functionalized

Entry	Substrate	Alkyl moiety	<i>m/z</i>	
1	1	Methyl-	402.2 [M+H]	
2	1	Benzyl-	478.2 [M+H]	
3	1	2-(Morpholin-1-yl)ethyl-	501.2 [M+H]	
4	1	2-(Pyrid-2-yl)ethyl-	493.2 [M+H]	
5	2	2-(Morpholin-1-yl)ethyl	479.2 [M+H]	
6	2	2-( <i>N,N</i> -Diethylamino)ethyl-	465.3 [M+H]	
7	3	2-(Morpholin-1-yl)ethyl-	710.3 [M+H]	
8	4	2-(Pyrid-2-yl)ethyl-	531.2 [M+H]	
9	5	2-( <i>N,N</i> -Diethylamino)ethyl-	483.3 [M+H]	
10	6	Methyl-	924.8 [M+H]	
11	6	Amino-PEG-200	1113.9 [M+H]	
12	7	Methyl-	1066.2 [M+3H] <sup>3</sup>	
13	7	Allyl-	1074.9 [M+3H] <sup>3</sup>	
14	7	Benzyl-	1091.6 [M+3H] <sup>3</sup>	
15	8	Methyl-	760.4 [M+2H] <sup>2</sup>	

Scheme 2. Derivatization of amino acids and peptides and transfer of protecting groups by polymer-bound triazenes.

derivatives. The method allows the introduction of protecting groups such as methyl-, allyl-, and benzyl- as well as the introduction of basic groups (*e.g.* 2-(*N,N*-diethylamino)ethyl- or 2-(morpholin-1-yl)ethyl-) yielding polar products that are easily protonated, thus providing an excellent label for ES-MS analysis. Furthermore, we were able to prepare an amino-PEG-200 labelled Pam<sub>3</sub>Cys-OH making this lipopeptide compatible with a wider range of polar solvents and substrates. The smooth C-terminal methylation of peptides with polymer-bound methyltriazene is an important tool for peptide derivatization for GC-MS.

### Acknowledgments

J. R. thanks Prof. M. E. Maier, Tübingen, the Strukturfonds of the University of Tübingen, and Merck KGaA, Darmstadt, Germany for financial support. J. S. and T. S. received a grant from the DFG Graduiertenkolleg Analytische Chemie.

### References

1. Rademann, J., Smerdka, J., Jung, G., Grosche, P., Schmid, D. *Angew. Chem.* **113**, 390–393 (2001); *Angew. Chem., Int. Ed.* **40**, 381–385 (2001).
2. Jung, G. (Ed.) *Combinatorial Chemistry, Synthesis, Analysis, Screening*, Wiley-VCH, Weinheim, 1999.

## Oxidation of Threonine and Serine Residues on Solid-Phase: Pyrazine Formation by Dess–Martin Periodinane Oxidation

Caspar Christensen and Morten Meldal

Carlsberg Research Center, Gamle Carlsberg Vej 10, DK-2500 Valby, Denmark

### Introduction

In recent years, solid phase synthesis has emerged as a powerful tool for creating large numbers of highly diverse compounds for utilization in various screening protocols. Libraries of organic molecules and peptides have proven to be highly efficient for the discovery process of new therapeutic lead compounds [1]. During the course of studies on carbonyl-formation on solid phase [2], we were interested in the oxidation of threonine and serine residues in a peptide on solid phase for the cyclization to a pyrazine ring. Dess–Martin periodinane (DMP) has been used for facile and efficient oxidations of primary and secondary alcohols to aldehydes and ketones, respectively, in solution [3]. It was expected that applying the Dess–Martin periodinane oxidation on solid phase would result in a novel pyrazine formation when a penultimate N-terminated threonine or serine was oxidized.

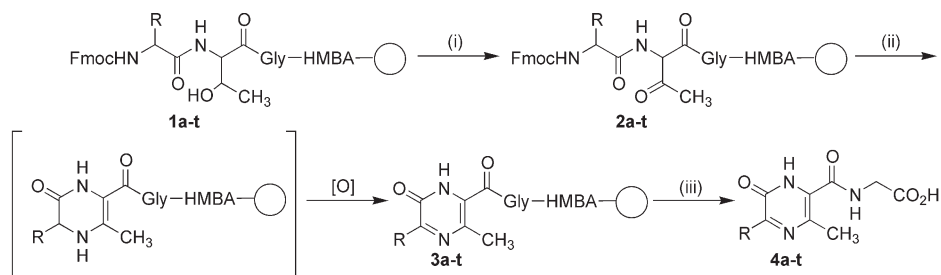


Fig. 1. Formation of pyrazine by oxidation. (i) Dess–Martin periodinane (DMP) (7.5 eq.) in  $\text{CH}_3\text{CN}$ , overnight; (ii) 20% Pip/DMF, then TFA (95%)/TIPS (2.5%) where necessary; (iii) NaOH (0.1 M).

### Results and Discussion

All solid phase reactions were performed on PEGA<sub>800</sub>. The oxidation of the  $\beta$ -hydroxy functionality of either the threonine or serine residue was investigated in a tripeptide containing an N-terminal phenylalanine, a threonine or serine residue, and a glycine, which was attached to the base labile HMBA (4-hydroxymethylbenzoic acid) linker (Figure 1). Oxidation with DMP in acetonitrile overnight proved to be optimal. Negative Kaiser tests were observed immediately after the removal of the Fmoc-group indicating a fast imine formation of the N-terminal amino group with the  $\beta$ -keto group of the adjacent amino acid residue. Only the threonine oxidation products formed a pyrazine ring. The N-terminal positions were randomised with the naturally occurring amino acids or DAP (diamino propanoic acid) and the pyrazine formation was tested (Table 1). The 6-membered 1,6-dihydro-1H-pyrazin-2-one was never isolated due to a fast air oxidation to 1H-pyrazin-2-one. The Boc-protected lysine or DAP residue af-

Table 1. Successful conversion to the 1*H*-pyrazin-2-one moiety.

Compound	Amino	ES-MS	Pyrazine
<b>3a</b>	Gly	211.9/212.1	65
<b>3b</b>	Ala	226.0/226.1	76
<b>3c</b>	Val	254.1/254.1	64
<b>3d</b>	Leu	268.0/268.1	65
<b>3e</b>	Ile	268.1/268.1	59
<b>3f</b>	Glu( <sup>t</sup> Bu)	282.1/282.1 <sup>a</sup>	91
<b>3g</b>	Gln(Trt)	–/283.1	88
<b>3h</b>	Asp( <sup>t</sup> Bu)	–/270.1	0
<b>3i</b>	Asn(Trt)	–/269.1	0
<b>3j</b>	Lys(Boc)	283.1/283.1	73
<b>3k</b>	Arg(Pmc/Boc <sub>2</sub> )	–/325.2	0
<b>3l</b>	His(Trt)	292.0/292.1	45
<b>3m</b>	Trp(Boc)	363.2 <sup>b</sup> /341.1	0
<b>3n</b>	Ser( <sup>t</sup> Bu)	–/242.2	0
<b>3o</b>	Thr( <sup>t</sup> Bu)	–/256.1	57
<b>3p</b>	Phe	302.0/302.1	>95
<b>3q</b>	Tyr( <sup>t</sup> Bu)	–/318.1	0
<b>3r</b>	Cys(Trt)	–/258.1	0
<b>3s</b>	Met	–/272.1	0
<b>3t</b>	DAP(Boc)	241.0/241.1	26

<sup>a</sup> Negative mode. <sup>b</sup> Two peaks corresponding to oxidation.

forded an amino functionality which served for further peptide synthesis or reacted with other acylating agents upon deprotection.

In conclusion, we have demonstrated a new method for the oxidation of threonine and serine residues that are adjacent to an *N*-terminal amino residue on solid phase. The cyclization to the substituted aromatic 1*H*-pyrazin-2-one has been observed for oxidized threonine residues in moderate to very good yields. Further investigations are underway to elucidate the potential of the 1*H*-pyrazin-2-one formation in libraries for screening for potential drug candidates.

### Acknowledgments

This work was supported by the Danish National Research Foundation and Osteopro A/S.

### References

1. Jung, G. *Combinatorial Peptide and Non-Peptide Libraries: A Handbook*. VCH, Weinheim, New York, Basel, Cambridge, Tokyo, 1996.
2. (a) Papanikos, A., et al. *J. Am. Chem. Soc.* **123**, 2176 (2001). (b) Groth, T., Meldal, M. *J. Comb. Chem.* **3**, 34 (2001). (c) Graven, A., et al. *J. Chem. Soc., Perkin Trans. 1* **6**, 955 (2000).
3. Dess, D.B., Martin, J.C. *J. Org. Chem.* **48**, 4155 (1983).

## A Novel Solid Phase Approach to Thioether Cyclized Peptides: Discovery of Mouse Melanocortin-1 Receptor Agonists

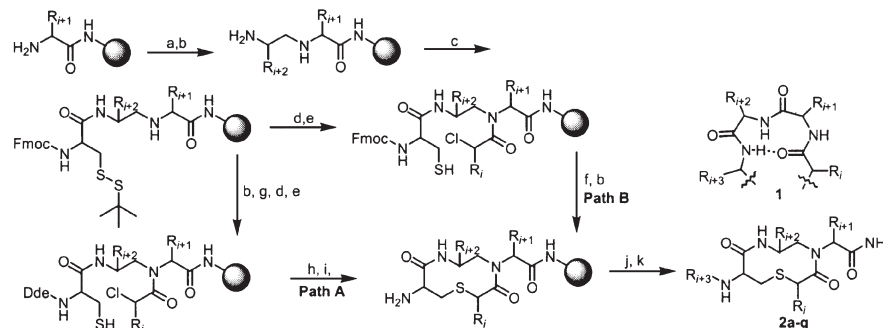
Jon Bondebjerg<sup>1</sup>, Morten Meldal<sup>1</sup>, Rayna M. Bauzo<sup>2</sup> and  
 Carrie Haskell-Luevano<sup>2</sup>

<sup>1</sup>Carlsberg Laboratory, Department of Chemistry, 2500 Valby, Denmark

<sup>2</sup>Department of Medicinal Chemistry, University of Florida, Gainesville, FL 32610-0485, USA

### Introduction

The  $\beta$ -turn **1** is both one of the most abundant motifs of peptide and protein secondary structure, and one of the key recognition elements in biological systems. In recent years the design of conformationally constrained peptidomimetics and small molecule  $\beta$ -turn mimics has been pursued with significant effort. Such peptidomimetic scaffolds can provide potential drug leads, as well as a better understanding of molecular recognition. We have prepared a range of novel heterocyclic peptidomimetics with the general structure **2** (Scheme 1, Figure 1, Table 1).



Scheme 1. Reagents and conditions: Rink-NH-PEGA<sub>800</sub> resin a) Fmoc-AA-H, NaBH<sub>3</sub>CN, AcOH/DMF; b) 20% piperidine/DMF; c) Fmoc-Cys(SBu<sup>t</sup>)-OH, TBTU, NEM, DMF; d) Cl(R<sub>i</sub>)CHCOX, base, DCM; e) Bu<sub>3</sub>P/H<sub>2</sub>O/THF; f) NEM, DMF,  $\Delta$ ; g) 2-acetyldimedone, DMF; h) DBU, DMF; i) 3% hydrazine/DMF; j) R<sub>i+3</sub>CHO, NaBH<sub>3</sub>CN, AcOH/DMF; k) TFA/TIPS.

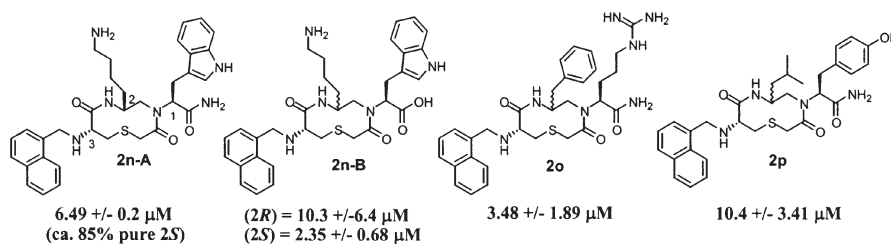


Fig. 1. EC<sub>50</sub> values for HPLC purified compounds tested for agonist activity at the mouse melanocortin-1 receptor [1] (mMC1R), using a  $\beta$ -galactosidase bioassay [2,3]. The results were determined from at least three independent experiments. **2o** and **2p** were both tested as a mixture of isomers.

Table 1. Synthesis of scaffold 2.

	R <sub>i</sub> <sup>a</sup>	R <sub>i+1</sub> <sup>a</sup>	R <sub>i+2</sub> <sup>a</sup>	R <sub>i+3</sub> <sup>a</sup>	Purity <sup>b</sup> (crude)	MS(calc./found) (MH <sup>+</sup> )	Path
<b>2a</b>	H	Nap	D-Lys(Boc)	Napht	58	612.29/612.02	A
<b>2b</b>	H	Nap	Lys(Boc)	Napht	64	612.29/612.10	A
<b>2c</b>	H	Nap	Arg(Boc) <sub>2</sub>	Napht	55	640.30/640.03	A
<b>2d</b>	H	Phe	D-Lys(Boc)	Napht	66	562.28/562.28	A
<b>2e</b>	H	Phe	Lys(Boc)	Napht	75	562.28/562.40	A
<b>2f</b>	H	Phe	Pro <sup>c,d</sup>	Napht	54	531.24/531.22	A
<b>2g</b>	C <sub>6</sub> H <sub>5</sub>	Phe	Gly <sup>d,e</sup>	H	42	427.53/427.22	A
<b>2h</b>	H	Trp(Boc)	Pro <sup>c,d</sup>	Napht	55	570.25/570.04	A
<b>2i</b>	H	Trp(Boc)	D-Lys(Boc)	Napht	71	601.29/601.32	A
<b>2j</b>	H	Tyr(Bu <sup>†</sup> )	D-Lys(Boc)	Napht	73	578.27/578.17	A
<b>2k</b>	H	Tyr(Bu <sup>†</sup> )	Lys(Boc)	Napht	83	578.27/578.21	A
<b>2l</b>	H	Tyr(Bu <sup>†</sup> )	Pro <sup>c,d</sup>	Napht	74	547.23/548.10	A
<b>2m</b>	H	FFG <sup>g</sup>	Gly <sup>d,e</sup>	Aloc	65	639.25/639.20	A <sup>h</sup>
<b>2n</b>	H	Trp(Boc)	Lys(Boc)	Napht	75	601.29/601.24	B
<b>2o</b>	H	Arg(Pmc)	Phe	Napht	57 <sup>i</sup>	450.22/451.13 <sup>i</sup>	B
<b>2p</b>	H	Tyr(Bu <sup>†</sup> )	Leu	Napht	52 <sup>i</sup>	423.20/424.14 <sup>i</sup>	B
<b>2q</b>	H	FLG <sup>g</sup>	Phe	Phe	88	758.36/758.40	B

Nap = 1-naphthylalanine; Napht = 1-naphthyl; Aloc = allyloxycarbonyl

<sup>a</sup> The three letter code refers to the side chain of the starting amino acid. <sup>b</sup> Determined by RP-HPLC monitored at 215 nm. The products were obtained as a diastereomeric mixture; furthermore MALDI-TOF MS analysis revealed that partial hydrolysis of the C-terminal amide occurred during TFA cleavage. <sup>c</sup> The reduced bond was temporarily protected with Aloc.

<sup>d</sup> Fmoc-Cys(Mmt)-OH used instead of Fmoc-Cys(SBu<sup>†</sup>)-OH. <sup>e</sup> Reduced bond introduced as the protected dipeptide building block. <sup>f</sup> Contains a D-Cys. <sup>g</sup> One letter code for amino acids.

<sup>h</sup> Cyclization performed from Aloc instead of Dde. <sup>i</sup> Determined prior to introduction of R<sub>i+3</sub>

## Results and Discussion

NMR studies revealed that **2n** existed as a mixture of three rotamers/conformers at room temperature. Heating caused coalescence of the isomeric resonances.

In conclusion we have developed a solid phase approach to the novel combinatorial scaffold **2**. The overall crude purity is moderate to very good, and the compounds showed agonist activity at the mouse melanocortin-1 receptor in the low micromolar range. The methodology is currently being expanded to larger cyclic structures for the use as a general approach to potential disulfide bond mimetics of bioactive peptides.

## Acknowledgments

This work was supported by the Danish National Research Foundation.

## References

1. Cone, R.D., Lu, D., Koppula, S., Vage, D.I., Klungland, H., Boston, B., Chen, W., Orth, D.N., Pouton, C., Kesterton, R.A. *Recent Prog. Horm. Res.* **51**, 287–318 (1996).
2. Chen, W., Shields, T.S., Stork, P.J.S., Cone, R.D. *Anal. Biochem.* **226**, 349–354 (1995)
3. Haskell-Luevano, C., Rosenquist, Å., Sours, A., Kong, K., Ellman, J., Cone, R.D. *J. Med. Chem.* **42**, 4380–4387 (1999).

## Bifurcated Dipeptide Schiff Bases as Ligands for Enantioselective Catalysis: Micro-Metalloenzymes

Robin Polt, Brian Dangel, Bhaskar Tadikonda and Brian Kelly

Department of Chemistry, University of Arizona, Tucson, AZ 85721, USA

### Introduction

Enantioselective catalysis mediated by transition metals complexed to enantiomerically pure ligands has become an important feature in organic synthesis. While numerous ligands have been designed for this purpose, and many have used amino acids as a source of chirality, only a very few (*c.f.* Belokon [1]) have used amino acids or peptides directly for this purpose. We have discovered that the use of highly hindered benzophenone imines as N-terminal capping groups imparts a chiral “twist” to the resulting transition metal complexes [2], and that this feature can be exploited to produce enantioselective catalysts. Use of Merrifield- or Wang-type resins and solid-phase peptide synthesis allows for the facile construction of ligand arrays, which facilitates “catalyst discovery” *via* parallel or combinatorial approaches.

### Results and Discussion

Construction of the linkers was accomplished from Merrifield resin, or from bromo-Wang resin (Figure 1). Displacement of chloride, or bromide with the cesium salt of *para*-cyanophenol can be monitored by elemental analysis of the resin for halide, or by IR (CN stretch). Addition of ArMgBr can be monitored by IR as well.

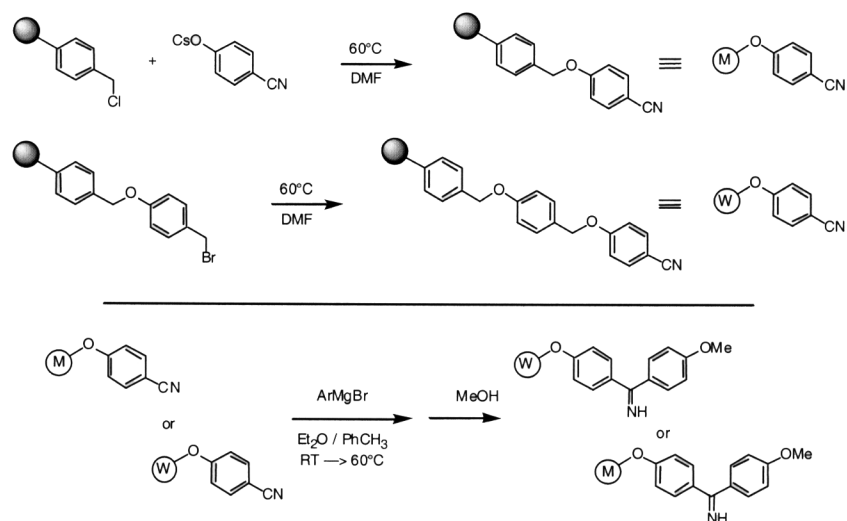


Fig. 1. Displacement by cesium phenoxides and Grignard addition is essentially quantitative.

Condensation of a Phe<sub>2</sub>-, Ala<sub>2</sub>-, or Val<sub>2</sub>-substituted phenylenediamine followed by “capping” with Ph<sub>2</sub>C=NH provided 3 sets of chiral ligands, with pseudo-C<sub>2</sub> symmetry (Figure 2). Both condensation reactions were catalyzed with camphorsulfonic acid. The required bis-acylated diamines were produced using classical methods with the appropriate *t*-Boc-protected amino acids and *o*-phenylenediamine.

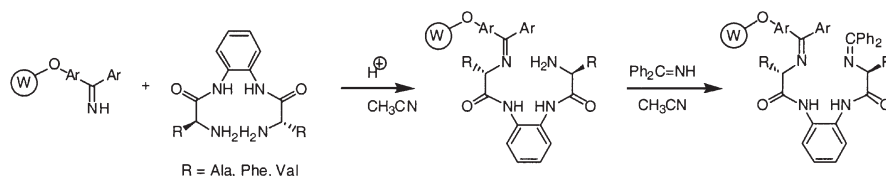


Fig. 2. Acid-catalyzed condensation of the bifurcated dipeptides and capping with  $Ph_2C=NH$ .

Treatment of these resin-bound ligands with  $NiCl_2$ ,  $CuBr_2$ ,  $CoCl_2$  or  $Et_2Zn$  at 0 °C (Cu and Co) or 60 °C (Ni and Zn) resulted in the insertion of the transition metal, and a profound color change for Ni, Cu and Co. For the Zn-complex, addition of an aliphatic or aromatic aldehyde and a dialkylzinc at 0 °C resulted in efficient conversion of the aldehyde to the corresponding 2° alcohol with high enantioselectivity (85–91% e.e. for Phe and Val), and lower e.e.'s for Ala (Figure 3) [3]. Further work with this chemistry has led to approaches for the synthesis of ligand arrays ( $R^1 \neq R^2$ ) with additional axial ligand binding sites for the transition metal, cleavage of the complexes, and regeneration of the ketimine linker.

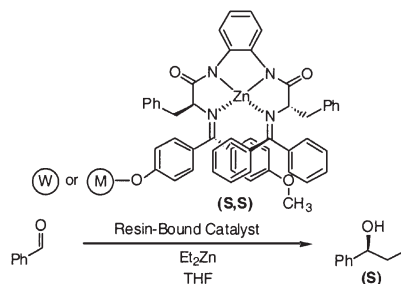


Fig. 3. Catalysis of the Soai Reaction with resin-bound Zn-complex ( $\approx 3\%$  catalyst).

## Acknowledgments

We would like to thank the National Science Foundation and the U.S. Army for support of this work.

## References

1. Belokon, Y.N., Chernoglazova, N.I., Kochetkov, C.A., Garbalinskaya, N.S., Belikov, V.M. *J. Chem. Soc., Chem. Commun.* 171–172 (1985).
2. Dangel, B., Clarke, M.; Haley, J., Sames, D., Polt, R. *J. Am. Chem. Soc.* **119**, 10865–10866 (1997).
3. Dangel, B.D., Polt, R. *Org. Lett.* **2**, 3003–3006 (2000).

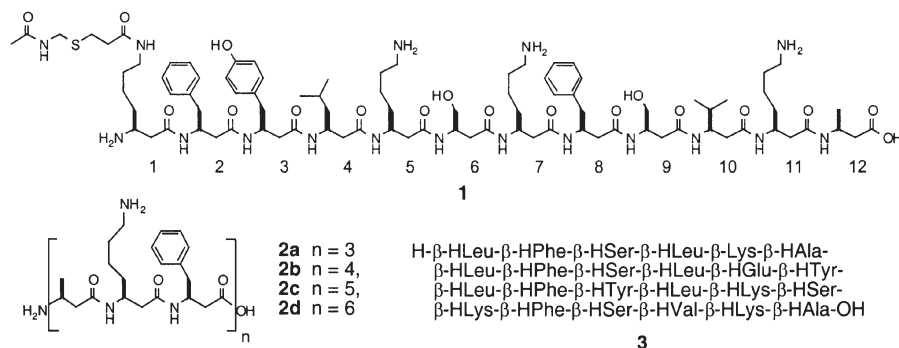
## Recent Advances in the Solid-Phase Synthesis of Long-Chain $\beta$ -Peptides

Jens Frackenkohl, Jürg V. Schreiber, Per I. Arvidsson and  
 Dieter Seebach

*Laboratorium für Organische Chemie der Eidgenössischen Technischen Hochschule,  
 CH-8092 Zürich, Switzerland*

### Introduction

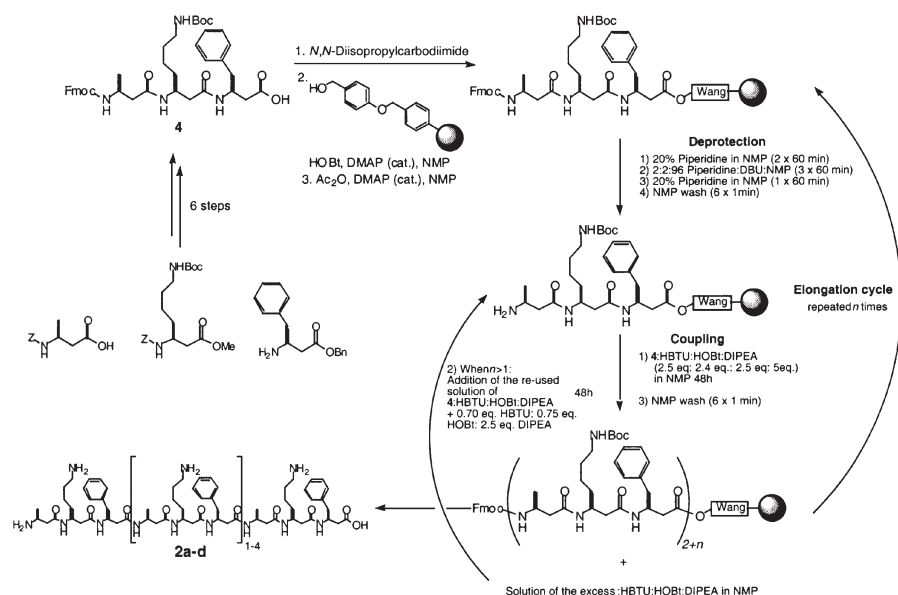
$\beta$ -Peptides built of homologated amino acids with proteinogenic side chains fold to secondary structures with as few as six residues [1]. We were interested to find out up to which chain length these  $\beta$ -peptidic structures are stable in solution as  $\alpha$ -peptidic helices, which rarely exceed chain lengths of 25 residues in proteins. Several problems had to be solved on the way to larger  $\beta$ -peptides. All  $\beta^3$ -peptides with non-functionalized or protected functionalized side-chains and with terminal protection become insoluble in organic solvents and in  $H_2O$  with increasing chain lengths. Therefore, sequential synthesis or fragment coupling in solution is prevented.



### Results and Discussion

Until recently, solid-phase synthesis of  $\beta$ -peptides following the Fmoc strategy was complicated [2]. This problem has now been solved by use of stronger base and longer reaction times for *N*-deprotection and coupling. Thus, the method of choice now is the solid-phase synthesis of  $\beta$ -peptides with protected functionalized side chains and complete deprotection of all functional groups in the final step of detachment from the resin [3]. This procedure can also be applied to solid-phase fragment coupling and leads to  $\beta$ -peptides with excellent solubility in  $H_2O$  and MeOH. To test the improved synthetic methodology and the tendency of large  $\beta$ -peptides for folding, we have synthesized dodecapeptide **1** and tetracosapeptide **3** by coupling single amino acids and the series of homologous peptides **2a–2d** by coupling  $\beta$ -peptidic triades [4]. Pentadecapeptide **2c** had to be prepared on a relatively large scale as it was used for *in vivo* studies. The repeating pattern of the sequence made us consider a combined solution- and solid-phase-approach. Therefore,  $\beta$ -tripeptide precursor Fmoc-( $\beta$ -HAla- $\beta$ -HLys(Boc)- $\beta$ -HPhe)-OH **4** was synthesized in eight steps from the corresponding  $\alpha$ -amino acids with an overall yield of 60%. As outlined in Scheme 1, Fmoc-protected  $\beta$ -tripeptide **4** was anchored to Wang resin, and the degree of anchoring was determined to be 0.50 mmol/g. In the next steps, the Fmoc-group was removed using a

deprotection sequence with piperidine and DBU in NMP as the solvent. Coupling of the tripeptide building blocks **4** was performed using HBTU, HOBt and DIPEA. To keep the material consumption of the tripeptide to a minimum, the coupling mixture from the previous step was reintroduced. This procedure of elongation and protection was then repeated until the desired chain length was reached. Standard TFA cleavage and precipitation with Et<sub>2</sub>O afforded the crude peptide as the TFA salt.



Scheme 1. Combined solution and solid-phase synthesis of  $\beta$ -peptides **2a–2d**.

It is thus demonstrated that we have the tools at hand to synthesize pure  $\beta$ -peptides of considerable chain length and complexity.

### Acknowledgments

We thank the Swedish Foundation for International Cooperation in Research and Higher Education (STINT) (P. A.) and the Deutscher Akademischer Austauschdienst (Hochschulsonderprogramm III) (J. F.) for Postdoctoral fellowships and Novartis Stipendienfonds for a scholarship granted to J.V.S.

### References

1. a) Seebach, D., Matthews, J.L. *J. Chem. Soc., Chem. Commun.* 2015 (1997); b) Gellman, S.H. *Acc. Chem. Res.* **31**, 173 (1998); c) Gademann, K., Hintermann, T., Schreiber, J.V. *Curr. Med. Chem.* **6**, 905 (1999).
2. Abele, S., Guichard, G., Seebach D. *Helv. Chim. Acta* **81**, 2141 (1998).
3. Schreiber, J.V., Seebach, D. *Helv. Chim. Acta* **83**, 3139 (2000).
4. Seebach, D., Schreiber, J.V., Arvidsson, P.I., Frackenhohl, J. *Helv. Chim. Acta.* **84**, 271 (2001).

## Fully Automated Parallel Oligonucleotide Synthesizer

Michal Lebl<sup>1,2</sup>, Christine Burger<sup>2</sup>, Brett Ellman<sup>2</sup>, David Heiner<sup>2</sup>,  
Georges Ibrahim<sup>2</sup>, Aaron Jones<sup>2</sup>, Mark Nibbe<sup>2</sup>, Jaylynn Pires<sup>2</sup>,  
Petr Mudra<sup>3</sup>, Vít Pokorný<sup>3</sup>, Pavel Poncar<sup>3</sup> and Karel Ženíšek<sup>3</sup>

<sup>1</sup>Spyder Instruments Inc., San Diego, CA 92121, USA

<sup>2</sup>Illumina, Inc., San Diego, CA 92121, USA

<sup>3</sup>Institute of Organic Chemistry and Biochemistry, 166 10 Prague 6, Czech Republic

### Introduction

The oligonucleotide and peptide synthesis technology is of major strategic importance in the field of genomics and proteomics. Commercially available single channel synthesizers cannot satisfy the demand of emerging technologies. Currently, there are several instruments for parallel synthesis of oligonucleotides such as: (i) a 96-channel instrument based on a microtiter plate format developed by scientists at Stanford University [1]; (ii) PolyPlex machine produced by the company GeneMachines [2]; or synthesizer using two microtiterplates for simultaneous synthesis of 192 oligonucleotides, developed at The University of Texas Southwestern Medical Center at Dallas, and sold under name MerMade by company BioAutomation [3]. While these technologies meet the modest requirements of most experiments today, they are inadequate for the manufacturing needs looming in the very near future. Current synthesis technologies do not meet the need for manufacturing large numbers of oligonucleotides (tens of thousands to millions of sequences) cost-effectively. Our goal was to fill this gap and build the parallel (and economical) synthesizer capable of preparation of needed numbers of oligonucleotides.

### Results and Discussion

We have devised a new technological concept for the automation of the solid-phase synthesis of large compound array [4]. The key feature of this technology is a new method for separation of the solid support from reagent solutions, termed “tilted plate centrifugation”, which uses centrifugation as a means of liquid removal in conjunction with the use of tilted microtiter plates as reaction vessels. The plates are mounted on a centrifugal plate and slightly tilted down towards the center of centrifugation, thus generating a pocket in each well, in which the solid support is collected during centrifugation, while the supernatant solutions are expelled from the wells. An essential feature of this approach is that well-to-well cross-contamination with reagent solution or resin is avoided by the fact that the plates are tilted, while the direction of centrifugation is horizontal. Consequently, any liquid or resin expelled from the wells is either captured in the inter-well space of the plate, or collected on the wall of the centrifugal drum. The fact that the cross contamination is not an issue we have proven by analyzing all products prepared on the microtiterplate by HPLC/MS.

We have built high-throughput synthesizer “Oligator™ 768” (Figure 1). Wash solutions and reagents common to all synthesized species are delivered automatically through a multichannel distributor connected to a serially linked four-port selector valves. Building blocks and other specific reagents are delivered individually to the respective wells by distribution through the banks of solenoids. An array of nozzles is placed on the actuator (single axis robotic arm). Each nozzle in the array is connected through the solenoid valve to a pressurized bottle (argon, 0.2 atm) and can be positioned (as a part of the array) above the particular well of a given microtiterplate. We

*Lebl et al.*

are using four arrays of eight nozzles for the delivery of four phosphoramidites and one array of eight nozzles for the delivery of the activator solution. Each array serves in parallel the wells of one column of microtiterplate. The arrays are placed in the grid, which covers five columns of the microtiterplate. The oligonucleotide synthesizer requires extremely fast building block and reagent delivery since prolonged times may destroy the prepared intermediate. Due to the fact that all five arrays of nozzles can be operated at the same time, the delivery of the reagents is fast – one plate can be serviced in 8 s. The synthesis is performed under inert atmosphere.

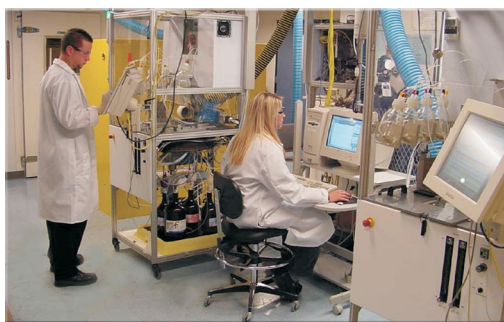


*Fig. 1. Prototypes of second generation Oligator™ 768 being tested at Illumina, Inc.*

Oligator™ 768 was tested in the synthesis of about 100,000 individual oligonucleotides of the lengths spanning from 20 bases up to 85 bases. Oligonucleotides were analyzed by ion exchange and reversed phase HPLC, gel electrophoresis and mass spectroscopy. As the ion exchange HPLC was shown to separate full-length oligonucleotide from the  $n - 1$  product, we were able to calculate step coupling yield of most of the products. Analysis of average step coupling yield showed 98.9%, which is above the industry-wide accepted value of 98%. Multifacility survey of 71 DNA core facilities have shown that only 85% of tested laboratories provided products with average coupling efficiency higher than 98% [5].

In conclusion, we have designed and built automated synthesizers using the tilted plate centrifugation technology. Eight microtiterplates are processed simultaneously, providing thus a synthesizer with a capacity of 768 parallel syntheses. The instruments are capable of unattended continuous operation, providing thus a capacity of close to a million of 20-mer oligonucleotides in a year per instrument.

## References

1. Lashkari, D.A., Hunickesmith, S.P., Norgren, R.M., Davis, R.W., Brennan, T. *Proc. Natl. Acad. Sci. USA* **92**, 7912–7915 (1995).
2. <http://www.genemachines.com/PolyPlex.html>.
3. Rayner, S., Brignac, S., Bumeister, R., Belosudtsev, Y., Ward, T., Grant, O., O'Brie, K., Evans, G.A., Garner, H.R. *Genome Res.* **8**, 741–747 (1998).
4. Lebl, M. *Bioorg. Med. Chem. Lett.* **9**, 1305–1310 (1999).
5. Pon, R.T., Buck, G.A., Hager, K.M., Naewe, C.W., Niece, R.L., Robertson, M, Smith, A.J. *BioTechniques* **21**, 680–685 (1996).

## **N to C Solid Phase Organic Synthesis of Peptidic and Peptidomimetic Derivatives Using 9-Fluorenylmethyl Esters**

**Sandrine A. M. Mérette, Christopher A. Goodwin, Michael F. Scully  
and John J. Deadman**

*Thrombosis Research Institute, Drug Discovery Section, Emmanuel Kaye Building, London,  
SW3 6LR, UK*

### **Introduction**

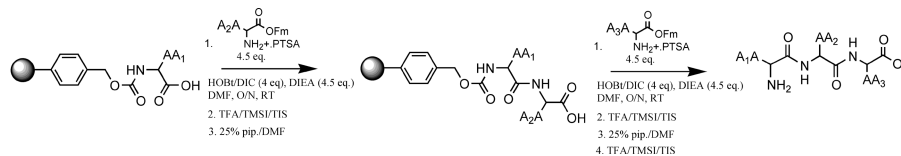
This presents the new application of our work utilizing 9-fluorenylmethyl esters (OFm) as novel protection strategy for the solid phase *N* to *C* synthesis of oligomeric peptides and peptidomimetics.

### **Results and Discussion**

9-Fluorenylmethyl esters [1] were prepared in good to excellent yields (25–99%) by adding 9-fluorenylmethylchloroformate to an ice-cooled, stirring solution of *N*-Boc protected amino acid and DIPEA in dry DCM. After 5 min, DMAP was added and the reaction medium left to stir for 30 to 120 min at 0 °C. *N*-Boc deprotection was achieved quantitatively using TFA (100%)/PTSA to yield the amines as PTSA salts.

PTSA·Leu-OFm was coupled to Wang-Asp(O-*t*Bu)-OH using different coupling reagents and the reaction times were varied to determine the best coupling conditions. In this case, the most effective coupling reagent was HOBt/DIC, which gave H-Asp-Leu-OFm in 44% yield after HPLC purification.

The following sequences were synthesised using the HOBt/DIC method (Scheme 1):  
1 – Phe-Asn-Arg; 2 – Phe-Ala-Lys; 3 – Asp-Tyr-Lys; 4 – Asp-Leu-Glu; 5 – Asn-Phe-His.



*Scheme 1. Synthesis of tripeptides using HOBt/DIC and OFm esters.*

The first unprotected amino acid (H-AA<sub>1</sub>(PG)-OH) was coupled to the Wang resin using HMPA/DMF at 80 °C. The second and the third amino acid esters were coupled using the HOBt/DIC method (Scheme 1). Yields were determined after cleavage and HPLC purification of the AA<sub>1</sub>-AA<sub>2</sub>-OFm and AA<sub>1</sub>-AA<sub>2</sub>-AA<sub>3</sub>-OFm (Table 1). The dipeptides and tripeptides were successfully synthesised in low to moderate yields using the Wang resin. Changing the solid support to a PAL-PEG-PS resin (using the side chain of Z-Asp-OFm as linker) did not lead to better yields. This method was applied to the preparation of aminoboronate, aminophosphonate and anilide derivatives [2].

The rate of deprotection of the OFm esters, using Boc-Phe-OFm and Boc-Tyr(OAll)-OFm, was studied to determine the kinetics of the reaction [3]. Both esters (100 mg) were dissolved in x% (either 5, 25 or 50) piperidine/DMF solution (1ml) and the deprotection was followed by TLC [4]. 25% Piperidine in DMF for 20 min was needed to convert the ester to the acid. These findings were applied to the solid phase chemistry, where the resin-bound esters were subjected to a 25% piperidine/DMF solution for one hour.

Table 1. Coupling efficiency of the OFm esters on SP.

Sequence	ES-MS	Theo.m (mg)	Exp. m (mg) <sup>b</sup>	Yield, %
Phe-Ala-OFm	414.3	13.1	5.2	40
Phe-Asn-OFm	475.2	15	3.6	24
Asn-Phe-OFm	475.2	11.4	8.6	75
Asp-Leu-OFm	424.0	15.1	5.2	34
Asp-Tyr-OFm	514.3	18.3	6.5	36
Phe-Ala-Lys-OFm	542.5	7.7 <sup>a</sup>	3.4	44
Phe-Asn-Arg-OFm	613.7	5.2 <sup>a</sup>	3.1	60
Asn-Phe-His-OFm	594.4	10.7 <sup>a</sup>	2.55	24
Asp-Leu-Glu-OFm	553.4	6.7 <sup>a</sup>	2.8	42
Asp-Tyr-Lys-OFm	602.4	7.7 <sup>a</sup>	0.8	10

<sup>a</sup> Taking into account the yield of the first coupling. <sup>b</sup> Value obtained after HPLC purification.

Z/Bzl containing peptides were deprotected and cleaved in a one-pot reaction, where the resin samples (100 mg) were subjected to a TMSI (trimethylsilyl-iodide)/TFA/TIS cocktail mixture [5]. Up to 3 Z/Bzl groups could be deprotected, on both Wang and PAL-PEG-PS resins, using 18 equivalents of TMSI for 4 h at room temperature.

### Conclusion

These preliminary results show that OFm esters can be used for peptidic and peptidomimetic SPS. Deprotection of Z/Bzl groups on SP can be achieved with TMSI.

### References

1. Mérette, S.A.M., Burd, A., Deadman, J.J. *Tetrahedron Lett.* **40**, 753–754 (1999).
2. Mérette, S.A.M., Burd, A.P., Teakle, N., Scully, M.F., Kakkar, V.V., Deadman, J.J., In R. Epton (Ed.) *Innovation and Perspectives in Solid Phase Synthesis & Combinatorial Libraries*, Mayflower Scientific, 2001, in press.
3. Bednarek, M.A., Bodansky, M. *Int. J. Pept. Protein Res.* **21**, 196–201 (1983).
4. Albericio, F., Nicolás, E., Rizo, J., Ruiz-Gayo, M., Pedroso, E., Giralt, E. *Synthesis* 119–122 (1990).
5. Lott, R.S., Chauhan, V.S., Stammer, C.H. *J. Chem. Soc., Chem. Commun.* 495–496 (1979).

**Analytical and Biophysical Methods,  
Peptides and Proteins Folding,  
De Novo Design of Peptides and Proteins**



## **A New Method to Quantify the Swelling Properties of Polymer Beads Used in Solid Phase Peptide Synthesis (SPPS)**

**Martin J. Sellers and Peter J. Heggs**

*Chemical Engineering Department, UMIST, Manchester, M60 1QD, UK*

### **Introduction**

The swelling properties of cross-linked polymer beads used as supports in solid phase peptide synthesis (SPPS) are important to the efficiency of the process and the purity of the product. Two of the important swelling properties are the volume to which the solid support will swell when contacted with solvent and how long the process requires to reach equilibrium [1]. If the swelling properties change at any stage, the reaction rate and ability to access every reactive site could be hampered. The swelling properties of the solid support are known to change throughout the synthesis, but an exact correlation is unknown. The technique highlighted here could be used to determine the effect of a change in the solvent concentration and the addition of an amino acid to the solid support on the swollen volume. The most obvious physical property of the solid support is the volume to which it swells when contacted with solvent. When the solid support is contacted with solvent, the solid support will swell to produce a gel phase made up of individual swollen beads. The swelling properties of the gel phase must be determined to be able to understand the process of SPPS. The gel phase must be maintained in a highly swollen state to allow the active species to diffuse to the reactive sites within the bead and to remove the by-products and excess reagents within the swollen bead [2].

Each individual swollen bead can be considered an individual reactor, as each bead has a different concentration of reactive sites and active species with a micro-litre volume. There are three different process configurations that supply solvent and active species to the individual micro-reactors, these are batch, semi-continuous and continuous flow synthesis. If the physical properties of the gel phase can be measured, then the process can be understood and optimized. The traditional method to measure the swelling properties of the solid support is very inaccurate. The general technique is to add a mass (1 g) of the polymer beads to an excess amount (20 ml) of solvent. The beads are assumed to have reached an equilibrium swelling when there is a separate liquid phase. The accuracy of the measurement of the volume of the gel phase is approximately 0.5 ml. The error associated with the volume of the gel could be enhanced due to the way the beads are packed within the column. The free space within the packed bed could vary from 26 to 45%, depending on the packing structure. The volume of the packed bed could range from 10 to 13.5 ml for 26 and 45% free space, respectively.

A more accurate method would be, to determine the swelling ratio of individual beads. The swelling ratio is the ratio of the swollen diameter of the beads to the initial (or dry) diameter. The addition of solvent to the solid support produces a significant change in the volume of the beads; this volume change can cause the beads to move across the surface. To reduce the movement of the beads, a suitable immobilization technique must be adopted. The technique to measure the swelling ratio of a sample of beads is to place a sample of the dry beads onto the surface of a porous material. A map of the surface is then made to determine the exact position of each individual bead. The solvent is added to the solid support by inducing it to flow up through the

pores and swell the beads. Once all of the beads are fully swollen, the surface is re-mapped to determine the exact position of the swollen beads. The position of the dry and swollen beads are compared, and the swelling ratio is measured as long as the following criteria are adhered to: (i) The beads are not floating and are not part of a large aggregate; (ii) The beads have not moved more than 1000  $\mu\text{m}$  along the surface; (iii) The solvent level is above the height of the largest swollen beads; (iv) Ensure the beads are surrounded by the same neighbours.

### Results and Discussion

The swelling ratios for three different combinations of solid support and solvent have been measured. The three different gel phases are: (i) Red beads (polyacrylamide treated with trinitrobenzene sulfonic acid (TNBSA)) swollen in dimethylformamide (DMF); (ii) Red beads swollen in dichloromethane (DCM); (iii) Magnetic beads (polystyrene impregnated with magnetite) swollen in DCM.

As shown in Table 1, there is a significant difference in the determined experimental swelling ratio and the equivalent swelling ratio calculated from the traditional method. The new technique determined the swollen volume of an individual bead, rather than the volume occupied by a swollen bead and excess solvent. This technique could also be used to determine the effect of a change in solvent concentration or the addition of a specific amino acid residue on the swollen volume. The experimental swelling ratio shows the same trend in the swollen volume as the traditional method. The red beads are swollen more in DCM than in DMF, and the magnetic beads are swollen to a higher extent than the red beads in DCM. The magnetic beads swell more than the red beads in DCM, since the magnetic beads have a lower equivalent percentage cross-linking. The main conclusions from this work are: (i) The new method to determine the swollen volume of the gel phase can accurately measure the swelling ratio of the unloaded solid support swollen in a variety of solvents; (ii) The swelling ratio of the solid support is not proportional to the initial diameter of the dry beads; (iii) The swelling ratio is different for the different combinations of solid support and solvent; (iv) The experimental swelling ratio follows the same trend, as that observed with the traditional swelling test.

Table 1. Swelling ratio for the traditional swelling method and the new swelling ratio experiment.

	Gel phase		
	Red beads	Red beads	Magnetic beads
Solid Support	Red beads	Red beads	Magnetic beads
Solvent	DMF	DCM	DCM
Swelling ratio (SR)	1.58	1.6	1.7
No. of beads	335	502	62
Traditional swelling (ml/g)	17	20	22
Equivalent SR	1.8	2.1	2.3

### References

1. Sellers, M.J., Heggs, P.J. *Proceedings of the 26th European peptide symposium*, 2000.
2. Hodge, P. *Chem. Soc. Rev.* **26**, 417–424 (1997).

## **A Novel High Throughput Analysis of Total Nitrogen Content by a Colorimetric Method**

**Kiyoshi Nokihara<sup>1</sup> and Tadashi Yasuhara<sup>2</sup>**

<sup>1</sup>*Shimadzu Scientific Research Inc., Kyoto 604-8511, Japan*

<sup>2</sup>*Tokyo University of Agriculture, Tokyo 156-0054, Japan*

### **Introduction**

Determination of total nitrogen amounts is routinely carried out for the quality control of pharmaceutical products especially proteins and food products. For this purpose a method originally developed by Kjeldahl [1] has been widely used over 100 years, in which ammonia generated during decomposition is titrated. This classical method is not practical for a large number of samples as it requires the use of specially designed fragile and expensive glassware, and fume hoods because of the generation of toxic gases. We have developed a novel system designated the "Nitro-Ace" for the determination of the total nitrogen content of proteins and peptides using a colorimetric method in high-throughput technology. To realize routine analyses a novel reactor for decomposition of multiple samples was designed.

### **Results and Discussion**

The reactor was designed basically from that used for combinatorial chemistry and has a capacity for handling 25 sample vials simultaneously. For high throughput decomposition a shaking component (up to 1000 rpm) together with a heating block (200 °C) for the bottom and cooling unit (circulated a chilled liquid) for the upper part of the vials is incorporated to allow efficient decomposition. The reaction conditions can be controlled precisely with a microprocessor (Figure 1). The sample and a mixture of K<sub>2</sub>SO<sub>4</sub> and CuSO<sub>4</sub>, added as an accelerator of the decomposition, were placed in a glass vial with a screw cap and septum. A mixture of sulfuric acid and hydrogen peroxide was added and decomposition was terminated after 15 min. The mixture was cooled to room temperature and neutralized with 1 M Na<sub>2</sub>CO<sub>3</sub>. The remaining excess hydrogen peroxide was removed with MnO<sub>2</sub> and then diluted with water.

The resulting solution was serially diluted and pipetted into a 96-well titer plate, in which each well was filled with n-heptane before sample loading, which was used to avoid diffusion of ammonia gas from wells. Coloration originally reported in [2] was improved and the following two reagent systems were developed: Reagent 1 consists of phenol and sodium pentacyanonitrosyl ferrate dihydrate in water and reagent 2 was prepared from sodium hypochloride and NaOH in water. Colorimetric analyses were performed with a conventional titerplate at 640 nm. The optimal conditions for the coloring reaction were 40–50 °C with a reaction time of 30–40 min.

Under these conditions the calibration profile was obtained by using standard NH<sub>4</sub>Cl solutions to give a correlation coefficient of 0.9942, which indicated the high reliability of the method. Additionally, the standard reference material (P/N 1548a, Typical Diet purchased from the US Department of Commerce, National Institute of Standards and Technology) was analyzed to show small deviations (CV: 1.72, standard deviation: 0.052). As applications of the present method, two different food samples (20 mg), roasted and ground soy beans used for Japanese delicatessen and All-bran® (Kellogg's Japan Co. Ltd.), were analyzed. The results obtained were reproducible and corresponded to those indicated by the manufactures.



Fig. 1. The reactor constructed in the present study.

Nitrogen content often reflects the efficiency of protein uptake through digestion. Hence such analyses are particularly important in feeding. The excrements (20 mg) of eight individual hamsters were collected, dried, milled and analyzed. The classic Kjeldahl method requires 1–2 g of excrements while the present method requires much less (1/50–1/100 times) and is considerably quicker in both drying and sample determination.

We have developed a sensitive and reproducible quantitative analytical system for nitrogen content determination. The present method is rapid, facile, economical and thus can be used to replace the conventional Kjeldahl method. As it has high throughput capabilities this is a powerful tool for the analysis of digestion efficiency of feed in the field of animal husbandry in addition to quality control of protein samples. Using a 25-position reactor the method allows more than 250 samples to be run daily.

#### References

1. Kjeldahl, J. Z. *Anal. Chem.* **22**, 366–382 (1883).
2. Sugano, S., Fukui, S., Naito, S., Kaneko, M. *Hygienic Chem.* **14**, 280–284 (1968).

## Conformational Studies of Cyclotetrapeptides [Xaa-D-Ala]<sub>2</sub> by NMR, CD and Molecular Modeling

Maria Ngu-Schwemlein<sup>1</sup>, Toni Bowie<sup>1</sup>, Rebecca Eden<sup>1</sup> and Frank Zhou<sup>2</sup>

<sup>1</sup>Department of Chemistry, Southern University, Baton Rouge, LA 70813, USA

<sup>2</sup>Department of Chemistry, Louisiana State University, Baton Rouge, LA 70803, USA

### Introduction

Small cyclopeptides are attractive molecular scaffoldings with reasonable rigidity and can be used as molecular templates for studies involving molecular recognition. Indeed, macrocyclic peptides have been investigated as probes to study molecular recognition by biomolecules, as well as ligands for metal ions. Nature also utilizes the peptide backbone to design ionophores, toxins and antibiotics, such as tentoxin, AM toxin, Gramicidin S and the depsipeptide, Valinomycin. Various different amino acid residues have been incorporated into small cyclic peptides in order to investigate their structural role, including the induction of specific peptide turns and the adoption of thermodynamically favored conformation(s) [1,2].

We have synthesized three cyclotetrapeptides consisting of alternating L- and D-residues, where the D-residue is Ala, to conduct conformational studies of such small peptides with this primary structural motif. Here we report the solution conformational analysis of these peptides by NMR, CD and a theoretical conformational sampling of the secondary structure of this cyclotetrapeptide backbone.

### Results and Discussion

We have synthesized three cyclotetrapeptides, c[Leu-D-Ala-Xaa-D-Ala], where Xaa is Leu (**P1**), Lys (**P2**) and Glu (**P3**), by cyclization of the pentafluorophenyl ester of the linear precursor using the Schmidt method [3]. Peptides were purified by reversed phase HPLC and characterized by MALDI-MS. Sequential assignments of all <sup>1</sup>H and <sup>13</sup>C resonances were accomplished by through bond connectivities from HSQC and HMBC spectra. In the <sup>1</sup>H and <sup>13</sup>C NMR spectra of **P1**, the number of resonances was half of the total counts, indicating a C<sub>2</sub> symmetric conformation. Phi angle (φ) constraints from <sup>3</sup>J<sub>NH $\alpha$</sub>  coupling constants, as calculated from the Karplus equation using Pardi's constants, yielded similar values for all three cyclotetrapeptides (Table 1). 2D NOESY and ROESY NMR spectra showed strong H <sub>$\alpha$</sub> (i) and NH(i+1) cross peaks for all four residues in **P1**, **P2** and **P3**, indicative of trans peptide bonds. All amide proton chemical shifts for **P1**, **P2** and **P3** exhibited linear dependence on temperature,

Table 1. Phi angle (φ) constraints from <sup>3</sup>J<sub>NH $\alpha$</sub>  coupling constants.

Peptide		Residue			
		Leu1	Ala2	Xaa3	Ala4
c[Leu-D-Ala- <b>Leu</b> -D-Ala], <b>P1</b>	<sup>3</sup> J <sub>NH<math>\alpha</math></sub>	9.93	9.52	9.93	9.52
	φ(±20°)	-120°	-110/-130°	-120°	-110/-130°
c[Leu-D-Ala- <b>Lys</b> -D-Ala], <b>P2</b>	<sup>3</sup> J <sub>NH<math>\alpha</math></sub>	9.44	8.74	9.50	8.84
	φ(±20°)	-110/-130°	-100/-140°	-110/-130°	-100/-140°
c[Leu-D-Ala- <b>Glu</b> -D-Ala], <b>P3</b>	<sup>3</sup> J <sub>NH<math>\alpha</math></sub>	9.45	8.56	9.47	8.82
	φ(±20°)	-110/-130°	-100/-140°	-110/-130°	-100/-140°

suggesting no conformational changes was occurring with increasing temperature. Temperature coefficients of amide protons in these peptides show consistently low values for the L-residue amide protons ( $-\Delta\delta/\Delta T$  ranged from 3.1 to 3.7 ppb/K). Higher temperature shifts were observed for the D-Ala amide protons ( $-\Delta\delta/\Delta T$  ranged from 5.1 to 9.8 ppb/K). However, amide proton signal broadening was observed for all residues in **P1**, **P2** and **P3**, indicating that they are all solvent accessible.

CD spectra of these peptides show characteristic positive CD bands at *ca* 210 and 222 nm in water, methanol and trifluoroethanol. Small CD/temp. effect was observed with isodichroic points, consistent with conformational stability and a well populated cyclotetrapeptide energy state (Figure 1). Conformational sampling by directed Monte Carlo searches, following ring rotation by “torsional flexing” motion [4], using the AMBER force field as implemented in HyperChem 5.1 yielded a low energy conformer with *trans* peptide bonds and negative values for all four phi angles where all carbonyl oxygen pointing to one side of the cyclopeptide backbone.

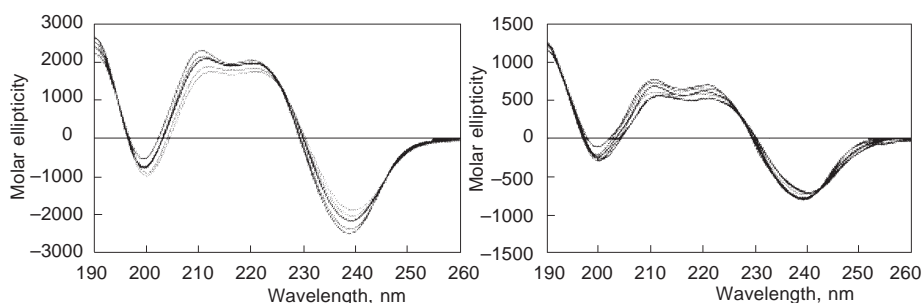


Fig. 1. Variable temperature CD of **P1** (left) and **P2** (right) at 0, 20, 40, 60, 80, 90 °C.

Cyclotetrapeptides, **P1**, **P2** and **P3** consisting of residues with alternating L- and D-configuration, where the D-residue is Ala, share a similar low energy peptide backbone energy state. This reasonably rigid cyclic peptide scaffolding may effectively be used as a molecular template for further functionalization.

#### Acknowledgments

We thank Dr. Stephen Macha for MALDI mass spectrometry analysis and Dr. Katherine Wu for initiating the structural studies of **P1** by NMR. This research was funded by a NSF-RUI grant.

#### References

1. Eyles, S.J., Gierasch, L.M. *J. Mol. Biol.* **301**, 737 (2000).
2. Nikiforovich, G., Kover, K., Zhang, W.-J., Marshall, G. *J. Am. Chem. Soc.* **122**, 3262–3273 (2000).
3. Schmidt, U., Lieberknecht, A., Griesser, H., Tabiersky, J. *J. Org. Chem.* **47**, 3261 (1982).
4. Kolossvary, I., Guida, W.C. *J. Comput. Chem.* **14**, 691 (1993).

## Conformation of $\beta^3$ -Residues-Containing Cyclic Pentapeptide Analogues of the Antitumoral Astin Family

Filomena Rossi<sup>1</sup>, Antonia De Capua<sup>1</sup>, Giancarlo Zanotti<sup>2</sup>,  
Teodorico Tancredi<sup>3</sup>, Pietro Amodeo<sup>3</sup>, Gabriella Saviano<sup>4</sup>,  
Michele Saviano<sup>1</sup>, Rosa Iacovino<sup>1</sup> and Ettore Benedetti<sup>1</sup>

<sup>1</sup>*Biocrystallography Research Center, CNR, and Biological Chemistry Department, University of Naples "Federico II", 80134, Naples, Italy*

<sup>2</sup>*CCF, CNR, University of Rome "La Sapienza", 00185, Rome, Italy*

<sup>3</sup>*Istituto Chimica MIB, CNR, 80072, Arco Felice, Italy*

<sup>4</sup>*DISTAT, University of Molise, 86170, Isernia, Italy*

### Introduction

The cyclopentapeptides of the astin family contain several uncoded amino acids, namely (–)-(3*S*,4*R*)-dichloroproline,  $\beta^3$ -*homo*-phenylalanine,  $\alpha$ -aminobutyric acid (Abu), and *allo*-threonine. The astins, isolated from the plant roots *Aster tataricus*, exhibit antitumor activity (Sarcoma 180 A), but the potential applications of this biological behaviour remain to be further investigated. Conformational studies of astin A, B and C were carried out by a combination of X-ray, NMR and computational techniques [1]. The results indicate that the backbone conformation of astin A and C, with lower activity, is different from that of astin B. Therefore, both the backbone conformation and a *cis* linkage shown by the 3,4-dichlorinated proline residue, were considered to play an important role in the antitumor activity of these molecules [2]. The development of efficient synthetic procedures for preparation of  $\beta^3$ -H residues and of *cis*-3,4-dihydroxyproline, as well as (–)-(3*S*,4*R*)-dichloroproline [3], has brought new interest in the structure-activity relationships of astin analogs. With the aim to further understand the structural and conformational requirements for activity and possibly the mechanism of action of these molecules, we have focused our attention on several cyclic pentapeptide related to astin G [4], which presents in its 16-membered ring the sequence Pro-*allo*-Thr-Ser- $\beta^3$ -HPhe-Abu. The structural results of two synthetic astin G related cyclopentapeptides c-(Pro-Thr-Aib- $\beta^3$ -HPhe-Abu) (**I**) and c-(Pro-Thr-Aib- $\beta^3$ -HPhg-Abu) (**II**) are reported.

### Results and Discussion

The linear pentapeptide precursors Z-Abu-Pro-Thr-Aib-X-OMe (Xxx =  $\beta^3$ -HPhe and  $\beta^3$ -HPhg) have been synthesized by classical methods in solution. Couplings were performed by the mixed anhydride, or the DCCI/HOBt procedures (*N,N'*-dicyclohexylcarbodiimide/1-hydroxybenzotriazole), when the Aib moiety was involved). Removal of the Z group was achieved using H<sub>2</sub> and a palladium/charcoal catalyst, while removal of the OMe was performed with aqueous sodium hydroxide in methanol. For cyclization of both linear peptides (1.25 · 10<sup>–3</sup> M) we have applied the mixed anhydride method in THF/DMF (1 : 2 v/v). The pure cyclopentapeptides (**I**) (yield 21%, MH<sup>+</sup> 530) and (**II**) (yield 13%, MH<sup>+</sup> 516) were characterized by HPLC and Maldi-TOF techniques.

The solid-state conformation of c-(Pro-Thr-Aib- $\beta^3$ -HPhe-Abu) (**I**) (Figure 1) has been determined by X-ray diffraction analysis. The structure was solved by direct methods (SIR97) and refined using the SHELX97 program. Structural comparison between natural astins and compound (**I**) shows that the conformational similarity be-

Rossi et al.

tween all molecules is limited to the region of the *cis* Xxx-Pro peptide bond. Unlike astin B, peptide (**I**) does not show any intramolecular H-bond in the solid state

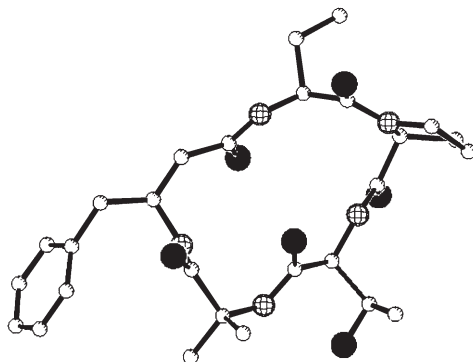


Fig. 1. X-Ray diffraction structure of *c*-(Pro-Thr-Aib- $\beta^3$ -H Phe-Abu) (**I**).

The NMR solution study of the two cyclopentapeptides (**I**) and (**II**) has been carried out at 300 K in acetonitrile. The conformation of the two analogues has been determined *via* 2D homo- and heteronuclear NMR experiments. The NMR data of both cyclopentapeptides (**I**) and (**II**) are compatible with an equilibrium in solution involving two (for compound **II**) or three (for compound **I**) major conformers. The first conformer (A) is very similar to the X-ray structure found for compound (**I**), while the second (B) is characterized by a  $\gamma$ -turn centered on Aib<sup>3</sup> with an H-bond pattern involving the NHs of  $\beta^3$ -H Phe<sup>4</sup> and Thr<sup>2</sup>. All residues of compound (**I**), except residue 4, give rise to a third conformer very reminiscent of that found in astin B.

#### Acknowledgments

The authors gratefully acknowledge Ministry of University and of the Scientific and Technological Research (M.U.R.S.T.) and the National Council of Research (C.N.R.) of Italy for their continuous and generous support to this research.

#### References

1. Morita, H., Nagashima, S., Takeya, K., Itokawa, H., Itaka, Y. *Tetrahedron* **51**, 1121–1132 (1995).
2. Morita, H., Nagashima, S., Takeya, K., Itokawa, H. *Chem. Pharm. Bull.* **41**, 992–993 (1993).
3. Schumacher, K.K., Jiang, J., Joullié, M.M. *Tetrahedron: Asymmetry* **9**, 47–53 (1998).
4. Schumacker, K.K., Hauze, D.B., Jiange, J., Szewczyk, J., Reddy, F.E., Davis, P.A., Joullié, M.M. *Tetrahedron Lett.* **40**, 455–458 (1999).

## Structure-Activity Relationship of Antimicrobial Peptide, Gaegurin 4, Isolated from Korean Frog

Sang-Ho Park and Bong-Jin Lee

College of Pharmacy, Seoul National University, Seoul, 151-742, Korea

### Introduction

Gaegurin 4 is a 37-residue antimicrobial peptide isolated from the skin of a Korean frog, *Rana rugosa*. It shows a broad range of activity against prokaryotic cells, but very little hemolytic activity against human red blood cells [1]. Using circular dichroism and NMR spectroscopy, we have determined the solution structure of gaegurin 4 [2]. In the present study, we determined the structure of this peptide bound to sodium dodecyl sulfate micelles and investigated the structure-activity relationship of this peptide by comparing the structure and physicochemical properties with other known antimicrobial peptides.

### Results and Discussion

CD investigation revealed that gaegurin 4 adopts mainly an  $\alpha$ -helical conformation in trifluoroethanol (TFE)/water solution, dodecylphosphocholine and in sodium dodecyl sulfate (SDS) micelles. By using homonuclear and heteronuclear NMR experiments, its structures in TFE/water solution and SDS micelles, respectively, were determined. The calculated structures of gaegurin 4 in both environments consisted of two amphipathic  $\alpha$ -helices covering residues 2–10 and residues 16–32. These two helices are connected by a flexible loop spanning residues 11–15. It could be supposed that the structure of gaegurin 4 bound to SDS micelles is more rigid than that of gaegurin 4 in TFE/water solution. However, the loop region is flexible, suggesting that gaegurin 4 bound to SDS micelles behaves dynamically. Figure 1 shows that there is no contact between the helices, which allows an independent movement of both helices at an angle of about 60–120°.

The topology of the overall secondary structure of gaegurin 4 is similar to that of cecropin A, a 37-residue antimicrobial peptide isolated from insects [3]. This peptide contains two amphipathic helices covering residues 5–21, and residues 24–37.

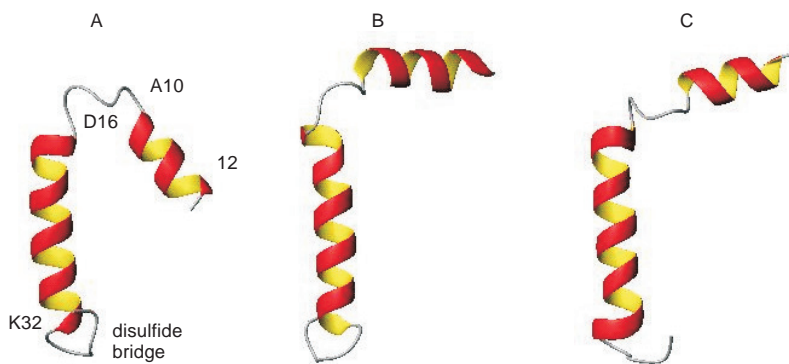


Fig. 1. Representative structures of gaegurin 4 bound to SDS micelles. Both helices are located at angle of about 60° (A), 90° (B), 120° (C) each other.

Cecropins are known to bind parallel to lipid membrane surfaces, and their antimicrobial activity is due to the formation of large ionophores in bacterial cell membranes [4]. The ionophoric property of gaegurin 4 is also likely to contribute to its antimicrobial activity by forming voltage-dependent and cation-selective pores in planar lipid bilayers [5]. In the hydropathy plot (Figure 2), the N-terminal helix of two turns of gaegurin 4 shows a typical amphipathic character, and the C-terminal helix of

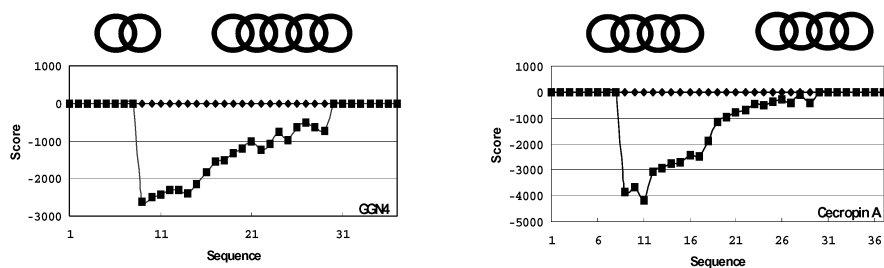


Fig. 2. Hydropathy plot of gaegurin 4 (left) and cecropin A (right). The helical representations obtained from the NMR data indicate the location of the two helices, respectively.

4–5 turns shows a relatively hydrophobic character. The hydropathy plot of cecropin A is also similar to that of gaegurin 4.

From the solution structure and the physicochemical properties of gaegurin 4, it could be suggested that the mechanism of antimicrobial activity of GGN4 is similar to that of cecropin A, despite of differences in the amino-acid sequence and species.

#### Acknowledgments

This study was supported by a grant (HMP-00-B-20900-0096) of the Good Health R & D Project, Ministry of Health & Welfare, R.O.K.

#### References

1. Park, J.M., et al. *Biochem. Biophys. Res. Commun.* **205**, 948–954 (1994).
2. Park, S.H., et al. *Eur. J. Biochem.* **267**, 2695–2704 (2000).
3. Steiner, H., et al. *Nature* **292**, 246–248 (1981).
4. Gazit, E., Boman, A., Boman, H.G., Shai, Y. *Biochemistry* **34**, 11479–11488 (1995).
5. Kim, H.J., et al. *J. Pept. Res.* **53**, 1–7 (1999).

## Tethering of the Proximal Region of the Angiotensin II Receptor (AT<sub>1A</sub>) C-Terminus to the Cell Membrane

**Henriette Mozsolits<sup>1</sup>, Sharon Unabia<sup>1</sup>, Walter G. Thomas<sup>2</sup>  
 and Marie-Isabel Aguilar<sup>1</sup>**

<sup>1</sup>*Department of Biochemistry and Molecular Biology, PO Box 13D, Monash University,  
 Clayton, Vic 3800, Australia*

<sup>2</sup>*Baker Medical Research Institute, PO Box 6492 Melbourne, Vic 8008, Australia*

### Introduction

The type 1 angiotensin receptor (AT<sub>1A</sub>) is a 359 amino acid G protein-coupled receptor that mediates the important cardiovascular and homeostatic actions of the peptide hormone angiotensin II (AngII) [1]. The 54 amino acid carboxyl-terminus (Leu<sup>305</sup> to Glu<sup>359</sup>) of the AT<sub>1A</sub> receptor interacts with, and activates, G proteins and other signalling molecules, indicating a contribution to receptor activation, while the identification of phosphorylation sites and internalisation motifs suggest a key role in receptor regulation [2]. The C-terminus of the type I angiotensin II receptor (AT<sub>1A</sub>) is thus a focal point for receptor activation and deactivation. Synthetic peptides corresponding to the membrane-proximal region of the C-terminus adopt a helical structure in hydrophobic environments [3], which may relate to the capacity of this region to act as an important switch site *in vivo*. In order to explore this hypothesis, we examined whether this basic-charged, amphipathic  $\alpha$ -helical region can interact with lipid components in the cell membrane and thereby modulate local receptor structure.

### Results and Discussion

Surface plasmon resonance was used to examine the membrane-binding behaviour of two synthetic peptides with immobilized liposomes composed of either dimyristoyl L- $\alpha$ -phosphatidyl-DL-glycerol (DMPG) or dimyristoyl L- $\alpha$ -phosphatidylcholine (DMPC) [4]. The sequences of the peptides are listed in Table 1.

Comparative experimental sensorgrams of the binding of each peptide to DMPG and DMPC are shown in Figure 1. A synthetic peptide corresponding to the proximal region of the AT<sub>1A</sub> receptor carboxyl-terminus (Leu<sup>305</sup> to Lys<sup>325</sup>) (AT) was shown by surface plasmon resonance to bind specifically and with high affinity to the negatively charged lipid DMPG but poorly to the zwitterionic lipid DMPC. In contrast, a peptide analog possessing substitutions at four lysine residues (corresponding to Lys<sup>307,308,310,311</sup>) (LGJ) displayed poor association with either lipid, indicating a crucial anionic component to the interaction.

Circular dichroism analysis revealed that both the wild type and substituted peptides possessed  $\alpha$ -helical propensity in methanol and trifluoroethanol, while the wild type peptide also adopted helical structure in DMPG and DMPC liposomes. In contrast, the substituted peptide adopted a mixture of sheet and structure in both liposomes (data not shown).

*Table 1. Amino acid sequence of synthetic peptides.*

Peptide	Sequence	Average hydrophobicity	Hydrophobic moment
AT	LGKKFKKYFLQLLKYIPPKAK	0.93	1.04
LGJ	LGJJFJJYFLQLLKYIPPKAK	1.95	0.51

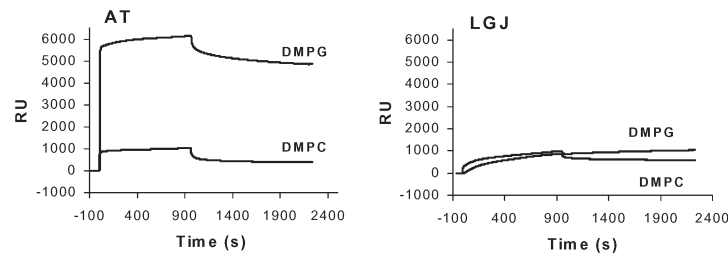


Fig. 1. Comparative sensorgrams for AT and LGJ peptides binding to DMPC and DMPG liposomes.

We therefore propose a model for the AT<sub>1A</sub> receptor, in which the proximal carboxyl-terminus binds specifically to anionic regions of the cell membrane. This occurs first through electrostatic interactions, followed by reorientation of the peptide to allow hydrophobic interactions to anchor the peptide at the interfacial region of the membrane. Removal of four lysine residues (Lys<sup>307,308,310,311</sup>) significantly affected the binding behaviour of the AT peptide, resulting in the loss of DMPG-specific binding through elimination of the initial rapid phase of binding associated with electrostatic interactions. Thus, the cytoplasmic region of the AT<sub>1A</sub> receptor may not extend into the cytoplasm, but is rather tethered to the cell membrane lipids, so that the axis of the helix runs parallel to the membrane surface. This orientation of the helix relative to the membrane is supported by the recent X-ray structure of bovine rhodopsin receptor [5].

## References

1. de Gasparo, M., Catt, K.J., Inagami, T., Wright, J.W., Unger, T. *Pharmacol. Rev.* **52**, 415–472 (2000).
2. Thomas, W.G. *Regul. Pept.* **79**, 9–23 (1999).
3. Franzoni, L., Nicastro, G., Pertinhez, T.A., Tato, M., Nakaie, C.R., Paiva, A.C., Schreier, S., Spisni, A. *J. Biol. Chem.* **272**, 9734–41 (1997).
4. Mozsolits, H., Wirth, H.-J., Werkmeister, J., Aguilar, M.I. *Biochim. Biophys. Acta* **1512**, 64–76 (2001).
5. Palczewski, K., Kumasaka, T., Hori, T., Behnke, C.A., Motoshima, H., Fox, B.A., Le Trong, I., Teller, D.C., Okada, T., Stenkamp, R.E., Yamamoto, M., Miyano, M. *Science* **289**, 739–45 (2000).

## Amide I Frequency as a Probe of Tertiary Structure: FTIR Studies of Helix Bundle Peptides

Karen Monteiro, Wendy Barber-Armstrong and Sean M. Decatur

Department of Chemistry, Mount Holyoke College, S. Hadley, MA 01075, USA

### Introduction

Infrared spectroscopy is extensively used to determine secondary structure content of peptides and proteins. The frequency, intensity, and line width of the amide I band of a peptide are commonly used to distinguish between alpha helix, beta sheet, and random coil [1]. However, tertiary structure also plays a role in determining IR spectral features. The amide I band is dependent on solvent environment; amide I frequencies of peptides which are exposed to water (and hydrogen bonded with solvent) can be distinguished from those in nonpolar environments [2]. However, there have been no systematic studies of the effects of tertiary structure changes on the amide I' band of a polypeptide.

In this study, we report a detailed FTIR study of the helix-turn-helix peptide Z34C, a 34 residue helix-turn-helix peptide with a sequence engineered based on the A domain of protein B [3]. Z34C features two cysteine residues, one at the C terminus and one near the N-terminus. Oxidation of these cysteines to form a disulfide bond stabilizes the structure of the peptide by restricting its flexibility. This is an ideal model system for investigating the effect of subtle changes in tertiary structure on the amide I' band: by comparing the spectra of the reduced and disulfide bonded peptides, we can determine the differences in amide I' bands of peptides as they become increasingly more "molten globule" like.

### Results and Discussion

FTIR spectra for Z34C and Z34CSS are shown in Figure 1; parameters for the amide I' band are summarized in Table 1. Short peptides which form stable, single alpha helices in solution give amide I' bands with frequency  $\approx 1633 \text{ cm}^{-1}$  [2,4,5]. By comparison, the amide I' frequencies of both Z34C and Z34CSS are  $\approx 1655 \text{ cm}^{-1}$ . The higher frequency in the helix-turn-helix peptide is due to the differences in solvation: the presence of a water-excluded core reduces hydrogen bonding between the helix backbone and solvent; this results in an increase in frequency.

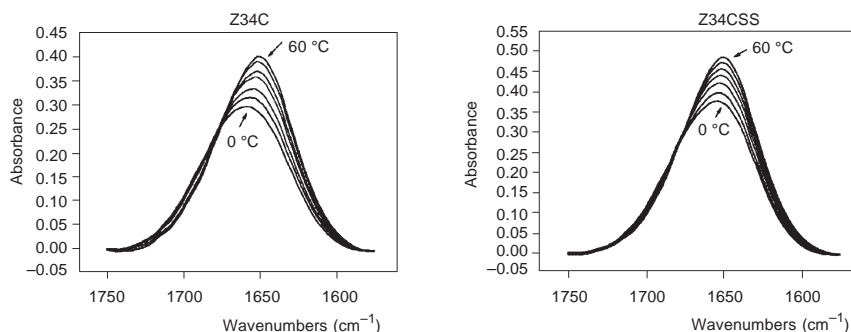


Fig. 1. Temperature dependencies of FTIR spectra of Z34C and Z34CSS.

Table 1. Parameters for the amide I' band of Z34C and Z34CSS.

Peptide	Temperature (°C)	Amide I' frequency (cm <sup>-1</sup> )	Amide I' band width (cm <sup>-1</sup> )
Z34C	0	1660	66.5
Z34CSS	0	1655	59
Z34C	60	1651	58
Z34CSS	60	1651	58

Z34C at 0 °C has a much broader amide I' band than the disulfide boded Z34CSS. The difference in line width is likely due to conformational flexibility of the reduced peptide; the presence of a large ensemble of tertiary conformations may result in the broader bandwidth. This suggests that the amide I' band may be a sensitive probe of tertiary structure flexibility, which may make it a useful probe for molten globule states in partially folded polypeptides. At 65 °C, where both Z34C and Z34CSS are random coil (according to CD data), the amide I' bands of the two peptides have similar frequency and bandwidth.

When specific residues within the peptide are <sup>13</sup>C labeled, the isotope-shifted amide I' band becomes a residue-specific probe of peptide structure [6–8]. By labeling amino acids, which are buried or exposed in the helix bundle, tertiary structure can be probed at the residue level using FTIR spectroscopy. These studies are currently underway.

#### Acknowledgments

This work is supported by an NSF CAREER grant (9984844) and an NIH AREA grant (GM661588) to S. M. D. The peptide synthesizer and circular dichroism spectrometer were purchased with NSF MRI grants.

#### References

1. Surewicz, W.K., Mantsch, H.H., Chapman, D. *Biochemistry* **32**, 389–394 (1993).
2. Williams, S., Causgrove, T.P., Gilmanishin, R., Fang, K.S., Callendar, R.H., Woodruff, W.H., Dyer, R.B. *Biochemistry* **35**, 691–697 (1996).
3. Starovasnik, M.A., Braisted, A.C., Wells, J.A. *Proc. Natl. Acad. Sci. USA* **94**, 10080–10085 (1997).
4. Graff, D.K., Pastran-Rios, B., Venyaminov, S. Yu., Prendergast, F.G. *J. Am. Chem. Soc.* **119**, 11282–11294 (1997).
5. Yoder, G., Pancoska, P., Keiderling, T.A. *J. Am. Chem. Soc.* **36**, 15123–15133 (1997).
6. Decatur, S.M., Antonic, J. *J. Am. Chem. Soc.* **121**, 11914–11915 (1999).
7. Decatur, S.M. *Biopolymers* **54**, 180–185 (2000).
8. Silva, R.A.G.D., Kubelka, J., Bour, P., Decatur, S.M., Keiderling, T.A. *Proc. Natl. Acad. Sci. USA* **97**, 8318–8323 (2000).

## **Coupled Plasmon Waveguide Resonance Studies of Agonist/Antagonist Binding to the Human $\delta$ -Opioid Receptor Provide New Structural Insights Into the Three-State Model for Receptor–Ligand Interactions**

**Z. Salamon<sup>1</sup>, I. Alves<sup>1</sup>, S. Cowell<sup>2</sup>, V. J. Hruby<sup>1,2</sup> and G. Tollin<sup>1,2</sup>**

*Departments of <sup>1</sup>Biochemistry and <sup>2</sup>Chemistry, University of Arizona, Tucson, AZ 85721, USA*

### **Introduction**

Traditional methods in pharmacology characterize a ligand by its binding to a receptor and/or the subsequent second messenger response. No information on the direct conformational changes of the receptor in response to the ligand is obtained. Using a new method, coupled plasmon-waveguide resonance spectroscopy, structural changes of the human  $\delta$ -opioid receptor immobilized in a lipid bilayer accompanying the binding of agonists and antagonists have been investigated. This highly sensitive technique directly monitors mass density, conformation, and molecular orientation changes occurring in anisotropic thin films. The extent of conformational change versus the amount of ligand allows determination of binding constants that are in good agreement with published values for the same ligands.

### **Results and Discussion**

The human  $\delta$ -opioid receptor was incorporated into a preformed lipid membrane deposited on the hydrophilic surface of the silica film by adding small aliquots of a concentrated solution of the human  $\delta$ -opioid receptor solubilized in 30 mM octylglucoside to the aqueous compartment of the CPWR cell, thereby diluting the detergent to a final concentration below its critical micelle concentration. Then binding of the highly selective agonist DPDPE (c[D-Pen<sup>2</sup>, D-Pen<sup>5</sup>]-enkephalin) was performed. Demonstration of the reversal of binding using the selective antagonist naltrindol (NTI) was accomplished as well as evaluation of the conformational changes in the receptor structure that accompany these binding interactions. CPWR spectra were obtained for experiments in which agonist is added to the receptor-containing CPWR cell first, followed by antagonist addition as well as experiments in which antagonist is added first, followed by agonist. Results of the described experiments in terms of membrane thickness changes, refractive index anisotropy and binding constants are presented in Figures 1a and 1b, respectively.

Results presented in Figure 1a demonstrate that DPDPE increases both the thickness and the anisotropy of the receptor. Subsequent addition of naltrindole causes a further increase in anisotropy, without any change in thickness. Figure 1b shows that the addition of the antagonist (NTI) causes an increase in the anisotropy of the receptor while the thickness does not increase. Upon subsequent addition of the agonist (DPDPE), there is a marked increase in the receptor thickness with a slight decrease in anisotropy.

As can be seen, although both agonist and antagonist binding to the receptor cause increases in molecular ordering within the proteolipid membrane, only agonist binding induces an increase in thickness and molecular packing density of the membrane. This is a consequence of mass movements perpendicular and parallel to the plane of the bilayer occurring within the lipid and receptor components. These results are consistent with models of receptor function that involve changes in the orientation of trans-

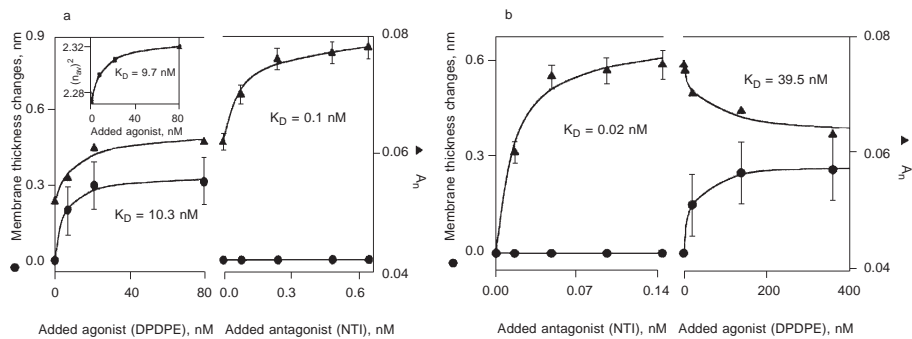


Fig. 1 (a,b). Average thickness (circles) and refractive index anisotropy (triangles) values for the proteolipid membrane containing a saturating amount of the opioid receptor as a function of the agonist and antagonist concentration. Insert shows the square of the average refractive index of the proteolipid membrane proportional to mass as a function of agonist concentration. Solid lines represent nonlinear least squares fits to hyperbolic function from which the binding constants ( $K_D$ ) were obtained.

membrane helices. Thus one can distinguish agonists from antagonists and inverse agonists ligands directly without the presence of G-proteins.

#### Acknowledgments

Supported by grants from the VP for Research, University of Arizona (to GT and VJH), the N.S.F. (MCB-9904753, to GT and ZS), the U.S.P.H.S., and the N.I.D.A. (DA-06284, to VJH), and a U.S.P.H.S. Postdoctoral fellowship (DA-05787, to SC).

#### References

1. Salamon, Z., Cowell, S., Varga, E., Yamamura, H., Hruby, V., Tollin, G. *Biophys. J.* **79**, 2463–2474 (2000).

## Structure Elucidation of Peptides with Unnatural Amino Acids Using an Automated Protein Sequencer

Ruiwu Liu and Kit S. Lam

*Division of Hematology and Oncology, Department of Internal Medicine, UC Davis Cancer  
Center, University of California Davis, Sacramento, CA 95817, USA*

### Introduction

The use of automatic Edman microsequencing to determine the primary structure of peptides or proteins containing 20 eukaryotic natural amino acids is now routine. However, the ability to readily sequence peptides containing multiple unnatural amino acids remains elusive. We recently reported on the elution profile of 35 PTH-derivatives of unnatural  $\alpha$ -amino acids on an ABI microsequencer [1]. A random “one-bead one-compound” tripeptide library containing 19 natural amino acids (cysteine excluded) plus 14 unnatural amino acids was synthesized and screened for streptavidin-binding ligands. The positive peptide beads were isolated and microsequenced using the modified elution gradient. A novel motif of Bpa-Phe(4-X)-Aib (wherein X = H, OH, or CH<sub>3</sub>) was identified. To increase the structural diversity of peptide libraries, development of a method for Edman microsequencing of peptides containing additional unnatural amino acids is necessary.

### Results and Discussion

In order to sequence unnatural amino acids that are more hydrophobic than natural ones, we modified the gradient program by extending the elution time from a total of 22 to 28 min prior to washing the column with 90% solvent B (88% acetonitrile/12% isopropanol v/v). The first 18 min of the gradient profile is identical to that recommended by the manufacturer. This ensures the elution profile of all 20 PTH-natural amino acids remains unchanged and that they can be read automatically using the existing software in the protein sequencer. To get better separation of PTH-amino acids near the region of PTH-His and PTH-Arg, we increased the buffer concentration by adding an additional 5 mL of Premix buffer concentrate per liter of solvent A3 (3.5% tetrahydrofuran/water).

Under the same sequencing conditions, we found that the variation in retention time (RT) of each individual PTH-amino acid was below 0.05 min. Therefore, distinguishing two amino acids with  $\Delta$ RT greater than 0.10 min is not difficult. When the column or bottle of mobile phase is changed, larger shifts of the PTH-amino acid elution positions may occur. It is therefore necessary to run an external reference standard containing both natural and unnatural amino acids. We can manually identify each amino acid by comparing the RT with the external reference. PTH-amino acids of the external reference standard are generated *in situ* by placing amino acids mixture that are covalently coupled to beads in the sequencing cartridge and let the sequencer run through one sequencing cycle. Amino acid beads are prepared by coupling a mixture of Fmoc-unnatural and Fmoc-natural amino acids to the TentaGel-NH<sub>2</sub> beads in a one-pot reaction, with subsequent Fmoc and side-chain deprotection, resulting in all amino acids covalently attached to each bead.

Table 1 summarizes the RT of 75 PTH derivatives of both natural and unnatural amino acids. Through this table, one can easily pick 40–45 amino acids, with  $\Delta$ RT greater than 0.10 min, as building blocks. This greatly increases the diversity of the peptide libraries one can generate.

Table 1. RT of PTH-amino acids (natural and unnatural) on an ABI protein sequencer.

AA	RT	AA	RT	AA	RT	AA	RT	AA	RT
Asp	4.17	Ala	8.37	Acp	14.78	Phe	17.24	Phe(4-N <sub>3</sub> )	20.83
Acpc	4.59	4-Pal	8.59	Phe(4-CN)	14.81	Phe(4-NO <sub>2</sub> )	17.27	Aic	20.89
Asn	4.70	3-Pal	8.71	Nva	14.82	Bug	17.65	Phe(3-Cl)	21.13
Ser	5.34	Hyp	8.75	DPTU	15.32	Dpr(Z)	17.72	HoPhe	21.66
Gln	5.61	Acdt	8.81	PMTC	15.52	Ile	17.76	Chg	21.86
Thr	5.85	Ahch	9.23	Thi	15.61	Lys	18.05	Bta	22.01
HoSer	5.95	Akch	9.95	Tyr(3-NO <sub>2</sub> )	15.62	Ach	18.13	Bpa	22.11
Cit	6.07	Pra	10.01	Dpr	15.75	Leu	18.36	Nal-2	22.41
Gly	6.11	Actp	10.03	Lys(Bz)	15.79	Tyr(di Br)	18.43	Nal-1	22.65
Glu	6.49	Arg	10.13	Dbu	16.32	Nle	18.88	Ana	22.72
DMPTU	6.83	Tyr	10.50	Thz	16.46	Phe(4-NH <sub>2</sub> )	18.97	Phe(di Cl)	23.23
HoCit	6.98	Aib	10.90	Trp	16.48	3-Apc	19.19	Hyp(Bzl)	23.31
Hyp	7.57	Abu	10.99	Tyr(Me)	16.66	4-Apc	19.22	Cha	23.98
Aad	7.80	Pro	13.02	DPU	16.76	App	20.05	Dpa	24.02
His	8.08	Met	13.70	Orn	16.83	Phe(4-Me)	20.38	Dpg	27.17
Lys(Ac)	8.13	Val	14.03	Phg	17.09	Tyr(di I)	20.67		

Natural amino acids are designated by the standard three-letter code. Other abbreviations: Acpc, 1-aminocyclopropane-1-carboxylic acid; HoSer, homoserine; Cit, citrulline; DMPTU, dimethylphenylthiourea; HoCit, homocitrulline; Hyp, hydroxyproline; Aad,  $\alpha$ -aminohexanedioic acid; Lys(Ac),  $\epsilon$ -acetyl lysine; 4-Pal, 3-(4-pyridyl)alanine; 3-Pal, 3-(3-pyridyl)alanine; Acdt, 4-amino-4-carboxy-1,1-dioxo-tetrahydrothiopyran; Ahch, 1-amino-1-(4-hydroxycyclohexyl)carboxylic acid; Akch, 1-amino-1-(4-ketocyclohexyl)carboxylic acid; Pra, propargylglycine; Actp, 4-amino-4-carboxytetrahydropyran; Aib,  $\alpha$ -aminoisobutyric acid; Abu,  $\alpha$ -aminobutyric acid; Acp, 1-amino-1-cyclopentane carboxylic acid; Phe(4-CN), 4-cyanophenylalanine; Nva, norvaline; DPTU, diphenylthiourea; PMTC, phenylisothiocyanate-methanol adduct; Thi, 3-(2-thienyl)alanine; Tyr(3-NO<sub>2</sub>), 3-nitrotyrosine; Dpr,  $\alpha,\beta$ -diaminopropionic acid; Lys(Bz),  $\epsilon$ -benzoyllysine; Dbu,  $\alpha,\gamma$ -diaminopropionic acid; Thz, thiazolidine-4-carboxylic acid; Tyr(Me), O-methyltyrosine; DPU, diphenylurea; Orn, ornithine; Phg, phenylglycine; Phe(4-NO<sub>2</sub>), 4-nitrophenylalanine; Bug,  $\alpha$ -tert-butylglycine; Dpr(Z),  $\beta$ -benzyloxycarbonyl; Ach, 1-amino-1-cyclohexane carboxylic acid; Tyr(diBr), 3,5-dibromotyrosine; Nle, norleucine; Phe(4-NH<sub>2</sub>), 4-aminophenylalanine; 3-Apc, 1-amino-1-(3-piperidinyl)carboxylic acid; 4-Apc, 1-amino-1-(4-piperidinyl)carboxylic acid; App, 2-amino-3-(4-piperidinyl) propionic acid; Phe(4-Me), 4-methylphenylalanine; Tyr(diI), 3,5-diiodotyrosine; Phe(4-N<sub>3</sub>), 4-azidophenylalanine; Aic, 2-aminoindane-2-carboxylic acid; Phe(3-Cl), 3-chlorophenylalanine; HoPhe, homophenylalanine; Chg,  $\alpha$ -cyclohexylglycine; Bta, 3-benzothienyllalanine; Bpa, 4-benzoylphenylalanine; Nal-2, 3-(2-naphthyl)alanine; Nal-1, 3-(1-naphthyl)alanine; Ana, 2-amino-2-naphthylacetic acid; Phe(di Cl), 3,4-di chlorophenylalanine; Hyp(Bzl), O-benzyl-hydroxyproline; Cha, cyclohexylalanine; Dpa, 3,3-diphenylalanine; Dpg, di-n-propylglycine.

### Acknowledgments

This work was supported by grants NIH CA78868, 78909, 86364, and NSF MCB 950621.

### References

1. Liu, R., Lam, K.S. *Anal. Biochem.* **295**, 9–16 (2001).

## **Structural Study of the Pro-Sequence of Protegrin-3**

**Jean-Frédéric Sanchez<sup>1</sup>, Yin-Shan Yang<sup>1</sup>, François Hoh<sup>1</sup>,  
Marie-Paule Strub<sup>1</sup>, Christian Dumas<sup>1</sup>, Jean-Marc Strub<sup>2</sup>,  
Alain Van Dorsselaer<sup>2</sup>, Robert Lehrer<sup>3</sup>, Tomas Ganz<sup>3</sup>,  
Alain Chavanieu<sup>1</sup>, Bernard Calas<sup>1</sup> and André Aumelas<sup>1</sup>**

<sup>1</sup>*Centre de Biochimie Structurale, UMR 5048 CNRS-UMI UMR 554 INSERM-UMI,  
Faculté de Pharmacie, 34060 Montpellier Cedex 02, France*

<sup>2</sup>*Laboratoire de Spectrométrie de Masse Bio-Organique, Faculté de Chimie,  
67000 Strasbourg, France*

<sup>3</sup>*Department of Medicine, Center for the Health Sciences, Los Angeles, CA 90095, USA*

### **Introduction**

Protegrins (PG-1 to 5) are a family of five short antibacterial peptides (16-18 residues) characterized by their high content in cysteine and arginine residues which adopt a  $\beta$ -sheet structure stabilized by two disulfide bridges [1]. Protegrins are initially produced as an inactive precursor protein of 149 residues which consists of a peptide signal (1-28), a pro-sequence (ProS) of 101 residues (29-130) and the protegrin sequence (131-147/148) [2]. The active protegrin is released by cleavage of the V<sup>130</sup>R<sup>131</sup> amide bond by an elastase-like enzyme [3]. Electrostatic interactions between PG-3 and its pro-sequence are supposed to suppress the antibacterial activity of PG-3. Interestingly, very similar pro-sequences are encountered in more than 15 antibacterial peptides of unrelated structures and are referred to as a cathelicidin motif [4,5]. The three-dimensional structure of this wide spread motif which contains two conserved disulfide bonds (85-96 and 107-124 in ProS) is not yet known. Despite a low sequence similarity (20%) with the chicken cystatin, a similar fold was hypothesized for the cathelicidin motif. This investigation was designed to determine the three-dimensional structure of ProS (the cathelicidin motif) as well as its interactions with PG supposed to be responsible for the loss of the antibacterial activity of PG-3. Here, we report the over-expression of the ProS and preliminary results of its structural study.

### **Results and Discussion**

ProS was overexpressed in *E. coli* by using the Tag-His/thrombin site/ProS construct. The tagged protein was purified on a nickel column, and the ProS protein obtained after thrombin cleavage was characterized by mass spectrometry. The presence of the two disulfide bonds was confirmed by the unchanged molecular weight measured after treatment with the 4-Vinylpyridine, a selective thiol alkylating reagent. Unexpectedly, as shown in Figure 1, NMR spectra were reversibly altered by pH, suggesting a pH-induced conformational change. The spectrum in neutral conditions indicates the presence of two conformations in the 55/45 ratio whereas at pH 3.0 this ratio is around 90/10. The simultaneous observation of the signals of the two conformations indicates that they are in slow exchange on the 1H chemical shift time scale.

Homonuclear and heteronuclear 2D and 3D NMR experiments were recorded at pH 3.0 and 7.0. The partial assignment of the 2D homonuclear and 3D heteronuclear spectra was carried out. Based on  $d_{NN}$  NOEs, it clearly appeared that the N-terminal sequence spanning residues 28-49 adopted an helical structure. Moreover, the observation of numerous  $d_{\alpha\alpha}$  NOEs allowed to identify residues involved into a four-stranded  $\beta$ -sheet. The amount of secondary structure is in agreement with that calculated from the CD spectrum. Despite the presence of two conformations, we re-

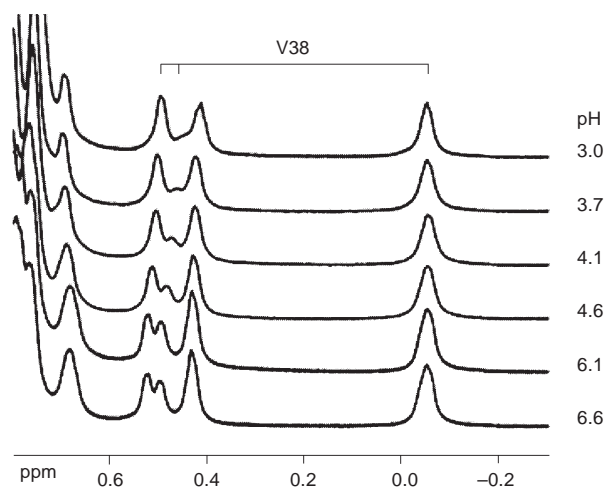


Fig. 1. NMR spectra of ProS as a function of pH. The methyl signals of the V<sup>38</sup> were used to monitor the pH-induced conformational change.

cently obtained diffraction quality crystals and X-ray data at 1.9 Å resolution were collected at the ESRF. Processing of X-ray data and modeling of NMR data are in progress.

We hope that the structure of the cathelicidin motif of the PG precursor will be helpful to identify the interactions between the ProS and PG peptides which are responsible for their inactivation. Moreover, this structural knowledge could be extended to other antimicrobial precursors built on the same scheme.

## References

1. Aumelas, A., Mangoni, M., Roumestand, C., Chiche, L., Despaux, E., Grassy, G., Calas, B., Chavanieu, A. *Eur. J. Biochem.* **237**, 574–583 (1996).
2. Zhao, C., Ganz, T., Lehrer, R.I. *FEBS Lett.* **368**, 197–202 (1995).
3. Panyutich, A., Shi, J., Boutz, P.L., Zhao, C., Ganz, T. *Infect. Immun.* **65**, 978–985 (1997).
4. Storici, P., Tossi, A., Lenarcic, B., Romeo, D. *Eur. J. Biochem.* **238**, 769–776 (1996).
5. Gennaro, R., Zanetti, M. *Biopolymers* **55**, 31–49 (2000).

## **$\alpha$ -Helix Stabilizing Aromatic-Backbone Interactions**

**Gergely Tóth<sup>1</sup>, Katalin E. Kövér<sup>2</sup>, Jonathan Hirst<sup>3</sup>, Richard F. Murphy<sup>1</sup>  
and Sándor Lovas<sup>1</sup>**

<sup>1</sup>*Department of Biomedical Sciences, Creighton University, Omaha, NE 68178, USA*

<sup>2</sup>*Department of Inorganic and Analytical Chemistry, University of Debrecen,  
H-4010 Debrecen, Hungary*

<sup>3</sup>*School of Chemistry, University of Nottingham, Nottingham, NG72RD, UK*

### **Introduction**

Weakly polar interactions can occur between aromatic side chains of amino acids and groups with hydrogen bond-donating potential [1]. For example, aromatic rings in polypeptides can interact with hydrogens of backbone amides (Ar-HN interactions) and with hydrogens of CH<sub>n</sub> groups ( $\pi$ -HC interactions). Side chain-side chain and side chain-backbone interactions affect the stability of  $\alpha$ -helices. Weakly polar interactions between side chains of  $\alpha$ -helical residues have been shown to enhance  $\alpha$ -helix stability [2]. Side chain hydroxyl group-backbone interactions in  $\alpha$ -helices in the N<sub>cap</sub> and N-terminal positions are considered to stabilize and nucleate the  $\alpha$ -helix, whereas they have the opposite effect in the inner and C-terminal positions of the helix [3]. Interactions between the aromatic ring and the backbone also occur in  $\alpha$ -helices in proteins [1] where aromatic rings interact with neighboring backbone amides.

In this study the effect of the interaction between the aromatic side chain of Tyr and the helical backbone on  $\alpha$ -helix stability is investigated. The aromatic-backbone interactions were analyzed in  $\alpha$ -helices of proteins and in Ala-based  $\alpha$ -helical model peptides using circular dichroism (CD), 1D and 2D <sup>1</sup>H NMR spectroscopy, molecular dynamics (MD) and CD calculations. The effects of aromatic-backbone interactions on the helix propensity of Tyr compared with Ala are discussed.

### **Results and Discussion**

The proximity of the aromatic side chain ring to the backbone carbonyl groups can cause the coupling of the  $n\pi^*$  transitions of the carbonyl group with the  $\pi\pi^*$  transitions of the aromatic group. First principle calculations of the CD spectra [4] of peptide structures from MD trajectories showed that the tyrosine transitions can change the mean molar residue ellipticity at 220 nm in the range  $-15000$  to  $12000$  deg cm<sup>2</sup> dmol<sup>-1</sup>. For most conformations this is  $1000$ – $3000$  deg cm<sup>2</sup> dmol<sup>-1</sup>, thus, estimates of helicity derived from  $[\theta]_{222}$  for tyrosine-containing peptides tend to under estimate the helical content of the peptide.

The minima in mean molar residue ellipticity around 222 and 205 nm were indicative of helical secondary structure in the far UV CD spectra of **Y0–Y6** (Table 1). To calculate the fractional helicity (FH<sup>CD</sup>) of the peptides, the contribution of the aromatic side chain to their CD spectra at 222 nm had to be determined. Thus, CD spectra of peptides in increasing concentrations of TFE were recorded. The highest negative value of  $[\theta]_{222}$  was taken as the maximum mean molar residue ellipticity ( $[\theta_{\infty}]_{222}$ ) corresponding to the 100%  $\alpha$ -helical structure. The CD data indicate that peptides containing Tyr are less helical than is **Y0**. The <sup>1</sup>H NMR <sup>3</sup>J<sub>HN $\alpha$  coupling constant is related to torsion angle  $\phi$  and, thus, from the <sup>3</sup>J<sub>HN $\alpha$  coupling constants of subsequent residues, the secondary structure of a polypeptide chain can be deduced.</sub></sub>

Fractional helical content (FH<sup>NMR</sup><sub>3/JHN $\alpha$</sub> , Table 1), calculated from the <sup>3</sup>J<sub>HN $\alpha$</sub>  coupling constants, suggest that **Y3** and **Y4** are as helical as **Y0**, while **Y5** and **Y6** are less than

Table 1. CD and NMR analyses of peptides **Y0–Y6**.

Peptide	Amino Acid Sequence	$[\Theta]_{222}^{222}$ (deg cm <sup>2</sup> dmol <sup>-1</sup> )	FH <sup>CD</sup>	FH <sup>NMR</sup> <sub>3JHN<math>\alpha</math></sub>
<b>Y0</b>	Ac-AAAAAAEAAKA-NH <sub>2</sub>	-21465	0.62	0.57
<b>Y1</b>	Ac-YAAAAAAEAAKA-NH <sub>2</sub>	-7123	0.50	0.53
<b>Y2</b>	Ac-AYAAAAEAAKA-NH <sub>2</sub>	-6438	0.53	0.47
<b>Y3</b>	Ac-AAYAAAAEAAKA-NH <sub>2</sub>	-5764	0.46	0.58
<b>Y4</b>	Ac-AAAYAAEAAKA-NH <sub>2</sub>	-7359	0.57	0.58
<b>Y5</b>	Ac-AAAAYAAEAAKA-NH <sub>2</sub>	-4351	0.34	0.23
<b>Y6</b>	Ac-AAAAAYAEAAKA-NH <sub>2</sub>	-5714	0.45	0.23

FH<sup>NMR</sup><sub>3JHN $\alpha$</sub>  was calculated from NMR data using the method described by Lacroix and co-workers [5].

50% as helical as **Y0**. <sup>1</sup>H NMR NOE crosspeaks between hydrogens of the aromatic ring of Tyr and backbone amide hydrogens could be due to the orientation of the aromatic ring and its proximity to the backbone. From the MD simulations, NOEs between 2,6 hydrogens of the aromatic ring and *i*, *i+1* amide hydrogens in both *trans* and *gauche* orientations were detected. This is in agreement with the experimental results since NOE crosspeaks between protons of the aromatic ring and the (*i*) and (*i+1*) amide protons were found in all peptides.

In  $\alpha$ -helical structures of the peptides, different types of weakly polar interactions were detected. In *trans* orientation of the Tyr side chain, Ar(*i*)-HN(*i+4*) and  $\pi$ (*i*)-CH(*i+1* and *i+4*) interactions occurred most often. Furthermore, in *gauche* orientation, Ar(*i*)-HN(*i* and *i-4*) and  $\pi$ (*i*)-CH(*i*, *i-3* and *i+4*) interactions were detected. In both orientations, interactions between some backbone carbonyl groups and the aromatic ring of Tyr was also observed.

Side chain interference with solvation of peptide backbone groups is a major determinant of helical propensities [6,7]. With the *trans* orientation of the Tyr side chain, the solvent accessible surface area (SASA) of backbone carbonyl and amide groups in position *i* and *i+4* were approximately 80% lower than with the *gauche* orientation. With the *gauche* orientation of the Tyr side chain in **Y4**, **Y5** and **Y6**, the SASAs of backbone carbonyl and backbone amide groups in position *i-4* and *i*, respectively, were about 90% lower than with the *trans* orientation.

The interaction energy of the hydroxyphenyl group of Tyr with the  $\alpha$ -helical polypeptide backbone was calculated (Table 2). Depending on the torsion angles  $\chi^1$  and  $\chi^2$  of the aromatic residue, the interaction energy of the aromatic ring and the  $\alpha$ -helical backbone is dominated by the Ar-HN interaction, the  $\pi$ -CH interaction and the aromatic-carbonyl (Ar-CO) interaction. The difference between interaction energies in selected  $\alpha$ -helical structures of **Y5**, **Y6** and in inner positions of  $\alpha$ -helical fragments of proteins may result from the interactions of the aromatic side chain with other side chains in the  $\alpha$ -helix or with nearby side chains in the protein. The large differences seen in the CD spectra intensity of **Y1–Y6** and **Y0** are partially attributable to the contribution of the aromatic ring of Tyr. In determining FH<sup>CD</sup> of **Y1–Y6**, it was assumed that the contribution of the aromatic ring to the CD spectra is independent of the extent of helicity of the peptides. Thus, FH<sup>CD</sup> values in Table 1 might have relatively

## Analytical Methods

large errors. The lower helicity of **Y5** and **Y6** than of **Y1–Y4**, indicated by  $\text{FH}_{3\text{JHN}\alpha}^{\text{NMR}}$  can be attributed to a different degree of solvation of the backbone amide group of Tyr in the N-terminal than in the inner part of the helix. The attractive interaction between the aromatic ring and the backbone stabilizes the  $\alpha$ -helical structure of the peptides. The origin of the aromatic-backbone interaction in  $\alpha$ -helices is the sum of several noncovalent interactions, such as Ar-HN,  $\pi$ -HC and Ar-CO interactions. These are weak separately but, in combination, they can have strong influence on the stability of polypeptide structure and contribute to the intrinsic helix propensity of Tyr at a given position in the helix.

Table 2. Interaction energy (in  $\text{kcal mol}^{-1}$ ) between the side chain aromatic group of Tyr, Phe and Trp and backbone in selected  $\alpha$ -helical structures of **Y1–Y6** and in inner positions of  $\alpha$ -helical protein fragments\*. Interaction energies were calculated with the modified GROMOS87 force field using the GROMACS program.

Peptides	<i>trans</i>	<i>gauche</i>	Average
<b>Y1</b>	$-3.90 \pm 1.23$	$-2.30 \pm 0.56$	$-3.74 \pm 1.28$
<b>Y2</b>	$-3.36 \pm 0.85$	$-3.07 \pm 0.86$	$-3.20 \pm 0.87$
<b>Y3</b>	$-3.20 \pm 0.43$	$-3.50 \pm 0.29$	$-3.20 \pm 0.43$
<b>Y4</b>	$-3.53 \pm 0.52$	$-3.61 \pm 0.49$	$-3.54 \pm 0.54$
<b>Y5</b>	$-3.97 \pm 0.77$	$-4.97 \pm 1.20$	$-4.38 \pm 1.09$
<b>Y6</b>	$-3.44 \pm 0.42$	$-4.15 \pm 0.63$	$-3.75 \pm 0.68$
Tyr*	$-2.25 \pm 1.12$	$-2.06 \pm 1.83$	$-2.18 \pm 1.33$
Phe*	$-3.18 \pm 1.29$	$-2.86 \pm 1.91$	$-3.06 \pm 1.56$
Trp*	$-6.43 \pm 1.22$	$-5.78 \pm 1.02$	$-6.21 \pm 1.19$

## Acknowledgments

This work was supported by the NSF (EPS-9720643) and the Carpenter Endowed Chair in Biochemistry, Creighton University. K. E. K. thanks the National Research Foundation for financial support (OTKA T 029089 and T 034515). J. D. H. thanks the BBSRC of the U.K. for support (grant number 42/B15240).

## References

1. Tóth, G., et al. *Proteins: Struct. Funct. Genet.* **43**, 373–381 (2001).
2. Padmanabhan, S., et al. *Biochemistry* **37**, 17318–17330 (1998).
3. Vijayakumar, M., et al. *Proteins: Struct. Funct. Genet.* **34**, 497–507 (1999).
4. Besley, N.A., Hirst, J.D. *J. Am. Chem. Soc.* **121**, 9636–9644 (1999).
5. Lacroix, E., Viguera, A.R., Serrano, L. *J. Mol. Biol.* **284**, 173–91 (1998).
6. Avbelj, F., Luo, P., Baldwin, R.L. *PNAS USA* **97**, 10786–10791 (2000).
7. Levy, Y., Jortner, J., Becker, O.M. *PNAS USA* **95**, 2188–2193 (2000).

## Solution Structure of Oligopeptides–Copper(II) Complexes

Ilze Vosekalna<sup>1</sup>, Bela Gyurcsik<sup>2</sup> and Erik Larsen<sup>3</sup>

<sup>1</sup>*Institute of Organic Synthesis, Riga, LV 1006, Latvia*

<sup>2</sup>*Department of Inorganic and Analytical Chemistry, Szeged University, Szeged, H-6701, Hungary*

<sup>3</sup>*Chemistry Department, The Royal Veterinary and Agricultural University, Frederiksberg C, 1871, Denmark*

### Introduction

Combined potentiometric and spectroscopic studies on the solution equilibria of the copper(II) ion and various hexapeptide-containing systems revealed that CD measurements in the copper(II) d-d transition region are useful for the determination of the coordinating donor groups of the ligand molecules, *i.e.* the coordination structure [1]. The systematic variation of the place of amino acids with coordinating and non-coordinating side chains in the amino acid sequence as well as the presence and the absence of these resulted in series of CD spectra, the comparison of which gave us the primary information on the coordination mode. The additivity of the chiral contributions of the ligands to the optical activity in the d-d bands have been suggested for some copper(II) tripeptide complexes, assuming that only one complex species exists in the measured solution under specified conditions [2]. But published molar CD spectra are mostly not molar regarding the individual complex species, but characteristic for a mixture of several coexisting species. The relatively good agreement of the spectra of the above mentioned tripeptide systems encouraged us to perform measurements in the systems containing copper(II) and glycine-L-alanine tripeptides of various sequences, such as Gly-Gly-Ala, Gly-Ala-Gly, Ala-Gly-Gly and Ala-Ala-Ala.

### Results and Discussion

The concentration distribution diagrams were obtained by the thorough potentiometric and spectrophotometric titrations performed at the same time in the same solution with an ABU autoburette and an Ocean Optics fiber optic spectrometer. On the basis of these we calculated the molar CD for the individual complex species, which did not necessarily exist separately and in 100% of the solutions. These results allowed us to assign the CD spectra to two types of the species with the compositions of  $\text{CuLH}_{-1}$  and  $\text{CuLH}_{-2}$  where L denotes the ligand molecule deprotonated at the carboxylate and amino groups (charges are omitted for simplicity) and where the negative index of the proton is devoted to the deprotonation of the ligand molecule at the peptide group(s) as a consequence of the coordination to the metal ion. The sign and intensity of the spectra are well related to the chirality and distance of the chiral centre(s) in the peptide from the metal ion chromophore and the stability of the metal complexes, and are additive within the experimental error in both cases: the sum of the CD spectra of the Gly-Gly-Ala, Gly-Ala-Gly and Ala-Gly-Gly complexes equals to the spectra of Ala-Ala-Ala complexes (Figure 1).

Other structural methods as *e.g.* X-ray diffractometry, show that the coordination mode of tripeptides around copper(II) ion is square planar, thus the main chiral contribution is the vicinal chirality. The evaluation of only the potentiometric measurements, resulted in the involvement of further species as  $\text{CuL}$  in the acidic and  $\text{CuLH}_{-3}$  in the basic pH region in relatively low concentrations without significant effect on the species distribution of the earlier two species. The stability constants were comparable to those values from the literature. However, nor reliable CD spectra could be calcu-

lated neither the additivity could be applied for these two species, therefore their existence is not supported.

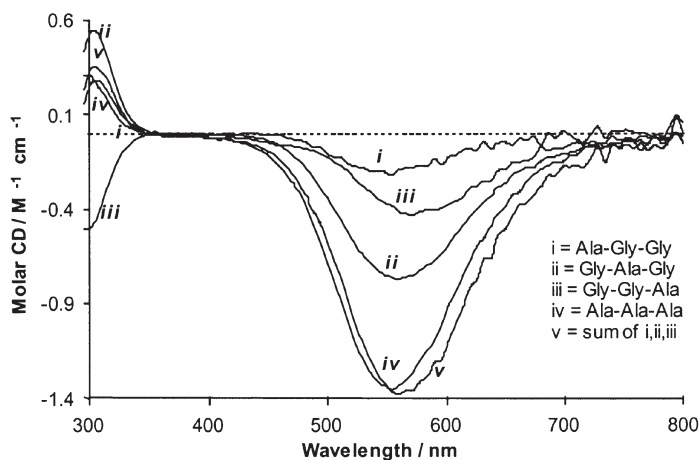


Fig. 1. CD spectra of the tripeptide-Cu(II) complexes.

Further investigations started with more complex systems. Glycine, L-alanine and L-histidine will be combined in the tripeptide sequences, since L-histidine moiety plays an exceptional role from the coordination chemistry point of view of peptides and proteins, which is due to the ability of the imidazol nitrogen(s) in the amino acid side chain to serve as a primary binding site – an anchor – for most metal ions in biological systems.

## References

1. Gyurcsik, B., Vosekalna, I., Larsen, E. *Acta Chem. Scand.* **51**, 49–58 (1997).
2. Sigel, H., Martin, R.B. *Chem. Rev.* **82**, 385–394 (1982).

## Development of Antibodies Against Conjugated Benzophenone, as a Tool in Photoaffinity Crosslinking Studies

Dror Yahalom, Michael Rosenblatt and Michael Chorev

*Division of Bone and Mineral Metabolism, Charles A. Dana and Thorndike Laboratories,  
Department of Medicine, Beth Israel Deaconess Medical Center and Harvard Medical School,  
Boston, Massachusetts 02215, USA*

### Introduction

The photoaffinity scanning (PAS) methodology is widely used for mapping the bimolecular ligand-acceptor interface. In the case of G protein-coupled receptors (GPCR's), which are not yet amenable to either NMR or X-ray analysis, the benzophenone-based PAS approach is almost the only direct method to gain insight on the contact sites between ligands and their cognate receptors. Identification of the contact sites is based on the analysis of the enzymatic and chemical fragmentation patterns of the radiolabeled ligand-receptor photoconjugate. Efficient and specific isolation of the radiolabeled ligand-receptor photoconjugate and photoconjugated fragments is detrimental for generating the quantities of highly pure material needed for sequencing or mass-spectrometric analysis. To this end, we undertook the development of antibodies that will identify the benzhydrol moiety (BH) obtained from the photophore, the benzophenone (BP) moiety, upon photoinsertion reaction at the contact site. Such antibodies will discriminate between and separate the conjugated from the non-conjugated species, and provide a universal affinity purification tool for the BP-based PAS approach. If successful, the use of anti-BH polyclonal antibodies will provide access to less stringent experimental design, eliminate the need for radiotagging, and facilitating access to a wider range of analytical instrumentation.

### Results and Discussion

The design of the antigen for immunization aimed to maximize the versatility of recognizable conjugated sites of the BH hapten. The antigen was generated by photocrosslinking a BP-containing molecule to carrier proteins such as BSA, KLH, ovalbumin and phosphorylase B (Figure 1). This non-targeted and non-specific photo-insertion of the BP-derived triplet biradical into the carrier protein will occur at amino acid residues susceptible to this reaction. Therefore, the presentation of the BH hapten is anticipated to cover the whole spectrum of amino acid residue-BH adducts that may be generated in different BP-based PAS experiments.

The BP moiety was introduced as the N-Su-Bpa-OH (N-Su-*p*-benzoyl-phenylalanine). The succinylation enhanced the water-solubility of Bpa, and when needed al-

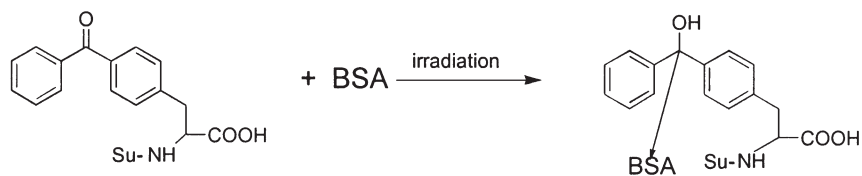


Fig. 1. Photoconjugation reaction of N-Su-Bpa-OH to BSA resulted in the BSA-BH antigen that was used for immunization. The molecular ratio of BH to BSA was 28 : 1.

lowed radiotagging by employing  $^{14}\text{C}$ -succinic anhydride. Photoconjugation in the presence of  $^{14}\text{C}$ -N-Su-Bpa-OH allowed quantifying the molecular ratio of carrier protein to hapten, *e.g.* BSA-BH (1 : 28). The incorporation of hapten into the carrier protein was assessed by the increase in molecular weight as monitored by PAGE analysis. Photoconjugation with other BP-containing ligands were carried out in a similar manner.

Anti-BSA-BH polyclonal antibodies were raised in rabbits and analyzed by ELISA employing microarray plates coated with carrier protein-BH conjugates and detected by alkaline phosphatase-tagged secondary (goat anti-rabbit IgG) antibodies.

These studies led to the following observations: 1) Both BSA and BSA-BH are recognized by the anti-BSA-BH antibodies with a high titer (1 : 25,000). 2) KLH-BH and ovalbumin-BH, but not KLH and ovalbumin, are recognized by diluted antisera. Thus, the antisera specifically recognize the BH hapten moiety. 3) The [N-Su-Ala-Bpa-Asp-OH]-KLH, a tripeptide photoconjugate, is also recognized by the antisera. This conjugate, with a molecular ratio of 1 : 60 (KLH : tripeptide) was better detected by the antisera than the KLH-BH conjugate with a molecular ratio of 1 : 135 (KLH : BH). 4) The [N-Su-Ala-Bpa-Asp-OH]-phosphorylase B (MW 97 kDa) photoconjugate (molecular ratio about 1 : 1) is also identified by the anti-BSA-BH antibodies. This later observation is of a particular significance, suggesting that these antibodies will also identify GPCR's, which are similar in size to phosphorylase B and conjugated to a single molecule of BP-containing ligand. 5) We were very encouraged by the capacity of the anti-BSA-BH polyclonal antibodies to identify specifically the  $[\text{Bpa}^3]\text{PTH}(1-34)$  (a parathyroid hormone derivative) photoconjugated to KLH (~400 kDa) (molecular ratio peptide : KLH is 0.6 as quantified by incorporating the radioiodinated peptide).

Purification of the crude anti-BSA-BH polyclonal antibodies using a BSA-affinity column resulted in a fraction of antibodies with high affinities towards BSA-BH and KLH-BH conjugates and insignificant affinity towards BSA. Interestingly, the [N-Su-Ala-Bpa-Asp-OH]-KLH photoconjugate was recognized only by the BSA-affinity retained fraction, but not by the affinity purified one. Apparently, our purification strategy has narrowed substantially the essential diversity to recognize a wide range of BH-containing epitopes. Therefore, in our future experiments we will use the crude antisera. However, since it presents cross-BSA reactivity, we will have to eliminate BSA from our photoconjugated systems.

In conclusion, we have generated antisera that recognize various BP-containing amino acids and peptides photoconjugated to different carrier proteins. The recognition is specific to the benzhydrol (BH) moiety. The sensitivity of detection, as tested by ELISA, is high enough to detect a single BH moiety on large proteins. These antisera have the properties that may yield a potential tool for purification of ligand-GPCR conjugates and their conjugated fragments produced during PAS. We are currently testing the antisera in affinity chromatography and immunoprecipitation of BP-based conjugates of the parathyroid hormone and its cognate GPCR.

## Monitoring Peptide-Induced Liposome Breakdown with Fluorescence Correlation Spectroscopy

Susanne Gangl<sup>1</sup>, M. Knapp<sup>1</sup>, S. Kuepcue<sup>2</sup>, G. Koehler<sup>1</sup> and Jack Blazyk<sup>3</sup>

<sup>1</sup>Institute for Theoretical Chemistry and Structural Biology, University of Vienna  
 and Austrian Society for Aerospace Medicine, Vienna, Austria

<sup>2</sup>Zentrum für Ultrastrukturforschung, Ludwig Boltzmann-Institut, Universität für Bodenkultur,  
 Vienna, Austria

<sup>3</sup>Department of Biomedical Sciences, College of Osteopathic Medicine, and Department  
 of Chemistry and Biochemistry, Ohio University, Athens, OH 45701, USA

### Introduction

The resistance of various bacterial strains against conventional antibiotics has increased rapidly, leading to enhanced interest in antimicrobial peptides [1]. The bacteriolytic activity of linear, cationic and cystein-free antimicrobial peptides stems primarily from their ability to perturb the lipid bilayer structure of membranes, and is not related to binding to a specific protein receptor site. The antimicrobial peptides magainin and peptidyl-glycyl-leucine-carboxamide (PGLa) were isolated from frog skin [2]. A common feature of these peptides is their propensity to form amphipathic  $\alpha$ -helices, *i.e.* helices with polar and nonpolar groups on opposite faces of the helix.

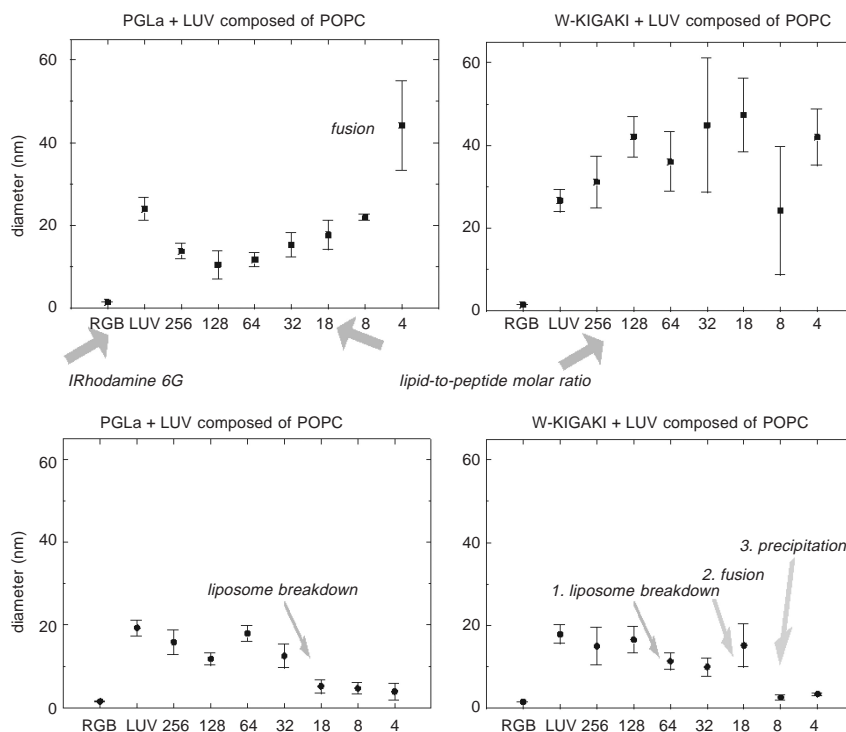


Fig. 1. Effect of PGLa and W-KIGAKI on large unilamellar vesicles (LUV) composed of POPC and POPG.

The effect of PGLa and two derivatives of PGLa on liposomes containing fluorescent lipids is investigated by fluorescence correlation spectroscopy (FCS). Diffusion coefficients derived from FCS give insight into the size distribution of liposomes and membrane fragments. Information on peptide-induced micellization, precipitation and/or fusion of membrane-fragments contributes to a better understanding of the mechanism of how peptides can distinguish between various membrane surfaces.

### **Results and Discussion**

PGLa and W-PGLa [3] adopt an  $\alpha$ -helix when bound to a membrane. W-KIGAKI is a novel linear amphipathic  $\beta$ -sheet antimicrobial peptide with enhanced selectivity for bacterial lipids [4].

Large unilamellar vesicles (LUV) composed of POPC remain intact up to lipid-to-peptide molar ratios of 16. The average size of liposomes decreases in the presence of PGLa, but increases in the presence of the  $\beta$ -sheet antimicrobial peptide W-KIGAKI. Liposomes composed of the negatively charged lipid POPG are destroyed by both the  $\alpha$ -helical and the  $\beta$ -sheet antimicrobial peptides (Figure 1).

The  $\beta$ -sheet antimicrobial peptide induces extensive fusion of liposomes composed of POPG at lipid-to-peptide molar ratios around 20. Large precipitates are not detected by FCS, but are clearly visible by eye and by freeze fracture electron microscopy.

Fluorescence correlation spectroscopy is shown to be a sensitive technique to follow membrane disruption, and to determine the size distribution of liposomes and membrane fragments.

### **Acknowledgments**

Financial support from the Austrian Society of Aerospace Medicine and from the Austrian Academy of Sciences to S. G. (APART-DOC) are gratefully acknowledged.

### **References**

1. Lohner, K. (Ed.), Staudegger, E., In *Development of Novel Antimicrobial Agents: Emerging Strategies*, Horizon Scientific Press, Norfolk, UK, 2000, p. 1.
2. Zasloff, M. *Proc. Natl. Acad. Sci. USA* **84**, 5449–5453 (1987).
3. Pérez-Payá, E., Houghten, R.A., Blondelle, S.E. *J. Biol. Chem.* **271**, 4120–4126 (1996).
4. Blazyk, J., Wiegand, R., Klein, J., Hammer, J., Epand, R.M., Epand, R.F., Maloy, L.W., Prasad Kari, U.P. *J. Biol. Chem.* **276**, 27899–27906 (2001).

## NMR Structural Investigation of a $\beta^3$ -Dodecapeptide with Proteinogenic Side Chains in MeOH and Water

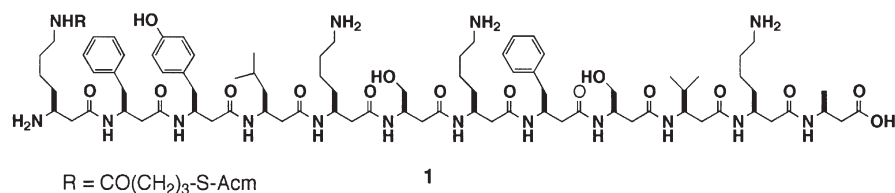
Touraj Etezady-Esfarjani<sup>1</sup>, Christian Hilty<sup>1</sup>, Kurt Wüthrich<sup>1</sup>,  
Magnus Rueping<sup>2</sup> and Dieter Seebach<sup>2</sup>

<sup>1</sup>*Institut für Molekularbiologie und Biophysik, Eidgenössische Technische Hochschule,  
CH-8093 Zürich, Switzerland*

<sup>2</sup>*Laboratorium für Organische Chemie, Eidgenössische Technische Hochschule,  
Universitätstrasse 16, CH-8092 Zürich, Switzerland*

### Introduction

Oligomers of  $\beta$ -amino acids ( $\beta$ -Peptides) have made their debut as a promising class of peptidomimetics. They have been shown to fold into well-ordered secondary structures, such as helices, turns and sheets [1]. Their wide structural diversity, together with the finding that  $\beta$ -peptides are resistant to degradation by peptidases, make them interesting for pharmaceutical applications [2,3]. Short  $\beta$ -peptides built from  $\alpha$ -amino acid homologs (insertion of a methylene group) form a left handed  $3_{14}$ -helix in MeOH. We wondered whether  $\beta^3$ -peptides with longer chain lengths would still form stable secondary structures in MeOH, or whether they would even form a  $3_{14}$ -helix that is stable in water. Therefore the  $\beta^3$ -dodecapeptide **1** was investigated by two-dimensional homonuclear NMR spectroscopy in MeOH and water.



### Results and Discussion

The spectra recorded in methanol at 800 MHz showed good separation of all signals and revealed that the  $\beta^3$ -dodecapeptide **1** adopts a well defined left-handed  $3_{14}$ -helical structure with eight 14-membered H-bonded rings and a *ca* 5 Å pitch. All NOEs typical for a  $3_{14}$  helix (Figure 1) are indeed found in the NOESY spectra recorded with a mixing time of 150 ms. The NMR spectra recorded in aqueous solution showed more spectral overlap, but still allowed for complete resonance assignments. No NOEs typical for a  $3_{14}$  helix were observed in the NOESY spectra measured in aqueous solution.

Only sequential NOEs  $d(\text{NH}_i, \beta_{i+1})$ , which are not compatible with any helical structure were observed, suggesting that the  $\beta^3$ -peptide **1** adopts an extended or elongated conformation in water.

The investigation shows that the  $\beta^3$ -dodecapeptide **1** adopts different conformations in MeOH and water. It will be interesting to see whether methanol/water mixtures lead to partially helical conformations, and whether the introduction of side chains which are able to form salt-bridges would stabilize the helix in water [4].

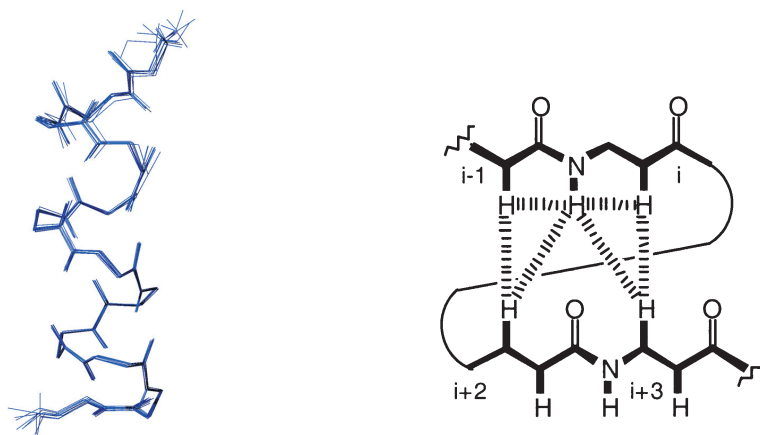


Fig. 1. Bundle of 10 structures obtained from the calculation using the NOE distance restraints (left). Schematic NOE pattern observed for  $3_{14}$ -helical conformations.  $\text{NH}_i$  shows strong NOEs to the protons  $\text{H}_{\alpha\text{-C}(\alpha)_{i-1,i}}$  and NOEs of medium strength to  $\text{H-C}(\beta)_{i+2,i+3}$  (right).

## References

1. Stigers, K.D., Soth, M.J., Nowick, J.S. *Curr. Opin. Chem. Biol.* **3**, 714 (1999).
2. Gademann, K., Ernst, M., Hoyer, D., Seebach, D. *Angew. Chem.* **111**, 1700 (1999).
3. Porter, E.A., Wang, X., Lee, H.S., Weisblum, B., Gellman, S.H. *Nature* **404**, 565 (2000).
4. Arvidsson, P.I., Rueping, M., Seebach, D. *Chem. Commun.* **5**, 649 (2001).

## Conformational Studies on a Synthetic Peptide with Prolactin-Releasing Activity in a Membrane Mimetic Environment

A. Di Fenza<sup>1</sup>, S. Albrizio<sup>2</sup>, A. D'Ursi<sup>1</sup>, D. Picone<sup>3</sup> and P. Rovero<sup>1</sup>

<sup>1</sup>Dipartimento di Scienze Farmaceutiche, Università di Salerno, Fisciano, Italy

<sup>2</sup>Dipartimento di Chimica Farmaceutica e Tossicologica, Università Federico II di Napoli, Napoli, Italy

<sup>3</sup>Dipartimento di Chimica, Università Federico II di Napoli, Napoli, Italy

### Introduction

Prolactin is an anterior pituitary hormone important in pregnancy and lactation in mammals. It is involved in the development of the mammary glands and the promotion of milk synthesis. Although several hypothalamic peptide hormones that regulate the secretion of anterior pituitary hormones have been identified, none of these is able to regulate the release of prolactin in a specific manner. Recently, a novel bioactive peptide, named prolactin-releasing factor, PrRP, has been isolated from bovine hypothalamic tissues as a ligand of an orphan seven-transmembrane-domain receptors hGR3 [1]. PrRP has been shown to play a central role in PRL secretion, both *in vitro* and, in rats, *in vivo*. It generates two forms of mature peptides as naturally occurring endogenous ligands, named PrRP31 (S R T H R H S M E I R T P D I N P A W Y A S R G I R P V G R F-NH<sub>2</sub>) and PrRP20 (T P D I N P A W Y A S R G I R P V G R F-NH<sub>2</sub>), respectively, that exhibit the same activities with respect to the whole protein. Herein, we describe the conformational analysis of PrRP20 by NMR spectroscopy and molecular modeling methods.

### Results and Discussion

A whole set of 1D and 2D protonic spectra was recorded in water and in water/sodium dodecylsulfate (SDS). The solvent for NMR analysis was chosen with the aim to reproduce a biologically significant environment, and to create conditions able to favor the prevailing of ordered conformers in solution over extended and/or disordered ones. Accordingly, since PrP20 acts through a specific interaction with a membrane receptor, we used SDS micelles as a biological membranes-mimicking environment [2]. DQF-COSY, TOCSY and NOESY experiments were recorded on a Bruker 600 MHz at 300 K. The complete <sup>1</sup>H chemical shift assignment of PrRP20 was achieved accord-

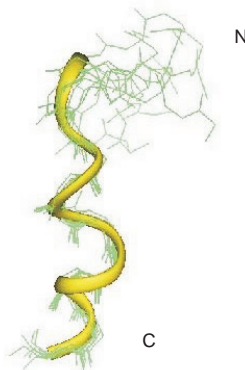


Fig. 1. Superposition of the 10 final structures of PrRP20.

ing to the Wüthrich procedure [3]. All NMR data revealed that PrRP20 is mainly unstructured in aqueous solution, while it clearly adopts a helical conformation in the presence of SDS micelles.

Three-dimensional structures were calculated by simulated annealing in torsion angle space, and restrained molecular dynamics methods based on 362 NOE derived restraints, using the DYANA software package [4]. Among 50 calculated structures, the 20 structures with the lowest values of their target function were subjected to further procedures of minimization with the SANDER module of AMBER 5.0 software using the DYANA derived restraints. Figure 1 shows the best 10 final structures of PrRP20. They are characterised by the common conformation in the C-terminal part, which converges to a 310-helical arrangement (RMSD = 0.4, calculated on backbone heavy atoms N, C $\alpha$ , C'O of residues 11-19).

The conformational characterization of PrRP20 represents a key step for the determination of the structural requirements necessary to activate hGR3 receptor, and represents the basis for the design of pharmacologically significant peptidomimetic agonists. On the other hand, recent studies report other potential actions of PrRP20, *e.g.*, as neuromodulator in the central nervous system [5]. In such a context, the understanding of structural determinants of the receptor/ligand interaction provides new insights to classify PrRP with its receptor, and to define their physiological role.

## References

1. Hinuma, S., Habata, Y., Fujii, R., Kawamata, Y., Hosoya, M., Fukusumi, S., Kitada, C., Masuo, Y., Asano, T., Matsumoto, H., Sekiguchi, M., Kurokawa, T., Nishimura, O., Onda, H., Fujino, M. *Nature* **393**, 272–276 (1998).
2. Blondelle, S.E., Forood, B., Houghten, R.A., Perez-Paya, E. *Biopolymers* **42**, 489–498 (1997).
3. Wüthrich, K., In *NMR of Proteins and Nucleic Acids*, John Wiley & Sons, Inc. (Eds), New York, 1986.
4. Guntert, P., Mumenthaler, C., Wüthrich, K. *J. Mol. Biol.* **273**, 283–298 (1997).
5. Samson, W.K., Resch, T.Z., Murphy, T.C. *Brain Res.* **858**, 18–25 (2000).

## **Analysis and Characterization of Combinatorial Mixtures of Mucin-2 Antigen Peptides**

**Emöke Windberg<sup>1</sup>, Ferenc Hudecz<sup>1</sup>, Andreas Marquardt<sup>2</sup>, Szilvia Bösze<sup>1</sup>,  
Ferenc Sebestyén<sup>3</sup>, Hedvig Medzihradszky-Schweiger<sup>1</sup>  
and Michael Przybylski<sup>2</sup>**

<sup>1</sup>*Research Group of Peptide Chemistry, Hungarian Academy of Sciences,  
Budapest 112, H-1518, Hungary*

<sup>2</sup>*Department of Analytical Chemistry, University of Konstanz, Konstanz, Germany*

<sup>3</sup>*Department of Organic Chemistry, Eötvös L. University, Budapest, Hungary*

### **Introduction**

An epitope motif, TX<sup>1</sup>TX<sup>2</sup>T, of mucin-2 glycoprotein was identified by means of a monoclonal antibody, Mab 994 raised against a synthetic mucin-derived 13-mer peptide-conjugate [1,2]. For determination of the epitope sequence recognised with highest affinity by the antibody, a combinatorial approach was applied. We have prepared 19 sub-libraries (TATX<sup>2</sup>T, TDTX<sup>2</sup>T, TYTX<sup>2</sup>T) with portioning-mixing technique [3] using Boc/Bzl chemistry. Each library contained one pre-selected amino acid in position X<sup>1</sup> and all proteinogenic amino acids, except Cys, in position X<sup>2</sup> [1]. Antibody binding of sub-libraries was most profound when Gln was at the X<sup>1</sup> position. 19 individual peptides corresponding to the TQTX<sup>2</sup>T sub-library were synthesised and tested. Binding data showed that apart from the native TQTPT peptide other compounds (*e.g.*, TQTAT) were also recognised [4]. For the analytical characterization of the TQTX<sup>2</sup>T sub-library MALDI-TOF-MS and ultrahigh-resolution ESI-FTICR-MS as well as amino acid analysis were applied (cysteine was omitted for practical reasons). Shorter libraries corresponding to X<sup>2</sup>T and TX<sup>2</sup>T were also produced for amino acid analysis. To evaluate the resolution power of these MS methods we have prepared and tested “artificial” peptide mixtures of different complexity by mixing 6, 10, or 19 individual peptides corresponding to the TQTX<sup>2</sup>T. Thus equimolar mixtures of pentapeptides were analysed and compared with the combinatorial mixture.

### **Results and Discussion**

Amino acid analysis results showed that all amino acids in X<sup>2</sup> position were built in. The data obtained from the sub-libraries with short peptides (X<sup>2</sup>T and TX<sup>2</sup>T) corresponding to TQTX<sup>2</sup>T are much more reliable as compared to those of the TQTX<sup>2</sup>T mixture. We have concluded that peptide mixtures could be characterized also by amino acid analysis by reduction of the length of the peptides if X amino acid is in the second position. The TQTX<sup>2</sup>T sub-library and the “artificial” mixtures with different complexity (6, 10 and 19 components) were subjected to mass spectrometrical measurements. MALDI-TOF-MS was capable to detect all components in the 6- and 10-member mixture, while this method failed to identify 19 components. Each component of this mixture could be fully identified only by ESI-FTICR-MS. This method resolved all mixtures and detected apart from the all signals of the protonated molecule ions also all of the sodiated TQTX<sup>2</sup>T peptide signals (Table 1). The high resolution ESI-FTICR-MS was able to distinguish all of the components also in the TQTX<sup>2</sup>T sub-library. Interestingly the combinatorial mixture contained only protonated molecule ions. Isobaric pentapeptides, TQTIT and TQTLT, gave only one signal with double intensity. We have distinguished even between the monoisotopic molecular masses of TQTKT and TQTQT pentapeptides ( $\Delta m = 0.0364$  amu).

Table 1. Molecular masses of the 19 TQTX<sup>2</sup>T peptides of the peptide mixture (ESI-FTICR-MS).

Peptide	[M + H] <sup>+</sup> <sub>calc.</sub>	[M + H] <sup>+</sup> <sub>exp.</sub>	Δm/ppm	[M + Na] <sup>+</sup> <sub>calc.</sub>	[M + Na] <sup>+</sup> <sub>exp.</sub>	Δm/ppm
TQTAT	521.2566	521.2533	6.3	543.2385	543.2369	3.0
TQTDT	565.2464	565.2453	1.9	587.2283	587.2264	3.3
TQTET	579.2621	579.2602	3.2	601.2440	601.2431	1.5
TQTFT	597.2879	597.2864	2.5	619.2698	619.2681	2.8
TQTGT	507.2409	507.2393	3.2	529.2229	529.2211	3.3
TQTHT	587.2784	587.2764	3.4	609.2603	609.2577	4.3
TQTIT	563.3035	563.3017	3.2	585.2855	585.2842	2.2
TQTKT	578.3144	578.3127	3.0	600.2964	600.2969	0.9
TQTLT	563.3055	563.3017	3.2	585.2855	585.2842	2.2
TQTMT	581.2599	581.2586	2.3	603.2419	603.2406	2.1
TQTNT	564.2624	564.2609	2.6	586.2443	586.2420	4.0
TQTPT	547.2722	547.2704	3.3	569.2542	569.2524	3.1
TQTQT	578.2780	578.2759	3.7	600.2600	600.2592	1.3
TQTRT	606.3206	606.3187	3.1	628.3025	628.3002	3.7
TQTST	537.2515	537.2498	3.1	559.2334	559.2312	4.0
TQTTT	551.2671	551.2658	2.4	573.2491	573.2470	3.6
TQTVT	549.2879	549.2862	3.0	571.2698	571.2679	3.4
TQTWT	636.2988	636.2961	4.2	658.2807	658.2800	1.1
TQTYT	613.2828	613.2801	4.4	635.2647	635.2614	5.2

### Acknowledgments

This work was supported by grants from the Ministry of Education (Hungary) FKFP 0101/97 and 0229/99, and the Deutsche Forschungsgemeinschaft (Bonn, Germany). Thanks are due to Eszter Illyés and Andrea Kiss for their contributions to the synthesis.

### References

1. Uray, K., Kele, P., Windberg, E., Illyés, E., Medzihradsky-Schweiger, H., Sebestyén, F., Price, M.R., Hudecz, F., In Bajusz, S. and Hudecz, F. (Eds.) *Peptides 1998 (Proceedings of the 25th European Peptide Symposium)*, Akadémiai Kiadó, Budapest, 1999, pp. 638–639.
2. Durrant, L.G., Jacobs, E., Price, M.R. *Eur. J. Cancer* **30A**, 355–391 (1994).
3. Furka, Á., Sebestyén, F., Asgedom, M., Dibó, G. *Int. J. Pept. Protein Res.* **37**, 487–492 (1991).
4. Hudecz, F., Uray, K., Windberg, E., Illyés, E., Majer, Zs., Price, M.R., Sebestyén, F., In Epton, R. (Ed.) *Innovation and Perspectives in Solid Phase Synthesis & Combinatorial Libraries 1999*, Mayflower Worldwide, Birmingham, 2001, pp. 169–172.

## High Throughput Validation and Quantitation of Synthetic Peptides *via* LC-MS

Lin Chen, Michael James, Brian Korenstein, Brian Miller  
and J. Mark Carter

AxCell Biosciences, Newtown, PA 18940-1721, USA

### Introduction

In support of our high throughput parallel peptide synthesis, which produces over 1000 synthetic peptide ligands per month, we have developed a high throughput method for validation and quantitation of synthetic peptides. This method includes automated LC-MS analysis, data processing, and sample purification steps. We were able to achieve high throughput while retaining sufficient sensitivity and resolution to accomplish characterization. At both analytical and semi-prep scale, data analysis and sample tracking were automated using a blend of proprietary and manufacturers' software.

### Results and Discussion

Our LC-MS system is equipped with a LEAP (Carrboro, NC) HTS auto sampler with capacity of six deepwell microplates, a Shimadzu (Columbia, MD) VP series HPLC system, and a PE Sciex (Toronto) API 165 (single quadrupole) mass spectrometer. With two Phenomenex (Torrance, CA)  $30 \times 1.0$  mm Luna  $3 \mu$  C8 columns at  $50^\circ\text{C}$ , one column analyzed the sample while the other column was re-equilibrated off line by a third aqueous solvent pump. The HPLC traces were monitored by total ion count (TIC) and by UV. A dansyl fluoro/chromophore (330 nm) was tagged on every peptide through a spacer lysine side chain to facilitate detection and quantitation. Including column washing (1 min), method loading, and sample injection, we achieved LC-MS analysis of peptides at the rate of 7 min/sample (Figure 1).

The data generated by LC-MS were analyzed using PE Sciex BioMultiview software. High throughput was facilitated by automated data analysis software developed

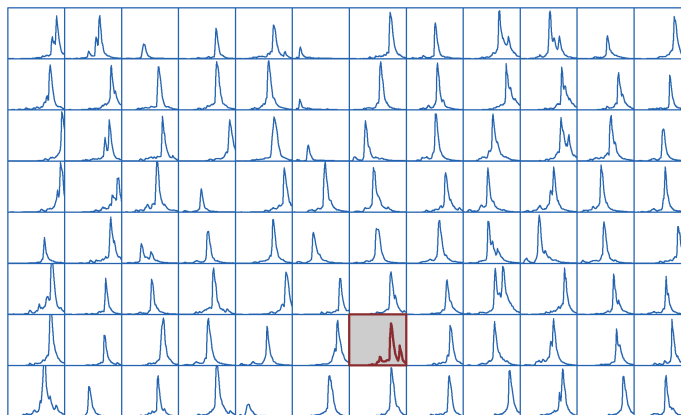


Fig. 1. Total ion count (LC-MS) profiles of 96 peptide samples analyzed in 11 h. Samples: 1–20  $\mu\text{g}$  crude peptide in  $1.0 \mu\text{L}$  water/acetonitrile/acetic acid (80 : 10 : 10). Gradient: 0–60% B in 5 min,  $350 \mu\text{L}/\text{min}$  (A = 0.1% acetic acid in water, B = 0.1% acetic acid in methanol).

in house. For each peptide sample:  $(M + H)^+/Z$  was extracted from MS data and compared to the expected mass for that sample, as calculated from its sequence. If the main peak observed in the MS matched the expected MW value for the peptide, the UV absorbance trace was integrated to determine purity and yield. The percent area of the correctly identified peak, corresponding to the desired  $(M + H)^+$  in the total integrated area, reflected the purity of the peptide. Yield was determined from the absolute absorbance of that peak as compared to a standard curve. Samples not achieving the established purity threshold (85%) were flagged in the database for subsequent purification. It took less than 10 min to accomplish automated data analysis for 96 LC-MS data files, determining both purity and yield.

When necessary, we purified crude peptide samples using two identical Gilson (Middleton, WI) HPLC systems equipped with model 215 liquid handlers for sample injection and fraction collection. Similar to our LC-MS system, each Gilson HPLC system was equipped with two Varian (Palo Alto) 25 cm  $\times$  1.0 cm Dynamax 5  $\mu$  300 Å C8 columns. A sample of 1–20 mg crude peptide in 1.0 mL water/acetonitrile/acetic acid (80 : 10 : 10) was separated with a gradient of 10–40% B to 25–55% B (determined by retention time in LC-MS analysis) in 20 min at 4 mL/min (A = 0.1% TFA in water, B = 0.1% TFA in acetonitrile). While one column separated the sample, the other column was re-equilibrated off line. 0.5 mL fractions were collected while the UV (215 nm) absorbance exceeded a threshold of 0.1 AU. After separation the fractions were pooled for LC-MS re-analysis. Including column washing (5 min), method loading, and sample injection, it took one day to separate 50 samples with each system.

In summary, we have developed a high throughput method for peptide validation and quantitation in support of high throughput synthesis. Key instrument techniques included handling all samples in microplates, column switching on both analytical and semi-preparative scale HPLC systems, and the use of 1.0 mm ID columns at elevated temperature for LC-MS. Also critical was our development of a robust rapid gradient reverse phase analytical separation for LC-MS that is optimized for throughput and achieves sufficient resolution power by the synergistic application of MS selectivity. Our LC-MS analysis achieved the rate of about 200 samples per day, and each purification system allowed us to purify up to 50 samples per day. Another key feature for maximum laboratory throughput was proprietary automated data analysis software developed. This accelerated the processing of LC-MS data, so that it took less than 10 min to perform data analysis of 96 peptide samples and linked selection of the optimal gradient for purification to the retention time values observed in analytical LC-MS.

## **Synthesis and Solution Three-Dimensional Structure of the Immunodominant Region of Protein G of Human RSV**

**A. Beck<sup>1</sup>, M. Sugawara<sup>2</sup>, J. Czaplicki<sup>2</sup>, C. Klinguer-Hamour<sup>1</sup>,  
J.-F. Haeuw<sup>1</sup>, T. Nguyen<sup>1</sup>, A. Van Dorsselaer<sup>3</sup>, J.-Y. Bonnefoy<sup>1</sup>  
and A. Milon<sup>2</sup>**

<sup>1</sup>*Centre d'Immunologie Pierre Fabre, F74164 Saint-Julien-en-Genevois, France*

<sup>2</sup>*IPBS-CNRS, F-31077 Toulouse, France*

<sup>3</sup>*ECPM-CNRS, F-67000 Strasbourg, France*

### **Introduction**

Human Respiratory Syncytial Virus (hRSV) is a major pathogen responsible for bronchiolitis and severe pulmonary disease. BBG2Na is a promising subunit vaccine candidate against this pathogen [1]. It is a well defined recombinant protein [2], composed of G2Na(130-230), the central domain of RSV G glycoprotein [3] and BB, an albumin binding domain of streptococcal protein G [4]. The G2Na part contains 4 Cys and several protective epitopes [5], while the BB part has shown carrier properties [4]. Phase I and II clinical trials were very promising [6], and phase III is on going. BBG2Na (pI = 9.3) was recently shown to be strongly adsorbed by  $\text{AlPO}_4$  (pZ<sub>0</sub> = 4.0) and surprisingly by  $\text{Al}(\text{OH})_3$  (pZ<sub>0</sub> = 11.1) [7]. These unexpected properties could be due to the presence of 2 independent structural domains with opposite charges (BB, pI = 5.5 and G2Na, pI = 10.0) that is not reflected by the pI of the whole protein. G2Na(130-230) was generated by CNBr cleavage of BBG2Na and purified. The Cys pairings were established after enzymatic digestion and LC-MS. On the other hand, all 3 possible isomers of the 4 Cys containing peptide G4a(172-187) were obtained using various oxidation conditions [3]. G4a(Cys<sup>173</sup>-Cys<sup>186</sup>/Cys<sup>176</sup>-Cys<sup>183</sup>), which corresponded to the native isomer, was investigated by 2D NMR in solution and a three-dimensional structure was established by molecular modeling.

### **Results and Discussion**

#### *Proteins BBG2Na, G2Na Production and Disulfide Bridge Analysis by MS*

Gene assembly, vector constructions and expression of BBG2Na were undertaken as previously described [3]. The protein was produced in *E. coli*. The primary structure of BBG2Na (349 AA; 38672 Da) was confirmed by LC-MS of the trypsin peptide map [3]. G2Na (103 AA; 11703 Da) was obtained after chemical cleavage of BBG2Na by CNBr [8], digested by Asp-N [8] and analyzed by LC-MS. Peptide D3(166-213) which contained the 4 Cys, was further digested with thermolysin [8] and analyzed by LC-MS. The disulfide pairing found was in agreement with the RSV protein G native one.

#### *G4a (1-2/3-4), (1-3/2-4), (1-4/2-3) Synthesis and Disulfide Bridge Analysis by MS*

Peptides G4a (hRSV-A subgroup G protein, [172-187]) were used as a model for oxidation and disulfide assignment. Using solid phase peptide synthesis, the reduced version was obtained with good homogeneity (1740.09). The raw peptide G4a-red was submitted to 4 different oxidation conditions [3]. The DMSO oxidation resulted in 3 main peaks (34/42/24 ratio) easily separated by HPLC. Using thermolysin, which catalyses the hydrolysis of peptide bonds involving the amino groups of hydrophobic residues [8], new fragments were obtained for each previously isolated isomer. These fragments were analyzed by LC-MS: G4a-ox1 peptide was identified as G4a(1-3/2-4) isomer, G4a-ox2 as G4a(1-4/2-3) and G4a-ox3 as G4a(1-2/3-4) [3].

## Analytical Methods

**G4a (1-4)/(2-3) Three-Dimensional Structure Determination by NMR Spectroscopy**  
2D-Nuclear Overhauser effect spectroscopy (NOESY) and total correlation spectroscopy (TOCSY) experiments were recorded on a Bruker DMX 500 MHz spectrometer (T = 285 K; pH = 4.6; NOESY: mixing time 100, 200 and 400 ms; TOCSY: mixing time 25 and 70 ms). The sample was obtained with 1 mM peptide in H<sub>2</sub>O/D<sub>2</sub>O (90 : 10) and in 99.9% D<sub>2</sub>O for determination of slow exchange NH experiment. Simulated annealing was coupled with molecular dynamics (simulation time: 260 ps) [9]. Force field: CVFF integrated in the Discover program (Insight II, MSI Inc.) The disulfide bridges were assigned as Cys<sup>173</sup>-Cys<sup>186</sup> and Cys<sup>176</sup>-Cys<sup>183</sup> on the basis of long range NOEs probably forming a surface exposed loop.

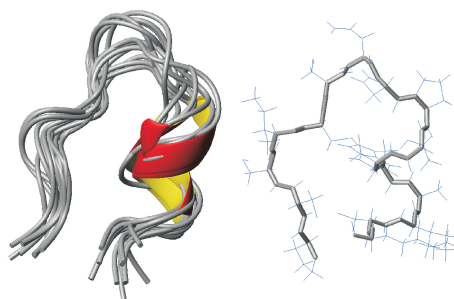


Fig. 1. G4a (1-4)/(2-3) three-dimensional structure determined by NMR spectroscopy.

## Conclusion

The cysteine pairings of BBG2Na, G2Na and G4a were established after chemical cleavage, enzymatic digestion and LC-MS analysis. The three-dimensional solution structure of the immunodominant central conserved region of the G protein of human RSV A [G4a(Cys<sup>173</sup>-Cys<sup>186</sup>/Cys<sup>176</sup>-Cys<sup>183</sup>)] was determined by NMR. It is composed by a compact assembly forming a cysteine noose similar to those of the homologous protein of the bovine RSV that may be important in receptor binding specificity [10]. Further structural studies of G2Na and BBG2Na hRSV candidate vaccine are ongoing.

## References

1. Goetsch, L., et al. *Vaccine* **18**, 2648–2655 (2000).
2. Dagouassat, N., et al. *J. Immunol. Methods* **251**, 151–159 (2001).
3. Beck, A., et al. *J. Peptide Res.* **55**, 24–35 (2000).
4. Libon, C., et al. *Vaccine* **17**, 406–414 (1999).
5. Power, U., et al. *Vaccine* **19**, 2345–2351 (2001).
6. Le Cam, N., et al. *40th ICAAC Abstracts*, Washington, DC, 2000, 493.
7. Dagouassat, N., et al. *Vaccine* **19**, 4143–4152 (2001).
8. Allen, G., In *Sequencing of Proteins and Peptides*, Elsevier, Amsterdam, 1989, pp. 73–175.
9. Nilges, M., et al. *FEBS Lett.* **239**, 129–136 (1988).
10. Doreleijers, J.F., et al. *Biochemistry* **35**, 14684–14688 (1996).

## Role of Residues in Position 2 and 7 on the Conformation of the N-Terminal Apamin Loop

André Aumelas<sup>1</sup>, Léo Barry<sup>2</sup>, Marie France Martin-Eauclaire<sup>3</sup> and  
 Dung Le-Nguyen<sup>2</sup>

<sup>1</sup>Centre de Biochimie Structurale, UMR 5048, U414 INSERM, Université Montpellier 1,  
 Faculté de Pharmacie, 34060 Montpellier Cedex 02, France

<sup>2</sup>INSERM U 376, CHU Arnaud de Villeneuve, 34295 Montpellier, Cedex 05, France

<sup>3</sup>CNRS UMR 6560, Faculté de Médecine secteur Nord, Institut Jean Roche,  
 Université de la Méditerranée, Cedex 20, Marseille, France

### Introduction

The solution structure of the bee venom neurotoxin apamin (18 residues and C<sup>1</sup>–C<sup>11</sup> and C<sup>3</sup>–C<sup>15</sup> disulfide bridges) has been determined by <sup>1</sup>H NMR and mainly consists of a β-turn (residues 2–5) and of an α-helix (residues 9–17) [1]. In addition, it has been shown that the deprotonation of the Glu<sup>7</sup> side chain induces both a dramatic downfield shift and an unexpected line broadening of the amide signals of Glu<sup>7</sup> and Asn<sup>2</sup>, although no major structural change occurs for the global structure of apamin. This downfield shift is partially reversed above pH 6 [2]. To demonstrate the role of the Glu<sup>7</sup> on the conformation of the N-terminal loop, the [Glu<sup>7</sup>Gln] and [Glu<sup>7</sup>Asp] analogues, in which the carboxyl group was either removed or brought closer to the backbone, and the [N-acetyl] analogue were synthesized. Similarly, to evaluate the role of the Asn<sup>2</sup> side chain in the hydrogen bond network, the [Asn<sup>2</sup>Abu] analogue in which the Asn<sup>2</sup> side chain was replaced by a hydrophobic one was synthesized. The <sup>1</sup>H NMR study as a function of pH of all these analogues was carried out. Moreover, their binding affinities for the apamin receptor were measured.

### Results and Discussion

All the analogues were synthesized by the solid phase strategy and their air-oxidation yielded only the native disulfide pattern. Their ability to inhibit the <sup>125</sup>I-apamin binding on rat brain P2 fraction were measured (Table 1). All analogues behave like apamin and are able to completely displace the <sup>125</sup>I-apamin from its binding site. The dose/response (IC<sub>50</sub>) of [Glu<sup>7</sup>Gln] and [N-acetyl] analogues is similar to that of apamin, whereas that of the [Asn<sup>2</sup>Abu] and [Glu<sup>7</sup>Asp] analogues is slightly less potent, *i.e.* 1 and 5 pM, respectively.

For each analogue, spectra as a function of the pH were recorded in the pH 2–5 range to evaluate the sensitivity of both amides in position 2 and 7 and of the cis/trans ratio of the Ala<sup>5</sup>–Pro<sup>6</sup> amide bond to the ionization of the Glu<sup>7</sup> or Asp<sup>7</sup> carboxyl group.

Table 1. IC<sub>50</sub> values measured for apamin analogues on rat P2 fraction.

Analogues	IC <sub>50</sub> (pM)	Relative binding potency (%)
Apamin	0.5	100
[N-acetyl]	0.5	100
[Glu <sup>7</sup> Gln]	0.5	100
[Glu <sup>7</sup> Asp]	5	10
[Asn <sup>2</sup> Abu]	1	50

Among the fully potent analogues, the *N*-acetylated apamin behaves similarly to the parent peptide and the spectra of the [Glu<sup>7</sup>Gln] analogue are practically insensitive to pH due to the absence of carboxyl group.

For the [Glu<sup>7</sup>Asp] analogue, which only retains 10% of the relative binding potency of apamin, no *cis* conformation was detected and the Asn<sup>2</sup> amide signal was almost insensitive to pH change. This suggests that in apamin the Glu<sup>7</sup> carboxylate group is located in the proximity of Asn<sup>2</sup> amide proton. Therefore, this later experiences the change of the ionization state of the Glu<sup>7</sup> carboxyl group. In contrast, the Asp<sup>7</sup> side chain seems to be too short and too constrained to induce similar effects.

For the [Asn<sup>2</sup>Abu] analogue, a similar pH sensitivity to that observed for apamin was measured for Abu<sup>2</sup> and Glu<sup>7</sup> amide signals (Figure 1). In contrast, the *cis/trans* ratio was significantly different since it moves from around 65/35 to 10/90 from pH 2 to pH 5 instead of 12/88 to 0/100 for apamin. From these results we conclude that the Asn<sup>2</sup> side chain is involved in a hydrogen bond network which favors the *trans* conformation. In the absence of this hydrogen bond network, as in the case of the Asn<sup>2</sup>Abu analogue, 10 and 65% of *cis* conformation were observed at pH 5.0 and 2.0, respectively.

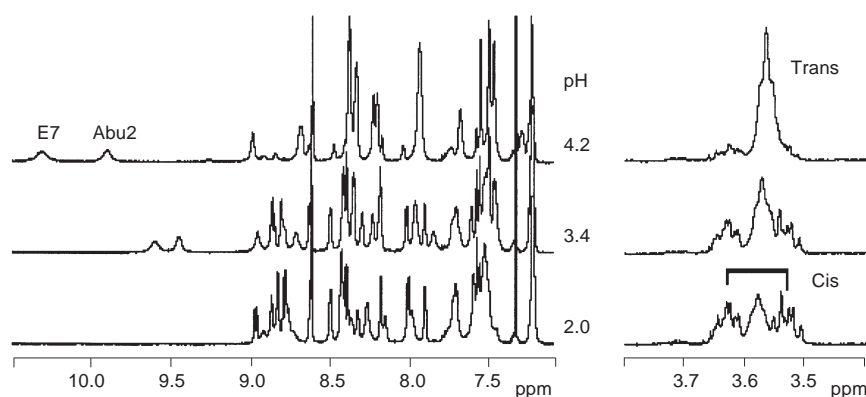


Fig. 1. Amide area (left) and Pro<sup>6</sup> delta signals (right) of <sup>1</sup>H NMR spectra of the [Asn<sup>2</sup>Abu]-apamin analogue recorded as a function of pH (H<sub>2</sub>O, 300 K).

These results suggest that the Glu<sup>7</sup> carboxylate group and the Asn<sup>2</sup> side chains have a cooperative role in the stabilization of the *trans* conformation of the N-terminal apamin loop. Nevertheless, although these conformational changes do not modify the global structure of apamin, they do modify the interface between the N-terminal loop and the helix, and therefore could be responsible for the decrease of the IC<sub>50</sub> value that we have measured.

## References

1. Pease, J.H., Wemmer, D.E. *Biochemistry* **157**, 269–274 (1988).
2. Dempsey, C.E. *Biochemistry* **25**, 3904–3911 (1986).

## **Conformational Study of [desHis<sup>1</sup>, desPhe<sup>6</sup>, Glu<sup>9</sup>]glucagon-NH<sub>2</sub> by 2D-NMR Spectroscopy in the Presence of Perdeuterated Dodecylphosphocholine**

**Jung-Mo Ahn, Neil E. Jacobsen, Michael F. Brown and Victor J. Hruby**

*Department of Chemistry, University of Arizona, Tucson, Arizona, 85721, USA*

### **Introduction**

Many peptide hormones are extremely flexible, and thus, possess many different conformations in solution. Therefore, a deep knowledge of the conformational behavior of these peptides is beneficial to understanding their biological activity. Glucagon is a 29 amino acid peptide hormone that is secreted by the  $\alpha$ -cells of the pancreas, and interacts with specific receptors located in various organs, especially the liver and fat cells. Its primary function is to initiate glucose production by stimulating glycogenolysis and gluconeogenesis in hepatocytes and lipolysis in adipocytes. The observation of higher levels of glucagon in diabetic patients [1] suggests a potential use of glucagon antagonists as therapeutics. Therefore, several glucagon antagonists have been developed in order to evaluate the role of glucagon in diabetes mellitus [2–4]. Among them, [desHis<sup>1</sup>, desPhe<sup>6</sup>, Glu<sup>9</sup>]glucagon-NH<sub>2</sub> [5] clearly demonstrated potent antagonist activity without any partial agonism even at extremely high concentrations [6]. While it has been demonstrated by X-ray crystallography that the enhanced biological activity may have resulted from an extended helical conformation in the C-terminal region of the superagonist, [Lys<sup>17,18</sup>,Glu<sup>21</sup>]glucagon [7], it is not clear why modifications at the N-terminal region converts glucagon into an antagonist. Therefore, 2D-NMR technique were used in this study to examine the conformation of the glucagon antagonist, [desHis<sup>1</sup>, desPhe<sup>6</sup>, Glu<sup>9</sup>]glucagon-NH<sub>2</sub>.

### **Results and Discussion**

Since the glucagon receptor is localized on the cell membranes, perdeuterated dodecylphosphocholine (DPC) micelles were used to provide the lipid/water interface. In this study, the 500 MHz TOCSY, DQF-COSY, and NOESY spectra of the glucagon antagonist in a perdeuterated DPC micelle solution were acquired at pH 6.0 and 37 °C. The chemical shifts of the protons in the molecule were assigned, and a large number of NOE cross peaks were quantitated and used for restrained simulated annealing. As expected from medium-range NOE pattern, the restrained simulated annealing using 332 distance restraints and 16 torsion angle constraints displayed a well-organized  $\alpha$ -helical conformation in the C-terminal region. This amphiphilic C-terminal  $\alpha$ -helical structure is comprised of the residues 17–29, and contained a hydrophobic patch which was organized with the side chains of Phe<sup>22</sup>, Val<sup>23</sup>, Leu<sup>26</sup>, Trp<sup>25</sup>, and Met<sup>27</sup>. The second hydrophobic patch, which is constructed with Tyr<sup>10,13</sup> and Leu<sup>14</sup>, is connected by a turn involving the short segment containing residues 14–16. The hydrophobic patch in the middle region is located on the same side of the molecule as the C-terminal hydrophobic patch, and presumably resulted from an interaction with lipophilic surface of micelles. The final segment of residues 2–9 appears to be flexible, and an extended conformation was found between Gly<sup>4</sup> and Thr<sup>5</sup>.

Since the glucagon antagonist used for this study has modifications only in the N-terminal region, the observed flexibility of the N-terminal part of the molecule places limitations on interpretation. However, one distinct difference in the conformation of

### Analytical Methods

the antagonist was observed in this region, a close proximity of Ser<sup>2</sup> and Glu<sup>9</sup> in the antagonist was seen in the NOE experiment. This proximity was presumably achieved by a salt bridge between an N-terminal ammonium group of Ser<sup>2</sup> and a carboxylate group of Glu<sup>9</sup> (Figure 1), and this was not present in the conformation of native glucagon determined by X-ray crystallography [8] and by 2D-NMR spectroscopy [9].

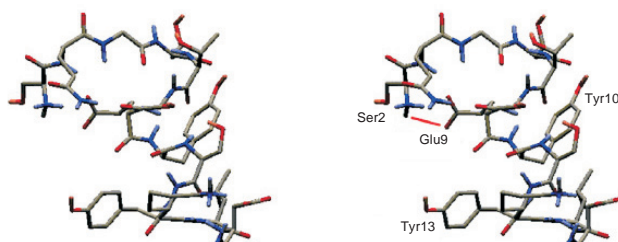


Fig. 1. Stereoview of the glucagon antagonist from restrained simulated annealing.

Since the glucagon antagonist does not contain Phe<sup>6</sup>, which may reinforce the hydrophobic patch in the middle region, the deletion of Phe<sup>6</sup> apparently enhances the formation of the salt bridge between Ser<sup>2</sup> and Glu<sup>9</sup>. Also, the substitution of Glu for Asp at the position 9 extends the side chain carboxylate group further from the backbone and helps fortify the salt bridge. These results suggest that the potent antagonist activity is a consequence of structural changes that lead to an N-terminal conformation that does not allow the ligand-receptor interactions essential for the structural changes in the receptor that are required for transduction. Further conformational constraints in the N-terminal region should provide new insights in this regard.

### Acknowledgments

Supported by a grant from U. S. Public Health Service DK-21085.

### References

1. Unger, R.H. *Metabolism* **27**, 1691–1709 (1978).
2. Hruby, V.J. *Mol. Cell. Biochem.* **44**, 49–64 (1982).
3. Hruby, V.J., et al. *Biopolymers* **25**, S135–S155 (1986).
4. Hruby, V.J. In Bittar E.E. and Bittar, N. (Eds.) *Principles of Medical Biology*. JAI Press, Greenwich, 1997, p. 387–401.
5. Azizeh, B.Y., et al. *Bioorg. Med. Chem. Lett.* **5**, 1849–1852 (1995).
6. Van Tine, B.A., et al. *Endocrinology* **137**, 3316–3322 (1996).
7. Sturm, N.S., et al. *J. Med. Chem.* **41**, 2693–2700 (1998).
8. Sasaki, K., et al. *Nature* **257**, 751–757 (1975).
9. Braun, W., Wider, G., Lee, K.H., Wüthrich, K. *J. Mol. Biol.* **169**, 921–948 (1983).

## Molecular Modeling Study of the $\beta$ -Turn-Type Reversals Involved in 3D Structure of IFABP

Gregory V. Nikiforovich and Carl Frieden

Department of Biochemistry and Molecular Biophysics, Washington University, St. Louis,  
MO 63110, USA

### Introduction

The intestinal fatty acid binding protein (IFABP) consists of ten  $\beta$ -strand fragments and two small  $\alpha$ -helical fragments packed in a general  $\beta$ -sheet 3D structure (see the PDB entry 1IFC). This study presents the results of energy calculations for the isolated IFABP hexapeptide fragments 42-47 (G44), 62-67 (G65), 71-76 (G75), 84-89 (G86), 108-113 (G110) and 118-123 (G121), as well as for the same fragments in mutants obtained by the G/V mutations [1]. The sets of low-energy conformers for these fragments may be regarded as the statistical ensembles of 3D structures accessible to the fragments during process of protein folding.

### Results and Discussion

All obtained results and calculated parameters are summarized in Table 1. For all unconstrained G\* and G\*V hexapeptides (\* = 44, 65, 75, 86, 110 and 121),  $N_{\text{low}}$  low-energy backbone conformers ( $\Delta E \leq 6$  kcal/mol) were found by considering all combinations of local energy minima for individual residues (according to [2]), except for the first and last residues, where only extended conformations were considered. The ECEPP force field [3,4] was used. Spatial positions of side chains were optimized by the algorithm described earlier [5]. For each hexapeptide,  $N_{\text{turn}}$  low-energy conformers formed a turn reversal without any additionally induced constraints, which corresponds to a model where the turns fold independently, *i.e.*, in a non-cooperative manner. (The turn reversal was defined as a conformer with the rmsd value  $\leq 1.5$  Å for C $\alpha$  atoms flanking the first and last peptide groups of the fragment.) The value  $P_{\text{turn}} = N_{\text{turn}}/N_{\text{low}}$  may be regarded as probability for an ensemble of low-energy conformers to form a turn without any induced constraints, and the value  $S_{\text{turn}} = (P_{\text{turn}})_{\text{Gly}}/(P_{\text{turn}})_{\text{Val}}$  as the ratio that shows tendency of increased or decreased refolding rates for the G/V mutants compared to WT: the larger  $S_{\text{turn}}$ , the slower the refolding process.

The  $S_{\text{turn}}$  values calculated in Table 1 suggest that the G75V mutant should possess the slowest refolding rate out of all G/V mutants considered in this study. However, it is not in agreement with the experimental data [1]. Therefore, ensembles of low-energy conformers of the unconstrained hexapeptide should be reconsidered by introducing elements accounting for cooperativity, *i.e.*, for influence of the entire IFABP protein.

Additional constraints (parabolic potentials) were added to conformational energy to maintain the distances between C $\alpha$  atoms flanking the first and last peptide groups of the fragments close to those in the X-ray structure of IFABP. For each hexapeptide,  $N_{\text{real}}$  low-energy conformers were found. The conformers closely matching the X-ray structure of IFABP (the rmsd value for all C $\alpha$  atoms  $\leq 1$  Å) were found for all G\* fragments except the G75 hexapeptide that possessed slightly different turn structures. Some low-energy conformers for the constrained G65V, G75V and G121V hexapeptides also match the X-ray structure, which is in good agreement with the experimental data on ligand binding to the G/V mutants [1]. The calculated ratio  $S_{\text{real}} = (N_{\text{real}})_{\text{Gly}}/(N_{\text{real}})_{\text{Val}}$  defines the same tendency of increased or decreased refolding

Table 1. Parameters calculated for the hexapeptide fragments of IFABP and its mutants.

Fragment	Unconstrained hexapeptides				Constrained hexapeptides		Experimental refolding rates [1]
	$N_{\text{low}}$	$N_{\text{turn}}$	$P_{\text{turn}}$	$S_{\text{turn}}$	$N_{\text{real}}$	$S_{\text{real}}$	
G44	92	26	0.28		8		
G44V	67	9	0.13	2.10	10	0.80	unchanged
G65	143	34	0.24		49		
G65V	81	19	0.23	1.02	28	1.75	unchanged
G75	80	14	0.17		10		
G75V	41	1	0.02	<b>7.29</b>	10	1.00	unchanged
G86	73	15	0.20		17		
G86V	43	3	0.07	2.93	9	1.89	unchanged
G110	28	9	0.32		8		
G110V	38	8	0.21	1.53	2	<b>4.00</b>	<b>slow</b>
G121	116	15	0.13		18		
G121V	21	1	0.05	2.69	4	<b>4.50</b>	<b>slow</b>

rates for the G/V mutants compared to WT as the  $S_{\text{turn}}$  value. According to the  $S_{\text{real}}$  values in Table 1, the G110V and G121V mutants possess the slowest refolding rate out of all G/V mutants considered in this study, which agrees with the experimental data [1]. Therefore, our results support the cooperative model of forming the local  $\beta$ -turn reversals during folding of IFABP and its mutants.

#### Acknowledgments

This work was supported by the NIH grants GM 53630 and DK 13332.

#### References

1. Kim, K., Frieden, C. *Protein Sci.* **7**, 1821–1828 (1998).
2. Zimmerman, S.S., Scheraga, H.A. *Biopolymers* **16**, 811–843 (1977).
3. Nemethy, G., Pottle, M.S., Scheraga, H.A. *J. Phys. Chem.* **87**, 1883–1887 (1983).
4. Dunfield, L.G., Burgess, A.W., Scheraga, H.A. *J. Phys. Chem.* **82**, 2609–2616 (1978).
5. Nikiforovich, G.V., Hruby, V.J., Prakash, O., Gehrig, C.A. *Biopolymers* **31**, 941–955 (1991).

## **Structural Features of Short, Linear Peptides in Solution by Fluorescence and Molecular Mechanics Studies**

**Basilio Pispisa<sup>1</sup>, Claudia Mazzuca<sup>1</sup>, Lorenzo Stella<sup>1</sup>, Mariano Venanzi<sup>1</sup>,  
Antonio Palleschi<sup>1</sup>, Fernando Formaggio<sup>2</sup>, Claudio Toniolo<sup>2</sup>  
and Quirinus B. Broxterman<sup>3</sup>**

<sup>1</sup>*Dipartimento di Scienze e Tecnologie Chimiche, Università di Roma Tor Vergata,  
00133 Roma, Italy*

<sup>2</sup>*Centro di Studio sui Biopolimeri, C.N.R., Dipartimento di Chimica Organica,  
Università di Padova, 35131 Padova, Italy*

<sup>3</sup>*DSM Research, Organic Chemistry and Biotechnology Section, 6160 MD Geleen,  
The Netherlands*

### **Introduction**

One important goal of solution chemistry is currently a quick identification of the structural features and conformational equilibria of a given compound in solution. This is especially true for peptide chemistry, owing to the increasing importance of this type of compounds in a number of fields, spanning from pharmaceuticals to enzyme mimetics. Even NMR studies do not always lead to a unique interpretation of the conformational features of peptides in solution. Indeed, these studies are often made difficult by the large conformational changes occurring rapidly on the NMR time scale, so that the NMR observables and the restraints developed from them are only consistent with an average structure that may not even exist [1]. By combining time-resolved fluorescence data with molecular mechanics results we were able to determine the most relevant structural features of a number of short, ordered peptides in solution [2], as exemplified below for a series of foldamers having the general formula  $F[(\alpha\text{Me})\text{Val}]_r\text{-T}[(\alpha\text{Me})\text{Val}]_2\text{NHtBu}$ , where  $(\alpha\text{Me})\text{Val} = \text{C}^\alpha\text{-methylvaline}$ ,  $r = 0\text{-}3$ ,  $F$  (= Fmoc) is a fluorophoric  $\text{N}^\alpha$ -protecting group, and  $T$  (= Toac) a nitroxide-based  $\alpha$ -amino acid quencher.

### **Results and Discussion**

According to IR and CD spectra, the longest term of the series ( $r = 3$ ) attains a  $3_{10}$ -helical structure, while the other peptides populate an intramolecularly H-bonded,  $3_{10}$ -helix-like conformation affected by helical distortions, which are enhanced by the shortness of the backbone chain. Such distortions are reflected in both the energy of the stretching mode and the molar extinction coefficient of the H-bonded N-H groups, the former being higher and the latter smaller than those of a canonical  $3_{10}$ -helix.

Steady-state and time-resolved fluorescence measurements in methanol show a strong quenching of Fmoc by the Toac residue, located at different helix positions, depending on the  $r$  value. Comparison of quenching efficiencies and lifetime pre-exponents with those theoretically obtained from the deepest energy minimum conformers [3], assuming a fluorescence resonance energy transfer (FRET) mechanism, is satisfactory.

The computed structures exhibit a compact arrangement, which accounts for the few sterically favored conformations for each peptide, in full agreement with the time-resolved fluorescence data. Orientational effects between the probes had to be taken into account for a correct interpretation of the fluorescence decay results, implying that interconversion among conformational substates involving the probes is slower than the characteristic time of the energy transfer (around 8 ns).

## Analytical Methods

The use of solvent with different polarity does not alter the foregoing findings, supporting the idea that the foldamers examined populate a few, highly compact structures in solution. Figure 1 illustrates the most favored conformer of the shortest term of the series ( $r = 0$ ). The agreement between both the quenching efficiency ( $E_{\text{calcd}} = 0.98$ ,  $E_{\text{exp}} = 0.96$ ) and population ( $P_{\text{calcd}} = 0.89$ ,  $P_{\text{exp}} \equiv \alpha_1 = 0.94$ ) of this conformer and the same parameters experimentally determined from time-resolved measurements is excellent, emphasizing the idea that this conformation is a good representation of the structure populating the methanol solution.

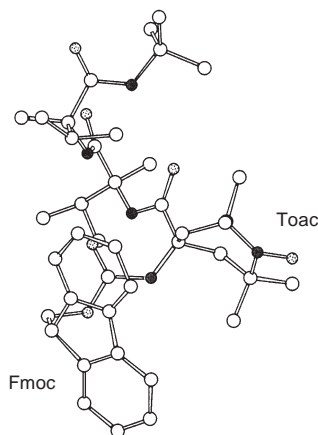


Fig. 1. Deepest energy minimum structure for F-T-[( $\alpha$ Me)Val]<sub>2</sub>NHtBu ( $r = 0$ ), from molecular mechanics calculations. The backbone chain is in the right-handed 3<sub>10</sub>-helical conformation, and is viewed perpendicularly to the helical axis.

## Acknowledgments

We thank C.N.R. for a partial financial support.

## References

1. Mierke, D.F., Kurz, M., Kessler, H. *J. Am. Chem. Soc.* **116**, 1042–1049 (1994).
2. Pispisa, B., Stella, L., Venanzi, M., Palleschi, A., Marchiori, F., Polese, A., Toniolo, C. *Biopolymers* **53**, 169–181 (2000).
3. Pispisa, B., Stella, L., Venanzi, M., Palleschi, A., Viappiani, C., Polese, A., Formaggio, F., Toniolo, C. *Macromolecules* **33**, 906–915 (2000).

## Influence of Stereochemistry of the Preceding Acyl Residue on the *cis/trans* Ratio of the Proline Peptide Bond

Matej Breznik<sup>1</sup>, Simona Golič Grdadolnik<sup>2</sup>, Gerald Giester<sup>3</sup>, Ivan Leban<sup>4</sup>  
and Danijel Kikelj<sup>1</sup>

<sup>1</sup>University of Ljubljana, Faculty of Pharmacy, SI-1000 Ljubljana, Slovenia

<sup>2</sup>National Institute of Chemistry, SI-1000 Ljubljana, Slovenia

<sup>3</sup>Institut für Mineralogie und Kristallographie, Geozentrum, Universität Wien,  
A-1090 Wien, Austria

<sup>4</sup>University of Ljubljana, Faculty of Chemistry and Chemical Technology,  
SI-1000 Ljubljana, Slovenia

### Introduction

Naturally occurring amino acids form predominantly *trans* peptide bonds, with the exception of proline whose ability to form *cis* peptide bonds and undergo *cis/trans* isomerization is well known [1]. The isomerization barrier of the acyl-Pro bond in proline containing molecules is lowered from *ca* 20 kcal/mol to *ca* 13 kcal/mol due to concomitant pyrrolidine puckering changes; additionally, the *trans* bond, involving a nitrogen atom of the pyrrolidine ring, is favored only slightly (*ca* 2 kcal/mol) over the *cis* bond [2]. Here we report the synthesis, X-ray structure analysis, and NMR conformational study of **1** and the corresponding diastereomer **2**, providing evidence that the (2*S*)-2,6-dimethyl-3-oxo-3,4-dihydro-2*H*-1,4-benzoxazin-2-carbonyl moiety constrains the acyl-Pro bond of **1** to *trans*.

### Results and Discussion

**Synthesis.** Coupling of racemic 2,6-dimethyl-3-oxo-3,4-dihydro-2*H*-1,4-benzoxazine-2-carboxylic acid [3] with (*S*)-ProOBn afforded a mixture of diastereomers **1** and **2** (Figure 1) which were separated by column chromatography. The diastereomer **1** was also prepared by a stereoselective synthesis *via* PLE catalysed hydrolysis of dimethyl 2-methyl-2-(4-methyl-2-nitrophenoxy)malonate [4a]. Palladium catalysed reduction and concomitant cyclization of resulting acid [4b] after EDC-catalysed coupling with (*S*)-ProOBn yielded **1**.

**Crystallographic analysis.** According to crystallographic data [5] the molecule **1** contains a *trans* proline peptide bond, whereas the peptide bond in molecule **2** is *cis* (Figure 1).

**Solution structures.** For **1** only one set of resonances was observed in <sup>1</sup>H NMR spectra, demonstrating the existence of a single conformation of the proline peptide bond in DMSO-*d*<sub>6</sub> solution. On the basis of NOEs that were observed for **1** between δCH<sub>2</sub>Pro/C<sup>2</sup>-CH<sub>3</sub> and δCH<sub>2</sub>Pro/HetC<sup>8</sup>H, we could assign the conformation of the peptide bond to *trans* (Figure 1). Two distinct sets of signals were observed in the one-dimensional <sup>1</sup>H spectrum of **2** with relative populations of 28 and 72%, indicating the existence of two conformations of proline peptide bond in DMSO-*d*<sub>6</sub> solution at 302 K. For the more abundant species, NOE peaks were observed between δCH<sub>2</sub>Pro/C<sup>2</sup>-CH<sub>3</sub> and δCH<sub>2</sub>Pro/HetC<sup>8</sup>H, characterizing the *trans* conformation. No NOEs were found for the less abundant species, indicating that the proline peptide bond of the species in solution adopts the *cis* conformation.

The pyrrolidine ring puckering of all the structures obtained in solution and solid state was C<sup>β</sup>-exo/C<sup>γ</sup>-endo, indicating that this most favourable conformation is not affected by any structural changes.

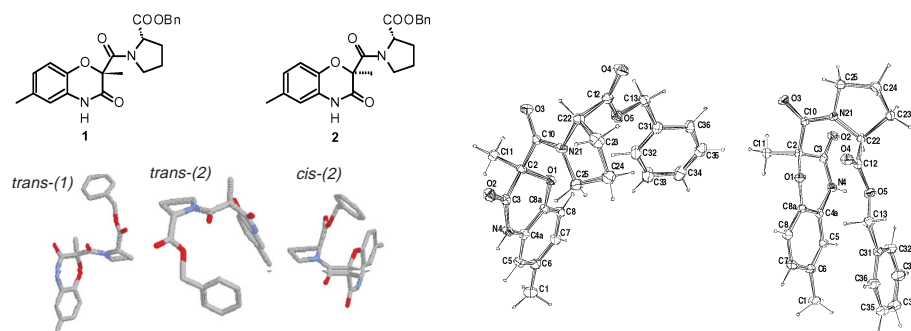


Fig. 1. Solution structures of **1** and **2** as observed in DMSO (left). Structures of **1** (middle) and **2** (right) showing the atomic numbering scheme (ellipsoids are drawn at 30% probability level).

Conformational analysis together with crystallographic analysis of **1** proved that the compound exhibits only *trans* conformation of the proline peptide bond. On the other hand the solution structure of **2** revealed a mixture of 72% *trans* and 28% *cis* conformer, whereas crystallographic analysis of **2** showed that only the *cis* conformation is present in the crystalline state (Figure 1). It is evident that in these cases, the conformation of the proline peptide bond depends on the chirality of the acyl residue.

In conclusion, an important feature of our finding is that the conformation of the proline peptide bond in acyl-Pro molecules can be constrained to *trans* by chirality of the acyl residue without modification of the proline.

#### Acknowledgments

The financial support of the Ministry of Science and Technology, Republic of Slovenia, through grants PS-511-103 and PS-787-502 is gratefully acknowledged.

#### References

1. (a) Brandts, J.F., Halvorson, H.R., Brennan, M. *Biochemistry* **14**, 4953–4963 (1975).  
(b) Schmid, F.X. *Annu. Rev. Biophys. Biomol. Struct.* **22**, 123–143 (1993).
2. (a) Schulz, G.E., Schirmer, R.H. *Principles of Protein Structure*, Springer-Verlag, New York, 1961, p. 25. (b) Tonelli, E.A. *J. Am. Chem. Soc.* **95**, 5946–5948 (1973).
3. Kikelj, D., Suhadolc, E., Urleb, U., Žbontar U. *J. Heterocycl. Chem.* **30**, 597–602 (1993).
4. (a) Breznik, M., Kikelj, D. *Tetrahedron: Asymmetry* **8**, 425–434 (1997). (b) Breznik, M., Hrast, V., Mrcina, A., Kikelj D. *Tetrahedron: Asymmetry* **10**, 153–167 (1999).
5. Cambridge Crystallographic Data Centre: No. CCDC-163847 and CCDC-163848.

## **The Influence of the Surrounding Media on the Structural Propensities of Amino Acid Residues in Proteins**

**Alex Rubinstein and Simon Sherman**

*The Eppley Institute for Research in Cancer and Allied Diseases, the University of Nebraska  
 Medical Center, Omaha, NE 68198-6805, USA*

### **Introduction**

We have shown [1] that the intrinsic ( $\phi, \psi$ ) conformational propensities of amino acid residues in a coil state, and the corresponding structural propensities of the same type of residues to form the equivalent secondary structures, strongly depend on the residue type and their solvent accessibility. For residues in the interior and exterior of proteins, very strong correlations ( $>0.9$ ) between these propensities were found. It suggests that non-covalent intraresidual interactions, in particular, electrostatic interactions, could make a crucial contribution to amino acid conformational propensities and predetermine propensities of the residue to be involved in the formation of secondary structures. To test this hypothesis, the pair wise electrostatic interactions (PEI) of the charges in a system that models the interface between a protein and aqueous solvent, containing mobile free ions, were calculated. The concept of non-local (NL) electrostatics for interfacial electrochemical systems [2,3] were used to investigate the contribution of the solvent orientational polarization, correlated by the network of hydrogen bonds, and the effect of the ionic strength on the PEI in proteins.

### **Results and Discussion**

To estimate the influence of the surrounding media on the PEI of charges that are in different proximity to the protein surface, we calculated the interactions of two point charges in a system that models the interface between a protein and a solution, using the concept of NL electrostatics for medium with interface. The NL electrostatics is the generalization of the classical electrostatics  $\mathbf{D} = \epsilon * \mathbf{E}$  between the induction  $\mathbf{D}$  and electric field  $\mathbf{E}$ :

$$\mathbf{D}(\mathbf{r}) = \epsilon(\mathbf{r} - \mathbf{r}') * \mathbf{E}(\mathbf{r}') * d\mathbf{r}'.$$

The kernel  $\epsilon(\mathbf{r} - \mathbf{r}')$  is a function determined by the medium structure [3]. Neglecting the effects of a dielectric saturation of the water and quantum short-range ionic forces as well as using the “sharp-boundary” model [3–5] one can state the PEI energy at the interface in terms of the Fourier-transform  $\epsilon_1(\mathbf{k})$  and  $\epsilon_2(\mathbf{k})$  of the dielectric functions  $\epsilon_1(\mathbf{r} - \mathbf{r}')$  and  $\epsilon_2(\mathbf{r} - \mathbf{r}')$ , characterizing the bulk properties of the media in contact. In the system of cylindrical coordinates  $(\mathbf{R}, Z)$ , a flat interface between protein-like media ( $Z > 0$ ) and a solution ( $Z < 0$ ) was considered, and

$$\epsilon_1(\mathbf{k}) = \epsilon_1 = 4.0 \quad \text{and} \quad \epsilon_2(\mathbf{k}) = \epsilon_2 + (\epsilon_s - \epsilon_2)/(1 + L^2 * \mathbf{k}^2 * \epsilon_s/\epsilon_2) + \epsilon_s * \chi_s^{-1}/\mathbf{k}^2$$

were used as approximations for the dielectric functions of these two media. Here,  $\epsilon_2$  and  $\epsilon_s$  are short- and long-wavelength dielectric constants of the solvent at room temperature;  $\chi_s^{-1}$  – the Debye screening length; and  $L$  – the correlation length of water dipoles. Numerical calculations of the PEI energy  $U(\mathbf{R}, Z = Z_0)$  for two charges, located at identical distances  $Z_0$  from the interface are shown in the Figure 1.

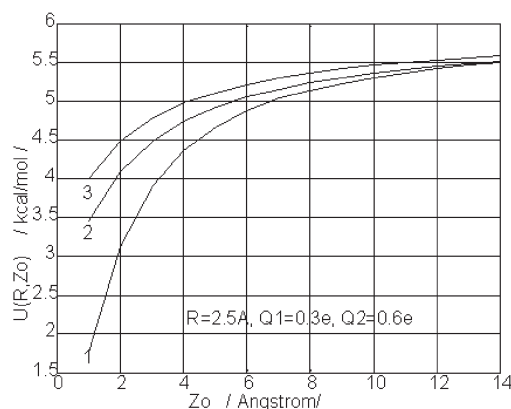


Fig. 1. Dependence of the PEI energy between two charges immersed into the protein-like uniform dielectric media as a function of distance,  $Z_0$ , from the interface with the solvent. Calculations were made for several solvent models: model with uniform dielectric ( $\epsilon_s = 78.3$ ) without mobile free ions (1), model with water structure ( $\epsilon_2 = 6.0$ ,  $\epsilon_s = 78.3$ ,  $L = 5.0$  Å) and with (2) and without (3) Debye screening by mobile free ions ( $\chi_s^{-1} = 13.6$  Å).

This figure shows that: (i) the PEI energy between charges located in a close proximity ( $Z_0 < 3.0$  Å) to the interface with a solvent is significantly underestimated by a classical model (1) and (ii) there are significant differences between the PEI energy when the charges are remote ( $Z_0 > 6.0$  Å) vs proximate ( $Z_0 < 3.0$  Å) to this interface. These results clearly illustrate that on some characteristic distances from the interface the value and character of the PEI might be changed significantly. These distances are determined by physical parameters of the system. Applying these observations to the problem of protein folding, one can conclude that the dependence of both conformational and structural propensities upon residue solvent accessibility may be due to the different dielectric properties of the media in the exterior and interior of proteins. Thus, by the screening effect, the surrounding media could play an important role in  $(\phi, \psi)$  intrinsic conformational propensities of amino acid residues, predetermining propensities of the residues to be involved in the formation of secondary structures of protein molecules.

#### Acknowledgments

We acknowledge the use of the Bioinformatics Shared Resource of the UNMC Eppley Cancer Center supported by Cancer Center Support grant P30 CA36727.

#### References

1. Rubinstein, A., Shats, O., Sclove, S., Vaisman, I., Sherman, S. *Protein Sci.* **9**, Suppl. 1, 71 (2000).
2. Kornishev, A., Rubinstein, A., Vorotintsev, M. *J. Phys. C: Solid State Phys.* **11**, 3307–3322 (1978).
3. Kornishev, A. *Electrochim. Acta* **26**, 1–20 (1981).
4. Rubinstein, A. *Phys. Status Solidi B* **120**, 65–76 (1983).
5. Rubinstein, A. *Sov. Electrochem.* **22**, 184–192 (1986).

## CD Evidence of the Conformational Transitions in rMOG[1-125] in the Presence of Membrane Mimicking Detergents

Maria Ngu-Schwemlein<sup>1</sup>, Michelle Corzette<sup>2</sup>, Rod Balhorn<sup>2</sup>  
 and Monique Cosman<sup>2</sup>

<sup>1</sup>Department of Chemistry, Southern University, Baton Rouge, LA 70813, USA

<sup>2</sup>Biology and Biotechnology Research Program, Lawrence Livermore National Laboratory,  
 Livermore, CA 94551, USA

### Introduction

Myelin oligodendrocyte glycoprotein (MOG), an integral glycoprotein associated with the myelin in brain nerve fibers, has recently been implicated as a prime autoantigen leading to autoimmune demyelination in animal models (experimental autoimmune encephalomyelitis, EAE). Immunization of animal models, including mice and marmosets, with rMOG led to the manifestation of a disease similar to multiple sclerosis (MS) – demyelination mediated by autoantibodies directed against the extracellular domain of MOG (MOG[1-125]) [1]. The extracellular location of MOG has been identified as a member of the immunoglobulin superfamily by Gardinier *et al.* [2]. The amino acid sequence of rat MOG[1-125] (139 residues) is as follows;

MRGS–FRVIGPGHPIRALVGDEAELPCRISPGKNATGMEVGWYRSPFSRVVHL  
 YRNGKDQDAEQAPEYRGRTELLKESIGEGKVALRIQNVRESDEGGYTCTFERDH  
 SYQEEAAVELKVEDPFYWINPG–RSQSHHHHHH.

In the myelin membranes, the ratio of neutral to anionic lipids is approximately 4 : 1. To better understand the conformational stability of this extracellular domain of MOG, we investigated the interaction of rMOG [1-125] with trifluoroethanol (TFE), sodium lauryl sulfate (SDS), neutral detergents, dodecylphosphocholine (DPC) and palmitoyllysophosphocholine (LPCP), and an anionic detergent, palmitoyllysophosphatidic acid (LPAP) by CD spectroscopy. The stability and conformational change(s) of MOG [1-125] in the presence of different lipid detergents are reported.

### Results and Discussion

The non-glycosylated extracellular domain of rMOG[1-125] has previously been cloned into a pQE12 vector (MRGS at the N-termini and a RSQSHHHHHH-tag at the C-termini). In this study, the expression of the soluble form of rMOG[1-125] was obtained in an *E. coli* M15(pRep4) host (1 mg/L in LB). The purity was analyzed on a

*Table 1. Relative mole percent of  $\alpha$  helicity in rMOG[1-125] in the presence of detergents or TFE at 25 °C, pH 7.5, in 10 mM phosphate buffer containing 5 mM  $\beta$  mercaptoethanol.*

Additive <sup>a</sup>	Relative mole $\alpha$ -helix <sup>b</sup>
Dodecylphosphocholine (DPC)	9
Palmitoyllysophosphocholine (LPCP)	9
Palmitoyllysophosphatidic acid (LPAP)	15
Sodium lauryl sulfate (SDS)	12
45% Trifluoroethanol (TFE)	20
No additive	9

<sup>a</sup> The molar ratio of detergent/rMOG[1-125] is 200 : 1. <sup>b</sup> Values were obtained by a theoretical fit using the CD deconvolution program, CDNN.

10% SDS PAGE and ascertained by a major band at 15.9 kD, which was confirmed by Western blot with mAb 6×His as well as staining with a fluorescent 6×His Protein Tag.

At pH 7.5, the CD spectrum of rMOG[1-125] shows a maximum at *ca* 195 nm and a minimum at 217 nm, typical of  $\beta$  sheet characteristics (Figure 1). Following titration with TFE (10–60%) or anionic detergents, LPAP and SDS, negative maxima at 208 and 222 nm were enhanced indicating a conformational transition from a predominantly  $\beta$  sheet to an increasing composition of  $\alpha$  helicity. However, titration with neutral detergents, DPC and LPCP did not show any significant change in the CD (Table 1). Variable temperature CD of this protein (30–90 °C) showed thermal unfolding at and above 70 °C, which was significantly reduced in the presence of DPC or LPAP.

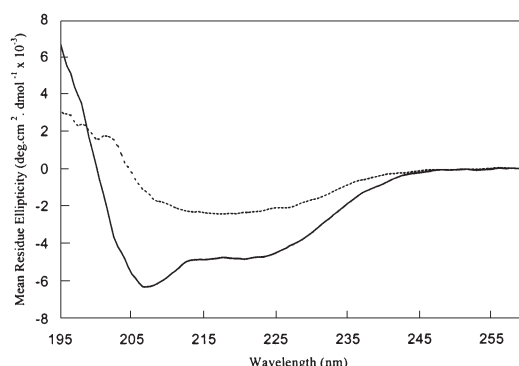


Fig. 1. rMOG[1-125] (0.17 mg/ml) in 10 mM phosphate at pH 7.5 at 25 °C, (....) ( $\beta$ -form) and in the presence of 2 mM LPAP, (—) ( $\alpha$ -form). A theoretical fit to the CD spectrum yielded *ca* 9%  $\alpha$ -helix and 38%  $\beta$ -antiparallel sheet, and *ca* 15%  $\alpha$ -helix and 27%  $\beta$ -antiparallel sheet, for the  $\beta$ -form and  $\alpha$ -form, respectively.

The CD data in this study provide evidence that rMOG[1-125] is a protein that can undergo conformational transition depending on its microenvironment and that there are discrete interaction sites on the protein for neutral and anionic micellar detergents.

#### Acknowledgments

M. N-S. thanks Kevin Thornton for helpful discussions, and acknowledges financial support from the DOE and OBER MI Faculty Research Participation Program.

#### References

1. Genain, C.P., Cannella, B., Hauser, S.L., Raine, C.S. *Nat. Med.* **5**, 170–175(1999).
2. Gardinier, M.V., Amiguet, C., Linington, C., Matthieu, J.-M. *J. Neurosci. Res.* **33**, 177–187 (1992).

## Coacervation and CD and FT-IR Spectroscopic Studies of Elastin-Derived Polypentapeptide and Its Analogs

Kouji Okamoto<sup>1</sup>, Yoshiteru Fukumoto<sup>1</sup>, Iori Maeda<sup>1</sup>, Elemer Vass<sup>2</sup>,  
 Zsuzsanna Majer<sup>2</sup>, Gabor Dibo<sup>2</sup> and Miklos Hollosi<sup>2</sup>

<sup>1</sup>Department of Biochemical Engineering and Science, Kyushu Institute of Technology,  
 Iizuka, Fukuoka 820-8502, Japan

<sup>2</sup>Department of Organic Chemistry, Eötvös University, H-1518 Budapest, Hungary

### Introduction

Elastin imparts elasticity to elastic tissues such as arterial walls, lungs, ligaments, and skin. *In vivo*, tropoelastin, a precursor of insoluble elastin, self-associates with appropriate alignment in extracellular spaces, followed by cross-linking to form elastin. The self-association of tropoelastin molecules is the most significant step in the process of elastin biosynthesis, termed coacervation *in vitro*. The polypentapeptide (VPGVG)<sub>n</sub>, one of the repeating peptide sequences in the elastin molecule, is the most striking primary structural feature of elastin. In order to clarify the molecular mechanism of coacervation, we synthesized the polypentapeptide (V<sup>1</sup>P<sup>2</sup>G<sup>3</sup>V<sup>4</sup>G<sup>5</sup>)<sub>n</sub> and its three analogs (Figure 1) – (V<sup>1</sup>P<sup>2</sup>G<sup>3</sup>V<sup>4</sup>)<sub>n</sub> in which Gly<sup>5</sup> is deleted, (V<sup>1</sup>P<sup>2</sup>G<sup>3</sup>)<sub>n</sub> in which both Gly<sup>5</sup> and Val<sup>4</sup> are deleted, and (P<sup>2</sup>G<sup>3</sup>V<sup>4</sup>G<sup>5</sup>)<sub>n</sub> in which Val<sup>1</sup> is deleted. The coacervation properties and conformational analyses of these polypeptides were investigated.

### Results and Discussion

As shown in Figure 2, it was found from the temperature profiles for coacervation of elastin-derived polypentapeptide and its analogs that the coacervation property of (VPGVG)<sub>n</sub> was completely reversible, which agrees with a previous report [1], but those of (VPGV)<sub>n</sub> and (VPG)<sub>n</sub> were incompletely reversible with weaker intensities of turbidity. However, no coacervation was observed for (PGVG)<sub>n</sub>. These results suggest that Val<sup>1</sup> residue is essential for the onset of coacervation and that Gly<sup>5</sup> and Val<sup>4</sup> residues, and notably Val<sup>4</sup> residue, are important for the process of coacervation, that is, the reversibility of coacervation and the intensity of turbidity. Coacervation is the process of intramolecular and intermolecular hydrophobic associations. The hydrophobic side chain of Val<sup>1</sup> residue is likely to interact with the hydrophobic side chain of adjacent Pro<sup>2</sup> residue intramolecularly, and the hydrophobic side chains of Val<sup>4</sup> residues interact with each other both intra- and intermolecularly. It has been reported by Urry *et al.* [2] that the hydrophobic interaction between the side chains of Val<sup>1</sup> and Pro<sup>2</sup> residues of the elastin-derived polytetrapeptide (V<sup>1</sup>P<sup>2</sup>G<sup>3</sup>G<sup>4</sup>)<sub>n</sub> is important for the onset of coacervation.

It was shown from CD studies of elastin-derived polypentapeptide and its analogs that the spectrum of (VPGV)<sub>n</sub> was similar to that of (VPGVG)<sub>n</sub> suggesting a predomi-

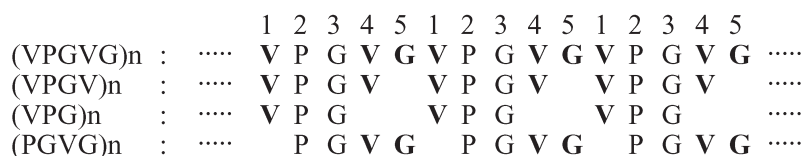


Fig. 1. Elastin-derived polypentapeptide and its analogs.

nant type II  $\beta$ -turn structure, which is characterized by a spectrum (a negative band between 230 and 220 nm, a positive band above 200 nm, and a second negative band around 190 nm) as reported in (VPGVG)<sub>n</sub> by Urry *et al.* [3]. The spectrum of (VPG)<sub>n</sub> was somewhat different from that of (VPGVG)<sub>n</sub> except for a negative band between 230 and 220 nm. The spectrum of (PGVG)<sub>n</sub> was distinct from that of (VPGVG)<sub>n</sub> suggesting an unordered structure, which is characterized by a spectrum with a strong negative band below 200 nm.

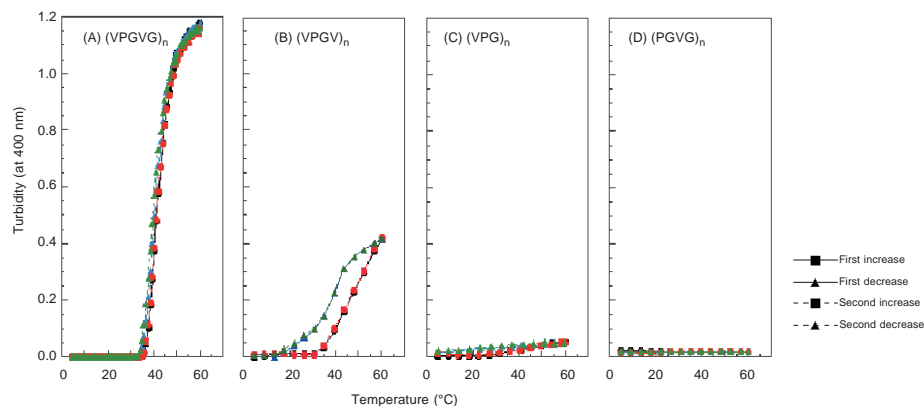


Fig. 2. Temperature profiles for coacervation of elastin-derived polypentapeptide and its analogs.

These results observed in CD studies were confirmed by FT-IR studies. The spectra of (VPGV)<sub>n</sub> and (VPG)<sub>n</sub> were similar to that of (VPGVG)<sub>n</sub> in which the bands around 1656, 1633, and 1680 cm<sup>-1</sup> are attributed to a helix, C=O groups involved in hydrogen bonds that stabilize the turn, and C=O groups that are not hydrogen bonded and are sterically constrained, respectively.

## References

1. Kaibara, K., Akinari, Y., Okamoto, K., Uemura, Y., Yamamoto, S., Kodama, H., Kondo, M. *Biopolymers* **39**, 189–198 (1996).
2. Urry, D.W., Khaled, M.A., Rapaka, R.S., Okamoto, K. *Biochem. Biophys. Res. Commun.* **79**, 700–706 (1977).
3. Urry, D.W., Long, M.M., Cox, B.A., Ohnishi, T., Mitchell, L.W., Yacobs, H. *Biochim. Biophys. Acta* **371**, 597–602 (1974).

## Conformational Analysis of Human Calcitonin in Aqueous Solution and Comparison with a Highly Potent Lactam-Bridged Analogue

C. M. McIntosh<sup>1</sup>, K. S. Rotondi<sup>1</sup>, M. Dhanasekaran<sup>2</sup>, K. Gunasekaran<sup>2</sup>,  
A. Kazantzis<sup>3</sup>, A. Kapurniotu<sup>3</sup> and L. M. Gierasch<sup>1,2</sup>

<sup>1</sup>Department of Chemistry, University of Massachusetts, Amherst, MA 01003, USA

<sup>2</sup>Department of Biochemistry & Molecular Biology, University of Massachusetts, Amherst,  
MA 01003, USA

<sup>3</sup>Physiological Chemical Institute, University of Tübingen, Tübingen, D-72076, Germany

### Introduction

Human calcitonin (hCt) is a peptide hormone of 32 amino acid residues that plays a central role in calcium metabolism [1,2]. The receptor-bound conformation of hCt has not yet been determined. In an effort to understand the bioactive conformation of hCt we have recently designed a lactam-bridged hCt analogue with the structure cyclo<sup>17,21</sup>-[Asp<sup>17</sup>,Orn<sup>21</sup>]hCt (**1**) and found it to be 400-times more potent than hCt and 4-times more potent than salmon Ct (sCt) in the *in vivo* hypocalcemic assay in mice, making this the most potent known hCt analogue [3]. By contrast, a linear control peptide [Asp<sup>17</sup>,Orn<sup>21</sup>]hCt (**2**) showed similar *in vivo* potency to hCt [3]. These results suggested that the conformation of **1** may correspond to a bioactive conformation of hCt [3]. Here, we present studies on the solution conformation of hCt and **1** based on NMR in combination with molecular modeling and CD spectroscopy. We also present data on the hCt receptor-binding affinity of **1** as compared to **2**, hCt and sCt.

### Results and Discussion

In the hCt receptor-binding assay in the human breast cancer cell line T47D, **1** exhibited approximately a 4-fold increased binding affinity as compared to hCt and was somewhat less potent than sCt. sCt, the most potent native Ct known, showed a roughly 6-fold higher binding affinity than hCt. By contrast, essentially no binding was observed for **2**. Enhanced receptor binding for **1** supports the notion that the structural and conformational features introduced by cyclization between residues 17 to 21 play a role in both receptor binding and *in vivo* bioactivity and, moreover, that the cyclic constraint stabilizes a bioactive conformation. Molecular modeling of the lactam bridge region of **1** suggests that the bridge constraint can be accommodated in either a helical backbone conformation or a set of consecutive  $\beta$ -turns. NMR analysis of heptapeptides corresponding to residues 16 to 22, with and without side-chain cyclization, did not show a clear local conformational bias from the lactam bridge. Hence, we concluded that the influence of the bridge should be evaluated in the context of the full-length calcitonin analogues.

CD spectra of both hCt and **1** in water show a low content of stable secondary structure. Addition of either TFE or SDS led to enhanced helical content, but to a similar extent for hCt and **1**. Based on analysis of nuclear Overhauser effects from 2D NOESY spectra, both full-length hCt and **1** display a nascent helical fold in aqueous solution from residues 6 to 21. The deviations of  $\alpha$ -proton chemical shifts from "random coil" values (the so-called chemical shift index [4]) (Figure 1) reinforce the conclusion that the two peptides have very similar conformational distributions in aqueous solution, with **1** somewhat more structured in the region of the lactam bridge. Note that a negative  $\Delta\delta$  deflection signifies a conformational bias towards helix, while

positive implies extended. Clearly, the conformations of both peptides are constrained by the disulfide-closed ring in the N-terminal region, and both are largely unstructured from proline 23 to the C-terminus. These observations are consistent with reported conformational behaviors of various calcitonins in structure-promoting solvents [e.g., 5,6]. We conclude that the conformational constraint imposed by cyclization only slightly favors a helical structure, which has been postulated to be important for bioactivity [7]; however, this result must be reconciled with the substantially higher *in vivo* activity of **1** as compared to hCt. Therefore, we are carrying out NMR studies in structure-promoting solvents to assess more fully the impact of the lactam bridge.

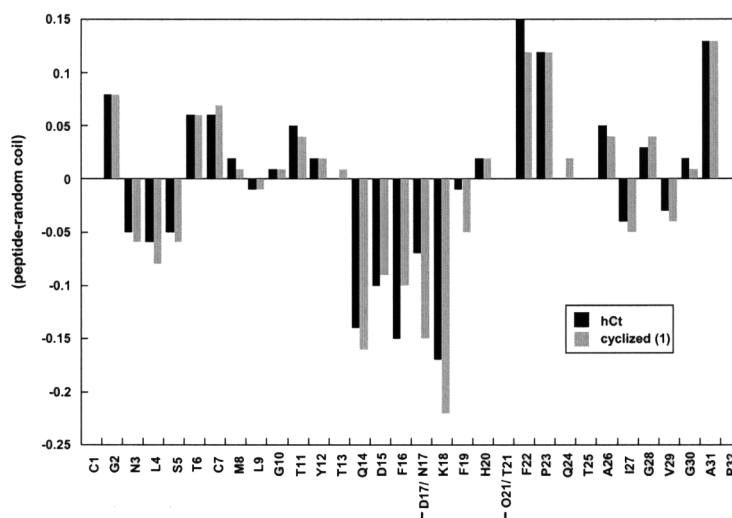


Fig. 1.  $\alpha$ H chemical shift deviations from random coil [4].

### Acknowledgments

We thank J. Bernhagen for help with the receptor-binding assays. Supported by grants Ka 979/2-2 (DFG, to A. K.) and GM27616 (NIH, to L. M. G.).

### References

1. Guttman, S. In Pecile, A. (Ed.) *Calcitonin 1980: Chemistry, Physiology, Pharmacology, and Clinical Aspects*, Excerpta Medica, Amsterdam, 1981, pp. 11–24.
2. Azria, M. *The Calcitonins: Physiology and Pharmacology*, Karger, Basel, 1989, pp. 3–21.
3. Kapurniotu, A., Kaye, R., Taylor, J.W., Voelter, W. *Eur. J. Biochem.* **265**, 606–618 (1999).
4. Schwarzing, S., Kroon, G.J.A., Foss, T.R., Chung, J., Wright, P.E., Dyson, H.J. *J. Am. Chem. Soc.* **123**, 2970–2978 (2001).
5. Ogawa, K., Nishimura, S., Uchiyama, S., Kobayashi, K., Kyogoku, Y., Hayashi, M., Kobayashi, Y. *Eur. J. Biochem.* **257**, 331–336 (1998).
6. Amodeo, P., Motta, A., Strazzullo, G., Morelli, M. *J. Biomol. NMR* **13**, 161–174 (1999).
7. Epand, R.M., Epand, R.F., Orlowski, R.C. *Int. J. Pept. Protein Res.* **25**, 105–111 (1985).

## Conformational Studies of a Glycopeptide Recognized with High Affinity by Autoantibodies in Multiple Sclerosis

Alfonso Carotenuto<sup>1</sup>, Armida Di Fenza<sup>1</sup>, Elena Nardi<sup>2</sup>, Anna M. Papini<sup>2</sup>  
and Paolo Rovero<sup>1</sup>

<sup>1</sup>Department of Pharmaceutical Sciences, University of Salerno, I-84084 Fisciano, Italy

<sup>2</sup>Department of Organic Chemistry "Ugo Schiff", University of Firenze, I-50019 Firenze, Italy

### Introduction

Myelin oligodendrocyte glycoprotein (MOG), a minor myelin component, is an important central-nervous system-specific target autoantigen for primary demyelination in autoimmune diseases like multiple sclerosis (MS). It has been described that glycosylation of a MOG peptide epitope improved the detection of specific autoantibodies in sera of MS patients [1]. We have recently found that the specific antibody recognition of this peptide is most likely driven by direct interactions of the antibody binding site with the Asn-linked sugar moiety and then stabilized by putative specific peptide–antibody interactions [2]. We have subsequently prepared and characterized a new 21-mer MOG derived glycopeptide *N*7 (H-Thr-Pro-Arg-Val-Glu-Arg-Asn(Glc)-Gly-His-Ser-Val-Phe-Leu-Ala-Pro-Tyr-Gly-Trp-Met-Val-Lys-OH – **1**) showing enhanced affinity for MS autoantibodies in ELISA experiments compared to the native *N*-glycosylated MOG peptide epitope Asn<sup>31</sup>(Glc)hMOG(30-50). Thus, the peptide (**1**) is a synthetic antigen able to detect pathogenic demyelinating autoantibodies in MS patients and, most importantly, it can be used as a template for the design of a new generation of drugs capable of specific blockage of circulating autoantibodies in patients affected by MS. In view of this goal, we describe here a conformational analysis of this peptide, and of its unglycosylated and inactive counterpart (H-Thr-Pro-Arg-Val-Glu-Arg-Asn-Gly-His-Ser-Val-Phe-Leu-Ala-Pro-Tyr-Gly-Trp-Met-Val-Lys-OH – **2**).

### Results and Discussion

Peptides **1** and **2** were analyzed in water and in water/HFA 1 : 1 v/v (HFA: hexafluoroacetone trihydrate) solutions. Almost complete <sup>1</sup>H NMR assignments were obtained by the combined use of DQF-COSY, TOCSY, NOESY spectra in both these environments. NMR data indicated that the two peptides sample a broad range of conformations in H<sub>2</sub>O solution. In water/HFA solution the two peptides adopt a more structured conformation. Diagnostic NOE contacts, and the shifts observed for CαH resonances compared to random coil peptides [3], indicate that the structures of the two peptides are very similar and consist of a β-hairpin in the region encompassing residues 2-14 with a turn at positions N<sup>7</sup>-G<sup>8</sup>. The same data indicate the presence of a helix in the C-terminal region.

For a quantitative analysis, NOE derived constraints were used as input for a structure calculation as implemented in the program Dyana [4]. For each peptide 100 structures were calculated, 10 of which were selected on the basis of low overall target function score. The selected structures were subjected to unrestrained energy minimization with the program DISCOVER (Molecular Simulation, Inc). The analysis of the optimized structures showed a preferred *type I'* β-turn conformation at the glycosylation site flanked by two short extended regions. Furthermore, an α-helix structure is present at the C-terminal side (Figure 1). Based on the obtained structures, we have designed and synthesized cyclic analogs in which the side chains of the resi-

dues 5 and 10, which appeared spatially close in the calculated structures, have been linked by a lactam bridge. The molecules are now under biological and spectroscopic investigation.

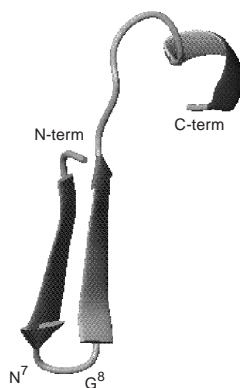


Fig. 1. Ribbon diagram of the lowest energy structure of peptide 1.

In conclusion, peptides **1** and **2** adopt virtually indistinguishable structures, again underlining the role of the sugar moiety in the antibody recognition. In peptide **1**, the *N*-glycosylated Asn<sup>7</sup> residue results to be part of a  $\beta$ -hairpin consisting of a type I'  $\beta$ -turn and two short extended flanking regions; a defined  $\alpha$ -helix at the C-terminal region is also observed (Figure 1). It can be hypothesized that the enhanced affinity for MS autoantibodies showed by this peptide compared to the unstructured Asn<sup>31</sup>(Glc)hMOG(30-50) peptide depend on these structural features. New constrained mimic peptides are currently under investigation.

## References

1. Mazzucco, S., Mata, S., Vergelli, M., Fiorese, R., Nardi, E., Mazzanti, B., Chelli, M., Lolli, F., Ginanneschi, M., Pinto, F., Massacesi, L., Papini, A.M. *Bioorg. Med. Chem. Lett.* **9**, 167–172 (1999).
2. Carotenuto, A., D'Ursi, A.M., Nardi, E., Papini, A.M., Rovero, P. *J. Med. Chem.* **44**, 2378–2381 (2001).
3. Wishart, D., Sykes, B., Richards, F. *Biochemistry* **31**, 1647–1651 (1992).
4. Guntert, P., Mumenthaler, C., Wüthrich, K. *J. Mol. Biol.* **273**, 283–298 (1997).

## Human Relaxin Chain Combination and Folding

Jian-Guo Tang<sup>1</sup>, Geoffrey W. Tregear<sup>2</sup> and John D. Wade<sup>2</sup>

<sup>1</sup>College of Life Sciences, Peking University, Beijing 100871, China

<sup>2</sup>Howard Florey Institute of Experimental Physiology and Medicine, University of Melbourne,  
 Victoria 3010, Australia

### Introduction

Relaxin is a bona fide member of the insulin superfamily and consists of two peptide chains, A- and B- (24- and 29-residues respectively), that are held together by three disulfide bonds in the exact disposition as in insulin (Figure 1). In most mammalian species, relaxin is produced principally in the corpus luteum during pregnancy and has a key role in the reproductive process. More recently, alternative roles have been postulated including one in the CNS to regulate fluid balance [1]. Acquisition of human relaxin for structural and biological study has usually been achieved by chemical synthesis of the two chains followed by their combination in solution at high pH [2]. Yields are variable and low, due, in part, to the poor solubility of the B-chain. Other methods of relaxin production have been developed, including via recombinant DNA expression of the individual chains, as well as a prorelaxin approach using a reduced size C-peptide between the two chains.

Although the insulin folding and oxidation pathway has been extensively studied [3], very little is known about the corresponding pathway for relaxin and other members of the insulin superfamily. Consequently, in this study, we have systematically re-examined the mechanics of the two-chain combination process to determine if the disulfide bond formation and subsequent peptide folding pathway of relaxin are similar.

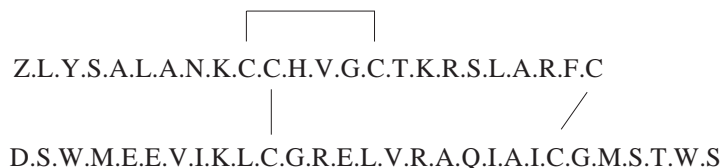


Fig. 1. Primary structure of human Gene 2 relaxin.

### Results and Discussion

Use of synthetic A-chain analogues containing specific Cys → Ser replacements allowed determination of relative rates of disulfide bond formation both within the A-chain and B-chain alone and between the two chains themselves. The first stable reaction intermediate to form is a bis-cyclic A-chain in which the intramolecular disulfide bond forms first. Small quantities of mismatched monomeric disulfide isomers of A-chain also form but do not combine with the B-chain. The rate of oxidation of the B-chain alone is much slower than the A-chain. The bis-cyclic A-chain then rapidly combines with the S-reduced B-chain to produce the two-chain peptide. It remains unknown which of the two intramolecular disulfide bonds forms first. In the absence of an intramolecular A-chain disulfide, little pairing with the B-chain occurs. This further confirmed that the rate limiting step for the folding of relaxin was the formation of the intra-A-chain disulfide bond. The rate and yield of combination was largely unaffected by temperatures below ambient but poor at 37 °C (data not shown).

## Analytical Methods

Our results suggest that in the case of the human Gene 2 relaxin, the chain folding and combination pathway is similar to that of insulin [4]. When optimized conditions were employed for the combination of relaxin B-chain with A-chains from other insulin-like peptides including ovine and human relaxin-like factors (RLFs), successful acquisition of hybrid molecules was achieved (Figure 2). This suggests that the folding pathway is likely to be similar for all members of the insulin superfamily.

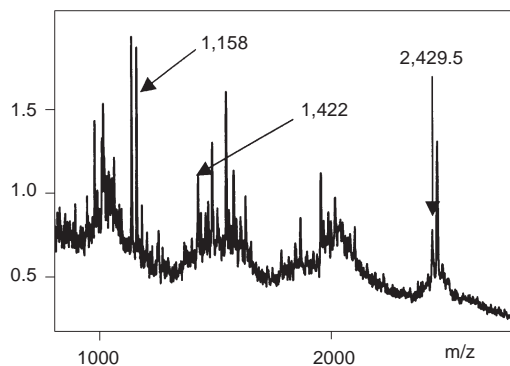


Fig. 2. MALDI-TOF mass spectrum of the tryptic digest of the product from combination of synthetic ovine RLF A-chain with synthetic H2 relaxin B-chain. Theoretical  $MH^+$  values: B(1–9), 1,158; A(9–17)/B(10–13), 1,422; and A(18–26)/B(18–30), 2,432.6.

## Acknowledgments

The work carried out at the Howard Florey Institute was supported by an Institute block grant (reg. key #983001) from the NHMRC. We thank the China Scholarship Council for receipt of a traveling award to J-G.T. to enable him to undertake studies at the Howard Florey Institute. We thank K. Smith (HFI) for provision of ovine RLF A-chain.

## References

1. Sherwood, O.D. In Knobil, E., Neill, J.D. (Eds.) *The Physiology of Reproduction*. Raven Press, 2nd ed., New York, 1994, p. 861.
2. Wade, J.D., Tregear, G.W. *Methods Enzymol.* **289**, 637–646 (1997).
3. Markussen, J. *Int. J. Pept. Protein Res.* **25**, 431–437 (1985).
4. Yuan, Y., Wang, Z-H., Tang, J-G. *Biochem. J.* **343**, 139–144 (1999).

## Effects of Human Leptin Fragments in Hypothalamic Nucleus C-Fos Expression

Vani X. Oliveira Jr.<sup>1</sup>, M. Terêsa M. Miranda<sup>2</sup>, Jackson C. Bittencourt<sup>3</sup>,  
 Carol F. Elias<sup>3</sup> and Antonio Miranda<sup>1</sup>

<sup>1</sup>Department of Biophysics, UNIFESP, 04044-020

<sup>2</sup>Department of Biochemistry, IQ-USP, 05508-900

<sup>3</sup>Department of Anatomy, ICB-USP, 05508-900, São Paulo, Brazil

### Introduction

The product of the *ob* gene is a protein hormone mainly secreted by the adipose tissue denoted leptin. Among many other effects, leptin provides signals to the brain about the amount of body fat stores and acts to reduce food intake and increase the energy expenditure. The weight-reducing effects of leptin are likely mediated through interaction with a specific cytokine family receptor. Leptin receptor mRNA is found in many hypothalamic regions including arcuate, paraventricular and ventromedial nuclei. In addition, Fos expression, an important tool for mapping neuronal activation, has also been observed in hypothalamic areas following leptin administration. The major goal of our work is to identify regions in the leptin molecule responsible for its important bioactivities. Thus, we have designed, synthesized and studied a few leptin fragments containing 17 to 25 amino acid residues.

### Results and Discussion

For the fragments design we took into account previous data employing synthetic peptides [1,2] and, also, the secondary structure of human leptin [3]. Fragments I, III, IV and VI listed in Table 1 present an  $\alpha$ -helical conformation in the intact protein molecule, feature that has been used to suggest that the leptin is a member of the short-helix subfamily of cytokine folds. Fragments II and V are two loops encompassing Thr<sup>27</sup>-Thr<sup>50</sup> (I–III) and Ser<sup>95</sup>-Tyr<sup>119</sup> (IV–VI)]. The syntheses were carried out by the SPPS method using MBHA resin and *t*-Boc strategy [4]. The crude materials were purified by RP-HPLC and characterized by LC/MS. The final products were tested for their ability to induce Fos-like immunoreactivity (Fos-IR) in the brain of adult male rats [5]. As it can be observed in Figure 1, fragments **I** and **V** induced Fos-IR in the paraventricular nucleus of the hypothalamus and in the lateral arcuate nucleus. However, no similar ability was observed for the other four synthetic fragments. These results suggest that fragments **I** and **V** were recognized by leptin receptors present in those areas of the brain. Interestingly, these two peptides encompass the regions from

Table 1. Leptin fragments studied.

No.	Fragment	Sequence
<b>I</b>	Leptin <sub>2–26</sub>	Ac-PIQKVQDDTKTLIKTIVTRINDISH-HN <sub>2</sub>
<b>II</b>	Leptin <sub>27–50</sub>	Ac-TQSVSSKQKVTGLDFIPGLHPILT-HN <sub>2</sub>
<b>III</b>	Leptin <sub>51–67</sub>	Ac-LSKMDQTLAVYQQILTS-HN <sub>2</sub>
<b>IV</b>	Leptin <sub>71–94</sub>	Ac-RNVIQISNDLENLRDLLHVLAFSK-HN <sub>2</sub>
<b>V</b>	[Ser <sup>96</sup> ]-Leptin <sub>95–119</sub>	Ac-SSHLPWASGLETLDLGLGGVLEASGY-HN <sub>2</sub>
<b>VI</b>	Leptin <sub>120–143</sub>	Ac-STEVVALSRLQGSLQDMLWQLDLS-HN <sub>2</sub>

which Samson *et al.* [1] and Grasso *et al.* [2], respectively, obtained peptides able to reduce food intake. Although our peptide fragments design needs refinement, this kind of strategy may offer the basis for the development of leptin-related compounds having potential application in human or veterinary medicine.

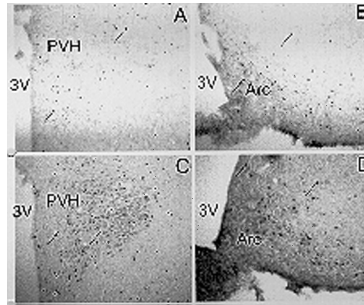


*Fig. 1. Fos-IR distribution in hypothalamic nucleus in response to leptin fragments injections. Photomicrography A and B: neurons activated by fragment I. Photomicrography C and D: neurons activated by fragment V.*

### Acknowledgments

This work has been supported by grants and fellowships from CNPq and FAPESP.

### References

1. Samson, W.K., Murphy, T.C., Robison, D., Vargas, T., Tau, E., Chang, J.K. *Endocrinology* **137**, 5182–5185 (1996).
2. Grasso, P., Leinung, M.C., Ingher, S.P., Lee, D.W. *Endocrinology* **138**, 1413–1418 (1997).
3. Kline, A.D., Becker, G.W., Churgay, L.M., Landen, B.E., Martin, D.K., Muth, W.L., Rathnachalam R., Richardson, J.M., Schoner, B., Ulmer, M., Hale, J.E. *FEBS Lett.* **407**, 239–242 (1997).
4. Miranda, A., Koerber, S.C., Gulyas, J., Lahrichi, S.L., Craig, A.G., Corrigan, A., Hagler, A., Rivier, C., Vale, W., Rivier, J. *J. Med. Chem.* **37**, 1450–1459 (1994).
5. Elias, C.F., Lee, C., Kelly, J., Aschkenasi, C., Ahima, R.S., Bjorbaek, C., Flier, J.S., Saper, C.B., Elmquist, J.K. *Neuron* **23**, 775–786 (1999).

## **Introduction of Temperature-Sensitive Elastin-Based Switches to Stabilize Globular Proteins**

**Bin Li, Darwin O. V. Alonso and Valerie Daggett**

*Department of Medicinal Chemistry, University of Washington, Seattle, WA 98195, USA*

### **Introduction**

Elastin and elastin-based peptides display a temperature-dependent conformational transition from a less to a more ordered state upon increasing temperature [1]. This inverse temperature behavior has been attributed to hydrophobic collapse and expulsion of water molecules associated with the non-polar side-chains of the polymer by both experimental [1] and simulation [2] studies. In addition, studies by Reiersen *et al.* [3] of various elastin monomers (VPGVG) suggest that short elastin-based peptides exhibit the same behavior as elastin. Also, an engineered protein A mini-domain containing an elastin turn exhibits reversible temperature-controlled IgG binding [4]. Following along these lines, we now ask whether an elastin-based turn can serve as a temperature-sensitive switch when engineered into a globular protein such that its conformational behavior and stability can be controlled. We investigated this possibility using molecular dynamic simulations. These simulations suggest that it is possible to introduce an “inverse temperature transition” and/or stabilize a globular protein at higher temperature, by replacing a turn in the target protein with an elastin-like turn (VPGVG).

### **Results and Discussion**

We swapped two turn-segments comprised of residues 23-28 and 33-37 in chymotrypsin inhibitor 2 (CI2) to the elastin-based turns AVPGVG and VPGVG, respectively. Molecular dynamics simulations were performed with wild-type CI2, switch (23-28) and switch(33-37) as the starting structures, each for 10 ns at 10 and 40 °C (below and above elastin’s transition temperature). The inverse temperature transition can be found in various properties averaged over the last nanosecond of the simulations. As shown in Table 1, the number of contacts, solvent accessible surface area and main-chain/main-chain hydrogen bonding all exhibit inverse trends after switching. The radius of gyration retained relatively low in all the simulations, indicating that CI2 retains most of its native-like features at these temperatures. The switch (23-28) protein at 40 °C had the lowest C $\alpha$  root-mean-square deviation (RMSD) from the X-ray structure of wild-type CI2. In fact, the C $\alpha$  of this construct at high temperature is lower than the wild-type protein at 10 °C. The helix in the switch(33-37) simulation at 10 °C rotated about 90° from its starting position. It is surprising that swapping some turn residues can cause such a large structural change at this low temperature. On the other hand, the final structure of the switch(33-37) simulation at 40 °C retained the overall structural features of native CI2.

Overall, our simulations suggest that introducing an elastin-based turn into a globular protein can dramatically change the protein’s thermal behavior – wild-type CI2 became less stable as the temperature increased, but both of the switched CI2 simulations were more stable at higher temperature after introduction of the elastin-based turn. In addition, previous experiments established that the introduction of an elastin peptide into a 34 amino acid cyclo-peptide (mini-protein A with a disulfide bond) causes an inverse temperature transition. Here, the target molecule is CI2, a 64-residue globular protein devoid of disulfide bonds. We obtained the same general

## Analytical Methods

temperature-dependent behavior with CI2. Therefore, it is possible to insert short elastin-based peptides into peptides and globular proteins that might be useful for improving upon protein stability and for designing temperature-based conformational biosensors.

Table 1. Average properties of wild-type and modified CI2 over the final ns.

	Wide-type		Switch(23–28)		Switch(33–37)	
	10 °C	40 °C	10 °C	40 °C	10 °C	40 °C
C $\alpha$ RMSD <sup>a</sup>	1.87	2.35	2.30	1.60	4.65	2.64
# of total contacts	254	225	246	245	222	243
# of non-polar contacts	73	57	63	68	59	66
Radius of gyration (Å)	11.0	11.3	11.1	11.1	11.9	11.2
Total SASA <sup>b</sup> (Å <sup>2</sup> )	4738	5163	4850	4733	5320	4757
Non-polar ASA (Å <sup>2</sup> )	3067	3261	3148	3037	330	2911
# of mc-mc HB <sup>c</sup>	23	16	22	20	16	21

<sup>a</sup> C $\alpha$  RMSD: C $\alpha$  root-mean-square deviation; <sup>b</sup> SASA: solvent-accessible surface area; <sup>c</sup> HB: hydrogen bond.

## Acknowledgments

We are grateful for financial support from the Office of Naval Research (N00014-98-1-0477).

## References

1. Urry, D.W. *J. Protein Chem.* **7**, 1–34 (1988).
2. Li, B., Alonso, D.O.V., Daggett, V. *J. Mol. Biol.* **305**, 581–592 (2001).
3. Reiersen, H., Clarke, A.R., Rees, A.R. *J. Mol. Biol.* **283**, 255–264 (1998).
4. Reiersen, H., Rees, A.R. *Biochemistry* **38**, 14897–14905 (1999).

## A Short-Range Interaction of the *cis-trans* Urea Motif in Ureapeptides

Michel Marraud<sup>1</sup>, Christine Hemmerlin<sup>1</sup>, Claude Didierjean<sup>2</sup>,  
 André Aubry<sup>2</sup>, Vincent Semetey<sup>3</sup>, Arnaud-Pierre Schaffner<sup>3</sup>,  
 Jean-Paul Briand<sup>3</sup> and Gilles Guichard<sup>3</sup>

<sup>1</sup>LCPM, UMR CNRS-INPL 7568, ENSIC-INPL, BP 451, 54001 Nancy, France

<sup>2</sup>LCM3B, ESA-CNRS 7036, UHP, BP 239, 54506 Vandoeuvre, France

<sup>3</sup>Laboratoire de Chimie Immunologique, UPR CNRS 9021, 67084 Strasbourg, France

### Introduction

The urea motif is known to promote particular structures, such as  $\beta$ -like sheets, in which the chains exchange multiple intermolecular H-bonds between all-*trans* urea groups [1]. Preliminary studies in  $\text{CHCl}_3$  on the  $\alpha$ -acylamino ureas Boc-*g*Xaa-CO-NHR **1**, where *g*Xaa denotes a *gem*-diamino residue, have revealed a structure folded by the  $\text{NH}\cdots\text{O}$  H-bond closing an 8-membered cycle, in which the urea fragment adopts the *cis-trans* conformation, and that we name a urea-turn [2]. Investigations have been extended to the urea-containing dipeptides **2**, **2'**, **3** and **4** by considering the N-H and C=O stretching frequencies, the NH proton solvent-accessibility and the NOE data.

### Results and Discussion

The investigated derivatives (Figure 1) have been obtained from *O*-succinimidyl carbamates of *N*-Boc-*gem*-diamino residues [3].

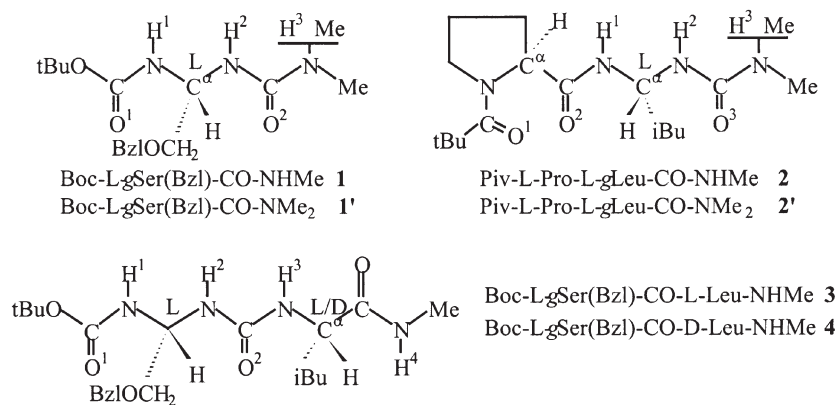


Fig. 1. Investigated ureapeptides.

Due to proline, **2** assumes in the solid state a globally folded molecular conformation with an all-*trans* urea motif. In  $\text{CH}_2\text{Cl}_2$ , both **1** and **2** exhibit the same NH absorption at a low IR frequency, which disappears for **1'** and **2'** where H<sup>3</sup> is replaced by a methyl, and a strong  $\text{NH}^3/\text{C}^\alpha\text{H}$  NOE cross-peak which denotes a *cis-trans* urea motif. In  $\text{CDCl}_3/\text{DMSO}$  mixtures, the solvent sensitivities of the urea NH proton resonances for **2** are quite similar to those for **1**, *i.e.* NH<sup>2</sup> exposed to DMSO and NH<sup>3</sup> protected from DMSO. Then the urea motif in **2** has the same conformation as in **1** and accommodates the urea-turn, independent of the preceding proline residue.

The same holds true for **3** and **4**, where the urea fragment is inserted between two peptide bonds. The IR spectrum displays the same low frequency as for **1**, and the solvent sensitivity for the  $\text{NH}^1$ ,  $\text{NH}^2$  and  $\text{NH}^3$  proton resonances are quite similar to those for **1**, **3** and **4**. The high solvent sensitivity for  $\text{NH}^4$  for both **3** and **4** denote a free amide NH. Furthermore, the variations for the NH signals for **3** and **4** in  $\text{CDCl}_3/\text{DMSO}$  mixtures are practically superimposed, indicating that the urea-turn occurs independently of the chirality of the adjacent amino acid residues.

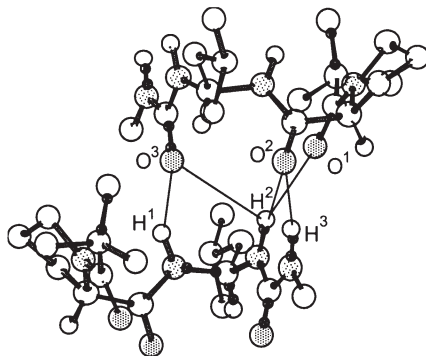


Fig. 2. Crystal molecular structure of **2**. The molecules are connected by a complex network of 2 close  $\text{H}\cdots\text{O}$  contacts ( $\text{H}^1\cdots\text{O}^3 = 2.03 \text{ \AA}$ ,  $\text{H}^3\cdots\text{O}^2 = 1.83 \text{ \AA}$ ) and 3 loose  $\text{H}\cdots\text{O}$  contacts ( $\text{H}^2\cdots\text{O}^1 = 2.67 \text{ \AA}$ ,  $\text{H}^2\cdots\text{O}^2 = 2.66 \text{ \AA}$ ,  $\text{H}^2\cdots\text{O}^3 = 2.98 \text{ \AA}$ ).

When inserted in a peptide chain, the flexible urea motif assumes the all-*trans* conformation in the solid state with intermolecular H-bonds, and the *cis-trans* conformation in solution where it is engaged in an intramolecular H-bond closing an 8-membered cycle that we call a urea-turn (Figure 2). This folded structure is observed in all the ureapeptides that we have investigated so far, independent of the presence and the chirality of the contiguous amino acid residues.

## References

1. Nowick, J.S. *Acc. Chem. Res.* **32**, 287–296 (1999).
2. Martinez, J., Fehrentz, J.A. (Eds.) *Peptides 2000 (Proceedings of the 26th European Peptide Symposium)*, EDK, Paris, 2001, p. 503.
3. Guichard, G., Semetey, V., Didierjean, C., Aubry, A., Briand, J.-P., Rodriguez, M. *J. Org. Chem.* **64**, 8702–8705 (1999).

## A New N-Terminal Helix Capping Box

Toshimasa Yamazaki<sup>1</sup>, Etsuko Katoh<sup>1</sup>, Tomohisa Hatta<sup>1</sup>,  
Teruhisa Tomari<sup>2</sup>, Sakurako Tashiro<sup>2</sup>, Heisaburo Shindo<sup>2</sup>  
and Takeshi Mizuno<sup>3</sup>

<sup>1</sup>Department of Biochemistry, National Institute of Agrobiological Sciences, 2-1-2 Kannondai,  
Tsukuba, Ibaraki 305-8602, Japan

<sup>2</sup>School of Pharmacy, Tokyo University of Pharmacy and Life Science, Hachioji,  
Tokyo 192-0392, Japan

<sup>3</sup>Laboratory of Molecular Microbiology, School of Agriculture, Nagoya University,  
Chigusa-ku, Nagoya, 464-8601, Japan

### Introduction

The  $\alpha$ -helix is one of the fundamental structural elements for three-dimensional structures of proteins, and is widely used for structure-based design of biologically active peptides. Several local motifs at  $\alpha$ -helix ends have been identified and experimentally characterized, such as the *Schellman* [1] and the *Pro-capping* [2] motifs at the C-terminus, and the *Capping box* [3], the *Hydrophobic staple* [4], and the *Pro-box* [5] at the N-terminus. In general, these local motifs are composed of two or more residues, and stabilize the  $\alpha$ -helix through various types of hydrogen bonds and hydrophobic interactions.

During NMR studies of YhhP, a small protein of 81 amino acid residues implicated in *Escherichia coli* cell division, we have identified a novel N-terminal helix capping box of the six-residue LxCPxP sequence [6,7]. Although YhhP shows no homology in primary sequence to any protein of known functions, a variety of microorganisms have similar proteins, all of which contain a common CPxP sequence motif in the N-terminal region. In this study, we have prepared several point mutants of YhhP employing rational site-directed mutagenesis to further investigate the role of the LxCPxP N-terminal helix capping box on the YhhP structure and function.

### Results and Discussion

The high-resolution three-dimensional structure of YhhP in solution was determined by a hybrid distance geometry-dynamical simulated annealing method based on 1655 experimental restraints derived from NMR spectroscopy. It folds into a compact two-layered  $\alpha/\beta$ -sandwich structure with a  $\beta\alpha\beta\alpha\beta\beta$  fold, comprising a mixed four-stranded  $\beta$ -sheet (strand  $\beta$ 1, residues 10-13;  $\beta$ 2, 37-43;  $\beta$ 3, 62-67;  $\beta$ 4, 73-80) stacked against two  $\alpha$ -helices ( $\alpha$ 1, residues 20-31;  $\alpha$ 2, 48-59) (Figure 1). The  $\alpha$ 1-helix does not contain a typical N-capping box, rather it is stabilized by a hydrogen bond from Glu21 NH to Arg18 backbone C=O at the N-terminus of the helix. The geometry of this hydrogen bond is nearly ideal, and is achieved because of the presence of a *cis*-proline at position 20. In addition, two separated hydrophobic contacts, one mediated by Leu17, Pro22 and C <sup>$\beta$</sup> H<sub>2</sub> group of Glu21, and the other by Cys19 and Pro20, stabilize the N-terminal structure of this helix (Figure 1). Hence these observations suggest the novel result that the six-residue sequence, LxCPxP, can serve as an N-capping box for the  $\alpha$ -helix.

In order to investigate a specific role of each amino acid residue within the LxCPxP box on the YhhP structure and function, we prepared a series of YhhP point mutants, L17A, C19S, E21A, P20A, P22A, and P20A/P22A. Mutational effects on the function were determined by examining an ability of the mutant to suppress the phenotype of

YhhP deficient ( $\Delta yhhP$ ) cells. Three-dimensional structures of the mutant proteins and their stability were analyzed by CD and NMR spectroscopy. The L17A and C19S mutants were designed to respectively examine importance of the Leu17/Pro22/Glu21- ( $C^\beta H_2$ ) and the Cys19/Pro20 hydrophobic interactions on the  $\alpha$ -helix stability. We expected that the E21A mutant has essentially the same three-dimensional structure and stability as its parent protein because the  $C^\beta H_3$  side chain of alanine is almost equivalent in size as the  $C^\beta H_2$  group of Glu21. However, this mutant should provide crucial information regarding the biological importance of Glu21 side chain carboxyl group previously proposed by our genetic study [6]. The P20A and P20A/P22A mutants should provide insight into the role of the *cis* peptide bond in the LxCPxP box, because the *cis* configuration of the Cys-Pro peptide bond in the wild-type YhhP is predicted to convert into *trans* in these mutants.

None of the substitutions introduced at positions 17, 19, and 21 were associated with any detectable changes in CD spectra. In fact, all the CD spectra of these mutants are superimposable with that of their parent protein. In addition, NMR analyses revealed that these mutants possess all the structural characteristics of the wild-type YhhP, including the *cis* peptide bond between residues 19 and 20. These results strongly indicate that solution structures of the L17A, C19S and E21A are essentially the same as the wild-type YhhP. Interestingly, however, the L17A mutant displays significantly reduced stability against guanidine hydrochloride (GnHCl) induced denaturation while the C19S and E21A mutants show nearly the same stability as their parent protein. Denaturation midpoints ( $C_m$ ) were observed at 1.84 M GnHCl for the wild-type YhhP, 1.34 M for L17A, 1.81 M for C19S, and 1.73 M for E21A. These values were obtained by fitting the denaturation curves to the two-state model between the native and unfolded states. The reduced stability observed for the L17A mutant indicates that the hydrophobic interactions mediated by the Leu117 and Pro22 side chains as well as the Glu21  $C^\beta H_2$  group have a significant role in the  $\alpha 1$ -helix stability. In contrast, the Cys19/Pro20 hydrophobic interactions have little contribution to the stability of the same helix. It should be noted that the C19S and E21A mutants lose the ability to suppress the phenotype of the  $\Delta yhhP$  cells. These results suggest that the Cys19 S<sup>7</sup>H and the Glu21 carboxyl groups are important for the YhhP function.

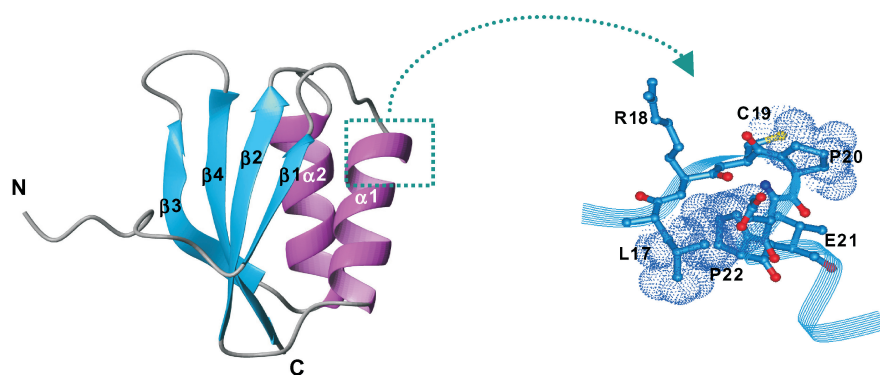


Fig. 1. A ribbon diagram of the energy-minimized average structure of YhhP, and a close-up view of the N-terminal structure of helix  $\alpha 1$  where the Cys19-Pro20 peptide bond assumes a *cis* configuration.

Substitutions of prolines at position 20 or/and 22 with alanine caused small, but critical structural changes around the N-terminal region of the  $\alpha$ 1-helix. As expected, the *cis* peptide bond between residues 19 and 20 in the wild-type YhhP was converted into *trans* in the P20A. More importantly, this mutant has a shortened  $\alpha$ 1-helix (residues 22–31) by two residues as compared with the wild-type YhhP, and has no hydrogen bond between the Glu21 NH and the Arg18 backbone C=O groups. According to these structural changes, the P20A mutant is less stable against GnHCl denaturation ( $C_m = 1.43$  M) than its parent protein. The P20A/P22A mutant, in which both prolines at positions 20 and 22 are replaced by alanines, also has a *trans* peptide bond between residues 19 and 20 as P20A. On the contrary to the P20A mutant, however, the P20A/P22A mutant has an elongated  $\alpha$ 1-helix (residues 19–31) by one residue, accompanied with a newly formed hydrogen bond from Ala22 NH to Arg18 backbone C=O. Resultantly, the P20A/P22A mutant shows higher stability with the  $C_m$  value of 2.27 M. The P22A mutant provided interesting information regarding roles of prolines in the LxCPxP capping box. This mutant shows distinctly separated two sets of signals on NMR spectra with a ratio of 2 : 1. The configuration of the Cys19-Pro20 peptide bond is *trans* in the major isomer while *cis* in the minor one. In addition, the solution structure of the major isomer is nearly identical to that of the P20A/P22A mutant while the solution structure of the minor isomer is essentially the same as that of the wild-type YhhP. These results strongly indicate that both prolines within the LxCPxP box are required to determine the N-terminus of the YhhP  $\alpha$ 1-helix.

In summary, we have identified a novel N-terminal  $\alpha$ -helix capping box composed of the six-residue L(N'')-x(N')-C(Ncap)-P(N1)-x(N2)-P(N3) sequence where the Cys-Pro peptide bond assumes a *cis* configuration. Both the Pro residues are significantly important in defining the N-terminus of the helix, which is the first proline, P(N1). The LxCPxP box stabilizes the helix mainly by the hydrogen bond from x(N2) NH to x(N') C=O and the L(N'')/P(N3)/x(N2) hydrophobic interactions. We hope that the new N-terminal helix capping box could increase possibility and variability for structure-based design of bioactive peptides and functional proteins.

### Acknowledgments

This work was supported by a grant from the Bio-oriented Technology Research Advancement Institution, Japan to T. Y.

### References

1. Schellman, C., In Jaenicke, R. (Ed.) *Protein Folding*, New York, 1980, pp. 53–61.
2. Prieto, J., Serrano, L. *J. Mol. Biol.* **274**, 276–288 (1997).
3. Harper, E.T., Rose, G.D. *Biochemistry* **32**, 7605–7609 (1993).
4. Munoz, V., Blanco, F.J., Serrano, L. *Nat. Struct. Biol.* **2**, 380–385 (1995).
5. Viguera, A.R., Serrano, L. *Protein Sci.* **8**, 1733–1742 (1999).
6. Katoh, E., Hatta, T., Shindo, H., Ishii, Y., Yamazda, H., Mizuno, T., Yamazaki, T. *J. Mol. Biol.* **304**, 219–229 (2000).
7. Ishi, Y., Yamada, H., Yamashino, Y., Ohashi, K., Katoh, E., Shindo, H., Yamazaki, T., Mizuno, T. *Biosci. Biotechnol. Biochem.* **64**, 799–807 (2000).

## The Determination of Helix Stability Coefficients Using D-Amino Acid Substitutions in the non-Polar Face of an Amphipathic $\alpha$ -Helical Model Peptide

Yuxin Chen, Colin T. Mant and Robert S. Hodges

Department of Biochemistry, University of Alberta, Edmonton, T6G 2H7, Canada and  
Department of Biochemistry and Molecular Genetics, University of Colorado Health Sciences  
Center, Denver, CO 80262, USA

### Introduction

The helix-destabilizing properties of D-amino acids [1] offer a systematic approach to the controlled destabilization of  $\alpha$ -helical structure in benign, aqueous medium, whilst retaining the ability to refold into a fully helical structure in a more hydrophobic environment. In the present study, each of the D-amino acids was substituted into the center of the non-polar face of an 18-residue  $\alpha$ -helical synthetic model peptide (Figure 1) and their effect on helical stability subsequently characterized by temperature denaturation monitored by circular dichroism (CD).

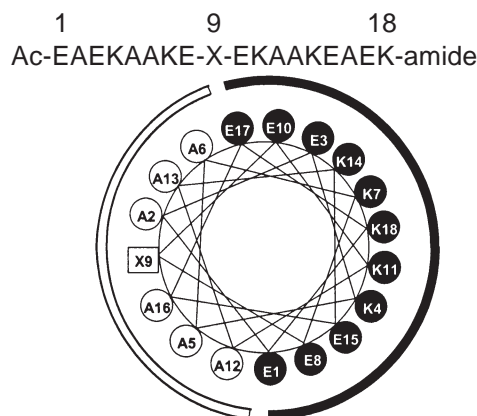


Fig. 1. Sequence (top) and helical wheel representation (bottom) of the "host" peptide. The hydrophobic face (Ala-face) is indicated as an open arc and the hydrophilic face as a solid arc. The substitution ("guest") site is at position 9 (boxed) of the hydrophobic face.

### Results and Discussion

We have demonstrated (data not shown) that all single D-amino acid substitutions in the model peptide prevent  $\alpha$ -helical formation in benign medium. Both the L- and D-substituted analogs were generally fully helical in hydrophobic medium (40% trifluoroethanol [TFE]; data not shown), with the D-isomers clearly destabilizing secondary structure (Table 1). For the L-series analogs,  $\alpha$ -helical stability generally decreased with decreasing hydrophobicity of the substituted side-chain (Table 1) [2]. In contrast, there was no clear pattern to the helix-destabilizing tendencies of the D-enantiomers, although the hydrophobic  $\beta$ -branched side-chains of Val and Ile exhibited a disproportionate effect on helix destabilization compared to their L-counterparts.

Table 1. Amino acid helix stability and stereochemistry coefficients.

Stability coefficients <sup>a</sup>				Stereochemistry coefficients <sup>b</sup>	
L-Amino Acid	$\Delta t_m$ (°C)	D-Amino Acid	$\Delta t_m$ (°C)	Amino Acid	$\Delta t'_m$ (°C)
Leu	30.5	Phe	9.0	Ile	34.5
Ile	26.0	Trp	6.5	Val	30.0
Met	25.5	Leu	6.5	Ala	24.5
Val	23.5	Met	3.5	Leu	24.0
Phe	22.5	Thr	3.5	Met	22.0
Ala	20.5	Asn	2.0	Arg	19.0
Trp	17.5	Tyr	1.5	Lys	18.5
Gln	17.5	Gln	0.5	Cys	17.5
Tyr	16.5	Gly	0	Gln	17.0
Arg	16.5	His	−0.5	Tyr	15.0
Cys	16.0	Cys	−1.5	Ser	14.0
Lys	15.5	Arg	−2.5	Phe	13.5
Thr	11.0	Lys	−3.0	His	11.5
Ser	11.0	Ser	−3.0	Trp	11.0
His	11.0	Ala	−4.0	Glu	11.0
Asn	9.5	Val	−6.5	Thr	7.5
Glu	2.0	Ile	−8.5	Asn	7.5
Gly	0	Glu	−9.0	Asp	1.0
Asp	−8.5	Asp	−9.5	Gly	0

<sup>a</sup>  $t_m$  is defined as the temperature when 50% of helical structure is denatured compared with the fully folded conformation of the peptide in 40% TFE at 5 °C and pH 7.0; a helix stability coefficient ( $\Delta t_m$ ) is defined as the difference of  $t_m$  value between a peptide analog and the Gly peptide. <sup>b</sup> Stereochemistry stability coefficients ( $\Delta t'_m$ ) are defined as the difference in  $t_m$  value between L- and D-diastereomeric peptide pairs.

From Table 1, amino acid helix stability coefficients ( $\Delta t_m$ ) quantify the ability of a specific L- or D-amino acid to stabilize or destabilize  $\alpha$ -helical structure; stereochemistry coefficients ( $\Delta t'_m$ ) express the destabilizing effects of L- to D-enantiomeric substitutions on helix stability. In conclusion, we believe such coefficients promise to prove valuable both for protein structure-function studies as well as for de novo design of model antimicrobial peptides.

### Acknowledgments

Y. C. was the recipient of a travel award from APS. This work is supported by CIHR (Canada) and grant GM-61855 (NIH) (R. S. H.).

### References

1. Rothemund, S., Krause, E., Beyermann, M., Dathe, M., Bienert, M., Hodges, R.S., Sykes, B.D., Sonnischen, F.D. *Peptide Res.* **9**, 79–87 (1996).
2. Monera, O.D., Sereda, T.J., Zhou, N.E., Kay, C.M., Hodges, R.S. *J. Peptide Sci.* **1**, 319–329 (1995).

## NMR-Based Studies of a Collagenous Substrate of Collagenase

Stella Fiori and Luis Moroder

*Max-Planck-Institut für Biochemie, Martinsried, 82152, Germany*

### Introduction

The highly selective cleavage of collagen type I by collagenases at the specific locus is thought to derive from a softened triple helical fold that allows partial unfolding of the natural substrate by the enzyme sub-domains prior to proteolysis [1]. However, a two-step thermal denaturation corresponding to different conformational tendencies of the cleavage site and adjacent portions of the molecule could not, so far, be observed.

A synthetic heterotrimer containing the collagenase cleavage site of collagen type I (Figure 1) was analyzed by NMR spectroscopy in order to determine the possibly structural basis of the high specificity of the enzymatic degradation. The peptide is crosslinked at the C-terminus by a cystine-knot and extended N-terminally with five Gly-Pro-Hyp repeats, whereby two mutations, *i.e.* Gln23Asn in the  $\alpha 1$  chain and Val27Phe in the  $\alpha 1'$  chain, were purposely performed to facilitate signal assignment of NMR spectra [2,3].

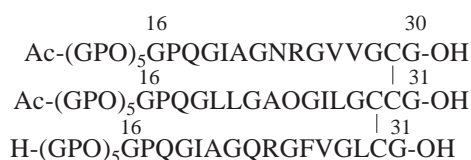


*Fig. 1. Synthetic heterotrimer.*

The molecule acts as a collagen-like substrate in its kinetics of proteolysis by the collagenases MMP1, MMP8 and MMP-13 [4], and thus mimics in all aspects the conformational properties of the functional epitope, both in the native and denatured state.

### Results and Discussion

Temperature gradients of the amide protons (277–285 K), as monitored by  $^1\text{H}$ -TOCSY experiments, clearly reveal the absence of interchain H-bonds from Gly<sup>16</sup> to the C-terminus ( $-\Delta\text{ppb}/\Delta T$  ranging from 5.00 to 10.00). The H $\rightarrow$ D exchange experiments support these observations, since all amide protons of these residues exchange similarly fast. Conversely, the Gly NH signals of the (GPO)<sub>5</sub> portion of the molecule are only slightly affected by the temperature excursion ( $-\Delta\text{ppb}/\Delta T$  3.71), and were found to exchange very slowly. These data are consistent with a tight triple helical fold in the N-terminal segment and a lack of this super-coiled structure in the central and C-terminal portion of the heterotrimer. These results provide a strong evidence of the coexistence of two structural domains in the collagen model peptide (Figure 2).

In order to better understand the molecular basis of the melting transition as observed by CD spectroscopy [3], the proton exchange of the H-bound protons (signal at 7.71 ppm) was measured in temperature dependency starting from the state reached after 36 h of exchange at 277 K. A sharp transition tracking very closely the CD melting curve and exhibiting a nearly identical  $T_m$  of 304 K as in CD was obtained by step-wise heating the sample at fixed times. Since insignificant exchange occurs in the triple helical state (data not shown), the initial plateau results from the absence of

measurable exchange at  $T \ll T_m$ , and indicates a triple helical structure. Conversely, the final plateau results from the completed exchange at  $T \gg T_m$ , and indicates a less ordered state. Thus, the transition describes the unfolding process of the triple helical domain of the molecule and its similarity to the CD melting curve clearly suggests that primarily this region contributes to the melting of the molecular structure observed by CD.

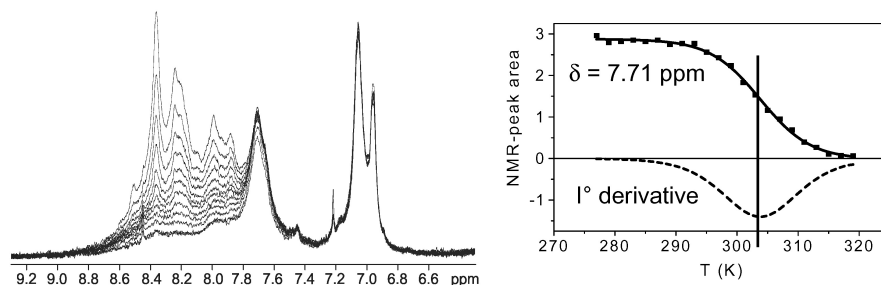


Fig. 2. Left: Amide proton exchange profile of the peptide during the first 36 h. The signal at  $\delta = 7.71$  ppm corresponds to the slowly exchanging Gly NH protons of the GPO portion of the peptide, while the signal around 7 ppm corresponds to the aromatic protons of Phe. Right: Thermal denaturation of the sole triple helical domain, as monitored by H $\rightarrow$ D proton exchange.

The results support the hypothesis of a non-triple helical structure of the collagenase cleavage site that allows successive trapping of the single strands through concerted action of the active site cleft and the hemopexin domains, as previously suggested by BIAcore experiments [4]. Moreover, the unfolding of the collagen triple helix was found to follow a non-two-state transition model, through formation of an intermediate, possibly corresponding to a poly-Pro II fold of the single strands, was observed.

### Acknowledgments

The project was supported by the SFB 533 of the Ludwig-Maximilian University of Munich.

### References

1. Fields, G.B. *Connect. Tissue Res.* **3**, 235–243 (1995).
2. Ottil, J., Battistutta, R., Pieper, M., Tschesche, H., Bode, W., Kühn, K., Moroder, L. *FEBS Lett.* **398**, 31–36 (1996).
3. Ottil, J., Moroder, L. *J. Am. Chem. Soc.* **121**, 653–661 (1999).
4. Ottil, J., Gabriel, D., Murphy, G., Knäuper, V., Tominaga, Y., Nagase, H., Kröger, M., Tschesche, H., Bode, W., Moroder, L. *Chem. Biol.* **7**, 119–132 (2000).

## Conformational Analysis of Model Polypeptides Having Repetitive Xaa-Pro Sequences

Yoshiaki Hirano<sup>1,2</sup>, Masashi Shimoda<sup>1</sup>, Masahiro Hattori<sup>2</sup>,  
Masahito Oka<sup>3</sup> and Toshio Hayashi<sup>3</sup>

<sup>1</sup>Department of Applied Chemistry, Faculty of Engineering

<sup>2</sup>Bio Venture Center, Osaka Institute of Technology, Osaka 535-8585, Japan

<sup>3</sup>Research Institute for Advance Science and Technology, Osaka Prefecture University,  
Osaka 599-8570, Japan

### Introduction

Recently, several repetitive Xaa-Pro sequences have been found in proteins, *e.g.*, Ala-Pro in myosin, Glu-Pro in procyclin, Glu-Pro and Lys-Pro in tonB protein, Arg-Pro in glycoprotein of pseudorabies virus. It is believed that such a repetitive domain forms a specific conformation relating to the molecular functions of these proteins. We are interested in investigating the conformations of the repetitive portion composed of the Xaa-Pro sequence. In this work, poly(Xaa-Pro) (Xaa = Ala, Arg, Lys, Asp, and Glu) were selected as model periodic polypeptides for the repetitive Xaa-Pro sequence of these proteins.

### Results and Discussion

The repetitive unit of Xaa-Pro and Xaa-Pro-Xaa-Pro were synthesized by liquid phase procedure and poly(Xaa-Pro) was polymerized with diphenylphosphoryl azide (DPPA). The averaged molecular weights of poly(Xaa-Pro) were estimated by gel permeation chromatography (GPC) measurement (converted to PEG standard) and MALDI-TOF-MS. These peptides were characterized by MALDI-TOF-MS, amino acid analysis and elemental analysis.

The CD measurements were carried out in H<sub>2</sub>O, TFE and buffer solution. The CD spectra of poly(Xaa-Pro) in TFE and in H<sub>2</sub>O are shown in Figures 1A and 1B, respectively. The CD spectra pattern in TFE is clearly different from those in H<sub>2</sub>O. For the case of poly(Arg-Pro) and poly(Asp-Pro), their spectra show a negative bands at 210 nm and the tendency forming a positive band at around 190 nm in TFE indicating that poly(Arg-Pro) and poly(Asp-Pro) form a new type helical conformation in TFE at 25 °C. As shown in Figure 1 (B), the CD spectra of poly(Arg-Pro) and poly(Glu-Pro) showed a negative broad band around 200 nm in H<sub>2</sub>O. These results also suggest that

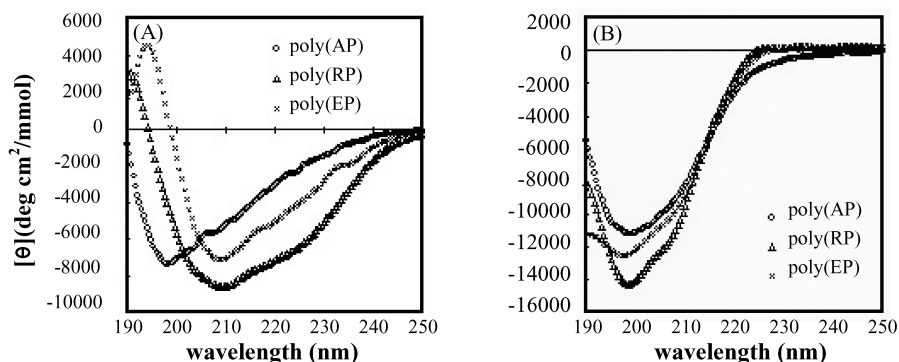


Fig. 1. Circular dichroism spectra of poly (Xaa-Pro) in TFE (A) and H<sub>2</sub>O (B).

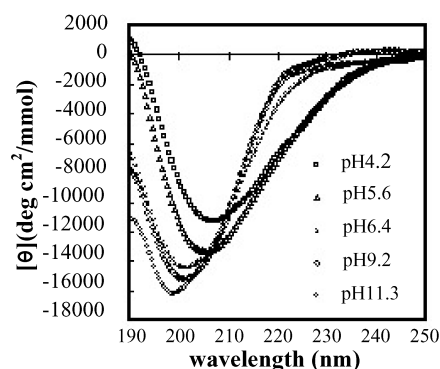


Fig. 2. Circular dichroism spectra of poly(Asp-Pro).

poly(Arg-Pro) and poly(Glu-Pro) take a new helical conformation resemble to the polyproline-II structure, *i.e.*, polyproline-II like structure. Poly(Ala-Pro) presents a strong negative band at around 200 nm and shoulders at around 205, 210 nm in TFE and in H<sub>2</sub>O. These spectra suggested that poly(Ala-Pro) take the polyproline-II like structure [1].

The CD spectra of poly(Asp-Pro) in Figure 2 showed a negative band at 200 nm in buffer solution. The negative bands at 210 nm clearly appeared with a decrease in pH, then a negative band at 200 nm disappeared. The CD spectra of poly(Asp-Pro) under the low pH condition are resembled to those of poly(Xaa-Pro) in TFE. However, the CD spectra of poly(Arg-Pro) whose side-chain groups are ionized under the low pH condition show the reverse dependency on pH. These results suggest that poly(Asp-Pro) and poly(Arg-Pro) change their conformations from the charged random-coils to the new helical structures with a decrease in number of ionized side-chain groups [2]. The above results indicate that poly(Xaa-Pro) forms the new helical structures, and the type of helix is changed with the type of Xaa residues and external environments such as solvents or pH. These results correspond to the theoretical results that poly(Xaa-Pro) have various new secondary structures as the local minimum conformations whose relative stability is changed depending on their repetitive amino acid sequences [3,4].

## References

1. Niidome, T., Mihara, H., Oka, M., Hayashi, T., Sakai, T., Yoshida, K., Aoyagi, H. *J. Peptide Res.* **51**, 337–345 (1998).
2. Hirano, Y., Shimoda, M., Hattori, M., Oka, M., Hayashi, T. *Peptide Sci.* **2000**, 337–340 (2000).
3. Oka, M., Nakajima, A. *Polym. Bull.* **33**, 693–699 (1994).
4. Sugimori, S., Iwai, I., Ohashi, K., Okuyama, H., Kitamura, M., Hattori, M., Fujimura, H., Ishikawa, Y., Hirano, Y., Oka, M., Nishinaga, A. *Peptide Chem.* **1994**, 397–400 (1995).

## The Role of Unstructured Highly Charged Regions on the Stability and Specificity of Dimerization of Two-Stranded $\alpha$ -Helical Coiled-Coils: Neck Region of Kinesin-Like Motor Protein Kif3A

Mundeep S. Chana, Brian P. Tripet and Robert S. Hodges

<sup>1</sup>Department of Biochemistry, University of Alberta, Edmonton, Alberta, T6G 2H7, Canada

<sup>2</sup>Department of Biochemistry and Molecular Genetics, University of Colorado Health Sciences Center, Denver, CO 80262, USA

### Introduction

Many of the kinesin-like motor proteins function as homo or heterodimeric molecules. Interestingly, many of these molecules have conserved regions following their globular head domains referred to as the neck and linker regions [1]. The neck region is thought to play a critical role in motor function, while the linker region is thought to specify heterodimer formation for the heterodimeric motor proteins [2]. This study was designed to elucidate whether preferential heterodimer formation can be attributed to the linker regions, rich in charged residues that follow the neck region of some kinesin-like motor proteins.

### Results and Discussion

We have observed that the region (356-377) directly N-terminal to the charged linker region in Kif3A can form an autonomously folded homo-two-stranded  $\alpha$ -helical coiled-coil or a hetero-two-stranded coiled-coil with a similar region in the protein Kif3B (351-373). To examine the role of highly charged regions on the specificity of heterodimer formation as well as the stability of the resulting coiled-coil, we synthesized the Kif3A neck coiled-coil (356-377) with the highly charged negative region (378-395) or a highly charged positive region (403-416) C-terminal to the coiled-coil (Figure 1).

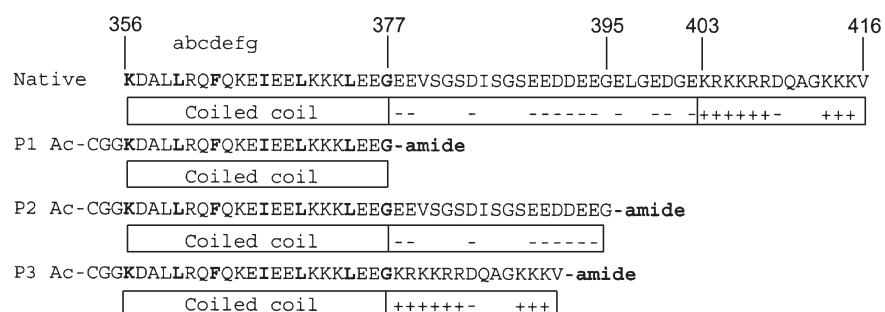
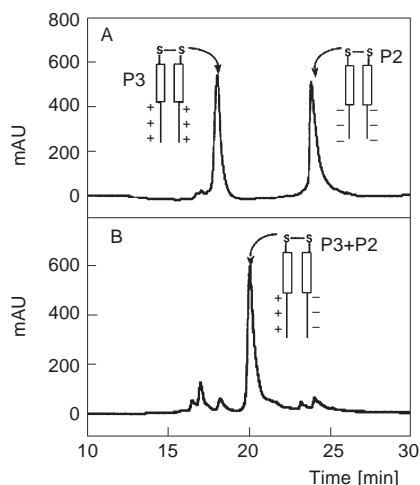


Fig. 1. Sequences of peptides P1, P2, and P3 used in the study.

We added an N-terminal CGG linker to prepare disulfide-bridged peptides for redox equilibrium experiments, and to remove the monomer-dimer equilibrium for stability determinations. In the redox equilibrium experiments the two homostranded coiled-coils (Figure 2A) were mixed in a 1 : 1 ratio in the presence of a 10 $\times$  molar excess of reduced and oxidized glutathione at pH 7.0. The formation of the P2 + P3 heterostranded coiled-coil was monitored by RP-HPLC. Equilibrium was reached in 5 min.

This result suggests that the oppositely charged regions give specificity and drive the reaction to form the hetero-two-stranded product. A stability analysis of the homo- and heterostranded peptides are shown in Panel C. Since GdnHCl masks electrostatic interactions, repulsions or attractions [3], and the coiled-coil region is identical in all peptides, the denaturation midpoints were essentially identical (~2.9 M); the stability results reflect the stability of the coiled-coil's hydrophobic core. Urea, an uncharged



C. Coiled-coil Stability Data.

Peptide	[GdnHCl] <sub>1/2</sub> (M)	[Urea] <sub>1/2</sub> (M)
P1	2.9	5.9
P2	2.8	3.8
P3	2.9	6.9
P3+P2	3.0	7.2

Fig. 2. RP-HPLC profile of the two disulfide-bridged, homostranded coiled-coils at time zero in the redox equilibrium experiment (Panel A), and the resulting disulfide-bridged heterostranded coiled-coil at equilibrium (Panel B). Panel C shows the chemical denaturation transition midpoints from circular dichroism studies of homostranded coiled-coils (P1, P2, and P3) and the heterostranded coiled-coil (P2 + P3).

denaturant, does not mask electrostatic interactions [3] and so the stability results reflect interactions of the charged regions on the stability of the coiled-coil. The negatively charged regions destabilize the homostranded coiled-coil (compare P1, 5.9 M to P2, 3.8 M, panel C), while the positively charged regions stabilized the coiled-coil (compare P1, 5.9 M to P3, 6.9 M, panel C). The hetero-two-stranded peptide exhibits stability (urea<sub>1/2</sub> value of 7.2 M) similar to the most stable homostranded peptide. Thus the oppositely charged regions bring specificity without any loss of stability.

### Acknowledgments

M. C. is supported by the Province of Alberta. This research was supported by the Canadian Institutes of Health Research, and the University of Colorado Health Sciences Center.

### References

1. Vale, R.D., Fletterick, R.J. *Annu. Rev. Cell Dev. Biol.* **13**, 745–777 (1997).
2. Rashid, D.J., Wedaman, K.P., Scholey, J.M. *J. Mol. Biol.* **252**, 157–162 (1995).
3. Monera, O.D., Kay, C.M., Hodges, R.S. *Protein Sci.* **3**, 1984–1991 (1994).

## A Leu-Thr-Trp-Lys “Lock” Stabilizes the N-Terminus of the Kinesin Neck Coiled-Coil

Brian Tripet and Robert S. Hodges

Department of Biochemistry and Molecular Genetics, University of Colorado Health Sciences  
 Center, Denver, CO 80262, USA

### Introduction

Conventional kinesin is a dimeric motor protein that transports intracellular vesicles along microtubules. Conventional kinesin is unique in that a single motor molecule can move for several micrometers along a microtubule without dissociating. The ability of kinesin to move processively is thought to arise from a “hand-over-hand” stepping mechanism in which the rear motor domain head is moved forward through a large conformational change within its neck linker region. Recently, studies investigating the molecular details of motility have advanced two models to account for this large structural change; 1) an unzipping/rezipping of the beta-sheet region of the neck linker against the motor domain head [1], and 2) an unwinding/rewinding of the neck coiled-coil [2]. In this study we investigate what unique structural features exist within the neck region coiled-coil that are likely to be important for triggering the coiled-coil to either unwind and/or re-wind during motility.

### Results and Discussion

We prepared 4 synthetic peptide analogs of the native human kinesin neck region (residues 330-369, Figure 1) and analyzed their secondary structure content and stability by CD spectroscopy.

Kinesin Neck Region		
330	369	
<div> <div>beta-linker</div> <div>coiled-coil</div> </div>		<u><math>\Delta\Delta G</math>(kcal/mol)</u>
Ac-CVNVELT AEQWKK-----amide		--
Ac-CVNVE <b>G</b> T AEQWKK-----amide		1.5
Ac-CVNVE <b>GG</b> AEQWKK-----amide		1.9
Ac-CVNVELT AEQW <b>A</b> K-----amide		1.2

Fig. 1. Sequences of human kinesin peptides used in this study. Peptide #1 represents native human kinesin sequence. Boxed residues indicate substituted residues from the native sequence.  $\Delta\Delta G$  is the change in stability between the mutant peptide and that of the native sequence. These peptides were synthesized by solid phase methodology using *t*Boc-chemistry.

Substitution of the two N-terminal residues, Leu 335 and Thr 336, to glycine resulted in a dramatic decrease in stability of the coiled-coil region despite the fact that these residues do not occur within the coiled-coil. Analysis of the X-ray crystal structure of kinesin (Figure 2) revealed that these stabilizing effects are a result of the residues acting as a hydrophobic staple (i to i+5) and N-cap (i to i+3) helix capping residues. Additionally substitution of Lys 341 to Ala also resulted in a dramatic decrease in stability of the coiled-coil neck region. Thus the inter-molecular side chain packing interactions occurring between Lys 341 and Trp 340 (Figure 2) are also critical for maintaining the tight association and folding of the first heptad of the coiled-coil region. Since large conformational changes are occurring within the beta-linker region of the neck [1], and that these important stabilizing interactions

herein are located outside of the hydrophobic core of the coiled-coil and within the beta-linker region, this would suggest that modulation of such interactions in their native setting could easily cause unfolding of the kinesin neck coiled-coil. Hence, we conclude that the kinesin neck coiled-coil may participate in the mechanism of kinesin motility by temporarily unfolding via modulation of the Leu-Thr-Trp-Lys lock residues thereby facilitating kinesin's placement onto the next microtubule binding site.

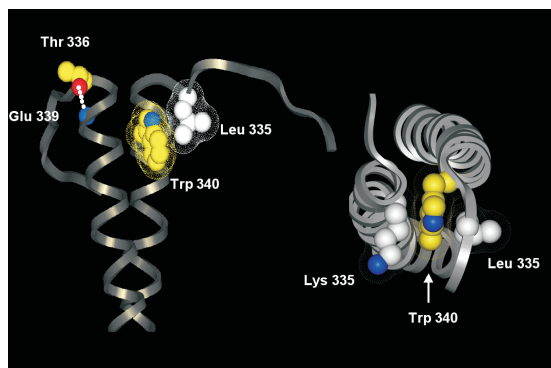


*Fig. 2. Molecular interactions at the N-terminus of the kinesin neck region. The X-ray crystallographic coordinates of dimeric rat brain kinesin were used (PDB#3KIN). Left, depiction of the hydrogen bonding and surface interactions of the N-cap and hydrophobic staple interactions between Thr 336 and Glu 339, and Leu 335 and Trp 340, respectively. Right, surface interactions occurring between Lys 341, Trp 340 and Leu 335.*

### Acknowledgments

This research was supported by the University of Colorado Health Sciences Center.

### References

1. Rice, S., Lin, A.W., Safer, D., Hart, C.L., Naber, N., Carragher, B.O., Cain, S.M., Pechatnikova, E., Wilson-Kubalek, E.M., Whittaker, M., Pate, E., Cooke, R., Taylor, E.W., Milligan, R.A., Vale, R.D. *Nature* **402**, 778–784 (1999).
2. Tripet, B., Vale, R.D., Hodges, R.S. *J. Biol. Chem.* **272**, 8946–8956 (1997).
3. Aurora, R., Rose, G.D. *Protein Sci.* **7**, 21–38 (1998).

## **Template-Assisted Stabilization of a Short HIV-1 gp41 Inner-Core Coiled-Coil Peptide**

**Edelmira Cabezas and Arnold C. Satterthwait**

*The Burnham Institute, La Jolla, CA 92037, USA*

### **Introduction**

The HIV-1 envelope glycoprotein is a heterodimer consisting of a surface subunit gp120 and a transmembrane subunit gp41. Gp120 is responsible for binding to CD4 and a chemokine receptor on the T cell surface while gp41 promotes viral entry by mediating the fusion of viral and cellular membranes. When HIV-1 binds to CD4 on the surface of a T cell, it triggers a conformational change that transiently exposes a long parallel trimeric coiled coil formed from the heptad repeat 1 (HR1) region of three intertwined gp41 subunits. The gp41 coiled coil is hypothesized to drive fusion and has become a target for drug and vaccine development [1].

Using the TASP concept [2], we designed a trilycine-based template for stabilizing peptides as parallel, trimeric coiled coils and tested it by covalently assembling three copies of a short HR1 peptide from the MN sequence. The HR1 peptide was then systematically substituted with amino acids to improve helix and coiled coil stability and the effects determined by comparing the helicities of corresponding pairs of linear and templated trimeric HR1 peptides using CD spectroscopy.

### **Results and Discussion**

Table 1 shows four HR1 peptides (1-4) and the corresponding trimers (1T-4T) synthesized for this study. Peptide 1 corresponds to the MN sequence with Gln/Leu and Leu/Ala substitutions, peptide 2 adds an additional Gly/Ala substitution, peptide 3 was substituted with Val and Leu at the first (a residue) and fourth (d residue) interface residues (VaLd) of the heptad repeat and peptide 4 combines the Gly/Ala and VaLd substitutions. The Gly/Ala substitution was made to improve helix stability and was the only residue other than Leu/Ala on the exposed face of the targeted coiled coil structure that was replaced. Prior work with another peptide had shown that VaLd substitutions converted it to a highly stable, parallel, trimeric coiled coil [3,4].

The HR1 peptides and trilycine template were synthesized on Rink amide resin with an ACT multiple peptide synthesizer using standard Fmoc chemistry. The purified peptides were linked to the template according to a procedure that has been described [5]. The thiol groups of HR1 C-terminal cysteine peptides were used to displace chloride from the chloroacetylated lysine side chains of the templates, Ac-K(AcCl)GK-(AcCl)GK(AcCl)-NH<sub>2</sub>, or Ac-K(AcCl)GK(AcCl)GK(AcCl)C(Acm)-NH<sub>2</sub> to give the trimers. The yields of the purified trimers were ~70%. The peptides were confirmed by MALDI-TOF mass spectrometry. The helical content of the peptides was assessed using CD spectroscopy and are reported as relative helicities (Table 1) based on molar ellipticities [Θ] at 222 nm for 40 μM HR1 peptide (40/3 μM of trimer) in water at pH 7.0, 25 °C.

The “wild-type” HR1 peptides (1 and 3) showed low helical content which improved somewhat for the Gly/Ala substituted peptides (2 and 4). The “wild-type” trimeric peptide (1T) also showed low helix content. When each of the HR1 arms on 1T was Gly/Ala substituted to give 2T, an improvement in helicity surpassing that for peptide 2 was observed implying a cooperative effect. When 1T was substituted with VaLd to give 3T, a major improvement in helicity was observed compared with pep-

tide 3 consistent with the stabilization of a coiled coil. When 3T was further modified with a Gly/Ala substitution to give 4T, helicity improved again to yield a highly helical trimer ( $[\Theta]_{222} \approx 20,000$ ). The coiled coil stabilized by 4T could be from the monomer, from a dimer of 4T or from higher order structure(s). To test for intermolecular associations, the molar ellipticity of 4T was examined between 4  $\mu\text{M}$  and 100  $\mu\text{M}$ . No change in molar ellipticity was observed. The midpoint of the thermal denaturation curve for 4T was  $>90^\circ\text{C}$  indicating considerable stability. Taken together, the data suggest that 4T stabilizes the HR1 substituted peptide as a parallel, trimeric coiled coil monomer.

Table 1. Helicity values for HR1 peptides and corresponding templated trimers.

Peptide	Relative helicity
1 <u>ALQHA</u> <u>LQLTVWGIKQLQ</u> ARC	0.19
1T     3 ( <u>ALQHA</u> <u>LQLTVWGIKQLQ</u> ARC ) KGKGK	0.15
2 <u>ALQHA</u> <u>LQLTVWAIKQLQ</u> ARC	0.29
2T     3 ( <u>ALQHA</u> <u>LQLTVWAIKQLQ</u> ARC ) KGKGK (Acm)	0.72
3 <u>ALQH</u> <u>AVQLLVWGVKQLQ</u> ARC	0.16
3T     3 ( <u>ALQH</u> <u>AVQLLVWGVKQLQ</u> ARC ) KGKGK	0.90
4 <u>ALQH</u> <u>AVQLLVWAVKQLQ</u> ARC	0.38
4T     3 ( <u>ALQH</u> <u>AVQLLVWAVKQLQ</u> ARC ) KGKGK (Acm)	1.00

HR1 peptide sequences indicating **a** and **d** interface residues of the heptad repeat positions (**bold**) and substituted residues (underlined). Peptides and trilisine template were N-terminally acetylated and C-terminally amidated. Acm is a S-acetamidomethyl protecting group.

## Acknowledgments

This work was supported by the National Institutes of Health (AI46235).

## References

1. Root, M.J., Kay, M.S., Kim, P.S. *Science* **291**, 884–888 (2001).
2. Mutter M., Vuilleumier S. *Angew. Chem., Int. Ed. Engl.* **28**, 535–554 (1989).
3. Boice, J.A., Dieckmann, G.R., DeGrado, W.F., Fairman, R. *Biochemistry* **35**, 14480–14485 (1996).
4. Ogiwara, N.L., Weiss, M.S., DeGrado, W.F., Eisenberg, D. *Protein Sci.* **6**, 80–88 (1997).
5. Cabezas, E., Wang, M., Parren, P.W.H.I., Stanfield, R.L., Satterthwait, A.C. *Biochemistry* **39**, 14377–14391 (2000).

## **STABLECOIL: An Algorithm Designed to Predict the Location and Relative Stability of Coiled-Coils in Native Protein Sequences**

**Brian Tripet and Robert S. Hodges**

*Department of Biochemistry and Molecular Genetics, University of Colorado Health Science Center, Denver, CO 80226, USA*

### **Introduction**

The  $\alpha$ -helical coiled-coil is a ubiquitous protein-folding motif important for mediating the oligomerization state of proteins. Its sequence is characterized by a 7-residue repeat (denoted **abcdefg**, where **a** and **d** are hydrophobic residues), which is very amenable to sequence-based structure prediction. For example, early analysis of the frequency of occurrence of residues found within cytoskeletal and intracellular coiled-coil containing proteins allowed algorithms to be designed to predict this structural motif *e.g.* COILS [1] and PAIRCOILS [2]. Here we describe a new algorithm, STABLECOIL, which not only predicts the location of coiled-coils within native protein sequences but has the added advantage of predicting stability fluctuations along the length of the coiled-coil. This method is based entirely upon physico-chemical parameters (*i.e.* stability coefficients) rather than statistical frequency of occurrence.

### **Results and Discussion**

The predictive method is based on the ability of amino acid sequence regions to score above pre-defined cut-off values using various sized window widths (*e.g.* 21, 28, 35 and 42). Scores are tabulated iteratively using  $\alpha$ -helical propensity values [3] for the positions **b**, **c**, **e**, **f**, **g** and hydrophobic core stability values [4,5] for the positions **a** and **d**. A weighting of  $\approx 2.3$ -fold is given to positions **a** and **d** over that of the other positions based on experimental results [6]. Data output is displayed graphically by plotting the cumulative score of the window width *versus* the residue number. In order to derive the individual cut-off values for each window width, a data set of 20 crystal structures containing different lengths of coiled-coils were analyzed. Averages of the scores of these known coiled-coils gave cut-off values of 21, 27, 32.5 and 38 kcal/mol for the window widths 21, 28, 35 and 42 residues, respectively. To determine the overall accuracy and robustness of the program, analysis of a larger data set of >65 crystal structures containing coiled-coil structures was performed. The results were able to show STABLECOIL could accurately predict the location of each coiled-coil region as well as its correct reading frame and respective size. A representative output plot for a 35-residue window width of the human kinesin sequence is shown in Figure 1, panel A.

Because data is output for each of the 7 possible reading frames, changes in the frame throughout the length of long coiled-coils can be easily observed (*i.e.* stutters and stammers). For example, in the human kinesin C-terminal stalk domain, the reading frame switches 5 times (Figure 1, panel A) thus indicating hinge locations or different domains.

STABLECOIL also allows for the use of a 7-residue window width to generate a "stability profile" plot of the predicted coiled-coil region (Figure 1, panel B). The stability fluctuates dramatically throughout the tropomyosin sequence with the stability troughs correlating strongly with the location of non-ideal residues within the hydrophobic core.

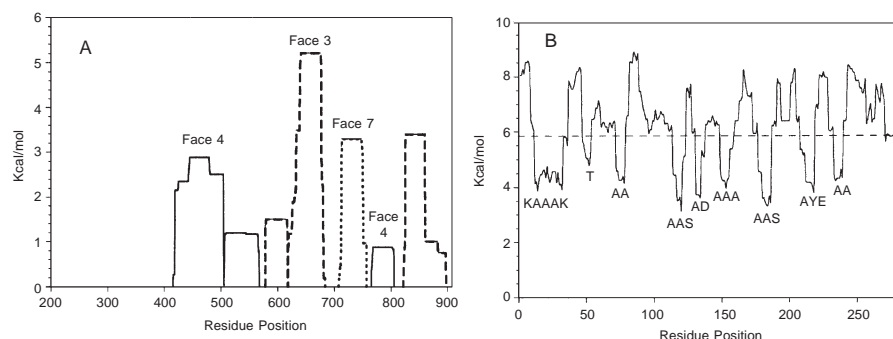


Fig. 1. Output from the STABLECOIL program. Panel A: Plot of the 7 reading frames of the human kinesin sequence using a 35 residue window width. Different line patterns denote the hydrophobic face from different reading frames. Panel B: 7-residue window width stability profile plot of rabbit skeletal tropomyosin sequence. Inset letters denote the location of non-ideal hydrophobic core residues which occur in the trough regions of the stability profile plot.

Overall, STABLECOIL appears to be a robust program that should make a major contribution as a sequence motif searching and analysis tool.

#### Acknowledgments

This research was supported by the Canadian Institute of Health Research, Protein Engineering Network of Centers of Excellence and University of Colorado Health Sciences Center.

#### References

1. Lupas, A., Van Dyke, M., Stock, J. *Science* **252**, 1162–1164 (1991).
2. Berger, B., Wilson, D.B., Wolf, E., Tonchev, T., Milla, M., Kim, P.S. *Proc. Natl. Acad. Sci. U.S.A.* **92**, 8259–8263 (1995).
3. Zhou, N.E., Monera, O.D., Kay, C.M., Hodges, R.S. *Protein Pept. Lett.* **1**, 114–119 (1994).
4. Wagschal, K., Tripet, B., Lavigne, P., Mant, C., Hodges, R.S. *Protein Sci.* **8**, 2312–2329 (1999).
5. Tripet, B., Wagschal, K., Lavigne, P., Mant, C.T., Hodges, R.S. *J. Mol. Biol.* **300**, 377–402 (2000).
6. Kwok, S.C., Mant, C.T., Hodges, R.S. *Peptides* 34–35 (1998).

## **Stabilization of Helical Conformation in Model Peptides by 2,2,2-Trifluoroethanol: An FTIR Study**

**Wendy Barber-Armstrong, Mohini Sridharan and Sean M. Decatur**

*Department of Chemistry, Mount Holyoke College, S. Hadley, MA 01075, USA*

### **Introduction**

Despite the widespread use of TFE as a helix-stabilizing agent, the mechanism of its action is still widely debated. While mechanisms in which TFE binds to residues in the helical conformation and stabilizes the structure have been proposed [1], there is no evidence for direct interactions between TFE and hydrophobic side chains [2]. Alternatively, recent explanations of the TFE effect have focussed on the impact of TFE on the structure of water and its solvation of peptide groups. Three different mechanisms of helix stabilization by TFE involving solvation effect have been proposed. Based on studies of the effect of TFE on the conformation of alanine-rich helical peptides and intramolecular hydrogen bonding in salicylic acid, Luo and Baldwin proposed that desolvation of the backbone carbonyls in a helix strengthens intrahelical hydrogen bonding; the stronger hydrogen bonding increases the enthalpic stability of the helix *versus* random coil in TFE/water mixtures [3]. In studies of coiled-coil peptides, Kenstis and Sosnick have proposed that the increased solvent structure in TFE/water mixtures (as opposed to pure water) raises the energy of solvation of peptide backbone groups in the unfolded state; this indirectly enhances the stability of the helical state [4]. Recently, Cammers-Goodwin and co-workers have proposed that in pure water, there is a greater ordering of the solvent shell around the helix compared to the coil state, resulting in an unfavorable entropic change; by disrupting hydrogen bonding between the helix backbone and solvent, TFE reduces the solvent ordering which occurs upon helix formation, stabilizing the helix relative to the coil state [5].

FTIR spectroscopy can be a valuable tool for characterizing the impact of TFE. While analysis of the amide I band is commonly used to elucidate the secondary structure of polypeptides, amide I modes of the helical peptides should be sensitive to both *conformation* and *solvation*; the frequency of the amide I band should be sensitive to environmental factors such as hydrogen bonding between water and the backbone carbonyl. This makes FTIR an ideal tool for probing the mechanism of helix induction by TFE: by analysis of the amide I band frequency as a function of %TFE in solution, spectroscopic evidence for desolvation of the helix backbone can be obtained.

We report the FTIR spectra of an alanine rich helical peptide (Ac-AAAKK-AAAKKAAAKAAAY-NH<sub>2</sub>) as a function of temperature and TFE. At low temperatures, this peptide is highly helical, as indicated by ultraviolet circular dichroism, FTIR spectroscopy, and vibrational circular dichroism. At higher temperatures, the peptide melts to a random coil conformation [6,7].

### **Results and Discussion**

At 0 °C and 0% TFE, the amide I' frequency for the peptide is at 1632 cm<sup>-1</sup>, typical for a helical peptide fully solvated by water [6,7]. At 0 °C and 60% TFE, the frequency of the amide I has shifted up to 1642 cm<sup>-1</sup>. This shift in amide I' frequency does not correspond to a change in secondary structure; CD spectra indicate that the peptide is highly helical at all TFE concentrations at 0 °C. This shift is consistent with a decrease in backbone-solvent hydrogen bonding; as hydrogen bonding decreases, the carbonyl bond order increases. Thus, we conclude that as % TFE increases, hydrogen bonding

between helix backbone and solvent decreases. At 65 °C, where the peptide is primarily random coil, the amide I' frequency is independent of % TFE (Figure 1). This suggests that solvent-backbone interactions in the random coil peptide are not perturbed by the presence of TFE.

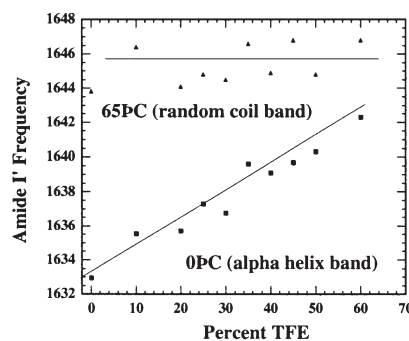


Fig. 1. Dependency of amide I frequency on the content of TFE.

Our results suggest that TFE acts to stabilize alpha helices by disrupting the hydrogen bonding between water and the helix backbone. This effect of TFE on water-backbone hydrogen bonding is specific to the helix state; our results suggest that TFE does not have a significant impact on backbone-solvent hydrogen bonding for the random coil peptide. This is consistent with other observations in the literature, which argue that the polarization of the backbone carbonyl within an alpha helix makes a better hydrogen bond acceptor than the carbonyl of a random coil peptide [5]. A reduction in water-backbone hydrogen bonding also reduces ordering of a solvent shell around the helix, and is entropically favorable. Thus, the specific effect of TFE on the helix backbone-solvent interactions may significantly reduce the entropic cost of helix formation, and this may underlie the helix induction effect of TFE.

These results also demonstrate the value of FTIR in elucidating peptide-solvent interactions. By simultaneously probing secondary structure and backbone solvation, FTIR may also be a valuable probe of tertiary structure in polypeptides. Moreover, they also warn of the dangers of interpreting amide I frequency of polypeptides solely in terms of secondary structure.

### Acknowledgments

This work is supported by an NSF CAREER grant (9984844) and an NIH AREA grant (GM661588) to SMD. The peptide synthesizer and circular dichroism spectrometer were purchased with NSF MRI grants. MS was a recipient of a Howard Hughes Medical Institute Undergraduate Fellowship.

### References

1. Jasanoff, A., Fersht, A.R. *Biochemistry* **33**, 2129–213 (1994).
2. Storrs, R.W., Truckses, D., Wemmer, D.E. *Biopolymers* **32**, 1695–1702 (1992).
3. Luo, P., Baldwin, R.L. *Proc. Natl. Acad. Sci. USA* **96**, 4930–4935 (1999).
4. Kenstis, A., Sosnick, T.R. *Biochemistry* **37**, 14613–14622 (1998).
5. Walgers, R., Lee, T.C., Cammers-Goodwin, A. *J. Am. Chem. Soc.* **120**, 5073–5079 (1998).
6. Decatur, S.M. *Biopolymers* **54**, 180–185 (2000).
7. Silva, R.A.G.D., Kubelka, J., Bour, P., Decatur, S.M., Keiderling, T.A. *Proc. Natl. Acad. Sci. USA* **97**, 8318–8323 (2000).

## Peptides Based on Daf, the First Rigid, Transition-Metal Receptor: $C^{\alpha,\alpha}$ -Disubstituted Glycine

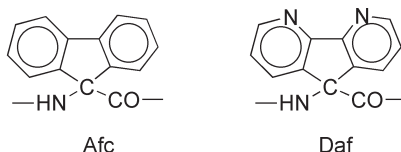
Marco Crisma<sup>1</sup>, Cristina Peggion<sup>1</sup>, Fernando Formaggio<sup>1</sup>, Claudio Toniolo<sup>1</sup>,  
Karen Wright<sup>2</sup>, Michel Wakselman<sup>2</sup> and Jean-Paul Mazaleyrat<sup>2</sup>

<sup>1</sup>Biopolymer Research Center, CNR, Department of Organic Chemistry, University of Padova,  
35131 Padova, Italy

<sup>2</sup>SIRCOB, ESA CNRS 8086, Bât. Lavoisier, University of Versailles, 78035 Versailles, France

### Introduction

The conformationally constrained  $C^{\alpha,\alpha}$ -symmetrically disubstituted glycyl residues are among the simplest and most widely used structural units in the construction of peptides with a predetermined secondary structure. In this connection, we have previously shown, *inter alia*, that the tendency of 9-aminofluorene-9-carboxylic acid (Afc) peptides to give folded/helical structures is rather low [1–3]. We present here the synthesis of terminally protected peptides from the Afc diaza-analogue 9-amino-4,5-diazafluorene-9-carboxylic acid (Daf) and the results of a conformational study of Ala/Daf, Gly/Daf and Aib/Gly/Daf peptides to the nonamer level.



### Results and Discussion

To avoid decarboxylation, coupling at the Daf C-terminus was performed *via* the acylazide method. Coupling at the Daf N-terminus was accomplished either by using a mixed anhydride or, more efficiently, a urethane-protected NCA. Peptides with internal Daf residues were obtained by the segment condensation approach *via* EDC/HOAt C-activation.

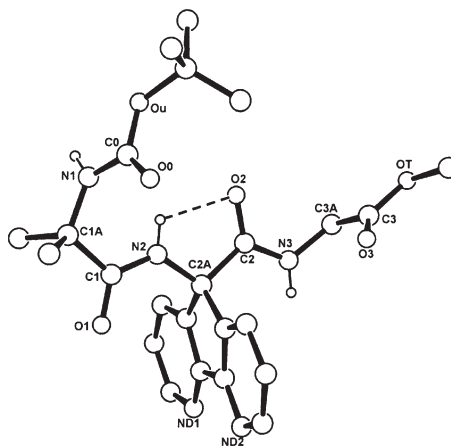


Fig. 1. X-Ray diffraction structure of Boc-Aib-Daf-Gly-OMe. The fully-extended ( $C_5$ ) conformation adopted by the central Daf residue is clearly seen.

***Crisma et al.***

FT-IR absorption,  $^1\text{H}$  NMR, and X-ray diffraction (one example of the latter technique is illustrated in Figure 1) analyses indicate that the structural preferences of Daf peptides closely match those of the related Afc peptides [all favor both the fully-extended ( $\text{C}_5$ ) conformation and the folded/helical conformations]. Spectroscopic (UV absorption, fluorescence, CD) characterization of this novel tricyclic heteroaromatic  $\text{C}^{\alpha,\alpha}$ -disubstituted glycine was also performed. Finally, preliminary conformational data and membrane activity measurements were obtained for an analog of the lipopeptaibol antibiotic [L-Leu $^{11}$ -OMe] trichogin GA IV, in which a Daf residue was synthetically incorporated in position 1 (replacing the native Aib residue).

**References**

1. Savrda, J., Mazaleyrat, J.-P., Wakselman, M., Formaggio, F., Crisma, M., Toniolo, C. *J. Pept. Sci.* **5**, 61–74 (1999).
2. Crisma, M., Formaggio, F., Mezzato, S., Toniolo, C., Savrda, J., Mazaleyrat, J.-P., Wakselman, M. *Lett. Pept. Sci.* **7**, 123–131 (2000).
3. Lombardi, A., De Simone, G., Galdiero, S., Nastri, F., Di Costanzo, L., Makihira, K., Yamada, T., Pavone, V. *Biopolymers* **53**, 150–160 (2000).

## Allyl-Based, C<sup>α</sup>-Methylated $\alpha$ -Amino Acids in the Side-Chain to Side-Chain Ring-Closing Metathesis Reaction of $\beta$ -Turn/ $3_{10}$ -Helical Peptides

Claudio Toniolo<sup>1</sup>, Marco Crisma<sup>1</sup>, Fernando Formaggio<sup>1</sup>, Cristina Peggion<sup>1</sup>, Quirinus B. Broxterman<sup>2</sup>, Bernard Kaptein<sup>2</sup>, Hans E. Schoemaker<sup>2</sup>, Floris P.J.T. Rutjes<sup>3</sup>, Johan J.N. Veerman<sup>4</sup>, Rosa Maria Vitale<sup>5</sup>, Ettore Benedetti<sup>6</sup> and Michele Saviano<sup>6</sup>

<sup>1</sup>Biopolymer Research Center, CNR, Department of Organic Chemistry, University of Padova, 35131 Padova, Italy

<sup>2</sup>DSM Research, Organic Chemistry and Biotechnology Section, 6160 MD Geleen, The Netherlands

<sup>3</sup>Department of Organic Chemistry, University of Nijmegen, 6525 ED Nijmegen, The Netherlands

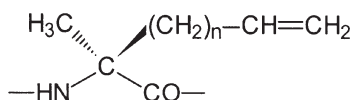
<sup>4</sup>Institute of Molecular Chemistry, University of Amsterdam, 1018 WS Amsterdam, The Netherlands

<sup>5</sup>Department of Environmental Sciences, 2nd University of Naples, 81100 Caserta, Italy

<sup>6</sup>Biocrystallography Research Center, CNR, Department of Chemistry, University of Naples "Federico II", 80134 Naples, Italy

### Introduction

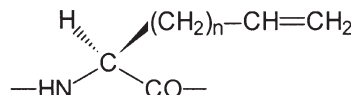
Recently, Verdine and coworkers experimentally investigated the olefin side-chain to side-chain ring-closing metathesis (RCM) reaction in  $\alpha$ -helical peptides with two allyl-based, C<sup>α</sup>-methylated  $\alpha$ -amino acids of various side-chain length incorporated at the *i*, *i*+4 and *i*+7 positions [1]. Here we describe our theoretical and experimental findings on the extension of the Verdine's approach to  $\beta$ -turn/ $3_{10}$ -helical peptides where the allyl-based, C<sup>α</sup>-methylated  $\alpha$ -amino acids are inserted at the *i*, *i*+3 positions.



*n* = 1 Mag

*n* = 2 hMag

*n* = 3 hhMag



*n* = 1 Agl

*n* = 2 hAgl

*n* = 3 hhAgl

### Results and Discussion

Our energy calculations indicate that two side chains of the type  $-(CH_2)_3-CH=CH_2$  (hhMag or hhAgl) represent the minimal length requirement to produce stable macrocycles based on an unperturbed peptide  $3_{10}$ -helix *via* RCM. Our experimental findings indirectly support the above conclusions in the sense that none of the *bis* C<sup>α</sup>-methyl, C<sup>α</sup>-allylglycine (Mag)-containing,  $\beta$ -turn/ $3_{10}$ -helical peptides examined underwent RCM. Conversely, we achieved RCM to a high extent with a peptide having the sequence RCO-Agl-Pro-Aib-Mag-NHR' (for RCM of related peptides, see ref. [2]).

By FT-IR absorption (Figure 1) and <sup>1</sup>H NMR we showed that this N<sup>α</sup>-acylated tetrapeptide amide is highly folded in a  $\beta$ -turn conformation. These results clearly indicate that, if the side chains of the partner residues are too short, RCM may be achieved only for peptides having an allyl-based, non-helix supporting,

**Toniolo et al.**

C<sup>α</sup>-trisubstituted α-amino acid in position 1, *i.e.* outside the rigid, central β-turn structure.

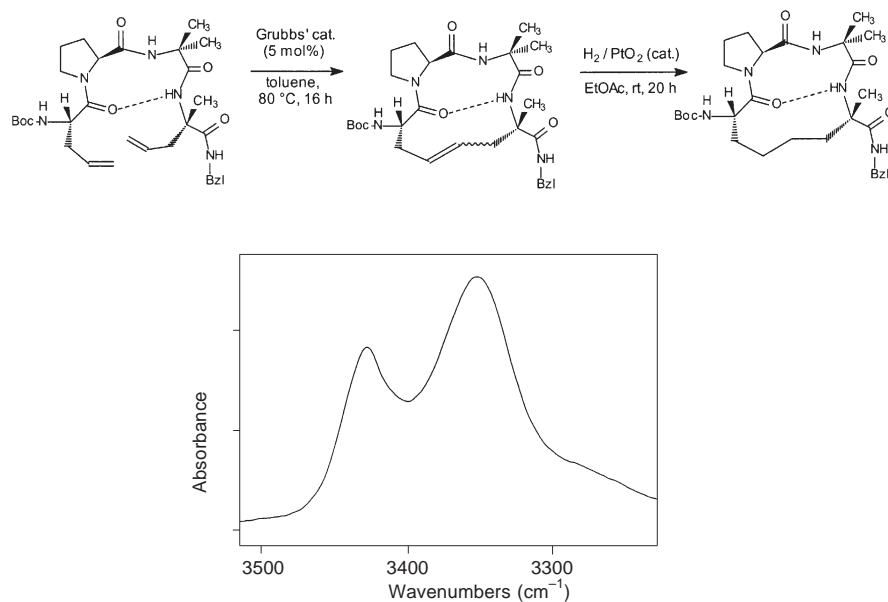


Fig. 1. FT-IR absorption spectrum in the N–H stretching region of the β-turn forming, N<sup>α</sup>-acylated tetrapeptide amide Boc-Agl-Pro-Aib-Mag-NHBzl in CDCl<sub>3</sub> solution (conc. 1 mM).

## References

1. Schafmeister, C.E., Po, J., Verdine, G.L. *J. Am. Chem. Soc.* **122**, 5891–5892 (2000).
2. Miller, S.J., Blackwell, H.E., Grubbs, R.H. *J. Am. Chem. Soc.* **118**, 9606–9614 (1996).

## Synthesis and Conformational Analysis of Polypeptides Having Repetitive Xaa-Pro-Pro Sequences

Masahito Oka<sup>1</sup>, Masahiro Wakahara<sup>1</sup>, Tatsuya Nakamura<sup>1</sup>,  
Yuichi Onoda<sup>1</sup>, Toshio Hayashi<sup>1</sup> and Yoshiaki Hirano<sup>2</sup>

<sup>1</sup>Research Institute for Advanced Science and Technology, Osaka Prefecture University, Sakai, Osaka, 599-8570, Japan

<sup>2</sup>Department of Applied Chemistry, Osaka Institute of Technology, Omiya, Osaka, 535-8585, Japan

### Introduction

It has been theoretically shown that periodic polypeptides containing Pro residues take specific helical conformations caused by the characteristic conformational properties of the Pro residue [1–3]. From the viewpoint of designing the functional polypeptides, such specific helical conformations are very interesting ones as the basic backbone conformations for constructing the functional site of the molecule. In this work, as one of such fundamental trials, conformational analysis of polypeptides having the repetitive Xaa-Pro-Pro sequences was performed by experimental and theoretical method.

### Results and Discussion

(Ala-Pro-Pro)<sub>n</sub> (n = 2, 3, 4) and (Leu-Pro-Pro)<sub>n</sub> (n = 2, 3, 4) were synthesized by the solid phase procedure. Crude peptides were purified by HPLC. CD spectra were measured in water, methanol, and trifluoroethanol (TFE). Molecular mechanics calculations used ECEPP and Powell minimization procedure for the whole conformational space of polypeptides.

The CD spectra of (Ala-Pro-Pro)<sub>4</sub> in water present a strong negative band at 202 nm and a weak positive band around 226 nm at 5 °C. These CD spectra patterns correspond to those of the polyproline-II structure. By increasing temperature up to 55 °C, the negative band shifts to 203 nm with decreasing the molar ellipticity, and the positive band also shifts to around 229 nm, then disappears at 55 °C. These results indicate that (Ala-Pro-Pro)<sub>4</sub> takes the polyproline-II structure in water, and increasing temperature causes the conformational change of (Ala-Pro-Pro)<sub>4</sub>. (Ala-Pro-Pro)<sub>3</sub> and (Ala-Pro-Pro)<sub>2</sub> also present similar CD spectra to those of (Ala-Pro-Pro)<sub>4</sub> in spite of decreasing their molar ellipticity. In methanol, the CD spectra of (Ala-Pro-Pro)<sub>4</sub> present a strong negative band at 202 nm and a weak positive band around 226 nm, which indicates that (Ala-Pro-Pro)<sub>4</sub> also takes the polyproline-II structure in methanol. However, the CD spectra of (Ala-Pro-Pro)<sub>4</sub> in TFE present a different CD pattern from those in water and methanol. That is, the strong negative band shifts to 200 nm with decreasing the molar ellipticity, and the positive band around 226 nm disappears, and a new weak negative band around 230 nm appears. This new band was also found in the CD spectra in TFE of poly(Arg-Pro-Pro-Phe), which is a model polypeptide of bactenecin 5 [4], suggesting strong possibility of new secondary structure in the periodic polypeptides having Pro residue as a repetitive amino-acid component. The CD spectra of (Leu-Pro-Pro)<sub>4</sub> in water present a strong negative band at 200 nm, a weak positive band around 225 nm and a weak negative band around 238 nm at 5 °C. By increasing temperature to 55 °C, the negative band shifts to 202 nm with decreasing the molar ellipticity, and the positive band shifts to around 227 nm, then disappears at 55 °C. These results indicate that (Leu-Pro-Pro)<sub>4</sub> takes the polyproline-II structure in water, and increasing temperature causes the conformational change of (Ala-Pro-Pro)<sub>4</sub>. In methanol, the CD spectra of (Leu-Pro-Pro)<sub>4</sub> present a strong negative band at 201 nm

and a weak positive band around 225 nm, which correspond to those of the polyproline-II structure. However, the molar ellipticity of the positive band is greater than that of typical polyproline-II structure. The CD spectra of (Leu-Pro-Pro)<sub>4</sub> in TFE present a different CD pattern from those in water and methanol. That is, the strong negative band shifts to 199 nm with decreasing the molar ellipticity, and the positive band around 226 nm disappears, then, a weak negative band around 230 nm appears whose molar ellipticity increases in comparison with that of (Ala-Pro-Pro)<sub>4</sub> in TFE, suggesting that a new secondary structure which would be formed in TFE solution of (Ala-Pro-Pro)<sub>4</sub> is stabilized by the amino-acid substitution of Ala residue for Leu residue.

The molecular-mechanics calculation showed that there are 34 and 80 helical conformations with  $\Delta E_{\text{res}}$  ( $\Delta E$  per residue;  $\Delta E$  is the energy difference from the global – minimum energy) less than 5 kcal/mol for poly(Ala-Pro-Pro) and poly(Leu-Pro-Pro), respectively. The lowest-energy conformation of poly(Ala-Pro-Pro) is a right-handed  $\beta^{13.5}$ -helix which is stabilized by strong inter-residue interactions between adjacent helix loops. The second lowest-energy conformation is a  $\gamma$ -helix ( $\Delta E_{\text{res}} = 0.17$  kcal/mol) with 0.16 nm helix pitch, and most of stable conformations are also  $\gamma$ -helices which have different helix pitch. Several of them have the conformational feature resembling the polyproline-II structure. For example, the 4th lowest-energy conformation ( $\Delta E_{\text{res}} = 0.61$  kcal/mol), which is categorized into a  $\gamma$ -helix, has 0.31 nm helix pitch. This value almost corresponds to that of the polyproline-II structure (0.30 nm). A typical polyproline-II structure is found as the 12th lowest-energy conformation with  $\Delta E_{\text{res}} = 1.49$  kcal/mol. No  $\alpha$ -helical conformations are found as stable helical conformations. The lowest-energy conformation of poly(Leu-Pro-Pro) is a  $\gamma$ -helix with 0.24 nm helix pitch, and most of stable conformations are also  $\gamma$ -helices which have different helix pitch. Several of them have the conformational feature resembling the polyproline-II structure as well as the case of poly(Ala-Pro-Pro). For example, the 4th lowest-energy conformation ( $\Delta E_{\text{res}} = 0.38$  kcal/mol) whose backbone conformation corresponds to the 4th lowest-energy one of poly(Ala-Pro-Pro), has 0.30 nm helix pitch. A typical polyproline-II structure is found as the 43th lowest-energy conformation with  $\Delta E_{\text{res}} = 2.67$  kcal/mol. No  $\alpha$ -helical conformations are also found as stable helical conformations.

Calculated results indicate that polyproline-II structure is a stable helical conformation of poly(Ala-Pro-Pro) and poly(Leu-Pro-Pro). However, it is also shown that non-polyproline-II or polyproline-II-like helical conformations are also energetically favorable ones. These results strongly support the CD spectra which suggest the possibility of new helical conformations formed in the TFE solutions of poly(Ala-Pro-Pro) and poly(Leu-Pro-Pro).

## References

1. Oka, M., Baba, Y., Kagemoto, Y., Nakajima, A. *Polym. J.* **22**, 555–558 (1990).
2. Oka, M., Nakajima, A. *Polym. Bull.* **30**, 647–654 (1993).
3. Oka, M., Nakajima, A. *Polym. Bull.* **33**, 693–699 (1994).
4. Niidome, T., Mihara, H., Oka, M., Hayashi, T., Saiki, T., Yoshida, K., Aoyagi, H. *J. Peptide Res.* **51**, 337–345 (1998).

## Biophysical Studies of a Proline-Rich Peptide from the Coral Bleach Pathogen *Vibrio shiloi*

Sanjay K. Khare<sup>1</sup>, Boris Arshava<sup>1</sup>, Ehud Banin<sup>2</sup>, Eugene Rosenberg<sup>2</sup>  
and Fred Naider<sup>1</sup>

<sup>1</sup>Department of Chemistry, College of Staten Island, CUNY, Staten Island, NY-10314, USA

<sup>2</sup>Department of Molecular Microbiology & Biotechnology, Tel Aviv University,  
Ramat Aviv, Israel 69978

### Introduction

Coral reef communities are an important part of the marine ecosystem. They are highly reproductive and apart from the tropical rain forest, there is no natural environment so rich in species diversity as the marine coral reef. During last two decades, there have been an increasing number of reports of disease of corals referred to as coral bleaching, which breaks the symbiotic association between the coral hosts and their photosynthetic micro algal endosymbionts known as zooxanthellae. In an attempt to reveal the actual mechanism behind coral bleaching earlier we documented that a pathogenic bacterium *Vibrio shiloi* was the causative agent involved in the coral bleaching [1]. This coral pathogen (*V. shiloi*) produces an array of extracellular material that can inhibit photosynthesis, bleach and lyse zooxanthellae. Recently we isolated a proline-rich dodecapeptide (PYPVYAPPPVVP) from *Vibrio shiloi* named Toxin P and its structure and activity was confirmed by chemical synthesis [2]. The detail conformational analysis of synthetic Toxin P was carried out using CD and NMR in various media including membrane mimetic environments.

### Results and Discussion

In order to establish the structure of Toxin P and reveal the facts behind coral bleaching, detailed CD studies of this peptide were carried out under a variety of experimental conditions. The CD spectrum of Toxin P (Figure 1) exhibits a strong negative band at 208 nm ( $[\Phi] = -55000 \text{ deg cm}^2 \text{ decimole}^{-1}$ ) and a weak positive band at 230 nm ( $[\Phi] = 3000 \text{ deg cm}^2 \text{ decimole}^{-1}$ ) in water. This spectrum manifests the essential characteristics of the CD spectrum of a polyproline II structure [3–5]. Very similar CD

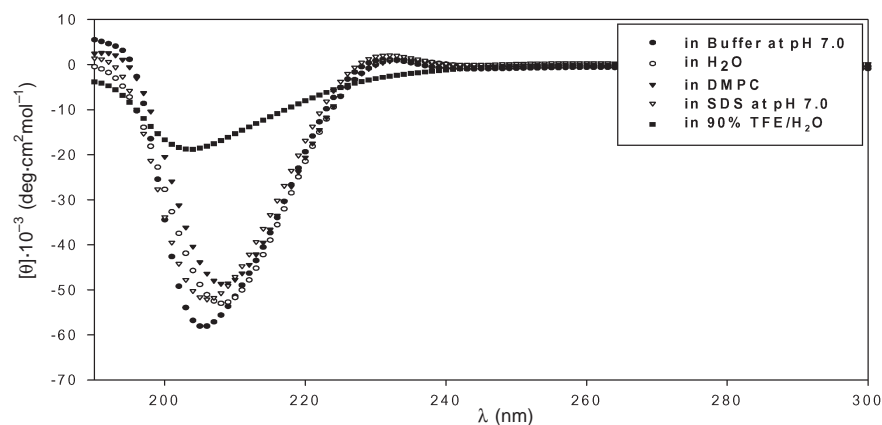


Fig. 1. CD of synthetic Toxin P in various media at 25 °C.

patterns were observed for Toxin P in aqueous buffer at pH 7.0, and in the presence of SDS micelles and DMPC vesicles. In contrast in 90% trifluoroethanol/water a marked decrease in the negative minimum is observed and the 230 nm band, characteristic of polyproline II, disappears. The latter band is generally considered to be a unique feature of the conformation because thermal denaturation of polyproline II containing proteins and peptides usually leads to complete loss of the positive band with only minor changes in the position of the negative band. Temperature dependence studies of the CD of Toxin P were carried out in the presence of SDS micelles or DMPC vesicles. At higher temperatures the Cotton effects at both 205 and 230 nm decrease markedly indicating that the elevated temperature increases the flexibility of Toxin P and likely decreases the poly proline II-like character of this peptide. Recently we reported [2] that natural and synthetic Toxin P inhibit the photosynthesis of zooxanthellae significantly and it suggested that this peptide bound avidly to zooxanthellae promoting inhibition by exogenous  $\text{NH}_4\text{Cl}$ . It was postulated that the peptide influenced  $\text{NH}_3$  influx into the microorganism. CD analysis in a basic environment including  $\text{NH}_3$  indicate that  $\text{NH}_3$  has major impact on the structure of Toxin P structure shifting the CD pattern polyproline II-like that of an unstructured peptide. Further analysis is necessary to discern whether this structural change of Toxin P is related to the transport of  $\text{NH}_3$  into cells, which ultimately results in coral bleaching.

Complete proton assignment of all residue of the coral bleach peptide was accomplished by combined use of 2D-TOCSY and NOESY spectra. The configuration of the prolyl residue in the dodecapeptide was determined by measuring the interproton distance between the  $\alpha\text{H}$  of the preceding residue and the proline  $\alpha\text{H}$ - and  $\delta\text{H}$ -protons. Strong  $\alpha\text{CH}$  to  $\delta\text{CH}_2$  (i, i+1) NOE cross peaks were observed for all prolyl residue in the NOESY spectra at 10 and 25 °C. These results are consistent with a *trans* peptide bond for the prolyl residues in Toxin P, consistent with the polyproline II structure. In summary CD and NMR results strongly indicates that the Toxin P dodecapeptide adopts the polyproline II structure in polar solvents and in the presence of detergents and lipids. Organic solvents tend to increase the flexibility of the peptide. Studies are in progress to determine whether the dodecapeptide binds ammonia and directly facilitates its passage into the cells.

#### **Acknowledgments**

The above work has been supported by grants GM 22086 from NIH.

#### **References**

1. Kusmaro, A., Loya, Y., Fine, M., Rosenberg, E. *Nature* **380**, 396 (1996).
2. Banin, E., Khare, S.K., Naider, F., Rosenberg, E. *Appl. Env. Microbio* **67**, 1536–1541 (2001).
3. Rabanal, F., Ludevid, M.D., Pons, M., Giralt, E. *Biopolymers* **33**, 1019–1028 (1993).
4. Dalcol, I., Pons, M., Ludevid, M.D., Giralt, E. *J. Org. Chem.* **61**, 6775–6782 (1996).
5. Ma, K., Kan, L.-S., Wang, K. *Biochemistry* **40**, 3427–3438 (2001).

## Lactam-Bridged and Disulfide-Bridged Peptide Mimic of a Stable $\alpha$ -Helical Folded Protein

Stanley C. Kwok, Colin T. Mant and Robert S. Hodges

*Department of Biochemistry and the Medical Research Council of Canada Group in Protein Structure and Function, University of Alberta, Edmonton, Alberta T6G 2H7, Canada and Department of Biochemistry and Molecular Genetics, University of Colorado Health Sciences Center, Denver, CO 80262, USA*

### Introduction

A conformationally-restricted lactam-bridged and disulfide-bridged  $\alpha$ -helical coiled-coil model peptide was designed to create a very small, yet good mimic of a stable folded protein, allowing investigation of the effects of amino acid substitutions at positions **e** and **g** of the heptad repeat on overall protein stability and oligomerization state. The residues in positions **e** and **g** are in a unique microenvironment, being solvent-exposed on the one hand and in close proximity to the hydrophobic core residues in positions **a** and **d** on the other (Figure 1). Thus, their contributions to protein stability may be significantly different from the intrinsic helical propensity contributions of fully surface-exposed residues, *i.e.*, positions **b**, **c** and **f**. This preliminary study investigates the contribution of four residues (Gly, Ala, Leu, Lys) at positions **e** and **g** to stability and oligomerization state of our model protein.

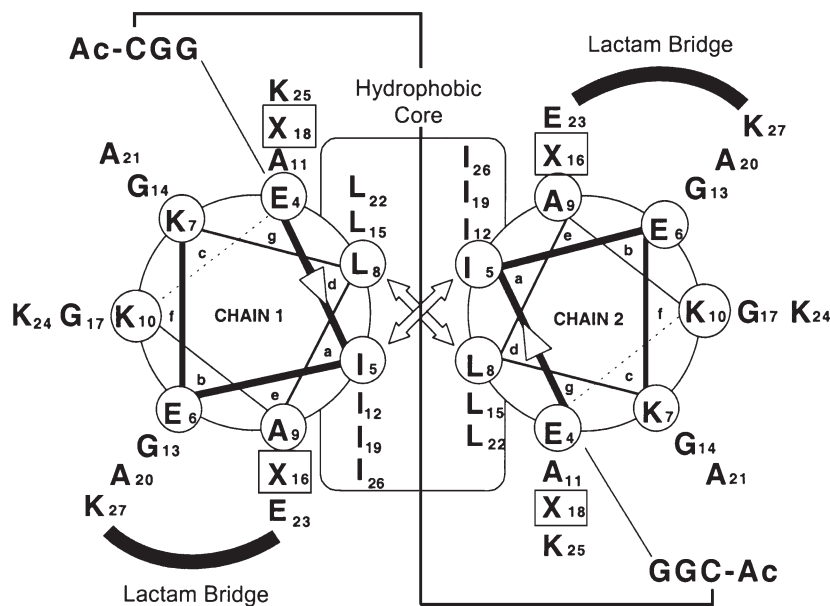


Fig. 1. Helical wheel representation of the interchain disulfide-bridged and intrachain lactam-bridged stabilized coiled-coil sequence. Lactam bridges are formed between Glu23 and Lys27. Identical amino acid substitutions are made at both positions **e** and **g** (residues 16 and 18, respectively).

## Results and Discussion

Residue substitutions were chosen based on the following criteria: (1) Gly and Ala for the lowest and highest helical propensity contribution to stability [1]; (2) Leu as a large hydrophobic residue; (3) Lys as a hydrophilic, charged residue. All four analogs were fully folded into an  $\alpha$ -helical structure in benign medium (Table 1).

Table 1. Biophysical data for selected peptide analogs.

Amino acid <sup>a</sup>	$[\theta]_{222}^b$	Helical <sup>c</sup> propensity	$[\text{Gdn}\cdot\text{HCl}]_{1/2}^d$ (M)	Observed <sup>e</sup> stability	Apparent <sup>f</sup> MW	Ratio to <sup>g</sup> monomer
Gly	−30 500	0	2.3	0	16 700	3.15
Ala	−31 900	−0.96	4.0	4.1	16 500	3.08
Leu	−32 800	−0.81	5.2	6.7	16 900	3.06
Lys	−31 800	−0.70	4.2	4.0	11 100	2.19

<sup>a</sup> Amino acid at positions **e** and **g** (Figure 1); <sup>b</sup> mean residue ellipticities ( $\text{deg cm}^2 \text{dmol}^{-1}$ ) of peptides in 50 mM aq. phosphate/0.1 M KCl, pH 7.0; <sup>c</sup> expressed as  $\Delta\Delta G$  ( $\text{kcal mol}^{-1}$ ), the difference in free energy of  $\alpha$ -helix formation relative to Gly from a monomeric helix [1]; <sup>d</sup> GdnHCl concentration at which half of the  $\alpha$ -helix is unfolded; <sup>e</sup>  $\Delta\Delta G$  ( $\text{kcal mol}^{-1}$ ) between the Gly peptide and the specified analog; <sup>f</sup> obtained from sedimentation equilibrium analysis; <sup>g</sup> apparent MW/calculated monomeric weight.

Helical propensity data show that Ala contributes more to stability than Leu (values of −0.96 and −0.81, respectively, *i.e.*, a difference of 0.15 kcal/mol/residue). However, with Leu in positions **e** and **g**, we observe the reverse effect on stability: compare  $\Delta\Delta G$  values of 6.7 and 4.1 kcal/mol for Leu- and Ala-peptides, respectively, *i.e.*, a difference of 0.65 kcal/mol/residue. Thus, this hydrophobic effect with the hydrophobic core residues at positions **a** and **d** is of major importance quantitatively to stability in the case of large hydrophobes compared to helical propensity effects. Sedimentation equilibrium analyses showed that the Gly-, Ala- and Leu-substituted analogs formed a trimer, whereas the analog substituted with Lys was a dimer (Table 1). These results suggest that residues at positions **e** and **g** can influence oligomerization state. Characterization of the effects of all 20 amino acids on these positions will further our understanding of protein folding and stability, as well as aid in the design of multimeric helical proteins.

## Acknowledgments

S.C.K. is the recipient of a Natural Sciences and Engineering Research Council of Canada postgraduate scholarship and Alberta Heritage Foundation of Medical Research scholarship. We thank M. Genest and J. Labrecque for technical help.

## References

1. Zhou, N.E., Monera, O.D., Kay, C.M., Hodges, R.S. *Protein Pept. Lett.* **1**, 114–119 (1994).

## **Stabilization of the Triple Helix of Collagen Peptides Using Fluoroproline and/or Triacid Scaffolds**

**Erik T. Rump<sup>1,2,3</sup>, Dirk T. S. Rijkers<sup>2</sup>, Philip G. de Groot<sup>1</sup>  
and Rob M. J. Liskamp<sup>2</sup>**

<sup>1</sup>*Department of Haematology, University Medical Center Utrecht, The Netherlands*

<sup>2</sup>*Department of Medicinal Chemistry, Utrecht Institute for Pharmaceutical Sciences,  
Utrecht University, The Netherlands*

<sup>3</sup>*Present address: Organon Teknika B.V. Boseind 15, 5281 RM Boxtel, The Netherlands*

### **Introduction**

The collagen triple helix is composed of three separate peptide chains, which are staggered by one residue and intertwine to form a right-handed triple helix [1]. The primary structure of these peptides is characterized by trimeric repeating units X-Y-G, where X and Y can be any amino acid. One trimer, Pro-Hyp-Gly (Hyp = hydroxyproline) or POG is found most prominently in native collagen. In order to induce folding of short collagen peptides into a stable triple helical structure, such peptides were coupled via their N-terminus to triacid scaffolds. The triple helical conformation of collagen molecules is of crucial importance since it is thought to be essential for recognition by its ligand [1]. A synthetic collagen mimic that meets this structural feature can therefore serve as a valuable tool to investigate blood platelet–collagen interactions under physiological conditions. Such structures should possess melting temperatures ( $T_m$ 's) above 37 °C.

### **Results and Discussion**

The collagen model peptides  $H-G_n(POG)_5-NH_2$  ( $n = 1, 2$ ) were synthesized by standard Fmoc-chemistry. Fmoc-POG-OH was synthesized to introduce the POG repeats by segment condensation. The model peptide ( $n = 2$ ) was coupled to a new cone-shaped triacid scaffold based upon a cyclotrimertrilene [2] unit (CTV), as well as to Kemp's triacid (KTA) [3]. After assembly and purification by RP-HPLC, the structures were analyzed by CD and mass spectroscopy. The new scaffold stabilized the triple helix of the peptides significantly. The melting temperature ( $T_m$ ) increased from 10 °C for the non-assembled peptide, to 58 °C for the CTV-assembled compound. The two assembled CTV-diastereomers (P- and M-CTV) were separated, and the structures had different  $T_m$ 's: 58 and 55 °C. To discriminate between the two CTV-diastereomers, the CTV-triacid isomers were separated and coupled as a chiral scaffold to the collagen model peptide  $H-G_2-(POG)_5-NH_2$ . CD analysis of these compounds showed that both structures adopted a triple helical conformation. However, P-CTV was favoured over M-CTV as a collagen scaffold, since the P-CTV-assembled compound showed the highest thermal stability ( $T_m = 58$  °C). The triple helix-stabilizing properties of the CTV triacid and KTA( $G-OH$ )<sub>3</sub> were also investigated with a unique blood platelet-binding sequence [4]. After assembly of the peptide  $H-G-(POG)_2-FOGE(All)RGVE(All)G-(POG)_2-NH_2$ , and deprotection, CD analysis showed that both scaffolds stabilized the triple helix of the peptides significantly. The  $T_m$ 's were 19 °C for the CTV- and 20 °C for the KTA-assembled compound, compared to <4 °C for the non-assembled peptide. In addition to stabilization by scaffold structures, a stabilization of the peptide by replacing hydroxyprolines in the flanking regions by *trans*-4-fluoroprolines ( $F_O$ ) was investigated. To introduce the fluoroprolines, Fmoc- $P^F$ OG-OH was synthesized. This tripeptide was used as a build-

**Rump et al.**

ing block during solid phase peptide synthesis. CD analysis of KTA[G<sub>2</sub>-(P<sup>F</sup>OG)<sub>3</sub>-FOGERGVEG-(P<sup>F</sup>OG)<sub>3</sub>-NH<sub>2</sub>]<sub>3</sub> revealed that a further stabilization could be reached: T<sub>m</sub> = 42 °C (Figure 1).

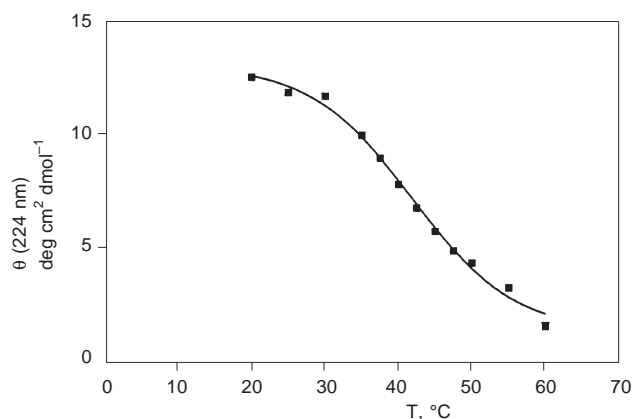


Fig. 1. CD melting curve of KTA[G<sub>2</sub>-(P<sup>F</sup>OG)<sub>3</sub>-FOGERGVEG-(P<sup>F</sup>OG)<sub>3</sub>-NH<sub>2</sub>]<sub>3</sub>. The collagen mimic was dissolved in 10 mM AcOH at a concentration of 0.5 mg/mL.

In conclusion, we demonstrated that a significant stabilization of the triple helical structure of collagen peptides using either CTV or KTA as a scaffold can be achieved. Moreover, a combined use of a scaffold and fluoroprolines led to a very stable collagen mimic composed of three short collagen peptides. These collagen mimics can be used to investigate blood platelet–collagen interactions.

#### Acknowledgments

This project was supported by grant PL 963517 of the European Commission.

#### References

1. Barnes, M. *Biopolymers* **40**, 383–397 (1996).
2. Canceill, J., Collet, A., Gbard J., Gottarelli, G., Spada, G.P. *J. Am. Chem. Soc.* **107**, 1299–1308 (1985).
3. Goodman, M., Feng, Y., Melacini, G., Taulane, J.P. *J. Am. Chem. Soc.* **118**, 5156–5157 (1996).
4. Knight, C.G., Morton, L.F., Peachey, A.R., Tuckwell, D.S., Farndale, R.W., Barnes M.J. *J. Biol. Chem.* **275**, 35–40 (2000).

## **Conformational Studies of O-Glycosylated 15-Residue Peptide from the Human Mucin (MUC1) Protein Core**

**Simon Sherman, Leo Kinarsky and Alex Rubinstein**

*Eppley Institute for Research in Cancer and Allied Diseases, University of Nebraska  
Medical Center, Omaha, NE 68198-6805, USA*

### **Introduction**

Certain MUC1 epitopes are detected on MUC1 glycoproteins from malignant cells as opposed to normal cells. The expression of the mucin epitopes appears to be due to the aberrant glycosylation in the tumors resulting in the excessive exposure of the MUC1 protein core on the cell surface. The truncated oligosaccharides of the tumor-derived mucin facilitate antibody binding to this epitope by unmasking the portion of the protein core that is involved in the antibody recognition. A polypeptide fragment APDTRP is known as an immunodominant (ID) region of the MUC1 protein core. To establish a structural rationale for the development of peptide-based tumor markers and vaccines, conformations of the 15-residue peptide PPAHGVTSAPDTRPA and its glycosylated counterpart with GalNAc residue attached at T7 position were studied by molecular dynamics (MD) simulations. The MD simulations in explicit water with and without NMR-derived constraints [1] were used to elucidate the effect of *O*-glycosylation on conformational propensities of a peptide backbone. Structural propensities of the peptide backbone for the APDTRP fragment were compared with a published crystal structure [2] of the breast tumor-specific antibody SM3 complexed with a 13-residue MUC1 peptide antigen that included this ID region.

### **Results and Discussion**

Representatives of the four structural clusters, which were previously defined from the NMR studies [1], were taken for MD simulations. Two clusters included a mix of conformers of the glycosylated and nonglycosylated peptides, while two other clusters represented conformers of either only glycosylated or nonglycosylated peptides. MD simulations were performed using the SANDER module of the AMBER 6 package. The updated version of the GLYCAM parameters [3,4] for sugar atoms were kindly provided by Dr. R. Woods. The peptide structures were solvated in a periodic box of water that was extended in each direction in order to have at least 10 Å from the box wall to any atom of the solute. Constant pressure simulations (NPT) were run at 278 K with a step size of 1 fs using the SHAKE algorithm. Electrostatic interactions were computed with the Particle Mesh Ewald method implemented in SANDER. The Lennard–Jones interactions were calculated with a 10.0 Å cutoff value. After the initial 1000 steps of energy minimization, the system was equilibrated during 250 ps of MD runs with the gradual relaxing of the positional and NMR constraints. Finally, the productive MD simulations were run for 200 ps for each structure. Results were analyzed with the CARNAL module of AMBER 6 and the graphical tools of the SYBYL 6.6 package (TRIPOS, Inc.). All calculations were performed on a SGI O2 workstation with R5000 CPU and by an optimized version of the SANDER on a Beowulf cluster containing 5 × Dell PowerEdge 1400 servers with 2 × 933 MHz CPUs, 512 MB RAM using MPICH 1.2. After equilibration, the total energy of the system remained stable through the MD simulations. Structural propensities of the cluster representatives for the glycosylated and nonglycosylated peptides were monitored by measuring several structural parameters of the peptide backbone shape. Angles between virtual

bonds  $C^\alpha(6)-C^\alpha(9)-C^\alpha(13)$ ,  $C^\alpha(5)-C^\alpha(6)-C^\alpha(8)$ ,  $C^\alpha(11)-C^\alpha(12)-C^\alpha(14)$  and distances between  $C^\alpha(6)-C^\alpha(13)$ ,  $C^\alpha(5)-C^\alpha(8)$ ,  $C^\alpha(6)-C^\alpha(9)$ ,  $C^\alpha(9)-C^\alpha(13)$ , and  $C^\alpha(11)-C^\alpha(14)$  were used to test the backbone shape of the G5-P14 region and its fragments that included the ID region. Structural propensities of the particular residues were monitored by a comparison of conformational distributions of the ( $\phi$ ,  $\psi$ ) angles on the Ramachandran plots. The MD simulations revealed structural similarities between glycosylated and nonglycosylated peptides, as well as distinct structural features of the peptide backbone specific for either the nonglycosylated or the glycosylated peptide. Both peptides demonstrated mostly extended conformations of the G5-P14 region with the  $C^\alpha(6)-C^\alpha(9)-C^\alpha(13)$  angles about  $150-160^\circ$  and characteristic distances of  $C^\alpha(6)-C^\alpha(13)$  bigger than 16 Å. Glycosylation slightly affected structural propensities of the V6-A9 region that exhibited more extended conformations for the glycosylated peptide. It is consistent with the distinct conformational differences in the ( $\phi$ ,  $\psi$ ) distributions on the Ramachandran plots for the T7 residue observed between the glycosylated and nonglycosylated peptide. The glycosylated peptide demonstrated only extended ( $\psi > 150^\circ$ ) conformations of T7, while for the nonglycosylated peptide were allowed both extended and twisted ( $\psi < -30^\circ$ ) conformations. The root-mean-square deviations (RMSD) of the backbone atoms ( $C^\alpha$ , C, N) for the APDTRP fragment were used to evaluate the difference between the calculated and crystal structures. A comparison of the results of MD simulations with the X-ray structure of the ID region [2] revealed distinct structural similarities that were enhanced by glycosylation of the remote T7 residue. The averaged population of the MD structures with RMSD less than 1 Å were shifted from approximately 10% for the nonglycosylated peptide to more than 30% for the glycosylated peptides. This shift caused by glycosylation should be taken into consideration for a design of new MUC1-like immunogenic peptides with enhanced immunogenicity.

#### Acknowledgments

We thank Dr. R. Woods for an updated version of the GLYCAM parameters. This work was partially supported by NIH grants 1RO1 CA69234 and 1RO1 CA84106. The Molecular Modeling Core Facility of the UNMC Eppley Cancer Center used in this work is supported by Cancer Center Support grant P30 CA36727.

#### References

1. Kirnarsky, L., Prakash, O., Vogen, S., Nomoto, M., Hollingsworth, M.A., Sherman, S. *Biochemistry* **39**, 12076–12082 (2000).
2. Dokurno, P., Bates, P.A., Band, H.A., Stewart, L.M.D., Lally, J.M., Burchell, J.M., Taylor-Papadimitriou, J., Snary, D., Sternberg, M.J.E., Freemont, P.S. *J. Mol. Biol.* **284**, 713–728 (1998).
3. Woods, R.J., Dwek, R.A., Edge, C.J., Fraser-Reid, B. *J. Phys. Chem.* **99**, 3832–3846 (1995).
4. Woods, R.J., Chappelle, R. *THEOCHEM* **527**, 149–156 (2000).

## Folding of $\beta$ - and $\gamma$ -Peptides – the Influence of Substitution Patterns on the Formation of Secondary Structures

Magnus Rueping, Bernhard Jaun and Dieter Seebach

Laboratorium für Organische Chemie, Eidgenössische Technische Hochschule,  
CH-8092 Zürich, Switzerland

### Introduction

In recent years, peptides consisting of non- $\alpha$ -amino acids have attracted great attention [1]. It was found, that oligomers consisting exclusively of  $\beta$ - and of  $\gamma$ -amino acids can adopt stable secondary structures in solution and in the solid state. A wealth of well-ordered secondary structures such as helices, sheets and turns has been discovered [2]. In addition, these  $\beta$ - and  $\gamma$ -peptides have proven to be stable against the degradation by peptidases [3] and are therefore promising peptidomimetics [4].

### Results and Discussion

It was shown by NMR investigations that  $\beta$ -peptides consisting only of  $\beta^2$ - or  $\beta^3$ -amino acids fold into a  $3_{14}$ -helical structure in methanol. The mixed  $\beta^2/\beta^3$ -peptide **1** (Figure 1), however, forms a helix with alternating 12- and 10-membered hydrogen-bonded rings (12/10/12-helix) [5]. Therefore, it was of interest to see, if the mixed  $\beta^3/\beta^2$ -peptide **2** would also adopt a 12/10/12-helix in solution.

The investigation shows that the Boc-protected  $\beta^3/\beta^2$ -peptide **2** adopts the same conformation in MeOH as the unprotected  $\beta^2/\beta^3$ -peptide **1**.

While there is a lot of activity in the field of  $\beta$ -peptides, their homologs, the  $\gamma$ -peptides, have received much less attention. The observation that  $\gamma^{2,3,4}$ -hexapeptide **3** (Figure 2) adopts a well defined (*M*)-2.6<sub>14</sub>-helix in solution [6] led us to examining the stability of the helix.

We measured 1D-<sup>1</sup>H NMR spectra in CD<sub>3</sub>OH up to 120 °C in a sealed NMR-tube to study the stability of this helix with increasing temperature. The data (Figure 2) indicate that the 2.6<sub>14</sub>-helix is still present to large extent at 90 °C. The large NH, C( $\gamma$ )H coupling constants decrease only slightly with increasing temperature and the dispersion of the chemical shifts for the NH-protons is still large. These results show that  $\gamma^{2,3,4}$ -peptides adopt very stable 2.6<sub>14</sub>-helices and that there is no evidence for a cooperative unfolding, melting or breakup of the structure.

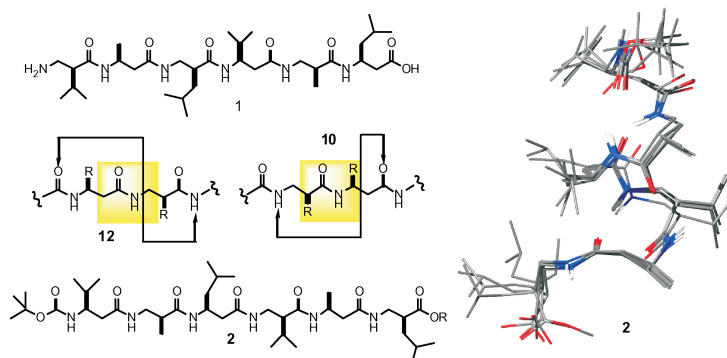


Fig. 1. Left: Formulae of mixed  $\beta^{2/3}$ -peptides, which fold into a helix, with alternating 12- and 10-membered hydrogen-bonded rings. Right: NMR structure of **2** in MeOH.

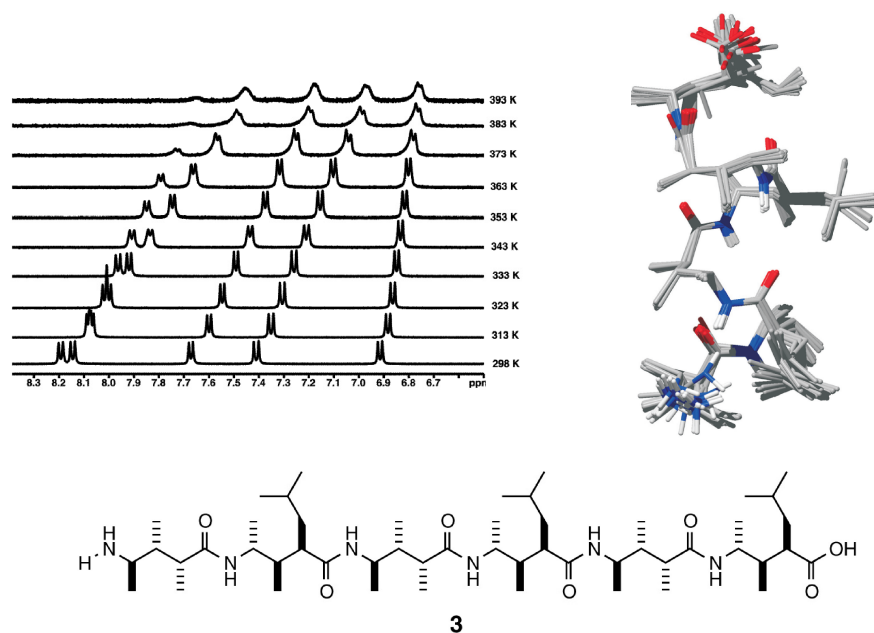


Fig. 2. (M)-2.6<sub>14</sub> helical solution structure of γ<sup>2,3,4</sup>-hexapeptide **3** and temperature dependent NMR measurements up to 120 °C.

## References

1. Baron, E.A., Zuckermann, R.N. *Curr. Opin. Chem. Biol.* **3**, 714 (1999).
2. Seebach, D., Matthews, J.L. *Chem. Commun.* 2015 (1997).
3. Frackenhohl, J., Arvidsson, P.I., Schreiber, J.V., Seebach, D. *ChemBioChem* **2**, 445 (2001).
4. Gademann, K., Ernst, M., Hoyer, D., Seebach, D. *Angew. Chem.* **111**, 1700 (1999).
5. Porter, E.A., Wang, X., Lee, H.S., Weisblum, B., Gellman, S.H. *Nature* **404**, 565 (2000).
6. (a) Seebach, D., Abele, S., Gademann, K., Guichard, G., Hintermann, T., Jaun, B., Matthews, J.L., Schreiber, J.V., Oberer, J.V., Hommel, U., Widmer, H. *Helv. Chim. Acta* **81**, 932 (1998). (b) Seebach, D., Brenner, M., Rueping, M., Schweizer, B., Jaun, B. *Chem. Commun.* 649 (2001).

## The $\beta$ -Methyne of Ile3 in the Propeptide Region of Prouroguanylin is Crucial for Chaperone Function in the Folding of the Mature Peptide, Uroguanylin

Yuji Hidaka, Chisei Shimono and Yasutsugu Shimonishi

*Institute for Protein Research, Osaka University, Suita, Osaka 565-0871, Japan*

### Introduction

A number of peptide hormones are expressed *in vivo* in the form of prepropeptides, which are subsequently processed into the biologically active mature peptides. However, the aspects of the specific role of the propeptide region remain obscure. We previously reported that uroguanylin, an endogenous ligand of guanylyl cyclase C [1], is folded into the native conformation via assistance by its propeptide region, which plays the role of an intra-molecular chaperone [2]. Our recent studies showed that the N-terminal region of prouroguanylin is important in the folding of the mature peptide, uroguanylin [3]. To further investigate the sites which are essential for the chaperone function in the N-terminal region of prouroguanylin, mutant proteins, in which the N-terminal amino acid residues were individually replaced by Gly or Ala residues (Figure 1), were prepared and their folding was examined.

wild type	V	Y	I	Q	Y	Q	G	-	-
V1G	G	-	-	-	-	-	-	-	-
Y2G	-	G	-	-	-	-	-	-	-
I3G	-	-	G	-	-	-	-	-	-
Q4G	-	-	-	G	-	-	-	-	-
Y5G	-	-	-	-	G	-	-	-	-
Q6G	-	-	-	-	-	G	-	-	-
V1A	A	-	-	-	-	-	-	-	-
I3A	-	-	A	-	-	-	-	-	-

Fig. 1. N-terminal amino acid sequences of the mutant proteins.

### Results and Discussion

We previously reported that the six N-terminal residues of the propeptide region of prouroguanylin play a critical role in the folding of the mature peptide, uroguanylin [3]. However, the tertiary (and secondary) structure of prouroguanylin and the role of the N-terminal amino acid residues in this folding have not yet been determined. NMR studies of proguanylin, which is homologous to prouroguanylin, revealed that the N-terminal region of the propeptide is in close proximity to the C-terminal mature region [4], suggesting that the N-terminal region might play a role in regulating the folding of the mature region. To further investigate the role of the N-terminal amino acid residues in the folding process of prouroguanylin, each of the amino acid residues from positions 1 to 6 of prouroguanylin were individually mutated to Gly or Ala residues by recombinant techniques, as shown in Figure 1.

The mutant proteins were expressed by *E. coli*, purified as reduced forms by HPLC, and oxidatively folded in the presence of 2 mM GSH and 1 mM GSSG. All mutant proteins contained an extra Met residue at the N-termini, but the presence of this resi-

due had no effect on the native folding of prouroguanylin, as has been previously reported [3].

The replacement of Tyr2, Gln4, Tyr5, Gln6 to a Gly residue (Y2G, Q4G, Y5G, and Q6G, respectively) did not significantly affect the construction of the native conformation or the disulfide pairings of prouroguanylin, indicating that the side chains of those amino acid residues do not directly interact with the mature region, uroguanylin. However, the mutation of the Val1 and Ile3 residues to a Gly residue (V1G and I3G, respectively) had a significant effect on folding. In particular, the replacement of Ile3 with a Gly residue resulted in the complete lack of chaperone function of the propeptide region.

To estimate the role of the side chain of the Val1 and Ile3 residues, the folding of mutants V1A and I3A were also examined. Both mutant proteins were efficiently folded to the native conformation. These data suggest that the methyne groups at the  $\beta$ -position of Val1 and Ile3 play a crucial role in the folding of prouroguanylin.

In order to obtain structural information on the folding of prouroguanylin, CD spectra of the mutants V1G, V1A, I3G, and I3A were obtained. The mutants V1G, V1A, and I3A showed CD spectra which were similar to that of the wild type of prouroguanylin. However, the degree of  $\alpha$ -helicity in the propeptide region of the mutant I3G was dramatically decreased. These findings indicate that the  $\beta$ -methyne of Ile3 contributes to the thermodynamic stability of the propeptide region. Alternatively, the  $\beta$ -methyne of Ile3 may directly interact with the mature region to fold the native tertiary structure of prouroguanylin, resulting in the formation of  $\alpha$ -helices in the propeptide region.

In conclusion, the presence of the  $\beta$ -methyne of Ile3 is absolutely required for the correct folding of prouroguanylin.

#### **Acknowledgments**

We thank Dr. K. Yutani for the measurements of CD spectra. The use of the facility at the Radio-isotope Research Center of Osaka University is also acknowledged.

#### **References**

1. Hamra, F.K., et al. *Proc. Natl. Acad. Sci. U.S.A.* **90**, 10464–10468 (1993).
2. Hidaka, Y., Ohno, M., Hemmasi, B., Hill, O., Forssmann, W.-G., Shimonishi, Y. *Biochemistry* **37**, 8498–8507 (1998).
3. Hidaka, Y., Shimonishi, C., Ohno, M., Okumura, N., Adermann, K., Forssmann, W.-G., Shimonishi, Y. *J. Biol. Chem.* **275**, 25155–25162 (2000).
4. Schulz, A., Marx, U.C., Hidaka, Y., Shimonishi, Y., Rosch, P., Forssmann, W.-G., Adermann, K. *Protein Sci.* **8**, 1850–1859 (1999).

## **Solution Structure of the Macrocyclic Squash Trypsin Inhibitor MCoTI-II, the First Member of a New Family of Cyclic Knottins**

**Annie Heitz<sup>1</sup>, Jean-François Hernandez<sup>2</sup>, Jean Gagnon<sup>2</sup>,  
Thai Trinh Hong<sup>3</sup>, Châu T.T. Pham<sup>3</sup>, Tuyet M. Nguyen<sup>3</sup>,  
Dung Le-Nguyen<sup>4</sup> and Laurent Chiche<sup>1</sup>**

<sup>1</sup>*Centre de Biochimie Structurale, UMR 5048 CNRS-UMI/UMR 554 INSERM/UMI,  
Montpellier, France*

<sup>2</sup>*Institut de Biologie Structurale Jean-Pierre Ebel (CEA/CNRS), Grenoble, France*

<sup>3</sup>*Centre of Biotechnology, National University of Vietnam, Hanoi, Vietnam*

<sup>4</sup>*INSERM U376 Montpellier, France*

### **Introduction**

Squash trypsin inhibitors are small disulfide-rich proteins (28-30 residues, 6 cysteines). Their 3D structures revealed that one disulfide crosses the macrocycle formed by the other two disulfide bridges and the interconnecting backbone, hence the term “knottins”. This particular topology has been found in a number of cystine-rich peptides with diverse biological activities isolated from plants or animals. Several of these peptides, such as kalata B1, circulin A and B and Cycloviolacin O1, display macrocyclic structures. These cyclic knottins were grouped in two subfamilies following sequence comparison [1]. To date, all the reported squash trypsin inhibitors have a linear structure. We recently isolated several cyclic squash trypsin inhibitors from *Momordica cochinchinensis* seeds [2]. MCoTI-II is the most abundant and its primary structure has been identified as *cyclo*-(S<sup>1</sup> G S D G G V C P K<sup>10</sup> I L K K C R R D S D<sup>20</sup> C P G A C I C R G N<sup>30</sup> G Y C G). Here we report the NMR and molecular modeling studies of this peptide.

### **Results and Discussion**

The NMR study was performed on a 2.5 mM aqueous solution at pH 3.4. <sup>1</sup>H and <sup>13</sup>C resonance assignment was achieved using COSY, TOCSY, NOESY and <sup>1</sup>H-<sup>13</sup>C HSQC experiments. 86 sequential and 171 medium and long range distance constraints as well as 9  $\phi$  and 10  $\chi$ 1 dihedral angles were used to generate 1000 3D structures using the DYANA program. The 30 best structures obtained were further refined with the AMBER 6 program and displayed with the program MOLMOL 2K.1. Refined structures satisfy the NMR data with no distance and dihedral violations equal or larger than 0.2 Å and 5°, respectively. The 3D structure of MCoTI-II is well resolved with a very low RMS deviation of 0.3 Å for superimposition of backbone atoms of core residues 13-33. The inhibitory loop (residues 8 to 12) displays rather low RMS deviations (< 1 Å). The sequence that links the residues corresponding to the C- and N- termini in the non-cyclic squash inhibitors (C-to-N linker) displays the highest RMS deviations and constitutes the most flexible part of the molecule.

The conformation of MCoTI-II closest to the average has been superimposed onto the X-ray structure of the non-cyclic squash trypsin inhibitor CPTI-II in complex with trypsin. CPTI-II has been selected for comparison because its sequence is closer to MCoTI-II compared to the other squash inhibitors with known 3D structures. The two structures are strikingly similar, with low RMS deviations (0.8 Å) for backbone superimposition of residues 7-34 corresponding to the entire sequence of CPTI-II.

The conformation of MCoTI-II has also been compared to the 3D structure of kalata B1 (Figure 1). Although the global fold is similar, clear differences are appar-

ent. Only one disulfide bridge (Cys<sup>15</sup>-Cys<sup>27</sup>) is structurally superimposable. The Cys<sup>21</sup>-Cys<sup>33</sup> disulfide bridge is slightly different and only Cys<sup>33</sup> is well conserved between the two structures. The Cys<sup>8</sup>-Cys<sup>25</sup> disulfide bridge is the most largely displaced, although Cys<sup>25</sup> is well conserved between the two structures. This is in clear

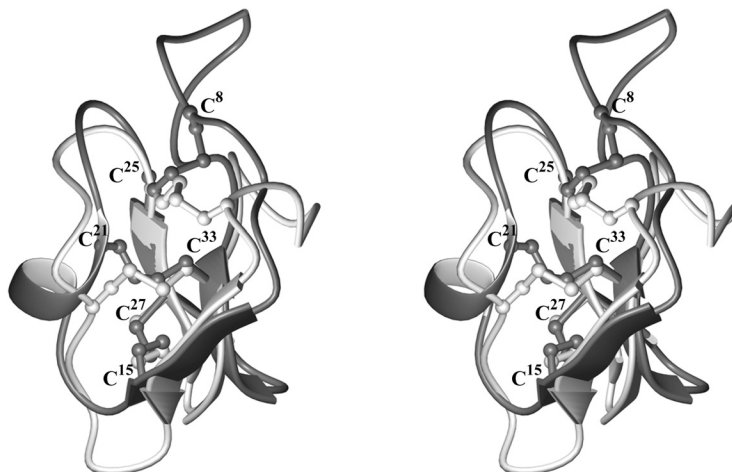


Fig. 1. Schematic stereoview of MCoTI-II (dark grey) superimposed onto kalata B1 (light grey).  $\beta$ -strands are shown as flat arrows and the  $3_{10}$  helix in MCoTI-II is shown as a flat ribbon.

relation with the large displacement of the C-to-N linker. Despite the spatial modification of the linker, the structurally conserved region corresponds to the anti-parallel triple-stranded  $\beta$ -sheet, which is the elementary CSB motif (Cystine Stabilized Beta-sheet motif) [3]. This comparison led to a structural sequence alignment shown in Figure 2.

<b>MCoTI-II</b>	SG---SDGGVCPKILKKC--RRDSD---CPGACICRNGYCG
<b>kalata B1</b>	RNGLP-----VCGETCVGGT--C---NTPGCTCS-WPVCT
<b>circulin A</b>	RNGIP-----CGESCWIP--C-ISAALGCSCK-NKVCY
<b>cycloviolacin O1</b>	-NGIP-----CAESCVYIP--CTVTALLGCSCS-NRVCY

Fig. 2. Structural alignment between MCoTI-II and cyclic knottins. The conserved anti-parallel triple-stranded  $\beta$ -sheet is shown by arrow.

Despite no significant sequence similarity between MCoTI-II and cyclic knottins, all peptides display a cystine knot, a cyclic backbone and the same elementary structural motif. For these reasons MCoTI-II can be considered as a member of a new family of cyclic knottins.

## References

1. Craik, D.J., Daly, N.L., Bond, T., Waite, C. *J. Mol. Biol.* **294**, 1327–1336 (1999).
2. Hernandez, J.F., et al. *Biochemistry* **39**, 5722–5730 (2000).
3. Heitz, A., Le-Nguyen, D., Chiche, L. *Biochemistry* **38**, 10615–10625 (1999).

## **Delineation of Structural Constraints Imposed by a Dimerizer Peptide When Grafted Onto the Terminal Ends of a Test Peptide**

**Tarikere L. Gururaja<sup>1</sup>, Gowda A. Naganagowda<sup>2</sup>, Donald G. Payan<sup>1</sup>  
and Dave Anderson<sup>1</sup>**

<sup>1</sup>*Protein Chemistry, Rigel Pharmaceuticals Inc., South San Francisco, CA 94080, USA*

<sup>2</sup>*Sophisticated Instrument Facility, Indian Institute of Science, Bangalore 560012, India*

### **Introduction**

Compared to linear peptides, constrained and/or cyclic peptides have many valuable features, including enhanced stability to proteolysis and a restricted conformation space that can result in a higher binding affinity for cognate binding proteins [1]. Retroviral expression of constrained structures having disulfide linkages in live cells may be more difficult due to high levels (mM) of reduced glutathione and the active reduction of these bonds by thioredoxin reductase. To circumvent this problem, we have developed a novel method wherein fusion of short peptide sequences having good self affinity ( $\mu$ M range) to each end of a random peptide will allow the folding of peptide library members into compact structures without the formation of disulfide bonds [2]. During this study, one problem was the solubility of the resulting peptide. Introduction of more charged residues around the hydrophobic core, FLIV of the dimerizer sequence alleviated this problem. As a proof of concept, using a 18mer sequence derived from the protease contact loop of barley chymotrypsin inhibitor 2 (Ci2b) [3], we tested the solubility as well as the structural stability by anchoring two *de novo* designed dimerizer sequences, KKKFLIVKKK and EEEFLIVEEE, respectively to the N- and C-terminus. We found that the resulting structure (38mer) was more soluble compared to other dimerizer peptides and significantly resistant to high levels of elastase than the disulfide-cyclized 18mer, which in turn is less readily proteolyzed than the linear 18mer. Here we report the structural features of this newly designed mini-protein domain (38mer-dimerizer peptide) determined by CD and NMR.

### **Results and Discussion**

The two test peptides, KKKFLIVKKK-VGTIVTMEYRIDRTRSFV-EEEFLIVEEE (38mer-dimerizer model peptide) and VGTIVTMEYRIDRTRSFV (Ci2b 18mer insert only) used in this study were synthesized, purified and characterized following conventional methods. Figure 1A shows the CD spectra of 18mer insert derived from Ci2b as well as the dimerizer peptide (38mer) recorded in phosphate buffer (pH 7.5) at 25 °C. The two peptides appear to have different conformations. The 18mer showed a random coil structure characterized by a broad negative band around 200 nm. The newly designed peptide scaffold with two dimerizer sequences at the terminal ends showed a mixture of  $\beta$ -sheet and  $\beta$ -turn structures which is characterized by a broad negative band around 225 nm and a positive band around 195 nm. This data suggests that the added dimerizer sequences such as KKKFLIVKKK and EEEFLIVEEE respectively at N- and C-terminus of the 18mer insert may have folded the peptide into a more ordered structure. Figure 1B depicts the effect of pH on the ellipticity of the circular dichroism (CD) signal for the 38mer peptide. At all pH, the 18mer sequence exhibited a random coil conformation (data not shown). At pH 3.5, the 38mer peptide showed a broad positive  $\pi$ - $\pi^*$  band around 195 nm and a negative  $n$ - $\pi^*$  band centered around 220 nm, which suggests a  $\beta$ -strand conformation with minor population of dis-

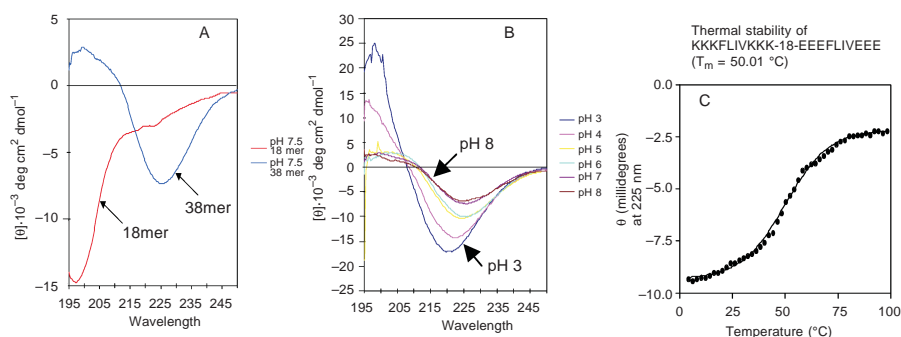


Fig. 1. Structural determinations of dimerizer peptide.

ordered polypeptide chain. As the pH of the peptide solution increased, the CD bands showed a progressive shift (red shift) of the negative band from 220 to ~225 nm with a decreased ellipticity of the positive  $\pi$ - $\pi^*$  band at 195 nm. This transition of secondary structure as a function of pH clearly indicates the internal flexibility of the peptide owing to a change in  $pK_a$  of the side chains leading to partial disruption of ionic interactions. Upon addition of the structure stabilizing organic cosolvent TFE, the secondary structure of the 38mer peptide didn't change, suggesting that the peptide may have already a stable structure before cosolvent addition. The basic and acidic ends of this peptide may form intermolecular salt bridges and thus promote internal association. Such an observation has been reported in the case of a polyglutamine repeat, Ac-DD-Q15-KK-NH<sub>2</sub> [4]. Thermal denaturation studies by CD gave  $T_m$  of 50.01 °C (Figure 1C) suggesting a thermodynamic stability similar to that of many proteins [5]. To better understand the structural features of this dimerizer peptide construct, we also undertook studies by high field NMR spectroscopy. From the preliminary NMR data, it appears that the 38mer peptide might contain a minor population of ordered structure in DMSO based on the peak resolution obtained in the amide region (1D and 2D NMR spectrum, data not shown). Under aqueous conditions, the peptide seems to contain  $\beta$ -sheet like structure, which is more pronounced when concentration of the sample increases. This data is consistent with our CD data.

### Acknowledgments

We thank Dr. Richard Scheller (Stanford University, CA) for use of the Aviv Circular Dichroism spectropolarimeter and Rigel Pharmaceuticals Inc. for financial support.

### References

1. Ladner, R.C. *Trends Biotechnol.* **13**, 426–430 (1995).
2. Gururaja, T.L., Narasimhamurthy, S., Payan, D.G., Anderson, D.C. *Chem. Biol.* **7**, 515–527 (2000).
3. McPhalen, C.A., James, M.N. *Biochemistry* **26**, 261–269 (1987).
4. Altschuler, E.L., Hud, N.V., Mazrimas, J.A., Rupp, B. *FEBS Lett.* **472**, 166–168 (2000).
5. Vogt, G., Woell, S., Argos, P. *J. Mol. Biol.* **269**, 631–643 (1997).

## Local and Long-Range Sequence Contributions to the Folding of a Predominantly $\beta$ -Sheet Protein

Lila M. Gierasch<sup>1,2</sup>, Kenneth S. Rotondi<sup>2</sup>, Kannan Gunasekaran<sup>1</sup>,  
Jennifer A. Habink<sup>2</sup> and Arnold T. Hagler<sup>2</sup>

<sup>1</sup>Department of Biochemistry & Molecular Biology; and <sup>2</sup>Department of Chemistry,  
University of Massachusetts, Amherst, MA 01003, USA

### Introduction

Understanding how a linear sequence of amino acids guides acquisition of the native state of a protein – the protein folding problem – is key to interpreting information present in the human genome and to developing therapeutic approaches to diseases caused by protein misfolding. While considerable progress has been made in elucidating the interplay of local and long-range forces in the folding of  $\alpha$ -helical proteins, such understanding has lagged for primarily  $\beta$ -sheet proteins [1]. We have undertaken studies aimed at determining the roles of local and global sequence information in the folding of the predominantly  $\beta$ -sheet protein, cellular retinoic acid binding protein I (CRABP I). CRABP I is a 136 residue  $\beta$ -clamshell protein (Figure 1) whose physiological role is the sequestration and transport of the hydrophobic ligand retinoic acid. CRABP I is a member of the large family of intracellular lipid binding proteins (iLBPs) [2], which contains 52 members with sequence identity greater than 30% with respect to CRABP I. Past work in our laboratory using stopped-flow (SF) mixing to follow the fluorescence of CRABP I has allowed us to define a series of kinetic phases from the urea-denatured conformational ensemble to the native fold [3]. Within the  $\approx 10$  ms dead time of the SF instrument, the unfolded ensemble forms a hydrophobically collapsed state with considerable secondary structure. The presence of significant secondary structure along with hydrophobic collapse suggests that both global and local forces are acting in the earliest folding events. We have previously shown that the formation of the helix-turn-helix sub-domain of CRABP I is dictated by local sequence, since a 30-residue peptide fragment adopts a native-like structure [4]. We anticipate that turns in CRABP I will also be determined by local sequence, such that the tendency for turns to form could limit the conformational space available to the peptide chain in the early folding phases. Subsequent kinetic phases likely arise as the

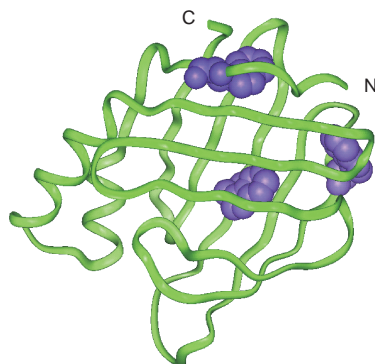


Fig. 1. CRABPI with its intrinsic tryptophans (PDB coordinate code 1CBB).

conformational ensemble forms longer-range contacts that specify native topology ( $\approx 100$  ms) and finally native interstrand hydrogen bonds and tertiary structure (1 s).

Here, we describe our identification of a well-defined sub-millisecond kinetic phase for the earliest hydrophobic collapse step of CRABP I, made possible through the use of a recently developed rapid mixer [5]. Next, we discuss a comparative study of peptide fragments corresponding to the turns in CRABP I and implications for the early steps in folding. Lastly, we summarize results of an analysis of sequences and structures for CRABP I and homologues, which enabled us to identify a network of conserved pairwise hydrophobic interactions that is likely to specify native-like global topology.

### Results and Discussion

A variant of CRABP I (W87F, R131Q), which contains only two of the three intrinsic tryptophans (7 and 109) and a stabilizing mutation, was designed and found to be robust in refolding studies and to yield a large fluorescence signal during the earliest folding events. Dilution of this mutant into folding conditions in the ultra-fast mixer developed by Shastry and Roder [5] revealed a well-defined 250  $\mu$ s kinetic phase. All fluorescence intensity change from denatured to native protein is accounted for by the combination of this phase with previously observed  $\approx 100$  ms, 1 s, and the minor  $\approx 15$  s phases. Hence, our kinetic experiments are now able to describe fully the folding energy landscape of CRABP I.

A major question emerges from the identification of a well-defined early collapse event in CRABP I: What sequence information is guiding the ensemble of unfolded states to a more restricted set of collapsed species that are competent to fold productively? To assess the importance of local sequence in these early stages of folding, we compared the behavior of seven short peptides corresponding to the turns of CRABP I by NMR. (A preliminary description of this work was published previously [6].) The fragments derived from turns III and IV are unique among those analyzed in that they exhibited a number of indicators of native-like conformation in their ensembles. For example, amide proton resonances from E69 and R79 in fragments III and IV, respectively, show reduced temperature coefficients, consistent with expectations for native-like turns. Additionally, the magnitudes and patterns of rotating-frame Overhauser enhancements (ROEs) (Figure 2) from turns III and IV are indicative of a substantial population of native-like turn conformers in their ensembles. In addition, these were

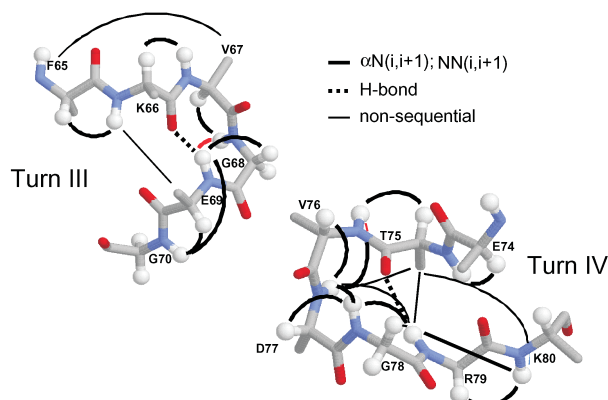


Fig. 2. Indicators of native-like turns in short peptides derived from CRABP I.

the only fragments to exhibit non-sequential ROEs. The turn III fragment exhibited a side-chain to side-chain ROE between F65  $\epsilon$  and V67  $\gamma$  protons, suggesting a role for local sequence hydrophobic clustering in early folding events, as well as a cross-strand ROE between the K66 NH and the E69  $\beta$  protons. In the turn IV peptide, ROEs between the T75 $\beta$  proton and the D77 NH and between the D77 and R79 NH protons establish the presence of a population of conformers with native conformation through the turn.

Also noteworthy is the higher than average (45%) sequence conservation of turns III and IV – 54 and 72%, respectively – when CRABP I was compared to the 52 iLBPs with 30% or higher sequence identity. No other turn was found to display conservation above the overall average. We thus conclude that the local bias towards a native-like conformation in turns III and IV is an important feature of the CRABP I primary structure and is likely to play a role in early folding events.

In order to take advantage of the large number of structural homologues of CRABP I and to seek insights into long-range interactions important for folding of iLBPs, we developed a simple algorithm to identify correlated pair-wise interactions. In this analysis, we identified residue pairs in contact, then examined these pairs in a multiple sequence alignment of the iLBP family for their correlated mutational behavior, based on classification of the side chains as polar or hydrophobic. We scored correlation of pair-wise variations by assuming that a bias towards maintaining the nature of the interaction (hydrophobic–hydrophobic or polar–polar) reflects a non-random mutational trend to preserve a favorable contact. This approach identifies a number of residues that make up a hydrophobic cluster, which likely plays a role in folding. Importantly, a small number of residues (F3, W7, I43, F50, F65, V67, P85, W87, I93, L119) participate in multiple conserved hydrophobic interactions, suggesting a key role for these sites in the structure and folding of iLBPs.

Our current efforts are directed at determining the point in the folding pathway of CRABP I at which these interactions form. A crucial question to be answered by this research is the extent to which the initial hydrophobic collapse is specific. Alternatively, the key hydrophobic interactions may play roles later, either by restricting the conformational ensemble to native topology in the  $\approx 100$  ms kinetic phase or by narrowing the ensemble at the point of formation of close native packing contacts in the 1 s kinetic phase.

### Acknowledgments

We thank Linda F. Rotondi for synthesis and purification of the peptide fragments, as well as Rama Shastry and Heinrich Roder for assistance with the ultra-fast mixing apparatus. Supported by NIH grant GM 27616; K.S.R and J.A.H. supported in part by NIH pre-doctoral training grant GM 08515.

### References

1. Capaldi, A., Radford, S.E. *Curr. Opin. Struct. Biol.* **8**, 86–92 (1998).
2. Banaszak, L., Winter, N., Xu, Z., Bernlohr, D.A., Cown, S., Jones, T.A. *Adv. Protein Chem.* **45**, 89–151 (1994).
3. Clark, P.L., Liu, Z.-P., Zhang, J., Gierasch, L.M. *Protein Science* **5**, 1108–1117 (1996).
4. Sukumar, M., Gierasch, L.M. *Folding & Design* **2**, 211–222 (1997).
5. Shastry, M.C.R., Luck, S.D., Roder, H. *Biophys. J.* **74**, 2714–2721 (1998).
6. Rotondi, K.S., Gunasekaran, K., Gierasch, L.M., In Fields, G.B., Tam, J.P., and Barany, G. (Eds.) *Peptides for the New Millennium (Proceedings of the 16th American Peptide Symposium)*, Kluwer, Dordrecht, 2000, p. 32.

### 3D Models for Conformational States of the V3 and V1/V2 Loops in gp120/CD4/Antibody Complex

Stan Galaktionov, Gregory V. Nikiforovich and Garland R. Marshall

Department of Biochemistry and Molecular Biophysics, Washington University, St. Louis, MO 63110, USA

#### Introduction

The X-ray structure of the ternary complex of an engineered “core” gp120, CD4 and an antibody [1] does not contain the hypervariable V3 and V1/V2 loops (the gp120<sub>298-331</sub> and gp120<sub>126-196</sub> fragments, respectively). These loops are extremely important in HIV function. We have restored several feasible 3D structures of these loops in gp120 applying a computational approach based on residue-residue contact matrices.

#### Results and Discussion

3D structures of the V3 and V1/V2 loops were restored by the procedure described elsewhere [2] that consists of the following steps: (i) prediction of coordination numbers for each loop residue (*i.e.*, the numbers of contacts between loop residues within the loop and with the “core” residues), a contact being defined as the  $C_i^\alpha - C_j^\alpha$  distance  $< 8 \text{ \AA}$ ; (ii) calculation of *a priori* probabilities of residue-residue contacts as functions of coordination numbers; (iii) calculation of the residue-residue contact matrices under conditions that ensure generation of matrices corresponding to sterically consistent 3D structures with appropriate protein density only; (iv) prediction of the matrices of inter-residue distances from the contact matrices; (v) restoring possible 3D structures of  $C^\alpha$ -traces for the loops by a distance geometry algorithm starting from predicted inter-residue distances; (vi) generating additional possible  $C^\alpha$ -traces by finding subfragments that are mirror images of a given 3D structure still in compliance with the contact matrix.

The above procedure resulted in the reconstruction of 8 different  $C^\alpha$ -traces for the loop V1/V2 and 6 different conformers for the loop V3. Figure 1 depicts the 3D structure of gp120 with both restored loops (the calculated loop structures of type 1 are shown). In all 8 structures predicted for the V1/V2 loop, there are contacts of loop res-

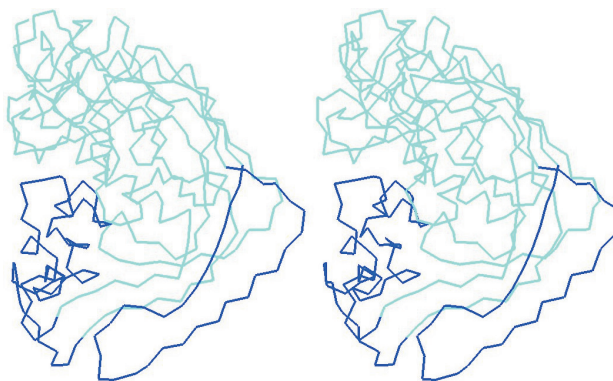


Fig. 1. Stereoview of 3D structure of gp120 with restored V3 (right) and V1/V2 (left) loops. In both cases, the calculated structures of type 1 are presented. Loops are shown in black.

idues with 10 to 25 out of 26 residues of the “core” gp120 that are in direct contact with CD4 according to the X-ray structure of the gp120/CD4/antibody complex [1]. For instance, the V1/V2 loop structure of type 1 contacts 25 out of the 26 mentioned residues of the “core” gp120, namely L125, D279, N280, A281, T283, S365, G366, G367, D368, E370, I371, N425, M426, W427, Q428, K429, V430, T455, R456, D457, G458, R469, G472, G473 and D474. Residues in the various structures of the V3 loop contact from 11-13 out of the 15 residues of the “core” gp120 that have been suggested to contact the co-receptor (CCR5) according to site-directed mutagenesis [3].

The V3 loop structure of type 1 contacts K121, T123, H330, R419, I420, K421, Q422, P437, P438, S440, G441, Q442 and R444.

The restored structures of the V1/V2 loop very effectively shield the gp120 cavity that is occupied by CD4 in the X-ray structure of the gp120/CD4/antibody complex, whereas the restored structures of the V3 loop cover the gp120 surface that presumably binds the HIV co-receptor. These observations validate the results of our calculations, since they are in agreement with the widely accepted hypothesis describing the HIV binding to the cell membrane (*e.g.*, [4]). First, CD4 binds gp120 on the viral envelope displacing the V1/V2 loop from the surface of gp120. This binding induces conformational changes in gp120 including movement of the V3 loop, which exposes the co-receptor-binding sites of gp120. It is noteworthy also that the computational approach based on the residue-residue contact matrices was able to restore large loops on the protein surface (up to 69 residues, as in the V1/V2 loop).

### **Acknowledgments**

This work was supported by the NIH grant GM 53630.

### **References**

1. Kwong, P.D., Wyatt, R., Robinson, J., Sweet, R.W., Sodroski, R., Hendrickson, W.A. *Nature* **393**, 648–659 (1998).
2. Galaktionov, S., Nikiforovich, G.V., Marshall, G.R. *Biopolymers (Pept. Sci.)* **60**, No. 2, in press (2001).
3. Rizzuto, C.D., Wyatt, R., Hernández-Ramos, N., Sun, Y., Kwong, P., Hendrickson, W.A., Sodroski, J. *Science* **280**, 1949–1953 (1998).
4. Berger, E.A., Murphy, P.M., Farber, J.M. *Annu. Rev. Immunol.* **17**, 657–700 (1999).

## Structure and Dynamics of Ribosome Recycling Factor

Takuya Yoshida, Susumu Uchiyama, Hiroaki Nakano  
and Yuji Kobayashi

*Graduate School of Pharmaceutical Sciences, Osaka University, Suita, Osaka 565-0871, Japan*

### Introduction

Ribosome recycling factor (RRF) catalyzes the disassembly of the post termination complex, which consists of ribosome, mRNA and deacylated tRNA, to allow recycling of ribosome for the next round of protein synthesis [1]. Recently, three-dimensional structures of RRF from several bacteria were determined by crystallography and NMR [2–5]. RRF consists of two domains and have a characteristic L-shaped overall structure, which has been suggested to mimic tRNA. Regarding the relative orientations of two domains, differences among the RRFs are found. In particular, the bending angle between domains of *E. coli* RRF is significantly larger than those of other RRFs. Our previous NMR study [5] has indicated that such differences originated from the flexibility of the joint region. Although the detailed mechanism of ribosome recycling is not established, the importance of the fluctuation in domain orientations was suggested from some molecular biological studies. To better understand the recycling step, we have characterized the inter-domain orientation and dynamics of *E. coli* RRF and *T. maritima* RRF in solution.

### Results and Discussion

The  $^{15}\text{N}$  and/or  $^{13}\text{C}$  enriched NMR samples of *E. coli* RRF and *T. maritima* RRF were prepared in the same manner described previously [3], except that the minimum medium with nitrogen and/or carbon source was used. All NMR experiments were carried out at 30 °C on Varian INOVA600 spectrometer. NMR signal assignments were obtained by a well-established sequence specific assignment strategy using triple resonance experiments. The backbone  $^{15}\text{N}$  relaxation parameters comprising the  $^{15}\text{N}$  longitudinal relaxation time  $T_1$ , transverse relaxation time  $T_2$  and  $^{15}\text{N}\{-^1\text{H}\}$  NOE, were measured using HSQC type pulse sequence. The relaxation decay curves were sampled at six time points for  $T_1$  and  $T_2$  measurements. To determine the relative orientation of domains of *E. coli* RRF, the rotational diffusion constants for whole molecule and the orientation of the unique axis of the rotational diffusion tensor for each domain were searched to optimize the agreement between the observed  $^{15}\text{N}$   $T_1/T_2$  ratios and ratios predicted from structure determined by crystallography [3] (PDB : 1EK8). Only well-resolved residues in HSQC spectra belonging to the well-defined secondary structure were used for the analysis. Residues that showed low  $^{15}\text{N}\{-^1\text{H}\}$  NOE values ( $<0.65$ ) were excluded in the analysis. From the analysis for a total of 79 residues, the effective correlation time and anisotropy were determined as 15.5 and 2.1 ns, respectively. Interestingly, the angle between the unique axis determined for domain I and that for domain II was 71 degrees. Assuming that RRF molecule tumbles as a rigid body in solution, the unique axis determined from the data of domain I should be parallel to that from domain II data. Therefore, it was suggested that the relative orientation of domains of *E. coli* RRF in solution is different to that in crystal structure. The statistical F-test indicated that the model used in this study was a significant improvement over the model where the unique axis for whole molecule was used ( $p < 1 \cdot 10^{-5}$ ). Although the relaxation data cannot distinguish between orientations that relate individual domains by an axial symmetry transformation, substantial steric restrictions on

the possible arrangement of domains are imposed. One possible relative orientation between domains is shown in Figure 1b. It is noteworthy that the suggested domain orientation is very similar to that of the reported structures of RRF except for that of *E. coli*. This picture suggests that *E. coli* RRF maintains the characteristic tRNA-like conformation in solution. The reported structure of *E. coli* RRF might be biased by packing force or binding of detergent molecule in the crystal lattice, as discussed in [5]. The  $^{15}\text{N}\{-^1\text{H}\}$  heteronuclear NOE data suggest that the joint region and Domain II of *E. coli* RRF are more flexible than those of *T. maritima* RRF. The joint region of *E. coli* RRF may contribute to the fluctuation in the orientation of two domains.

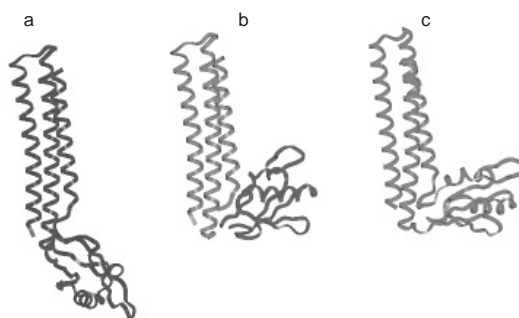


Fig. 1. (a) Crystal structure of *E. coli* RRF [3]. (b) Model structure for *E. coli* RRF in solution obtained from NMR relaxation anisotropy. (c) Crystal structure of *T. maritima* RRF [2].

## References

1. Kaji, A., Hirokawa, G., In Garrett, R.A., Douthwaite, S.R., Liljas, A., Matheson, A.T., Moore, P.B., and Noller, H.F., (Eds.) *The Ribosome: Structure, Function, Antibiotics and Cellular Interactions*, ASM Press, Washington, DC, 2000, pp. 527–539.
2. Selmer, M., Al-Karadaghi, S., Hirokawa, G., Kaji, A., Liljas, A. *Science* **286**, 2349–2352 (1999).
3. Kim, K.K., Min, K., Suh, S.W. *EMBO J.* **19**, 2362–2370 (2000).
4. Toyoda, T., Tin, O.F., Ito, K., Fujiwara, T., Kumasaki, T., Yamamoto, M., Garber, M.B., Nakamura, Y. *RNA* **6**, 1432–1444 (2000).
5. Yoshida, T., Uchiyama, S., Nakano, H., Kashimori, H., Kijima, H., Ohshima, T., Saihara, Y., Ishino, T., Shimahara, H., Yoshida, T., Yokose, K., Ohkubo, T., Kaji, A., Kobayashi, Y. *Biochemistry* **40**, 2387–2396 (2001).

## Peptide Models for Studying Autonomous Folding of Subdomain Sections of Protein Molecules

Gerardo Byk<sup>1</sup>, Dikla Engel<sup>1</sup>, Vardah Ittah<sup>2</sup> and Elisha Haas<sup>2</sup>

<sup>1</sup>Department of Chemistry, Bar Ilan University, Ramat Gan-52900, Israel

<sup>2</sup>Faculty of Life Science, Bar Ilan University, Ramat Gan-52900, Israel

### Introduction

Polypeptide segments are the elementary folding units of globular proteins. Relatively short synthetic polypeptide segments are essential models for the investigation of the mechanism of folding of globular proteins. The search for intermediate, partially folded states of proteins, or their fragments, is a central issue in the protein folding problem. In order to be able to characterize partially folded states, it is essential to be able to characterize the conformation of polypeptide segments in the presumably unfolded (statistical coil) and fully folded states. To this end, a series of model polypeptide segments, labeled by pairs of fluorescent probes, were prepared and characterized by means of time resolved dynamic non-radiative fluorescence energy transfer (FRET) measurements.

The first model oligopeptide, designed as a model for the rigid fully folded state, was a pair of polyproline molecules containing 9 and 14 Pro residues, respectively. Each peptide was labeled at its ends by a donor (naphthylalanine) and an acceptor (aminocoumarine, M1410) of excitation energy, and the time resolved FRET measurements show that the flexibility of the folded conformation depends on the length of the polypeptide.

### Results and Discussion

The fluorescence spectra of a peptide of the sequence (pro)<sub>9</sub>-naphthylalanine is shown in Figure 1. The results of a time resolved experiment are shown in Figure 2. Note the reduction of the donor fluorescence lifetime, due to the FRET. The global analysis of the time resolved FRET experiments yields the end-to-end distance distributions for the peptide. The results are shown in Figures 3 and 4.

Figure 3 shows a narrow distribution with a mean distance of  $23 \pm 1$  Å which is larger than the length expected for an all cis-proline peptide. The longer peptide, which contains 14 proline residues showed correspondingly longer end-to-end distance, but significantly wider width of the distribution. Figure 4 shows that the mean of the distribution is only slightly changed by the addition of 6 M GUHCl. Figure 5 shows the far UV CD spectrum of the labeled Pro<sub>9</sub> peptide. Surprisingly, the CD spec-

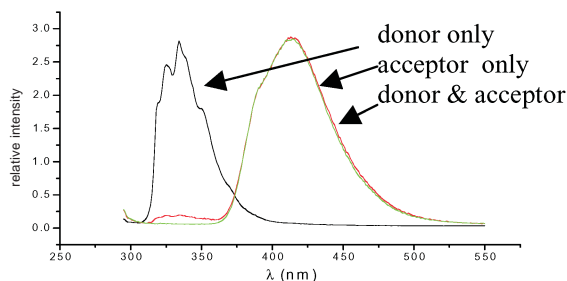


Fig. 1. Fluorescence spectra of double labeled Pro<sub>9</sub>.

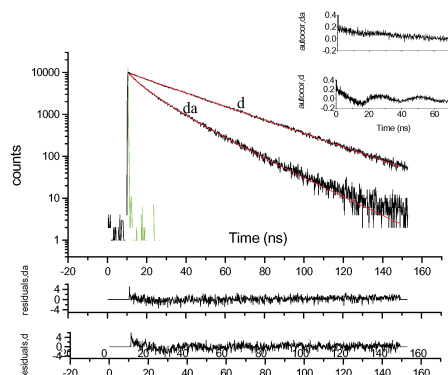


Fig. 2. Decay curves of the donor fluorescence attached to a peptide that has no acceptor (upper trace) and of the same peptide labeled by both donor and acceptor in 6 M GuHCl, at 40 °C.

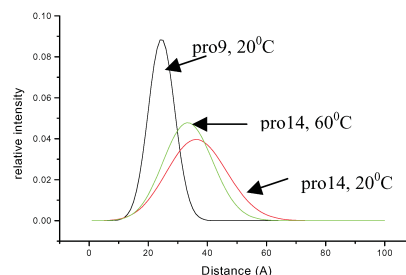


Fig. 3. End to End Distance Distribution of Pro9 and Pro14 peptides in 0.1 M Tris pH 8.

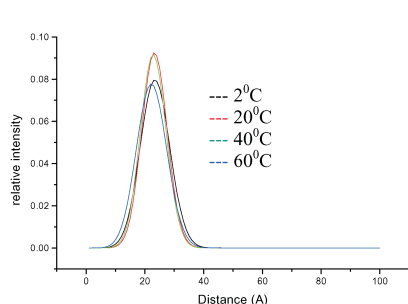


Fig. 4. End to End Distance Distribution of Pro<sub>9</sub> peptide in 0.1 M Tris pH 8 + 6 M GUHCl.

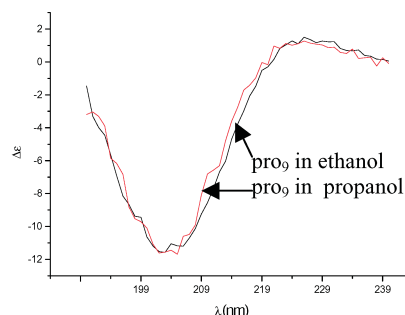


Fig. 5. CD spectra of Pro<sub>9</sub>.

trum resembles that of an all trans polyproline, while the end-to-end distance is closer to the all cis-polyproline.

The synthetic proline peptides can be used as reference for an ordered state of peptide segment in applications of time-resolved FRET measurements.

The distribution of the end-to-end length of the peptides shows increased flexibility of the structure at longer chain length, despite the expected increased cooperativity.

The end-to-end distance distribution obtained by the present experiments is closer to the all cis-proline peptides, although the mean value is larger than expected.

## Acknowledgments

This research was supported by an internal grant of Bar Ilan University.

## References

1. Ittah, V., Haas, E. *Biochemistry* **34**, 4493–4506 (1995).
2. Haas, E. *IEEE JSTQE* **2**, 1088–1106 (1996).

## Towards New Designed Proteins: Oxime Ligation of Core Modules

Natalia Carulla<sup>1</sup>, Clare Woodward<sup>2</sup> and George Barany<sup>1</sup>

<sup>1</sup>Department of Chemistry, University of Minnesota, Minneapolis, MN 55455, USA

<sup>2</sup>Department of Biochemistry, Molecular Biology, and Biophysics, University of Minnesota,  
St. Paul, MN 55108, USA

### Introduction

A 25-residue disulfide-cross-linked peptide, termed “oxidized core module” (OxCM), that includes essentially all of the secondary structural elements of bovine pancreatic trypsin inhibitor (BPTI) most refractory to hydrogen exchange, was shown previously to favor native-like  $\beta$ -sheet structure [1]. The present work prepares to explore the hypothesis that the energies of native-like conformations, relative to other possible conformations, could be decreased further by covalent linkage of two OxCMs. Such a design strategy is particularly suited for this system since the full-length protein, *i.e.*, BPTI, undergoes rapid association-dissociation to dimeric forms in solution [2,3]. Further, molecular modeling studies on dimeric BPTI indicate that the residues at the hydrophobic monomer-monomer interface are primarily in the OxCM [4].

The chemistry chosen to link two OxCMs is oxime-forming ligation [5]. The chosen dimerization chemistry accommodates changes in the position of the cross-link (Figures 1a, 1b) and variations in the length of the cross-link (Figures 1b–1f). Thus, six examples of OxCM dimers were synthesized. One-dimensional proton (1D <sup>1</sup>H) NMR was used as a qualitative criterion to gauge the extent of conformational families present in each OxCM dimer (Figure 1). Three dimers showed considerable chemical shift dispersion, and one of them is amenable for further structural characterization by multi-dimensional homo- and heteronuclear NMR methods.

### Results and Discussion

All dimers have Arg<sup>17</sup> replaced in monomer I, which contributes the (aminoxy)acetyl (Aoa or U) component of the oxime linkage. In one set of studies (Figures 1a, 1b), the “matching” residue replaced in monomer II, that would contribute the glyoxylyl (Gxy or J) functionality, was either Leu<sup>29</sup> or Asn<sup>24</sup>. NMR studies show that the dimer with the oxime linkage between residue 17 in monomer I and residue 24 in monomer II, *i.e.*, I<sub>R17K(U)</sub>–II<sub>N24K(J)</sub> (Figure 1a), has less chemical shift dispersion than the dimer with the oxime linkage between residue 17 in monomer I and residue 29 in monomer II, *i.e.*, I<sub>R17K(U)</sub>–II<sub>L29K(J)</sub> (Figure 1b). A further set of studies (Figures 1b–1f) kept constant the preferred cross-linkage site, but varied the cross-linking length from 10 to 22 atoms ( $\alpha$ -carbon of position 17 in monomer I to  $\alpha$ -carbon of position 29 in monomer II). Although intuition suggests that self-association between covalently joined monomers might be improved if they were closer, experiments proved otherwise. 1D <sup>1</sup>H NMR spectra of I<sub>R17Z(U)</sub>–II<sub>L29Z(J)</sub> (Figure 1c) and I<sub>R17Z(U)</sub>–II<sub>L29K(J)</sub> (Figure 1d) show broad linewidths and reduced chemical shift dispersion. 1D <sup>1</sup>H NMR spectra of I<sub>R17K(U)</sub>–II<sub>L29K(JG)</sub> (Figure 1e) and I<sub>R17K(UG)</sub>–II<sub>L29K(JG)</sub> (Figure 1f) show narrower linewidths and similar chemical shift dispersion, by comparison to I<sub>R17K(U)</sub>–II<sub>L29K(J)</sub>, demonstrating the advantages of a longer cross-link.

Although I<sub>R17K(U)</sub>–II<sub>L29K(J)</sub> was the first dimer that gave evidence of folded structure beyond that inherent in the OxCM monomer, further structural characterization was stymied by the fact that relatively few cross-peaks were observed in TOCSY spectra. The iterative development of dimers to date culminates with I<sub>R17K(UG)</sub>–II<sub>L29K(JG)</sub> (Figure 1f),

the TOCSY spectra of which show considerably more cross-peaks. Current structural characterization of  $I_{R17K(UG)}-II_{L29K(JG)}$  suggests that this molecule exists in a folded state at 1 °C, and is globally unfolded at 55 °C.

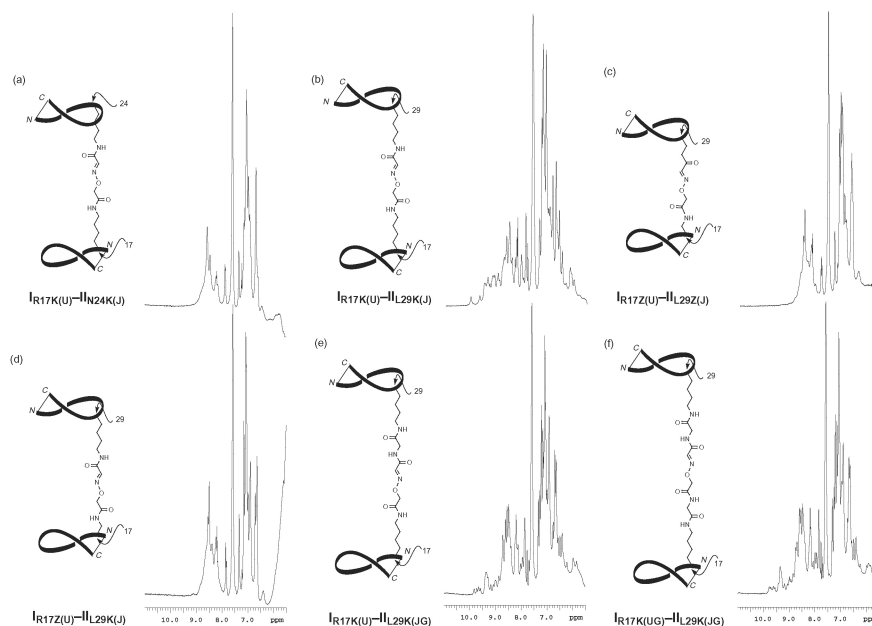


Fig. 1. Within each panel, the left side shows schematic representation of, and nomenclature system for, the six OxCM covalent dimers synthesized in this work, emphasizing (a, b) different positions of the cross-link and (b–f) different length cross-links between the monomers. Each solid bold ribbon depicts an OxCM, and the spanning disulfide bond between Mpa<sup>14</sup> and Cys<sup>38</sup> is indicated by the solid line connecting the N- and C-termini. Arrows indicate residue numbers that are connected; the type I monomer is drawn directly beneath the type II monomer in all representations. All atoms in the cross-links, starting with the  $\beta$ -carbons, are shown. The right side of each panel shows aromatic and amide regions of 1D <sup>1</sup>H NMR spectra at 600 MHz, obtained at pH 2 and 5 °C for the indicated OxCM dimers.

## Acknowledgments

Supported by the National Institutes of Health, Grant GM 51628 (G. B. and C. W.).

## References

1. Carulla, N., Woodward, C., Barany, G. *Biochemistry* **39**, 7927–7937 (2000).
2. Gallagher, W.H., Woodward, C.K. *Biopolymers* **28**, 2001–2024 (1989).
3. Ilyina, E., Roongta, V., Pan, H., Woodward, C., Mayo, K.H. *Biochemistry* **36**, 3383–3388 (1997).
4. Zielenkiewicz, P., Georgalis, Y., Saenger, W. *Biopolymers* **31**, 1347–1349 (1991).
5. Rose, K. *J. Am. Chem. Soc.* **116**, 30–33 (1994).

## Do Bioactive Peptides Display Native-Like Conformations When Bound to a Solid Support?

Alberto Bianco<sup>1</sup>, Julien Furrer<sup>2</sup>, Martial Piotto<sup>3</sup>, Maryse Bourdonneau<sup>3</sup>,  
David Limal<sup>4</sup>, Gilles Guichard<sup>1</sup>, Karim Elbayed<sup>2</sup>, Jésus Raya<sup>2</sup>  
and Jean-Paul Briand<sup>1</sup>

<sup>1</sup>*Institut de Biologie Moléculaire et Cellulaire, UPR 9021 CNRS, 67084 Strasbourg, France*

<sup>2</sup>*Institut de Chimie, UMR 7510 CNRS-Bruker, Université Louis Pasteur,  
67084 Strasbourg, France*

<sup>3</sup>*UMR 7510 CNRS-Bruker, 67160 Wissembourg, France*

<sup>4</sup>*Laboratoire de Chimie Macromoléculaire, ENSCMu, 68093 Mulhouse, France*

### Introduction

High-resolution magic angle spinning (HRMAS) NMR spectroscopy is a very promising technique in the field of solid phase organic chemistry for the analysis of resin-bound compounds, including small molecules and peptides [1,2]. We have successfully applied HRMAS NMR to the conformational study of bioactive peptides covalently attached to different resins [3]. The combination of the swelling and solvation properties of resin-bound peptides with the chemico-physical nature of the solid supports plays a fundamental role in the characterization of such conjugates by HRMAS technique. The secondary structure adopted by the sequence <sup>141</sup>GSGVVRGDFGSLAPRVARQL<sup>159</sup>, which delineates the major antigenic site of the viral protein VP1 of foot-and-mouth disease virus (FMDV), bound to three different types of resin, namely MBHA, PEGA and POEPOP, has been determined and compared with that of the same peptide free in solution.

### Results and Discussion

A series of homonuclear and heteronuclear 2D experiments was performed for the complete assignment of the peptide resonances and the qualitative characterization of the peptide folding. The identification of the 141-159 FMDV residues on the three different resins is shown in Figure 1 (the amino acids are numbered from 1 to 19).

The peptide analyzed in this study displays similar conformational behavior on the three different resins. POEPOP-bound FMDV epitope, swollen in DMF-*d*<sub>7</sub>, is able to fold into a regular helical structure, encompassing the C-terminal domain from residues 152 to 159. This conformation is very close to the secondary structure adopted by the free peptide in solution of 2,2,2-TFE [4]. The same helical folding also character-

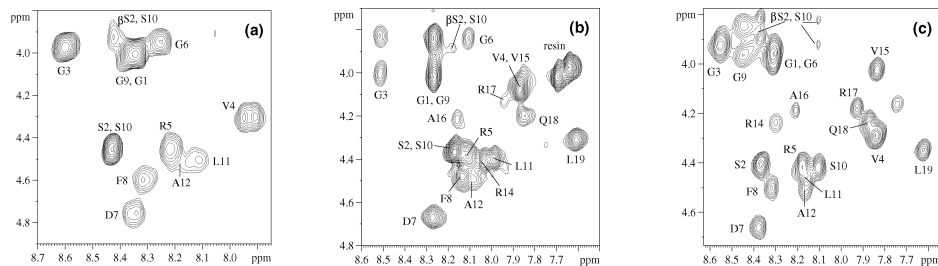


Fig. 1. Fingerprint region of the HRMAS TOCSY NMR spectra of 141-159 FMDV peptide bound to MBHA resin (a), PEGA resin (b) and POEPOP resin (c), swollen in DMF-*d*<sub>7</sub>.

izes part of the G-H loop in the crystal structure of the entire VP1 FMDV protein from different virus serotypes [5,6]. A change in the folding was observed when the peptide-POEPOP conjugate was swollen in aqueous solution. Similar conformational features were displayed by the free FMDV peptide previously studied in water [7]. For the MBHA-resin bound FMDV peptide swollen in deuterated dimethylformamide, the seven C-terminal residues could not be identified due to a strong lack of mobility ascribed to the interaction of this particular sequence, in a folded or unfolded structure, with the aromatic core of the resin. In the case of the PEGA-bound FMDV peptide, the NOES suggested only a propensity towards a folded helical structure.

This study clearly shows that a bioactive peptide bound to a solid support is able to fold into an ordered helical conformation. The possibility of studying ordered secondary and tertiary structures directly on the solid support by HRMAS can be extended to other biologically relevant peptides and proteins, and to new synthetic oligomers.

### Acknowledgments

This work was supported by a grant from EC (No. Fair 5-CT-3577).

### References

1. Bianco, A., Furrer, J., Limal, D., Guichard, G., Elbayed, K., Raya, J., Piotto, M., Briand, J.-P. *J. Comb. Chem.* **2**, 681–690 (2000).
2. Keifer, P.A. *Drug Discovery Today* **2**, 468–478 (1997).
3. Furrer, J., Piotto, M., Bourdonneau, M., Limal, D., Guichard, G., Elbayed, K., Raya, J., Briand, J.-P., Bianco, A. *J. Am. Chem. Soc.* **123**, 4130–4138 (2001).
4. Pegna, M., Molinari, H., Zetta, L., Melacini, G., Gibbons, W.A., Brown, F., Rowland, D., Chan, E., Mascagni, P. *J. Peptide Sci.* **2**, 91–105 (1996).
5. Logan, D., Abu-Ghazaleh, R., Blakemore, W., Curry, S., Jackson, T., King, A., Lea, S., Lewis, R., Newman, J., Parry, N., Rowlands, D.J., Stuart, D., Fry, E. *Nature* **362**, 566–568 (1993).
6. Hewat, E.A., Verdaguer, N., Fita, I., Blakemore, W., Brookes S., King A., Newman, J., Domingo, E., Mateu, M.G., Stuart, D.I. *EMBO J.* **16**, 1492–1500 (1997).
7. Petit, M.-C., Benkirane, N., Guichard, G., Phan Chan Du, A., Marraud, M., Cung, M. T., Briand, J.-P., Muller, S. *J. Biol. Chem.* **274**, 3686–3692 (1999).

## Direct Observation of Backbone Hydrogen Bonding in the Folding Transition of Chymotrypsin Inhibitor 2 (CI2)

Gangamani S. Beligere<sup>1</sup>, Radha Plachikkat<sup>2</sup> and Philip E. Dawson<sup>1</sup>

<sup>1</sup>Department of Cell Biology and <sup>2</sup>Department of Molecular Biology  
 The Scripps Research Institute, La Jolla, CA 92037, USA

### Introduction

Protein folding is a complex process in which a polypeptide chain is converted to a native structure by multiple non-covalent interactions [1]. The role of side chains in the process of folding is determined by thermodynamic and kinetic analysis using site directed mutagenesis. An intriguing question in protein folding is how the secondary structure is formed during the folding process, and its relationship to the formation of tertiary interactions. In the case of small single domain proteins such as Chymotrypsin Inhibitor 2 (CI2), it has been established through site directed mutagenesis and kinetic analysis [2], that both secondary structure and tertiary interactions are present in the transition state ensemble. Since the side chain modifications only indirectly probes secondary structure, the objective of this work is to directly alter the peptide backbone using ester by incorporating  $\alpha$ -hydroxy acids into the protein.

### Results and Discussion

CI2 and its ester analogues were synthesized using solid phase peptide synthesis combined with ligation [3]. During the chain assembly, four  $\alpha$ -hydroxy acids were incorporated: (*S*)-lactic acid (at residues 16 and 22) and (*S*)-2-hydroxyisovaleric acid (at residues 13 and 19). The amide couplings were carried out using standard *in situ* neutralization cycles for Boc SPPS using HBTU/DIEA. The hydroxy acids were coupled using DIC/HOBt/NME without hydroxyl protection and ester bonds were formed using DIC/DMAPI in CH<sub>2</sub>Cl<sub>2</sub> [4]. The resulting ester containing CI2(1-39)-COSY peptide was purified by HPLC in good recovered yield (30–35%). The full-length CI2 polypeptide was assembled by conformationally-assisted ligation of the ester

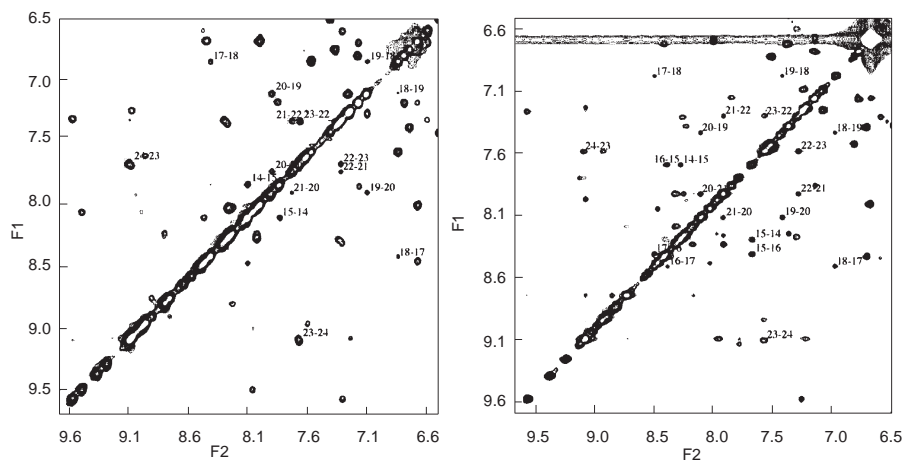


Fig. 1. 2D-NOESY where in the NH–NH(*i*, *i*+1) connectivities in the  $\alpha$ -helix region of the protein are labeled.

CI2(1-39)-COSY peptide with a peptide corresponding to CI2(40-64). This strategy takes advantage of the observation that CI2 fragments self-associate to form a native-like tertiary structure.

An ester in the middle of the helix perturbs two hydrogen bond but still maintains the conformation preferences of the helix. This is shown in Figure 1 where the NH–NH (i, i+1) connectivity of the helix is observed. The 15-16 and 16-17 are missing as expected but all other cross-peaks are present, this suggests that the  $\alpha$ -helix is intact.

The thermodynamic stabilities of the ester containing proteins were determined by guanidium hydrochloride induced denaturation studies using tryptophan fluorescence. Introduction of ester in the middle of the helix destabilises the protein by 2 kcal/mol. At the terminal it is 0.5–1 kcal/mol in case of CI2 analogues. Kinetics of folding was analyzed by following the rate of folding and unfolding as a function of time at different denaturation concentrations. The ester substituted analogues are destabilized due to decreased folding rates implying high energetic contribution to folding rates compared to the unfolding rates.

These studies suggests that the backbone H-bonds of the entire helix are partially formed in the transition state for CI2 refolding.

### **Acknowledgments**

We thank Jeff Kelly and Xin Jiang for assistance use of stopped flow spectrofluorometer. This work was supported by grant the Sloan Foundation, Skaggs Institute of Chemical Biology and NIH GM 59380.

### **References**

1. Dobson, C.M., Sali, A., Karplus, M. *Angew. Chem., Int. Ed.* **37**, 868–893 (1999).
2. Itzhaki, L.S., Otzen, D.E., Fersht, A.R. *J. Mol. Biol.* **254**, 260–288 (1995).
3. Beligere, G.S., Dawson, P.E. *J. Am. Chem. Soc.* **121**, 6332–6333 (1999).
4. Bramson, H.N., Thomas, N.E., Kaiser, E.T. *J. Biol. Chem.* **260**, 15452–15457 (1985).

## Optimizing Aqueous Fold Stability for Short Polypeptides: 20 Residue Miniprotein Constructs That Melt as High as at 61 °C

Niels H. Andersen, Bipasha Barua, R. Matthew Fesinmeyer  
 and Jonathan Neidigh

*Department of Chemistry, University of Washington, Seattle, WA 98195, USA*

### Introduction

There has been significant research activity directed at designing peptide sequences that are short but still display the folding cooperativity of proteins and the development of spectroscopic methods for assessing cooperativity [1]. Miniproteins as small 26-residues [2] and  $\beta$ -hairpin sequences that are relatively well-folded [3,4] have been reported. There was even a report of a 20 residue  $\beta$ -sheet, betanova [5]. Subsequent studies [6] indicate that betanova is less than 10% folded in water. As a result we adopted the production of 20 residue systems that are folded in water as a goal in our effort to define the features required for miniprotein stability. We have previously reported [7] that truncation and mutation of a sequence found in exendin-4 (a 39-residue peptide from Gila monster saliva) resulted in soluble 20-mer miniproteins that are fully (>90%) folded in water. Herein, we present the experiments that define the features required for fold stability and the extent of folding cooperativity displayed by these systems.

### Results and Discussion

The NMR structure ensemble derived for exendin-4 in 30 vol.% TFE/water [8] suggested that the burial of the indole ring of Trp in a cage comprised of prolines, a leucine and a phenyl ring was the key feature of the fold, which we have designated as the Trp-cage motif [7]. The first 20-mer produced (mini-**3a**) was nearly as well-folded in 30% TFE displaying extreme upfield ring current shifts (for examples, see Table 2) for the  $\alpha$  protons of Leu<sup>7</sup>, Gly<sup>11</sup>, and Pro<sup>18</sup>, the  $\delta$  protons of Pro<sup>19</sup> and also the  $\beta$ 3 and  $\gamma$ 3 protons of Pro<sup>18</sup>. Based on the diminished chemical shift deviations observed, mini-**3a** is only 38% folded in water even at 8 °C. The serial improvements in the folding of the Trp-cage motif are given in Table 1.

Mini-**10b** has a more stable tertiary structure than any native or designed polypeptide sequence of  $\leq 40$  residue length. The factors that contributed are discussed below.

*Table 1. Properties of Trp-cage motif peptides.*

Mini #	Sequence	% folded <sup>a</sup>	T <sub>m</sub> (at pH 7), °C
<b>3a</b>	NLFIEWLKNGGPSSGAPPPS	38	
<b>5a</b>	NLFIQWLKDGGPSSGRPPPS	94	31
<b>5b</b>	NLYIQWLKDGGPSSGRPPPS	98.5	43.5
<b>8a</b>	NLYAQWLKDGGPSSGRPPPS	99	49
<b>8b</b>	DLYAQWLKDGGPSSGRPPPS	99 +	55
<b>10b</b>	DAYAQLKDGGPSSGRPPPS	99.74	61

<sup>a</sup> The percent folded estimates are from NMR shifts except for those in excess of 90%, which are based on NH exchange protection.

## Analytical Methods

Titration reveals that a D9/R16 “salt bridge” provides *ca* 1.5 kcal of fold stabilization (for example, the  $T_m$  of mini-**8a** drops to 30 °C at pH 2.5). This feature was introduced at the stage of mini-**5a**. The importance of the Trp residue sidechain to fold stability was assessed by preparing mutants of mini-**5b** with the Trp replaced by His, Phe and both regioisomers of naphthylalanine. For the His and Phe mutants, the folded population drops below 10% in water (see Figure 1). However, a naphthalene ring can replace the indole ring with only a modest loss in folding. The most important hydrophobic interactions are between the Y3/W6 sidechains and P18/P19 rings.

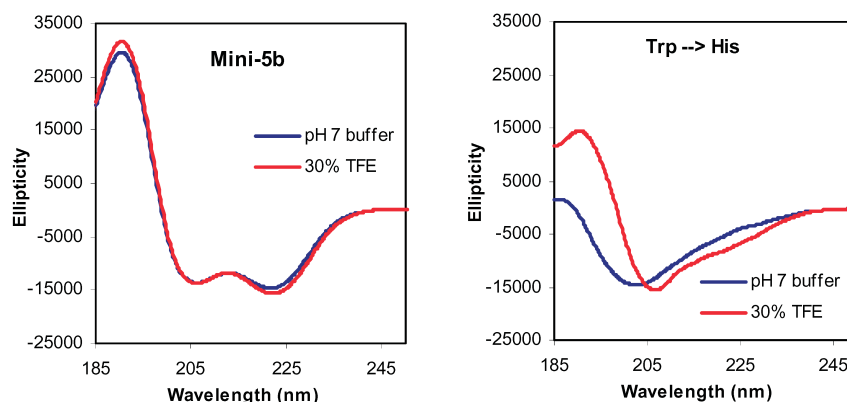


Fig. 1. CD comparison of mini-**5b** (left panel) and its W6H mutant (right panel); in each panel the CD spectra observed in pH 7 aqueous buffer and in 30% TFE are shown.

We attribute most of the additional stabilization obtained beyond the mini-**5b** stage to the reduction of the entropic advantage of unfolding – the L2A and I4A mutations are examples. Efforts to improve water solubility of Trp-fold peptides by replacing the solvent exposed proline (P17) with polar residues provided another example of  $\Delta S_U$  effects and also revealed residual structural features in the unfolded state ensemble. Some the systems examined in this context appear below.

Mini- <b>1b</b>	SEDEAV	RLFIEWLKNGGPSSGAPPPSNH <sub>2</sub>
Mini- <b>1c</b>	SEDEAV	RLFIEWLKNGGPSSGADPPS
Mini- <b>1d</b>	SEDEAV	RLFIEWLKNGGPSSGAD
Mini- <b>11</b>		DLYAQWLKDGGPSK

The clearest evidence for folding and structure (*e.g.*, the extent of Trp-cage formation, the fractional helicity, and any residual ring current effects in the unfolded state ensemble) comes from chemical shift deviations (CSDs). Trp-cage formation can be monitored by the upfield displacement of P18 and P19 resonances, of which P18 $\alpha$  has been selected for this account. Other resonances which display notable upfield shifts are also included in Table 1. Mini-**10b** is used as the representative of the fully folded Trp-cage. Mini-**1d** serves as a model system for complete helix formation (from the N-terminus to K8) with no possibility of cage formation, since the P18/P19 unit that docks onto the aromatic rings is absent. The CSDs for P18 $\alpha$  indicate that the P17D mutation (**1b** versus **1c**) reduces the Trp-cage population from 0.81 to 0.51 in 30% TFE and from 0.43 to 0.21 in water. This reduction in folding is attributed to the greater backbone entropy of Asp relative to Pro in the unfolded state.

The other intriguing feature in Table 2 is the observation that Pro1283 and Gly11 $\alpha$ 2 actually move upfield in the mutants that display reduced Trp-cage populations. This is also observed during thermal melts of mini-**5b**, -**8a** and -**10b**. Apparently, Pro1283 is, on average, more deeply in the shielding cone of the indole ring in the unfolded state ensemble. Our current model of the transition appears in Figure 2.

Table 2. CSDs of selected miniproteins and models in 30% TFE and water. All shifts are up-field from the random coil values and are given in ppm.

<i>in 30% TFE</i>	Mini- <b>10b</b>	Mini- <b>1b</b>	Mini- <b>1c</b>	Mini- <b>1d</b>	Mini- <b>11</b>
Pro18 $\alpha$	2.26	1.82	1.12	n.a.	n.a.
Gly11 $\alpha$ 2	3.55	3.02	2.44	1.74	1.04
Gly11 $\alpha$ 3	1.09	1.44	1.37	1.21	0.93
Pro1283	0.30	0.69	0.87	0.84	0.72
<i>In water</i>					
Pro-18 $\alpha$	2.29	0.98	0.48	n.a.	n.a.
Gly11 $\alpha$ 2	3.50	1.65	1.36	1.08	0.33
Gly11 $\alpha$ 3	0.97	0.95	0.87	0.79	0.22
Pro1283	0.22	0.72	0.77	0.73	0.33

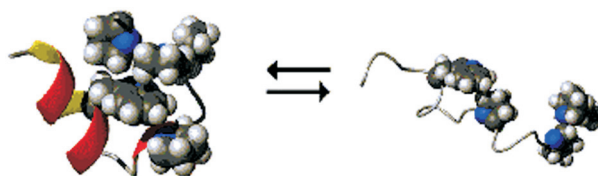


Fig. 2. Model of the folding transition.

## Acknowledgments

This research was supported by grant GM59658 from the National Institutes of Health.

## References

1. Andersen, N.H., Neidigh, J.W., Harris, S.M., Chen, C., Lee, G.M., Liu, Z., Tong, H. *J. Am. Chem. Soc.* **119**, 8547–8561 (1997).
2. Dahiyat, B.I., Mayo, S.L. *Science* **278**, 82–87 (1997).
3. Maynard, A.J., Sharman, G.J., Searle, M.S. *J. Am. Chem. Soc.* **120**, 1996–2007 (1998).
4. Andersen, N.H., Dyer, R.B., Fesinmeyer, R.M., Gai, F., Liu, Z., Neidigh, J.W., Tong, H. *J. Am. Chem. Soc.* **121**, 9879–9880 (1999).
5. Kortemme, T., Ramírez-Alvarado, M., Serrano, L. *Science* **281**, 253–256 (1998).
6. López de la Paz, M., Lacroix, E., Ramírez-Alvarado, M., Serrano, L. *J. Mol. Biol.* **312**, 229–246 (2001).
7. Andersen, N.H., Fesinmeyer, R.M., Neidigh, J.W., Barua, B., In Martinez J. and Fehrentz, J-A. (Eds.) *Peptides 2000 (Proceedings of the 26th European Peptide Symposium)*, EDK, Paris, 2001, p. 45–46.
8. Neidigh, J.W., Fesinmeyer, R.M., Prickett, K.S., Andersen, N.H. *Biochemistry* **40**, 13188–13200 (2001).

## Synthetic Approach to Study the Effects of $\beta$ -Turn Residues on the Structure and Folding of Bovine Pancreatic Trypsin Inhibitor (BPTI)

Judit Tulla<sup>1</sup>, Clare Woodward<sup>2</sup> and George Barany<sup>1</sup>

<sup>1</sup>Department of Chemistry, University of Minnesota, Minneapolis, Minnesota, 55455, USA

<sup>2</sup>Department of Biochemistry, Molecular Biology, and Biophysics, University of Minnesota,  
St. Paul, Minnesota, 55108, USA

### Introduction

Previous work from our laboratory has established a system for accessing partially folded conformational ensembles of bovine pancreatic trypsin inhibitor (BPTI), based on the replacement of Cys 5, 30, 51, and 55 by  $\alpha$ -amino-*n*-butyric acid (Abu), while retaining the disulfide between Cys 14 and 38 [1]. Several observations in the aforementioned  $[14-38]_{\text{Abu}}$  system suggest that the type I  $\beta$ -turn ( $A^{25}K^{26}A^{27}G^{28}$ ) connecting the two core strands of the antiparallel  $\beta$ -sheet (residues 18-24 and 29-35) is the main site for initiation of folding of BPTI [2]. For the present work, two analogues of  $[14-38]_{\text{Abu}}$  have been synthesized in which turn residues at positions 26, 27, and 28 were altered to maximize amino acid positional potentials for  $\beta$ -turns [3]. One analogue,  $P^{26},D^{27}[14-38]_{\text{Abu}}$ , has at three positions (including the natural G28) residues with the highest potential for a type I  $\beta$ -turn. In a second analogue,  $N^{26},G^{27},K^{28}[14-38]_{\text{Abu}}$ , residues with the highest potential for a type I'  $\beta$ -turn have been introduced. Type I'  $\beta$ -turns are most common for  $\beta$ -hairpins [4].

### Results and Discussion

The CD spectrum in the far UV for  $[14-38]_{\text{Abu}}$  shows a negative ellipticity at 220 nm that arises from secondary structure, and a strong minimum around 202 nm characteristic for BPTI and attributed to tertiary contacts of aromatic groups (Figure 1). Both synthesized analogues show loss of negative ellipticity at 220 nm, consistent with more unfolded states. However, the analogue  $P^{26},D^{27}[14-38]_{\text{Abu}}$  shows increased negative ellipticity at 220 nm, indicative of non-random structure, with respect to  $[R]_{\text{Abu}}$ , a known unfolded state where all six Cys are replaced by Abu [5].

The CD spectrum in the near UV of analogue  $P^{26},D^{27}[14-38]_{\text{Abu}}$  shows the same overall shape as  $[14-38]_{\text{Abu}}$ , but with a reduced signal at 277 nm indicating that approximately 75% of the tertiary structure is lost. Analogue  $N^{26},G^{27},K^{28}[14-38]_{\text{Abu}}$  also

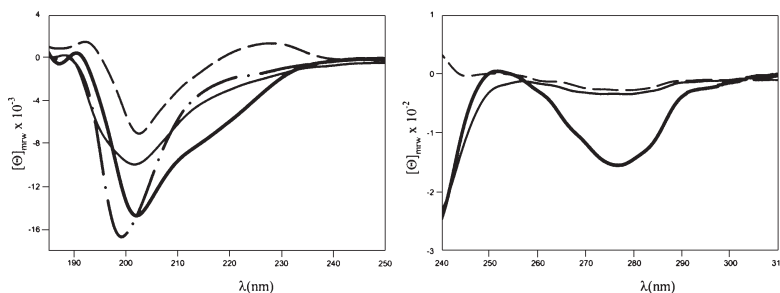


Fig. 1. Far and near UV CD of  $[14-38]_{\text{Abu}}$  (thick solid line),  $P^{26},D^{27}[14-38]_{\text{Abu}}$  (thin solid line),  $N^{26},G^{27},K^{28}[14-38]_{\text{Abu}}$  (dashed line), and  $[R]_{\text{Abu}}$  (dash-dotted line).

shows less tertiary structure than the parent protein, but the different shape suggests that any structure in the analogue is non-native.

One-dimensional  $^1\text{H}$  NMR spectra of  $[14-38]_{\text{Abu}}$  at pH 4.6 and 1  $^{\circ}\text{C}$  contain resolved downfield resonances which are characteristic of native BPTI (Figure 2). Analogue  $\text{P}^{26},\text{D}^{27}[14-38]_{\text{Abu}}$  shows the same native downfield resonances, but they are less intense suggesting that there is a greater population of unfolded conformations. On the other hand, analogue  $\text{N}^{26},\text{G}^{27},\text{K}^{28}[14-38]_{\text{Abu}}$  does not show any downfield resonances, consistent with a more unfolded and non-native like conformation.

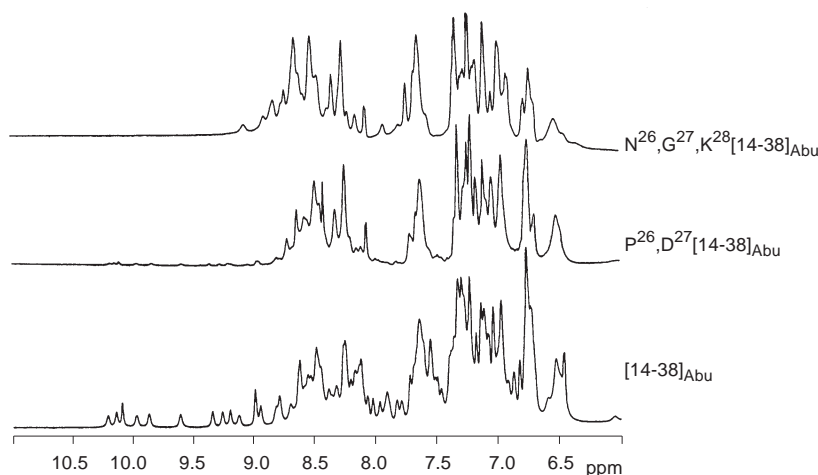


Fig. 2.  $^1\text{H}$  NMR spectra at pH 4.6 and 1  $^{\circ}\text{C}$ .

Results presented here suggest that under conditions where  $[14-38]_{\text{Abu}}$  retains the native core, the attempted stabilization of the type I  $\beta$ -turn results in a smaller population of partially folded conformations than in the parent protein. The analogue designed using rules to promote a type I'  $\beta$ -turn results in loss of detectable native-like structure.

#### Acknowledgments

We thank Natalia Carulla for helpful discussions, and NIH grant GM 51628 (G. B. and C. W.) for support.

#### References

1. Ferrer, M., Barany, G., Woodward, C. *Nat. Struct. Biol.* **2**, 211–217 (1995).
2. Barbar, E., Barany, G., Woodward, C. *Biochemistry* **34**, 11423–11434 (1995).
3. Hutchinson, E.G., Thornton, J.M. *Protein Sci.* **3**, 2207–2216 (1994).
4. Chou, P.Y., Fasman, G.D. *J. Mol. Biol.* **115**, 135–175 (1977).
5. Pan, H., Barbar, E., Barany, G., Woodward, C. *Biochemistry* **34**, 13974–13981 (1995).

## **NMR Solution Structure of B-Motif, a Signature Motif of Type-B Response Regulators for His-to-Asp Phosphorelay Signal Transduction System, and Its Interactions with DNA**

**Kazuo Hosoda<sup>1</sup>, Etsuko Katoh<sup>1</sup>, Tomohisa Hatta<sup>1</sup>, Takeshi Mizuno<sup>2</sup>  
and Toshimasa Yamazaki<sup>1</sup>**

<sup>1</sup>*Department of Biochemistry, National Institute of Agrobiological Sciences, 2-1-2 Kannondai, Tsukuba, Ibaraki 305-8602, Japan*

<sup>2</sup>*Laboratory of Molecular Microbiology, School of Agriculture, Nagoya University, Chigusa-ku, Nagoya 464-8601, Japan*

### **Introduction**

His-to-Asp phosphorelay mechanisms are evolutionary-conserved powerful biological tactics for intracellular signal transduction. Such a phosphorelay is generally made up of “sensor histidine kinase”, “response regulator” and “histidine-containing transmitter”. In higher plant, *Arabidopsis thaliana*, the same mechanism is involved in propagation of environmental stimuli. Recent studies have revealed that this higher plant has, at least, 20 members of the family of response regulators that can be classified into two distinct subtypes (type-A and type-B) [1]. Type-B regulators have a common motif (B-motif) consisting of *ca* 60–70 amino acids in their C-terminal extensions after the receiver domain. The B-motif shows a weak, limited similarity in primary sequence to Myb-related domains found in various transcription factors, but its precise function has not been yet identified. Here we present the three-dimensional solution structure of B-motif determined by NMR spectroscopy. Comparison of the structure with other proteins which have known biological functions suggests that B-motif functions by binding to a DNA target. We have experimentally confirmed our structure-based hypothesis, and have identified a target DNA sequence. In addition, we have identified DNA-binding sites of B-motif by analyzing NMR chemical shift changes upon complex formation with the target DNA.

### **Results and Discussion**

Sequence-specific resonance assignments of B-motif, a conserved signature sequence of the family of type-B response regulators in *Arabidopsis thaliana*, were achieved according to the conventional NMR method. NMR solution structures of this motif were calculated using the hybrid distance geometry-dynamical simulated annealing method as contained in X-PLOR 3.1. B-Motif assumes a three-helical structure containing a helix-turn-helix (HTH) motif, which is one of the fundamental DNA-recognition units observed in many DNA-binding proteins such as protooncogene product (c-Myb) [2], telomeric repeat-binding factor, and engrailed homeodomain (ENG) [3] (Figure 1). B-motif has a positively charged surface around the HTH motif as observed in these DNA-binding proteins.

B-motif displays the highest similarity to ENG in two aspects, (a) the length of  $\alpha$ 3-helix and (b) existence of the basic residue rich N-terminal region before  $\alpha$ 1-helix. Although homology in the primary sequence between B-motif and ENG is only 15%, most of the identical amino acid residues are observed in  $\alpha$ 3-helix and the N-terminal region. Interestingly, ENG binds to its target DNA as a monomer using these two regions. The  $\alpha$ 3-helix binds in the major groove of DNA and provides sequence specific interactions with DNA bases. The N-terminal flexible arm binds in the minor groove

on the opposite side of the DNA molecule and makes nonspecific interactions with DNA phosphate groups.

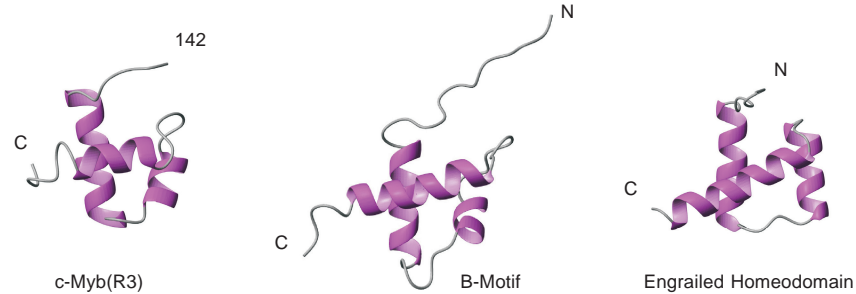


Fig. 1. Comparison of the free B-motif with the DNA-bound forms of engrailed homeodomain (ENG) and c-Myb R3-repeat.

Based upon these findings, we have proposed a structure-based hypothesis that B-motif serves as a nuclear-localizing DNA-binding domain (so-called the output domain), and experimentally confirmed that this motif binds to a DNA target whose core consensus sequence is most likely AGATT.

The DNA-binding sites of B-motif in solution were identified by analyzing NMR chemical shift perturbation upon complex formation with 12bp DNA, GCAAGATTCGGC. Examination of chemical shift changes in the course of titration with DNA revealed that the stoichiometry of the B-motif/DNA complex is 1 : 1. Large chemical shift changes occurred mainly in  $\alpha$ 3-helix and the N-terminal region when B-motif was titrated into DNA. Taking these results into consideration, we have built a model of the B-motif/DNA complex, showing similar binding mode as the ENG/DNA complex. In order to understand binding mechanisms of B-motif to DNA more precisely, we are currently determining the three-dimensional solution structure of the B-motif/DNA complex.

#### Acknowledgments

This work was supported by a grant from the Biooriented Technology Research Advancement Institution, Japan to T. Y.

#### References

1. Imamura, A., Hanaki, N., Nakamura, A., Suzuki, T., Taniguchi, M., Kiba, T., Ueguchi, C., Sugiyama, T., Mizuno, T. *Plant Cell Physiol.* **40**, 733–742 (1999).
2. Ogata K., Morikawa S., Nakamura, H., Sekikawa, A., Inoue, T., Kanai, H., Sarai, A., Ishii, S., Nishimura, Y. *Cell* **79**, 639–648 (1994).
3. Kissinger, C.R., Liu, B., Martin-Blanco, E., Kornberg, T.B., Pabo, C.O. *Cell* **63**, 579–590 (1990).

## Synthesis and Characterization of the Pain-Killing Peptide *Grammostola spatulata* Analgesic Factor (GsAF-1) Containing Three Disulfide Bonds

Rong-qiang Liu<sup>1</sup>, Robert T. Jacobs<sup>2</sup>, Russell C. Spreen<sup>2</sup>  
and George Barany<sup>1</sup>

<sup>1</sup>Department of Chemistry, University of Minnesota, Minneapolis, MN 55455, USA

<sup>2</sup>AstraZeneca Pharmaceuticals LP, Wilmington, DE 19850, USA

### Introduction

Recent work at AstraZeneca resulted in the discovery of novel pain-killing peptides from the venom of the Chilean pink tarantula [1–3]. These peptides, designated *Grammostola spatulata* analgesic factors (GsAF), were found effective in a variety of animal models of moderate-to-severe pain. They were also found to exhibit activity in models of neuropathic pain, and as such represent a potentially interesting approach to the amelioration of pain associated with cancer and the post-operative surgical period.

The limited supply of GsAF peptides from the natural spider venom source makes evident a need for synthetic materials for further biological study. A synthetic approach would also facilitate labeling which could allow identification of the biological target(s) of these peptides, as well as systematic analogue work to define structure-activity relationships. Reported herein is an efficient synthesis of the linear GsAF-1 peptide, along with initial results aimed at reproducing the natural folded array of three disulfide bonds.

### Results and Discussion

A combination of amino acid analysis, enzymatic cleavage, and mass spectroscopic studies permitted determination of the primary amino acid sequence of the GsAF peptides. Additional reduction/thiol labeling techniques supported the disulfide bond connectivity depicted in Figure 1. Structures were further supported by extensive NMR experiments.

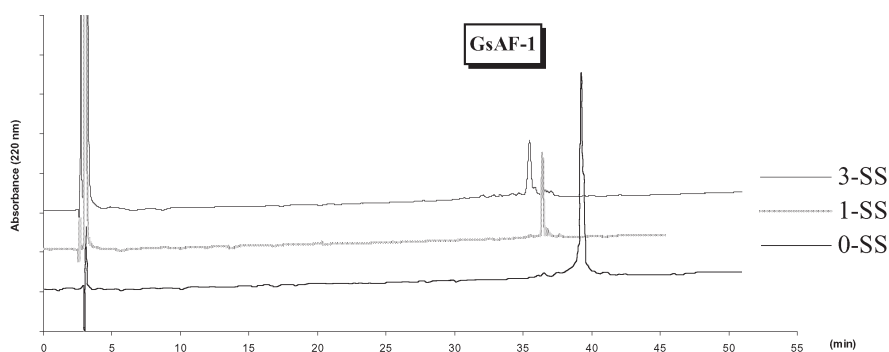
Assembly of the GsAF-1 primary sequence was performed using automated Fmoc solid-phase synthesis chemistry starting with a PAL-PEG-PS resin (0.7 g, 0.15 mmol/g). Side-chain protecting groups included Boc for Lys and Trp, *t*Bu for Asp, Glu, Ser, Thr, and Tyr, Pbf for Arg, and Trt, Mmt, Xan, and/or Acn for Cys. Initial work with HBTU/HOBt/DIEA in DMF for 30 min coupling cycles gave highly heterogeneous crude products. Substantially better initial purities and yields were obtained when the coupling protocol was switched to HATU/HOAt/DIEA in DMF for 2 h. Linear peptides were released from the support (1.3 g) by treatment with TFA–PhOH–H<sub>2</sub>O–thioanisole–EDT (82.5 : 5 : 5 : 5 : 2.5) (Reagent K) for 1.5 h (95% cleavage yield) and purified by careful semi-preparative reversed-phased HPLC (≈35% isolated, purified yield).



Fig. 1. Amino acid sequence and disulfide bond connectivity of GsAF-1.

In order to establish the fully folded structure of GsAF-1 from linear precursors, several strategies were explored as dictated by the initial combination of Cys protecting groups. The purified linear GsAF-1 with six free thiols, when treated with 10% DMSO at pH 7, gave only intractable oligomers and polymers. Similar poor results were obtained upon attempted DMSO oxidation of a GsAF-1 precursor with four free thiols (corresponding to Cys at positions 2, 15, 16, and 25) and two Cys(Acm) (at positions 9 and 21).

The most promising strategy (Figure 2) devised to date was a two-step oxidation procedure applied to a GsAF-1 linear precursor with two free Cys (at position 9 and 21; originally protected by Trt) and four Cys(Acm) (at positions 2, 15, 16, and 25). The first disulfide bridge formed rather cleanly (>80%) by DMSO treatment at pH 7, or upon aeration of an aqueous solution. In the former case, the peptide was purified by HPLC; in the later case, the peptide was lyophilized directly. Next, the peptide was dissolved (at 1.0 mg/mL) in HOAc–H<sub>2</sub>O (1 : 1), and I<sub>2</sub> (10 eq. based on Acm groups) was added for 0.5 h at 0 °C to form the remaining disulfide (≈60% conversion starting material to product). At 25 °C, starting peptide was consumed in the I<sub>2</sub> step, but desired product did not form.



*Fig. 2. Analytical C-18 reversed-phase HPLC monitoring of three stages of preferred GsAF-1 synthesis described in above paragraph. Each material shown was purified by semi-preparative HPLC, and gave the correct molecular weight by LC-MS.*

In conclusion, we have optimized an efficient Fmoc solid-phase protocol to synthesize linear GsAF-1, which includes sensitive residues such as Trp and Met. Carefully optimized oxidation conditions, associated with an appropriate cysteine protection strategy, gave a pure GsAF sample.

## References

1. Lampe, R.A., Sachs, F., US Patent 5,756,663, May 26, 1998.
2. Lampe, R.A. US Patent 5,776,896, July 7, 1998.
3. Lampe, R.A. US Patent 5,807,821, Sept. 15, 1998.

## Molecular Modeling: Indispensable Tool at the Interface Between Structural Analysis and Molecular Design

Christian Lehmann

University of Lausanne, Institute of Organic Chemistry, BCH-Dorigny, CH-1015 Lausanne, Switzerland

### Introduction

As exemplified by last centuries milestone rationalization of particular peptidic and nucleic acid biomolecular fibre diffraction patterns through their helical conformation models [1], the interpretation of structural data has always stood at the onset of any molecular modeling endeavor. Ever since structural information encompassing low molecular weight peptides [2] as well as macromolecular protein structures [3] has been rapidly growing, computer-assisted tools for structure analysis, comparison and design will become more and more important. The present communication features results obtained with a recently introduced software suite [4] based on a united atom force field approach originally developed for structure modeling in medicinal chemistry [5].

### Results and Discussion

The force-field equation applied and parametrized for a large number of low-molecular weight compounds (for details *cf.* [5]) uses standard harmonical energy expressions for bond  $E_b$  and valence  $E_v$  energies, alternating dihedral angular energy terms  $E_d$  taking into account rotation about single bonds, quadratic pyramidal energy restoration terms  $E_p$ , modulation of the dihedral energy term by a 1–4 non-bonding interaction expression  $E_{14}$  reflecting gauche/trans effects, followed by non-bonding longer-distance interaction  $E_{1n}$  as well as directed hydrogen bonding potential energy terms  $E_{hb}$ . Minimization in the force field of the exemplary GCN4 X-ray structure [6], which contains in the same complex both peptidic and nucleic acid domains (*cf.* Figure 1), results in a superimposable energy minimum structure with RMSD of the  $C_\alpha$  and  $C1'$  centers of 1.72 Å, a value which lies within the resolution band of the X-ray structure (resolved at 2.90 Å, *cf.* [6]).

$$\begin{aligned}
 E_{\text{MAB}} = & E_b + E_v + E_d + E_p + E_{14} + E_{1n} + E_{hb} = \\
 & \sum A_{bi}(\mathbf{b}_i - \mathbf{b}_{0i})^2 + \sum A_{vi}(\mathbf{v}_i - \mathbf{v}_{0i})^2 \\
 & + 1/2 \sum \sum D_{ki}[\cos(\mathbf{m}_{ki}\phi_i - \phi_{ki}) - 1] \\
 & + \sum A_{pi}p_i^2 + A_{14} \sum [\mathbf{R}(\mathbf{r}_p)]^4 \\
 & + 1/7 \sum e_{m,ij} \{[\mathbf{R}(\mathbf{r}_{ij})]^{16} - 8[\mathbf{R}(\mathbf{r}_{ij})]^2\} \\
 & + A_h \mathbf{B}_r(\mathbf{r}) \Theta_d(\mathbf{r}_-) \Theta_a(\mathbf{r})
 \end{aligned}$$

Extensive conformational analysis of homo- as well as heterochiral cyclodecapeptides of the type described in Figure 2 leads to the conclusion that the stereochemical laws which determine low molecular weight peptide structures are the same as the ones observed in high molecular weight proteins. As minimum energy structural types in the force field were identified backbone folds resembling the one of the natural cyclodecapeptide paradigm gramicidin S [7] for heterochiral template substrates spanned by type II' mirror image turns (termed "GrS\_like"), however, for homochiral ("GrS\_unlike") type II cyclodecapeptides, subtle energy differences within the

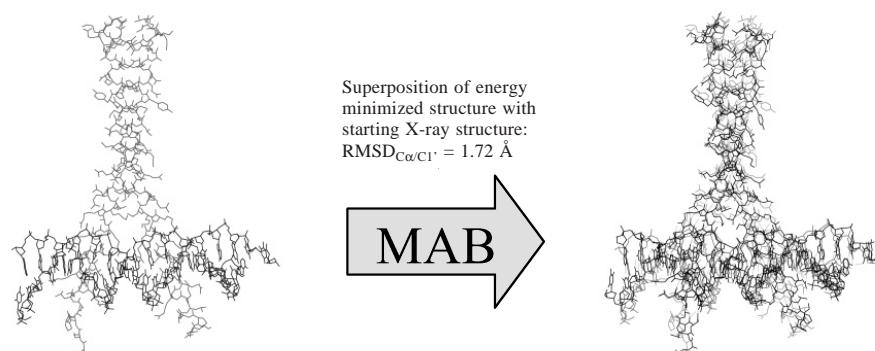


Fig. 1. Energy minimization of the GCN4 protein-DNA complex in the MAB force field.

*L*-peptidic framework result in ambiguously determined backbone conformations, the antiparallel  $\beta$ -sheet being of a metastable nature [9]. The two backbone types have been described now with redundant data sets both in solution as well as in the crystalline state (*cf.* [10] and references cited therein).

In extension of these conformational analysis results an energy minimized complex of the in Figure 3 depicted  $\beta$ -sheet transcription factor/DNA complex maintains its characteristic GrS\_like left-handed twist in complete congruence with the conformation required for adjustment to the DNA major groove curvature – a feature which is in close agreement with preliminary spectroscopical data observed in this series [12]. The presented examples show the value of our force-field approach for small as well as large molecules – correctly reflecting their conformation within a macromolecular complex or as adopted intrinsically by the stereochemical properties of the substrate molecules themselves.

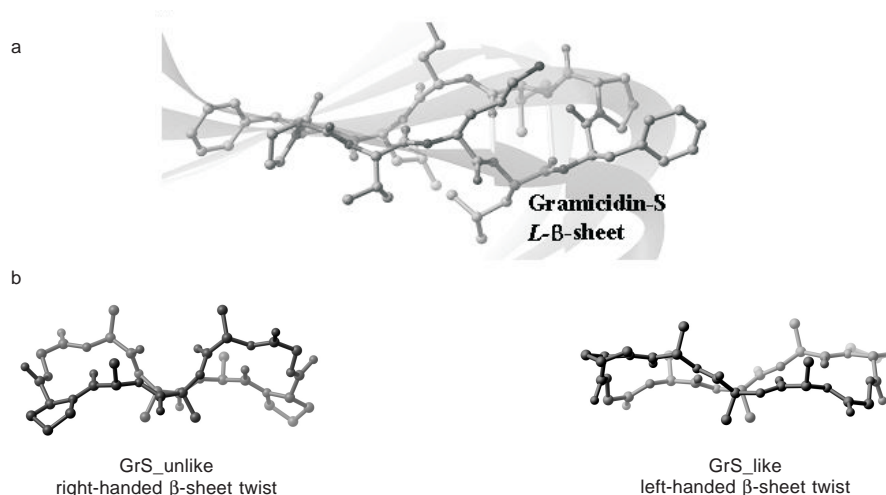


Fig. 2. a) GrS\_like *L*- $\beta$ -sheet twist as exemplified by superposition of Gramicidin S [7] unto the ribbon-trace of the  $\beta$ -sheet multidomain protein TRAP [8]; b) homochiral *c*(PGAAA)<sub>2</sub> GrS\_unlike and heterochiral *c*(PGAAA)<sub>2</sub> GrS\_like  $\beta$ -sheet backbone templates energy minimized in the MAB force field (the models were rendered using the “Ribbons” program [13]).

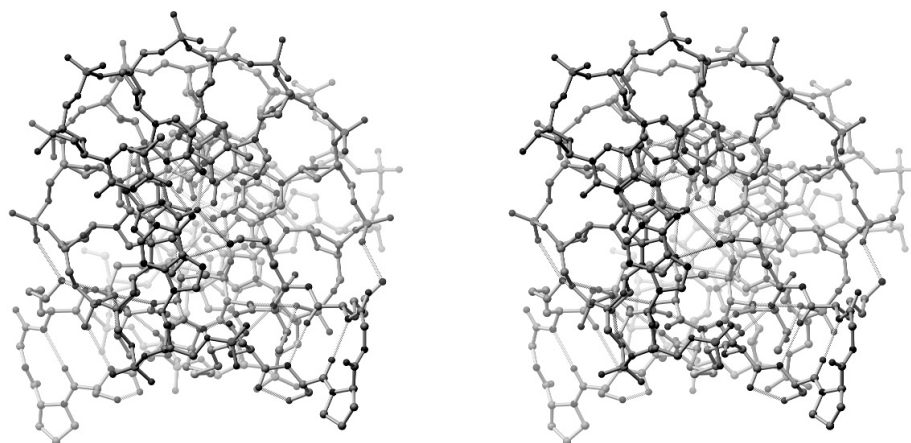


Fig. 3. Stereoprojection along the DNA helix axis of a modeled complex between a mimetic of the Met-repressor [11] and its operator-box.

#### References

1. (a) Franklin, R.E., Gosling, R.G. *Nature* **171**, 740–741 (1953). (b) Wilkins, M.H.F., Stokes, A.R., Wilson, H.R. *Nature* **171**, 738–740 (1953). (c) Cochran, W., Crick, F.H.C., Vand, V. *Acta Crystallogr.* **5**, 501; 581 (1952). (d) Watson, J.D., Crick, F.H.C. *Nature* **171**, 737–738 (1953).
2. Protein Database: <http://www.rcsb.org/>
3. Cambridge Crystallographic Data Centre: <http://www.ccdc.cam.ac.uk/>; Zürich mirror: <http://sixray.ethz.ch/csdeth.html>
4. Gerber, P.R.: MOLOC – A Molecular Design Software Suite: <http://www.moloc.ch>
5. Gerber, P.R., Müller, K. *J. Comput.-Aided Mol. Design* **9**, 251–268 (1995).
6. Ellenberger, T.E., et al. *Cell* **71**, 1223–1237 (1992).
7. Hull, S.E., et al. *Nature* **275**, 206 (1978).
8. Antson, A.A., et al. *Nature* **401**, 235–243 (1999).
9. Nikiforovich, G.V., Mutter, M., Lehmann, C. *Biopolymers* **50**, 361–372 (1999).
10. Peluso, S., et al. *ChemBioChem* **2**, 432–437 (2001).
11. Somers, W.S., Phillips, S.E.V. *Nature* **359**, 387–393 (1992).
12. Wu, B.Y., Hurley, L.H. In Tam, J.P. and Kaumaya, P.T.P. (Eds.) *Peptides: Frontiers of Peptide Science (Proceedings of the 15th American Peptide Symposium)*, Kluwer, Dordrecht, 1999, p. 383.
13. Carson, M., Ribbons *Methods Enzymol.* **277**, 493–505 (1997).

## Molecular Modeling and Binding Energy Calculations for Drug Resistant Mutations in HIV-1 Protease-Inhibitor Complexes

Mark D. Shenderovich, Vladimir Tseitin, Cindy L. Fisher and  
 Kalyanaraman Ramnarayan

*Structural Bioinformatics Inc., San Diego, CA 92127, USA*

### Introduction

HIV-1 protease (Pr) processes polypeptide gene products into structural proteins and enzymes essential for maturation and infectivity of the virus. HIV-1 Pr inhibitors (PrI) developed by high-throughput screening and structure-based drug design have shown significant promise in anti-AIDS therapy [1]. However, the clinical effectiveness of PrIs is limited by rapid emergence of drug-resistant mutations [2]. Pr variants resistant to a particular PrI first occur by mutation of amino acids close to the drug-binding site, which then are accompanied with compensatory mutations at more distant amino acids. The primary resistant mutations usually result in significant decrease of the inhibitor binding affinity [3]. The aim of this study was to develop and validate a computational protocol for modeling of the 3D structures of mutant HIV Pr-inhibitor complexes and for estimation of changes in PrI binding affinities upon mutations.

### Results and Discussion

Models of the wild-type (WT) HIV-1 protease complexes with FDA-approved PrIs were built from their X-ray crystal structures (see Table 1) using a modified ECEPP/3 [4] force field. The crystal structures were refined by Monte Carlo simulations [5] with minimization including flexible ligands and variable Pr side chains located within 7.0 Å of the ligand. Mutations were introduced into the WT complexes in the order of increasing distance from the ligand. The mutant side chains were locally optimized by a systematic search procedure, and the mutant complexes were further refined by energy minimization involving the ligand, the Pr binding site residues, and residues close to mutation sites. Molecular modeling was performed with the ICM 2.7 program [6,7]. Binding energies of PrI were estimated as  $E_{\text{bind}} = E_0 + E_{\text{compl}} - E_{\text{ligand}} - E_{\text{prot}}$ , where  $E_0$  is an adjustable constant,  $E_{\text{compl}}$  is the energy of the complex,  $E_{\text{ligand}}$  and  $E_{\text{prot}}$  are the energies of the ligand and protein when separated. The binding energy function included ECEPP/3 van der Waals and hydrogen-bonding terms [4], exact-boundary electrostatics with  $\epsilon = 8.0$  [8], and side-chain entropy [5]. Calculated changes in binding energy,  $\Delta E_{\text{bind}}(\text{calc}) = E_{\text{bind}}(\text{wt}) - E_{\text{bind}}(\text{mut})$  were correlated to the experimental

*Table 1. Correlation between experimental and calculated binding energies for HIV-1 protease inhibitors.*

HIV PR inhibitor	PDB ID of crystal complex	Experimental data points	Correlation coefficient, R	S.D. of $\Delta E_{\text{bind}}^a$ , kcal/mol
Saquinavir (SQV)	1HXB	18	0.84	0.68
Indinavir (IDV)	1HSG	17	0.83	0.65
Ritonavir (RTV)	1HXX	12	0.90	0.72
Amprenavir (APV)	1HPV	15	0.90	0.54

<sup>a</sup> Standard deviation of calculated  $\Delta E_{\text{bind}}$  from the correlation line.

binding free energies  $\Delta\Delta G_{\text{bind}} = -RT \ln(K_{i,\text{mut}}/K_{i,\text{wt}})$  estimated from  $K_i$  values available in the literature.

The correlations obtained for four clinically available PrI are characterized in Table 1. The correlation coefficients  $R = 0.8$  to  $0.9$  manifest statistically significant correlations between calculated and experimental changes in binding energy of the four PrIs upon mutations. The standard deviations shown in last column of Table 1 suggest that the correlations can reliably predict major (more than 10-fold) increases in  $K_i$ , which are associated with primary resistant mutations [3]. In fact, our calculations were able to recognize mutations resistant to a particular PrI (G48V for saquinavir, V82A for ritonavir and indinavir, I50V for amprenavir) by a significant increase in binding energy ( $\Delta E_{\text{bind}} > 2.0$  kcal/mol).

The computational mutagenesis procedures were further validated with multiple-mutation HIV Pr variants from clinical isolates. Condra *et al.* [9] have measured indinavir concentrations  $IC_{95}$  for more than 50 viral isolates taken from 21 patients at different stages of treatment with the drug. Each isolate contained several variant HIV protease genes. In total, 315 amino acid sequences were used to build mutant Pr-IDV complexes from two models of the WT complex, one with mono-protonated and the other with di-protonated IDV. For correlation with experimental  $IC_{95}$  values, average  $\langle\Delta E_{\text{bind}}\rangle$  values per viral isolate were calculated by minimization of the least square deviations between experimental and calculated values. Statistically significant correlations with the coefficients  $R = 0.79$  and  $0.74$  were obtained for the models of mutant Pr complexes with the two different charge states of IDV. The computational mutagenesis approach can be used to predict mutations that may be resistant to newly designed HIV Pr inhibitors.

### Acknowledgments

The authors are grateful to Dr. Patrick Hess and Dr. Ron Kagan from Quest Diagnostics Inc., San Juan Capistrano, CA, U.S.A., for valuable discussion of the results of this study.

### References

1. Tomasselli, A.G., Heinrikson, R.L. *Biochim. Biophys. Acta* **1477**, 189–214 (2000).
2. Boden, D., Markowitz, M. *Antimicrob. Agents Chemother.* **42**, 2775–2783 (1998).
3. Gulnik, S.V., Suvorov, L.I., Liu, B., Yu, B., Anderson, B., Mitsuya, H., Erickson, J.W. *Biochemistry* **34**, 9282–9287 (1995).
4. Abagyan, R., Totrov, M. *J. Mol. Biol.* **235**, 983–1002 (1994).
5. Némethy, G., Gibson, K.D., Palmer, K.A., Yoong, C.N., Paterlini, G., Zagari, A., Rumsey, S., Scheraga, H.A. *J. Phys. Chem.* **96**, 6472–6484 (1992).
6. Abagyan, R.A., Totrov, M., Kuznetsov, D. *J. Comput. Chem.* **15**, 488–506 (1994).
7. *ICM Version 2.7, User's Manual*. Molsoft, L.L.C., San Diego, CA, 1999.
8. Schapira M, Totrov M, Abagyan R. *J. Mol. Recogn.* **12**, 177–186 (1999).
9. Condra, J.H., Holderer, D.J., Schleif, W.A., Blahy, O.M., Danovich, R.M., Gabryelski, L.J., et al. *J. Virol.* **70**, 8270–8276 (1996).

## **Electrostatic and Hydrophobic Nature of the Binding of Gelsolin 135-142 and Gelsolin 150-169 Fragments to the PIP2-Containing Lipid Bilayer**

**Inta Liepina<sup>1</sup>, Cezary Czaplewski<sup>2</sup>, Paul Janmey<sup>3</sup> and Adam Liwo<sup>2</sup>**

<sup>1</sup>*Latvian Institute of Organic Synthesis, Riga, LV1006, Latvia*

<sup>2</sup>*Faculty of Chemistry, University of Gdańsk, 80-952 Gdańsk, Poland*

<sup>3</sup>*Institute of Medicine and Engineering, University of Pennsylvania,  
Philadelphia, PA 19104, USA*

### **Introduction**

Gelsolin is a  $\text{Ca}^{2+}$ -activated and phosphoinositide-regulated cytoskeletal actin-binding-and-severing protein, responsible for the cell shape and motility [1]. Two fragments of gelsolin sequence 150-169: **KHVVPNEVVVQRLFQVKGR** (G150-169), and 135-142: **KSGLKYKK** (G135-142), respectively, are involved in the binding of this protein to actin and the cellular messenger phosphatidylinositol 4,5-bisphosphate (PIP2) occurring in the inner side of the cell membrane. The binding of gelsolin peptides G135-142 and G150-169 to a cluster of four PIP2 molecules in a dimyristoyl-phosphatidylcholine (DMPC) lipid (PIP2 lipid) was investigated by means of molecular-dynamics (MD) simulations.

### **Results and Discussion**

Initially, the electrostatically driven Monte Carlo (EDMC) [2] method with the ECEPP/3 [3] force field was used to find the low-energy conformations of G150-169 and G135-142, which were taken as the starting conformations for MD simulations. Four and seven representative low-energy structures were found for G150-169 and G135-142, respectively. All of the four low-energy structures of the G150-169 comprise  $\alpha$ -helical part, but the global-minimum structure possesses the largest  $\alpha$ -helical fragment (from Val<sup>4</sup> to Arg<sup>20</sup>). The positively charged side chains of this structure are largely grouped on one side of the helix while the hydrophobic residues form a hydrophobic twine around the molecule. All seven low-energy structures of G135-142 contain  $\alpha$ -helical segments. The lowest-energy conformations of both peptides were subsequently subjected to 1600 ps MD simulations with the AMBER 4.1 [4] force field. The simulations were carried out in a periodic box consisting of a lipid bilayer immersed in water and containing a cluster of four PIP2 molecules per unit.

After 10 ps of MD simulations short-time binding of the Arg<sup>12</sup> side chain of G150-169 to PIP2 molecule cluster occurred; it was quickly disrupted by thermal motions. The binding occurred again on the 980th ps *via* hydrogen bonding of the Lys<sup>1</sup> side chain and the N-terminus of G150-169 to the oxygen atoms of the PIP2 monophosphate groups. It is interesting to note that PIP2 bound to G150-169 mainly through phosphomonoester groups in the 4th and the 5th position of the inositol ring, although 1-phosphodiester group was involved in the binding for a short time. The hydrogen bonds existed for 65 ps, then they were broken, and reformed after next 24 ps. On the 1108th ps of the MD run the arachidonate tail of one of the PIP2 molecules formed a hydrophobic bond with the Val<sup>4</sup> residue of G150-169, while the stearate tail of another PIP2 molecule interacted with the Val<sup>3</sup>, Pro<sup>5</sup>, and Val<sup>8</sup> residues. Consequently, two of the four PIP2 molecules of the cluster had partly left the lipid bilayer disrupting the structure of the lipid membrane. Similar events occurred for G135-142. Thus, the binding of the PIP2 molecules to both gelsolin-based peptides showed both

electrostatic and hydrophobic nature. The N-terminal residues of G150-169, which are involved in the binding, tended to accept extended conformations while the C-terminal part residues formed an  $\alpha$ -helix or a  $3_{10}$ -helix.

To prove that pulling the PIP2 molecules out of the lipid membrane was caused by interaction with gelsolin peptides, a 2000 ps MD simulation of the PIP2 lipid bilayer without G150-169 or G135-142 was carried out. It was shown that the structure of the membrane remained reasonably conserved. All fatty acid tails of the four PIP2 molecules remained in the lipid during the simulation time, only already after 300 ps of simulation the negatively-charged phosphate groups of the PIP2 molecules moved towards the water phase, thus locally curving the lipid. This lipid convex curvature could help in interaction of PIP2 molecules with gelsolin peptides or gelsolin. The negatively charged phosphate heads of the PIP2 cluster were kept together by water bridges between the oxygen atoms.

The binding of G150-169 to free PIP2 molecules in water was also investigated. G159-160 and two PIP2 molecules were placed in a periodic water box and subjected to a 2200 ps of MD simulation. The peptide formed both salt bridges and hydrophobic contacts with PIP2 after 850 ps of MD simulation. The complex subsequently dissociated, reformed after 1293 ps of total simulation time, and finally dissociated.

It can be concluded that (1) the binding of G150-169 or G135-142 to the PIP2 molecules has electrostatic and hydrophobic nature: electrostatic interactions occur between the lysine and arginine residues of the peptides and the phosphate groups of the PIP2 molecules, while hydrophobic interactions occur between the hydrophobic residues of the peptides and the fatty-acid tails of PIP2; (2) the binding to the PIP2 lipid bilayer disrupts the structure of the membrane, pulling out the PIP2 molecules and forming hydrophobic bonds between nonpolar side chains of the peptide and the fatty-acid tails of PIP2.

### Acknowledgments

This work was supported by NATO Collaborative Linkage Grant LST.CLG.976647 and grant 127/E-335/S/2000 from the Polish State Committee for Scientific Research (KBN). Calculations were carried out using the resources and software at the Computer Center of the Academic Metropolitan Network (CI TASK) in Gdańsk, Poland and Interdisciplinary Center of Mathematical and Computer Modeling (ICM) in Warsaw, Poland.

### References

1. Janmey, P.A., Xian, W., Flanagan, L.A. *Chem. Phys. Lipids* **101**, 93–107 (1999).
2. Ripoll, D.R., Scheraga H.A. *Biopolymers* **30**, 165–176 (1990).
3. Nemethy, G., Gibson, K.D., Palmer, K.A., Yoon, C.N., Paterlini, G., Zagari, A., Rumsey, S., Scheraga, H.A. *J. Phys. Chem.* **96**, 6472–6484 (1992).
4. Weiner, S.J., Kolman, P.A., Nguyen, D.T., Case D.A. *J. Comput. Chem.* **7**, 230–252 (1986).

## **Prediction of Antibody Complexes with Rationally-Designed and Library-Derived Cyclic Peptides: A Computer Modeling Study**

**Tobias Knaute, Livia Otte and Rudolf Volkmer-Engert**

*Institute of Medical Immunology, University Clinic Charité, Humboldt University of Berlin,  
Berlin, 10098, Germany*

### **Introduction**

The complexity of peptide conformational space poses a great obstacle for the correct prediction of three-dimensional peptide structures in complex with proteins. We have investigated the predictability of linear and cyclic peptides that were derived from combinatorial libraries as well as designed rationally *in silico*. Linear peptides in general performed poorly in respect to simulation convergence, accuracy and reproducibility. So does conformational constraining of peptides raise the chances of correctly predicting the bound conformation by molecular modeling techniques?

### **Results and Discussion**

In a first set of experiments, the binding conformation of the small cyclic epitope cyclo(N $\alpha$ -C $\delta_7$ )SHFNEYE in complex with the anti-TGF $\alpha$  antibody tAB2 [1] was correctly identified in several independent Monte-Carlo global optimization calculations using the ICM method [2]. Starting from a random conformation,  $10^8$  function calls were invoked during each run with local energy minimization after every random move. The antibody was present as a set of five grid potentials during the conformational sampling and the peptide was totally flexibilized with the pseudo-peptide bond accounted for by strong distance restraints.

To further test the performance of constrained peptides, we have designed a set of cyclic derivatives of the linear peptide GLYEWGGARIT, which was shown to be bound in an *a priori* bent conformation to the monoclonal anti-p24 (HIV-1) antibody CB4-1 [3] (PDB code 1CFS). These cyclic constructs carry either a disulfide or side-chain amide linkage to covalently replace a hydrogen bond between the arginine guanidino group and the N-terminal glycine carbonyl observed in the template peptide. Length adjustment was achieved by inserting L- or D-prolines into the linker region.

The cyclic derivatives were subjected to global conformational searches as described above. Of five independent simulations for each peptide with random initial conformations, three converged for the amide-bridged entities and two for the disulfide-linked peptides, owing to the more flexible nature of the S-S bond. The low-energy structures revealed very similar conformations and antibody contacts in respect to the linear template peptide. These findings are supported by binding studies and substitutional analyses (Table 1).

In addition, we suggest a complex structure for the cyclic peptide cyclo-(S $\gamma_1$ -S $\gamma_{11}$ )CNQLFNTTPSC, identified from a phage display library as binding to the anti-cholera toxin antibody TE33 [4]. Two out of five docking simulations converged into a conformation that showed surprising similarity to the backbone arrangement of the unhomologous linear wt epitope VPGSQHID (PDB code 1TET). The model is in good agreement with the substitutional analysis of the peptide.

Libraries with cyclic peptides can be easily designed and synthesized. Our study shows that conformationally constraining peptides can lead to an increased predictability of the bound conformation by molecular modeling beside other potential benefits such as higher binding affinity and lower degradation rates.

Table 1. Designed cyclic peptides: CB4-1 binding constants and deviation after docking.

Peptide <sup>a</sup>	IC <sub>50</sub> (M) <sup>b</sup>	Lowest R.m.s.d. (Å) <sup>c</sup>
Template: GLYEWGGARIT	$2.7 \cdot 10^{-7}$	–
<u>C</u> PGLYEWGG <u>A</u> CIT	$1.8 \cdot 10^{-7}$	1.43
<u>C</u> PpLYEWGG <u>A</u> CIT	$1.6 \cdot 10^{-7}$	1.30
<u>D</u> GLYEWGG <u>A</u> KIT	n.d.	1.39
<u>D</u> pLYEWGG <u>A</u> KIT	$2.5 \cdot 10^{-7}$	1.59
<u>D</u> pLYEWGGV <u>K</u> IT	$9.2 \cdot 10^{-8}$	n.d.

<sup>a</sup> Linker residues underlined. Only side chain cyclization was applied. <sup>b</sup> Determined by competitive ELISA (against p24). <sup>c</sup> Root mean square deviation (r.m.s.d.) of backbone heavy atoms between identical residues; in respect to the template peptide.

### Acknowledgments

We thank Ruben Abagyan, Brian Marsden and Jens Schneider-Mergener. We are also indebted to Ines Kretzschmar and Christiane Landgraf. Supported by Deutsche Forschungsgemeinschaft.

### References

1. Winkler, D., Stigler, R.D., Hellwig, J., Hoffmann, B., Schneider-Mergener, J. *Peptides: Chem. Struct. Biol.* 315 (1996).
2. Abagyan, R., Totrov, M. *J. Mol. Biol.* **235**, 983 (1994).
3. Keitel, T., Kramer, A., Wessner, H., Scholz, C., Schneider-Mergener, J., Höhne, W. *Cell* **91**, 811 (1997).
4. Otte, L., Ivascu, C., Kramer, A., Dong, L., Schneider-Mergener, J. *Proc. 26th European Peptide Symposium* 707 (2000).

## **Ligand–Receptor Interactions Regulating Cell Trafficking and Signaling of the Human PTH1Rc: An *in Silica* Examination**

**Luca Monticelli<sup>1</sup>, Stefano Mammi<sup>1</sup>, Evaristo Peggion<sup>1</sup>, Serge Ferrari<sup>2</sup>, Michael Rosenblatt<sup>2</sup>, Michael Chorev<sup>2</sup>, Alessandro Bisello<sup>3</sup> and Dale F. Mierke<sup>4</sup>**

<sup>1</sup>*Department of Organic Chemistry, University of Padova and Biopolymers Research Center, C.N.R., Padova, I-35131, Italy*

<sup>2</sup>*Division of Bone and Mineral Metabolism, Charles A. Dana and Thorndike Laboratories, Department of Medicine, Beth Israel Deaconess Medical Center and Harvard Medical School, Boston, MA 02215, USA*

<sup>3</sup>*Department of Medicine, University of Pittsburgh, Pittsburgh, PA 15261, USA*

<sup>4</sup>*Department of Molecular Pharmacology, Brown University, Providence, RI 02912, USA*

### **Introduction**

Desensitization of G-protein coupled receptors is a fundamental mechanism regulating the cellular response to agonists. It was recently demonstrated that stimulation of the human parathyroid hormone (PTH)/parathyroid hormone related protein (PTHrP) receptor (PTH1Rc) by its cognate agonists, *e.g.*, PTH(1-34), triggers the rapid internalization of ligand-receptor complexes, while the interaction of the receptor with antagonists, *e.g.*, PTH(7-34), does not [1].

Internalization of PTH1Rc and other GPCRs is dependent upon  $\beta$ -arrestin2, which has been shown to be responsible for the rapid desensitization of cAMP signaling. Nevertheless, the detailed mechanism of transduction of agonist binding into coupling to G protein, recruitment of effectors such as  $\beta$ -arrestin2 and receptor internalization is not known.

Trafficking of rhodamine-labeled PTH1Rc agonists and antagonists, and GFP-tagged  $\beta$ -arrestin2 was monitored in real time in HEK-293 cells stably expressing the hPTH1Rc [1,2]. We recently found that Bpa<sup>1</sup>-PTHrP(1-36), a G<sub>s</sub>-signaling-selective agonist, has a protracted stimulation of cAMP accumulation, which does not result in either mobilization of  $\beta$ -arrestin2 or receptor internalization.

### **Results and Discussion**

In an effort to characterize the different ligand binding modes in the PTH-PTH1Rc system, we developed molecular models for the complexes of the receptor with wild type and modified ligands. These models incorporate conformational features of several PTH1Rc fragments as determined by NMR [3–5], as well as the conformational features of the hormone in a membrane-mimicking environment [6], the arrangement of the transmembrane (TM) helices based on the X-ray structure of rhodopsin [7], and the contact points provided by photoaffinity cross-linking studies [8–11].

These models were utilized as starting structures for extensive molecular dynamics (MD) simulations carried out with the Gromacs package [13,14]; starting structures for the receptors in the different complexes were almost identical; RMSD calculated on the backbone atoms in the transmembrane region was less than 0.2 Å.

MD simulations were carried out in three steps:

1. Soaking of the complex in a three-layer simulation cell (H<sub>2</sub>O/decane/H<sub>2</sub>O), which simulates the membrane environment [12], followed by energy minimization.
2. Position restrained MD (50 ps) for the equilibration of the solvent system.
3. Restrained MD (600–900 ps), with temperature and pressure coupling.

To compare the structures of the ligand–receptor complexes with the native and modified hormones, we calculated the average coordinates during the last 200–300 ps of MD simulation and obtained a representative structure for each complex by energy minimization. We also calculated the RMSD for the backbone atoms of the transmembrane region during each simulation and the RMSD between the starting and the representative structures for each complex. The structures of the native complexes [ligands: PTH(1-34) and PTHrP(1-36)] are stable during all the simulations (the RMSD between starting and final structures was less than 1.5 Å), while the complexes with modified ligands [PTHrP(2-36) and Bpa<sup>1</sup>-PTHrP(1-36)] undergo structural transitions during the simulations. The RMSD between the representative structures of a wild type complex and a modified-ligand complex was always bigger than 2.5 Å.

Each pair and each triplet of transmembrane helices was superimposed in 2 complexes, *i.e.*, one wild type and one modified-ligand complex. Considering the representative structures, TM1 and TM2 overlap with a small RMSD in most of the pairs of complexes. In most of the simulations, superposition of the backbone atoms of TM1 and TM2 resulted in the relative displacement of the other TM helices, especially TM5, TM6, the third intracellular loop and the third extracellular loop.

In conclusion, the molecular models described here allow for atomic insight into the agonist-associated PTH1Rc conformation responsible for the interaction with  $\beta$ -arrestin2. The analysis of the motions of the receptor domains indicates that the Ser<sup>1</sup> modification, as well as its deletion, lead to major changes in the relative position of transmembrane helices. The direction and extent of the relative displacements were different in each simulation, but resulted in remarkable conformational changes of the third extracellular loop and of the third cytoplasmic loop. The third intracellular loop is known to have a significant role in the interaction with the G protein in many GPCR systems [15–18].

Based on the dynamic properties of our models, we hypothesize that the Bpa substitution or deletion of the residue in position 1 of the PTHrP hormone alters the coupling of PTH1Rc to  $\beta$ -arrestin2 *via* a mechanism involving a conformational change in the third intracellular loop.

## References

1. Ferrari, S.L., Bisello, A., et al. *J. Biol. Chem.* **274**, 29968–29975 (1999).
2. Ferrari, S.L., Bisello, A. *Mol. Endocrinol.* **15**, 149–163 (2001).
3. Pellegrini, M., Mierke, D.M., et al. *Biochemistry* **37**, 12737–12743 (1998).
4. Pellegrini, M., Mierke, D.M., et al. *Biopolymers* **40**, 653–666 (1997).
5. Piserchio, A., Mierke, D.M., et al. *Biochemistry* **39**, 8153–8161 (2000).
6. Pellegrini, M., Mierke, D.M., et al. *J. Biol. Chem.* **273**, 10420–10427 (1998).
7. Palczewski, K., et al. *Science* **289**, 739–745 (2000).
8. Bisello, A., Chorev, M., et al. *J. Biol. Chem.* **273**, 22498–22505 (1998).
9. Carter, P.H., Gardella, T.J., et al. *J. Biol. Chem.* **274**, 31955–31960 (1999).
10. Greenberg, Z., Chorev, M., et al. *Biochemistry* **39**, 8142–8152 (2000).
11. Behar, V., Chorev, M., et al. *J. Biol. Chem.* **275**, 9–17 (2000).
12. Van Buuren, A.R., Berendsen, H.J.C., et al. *J. Phys. Chem.* **97**, 9206–9212 (1993).
13. Berendsen, H.J.C., van der Spoel, D., et al. *Comput. Phys. Commun.* **91**, 43–56 (1995).
14. Hess, B., et al. *J. Comput. Chem.* **18**, 1463–1472 (1997).
15. Wong, S.K.F., Parker, E.M., Ross, E.M. *J. Biol. Chem.* **265**, 6219–6224 (1990).
16. Cotecchia, S., et al. *J. Biol. Chem.* **267**, 1633–1639 (1992).
17. Wong, S.K.F., Ross, E.M. *J. Biol. Chem.* **269**, 18968–18976 (1994).
18. Okamoto, T., et al. *Cell* **67**, 723–730 (1991).

## Theoretical Design of $\alpha$ -Hairpin Structures

Masahito Oka and Toshio Hayashi

*Research Institute for Advanced Science and Technology, Osaka Prefecture University,  
Sakai, Osaka, 599-8570, Japan*

### Introduction

The  $\alpha$ -hairpin structure is one of the fundamental motifs, which are commonly found in native proteins, and is also interesting as a fundamental super secondary structure for designing the backbone structures of the artificial proteins [1–3]. In this work, we tried to introduce electrostatic interactions and a disulfide linkage for stabilizing the  $\alpha$ -hairpin structure based on the molecular mechanics calculation and minimization procedure.

### Results and Discussion

A total of 138 polypeptides, Ac-(Ala)(20-m)-Lys-(Ala)(m-1)-Gly-Gly-Gly-(Ala)(n-1)-Glu-(Ala)(20-n)-NHMe(m = 20, n = 20-16; m = 19, n = 20-16; m = 18, n = 20-15; m = 17, n = 20-14; m = 16, n = 20-13; m = 13, n = 16-10; m = 12, n = 15-9; m = 11, n = 14-8; m = 10, n = 13-5; m = 3, n = 7-1) having charged Lys and Glu residues, and Ac-(Ala)(20-m)-Cys-(Ala)(m-1)-Gly-Gly-Gly-(Ala)(n-1)-Cys-(Ala)(20-n)-NHMe(m = 20, n = 20-17; m = 19, n = 20-16; m = 18, n = 20-15; m = 17, n = 20-14; m = 16, n = 19-13; m = 13, n = 16-10; m = 12, n = 15-9; m = 11, n = 14-8; m = 10, n = 14-6; m = 3, n = 7-1; m = 1, n = 5-1) having a disulfide bond between two Cys residues were selected as model polypeptides. Moreover, Ac-(Ala)(20-m)-Glu-(Ala)(m-1)-Gly-Gly-Gly-(Ala)(n-1)-Lys-(Ala)(20-n)-NHMe(m = 19, n = 18-16) and Ac-(Ala)(15-m)-Cys-(Ala)(m-1)-Gly-Gly-Gly-(Ala)(n-1)-Cys-(Ala)(15-n)-NHMe(m = 10, n = 11-9) were also selected to estimate the effects of amino-acid exchange between Lys and Glu residues and the helix length on the stability of  $\alpha$ -hairpin structure, respectively. All conformational energy calculations were carried out with ECEPP and Powell minimization procedure. During minimization, all ( $\phi$ ,  $\psi$ ) of Gly, ( $\phi$ ,  $\psi$ ,  $\chi^1$ ,  $\chi^2$ ,  $\chi^3$ ,  $\chi^4$ ,  $\chi^5$ ) of Lys and ( $\phi$ ,  $\psi$ ,  $\chi^1$ ,  $\chi^2$ ,  $\chi^3$ ,  $\chi^{4,2}$ ) of Glu were allowed to vary. ( $\phi$ ,  $\psi$ ,  $\chi^1$ ) of Ala were fixed to those of the energy minimum in the  $\alpha$ -helical region of poly(Ala), and all other backbone dihedral angles were fixed to 180°. All local energy minima of Ac-Gly-Gly-Gly-NHMe obtained in the previous work [1] were used as starting conformation for the -Gly-Gly-Gly-portion. All local energy minima of the Lys and Glu residues whose ( $\phi$ ,  $\psi$ ) are those of the  $\alpha$ -helical region were used as starting conformation for the Lys and Glu residues, respectively. Then, all combination of above local minima of Ac-Gly-Gly-Gly-NHMe and the Lys and Glu residues were used as the starting conformation for each polypeptide.

Calculated results indicate that  $\alpha$ -hairpin structures are stabilized by introduction of a pair of Lys and Glu residues having ionized side-chain groups on the polypeptide for 37 (m,n)-pairs [m = 20, n = 19-17; m = 19, n = 20, 17, 16; m = 18, n = 20, 17, 16; m = 17, n = 20-17, 15, 14; m = 16, n = 18, 15; m = 13, n = 15, 14, 11; m = 12, n = 13, 10, 9; m = 11, n = 14, 13, 10, 9; m = 10, n = 12-10, 8, 7; m = 3, 6-3, 1] among 66 (m,n)-pairs investigated in this work. Their stabilization energy shows about 1 kcal/mol increase in comparison with that for the Ala-residue approximation [1]. For each case of these 37 (m,n)-pairs, all stable local minima show the standard orientation angle between two  $\alpha$ -helices in spite of each of them has a different local conformation of the side-chain or the Gly-Gly-Gly loop portion. It means that  $\alpha$ -hairpin structures are not

rigid conformations. They fluctuate among many local minima by changing local conformations of the side-chain or the loop portion in keeping the orientation angle around its standard value.

Calculated results also indicate that a disulfide-linkage between two helices stabilizes the  $\alpha$ -hairpin structure. However, because of the strong restriction caused by the formation of a disulfide bond, the positions introducing two Cys residues are more specific than those introducing a pair of Lys and Glu residues. Only 7 (m,n)-pairs, *i.e.*, (18,18), (18,17), (17,18), (11,10), (10,10), (3,4) and (3,3), were found as suitable position for stabilizing the standard  $\alpha$ -hairpin structure. For each case of these 7 (m,n)-pairs, the local minima which have standard orientation angle were also found as stable minima. However, number of them is smaller than those for introduction of the Lys-Glu pair because of the strong restriction of disulfide-linkage. It means that the  $\alpha$ -hairpin structure, which is stabilized by a disulfide-linkage, is not so fluctuating as that formed by introducing the Lys-Glu pair.

For the case of (m = 19, n = 18-16), stable local minima of Ac-(Ala)(20-m)-Glu-(Ala)(m-1)-Gly-Gly-Gly-(Ala)(n-1)-Lys-(Ala)(20-n)-NHMe almost correspond to those of Ac-(Ala)(20-m)-Lys-(Ala)(m-1)-Gly-Gly-Gly-(Ala)(n-1)-Glu-(Ala)(20-n)-NHMe. These results indicate that the interaction mode of two helices is not influenced by the amino-acid exchange between Lys and Glu. That is, the change of the relative positions of side-chain group is compensated by the large freedom of side chain.

The results for Ac-(Ala)(15-m)-Cys-(Ala)(m-1)-Gly-Gly-Gly-(Ala)(n-1)-Cys-(Ala)(15-n)-NHMe (m = 10, n = 11-9) indicate that the change of the length of  $\alpha$ -helices causes the change of the packing mode of two  $\alpha$ -helices. For example, for the case of (m,n) = (10,10), the orientation angle between two 15-residue helices deviates about 20° from the standard orientation angle between 20-residue helices, suggesting that the helix length is a important factor for designing the  $\alpha$ -hairpin structure by introducing the disulfide linkage.

Above results indicate that  $\alpha$ -hairpin structures are stabilized by introducing adequate electrostatic interactions between a pair of Lys and Glu residues or a disulfide bond between a pair of Cys residues. However, those results also indicate that it is very important to select the suitable positions for introducing such residues. Especially, for the case of the disulfide linkage, the suitable position is more specific than that for the electrostatic interactions because of the high constraint caused by the disulfide linkage. These results indicate the important roles of theoretical design that decides the suitable position for introducing a pair of Lys and Glu residues or a pair of Cys residues on the polypeptides.

## References

1. Ishikawa, Y., Oka, M., Hayashi, T., Nishinaga, A. *Polym. J.* **28**, 86–90 (1996).
2. Oka, M., Hayashi, T., Ishikawa, Y., Hirano, Y. *Pept. Sci.* **1998**, 361–364 (1999).
3. Oka, M., Hayashi, T., Ishikawa, Y., Hirano, Y. *Pept. Sci.* **1998**, 365–368 (1999).

## **Application of a Detailed Energy Surface to Homology Modeling of the $\omega$ -Conotoxin Family**

**Michael J. Dudek and K. Ramnarayan**

*Structural Bioinformatics Inc., San Diego, CA 92127, USA*

### **Introduction**

$\omega$ -Conotoxins are a family of neurotoxic peptides (24 to 31 residues) isolated from the venoms of marine snails of the genus *Conus*. They act in vertebrates by selectively blocking voltage-sensitive calcium channels. They are being explored as a new class of therapeutics for pain management. Of the 16 known family members, 7 have NMR structures available. As a first step in a project to correlate changes in peptide surface structure with changes in binding activity and function, we carried out, for the remaining 9 family members, a procedure of homology-constrained global energy minimization over a detailed protein energy surface. Sequence identities to the most similar NMR-determined family member range from 27 to 76%. The homology modeling methodologies of sequence alignment and template substitution were followed by global energy minimization, accomplished by cycling through a sequence of conformational searches of 7-residue segments that together span the entire protein chain. Increases in model accuracy with application of global energy minimization are inferred by tracking a collection of properties including distributions of backbone torsion angles ( $\phi$ ,  $\psi$ , and  $\omega$ ), fraction of non-rotameric side chain conformations, internal cavities, buried charges, unpaired hydrogen bond donors and acceptors, Miyazawa-Jernigan contact energy, and exposed hydrophobic surface area.

The energy surface, which has been described previously [1–3], is based on a non-standard collection of detailed functional forms. These include a distributed atomic multipole representation of the electrostatic component, a buf14-7 representation of the repulsion + dispersion component, a 2-dimensional fourier series representation of the intrinsic torsional component, and a hydration shell model representation of the hydrophobic contribution to hydration free energy. The remainder of hydration free energy is obtained as the energetic effect of a continuous dielectric medium. Initial validation of the energy surface [3] was through applications of global energy minimization to seven-residue surface segments of protein crystal structures. For nine of ten predictions, the native backbone conformation was identified correctly (to within 1 Å RMSD). The origin of the one incorrect prediction (Loop 68-74 of Lysozyme) is most likely the inability of the dielectric continuum model to account for two water molecules that are partially buried, along with an Asp side chain, in the crystal structure. The predicted structure collapses into the cavity that is occupied in the crystal by the buried water.

The conformational search program [1,3] was originally developed for applications to protein segments ranging in length from 5–15 residues, and has recently been extended to enable applications to up to eight interacting segments. For a given protein segment (or collection of interacting segments), the program first generates a large collection of starting conformations that covers uniformly the space of possible deformations, then executes a series of fast screening operations followed by local energy minimization.

## Results and Discussion

For 6 of 7 template NMR structures, backbone RMSD after global energy minimization is  $\sim 1$  Å, reflecting only small conformational shifts. For the 9 homology models, RMSD from an experimental structure is not available as a measure of correctness. As a substitute, a collection of 8 coarse-grained properties was chosen such that the properties tend to reach near-optimal values in native protein structures yet are not directly related to underlying energy function components. Comparison of these properties before and after global energy minimization shows improvement in every property more often than decline. All of the properties monitored with the exception of contact energy measure defects in structure and are orthogonal to one another. An average defect energy was defined by assigning to each type of defect an appropriate energy penalty, summing over defects, then averaging over residues in the chain. This balanced, combined measure (Table 1) shows more consistent improvement with application of global energy minimization than any individual property. Consistent with the broad range in binding activity that is observed experimentally [4], a large variation is observed within the  $\omega$ -conotoxin family in the pattern of electrostatic forces at the peptide surfaces.

As measured by a collection of 8 coarse-grained properties, conformational search guided by a detailed energy surface appears able to add structural information to that ordinarily obtainable from sequence homology. If this ability to add structural information can be further demonstrated, the procedure used in this work could become a useful foundation for automating and extending comparative modeling.

Table 1. Defect energy changes with global energy minimization.

Conotoxin <sup>a</sup>	Defect energy <sup>b</sup>	Conotoxin	Defect energy
cxoa_conma <sup>c</sup>	3.26(−.38)	cxoa_conpe	2.33(+.17)
cxo6_conge	2.52(−.27)	cxob_conpe	2.95(−.50)
cxo7_conte	3.11(−.87)	cxod_conma	2.13(−.50)
cxob_const	2.31(−.12)	cxob_conma	2.54(+.20)
cxoc_conma	1.83(+.33)	cxoa_const	2.64(−.70)
q9xzk2	2.26(+.22)	q9xzl5	2.09(−.21)
q9ub25	2.39(−.77)	q9xzl4	2.07(−.10)
cxo7_conge	2.50(−.34)	q9ub26	2.64(−.63)

<sup>a</sup> SWISS-PROT/TrEMBL entries. <sup>b</sup> Energy per residue (kcal/mol). <sup>c</sup> Left and right values correspond to initial (NMR or substituted template) and final (converged) structures, respectively.

## References

1. Dudek, M.J., Scheraga, H.A. *J. Comp. Chem.* **11**, 121–151 (1990).
2. Dudek, M.J., Ponder, J.W. *J. Comp. Chem.* **16**, 791–816 (1995).
3. Dudek, M.J., Ramnarayan, K., Ponder, J.W. *J. Comp. Chem.* **19**, 548–573 (1998).
4. Nielsen, K.J., Schroeder, T., Lewis, R. *J. Mol. Recognit.* **13**, 55–70 (2000).

## DARWINIZER<sup>®</sup> – a Computer Based Method for Peptide and Peptidomimetics Design

Matthias Filter and Paul Wrede

CallistoGen AG, Hennigsdorf, D-16761, Germany

### Introduction

Due to the metabolic instability of peptides, the design of modified isofunctional peptidomimetics is an adequate approach toward their application in pharmacology. DARWINIZER<sup>®</sup> is a computer-based tool for the *de novo* design of modified peptide structures. DARWINIZER<sup>®</sup> is an extension of the PepHarvester<sup>®</sup> and SME<sup>®</sup> algorithm [1–3] including non-canonical amino acids.

### Results and Discussion

Peptide design can be considered an optimization task. For any systematic optimization, the principle of strong causality has to be fulfilled [1]. DARWINIZER<sup>®</sup> starts with a single known peptide, and by an iterative process of mutation, selection and *in vitro* screening, a new peptide is obtained after a few generations.

Therefore, the Darwinizer<sup>®</sup> algorithm consists of 5 consecutive steps:

- i) identification of a seed peptide with certain biological activity;
- ii) generation of a focused peptide library with gaussian distance distribution and user-defined mutability and variant number;
- iii) synthesis and testing of the peptide library in a biological assay;
- iv) training of an artificial neural network (ANN) with data from iii) as quantitative sequence–activity relationship (QSAR) model;
- v) *de novo* design of peptides and peptidomimetics with improved activities according to the QSAR model by simulated molecular evolution (SME<sup>®</sup>).

Within this strategy, steps i) to iv) lead to an optimal QSAR model as a fitness function for the design cycle. A prerequisite to the model generation is the selection of appropriate descriptors, reflecting the physicochemical and structural properties of non-canonical amino acids [5].

For navigation through the sequence space during the *in machina* optimization process (step v), only the offspring variants are considered for selection. To show the efficiency of the DARWINIZER<sup>®</sup> approach we applied this technology to substrate optimization of Caspase-3, since this enzyme plays a central role in apoptosis.

The sequence VDQMDGW [6] was used as a seed peptide for generating a focused peptide library (step ii). Figure 1a shows the distance to seed distribution and Figure 1b the substrate cleavage rate to distance to seed distribution of the *in vitro* screening

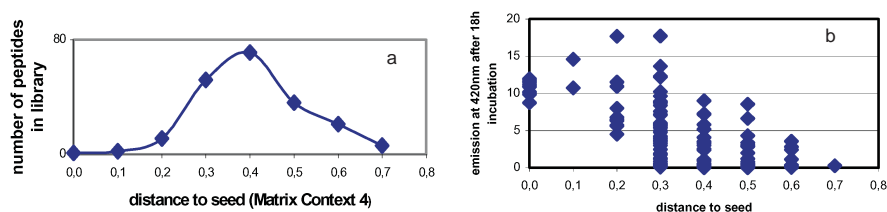


Fig. 1. Caspase 3. a) distance to seed distribution; b) signal in Protease-spot assay vs. distance to seed.

(step iii) using a ProteaseSpot assay [4] (assay performed by Jerini biotools GmbH; Germany).

These data were the basis for QSAR modeling using ANN. Figure 2a shows a representation of the observed cleavage rate after 18h of incubation with Caspase-3 over the first two principal components of the peptide sequence encoded by the 5 z-scales published in [5]. Figure 2b shows the output values of the QSAR model for the same data set. This is consistent with the observed correlation coefficient [7] of  $CC > 0.95$  for both the test and training set.

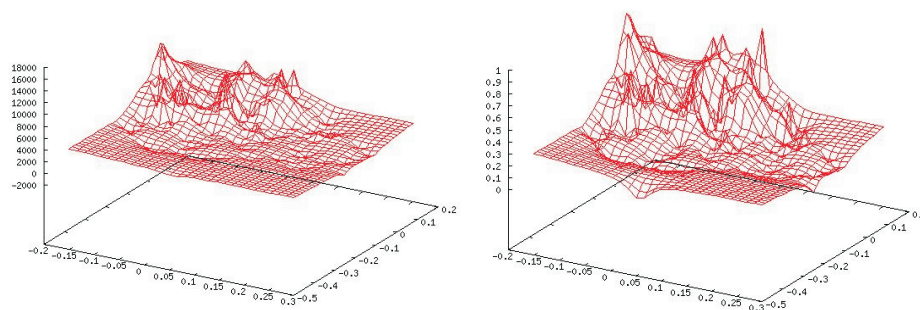


Fig. 2. Fitness landscape of ProteaseSpot assay results (left) and QSAR model (right).

During the *in machina* optimization process the sequence HDRRDGY was obtained. This peptide sequence is currently synthesized and will be tested for activity.

As the DARWINIZER® approach can also handle non-canonical amino acids, the next step will be the design of a peptide substrate for Caspase-3 containing non-canonical amino acids.

#### References:

1. Schneider, G., Wrede, P. *Biophys. J.* **66**, 335–344 (1994).
2. Wrede, P., Landt, O., Klages, S., Fatemi, A., Hahn, U., Schneider, G. *Biochemistry* **37**, 3588–3593 (1998).
3. Wrede, P., Schneider, G., Eds., *Concepts in Protein Engineering and Design*, 1994.
4. Hilpert, K., Hansen, G., Wessner, H., Schneider-Mergener, J., Hohne, W. *J. Biochem. (Tokyo)* **128**, 1051–1057 (2000).
5. Sandberg, M., Eriksson, L., Jonsson, J., Sjostrom, M., Wold, S. *J. Med. Chem.* **41**, 2481–2491 (1998).
6. Talanian, R.V., Quinlan, C., Trautz, S., Hackett, M.C., Mankovich, J.A., Banach, D., Ghayur, T., Brady, K.D., Wong, W.W. *J. Biol. Chem.* **272**, 9677–9682 (1997).
7. Matthews, B.W. *Biochim. Biophys. Acta* **405**, 442–451 (1975).

## Proline: A Key Building Block in “de novo” Designed Peptide Molecules

Ernest Giralt, Miriam Royo, Marcelo Kogan, Laia Crespo, Glòria Sanclimens, Josep Farrera, Miquel Pons and Fernando Albericio

Department of Organic Chemistry, University of Barcelona, Barcelona, E-08028, Spain

### Introduction

Proline is unique among the proteinogenic amino acids in that it has a disubstituted amino group. Living systems have taken advantage of this in a variety of ways, especially in molecular recognition processes [1]. Could proline play a special role in the “de novo” design of peptides or proteins? Recent work that we present here indicates that this could indeed be the case.

### Results and Discussion

It is very well known that polyproline peptides can adopt two different helical conformations in solution: polyproline I (PPI) and polyproline II (PPII). *n*-Propanol, acetonitrile, and other less acidic solvents generally favor the formation of a right-handed and compact helical structure (PPI); on the other hand water, acetic acid, and other acidic solvents favor the formation of a left-handed and extended helical structure (PPII) [2].

Peptide dendrimer chemistry is not very well developed [3]. The pioneering work of Tam *et al.* [4] has not been followed by a significant number of peptide dendrimers, probably due to synthetic difficulties. It is our aim to develop an efficient all-solid-phase approach for dendrimer synthesis and, concomitantly, to supply the conformational plasticity of polyproline to dendritic molecules. In Figure 1 we present two ex-

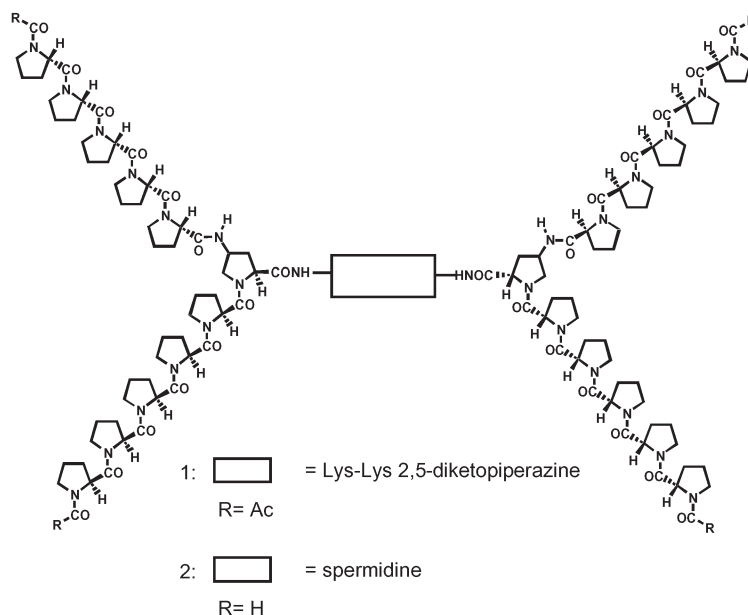


Fig. 1. Polyproline dendrimers.

amples of polyproline dendrimers (compounds **1** and **2**), synthesized by solid-phase, using polyproline peptides as building blocks, *cis*- $\gamma$ -amino-L-proline as branching unit and two different cores: spermidine and a Lys-Lys 2,5-diketopiperazine. *cis*- $\gamma$ -Amino-L-proline can be substituted by a 2-imidazolidine carboxylic acid, which can also act as a core. The conformational plasticity of one of this dendrimers based on polyproline helices is illustrated in Figure 2.

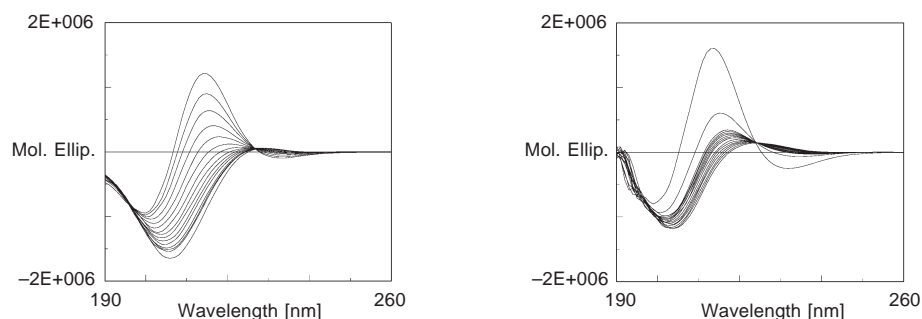


Fig. 2. Representative smoothed CD spectra recorded during: left PPI  $\rightarrow$  PPII isomerization ( $t_{90\%} \approx 3$  h), right PPII  $\rightarrow$  PPI isomerization ( $t_{90\%} \approx 10$  h) of a dendrimer in *n*-propanol/water (99.5 : 0.5, v/v) at 25 °C.

*cis*- $\gamma$ -Amino-L-proline, which we have used as dendrimer branching unit, has also been used as scaffold for the synthesis of functionalized  $\gamma$ -peptides. The advantages of our  $\gamma$ -peptides compared with those previously reported [5–7] are: i) the cyclic structure of the building block supplies conformational rigidity to the  $\gamma$ -peptide; ii) the secondary amino group allows the incorporation of a wide variety of functional groups; and iii) the orthogonally protected *cis*- $\gamma$ -amino-L-proline ( $\alpha$ -Boc,  $\gamma$ -Fmoc) allows an easy and efficient all-solid-phase synthesis to these novel compounds.

Figure 3 shows the structures of some of the compounds recently synthesized in our laboratory. The basic  $\gamma$ -peptide backbone is decorated with pending groups that mimic the side chains of the proteinogenic  $\alpha$ -amino acids Ala, Leu or Phe. As mentioned above, polyproline chains adopt helical left-handed structures in water (PPII). These structures present a periodicity of 3 residues per turn [2]. A PPII molecule displaying

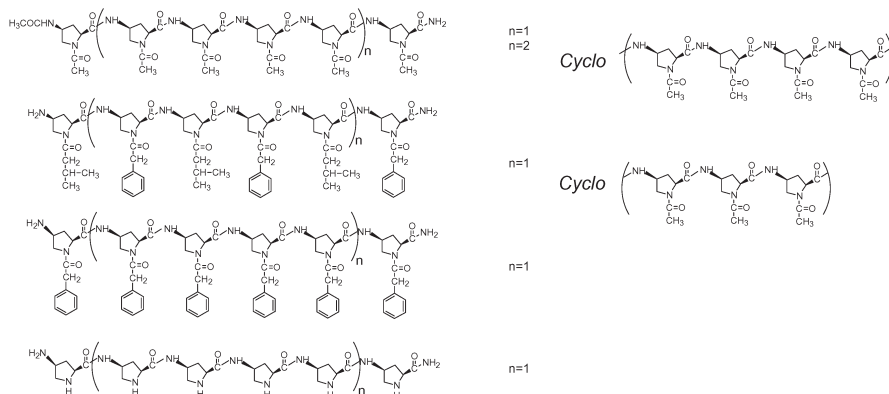


Fig. 3.  $\gamma$ -Peptide structures.

hydrophilic residues at positions  $i/i+3/i+6/i+9\dots$  and hydrophobic residues at positions  $i+2/i+4/i+5/i+7/i+8/i+10\dots$  would be a new type of amphipathic helix. This type of helix is found in the N-terminal domain of  $\gamma$ -zein of maize, and is formed by a repetitive sequence  $(VHLPPP)_8$  (Figure 4) [2]. In our laboratory we have synthesized different oligomers of general formula  $(VHLPPP)_n$  ( $n = 1, 3, 5, 8$ ) [8]. We have thoroughly studied these molecules in solution and have found that they: i) adopt PPII conformations; ii) are tensioactives; and iii) self-aggregate. Finally, we have proved that the amphipathic character of the individual molecules, generating very well defined structures, governs the self-aggregation mechanism. Studies by atomic force microscopy and electronic microscopy show the formation of tubular structures with very well defined diameters.

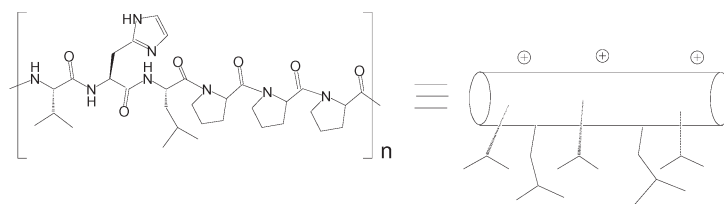


Fig. 4. Representation of the  $(VHLPPP)_n$  oligomers.

In summary, we have synthesized a wide variety of compounds based on proline. Our future research is focused not only in the physical properties of these compounds but also in their applicability, especially in drug delivery.

#### Acknowledgments

This work was supported by Marató de TV3, DGICYT (BIO 99-0484) and Generalitat de Catalunya (Grups Consolidats (1999 SGR 0042) and Centre de Referencia en Biotecnologia).

#### References

1. Williamson, P. *Biochem. J.* **297**, 249–260 (1994).
2. Rabanal, F., Ludevid, M.D., Pons, M., Giralt, E. *Biopolymers* **33**, 1019–1028 (1993).
3. Newkome, G.R., Moorefield, C.N., Vögtle, F. *Dendritic Molecules: Concepts, Synthesis, Perspectives*, VCH, Weinheim, 1996.
4. Tam, J.P. *Proc Natl. Acad. Sci. U.S.A.* **85**, 5409–5413 (1988).
5. Seebach, D., Brenner, M., Rueping, M., Schweizer, B., Jaun, B. *Chem. Commun.* 207–208 (2001).
6. Chung, Y.J., Huck, B.R., Christianson, L.A., Stauger, H.E., Krauthauser, S., Powell, D.R., Gellman, S.H. *J. Am. Chem. Soc.* **122**, 3995–4004 (2000).
7. Hanessian, S., Luo, X.H., Schaum, R. *Tetrahedron Lett.* **40**, 4925–4929 (1999).
8. Dalcol, I., Rabanal, F., Ludevid, M.D., Albericio, F., Giralt, E. *J. Org. Chem.* **60**, 7575–7581 (1995).

## **Complementary Assembly of Heterogeneous Multiple Peptides into Amyloid Fibrils with $\alpha$ - $\beta$ Structural Transitions**

**Yuta Takahashi<sup>1</sup>, Akihiko Ueno<sup>1</sup> and Hisakazu Mihara<sup>1,2</sup>**

<sup>1</sup>*Department of Bioengineering, Graduate School of Bioscience and Biotechnology,  
Tokyo Institute of Technology, Tokyo, Japan*

<sup>2</sup>*PRESTO, Japan Science and Technology Corporation, Yokohama 226-8501, Japan*

### **Introduction**

An improved understanding of protein misfolding and off-pathway aggregation is critical to the study of proteins related to amyloid diseases such as Alzheimer's and prion [1–6]. The pathway of protein misfolding involves a conformational transition, for example, from  $\alpha$ -helix to  $\beta$ -sheet. This transition is especially apparent in the transformation of the  $\alpha$ -helix-rich cellular form of the prion protein (PrP<sup>C</sup>) to the scrapie isoform with a higher  $\beta$ -sheet content (PrP<sup>Sc</sup>), which assembles into amyloid fibrils [3]. In general, one cause of protein misfolding and transformation is thought to be the exposure of the hydrophobic region of proteins in an unstable form to water environments, and the formation of aggregates that follows. A simplified model peptide can lead to a better understanding of the process by which misfolding and aggregation occur.

Recently, we have reported the design and synthesis of peptides undergoing a self-initiated  $\alpha$ -to- $\beta$  structural transition and amyloid fibril formation [7–12]. The N-termini of the peptides were modified with hydrophobic groups such as adamantanecarbonyl or octanoyl groups as exposed hydrophobic nucleation domains. We have also carried out mutational analyses for the charged residues (E, K) of the parent sequence. It has been shown that peptides, which originally do not have the ability, are able to self-assemble into the fibrils if the complementary peptide coexists. Furthermore, we attempted to assemble three or four peptide species complementarily and heterogeneously into amyloid fibrils.

### **Results and Discussion**

According to the previous studies [7–11], a peptide composed of two amphiphilic  $\alpha$ -helices was designed and the N-termini were acylated with the 1-adamantanecarbonyl (Ad-) group. The two- $\alpha$ -helix part was constructed from amino acid sequences of coiled-coil proteins, which had heptad repeats (abcdefg)<sub>n</sub> with hydrophobic residues at the a and d positions (Figure 1a). However, the peptide sequence also has the potential to form an amphiphilic  $\beta$ -strand in which hydrophobic residues and charged residues are separated on different faces of each heptad. We have synthesized a complete set of sixteen peptides with substitutions at the charged residues (E and K at X1–X4 positions) [12]. The conformational transition was evaluated by CD spectra and the amyloid formation was analyzed by transmission electron microscopy and thioflavin T binding assay.

Among the sixteen peptides examined, only four neutral peptides (6.EEKK, 7.EKEK (parent sequence), 10.KEKE, and 11.KKEE) showed structural transitions to  $\beta$ -sheet and homogeneous amyloid fibril formation. This result suggests that the charge neutralization is not sufficient for the fibril formation with a  $\beta$ -sheet structure and that the positions of positive and negative charges are critical for the well-organized assembly of the  $\beta$ -strands in the amyloid. None of the negatively (1.EEEE to 5.KEEE) or positively-charged peptides (12.EKKK to 16.KKKK) was able to form the amyloid fibrils, indicating that they disfavored intermolecular associ-

ation. All combinations of the equimolar mixtures of two of sixteen peptides (120 combinations) were examined employing the thioflavin T binding analysis to determine whether there are complementary pairings for the amyloid formation (Figure 1b). It has become clear that there are complementary pairings of the peptides for the fibril formation. The combinations are 2.EEEK/12.EKKK, 3.EEKE/13.KEEK, 4.EKEE/14.KKEK and 5.KEEE/15.KKKE. This result implies that two kinds of the  $\beta$ -strands would be arrayed in an antiparallel manner to form ion pairs in the fibrils [12].

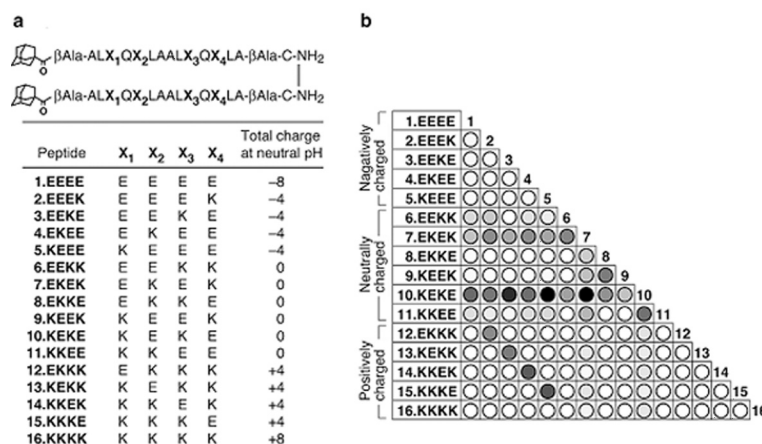


Fig. 1. Structure of sixteen peptides with substitutions of charged residues at X1–X4 (a), and the thioflavin T assay of combinations of the equimolar mixtures of two of sixteen peptides (120 combinations) (b). The darkness of the circles indicates the fluorescence intensity of thioflavin T.

Furthermore, in the library, the complementary triplets or quadruplets that heterogeneously assemble into the fibrils with three or four different peptides were identified. In the mixed screening of two peptides from 2.EEEK–5.KEEE (carrying –4 net charges) together with a peptide 16.KKKK (carrying +8 net charges), we found two combinations, 2.EEEK/4.EKEE/16.KKKK and 3.EEKE/5.KEEE/16.KKKK, are fibril-forming complementary triplets. Moreover, it was found that two quadruplets, 2.EEEK/5.KEEE/8.EKKE/16.KKKK and 3.EEKE/4.EKEE/9.KEEK/16.KKKK, possess an outstanding ability to form amyloid fibrils among four-peptides combinations.

In conclusion, it has been shown that the peptides, which originally do not have the ability to form the fibrils, are able to self-assemble into the fibrils if the complementary peptide coexists. The charged residues are determinants of regulating the amyloid fibril formation. According to this finding, we present the construction of amyloid fibrils involving three or four peptide species complementarily assembled. This method makes possible the sequential array of multiple kinds of functional groups and their site-specific incorporation into the predeterminable fibrous scaffold. The results obtained here may provide insights into studies on a number of amyloidosis-related mutant proteins, as well as a structural basis of well-organized self-assembling peptides and proteins.

### Acknowledgments

This work was supported in part by the Tokyo Ohka Foundation for the promotion of science and technology.

**References**

1. Fink, A.L. *Fold. Des.* **3**, R9–R23 (1998).
2. Dobson, C.M. *Trends Biochem. Sci.* **24**, 329–332 (1999).
3. Cohen, F.E., Prusiner, S.B. *Annu. Rev. Biochem.* **67**, 793–819 (1998).
4. Harper, J.D., Lansbury, P.T., Jr. *Annu. Rev. Biochem.* **66**, 385–407 (1997).
5. Kelly, J.W. *Curr. Opin. Struct. Biol.* **8**, 101–106 (1998).
6. Mihara, H., Takahashi, Y. *Curr. Opin. Struct. Biol.* **7**, 501–508 (1997).
7. Takahashi, Y., Ueno, A., Mihara, H. *Chem. Eur. J.* **4**, 2475–2484 (1998).
8. Takahashi, Y., Ueno, A., Mihara, H. *Bioorg. Med. Chem.* **7**, 177–185 (1999).
9. Takahashi, Y., Ueno, A., Mihara, H. *Peptide Science 1999 (Proceedings of the 36th Japanese Peptide Symposium)*, The Japanese Peptide Society, Osaka, 2000, pp. 57–60.
10. Takahashi, Y., Yamashita, T., Ueno, A., Mihara, H. *Tetrahedron* **56**, 7011–7018 (2000).
11. Takahashi, Y., Ueno, A., Mihara, H. *Structure* **8**, 915–925 (2000).
12. Takahashi, Y., Ueno, A., Mihara, H. *ChemBioChem* **2**, 75–79 (2001).

## Conformational Uniqueness *via* Designed Ion Pairs

Juliana K. Gill and Joel P. Schneider

Department of Chemistry, University of Delaware, Newark, DE 19716, USA

### Introduction

GCN4-p1 is a 33 amino acid peptide derived from the leucine zipper region of the protein GCN4. In solution, this peptide adopts a two stranded parallel coiled coil whose conformation is specified by the formation of a single buried H-bond between two asparagine residues located at position 16 of each helix [1,2]. It has been shown that an N16D mutant of GCN4-p1 will specifically form a heterodimer with an N16dap (diaminopropionic acid) mutant through formation of a single buried salt-bridge between the Asp and Dap sidechains. The free energy advantage for the formation of this heterodimer over any possible homodimers ( $\Delta\Delta G_{\text{specificity}}$ ) is 1.6 kcal/mol, indicating that a single buried salt bridge can specify the desired heterodimeric fold to an impressive degree. However, this heterodimer is about 2 kcal/mol less stable than wild-type GCN4-p1. This difference in thermodynamic stability is attributed to an increase in desolvation energy during the folding of the heterodimer as compared to GCN4-p1 [3]. (It is more difficult to desolvate charged side chains upon folding than the neutral asparagine side chains.) In order to circumvent the energetic cost of desolvation upon heterodimer formation, a novel basic amino acid having a side chain with increased hydrophobicity has been synthesized. A heterodimer formed between an N16D mutant and an N16mmdap (monomethylated dap) mutant shows increased thermal stability, demonstrating that by increasing the hydrophobicity of the basic side chain involved in salt bridge formation, a more stable heterodimer can be realized.

### Results and Discussion

A  $N_{\alpha}$ -Fmoc,  $N_{\beta}$ -methyl diaminopropionic acid (Mmdap) residue was synthesized from Z-serine by first forming the  $\beta$ -lactone using Mitsunobu chemistry followed by ring opening with trimethylsilyl-monomethyl amine (Figure 1) [4]. This residue was then suitably protected for Fmoc-based solid phase peptide synthesis and incorporated into

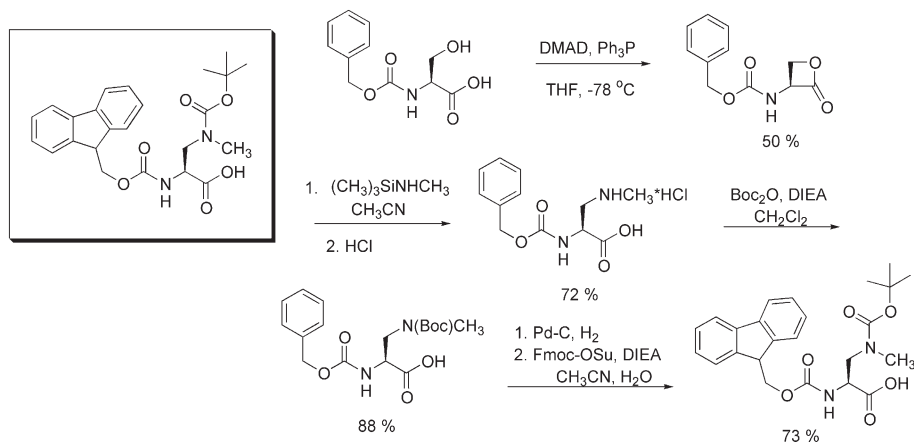


Fig. 1. Synthesis of  $N_{\alpha}$ -Fmoc,  $N_{\beta}$ -Boc,  $N_{\beta}$ -monomethyldiaminopropionic acid.

the following sequence of GCN4-p1 at position 16. (Ac-RMKQLED SKVEELLSKXY HLENEVARLKKLVGER-CONH<sub>2</sub>) A series of mutants were prepared where **X** = D, Dap, or Mmdap, affording the corresponding peptides: Asp-p1, Dap-p1 and Mmdap-p1. The pH-dependent folding of each peptide was determined by circular dichroism spectrometry. Figure 2 shows that these mutant peptides form folded homo-oligomers at pH's where the side chain at position 16 is neutral. The peptides are unfolded when their side chains are charged. Importantly, further studies indicate that equimolar mixtures of Asp-p1 and Mmdap-p1 (or Dap-p1) at pH 6 support heterodimer formation. For example, CD experiments where the mole-fraction of Mmdap-p1 (or Dap-p1) is varied from 0 to 1 resulted in a chevron shaped plot of  $\theta_{222}$  vs mole fraction with a minima at 0.5 indicating a 1 : 1 stoichiometry for both the Asp-p1 : Mmdap-p1 and Asp-p1 : Dap-p1 heterodimers. Analytical sedimentation ultracentrifugation experiments confirmed the dimeric nature of these hetero-oligomers.

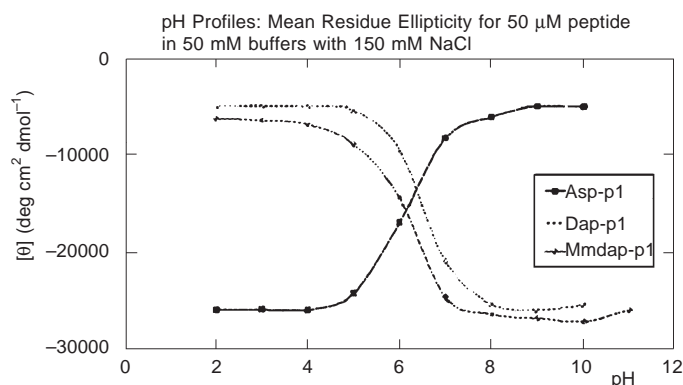


Fig. 2. The pH dependence of folding for the mutant peptides.

The thermodynamic stabilities of both the Asp-p1 : Mmdap-p1 and Asp-p1 : Dap-p1 heterodimers were determined by fitting the concentration and temperature dependence of their CD spectra to the Gibbs-Helmholtz equation. These thermal denaturation experiments indicate that the  $\Delta\Delta G_{\text{specificity}}$ 's calculated for the heterodimers are equivalent, and that the Asp-p1 : Mmdap-p1 heterodimer is approximately 0.6 kcal/mol more stable than the Asp-p1 : Dap-p1 heterodimer. This study demonstrates that a basic non-natural amino acid having a shortened side chain with increased hydrophobicity is capable of stabilizing a buried salt bridge without affecting the specificity of the protein fold.

### Acknowledgments

We would like to thank Dan Camac and the structural biology group at DuPont Pharmaceutical, Jim Lear at the University of Pennsylvania for "energetic" discussions, and the University of Delaware for financial support.

### References

1. Harbury, P.B., Zhang, T., Kim, P.S., Alber, T. *Science* **262**, 1401 (1993).
2. Gonzalez, L., Brosn, R.A., Richardson, D., Alber, T. *Nat. Struct. Biol.* **250**, 669 (1996).
3. Schneider, J.P., Lear, J.D., DeGrado, W.F. *J. Am. Chem. Soc.* **119**, 5742 (1997).
4. Ratemi, E.S., Vederas, J.C. *Tetrahedron Lett.* **35**, 7605 (1994).

## Design, Synthesis and Incorporation in Peptides of a $\beta$ -Turn Mimetic

Selvasekaran Janardhanam, Devan Balachari and Krishnan P. Nambiar

*Department of Chemistry, University of California, Davis, CA 95616, USA*

### Introduction

Designing peptides and proteins that fold into predetermined secondary structures is a challenging biochemical problem.  $\alpha$ -Helix,  $\beta$ -ribbon and turns are landmark protein secondary structures. While major advances have been made in the design of  $\alpha$ -helices, designing water-soluble  $\beta$ -ribbon structures and turns are under active investigation. Several unnatural turn structures have been designed for incorporation into peptides to enhance their folding to yield  $\beta$ -ribbon structures [1–5]. Most of these models involve complex ring systems, which require multistep synthesis. Using model building and computer graphics, we designed a simple  $\beta$ -turn mimic (Figure 1) using three simple building blocks,  $\beta$ -alanine, 3-amino-5-nitrobenzoic acid and sarcosine. Our model forms a nice hydrophobic interior while assuming a  $\beta$ -turn structure. We reasoned this to be quite favorable in aqueous solution.

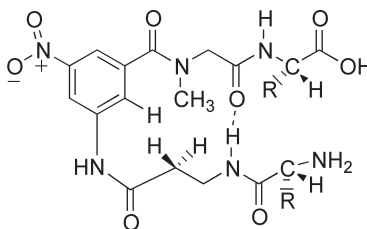


Fig. 1. Structure of the  $\beta$ -turn mimic.

### Results and Discussion

In earlier reports, we had shown that a strain-free disulfide bridge formed between the side chains of higher homologs of cysteine are much better in stabilizing  $\beta$ -ribbon structures as compared to cystine peptides [6,7]. Our results clearly show that a longer strain-free disulfide bridge between two peptide strands is much more efficient in stabilizing the  $\beta$ -ribbon structure of the peptide dimer as compared to an intramolecular cystine disulfide bridge.

The design of the turn structure allows clustering of the hydrophobic residues in the interior of the molecule, while the polar residues point outwards into the aqueous environment. The components of our turn structure are amino acids and hence it can be incorporated in the peptide sequence using standard solid-phase peptide synthesis. The incorporation of the turn structure in the middle of a peptide would orient the two halves of the peptide to form the hydrogen bonds characteristic of an antiparallel  $\beta$ -sheet. We synthesized a short peptide (T-V-hC-M-T-M-E- $\beta$ A-ANB-Sar-K-M-T-M-hC-Y-V) incorporating the turn structure using solid-phase methods and Fmoc chemistry, and purified it using reversed phase HPLC. CD spectroscopy indicates typical  $\beta$ -ribbon structure (Figure 2). Detailed structure determination using 2D-NMR spectroscopy is underway.

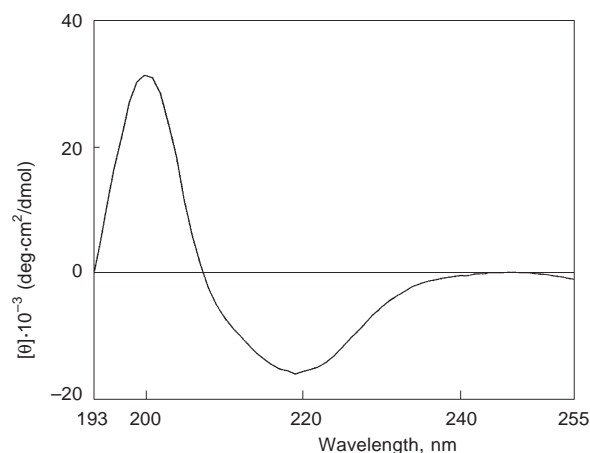


Fig. 2. CD spectrum of 5  $\mu$ M solution of the peptide [T-V-hC-M-T-M-E- $\beta$ A-ANB-Sar-K-M-T-M-hC-Y-V] in aqueous solution at 0  $^{\circ}$ C.

### Acknowledgments

This research was supported by NIH grant GM 39822.

### References

1. Wang, W., Xiong, C., Hraby, V.J. *Tetrahedron Lett.* **42**, 3159–3161 (2001).
2. Halab, L., Gosselin, F., Lubell, W.D. *Biopolymers* **55**, 101–122 (2000).
3. Neslooney, C.L., Kelly, J.W. *J. Am. Chem. Soc.* **118**, 5836–5845 (1996).
4. Nowick, J.S., Holmes, D.L., Mackin, G., Noronha, G., Shaka, A.J., Smith, E.M. *J. Am. Chem. Soc.* **118**, 2764–2765 (1996).
5. Kemp, D.S., Li, Z.Q. *Tetrahedron Lett.* **36**, 4175–4178 (1995).
6. Aberle, A.M., Reddy, H.K., Heeb, N.V., Nambiar, K.P. *Biochem. Biophys. Res. Commun.* **200**, 102–107 (1994).
7. Nambiar, K.P., Janardhanam, S., Balachari, D., In G.B. Fields, J.P. Tam, and G. Barany (Eds) *Peptides for the New Millenium, Proceedings of the 16th American Peptide Symposium*, Kluwer Academic Publishers, 2000, p. 311.

## Evaluating PERMs as Protein Mimics

Arno F. Spatola<sup>1</sup>, Anne-Marie Leduc<sup>1</sup>, James L. Wittliff<sup>2</sup>  
and K. Grant Taylor<sup>1</sup>

<sup>1</sup>Department of Chemistry and <sup>2</sup>Department of Biochemistry and Molecular Biology and  
the Institute for Molecular Diversity and Drug Design,  
University of Louisville, Louisville, KY 40292, USA

### Introduction

The post-proteomic era promises a resurgence in protein-based drug design. While genetic engineering may provide improved proteins at a modest bulk cost, at least three chemistry-based approaches will also be competitive. These include a) protein ligation, as exemplified by the work of Kent [1] and Tam [2]; b) genetic reengineering, which can remarkably modify the ribosomal apparatus to allow the incorporation of unusual amino acids into a desired structure (Schultz *et al.* [3]); and c) protein mimetics, in which simpler organic molecules may replace proteins as agonists, antagonists, or even as catalases.

### Results and Discussion

As our first example of protein mimetics, we have selected the nuclear receptor-coactivator interactions, which represent an attractive alternative option for transcriptional control. Nuclear receptors, including the estrogen, androgen, progesterone, glucocorticoid, mineralocorticoid, and a growing number of orphan receptors, are important drug targets [4]. Most are non-peptidic, such as tamoxifen – the anti-cancer agent – or raloxifene, used to retard osteoporosis. But with the discovery of nuclear receptor-modulating proteins known as coactivators and corepressors, came the potential to disrupt normal cell functions through modification of protein-protein interactions.

Virtually all nuclear receptors have several activation factor domains [5,6], one of which is specific for a ubiquitous coactivator pentapeptide sequence known as the NR box [7,8]. The most common fragment, LXXLL, becomes an ideal candidate for protein mimicry design, particularly if the replacement retains the required three-dimensional structure of the parent coactivator-binding surface [9].

An X-ray structure by Shiau *et al.* [10] revealed the  $\alpha$ -helical orientation of an LXXLL peptide bound to ligand-activated estrogen receptor  $\alpha$ . Based on this finding, we have designed and synthesized linear and cyclic peptides intended to replicate the LXXLL structure while reducing the molecule to a minimally productive size. In analogy to SERMs (selective estrogen response modifiers), we term these compounds PERMs for peptidomimetic estrogen receptor modulators. Our studies have led to the following conclusions:

- While short linear peptides are flexible or form  $\beta$ -sheets, molecular modelling confirmed that certain cyclic structures can best retain an  $\alpha$ -helical orientation.
- While *i, i+4* cyclic amides [11,12] and *i, i+3* disulfide bridges [13] have been used to lock in the  $\alpha$ -helix conformation, the best fit with the LXXLL compounds corresponded to an *i, i+3* disulfide with D-Cys and L-Cys.
- Short peptides and pseudopeptides based on LXXLL and LX $\Psi$ [CH<sub>2</sub>NH]XLL showed no activity on steroid-based gel shift and supershift bioassays [14].

Our initial studies confirm that the cyclic structures are exceptionally promising as protein mimics. Further efforts will focus on structural modifications to make the pep-

tide molecules more “drug-like”, lock-in receptor selectivity, and improve membrane permeability.

### **Acknowledgments**

We thank Tom Burris of Lilly Research Laboratories and V. Narayanan of the National Cancer Institute for providing biological assays for this research, and John Trent of the J. Graham Brown Cancer Center at the University of Louisville for invaluable assistance with molecular modelling.

### **References**

1. Dawson, P.E., Muir, T.W., Clark-Lewis, I., Kent, S.R.H. *Science* **266**, 776 (1994).
2. Liu, C.F., Tam, J.P. *J. Am. Chem. Soc.* **116**, 4149 (1994).
3. Cornish, V.W., Mendel, D., Schultz, P. *Angew. Chem., Int. Ed. Engl.* **34**, 621–633 (1995).
4. Burris, T.P., McCabe, E.R.B. (Eds.) *Nuclear Receptors and Genetic Disease*, Academic Press, San Diego, 2001.
5. O'Malley, B. *Mol. Endocrinol.* **4**, 363–369 (1990).
6. Klinge, C.M. *Steroids* **65**, 227–251 (2000).
7. Heery, D.M., Kalkhoven, E., Horare, S., Parker, M.G. *Nature* **387**, 733–736 (1997).
8. Torchia, J., Glass, C., Rosenfeld, M.G. *Curr. Opin. Cell Biol.* **10**, 373–383 (1998).
9. Norris, J.D., Paige, L.A., Christensen, D.J., Chang, C.-Y., Huacani, M.R., Fan, D., Hamilton, P.T., Fowlkes, D.M., McDonnell, D.P. *Science* **285**, 744–746 (1999).
10. Shiau, A.K., Barstad, D., Loria, P.M., Cheng, L., Kushner, D.J., Agard, D.A., Green, G.L. *Cell* **95**, 927–937 (1998).
11. Felix, A.M., Heimer, E.P., Wang, C.-T., Lambros, T.J., Fournier, A., Mowles, T.F., Maines, S., Campbell, R.M., Wegrzynski, B.B., Toome, V., Fry, D.C., Madison, V.S. *Int. J. Pept. Protein Res.* **112**, 6046 (1990).
12. Osapay, G., Taylor, J.W. *J. Am. Chem. Soc.* **112**, 6046 (1990).
13. Pellegrini, M., Royo, M., Chorev, M., Mierke, D.F. *J. Peptide Res.* **49**, 404–414 (1997).
14. Wittliff, J.L., Wenz, L.L., Dong, J., Nawaz, Z., Butt, T.R. *J. Biol. Chem.* **265**, 22016–22022 (1990).

## Amphipathic Stabilization of the $3_{10}$ -/ $\alpha$ -Helix Equilibrium in Synthetic Peptides Rich in $C^\alpha, C^\alpha$ -Disubstituted Glycines

Lars G. J. Hammarström, Ted J. Gauthier and Mark L. McLaughlin

Louisiana State University, Department of Chemistry, Baton Rouge, LA 70803, USA

### Introduction

The ability to design desired secondary peptide structure *a priori* from specific amino acid sequence is a major goal in peptide studies. In particular, influences on the  $3_{10}$ -/ $\alpha$ -helical equilibrium have gained considerable recent interest [1]. The ability to understand and control the  $3_{10}$ -/ $\alpha$ -helix equilibrium is desirable in the development of peptide design research. We have synthesized a series of closely related deca-meric peptides in order to determine to what extent amphipathic character plays a role in helix conformation preference in amphipathic environments (Table 1).

Table 1. Peptides designed to be perfectly amphipathic as an  $\alpha$ -helix (Pi-10, Ach-10 $\alpha$  and Cyh-10) and perfectly amphipathic as a  $3_{10}$ -helix. (Ipi-10, Ach-10 and Ich-10).

Peptide	Sequence	Design
Pi-10	H-Aib <sup>a</sup> -Aib-Api <sup>b</sup> -Lys <sup>c</sup> -Aib-Aib-Api-Lys-Aib-Aib-NH <sub>2</sub>	$\alpha$
Ipi-10	H-Api-Aib-Aib-Lys-Aib-Aib-Lys-Aib-Aib-Api-NH <sub>2</sub>	$3_{10}$
Ach-10 $\alpha$	H-Ac <sub>6</sub> c <sup>d</sup> -Aib-Lys-Api-Aib-Ac <sub>6</sub> c-Api-Lys-Ac <sub>6</sub> c-Aib-NH <sub>2</sub>	$\alpha$
Ach-10	H-Api-Aib-Ac <sub>6</sub> c-Lys-Ac <sub>6</sub> c-Aib-Lys-Aib-Ac <sub>6</sub> c-Api-NH <sub>2</sub>	$3_{10}$
Cyh-10	H-Ac <sub>6</sub> c-Ac <sub>6</sub> c-Api-Lys-Ac <sub>6</sub> c-Ac <sub>6</sub> c-Api-Lys-Ac <sub>6</sub> c-Ac <sub>6</sub> c-NH <sub>2</sub>	$\alpha$
Ich-10	H-Api-Ac <sub>6</sub> c-Ac <sub>6</sub> c-Lys-Ac <sub>6</sub> c-Ac <sub>6</sub> c-Lys-Ac <sub>6</sub> c-Ac <sub>6</sub> c-Api-NH <sub>2</sub>	$3_{10}$

<sup>a</sup> Aib: 2-aminoisobutyric acid; <sup>b</sup> Api: 4-aminopiperidine-4-carboxylic acid; <sup>c</sup> The incorporation of 20% L-lysine (Lys) allows for CD spectroscopic determination of peptide secondary structure by inducing right-handed helix formation. <sup>d</sup> Ac<sub>6</sub>c: 1-amino-1-cyclohexanoic acid.

### Results and Discussion

By studying the helical wheel cross sections of the peptides in their  $\alpha$ - and  $3_{10}$ -helical conformations, it is apparent that amphipathicity is maximized when the peptides have continuous hydrophobic and hydrophilic faces. Otherwise hydrophilic residues are distributed throughout the cross-section of the helix. This work tests the hypothesis that synthetic helical peptides “prefer” maximized amphipathicity, and applies it as a helix design principle. The general sequence of peptides designed to be  $\alpha$ -helical is: H-N-N-P-P-N-N-P-P-N-N-NH<sub>2</sub>; (N = non-polar residues; P = polar residues) and the  $3_{10}$ -helical peptides have the sequence: H-P-N-N-P-N-N-P-N-N-P-NH<sub>2</sub>. Peptides that adopt the  $\alpha$ -helical amphipathic distribution are less amphipathic in the  $3_{10}$ -helical conformation and *vice versa*, (Figure 1). Since the sequence permutation isomer pairs contain the same amino acids in varying sequences, it is likely that the helical conformation adopted is primarily based on preferential formation of amphipathic structures.

The most prominent  $3_{10}$ -helical character for both Ipi-10 and Ach-10 was observed in SDS micelles (Figure 2), indicating that an amphipathic environment strongly favors the more amphipathic secondary structure of the peptide. Unexpectedly, Ich-10 failed to show this same transition. Ich-10 forms an  $\alpha$ -helix in all solvent systems tested. This may be due to steric interactions between adjacent cyclic moieties of Ac<sub>6</sub>c

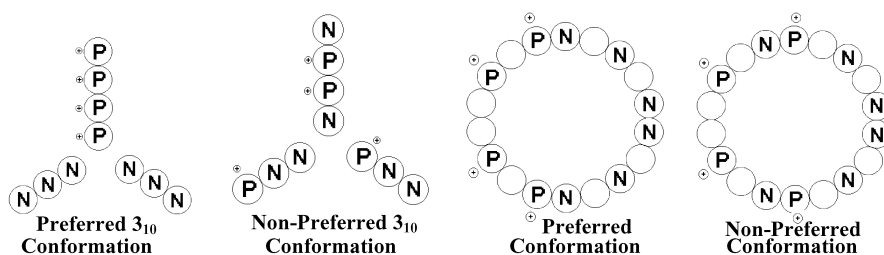


Fig. 1. Helical wheel cross-sections of empirical peptide sequences in their preferred conformation and non-preferred conformations. **P** designates ionizable polar amino acid residues (Lys or Arg); **N** designates non-polar residues (Aib or Ac<sub>6</sub>c). Empty circles represent non-occupied locations in the alpha helical wheel.

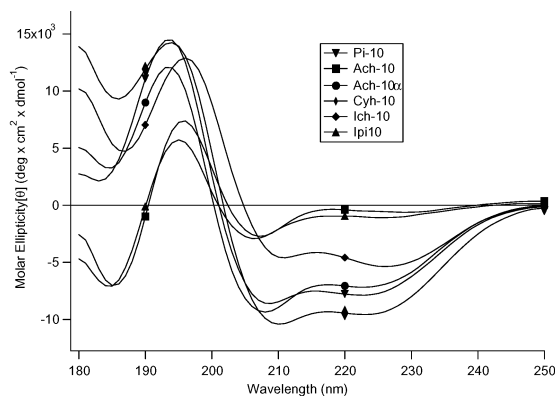


Fig. 2. ECD spectra of designed peptides in 25 mM SDS micelles.

in the tightly wound  $3_{10}$ -helix. A transition to  $\alpha$ -helix would relieve this stress by increasing the diameter of the helix, and staggering cyclic groups [2].

It is interesting to note the prominent negative maximum present at 185 nm for both of the  $3_{10}$ -helices in SDS micelles. This maximum is not found in any of the designed  $\alpha$ -helical peptides, nor is it apparent in the permutation isomers of Ipi-10 and Ach-10. Thus, one must assume that this band is due to peptide conformation and not an effect of solvent or residue absorption. It may be an important factor in the interpretation of  $3_{10}$ - vs.  $\alpha$ -helical segments, but a larger basis set of water-soluble  $3_{10}$ -helices is needed before anything can be said definitively.

#### Acknowledgments

The authors wish to thank Dr. Robert P. Hammer and Martha Juban of the Louisiana State University Protein Facility. This work was supported by NIH GM 56835.

#### References

1. Bolin, K.A., Millhauser, G.L. *Acc. Chem. Res.* **32**, 1027–1033 (1999).
2. Sun, J.K., Doig, A.J. *Protein Sci.* **7**, 2374–2383 (1998).

## Design, Synthesis and Characterization of Novel Scaffold-Assembled Collagen Mimetics

Garth A. Kinberger and Murray Goodman

Department of Chemistry and Biochemistry, University of California, San Diego,  
 CA 92093, USA

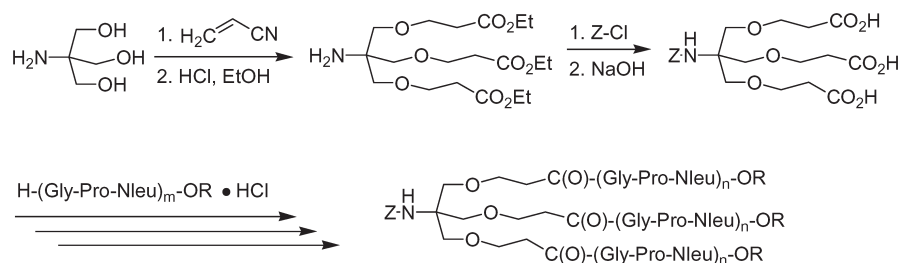
### Introduction

In collagen mimetic research we have demonstrated the successful incorporation of *N*-isobutyl glycine (Nleu) into triple helical collagen-like peptides composed of Gly-Nleu-Pro and Gly-Pro-Nleu sequences [1]. In addition, scaffolds (templates) have been employed by us to enhance the formation and stability of triple helices [2]. In this brief communication we report the utilization of a new scaffold for collagen mimetic synthesis. This scaffold, synthesized from the biological buffer TRIS (tris-(hydroxymethyl)aminomethane), possesses three carboxylic acid moieties for attachment to the N-terminus of peptide chains and a free amine for reaction at surfaces or with core structures (Scheme 1) [3]. This scaffold allows us to prepare novel collagen-based biomaterials.

### Results and Discussion

Collagen-like peptides composed of the sequence Gly-Pro-Nleu have been assembled on the TRIS scaffold (Scheme 1). Molecules with chain lengths of 1, 3, 5, 7 and 10 have been prepared which were investigated by HPLC and mass spectrometry MALDI-TOF. Triple helicity was determined by circular dichroism (CD). The midpoint of the temperature dependence of optical rotations established the melting temperatures ( $T_m$ ). The CD and optical rotation studies of these molecules were initially carried out in water. Triple helicities were also determined in 2 : 1 ethylene glycol : water (EG : H<sub>2</sub>O). The triple helices are generally more stable in this solvent system.

We have recently embarked on a program of dendrimer synthesis, which involves linking the free amine of the TRIS-assembled collagen mimetic structures to a core molecule such as trimesic acid. The dendrimer shown in Figure 1 represents our initial success in building these star-like structures. In EG : H<sub>2</sub>O 2 : 1 the dendrimer exhibits enhanced stability of the triple helices compared to TRIS-terminated analogs of similar length.



*Scheme 1. Synthesis of the TRIS scaffold and the subsequent attachment of peptidomimetic chains where R is Me or Et, m is 1, 2 or 5 and n is 1, 3, 5, 7 and 10.*

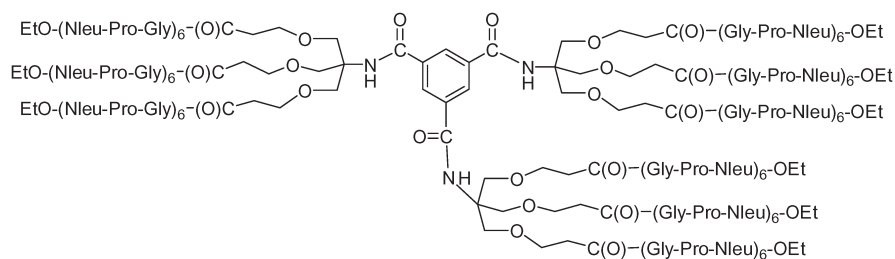


Fig. 1. A collagen mimetic dendrimer assembled upon a trimesic acid core structure.

### Acknowledgments

We thank the NSF Biomaterials division for financial support.

### References

1. Feng, Y., Melacini, G., Taulane, J.P., Goodman, M. *Biopolymers* **39**, 859–872 (1996).
2. Feng, Y., Melacini, G., Taulane, J.P., Goodman, M. *J. Am. Chem. Soc.* **118**, 10351–10358 (1996).
3. Newkome, G.R., Lin, X. *Macromolecules* **24**, 1443–1444 (1991).

## **Design and Synthesis of a Mini-Prorelaxin Model**

**Marc Mathieu, Nicola F. Dawson, John D. Wade  
and Geoffrey W. Tregear**

*Howard Florey Institute of Physiology and Medicine, University of Melbourne, Victoria 3010,  
Australia*

### **Introduction**

Relaxin is a two-chain peptide that shares several common features with insulin, such as size, chain structure and the cross-linking pattern. It is produced principally by the ovaries during pregnancy and has three major biological effects: (1) it decreases connective tissue formation (antifibrotic); (2) it promotes blood vessel formation (pro-angiogenic); and (3) it dilates blood vessels (vasodilatory). As a naturally occurring hormone, relaxin may serve as a treatment for a variety of disorders, such as infertility, peripheral arterial disease, cardiovascular disease, and other systemic diseases. The hormone is synthesised as a single-chain precursor, prorelaxin (as for insulin), and produced by proteolytic processing by enzymes [1].

In order to develop human relaxin analogues for possible therapeutic use and to bypass the currently-employed two chain folding process, we have investigated the use of a short connecting C-peptide between the A- and B-chains which would still allow proper refolding [2,3]. For the assembly of the long single-chain peptide, we chose the native chemical ligation approach that enables the selective coupling in aqueous solutions of unprotected peptide fragments through highly chemoselective reactions prior to folding [4]. A considerable advantage of this approach is the great flexibility regarding the choice of the individual fragments.

### **Results and Discussion**

For the design of our model, we took into account previous work done on relaxin and insulin [2,5]. The sequence was chosen by including all peptide domains of the native protein important for biological activity based on structure-function studies [6]. From the crystal structure of relaxin, it was determined that the N-terminus of the B-chain was only about 10 Å away from the C-terminus of the A-chain, 5 Å closer than in the regular B-C-A model. For this reason we undertook the synthesis of the inverted form (A-C-B), compared to the native (B-C-A), in which a short connecting C-peptide was used. This peptide also restrains to some degree the flexibility of the molecule.

Peptides 1 and 2 were prepared by manual Boc solid-phase peptide synthesis; their C-terminal thioester linker was prepared as previously described [7]. The N-terminal biotin label on peptide 1 was introduced using the standard acylation protocols. The N-terminal protecting group on peptide 2 was introduced by treating the peptide with 2-methylsulfonyl ethyl 4-nitrophenyl carbonate for 1 h in DMF/5% DIEA. Peptide 3 was prepared by automatic continuous-flow Fmoc solid-phase synthesis. The sequential ligation of unprotected fragments (Figure 1) was performed in 0.1 M phosphate buffer (pH 7.5) containing 4 M guanidine, 2% (v/v) benzylmercaptan and 2% (v/v) thiophenol. The N-terminal Msc protecting group on peptide 2 was removed by raising the ligation mixture to pH 13 with 1 N NaOH for a period of 10 min. All reactions were monitored by RP-HPLC and MALDI-MS, and intermediates were purified by preparative RP-HPLC. Yields (including the folding step) were in the lower range, due in part to the poor solubility of the individual peptides, and the corresponding ligation

products. It also appeared that some of the thioester peptides were unstable in the ligation buffers, and this affected the overall recovery as well.

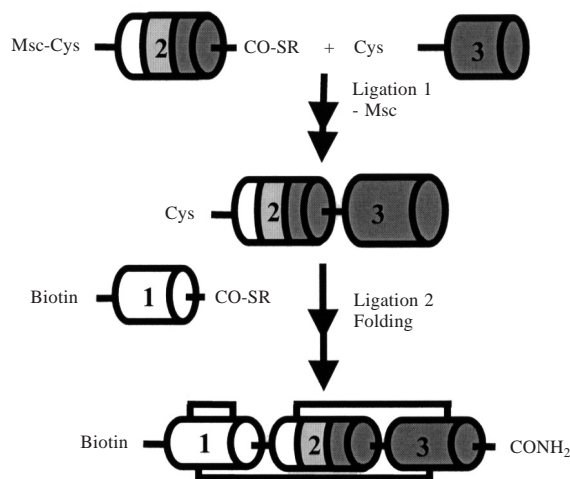


Fig. 1. Sequential chemical ligation of biotinylated mini-prorelaxin.

Future work will focus on (i) reducing the number of fragments, and (ii) enhancing the handling properties of the individual fragments through sequence modification.

## References

1. Sherwood, O.D. *The Physiology of Reproduction*, Raven Press, New York, 1994, p. 861.
2. Chang S.G., Kim, D.Y., Choi, K.D., Shin, J.M., Shin, H.C. *Biochem. J.* **329**, 631–635 (1998).
3. Vandlen, R., Winslow, J., Moffat, B., Rinderknecht, E. *Progress in Relaxin Research. Relaxin 1994*, Global Publication Services, Singapore, 1994, p. 59.
4. Dawson, P.E., Kent, S.B.H. *Ann. Rev. Biochem.* **69**, 923–960 (2000).
5. Heath, W.F., Belagaje, R.M., Brooke, G.S. *J. Biol. Chem.* **267**, 419–425 (1992).
6. Tan, Y.Y., Wade, J.D., Tregear, G.W., Summers, R.J. *Br. J. Pharm.* **123**, 762–770 (1998).
7. Hackeng T.L., Griffin, J.H., Dawson, P.E. *Proc. Natl. Acad. Sci. USA* **96**, 10068–10073 (1999).

## Site Specificity Metal Binding Affinity in C-Terminal of Calmodulin

Yiming Ye and Jenny J. Yang

*Department of Chemistry, Georgia State University, Atlanta, Georgia 30303, USA*

### Introduction

EF-hand proteins use the ubiquitous EF-hand calcium-binding motif to coordinate diverse cellular functions ranging from muscle control and neuronal signaling, to apoptosis and cell cycle control [1–3]. A classic EF-hand motif spans 29 residues and consists of a highly conserved calcium-binding loop flanked by two helices. All the calcium-binding ligands are located inside the 12-residue loop (EF-hand loop). Nearly all the EF-hand proteins contain at least two calcium-binding sites. The binding to calcium is highly co-operative. The trigger protein, calmodulin, regulates many biological processes by calcium-induced conformational change. It contains four EF-hand calcium-binding sites in two domains. Extensive studies have shown that the calcium binding affinity of the C-terminal is greater than that of the N-terminal.

The site-specific binding affinity of calmodulin is hampered by the multiple interactive metal ions and calcium-induced conformational change. In this study, we report our investigation of the intrinsic calcium binding affinity of C-terminal calcium-binding site III and IV by engineering isolated EF-hand motifs with Gly linkers in a scaffold protein, domain 1 of CD2-D1 (denoted as CAM-CD2-III-5G and CAM-CD2-IV-5G) (Figure 1). This novel approach allows us to focus specifically on the intrinsic binding ability of an individual EF-hand motif without the limitation of simplistic peptide models.



*Fig. 1. 3D structure of the host protein domain 1 of CD2. Loop III from calmodulin with glycine linkers was inserted into the host protein at the loop between C' and C''  $\beta$ -sheet. Previous studies have shown that this region can tolerate many mutations, while retaining the native conformation of the protein.*

### Results and Discussion

Our previous studies have shown that the insertion of EF-loop III of calmodulin into CD2-D1 with 3 Gly residues on each end does not change the native conformation of the host protein. The insertion of EF-loop IV into CD2-D1 was carried out using the similar mutagenesis procedure. The protein expression and purification of CAM-CD2-IV-5G are very similar to that of CAM-CD2-III-5G. The conformational analysis, monitored by far-UVCD, near-UVCD, fluorescence, and NMR, of CAM-CD2-

III-5G and CAM-CD2-IV-5G indicated that their secondary and tertiary structures are similar with that of host protein, domain 1 of CD2, suggesting that the insertion of calcium binding loop with Gly linker from calmodulin did not change the host protein conformation.

To monitor the metal binding in a protein, the fluorescence from the lanthanide ion  $\text{Tb}^{3+}$  is frequently used, because of similar effective ionic radii (0.98 and 1.06 Å for  $\text{Ca}^{2+}$  and  $\text{Tb}^{3+}$ , respectively), it is often used to effectively replace bound  $\text{Ca}(\text{II})$ . In addition, the modeling of CAM-CD2-III-5G and CAM-CD2-IV-5G shows that the distance between the metal binding site in the loop and a Tyr in position 8 of the loop is about 3 Å. Excited at 292 nm, we are able to observe the  $\text{Tb}(\text{III})$  energy transfer between Tyr and  $\text{Tb}(\text{III})$  at 545 nm with enhanced Tb fluorescence upon addition of  $\text{Tb}(\text{III})$ . The binding constant of CAM-CD2-III-5G can be obtained by fitting the fractional change of enhanced Tb fluorescence as a function of  $\text{Tb}(\text{III})$  concentration (assuming 1 : 1 protein and  $\text{Tb}(\text{III})$  binding).

Using the Trp fluorescence methods, we have examined the metal affinity of CAM-CD2-III-5G and CAM-CD2-IV-5G for  $\text{La}(\text{III})$ . The spectra of fluorescence shows that the fluorescence intensity of proteins is gradually decreasing with increasing  $\text{La}(\text{III})$  concentration without changing the emission maximum greatly, but in high  $\text{La}(\text{III})$  concentration (about 1 mM), the addition of  $\text{La}(\text{III})$  does change the emission maximum from 327 to 340 nm and the 340 nm is close to the free Trp amino acid emission maximum, suggesting that high  $\text{La}(\text{III})$  concentration would expose the buried Trp of the proteins. Under identical conditions, CAM-CD2-III-5G exhibits stronger metal binding affinities for both  $\text{La}(\text{III})$  and  $\text{Tb}(\text{III})$  than that of CAM-CD2-IV-5G. The binding affinity of  $\text{La}(\text{III})$  and  $\text{Tb}(\text{III})$  for CAM-CD2-III-5G are 59 and 2  $\mu\text{M}$  respectively; for CAM-CD2-IV-5G are 121 and 18  $\mu\text{M}$  respectively.

### Conclusion

The insertion of the C-terminal calcium binding loop III and IV of calmodulin into CD2-D1 (CAM-CD2-III-5G and CAM-CD2-IV-5G) retain the host protein's conformation, and they have high  $\text{Tb}(\text{III})$  and  $\text{La}(\text{III})$  binding affinity.

### Acknowledgments

We thank Dr. Yang's group for their helpful discussion. The study is supported in part by the NSF grant MCB-0092486 and NIH GM 62999-1 for JJY.

### References

1. Ikura, M. *Trends Biochem. Sci.* **21**, 14–17 (1996).
2. Kawasaki, H., Kretsinger, R.H., *Calcium-binding proteins 1: EF-hands. Protein Profile* **2**(4), 297–490 (1995).
3. Carafoli, E., Klee, C.B. (Eds.) *Calcium as a cellular regulator*, Oxford University Press, 1999.

## A Cassette Ribonuclease: Site Selective Cleavage of RNA by a Ribonuclease S-Bearing RNA-Recognition Segment

Shiroh Futaki, Michihiro Araki, Tatsuto Kiwada, Ikuhiko Nakase and Yukio Sugiura

*Institute for Chemical Research, Kyoto University, Uji, Kyoto 611-0011, Japan*

### Introduction

Elucidation of the two-dimensional and three-dimensional structures of RNA has recently been required in relation to their therapeutic potential as targets of RNA-oriented molecules, such as antisense nucleic acids and ribozymes. Structural elucidation of RNAs leads to an understanding of the replication mechanisms of RNA viruses, and also provides new target sites for antiviral drugs. We report here the creation of a novel Rnase, in which a conjugate of an RNA recognition peptide and the S-peptide were encapsulated as a cassette in RNase S (Figure 1A).

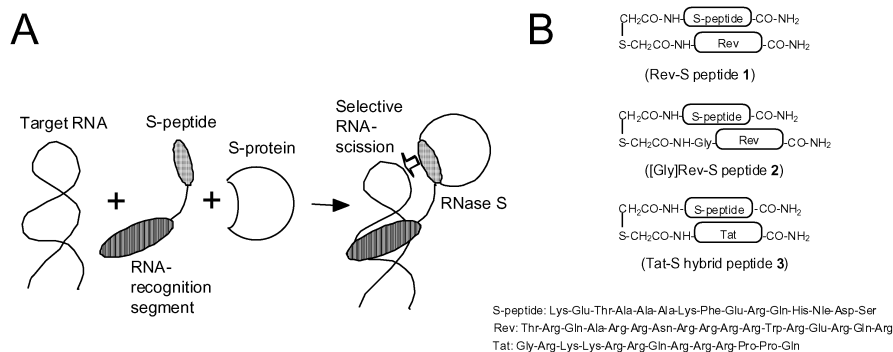


Fig. 1. The general concept of the "cassette" RNases (A) and design of the "cassette" peptides comprising an RNA-recognition segment and the S-peptide.

### Results and Discussion

The RNA binding segment derived from the HIV-1 Rev protein was selected as a model of the RNA recognition segment. The design of the cassette molecule, *i.e.*, the conjugate of the RRE-recognition peptide and the S-peptide (Rev-S peptide 1), is shown in Figure 1B. The sequence corresponding to the positions 34-50 of HIV-1 Rev was employed as the RNA-recognition peptide. Residues 1-15 of the S-peptide are sufficient to form a complex with the S-protein, while retaining the RNase activity. The N-termini of both peptides were connected so that the RNase S bearing the RNA-recognition segment is situated close to the RRE loop. Met13 in the original S-peptide was replaced with norleucine (Nle) for ease of handling. A conjugate with an additional Gly at the N-terminus of HIV-1 Rev-(34-50) ([Gly]Rev-S peptide 2), and a conjugate of the S-peptide with HIV-1 Tat-(48-60) (Tat-S peptide 3), which is another RNA-binding peptide specific for an RNA loop called Tat response element, were respectively designed to clarify the effect of the linkers and the RNA-recognition segments on the detection and cleavage of the target RNA by the cassette RNases.

We examined whether the Rev-S peptide 1 and S-protein form a complex for attachment to the RNA derived from the RRE and cleave it at a specific site. A truncated

## Analytical Methods

RNA derived from the stem-loop IIB of RRE, which contains the highest affinity Rev binding site, was employed as a model (Figure 2A). As shown in Figure 2B, the RNA was preferentially cleaved at a specific position by the complex of the Rev-S peptide **1** and the S-protein (lanes 6–8). Limited hydrolysis of the RNA by RNase T<sub>1</sub>, a G-specific RNase, gave a major cleavage band at a position corresponding to one base shorter than that for the above main cleavage band (Figure 2B, lane 2). As RNase T<sub>1</sub> hydrolyzes the single strand RNA much more preferentially than the double strand RNA, the cleavage site for the RNase T<sub>1</sub> treatment was deduced to be G adjacent to C54 (indicated by the bold arrow in Figure 2A). RNase S was reported to retain the pyrimidine preference in the RNA scission, even when the S-peptide was fused with other proteins. Taken together, it is most likely that the complex of the Rev-S peptide and the S-protein was cleaved at the 3' site of C in the RNA loop (Figure 2A, open arrow). Efficiency of the cleavage using the mixture of the Tat-S peptide **3** and the S-protein was much less than that by the mixture of the Rev-S peptide **1** and S-protein. The specificity of the cleavage in the mixture of the [Gly]Rev-S peptide **2** and S-protein was similar to the mixture of **1** and the S-protein. However, the efficiency of the cleavage is again less than that of the latter.

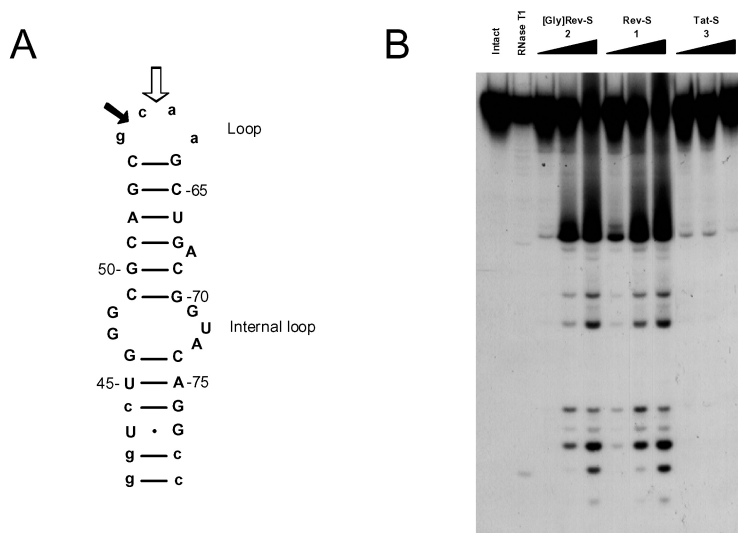


Fig. 2. Structure of RNA (A) and site-specificity in the hydrolysis of 5'-<sup>32</sup>P-end-labeled RRE RNA (B). Lane 1, intact RRE RNA; lane 2, RNA treated with RNase T<sub>1</sub>; lanes 3–11, RNA treated with the S-protein (1 nM) in the presence of the [Gly]Rev-S peptide **2**, Rev-S peptide **1**, and Tat-S peptide **3**, respectively. The concentration of conjugate **1**, **2**, and **3** was 1, 10, and 100 nM (from the left), respectively. 15% polyacrylamide gel was used for the electrophoresis.

In conclusion, we have demonstrated that the RNase S equipped with an RNA-recognition cassette worked as an efficient tool for the detection of a specific structure of RNA. These cassette RNases will be utilized as a powerful tool for uncovering the factors determining the structure-functional relationships of RNA.

## Protein Models on Carbohydrate Templates: Effect of the Template

Jesper Brask, Jan M. Dideriksen and Knud J. Jensen

Department of Chemistry, Technical University of Denmark, Building 201,  
Kgs. Lyngby, DK-2800, Denmark

### Introduction

*De novo* design is a valuable tool for the systematic study of factors controlling protein structure and function [1]. We have previously described [2–4] the concept of carbohydrates as templates for *de novo* design of protein models and introduced the terms carbopeptides and carboproteins for this class of template-assembled synthetic proteins [5]. The chemoselective oxime ligation [6] of tetraaminoxyacetyl functionalized carbohydrates and amphiphilic C-terminal peptide aldehydes provided carboproteins that fold to form 4- $\alpha$ -helix bundles according to CD spectroscopy and NMR H-D exchange studies [4].

### Results and Discussion

In order to investigate the contribution of the template to carboprotein structure and stability, templates **1**, **2**, and **3** were prepared from methyl  $\alpha$ -D-Galp, methyl  $\alpha$ -D-Glcp and methyl  $\alpha$ -D-Altp, respectively (Figure 1, left). The synthesis followed the procedure previously published for **1** [3].

Next, oxime ligations with the C-terminal hexadecapeptide aldehyde Ac-YEELLKKLEELLKKAG-H, **4**, provided carboproteins **5**, **6**, and **7** (structure illustrated for **5** in Figure 1, right). Reactions proceeded in aqueous acetate buffer, pH 4.76 over 2 h with 50% excess of peptide aldehyde **4**. The desired carboproteins were obtained in quantitative yields following preparative HPLC and lyophilization.

The design of peptide aldehyde **4** rested on the following principles: 1) A heptad repeat recently shown to form stable 4- $\alpha$ -helix bundles [7]; 2) An N-terminal Ac-Y moiety to avoid charge repulsion in the bundle and to facilitate concentration determination from UV-absorption; 3) A C-terminal AG-H moiety due to the large helix

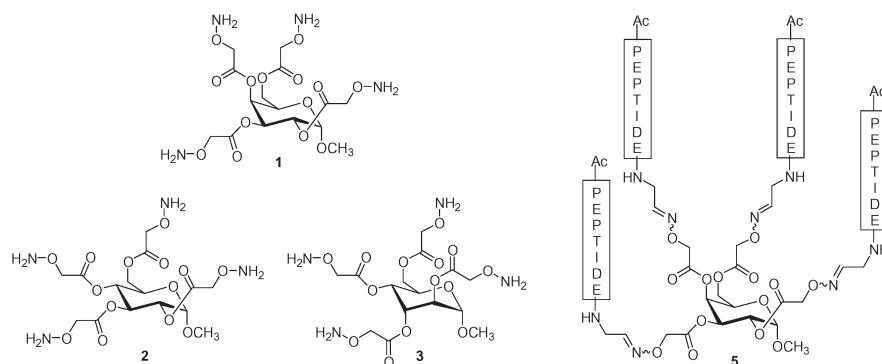


Fig. 1. (Left) Methyl  $\alpha$ -D-Galp, methyl  $\alpha$ -D-Glcp and methyl  $\alpha$ -D-Altp based templates **1**, **2**, and **3**, respectively. (Right) Carboprotein **5**, assembled on template **1**. The peptide sequence was -YEELLKKLEELLKKA-. The wavy lines indicate presence of E- and Z-isomers.

propensity of Ala and to avoid C-terminal racemization. The synthesis of **4** followed a BAL strategy [8].

The circular dichroism (CD) spectra of carboproteins **5**, **6**, and **7** confirmed the formation of helical structures. From  $[\theta]_{222}$  the helicity was calculated [9] to 65, 78, and 87% for **5**, **6**, and **7**, respectively (Table 1). As a control experiment, the CD spectra of the templates ligated with acetone or acetaldehyde were recorded. The observed molar ellipticities were insignificant and could not account for the differences in carboprotein helicity. Further biophysical studies are in progress.

Table 1. Summary of compound numbers and measured carboprotein helicities.

Carbohydrate	Galp	GlcP	Altp
Template	<b>1</b>	<b>2</b>	<b>3</b>
Carboprotein	<b>5</b>	<b>6</b>	<b>7</b>
Carboprotein helicity <sup>a</sup>	65%	78%	87%

<sup>a</sup> Calculated from  $[\theta]_{222}$ . CD spectra recorded in phosphate buffer, pH 7.0. Carboprotein concentration was 17–23  $\mu$ M, determined from Tyr UV absorption at 275 nm.

In conclusion, carboproteins **5**, **6**, and **7** were prepared from methyl  $\alpha$ -D-Galp, methyl  $\alpha$ -D-GlcP and methyl  $\alpha$ -D-Altp based templates, respectively. Biophysical studies of the three carboproteins are ongoing. Preliminary results indicate a significant and surprising [10] template effect on folding as **7** showed the highest degree of  $\alpha$ -helicity.

### Acknowledgments

We thank Anne Hector and Karen Jørgensen for MS and CD analyses. The Alfred Benzon Foundation is acknowledged for a Bøje Benzon Fellowship to K. J. J.

### References

1. DeGrado, W.F., Summa, C.M., Pavone, V., Nastri, F., Lombardi, A. *Annu. Rev. Biochem.* **68**, 779–819 (1999).
2. Jensen, K.J., Barany, G. *J. Peptide Res.* **56**, 3–11 (2000).
3. Brask, J., Jensen, K.J. *J. Peptide Sci.* **6**, 290–299 (2000).
4. Brask, J., Jensen, K.J. *Bioorg. Med. Chem. Lett.* **11**, 697–700 (2001).
5. Mutter, M., Vuilleumier, S. *Angew. Chem., Int. Ed. Engl.* **28**, 535–554 (1989).
6. Rose, K. *J. Am. Chem. Soc.* **116**, 30–33 (1994).
7. Mezo, A.R., Sherman, J.C. *J. Am. Chem. Soc.* **121**, 8983–8994 (1999).
8. Jensen, K.J., Alsina, J., Songster, M.F., Vágner, J., Albericio, F., Barany, G. *J. Am. Chem. Soc.* **120**, 5441–5452 (1998).
9. Chen, Y.-H., Yang, J.T., Chau, K.H. *Biochemistry* **13**, 3350–3359 (1974).
10. Wong, A.K., Jacobsen, M.P., Winzor, D.J., Fairlie, D.P. *J. Am. Chem. Soc.* **120**, 3836–3841 (1998).

## New Foldamers: Rigid Peptides with an Alternating *cis-trans* Amide Sequence

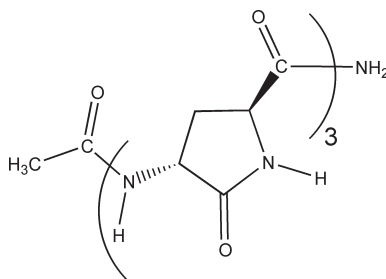
Marco Crisma<sup>1</sup>, Alessandro Moretto<sup>1</sup>, Claudio Toniolo<sup>1</sup>,  
Krzysztof Kaczmarek<sup>2</sup> and Janusz Zabrocki<sup>2</sup>

<sup>1</sup>Biopolymer Research Center, CNR, Department of Organic Chemistry, University of Padova,  
35131 Padova, Italy

<sup>2</sup>Institute of Organic Chemistry, Technical University of Lodz, 90-543 Lodz, Poland

### Introduction

The design of compounds that fold into a predictable and well defined 3D-structure ("foldamers") [1] can help us learn about self-assembly motifs and self-organization processes and tailor molecules with novel functions and properties. As part of a program aimed at evaluating homo-chiral and hetero-chiral amino- and carboxylic acid-substituted  $\gamma$ -lactams as conformationally constrained dipeptide building blocks, we synthesized by the solid-phase technique and solved by X-ray diffraction the crystal-state structure of the terminally blocked homo-trimer from (2*S*,4*R*)-4-amino-5-oxopyrrolidine-2-carboxylic acid.



Ac-[(*S,R*)-4aPy]<sub>3</sub>-NH<sub>2</sub>

### Results and Discussion

Conventional solid-phase peptide synthesis was used to construct the terminally blocked trimer Ac-[(*S,R*)-4aPy]<sub>3</sub>-NH<sub>2</sub>. In particular, we employed a methylbenzhydrylamine resin, HATU, as the coupling reagent, and 20% piperidine in DMF for Fmoc N $\alpha$ -deprotection. Acetylation of the terminal amino group was achieved by use of (Ac)<sub>2</sub>O/DIEA. The peptide was cleaved from the resin by HF treatment in the presence of 10% anisole at 0 °C for 60 min.

Figure 1 shows the X-ray diffraction structure of the trimer. Each *cis*-amide lactam ring and the *following trans* peptide unit are nearly perpendicular to each other, the angles between normals to each pair of average planes being found in the range 90.3  $\pm$  1.8°. However, the angles between normals to the average planes of each *cis*-amide lactam ring and the *preceding trans* peptide unit are 65.7(2)°, 89.8(2)°, and 61.2(3)° (beginning from the N-terminal lactam). Therefore, a strictly orthogonal arrangement of alternating *trans* and *cis* amide (peptide) units is observed along the central part of the trimeric molecule, whereas this arrangement is significantly distorted at either terminus.

## Analytical Methods

The molecules of  $\text{Ac}-[(S,R)\text{-4aPy}]_3\text{-NH}_2$  trihydrate lay nearly parallel to the  $bc$  plane, with the *trans* peptide units perpendicular to it. As a consequence, in the crystal packing mode the N-H and C=O groups of the *trans* peptide units are interconnected through either direct or water-mediated H-bonds to symmetry-related molecules along the  $a$  direction.

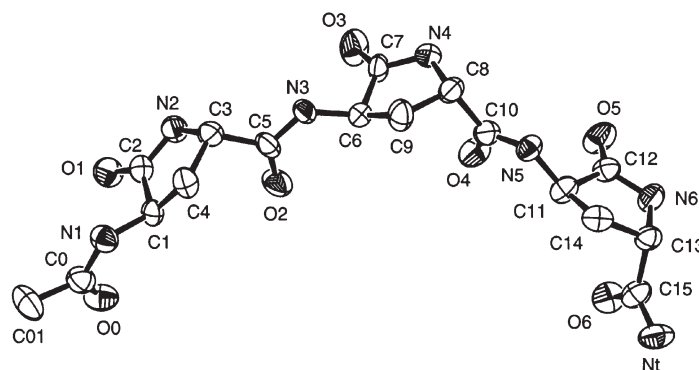


Fig. 1. X-Ray diffraction structure of  $\text{Ac}-[(S,R)\text{-4aPy}]_3\text{-NH}_2$ .

We have constructed a computer model of the *cis-trans* amide alternating foldameric structure based on the  $\phi, \psi$  torsion angles of the central, undistorted unit of the  $(S,R)$ -4aPy trimer. We find that the curved backbone will lead to the formation of a left-handed helical structure characterized by six  $(S,R)$ -4aPy residues per turn, a pitch of 13 Å, and a large hydrophilic cavity with an approximate 10 Å diameter. This rather elongated helix is not stabilized by any intramolecular N-H $\cdots$ O=C H-bond.

## References

1. Gellman, S.H. *Acc. Chem. Res.* **31**, 173–180 (1998).

## Design, Synthesis, and Conformational Studies of Short Peptides Containing C<sup>αα</sup>-Dipropylglycine and Dibenzylglycine

Yanwen Fu, Zhe Zhou, W. Dale Treleaven, Jorge Escobedo and  
 Robert P. Hammer

*Department of Chemistry, Louisiana State University, Baton Rouge, LA 70803, USA*

### Introduction

Non-proteinogenic C<sup>αα</sup>-disubstituted amino acid (ααAA) residues greatly restrict the number of conformations of peptides and thus induce distinct secondary structures, even in short peptides [1]. In this work several pentapeptides containing C<sup>αα</sup>-dipropylglycine (Dpg) and dibenzylglycine (Dbg) at alternating sequence positions and their L-norvaline (Nva) analogs were prepared. The design of these peptides is based on our models of amyloid β-sheet blocker peptides. Dpg and Dbg could accommodate energetically favored extended conformation [2] and thus induce the formation of β-sheet by self-aggregation.

DPG-1	Ac-Lys-Dpg-Tyr-Dpg-Lys-NH <sub>2</sub>
DPG-2	Ac-Glu-Dpg-Tyr-Dpg-Lys-NH <sub>2</sub>
DPG-3	Ac-Glu-Dpg-Tyr-Dpg-Glu-NH <sub>2</sub>
DPG-5	Ac-Glu-Dpg-Thr-Dpg-Lys-NH <sub>2</sub>
DBG-E	Ac-Lys-Dbg-Ala-Dpg-Glu-NH <sub>2</sub>
NVA-2	Ac-Glu-Nva-Tyr-Nva-Lys-NH <sub>2</sub>
NVA-5	Ac-Glu-Nva-Thr-Nva-Lys-NH <sub>2</sub>

### Results and Discussion

The peptides were prepared using Fmoc methodology with Fmoc-PAL-PEG-PS resin as a solid support. All coupling reactions except the acylation of the N-terminus of Dbg were carried out using PyAOP as coupling reagent. The pre-formed Fmoc-Lys(Boc)-symmetrical anhydride was used for acylation of N-terminus of Dbg [3]. Peptides were purified by reverse-phase HPLC and verified by MALDI-MS. The CD results for DPG-1, DPG-2 and DPG-3 (Table 1) suggest type II or I' β-turn like structure. The significant large ellipticity values for DPG-2 indicate a strong H-bonding in DPG-2 secondary structure. This assumption is supported by the CD studies of pH dependence of DPG-2 in buffer solution where the ellipticity dropped

*Table 1. CD data of the peptides.*

Peptide <sup>a</sup>	DPG-1	DPG-2	DPG-3	DBG-E	DPG-5	NVA-2	NVA-5
CD data <sup>b</sup>	185 (−17)	185 (−28)	188 (−24)	200 (−11)	190 (−5.0)	196 (−7.5)	196 (−6.8)
λ <sub>nm</sub> ([θ] <sub>ME</sub> )	200 (5.0)	200 (19.5)	202 (5.5)	227 (−2.5)	225 (−2.3)		
	230 (−3.5)	230 (−8.0)	230 (−7.0)				

<sup>a</sup> All CD experiments were performed with 100 μM of the peptide (peptide conc. was 250 μM for DPG-E and DPG-5) in 10 mM of pH 7.0 phosphate at 20 °C. <sup>b</sup> CD data were expressed as molar ellipticity ([θ] × 103) vs wavelength (nm).

gradually with the change of buffer from neutral to acidic condition. DPG-5 and DBG-E are likely to adopt both random coil and  $\beta$ -sheet or  $\beta$ -turn like structures indicated by the CD results, while peptide analogs NVA-2 and NVA-5 both adopt random coil structures as indicated by the unique negative band at 196 nm. In NMR studies of DPG-2, the observation of NOE crosspeaks  $d_{\alpha N}(\text{glu}^1, \text{dpg}^2)$  and  $d_{NN}(\text{dpg}^2, \text{tyr}^3)$  suggests a type II  $\beta$ -turn with an intramolecular H-bond between the acetyl carbonyl oxygen and the tyrosine NH (Figure 1). The observation of  $d_{NN}(\text{tyr}^3, \text{dpg}^4)$  and a depressed  $\text{dpg}^4$  NH temperature coefficient suggest another  $\beta$ -turn in residues  $\text{glu}^1$ - $\text{dpg}^4$ . Based on these data, a molecular model of DPG-2 was constructed (Sybyl)

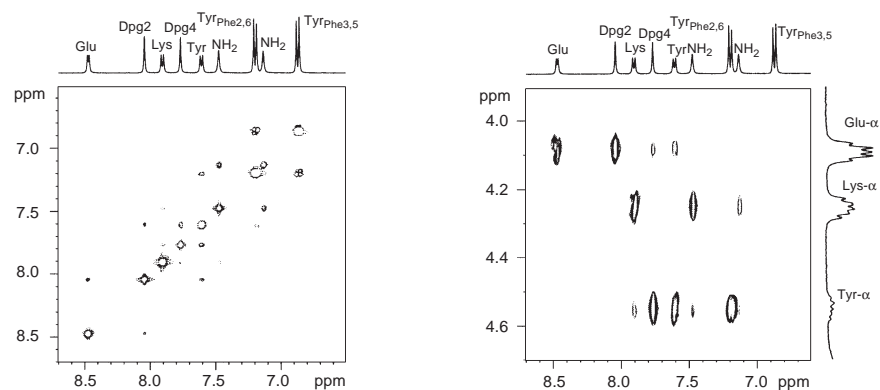


Fig. 1. Expansion of the ROESY spectrum of DPG-2 (10 mM) in 30 mM phosphate buffer, pH 7,  $\text{H}_2\text{O}$ - $\text{D}_2\text{O}$  (9:1): (left) amide-amide region; (right) amide- $\alpha$ -hydrogen region.

and minimized suggesting the two consecutive  $\beta$ -turns from the acetyl group through the  $\text{dpg}^4$  residue are type II and I', respectively (Figure 2, left). Similar CD and NMR analysis and modeling of DPG-5, suggests consecutive  $\beta$ -turns in residues Ac- $\text{dpg}^4$  as well as a type I  $\beta$ -turn from  $\text{thr}^3$  to the C-terminal  $\text{NH}^6$  (Figure 2, right).

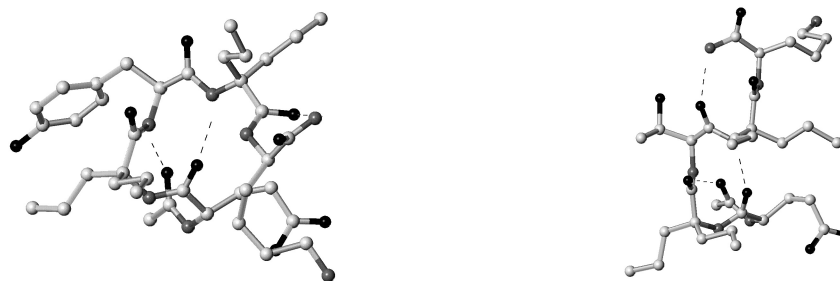


Fig. 2. Minimized NMR-derived molecular models of DPG-2 (left) and DPG-5 (right).

## References

1. Balam, P. *Curr. Opin. Struct. Biol.* **2**, 845–851, (1992).
2. Valle, G., Crisma, M., Bonora, G.M., Toniolo, C., Lelj, F., Barone, V., Hardy, P. M., Langran-Goldsmith, A., Maia, H.L.S. *J. Chem. Soc., Perkin Trans. 2*, **8**, 1481–1487 (1990).
3. Fu, Y.W., Hammarström, L.G.J., Miller, T.J., McLaughlin, M.L., Hammer, R.P. This Book.

## Bromo Tryptophan Based Antisickling Peptides: Design, Synthesis and Evaluation

M. Prabhakaran<sup>1</sup>, Seetharama A. Acharya<sup>2</sup>, Shabbir A. Khan<sup>3</sup>  
and K. Ramnarayan<sup>1</sup>

<sup>1</sup>Structural Bioinformatics, Inc, San Diego, CA 92127, USA

<sup>2</sup>Albert Einstein College Of Medicine, New York, NY 10461, USA

<sup>3</sup>Infinity Biotech, Upland, PA10911, USA

### Introduction

The polymerisation of deoxy sickle cell Haemoglobin (HbS) within the erythrocytes is the primary molecular event responsible for the patho-physiology of the sickle cell disease. From our theoretical analysis [1], we have found that deoxy sickle haemoglobin exhibits the potential for a limited number of small molecules binding sites in conformity with experimental results. From our theoretical binding studies we designed tripeptide analogs with increased flexibility as well as rigidity (Figure 1). These peptides were synthesised and the oxygen affinity and polymerisation of HbS in the presence of these compounds were measured.

5-Br-DL-Trp-Gly-5-Br-DL-Trp-amide

5-Br-DL-Trp-AiB-5-Br-DL-Trp-amide

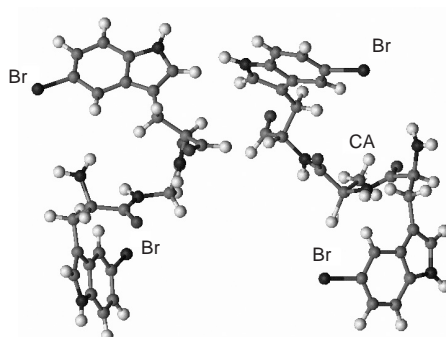


Fig. 1. Inhibitors used in the study.

### Results and Discussion

**Ligand docking and scoring** (Table 1): We have tried the tripeptide analogs for docking and scoring. The docking was done manually followed by simple minimization. Low temperature (100 °C) dynamics was then carried out for optimal docking. Maximum hydrophobic packing chemical complementarity guided by electrostatic component and the number of hydrogen bonds was achieved by many trials. The flexible Gly analog tops the list followed by AiB.

**Polymerization results** (Table 2): The brominated dipeptide and two dipeptide analogs were synthesized. They were tested for their effect on polymerization. The increase in solubility is a measure of their antigelling activity by increasing the solubility of HbS and thereby decreasing the polymerization. The flexible Gly tripeptide show enhanced activity in comparison with rigid AiB compound.

Table 1. Ligand docking and scoring results.

Ligand	Enthalpy (kcal/mol)	Free energy	Hydrogen bonds	Chemical complement	Packing loss (Å <sup>2</sup> )	Br–Br dist (Å)
Dipep	−36.1	−6.1	1	−9.1	684.1	11.8
Thr	−62.8	−4.8	3	−9.5	831.0	17.2
Val	−61.2	−4.7	1	−17.2	773.3	11.2
Gly	−79.1	−8.8	3	−25.8	847.6	10.9
Ser	−49.0	−6.4	2	−5.5	693.9	15.2
Cys	−38.2	−5.5	1	−5.6	625.2	12.6
Aib	−72.5	−7.7	4	−18.1	777.8	10.1

Table 2. Polymerization results.

Inhibitor (Peptide)	C <sub>sat</sub> (grams %)	Increase in solubility (%)
None	18	
Trp	19.5	8.3
5-Br-DL-Trp amide	23	27
5-Br-DL-Trp-5-Br-DL-Trp amide	27.5	33
5-Br-DL-Trp-Gly-5-Br-DL-Trp amide	32	78
5-Br-DL-Trp-Aib-5-Br-DL-Trp amide	29	66

## Conclusion

We have developed a method to predict the best possible binding sites for a given receptor. From our findings and from experimental evidence, we predict the best possible binding site for indole rings. We have developed tripeptide analogs as ligands at that site. These peptides, had a very limited influence on the oxygen affinity of HbS, but had a very strong inhibitory effect on the polymerization. In the presence of 2 equivalents of bromotryptophyl-glycyl-bromo-tryptophanamide, the solubility of deoxy HbS is nearly twice that of a control sample of deoxy HbS. This is the best inhibitory effect seen so far for any noncovalent inhibitor of the polymerization. Our iterative approach of design, synthesis and evaluation has led to a better antigelation compound for sickle cell haemoglobin.

## References

1. Manavalan, P., Prabhakaran, M., Johnson, M.E. *J. Mol. Biol.* **223**, 791–800 (1992).

## Synthesis, Redox and Structural Properties of Cystine-Cyclopeptides Containing the Active-Site of the Thioredoxin Superfamily

Chiara Cabrele, Stella Fiori, Stefano Pegoraro and Luis Moroder

Department of Bioorganic Chemistry, Max-Planck-Institute for Biochemistry,  
 Martinsried-Munich, D-82152, Germany

### Introduction

Thioredoxin (TRX), thioredoxin-reductase (TRR), protein disulfide isomerase (PDI) and glutaredoxin (GRX) belong to the TRX family of thiol-disulfide oxidoreductases [1]. The active-site sequence motif common to all members of this family is Cys-Xaa-Yaa-Cys. PDI is the strongest oxidant of the family ( $E_0 = -0.110$  V) and is known to be involved in *in vivo* oxidative folding of proteins. *In vitro* it catalyzes the refolding of reduced or scrambled RNase A [2].

In the present study, the structural and redox properties of related, conformationally restricted synthetic active-site fragments were investigated, and their ability to act as PDI-like protein folding catalysts was comparatively analyzed.

### Results and Discussion

In a previous study, the redox potentials of octapeptide fragments of the bis-(cysteinyl)-catalytic sites of TRX, TRR, GRX and PDI were determined [3]. The  $E_0$  values calculated by using glutathione (GSH/GSSG) as reference ( $E_0' = -0.240$  V) were in the range of  $-0.190$  V to  $-0.215$  V. In order to possibly obtain compounds with stronger oxidant character (PDI-mimetics), hexapeptides based on the active-site sequences of the four enzymes were *N*-to-*C* backbone cyclized and oxidized by air or di-*tert*-butyl-azodicarboxylate.

The redox potentials of the cystine-cyclopeptides were measured by equilibrating each peptide with excess GSH/GSSG or cysteine/cystine ( $E_0' = -0.223$  V [4]) at  $25^\circ\text{C}$  (the latter redox pair was chosen as an alternative to overcome experimental difficulties encountered for *cyclo*-TRX and *cyclo*-PDI when using glutathione). The redox mixtures at equilibrium were characterized by HPLC and ESI-MS. As shown in Table 1, the oxidant properties of the bis(cysteinyl) system were increased upon backbone cyclization, with *cyclo*-PDI exhibiting a redox potential of  $-0.13$  V, which is close to that of the native enzyme ( $-0.11$  V).

Table 1. Redox potentials of the enzymes of the TRX family and of the active-site fragments.

Amino acid sequence <sup>a</sup>		$E_0$ (V)		
		Enzyme <sup>b</sup>	Cystine-octapeptide <sup>b</sup>	Cystine-cyclohexapeptide
TRX-[H <sup>37</sup> ]- (31-38)	<b>WCGPCKHI</b>	-0.270	-0.190	-0.153 <sup>c</sup>
GRX-(10-17)	<b>GCPYCVRA</b>	-0.230	-0.215	-0.174 <sup>c</sup> (-0.179) <sup>d</sup>
TRR-(134-141)	<b>ACATCDGF</b>	-0.250	-0.210	-0.198 (-0.200) <sup>d</sup>
PDI-(35-42)	<b>WCGHCKAL</b>	-0.110	-0.205	-0.128 <sup>c</sup>

<sup>a</sup> The sequence of the cyclopeptides are in bold. <sup>b</sup> See reference 3. <sup>c</sup>  $E_0$  values calculated using  $E_0'$ (cysteine/cystine) =  $-0.223$  V. pH 7,  $25^\circ\text{C}$ . <sup>d</sup>  $E_0$  values calculated using  $E_0'$ (GSH/GSSG) =  $-0.240$  V. pH 7,  $25^\circ\text{C}$ .

## Analytical Methods

The NMR solution structures of the bicyclic compounds were determined in DMSO or DMF, due to limited solubility of *cyclo*-GRX in phosphate buffer. The active-site adopts a well-defined  $\beta$ -turn in *cyclo*-GRX, while three conformers were identified for *cyclo*-TRX containing a  $\beta$ -turn or a *pseudo*- $\gamma$ -turn. In contrast, no regular structural elements were found for *cyclo*-PDI. Interestingly, interactions between one sulfur atom of the disulfide bridge and backbone amide protons were observed for the two stronger oxidants, *i.e.* *cyclo*-TRX and *cyclo*-PDI (Figure 1).

In order to analyze whether the bicyclic peptides are capable of catalyzing oxidative protein refolding in a PDI-like manner, reactivation rates of reduced RNase A were determined in Tris-HCl buffer (pH 7.4) containing GSH/GSSG (5/1) with or without peptide. As shown in Figure 2, the initial refolding rate, as well as the yield of renatured enzyme, were enhanced upon addition of either *cyclo*-GRX or *cyclo*-PDI.

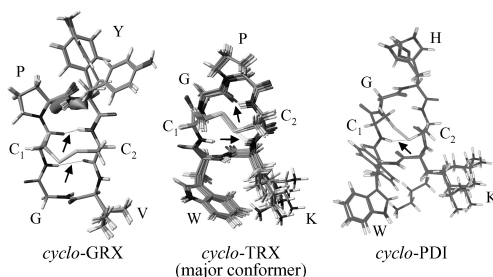


Fig. 1. NMR structures of *cyclo*-GRX in DMSO, *cyclo*-TRX and *cyclo*-PDI in DMF. The H-bonds are indicated by arrows.

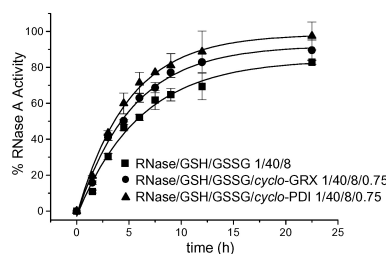


Fig. 2. Reactivation of reduced RNase A (24  $\mu$ M) in Tris buffer (pH 7.4) at 30  $^{\circ}$ C.

In conclusion, by conformationally constraining the peptide backbone, the oxidant character of the active-site fragments related to the TRX family and the catalytic effect on the oxidative refolding of RNase A were markedly improved.

## Acknowledgments

This work was supported by a Marie Curie postdoctoral fellowship.

## References

- Holmgren, A. *Annu. Rev. Biochem.* **54**, 237–271 (1985).
- Epstein, C.J., Goldberger, R.F., Anfinsen, C.B. *Cold Spring Harbor Symp. Quant. Biol.* **28**, 439–449 (1963).
- Siedler, F., Rudolph-Böhner, S., Doi, M., Musiol, H.J., Moroder, L. *Biochemistry* **32**, 7488–7495 (1993).
- Millis, K.K., Weaver, K.H., Rabenstein, D.L. *J. Org. Chem.* **58**, 4144–4146 (1993).

## Probing Backbone Flexibility Within the Active Site of Glutaredoxin 3

John W. Blankenship and Philip E. Dawson

*Departments of Chemistry and Cell Biology, and the Skaggs Institute of Chemical Biology,  
The Scripps Research Institute, La Jolla, CA 92037, USA*

### Introduction

Disulfide oxidoreductases such as thioredoxin and glutaredoxin are ubiquitous and used for a wide array of activities within the cell. The diversity of the redox potentials in these proteins is accommodated by the characteristic Cys-Xaa-Yaa-Cys active site disulfide. One of the less understood factors responsible for this diversity is the differential stability of the disulfide bond between different proteins in the family; formation of a disulfide bond can significantly stabilize or destabilize the protein [1,2]. Backbone flexibility has been shown to increase or decrease upon the formation of a disulfide bond depending on the family member [3,4]. To better determine the contribution of backbone flexibility within the active site to the redox potential, we have incorporated several unnatural imino acids that are variants of proline, azetidine (Aze) and pipecolic acid (Pip) in the place of proline (the *i*+2 position) in the active site of glutaredoxin 3. Both should alter the backbone flexibility within the active site, which has the characteristic sequence Cys-Pro-Tyr-Cys and approximates a Type I  $\beta$ -turn [5].

### Results and Discussion

Glutaredoxin 3 (C65Y)[6–8] was synthesized on a 0.8 mmol scale on a Pam-OCH<sub>2</sub>-Lys solid support using a Boc protecting scheme. The resin was split into three separate reaction vessels after the coupling of Tyr13 was complete, and Boc protected Azetidine, Proline, and Pipecolic acid were each activated and coupled to one batch of resin, after which the remainder of the natural sequence (Met1-Cys12) was successively coupled to each batch of resin. The peptide was N-terminally deprotected and neutralized, then deprotected and cleaved from the resin by treatment in anhydrous HF at 0 °C. HF was pumped off under vacuum, and the remaining peptide was precipitated in ether, dissolved in 30% acetic acid, lyophilized, then dissolved in a 1 M GuHCl, 0.1 M NaP<sub>i</sub> buffer at 1 mg/mL and left to stir under air exposure overnight. The resulting solution was then centrifuged at 8,000 RPM for 30 min, decanted, and filtered prior to being purified by RP-HPLC. Purity was monitored and confirmed by ES-MS and subsequent analytical HPLC runs of the purified material. Concentration was determined by the method of Gill and von Hippel [9].

The resulting purified proteins were dissolved in a degassed solution containing 100 mM NaP<sub>i</sub>, 1 mM ultrapure EDTA, pH 7.0, and diluted to a concentration of 50  $\mu$ M, where they were analyzed by circular dichroism. Wavelength scans (Figure 1) of the oxidized wildtype and mutant proteins reveal that all three fold and possess a similar amount of secondary structure. Preliminary thermal denaturation experiments (Figure 2) show that all three proteins fold by a two-state folding mechanism, and that they possess a similar slope, although there is a difference in melting temperature at the mid-point, suggesting that the enthalpy of the proteins in the oxidized state is relatively unaffected, but that the entropy of the proteins has changed.

Further characterization of the folding and redox potentials of these proteins is in process.

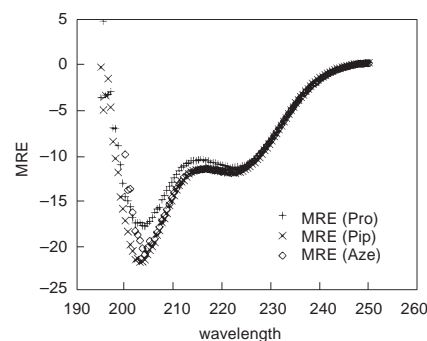


Fig. 1. CD spectra of oxidized Glutaredoxin 3 and mutants.

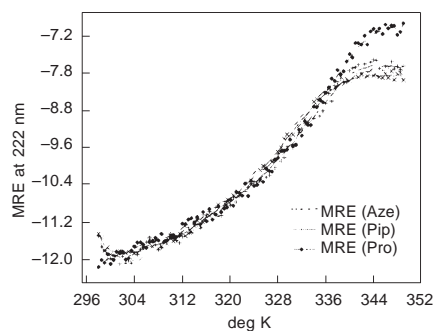


Fig. 2. Thermal denaturation of oxidized Glutaredoxin 3 and mutants.

### Acknowledgments

We thank Dr. Jeffery Kelly, Dr. Peter Wright, Dr. Jane Dyson, Dr. Ganga Beligere, Dr. Uma Manjappara, Linda Tennant and Songpon Deechongkit for technical assistance and equipment access. Supported by grant GM59380 and the Skaggs Institute of Chemical Biology.

### References

1. Lin, T.-Y., Kim, P.S. *Biochemistry* **28**, 5282–5287 (1989).
2. Sandberg, V.A., Kren, B., Fuchs, J.A., Woodward, C. *Biochemistry* **30**, 5475–5484 (1991).
3. Kelley, J.J., Caputo, T.M., Eaton, S.F., Laue, T.M., Bushweller, J.H. *Biochemistry* **36**, 5029–5044 (1997).
4. Rabenstein, D.L., Shi, T., Spain, S. *J. Am. Chem. Soc.* **122**, 2401–2402 (2000).
5. Nordstrand, K., Sandstrom, A., Aslund, F., Holmgren, A., Otting, G., Berndt, K.D. *J. Mol. Biol.* **303**, 423 (2000).
6. Aslund, F., Nordstrand, K., Berndt, K.D., Nikkola, M., Bergman, T., Ponstingl, H., Jornvall, H., Otting, G., Holmgren, A. *J. Biol. Chem.* **271**, 6736–6745 (1996).
7. Aslund, F., Ehn, B., Miranda-Vizuetta, A., Pueyo, C., Holmgren, A. *Proc. Natl. Acad. Sci. U.S.A.* **91**, 9813–9817 (1994).
8. Nordstrand, K., Aslund, F., Meunier, S., Holmgren, A., Otting, G., Berndt, K.D. *FEBS Lett.* **449**, 196–200 (1999).
9. Nordstrand, K., Aslund, F., Holmgren, A., Otting, G., Berndt, K.D. *J. Mol. Biol.* **286**, 541–552 (1999).
10. Aslund, F., Berndt, K.D., Holmgren, A. *J. Biol. Chem.* **272**, 30780–30786 (1997).
11. Gill, S.C., von Hippel, P.H. *Anal. Biochem.* **182**, 319–326 (1989).

## Homostranded and Heterostranded $\alpha$ -Helical Templates for Combinatorial Library Display: Differences in Stability and Solubility

Stephen M. Lu, Jennifer R. Litowski, Brian Tripet and Robert S. Hodges

Department of Biochemistry and Protein Engineering Network of Centres of Excellence,  
 University of Alberta, Edmonton, Alberta T6G 2S2, Canada and  
 Department of Biochemistry and Molecular Genetics, University of Colorado Health Sciences  
 Center, Denver, Colorado 80262

### Introduction

Peptide libraries are useful in the discovery of new drugs (agonists/antagonists) for novel targets. Successful library designs incorporate structural elements to restrict the conformation of the peptide chains. A two-stranded  $\alpha$ -helical coiled-coil is an excellent template for stabilizing  $\alpha$ -helical structure. Coiled-coils are characterized by repeating heptads  $(abcdefg)_n$  in which positions *a* and *d* are typically hydrophobic residues. We have previously studied a three heptad disulfide-bridged homostranded coiled-coil library containing two lactam bridges per strand [1]. With this design, we were able to show that the coiled-coil could mimic the binding of lipopolysaccharide to its antibody. In this study we describe a refinement by designing a hetero-two-stranded molecule incorporating a “backing strand” (denoted as BS) and a single library display strand (Figure 1A) and comparing this template to the original design.

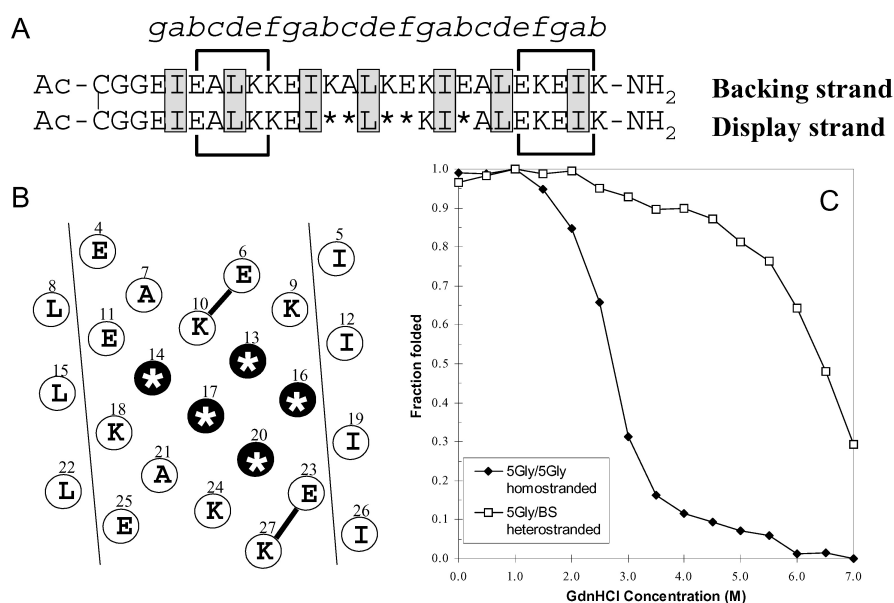


Fig. 1. A. The sequence of the disulfide-bridged hetero-two-stranded  $\alpha$ -helical coiled-coil template consisting of a backing strand and a library display strand, each stabilized by Glu-Lys lactam bridges (brackets). The hydrophobic core residues are shaded. B. Helical net diagram. The \* indicates the library positions on the helix surface. C. Comparison of stability of 5Gly homostranded and 5Gly/BS heterostranded coiled-coils.

The helical net diagram shows the clustering of the library positions to create a binding domain on the surface of the helix (Figure 1B).

### **Results and Discussion**

Three test sequences consisting of 5Gly, 5Ala and 5Leu residues in the library positions were chosen to represent a range of analogs with varying hydrophobicity and stability in the library display strand. The conformation of all constructs were assessed by circular dichroism spectroscopy (data not shown) and their stabilities were determined by guanidine hydrochloride (GdnHCl) denaturation. All constructs showed spectra typical of  $\alpha$ -helical coiled-coils with the exception of the 5Leu homo-two-stranded molecule, which was insoluble.

The 5Gly analog represents a sequence that is extremely destabilizing to  $\alpha$ -helical structure [2]. A comparison of the stability between the 5Gly homostranded molecule and the 5Gly/BS heterostranded molecule is shown in Figure 1C. The heterostranded molecule is significantly more stable with a  $[\text{GdnHCl}]_{1/2}$  value of 3.7 M greater than the homostranded molecule (6.5 M vs 2.8 M). This suggests that all library sequences will be more stable than the 5Gly/BS heterostranded coiled-coil.

The 5Ala analog was chosen to represent a sequence with high  $\alpha$ -helical propensity, while the 5Leu analog represents a very hydrophobic exposed sequence. The 5Ala/BS heterostranded molecule was so stable that even thermal denaturation measurements in 5 M GdnHCl were incomplete. The 5Leu homostranded molecule was insoluble, while 5Leu/BS was soluble and extremely stable, demonstrating the advantage of the backing strand to increase solubility.

The advantages of this heterostranded design are the dramatic improvement in stability of destabilizing sequences, improved solubility of hydrophobic sequences and a single display which eliminates the complications associated with dual display.

### **Acknowledgments**

We thank the University of Alberta and Protein Engineering Network of Centres of Excellence (Canada) and the University of Colorado Health Sciences Center for support.

### **References**

1. Houston, Jr., M., Wallace, A., Bianchi, E., Pessi, A., Hodges, R.S. *J. Mol. Biol.* **262**, 270–282 (1996).
2. Zhou, N.E., Monera, O.D., Kay, C.M., Hodges, R.S. *Protein Pept. Lett.* **1**, 114–119 (1994).

## Synthesis and Solution Structures of Cyclic Hexapeptides Cyclo(Pro-Leu-Xxx)<sub>2</sub>

Satoshi Osada<sup>1</sup>, Ryo Hayashi<sup>1</sup>, Taichi Yamashita<sup>1</sup>, Masahiro Yoshiki<sup>1</sup>,  
 Yuki Okamoto<sup>1</sup>, Toshihisa Ueda<sup>2</sup>, Hiroaki Kodama<sup>1</sup> and Michio Kondo<sup>1</sup>

<sup>1</sup>Department of Chemistry, Saga University, Saga 840-8502, Japan

<sup>2</sup>IFOC, Kyusyu University, Fukuoka 812-8581, Japan

### Introduction

Cyclic peptides are excellent models for reverse turns, and it is well established that the cyclic hexapeptides contain two  $\beta$ -turns. In our previous studies, we reported the conformation of cyclo(Pro-Leu-Gly)<sub>2</sub>, and also the influence of the two C $\alpha$  methyl groups of Aib on the formation of  $\beta$ -turns and overall conformation of cyclo-(Pro-Leu-Aib)<sub>2</sub> [1,2]. The structure of cyclo(Pro-Leu-Gly)<sub>2</sub> was comprised of two type I  $\beta$ -turns and the molecule had an overall C<sub>2</sub> symmetry. The cyclo(Pro-Leu-Aib)<sub>2</sub>, however, exhibited an asymmetrical conformation containing two different types of  $\beta$ -turn (type II' and type VI).

In the present study, to elucidate the side chain effect of Xxx on the type of  $\beta$ -turns, cyclic hexapeptides, cyclo(Pro-Leu-Xxx)<sub>2</sub>, containing D-Ala and D-Phe residues were synthesized by solution-phase methods. The solution structures of these peptides were investigated by <sup>1</sup>H NMR and CD measurements.

### Results and Discussion

Synthesis of cyclo(Pro-Leu-D-Phe)<sub>2</sub> is shown in the scheme in Figure 1. The tripeptide, which was prepared by a stepwise elongation, was activated by DCC-HONSu, deprotected by TFA, then cyclized under high dilution condition (3 mM in pyridine). The obtained crude product was purified by gel-filtration (Sephadex LH-20) or silica gel chromatography. The cyclic hexapeptide was characterized by HPLC, amino acid analysis, <sup>1</sup>H NMR and MALDI-TOF mass spectrometry.

Cyclo(Pro-Leu-D-Ala)<sub>2</sub> was also synthesized by cyclization of the respective linear peptides: Boc-Pro-Leu-D-Ala-OMe, Boc-Leu-D-Ala-Pro-OMe, Boc-D-Ala-Pro-Leu-OMe, and Boc-(Pro-Leu-D-Ala)<sub>2</sub>-OMe. In each case the yields were comparable and in general, the cyclic hexapeptides containing D-Ala and D-Phe units were obtained in relatively high yields. However, the L-Ala substituted peptide, cyclo(Pro-Leu-L-Ala)<sub>2</sub> was not obtained in pure form, as cyclization provided inseparable complex mixtures. This

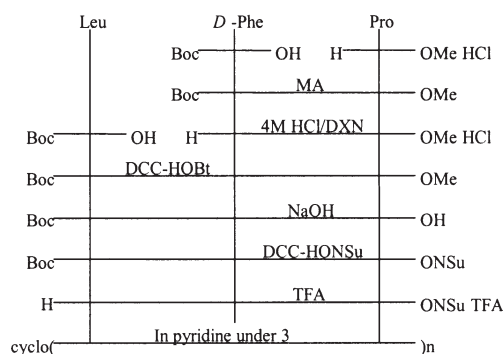


Fig. 1. Synthesis of cyclo(Pro-Leu-D-Phe)<sub>2</sub>.

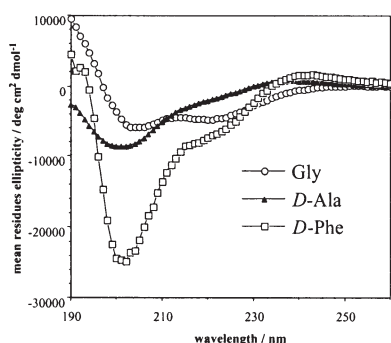


Fig. 2. CD spectra of cyclo(Pro-Leu-Xxx)<sub>2</sub>. Cyclo(Pro-Leu-D-Phe)<sub>2</sub> Peptide at 2 mM concentrations.

Table 1. Temperature coefficients of amide protons in DMSO-*d*<sub>6</sub>.

Cyclic peptides	Residues	$\Delta\delta/\Delta T$ ( $\cdot 10^{-3}$ ppm deg <sup>-1</sup> )
Cyclo(Pro-Leu-Gly):	Leu NH	6.80
	Gly NH	0.37
Cyclo(Pro-Leu-Aib):	Leu NH	0.69
	Aib NH	4.29
		6.66
Cyclo(Pro-Leu-D-Ala):	Leu NH	2.50
	D-Ala	2.40
Cyclo(Pro-Leu-D-Phe):	Leu NH	1.98
	D-Phe	4.68

result can be due to the conformational disadvantage of the L-Ala-containing linear peptides to form of cyclo(Pro-Leu-L-Ala)<sub>2</sub>.

Figure 2 shows the CD spectra of cyclo(Pro-Leu-Xxx)<sub>2</sub> (Xxx = Gly, D-Ala, and D-Phe). Cyclo(Pro-Leu-D-Phe)<sub>2</sub> is characterized as type II'  $\beta$ -turn, with the typical double-minima ellipticity at *ca* 200 and 220 nm and the positive ellipticity at shorter wavelengths. The spectrum of cyclo(Pro-Leu-D-Ala)<sub>2</sub> differs from that of cyclo(Pro-Leu-Gly)<sub>2</sub>, which was previously reported to form type I  $\beta$ -turns, but is rather similar (though with less intensity) in shape to that of cyclo(Pro-Leu-D-Phe)<sub>2</sub>.

The peptides, cyclo(Pro-Leu-D-Phe)<sub>2</sub> and cyclo(Pro-Leu-D-Ala)<sub>2</sub>, were also subjected to the temperature-dependent NMR experiments in DMSO-*d*<sub>6</sub>. The proton resonance of the four amide protons showed only two signals, an implication for the formation of symmetric structures in DMSO. The temperature coefficients of these amide protons in cyclic peptides are summarized in Table 1. In cyclo(Pro-Leu-D-Phe)<sub>2</sub>, temperature coefficient of the amide NH of D-Phe was higher than that of the NH of Leu, indicating that the amide NH of Leu are shielded from the solvent by intramolecular hydrogen bonds.

On the other hand, the temperature coefficient of Leu NH is similar to that of D-Ala NH in cyclo(Pro-Leu-D-Ala)<sub>2</sub>. This result can suggest that in cyclo(Pro-Leu-D-Ala)<sub>2</sub>, both Leu and D-Ala residues form weak intramolecular hydrogen bonds.

Previously, Gierasch *et al.* reported that the general sequence -Pro-L-Y-D-X- leads to formation of type II'  $\beta$ -turn in cyclic hexapeptides [3]. <sup>1</sup>H NMR and CD spectral results of cyclo(Pro-Leu-D-Phe)<sub>2</sub> agrees with this observation, however, cyclo(Pro-Leu-D-Ala)<sub>2</sub> does not seem to form type II'  $\beta$ -turns. The present study suggest that a subtle structural change in the D-amino acid at position 3 in cyclo(Pro-Leu-Xxx)<sub>2</sub> would lead to a global structural change.

### Acknowledgments

We would like to thank J. Wang for the peptide synthesis and related measurements.

### References

1. Wang, J., Osada, S., Kodama, H., Kato, T., Kondo, M. *Bull. Chem. Soc. Jpn.* **72**, 533–540 (1999).
2. Wang, J., Osada, S., Kodama, T., Kondo, M. *Bull. Chem. Soc. Jpn.* **73**, 1221–1226 (2000).
3. Gierasch, L.M., Deber, C.M., Madison, V., Niu, C., Blout, E.R. *Biochemistry* **20**, 4730–4738 (1981).

## Functional and Structural Comparisons of Linear and Dendritic Arrays of Polypeptides

Yi-An Lu, Jin-Long Yang and James P. Tam

*Department of Microbiology and Immunology, Vanderbilt University, Nashville, 37232, USA*

### Introduction

Bioactive biopolymers with repeating sequences are often found in nature. Polypeptides usually contain an array of linear repeats, whereas both linear and dendritic repeats are found in polysaccharides. To determine the functional and structural consequences of polypeptides in a dendritic array, we have designed dendritic polypeptides [1] and compared them to the linearly repeating polypeptides. Both series of polypeptides contain two to eight copies of tetrapeptides with BHHB motifs (B = basic amino acid, H = hydrophobic amino acid) derived from naturally occurring antimicrobials.

### Results and Discussion

Dendritic peptides are biopolymers of unusual architectures. The dendritic core consists of a divalent Lys core, whose  $\alpha$  and  $\epsilon$  amines double geometrically with each branching generation (Figure 1). We designed two to eight copies of the Arg-Leu-Tyr-Arg motif derived from tachyplesins and protegrins. Dendritic polypeptides and linearly repeating polypeptides were synthesized by Fmoc-chemistry on Fmoc-Rink amide MBHA resin. Peptides were assayed against Gram-negative, Gram-positive and fungi in high- and low-salt conditions [2] (Table 1).

Hemolytic activity and stability to proteolysis were also determined [3]. Dendritic peptides showed broad activity with minimal inhibition concentrations  $<1 \mu\text{M}$ . Compared to the corresponding series of linearly repeating polypeptides, the dendrimers are superior in antimicrobial potency, more stable to proteolysis, less toxic to human cells, and more easily synthesized chemically. Based on their size and charge similarities, the potency and activity spectrum of a tetravalent dendritic polypeptide is comparable to protegrins and tachyplesins, a family of potent antimicrobials containing 17 to 20 residues. These results suggest that the dendritic design of polypeptides presents an attractive approach for developing novel peptide antibiotics.

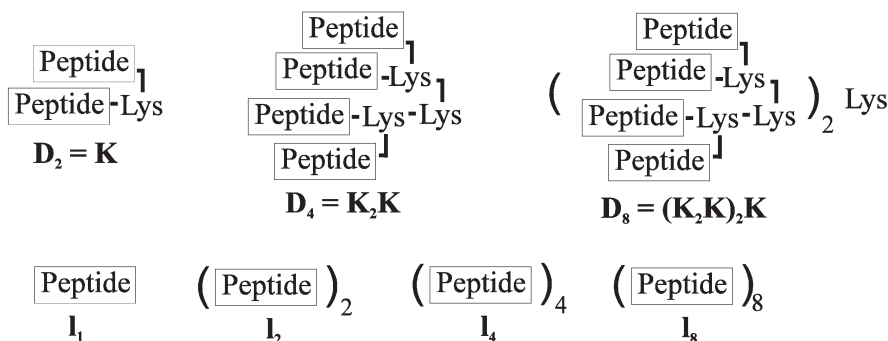


Fig. 1. Linear vs dendritic design.

Table 1. Antimicrobial activity of dendritic, linearly repeating peptides, tachyplesin and protegrin.

	MIC (μM)					
	<i>E. coli</i>		<i>S. aureus</i>		<i>C. albicans</i>	
	L-salt	H-salt	L-salt	H-salt	L-salt	H-salt
Linear peptide						
1 <sub>1</sub> RLYR	>500	>500	>500	>500	>500	>500
1 <sub>2</sub> (RLYR) <sub>2</sub>	39.0	33.6	8.1	17.5	9.0	17.4
1 <sub>4</sub> (RLYR) <sub>4</sub>	1.0	0.7	1.8	1.1	1.2	1.9
1 <sub>8</sub> (RLYR) <sub>8</sub>	4.2	3.9	3.4	4.2	4.1	9.8
Dendritic peptide						
D <sub>2</sub> RLYR	6.1	10.2	4.5	10.2	1.0	6.4
D <sub>4</sub> RLYR	0.6	0.7	0.8	0.6	0.8	0.8
D <sub>8</sub> RLYR	0.5	0.7	0.5	0.6	0.7	0.9
Tachyplesin	0.3	0.4	0.4	0.5	0.7	0.9
Protegrin	0.9	0.8	0.7	0.6	1.3	1.0

Experiments were performed in radial diffusion assay with underlay gel containing 1% agarose, 10 mM phosphate buffer with (High-salt) or without (Low-salt) 100 mM NaCl.

### Acknowledgments

This work was supported, in part, by Public Health Service NIH Grants AI46164 and GM57145.

### References

1. Tam, J.P. *Proc. Natl. Acad. Sci. USA* **85**, 5409–5413 (1988).
2. Lehrer, R.I., Rosenman, M., Harwing, S.S., Jackson, R., Eisenhauer, P. *J. Immunol Med.* **137**, 167–173 (1991).
3. Fehlbauer, P., Bulet, P., Michaut, L., Lagueux, M., Broekaert, W.F., Hetru, C., Hoffmann, J.A. *J. Biol. Chem.* **269**, 33159–33163 (1994).



**Biologically Active Peptides,  
Enzyme Inhibitors,  
Peptide Neurotoxins and Antibiotics,  
Peptidomimetics,  
Peptide and Peptidomimetic Therapeutics  
and Delivery**



## Synthetic Studies on the Antimicrobial Activity of Pleurocidin

Lenore M. Martin<sup>1</sup>, Khaled A. Elsaid<sup>2</sup>, Tarquin Dorrington<sup>3</sup>  
 and Marta Gómez-Chiarri<sup>4</sup>

<sup>1</sup>Department of Cell and Molecular Biology; <sup>2</sup>Department of Biomedical Sciences; <sup>3</sup>Graduate School of Oceanography; <sup>4</sup>Department of Fisheries, Animal and Veterinary Sciences, University of Rhode Island, Kingston, RI 02881, USA

### Introduction

*Vibrio anguillarum* infections result in huge economic losses in the aquaculture industry annually. Pleurocidin, an antimicrobial peptide (AMP) isolated in 1997 from winter flounder, exhibited MICs in the micromolar range against a wide variety of fish and human pathogens [1]. Studies have shown a correlation between antimicrobial activity and the charges, hydrophobicities, and hydrophobic moments of amphipathic peptides that are capable of adopting an  $\alpha$ -helical structure [2]. Although the C-terminal acid is the naturally-occurring form, synthetic pleurocidin amide is more potent and has been shown to protect coho salmon from vibriosis *in vivo* [3]. No additional increase in potency was obtained by adding a lysine at the N-terminus of pleurocidin amide to increase the positive charge on the peptide [3]. To characterize the structural determinants required for antimicrobial activity and to discover minimal sequences for genetic engineering, we synthesized pleurocidin amide and two new pleurocidin analogs LM4-1 and LM4-2 (see Figure 1). The analogs were truncated at the C-terminus to determine if any residues in this region could be deleted and yet retain activity. Peptide LM4-1 lacked seven C-terminal residues and also one of the pair of phenylalanines found at positions 5/6 in native pleurocidin. This deletion moved a positively-charged lysine pair up to positions 6/7, thereby giving the N-terminus of LM4-1 an amphipathic pattern similar to that responsible for helix formation in cecropin A [4]. AMPs were screened against *E. coli*, *V. anguillarum*, and *V. carchariae*.

<b>Cecropin A</b>	H-KWKLFFKKIEKVGQNIRDGIIKAGPAVAVVGQATQIAK-NH <sub>2</sub>
<b>LM4-1</b>	H-GWGSFFKKAHVGVK-NH <sub>2</sub>
<b>Pleurocidin</b>	H-GWGSFFKKAHVGVGKAAL <sup>1</sup> THYL-OH
<b>LM4-2</b>	H-GWGSFFKKAHVGVGKAAL-NH <sub>2</sub>

Fig. 1. Sequences of cecropin A, native pleurocidin and synthetic pleurocidin analogs

### Results and Discussion

Synthetic peptides pleurocidin amide (25 residues), LM4-1 ([des-F<sup>5</sup>]Pleurocidin 1-18 amide) and LM4-2 (pleurocidin 1-21 amide) were synthesized using Boc chemistry on MBHA (1.1 mmol/g, 1 g) resins in a CS-Bio peptide synthesizer. The N-terminal Boc-group was left on during removal of Dnp from His residues using thiophenol in DMF. Following low-high HF deprotection and cleavage with thiocresol and cresol scavengers, the crude peptides were extracted from the resin with 10% aqueous HOAc; material excluded from a Sephadex® G-25 column was pooled and lyophilized, then dissolved in water, and analyzed by C<sub>18</sub> RP-HPLC (Vydac 218TP54) with a gradient of 5–85% CH<sub>3</sub>CN in aq. 0.1% TFA. Pleurocidin amide eluted at 29%, LM4-1 at 27% and LM4-2 at 28% CH<sub>3</sub>CN. Purification was by preparative isocratic HPLC. MALDI-TOF MS of the purified peptides (Perseptive Biosystems Voyager DE STR, matrix  $\alpha$ -cyano-4-hydroxycinnamic acid, 0.7–5 kDa, calib.  $\pm$ 0.2%) gave the ex-

pected monoisotopic, +1, ions (M+H)<sup>+</sup> of pleurocidin amide (m/z 2709.61, calc. 2709.48), LM4-1 (m/z 1793.16, calc. 1793.00), and LM4-2 (m/z 2195.16, calc. 2195.23).

Antibacterial assays were performed by evaluating the ability of synthetic peptides to inhibit bacterial growth in cell cultures [5] (Table 1). Tachyplesin (Bachem, PA), a disulfide-stabilized AMP that acts via a different mechanism, was used as a control peptide. The intensities of the peptide peaks detected at 220 nm in the HPLC were used to determine peptide concentrations; extinction coefficients were calculated using the actual value determined for LM4-2 by AA anal. ( $\epsilon = \epsilon_{\text{LM4-2}} \times \# \text{ amide bonds}/22$ ). The peptides were assayed in triplicate at ten concentrations ranging from 200 to 0.2  $\mu\text{M}$ . Synthetic pleurocidin amide exhibited similar antibiotic activity to tachyplesin, with the desired activity against marine pathogens *V. anguillarum* and *V. carchariae*. Pleurocidin was not as potent against *E. coli* as it was against *V. anguillarum*. The pleurocidin analogs were an order of magnitude less active than the parent peptide, and this result indicated that the C-terminus of pleurocidin might play a role in stabilizing the helix. LM4-2 was more active than LM4-1, possibly indicating that Phe<sup>6</sup> is required for optimal helix formation and activity, however comparing the activities of LM4-1 and LM4-2 is complicated by the different lengths of their C-termini. The antibacterial activity of pleurocidin amide was not notably diminished in 1.5% NaCl, despite a lack of disulfide bonds to help stabilize the active conformation.

Table 1. Antibacterial activity of peptides.

Peptide	Minimum Bactericidal Concentration ( $\mu\text{M}$ ) <sup>a</sup>			
	CSMHB		CSMHB + 1.5% NaCl	
	<i>V. anguillarum</i>	<i>E. coli</i>	<i>V. anguillarum</i>	<i>V. carchariae</i>
Pleurocidin amide	25	100	100	100
LM4-1	>100	>200	>200	>100
LM4-2	100	200	>200	>100
Tachyplesin (control)	25	50	50	25

<sup>a</sup> MBC is the minimum peptide conc. where bacterial growth was not observed at 21 h.

## Acknowledgments

The work was funded by an USDA-NRICGP grant to L. Martin and M. Gómez-Chiarri.

## References

1. Cole, A.M., Weis, P., Diamond, G. *J. Biol. Chem.* **272**, 12008–12013 (1997).
2. Tossi, A., Sandri, L., Giangaspero, A. *Biopolymers* **55**, 4–30 (2000).
3. Jia, X., et al. *Appl. Environ. Microbiol.* **66**, 1928–1932 (2000).
4. Merrifield, R.B., Vizioli, L.D., Boman, H.G. *Biochem.* **21**, 5020–5031 (1982).
5. Alderman, D.J., Smith, P. *Aquaculture* **196**, 211 (2001).

## Disruption of the $\beta$ -Sheet Structure of Cyclic Peptides by Single Amino Acid Substitution: Influence on Prokaryotic and Eukaryotic Cell Viability

Darin L. Lee<sup>1</sup>, Susan W. Farmer<sup>2</sup>, Karin Pflegerl<sup>3</sup>,  
 Robert E. W. Hancock<sup>2</sup>, Michael L. Vasil<sup>4</sup> and Robert S. Hodges<sup>5</sup>

<sup>1</sup>Department of Biochemistry, University of Alberta, Edmonton, T6G 2H7, Canada

<sup>2</sup>Department of Microbiology, University of British Columbia, Vancouver, V6T 1Z3, Canada

<sup>3</sup>Institute of Applied Microbiology, University of Agricultural Sciences, Vienna, A-1190, Austria

<sup>4</sup>Department of Microbiology, University of Colorado,  
 Denver, CO 80262, USA

<sup>5</sup>Department of Biochemistry and Molecular Genetics, University of Colorado,  
 Denver, CO 80262, USA

### Introduction

We have studied the effect of ring size on cyclic  $\beta$ -sheet peptides and showed that we were able to dissociate antimicrobial activity from hemolytic activity [1]. The 14-residue peptide, GS14, displayed weak antimicrobial activity and strong hemolytic activity. In a subsequent study of GS14 analogs, we reversed this profile to create peptides with strong antimicrobial activity and weak hemolytic activity. Single amino acids within the GS14 sequence were substituted with their corresponding D- or L-enantiomers at all 14 ring positions. These analogs had reduced amphipathicity and disrupted  $\beta$ -sheet structure when compared to GS14 (represented in Figure 1, left) [2,3]. Of these analogs, the D-Lys substitution at position 4 (Figure 1, right) yielded the largest increase in therapeutic index (lytic specificity for prokaryotic vs eukaryotic cells) [3]. Here, we substitute other amino acids (both D- and L-enantiomers) at position 4 and study their influence on hemolytic and antimicrobial activity.

### Results and Discussion

All GS14X4 analogs with L-enantiomers (Leu, Phe, Tyr, Asn and Lys) did not disrupt  $\beta$ -sheet structure, exhibited weak to moderate antimicrobial activity, and strong hemolytic activity (data not shown). In contrast, D-substituted analogs exhibited a disrupted  $\beta$ -sheet structure (data not shown), and differences in biological activity de-

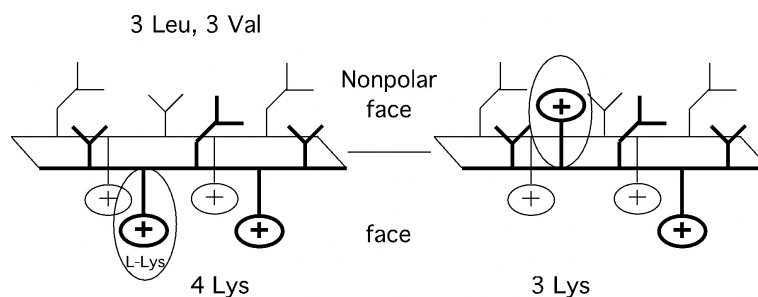


Fig. 1. Representations of GS14X4 analogs. L-amino acid substitutions project onto the polar face (left), while D-amino acids project onto the nonpolar face (right). Sequence: cyclo-VKLXVYPLKVKLYP, where X is the substitution site and D-residues are underlined.

pendent on the hydrophobicity of the substituted amino acid (Figure 2). Peptides with nonpolar amino acids (Leu and Phe) demonstrated strong hemolytic activity and weak antimicrobial activity towards Gram-negative bacteria (Figure 2, left), resulting in a poor therapeutic index (Figure 2, right). Of the peptides studied, the most polar D-substitution (D-Lys) had the strongest therapeutic index, indicating good activity specifically towards microbial membranes.

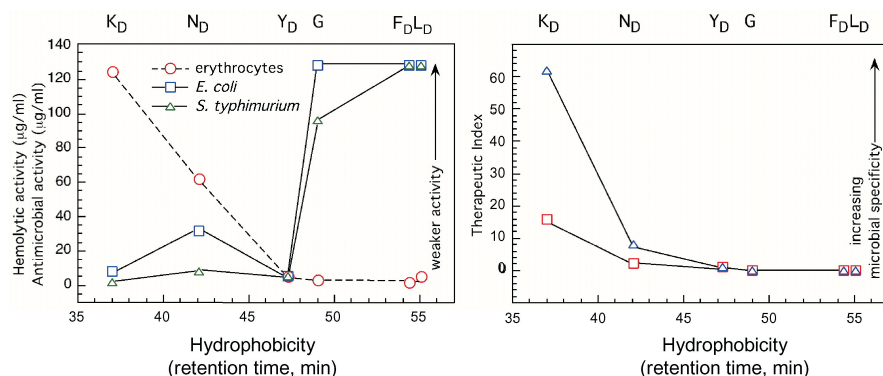


Fig. 2. Effect of GS14X4 nonpolar face hydrophobicity on biological activity. Left panel: hemolytic activity against human erythrocytes (dashed line) and antimicrobial activity (solid line) against *E. coli* UB1005 (squares) and *S. typhimurium* C610 (triangles) were plotted versus reversed-phase HPLC retention times of peptide analogs. Amino acid substitutions at position 4 are listed above their respective peptide retention times. One letter codes are used, with the subscript D denoting side chain stereochemistry. Right panel: therapeutic index (hemolytic activity ÷ antimicrobial activity) of GS14X4 peptides.

In conclusion, we have demonstrated here that differences in the hydrophobicity of the GS14X4 nonpolar face and disruption of  $\beta$ -sheet structure can influence the lytic specificity between prokaryotic and eukaryotic cells.

### Acknowledgments

D. L. is supported by scholarships from NSERC (Canada) and the Alberta Heritage Foundation for Medical Research, and travel awards from APS and the Mary Louise Imrie Graduate Student Award (University of Alberta). R. S. H. is supported by grant GM-61855 (NIH).

### References

1. Kondejewski, L.H., Farmer, S.W., Wishart, D.S., Kay, C.M., Hancock, R.E., Hodges, R.S. *J. Biol. Chem.* **271**, 25261–25268 (1996).
2. McInnes, C., Kondejewski, L.H., Sykes, B.D., Hodges, R.S. *J. Biol. Chem.* **275**, 14287–14294 (2000).
3. Kondejewski, L.H., Jelokhani-Niaraki, M., Farmer, S.W., Lix, B., Kay, C.M., Sykes, B.D., Hancock, R.E.W., Hodges, R.S. *J. Biol. Chem.* **274**, 13181–13192 (1999).

## **Relationship Between Amphipathic Secondary Structure and Activity in Model Linear Cationic Antimicrobial Peptides**

**Jack Blazyk<sup>1,2</sup>, Janet Hammer<sup>1</sup>, Yi Jin<sup>2</sup>, Yu Zhang<sup>2</sup> and Fang Zhu<sup>2</sup>**

<sup>1</sup>*Department of Biomedical Sciences, College of Osteopathic Medicine, Ohio University, Athens, OH 45701, USA*

<sup>2</sup>*Department of Chemistry and Biochemistry, Ohio University, Athens, OH 45701, USA*

### **Introduction**

Cationic peptides are a common component of many host defense systems [1]. Upon binding to the plasma membrane of target bacteria, many of these peptides can adopt a conformation that exhibits amphipathic character. The accumulation of peptides at the membrane surface eventually results in a breakdown of the permeability barrier in the target organism, resulting in cell death. Naturally occurring cationic antimicrobial peptides usually fall into one of two classes. Linear peptides such as magainins, PGLa and cecropins, adopt  $\alpha$ -helical structure, while cysteine-containing peptides such as defensins (constrained by intramolecular disulfide bonds) form  $\beta$ -sheet conformation in order to maximize amphipathicity. Recently we designed an 18-residue linear peptide, (KIGAKI)<sub>3</sub>-NH<sub>2</sub>, with no amphipathic propensity as an  $\alpha$ -helix, but a highly amphipathic  $\beta$ -sheet structure [2]. Although this peptide possesses similar antimicrobial activity to that of linear  $\alpha$ -helical peptides of comparable size, charge and hydrophobicity, it appears to be significantly more selective for bacterial membranes as compared to mammalian membranes. In this study, we examined the relationship between amphipathicity, secondary structure, antimicrobial activity, and lipid selectivity among a representative group of model peptides.

### **Results and Discussion**

First, we compared the structure and activity of a peptide capable of forming an amphipathic  $\alpha$ -helix with those of three peptides with amphipathic  $\beta$ -sheet potential.

KIAGKIA	KIAGKIAKIAGKIAKIAGKIA-NH <sub>2</sub>
KIGAKI	KIGAKIKIGAKIKIGAKI-NH <sub>2</sub>
KL-14	KLKLKLKWKLKLKL-NH <sub>2</sub>
KL-18	KLKLKLKWKLKLKLKLKL-NH <sub>2</sub>

CD and FTIR spectroscopy showed that all of these peptides exhibit the expected secondary structure (*i.e.*, the structure of KIAGKIA was  $\alpha$ -helical while that of the other peptides was  $\beta$ -sheet) in the presence of large unilamellar vesicles (LUV) containing the acidic lipid POPG. KIAGKIA and KIGAKI were equal in antimicrobial potency *vs E. coli*, *S. aureus* and *P. aeruginosa* with minimum inhibitory concentration (MIC) values of 8, 8 and 16  $\mu$ g/mL, respectively. KL-14 and KL-18 were less effective *vs E. coli* (MIC values of 32 and 64  $\mu$ g/mL, respectively).

The  $\alpha$ -helical peptide KIAGKIA was much better at inducing the leakage of calcein from mixed LUV containing POPG and POPC as compared to POPG and POPE. In contrast, the  $\beta$ -sheet peptide KIGAKI was more active when the neutral lipid was POPE instead of POPC. The other  $\beta$ -sheet peptides, KL-14 and KL-18, however, did not share this selectivity at neutral-to-acidic lipid ratios of 3 : 1 and 4 : 1. In spite of their weaker antimicrobial activity toward *E. coli*, KL-14 and KL-18 were more potent at releasing calcein from LUV composed of *E. coli* polar lipids. These peptides are

much less hydrophobic than either KIGAKI or KIAGKIA, which could be an important factor in interactions with the bacterial cell envelope.

In an effort to gain insight into the importance of amphipathicity independently of secondary structure, we compared the activity of two families of model peptides with identical charge and overall hydrophobicity but different degrees of amphipathic potential as either  $\alpha$ -helix or  $\beta$ -sheet. One family of five 18-residue peptides, based on a hexamer repeat containing two lysines, two isoleucines, one alanine, and one glycine, differs only in the placement of the lysines, resulting in a set of peptides with no amphipathic potential as an  $\alpha$ -helix but different levels of amphipathicity as a  $\beta$ -sheet. A second family of six 21-residue peptides, based on a heptamer repeat containing two lysines, two leucines, two alanines, and one glycine, also differs in the placement of the lysines, resulting in a set of peptides with varying amphipathic potential as  $\alpha$ -helix and a  $\beta$ -sheet. In addition, each peptide contains a single tryptophan (replacing an isoleucine or a leucine in the central region of the molecule) for fluorescence studies. The sequences of these peptides are:

1,2-Hept	KKLAGLAKKWAGLAKKLAGLA-NH <sub>2</sub>
1,3-Hept	KLKAGLAKWKAGLAKLKAGLA-NH <sub>2</sub>
1,4-Hept	KLAKGLAKWAGKLAKLAGKLA-NH <sub>2</sub>
1,5-Hept	KLAGKLAKWAGKLAKLAGKLA-NH <sub>2</sub>
1,6-Hept	KLAGLKAKWAGLKAKLAGLKA-NH <sub>2</sub>
1,7-Hept	KLAGLAKKWAGLAKKLAGLAK-NH <sub>2</sub>
1,2-Hex	KKIGAIAKKWGAIKKIGAI-NH <sub>2</sub>
1,3-Hex	KIKGAIKWKGAIKIKGAI-NH <sub>2</sub>
1,4-Hex	KIGKAIAKWGKAIKIGKAI-NH <sub>2</sub>
1,5-Hex	KIGAKIKWGAKIKIGAKI-NH <sub>2</sub>
1,6-Hex	KIGAIAKKWGAIKKIGAIK-NH <sub>2</sub>

Of these peptides, only 1,3-Hex and 1,5-Hex can form highly amphipathic  $\beta$ -sheet structure and 1,2-Hept, 1,4-Hept, 1,5-Hept and 1,7-Hept can adopt an amphipathic  $\alpha$ -helical conformation. These were the only peptides that demonstrated significant antimicrobial activity. A strong correlation was observed between amphipathic potential (as either an  $\alpha$ -helix or  $\beta$ -sheet) and antimicrobial potency. Further studies will explore the binding of these molecules to LUV of defined lipid composition and functional assessments including effects on membrane permeability of mammalian and bacterial cells in order to better understand the relationships among structure, activity and selectivity.

#### **Acknowledgments**

Supported by grant AI-47165 (National Institute of Allergy and Infectious Diseases).

#### **References**

1. Maloy, W.L. Kari, U.P. *Biopolymers* **37**, 105–122 (1995).
2. Blazyk, J., Wiegand, R., Klein, J., Hammer, J., Epand, R.M., Epand, R.F., Maloy, W.L. Kari, U.P. *J. Biol. Chem.* **276**, 27899–27906 (2001).

## Shedding Light on the Aglycon Formation of Glycopeptide Antibiotics

Daniel Bischoff<sup>1</sup>, Bojan Bister<sup>1</sup>, Stefan Weist<sup>1</sup>, Stefan Pelzer<sup>2</sup>, Alexandra Hölzel<sup>1</sup>, Graeme Nicholson<sup>1</sup>, Sigrid Stockert<sup>2</sup>, Wolfgang Wohlleben<sup>2</sup>, Günther Jung<sup>1</sup> and Roderich D. Süssmuth<sup>1</sup>

<sup>1</sup>Institute of Organic Chemistry, and <sup>2</sup>Institute of Microbiology/Biotechnology,  
University of Tübingen, 72076, Germany

### Introduction

Glycopeptide antibiotics, with vancomycin as the most prominent representative, have gained considerable interest over recent years. This is due to their function as antibiotics of last resort for infections of methicillin-resistant *Staphylococcus aureus* (MRSA) strains. The antibiotic activity of glycopeptides is based on the high specificity of the aglycon cavity towards the *N*-acyl-D-Ala-D-Ala-peptide motif of bacterial cell wall precursors as summarized in recent reviews [1,2]. First insights into the glycopeptide antibiotic biosynthesis have been obtained by sequencing the chloroeremomycin gene cluster of *Amycolatopsis orientalis* [3] and cloning and analyzing the balhimycin cluster of *Amycolatopsis mediterranei* [4]. We addressed our research to understand how nature assembles the side chain-cyclized aglycon cavity, which is an essential element of a whole class of natural compounds.

### Results and Discussion

Our studies focus on the biosynthesis gene cluster of balhimycin, a glycopeptide antibiotic of the vancomycin type, which is produced by *A. mediterranei*. Except for their glycosylation pattern, vancomycin and balhimycin are structurally identical. Targeted are three oxygenase genes (*oxyA/B/C*), which are supposed to encode the respective enzymes responsible for the aglycon formation from a linear heptapeptide precursor molecule [4]. From the generation of gene replacement and deletion mutants in the balhimycin biosynthesis gene cluster we were able to isolate peptides accumulated in the culture filtrates of these mutants. These peptides were purified and analyzed by ESI-MS, 2-D NMR experiments, Edman degradation and amino acid analysis. They are considered to be intermediates of the biosynthesis and thus give insight into the formation of the aglycon.

SP-1134, a heptapeptide previously characterized from a mutant, is possibly the linear precursor prior to the aglycon formation [5]. Recently, we isolated the intermediate SP-1132 with a molecular mass of 1132 Da from an *oxyA* mutant [6]. Compared to SP-1134, the mass difference of 2 Da corresponds to the loss of two hydrogen atoms *i.e.* one oxidation step performed by an oxygenase, presumably OxyB or OxyC. Edman degradation and supporting NMR studies of that compound revealed a monocyclic sidechain-bridged heptapeptide with a biarylether in the C-O-D ring system (Figure 1). We consider SP-1132 as a novel intermediate of the glycopeptide antibiotic biosynthesis. It is of particular relevance, that this result implies a stepwise crosslinking of the heptapeptide side chains in an ordered sequence.

Our present work gives further insight into important steps of the glycopeptide antibiotic biosynthesis. We suggest the following course for the complex biosynthesis of vancomycin-type glycopeptide antibiotics: 1. Formation of a linear heptapeptide precursor (SP-1134) *via* peptide synthetases (BpsA/B/C). 2. Conversion of SP-1134 to the aglycon upon the action of three oxygenases (OxyA/B/C). 3. Further modifications

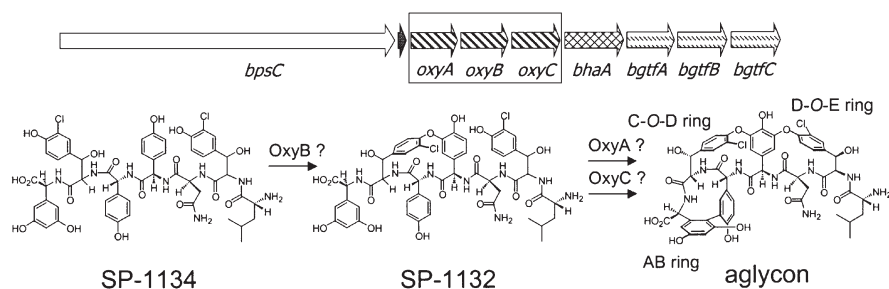


Fig. 1. Part of the balhimycin biosynthesis gene cluster and postulated scheme of the aglycon formation by the three oxygenases OxyA/B/C.

by glycosyltransferases (BgtfA/B/C) and an *N*-methyltransferase to furnish the glycopeptide antibiotic.

### Acknowledgments

R.D. Süssmuth is currently a recipient of a Feodor-Lynen Fellowship granted by the Alexander-von-Humboldt Foundation. This work was supported by the grant SFB 323 (Deutsche Forschungsgemeinschaft).

### References

1. Williams, D.H., Bardsley, B. *Angew. Chem., Int. Ed. Engl.* **38**, 1172–1193 (1999).
2. Nicolaou, K.C., Boddy, C.N.C., Bräse, S., Winssinger N. *Angew. Chem., Int. Ed. Engl.* **38**, 2096–2152 (1999).
3. van Wageningen, A.M.A., Kirkpatrick, P.N., Williams, D.H., Harris, B.R., Kershaw, J.K., Lennard, N.J., Jones, M., Jones, S.J.M., Solenberg, P.J. *Chem. Biol.* **5**, 155–162 (1998).
4. Pelzer, S., Süssmuth, R., Heckmann, D., Recktenwald, J., Huber, P., Jung, G., Wohlleben, W. *Antimicrob. Agents Chemother.* 1565–1573 (1999).
5. Süssmuth, R.D., Pelzer, S., Nicholson, G., Walk, T., Wohlleben, W., Jung, G. *Angew. Chem., Int. Ed. Engl.* **38**, 1976–1979 (1999).
6. Bischoff, D., Pelzer, S., Hölzel, A., Nicholson, G.J., Stockert, S., Wohlleben, W., Jung, G., Süssmuth, R.D. *Angew. Chem., Int. Ed. Engl.* **40**, 1693–1696 (2001).

## Synthesis of $\lambda$ -Conotoxins, a New Family of Conotoxins with Unique Disulfide Pattern

Kazuki Sato<sup>1</sup>, Yuko Sugahara<sup>1</sup>, R. Ashok Balaji<sup>2</sup>  
and P. Gopalakrishnakone<sup>2</sup>

<sup>1</sup>Faculty of Human Environmental Science, Fukuoka Women's University,  
Fukuoka 813-8529, Japan

<sup>2</sup>Faculty of Medicine, National University of Singapore, Singapore 117597

### Introduction

The peptide toxins (Conotoxins) obtained from the venom of predatory marine cone snails (genus *Conus*) are widely used as research tools in neuroscience and some are potential therapeutic agents. Conotoxins are classified based on their cystine motif and/or biological activity [1,2]. Recently, a new family of conotoxins named  $\lambda$ -conotoxin CMrVIA, CMrVIB, and CMrX were isolated and characterized from molluscivorous cone snail *Conus marmoreus* venom [3,4]. Although they have two-loop motif like  $\alpha$ -conotoxins, their disulfide pairings (C1-C4 and C2-C3) (Figure 1) are different from that of  $\alpha$ -conotoxins (C1-C3 and C2-C4). For the study of three-dimensional structure of these unique peptides, we tried to synthesize them in a large quantity by one-step random air oxidation instead of selective two-step disulfide bond formation strategy that we had taken to determine the disulfide pairings of  $\lambda$ -conotoxins.

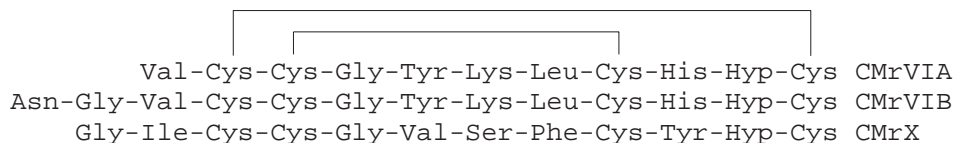


Fig. 1. Amino acid sequences of  $\lambda$ -conotoxins.

### Results and Discussion

The linear precursors of three  $\lambda$ -conotoxins with Trt groups for the protection of Cys residues were successfully assembled by the solid phase methodology of Fmoc chemistry. After TFA cleavage, crude linear peptides were diluted to the final peptide concentration of 0.05 mM and subjected to oxidative disulfide bond formation at room temperature for 3–5 days in 0.5 M ammonium acetate buffer (pH 8.0). The folding reaction was monitored by HPLC and stopped by lowering the pH of the solution to 3–4 with AcOH. The crude cyclic products were purified by successive chromatography on Sephadex G-25F, CM-cellulose CM-52, and preparative HPLC with an ODS column. The structure and purity of synthetic peptides were confirmed by analytical HPLC, amino acid analysis, and MALDI-TOF-MS measurements.

Random air oxidation of linear precursor of CMrVIA afforded three products with correct molecular weight indicating the formation of disulfide bond isomers. Peptide with native disulfide pairings was obtained as the most abundant component resulting in the improvement of overall isolation yield. The yield of native peptide was 18%, which was much higher than the previous yield (9%) with two-step selective strategy. SS isomer with  $\alpha$ -conotoxin-like C1-C3 and C2-C4 pairings was obtained in 9% yield and that with C1-C2 and C3-C4 pairings was also isolated in 5% yield.

Formation of disulfide bond isomers was not significant in the cyclization reaction of linear precursors of CMrVIB and CMrX. Overall yield of CMrX was 16%, which is higher than that (8%) in the previous method. However, CMrVIB afforded by-products with  $\alpha$ - and  $\beta$ -Asp-Gly sequence at their N-termini as major products due to formation and opening of succinimide derivatives. Purified CMrVIB was isolated in 5% yield, which was still satisfactory. In order to suppress this side reaction, we tried to use Boc-Asn at the final coupling step so that we can avoid the base treatment in the deprotection of Fmoc group. However, the yield was not improved, suggesting that the side reaction occurred in later steps.

In the present study we were able to obtain satisfactory amount of  $\lambda$ -conotoxins. Three-dimensional structure analysis of these peptides by NMR is currently in progress to obtain precise information on the role of unique disulfide bond pattern for the structure-activity relationships of  $\lambda$ -conotoxins.

#### **Acknowledgments**

This work was supported in part by a project grant from the Japan Health Science Foundation, Program for Promotion of Fundamental Studies in Health Sciences of Organization for Drug ADR Relief, R&D Promotion and Product Review of Japan.

#### **References**

1. Jones, R.M., Bulaj, G. *Curr. Opin. Drug Disc. Dev.* **3**, 141–154 (2000).
2. McIntosh, J.M., Olivera, B.M., Cruz, L.J. *Methods Enzymol.* **294**, 605–624 (1999).
3. Balaji, R.A., Ohtake, A., Sato, K., Gopalakrishnakone, P., Kini, R.M., Seow, K.T., Bay, B.H. *J. Biol. Chem.* **275**, 39516–39522 (2000).
4. Macintosh, J.M., Corpuz, G.O., Layer, R.T., Garrett, J.E., Wagstaff, J.D., Bulaj, G., Vyazcvikina, A., Yoshikami, D., Cruz, L.J., Olivera, B.M. *J. Biol. Chem.* **275**, 32391–32397 (2000).

## **Solution Conformation of an $\alpha$ -Conotoxin GI with a D-Tyr at Position 11**

**Do-Hyung Kim, Kyu-Hwan Park and Kyou-Hoon Han**

*Protein Engineering Laboratory, Korea Research Institute of Bioscience and Biotechnology,  
Taejeon, Korea*

### **Introduction**

$\alpha$ -Conotoxin GI is the first discovered among the conotoxin antagonists against nicotinic acetylcholine receptor (nAChR) [1]. Several studies have shown that a few residues in this toxin are responsible for receptor subtype selectivity, in particular,  $^9\text{Arg}$  and  $^{10}\text{His}$  [2,3]. Three-dimensional structures of this toxin determined independently by NMR spectroscopy [4,5] and X-ray crystallography [6] reveal that  $^9\text{Arg}$  and  $^{10}\text{His}$  in  $\alpha$ -conotoxin GI are fully exposed to the molecular surface and hence capable of contacting ligand-binding surface within nAChR. In a more recent study [7], several analogs of  $\alpha$ -conotoxin MI, another  $\alpha 3/5$  sub-family toxin that exhibits a similar activity as  $\alpha$ -conotoxin GI [8], that contain Ala, Trp, Met and His instead of  $^{12}\text{Tyr}$  (corresponding to  $^{11}\text{Tyr}$  in  $\alpha$ -conotoxin GI) have been tested for their activity. Results showed that only the Ala-substituted analog exhibited markedly different activity while the other three analogs with bulky hydrophobic sidechains had a similar activity as the wild type  $\alpha$ -conotoxin MI.

In order to understand such activity differences among different analogs of  $\alpha$ -conotoxin MI we have synthesized an analog of  $\alpha$ -conotoxin GI that has a D-Tyr at position 11 (GIDY henceforth) and have determined its three-dimensional structure using NMR spectroscopy and molecular modeling (Figure 1). The L-Tyr in the three-dimensional structure of  $\alpha$ -conotoxin GI/MI occupies a peculiar position so that its bulky hydrophobic aromatic ring helps  $\alpha$ -conotoxin GI/MI to maintain its overall structural topology by forming a hydrophobic core of the toxin molecule [4,5,9]. Hence, any mutation of this residue by an amino acid with a smaller sidechain is likely to alter the activity drastically by destabilizing the overall three-dimensional structure. Our results show that GIDY has a totally different overall topology from the wild type where critical residues such as  $^9\text{Arg}$  and  $^{10}\text{His}$  point opposite directions from those found in the wild type.

### **Results and Discussion**

GIDY was synthesized on an Applied Biosystems/Perkin Elmer 432A Synergy peptide synthesizer using FastMoc cycles (HBTU/piperidine activation, DMF/NMP/DMSO as

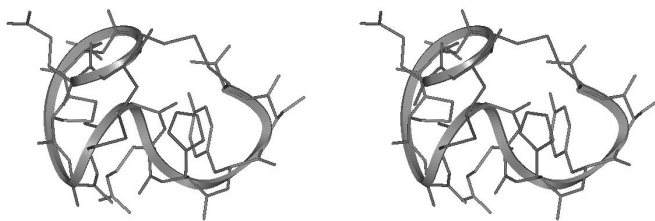


*Fig. 1. A representative structure of GIDY. The ribbon shows the peptide backbone.*

coupling solvent) and Synergy Fmoc-Amide resin. Purification of the peptide was performed using a preparative reversed-phase HPLC. A Kromasil KR-100-10-C8 (10 mm id  $\times$  250 mm, C8, 10  $\mu$ m, Akzo Nobel) column was used, with a linear gradient of 10% CH<sub>3</sub>CN to 20% CH<sub>3</sub>CN, 0.1% TFA over 20 column volumes.

Samples for NMR studies were prepared in 90% H<sub>2</sub>O/10% <sup>2</sup>H<sub>2</sub>O or 100% <sup>2</sup>H<sub>2</sub>O at pH 4.0 with a final sample concentration of 2 mM. NMR experiments were performed in a phase-sensitive mode using a Varian UNITY INOVA 600 spectrometer at 5, 15 and 25 °C.

### **Acknowledgments**

This work has been supported in part by NB1310 to K. Han from Ministry of Science and Technology of Korea.

### **References**

1. Gray, W.R., Luque, A., Olivera, B.M., Barrett, J., Cruz, L.J. *J. Biol. Chem.* **256**, 4734–4740 (1981).
2. Groebe, D.R., Gray, W.R., Abramson, S.N. *Biochemistry* **36**, 6469–6474 (1997).
3. Hann, R.M., Pagan, O.R., Gregory, L.M., Jacome, T., Eterovic, V.A. *Biochemistry* **36**, 9051–9056 (1997).
4. Gehrmann, J., Alewood, P.F., Craik, D.J. *J. Mol. Biol.* **278**, 401–415 (1998).
5. Maslennikov, I.V., Sobol, A.G., Gladky, K.V., Lugovskoy, A.A., Ostrovsky, A.G., Tsetlin, V.I., Ivanov, V.T., Arseniev, A.S. *Eur. J. Biochem.* **254**, 238–247 (1998).
6. Guddat, L.W., Martin, J.A., Shan, L., Edmunson, A.B., Gray, W.R. *Biochemistry* **35**, 11329–11335 (1996).
7. Jacobsen, R.B., DelaCruz, R.G., Grose, J.H., McIntosh, J.M., Yoshikami, D., Olivera, B.M. *Biochemistry* **38**, 13310–13315 (1999).
8. McIntosh, J.M., Cruz, L.J., Hunkapiller, M.W., Gray, W.R., Olivera, B.M. *Arch. Biochem. Biophys.* **218**, 329–334 (1982).
9. Gouda, H., Yamazaki, K., Hasegawa, J., Kobayashi, Y., Nishiuchi, Y., Sakakibara, S., Hirono, S. *Biochim. Biophys. Acta* **1343**, 327–334 (1997).

## Antimicrobial and Chemotactic Activities of $\omega$ -Conotoxin Cyclic Analogues

Jin-Long Yang, Yi-An Lu, Chengwei Wu and James P. Tam

Department of Microbiology and Immunology, University of Vanderbilt, Nashville,  
 TN 37232, USA





### Introduction

The family of  $\omega$ -conotoxins isolated from paralytic venomous of *Conus snails* has been known to be an antagonist of presynaptic N-type calcium ion channels. They share certain similarities to the newly discovered family of antimicrobial macrocyclic peptides found in plant [1]. Both are basic peptides with a four- $\beta$ -loop scaffold constrained by a cystine-knot disulfide motif. We have prepared three cyclic  $\omega$ -conotoxin analogues with different disulfide constraints to determine whether the open-chain  $\omega$ -conotoxins are microbicidal and whether their activity can be improved by end-to-end cyclic analogues mimicking the plant macrocycles. In addition, we have also determined their hemolytic and chemotactic activities attendant to membranolytic and defense mechanisms of antimicrobials.

### Results and Design

Solid-phase peptide synthesis method based on thia-zip cyclization [1] was employed to synthesize three cyclic analogues **cA1**–**cA3** based on  $\omega$ -conotoxin MVIIA, as shown in Table 1. The open-chain MVIIA contains three covalent constraints imposed by the cystine-knot motif while the cyclic analogues contain two or three constraints with an end-to-end lactam and one or two disulfide(s). The half-cystines in these analogues are replaced by the isosteric aminobutyric acids (Abu). Since the N- and

Table 1. Sequences and antimicrobial activity of native and cyclic  $\omega$ -conotoxin.

Peptide	Sequence	MIC ( $\mu$ M)		
		G <sup>-</sup> <i>E. coli</i>	G <sup>+</sup> <i>S. aureus</i>	Fungi <i>C. kefir</i>
MVIIA	 CKGKGAKCSRLMYDCCTGSCRSKGK	>500	>500	28.8
<b>cA1</b>	 CKGKGAKBSRLMYDCCTGSBRSGKCGS	9.56	11.2	2.40
<b>cA2</b>	 CKGKGAKBSRLMYDCCTGSBRSGKCGS	39.4	18.8	6.92
<b>cA3</b>	 CKGKGAKBSRLMYDCCTGSBRSGKCGS	11.4	21.1	5.02

Antimicrobial experiments were performed in radial diffusion assay with underlay gel containing 1% agarose and 10 mM phosphate buffer.

C-termini of MVIIA are not spatially close, computer modeling shows that the end-to-end cyclization of the native MVIIA to **cA1**–**cA3** imparts significant conformational changes even though their amino acid sequences are essentially similar.

The antimicrobial activity was determined in three test organisms by a two-stage radial diffusion assay under low-salt conditions [2]. MVIIA was completely inactive against both Gram-negative bacteria (*E. coli*) and Gram-positive bacteria (*S. aureus*), although it had marginally activity against fungi (*C. kefyr*). Analogue **cA1**, a cyclized MVIIA with two disulfides (Cys-1,16 and Cys-15,25), displayed significantly enhanced microbicidal activity against three test organisms with MICs of 2–11  $\mu$ M. Reducing the conformational constraint of **cA1** by replacing the Cys-15,25 disulfide by two Abu in **cA2** lowered its potency 2- to 4-fold. Replacing the Cys-1,16 disulfide pair by Abu in **cA3** also resulted in decreased antimicrobial activity compared to **cA1** against *S. aureus* and *C. kefyr*, while activity against *E. coli* was retained.

MVIIA showed low toxicity on human erythrocytes with an  $EC_{50}$  of 4210  $\mu$ M. Similarly, all three cyclic MVIIA analogues had low hemolytic activity with  $EC_{50}$ s of 1320–2650  $\mu$ M. MVIIA and its cyclic analogues were chemotactic (Figure 1). Chemotaxis based on monocyte migrations performed in microchemotaxis chamber [3] were **cA1** > **cA3** > **cA2** = MVIIA.

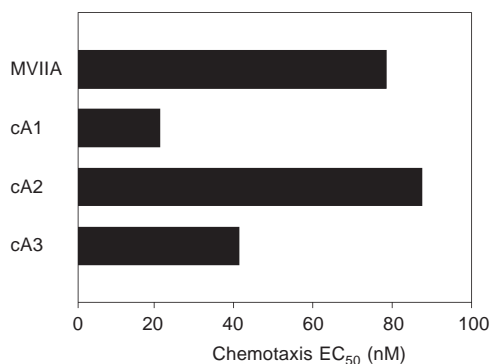


Fig. 1. Chemotactic potency of MVIIA and its cyclic analogs on monocytes.

In conclusions, the  $\omega$ -conotoxin MVIIA is essentially inactive as an antimicrobial. End-to-end cyclization of MVIIA produces analogues that are active and broad-spectrum antimicrobials. MVIIA and its cyclic analogues display low hemolytic toxicity against human erythrocytes and induce migration of monocytes. These results show that conotoxins can be used as a template for designing novel antimicrobials and chemokines.

#### Acknowledgments

This research was supported in part by PHS NIH Grant AI46164 and CA 36544.

#### References

1. Tam, J.P., Lu, Y-A., Yang, J-L., Chiu, K-W. *Proc. Natl. Acad. Sci. USA* **96**, 8913–8918 (1999).
2. Lehrer, R.I., Rosenman, M., Harwing, S.S., Jackson, R., Eisenbauer, P.J. *Immunol. Methods* **137**, 167–173 (1991).
3. Tam, J.P., Yu, Q., Yang, J-L. *J. Am. Chem. Soc.* **123**, 2487–2494 (2001).

## Synthesis of Parallel and Antiparallel Magainin 2 Dimers and Their Interaction with Lipid and Cell Membrane

**Takuro Niidome, Yuko Matsushita, Tomomitsu Hatakeyama and Haruhiko Aoyagi**

*Department of Applied Chemistry, Faculty of Engineering, Nagasaki University, Nagasaki 852-8521, Japan*

### Introduction

Magainin 2 (MG2) is a cationic amphiphilic peptide isolated from the skin of the African clawed frog (*Xenopus laevis*) and has antibacterial activity. MG2 was found to strongly interact with anionic phospholipid to form ion channels in lipid bilayers [1,2]. The synthesis and properties of parallel dimers [3,4] and antiparallel dimer of MG2 [5] have been successively reported. In this study, we synthesized two MG2 analogs, MG2-C and MG2-N, which have a linker of  $\beta$ Ala-Cys at the C-terminus and Cys- $\beta$ Ala at the N-terminus, respectively. Then, we prepared a parallel MG2 dimer (MG2-CC) from MG2-C and an antiparallel MG2 dimer (MG2-CN) from MG2-C and MG2-N (Figure 1), and investigated their properties and antibacterial activity.

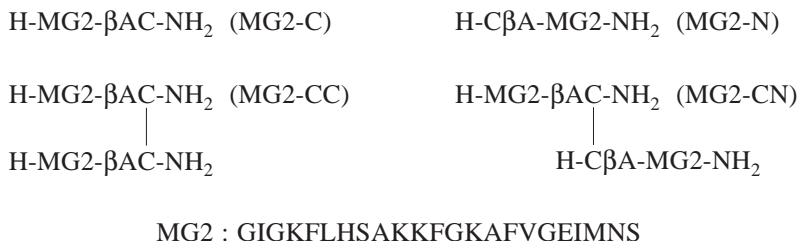


Fig. 1. Structures of synthetic peptides.

### Results and Discussion

Two monomers, MG2-C and MG2-N, were prepared using Fmoc-amino acids by standard solid phase synthesis. MG2-CC was obtained by air oxidation of MG2-C in a buffer solution (pH 8.0), whereas MG2-CN was obtained by S-S exchange reaction of MG2-N and MG2-C, which was activated with 2,2-dithiodipyridine. After purification by gel chromatography and RP-HPLC, identification of the products was performed by analytical RP-HPLC and MALDI-TOF-MS. CD measurement showed that all the peptides were random in aqueous solution and had moderate  $\alpha$ -helical content (35–65%) in the presence of neutral or anionic phospholipid vesicles. MG2-CN showed higher helicity than MG2-CC. Calcein leakage mediated by peptide from calcein-entrapped vesicles was performed to examine the peptide-lipid interaction. The leakage activity of the dimers was stronger than that of the corresponding monomers. For DOPC/DOPG (3 : 1) small unilamellar vesicles, MG2-CN showed slightly stronger activity than MG2-CC.

To evaluate biological activity of the peptides, their hemolytic activity was examined using rabbit blood cells. MG2-C, MG2-N and MG2 exhibited weak or negligible activity, whereas the activity of the dimers was fairly strong. This result suggests that dimerization of MG2 strengthens interaction of peptide-neutral lipid, because the

**Niidome et al.**

outer leaf of blood cell scarcely contains anionic lipid. The antibacterial activity of the peptides is shown in Table 1. MG2-CC and MG2-CN had strong activity against gram-positive and gram-negative bacteria. MG2-C showed activity very similar to that of MG2, whereas the activity of MG2-N was unexpectedly weak. The reason is currently unclear. It is clear, however, that interaction of peptide with lipid membrane was increased by dimerization of peptide. However, no significantly different properties or activities were found between the dimers, MG2-CC and MG2-CN.

*Table 1. Antibacterial activity of peptides.*

	Minimum inhibitory concentration ( $\mu\text{M}$ ) <sup>a</sup>				
	MG2	MG2-C	MG2-N	MG2-CC	MG2-CN
<i>S. aureus</i>	8	8	16	2	4
<i>B. subtilis</i>	8	8	32	2	4
<i>E. coli</i>	4	8	32	2	4
<i>P. aeruginosa</i>	8	4	32	1	2

<sup>a</sup> Method, liquid based assay; medium, tryptic soy broth medium (pH 7.4); inoculum size,  $10^4$  cells/ml.

**Acknowledgments**

This work was supported by a Grant-in-Aid from the Ministry of Education, Science, Sports and Culture of Japan.

**References**

1. Matsuzaki, K., Harada, M., Funakoshi, S., Fujii, N., Miyajima, K. *Biochim. Biophys. Acta* **1063**, 162–170 (1991).
2. Matsuzaki, K., Murase, O., Tokuda, H., Funakoshi, S., Fujii, N., Miyajima, K. *Biochemistry* **33**, 3342–3349 (1994).
3. Mukai, Y., Niidome, T., Hatakeyama, T., Aoyagi, H., In Fields, G.B., Tam, J.P., Barany, G. (Eds.) *Peptide for the New Millennium (Proceedings of the 16th American Peptide Symposium)*, Kluwer, Dordrecht, 2000, p. 756.
4. Kanegae, H., Okumura, S., Akao, S., Harata, K., Morii, H., In Shioiri, T., (Ed.) *Peptide Science 2000 (Proceedings of the 37th Japanese Peptide Symposium)*, The Japanese Peptide Society, Osaka, 2001, p. 377.
5. Hara, T., Kodama, H., Kondo, M., Wakamatsu, K., Takeda, A., Tachi, T., Matsuzaki, K., In Shioiri, T. (Ed.) *Peptide Science 2000 (Proceedings of the 37th Japanese Peptide Symposium)*, The Japanese Peptide Society, Osaka, 2001, p. 121.

## Interaction of the Antimicrobial Peptide PGLa and Its Ala-Substitution Analog with Membrane-Mimetic Systems

Sylvie E. Blondelle<sup>1</sup> and Karl Lohner<sup>2</sup>

<sup>1</sup>Torrey Pines Institute for Molecular Studies, San Diego, CA 92121, USA

<sup>2</sup>Institut für Biophysik und Röntgenstrukturforschung, Österreichische Akademie der Wissenschaften, Graz, A 8042, Austria

### Introduction

The rapid emergence of multi-resistant bacteria poses a major global health problem and calls for the development of antibiotics that bacteria have never seen before. The discovery of host defense peptides has opened new avenues for developing such drugs. Many of these peptides, while exhibiting random structure in solution, adopt an  $\alpha$ -helical conformation upon interaction with cell membranes and model membranes [1]. However, synthetic  $\alpha$ -helical peptides are often toxic to mammalian cells. A better understanding of the biophysical requirements for selective bacterial lysis to occur in regards to peptide induced structures, as well as their effect on lipid properties, is therefore needed for the de novo design of novel antimicrobial peptides. Using synthetic peptides having varying hydrophobic/hydrophilic amino acid distribution, we have investigated how a peptide's helicity and hydrophobicity affect its interaction with model membrane systems and how this correlates with the peptide activity.

### Results and Discussion

The biological activity and helicity of the antimicrobial frog skin peptide peptidyl-glycine-leucine-carboxamide (PGLa) and an alanine substitution analog (A-PGLa), which is characterized by lower hydrophobic moment and total hydrophobicity values, were investigated. As shown in Table 1, both peptides exhibit a similar content of  $\alpha$ -helix in the presence of liposomes mimicking bacterial cytoplasmic membranes, al-

Table 1. Biological activity and helicity of PGLa and A-PGLa.

	hydrophobicity	<i>E. aureus</i>		<i>E. coli</i>		erythrocyte	
		IC <sub>50</sub>	% helix <sup>a</sup>	IC <sub>50</sub>	% helix <sup>b</sup>	HD <sub>50</sub>	% helix <sup>c</sup>
PGLa	+0.89	26	56	10	60	>250	4
A-PGLa	-0.36	>125	70	>125	78	>250	4

The % helix are calculated from CD spectra in the presence of small unilamellar vesicles prepared using the following lipid ratio: <sup>a</sup> PG/DPG 95/5; <sup>b</sup> PE/PG/DPG 82/6/12; <sup>c</sup> PC/SM/cholesterol 37/37/25.

though only PGLa exhibits antimicrobial activity. Furthermore, neither of the two peptides exhibited hemolytic activity, which correlated with the absence of  $\alpha$ -helical conformation observed for the peptides in the presence of liposomes mimicking the outer leaflet of the erythrocyte membrane. In agreement with numerous studies aimed at correlating a peptide induced secondary structure and its antimicrobial activity, these results suggest that the induction of the  $\alpha$ -helical conformation is of less importance for the lytic activity of antimicrobial peptides as compared to hemolytic peptides.

The mode of membrane perturbation by the peptides was studied by means of microcalorimetry. As shown in Figure 1A, the phase behavior of vesicles composed of phosphatidylglycerol, a main component of bacterial membranes, was only markedly affected by PGLa. On the other hand, vesicles composed of phosphatidylcholine, a main component of erythrocyte outer leaflet were not affected by any of the two peptides (Figure 1B). These results agree with the antimicrobial activity observed only for PGLa and lack of hemolytic activity observed for the two peptides.

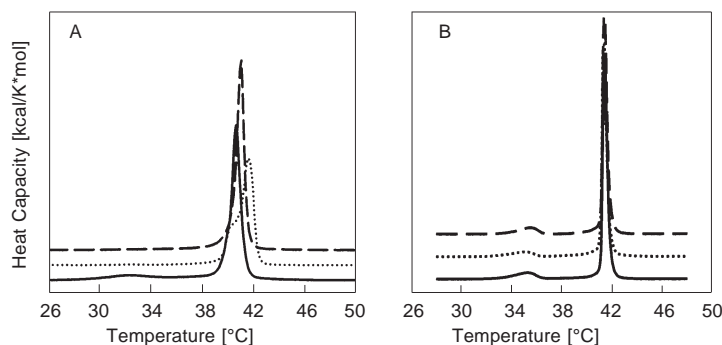


Fig. 1. Thermograms of (—) pure vesicles, and vesicles in the presence of (···) PGLa and (---) A-PGLa at a lipid:peptide molar ratio of 25 : 1. (A) DPPG, (B) DPPC.

In summary, the discrepancies in correlation between the induction into an  $\alpha$ -helical conformation and the peptide's hemolytic and antimicrobial activities may be partly due to the variations in the packing properties that exist between the respective lipid matrices. This results in different interfacial properties of the membranes, which can affect the mode of lipid-peptide interactions. For example, while phosphatidylcholine and sphingomyelin show complete miscibility [2], the major components of erythrocyte membranes, regions of immiscibility are observed in mixtures of phosphatidylethanolamine and phosphatidylglycerol [3], the major phospholipids in bacterial membranes. These differences can be explained based on the nature of the headgroups and the molecular geometry of the phospholipids. Therefore, it may be of significant importance to consider the microscopic differences that exist in the lateral organization, packing and/or mobility of lipids when studying the effect of cell membrane-mimetic lipids on the lytic activity of peptides.

#### Acknowledgments

This work was supported by grants from the Austrian Ministry of Science & Transportation and by grant No. 7190 from the Österreichische Nationalbank.

#### References

1. Blondelle, S.E., Lohner, K. *Biopolymer (Peptide Sci.)* **55**, 74–87 (2000).
2. Degovics, G., Latal, A., Prenner, E.J., Kriechbaum, M., Lohner, K. *J. Appl. Cryst.* **30**, 776–780 (1997).
3. Latal, A., Degovics, G., Lohner, K. *Chem. Phys. Lipids* **94**, 161 (1998).

## Antibacterial Activity Spectrum of Designed Pyrrhocoricin Analogs

Mare Cudic<sup>1</sup>, Philippe Bulet<sup>2</sup>, Goran Kragol<sup>1</sup> and Laszlo Otvos, Jr.<sup>1</sup>

<sup>1</sup>The Wistar Institute, Philadelphia, PA 19104, USA

<sup>2</sup>Institut de Biologie Moléculaire et Cellulaire, 67084 Strasbourg Cedex, France

### Introduction

Pyrrhocoricin, VDKGSYLPRPTPPRPIYNRN, a peptide isolated from the sap-sucking bug *Pyrrhocoris apterus* [1], exhibits potent *in vitro* antibacterial activity against Gram-negative strains [2], and protects mice from experimental *Escherichia coli* challenge [3]. However, at 50 mg/kg the peptide is toxic to compromised animals, a feature likely related to pyrrhocoricin's unspecific binding to the peptide-binding pocket of the 70 kDa heat shock protein [4]. A designed peptide analog, Chex-pyrrhocoricin-2-19-Dap(Ac) lacks the toxicity and shows good serum stability [3] but displays inferior *in vitro* efficacy. To obtain analogs suitable for pharmaceutical development, we synthesized a series of peptides based on the Chex-pyrrhocoricin-2-19-Dap(Ac) lead. Two dimeric and one tetrameric analog were made for lead optimization and five linear analogs were used for structure-activity studies. We also studied the environmental factors that deactivate otherwise potent antibacterial peptides during the *in vitro* efficacy assay procedure.

Pyrr-mod1:	VDKGRYLEAPTPPRPIYNRN
Pyrr-mod2:	VDKGRYLEAPTRPRPERNRK
Pyrr-mod3:	VDKGSYLPRPTPTPRPPIYNRN
Pyrr-mod4:	VDKGSYLPRPTPYSPRPPIYNRN
Pyrr-mod5:	VDKGSYLPRPTPTPRYRPIYNRN
Chex-Dap(Ac) dimer:	(XDKGSYLPRPTPPRPIYNR) <sub>2</sub> -Q-Z
Chex-Map tetramer:	(XDKGSYLPRPTPPRPIYNRN) <sub>4</sub> -Map scaffold
Chex-MeArg dimer:	(XDKGSYLPRPTPPRPIYN-MeR-N) <sub>2</sub> Q

where X: Chex, cyclohexane-1-carboxylic acid; Q: Dap, diamino-propionic acid; Z: Dap(Ac), monoacetyl-diamino-propionic acid; Map: multiple antigenic peptide.

### Results and Discussion

From Gram-negative strains, the backbone protected dimer killed the clinical isolate *E. coli* JC7623 with an MIC of 0.5  $\mu$ M (2.5  $\mu$ g/mL) in an assay where amoxicillin killed the same strain at 5  $\mu$ M (2  $\mu$ g/mL). The peptide was bacteriocidal at 1.2  $\mu$ M (6  $\mu$ g/mL). While amoxicillin was inactive against the streptomycin-resistant *E. coli* strain D31, the lead backbone protected dimeric peptide killed this strain with an MIC of 0.4  $\mu$ M (2  $\mu$ g/mL). Other established activities included MIC 2  $\mu$ M (9.5  $\mu$ g/mL) against the clinical isolate *Haemophilus influenzae* 233 in the liquid assay, and the decrease of the colony forming units to 15% of the original value in the killing assay within a 2 h period. The peptide was inactive against *Pseudomonas aeruginosa* up to 20  $\mu$ M. The non-backbone protected dimer killed five remarkably different *E. coli* strains with almost identical efficacy, indicating that the activity was not directed against the variable inner membrane. Other low micromolar activities included killing of *Klebsiella pneumoniae* and *Salmonella typhimurium*. The peptide was inactive against *Erwinia carotovora carotovora*. From Gram positives, the non-backbone protected analog

*Cudic et al.*

killed *Micrococcus luteus*, *Bacillus megaterium* and *Aerobacterium viridans*, but was inactive against *Staphylococcus aureus*, *Staphylococcus haemolyticus* and *Streptococcus pyogenes*. Fungi were also resistant to the dimer. Increasing the valency increased the efficacy against Gram-positive strains, indicating the need of multiple positive charges to penetrate the bacterial membranes.

Modified linear analogs containing substitutions in their N-terminal halves lost their activity against *E. coli*, indicating that the pharmacophore is located at the amino terminal region. While the removal of potential contact residues to the D-E helix region of *E. coli* DnaK, the proposed target sequence [4], was successful, no new contact residues with the homologous *S. aureus* DnaK protein could be established.

The antibacterial activity of the peptides was reduced upon increasing the temperature and the salt content of the liquid assay medium. The first finding may reflect the increased DnaK production of the bacteria at elevated temperatures. The second is indicative of the sensitivity of the assay. In general, validated assay protocols are concerned with the reproduction of bacteria in specific media and conditions most suitable for bacterial growth, conditions not present *in vivo* in mammals. A very fine-tuned balance of bacterial growth and medium composition has to be found to assay the true *in vitro* antibacterial efficacy of the peptides and peptidomimetics.

## References

1. Cociancich, S., Dupont, A., Hegy, G., Lanot, R., Holder, F., Hetru, C., Hoffmann, J.A., Bulet, P. *Biochem. J.* **300**, 567–575 (1994).
2. Hoffmann, R., Bulet, P., Urge, L., Otvos, L., Jr. *Biochim. Biophys. Acta* **1426**, 459–467 (1999).
3. Otvos, L., Jr., Bokonyi, K., Varga, I., Otvos, B.I., Hoffmann, R., Ertl, H.C.J., Wade, J.D., McManus, A.M., Craik, D.J., Bulet, P. *Protein Sci.* **9**, 742–749 (2000).
4. Kragol, G., Lovas, S., Varadi, G., Condie, B.A., Hoffmann, R., Otvos, L., Jr. *Biochemistry* **40**, 3016–3026 (2001).

## Importance of the Intramolecular Disulfide Bridges in the Biological Activity of Gomesin

Marcos A. Fázio<sup>1</sup>, Sirlei Daffre<sup>2</sup>, M. Terêsa M. Miranda<sup>3</sup>, Philippe Bulet<sup>4</sup>  
and Antonio Miranda<sup>1</sup>

<sup>1</sup>Depto de Biofísica, UNIFESP, 04044-020, São Paulo, São Paulo, Brasil

<sup>2</sup>Depto de Parasitologia, ICB-USP, 05508-900, São Paulo, São Paulo, Brasil

<sup>3</sup>Depto de Bioquímica, IQ-USP, 05508-900, São Paulo, São Paulo, Brasil

<sup>4</sup>Institut de Biologie Moléculaire et Cellulaire, Strasbourg Cedex 67084, France

### Introduction

Gomesin (*Gm*) is a potent cationic antimicrobial peptide isolated from hemocytes of tarantula spider *Acanthoscurria gomesiana*. It contains two intramolecular disulfide bridges Cys<sup>2-15</sup> and Cys<sup>6-11</sup>, a pyroglutamic acid as N-terminal residue and an amide in its C-terminal carboxyl group (PyrCRRLCYKQRCVITYCRGR-NH<sub>2</sub>), showing sequence similarities to tachyplesin and polyphemusin from horseshoe crabs, androctonin from scorpions and, also, to protegrins from porcine leukocytes. Such structural properties confer high stability to the molecule. This peptide exhibits a strong and broad activity spectrum, being effective against Gram-positive and Gram-negative bacteria, fungi and yeast [1]. Thus, gomesin appears to have an interesting potential for therapeutic application. The aim of the present work was to evaluate the importance of the disulfide bridges in *Gm* biological activity.

### Results and Discussion

Peptides were synthesized by the solid phase methodology using the t-Boc strategy on a MBHA-Resin [2]. After full deprotection and peptide cleavage from the resin in anhydrous HF (2 h at 0 °C), the crude products were cyclized by air oxidation at pH 6.8–7.0 during 72 h at 5 °C. Cyclization was monitored by RP-HPLC/MS. The crude peptides were purified by RP-HPLC and characterized by RP-HPLC/MS. The antibacterial and antifungal activities were determined by a liquid growth inhibition assay against *Micrococcus luteus* A-270, *Escherichia coli* SBS-363 and *Candida albicans* [3]. Microbial growth was assessed by an increase in A<sub>620</sub> after incubation. The minimal inhibitory concentration (MIC) was measured after 16 h incubation at 30 °C. MICs are expressed as the [a]–[b] interval of concentrations, where [a] is the highest concentration tested at which the microorganisms are growing and [b] is the lowest concentration that causes 100% growth inhibition. All the experiments were performed in triplicate. As it can be seen in Table 1, the monocyclic {[Cys(Acm)<sup>6,11</sup>]-, [Cys(Acm)<sup>2,15</sup>]-, [Ser<sup>6,11</sup>]- and [Ser<sup>2,15</sup>]-*Gm*} and the linear compounds {[Ser<sup>2,6,11,15</sup>]- and [Cys(Acm)<sup>2,6,11,15</sup>]-*Gm*} were found to be two- to eight-fold less active than the native gomesin in low salt concentration. Interestingly, the activities of [Ser<sup>2,6,11,15</sup>]- and [Cys(Acm)<sup>2,6,11,15</sup>]-*Gm* on *E. coli* were 16-fold lower than those observed on the other strains. When the antimicrobial assay was performed under physiological salt concentration (137 mM NaCl), the activity of the native gomesin on *Micrococcus luteus* and *Candida albicans* was slightly reduced while the same effect was not observed for *E. coli*. The monocyclic and linear analogues had their activities reduced from 2- to 8-fold. The main decrease were observed for the analogues [Ser<sup>2,6,11,15</sup>]-*Gm* and [Cys(Acm)<sup>2,6,11,15</sup>]-*Gm* which showed to be 32- and 64-fold less active than the native peptide against *E. coli*, respectively. Also, [Cys(Acm)<sup>2,6,11,15</sup>]-*Gm* was not active up to 127 µM against *Candida albicans*. It is important to note that despite the

fact that *Gm* analogues were less potent than the native molecule in terms of antimicrobial activity, they exhibited lower hemolytic activities than *Gm* (from 2- to 11-fold in 100  $\mu$ M of peptide concentration; data not shown). These results suggest that both disulfide bridges are important for the expression of gomesin biological activity and that there is some specificity of this antimicrobial peptide against certain microorganisms. Further studies are in progress in our laboratories in order to obtain more selective or active analogues or to extinguish any hemolytic activity.

Table 1. Antimicrobial activity of gomesin analogues.

	Minimum inhibitory concentration ( $\mu$ M)					
	<i>Micrococcus luteus</i>		<i>Escherichia coli</i>		<i>Candida albicans</i>	
	PB <sup>a</sup>	PB <sup>b</sup>	PB <sup>a</sup>	PB <sup>b</sup>	PDB <sup>c</sup>	PDB <sup>d</sup>
<i>Gm</i>	0.16–0.32	0.32–0.64	0.64–1.28	0.64–1.28	0.32–0.64	1.28–2.56
[Cys(Acm) <sup>6,11</sup> ]- <i>Gm</i>	0.64–1.28	1.28–2.56	1.28–2.56	2.56–5.12	0.64–1.28	5.12–10.25
[Cys(Acm) <sup>2,15</sup> ]- <i>Gm</i>	0.64–1.28	1.28–2.56	1.28–2.56	2.56–5.12	0.64–1.28	5.12–10.25
[Ser <sup>6,11</sup> ]- <i>Gm</i>	0.64–1.28	1.28–2.56	1.28–2.56	2.56–5.12	0.64–1.28	2.56–5.12
[Ser <sup>2,15</sup> ]- <i>Gm</i>	0.32–0.64	0.64–1.28	1.28–2.56	2.56–5.12	0.64–1.28	2.56–5.12
[Ser <sup>2,6,11,15</sup> ]- <i>Gm</i>	0.32–0.64	1.28–2.56	10.25–20.5	20.5–41.0	2.56–5.12	20.5–41.0
[Cys(Acm) <sup>2,6,11,15</sup> ]- <i>Gm</i>	0.64–1.28	2.56–5.12	10.25–20.5	41.0–82.0	2.56–5.12	ND <sup>e</sup>

<sup>a</sup> PB means Poor Broth nutrient medium (217 mOsM; 1.0 g Peptone + 86 mM NaCl in 100 mL of H<sub>2</sub>O). <sup>b</sup> PB (367 mOsM; 1.0 g Peptone + 137 mM NaCl in 100 mL of H<sub>2</sub>O). <sup>c</sup> PDB (Difco) means poor dextrose broth (79 mOsM; 1.2 g potato dextrose in 100 mL of H<sub>2</sub>O). <sup>d</sup> PDB (333 mOsM; 1.2 g potato dextrose in 100 mL of H<sub>2</sub>O + 137 mM NaCl). <sup>e</sup> ND means not detected activity until 127  $\mu$ M.

### Acknowledgments

This work was supported by grants and fellowships from CNPq and FAPESP.

### References

1. Silva Jr., P.I., Daffre, S., Bulet, P. *J. Biol. Chem.* **275**, 33464–33470 (2000).
2. Miranda, A., Koerber, S.C., Gulyas, J., Lahrichi, S.L., Craig, A.G., Corrigan, A., Hagler, A., Rivier, C., Vale, W., Rivier, J. *J. Med. Chem.* **37**, 1450–1459 (1994).
3. Bulet, P., Dimarcq, J.L., Hetru, C., Lagueux, M., Charlet, M., Hegy, G., Van Dorsselaer, A., Hoffmann, J.A. *J. Biol. Chem.* **268**, 14893–14897 (1993).

## **Variation in Ring Size of Cyclic Antimicrobial Peptides Results in Diversity and Selectivity of Biological Activity**

**Masood Jelokhani-Niaraki<sup>1,2</sup>, Leslie H. Kondejewski<sup>1</sup>, Cyril M. Kay<sup>1</sup>  
and Robert S. Hodges<sup>1,3</sup>**

<sup>1</sup>*Protein Engineering Network of Centres of Excellence, University of Alberta, Edmonton, Alberta, T6G 2S2, Canada*

<sup>2</sup>*Department of Chemistry, Brandon University, Brandon, Manitoba, R7A 6A9, Canada*

<sup>3</sup>*Department of Biochemistry and Molecular Genetics, University of Colorado Health Sciences Center, Denver, CO 80262, USA*

### **Introduction**

In continuing our efforts to understand the structure-function relationships in the cationic cyclic antimicrobial peptides [*e.g.*,1,2], the ring size was varied from 10 to 16 amino acids in a series of cyclic peptides based on the structure of GS10 (a decameric analog of the antimicrobial peptide gramicidin S) to study the effect of changes in peptide size, structure, hydrophobicity and amphipathicity on biological activity. Similar to gramicidin S, GS10 adopts a structure composed of an antiparallel  $\beta$ -sheet and two type II'  $\beta$ -turns, is highly hemolytic and also quite active against a broad spectrum of bacteria and fungi [2]. The diversity in physicochemical and biological properties of the designed cyclic peptides of this study reveals the complex nature of their mechanism of biological activity.

### **Results and Discussion**

Addition of alternating basic and hydrophobic amino acids to the original structural framework of GS10 generated a set of even-numbered ring sizes: (*dY* denotes D-Tyr).

GS10: cyclo-(VKL*d*YP<sup>5</sup>VKL*d*YP<sup>10</sup>); GS12: cyclo-(VKLK*d*YP<sup>6</sup>KVKL*d*YP<sup>12</sup>)

GS14: cyclo-(VKLKVK*d*YP<sup>7</sup>LKVKL*d*YP<sup>14</sup>)

GS16: cyclo-(VKLKVK*d*YP<sup>8</sup>KLKVKL*d*YP<sup>16</sup>)

In contrast to GS10, GS12 was only weakly to moderately active. GS14 was very hemolytic, but only weakly active against bacteria or fungi. GS16 was weakly hemolytic, and showed moderate to strong antimicrobial but weak antifungal activities. In certain environments, structure of GS14 was similar to GS10, whereas GS12 and GS16 were structurally different from GS10. The odd-numbered analogs (11-, 13- and 15-mers) had a variety of structures, and were derived from these four peptides either by addition or deletion of single basic (Lys) or hydrophobic (Leu or Val) amino acids: 11-mers (GS12-K<sup>4</sup>, GS12-K<sup>7</sup>, and GS12-L<sup>3</sup>); 13-mers (GS14-K<sup>4</sup>, GS14-L<sup>3</sup>, and GS14-V<sup>5</sup>); 15-mers (GS16-K<sup>4</sup>, GS16-K<sup>6</sup>, and GS16-V<sup>5</sup>).

For an easier comparison, peptides are divided into three groups. In the first group (GS10, 11 and 12 series), an increase in peptide hydrophobicity and amphipathicity (evaluated by the retention times on a reversed-phase HPLC column, and also the ratio of charged to hydrophobic amino acid residues in the peptide sequence) resulted in an increase in hemolytic, antibacterial and antifungal activities (Figure 1A). The CD spectra of the peptides in this series show different conformations between those of GS10 (highly amphipathic) and GS12 in aqueous and phospholipid membranes (*e.g.*, Figure 1B). In contrast to the first series, the peptides in the second group (GS13 and 14 series) exhibited a different activity profile. An increase in peptide hydrophobicity and amphipathicity resulted in an increase in the hemolytic and a decrease in the

antimicrobial activity. Despite their similar conformations in the aqueous media, the 13-mers adopted different conformations in lipid membranes.

Peptides in the last group (GS15 and 16 series) exhibited an increase in both hemolytic activity and antibacterial activity against Gram-positive bacteria with the increase in hydrophobicity and amphipathicity. In this latter series activities against Gram-negative bacteria and fungi were more selective and varied for different strains. Interestingly, peptides with the same hemolytic activity in this group had comparable conformations in aqueous and PC (phosphatidylcholine) vesicles. Moreover, these peptides caused fusion and aggregation of the negatively charged phosphatidylethanolamine/phosphatidylglycerol vesicles.

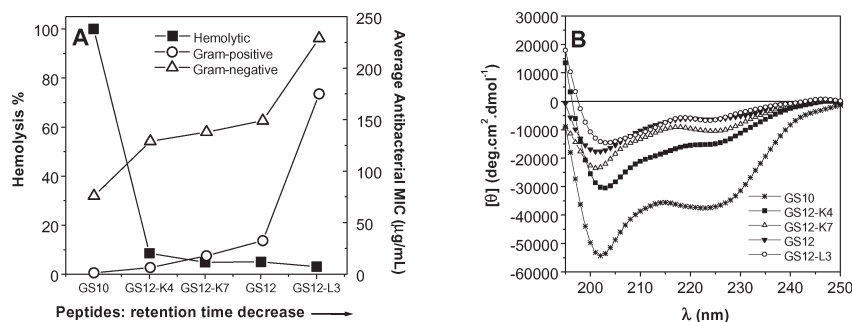


Fig. 1. Hemolytic and average antibacterial activity of GS10, 11 and 12 series (A), and their CD spectra in POPC (palmitoyl-oleoyl-phosphatidylcholine) vesicles at 25 °C (B).

In GS12 and the 11-mer peptides, the  $\beta$ -sheet structure was disrupted, which resulted in lower amphipathicity, reduced hemolytic activity, and a moderate degree of antimicrobial activity, compared to GS10 (Figure 1). The 13-mer peptides also had a disrupted  $\beta$ -sheet conformation. In contrast to the 11-mers and despite their comparable conformations in aqueous and PC membranes (a model for erythrocyte membranes), the hemolytic activity of the 13-mers was higher along with higher antimicrobial activity. Compared to GS10, The 15-mer peptides and GS16 had reduced hemolytic activity and there was a clear correlation between the conformations of the 15-mers in PC and their hemolytic activity, similar to the 11-mers (Figure 1B). Overall, diversity in the biological activity in the cationic cyclic peptides was closely correlated to their ring size, structure, hydrophobicity and amphipathicity. The cyclic peptides with smaller ring size showed less conformational flexibility, while larger peptides had less rigid conformations. Moreover, conformation of most of the studied peptides was different in different lipid environments and aqueous solutions, which accounts for their diversity in biological activity. It was also shown that peptides with different conformations might have comparable hemolytic and/or antimicrobial activity, while peptides with similar conformations might possess different biological activities. The results of this work clearly points to the complexities involved in design of novel efficient antimicrobial peptides.

## References

1. Kondejewski, L.H., Jelokhani-Niaraki, M., Farmer, S.W., Lix, B., Kay, C.M., Sykes, B.D., Hancock, R.E.W., Hodges, R.S. *J. Biol. Chem.* **274**, 13181–13192 (1999).
2. Jelokhani-Niaraki, M., Kondejewski, L.H., Farmer, S.W., Hancock, R.E.W., Kay, C.M., Hodges, R.S. *Biochem. J.* **349**, 747–755 (2000).

## $\alpha$ -Helical Glycopeptide Analgesics: $\beta$ -Endorphin Mimics with Good *in vivo* Potency

Michael M. Palian<sup>1</sup>, Nura Elmagbari<sup>2</sup>, Peg Davis<sup>3</sup>, Hong-Bing Wei<sup>3</sup>,  
 Richard Eggleton<sup>3</sup>, Frank Porecca<sup>3</sup>, Henry I. Yamamura<sup>3</sup>,  
 Victor J. Hruby<sup>1</sup>, Edward J. Bilsky<sup>2</sup> and Robin Polt<sup>1</sup>

<sup>1</sup>Department of Chemistry, University of Arizona, Tucson, AZ 85721, USA

<sup>2</sup>Department of Pharmacology, Arizona Health Sciences Center, Tucson, AZ 85726, USA

<sup>3</sup>Department of Biological Sciences, Univ. of Northern Colorado, Greeley, CO 8063, USA

### Introduction

Glycopeptide enkephalins [1] show potent analgesic activity *in vivo* [2], and are capable of penetrating the blood-brain barrier [3]. The opioids themselves represent a broad class of centrally acting ligands that may target the  $\delta$ ,  $\kappa$ , or  $\mu$  opioid receptors in the brain or the spinal column in order to produce pain relief, or other effects.

### Results and Discussion

The amphipathic  $\alpha$ -helix is a very common structural motif in nature. One could envision that these helices could be used as “addresses” by binding to the cellular membrane to direct the “message” segment along the membrane surface to its proper receptor, the opioids in this case. These may be thought of as dynorphin or endorphin mimics, possessing a Leu-enkephalin message segment with a synthetically engineered address segment controlling receptor specificity (Figure 1).

A fundamental question addressed was how glycosylated amino acid residues affect  $\alpha$ -helix formation. We observed that glycosyl amino acids did not destroy helicity in model  $\alpha$ -helices (Figure 2). It was concluded from these experiments that the amino acid sequence of the helix is more important to helicity than the glycosyl amino acid [4]. These observations provide the basis for the synthesis of the amphipathic  $\alpha$ -helical glycopeptides presented.

The first series of glycopeptides (Figure 3) was designed to possess three portions. First, an address segment, which was designed to be amphipathic,  $\alpha$ -helical, and lay parallel to the membrane normal. The message segment comprises the N-terminus and

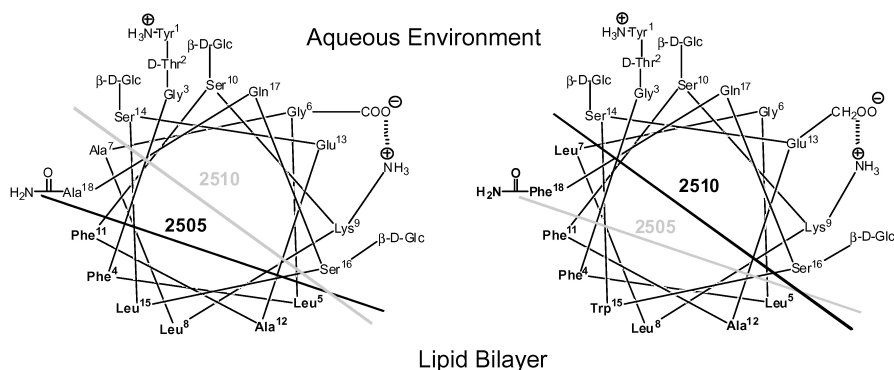


Fig. 1. Helical glycosylated “addresses,” e.g. MMP-2505 Tyr-DThr-Gly-Phe-Leu-Gly-Ala-Leu-Lys-Ser\*-Phe-Ala-Glu-Ser\*-Leu-Ser\*-Gln-Ala-CONH<sub>2</sub> and MMP-2510 Tyr-DThr-Gly-Phe-Leu-Gly-Leu-Leu-Lys-Ser\*-Phe-Ala-Glu-Ser\*-Trp-Ser\*-Gln-Phe-CONH<sub>2</sub> insert into lipid bilayers to orient the opioid “message” with respect to the membrane.

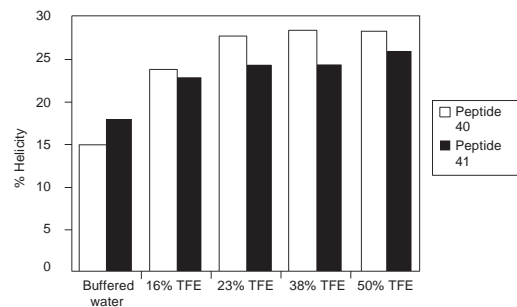


Fig. 2. Peptide 40 = AcNH-AEAAAKEASAKEAAKA-CONH<sub>2</sub>,  
Peptide 41 = AcNH-AEAAAKEAS\*AKEAAKA-CONH<sub>2</sub> S\* = Serine(α-Mannose).

will activate the opioid receptor. Finally, a glycine spacer (“helix breaker”) was incorporated to prevent any propagation of helicity from the address segment into the message segment. Glycine was only partially successful in this regard, and the helix appeared to include the Phe-Leu-Gly sequence.

Peptide	Message segment	Address Segment
2405	H <sub>2</sub> N-Tyr-DThr-Gly-Phe-Leu-	Gly-Glu-Leu-Ala-Ser*-Lys-Trp-Phe-Gln-Ala-Leu-Glu-CONH <sub>2</sub>
2410	H <sub>2</sub> N-Tyr-DThr-Gly-Phe-Leu-	Gly-Glu-Leu-Ala-Ser*-Lys-Trp-Phe-Gln-Ala-Leu-Glu-Ser*-CONH <sub>2</sub>
2415	H <sub>2</sub> N-Tyr-DThr-Gly-Phe-Leu-	Gly-Glu-Leu-Ala-Ser*-Lys-Trp-Phe-Gln-Ala-Leu-Glu-Ser*-Phe-CONH <sub>2</sub>
2420	H <sub>2</sub> N-Tyr-DThr-Gly-Phe-Leu-	Gly-Glu-Leu-Ala-Ser*-Lys-Trp-Phe-Gln-Ala-Leu-Glu-Ser*-Phe-Trp-CONH <sub>2</sub>
	1 2 3 4 5 6 7 8 9 10 11 12 13 14 15	
	H <sub>2</sub> N-Tyr-Gly-Gly-Phe-Leu	
	(native Leu-Enkephalin)	Ser* = Serine β-glucoside

Fig. 3. Structures of the 2400 series of enkephalins.

Circular dichroism and NMR experiments in SDS micelles and water were conducted on the 2400 series to explore two questions: 1) Is there a minimum length required for the formation of a stable α-helical in the address segment? 2) Can the α-helices provide potent analgesia, or is the address segment too large and impede receptor binding of the message segment (Figure 4)? CD experiments provided evidence that the all glycopeptides were largely unstructured in water, but highly helical in the presence of micelles. Furthermore, *in vivo* analgesia studies show that the glycopeptides can provide good analgesia. Glycopeptide 2410 has an A<sub>50</sub> (*i.c.v.*) value of 120 pmoles, ~20 times more potent than morphine itself, while retaining the delta-selectivity of the parent message segment.

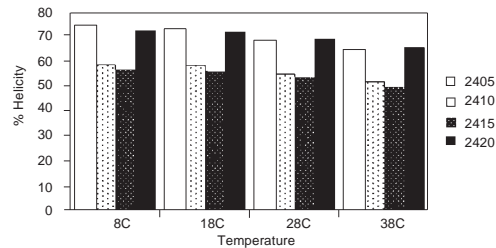


Fig. 4. %Helicity determined by circular dichroism at various temperatures.

### Biologically Active Peptides

While preliminary results of the 2400 series were encouraging, 3 of the 4 compounds in this series were not water-soluble. The 2500 series was synthesized to explore the optimal balance of lipophilicity and water solubility. This series used three glycosides per helix and increased in lipophilicity across the series.

The 2500 series (Figure 5) displayed many of the same properties as the 2400 series, but were much more water soluble. The helicity of the 2500 series was reduced, and helicity showed no clear correlation with analgesia *in vivo*. 2510 possessed only moderate helicity, yet was the most potent *i.c.v.*, ( $A_{50} = 28$  pmol/mouse *vs* 2,700 pmol/mouse for morphine). In addition, 2520 (most lipophilic) showed the lowest  $A_{50}$  *i.c.v.* value ( $A_{50} = 592$  pmol/mouse), but had the longest duration of action.

Message	Address
2505 Tyr-DThr-Gly-Phe-Leu-Gly-Ala-Leu-Lys-Ser*-Phe-Ala-Glu-Ser*-Leu-Ser*-Gln-Ala-CONH <sub>2</sub>	
2510 Tyr-DThr-Gly-Phe-Leu-Gly-Leu-Leu-Lys-Ser*-Phe-Ala-Glu-Ser*-Trp-Ser*-Gln-Phe-CONH <sub>2</sub>	
2515 Tyr-DThr-Gly-Phe-Leu-Gly-Lys-Ser*-Phe-Ala-Glu-Leu-Trp-Ser*-Gln-Phe-Leu-Ser*-CONH <sub>2</sub>	
2520 Tyr-DThr-Gly-Phe-Leu-Gly-Leu-Leu-Lys-Ser*-Phe-Trp-Glu-Ser*-Trp-Ser*-Gln-Phe-CONH <sub>2</sub>	

Fig. 5. 2500 Series bearing 3 glycosides per helix (Ser\* =  $\beta$ -glucoside of L-serine).

In conclusion, preliminary results of studies on  $\alpha$ -helical glycopeptide enkephalin analogs demonstrate that glycosylation does not necessarily destroy helicity and the resulting enkephalin analogs give excellent *in vivo* analgesia profiles [5].

## Acknowledgments

We thank the Arizona Disease Control Research Commission, NIDA, the A.R.C.S. Foundation and the U.S. Army for support.

## References

1. Mitchell, S.A., et al. *J. Org. Chem.* **66**, 2327–2342 (2001).
2. Bilsky, E.J., et al. *J. Med. Chem.* **43**, 2586–2590 (2000).
3. Egleton, R.D., et al. *Brain Research* **881**, 37–46 (2000).
4. Palian, M.M., Jacobsen, N., and Polt, R. *J. Peptide Res.* **58**, 1–12 (2001).
5. Palian, M.M., unpublished results.

## Efforts to Investigate the Conformational Changes of the Prion Protein by N-Glycosylation

Kristina Münnich<sup>1</sup>, Stefan Becker<sup>2</sup> and Christian Griesinger<sup>1,2</sup>

<sup>1</sup>Department of Organic Chemistry, University of Frankfurt, 60439 Frankfurt, Germany

<sup>2</sup>Max Planck Institute for Biophysical Chemistry, 37077 Goettingen, Germany

### Introduction

The prion protein, structurally very well investigated in its recombinant form [1], has two natural N-glycosylation sites, which evidently show some influence on the proteins' global structure. Biological tests and molecular dynamic studies indicate that the N-glycan chain hinders the conformational change from the normal form PrP<sup>c</sup> to the pathological form PrP<sup>Sc</sup> [2–4]. Moreover, the grade of prion glycosylation determines the path of prion pathogenesis. The prion proteins'  $\alpha$ -helical region SHA 172–194, containing the potential glycosylation site 181, was synthesized in the non glycosylated and glycosylated form in order to examine the influence of the N-glycan chain on the peptide backbone. NMR- and CD-studies reveal some influence of the sugar residue on the equilibrium between  $\alpha$ -helix and  $\beta$ -sheet structures (Figure 1). Based on these results, we are trying to express a labeled N-terminal recombinant fragment of the Syrian Hamster prion protein as a fusion protein with intein [5,6]. This fragment shall be ligated *via* chemical ligation [7,8] with a C-terminal peptide carrying N-terminally cysteine 179, and the glycosylation sites of the natural prion protein. The segmental labeling allows us to examine the effect of the glycosylation on the folding of the prion protein by NMR more easily.

### Results and Discussion

CD-measurements were performed with the non-glycosylated and glycosylated peptide SHA 172–194 at pH 5 and pH 7.5 in phosphate buffer (Figure 1). Shown are the pH-dependent conformational changes of the peptide induced by N-glycosylation.

Ligations of the unlabeled N-terminal prion fragment SHA 121–178 with the C-terminal non-glycosylated prion fragment SHA 179–231 were carried out success-

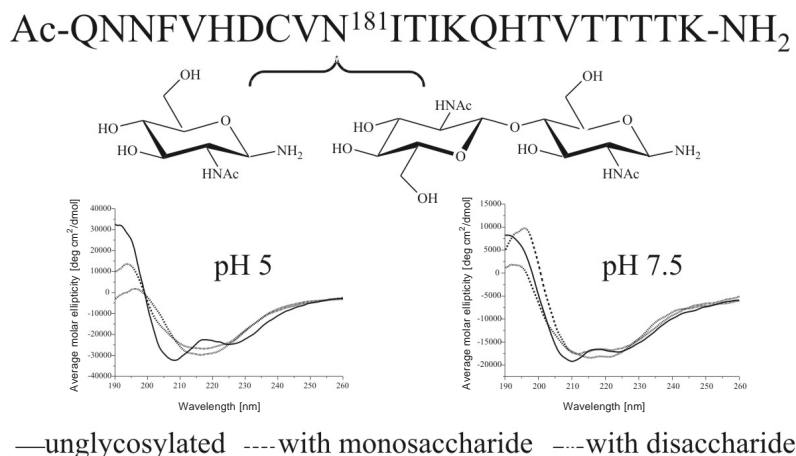


Fig. 1. CD-spectra of prion N-glycoprotein fragments (SHA Pr172–194) at different pH.

fully (Figure 2). Test ligations of shorter N-terminal prion fragments with C-terminal N-glycosylated prion fragments showed that the ligation works well despite the bulky sugar residues close to the ligation site.

The biochemical approach was to express the SHA PrPc fragment 121-178 with N-terminal Glutathione-S-Transferase fusion protein (26 kDa) and C-terminal intein GyrA from *Mycobacterium xenopi*-chitin binding domain (27 kDa). GST-fusion increases the expressed protein amounts, and decreases proteolytic degradation. A thiol-induced cleavage of the intein GyrA releases the PrPc-fragment with an activated thioester at the C-terminal carboxy group. The GST-PrPc-GyrA protein can be expressed in soluble form (60 kDa band) and purified with a Ni-Agarose column. Inevitably, intein autocleavage occurs up to 50% due to intein activity of GyrA, favored by the Asp residue at position 178 (35 kDa band) (Figure 2).

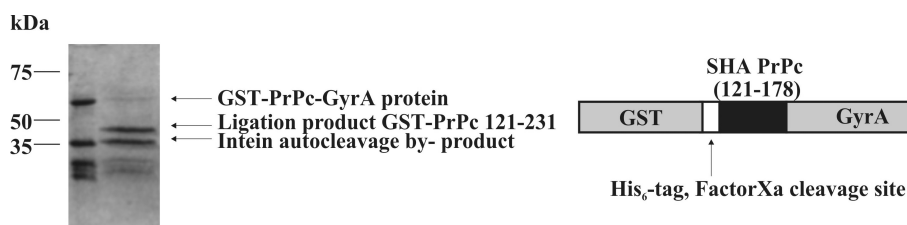


Fig. 2. SDS-page of ligations with the prion fusion protein GST-PrPc-GyrA and the fragment 179-231; (5 eq. of Pr179-231; 4% MESNA (w/v); 20 mM Tris, 1 mM EDTA, 0.5 M NaCl, pH 7.5; 37 °C; 2 d).

## References

1. Liu, H., Farr-Jones, S., Ulyanov, N.B., Llinas, M., Marqusee, S., Groth, D., Cohen, F.E., Prusiner, S.B., James T.L. *Biochemistry* **38**, 5362–5377 (1999).
2. Meyer, R.K., Lustig, A., Oesch, B., Fatzer, R., Zurbriggen, A., Vandevelde, M. *J. Biol. Chem.* **275**, 38081–38087 (2000).
3. Zuegg, J., Gready, J.E. *Glycobiology* **10**, 959–974 (2000).
4. Rudd, P.M., Wormald, M.R., Wing, D.R., Prusiner, S.B., Dwek, R.A. *Biochemistry* **40**, 3759–3766 (2001).
5. Völkel, D., Blankenfeldt, W., Schomburg, D. *Eur. J. Biochem.* **251**, 462–471 (1998).
6. Liemann, S., Glockshuber, R. *Biochemistry* **38**, 3258–3267 (1999).
7. Mizuno, M., Haneda, K., Iguchi, R., Muramoto, I., Kawakami, T., Aimoto, S., Yamamoto, K., Inazu, T. *J. Am. Chem. Soc.* **121**, 284–290 (1999).
8. Shin, Y., Winans, K.A., Backes, B.J., Kent, S.B.H., Ellman, J.A., Bertozzi, C.R. *J. Am. Chem. Soc.* **121**, 11684–11689 (1999).

## Glycation of Leucine-Enkephalin: Imidazolidinones and Amadori Compounds

Maja Roscic and Stefica Horvat

Department of Organic Chemistry and Biochemistry, Rudjer Boskovic Institute, P.O.Box 180,  
10002 Zagreb, CROATIA

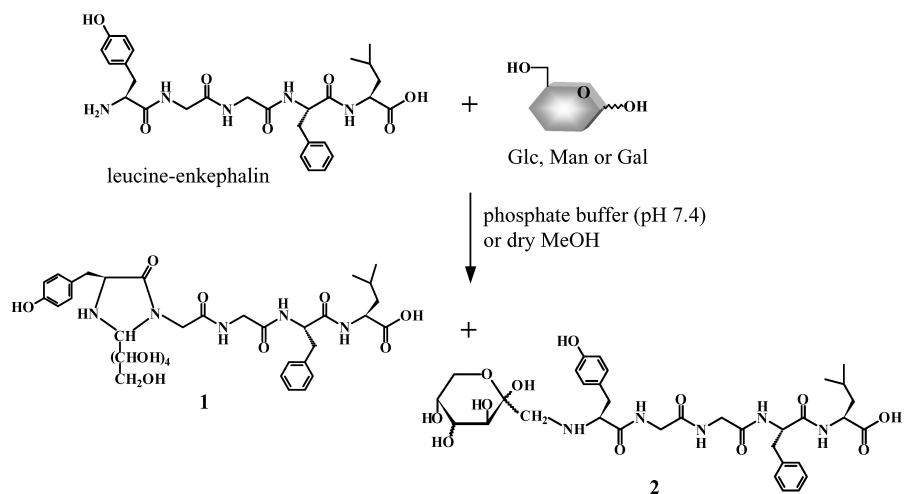
### Introduction

In view of the current research interest in non-enzymatic glycation reactions known to occur widely in biological systems, we have recently described the intramolecular cyclizations of monosaccharide esters in which the sugar moiety is linked, through the C-6 hydroxy group, to the C-terminal carboxy group of the endogenous opioid pentapeptide leucine-enkephalin (LE), leading to the bicyclic imidazolidinones [1–3], or bicyclic Amadori compounds [4]. In an effort to elucidate the properties and reactivity of the parent free sugars, we present the formation of leucine-enkephalin related “free hands” imidazolidinones, as well as Amadori compounds from D-glucose, D-mannose or D-galactose and leucine-enkephalin.

### Results and Discussion

Incubation of leucine-enkephalin and D-glucose, D-mannose or D-galactose in either dry MeOH or phosphate buffer (pH 7.4) as a solvent results in the formation of the corresponding “free hands” imidazolidinone **1** and Amadori compound **2** (Scheme 1).

We have studied the influence of solvent (methanol and phosphate buffer), temperature (37 and 50 °C) and of added base (NEM) on the rate of formation of these carbohydrate-peptide adducts. The graphical representation of the relative RP HPLC concentrations of the incubation mixtures, obtained by the reaction of leucine-enkephalin with free sugar (Glc, Man or Gal) in MeOH (LE : sugar : NEM = 1 : 15 : 5) and phosphate buffer (LE : sugar = 1 : 15) at 50 °C, after 2 days and 4 days, respectively, is given in Figure 1. The structural properties of the isolated products have been deduced from NMR spectroscopy.



*Scheme 1. Formation of imidazolidinone 1 and Amadori compound 2 by the reaction of leucine-enkephalin and free sugar (Glc, Man or Gal).*

## Biologically Active Peptides

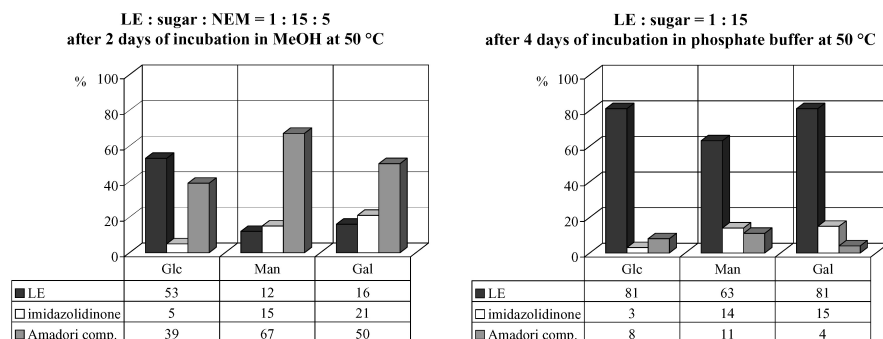


Fig. 1. Relative distribution of the products formed by the incubation of leucine-enkephalin and free sugar (Glc, Man or Gal) in MeOH and phosphate buffer. The relative concentrations were determined by RP HPLC.

In conclusion, we have demonstrated for the first time that free reducing sugars, such as D-glucose, D-mannose and D-galactose, can react non-enzymatically with leucine-enkephalin and generate, in addition to the Amadori compounds, novel carbohydrate-related imidazolidinones in either MeOH or phosphate buffer. The fact that phosphate buffer closely resembles the conditions of the physiological environment points to the possibility that similar carbohydrate-peptide adducts may also be generated in vivo.

### Acknowledgments

This work was supported by grant No. 00980704 from the Ministry of Science and Technology of Croatia.

### References

1. Horvat, S., Varga-Defterdarovic, L., Roscic, M., Horvat, J. *Chem. Commun.* 1663–1664 (1998).
2. Horvat, S., Roscic, M., Horvat, J. *Glycoconjugate J.* **16**, 391–398 (1999).
3. Varga-Defterdarovic, L., Vikić-Topić, D., Horvat, S. *J. Chem. Soc., Perkin Trans. 1* 2829–2834 (1999).
4. Horvat, S., Roscic, M., Varga-Defterdarovic, L., Horvat, J. *J. Chem. Soc., Perkin Trans. 1* 909–913 (1998).

## Solid-Phase Synthesis of Thio-Linked C-Terminal Glycopeptides via a Mitsunobu Reaction

John P. Malkinson and Robert A. Falconer

Department of Pharmaceutical and Biological Chemistry, The School of Pharmacy,  
University of London, London WC1N 1AX, UK

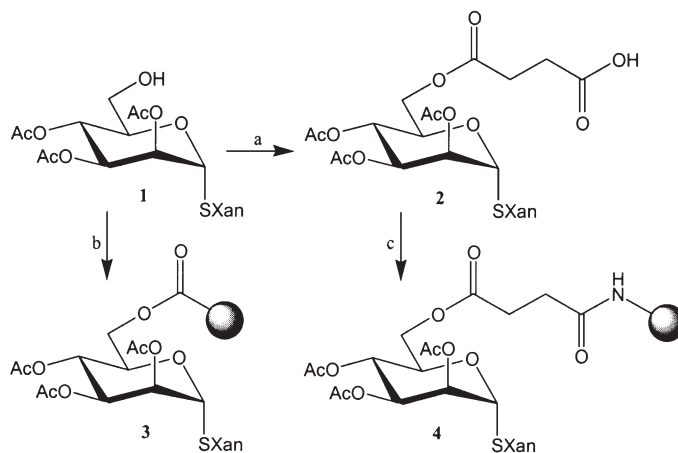
### Introduction

Of the large number of biologically active peptides known, relatively few have been exploited for routine clinical use, primarily as a consequence of their poor bio-availability and rapid enzymatic degradation. Glycosylation can be used as a means to address these problems, potentially allowing the glycopeptides produced to utilise active transport processes [1] and/or gain improved resistance to metabolism [2].

In order to allow the facile synthesis of glycopeptides, it is important to develop methods that are fully compatible with the well-established methodology of solid-phase peptide synthesis. We have previously reported a convenient method for the synthesis of *N*-linked C-terminal glycopeptides [3]. Thioglycosides also exhibit improved stability towards chemical and enzymatic hydrolysis compared to their *O*-glycoside isosteres, and have been prepared from 1-thiosugars and alcohols *via* a Mitsunobu condensation [4]. Here we report the use of this method for the solid-phase synthesis of *S*-linked C-terminal glycopeptides.

### Results and Discussion

9*H*-Xanthen-9-yl 2,3,4-tri-*O*-acetyl-1-thio- $\alpha$ -D-mannopyranoside (**1**) was prepared. This protected thioglycoside could be immobilised directly (through its free 6-position primary hydroxyl) onto a carboxypolystyrene resin by MSNT/*N*-methylimidazole mediated esterification [5]. Alternatively, reaction of the free hydroxyl with succinic anhydride afforded the free carboxyl-containing building block (**2**) that could be simply immobilised onto an amino-functionalised resin (Scheme 1).

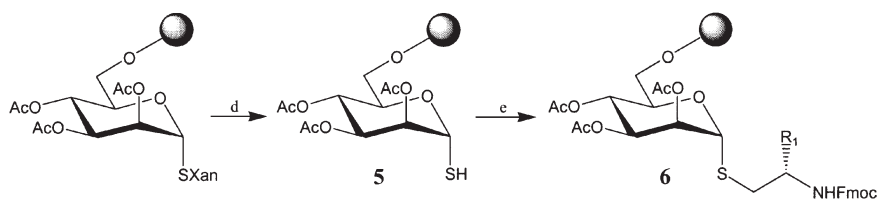


Scheme 1. Reagents and conditions: (a) Succinic anhydride, pyridine, DMAP, RT, 18 h; (b) Carboxypolystyrene resin, MSNT, MeIm,  $\text{CH}_2\text{Cl}_2$ ,  $3 \times 1$  h; (c) pMBHA resin, HBTU, HOBT, DIEA, DMF, 30 min.

### Biologically Active Peptides

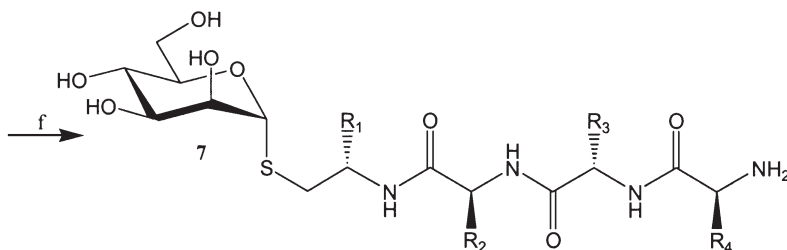
The amino-functionalised resin can be chosen to be either stable (*e.g.* *p*MBHA) or labile (*e.g.* Rink amide MBHA) to treatment with 95% TFA allowing synthetic flexibility in the cleavage/deprotection steps.

After immobilisation of the thioglycoside, the *S*-xanthenyl protecting group was selectively removed by treatment with 2% TFA in  $\text{CH}_2\text{Cl}_2$ , generating the resin-bound 1-thiosugar **5**. Mitsunobu condensation of resin-bound thiosugar **5** and excess *N*-Fmoc protected amino alcohol (prepared by the reduction of the corresponding *N* $^\alpha$ -protected amino acid) in the presence of triphenylphosphine and diethyl azodicarboxylate (DEAD) afforded the protected thioglycoside **6** (Scheme 2).



Scheme 2. Reagents and conditions: (d) TFA/TES/ $\text{CH}_2\text{Cl}_2$ ,  $2 \times 1$  h; (e) Fmoc-Xaa-ol,  $\text{PPh}_3$ , DEAD, THF, 3 h.

Following *N*-Fmoc deprotection, the *S*-linked glycopeptide sequence was extended using standard *N* $^\alpha$ -Fmoc strategy solid-phase peptide synthesis. Subsequent to final *N* $^\alpha$ -Fmoc deprotection, the glycopeptide (**7**) was removed from the solid-support by base-mediated cleavage, with simultaneous removal of the sugar *O*-acetyl protecting groups (Scheme 3).



Scheme 3. Reagents and conditions: (f)  $\text{NH}_3/\text{MeOH}$ , RT, 18 h.

Side-chain protecting groups can be removed prior to or after cleavage by treatment with TFA and appropriate scavengers.

### Acknowledgments

This work was supported by a CW Maplethorpe fellowship for J. M.

### References

1. Nomoto, M., et al. *J. Pharm. Sci.* **87**, 326 (1998).
2. Polt, R., et al. *Proc. Natl. Acad. Sci. USA* **91**, 7114 (1994).
3. Malkinson, J.P., et al. *J. Org. Chem.* **65**, 5249 (2000).
4. Falconer, R.A., et al. *Tetrahedron Lett.* **40**, 8663 (1999).
5. Nielsen, J., et al. *Tetrahedron Lett.* **46**, 8439 (1996).

## Synthesis of the Extracellular Ig Domain I (34-94) of Emmprin Carrying a Chitobiose Unit

Hironobu Hojo<sup>1,2</sup>, Jun Watabe<sup>1</sup>, Yoshiaki Nakahara<sup>1,2,3</sup>, Yuko Nakahara<sup>2,3</sup>, Yukishige Ito<sup>2,3</sup>, Kazuki Nabeshima<sup>4</sup> and Bryan P. Toole<sup>5</sup>

<sup>1</sup>Department of Applied Biochemistry, Tokai University, Kanagawa 259-1292, Japan

<sup>2</sup>The Institute of Physical and Chemical Research (RIKEN), Saitama 351-0198, Japan

<sup>3</sup>CREST, Japan Science and Technology Corporation (JST) and

<sup>4</sup>Department of Pathology, Miyazaki Medical College, Miyazaki 889-1692, Japan

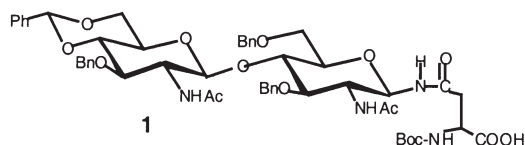
<sup>5</sup>Department of Anatomy and Cellular Biology, Tufts University School of Medicine, Boston, MA 02111, USA

### Introduction

Emmprin is a glycoprotein located on the surface of human tumor cells [1]. It belongs to the immunoglobulin (Ig) superfamily and stimulates nearby fibroblasts to produce matrix metalloproteinases (MMP), which play an essential role for tumor metastasis. The functional site of this activity is supposed to be the extracellular Ig domain I (34-94), which possesses an *N*-glycosylation site at Asn<sup>44</sup>. To analyze the effect of the glycosylation on its activity, as well as the mechanism of the stimulation of MMP production, we synthesized the Ig domain carrying chitobiose unit at Asn<sup>44</sup> by the thioester method [2]. The enhancement of MMP production by fibroblast cells were preliminary examined using synthetic Ig domain with (GlcNAc)<sub>0-2</sub> at Asn<sup>44</sup>.

### Results and Discussion

Emmprin (34-94) was divided at Gly<sup>58</sup>-Gly<sup>59</sup> and two peptide segments were prepared by the solid-phase method. In previous syntheses [2], peptide thioesters have been prepared by Boc strategy, since the thioester linkage is labile to piperidine treatment used for Fmoc strategy. However, the final acid treatment in Boc strategy would be strong enough to cleave most of glycosidic linkages. Thus, a key to realize the preparation of the domain is whether the peptide thioester carrying a chitobiose unit at Asn<sup>44</sup> can be synthesized by the Boc strategy. The route for its preparation is shown in Figure 1. Starting from Boc-Gly-SCH<sub>2</sub>CH<sub>2</sub>CO-Leu-OCH<sub>2</sub>-Pam-resin, peptide chain was elongated by an ABI 433A using Boc/HOBt/DCC. Asn<sup>44</sup> was introduced manually using Boc-Asn carrying benzyl-protected chitobiose **1** by DCC-HOBt method. After the chain elongation was completed, the protected peptide resin **2** was treated with HF.



The HPLC analysis of the crude peptide showed that the desired peptide **3** was successfully obtained in 12% yield. However, the chitobiose seems to have a moderate stability to HF, since GlcNAc-truncated peptide **4** was also obtained in 7.5% yield. To realize the complete retention of chitobiose unit, the deprotection conditions require further optimization. In this study, however, peptide **4** was also used to synthesize Ig domain with GlcNAc unit. The amino groups of peptides **3** and **4** were protected with Boc groups using Boc-OSu to obtain peptides **5**, **6** in yields of 73 and 92%, respectively. The C-terminal peptide Gly-Val-Val-Leu-Lys(Boc)-Glu-Asp-Ala-Leu-Pro-

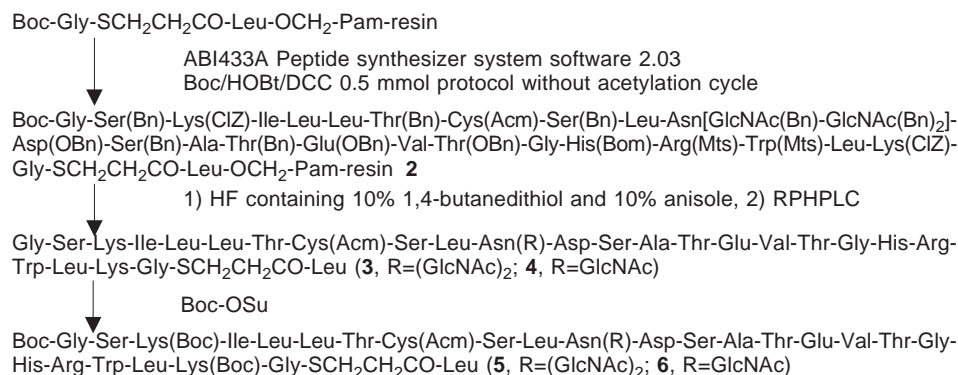


Fig. 1. Synthetic procedure for peptide thioester carrying (GlcNAc)<sub>1,2</sub>.

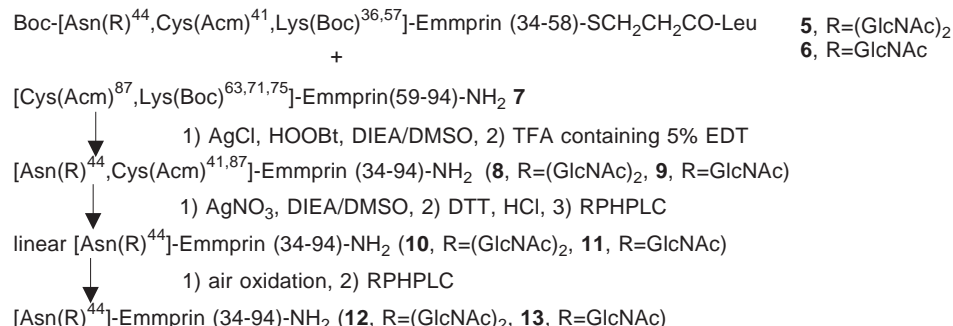


Fig. 2. Synthetic procedure for [Asn(GlcNAc)<sub>1,2</sub>]-Emmprin (34-94)-NH<sub>2</sub>.

Gly-Gln-Lys(Boc)-Thr-Glu-Phe-Lys(Boc)-Val-Asp-Ser-Asp-Asp-Gln-Trp-Gly-Glu-Tyr-Ser-Cys(Acm)-Val-Phe-Leu-Pro-Glu-Pro-Met-NH<sub>2</sub> **7** was prepared via a peptide segment synthesized on Fmoc-Rink amide MBHA-resin using *FastMoc* protocol in 8.9% yield.

Two segments were then condensed following the procedure of Kawakami et al. as shown in Figure 2 [2b]. Peptides **11** and **13** were dissolved in DMSO containing HOObt and DIEA and AgCl was added. The condensation was almost completed within 4 h without significant side reactions. The product was successively treated with TFA and AgNO<sub>3</sub> to remove all protecting groups. After HPLC purification, the peptide was air-oxidized in 1% AcONH<sub>4</sub> (pH 7.8) containing 20% DMSO. The Ig domain carrying a chitobiose unit **12** was successfully obtained after HPLC purification in 37% yield from peptide **7**. Following the same procedure, peptide **13** was obtained in 27% yield.

The stimulation of the MMP-2 production by fibroblast cells was analyzed by Western blotting. The results showed that the Ig domain itself had no stimulation activity, whereas peptide **13** and **12** stimulated about 5 and 8.5 times higher production of MMP-2. Thus, we demonstrated that the carbohydrate chain on Asn<sup>44</sup> plays an essential role for the stimulation of MMP production. Further biological studies are in progress.

## References

1. Nabeshima, K., Kataoka, H., Koono, M., Toole, B.P. In W. Hoeffler (Ed.) *Collagenases*, R.G. Landes Company, Texas, 1999, pp. 91–113.
2. (a) Aimoto, S. *Biopolymers (Peptide Science)* **51**, 247–265 (1999). (b) Kawakami, T., Yoshimura, S., Aimoto, S. *Tetrahedron Lett.* **39**, 7901–7904 (1998).

## Synthesis of Peptide- and Glycopeptide-Conjugates for Specific Drug Targeting

Shui-Tein Chen

*Institute of Biological Chemistry, Academia Sinica, Nankang, Taipei, 11529, Taiwan*

### Introduction

Mammalian liver cells possess a specific membrane-bound receptor (the asialoglycoprotein receptor, ASGPr), which recognizes terminal galactose/*N*-acetylgalactosamine residues, and require multivalency to achieve tight binding of ligands. A designed glycoside cluster containing three *N*-acetylgalactosamine moieties on Tyr-Glu-Glu, YEE(GalNAcAH)<sub>3</sub> **1** (Figure 1), which has sub-nanomolar binding constants for ASGPr, has been previously synthesized and successfully utilized in the delivery of gene to the parenchymal cells of the liver. We describe a new procedure for the synthesis of the cluster using protected GalNAc derivatives as building blocks by step-wise solid-phase method [1].

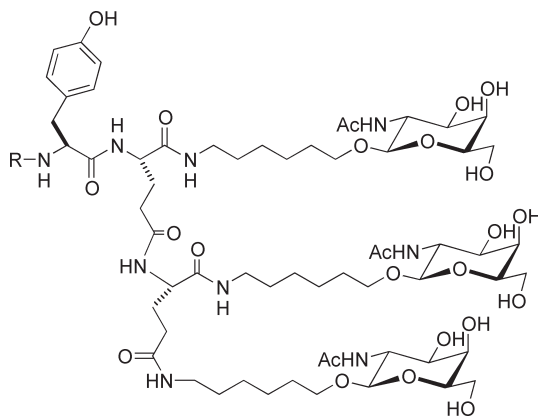


Fig. 1. Tyr-Glu-Glu, YEE(GalNAcAH)<sub>3</sub>.

Octreotide **2** (Figure 2), a metabolically stable somatostatin analog, inhibits the growth of tumor cells by binding to surface somatostatin receptors. The binding of somatostatin (SST) to their endogenous G-protein-coupled receptors was demonstrated to be followed by internalization of SST. Several reports have shown that a

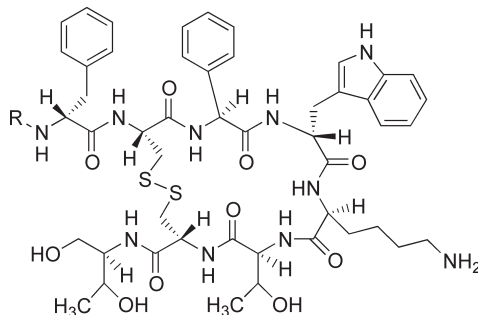


Fig. 2. Octreotide.

high density of somatostatin receptors (SSTR) was present on most hormone-secreting tissue tumors, together with the facile chemical synthesis, the long-acting SST analogue, octreotide, may be of practical value in developing tumor tracer and in serving as a carrier of cytotoxic antitumor drugs [2–5].

### **Results and Discussion**

An alternative route for the synthesis of the trivalent glucosidal cluster peptide has been described. The synthesis was carried out by the SPPS technique using Fmoc-( $\alpha$ -ah-GalNAcAc3)-glutamic acid as a building block. Compared with other methods used to synthesize the ASGP-R ligand, the synthesis of YEEE(ah-GalNAc)<sub>3</sub> represents a considerable improvement, mainly by simplifying the preparations of the starting material and by using solid phase peptide synthesis as the synthetic strategy. This enables a more efficient synthesis to be performed, and also provides a relatively efficient means for preparing close analogues and conjugation of drugs during the synthetic courses. The described procedure was used to synthesize compound YEEE-(GalNAcAH)<sub>3</sub>, which possesses comparable affinity to YEE, and derivatives with fatty acid, poly-lysine, fluorescein, and biotin conjugation to demonstrate its facility.

Fluorescein-labeled octreotide was internalized into the cytosol of human breast MCF-7 carcinoma cells *via* binding to somatostatin receptor (SSTRs) on the cell membrane. Octreotide-conjugated paclitaxel (taxol) was created by coupling taxol-succinate to N-terminal of octreotide. This conjugate maintains biological actions of taxol in inducing formation of tubulin bundles, eventually causing apoptosis of MCF-7 cells. Cytotoxicity of octreotide-conjugated taxol is mainly mediated by SSTR because octreotide pretreatment can remarkably rescue the induced cell death. In comparison with free taxol, this conjugate shows much less toxicity in CHO (Chinese hamster ovary) cells. Octreotide-conjugated taxol exerts the same antitumor effect of free taxol on stabilizing microtubule formation and inducing cell death. This conjugate triggers tumor cell apoptosis mediated by SSTRs and is exclusively toxic to SSTR expressing cells. Octreotide-conjugated taxol presents less toxicity to low-SSTR expressing cells than free taxol. These results strongly indicate that octreotide-conjugated taxol has cell selectivity and may be used as a targeting agent for cancer therapy.

### **References**

1. Jiaang, W.T., et. al. *Synlett* 797–800 (2000).
2. Huang, C.M., et. al. *Chem. Biol.* **7**, 453–461 (2000).
3. Hsieh, H.P., et al. *Bioorg. Med. Chem.* **7**, 1797–1803 (1999).
4. Wu, Y.T., et. al. *Tetrahedron Lett.* **39**, 1783–1784 (1998).
5. Hsieh, H.P., et. al. *Chem. Commun.* 649–650 (1998).

## Complexation of Peptidoglycan Intermediates by the Lipoglycopeptide Antibiotic Ramoplanin: Structural Requirements for Intermolecular Complexation and Fibril Formation

**Predrag Cudic, James Kranz, Douglas C. Behenna, Ryan G. Kruger,  
 A. Joshua Wand and Dewey G. McCafferty**

*Johnson Research Foundation and the Department of Biochemistry and Biophysics,  
 School of Medicine, University of Pennsylvania, Philadelphia, PA 19104-6059, USA*

### Introduction

For the past 50 years, bacterial infections have been effectively treated with antimicrobial agents [1]. However, the sudden rise in clinical cases of resistance to the antibiotic vancomycin, the antibiotic of last resort against Gram-positive bacteria [2], is a dismal reminder for the pressing need for new antimicrobials against these pathogens. The peptide antibiotic Ramoplanin **1**, a 17-residue lipoglycopeptide antibiotic obtained by fermentation of *Actinoplanes* ATCC 33076 [3], is a promising replacement for vancomycin since it is highly active against vancomycin-resistant *Enterococcus faecium* (VRE) and Gram-positive bacteria resistant to methicillin, erythromycin, and ampicillin. No resistance to Ramoplanin has been reported. Though it is known that Ramoplanin interrupts the conversion of peptidoglycan Lipid intermediate I to II and the crosslinking of Lipid II into mature peptidoglycan [4,5], the molecular basis of its mechanism is not clear. We report here on our studies of the molecular mechanism of action of the peptide antibiotic Ramoplanin.

### Results and Discussion

Independently, we [6] and others [4,5] have suggested that Ramoplanin **1** acts by forming a 1 : 1 inhibitory complex with Lipid intermediates I and II, membrane anchored peptidoglycan (PG) monomers. Complexation of PG monomers prevents their proper utilization into crosslinked peptidoglycan by cell membrane-associated glycosyltransferases. In solution, this high affinity complexation of Lipid intermediates **2–4** by Ramoplanin **1** produces conformational changes in the antibiotic, which lead to aggregation and formation of insoluble amyloid-like fibrils. To determine the structure of the inhibitory complex, a combination of NMR experiments and chemical synthesis of peptidoglycan intermediates **2–4** was employed (Figure 1). Addition of 20%

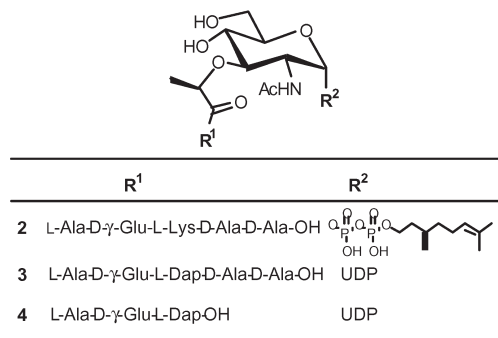


*Fig. 1. Structures of the peptidoglycan derivatives 2–4.*

dimethyl sulfoxide (DMSO) to the complex prevented fibril formation, yet preserved modest affinity for peptidoglycan intermediates, thus allowing for the determination of the dissociation constants and identification of the binding interface by 1D and 2D NMR methods. The dissociation constants for the complexes between the Ramoplanin **1** and peptidoglycan intermediates **2–4**, determined by  $^1\text{H}$  NMR titration experiment in 20% DMSO- $d_6$ /D $_2$ O solvent mixture, cover a range from 0.18 to 2.5 mM. By two dimensional NOESY experiments we have determined that Ramoplanin **1** utilizes an eight amino acid sequence (D-Orn-L-Hpg-D-*allo*-Thr-L-Hpg-D-Hpg-L-*allo*-Thr-L-Phe-D-Orn) to recognize the muramyl carbohydrate and adjacent pyrophosphosphate moieties of peptidoglycan, a different locus than the *N*-acyl-D-Ala-D-Ala dipeptide site targeted by vancomycin (Figure 2). Chemotherapeutics derived from this octapeptide recognition sequence may find future use as antibiotics against VRE and related infections.

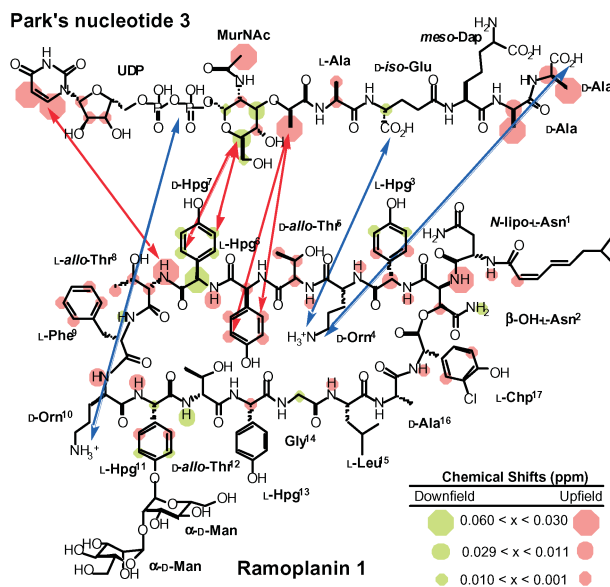


Fig. 2. Schematic presentation of the complex between Ramoplanin **1** and Park's nucleotide **7**. Salt bridges are shown by arrows 2, 7, and 8 (from the left), intermolecular NOEs are shown by arrows 1, 3, 4, 5, 6.

## References

- Gold, H.S., Moellering, R.C. *New Eng. J. Med.* **335**, 1445–1452 (1996).
- Malabarba, A. *Exp. Opin. Ther. Pat.* **6**, 627–644 (1996).
- Cavalleri, B., Pagani, H., Volpe, G., Selva, E., Parenti, F. *J. Antibiot.* **37**, 309–317 (1989).
- Somner, E.A., Reynolds, P.E. *Antimicrob. Agents Chemother.* **34**, 413–419 (1990).
- Lo, M.C., Men, H., Branstrom, A., Helm, J., Yao, N., Goldman, R., Walker, S. *J. Am. Chem. Soc.* **122**, 3540–3541 (2000).
- McCafferty, D.G., Cudic, P., Yu, M.K., Behenna, D.C., Kruger, R. *Curr. Opin. Chem. Biol.* **3**, 672–680 (1999).

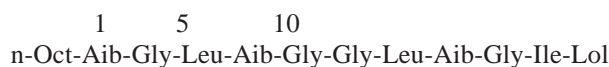
## Short Analogues of the Lipopeptaibol Trichogin GA IV

Marco Crisma, Cristina Peggion, Fernando Formaggio and  
Claudio Toniolo

*Biopolymer Research Center, CNR, Department of Organic Chemistry, University of Padova,  
35131 Padova, Italy*

### Introduction

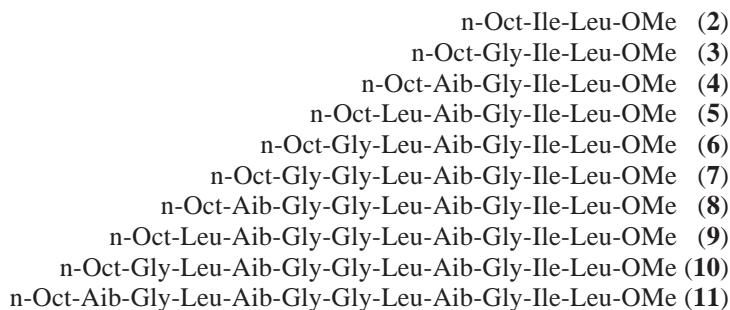
Lipopeptaibols are a unique group of membrane active peptides characterized by a linear sequence of 6–10 amino acid residues, a high proportion of the helix-forming Aib, an N-terminal fatty acyl group, and a C-terminal 1,2-amino alcohol. Trichogin GA IV,



where n-Oct is n-octanoyl and Lol is leucinol. The main component of the natural microheterogeneous mixture is a mixed  $3_{10}/\alpha$ -helical lipopeptaibol and is able to remarkably modify membrane permeability. We have already reported that at least six carbon atoms in the N $^{\alpha}$ -blocking fatty acyl moiety are required for significant membrane activity.

### Results and Discussion

To examine the role of the peptide main-chain length on the conformation and membrane activity of trichogin GA IV we have synthesized by solution methods the [Leu<sup>11</sup>-OMe] analogue (**11**) and all its short, N $^{\alpha}$ -octanoylated C-terminal sequences (**2–10**).



Membrane activity is already found at the level of the tetrapeptide (**4**) and progressively increases up to the undecapeptide (**11**) (Figure 1). The presence of the helicogenic Aib residue in the tetrapeptide (**4**) is essential for activity.

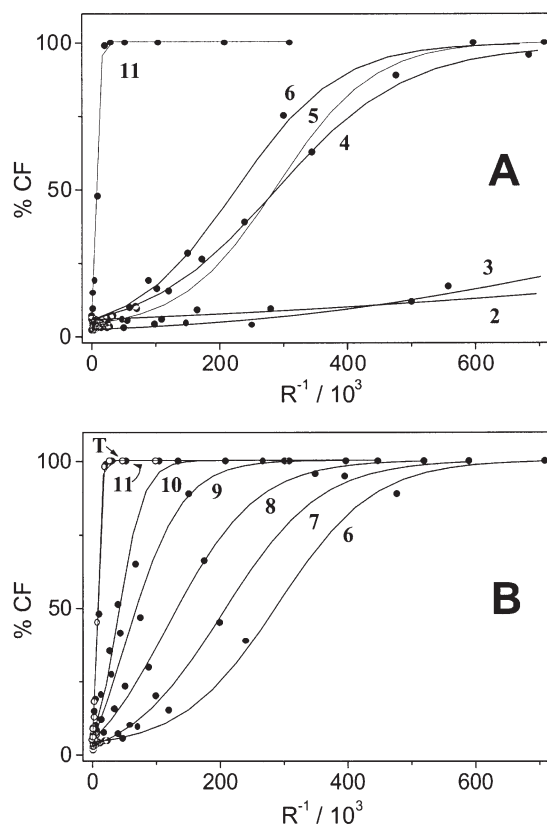


Fig. 1. Peptide induced carboxyfluorescein (CF) leakage at 20 min for different ratios  $R_i^{-1} = [\text{peptide}]/[\text{lipid}]$  from egg phosphatidylcholine/cholesterol (70:30) vesicles. (A) Peptides 2–6 and 11; (B) Peptides 6–11 and trichogin GA IV (T).

By FT-IR absorption,  $^1\text{H}$  NMR and X-ray diffraction we have also shown that partially folded forms characterize the short peptides, while the octa- and longer peptides (8–11) predominantly adopt helical structures.

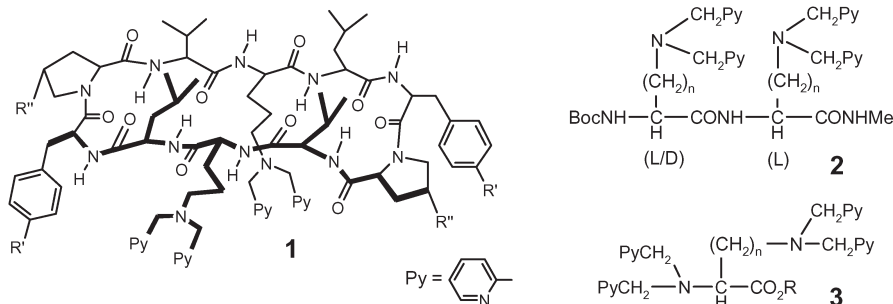
## Dinuclear Zinc(II) Complexes of Linear and Cyclic Peptides Containing Two Bis(2-pyridylmethyl)amino Groups as Catalysts for Hydrolysis of RNA Model Substrate

Masao Kawai, Hatsuo Yamamura, Nobuko Izuhara,  
Tomotsugu Kawaguchi, Ryoji Tanaka, Ryougo Akasaka,  
Yu-ichi Takahashi, Keiichi Yamada and Shuki Araki

Department of Applied Chemistry, Nagoya Institute of Technology, Nagoya, 466-8555, Japan

### Introduction

Various enzymes possess two metal ions in their active center and many models of the metalloenzymes were reported. Dinuclear Zn(II) complex of 2-pyridylmethyl (PyCH<sub>2</sub>) derivative of 2-hydroxypropanediamine, (PyCH<sub>2</sub>)<sub>2</sub>NCH<sub>2</sub>CH(OH)CH<sub>2</sub>N(CH<sub>2</sub>Py)<sub>2</sub>, was reported to promote cleavage of phosphodiester linkage of diribonucleotides, where synergistic effect of the two metal centers was considered to be essential [1]. Since the cyclic decapeptide gramicidin S (GS), cyclo(-Val-Orn-Leu-D-Phe-Pro-)<sub>2</sub>, possesses two Orn side chains located on one side of the stable antiparallel  $\beta$ -sheet plane, we prepared a GS derivative containing two bis(2-pyridylmethyl)amino groups, namely [Orn(PyCH<sub>2</sub>)<sub>2</sub><sup>2,2'</sup>]GS (**1**, R' = R'' = H). As expected, dinuclear Zn(II) complex of it effectively enhanced the cleavage of the phosphodiester linkage of 2-hydroxypropyl *p*-nitrophenyl phosphate (HPNP) as an RNA model substrate [2]. Here we will report the synthesis, Zn(II) ion-chelating behavior, and phosphodiester bond-cleaving activity for HPNP of the Zn(II) complexes of related cyclic and linear peptide derivatives.



### Results and Discussion

For the purpose of improving this metalloenzyme mimic **1** (R' = R'' = H)-Zn(II)<sub>2</sub>, hydroxy group-containing analogs of GS, namely [D-Tyr<sup>4,4'</sup>]GS and [Hyp<sup>5,5'</sup>]GS, were chosen as more versatile  $\beta$ -sheet frameworks since introduction of additional functionality such as substrate recognition and activity control could be possible by use of the OH groups. Protected [D-Tyr<sup>4,4'</sup>]GS and [Hyp<sup>5,5'</sup>]GS were prepared by solid-phase-synthesis and cyclization-cleavage method using Kaiser's oxime resin and were converted to the tetrakis(2-pyridylmethyl) derivatives, **1** (R' = OH, R'' = H) and **1** (R' = H, R'' = OAc) by NaBH<sub>3</sub>CN-reduction of the corresponding Schiff bases with PyCHO. Spectroscopic titration indicated the formation of transient 1 : 1 and stable 1 : 2 complexes of these derivatives with Zn(II) ions. Phosphodiester bond-hydrolyzing activity of the dinuclear Zn(II) complexes generated *in situ* were examined in 50%

CH<sub>3</sub>CN–20 mM HEPES buffer (pH 7) using HPNP as a substrate ([HPNP] = 0.25 mM, [Zn(II) complex] = 0.5 mM). Pseudo-first-order rate constants  $k'$  were obtained as  $2.2 \cdot 10^{-3}$  (4300) for **1** (R' = OH, R'' = H) and  $3.0 \cdot 10^{-3}$  (6000) for **1** (R' = H, R'' = OAc). The values in parentheses are relative activity  $k'/k'_0$  where  $k'_0$  refers to the rate in buffer solution without Zn(II) species. Since the activity of these complexes was comparable to that of **1** (R' = R'' = H)-Zn(II)<sub>2</sub> ( $k'/k'_0$  = 6500) [2], the OH-possessing analogs of GS could be considered as useful scaffolds for the preparation of ligands with various properties.

As more flexible and much simpler analogs of **1** (R' = R'' = H), Orn(PyCH<sub>2</sub>)<sub>2</sub> residue-containing diastereomeric dipeptide derivatives **2** (n = 3) and the corresponding Lys analogs **2** (n = 4) were synthesized. Dinuclear Zn(II) complex-mediated phosphate bond cleavage of HPNP was studied using these tetrakis(2-pyridylmethyl) derivatives as ligands. The  $k'/k'_0$  values of the Zn(II) complexes of diastereomeric **2** were 2400 (n = 3, L-L), 3800 (n = 3, D-L), 1200 (n = 4, L-L) and 1400 (n = 3, D-L), *i.e.*, diornithyl peptides showed higher activity than dilysyl peptides and D-L sequence showed higher activity than L-L sequences. Attempts to control dipeptide stereochemistry by host-guest interaction are being undertaken. Preliminary study with diastereomeric dialanyl model peptides possessing  $\beta$ -cyclodextrin and 1-adamantyl moieties at their termini indicated presence of notable interaction between these terminal groups. The results suggested the possibility of controlling conformation and activity of the functional dipeptide derivatives by the addition of an external guest molecule whose interaction with the host moiety could compete with the intramolecular interaction.

Bis(2-pyridylmethyl)amino group-containing derivatives of  $\alpha$ -amino acids and  $\alpha,\omega$ -diamino acids **3** were prepared by either dialkylation of primary amino group using PyCH<sub>2</sub>Cl or *via* Schiff bases with PyCHO. Saponification of an Ala derivative (PyCH<sub>2</sub>)<sub>2</sub>-L-Ala-OMe followed by coupling with H-Gly-OEt yielded bis(2-pyridylamino) group-containing dipeptide (PyCH<sub>2</sub>)<sub>2</sub>-L-Ala-Gly-OEt in good yield, showing versatility of these amino acid derivatives as building blocks for the preparation of the ligand moiety of phosphodiester-cleaving compounds. The Lys derivative **3** (n = 4, R = Et) was shown to form 1 : 2 complex with Zn(II) ions and the dinuclear metal complex cleaved the phosphate bond of HPNP ( $k'/k'_0$  = 370), but the breakdown of the ethyl ester moiety was also observed.

### Acknowledgments

The authors are grateful to Nikken Kagaku Co., Ltd. for the supply of GS·2HCl. This work was supported by a Grant-in-Aid for Scientific Research (No. 10650847) from the Ministry of Education, Science, Sports and Culture, Japan.

### References

1. Yashiro, M., Ishikubo, A., Komiyama, M. *J. Chem. Soc., Chem. Commun.* **1995**, 1793–1794 (1995).
2. Yamada, K., Takahashi, Y., Yamamura, H., Araki, S., Saito, K., Kawai, M. *J. Chem. Soc., Chem. Commun.* **2000**, 1315–1316 (2000).

## Construction of RNA-Binding Proteins Having Nucleobase Amino Acids Based on HIV-1 Nucleocapsid Protein

**Tsuyoshi Takahashi<sup>1</sup>, Akihiko Ueno<sup>1</sup> and Hisakazu Mihara<sup>1,2</sup>**

<sup>1</sup>Department of Bioengineering, Graduate School of Bioscience and Biotechnology,  
Tokyo Institute of Technology, Japan

<sup>2</sup>PRESTO, Japan Science Technology Corporation, Yokohama 226-8501, Japan

## Introduction

RNA-protein interaction plays important roles in nature [1]. In many cases, RNA-binding proteins target secondary structural domains such as hairpin loops, internal loops, and bulges of RNA [1]. For the sake of developing highly selective drugs against RNA, it is important to construct novel molecules that recognize highly structured RNA. For this purpose, we have attempted to design the peptides and proteins having the nucleobase moieties at the L- $\alpha$ -amino acid side chain (nucleobase amino acids; NBAs) [2], expecting that the recognition ability for RNA bases by NBAs can be utilized on peptide and protein conformation.

In this study, we designed and synthesized the proteins conjugated with NBA units based on the structure of HIV-1 nucleocapsid protein (NCp7). The binding affinities of the proteins with an RNA construct including the SL3 region of HIV-1  $\Psi$ -site were elucidated. This study has demonstrated that the NBA units incorporated into RNA-binding proteins can work as a factor for enhancing the RNA-binding affinity and specificity.

## Results and Discussion

HIV-1 NCp7 (55 residues) contains two CCHC (Cys-X<sub>2</sub>-Cys-X<sub>4</sub>-His-X<sub>4</sub>-Cys) type zinc knuckle domains (Figure 1) [3]. The domains are critical for viral replication and participate directly in genome recognition and encapsidation [4]. The HIV-1 Ψ-site contains four stem-loop structures, denoted SL1 through SL4. The 3D structure of the complex between NCp7 and SL3 RNA has been determined by NMR structural analyses [3]. In the NMR structure of NCp7–SL3 complex, Val13 and Lys14 of NCp7 are close to the G12 base in SL3 RNA, and Lys38 and Met46 are also in close positions to the G10 base. On this basis, the NBA-proteins, in which the Val13, Lys14, Lys38, and Met46 residues were replaced by 4-(cytosin-1-yl)-2S-aminobutyric acid (C<sub>NBA</sub>) and 4-(guanine-9-yl)-2S-aminobutyric acid (G<sub>NBA</sub>), were designed (Figure 1).

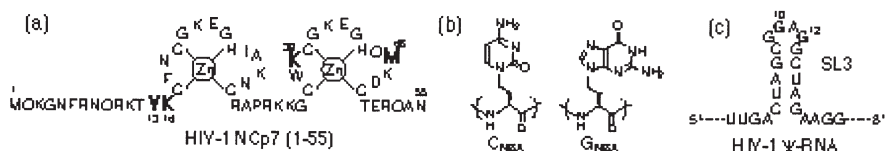


Fig. 1. (a) Structure of NCp7. (b) Structure of  $C_{NBA}$  and  $G_{NBA}$  residues. (c) Secondary structure of SL3 region of HIV-1  $\Psi$ -RNA.

The NBA-proteins were synthesized by the native chemical ligation, reported by Kent *et al.* [5], between the segment 1-35 residues (S1-Gly-COSR; R = CH<sub>2</sub>CH<sub>2</sub>COOEt) and the segment 36-55 residues (Cys-S2). The segment peptides were synthesized by the solid-phase method using Fmoc strategy. The chemical ligation was carried out in 0.1 M phosphate buffer (pH 7.5) containing 6 M guanidine hy-

drochloride and 4% thiophenol (v/v). The ligation products were purified by a semi-preparative RP-HPLC with high purity and good yield.

For the evaluation of the binding affinities of the NBA-proteins to SL3 RNA, a fluorescein-labeled RNA (SL3-Flu RNA) was prepared. The binding affinities were determined by fluorescence anisotropy measurements based on the fluorescein moiety of SL3-Flu RNA [2]. The dissociation constant ( $K_d$ ) of 551 nM was estimated from the anisotropy increase using an equation with 1 : 1 stoichiometry. The binding affinities of the NBA-proteins to SL3-Flu RNA were significantly dependent on the type and positions of NBA units. Especially, the protein, which possessed  $C_{NBA}$  and  $G_{NBA}$  units at 13th and 46th positions, respectively, bound to SL3-RNA, *ca* 9-fold stronger than NCp7 did. Furthermore, the binding affinities of this protein with two mutant RNAs, in which the G12 or G10 base in SL3-Flu RNA was replaced by adenine, were significantly decreased. These results suggest that the cytosine and guanine moieties incorporated into NCp7 can interact specifically with G12 and G10 bases in SL3-Flu RNA.

In summary, this study demonstrated that the conjugation strategy of the NBA units with protein is valuable for constructing novel molecules that recognize specific structure of RNA.

#### **Acknowledgments**

This work was supported in part by Research Fellowships of the Japan Society for the Promotion of Science for Young Scientists (T. T.).

#### **References**

1. Draper, D.E. *J. Mol. Biol.* **293**, 255–270 (1999).
2. Takahashi, T., Hamasaki, K., Ueno, A., Mihara, H. *Bioorg. Med. Chem.* **9**, 991–1000 (2001).
3. De Guzman, R.N., Wu, Z.R., Stalling, C.C., Pappalardo, L., Borer P.N., Summers, M.F. *Science* **279**, 384–388 (1998).
4. Coffin, J.M., Hughes, S.H., Varmus, H.E. *Retroviruses*, Cold Spring Harbor Laboratory Press, 1997.
5. Dawson, P.E., Muir, T.W., Clark-Lewis, I., Kent, S.B.H. *Science* **266**, 776–779 (1994).

## Screening of Peptides that Control Interaction Between Nucleobases from Peptide Libraries Based on Loop Structures

Mizuki Takahashi<sup>1</sup>, Akihiko Ueno<sup>1</sup> and Hisakazu Mihara<sup>1,2</sup>

<sup>1</sup>*Department of Bioengineering, Graduate School of Bioscience and Biotechnology,  
Tokyo Institute of Technology, Japan*

<sup>2</sup>*PRESTO, Japan Science and Technology Corporation, Yokohama 226-8501, Japan*

### Introduction

The combinatorial peptide library has been widely used as a useful tool for screening of the bioactive ligands and/or recognition motif against specific molecules [1]. The random peptide libraries, however, generally have considerable conformational flexibility, thus many kinds of conformationally restrained peptide libraries have been reported recently [2]. In this study, we constructed a unique conformationally-restricted peptide library using a loop structure as a structural scaffold and peptide nucleic acids (PNAs) as a recognition site. By using this structure, we carried out the effective screening of the amino acid sequences that control the interaction between nucleobases.

### Results and Discussion

In the designed peptide libraries, 3mer PNAs were conjugated with the C-terminus of a peptide structure to introduce a defined recognition site to their complementary DNA. The 3mer library sequence was placed at the N-terminus of the peptide connected *via* a loop sequence so as to be in close to the PNA-DNA complex and to affect the interaction between PNA and its complementary DNA (Figures 1a, 1b).

Designed libraries were synthesized using the spot-synthesis method as an individual spot on a cellulose membrane [3]. To detect the binding of DNA that has a complementary sequence to PNA, we used a biotinylated DNA and peroxidase-labeled streptavidin. Amount of bound DNA was estimated by brown color with 3,3',5,5'-tetramethylbenzidine as a substrate of peroxidase.

At first, the synthetic and detection methods were checked and the sequence of loop peptide designed to form a  $\beta$ -hairpin structure was selected from some candidates by the comparison of the results from the full library XXX with that from the reference sequence GGG, where X represents an equal distribution of 19 amino acids (20 natural amino acids except for Cys). The results indicated that the loop peptide sequences designed based on an antibody loop [4] showed a non-specific binding to DNA, which may be due to an Arg residue in the loop sequence. In contrast, the sequences based on the peptide designed to form a stable  $\beta$ -hairpin structure [5] showed a good contrast between XXX and GGG. Therefore, we used this 9mer sequence as a scaffold loop structure for the construction of the positional scanning library with  $(A_{PNA})_3$  sequence at the C-terminus.

In the first generation, the library sequence was OXX, where O represents 19 defined amino acids. In this series, the stronger binding of biotinylated  $(dT)_3$  was observed for positively charged amino acids such as Arg, Lys, His, as well as large hydrophobic amino acids such as Phe, Tyr at the O site. However, only the peptide which has Phe at the O position showed a weaker binding to biotinylated  $(dC)_3$ , indicating that this peptide has some specificity for  $(dT)_3$ , complementarily interacting to  $(A_{PNA})_3$  in the peptide (Figure 1c).

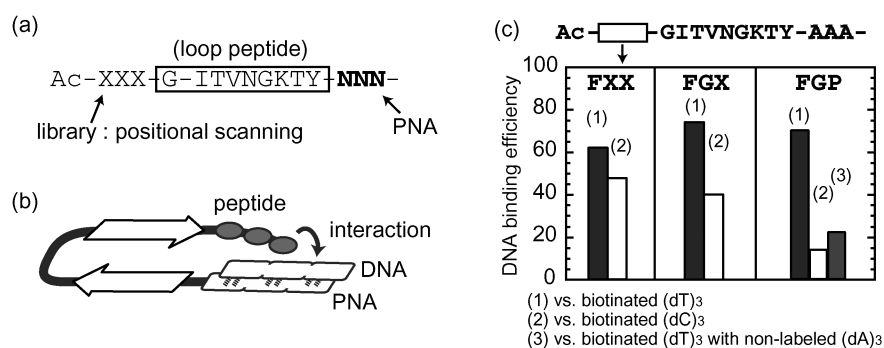


Fig. 1. Structure (a) and schematic representation (b) of designed library, and the DNA binding efficiency of the selected sequences (c). Reaction time for colorization is 5 min (for 1st and 2nd library; FXX and FGX) or 30 sec (for 3rd library; FGP).

According to this result, the second library which has FOX as the sequence was synthesized. In this position, the introduction of amino acids with a relatively small side chain such as Gly, Asn, Thr caused a good contrast of the results between biotinylated (dT)<sub>3</sub> and (dC)<sub>3</sub> as a ligand (Figure 1c). In this study, we selected Gly in this position to generate the next library.

The third library having FGO as the sequence was synthesized. From this library, FGP sequence was selected as the strongest binder of (dT)<sub>3</sub>. In contrast, this peptide showed a lower ability in the binding to (dC)<sub>3</sub>. Furthermore, the binding of biotinylated (dT)<sub>3</sub> to the FGP peptide was significantly inhibited by the coexistence of non-labeled (dA)<sub>3</sub> (Figure 1c), while no significant inhibition was observed for the peptides that have other amino acids at the O position. These results suggest that the selected FGP sequence has a higher specificity to enhance the interaction of A<sub>PNA</sub>-T<sub>DNA</sub> base pair. Although it was not clearly revealed how the selected sequence interacts with the A<sub>PNA</sub>-T<sub>DNA</sub> base pair, it was possibly suggested that the Pro and Gly residues may contribute to the structural suitability, while an aromatic ring in the side chain of Phe residue may interact to nucleobases directly.

In conclusion, we have demonstrated a unique conformationally-restricted peptide library using a loop structure as a structural scaffold. This library was used to screen the amino acid sequences that control the interaction between A<sub>PNA</sub>-T<sub>DNA</sub> trinucleobases. By using this PNA-peptide conjugate system, the binder to a specific base pair could be effectively obtained.

### Acknowledgments

This work was supported in part by the Tokyo Ohka Foundation for the promotion of science and technology.

### References

1. Lam, K.S., Lebl, M., Krchnak, V. *Chem. Rev.* **97**, 411–448 (1997).
2. Nygrenn, P.-Å., Uhlén, M. *Curr. Opin. Struct. Biol.* **7**, 463–469 (1997).
3. Frank, R. *Tetrahedron* **48**, 9217–9232 (1992).
4. Takahashi, M., Ueno, A., Mihara, H. *Chem. Eur. J.* **6**, 3196–3213 (2000).
5. Ramírez-Alvarado, M., Blanco, F. J., Serrano, L. *Nat. Struct. Biol.* **3**, 604–612 (1996).

## Preparation of a Site-Specifically Labeled Fluorescent Chemokine by Chemical Synthesis

Andrew E. Strong and Antonio S. Verdini

Department of Research and Development (Synthetic Peptides), RMF Dictagene SA,  
 Epalinges, 1066, Switzerland

### Introduction

Labeled biomolecules are of interest as biological tools, *e.g.* to follow the binding of a ligand to its receptor or to screen antagonists to that receptor. The labeling of peptides that are chemically synthesized is attractive as the development of orthogonal protecting groups allows the labeling to be site-specific. We were interested in developing a method for site-specific labeling of chemokines. Of particular interest was any effect that the length of the peptide would have on the coupling of the label to the side-chain, on the stability of the fluorescent label to the coupling and cleavage conditions, and on the folding of the peptide. We describe the preparation of the CC chemokine MCP-1(9-76), labeled at Lys<sup>75</sup> with fluorescein.

### Results and Discussion

The residue chosen for labeling was Lys<sup>75</sup> which, as a residue close to the C-terminal, was believed to be non-essential for binding or activity. Furthermore the Lys side chain can be easily modified by protecting the side-chain with an orthogonal protecting group such as Dde [1] then coupling the fluorescent label via a peptide bond.

The synthetic plan is outlined in Figure 1. Fmoc-Lys(Dde) was coupled to the Thr(O<sup>t</sup>Bu)-resin and the stepwise synthesis was completed using preactivated HOBt esters and standard protecting groups. At the end of the synthesis the N-terminal was protected with Boc<sub>2</sub>O-NMM in DMF. The side-chain of Lys<sup>75</sup> was Dde-deprotected with 2% NH<sub>2</sub>NH<sub>2</sub> in DMF. 5-Carboxyfluorescein (5-CF) was coupled with DIC-HOBt (3-fold excess over peptide-resin) in DMF for 2 h. After washing and drying the peptide was cleaved from the resin with a mixture of TFA and scavengers. However no ion of the expected molecular weight was observed in the mass spectrum. Neither did we observe the ion with *m/e* corresponding to peptide with Dde still at-

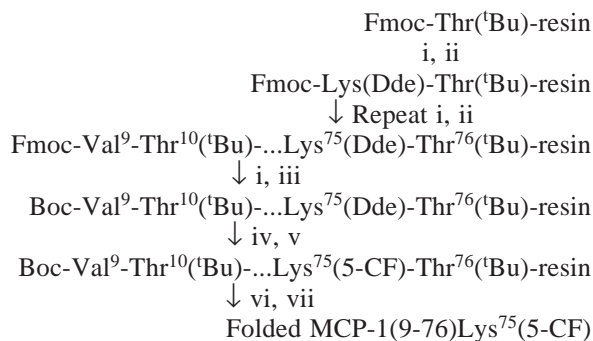


Fig. 1. Synthetic plan for the preparation of the labelled chemokine. i, 20% piperidine in DMF. ii, Couple Fmoc-Aaa-OH. iii, Boc<sub>2</sub>O-NMM in DMF. iv, 2% NH<sub>2</sub>NH<sub>2</sub> in DMF. v, 5-CF (5-carboxyfluorescein), coupling reagents (see Table 1). vi, Cleavage and purification. vii, Disulfide formation and purification.

tached, which indicated that the hydrazine treatment had deprotected Lys<sup>75</sup> but that the subsequent coupling reaction had failed.

We therefore studied other conditions for the coupling of 5-CF. Double-coupling, a greater excess of reagent and longer reaction times (Table 1, entries 2, 3, and 4) all failed to produce the desired labeled peptide when coupling with DIC-HOBt. Coupling was achieved using 3 eq. 5-CF with HBTU-HOBt in DMF with 6 eq. DIEA. After cleavage the crude product contained the desired labeled MCP-1(9-76), but was still contaminated with the unlabeled peptide. Following purification by RP-HPLC the ratio of labeled: unlabeled peptide was 1 : 9, indicating that there were still considerable problems with this coupling step. The linear, reduced MCP-1(9-76)-Lys<sup>75</sup>(CF) was folded using our novel folding method [2] to produce the oxidized target material in high purity following HPLC.

*Table 1. Summary of conditions for coupling 5-carboxyfluorescein to Lys<sup>75</sup> of MCP-1(9-76).*

Entry	Reagents	Excess	Time, h	%labeled
1	DIC-HOBt	1 × 3 eq.	2	n.d. <sup>a</sup>
2	DIC-HOBt	2 × 2.5 eq.	2	n.d.
3	DIC-HOBt	1 × 5 eq.	2	n.d.
4	DIC-HOBt	1 × 12 eq.	4	n.d.
5	HBTU-HOBt-DIEA	3 eq.	3	10

<sup>a</sup> Not determined.

In conclusion, we have obtained the target molecule, MCP-1(9-76) site specifically labeled at Lys<sup>75</sup> with fluorescein. The fluorophore was stable to the conditions of synthesis and cleavage as described above. The presence of the fluorescein derivative on this Lys side-chain did not prevent the chemokine folding and forming its two disulfide bonds. However the yield for coupling of the 5-CF was low using HBTU-HOBt-DIEA and essentially zero with DIC-HOBt. Future work to optimize this step could be attempted using a greater excess of reagents, longer reaction times, other coupling reagents, or different resins for the synthesis.

## References

1. Bycroft, B.W., Chan, W.C., Chhabra, S.R., Hone, N.D. *J. Chem. Soc., Chem. Commun.* 778 (1993).
2. Verdini, A.S., Roggero, M.A., Corradin, G., patent pending.

## Synthesis, Characterization, and Calorimetric Studies of a Series of Novel Bioconjugates for Selective Targeting of Microbubbles to GPIIb/IIIa Receptors on Vascular Thrombi

Patricia A. Schumann, Rachel M. Quigley, Varadarajan Ramaswami,  
Evan C. Unger and Terry O. Matsunaga

*ImaRx Therapeutics, Inc., Tucson, AZ 84719, USA*

### Introduction

Bioconjugate ligands have been used in our laboratory to target microbubbles to glycoprotein receptors for both diagnostic and therapeutic purposes. The purpose of the bioconjugates (Figure 1) are to: 1) anchor the molecule into the microbubble membrane, 2) provide overall flexibility for the ligand to “find” its target [1], and 3) provide a ligand selective for certain receptors [2]. However, in order for ligands to effectively direct the entire microbubble to a selective receptor, the bioconjugate must remain inserted into the microbubble membrane. Failure to do so could result in “free” bioconjugates acting as competitive receptor antagonists to microbubble or liposome binding. We have thus conducted a calorimetric study to determine the efficiency of insertion of a series of bioconjugates varying only in hydrocarbon tail length.

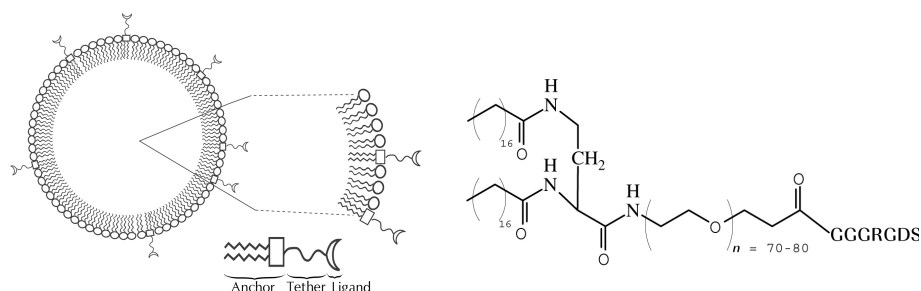


Fig. 1. The structure of the bioconjugate.

### Results and Discussion

All compounds were synthesized employing standard Fmoc coupling schemes. Removal from the resin was accomplished using standard TFA cleavage cocktails in the presence of scavengers. The crude bioconjugates were then desalted by membrane dialysis (1000 MWCO) and purified by reverse-phase HPLC. All structures were then characterized and confirmed by amino acid analysis, NMR, and MALDI mass spectrometry. Calorimetry was performed on a MicroCal MC-2 scanning calorimeter. Sample preparation was performed by mixing up to 9.6 mole % of the bioconjugate with dipalmitoylphosphatidylcholine (DPPC). Samples were suspended in 0.9% NaCl solution followed by six freeze-thaw cycles. Calorimetry was performed at a scanning rate of  $10\text{ }^{\circ}\text{C h}^{-1}$  through a temperature range from 20–50  $^{\circ}\text{C}$ .

Digital Scanning Calorimetry (DSC) can measure disruptions in the membrane packing order which results in changes in the calorimetric enthalpy. Thus, enthalpic measurements can indicate the effects of bioconjugate insertion into membranes. Broadened peaks in the right panel of Figure 2 indicate insertion of bioconjugate into the membrane.

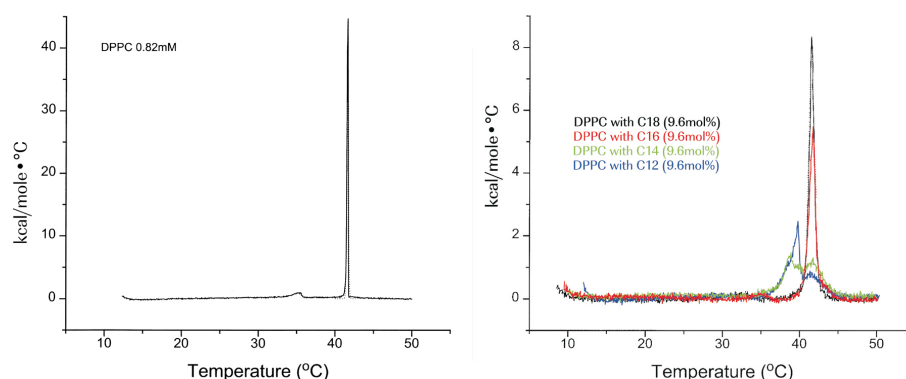


Fig. 2. Calorimetric scans of (left) DPPC liposome, and (right) DPPC liposome mixed with 9.6 mole % the diacyl-diaminobutyryl-PEG-GGGRGDS analogs.

The calorimetric enthalpy ( $\Delta H$  Cal) decreases with shorter chain lengths (Table 1). The CU follows the same trend. The peak width at half height increases with decreasing chain length.

Table 1. Calorimetric data for all four bioconjugates ( $n = 3$  for all samples) differing only in hydrocarbon tail length of the acyl moieties.

Samples	$T_m$ °C	$T_{1/2}$ °C	$\Delta H$ Cal (Kcal/mol °C)	$\Delta H$ van't Hoff (Kcal/mol °C)	CU	Mean particle size ( $\mu m$ )
DPPC	41.59	0.14	8.65	3290	394	>2
DPPC/C18 analog	41.55	0.70	7.67	803	105	>2
DPPC/C16 analog	41.15	1.14	6.95	487	70	0.8
DPPC/C14 analog	39.62	4.29	6.16	124	20	0.06
DPPC/C12 analog	38.37	2.77	5.86	143	25	0.1

## Conclusions

For proper targeting of microbubbles to selective receptors, bioconjugate ligands must efficiently insert into lipids without disruption of the membranes into mixed micellar components. Thus, the length of the inserting hydrocarbon tail may be critical for proper insertion. Sizing and calorimetric results indicate that bioconjugate ligands with 18-carbon chain lengths insert into the membrane without significant alteration in mean particle size. Shorter chains, especially 14- and 12-carbon lengths induce significant decreases in cooperative units as well as mean particle size. Data suggest that DPPC bilayers with bioconjugates of 14- and 12-carbon chain lengths disrupt bilayers into mixed-micellar components. Therefore, for targeting applications using liposomes or microbubbles, the anchoring should not be shorter than 16-carbons.

## References

1. Jeppesen, C., et al. *Science* **293**, 465–468 (2001).
2. Wu, Y., et al. *Invest. Radiol.* **33**, 12, 880–885 (1998).

## Energy and Electron Transfer Systems Built in Dendritic Poly(L-lysine)s

Louis A. Watanabe, Motonori Uchiyama, Yusuke Oniki, Tamaki Kato,  
Toru Arai and Norikazu Nishino

*Department of Applied Chemistry, Faculty of Engineering, Kyusyu Institute of Technology,  
Tobata, Kitakyusyu, 804-8550, Japan*

### Introduction

We previously reported the incorporation of a large number of free base- and Zn(II)-porphyrins near the surface of dendritic poly(L-lysine)s in a scramble fashion [1] and hemisphere fashion [2]. Each of the dendrimers showed fluorescence energy transfer from Zn(II)-porphyrin to free base-porphyrin with 85 and 43% efficiencies, respectively. In the present study, we combined eight Zn(II)-porphyrins and sixteen free base-porphyrins in double strata fashion on a dendritic poly(L-lysine) ((Zn8/Fb16)K62 in Figure 1). Namely, Zn(II)-porphyrins are placed near the core, while free base-porphyrins are scattered near the surface.

### Results and Discussion

The synthesis of (Zn8/Fb16)K62 was carried out according to the previous reports [1,2]. The dendrimers combining single species of porphyrin, (Zn8)K30 and (Fb16)K62 were also prepared as reference compounds (Figure 1).

The (Zn8/Fb16)K62 was subjected to the fluorescence measurements with the reference of equimolar mixture of (Zn8)K30 and (Fb16)K62 in DMF. As shown in Figure 2A, upon excitation at 560 nm for Q band of Zn(II)-porphyrin, the emission at 610 nm from Zn(II)-porphyrin was significantly quenched. Instead, the emissions from free base-porphyrin at 657 and 720 nm increased slightly. From the quenching at 610 nm, the energy transfer was estimated as 90%.

Furthermore, fluorescence lifetime of (Zn8/Fb16)K62 was measured. The double strata dendrimer showed fast quenching (thick line in Figure 2B) at a few nanoseconds. This fact suggests that the quenching is caused by intramolecular energy transfer from Zn(II)-porphyrins to free base-porphyrins. Thus, an efficient fluorescence energy transfer system could be built in a dendrimer by applying peptide chemistry. This system will be utilized by various combinations of groups with photo-electronic function.

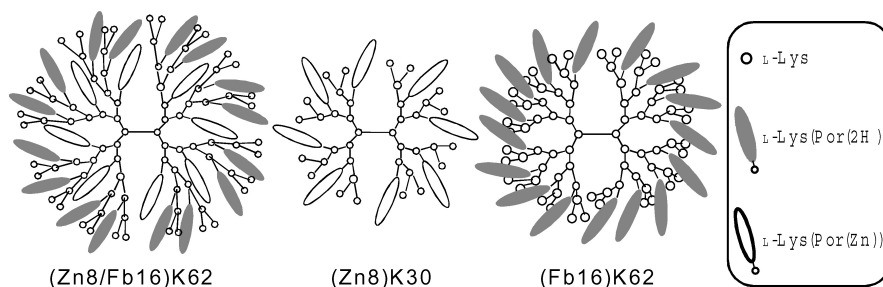


Fig. 1. Illustration of a double strata dendrimer and reference dendrimers.

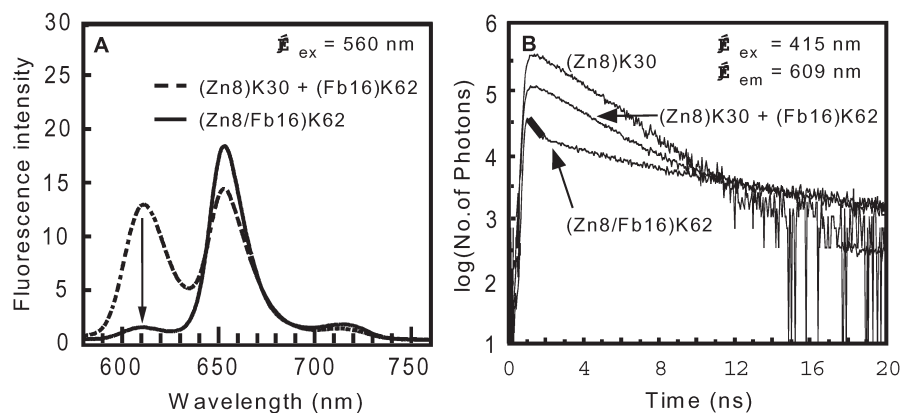


Fig. 2. Fluorescence spectra and fluorescence lifetime of the dendrimers combining porphyrins.

#### Acknowledgments

We thank Dr. Masahiko Sisido of Okayama University for the fluorescent lifetime measurements and his helpful discussion.

#### References

1. Kato, T., Uchiyama, M., Maruo, N., Arai, T., Nishino, N. *Chem. Lett.* 144–145 (2000).
2. Maruo, N., Uchiyama, M., Kato, T., Arai, T., Akisada, H., Nishino, N. *Chem. Commun.* 2057–2058 (1999).

## Design of Analogs of Trapoxin, Cyl-1, and Chlamydocin for MHC Class-I Molecule Up-Regulation

Norikazu Nishino<sup>1,2</sup>, Tamaki Kato<sup>1,2</sup>, Yasuhiko Komatsu<sup>2,3</sup> and Minoru Yoshida<sup>2,4</sup>

<sup>1</sup>Department of Applied Chemistry, Faculty of Engineering, Kyushu Institute of Technology,  
 Kitakyushu, 804-8550, Japan

<sup>2</sup>CREST Research Project, Japan Science and Technology Corporation and

<sup>3</sup>Pharmaceuticals & Biotechnology Laboratory, Japan Energy Corporation, Toda,  
 335-8502, Japan

<sup>4</sup>Department of Biotechnology, The University of Tokyo, Tokyo, 113-8657, Japan

### Introduction

Hydroxamic acid analogs of trapoxin, Cyl-1, and chlamydocin have been designed and synthesized as targeting molecules toward histone deacetylases (HDAC) [1,2]. These analogs resemble each other except the configurations of component amino acids. Trapoxin analog has LLLD configuration from its functional amino acid (L-Asu(NHOH)), while Cyl-1 analog and chlamydocin analog have LDLL and LxLD configuration, respectively. In order to apply these HDAC inhibitors for the regulation of cell affiliation and cell cycles, the efficient transportation into the cell nucleus is important. Using an assaying method [3] in which up-regulation of MHC class-I molecule could be measured as a result of HDAC inhibition, we found more active stereoisomers than the natural cyclic tetrapeptides.

In this study, focusing on the cyclic peptide framework of trapoxin, we designed and synthesized a number of stereoisomers of trapoxin hydroxamic acid analogs. They were subjected to both HDAC inhibition assay and MHC class-I molecule up-regulating assay.

### Results and Discussion

The stereoisomers of trapoxin B having LDLD (**7**) and LDLL (**3**) configuration inhibited HDAC with almost same high potency (Table 1). The retro-enantio DLDL analog

*Table 1. Inhibition of HDAC1, expression of MHC class-I molecules, and retention times of stereoisomers of trapoxin hydroxamic acid analogs.*

		HDAC1 inhibitory activity (nM)	MHC 2-fold up- regulation (nM)	Retention time (min)
<b>1</b>	<i>cyclo</i> (-L-Asu(NHOH)-L-Phe-L-Phe-D-Pro-)	13	98	16.1
<b>2</b>	<i>cyclo</i> (-L-Asu(NHOH)-L-Phe-D-Phe-L-Pro-)	130	>10000	17.6
<b>3</b>	<i>cyclo</i> (-L-Asu(NHOH)-D-Phe-L-Phe-L-Pro-)	2.2	560	18.5
<b>4</b>	<i>cyclo</i> (-D-Asu(NHOH)-L-Phe-L-Phe-L-Pro-)	1300	>10000	15.4
<b>5</b>	<i>cyclo</i> (-L-Asu(NHOH)-L-Phe-D-Phe-D-Pro-)	160	>10000	17.4
<b>6</b>	<i>cyclo</i> (-L-Asu(NHOH)-D-Phe-D-Phe-L-Pro-)	35	>10000	28.6
<b>7</b>	<i>cyclo</i> (-L-Asu(NHOH)-D-Phe-L-Phe-D-Pro-)	1.9	3.0	20.2
<b>8</b>	<i>cyclo</i> (-L-Asu(NHOH)-D-Phe-D-Phe-D-Pro-)	42	>10000	17.4
<b>9</b>	<i>cyclo</i> (-D-Asu(NHOH)-L-Pro-D-Phe-L-Phe-)	2.0	75	18.4

### Biologically Active Peptides

(**9**) also inhibited HDAC with almost same activity (Table 1). Other stereoisomers (LLLD and LLDL *etc.*) showed obviously poor activity than those three. Conformational analysis by NMR and MM2 calculation showed that these stereoisomers with high-HDAC inhibition activity have nearly the same side chain deployment (Figure 1). Other isomers having poor HDAC inhibition activity arranged their side chains differently. In the case of Pro scanning, *cyclo*(-L-Asu(NHOH)-D-Pro-L-Phe-D-Phe-) showed almost a half HDAC inhibitory activity of *cyclo*(-L-Asu(NHOH)-D-Phe-L-Phe-D-Pro-) (data not shown).

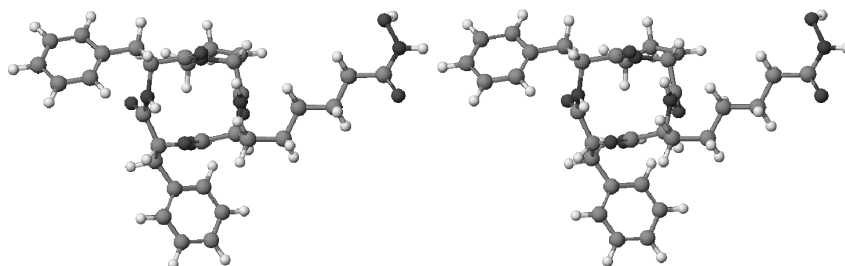


Fig. 1. Stereo drawing of *cyclo*(-L-Asu(NHOH)-D-Phe-L-Phe-D-Pro-) (**7**).

On the other hand, the isomer **7** having LDLD configuration showed nearly 200 times higher activity than the isomer **3** having LDLL configuration and 25 times higher activity than the retro-enantio LDLD analog **9** in the MHC assay. According to the HPLC retention time, isomer **7**, having high MHC activity, showed more hydrophobic nature than isomers **3** and **9**. This showed that the hydrophobicity of the cyclic tetrapeptide framework is also important for MHC activity.

### Acknowledgments

This work was supported by a research grant from the CREST Research Project, Japan Science and Technology Corporation.

### References

1. Furumai, R., Komatsu, Y., Nishino, N., Khochbin, S., Yoshida, M., Horinouchi, S. *Proc. Natl. Acad. Sci. USA* **98**, 87–92 (2001).
2. Komatsu, Y., Tomizaki, K.-Y., Tsukamoto, M., Kato, T., Nishino, N., Sato, S., Yamori, T., Tsuruo, T., Furumai, R., Yoshida, M., Horinouchi, S., Hayashi, H. *Cancer Res.* **61**, 4459–4466 (2001).
3. Komatsu, Y., Hayashi, H. *J. Antibiot.* **51**, 89–91 (1998).

## Backbone Assignment of Gyrase-B P24 Fragment and Its Interactions with the Inhibitor GR122222

Massimo Bellanda<sup>1</sup>, Stefano Mammi<sup>1</sup>, Evaristo Peggion<sup>1</sup>,  
Gottfried Otting<sup>2</sup>, Johan Weigelt<sup>2</sup>, Elisabetta Perdonà<sup>3</sup>, Enrico Domenici<sup>3</sup>  
and Carla Marchioro<sup>3</sup>

<sup>1</sup>Department of Organic Chemistry, University of Padova and Biopolymers Research Center,  
C.N.R., I-35131 Padova, Italy

<sup>2</sup>Department of Medical Biochemistry and Biophysics, Karolinska Institute, S-171 77,  
Stockholm, Sweden

<sup>3</sup>GlaxoSmithKline Research Center, I-37100, Verona, Italy

### Introduction

DNA topoisomerases are ubiquitous enzymes that control the topological state of DNA in cells. There are several classes of topoisomerases, each with distinct properties. Among them, bacterial DNA-gyrase is able to introduce negative supercoils into DNA in a reaction coupled to hydrolysis of ATP [1]. Gyrase is essential in all bacteria but it is not found in eukaryotes and is therefore a good target for antibiotics. Gyrase consists of 2 subunits GyrA and GyrB, the active enzyme being an A<sub>2</sub>B<sub>2</sub> complex. The ATPase reaction takes place in the B subunit and binding sites of different inhibitors have been localized in the N-terminal 24 kDa fragment of GyrB (P24). The X-ray structures of this fragment complexed with different ligands have been published [2] but structural studies in solution are scarce [3]. NMR provides useful tools to study the interactions of a protein with small substrates in solution but the first, demanding step required for this approach is the assignment of resonances, which must be achieved at least in part. In the present work, the fragment P24 from *E. coli* was investigated by heteronuclear NMR, both in the free form and as a complex with the cyclothialidine GR122222 [4] (Figure 1).

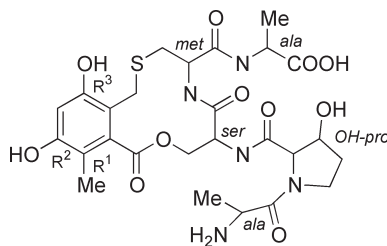


Fig. 1. Structure of GR122222.

### Results and Discussion

Triple resonance NMR experiments were initially performed on <sup>15</sup>N, <sup>13</sup>C uniformly labeled protein but the quality of the spectra proved to be very poor due to line broadening and only 20% of backbone resonances were unambiguously assigned using this sample. In order to overcome this problem, triply labeled protein (100% <sup>15</sup>N, 100% <sup>13</sup>C, 75% <sup>2</sup>H) was prepared. With this sample, the extent of the assignments is the following: 92% <sup>1</sup>H, <sup>15</sup>N of amide groups, 92% <sup>13</sup>CO, 90% <sup>13</sup>C<sup>α</sup>, 76% <sup>1</sup>H<sup>α</sup>, 78% <sup>13</sup>C<sup>β</sup>. The amide groups of some residues remain to be assigned, including the first 8 residues, I94, M95, L98, H99, G102, I134, Q135, H141, E183. The assigned <sup>15</sup>N-HSQC of the 24 kDa N-terminal gyrase B is shown in Figure 2.

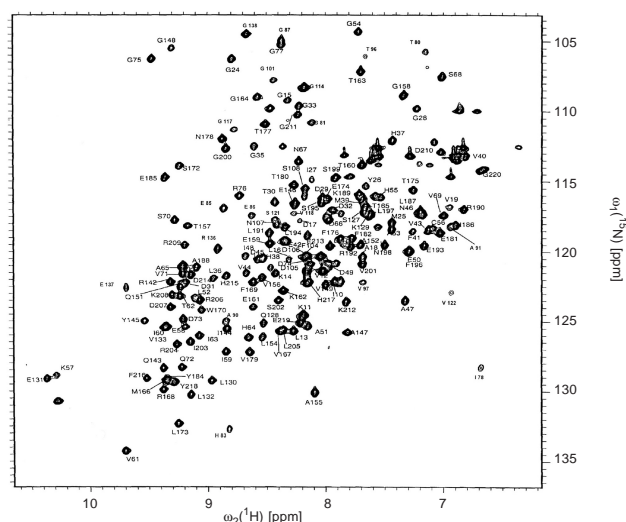


Fig. 2.  $^{15}\text{N}$ -HSQC of the 24 kDa N-terminal fragment of DNA gyrase B from *E. coli* recorded at 800 MHz. Only assignment of backbone amide groups is shown.

Secondary structural elements were estimated on the basis of Chemical Shift Index (CSI) [5] for  $^1\text{H}^\alpha$ ,  $^{13}\text{C}^\alpha$ ,  $^{13}\text{CO}$ ,  $^{13}\text{C}^\beta$  and a substantial agreement with the X-ray structure of the complexes with Novobiocin [2] and GR122222 [2] was found. The N-terminal helices seem to be less defined in solution. Long range NOEs detected in NOESY- $^{15}\text{N}$ -HSQC spectrum show the same topology for the  $\beta$  sheet as in the X-ray structure.

A significant shift of a large number of peaks in the  $^{15}\text{N}$ -HSQC spectrum was observed upon binding of GR122222. A new set of 3D heteronuclear experiments was acquired to allow assignment of this spectrum and 90% of the amide groups were assigned for the complex. Differential line-broadening was observed with respect to the spectrum of the free protein, indicating a different dynamic behavior of the backbone after binding of the ligand. In order to map the binding surface of the pentapeptide on the enzyme fragment, a weighted average chemical shift difference was calculated for the amide groups. Six of the assigned residues exhibit a shift larger than 3 standard deviations from the average and 15 others a shift between  $\sigma$  and  $3\sigma$ . Almost all these residues are clustered in a region comprising the crystallographic binding site. Comparison with the X-ray structure shows that, among the residues exhibiting a significant shift, V43, A47, G77, I78 are hydrophobic amino acids lining the ligand binding site while, N46, D73, H136 and T165 are involved in hydrogen bonding with GR122222.

## References

1. Wigley, D.B. *Annu. Rev. Biophys. Biomol. Struct.* **24**, 185–208 (1995).
2. Lewis, R.J., Singh, O.M., Smith, C.V., Skarzynski, T., Maxwell, A., Wonacott, A.J., Wigley, D.B. *EMBO J.* **15**, 1412–1420 (1996).
3. Klaus, W., Ross, A., Gsell, B., Senn, H. *J. Biomol. NMR* **16**, 357–358 (2000).
4. Oram, M., Dosanjh, B., Gormley, N.A., Smith, C.V., Fisher, L.M., Maxwell, T., Duncan, K. *Antimicrob. Agents Chemoter.* **40**, 473–476 (1996).
5. Wishart, D.S., Sykes, B.D. *J. Biomol. NMR* **4**, 171–180 (1994).

## Synthetic Progress Towards a TMC-95 Analogue as a Potential Proteasome Inhibitor

M. Angels Estiarte, Amy M. Elder and Daniel H. Rich

Department of Chemistry, University of Wisconsin-Madison, Madison, WI 53706, USA

### Introduction

Recently, four novel compounds, TMC 95A-D **1** ( $R_1, R_2 = \text{H or OH}$ ;  $R_3, R_4 = \text{H, OH or CH}_3$ ), have been isolated from the fermentation broth of *Apiospora montagnei* Sacc. TC 1093 [1,2], and shown to inhibit the 20S proteasome ( $\text{IC}_{50} = 5.4\text{--}60\text{ nM}$ ), an eukaryotic threonine protease responsible for the degradation of most cell proteins [3]. Increased levels of this enzyme and subsequent protein breakdown have been related to different diseases such as malaria, inflammation and cancer. Thus, inhibition of the proteasome is currently becoming a promising therapeutic target. In this work, we describe the synthetic approaches towards the synthesis of a novel indole analog **2** of the core of **1** to evaluate its possible activity as a proteasome inhibitor (Figure 1).

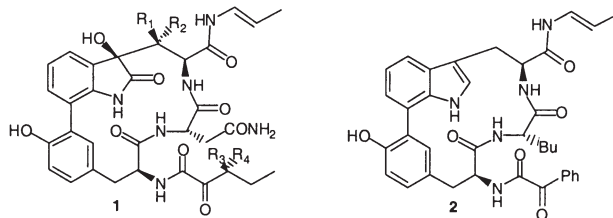


Fig. 1. Structure of TMC-95 and of the simplified analogue.

### Results and Discussion

Previously, we described the synthesis of the 16-membered DEF ring system of chloropeptin by using a biomimetic ring contraction of the 17-membered DEF ring system of complestatin. In acidic media, the biaryl junction migrates from the 6 to the 7 position of the indole ring. In order to evaluate the effect of the ring size on this migration, we decided to synthesize the TMC 95A-D analogue **2** (Figure 2).

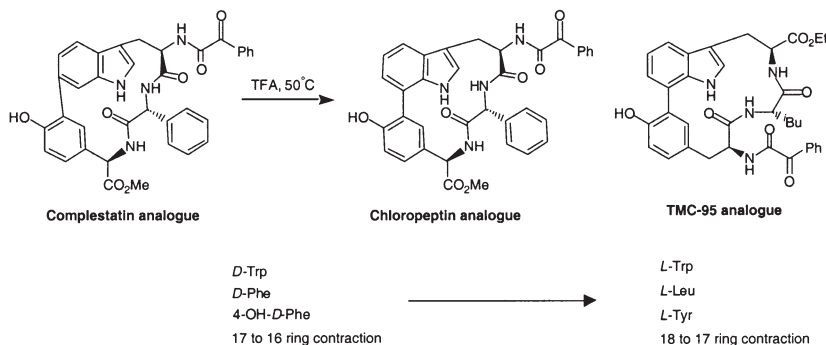
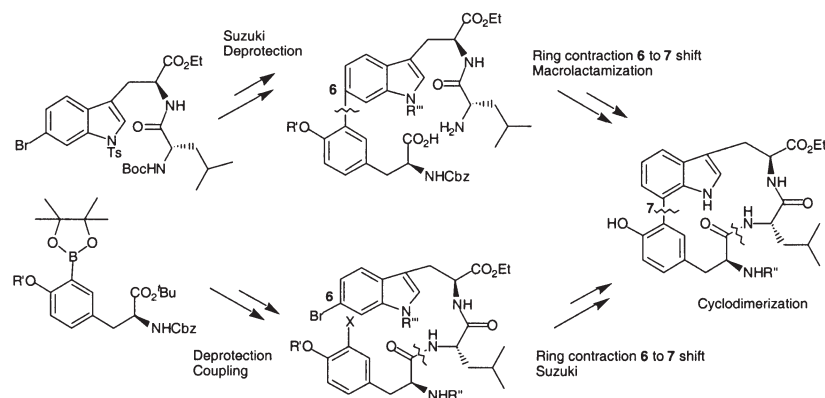


Fig. 2. Structural comparison of complestatin and chloropeptin with TMC-95 analogue.

## Biologically Active Peptides

One route utilizes a macrolactamization as the last step of the synthesis, while the second one utilizes an intramolecular palladium-catalyzed ring closure to the 18-membered ring system. The synthesis of the 18-membered ring proved to be more troublesome and, under high dilution conditions, tend to cyclodimerize easily.



Scheme 1. Synthetic approaches of the TMC-95 analogue.

## Acknowledgments

Supported by Spanish Government (M. A. E.) and NIH (GM 50113).

## References

1. Wójcik, C. *Drug Discov. Today* **4**, 188 (1999).
2. (a) Koguchi, Y., Kohno, J., Nisshio, M., Takahashi, K., Okuda, T., Komatsubara, S.J. *J. Antibiot.* **53**, 105 (2000). (b) Kohno, J., Koguchi, Y., Nisshio, M., Nakao, K., Kuroda, M., Shimizu, R., Ohnuki, T., Komatsubara, S.J. *J. Org. Chem.* **65**, 990 (2000).
3. (a) Ma, D., Wu, Q. *Tetrahedron Lett.* **41**, 9089 (2000). (b) Albrecht, B.K., Williams, R.M. *Tetrahedron Lett.* **42**, 2755 (2001). (c) Lin, S., Danishefsky, S.J. *Angew. Chem., Int. Ed.* **40**, 1967 (2001).
4. (a) Elder, A.M., Rich, D.H. *Org. Lett.* **1**, 1443 (1999). (b) Elder, A.M., Rich, D.H. *Org. Lett.* 2001, submitted.

## **Prime Site Binding Inhibitors of the Hepatitis C Virus NS3/4A Serine Protease**

**Elisabetta Bianchi, Paolo Ingallinella, Daniela Fattori, Sergio Altamura,  
Christian Steinkühler, Daniel Cicero, Renzo Bazzo,  
Riccardo Cortese and Antonello Pessi**

*Istituto di Ricerche di Biologia Molecolare P. Angeletti (IRBM), 00040 Pomezia (RM), Italy*

### **Introduction**

Infection by hepatitis C virus (HCV) is a leading cause of cirrhosis and liver cancer. Much effort for a therapy is currently devoted to the search of inhibitors of the serine protease NS3/4A, which is required for maturation of viral polyprotein.

For serine proteases in general, and NS3/4A in particular, the main determinants of ground-state substrate binding reside in the P-region [1]. Accordingly, potent peptide inhibitors derived from the cleaved substrate ("product inhibitors") have been developed [2]. By contrast, the P' region of the substrate, while being important for catalysis, contributes little to ground state binding [1]. This notwithstanding, binding pockets exist in the S' region, which can be exploited for active site-directed inhibition. We were recently able to develop subnanomolar decapeptide inhibitors, spanning the prime and non-prime subsites of the enzyme [3]. In addition to a previously optimized P<sub>6</sub>-P<sub>1</sub> sequence [2], these inhibitors include a P<sub>2</sub>'-P<sub>4</sub>' tripeptide fragment, which contributes >2000-fold gain in potency. While the binding mode of the non-prime fragment was found to be similar to the natural substrates, novel interactions were present in the prime site tripeptide. We therefore set to exploit these interactions for inhibitor design.

### **Results and Discussion**

Our strategy for the development of prime site-binding inhibitors was to combine two elements: i) the optimized tripeptide fragment from the above decapeptides, and ii) a fragment containing a carboxylic acid. In our design, this moiety would take advantage of interactions in the active site, similar to those previously established for the C-terminal carboxylate of peptide product inhibitors [3]. To select the right moiety we prepared a small combinatorial library of tripeptides, capped with a variety of constrained and unconstrained diacids, as shown in Figure 1. While a control library, based on the non-optimized P<sub>2</sub>'-P<sub>4</sub>' fragment of the NS4A/4B cleavage site (-Ser-His-Leu-NH<sub>2</sub>), did not yield any active compound, the combination of the optimized -Cha-Asp-Leu-NH<sub>2</sub> tripeptide with the cyclic diacid fragment X<sub>14</sub> (Figure 1) yielded an inhibitor with IC<sub>50</sub> = 54 μM. We then prepared multiple analogs of the initial lead, where we further investigated the N-terminal cyclic diacid, the side chains in position P<sub>2</sub>' and P<sub>3</sub>' and the C-terminal carboxyamide. The resulting SAR is summarized in Figure 2. The main features present in the prime region of the decapeptides [3] were maintained in these inhibitors. The optimal P<sub>2</sub>' residues were β-cyclohexylalanine (Cha) or phenylglycine (Phg), while a negative charge was required in P<sub>3</sub>'. Site-directed mutagenesis of the two potential basic contacts for this acid, Lys<sup>136</sup> and Arg<sup>109</sup>, indicated that the latter was responsible for the P<sub>3</sub>' preference, as observed for the decapeptide series [3]. The N-terminal carboxylate was also critical and could not be deleted nor neutralized. A tight SAR was observed for the cyclic moiety bearing the acid: only few fragments resulted in active compounds (Figure 2), 1,2-*trans*-cyclohexanedicarboxylic acid being the most potent (IC<sub>50</sub> = 15 μM).

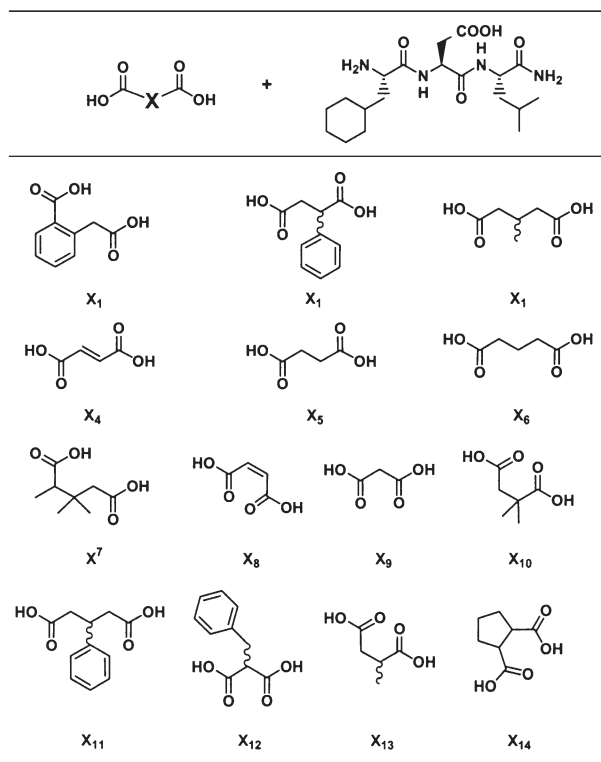


Fig. 1. Diacid building blocks used in the assembly of the prime-site inhibitor library. Due to the presence of isomers, a total of 26 different compounds were prepared.

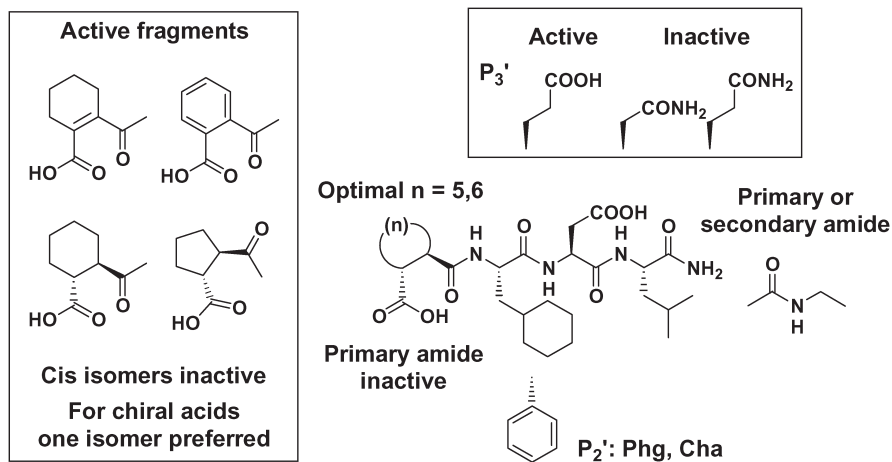


Fig. 2. Summary of the general features of SAR for the prime site-binding inhibitor selected from the combinatorial library.

In addition to the similarities with the decapeptide SAR, further proof of success for our design came from NMR experiments. Titration of the  $^{15}\text{N}$ -labeled enzyme with a representative inhibitor produced chemical shift variations of both the  $^1\text{H}$  and  $^{15}\text{N}$  nuclei of the backbone amide group, which were used to map the interaction surface between the enzyme and the inhibitor. This surface was found to include, as expected, the active site and the prime site of the protease.

In conclusion, the strategy and the compounds described here represent a promising new approach to inhibition of NS3/4A. Further optimization of the inhibitors with concomitant reduction of peptide character is in progress, and will be reported elsewhere. In addition, we wish to highlight that, unlike the several prime-site inhibitors developed for metalloproteases, the current work represents the first example of prime-site inhibitors of a *serine* protease. We believe it conceivable, to extend the course of action, used here for NS3/4A, to other enzymes. The needed starting point, a non-cleavable substrate analog, can be easily obtained by simply substituting the  $\text{P}_1'$  residue with proline or a D-amino acid [4]. The critical choice of the proper active site-binding fragment will of course depend on the particular enzyme under study. Interaction of a peptide carboxylate in the active site has been observed for other serine proteases, like thrombin and Sindbis virus protease [5], thus making an acidic moiety (akin to the NS3/4A case) a viable option.

A classical “serine trap” might be more indicated for other proteases, especially those displaying a “lock-and-key” catalytic machinery. In any case, combinatorial search of the best fragment should be used, to compensate for the inevitable uncertainties of the specific design.

### **Acknowledgments**

We wish to thank Victor G. Matassa and Raffaele De Francesco for useful criticism and discussion throughout this work.

### **References**

1. Urbani, A., Bianchi, E., Narjes, F., Tramontano, A., De Francesco, R., Steinkühler, C., Pessi, A. *J. Biol. Chem.* **272**, 9204 (1997).
2. Ingallinella, P., Altamura, S., Bianchi, E., Taliani, M., Ingenito, R., Cortese, R., De Francesco, R., Steinkühler, C., Pessi, A. *Biochemistry* **37**, 8906 (1998).
3. Ingallinella, P., Bianchi, E., Ingenito, R., Koch, U., Steinkühler, C., Altamura, S., Pessi, A. *Biochemistry* **39**, 12898 (2000).
4. Meldal, M., Svendsen, I., Juliano, L., Juliano, M.A., Del Nery, E. Scharfstein, J. *J. Peptide Sci.* **4**, 83 (1998).
5. Steinkühler, C., Biasiol, G., Brunetti, M., Urbani, A., Koch, U., Cortese, R., Pessi, A., De Francesco, R. *Biochemistry* **37**, 8899 (1998).

## Solution and Solid Phase Synthesis of Non-Peptide Peptidomimetic Aspartic Peptidase Inhibitors

Matthew G. Bursavich<sup>1</sup> and Daniel H. Rich<sup>1,2</sup>

<sup>1</sup>Department of Chemistry; <sup>2</sup>School of Pharmacy, University of Wisconsin-Madison, Madison, WI 53706, USA

### Introduction

A major research goal of medicinal chemistry is to design completely non-peptide scaffolds that mimic the topography and function of peptide-derived inhibitors. Researchers at Roche-Basel recently discovered novel topographical peptidomimetic inhibitors of the aspartic peptidases renin and plasmepsin based on a piperidine scaffold [1]. The aspartic peptidases are the current therapeutic targets for a variety of human diseases including AIDS, Alzheimer's disease, hypertension, and malaria. Consequently, the screening-based discovery of these non-peptide peptidomimetics constitutes a major advance for the development of medicinal compounds to treat these disease states. We have used the structure-generating program Growmol [2] to rationally design the related piperidine analogs **1** and **2** (Figure 1) that inhibit *Rhizopus chinensis* and porcine pepsin ( $IC_{50}$  2 and 0.2  $\mu$ M, respectively), two aspartic peptidases not inhibited in the Roche reports. We developed enantioselective syntheses of the piperidine scaffolds as well as a solid supported traceless functionalization method to provide quick access to analogs of these non-peptide peptidomimetic inhibitors.

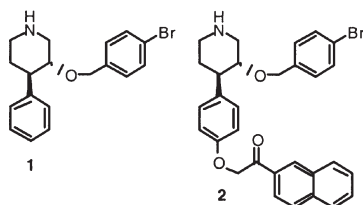
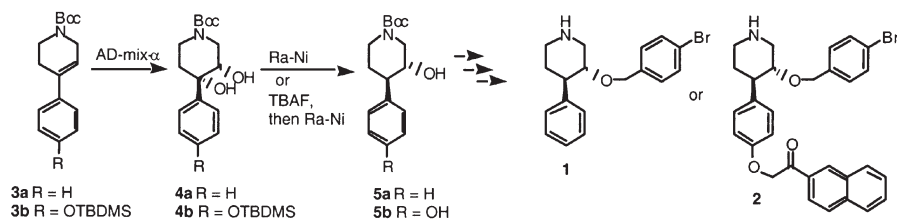


Fig. 1. Growmol generated piperidine-based aspartic peptidase inhibitors.

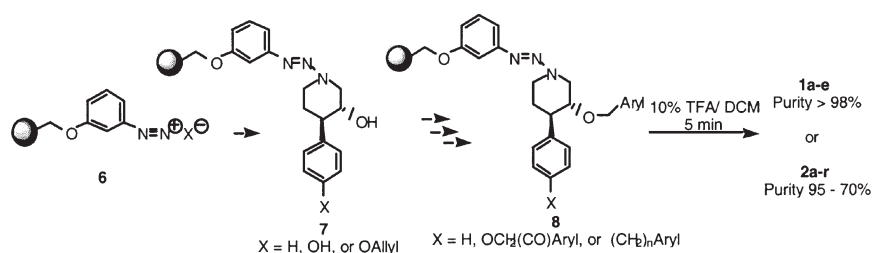
### Results and Discussion

We have developed a solid phase method to rapidly synthesize libraries of piperidine **1** and **2** analogs needed for further biological studies. The requisite piperidines **5** were first synthesized in solution *via* a two step process (Scheme 1) from the tetrahydropyridines **3** using Sharpless asymmetric dihydroxylation [3] followed by stereoselective reduction of the benzylic alcohol of **4** with Raney-nickel [4].



Scheme 1.

The solid phase synthesis utilized a traceless triazene linker strategy first reported by Brase and coworkers for amines [5]. The piperidine cores were reacted with the diazonium resin **6**, prepared in two steps from Merrifield resin, to generate the solid supported triazene **7**. Following subsequent functionalizations to generate **8** the piperidine-based aspartic peptidase inhibitors were liberated from the resin with a traceless cleavage in mild acid to afford **1a-e** or **2a-r** in both high yields and purities (Scheme 2). In those cases of lesser purity (<80%) the final products were further purified using a solid phase extraction method [6]. These piperidine analogs are currently under evaluation as potential inhibitors for a variety of therapeutically interesting aspartic peptidases. Interestingly, these piperidines are structurally related to the CNS active drug paroxetine and as such may become especially important at inhibiting aspartic peptidases located within the CNS.



Scheme 2.

### Acknowledgments

We thank Dr. George Flentke for providing *R. chinensis* pepsin and initial assistance with the biological assays, Dr. Chris West, Ken Satyshur and Regine Bohacek for assistance with molecular modeling, and Dr. Colin McMartin for the use of his software Flo-01. Supported by NIH (GM50113).

### References

- Oefner, C., Binggeli, A., Breu, V., Bur, D., Clozel, J.P., D'arcy, A., Dorn, A., Fischli, W., Gruninger, F., Guller, R., Hirth, G., Marki, H., Mathews, S., Miller, M., Ridley, R.G., Stadler, H., Viera, E., Wilhelm, M., Winkler, F., Wostl, W. *Chem. Biol.* **6**, 127–131 (1999).
- Bohacek, R.S., McMartin, C., Guida, W.C. *Med. Res. Rev.* **16**, 3–50 (1996).
- Sharpless, K.B., Amberg, W., Bennani, Y.L., Crispino, G.A., Hartung, J., Jeong, K.S., Kwong, H.L., Morikawa, K., Wang, Z.M., Xu, D., Zhang, X.L. *J. Org. Chem.* **57**, 2768–2771 (1992).
- Cope, A.C., McKervey, M.A., Weinshenker, N.M., Kinnel, R.B. *J. Org. Chem.* **35**, 2918–2923 (1970).
- Brase, S., Kobberling, J., Enders, D., Lazny, R., Wang, S., Brandtner, S. *Tetrahedron Lett.* **40**, 2105–2108 (1999).
- Parlow, J.J., Devraj, R.V., South, M.S. *Curr. Opin. Chem. Biol.* **3**, 320–326 (1999).

## Design and Synthesis of Novel Matrix Metalloproteinase Inhibitors

Jiayi Xu, Ding Wang and Qihan Zhang

College of Chemistry and Molecular Engineering, Peking University,  
 Beijing 100871, P.R. China

### Introduction

The matrix metalloproteinase (MMP) family includes the collagenases, gelatinases, and stromelysins [1,2]. MMPs are necessary for tissue remodeling and the healing cascade. However, the overexpression of MMP activity or the presence of MMP activity in healthy and uninjured areas can contribute to the pathophysiology of a variety of disease states and conditions [2]. In addition to tissue destruction and remodeling, MMPs are known to be essential for the growth of new blood vessels. This process of angiogenesis is essential for the vascularization and growth of tumors. Consequently, MMP inhibitors (MMPIs) are currently under investigation for their utility in slowing or halting the progression of tumor growth and metastasis.

### Results and Discussion

The MMPs are a family of zinc-binding metalloendopeptidases capable of degrading extracellular matrix components, including collagen, gelatin, myelin, laminin, fibronectin, and elastin. Recent X-ray crystallographic analyses of MMPs, with and without bound inhibitors [3], and *in vitro* SAR studies showed that the dipeptide-mimetic core of a hydroxamic acid based MMPIs are effective [4]. Based on these results novel MMPIs **1** containing sulfur, which is a favorable atom to coordinate to zinc, have been designed and synthesized. The synthetic approach is presented in Figure 1.

2-Thioalkyl/aryl succinic anhydrides **2** were prepared in yields ranging from 46 to 87.5% through Micheal addition of isopropanethiol or thiophenol to maleic anhydride in the presence of triethylamine. 2-Thioalkyl/aryl succinic acid monoesters **3**, which serve as structural mimetics of valine and phenylalanine, were obtained by selective alcoholysis with methanol or isopropanol.

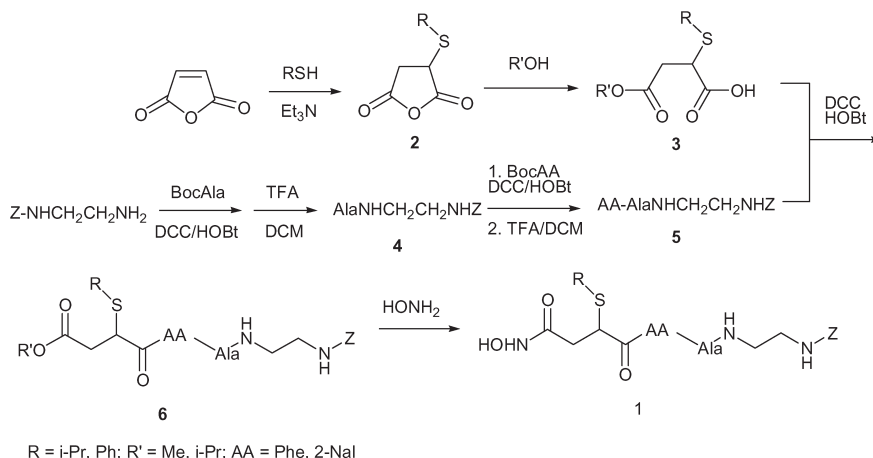


Fig. 1. Synthesis of novel matrix metalloproteinase inhibitors.

*Xu et al.*

*N*-Alanyl-*N'*-benzyloxycarbonyl-1,2-ethylenediamine **4** was synthesized from Boc-L-alanine and *N*-benzyloxycarbonyl-1,2-ethylenediamine in 85% yield. It was coupled to Boc-protected amino acids (L-phenylalanine and L-2-naphthylalanine) to yield dipeptide amide derivatives **5**. After coupling the dipeptides **5** with succinic monoester **3** and aminolysis with hydroxylamine, desired matrix metalloproteinase inhibitors **1** were obtained in satisfactory yields (summarized in Table 1). Bioassays on their inhibitory activity is in progress.

Table 1. Synthetic novel matrix metalloproteinase inhibitors.

Inhibitors	Yield (%)	
	R = i-Pr	R = Ph
HONHCOCH <sub>2</sub> CH(SR)COPheAlaNHCH <sub>2</sub> CH <sub>2</sub> NHZ	63	81
HONHCOCH <sub>2</sub> CH(SR)CONalAlaNHCH <sub>2</sub> CH <sub>2</sub> NHZ	42	47

### Acknowledgments

This work has been supported by grant 29772002 (NSFC).

### References

1. Morphy, J.R., Millican, T.A., Porter, J.R. *Curr. Med. Chem.* **2**, 743–762 (1995).
2. Wang, D., Xu, J.X. *Chem. Life* **19**, 189–192 (1999).
3. Dhanaraj, V., Ye, Q.Z., Johnson, L.L., Hupe, D.J., Ortwine, D.F., Dubar, J.B., Rubin, J.R., Pavlovsky, A., Humblet, C., Blundell, T.L. *Structure* **4**, 375–386 (1996).
4. Levy D.E., Lapierre, F., Liang, W.S., Ye, W.Q., Lange, C.W., Li, X.Y., Grobelny, D., Casabonne, M., Tyrrell, D., Holme, K., Nadzan, A., Galardy, R.E. *J. Med. Chem.* **41**, 199–223 (1998).
5. Xu, J.X., Wang, D., Zhang, Q.H., Huang, A.J. *Rapid Commun. Mass Spectrom.* **14**, 1746–1750 (2000).

## A Novel Continuous Assay for the Mechanistic Characterization of Histone Deacetylases and Homologues Using a Small Molecule Fluorescent Substrate

Jennifer L. Gronlund<sup>1</sup>, Michael K. Yu<sup>1</sup>, A. Melissa Concepcion<sup>1</sup>, Shu He<sup>1</sup>, Ravi Venkataramani<sup>1,2</sup>, Ronen Marmorstein<sup>1,2</sup> and Dewey G. McCafferty<sup>1</sup>

<sup>1</sup>The Department of Biochemistry and Biophysics and the Johnson Research Foundation

<sup>2</sup>The Department of Chemistry and the Wistar Institute, University of Pennsylvania, Philadelphia, PA 19104-6059, USA

### Introduction

DNA associated with histone proteins is organized into nucleosomes, which are then arranged into higher-order structures known as chromatin. The N-terminal tails of histone proteins are the sites of many different types of modifications including acetylation, phosphorylation, ubiquitination, and methylation, each of which plays a role in the dynamic remodeling of chromatin [1]. Acetylation of the  $\epsilon$ -amino group of specific lysine residues achieved by histone acetyltransferase (HAT) enzymes results in transcriptional activation and gene expression. Hyperacetylation is believed to enable transcription factors access to the DNA by neutralizing the positive charge on lysine residues that promotes tight association with the negatively charged phosphate backbone of DNA. On the other hand, hypoacetylation mediated by histone deacetylase (HDAC) enzymes is associated with repression of gene expression and the maintenance of transcriptionally silent chromatin. There are three different classes of HDAC enzymes, with class I/II being zinc dependent metallohydrolases and class III being NAD<sup>+</sup>-dependent transacetylases [2]. Hos3 is a prototypical member of the class I/II zinc dependent HDACs from *Saccharomyces cerevisiae*. HDACs have been shown to interact with, or be recruited by, many well-known tumor suppressors and oncogenes [3]. As a result, inhibitors of the HDAC function have been shown to be effective therapeutic agents for the treatment of human cancers [4,5].

### Results and Discussion

We have developed a novel continuous assay to study the catalytic hydrolytic mechanism of histone deacetylases by fluorescence spectrophotometry. 7-Acetoxycoumarin (7AC) was synthesized by acetylation of 7-hydroxycoumarin with acetic anhydride/pyridine (93% yield) and employed as a small molecule substrate to create the first continuous fluorescent assay for assessment of HDAC activity. Upon hydrolysis of the acetate ester, the 7-hydroxycoumarin fluorophore is released with a concomitant gain in solution fluorescence ( $\lambda_{\text{ex}} = 332 \text{ nm}$ ;  $\lambda_{\text{em}} = 447 \text{ nm}$ ) (Figure 1). The steady state kinetic parameters of yeast Hos3, as well as human HDAC2, AcuC1 (a closely-related HDAC homologue from *Aquifex aeolicus*), have been determined. All showed

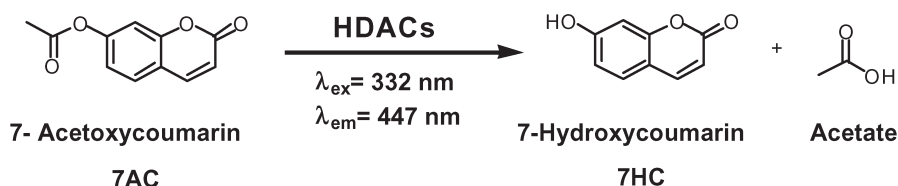


Fig. 1. A continuous fluorescent assay for assesment of HDAC activity.

similar  $K_M$  values against this substrate ranging from 74 to 88  $\mu\text{M}$ , while their respective  $k_{\text{cat}}$  values spanned 2 orders of magnitude, with human HDAC 2 exhibiting the lowest activity. Slight substrate inhibition was observed at substrate concentrations greater than 400  $\mu\text{M}$ .

This continuous assay was employed to further characterize the catalytic mechanism of yeast Hos3 using pH profile, solvent deuterium kinetic isotope effect, and proton inventory studies. The pH dependence of  $k_{\text{cat}}$  was bell-shaped and revealed the presence of two catalytically important ionizable groups at  $\text{p}K_A$  7.2 and  $\text{p}K_B$  8.9. Hos3 exhibited a normal solvent deuterium kinetic isotope effect with  $^{D_2O}V = 2.23$  and  $^{D_2O}V/K = 1.59$ . Further proton inventory measurements were conducted by varying the mole fraction of  $D_2O$  between 0 and 0.99 in 0.1 mol increments. Gross-Butler analysis of the inventory data revealed a linear slope consistent with a mechanistic interpretation of one in-flight proton transferred in the rate determining transition state.

The validity of 7AC as a surrogate substrate for Hos3 was examined by inhibition studies with known HDAC inhibitors trichostatin A (TSA) and butyrate (NaB) as well as with competition assays using a histone H4-derived acetylated peptide (residues 1-24). As anticipated, NaB displayed mixed-type inhibition with a  $K_i$  value of 12 mM. Trichostatin A was determined to be a tight-binding competitive inhibitor with a  $K_i$  value of 180 nM. Interestingly, histone H4 (1-24) hyperacetylated peptide showed apparent noncompetitive inhibition with a  $K_i$  value of 50  $\mu\text{M}$ . The magnitude of the observed  $K_i$  values are in accordance with literature reports. These data support the utility of 7AC as a substrate for evaluation of the catalytic mechanism of HDACs and for discovery of novel inhibitors *via* high-throughput methods.

## References

1. Spencer, V., Davie, J. *Gene* **240**, 1–12 (1999).
2. Gray, S., Ekstrom, T. *Exp. Cell Res.* **262**, 75–83 (2001).
3. Cress, W., Seto, E. *J. Cell. Physiol.* **184**, 1–16 (2000).
4. Marks, P., Richon, V., Rifkind, R. *J. Natl. Cancer Inst.* **92**, 1210–1216 (2000).
5. Vigushin, D., Ali, S., Pace, P., Mirsaidi, N., Ito, K., Adcock, I., Coombes, R. *Clin. Cancer Res.* **7**, 971–976 (2001).

## Peptide Inhibitors of $\alpha$ -Amylase Based on Tendamistat: Synthesis and Kinetic Studies

Deborah Heyl, Leo Lucas, Rebecca Himm, Jennifer Kappler,  
Jason Groom, Jeffrey Asbill, Jon Nzoma, Janice Lima and Mary Gillispie

Department of Chemistry, Eastern Michigan University, Ypsilanti, MI 48197, USA

### Introduction

Tendamistat is a tight-binding pseudo-irreversible inhibitor of mammalian  $\alpha$ -amylases with a KI value of  $9 \cdot 10^{-12}$  M [1,2]. The crystal structure of the  $\alpha$ -amylase-Tendamistat complex has been elucidated by X-ray techniques and nuclear magnetic resonance spectroscopy [3,4], revealing that only 15 of the 74 amino acids in the inhibitor (in 4 segments, shown below) actually interact directly with the enzyme binding site *via* hydrogen bonding and hydrophobic and electrostatic forces [5]. Our goal was to design smaller analogs of Tendamistat, which might be less immunogenic.

Segment 1: Tyr<sup>15</sup> Trp<sup>18</sup> Arg<sup>19</sup> Tyr<sup>20</sup>    Segment 2: Leu<sup>44</sup> Tyr<sup>46</sup>  
Segment 3: Gln<sup>52</sup> Ile<sup>53</sup> Thr<sup>54</sup> Thr<sup>55</sup>    Segment 4: Asp<sup>58</sup> Gly<sup>59</sup> Tyr<sup>60</sup> Ile<sup>61</sup> Gly<sup>62</sup>

### Results and Discussion

Our first target compounds (I and II, Figure 1) were comprised of all four segments. The N-terminus was acetylated and the C-terminus amidated to eliminate the unnaturally proximate charges in the peptide backbone. Novel "linker"  $\omega$ -amino acids were employed to connect the segments. However, these larger analogs precipitated in the test tube in the aqueous spectrophotometric activity assay.

We therefore designed slightly smaller analogs of 13 to 15 amino acids (III–VI, Figure 1), which retain what we feel are the barest essential elements of the structure of Tendamistat, with segment 2 and most of segment 3 cut out to improve solubility.

I: Ac-Y- **$\beta$ Ala**-WRY-**Ahx**-LSY-**Ahx**-QITT- **$\beta$ Ala**-DGYIG-NH<sub>2</sub>  
II: Ac-YQSWRY-**Ahx**-LSY-Ahx-QITTVGDGYIG-NH<sub>2</sub>  
III: Ac-YQSWRY- $\gamma$ **Abu**-TVGDGYIG-NH<sub>2</sub>  
IV: Ac-Y-**Ava**-WRY- $\gamma$ **Abu**-T-**Ava**-DGYIG-NH<sub>2</sub>  
V: Ac-Y-**Oct**-WRY-Ahx-T-**Oct**-DGYIG-NH<sub>2</sub>  
VI: Ac-YQSWRY-**Ahx**-TVGDGYIG-NH<sub>2</sub>

Fig. 1. Sequences of peptide inhibitors I–VI, with linkers in bold; abbreviations:  $\beta$ -alanine,  $\beta$ Ala;  $\gamma$ -aminobutyric acid,  $\gamma$ Abu; 6-aminohexanoic acid, Ahx; 5-aminopentanoic acid or aminovaleric acid, Ava; 8-aminooctanoic acid, Oct.

These analogs retain the required conserved Trp<sup>18</sup>Arg<sup>19</sup>Tyr<sup>20</sup> binding segment and other homologous amino acids (Thr<sup>55</sup>, Gly<sup>59</sup>, Tyr<sup>60</sup>) from related protein amylase inhibitors isolated from plant and bacterial species [5]. Since segment 4 helps to stabilize the important Trp-Arg-Tyr triplet [5], surrounding amino acids in segment 4 were also preserved. Distances between the binding segment pieces included in the inhibitor peptides were approximated with novel  $\omega$ -amino acids of similar length. In some cases, native dipeptide spacers were left intact, since their side chains may confer topographical influences. Linkers in V and VI are longer, to allow for more conformational flexibility and coiling in solution.

### Heyl et al.

Mean  $V_{\max}$  and  $K_m$  values ( $n = 24$ ) for  $\alpha$ -amylase in our assay system are  $1.21 \cdot 10^{-6}$  M/min and 9.63 mM, respectively. The smaller analogs III–VI inhibit the enzyme in the micromolar to millimolar range (Table 1), though not all data fit the expected kinetic model. In fact, only V, which was tested at low concentration, exhibits competitive inhibition; the others are uncompetitive. Inhibition is more pronounced at lower peptide analog concentrations, which may result from improved solubility. Plots of substrate concentration vs velocity for individual runs of some analogs appear sigmoidal in shape, indicating a possible allosteric effect. Moreover, early results suggest that the inhibitors may have different effects on the enzyme at different concentrations, perhaps fitting a two-site binding model. Visual observation, however, provides clear qualitative evidence of enzyme inhibition, as tubes containing the inhibitor are distinctively less yellow in color than the tubes without inhibitor. The most effective analogs thus far appear to be those that contain three linkers, rather than those retaining the native dipeptide spacers at two positions. Studies are underway at several different inhibitor, substrate and enzyme concentrations to further characterize the nature of the interaction.

Table 1. Physicochemical and kinetic data<sup>a</sup> for peptide inhibitors.

Compound	Mol. W.	Purity (%)	$K_I$ (nM)	Number of trials	Conc. of analog tested (nM)
I	2409.4	95	N.D.	–	–
II	2637.9	96	N.D.	–	–
III	1790.4	99	0.618	5	0.50–1.0
IV	1617.5	99	0.0316	5	0.25–0.50
V	1727.5	99	0.0287	3	0.020–0.10
VI	1818.4	99	0.767	3	0.25–1.3

<sup>a</sup> Determined from rate of cleavage of *p*-nitrophenyl- $\alpha$ -D-maltoside by porcine pancreatic  $\alpha$ -amylase, monitored at 405 nm over 15 min; HEPES buffer, pH 7.2; 30 °C.  $K_I$  values for some runs could not be determined since the reaction rate for several inhibited tubes was zero.

### Acknowledgments

This work was supported by PRF grant # 34911-B4 from the American Chemical Society and EMU Faculty Research Fellowship and Graduate School Support Awards.

### References

1. Aschauer, H., Vertesy, L., Nesemann, G., Braunitzer, G. *Hoppe-Seyler's Z. Physiol. Chem.* **364**, 1347–1356 (1983).
2. Vertesy, L., Odeing, V., Bender, R., Zepf, K., Nesemann, G. *Eur. J. Biochem.* **141**, 505–512 (1984).
3. Pflugrath, J.W., Wiegand, G., Huber, R., Vertesy, L. *J. Mol. Biol.* **189**, 383–386 (1986).
4. Kline, A.D., Braun, W., Wuthrich, K. *J. Mol. Biol.* **204**, 675–724 (1988).
5. Wiegand, G., Epp, O., Huber, R. *J. Mol. Biol.* **247**, 99–110 (1995).

## Structural Studies of the Complex Between Decapeptide Inhibitors and the Serine Protease NS3/4A of Hepatitis C Virus

Paolo Ingallinella<sup>1</sup>, Piero Pucci<sup>2</sup>, Fabrizio Dal Piaz<sup>2</sup>, Antonello Pessi<sup>1</sup>  
and Elisabetta Bianchi<sup>1</sup>

<sup>1</sup>*Istituto di Ricerche di Biologia Molecolare P. Angeletti (IRBM), 00040 Pomezia (RM), Italy*

<sup>2</sup>*CNR-Universita di Napoli Federico II, 80131 Napoli, Italy*

### Introduction

One of the most promising approaches to anti-HCV therapy is the development of inhibitors of the viral NS3/4A protease, which is essential for maturation of the viral polyprotein. Several substrate-derived inhibitors have been described [1], all taking advantage of binding to the S site of the enzyme. By studying the interaction of these inhibitors with NS3 [2], we showed that binding occurs according to an induced-fit mechanism. In the absence of a cofactor, multiple binding modes are apparent, while in the presence of a cofactor all P-inhibitors show the same binding mode with a small rearrangement in the NS3 structure, as suggested by CD spectroscopy. Inhibitor complex formation is associated with stabilization of the enzyme, as highlighted by limited proteolysis experiments.

We have recently developed P-P' decapeptide inhibitors of NS3 with affinities below the nanomolar range [3]. In the present study we have studied the interaction between NS3, NS4A and P-P' spanning decapeptide inhibitors and found that binding in the S' site of the enzyme is linked to additional structural changes, with a considerable impact on the stabilization of the enzyme.

### Results and Discussion

The complex of NS3 with the inhibitors shown in Table 1 was first studied by CD. The structural organization of the N-terminal domain, which contains the S' site is strongly dependent on complexation with 4A. In the absence of 4A, binding in the S' site of the enzyme can induce additional structural rearrangements of the protease tertiary structure, apart from those previously observed for the P inhibitors. This is

Table 1. Peptide inhibitors used in this study. IC<sub>50</sub> values are taken from reference [3].

No.	Peptide <sup>a</sup>	IC <sub>50</sub> , $\mu$ M
1	Ac-Asp-glu-Leu-Ile-Cha-Abu-(Me)Ala-Ser-His-Leu-NH <sub>2</sub>	5000
2	Ac-Asp-glu-Leu-Ile-Cha-Cys-Pro-Nle-Ser-Leu-NH <sub>2</sub>	10
3	Ac-Asp-glu-Leu-Ile-Cha-Cys-Pro-Cha-Asp-Leu-NH <sub>2</sub>	<0.2
4	Ac-Asp-glu-Leu-Ile-Cha-Cys-OH	15

<sup>a</sup> Abbreviations: Cha =  $\beta$ -cyclohexylalanine; glu = (D)Glu; N-methylation of the amide nitrogen is indicated as (Me).

shown in Figure 1 by changes in the near-UV CD region for NS3 complexes of inhibitors sharing the same P region and with various P' sequences (Pep 1–3) or lacking P' (Pep 4). In the absence of 4A, binding in the flexible S' site is linked to the stabilization of various states of the enzyme.

In the presence of 4A, binding in the pre-organized S' site produces additional structural rearrangements with respect to binding in the S site alone (Figure 1, right).

However, contrary to what was observed for P-inhibitors, for P-P' inhibitors binding can be accomplished by stabilizing slightly different states, depending on the different P' binding sequences.

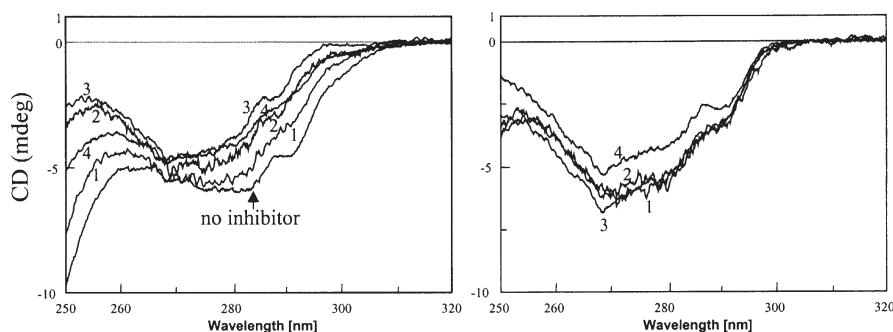


Fig. 1. Inhibitor-induced conformational change of NS3 (60  $\mu$ M) in 15% glycerol, 2% CHAPS, 3 mM DTT, phosphate buffer 50 mM, pH 7.5. (left) NS3 + inhibitors; (right) NS3/Pep4A + inhibitors (60  $\mu$ M); inhibitors 1–4 from Table 1. Pep4A, aa 21–34 of NS4A.

As previously observed for P-inhibitors, limited proteolysis-mass spectrometry experiments show that NS3/4A complex formation with P-P' decapeptide inhibitors is associated with an overall stabilization of the enzyme. Moreover, in the case of the optimized P' (Pep 3), complete protection is now observed for the N-terminal 28 residues of NS3, which are located near the NS4A binding site. These residues were found unordered in the NMR analysis of the single-chain NS3/4A complex and also the 4A co-factor was in slow exchange between the bound and free state [4]. In conclusion, by exploiting the binding potential of the prime site, we have developed a new class of competitive inhibitors. Our data now show that binding of these inhibitors is associated with a structural rearrangement and stabilization of the enzyme.

## References

1. Ingallinella, P., Altamura, S., Bianchi, E., Taliani, M., Ingenito, R., Cortese, R., De Francesco, R., Steinkühler, C., Pessi, A. *Biochemistry* **37**, 8906 (1998).
2. Bianchi, E., Orrù, S., Dal Piaz, F., Ingenito, R., Casbarra, A., Biasiol, G., Koch, U., Pucci, P., Pessi, A. *Biochemistry* **38**, 13844–13852 (1999).
3. Ingallinella, P., Bianchi, E., Ingenito, R., Koch, U., Steinkühler, C., Altamura, S., Pessi, A. *Biochemistry* **39**, 12898 (2000).
4. McCoy, M.A., Senior, M.M., Gesell, J.J., Ramanathan, L., Wyss, D.F. *J. Mol. Biol.* **305**, 1099 (2001).

## Synthesis and Activity of a Small Cyclic Protease Inhibitor from Sunflower Seeds, SFTI-1

Agnès M. Jaulent, Jeffrey D. McBride and Robin J. Leatherbarrow

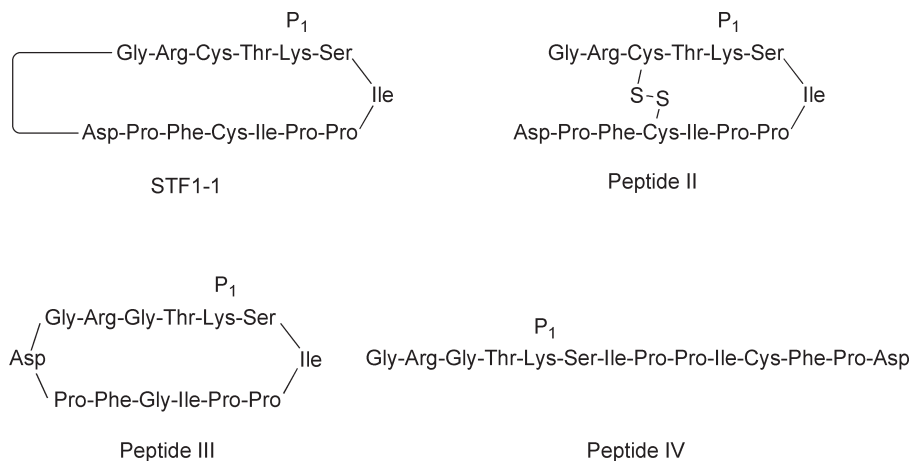
Department of Chemistry, Imperial College of Science Technology and Medicine,  
London, SW7 2AZ, UK

### Introduction

Proteinaceous proteinase inhibitors control proteases' proteolytic activity by preventing unwanted proteolysis. They are involved in important biological "housekeeping" functions such as blood clotting, inflammatory reactions *etc.* The BBI family are small serine protease inhibitors (60 to 90 amino acids) which are particularly abundant in leguminous and gramineous plants [1,2]. They contain 7 disulfide bridges and have a symmetrical double-headed structure. Each domain contains an independent canonical binding site of nine amino acid residues encapsulated in a disulfide bridge. Generally, the inhibitory activity is directed at either chymotrypsin/trypsin or trypsin/trypsin.

Recently, Luckett *et al.* [3] isolated and characterized the smallest plant proteinaceous protease inhibitor known to date, SFTI-1. It is a 14 amino acid residue peptide, very similar to the trypsin-inhibitory loop from the large Bowman Birk inhibitor proteins, but whilst Cys3 and Cys11 are disulfide-linked, extra-rigidity is conferred *via* a supplementary head-to-tail cyclisation between residues Gly1 and Asp14.

In order to assess the role of this extra-cyclisation in SFTI-1, its synthesis has been performed alongside with three other closely related peptides, which have systematic variations in their cyclisation. The activity of these inhibitors against bovine  $\beta$ -trypsin has been analysed.



### Results and Discussion

SFTI-1 was successfully synthesized using an on-resin cyclisation strategy, with an overall yield of 20%. All peptides were characterized by mass spectroscopy and found to be more than 95% pure by analytical reverse-phase HPLC. The Table 1 summarizes the competitive inhibition kinetic results against bovine  $\beta$ -trypsin.

Cyclic derivatives of SFTI-1 all display inhibitory activity. By contrast, the linear version, peptide IV, showed no inhibitory potential, as is also the case with those

based on BBI loops. Of the 3 cyclic versions, SFTI-1 is the most potent inhibitor. As demonstrated by Luckett *et al.* [3], its structure consists of 2 antiparallel  $\beta$ -strands, and can be seen as a combination of 2 loops: (i) The “*reactive loop*” consisting of the 9-residue disulfide-linked loop between residues Cys3 and Cys11; (ii) The “*cyclic loop*” comprising the 5-turn residues. An internal network of hydrogen bonds further stabilises the structure.

*Table 1. Inhibitory activity of synthetic peptides.*

Peptide	<i>SFTI-I</i> GRCTKSIPPICFPD	<i>Peptide II</i> GRCTKSIPPICFPD	<i>Peptide III</i> GRGTSKIPPIGFPD	<i>Peptide IV</i> GRGTSKIPPIGFPD
$K_i$ (nM)	0.3	1.2	27	> mM

SFTI-1 is a very potent trypsin inhibitor, with a  $K_i$  of 0.3 nM, better than most parent proteinaceous BBIs. *Peptide II* has only a disulfide constraint and displays a  $K_i$  value against trypsin lower to that of SFTI-1 but which lies within the range reported for BBI protein by this laboratory for cyclic BBI-derived peptides [Mc Bride *et al.*, in press]. *Peptide III*, lacking the inner disulfide bond but constrained by a head-to-tail cyclisation, is also a fairly potent trypsin inhibitor even if it cannot *a priori* be considered as obeying the standard mechanism for canonical inhibitors. This result corroborates those found by Flecker *et al.* [4]. This research group expressed BBI variants lacking only the inner disulfide bond, but found nevertheless similar  $K_i$ , thus suggesting the importance of the internal hydrogen networking.

The inhibitory constant,  $K_i$ , is a measure of the inhibitor’s affinity for its target enzyme and can be directly correlated to the free energy of binding, using the formula:  $\Delta G = -RT \ln K_i$ . This allows us to calculate the relative contribution in free energy granted by the head-to-tail cyclisation to be 3.4 kJ mol<sup>-1</sup>.

### Conclusions

SFTI-1 synthesis has been performed for the first time. The on-resin cyclisation strategy afforded an overall yield of 20%. SFTI-1 has been found to be indeed a very potent trypsin inhibitor displaying a subnanomolar inhibitory constant. The extra loop makes it a much better inhibitor than its BBI equivalent ( $K_i$  ratio of 4). It is worth noting as well that this very small rigid peptide is as good an inhibitor as a BBI protein.

### References

1. Birk, Y. *Int. J. Pept. Protein Res.* **25**, 113–131 (1985).
2. Prakash, *et al.* *J. Mol. Evol.* **42**, 560–569 (1996).
3. Luckett, S., *et al.* *J. Mol. Biol.* **290**, 525–533 (1999).
4. Flecker, P., *et al.* *Eur. J. Biochem.* **251**, 854–862 (1998).

## Different Types of P1 Residues in Peptide-Based Inhibitors of Hepatitis C Virus Full-Length NS3 Protease

Anja Johansson<sup>1</sup>, Eva Åkerblom<sup>1</sup>, Gunnar Lindeberg<sup>1</sup>, Anton Poliakov<sup>2</sup>,  
 U. Helena Danielsson<sup>2</sup> and Anders Hallberg<sup>1</sup>

<sup>1</sup>Department of Organic Pharmaceutical Chemistry, Uppsala University,  
 SE-751 23 Uppsala, Sweden

<sup>2</sup>Department of Biochemistry, Uppsala University, SE-751 23 Uppsala, Sweden

### Introduction

In a project aimed at the design and synthesis of inhibitors to the hepatitis C virus (HCV) NS3 serine protease, peptides containing different types of P1 residues were compared: 1) pentafluoroethyl ketones, since substrate-based peptides containing electrophilic groups in the P1 position are classical inhibitors of serine proteases; 2) tetrazoles, since HCV NS3 protease is uniquely inhibited by its N-terminal cleavage products [1] and tetrazoles are known metabolically stable bioisosteres for carboxylic acids; 3) ketotetrazoles, since peptide  $\alpha$ -ketoacids work as electrophilic inhibitors of the HCV NS3 protease [2] and  $\alpha$ -ketotetrazoles should serve as  $\alpha$ -ketoacid bioisosteres and; 4) carboxylic acids, as reference compounds.

### Results and Discussion

Seven different modified amino acid P1 building blocks have been prepared successfully (Figure 1).

The corresponding peptide inhibitors **5–11** (Figure 3) were prepared by N- to C-directed (inverse) SPPS [3] (Figure 2). The peptide analogues **12–14** (Figure 3), serving as reference substances, were prepared using standard SPPS.

Inhibition of HCV NS3 protease activity by compounds **5–14**, was thereafter determined in an in vitro assay system comprising the native bifunctional full-length NS3 (protease-helicase/NTPase) protein [4] (Table 1).

The inhibitory data obtained so far reveal that peptides encompassing any of the four types of P1 residues act as inhibitors of the full-length NS3 protease. Moreover,

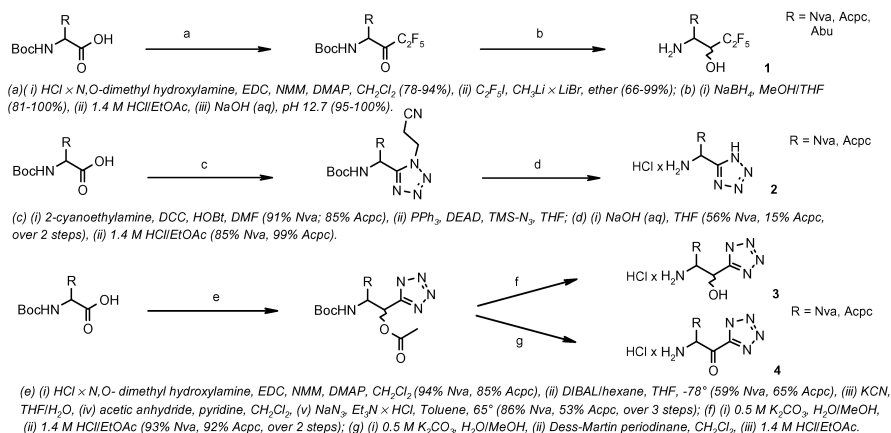


Fig. 1. Synthesis of the pentafluoroethyl ketone building blocks **1**, the tetrazole building blocks **2**, and the ketotetrazole building blocks **3** and **4**.

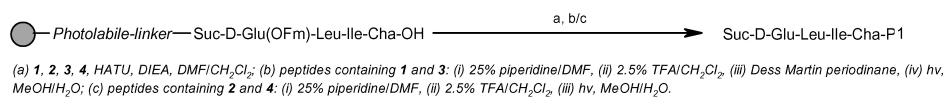


Fig. 2. Synthesis of peptide-based inhibitors using *N*- to *C*-directed (inverse) SPPS.

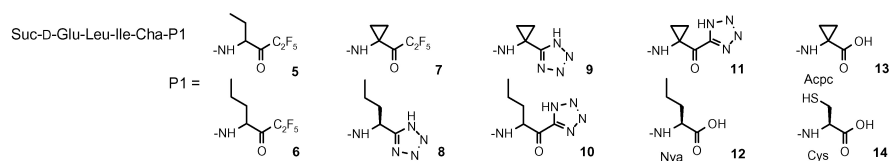


Fig. 3. Potential HCV NS3 protease inhibitors.

Table 1. Inhibition of HCV NS3 protease activity by compounds **5–14**, evaluated in an *in vitro* assay system comprising the full-length NS3 (protease-helicase/NTPase) protein.

Number	$K_i$ ( $\mu$ M) $\pm$ SD	Number	$K_i$ ( $\mu$ M) $\pm$ SD
<b>5</b>	2.0	<b>10</b>	n.d.
<b>6</b>	$2.9 \pm 0.3$	<b>11</b>	$13 \pm 2$
<b>7</b>	10% inhib. at 83 $\mu$ M	<b>12</b>	$1.9 \pm 0.1$
<b>8</b>	n.d.	<b>13</b>	$1.8 \pm 0.2$
<b>9</b>	50% inhib. at 83 $\mu$ M	<b>14</b>	$0.25 \pm 0.03$

cysteine, which is the amino acid found in the P1 position of the natural substrate, is superior. Further testing is necessary for evaluation of the tetrazole and ketotetrazole compounds, since the inhibitory potencies of peptides containing the cyclopropyl ring in the P1 residue are unpredictable.

## References

- Steinkühler, C., Biasiol, G., Brunetti, M., Urbani, A., Koch, U., Cortese, R., Pessi, A., De Francesco, R. *Biochemistry* **37**, 8899–8905 (1998).
- Narjes, F., Brunetti, M., Colarusso, S., Gerlach, B., Koch, U., Biasiol, G., Fattori, D., De Francesco, R., Matassa, V.G., Steinkühler, C. *Biochemistry* **39**, 1849–1861 (2000).
- Johansson, A., Åkerblom, E., Ersmark, K., Lindeberg, G., Hallberg, A. *J. Comb. Chem.* **2**, 496–507 (2000).
- Johansson, A., Hubatsch, I., Åkerblom, E., Lindeberg, G., Winiwarter, S., Danielson, U.H., Hallberg, A. *Bioorg. Med. Chem. Lett.* **11**, 203–206 (2001).

## **Development and Characterization of Potent Peptide Inhibitors of p60<sup>c-src</sup> PTK Using Pseudosubstrate-Based Inhibitor Design Approach**

**Jayesh R. Kamath, Ruiwu Liu, Amanda M. Enstrom, Gang Liu,  
Qiang Lou and Kit S. Lam**

*Division of Hematology and Oncology, Department of Internal Medicine, UC Davis Cancer  
Center, University of California Davis, Sacramento, CA 95817, USA*

### **Introduction**

The cytoplasmic protein p60<sup>c-src</sup> is a ubiquitous non-receptor protein tyrosine kinase (PTK) that is over-expressed and/or activated in several cancer types making it an important anti-cancer target [1]. In addition, c-src knockout mice have a phenotype consistent with osteopetrosis suggest that inhibitors against this enzyme may be therapeutic for osteoporosis. In the past few years, we have developed a pseudosubstrate-based inhibitor strategy [2,3] to target the peptide-substrate binding site of p60<sup>c-src</sup> PTK. This strategy has led to the identification of highly selective and potent inhibitors of p60<sup>c-src</sup> PTK [2]. By screening a random “one-bead one-compound” combinatorial peptide-bead library with a functional phosphorylation assay [4], we identified MIYKYYF as a very inefficient peptide substrate for this enzyme. However, MIYKYYF was found to be a moderately potent inhibitor ( $IC_{50} = 6 \mu M$ ) of p60<sup>c-src</sup> PTK using YIYGSFK ( $K_m = 55 \mu M$ ) as a substrate. In this study, we describe the development and characterization of potent pseudosubstrate-based inhibitors ( $IC_{50} = 0.14\text{--}0.6 \mu M$ ) of p60<sup>c-src</sup> PTK, using MIYKYYF as the template.

### **Results and Discussion**

SAR studies of the parent peptide MIYKYYF led to the identification of IYKYYF as an inhibitor with similar potency ( $IC_{50} = 8 \mu M$ ) as its parent peptide. The initial library screening from which MIYKYYF was identified, did not contain cysteine residues to avoid any intra or intermolecular disulfide bond formation. It has been suggested that targeting sulfhydryl groups of the enzyme p60<sup>c-src</sup> PTK might be critical for enzyme inhibition [5]. We found that the addition of just one cysteine residue to the amino terminus of IYKYYF increased the inhibitory potency of this peptide by more than twenty-fold. The peptide inhibitor, CIYKYYF, was determined to be a very potent inhibitor of p60<sup>c-src</sup> with an  $IC_{50}$  value of  $0.5 \mu M$ . Inhibition experiments conducted in the presence of a reducing agent, DTT (dithiothreitol), showed a ten-fold reduction in inhibitory potency of CIYKYYF. This suggests that disulfide bond formation between the Cys<sup>1</sup> of the peptide CIYKYYF and a cysteine residue at the enzyme active site (possibly Cys<sup>290</sup> or Cys<sup>299</sup>) might account for the improved potency of CIYKYYF. Further SAR studies suggest, at the N-terminus, the sulfhydryl group, the free N<sup>α</sup>-group, as well as the L-enantiomer of Cys<sup>1</sup> are critical for the improved inhibitory potency of the peptide CIYKYYF. “Alanine scan” and “Deletion scan” of this inhibitor led to the identification of a shorter hexa-peptide inhibitor, CIYKYY, with similar potency ( $IC_{50} = 0.6 \mu M$ ) as CIYKYYF. In CIYKYY, a possible cation- $\pi$  interaction between the aromatic residues (Tyr<sup>5</sup> and Tyr<sup>6</sup>) and the adjacent cationic Lys<sup>4</sup> might result in a constrained peptide structure. This is suggested by the gradual loss of inhibitory potency by truncation of the amino acid residues at the carboxyl terminus of CIYKYY. Replacement of L-isoleucine<sup>2</sup> of CIYKYY with unnatural amino acid

**Kamath et al.**

D-propargylglycine (pra) led to the development of the most potent inhibitor of this series, CpraYKYY ( $IC_{50} = 0.14 \mu M$ ) (Table 1). No improvement in inhibitory potency has been observed with the “Tyr<sup>3</sup> mimetic” analogues of CIYKYYF or CIYK, suggesting the possibility that the hydroxyl group of Tyr<sup>3</sup> might be important for certain critical interactions at the enzyme active site.

Table 1. Pseudosubstrate-based peptide inhibitors for p60<sup>c-src</sup> PTK.

Peptide structure <sup>a</sup>	IC <sub>50</sub> $\mu M$ <sup>b</sup>
CIYKYYF	0.5 $\pm$ 0.15
Ac-CIYKYYF	6.0 $\pm$ 1.1
cIYKYYF	5.9 $\pm$ 0.8
CIYKYY	0.6 $\pm$ 0.1
CIYK	15.0 $\pm$ 0.8
CI-(3,5-diI)Tyr-KYYF	1.1 $\pm$ 0.16
PenIYKYYF	1.3 $\pm$ 0.53
CpraYKYY	0.14 $\pm$ 0.08

<sup>a</sup> (3,5-diI)Tyr, 3,5-di-iodo L-tyrosine; Pen, L-Penicillamine; pra, D-propargylglycine; Ac, acetyl. <sup>b</sup> The values represent the mean of two to four independent experiments. The substrate used in these experiments was YIYGSFK at a concentration equal to its  $K_m$  (55  $\mu M$ ).

**Acknowledgments**

This work was supported by NSF grant MCB 9728399.

**References**

1. Al-Obeidi, F.A., Lam, K.S. *Oncogene* **19**, 5690–5701 (2000).
2. Alfaro-Lopez, J., Wei, Y., Phan, B., Kamath, J., Lou, Q., Lam, K.S., Hruby, V.J. *J. Med. Chem.* **41**, 2252–2260 (1998).
3. Lou, Q., Leftwich, M., McKay, R.T., Salmon, S.E., Rychetsky, L., Lam, K.S. *Cancer Res.* **57**, 1877–1888 (1997).
4. Lam, K.S., Wu, J.S., Lou, Q. *Int. J. Pept. Protein Res.* **45**, 587–592 (1995).
5. Uehara, Y., Murakami, Y., Sugimoto, Y., Mizuno, S. *Cancer Res.* **49**, 780–785 (1989).

## Use of $\beta$ -Amino Acids in the Design of Substrate-Based Peptidase Inhibitors

**R. A. Lew<sup>1</sup>, E. Boulos<sup>2</sup>, K. M. Stewart<sup>2</sup>, P. Perlmutter<sup>3</sup>, M. F. Harte<sup>3</sup>,  
 S. Bond<sup>3</sup>, S. B. Reeve<sup>1</sup>, M. U. Norman<sup>1</sup>, M. J. Lew<sup>4</sup>, M.-I. Aguilar<sup>2</sup>  
 and A. I. Smith<sup>1</sup>**

<sup>1</sup>*Baker Medical Research Institute, Melbourne, Victoria, Australia 8008*

<sup>2</sup>*Department of Biochemistry and Molecular Biology, Monash University, Clayton, Victoria, Australia 3800*

<sup>3</sup>*Department of Chemistry, Monash University, Clayton, Victoria, Australia 3800*

<sup>4</sup>*Department of Pharmacology, University of Melbourne, Victoria, Australia 3010*

### Introduction

$\beta$ -Amino acids contain an extra carbon between the amino and carboxy-termini; this modification renders the adjacent peptide bond resistant to hydrolysis [1,2]. We hypothesize that substitution of the residues at the scissile bond with  $\beta$ -amino acids can confer resistance to cleavage without necessarily abolishing binding to the enzyme. In the present study, we have synthesized a series of  $\beta$ -amino acid-substituted analogues of bradykinin (BK), and examined both their susceptibility to cleavage by and their ability to inhibit the soluble metalloendopeptidases EC 3.4.24.15 (EP24.15) and EC 3.4.24.16 (EP24.16) [3]. Our findings suggest that  $\beta$ -amino acid incorporation at the scissile bond completely prevents peptide hydrolysis with only minimal reduction in affinity for the enzyme.

### Results and Discussion

Bradykinin analogues containing a  $\beta$ -Gly either side of the cleavage site (Phe<sup>5</sup>-Ser<sup>6</sup>) or at residue 7 were completely resistant to hydrolysis by recombinant EP24.15 and EP24.16 (Table I). However, some affinity for the peptidases, particularly EP24.15, was retained, as demonstrated by inhibition of cleavage of a quenched fluorescent substrate. With one exception (see below),  $\beta$ -Gly substitution at other residues did not prevent hydrolysis; indeed, some analogues were more efficiently degraded than BK itself. Furthermore, differences between the peptidases in the cleavage rates and/or the inhibition constants of certain analogues were observed, suggesting subtle differences in substrate specificity. In particular,  $\beta$ -Gly<sup>8</sup> was neither a substrate nor an inhibitor of EP24.15, whilst its cleavage by EP24.16 was retained.

*Table 1.  $\beta$ -Amino acid containing analogues of bradykinin are resistant to degradation by, but can still inhibit EP24.15 and EP24.16.*

Peptide	EP24.15		EP24.16	
	Degradation	IC <sub>50</sub> ( $\mu$ M)	Degradation	IC <sub>50</sub> ( $\mu$ M)
BK	++	8	++	7
$\beta$ Gly <sup>5</sup> BK	0	28	0	40
$\beta$ Gly <sup>6</sup> BK	0	28	0	>40
$\beta$ Gly <sup>7</sup> BK	0	>40	0	>40
$\beta$ -C3-L-Phe <sup>5</sup> BK	0	20	0	20
$\beta$ -C3-D-Phe <sup>5</sup> BK	0	12	0	>40

Substitution with the  $\beta$ -congener of the native amino acid residue at the cleavage site (*i.e.*,  $\beta$ -Phe<sup>5</sup> or  $\beta$ -Ser<sup>6</sup>) also prevented hydrolysis by both peptidases. Again, affinity for EP24.15 was retained, with the best analogues ( $\beta$ -C3-L-Phe<sup>5</sup>-BK and  $\beta$ -C3-D-Phe<sup>5</sup>-BK) displaying IC<sub>50</sub> values less than 3-fold greater than BK itself (Figure 1). These analogues were less effective inhibitors of EP24.16 (Figure 1), again emphasising substrate differences between these closely related peptidases.

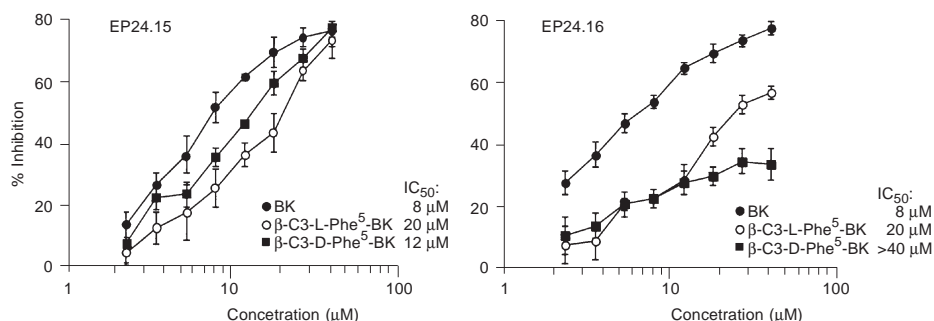


Fig. 1. Inhibition of EP24.15 and EP24.16 by bradykinin (BK),  $\beta$ -C3-L-Phe<sup>5</sup>-BK and  $\beta$ -C3-D-Phe<sup>5</sup>-BK.

Finally, both  $\beta$ -C3-L-Phe<sup>5</sup>-BK and  $\beta$ -C3-D-Phe<sup>5</sup>-BK retained some affinity for the bradykinin B<sub>2</sub> receptor, as assessed by relaxation of pig coronary artery segments pre-contracted with a thromboxane mimetic. However, potencies were several orders of magnitude lower than bradykinin itself (pEC<sub>50</sub>  $\pm$  s.e.m. = 9.08  $\pm$  0.10, 6.25  $\pm$  0.12, and 5.54  $\pm$  0.21 for BK,  $\beta$ -C3-L-Phe<sup>5</sup>-BK, and  $\beta$ -C3-D-Phe<sup>5</sup>-BK, respectively).

In conclusion, the present study demonstrates that peptide substrates containing a  $\beta$ -amino acid at the scissile bond are capable of inhibiting the peptidase without being cleaved. This observation negates previous assumptions that the resistance of  $\beta$ -amino acid-containing peptides to hydrolysis results solely from a lack of binding. Incorporation of  $\beta$ -amino acids thus represents a novel peptidomimetic element with potential utility in the development of specific peptidase inhibitors.

#### Acknowledgments

This study was supported by the National Health and Medical Research Council of Australia, and the Department of Industry, Science and Resources of Australia.

#### References

1. Hintermann, T., Seebach, D. *Chimia* **51**, 244–247 (1997).
2. Seebach, D., Abele, S., Schreiber, J.V., Martinoni, B., Nussbaum, A.K., Schild, H., Schulz, H., Hennecke, H., Woessner, R., Bitsch, F. *Chimia* **52**, 734–739 (1998).
3. Barrett, A.J., Brown, M.A., Dando, P.M., Knight, C.G., McKie, N., Rawlings, N.D., Serizawa, A. *Methods Enzymol.* **248**, 529–556 (1995).

## Bivalent Inhibition of Human $\beta$ -Tryptase: Probing the Distance Between Neighbouring Subunits by Dibasic Inhibitors

Norbert Schaschke<sup>1</sup>, Andreas Dominik<sup>2</sup>, Gabriele Matschiner<sup>3</sup>  
and Christian P. Sommerhoff<sup>3</sup>

<sup>1</sup>Max-Planck-Institut für Biochemie, D-82152 Martinsried, Germany

<sup>2</sup>Byk Gulden Lomborg Chemische Fabrik GmbH, D-78467 Konstanz, Germany

<sup>3</sup>Abteilung für Klinische Chemie und Klinische Biochemie in der Chirurgischen Klinik und Poliklinik der LMU München, D-80336 München, Germany

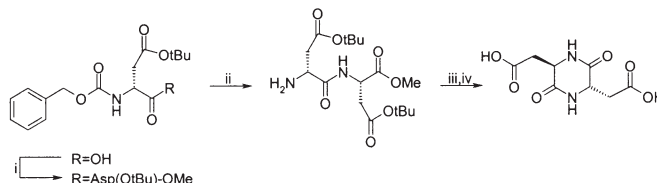
### Introduction

Human  $\beta$ -tryptase is a mast cell specific serine protease [1,2] with a unique tetrameric architecture, as recently revealed by X-ray crystallography [3,4]. The enzyme consists of four quasi equivalent subunits (A, B, C, and D) each with trypsin-like activity. Therefore,  $\beta$ -tryptase represents an array of four negatively charged S1 pockets with an defined spatial arrangement. In detail, the distance between the specificity pockets of subunits A/D and B/C within the tetramer is 33 Å, respectively, whereas the distances between the S1 subsites of subunits A/C and B/D as well as A/B and C/D comprise 45 Å. Thus, this protease should act as a molecular ruler capable of recognizing dibasic inhibitors of appropriate length. To prove the concept of a molecular ruler, we have synthesized an array of structurally related dibasic compounds by systematically increasing the distance between the positively charged head groups to address, in particular, the subunit pairs A/D and B/C, respectively.

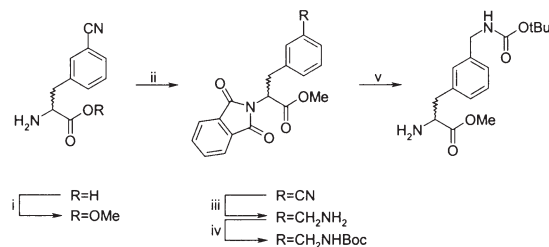
### Results and Discussion

As potential binding heads for  $\beta$ -tryptase that mimic arginine, 3- and 4-aminomethyl-phenylalanine were investigated. Due to 15 times higher inhibitory potency of Ac-DL-Phe(3-H<sub>2</sub>N-CH<sub>2</sub>)-OMe ( $K_i$  = 13.7  $\mu$ M) in comparison to Ac-DL-Phe(4-H<sub>2</sub>N-CH<sub>2</sub>)-OMe ( $K_i$  = 213  $\mu$ M), the more potent *meta*-derivative was used for the present study. As central scaffold for displaying the binding heads, diketopiperazines were chosen, in particular, those derived from aspartic and glutamic acid as well as mixed ones to reduce to a minimum the contribution to the total spacer length. By inspecting the X-ray structure of the  $\beta$ -tryptase tetramer, diketopiperazines with *trans*-geometry, *i.e.*, those consisting of a D- and an L-amino acid, were expected to allow a better positioning of the binding heads into the neighbouring S1 subsites of subunit pairs A/D and B/C, respectively. These were used for the distance scan and additional spacing was achieved with  $\omega$ -amino acids.

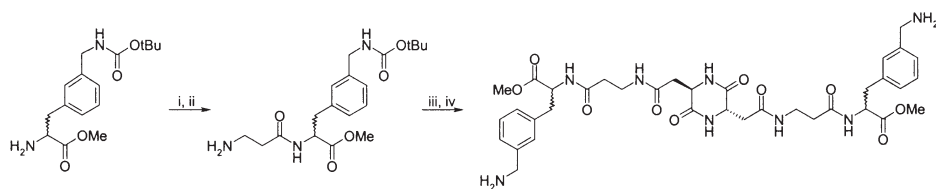
In Schemes 1–3 the synthesis of compound **4** is outlined as a representative for the whole set of inhibitors. All inhibitors were fully characterized by ESI-MS and HPLC, some of them additionally by NMR.



Scheme 1. Synthesis of the scaffold. Reaction conditions: (i) *H*-L-Asp(OtBu)-OMe/DIEA/EDC/HOBt, CHCl<sub>3</sub>; (ii) 10% Pd-C/H<sub>2</sub>, MeOH; (iii) T, MeOH; (iv) 95% aq. TFA, 0 °C  $\rightarrow$  RT.



Scheme 2. Synthesis of the head group. Reaction conditions: (i)  $\text{MeOH}/\text{SOCl}_2$ ,  $-5\text{ }^\circ\text{C}$ ; (ii)  $N$ -ethoxycarbonylphthalimide/ $\text{Na}_2\text{CO}_3$ , dioxane/ $\text{H}_2\text{O}$  (1 : 1); (iii) 10%  $\text{Pd-C}/\text{H}_2$ ,  $\text{AcOH}$ ; (iv)  $(\text{Boc})_2\text{O}/\text{NaHCO}_3$ , dioxane/ $\text{H}_2\text{O}$  (1 : 1); (v)  $\text{H}_2\text{N-NH}_2 \times \text{AcOH}$ ,  $\text{MeOH}$ ,  $50\text{ }^\circ\text{C}$ .



Scheme 3. Synthesis of the dibasic inhibitor **4**. Reaction conditions: (i)  $Z$ - $\beta$ -Ala-OH/DIEA/EDC/HOBt,  $\text{DMF}$ ; (ii) 10%  $\text{Pd-C}/\text{H}_2$ ,  $\text{MeOH}$ ; (iii)  $c[\text{D-Asp-L-Asp}]/\text{DIEA/EDC/HOBt}$ ,  $\text{DMF}$ ; (iv) 95% aq.  $\text{TFA}$ ,  $0\text{ }^\circ\text{C} \rightarrow \text{RT}$ .

The inhibition data for the series of dibasic inhibitors against the  $\beta$ -tryptase tetramer are summarized in Table 1. A comparison of the  $K_i$ -values clearly shows a SAR between the distance of the binding heads and the affinity of the inhibitors. The dibasic inhibitor **1** with the shortest distance between the terminal amino groups dis-

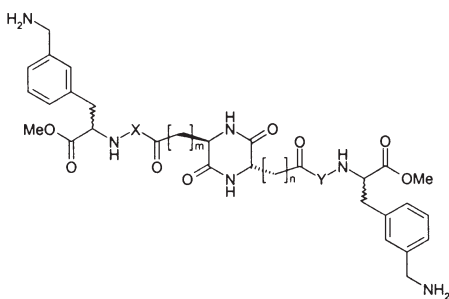


Table 1.  $K_i$ -values of the dibasic inhibitors.

Comp.	m	n	X	Y	Number of bonds between the amino groups	$K_i$ [ $\mu\text{M}$ ]
<b>1</b>	2	2	—	—	25	2.4
<b>2</b>	1	2	Gly	—	27	0.18
<b>3</b>	1	1	Gly	Gly	29	0.018
<b>4</b>	1	1	$\beta$ -Ala	$\beta$ -Ala	31	0.010
<b>5</b>	1	1	4-Abu	4-Abu	33	0.35

plays almost the same inhibitory potency as the head group (2.4  $\mu\text{M}$  vs 13.7  $\mu\text{M}$ , respectively), whereas a further increase of the distance is accompanied by a strong increase in the affinity of the inhibitors. The maximum of cooperativity, *i.e.*, a 1370 times more potent inhibitor in comparison to the binding head, is realized with **4**.

Furthermore, the inhibitors were subjected to a new modeling program which allows the docking of bivalent inhibitors. Two of the possible diastereomers (namely the *S,S*- and *R,R*-compound; the absolute stereochemistry refers to the head groups, respectively) of each inhibitor were docked. Both diastereomers of inhibitor **1** and the *R,R*-diastereomer of inhibitor **2** were classified as compounds unable to bind in a bivalent manner, whereas the other diastereomers of the series are assigned by the program as bivalent binders. These results are in full agreement with the SAR derived from inhibition kinetics.

#### **Acknowledgments**

This study was supported by grants A2 and B6 of the SFB 469 (LMU Munich) and by Byk Gulden, Konstanz, Germany with a postdoctoral grant for N.S.

#### **References**

1. Johnson, D.A., In Barrett, A.J., Rawlings, N.D. and Woessner, J.F. (Eds.) *Handbook of Proteolytic Enzymes*, Academic Press, San Diego, 1998, p. 70.
2. Sommerhoff, C.P., Bode, W., Matschiner, G., Bergner, A., Fritz, H. *Biochim. Biophys. Acta* **1477**, 75–89 (2000).
3. Barbosa Pereira, P.J., Bergner, A., Macedo-Ribeiro, S., Huber, R., Matschiner, G., Fritz, H., Sommerhoff, C.P., Bode, W. *Nature* **392**, 306–311 (1998).
4. Sommerhoff, C.P., Bode, W., Barbosa Pereira, P.J., Stubbs, M.T., Stürzebecher, J., Piechottka, G.P., Matschiner, G., Bergner, A. *Proc. Natl. Acad. Sci. U.S.A.* **96**, 10984–10991 (1999).

## **A Highly Selective Cell Permeable Peptide Inhibitor of Proprotein Convertase 1: Design, Synthesis and Biological Evaluation in Cellular PC1-Mediated Proteolysis**

**Ajoy Basak<sup>1</sup>, Peter Koch<sup>1</sup>, Marcel Dupelle<sup>1</sup>, Francine Sirois<sup>1</sup>,  
Michel Chrétien<sup>1</sup>, Nabil G. Seidah<sup>2</sup> and Majambu Mbikay<sup>1</sup>**

<sup>1</sup>Laboratory of Diseases of Aging, Ottawa Health Research Institute, Loeb Campus,  
University of Ottawa, Ottawa, ON, K1Y 4K9, Canada

<sup>2</sup>Laboratory of Biochemical Neuroendocrinology, Clinical Research Institute of Montreal,  
Montreal, QC, H2W 1R7, Canada

### **Introduction**

Hormonal peptides, neuropeptides, growth factors, receptors, bacterial toxins, viral glycoproteins and many biologically active proteins are generated as their precursors that must undergo proteolytic cleavages in order to be active. The delicate balance between these cleaved functional proteins and their precursors is the key element for normal growth, function, metabolism, development, and in pathophysiologic conditions [1,2]. These cleavage sites are generally composed of a pair of basic amino acids (aa) within the consensus sequence **R/K/H-(X)<sub>n</sub>-R↓** (n = 0, 2, 4 or 6, X = any aa except Cys). These cleavages are mostly performed by a family of Ca<sup>+2</sup>-dependent serine proteases called Proprotein Convertases (PCs) related to bacterial subtilisin and yeast kexin [1]. PC1 is the first member of this family that mediates the processing of neural and endocrine precursor proteins, such as proopiomelanocortin (POMC) found in the secretory pathway [1,2]. PC1 activity was selectively regulated by grannin neuroendocrine protein, proSAAS [2]. The PC1-inhibitory property of proSAAS is confined within a short peptide segment near the C-terminus that contains the critical **KR<sup>244</sup>** motif [2–4]. In this article, we present kinetic evaluation of the specificity and potency of PC1-inhibition by a 12-mer h(human) proSAAS peptide and its mutants. The specificity and potency of these peptides were also tested against other PCs and compared with that of r (rat) proSAAS<sup>221-254</sup>, known as PenLen, the major processing form of proSAAS in rat brain [4]. In an effort to enhance the cell translocation ability, the most potent PC1 inhibitor was conjugated to R<sub>8</sub> at the N-terminus *via* a 14-atom linker and tested for its antiprotease activity in cellular PC1-mediated processing of POMC [1,2]. Previous studies indicated that Arg-rich peptides, such as HIV-tat<sup>48-60</sup>, HIV-rev<sup>34-50</sup>, and polyarginines (with 6-8 residues) can efficiently permeate through the cell membrane and carry exogenous proteins, drugs, or ion beads chemically linked to them [5].

### **Results and Discussion**

*Peptide design and inhibition parameters.* Based on earlier studies (4-6), we selected the conserved 12mer h/r proSAAS<sup>235-246</sup> peptide for detailed kinetic analysis and positional scanning. Table 1 lists all 19 peptides that include the wild type sequence and its 11 Ala derivatives, 3 Lys mutants at P1, P4 and [P1 + P4] and a [P3 + P5] double Ala mutant, as well as PenLen. The measured K<sub>i</sub> (inhibition constant) of proSAAS peptides against PC1 and in some cases against furin, PC5 and PC7 are shown in Table 1. The true competitive nature of inhibition of PC1 by proSAAS peptides was demonstrated by Dixon plots and by the observed linear increase of IC<sub>50</sub> with substrate concentration [3]. ProSAAS<sup>235-244</sup> was the most powerful PC1 inhibitor (K<sub>i</sub> ≈ 9.1 nM), being >5-fold more potent than the C-terminally extended proSAAS<sup>235-246</sup>

## Biologically Active Peptides

Table 1. Inhibition constant ( $K_i$  nM  $\pm$  SD) of proSAAS peptides against PC1, furin, PC5 and PC7.

Peptides		PC1	furin	PC5	PC7	PC1 : furin : PC5 : PC7
dSAAS <sup>235-244</sup> <sub>dextro</sub>	VLGALLRVKR	122000 $\pm$ 11900				
SAAS <sup>235-244</sup>	VLGALLRVKR	<u>9<math>\pm</math>0.5</u>	261 $\pm$ 44	317 $\pm$ 9	940 $\pm$ 32	1 : 29 : 35 : 103
SAAS <sup>235-246</sup>	VLGALLRVKRLE	51 $\pm$ 3.8	39400 $\pm$ 4300	100000 $\pm$ 7000	4750 $\pm$ 95	1 : 780 : 1980 : 94
SAAS <sup>235-246</sup> P2'A	VLGALLRVKR <u>L</u> A	293 $\pm$ 12	4399 $\pm$ 220	35963 $\pm$ 1438	1667 $\pm$ 67	1 : 15 : 123 : 6
SAAS <sup>235-246</sup> P1'A	VLGALLRVKR <u>A</u> E	1024 $\pm$ 40	1280 $\pm$ 120	231000 $\pm$ 21600	2330 $\pm$ 330	1 : 1 : 181 : 2
SAAS <sup>235-246</sup> P1A	VLGALLRVK <u>A</u> LE	509000 $\pm$ 15270				
SAAS <sup>235-246</sup> P2A	VLGALLRV <u>A</u> RLE	4503 $\pm$ 30				
SAAS <sup>235-246</sup> P3A	VLGALLR <u>A</u> KRLE	360 $\pm$ 72	92000 $\pm$ 8000	335000 $\pm$ 40000	484 $\pm$ 34	1 : 274 : 931 : 1
SAAS <sup>235-246</sup> P4A	VLGALL <u>A</u> VKRLE	286 $\pm$ 34				
SAAS <sup>235-246</sup> P5A	VLGAL <u>A</u> RVKRLE	172 $\pm$ 41				
SAAS <sup>235-246</sup> P6A	VLGA <u>A</u> LRVKRLE	58 $\pm$ 16				
SAAS <sup>235-246</sup> P8A	VL <u>A</u> ALLRVKRLE	143 $\pm$ 24				
SAAS <sup>235-246</sup> P9A	V <u>A</u> GALLRVKRLE	737 $\pm$ 110				
SAAS <sup>235-246</sup> P10A	<u>A</u> LGALLRVKRLE	177 $\pm$ 6.6				
SAAS <sup>235-246</sup> P1K	VLGALLRVK <u>K</u> LE	1530 $\pm$ 198				
SAAS <sup>235-246</sup> P4K	VLGALL <u>K</u> VKRLE	177500 $\pm$ 3020				
SAAS <sup>235-246</sup> P1KP4K	VLGALL <u>K</u> VK <u>K</u> LE	N.I.(185 $\mu$ M)				
SAAS <sup>235-246</sup> P3AP5A	VLGAL <u>A</u> R <u>A</u> KRLE	13700 $\pm$ 1200	127 $\pm$ 30	27700 $\pm$ 720	10817 $\pm$ 4541	1 : 1 : 218 : 85
PenLen[rsAAS <sup>221-254</sup> ]		119 $\pm$ 1.5	19300 $\pm$ 1800	1400 $\pm$ 200	4630 $\pm$ 600	1 : 162 : 12 : 39
AVDQDLGPEVPPENVLGALLRVKRLNSSPQAPA						

( $K_i \approx 50.5$  nM). PenLen ( $K_i \approx 120$  nM) is nearly 3- and 13-fold less efficient than proSAAS<sup>235-246</sup> and proSAAS<sup>235-244</sup>, respectively. The extent of PC1 inhibition by proSAAS peptides is sensitive to the pre-incubation time preceding substrate addition. Accordingly, for a fixed inhibitor concentration, a 15 min pre-incubation period of enzyme and inhibitor is necessary for maximal PC1 inhibition. The progress curves in the presence of various concentrations of proSAAS<sup>235-244</sup> indicated a slow and tight binding inhibition. This type of binding is also deduced from the characteristic observation that  $IC_{50}$  of proSAAS<sup>235-244</sup> increased linearly with the enzyme amount [3].

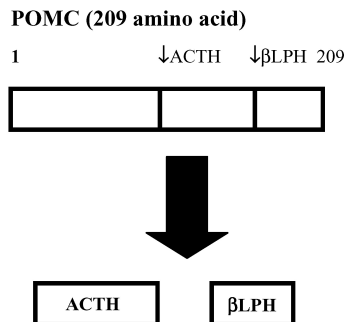


Fig. 1. POMC processing by PC1.

**Digestion of proSAAS peptides by PCs.** ProSAAS<sup>235-246</sup> was found to behave as a competitive substrate being cleaved by PC1 at VLGALLRVKR<sup>244</sup>↓LE. However, it is cleaved best by PACE4 and least by PC1, but PenLen containing this peptide in its internal sequence is most efficiently cleaved by PC1, and not at all by either PC5 or PC7.

**Cell permeable PC-inhibitors.** The highly potent and selective PC1 inhibitor proSAAS<sup>235-244</sup> was conjugated *via* a linker to R<sub>8</sub> as indicated: RRRRRR-εAhx-εAhx-VLGALLRVKR (εAhx = ε amino hexanoic acid). This peptide, when added exogenously to AtT-20 cells, was able to block PC1-induced *ex vivo* cleavage of POMC into ACTH and β-LPH (Figure 1). The data was compared with those of nonconjugated proSAAS<sup>235-244</sup>, as well as poor PC1 inhibitors (Figure 2). R<sub>8</sub>-containing peptide at 50 μM concentration can block this cleavage by nearly 2-fold, while the rest of the peptides exhibited no effect. Similar results were achieved with S<sup>35</sup>-labeled AtT-20 cell lines.

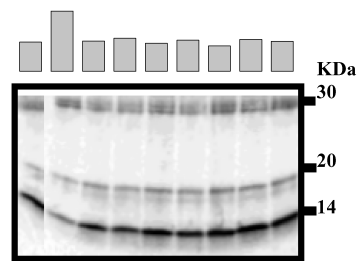


Fig. 2. Western blot analysis on AtT-20 cell medium in presence and absence of various SAAS peptides (50 μM). From left: control, R<sub>8</sub>SAAS<sup>235-244</sup> 2 h, SAAS<sup>235-244</sup> 2 h, 4 h, 6 h, SAAS<sup>235-246</sup>PIA 2 h, 4 h, dextro SAAS<sup>235-244</sup> 2 h, 4 h. The bar indicates the ratio of band density of POMC and β-LPH. The black lines on the right represent the markers of molecular weights 30, 20 and 14 kDa (top to bottom).

In conclusion, our data suggests that conjugation of polyarginine can be used as a promising strategy to deliver inhibitors across the cell membrane. (CIHR and NSERC fund).

## References

1. Seidah, N.G. Chrétien, M. *Brain Res.* **848**, 45–62 (1999).
2. Fricker, L.D., McKinzie, A.A., Sun, J., Curran, E., Qian, Y., Yan, L., Patterson, S.D., Courchesne, P.L., Richards, B., Levin, N., Mzhavia, N., Devi, L.A., Douglass, J. *J. Neurosci.* **20**, 639–648 (2000).
3. Apletalina, E.V., Juliano, M.A., Juliano, L., Lindberg, I. *Biochem. Biophys. Res. Commun.* **267**, 940–942 (2000).
4. Mzhavia, N., Berman, Y., Che, F.Y., Fricker, L.D., Devi, L.A. *J. Biol. Chem.* **276**, 6207–6213 (2001).
5. Futaki, S., Suzuki, T., Ohashi, W., Yagami, T., Tanaka, S., Ueda, K., Sugiura, Y. *J. Biol. Chem.* **276**, 5836–5840 (2001).

## Bicyclic Peptide Inhibitors of an Epithelial Cell-Derived Transmembrane Protease, Matriptase

Peter P. Roller<sup>1</sup>, Ya-Qiu Long<sup>1</sup>, Peng Li<sup>1</sup>, Sheau-Ling Lee<sup>2</sup>,  
Chen-Yong Lin<sup>2</sup>, Istvan Enyedy<sup>2</sup>, Shaomeng Wang<sup>2</sup>  
and Robert B. Dickson<sup>2</sup>

<sup>1</sup>Laboratory of Medicinal Chemistry, National Cancer Institute, NIH, FCRDC, 376/208,  
Frederick, MD 21702, USA

<sup>2</sup>Lombardi Cancer Center, Georgetown University Medical Center,  
Washington, DC 20007, USA

### Introduction

Matriptase is a recently identified type II transmembrane protease that is found on the surface of epithelial cells [1,2]. It is overexpressed in most cancer cells, including human breast cancer cells. It is a multidomain protein with a C-terminal extracellular region containing the protease domain. It activates urokinase-type of plasminogen activator (uPA), and the protease activated receptor (Par-2). It has been demonstrated that matriptase can proteolytically activate hepatocyte growth factor (HGF/Scatter Factor) to its active form, and thus it may function in epithelial cell migration, cancer invasion and metastasis [2]. Developing inhibitors of matriptase provides for a therapeutic approach to metastatic diseases, and in particular, cancer.

We have chosen the recently isolated natural product, SFTI-1 (Sunflower Trypsin Inhibitor-1) [3], as a prototype inhibitor of matriptase (Figure 1). The structure of SFTI-1 was elucidated using X-ray crystallography. It is a 14 amino acid long backbone cyclized peptide, bisected with a single cystine disulfide bridge. It was reported to possess very potent inhibitory activity to serine proteases [3]. We report here the synthesis and further characterization of this inhibitor for its inhibitory effectiveness on matriptase.

### Results and Discussion

SFTI-1 was synthesized using Fmoc chemistry based protocols. The linear peptide was assembled on a Rink acid resin. Gly is attached as the first amino acid on the resin, in order to avoid racemization during the synthesis. The side chain protected peptide was cleaved from the resin with 2% TFA, and the peptide was cyclized with HATU/HOAt/DIEA/ DMF. The protective groups were removed with TES-TFA-H<sub>2</sub>O. The bicyclic peptide, SFTI-1, was generated by air oxidation of the two cysteines in weakly basic medium. This approach also provided us the methodology to prepare a variety of analogs for SAR studies. Enzyme inhibitory assays were carried out with

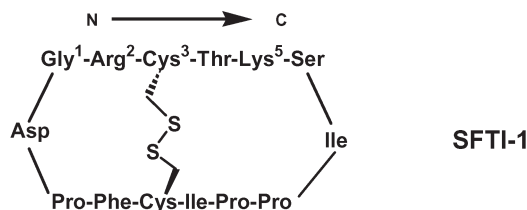


Fig. 1. Structure of SFTI-1.

matriptase proteolysis assay using the fluorescent substrate, N-t-Boc-Gln-Ala-Arg-AMC [2].  $K_i$  values were determined using Dixon plots (Table 1).

Results show that the synthetic SFTI-1 inhibited matriptase at 1 nM concentration, and it was equally inhibitory to trypsin. It was much less potent against the serum protein, thrombin, and essentially non-inhibitory to uPA [4].

*Table 1. Protease inhibitory properties of SFTI-1.*

Protease	$K_i$ (nM)
Matriptase	0.92
Trypsin	1.06
Thrombin	5 050
uPA	500 000

In order to establish a rational basis for selective inhibitor design, we carried out homology modeling to build the 3D structure of matriptase complexed with SFTI-1. Matriptase has a 34% amino acid identity and 53% similarity to thrombin. In addition, the X-ray structure of SFTI-1 complexed with trypsin was available for the initial homology modeling [3]. This structural model suggests that the two basic amino acids, Lys<sup>5</sup> and Arg<sup>2</sup> of SFTI-1 provide important interactions, within the catalytic cavity of matriptase. Lys<sup>5</sup> of SFTI-1 binds to the S1 pocket of the enzyme. Arg<sup>2</sup> forms an H-bond with the main chain carbonyl of Phe706, and interacts with Phe708 and Phe706 sidechains of matriptase through  $\pi$ -cation interactions. Since the homology modeling based distance geometries are taken only as approximate, SAR studies will be performed to optimize the effectiveness of Lys<sup>5</sup> and Arg<sup>2</sup> sidechains, in particular. Efforts are also focused on replacing the cystine disulfide linkage of the peptide with redox stable thioether and olefinic bisecting bridges.

SFTI-1 is a rigid molecule with an extensive network of intramolecular hydrogen bonds. It is proteolytically stable on account of its rigid architecture, and this makes it well suited for evaluation in cells for inhibitory effectiveness on the activation of the latent form of HGF. SFTI-1 and its analogs may well be suitable for inhibitory studies of metastatic tumors in animal models also.

### Acknowledgments

We thank for the support by a Department of Defense Fellowship DAMD 17-00-1-0269, to S.-L. Lee.

### References

1. Lin, C.-Y., Wang, J.-K., Torri, J., Dou, L., Sang, Q.A., Dickson, R.B. *J. Biol. Chem.* **272**, 9147–9152 (1997).
2. Lee, S.-L., Dickson, R.B., Lin, C.-Y. *J. Biol. Chem.* **275**, 36720–36725 (2000).
3. Luckett, S., Santiago-Garcia, R., Barker, J.J., Konarev, A.V., Shewry, P.R., Clarke, A.R., Brady, R.L. *J. Mol. Biol.* **290**, 525–533 (1999).
4. Long, Y.-Q., Lee, S.-L., Lin, C.-Y., Enyedy, I., Wang, S., Li, P., Dickson, R.B., Roller, P.P. *Bioorg. Med. Chem. Lett.* **11**, 2515–2519 (2001).

## Probing the Substrate Specificity of Hepatitis C Virus Nonstructural 3 Protein Serine Protease by Intramolecularly Quenched Fluorogenic Peptide Substrates

Addy Po<sup>1</sup>, Morgan Martin<sup>1</sup>, Martin Richer<sup>1</sup>, Maria A. Juliano<sup>2</sup>,  
 Luiz Juliano<sup>2</sup> and François Jean<sup>1</sup>

<sup>1</sup>Department of Microbiology and Immunology, University of British Columbia, Vancouver,  
 V6T 1Z3, Canada

<sup>2</sup>Department of Biophysics, Escola Paulista de Medicina, Universidade Federal de Sao Paulo,  
 Sao Paulo, 04044-020, Brazil

### Introduction

Recent information about the incidence of Hepatitis C (HCV) around the world clearly indicates that the virus is a major public health issue: the estimated worldwide prevalence is approximately 1% [1]. The need to rapidly identify new therapeutic approaches has resulted in intensive study of the molecular properties of this virus, yet thus far no efficient therapy or vaccine exists. Currently, one of the most promising approaches to anti-HCV therapy is the development of inhibitors of the virally encoded serine protease, nonstructural 3 (NS3) [1]. Elucidating the substrate specificity of the HCV NS3 protease is important for the development of high-throughput assays (HTA) for random screening of HCV protease inhibitors and for rational design of HCV protease-specific inhibitors [2]. As a first step towards the realization of these aims, we report here our progress in probing the substrate specificity of two HCV NS3 variants, ΔNS3 [3] and full-length (FL) NS3 [4], with intramolecularly-quenched fluorogenic peptide substrates (IQFS) [5], based on fluorescence resonance energy transfer (FRET) between the donor/acceptor couple (Abz, EDDnp; Figure 1A and [6]). Cleavage of a FRET substrate by an enzyme separates the fluorophore from the quenching group, which results in the generation of a fluorescence signal (Figure 1 and [5,6]).

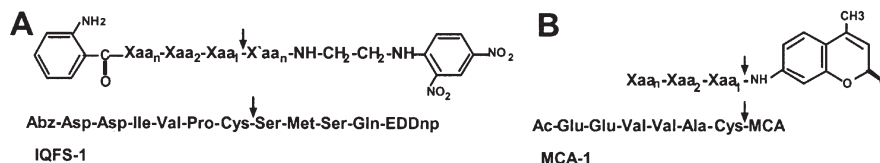


Fig. 1. Chemical structures of IQFS-1 and MCA-1. (A) IQFS-1 was synthesized by solid-phase peptide synthesis based on Fmoc chemistry [6]. The fluorescent ortho-aminobenzoic acid (Abz) is efficiently quenched by long-range resonance energy transfer to the [N-(ethylenediamine)-2,4-dinitrophenyl amide] (EDDnp) moiety. (B) MCA-1. Peptidyl 4-methyl-7-coumarylamide (MCA). (Xaa = any amino acid; Arrow = cleavage site).

### Results and Discussion

Synthetic peptide substrates based on the natural cleavage sites of the HCV NS polypeptide are currently in use for the biochemical characterization of HCV NS3 protease and the screening of protease inhibitors [2]. Here, we report a new high-throughput assay of the HCV NS3 protease/NS4A peptide cofactor complex (Figure 2) based on intramolecular FRET between the donor/acceptor couple Abz/EDDnp [3,4].

In contrast with the commercially available peptidyl-coumarinamide substrate MCA-1 (Figure 2A), in which the P' portion is replaced with a coumarinamide moiety (Figure 1B), the IQFS synthesized in this study (IQFS-1) (Figure 1A) allowed efficient detection of the FLNS3 protease/NS4A complex activity (Figure 2B and 2C).

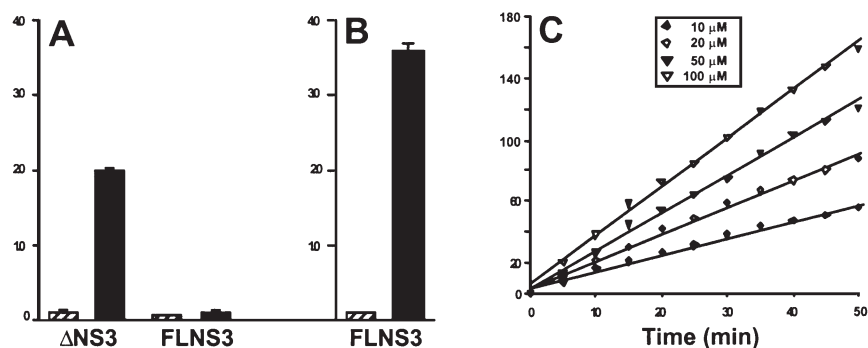


Fig. 2. Discrepancy is observed for NS3 variants in the efficiency of cleavage of (A) MCA-1 and (B) IQFS-1. The enzyme reaction was carried out as described previously [3,4] using 100  $\mu$ M of fluorogenic substrates in the absence (open bars) or presence (filled bars) of 15  $\mu$ M of NS4A-derived peptide cofactor: In vitro, NS3 can be activated by addition of peptide-harboring residues 21-34 of the HCV NS4A cofactor (Pep4AK) [4]. (C) Continuous monitoring of the progress of hydrolysis of IQFS-1 by FLNS3 protease/NS4A complex using 10, 20, 50 and 100  $\mu$ M of IQFS-1 and a fluorescence plate reader.

## Conclusions

We have now developed a FRET substrate suitable for the continuous monitoring of HCV NS3 protease/NS4A complex activity for both  $\Delta$ NS3 and bifunctional protease-helicase FLNS3. In contrast to fluorogenic and chromogenic ester substrates, this new IQFS based on the HCV NS5A/5B junction is well suited for the screening and detailed mechanistic studies of all types of inhibitors, including molecules that compete for the more distal P' sites [2,5]. Therefore, IQFS-1 will be a useful tool for identifying and developing HCV NS3 protease-specific inhibitors.

## Acknowledgments

We are grateful to Dr. N. Kakiuchi and Dr. P. Gallinari for the gift of the plasmids pHisB $\Delta$ NS3 and pETNS3FL, respectively. The authors thank Laura Willihnganz for the artwork. This work was supported by a CIHR/Health Canada Research Initiative on Hepatitis C operating grant (F. Jean: 22R90329). F. Jean is a CIHR/Health Canada Scholar.

## References

1. Bartenschlager, R., Lohman, V. *J. Gen. Virol.* **81**, 1631–1648 (2000).
2. Pessi, A. *J. Peptide Sci.* **7**, 2–14 (2001).
3. Vishnuvardhan, D., et al., Nishikawa, S. *FEBS Lett.* **402**, 209–212 (1997).
4. Gallinari, P., et al., De Francesco, R. *Biochemistry* **38**, 5620–5632 (1999).
5. Jean, F., et al., Lazure, C. *Biochem. J.* **307**, 689–695 (1995).
6. Oliveira, V., et al., Juliano, L. *Anal. Biochem.* **292**, 257–265 (2001).

## **Characterization of the *Staphylococcus aureus* Sortase Transpeptidase: A Novel Target for the Development of Chemotherapeutics Against Gram-Positive Bacteria**

**Ryan Kruger, Scott Pesiridis and Dewey G. McCafferty**

*Johnson Research Foundation and the Department of Biochemistry and Biophysics,  
University of Pennsylvania, Philadelphia, PA 19104-6059, USA*

### **Introduction**

Antibiotic resistance is becoming an ever more pressing problem as vancomycin resistant *Staphylococcus aureus* infections are becoming common in hospital acquired infections. To combat these resistant microbes, novel targets that provide new routes to treatment will be necessary. One avenue of therapy would involve preventing bacterial colonization by removing the ability of bacteria to become adherent to endothelial tissue. The *S. aureus* Sortase enzyme (SrtA) is a membrane-associated cell wall transpeptidase that covalently anchors protein virulence factors to the outer surface of the bacterial peptidoglycan. Cell wall-anchored virulence proteins are involved in a myriad of functions such as: (1) capture and presentation of immunoglobulins for evasion of host immune defenses (e.g. Protein A) (2) modulation of adhesion to endothelial tissue (e.g. fibronectin-binding protein) (3) adherence to plastics found in intercranial shunts and indwelling catheters. Common to these virulence factors is a highly conserved C-terminal LPXTG sequence, the recognition site for Sortase. In *S. aureus*, Sortase cleaves the Thr-Gly peptide bond within LPXTG and creates a new peptide bond with the amino terminus of a peptidoglycan Gly5 pentapeptide bridging sequence [1]. Genetic deletion of Sortase in both *S. aureus* [2] and *Streptococcus gordonii* [3] results in bacteria with markedly reduced capacity for colonization. Here we report results from the *in vitro* characterization of Sortase activity and inhibition.

### **Results and Discussion**

To investigate the mechanism and substrate specificity of Sortase, we have cloned, overproduced, and purified to homogeneity *S. aureus* Sortase containing an N-terminal deletion of the membrane anchor, SrtA<sub>ΔN33</sub>. To monitor the enzymatic activity, we have developed both a novel fluorescence-quenching assay using peptides derived from the LPXTG and GGGGG motifs with anthranilic acid (Abz) and *meta*-nitrotyrosine (m-NO<sub>2</sub>Tyr) as the partner LPXTG-containing fluorophore and quencher as well as a more robust HPLC assay using a 2,4-dinitrophenyl (Dnp) labeled substrate.

Through the use of a Dnp-labeled substrate (Dnp-AQALPETGEE-OH) and an HPLC based assay, kinetic information on the reaction catalyzed by sortase (Table 1) was obtained. A  $K_M$  of 31.78  $\mu M$  for pentaglycine and a  $K_M$  of 5.68 mM for the DNP-labeled peptide were observed. The  $k_{cat}$  of the reaction was  $1.3 \cdot 10^{-3} s^{-1}$ . These values are in stark contrast to those previously reported using the fluorescence quenching substrate dabsyl-QALPETGEE-edans [5], with our  $k_{cat}$  being over 500-fold higher. We attribute these differences to the inability to observe the reaction at high substrate concentrations using a fluorometric assay due to inner filter effect limitations.

Bisubstrate experiments aimed at determining the order of addition of substrates and release of products were performed. The result of varying each substrate concentration while holding the other constant is a pattern of lines consistent with noncom-

Table 1. Kinetic parameters of the Sortase catalyzed transpeptidation reaction.

DnpAQALPETGEE-OH	$K_M^A$	$K_M^B$	$V_{max}$	$k_{cat}$	$k_{cat}/K_M^A$	$k_{cat}/K_M^B$
	5.68 mM	31.78 $\mu$ M	113.12 nM/sec	$1.3 \cdot 10^{-3}$ $\text{sec}^{-1}$	$2.3 \cdot 10^{-7}$ $\mu\text{M}^{-1} \text{sec}^{-1}$	$4.1 \cdot 10^{-5}$ $\mu\text{M}^{-1} \text{sec}^{-1}$

petitive behavior. While this rules out a ping-pong mechanism, further studies using product inhibitors are necessary to distinguish between a random and an ordered mechanism.

We have also prepared the phosphinate octapeptide  $\text{NH}_2\text{-ALPEA}\Psi(\text{PO}_2\text{HCH}_2)\text{GEE-OH}$  by solid phase methods [4] as a transition state mimic of the Thr-Gly scissile bond. (Figure 1). This phosphinate peptide mimetic exhibited inhibition with a  $K_I$  equal to 2.5 mM. As demonstrated by its poor inhibition, the transition state may not be accurately mimicked by this molecule. Present efforts are directed towards the design and synthesis of inhibitors based on the pentaglycine substrate and will include reactive electrophiles targeted at the putative reactive site cysteine 184. NMR characterization of the substrate and inhibitor-bound conformation of the enzyme to assist in structure-based inhibitor design is presently underway.

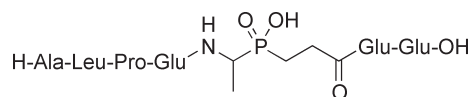


Fig. 1.  $\text{NH}_2\text{-ALPEA}\Psi(\text{PO}_2\text{HCH}_2)\text{GEE-OH}$ .

The development of our HPLC assay and our discovery of the improved kinetic parameters will allow us to complete the chemical and kinetic mechanism of Sortase rapidly and efficiently. This information will open the door to the development of antibiotics that will target the pathogenicity of previously untreatable infections such as multidrug resistant *Staphylococcus aureus* and other Gram-positive infections.

## References

1. Mazmanian, S.K., Liu, G., Ton-That, H., Schneewind, O. *Science* **285**, 760–763 (1999).
2. Mazmanian, S.K., Liu, G., Jensen, E.R., Lenoy, E., Schneewind, O. *PNAS* **97**, 5510–5515 (2000).
3. Bolken, T.C., Franke, C.A., Jones, K.F., Zeller, G.O., Jones, C.H., Dutton, E.K., Hruby, D.E. *Infect. Immun.* **69**, 75–80 (2001).
4. Buchardt, J., Meldal, M. *J. Chem. Soc., Perkin Trans. I* 3306–3310 (2000).
5. Ton-That, H., Mazmanian, S.J., Faull, K.F., Schneewind, O. *J. Biol. Chem.* **275**, 9876–9881 (2000).

## **Cyclic Octapeptide Inhibitors of the Acetylcholinesterase Peripheral Site: Implications for Inhibition of Nerve Toxins**

**Peteris Romanovskis<sup>1</sup>, Terrone L. Rosenberry<sup>2</sup>, Bernadette Cusack<sup>2</sup>  
and Arno F. Spatola<sup>1</sup>**

<sup>1</sup>*Department of Chemistry and the Institute for Molecular Diversity and Drug Design,  
University of Louisville, Louisville, KY 40292, USA*

<sup>2</sup>*Department of Neuroscience at Mayo Clinic, Jacksonville, FL 32224, USA*

### **Introduction**

The primary physiological role of acetylcholinesterase (AChE) is to hydrolyze the neurotransmitter acetylcholine at cholinergic synapses. AChE is among the most efficient enzymes, with a turnover number of  $>10^4 \text{ s}^{-1}$  [1]. Ligand binding studies and X-ray crystallography have focused on the structural basis for the enzyme's high catalytic efficiency and revealed that the AChE active site consists of a narrow gorge some 20 Å deep with two separate ligand binding sites: an *acylation site* at the bottom of the gorge where substrate hydrolysis occurs, and a *peripheral site* at the gorge mouth.

Recently the fasciculins, a family of similar snake venom neurotoxins from green mambas (genus *Dendroaspis*) have been identified as new, very effective probes of the AChE active site with affinity levels of the native toxin reaching  $K_i = 10\text{--}100 \text{ pM}$ . Fasciculins contain 61 amino acids and 4 disulfide bonds, with three loops protruding from a central core. Fasciculins interact with the peripheral site of AChE at the rim of the gorge, but this interaction does not totally exclude/prevent access of ligands to the catalytic site.

Our goal has been to design an inhibitor that will bind to the peripheral site and exclude toxic organophosphorylating agents from the acylation site while interfering minimally with acetylcholine passage.

### **Results and Discussion**

Our initial efforts focused on large libraries of several hundred cyclic peptides with random amino acid sequences. Several sets of peptides indicated AChE binding at high total peptide concentrations (100  $\mu\text{M}$ ), and common features began to emerge:

- 1) Most of the libraries that gave positive results possessed amino acid sequences with positively charged residues;
- 2) There was a clear preference in binding and inhibitory activity for libraries with 7- and 8-residue cyclic peptides.

With this information we initiated the direct design of the next series of cyclic compound libraries using loop II of fasciculin: cyclo(-Arg-Arg-His-Pro-Pro-Lys-Met-Xxx-), where Xxx stands for the amino acid residue that is used for the side chain attachment during the on-resin synthesis and cyclization (Asn or Gln) [2]. A related study using disulfide bridged peptides has also been reported [3]. Closer examination of the AChE – fasciculin crystal structure indicated that Arg<sup>2</sup>, Lys<sup>6</sup>, and Xxx do not make direct contact with the enzyme surface. We varied these residues and others to evaluate the effect of different side chains or peptide linkages on cyclic peptide activity. In addition, novel side chains (Nle, Nal, and C-alpha-methyl-Nal) were inserted in an attempt to improve inhibitor potency by altering peptide hydrophobicity and conformational flexibility. Inhibitory peptides identified as promising candidates from initial screening assays were analyzed to determine their  $K_i$  for AChE (Table 1).

Table 1. Inhibitory activity of promising peptides.

Octapeptide inhibitors at the AChE peripheral site												
Peptide sequence								Percent inhibition, initial screen				K <sub>i</sub> μM
1	2	3	4	5	6	7	8	Activity		Fas binding		
Fasciculin (27-34)								10 μM	1 μM	10 μM	1 μM	
R	R	H	P	P	K	M	V					
cyclic peptides												
R	L-Nal	H	P	P	K	M	Q	79	40	52	14	0.2
R	A	H	P	P	K	L-Nal	Q	78	28	62	23	1
R	A	H	P	P	K	D-Nal	Q	68	21	50	7	1.5
R	D-Nal	H	P	P	K	M	Q	65	27	54	27	1.1
R	A	H	P	P	K	M	Q	51	16	53	36	2
R	A	H	P	P	K	M	N	29	5	15	0	64
linear peptide												
R	A	H	P	P	K	Nle	Q	18	12	20	26	14.4

The main results can be summarized as follows: synthetic linear and cyclic octapeptides corresponding to fasciculin fragment 27-34 (loop II) effectively inhibit AChE in the micromolar concentration range. In all cases the cyclic analogues proved more potent inhibitors than their linear counterparts. Cyclic analogues obtained through Gln side chain attachment show greater inhibitory potency than those formed through Asn side chain attachment. Introduction of hydrophobic Nal residues at certain octapeptide positions represents the best choice at present for the increase of the AChE inhibitory potency of the compounds.

#### Acknowledgments

Supported by NIH GM 33376 and US Army DAMD 17-98-2-8019.

#### References

1. Rosenberry, T.L. *Adv. Enzymol. Relat. Areas Mol. Biol.* **43**, 103–218 (1975).
2. Spatola, A.F., Romanovskis, P. *The Amide Linkage: Selected Structural Aspects in Chemistry, Biochemistry and Material Science*, Greenberg, A., Breneman, C.M., Liebman, J.F., John Wiley, New York, 2000, pp. 519–564.
3. Falkenstein, R.C., Pena, C. *Biochim. Biophys. Acta* **1340**, 143–151 (1997); *J. Protein Chem.* **18**, 233–238 (1999).

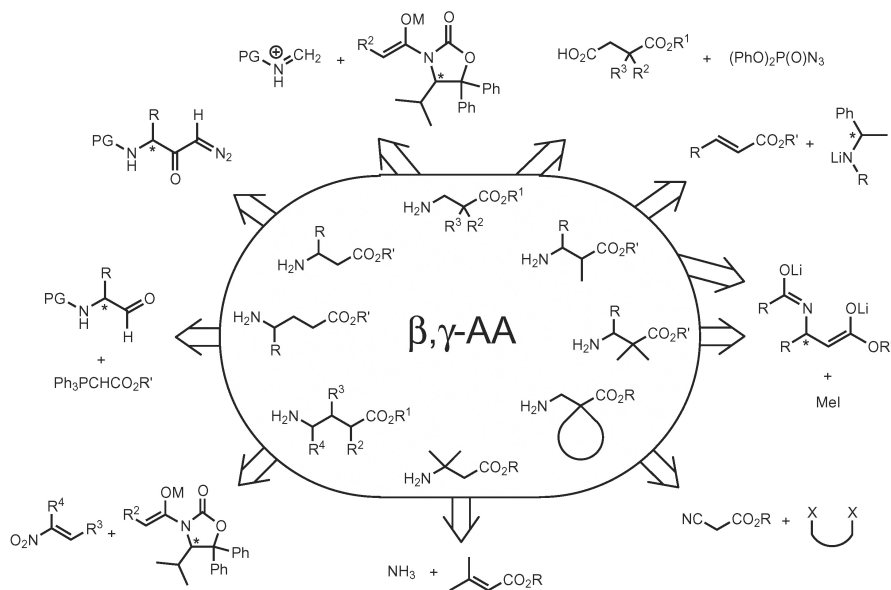
# Homologs of Amino Acids and Explorations into the Worlds of $\beta$ - and $\gamma$ -Peptides

Dieter Seebach

*Laboratorium für Organische Chemie, Eidgenössische Technische Hochschule,  
CH-8092 Zürich, Switzerland*

Six years ago we initiated a project, which originated from our work on the biopolymer and on oligomers built from  $\beta$ -hydroxybutanoic acid (PHB, OHB) [1]. The question arose: *what happens upon insertion of one or two  $\text{CH}_2$  groups in the backbone of each and every amino acid residue of a peptide?* The uniform answer of the specialists in the field of peptides and proteins was: *chaos!*

To test the idea, we synthesized the homologues of the proteinogenic  $\alpha$ -amino acids, the  $\beta$ - and  $\gamma$ -amino acids by known methods (Scheme 1).



*Scheme 1. Methods for synthesis of amino acid homologues.*

These homologues were assembled to the corresponding  $\beta$ - and  $\gamma$ -peptides by the established techniques of protecting, activating, coupling (step-by-step, or fragments; on solid phase, manually or by machine), deprotecting, and HPLC purifying. Identification of the resulting peptide analogs was achieved using MS, CD, NMR, and X-ray methods, as with  $\alpha$ -peptides and proteins. In the five years since our first paper [2] we have shown that  $\beta$ - and  $\gamma$ -peptides, like their natural  $\alpha$ -peptidic models, fold to helices [3], turns [4] and hair-pins [5], and form pleated sheets [5], as well as stacks of cyclic derivatives [6] (Figure 1).

The actual shapes, sizes, dimensions, and polarities of these secondary structures are, however, totally different in the homologous series. Thus, when we go from L- $\alpha$ - to L- $\beta^3$ - to L- $\gamma^4$ -amino acid residues, the helices of the resulting peptides are 3.6<sub>13</sub>, 3<sub>14</sub>,

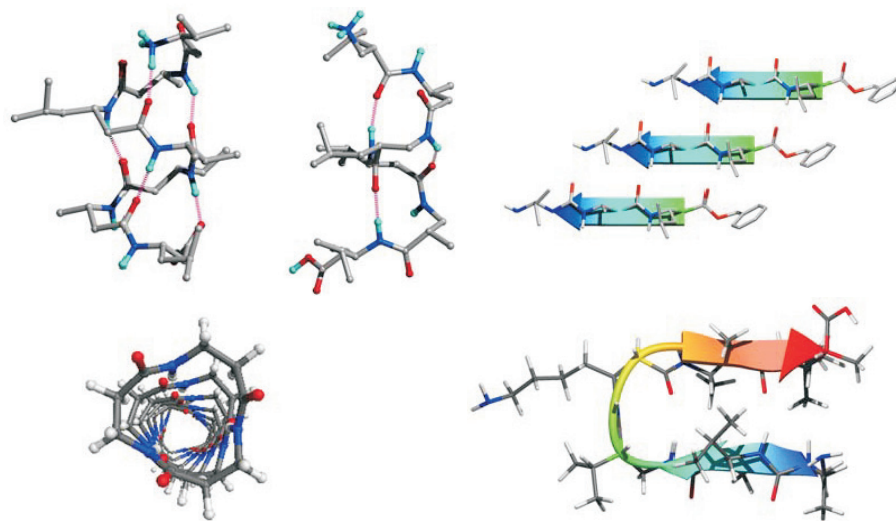


Fig. 1. Secondary structures formed by  $\beta$ - and  $\gamma$ -peptides.

and  $2.6_{14}$ , their handedness reverses from right to left to right, and their dipoles run from N $\rightarrow$ C, C $\rightarrow$ N, and N $\rightarrow$ C terminus, respectively (Figure 2).

The most surprising fact, at first sight, is, however, that the stability of the helix increases from  $\alpha$ - to  $\beta$ - to  $\gamma$ -peptides: it takes six  $\beta$ - and only four  $\gamma$ -amino acid residues to detect the helices in MeOH or H<sub>2</sub>O solution [7,8]. We are now able to design simple

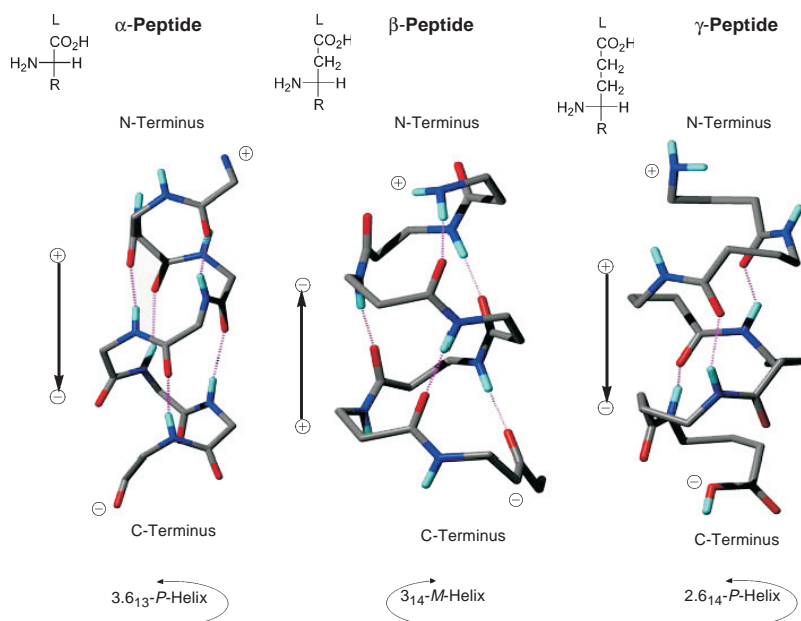


Fig. 2. Handedness of helices formed by  $\alpha$ -,  $\beta$ -, and  $\gamma$ -peptides.

$\beta$ -hexapeptides (from homologated proteinogenic amino acid residues [9]) that form either one of two helices (the  $3_{14}$  or a 12/10 helix) or, else, a hairpin.

Like in the “ $\alpha$ -world”, the  $3_{14}$  helix of  $\beta$ -peptides can be “fixed” by a disulfide clamp [10], stabilized by a salt bridge between charged side chains [11], or rendered amphiphilic by proper placement of polar and non-polar side chains [12]. So-called “ $\beta$ II turns” of  $\alpha$ -peptides are usually part of longer chains and/or require special amino acids (a D-amino acid, a glycine, a proline); with  $\beta$ - and  $\gamma$ -peptides four [4] and two [13] residues, respectively, suffice for the turn to be seen by NMR spectroscopy.

Most remarkably, the homo-peptides are absolutely stable against peptidases, as demonstrated in *ca* 300 tests with a series of 15 peptide-cleaving enzymes and 36 different linear and cyclic  $\beta$ - and  $\gamma$ -peptides (consisting of 2 to 15 residues) [14]. This property, together with the fact that functionalized side chains on turns can be arranged in identical geometries with  $\alpha$ -,  $\beta$ - and  $\gamma$ -peptidic backbones [4,13], and that amphipathic helices of  $\alpha$ -peptides can be mimicked by  $\beta$ -peptides [12], renders the novel peptides, presented here, “hot” candidates for drugs, an aspect which is actively pursued in pharmaceutical companies [4,15].

## References

1. Seebach, D., Fritz, M.G. *Int. J. Biol. Macromol.* **25**, 217–236 (1999).
2. Seebach, D., Overhand, M., Kühnle, F.N.M., et al. *Helv. Chim. Acta* **79**, 913 (1996).
3. Seebach, D., Abele, S., Gademann, K., et al. *Helv. Chim. Acta* **81**, 932 (1998).
4. Gademann, K., Kimmerlin, T., Hoyer, D., Seebach, D. *J. Med. Chem.* (2001), in press.
5. Seebach, D., Abele, S., Gademann, K., Jaun, B. *Angew. Chem.* **111**, 1700 (1999).
6. (a) Seebach, D., Matthews, J.L., Meden, A., Wessels, T., Baerlocher, C., McCusker, C.L. *Helv. Chim. Acta* **80**, 173 (1997). (b) Le, H.B., Hintermann, T., Wessels, T., Gan, Z., Seebach, D., Ernst, R.R. *Helv. Chim. Acta* **84**, 187 (2001).
7. Seebach, D., Schreiber, J.V., Abele, S., Daura, X., van Gunsteren, W.F. *Helv. Chim. Acta* **83**, 34 (2000).
8. (a) Hintermann, T., Gademann, K., Jaun, B., Seebach, D. *Helv. Chim. Acta* **81**, 983 (1998). (b) Hanessian, S., Luo, X., Schaum, R., Michnick, S. *J. Am. Chem. Soc.* **120**, 8569.
9. For  $\beta$ -peptides with conformationally restricted backbones see: Gellman, S.H. *Acc. Chem. Res.* **31**, 173 (1998).
10. (a) Rueping, M., Jaun, B., Seebach, D. *Chem. Commun.* **22**, 2267 (2000). (b) Jacobi, A., Seebach, D. *Helv. Chim. Acta* **82**, 1150 (1999).
11. Arvidsson, P.I., Rueping, M., Seebach, D. *Chem. Commun.* **7**, 649 (2001).
12. (a) Werder, M., Hauser, H., Abele, S., Seebach, D. *Helv. Chim. Acta* **82**, 1774 (1999). (b) Schreiber, J.V., Seebach, D. *Helv. Chim. Acta* **83**, 3139 (2000).
13. Brenner, M., Seebach, D. *Helv. Chim. Acta* (2001), in press.
14. Frackenhohl, J., Arvidsson, P.I., Schreiber, J.V., Seebach, D. *ChemBioChem* **2**, 445 (2001).
15. Arvidsson, P.I., Frackenhohl, J., Ryder, N.S., Liechty, B., Petersen, F., Zimmermann, H., Camenisch, G.P., Woessner, R., Seebach, D. *ChemBioChem* (2001), submitted.

## Designed Amino Acids That Induce $\beta$ -Sheet Folding and $\beta$ -Sheet Interactions in Peptides

James S. Nowick<sup>1</sup>, Kit S. Lam<sup>2</sup>, Chris M. Gothard<sup>1</sup>, Jeffrey K. Huon<sup>1</sup>,  
William E. Kemnitzer<sup>1</sup>, Tatyana Khasanova<sup>1</sup>, Hong Woo Kim<sup>1</sup>, Ruiwu  
Liu<sup>2</sup>, Santanu Maitra<sup>1</sup>, Hao T. Mee<sup>1</sup> and Kimberly D. Stigers<sup>1</sup>

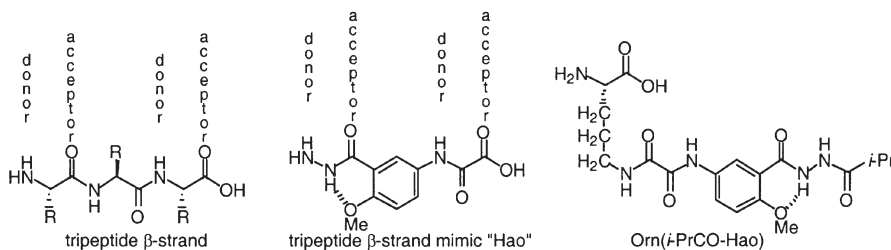
<sup>1</sup>Department of Chemistry, University of California, Irvine, Irvine, CA 92697-2025, USA

<sup>2</sup>Department of Internal Medicine, University of California Davis Cancer Center,  
Sacramento, CA 95817, USA

### Introduction

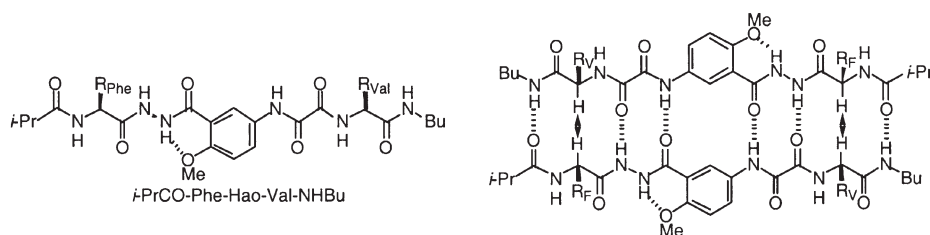
For the past several years, our research laboratory has been developing chemical models of protein  $\beta$ -sheets in which molecular templates induce  $\beta$ -sheet structure in attached peptide strands [1]. We have termed these structures *artificial  $\beta$ -sheets* and call the templates a molecular *scaffold* and a  *$\beta$ -strand mimic* to reflect their structural roles. The molecular scaffold holds the peptide and peptidomimetic groups in proximity; the  $\beta$ -strand mimic duplicates the hydrogen-bonding functionality of a peptide  $\beta$ -strand and helps align the peptide strand by hydrogen bonding to it. A few years ago, we asked the deceptively simple question: "What happens when we move the  $\beta$ -strand mimic to the bottom edge of an artificial  $\beta$ -sheet?" [2] Its answer proved both exciting and significant. Not only did the molecules fold to adopt  $\beta$ -sheet-like structures, but these structures also formed well-defined hydrogen-bonded dimers in chloroform solution. This result is noteworthy, both because peptides generally do not form well-defined dimers (they aggregate) and because many proteins do.

$\beta$ -Sheet formation between proteins is an important (and under-recognized) mode of protein-protein interaction, which occurs in various protein dimers, in interactions between different proteins, and in peptide and protein aggregates [3]. Our finding of chemical model systems that mimic these interactions opens the door to the development of compounds that control them. At this point, we recognized that the  $\beta$ -strand mimic of the artificial  $\beta$ -sheet that dimerized could be envisioned as an unnatural amino acid that mimicked the hydrogen-bonding functionality of one edge of a tripeptide  $\beta$ -strand. We termed this amino acid *Hao* to reflect that it is composed of hydrazine, 5-amino-2-methoxybenzoic acid, and oxalic acid components, and we set out to study its synthetic and structural properties [4]. This paper describes the development of the designed amino acid *Hao* and a second designed amino acid *Orn(i-PrCO-Hao)* and discusses their incorporation into peptides.



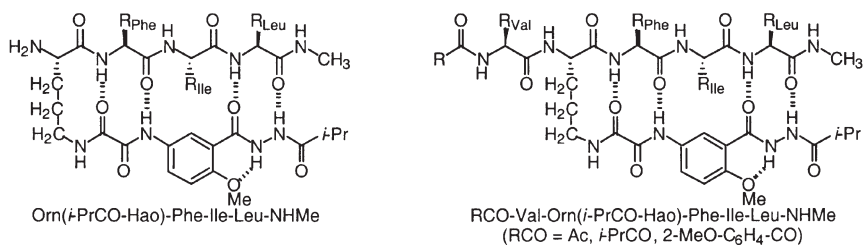
## Results and Discussion

For use in standard Fmoc-based solid-phase peptide synthesis, we developed a version of the Hao amino acid that is protected with the more soluble di-*tert*-butyl Fmoc-analogue, Fmoc\* [5]. We also developed a Boc-protected version of Hao, which is compatible with standard Boc-based peptide synthesis. Fmoc\*-Hao works well with carbodiimide coupling agents and HOBt in standard solid-phase peptide synthesis, although its coupling is slightly less efficient than that of regular amino acids. The Hao-containing peptide *i*-PrCO-Phe-Hao-Val-NHBu was successfully synthesized on PEG-PS-PAL resin using Fmoc\*-Hao and in solution using Boc-Hao.



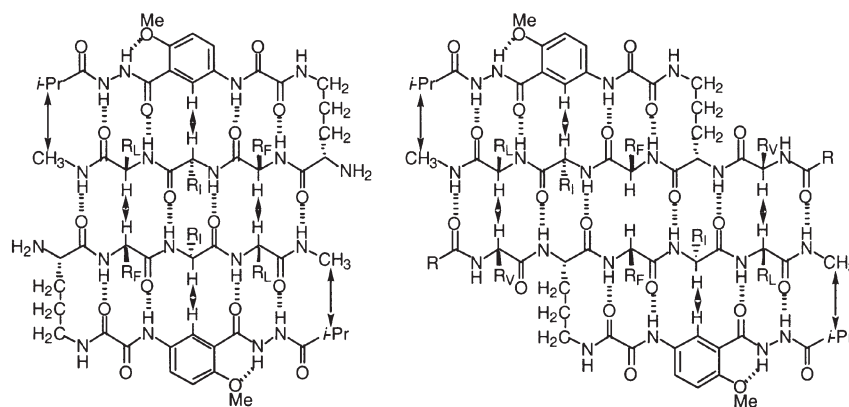
$^1\text{H}$  NMR titration and Tr-ROESY studies reveal that Hao-containing peptides form  $\beta$ -sheet-like hydrogen-bonded dimers. The peptide *i*-PrCO-Phe-Hao-Val-NHBu is fully dimerized in  $\text{CDCl}_3$  solution ( $K_{\text{dim}} \approx 10^6 \text{ M}^{-1}$ ) and exhibits a strong intermolecular NOE between the Phe and Val  $\alpha$ -protons associated with dimer formation (shown with arrows, above right). In the more competitive solvent 10%  $\text{CD}_3\text{OD}-\text{CDCl}_3$ ,  $K_{\text{dim}} = 900 \text{ M}^{-1}$ .

By making a series of small changes to the original artificial  $\beta$ -sheet that dimerized, we discovered that it was possible to retain its folding and dimerization properties while consolidating the molecular scaffold and  $\beta$ -strand mimic into a single amino acid. The resulting Orn(*i*-PrCO-Hao) amino acid acts as a molecular splint to help enforce  $\beta$ -sheet-like structure in peptides. Peptides with appended Orn(*i*-PrCO-Hao) groups (*e.g.*, Orn(*i*-PrCO-Hao)-Phe-Ile-Leu-NHMe) are readily synthesized on solid support from Boc-Orn(Fmoc)-OH and *i*-PrCO-Hao-OH, while peptides that incorporate Orn(*i*-PrCO-Hao) groups (*e.g.*, RCO-Val-Orn(*i*-PrCO-Hao)-Phe-Ile-Leu-NHMe) are readily synthesized on solid support from Fmoc-Orn(*i*-PrCO-Hao)-OH.



$^1\text{H}$  NMR Tr-ROESY studies establish that Orn(*i*-PrCO-Hao)-Phe-Ile-Leu-NHMe and RCO-Val-Orn(*i*-PrCO-Hao)-Phe-Ile-Leu-NHMe fold into  $\beta$ -sheet-like structures that form  $\beta$ -sheet-like hydrogen-bonded dimers in  $\text{CDCl}_3$  solution. These dimers are shown below; the arrows represent key interstrand NOEs. Tr-ROESY studies also es-

establish that the TFA salt of Orn(i-PrCO-Hao)-Phe-Ile-Leu-NHMe folds but does not dimerize in the competitive solvent CD<sub>3</sub>OD.



### Conclusions and Future Directions

$\beta$ -Sheet interactions between proteins are important and widespread. Peptides containing the unnatural amino acids Hao and Orn(i-PrCO-Hao) exhibit similar interactions: Hao-containing peptides form well-defined, hydrogen-bonded,  $\beta$ -sheet dimers; Orn(i-PrCO-Hao)-containing peptides fold into  $\beta$ -sheet-like structures that also form well-defined, hydrogen-bonded,  $\beta$ -sheet dimers. These peptides are readily prepared from Hao, i-PrCO-Hao, or Orn(i-PrCO-Hao) by solid-phase peptide synthesis. The modular design and ease of synthesis afforded by these unnatural amino acids allow rapid evaluation of new structures and ideas. Future studies seek to develop peptides that contain Hao or Orn(i-PrCO-Hao), bind proteins in water through  $\beta$ -sheet interactions, and block protein-protein interactions. By studying  $\beta$ -sheet interactions among chemical model systems and proteins, we aim to eventually develop drugs that control these important protein interactions.

### Acknowledgments

The authors thank the following agencies for support in the form of grants and awards: NIH (GM-49076), NSF (CHE-9813105), Camille and Henry Dreyfus Foundation, Alfred P. Sloan Foundation, and American Chemical Society.

### References

1. Nowick, J.S. *Acc. Chem. Res.* **32**, 287–296 (1999).
2. Nowick, J.S., Tsai, J.H., Bui, Q.-C.D., Maitra, S. *J. Am. Chem. Soc.* **121**, 8409–8410 (1999).
3. Maitra, S., Nowick, J.S., In Greenberg, A., Breneman, C.M., Liebman, J.F. (Eds.) *The Amide Linkage: Structural Significance in Chemistry, Biochemistry, and Materials Science*, Wiley, New York, 2000, Chapter 15.
4. Nowick, J.S., Chung, D.M., Maitra, K., Maitra, S., Stigers, K.D., Sun, Y. *J. Am. Chem. Soc.* **122**, 7654–7661 (2000).
5. Stigers, K.D., Koutroulis, M.R., Chung, D.M., Nowick, J.S. *J. Org. Chem.* **65**, 3858–3860 (2000).

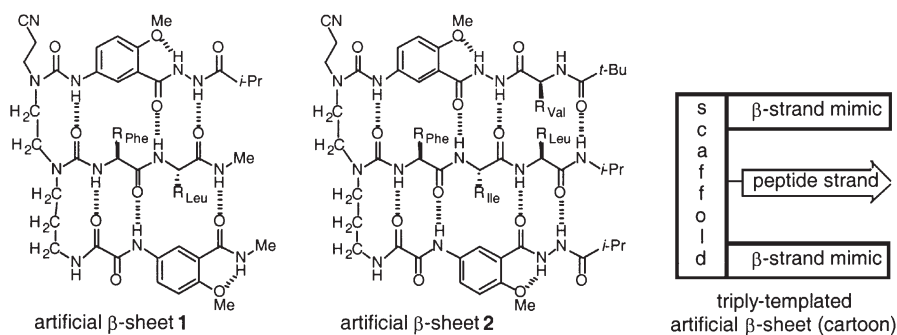
## Triply-Templated Artificial $\beta$ -Sheets

James S. Nowick, Jennifer M. Cary, James H. Tsai and Wade A. Russu

Department of Chemistry, University of California, Irvine, Irvine, CA 92697-2025, USA

### Introduction

Chemical models of protein secondary structures provide insight into protein structure and interactions and can serve as useful peptidomimetic building blocks. With the goal of studying protein folding and recognition, our research group has developed chemical models of protein  $\beta$ -sheets that consist of molecular templates and attached peptide strands [1]. We have previously created artificial  $\beta$ -sheets of this sort that contain one or two molecular templates [2–7]. Here, we describe artificial  $\beta$ -sheets **1** and **2**, which contain three molecular templates [8].



### Results and Discussion

Artificial  $\beta$ -sheets **1** and **2** were synthesized by assembling their triamine backbones,  $\beta$ -strand mimics, and peptide strands in an appropriate fashion and were studied by  $^1\text{H}$  NMR spectroscopy. Interstrand NOEs provide compelling evidence that **1** and **2** fold into  $\beta$ -sheet-like structures in  $\text{CDCl}_3$  solution. Notably, both compounds exhibit characteristic NOEs between the upper  $\beta$ -strand mimic and the middle peptide strand and between the middle peptide strand and the lower  $\beta$ -strand mimic. These NOEs, which are illustrated in Figure 1, reflect proximity between the strands. Additional evidence for  $\beta$ -sheet-like conformations of **1** and **2** come from the intrastrand NOEs and coupling constants of the peptide strands: The interresidue NOEs between the NH and  $\alpha$ -protons are relatively strong; the intrasidue NOEs between the NH and  $\alpha$ -protons are relatively weak; and the  $^3J_{\text{HN}\alpha}$  coupling constants are large (8.8–10.8 Hz). Further evidence for the folded  $\beta$ -sheet-like structures of **1** and **2** comes from the chemical shifts of the NH and  $\alpha$ -protons: The NH resonances appear substantially downfield of suitable controls, reflecting their participation in a  $\beta$ -sheet-like pattern of hydrogen bonding; the  $\alpha$ -protons of the amino acid groups are downfield of values characteristic of random coils. Comparison of the chemical shifts of the NH and  $\alpha$ -protons of triply-stranded artificial  $\beta$ -sheets **1** and **2** to those of doubly-stranded homologues lacking either the upper or lower  $\beta$ -strand mimic suggests that the triply-stranded compounds are better folded [5–7].

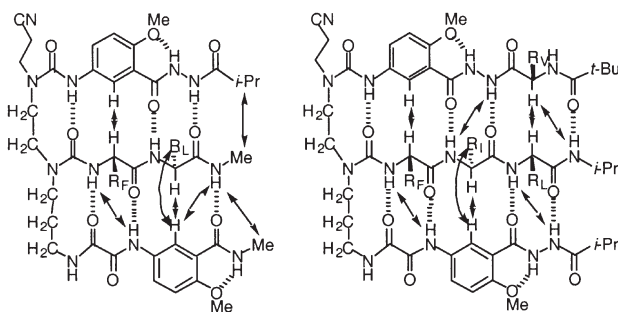


Fig. 1. Key interstrand NOEs observed in artificial  $\beta$ -sheets **1** and **2**.

## Conclusion

These studies establish that three molecular templates can be combined with peptide strands to form compounds that fold to resemble three-stranded protein  $\beta$ -sheets and further support our modular approach to the creation of protein like structures. In future studies, we plan to modify these triply-templated structures to develop molecular receptors for peptides.

## Acknowledgments

The authors thank the NSF for grant support (CHE-9813105). J.S.N. thanks the following agencies for support in the form of awards: the Camille and Henry Dreyfus Foundation (Teacher-Scholar Award), the Alfred P. Sloan Foundation (Alfred P. Sloan Research Fellowship), and the American Chemical Society (Arthur C. Cope Scholar Award). J.M.C. thanks Allergan, Inc. for fellowship support. J.H.T. thanks the Chao Family Comprehensive Cancer Center Functional Genomics Program for training grant support. W.A.R. thanks the NIH for training grant support (5 T32 CA09054).

## References

1. Nowick, J.S. *Acc. Chem. Res.* **32**, 287–296 (1999).
2. Nowick, J.S., Smith, E.M., Noronha, G. *J. Org. Chem.* **60**, 7386–7387 (1995).
3. Nowick, J.S., Holmes, D.L., Mackin, G., Noronha, G., Shaka, A.J., Smith, E.M. *J. Am. Chem. Soc.* **118**, 2764–2765 (1996).
4. Nowick, J.S., Pairish, M., Lee, I.Q., Holmes, D.L., Ziller, J.W. *J. Am. Chem. Soc.* **119**, 5413–5424 (1997).
5. Nowick, J.S., Holmes, D.L., Smith, E.M., Shaka, A.J. *J. Org. Chem.* **62**, 7906–7907 (1997).
6. Tsai, J.H., Waldman, A.S., Nowick, J.S. *Bioorg. Med. Chem.* **7**, 29–38 (1999).
7. Nowick, J.S., Tsai, J.H., Bui, Q.-C.D., Maitra, S. *J. Am. Chem. Soc.* **121**, 8409–8410 (1999).
8. Nowick, J.S., Cary, J.M., Tsai, J.H. *J. Am. Chem. Soc.* **123**, 5176–5180 (2001).

## Stepwise Peptide–Peptoid Transformation *via* SPOT Synthesis

Ulrich Reineke<sup>1</sup>, Berit Hoffmann<sup>2</sup>, Thomas Ast<sup>1,2</sup>, Thomas Polakowski<sup>1</sup>,  
Jens Schneider-Mergener<sup>1,2</sup> and Rudolf Volkmer-Engert<sup>2</sup>

<sup>1</sup>Jerini AG, 12489 Berlin, Germany

<sup>2</sup>Institut für Medizinische Immunologie, Charité, Humboldt-Universität zu Berlin,  
10098 Berlin, Germany

### Introduction

Bioactive peptides are promising lead structures for the development of novel drugs. However, peptides have many drawbacks for their direct use as therapeutics such as degradation by proteases and low bioavailability. These limitations can be overcome by their transformation into peptidomimetics.

Here we report the systematic and stepwise transformation of the linear peptide epitope VVSHFND recognized by the anti-transforming growth factor  $\alpha$  (TGF $\alpha$ ) monoclonal antibody Tab2 [1] into peptide–peptoid hybrids (peptomers) and finally peptoids while preserving binding to the antibody paratope. This was achieved using the SPOT synthesis technique [2–4], which is a rapid and easy method for the generation of arrays of peptides, peptomers [5], peptoids, and other small organic compounds on planar surfaces such as cellulose or polypropylene membranes. The key experiment for this transformation is the so-called substitutional analysis in which each position – but only one at a time – is exchanged by a set of different peptoid building blocks resulting in a peptomer array. After binding assays with peroxidase-labeled Tab2 best binding peptomers were selected and subjected to a successive transformation (Figure 1).

### Results and Discussion

The peptomer assembly *via* SPOT synthesis on planar surfaces requires the efficient parallel incorporation of peptoid and peptide building blocks which was previously described by Ast *et al.* [5]. In order to transform the peptide epitope VVSHFND into a peptoid, a substitutional analysis of the wild-type peptide was performed exchanging every position by a set of 30 peptoid building blocks. Thus, an array of 210 different peptide–peptoid hybrids with one peptoidic and 6 peptidic residues each was synthesized and tested for binding by Tab2. One of the functional peptomers was selected for a subsequent substitutional analysis transforming one of the remaining amino acids into a peptoid building block. This transformation process was continued iteratively until a full peptoid was identified. Because this peptoid displayed reduced Tab2 binding, a final substitutional analysis was carried out to re-optimize those residues which have been transformed in the beginning of the process.

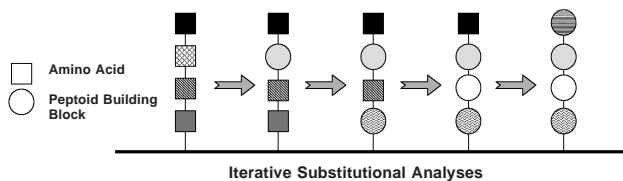


Fig. 1. Scheme of the peptide–peptoid transformation.

Chosen compounds of each transformation step were resynthesized, purified by HPLC, and dissociation constants of the complexes with Tab2 were determined by BIAcore. In addition, competition ELISAs with the N-terminal fragment of TGF $\alpha$  comprising the antibody epitope revealed a specific binding of the peptomers and peptoids to the Tab2 paratope. The starting peptide ( $K_D = 6.4 \cdot 10^{-8}$  M) and one of the peptoids ( $K_D = 2.0 \cdot 10^{-7}$  M) are shown in Figure 2.

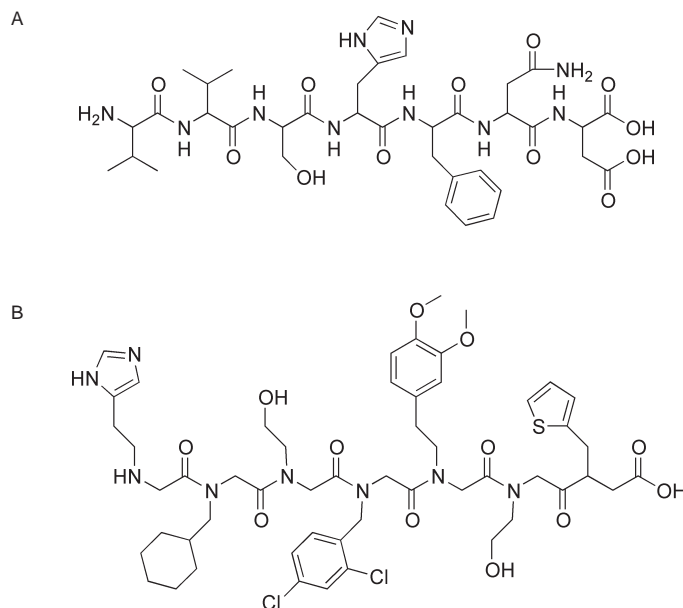


Fig. 2. Structures of the starting peptide VVSHFND (A) and one of the peptoids (B) resulting from the transformation process.

In general, the transformation of peptides into peptoids is greatly facilitated by SPOT synthesis, since large numbers of peptide-derived peptomers and peptoids can be synthesized and screened for binding in a highly parallel and rapid manner. Interestingly, our process leads to peptoids with completely different side chains in comparison to the starting peptide despite using building blocks with characteristics like natural amino acids.

## References

1. Hahn, M., Winker, D., Welfle, K., Misselwitz, R., Welfle, H., Wessner, H., Zahn, G., Scholz, C., Seifert, M., Hawkins, R., Schneider-Mergener, J., Höhne, W. *J. Mol. Biol.* **314**, 293–309 (2001).
2. Frank, R. *Tetrahedron* **48**, 9217–9232 (1992).
3. Wenschuh, H., Volkmer-Engert, R., Schmidt, M., Schulz, M., Schneider-Mergener, J., Reineke, U. *Biopolymers (Peptide Sci.)* **55**, 188–206 (2000).
4. Reineke, U., Volkmer-Engert, R., Schneider-Mergener, J. *Curr. Opin. Biotechnol.* **12**, 59–64 (2001).
5. Ast, T., Heine, N., Germeroth, L., Schneider-Mergener, J., Wenschuh, H. *Tetrahedron Lett.* **40**, 4317–4318 (1999).

## SPOT Synthesis of 1,3,5-Trisubstituted Hydantoins on Cellulose Membranes

Niklas Heine<sup>1</sup>, Jens Schneider-Mergener<sup>2</sup> and Holger Wenschuh<sup>2</sup>

<sup>1</sup>*Institut für Medizinische Immunologie, Charité, Humboldt-Universität,  
 D-10117 Berlin, Germany*

<sup>2</sup>*Jerini AG, D-12489 Berlin, Germany*

### Introduction

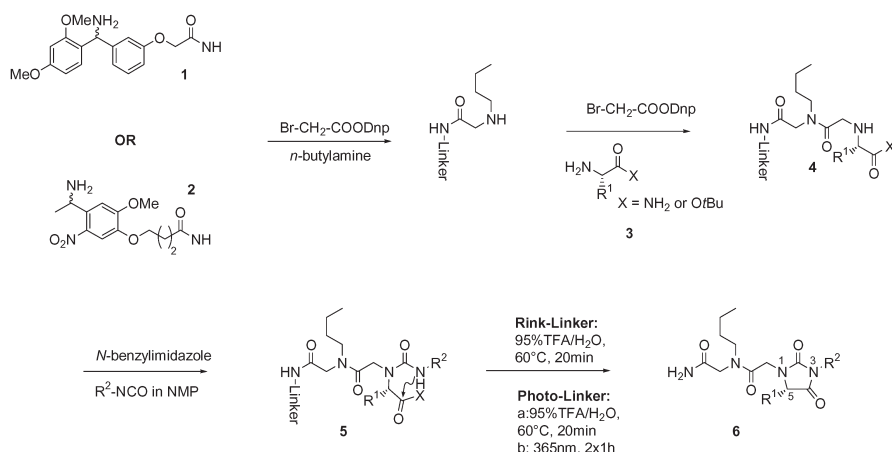
The SPOT synthesis concept on cellulose membranes a powerful method for the synthesis of peptide libraries [1] and effective screening of the membrane bound compounds by binding assays [2,3] was recently extended to the assembly of peptidomimetics, glycoconjugates, and small organic molecules [4–6]. The present article reports on an additional application, namely the generation of hydantoins [7] using coherent cellulose membranes as solid phase carriers.

### Results and Discussion

The hydantoin synthesis procedure described in this communication is based on a modified synthesis protocol for peptoids on planar membrane supports using the SPOT synthesis concept. First, linear dipeptoid precursors **4** were assembled on a linker modified cellulose membrane (Rink- **1** or photo- **2** linker) as reported recently (Scheme 1) [4a]. After reaction of the N-terminal amino functions with isocyanates R<sup>2</sup>-NCO the formed ureas **5** were cyclized under acidic conditions (95% TFA in water, 10–20 min, 60 °C) yielding the hydantoins either in solution (Rink-linker) or covalently linked (photo-linker) to the membrane applicable for solid phase binding assays. Analysis of the latter compounds was achieved after irradiating the dried membrane at 365 nm and dissolving the released hydantoins **6** with buffer.

The synthesis approach was applied to several hydantoins **6** using amino acid derivatives **3** differing in their sterical demand as well as various isocyanates for the introduction of aryl and alkyl substituents in the 3-position (Table 1).

In conclusion, it could be shown that the SPOT synthesis approach is applicable to the efficient synthesis of diverse hydantoin arrays enabling combinatorial substitutions



Scheme 1. SPOT synthesis of hydantoins on linker modified cellulose membranes.

Table 1. Hydantoin derivatives **7** obtained according to Scheme 1.

Entry	R <sup>1</sup>	X	(=H-AA-X) <b>3</b>	Solvent [conc.] of <b>3</b>	R <sup>2</sup>	Purity <b>6</b> [%] <sup>a</sup>
a	•-H	NH <sub>2</sub>	(=H-Gly-NH <sub>2</sub> )	H <sub>2</sub> O [5.0 M] <sup>b</sup>	Ph	81 <sup>c</sup>
b	•-H	OtBu	(=H-Gly-OtBu)	H <sub>2</sub> O [2.5 M] <sup>b</sup>	Ph	79 <sup>d</sup>
c	•-Me	NH <sub>2</sub>	(=H-Ala-NH <sub>2</sub> )	H <sub>2</sub> O [5.0 M] <sup>b</sup>	Ph	86 <sup>c</sup>
d	•-CH <sub>2</sub> CH <sub>3</sub>	NH <sub>2</sub>	(=H-Leu-NH <sub>2</sub> )	H <sub>2</sub> O [5.0 M] <sup>b</sup>	Ph	76 <sup>d</sup>
e	•-CH <sub>2</sub> CH <sub>2</sub> CH <sub>3</sub>	OtBu	(=H-Ile-OtBu)	NMP [1.0 M]	Ph	54 <sup>d</sup>
f	•-H	NH <sub>2</sub>	(=H-Gly-NH <sub>2</sub> )	H <sub>2</sub> O [5.0 M] <sup>b</sup>	<i>n</i> -Bu	82 <sup>c</sup>
G	•-Me	NH <sub>2</sub>	(=H-Ala-NH <sub>2</sub> )	H <sub>2</sub> O [5.0 M] <sup>b</sup>	<i>n</i> -Bu	70 <sup>d</sup>

<sup>a</sup> HPLC (220 nm); <sup>b</sup> 0.05 % Tween® 20 added; <sup>c</sup> photo-linker **2**; <sup>d</sup> Rink-linker **1**.

in the 1-, 3-, and 5-positions of the heterocycle. The development of an efficient hydantoin synthesis protocol on planar membrane supports extends the scope of the SPOT synthesis technique to small organic molecules previously not readily accessible by this method.

#### Acknowledgments

This work was supported by a grant from the Fonds der Chemischen Industrie.

#### References

1. Frank, R. *Tetrahedron* **48**, 9217–9232 (1992).
2. Wenschuh, H., Volkmer-Engert, R., Schmidt, M., Schulz, M., Schneider-Mergener, J., Reineke, U. *Biopolymers* **55**, 188–206 (2000).
3. Reineke, U., Volkmer-Engert, R., Schneider-Mergener, J. *Curr. Opin. Biotechnol.* **12**, 59–64 (2001).
4. Ast, T., Heine, N., Germeroth, L., Schneider-Mergener, J., Wenschuh, H. *Tetrahedron Lett.* **40**, 4317–4318 (1999).
5. Scharn, D., Germeroth, L., Schneider-Mergener, J., Wenschuh, H. *J. Org. Chem.* **66**, 507–513 (2000).
6. Scharn, D., Wenschuh, H., Reineke, U., Schneider-Mergener, J., Germeroth, L. *J. Comb. Chem.* **2**, 361–370 (2000).
7. Park, K.-H., Kurth, M.J. *Tetrahedron Lett.* **41**, 7409–7413 (2000).

## Synthesis and CD Spectra of $\beta^2$ -(3-Aza-peptides)

Gérald Lelais and Dieter Seebach

Laboratorium für Organische Chemie der Eidgenössischen Technischen Hochschule,  
 ETH Zentrum, 8092 Zürich, Switzerland

### Introduction

It has been demonstrated that short oligomers derived from  $\beta$ -amino acids ( $\beta$ -peptides) can fold into well-ordered secondary structures like helices, turns and sheets [1]. Furthermore, they show an outstanding stability against a large range of proteases [2], and are thus promising candidates as peptidomimetics in drug design. During the search for new secondary structures we envisaged the replacement of the  $C^\beta$   $CH_2$  groups of  $\beta$ -peptides by NR, which leads to  $\beta^2$ -(3-aza-peptides). These new types of peptides are of great interest, since they might form additional H-bonds *via* their  $sp^3$ -nitrogens. The  $sp^3$ -nitrogen might act as a H-bond acceptor, or as a H-bond donor. Recently, quantum-chemical calculations carried out on unsubstituted  $\beta$ -3-aza-peptides by Günther and Hofmann [3] have suggested the presence of helical secondary structures.

### Results and Discussion

In order to compare the structure and stability of the  $\beta^2$ -3-aza-peptides to their known  $\beta$ -peptide analogs [4], we synthesized the  $\beta^2$ -3-aza-peptides **1–4** with Val, Ala, and Leu side chains (Figure 1).

The  $\beta^2$ -3-aza-amino acids were prepared from the natural  $\alpha$ -amino acids *via* an amination reaction, following a procedure described by Collet *et al.* [5]. Since conventional peptide coupling conditions failed to give the desired products, the use of strong coupling reagents was necessary.

Synthesis of the di- and tripeptide was achieved with good yields and negligible epimerization using HATU in  $CH_2Cl_2$  or in DMF. Subsequent coupling to give the hexapeptide, using BOPCl, led to the fully protected  $\beta^2$ -3-aza-hexapeptide **3** in reasonable yield. Benzyl deprotection, leading to the  $\beta^2$ -3-aza-peptides **2** and **4**, could be carried out by catalytic hydrogenolysis (Pd/C and  $H_2$ ) without cleavage of N,N bonds.

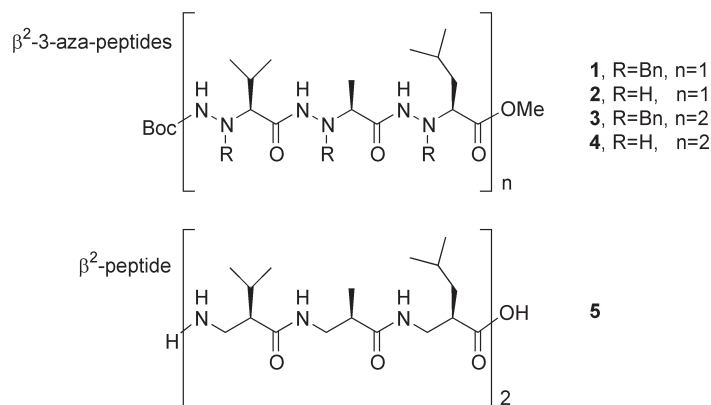


Fig. 1.  $\beta^2$ -3-Aza-peptides **1–4** and the analogous  $\beta^2$ -peptide **5**.

As a first step in probing the existence of secondary structures, CD spectra (0.2 mM solutions) of the peptides **1–4** have been measured (Figure 2).

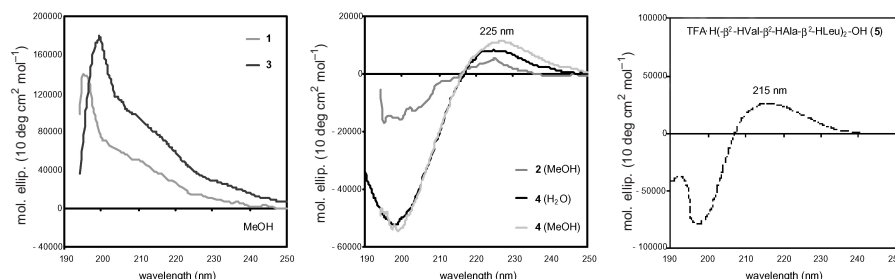


Fig. 2. CD spectra (0.2 mM solutions) of the  $\beta^2$ -3-aza-peptides **1–4** and of the analogous  $\beta^2$ -peptide **5**. Molar ellipticity  $\theta$  in  $10 \text{ deg cm}^2 \text{ mol}^{-1}$  (non-normalized).

Surprisingly, the CD spectra of tripeptides **1** and **2** have a pattern similar to that of hexapeptides **3** and **4**, indicating that oligomers derived from as little as three  $\beta^2$ -3-aza-amino acids might already adopt a secondary structure. The fully protected  $\beta^2$ -3-aza-peptides **1** and **3** show an *all*-positive curve with a shoulder at *ca* 210 nm and an intensive maximum at *ca* 198 nm. In contrast, the CD spectra of the debenzylated  $\beta^2$ -3-aza-peptides **2** and **4** are similar to that obtained for the  $\beta^2$ -peptide **5**, even though the value of the positive molar ellipticity is red-shifted by about 10 nm. The CD spectra of **4** were measured in MeOH, as well as in water (at different pH-values), and they are almost superimposable at all pH values tested.

In order to obtain information about the secondary structure of these new peptide analogs, 2D-NMR measurements are currently underway.

## References

1. Seebach, D., Matthews, J.L. *Chem. Commun.* 2015–2022 (1997).
2. Frackenpohl, J., Arvidsson, P.I., Schreiber, J.V., Seebach, D. *ChemBiochem* **2**, 445–455 (2001).
3. Günther, R., Hofmann, H.-J. *J. Am. Chem. Soc.* **123**, 247–255 (2001).
4. Hintermann, T., Seebach, D. *Synlett* 437–438 (1997).
5. Collet, A., Vidal, J., Hannachi, J.-C., Guy, L. *Brevet français* 95/10685 (1995); PCT WO 97/09303 (1997).

## Preferred Conformations of Azaamino Acids

Dong-Kyu Shin<sup>1</sup>, Ho-Jin Lee<sup>2</sup>, Kang-Bong Lee<sup>2</sup>, Young-Sang Choi<sup>3</sup>,  
Chang-Ju Yoon<sup>4</sup> and Seonggu Ro<sup>1</sup>

<sup>1</sup>CrystalGenomics, Inc., Daejeon, 305-390, Korea

<sup>2</sup>Advanced Analysis Center, KIST, Seoul 136-791, Korea

<sup>3</sup>Department of Chemistry, Korea University, Seoul 136-701, Korea

<sup>4</sup>Department of Chemistry The Catholic University of Korea, Pucheon 420-743, Korea

### Introduction

Azaamino acids are formed by the replacement of the  $\alpha$ -carbon of amino acids with a nitrogen atom. They contain no extra functional group(s) unlike other constrained amino acids, and we believe that the azaamino acid is highly constrained because the  $N^\alpha$ -C(O) bond has a double bond character in the urea-type structure. Moreover, when the azaamino acid is incorporated into peptides, the N-N $^\alpha$  bond of azaamino acids is between amide and urea. Since the amide and urea are quite planar, rotation of this bond is restrained. Thus, azaamino acids in peptides have unique conformational preference and their preferred ( $\phi$ ,  $\psi$ ) torsion angles are different from natural amino acids. In spite of wide usage and interesting conformational characteristics of azaamino acids, their conformational studies have not been extensively carried out. Aubry, Boussard and Marraud have made major contributions to this area carrying out crystallographic and spectroscopic studies. We also have studied the conformational preference of azaamino acids using computational methods and NMR spectroscopy. In this paper, we report the results of *ab initio* studies of model peptides containing 6 representative azaamino acids: Ac-AzGly-NHMe (acetyl azaglycine-*N*-methylamide), Ac-AzAla-NHMe (acetyl azaalanine-*N*-methylamide), Ac-AzLeu-NHMe (acetyl aza-leucine-*N*-methylamide), Ac-AzPhe-NHMe (acetyl azaphenylalanine-*N*-methylamide), Ac-AzAsn-NHMe (acetyl azaasparagine-*N*-methylamide) and Ac-AzPro-NHMe (acetyl azaproline-*N*-methylamide).

### Results and Discussion

For all the model peptides, we carried out the conformational search by molecular mechanical methods and fully optimized with the 3-21G\* and 6-31G\*\* basis sets. Each of the resulting conformations were classified and analyzed.

The  $\phi$  angle is the rotational status of N-N $^\alpha$  bond that connects acetyl amide and methyl urea. Since the amide and urea are quite planar, the bond was expected to show unique conformational constraints. In all cases, preferred torsion angles for N-N $^\alpha$  bond ( $\phi$ ) of the azaamino acid are about  $-90^\circ$  or  $90^\circ$  ( $\pm 30^\circ$ ). These results indicated that Ac-NH and -N(R)-C(O)-NHMe are perpendicular. The stability of these angles can be explained by the repulsion of lone pairs on the nitrogens. The orientations of the lone pairs on these nitrogens are vertical to the amide and urea planes, respectively. Thus, to minimize repulsion between these two lone pairs, they assume a geometry in which they are perpendicular to each other. In the optimized conformations, the  $\psi$  angle assumes about  $0^\circ \pm 30^\circ$  or  $180^\circ \pm 30^\circ$ , *cis* and *trans*. These angles originated from the partially double bond character of N $^\alpha$ (R)-C(O) bond.

In terms of backbone conformation, the azaamino acid prefers to adopt 3 conformations. In the first conformation,  $\phi$  and  $\psi$  torsion angles are about  $\pm 90^\circ \pm 30^\circ$ , and  $0^\circ \pm 30^\circ$ , respectively. This conformation is similar to the conformation appeared in the  $i+2$  position of typical  $\beta$ -I turn ( $\phi_{i+1} = -60^\circ$ ,  $\psi_{i+1} = -30^\circ$ ,  $\phi_{i+2} = -90^\circ$ ,  $\psi_{i+2} = 0^\circ$ ) and  $\beta$ -II

turn ( $\phi_{i+1} = -60^\circ$ ,  $\psi_{i+1} = 120^\circ$ ,  $\phi_{i+2} = 80^\circ$ ,  $\psi_{i+2} = 0^\circ$ ). Additionally, when the amide between  $i+1$  and  $i+2$  residues is in a *cis* configuration (the case of AzPro), such preference fit to the  $i+2$  position of typical  $\beta$ -VI turn ( $\phi_{i+1} = -60^\circ$ ,  $\psi_{i+1} = 120^\circ$ ,  $\phi_{i+2} = 90^\circ$ ,  $\psi_{i+2} = 0^\circ$ ). In the second conformation,  $\phi$  and  $\psi$  torsion angles are about  $\pm 80^\circ \pm 15^\circ$  and  $180^\circ \pm 15^\circ$ , respectively. The  $\phi$  angle in these conformations is also close to  $\pm 90^\circ$  and the  $\psi$  angle is about  $180^\circ$ . This conformation is similar to polyglycine II and poly(L-proline) II conformations in which ( $\phi$ ,  $\psi$ ) torsion angles are  $(-80^\circ, 150^\circ)$  and  $(-78^\circ, 149^\circ)$ , respectively. In the third conformation,  $\phi$  and  $\psi$  torsion angles are about  $\pm 90^\circ \pm 10^\circ$  and  $30^\circ \pm 10^\circ$ . This conformation is similar to the first conformation, but it includes hydrogen bonding between acetyl C=O and terminal NH proton forming 7-membered ring ( $\gamma$ -turn). Usually, such conformation is the lowest energy conformation in most of amino acids. However, this is the least stable conformation among the three preferred conformations of azaamino acids.

The side chain of azaamino acids preferentially adopts one or two angle(s) between  $\pm 70^\circ$  and  $\pm 120^\circ$ . Since N–N $^\alpha$  bond ( $\phi$ ) of the azaamino acid adopt about  $\pm 90^\circ$ , always, the N $^\alpha$ –C $^\beta$  bond is perpendicular to the Ac–NH amide. Thus, the side chain functional group positions in the same side of carbonyl oxygen or NH proton of Ac–NH amide. When an aromatic or aliphatic side chain is in the same side of carbonyl oxygen, the resulting conformation is unstable because of steric bump between the carbonyl oxygen and the side chain functional group. On the other hand, when the side chain contains a hydrogen bond donor for carbonyl oxygen, the resulting conformation is quite stable. These results indicate that side chain conformations of azaamino acids are dependent on the side chain functional group and backbone conformation. Moreover, their conformational preference is different from that of usual amino acids.

To confirm our results, we have carried out designs, synthesis and conformational studies of model azapeptides such as Boc-Ala-Phe-AzLeu-Ala-OMe, Boc-Phe-AzLeu-Ala-OMe and Ac-Aib-AzGly-NH $_2$  [1–3]. All of these peptides clearly show conformational preference to adopt a  $\beta$ -turn conformation in solution. In these cases, the azaamino acids adopt the conformation similar to the first conformation. Such conformational preference is not possible in tri- or tetra-peptides that consist of usual amino acids. We believe these results are important for the design of useful molecules containing azaamino acids for drug discovery and peptide nanotechnology.

### Acknowledgments

Supported by a Korea University grant 2001 to Y.-S. Choi.

### References

1. Lee, H.-J., Ahn, I.-A., Ro, S., Choi, K.-H., Choi, Y.-S., Lee, K.-B. *J. Peptide Res.* **56**, 35–43 (2000).
2. Lee, H.-J., Choi, K.-H., Ahn, I.-A., Ro, S., Jang, H.G., Choi, Y.-S., Lee, K.-B. *J. Mol. Struct.* **569**, 43–54 (2001).
3. Ro, S., Lee, H.-J., Ahn, I.-A., Shin, D.K., Lee, K.-B., Yoon, C.-J., Choi, Y.-S. *Bioorg. Med. Chem.* **9**, 1837–1841 (2001).

## Higher Anti-HIV-1 Activity of Peptides Derived from gp41 Carboxyl-Terminal Coiled Coil Structure of HIV-1 89.6 Strain

Myung Kyu Lee, Jeong Kon Seo, Hee Kyung Kim, Ju Hyun Cho  
 and Kil Lyong Kim

*Protein Engineering Laboratory, Peptide Research National Laboratory, Korea Research  
 Institute of Bioscience and Biotechnology, Yusong Taejon 305-600, Korea*

### Introduction

The envelope glycoprotein (Env) of HIV-1 mediates virus entry into the target cells. Gp120 binds with CD4 and a chemokine receptor (coreceptor). The binding between Env and coreceptor determines the host tropism of HIV-1 (R5 tropic-CCR5, X4 tropic-CXCR4 and R5X4 tropic-CCR5 and CXCR4) [1]. These interactions trigger gp41 to promote fusion via the insertion of the fusion peptide into the host membrane, and then the two heptad repeated sequences of gp41 form a trimeric coiled coil structure [2]. The coiled coil structure is considered to induce membrane fusion between viral and host membranes. Interestingly the C-peptides, C34 [2] and T20 [3], derived from the C-terminal heptad repeated sequence of HIV-1<sub>LAI</sub> strongly inhibit HIV-1 infection by disrupting formation of the coiled coil structure. In this study, we tried to find more potent peptides derived from various HIV-1 strains.

### Results and Discussion

We synthesized C34, C28 and T20 peptides derived from various HIV-1 strains (Table 1). Anti-HIV-1 activities of the C34 peptides derived from various HIV-1 strains were studied using various HIV-1/MuLV pseudotypes [4]. Interestingly, X4 or R5X4 tropic HIV-1s were more susceptible for those peptides (Table 2). C34-89.6 derived from the HIV-1 89.6 strain showed the most potent anti-HIV-1 activity as compared to the other HIV-1 strains used. The N-terminal half of C34-89.6 is more negatively charged (−3), whereas its C-terminal half is more positively charged (+3) compared with other C34. It was found that the C-terminal region of C34-89.6 was more critical than the

*Table 1. Amino acid sequences used derived from C-terminal coiled coil structure.*

Peptide	Amino Acid Sequence
C34-BaL	WMEWDREINNYTSIIYSLIEESQNQQWKNEQEELL
C34-89.6	WMEWEREIDNYTDYIYDLLEKSQTQQWKNEKELL
C34-LAI	WMEWDREINNYTSLIHSLIEESQNQQWKNEQEELL
C34-89.6/LAI	WMEWEREIDNYTDYIYDLIEESQNQQWKNEQEELL
C34-LAI/89.6	WMEWDREINNYTSLIHSLLEKSQTQQWKNEKELL
C28-89.6A	WMEWEREIDNYTDYIYDLLEKSQTQQWKN-NH <sub>2</sub>
C28-89.6B	WEREIDNYTDYIYDLLEKSQTQQWKNEK-NH <sub>2</sub>
C28-89.6C	EIDNYTDYIYDLLEKSQTQQWKNEKELL-NH <sub>2</sub>
C28-LAI-C	EINNYTSLIHSLIEESQNQQWKNEQEELL-NH <sub>2</sub>
T20-89.6	YTDYIYDLLEKSQTQQWKNEKELLELDKWASLWNWF
T20-LAI	YTSLIHSLIEESQNQQWKNEQEELLELDKWASLWNWF

N-terminal region. The chimeric C34 peptide C34-IIIB/89.6 showed stronger activity than C34-89.6/LAI. The C-terminal deleted peptide (C28-89.6A) of C34-89.6 elicited no anti-HIV-1 activity, while the peptide (C28-89.6C) with the N-terminal deletion showed some activity. However, C28-LAI-C with the N-terminal deletion of C34-LAI showed no activity. T20-89.6 having the C-terminal half sequence of C34-89.6 showed 3-5 times higher activity than that of C34-LAI. These results suggest that the C-terminal half of C34-89.6 may be related to its higher anti-HIV-1 activity and the C-peptide derived from HIV-1<sub>89.6</sub> is a good target for the development of an anti-HIV-1 peptide than that of HIV-1<sub>LAI</sub>. Even though the propensity of  $\alpha$ -helical structure of the C-peptide is important for anti-HIV-1 activity, no critical difference among the peptide secondary structures was found.

Table 2. Inhibition of various peptides against infection of the HIV-1/MuLV pseudotypes to the target cells, HOS-CD4-CCR5 or HOS-CD4-CXCR4.

Peptide	50% Inhibition Concentration (IC <sub>50</sub> , nM)				
	AD8 <sup>a</sup> /CCR5 <sup>b</sup>	BaL/CCR5	89.6/CCR5	89.6/CXCR4	LAI/CXCR4
C34-BaL	193.1	78.0	43.6	21.2	24.3
C34-89.6	17.5	7.8	3.5	2.4	0.94
C34-LAI	45.4	26.3	8.7	5.9	2.2
C34-89.6/LAI	49.2	26.8	nd	nd	nd
C34-LAI/89.6	27.8	7.7	nd	nd	nd
C28-89.6A	nd	ND	nd	nd	nd
C28-89.6B	nd	4500	nd	nd	nd
C28-89.6C	nd	1700	nd	nd	nd
C28-LAI-C	nd	ND	nd	nd	nd
T20-89.6	69.6	38.7	nd	nd	nd
T20-LAI	190.2	176.8	nd	nd	nd

<sup>a</sup> AD8, HIV-1 strain (HIV-1<sub>AD8</sub>) of the pseudotype; <sup>b</sup> the target cells (HOS-CD4-CCR5) used; nd: not determined; ND, not detectable at 10,000 nM

## Acknowledgments

Supported by grants NL1010 and NLM0010012 (Korea Ministry of Science and Technology).

## References

1. Moore, J.P., Trkola, A., Dragic, T. *Curr. Opin. Immunol.* **9**, 551–562 (1997).
2. Chan, D.C., Fass, D., Berger, J.M., Kim, P.S. *Cell* **89**, 263–273 (1997).
3. Wild, C.T., Shugars, D.C., Greenwell, T.K., McDanal, C.B., Matthews, T.J. *Proc. Natl. Acad. Sci. U.S.A.* **91**, 9770–9774 (1994).
4. Schnierle, B.S., Stitz, J., Bosch, V., Nocken, F., Merget-Millitzer, H., Engelstadter, M., Kurth, R., Groner, B., Cichutek, K. *Proc. Natl. Acad. Sci. U.S.A.* **94**, 8640–8645 (1997).

## Synthetic Approach to Dipeptide Mimetics Based on Aminoacyl Incorporation Reaction

Alexey N. Chulin, Igor L. Rodionov and Vadim T. Ivanov

*Laboratory of Peptide Chemistry, Branch of Shemyakin–Ovchinnikov Institute of Bioorganic Chemistry, Pushchino, Moscow Region, 142290, Russian Federation*

### Introduction

Actual progress in the area of modern drug design is largely dependent on the practical accessibility of a variety of small molecule mimetics of naturally occurring biomolecules, which command increasing interest of researchers involved in drug discovery technology.

Aminoacyl incorporation (insertion) reaction (Figure 1) discovered about 40 years ago [1] and studied using plain achiral models during the 1960's attracted our attention as a potential general synthetic approach to certain conformationally restricted dipeptides (dilactams) **III**.

Although usefulness of these bifunctional building blocks for introducing particular structural modifications into peptide molecules was recognized more than 10 years ago [2,3], they are not commonly available for modern molecular designers. Notably, only 8 representatives of bridged dipeptides **III** have been described so far [2–5], and only once aminoacyl incorporation route has been utilized [2].

### Results and Discussion

Aminoacyl incorporation is effectively a ring enlargement, mediated by bicyclic azacyclols **II**, which results in intramolecular acyl transfer to nucleophilic functions Nu = NH, S, O (Figure 1). The key intermediates **I** having internal imide moiety represent the poorly accessible and unexplored class of non-typical peptides, therefore our initial efforts were focused on practical evaluation of different synthetic approaches to **I**. Scope and limitations of the following methods were studied:

- direct acylation of sodium derivative of pGlu-OR [6];
- pyrrolidone ring closure in dipeptides R'-Xaa-Glu(OX)-OR *via* activation of side-chain carboxylic group of glutamic acid;
- selective oxidation of proline moiety in related dipeptides Boc-Xaa-Pro-OBu-t by RuO<sub>2</sub>/NaIO<sub>4</sub> [7].

Using the above methods a variety of protected aminoacylated pyroglutamates were obtained:



(Xaa = Gly, Ala, β-Ala, Ser, Thr, Cys, Asp, Glu, Lys, Orn, Dab, Dpr, i-Gln, 4-substituted salicylic acids and anthranilic acid.

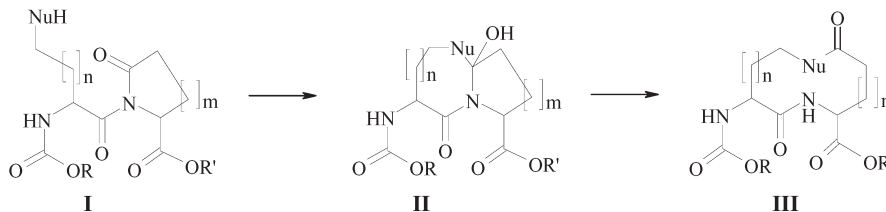


Fig. 1. Aminoacyl incorporation reaction.

Release of nucleophilic functions in **I** followed by exposure to basic conditions in many cases resulted in expected aminoacyl incorporation. In this way, a number of 10–12 membered cycles **III** were obtained in 35–70% yield and characterized by NMR and MS data. However, stable azacyclols **II**, but not 9-membered **III** were isolated according to NMR data. Figure 2 shows the types of cyclic molecules obtained within the frame of the present study.

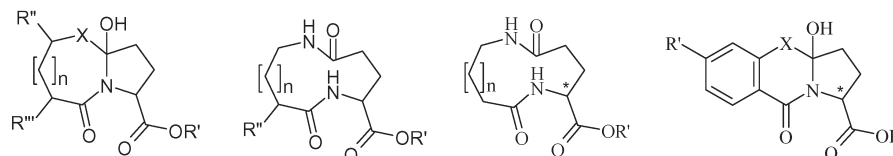


Fig. 2. Types of obtained structures.

Notably, we were not able to promote incorporation of  $\alpha$ -NH<sub>2</sub> groups of amino acids, SH groups in cysteinylpyroglutamates, nor phenolic hydroxy groups in the case of all salicylic acid derivatives studied. Unlike direct cyclization technique, aminoacyl incorporation yields no oligomerization by-products, but sometimes is accompanied by formation of two lactams due to participation of the alternative carbonyl group of imido moiety.

In conclusion, aminoacyl incorporation reaction provides an easy access to otherwise poorly accessible bifunctional bridged dipeptides **III** and **II**.

#### Acknowledgments

Alexey Chulin's participation in 17 APS/2 IPS was sponsored by APS Travel Grant Committee and AnaSpec Co, which is gratefully acknowledged.

#### References

1. Brenner, M., Zimmermann, J.P., Wehrmueller, J., Quitt, P., Photaki, I. *Experientia* **11**, 397–399 (1955).
2. Kemp, D.S., Stites, W.E. *Tetrahedron Lett.* **29**, 5057–5060 (1988).
3. Manesis, N., Goodman, M. *J. Org. Chem.* **52**, 5331–5341 (1987).
4. Kumar, A., Singh, M., Chauhan, V.S. *Indian J. Chem.* **25B**, 230–232 (1986).
5. Heavner, G.A., Audhya, T., Doyle, D., Tioeng, F.S., Goldstein, G. *Int. J. Pept. Protein Res.* **37**, 198–209 (1991).
6. Johnson, A.L., Price, W.A., Wong, P.C., Vavala, R.F., Stump, J.M. *J. Med. Chem.* **28**, 1596–1602 (1985).
7. Yoshifujui, S., Tanaka, K., Kawai, T., Nitta, Y. *Chem. Pharm. Bull.* **34**, 3873–3878 (1986).

## Convenient Conversion of Amino Acids to Their *N*-Hydroxylated Derivatives on a Solid Support: Synthesis of Hydroxamate-Based Pseudo-Peptides

Yunpeng Ye and Garland R. Marshall

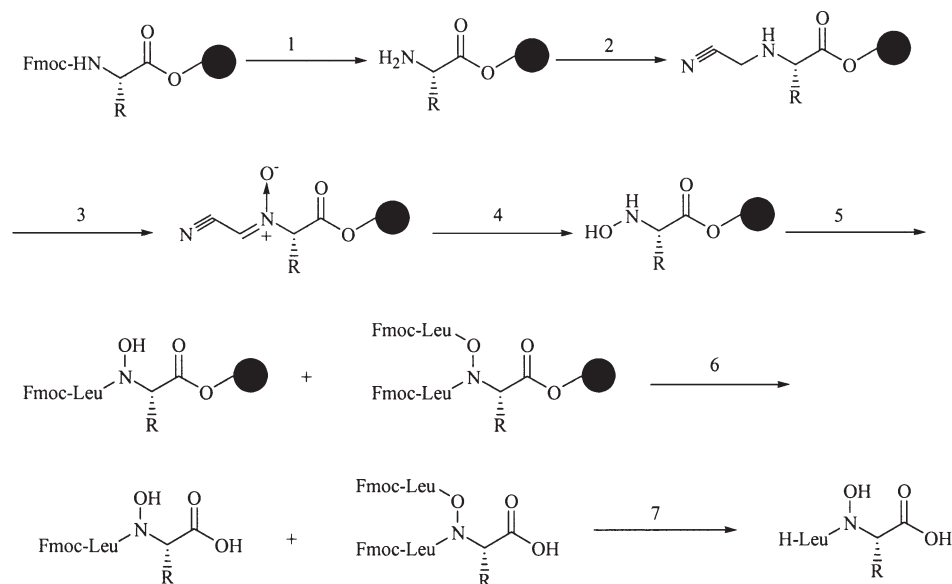
Biochemistry and Molecular Biophysics, Washington University School of Medicine,  
 660 S. Euclid Avenue, St. Louis, MO 63110, USA

### Introduction

*N*-Hydroxyl-substituted amino acid derivatives are key building blocks for synthesis of hydroxamate-based pseudo-peptides. They have potentially important applications in the synthesis of peptidomimetics, enzyme inhibitors, natural products, and in combinatorial chemistry. Several methods for synthesis of *N*-hydroxylamino acid derivatives in solution have been reported. But no method has been reported to our knowledge for the direct conversion of amino acids to their *N*-hydroxyl-substituted derivatives on a solid support. In our continuing efforts to constructing a library of metal-binding, hydroxamate-based pseudopeptide, we have been interested in developing a protocol for efficient conversion of amino acids to their corresponding *N*-hydroxylated derivatives on a solid support.

### Results and Discussion

The solid phase synthesis of *N*-hydroxyl amino acids was predicated on a reported solution phase method [1] that includes the following three major steps: 1. monocyano-methylation of a primary amine with  $\text{NCCH}_2\text{Br}$ ; 2. oxidation with *m*-CPBA; and 3.



1. Piperidine/DMF (20%); 2.  $\text{NCCH}_2\text{Br}$ /DIEA/DMF; 3. *m*-CPBA/DCM; 4.  $\text{NH}_2\text{OH}\cdot\text{HCl}$ /DMF, 60 °C;  
 5. Fmoc-Leu-Cl/AgCN/Toluene; 6. TFA; 7. Piperidine/DMF (20%).

Fig. 1. Conversion of amino acids to their *N*-hydroxylated derivatives on Wang resin and their incorporation into peptides.

*Ye et al.*

hydroxylaminolysis with  $\text{NH}_2\text{OH}\cdot\text{HCl}$  at 60 °C. We have successfully adapted this method for the conversion of a series of amino acids including Glu, Phe, Lys, Gln, Leu, and Ser to their *N*-hydroxylated derivatives on Wang resin with a total yields of 60–70% (Figure1). According to ESI-MS analysis, we deduced that some byproducts may result from *N,N*-dicyanomethylation.

The resin-bound *N*-hydroxylated amino acid derivatives were efficiently incorporated into peptides by reacting with Fmoc-AA-Cl/AgCN in toluene [2]. When 5 equiv. of Fmoc-Leu-Cl were used, the major product was found to be the mono-(Fmoc-Leu) substituted product Fmoc-Leu- $\Psi[\text{CON}(\text{OH})]\text{X}_{\text{AA}}\text{OH}$  (**1**) together with the minor *N,O*-bis(Fmoc-Leu) derivative Fmoc-Leu- $\Psi[\text{CON}(\text{O-Leu-Fmoc})]\text{X}_{\text{AA}}\text{OH}$  (**2**). **1** and **2** were deprotected with piperidine/DMF (20%) to afford the pseudo-peptide H-Leu- $\Psi[\text{CON}(\text{OH})]\text{X}_{\text{AA}}\text{OH}$ . As exemplified by the preparation of Fmoc-protected *N*-hydroxyl Glu(OH)-OH *via* a reaction with Fmoc-Cl, *N*-hydroxyl-amino acids can be changed into their Fmoc-protected derivatives **3**. Compounds **1**, **2**, and **3** can serve as building blocks in solid-phase synthesis. HO-Phe-Phe-NH<sub>2</sub>, Fmoc-Leu $\Psi$ (CONOH)-Phe-Phe-NH<sub>2</sub>, and H-Leu $\Psi$ (CONOH)-Phe-Phe-NH<sub>2</sub> were synthesized on Fmoc amide MBHA resin similarly, demonstrating that this protocol is also compatible with the amide resin.

Based on these results, site-specific *N*-hydroxylation of peptides and efficient solid-phase synthesis of a hydroxamate-based pseudo-peptide library appears feasible and is currently under investigation.

### Acknowledgments

The authors acknowledge support for this research from NIH Grants EY12113 and GM53630. The Washington University Mass Spectroscopy Resource Center supported by NIH (RR00954) was utilized to characterize the peptides synthesized as part of this study.

### References

1. Tokuyama, H., Kuboyama, T., Amano, A., Yamashita, T., Fukuyama, T.A. *Synthesis* 1299–1304 (2000).
2. Perlow, D.S., Erb, J.M., Gould, N.P., Tung, R.D., Freidinger, R.M., Williams, P.D., Veber, D.F. *J. Org. Chem.* **57**, 4394–4400 (1992).

## Peptide Bond Modification for Metal Coordination:

### 1. Metal-Binding Properties of Hydroxamate-Based Pseudo-Peptides

Yunpeng Ye and Garland R. Marshall

*Department of Biochemistry and Molecular Biophysics, Washington University School of Medicine, St. Louis, MO 63110, USA*

#### Introduction

Most reports in the literatures focus on metal-peptide complexes utilizing sites on the peptide side chains, *i.e.* the amino group, imidazole ring, carboxylic acid group, phenol group, *etc.* In our efforts to developing peptides with high metal-binding affinity and selectivity, we have targeted synthesis of siderophore-like peptides with backbone metal chelation through modification of the peptide amide bond. This would leave the side chains free to interact with receptors while the backbone would be preorganized during metal complexation. In this work we focused on the design, synthesis, and metal-binding properties of a hydroxamate-based pseudo-peptide library.

#### Results and Discussion

**Design and synthesis:** We initially chose to design the following novel dihydroxamate-containing pseudo-oligopeptides:  $X_{AA1}-\Psi[\text{CON}(\text{OH})]-X_{AA2}\cdots X_{AAn}-\text{NH}(\text{OH})$ . Several strategies for synthesis of the designed pseudo-peptides have been developed based on *N*-hydroxylamino acid derivatives as building blocks. *N*-benzyloxy-L- $\alpha$ -phenylalanine synthesized from the corresponding hydroxyl analog [1] was incorporated into peptides by reacting with Fmoc-amino acid chloride/AgCN in toluene [2]. The resulting pseudo-tripeptide Fmoc-AA<sub>1</sub>- $\Psi\{\text{CON}(\text{OBz})\}$ -Phe-AA<sub>3</sub>-OBu<sup>t</sup> were further deblocked with piperidine/DMF or TFA/DCM to afford two modules which were used to assemble the target compounds in solution or on a solid support. The protecting *O*-benzyl groups were removed with HCOONH<sub>4</sub> in the presence of Pd/C (5%) in CH<sub>3</sub>OH [3]. A library of mono-, di-, and trihydroxamate-containing linear and cyclic pseudo-peptides have been constructed in order to establish the relationship between the structure and metal binding properties of hydroxamate-based pseudopeptides. Table 1 showed some of the synthesized compounds.

**Metal-Binding Properties:** ESI-MS was used to screen the metal-binding properties of all the compounds and the relative ion abundances in a metal-competition assay were measured. All ligands exhibited a clear preference for binding with iron. The results revealed some significant information about the structure-metal-binding relationship. 1. **9>8**: cyclization can significantly improve the binding affinities of this type of ligand; 2. **5>4**, **4>1**, and **9>7**: the results indicate the importance of the distance between the two hydroxamate groups as a suitable distance allows adjustment of the bidentate hydroxamate groups to the geometry required for metal coordination; 3. **1>11**: the introduced two hydroxamate groups cooperate in coordination to efficiently improve the binding affinity; 4. **10>5**, **3>2**, and **3>4**: the steric hindrance of -(CONOH)-neighboring groups could exert an influence on the metal-binding properties; 5. **2>4**: this suggested the phenyl group may cooperate in the metal coordination. 6. **9>12** and **9>13**: high metal-binding selectivity and affinity are attainable with the dihydroxamate-containing oligopeptide system.

*Table 1. Example of some synthesized peptides from the library.*

Entry	Sequence
1	H-Leu-Ψ[CON(OH)]-Phe-Ala-NHOH
2	H-Val-Ψ[CON(OH)]-Phe-Ala-Leu-NHOH
3	H-Val-Ψ[CON(OH)]-Gly-Ala-Leu-NHOH
4	H-Val-Ψ[CON(OH)]-Ala-Ala-Leu-NHOH
5	H-Val-Ψ[CON(OH)]-Phe-Ala-Pro-Leu-NHOH
6	H-{Leu-Ψ[CON(OH)]-Phe-Ala} <sub>2</sub> -OH
7	Cyclo-{Leu-Ψ[CON(OH)]-Phe-Ala} <sub>2</sub>
8	H-{Leu-Ψ[CON(OH)]-Phe-Ala-Pro} <sub>2</sub> -OH
9	Cyclo-{Leu-Ψ[CON(OH)]-Phe-Ala-Pro} <sub>2</sub>
10	H-Leu-Ψ[CON(OH)]-Phe-Ala-Pro-Leu-NHOH
11	H-Leu-Ψ[CON(OH)]-Phe-Ala-OH
12	H-{Leu-Ψ[CON(OH)]-Phe-Ala-Pro} <sub>3</sub> -OH
13	H-{Leu-Ψ[CON(OH)]-Phe-Ala-Pro} <sub>2</sub> -Leu-NHOH

### Acknowledgments

The authors acknowledge support for this research from NIH Grant EY12113. The Washington University Mass Spectroscopy Resource Center supported by NIH (RR00954) was utilized to characterize the peptides synthesized as part of this study.

### References

1. Feenstra, R.W., Stokkingreef, E.H.M., Nivard, R.J.F., Ottenheijm, H.C.J. *Tetrahedron Lett.* **28**, 1215–1218 (1987).
2. Perlow, D.S., Erb, J.M., Gould, N.P., Tung, R.D., Freidinger, R.M., Williams, P.D., Veber, D.F. *J. Org. Chem.* **57**, 4394–4400 (1992).
3. Olsen, R.K., Ramasamy, K. *J. Org. Chem.* **50**, 2264–2271 (1985).

## Peptide Bond Modification for Metal Coordination: 2. Metal-Binding Properties of Peptide-Derived Pentaaza-Macrocyclic Templates

Yunpeng Ye<sup>1</sup>, Garland R. Marshall<sup>1</sup>, Ron Smith<sup>2</sup>, Craig Durmstorff<sup>2</sup>  
and Urszula Slomczynska<sup>2</sup>

<sup>1</sup>Department of Biochemistry and Molecular Biophysics, Washington University  
School of Medicine, St. Louis, MO 63110, USA

<sup>2</sup>MetaPhore Pharmaceuticals, Inc., St. Louis, MO 63114, USA

### Introduction

Conformation templates have been applied to elucidation of receptor-bound conformation, design of peptidomimetics, construction of combinatorial libraries, and *de novo* peptide and protein design. We are exploring pentaaza-macrocyclic templates (Figure 1) in conjunction with metal coordination as a means to preorganize peptides for probing molecular recognition. One consideration is that the peptide backbone of cyclic pentapeptides, used by the Kessler group and others as receptor probes, can be readily transformed to chiral pentaaza-macrocycles *via* selective reductions of the amide bonds [1] with side chains displayed around the macrocyclic scaffold in a defined geometrical manner. In addition, the pentaazamacrocycle is an excellent ligand system for coordination of various metals [2] that can preorganize the molecular structures even further to help define the conformation responsible for biological activity. We are also exploring the effects of the chiral pendant side chains on the metal-binding properties and related molecular recognition of the azacrown scaffold.

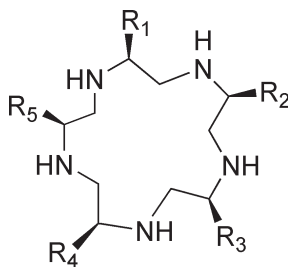


Fig. 1. The general structure of peptide-derived pentaazamacrocyclic template.

### Results and Discussion

As an initial part of our project, a series of cyclic pentapeptide precursors containing Ala, Leu, Phe, His, Tyr, Lys, Met, Cys,  $\beta$ -Ala, D-Phe, D-Ala, and (D)-Leu residues were prepared from their corresponding linear analogs using PyBOP as a coupling reagent in presence of HOBT and DIEA in DMF/DCM solution. After purified by flash column chromatography, the cyclic peptides were reduced by refluxing in a solution of  $\text{LiAlH}_4/\text{THF}$  (1 M) overnight to afford the desired products that were purified using HPLC and identified using ESI-MS. Some representative compounds of the synthesized library are listed in Table 1.

As some pentaaza-crown-Mn(II) complexes have been reported to exhibit very significant SOD mimetic activities, we focused on the Mn(II) binding properties. All

Table 1. Positive-ion ESI-MS data for some synthesized peptide-derived pentaaza-macrocyclic templates and their  $Mn^{2+}$  complexes.

Entry	Structure	ESI-MS	
		$[L + H]^+$	$[L + Mn-Cl]^+$
1	Pentaaza-cyclo [Ala-Cys(4MBZ)-Leu-Leu-Phe] <sup>a</sup>	582.3	671.5
2	Pentaaza-cyclo [Ala-Met-Leu-Leu-Phe]	506.3	595.5
3	Pentaaza-cyclo [Cys(4MBZ)-Cys(4MBZ)-Leu-Leu-Phe]	718.3	807.6
4	Pentaaza-cyclo [Ala-Tyr(Bz)-Leu-Leu-Phe]	628.4	717.6
5	Pentaaza-cyclo [Ala-Tyr-Leu-Leu-Phe]	538.3	627.3
6	Pentaaza-cyclo [Ala-His(Bom)-Leu-Leu-Phe]	632.4	721.6
7	Pentaaza-cyclo [(β)-Ala-Tyr(Bz)-Leu-Leu-Phe]	628.4	717.6
8	Pentaaza-cyclo [(β)-Ala-Tyr-Leu-Leu-Phe]	538.3	717.6
9	Pentaaza-cyclo [Ala-Lys-Leu-Leu-Phe]	503.6	637.7

<sup>a</sup> Pentaaza-cyclo [Ala-Cys(4MBZ)-Leu-Leu-Phe] refers to the pentaazamacrocyclic product from reducing the corresponding cyclo [Ala-Cys(4MBZ)-Leu-Leu-Phe]. All compounds are designated similarly.

the synthesized compounds coordinated with  $MnCl_2$  in methanol to form the 1 : 1 Mn(II) complexes with very high ion abundances in ESI-MS spectra (Table 1). Competition studies were carried out to compare their binding properties and revealed that the relative binding affinities of the ligands are in the following order: L2  $\approx$  L1, L1 > L3, L5 > L4, and L5 > L2, indicating that the side chains may have significant influences on the metal coordination. The ligands can also bind with other metal ions such as Cu(II), Zn(II), Ni(II), and Cd(II) strongly to form very stable and identifiable coordination species with the characteristic isotope clusters in ESI-MS spectra.

The effects of side chains, especially metal binding phenol, imidazole, methylthio, and amino groups which originate from the corresponding amino acid residues such as tyrosine, histidine, methionine, and lysine should be taken into account in further molecular design.

### Acknowledgments

The authors acknowledge support for this research from NIH Grants EY12113 and GM53630. The Washington University Mass Spectroscopy Resource Center supported by NIH (RR00954) was utilized to characterize the peptides synthesized as part of this study.

### References

1. Neumann, W.L., Franklin, G.W., Sample, K.R., Aston, K.W., Weiss, R.H., Riley, D.P. *Tetrahedron Lett.* **38**, 779–782 (1997).
2. Riley, D.P., Weiss, R.H. *J. Am. Chem. Soc.* **116**, 387–388 (1994).

### Peptide Bond Modification for Metal Coordination: 3. Metal-Binding Properties of Phosphorus-Based Pseudo-peptides

Yunpeng Ye and Garland R. Marshall

Department of Biochemistry and Molecular Biophysics, Washington University  
 School of Medicine, St. Louis, MO 63110, USA

#### Introduction

Phosphorus-based peptidomimetics have been attractive target compounds during research and development of metalloproteinase inhibitors [1]. Their inhibiting activities are thought to be associated with mimicry of the metal-mediated transition state or tetrahedral-intermediate of the amide hydrolysis [2]. Because of the important roles of metal ions in the structures and functions of metalloproteinases, we envision that systematic investigation of the metal binding properties of phosphorus-based peptidomimetics should provide better understanding of their mechanism of action and assist the rational design of potent and specific inhibitors.

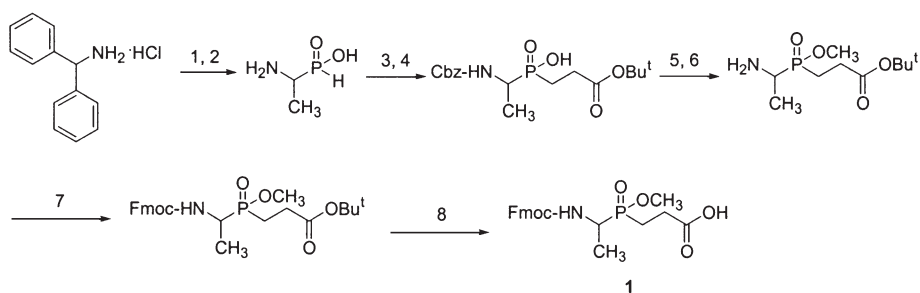
#### Results and Discussion

Based on our previous studies on metal binding hydroxamate-based pseudo-peptides, the following four novel linear and cyclic diphosphinic acid-based pseudo-peptides with a general structure of {AlaΨ[P(O)(OH)CH<sub>2</sub>]Gly---Linker---AlaΨ[P(O)(OH)CH<sub>2</sub>]Gly} were designed as models to explore the potential of phosphorus-containing moieties as metal binding sites in the pseudopeptides.

1. Ac-Ala-Ψ[P(O)(OH)CH<sub>2</sub>]Gly-Phe-Ala-Ψ[P(O)(OH)CH<sub>2</sub>]Gly-NH<sub>2</sub>
2. Ac-Ala-Ψ[P(O)(OH)CH<sub>2</sub>]Gly-Phe-Phe-Ala-Ψ[P(O)(OH)CH<sub>2</sub>]Gly-NH<sub>2</sub>
3. Cyclo{Ala-Ψ[P(O)(OH)CH<sub>2</sub>]Gly-Phe-Ala-Ψ[P(O)(OH)CH<sub>2</sub>]Gly-Phe}
4. Cyclo{Ala-Ψ[P(O)(OH)CH<sub>2</sub>]Gly-Phe-Phe-Ala-Ψ[P(O)(OH)CH<sub>2</sub>]Gly-Phe-Phe}

A Fmoc-protecting *pseudo*-dipeptide (Fmoc-(*R,S*)-AlaΨ[P(O)(OCH<sub>3</sub>)CH<sub>2</sub>]Gly, **1**) was first synthesized [3] as a module for solid phase assembly of the four designed compounds (Figure 1).

Compounds **1** and **2** were similarly assembled on Fmoc-Amide MBHA resin using conventional Fmoc chemistry. The linear peptidic precursors for compound **3** and **4**



1. CH<sub>3</sub>CHO, H<sub>2</sub>O, reflux, 1.5 h; 2. HCl solution (18%); 3. Cbz-Cl, Na<sub>2</sub>CO<sub>3</sub>, dioxane, H<sub>2</sub>O;
4. CH<sub>2</sub>=CHCOOBu<sup>t</sup>, CH<sub>3</sub>C[=NSi(CH<sub>3</sub>)<sub>3</sub>]OSi(CH<sub>3</sub>)<sub>3</sub>, CH<sub>3</sub>CN; 5. CH<sub>3</sub>OH, EDCI, DMAP;
6. Pd/C (10%), HCOONH<sub>4</sub>, CH<sub>3</sub>OH; 7. Fmoc-Cl, Na<sub>2</sub>CO<sub>3</sub>, dioxane, H<sub>2</sub>O; 8. TFA/DCM.

Fig. 1. Synthesis of Fmoc-protecting *pseudo*-dipeptide (Fmoc-(*R,S*)-AlaΨ[P(O)(OCH<sub>3</sub>)CH<sub>2</sub>]Gly, **1**).

were assembled starting from Fmoc-Phe Wang resin, cleaved with TFA, and cyclized in solution in the presence of PyBOP/HOBt/DIEA. Finally hydrolysis of the methyl esters using LiOH in dioxane/H<sub>2</sub>O afforded the desired products. All the crude products were purified with HPLC. As estimated, the products were in the diastereoisomeric forms and showed a cluster of peaks in HPLC profiles.

Some results of the metal binding study using ESI-MS are tabulated in Table 1. It was found that all the di-phosphinic based pseudo peptides exhibited high binding affinity and selectivity for Fe<sup>3+</sup> and Fe<sup>2+</sup> among the metal ions Cu<sup>2+</sup>, Zn<sup>2+</sup>, Fe<sup>3+</sup>, Co<sup>2+</sup>, Ni<sup>2+</sup>, Cd<sup>2+</sup>, Fe<sup>2+</sup> and Mn<sup>2+</sup>, indicating that the phosphinic moiety may be a highly selective ligand for iron ion coordination. Competition binding assays revealed that their iron(III) binding affinities were in the following order: 1. **1**  $\approx$  **2** and **4** > **3**, suggesting that the 8-atom length between two phosphinic groups in a linear ligand may provide enough conformational flexibility for iron coordination but a longer length between two phosphinic groups in a cyclic ligand may be essential to maintain high metal binding affinity; 2. **2**  $\approx$  **4**, indicating that cyclization may not make significant contributions to the binding affinity.

Table 1. The relative binding  $\{[Ligand+M^{n+}]/([Ligand+M^{n+}] + [Ligand])\}$ , % from positive-ion ESI-MS for solutions of Ligand 1 and 2 with different metal ions at a ligand-to-metal molar ratio of 1 : 2 in CH<sub>3</sub>OH.

Ligand	Cu <sup>2+</sup>	Mn <sup>2+</sup>	Zn <sup>2+</sup>	Ni <sup>2+</sup>	Co <sup>2+</sup>	Fe <sup>2+</sup>	Cd <sup>2+</sup>	Fe <sup>3+</sup>
1	58.6	66.5	53.1	34.6	57.6	94.3	27.0	99
2	54.5	77.3	45.6	51.8	60.5	94.9	31.3	99.0

The capacity of the phosphinic acid moiety as chelation sites in peptides has been demonstrated and its further application to the development of metal-binding peptides is in progress.

### Acknowledgments

The authors acknowledge support for this research from NIH Grants EY12113 and GM53630. The Washington University Mass Spectroscopy Resource Center supported by NIH (RR00954) was utilized to characterize the peptides synthesized as part of this study.

### References

1. Buchardt, J., Ferreras, M., Krog-Jensen, C., Delaisse, J.-M., Foged, N.T., Meldal, M. *Chem. Eur. J.* **5**, 2877–2884 (1999).
2. Morgan, B.P., Scholtz, J.M., Ballinger, M.D., Zipkin, I.D., Bartlett, P.A. *J. Am. Chem. Soc.* **113**, 297–307 (1991).
3. Baylis, E.K., Campbell, C.D., Dingwall, J.G. *J. Chem. Soc., Perkin Trans. 1* 2845–2853 (1984).

## Mimicry of the Backbone and Side-Chain Geometry of Peptide Turns: Synthesis of Novel 4-Substituted Indolizidin-9-one Amino Acids

Jérôme Cluzeau and William D. Lubell

Université de Montréal, Département de Chimie, Montréal, Québec, H3C 3J7, Canada

### Introduction

Indolizidinone amino acids have served as  $\beta$ -turn mimics for exploring conformation-activity relationships in natural peptides [1]. Focus has been particularly placed on mimicry of peptides containing aromatic residues within turn regions because of their importance in various recognition events. For example, 4- and 7-benzyl-indolizidin-2-one amino acid analogs **1** and **2** have been respectively used to synthesize ligands of the tachykinin and opioid receptors [2,3]. Similarly, indolizidin-9-one amino acid **3** has served in the synthesis of potent gramicidin S antibiotic peptides [4]. Interested in expanding the variety of indolizidinone amino acids possessing aromatic side-chains, we have now developed a new means for synthesizing 4-aryl-indolizidin-9-one amino acids **4**.

### Results and Discussion

Azelate **5** was synthesized from aspartic acid in 6 steps and 62% overall yield on 15g scale by a route featuring the Horner-Emmons olefination of  $\beta$ -aldehyde and  $\beta$ -ketophosphonate components from  $\alpha$ -*tert*-butyl  $\gamma$ -methyl *N*-(PhF)aspartate [5]. Conjugate addition reactions on enone **5** were explored using aromatic organometallic reagents to provide 6-arylazelates **6a** and **6b** (Table 1) [6]. Aryl Grignard reagents furnished predominantly product with 6*S* stereochemistry in high yield and good selectivity. On the other hand, higher-order aryl cuprates added in high yield with a preference for producing the 6*R* stereoisomer albeit with lower diastereoselectivity. Separation of a 1.5 to 1 mixture of 6*R* and 6*S* diastereomers was accomplished using a ternary eluant composed of toluene : *iso*-octane : *iso*-propyl ether (45:45:10) and gave 57% of (6*R*)-**6a** and 36% of (6*S*)-**6a**.

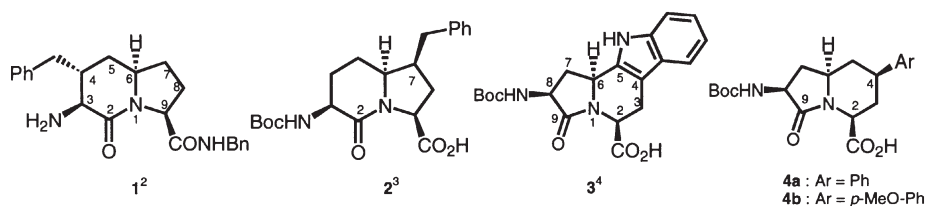
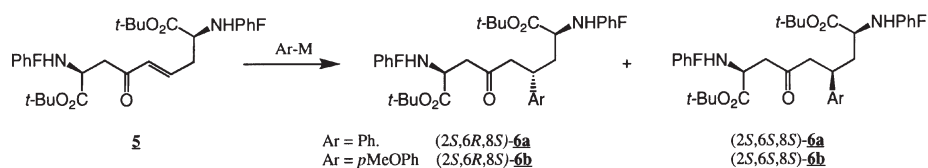


Figure 1. Example of arylindolizidinone amino acids.

4-Phenylindolizidin-9-one **7** was synthesized using our reductive amination / lactam cyclization protocol on (6*R*)-**6a**. Treatment of 6*R*-**6a** in 9:1 EtOH:AcOH with Pd/C under 7 atm of H<sub>2</sub> caused cleavage of the PhF groups, intramolecular imine formation and reduction of the protonated imine to furnish a disubstituted pipercolate intermediate. Removal of the *tert*-butyl ester with concurrent reprotection as methyl ester was accomplished using *p*-TsOH in 10:1 toluene:MeOH. Arylindolizidinones (6*R*)-**7** and (6*S*)-**7** were finally isolated in 46 and 10% respective overall yields after lactam cyclization with *p*TsOH·NEt<sub>3</sub> in toluene, amine protection with Boc<sub>2</sub>O and Et<sub>3</sub>N in DCM and purification by chromatography on silica gel (hexane : *i*-Pr<sub>2</sub>O : *i*-PrOH, 85 : 10 : 5).



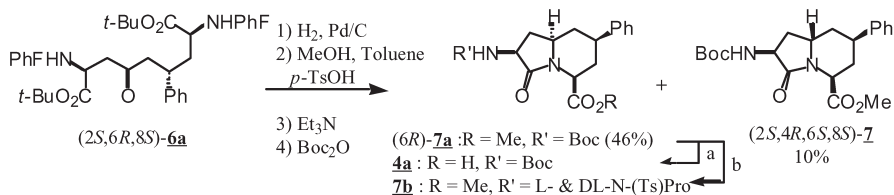
Scheme 1.

The relative stereochemistry of the (6*R*)- and (6*S*)-**7** as well as their linear ketone counterparts were assigned based on 1D and 2D (COSY, NOESY) <sup>1</sup>H NMR data. In the spectra of (6*R*)-**7**, NOE was observed between H<sup>6</sup> and both H<sup>8</sup> and H<sup>4</sup>. In the case of (6*S*)-**7**, no similar NOE was observed which was compatible with the coupling constant data and the convex configuration. The enantiomeric purity of (6*R*)-**7** was evalu-

Table 1. Selectivity of 1,4-addition reactions on enone **5**.

Ar-M	Solvent	Yields (%)	Product	Ratio (6 <i>R</i> /6 <i>S</i> )
PhMgBr	Et <sub>2</sub> O/THF	96	<b>6a</b>	1/9
Ph <sub>2</sub> CuCu(MgBr) <sub>2</sub>	THF	98	<b>6a</b>	1.5/1
( <i>p</i> -MeO-Ph)MgBr	THF	82	<b>6b</b>	1/9
( <i>p</i> -MeO-Ph) <sub>2</sub> CuCNMgBr	THF	98	<b>6b</b>	1.6/1

ated after conversion to diastereomeric N-(*p*-Ts)proline amide **7b**. By measuring the diastereomeric methyl ester singlets at 3.66 and 3.64 ppm in C<sub>6</sub>D<sub>6</sub> using <sup>1</sup>H NMR spectroscopy, amides **7b** were shown to be of 99% de. N-(Boc) amino acid **4a** was synthesized by hydrolysis of ester (6*R*)-**7a** using TMSOK in Et<sub>2</sub>O in 98% yield.



Scheme 2. Synthesis of a 4-Aryl Indolizidin-9-one amino esters **7**: a. TMSOK, Et<sub>2</sub>O (99%); b. i: TFA, CH<sub>2</sub>Cl<sub>2</sub>, ii: L and DL N-(*p*-Ts)-Pro-Cl (93%, 2 steps).

### Acknowledgments

This research was supported by NSERC (Canada) and by the Ministère de l'Éducation du Québec

### References

- Hanessian, S., et al. *Tetrahedron* **53**, 12789 (1997).
- Hanessian, S., Ronan, B., Laoui, A. *Bioorg. Med. Chem. Lett.* **4**, 1397 (1994).
- Polyak, F., Lubell, W.D. In Bajusz, S., Hudecz, F. (Eds.) *Peptides (Proceedings of the 25th European Peptide Symposium)*, 1998, p.688.
- Andreu, D. et al. *J. Am. Chem. Soc.* **119**, 10579 (1997).
- Gosselin, F., Lubell, W.D. *J. Org. Chem.* **63**, 7463 (1998).
- Organocopper Reagents, A Practical Approach*, Richard J.K.T. (Eds), 1994.

## Employing the Steric Interactions of 5-*tert*-Butylproline to Control Peptide Folding and Biology

Liliane Halab, Laurent Bélec and William D. Lubell

Université de Montréal, Département de chimie, Montréal, Québec, Canada H3C 3J7

### Introduction

Detailed analysis of the structural requirements for peptide biological activity is important for understanding mechanisms of action at the molecular level. Towards this goal, the geometrical prerequisites for peptide function may be ascertained by the use of steric interactions to restrain side-chain and backbone conformations. Steric interactions of alkyl-substituted amino acids such as linear  $\alpha$ - and  $\beta$ -methyl amino acids, various alkyl substituted pyrrolidines and their oxazolidine and thiazolidine counterparts, all have been used to restrict peptide secondary structure [1].

Our laboratory has developed efficient syntheses of (2*S*,5*S*)- and (2*S*,5*R*)-*N*-BOC-5-*tert*-butylprolines for studying the effect of steric bulk at the 5-position of a prolyl residue in peptides [1,2]. In *N*-acetyl proline *N'*-methanamides, the 5-*tert*-butyl substituent disfavored the prolyl amide *trans*-isomer and increased the *cis*-isomer population [3]. Furthermore, (2*S*,5*R*)-*N*-acetyl-5-*tert*-butylproline *N'*-methanamide showed a 3.9 kcal/mol lower barrier for isomerization of its prolyl amide bond relative to its (2*S*,5*S*)-isomer and natural proline counterpart [3]. The stabilization of type VI  $\beta$ -turn conformations by (2*S*,5*R*)-5-*tert*-butylproline (5-*t*BuPro) was next demonstrated by incorporation of D- and L-amino acids at the *N*-terminal of Ac-Xaa-5-*t*BuPro-NHMe [4,5]. Predominant prolyl amide *cis*-isomer populations have been observed in CDCl<sub>3</sub>, DMSO and water by NMR spectroscopy indicative of the steric interactions between the *tert*-butyl substituent and the *N*-terminal residue disfavoring the prolyl amide *trans*-isomer. The stereochemistry of the *N*-terminal residue in the 5-*t*BuPro-peptides was shown to exhibit a significant effect on their conformation. Dipeptides Ac-Xaa-5-*t*BuPro-NHMe adopted type VIa and type VIb  $\beta$ -turn conformations when the *N*-terminal amino acid (Xaa) possessed respectively L- and D-configuration as shown by NMR, circular dichroism and X-ray analysis [4,5]. In addition, the polyproline type II all *trans*-isomer geometry was destabilized at local positions on incorporation of 5-*t*BuPro into polyproline hexamers that may mimic the transitional intermediates involved in type II to type I helical interconversion [6].

The conformational requirements for biological activity of the neurohypophyseal hormone oxytocin (OT) were studied by using 5-*t*BuPro to offset the dynamic equilibrium about its Cys<sup>6</sup>-Pro<sup>7</sup> amide in water. The impact of the steric interaction of 5-*t*BuPro in oxytocin has been measured so far as a 2-3.5 fold augmentation of the prolyl amide *cis*-isomer population in a series of analogs of OT, Mpa<sup>1</sup>-OT (a potent agonist), and dPen<sup>1</sup>-OT (an antagonist, Figure 1) [7,8]. Additional steric interactions were introduced by replacement of Pen<sup>6</sup> for Cys<sup>6</sup>. The prolyl amide *cis*-isomer population of oxytocin has been measured at 10% in water [9]. Conformational studies on the C-terminal tetrapeptide of oxytocin, *S*-benzyl-L-cysteinyl-L-prolyl-L-leucyl-glycinamide, by <sup>1</sup>H NMR spectroscopy in DMSO, showed nearly equal populations of prolyl amide *cis*- and *trans*-isomer [10]. Similarly, in all the 5-*t*BuPro<sup>7</sup> analogs, lower populations of *cis*-isomer were observed relative to linear model peptides containing Cys-5-*t*BuPro and Pen-5-*t*BuPro residues. The steric effects of the 5-*t*BuPro residue in the peptide may be modulated by factors that have been postulated to offset the prolyl amide iso-

mer equilibrium in oxytocin [11]. In the 5-*t*BuPro<sup>7</sup>-OT series, increased *cis*-isomer population was always correlated with a reduction in agonistic potency and binding affinity for agonist analogs. In antagonist analogs, greater *cis*-isomer populations were in accord with maintained or increased antagonistic potency and binding affinity [7,8]. Although *cis*-isomer populations were only augmented up to 35% in the 5-*t*BuPro analogs, several potent antagonists were synthesized that may serve as models for evaluating the conformational requirements for inhibitory action at the oxytocin receptor.

## Results and Discussion

The influence of sequence on turn geometry and the propensity for type VI  $\beta$ -turns to nucleate hairpins have recently been explored in water by varying the amino acid residues adjacent to 5-*t*BuPro in dipeptide and tetrapeptide analogs.

Dipeptides Ac-Xaa-5-*t*BuPro-NHMe were synthesized with aromatic and hydrogen-bond donor and acceptor residues (Xaa) and their populations were measured in water by NMR spectroscopy: Xaa (% *cis*), Asp (51%), Asn (59%), Ser (68%), Ala (79%), Phe (90%), Tyr (92%), Trp (96%). As observed for linear prolyl peptides, the highest *cis*-isomer populations were observed with aromatic amino acid residues (Xaa) in water, DMSO and chloroform. Relative to their aliphatic and aromatic amino acid counterparts, hydrogen-bond donor and acceptor residues gave lower *cis*-isomer populations. Screening of protein data banks has shown that natural peptides possessing Xaa-Pro residues, where Xaa = hydrogen-bond donor or acceptor, prefer to adopt a type I  $\beta$ -turn conformation with proline at the *i* + 1 residue [12].

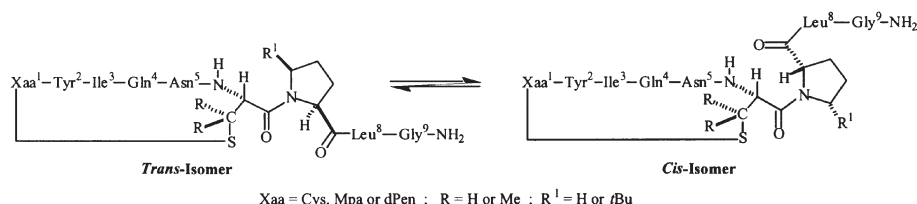


Fig. 1. Oxytocin prolyl amide isomers.

In tetrapeptides Ac-Ala-Xaa-5-*t*BuPro-Yaa-ZMe (Xaa = Ala, Leu, Phe; Yaa = Ala, Leu, Val, Phe and Z = O, NH), aromatic residues at the *N*-terminal and small alkyl substituents at the *C*-terminal of ester analogs led to the highest *cis*-isomer populations in water. Although  $\beta$ -alkyl branched and aromatic residues at the *C*-terminal of natural prolyl peptides favor *cis*-isomer conformations, in 5-*t*BuPro-tetrapeptides, smaller *cis*-isomer populations were obtained with increased steric bulk at the *C*-terminal residue. Interactions between the *tert*-butyl group of 5-*t*BuPro and the side-chain of the *C*-terminal residue appear to disfavor the *cis*-isomer conformation. Among the modifications to the 5-*t*BuPro-tetrapeptides, the most significant increases in *cis*-isomer population were obtained on conversion of the *N'*-methylamide to a methyl ester. This augmentation may be rooted in the removal of a competitive hydrogen-bonding conformation favoring the prolyl amide *trans*-isomer.

Combining the factors favoring prolyl amide *cis*-isomer geometry, we synthesized Ac-Ala-Phe-5-*t*BuPro-Ala-OMe, which exhibited 84% *cis*-amide isomer, the highest *cis*-isomer population we have observed for a linear tetrapeptide in water. Similar fac-

tors are now being considered as a means for augmenting prolyl amide *cis*-isomer population in biologically relevant peptides such as oxytocin.

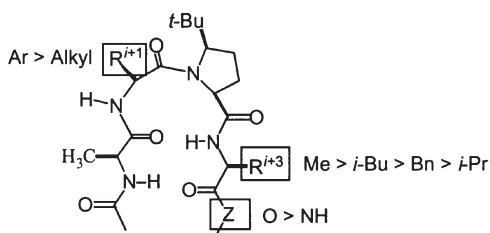


Fig. 2. Relation of *cis*-isomer population with sequence.

### Acknowledgments

This research was supported by NSERC (Canada) and the Ministère de l'Éducation du Québec.

### References

1. Halab, L., Bélec, L., Lubell, W.D. *Tetrahedron* **57**, 6439–6446 (2001), and references 1–38 therein.
2. Beausoleil, E., L'Archevêque, B., Bélec, L., Atfani, M., Lubell, W.D. *J. Org. Chem.* **61**, 9447–9454 (1996).
3. Beausoleil, E., Lubell, W.D. *J. Am. Chem. Soc.* **118**, 12902–12908 (1996).
4. Halab, L., Lubell, W.D. *J. Org. Chem.* **64**, 3312–3321 (1999).
5. Halab, L., Lubell, W.D. *J. Peptide Sci.* **7**, 92–104 (2000).
6. Beausoleil, E., Lubell, W.D. *Biopolymers* **53**, 249–256 (2000).
7. Bélec, L., Slaninová, J., Lubell, W.D. *J. Med. Chem.* **43**, 1448–1455 (2000).
8. Bélec, L., Maletinska, L., Slaninová, J., Lubell, W.D. *J. Peptide Res.* **58**, 263–273 (2001).
9. Hruby, V.J., Brewster, A.I., Glasel, J.A. *Proc. Natl. Acad. Sci. U.S.A.* **68**, 450–453 (1971).
10. Larive, C.K., Guerra, L., Rabenstein, D.L. *J. Am. Chem. Soc.* **114**, 7331–7337 (1992).
11. Larive, C.K., Rabenstein D.L. *J. Am. Chem. Soc.* **115**, 2833–2836 (1993).
12. Wilmot, C.M., Thornton, J.M. *J. Mol. Biol.* **203**, 221–232 (1988).

## Synthesis of $\beta$ -Turn Mimetics: [5,5]-Fused Bicyclic $\gamma$ -Lactam Dipeptide Analogues

Xuyuan Gu, Wei Qiu, Jinfa Ying, John M. Ndungu and Victor J. Hruby

Department of Chemistry, The University of Arizona, Tucson, AZ, 85721, USA

### Introduction

The “secondary structure approach” to the *de novo* design of peptide mimetics is guided by the simple elegance which nature has employed in the molecular architecture of peptide and protein species [1].  $\beta$ -Turns offer the significant synthetic advantage that they are relatively compact and in principle can be more readily mimicked by conformationally constrained or rigidified small organic molecules. To truly mimic different types of  $\beta$ -turns requires stereo- and enantiocontrolled introduction of a minimum of four asymmetric centers, with different backbone geometry and side chain topography. Among the interesting approaches toward  $\beta$ -turn mimetics, the design of azabicycloalkane amino acids have been shown to have unique potential advantages, and numerous bicyclic derivatives of this general class have been synthesized [2]. Although  $\beta$ -lactam bicyclic analogues have well-known antibacterial activities, most  $\gamma$ -lactams without appropriate side chain moieties have not shown significant biological activities. Obviously, side chains play important roles in  $\beta$ -turns and we have proposed [3], that introduction of side-chains on the bicyclic scaffold would generate expected biological activities. Here we report a simple but potentially general method to generate in 5 steps [5,5]-bicyclic dipeptide, which not only have both C- and N-terminals but also have side chain groups on both rings.

### Results and Discussion

Starting from N-protected glycine, esterification with cinnamyl alcohol provided **3** (Figure 1) in excellent yield (98%). The typical Kazmaier-Claisen rearrangement generated highly diastereoselective  $\beta$ -vinyl phenylalanines **4** in large scales. Only one diastereomer was observed in  $^1\text{H}$  NMR spectrum. Osmylation followed by oxidation cleavage generated the aldehyde. The lack of an aldehyde-H in  $^1\text{H}$  NMR indicated the formation of hemiacetal **5**. After work up, the aldehyde was used directly to react with  $\beta$ -mercapto amino acids [4]. The thiazolidine formation was performed under very

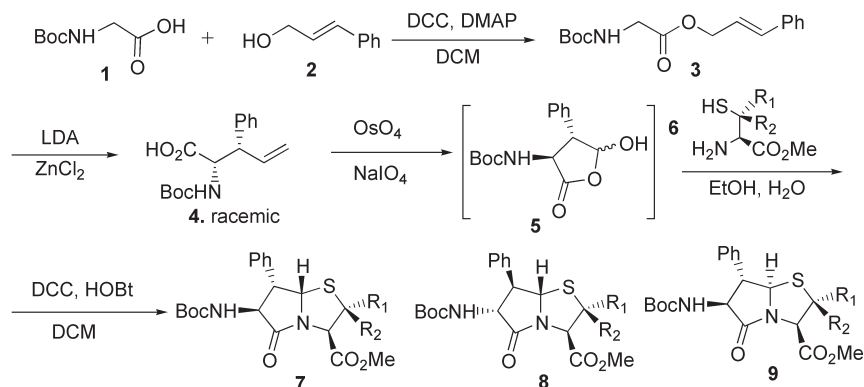


Fig.1. The syntheses of [5,5]-fused bicyclic  $\gamma$ -lactam dipeptide.

mild reaction conditions to give products with a 2,5-*trans* relationship, which is preferred to the 2,5-*cis* due to steric effects. Bicyclization was completed by use of a typical amide coupling reagent to give a [5,5]-fused bicyclic  $\gamma$ -lactam dipeptides in 5 steps and overall 31–66% yield. Because racemic  $\beta$ -vinyl phenylalanine and enantiomerically pure  $\beta$ -thio amino acids were used, two or three diastereomers were generated. Fortunately, all these isomers can be isolated and purified by liquid chromatography.

*Table 1. The results of bicyclization of  $\gamma$ -lactam dipeptide.*

	Starting material		Three-step yield	Product ratio		
	R <sub>1</sub>	R <sub>2</sub>		<b>7</b>	<b>8</b>	<b>9</b>
<b>6a</b>	H	H	77	32	48	20
<b>6b</b> *	Me	Me	70	30	58	12
<b>6c</b> *	H	Me	40	50	50	

*Penicillamine methyl ester was prepared from penicillamine (gaseous HCl in distilled methanol). The synthesis of methyl  $\beta$ -thio- $\alpha$ -amino butyrate will be published elsewhere.*

Another method starting from  $\beta$ -vinyl phenylalanine methyl ester leading to the fused bicyclic compounds in one step (in refluxing pyridine) or in two steps (monocyclization in EtOH and H<sub>2</sub>O followed by heating in DMF) was not successful due to the instability of the aldehyde under these reaction conditions [5]. The formation of a hemiacetal in this case is thought to be important [6]. The stereo-structure of **8a** was determined by deprotection of N-Boc and attachment of the N-Cbz protecting group. The X-ray crystal structure of N-Cbz of **8a** has been published in our previous paper [4]. All the other structures are characterized by either X-ray and nOe spectrum. In our future work, we are focusing on the [6,5]-bicyclic formation and other analogue syntheses and their application to short peptides with important biological activities.

#### Acknowledgments

This work was supported by grants from the U.S. Public Health Service and NIDA DK 17420 and DA 13449.

#### References

1. Nakanishi, H., Kahn, M. In *Bioorganic Chemistry: Peptides and Proteins*; Hecht, S.M., Ed.; Oxford University Press: London, 1998; pp. 395–419.
2. Hanessian, S., McNaughton-Smith, G., Lombart, H-G., Lubell, W.D. *Tetrahedron* **53**, 12789–12845 (1997).
3. Qiu, W., Gu, X., Soloshonok, V.A., Carducci, M.D., Hruby, V.J. *Tetrahedron Lett.* **42**, 145–148(2001).
4. Baldwin, J.E., Adlington, R.M., Bryans, J.S., Lloyd, M.D., Sewell, T.J., Schofield, C.J. *Tetrahedron* **53**, 7011–7020 (1997).
5. (a) Nagai, U., Sato, K., Nakamura, R., Kato, R. *Tetrahedron* **49**, 3577–3592 (1993); (b) Baldwin, J.E., Lee, V., Schofield, C.J. *Heterocycles* **34**, 903–906 (1992).
6. Banfi, L., Guanti, G, Riva, R. *Tetrahedron* **52**, 13493–13512 (1996).

## Pyridine as a Tripeptidomimetic Scaffold

Stina Saitton<sup>1,2</sup>, Jan Kihlberg<sup>1</sup> and Kristina Luthman<sup>2,3</sup>

<sup>1</sup>Umeå University, Organic Chemistry, SE-901 87 Umeå, Sweden

<sup>2</sup>University of Tromsø, Institute of Pharmacy, NO-9037 Tromsø, Norway

<sup>3</sup>Göteborg University, Department of Chemistry, SE-412 96 Göteborg, Sweden

### Introduction

There are several short peptides that are biologically active and hence of interest for drug development. One major limitation preventing oral administration of these compounds is the instability of amide bonds towards enzymatic degradation. Therefore, compounds that mimic the effect of peptides but lack the peptide structure are of great interest [1]. One approach towards so called peptidomimetics is to use a cyclic structure as a scaffold to which different pharmacophoric groups, supposedly amino acid side chains, can be attached.

We are interested in the development of a general tripeptidomimetic scaffold both for mimicry and investigation of various tripeptides and tripeptide segments. Molecular mechanics based conformational analysis and semi-empirical calculations (AM1) of electrostatics were performed on Ac-Ala-Ala-Ala-NHMe, to represent a general tripeptide, and two examples of mimetics (Figure 1) were identified. This led to our suggestion of a 2,3,4-trisubstituted pyridine (**1**) as a scaffold to which the different amino acid side chains are attached.

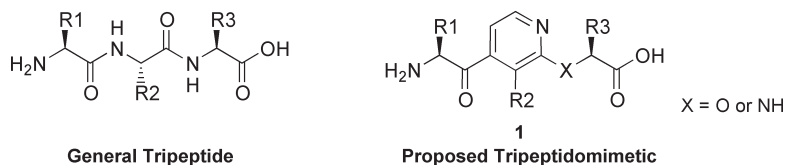


Fig. 1. A general tripeptide and the proposed tripeptidomimetic based on a pyridine scaffold. R<sub>1</sub>–R<sub>3</sub> represent different amino acid side chains.

### Results and Discussion

The synthesis of a tripeptidomimetic based on pyridine started with the functionalized scaffold **2** that was synthesized in two steps starting from 2-fluoropyridine according to the procedure by Quéguiner and co-workers [2]. In the first step, treatment with LDA was followed by addition of iodine to afford 2-fluoro-3-iodo-pyridine in 78% yield. In the second step, treatment with LDA was accompanied with a migration of iodine to the 4-position to produce a more stable anion, which by reaction with methyl iodide gave 2-fluoro-4-iodo-3-methylpyridine (**2**) in 89% yield (Figure 2).

The third amino acid moiety was attached at the 2-position of pyridine by a nucleophilic substitution reaction. Reaction of methyl-L-lactate with NaH, followed by addition of the functionalized scaffold **2** afforded racemic **3** in 80% yield.

Coupling of the first amino acid moiety was accomplished by a Grignard reaction [3]. Reaction of the pyridine derivative with iPrMgCl followed by addition of Boc-protected prolinal [4] produced a crude mixture of the alcohols **4** which was treated with Jones'

reagent to afford **5** in 77% yield over 2 steps. Deprotection of the ethyl ester with LiOH and the Boc-group with TFA finally afforded the desired tripeptidomimetic **6**.

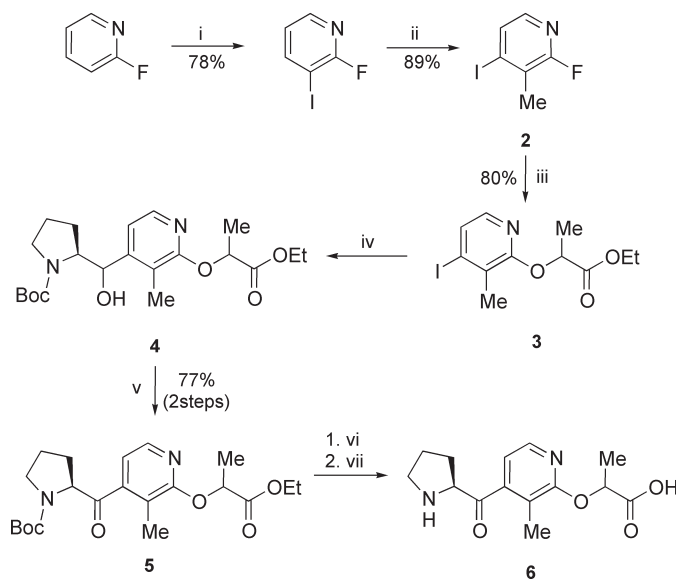


Fig. 2. Reaction conditions: (i) 1. LDA, THF, -78 °C, 4 h; 2. I<sub>2</sub>, -78 °C, 1 h. (ii) 1. LDA, THF, -78 °C, 1 h; 2. MeI, -78 °C, 2 h. (iii) NaH, Ethyl-L-lactate, THF, 60 °C, overnight. (iv) 1. iPrMgCl, THF, -40 °C, 2 h; 2. Boc-Pro-CHO, -40 °C, 1 h. (v) Jones' reagent, acetone, 0 °C, 1 h. (vi) 1. LiOH, THF/H<sub>2</sub>O, 25 °C, overnight. (vii) TFA, CH<sub>2</sub>Cl<sub>2</sub>, 25 °C, 1.5 h.

In summary, a novel pyridine-based peptidomimetic scaffold has been designed and used in a synthesized tripeptidomimetic. We are presently working on achieving stereoselectivity in the nucleophilic substitution reaction. Further work will reveal the generality of the synthetic strategy and the ability of the pyridine scaffold to mimic various tripeptides.

### Acknowledgments

We thank the Norwegian Research Council for providing financial support for this project and Dr Roeland C. Vollinga for the design work.

### References

1. Pauletti, G.M., Gangwar, S., Siahaan, T.J., Aubé, J., Borchardt, R.T. *Adv. Drug Delivery Rev.* **27**, 235 (1997).
2. Rocca, P., Cochennec, C., Marsais, F., Thomas-dit-Dumont, L., Mallet, M., Godard, A., Quéguiner, G. *J. Org. Chem.* **58**, 7832 (1993) and references therein.
3. Trécourt, F., Breton, G., Bonnet, V., Mongin, F., Marsais, F., Quéguiner, G. *Tetrahedron* **56**, 1349 (2000).
4. Fehrentz, J.A., Castro, B. *Synthesis* 676 (1983).

## Synthesis of Fluoroalkene Dipeptide Isosteres Utilizing Organometallic Reagents

Akira Otaka, Hideaki Watanabe, Junko Watanabe, Hirokazu Tamamura and Nobutaka Fujii

Graduate School of Pharmaceutical Sciences, Kyoto University, Sakyo-ku,  
 Kyoto 606-8501, Japan

### Introduction

Dipeptide isosteres possessing nonhydrolyzable scaffolds as replacements for scissile peptide bonds represent important constituents in peptidomimetics for medicinal and/or biological use. Among these, (*E*)-alkene dipeptide isosteres, Xaa1-Ψ[(*E*)-CH=CH]-Xaa2 (**1**), feature three-dimensional structures closely approximating parent peptide bonds; however, certain intrinsic properties of amide bonds such as dipole interaction and hydrogen bonding are lacking. Therefore, (*Z*)-fluoroalkene dipeptide isosteres, Xaa1-Ψ[(*Z*)-CF=CH]-Xaa2 (**2**), have gained significant attention as potentially superior mimetics to (*E*)-alkene type isosteres [1] (Figure 1).

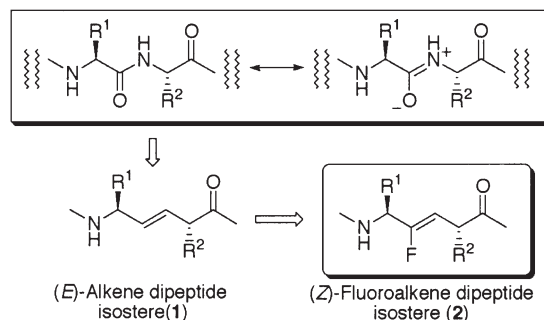
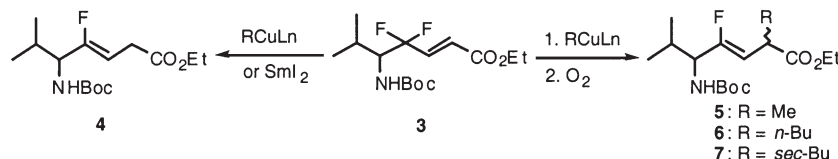


Fig. 1. Alkene-type dipeptide isosteres.

During the course of investigations on the synthesis of nonhydrolyzable phosphothreonine mimetics [2], we found that reaction of  $\gamma$ -phosphono- $\gamma,\gamma$ -difluoro- $\alpha,\beta$ -enoates with organocopper reagents afforded reduction products,  $\gamma$ -phosphono- $\gamma$ -fluoro- $\beta,\gamma$ -enoates [3]. Subsequently we applied the organocopper-mediated reduction to the synthesis of Xaa-Gly type (*Z*)-fluoroalkene dipeptide isosteres (Scheme 1, **3** to **4**) [4]. Although such copper-mediated methodologies provide new access to the fluoroalkene isosteres, the resulting products have been limited to Xaa-Gly type isosteres. Here, we examined the feasibility of copper-mediated procedures for the



Scheme 1. Synthesis of fluoroalkene dipeptide isosteres using organometallic reagents.

synthesis of  $\alpha$ -substituted (Z)-fluoroalkene dipeptide isosteres and the usefulness of other organometallic reagents for the synthesis of the isosteres.

### Results and Discussion

We explored methodology for  $\alpha$ -alkylation based on reaction mechanisms of the copper-mediated reduction. Recently, Yamamoto *et al.* reported that single electron transfer (SET) from  $\text{MeCuLn}$  ( $\text{Ln}$  = ligand) to a substrate, is involved with a highly electrophilic substrate in the formation of corresponding reduction products [5]. In this process, single electron transfer to the substrate give stable Cu(I) or Cu(II) intermediate which are quenched with  $\text{H}^+$  to yield the reduction product. Alternatively, oxidation with  $\text{O}_2$  to unstable Cu(III) species affords the Me substituted product *via* reductive elimination. This work prompted us to envision that the formation of reduction products from highly electrophilic  $\gamma,\gamma$ -difluoro- $\alpha,\beta$ -enoates with organocopper reagents, would be likely to proceed *via* the SET mechanism. Treatment of **3** with  $\text{Me}_2\text{Cu}(\text{CN})\text{Li}_2 \cdot 2\text{LiBr} \cdot 2\text{LiCl}$  in  $\text{Et}_2\text{O}$ –THF at  $-78^\circ\text{C}$  under an Ar atmosphere for 4 min followed by reaction under an  $\text{O}_2$  atmosphere at  $-78^\circ\text{C}$  for 20 min, proceeded non-stereoselectively to afford the corresponding  $\alpha$ -methylated product (**5**) in 64% isolated yield. The use of higher order species ( $\text{Me}_3\text{Cu}(\text{CN})\text{Li}_3$ ) improved the yield (74%). Reaction with other alkyl copper reagents derived from *n*-BuLi or *sec*-BuLi, followed by  $\text{O}_2$  oxidation, gave the  $\alpha$ -substituted products (**6** or **7**) in moderate yields (54 and 45%, respectively, Scheme 1).

Samarium(II) iodide ( $\text{SmI}_2$ ) has been well recognized as a powerful one-electron reducing agent capable of meeting the intensifying demands of synthetic organic chemistry [6]. Taking account of our mechanistic insight into the organocopper-mediated reduction, we speculated that  $\text{SmI}_2$  would be also applicable to the reduction of  $\gamma,\gamma$ -difluoro- $\alpha,\beta$ -enoates to give fluoroalkene dipeptide isosteres. Based on this assumption, the enoate (**3**) was subjected to  $\text{SmI}_2$ -mediated reduction ( $\text{SmI}_2$  in THF at  $4^\circ\text{C}$  for 30 min) to afford a desired (Z)-fluoroalkene isoster (**4**) in 80% isolated yield (Scheme 1).

In summary, we have developed a new route to  $\alpha$ -substituted fluoroalkene dipeptide isosteres using organocopper reagents. Furthermore,  $\text{SmI}_2$  was proved to be useful reagent for the synthesis of fluoroalkene isosteres.

### References

1. Welch, J.T., Allmendinger, T., In Kazmierski, W.M. (Eds.) *Peptidomimetics Protocols*, Humana Press, 1999, p. 357–384.
2. Otaka, A., Mitsuyama, E., Kinoshita, T., Tamamura, H., Fujii, N. *J. Org. Chem.* **65**, 4888–4899 (2000).
3. Otaka, A., Mitsuyama, E., Watanabe, H., Tamamura, H., Fujii, N. *Chem. Commun.* 1081–1082 (2000).
4. Otaka, A., Watanabe, H., Mitsuyama, E., Yukimasa, A., Tamamura, H., Fujii, N. *Tetrahedron Lett.* **42**, 285–287 (2001).
5. Chounan, Y., Ibuka, T., Yamamoto, Y. *J. Chem. Soc., Chem. Commun.* 2003–2004 (1994).
6. Molander, G. A., Harris, C.R. *Tetrahedron* **54**, 3321–3354 (1998).

## Synthesis of Peptide Mimetics and Amino Acid Mimetics Bearing Aminoxy Instead of Amino Group

Toratane Munegumi, Tokanori Yoshii, Masahide Nakamura  
 and Kunie Sakurai

*Department of Materials Chemistry and Bioengineering, Oyama National College  
 of Technology, 771 Nakakuki, Oyama, 323-0806, Tochigi, Japan*

### Introduction

The compounds composed of sequential units different than amino acids might have different functionality from those of peptides. In this study, we have chosen a structure (–N–O–C–C–) as one of the sequential units and attempted to prepare the building blocks analogous to amino acids in peptides. Those building blocks, amino acid mimetics, bear an aminoxy group (H<sub>2</sub>N–O–) instead of the α-amino group (H<sub>2</sub>N–) in amino acids. Such new amino acid mimetics and the peptide mimetics constructed from those would be interesting in the studies of chemical reactivity and structure as well as bioactivity.

### Results and Discussion

The syntheses of the amino acid mimetics **4a–d** were carried out by the hydrolysis of the compounds **3a–d** (5–40 mmol) prepared by the reactions between *N*-hydroxyphthalimide **1a–d** and 2-bromocarboxylic acids **2** [1].

Compounds **3a–d** and amino acid mimetics **4a–d** were obtained in the yield of 54–84% and more than 89%, respectively. Protection of compounds **4a–c** (10 mmol) was carried out by di-*t*-butyldicarbonate to give *N*-Boc-derivatives **5a–c**. The results in Table 1 showed that the mimetics can be prepared easily and transformed to their *N*-Boc protected forms.

The pK<sub>a</sub> of an amino acid mimetic (**4b**) was measured by the titration using 1 M NaOH. The pK<sub>a</sub> value of the conjugated acid of the aminoxy group in **4b** was 4.8 at 25 °C. The value was lower than that of alanine (pK<sub>a</sub> = 9.9). On the other hand, the pK<sub>a</sub> values of the carboxyl groups of the mimetic (**4b**) and alanine were almost the same (pK<sub>a</sub> = 2.3). The different pK<sub>a</sub> value of the mimetics from that of amino acids might affect the reactivity of the compounds. However, the acidity difference did not have an effect on the Boc-derivatization of the mimetics.

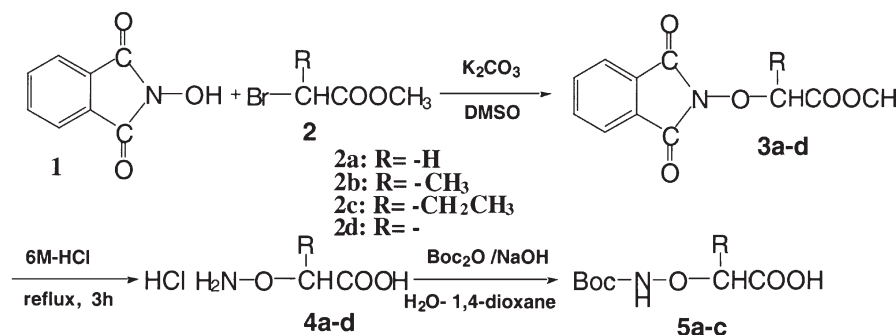


Fig. 1. Synthesis of amino acid mimetics and their *N*-Boc-derivatives.

*Table 1. Synthesis of amino acid mimetics and N-Boc-derivatives.*

Substituent group	<b>3</b>		<b>4</b>		<b>5</b>	
	Yield (%)	Mp (°C)	Yield (%)	Mp (°C)	Yield (%)	Mp (°C)
<b>a</b> (R = H)	69	138–139	99	146	95	109–111
<b>b</b> (R = CH <sub>3</sub> )	84	64–66	89	157–159	96	85–87
<b>c</b> (R = CH <sub>2</sub> CH <sub>3</sub> )	76	75–76	99	121–125	93	80–82
<b>d</b> (R = Ph)	54	126–128	92	169–170		

The synthesis of peptide mimetics was tested by the coupling between *N*-hydroxysuccinimide ester of **4a** and **5c** in CH<sub>3</sub>CN–H<sub>2</sub>O to give a peptide mimetic compound (Boc-NHO-CH<sub>2</sub>-CO-NHO-CH(CH<sub>2</sub>CH<sub>3</sub>)-COOH, oil, 80%).

The racemic phthalimide derivative (**3d**) of the racemic amino acid mimetic (**4d**) was resolved into the enantiomers by HPLC equipped with a chiral column OA-7000 (Sumitomo). However, other racemic phthalimide derivatives (**3a–c**) were not resolved by this method.

## References

1. Fujii, T., Wu, C.C., Yamada, S. *Chem. Pharm. Bull.* **15**, 345–349 (1967).

## Design and Synthesis of Amide Isosteres of Phe-Gly: Potential Peptidomimetic Ligands for the Intestinal Oligopeptide Transporter PepT1

Jon Våbenø<sup>1</sup>, Magnus Brisander<sup>1</sup>, Weiqing Chen<sup>2</sup>, Ronald T. Borchardt<sup>2</sup>  
 and Kristina Luthman<sup>1,3</sup>

<sup>1</sup>Department of Medicinal Chemistry, University of Tromsø, N-9037 Tromsø, Norway

<sup>2</sup>Department of Pharmaceutical Chemistry, University of Kansas, Lawrence, Kansas 66047, USA

<sup>3</sup>Göteborg University, Department of Chemistry, SE-412 96 Göteborg, Sweden

### Introduction

The transport of di- and tripeptides across the intestinal epithelium is an active process mediated by the oligopeptide transporter PepT1 [1]. Oligopeptides transported by PepT1 should preferably consist of 2–3 amino acids. The possible use of this transporter for transport of drugs requires knowledge of which structural modifications that can be made on the peptidomimetics without losing affinity for PepT1. We have synthesized Phe-Gly peptidomimetics in which the amide bond has been replaced by isosteric moieties, which have been designed to have similar (a) geometrical properties, (b) conformational flexibility and/or (c) electrostatic and hydrogen bonding properties as the amide bond.

Several models for binding to the transporter have been suggested. Bailey [2] has proposed a model indicating the relative orientation of the different groups of a peptide. For dipeptides, it is suggested that the bond to the terminal carboxylate group should be oriented 60° relative to the plane of the amide bond. If this theory is correct, the more flexible dipeptidomimetics should be preferred by the transporter because of their ability to adopt this conformation.

### Results and Discussion

The synthetic strategy is outlined in Figure 1. The key intermediate **3** was prepared by a Wadsworth–Emmons reaction by treatment of the phosphonate **2** with *tert*-butyl glyoxylate, triethylamine and lithium chloride.

To obtain the two alcohols **5** and **6**, a variety of reducing agents have been investigated to achieve diastereoselective reductions. The ratio of **5** : **6** varied between 3 : 1 ((*S*)-CBS, BH<sub>3</sub>·THF) and 1 : 14 (NB-Enantride). The resulting mixtures were separated by straight phase HPLC.

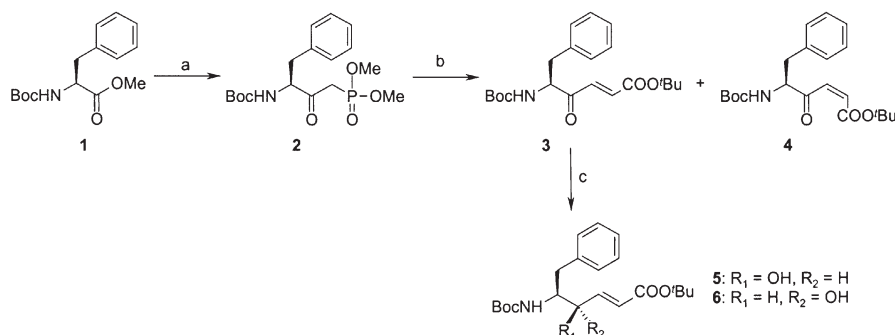


Fig. 1. Synthetic strategy; reagents and conditions: (a)  $\text{LiCH}_2\text{PO}(\text{OMe})_2$  (3 eq), THF,  $-78^\circ\text{C}$ . (b)  $t\text{BuOOC-CHO}$ , LiCl,  $\text{Et}_3\text{N}$ ,  $\text{CH}_3\text{CN}$ ,  $-10^\circ\text{C}$ . (c) (*S*)-CBS,  $\text{BH}_3\cdot\text{THF}$  or NB-Enantride.

### Biologically Active Peptides

Deprotection of **3**, **4**, **5** and **6** with TFA in  $\text{CH}_2\text{Cl}_2$  followed by purification by reversed phase HPLC, afforded the trifluoroacetate salts of compounds **7**, **8**, **9** and **10**, respectively (Figure 2).

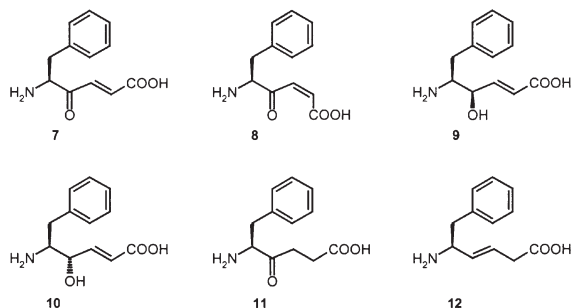


Fig. 2. Structures of the synthesized Phe-Gly mimetics [3].

Preliminary transport studies on Caco-2 cells of alcohols **9** and **10**, the saturated ketone **11** and alkene **12** [3], have shown that these compounds differ both in their affinity for, and transport by PepT1. The alcohols bind to PepT1 (**10** > **9**), but are not transported to any significant extent. Ketone **11** is both binding and transported. Alkene **12** does not bind, but seems to be passively transported.

Thus, it seems as the amide carbonyl group is important for recognition, binding and efficient transport of these compounds by PepT1. The test results for the unsaturated ketones **7** and **8** will provide useful information about the importance of flexibility and of the orientation of the carboxylate group.

### Acknowledgments

We gratefully acknowledge Dr. Tore Lejon for valuable discussions and advice. We also thank the Norwegian Research Council for providing financial support for this project.

### References

1. Fei, Y.J., Kanai, Y., Nussberger, S., Ganapathy, V., Leibach, F.H., Romero, M.F., Singh, S.K., Boron, W.F., Hediger, M.A. *Nature* **368**, 563–566 (1994).
2. Bailey, P.D., Boyd, C.A.R., Bronk, J.R., Collier, I.D., Meredith, D., Morgan, K.M., Temple, C.S. *Angew. Chem., Int. Ed. Engl.* **39**, 506–508 (2000).
3. Compounds **9–12** were synthesized by Silje Grinde. Described in “*Design og syntese av dipeptidomimetika som ligand for transport-molekylet PepT1*”, Diploma work, University of Tromsø, Norway, 1999.

## $\beta$ -D-Mannose Based Peptidomimetics in the Design of $\alpha_4\beta_1$ and $\alpha_4\beta_7$ Antagonists

Jürgen Boer<sup>1</sup>, Elsa Locardi<sup>1</sup>, Anja Schuster<sup>2</sup>, Bernhard Holzmann<sup>2</sup> and Horst Kessler<sup>1</sup>

<sup>1</sup>Institut für Organische Chemie und Biochemie, Technische Universität München, Garching, 85747, Germany

<sup>2</sup>Institut für Medizinische Mikrobiologie, Immunologie und Hygiene, Technische Universität München, München, 81675, Germany

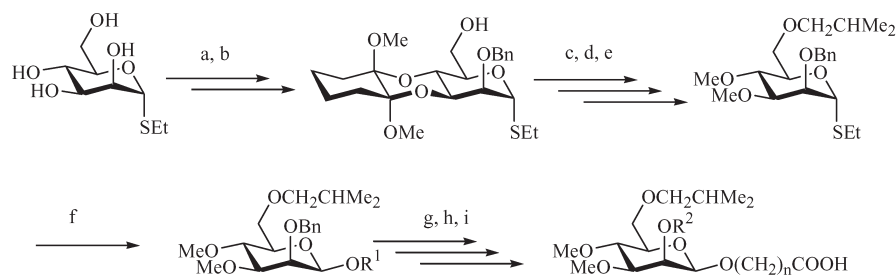
### Introduction

Interfering protein-protein interaction by small non-peptidic molecules is one of the great challenges in medicinal chemistry. The use of rigid scaffolds to generate peptidomimetics was first proposed by Farmer [1]. Carbohydrate moieties as scaffolds were first introduced by Hirschmann and Nicolaou [2].

We present herein the design, synthesis and biological evaluation of  $\beta$ -D-mannose based non-peptidic mimetics of the vascular cell adhesion molecule-1 (VCAM-1), and of the mucosal addressin cell adhesion molecule-1 (MAdCAM-1), which are the natural ligands of  $\alpha_4\beta_1$  and  $\alpha_4\beta_7$  integrin receptors [3,4]. Similar recognition motifs were identified for these ligands: Ile-Asp-Ser-Pro (IDSP) in VCAM-1 and Leu-Asp-Thr (LDT) in MAdCAM-1. The pharmacophoric side chains were anchored on a  $\beta$ -D-mannose core in a rational combinatorial approach. The design originated from the conformation in solution of cyclic hexapeptides recently developed in our group as potent and selective inhibitors of the MAdCAM-1/ $\alpha_4\beta_7$  integrin interaction [5].

### Results and Discussion

The pharmacophoric side chains present in the natural ligands were attached *via* ether linkages to the sugar core at position 6, 1 and 2. The synthetic protocol is shown in Scheme 1. The final components **1–8** were synthesized in nine steps starting from ethyl thio- $\alpha$ -D-mannopyranoside. The key steps in our synthetic strategy was the selective protection of the 3 and 4 position of the mannose ring using the cyclohexane-



Scheme 1. a) CDA, CSA, TMOF, MeOH (55%); b) BnBr, KOH, DMSO (75%); c) BrCH<sub>2</sub>CHMe<sub>2</sub>, KOH, DMSO (89%); d) 90% TFA (73%); e) MeI, KOH, DMSO (75%); f) Br<sub>2</sub>, DCM, 0 °C then R<sup>1</sup>OH, Ag<sub>2</sub>CO<sub>3</sub>, DCM, RT. R<sup>1</sup> = CH<sub>2</sub>CH(OMe)<sub>2</sub>; R<sup>1</sup> = CH<sub>2</sub>CH<sub>2</sub>CH(OEt)<sub>2</sub>; g) 10% Pd/C, H<sub>2</sub> then BrR<sup>2</sup>(-OBn), KOH, DMSO; h) 2 N HCl, THF, RT then NaClO<sub>2</sub>, 2-methyl-2-butene, *t*-BuOH, NaH<sub>2</sub>PO<sub>4</sub>, H<sub>2</sub>O, RT; i) 10% Pd/C, H<sub>2</sub>, MeOH. **1**: R<sup>2</sup> = CH<sub>2</sub>CH<sub>2</sub>OH, *n* = 1; **2**: R<sup>2</sup> = CH<sub>2</sub>CH<sub>2</sub>CH<sub>2</sub>OH, *n* = 1; **3**, **4**: R<sup>2</sup> = CH<sub>2</sub>CH(OH)CH<sub>3</sub>, *n* = 1; **5**: R<sup>2</sup> = CH<sub>2</sub>CH<sub>2</sub>OH, *n* = 2; **6**: R<sup>2</sup> = CH<sub>2</sub>CH<sub>2</sub>CH<sub>2</sub>OH, *n* = 2; **7**, **8**: R<sup>2</sup> = CH<sub>2</sub>CH(OH)CH<sub>3</sub>, *n* = 2.

1,2-diacetal (CDA) [6] and the subsequent benzylation in 2 position due to the steric hindrance of the primary alcohol in 6 position [7]. The orthogonal protecting groups were successively cleaved and replaced by the pharmacophoric groups. Short interproton distances H1–H5 and H1–H3 in the NOESY spectra confirmed the formation of the  $\beta$ -anomer. Heteronuclear one-bond coupling constants at the anomeric center  $^1J_{C1,H1}$  were also used to confirm the configuration at the anomeric center [8].

The biological evaluation of the carbohydrate protein-mimetics **1–8** was done by cell adhesion experiments. The binding of Jurkat ( $\alpha_4\beta_1^+$ ,  $\alpha_4\beta_7^-$ ) and 38- $\beta$ 7 lymphoma cells to immobilized VCAM-1 as well as the binding of 38- $\beta$ 7 lymphoma cells to immobilized MAdCAM-Ig fusion protein were examined after incubation of these cells with our mannose derivatives.

The incorporation of a Leu-Asp-Ser mimetic onto the  $\beta$ -mannose scaffold at position 6, 1 and 2, respectively, led to inhibitory activity towards the VCAM-1/ $\alpha_4\beta_1$  integrin interaction [9]. Compound **1** inhibits selectively 70% of Jurkat cell adhesion to VCAM-1. The compounds **2–8** in all assays do not exhibit significant biological activity. No inhibition of the MAdCAM-1/ $\alpha_4\beta_7$  was found for all the sugar derivatives.

These data demonstrate that the amide groups are not involved in the VCAM-1/ $\alpha_4\beta_1$  integrin interaction or contribute only marginally. This class of protein-mimetics represents a promising candidate for drug development since it overcomes the limitations of peptidic drugs, generally associated with mediocre absorption, poor oral bioavailability and poor metabolic stability amongst other factors. Further investigations on this field are currently in progress in our group.

## References

1. Farmer, P.S. *Drug Design*, Academic Press, New York, 1980.
2. Hirschmann, R., Nicolaou, K.C., et al. *J. Am. Chem. Soc.* **114**, 9217–9218 (1992).
3. Kilger, G., Holzmann, B. *J. Mol. Med.* **73**, 347–354 (1995).
4. Berlin, C., Berg, E.L., Briskin, M.J., Andrew, D.P., Kilshaw, P.J., Holzmann, B., Weissman, I.L., Hamann, A., Butcher, E.C. *Cell* **74**, 185–195 (1993).
5. Boer, J., Gottschling, D., Schuster, A., Semmrich, M., Holzmann, B., Kessler, H. *J. Med. Chem.* **44**, 2586–2592 (2001).
6. Douglas, N.L., Ley, S.V., Osborn, H.M.I., Owen, D.R., Priepke, H.W.M., Warriner, S.L. *Synlett* **8**, 793–795 (1996).
7. Felix, A.M., Heimer, E.P., Lambros, T.J., Tzougraki, C., Meienhofer, J. *J. Org. Chem.* **43**, 4194–4196 (1978).
8. Weingart, R., Schmidt, R.R. *Tetrahedron Lett.* **41**, 8753–8758 (2000).
9. Boer, J., Gottschling, D., Schuster, A., Holzmann, B., Kessler, H. *Angew. Chem., Int. Ed.* **40**, 3870–3873 (2001).

## Design, Synthesis and Modulation of Angiogenesis by Thrombin Receptor Non-Peptide Antagonists

Kostas A. Alexopoulos<sup>1</sup>, Michael Maragoudakis<sup>2</sup> and John M. Matsoukas<sup>1</sup>

<sup>1</sup>Department of Chemistry, University of Patras, 26500 Patras, Greece

<sup>2</sup>Department of Pharmacology, Medical School, University of Patras,  
26110 Rio, Patras, Greece

### Introduction

The angiogenic action of thrombin has been shown to be mediated by activation of the thrombin receptor. The thrombin receptor (PAR-1) is activated by serine protease cleavage of its extracellular N-terminus to expose an agonist peptide ligand which is tethered to the receptor itself. Synthetic peptides containing the agonist motif, such as SFLLR for human PAR-1, are capable of causing full receptor activation. From extensive structure-activity studies (SAR) we proposed a curved backbone for the active form of SFLLR, in which the Phe and Arg residues cluster together to form a primary pharmacophore motif. Spatial relationships between the important Phe and Arg functional groups of the PAR-1 agonist peptide SFLLR were employed to design and synthesize candidate ligands with appropriate groups attached to a rigid molecular template. Herein, we report the design, synthesis and effects of potent non-peptide PAR-1 antagonists on angiogenesis in the chorioallantoic membrane (CAM) system, which have therapeutic potential for treating cancer and other angiogenic diseases.

### Results and Discussion

We have initiated an effort in developing thrombin receptor non-peptide mimetics based on our observation that thrombin receptor activating peptides (TRAPs) can mimic the effect of thrombin on angiogenesis. In our studies, cyclization of TRAPs [1] confirmed that a Phe/Arg relative conformation is important in triggering the receptor, which suggests that a comparable cyclic conformation may be responsible for the interaction of linear TRAPs with the thrombin receptor as well.

Based on this model, we have synthesized a number of novel small-molecule non-peptide TRAP analogues [2], which were bioassayed for their angiogenic activity [3]. These compounds carry the essential pharmacophoric groups of the native pentapeptide SFLLR (Phe and Arg) incorporated onto a piperazine scaffold.

In this work we report the effects of compound **1** (Figure 1) in the CAM system of angiogenesis. This analogue, at 90 nmoles/disc, inhibited angiogenesis as evidenced by morphological evaluation and the extent of collagenous protein biosynthesis under

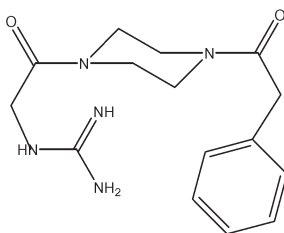


Fig. 1. 1-Phenylacetyl-4-(2-guanidoacetyl)piperazine (compound **1**): a novel thrombin receptor non-peptide analogue.

the disc containing the test compound as compared to controls (Table 1). When used in combination, 90 nmoles of this compound with thrombin (1.0 IU/disc) completely abolished the angiogenic effect of thrombin [3].

*Table 1. Inhibition of angiogenesis by thrombin receptor antagonist in the CAM system.*

Treatment	Collagenous protein biosynthesis, %
Thrombin (n = 10)	34 ± 9
Compound <b>1</b> (n = 10)	-11 ± 4
Thrombin + compound <b>1</b> (n = 10)	-19 ± 7

In addition, the synthetic antagonist compound **1** was evaluated for its effect on endothelial cell progelatinase A activation. This metalloproteinase is secreted in the growth medium of human umbilical cord endothelial cells (HUVECS) in culture and appears at 72 KDa collagenolytic zone in zymograms. A second zone appears at 62 KDa corresponding to the activated form of progelatinase A. Under control conditions the activated gelatinase (62 KDa) was about 8% of the 72 KDa zone. When the HUVECS are treated with thrombin (1.0 IU/ml), for 24 h, the 62 KDa zone increased to an extent of approximately 40% of the 72 KDa zone [3]. Compound **1** completely abolishes gelatinase A activation by thrombin.

The piperazine derivative we have evaluated provides for lead compounds with optimized thrombin-receptor antagonist features. The goal is to synthesize compounds that are specific, non-toxic and active *in vivo* for therapeutic applications in cancer and other angiogenic diseases.

#### **Acknowledgments**

This work was supported by the Ministry of Development of Greece (GSRT, EΠET II, 115), and the Ministry of Education (EPEAK).

#### **References**

1. Alexopoulos, K., Panagiotopoulos, D., Fatseas, P., Mavromoustakos, T., Mihailescu, S., Paredes-Carbajal, M., Mascher, D., Matsoukas, J. *J. Med. Chem.* **44**, 328–339 (2001).
2. Alexopoulos, K., Fatseas, P., Melissari, E., Vlahakos, D., Smith, J., Mavromoustakos, T., Saifeddine, M., Moore, G., Hollenberg M., Matsoukas, J. *Bioorg. Med. Chem.* **7**, 1033–1041 (1999)
3. Maragoudakis, M., Kraniti, N., Missirlis, E., Alexopoulos, K., Matsoukas, J. *Endothelium*, in press (2001).

## Development of Endomorphin Derivatives with Dual Functions and Studies on Their Three-Dimensional Structure

**Yoshio Fujita<sup>1</sup>, Motohiro Takahashi<sup>1</sup>, Toshio Yokoi<sup>1,2</sup>, Yuko Tsuda<sup>1,2</sup>,  
 Lawrence H. Lazarus<sup>3</sup>, Sharon D. Bryant<sup>3</sup>, Akihiro Anbo<sup>4</sup>,  
 Yusuke Sasaki<sup>4</sup> and Yoshio Okada<sup>1,2</sup>**

<sup>1</sup>*Faculty of Pharmaceutical Sciences and* <sup>2</sup>*High Technology Research Center, Kobe Gakuin University, Nishi-ku, Kobe 651-2180, Japan*

<sup>3</sup>*Peptides Neurochemistry, LCBRA, National Institute of Environmental Health Sciences, Research Triangle Park, NC 27709, USA*

<sup>4</sup>*Tohoku Pharmaceutical University, Komatsushima, 44-1, Aoba-ku, Sendai 981-8558, Japan*

### Introduction

The G-protein coupled  $\delta$ -,  $\kappa$ -,  $\mu$ -opioid receptors and their endogenous ligands primarily are involved in the modulation and perception of pain. In this regard, highly selective endogenous  $\mu$ -opioid receptor ligands, endomorphin-1 (H-Tyr-Pro-Trp-Phe-NH<sub>2</sub>) and endomorphin-2 (H-Tyr-Pro-Phe-Phe-NH<sub>2</sub>) [1], and their analogues may provide a powerful molecular platform to examine  $\mu$  opioid pathways throughout the body and to pave the way for development of novel type drugs for controlling pain. Since the Tyr-Pro-Phe sequence is required for binding to  $\mu$ -opioid receptors [2], we designed and synthesized opioidmimetics containing Tyr-Pro-Phe-NH-X sequences, and analyzed their receptor binding profiles and three dimensional solution structure by <sup>1</sup>H NMR.

### Results and Discussion

All compounds were prepared by solution methods. Purity was assessed by HPLC and mass spectrometry. The use of 2',6'-dimethyl-L-tyrosine (Dmt) instead of Tyr<sup>1</sup> increased binding activity significantly. As shown in Table 1, Dmt-Pro-Phe-NH-5-Quinoline and Dmt-Pro-Phe-NH-5-Isoquinoline exhibited potent  $\mu$ -opioid receptor binding with K<sub>i</sub> values of 0.11 nM and 0.19 nM, respectively, with 10- to 20-fold greater activity than the endomorphins. As shown in Table 2, Dmt-Pro-Phe-NH-5-Quinoline is also an excellent  $\mu$ - and  $\delta$ -agonist, although it exhibits a weak antagonist activity with pA<sub>2</sub> value of 5.88. These compounds are mixed agonist/antagonist for  $\delta$ -receptor. Figure 1 shows a stereoview of H-Dmt-Pro-Phe-NH-6-Quinoline based on NMR data.

*Table 1. Receptor affinity of endomorphin analogues.*

Endomorphin analogues	Receptor binding, K <sub>i</sub> (nM)		Selectivity
	$\delta$	$\mu$	
Dmt-Pro-Phe-NH-1-Naphthalene	19.86 $\pm$ 3.0	0.30 $\pm$ 0.03	68
Dmt-Pro-Phe-NH-3-Quinoline	190.4 $\pm$ 22.2	0.33 $\pm$ 0.02	580
Dmt-Pro-Phe-NH-5-Quinoline	30.0 $\pm$ 3.8	0.106 $\pm$ 0.014	283
Dmt-Pro-Phe-NH-6-Quinoline	46.6 $\pm$ 2.4	0.22 $\pm$ 0.038	212
Dmt-Pro-Phe-NH-8-Quinoline	33.14 $\pm$ 1.71	0.486 $\pm$ 0.1	68
Dmt-Pro-Phe-NH-5-Isoquinoline	98.33 $\pm$ 8.8	0.190 $\pm$ 0.1	517

## Biologically Active Peptides

Table 2. Pharmacological activity of endomorphin analogues in vitro.

Endomorphin analogues	GPI IC <sub>50</sub> (nM)	MVD IC <sub>50</sub> (nM)	pA <sub>2</sub> vs DADLE
Dmt-Pro-Phe-NH-1-Naphthalene	0.494 ± 0.18	5.47 ± 1.01	—
Dmt-Pro-Phe-NH-3-Quinoline	9.14 ± 0.81	>10 000	6.01
Dmt-Pro-Phe-NH-5-Quinoline	0.256 ± 0.04	0.616 ± 0.165	5.88
Dmt-Pro-Phe-NH-6-Quinoline	6.21 ± 3.1	>10 000	5.41
Dmt-Pro-Phe-NH-8-Quinoline	44.5 ± 11.0	2 981 ± 685	5.87
Dmt-Pro-Phe-NH-5-Isoquinoline	0.939 ± 0.112	>10 000	6.14



Fig. 1. Stereoview of H-Dmt-Pro-Phe-NH-6-Quinoline based on NMR data.

## References

1. Zadina, J.E., Hackler, L., Ge, L.J., Kastin, A.B. *Nature* **386**, 499–502 (1997).
2. Okada, Y., Fukumizu, A., Takahashi, M., Shimizu, Y., Tsuda, Y., Bryant, S.D., Lazarus, L.H. *Biochem. Biophys. Res. Commun.* **276**, 7–11 (2000).

## Stereoselective Synthesis of Tyr $\psi$ [CH<sub>2</sub>O]Phe and Tyr $\psi$ [CH<sub>2</sub>O]Ile, Methylene-oxy Analogs of Oxytocin and [8-Arginine]Vasopressin

Jan Mařík, Jan Hlaváček, Miloš Buděšínský and Jiřina Slaninová

*Institute of Organic Chemistry and Biochemistry, Academy of Sciences of the Czech Republic,  
 166 10 Prague, Czech Republic*

### Introduction

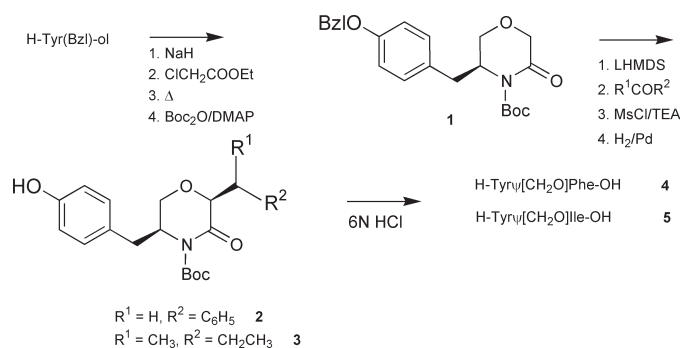
Methylene-oxy replacement  $\psi$ [CH<sub>2</sub>O] of the peptide bond provides flexible, lipophilic surrogates with enhanced metabolic stability. Moreover the geometry of the methylene-oxy surrogates resembles the geometry of the peptide bond in extended conformation [1,2].

### Results and Discussion

The synthesis of the pseudodipeptides (Scheme 1) was started with side chain protected aminoalcohol, derived from natural amino acid H-Tyr(Bzl)-OH, which was converted to the N-protected morpholin-3-one **1** in four steps. An aldol condensation of this compound with benzaldehyde or methylethylketone provided 2,5-disubstituted morpholin-3-ones **2**, **3** in good yields. Following dehydration, stereoselective hydrogenation and hydrolysis of the lactam gave desired pseudodipeptides **4**, **5**. In the case of H-Tyr $\psi$ [CH<sub>2</sub>O]Ile-OH **5** a mixture of two diastereomers was isolated, in other words we obtained a mixture of isoleucine and alloisoleucine analogs.

Using Fmoc methodology, the oxytocin and [8-arginine]vasopressin pseudononapeptides were synthesized on the Rink amide resin and were purified on preparative HPLC.

The newly synthesized analogs [Tyr $\psi$ [CH<sub>2</sub>O]Ile<sup>2-3</sup>]OT and [Tyr $\psi$ [CH<sub>2</sub>O]Phe<sup>2-3</sup>, Arg<sup>8</sup>]VP possess neither uterotonic nor pressoric and antidiuretic activities. These results might be explained by the significant conformational change in the 20-membered disulfide ring as a consequence of a missing hydrogen bond between the Tyr-2 carbonyl and Asn-5 amide nitrogen. This H-bond is suggested to be one of the conformational control elements in the biologically active conformation of oxytocin and vasopressin [3]. Similar results in terms of biological activity were obtained with methylene-amino analogs of oxytocin and [8-arginine]vasopressin [4].



*Scheme 1. Synthesis of pseudodipeptides.*

### ***Biologically Active Peptides***

Temperature coefficients of backbone amide proton NMR chemical shifts were measured and revealed the increased flexibility of the macrocyclic ring. Furthermore, some NOE contacts present in the parent peptides were not observed in methylene-oxy analogs. Namely, the NOE contact between  $\alpha$ -CH of Cys-1 and Cys-6 in the molecule arginine vasopressin and  $\alpha$ -CH of Tyr-2 and Asn-5 in oxytocin.

#### **Acknowledgments**

We thank Dr. Martin Flegel (PolyPeptide Laboratories, Prague) for providing the oxytocin and arginine vasopressin samples for NMR experiments. This work is a part of the research project No. Z4 055 905 and was supported by grant 203/98/1330 of the Grant Agency of the Czech Republic.

#### **References**

1. Roubini E., Laufer R., Gilon C., Selinger Z., Roques B.P., Chorev M. *J. Med. Chem.* **34**, 2430 (1991).
2. Norman, B.H., Kroin J.S. *J. Org. Chem.* **61**, 4990 (1996).
3. Jošt K., Lebl M., Brtník F. in: *Handbook of Neurohypophyseal Hormone Analogs*, Vol. II/2; CRC Press, Inc. Boca Raton, Florida, 1987.
4. Slaninová J., Lebl M. Unpublished results.

## Exploration of the DTrp-NMeLys Motif in the Search for Potent Somatostatin Antagonists

W. G. Rajeswaran<sup>1</sup>, William A. Murphy<sup>1</sup>, John E. Taylor<sup>2</sup> and David H. Coy<sup>1</sup>

<sup>1</sup>Peptide Research Labs, SL 12, Department of Medicine, Tulane University Health

Sciences Center, New Orleans, LA 70112, USA

<sup>2</sup>Biomeasure Inc., Milford, MA 01757, USA

### Introduction

Somatostatin (SRIF), a tetradecapeptide discovered by Brazeau *et al.* [1] has been shown to have potent inhibitory effects on various secretory processes in tissues such as pituitary, pancreas or gastrointestinal tract. These biological effects of SRIF, all inhibitory in nature, are elicited through a series of G protein coupled receptors, of which five different subtypes have been characterized (sst<sub>1</sub>-sst<sub>5</sub>). It has been demonstrated that the Trp<sup>8</sup>-Lys<sup>9</sup> residues are required for receptor recognition and bioactivity [2]. Previous studies [3] from this laboratory showed that N $\alpha$ -methylation at Lys<sup>9</sup> in the peptide sequence Cpa-cyclo[DCys-Tyr-DTrp-Lys-Thr-Cys]-Nal-NH<sub>2</sub>, increased the GH release inhibitory potency and also type 5 affinity. Therefore, it was decided to exploit this motif further in the search for additional potent antagonists.

### Results and Discussion

Synthetic analogues were tested for their ability to inhibit somatostatin-inhibited GH release from rat pituitary cells in culture and to displace <sup>125</sup>I-labeled somatostatin from CHO cells transfected with the 5 known human somatostatin receptors (Table 1). Several interesting observations resulted from the study. Replacement of lipophilic Nal<sup>12</sup> at the C-terminus with a hydrophilic His<sup>12</sup> resulted in increased affinity and selectivity for the type 2 receptor. When the C-terminus was replaced by Tyr<sup>12</sup>, it resulted in high selectivity for sst<sub>2</sub>, but with decreased affinity and potency. Substitution of Bip<sup>12</sup> and Fpa<sup>5</sup> resulted in the high type 2 selectivity and GH release potency. Thr<sup>12</sup> and Tyr<sup>7</sup> substitution gave the peptide with increased affinity for the type 2 receptor and also with better GH release potency. Replacement of Cpa<sup>5</sup> with Iph<sup>5</sup> did not affect the affinity for the type 2 receptor much, but it decreased the GH release potency by 6 fold. His<sup>7</sup> substitution in the previously reported [3] most potent peptide sequence retained the potency and affinity for the type 2 receptor with little decrease in the selectivity. However, a large halogen substituted aromatic amino acid, Iph<sup>7</sup> decreased the affinity and potency for GH release by about 20-fold. Apa<sup>7</sup> substitution in the C-terminus D-Trp<sup>12</sup> peptide sequence retained the affinity for type 2 but lost 3-fold GH release potency. In an extended cyclic system, methylation at Lys<sup>9</sup> yielded an analogue with high selectivity for type 3 receptors.

Conformational restriction, imposed by a second cyclization of the side chains of Dap residues at both the N- and C-terminus using the succinic moiety as a linker, destroyed the affinity for all the subtypes. A bicyclic analogue was synthesized by selective cyclization of the C- and N-terminus Cys residues. Biological evaluation of this analogue revealed that it had poor affinity for type 2 receptors.

Having studied the effect of substitution of various residues at both the sides of active center and also conformational restriction by bicyclic analogue formation, it was decided to explore the effect of dimerization of the peptide ligands using linkers of varied flexibility and hydrophilicity. In the first experiment 4,4'-biphenyldicarboxylic acid was used to generate a bivalent peptide ligand on the resin. Biological evaluation

*Table 1. Binding affinities for the cloned human sst1-5 receptors and rat pituitary antagonist data.*

No.	N-Me Sequence	hsst <sub>1</sub> K <sub>1</sub> ±SEM (nM)	hsst <sub>2</sub> K <sub>1</sub> ±SEM (nM)	hsst <sub>3</sub> K <sub>1</sub> ±SEM (nM)	hsst <sub>4</sub> K <sub>1</sub> ±SEM (nM)	hsst <sub>5</sub> K <sub>1</sub> ±SEM (nM)	Antagonist IC <sub>50</sub> ±SEM (nM)
1	Cpa-cyclo(DCys-Tyr-DTrp-NMeLys-Thr-Cys)-His-NH <sub>2</sub>	1000	1.48	124.9	1000	226±15	10±2.6
2	Cpa-cyclo(DCys-Pal-DTrp-NMeLys-Thr-Cys)-His-NH <sub>2</sub>	1000	5.57±0.6	58	nd	1000	13.0±0.6
3	Cpa-cyclo(DCys-Pal-DTrp-NMeLys-Abu-Cys)-His-NH <sub>2</sub>	1286	24.8±2.2	106	nd	1000	83±9
4	Cpa-cyclo(DCys-Tyr-DTrp-NMeLys-Thr-Cys)-Tyr-NH <sub>2</sub>	1000	26.3±5.6	1000	1000	1000	70.8±34
5	Fpa-cyclo(DCys-Tyr-DTrp-NMeLys-Thr-Cys)-Bip-NH <sub>2</sub>	1000	8.05±3.1	336	1000	229	1.1±0.0
6	Cpa-cyclo(DCys-Tyr-DTrp-NMeLys-Abu-Cys)-Thr-NH <sub>2</sub>	1000	16.5±1.8	114±13.5	1000	226±108	23.4±0.7
7	Nal-cyclo(DCys-Tyr-DTrp-NMeLys-Abu-Cys)-Thr-NH <sub>2</sub>	1000	35±8.2	198±13.5	364	96.4±23	Weak agonist
8	Iph-cyclo(DCys-Tyr-DTrp-NMeLys-Thr-Cys)-Nal-NH <sub>2</sub>	1000	6.8±0.6	85.3±37	1000	48.3±16	3.5±1.6
9	Cpa-cyclo(DCys-His-DTrp-NMeLys-Thr-Cys)-Nal-NH <sub>2</sub>	1000	6.07±0.3	36.8±3.2	1000	51.1±8.2	0.9±0.3
10	Cpa-cyclo(DCys-Iph-DTrp-NMeLys-Thr-Cys)-Nal-NH <sub>2</sub>	1000	86±33	439±32	1000	1000	11±3.3
11	Cpa-cyclo(DCys-Npa-DTrp-NMeLys-Thr-Cys)-Nal-NH <sub>2</sub>	1000	24.5±14	109±20	1000	441	1.1±0.3
12	Cpa-cyclo(DCys-Apa-DTrp-NMeLys-Thr-Cys)- DTrp-NH <sub>2</sub>	1000	4.4±1.1	99.5±19	1000	37.9	1.6±0.4
13	Cpa-cyclo(DCys-Tyr-DTrp-NMeLys-Thr-Cys)-DTrp-NH <sub>2</sub>	1000	12.4±6.2	129±27	1000	267	0.9±0.1
14	Cyclo(DCys-DPhe-Tyr-DTrp-NMeLys-Thr-Phe-Cys)NH <sub>2</sub>	1000	581	38.9	1000	1000	nd
15	Cyclo[Cys-cyclo(DCys-Tyr-DTrp-NMeLys-Thr- Cys)-Cys]-NH <sub>2</sub>	1000	301±170	1000	837±162	1000	nd
16	4,4'-Biphenyldicarbonyl-[HN-Y] <sub>2</sub>	1000	830±24	1000	1000	1000	nd
17	X-Ahp-Z	1000	34.7±3.6	137±7.6	1000	1000	24.9±4.1

*X = Cpa-cyclo(DCys-Tyr-DTrp-NMeLys-Thr-Cys)Nal; Y = Cpa-cyclo(DCys-Tyr-DTrp-NMeLys-Thr-Cys)-Nal-NH<sub>2</sub>; Z = Cpa-cyclo(DCys-Tyr-DTrp-NMeLys-Thr-Cys)-Nal-NH<sub>2</sub>.*

of this peptide revealed that it lost affinity for all the subtypes. In another approach towards a generating a bivalent ligand, the C-terminus of one pharmacophore was connected to the N-terminus of the other using 6-aminohexanoic acid as a linking agent. The generated bivalent peptide ligand bound to type 2 receptor with good selectivity, but it was 34-fold less potent than the monovalent ligand in the GH release assay. Further work is in progress in this area to find suitable spacers between two pharmacophores which impart selectivity for the 5 receptors.

### Acknowledgments

We thank Ms. Etchie Yauger for amino acid analysis and Ms. Vienna Mackey for her assistance with the *in vitro* antagonist assay.

### References

1. Brazeau, P., Vale, W., Burgus, R., Ling, N., Butscher, M., Rivier, J., Guillemin, R. *Science* **179**, 77–79 (1973).
2. Bass, R.T., Buckwalter, B.L., Patel, B.P., Pausch, M.H., Price, L.A., Strnad, J., Hadcock, J.R. *Mol. Pharmacol.* **51**, 170 (1997).
3. Rajeswaran, W.G., Hocart, S.J., Murphy, W.A., Taylor J.E., Coy, D.H. *J. Med. Chem.* **44**, 1305 (2001).

## Synthesis and Biological Evaluation of Mixed $\beta^2/\beta^3$ -Dipeptides as Somatostatin Analogs

T. Kimmerlin<sup>1</sup>, D. Hoyer<sup>2</sup> and D. Seebach<sup>1</sup>

<sup>1</sup>Laboratorium für Organische Chemie der Eidgenössischen Technischen Hochschule,  
ETH-Zentrum, 8092 Zürich, Switzerland

<sup>2</sup>Nervous System Research, S-386-745, Novartis Pharma AG, 4002 Basel, Switzerland

### Introduction

Somatostatin (somatotropin release-inhibiting factor, SRIF) is a widely distributed tetradecapeptide with multiple functions, including modulation of secretion of growth hormone, insulin, glucagon, and gastric acid. The mechanism of action of somatostatin is mediated by specific membrane receptors, and to date five individual receptor subtypes have been characterized and cloned (hsst1-5). Extensive studies with synthetic Somatostatin analogues have established that the key pharmacophoric element of SRIF<sub>14</sub> includes Phe<sup>7</sup>-Trp<sup>8</sup>-Lys<sup>9</sup>-Thr<sup>10</sup>, which comprise a  $\beta$ -turn [1]. This secondary structural motif is often encountered in biologically active peptides, and is therefore an important target for mimicry in medicinal chemistry. Herein we report the synthesis and the biological evaluation of  $\beta^2/\beta^3$ -mixed dipeptides as mimics of the crucial  $\beta$ -turn region present in somatostatin.

### Results and Discussion

It has been shown that the central Lys and Trp residues in somatostatin are a prerequisite for high biological activity. Therefore, dipeptides **1**, **2**, and **3**, containing the  $\beta^2$ -HLys $\beta^3$ -HTrp sequence, a  $\beta$ -hydroxybutyric acid at the N-terminus and an amide with aromatic group at the C-terminus, were chosen as targets for a potential Somatostatin analogue. Cbz-(S)- $\beta^2$ -HLys(Boc)-OH was obtained as previously reported [2], and the dipeptides were synthesized in solution. The crude  $\beta$ -dipeptides were purified by reverse-phase HPLC.

The three dipeptides have been tested for specific binding to the five cloned human somatostatin receptors (hsst<sub>1-5</sub>), expressed in CCL-39 cell lines. Binding affinities for

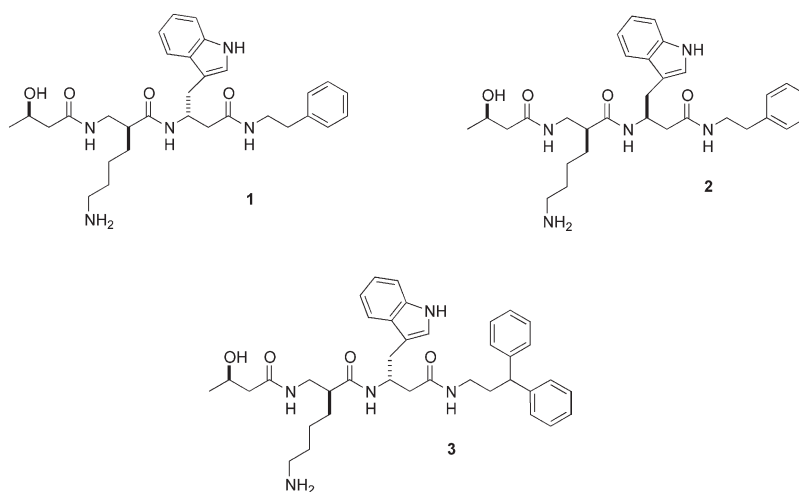


Table 1.  $pK_D$  values for  $\beta$ -peptides **1**, **2**, **3** at the five *hsst* expressed in CCL-39 cells measured by radioligand binding assays using LTT-SRIF<sub>28</sub> as radioligand.

	<b>1</b>	<b>2</b>	<b>3</b>	Octreotide	SRIF <sub>14</sub>
hsst <sub>1</sub>	4.25	4.93	4.75	6.45	9.08
hsst <sub>2</sub>	<5	<5	<5	9.11	10.06
hsst <sub>3</sub>	<5	<5	<5	8.6	9.67
hsst <sub>4</sub>	5.63	7.13	5.58	5.76	8.39
hsst <sub>5</sub>	<5	<5	<5	7.31	9.01

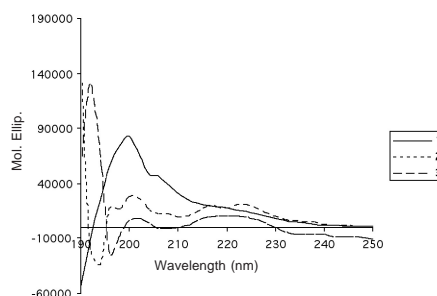
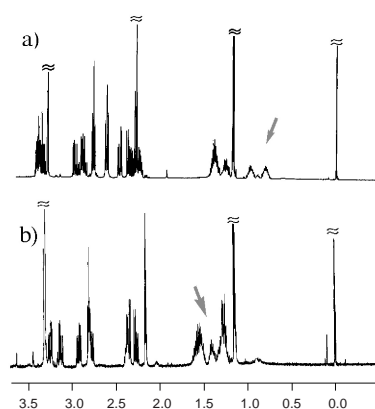


Fig. 1. <sup>1</sup>H NMR spectra of *b*-dipeptides a) **2**, b) **3**. Fig. 2. CD spectra in MeOH (0.2 nm).

hsst<sub>1-5</sub> were determined by the displacement of [<sup>125</sup>I]LTT-SRIF<sub>28</sub> from the corresponding receptors. The affinities are reported as  $pK_D$  values. As shown in Table 1, the  $\beta^2/\beta^3$ -dipeptide **2** binds to *hsst*<sub>4</sub> with an excellent  $K_D$  value of 74 nM and a high selectivity for *hsst*<sub>4</sub> over the other subtypes.

Full structural characterization of dipeptide **2** has not been achieved yet. However, the upfield shift observed for the C( $\gamma$ )-H protons in **2** by one-dimensional NMR spectroscopy (Figure 1) is highly instructive. Indeed, it has been proven that an upfield shift of these protons in active somatostatin analogs relative to the chemical shift of these protons in a random coil structure is due to the close spatial proximity of the Trp and Lys side chains within the  $\beta$ -turn [3]. The CD-pattern of **2** displaying a maximum at 200 nm (Figure 2) is another indication of a turn type-structure.

We have shown that a mixed (*S*)- $\beta^2$ /(*S*)- $\beta^3$ -dipeptide can fold into a turn-type structure, thus mimicking a natural cyclo- $\alpha$ -peptide with high biological activity. This result clearly demonstrates the potential of  $\beta$ -peptides as peptidomimetics.

## References

1. Melacini, G., Zhu, Q., Osapay, G., Goodman, M. *J. Med. Chem.* **40**, 2252 (1997).
2. Gademann, K., Kimmerlin, T., Hoyer, D., Seebach, D. *J. Med. Chem.*, in press.
3. (a) Wynants, C., Tourwe, D., Kazmierski, W., Hruby, V.J., Van Binst, G. *Eur. J. Biochem.* **185**, 371 (1989). (b) Freidinger, R.M., Perlow, D.S., Randall, W.C., Saperstein, R., Arison, B.H., Veber, D.F. *Int. J. Pept. Protein Res.* **23**, 142 (1984).

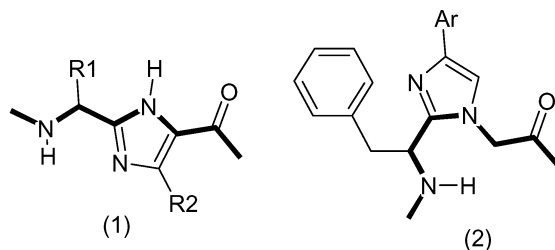
## Cyclic Peptides Related to Somatostatin Containing a Novel Imidazole Derived *cis*-Amide Mimetic

Tom Gordon, John Eynon, John Taylor, Michael Culler  
and Barry Morgan

Biomeasure Inc., Milford, MA 02038, USA

### Introduction

The design of structural fragments that mimic specific aspects of peptide secondary structure is a continuing challenge to medicinal chemists. We wish to describe a novel approach to *cis* amide mimicry employing an extension of our "peptide azole" concept [1] (1). We now demonstrate that this concept can be extended to mimic a *cis* amide bond (2), by modifying the substitution pattern of the imidazole. These *cis* amide mimics can be readily assembled by alkylation of a protected 2-(aminomethyl) imidazole with bromoacetate.



We tested the applicability of the new mimetic in a series of cyclic "hexapeptides" related to familiar somatostatin (SS) agonists such as seglitide (analog 2). Introduction of fragment (2) into peptides was achieved by a repetitive solution strategy for peptide synthesis. Cyclisation was carried out by activation of the "glycine" carboxyl group of (2), yielding the desired cyclic peptides in excellent yield. The peptides were purified by reverse phase HPLC and lyophilized prior to biological testing.

### Results and Discussion

The biological effects of SS are mediated through five distinct G protein-coupled receptor subtypes (SSTR<sub>1-5</sub>) [2]. The analogs were assessed for binding affinity at hSSTR1 through 5 using membrane preparations of hSSTRs expressed in CHO cells. Radiolabelled seglitide was used as a radioligand, and K<sub>i</sub> values calculated by a standard protocol (Table 1). The quoted values were the mean of at least three determinations. The new *cis* amide surrogate (2) was incorporated into cyclic peptide structures designed to probe agonist activity at hSSTR2 and hSSTR5.

A target series designed to mimic hSSTR2 selective ligands were based on cyclohexapeptides containing N-MeAla (sequence 2). This series include some of the most potent and selective hSSTR2 ligands known, with K<sub>i</sub> values around 0.1 nM. In terms of affinity at hSSTRs the prototype azole linked peptide 1 was found to be potent and very similar in profile to the corresponding cyclohexapeptide sequence 2. We suggest that these data provide a good basis to support the thesis that this new imidazole based linkage is an excellent surrogate for a *cis* amide bond, and validates the imidazole linker strategy.

The imidazole linker was also evaluated in a *O*-benzyl Tyr (Ybz) substituted cyclo-CXwKXC template (see WO 97/01579), which has potency and modest selec-

Table 1. Binding constants of studied analogs.

		Subst. <sup>a</sup>	Ki, nM, hSSTR				
Imidazole			1	2	3	4	5
1	Gly Tyr trp Lys Val Phe	3-MeO	>1000	1.1	986		264
2	MeA Tyr trp Lys Val Phe		>1000	0.14	82		15.6
3	Gly Trp trp Lys Ybz Phe	H	514	>1000	702	>1000	7.9
4	Gaba Trp trp Lys Ybz Phe	3-HO	68	>1000	224	127	74

<sup>a</sup> C4-phenyl substituent.

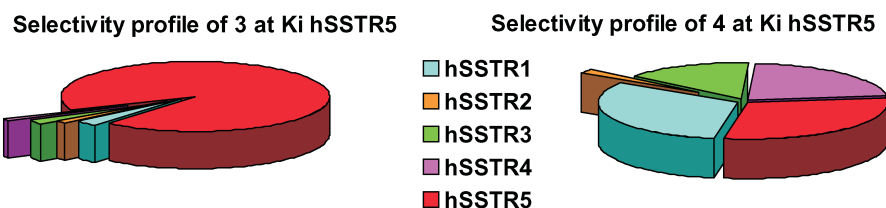


Fig. 1. Selectivity profiles of analogs 3 and 4.

tivity for hSSTR5. In this case, incorporation of the imidazole *cis* amide surrogate, Phe⇒Trp substitution, and conversion to the 4-H analog at the imidazole aryl substituent yielded sequence 3, which was a potent and highly selective hSSTR5 ligand. This selectivity can be seen from the receptor occupancy pie chart calculated at the hSSTR5 Ki (Figure 1). An increase in imidazole linker length by two carbon atoms (Gly⇒Gaba) and modification to the 4-HO-phenyl imidazole yielded analog 4 which had an interesting profile in that it showed moderate potency at hSSTR1, 3, 4 and 5 (Ki's in the range 70–200 nM), while having little affinity at hSSTR2. We suggest that analog 4 would be a useful prototype ligand for exploring the utility of a hSSTR “panagonist”, without the GH inhibitory effect associated with efficacy at hSSTR2.

To summarize, analog 1 containing a new *cis* amide mimetic was designed, and found to have high affinity for hSSTR2. This compares well to the hSSTR2 Ki for the corresponding cyclohexapeptide 2, known to assume a *cis* amide conformation. In addition, the high hSSTR2 selectivity profile shown by analog 1 is identical to that of analog 2, suggesting that, from a receptor site perspective, the imidazole is an excellent surrogate for the *cis* amide bond of analog 2.

In a second series containing the new *cis* amide mimetic, we were able to develop a compound with potency and selectivity at hSSTR5 (analog 3), and a lead with a broader affinity profile for hSSTRs, but lacking hSSTR2 affinity (analog 4).

We conclude that the imidazole *cis* dipeptide surrogate [3] has been validated from a pharmacological perspective, and has the potential to be a valuable addition to the range of modifications available to chemists and biologists interested in the structure- and conformation-activity relationships of peptides.

## References

1. Gordon, T., et al. *Bioorg. Med. Chem. Lett.* **3**, 915–920 (1993).
2. Reisine, T., Bell, G.I. *Endocr. Rev.* **16**, 427–442 (1995).
3. Similar approach using a tetrazole linker has been described: see Beusen, D.D., et al. *Biopolymers* **36**, 181–200 (1995) and references therein.

## Human Somatostatin Receptor Specificity of Backbone-Cyclic Analogs Containing Novel Sulfur Building Units

Sharon Gazal<sup>1</sup>, Gary Gellerman<sup>2</sup>, Ofer Ziv<sup>2</sup>, Olga Karpov<sup>2</sup>,  
 Pninit Litman<sup>2</sup>, Moshe Bracha<sup>2</sup>, Michel Afargan<sup>2</sup> and Chaim Gilon<sup>1</sup>

<sup>1</sup>Department of Organic Chemistry, Hebrew University, Jerusalem, 91904 Israel

<sup>2</sup>Peptor Ltd., Kiryat Weizmann, Rehovot, 76326 Israel

### Introduction

This work describes the synthesis and the biological properties of novel disulfide bridged backbone cyclic somatostatin analogs. These analogs were prepared in order to investigate the influence of the ring size and ring chemistry on the binding profile of a parent analog named PTR 3173. PTR 3173 is 1000-fold more potent in the *in vivo* inhibition of growth hormone (GH) than of glucagon and 10,000-fold more potent inhibitor of GH than of insulin release. This unique pharmacological property is ascribed to the unique binding profile of PTR 3173, and it has been suggested that the binding profile, namely, binding to a specific combination of somatostatin receptors and not to a single receptor determines the physiological properties of the discussed SST analog [1]. These disulfide-bridged analogs of PTR 3173 possess the same pharmacophore as their parent analog, but the lactam bridge of PTR 3173 was replaced by backbone disulfide bridge (Figure 1) [2].

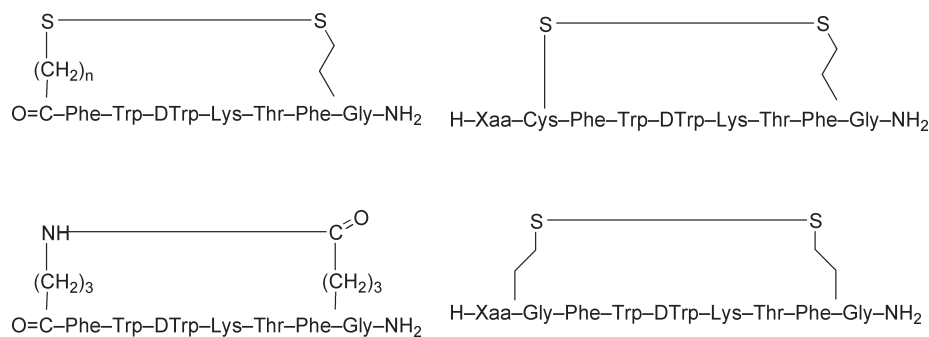


Fig. 1. Disulfide-bridged analogs of PTR 3173.

### Results and Discussion

The utilization of a novel class of sulfur containing N-alkylated amino acid building units enabled the preparation of this novel class of disulfide-bridged, backbone-cyclic analogs. This class of alkylated amino acids contains an acm protected sulfur moiety that enables the convenient on-resin deprotection oxidation using I<sub>2</sub> as an oxidizing agent.

The IC<sub>50</sub> values of the disulfide-bridged, backbone-cyclic analogs and PTR 3173 are given in Table 1. It was found that disulfide-bridged analogs of PTR 3173 possessed increased selectivity to hsst2 and 5, however, they exhibited weaker affinity to hsst4 compared to PTR 3173. These studies suggest the effect of ring chemistry, ring size, and ring position of the peptide template on receptor binding selectivity. These

### Biologically Active Peptides

disulfide-bridged analogs were also highly resistant to a broad spectrum of proteolytic activity (rat renal homogenate) compared to somatostatin that was degraded within a few minutes.

Table 1.  $IC_{50}$  values (nM) of the displacement of [ $^{125}I$ ] Tyr<sup>11</sup> SRIF-14 binding by PTR 3173 and the various analogs containing a disulfide bridge.

Peptide	hsst1	hsst2	hsst3	hsst4	hsst5
PTR 3173	>1000	3	>100	7	1
PTR 3211	>1000	28.7	15.6	>100	1.3
PTR 3217	>1000	1.3	>100	>100	2.8
PTR 3197	>1000	5.2	40.7	41.1	1.2
PTR 3207	>1000	12.8	>100	35.9	4.5
PTR 3213	>1000	4.1	>100	49.5	7.8
PTR 3219	>1000	2.5	>100	>100	18.2
PTR 3221	>1000	8.4	>100	61.8	91

### References

1. Afargan, M., Janson, E.T., Gelerman, G., Rosenfeld, R., Ziv, O., Karpov, O., Wolf, A., Bracha, M., Shohat, D., Liapakis, G., Gilon, C., Hoffman, A., Stephensky, D., Oberg, K. *Endocrinology* **142**, 477–486 (2001).
2. Andreu, D., Albericio, F., Sole', N.A., Munson, M.C., Ferrer, M., Barany, G., In Pennington, M.W. and Dunn, B.M. (Eds.) *Methods in Molecular Biology*, Humana Press, Totowa, 1994, p. 91.

## Linear and Cyclic Thr<sup>6</sup>-Bradykinin Analogues Containing *N*-Benzylglycine as a Replacement for Residues Phe<sup>5</sup> and Phe<sup>8</sup>

Marina Gobbo<sup>1</sup>, Laura Biondi<sup>1</sup>, Fernando Filira<sup>1</sup>, Barbara Scolaro<sup>1</sup>,  
Raniero Rocchi<sup>1</sup> and Tom Piek<sup>2</sup>

<sup>1</sup>Department of Organic Chemistry, Biopolymer Research Centre, C.N.R., University of  
Padova, Padova 35131, Italy

<sup>2</sup>Department of Pharmacology, University of Amsterdam, Amsterdam 1105 AZ,  
The Netherlands

### Introduction

*N*-Benzylglycine (Nphe) is an achiral structural isomer of phenylalanine that may be useful as an amino acid replacement in SAR studies. The first incorporation of Nphe into a biologically active peptide was reported by using bradykinin (BK) [1]. In continuation of our investigations on the structure-activity relationship of BK and BK analogues [2] we focused our attention on Thr<sup>6</sup>-BK (H-Arg-Pro-Pro-Gly-Phe-Thr-Pro-Phe-Arg-OH), a native kinin discovered in the venom of a solitary wasp and present also in ant venom and in frog skin. Thr<sup>6</sup>-BK proved to be about 10 times more potent than BK in the insect central nervous system [3] as well as in stimulating smooth muscle contraction [4]. The structural analysis of Thr<sup>6</sup>-BK and its analogues is made particularly interesting by the fact that despite the high sequence homology with native BK (only one conservative substitution: Ser<sup>6</sup>/Thr<sup>6</sup>) there is a marked and significant difference in the biological profile of the two peptides. The conformation of the native Thr<sup>6</sup>-BK has been already investigated in DMSO by NMR spectroscopy and computer simulations [5]. We report in this communication the synthesis and some preliminary pharmacological experiments and structural investigations of new linear and cyclic Thr<sup>6</sup>-BK analogues in which either one or both the Phe residues in the peptide sequence have been substituted by *N*-benzylglycine.

### Results and Discussion

Solid phase synthesis of linear peptides Nphe<sup>5</sup>,Thr<sup>6</sup>-BK (**I**), Nphe<sup>8</sup>,Thr<sup>6</sup>-BK (**II**) and Nphe<sup>5</sup>,Nphe<sup>8</sup>,Thr<sup>6</sup>-BK (**III**) was performed by the Fmoc chemistry and started with Fmoc-Arg(Pmc)-HMP resin. The solid phase procedure was also used for preparation of three nonapeptides covering the entire sequences of **I**, **II** and **III**, with glycine as the C-terminal residue, which were cyclized at room temperature in the presence of HATU and HOAt, fully deblocked and purified by semipreparative HPLC. The resulting cyclic peptides Nphe<sup>5</sup>,Thr<sup>6</sup>-BK (**Ia**), cyclo Nphe<sup>8</sup>,Thr<sup>6</sup>-BK (**IIa**) and cyclo Nphe<sup>5</sup>,Nphe<sup>8</sup>,Thr<sup>6</sup>-BK (**IIIa**) were characterized by amino acid analysis, optical rotation, analytical HPLC and mass spectrometry. The conformational features of the synthetic Thr<sup>6</sup>-BK analogues were investigated by FT-IR in the solid state (KBr, linear and cyclic peptides) as well as in TFE solution (linear peptides) and CD measurements in water, TFE and SDS aqueous solution. The solid state FT-IR spectra of both the linear and cyclic peptides in the 1800–1500 cm<sup>-1</sup> region are consistent with  $\beta$ -turn structures stabilized by 1 $\leftarrow$ 4 intramolecular H bonds [6] and with  $\gamma$ -turn structures with a proline residue in (i + 1) position [7]. The FT-IR spectra in TFE solution suggest that the organic solvent stabilize the  $\beta$ -turns and that the Phe/Nphe substitution gradually increases the  $\beta$ -turn structures in the order **III** > **II** > **I** > Thr<sup>6</sup>-BK.

The features of the aqueous CD spectra of linear peptides over the 250–185 nm region, could indicate the presence of more ordered or more rigid structures in the order

Thr<sup>6</sup> < **I** < **II** < **III**. Peptide **III** assumes a polyproline II type structure characterized by a strong negative band at 203 nm and a weak, broad positive band at 225 nm [8]. Quite similar features were shown by the CD spectra in SDS solution. In TFE significant amounts of type I  $\beta$  turns were present in Thr<sup>6</sup>-BK and **I** (class C-like spectrum) [9] and type II  $\beta$  turn structures could be present in **II** and **III** (type B structure) [9]. In the examined solvents the CD spectra of cyclo Thr<sup>6</sup>-BK and **Ia** showed prevailing class C character. Those of **IIa** and **IIIa** corresponded to type II  $\beta$  turns.

Preliminary pharmacological experiments on isolated preparation of rat duodenum [3] confirmed earlier findings. Thr<sup>6</sup>-BK is more potent than BK and cyclo Thr<sup>6</sup>-BK and cyclo-BK are less active but equally potent [4]. The linear analogues Nphe<sup>5</sup>,Thr<sup>6</sup>-BK,Nphe<sup>8</sup>,Thr<sup>6</sup>-BK and Nphe<sup>5</sup>,Nphe<sup>8</sup>,Thr<sup>6</sup>-BK are practically inactive. The situation observed for the cyclic peptides is quite different. **IIa** and **IIIa** are inactive but **Ia** showed a potency, which is in the same order of magnitude ( $EC_{50} \approx 10^{-8}$ ) as for cyclo-BK and cyclo Thr<sup>6</sup>-BK suggesting that, at least in the cyclic derivatives, the presence of an  $\alpha$ -amino acid residue in position 5 is not essential.

### Acknowledgments

Financial support from the National Research Council (Progetto finalizzato "Biotecnologie") and MURST of Italy is gratefully acknowledged.

### References

1. Young, J.D., Mitchell, A.R., In Rivier, J.E. and Marshall, G.R. (Eds) *Peptides: Chemistry, Structure and Biology (Proceedings of the 11th American Peptide Symposium)*, Escom, Leiden, The Netherlands, 1990, p. 155.
2. Gobbo, M., Biondi, L., Filira, F., Rocchi, R., Piek, T. *Lett. Peptide Sci.* **7**, 171–178 (2000).
3. Piek, T. *Toxicon* **29**, 139–149 (1991) and references therein.
4. Gobbo, M., Biondi, L., Filira, F., Piek, T., Rocchi, R. *Int. J. Pept. Protein Res.* **45**, 459–465 (1995).
5. Pellegrini, M., Gobbo, M., Rocchi, R., Peggion, E., Mammi, S., Mierke, D.F. *Biopolym. Peptide Sci.* **40**, 561–569 (1997).
6. Mantsch, H.H., Perczel, A., Hollosi, M., Fasman, G.D. *Biopolymers* **33**, 201–207 (1993).
7. Shaw, R.A., Perczel, A., Mantsch, H.H., Fasman, G.D. *J. Mol. Struct.* **324**, 143–150 (1994).
8. Helbeque, H., Loucheux-Lefebvre, *Int. J. Pept. Protein Res.* **19**, 94–101 (1982).
9. Woody, R.W., In Blout, E.R., Boverly, F.A., Lotan N., Goodman M. (Eds) *Peptides, Polypeptides and Proteins*, Wiley, New York, USA, 1974, pp. 338–360.

## **Design, Synthesis and Conformational Analysis of Human Urotensin II (U-II) Analogues with Lactam Bridge**

**Paolo Grieco, Riccardo Patacchini, Alfonso Carotenuto, Carlo A. Maggi, Ettore Novellino and Paolo Rovero**

*Dipartimento di Chimica Farmaceutica e Toss. Università di Napoli "Federico II",  
80131-Napoli, Dipartimento di Scienze Farmaceutiche, Università di Salerno Fisciano (SA),  
Italy and Menarini Ricerche SpA, 50131 Firenze, Italy*

### **Introduction**

Urotensin II (U-II), a cyclic neuropeptide with potent vasoconstrictor activity, has been originally isolated from the urophysis of the fish goby. Several structural forms of U-II, showing a disulfide bridge between cysteines, have been reported in different species of fish and amphibian, with variation occurring in the first five to seven N-terminal amino acids, while the C-terminal cyclic hexapeptide sequence is conserved in all species [1,2]. The recent cloning of the U-II precursor in frog and human has demonstrated that the peptide is not restricted to the fish urophysis, but is also expressed in the central nervous system of tetrapods. The identification of a human G protein-coupled receptor homologous to rat GPR14, expressed predominantly in cardiovascular tissue, has demonstrated that U-II is an endogenous ligand of this orphan receptor. Human U-II is an 11 amino acids peptide that retains the cyclohexapeptide sequence typical of this family (GluThrProAspCysPheTrpLysTyrCysVal). The cyclic sequence of U-II is the biologically active fragment, and it has been suggested that the conformation of the disulfide loop might modulate the activity of the molecule [3,4]. U-II is partially homologous and analogous to somatostatin, a peptide whose disulfide bridge is known to be important for activity.

In order to elucidate the importance of the disulfide bridge in U-II, we synthesized a series of analogues where the disulfide bridge is replaced by a lactam bridge. Here we report the design and synthesis of these new lactam analogues, along with preliminary biological and conformational data.

H-Glu-Thr-Pro-Asp-[Cys-Phe-Trp-Lys-Tyr-Cys]-Val-OH	U-II
H-Asp-[Lys-Phe-Trp-Lys-Tyr-Asp]-Val-OH	UPG-I
Ac-Asp-[Lys-Phe-Trp-Lys-Tyr-Asp]-Val-OH	UPG-II
H-Asp-[Asp-Phe-Trp-Lys-Tyr-Lys]-Val-OH	UPG-III
Ac-Asp-[Asp-Phe-Trp-Lys-Tyr-Lys]-Val-OH	UPG-IV
H-Glu-Thr-Pro-Asp-[Lys-Phe-Trp-Lys-Tyr-Asp]-Val-OH	UPG-V
H-Asp-[Dap-Phe-Trp-Lys-Tyr-Asp]-Val-OH	UPG-VI

### **Results and Discussion**

In the design of the new analogues we have focused our structural modifications on the disulfide bridge, which was replaced by an amide bond. We also decided to investigate the effect of ring size on the pharmacological activity, choosing as a starting point the minimal framework of U-II, namely U-II (4-11), that previous work has indicated to be important for the activity. UPG-VI induced efficacious contractions in the rat isolated thoracic aorta ( $EC_{50} = 30$  nM), while all other tested compounds were inactive as agonists or antagonists up to a concentration of 10 nM. In the same conditions hU-II showed an  $EC_{50}$  of 5.7 nM. The conformational analysis of one of the lactam analogues (UPG-IV) indicates that the core region of this peptide is highly or-

dered, and a good overlap with the corresponding region of U-II is observed. The solution structures of U-II and of the cyclic analog UPG-IV were determined by NMR analysis and MD calculations. In Figure 1 is shown the superposition of the mean structures of U-II and UPG-IV. The structures of both peptides are well defined in the cyclic region, which are folded to form closed loops.

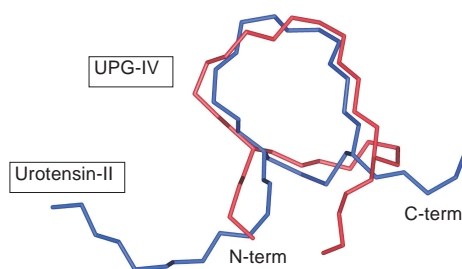


*Fig.1. Structures of U-II and UPG-IV determined by NMR.*

However, the lack of activity of this compound indicates that the disulfide bridge may be important for biological activity, as already demonstrated in the case of analogous peptides, such as somatostatin. On the other hand, preliminary data shows that a reduction of the dimension of the lactam bridge could restore limited activity (see UPG-VI). Further studies are under progress to shed light on this point.

#### **References**

1. Ames, R.A., Sarau, H.M., et. al. *Nature* **401**, 282 (1999).
2. Davenport, A.P., Maguire, J.J. *TiPS* **21**, 80 (2000).
3. Itoh, H., Itoh, Y., Rivier, J., Lederis, K. *Am. J. Physiol.* **252**, R361 (1987).
4. Bhaskaran, R., Arunkumar, A.I., Yu, C. *BBA* **1199**, 115 (1994).

## PACAP27 Analogues Incorporating Type II/II' $\beta$ -Turn Mimetics

**Rosario González-Muñoz<sup>1</sup>, Mercedes Martín-Martínez<sup>1</sup>, Cesare Granata<sup>2</sup>,  
Eliandre de Oliveira<sup>2</sup>, Clara M. Santiveri<sup>3</sup>, Carlos González<sup>3</sup>,  
Diana Frechilla<sup>4</sup>, Rosario Herranz<sup>1</sup>, M. Teresa García-López<sup>1</sup>,  
Joaquín Del Río<sup>4</sup>, M. Angeles Jiménez<sup>3</sup> and David Andreu<sup>2</sup>**

<sup>1</sup>*Institute of Medicinal Chemistry, CSIC, 28006 Madrid, Spain*

<sup>2</sup>Department of Organic Chemistry, University of Barcelona, 08028 Barcelona, Spain

<sup>3</sup>*Institute of Structure of Matter, CSIC, 28006 Madrid, Spain*

<sup>4</sup>University of Navarre, 31008 Pamplona, Spain

## Introduction

Pituitary adenyl cyclase-activating peptide (PACAP) is a member of the superfamily of regulatory peptides including secretin, glucagon, VIP and GRF [1]. It exists in two bioactive forms, PACAP38 and its shortened version, PACAP27. Both exert their action through specific binding to three classes of receptors: PAC<sub>1</sub>, with higher affinity for PACAP than VIP, and VPAC<sub>1</sub>/VPAC<sub>2</sub>, which recognize PACAP38, PACAP27 and VIP with similar affinity. Although some ligands for these receptors have been described [2–4], there is still a need for specific, potent, preferably peptidomimetic agonists and antagonists of VIP/PACAP. In this regard, reliable data on the 3D conformation of PACAP are essential. Two different solution structures for PACAP27 have been proposed: i) in TFE [5], a disordered N-terminus followed by a  $\alpha$ -helical stretch spanning residues S9-V26, with a discontinuity between K20 and K21; ii) in 25% MeOH [6], a type II  $\beta$ -turn at S9-R12, and two helices spanning R12-K20 and Y22-A24. Compared to VIP, PACAP27 would have distinct conformational properties, regarding position and shape of the helix, plus the possibility of a unique  $\beta$ -turn-like motif. Since minor conformational changes between VIP and PACAP may contribute to receptor selectivity, increasing the rigidity of these peptides by incorporation of well-defined secondary structure motifs is a first step in the development of selective analogues. Based on our previous experience in  $\beta$ -turn mimetics [7,8], we have studied the structural and biological properties of the conformationally restricted analogue **1**, where the putative S9-R12  $\beta$ -turn is fixed by replacement of the Y10-S11 dipeptide with S-IBTM, an efficient type II mimetic. For comparison, analogue **2**, containing the type II'  $\beta$ -turn mimetic R-IBTM, was also evaluated (Figure 1).

PACAP 27	HSDGIFTDS Y <sup>10</sup> S <sup>11</sup> RYRKQMAVKKYLA AVL-NH <sub>2</sub>
[S-IBTM <sup>10,11</sup> ]PACAP27 (1)	HSDGIFTDS[S-IBTM]RYRKQMAVKKYLA AVL-NH <sub>2</sub>
[R-IBTM <sup>10,11</sup> ]PACAP27 (2)	HSDGIFTDS[R-IBTM]RYRKQMAVKKYLA AVL-NH <sub>2</sub>

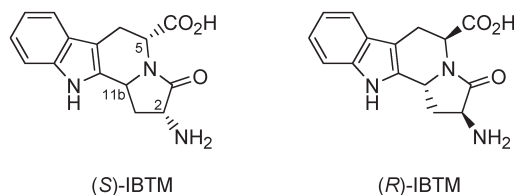


Fig. 1. Structures of PACAP27 and two analogues.

## Results and Discussion

Peptides were synthesized by Boc solid phase methods. The structure of PACAP and **1** in water and in 30% TFE was investigated by 2D NMR. In water, large negative  $\Delta\delta_{\text{C}\alpha\text{H}}$  values were observed for both peptides, suggesting the presence of a helical structure spanning residues T7-L27. The few non-sequential NOEs that could be unambiguously identified for the two peptides were all compatible with a helix. Experimental data provided no evidence for the previously proposed  $\beta$ -turn conformation at S9-R12. The helix length of PACAP27 coincided with the AGADIR prediction, though the experimental population (estimated from  $\Delta\delta_{\text{C}\alpha\text{H}}$  values for the T7-L27 segment) was higher than predicted (39 vs 15%). In TFE, as expected, the helix populations of PACAP27 and **1** increased to 73 and 67%, respectively, and spanned approximately the same region (residues 9-27). The distance constraints derived from the experimental NOEs were used in structure calculations. Sequential NOEs, except helix-characteristic  $d_{\text{NN}(i,i+1)}$ , were excluded from the calculation, because of the contribution of random coil conformations to their intensity. The calculated structures displayed a well-defined helix over residues 9-27 and a disordered N-terminus. Backbone RMSDs for the 20 best-scoring conformers were  $0.3 \pm 0.1$  Å and  $0.5 \pm 0.2$  Å for PACAP and **1**, respectively. In **1**, the helix is slightly distorted around the IBTM moiety relative to the native peptide, with the side chains of R12 adopting different orientations. Globally, however, both peptides are substantially similar in structure under the two solution conditions examined.

In radioligand assays, **1** and **2** showed lower affinity for VPAC<sub>1</sub>/VPAC<sub>2</sub> receptors than PACAP ( $\mu\text{M}$  vs  $\sim\text{nM}$  range). The observed conformational differences between **1** and PACAP27 could account, at least in part, for the decreased binding of these restricted mobility analogues. On the other hand, the fact that **1** lacks side chains such as Y10, known to play an important role in receptor recognition in VIP, may also contribute to the lower affinity. Incorporation of  $\beta$ -turn mimetics bearing Tyr and Ser side chains would be required to evaluate the relative contribution of these possible factors.

## References

1. Vaudry, D., González, B.J., Basille, M., Yon, L., Fournier, A., Vaudry, H. *Pharmacol. Rev.* **52**, 269–324 (2000).
2. Gourlet, P., Vandermeers, A., Vertongen, P., Rathe, J., De Neef, P., Cnudde, J., Waelbroeck, M., Robberecht, P. *Peptides* **18**, 1539–1545 (1997).
3. Xia, M., Sreedharan, S.P., Bolin, D.R., Gaufo, G.O., Goetzl, E.J. *J. Pharmacol. Exp. Ther.* **281**, 629–633 (1997).
4. Dickinson, T., Fleetwood-Walker, S.M., Mitchell, R., Lutz, E.M. *Neuropeptides* **31**, 175–185 (1997).
5. Wray, V., Kakoschke, C., Nokihara, K., Naruse, S. *Biochemistry* **32**, 5832–5841 (1993).
6. Inooka, H., Endo, S., Kitada, C., Mizuta, E., Fujino, M. *Int. J. Peptide Protein Res.* **40**, 456–464 (1992).
7. De la Figuera, N., Alkorta, I., García-López, M.T., Herranz, R., González-Muñiz, R. *Tetrahedron* **51**, 7841–7856 (1995).
8. Andreu, D., Ruiz, S., Carreño, C., Alsina, J., Albericio, F., Jiménez, M.A., De la Figuera, N., Herranz, R., García-López, M.T., González-Muñiz, R. *J. Am. Chem. Soc.* **119**, 10579–10586 (1997).

## Bicyclic $\beta$ -Strand Templates: Epimerization and Biological Activity of Non-Electrophilic Serine Protease Inhibitors

Jan Urban<sup>1</sup>, Hiroshi Nakanishi<sup>1,2</sup>, Cyprian O. Ogbu<sup>1</sup>, Geoffrey Kozu<sup>1</sup>,  
 Kenneth Farber<sup>1</sup>, Polina Kazavchinskaya<sup>1</sup> and Min S. Lee<sup>1,2</sup>

<sup>1</sup>Molecumetics Ltd., 2023 120th Ave., N.E. Ste. 400, Bellevue, WA 98005, USA

<sup>2</sup>Department of Pathobiology, SC-38, University of Washington, Seattle, WA 98195, USA

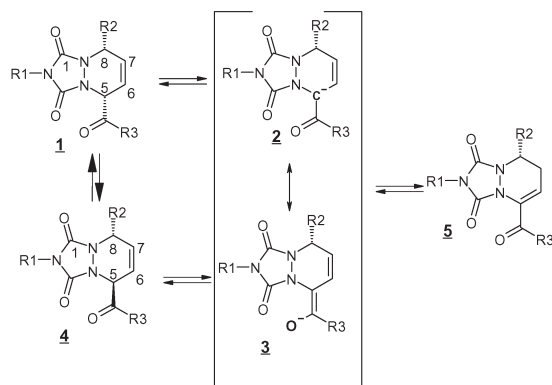
### Introduction

Previously, we have demonstrated the utility of Diels-Alder cycloaddition in the solid-phase organic synthesis of proteolytic enzyme inhibitors [1]. In the reported syntheses of  $\beta$ -strand mimetics using this methodology, the assumption was that the classic concerted addition of the diene resulted in two enantiomers with the *cis* configuration. The C5 position of the  $\beta$ -strand mimetic corresponding to the C $\alpha$  position of the natural amino acid now appears to be epimerizable, either under basic conditions, or elevated temperature. The resulting template enantiomers could have different biological activities as a result of different presentation of side chains, but also as a result of overall change in the conformation of template.

### Results and Discussion

The epimerization of template **1** seems to be a rather fast reaction, compared to its analogous amino acids. Deprotonation at C-5 first provides intermediates **2** and **3**. These can then reprotonate, producing either product **4**, or starting material **1** (Scheme 1). This process can be achieved by treatment with base [2] or by heating at 100 °C [3]. Shifting of the double bond into conjugation (**5**) is more prevalent at higher temperatures (>130 °C), and extended reaction times (several days in 25% piperidine/DMF). Templates with bulky substituents at C-8 appear to be more prone to this process. In order to determine the actual center of epimerization, we have conducted similar experiments in deuterated solvents (Piperidine-d<sub>11</sub>/DMF-d<sub>7</sub>, THF-CD<sub>3</sub>OD-DBU, trichloroacetic acid-*d*). Under all conditions, the proton at C-5 was exchanged for deuterium. Deuterium was not incorporated at other positions.

Effects of *cis*- and *trans*-isomers on the template conformation: Monte Carlo conformational searches were carried out for  $\beta$ -strand templates **1** and **4** and their saturated analogues. The global minimum energy structures were then superimposed at the



Scheme 1

two anchoring points to the serine proteases active site (amide nitrogen from C5 and urazole oxygen from C3) (Figure 1). The resulting conformational differences explain very well the observed activity differences for the *cis*- and *trans*-isomers on thrombin and trypsin.

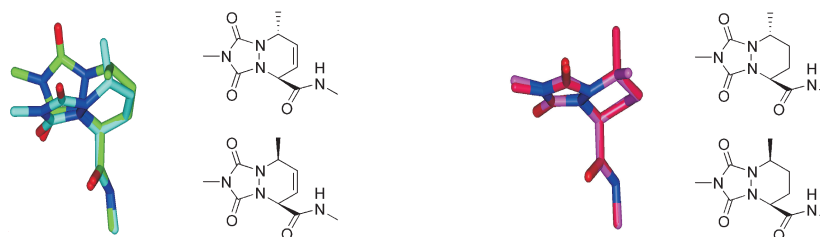
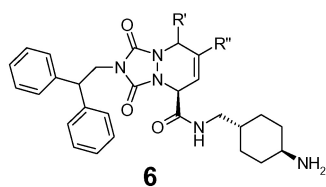


Fig. 1. Overlay of *cis* and *trans* configuration of unsaturated and saturated templates.

The results of the *in vitro* assays of the inhibition of thrombin and trypsin (Table 1) show the most active inhibitors for thrombin are, as expected, the 8-unsubstituted analogs. The primary reason for this is the 60A-D insertion loop that resides above the active site of thrombin and is responsible for the enzyme selectivity compared to trypsin and other serine proteases. Among the C-8 substituted inhibitors, there is a significant difference in activities between the *cis* and *trans* analogues of the unsaturated, but not saturated template. This can be explained by a conformational change of the template, and the related position change of the side chain corresponding to the P3 group (diphenylethyl;  $\approx 25^\circ$  difference between *cis/trans* for the unsaturated, but only  $2^\circ$  for saturated template, Figure 1). This is likely the reason why the relative differences in the thrombin inhibitor activity of *trans*-8-methyl to *cis*-8-methyl compound **6** is 40-fold while for 6,7-dihydro-8-methyl is only a 4-fold.



Ki (nM)					
Trypsin	320	310	1,000	280	330
Thrombin	0.1	1.2	15	0.4	16
Ki (nM)					
Trypsin	2500	3400	3,000	6600	2,400
Thrombin	2.0	44	80	22	90

Table 1. Activities of selected analogs of compound **6** against trypsin and thrombin.

## Conclusion

*Cis/trans* isomerization of the scaffold has significant impact on the biological activities of prepared inhibitors. Fortunately, both isomers are easily accessible. Where the *cis*-isomer is needed, its synthesis has to be designed so that basic treatments are minimized or avoided after the cycloaddition step.

## References and Notes

1. Cyprian, O., Ogbu, et al. *Bioorg. Med. Chem. Lett.* **8**, 2321 (1998).
2. 25% piperidine/DMF,  $T_{1/2} \approx 8$  min; DBU/MeOH/THF complete in <60 min; aqueous solution pH 13, complete in <3 h; aqueous solution pH 11, complete in <3 d.
3. In neat TCA, chloroacetic acid or diethyleneglycol  $T_{1/2} \approx 4$  to 6 h).

## Design, Synthesis and Biological Evaluation of Pilicides: Inhibitors of Pilus Assembly in Pathogenic Bacteria

Andreas Larsson<sup>1</sup>, Hans Emtenäs<sup>1</sup>, Anette Svensson<sup>2</sup>, Jerome S. Pinkner<sup>3</sup>,  
 Scott J. Hultgren<sup>3</sup>, Fredrik Almqvist<sup>1</sup> and Jan Kihlberg<sup>1</sup>

<sup>1</sup>Department of Organic Chemistry, Umeå University, SE-901 87 Umeå, Sweden

<sup>2</sup>Department of Organic Chemistry 2, Lund Institute of Technology, Lund University,  
 SE-221 00 Lund, Sweden

<sup>3</sup>Department of Molecular Microbiology, Washington University, School of Medicine,  
 St. Louis, MO 63110, USA

### Introduction

Due to bacterial resistance, there is a constant struggle to get new treatments for bacterial diseases. A wide range of pathogenic gram-negative bacteria such as *E. coli*, *K. pneumonia* and *Y. Pestis* assembles hair-like adhesive protein filaments called pili on their surfaces. These organelles mediate attachment to the host-cell during microbial invasion. The stabilization and transportation of pilus subunits through the periplasmic compartment by a periplasmic chaperone is crucial in pilus assembly. Inhibition of the chaperone/subunit complex, thus preventing pilus assembly, appears to be a good target for development of a new antibacterial drug.

### Results and Discussion

A crystal structure of the complex between the periplasmic chaperone PapD, involved in assembly of P Pili in uropathogenic *E. coli*, and a 19-mer peptide corresponding to the C-terminus of the adhesin PapG [1] has been used to develop two classes of

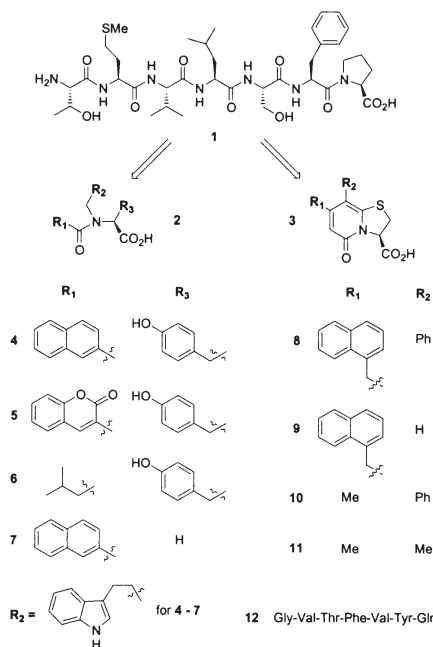


Fig. 1. Libraries of amino acid derivatives 2 and 2-pyridinones 3.

*Table 1. Biological evaluation of Pilicides.*

Peptide/pilicide	Calculated affinity ( $-\log K_{dis}$ )	Norm. response for PapD (%)	Norm. response for FimC (%)	CH complex dissociation (%)
4	10.8	57	47	15
5	10.1	36	21	8
6	9.5	14	20	0
7	8.9	19	23	5
8	10	100	100	86
9	8.7	18	23	7
10	8.3	12	16	5
11	7.1	7	20	1
1	–	25	10	–
12	–	19	11	–

peptidomimetics, amino acid derivatives **2** and 2-pyridinones **3**, as potential inhibitors of the chaperone/subunit complex by rational drug design.

Two different synthetic routes that makes it possible to obtain statistically diverse libraries (Figure 1) through combinatorial synthesis of the two classes have been developed.

The amino acid derivatives are synthesized through an *N*-alkylation of an amino acid followed by acylation of the resulting secondary amine [2]. The 2-pyridinones are obtained in five steps through a novel procedure based on use of acid chlorides and nitriles as starting materials [3].

Two small libraries of **2** and **3** were selected, based on their binding affinities for PapD predicted in VALIDATE [4], and tested for direct binding to PapD and FimC with surface plasmon resonance using a Biacore 3000 instrument (Table 1, columns 2–4) [5]. Their ability to dissociate a FimC/FimH complex was also determined (Table 1, column 5) [5]. Within both the amino acid derivatives **2** and the 2-pyridinones **3** compounds, which bind to periplasmic chaperones and even dissociate chaperone – pilus subunit complexes, were found. Hence these generic structures constitute leads for development of a novel type of antibacterial agent that prevents bacterial colonization of host tissue by interfering with chaperone-mediated pilus assembly.

### Acknowledgments

We thank Professor Garland R. Marshall for helpful discussions. We are grateful to the Swedish Natural Science Research Council, the Knut and Alice Wallenberg Foundation and the Foundation for technology transfer in Umeå, Active Biotech and the Swedish Research Council for Engineering Sciences for financial support.

### References

1. Kuehn, M.J., et al. *Science* **262**, 1234–1241 (1993).
2. Head, R. D., et al. *J. Am. Chem. Soc.* **118**, 3959–3969 (1996).
3. Svensson, A., et al. *J. Comb. Chem.* **2**, 736–748 (2000).
4. Emtenäs, H., et al.: Submitted.
5. Svensson, A., et al.: Submitted.

## Phenylahistin, a Small Dipeptidic Colchicine-Like Anti-Microtubule Agent: Total Synthesis and SAR Study of the Derivatives

Yoshio Hayashi<sup>1</sup>, Sumie Orikasa<sup>1</sup>, Koji Tanaka<sup>1</sup>, Kaneo Kanoh<sup>2</sup>  
and Yoshiaki Kiso<sup>1</sup>

<sup>1</sup>Department of Medicinal Chemistry, Center for Frontier Research in Medicinal Science,  
Kyoto Pharmaceutical University, Yamashina-Ku, Kyoto 607-8412, Japan

<sup>2</sup>Shimizu Laboratories, Marine Biotechnology Institute, Shimizu, Shizuoka, 424-0037, Japan

### Introduction

Phenylahistin (**1**), a fungal metabolite from *Aspergillus ustus* NSC-F038, belongs to a new class of peptidic colchicine-like microtubule-binding agents that exhibits cytotoxic activity against a wide variety of tumor cell lines [1]. (–)-Phenylahistin (–)-**1**, a diketopiperazine derivative, consists of L-phenylalanine and a unique isoprenylated dehydrohistidine residue with a quaternary carbon at the 5-position of the imidazole ring. To develop more potent anti-tumor agents based on this diketopiperazine derivative, it is important to elucidate the structural components necessary for the anti-microtubule activity of (–)-**1**. The total synthesis of **1** will establish the synthetic route for its derivatives.

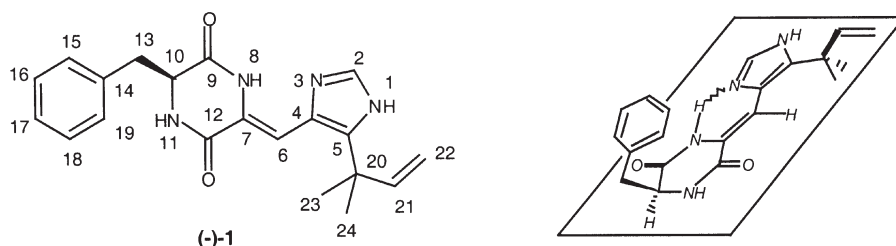


Fig. 1. Pseudo-tricyclic structure of (–)-**1** necessary for anti-microtubule activity.

### Results and Discussion

We demonstrated that (–)-**1**, which is the biologically active form with the L-Phe residue, exhibited colchicine-like inhibition of microtubule polymerization ( $IC_{50} = 25 \mu M$ ). This inhibitory activity of (–)-**1** was similar to that of colchicine ( $IC_{50} = 16 \mu M$ ). The hydrophilic nature of (–)-**1** seemed attractive for the development of potent anti-microtubule agents with appropriate water solubility, because Taxol, a clinically available anti-microtubule agent used in cancer treatment, is highly insoluble in aqueous media.

From the X-ray and NMR analyses of **1**, the stereochemistry of the C6-C7 double bond was confirmed to be Z, and the presence of a hydrogen bond between N8-H and N3 was noted. This result suggested that the two heterocycles, *i.e.*, the diketopiperazine and imidazole rings, were fixed in the same plane by forming a pseudo-tricyclic structure. The benzyl group of the Phe residue was located out of this plane and over the diketopiperazine ring, in a conformation which is reported as most energetically favorable for a diketopiperazine with an aromatic amino acid residue. These findings indicate that the conformation of **1** is highly restricted.

To determine the effect of the rigid conformation of phenylahistin on the binding to the microtubule protein, our efforts were focused on the preliminary modification of (–)-**1**, such as reduction of olefin structures, and methylation of nitrogen atoms. From the biological evaluation of these derivatives, we found that a planar pseudo-tricyclic structure of phenylahistin was important for the anti-microtubule activity [2]. This biologically important template of phenylahistin suggested two attractive sites for further modification to develop more potent antitumor agents, *i.e.*, the side chain of the Phe residue and the 5-position of the imidazole ring.

Accordingly, to establish a suitable synthetic route for preparing phenylahistin derivatives, total syntheses of (–)-**1** and its closely related derivative aurantiamine (**2**) were carried out. These compounds were successfully synthesized with total yields of 1 and 3%, respectively, starting from ethyl isobutyrate through 10 steps [3]. Synthetic compounds were characterized using spectroscopic techniques, and they were found to be identical to those for the natural products. From the assay on the cytotoxic effect on P388 cell proliferation, the activity of the synthetic (–)-**1** was similar to that of native (–)-**1**, while (–)-**2** was 40 times less potent than (–)-**1**.

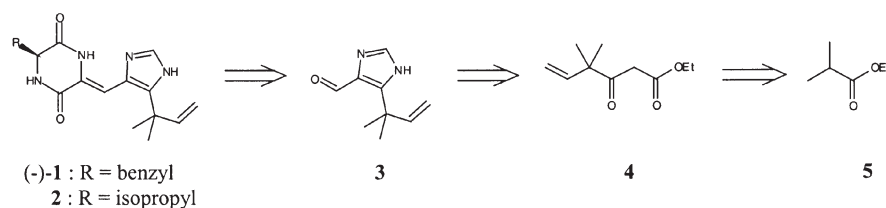


Fig. 2. Retrosynthetic analysis of phenylahistin and aurantiamine.

By utilizing this established synthetic route, we synthesized several derivatives of (–)-**1**, whose substituent at the 5-position of the imidazole ring was modified with different alkyl chains, to determine the effect of this moiety on the biological activity. From the evaluation of derivatives, it is suggested that the existence of the *gem*-dimethyl structure at this position is important to elicit higher cytotoxic activity.

Further derivatization of (–)-**1** using the above synthetic method will contribute to a better understanding of the structure-activity relationship of phenylahistin and to develop more potent antitumor agents based on the diketopiperazine structure. Studies in this regard are in progress.

## References

1. Kanoh, K., Kohno, S., Katada, J., Hayashi, Y. Muramatsu, M., Uno, I. *Biosci. Biotechnol. Biochem.* **63**, 1130–1133 (1999).
2. Kanoh, K., Kohno, S., Katada, J., Takahashi, J., Uno, I., Hayashi, Y. *Bioorg. Med. Chem.* **7**, 1451–1457 (1999).
3. Hayashi, Y., Orikasa, S., Tanaka, K., Kanoh, K., Kiso, Y. *J. Org. Chem.* **65**, 8402–8405 (2000).

## New Antiproliferative Agents from a Peptidomimetic Library

László Örfi<sup>1</sup>, Györgyi Bökönyi<sup>2</sup>, Anikó Horváth<sup>2</sup>, Richard A. Houghten<sup>3</sup>,  
John M. Ostresh<sup>3</sup>, István Teplán<sup>2</sup> and György Kéri<sup>2</sup>

<sup>1</sup>Department of Pharmaceutical Chemistry, Semmelweis University, Budapest, 1092, Hungary

<sup>2</sup>Department of Medical Chemistry, Semmelweis University, Budapest, 1088, Hungary

<sup>3</sup>Torrey Pines Institute for Molecular Studies, San Diego, CA 92121, USA

### Introduction

It is known that chiral ATP analogue quinazolines show selective Epidermal Growth Factor Receptor Tyrosine Kinase (EGFR TK) inhibitory activity depending on the chirality of the molecule [1]. We have developed new types of chiral quinazoline derivatives by synthesising quinazolyl amino acid derivatives (Figure 1, Library "A") varying the nature and the configuration of the amino acid residue (-NH-R1) and/or the substituents of the benzene ring (R2). A similar library was developed when we substituted 2-bromoethyl quinazolinone derivatives (Figure 1, Library "B") with different amino acids (-NH-R1). Compounds from Library "B" were condensed with a series of aromatic aldehydes giving Library "C" [2]. The aim of our work was to study how the antitumour activity is influenced by the nature of the applied amino acids and the substituents of the quinazoline's benzene ring. Antiproliferative activity of Library "A" compounds have been measured in MTT assay (Figure 2).

### Results and Discussion

**Synthesis:** Three libraries were developed using SPPS with the tea-bag method [3].

**Library "A":** The amino acids were coupled as their Fmoc-derivatives to Rink-amide resin. After removing the Fmoc-protecting groups from the amino acids the amino groups were alkylated by a series of 4-chloro-quinazoline derivatives in DMSO at 80 °C. Products were cleaved by TFA.

**Library "B":** The amino acids were coupled to MBHA resin as their Boc-derivatives. After removing the Boc-protecting group the bags were selected and grouped for coupling reaction with the appropriate Br-quinazolinone derivatives. Br-quinazolinone derivatives were prepared from their anthranilic acid derivatives. The coupling of the amino acids and the Br-quinazolinone derivatives were carried out in DMF at 155 °C.

**Library "C" (mixtures):** Quinazolyl amino acid derivatives in the "B" library were mixed and splitted into 30 equal parts and cyclised with a series of benzaldehydes in DMSO at 160 °C. We have used the same control compounds in each cyclisations (R1: Ala, Phe, Tyr; R2: H).

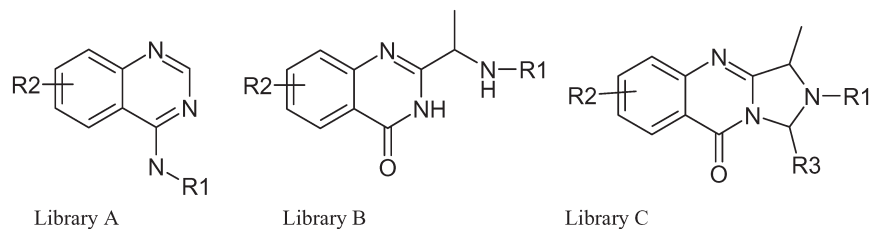


Fig. 1. General structures of the synthesized quinazoline libraries.

### Biologically Active Peptides

After the reaction was completed, the products were cleaved from the resin by HF. The yields of the synthetic procedures were between 30–70% of the theoretical. The structures were validated by HPLC-MS.

MTT test: The antiproliferative activity of analogues was measured by MTT test [4] on M1 human melanoma cell lines at 50  $\mu\text{g}$  and 250  $\mu\text{g}$  doses after 24 h incubation.

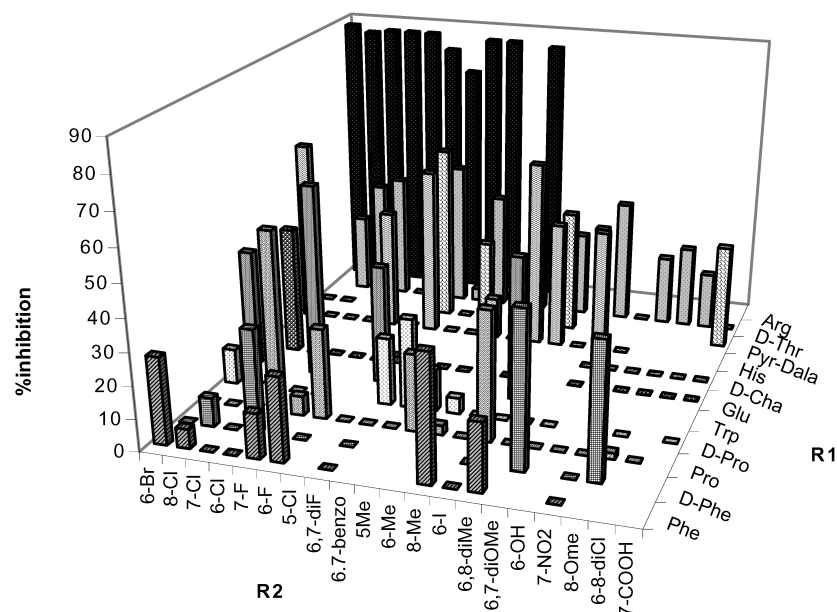


Fig. 2. MTT test results of Library "A" at 50  $\mu\text{g}$  concentrations.

### Conclusions

Biological testing of 220 compounds from library "A" resulted in 33 hits. New conjugates which contain both the L- and the D-amino acids in the same series are under investigation to study the influence of the chirality of the amino acid upon the antiproliferative activity of the compound. The remaining part of Library "A" as well as Library "B" and "C" are under biological testing. Three (Arg) derivatives were selected as potential leads for further development.

### Acknowledgments

This work was supported by the US-Hungarian Science & Technology Transfer Grant.

### References

1. Bridges, A.J., et al. *Bioorg. Med. Chem.* **3**, 1651 (1995).
2. Hirth, P., et al. U.S. Patent 5,990,141.
3. Houghten, R.A., et al. *Proc. Natl. Acad. Sci. U.S.A.* **82**, 5131 (1985).
4. Martin, A., Clynes, M. *Cytotechnology* **11**, 49–58 (1993).

## Development of New Analogs of the Highly Potent Anti-Cancer Compound BKM-570

Lajos Gera<sup>1,3</sup>, Daniel C. Chan<sup>2,3</sup>, Barbara Helfrich<sup>2</sup>, Paul A. Bunn, Jr.<sup>2,3</sup>,  
 Eunice J. York<sup>1</sup> and John M. Stewart<sup>1,2,3</sup>

<sup>1</sup>Department of Biochemistry and Molecular Genetics, University of Colorado Medical School,  
 Denver, CO 80262, USA

<sup>2</sup>Cancer Center, University of Colorado Medical School, Denver, CO 80262, USA

<sup>3</sup>Carcinex Inc., Boulder, CO 80301, USA

### Introduction

Some peptide hormones (bombesin-like peptides, bradykinin, *etc.*) have been identified as growth factors in human cancer. Furthermore, many neuropeptide receptors expressed in small cell lung cancer (SCLC) cells have a general ability to stimulate intracellular Ca<sup>2+</sup> mobilization, a process linked to the proliferation of SCLC. Our highly potent B<sub>1</sub> and B<sub>2</sub> receptor antagonist peptide, B9430 (DArg-Arg-Pro-Hyp-Gly-Igl-Ser-DIgl-Oic-Arg) (Igl =  $\alpha$ -(2-indanyl)glycine; Oic = octahydroindole-2-carboxylic acid), blocked Ca<sup>2+</sup> mobilization by bradykinin but did not inhibit the growth of SCLC. However, dimers of B9430 with appropriate linkers at the amino terminus or *N*-acylated analogs are potent cytotoxic agents for SCLC cells *in vitro* and *in vivo* [1]. Based on these structures, we developed a highly potent anti-cancer mimetic, BKM-570 (Figure 1), which showed impressive growth inhibition of SCLC *in vitro* and *in vivo* in nude mice [2]. We have now synthesized a number of analogs of this simple acyl tyrosine amide for structure-activity studies. The newly developed BKM-1110, 2,3,4,5,6-pentafluorocinnamoyl-[(4-cyano)-L-phenylalanine] *N*-(2,2,6,6-tetramethyl-4-piperidyl)amide, (F5c-PCNF-Atmp) (Figure 1) is twice as potent *in vitro* (ED<sub>50</sub> = 0.95  $\mu$ M on SHP-77 SCLC cells) as BKM-570 (Table 1).

### Results and Discussion

Peptides and mimetics were prepared using solution or solid phase methods, purified by HPLC and characterized by TLC, LDMS and amino acid analysis. BOP-HOBt was

Table 1. Structures and activities of selected compounds.

Number	Structure <sup>a</sup>	SCLC <sup>b</sup>	GPI <sup>c</sup>
B9430	DArg-Arg-Pro-Hyp-Gly-Igl-Ser-DIgl-Oic-Arg	120	8.2
B9870	SUIM-(B9430) <sub>2</sub>	0.15	8.4
BKM-570	F5c-OC2Y-Atmp	1.8	5.6
BKM-578	F5c-Tyr(SO <sub>3</sub> H)-Atmp	inactive	4.7
BKM-1054	F5c-F5F-Atmp	4.6	5.3
BKM-1108	F5c-D-OC2Y-Atmp	inactive	
BKM-1110	F5c-PCNF-Atmp	0.95	

<sup>a</sup> Abbreviations: Atmp = 4-amino-2,2,6,6-tetramethylpiperidine, F5c = pentafluorocinnamoyl, F5F = pentafluorophenylalanine, OC2Y = O-2,6-dichlorobenzyltyrosine, PCNF = 4-cyano-phenylalanine, SUIM = suberimidyl. <sup>b</sup> ED<sub>50</sub> ( $\mu$ M) for cytotoxicity by MTT test for SHP-77 SCLC *in vitro*. <sup>c</sup> pA<sub>2</sub> for bradykinin antagonist activity on isolated guinea pig ileum.

### Biologically Active Peptides

used for coupling of normal amino acids, and HATU was used for sterically hindered residues.

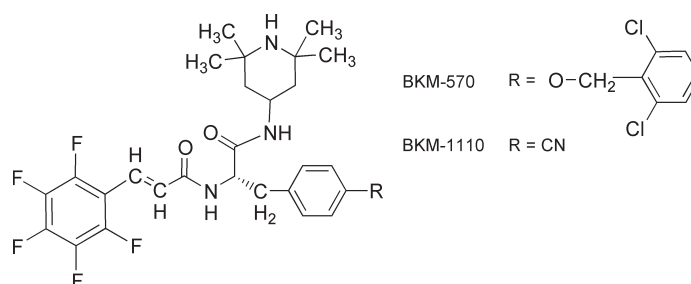


Fig. 1. BKM-570 (F5c-OC2Y-Atmp) and BKM-1110 (F5c-PCNF-Atmp).

In this study, our plan was to examine the structure-activity relationships for anti-cancer activity of analogs of BKM-570. We have systematically incorporated different, usual, or unusual amino acids with bulky acylating and amide groups. Interestingly, a very simple modification of BKM-570, replacement of the L-amino acid, (*O*-2,6-dichlorobenzyl)-L-tyrosine with the D-amino acid which is only a configurational change, eliminated the anti-cancer activity of BKM-1108 *in vitro*. We synthesized numerous analogs replacing the *O*-2,6-dichlorobenzyltyrosine with tyrosine, substituted tyrosines, phenylalanine derivatives and conformationally restricted phenylalanine analogs. Based on these amino acid substitutions, the most active anti-cancer compound is BKM-1110 (ED<sub>50</sub> = 0.95 μM). The requirements concerning the nature of the amino acid appear to be bulk and hydrophobicity.

B9870 has been accepted by the U.S. National Cancer Institute for drug development. BKM-570 has anti-cancer activity (91% inhibition) superior to the widely used highly toxic chemotherapeutic drug cisplatin (60% inhibition) *in vivo*. We have developed BKM-1110, which is the most potent analog of BKM-570 *in vitro*.

### Acknowledgments

We thank Robert Congdon for assistance with chemistry and the US NIH for support (grants HL-26284 and #1R43CA78154).

### References

1. Stewart, J.M., Gera, L., York, E.J., Chan, D.C., Whalley, E.J., Bunn, P.A., Jr., Vavrek, R.J. *Biol. Chem.* **382**, 37–41 (2001).
2. Gera, L., Chan, D.C., Helfrich, B., Bunn, P.A., Jr., York, E.J., Stewart, J.M., In Martinez, J. and Fehrentz, J-A. (Eds.) *Peptides 2000 (Proceedings of the 26th European Peptide Symposium)*, EDK, Paris, 2001, p. 637.

## **Design and Synthesis of a Selective PSA Cleavable Peptide-Doxorubicin Prodrug Which Targets PSA Positive Tumor Cells**

**Victor M. Garsky, Patricia K. Lumma, Dong-Mei Feng, Jenny Wai, Mohinder K. Sardana, Harri Ramjit, Bradley K. Wong, Allen Oliff, Raymond E. Jones, Deborah DeFeo-Jones and Roger M. Freidinger**

*Merck Research Laboratories, West Point, PA 19486, USA*

### **Introduction**

Prostate cancer is the second leading cause of cancer mortality in males. It is estimated that 37,000 men died of prostate carcinoma in the United States in 1999 [1]. While cancer that is confined to the prostate can be treated with surgery or radiation, the prognosis for metastatic disease is poor.

Doxorubicin (Dox) has limited utility in prostate cancer due to systemic toxicities, consisting primarily of cardiotoxicity and myelosuppression [2]. The administration of a prodrug of Dox, designed to permit selective activation by the tumor, would reduce general systemic exposure to the active drug and would thereby increase the therapeutic index. This strategy in turn will permit delivery of an increased amount of active drug to the target site, thereby increasing efficacy.

We, as well as others, have considered using the enzyme prostate specific antigen (PSA) to convert an inactive Dox prodrug into the active drug at the site of the tumor [3–5]. PSA is a serine protease with chymotrypsin-like activity that is a member of the kallikrein gene family [6,7]. PSA's putative physiological role is the liquefaction of semen by virtue of its ability to cleave the seminal fluid proteins semenogelins I and II [8]. Importantly, PSA which is secreted into systemic circulation lacks enzymatic activity because it forms a complex with  $\alpha_1$ -antichymotrypsin and  $\alpha_2$ -macroglobulin [9,10]. The use of a prodrug which is cleaved by the enzyme PSA should in principle produce high localized concentration of the cytotoxic agent at the tumor site while limiting systemic exposure to the active drug.

### **Results and Discussion**

The initial steps in designing the potential Dox prodrug were to identify a functionality of Dox that when coupled to a peptide fragment would yield a biologically inactive (*i.e.* non-cytotoxic) compound, and secondly, to identify a peptide which, when coupled to Dox, would be converted by PSA into the active drug, Dox. The coupling of the tripeptide, Ac(Ala)<sub>3</sub>-OH, with the amino group of Dox to form Ac-(Ala)<sub>3</sub>-Dox satisfied the first of the above criteria.

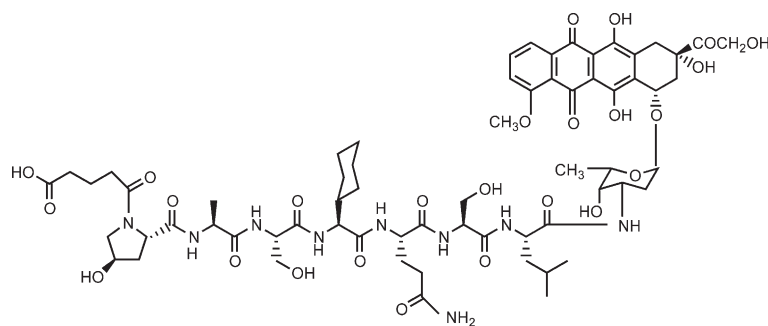
The identification of an appropriate substrate resulted from cleavage maps following PSA treatment of PSA's physiological substrate, semenogelin I. The most efficient cleavage site from recombinant semenogelin I occurs between Gln<sup>349</sup> and Ser<sup>350</sup>. Systematic modification, through the use of chemically synthesized nineteen component peptide libraries at P1'-P4' and point substitution SAR studies of the amino acid residues flanking the P1-P4 cleavage site, led to the design of short peptides which were efficiently hydrolyzed by PSA.

Dox-peptide conjugates were prepared based on, in part, structural data derived from the peptide optimization studies. Synthesis of the peptide-Dox conjugates utilized a combination of solid-phase and solution chemistries. The conjugates were optimized for maximal PSA T<sub>1/2</sub> cleavage rates, selectivity for PSA-secreting tumor cells, and efficacy in nude mouse xenograft studies using PSA-secreting human LNCaP

prostate cancer cells. From these studies **1** was found to have the most favorable profile of physical and biological properties (Figure 1).

Compound **1** is effectively digested by the human PSA enzyme with a  $T_{1/2}$  of 30 min while resisting digestion by human proteases in whole blood or plasma. **1** exhibits a >20-fold selectivity for killing PSA-producing prostate cancer cells *versus* non-PSA producing cancer cells in cell culture. In nude mouse xenograft studies using human LNCaP prostate cancer cells that secrete PSA, **1** demonstrates dramatically improved anti-tumor activity compared to doxorubicin or Leu-Dox as measured by circulating PSA levels and tumor weights [5]. Additionally, Ac-Orn-Ala-Ser-Tyr-D-Gln-Ser-Leu-Dox, which is a peptide-Dox conjugate that is not cleaved by PSA, was evaluated and found not to exhibit antitumor activity more effective than free Dox against LNCaP tumors [5].

The PSA peptide-Dox conjugate, **1**, is intended as an intravenous anticancer agent for the treatment of hormone refractory prostate cancer. **1** is a prostate-targeted pro-drug that is itself less toxic than the parent drug until activated by proteolytic cleavage to its active moieties, Leu-Dox and Dox. The initial step in this activation is preferentially carried out by the serine protease PSA which is expressed in prostate epithelial tissue but is not found at significant levels in other tissues. Subsequent removal of Ser and Leu is mediated by amino peptidases. Additional data supporting tumor selective delivery of Dox by the PSA targeted peptide conjugate, **1**, in a nude mouse xenograft model of human prostate cancer, was recently presented [11]. In theory, **1** should circulate freely in the body and be preferentially activated at sites of prostate cancer tissue, including metastatic foci, by PSA. Therefore, **1** should exhibit better antitumor activity against prostate cancers than free Dox without enhanced toxicities.



Glutaryl-Hyp-Ala-Ser-Chg-Gln-Ser-Leu-Dox (**1**)

Fig. 1. Structure of peptide-Dox conjugate.

## References

1. Landis, S.H., Murray, T., Bolden, S., Wingo, P.A. *CA Cancer J. Clin.* **49**, 8–31 (1999).
2. Raghavan, D., Koczwara, B., Javle, M. *Eur. J. Cancer* **33**, 566–574 (1997).
3. DeFeo-Jones, D., Feng, D.-M., Garsky, V.M., Jones, R.E., Oliff, A.I., *Novel Oligopeptides for Diagnosis and Treatment of Prostate Cancer*, PCT Int. Appl. 1996, p. 141.
4. Khan, S.R. Denmeade, S.R. *The Prostate* **45**, 80–83 (2000).
5. DeFeo-Jones, D., Garsky, V.M., Wong, B.K., Feng, D.-M., Bolyar, T., Haskell, K., Kiefer, D.M., Leander, K., McAvoy, E., Lumma, P., Wai, J., Senderak, E.T., Motzel, S.L., Keenan, K., Van Zwieten, M., Lin, J.H., Freidinger, R.M., Huff, J.R., Oliff, A., Jones, R.E. *Nat. Med.* **6**, 1248–1252 (2000).

**Garsky et al.**

6. Lilja, H. *J. Clin. Invest.* **76**, 1899-1903 (1985).
7. Akiyama, K., Nakamura, T., Iwanaza, S., Hara, M. *FEB Lett.* **235**, 168-172 (1987).
8. Lilja, H., Abrahamson, P., Lundwall, A. *J. Biol. Chem.* **264**, 1894-1900 (1989).
9. Lilja, H., Christensson, A., Dahlen, U., Matikainen, M., Nilsson, O., Pettersson, K., Lovgren, T. *Clin. Chem.* **37**, 1618-1625 (1991).
10. Otto, A., Bar, J., Birkenmeier, G. *J. Urol.* **159**, 297-303 (1998).
11. Wong, B.K., DeFeo-Jones, D., Jones, R.E., Garsky, V.M., Feng, D-M., Oliff, A., Chiba, M., Ellis, J.D., Lin, J.H. *Drug Metab. Dispos.* **29**, 313-318 (2001).

## Peptidic Inhibitors for Protein–Protein Interactions at Cell Surfaces

Horst Kessler<sup>1</sup>, Jürgen Boer<sup>1</sup>, Dirk Gottschling<sup>1</sup>, Niko Schmiedeberg<sup>1</sup>,  
Christian Rölz<sup>1</sup>, Vincent Truffault<sup>1</sup>, Bernhard Holzmann<sup>2</sup>,  
Anja Schuster<sup>2</sup>, Markus Bürgle<sup>3</sup>, Olaf Wilhelm<sup>3</sup>, Viktor Magdolen<sup>4</sup>  
and Manfred Schmitt<sup>4</sup>

<sup>1</sup>Institut für Organische Chemie und Biochemie, Technische Universität München,  
Garching, 85747, Germany

<sup>2</sup>Institut für Medizinische Mikrobiologie, Immunologie und Hygiene, Technische Universität  
München, München, 81675, Germany

<sup>3</sup>Wilex Biotechnology AG, München, Germany

<sup>4</sup>Frauenklinik rechts der Isar, Technische Universität München, München, Germany

### Introduction

Interactions at cell surfaces are involved in a number of regulatory functions in living systems and therefore represent interesting drug targets such as the development of cyclic peptides and peptidomimetics of the RGD sequence [1]. Here we present two further examples diminishing a protein sequence into cyclic peptides with improved affinity, selectivity and enhanced proteolytic stability.

### Results and Discussion

The serine protease urokinase-type plasminogen activator (uPA) is implicated in tissue remodelling, cell migration, wound healing and metastasis. uPA binds with high affinity to a specific cell-surface receptor (uPAR; CD87). Modulation of cell-associated uPA-activity by binding of uPA or its N-terminal fragment (ATF) to uPAR resulted in significant reduction of the invasive capacity of tumor cells [2].

We have previously shown, that the N-terminal fragment of uPA can be shortened to a 13 membered cyclic peptide *cyclo*[19,31]-uPA<sub>19-31</sub> **1**, mimicking the receptor binding region of uPA [3]. A further reduction of size was achieved by alanine scan and subsequent shift of the disulfide group to result in the peptide *cyclo*[21,29][Cys<sup>21,29</sup>]-uPA<sub>21-30</sub> **2** [4]. For optimal activity the D-Cys<sup>21</sup> epimer **3** was derived as a consequence of a D-XAA scan and is thereby the most active synthetic

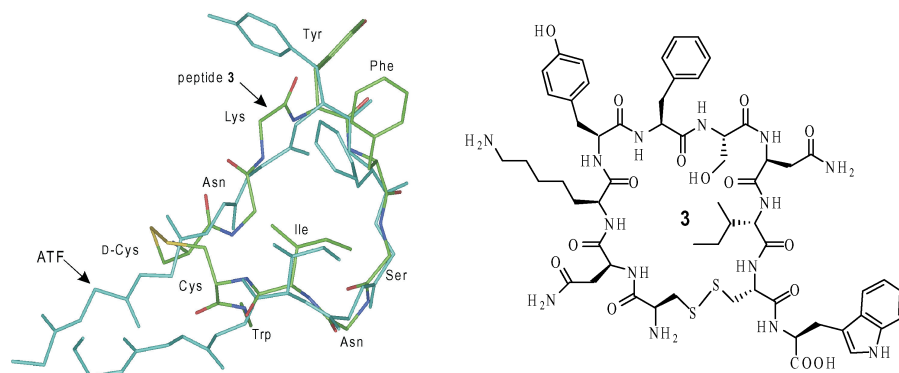
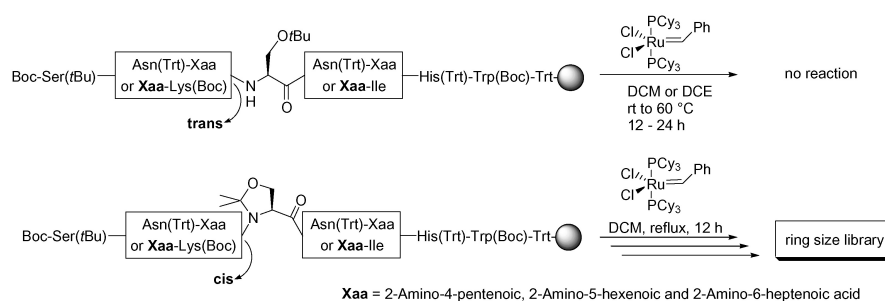


Fig. 1. Solution structures of *cyclo*[21,29][D-Cys<sup>21</sup>Cys<sup>29</sup>]-uPA<sub>21-30</sub> **3** in H<sub>2</sub>O and ATF.

uPAR antagonist ( $IC_{50} = 31$  nM,  $ATF \approx 20$  nM, determined in *flow cytometry*) published so far. The NMR derived conformation of **3** in  $H_2O$  exhibits a striking similarity to the  $\omega$  loop found by Hansen *et al.* in the amino terminal fragment of uPA itself (Figure 1) [3].

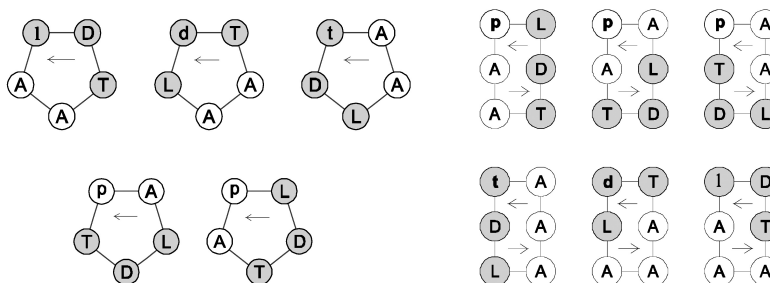
Sensitivity to proteolytic cleavage could be removed by substitution of Lys<sup>23</sup> and Tyr<sup>24</sup> for several noncoding amino acids (Nle, Orn, Nal, Cha). These modifications finally lead to the peptide *cyclo*[21,29][D-Cys<sup>21</sup>Nle<sup>23</sup>Cys<sup>29</sup>]-uPA<sub>21-30</sub> **4** with high affinity to uPAR ( $IC_{50} = 68$  nM) and resistance towards proteolytic cleavage in serum, whole blood and even plasmin.

Substitutions of the disulfide bridge by hydrocarbon linkers were attempted *via* ring closing metathesis reaction (RCM) using amino acids with olefinic side chains. It turned out, that the RCM did not run at all under conventional conditions with several model peptides derived from uPA<sub>21-30</sub>. In order to suppress the formation of restraining secondary structures in the peptide chain we introduced the reversible backbone protection ( $\Psi^{Me,Me}_{pro}$ ) at position Ser<sup>26</sup> to enforce a cisoid conformation [4]. This strategy enabled RCM in almost all cases shown below with nearly quantitative conversion rates (Scheme 1).



Scheme 1. Reversible backbone protection enables combinatorial RCM with peptides on solid phase.

Previously we have shown that RGD peptides can be optimised with respect to selectivity and activity by “spatial screening” [1]. Here we used the same procedure for ligands of  $\alpha 4\beta 1$ - and  $\alpha 4\beta 7$ -integrins.  $\alpha 4\beta 1$ -integrins bind *via* the QIDSP-sequence to VCAM-1 [7]. All isomers of a stereochemical library of cyclic hexapeptides did not inhibit the  $\alpha 4\beta 1$ /VCAM-1 interactions.



Scheme 2. Arrangement of the bioactive LDT motif in cyclic penta- and hexapeptides with one structure inducing amino acid (D-amino acid).

The LDT motif in MAdCAM-1 is the binding sequence for  $\alpha 4\beta 7$ -integrins [8]. From stereochemical cyclic peptide libraries we found *cyclo*(LDTApA) as selective and active ligand for  $\alpha 4\beta 7$ -integrins (Scheme 2). Stepwise optimisation of all positions in this cyclopeptide resulted in a new lead structure *cyclo*(LDTDpF). The introduction of an N-terminal hydrophobic amino acid like phenylalanine increased dramatically the biological activity. This ligand is selective for  $\alpha 4\beta 7$ -integrins and does not inhibit  $\alpha 4\beta 1$ /VCAM-1 interactions [9].

We determined the conformation of this peptide by NMR spectroscopy. The pharmacophoric sidechains were subsequently put onto a mannose scaffold (see Boer *et al.* in this book).

### Conclusion

We were able to demonstrate that protein subsequences can be used as starting point for the development of highly selective and active ligands for the inhibition of protein-protein interactions. Their further development to non-peptidic drugs is a next challenge, which has already successfully achieved in part.

### References

1. Haubner, R., Finsinger, D., Kessler, H. *Angew. Chem., Int. Ed. Engl.* **36**, 1374–1389 (1997).
2. Schmitt, M., Wilhelm, O.G., Reuning, U., Krüger, A., Harbeck, N., Lengyel, E., Graeff, H., Gänsbacher, B., Kessler, H., Bürgle, M., Stürzebecher, J., Sperl, S., Magdolen, V. *Thromb. Haemostasis* **78**, 285–296 (2000).
3. Bürgle, M., Koppitz, M., Riemer, C., Kessler, H., König, B., Weidle, U.H., Kellermann, J., Lottspeich, F., Graeff, H., Schmitt, M., Goretzki, L., Reuning, U., Wilhelm, O., Magdolen, V. *Biol. Chem.* **378**, 231–237 (1997).
4. Schmiedeberg, N., Bürgle, M., Wilhelm, O., Lottspeich, F., Graeff, H., Schmitt, M., Magdolen, V., Kessler, H., In Fields, G.B., Tam, J.P., and Barany, G. (Eds.) *Peptides for the New Millennium (Proceedings of the 16th American Peptide Symposium, Kluwer, Dordrecht, 1999, pp. 543–545.*
5. Hansen, A.P., Petros, A.M., Meadows, R.P., Nettesheim, D.G., Mazar, A.P., Olejniczak, E.T., Xu, R.X., Pederson, T.M., Henkin, J., Fesik, S.W. *Biochemistry* **33**, 4847–4864 (1994).
6. Dumy, P., Keller, M., Ryan, D.E., Rohwedder, B., Wöhr, T., Mutter, M. *J. Am. Chem. Soc.* **119**, 918–925 (1997).
7. Kilger, G., Holzmann, B. *J. Mol. Med.* **73**, 347–354 (1995).
8. Viney, J.L., Fong, S. *Chem. Immunol.* **71**, 64–76 (1998).
9. Boer, J., Gottschling, D., Schuster, A., Semmrich, M., Holzmann, B., Kessler, H. *J. Med. Chem.* **44**, 2586–2592 (2001).

## Prodrug Forms of Peptidomimetic HIV Protease Inhibitors Using Intramolecular Cyclization Reaction

Yoshiaki Kiso, Hikaru Matsumoto, Tomonori Hamawaki, Youhei Sohma, Tooru Kimura and Yoshio Hayashi

Department of Medicinal Chemistry, Center for Frontier Research in Medicinal Science,  
 Kyoto Pharmaceutical University, Yamashina-ku, Kyoto 607-8412, Japan

### Introduction

The human immunodeficiency virus (HIV) contains an aspartic protease known to be essential for retroviral maturation and replication. On the basis of the substrate transition state, we have studied HIV-1 protease inhibitors containing an unnatural amino acid, (2*S*,3*S*)-3-amino-2-hydroxy-4-phenylbutyric acid, named allophenylnorstatine with a hydroxymethylcarbonyl (HMC) isostere. We reported small dipeptide-based HIV-1 protease inhibitors containing the HMC isostere [1]. In order to enhance the anti-HIV activity and improve the physicochemical characteristics, we designed and synthesized prodrug forms of a peptidomimetic HIV protease inhibitor, KNI-727, conjugated with a nucleoside reverse transcriptase inhibitor, AZT [2,3].

### Results and Discussion

For conjugation, a series of linkers that connect the two different classes of inhibitors have been investigated. Conjugates using a succinyl amino acid linker were shown to cause the faster release of the parent components *via* the spontaneous imide formation compared to conjugates using a glutaryl amino acid linker, as expected from the energetically favorable cyclization to the five-membered ring. Among the double-drugs, KNI-1039 with a glutaryl-glycine linker exhibited extremely potent anti-HIV activity compared with that of the individual components (Table 1). Double-drug KNI-1039 was relatively stable in culture medium, whereas it regenerated active species in cell homogenate [3].

In addition, we synthesized a series of highly water-soluble prodrugs of an HIV protease inhibitor, KNI-727 (**1**), containing tandem-linked two auxiliary units, a

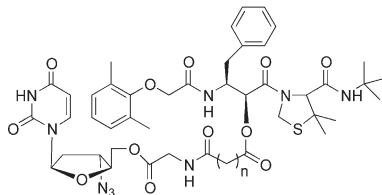


Table 1. Antiviral activities of hybrid-type anti-HIV agents.

Compound	n	ED <sub>50</sub> HIV-1 <sub>IIIB</sub> /Molt-4	Relative potency	t <sub>1/2</sub> <sup>a</sup> (h)
KNI-1038	2	5.3 nM	1.2	0.7
KNI-1039	3	0.1 nM	62	12
<b>KNI-727</b>	—	92.0 nM	0.07	—
<b>AZT</b>	—	6.2 nM	1.0	—

<sup>a</sup> t<sub>1/2</sub> is the time required for 50% release of KNI-727 at 37 °C in phosphate buffered saline (pH 7.4).

## Biologically Active Peptides

solubilizing moiety and a self-cleavable spacer (Table 2). Prodrugs with an ionized amino group at the solubilizing moiety exhibited a remarkable increase of water-solubility ( $>10^4$  fold) compared to the parent drug **1** [4]. These prodrugs released **1** not enzymatically, but chemically *via* an intramolecular cyclization-elimination reaction through an imide formation in physiological conditions. Diversified rates of parent drug release were observed when the chemical structure of both the solubilizing and the spacer moieties were modified. This new approach for water-soluble prodrugs will enable to control chemically the release of parent drug as well as to maintain high water-solubility.

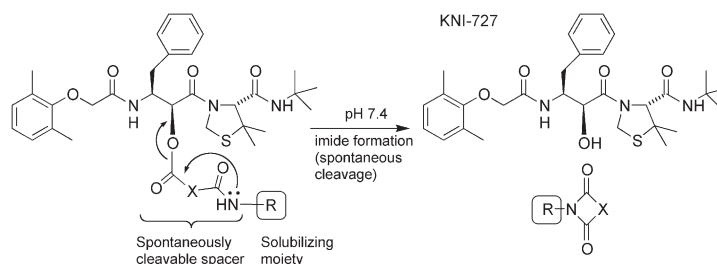


Table 2. Water-solubility and disintegration rate of prodrugs.

Compound	X	R	Water-solubility		$t_{1/2}^a$ min
			mg/mL	relative	
<b>1</b> (KNI-727)	—	—	$11.1 \cdot 10^{-3}$	1.0	—
<b>2*</b>	—	—	$16.4 \cdot 10^{-3}$	1.3	Stable
<b>3</b>	$-\text{CH}_2\text{CH}_2-$	H	$89.5 \cdot 10^{-3}$	8.1	960 (16 h)
<b>4</b>	$-\text{CH}_2\text{CH}_2-$	$-\text{CH}_2\text{COOH}$	$73.5 \cdot 10^{-3}$	6.6	1 122 (19 h)
<b>5</b>	$-\text{CH}_2\text{CH}_2-$	$-(\text{CH}_2)_2\text{COOH}$	N.D.	N.D.	1 008 (17 h)
<b>6</b>	$-\text{CH}_2\text{CH}_2-$	$-\text{CH}_2\text{CONH}_2$	$210 \cdot 10^{-3}$	18.9	20
<b>7</b> (KNI-1511)	$-\text{CH}_2\text{CH}_2-$	$-(\text{CH}_2)_2\text{NH}_2 \cdot \text{HCl}$	115.4	10 400	21
<b>8</b>	$-\text{CH}_2\text{CH}_2\text{CH}_2-$	$-(\text{CH}_2)_2\text{NH}_2 \cdot \text{HCl}$	56.9	5 130	1 680 (28 h)
<b>9</b> (KNI-1515)	$-\text{CH}_2\text{C}(\text{Me})_2-$	$-(\text{CH}_2)_2\text{NH}_2 \cdot \text{HCl}$	136.7	12 320	<1
<b>10</b>	$\text{C}(\text{Me})_2\text{CH}_2-$	$-(\text{CH}_2)_2\text{NH}_2 \cdot \text{HCl}$	N.D.	N.D.	<1
<b>11</b>	$-\text{CH}_2\text{CH}_2-$	$-(\text{CH}_2)_2\text{N}(\text{CH}_3)_2 \cdot \text{HCl}$	171.5	15 450	11

\* KNI-727-hemisuccinate. <sup>a</sup>  $t_{1/2}$  is the time required for 50% release of KNI-727 at 37 °C in phosphate buffered saline (pH 7.4).

## References

1. Kiso, Y., Matsumoto, H., Mizumoto, S., Kimura, T., Fujiwara, Y., Akaji, K. *Biopolymers* **51**, 59–68 (1999).
2. (a) Kimura, T., Matsumoto, H., Matsuda, T., Hamawaki, T., Akaji, K., Kiso, Y. *Bioorg. Med. Chem. Lett.* **9**, 803–806 (1999). (b) Matsumoto, H., Matsuda, T., Nakata, S., Mitoguchi, T., Kimura, T., Hayashi, Y., Kiso, Y. *Bioorg. Med. Chem.* **9**, 417–430 (2001).
3. (a) Matsumoto, H., Hamawaki, T., Ota, H., Kimura, T., Goto, T., Sano, K., Hayashi, Y., Kiso, Y. *Bioorg. Med. Chem. Lett.* **10**, 1227–1231 (2000). (b) Matsumoto, H., Kimura, T., Hamawaki, T., Kumagai, A., Goto, T., Sano, T., Hayashi, Y., Kiso, Y. *Bioorg. Med. Chem.* **9**, 1589–1600 (2001).
4. Matsumoto, H., Sohma, Y., Kimura, T., Hayashi, Y., Kiso, Y. *Bioorg. Med. Chem. Lett.* **11**, 605–609 (2001).

## **Effect of Poly[L-Lysine] Based Polymer Polypeptides on Chemotaxis and Phagocytosis of the Unicellular *Tetrahymena pyriformis* GL**

**Rita Szabó<sup>1</sup>, Éva Pállinger<sup>2</sup>, Gábor Mező<sup>1</sup>, László Köhidai<sup>2</sup>  
and Ferenc Hudecz<sup>1</sup>**

<sup>1</sup>Research Group of Peptide Chemistry, Hungarian Academy of Sciences Budapest,  
H-1518, Hungary

<sup>2</sup>Department of Genetics, Cell- and Immunobiology, Semmelweis University, Budapest,  
H-1445, Hungary

### **Introduction**

Branched chain polymeric polypeptides with poly[L-lysine] core (poly[Lys(DL-Ala<sub>m</sub>-X<sub>i</sub>)] = XAK) have been used for a long time as macromolecular carriers of different drugs and peptide epitopes. Earlier studies have demonstrated, that charge and polarity of the amino acid constituents of the side-chains influence conformation in solution, phospholipid membrane interaction, biological properties like cytotoxicity and immunoreactivity and *in vivo* biodistribution [1–3].

Chemotactic properties and the modulation of phagocytosis of relevant cells could be considered as essential features of polymeric polypeptides to be used as carriers. In order to establish structure-function relationship, we have prepared polypeptides with different side chain structure. Polycationic poly[L-Lys], poly[Lys(X<sub>i</sub>)], where X = His (H<sub>i</sub>K), Pro (P<sub>i</sub>K) and poly[Lys(X<sub>i</sub>-DL-Ala<sub>m</sub>)], where X = Thr (TAK), polyanionic poly[Lys(X<sub>i</sub>-DL-Ala<sub>m</sub>)], where X = AcGlu (AcEAK) and amphoteric poly[Lys(X<sub>i</sub>)], where X = Glu (E<sub>i</sub>K) were synthesized and tested using a unicellular model organism. The eukaryotic, ciliated protozoan *Tetrahymena pyriformis* GL is a popular model of cell-physiological experiments and hormone-receptor studies. It possesses several similarities (receptors and second messengers *e.g.* phosphatidylinositol system) to the higher ranks of phylogeny. These cells also produce, store and secrete hormone-like molecules.

### **Results and Discussion**

Chemotactic activity of these polypeptides was studied by a modified two-chambers capillary technique using incubation time of 20 min [4]. Changes in chemotactic ability of the new generations of unicellular population after chemotactic selection with polymers were investigated [5]. Our results indicate, that polymers depending on their side chain structure could exhibit repellent (negative) or attractant (positive) chemotactic properties. Two polymers, P<sub>i</sub>K and H<sub>i</sub>K displayed chemo-attractant effect (Figure 1A), while poly[L-lysine] with free ε-amino groups, polyanionic AcEAK, and amphoteric E<sub>i</sub>K (Figure 1B) proved to be chemo-repellent in a wide range of concentration (0.02–2.0 µg/mL).

For selection experiments the two chemo-attractant polypeptides were chosen. The chemotaxis of *Tetrahymena* cells selected by the polymers or by buffer solution were tested in the presence of P<sub>i</sub>K, H<sub>i</sub>K or buffer and  $Ch_{sel} = (C/C^*S/S)/(S/C^*C/S)$  values were calculated. As indicated by these values ( $Ch_{sel} = 0.88$  for P<sub>i</sub>K;  $Ch_{sel} = 0.67$  for H<sub>i</sub>K), no positive selection effect could be observed. This finding might indicate that chemotactic properties of these polymers are not related to inherited chemotaxis-receptor.

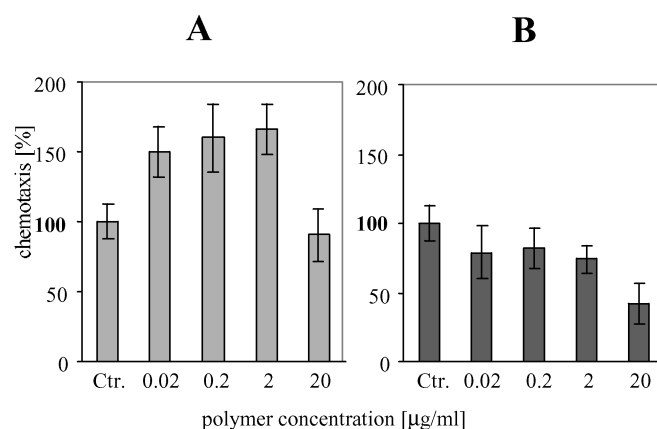


Fig. 1. Effect of H<sub>7</sub>K (A) and E<sub>7</sub>K (B) on chemotaxis of *Tetrahymena pyroformis* GL.

Influence of polymer polypeptides on phagocytosis of FITC-labeled *E. coli* bacterium or Chinese-ink test particles was determined by flow-cytometry [6]. We found that phagocytotic activity of *Tetrahymena* cells were elevated by 7–10% at low concentration, however even at the highest concentration (2 µg/mL) studied we have detected also 5–12% increase. Data suggest that polypeptides studied had no significant effect on the phagocytosis of *Tetrahymena* cells.

#### Acknowledgments

This work was supported by grants from OTKA No. T-032533 and T-030838.

#### References

1. Hudecz, F., Nagy, I.B., Kóczán, Gy., Alsina, M.A., Reig, F., In Chiellini, E., Sunamoto, J., Migliaresi, C., Ottenbrite, and R.M., Cohn, D. (Eds.) *Biomedical Polymers and Polymer Therapeutics*, Kluwer Academic/Plenum Publishers, New York, 2001, p. 103.
2. Hudecz, F., Gaál, D., Kurucz, I., Lányi, Á., Kovács, A.L., Mezö, G., Rajnavölgyi, É., Szekerke, M. *J. Controlled Release* **19**, 231–244 (1992).
3. Hudecz, F. *Anti-Cancer Drugs* **6**, 171–193 (1995).
4. Köhidai, L., Lemberkovits, É., Csaba, G. *Acta Protozool.* **34**, 181–185 (1995).
5. Köhidai, L., Csaba, G. *Comp. Biochem. Physiol.* **126C**, 1–9 (2000).
6. Esparza, B., Sánchez, H., Ruiz, M., Barranquero, M., Sabino, F., Merino, F. *Immunol. Invest.* **25**, 185–190 (1996).

## **Costimulatory Blockade by CD28 Peptide Mimics: Suppression of Experimental Autoimmune Encephalomyelitis**

**Mythily Srinivasan<sup>1</sup>, Ingrid E. Gienapp<sup>2</sup>, Connie J. Rogers<sup>2</sup>,  
Caroline C. Whitacre<sup>2,5</sup> and Pravin T. P. Kaumaya<sup>1,3,4,5,6</sup>**

<sup>1</sup>Department of Microbiology; <sup>2</sup>Department of Molecular Virology, Immunology and Medical Genetics; <sup>3</sup>Department of Obstetrics and Gynecology; <sup>4</sup>Molecular and Cellular Biochemistry  
<sup>5</sup>College of Medicine; and <sup>6</sup>The Arthur G James Comprehensive Cancer Center, The Ohio State University, Columbus, OH 43210, USA

### **Introduction**

Multiple sclerosis (MS) is a demyelinating disease of the central nervous system (CNS) characterized by destruction of myelin accompanied by inflammation. Experimental autoimmune encephalomyelitis (EAE) shares many of the clinical and histopathological features and serves as an animal model for MS. Considerable evidence indicate a critical role for the B7:CD28/CTLA-4 interactions in the pathogenesis of EAE and MS. Targeting this pathway *in vivo* represents a method for selective immunosuppression of antigen specific T cells while majority of the T cells are not affected [1].

Knowledge about the molecular topology of the interacting surface can be used for developing antagonists of protein-protein interactions. For example, a peptide analog derived from the CDR-3 like region of CD4 inhibits T-cell responses. The premise is that the side-chain functional groups of the key residues of the binding epitope can be transferred on to a much smaller fragment without loss of binding efficiency [2]. In the present study, we evaluated the therapeutic efficacy of a peptide antagonist for the B7:CD28 interactions. Based on the differences in the kinetics of interaction of CD28 and CTLA-4 with B7 ligands, we hypothesized that a peptide derived from the ligand binding region of CD28 will selectively block B7:CD28 interactions without affecting the higher affinity B7:CTLA-4 interactions [3].

### **Results and Discussion**

The combined results of the mutagenesis studies and the molecular modeling of CD28 ECD were adapted in the design of a 20-residue CD28 peptide mimic encompassing the "MYPPPY" motif and the delineated flanking sequence. The synthetic CD28 peptide was acetylated and amidated (EL-CD28) to mimic the termini of the ligand binding epitope of the parent CD28 molecule. A retro-inverso isomer of the CD28 peptide mimic (RI-CD28) with a structural equivalence to the parent peptide was designed and synthesized to circumvent the problem of rapid proteolytic degradation *in vivo* [4]. The peptides used in this study are summarized in Table 1. By surface plasmon resonance, we show that both the EL-CD28 and RI-CD28 peptide mimics compete effectively with the extracellular domain of CD28 to bind B7-1 and selectively block B7:CD28 interaction [5] (Figure 1). We have also demonstrated by circular dichroism measurements that the CD28 peptides adopt a polyproline Type II structure (data not shown).

Groups of B10.PL mice immunized with MBP in CFA which simultaneously received intravenously the EL-CD28 or RI-CD28 peptides showed significantly reduced disease severity as compared to the control CD28 peptides or PBS treated mice (Table 2). Furthermore, when the EL-CD28 and RI-CD28 peptide mimics were administered during acute disease, a dramatic improvement of clinical signs of EAE was

Table 1. Amino acid sequences of synthetic CD28 and control peptides.

Abbreviation	Sequence
L-CD28	NH <sub>2</sub> KIEFMYPYPPYLDNERSNGTICOOH
EL-CD28	CH <sub>3</sub> CO-L[KIEFMYPYPPYLDNERSNGTI]-CONH <sub>2</sub>
RI-CD28	CH <sub>3</sub> CO-D[ITGNSRENDLYPPPYMFEIK]-CONH <sub>2</sub>
D-CD28	CH <sub>3</sub> CO-D[KIEFMYPYPPYLDNERSNGTI]CONH <sub>2</sub>
RL-CD28	CH <sub>3</sub> CO-L[ITGNSRENDLYPPPYMFEIK]-CONH <sub>2</sub>

Italicized L and D refer to L and D amino acid residues respectively.

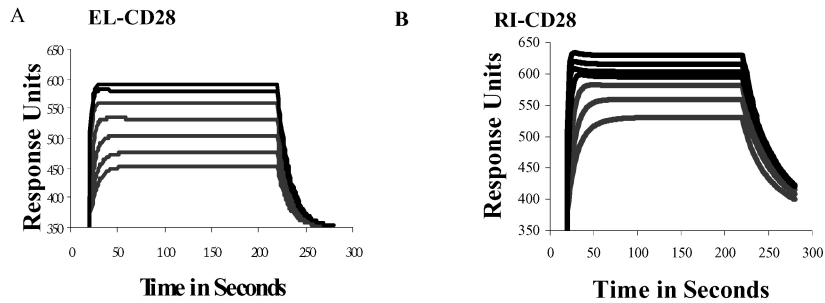


Fig. 1. An overlay of sensograms obtained from injections of a mixture of constant concentration of CD28-Ig (top curve in 2A and 2B) with increasing concentrations of EL-CD28 (2A) or RI-CD28 (2B) over a flow cell with bound B7-1Ig. The response of CD28-Ig binding decreases with increasing concentrations of EL-CD28 (A) or RI-CD28 (B) peptide.

Table 2. B10.PL mice were immunized with MBP in CFA and injected with pertussis toxin i.p. on the day of immunization and 2 days later. Animals received a single i.v. injection of 500 µg of EL-CD28, RI-CD28 peptide, control (L-CD28, RL-CD28 and D-CD28) peptides in sterile PBS, or sterile PBS alone on the day of immunization (Group I) or fourteen days later (Group II). The severity of EAE as measured by the mean cumulative score divided by the number of days observed is significantly reduced in EL-CD28 and RI-CD28 peptide treated mice as compared to control mice in both the treatment schedules.

		PBS	L-CD28	EL-CD28	EL-CD28	RI-CD28	D-CD28
Group I	mean cumulative	1.9 ± 0.2	1.8 ± 0.1	1.1 ± 0.3	0.7 ± 0.3	1.7 ± 0.1	2.0 ± 0.4
Group II	score per day	3.1 ± 1.0	2.8 ± 1.5	1.9 ± 0.1	1.8 ± 0.9	2.6 ± 0.1	2.6 ± 0.1

observed. This could be attributed to suppression of ongoing disease by peripheral deletion of antigen specific CD4<sup>+</sup> T cells (Table 2). Using anti-CD28 Fab, Perrin *et al.*, have shown similar protection against EAE [6].

## Reference

1. Karandikar, N.J., Vabderlugt, C.L., Bluestone, J.A., Miller, S.D. *J. Immunol.* **155**, 4521–4521 (1995).
2. Huang, Z., Li, S., Korngold, R. *Biopolymers* **43**, 367–372 (1997).
3. Bajorath, J., Metzler, W.J., Linsley, P.S. *J. Mol. Graph. Model* **15**, 135–138 (1997).
4. Chorev, M., Goodman, M. *Trends Biotechnol.* **13**, 438–440 (1995).
5. Karlsson, R. *Ann. Biochem.* **221**, 142–144 (1994).
6. Perrin, P.J., June, C.H., Maldonado, J.H., Ratts, R.B., Racke, M.K. *J. Immunol.* **163**, 1704–1707 (1991).

## Design and Synthesis of an Amide-Linked Angiotensin II Analogue with 3,5 Side Chain Bridge: Structural Resemblance of Ring Cluster Conformation with AT<sub>1</sub> Non-Peptide Antagonists

Panagiota Roumelioti<sup>1</sup>, Ludmila Polevaya<sup>2</sup>, Nektarios Giatas<sup>1</sup>,  
 Anastasia Zoga<sup>3</sup>, Ilze Mutule<sup>2</sup>, Tatjana Keivish<sup>2</sup>,  
 Thomas Mavromoustakos<sup>4</sup>, Panagiotis Zoumpoulakis<sup>4</sup>,  
 Demetrios Vlahakos<sup>3</sup> and John Matsoukas<sup>1</sup>

<sup>1</sup>Department of Chemistry, University of Patras, Patras, Greece

<sup>2</sup>Laboratory of Peptide Chemistry, Latvian Institute of Organic Synthesis, Riga, Latvia

<sup>3</sup>Onassis Cardiac Surgery Center, Athens, Greece

<sup>4</sup>Institute of Organic and Pharmaceutical Chemistry, The National Hellenic Research Foundation, Athens, Greece

### Introduction

The novel amide linked Angiotensin II cyclic analogue c-(3,5)-[Sar<sup>1</sup>-Lys<sup>3</sup>-Glu<sup>5</sup>-Ile<sup>8</sup>]-ANG II (Figure 1) has been designed, synthesized and bioassayed in anesthetized rabbits. The aim of this work was to investigate furthermore the role of a ring cluster receptor conformation in agonist activity and shed light to intriguing differences in activity and conformation upon replacement of aromatic residue Phe with aliphatic Ile. This replacement produces an antagonist, and the cyclization between 3 and 5 positions does not affect the antagonist activity. The constrained cyclic analogue with a lactam amide bridge linking a Lys-Glu pair at positions 3 and 5 and Ile at position 8, was synthesized by solution procedure using the maximum protection strategy. NMR spectroscopy coupled with computational analysis was performed in order to establish the significance of  $\pi^*-\pi^*$  interactions. In addition, conformational analysis of non-peptide AT<sub>1</sub> antagonists is performed in an attempt to study their stereoelectronic similarities with such a cluster.

### Results and Discussion

Our interest in the conformational model of angiotensin II, which could be used as a basis for the synthesis of non-peptide receptor antagonists, prompted us to design and synthesize the cyclic analogue of angiotensin II, c-(3,5)-[Sar<sup>1</sup>-Lys<sup>3</sup>-Glu<sup>5</sup>-Ile<sup>8</sup>]-ANG II.

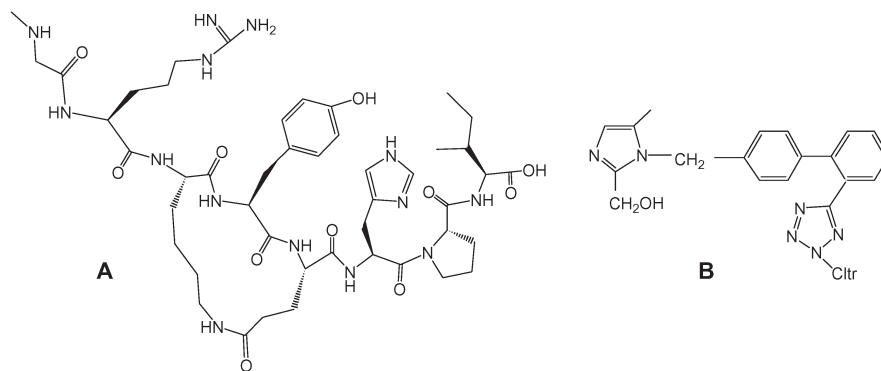


Fig. 1. Structure c-(3,5)-[Sar<sup>1</sup>-Lys<sup>3</sup>-Glu<sup>5</sup>-Ile<sup>8</sup>]-ANG II (A) and 5-methyl-2-hydroxymethyl-1-[[2'-(N-triphenylmethyl)tetrazol-5-yl]biphenyl-4-yl]methyl]imidazole (B).

Design of compound was based on previous SAR and NMR studies, which has shown that residues 3 and 5 are the least important for activity and therefore could be used to create an amide link without disturbing the ring cluster conformation [1,2]. This analogue can potentially pertain the angiotensin II conformational characteristics (i.e. backbone bend and aromatic ring clustering). Cyclization was achieved by forming an amide-linkage between the  $\text{-NH}_2$  and  $\text{-COOH}$  side chain groups of Lys and Glu residues at positions 3 and 5, respectively, which are the least important for activity [3]. Our findings indicate the importance of a Phe ring at position 8 for integration of a ring cluster receptor conformation and activity. Superimposition of non-peptide  $\text{AT}_1$  antagonists with the cyclic analogue were performed in an attempt to reveal the similarities of the C-terminal segment with specific structural features of  $\text{AT}_1$  antagonists. Based on NMR spectroscopy coupled with computational analysis comparisons between ring cluster and  $\text{AT}_1$  antagonists, we have designed and synthesized by novel methods a non-peptide mimetic, 5-methyl-2-hydroxymethyl-1-[[2'-[(*N*-triphenylmethyl)tetrazol-5-yl]biphenyl-4-yl]methyl]imidazole (Figure 1). This mimetic was found to be an active inhibitor of angiotensin II induced hypertension when tested in the rat uterus assay and in anesthetized rabbits.

#### **Acknowledgments**

This work was supported by the European Social Fund and the Ministry of Development of Greece (GSRT, PENED 99/ED-349, EPET II/115), and the Ministry of Education (EPEAEK). Also by NATO grant (HTECHLG 974548), the Latvian Science Council grant (96.0726) and the Latvian National Scientific Program (ZP-10).

#### **References**

1. Matsoukas, J., Hondrelis, J., Keramida, M., Mavromoustakos, T., Makriyannis, A., Yamdagni, R., Wu, Q., Moore, G.J. *J. Biol. Chem.* **269**, 5303–5311 (1994).
2. Matsoukas, J., Ancans, J., Mavromoustakos, T., Roumelioti, P., Vlahakos, D.V., Yamdagni, R., Wu, Q., Moore, G.J. *Bioorg. Med. Chem.* **8**, 1–10 (2000).
3. Zhang, W.J., Nikiforovich, G.V., Perodin, J., Richard, D.E., Escher, E., Marshall, G.R. *J. Med. Chem.* **39**, 2738–2744 (1996).

## Sustained Delivery of an ApolipoproteinE Peptidomimetic Lowers Serum Cholesterol Levels in Dyslipidemic Mice

Mysore P. Ramprasad<sup>1</sup>, Arjang Amini<sup>1</sup>, Nandini Katre<sup>1</sup>, David Garber<sup>2</sup>,  
Manjula Chadda<sup>2</sup> and G. M. Anantharamaiah<sup>2</sup>

<sup>1</sup>SkyePharma Inc., San Diego, CA 92121, USA

<sup>2</sup>The University of Alabama, Birmingham Medical Center, Birmingham, AL 35294, USA

### Introduction

Receptor-mediated removal of LPs by the liver is predominantly mediated by apolipoproteinE. Recent data show that a novel dual domain peptide (hE-18A) containing the 10-residue receptor-binding domain of human apoE, and a model class A amphipathic helix (18A), can associate with low density and very low density lipoproteins (LDL, VLDL) and enhance their uptake and degradation by HepG2 cells; and further, causes a dramatic reduction in plasma cholesterol levels in apoE-null mice [1,2]. These results provide the basis for developing sustained-release vehicles for this novel peptide as an alternate form of treatment for hypercholesterolemia and hypertriglyceridemia. We encapsulated this peptide into a multivesicular liposome (MVL) depot-delivery system (DepoFoam™) [3], and evaluated its sustained-release properties *in vitro* and its pharmacodynamic effects in a dyslipidemic mouse model.

### Results and Discussion

We successfully encapsulated the hE-18A peptide in MVL at >90% efficiency and achieved favorable drug loading between 2 to 4 mg/ml. The process of manufacture did not cause any detectable degradation or modification of the peptide, resulting in maintenance of its lipoprotein-associating activity. *In vitro* plasma release assays indicated sustained release of the peptide from DepoFoam particles over 7 days. Agarose gel electrophoresis followed by Western blotting established that the hE-18A peptide released into plasma, specifically associated with LDL and VLDL.

The pharmacodynamic response of the DepoE-18A formulation was evaluated after a single subcutaneous injection of 30 mg/kg encapsulated peptide in apoE-null mice. The *in vivo* data obtained in these mice (Figure 1) were consistent with the *in vitro* release profile of the peptide in plasma, and demonstrated that there was a gradual decrease in the total serum cholesterol levels with time, with a cumulative decrease of

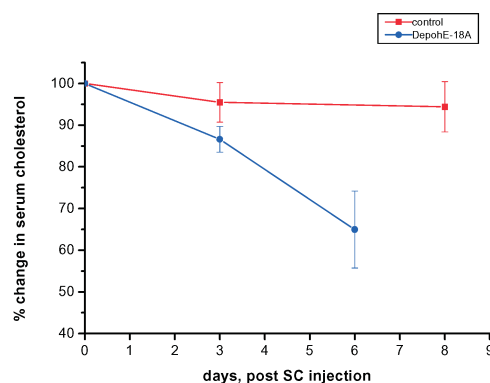


Fig. 1. The pharmacodynamic response of the DepoE-18A formulation.

25 to 48% by day 6 in the Depo-peptide treated mice. Serum lipoprotein profile analyses showed a steady decrease primarily in the VLDL/remnant fraction.

In contrast, the serum cholesterol levels in the saline treated control animals were relatively constant through this same period. Injection of the free peptide at 30 mg/kg resulted in a rapid reduction of serum cholesterol levels, averaging 50% decrease at 4 h, after which there was a rapid decline in efficacy and restoration of cholesterol levels to greater than 90% of starting levels by day 2 (Figure 2). Administration of the DepoFoam vehicle containing no peptide, like the saline control, resulted in little change in cholesterol levels (data not shown), suggesting that the sustained reduction in cholesterol levels seen with the DepoE-18A treatment was mediated by the slow release of the encapsulated peptide.

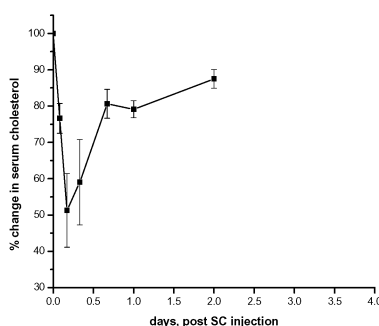


Fig. 2. The response to the injection of free peptide.

The DepoFoam technology is highly versatile and has been demonstrated to efficiently deliver several molecules in a sustained manner, including peptides and proteins [4], without burst release. The biological activity of the peptide is retained after encapsulation, and the encapsulated molecules can be efficiently extracted for structural and biological characterization. Taken together, this technology is highly applicable for the sustained delivery of several peptidomimetics, including those containing significant hydrophobic regions.

#### Acknowledgments

We thank Sam Hernandez, SkyePharma, for his invaluable technical assistance with cholesterol analyses. We are grateful to Mario Flores and Maria Esguerra, SkyePharma, for conducting the animal experiments.

#### References

1. Datta, G., Chadda, M., Garber, D.W., Chung, B.H., Tyler, E.M., Dashti, N., Bradley, W.A., Gianturco, S.H., Anantharamaiah, G.M. *Biochemistry (USA)* **39**, 213–220 (2000).
2. Datta, G., Garber, DW., Chung, B.H., Chadda, M., Dashti, N., Bradley, W.A., Gianturco, S.H., Anantharamaiah, G.M. *J. Lipid Res.* **42**, 959–966 (2001).
3. Kim, S. *Methods Neurosci.* **21**, 118–131 (1994).
4. Ye, Q., Asherman, J., Stevenson, M., Brownson, E., Katre, N.V. *J. Controlled Release* **64**, 155–166 (2000).

## Design, Synthesis and Biological Evaluation of Novel Non-Peptide Opioid Ligands for Human Pain

Xuejun Tang, Xuyuan Gu, Jinfa Ying, Vadim A. Soloshonok and Victor J. Hruby

*Department of Chemistry, University of Arizona, Tucson, AZ 85721, USA*

### Introduction

To find therapeutics for human pain with efficacy but without the side effects which accompany morphine-related drugs is a critical need. Based on extensive structure-activity studies of cyclic enkephalins, we have designed and synthesized a series of conformationally constrained peptide analogues such as [(2*S*,3*R*)-TMT1]-DPDPE, which are essentially specific for the  $\delta$ -opioid receptor [1]. Aiming to transfer the pharmacophores in these peptide ligands to a non-peptide scaffold and to maintain the high binding affinity and biological activities at the  $\delta$ -receptor, first and second generation non-peptide ligands were successfully designed with the aid of computer modeling [2,3]. In an effort to optimize these ligands, we present some newly designed ligands such as **6–11** that are based on computer modeling and our understanding of current successful examples like SL-3111.

### Results and Discussion

Our design is based on the model in Figure 1. The major parameter under consideration is the spatial distance between the two key pharmacophores, the phenyl ring of the benzyl group and the phenol ring. From the model, it was found that the characteristic distance is  $7.5 \pm 1.5$  Å. Also it is necessary to place these pharmacophores on a six-membered ring with 2 key basic nitrogen atoms for effective binding. Our first and second generation ligands have been designed to explore various structural features on the scaffold and pharmacophores [2,3]. Based on these studies, it was demonstrated that the six-member ring is a pivotal structural feature. Even though our so-far most successful example SL-3111 (**1**) has shown very good selectivity for the  $\delta$ -receptor over  $\mu$ -receptor, it still needs some modifications [2]. Therefore we designed a series

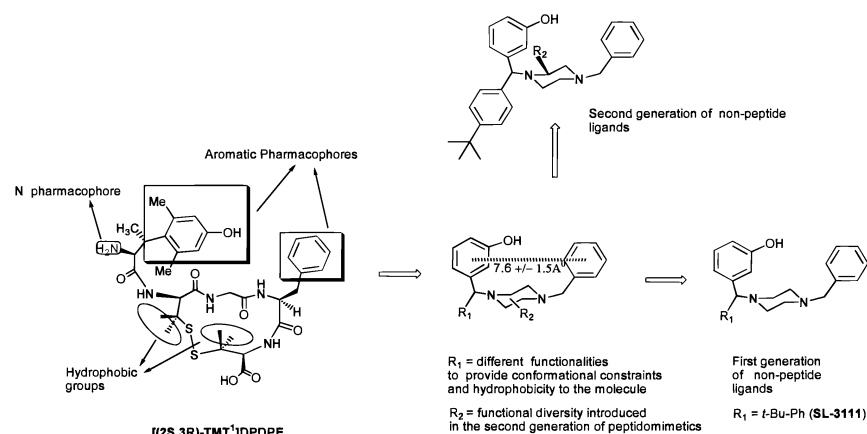


Fig. 1. A model for rational design of non-peptide petidomimetics for  $\delta$ -opioid receptor.

of analogues with structure features like **6–11**. These types of analogues can be reached through diketopiperazines (Figure 2). Based on computer modeling the key distance is still in the correct range. After reduction, the piperazine structure can be modified by alkylation or amidation to give structures like **6–11** (Figure 2 and structures below).

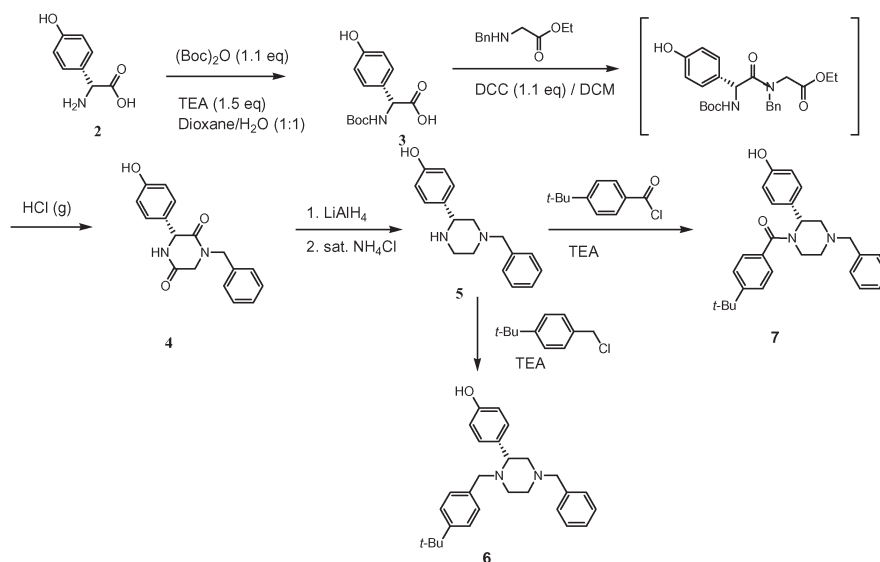
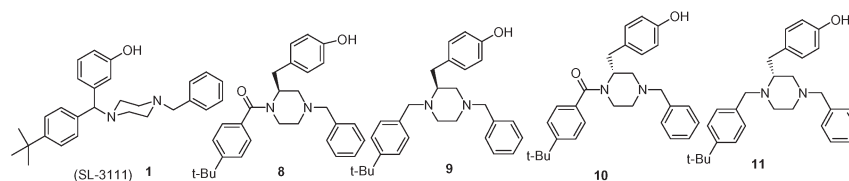


Fig. 2. Synthesis of designed compounds.



## Acknowledgments

The work was supported by USPHS and NIDA (Grants DA 06248 and DA 13449). The views expressed are those of the authors and not necessarily the USPHS.

## References

1. Hruby, V.J., Yumamura, H.I., Porreca, F. *Ann. N.Y. Acad. Sci.* **757**, 7 (1995).
2. Liao, S., Alfaro-Lopez, J., Shendrovich, M.D., Hosohata, K., Yumamura, H.I., Hruby, V.J. *J. Med. Chem.* **41**, 4767 (1998).
3. Alfaro-Lopez, J., Okayama, T., Hosohata, K., Davis, P., Porreca, F., Yamamura, H.I., Hruby, V.J. *J. Med. Chem.* **42**, 5359 (1999).

## Design and Synthesis of Novel Pure Motilin Antagonists

Masayuki Haramura<sup>1</sup>, Akira Okamachi<sup>2</sup>, Kouichi Tsuzuki<sup>2</sup>, Kenji Yogo<sup>2</sup>,  
 Makoto Ikuta<sup>2</sup>, Toshiro Kozono<sup>2</sup>, Hisanori Takanashi<sup>1</sup> and  
 Eigoro Murayama<sup>2</sup>

<sup>1</sup>Chugai Biopharmaceuticals, Inc., San Diego, CA 92121, USA

<sup>2</sup>Chugai Pharmaceutical Co., Ltd., Shizuoka, 412-8513, Japan

### Introduction

Motilin is a 22 amino acid gastrointestinal (GI) peptide which stimulates contractile activity of gastrointestinal smooth muscle. Recently, it was suggested that motilin may be involved in the production of some GI symptoms, such as early satiety, abdominal distention, nausea, vomiting, and anorexia, suggesting that motilin antagonists may have clinical applications.

We recently found that Tyr<sup>3</sup> porcine motilin 1-4 fragment peptide H-Phe-Val-Tyr-Ile-NH<sub>2</sub> (**I**) has an affinity of 11  $\mu$ M (IC<sub>50</sub>) for the motilin receptor, but is devoid of contractile effects (unpublished data). Based on this result, **I** was thought to be either a metabolically unstable agonist, even in a contraction assay, or an antagonist. However metabolic inactivation of similar motilin tetra-peptides was not observed in the assay system (unpublished data). Based on this result, **I** was hypothesized to be a motilin receptor antagonist. We have, therefore, focused on the design and synthesis of more potent motilin antagonists *via* enhancement of the binding activity of this tetra-peptide.

We anticipated that appropriate conformational restriction of **I**, through cyclization, would result in the formation of improved motilin receptor antagonists. Phe<sup>1</sup> is very important for binding as its substitution by alanine in motilin partial peptides causes the binding affinity to drop more than 100-fold [1,2]. The next residue, Val<sup>2</sup> does not seem to be part of the motilin pharmacophore, which involves residues 1, 4 and 7 [1,2]. Residue 7 is a Tyr, and our fragment contained a Tyr in position 3. Based on these considerations, we hypothesized that a cyclic peptide, connecting the side chain of the second residue with the C-terminus of the peptide, would bind tightly to MTL-R. Therefore, we focused our effort on the design and synthesis of cyclic peptides. In addition, we studied the modification of Tyr in these cyclic peptides with an aim of enhancing the binding activity.

Table 1. Structures, contractile activity and binding activity of cyclic peptides.

No.	Compound	Binding activity IC <sub>50</sub> (nM)	Contractile activity	
			EC <sub>50</sub> (nM)	pA <sub>2</sub>
1	H-Phe-c[N <sup>ε</sup> -Lys-Tyr-βAla-]	25 000	>100 000	4.05 ± 0.07
2	H-Phe-c[N <sup>ε</sup> -Lys-Tyr(O-tBu)-βAla-]	7 500	—	—
3	H-Phe-c[N <sup>ε</sup> -Lys-Tyr(3-tBu)-βAla-]	10	>100 000	7.37 ± 0.24

### Results and Discussion

The cyclic tetrapeptides were synthesized using Fmoc solid phase methodology, followed by cyclization between N<sup>ε</sup>-Lys and C-terminus with Bop reagent. The cyclic peptides were tested for binding activity to the motilin receptor (MTL-R) and for smooth muscle contractile activity in rabbit smooth muscle.

All peptides showed binding affinity, but those with an alkyl-substituted Tyr residue were more effective than the one compound with the non-substituted Tyr (compound **1**). This result suggested that the alkyl substituent on Tyr<sup>3</sup> contributes to an interaction with the MTL-R. Especially the 3-*tert*-butyl substituted Tyr derivatives (compound **3**) showed good binding affinity. Compound **3** bound to MTL-R with an IC<sub>50</sub> of 10 nM.

Importantly, the antagonistic activity of these compounds in the contractile assay correlated with their binding activity, and no contractile activity was observed even at high concentration (>100 µM). Thus, 3-*tert*-butyl substituted Tyr derivative (compound **3**) showed good antagonistic activity, with pA<sub>2</sub> values of 7.37 ± 0.24 in the rabbit duodenum contractile assay. Compound **3** (GM-109), which has the highest binding activity (pK<sub>i</sub> value: 7.99 ± 0.04), showed antagonism in an *in vivo* assay in dog [3]. It has also been reported that compound **3** (GM-109) antagonizes motilin induced calcium signaling in TE671 cells (a cell line of human cerebellar origin) [4] and in cultured myocytes from the human colon [5]. In these systems compound **3** (GM-109) did not show any agonist activity.

In conclusion, we designed and synthesized potent cyclic peptide motilin antagonists based on the structure H-Phe-c[-N<sup>ε</sup>-Lys-Tyr-βAla-]. Substitution of Tyr with 3-*tert*-butyl Tyr strongly increases potency. These antagonists should be useful for the investigation of the role of motilin, and may find application in diseases associated with increased motilin secretion.

#### Acknowledgments

We thank Dr. Theo L. Peeters, Dr. Hiroharu Matsuoka and Dr. Thomas Arrhenius for their helpful advice.

#### References

1. Peeters, T.L., Macielag, M.J., Depoortere, I., Konteatis, Z.D., Florance, J.R., Lessor, R.A., Galdes, A. *Peptides* **13**, 1103–1107 (1992).
2. Haramura, M., Tsuzuki, K., Okamachi, A., Yogo, K., Ikuta, M. Kozono, T., Takanashi, H., Murayama, E. *Chem. Pharm. Bull.* **47**, 1555–1559 (1999).
3. Takanashi, H., Yogo, K., Ozaki, K., Akima, M., Koga, H., Nabata, H. *Gastroenterology* **108**, A697 (1995).
4. Thielemans, L., Depoortere, I., Van Assche, G., Bender, E., Peeters, T.L. *Brain Res.* **23**, 119–128 (2001).
5. Van Assche, G., Depoortere, I., Thijs, T., Missiaen, L., Penninckx, F., Takanashi, H., Geboes, K., Janssens, J., Peeters, T.L. *Neurogastroenterol Motil.* **13**, 27–35 (2001).

## Active Somatostatin Analogues Containing Sugar Amino Acids

Sibylle A. W. Gruner<sup>1</sup>, Horst Kessler<sup>1</sup>, Gyorgy Kéri<sup>2</sup> and Aniko Venetianer<sup>3</sup>

<sup>1</sup>Novaspin Biotech GmbH, and Institut für Organische Chemie und Biochemie  
der TU München, 85748 Garching, Germany

<sup>2</sup>Department of Medicinal Chemistry, Semmelweis Medicinal University,  
H-1444 Budapest 8, Hungary

<sup>3</sup>Institute of Genetics, Biological Research Center, Hungarian Academy of Sciences,  
6726 Szeged, Hungary

### Introduction

Sugar Amino Acids (SAAs) are sugar moieties containing at least one amino as well as at least one carboxyl group [1]. Their oligomers represent chimeras between the two big classes of biopolymers, the carbohydrates and proteins. They therefore have been used as both, carbohydrate and peptidomimetics [2]. SAAs have been used in our laboratory mainly as turnmimics. We also applied SAAs to improve bioavailability and selectivity by functionalizing the carbohydrate skeleton.

### Results and Discussion

In this work we present the development of new, SAA-containing somatostatin analogues [3]. A library of compounds containing different furanoid and pyranoid SAAs has been synthesized (Figure 1). Hereby the skeleton and the functional groups of the SAAs as well as the amino acids of the peptide backbone have been optimized.

Some SAA containing somatostatin analogues induce apoptosis most effectively. Remarkably analogues containing D- and L-tryptophan are both active. The simple and straightforward synthesis of SAAs **1** and **2**, which serve as structure inducing templates in our compounds, is shown in Scheme 1. Both were synthesized *via* the azides **6** and **7**. The crucial step is the azidolysis of the triflate activated diacetoneglucose. Considerably higher yields than given in references [4–6] were obtained, by using the cheaper and less hazardous reagents NaN<sub>3</sub> and catalytic amounts of Bu<sub>4</sub>NCl. Azidolysis is followed by quantitative deprotection of the exocyclic hydroxyl groups using acetic acid [7]. In a one-pot reaction the azide was reduced and simultaneously Fmoc-protected yielding about 70% of the Fmoc-protected amine.

To prevent decarboxylation during TEMPO oxidation, it is crucial to avoid too basic conditions, and to keep the temperature below 0 °C.

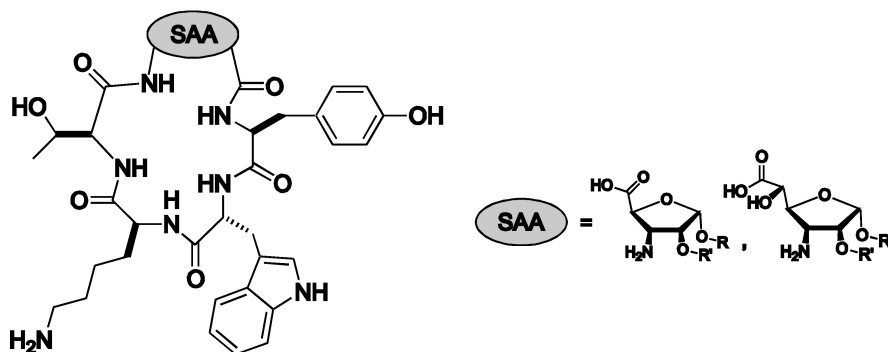
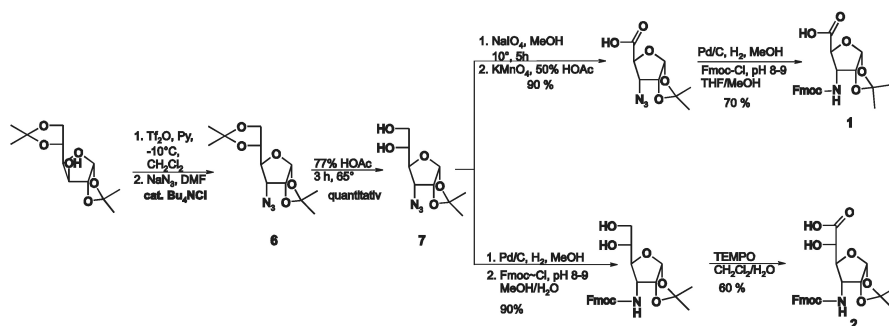


Fig. 1. SAA containing somatostatin analogues. R, R', R'' = H, Bn, or ketal groups.



Scheme 1. Synthesis of structure inducing furanoid SAAs 1 and 2.

## References

1. Lohof, E., Burkhart, F., Born, M.A., Planker, E., Kessler, H., In Abell, A. (Ed.) *Advances in Amino Acid Mimetics and Peptidomimetics*, Vol. 2, JAI Press Inc., Stanford, 1999, p. 263.
2. Gruner, S.A.W., Locardi, E., Kessler, H. *Chem. Rev., Special issue "Glycobiology"* April (2002).
3. Gruner, S.A.W., Kéri, G., Schwab, R., Venetianer, A., Kessler, H. *Org. Lett.* **3**, 3723 (2001).
4. Daley, L., Monneret, C., Gautier, C., Roger, P. *Tetrahedron Lett.* **33**, 3749 (1992).
5. Fernández, J.M.G., Mellet, C.O., Blanco, J.L.J., Fuentes, J. *J. Org. Chem.* **59**, 5565 (1994).
6. Baer, H.H., Gan, Y. *Carbohydr. Res.* **210**, 233 (1991).
7. Kulinkovich, L.N., Timoshchuk, V.A. *J. Gen. Chem. USSR (Engl. Transl.)* **53**, 1917 (1983).

## A Potent Non-Peptide Inhibitor of Anthrax Lethal Factor

Venkatachalapathi V. Yalamoori<sup>1</sup>, M. G. de Luna<sup>1</sup>, D. H. Rideout<sup>1</sup>,  
 M. D. Shenderovich<sup>1</sup>, J. H. Zheng<sup>1</sup>, N. Duesberry<sup>2</sup>, S. H. Leppla<sup>3</sup>,  
 C. S. Niemeyer<sup>1</sup>, J. Sun<sup>1</sup> and K. Ramnarayan<sup>1</sup>

<sup>1</sup>Structural Bioinformatics, Inc. San Diego, CA 92127, USA

<sup>2</sup>NCI, Frederick, MD 21702, USA

<sup>3</sup>NIDR-NIH, Bethesda, MD 20892, USA

### Introduction

*Bacillus anthracis*, the cause of anthrax, poses a considerable danger because of its potential use as a weapon by military organizations and terrorist groups. Respiratory anthrax infections are almost invariably fatal despite antibiotic treatment. Anthrax lethal factor (LF) is a zinc metalloprotease [1] that cleaves mitogen-activating protein kinase kinase 1 and 2 (MAPKK1 and MAPKK2) followed by a series of biological reactions that leads to death [2]. Existing vaccines provide no protection against certain strains of *Bacillus anthracis*. The most potent inhibitor currently known is too weak to be useful *in vivo* [1]. A potent, non-peptide inhibitor of LF could be used to ameliorate and prevent the lethal effects of anthrax. Our approach involves identifying small molecules that mimic the substrate MAPKK1 in the calculated MAPKK/LF complex, which differs from traditional rational drug design methods.

### Results and Discussion

Structural Bioinformatic's (SBI) core technology includes an augmented homology modeling procedure to derive three-dimensional models of proteins starting with protein sequence data. The flowchart of the protein modeling process is shown in Figure 1. The modeling process has been used to develop a model for MAPKK1 at atomic resolution. Protein kinase A (PKA) for which a high-resolution X-ray crystal structure was available in the Protein Data Bank, has a sequence identity of 28% to MAPKK1, was used as a template. The initial model was then refined using molecular mechanics and molecular dynamics protocols. The resultant model was then used to design inhibitors to LF, by a computational analysis of the dynamic trajectory of the MAPKK1, particularly at the LF binding site and deriving dynamic pharmacophore templates (DynaPharms<sup>TM</sup>). These DynaPharms are then used to search databases of virtual com-

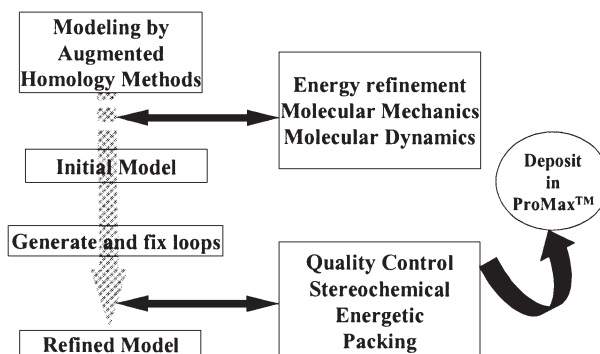


Fig. 1. SBI Modeling procedure.

### Biologically Active Peptides

binatorial libraries. A focused library was constructed based on the pharmacophoric requirements of the LF binding site, and this was used to derive inhibitors for synthesis and subsequent screening.

The peptide cleavage assay for LF, using the peptide ELYENKPRRPYIL [1], was too slow to be useful. Instead, a His-tagged MAPKK1 was used as a substrate as it was cleaved more rapidly. Two methods were used to determine the inhibition of cleavage of MAPKK1. In the first, the rate of MAPKK1 cleavage by LF was measured using a Western Blot-based gel assay. Initially, LF was pre-incubated for 30 min at 30 °C with either inhibitor or vehicle (DMSO). His-MAPKK1 was then added, and the reaction incubated for an additional 30 min at 30 °C. The protein products were separated by 14% SDS-PAGE and immunoblotted with an antibody to MAPKK1. SCION Image software was used for quantification. The second method used an ELISA assay to detect uncleaved substrates and calculate percentage inhibition. The inhibition activities of representative compounds from the 70 that were tested, including some known inhibitors, are shown in Table 1.

Table 1. Inhibition activities of representative compounds.

Sample	Western Blot IC <sub>50</sub> , $\mu$ M	Elias IC <sub>50</sub> , $\mu$ M
SBI-005737	16.5	6.0
SBI-005738	43.0	70.0
SBI-005739	18.0	15.0
SBI-005803	3.6	10.0
SBI-005804	2.6	ND
SBI-003133	>100	100
SBI-010045	ND	8.0
SBI-010233	ND	12.0
SBI-010236	ND	5.0
Zincov	>100	>100
Tyrosine Hydroxamic acid	>100	330
Phenylalanine Hydroxamic acid	>100	160

ND, Not determined.

### Conclusion

In this ongoing project in our laboratory, we have achieved a greater than 40-fold decrease in IC<sub>50</sub> values for SBI 5804 of the inhibition of cleavage of MAPKK1 by Anthrax Lethal Factor.

### Acknowledgments

Supported by SBIR grant # R43AI45237-01 from NIH-NIAID.

### References

1. Hammond, S.E., Hanna P.S. *Infect. Immun.* **66**, 2374 (1998).
2. Duesbery, N.S., et. al. *Science* **280**, 734–737 (1998).

## Highly Potent Analogs of Human Parathyroid Hormone and Human Parathyroid Hormone-Related Protein

Jesse Z. Dong<sup>1</sup>, Yeelana Shen<sup>1</sup>, Michael Culler<sup>1</sup>, John E. Taylor<sup>1</sup>,  
 Chee-Wai Woon<sup>1</sup>, Jean-Jacques Legrand<sup>2</sup>, Barry Morgan<sup>1</sup>,  
 Michael Chorev<sup>3</sup>, Michael Rosenblatt<sup>3</sup>, Chizu Nakamoto<sup>3</sup> and  
 Jacques-Pierre Moreau<sup>1</sup>

<sup>1</sup>Biomeasure Incorporated/Beaufour-IPSEN, Milford, MA 01757, USA

<sup>2</sup>Beaufour-IPSEN Pharma, Paris, France

<sup>3</sup>Beth Israel Deaconess Medical Center, Harvard Medical School, Boston, MA 02215, USA

### Introduction

It is well established that intermittently administered human parathyroid hormone, hPTH(1-84), and its fragment hPTH(1-34) effectively increase bone mass in animals and humans. Because of its unique bone anabolic effect, PTH is considered a potential therapeutic agent for the treatment of osteoporosis. However, the native hPTH(1-84) and its fragment hPTH(1-34) have a relatively narrow therapeutic index, above which they can cause bone resorption and hypercalcemia. To address this problem, we have designed and identified novel PTH/PTHrP analogs that have a wider therapeutic index.

### Results and Discussion

NMR studies have indicated that in aqueous solution, the major conformational features of hPTH(1-34) are two amphiphilic  $\alpha$ -helices at the N- and C-termini [1]. We hypothesized that the C-terminal amphiphilic  $\alpha$ -helix has membrane association property, which modulates and promotes hormone-receptor interaction. One approach to increase the receptor binding affinity of PTH(1-34) is to enhance its membrane affinity by stabilizing the C-terminal  $\alpha$ -helix. It has been reported that C $^{\alpha,\alpha}$ -symmetrically disubstituted glycines have the tendency to induce and stabilize  $\alpha$ -helix in peptides [2]. From this class of amino acids, aminoisobutyric acid (Aib) and 1-aminocyclohexane-1-carboxylic acid (A6c) were chosen in our PTH analog design. Of this new class of hPTH(1-34) analogs that contain Aib and A6c in the C-terminal  $\alpha$ -helix, compound **1** is highly potent in stimulating cAMP production *in vitro* (Table 1).

Table 1. Biological activity in production of cAMP in human osteosarcoma cells.

Peptide	cAMP(EC <sub>50</sub> , nM)	Sequences
<b>1</b>	0.3	[A6c <sup>24</sup> ,Leu <sup>27</sup> ,Aib <sup>29</sup> ]hPTH(1-34)NH <sub>2</sub>
<b>2</b>	0.5	[Glu <sup>22,25</sup> ,Leu <sup>23,31</sup> ,Lys <sup>26,30</sup> ,A6c <sup>28</sup> ,Aib <sup>29</sup> ]hPTHrP(1-34)NH <sub>2</sub>
<b>3</b>	0.3	[A6c <sup>22,24,27</sup> ,Leu <sup>23,28,31</sup> ,Glu <sup>25</sup> ,Lys <sup>26,30</sup> ,Aib <sup>29</sup> ]hPTHrP(1-34)NH <sub>2</sub>
<b>4</b>	0.4	[Cha <sup>22</sup> ,A6c <sup>23</sup> ,Glu <sup>25</sup> ,Lys <sup>26,30</sup> ,Leu <sup>28,31</sup> ,Aib <sup>29</sup> ]hPTHrP(1-34)NH <sub>2</sub>
<b>5</b>	0.4	[Cha <sup>22</sup> ,Leu <sup>23,28,31</sup> ,A6c <sup>24,27</sup> ,Glu <sup>25</sup> ,Lys <sup>26,30</sup> ,Aib <sup>29</sup> ]hPTHrP(1-34)NH <sub>2</sub>
<b>6</b>	0.4	[Glu <sup>22</sup> ,Leu <sup>23,28,31</sup> ,A6c <sup>24,27</sup> ,Lys <sup>25,26</sup> ,Aib <sup>29</sup> ]hPTHrP(1-34)NH <sub>2</sub>
<b>7</b>	0.3	[Glu <sup>22</sup> ,Cha <sup>23</sup> ,A6c <sup>24</sup> ,Lys <sup>25,26</sup> ,Leu <sup>28</sup> ,Aib <sup>29</sup> ]hPTHrP(1-34)NH <sub>2</sub>
<b>8</b>	0.3	[Glu <sup>22,25</sup> ,Leu <sup>23,28,31</sup> ,Aib <sup>29</sup> ,Lys <sup>26,30</sup> ]hPTHrP(1-34)NH <sub>2</sub>
hPTH(1-34)OH	4.0	

We further extended this strategy for the design of analogs of human parathyroid hormone related-protein (hPTHrP), a peptide that is structurally and functionally similar to hPTH. In this series of hPTHrP(1-34) analogs, A6c was employed to systematically replace Phe23, Leu24, Leu27 and Ile28 residues located in the hydrophobic face of the C-terminal amphiphilic  $\alpha$ -helix, while Aib was adopted to substitute Ala29 in the hydrophilic face of the  $\alpha$ -helix. Cyclohexylalanine (Cha), a bulky hydrophobic amino acid, was inserted into positions 22 or 23 to increase the hydrophobic interaction between the  $\alpha$ -helix and membrane. The analogs with such modifications are highly potent in inducing cAMP formation *in vitro* (Table 1). It was found that negatively charged Glu30 in the hydrophilic face of the  $\alpha$ -helix can be replaced by positively charged Lys without losing *in vitro* activity (compounds **2**, **3**, **4**, **5** and **8**), indicating that Glu30 is not directly involved in the receptor binding. His25 residue in the hydrophilic face can be substituted with either positively charged Lys or negatively charged Glu without losing potency (compounds **2–8**).

These novel hPTH and hPTHrP analogs were screened in rats for their ability of elevating blood calcium concentration. It was observed that compound **8** has much lower tendency to mobilize calcium than hPTH(1-34), a property that would contribute to a wider therapeutic index [3]. The lower calcium mobilizing ability of this analog was further confirmed in primate studies [4].

The bone anabolic effect of compound **8** was evaluated in ovariectomized (OVX), osteopenic rats and monkeys. It was demonstrated that compound **8** is about 2-fold more efficacious than hPTH(1-34) in restoring femoral bone mineral density (BMD) in the OVX, osteopenic rats [3]. Compound **8**, at the doses of 1 and 10  $\mu\text{g/kg/day}$ , significantly enhanced bone formation at trabecular sites without impact on the cortical porosity in old, OVX, osteopenic, cynomolgus monkeys [4].

In conclusion, a new series of novel and highly potent hPTH/hPTHrP analogs have been designed and synthesized. Among them, compound **8** is a potent bone anabolic agent with a wider safety margin than native hPTH(1-34).

## References

1. Pellegrini, M., et al. *J. Biol. Chem.* **273**, 10420–10427 (1998).
2. Toniolo, C. *Janssen Chim. Acta* **11**, 10–16 (1993).
3. Culler, M.D., et al. *Am. Soc. Bone Mineral Res. 23rd Annual Meeting*, abstract, 2001.
4. Legrand, J-J., et al. *Am. Soc. Bone Mineral Res. 23rd Annual Meeting*, abstract, 2001.

## Glucagon-Like Peptide-1 Analogs with Significantly Improved *in vivo* Activity

Jesse Z. Dong, Yeelana Shen, John E. Taylor, Michael Culler, Chee-Wai Woon,  
 Barry Morgan, Steve Skinner and Jacques-Pierre Moreau

Biomeasure Incorporated/Beaufour-IPSEN, Milford, MA 01757, USA

### Introduction

Glucagon-like peptide-1 (GLP-1), a potent and strictly glucose-dependent insulinotropic agent, has received increasing attention as a possible new treatment for type 2 diabetes. Although its effectiveness in type 2 diabetes patients has been demonstrated in clinical evaluations, the potential use of the native GLP-1 as a therapeutic agent is greatly hampered by its short plasma half-life. Physiologically, GLP-1 is rapidly degraded by endoproteases. Here we report that a series of novel human GLP-1 (hGLP-1) analogs have been designed and synthesized, which have greatly improved plasma half-life and significantly enhanced *in vivo* activity.

### Results and Discussion

One of the enzymes that are responsible for the fast degradation of GLP-1 *in vivo* is DPP-IV, which cleaves the amide bond between Ala8 and Glu9 at the N-terminus of hGLP-1 [1]. To prevent this enzymatic cleavage, we replaced Ala8 with some unnatural amino acids, including *N*-methyl-D-alanine (N-Me-D-Ala), 1-aminocyclopentane-1-carboxylic acid (A5c), and aminoisobutyric acid (Aib). These sterically hindered amino acids make the peptide bond between positions 8 and 9 less accessible to the enzyme, yielding analogs with greater DPP-IV resistance (compounds **1**, **2**, and **3**, Table 1).

Knowing that the amide bond between Lys34 and Gly35 of hGLP-1(1-36)NH<sub>2</sub> may also be cleaved *in vivo* [2], we further substituted the C-terminal Gly35 residue with Aib or  $\beta$ -alanine ( $\beta$ -Ala) with the goal of protecting the peptide bond. The resulting analogs bearing modifications at both positions 8 and 35 (compounds **4–8**, Table 1) have much longer plasma half-life than mono-substituted compounds **1**, **2** and **3**. These

Table 1. hGLP-1 receptor binding affinity and rat plasma half-life.

Peptide	hGLP-1 <sup>a</sup> Ki (nM)	Rat plasma T1/2 (h)	Sequence
hGLP-1(7-36)NH <sub>2</sub>	1.09	0.84	
<b>1</b>	1.13	4.35	[N-Me-D-Ala <sup>8</sup> ]hGLP-1(7-36)NH <sub>2</sub>
<b>2</b>	7.23	4.86	[A5c <sup>8</sup> ]hGLP-1(7-36)NH <sub>2</sub>
<b>3</b>	0.64	4.52	[Aib <sup>8</sup> ]hGLP-1(7-36)NH <sub>2</sub>
<b>4</b>	0.95	9.76	[Aib <sup>8,35</sup> ]hGLP-1(7-36)NH <sub>2</sub>
<b>5</b>	1.26	8.34	[Aib <sup>8</sup> , $\beta$ -Ala <sup>35</sup> ]hGLP-1(7-36)NH <sub>2</sub>
<b>6</b>	1.39	17.6	[Aib <sup>8,35</sup> ,Phe <sup>31</sup> ]hGLP-1(7-36)NH <sub>2</sub>
<b>7</b>	1.77	7.40	[Aib <sup>8</sup> ,Phe <sup>31</sup> , $\beta$ -Ala <sup>35</sup> ]hGLP-1(7-36)NH <sub>2</sub>
<b>8</b>	2.12	8.91	[Aib <sup>8,35</sup> ,Arg <sup>26,34</sup> ,Phe <sup>31</sup> ]hGLP-1(7-36)NH <sub>2</sub>

<sup>a</sup> The assays were done in CHO-K1 cells expressing the human recombinant GLP-1 receptor.

novel hGLP-1 analogs with modifications at positions 8 and 35 also retain receptor potency of the native hGLP-1 (Table 1). Replacement of Trp31 by chemically more stable Phe does not significantly influence receptor affinity (compounds **6** and **7**).

The *in vivo* studies of this new series of hGLP-1 analogs in normal Sprague–Dawley rats demonstrated that the efficacy of the analogs, in terms of the glucose-dependent stimulation of insulin secretion, is highly correlated with their *in vitro* plasma half-life [3]. Among these analogs, compound **4** enhanced the insulin response to elevated glucose with a calculated ED<sub>50</sub> at 16.0 pmol/kg, compared to that of the native hGLP-1(7-36)NH<sub>2</sub> at 121 pmol/kg [4]. This 7.6-fold increase in efficacy is likely due to its enhanced enzymatic stability, resulting in an increased circulating half-life. In studies utilizing the *db/db* mouse, intraperitoneal administration of compound **4** at 5–50 nmol/kg to 5-week old animals produced a dose-dependent reduction in blood glucose monitored over a 5-h period [4].

In conclusion, we have designed and synthesized a novel class of GLP-1 analogs that have substantially enhanced plasma half-life, while retaining full receptor potency of the native hormone. The representative analog, compound **4**, is significantly more efficacious than hGLP-1 *in vivo*, and is effective in lowering blood glucose in the *db/db* mouse model of type 2 diabetes.

## References

1. Mentlein, R., Gallwitz, B., Schmidt, W.E. *Eur. J. Biochem.* **214**, 829–835 (1993).
2. Tammem, H., Forssmann, W.-G., Richter, R. *J. Chromatogr. A* **852**, 285–295 (1999).
3. Culler, M.D., et al. *83rd Annual Meeting of the Endocrine Society*, abstract P1-353, 2001.
4. Culler, M.D., et al. *83rd Annual Meeting of the Endocrine Society*, abstract P1-360, 2001.

## Neuropeptide Y (NPY) Y1 Receptor Antagonists

V.C. Dhawan<sup>1</sup>, D.E. Mullins<sup>2</sup>, W.T. Chance<sup>1</sup>, S. Sheriff<sup>1</sup>, M. Guzzi<sup>2</sup>,  
E.M. Parker<sup>2</sup> and A. Balasubramaniam<sup>1</sup>

<sup>1</sup>*Surgery, University of Cincinnati Medical Center, Cincinnati, OH, USA*

<sup>2</sup>*CNS and Cardiovascular Research, Schering-Plough Research Institute, Kenilworth, NJ, USA*

### Introduction

Neuropeptide Y (NPY), a 36-residue peptide amide isolated originally from porcine brain, exhibits a wide spectrum of central and peripheral activities mediated by at least six receptor subtypes denoted as Y1, Y2, Y3, Y4, Y5 and Y6 [1]. Investigations to date have implicated NPY in the pathophysiology of a number of diseases including feeding disorders, seizures, anxiety, hypertension and diabetes. To aid in the determination of the receptor subtype(s) mediating these effects of NPY, efforts have been made to develop highly potent and selective ligands for various NPY receptors. One of these compounds, GR231118, exhibited subnanomolar affinity to Y1 receptors [2], and has therefore been widely used in defining the role and distribution of Y1 receptors. However, our recent investigations revealed that both GR231118 and its parent compound, BW1911U90, exhibit potent agonist activity at the Y4 receptors [3]. This paper describes the SAR studies with BW1911U90 that have resulted in the development of a series of potent and selective Y1 receptor antagonists.

### Results and Discussion

Replacing the C-terminal amide with a methyl ester or introducing  $\Psi(\text{CH}_2\text{-NH})^{35-36}$  in BW1911U90 resulted in two analogs, BVD-10 and BVD-29, respectively, both of which exhibited greater selectivity for Y1 receptors than BW1911U90 (Table 1). However, both BVD-10 and BVD-29 exhibited 5–7 times lower affinity for Y1 receptors than BW1911U90. Dimerization of these monomers *via* Cys<sup>31</sup> as in BVD-21 and BVD-30 restored the Y1 affinities. Moreover, these analogs retained sufficient selectivity for Y1 receptors. The corresponding C-terminal methyl ester and the  $\Psi(\text{CH}_2\text{-NH})^{35-36}$  analogs of GR231118, BVD-11 and BVD-42, respectively, retained the subnanomolar affinity for Y1 receptors, and exhibited higher selectivity for Y1 relative to Y2, Y4 and Y5 receptors than GR231118. In the cAMP assay, BVD-11, BVD-21, BVD-30 and BVD-46 exhibited no agonist activity in cells expressing Y1 receptors, but antagonized NPY effects in these cells with a rank order of potency of BVD-11 ( $K_b = 0.19 \pm 0.01$  nM) > BVD-42 ( $0.58 \pm 0.10$ ) > BVD-30 ( $0.79 \pm 0.09$ ) > BVD-21 ( $2.30 \pm 0.58$ ). These analogs exhibited no agonist activity in Y2, Y4 and Y5 cells at concentrations < 20000 nM. Moreover, none of these peptides exhibited Y4 antagonistic activities at a concentration of 100 nM.

Since Y1 receptors have been implicated in NPY-induced feeding, we chose BVD-11, the most potent Y1 antagonist in this series, to investigate these effects. Pre-treatment with intrahypothalamic (iht)-BVD-11 (8.4 nmol) significantly attenuated the 1 h food intake induced by iht-NPY (0.17 nmol) in satiated rats. On the other hand, iht injection of BVD-11 (8.4 or 12.6 nmol) significantly attenuated food intake in schedule-fed rats 1, 2 and 4 h after the injection. It appears therefore that the effects of the Y1 receptor antagonist is more pronounced in fasted rats than in NPY-treated satiated rats. These observations are in agreement with previous findings [4]. In summary, we have successfully dissociated the Y4 activity in BW1911U90 and GR231118, and synthesized a series of highly selective and potent Y1 selective antag-

### Biologically Active Peptides

onists. These analogs could be used to detect or attenuate Y1 mediated activities without any undue concerns about interactions with other receptor subtypes, especially in *in vivo* models.

Table 1. Structures and “Y” - receptor affinities ( $K_i$  nM) of C-terminal nonapeptide monomer and dimer analogs of NPY.

	Structure	Y1	Y2	Y4	Y5
	NPY	0.52±0.02	0.23±0.02	0.079±0.003	2.21±0.03
BW1911U90	Ile-Asn-Pro-Ile-Tyr-Arg-Leu-Arg-Tyr-NH <sub>2</sub>	5.0±0.46	11.3±3.8	5.8±0.91	>1,000
BVD-10	Ile-Asn-Pro-Ile-Tyr-Arg-Leu-Arg-Tyr-OMe	25.7±5.9	1420±191	2403±368	7100±380
BVD-29	Ile-Asn-Pro-Ile-Tyr-Arg-Leu-Arg-(CH <sub>2</sub> -NH)-Tyr-NH <sub>2</sub>	34.8±5.8	1650±114	3737±182	5080±940
BVD-21	Ile-Asn-Pro-Cys-Tyr-Arg-Leu-Arg-Tyr-OMe	4.8±1.1	1120±15	99±3	464±17
	Ile-Asn-Pro-Cys-Tyr-Arg-Leu-Arg-Tyr-OMe				
BVD-30	Ile-Asn-Pro-Cys-Tyr-Arg-Leu-Arg-(CH <sub>2</sub> -NH)-Tyr-NH <sub>2</sub>	2.3±0.5	822±78	65±5	2340±370
	Ile-Asn-Pro-Cys-Tyr-Arg-Leu-Arg-(CH <sub>2</sub> -NH)-Tyr-NH <sub>2</sub>				
GR231118	Ile-Glu-Pro-Dpr-Tyr-Arg-Leu-Arg-Tyr-NH <sub>2</sub>	0.07±0.01	55±21	0.26±0.08	115±29
	Ile-Glu-Pro-Dpr-Tyr-Arg-Leu-Arg-Tyr-NH <sub>2</sub>				
BVD-11	Ile-Glu-Pro-Dpr-Tyr-Arg-Leu-Arg-Tyr-OMe	0.27±0.01	1036±116	33.4±1.7	662±49
	Ile-Glu-Pro-Dpr-Tyr-Arg-Leu-Arg-Tyr-OMe				
BVD-42	Ile-Glu-Pro-Dpr-Tyr-Arg-Leu-Arg-(CH <sub>2</sub> -NH)-Tyr-NH <sub>2</sub>	0.46±0.12	624±69	65.5±1.9	7890±243
	Ile-Glu-Pro-Dpr-Tyr-Arg-Leu-Arg-(CH <sub>2</sub> -NH)-Tyr-NH <sub>2</sub>				

### Acknowledgments

Supported in part by grants GM47122 and DK53548 (National Institutes of Health).

### References

1. Balasubramaniam, A. *Peptides* **18**, 445–457 (1997).
2. Daniels, A.J., Matthews, J., Slepetis, R.J., et al. *Proc. Natl. Acad. Sci. U.S.A.* **92**, 9067–9071 (1995).
3. Parker, E.M., Babji, C.K., Balasubramaniam, A., et al. *Eur. J. Pharmacol.* **349**, 97–105 (1998).
4. Inui, A. *Trends Pharmacol. Sci.* **20**, 43–46 (1999).

## Template-Directed Ligation of Peptides with Nucleobase Amino Acids

Sachiko Matsumura<sup>1</sup>, Akihiko Ueno<sup>1</sup> and Hisakazu Mihara<sup>1,2</sup>

<sup>1</sup>Department of Bioengineering, Graduate School of Bioscience and Biotechnology,  
 Tokyo Institute of Technology, Yokohama 226-8051, Japan

<sup>2</sup>PRESTO, Japan Science and Technology Corporation, Yokohama 226-8501, Japan

### Introduction

Complementary recognition is a basis of a variety of biological and chemical phenomena. In DNA and RNA, the complementarity derived from the interaction between nucleobases develops the specific structures and functions. To apply the complementarity in the *de novo* peptide design, we have attempted to use nucleobase interaction in peptides, because the combination of the recognition ability of nucleobases and the peptide tertiary structure should provide an artificial peptide with a novel character. To introduce nucleobases in the peptide structure, we employed artificial L- $\alpha$ -amino acids having a nucleobase unit at the side chain (nucleobase amino acids; NBAs) [1,2]. In a two-stranded  $\alpha$ -helix, the specific interaction between nucleobases was found to function as a stabilizing factor [3]. In this study, we have attempted to apply the nucleobase interaction to a template-directed self-replicating peptide system based on a coiled-coil structural motif [4,5]. The effect of the nucleobase interaction on the template-directed peptide ligation was examined.

### Results and Discussion

The peptides used in this study were designed based on the peptide K1K2 of Yao *et al.* (Figure 1) [5]. The K1K2 peptide (named LysLys-Tp in this study) was designed to form a coiled-coil structure containing Leu residues at the a and d positions and Lys residues at the e and g positions of the helical heptad repeats. The two fragments, the thioester-containing fragment LysLys-N<sub>f</sub> and the nucleophilic fragment LysLys-C<sub>f</sub> having a free Cys residue at its N-terminus, were known to produce LysLys-T<sub>p</sub> following the native chemical ligation strategy developed by Kent [6]. In this self-replicating system, the hydrophobic interface provides interhelical recognition, promoting an effective condensation reaction. The charged residues at the e and g positions adjust the association of fragment peptides on the template peptide depending on the environmental condition, affecting the reaction efficiency. On the basis of this system, to examine the advantage of a nucleobase-complementarity in the peptide recognition, we introduced nucleobases at the side chains as additional interactions. TNBA and ANBA were incorporated at the g and g' positions instead of Lys, because the base pair inter-

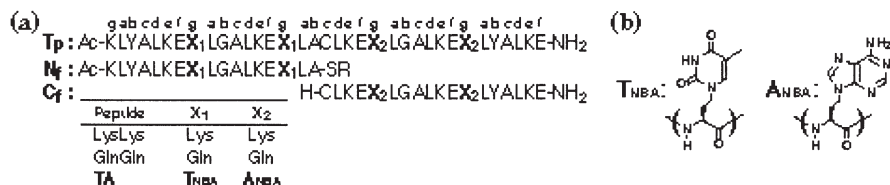


Fig. 1. (a) Sequences of the designed peptides. T<sub>p</sub>: template (product) peptide, N<sub>f</sub>: N-terminus fragment, and C<sub>f</sub>: C-terminus fragment. (b) Structures of TNBA and ANBA.

action is expected as interhelical interaction in antiparallel coiled-coils. The NBA-combined peptides (TA) were designed to form two base pairs between a template (TA-T<sub>p</sub>) and each of two fragments (TA-N<sub>f</sub> and TA-C<sub>f</sub>). To check the effect of charged residues, we also designed peptides possessing Gln at the g and g' positions (GlnGln).

The designed peptides were synthesized by the solid-phase method using Fmoc strategy. To introduce TNBA and ANBA to the Fmoc protocols, *N*-Fmoc-TNBA-OH and *N*-Fmoc-ANBA(Z)-OH were prepared [1]. The condensation reactions between two fragments in the presence of various amounts of template peptides were carried out in a buffer (pH 7.5) containing 1% (v/v) 3-mercaptopropionic acid ethyl ester at 22 °C, and the product formation was analyzed by reversed-phase HPLC.

The amide bond formation was promoted by the presence of the template peptide like a reported system. In the cases of LysLys and GlnGln, however, product formation was very suppressed in the condition used in this study. On the other hand, efficient condensation was observed in the TA system. This observation implied that the T-A interaction might facilitate the assembly of fragment peptides on the template peptide.

Circular dichroism measurements provided a structural speculation with respect to association of fragment and template peptides. Spectra of an equimolar mixture of two fragments showed mostly a random coil conformation in all systems in this study, suggesting preorganization between the two fragments had not occurred. In the case of the TA system, however, the fragments were induced to take an  $\alpha$ -helical conformation by addition of a template peptide, indicating that coiled-coil formation was organized with two fragments and a template. The effective coiled-coil formation might accelerate the ligation.

In conclusion, nucleobases introduced at the amino acid side chains in coiled-coils were found to function as interhelical recognition units. The interaction between nucleobases effectively enhanced the template-directed peptide formation. These results imply that NBAs are useful for producing a self-complementary interaction in peptide.

## References

1. Takahashi, T., Hamasaki, K., Ueno, A., Mihara, H. *Bioorg. Med. Chem.* **9**, 991–1000 (2001).
2. Takahashi, T., Hamasaki, K., Kumagai, I., Ueno, A., Mihara, H. *Chem. Commun.* 349–350 (2000).
3. Matsumura, S., Ueno, A., Mihara, H. *Chem. Commun.* 1615–1616 (2000).
4. Lee, D.H., Granja, J.R., Martinez, J.A., Severin, K., Ghadiri, M.R. *Nature* **382**, 525–528 (1996).
5. Yao, S., Ghosh, I., Zutshi, R., Chmielewski, J. *Angew. Chem., Int. Ed. Engl.* **37**, 478–481 (1998).
6. Dawson, P.E., Muir, T.W., Clark-Lewis, I., Kent, S.B.H. *Science* **266**, 776–779 (1994).

## **A General New Concept for the Development of Opioid Peptide Derived $\mu$ -, $\delta$ - and $\kappa$ -Antagonists**

**Peter W. Schiller, Yixin Lu, Grazyna Weltrowska, Irena Berezowska,  
Brian C. Wilkes, Thi M.-D. Nguyen, Nga N. Chung and Carole Lemieux**

*Laboratory of Chemical Biology and Peptide Research, Clinical Research Institute of Montreal,  
Montreal, Quebec, Canada H2W 1R7*

### **Introduction**

For decades, it has been assumed that a positively charged nitrogen in opioid compounds is a necessary requirement for binding to their receptors. In a recent study, both somatostatin-derived cyclic hexapeptides lacking a positive charge and a neutral, cyclic des-amino analogue of  $\beta$ -casomorphin, containing 3-(2,6-dimethyl-4-hydroxyphenyl)propanoic acid (Dhp) in place of Tyr<sup>1</sup>, were shown to be  $\delta$ -opioid antagonists with moderate  $\delta$  receptor binding affinity [1]. Subsequently, we prepared an analogue of the potent enkephalin analogue H-Dmt-D-Ala-Gly-Phe-Leu-NH<sub>2</sub>, in which the amino group was replaced with the neutral and almost isosteric methyl group [2]. This was achieved by replacement of Dmt with (2*S*)-2-methyl-3-(2,6-dimethyl-4-hydroxyphenyl)propanoic acid ((2*S*)-Mdp), for which a stereospecific synthesis based on Evans chiral enol chemistry was developed [2]. The resulting peptide, (2*S*)-Mdp-D-Ala-Gly-Phe-Leu-NH<sub>2</sub>, turned out to be a quite potent  $\delta$  antagonist ( $K_e$  = 28 nM) in the mouse vas deferens (MVD) assay and a less potent  $\mu$  antagonist ( $K_e$  = 154 nM) in the guinea pig ileum (GPI) assay. In view of this interesting conversion of an agonist into an antagonist at both  $\delta$  and  $\mu$  receptors, it was of interest to prepare and examine analogues of a number of key opioid peptides that lack an N-terminal amino group and contain two methyl groups at the 2',6'-positions of Tyr<sup>1</sup>. Here we describe the syntheses and *in vitro* opioid activity profiles of Dmt<sup>1</sup>-analogues of the potent, cyclic opioid peptide agonist H-Tyr-c[D-Cys-Gly-Phe(*p*NO<sub>2</sub>)-D-Cys]NH<sub>2</sub> [3], in which the N-terminal amino group was either deleted or replaced with a methyl, ethyl, cyclohexyl, or phenyl group. Furthermore, we report on our successful attempt to convert selective  $\kappa$ -,  $\delta$ - and  $\mu$ -opioid agonist peptides into selective  $\kappa$ -,  $\delta$ - and  $\mu$ -opioid antagonists, respectively, by replacement of Tyr<sup>1</sup> with (2*S*)-Mdp or Dhp.

### **Results and Discussion**

The replacement of the amino group in H-Dmt-c[D-Cys-Gly-Phe(*p*NO<sub>2</sub>)-D-Cys]NH<sub>2</sub> with an ethyl, cyclohexyl or phenyl group required stereoselective syntheses of (2*S*)-2-ethyl-3-(2,6-dimethyl-4-hydroxyphenyl)propanoic acid ((2*S*)-Edp), (2*R*)-2-cyclohexyl-3-(2,6-dimethyl-4-hydroxyphenyl)propanoic acid ((2*R*)-Cdp) and (2*R*)-2-phenyl-3-(2,6-dimethyl-4-hydroxyphenyl)propanoic acid ((2*R*)-Pdp). (2*S*)-Edp was synthesized using a synthetic scheme analogous to that developed for the preparation of (2*S*)-Mdp [2]. A different synthetic scheme using again Evans' 4-benzyl-2-oxazolidinone chiral auxiliary was developed for the stereospecific syntheses of (2*R*)-Cdp and (2*R*)-Pdp [4]. Linear peptides were prepared by the solid-phase method and the various cyclic peptide analogues were synthesized by a combination of solid-phase and solution techniques. The *in vitro* opioid activity profiles of the peptides were determined in the GPI and MVD assays and in  $\mu$ -,  $\delta$ - and  $\kappa$ -opioid receptor selective binding assays.

The Dhp<sup>1</sup>-analogue of H-Dmt-c[D-Cys-Gly-Phe(*p*NO<sub>2</sub>)-D-Cys]NH<sub>2</sub> displayed high  $\mu$  antagonist activity in the GPI assay and was a somewhat less potent  $\delta$  antagonist in

the MVD assay (Table 1). Interestingly, deletion of the 2',6'-dimethyl groups in the latter compound, as achieved by replacement of Dhp with 3-(4-hydroxyphenyl)propanoic acid (Hpp), resulted in a compound, Hpp-c[D-Cys-Gly-Phe(*p*NO<sub>2</sub>)-D-Cys]NH<sub>2</sub>, which showed relatively weak  $\mu$  and  $\delta$  receptor binding affinities and partial  $\mu$  and  $\delta$  agonist properties (the maximal inhibition of the electrically evoked contractions determined in the GPI and MVD assays was 50 and 80%, respectively). This result indicates that the two methyl groups in the 2',6'-positions of Dhp in Dhp-c[D-Cys-Gly-Phe(*p*NO<sub>2</sub>)-D-Cys]NH<sub>2</sub> play an important role in the peptide's binding to and stabilization of inactive receptor conformations, resulting in the observed antagonism. Substitution of the amino function with a methyl group produced a compound, (2*S*)-Mdp-c[D-Cys-Gly-Phe(*p*NO<sub>2</sub>)-D-Cys]NH<sub>2</sub>, showing  $K_e$  values of 1.78 and 3.48 nM at the  $\mu$  and  $\delta$  receptor, respectively (Table 1), as well as a low  $K_e^{\kappa}$  value (6.41 nM, determined against the selective  $\kappa$  agonist U50,488 in the GPI assay). This result suggests that elimination of the positively charged amino group in combination with 2',6'-dimethylation of the Tyr<sup>1</sup> aromatic ring may represent a generally applicable structural modification to convert opioid agonist peptides into antagonists at all three receptors. In comparison with its parent peptide H-Dmt-c[D-Cys-Gly-Phe(*p*NO<sub>2</sub>)-D-Cys]NH<sub>2</sub>, the (2*S*)-Mdp<sup>1</sup>-analogue has about 9-fold lower  $\mu$  receptor binding affinity (Table 1) which corresponds to a 1.3 kcal/mole reduction in binding interaction energy. An analogue containing a reduced amide bond between the (2*S*)-Mdp<sup>1</sup> and D-Cys<sup>2</sup> residues was an even more potent antagonist with  $K_e$  values and receptor binding affinities in the subnanomolar range at both  $\mu$  and  $\delta$  receptors. The cyclic (2*S*)-Edp<sup>1</sup>-, (2*R*)-Cdp<sup>1</sup>- and (2*R*)-Pdp<sup>1</sup>-analogues all showed high  $\mu$  and  $\delta$  receptor binding affinities and high  $\mu$  and  $\delta$  antagonist activities. Furthermore, the (2*R*)-Cdp<sup>1</sup>- and (2*R*)-Pdp<sup>1</sup>-analogues also displayed very high  $\kappa$  antagonist activity with  $K_e^{\kappa}$  values of 2.74 and 1.72 nM, respectively. In comparison with the H-Tyr-c[D-Cys-Gly-Phe(*p*NO<sub>2</sub>)-D-Cys-NH<sub>2</sub>] parent peptide, these compounds have much increased lipophilic character and, therefore, may have an improved ability to cross the blood-brain barrier.

*Table 1. In vitro opioid activity profiles of H-Dmt-c[D-Cys-Gly-Phe(*p*NO<sub>2</sub>)-D-Cys]NH<sub>2</sub>-derived antagonists.*

Compound	GPI $K_e$ , nM <sup>a</sup>	MVD $K_e$ , nM <sup>b</sup>	Receptor binding <sup>c</sup>	
			$K_i^{\mu}$ , nM	$K_i^{\delta}$ , nM
Dhp-c[D-Cys-Gly-Phe( <i>p</i> NO <sub>2</sub> )-D-Cys]NH <sub>2</sub>	3.68	63.3	4.79	11.6
Hpp-c[D-Cys-Gly-Phe( <i>p</i> NO <sub>2</sub> )-D-Cys]NH <sub>2</sub>	P.A. <sup>d</sup>	P.A. <sup>d</sup>	487	420
(2 <i>S</i> )-Mdp-c[D-Cys-Gly-Phe( <i>p</i> NO <sub>2</sub> )-D-Cys]NH <sub>2</sub>	1.48	3.48	2.23	3.16
(2 <i>S</i> )-Mdp $\psi$ [CH <sub>2</sub> NH]c[D-Cys-Gly-Phe( <i>p</i> NO <sub>2</sub> )-D-Cys]NH <sub>2</sub>	0.594	0.595	0.401	0.328
(2 <i>S</i> )-Edp-c[D-Cys-Gly-Phe( <i>p</i> NO <sub>2</sub> )-D-Cys]NH <sub>2</sub>	7.03	4.61	0.930	2.11
(2 <i>R</i> )-Cdp-c[D-Cys-Gly-Phe( <i>p</i> NO <sub>2</sub> )-D-Cys]NH <sub>2</sub>	2.21	26.0	2.64	10.0
(2 <i>R</i> )-Pdp-c[D-Cys-Gly-Phe( <i>p</i> NO <sub>2</sub> )-D-Cys]NH <sub>2</sub>	1.70	7.72	1.35	1.78
H-Dmt-c[D-Cys-Gly-Phe( <i>p</i> NO <sub>2</sub> )-D-Cys]NH <sub>2</sub>	0.541 <sup>e</sup>	0.182 <sup>e</sup>	0.247	0.704

<sup>a</sup> Determined against TAPP; <sup>b</sup> Determined against DPDPE; <sup>c</sup> Displacement of [<sup>3</sup>H]DAMGO ( $\mu$ -selective) and [<sup>3</sup>H]DSLET ( $\delta$ -selective) from rat brain membrane binding sites; <sup>d</sup> Partial agonist; <sup>e</sup> Value indicates IC<sub>50</sub> of agonist effect.

Deletion of the N-terminal amino group of the dynorphin A (Dyn A) analogue [Dmt<sup>1</sup>]Dyn A(1-11)-NH<sub>2</sub> led to a compound, [Dhp<sup>1</sup>]Dyn A(1-11)-NH<sub>2</sub>, which showed quite high  $\kappa$  antagonist potency in the GPI assay and significant preference for  $\kappa$  receptors over  $\mu$  and  $\delta$  receptors in the receptor binding assays (Table 2). The analogue [(2*S*)-Mdp<sup>1</sup>]Dyn A(1-11)-NH<sub>2</sub> (dynantini) turned out to be a highly potent  $\kappa$  antagonist with a  $K_e^\kappa$  value of 0.632 nM and a  $K_i^\kappa$  of 0.823 nM in the receptor binding assay. Dynantini is a highly selective  $\kappa$  antagonist, as indicated by both the ratios of  $K_e$  values determined against  $\kappa$ ,  $\mu$  and  $\delta$  agonists, and the ratios of the  $\kappa$ ,  $\mu$  and  $\delta$  receptor binding affinity constants. It is interesting to note that it displays much higher  $\kappa$  selectivity than the Dyn A(1-11)-NH<sub>2</sub> parent peptide, for which a  $K_i$  ratio ( $\kappa/\mu/\delta$ ) of 1/8/155 was determined. Dynantini is the first highly potent and selective Dyn A-derived  $\kappa$  antagonist known and is about 10 times more  $\kappa$ -selective than the non-peptide  $\kappa$  antagonist norbinaltorphimine. Replacement of Tyr<sup>1</sup> in the selective  $\delta$  opioid agonist H-Tyr-c[D-Pen-Gly-Phe(*p*F)-Pen]-Phe-OH [5] with (2*S*)-Mdp resulted in a compound with high  $\delta$  antagonist activity ( $K_e^\delta = 0.785$  nM in the MVD assay) and excellent  $\delta$  receptor binding selectivity ( $K_i^\mu/K_i^\delta = 175$ ). Finally, the (2*S*)-Mdp<sup>1</sup>-analogue of the  $\mu$  agonist peptide cyclo(*N* <sup>$\epsilon$</sup> ,*N* <sup>$\beta$</sup> -carbonyl-D-Lys<sup>2</sup>,A<sub>2</sub>bu<sup>5</sup>)enkephalinamide [6] turned out to be a selective  $\mu$  antagonist ( $K_e^\mu = 34.6$  nM;  $K_e^\delta = 5170$  nM).

Table 2.  $\kappa$  Antagonist activities and  $\kappa$  receptor binding selectivities of dynorphin A-derived antagonists.

Compound	GPI and MVD assays		Receptor binding assays <sup>c</sup>	
	$K_e^\kappa$ , nM	$K_e$ ratio( $\kappa/\mu/\delta$ ) <sup>b</sup>	$K_i^\kappa$ , nM	$K_i$ ratio ( $\kappa/\mu/\delta$ )
[Dhp <sup>1</sup> ]Dyn A(1-11)-NH <sub>2</sub>	17.4	1/26/305	3.49	1/8/35
[(2 <i>S</i> )-Mdp <sup>1</sup> ]Dyn A(1-11)-NH <sub>2</sub>	0.632	1/1460/5090	0.823	1/259/198
norbinaltorphimine	0.368	1/71/25	0.811	1/35/22

<sup>a</sup> Determined against Dyn A(1-13); <sup>b</sup>  $K_e^\mu$  was determined against the  $\mu$  agonist TAPP in the GPI assay and  $K_e^\delta$  was determined against the  $\delta$  agonist DPDPE in the MVD assay; <sup>c</sup> Displacement of [<sup>3</sup>H]U69,593 ( $\kappa$ -selective) from guinea pig brain membrane binding sites, and of [<sup>3</sup>H]DAMGO ( $\mu$ -selective) and [<sup>3</sup>H]DSLET ( $\delta$ -selective) from rat brain membrane binding sites.

## References

- Schiller, P.W., Berezowska, I., Nguyen, T.M.-D., Schmidt, R., Lemieux, C., Chung, N.N., Falcone-Hindley, M.L., Yao, W., Liu, J., Iwama, S., Smith, III, A.B., Hirschmann, R. *J. Med. Chem.* **43**, 551–559 (2000).
- Lu, Y., Weltrowska, G., Lemieux, C., Chung, N.N., Schiller, P.W. *Bioorg. Med. Chem. Lett.* **11**, 323–325 (2001).
- Schiller, P.W., DiMaio, J., In Hruby, V.J., Rich, D.H. (Eds.) *Peptides: Structure and Function (Proceedings of the 8th American Peptide Symposium)*, Pierce Chemical Company, Rockford, IL, 1983, p. 269.
- Lu, Y., Schiller, P.W. *Synthesis*, in press.
- Hruby, V.J., Baratosz-Bechowski, H., Davis, P., Slaninova, J., Zalewska, T., Stropova, D., Porreca, F., Yamamura, H.I. *J. Med. Chem.* **40**, 3957–3962 (1997).
- Pawlak, D., Oleszczuk, M., Wojcik, J., Pachulska, M., Chung, N.N., Schiller, P.W., Izdebski, J. *J. Peptide Sci.* **7**, 128–140 (2001).

## **Synthesis and Pharmacological Activity of Dmt-Tic Analogs with Highly Potent Agonist and Antagonist/Agonist Opioid Activity**

**Remo Guerrini<sup>1</sup>, Gianfranco Balboni<sup>2</sup>, Daniela Rizzi<sup>3</sup>, Girolamo Calo<sup>3</sup>, Sharon D. Bryant<sup>4</sup>, Lawrence H. Lazarus<sup>4</sup> and Severo Salvadori<sup>1</sup>**

<sup>1</sup>*Department of Pharmaceutical Sciences, University of Ferrara, 44-100 Ferrara, Italy*

<sup>2</sup>*Department of Toxicology, University of Cagliari, I-09126 Cagliari, Italy*

<sup>3</sup>*Department of Experimental and Clinical Medicine, Section of Pharmacology, University of Ferrara, 44-100 Ferrara, Italy*

<sup>4</sup>*Peptide Neurochemistry, LCBRA, Research Triangle Park, NC 27707, USA*

### **Introduction**

Several synthetic peptides containing L-1,2,3,4-tetrahydroisoquinoline-3-carboxylic acid (L-Tic) in the second position show  $\delta$ -selective opioid antagonist activity [1]. We have reported that enhancement of  $\delta$ -opioid antagonist potency was achieved by synthetic di- and tri-peptides in which Tyr<sup>1</sup> was substituted by 2,6-dimethyl-L-tyrosine (Dmt) [2]. Recently, Schiller *et al.* [3] reported the development of novel  $\delta$  opioid agonists structurally derived from the prototype  $\delta$  antagonist TIPP (H-Tyr-Tic-Phe-Phe-OH). In the present investigation, we modified the selective  $\delta$  antagonist Dmt-Tic, and identified highly potent  $\delta$  opioid agonists and  $\delta$  opioid antagonists/ $\mu$  agonists.

### **Results and Discussion**

The results of *in vitro* opioid activities of the synthesized Dmt-Tic analogues are reported in Table 1. The dipeptide derivative Dmt-Tic-NH-CH<sub>2</sub>-Bid (compound 1) was found to be a highly potent  $\delta$  agonist in the mVD and a moderately potent  $\mu$  agonist in the gpI assay. Thus, the insertion of a second pharmacophore structured as a Bid at the proper distance (NH-CH<sub>2</sub>) from the  $\delta$  antagonist pharmacophore Dmt-Tic converts the dipeptide into a potent  $\delta$  agonist and moderately potent  $\mu$  agonist. The corresponding analog Dmt-Tic-Gly-NH-Ph (compound 2), where an *N*-phenyl amide function at the C-terminal replaces 1*H*-benzimidazol-2-yl nucleus, shows a similar pharmacological behaviour, with however less potency (by 25-fold) in the mVD and increased activity (by 11-fold) in the gpI assay giving an equally potent  $\mu/\delta$  agonist. These functional results are confirmed by the receptor binding assays of these compounds. Increasing the distance between the Dmt-Tic pharmacophore and Bid with an additional methylene group (CH<sub>2</sub>) or with a glycine residue (NH-CH<sub>2</sub>-CO), yields the analogs Dmt-Tic-NH-(CH<sub>2</sub>)<sub>2</sub>-Bid and Dmt-Tic-Gly-NH-CH<sub>2</sub>-Bid (compounds 3 and 4), which maintain high  $\delta$  affinity but decrease  $\mu$  receptor binding (by 10- to 40-fold). Based on the *in vitro* assays these analogs show potent  $\delta$  antagonist activity (pA<sub>2</sub> 8.32 and 9.0) and a weak  $\mu$  agonist activity. Finally, the last compound Dmt-Tic-Gly-NH-CH<sub>2</sub>-Ph (compound 5), in which the *N*-benzyl amide pharmacophore replaces the *N*-phenyl amide thus increasing the distance from the Dmt-Tic, maintains high opioid receptor binding and it behaves as an extraordinary potent  $\delta$  antagonist (pA<sub>2</sub> 9.25) in the mVD and excellent agonist (pEC<sub>50</sub> 8.37) in the gpI assay.

From these results we can make the following conclusions: a) a further pharmacophore (Bid, *N*-phenyl- and *N*-benzyl amide) at the C-terminal of the  $\delta$  antagonist Dmt-Tic drastically increases  $\mu$  receptor affinity and induces agonist activity in the gpI; b) in the mVD assay the compounds are agonists only when the second pharmacophore (Bid or *N*-phenyl amide) is located at a minimal distance from the aro-

matic nuclei Dmt-Tic (compounds 1 and 2); c) comparing the  $\delta$  agonist activity of compounds 1 and 2, a second pharmacophore, chemically structured as a 1*H*-benzimidazol-2-yl, is better than an *N*-phenyl amide function for the activation of the  $\delta$  opioid receptor.

Table 1. *In vitro* opioid activities of Dmt-Tic analogues.

Compounds	Receptor binding assay <sup>a</sup>		mVD pEC <sub>50</sub>	pA <sub>2</sub> <sup>b</sup>	gpl pEC <sub>50</sub>
	Ki <sup>δ</sup> , nM	Ki <sup>μ</sup> , nM			
1) Dmt-Tic-NH-CH <sub>2</sub> -Bidc	0.035	0.5	9.90		7.57
2) Dmt-Tic-Gly-NH-Phd	0.042	0.15	8.52		8.59
3) Dmt-Tic-NH-CH <sub>2</sub> -CH <sub>2</sub> -Bid	0.067	5.49		8.32	6.97
4) Dmt-Tic-Gly-NH-CH <sub>2</sub> -Bid	0.058	20.5		9.00	6.45
5) Dmt-Tic-Gly-NH-CH <sub>2</sub> -Ph	0.031	0.19		9.25	8.57

<sup>a</sup> Displacement of [<sup>3</sup>H]DAGO and [<sup>3</sup>H]DPDPE from rat brain synaptosomal preparations (P2).

<sup>b</sup> The antagonism was tested using deltorphin I as agonist. <sup>c</sup> Bid is a 1*H*-benzimidazol-2-yl. <sup>d</sup> Ph is a phenyl.

## References

- Schiller, P.W., Weltrowska, G., Berezowska, I., Nguyen, Thi M.-D., Wilkes, B.C., Lemieux, C., Chung, N.N. *Biopolymers (Peptide Science)* **51**, 411–425 (1999).
- Salvadori, S., Attila, M., Balboni, G., Bianchi, C., Bryant, S.D., Crescenzi, O., Guerrini, R., Picone, D., Tancredi, T., Temussi, P.A., Lazarus, L.H. *Mol. Med.* **1**, 678–689 (1995).
- Schiller, P.W., Weltrowska, G., Schmidt, R., Berezowska, I., Nguyen, Thi M.-D., Lemieux, C., Chung, N.N., Carpenter, K.A., Wilkes, B.C. *J. Recept. Sign. Trans. Res.* **19**, 573–588 (1999).

## **A Novel Cyclic Opioid Peptide Antagonist Containing a Hydroxy Group in Place of the N-Terminal Amino Function**

**Grazyna Weltrowska, Carole Lemieux, Nga N. Chung and Peter W. Schiller**

*Laboratory of Chemical Biology and Peptide Research, Clinical Research Institute of Montreal, Montreal, Quebec, H2W 1R7, Canada*

### **Introduction**

Since a positively charged N-terminal amino group in opioid peptides is generally thought to be of crucial importance for their interaction with opioid receptors, it is of interest to determine the effect on biological activity of its elimination or replacement with other groups. Recently, we prepared a des-amino analogue of the potent cyclic  $\beta$ -casomorphin-derived peptide H-Dmt-c[D-Orn-2-Nal-D-Pro-Gly] (Dmt = 2',6'-dimethyl-tyrosine) [1]. The Dmt<sup>1</sup>-analogue was chosen as parent peptide because substitution of Dmt for Tyr<sup>1</sup> in opioid peptides is known to generally result in significantly enhanced  $\mu$  and  $\delta$  opioid receptor binding affinities [2]. The preparation of the des-amino peptide required the synthesis of 3-(4-hydroxy-2,6-dimethylphenyl)propanoic acid (Dhp) [1]. Interestingly, Dhp-[D-Orn-2-Nal-D-Pro-Gly] turned out to be a  $\delta$  and  $\mu$  opioid antagonist with moderate receptor binding affinities, indicating that a positively charged N-terminal amino group is not a *conditio sine qua non* for binding to  $\delta$  and  $\mu$  opioid receptors. To further examine the role of the N-terminal amino group in opioid peptides on receptor binding and signal transduction, its replacement with a hydroxyl group is of interest. This can be achieved by replacement of Tyr<sup>1</sup> with (2*S*)-2-hydroxy-3-(2,6-dimethyl-4-hydroxyphenyl)propanoic acid [(2*S*)-Hdp]. Here we describe the syntheses of the (2*S*)-Hdp<sup>1</sup>- and (2*R*)-Hdp<sup>1</sup>-analogues of the potent cyclic opioid peptide agonist H-Tyr-c[D-Cys-Gly-Phe(*p*NO<sub>2</sub>)-D-Cys]NH<sub>2</sub> [3] and their *in vitro* opioid activity profiles in comparison with that of the corresponding des-amino analogue.

### **Results and Discussion**

(2*S*)-Hdp and racemic (2*R*,2*S*)-Hdp were prepared from L-Dmt and racemic D,L-Dmt, respectively, by nitrous acid deamination, essentially by following a protocol that had been used for the synthesis of L-hydroxyphenyllactic acid from L-tyrosine [4]. The C-terminal tetrapeptide of the target compounds was prepared by solid-phase synthesis on a benzhydrylamine resin using the Boc protection strategy and Ac<sub>2</sub>O protection of the Cys side chains. After cleavage from the resin by HF/anisole treatment, disulfide bond formation was carried out in solution, followed by DIC coupling of (2*S*)-Hdp or (2*R*,2*S*)-Hdp. Peptides were purified by reversed-phase HPLC and structures were confirmed by FAB-MS. The (2*R*)-Hdp<sup>1</sup> and (2*S*)-Hdp<sup>1</sup> diastereomeric peptides were easily separated by preparative reversed-phase HPLC.

The (2*S*)-Hdp<sup>1</sup>-analogue showed high  $\mu$  and  $\delta$  receptor binding affinities in the receptor binding assays (Table 1) and weak  $\kappa$  receptor affinity ( $K_i^{\kappa} = 408$  nM) in a binding assay based on displacement of [<sup>3</sup>H]U69,593 from guinea pig brain membrane binding sites. In the guinea pig ileum (GPI) assay this compound turned out to be a quite potent  $\mu$  opioid antagonist ( $K_e = 9.55$  nM) and it was a somewhat less potent  $\delta$  antagonist ( $K_e = 28.0$  nM) in the mouse vas deferens (MVD) assay. In comparison with the corresponding des-amino analogue, Dhp-c-[D-Cys-Gly-Phe(*p*NO<sub>2</sub>)-D-Cys]NH<sub>2</sub>, it showed somewhat higher  $\mu$  and  $\delta$  receptor binding affinities and higher  $\delta$  antagonist activity, but slightly lower  $\mu$  antagonist activity. The diastereomeric pep-

tide (2R)-Hdp-c[D-Cys-Gly-Phe(*p*NO<sub>2</sub>-D-Cys)NH<sub>2</sub>] was also a  $\mu$  and  $\delta$  opioid antagonist with about 10–20-fold lower potency than the (2S)-Hdp<sup>1</sup>-peptide. This potency relationship is parallel to the one generally observed in the case of opioid agonist peptides, where L-Tyr<sup>1</sup>-containing peptides are always more potent agonists than their D-Tyr<sup>1</sup>-containing diastereomers. The obtained results confirm that elimination of the positively charged amino group in combination with 2',6'-dimethylation of the Tyr<sup>1</sup> aromatic ring may represent a generally applicable structural modification to convert agonist opioid peptides into antagonists. Since both the –OH and the –NH<sub>3</sub><sup>+</sup> group have hydrogen bonding capability, these results suggest that a salt bridge between the positively charged amino group of the agonist peptide and a negatively charged receptor moiety rather than hydrogen bonding may be the crucial determinant for agonist activity.

Table 1. *In vitro* opioid activity profiles of cyclic opioid peptide antagonists.

Compound	GPI	MVD	Receptor binding <sup>c</sup>	
	K <sub>e</sub> , nM <sup>a</sup>	K <sub>e</sub> , nM <sup>b</sup>	K <sub>i</sub> <sup><math>\mu</math></sup> , nM	K <sub>i</sub> <sup><math>\delta</math></sup> , nM
(2S)-Hdp-c[D-Cys-Gly-Phe( <i>p</i> NO <sub>2</sub> )-D-Cys]NH <sub>2</sub>	9.55	28.0	0.579	2.66
(2R)-Hdp-c[D-Cys-Gly-Phe( <i>p</i> NO <sub>2</sub> )-D-Cys]NH <sub>2</sub>	120	628	7.60	88.5
Dhp-c[D-Cys-Gly-Phe( <i>p</i> NO <sub>2</sub> )-D-Cys]NH <sub>2</sub>	3.68	63.3	4.79	11.6

<sup>a</sup>Determined against TAPP, <sup>b</sup>Determined against DPDPE, <sup>c</sup>Displacement of [<sup>3</sup>H]DAMGO ( $\mu$ -selective) and [<sup>3</sup>H]DSLET ( $\delta$ -selective) from rat brain membrane binding sites.

### Acknowledgments

This work was supported by grants from the Canadian Institutes of Health Research (MT-5655) and the U.S. National Institutes of Health (DA-04443).

### References

- Schiller, P.W., Berezowska, I., Nguyen, T.M.-D., Schmidt, R., Lemieux, C., Chung, N.N., Falcone-Hindley, M.L., Yao, W., Lin, J., Iwama, S., Smith, III, A.B., Hirschmann, R. *J. Med. Chem.* **43**, 551–559 (2000).
- Hansen, D.W., Stapelfeld, A., Savage, M.A., Reichmann, M., Hamond, D.L., Haaseth, R.C., Mosberg, H.I. *J. Med. Chem.* **35**, 684–687 (1992).
- Schiller, P.W., DiMaio, J., In Hruby, V.J. and Rich, D.H. (Eds.) *Peptides: Structure and Function (Proceedings of the 8th American Peptide Symposium)*, Pierce Chemical Company, Rockford, IL, 1983, p. 269.
- Kotake, Y. *Hoppe-Seyler's Z. Physiol. Chem.* **65**, 397–401 (1910).

## Modifications of the Tic Residue in TIPP-Peptides

D. Tourwé<sup>1</sup>, S. Van Cauwenberghe<sup>1</sup>, K. Vanommeslaeghe<sup>1</sup>,  
E. Mannekens<sup>1</sup>, P. Geerlings<sup>2</sup>, G. Toth<sup>3</sup>, A. Péter<sup>4</sup> and J. Csombos<sup>4</sup>

<sup>1</sup>Departments of Organic Chemistry, Vrije Universiteit Brussel, B-1050 Brussels, Belgium

<sup>2</sup>General Chemistry, Vrije Universiteit Brussel, B-1050 Brussels, Belgium

<sup>3</sup>Biological Research Center and

<sup>4</sup>University of Szeged, H-6720 Szeged, Hungary

### Introduction

H-Tyr-Tic-Phe-Phe-OH (TIPP) is a potent and selective  $\delta$ -opioid antagonist developed by P. Schiller. Its  $\delta$ -antagonist properties are related to the cyclic nature of the Tic residue. In the proposed bioactive conformation, the aromatic ring of Tic overlaps with the indole ring of the non-peptide  $\delta$ -antagonist naltrindole (NTI) [1]. We have prepared several Tic analogs having modifications in the saturated ring **1**, **2** or in the aromatic part **3**, **4** (Figure 1).

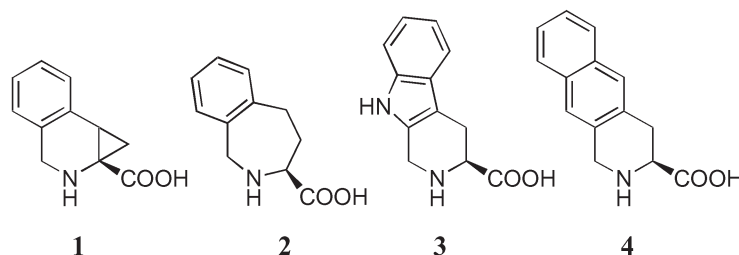


Fig. 1. Tic-analogs.

### Results and Discussion

The new amino acids **1** and **2** were prepared by cyclopropanation of  $\alpha,\beta$ -dehydro-Tic [2] and by sigmatropic rearrangement of 2,3-methano-Phe with formaldehyde [3] respectively. Compounds **3** and **4** were prepared according to published procedures [4,5]. Since **1**, **2** and **4** were racemates, after incorporation into the tetrapeptides, the resulting diastereomeric TIPP-analogs were separated by HPLC.

The  $\delta$ -receptor affinities of TIPP-analogs containing the modifications **1**, **2** and **3** were all in the micromolar range, whereas that of the most active isomer of **4** was 83 nM. Molecular modelling of the tripeptide TIP-analogs containing modified Tics **1**–**4** with (3*S*) configuration was performed using the Sybyl software as described by Wilkes [1]. The ring search identified one low energy conformer for **1** ( $\chi_1 = -5.4^\circ$ ) and four for **2** ( $\chi_1 = 41.4, -41.9, 59.7, -44.7^\circ$ ), whereas the usual gauche(+) and gauche(–) conformers were found for **3** and **4**. A systematic search procedure identified the low energy conformations for the tripeptide analogs. Those showing the best overlap with NTI using a three point overlap (Tyr N $\alpha$ , centroids of phenolic ring and Tic benzene) were identified (Figure 2). The quality of the overlap was compared to that for native TIP [1]. In Tyr-(**1**)-Phe and in Tyr-(**2**)-Phe, overlap and coplanarity of the Tyr phenolic rings was less satisfactory than in TIP, and the carbonyl linking the Tic-analog to Phe was oriented completely differently. In Tyr-(**3**)-Phe, the overall conformation was very similar to that in TIP, the indole ring was coplanar with the corresponding indole in NTI, and the Phe orientation was unchanged. The Tyr phenolic ring was coplanar

with that in NTI, but the distance between the aromatic pharmacophores was slightly larger. In Tyr-(4)-Phe, the most active analog, this distance was maintained, although the extra benzene ring compared to Tic, caused a less satisfactory overall overlap of the peptide backbone with NTI, which could explain its lower  $\delta$ -affinity. These data suggest that the exact distance between the aromatic rings in TIP and the positioning of the phenolic group are crucial for  $\delta$ -affinity. The positioning of the Tic carbonyl, which also determines the orientation of the Phe residue, appears to play an important role as well.

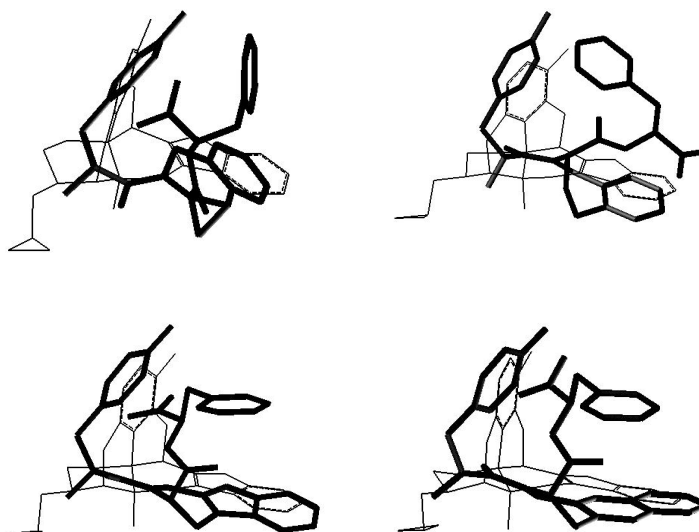


Fig. 2. Overlap of TIP-analogs with NTI: from left to right: T(1)P, T(2)P, T(3)P and T(4)P.

#### Acknowledgments

We thank Dr. A. Borsodi, Biological Research Center, Szeged, Hungary and Dr. M. Jurzak, Janssen Research Foundation, Beerse, Belgium for the binding assays. Supported by grant AWI-BIL00/52 and FWO.

#### References

1. Wilkes, B.C., Schiller, P.W. *Biopolymers* **37**, 391 (1995).
2. Csombos, J., Aelterman, W., Tkachev, A., Martins, J.C., Tourwé, D., Péter, A., Toth, G., Fülöp, F., De Kimpe, N. *J. Org. Chem.* **65**, 5469 (2000).
3. Martins, J.C., Van Rompaey, K., Wittmann, G., Tömböly, C., Tóth, G., De Kimpe, N., Tourwé, D. *J. Org. Chem.* **66**, 2884 (2001).
4. Iterbeke, K., Laus, G., Verheyden, P., Tourwé, D. *Lett. Peptide Sci.* **5**, 121 (1998).
5. Wang, C., Mosberg, H.I. *Tetrahedron Lett.* **36**, 3623 (1995).

## Structure–Activity Relationships of Linear and Cyclic Nociceptin Analogues and Conformational Analysis by CD and NMR Spectroscopy

Ralf Schmidt<sup>1</sup>, Ibtihal Fadhil<sup>1</sup>, Katharine Carpenter<sup>1</sup>,  
Joanne Butterworth<sup>2</sup> and Kemal Payza<sup>2</sup>

<sup>1</sup>Department of Chemistry, and <sup>2</sup>Department of Pharmacology, AstraZeneca R&D Montreal,  
St. Laurent, Quebec, Canada H4S 1Z9

### Introduction

The heptadecapeptide nociceptin was identified as the ligand for the ORL1 (opioid receptor-like 1) receptor, which shares 60% sequence homology with the  $\kappa$  opioid receptor. In contrast to the opioid peptides, the aromatic amino acid in position 1 can be substituted by non-aromatic residues, whereas the one in the 4-position is crucial for receptor binding [1]. To establish the structural requirements for binding and activation, the latter position residue was substituted by a variety of aromatic amino acids using nociceptin(1-13)-NH<sub>2</sub> (NC-13) as parent peptide. Additionally, a series of cyclic analogs was designed in order to stabilize helical structures, and probe their contribution to the bio-active conformation, since analysis of the CD spectra of NC-13 revealed the existence of secondary structures.

### Results and Discussion

Peptides were assembled by automated solid-phase synthesis on Rink-Amide-MBHA resin following standard protocols. Cyclic peptides were obtained by on-resin cyclization of the *N*<sup>α</sup>-Fmoc protected linear precursors with PyBOP. The homogeneity of the final products was found to be >98% by analytical HPLC, and the identity confirmed by ES-TOF-MS and NMR. The receptor affinity and the functional activity of the peptides were determined in assays based on displacement of radio-iodinated [Tyr<sup>14</sup>]nociceptin and in the GTPγ[<sup>35</sup>S] assay using mouse brain membranes.

The amino acid substitutions at the 4-position clearly demonstrated that other aromatic residues could not easily replace Phe<sup>4</sup> (Table 1). Subnanomolar receptor affinities and full agonism were only obtained for Trp (data not shown) and to a lesser extent for *N*-methylphenylalanine (**2**), 2-naphthyl- (**3**) and 1-naphthylalanine (**4**), benzothienylalanine (**5**) and *O*-methyltyrosine (**6**). Interestingly, changing the distance between the phenyl ring and the peptide backbone resulted in more than 100-fold reduced binding affinity (phenylglycine, homophenylalanine, data not shown).

Analogues with i(i+4) and i(i+3) side chain to side chain cyclization known to stabilize helical structures [2] were designed by keeping the crucial basic residues in the “address” region unchanged [1]. Cyclization between positions 7 and 10 or 11, respectively, were detrimental for receptor binding and activation, but c[Asp<sup>6</sup>,Lys<sup>10</sup>]NC-13 (analogue **7**) possessed pharmacological properties similar to the parent peptide. Changing the direction of the side chain amide bond (analogue **11**), as well as reversal of the chirality in position 10 (analogue **12**), were well tolerated. Remarkably, these conformationally constrained compounds displayed higher binding affinity and improved *in vitro* activity. In contrast, introduction of a D-amino acid at the 6-position led to a dramatic loss of receptor affinity and activity (analogue **10**).

CD and NMR experiments were performed using micelles to mimic the receptor environment. The CD spectra of all active cyclic analogues revealed an increase in heli-

Table 1. Receptor affinities and activities of linear and cyclic nociceptin analogs.

Peptide	Binding assay		Functional assay
	IC <sub>50</sub> [nM]	Relative affinity	EC <sub>50</sub> [nM]
<b>1</b> Noc(1-13)-NH <sub>2</sub> (NC-13)	0.0396	100	4.70
<b>2</b> [MePhe <sup>4</sup> ]NC-13	0.127	31	29.2
<b>3</b> [2NaI <sup>4</sup> ]NC-13	0.502	7.9	42.5
<b>4</b> [1NaI <sup>4</sup> ]NC-13	0.370	11	48.6
<b>5</b> [Bta <sup>4</sup> ]NC-13	0.161	25	47.5
<b>6</b> [Tyr(Me) <sup>4</sup> ]NC-13	0.810	4.9	85.8
<b>7</b> c[Asp <sup>6</sup> ,Lys <sup>10</sup> ]NC-13	0.0187	210	1.34
<b>8</b> c[Asp <sup>7</sup> ,Lys <sup>11</sup> ]NC-13	0.127	32	44.0
<b>9</b> c[Asp <sup>7</sup> ,Lys <sup>10</sup> ]NC-13	0.846	4.7	356
<b>10</b> c[D-Asp <sup>6</sup> ,Lys <sup>10</sup> ]NC-13	9.14	0.43	583 (72%) <sup>a</sup>
<b>11</b> c[Lys <sup>6</sup> ,Asp <sup>10</sup> ]NC-13	0.0167	240	3.03
<b>12</b> c[Lys <sup>6</sup> ,D-Asp <sup>10</sup> ]NC-13	0.00725	550	0.934

<sup>a</sup>  $E_{max}$  for partial agonist in parentheses.

cal content, whereas the constrained inactive analogs showed less or no secondary structure. In NMR studies an observed density of four or more  $\alpha$ H chemical shift displacements greater than 0.1 ppm upfield from random coil values indicates a region of  $\alpha$  helical structure. In analog **7**, the helical conformation spanned the entire sequence. In contrast, the low-affinity ligand **10** displayed some helical structure, but the overall helical stability was much reduced compared to that of the high-affinity compound **7**. In the NOESY spectra, the large number of medium range NOEs observed for analog **7** reflected its stable helical conformation, whereas the comparatively sparse number of medium range NOEs observed for analog **10** confirmed its lower helix stability.

In conclusion, this study demonstrated the importance of the chemical nature of the aromatic side chain at position 4 of nociceptin(1-13)-NH<sub>2</sub> analogs, since only minor changes were tolerated. Furthermore, i(i+4) side chain cyclization between positions 6 and 10 resulted not only in analogs with an extended and stable helix, but also in compounds with improved pharmacological properties. This observation indicates that a helical structure of the ligand might provide an important contribution for the effective ligand-receptor interaction, and possibly represent the bio-active conformation of the peptide.

## References

- Guerrini, R., Calo, G., Rizzi, A., Bianchi, C., Lazarus, L.H., Salvadori, S., Temussi, P.A., Regoli, D. *J. Med. Chem.* **40**, 1789–1793 (1997).
- Carpenter, K.A., Schmidt, R., Yu, S.Y., Hodzic, L., Pou, C., Payza, K., Godbout, C., Brown, W., Roberts, E. *Biochemistry* **38**, 15295–15304 (1999).

## Design and Synthesis of Dynorphin A-(1-11) Analogs with C-Terminal Modifications and Evaluation of their Opioid Activity

Kshitij A. Patkar<sup>1</sup>, Thomas F. Murray<sup>2</sup> and Jane V. Aldrich<sup>2</sup>

<sup>1</sup>Department of Pharmaceutical Sciences, School of Pharmacy, University of Maryland, Baltimore, MD 21201, USA

<sup>2</sup>College of Veterinary Medicine, University of Georgia, Athens, GA 30602, USA

### Introduction

Dynorphin A (Dyn A) is a natural kappa opioid receptor ( $\kappa$ ) agonist that contains a characteristic tetrapeptide sequence Tyr-Gly-Gly-Phe at the N-terminus termed the "message" sequence, followed by a unique C-terminal sequence termed the "address" [1]. The message sequence is proposed to confer opioid activity, whereas the address sequence is thought to impart high affinity for  $\kappa$  opioid receptors. However, the structural and conformational requirements for antagonist activity as opposed to agonist activity are not clear from the structure-activity relationship (SAR) studies of Dyn A.

### Dyn A-(1-11): Tyr-Gly-Gly-Phe-Leu-Arg-Arg-Ile-Arg-Pro-Lys

In our laboratory, examination of the effect of N-terminal alkylation on opioid receptor affinity, selectivity and efficacy led to the synthesis of [*N* $^{\alpha}$ -benzyl-Tyr<sup>1</sup>,D-Pro<sup>10</sup>]Dyn A-(1-11)OH (**1**), which was a weak agonist in the guinea pig ileum (GPI) assay [2] and a partial agonist in the adenylyl cyclase assay [3]. The previous report of C-terminally modified [Phe<sup>1</sup>]Dyn A-(1-11) analogs with widely varying potencies in the GPI in spite of similar affinities in binding assays[4] suggested that C-terminus of Dyn A could affect receptor activation. To assess this hypothesis, we designed and synthesized several [*N* $^{\alpha}$ -benzylTyr<sup>1</sup>]Dyn A-(1-11) (**2**) analogs with various modifications (*N* $^{\alpha}$ -MeArg<sup>7</sup>,D-Ala<sup>8</sup>,D-Pro<sup>10</sup>) that have been utilized individually in a number of previous SAR studies on Dyn A and evaluated the analogs for opioid receptor affinity and efficacy.

### Results and Discussion

The peptides were synthesized by solid phase peptide synthesis using the Fmoc synthetic protocol and standard coupling reagents. *N* $^{\alpha}$ -Benzyltyrosine was synthesized by reductive amination of tyrosine *t*-butyl ester with benzaldehyde, followed by TFA deprotection. The affinities of the peptides were determined in radioligand binding assays using [<sup>3</sup>H]diprenorphine, [<sup>1</sup>H]DAMGO and [<sup>3</sup>H]DPDPE, respectively, for cloned  $\kappa$ ,  $\mu$  and  $\delta$  opioid receptors stably expressed in Chinese hamster ovary cells [5] (Table 1).

Table 1. Opioid receptor binding affinities of selected Dyn A-(1-11) analogs.

Peptide	Kappa K <sub>i</sub> (nM $\pm$ SEM)	K <sub>i</sub> Ratio ( $\kappa/\mu/\delta$ )
1. [ <i>N</i> -benzylTyr <sup>1</sup> ,D-Pro <sup>10</sup> ]Dyn A-(1-11)OH	26.2 $\pm$ 1.60	1/10/60
2. [ <i>N</i> -benzylTyr <sup>1</sup> ]Dyn A-(1-11)OH	20.0 $\pm$ 6.1	1/9/33
3. [ <i>N</i> -benzylTyr <sup>1</sup> ]Dyn A-(1-11)NH <sub>2</sub>	8.17 $\pm$ 2.16	1/10
4. [ <i>N</i> -benzylTyr <sup>1</sup> ,D-Pro <sup>10</sup> ]Dyn A-(1-11)NH <sub>2</sub>	4.56 $\pm$ 0.40	1/9/32
5. [ <i>N</i> -benzylTyr <sup>1</sup> , <i>N</i> -MeArg <sup>7</sup> ,D-Ala <sup>8</sup> ,D-Pro <sup>10</sup> ]Dyn A-(1-11)NH <sub>2</sub>	4.41 $\pm$ 0.07	1/17/166
6. Dyn A-(1-11)NH <sub>2</sub>	0.07 $\pm$ 0.01	1/26/88

$N^\alpha$ -Benzoylation of Dyn A-(1-11)NH<sub>2</sub> resulted in a decrease in  $\kappa$  receptor affinity. The most influential modification in the C-terminus was C-terminal amidation (analogs **3–5**) that resulted in a significant increase in affinity for  $\kappa$  opioid receptors. Further incorporation of multiple substitutions in positions 7, 8 and/ or 10 caused an additional small increase in the  $\kappa$  receptor affinity. The efficacy of these compounds was evaluated in an adenylyl cyclase assay [3] also using cloned rat  $\kappa$  opioid receptors. Preliminary results indicated that these analogs were all partial agonists at  $\kappa$  opioid receptors with fairly similar efficacies (70–94% of the inhibition of Dyn A-(1-13)NH<sub>2</sub> at 10  $\mu$ M). These results indicate that the C-terminus can tolerate a variety of modifications in the “address” sequence. These [ $N^\alpha$ -benzylTyr<sup>1</sup>]Dyn A-(1-11) analogs are undergoing further pharmacological evaluation and information from these assays will be used in the design of additional analogs.

#### **Acknowledgments**

The authors would like to thank Jennif Chandler and B. Miranda Thomas for performing the pharmacological assays of the synthesized peptides. This research was supported by NIDA grant R01 DA05195.

#### **References**

1. Chavkin, C., Goldstein, A. *Proc. Natl. Acad. Sci. USA* **78**, 6543–6547 (1981).
2. Choi, H., Murray, T., DeLander, G., Schmidtt, W., Aldrich, J. *J. Med. Chem.* **40**, 2733–2339 (1997).
3. Sonderstrom, K., Choi, H., Berman, F.W., Aldrich, J.V., Murray, T.F. *Eur. J. Pharmacol.* **338**, 191–197 (1997).
4. Kawasaki, A., Knapp, R.J., Walton, A., Wire, W.S., Zaleska, T., Yamamura, H.I., Porecca, F., Burks, T.F., Hruby, V.J. *Int. J. Peptide Protein Res.* **42**, 411–419 (1993).
5. Arttamangkul, S., Ishmael, J.E., Murray, T.F., Grady, D.K., DeLander, G.E., Kieffer, B.L., Aldrich, J.V. *J. Med. Chem.* **40**, 1211–1218 (1997).

## **C-Terminal Structure-Activity Relationships for the Novel Opioid Peptide JVA-901 (Venorphin)**

**Christy A. Sasiela<sup>1</sup>, Marco A. Bennett<sup>1</sup>, Thomas F. Murray<sup>2</sup>  
and Jane V. Aldrich<sup>1</sup>**

<sup>1</sup>*Department of Pharmaceutical Sciences, University of Maryland School of Pharmacy,  
Baltimore, MD 21201, USA*

<sup>2</sup>*Department of Physiology and Pharmacology, College of Veterinary Medicine,  
University of Georgia, Athens, GA 30602, USA*

### **Introduction**

We previously reported a novel kappa opioid receptor antagonist JVA 901, now named venorphin, which was designed as a chimeric construct of a cobra venom tetrapeptide and [D-Ala<sup>8</sup>]dynorphin A(1-11)NH<sub>2</sub> [1]. The N-terminal region of this new peptide exhibits structure-activity relationships (SAR) distinctly different from that of [D-Ala<sup>8</sup>]dynorphin A(1-11)NH<sub>2</sub> [2]. Herein we explore the SAR of the C-terminal region of venorphin.

<b>Venorphin</b>	Ac-Tyr-Lys-Trp-Trp-Leu-Arg-Arg-D-Ala-Arg-Pro-Lys-NH <sub>2</sub>
<b>Dyn A(1-11)amide</b>	H-Tyr-Gly-Gly-Phe-Leu-Arg-Arg-Ile-Arg-Pro-Lys-NH <sub>2</sub>

### **Results and Discussion**

The peptides were assembled on a PAL-PEG-PS resin using the standard Fmoc synthetic protocol with HBTU as the coupling reagent and were purified to >98% purity by reversed phase HPLC. Radioligand binding assays were performed using cloned opioid receptors expressed in Chinese hamster ovary (CHO) cells [3].

The alanine scan indicates that residue 9 is the most critical C-terminal position for retention of kappa opioid receptor (KOP) affinity, with a 10-fold decrease in affinity for KOP and a concomitant 3-fold decrease in selectivity upon replacement with alanine (Table 1). Interestingly, replacement of the constrained Pro in the native dynorphin A (DynA) sequence with alanine did not affect either affinity or selectivity of venorphin for KOP. The truncation study confirms the importance of residue 9 within venorphin; significant affinity (13-fold relative to the parent peptide) for KOP was lost with removal of this residue. Substitutions have also been incorporated into position 8 of venorphin. Incorporation of Ile, as found in this position of Dyn A, decreased the KOP affinity of the peptide. Incorporation of an additional basic residue, either Lys or Arg, in this position, however, increased affinity relative to the Ile<sup>8</sup> analogue, resulting in peptides with KOP affinity similar to that of venorphin and with slightly higher selectivity for KOP than the parent peptide.

Although based upon the structure of [D-Ala<sup>8</sup>]Dyn A(1-11)NH<sub>2</sub>, venorphin does not possess the same SAR as this peptide. The important residue in the C-terminus of venorphin for KOP affinity is Arg<sup>9</sup>; replacement of this residue in the Ala scan or removal in the truncation study caused a large decrease in affinity for KOP. This residue is not critical for Dyn A binding to KOP [4]. The differences in SAR suggest that the two peptides have different binding modes for KOP. Future work with this peptide and with other Dyn A analogues may further elucidate the binding sites for novel KOP ligands such as venorphin.

Table 1. KOP binding affinity and selectivity ratios for venorphin analogues.

Peptide sequence	Modification	K <sub>i</sub> KOP±SEM (nM)	K <sub>i</sub> ratio KOP/MOP/DOP
Ac-YKWWLRRaRPK-NH <sub>2</sub>	Venorphin	19.8 ± 5.2	1/13/270
Ac-YKWWLRRaAPK-NH <sub>2</sub>	[Ala <sup>9</sup> ]	212 ± 42	1/4.5/>47
Ac-YKWWLRRaRAK-NH <sub>2</sub>	[Ala <sup>10</sup> ]	14.7 ± 1.1	1/24/>680
Ac-YKWWLRRaRP-NH <sub>2</sub>	(1–10)	38.8 ± 2.8	1/18/>260
Ac-YKWWLRRaR-NH <sub>2</sub>	(1–9)	38.9 ± 2.0	1/7.0/>260
Ac-YKWWLRRa-NH <sub>2</sub>	(1–8)	264 ± 32	1/4.2/>38
Ac-YKWWLRRIRPK-NH <sub>2</sub>	[Ile <sup>8</sup> ]	43.5 ± 7.1	1/6.8/100
Ac-YKWWLRRKRPK-NH <sub>2</sub>	[Lys <sup>8</sup> ]	14.0 ± 2.0	1/21/580
Ac-YKWWLRRRRPK-NH <sub>2</sub>	[Arg <sup>8</sup> ]	15.6 ± 3.6	1/27/360

### Acknowledgments

We thank Jennif Chandler and B. Marinda Thomas for performing the binding assays. This work was supported by NIDA grants RO1DA-05195 and F31DA-06049 (C. Sasiela) and by an American Foundation for Pharmaceutical Education Predoctoral Fellowship (C. Sasiela).

### References

1. Wan, Q., Murray, T.F., Aldrich, J.V. *J. Med. Chem.* **42**, 3011–3013 (1999).
2. Aldrich, J.V., Sasiela, C.A., Wan, Q., Murray, T.F., manuscript in preparation.
3. Attamangkul, S., Ishmael, J.E., Murray, T.F., Grandy, D.K., DeLander, G.E., Keiffer, B.L., Aldrich, J.V. *J. Med. Chem.* **40**, 1211 (1997).
4. Turcotte, A., Lalonde, J.M., St. Pirerre, J.M., Lemaire, S. *Int. J. Peptide Protein Res.* **23**, 361–367 (1984).

## **Design and Synthesis of Bifunctional Peptides: Antagonists at CCKA/CCKB Receptors and Agonists at $\mu/\delta$ Opioid Receptors**

**Richard S. Agnes<sup>1</sup>, Yeon Sun Lee<sup>1</sup>, Peg Davis<sup>2</sup>, Shou-Wu Ma<sup>2</sup>,  
Josephine Lai<sup>2</sup>, Frank Porreca<sup>2</sup> and Victor J. Hruby<sup>1</sup>**

<sup>1</sup>*Department of Chemistry, University of Arizona, Tucson, AZ 85721, USA*

<sup>2</sup>*Department of Pharmacology, University of Arizona, Tucson, AZ 85719, USA*

### **Introduction**

Endogenous CCK has been demonstrated to exhibit anti-opioid effects, particularly in the spinal cord [1]. We have hypothesized that the development of novel ligands which possess properties as antagonists at CCK receptors, and as agonists at opioid receptors within the same molecule would present a significant therapeutic advantage in the treatment of pain states refractory to commonly employed opioids such as morphine. Our research has been aimed at the development of ligands that could interact simultaneously and potently with opioid receptors as agonists and with CCK receptors as antagonists.

### **Results and Discussion**

We designed two different types of ligands for binding to opioid and CCK receptors. The first structure was based on overlapping the known opioid and CCK pharmacophores in a single linear peptide. SNF-9007 (Asp-Tyr-D-Phe-Gly-Trp-NMeNle-Asp-Phe-NH<sub>2</sub>) which is a highly potent CCKB and a weak opioid  $\delta$  ligand [2], was modified by removing the N-terminal Asp residue to expose a free N-terminal Tyr, which is a known pharmacophore important for binding to opioid receptors [3]. The other structure added a known CCK pharmacophore to the opioid pharmacophore via a hydrazide linkage. For the opioid agonist, we chose the pharmacophore in the half structure of biphalin (Tyr-D-Ala-Gly-Phe-NH-), which has remarkable efficacy at both  $\delta$  and  $\mu$  opioid receptors [4]. For the CCK antagonist pharmacophore, we chose the C-terminal CCK (30–33) (Trp-Met [or Nle]-Asp-Phe-NH-) with D-Trp instead of L-Trp [5].

**1** Tyr-D-Phe-Gly-Trp-NMeNle-Asp-Phe-NH<sub>2</sub>

**2** Tyr-Gly-Gly-Trp-NMeNle-Asp-Phe-NH<sub>2</sub>

**3** Tyr-D-Ala-Gly-Phe-NH-NH-Phe-Asp-Nle-D-Trp-Boc

The general strategy for the synthesis of the designed analogues was stepwise coupling by SPPS or LPPS. **1** and **2** were prepared by standard SPPS using Fmoc/*t*-Bu chemistry, and **3** by LPPS using Boc/Bzl chemistry in good yields. During the chain elongation in solution of unsymmetrical hydrazide linked peptide **3**, crude peptides were isolated from appropriate solvents to give peptides with high purity.

Compounds **1** and **2** showed higher affinity for both hCCK<sub>B</sub> receptor and  $\delta/\mu$  opioid receptors than SNF-9007 (Table 1). **1–3** showed moderate agonist activities at  $\delta$  opioid receptor, and antagonist activities at CCK receptors (Table 2). In conclusion, it is possible to build agonist function for opioid receptors and antagonist function for CCK receptors in a single structure. Furthermore it is promising that two different pharmacophores can be designed into one structure by rational design.

Table 1. Binding Affinities for the CCK and Opioid Receptor Types.

	hCCK <sub>A</sub> (nM)	hCCK <sub>B</sub> (nM)	hDOR (nM)	rMOR (nM)
	[ <sup>125</sup> I]CCK-8	[ <sup>125</sup> I]CCK-8	[ <sup>3</sup> H]DPDPE	[ <sup>3</sup> H]DAMGO
1	>10000	2.1	6.8	136
2	871	1.3	20.3	612
SNF-9007	n/d <sup>a</sup>	2.1	253	5200
CCK-8 (ns)	n/d <sup>a</sup>	125 <sup>b</sup>	2500 <sup>b,c</sup>	>40000 <sup>b</sup>

<sup>a</sup> n/d: not determined; <sup>b</sup> Binding affinities were measured using guinea pig brain membranes; <sup>c</sup> reference 2

Table 2. Biological activities at mouse vas deferens and guinea pig ileum assays.

	IC <sub>50</sub> GPI agonist <sup>a</sup>	IC <sub>50</sub> GPI agonist <sup>b</sup>	IC <sub>50</sub> MVD (δ) (nM)	Effects in the MVD
1	0%	11 fold	65	ICI sensitive
2	0%	3 fold	297	Slightly ICI sensitive
3	0%	5 fold	24 <sup>c</sup>	ICI sensitive

<sup>a</sup> at 1 μM; <sup>b</sup> 1 μM shift CCK<sub>8</sub>(s); <sup>c</sup> with peptidase inhibitor cocktail 2.137

## Acknowledgments

The financial support from the National Institute of Drug Abuse (DA 12394) is gratefully acknowledged.

## References

1. Noble, F., Roques, B.P. *Progress in Neurobiology* **58**, 349–379 (1999).
2. Slaninova, J., Knapp, R.J., Wu, J., Fang, S.N., Kramer, T., Hruby, V.J., Yamamura, H.I. *Eur. J. Pharmacol.* **200**, 195–198 (1991).
3. Hruby, V.J., Agnes, R.S., *Biopolymers (Peptide Science)* **51**, 391–410 (2000).
4. Horan, P.J., Mattia, A., Bilsky, E.J., Weber, S.J., Davis, T.P., Yamamura, H.I., Malatynska, E., Applyard, S.M., Slaninova, J., Misicka, A., Lipkowski, A.W., Hruby, V.J., Porreca, F. *J. Pharmacol. Ep. Ther.* **265**, 1446–1454 (1993).
5. Horwell, D.C., Beeby, A., Clark, C.R., Hughes, J. *J. Med. Chem.* **30**, 729–732 (1987).

## **Role of the C-Terminal and Central Region of Gastrin for Recognition by the Human CCK<sub>2</sub> Receptor**

**Shawn I. Ahmed, Felice Wibowo, Dmitry S. Gembitsky,  
Richard F. Murphy and Sándor Lovas**

*Department of Biomedical Sciences, Creighton University School of Medicine, Omaha,  
NE 68178, USA*

### **Introduction**

The effects of gastrin are mediated through the cholecystokinin-2 (CCK<sub>2</sub>) receptor, which has been cloned from a number of sources and found to possess an overall amino acid identity of 72% [1]. CD and NMR spectroscopy have identified a  $\beta$ -turn from residues 11-14, which may be important for receptor recognition [2,3]. Structure-activity studies using rodents have shown that the C-terminal Phe is important for agonist activity. Removal of Phe<sup>17</sup> results in peptides that act as antagonists of gastrin-induced acid secretion in rats [4]. Interspecies differences, however, bring into question the relevance of such findings with regard to humans. In the current study, the importance of the C-terminal Phe and putative  $\beta$ -turn of gastrin for binding to the human CCK<sub>2</sub> receptor was examined. The C-terminal heptapeptide [Leu<sup>15</sup>]G(11-17), with the sequence Ala-Tyr-Gly-Trp-Leu-Asp-Phe-NH<sub>2</sub>, was used as the basis for this study. Two sets of analogs were synthesized involving either substitution of Gly<sup>13</sup> with constrained amino acids or removal or replacement of Phe<sup>17</sup> (Table 1). Binding of the peptides to human CCK<sub>2</sub> receptors stably expressed in CHO cells was examined in competition with [<sup>3</sup>H-propionyl]CCK-8. Structures of [Leu<sup>15</sup>]G(11-17), [Pro<sup>13</sup>,Leu<sup>15</sup>]G(11-17), and [Aib<sup>13</sup>,Leu<sup>15</sup>]G(11-17) were simulated by MD using the GROMACS 2.0 package.

### **Results and Discussion**

Table 1 lists the peptides synthesized and their binding affinities. [<sup>3</sup>H]CCK-8 bound in a saturable and displaceable manner with a K<sub>d</sub> of 1.54 nM. Removal of Phe<sup>17</sup> resulted in an analog that did not compete with [<sup>3</sup>H]CCK-8 at concentrations up to 0.1 mM. This shows the importance of the Phe for interaction with the human receptor, whereas corresponding analogs bind to the rat CCK<sub>2</sub> receptor as antagonists [4]. Substitution in the *para*-position of the aromatic ring of Phe<sup>17</sup> did not significantly affect binding. Replacement of Phe<sup>17</sup> with either Tic or D-Phe resulted in a marked decrease in binding affinity. Replacement with either Ala, Abu, Val, or Leu resulted in a loss of affinity. Introduction of the bulkier Cha results in significant affinity, although lower than that of [Leu<sup>15</sup>]G(11-17). Introduction of Trp at position 17 resulted in a peptide with affinity close to that of [Leu<sup>15</sup>]G(11-17).

Replacement of Gly<sup>13</sup> with constrained amino acids is well tolerated. Increasing tendency of [Aib<sup>13</sup>,Leu<sup>15</sup>]G(11-17), [Leu<sup>15</sup>]G(11-17), and [Pro<sup>13</sup>,Leu<sup>15</sup>]G(11-17) to form turn and bend structure at residues 11-14 during the time course of the MD simulation correlated with increasing affinity for the receptor.

The results suggest the presence of a  $\beta$ -turn at residues 11-14 in the active conformation of gastrin. In addition, this study demonstrated the importance of phenylalanine at position 17 of gastrin for binding to the human CCK<sub>2</sub> receptor. Therefore, des-Phe analogs of gastrin would not be appropriate for the development of antagonists for the human CCK<sub>2</sub> receptor.

Table 1. Competition binding results.

Peptide	Log IC <sub>50</sub> ± SEM (n = 3)	K <sub>i</sub> /nM
[Leu <sup>15</sup> ]G17	-7.80 ± 0.03	13
[Pro <sup>13</sup> ,Leu <sup>15</sup> ]G(11-17)	-7.10 ± 0.08	60
Ac[Leu <sup>15</sup> ]G(11-17)	-7.01 ± 0.18	93
[Leu <sup>15</sup> ,p-NH <sub>2</sub> -Phe <sup>17</sup> ]G(11-17)	-7.01 ± 0.22	94
[Leu <sup>15</sup> ,Trp <sup>17</sup> ]G(11-17)	-6.82 ± 0.04	132
[Leu <sup>15</sup> ]G(11-17)	-6.72 ± 0.11	142
[Leu <sup>15</sup> ,p-F-Phe <sup>17</sup> ]G(11-17)	-6.77 ± 0.10	146
Ac[γ-Lac <sup>13</sup> ,Leu <sup>15</sup> ]G(11-17)	-6.69 ± 0.18	153
[Acc <sup>13</sup> ,Leu <sup>15</sup> ]G(11-17)	-6.69 ± 0.09	156
[Leu <sup>15</sup> ,p-Br-Phe <sup>17</sup> ]G(11-17)	-6.68 ± 0.07	157
[Leu <sup>15</sup> ,Tyr <sup>17</sup> ]G(11-17)	-6.43 ± 0.13	279
[Leu <sup>15</sup> ,p-NO <sub>2</sub> -Phe <sup>17</sup> ]G(11-17)	-6.40 ± 0.04	302
[Leu <sup>15</sup> ,p-CH <sub>3</sub> -Phe <sup>17</sup> ]G(11-17)	-6.40 ± 0.01	314
[Aib <sup>13</sup> ,Leu <sup>15</sup> ]G(11-17)	-6.40 ± 0.14	323
[Leu <sup>15</sup> ,p-Cl-Phe <sup>17</sup> ]G(11-17)	-6.40 ± 0.10	352
[Leu <sup>15</sup> ,p-I-Phe <sup>17</sup> ]G(11-17)	-6.29 ± 0.09	381
[Leu <sup>15</sup> ,Cha <sup>17</sup> ]G(11-17)	-6.11 ± 0.07	556
[Leu <sup>15</sup> ,Tic <sup>17</sup> ]G(11-17)	-5.36 ± 0.10	3304
[Leu <sup>15</sup> ,D-Phe <sup>17</sup> ]G(11-17)	-4.59 ± 0.23	19470
Ac[Leu <sup>15</sup> ]G(11-16)NH <sub>2</sub>	–	nb <sup>a</sup>
[Leu <sup>15</sup> ,Ala <sup>17</sup> ]G(11-17)	–	nb
[Leu <sup>15</sup> ,Abu <sup>17</sup> ]G(11-17)	–	nb
[Leu <sup>15</sup> ,Val <sup>17</sup> ]G(11-17)	–	nb
[Leu <sup>15</sup> ,Leu <sup>17</sup> ]G(11-17)	–	nb

<sup>a</sup> nb, no binding.

### Acknowledgments

This work was supported by a grant from the NSF (EPS-9720643) and the Carpenter Endowed Chair in Biochemistry, Creighton University.

### References

1. Noble, J., Wank, S.A., Crawley, J.N., Bradwejn, J., Seroogy, K.B., Hamon, M., Roques, B.P. *Pharmacol. Rev.* **51**, 745–781 (1999).
2. Mammi, S., Goodman, M., Peggion, E., Foffani, M.T., Moroder, L., Wuensch, E. *Int. J. Pept. Protein Res.* **27**, 145–152 (1986).
3. Peggion, E., Foffani, M.T. *Biopolymers* **24**, 647–666 (1985).
4. Martinez, J., Magous, R., Lignon, M.-F., Laur, J., Castro, B., Bali, J.-P. *J. Med. Chem.* **27**, 1597–1601 (1984).

## **Structure and Peptide Binding Specificity of the SH3 and SH2 Domain from a Self-Regulated Protein Tyrosine Kinase – BTK**

**Jya-Wei Cheng, Shiou-Ru Tzeng and Ming-Tao Pai**

*Department of Life Science, National Tsing Hua University, Hsinchu, 300, Taiwan, R.O.C.*

### **Introduction**

The cytoplasmic tyrosine kinase, Bruto's tyrosine kinase (BTK), was found to play a central role in B cell proliferation and differentiation. BTK, along with Tec, Ltk and Atk, belong to a small family of tyrosine kinases (the Tec family) that share common structural features. However, little is known about their biological roles. BTK contains an N-terminal PH domain, an SH2 domain, an SH3 domain and a kinase domain. Mutations or deletions within these domains are responsible for X-linked agammaglobulinemia (XLA), an inherited immunodeficiency disease [1]. The SH3 and SH2 domains are small protein modules that mediate protein-protein interactions and are found in many proteins involved in intracellular signal transduction. It was shown that the BTK SH2 domain is essential for phospholipase C- $\gamma$  phosphorylation; mutations in this domain lead to XLA. Recently, the B-cell linker protein (BLNK, also called SLP-65) was found to interact with the SH2 domain of BTK, and this association is required for the activation of phospholipase C- $\gamma$  [2,3]. However, the molecular basis for the interaction between the BTK SH2 domain and BLNK and the cause of XLA remain unclear. Although the structures of BTK SH3 domain and its complex with proline-rich peptides have been solved by NMR [4,5], little is known about the structure and peptide binding specificity for the SH2 domain of BTK. In order to understand the role of BTK in B cell development, in here, we report the structure and peptide binding specificity of the SH3 and SH2 domains of the self-regulated protein tyrosine kinase – BTK. Our results provide a molecular basis for understanding the role of the BTK SH2 domain in XLA.

### **Results and Discussion**

Songyang *et al.* used a phosphopeptide library to determine the peptide binding specificity of SH2 domains [6]. They have found that one group of the SH2 domains (Src, Fyn, Lck, Abl, Nck, *etc.*) binds preferably with the general motif pTyr-hydrophilic-hydrophilic-hydrophobic, while the other group (PLC- $\gamma$ 1, p85, Shc, and SHPTP2) selects the pTyr-hydrophobic-X-hydrophobic motif. We synthesized several phosphotyrosine-containing peptides according to the specific recognition sequences for Src, Nck, p85 N- and C-terminal, PLC- $\gamma$ 1 N- and C-terminal SH2 domains. We examined the association and dissociation of these phosphopeptides with the BTK SH2 domain using surface plasmon resonance. The dissociation constants ( $K_D$ ) obtained were in the low  $\mu$ M range in accordance with other studies [7]. It can be found from [7] that the BTK SH2 domain binds the phosphopeptides in the order of pYEEI > pYDEP > pYMEM > pYLDL > pYIIP. Thus, the optimal binding sequence for BTK SH2 domain is pTyr-hydrophilic-hydrophilic-hydrophobic.

Based on these results and the amino acid sequences of BLNK, the most possible BTK SH2 domain binding sites in BLNK are predicted to be pYENP (Y72) and pYEPP (Y96). Recently, the Itk SH2 domain (also a Tec family kinase) binding sites in SLP-76 were mapped to be pYESP (Y113), pYESP (Y128) and pYEPP (Y145) using oriented peptide library screening. These possible Itk SH2 domain binding sites in SLP-76 are in accordance with the pYENP and pYEPP sites in BLNK. Also, the bind-

**Cheng et al.**

ing specificity between BTK and BLNK may not only come from the BTK SH2 domain alone. Interestingly, there is also a putative SH3 domain binding site in BLNK and SLP-76 that is adjacent to the Itk and BTK SH2 domain binding site. The presence of adjacent binding sites for Btk SH3 and SH2 domains suggested that BLNK could bind synergistically to the Btk SH3 and SH2 domains. We have successfully cloned and expressed BTK SH3-SH2 dual domain protein. CD experiments indicated that BTK SH3-SH2 dual domain is as stable as BTK SH2 domain. The binding studies on the interactions between BLNK and BTK SH3-SH2 dual domain protein is in progress.

**Acknowledgments**

This work is supported by grants from the National Science Council, ROC (NSC89-2113-M-007-015) and from VTY Joint Research Program, Tsou's Foundation (VTY88-P4-30)..

**References**

1. Vihinen, M., Iwata, T., Kinnon, C., Kwan, S.P., Ochs, H.D., Vorechovsky, I. Smith, C.I.E. *Nucleic Acids Res.* **24**, 160–166 (1996).
2. Hashimoto, S., Iwamatsu, A., Ishiai, M., Okawa, K., Yamadori, T., Matsushita, M., Baba, Y., Kishimoto, T., Kurosaki, T. Tsukada, S. *Blood* **94**, 2357–2364 (1999).
3. Su, Y.W., Zhang, Y., Schweikert, J., Koretzky, G.A., Reth, M., Wienands, J. *Eur. J. Immunol.* **29**, 3702–3711 (1999).
4. Hansson, H., Mattsson, P.T., Allard, P., Haapaniemi, P., Vihinen, M., Smith, C.I., Hard, T. *Biochemistry* **37**, 2912–2924 (1998).
5. Tzeng, S.R., Lou, Y.C., Pai, M.T., Cheng, J.W. *J. Biomol. NMR* **16**, 303–312 (2000).
6. Songyang, Z., Shoelson, S.E., Chaudhari, M., Gish, G., Pawson, T., Haser, W.G., King, F., Roberts, T., Ratnofsky, S., Lechleider, R.J., Neel, B.G., Birge, R.B., Fajardo, E.J., Chou, C.M., Hanafusa, H., Schaffhausen, B., Cantley, L.C. *Cell* **72**, 767–778 (1993).
7. Tzeng, S.R., Pai, M.T., Lung, F.D., Wu, C.W., Roller, P.P., Lei, B., Wei, C.J., Tu, S.C., Chen, S.H., Soong, W.J., Cheng, J.W. *Protein Sci.* **9**, 2377–2385 (2000).

## Pseudoprolines for Studying Bioactive *cis*-Prolyl Conformations

Angela Wittelsberger<sup>1</sup>, Luc Patiny<sup>1</sup>, Jiřina Slaninová<sup>2</sup> and Manfred Mutter<sup>1</sup>

<sup>1</sup>Institute of Organic Chemistry, University of Lausanne, 1015 Lausanne, Switzerland

<sup>2</sup>Institute of Organic Chemistry and Biochemistry, Academy of Sciences of the Czech Republic,  
 166 10 Prague, Czech Republic

### Introduction

*Cis*-prolyl conformations are recently found to play significant roles in recognition processes among proteins. Here, we present several applications in which pseudoprolines ( $\Psi$ Pro) were used to experimentally target hypothetical bioactive *cis* conformations. The pseudoproline 2,2-dimethyl-1,3-thiazolidine-4-carboxylic acid (Cys( $\Psi^{\text{Me,Me}}$ pro), **I**) represents a highly effective *cis*-proline mimic. Its introduction in short model peptides as well as longer bioactive sequences derived from loop and recognition motifs of different proteins showed that it induces a *cis*-content in Xaa<sub>i-1</sub>- $\Psi$ Pro<sub>i</sub> imide bonds of close to 100% [1,2]. On the other hand, the impact of the C2-substituents of  $\Psi$ Pro can be delineated by comparison with unsubstituted analogs (R = H).

### Results and Discussion

For example, new insights into a structure/activity relationship of the peptide hormone oxytocin were obtained. Incorporation of a pseudoproline *cis*-mimic at position 7 of the hormone yielded the analog [Cys( $\Psi^{\text{Me,Me}}$ pro)]<sup>7</sup>oxytocin (**IIa**, Figure 1) that showed a 95% induction of the *cis* peptide bond conformation between Cys<sup>6</sup> and  $\Psi$ Pro<sup>7</sup>, calculated from one- and two-dimensional NMR spectra in water and DMSO. Secondly, the impact of the dimethyl moiety regarding conformation and bioactivity was investigated through the synthesis of the corresponding dihydro compound, [Cys( $\Psi^{\text{H,H}}$ pro)]<sup>7</sup>oxytocin (**IIb**, Figure 1).

Biological tests of the uterotonic activity, the pressor activity, and the binding affinity to the rat and human uterus membrane were carried out with the analogs. As a most significant result, no antagonistic activity was found for the *cis*-constrained analog

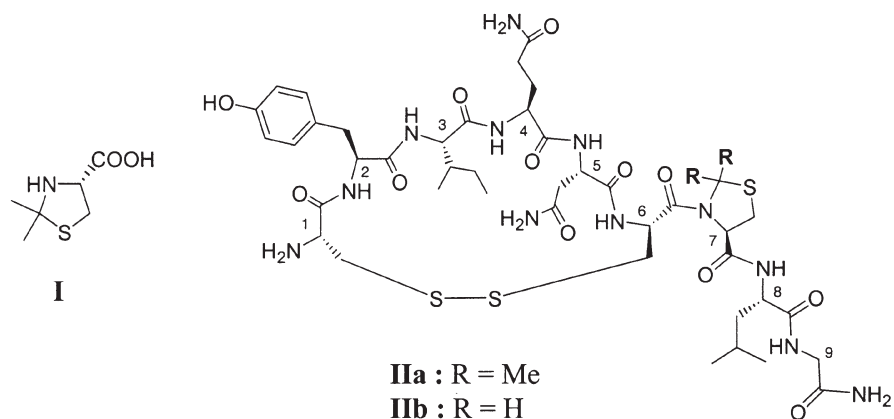


Fig. 1. The novel *cis*-mimic 2,2-dimethyl-1,3-thiazolidine-4-carboxylic acid ( $\Psi$ Pro, **I**) and the  $\Psi$ Pro-containing oxytocin analogs **IIa** and **IIb**.

**IIa**, indicating that a *cis* conformation between residues 6 and 7 of the molecule is not decisive for antagonistic activity, as might have been suggested from recent results in the literature [3]. However, the about 10-fold reduction in agonistic activity of [Cys( $\Psi^{\text{Me,Me}}$ pro)]<sup>7</sup>oxytocin (**IIa**) compared to oxytocin itself is consistent with the reduction of the *trans* conformation from 90% for oxytocin to 5% for compound **IIa** (Table 1). In contrast to the reduced oxytocin activity, compound **IIa** kept a high binding affinity for the uterus membrane, with  $K_i$  values of 8.0 nM and 0.9 nM for the rat and the human uterus receptor, respectively (Table 1).

Table 1. Biological activities obtained for the oxytocin analogs **IIa** and **IIb**.

Compound	Cis-content in water (%)	Oxytocic activity (IU/mg)	Vasopressic activity (IU/mg)	$K_i$ to uterus membrane (nM)	
				Rat	Human
[Cys( $\Psi^{\text{Me,Me}}$ pro)] <sup>7</sup> OT ( <b>IIa</b> )	95	31.8±2.0	0	8.0	0.88
[Cys( $\Psi^{\text{H,H}}$ pro)] <sup>7</sup> OT ( <b>IIb</b> )	6–7	1010±88	2.4±0.4	1.5	0.066
Oxytocin (OT)	10	450	5	3.7	1.4

Comparison of the biological activities of **IIa**, **IIb**, and oxytocin itself, and relation to the *cis*-contents obtained from NMR analysis allowed to draw new conclusions regarding the *cis/trans* conformational impact of the Cys<sup>6</sup>-Pro<sup>7</sup> peptide bond.

#### Acknowledgments

We thank Dr. Claude Barberis for testing our analogs for their binding affinity to the human uterus membrane receptor. This work was supported by the Swiss National Science Foundation.

#### References

1. Dumy, P., Keller, M., Ryan, D.E., Rohwedder, B., Wöhr, T., Mutter, M. *J. Am. Chem. Soc.* **119**, 918–925 (1997).
2. Wittelsberger, A., Keller, M., Scarpellino, L., Patiny, L., Acha-Orbea, H., Mutter, M. *Angew. Chem., Int. Ed.* **39**, 6, 1111–1115 (2000).
3. Belec, L., Slaninova, J., Lubell, W.D. *J. Med. Chem.* **43**, 1448–1455 (2000).

## Design of Oxytocin Antagonists Which Are More Selective than Atosiban in Rat Bioassays and in Human Receptor Assays

Stoytcho Stoev<sup>1</sup>, Ling Ling Cheng<sup>1</sup>, Maurice Manning<sup>1</sup>, N. C. Wo<sup>2</sup>,  
 W. Y. Chan<sup>2</sup>, Thierry Durroux<sup>3</sup> and Claude Barberis<sup>3</sup>

<sup>1</sup>Department of Biochemistry and Molecular Biology, Medical College of Ohio, Toledo, OH 43614, USA

<sup>2</sup>Department of Pharmacology, Cornell University Medical College, New York, NY 10021, USA

<sup>3</sup>INSERM U469 Endocrinologie moléculaire: Signalisation cellulaire et pathologie,  
 Montpellier, France

### Introduction

Preterm birth is the single largest cause of neonatal morbidity and death [1]. Oxytocin antagonists have been extensively studied as possible therapeutic agents for the treatment of premature labor [2]. The oxytocin antagonist (OTA) atosiban ([1-deamino, D-Tyr(Et)<sup>2</sup>,Thr<sup>4</sup>]OVT) has been shown to be an effective tocolytic for the treatment of pre-term labor [3]. Atosiban is in fact the only OTA (peptide or nonpeptide) approved for clinical use (in Europe) [4]. Atosiban is however far from an ideal OTA. It is highly nonselective for OT receptors *versus* vasopressin (VP) V<sub>1a</sub> receptors. In the rat it is only 8 times more potent as an OTA than as a V<sub>1a</sub> antagonist *in vivo* [5]. However, in humans its affinity for V<sub>1a</sub> receptors is 100 times greater than for OT receptors [6]. It is thus a strikingly more potent V<sub>1a</sub> antagonist than an OTA in humans. We have shown that V<sub>1a</sub> antagonism is an undesirable side effect in OTAs [7]. Here we report the synthesis and some pharmacological properties of the following six L-Thi<sup>2</sup>/D-Thi<sup>2</sup> (where Thi = β-thienylalanine) OTAs: **1** d(CH<sub>2</sub>)<sub>5</sub>[Thi<sup>2</sup>,Thr<sup>4</sup>,Tyr-NH<sub>2</sub><sup>9</sup>]OVT, **2** d(CH<sub>2</sub>)<sub>5</sub>[D-Thi<sup>2</sup>,Thr<sup>4</sup>,Tyr-NH<sub>2</sub><sup>9</sup>]OVT, **3** d(CH<sub>2</sub>)<sub>5</sub>[Thi<sup>2</sup>,Thr<sup>4</sup>,Eda<sup>9</sup>]OVT, **4** d(CH<sub>2</sub>)<sub>5</sub>[D-Thi<sup>2</sup>,Thr<sup>4</sup>,Eda<sup>9</sup>]OVT, **5** d(CH<sub>2</sub>)<sub>5</sub>[Thi<sup>2</sup>,Thr<sup>4</sup>,Eda<sup>9</sup>←Tyr<sup>10</sup>]OVT, **6** d(CH<sub>2</sub>)<sub>5</sub>[D-Thi<sup>2</sup>,Thr<sup>4</sup>,Eda<sup>9</sup>←Tyr<sup>10</sup>]OVT; all of which are more selective than atosiban in rat bioassays and in human receptor assays.

Table 1. L- and D-Thi<sup>2</sup> OT antagonists (1–6) are more selective than Atosiban in rat bioassays and in human receptor assays.

Peptide <sup>c</sup>	Anti-OT In vivo	Anti-V <sub>1a</sub>	Anti-OT selec- tivity	Selec- tivity vs Atosiban	hOTR	hV <sub>1a</sub> R	hReceptor selectivity	hReceptor selectivity vs Atosiban
	ED <sup>a</sup>	ED <sup>a</sup>	ED ratio <sup>b</sup>		Ki (nM)	Ki (nM)	V <sub>1a</sub> R/OTR	
Atosiban	5.95	48.5	8	1	41	0.40	0.01	1
1	8.18	~700	~82	10.2	–	–	–	–
2	4.55	~700	~147	18.4	28.6	104	3.6	360
3	8.41	~700	~83	10.4	599	416	0.7	70
4	10.3	112.8	11	1.4	–	–	–	–
5	12.1	375.7	31	3.9	–	–	–	–
6	6.34	269	42	5.3	70.7	224	3.2	320

<sup>a</sup> The effective dose (ED) is defined as the dose (in nanomoles/kilogram) of antagonist that reduces the response to 2× units of agonist administered in the absence of antagonist; <sup>b</sup> ED ratio = antivasopressor ED/antioxytocic ED; <sup>c</sup> For structures see text.

### Results and Discussion

The pharmacological properties in the rat bioassays and in human OT receptor binding assays of the six new OTAs and those of atosiban are presented in Table 1. All six new OTAs exhibit *in vivo* anti-OT activity, as measured by their effective doses (EDs), in the same range as atosiban. All however exhibit significantly diminished anti-V<sub>1a</sub> potencies (EDs) compared to atosiban. Thus they exhibit gains in anti-OT/anti-V<sub>1a</sub> selectivity in the rat of 1.4 to 18.4. With a K<sub>i</sub> = 28.6 nM, OTA 2 possess a higher affinity for the human OT receptor than atosiban (K<sub>i</sub> = 41 nM). Peptides **2**, **3**, and **6** exhibit significantly lower affinities for the human V<sub>1a</sub> receptor than atosiban. (K<sub>i</sub> = 0.40 nM) and thus exhibit striking gains of 360, 70 and 320 in hOTR/hV<sub>1a</sub>R selectivity compared to atosiban. Since peptide **2** is both a more potent and more selective OTA than atosiban, it clearly possesses a much safer pharmacological profile as a tocolytic agent than atosiban.

These findings offer promising clues for the design of more potent and selective OTAs for development as potential tocolytic agents for the prevention of premature labor.

### Acknowledgments

We thank Ms Suzanne Payne for expert help in the preparation of this manuscript and NIH Grant GM-25280.

### References

1. Adams, M.M. *JAMA* **273**, 730–740 (1995).
2. Goodwin, T.M., Zograbyan, A. *Emerging Concepts in Perinatal Endocrinology* **25**, 859–871 (1998).
3. Romero, R., Sibai, B.M., Sanches-Ramos, L., Valenzuela, G.J., Veille, J-C., Tabor, B., Perry, K.G., Varner, M., Murphy, G., Lane, R., Smith, J., Shangold, G., Creasy, G.V. *Am. J. Obstet. Gynecol.* **182**, 1173–1183 (2000).
4. *Pharm. J.* **264**, 7–100, 871 (2000).
5. Manning, M., Miteva, K., Pancheva, S., Stoev, S., Wo, N.C., Chan, W.Y. *Int. J. Pept. Protein Res.* **46**, 244–252 (1995).
6. Barberis, C., Morin, D., Durroux, T., Mouillac, B., Guillon, G., Hibert, M., Tribollet, E., Manning, M. *Drug News Persp.* **12**, 279–292 (1999).
7. Chan, W.Y., Wo, N.C., Manning, M. *Am. J. Obstet. Gynecol.* **175**, 1331–1335 (1996).

## Highly Selective Cyclic Peptides for Human Melanocortin-4 Receptor (MC-4 R): Design, Synthesis, Bioactive Conformation, and Pharmacological Evaluation as an Anti-Obesity Agent

Waleed Danho, Joseph Swistok, Adrian Cheung, Xin-Jie Chu, Yao Wang, Li Chen, David Bartkovitz, Vijay Gore, Lida Qi, David Fry, David Greeley, Hongmao Sun, Jeanmarie Guenot, Lucia Franco, Grazyna Kurylko, Leonid Rumennik and Keith Yagaloff

*Roche Research Center, Hoffmann-La Roche Inc. Nutley, NJ 07110, USA*

### Introduction

Melanocortin (MC) peptides  $\alpha$ -,  $\beta$ -, and  $\gamma$ -MSH and adreno-corticotrophic hormone (ACTH) are a group of neuropeptides derived from pro-opiomelanocortin hormone (POMC). The physiological actions of these peptides are mediated through five (MCR-1-5) seven-transmembrane G-protein-coupled receptor subtypes. The MSH peptides have been implicated in numerous biological functions [1] including regulation of skin pigmentation, regulation of steroid production, modulation of the immune response, thermo-regulation and obesity [2]. Clarification of the role of melanocortin receptor subtypes, in particular the recently discovered MC-3, MC-4 and MC-5 receptors, has been hampered by the lack of selective peptide ligands. However, recent studies on MCR knockout animals demonstrated that the MC-4 receptor is involved in regulation of feeding. MCR-4 knockout mice display an obesity phenotype that includes maturity onset obesity, hyperglycemia, and hyperinsulinemia. Moreover, it has been reported that a *non-selective* cyclic MCR-4 peptide agonist (MT II) inhibits food intake when given *icv* to mice [3]. Consequently, a potent and *selective* MC-4R agonist is regarded as potentially useful in therapeutic approaches to obesity management. The goal of this work was to identify a selective MCR-4 cyclic peptide agonist for use as a pharmacological tool in obesity and feeding studies and to develop a pharmacophore model applicable to structure-based drug design.

### Results and Discussion

Extensive structure-activity studies on the cyclic peptide MT II [Ac-Nle-cyclo-(Asp-Lys)(Asp-His-(D)Phe-Arg-Trp-Lys)-NH<sub>2</sub>] suggest that the [His-(D)Phe-Arg-Trp] is regarded as an "active site" essential to the interaction of the ligand with its receptors [4]. Our more detailed structure-activity studies on MT II identified that the side chains of the aromatic residues (D)Phe and Trp are critical for the binding of MT II and agonist activity, but the basic hydrophilic residues His and Arg are less important. Since our first goal was to identify a selective MC-4 R peptide agonist, we systematically replaced each of the four "core amino acids" with conformationally constrained amino acids and evaluated the analogs in binding and intercellular cAMP assays at the human MC-1, MC-3, MC-4 and MC-5 receptors. The results of this detailed structure-activity evaluation demonstrated that the amino acid position occupied by *His* is the most critical position responsible for the selectivity of MC-4 *versus* the other MC-receptors. Replacement of His with conformationally constrained 2-Aminotetraline-2-carboxylic acid (Atc) and the novel amino acids 1-Amino-4-phenylcyclohexane-carboxylic acid (APC) and 4-Aminophenylpiperidine-4-carboxylic acid (APPC) (Figure 1) resulted in highly MC-4 selective peptides (Table 1).

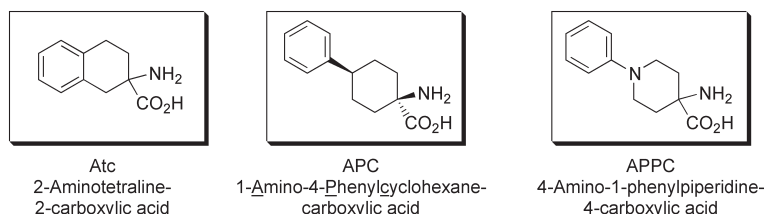


Fig. 1. Structures of Atc, APC and APPC.

Table 1. MC-4 selective peptides.

Compound	MC-4 Agonist nM	MC-1 Agonist nM	MC-3 Agonist nM	MC-5 Agonist nM
Ac-Nle-cyclo(D-K)-Asp-His-(D)Phe-Arg-Trp-Lys-NH <sub>2</sub> (MT II) <sup>a</sup>	0.6	0.6	25	25
Penta-cyclo(D-K)-Asp-His-(D)Phe-Arg-Trp-Lys-NH <sub>2</sub>	0.9	0.4	25	25
Penta-cyclo(D-K)-Asp-(D,L)Atc-(D)Phe-Arg-Trp-Lys-NH <sub>2</sub>	65	903	999.999	51% <sup>b</sup>
Penta-cyclo(D-K)-Asp-5-Br(D)Atc-(D)Phe-Arg-Trp-Lys-NH <sub>2</sub>	41	772 (PA) <sup>c</sup>	999.999	75%
Penta-cyclo(D-K)-Asp-5-Br(L)Atc-(D)Phe-Arg-Trp-Lys-NH <sub>2</sub>	15	1289 (PA)	1752 (PA)	85%
Penta-cyclo(D-K)-Asp-5-Cl(D)Atc-(D)Phe-Arg-Trp-Lys-NH <sub>2</sub>	40	1366 (PA)	999.999	38%
Penta-cyclo(D-K)-Asp-5-Cl(L)Atc-(D)Phe-Arg-Trp-Lys-NH <sub>2</sub>	4	2130 (PA)	25%	75%
Penta-cyclo(D-K)-Asp-5-MeO(D,L)Atc-(D)Phe-Arg-Trp-Lys-NH <sub>2</sub>	5	737	30%	462
Penta-cyclo(D-K)-Asp- <i>cis</i> Apc-(D)Phe-Arg-Trp-Lys-NH <sub>2</sub>	9	654	55 (PA)	805
Penta-cyclo(D-K)-Asp- <i>trans</i> Apc-(D)Phe-Arg-Trp-Lys-NH <sub>2</sub>	757	349	ND <sup>d</sup>	ND
Penta-cyclo(D-K)-Asp-4-MeOApc-(D)Phe-Arg-Trp-Lys-NH <sub>2</sub>	8.4	999.999	30%	54%
Penta-cyclo(D-K)-Asp-4-EtO Apc-(D)Phe-Arg-Trp-Lys-NH <sub>2</sub>	20	999.999	31%	57%
Penta-cyclo(D-K)-Asp-4-Me Apc-(D)Phe-Arg-Trp-Lys-NH <sub>2</sub>	2.2	796	ND <sup>e</sup>	ND
Penta-cyclo(D-K)-Asp-3-Me Apc-(D)Phe-Arg-Trp-Lys-NH <sub>2</sub>	1.5	76	ND	ND
Penta-cyclo(D-K)-Asp-4-Cl Apc-(D)Phe-Arg-Trp-Lys-NH <sub>2</sub>	2.2	796	ND	ND
Penta-cyclo(D-K)-Asp-Apc-(D)Phe-Ala-Trp-Lys-NH <sub>2</sub>	213	70%	32%	999.999
Penta-cyclo(D-K)-Asp-Apc-(D)Phe-Cit-Trp-Lys-NH <sub>2</sub>	23	999.999	26%	23%
Penta-cyclo(D-K)-Asp-Apc-(D)Phe-Arg-(2 <i>S</i> ,3 <i>S</i> )β- <i>methyl</i> Trp-Lys-NH <sub>2</sub>	11	700	ND	ND
Penta-cyclo(D-K)-Asp-Appc-(D)Phe-Arg-Trp-Lys-NH <sub>2</sub>	3.6	268	442	470
Penta-cyclo(D-K)-Asp-4-Me Appc-(D)Phe-Arg-Trp-Lys-NH <sub>2</sub>	6.3	770	61%	118
Penta-cyclo(D-K)-Asp-4-PhO Appc-(D)Phe-Arg-Trp-Lys-NH <sub>2</sub>	7	803 (PA)	50	600

<sup>a</sup> The linear peptides were synthesized by solid phase peptide synthesis and purified by HPLC. The cyclization was carried out in solution (DMF) using (Benzotriazole-1-yl-oxy) tris(dimethylamino)phosphonium hexafluorophosphate [BOP] as coupling reagent. The cyclic peptides were purified by HPLC and characterized by LC/MS. <sup>b</sup> [% stimulation at 50 μM.]

<sup>c</sup> PA = Partial Agonist, <sup>d</sup> ND = Not determined.

Our second goal was to determine the three-dimensional conformations of selected cyclic peptides in DMSO by NMR using established procedures of constrained molecular dynamics calculations incorporating NOE-derived interproton distances. For the backbone, a correlation was discovered between high potency and the presence of a β turn at positions corresponding to Asp-His-(D)Phe-Arg in the parent sequence. For the side chains, optimal positions for potency and selectivity were discerned by examining peptides containing constrained amino acid derivatives. At the His position, the APC replacement was found to be quite rigid, locked into a single conformation, that appar-

ently confers selectivity by providing a non-adjustable protrusion which is compatible only with the MC-4 receptor binding site and not with the others. At the Trp position, methyl substitutions on the beta carbon were found to rigidify the position of the side chain, with the (2*S*,3*S*) configuration being the most favorable for activity. The conformation of the most rigid peptide Penta-cyclo(D-K)-Asp-Apc-(D)Phe-Arg-(2*S*,3*S*)β-methylTrp-Lys-NH<sub>2</sub> is shown in Figure 2.

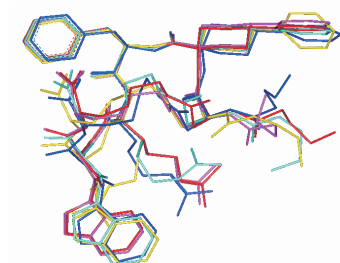


Fig. 2. Structure of Penta-cyclo(D-K)-Asp-Apc-(D)Phe-Arg-(2*S*,3*S*)β-methylTrp-Lys-NH<sub>2</sub> determined by NMR. A superposition of five calculated low energy structures is shown.

Our third goal was to determine the *in vivo* efficacy of the cyclic peptides. IP administration of MC-4 agonist peptide, Penta-cyclo(D-K)-Asp-Apc-(D) Phe-Arg-Trp-Lys-NH<sub>2</sub> causes reduction in food intake in *ob/ob* mice (Figure 3A), an effect not observed in MC-4 KO mice (Figure 3B). Moreover chronic IP or IN administration of this peptide in *ob/ob* mice over 37 days resulted in a 10% reduction of body weight.

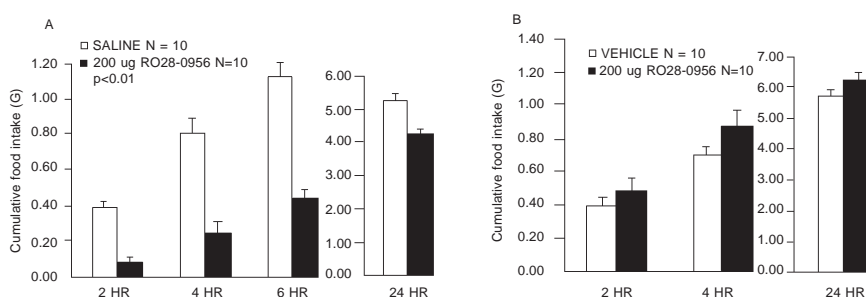


Fig. 3. Effect of: Penta-cyclo(D-K)-Asp-Apc-(D)Phe-Arg-Trp-Lys-NH<sub>2</sub> on food intake in (A) *ob/ob* mice and (B) MC-4 R KO mice.

In conclusion, we have identified potent, highly selective MC-4 cyclic peptides. Their bioactive conformation was determined, and their *in vivo* efficacy in *ob/ob* mice was established.

## References

1. Hruby, V.J., Wilkes, B.C., Cody, W.L., Sawyer, T.K., Hadley, M.E. *Pept. Protein Rev.* **3**, 1–64 (1984).
2. Lu, D., Willard, D., Patel, I.R., Kadwell, S., Overton, L., Kost, T., Luther, M., Chen, W., Yowchik, R.P., Wilkison, W.O., Cone, R.D. *Nature* **385**, 799–802 (1997).
3. Fan, W., Boston, B.A., Kesterson, R.A., Hruby, V.J., Cone, R. *Nature* **385**, 165–168 (1997).
4. Al-Obeidi, F., de L. Castrucci, A.M., Hadley, M.E., Hruby, V.J. *J. Med. Chem.* **32**, 2555–2561 (1998).

## **SAR of Melanin-concentration Hormone (MCH), an Important Regulatory Hormone in Feeding Behavior**

**Waleed Danho, Joseph Swistok, Wajiha Khan, Theresa Truitt,  
Anthony Aglione, Ralph Garippa, Kui Xu, Yingsi Chen, Qing Xiang,  
Jarema Kochan and Fiorenza Falcioni**

*Roche Research Center, Hoffmann-La Roche Inc. Nutley, NJ 07110, USA*

### **Introduction**

Melanin-concentrating hormone is a cyclic hypothalamic neuropeptide [NH<sub>2</sub>-Asp-Phe-Asp-Met-Leu-Arg-Cys-Met-Leu-Gly-Arg-Val-Tyr-Arg-Pro-Cys-Trp-Gln-Val-COOH cyclo Cys-Cys (7-16)] that was first characterized in *chum* salmon pituitary as a hormone responsible for color changes in response to environmental stimuli [1]. In mammals, MCH appears to have evolved into an important regulatory hormone in feeding behavior [2]. The MCH peptide is expressed in the hypothalamus, a region involved in energy balance and food intake. In the hypothalamus, MCH mRNA is overexpressed and upregulated during fasting in ob/ob mice and rats. Intra-cerebroventricular injections of MCH promote feeding in mice and rats. Transgenic mice (Tg) lacking the MCH gene are lean and hypophagic, while Tg mice overexpressing MCH in the hypothalamus are hyperphagic, obese, and insulin resistant. Consequently, a potent MCH antagonist is regarded as potentially useful in therapeutic approaches to obesity management. Efforts to identify the ligands for orphan GPCRs have recently led to the discovery of the receptor for MCH [3,4]. Receptor cloning and identification of functional assays for MCHR1 receptor allow the study of receptor/ligand interaction. One possible strategy consists of chemical modifications of the natural ligand (MCH) including: N- and C-termini truncations, Ala substitutions, D-amino acid replacements, and ring size variations, with the goal to identify the critical amino acid residues responsible for agonist or antagonist activity. Here, we describe a detailed SAR of MCH peptides on MCHR1.

### **Results and Discussion**

A total of 50 analogues were synthesized by solid phase peptide synthesis. All peptides were used as tools to establish the MCH/MCH-R1 relationship both as agonist or antagonist. Competition binding assays were used to determine the IC<sub>50</sub> values for MCH and analogues at the receptor. The peptide analogues were also tested in a functional cell based assay (calcium release measurement using FLIPR technology) for their ability to function as agonist or antagonist of the MCH receptor. Truncations at either the carboxyl or amino terminus resulted in no loss in agonist activity, indicating that Trp-Gln-Val-OH (position 16-19) and H-Asp-Phe-Asp-Met-Leu (position 1-5) were not essential for full agonist activity. The minimum peptide analog retaining the agonist activity is (6-16) Arg-cyclo (Cys7-Cys16) (Arg-Cys-Met-Leu-Gly-Arg-Val-Tyr-Arg-Pro-Cys). The Ala-scan of MCH indicates a mandatory side chain at Arg 11, Tyr 13 and to a lesser extent at Met 8 and Arg 6 for agonist activity. The replacement of other amino acids by Ala did not abolish the biological activity, suggesting the importance of Met 8, Arg 11, Tyr 13, for agonist activity within the ring structure of MCH (8-15). The (D) amino acid scan of MCH indicates that inversion of the chirality of the amino acids Met 8, Leu 9, Arg 11, Val 12, Tyr 13 Arg 14 and Pro 15 resulted in loss of agonist activity, suggesting the importance of chirality of the amino acids within the ring structure of MCH (8-15).

### Biologically Active Peptides

The presence of the cyclic structure (cyclo 7-16) is critical for agonist activity since the linear analogue of MCH, in which both Cys residues were replaced by Ser was not active. Attempts to reduce the number of amino acids in the (7-16) ring resulted in inactive analogues, suggesting the importance of the cyclic structure of (7-16) for agonist/antagonist activity. Table 1 summarizes the Ala and (D) scan within the core sequence (8-15) of MCH.

Table 1. Ala and (D) substitution of the MCH-Core sequence: [(Cys-Cys) (7-16) (Met-Leu-Gly-Arg-Val-Tyr-Arg-Pro) (8-15)]

Cmpound	Ala substitution EC <sub>50</sub> nM	(D) substitution IC <sub>50</sub> nM
H-Cys- <b>Met</b> -Leu-Gly Arg-Val-Tyr-Arg-Pro-Cys	P. agonist	Inactive
H-Cys-Met- <b>Leu</b> -Gly Arg-Val-Tyr-Arg-Pro-Cys	Agonist (303 nM)	Antagonist (2200 nM)
H-Cys-Met-Leu- <b>Gly</b> Arg-Val-Tyr-Arg-Pro-Cys	Agonist (573 nM)	
H-Cys-Met-Leu-Gly <b>Arg</b> -Val-Tyr-Arg-Pro-Cys	Inactive	Antagonist (740 nM)
H-Cys-Met-Leu-Gly Arg- <b>Val</b> -Tyr-Arg-Pro-Cys	Agonist (630 nM)	Antagonist (1620 nM)
H-Cys-Met-Leu-Gly Arg-Val- <b>Tyr</b> -Arg-Pro-Cys	Inactive	P. agonist (1150 nM)
H-Cys-Met-Leu-Gly Arg-Val-Tyr- <b>Arg</b> -Pro-Cys	Agonist (305 nM)	Antagonist (1520 nM)
H-Cys-Met-Leu-Gly Arg-Val-Tyr-Arg- <b>Pro</b> -Cys	Agonist (351 nM)	Antagonist (2000 nM)

In conclusion, we have identified the amino acid residues important for agonist/antagonist activity of the MCH peptide on MCHR1. Exploitation of this information should open the way for the design of more potent MCH peptide antagonists.

### References

1. Kawauchi, H., Kawazoe, I., Tsubokawa, M., Kishida, M., Baker, B.I. *Nature* **305**, 321–323 (1983).
2. Tritos, N.A., Maratos-Flier, E. *Neuropeptides* **33**, 339–349 (1999).
3. Chambers, J., Ames, R.S., Bergsma, D., Muir, A., Fitzgerald, L.R., Hervieu, G., Dytko, G.M., Foley, J., Martin, J., Liu, W.S., Park, J., Ellis, C., Ganguly, S., Konchar S., Cluderay, J., Leslie, R; Wilson, S., Sarau, H.M. *Nature* **400**, 261–265 (1999).
4. Saito, Y., Nothacker, H.P., Wang, Z., Lin, S.H.S., Leslie, F., Civelli, O. *Nature* **400**, 265–269 (1999).

## Structure-Activity Relationship Studies (SAR) of Melanocortin Agonists Central His-Phe-Arg-Trp Sequence

Jerry Ryan Holder, Rayna M. Bauzo, Zhimin Xiang  
and Carrie Haskell-Luevano

*University of Florida, Department of Medicinal Chemistry, Gainesville, FL 32610, USA*

### Introduction

Obesity and obesity related diseases affect millions of people in the United States and other countries. The melanocortin (MC) system contains genetic factors that have been demonstrated to be involved in obesity. The melanocortin receptor system is a GPCR pathway that consist of five receptor subtypes (MC1R-MC5R). The MC4 receptor subtype is expressed in the brain and is involved in the regulation of energy homeostasis and feeding behavior [1]. The endogenous melanocortin agonists are derived from posttranslational processing of the POMC gene transcript, and contain the central His-Phe-Arg-Trp sequence [2]. The His<sup>6</sup>-Phe<sup>7</sup>-Arg<sup>8</sup>-Trp<sup>9</sup> ( $\alpha$ -MSH numbering) sequence is the minimal sequence required for activity at the MC4R [2]. To further investigate the role of the His-Phe-Arg-Trp amino acids in receptor activity, 60 positionally modified tetrapeptides were synthesized, purified and characterized at the mouse MC4R [3,4].

### Results and Discussion

The SAR and Alanine scanning studies of the MC agonists His-Phe-Arg-Trp sequence has further validated the importance of these amino acid residues in activity at the MC4R. Substitution of the four A.A. residues with alanine resulted in decreased activity (Table 1). The chirality of positions 6, 7 and 9 was determined to be important for activity at the MC4R. At the 6 and 9 positions amino acids with L-chirality had decreased EC<sub>50</sub> values compared with the corresponding D-isomers. Amino acids in the 7 position had lower EC<sub>50</sub> values when the D-isomers were used in place of the L-isomers. The Arg<sup>8</sup> residue was determined to have a critical role in MC4R activity.

Peptide synthesis was performed using standard Fmoc methodology on an automated synthesizer (Advanced ChemTech 440MOS, Louisville, KY). The peptides were assembled on Rink-amide-MBHA resin (Peptides International). All reagents were ACS grade or better. The crude peptide yields ranged from 60 to 90% of the theoretical yields. The purified peptide was >95% pure as determined by analytical RP-HPLC

*Table 1. Functional activity of Ac-His-Phe-Arg-Trp-NH<sub>2</sub> tetrapeptide analogues.*

Peptide	Sequence	EC <sub>50</sub> (nM)	Fold difference
1	Ac- <b>His</b> -DPhe-Arg-Trp-NH <sub>2</sub>	15 ± 3.2	1.0
2	Ac-His- <b>Phe</b> -Arg-Trp-NH <sub>2</sub>	2100 ± 380	140
3	Ac- <b>Ala</b> -DPhe-Arg-Trp-NH <sub>2</sub>	750 ± 64	50
4	Ac-His- <b>Ala</b> -Arg-Trp-NH <sub>2</sub>	NR*	
5	Ac-His-DPhe- <b>Ala</b> -Trp-NH <sub>2</sub>	23000 ± 4000	2500
6	Ac-His-DPhe-Arg- <b>Ala</b> -NH <sub>2</sub>	NR*	

*The indicated errors represent the standard error of the mean determined from at least three independent experiments. \* Indicates no agonist or antagonist activity was observed.*

and had the correct molecular mass (University of Florida protein core facility). Peptides were pharmacologically characterized using stable cell lines expressing mouse MC4R. The functional bioassay is a 96-well colorimetric CRE- $\beta$ -galactosidase reporter gene assay and data was collected in at least three independent experiments.

#### **Acknowledgments**

Supported by NIH grant R01DK57080, and CHL is a recipient of a Burroughs Wellcome Fund Career Award in the Biomedical Sciences

#### **References**

1. Huszar, D., Lynch, C.A., Fairchild-Huntress, V., Dunmore, J.H., Smith, F.J., Kesterson, R.A., Boston, B.A., Fang, Q., Berkemeir, L.R., Gu, W., Cone, R.D., Campfield, L.A., Lee, F. *Cell* **88**, 131–141 (1997).
2. Haskell-Luevano, C., Holder, J.R., Monck, E.K., Bauzo, R.M. *J. Med. Chem.* **44**, 2247–2252 (2001).
3. Yang, Y., Fong, T.M., Dickinson, C.J., Mao, C., Li, J.Y., Tota, M.R., Mosley, R., Van Der Ploeg, L.H., Gantz, I. *Biochemistry* **39**, 14900–14911 (2000).
4. Haskell-Luevano, C., Cone, R.D., Monck, E.M., Wan, Y.-P. *Biochemistry* **40**, 6164–6179 (2001).

## The Development of a Novel Highly Selective and Potent Agonist for Human Melanocortin 4 Receptor

Malcolm Kavarana, M. Cai, D. Trivedi, G. Han and Victor J. Hruby

Department of Chemistry, 1306 University Blvd., University of Arizona, Tucson, AZ 85721, USA

### Introduction

$\alpha$ -,  $\beta$ -, and  $\gamma$ -MSH, along with adrenocorticotrophic hormones form a group of endogenous neuropeptides that regulate several key biological functions *via* five melanocortin (MC1R-MC5R) seven transmembrane G-protein coupled receptors (GPCR). Recent studies have indicated that in humans, the MC4R plays an important role in controlling feeding behavior and energy homeostasis [1,2]. These studies have further shown that agonists at hMC4R promote a feeling of satiety, while antagonists induce feeding. Thus selective agonists at this receptor could find therapeutic applications as anti-obesity drugs. This work discusses the development of the first highly selective and potent agonist MK-1 ( $c[(O)C-CH_2-CH_2-C(O)-His^6-D-Phe^7-Arg^8-Trp^9-Lys^{10}]-NH_2$ ), at the human MC4 receptor *versus* the other three hMCR's (hMC1, hMC3 and hMC5) respectively.

### Results and Discussion

Peptide MK-1 is a modified cyclic lactam analogue of the potent but non-selective agonist MT-II, [(Ac-Nle<sup>4</sup>-cyclo(5 $\beta$ →10 $\epsilon$ )(Asp<sup>5</sup>-His<sup>6</sup>-D-Phe<sup>7</sup>-Arg<sup>8</sup>-Trp<sup>9</sup>-Lys<sup>10</sup>)-amide]. MK-1 has the same message sequence as MT-II; however, unlike MT-II, cyclization in MK-1 is *via* a succinyl linker between the  $\alpha$ -amino group of histidine at the N-terminus and the  $\epsilon$ -amino group of lysine at the C-terminus.

*Binding studies:* *In-vitro* competitive binding studies indicate that MK-1 binds to hMC4R with an IC<sub>50</sub> value comparable to MT-II (Table I). These studies also showed that MK-1 was  $\approx$ 700-fold more selective at the hMC4R than at hMC1R (hMC4R IC<sub>50</sub> MK-1 = 5.96 nM and hMC1R IC<sub>50</sub> MK-1 = 4200 nM) and 50-120-fold more selective at hMC4R *versus* hMC3 and hMC5 receptors, respectively (Table II). However, the IC<sub>50</sub> values for MT-II at all four receptors is nearly the same. Substituting Arg<sup>8</sup>, D-Phe<sup>7</sup> and His<sup>6</sup> in the message sequence of MK-1 by alanine gave analogues that bind poorly to the hMC4R. In addition, replacing the D-Phe<sup>7</sup> residue in MK-1 by D-(2')Nal<sup>7</sup> (MK-2), resulted in a 20-fold decrease in the IC<sub>50</sub> value of MK-2 at

Table I. *In-vitro* binding and second messenger assays of the cyclic analogues to various human melanocortin receptors.

Peptides	hMC3R		hMC4R		hMC5R	
	IC <sub>50</sub> nM	EC <sub>50</sub> nM	IC <sub>50</sub> nM	EC <sub>50</sub> nM	IC <sub>50</sub> nM	EC <sub>50</sub> nM
MK-1	332.0	70	5.96	1.55	710.0	61.5
MK-2	21.5	81.9	103.0	282	155.0	148
MK-3	6.67	3.75	51.0	450	6120	120
MT-II	1.52	1.85	6.86	1.85	7.47	1.85

MK-1 =  $c[(O)C-CH_2-CH_2-C(O)-His^6-D-Phe^7-Arg^8-Trp^9-Lys^{10}]-NH_2$ ;

MK-2 =  $c[(O)C-CH_2-CH_2-C(O)-His^6-D-(2')Nal^7-Arg^8-Trp^9-Lys^{10}]-NH_2$ ;

MK-3 =  $c[(O)C-C_6H_4-C(O)-His^6-D-(2')Nal^7-Arg^8-Trp^9-Lys^{10}]-NH_2$ .

hMC4R (Table I). Interestingly, this bulky residue is better accommodated at the hMC3R receptor as is evident by the lower IC<sub>50</sub> value of analogue MK-2 at this receptor (hMC4R IC<sub>50</sub> MK-2 = 103 nM and hMC3R IC<sub>50</sub> MK-2 = 21.5 nM). Furthermore, replacing the succinyl linker of MK-2 with a bulky hydrophobic phthalic acid linker gave analogue MK-3, which binds to the hMC3R ≈8-fold more tightly than to the hMC4R (hMC4R IC<sub>50</sub> MK-3 = 51 nM and hMC3R IC<sub>50</sub> MK-3 = 6.67 nM). These results suggest that the active site of hMC3R is better able to accommodate bulky groups *versus* the hMC4 receptor, and that hydrophobic interactions may be more important in binding to the hMC3 receptor.

**Biological activity:** In order to test the *in-vitro* potency of MK-1 and its analogues at the human MCR's, the ability of these ligands to stimulate or suppress the production of c-AMP was determined using the standard superpotent agonist MT-II as the control (Table II). These studies showed that MK-1 was a superpotent agonist at hMC4R with an EC<sub>50</sub> value comparable to MT-II. However, MK-1 is a weak agonist at the hMC1, hMC3 and hMC5 receptors with EC<sub>50</sub> values ≈30-fold greater than MT-II at these receptors. An interesting observation from the *in-vitro* biological assays was the finding that MK-3 (D-Phe<sup>7</sup>(D-(2')Nal<sup>7</sup> and succinyl→phthalic linker) is a weak inverse agonist at hMC4R. To our knowledge MK-3 represents the first example of an inverse agonist at the hMC4R, and could have important therapeutic applications, such as down regulation of constitutively active MC4 receptors in disease states such as anorexia.

*Table II. Selectivity of the cyclic analogues to hMC4R versus hMC1R, hMC3R and hMC5R.*

Peptides	hMC1R/hMC4R	hMC3R/hMC4R	hMC5R/hMC4R
MK-1	700.0	55.0	118.0
MK-2	n.d.	0.21	1.5
MK-3	n.d.	0.13	120

*n.d.* = not determined.

### Acknowledgments

The authors would like to thank the USPHS, Grant DR-17420, for financial support.

### References

1. Yang, Y., Fong, T.M., Dickinson, C.J., Mao, C., Li, J.Y., Tota, M.R., Mosley, R., Van der Ploeg, L.H.T., Gantz, I. *Biochemistry* **39**, 14900–14911 (2000).
2. Fan, W., Boston, B.A., Kesterson, R.A., Hruby, V.J., Cone, R.D. *Nature* **385**, 165–168 (1997).

## Synthesis and NMR Characterization of Melanin-Concentrating Hormone

Rosa Maria Vitale<sup>1</sup>, Laura Zaccaro<sup>2</sup>, Benedetto Di Blasio<sup>1</sup>,  
Roberto Fattorusso<sup>1</sup>, Carla Isernia<sup>1</sup>, Pietro Amodeo<sup>3</sup>, Ettore Benedetti<sup>2</sup>,  
Michele Saviano<sup>2</sup> and Carlo Pedone<sup>2</sup>

<sup>1</sup>Department of Environmental Sciences, 2nd University of Naples, Caserta, 81100, Italy

<sup>2</sup>Biocrystallography Research Center, University of Naples "Federico II",  
Naples, 80134, Italy

<sup>3</sup>Istituto Chimica MIB-CNR, Arco Felice, 80072, Italy

### Introduction

Melanin-concentrating hormone (MCH), a hypothalamic cyclic peptide, was identified initially in teleost fish as a regulator of pigmentary changes in background adaptation. MCH was later also found in mammals to be a regulator of feeding and energy homeostasis. The conformational analysis of human MCH (a heterodetic cyclic nonadecapeptide) is the object of considerable interest with the aim of gaining insight into a possible bioactive conformation through the development of structure–activity relationships. In fact, it has been found that the MCH binding sites on mammalian cells are overexpressed, particularly, on skin carcinoma cells [1].

### Results and Discussion

MCH was synthesized by the solid phase method using Fmoc chemistry on 2-chlorotrityl chloride resin. The N- $\alpha$ -amino acids were activated *in situ* according to the standard PyBop/HOBt/DIEA procedure. The peptidyl-resin was treated with a mixture of TFA and scavengers to cleave the peptide from the resin. The crude product was purified by preparative RP-HPLC. Cyclization of the linear peptide was performed by air oxidation, followed by RP-HPLC and MALDI-TOF techniques in order to evaluate the purity and the identity of the final product.

The conformational properties of MCH peptide were investigated by mono- and two-dimensional NMR experiments in 1 : 1 CD<sub>3</sub>CN/H<sub>2</sub>O, by Distance Geometry and Molecular Dynamics procedures, and by CD technique in the same solvent conditions used for NMR.

The CD data were collected in the 260–190 nm range. The deconvolution of the spectrum *via* a neural network approach resulted in 18.3 and 22.4% of helical and turn content, respectively.

The NMR experimental data demonstrate that human Melanin Concentrating Hormone in a water/acetonitrile mixture presents a well-defined structure. Computational analysis shows that the cyclic peptide in all clusters presents an  $\alpha$ -helix structure in the region 2–5 outside the heterodetic cycle, and an  $\alpha/3_{10}$  helix structure in the region 8–12 inside the cycle (Figure 1). The two clusters present different conformational behaviour in the C-terminal part: a random coil conformation and an  $\alpha$ -helical structure. A careful comparison of the two clusters shows that these structures are substantially different from that reported by Brown and coworkers [2]. This model was recently used to perform a molecular characterization of the Melanin Concentrating Hormone/Receptor complex [3], and to identify the critical residues for binding and activation.

In summary, our findings emphasize the necessity to critically revise the proposed MCH/Receptor complex model.

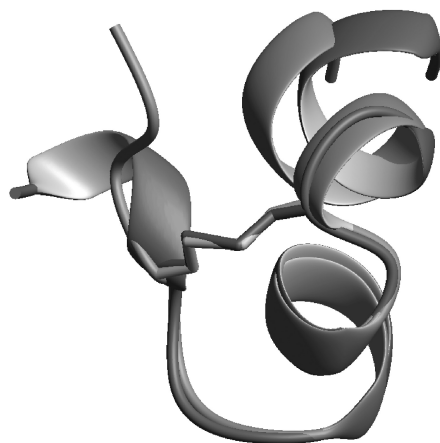


*Fig. 1. Cartoon models of the representative structures of the main clusters for MCH as obtained after restrained cartesian-space simulated annealing.*

#### **Acknowledgments**

The authors gratefully acknowledge the Ministry of University and of the Scientific and Technological Research (M.U.R.S.T.), and the National Council of Research (C.N.R.) of Italy for their continuous and generous support to this research.

#### **References**

1. Burgaud, J.-L., Poosti, R., Fehrentz, J.-A., Martinez, J., Nahon, J.-L. *Biochem. Biophys. Res. Commun.* **241**, 622–629 (1997).
2. Brown, D.W., Campbell, M.M., Kinsman, R.G., White, P.D., Moss, C.A., Osguthorpe, D.J., Paul, P.K.C., Kaker, B.I. *Biopolymers* **29**, 609–622 (1990).
3. Macdonald, D., Murgo, N., Zhang, R., Durkin, J.P., Yao, X., Strader, C.D., Graziano, M.P. *Mol. Pharm.* **58**, 217–224 (2000).

## **Synergism Between Agouti Protein Fragment 91-131 and Melanin Concentrating Hormone**

**Alex N. Eberle<sup>1</sup>, Jozsef Bódi<sup>2</sup>, György Orosz<sup>2</sup>, Helga Süli-Vargha<sup>2</sup>,  
Verena Jäggin<sup>1</sup> and Urs Zumsteg<sup>1</sup>**

<sup>1</sup>*Laboratory of Endocrinology, Department of Research, University Hospital and University Children's Hospital, CH-4059 Basel, Switzerland*

<sup>2</sup>*Research Group of Peptide Chemistry, Hungarian Academy of Sciences, H-1518 Budapest, Hungary*

### **Introduction**

Murine *agouti* protein (AP) is a 131-amino acid cysteine-rich peptide responsible for the induction of pheomelanin production in melanocytes [1]. Overexpression and ubiquitous secretion of AP in mice carrying the lethal yellow *A<sup>y</sup>* mutation leads to a bright yellow coat and obesity [1]. AP antagonizes  $\alpha$ -melanocyte-stimulating hormone ( $\alpha$ -MSH) at the melanocortin-1 receptor (MC1-R) and hence inhibits MSH-induced cAMP formation and melanin synthesis. AP was also shown to exhibit some MSH-agonist effects (*e.g.* receptor down-regulation) and to display the characteristics of an inverse agonist [2]. The finding that the C-terminal cysteine-rich fragment of AP is sufficient for  $\alpha$ -MSH antagonism and the observation that AP evokes biological effects independent from  $\alpha$ -MSH antagonism have prompted us to study the biological characteristics of a C-terminal AP fragment in assays typical for both types of action of AP. We have selected the mouse AP<sub>91-131</sub> fragment which does not contain Val<sup>83</sup>, a crucial residue for the bioactivity of native AP. Also, we were interested in whether melanin-concentrating hormone (MCH), a physiological antagonist of  $\alpha$ -MSH and inducer of food intake [3], exerts any synergistic effects on AP<sub>91-131</sub> action. In a previous report, the strategy of the chemical synthesis of AP<sub>91-131</sub> had been described [4]. Here we report the biological data obtained with this AP fragment. The salient finding is that the C-terminal part of AP mediates both antagonist and agonist activities, and that MCH potentiates the antagonist activity of AP<sub>91-131</sub>.

### **Results and Discussion**

Antagonist and agonist activities of AP<sub>91-131</sub> at the MC1-R were assessed using B16-F1 mouse melanoma cells *in vitro* and the following assay systems: (i) receptor binding, (ii) adenylyate cyclase, (iii) tyrosinase, (iv) melanin production, and (v) cell proliferation. In competition binding studies AP<sub>91-131</sub> was about 3-fold less potent than the natural agonist  $\alpha$ -melanocyte-stimulating hormone ( $\alpha$ -MSH) in displacing the radioligand [<sup>125</sup>I]-[Nle<sup>4</sup>, D-Phe<sup>7</sup>]- $\alpha$ -MSH ( $K_i$  6.5  $\pm$  0.8 nmol/l).  $\alpha$ -MSH-induced tyrosinase activation and melanin production were completely inhibited by a 100-fold higher concentration of AP<sub>91-131</sub>; the IC<sub>50</sub> values for AP<sub>91-131</sub> in the two assay systems were 91  $\pm$  22 nM and 95  $\pm$  15 nM, respectively. Basal melanin production and adenylyate cyclase activity in the absence of agonist were decreased by AP<sub>91-131</sub> with IC<sub>50</sub> values of 9.6  $\pm$  1.8 nM and 5.0  $\pm$  2.4 nM, respectively. This indicates inverse agonist activity of AP<sub>91-131</sub> similar to that of native AP. The presence of 10 nM MCH slightly but significantly potentiated the inhibitory activity of AP<sub>91-131</sub> in the adenylyate cyclase and melanin assays (Figure 1). On the other hand, AP<sub>91-131</sub> inhibited cell growth similar to  $\alpha$ -MSH (IC<sub>50</sub> 11.0  $\pm$  2.1 nM; maximal inhibition 1.8-fold higher than that of  $\alpha$ -MSH). Furthermore, MC1-R was down-regulated by AP<sub>91-131</sub> with about the same potency and time-course as with  $\alpha$ -MSH. These results demonstrate that AP<sub>91-131</sub> dis-

plays both agonist and antagonist activities at the MC1-R, and hence it is the cysteine-rich region of agouti protein which inhibits and mimics the different  $\alpha$ -MSH functions, most likely by simultaneous modulation of different intracellular signalling pathways. MCH displays synergistic effects on the MSH-antagonist activity of AP<sub>91-131</sub>.

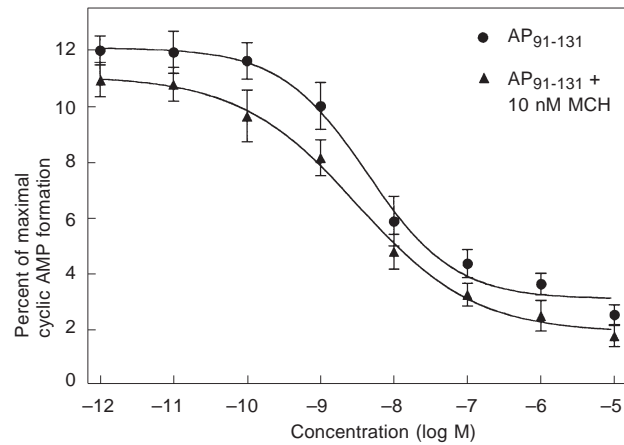


Fig. 1. Potentiation of inverse agonism of AP<sub>91-131</sub> by 10 nM MCH when tested with the adenylate cyclase assay using B16-F1 mouse melanoma cell membranes (three experiments  $\pm$  SD).

## References

1. Wilson, B.D., Ollmann, M.M., Barsh, G.S. *Mol. Med. Today* **5**, 250–256 (1999).
2. Siegrist, W., Drozd, R., Cotti, R., Willard, D.H., Wilkison, W.O., Eberle, A.N. *J. Recept. Signal Transd. Res.* **17**, 75–98 (1997).
3. Tritos, N.A., Maratos-Flier, E. *Neuropeptides* **33**, 339–349 (1999).
4. Bódi, J., Süli-Vargha, H., Ludányi, K., Vékey, K., Orosz, G. *Tetrahedron Lett.* **38**, 3293–3296 (1997).

## Development of a Human Growth Hormone Peptide Analogue AOD9604 into an Anti-Obesity Drug

Woei-Jia Jiang, Robert Gianello, Mark Heffernan, Esra Ogru,  
 Roksan Libinaki and Frank Ng

*Obesity and Diabetes Laboratories Department of Biochemistry and Molecular Biology,  
 Monash University, Victoria 3800, Australia*

### Introduction

Previous studies from our laboratory have identified that a carboxy-terminal fragment of the human growth hormone (hGH), hGH(177-191), is the lipolytic/anti-lipogenic domain of intact hGH [1]. By targeting the key enzymes involved in lipid metabolism, hGH(177-191) is able to increase lipolysis, and decrease lipogenesis in adipose tissue, resulting in reduction of body weight gain in obese rodent models. In view of its significant clinical potential, the aim of our study is to develop the peptide into a drug for the treatment of human obesity. A series of peptide analogues of hGH(177-191) were designed, synthesized and studied for the structure-activity relationship.

### Results and Discussion

Peptide analogues of hGH(177-191), as listed in Table 1, were prepared using Fmoc-amino acids by usual solid phase synthesis. After cleavage and purification, the Cys(Acm)<sup>182,189</sup>-hGH peptides were cyclized by an one-step oxidation by excess iodine (4.5-folds) in an acetic acid–water solution (80/20, v/v) for 60 min at room temperature. A final RP-HPLC purification was conducted and structure of the products were confirmed by ESI-MS.

*Table 1. In vitro effects of hGH(177-191) peptide and its analogues (0.3 μM) on lipogenesis.*

Peptide <sup>a</sup>	Lipogenesis (pmol/mg tissue/min) <sup>b</sup>
LRIVQCRSVEGSCGF	3.02 ± 0.17*
YLRLVQCRSVEGSCGF	2.48 ± 0.07*
IVQCRSVEGSCGF	3.89 ± 0.19
LRIVQCRSVEGSC	3.64 ± 0.22
LRIVQARSVEGSCGF	3.78 ± 0.23
Buffer	4.05 ± 0.22

<sup>a</sup> These peptides were in cyclic disulfide form, except for Ala<sup>182</sup>-hGH(177-191). <sup>b</sup> Mean ± SEM of 25 replicates. The Student t-test was used for statistics. Groups were accepted as significant to the control, if P values <0.05 and then denoted by \*.

To evaluate biological activity of the peptides, their inhibitory effects on lipid synthesis was examined using the *in vitro* lipogenesis assay. Results (Table 1) indicated that the length and the disulfide bond of hGH(177-191) were crucial for it to retain biological activities. Truncated analogues with deletion from either N- or C-terminus showed dramatic loss in activity. Ala<sup>182</sup>-hGH(177-191), a linear analogue, is also less active. On the other hand, Tyr<sup>176</sup>-hGH(176-191), coded as AOD9604 [2], demonstrated a 52.4% increase in the *in vitro* bioactivity. Further studies in animals with AOD9604 demonstrated its specific *in vivo* activity (Table 2). Long-term treatment of C57BL/6J (ob/ob) mice with AOD9604 (500 μg/kg/day) had a marked effect on re-

### Biologically Active Peptides

ducing the body weight gain and total body triglyceride after chronic oral administration. No significant change in tibia bone length in animals was observed between the treated and control groups. Unlike the intact hGH, data indicated that AOD9604 had no effect on bone growth.

Table 2. Effects of chronic treatment with AOD9604 (500 µg/kg body weight/day) or saline by oral administration for 88 days in C57BL/6J (ob/ob) mice. Data = Mean ± SEM.

Item	Group	
	Control (n = 6)	Treated (n = 10)
Body weight gain (gram)	11.0 ± 1.0	7.8 ± 0.5*
Total body triglyceride <sup>a</sup> (%)	21.27 ± 1.22	16.28 ± 0.68*
Length of tibia <sup>b</sup> (mm)	17.29 ± 0.09	17.10 ± 0.09

<sup>a</sup> Animals were blended and digested on Day 88. The total triglycerides present in each animal was measured and expressed as the percentage of the animal total body weight. <sup>b</sup> The two hind legs were taken from each animal on Day 88. The tibia bones were dissected out and any remaining tissue was removed. Bones were aligned and scanned at 300% zoom and 600 dpi. The scanned images were then analyzed using Microcomputer Imaging Device (CMCID5, Imaging research Inc., Canada) to give measurements of the bone lengths.

Preclinical toxicology of AOD9604 was successfully completed in late 2000 with no unfavorable side effect observed. The Phase I human clinical trials of AOD9604 are currently underway in UK.

### Acknowledgments

This project is funded by Metabolic Pharmaceuticals Limited, Australia.

### References

1. Ng, F., Natera, S., Jiang, W.-J. *US Patent No. 5,869,452* (1999).
2. Ng, F., Jiang, W.-J. *Int. Patent Appl. PCT/AU98/00724*. Published and grant pending.

## Rational Approach to Stable, Universal Somatostatin Analogues with Superior Therapeutic Potential

Ian Lewis, Wilfried Bauer, Rainer Albert, Nagarajan Chandramouli,  
Janos Pless, Günter Engel, Gisbert Weckbecker and Christian Bruns

*Novartis Pharma Preclinical Research Department, Basel, CH-4002, Switzerland*

### Introduction

The unique pharmacological effects mediated by SRIF-14 [1] are derived from its universal high affinity binding to all somatostatin receptor subtypes sst1-5. Until now, somatostatin analogues used in the clinic have exhibited high affinity binding only to sst2 and sst5. The goal of this research was to discover a small, stable SRIF mimic exhibiting universal high affinity binding to sst1-5.

### Methods

Cyclohexapeptide analogues such as SOM230, were synthesised on solid phase using Fmoc/tBu strategy and the SASRIN® linker prior to cyclisation in solution. In contrast, octapeptide analogues of SMS 201-995 (octreotide) [2] were synthesised on solid phase using Fmoc/tBu strategy and the [4-[4-methyl-5-[(fluorenylmethoxycarbonyl)-amino]-1,3-dioxan-2-yl]phenoxy]-acetic acid linker and cyclised in solution.

### Results and Discussion

A rational approach capitalising on structure activity relationships has led to the discovery of SOM230, a novel, stable cyclohexapeptide somatostatin analogue which exhibits unique binding to human somatostatin receptors (sst1-5). This approach has been based on transposing functional groups from SRIF-14 into octapeptide and cyclohexapeptide templates. Initially, a wealth of structure-activity information was obtained by preparing stable SRIF-14 “Ala-Scan” analogues, in the form of the C-terminal amides and investigating their binding to SRIF receptor subtypes sst1-5. This rational study revealed that Lys<sup>4</sup>, Phe<sup>6</sup>, Phe<sup>7</sup> and Phe<sup>11</sup> are pivotal residues responsible for the universal binding to sst1-5 exhibited by SRIF-14.

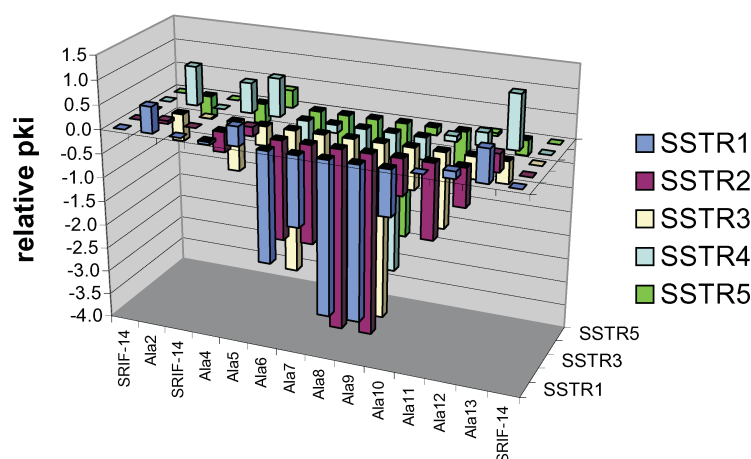


Fig. 1. Binding to SRIF receptor subtypes of SRIF-14 “Ala-Scan” analogues.

Figure 2 illustrates the structure of the new cyclohexapeptide analogue, SOM230. Structural elements such as Lys<sup>4</sup>, Phe<sup>6</sup>, Phe<sup>7</sup> and Phe<sup>11</sup> from SRIF-14 have been transposed into the reduced size, stable cyclohexapeptide template in the form of the 2-aminoethyl-carbamoyl-oxy-Pro<sup>6</sup>, Phg<sup>7</sup> and Tyr(Bzl)<sup>10</sup> where the numbering refers to the positions in native somatostatin. Figure 3 compares the high affinity binding to sst1, sst2, sst3 and sst5 exhibited by SOM230 compared to the full universal high affinity binding profile of SRIF-14.

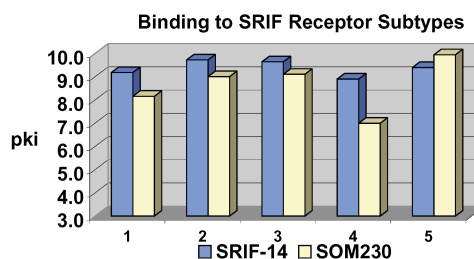
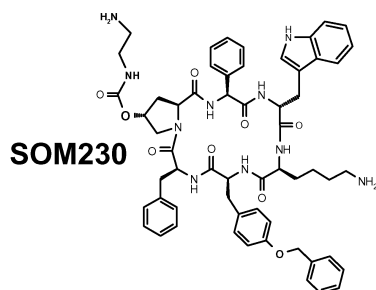


Fig. 2. Structure of SOM230.

Fig. 3. Binding to SRIF receptor subtypes.

Subsequent to assembly, cyclisation and deprotection, cyclohexapeptides were purified by reversed phase HPLC prior to pharmacological profiling. Typical preparative HPLC-MS purification of SOM230 is shown in Figure 4.

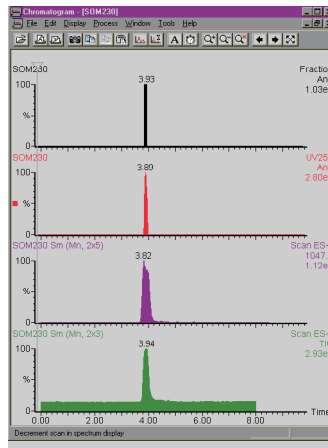


Fig. 4. HPLC-MS Purification of SOM230.

Figure 5 illustrates the full palette of selectivities that can be obtained utilising the cyclohexapeptide template. PKF 226-969, incorporating Tyr<sup>7</sup>, exhibits potentiation of affinity to sst3 and sst5, whereas PKF 227-111, incorporating Arg<sup>7</sup>, exhibits reduced affinities for sst1-4 with increasing selectivity for sst5, as shown in Figure 6.

Importantly, SOM230 exhibits at 30 times higher binding affinity to sst1 and a 40 times higher binding affinity to sst5 than SMS 201-995. In rats, SOM230 potently suppressed GH secretion with superior efficacy as compared to octreotide, measured

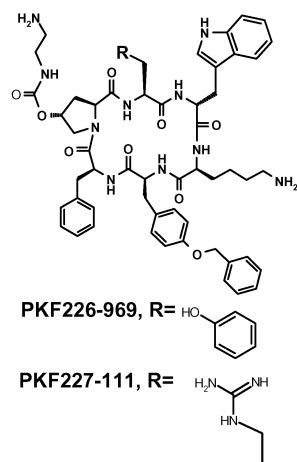


Fig. 5. Structural comparison.

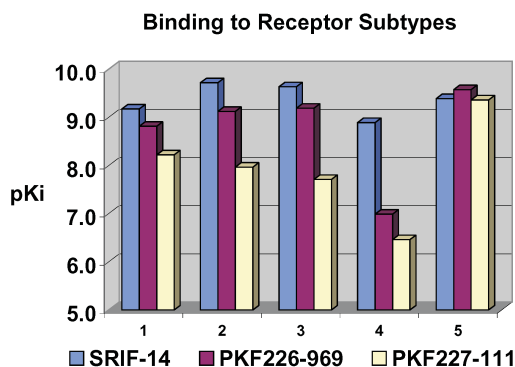


Fig. 6. Binding to SRIF receptor subtypes.

6 h after injection. Furthermore, in rats, and rhesus and cynomolgus monkeys, SOM230 potently decreased plasma IGF-1 levels.

### Conclusion

SOM230 is a new somatostatin analog with a unique binding profile for SRIF receptor subtypes and a superior inhibitory effect on the GH/IGF-1 axis. Clinical testing will start soon to determine its inhibitory profile in man.

### Acknowledgments

The technical support of S. Arnold, Ch. Bourquin, F. Kessler, J. Meisburger, A. Simon and A. Stich is gratefully acknowledged.

### Dedication

This research is dedicated to Professor B. Merrifield on the occasion of his 80th birthday.

### References

1. Brazeau, P., Vale, W., Burgus, R., Ling, N., Butcher, M., Rivier, J., Guillemin, R. *Science* **179**, 77–79 (1973).
2. Bauer, W., Briner, U., Doepfner, W., Haller, R., Huguenin, R., Marbach, P., Petcher, T., Pless, J. *Life Sci.* **31**, 1134–1140 (1980).

## N-Methyl Scan of a sst1-Selective Somatostatin (SRIF) Analog

Judit Erchegyi<sup>1</sup>, Carl Hoeger<sup>1</sup>, Sandra Wenger<sup>2</sup>, Beatrice Waser<sup>2</sup>,  
 Jean-Claude Schaer<sup>2</sup>, Jean Claude Reubi<sup>2</sup> and Jean E. Rivier<sup>1</sup>

<sup>1</sup>The Clayton Foundation Laboratories for Peptide Biology, The Salk Institute, La Jolla,  
 CA 92037, USA

<sup>2</sup>Division of Cell Biology and Experimental Cancer Research, Institute of Pathology,  
 University of Berne, Switzerland

### Introduction

Tyrosine residue substitutions at position 2, 7 and 11 in des-AA<sup>1,2,5</sup>-[D-Trp<sup>8</sup>,IAMP<sup>9</sup>]-SRIF (CH-275) resulted in peptides not only with improved affinity and selectivity for sst1, but suitable for radioiodination as well [1]. Here, we present the effect of methylation of the backbone nitrogen of all residues in des-AA<sup>1,2,5</sup>-[D2Nal<sup>8</sup>,IAMP<sup>9</sup>]-SRIF (**2**) (Table 1) on receptor binding affinity. N<sup>α</sup>-Methyl amino acid substitutions may limit conformational freedom of a peptide, block its proteolytic enzyme cleavage sites, and as a result yield analogs with increased potency and selectivity [2,3].

### Results and Discussion

Peptides were synthesized using SPPS and analyzed for receptor binding affinity to pellet sections of sst1-sst5-expressing cells. N<sup>α</sup>-Methylation in **3–12** was achieved on the resin according to published procedures [4,5]. This approach was not applicable for the synthesis of **13** and inadequate (poor yield) for that of **12**. As experienced by others [6], steric hindrance may cause the poor reactivity of the nitrogen at or near the C-terminus adjacent to the resin. By extending the C-terminus of our target peptide by 2 or 3 lysines, respectively, N-methylation of Ser<sup>13</sup> and Cys<sup>14</sup> became possible. After

Table 1. Binding affinities at the five human SRIF receptors. Mean of two or more experiments.

Compound	IC <sub>50</sub> (nM)				
	sst1	sst2	sst3	sst4	sst5
<b>1</b> Somatostatin-28	4.2	2.4	5.3	4.0	4.4
<b>2</b> Des-AA <sup>1,2,5</sup> -[D2Nal <sup>8</sup> ,IAMP <sup>9</sup> ]-SRIF	100 ± 32	>1000	>1000	>1000	>10K
<b>3</b> Des-AA <sup>1,2,5</sup> -[(NMe)Cys <sup>3</sup> ,D2Nal <sup>8</sup> ,IAMP <sup>9</sup> ]-SRIF	99.8 ± 52	>1000	>1000	>10K	>10K
<b>4</b> Des-AA <sup>1,2,5</sup> -[(NMe)Lys <sup>4</sup> ,D2Nal <sup>8</sup> ,IAMP <sup>9</sup> ]-SRIF	292 ± 129	>1000	990	>10K	>1000
<b>5</b> Des-AA <sup>1,2,5</sup> -[(NMe)Phe <sup>6</sup> ,D2Nal <sup>8</sup> ,IAMP <sup>9</sup> ]-SRIF	>1000	>1000	>1000	>10K	>10K
<b>6</b> Des-AA <sup>1,2,5</sup> -[(NMe)Phe <sup>7</sup> ,D2Nal <sup>8</sup> ,IAMP <sup>9</sup> ]-SRIF	>1000	>1000	>1000	>1000	>1000
<b>7</b> Des-AA <sup>1,2,5</sup> -[(NMe)D2Nal <sup>8</sup> ,IAMP <sup>9</sup> ]-SRIF	325 ± 135	>10K	>1000	>1000	>10K
<b>8</b> Des-AA <sup>1,2,5</sup> -[D2Nal <sup>8</sup> ,(NMe)IAMP <sup>9</sup> ]-SRIF	43 ± 13	>1000	>1000	>1000	>10K
<b>9</b> Des-AA <sup>1,2,5</sup> -[D2Nal <sup>8</sup> ,IAMP <sup>9</sup> ,(NMe)Thr <sup>10</sup> ]-SRIF	>1000	>1000	>10K	>10K	>10K
<b>10</b> Des-AA <sup>1,2,5</sup> -[D2Nal <sup>8</sup> ,IAMP <sup>9</sup> ,(NMe)Phe <sup>11</sup> ]-SRIF	620	>1000	>1000	>10K	>1000
<b>11</b> Des-AA <sup>1,2,5</sup> -[D2Nal <sup>8</sup> ,IAMP <sup>9</sup> ,(NMe)Thr <sup>12</sup> ]-SRIF	170	>1000	>1000	400	>10K
<b>12</b> Des-AA <sup>1,2,5</sup> -[D2Nal <sup>8</sup> ,IAMP <sup>9</sup> ,(NMe)Ser <sup>13</sup> ]-SRIF	65 ± 19	>1000	>1000	>10K	>1000
<b>13</b> Des-AA <sup>1,2,5</sup> -[D2Nal <sup>8</sup> ,IAMP <sup>9</sup> ,(NMe)Cys <sup>14</sup> ]-SRIF	290	>1000	>1000	>10K	>1000

cleavage, oxidization and purification, hydrolysis with Carboxypeptidase B gave the targeted peptide (**12**, **13**) in excellent yields. Analog **2** binds to sst1 with slightly less affinity than CH-275 [1], yet is more selective since its binding is less than 1/1000 that of SRIF-28 (**1**) to the other four receptors. *N*-Methylation resulted in loss of sst1-affinity in all analogs but **3**, **8** and **12** with little influence on selectivity. The binding affinities of des-AA<sup>1,2,5</sup>-[D2Nal<sup>8</sup>,Iamp<sup>9</sup>]-SRIF (**2**), des-AA<sup>1,2,5</sup>-[(NMe)Cys<sup>3</sup>,D2Nal<sup>8</sup>,Iamp<sup>9</sup>]-SRIF (**3**), des-AA<sup>1,2,5</sup>-[D2Nal<sup>8</sup>,(NMe)Iamp<sup>9</sup>]-SRIF (**8**) and des-AA<sup>1,2,5</sup>-D2Nal<sup>8</sup>,Iamp<sup>9</sup>,(NMe)Ser<sup>13</sup>]-SRIF (**12**) are about 1/25, 1/25, 1/10 and 1/15 that of SRIF-28 (**1**) to sst1, respectively.

In conclusion, our new strategy that allowed the synthesis of *N*<sup>α</sup>-methylated peptides at or near their C-terminus can be applied to the synthesis of other peptides where the *N*<sup>α</sup>-methylated and adequately protected amino acid is not available or where methylation cannot be achieved using presently available strategies. *N*-Methylation of Iamp<sup>9</sup> yielded **8** with 2-fold enhanced binding affinity and selectivity for sst1 over that of the parent **2**. Structurally, *N*-methylation is attractive as it constrains conformations by limiting rotational freedom of amino acid sidechains. With the ultimate goal of determining the structural basis of ssts' binding and activation mechanism, *N*-methylation becomes a very significant means of constraining peptide conformation.

#### Acknowledgments

This work was supported in part by NIH grant DK 50124 and the Hearst Foundation.

#### References

1. Rivier, J.E., Hoeger, C., Erchegeyi, J., Gulyas, J., DeBoard, R., Craig, A.G., Koerber, S.C., Wenger, S., Waser, B., Schaer, J.-C., Reubi, J.C. *J. Med. Chem.* **44**, 2238–2246 (2001).
2. Ali, F.E., Bennett, D.B., Calvo, R.R., Elliott, J.D., Hwang, S.-M., Ku, T.W., Lago, M.A., Nichols, A.J., Romoff, T.T., Shah, D.H., Vasko, J.A., Wong, A.S., Yellin, T.O., Yuan, C.-K., Samanen, J.M. *J. Med. Chem.* **37**, 769–780 (1994).
3. Schmidt, R., Kalman, A., Chung, N.N., Lemieux, C., Horvath, C., Schiller, P.W. *Int. J. Pept. Protein Res.* **46**, 47–55 (1995).
4. Kaljuste, K., Unden, A. *Int. J. Pept. Protein Res.* **42**, 118–124 (1993).
5. Miller, S.C., Scanlan, T.S. *J. Am. Chem. Soc.* **119**, 2301–2302 (1997).
6. Rajeswaran, W.G., Hocart, S.J., Murphy, W.A., Taylor, J.E., Coy, D.H. *J. Med. Chem.* **44**, 1305–1311 (2001).

## Exploring the “Double-Ring” Motif in Bradykinin Antagonists

Eunice J. York<sup>1</sup>, Daniel C. Chan<sup>2</sup>, Barbara Helfrich<sup>2</sup>,  
 Paul A. Bunn, Jr.<sup>2</sup>, Lajos Gera<sup>1</sup> and John M. Stewart<sup>1</sup>

<sup>1</sup>Department of Biochemistry and Molecular Genetics and

<sup>2</sup>University of Colorado Cancer Center, University of Colorado Health Sciences Center,  
 Denver, CO 80262, USA

### Introduction

Bradykinin (BK; Arg-Pro-Pro-Gly-Phe-Ser-Pro-Phe-Arg) is a primary mediator of inflammation, enhances tissue permeability and is also a growth factor for many lung and prostate cancers. Antagonists of BK such as B9870, the suberimidyl dimer of the potent BK antagonist B9430 [1] (see Table 1 for structures) and other neuropeptides have been used for treatment of small cell lung carcinoma (SCLC) *in vitro* and in nude mice and have aroused much interest for the development of anti-cancer drugs.

Table 1. Activities of bradykinin antagonist analogs.

Number	Structure <sup>a</sup>	Biological Activity	
		GPI <sup>b</sup>	SCLC <sup>c</sup>
HOE140	DArg-Arg-Pro-Hyp-Gly-Thi-Ser-DTic-Oic-Arg	7.8	150
B9430	DArg-Arg-Pro-Hyp-Gly-Igl-Ser-DIgl-Oic-Arg	7.9	120
B10238	F5c-DArg-Arg-Pro-Hyp-Gly-Igl-Ser-DIgl-Oic-Arg	8.1 (LT)	50
B9870	Suim-(DArg-Arg-Pro-Hyp-Gly-Igl-Ser-DIgl-Oic-Arg) <sub>2</sub>	7.6	1.5
B10448	F5c-DArg <sup>0</sup> -Hyp <sup>3</sup> -Igl <sup>5</sup> -DIgl <sup>7</sup> -Oic <sup>8</sup> -Dip <sup>10</sup> (NH <sub>2</sub> )-BK	Inact	3.8
B10496	F5c-DArg <sup>0</sup> -Hyp <sup>3</sup> -PFF <sup>5,8</sup> -DF5F <sup>7</sup> -DDip <sup>10</sup> (NH <sub>2</sub> )-BK	Inact	4.2
B10526	Bcpa-DArg <sup>0</sup> -Hyp <sup>3</sup> -Thi <sup>5</sup> -DDip <sup>7</sup> -F5F <sup>8</sup> -BK	–	6.4
B10528	Tf2c-DArg <sup>0</sup> -Hyp <sup>3</sup> -Thi <sup>5</sup> -DDip <sup>7</sup> -F5F <sup>8</sup> -BK	–	7.8
B10530	Bipa-DArg <sup>0</sup> -Hyp <sup>3</sup> -Thi <sup>5</sup> -DDip <sup>7</sup> -F5F <sup>8</sup> -BK	–	12
B10524	F5c-DArg <sup>0</sup> -Hyp <sup>3</sup> -Igl <sup>5</sup> -DIgl <sup>7</sup> -PIF <sup>8</sup> -BK	–	12.5
B10396	F5c-DArg <sup>0</sup> -Hyp <sup>3</sup> -Igl <sup>5</sup> -DIgl <sup>7</sup> -PFF <sup>8</sup> -BK	6.2	14
B10534	F5c-DArg <sup>0</sup> -Hyp <sup>3</sup> -Thi <sup>5</sup> -DBip <sup>7</sup> -F5F <sup>8</sup> -BK	–	18
B10518	α-DDD-(Lys-DArg <sup>0</sup> -Hyp <sup>3</sup> -Thi <sup>5</sup> -DDip <sup>7</sup> -F5F <sup>8</sup> -BK) <sub>2</sub>	Inact	2.1
B10504	α-DDD-(DArg <sup>0</sup> -Hyp <sup>3</sup> -Thi <sup>5</sup> -DDip <sup>7</sup> -F5F <sup>8</sup> -BK) <sub>2</sub>	Inact	4.0
B10432	DDD-(Dip-DArg <sup>0</sup> -Hyp <sup>3</sup> -Igl <sup>5</sup> -DIgl <sup>7</sup> -Oic <sup>8</sup> -BK) <sub>2</sub>	5.9 (LT)	5.2
B10510	DDD-(DDip-DArg <sup>0</sup> -Hyp <sup>3</sup> -Thi <sup>5</sup> -DIgl <sup>7</sup> -PFF <sup>8</sup> -BK) <sub>2</sub>	–	6.2

<sup>a</sup> Abbreviations: Inact = inactive; LT = long term; Ac = acetyl; Bcpa = bis(4-chlorophenyl)-acetyl; Bip = biphenylalanine; Bipa = 4-biphenylacetyl; DDD = dodecanedioyl; Dip = 3,3-diphenylalanine; 33Dp = 3,3-diphenylpropionyl; F5c = 2,3,4,5,6-pentafluorocinnamoyl; F5F = pentafluorophenylalanine; Hyp = trans-4-hydroxyproline; Igl = α-2-indanylglycine; Oic = octahydroindole-2-carboxylic acid; PFF = p-fluorophenylalanine; PIF = p-iodophenylalanine; SUIM = suberimidyl; Tf2c = trans-3,5-bis(trifluoromethyl)cinnamoyl; Thi = β-2-thienylalanine; Tic = 1,2,3,4-tetrahydroisoquinoline-3-carboxylic acid. <sup>b</sup>pA<sub>2</sub> for bradykinin antagonist activity on isolated guinea pig ileum. <sup>c</sup>ED<sub>50</sub> (μM) for cytotoxicity by MTT test for SHP-77 SCLC *in vitro*.

BK receptors belong to the G protein-coupled receptor family. A common accessory binding site for peptide and non-peptide antagonists on these receptors is thought to be hydrophobic. A “double-ring” motif of aromatic, heterocyclic or aliphatic ring systems on the antagonist has a strong affinity for this binding site [2]. These similar hydrophobic structures can provide the basis for drug design for specific receptors; the key is finding the proper specificity. The improved potency of the “second- and third-generation” bradykinin antagonists, HOE 140 [3] and B9430, may be due, in part, to incorporation of the double-ring systems of Tic, Oic and Igl.

This work presents anti-BK and anti-cancer activities of a series of peptides that explores this motif. The extended double-ring of biphenylalanine (Bip) and the benzhydryl-like diphenylalanine (Dip) have been used previously to replace arginine at position 1 in “first generation” BK antagonists [4].

### Results and Discussion

Structures and activities of representative peptides are presented in Table 1. GPI potency does not correlate with activity against SCLC. None of the “double-ring” amino acid and acyl group substitutions in BK antagonists improve anti-BK activity over that of B9430 and B10238. The best antagonists have  $pA_2 = 7.0$ – $7.4$  and involve N-terminal modifications of B9430 (33Dp, Ac-F5F, Ac-DF5F and Ac-Dip). In contrast, several substitutions have been remarkably successful in improving anti-cancer activity of monomeric peptides *in vitro*. Our most potent monomers are B10488 ( $ED_{50} = 3.8 \mu M$ ) and B10496 ( $ED_{50} = 4.2 \mu M$ ), which have Dip-amide and D-Dip amide, respectively, at the C-terminal and are about 12 times more potent than B10238. Two benzhydryl-type groups are tolerated as shown by the D-Dip analog B10526 ( $ED_{50} = 6.4 \mu M$ ), where the acyl group Bcpa increased the killing of SCLC 4-fold over that of F5c. C-terminal amides are not expected to have anti-BK activity.

Dimerization of several of the monomers with DDD has also been successful for anti-cancer activity. The dimer B10518, with D-Dip in position 7, has an  $ED_{50}$  of  $2.1 \mu M$  and is almost as potent as B9870.

### Acknowledgments

We thank Robert Congdon and Lisa Swize for assistance in synthesis and purification and Vitalija Simkeviciene, Lila Sawaged and Lisa Swize for biological assays on guinea pig ileum. Supported by NIH grants HL-26284 and CA-86581.

### References

1. Gera, L., Stewart, J.M., Whalley, E.T., Burkard, M., Zuzack, J.S. *Immunopharmacol.* **33**, 178–182 (1996).
2. Ariens, E.J., Beld, A.J., Rodrigues, J.F., Simones, A.M., In O'Brien, R.D. (Ed.) *The Receptors: A Comprehensive Treatise*, Plenum, New York, 1979, p. 33.
3. Hock, F.J., Wirth, K., Albus, U., Linz, W., Gerhards, H.J., Weimer, G., Henke, S., Breipohl, G., Konig, W., Knolle, J., Scholkens, B.A. *Br. J. Pharmacol.* **102**, 769–773 (1991).
4. Hsieh, K.H., Stewart, J.M. *J. Peptide Res.* **54**, 23–31 (1999).

## Conformational Studies of Angiotensin II Cyclic Analogues

Vani X. Oliveira, Jr.<sup>1</sup>, Shirley Schreier<sup>2</sup>, Fabio Casallanovo<sup>2</sup>,  
 Therezinha B. Paiva<sup>1</sup>, Antonio C. M. Paiva<sup>1</sup> and Antonio Miranda<sup>1</sup>

<sup>1</sup>Department of Biophysics, UNIFESP, 04044-020 and

<sup>2</sup>Department of Biochemistry, IQ-USP, 05508-900, São Paulo, Brazil

### Introduction

Angiotensin II (AII) is an octapeptide, produced in the blood as a result of two different enzymatic hydrolyses, which occur in the renal hypertensor system. Among many others pharmacological properties, angiotensin II exerts its effects in the smooth and visceral muscles, peripheral and central nervous system and in the induction of aldosterone releasing from the cortex adrenal gland. As a potent pressor agent it plays an important role in the blood pressure regulation. Many efforts have been done in order to establish the AII receptor-bound conformation. As the molecule is very flexible in solution, one of the most successful strategies is the use of conformationally constrained AII analogues by disulfide [1,2] or lactam bridges [3,4].

Recently, we have scanned the whole A<sub>II</sub> sequence with i-(i+2) and i-(i+3) lactam bridge consisting of the Asp-(X)<sub>n</sub>-Lys scaffold. All the analogues contained the main functional groups that are important for AII activity (*i.e.* Tyr, His, and Phe side-chains and the C-terminal carboxyl group) and presented low agonistic activity in three different bioassays (guinea-pig ileum and rat uterus and in the rat blood pressure). Cyclo(0-1a)-[Asp<sup>0</sup>,endo-Lys<sup>1a</sup>]-A<sub>II</sub> and [Asp<sup>0</sup>,endo-Lys<sup>1a</sup>]-A<sub>II</sub> were the only exceptions since they retained 5 and 10% of the activity of the A<sub>II</sub>, respectively (data not shown). Based on these data and those obtained by Matsoukas *et al.* with the analogue cyclo(3-5)[Sar<sup>1</sup>,Asp<sup>3</sup>,Lys<sup>5</sup>]-A<sub>II</sub> [3] we have designed a new series of monocyclic angiotensin II analogues.

Table 1. Relative potencies for the A<sub>II</sub> cyclic analogues.

No.	Name	Relative Potency <sup>a</sup>		
		Guinea pig Ileum	Rat Uterus	Rat Blood pressure
1	Cyclo(0-1a)-[Asp <sup>0</sup> ,endo-DLys <sup>1a</sup> ]-AII	4.7	2.3	6.5
2	Cyclo(0-1a)-[DAsp <sup>0</sup> ,endo-DLys <sup>1a</sup> ]-AII	3.9	3.3	5.1
3	Cyclo(0-1a)-[Glu <sup>0</sup> ,endo-Lys <sup>1a</sup> ]-AII	9.5	9.0	10.8
4	Cyclo(0-1a)-[Asp <sup>0</sup> ,endo-Orn <sup>1a</sup> ]-AII	4.4	3.8	4.0
5	Cyclo(0-1a)-[Glu <sup>0</sup> ,endo-Orn <sup>1a</sup> ]-AII	9.9	9.7	9.9
6	Cyclo(3a-4a)-[Sar <sup>1</sup> ,endo-Asp <sup>3a</sup> ,endo-Lys <sup>4a</sup> ]-AII	<0.1	NA <sup>b</sup>	0.1
7	Cyclo(3a-4a)-[Sar <sup>1</sup> ,endo-Asp <sup>3a</sup> ,endo-Orn <sup>4a</sup> ]-AII	<0.1	0.1	0.3
8	Cyclo(3a-4a)-[Sar <sup>1</sup> ,endo-Glu <sup>3a</sup> ,endo-Lys <sup>4a</sup> ]-AII	NA <sup>b</sup>	<0.1	4.8
9	Cyclo(3a-4a)-[Sar <sup>1</sup> ,endo-Glu <sup>3a</sup> ,endo-Orn <sup>4a</sup> ]-AII	0.4	0.1	NA <sup>b</sup>
10	Cyclo(3-4a)-[Sar <sup>1</sup> ,Asp <sup>3a</sup> ,endo-Lys <sup>4a</sup> ]-AII	NA <sup>b</sup>	<0.1	NA <sup>b</sup>
11	Cyclo(3a-5)-[Sar <sup>1</sup> ,endo-Asp <sup>3a</sup> ,Lys <sup>5</sup> ]-AII	0.1	0.6	2.7

<sup>a</sup> Data reported as a percentage of the angiotensin II activity; <sup>b</sup>No activity detected (limit concentration = 10<sup>-5</sup> M).

## Results and Discussion

The peptides listed in Table 1 were synthesized by solid-phase methodology, using *t*-Boc strategy on a chloromethylated resin [5]. Solid phase side-chain to side-chain cyclization of the peptides on the resin were performed by BOP/DIEA [5]. The peptides were purified by RP-HPLC, characterized by RP-HPLC, capillary zone electrophoresis, amino acid analysis and mass spectrometry. Biological activities were assayed on rat blood pressure and on the isolated smooth muscles from guinea-pig ileum and rat uterus.

Out of the 11 analogues that were tested, only two, {cyclo(0-1a)[Glu<sup>0</sup>,endo-(Orn<sup>1a</sup>)]-A<sub>II</sub> and cyclo(0-1a)[Glu<sup>0</sup>,endo-(Lys<sup>1a</sup>)]-A<sub>II</sub>, were found to have around 10% of the A<sub>II</sub> activity. We also did not observe any antagonistic activity of the analogues. Because the corresponding linear analogues proved to be virtually inactive, our interpretation of the potency decrease is that the introduction of the side chain to side chain bridging element was not sufficient to induce or stabilize a bioactive conformation in the receptor environment. A careful optimization of bridge length and chirality is critical for the recognition and binding with the A<sub>II</sub> receptors.

## Acknowledgments

This study has been supported by CNPq and FAPESP.

## References

1. Zhang, W.J., Nikiforovich, G.V., Pérodin, J., Richard, D.E., Escher, E., Marshal, G.R. *J. Med. Chem.* **39**, 2738–2744 (1996).
2. Lindman, S., Lindeberg, G., Gogoll, A., Nyberg, F., Karlen, A., Hallberg, A. *Bioorg. Med. Chem.* **9**, 763–772 (2001).
3. Matsoukas, J.M., Hondrelis, J., Agelis, G., Barlos, K., Gatos, D., Ganter, R., Moore, D., Moore, G.J. *J. Med. Chem.* **37**, 2958–2969 (1994).
4. Matsoukas, J.M., Plevaya, L., Ancans, J., Mavromoustakos, T., Kolocouris, A., Roumelioti, P., Vlahakos, D.V., Yamdagni, R., Wu, Q., Moore, G.J. *Bioorg. Med. Chem.* **8**, 1–10 (2000).
5. Miranda, A., Koerber, S.C., Gulyas, J., Lahrichi, S.L., Craig, A.G., Corrigan, A., Hagler, A., Rivier, C., Vale, W., Rivier, J. *J. Med. Chem.* **37**, 1450–1459 (1994).

## Identification of Key-Residues of Urotensin II, a Potent Mammalian Vasoconstrictor

A. Brkovic, P. Lampron, M. Létourneau and A. Fournier

Centre de recherche en santé humaine, INRS/Institut Armand-Frappier, Université du Québec,  
245 boul. Hymus, Pointe-Claire, Qc, Canada H9R 1G6

### Introduction

Nearly 20 years ago, urotensin II (UT-II), a cyclic dodecapeptide, was originally isolated from fish urophysis (Figure 1). Recently, UT-II was identified in amphibians, small rodents and humans [1]. Human UT-II appeared as a 11 amino acid neuro-peptide containing a cyclic hexapeptide identical to that present in fish, amphibians and rodents. *In vitro*, hUT-II demonstrated a potent vasoconstricting activity in the rat thoracic aorta bioassay [2]. In fact, this peptide is now identified as the most potent vasoconstrictor ever reported. *In vivo*, hUT-II appears to modulate cardiovascular homeostasis since administration of hUT-II to monkeys provokes a diminution of myocardial contractility. Little is known about the role of the primary structure. However, previous studies have shown that the hexapeptide (6-11) would be essential for the activity of hUT-II [3]. Thus, the aim of our study was to determine the relationship between the amino acid sequence of hUT-II and its constricting activity.

### Results and Discussion

Table 1 shows the EC<sub>50</sub> values for the analogs obtained after an "Ala-scan", as well as for six additional hUT-II analogs. [Ala<sup>6</sup>]-, [Ala<sup>9</sup>]- and [Ala<sup>11</sup>]hUT-II demonstrated reduced vasoconstricting activity, while [Ala<sup>7</sup>]- and [Ala<sup>8</sup>]- showed no biological activity, nor affinity for the receptor. Therefore, position 7 and 8, which correspond to a tryptophan and a lysine residue, respectively, are crucial for biological activity. Thus, any substitution of the amino acids from the hexapeptide (5-11), with an alanine, led to an important loss of biological activity. These results support a previous study, which demonstrated that the cyclic segment (5-11) is essential and sufficient to maintain a full vasoconstrictor activity [3]. On the contrary, the N-terminal amino acids appeared less crucial for biological activity. This was shown with [Ala<sup>1</sup>]-, [Ala<sup>2</sup>]-, [Ala<sup>3</sup>]- and [Ala<sup>4</sup>]hUT-II, which demonstrated similar or only slightly reduced potencies when compared to hUT-II.

In order to further document these data, hUT-II(5-11) and [Ala<sup>1,2,3,4</sup>]hUT-II were synthesized and tested for their biological activities. Interestingly, hUT-II(5-11) was 400-fold less potent than hUT-II, while [Ala<sup>1,2,3,4</sup>]hUT-II maintained a very significant potency, being only 5-fold less potent than the parent molecule. These data suggest that a N-terminal segment is necessary in order to maintain significant activity. Possibly, a N-terminal segment favors the stabilization of the hexapeptide core, thus allowing a better interaction with the receptor. Rat UT-II, which possesses three additional amino acids, is equipotent to hUT-II, but shows an important loss of efficacy. In addition,

- a) H-Glu-Thr-Pro-Asp-Cys-Phe-Trp-Lys-Tyr-Cys-Val-OH
- b) H-Gln-His-Gly-Thr-Ala-Pro-Glu-Cys-Phe-Trp-Lys-Tyr-Cys-Ile-OH
- c) H-Ala-Gly-Thr-Ala-Asp-Cys-Phe-Trp-Lys-Tyr-Cys-Val-OH

Fig. 1. Amino acid sequence for (a) human UT-II, (b) rat UT-II and (c) fish UT-II.

Table 1. Vasoconstrictor activity of hUT-II and analogs.

Analog <sup>a</sup>	EC <sub>50</sub> (nM)	Efficacy (%) <sup>b</sup>
hUT-II	1.5	104
[Ala <sup>1</sup> ]hUT-II	1.4	104
[Ala <sup>2</sup> ]hUT-II	1.3	104
[Ala <sup>3</sup> ]hUT-II	12.7	100
[Ala <sup>4</sup> ]hUT-II	10.0	77
[Ala <sup>6</sup> ]hUT-II	2260	70
[Ala <sup>7</sup> ]hUT-II	>10 <sup>5</sup>	n.d.
[Ala <sup>8</sup> ]hUT-II	>10 <sup>5</sup>	n.d.
[Ala <sup>9</sup> ]hUT-II	691	46
[Ala <sup>11</sup> ]hUT-II	177	62
hUT-II(5-11)	600	28
hUT-II-CONH <sub>2</sub>	29	71
[Ala <sup>1,2,3,4</sup> ]hUT-II	7.6	46
[His] <sup>7</sup> hUT-II	2600	51
[Ala <sup>6</sup> ,Phe <sup>7</sup> ,Trp <sup>8</sup> ,Lys <sup>9</sup> ,Tyr <sup>10</sup> ,Cys <sup>11</sup> ,Val <sup>12</sup> ]hUT-II	2500	34
ratUT-II	7.6	44

<sup>a</sup> Synthesized by solid-phase method using the FMOC chemistry. <sup>b</sup> % of contraction of 10<sup>-5</sup> M or less in comparison to the response obtained with 80 mM KCl.

tion, hUT-II-CONH<sub>2</sub> exhibited only a slight decrease of potency, suggesting that the carboxy-terminus is not crucial for vasoconstricting activity. Finally, [His<sup>7</sup>]hUT-II, and [Ala<sup>6</sup>,Phe<sup>7</sup>,Trp<sup>8</sup>,Lys<sup>9</sup>,Tyr<sup>10</sup>,Cys<sup>11</sup>,Val<sup>12</sup>]hUT-II were weak agonists. The size of the cyclic core, as well as the aromaticity of Trp<sup>7</sup>, could also be key structures for the activity.

### Acknowledgments

Supported by the Canadian Institutes of Health Research and the Heart and Stroke Foundation. A. B. and P. L. are recipients of NSERC studentships. A. F. is Chercheur National from the Fonds de la recherche en santé du Québec. A. B. is the recipient of a travel grant from the APS organization.

### References

1. Coulouarn, Y., Lihmann, I., Jegou, S., Anouar, Y., Tostivint, H., Beauvillain, J.C., Conlon, J.M., Bern, H.A., Vaudry H. *Proc. Natl. Acad. Sci. USA* **95**, 15803–15808 (1998).
2. Itoh, H., Itoh, Y., Rivier, J., Lederis, K. *Am. J. Physiol.* **252**, 361–366 (1987).
3. Perkins, T.D., Bansal, S., Barlow, D.J. *Biochem. Soc. Trans.* **18**, 918–919 (1990).

## Structure–Activity Studies on the Corticotropin Releasing Factor Antagonist Astressin, Minimal Sequence Necessary for Antagonistic Activity: Implications for a New Pharmacophoric Model

Dirk T. S. Rijkers<sup>1</sup>, Jack A. J. den Hartog<sup>2</sup> and Rob M. J. Liskamp<sup>1</sup>

<sup>1</sup>Department of Medicinal Chemistry, Faculty of Pharmacy, Utrecht Institute for Pharmaceutical Sciences, Utrecht University, 3508 TB Utrecht, The Netherlands

<sup>2</sup>Solvay Pharmaceuticals, Research Laboratories, Weesp, The Netherlands

### Introduction

Corticotropin Releasing Factor (CRF) is an important physiological regulator of the body response to stressful stimuli [1]. Over-expression of CRF is involved in endocrine, neurologic and psychiatric diseases such as feeding disorders, major depression and anxiety-related disorders. To obtain more insight into the physiological role of CRF, potent peptide antagonists have recently been developed mainly based on the amino acid sequence of CRF, which ultimately led to the discovery of astressin, one of the most potent peptide-based CRF antagonists reported until now [2].

The presently known small molecule non-peptide CRF antagonists [3] are found by library screening and their narrow structure activity relationship, emphasizes the need for new lead structures [4]. Herein we describe our approach to design new lead structures for CRF antagonists in which the lactam moiety of astressin forms a scaffold to present the pharmacophoric residues in the correct three-dimensional position.

### Results and Discussion

To elucidate which amino acid residues were required for CRF antagonistic activity, astressin was systematically truncated: C-terminally, N-terminally and C/N-terminally truncated derivatives were synthesized to unravel the importance of the C- or N-terminus or a combination of them. To probe the possibility of a discontinuous epitope in which merely sequences at both the C- and N-termini of astressin interact with the receptor, a centrally truncated series was synthesized. It was found that the cyclic constraint is of utmost importance for the biological activity. Furthermore, the C-terminal deletion study revealed the importance of the Ile<sup>41</sup> residue. In line with this observation, truncation at both termini of astressin resulted in inactive compounds. Central truncation of astressin also proved deleterious for the biological activity. Noteworthy, and most surprising, was the fact that when astressin was shortened from its N-terminus, the CRF antagonistic activity sharply decreased, but restored – although it did not regain the activity of full length astressin – if the peptide was further shortened by 16 to 19 amino acid residues. These deletion studies ultimately resulted in two peptides: Ac(27-41)C **1** and Ac(30-41)C **2**, which were substantially smaller in size than astressin but retained CRF antagonistic activity *in vitro* (astressin: IC<sub>50</sub> 0.8 nM, K<sub>i</sub> 0.6 nM; **1**: IC<sub>50</sub> 40 nM, K<sub>i</sub> 2.8 nM) as well as *in vivo* (astressin: IC<sub>50</sub> 0.03 mg/kg i.v.; **1**: IC<sub>50</sub> 1 mg/kg i.v.) [5].

Astressin derivative **1** was further truncated and used for an alanine scan, a D-amino acid scan and a lactam bridge scan to arrive at the smallest active derivative in which secondary structure elements stabilize the bio-active conformation. Unfortunately, these efforts did not result in active compounds and it was concluded that **1** was the smallest peptide that retained CRF antagonistic activity.

NMR and CD studies showed us that a stretched  $\alpha$ -helix represents the bio-active conformation of **1**. The biological data together with the structural studies imply a new pharmacophoric model of peptide-based CRF antagonists (Figure 1). Furthermore, scaffolding to mimic secondary structure, as shown successfully with somatostatin and melanocortin, failed with CRF antagonists.

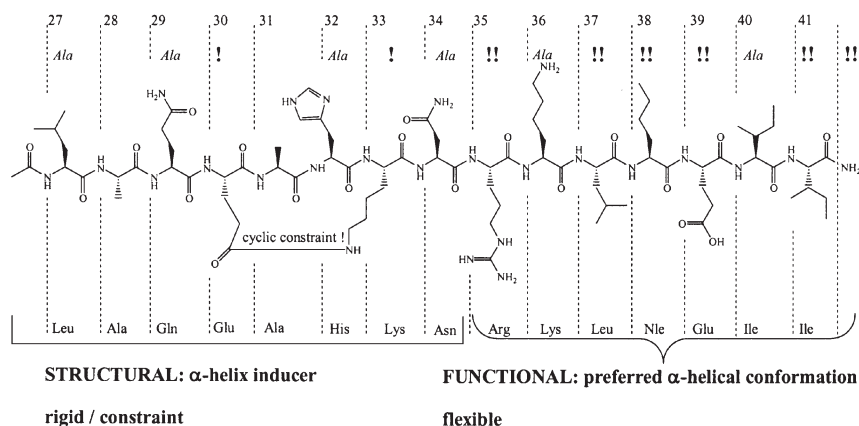


Fig. 1. Proposed pharmacophoric model of a peptide-based CRF antagonist: Ac(27-41)C **1**. Ala: alanine substitution allowed, !/!! important/necessary for activity.

## Acknowledgments

This research was financed by a strategic alliance between Solvay Pharmaceuticals, the Ministry of Economic Affairs and Utrecht University, The Netherlands.

## References

1. Vale, W., Spiess, J., Rivier, C., Rivier, J. *Science* **213**, 1394–1397 (1981).
2. Gulyas, J., Rivier, C., Perrin, M., Koerber, S.C., Sutton, S., Corrigan, A., Lahrachi, S.L., Craig, A.G., Vale, W., Rivier, J. *Proc. Natl. Acad. Sci. USA* **92**, 10575–1079 (1995).
3. Gilligan, P.J., Robertson, D.W., Zaczek, R. *J. Med. Chem.* **43**, 1641–1660 (2000).
4. Keller, P.A., Bowman, M., Dang, K.H., Garner, J., Leach, S.P., Smith, R., McGluskey, A. *J. Med. Chem.* **42**, 2352–2357 (1999).
5. Rijkers, D.T.S., den Hartog, J.A.J., Liskamp, R.M.J. WO 0129086.

## Solid-Phase Synthesis and Radiolabeling of a Bombesin Peptide Analog for Diagnostic Imaging of Tumors: A Preliminary Report

Subhani M. Okarvi

King Faisal Specialist Hospital and Research Centre, Cyclotron and Radiopharmaceuticals  
 Department, MBC-03, Riyadh 11211, Saudi Arabia

### Introduction

Radiolabeled receptor-binding peptides have emerged as a clinically useful class of radiopharmaceuticals. The high binding affinity for its receptor facilitates retention of the peptide in receptor-expressing tissues while its relatively smaller size (compared to proteins and antibodies) results in rapid clearance from the blood and other non-target tissues [1]. Receptor-binding peptides labeled with  $\gamma$ -emitters can be used to visualize receptor-positive cells *in vivo*. Bombesin (BN) is a 14-amino acid peptide that binds to its receptor with high affinity. Specific receptors for BN have been identified on a variety of tumors including lung, breast, pancreas and prostate. BN receptors on various cancer cells may be important for the early diagnosis of cancers [2]. The aim of this study was to synthesize and evaluate a bombesin analog coupled to a chelating agent MAG3 (mercaptoacetyltriglycine) for labeling with  $^{99m}\text{Tc}$  for diagnostic imaging.

### Results and Discussion

We have synthesized a novel MAG<sub>3</sub>-bombesin analog by the solid-phase peptide synthesis technique (using N- $\alpha$ -Fmoc protection and HBTU coupling-standard methods of solid-phase peptide chemistry for protection and activation). It has been shown that

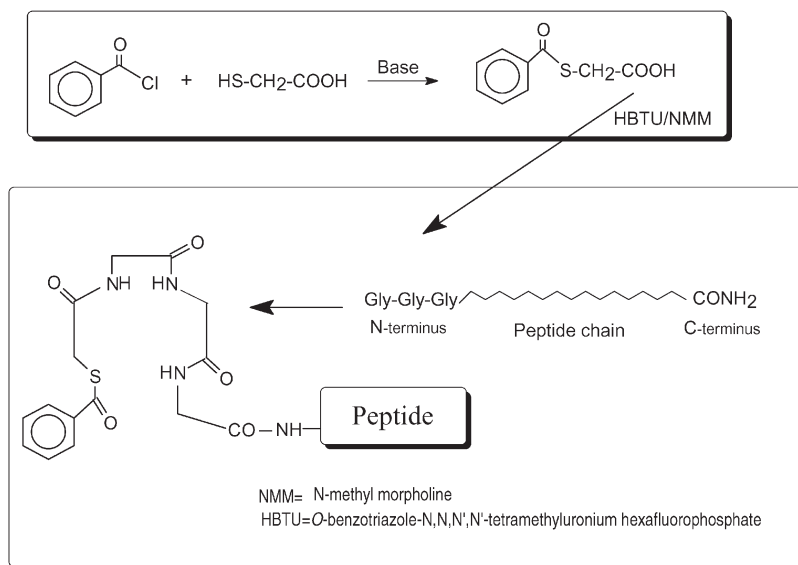


Fig. 1. Preparation of S-benzoyl-MAG<sub>3</sub>-bombesin (6-14) peptide analog i.e., C<sub>6</sub>H<sub>5</sub>-CO-(Gly)<sub>3</sub>-D-Asp-D-Phe-D-Gln-Trp-Ala-Val-Gly-D-Phe-Leu-Met-NH<sub>2</sub> by the solid-phase peptide synthesis method.

## Okarvi

the C-terminal 7 to 14 amino acid sequence (*i.e.*, Trp-Ala-Val-Gly-His-Leu-Met-NH<sub>2</sub>) is necessary for retaining receptor-binding affinity of bombesin-like peptides [3]. This means a suitable chelating moiety can be introduced at the N-terminal region of the bombesin-like peptide, which is not involved in receptor binding. The site-specific introduction results in minimal interference with the receptor binding-site of the bombesin analog. We have prepared a bombesin (6-14 amino acid sequence) analog coupled to MAG<sub>3</sub> with a D-Asp spacer inserted between the receptor binding-site of the peptide and the <sup>99m</sup>Tc chelation site. A triglycine (Gly<sub>3</sub>) N-terminal tail was added to the bombesin template to facilitate synthesis of MAG<sub>3</sub> moiety. Upon completion of synthesis the N-terminal Fmoc group was removed and the peptide-resin was washed to prepare for acylation with *S*-benzoyl mercaptoacetic acid that was activated and manually coupled to the free N-terminus of the Gly<sub>3</sub> peptide chain using standard HBTU activation. This addition step completed the synthesis of MAG<sub>3</sub> moiety and yielded the thiol-protected MAG<sub>3</sub>-bombesin peptide analog (Figure 1). The identity of the peptide was confirmed by mass spectrometry.

Radiolabeling with <sup>99m</sup>Tc was performed using stannous tartrate as an intermediate complexing agent. The radio-HPLC analysis (reversed-phase C18 column with TFA/H<sub>2</sub>O and TFA/CH<sub>3</sub>CN solvents gradient system) revealed that a single <sup>99m</sup>Tc-species is formed when labeling with <sup>99m</sup>Tc is performed under alkaline (basic) conditions (pH 11 or 12). It was found that the radiochemical purity could be improved significantly by adding 100 µL of 5% ascorbic acid (anti-oxidant) to the reaction mixture. *In vivo* biodistribution in normal mice was performed at different time intervals after the intravenous injection of 100 µL (4 µCi) of HPLC purified <sup>99m</sup>Tc-MAG<sub>3</sub>-bombesin conjugate. The preliminary biodistribution results indicate a high accumulation and retention of radioactivity in the liver and intestines. In conclusion, the data suggest that the solid-phase synthesis approach permit simple, site-specific and facile introduction of a chelating moiety directly into the targeting peptide without interfering with its receptor-binding region. The peptide examined in this study has the ability to label efficiently with <sup>99m</sup>Tc by stannous tartrate exchange method. Detailed biological evaluation in healthy and tumor-bearing animals is needed in order to elucidate the full potential of the <sup>99m</sup>Tc-MAG<sub>3</sub>-bombesin analog for tumor imaging.

## Acknowledgments

This work is supported by the KFSH&RC RAC grant# 990026.

## References

1. Okarvi, S.M. *Nucl. Med. Commun.* **20**, 1093–1112 (1999).
2. Baidoo, K.E., Lin, K.S., Zhan, Y., et al. *Bioconjugate Chem.* **9**, 218–225 (1999).
3. Karra, S.R., Schibli, R., Gali, H., et al. *Bioconjugate Chem.* **10**, 254–260 (1999).

## Investigation on the Structural Requirements for Binding Integrin $\alpha_{\text{IIb}}\beta_3$

Silke Schabbert<sup>1</sup>, Elsa Locardi<sup>1</sup>, Ralph-Heiko Mattern<sup>2</sup>,  
Michael D. Pierschbacher<sup>2</sup>, Shaokai Jiang<sup>1</sup> and Murray Goodman<sup>1</sup>

<sup>1</sup>Department of Chemistry and Biochemistry, University of California at San Diego, La Jolla,  
CA 92093-0343, USA

<sup>2</sup>Integra LifeSciences Corp. Corporate Research Center, San Diego, CA 92121, USA

### Introduction

Since the discovery of the cell adhesion sequence Arg-Gly-Asp (RGD) in fibronectin [1], it has been shown that the RGD sequence serves as a binding site of many adhesion proteins to integrin receptors [2]. The RGD sequence incorporated into small peptides can mimic these adhesion proteins, and can regulate cell-cell and cell-matrix interaction. It has been demonstrated very early that the conformation of such peptides, and the way the RGD portion is presented to the receptor, have a tremendous influence on potency and integrin selectivity [3]. The integrin  $\alpha_{\text{IIb}}\beta_3$  plays a major role in platelet aggregation and is the most thoroughly studied integrin receptor. The receptor  $\alpha_v\beta_3$  is a related integrin containing the same  $\beta_3$  subunit and has attracted considerable interest due to its possible involvement in osteoporosis, angiogenic ocular disorders, and cancer.

### Results and Discussion

NMR studies on the receptor-bound conformation and side chain restrictions by synthetic modifications were used to gain insight into the structural requirements for binding to the  $\alpha_{\text{IIb}}\beta_3$  and  $\alpha_v\beta_3$  receptor.

The conformations of the <sup>15</sup>N labeled cyclic heptapeptides c[Mpa-<sup>15</sup>N-Arg<sup>1</sup>-<sup>15</sup>N-Gly<sup>2</sup>-<sup>15</sup>N-Asp<sup>3</sup>-<sup>15</sup>N-Phe<sup>4</sup>-<sup>15</sup>N-Arg<sup>5</sup>-Cys]NH<sub>2</sub> (**Phe-Arg** analog) and c[Mpa-<sup>15</sup>N-Arg<sup>1</sup>-<sup>15</sup>N-Gly<sup>2</sup>-<sup>15</sup>N-Asp<sup>3</sup>-<sup>15</sup>N-Asp<sup>4</sup>-<sup>15</sup>N-Val<sup>5</sup>-Cys]NH<sub>2</sub> (**Asp-Val** analog) in the presence of  $\alpha_{\text{IIb}}\beta_3$  receptor were studied by NMR using transfer NOE techniques and <sup>15</sup>N-editing of the spectra (Mpa denotes 3-mercaptopropionic acid). Computer simulations of these peptides using NMR data resulted in conformations that contain a  $\beta$ -turn spanning residues Arg<sup>1</sup> and Gly<sup>2</sup> for both peptides. Figure 1 demonstrates the superposition of representative structures of the two analogs. To probe our model further and to refine the conformational requirements for binding, a series of peptidomimetics

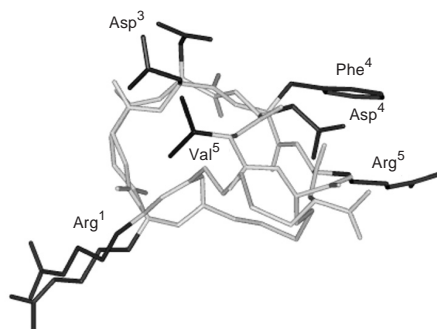


Fig. 1. Superposition of the **Phe-Arg** and the **Asp-Val** analogs.

Table 1. Binding affinities of selected peptides to the integrin receptors  $\alpha_{IIb}\beta_3$  and  $\alpha_v\beta_3$ .

Compound	$\alpha_v\beta_3$ IC <sub>50</sub> (nM)	$\alpha_{IIb}\beta_3$ IC <sub>50</sub> (nM)
Ac-c[Cys-Arg-Gly- $\beta$ (S) <b>Me-Asp</b> -Tyr(Me)-Arg-Cys]NH <sub>2</sub>	29.7	145
Ac-c[Cys-Arg-Gly- $\beta$ (R) <b>Me-Asp</b> -Tyr(Me)-Arg-Cys]NH <sub>2</sub>	2110	4480
Ac-c[Cys-Arg-Gly- $\beta$ (S) <b>Me-Asp</b> -Asp-Val-Cys]NH <sub>2</sub>	304	228
Ac-c[Cys-Arg-Gly- $\beta$ (R) <b>Me-Asp</b> -Asp-Val-Cys]NH <sub>2</sub>	4050	>10000
Ac-c[Cys-Arg-Gly- $\beta$ (S) <b>Me-Asp</b> -Thr-Tic-Cys]NH <sub>2</sub>	4.49	186
Ac-c[Cys-Arg-Gly- $\beta$ (R) <b>Me-Asp</b> -Thr-Tic-Cys]NH <sub>2</sub>	1620	>10000

containing  $\beta$ -methylated Asp residues was synthesized and tested for binding to the  $\alpha_{IIb}\beta_3$  and  $\alpha_v\beta_3$  receptors (Table 1). Treatment of a  $N^\alpha$ -Phenylfluorenyl-Asp(OBu<sup>t</sup>)-OBzl with LiHMDS results in the formation of the enolate at  $\beta$ -carbonyl carbon allowing methylation of the  $\beta$ -position with methyl iodide without alkylation or epimerization of the  $\alpha$ -carbon. A mixture of both  $\beta$ -methylated diastereomers was formed, whose stereochemistry was established subsequently. After removal of the benzyl group and the PhF protecting group by hydrogenation we were able to separate the diastereomers on silica gel using a mixture of ethyl acetate, isopropanol and water (8 : 2 : 1) as eluent. Significant differences in binding to the  $\alpha_{IIb}\beta_3$  and  $\alpha_v\beta_3$  of  $\beta$ -methylated Asp residues with (*R*) and (*S*) configurations at C <sup>$\beta$</sup>  were observed (Table 1). While the compounds containing (*S*)  $\beta$ -methylated Asp residues bind to the receptors approximately as potently as the unmethylated parent compounds, the compounds containing the (*R*)  $\beta$ -methylated Asp residues have drastically reduced binding affinities. These results suggest that the three-dimensional arrangement required for binding to the  $\alpha_{IIb}\beta_3$  and  $\alpha_v\beta_3$  receptors is not accessible for compounds containing the (*R*)  $\beta$ -methylated Asp residue, but can be adopted in compounds containing the (*S*)  $\beta$ -methylated Asp residue.

These results provide important guidelines for the design of novel potent RGD peptidomimetics.

### Acknowledgments

This research has been supported by grant R44DK51938.

### References

1. Ruoslahti, E., Pierschbacher, M.D. *Nature* **309**, 30–33 (1984).
2. Ruoslahti, E., Pierschbacher, M.D. *Proc. Natl. Acad. Sci. U.S.A.* **81**, 5985–5988 (1984).
3. Pierschbacher, M.D., Ruoslahti, E. *J. Biol. Chem.* **262**, 17294–17298 (1987).

## Linear and Cyclic Peptides for Integrin $\alpha_v\beta_6$ Inhibition

Gunther Zischinsky<sup>1</sup>, Ulrich Groth<sup>1</sup>, Beate Diefenbach<sup>2</sup> and  
Alfred Jonczyk<sup>2</sup>

<sup>1</sup>Faculty of Chemistry, University of Konstanz, Germany

<sup>2</sup>Preclinical Research, Merck KGaA, Darmstadt, Germany

### Introduction

The integrin  $\alpha_v\beta_6$  is a member of a family of non-covalent heterodimeric cell adhesion receptors, which take part in processes including cell adhesion and migration. It is known to bind to the natural ligands fibronectin and tenascin, and is predominantly found on epithelial cells [1]. Its expression was found upregulated in wound healing and inflammation [2]. Involvement of this integrin in development and metastasis of tumors from epithelial origin has been suggested [3]. Recently, peptides containing the motive XXDLXXLX were published to bind to integrin  $\alpha_v\beta_6$  [4]. Here, a more detailed pharmacophore definition and first steps of optimisation are reported.

### Results and Discussion

N-terminally acetylated peptide amides were synthesized in parallel following Fmoc-chemistry on Sieber-resin with TFA/water/TIS cleavage and purification *via* preparative RP-HPLC. Purity was ensured by analytical HPLC and capillary electrophoresis. Accurate constitution was confirmed by FAB-MS. An integrin-ligand competition assay was performed as described [4] and  $IC_{50}$ -values were determined. For our investigations, the peptide Ac-RTDLDSLRL-NH<sub>2</sub> was selected as starting point, as it had good affinity to integrin  $\alpha_v\beta_6$  ( $IC_{50} \approx 100$  nM).

It was found that neither Arg(1) nor Asp(3) could be exchanged by any other natural amino acid without dramatic loss of affinity to  $\alpha_v\beta_6$ . In position 2, in addition to glycine, serine and threonine showed surprising high potency. This is an interesting finding since  $\alpha_v$ -integrin recognition is usually restricted to RGD-ligands. As predicted by the DLXXL-motive it was not possible to substitute leucine in position 4 and 7 by other hydrophobic amino acids. Amino acids in positions 5 and 6 seem to function as a spacer, since alanine or glycine could be introduced there with almost no change in inhibition properties. It could be shown that the distance provided by two  $\alpha$ -amino acid residues is optimal. Both, shortening and elongation of the spacer led to drastic decline of affinity. In position 8 basic amino acids were found to be superior over other ones. Arginine and lysine are of similar effectiveness, suggesting that a positive charge is needed in this position.

A D-amino acid scan showed that in most positions the D-enantiomers caused loss of potency of approximately one order of magnitude. On the other hand, enhanced affinity was found for D-Asp(5) and D-Ser(6). First, D-amino acids are known to cause  $\beta$ -turns in position  $i+3$ . Here, in consequence D-Asp(5) would support a  $\beta$ -turn in RTDL. Second, in peptides with D-Asp(5) the non-RGD-sequence Ac-RTDLdSLRL-NH<sub>2</sub> ( $IC_{50} \approx 8$  nM) is about twice as potent as the corresponding RGD-peptide Ac-RGDLdSLRL-NH<sub>2</sub> ( $IC_{50} \approx 20$  nM).

In our efforts to develop potent integrin  $\alpha_v\beta_6$  inhibitors, peptides were cyclized to increase rigidity and proteolytic stability. However, by direct terminal backbone cyclization of the sequence RGDLdALR, affinity dropped by more than one order of magnitude (Figure 1,  $n = 0$ ). On the other hand, ring enlargement by successive introduction of several glycyll moieties between the former termini led to a stepwise im-

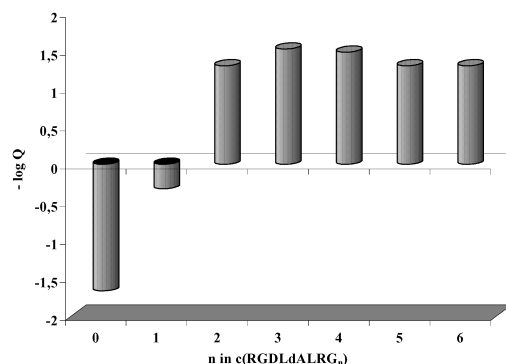


Fig. 1. Ring enlargement in c(RGDLdALRG<sub>n</sub>) Terminal backbone cyclization of the RGDLdALR-sequence ( $n = 0$ ) followed by successive incorporation of several glycyl moieties ( $n = 1-6$ ) as spacers.  $Q = IC_{50}(c(RGDLdALRG_n))/IC_{50}(Ac-RGDLdALR-NH_2)$ .

provement of potency culminating in a 1000-fold improved  $IC_{50}$ -value with the third glycine ( $IC_{50} \approx 1$  nM).

To elucidate whether these peptides are suitable as tools for *in vivo* experiments, plasma stability of selected peptides were examined. For this, peptides were incubated in human blood plasma containing pyridine as an internal standard. The decline of HPLC-peak area was monitored with time. The control peptide Fmoc-GGGRGDSPK-OH was completely degraded within 6 h. Peak areas of cyclic peptides c(RTDLdALRGGG) and c(RGDLdALRGGG) showed only slight decline within 30 h, but no degradation products were found.

### Conclusion

An octapeptide was optimized for integrin  $\alpha_v\beta_6$  inhibition. The best linear derivative was the non-RGD peptide Ac-RTDLdSLR-NH<sub>2</sub>. Cyclization, which was successfully used to improve the affinity of the linear peptide required some ring enlargement by introduction of spacers. The  $IC_{50}$ -values for the best cyclic peptides was improved by three orders of magnitude to about 1 nM. Furthermore, selected cyclic peptides proved to be stable in human blood plasma with half live-times of more than 30 h. Therefore, these may be used as tools to elucidate the role of integrin  $\alpha_v\beta_6$  *in vivo*.

### References

1. Busk, M., Pytela, R., Sheppard, D. *J. Biol. Chem.* **267**, 5790–96 (1992).
2. Zambruno, G., et al. *J. Biol. Chem.* **129**, 853–865 (1995).
3. Agrez, M., Chen, A., Cone, R.I., Pytela, R., Sheppard, D. *Cell. Biol.* **127**, 547–556 (1994).
4. Kraft, S., et al. *J. Biol. Chem.* **247**, 1979–1985 (1999).

## **The Synthesis of Collagen Peptides and Characterization of Their Inhibitory Effects on the Collagen Binding Activities of Integrins $\alpha_1\beta_1$ and $\alpha_2\beta_1$**

**Sivashankarappa Gurusiddappa<sup>1</sup>, Yi Xu<sup>1</sup>, Rebecca L. Rich<sup>1</sup>, Rick T. Owens<sup>1</sup>, Douglas R. Keene<sup>2</sup>, Richard Mayne<sup>3</sup>, Agneta Höök<sup>1</sup> and Magnus Höök<sup>1</sup>**

<sup>1</sup>*Center for Extracellular Matrix Biology, Institute of Biosciences and Technology, Texas A&M University, Houston, TX 77030, USA*

<sup>2</sup>*Shriners Hospital for Children, Portland, Oregon 97201, USA*

<sup>3</sup>*Department of Cell Biology, University of Alabama at Birmingham, Birmingham, AL 35294, USA*

### **Introduction**

Integrins  $\alpha_1\beta_1$  and  $\alpha_2\beta_1$  are two major eukaryotic collagen receptors. Binding to collagen is primarily due to an A-domain located near the N-terminus of the alpha chains ( $\alpha_1A$  and  $\alpha_2A$ ) [1,2] and requires the triple helical conformation of collagen and the presence of divalent cations such as  $Mg^{2+}$  or  $Mn^{2+}$ . Here we report the identification of three high affinity binding sites in type I collagen for both A domains, two of which were further confirmed using synthetic collagen peptides that adopt triple-helical conformation.

### **Results and Discussion**

Recombinant  $\alpha_1A$  and  $\alpha_2A$  were expressed in a His-tag fusion expression vector (pQE30) in *Escherichia coli* and purified using  $Ni^{++}$  affinity chromatography. The binding of the A domains to type I collagen was analyzed using surface plasmon resonance (SPR) technique in a Biacore system. The results showed that  $\alpha_2A$  exhibited only one detectable class of binding sites in type I collagen, with a  $K_D$  of  $\sim 10 \mu M$  at  $\sim 3$  binding sites per collagen molecule, whereas  $\alpha_1A$  exhibited at least two classes of binding sites with the highest affinity class having a  $K_D$  of  $0.09 \pm 0.06 \mu M$  at  $2.5 \pm 0.5$  binding sites per collagen molecule [3]. We further demonstrate that  $\alpha_1A$  and  $\alpha_2A$  competed with each other for binding to type I collagen in enzyme-linked immunosorbent assay (ELISA), suggesting that the high affinity binding sites in collagen for the two A domains overlap or are adjacent to each other.

In order to identify the high affinity binding sites, we incubated type I procollagen with either  $\alpha_1A$  and  $\alpha_2A$  and imaged the binding sites by electron microscopy after rotary shadowing. Morphometric analyses indicated three major binding regions (near the N-terminus, in the middle part, and near the C-terminus) along the collagen molecule for both A domains, consistent with the SPR results. The positions of the respective binding regions for  $\alpha_1A$  and  $\alpha_2A$  were overlapping with or adjacent to each other, consistent with the ELISA results.

Analysis of the amino acid sequences of the two chains of type I collagen revealed that GER containing motifs are present at each of the binding regions and notably, the central region contains the GFOGER sequence, which was previously identified as a high affinity binding site for both  $\alpha_1A$  and  $\alpha_2A$  [4-6]. We then synthesized the three peptides using the GER containing sequences of the  $\alpha_1$  chain of type I collagen in each of the three regions (Table 1), as well as a generic peptide. The synthesis was performed using a solid phase method on a TentaGel R RAM resin using Fmoc chem-

istry. The peptides were released from the resin and the cleaved peptides were analyzed by reverse-phase HPLC.

Table 1. Amino acid sequences of the synthetic collagen peptides.

Peptide	Sequence (N-C)
I	(GPO) <sub>4</sub> GLOGERGRO(GPO) <sub>4</sub> <sup>a</sup>
II	(GPO) <sub>4</sub> GFOGERGVQ(GPO) <sub>4</sub>
III	(GPO) <sub>4</sub> GASGERGPO(GPO) <sub>4</sub>
Generic	(GPO) <sub>11</sub>

<sup>a</sup> O indicates hydroxyproline.

To examine the ability of these peptides to form triple-helix in solution, we used circular dichroism spectroscopy. A positive maximum at 220–225 nm indicates the presence of collagen triple-helix. Each of four peptides exhibited a characteristic maximum at 220–225 nm when measured at 4 and 25 °C. At denaturing temperature (70 °C), the positive maxima disappeared. These indicated that the linear peptides were able to form triple helix at both 4 and 25 °C. The denatured peptides could renature and form triple helical structures after the solution was cooled to 4 °C, as indicated by the reappearance of the positive maxima.

To examine the ability of these peptides to inhibit the binding of  $\alpha_1$ A and  $\alpha_2$ A to type I collagen, we performed competition ELISAs where type I collagen was immobilized in microtiter wells. Collagen peptides I and II effectively inhibited the binding of both A domains in a dose-dependent manner, while peptide III did so moderately. The generic peptide did not show any inhibitory effect. These results suggested that peptide I represents a newly discovered native high affinity site for  $\alpha_1$ A and  $\alpha_2$ A, while peptide III is recognized by the A-domains but does not represent a high affinity site.

### Acknowledgments

This work was supported by NIH grant No. AR44415 to Magnus Höök, AR30481 to Richard Mayne, and an Arthritis Foundation postdoctoral fellowship award to Yi Xu.

### References

1. Calderwood, D.A., et al. *J. Biol. Chem.* **272**, 12311–12317 (1997).
2. Dickeson, S.K., Walsh, J.J., Santoro, S.A. *J. Biol. Chem.* **272**, 7661–7668 (1997).
3. Rich, R.L., Deivanayagam, C.C.S., Owens, R.T., Carson, M., Höök, A., Moore, D., Symerski, J., Yang, V.W.-C., Narayana, S.V.L., Höök, M. *J. Biol. Chem.* **274**, 24906–24913 (1999).
4. Knight, C.G., Morton, L.F., Onley, D.J., Peachey, A.R., Messent, A.J., Smethurst, P.A., Tuckwell, D.S., Farndale, R.W., Barnes, M.J. *J. Biol. Chem.* **273**, 33287–33294 (1998).
5. Knight, C.G., Morton, L.F., Peachey, A.R., Tuckwell, D.S., Farndale, R.W., Barnes, M.J. *J. Biol. Chem.* **275**, 35–40 (2000).
6. Emsley, J., Knight, C.G., Farndale, R.W., Barnes, M.J., Liddington, R.C. *Cell* **100**, 47–56 (2000).

## **Probing the Importance of the N-Terminal Helix of Parathyroid Hormone: Introduction of Cyclohexylalanine to Tether to the Membrane**

**Maria Pellegrini<sup>1,2</sup>, Andrea Piserchio<sup>3</sup>, Dale F. Mierke<sup>1,3</sup> and Jesse Dong<sup>4</sup>**

<sup>1</sup>*Molecular Pharmacology, Physiology & Biotechnology, Brown University, Providence, RI 02912, USA*

<sup>2</sup>*Abbott Bioresearch Center, Worcester, MA 01605, USA*

<sup>3</sup>*Department of Chemistry, Brown University, Providence, RI 02912, USA*

<sup>4</sup>*Biomeasure, Inc./Beaufour-ISPEN group, Medford, MA 01757, USA*

### **Introduction**

We have previously described the structural features of parathyroid hormone (PTH) as determined by high-resolution NMR under a number of different conditions, including the membrane mimetic environment of dodecylphosphocholine (DPC) micelles [1]. The structure of PTH consisted of a C-terminal helix extending from Glu<sup>19</sup>-Asn<sup>33</sup>, which is important for binding, and a N-terminal helix from residues Ser<sup>3</sup>-Asn<sup>10</sup>, which is responsible for activation of the PTH receptor. Based on a series of titrations with a relaxation-inducing lipid, the N-terminal helix was observed to be closely associated with the membrane surface. To further examine the importance of the interaction of the N-terminus with the membrane surface, we have undertaken the structural characterization of PTH containing cyclohexylalanine (Cha) at positions 7 and 11, replacing the naturally occurring leucines at these positions. Here, we present the results from our NMR-based structural investigation of this PTH analog, [Cha<sup>7,11</sup>]hPTH(1-34)NH<sub>2</sub>.

### **Results and Discussion**

The peptide [Cha<sup>7,11</sup>]hPTH(1-34)NH<sub>2</sub> (2 mM) was examined in the presence of DPC (120 mM) at pH 6.5 (uncorrected for deuterium effect) at 500 and 600 MHz on Varian Unity and Bruker Avance instruments. There was a significant broadening of the resonances upon the addition of DPC, clearly indicating tight association with the zwitterionic, phosphocholine head group of the micelle. The NMR resonance assignments were obtained using standard procedures of TOCSY spectra for spin system identification and NOESY for sequential assignment of the amino acids. A plot of the secondary shifts was obtained by subtracting the chemical shift values for "random coil" peptides from the values observed here. This plot clearly indicated two  $\alpha$ -helices for [Cha<sup>7,11</sup>]hPTH(1-34)NH<sub>2</sub>. The C-terminal helix, encompassing residues S<sup>16</sup>-H<sup>32</sup>, is very similar to that previously observed for PTH. In contrast, we observed a great extension and stabilization of the N-terminal helix of [Cha<sup>7,11</sup>]hPTH(1-34)NH<sub>2</sub> in comparison to that for PTH, the N-terminal helix extends from V<sup>2</sup>-L<sup>15</sup>. Analysis of the NOEs confirmed the secondary shift analysis. A large number of NOEs in the N-terminal portion of the peptide are observed. Many of these NOEs are absent, or very weak, in the spectra collected (under identical conditions) for PTH. Therefore, the incorporation of Cha to replace Leu at the 7 and 11 positions has a dramatic effect on the helicity of the peptide.

Following procedures previously utilized in our laboratories [2], we have examined the topological display of the peptide with respect to the micelle surface. The method utilizes the titration of a doxyl-containing long-chain acid, which is readily incorporated into the micelle environment, and careful monitoring of the broadening of the NMR sig-

nals. Based on these results, we found that both  $\alpha$ -helices of [Cha<sup>7,11</sup>]hPTH(1-34)NH<sub>2</sub> are closely associated with the lipid surface of the micelle. The association of the N-terminal helix of [Cha<sup>7,11</sup>]hPTH(1-34)NH<sub>2</sub> to the micelle surface is much greater than that for PTH, as expected based on the increased hydrophobicity of Cha over Leu.

The structural consequences of replacing Leu<sup>7,11</sup> with Cha<sup>7,11</sup> in PTH is an extension of both the N- and C-terminal helices (although the latter to a smaller extent). This results in a small, non-helical region approximately in the middle of the 34-residue peptide. The fact that [Cha<sup>7,11</sup>]hPTH(1-34)NH<sub>2</sub> is *ca.* 6 times more active than PTH may indicate that the stabilization of the N-terminal helix is required for biological function. The extension of the two helices is similar in many regards to the X-ray structure of PTH, in which packing of two PTH molecules within the unit cell produces a structure, which is entirely helical [3]. Importantly, our NMR data clearly indicates a centrally located region of undefined structure, which we have previously postulated to be important for binding and activation of the PTH receptor [4].

## References

1. Pellegrini, M., Royo, M., Rosenblatt, M., Chorev, M., Mierke, D.F. *J. Biol. Chem.* **273**, 10420–10427 (1998).
2. Pellegrini, M., Tancredi, M., Rovero, P., Mierke, D.F. *J. Med. Chem.* **42**, 3369–3377 (1999).
3. Jin, L., Briggs S.L., Chandrasekhar, S., Chirgadze, N.Y., Clawson, D.K., Schevitz, R.W., Smiley, D.L., Tashjian, A.H., Zhang F. *J. Biol. Chem.* **275**, 27238–27244 (2000).
4. Mierke, D.F., Maretto, S., Schievano, E., DeLuca, D., Bisello, A., Rosenblatt, M., Peggion, E., Chorev, M. *Biochemistry* **36**, 10372–10383 (1997).

## Structure–Function Relationship Studies on Parathyroid Hormone (PTH) 1-34 Analogs Containing $\beta$ -Amino Acid Residues in Positions 11, 12, and 13

Evaristo Peggion<sup>1</sup>, Stefano Mammi<sup>1</sup>, Elisabetta Schievano<sup>1</sup>,  
 Laura Silvestri<sup>1</sup>, Lukas Scheibler<sup>2</sup>, Martina Corich<sup>2</sup>, Alessandro Bisello<sup>2</sup>,  
 Michael Rosenblatt<sup>2</sup> and Michael Chorev<sup>2</sup>

<sup>1</sup>Department of Organic Chemistry, University of Padova, Padova, I-35131, Italy

<sup>2</sup>Division of Bone and Mineral Metabolism, Beth Israel Deaconess Medical Center, Harvard Medical School, Boston, MA 02215, USA

### Introduction

Parathyroid hormone (PTH) is an 84 amino acid residue peptide, which plays a key physiological role in the regulation of calcium levels in serum. Virtually, all bone-relevant activities of PTH are encoded in the fully active N-terminal 1-34 sequence [1]. On the basis of our previous results on a series of active and inactive analogs of the PTH(1-34) [2], we suggested that the structural elements essential for biological activity are an N-terminal and a C-terminal helical segments connected by hinges or flexible points around positions 12 and 19. To probe this hypothesis, in the present work we synthesized by solid phase methods, and characterized the following bPTH(1-34) analogs containing  $\beta$ -amino acid residues at positions 11, 12 and 13.

- I:** [Nle<sup>8,18</sup>,  $\beta$ -Ala<sup>11</sup>, Nal<sup>23</sup>, Tyr<sup>34</sup>]bPTH(1-34)NH<sub>2</sub>  
**II:** [Nle<sup>8,18</sup>,  $\beta$ -hLeu<sup>11</sup>, Nal<sup>23</sup>, Tyr<sup>34</sup>]bPTH(1-34)NH<sub>2</sub>  
**III:** [Nle<sup>8,18</sup>,  $\beta$ -Ala<sup>12</sup>, Nal<sup>23</sup>, Tyr<sup>34</sup>]bPTH(1-34)NH<sub>2</sub>  
**IV:** [Nle<sup>8,18</sup>,  $\beta$ -Ala<sup>13</sup>, Nal<sup>23</sup>, Tyr<sup>34</sup>]bPTH(1-34)NH<sub>2</sub>

### Results and Discussion

The results of the biological characterization of the analogs, including binding affinity and efficacy in stimulating cAMP, are reported in Table 1.

Analog **I**, containing  $\beta$ -Ala at position 11, is inactive, while reintroduction of the Leu side-chain, present at this position in the native sequence, in the form of  $\beta$ -homo-Leu in analog **II** leads to a partial recovery of biological activity and binding capacity. Finally, analogs **III** and **IV** containing  $\beta$ -Ala residues at positions 12 and 13 respectively, are fully active. The conformational properties of the four analogs in aqueous solution containing dodecylphosphocholine (DPC) micelles were studied by CD, 2D-NMR and molecular dynamics calculations. The CD spectra of analog **I** in aqueous solution in the presence of increasing concentrations of DPC are shown in Figure 1.

Table 1. Results of biological activity and binding assay test.

Analog	EC <sub>50</sub> (nM) <sup>a</sup>	IC <sub>50</sub> (nM) <sup>b</sup>
[Nle <sup>8,18</sup> , Nal <sup>23</sup> , Tyr <sup>34</sup> ]bPTH(1-34)NH <sub>2</sub>	0.85 ± 0.15	12 ± 0.5
<b>I</b> [Nle <sup>8,18</sup> , $\beta$ -Ala <sup>11</sup> , Nal <sup>23</sup> , Tyr <sup>34</sup> ]bPTH(1-34)NH <sub>2</sub>	500	1000
<b>II</b> [Nle <sup>8,18</sup> , $\beta$ -hLeu <sup>11</sup> , Nal <sup>23</sup> , Tyr <sup>34</sup> ]bPTH(1-34)NH <sub>2</sub>	50 ± 1.5	80
<b>III</b> [Nle <sup>8,18</sup> , $\beta$ -Ala <sup>12</sup> , Nal <sup>23</sup> , Tyr <sup>34</sup> ]bPTH(1-34)NH <sub>2</sub>	0.7 ± 0.07	150 ± 13
<b>IV</b> [Nle <sup>8,18</sup> , $\beta$ -Ala <sup>13</sup> , Nal <sup>23</sup> , Tyr <sup>34</sup> ]bPTH(1-34)NH <sub>2</sub>	0.3 ± 0.1	23 ± 1

<sup>a</sup> Stimulation of adenylyl cyclase activity; <sup>b</sup> competition of <sup>125</sup>I-PTH-(1-34) binding.

Increase of the detergent concentration results in the formation of  $\alpha$ -helical structure. Practically identical results were obtained with the other analogs. Thus, the sequence modifications introduced in the four analogs do not have major effects on the chiroptical properties. In all cases the set of spectra fit the same isodichroic point typical of the coil-helix equilibrium. The maximum helix content formed in the presence of DPC micelles is of the order of 30–35% in all analogs. The chemical shift differences of the  $\alpha$ CH proton resonances with respect to the corresponding random coil values, obtained from the NMR analysis, are reported in Figure 2. Two stretches of  $\alpha$ -helix at the N- and C-termini are identified by negative values of 0.1 ppm or higher. The helix is clearly interrupted around position 12 and there is an additional minimum around position 19, which might indicate the presence of a bend or kink of the C-terminal helix. Analogs **I** and **II** are conformationally indistinguishable. Thus, the partial recovery of binding affinity and biological activity of the  $\beta$ -*homo*-Leu contain-

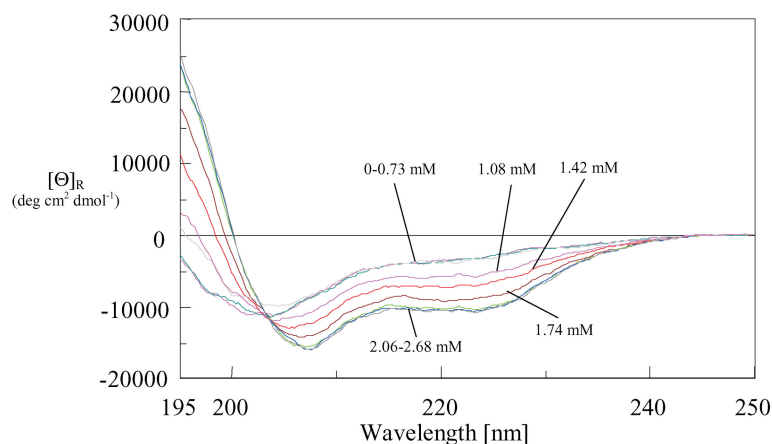


Fig. 1. CD spectra of analog **I** in aqueous solution  $c = 0.0491$  mM containing increasing concentrations of DPC (indicated). The maximum helix content is formed at 2.06 mM DPC.

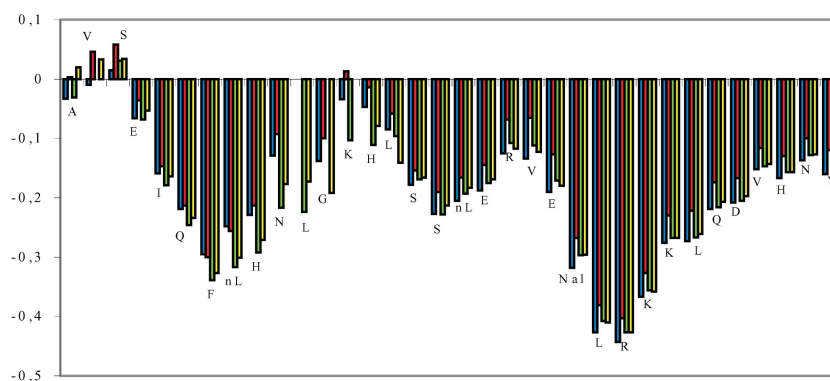


Fig. 2. Chemical shift differences (ppm) of  $\alpha$ H protons relative to the random coil values of analogs **I** (blue), **II** (red), **III** (green), and **IV** (yellow).

ing analog **II** must be due to the re-introduction of the Leu side-chain moiety, as in the native sequence. This side-chain should be therefore involved in a crucial interaction with a complementary site at the receptor. The chemical shift difference profile of analog **III** reveals a small but detectable difference with respect to the first two analogs. The more negative values indicate a higher stability of the N-terminal helix and a more extended C-terminal helical segment which starts from Lys<sup>13</sup>. The chemical shift difference profile of analog **IV** is identical to that of analog **III**. The stability of the N-terminal helix of these fully active analogs is higher than in analogs **I** and **II**. Taken together, these findings underline the importance of the stability of the N-terminal helix and of the Leu<sup>11</sup> side-chain for bioactivity. The ensemble of sequential and medium range NOESY connectivities, obtained from NOESY experiments are consistent with the results of the secondary chemical shift. Medium range ( $i, i+3$ ) connectivities are present in the C-terminal and, to a lesser extent, in the N-terminal regions, indicating the presence of two helical segments, the C-terminal one being more stable (data not shown).

Interestingly, ( $i, i+3$ ) and ( $i, i+2$ ) NOE connectivities, usually indicative of  $3_{10}$ -helices or turn-like structures were observed in the segment 10-14 comprising the  $\beta$ -amino acid residues. Taken together, these findings show that these sequence modifications do not induce a disordered structure in this position of the sequence. Most important, no long-range connectivity was found in any of the four analogs. There is therefore no evidence of a folded, U-shaped conformation in which the two terminal helical segments are in close proximity, as suggested in early work [3]. Inter-proton distances obtained from integration of the NOESY spectra were used in structure calculations using the simulated annealing protocol of the X-PLOR program. The ensembles of the calculated low energy structures of all analogs converge to the  $\alpha$ -helical conformation in the N- and C-terminal regions. The results presented in this work confirm the importance of the conformational stability of the N-terminal helix for bioactivity. The structural details around the putative hinge or bend positions 12 and 19 must be further investigated in order to assess unambiguously their role in the biological function.

#### **Acknowledgments**

We acknowledge the support of C.N.R, Italy and, in part, of NIH, grant RO1-DK47940.

#### **References**

1. Chorev, M., Rosenblatt, M., In Bilezikian, J.P., Levine, M.A., and Marcus, R. (Eds.) *The Parathyroids*, Raven Press, New York, 1994, pp. 139–156.
2. Peggion, E., Mammi, S., Schievano, E., Behar, V., Rosenblatt, M., Chorev, M. *Biopolymers* **50**, 525–535 (1999) and references therein.
3. Cohen, F.E., Stewler, G.J., Bradley, M.S., Carlquist, M., Nilsson, M., Ericsson, M., Ciardelli, T.L., Nissenson, R.A. *J. Biol. Chem.* **266**, 1997–2004 (1991).

## Local Conformation Around Position 12 of the (1-34) Fragment of Parathyroid Hormone Probed by Substitution with Aib Residues

Evaristo Peggion<sup>1</sup>, Stefano Mammi<sup>1</sup>, Elisabetta Schievano<sup>1</sup>,  
 Laura Silvestri<sup>1</sup>, Lukas Scheibler<sup>2</sup>, Martina Corich<sup>2</sup>, Alessandro Bisello<sup>2</sup>,  
 Michael Rosenblatt<sup>2</sup> and Michael Chorev<sup>2</sup>

<sup>1</sup>Department of Organic Chemistry, University of Padova and Biopolymers Research Center,  
 C.N.R., Padova, I-35131, Italy

<sup>2</sup>Division of Bone and Mineral Metabolism, Charles A. Dana and Thorndike Laboratories,  
 Department of Medicine, Beth Israel Deaconess Medical Center and Harvard Medical School,  
 Boston, MA 02215, USA

### Introduction

Parathyroid hormone (PTH) controls the homeostasis of calcium ions in the blood. Its N-terminal 1-34 fragment is sufficient to reproduce all the physiological functions elicited by the intact hormone. The biologically relevant conformation of PTH(1-34) is thought to include two critical points of flexibility around residue 12 and residue 19 [1]. These two hinges are believed to connect two  $\alpha$ -helical regions at either end of the molecule. In order to assess the relationship between biological activity and local conformation around Gly<sup>12</sup>, we prepared and studied several PTH(1-34) analogs containing Aib residues: [Aib<sup>11</sup>], [Aib<sup>12</sup>], [Aib<sup>11,12</sup>] or [Aib<sup>12,13</sup>].

### Results and Discussion

In Table 1, the data of binding affinity and adenylyl cyclase (AC) stimulation are reported for the Aib-containing analogs and the parent PTH(1-34) derived compound. Substitution with Aib residues in position 11 (analog **I**), or in positions 11 and 12 (analog **III**) results in loss of binding capacity and a substantial reduction of biological activity compared to the parent compound. Both binding affinity and AC stimulation activity are largely restored when the Aib residues are introduced in position 12 (analog **II**) or in position 12 and 13 (analog **IV**).

The conformational properties of the four analogs in aqueous solution containing dodecylphosphocholine (DPC) micelles were studied by CD, 2D-NMR and molecular dynamics calculations. The CD spectra of analog **I**, **II** and **IV** in aqueous solution in the presence of increasing concentrations of DPC show helix formation at DPC concentration above c.m.c. All spectra fit the same isodichroic point typical of the coil-helix equilibrium. The maximum helix content in the presence of DPC micelles is

Table 1. Biological activity and binding affinity data in HEK293 cells stably expressing the recombinant human PTH1Rc.

Analog	EC <sub>50</sub> (nM) <sup>a</sup>	IC <sub>50</sub> (nM) <sup>b</sup>
[Nle <sup>8,18</sup> , Nal <sup>23</sup> , Tyr <sup>34</sup> ]bPTH(1-34)-NH <sub>2</sub>	0.85 ± 0.15	16 ± 4
<b>I</b> [Nle <sup>8,18</sup> , Aib <sup>11</sup> , Nal <sup>23</sup> , Tyr <sup>34</sup> ]bPTH(1-34)-NH <sub>2</sub>	4.2 ± 0.2	>1000
<b>II</b> [Nle <sup>8,18</sup> , Aib <sup>12</sup> , Nal <sup>23</sup> , Tyr <sup>34</sup> ]bPTH(1-34)-NH <sub>2</sub>	0.35 ± 0.15	65 ± 10
<b>III</b> [Nle <sup>8,18</sup> , Aib <sup>11,12</sup> , Nal <sup>23</sup> , Tyr <sup>34</sup> ]bPTH(1-34)-NH <sub>2</sub>	5 ± 1	653 ± 8
<b>IV</b> [Nle <sup>8,18</sup> , Aib <sup>12,13</sup> , Nal <sup>23</sup> , Tyr <sup>34</sup> ]bPTH(1-34)-NH <sub>2</sub>	0.20 ± 0.05	36 ± 4

<sup>a</sup> Stimulation of adenylyl cyclase activity; <sup>b</sup> competition of <sup>125</sup>I-PTH(1-34) binding.

of the order of 42%. The results obtained with analog **III** are qualitatively very similar. However, the maximum helix content at saturation conditions is about 30%, *i.e.*, lower than in the other analogs. Taken together, these results indicate that the shift of the Aib substitution from positions 11 and 12 to 12 and 13 enhances the conformational preference towards the  $\alpha$ -helix.

From chemical shift difference of the  $\alpha$ CH proton resonances with respect to the corresponding random coil values obtained from the NMR analysis, two stretches of  $\alpha$ -helix at the N- and C-termini are identified by negative values of 0.1 ppm or higher (Figure 1). In all analogs, the helix is clearly interrupted around position 12. The  $\alpha$ CH proton chemical shifts indicate an increased stability of both helices relative to the parent peptide for all analogs except analog **I**, which shows less negative values in the region 8–15. Interestingly, in all the peptides examined there is an additional minimum around position 20, which is more pronounced than in the parent peptide and might indicate the presence of a bend or kink of the C-terminal helix.

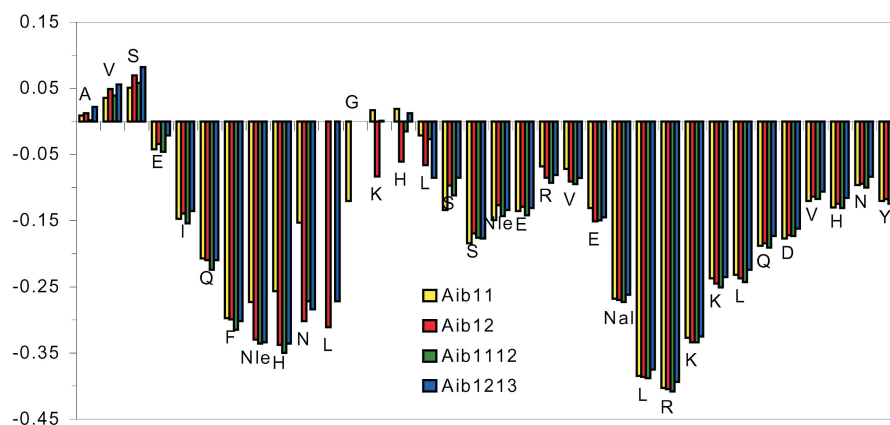


Fig. 1. Chemical shift differences of the  $C\alpha$  protons of the four peptides investigated in aqueous solution in the presence of DPC micelles.

Consistent with the results obtained with the  $\beta$ -amino acid containing analogs, the lack of binding affinity and lower biological activity in analogs **I** and **III** must be due to the elimination of the Leu side-chain moiety in position 11, as present in the native sequence. In the case of analog **I**, the lower stability of the N-terminal helix must also play a role.

The patterns of sequential and medium range NOESY connectivities corroborate the interpretation of the chemical shift data. In summary, the importance for biological activity of the stability of the N-terminal helix, which is enhanced by the Aib substitutions, and of the Leu side-chain at position 11 of the native sequence are confirmed.

## References

1. Peggion, E., Mammi, S., Schievano, E., Behar, V., Rosenblatt, M., Chorev, M. *Biopolymers* **50**, 525 (1999) and references therein.

## Positional Cyclization Scanning: A New Method to Evaluate the Bioactive Conformation of Glucagon

Jung-Mo Ahn, Dev Trivedi, Peter M. Gitu, Matthew Medeiros,  
 Jennifer R. Swift and Victor J. Hruby

*Department of Chemistry, University of Arizona, Tucson, Arizona, 85721, USA*

### Introduction

Glucagon is a polypeptide hormone, which consists of 29 amino acid residues. Secreted from pancreas, it has an importance role in glucose homeostasis. The conformation of glucagon has been examined by various biophysical methods including X-ray crystallography [1] and 2D-NMR spectroscopy [2]. Although an amphiphilic helical conformation was observed at the C-terminal region of glucagon by both methods, the rest of the molecule displayed different conformations depending on the method used to examine them. The glucagon receptor is a G protein-coupled receptor (GPCR) which resides on the membrane surface, and unfortunately, it is still extremely difficult to examine a bioactive conformation of a ligand when it binds to its receptor. Therefore, in an attempt to obtain information about the bioactive conformation of glucagon, a new approach, "positional cyclization scanning", was developed to determine secondary structures in the bioactive conformation.

### Results and Discussion

Positional cyclization scanning (Figure 1) consists of a series of structure-activity relationship studies using conformational restrictions to stabilize secondary structures by conformational restrictions at defined regions of a target ligand. Synthesis of a conformationally constrained analogue and the result of receptor binding assay determines whether a certain secondary structure is required by the receptor for the region where the conformational restriction is imposed. By introducing secondary structures throughout the sequence of glucagon, and examining the affinity of these ligands in receptor binding assays, the bioactive conformation of glucagon can be derived indirectly. The conformational restrictions used in this investigation are disulfide bridges between Cys<sup>i</sup>-Cys<sup>i+5</sup> for turns, and lactam bridges between Lys<sup>i</sup>-Glu<sup>i+4</sup> for  $\alpha$ -helices. The choice of the residues and their positions for the conformational restrictions were based on the previous SAR studies of glucagon [3,4]. The decreased binding affinities of all cyclic glucagon analogues containing disulfide bridges suggest that turn confor-

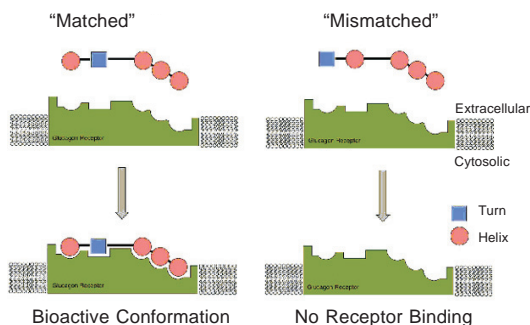


Fig. 1. Structure of cyclo(-RGDfK-)-MAG3 conjugate.

*Table 1. Biological activities of the conformationally restricted glucagon analogues.*

Compound	Receptor Binding		Adenylate Cyclase Activity		
	IC <sub>50</sub> (nM)	Relative Binding (%)	EC <sub>50</sub> (nM)	Maximum Stimulation (%)	pA <sub>2</sub>
Glucagon	1.5	100	5.9	100	-
1 [Cys <sup>2,7</sup> ]Glucagon-NH <sub>2</sub>	5.6	27	41.8	50	-
2 c[Cys <sup>2,7</sup> ]Glucagon-NH <sub>2</sub>	101	1.5	9200	23	-
3 [Cys <sup>4,9</sup> ]Glucagon-NH <sub>2</sub>	3.6	42	295	18	-
4 c[Cys <sup>4,9</sup> ]Glucagon-NH <sub>2</sub>	84.5	1.7	295	7.5	-
5 [Cys <sup>7,12</sup> ]Glucagon-NH <sub>2</sub>	6.4	23	59	100	-
6 c[Cys <sup>7,12</sup> ]Glucagon-NH <sub>2</sub>	558	0.27	5900	53	-
7 [Cys <sup>14,19</sup> ]Glucagon-NH <sub>2</sub>	13.7	11	236	100	-
8 c[Cys <sup>14,19</sup> ]Glucagon-NH <sub>2</sub>	562	0.27	7500	30	-
9 c[Lys <sup>3</sup> ,Glu <sup>7</sup> ]Glucagon-NH <sub>2</sub>	6.0	25	i.a.	-	8.28
10 c[Lys <sup>5</sup> ,Glu <sup>9</sup> ]Glucagon-NH <sub>2</sub>	0.20	760	390	12	8.26
11 c[Lys <sup>7</sup> ,Glu <sup>11</sup> ]Glucagon-NH <sub>2</sub>	13.6	11	47	17	-
12 c[Lys <sup>9</sup> ,Glu <sup>13</sup> ]Glucagon-NH <sub>2</sub>	652	0.23	23	19	-
13 c[Lys <sup>13</sup> ,Glu <sup>17</sup> ]Glucagon-NH <sub>2</sub>	1.7	87	6.3	85	-
14 c[Lys <sup>17</sup> ,Glu <sup>21</sup> ]Glucagon-NH <sub>2</sub>	0.24	630	0.27	98	-

mations in the N-terminal region and between residues 14-19 are unlikely in the bioactive conformations. These results indicate that the earlier prediction [5] of  $\beta$ -turns between positions 2-5 and 14-19 seems to be invalid. On the other hand, the predominant helical conformations in the N-terminal region and in residues 13-29 can be proposed by the increased binding affinities of the cyclic glucagon analogues containing lactam bridges. Helical conformations in the N-terminal region were not observed in any previous studies [1,2]. As a result, a new bioactive conformation of glucagon determined in this study consists of two helical segments which are connected by a non-helical segment between positions 10-13. Most of the peptides, except for analogues **9** and **10**, are found to be agonists, and analogue **14** displayed extremely potent adenylate cyclase activity (a 21-fold increase compared to glucagon). This enormous increase seems to result from the improved binding affinity by the formation of the lactam bridge between positions 17 and 21. On the other hand, the glucagon analogues with lactam bridges in the N-terminal region (analogues **9** and **10**) showed no or very minor adenylate cyclase activity, and these analogues demonstrated potent antagonism ( $pA_2 = 8.28$  and  $8.26$ , respectively).

### Acknowledgments

Supported by a grant from U. S. Public Health Service DK-21085.

### References

1. Sasaki, K., Dockerill, S., Adamiak, D.A., Tickle, I.J., Blundell, T. *Nature* **257**, 751–757 (1975).
2. Braun, W., Wider, G., Lee, K.H., Wüthrich, K. *J. Mol. Biol.* **169**, 921–948 (1983).
3. Hruby, V.J. *Mol. Cell. Biochem.* **44**, 49–64 (1982).
4. Hruby, V.J., Krstenansky, J.L., Gysin, B., Pelton, J.T., Trivedi, D., McKee, R.L. *Biopolymers* **25**, S135–S155 (1986).
5. Korn, A.P., Ottensmeyer, F.P. *J. Theor. Biol.* **105**, 403–425 (1983).

## **Age-Related Decreases of Calcitonin Gene-Related Peptide (CGRP)-Induced Hypotension *in vivo* and Vasorelaxant Responses *in vitro* in Rats**

**Gabriel H. H. Chan and Ronald R. Fiscus**

*Department of Physiology, Faculty of Medicine, Epithelial Cell Biology Research Center & Center for Gerontology and Geriatrics, The Chinese University of Hong Kong, Shatin, New Territories, Hong Kong*

### **Introduction**

CGRP is a 37 amino-acid neuropeptide and is reported to be the most potent endogenous vasodilator ever found [1,2]. CGRP causes both endothelium-independent and endothelium-dependent vasorelaxations, depending on the type of blood vessel [2]. The endothelium-dependent vasorelaxations are known to be mediated by nitric oxide (NO) released from endothelial cells and NO-dependent elevations of both cAMP and cGMP levels in vascular smooth muscle cells (VSMCs) [3]. CGRP also has anti-proliferative effects on VSMC [4], which may help in the prevention of the development of atherosclerosis. Blocking of the CGRP gene is associated with hypertension [5]. Thus, a decrease in CGRP's vascular actions, as for example during aging, may lead to atherosclerosis and hypertension. Interestingly, both the vasodilator and anti-proliferative effects of CGRP are synergistically enhanced by NO [6,7]. In general, the production of NO in blood vessels decreases during the aging process [8]. We have hypothesized that the vasodilatory and anti-proliferative actions of CGRP may substantially decrease during aging. The purpose of the present study is to examine the effect of aging on CGRP-induced hypotensive response *in vivo* and vascular responses to CGRP *in vitro*.

### **Results and Discussion**

The vasorelaxations *in vitro* induced by CGRP decreased significantly with advancing age of 28-month-old male rats in both thoracic aorta (reduced to 40% of response in 3-month-old controls) and caudal arteries (reduced to 55% of response in 3-month-old controls). These two blood vessels showed endothelium-dependent and endothelium-independent vasorelaxations, respectively. CGRP-induced hypotension *in vivo* was also significantly decreased in aged animals in both male (48% of control hypotension) and female (35% of control hypotension) rats.

Loss of NO production during aging may contribute to the diminished CGRP-induced vasorelaxant and hypotensive responses in elderly animals because there is a reduction of NO production with aging that may also diminish the responses to CGRP, which are known to be synergistically enhanced by NO in aortic rings [6] and cultured VSMCs [7].

CGRP-induced vasodilations may be influenced by sex steroid hormones, which are known to diminish during aging [8]. Also, Fiscus and Ming [8] have hypothesized that normal glucose levels can lead to glycosylation of proteins and receptors that may cause altered receptor function and subsequent loss of normal vascular responses as part of the aging process. Thus, during aging, glycosylation of CGRP receptors or other proteins involved in the signal transduction pathway of CGRP-induced vasodilations may lead to attenuation of the CGRP-induced hypotensive and vasorelaxant responses.

In conclusion, the results of the present study indicate that endothelium-dependent relaxations in aortic rings and endothelium-independent relaxations in caudal arterial rings in response to CGRP are greatly decreased in elderly male rats. Furthermore, the results indicated that the CGRP-induced hypotensive responses *in vivo* are also severely impaired in older rats, both female and male, as compared to young ones.

#### **Acknowledgments**

This work was supported by a Direct Grant for Research from the Research Grants Council of Hong Kong awarded to R.R. Fiscus. We would like to give special thanks to Dr. Anthony James, Director of the Laboratory Animal Services Center at The Chinese University of Hong Kong and workers of this center for helpful advice and technical assistance.

#### **References**

1. Wimalawansa, S.J. *Endocr. Rev.* **17**, 533–582 (1996).
2. Fiscus, R.R. *Semin. Thromb. Hemostasis Suppl.* **14**, 12–22 (1988).
3. Fiscus, R.R., Zhou, H.L., Wang, X., Han, C., Ali, S., Joyce, C.D., Murad, F. *Neuropeptides* **20**, 133–143 (1991).
4. Li, Y., Fiscus, R.R., Wu, J., Yang, L., Wang, X. *Neuropeptides* **31**, 503–509 (1997).
5. Gangula, P.R., Zhao, H., Supowit, S.C., Wimalawansa, S.J., Dipette, D., Westlund, K.N., Gagel, R.F., Yallampalli, C. *Hypertension* **35**, 470–475 (2000).
6. Fiscus, R.R., Hao, H., Wang, X., Arden, W.A., Diana, J.N. *Neuropeptides* **26**, 133–144 (1994).
7. Wang, X., Wang, W., Li, Y., Bai, Y., Fiscus, R.R. *J. Mol. Cell. Cardiol.* **31**, 1599–1606 (1999).
8. Fiscus, R.R., Ming, S.K., In Weng, S.P., Ming, K.T., Shiu, K.W. (Eds.), *Medicine and Surgery in the Elderly Person: Biology of Ageing*, Armour Publishing Pte Ltd., Singapore, 2000, pp. 29–42.

## A Novel Series of Growth Hormone Secretagogues

Vincent Guerlavais<sup>1</sup>, Damien Boeglin, Jean-Alain Fehrentz<sup>1</sup>,  
Romano Deghenghi<sup>2</sup>, Vittorio Locatelli<sup>3</sup>, Giampiero Muccioli<sup>4</sup>  
and Jean Martinez

<sup>1</sup>Laboratoire des Aminoacides, Peptides et Protéines (LAPP), UMR 5810, Universités  
Montpellier I et II, Faculté de Pharmacie, 34060 Montpellier Cédex 2, France

<sup>2</sup>EUROPEPTIDES, member of the Zentaris Group, 95108 Argenteuil Cedex, France

<sup>3</sup>Dept. of Pharmacology, School of Medicine, University of Milan, 20129 Milan, Italy

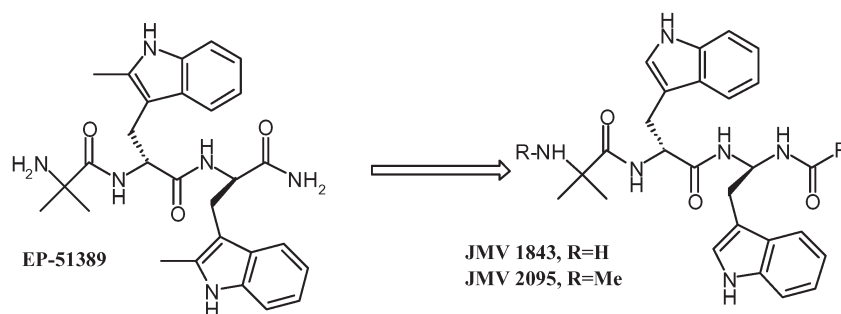
<sup>4</sup>Anatomy, Pharmacology and Forensic Medicine, University of Turin, Italy

### Introduction

Growth Hormone (GH), secreted by the pituitary gland, acts directly or indirectly on the peripheral organs by stimulating the synthesis of growth factors (insulin-like growth factor-I or IGF-I). The direct action of GH is of a type referred to as anti-insulinic, which favours lipolysis at the level of adipose tissues. Through its action on IGF-I (somatomein C) synthesis and secretion, GH stimulates growth of cartilage and bones, protein synthesis and cellular proliferation in multiple peripheral organs, including muscles and skin. Through its biological activity, GH participates within adults in the maintenance of a protein anabolism state, and plays a primary role in the tissue regeneration phenomenon after a trauma.

Growth Hormone secretion is regulated by two hypothalamic peptides: GH-releasing hormone (GHRH), which exerts a stimulatory effect on GH release, and somatostatin, which exhibits an inhibitory influence. In the last few years, several investigators have demonstrated that GH secretion can also be stimulated by synthetic oligopeptides, termed GH-releasing peptides (GHRPs), such as Hexarelin (His-2-Me-D-Trp-Ala-Trp-D-Phe-Lys-NH<sub>2</sub>) [1]. These compounds act through a mechanism which is distinct from that of GHRH [2] and by interacting with specific receptors localized in the hypothalamus and pituitary gland [3].

In a preliminary study the hexapeptide Hexarelin was downsized to give, among others, a tripeptide, compound EP-51389, subcutaneously more potent than Hexarelin in an infant rat model and orally active in dogs and in humans. We present here the synthesis and biological evaluation of a new class of orally bioavailable pseudotriptide analogs of EP-51389 (Scheme 1).



Scheme 1. Synthesis of pseudotriptide analogs of EP-51389.

## Results and Discussion

A number of our compounds were found to be efficacious in elevating plasma GH in the rat (Table 1); our best compounds showed comparable and even higher activity than Hexarelin when tested on dogs by oral route. Growth Hormone secretagogues are currently undergoing clinical evaluation as alternatives to growth hormone replacement therapy. Some of our compounds have been selected as candidates for further development.

*Table 1. Biological activity.*

Code JMV	N-terminus	Structure	C-terminus	JMV/Hexarelin <sup>a</sup>	IC50 (nM) <sup>b</sup>
1843	H-Aib	D-Trp-D-gTrp	formyl	1.31	14.6±0.2
1925	N-Me-Aib	“	“	0.82	n.d.
1926	H-Aib	“	acetyl	0.87	n.d.
1927	N-Me-Aib	“	“	1.38	n.d.
2141	H-Aib	“	CO-NH-Et	2.18	12.2±0.5
2142	N-Me-Aib	“	“	1.04	n.d.
2022	H-Aib	“	CO-4-piperidine	1.12	n.d.
2094	N-Me-Aib	“	“	0.85	n.d.
2096	H-Aib	D-Trp-N-Me-D-gTrp	acetyl	0.65	n.d.
2095	N-Me-Aib	“	“	1.25	n.d.

<sup>a</sup> *In vivo* activity ratio in rat: GH cc in ng/mL produced by 300 µg of JMV/ GH cc in ng/mL produced by 300 µg of Hexarelin. <sup>b</sup> Inhibition of specific binding of <sup>125</sup>I-ghrelin in human hypothalamus.

## References

1. Torsello, A., Battisti, C., Deghenghi, R., Müller, M.M., Locatelli, V. *Life Sciences* **18**, 1321 (1994).
2. Bercu, B., Walker, R.F. (Eds.) In *Xenobiotic Growth Hormone Secretagogues*, Bowers, C. Y., New York 1996, p. 9.
3. Muccioli, G., Ghé, C., Ghigo, M.C., Papotti, M., Arvat, E., Boghen, M., Nilsson, M., Deghenghi, R., Ong, H., Ghigo, E. *J. Endocrinology* **157**, 99 (1998).

## **Chimeric Mastoparans: Biological Probes and Designer Secretagogues**

**Michelle Farquhar<sup>1</sup>, Ursel Soomets<sup>2</sup>, Ashley Martin<sup>1</sup>, Ülo Langel<sup>2</sup>  
and John Howl<sup>1</sup>**

<sup>1</sup>*Molecular Pharmacology Group, School of Health Sciences,  
University of Wolverhampton, UK*

<sup>2</sup>*Department of Neurochemistry and Neurotoxicology, Stockholm University, Sweden*

### **Introduction**

Mastoparan (MP), an amphiphilic tetradecapeptide component of wasp venom, is able to directly activate G proteins and stimulate mast cell degranulation in a receptor-independent manner [1]. Chimeric peptides combine two or more bioactive modules in a single molecule. Previous studies have demonstrated that MP-containing chimeric constructs exhibit G protein-coupled receptor (GPCR)-independent actions dissimilar to those of their individual components [2].

Utilizing the RBL-2H3 cell line, a proven model for mucosal mast cells [3], the abilities of various MP-containing chimeras to stimulate secretion of both 5-hydroxytryptamine (5-HT) and  $\beta$ -hexosaminidase, and to activate Phospholipase D (PLD), were determined. Previously reported chimeras combining human calcitonin-gene-related peptide and MP (M432, M435, M436) were compared with constructs combining MP with galanin (galparan) and a  $V_{1a}$ -selective vasopressin antagonist (M391), all of which are potent insulin secretagogues [4–6]. Novel chimeric constructs were also synthesized combining sequences shown to modulate secretion with MP (SFLLR-MP, QLKK-MP, ZGF-MP) and the tandem homodimer MP-MP [7–9].

### **Results and Discussion**

All of the peptides stimulated 5-HT and  $\beta$ -hexosaminidase secretion and activated PLD, an enzyme involved in the regulated secretory pathway (Table 1) [10]. The chimeric MP analogues M435 and M436 significantly stimulated secretion of 5-HT displaying higher potency than MP. In comparison all the other peptides were relatively weak 5-HT secretagogues. ZGF-MP, SFLLR-MP, galparan, M391 and MP-MP were selective, high efficacy  $\beta$ -hexosaminidase secretagogues. Low efficacy secretagogues QLKK-MP and M432 were weak stimulators of both 5-HT and  $\beta$ -hexosaminidase secretion. These data indicate that MP-containing chimeric peptides act as differential secretagogues and suggest that secretion of 5-HT and  $\beta$ -hexosaminidase is regulated by subtly different mechanisms.

The efficacy of the peptides to activate PLD was compared with their secretory activities. These data indicate there is no correlation between PLD activation and 5-HT secretion. Potent 5-HT secretagogues M435 and M436 are weak activators of PLD whereas peptides that are weak 5-HT secretagogues significantly activate PLD. However, the results indicate a clear correlation between PLD activation and  $\beta$ -hexosaminidase secretion. Chimeric MP-analogues that potently stimulate  $\beta$ -hexosaminidase secretion are significant activators of PLD whereas weak stimulators of  $\beta$ -hexosaminidase do not significantly activate PLD. This would indicate that peptide-induced PLD activity is involved in the secretory mechanism leading to the secretion of  $\beta$ -hexosaminidase, a secretory granule enzyme. In conclusion, some chimeric MP analogues are differential secretagogues able to discriminate between and preferentially

### Biologically Active Peptides

activate either 5-HT or  $\beta$ -hexosaminidase secretion. Peptide-induced activation of PLD correlates with secretion of  $\beta$ -hexosaminidase, but not 5-HT.

Table 1. Structures of chimeric MP analogues compared in this study. Data indicate response activity at a concentration of  $3 \cdot 10^{-5}$  M. Data are means of three separate experiments.

Peptide, amino acid sequence	5-HT secretion	$\beta$ -Hexosaminidase secretion	PLD activity
<b>MP</b> , INLKALAALAKKIL-NH <sub>2</sub>	12.86	7.46	2.85
<b>M432</b> , INLKALAALAKKILVPTNVGSKAF-NH <sub>2</sub>	3.07	1.70	1.36
<b>M435</b> , ACDTATCVTHRLAGLINLKALAALAKKIL-NH <sub>2</sub>	14.26	7.73	1.75
<b>M436</b> , INLKALAALAKKILVTHRLAGLLSRVPTNVGSKAF-NH <sub>2</sub>	13.97	4.31	1.20
<b>Galparan</b> , GWTLNSAGYLLGPIINLKALAALAKKIL-NH <sub>2</sub>	4.89	7.97	5.39
<b>M391</b> , PhaaD-Y(Me)FQNRPRYεAhxINLKALAALAKKIL-NH <sub>2</sub>	5.65	6.93	5.07
<b>MP-MP</b> , INLKALAALAKKILINLKALAALAKKIL-NH <sub>2</sub>	2.91	6.30	3.73
<b>OLKK-MP</b> , QLKKINLKALAALAKKIL-NH <sub>2</sub>	1.78	3.17	1.84
<b>SFLLR-MP</b> , SFLLRINLKALAALAKKIL-NH <sub>2</sub>	2.89	7.81	4.21
<b>ZGF-MP</b> , ZGFINLKALAALAKKIL-NH <sub>2</sub>	3.54	9.75	5.08

### Acknowledgments

We thank the APS and Biochemical Society for travel grants awarded to M. F.

### References

1. Mousli, M., et al. *Trends Pharmacol. Sci.* **11**, 358–362 (1990).
2. Consolo, S., et al. *Brain Res.* **756**, 174–178 (1997).
3. Ludowyke, R.I., Peleg, I., Beaven, M.A., Aldstein, R.S. *J. Biol. Chem.* **264**, 12492–12501 (1989).
4. Poyner, D.R., Soomets, U., Howitt, S.G., Langel, Ü. *Br. J. Pharmacol.* **124**, 1659–1666 (1998).
5. Östenson, C-G., Zaitsev, S., Berggren, P-G., Efendic, S., Langel, Ü., Bartfai, T. *Endocrinology* **138**, 3308–3313 (1997).
6. Hällbrink, M., Saar, K., Östenson, C-G., Soomets, U., Efendic, S., Howl, J., Wheatley, M., Zorko, M., Langel, Ü. *Regul. Pept.* **82**, 45–51 (1999).
7. Scarborough, R.M., Naughton, M.A., Teng, W., Hung, D.T., Rose, J., Vu, T.K.H., Wheaton, V.I., Turck, C.W., Coughlin, S.R. *J. Biol. Chem.* **267**, 13146–13149 (1992).
8. Wu, D., Jiang, H., Katz, A., Simon, M.I. *J. Biol. Chem.* **268**, 3704–3709 (1993).
9. Mundi, D.I., Strittmatter, W.J. *Cell* **40**, 645–656 (1985).
10. Cissel, D.S., Fraudorfer, P.F., Beaven, M.A. *J. Pharmacol. Exp. Ther.* **285**, 110–118 (1998).

## Design of Cyclic $\alpha$ -Defensin Dimers as Channel Forming BuildingBlocks

Qitao Yu, Jin-Long Yang and James P. Tam

Department of Microbiology and Immunology, Vanderbilt University,  
 Nashville, TN 37232, USA

### Introduction

Defensins exhibit antimicrobial activity toward bacteria, yeast, fungi and enveloped viruses. Studies indicate that the microbe killing activity is related to their pore forming and membrane permeabilizing properties [1]. Also, the microbicidal activities of defensins are salt sensitive. This leads to the hypothesis that salt-sensitivity of defensins may exacerbate certain pathological conditions such as those found in cystic fibrosis in which the NaCl concentration on lung mucosal surface is increased to a level that inactivates endogenous defensins.

*In vivo*, defensins are stored in granules in high concentration. After releasing from granules, defensins are rapidly dissociated as monomers under physiological conditions, but self assemble on microbial surfaces to form channels to exert their microbicidal activity. The crystal structure of a rabbit defensin shows that the building block for the pore formation is a dimer [2].

Structurally, defensins contain three anti-parallel  $\beta$ -strands and clusters of hydrophobic and charged regions in their folded forms. Their N- and C-termini are at a close proximity by an end-to-end disulfide linkage. Our previous work suggested that the end-to-end cyclic structure with a triple  $\beta$ -stranded framework was sufficient to retain the molecular conformation required for biological activity [3]. These structural and mechanistic insights provide a rational design for dimeric defensins to improve their antimicrobial property.

### Results and Discussion

Eight homo- and hetero-dimers were designed and prepared. In all analogs, the 1,6-disulfide bond in natural NP-1 were replaced with two Gly and the N- and C-termini were covalently linked as a peptide bond [4]. All other Cystine pairs were replaced with Gly residues. Dimers were formed *via* a covalent disulfide linkage (Figure 1) [5].

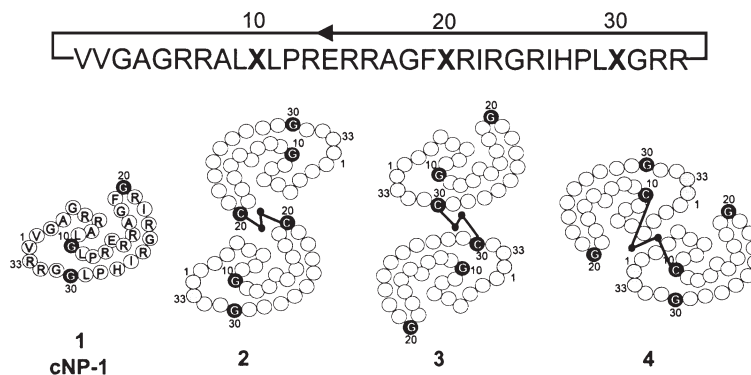


Fig. 1. Sequences and schematic representations of cyclic defensin cNP-1 (1) and selected dimers. Amino acids are numbered based on rabbit NP-1. X are Cys used for dimer formation. The dimeric disulfide bond are represented by zigzag.

### Biologically Active Peptides

Our results show that all dimers are substantially more active against three Gram-positive, four Gram-negative and three fungi as well as less salt-sensitive than either the natural defensin NP-1 or their corresponding synthetic cyclic analogue cNP-1 (Table 1). The dimeric or tetrameric design may provide a useful concept to improve the microbicidal activity of pore-forming, naturally occurring antimicrobial peptides.

Table 1. Antimicrobial activity of cNP-1 and selected dimers.

Peptide	Salt <sup>a</sup>	Mean MIC (μM)		
		Gram-negative bacteria <sup>b</sup>	Gram-positive bacteria <sup>b</sup>	fungi <sup>b</sup>
1 (cNP-1)	L	4.2	4.9	2.4
	H	14.9	14.1	20.7
2	L	1.3	0.74	1.0
	H	2.0	3.9	8.2
3	L	0.8	1.0	1.0
	H	1.5	1.0	8.5
4	L	0.6	0.6	0.6
	H	1.7	2.8	18.0

<sup>a</sup> Experiments were performed via the radial diffusion assay with an underlay gel containing 1% agarose and 10 mM phosphate buffer with (high salt, H) or without (low salt, L) 100 mM NaCl. <sup>b</sup> Gram-negative bacteria: *E. coli*, *P. aeruginosa*, *Pr. vulgaris*, *K. oxytoca*; Gram-positive bacteria: *S. aureus*, *M. luteus*, *E. faecalis*, fungi: *C. albicans*, *C. kefyr*, *C. tropicalis*.

### Acknowledgments

This work was in part supported by US public Health Service NIH Grant CA 36544, AI 37965.

### References

1. Ganz, T., Lehrer, R.I. *Curr. Opin. Immunol.* **10**, 41–44 (1998).
2. Hill, C.P., Yee, J., Selsted, M.E., Eisenberg, D. *Science* **251**, 1481–1485 (1991).
3. Yu, Q., Lehrer, R.I., Tam, J.P. *J. Biol. Chem.* **275**, 3943–3949 (2000).
4. Tam, J.P., Lu, Y.A., Liu, C.-F., Shao, J. *Proc. Natl. Acad. Sci. USA* **92**, 12458–12489 (1995).
5. Rabanal, F., DeGrado, W.F., Dutton, P.L. *Tetrahedron Lett.* **37**, 1347–1350 (1996).

## The Effect of Multiple Substitution of Aliphatic Amino Acids on the Structure, Function and Mode of Action of Lytic Peptides

Dorit Avrahami, Ziv Oren and Yechiel Shai

*Department of Biological Chemistry. The Weizmann Institute of Science, Rehovot, 76100 Israel*

### Introduction

Membrane-active polypeptides such as hormones, signal sequences, and lytic peptides initially bind to the membrane by electrostatic attraction and hydrophobic partitioning between water and lipid bilayers. Antimicrobial peptides have served as an important model for these studies [1,2]. To date, the contribution of hydrophobic amino acids in cell lysis by antimicrobial peptides has not been systematically analyzed, since many of these peptides aggregate and inactivate in solution. In this study, we synthesized a group of model amphipathic all-L amino acid peptides and their diastereomers, composed of lysines and one of the following aliphatic amino acids: Gly, Ala, Val, Ile, or Leu. The effect of the aliphatic amino acids on the binding, structure, membrane localization, and mode of action of the peptides was investigated.

### Results and Discussion

The results reveal that the peptides containing the most hydrophobic amino acids (L, I, V) are highly hemolytic, whereas their diastereomers are substantially less hemolytic (Table 1). All the diastereomers were monomers and unstructured in solution, but adopted distinct structures upon membrane binding, as revealed by Fourier-transform infrared spectroscopy (FTIR). Remarkably, only the diastereomers showed a direct correlation between their hydrophobicity, propensity to form a helical/dynamic-helical structure, and membrane permeating and antibacterial activities, despite the fact that they contained 30% D-amino acids. Interestingly, whereas all the peptide seems to bind initially on the surface of the membrane in a "carpet" like manner [3], efficient membrane permeation can proceed through different mechanisms depending on the

Table 1. Minimal inhibitory concentration ( $\mu\text{M}$ ) and hemolytic activity of the peptides.

Peptide designation	Minimal inhibitory concentration ( $\mu\text{M}$ ) <sup>a</sup>				% Hemolysis at 50 $\mu\text{M}$ peptide
	<i>E. coli</i> (ATCC 25922)	<i>P. aeruginosa</i> (ATCC 27853)	<i>B. subtilis</i> (ATCC 6051)	<i>S. aureus su</i> (ATCC 25922)	
K <sub>4</sub> G <sub>7</sub> W	200	200	200	200	0
K <sub>4</sub> A <sub>7</sub> W	200	200	200	200	0
K <sub>4</sub> V <sub>7</sub> W	70	100	2.8	150	27
K <sub>4</sub> I <sub>7</sub> W	150	>200	30	200	56
K <sub>4</sub> L <sub>7</sub> W	12.5	>200	1.25	18.1	93
K <sub>4</sub> A <sub>3a4</sub> W	>200	>200	>200	>200	0
K <sub>4</sub> V <sub>3a4</sub> W	150	>200	60	>200	2
K <sub>4</sub> I <sub>3a4</sub> W	19.3	>200	3.5	>200	6.4
K <sub>4</sub> L <sub>3a4</sub> W	15	7.5	1.25	30	13

<sup>a</sup> Results are the mean of three independent experiments, each performed in duplicates with a standard deviation not exceeding 20%.

### Biologically Active Peptides

aliphatic amino acid present. Moreover, by using transmission electron microscopy we found that the Leu-containing diastereomeric peptide caused micellization of lipid vesicles (Figure 1) and possibly of bacterial membranes. In contrast, the Ile-containing diastereomeric peptide fused model membranes and irregularly disrupted bacterial membranes, presumably due to its hydrophobic interaction with the membrane acyl chain region, as revealed by ATR-FTIR spectroscopy. Taken together, our results reveal that membrane permeation can proceed *via* different mechanisms depending on the amino acid composition.

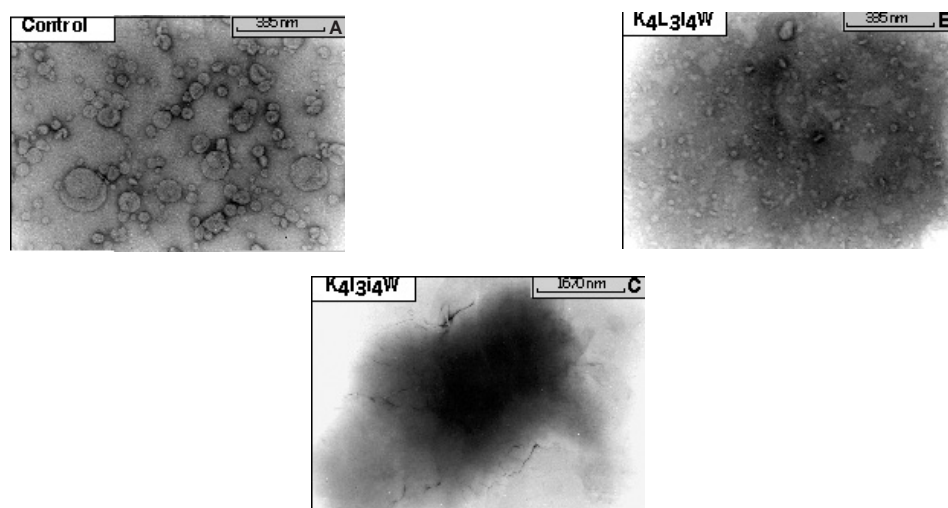


Fig. 1. Electron micrographs of negatively stained LUV composed of PE/PG (7 : 3 w/w) in the absence (Panel A), or in the presence of  $K_4L_3I_4W$  (peptide : lipid molar ratio 1 : 10, Panel B) or  $K_4I_3I_4W$  (peptide : lipid molar ratio 1 : 25, Panel C) peptides.

### References

1. Hancock, R.E., Lehrer, R. *Trends Biotechnol.* **16**, 82–88 (1998).
2. Oren, Z., Shai, Y. *Biopolymers* **47**, 451–463 (1998).
3. Shai, Y. *Trends Biochem. Sci.* **20**, 460–464 (1995).

## **Three-Dimensional Structure of Big Defensin, a Novel Antimicrobial Peptide Isolated from Horseshoe Crab**

**Naoki Fujitani<sup>1,2</sup>, Shun-ichiro Kawabata<sup>3,4,5</sup>, Tsukasa Osaki<sup>3</sup>,  
Makoto Demura<sup>1</sup>, Katsutoshi Nitta<sup>1</sup> and Keiichi Kawano<sup>2</sup>**

<sup>1</sup>*Division of Biological Sciences, Graduate School of Science, Hokkaido University,  
Sapporo 060-0810, Japan*

<sup>2</sup>*Faculty of Pharmaceutical Sciences, Toyama Medical and Pharmaceutical University,  
Toyama 930-0194, Japan*

<sup>3</sup>*Department of Biology, Kyushu University, Fukuoka 812-8581, Japan*

<sup>4</sup>*Core Research for Evolutional Science and Technology, Japan Science and Technology  
Corporation, Tokyo 101-0062, Japan*

<sup>5</sup>*Department of Molecular Biology, Graduate School of Medical Science, Kyushu University,  
Fukuoka 812-8582, Japan*

### **Introduction**

Big defensin is an antimicrobial peptide isolated from horseshoe crab (*Tachypleus tridentatus*) hemolymph and consists of a total of 79 amino acid residues. Although big defensin belongs to the family of defensin peptide with regard to homology of amino acid sequence, its molecular mass is significantly larger than other defensins, hence the name “big defensin”. The C-terminal region of big defensin composed of 37 amino acids shows homology with defensins, but the N-terminal region has no sequence homology with defensins. Big defensin shows strong antimicrobial activity against Gram-negative and Gram-positive bacteria. As a noteworthy character of this molecule, there is a functional difference between the N-terminal domain comprising residues 1 to 37 and the C-terminal domain comprising residues 38 to 79. The N-terminal hydrophobic fragment is more effective than the C-terminal fragment against Gram-positive bacteria. On the other hand, the C-terminal fragment shows more potent activity than the N-terminal fragment against Gram-negative bacteria [1,2].

In this study, we determined the solution structure of big defensin by NMR experiments and structure calculations. It was revealed that the N-terminal region consists of two  $\alpha$ -helices and the C-terminal region comprises a three-stranded antiparallel  $\beta$ -sheet. The domain structures form a striking contrast to each other and suggest that they reflect the difference of antimicrobial activity in each region.

### **Results and Discussion**

Two-dimensional NMR spectra were acquired for big defensin and signals were assigned completely except for N-terminal 1-15 residues region. The characteristic NOEs for  $\alpha$ -helix were found in the N-terminal domain of big defensin, and those for  $\beta$ -sheet were found in the C-terminal domain. This result suggests that the N- and C-terminal domains consist of  $\alpha$ -helix and  $\beta$ -sheet structures, respectively.

Three-dimensional structure of big defensin was calculated with 550 distance restraints and 32 dihedral angle restraints obtained by NMR experiments (Figure 1). From calculated structure, it was revealed that the N-terminal domain consists of two  $\alpha$ -helices (16-23, 38-34) and the C-terminal domain consists of a triple-stranded antiparallel  $\beta$ -sheet (51-54, 60-63 and 73-78). Both domains were connected by long flexible loop, and no long-range NOEs were observed between N- and C-terminal domains. The ensemble structure fitted in all region of this molecule was not obtained although each domain was converged well. This result supports the functional differ-

ence between domains. If the structure is stabilized by interactions between domains, each domain may not display the separate activity.

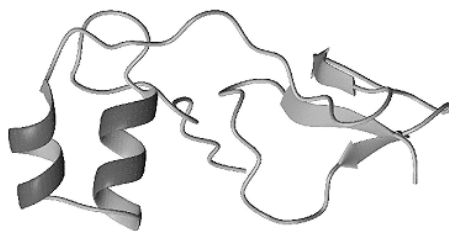


*Fig. 1. The lowest energy structure of big defensin.*

Interestingly, big defensin is the first reported peptide to have sequence homology with mammalian defensins. This study clarified that the structural homology is also recognized between the bovine  $\beta$ -defensin BNBD-12 and the C-terminal domain of big defensin (Figure 2). From the point of structure-function relationship, it is suggested that the mechanism for attacking Gram-negative bacteria may be similar for both molecules.

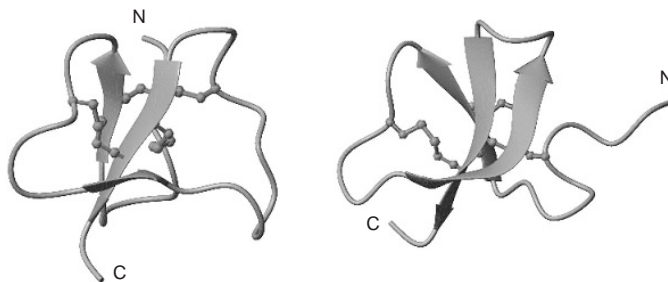


*Fig. 2. Structural comparison of big defensin and BNBD-12.*

## References

1. Saito, T., Kawabata, S., Shigenaga, T., Takayenoki, Y., Cho, J., Nakajima, H., Hirata, M., Iwanaga, S. *J. Biochem.* **117**, 1131–1137 (1995).
2. Iwanaga, S., Kawabata, S., Muta, T. *J. Biochem.* **123**, 1–15 (1998).

## Selective Bioactivity of Synthetic Amphipathic Peptides Against Murine Macrophages Infected with *Brucella abortus*

Lars G. J. Hammarström, Ted J. Gauthier and Mark L. McLaughlin

Louisiana State University, Department of Chemistry, Baton Rouge, LA 70803, USA

### Introduction

The efficacy of current antibiotics is declining at an alarming rate due to the proliferation of multi-drug resistant bacteria [1]. Synthetic antimicrobial peptides are currently being investigated as potential agents to address the increased need of antibiotics with different mechanism of action [2]. A series of short, synthetic, amphipathic peptides, incorporating high levels of C<sup>α</sup>,C<sup>α</sup>-disubstituted glycines (Table 1) have been prepared to determine their suitability as antimicrobial agents against the intracellular pathogen *Brucella abortus*. Though exhibiting low direct bioactivity against *B. abortus*, the peptides show a remarkable selectivity towards killing Murine peritoneal macrophages that have been infected with the pathogen *in vitro*. In all instances, the α-helical permutation isomers of the peptides exhibited higher selectivity and overall activity than the 3<sub>10</sub>-helical permutations. These results are being applied towards the development of therapeutic applications of synthetic peptides against intracellular pathogens of significant current interest, such as *M. tuberculosis*.

### Results and Discussion

Direct cytolytic activity against *B. abortus* was tested to verify that no significant cytotoxicity against the pathogen was observed under conditions similar to those of the studies of selective macrophage destruction. This was not surprising since it has been thoroughly documented that *B. abortus* is considerably more resistant to bactericidal cationic peptides than most Gram-negative bacteria [3].

*In vitro* studies, showing the selective killing of infected vs non-infected macrophages by the peptides, were performed using a strain of *B. abortus* containing a green fluorescent protein (GFP). Trypan blue exclusion was used to visualize dead macrophages. The optimum concentration for each peptide was established as the dosage at which maximum differentiation between infected macrophage killing and non-infected macrophage killing was observed. Cyh-10 was, by far, the most active

Table 1. Peptides designed to be perfectly amphipathic as an α-helix (Pi-10, Ach-10α and Cyh-10) and perfectly amphipathic as a 3<sub>10</sub>-helix (Ipi-10, Ach-10 and Ich-10).

Peptide	Sequence	Amphipathic Design
Pi-10	H-Aib <sup>a</sup> -Aib-Api <sup>b</sup> -Lys <sup>c</sup> -Aib-Aib-Api-Lys-Aib-Aib-NH <sub>2</sub>	α
Ipi-10	H-Api-Aib-Aib-Lys-Aib-Aib-Lys-Aib-Aib-Api-NH <sub>2</sub>	3 <sub>10</sub>
Ach-10α	H-Ac <sub>6</sub> c <sup>d</sup> -Aib-Lys-Api-Aib-Ac <sub>6</sub> c-Api-Lys-Ac <sub>6</sub> c-Aib-NH <sub>2</sub>	α
Ach-10	H-Api-Aib-Ac <sub>6</sub> c-Lys-Ac <sub>6</sub> c-Aib-Lys-Aib-Ac <sub>6</sub> c-Api-NH <sub>2</sub>	3 <sub>10</sub>
Cyh-10	H-Ac <sub>6</sub> c-Ac <sub>6</sub> c-Api-Lys-Ac <sub>6</sub> c-Ac <sub>6</sub> c-Api-Lys-Ac <sub>6</sub> c-Ac <sub>6</sub> c-NH <sub>2</sub>	α
Ich-10	H-Api-Ac <sub>6</sub> c-Ac <sub>6</sub> c-Lys-Ac <sub>6</sub> c-Ac <sub>6</sub> c-Lys-Ac <sub>6</sub> c-Ac <sub>6</sub> c-Api-NH <sub>2</sub>	3 <sub>10</sub>

<sup>a</sup> Aib: 2-aminoisobutyric acid; <sup>b</sup> Api: 4-aminopiperidine-4-carboxylic acid; <sup>c</sup> The incorporation of 20% L-lysine (Lys) allows for CD spectroscopic determination of peptide secondary structure by inducing right-handed helix formation. <sup>d</sup> Ac<sub>6</sub>c: 1-amino-1-cyclohexanoic acid.

peptide, showing an optimum concentration dose at 1–3  $\mu\text{M}$ . Ich-10 also showed activity at low concentrations. However, cytolytic activity was much lower than with Cyh-10, as was selectivity at all concentrations. In general, all peptides designed with the  $3_{10}$ -helix permutations showed significantly lower bioactivity and selectivity than their  $\alpha$ -helical counterparts (Table 2). However, the most dramatic effect was observed between Cyh-10 and Ich-10. This may be due to the lowered amphipathicity that is exhibited by Ich-10 in the  $\alpha$ -helical form. ECD studies show that Ich-10 does not adopt the designed  $3_{10}$ -helical conformation; rather it forms an  $\alpha$ -helix in membrane-mimetic environments [4].

Optimum concentrations decreased as the peptides increased in hydrophobicity, with the  $\alpha$ -helical permutation isomer retaining higher activity than the  $3_{10}$ -helical isomer. This may suggest that the  $\alpha$ -helical conformation is a more active membrane-disruption agent than a  $3_{10}$ -helical peptide of the same hydrophobicity. Overall efficacy of the peptides was established by peptide activity (% difference in infected vs non-infected killing at the optimum concentration)/optimum concentration dosage. As can be seen in Table 2, Cyh-10 and Ich-10 showed the highest efficacy. Ach-10 $\alpha$  and Pi-10 are the most interesting candidates for further study, as they retain high activity and relatively low cytotoxicity. It remains unclear why synthetic peptides of this family selectively destroy macrophages infected with intracellular pathogens, since macrophages, like other mammalian cells, are known to be relatively resistant to amphipathic peptides of this length.

Table 2. Activity summary of de novo peptides.

Peptide	Optimum Conc. ( $\mu\text{M}$ ) <sup>a</sup>	Activity <sup>b</sup>	Efficacy <sup>c</sup>
Pi-10	100	90	0.9
Ipi-10	200	25	0.13
Ach-10 $\alpha$	100	75	0.75
Ach-10	100	60	0.60
Cyh-10	3	95	31.67
Ich-10	20	40	2.0

<sup>a</sup> Optimum concentrations for each peptide were established as described above. <sup>b</sup> Activity = (% Infected killed – % Non-infected killed) at optimum conc. <sup>c</sup> Efficacy = Activity/Optimum Concentration.

### Acknowledgments

Authors wish to thank Fred Enright, Phil Elzer and Natha Booth of the LSU Veterinary Science Department, and Martha Juban of the LSU Protein Facility. This work was supported by the National Institute of Health grant GM 56835.

### References

1. Travis, J. *Science* **264**, 360–362 (1994).
2. Tossi, A., Sandri, L., Giangaspero, A. *Biopolymers* **55**, 4–30 (2000).
3. Martinez de Tejada, G., Pizarro-Cerda, J., Moreno, E., Moriyon, I. *Infect. Immun.* **63**, 3054–3061 (1995).
4. Hammarström, L. G. J., Gauthier, T. J., Hammer, R. P., McLaughlin, M. L. *J. Peptide Res.* **58**, 108–116 (2001).

## Antibacterial Peptides Derived from the C-Terminal Domain of the Hemolytic Lectin, CEL-III

Tomomitsu Hatakeyama, Tomoko Suenaga, Takuro Niidome  
and Haruhiko Aoyagi

Department of Applied Chemistry, Faculty of Engineering, Nagasaki University,  
Nagasaki 852-8521, Japan

### Introduction

CEL-III is a  $\text{Ca}^{2+}$ -dependent, galactose/*N*-acetylgalactosamine-specific lectin (carbohydrate-binding protein) isolated from a sea cucumber, *Cucumaria echinata*. In addition to carbohydrate-binding activity, this lectin also exhibits strong hemolytic activity [1] and cytotoxicity toward some cell lines [2] through forming ion-permeable pores in the cell membrane after binding to carbohydrate receptors [3]. The N-terminal regions of two-thirds of CEL-III are homologous to the sequence of the B-chains of ricin and abrin, plant lectins which are highly toxic, while the C-terminal region has relatively high hydrophobicity, and is thought to function as a pore-forming domain [4]. To elucidate the mechanism of pore-formation of CEL-III, we have synthesized peptides derived from the amino acid sequence of the C-terminal domain of CEL-III, and examined their properties and biological activities.

### Results and Discussion

We have synthesized three peptides corresponding to the sequences of the C-terminal region of CEL-III (Figure 1), P303 (position 303-322), P313 (position 313-332) and P332 (position 332-351). Far-UV circular dichroism spectra of these peptides showed almost random structure in Tris-buffered saline (TBS; 10 mM Tris-HCl, 0.15 M NaCl, pH 7.5). However, they exhibited typical  $\alpha$ -helical patterns in trifluoroethanol, suggesting that these peptides form  $\alpha$ -helices in hydrophobic environments, such as lipid membranes. These peptides were found to exert antibacterial activity toward some bacteria, such as *Bacillus subtilis*, *Staphylococcus aureus*, and *Pseudomonas aeruginosa*. Antibacterial activity was especially strong for P332. As shown in Figure 2, P332 showed the most effective inhibition to the growth of Gram-positive bacteria, *S. aureus* and *B. subtilis*. The growth was completely inhibited at 3.9  $\mu\text{g/ml}$  (*S. aureus*) and 31  $\mu\text{g/ml}$  (*B. subtilis*).

P303	H-KVSQQISNTISFSSTVTAGV-NH <sub>2</sub>
P313	H-SFSSTVTAGVAVEVSSTIEK-NH <sub>2</sub>
P332	H-KGVIFAKASVSVKVTASLSK-NH <sub>2</sub>

Fig. 1. Amino acid sequences of the peptides derived from the C-terminal domain of CEL-III.

Since such activity was thought to be caused by interaction between the peptide and the bacterial cell membrane, effects of the peptides on liposomes composed of dioleoyl phosphatidylcholine (DOPC) or dioleoyl phosphatidylcholine/dioleoyl phosphatidylglycerol (DOPC/DOPG) were examined. P332 effectively agglutinated DOPC/DOPG-liposomes, but not DOPC-liposomes, suggesting that the antibacterial activity of P332 is mediated by both electrostatic and hydrophobic interactions between the peptide and the cell membrane. P332 has four lysine residues spaced by 5-6

## Biologically Active Peptides

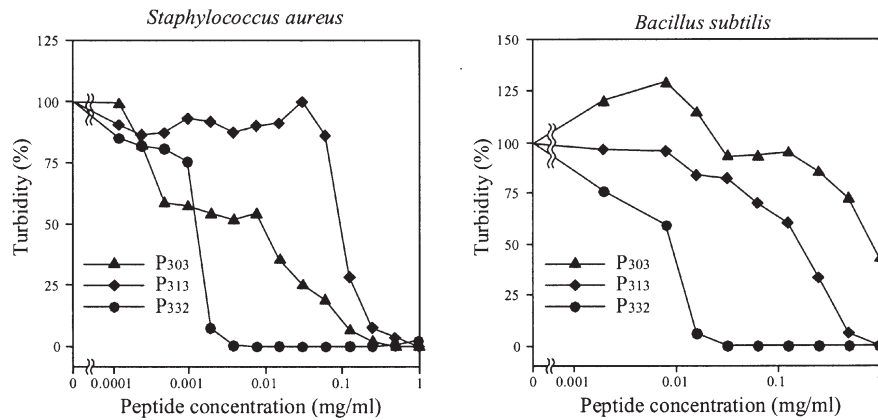


Fig. 2. Antibacterial activities of CEL-III-derived peptides.

residues, whereas the other two peptides have only one lysine residue at the N- or C-terminus. It appears possible that positively charged lysine side chains could be aligned along with  $\alpha$ -helical axis on the target membranes, leading to the perturbation of the bacterial membrane structure, and inhibition of cell growth. These results support that the C-terminal portion of CEL-III may play an important role in the hemolytic and cytotoxic activity through interaction with target cell membranes. It can also be expected that the structure of P332 may provide a clue to the design of new antibacterial peptides.

## References

1. Hatakeyama, T., Kohzaki, H., Nagatomo, H., Yamasaki, N. *J. Biochem.* **116**, 209–214 (1994).
2. Oda, T., Tsuru, M., Hatakeyama, T., Nagatomo, H., Muramatsu, T., Yamasaki, N. *J. Biochem.* **121**, 560–567 (1997).
3. Hatakeyama, T., Nagatomo, H., Yamasaki, N. *J. Biol. Chem.* **270**, 3560–3564 (1995).
4. Nakano, M., Tabata, S., Sugihara, K., Kouzuma, Y., Kimura, M., Yamasaki, N. *Biochim. Biophys. Acta* **1435**, 167–176 (1999).

## Low Molecular Weight $\psi$ [CH<sub>2</sub>NH] Pseudopeptides Yield Potent Antimicrobial Agents

David M. Vogel<sup>1</sup>, Sylvie Blondelle<sup>2</sup> and Arno F. Spatola<sup>1</sup>

<sup>1</sup>Department of Chemistry and the Institute for Molecular Diversity and Drug Design,  
University of Louisville, Louisville, KY 40292 USA

<sup>2</sup>Torrey Pines Institute for Molecular Studies, San Diego, CA 92121, USA

### Introduction

Emerging drug-resistant bacteria have rapidly increased the need for new antimicrobial drug leads. Random screening of peptide libraries generated through combinatorial synthesis led to three mixtures with promising antimicrobial activity. Deconvolution of these libraries led to several individual compounds active against methicillin-resistant *Staphylococcus aureus* (MRSA) and *Pseudomonas aeruginosa* (*P. aeruginosa*). Modifications were made in the most active sequences for structure activity studies.

### Results and Discussion

Based on an initial screen of peptide and pseudopeptide libraries (over 75 million compounds as mixtures), this work focused on a set of linear pseudopentapeptides having the structure H-Zzz $\psi$ [CH<sub>2</sub>NH]Yyy-Xxx-Phe $\psi$ [CH<sub>2</sub>NH] Leu-OH (where Zzz is either Phe, Tyr, or 2-Nal, and Yyy and Xxx are each a mixture of eight amino acids) [1]. These mixtures were found to be active against *P. aeruginosa* in the initial screen. Next, a positional scan approach [2] was used to narrow the set of active compounds. This involved the synthesis of forty-eight 8-component mixtures. Screening of these mixtures for antimicrobial activity against both *P. aeruginosa* and MRSA led to nine individual structures (where Zzz = 2-Nal, Yyy = Lys, Ile or Val, and Xxx = Met, Ser, or Phe). These were then synthesized along with analogs containing aminoisobutyric acid (Aib) and diethylglycine (Deg) (for either Yyy or Zzz) in an effort to add conformational constraint to these very flexible structures. A total of 21 single pseudopeptides were prepared and screened.

In a microdilution assay [3], all but two of the 21 structures were active against MRSA at 250  $\mu$ g/mL. However, only eight compounds exhibited activity against *P. aeruginosa* at the same concentration. Analogous pseudotetrapeptides (lacking the Nal residue) showed no detectable activity in either assay. Additionally, the toxicity of the most active compounds toward erythrocytes was determined as a first evaluation of the compounds' specificity toward bacterial cells. Unfortunately, the two most active antimicrobials (where Yyy-Xxx = Lys-Ser or Met-Aib) were the most hemolytic of the tested pseudopeptides (Table 1).

In an effort to derive a pharmacophore having potential therapeutic properties, inductive logic programming (ILP) analysis was then performed on the individual compounds having activity against *P. aeruginosa* [4,5]. Energy minimization failed to show that either Aib or Deg added significant constraint to these very flexible structures. A possible four-point pharmacophore was proposed from the ILP analysis. Based on these data, several modified compounds derived from the two most active sequences (where Yyy-Xxx = Lys-Ser or Met-Aib, Table 1) were synthesized. Modifications included deletion of charged sites (by acetylation of amines or amidation of C-terminus), incorporation of the rigid amino acids 3- and 4-aminomethyl benzoic acid (AMB), all D-amino acid sequences, removal of reduced amide bonds, and re-

### Biologically Active Peptides

placement of Met with Nle. Also, a set of pseudohexapeptides containing either an extra 2-Nal or Lys at the N-terminus, or an extra Leu or Lys at the C-terminus was synthesized. These variations altered the activity of the sequences with none of the modified compounds exhibiting greater antimicrobial activity relative to the two original sequences (Table 1). However, a number of these compounds showed little to no hemolytic activity at concentrations 5- to 10-fold greater than their antimicrobial doses. Further efforts are underway to develop compounds having an increased therapeutic index and, in turn a more favorable pharmacological profile as antimicrobial agents.

Table 1. Structure, antimicrobial activity and hemolytic activity of several pseudopeptides.

Structure	MRSA IC <sub>50</sub> μg/ml	P. aeruginosa IC <sub>50</sub> μg/ml	% hemolysis @ 250 μg/ml
H-2-Nalψ[CH <sub>2</sub> NH]Lys-Phe-Pheψ[CH <sub>2</sub> NH]Leu-OH	44	46	0
H-2-Nalψ[CH <sub>2</sub> NH]Ile-Val-Pheψ[CH <sub>2</sub> NH]Leu-OH	4.0	>250	34
H-2-Nalψ[CH <sub>2</sub> NH]Met-Aib-Pheψ[CH <sub>2</sub> NH]Leu-OH	3.5	29	94
H-2-Nalψ[CH <sub>2</sub> NH]Deg-Phe-Pheψ[CH <sub>2</sub> NH]Leu-OH	4.8	>250	39
H-2-Nalψ[CH <sub>2</sub> NH]Lys-Ser-Pheψ[CH <sub>2</sub> NH]Leu-OH	4.8	9.4	93
H-D-2-Nalψ[CH <sub>2</sub> NH]D-Lys-D-Ser-D-Pheψ[CH <sub>2</sub> NH]D-Leu-OH	8.6	12	18
H-2-Nalψ[CH <sub>2</sub> NH]Met-4-Amb-Pheψ[CH <sub>2</sub> NH]Leu-OH	17	175	20
H-2-Nal-2-Nalψ[CH <sub>2</sub> NH]Lys-Ser-Pheψ[CH <sub>2</sub> NH]Leu-OH	56	77	0
H-2-Nalψ[CH <sub>2</sub> NH]Lys-Ser-Pheψ[CH <sub>2</sub> NH]Leu-Lys-OH	9.5	19.1	50

### References

1. Wen, J.J., Spatola, A.F. *J. Peptide Res.* **49**, 3–14 (1997).
2. Pinilla, C., Appel, J.R., Blanc, P., Houghten, R.A. *Biotechniques* **13**, 901–905 (1992).
3. Blondelle, S.E., Takahashi, E., Weber, P.A., Houghten, R.A. *Antimicrob. Agents Chemother.* **38**, 2280–2286 (1994).
4. Page, D., Curtis, S., Graham, J.H., Spatola, A.F., In *Proceedings of the Seventh International Conference on Intelligent Systems*, The International Society for Computers and Their Applications, Paris, 1998, p. 60–63.
5. Spatola, A.F., Page, D., Vogel, D.M., Crozet, Y., Blondelle, S., In Fields, G.B., Tam, J.P., Barany, G. (Eds) *Peptides for the New Millennium (Proceedings of the Sixteenth American Peptide Symposium)*, Kluwer, Dordrecht, 2000, p. 738.

## Synthesis and Study of the Antimicrobial Action of Cecropin A-Melittin Hybrids with Aib Substitution

**Padmaja Juvvadi<sup>1</sup>, Satyanarayana Vunnam<sup>2</sup>, Barney Yoo<sup>3</sup>  
 and Bruce Merrifield**

*The Rockefeller University, New York, NY 10021, USA. Present Addresses:*

<sup>1</sup>*Xencor, Monrovia, CA 91016, USA*

<sup>2</sup>*Baxter Hyland Immuno, Duarte, CA 91010, USA*

<sup>3</sup>*Mount Sinai Medical School, New York, NY 10029, USA*

### Introduction

Cecropins [1] and melittins [2] are a group of potent antimicrobial peptides. The cecropin melittin analogs are highly antimicrobial [3], had antitumor activity [4] and cecropins are potent fungicides [5]. To understand the role of substitution of hydrophobic amino acids with hydrophilic amino acids and Aib, different substituted analogs were separately synthesized and their antimicrobial activity studied.

### Results and Discussion

Design and synthesis of cecropin-melittin hybrid analogs is of interest because of their high antimicrobial activity [3]. Substitution of V13 by hydrophilic amino acids in KWKLFFKKGAVLKVL-NH<sub>2</sub>, [CA(1-7)M(3-9)-NH<sub>2</sub>] and KWKLFFKKGAVLKVLT-NH<sub>2</sub>, [CA(1-7)M(3-10)-NH<sub>2</sub>] was expected to increase the antimicrobial activity by increasing the ability for the initial ionic interactions with the membrane. These analogs showed similar activity as CA(1-7)M(3-9) and CA(1-7)M(3-10) amides [6], against *Streptococcus pyogenes*. However, the substitutions resulted in the loss of activity against two other Gram-positive and Gram-negative bacteria tested (Table 1). Interest-

*Table 1. Lethal concentrations (μM) for cecropin-melittin analogs.*

Peptide amide	D21	OT97	Bs11	Sac1	Sp1
CA(1-7)M(3-9)	3.9	14	10	2.9	0.9
CA(1-7)M(3-10)	9.1	14	6.3	>200	1.2
CA(1-7)K13M(3-9)	17.9	354	36.5	354.7	1.8
CA(1-7)K13M(3-10)	18.3	354	23.3	354.7	1.6
Ac-CA(1-7)K13M(3-10)	37.9	354	55.1	354.7	1.8
CA(1-7)L12K13M(3-9)	2.1	128	3.5	354.7	0.64
CA(1-7)L12K13M(3-10)	1.4	203	4.2	167.6	0.69
Ac-CA(1-7)L12K13M(3-10)	5.4	169	4.0	222.6	0.49
CA(1-7)Aib12M(3-9)	1.1	45.1	1.9	28.3	0.44
Ac-CA(1-7)Aib12M(3-9)	2.6	54.7	3.8	58.1	0.60
CA(1-7)Aib12M(3-10)	1.02	36.6	2.7	56.1	0.57
Ac-CA(1-7)Aib12M(3-10)	2.4	45.4	4.6	78.7	0.68
CA(1-7)Aib13M(3-9)	8.5	354	12.1	157.7	0.71
Ac-CA(1-7)Aib13M(3-9)	15.5	354	11.8	354.7	0.50

<sup>a</sup> *Lethal concentrations calculated from inhibition zones on agarose plates seeded with the respective organisms: D21 = Escherichia coli; OT97 = Pseudomonas aeruginosa; Bs11 = Bacillus subtilis; Sp = Streptococcus pyogenes; Sac1 = Staphylococcus aureus.*

ingly, these analogs lost their  $\alpha$ -helical character, which correlates with our earlier observations that the higher the helical propensity the greater the antimicrobial activity [6]. Further the effect of interchanging the hydrophobic and hydrophilic groups at 12 and 13 positions (K12 to L12 & V13 to K13) was studied. These analogs, CA(1-7)L12K13M(3-9)-NH<sub>2</sub> and CA(1-7)L12K13M(3-10) amides showed similar activity as the parent analogs against *Escherichia coli*, *Bacillus subtilis*, *Staphylococcus aureus*, *S. pyogenes* and were inactive against *Pseudomonas aeruginosa* (Table 1). The presence of V13 appears important for antimicrobial activity and  $\alpha$ -helical propensity of these hybrid analogs.

To study the effect of Aib in the sequence, K12 was substituted by Aib12 in both [CA(1-7)M(3-9)] and [CA(1-7)M(3-10)] amides. These analogs showed improved activity (2-4 fold) against *E. coli*, *B. subtilis* and *S. pyogenes*, but were less active against *P. aeruginosa* and *Staph. aureus* (Table 1). The Aib analogs retained 25–40% of helicity determined by circular dichroism with increasing concentrations of hexafluoro isopropanol. Acetylation of the amino terminus showed no effect on the antimicrobial activity or the helical property.

All the peptides were synthesized by solid phase technique [7] and the homogeneity confirmed by analytical HPLC and their molecular weights determined by electrospray mass spectrometry.

### Conclusions

Our results showed that substitution of the hydrophilic amino acid at 12 position both in [CA(1-7)M(3-9)-NH<sub>2</sub>] and [CA(1-7)M(3-10)-NH<sub>2</sub>] by a hydrophobic group resulted in similar activity but substitution by Aib increased the antimicrobial activity. The effect of Aib substitution on the antimicrobial activity may be attributed to the increase of  $\alpha$ -helicity of the Aib substituted peptide analogs compared to other analogs synthesized.

### References

1. Hultmark, D., Steiner, H., Rasmunson, T., Boman, H.G. *Eur. J. Biochem.* **106**, 7–16 (1980).
2. Habermann, E., Jentsch, J. Hoppe-Seyler's *Z. Physiol. Chem.* **348**, 37–50 (1967).
3. Andreu, D., Ubach, J., Boman, A., Wahlin, B., Wade, D., Merrifield, R.B. *FEBS Lett.* **296**, 190–194 (1992).
4. Shin, S.Y., Kang, J.H., Hahn, K.S. *J. Peptide Res.* **53**, 82–90 (1999).
5. Andra, J., Berninghausen, O., Leippe, M. *Med. Microbiol. Immunol.* **189**, 169–173 (2001).
6. Juvvadi, P., Vunnam, S., Merrifield, E.L., Boman, H.G., Merrifield, R.B. *J. Peptide Sci.* **2**, 223–232 (1996).
7. Merrifield, R.B. *J. Am. Chem. Soc.* **85**, 2149–2154 (1963).

## Structure-Function Relationship of Gramicidin-Alamethicin Hybrid Analogs

Hiroaki Kodama<sup>1</sup>, Mitsukuni Shibue<sup>1</sup>, Kimiko Hashimoto<sup>1</sup>,  
 Hiroshi Yamaguchi<sup>1</sup>, Toshiaki Hara<sup>1</sup>, Masood Jelokhani-Niaraki<sup>2</sup>  
 and Michio Kondo<sup>1</sup>

<sup>1</sup>Department of Chemistry, Faculty of Science and Engineering, Saga University,  
 Saga 840-8502, Japan

<sup>2</sup>Department of Chemistry, Brandon University, Brandon, Manitoba, Canada R7A 6A9

### Introduction

Gramicidin is a 16-meric linear peptide, which is composed of alternating L- and D-amino acid residues and forms dimeric  $\beta^{6,4}$ -helical structures in biological membranes. Alamethicin is an Aib-containing peptide composed of 20 amino acids and consists of a dominantly  $\alpha$ -helical N-terminal and a central kinked region. Both peptides are potentially antimicrobial and form ion channel structures in cell membranes. We have previously reported of Aib-containing analogs of gramicidin (GAA and GBA) [1]. Both analogs formed stable helical structures in both organic and aqueous systems, and in phospholipid vesicles [1]. Moreover, GBA showed a multi-state channel-type activity, similar to that of alamethicin, in phospholipid bilayers [2].

In this study, by considering a widely found sequence in the Aib-containing peptaibols such as alamethicin, Gly-Leu-Aib-Pro, we have designed and synthesized an alamethicin analog (AB18-P) and two gramicidin-alamethicin hybrid analogs (AB18-W3 and AB18-PW3) (Figure 1). Similar to alamethicin, these peptides (except for AB18-W3) possess a central kink in the otherwise completely helical peptide structure.

AB18-P	Boc-A-B-A-B-A-B-A-B- <u>G-L-B-P</u> -A-B-A-B-A-B-OMey
AB18-W3	Boc-A-B-A-B-A-B-A-B- <u>A-B-A-B</u> -W-B-W-B-W-B-OPac
AB18-PW3	Boc-A-B-A-B-A-B-A-B- <u>G-L-B-P</u> -W-B-W-B-W-B-OPac

Fig. 1. Structures of synthetic peptides (B stands for Aib).

### Results and Discussion

All analogs were synthesized by solution-phase method. In order to avoid a side reaction by acid treatment, indole groups were protected by CHO group and monitored by UV spectra. Each fragment was synthesized by step-wise and fragment condensation method. CD spectra of the synthetic peptides were measured in TFE and EtOH (Figure 2). Due to the extremely low solubility of these peptides in aqueous environments, we were unable to measure their CD spectra in the aqueous medium and lipid vesicles. CD spectra of AB18-P showed a low content of  $\alpha$ -helical conformation, with a positive band around 193 nm, and negative bands around 208 and 225 nm. On the other hand, CD spectra of AB18-W3 exhibited an  $\alpha$ -helical structure together with a shoulder motif around 230 nm, which is due to the exciton interaction of Trp residues. Similarly, CD spectra of AB18-PW3 in both alcohols showed an  $\alpha$ -helical conformation with an unusual maximum at around 230 nm. CD spectra of both AB18-W3 and AB18-PW3 are clearly distorted due to the interaction of Trp residues at their C-terminals, and the typical minimum of the carbonyl  $n\pi^*$  transition of peptide group at around 222 nm is somehow concealed in this region (220–230 nm). The spectral difference between AB18-W3 and AB18-PW3 is possibly caused by the presence of

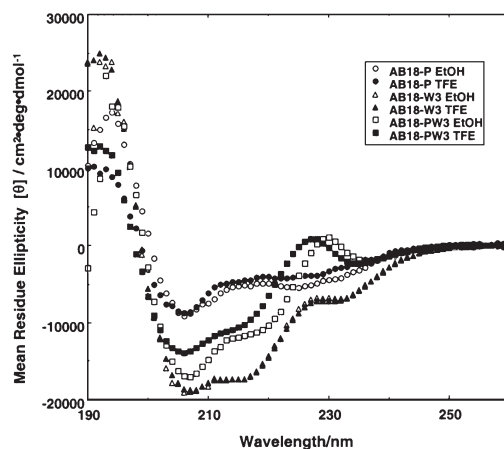


Fig. 2. CD spectra of AB18-P, W3 and PW3.

the Gly-Leu-Aib-Pro sequence incorporated in the central region of the latter. AB18-PW3 thus becomes more flexible at its C-terminal and is less helical than AB18-W3.

To evaluate the channel-forming properties of these peptides, we measured single-channel currents by the tip-dip patch clamp method (Figure 3). Conductance patterns of AB18-P in DPhPC lipid bilayers depict a single-state channel with a rapidly fluctuating open state. The open state of the channel has relatively long lifetimes and its conductance of  $\approx 130$  pS. In contrast, AB18-W3 channels have much shorter lifetimes and do not exhibit a dominantly single-state pattern. The average conductance of these channels are  $\approx 52$  pS (trimeric channel). On the other hand, AB18-PW3 forms dominantly single-state channels, similar to those of AB18-P. These channels have considerably long lifetimes with conductance of  $\approx 57$  pS (trimeric channels).

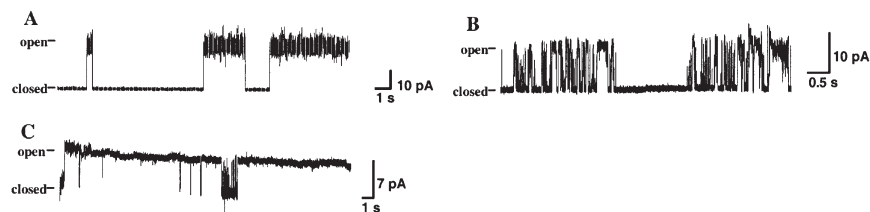


Fig. 3. Single channel fluctuations induced by AB18-P (at +200 mV) (A), AB18-W3 (at +100 mV) (B) and AB18-PW3 (at +200 mV) (C) in DPhPC lipid bilayers.

In conclusion, AB18-P, AB18-W3 and AB18-PW3 form helical conformations in alcoholic solvents as environments comparable to the hydrophobic core of lipid membranes. However, the CD spectra in AB18-W3 and AB18-PW3 are distorted (and sometimes misleading) as is the case for other Trp-containing peptides. Furthermore, all of these peptides form ion channels in DPhPC bilayers. Results of single-channel measurements suggest that the kink at the Gly-Leu-Aib-Pro sequence affects the C-terminal region, and remarkably increases the channel lifetime.

## References

1. Jelokhani-Niaraki, M., et al. *J. Chem. Soc., Perkin Trans. 2* 1187–1193 (1992).
2. Jelokhani-Niaraki, M., et al. *J. Chem. Soc., Perkin Trans. 2* 801–808 (1995).

## Biaryl-Bridged Lipopeptides from *Streptomyces* sp. T $\ddot{U}$ 6075

Dietmar G. Schmid<sup>1</sup>, Alexandra H $\ddot{o}$ ltzel<sup>1</sup>, Graeme J. Nicholson<sup>1</sup>,  
Stefan Stevanovic<sup>2</sup>, Judith Schimana<sup>3</sup>, Klaus Gebhardt<sup>3</sup>,  
Johannes M $\ddot{u}$ ller<sup>3</sup>, Hans-Peter Fiedler<sup>3</sup> and G $\ddot{u}$ nther Jung<sup>1</sup>

<sup>1</sup>Institut für Organische Chemie, Auf der Morgenstelle 18 and

<sup>2</sup>Institut für Zellbiologie, Abteilung Immunologie and

<sup>3</sup>Mikrobiologisches Institut, Universität T $\ddot{u}$ bingen, D-72076, Germany

### Introduction

HPLC-DAD screening for new metabolites [1] from *Streptomyces* sp. T $\ddot{U}$  6075 revealed two series of compounds composed of five colorless and seven yellow fractions. For structure elucidation, ES-FTICR-MS, chiral GC-MS, Edman sequencing, and NMR spectroscopy were used. The isolated compounds, termed arylomycins, represent the first example of lipopeptides containing biaryl-bridged amino acids. The majority of the arylomycins exhibit antimicrobial activity against Gram-positive bacteria.

### Results and Discussion

By ES-FTICR-MS, homologous compounds were found for each series in the mass range between 810 and 911 Da (Figure 1).

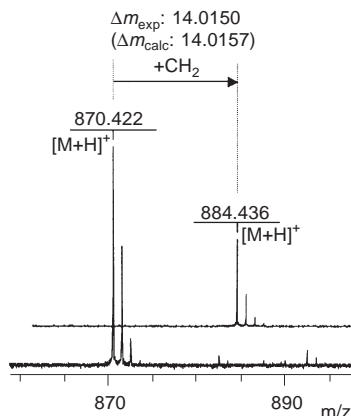


Fig. 1. ES-FTICR-mass spectra of two homologous compounds of the yellow series. The exact mass difference between the compounds identifies the methylene group.

The mass difference of 45 Da between corresponding compounds from the colorless (arylomycins A<sub>n</sub>) and the yellow series (arylomycins B<sub>n</sub>) indicated a nitro substitution of arylomycins B<sub>n</sub> (Δm<sub>exp</sub> = 44.9847; Δm<sub>calc</sub> = 44.9851).

The structures of two prominent compounds of each series, arylomycins A<sub>2</sub> (R = H, 824 Da) and B<sub>2</sub> (R = NO<sub>2</sub>, 869 Da), were elucidated in DMSO-*d*<sub>6</sub> and MeOH-*d*<sub>4</sub> solution by TOCSY, NOESY, CW-ROESY, HSQC, and HMBC experiments (Figure 2).

The proposed structure was confirmed by ES-FTICR-MS/MS- and -MS/MS/MS experiments. Due to the presence of *N*-methyl-serine, a significant b<sub>2</sub>-fragment was observed, which is typical for *N*-methylated peptides [2].

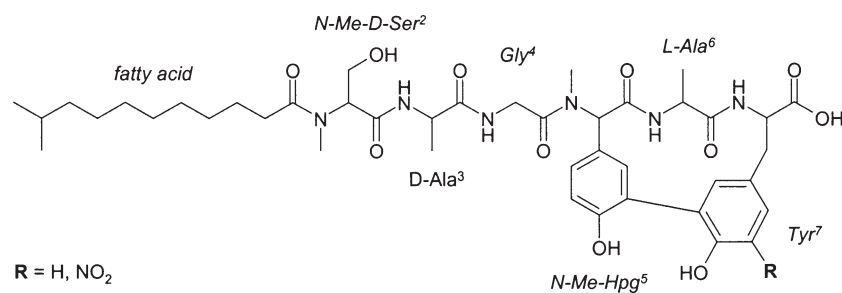


Fig. 2. Structure of arylomycins  $A_2$  and  $B_2$ .

Hydrolyzates of all fractions were analyzed for their fatty acid and amino acid composition by chiral GC-MS. An identical amino acid composition of L-alanine, D-alanine, glycine, *N*-methyl-D-serine, as well as the respective biaryl-bridged bis-amino acid fragment, was found in all fractions. Fatty acids from  $C_{11}$  to  $C_{15}$  comprising *n*, *iso*, and *anteiso* isomers were detected. To investigate the position of D-alanine and L-alanine, respectively, a partial hydrolysis to cleave mainly the fatty acid was performed on arylomycins  $A_2$  and  $B_2$ . The partial hydrolyzates were subjected to two cycles of Edman sequencing. The remaining Ala<sup>6</sup> residue in the residual cyclic tetrapeptides was identified as L-alanine in both arylomycins by total hydrolysis and subsequent chiral GC-MS analysis.

## References

1. Fiedler, H.-P. *Nat. Prod. Lett.* **2**, 119 (1993).
2. Vaisar, T., Urban, J. *J. Mass Spectrom.* **33**, 505 (1998).

## **Generation of Bioactive Peptides Derived from Caseins Using a *Lactobacillus helveticus* Strain**

**Marie-Claude Robert<sup>1,2</sup>, Anne Donnet-Hughes<sup>2</sup>  
and Marcel-Alexandre Juillerat<sup>2</sup>**

<sup>1</sup>*Faculty of Sciences, University of Lausanne, Lausanne, Switzerland*

<sup>2</sup>*Nestec Ltd., Nestlé Research Center, Lausanne, Switzerland*

### **Introduction**

Bovine milk is known to contain a number of peptide fractions that can affect physiological functions. Bioactive peptides have to be hydrolytically derived from native proteins. Various biological effects of peptides generated upon *in vitro* enzymatic or *in vivo* gastrointestinal digests have been demonstrated [1].

The beneficial effects of lactic acid bacteria and cultured dairy products on the nutrition and health of animals and humans have been well studied in recent years [2]. Strains of lactic acid bacteria that grow well in milk are usually proteolytic and it has been suggested that lactic acid bacteria possessing this activity generate bioactive peptides.

### **Results and Discussion**

The bacterial strain used in this study was initially grown in milk before incubation of whole cells with a pure casein solution. Caseinolytic activity was higher when the cells were grown in milk rather than MRS, thus favouring the generation of potentially bioactive, low molecular weight peptides.

Whole casein hydrolysates were subjected to size exclusion chromatography. The chromatogram showed a more extensive hydrolysis after a few hours, confirming the SDS-electrophoresis data. Fractions of small peptides (5'–1'000 Da) and peptides >1'000 Da were collected. These two fractions were selected for further purification by reversed phase chromatography. Altogether, thirty-two fractions were collected in the second purification step and subsequently analysed. Mass spectrometric identification was performed using Sequest searching of MS/MS fragmentation data acquired on a Finnigan Mat LCQ quadrupole ion trap mass spectrometer.

Several peptides inhibiting the angiotensin-converting enzyme (ACE) were identified in the hydrolysates: RPKHPI, RPKHPIKHQ, AYFYPE, TTMPLW derived from  $\alpha_{s1}$ -casein; MKPWIQPK from  $\alpha_{s2}$ -casein; DKIHPI, HKEMPFKYPVEPF, HLPLP, LHLPLP, ENLHLPLP, NLHLP, LQSW, KAVPYPQ, AVPYPQ, KVLVPQ, RDMIQAF, YQEPVL, YQEPVLGPVRGPFPIIV from  $\beta$ -casein and VIESPPEIN from  $\kappa$ -casein. Two peptides with potential opioid activity [1] were identified: one from  $\alpha_{s1}$ -casein (YLGYLE) and the other from  $\kappa$ -casein (YIPIQYVLSR). Three peptides (LLY from  $\beta$ -casein, RPKHPIKHQGLPQEVNENLLRF and TTMPLW from  $\alpha_{s1}$ -casein) previously described in the literature as immunomodulating and antibacterial, were also identified among the peptides present in the hydrolysates [3–9].

We have shown in this study that *Lactobacillus helveticus* NCC 619 was able to produce a library of peptides which are potentially biologically active. We observed that the amount of peptides present in the hydrolysates was sufficient to significantly inhibit ACE activity (Figure 1). Furthermore, some fractions inhibited the proliferation of the human intestinal carcinoma epithelial cell line, HT-29 (Figure 2).

Further fractionation will permit the identification and purification of the biologically active peptides.

### Biologically Active Peptides

As previously shown for *Lb. helveticus* CP790 strain [3], we have found that the strongly proteolytic *Lb. helveticus* NCC619 strain is able to generate antihypertensive peptides as well as peptides which modulate proliferation of intestinal epithelial cells *in vitro*. Moreover, during casein hydrolysis, the same strain generated peptides which have been identified as having antibacterial, immunomodulating and opioid properties.

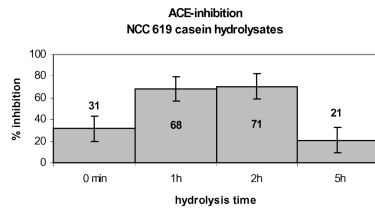


Fig. 1. ACE inhibitory activity of NCC 619 casein hydrolysates.

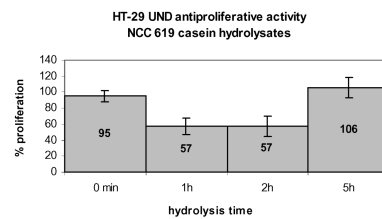


Fig. 2. HT-29 UND antiproliferative activity of NCC 619 casein hydrolysates.

### References

1. Meisel, H. *Livestock Production Sci.* **50**, 125–138 (1997).
2. Harwalkar, V.R., McMahon, D.J. *J. Dairy Sci.* **76**, 300–310 (1993).
3. Yamamoto, N., et al. *J. Dairy Sci.* **77**, 917–922 (1994).
4. Lahov, E., Regelson, W. *Food Chem. Toxicol.* **34**, 131–145 (1996).
5. Pihlanto, L.A., et al. *Int. Dairy J.* **8**, 325–331 (1998).
6. Maeno, M., et al. *J. Dairy Sci.* **79**, 1316–1321 (1996).
7. Gobetti, M., et al. *Appl. Environ. Microbiol.* **66**, 3898–3904 (2000).
8. Kohmura, M., et al. *Agric. Biol. Chem.* **53**, 2107–2114 (1989).
9. Migliore-Samour, D., et al. *Dairy Res.* **56**, 357–362 (1989).

## Bioactive Peptides Produced by a Strain of *Lactobacillus plantarum*: Characterization and Partial Purification

Diana M. Müller<sup>1</sup>, Marta S. Carrasco<sup>2</sup>, Arturo Simonetta<sup>2</sup>  
and Georgina G. Tonarelli<sup>1</sup>

<sup>1</sup>Dpto. de Química Orgánica, Facultad de Bioquímica and

<sup>2</sup>Cát. Microbiología, Dpto. Ing. en Alimentos, Facultad de Ingeniería Química  
Universidad Nacional del Litoral, 3000, Santa Fe, Argentina

### Introduction

Bacteriocins produced by lactic acid bacteria (LAB) are proteins or peptides with inhibitory activity against related and non related species, associated with food spoilage and food borne illnesses. The aim of this study was to purify and characterize bacteriocins produced by a strain of *Lactobacillus plantarum* [1].

### Results and Discussion

*Lactobacillus plantarum* Lp31 was isolated from Argentinian dry-fermented sausages, and when grown at 37 °C for 16–20 h in MRS broth produced antimicrobial compounds. The antimicrobial activity was completely lost after treatment with trypsin, papaine and pepsin. This activity was only partially affected by treatment with lysozyme, aminoglycosidase and alpha-amylase. The inhibitory activity was found to be stable at pH levels between 4.5 and 6.5, and not reduced by catalase and heat treatment at 100 °C for 10 and 30 min, but was destroyed by ethanol.

According to these preliminary tests, the active compounds evidenced a proteinaceous nature, and were heat-resistant like most of the known bacteriocin substances produced by lactic acid bacteria [2,3]. It will be necessary to perform additional studies in order to determine the presence and influence of a glycosidic moiety in the active compounds on the inhibitory activity.

Two active fractions, IIA and IIB, were obtained from a crude cell-free supernatant, concentrated under vacuum and purified by solid phase extraction and gel filtration chromatography [4]. Both Fractions IIA and IIB consisted of hydrophilic peptides of low molecular weights: within 1200–1300 Da range for IIA, and 600–800 Da for IIB, as determined by MALDI MS. It is interesting to mention that the bacteriocins described here fall into the range of the lowest molecular weights reported. Bacteriocins produced by *Lactobacillus plantarum* Lp31 have proved to be effective against Gram-negative and Gram-positive bacteria. By the application of the well-diffusion assay against six sensitive bacterial species (*Pseudomonas* sp., *Staphylococcus aureus*, *Bacillus cereus*, *Listeria monocytogenes*, *Bacillus megaterium* and *Bacillus subtilis*) it was shown that fraction IIA has strong antimicrobial activity. A bactericidal effect of

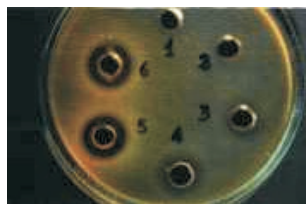


Fig. 1. Inhibition of *Pseudomonas* sp. by Fraction IIA (bactericidal effect wells 5, 6) and Fraction IIB (bacteriostatic effect wells 3, 4) by the agar well-diffusion assay.

fraction IIA, a bacteriostatic effect of fraction IIB and a synergic action of the mixture was observed by inhibition tests of a growing culture [2] of *Pseudomonas sp.* Since they may play an important role in natural preservation of different foods, we are focusing our efforts to elucidate the structure of the isolated compounds.

#### **Acknowledgments**

We wish to thank Prof. David Andreu for his contribution with mass spectrometry analyses and scientific support and to our coworkers from Departamento de Química Orgánica (Facultad de Bioquímica) and Cát. Microbiología, Dpto. Ing. en Alimentos (Facultad de Ing. Química), Universidad Nacional del Litoral.

#### **References**

1. Carrasco, M.S., Scarinci, H.E., Simonetta, A. *Microbiologie-Aliments-Nutrition* **15**, 299–305 (1997).
2. Jiménez Díaz, R., Ruíz-Barba, J.L., Cathcart, D.P., Holo, H., Nes, I.F., Sletten, K.H. *Appl. Environ. Microbiol.* **61**, 4459–4463 (1995).
3. Aktypis, A., Kalantzopoulos, G., Huis in't Veld, J.H.J., ten Brink, B. *J. Appl. Microbiol.* **84**, 568–576 (1998).
4. Suma, K., Misra, M.C., Varadaraj, M.C. *J. Food Microbiol.* **40**, 17–25 (1998).

## Stilboflavins, a Natural Peptaibol Library from the Mold *Stilbella flavipes*

Hans Brückner and Andreas Jaworski

Interdisciplinary Research Center, Department of Food Sciences, Justus-Liebig-University,  
35392 Giessen, Germany

### Introduction

We have recently reported on the isolation of a mixture of polypeptides of the peptaibol group from the mold *Stilbella flavipes*, strain CBS 146.81 [1]. Groups of peptides isolated by preparative TLC were named stilboflavins (SF) A, B, and C. The sequences of SF B were investigated by ESI-MS, GC-MS and quantitative amino acid analysis and shown to represent a mixture of 10 microheterogeneous *N*-acetylated 20-residue peptides distinguished by exchange of certain amino acids, as well as C-terminal amino alcohols, valinol, leucinol and isoleucinol. We now report on the sequences of SF A peptides and their relation to SF B peptides. For full details we refer to the literature [2].

### Results and Discussion

The HPLC elution profile of SF A peptides is shown in Figure 1. For TLC see reference [1]. Structures of SF A were determined in analogy to SF B peptides [1,2]. The peptides representing SF C are still under investigation. The sequences of seven peptides, accounting for 92.6% of SF A peptides (retention time indicated by arrows in Figure 1), are represented in Figure 2. As can be seen, the peptide groups are distinguished from each other by exchange of Gln-18/Glu-18, resulting in acidic SF A peptides and neutral SF B peptides. This explains separability on silica gel. Peptaibols SF A1, A2, A4, A5 and A7 correspond to peptides SF B1, B2, B4, B5 and B7 (with the exception of the Gln/Glu exchange). The peptide eluting just before SF A4 is named SF A3, as it differs from SF B3 by Ala-6/Aib-6 exchange as well as Gln-18/Glu-18 exchange. The C-terminal amino alcohol of SF A6, designated Xol, could not be de-

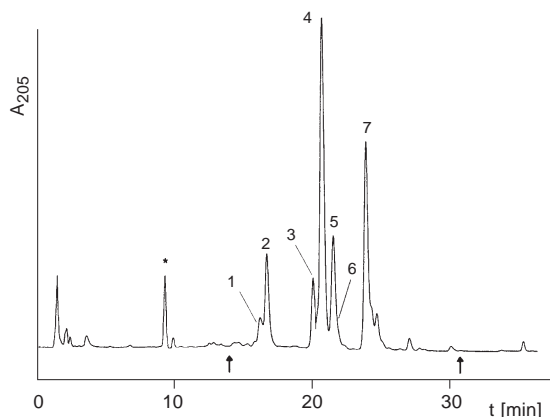


Fig. 1. HPLC elution profile of SF A peptide mixture isolated by TLC. Numbers refer to SF A sequences shown in Figure 2; asterisk, non-peptidic impurity. Chromatography: Superspher 100 RP-18, 4  $\mu$ m; 250 mm  $\times$  4 mm i.d.; gradient elution (A) MeOH/water/MeCN/TFA 38/38/24/0.1; (B) MeOH/MeCN/TFA 1/1/0.1.

## Biologically Active Peptides

terminated with certainty. Notably, the natural mixture of stilboflavins might be considered as a fungal peptaibol library [3]. Production of peptide antibiotics by species of *Stilbella* is of interest since peptaibol producing species such as *Stilbella aciculosa* have been recognized as potential biocontrol fungi against phytopathogenic fungi *cf.* [4]. Further, we have recently shown that *Stilbella erythrocephala* and *Stilbella fimetaria* are capable of producing microheterogeneous 16-residue peptaibols anti-amoebins [4].

SFA	1	2	3	4	5	6	7	8	9	10	11	12	13	14	15	16	17	18	19	20	%
1	Ac	U	P	U	A	U	<b>A</b>	Q	U	<b>V</b>	U	G	U	<b>U</b>	P	V	U	<b>E</b>	Q	<b>Vol</b>	3.4
2	Ac	U	P	U	A	U	<b>A</b>	Q	U	<b>L</b>	U	G	U	<b>U</b>	P	V	U	<b>E</b>	Q	<b>Vol</b>	10.3
3	Ac	U	P	U	A	U	<b>U</b>	Q	U	<b>V</b>	U	G	U	<b>A</b>	P	V	U	<b>E</b>	Q	<b>Lol</b>	6.2
4	Ac	U	P	U	A	U	<b>A</b>	Q	U	<b>L</b>	U	G	U	<b>U</b>	P	V	U	<b>E</b>	Q	<b>Lol</b>	34.8
5	Ac	U	P	U	A	U	<b>U</b>	Q	U	<b>L</b>	U	G	U	<b>U</b>	P	V	U	<b>E</b>	Q	<b>Vol</b>	8.3
6	Ac	U	P	U	A	U	<b>A</b>	Q	U	<b>L</b>	U	G	U	<b>U</b>	P	V	U	<b>E</b>	Q	<b>Xol</b>	6.0
7	Ac	U	P	U	A	U	<b>U</b>	Q	U	<b>L</b>	U	G	U	<b>U</b>	P	V	U	<b>E</b>	Q	<b>Lol</b>	23.6
SFB	1	2	3	4	5	6	7	8	9	10	11	12	13	14	15	16	17	18	Q	20	%
1	Ac	U	P	U	A	U	<b>A</b>	Q	U	<b>V</b>	U	G	U	<b>U</b>	P	V	U	<b>Q</b>	Q	<b>Vol</b>	2.5
2	Ac	U	P	U	A	U	<b>A</b>	Q	U	<b>L</b>	U	G	U	<b>U</b>	P	V	U	<b>Q</b>	Q	<b>Vol</b>	6.5
3	Ac	U	P	U	A	U	<b>A</b>	Q	U	<b>V</b>	U	G	U	<b>U</b>	P	V	U	<b>Q</b>	Q	<b>Lol</b>	4.4
4	Ac	U	P	U	A	U	<b>A</b>	Q	U	<b>L</b>	U	G	U	<b>U</b>	P	V	U	<b>Q</b>	Q	<b>Lol</b>	13.7
5	Ac	U	P	U	A	U	<b>U</b>	Q	U	<b>L</b>	U	G	U	<b>U</b>	P	V	U	<b>Q</b>	Q	<b>Vol</b>	17.6
6	Ac	U	P	U	A	U	<b>U</b>	Q	U	<b>V</b>	U	G	U	<b>U</b>	P	V	U	<b>Q</b>	Q	<b>Vol</b>	3.3
7	Ac	U	P	U	A	U	<b>U</b>	Q	U	<b>L</b>	U	G	U	<b>U</b>	P	V	U	<b>Q</b>	Q	<b>Lol</b>	35.1
8	Ac	U	P	U	A	U	<b>U</b>	Q	U	<b>V</b>	U	G	U	<b>U</b>	P	V	U	<b>Q</b>	Q	<b>Lol</b>	6.1
9	Ac	U	P	U	A	U	<b>U</b>	Q	U	<b>L</b>	U	G	U	<b>U</b>	P	V	U	<b>Q</b>	Q	<b>Iol</b>	4.3
10	Ac	U	P	U	A	U	<b>U</b>	Q	U	<b>V</b>	U	G	U	<b>U</b>	P	V	U	<b>Q</b>	Q	<b>Iol</b>	1.6

Fig. 2. Sequences (one-letter-nomenclature) of stilboflavin (SF) A and B peptides. Chiral amino acids and amino alcohols are of the L-configuration; U = Aib, Vol = valinol, Lol = leucinol; Iol = isoleucinol, Xol = leucinol or isoleucinol; (%) refers to relative amounts of peptides calculated from total of peak areas indicated by arrows in HPLC. Bold letters indicate amino acid exchange.

## References

1. Jaworski, A., Brückner, H., In Martinez, J. and Fehrentz, J.-A. (Eds). *Peptides 2000 (Proceedings of the Twenty-Sixth European Peptide Symposium)*, Édition EDK, Paris, 2001, p. 657–658.
2. Jaworski, A., Brückner, H. *J. Pept. Sci.* **7**, 433–447 (2001).
3. Jung, G. (Ed.) *Combinatorial Peptide and Nonpeptide Libraries*. VCH-Publishers, Weinheim, Germany, 1996.
4. Jaworski, A., Brückner, H. *J. Pept. Sci.* **6**, 149–167 (2000).

## Cyclic Analogues of the Insect Antimicrobial Peptides Drosocin and Apidaecin

Marina Gobbo<sup>1</sup>, Monica Benincasa<sup>2</sup>, Laura Biondi<sup>1</sup>, Fernando Filira<sup>1</sup>,  
 Renato Gennaro<sup>2</sup> and Raniero Rocchi<sup>1</sup>

<sup>1</sup>*Centro di Studio sui Biopolimeri del C. N. R. , Dipartimento di Chimica Organica, Università di Padova, Padova, I-35131, Italy*

<sup>2</sup>*Dipartimento di Biochimica, Biofisica e Chimica delle Macromolecole, Università di Trieste, Trieste, I-34127, Italy*

### Introduction

Most antimicrobial peptides kill bacteria by acting on the cell membrane. A direct correlation between the antibiotic effect and the ability to permeabilize has been found, for example, for magainins, cecropins and dermaseptins [1]. Several alternative pathways have, however, been proposed as the killing mechanism for other antimicrobial peptides [2], sometimes requiring the recognition of a specific bacterial target. Recent results upheld the model of permease/transporter-mediated uptake in bacterial cells [3] for three small proline-rich peptides: apidaecin, drosocin and pyrrhocoricin, originally isolated from insects [4]. Information about the bioactive conformation of these peptides are thus fundamental to elucidate their mechanism of action. A popular approach to better define the structural features required for an effective binding of the peptide to the receptor/docking molecule, is to restrict its conformational freedom by introducing some conformational constraints, e.g. cyclization.

We have synthesized the head-to-tail cyclic analogues of drosocin (unglycosylated) and apidaecin Ib (Figure 1) and compared the results of their antibacterial activity with those of the unmodified linear peptides. Synthesis and antibacterial activity of cyclic analogues of pyrrhocoricin have been already published [5]. To mimic the cyclic antimicrobial peptides containing a single disulfide bond, the synthetic Cys<sup>7</sup>,Cys<sup>12</sup>-[Thr<sup>11</sup>]drosocin analogue was oxidized yielding the drosocin analogue **V**.

### Results and Discussion

Head-to-tail cyclic peptides were obtained by cyclization in solution of the corresponding side-chain protected linear peptides, covering the entire peptide sequence, previously assembled on the solid phase (Sasrin resin, Fmoc/*t*-butyl chemistry). To prevent the risk of racemization in the cyclization step, glycine was the C-terminal residue. Cyclization was carried out in DMF or in DCM, by using different coupling reagents (TBTU/HOBT, PyBOP), under high-dilution conditions (concentration of the linear peptide was 10<sup>-3</sup> M). Cyclic drosocin **I** was obtained, after removal of side

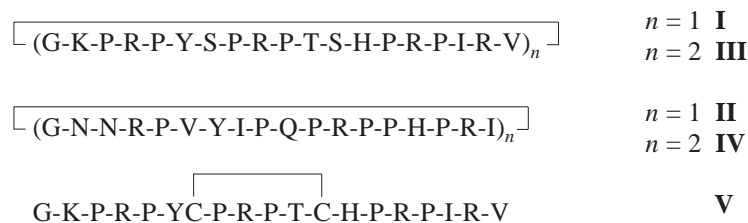


Fig. 1. Cyclic analogues of drosocin (**I**, **III** and **V**) and apidaecin (**II** and **IV**).

chain protecting groups (TFA/phenol/H<sub>2</sub>O/TES 90 : 5 : 2.5 : 2.5) and HPLC purification, in 50–60% yield together with a small amount of cyclo dimer **III** (<10% in weight, independently from the reaction condition). Cyclization of the protected apidaecin precursor, in DMF, yielded, after deprotection and purification, 65–70% of the cyclic peptide **III** and less than 10% of the cyclo dimer **IV**. On the contrary, when the reaction was carried out in DCM, the amount of cyclo dimer was comparable to that of the cyclo monomer. Probably the poor capacity of the solvent to “solvate” the peptide chains favoured the formation of  $\beta$ -sheet like structures responsible for oligomerization [6]. The heterodetic cyclic drosocin **V** was obtained by air oxidation of the fully deprotected Cys<sup>7</sup>,Cys<sup>12</sup>-[Thr<sup>11</sup>]drosocin analogue, previously synthesized on solid phase (Wang resin). Formation of the disulfide bond (peptide concentration 1 mg/ml in 0.1 M NH<sub>4</sub>HCO<sub>3</sub>) took about 40 h. Compounds **I–V** were purified by semi-preparative HPLC and characterized by amino acid analysis and MALDI-TOF or ESI-MS.

The antimicrobial activity was tested against a panel of Gram-negative bacteria (*E. coli*, *S. enteritidis*, *K. pneumoniae*, *P. aeruginosa*, *S. typhimurium* and *A. baumannii* strains) by the microdilution susceptibility test in microtiter plates. All cyclic drosocin derivatives and cyclo apidaecin were inactive up to a concentration exceeding at least 8 times the MIC of the parent natural peptide. Only the cyclo dimer of apidaecin **IV** was partially active against some bacterial strains, at concentrations similar to or slightly higher than the MIC values of linear apidaecin (*E. coli* ATCC 25922 and O18 : K1 : H7, *S. typhimurium* ATCC 14028) or higher (*E. coli* D22 and *K. pneumoniae* 22).

The loss of antibacterial activity of the monomeric cyclic analogues of drosocin and apidaecin demonstrate that constrained analogues do not represent the bioactive conformation of these antimicrobial peptides, as already shown for pyrrhocoricin [7]. Larger cycles, such as the cyclo dimer of apidaecin or an extended cyclic analogue of pyrrhocoricin [7], can preserve the antimicrobial activity probably because they allow an extended domain in the central part of the peptide. This structural hypothesis is supported by the NMR conformational studies recently reported for drosocin and pyrrhocoricin [4].

### Acknowledgments

Financial support from the National Research Council (Target Project on Biotechnology) and MURST of Italy is gratefully acknowledged.

### References

1. Oren, Z., Shai, Y. *Biopolymers* **47**, 451–463 (1998).
2. Andreu, D., Rivas, L. *Biopolymers* **47**, 415–433 (1998).
3. (a) Castle, M., et al. *J. Biol. Chem.* **274**, 32555–32564 (1999). (b) Otvos, L., Jr., et al. *Biochemistry* **39**, 14150–14159 (2000).
4. Otvos, L., Jr. *J. Peptide Sci.* **6**, 497–511 (2000).
5. Cudic, M., et al., In Martinez, J. and Fehrentz, J.A. (Eds.) *Peptides 2000 (Proceedings of the 26th European Peptide Symposium)*, Edition EDK, Paris, 2001, p. 204.
6. Bodansky, M. *Principles of Peptide Synthesis*. Springer-Verlag, Berlin 1984, pp. 217–222.
7. Otvos, L., Jr., et al. *Protein Sci.* **9**, 742 (2000).

## **Interaction of Antithrombin III-Binding Domain in Heparins with Novel Heparin Binding Peptides**

**Satomi Onoue<sup>1,2</sup>, Yoshitaka Nemoto<sup>1,3</sup>, Takahiro Mizumoto<sup>1</sup>,  
Sunao Harada<sup>1</sup>, Takehiko Yajima<sup>2</sup> and Kazuhisa Kashimoto<sup>1</sup>**

<sup>1</sup>*Health Science Division, ITOHAM FOODS INC, Moriya, Ibaraki, 302-0104, Japan*

<sup>2</sup>*Analytical Sciences, School of Pharmaceutical Sciences Toho University, Chiba,  
274-8510, Japan*

<sup>3</sup>*American Peptide Company, Sunnyvale, CA 94086, USA*

### **Introduction**

Antithrombin III (AT III), a member of the serpin family, is a plasma glycoprotein consisting of 432 amino acids [1], and it acts as the key regulatory elements in the blood coagulation cascade acting as an inhibitor of thrombin, factor Xa, and other serine protease factors [2]. In the presence of heparin, the biological activity of AT III toward these serine proteases is enhanced [3], therefore this highly sulfated polysaccharide has been clinically used as an anticoagulant. The inhibitory effect of heparin on blood coagulation may be classified into two distinct types; factor Xa type and factor IIa type [4]. Whereas normal heparin with high molecular weight is able to interact with both types, a decrease in molecular weight is well-correlated with a decrease in activity toward the factor IIa type [5]. These heparins have a pentasaccharidic AT III-binding site, and this fragment is essential for the inhibition of factor Xa-mediated coagulation, not for factor IIa type. With respect to the binding domain of AT III to heparin, at least three binding regions are reported, however the critical binding site with pentasaccharide was not characterized. Therefore, we investigated the binding sequence in AT III with use of physicochemical and biochemical methods, and we previously reported that the region around 120–140 sequence in AT III plays an important and indispensable role in heparin-mediated anticoagulation [6]. In this investigation, we developed a new analogue of heparin-binding peptide (HBP) which has a strong affinity to heparin as well as an antagonistic effect on heparins.

### **Results and Discussion**

We prepared the HBPs (Table 1) using manual solid-phase technology, and HBP-1, HBP-2 and HBP-4 correspond to the reported heparin interactive region in AT III, HBP-7–11 are derivatives of HBP-4. With respect to the new derivatives, the free Cys residues readily react among themselves, therefore the Cys in HBP-4 was modified into the Ser residue. In addition, the binding of HBP with heparin should be associated with the interaction of cationic amino acid residues in HBPs with an anionic functional group in heparins such as the *O*-sulfate and carboxyl groups, and this was supported by a high correlation coefficient ( $r = 0.96$ ) estimated between the binding potency and the electric charge of HBPs. Upon these new findings, we prepared the HBP-10 and 11 in order to enhance their binding activity toward heparin, which have many Arg residues instead of Lys residues.

Heparin showed a strong inhibition of factor Xa in the blood coagulation cascade, and the addition of HBPs gave a significant protection of factor Xa activity. This means that HBPs have an inhibitory effect on heparin binding to AT III. At the concentration of  $10^{-5}$  M, significant differences ( $P < 0.05$ ) in the protective effect on factor Xa activity were confirmed between the control (no-HBPs) and HBPs. HBPs without AT III showed no effect on factor Xa activity. We confirmed the high activity

*Table 1. Sequence of synthetic heparin binding peptides (HBPs).*

Peptides	1	5	10	15														
HBP-1	K	I	P	E	A	T	N	R	R	V	W	E	L	S	K	A	*	
HBP-2	P	K	P	E	K	S	L	A	K	V	E	K	E	L	T	P	*	
HBP-4	F	A	K	L	N	C	R	L	Y	R	K	A	N	K	S	S	K	
HBP-7	F	A	K	L	N	S	R	L	Y	R	K	A	N	K	S	S	K	*
HBP-8	F	A	K	L	N	S	R	L	Y	R	K	A	N	K	S	S	K	
HBP-9	Ac-	F	A	K	L	N	S	R	L	Y	R	K	A	N	K	S	S	K
HBP-10	F	A	R	L	N	S	R	L	Y	R	R	A	N	R	S	S	R	*
HBP-11	F	A	R	L	N	C	R	L	Y	R	R	A	N	R	S	S	R	*

Syntheses of all heparin binding peptides were achieved by the solid-phase strategy employing optimal side-chain protection. \*, amidated in C-terminus.

in HBP-4 in comparison with HBP-1 and 2, and this potent antagonistic effect of HBP-4 was dramatically reduced by the modification of Cys to Ser (HBP-7–10). On the other hand, HBP-11, HBP-4 derivative having a lot of Arg residues instead of Lys residues, showed the highest activity of all tested peptides.

We also examined the binding potency of HBPs to heparin by the evaluation of elution behavior of HBPs from the heparin-agarose affinity column, and they eluted from the affinity column at the concentration of 650–750 mM Na<sub>2</sub>SO<sub>4</sub>. The conversion of Cys to Ser did not show significant changes in their affinity toward heparins, whereas this modification was effective in the protective effects of HBP-4 on heparin-induced inhibition of factor Xa activity. From the indicated results, there is the probability that the Cys residue in HBP-4 related compounds is essential for their activity, and that localized basic side-chains in the HBPs interact with the negatively charged group of heparin, in particular, *O*-sulfate and hexuronic acid moieties.

In this investigation, we clarified the structure–activity relationship of HBPs, and we obtained a new analogue of HBP-4 having strong inhibitory effects on the anti-factor Xa activity of heparins and high binding potency to heparins.

## References

1. Smith, J.W., Knauer, D.J. *Anal. Biochem.* **160**, 105–114 (1987).
2. Owen, W.S., Penich, G.D., Yodar, E., Pool, B.L. *Thromb. Haemostasis* **35**, 87–95 (1976).
3. Fish, W.W., Bjork, I. *Eur. J. Biochem.* **101**, 31–38 (1979).
4. Holmer, E., Kurachi, K., Soderstrom, G. *Biochem. J.* **193**, 395–400 (1981).
5. Sinay, P., Jacquinet, J.C., Petitou, M., Duchaussoy, P., Lederman, I., Choay, J., Torri, G. *Carbohydr. Res.* **132**, C5 (1984).
6. Onoue, S., Uda, T., Harada, S., Nemoto, Y., Yatohgo, T., Yajima, T., Kashimoto, K. *Peptide Sci.* **2000**, 163–166 (2001).

## **Antithrombin III-Derived Novel Heparin Binding Peptides Have an Antagonistic Effect on Heparins**

**Satomi Onoue<sup>1,2</sup>, Sunao Harada<sup>1</sup>, Yoshitaka Nemoto<sup>1,3</sup>, Takehiko Yajima<sup>2</sup>  
and Kazuhisa Kashimoto<sup>1</sup>**

<sup>1</sup>*Health Science Division, ITOHAM FOODS INC, Moriya, Ibaraki, 302-0104, Japan*

<sup>2</sup>*Analytical Sciences, School of Pharmaceutical Sciences Toho University, Chiba,  
274-8510, Japan*

<sup>3</sup>*American Peptide Company, Sunnyvale, CA 94086, USA*

### **Introduction**

Heparin is a highly sulfated, linear polysaccharide that has been used clinically in order to prevent the recurrence of venous thromboembolism because of its anticoagulant effect [1]. In the blood coagulation cascade, it binds with antithrombin III (AT III) [2], a serine protease inhibitor, and the reaction of AT III with serine proteases such as thrombin and factor Xa is dramatically accelerated [3]. It has been well established that there is a critical pentasaccharidic sequence in heparin named as an antithrombin-binding domain (A-domain) [4], which exhibits a high affinity to hAT III. The binding of A-domain to AT III strongly increases the inhibitory activity of AT III toward factor Xa, although not toward factor IIa [5]. On the other hand, the binding of AT III to another sequence, *i.e.* the thrombin-binding domain (T-domain) coupled to the A-domain in heparin causes an inhibitory effect on hAT III toward factor IIa. In the heparinotherapy, the T-domain in heparin caused significant side effects such as thrombocytopaenia and haemorrhages. Therefore, attention has been drawn to the structure and activity of the A-domain, and a lot of work has already been carried out to identify the high affinity binding site for the A-domain of heparin in AT III. However, these investigations are not sufficient to characterize the heparin-binding site. It is the purpose of this study to clarify, with use of a novel physicochemical and biochemical method, the heparin binding sites of AT III in relation to the inhibition of coagulation involving factor Xa. In addition, the use of synthetic peptides related to the heparin-binding sites of AT III led us to the successful development of a novel purification method by affinity chromatography for a highly active moiety of heparin molecules.

### **Results and Discussion**

The CD spectral analysis of HBPs (Table 1) showed that they were unordered in aqueous solution but became somewhat structured in the presence of 50% methanol. These helical components were confirmed in the corresponding sequences of AT III molecule obtained from slowly quenched simulated annealing calculation, hence the structures of synthetic HBPs were considered to be almost similar with those in AT III.

The binding activity of each HBP was estimated both by the absolute retention time in heparin-agarose affinity column HPLC system and by the salt concentration in the corresponding eluates, and HBPs were eluted from the heparin-agarose column over the concentration of salt range of 520–700 mM. The binding activity of them correlated well with the electric charge of HBPs, and this result indicated the existence of ionic interaction in the binding mechanism of HBPs to heparin.

We also examined the inhibitory effects of HBPs on heparins binding to AT III, and the catalytic activity of heparins coupled with AT III can be measured by assaying residual factor Xa activity using a chromogenic substrate in the presences of AT III and

### Biologically Active Peptides

factor Xa in excess. The addition of HBP-3 and 4 at the final concentration of  $10^{-5}$  M gave a similar potent protection of factor Xa activity, and less protection was observed with other HBPs at the concentrations examined. These results indicated that HBP-3 and 4 bind specifically to the active sequence of heparins.

*Table 1. Sequence of synthetic heparin binding peptides (HBPs). Peptide syntheses were performed by manual solid-phase technology employing optimal side-chain protection. The HBPs with asterisk are amidated in C-terminus.*

Peptides	1	5	10	15
HBP-1-1	K	I P E A T N R R V W E L S K A *		
HBP-1-2	I	P E A T N R R V W E L S K A *		
HBP-1-3	E	A T N R R V W E L S K A *		
HBP-1-4	R	R V W E L S K A *		
HBP-2	P	K P E K S L A K V E K E L T P *		
HBP-3	F	A K L N C R L Y R K A N K S S K L V		
HBP-4	F	A K L N C R L Y R K A N K S S K		
HBP-5	F	A K L N C R L Y R K A N A S S K		
HBP-6	F	A K L N C R L Y R A K S S N L K		

On the basis of the result that HBP-4 had a high affinity to the heparins and a potent inhibitory effect on heparins binding to AT III, we prepared the HBP-4-coupled cellulofine column for affinity chromatography of highly active moiety in heparins. With the use of this affinity column, the polysaccharides with potent anticoagulant activity could be fractionated, and they were eluted with high concentrations of  $\text{Na}_2\text{SO}_4$ . These highly active moieties of heparin are expected to be clinically valuable as an antithrombotic agent without significant side effects such as hemorrhages and thrombocytopaenia. This result also provided further evidence that HBP-4, corresponding to the consensus sequences from position 123 to 139 in AT III molecule, has a potent binding activity to the active moieties in heparins.

In conclusion, we succeeded in characterizing the proposed heparin-binding sites of hAT III using synthetic peptides. The synthetic peptides that related to the proposed heparin-binding sites of hAT III were also used for the development of an efficient method of LMW-heparin preparation.

### References

1. Casu, B. *Adv. Carbohydr. Chem. Biochem.* **43**, 51–134 (1985).
2. Smith, J.W., Knauer, D.J. *Anal. Biochem.* **160**, 105–114 (1987).
3. Jordon, R.E., Oosta, G.M., Gardner, W.T., Rosenberg, R.D. *J. Biol. Chem.* **55**, 10081–10090 (1980).
4. Riesenfeld, J., Thunberg, L., Hook, M., Lindahl, U. *J. Biol. Chem.* **256**, 2389–2394 (1981).
5. Holmer, E., Kurachi, K., Soderstrom, G. *Biochem. J.* **193**, 395–400 (1981).

## **The Octapeptide (Fragment of Differentiation Factor HLDF) Exhibits Nuclease Activity and Induces Apoptosis**

**Valery M. Lipkin<sup>1</sup>, Svetlana M. Dranitsina<sup>1</sup>, Igor I. Babichenko<sup>2</sup>,  
Igor L. Rodionov<sup>3</sup>, Ludmila K. Baidakova<sup>3</sup> and Irina A. Kostanyan<sup>1</sup>**

<sup>1</sup>*Shemyakin-Ovchinnikov Institute of Bioorganic Chemistry, Russian Academy of Sciences,  
Moscow, 117871 Russia*

<sup>2</sup>*University of Peoples' Friendship, Moscow, 117198 Russia*

<sup>3</sup>*Shemyakin-Ovchinnikov Institute of Bioorganic Chemistry (Pushchino Branch),  
Russian Academy of Sciences, Pushchino, Moscow region, 142292 Russia*

### **Introduction**

Previously, we isolated the differentiation factor HLDF of 8.2 kDa molecular mass from the culture medium of the promyelocyte human leukemia cells (HL-60) treated with *all-E*-retinoic acid and characterized it as the factor differentiating these cells into granulocytes [1]. A search in the EMBL computer database ([www.embl-heidelberg.de](http://www.embl-heidelberg.de)) revealed a significant homology between the cDNA sequence of the differentiation factor and that of the S21 ribosomal protein [2]. However, no homology was observed between the primary structures of the mature proteins, since two nucleotides, G in position 112 and C in position 224, in the cDNA of RPS21 are deleted from that of the HLDF precursor. As a result of these point mutations, the mature differentiation factor and the S21 ribosomal protein were the translation products from different reading frames. In earlier studies, we have shown that the hexapeptide fragment of the HLDF: TGENHR (HLDF-6) fully reproduces the differentiating and antiproliferative activities of the native HLDF in experiments on the HL-60 cells. It was also found using a model of transplantable NSO myeloma that HLDF-6 has antitumor activity [3]. This study is devoted to the identification and the structure-function analysis of the HLDF fragment that exhibits DNA/RNA-hydrolyzing activity.

### **Results and Discussion**

All our attempts to produce the mature differentiation factor in different prokaryotic systems were unsuccessful. In all cases, the production of recombinant HLDF was extremely low, and, though several clones started its production, it completely stopped after time.

The amino acid sequence of HLDF was compared with those of some known DNA/RNA-binding or DNA/RNA-hydrolyzing enzymes, and its octapeptide fragment (RRWHRLKE, 31–38) showed a homology to their sequences. We supposed that the presence of this sequence (we named it as DNA-hydrolyzing fragment) in the differentiation factor was responsible for the cDNA hydrolysis that results in a low expression of this protein. To confirm our proposal, we have used the pET-pA translation vector containing the nucleotide insertion encoding the IgG-binding domain of protein A to construct the pET-pA1 plasmid involving the cDNA sequence encoding the DNA-hydrolyzing fragment. Only the starting pET-pA plasmid and the construct with the sequence encoding the inert peptide (pET-pAk) were expressed. Insertion into plasmid the cDNA sequence, encoding the DNA-hydrolyzing fragment inhibits the process of protein expression.

To determine the functional role of the DNA-hydrolyzing fragment of HLDF, we synthesized the octapeptide RRWHRLKE (HLDF-8) and several of its analogs and studied their biological activity. HLDF-8 was shown to cleave matrix and ribosomal

RNAs, linear DNA of phage  $\lambda$  and all the forms of plasmid DNA *in vitro*. HLDF-8 exhibits its activity at low ionic strength, at acidic pH values ( $<4.5$ ; levels at which the His residue is protonated), and in the presence of cations of bivalent metals ( $\text{Zn}^{2+}$  or  $\text{Mn}^{2+}$ ). The addition of  $\text{Mg}^{2+}$  ions to the incubation medium inhibited the nuclease activity of HLDF-8, which probably was caused by a destabilization of the formed peptide-DNA complex. It should be noted that HLDF-8 loses its DNA/RNA hydrolyzing activity when the NaCl concentration in the medium increases to 100 mM. Conditions of high ionic strength can disturb not only ionic interactions between the peptide and the sugar-phosphate DNA backbone but also stacking interactions between the aromatic tryptophan ring and pairs of complementary bases. We demonstrated that a synthetic analogue of peptide-8 devoid of the Trp residue had no DNA-hydrolyzing activity.

HLDF (54 aa) and several large peptide fragments were synthesized for further studies. The peptides with the chain elongated at their C-termini exhibit changes in their hydrolyzing activity. For example, peptide containing 24 amino acids (HLDF-24) gained the ability to cleave DNA not only in acidic medium (pH 4.5) but also in a neutral medium (pH 7.5). We found that the N-terminal Tyr residue was oxidized to 3,4-dihydroxyphenylalanine (DOPA) when peptide containing 25 amino acids (HLDF-25) interacted with DNA. The conversion of the Tyr residue to DOPA can take place in the presence of active forms of oxygen, and, therefore, we suppose that the cleavage of nucleic acids by HLDF peptides proceeds according to the free radical mechanism. To test the hypothesis, we incubated the pSp65 DNA plasmid with HLDF-8 in argon atmosphere under acidic pH values. It was found that the peptide exhibits no DNA-hydrolyzing activity in the absence of oxygen. The confirmation of the hypothesis proposed is the fact that the addition of 3%  $\text{NaN}_3$ , an interceptor of free radicals, to the reaction medium inhibits DNA hydrolysis.

The full-length synthetic HLDF ( $10^{-5}$  M) hydrolyzed the plasmid DNA both at acidic and neutral pH values, and even in the presence of 0.15 M NaCl (*i.e.*, under physiological conditions). Thus, we can convincingly conclude that the low level of the recombinant HLDF production was associated with its specific nuclease activity.

The penetration of the fluorescent-labeled HLDF-8 peptide into the HL-60 cells was investigated. The PITS-labeled peptide was initially bound to the cell membrane and then, after two hours, penetrated into the cells. Two types of the stained cells were found in the culture: a) with the fluorescent stained nuclei and b) with large cellular structures in the cytoplasm stained. Thus, two mechanisms for the penetration of HLDF-8 into a cell may be suggested: (i) direct penetration into the cell nucleus followed by DNA fragmentation and (ii) the initial penetration into the cytoplasm and subsequent participation of the cell elements (mitochondria and lysosomes) in the activation of apoptosis.

Owing to the HLDF-8 capacity to digest the nucleic acids *in vitro* and penetrate to the nuclei of cells, we have decided to observe the changes in nuclear DNA of HL-60 cells taking place after their incubation with the peptide. (In a control experiment the cells were treated with the actinomycin D – known as apoptosis inducer.) The substantial nuclear DNA degradation in HL-60 was found after its cultivation (12 h) with HLDF-8 ( $10^{-4}$  M).

An immunohistochemical staining of the HL-60 cells with the use of polyclonal antibodies to the synthetic HLDF demonstrated that nuclei of the cells differentiated by the action of retinoic acid or subjected to apoptosis by the treatment with C2-Cer for a day were specifically point-stained. More intensive staining was observed in the

case of cells suffering from apoptosis. These results allow us to assume that HLDF participates in apoptosis processes. HLDF-8 was examined for the ability to induce the apoptosis in the HL-60 cell line. The number of annexin-positive cells (*i.e.*, cells in which the apoptosis was induced) was reliably increased even after four hours of incubation with HLDF-8 ( $10^{-6}$  M) according to the cytofluorometry (double staining with the PITC-labeled annexin V and propidium iodide).

Thus, in addition to inducing cell differentiation, the function that had been originally found [1], HLDF exhibits the properties of an unspecific nuclease due to the existence of a DNA/RNA-hydrolyzing fragment in its structure. HLDF probably participates in the degradation of DNA and RNA molecules released by the cells subjected to destruction (for example, by necrotic cells). Moreover, there is every reason to suppose that HLDF also plays an important role in the induction of apoptosis, since HLDF-8, a part of its sequence, causes the programmed cell death. The pathway of cell development (apoptosis or differentiation) probably depends on their physiological state.

#### **Acknowledgments**

This research was supported by the International Scientific and Technology Center (project #463) and by the Russian Foundation for Basic Research (grant No 97-04-49462).

#### **References**

1. Kostanyan, I.A., Astapova, M.V., Starovoitova, E.V., Dranitsyna, S.M., Lipkin, V.M. *FEBS Lett.* **356**, 327–329 (1994).
2. Bhat, K., Morrison, S.G. *Nucleic Acids Res.* **21**, 2939 (1993).
3. Kostanyan, I.A., Astapova, M.V., Navolotskaya, E.V., Lepikhova, T.N., Dranitsyna, S.M., Telegin, G.B., Rodionov, I.L., Baidakova, L.K., Zolotarev, Yu.A., Molotkovskaya, I.M., Lipkin, V.M. *Bioorg. Khim.* **26**, 505–511 (2000).

## ***In vivo* Proteolytic Hemoglobin Products as Tissue Growth Promoters**

**Olga V. Sazonova, Elena Yu. Blishchenko, Sergei V. Khaidukov,  
Andrei A. Karelin and Vadim T. Ivanov**

*Shemyakin-Ovchinnikov Institute of Bioorganic Chemistry, 117997 Moscow, V-437, GSP,  
Russia*

### **Introduction**

It is well known that growth factors are responsible for maintenance of cell proliferation *in vitro* and *in vivo*. At the same time, the ability to stimulate cell proliferation *in vitro* was demonstrated for endogenous fragments of functional proteins, defined earlier as components of tissue-specific peptide pools [1]. Neokytorphin, the  $\alpha$ -globin (137-141) fragment, has been shown earlier to stimulate proliferation of L929 transformed murine fibroblasts and brown preadipocytes independently on the presence of fetal bovine serum (FBS) [2–4]. We have studied the *in vitro* proliferative effects of the peptides corresponding to the  $\alpha$ -globin (133-141) segment, and on the basis of the data obtained suggested their function in the organism.

### **Results and Discussion**

Eight fragments of  $\alpha$ -globin (133-141) segment, including seven endogenous peptides and one synthetic analogue [ $\alpha$ -(133-141),  $\alpha$ -(134-141),  $\alpha$ -(134-140),  $\alpha$ -(133-138),  $\alpha$ -(137-140),  $\alpha$ -(137-141) and TS] were tested for their ability to stimulate L929 cell proliferation in serum-free culture medium. The activity was determined in 0.01–1  $\mu$ M concentration range after 24 h of co-incubation. All peptides exhibited a reliable proliferative activity ranging from 25 to 50%, the maximal effects (40–50%) being exhibited by  $\alpha$ -(134-141),  $\alpha$ -(134-140) and  $\alpha$ -(133-138). The activity of  $\alpha$ -(137-140) and  $\alpha$ -(134-140) was less than that of the corresponding peptides containing C-terminal Arg, indicating that removal of C-terminal Arg reduces proliferative activity. Two peptides,  $\alpha$ -(137-141) and  $\alpha$ -(134-141), stimulate proliferation of M3 murine melanoma and MEF murine embryonic fibroblasts (Figure 1).  $\alpha$ -(137-141) is more potent in stimulation of the normal fibroblast proliferation, whereas  $\alpha$ -(134-141) more effectively stimulates proliferation of corresponding tumor (L929) cells. The  $\alpha$ -(137-141) and  $\alpha$ -(134-141) were shown to support viability of M3, L929 cells and the cells of primary cultures of murine red bone marrow cells and spleen cells for 48–96 h; the increase of survived cells ranged from 28 to 85% as compared to the negative control. Using flow cytometry analysis, we have demonstrated that the cell supportive activity in serum deprivation conditions is directly due to the ability of the peptides to maintain cell proliferation in the absence of growth factors.

The dependence of the action of the peptides  $\alpha$ -(137-141) and  $\alpha$ -(134-141) on the initial cell density was studied in tumor (L929) and normal (MEF) fibroblasts in a tissue regeneration *in vitro* model. In the absence of FBS, both peptides stimulated cell proliferation independently of cell density. In the presence of 10% FBS,  $\alpha$ -(134-141) effectively increases the rate of proliferation, its effect being maximal at lower cell density. In contrast, the growth stimulatory effect of  $\alpha$ -(137-141) was detected at quite narrow cell density range, corresponding to “damaged tissue”. The data obtained point to the complementary growth stimulatory effect of different peptides derived from the  $\alpha$ -(133-141) segment. Summarizing, the results obtained speak of the ability of the peptides to replace growth factors in the case of their lack or deficiency and to act

additively to growth factors, probably, participating in tissue regeneration *in vivo*. On the other hand, the ability to effectively stimulate proliferation of tumor cells together with the data on accumulation of neokytorphin in lung carcinoma tissues [5] could indicate involvement of proliferative pool components in tumor progression.

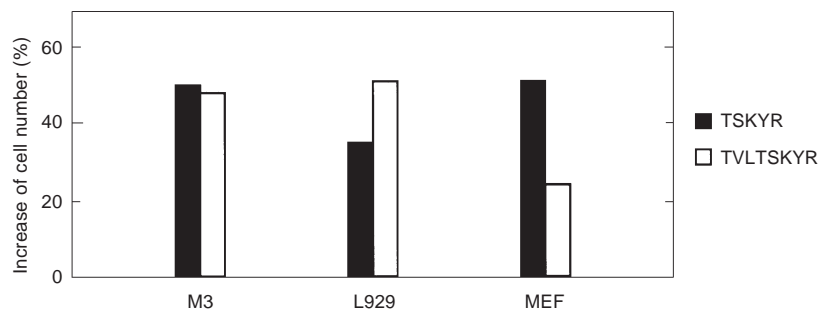


Fig. 1. Effects of  $\alpha$ -globin fragments (137-141) and (134-141) in cell cultures of various origin. The values are reliable with  $p \leq 0.05$ .

#### Acknowledgments

Supported by grants from the U.S. Civilian Research and Development Foundation (CRDF) (#TGP-256); and from the Russian Foundation for Basic Research (#00-04-48639).

#### References

1. Ivanov, V., Karelin, A., Blischenko, E., Philippova, M., Nazimov, I. *Pure Appl. Chem.* **70**, 67–74 (1998).
2. Blishchenko, E.Yu., Mernenko, O.A., Yatskin, O.N., Ziganshin, R.H., Phillipova, M. M., Karelin, A.A., Ivanov, V.T. *Biochem. Biophys. Res. Commun.* **224**, 721–727 (1996).
3. Blishchenko, E.Yu., Mernenko, O.A., Yatskin, O.N., Ziganshin, R.H., Phillipova, M.M., Karelin, A.A., Ivanov, V.T. *FEBS Lett.* **414**, 125–128 (1997).
4. Bronnikov, G., Dolgacheva, L., Zhang, Sh., Galitovskaya, E., Kramarova, L., Zinchenko, V. *FEBS Lett.* **407**, 73–77 (1997).
5. Zhu, Y.X., His, K.L., Chen, Z.G., Zhang, H.L., Wu, S.X., Zhang, S.Y., Fang, P.F., Guo, S.Y., Kao, Y.S., Tsou, K. *FEBS Lett.* **208**, 253–257 (1986).

## Synthesis and Pharmacological Activity of Superagonists of the ORL1 Receptor

Severo Salvadori<sup>1</sup>, Remo Guerrini<sup>1</sup>, Roberto Tomatis<sup>1</sup>, Girolamo Calo<sup>2</sup>,  
 Raffaella Bigoni<sup>2</sup>, Anna Rizzi<sup>2</sup>, Daniela Rizzi<sup>2</sup> and Domenico Regoli<sup>2</sup>

<sup>1</sup>Department of Pharmaceutical Sciences and

<sup>2</sup>Department of Experimental and Clinical Medicine, Section of Pharmacology, University of  
 Ferrara, 44-100 Ferrara, Italy

### Introduction

Nociceptin (NC)/orphanin FQ (H-Phe-Gly-Gly-Phe-Thr-Gly-Ala-Arg-Lys-Ser-Ala-Arg-Lys-Leu-Ala-Asn-Gln-OH) is a neuropeptide, which modulates several biological functions by activating the ORL1 receptor [1]. In the past years, we have performed systematic structure activity studies on NC that have established: a) NC residues 1-13 are sufficient both for high ORL1 receptor binding and biological activity; b) The basic residues in the C-terminal sequence, especially Arg<sup>8</sup>, appear to be instrumental for ORL1 receptor recognition; c) Contrary to opioid peptides, which strictly require Tyr<sup>1</sup> for opioid receptor activation, the active core of NC that stimulates the ORL1 receptor, is the Phe<sup>4</sup>; d) Specific changes of the N-terminal sequence, especially at Phe<sup>1</sup>, led to the discovery of a partial agonist, [Phe<sup>1</sup>Ψ(CH<sub>2</sub>-NH)Gly<sub>2</sub>]NC(1-13)-NH<sub>2</sub>, and [Nphe<sup>1</sup>]NC(1-13)-NH<sub>2</sub>, a pure antagonist of the ORL1 receptor [2]. In the present investigation, we describe the effect of substitutions with a halogen series of the Phe<sup>4</sup> aromatic side chain of the NC(1-13)-NH<sub>2</sub>, and identification of new ligands, which behave as superagonists of the ORL1 receptor.

### Results and Discussion

Peptides described here were prepared by solid-phase method on a PAL-PEG-PS-resin. Their pharmacological effects in the electrically stimulated mouse vas deferens are summarized in Table 1. All of the p-xPhe<sup>4</sup> analogues are agonists in the mouse vas deferens assay, and their potencies depend on the type of halogen. The fluoro-analog (comp. 4) was found to be 5-fold more potent than the reference NC(1-13)-NH<sub>2</sub>, while other para halogenated Phe<sup>4</sup> derivatives (comp. 1-3) showed

Table 1. Effects of NC(1-13)-NH<sub>2</sub> analogues in the electrically stimulated mouse vas deferens.

No.	Compound	Agonist	
		pEC <sub>50</sub> (CL <sub>95%</sub> )	E <sub>max</sub>
	NC(1-13)-NH <sub>2</sub>	7.49 (0.11)	-82 ± 3%
1	[(pCl)Phe <sup>4</sup> ]NC(1-13)NH <sub>2</sub>	7.09 (0.32)	-82 ± 5%
2	[(pBr)Phe <sup>4</sup> ]NC(1-13)NH <sub>2</sub>	6.68 (0.27)	-85 ± 3%
3	[(pI)Phe <sup>4</sup> ]NC(1-13)NH <sub>2</sub>	6.13 (0.34)	-76 ± 5%
4	[(pF)Phe <sup>4</sup> ]NC(1-13)NH <sub>2</sub>	8.19 (0.25)	-85 ± 2%
5	[(mF)Phe <sup>4</sup> ]NC(1-13)NH <sub>2</sub>	8.03 (0.30)	-90 ± 6%
6	[(oF)Phe <sup>4</sup> ]NC(1-13)NH <sub>2</sub>	7.48 (0.54)	-94 ± 2%

pEC<sub>50</sub>, the negative logarithm to base 10 of the molar concentration of an agonist that produces 50% of the maximal possible effect.

*Salvadori et al.*

lower potencies (from 2- to 30-fold) than the reference NC(1-13)-NH<sub>2</sub>. Analogues with fluorine in meta (comp. 5) or ortho position (comp. 6), are less potent than [(pF)Phe<sup>4</sup>]NC(1-13)-NH<sub>2</sub>. The ORL1 receptor potency of the para-halogenated Phe<sup>4</sup> analogues is positively correlated to the electronegativity of the substituents; *i.e.* the higher the electronegativity of the substituent, the higher the potency of the compound, while the lipophilicity and steric hinderance of the halogen decreased the biological activity. In the halogen series, substituent with the highest electronegativity (F), lowest lipophilicity, and smallest size was present in the most active NC analogues. On the other hand, the fluorine atom has a lone electron pair that is able to accept, but not give hydrogen bonds, and this chemical property could be important for ORL1 receptor interaction and activation. The results of our studies clearly demonstrate the importance of the Phe<sup>4</sup> pharmacophore of NC, and led to the identification of superagonists of the ORL1 receptor.

### References

1. Calo, G., Guerrini, R., Rizzi, A., Salvadori, S., Regoli, D. *Br. J. Pharmacol.* **129**, 1261–1283 (2000).
2. Guerrini, R., Calo, G., Rizzi, A., Bigoni, R., Rizzi, D., Regoli, D., Salvadori, S. *Peptides* **21**, 923–933 (2000).

## Rational Designing of CXCR-4 Agonists and Antagonists: Synthesis of Novel Cyclam Derivatives of Stromal Cell-Derived Factor (SDF-1)

A. Merzouk<sup>1</sup>, C. Tudan<sup>1</sup>, L. Arab<sup>1</sup>, S. Chahal<sup>1</sup>, G. E. Willick<sup>2</sup>  
 and H. Salari<sup>1</sup>

<sup>1</sup>Chemokine Therapeutics Corp., Research Laboratory, Vancouver, V6T 1Z3, Canada

<sup>2</sup>Institute of Biological Sciences, National Research Council of Canada, Ottawa, K1A 0R6, Canada

### Introduction

Stromal cell-derived factor (SDF-1) is a primordial chemokine of the CXC subfamily and has multiple biological activities on a variety of cell types [1]. SDF-1 is of unique interest because it is the only chemokine that regulates the cycling of both long-term culture initiating and primitive erythroid and granulopoietic colony-forming cells [2]. The N-terminus of SDF-1 is a critical site for CXCR4 receptor binding and activation [3]. We describe here new, active, truncated analogues of SDF-1 [4]. These peptides have the N-terminal region (residues 1–14) linked to the C-terminal (residues 55–67)  $\alpha$ -helix. A four-glycine linker approximates the distance between these C-terminal and N-terminal regions in the native folded SDF-1. In this study some of these 31-residue analogues are cyclized by lactamization between residues K20-E24 or residues E24-K28. All of these analogues showed enhanced *in vitro* biological activity, especially the cyclized ones.

### Results and Discussion

Both the N-terminal and C-terminal regions of SDF-1 **I** (Figure 1) are important for receptor binding and signaling [3,4]. The C-terminal region alone does not display any binding activity but it can bind to a GAG matrix. This may increase its local concentration and display it in the correct conformation towards the CXCR4 receptor. The

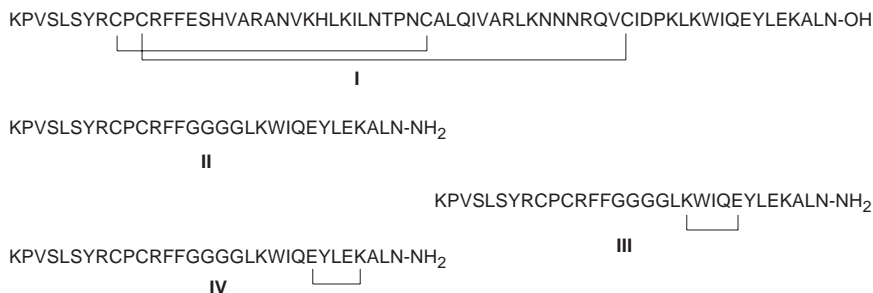


Fig. 1. Primary structure of peptide analogues.

amphiphilic  $\alpha$ -helix seems to be important for GAG binding. Lactam formation on the polar side face has been shown to increase activity and bioavailability in hormones such as PTH [5]. The truncated linear form of SDF (**II**) was cyclized by lactam formation between the side chains of either K20 and E24 (**III**) or E24 and K28 (**IV**).

The corresponding antagonist analogues, having P2G replacements were also prepared (results not shown).

The CD data indicated that analogue **III**, cyclized between K20 and E24 had 2–3 extra residues in  $\alpha$ -helix, compared to the linear form, as shown by the  $\theta_{222}$  values

(Table 1). The  $\theta_{222}$  to  $\theta_{209}$  ratio has a value of about 1.1 in a perfect  $\alpha$ -helix model. This value changes only slightly in the analogues **III** cyclized between residues 20 and 24, even though there is an increase in the length of the  $\alpha$ -helix. In contrast, cyclization between residues 24 and 28 **IV** affects only slightly the helical content of the analogue but results in a clearly more classical  $\alpha$ -helical structure.

Table 1. CD helical parameters and in vitro activities of SDF-1 analogues.

Peptide	$\theta_{222}/\theta_{209}$	Estimated residues <sup>a</sup>	Binding, nM	Assay [ $\text{Ca}^{2+}$ ]I, nM
			EC <sub>50</sub>	EC <sub>50</sub>
<b>I</b>	–	–	60.5	26.56
<b>II</b>	0.81	7	28960	–
<b>III</b>	0.86	10	1375	147.92
<b>IV</b>	0.98	8	1388	106.25

<sup>a</sup> Estimated as in reference [5].

The calcium release activities, as measured by EC<sub>50</sub> values, were clearly higher in the analogue cyclized between residues 24 and 28, resulting in this analogue having activities approaching that of the full length molecule. These data show that cyclization between residues 24 and 28 stabilized  $\alpha$ -helical structure approximating that found in the hormone-receptor complex, and demonstrate that this structure is similar to a classical  $\alpha$ -helix. Furthermore, these data show that the large intervening sequence of SDF-1 is not essential for the receptor binding. The structure of SDF that binds to the receptor is strikingly similar to that observed in the family of receptors that includes PTH, VIP, PACAP, glucagon, and secretin [5].

### Acknowledgments

We thank Mr Jean-Rene Barbier (National Research Council) for help with peptide synthesis and purification. Work was partly supported by the National Research Council of Canada Industrial Research Assistance Program.

### References

1. a) Nagasawa, T., Kikutani, H., Kishimoto, T. *Proc. Natl. Acad. Sci. U.S.A.* **91**, 2305–2309 (1994). b) Aiuti, A., Springer, T.A. *J. Exp. Med.* **184**, 1101–1109 (1996).
2. Cashman, J.D., et al. *Blood* **94**, 3722–3729 (1999).
3. Loetscher, P., et al. *J. Biol. Chem.* **273**, 22279–22283 (1998).
4. Luo, J., et al. *Biochem. Biophys. Res. Commun.* **264**, 42–47 (1999).
5. Barbier, J.R., et al. *J. Med. Chem.* **40**, 1373–1380 (1997).

## A Computational Study of Conformational Properties for *N*-Methylated Azapeptide Models

Ho-Jin Lee<sup>1</sup>, Dong-Kyu Shin<sup>2</sup>, Young-Sang Choi<sup>3</sup>, Chang-Ju Yoon<sup>4</sup>,  
 Kang-Bong Lee<sup>1</sup> and Seonggu Ro<sup>2</sup>

<sup>1</sup>Advanced Analysis Center, KIST, Seoul 136-791, South Korea

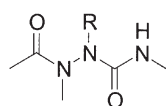
<sup>2</sup>CrystalGenomics, Inc. 461-6, Jeonmin-dong, Yusong-gu, Taejeon 305-390, South Korea

<sup>3</sup>Department of Chemistry, Korea University, Seoul 136-701, South Korea

<sup>4</sup>Department of Chemistry, The Catholic University of Korea, Pucheon 420-743, South Korea

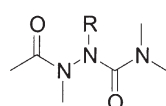
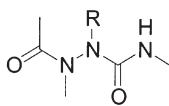
### Introduction

The modification of peptide structures is a general strategy in drug design to increase the resistance to physiological degradation and decrease the conformational flexibility. Among these modifications, azaamino acids are promising peptidomimetic compounds, which are formed by the replacement of an  $\alpha$ -carbon of amino acids with a nitrogen atom. Azaamino acids also could be prepared relatively easily with retention of the side chain in the normal amino acid. Recently, our laboratories reported torsion angle based design, solid phase synthesis and conformational study of a  $\beta$ -I turn adopting peptidomimetic template [1]. During these studies, we found that besides  $N^\alpha$ , two other nitrogens of an azaamino acid can be alkylated. To understand the effects of such alkylation on the conformation of azaamino acid is critical for the design of conformation directed combinatorial libraries. Thus, we carried out computational studies of model azapeptides in which methyl groups are systematically incorporated, Ac-Sar-NHMe (1), Ac-(NMe)AzAla-NHMe (2), Ac-Sar-NMe<sub>2</sub> (3) and Ac-(NMe)AzAla-NMe<sub>2</sub> (4).



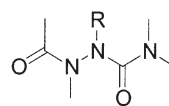
R=H, Ac-AzSar-NHMe (1)

R=CH<sub>3</sub>, Ac-NMe-AzAla-NHMe (2)



R=H, Ac-AzSar-NHMe (3)

R=CH<sub>3</sub>, Ac-NMe-AzAla-NHMe (4)



### Results and Discussion

The potential energy surfaces (PESs) of the models were generated by rotating two key dihedral angles  $\phi$  and  $\psi$  with an increment of 30° at the HF/6-31G\* level of theory. During this rotation, one of *cis* or *trans* configurations of acetyl amide was fixed. Then, the resulting conformations were fully optimized at the B3LYP/6-31G\* level.

The PESs of 1 and 2 are symmetric, thus we only discuss one half of the PES. The low-energy conformations of 1 and 2 are located in the right-handed region ( $\phi \approx -90 \pm 30^\circ$ ,  $\psi \approx 0 \pm 30^\circ$ ) and polyproline II regions ( $\phi \approx -90 \pm 30^\circ$ ,  $\psi \approx 180 \pm 30^\circ$ ). This shows that the *N*-methylation in the azaamino acids might not alter the conformational preferences of azaamino acids significantly, however, would be limited to the stereochemically allowed regions more than azaamino acids [2]. Interestingly, the PESs of the *trans* and *cis* form for compound 1 and 2 are similar, which demonstrates that the conformational properties of  $\phi$  ( $N-N^\alpha$ ) and  $\psi$  ( $N^\alpha-C$ ) are determined by the repulsion between nitrogen lone pairs and amide conjugated effect in urea-type structure, respectively [3].

The B3LYP/6-31G\* minima of the model **1** are four. They include conformation **1a**: ( $\omega_0, \phi_1, \psi_1, \omega_1$ ) = ( $-171^\circ, -94^\circ, -22^\circ, 176^\circ$ ), conformation **1b**: ( $175^\circ, -84^\circ, 166^\circ, 172^\circ$ ), conformation **1c**: ( $12^\circ, -122^\circ, 23^\circ, 174^\circ$ ), and conformation **1d**: ( $-8^\circ, -93^\circ, -165^\circ, -169^\circ$ ). The B3LYP/6-31G\* minima of the model **2** are also four including conformation **2a**: ( $\omega_0, \phi_1, \psi_1, \omega_1$ ) = ( $-171^\circ, -92^\circ, -9^\circ, 173^\circ$ ), conformation **2b**: ( $172^\circ, -70^\circ, 160^\circ, 178^\circ$ ), conformation **2c**: ( $12^\circ, -114^\circ, 15^\circ, 174^\circ$ ), and conformation **2d**: ( $-10^\circ, -84^\circ, -165^\circ, -178^\circ$ ). The global minima of the model azapeptides **1** and **2** are the conformations **1c** and **2c**, respectively. These conformations are found at the i+2 position of  $\beta$ -VI turn structure. These results were supported by the X-ray structure of Boc-Ala-(NMe)AzAla-Ala-NhiPr, which adopts a  $\beta$ -VI turn [4].

Furthermore, we carried out systematic conformational search and optimization of model compounds, Ac-AzSar-NMe<sub>2</sub> (**3**) and Ac-NMe-AzAla-NMe<sub>2</sub> (**4**), in which methyl group is incorporated at the following amide of azaamino acid. Interestingly in the B3LYP/6-31G\* minima of **3** and **4** includes the  $3_{10}$  helix or  $\beta$ -III turn structures. Their torsion angles ( $\omega_0, \phi_1, \psi_1, \omega_1$ ) are ( $-173^\circ, -66^\circ, -43^\circ, 174^\circ$ ) and ( $-173^\circ, -63^\circ, -40^\circ, 171^\circ$ ) for **3** and **4**, respectively. Such conformation is not observed among the conformations of **1** and **2**, but it was observed in the preferred conformations of Ac-AzAla-NMe<sub>2</sub>. Thus, it may originate from the methylation of the amide group of following azaamino acid in peptides.

## Conclusions

We analyzed the conformational properties of four model azapeptides in which methyl groups were systematically incorporated. The results show that incorporation of *N*-methylated azaamino acids, when coupled to primary amine, can stabilize  $\beta$ -VI turn in peptides. Moreover, when *N*-methylated azaamino acids are coupled to secondary amine (methylation at the amide following azaamino acids), the  $3_{10}$  helix or  $\beta$ -III turn structures can be generated. Currently, extensive quantum mechanical calculations of the above and other related azapeptides are in progress in our laboratories to obtain useful information for design of new drugs and molecular machine containing azaamino acids.

## Acknowledgments

Supported by a Korea University grant 2001 to Y.-S. Choi.

## References

1. Ro, S., Lee, H.-J., Ahn, I.-A., Shin, D.K., Lee, K.-B., Yoon, C.-J., Choi, Y.-S. *Bioorg. Med. Chem.* **9**, 1837–1841 (2001).
2. Lee, H.-J., Song, J.-W., Choi, Y.-S., Ro, S., Yoon, C.-J. *Phys. Chem. Chem. Phys.* **3**, 1693–1698 (2001).
3. Ro, S., Yoon, C.-J. *Z. Phys. Chem.* **214**, 1699–1706 (2000).
4. Zouikri, M., Vicherat, A., Aubry, A. Marraud, M., Boussard, G. *J. Peptide Res.* **52**, 19–26 (1998).

## Structural Requirements of Non-Mammalian Vasodilatory Peptide Maxadilan, an Excellent Agonist of PACAP Type 1 Receptors

Kiyoshi Nokihara<sup>1</sup>, Yoshihiro Nakata<sup>2</sup>, Ethan Lerner<sup>3</sup>,  
 Tadashi Yasuhara<sup>4</sup> and Victor Wray<sup>5</sup>

<sup>1</sup>Shimadzu Scientific Research Inc., Kyoto, 8511 Japan

<sup>2</sup>Hiroshima University, Hiroshima, 734-8551 Japan

<sup>3</sup>MGH, Harvard Medical School, Charlestown, MA 02129, USA

<sup>4</sup>Tokyo University of Agriculture, Tokyo 156-0054 Japan

<sup>5</sup>GBF, Braunschweig, 38124, Germany

### Introduction

Maxadilan (Maxa), isolated from salivary gland lysates of the blood feeding sand fly, *Lutzomyia longipalpis*, consists of 61 amino acid residues with two disulfide bridges and is a potent vasodilator. This particular non-mammalian derived peptide is an agonist of the PACAP type I receptor (PAC1) although it has no primary structure similarity [1]. PACAP has been implicated in a number of physiologic processes, although the absence of type-specific receptor agonists and antagonists hinders progress in further biochemical studies. Hence, Maxa and its related peptides may provide useful tool for physiological studies on the PACAP receptor system and new insights into the pathophysiology of skin diseases. The action of Maxa is an endothelium-independent vasodilator with immunomodulatory properties that binds to the PAC1 inducing the accumulation of intracellular cAMP and subsequent vasodilatation. Previously we have synthesized PACAP/VIP related peptide libraries, elucidated their solution structures and compared their biological actions [2,3]. In the present study we have investigated the structural requirements of Maxa-PAC 1 system by the use of Maxa-libraries.

### Results and Discussion

We have constructed Maxa-libraries that include the wild type Maxa (two disulfides position 1-5 and 14-51), mono disulfide, disulfide isomers and linear peptides (without disulfides), C-terminal fragments with or without disulfide, C-terminal dimer, middle fragments with a disulfide, N-terminal fragments with or without a disulfide, N-terminal dimer, peptides without the middle segment (different size) with a disulfide (N-linked to C-terminal fragment), different size of two peptide chains connected with disulfide bond corresponding to the wild type (between 14-51), and tyrosinated mutants (N<sup>α</sup>-Tyr and Tyr<sup>7</sup>) which exhibited full potency. Figure 1 illustrates the designed Maxa-libraries constructed in the present study.

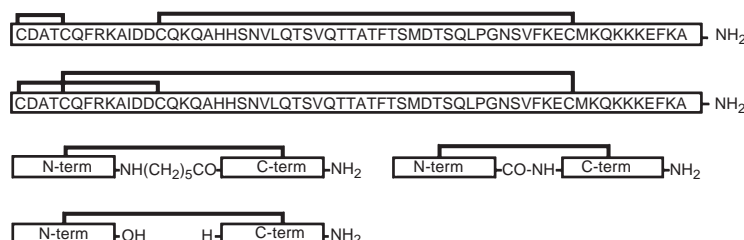


Fig. 1. Maxa-libraries designed and prepared the present study.

The syntheses were performed by the improved highly efficient protocol [4], although the “difficult sequences” was envisaged particularly in the middle region of Maxa. After cleavage, regio-specific disulfide(s) were formed by oxidation and de-salted. After purification by two modes of preparative HPLC (ion-exchange followed by RP-C18) the resulting materials were assessed by ion-trap LC-MS, MALDI-TOF-MS in addition to the Edman-Sequencing (disulfide forms), and amino acid analysis (peptide content). Biological actions were characterized by binding assays using rat brain membranes and cAMP assays were carried out in addition to analyses using melanophore technology, which is effective for functional analysis of GPCR ligands. The effects of the present libraries on PACAP induced cAMP accumulation in PC12 cells were also studied.

Of the three possible disulfide isomers, with S–S 1-5/14-51, 1-14/5-51, and 1-51/5-14, only the first two could be synthesized, although single disulfide derivatives (S–S between 14-51, 5-14 and 5-51) could be prepared. It is predicted that the residue 1 is not close to residue 51 in the active molecule.

The biological assays show that the N- and C-terminal fragments as well as central fragments with a disulfide (14-51) do not bind. The first disulfide is not essential in recognition, while the flexibility of both termini of the molecule plays an important role for recognition. Since the middle-region deleted mini-Maxa showed binding, the binding sites are most likely situated in fragments 7-14 and 40-61. The recognition core of PAC1 is the N-terminal region up to position 20 and the C-terminal region from 45. Antagonistic effects were observed in a two-chain peptide 1-23 and 43-61 linked with a disulfide bridge between 14-51. Similar results were reported recently in [5]. The two chain linked mutant possessing fragment 1-18 instead of 1-23 showed weaker binding. The dimers of the N- and C-terminal fragments show weak binding. The N-terminal region connected to the C-terminal region *via* an amino hexanoic acid showed weak agonistic effects whose magnitude depends on the size of the fragment. The detailed biological significance will be published elsewhere.

### Acknowledgments

A part of the present study was supported by a grant from the Ministry of Education, Science, and Culture, Japan. We thank T. Kasama, Tokyo Medical and Dental University, for MALDI-TOF-MS, and S. Shimizu and S. Yamamoto, Shimadzu Scientific Research, for their assistance.

### References

1. Moro, O., Lerner, E.A. *J. Biol. Chem.* **272**, 966–970 (1997).
2. Nokihara, K., Naruse, S., Ando, E., Wei, M., Ozaki, T., Wray, V., In Ramage, R. and Epton, R. (Eds) *Peptides 1996 (Proceedings of the 24th European Peptide Symposium)*, Mayflower Scientific., Birmingham, U.K., 1998, p. 63.
3. Wray, V., Blankenfeldt, W., Nokihara, K., Naruse, S., In Ramage, R. and Epton, R. (Eds) *Peptides 1996 (Proceedings of the 24th European Peptide Symposium)*, Mayflower Scientific., Birmingham, U.K., 1998, p. 921.
4. Nokihara, K., Yasuhara, T., Nakata, Y., Wray, V., In Epton, R. (Ed.) *Innovation and Perspectives in Solid-Phase Synthesis and Combinatorial Libraries 2000 (Proceedings of the 6th International Symposium)*, Mayflower Scientific., Birmingham, U.K., in press.
5. Moro, O., et al. *J. Biol. Chem.* **274**, 23103–23110 (1999).

## Effect of Deficiency of Cytochrome C Oxidase Assembly Peptide Cox17p on Mitochondrial Functions and Respiratory-Chain in Mice

Yoshinori Takahashi, Koichiro Kako, Hidenori Arai, Akio Takehara  
and Eisuke Munekata

Institute of Applied Biochemistry, University of Tsukuba, Tsukuba, 305-8572, Japan

### Introduction

A gel filtration fraction of porcine heart extract promoted the survival of NIH3T3 fibroblast cells in serum-free medium [1]. In addition to the porcine peptide [1], human, rat [2], and mouse [2] Cox17p homologues have been discovered to date (Figure 1). Although it has been believed that Cox17p guides Cu to mitochondria for insertion into cytochrome c oxidase (COX) in yeast, its physiological role in mammals is unknown. Recently, we have found that expression levels of Cox17p mRNA are high in mouse heart, kidney, brain and some endocrine cell lines, but quite low in small intestine, liver and some fibroblast cell lines [2]. Using the GST-fusion protein technology, we show that the GST-mCox17p (mouse Cox17p) binds copper at the putative metal-binding motif (-KPCCXC-) *in vitro* [3]. We have isolated *COX17* genomic DNA and shown that transcription factors Sp1 and NRF-1 drive the basal transcription of this gene [4]. Since our goal is to determine the physiological function of this novel peptide, we hypothesized that mammalian Cox17p peptide delivers intracellular Cu to the cuproenzymes, such as COX.

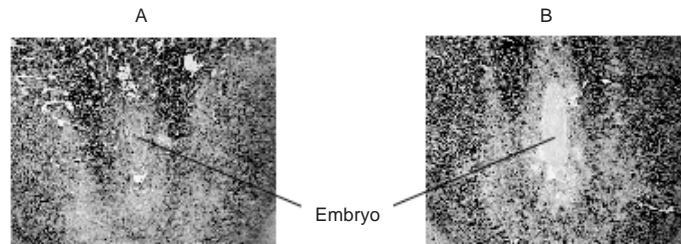
10 20 30 40 50 60 63  
MPGLAAASPAPPEAQEKPL**KPCCAC**PETKKARDACIEKGEEHCGHLIEAHKECMRALGFKI

Fig. 1. Primary structure of mouse Cox17p. The putative metal-binding motif is (KPCCXC) shown in bold.

### Results and Discussion

To examine the function of Cox17p *in vivo*, we investigated the effect of targeted disruption of the *COX17* gene. Targeting vector was constructed to delete almost all of the Cox17p peptide coding region and used to obtain heterozygote *COX17* (+/-). Progeny from intercrosses of *COX17* (+/-) mice were analyzed for genotype at 3 weeks after birth and the ratio of wild-type *COX17* (+/+) to *COX17* (+/-) littermates was 1.0 : 1.9 indicative of an embryonic lethal phenotype associated with the *COX17* (-/-) genotypes. The stage of embryonic death associated with *COX17* loss of function was investigated by determining the genotypes of embryos between 10 and 14 days postcoitus (dpc). No *COX17* (-/-) fetuses were found in this term and the ratio of *COX17* (+/+) to *COX17* (+/-) fetuses was 1.0 : 2.5. Therefore, we performed PCR to genotype presomite stage embryo. Among 11 fetuses isolated at 6.5 dpc, two were *COX17* (+/+), seven were *COX17* (+/-), and two were *COX17* (-/-), in close agreement with the expected ratio for Mendelian inheritance. Thus, homozygous null mutations in *COX17* result in lethality between embryonic days 6.5 and 10. To determine whether Cox17p is functional in presomite embryos, COX histochemical study was performed. Surprisingly, among 11 embryos isolated at 6.5 dpc, three embryos showed severe reductions in COX enzyme activity in the whole body (Figure 2).

According to the genotype ratio at this stage, these embryos must have been homozygous mutants, but they seemed to be viable and morphologically normal (Figure 2). In general, formation of heart, skeletal muscle and kidney (which are all derived from mesoderm) start around 7-9 dpc. Since Cox17p mRNA is also highly expressed in these organs in adults, Cox17p may be involved in not only cellular respiration but also development of these organs in early embryogenesis; further study is required to substantiate this speculation.



*Fig. 2. Histochemical staining of embryo serial sections to detect COX enzyme activities. (A) Putative wild type (+/+) or heterozygote (+/-) and (B) homozygote (-/-).*

#### **Acknowledgments**

We thank Ms. Yoshiko Inada, Ms. Sachiko Dobashi, and Mr. Takashi Onodera for their skilled technical assistances. This work was supported in part by grants from the Ministry of Education, Science, Sports and Culture of Japan, and University of Tsukuba Research Projects.

#### **References**

1. Takenouchi, T., Fujimoto, M., Shimamoto, A., Munekata, E. *Biochim. Biophys. Acta* **1472**, 498–508 (1999).
2. Kako, K., Tsumori, K., Ohmasa, Y., Takahashi, Y., Munekata, E. *Eur. J. Biochem.* **267**, 1–9 (2000).
3. Kako, K., unpublished data.
4. Takahashi, Y., unpublished data.

## Circadian Rhythm Pacemaker Neuropeptide “PDF” in Nocturnal Insect Cricket *Gryllus bimaculatus*: cDNA Cloning, mRNA Expression, and Nuclear Localization

Yoshiro Chuman<sup>1</sup>, Ayami Matsushima<sup>1</sup>, Yasuyuki Shimohigashi<sup>1</sup> and Miki Shimohigashi<sup>2</sup>

<sup>1</sup>Laboratory of Structure-Function Biochemistry, Faculty and Graduate School of Sciences, Kyushu University, Fukuoka 812-8581, Japan

<sup>2</sup>Division of Biology, Faculty of Science, Fukuoka University, Fukuoka 814-0180, Japan

### Introduction

Pigment-dispersing factor (PDF) has recently been reported to be a principal circadian neuromodulator involved in transmitting circadian rhythms of daily locomotion in insects. In *Drosophila*, PDF functions in some of the neurons expressing the clock genes *period*, *timeless*, *Clock*, and *cycle*, and clock genes in turn regulate *pdf* gene expression [1]. To date, investigations on circadian clocks have been performed mainly on diurnal animals such as *Drosophila* and humans. However, many species are nocturnal, and perhaps different systems of modulation either generate or edit diurnal and nocturnal behavioral profiles. In the present study, we have carried out the cDNA cloning of PDF from adult brains of the cricket *Gryllus bimaculatus*, whose behavioral activity manifests nocturnal rhythmicity. We cloned a cDNA encoding PDF in the brain of a nocturnal insect, the cricket *Gryllus bimaculatus*, and found that an isolated clone codes for an extraordinary short precursor protein. This prompted us to carry out a series of gene-based and peptide-based examinations for characterization of this novel PDF precursor.

### Results and Discussion

For cDNA cloning, mRNA was isolated from heads of the adult crickets maintained in a light/dark (LD) 12 : 12 photoperiod at 27 °C. Combined results from the 3'RACE and cRACE methods determined the full length of cDNA clone comprising 310 bp with a precursor protein of 43 amino acid residues. The cDNA sequence was further confirmed by RT-PCR using primers set for both 5'-UTR and 3'-UTR to amplify the full-length PDF cDNA. It should be noted that this size of PDF precursor is considerably smaller than those of other insects, which contain for example 102 amino acid residues for *Drosophila melanogaster* [2], and 89 amino acid residues for *Romalea microptera* (GenBank). It was found that the clarified sequence of *G. bimaculatus* PDF, NSEIINSLGLPKVLNDA-amide, is identical with that of *Acheta domesticus* (Figure 1). The structure of *G. bimaculatus* PDF itself exhibits a high level of sequence identity (78–100%) and similarity (89–100%) when compared with PDFs of other insects (Figure 1). When analyzed by the computer-assisted signal peptide prediction method for eukaryotic sequences, no distinct sequence was indicated as a signal (data not shown). The initiation sequence MARRARFEAN of the *G. bimaculatus* PDF resembles the sequences of nuclear localization signals (NLS) previously reported.

When we calculated the score that distinguishes the tendency of a peptide to translocate either to the nucleus or to the cytoplasm, using the network system, the 1-22 initiation sequence of the *G. bimaculatus* PDF precursor was judged to have a higher likelihood of being in the nucleus (about 48%) than in the cytoplasm (about

**Chuman et al.**

22%). For anatomical analysis of PDF immunoreactive cells, confocal microscopy was first used on whole-mount immunostains. The optic lobes of *G. bimaculatus* revealed PDF-immunoreactive neurons in both the medulla and lamina neuropiles. Among the strongly immunoreactive lamina PDF neurons, we identified by electron microscopy cells having distinct staining that is not only cytoplasmic but also nuclear. To confirm the nuclear localization of PDF peptide, we prepared mRNAs to express the proteins fused with green fluorescent protein (GFP) at the either N- or C-terminus of PDF precursor protein. It was found that only PDF protein GFP-fused at the C-terminus, but not at the N-terminus, is translocated into the nucleus.

**Insect PDFs**

<i>Gryllus bimaculatus</i>	NSEIINSLGLPKVLNDA-NH <sub>2</sub>
<i>Acheta domesticus</i>	NSEIINSLGLPKVLNDA-NH <sub>2</sub>
<i>Romalea microptera</i>	NSEIINSLGLPKLLNDA-NH <sub>2</sub>
<i>Periplaneta americana</i>	NSELINSLGLPKVLNDA-NH <sub>2</sub>
<i>Drosophila melanogaster</i>	NSELINSLSLPKNMNDA-NH <sub>2</sub>

**Crustacean  $\beta$ -PDHs**

<i>Uca pugilator</i>	NSELINSILGLPKVMNDA-NH <sub>2</sub>
<i>Procambarus clarkii</i>	NSELINSILGLPKVMNEA-NH <sub>2</sub>
<i>Penaeus aztecus</i>	NSELINSLGIPKVMNDA-NH <sub>2</sub>
<i>Penaeus japonicus I</i>	NSELINSLGIPKVMTDA-NH <sub>2</sub>
<i>Penaeus japonicus II</i>	NSELINSLGLPKFMIDA-NH <sub>2</sub>

*Fig. 1. Amino acid sequences of insect pigment-dispersing factors (PDFs) and crustacean  $\beta$ -pigment-dispersing hormones ( $\beta$ -PDHs).*

The *in situ* hybridization was carried out to identify the places where the mRNA is expressed. As observed by the immunochemical detection, the medulla and lamina cells in the optic lobes were found to express the *pdf*-gene. The rhythmicity of PDF was assessed by examining the temporal expression of mRNA. As reported for *Drosophila* PDF mRNA, we have found almost no significant rhythmicity in expressing PDF mRNA.

The present result is the first finding of PDF peptide itself in the nucleus, and suggests a fundamental role of PDF peptide *per se* in the circadian clock system.

**References**

1. Dunlap, J.C. *Cell* **96**, 271–290 (1999).
2. Park, J.H., Hall, J.C. *J. Biol. Rhythms* **13**, 219–228 (1998).

## **Design and Synthesis of the Hydroxamic Acid Variants Antitumorigenic and Antimetastatic Hydroxamate Based Ac-PHSXX'-NH<sub>2</sub> Sequences**

**Yingchuan Sun and Arno F. Spatola**

*Department of Chemistry and the Institute for Molecular Diversity and Drug Design,  
University of Louisville, Louisville, KY 40292, USA*

### **Introduction**

One of the best characterized integrin-ligand interactions is  $\alpha_5\beta_1$  binding to fibronectin (FN). The RGD sequence in the FN III domain 10 (FN10) is the key binding site for  $\alpha_5\beta_1$  integrin [1]. But the FN III domain 9 (FN9) also contributes importantly to adhesion, and the critical minimal sequence in this domain is a pentapeptide with the sequence PHSRN. Because this region has the potential to enhance overall binding to the integrin, the adhesive region in FN9 has been called the synergy site [2]. Livant and coworkers reported PHSRN sequence induced invasion through  $\alpha_5\beta_1$  integrin by interacting with the third NH<sub>2</sub> terminal domain of the  $\alpha_5$  chain, which forms a pocket that may contain a divalent cation [3–5]. PHSCN, a competitive inhibitor, blocked both PHSRN- and serum-induced invasion [5]. An acetylated, amidated PHSCN was 30-fold more potent. Thus, Ac-PHSCN-NH<sub>2</sub> may be a potent anti-tumorigenic and antimetastatic agent for postsurgical use prior to extensive metastasis [5].

We have designed and synthesized a new series of Ac-PHSXX'-NH<sub>2</sub> based hydroxamates, where X is the aspartic acid or glutamic acid incorporates a side chain hydroxamate moiety. The rationale for substituting cysteine with hydroxamate is that the latter has a high metal-binding ability and these analogs might reveal whether metal binding is an important consideration for the design of second-generation compounds. Hydroxamic acids have performed as a primary role in MMP inhibition studies since they can serve as bidentate ligands to block MMPs' central Zn(II) active site. Correspondingly, PHSCN was reported to inhibit the expression of specific metalloproteinase functioning in cell migration through the extracellular matrix [5].

### **Results and Discussion**

In order to produce hydroxamate analogs by solid phase methods, it would be convenient to have appropriately protected building blocks. Accordingly, we decided to prepare both aspartic acid and glutamic acid derived amino hydroxamates. In the synthesis of Boc-Asp(NHOBzl)-OH, Boc-Asp-OFm was prepared by the method previously described [6]. Boc-Asp-OFm was coupled to NH<sub>2</sub>OBzl with BOP and DIEA to afford Boc-Asp(NHOBzl)-OFm. After base deprotection of the Fm group, the aspartic acid hydroxamate building block Boc-Asp(NHOBzl)-OH was obtained in 97% purity and 65% yield (from Boc-Asp-OFm). Following a method we reported earlier [7], we synthesized Boc-Glu-OFm, which was then treated by the same method as Boc-Asp-OFm and afforded Boc-Glu(NHOBzl)-OH in 94% purity and 71% yield (from Boc-Glu-OFm).

We have described an effective method to prepare peptide hydroxamic acids on a solid support [8]. A residue bearing a protected carboxylic residue was introduced using orthogonally protected Asp/Glu derivatives. The side chain carboxylic group was modified by solid phase N to C amidation using an *O*-benzyl hydroxylamine. The

O-benzyl protection group can be removed concomitantly before or after the peptide resin cleavage to afford the functionalized hydroxamated side chain.

In the synthesis of Ac-PHSX(NHOH)X'-NH<sub>2</sub> analogs, Fmoc-Glu(O<sup>t</sup>Bu)-OH or Fmoc-Asp(O<sup>t</sup>Bu)-OH was incorporated onto X'-MBHA resin by in situ neutralization coupling to afford Fmoc-X(O<sup>t</sup>Bu)-X'-MBHA resin. TFA treatments deprotected the OtBu protecting group. Prior to the N to C coupling, the resin was neutralized with 10% DIEA/CH<sub>2</sub>Cl<sub>2</sub>, which effectively overcome the succinimide formation. BzlONH<sub>2</sub>·HCl was condensed with BOP and DIEA, which resulted in Fmoc-X(NHOBzl)-X'-MBHA resin. The remaining amino acids were coupled to the resin *via* routine Fmoc chemistry SPPS. After HF cleavage, the crude peptides were obtained. When tested with FeCl<sub>3</sub> test, the compounds gave the requisite pink positive hydroxamic acid test. Further analyzing involved proton NMR, which gave the characteristic pair of signals near 10 ppm indicating the NHOH moiety and MALDI-TOF MS which confirmed the expected masses. Efforts are underway to establish the detailed biological profiles of these analogs.

Table 1. Prepared peptide hydroxamic acids.

No.	Peptide hydroxamic acid	Peptide content in crude peptide (%) <sup>a</sup>	Yield (%) <sup>b</sup>	MW calcd	MW found (M+1) <sup>c</sup>
1	Ac-Pro-His-Ser-Glu(NHOH)-Leu-NH <sub>2</sub>	86	78	637.7	638.7
2	Ac-Pro-His-Ser-Glu(NHOH)-Asn-NH <sub>2</sub>	83	80	638.6	639.9
3	Ac-Pro-His-Ser-Asp(NHOH)-Asn-NH <sub>2</sub>	78	68	624.6	625.8

<sup>a</sup> Determined by RP-HPLC at  $\lambda = 220$  nm. <sup>b</sup> Calculated after RP-HPLC purification according to the initial substitution level (1.25 meq/g) on the pMBHA resin. <sup>c</sup> Obtained by MALDI-TOF MS.

## References

1. Pierschbacher, M.D., Ruoslahti, E. *Nature* **309**, 30–33 (1984).
2. Aota, S., Nomizu, M., Yamada, K.M. *J. Biol. Chem.* **269**, 24756–24761 (1994).
3. Mould, A.P., Askari, J.A., Aota, S., Yamada, K.M., Irie, A., Takada, Y., Mardon, H.J., Humphries, M.J. *J. Biol. Chem.* **272**, 17283–17292 (1997).
4. Mould, A.P., Garratt, A.N., Puzon-McLaughlin, W., Takada, Y., Humphries, M.J. *Biochem. J.* **331**, 821–828 (1998).
5. Livant, D.L., Brabec, R.K., Pienta, K.J., Allen, D.L., Kurachi, K., Markwart, S., Upadhyaya, A.J. *Cancer Res.* **60**, 309–320 (2000).
6. Spatola, A.F., Darlak, K., Romanovskis, P. *Tetrahedron Lett.* **37**, 591–594 (1996).
7. Romanovskis, P., Spatola, A.F. *J. Peptide Res.* **52**, 356–374 (1998).
8. Chen, J.J., Spatola, A.F. *Tetrahedron Lett.* **38**, 1511–1512 (1997).

## Design, Synthesis and Evaluation of Growth Regulating SDF-1 Peptides on Breast Carcinoma Cells

Megan K. Condon<sup>1</sup>, Christy A. Sasiela<sup>2</sup>, Angela H. Brodie<sup>3</sup> and Sandra C. Vigil-Cruz<sup>1,4</sup>

<sup>1</sup>Department of Pharmaceutical Sciences, University of Connecticut, Storrs, CT 06269, USA

<sup>2</sup>Department of Pharmaceutical Sciences and <sup>3</sup>Department of Pharmacology and Experimental Therapeutics, University of Maryland, Baltimore, MD 20201, USA

<sup>4</sup>Department of Medicinal Chemistry, University of Kansas, Lawrence, KS 66045, USA

### Introduction

Despite significant research advances, breast cancer is still the second leading cause of cancer deaths among American women [1]. Thus, new therapeutic modalities are desperately needed with different mechanisms of action from those currently available. The G-protein coupled CXCR4 chemokine receptor and stromal cell-derived factor-1 (SDF-1), the only known endogenous ligand for CXCR4, are overexpressed on the cell surface of both primary breast tumor cells and breast tumor cell lines [2]. However, neither CXCR4 nor SDF-1 are expressed in normal breast tissue [3]. By designing and synthesizing a series of small synthetic peptides as potential antagonists at CXCR4 and evaluating their antiproliferative activity in breast cancer cell lines, we are the first research group to evaluate the growth regulating effect of SDF-1 derived peptides on breast cancer cells and explore CXCR4 as a potential drug target for breast cancer.

### Results and Discussion

SDF-1-(1-17) was chosen for modification as it retains affinity for the CXCR4 receptor compared to the intact protein [4]. The lead compound included amidation to increase metabolic stability and Cys replacement with Abu,  $\alpha$ -aminobutyric acid, to prevent unwanted disulfide bond formation (**UU117**). Utilizing results of structure-activity relationship studies for inhibition of HIV-1 infectivity (presumably through CXCR4 receptor interaction) [5], analogues were designed to increase potency and impart antagonist activity to the lead compound. In an effort to increase potency, Cys9 was replaced with Phe (**FU117**), Leu5 with His (**HFU117**) [5], and Cys11 was substituted with Arg (**FR117**) [5,6]. The initial strategy to impart antagonist activity focused on truncation of the N-terminus (**FU317**) [5].

Our inaugural work demonstrates the ability of first generation peptide analogues to inhibit T47-D breast tumor cell proliferation. However, the peptides are active at a concentration of 10  $\mu$ M with approximately one-third the efficacy of 4-hydroxy-tamoxifen at 10 nM. The inhibition was determined by comparison to a diluent control (0% inhibition). Two analogues were selected for further evaluation to examine dose-dependent inhibition in both T47-D and MCF-7 cell lines (Figure 1). Although **FU117** and **HFU117** appeared to have similar potency in the preliminary screen, Leu5 was superior to His in the inhibition of breast tumor cell proliferation as demonstrated by the dose-response curve. In contrast, **HFU117** demonstrated only minimal inhibition (<10%) at high concentrations and **FU117** was inactive in MCF-7 cells (data not shown). However, the MCF-7 cell results demonstrate the peptides are not toxic at high concentrations to breast tumor cells.

The anti-proliferative effect of the analogues supports our hypothesis that the CXCR4 chemokine receptor is a viable drug design target for breast cancer. Further

ongoing studies include evaluation for CXCR4 receptor binding affinity and additional structure-activity relationship studies to enhance potency and efficacy of the peptides as well as signaling studies to ascertain agonist versus antagonist activity at CXCR4. The variance in effect between cell lines also suggests that further studies are needed, but the difference in efficacy is a reminder of the heterogeneity of the breast tumor cell population.

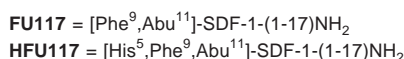
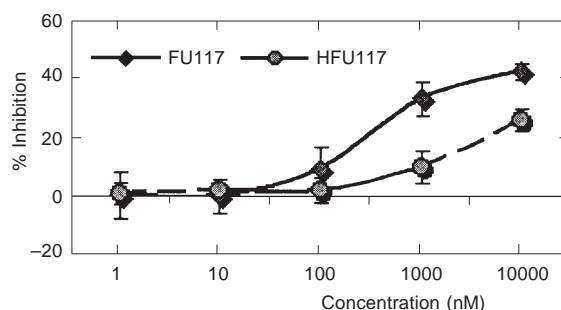


Fig. 1. Initial dose-response curves in T-47D cells for selected analogues.

## Acknowledgments

We acknowledge Lisa Popovich, Pharm.D. and Melissa Walczak for the synthesis and purification of FU317 and FR117, respectively. We thank New England Peptide, Inc. (Fitchburg, MA) for MALDI-TOF mass spectrometry and AAA Service Laboratory (Boring, OR) for amino acid analysis. This work was supported by the Pfizer Summer Undergraduate Research Fellowship (SURF) and the Karl A. Nieforth Summer Undergraduate Research Fellowship to M. K. C.

## References

1. Armstrong, K., Eisen, A., Weber, B. *NEJM* **342**, 564–571 (2000).
2. Müller, A., Homey, B., Soto, H., Ge, N., Catron, D., Buchanan, M., McClanahan, T., Murphy, E., Yuan, W., Wagner, S., Barrera, J., Mohar, A., Verástegui, E., Zlotnik, A. *Nature* **410**, 50–56 (2001).
3. Sehgal, A., Keener, C., Boynton, A., Warrick, J. *J. Surg. Oncol.* **69**, 99–104 (1998).
4. Loetscher, P., Gong, J.-H., Dewald, B., Baggiolini, M., Clark-Lewis, I. *J. Biol. Chem.* **273**, 22279–22283 (1998).
5. Heveker, N., Montes, M., Germeroth, L., Amara, A., Trautmann, M., Alizon, M., Schneider-Mergener, J. *Curr. Biol.* **8**, 369–376 (1998).
6. Luo, Z., Zhou, N., Luo, J., Hall, J., Huang, Z. *Biochem. Biophys. Res. Commun.* **263**, 691–695 (1999).

## Components of Tissue-Specific Peptide Pools as Negative Regulators of Cell Growth

Elena Yu. Blischenko<sup>1</sup>, Olga V. Sazonova<sup>1</sup>, Sergei V. Khaidukov<sup>1</sup>,  
Yury A. Sheikine<sup>2</sup>, Dmitry I. Sokolov<sup>2</sup>, Irina S. Freidlin<sup>2</sup>,  
Marina M. Philippova<sup>1</sup>, Andrei A. Karelin<sup>1</sup> and Vadim T. Ivanov<sup>1</sup>

<sup>1</sup>Institute of Bioorganic Chemistry, 117997 Moscow, B-437, GSP, Russia

<sup>2</sup>Institute of Experimental Medicine, Russian Academy of Medical Sciences, ul. Acad. Pavlov 12,  
197376 St. Petersburg, Russia

### Introduction

During the past decade, several hundred endogenous peptides proteolytically derived from proteins with an established *in vivo* function, such as hemoglobin,  $\beta$ -actin, cellular enzymes, etc. have been isolated from various tissue extracts and sequenced [1–5]. The tissue-specific and conservative sets of these peptides were defined earlier as tissue-specific peptide pools. *In vitro* studies of the biological activity of more than 100 peptides demonstrated that the majority of them are active, their effect being typically due to inhibition or stimulation of cell growth [3–5]. Below we represent the typical effects of the peptides exhibiting most pronounced growth inhibitory potency.

### Results and Discussion

Three endogenous peptides: Val-Val-hemorphin-5 ( $\beta$ -globin fragment (33-39) and  $\beta$ -actin fragments (75-90) and (68-77) were demonstrated to inhibit proliferation of tumor and normal cells. The antiproliferative effects were studied in a panel of tumor cell lines, including fresh and drug-resistant tumor cells and normal cells of different

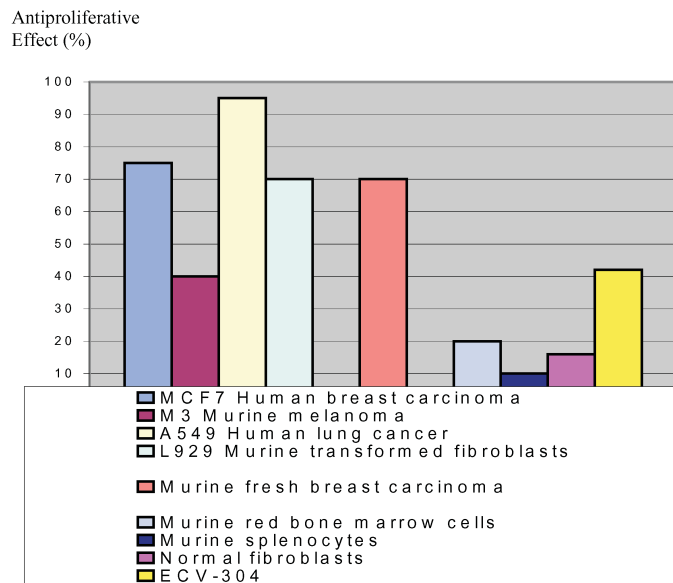


Fig. 1. Antiproliferative effects of VV-hemorphin-5 in tumor cells and normal cells. Tumor cells were incubated in the presence of  $10^{-6}$  M of the peptide for 96–120 h. After completion of the incubation procedure the cells were stained with sulforhodamine B dye.

origin. The peptides effectively suppress proliferation of L929 (murine transformed fibroblasts), M3 (murine melanoma), A549 (human lung carcinoma), HL-60 (human promyelocytic leukemia) and MCF7 (human breast carcinoma) tumor cells, being several fold less active in normal fibroblasts and primary cultures of murine red bone marrow and spleen cells (Figure 1). The mechanism of action of all studied peptides involves reversible arrest of cell cycle progression on one hand, and induction of reversible resistance of target cells to the following treatment by the same compound, on the other. Combined action of selected peptides with a standard cytostatic chemopreparation, epirubicin, was also studied. In that case the effect depends on application schedule and varies from inhibition of the cytostatic effect of the drug to its additive enhancement. The differences in the effects of peptides on epirubicin action were directly related to the ability of the peptides to induce reversible cell cycle arrest. One of most active peptides, VV-hemorphin-5, in combination with epirubicin prolonged the average lifetime of mice two-fold, and suppressed the tumor growth by 22% as compared with epirubicin alone in murine breast carcinoma model *in vivo*.

In summary, endogenous fragments of functional proteins exhibiting antiproliferative activities are considered as participants of cell growth regulation *in vivo*.

#### **Acknowledgments**

Supported by grants from the U.S. Civilian Research and Development Foundation (CRDF) (#TGP-256); and from Russian Foundation for Basic Research (#00-04-48639).

#### **References**

1. Blishchenko, E.Yu., Karelin A.A., Ivanov V.T. *Neurochem. Res.* **27**, 1119–1126 (1999).
2. Karelin, A.A., Philippova, M.M., Karelina, E.V., Strizhkov, B.N., Grishina, G.A., Nazimov, I.V., Ivanov, V.T. *J. Pept. Sci.* **4**, 211–225 (1998).
3. Ivanov, V.T., Karelin, A.A., Philippova, M.M., Blishchenko, E.Yu., Nazimov, I.V. *Pure Appl. Chem.* **70**, 67–74 (1998).
4. Karelin, A.A., Philippova, M.M., Yatskin, O.N., Kalinina, O.A., Nazimov, I.V., Blishchenko, E.Yu., Ivanov, V.T. *J. Pept. Sci.* **6**, 345–361 (2000).
5. Ivanov, V.T., Yatskin O.N., Kalinina O.A., Philippova, M.M., Karelin, A.A., Blishchenko, E.Yu. *Pure Appl. Chem.* **72**, 355–361 (2000).

## HPLC Analysis, Modeling, and Biological Studies of Antiproliferative Heterocyclic Carboxamides

János Seprődi<sup>1</sup>, Ferenc Hollósy<sup>1</sup>, Dániel Erős<sup>2</sup>, László Örfi<sup>2</sup>,  
István Teplán<sup>1</sup>, György Kéri<sup>1</sup> and Miklós Idei<sup>1</sup>

<sup>1</sup>Department of Medical Chemistry & Peptide Biochemistry Research Group,  
Semmelweis University, Budapest, Hungary

<sup>2</sup>Institute of Pharmaceutical Chemistry, Semmelweis University, Budapest, Hungary

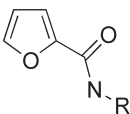
### Introduction

Reversed phase HPLC and MEKC [1] provide excellent possibilities to measure the hydrophobic properties of compounds, characterizing them directly from the chromatographic retention time. The aim in this respect is to estimate the hydrophobic character of the molecules on the basis of their retention factors ( $k'$ ) determined in various separation processes [1]. The expected biological activity of the compounds can be reliably predicted on the basis of the measured hydrophobicity data [2]. Another possibility is the use of highly sophisticated computer programs to calculate hydrophobicity on the basis of the structural moieties building up the molecule being investigated.

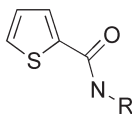
We have synthesized two dozen carboxamides in pairs (Table 1), a parallel S- and O-library which consist of tiophen and furan derivatives. Suitable isocratic HPLC and MEKC methods were worked out to separate of the molecules and to determine the retention factor ( $k'$ ). Furthermore, the hydrophobicity of carboxamides was characterized by a calculated clogP parameter predicted on their structural basis. To compare the experimentally obtained  $k'$  values and software calculated clogP data with the biological activities of the two sub-libraries, the antiproliferative activity of the molecules was investigated by MTT assay [3].

### Results and Discussion

As it can be seen in Table 1 a fairly good correlation was found between the measured and calculated hydrophobicity, and between the antiproliferative activity of the compounds in MTT test. The O-S exchange within the five-member ring resulted in a relatively large change in the retention factor of the molecules irrespective of the R substituents. The trend of change was the same in all molecule pairs: retention factors and clogP parameters in the tiophenyl sub-library were always higher than that in the furoyl sub-library. The comparison of the retention factors of the respective members of both libraries revealed that the replacement of O atom for S atom always resulted in an increase in clogP data with an average of  $0.552 \pm 0.03$  value. Moreover, the replacement of O for S increased not only the hydrophobicity of molecules but in most cases their cytotoxicity (antitumor activity), too.



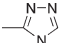
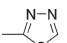
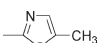
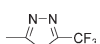
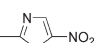
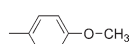
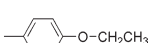
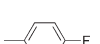
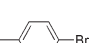
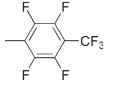
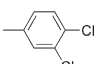
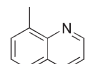
O-library



S-library

**Seprödi et al.**

**Table 1.** Measured ( $k'_{\text{HPLC}}$ ) and calculated (clogP) data of the hydrophobicity together with the biological  $\text{LD}_{50}$  values of carboxamides having different R groups.

#	R groups	$k'_{\text{HPLC}}$		clogP		$\text{LD}_{50}$	
		O	S	O	S	O	S
1		0.77	1.5	1.211	1.741	126	91
2		0.82	1.59	0.195	1.598	178	123
3		1.25	2.16	1.547	2.097	87	21
4		3.36	5.06	1.083	1.603	253	127
5		2.4	4.54	0.975	1.499	102	70
6		1.48	2.52	1.901	2.47	93	49
7		2.89	4.4	3.16	2.34	100	100
8		2.50	4.04	2.227	2.975	87	156
9		4.81	7.44	2.947	3.477	46	185
10		8.32	13.78	2.591	3.109	48	123
11		10.0	18.86	3.48	4.015	50	82
12		7.8	13.6	2.334	2.902	150	31

**Acknowledgments**

This work was supported by the Hungarian National Research Fund (T-26385, T-26388 and T-030263 OTKA, FKFP 386/2000).

**References**

1. Idei, M., Kiss, É., Kéri, Gy. *Electrophoresis* **17**, 762–765 (1996).
2. Idei, M., Györfy, E., Kiss, É., Őrfi, L., Seprödi, J., Tamás, B., Hollósy, F., Mészáros, Gy., Kéri, Gy. *Electrophoresis* **20**, 1561–1567 (1999).
3. Hollósy F., Mészáros Gy., Bökönyi Gy, Idei M., Seprödi A., Szende B., Kéri, Gy. *Anticancer Res.* **20**, 4563–4570 (2000).

## **Macrophage Chemotactic Response to Elastin-Derived VGVAPG and VGVPV Permutations: A Structure–Activity Relationship and Receptor Binding Assay**

**Maria Portia P. Briones<sup>1</sup>, Satsuki Kamisato<sup>1</sup>, Iori Maeda<sup>1</sup>,  
Noboru Takami<sup>2</sup> and Kouji Okamoto<sup>1</sup>**

<sup>1</sup>*Department of Biochemical Engineering and Science, Kyushu Institute of Technology,  
Iizuka, Fukuoka 820-8502, Japan*

<sup>2</sup>*RI Center, Fukuoka University School of Medicine, Fukuoka 814-0180, Japan*

### **Introduction**

Elastin, an insoluble component of the extracellular matrix, is considered as the core protein and insoluble part of the elastic fiber, which confers elasticity to extensible tissues such as the arterial walls, lungs, skin and elastic fibers. Elastin has unique repeating sequences in the hydrophobic region, including the pentapeptide VPGVG and the hexapeptide VGVAPG. Elastin in itself is considered biologically inactive, but when degraded renders elastin fragments or elastin peptides which interact with a variety of cell types to modulate cellular behavior. VGVAPG, for example has been found to induce chemotaxis in monocytes [1], fibroblasts [2] and cancer cells [3]. It is known that binding of extracellular matrix components to the cell membrane is mediated by specific receptor proteins that promote cellular attachment and display biological activity, such as chemotaxis. Our research was conducted according to this working hypothesis as prompted by our previous observation that the polyhexapeptide (VGVAPG)<sub>n</sub> was able to induce chemotactic response to macrophages, while the polypentapeptide (VPGVG)<sub>n</sub> failed to do so. This study was conducted with the aim of evaluating the potency of the hexapeptide VGVAPG and pentapeptide VGVPV permutations in inducing chemotaxis, identifying the receptor involved in the chemotactic activity, investigating whether VGVAPG could act as a ligand for the macrophage receptor, and determining the structure-activity relationship involved in this biological activity.

### **Results and Discussion**

A chemotaxis assay demonstrated that four among the six permutations were chemoattractants for macrophages. As presented in Table 1, VGVAPG, GVAPGV, VAPGVG and GVGVPV hexapeptides induced chemotaxis at  $10^{-9}$ ,  $10^{-8}$ ,  $10^{-10}$  and  $10^{-7}$  M, respectively. Results of the deactivation test of the four potent hexapeptides suggested the existence of a single receptor for these hexapeptide permutations (data not shown). Hence, we used VGVAPG in our next deactivation test, wherein, VGVAPG desensitized chemotactic response of macrophages to the pentapeptide VGVPV, the only active pentapeptide among the five permutations (Table 1), suggesting the possibility of chemotaxis induction through recognition of these chemotactic peptides by a single receptor. In addition, it was found out that these peptides were recognized by a receptor distinct from that which recognizes fMLP. Moreover, macrophages stimulated by VGVAPG demonstrated an enhancement in guanosine 3',5'-cyclic monophosphate (cGMP) level, reflecting an involvement of cGMP in the signaling mechanism of elastin hexapeptide VGVAPG-induced chemotaxis. Such a biological activity was found to be significantly inhibited in the presence of lactose (data not shown). This was in agreement with the observation of cGMP level reduction upon lactose treatment. In order to evaluate whether the receptor/s for the active hexapeptides and active pentapeptide is/are

Table 1. Chemotactic activity of hexapeptide VGVAPG and pentapeptide VGVP as tested in peritoneal rat macrophages.

Peptide	Biological activity	Concentration of optimal activity, [M]
VGVAPG	+	$1 \cdot 10^{-9}$
GVAPGV	+	$1 \cdot 10^{-8}$
VAPGVG	+	$1 \cdot 10^{-10}$
APGVGV	–	NA
PGVGVA	–	NA
GVGVAP	+	$1 \cdot 10^{-7}$
VGVP	+	$1 \cdot 10^{-9}$
GVPGV	–	NA
VPGVG	–	NA
PGGVG	–	NA
GVGV	–	NA

NA = no activity was observed from concentration range of  $1 \cdot 10^{-2}$  M to  $1 \cdot 10^{-12}$  M.

single or multiple, deactivation test was again employed and results showed that the receptor is single. Binding of VGVAPG to macrophages was studied using a tyrosinated analog (Y-VGVAPG), which indicated the presence of a single class of affinity binding site (data not shown). Crosslinking of the radiolabeled ligand to macrophages and analysis by electrophoresis suggested a 67 kilodalton and a 39 kilodalton proteins, both of which bind to VGVAPG, thus, suggesting the induction of chemotaxis by binding to a distinct cell receptor. Structural study of VGVAPG and VGVP permuta-tions using CD spectroscopy demonstrated that potent hexapeptides have no prefer-ence for structured conformations in the presence of phospholipid liposome DPPC (dipalmitoyl-DL- $\alpha$ -phosphatidylcholine). In contrast, the chemotactic pentapeptide VGVP assumed a folded conformation, most likely a type II  $\beta$  turn. The results do not suggest a clarified structural requirement for the chemotactic activity, hence fur-ther structural studies of these peptides in different lipid environments will be con-ducted.

## References

1. Senior, R.M., Mecham, R.P., Wrenn, D.S., Prasad, K.U., Urry, D.W. *J. Cell Biol.* **99**, 870 (1984).
2. Uemura, Y., Kamisato, S., Arima, K., Takami, N., Okamoto, K., In Kaumaya, P. and Hodges, R.S. (Eds) *Peptides; Chemistry, Structure and Biology*, Mayflower Scientific Ltd., 1996, pp. 412–413.
3. Blood, C.H., Zetter B.R. *J. Biol. Chem.* **264**, 10614–10620 (1989).

**Peptide Conjugates,  
Glycopeptides and Lipopeptides,  
Transmembrane Peptides and Proteins,  
Receptors and Receptor Interactions,  
Signal Transduction**



## **Analysis and Evaluation of Rational Designed Calcium Binding Sites in CD2**

**Wei Yang<sup>1</sup>, Hsiau-wei Lee<sup>2</sup> and Jenny J. Yang<sup>2</sup>**

<sup>1</sup>*Department of Biology and* <sup>2</sup>*Department of Chemistry, Center of Drug Design,  
Georgia State University, Atlanta, GA 30303, USA*

### **Introduction**

Calcium functions as a second messenger. It regulates different biological systems by interaction with proteins with different affinities in different biological environments. Calcium and calcium-binding proteins play central roles in intracellular signal transduction pathways and are associated with a wide-range of effects in health and disease [1]. To reveal the key factors for the calcium binding in proteins, rational design of de novo calcium-binding proteins has been carried out to overcome the drawbacks of natural calcium-binding proteins such as metal-metal interactions and conformational changes. Establishments of the parameters in programs and criteria in screening the output from the computer are the keys for successful design.

### **Results and Discussion**

Detailed surveys of known calcium-binding proteins have revealed that almost all of the ligands involved in calcium binding in proteins use oxygen atoms. The deviations in the Ca–O bond length are from 2.2 to 2.8 Å with a mean calcium-ligand distance of 2.42 Å. The most common calcium-binding site has pentagonal bipyramidal or distorted octahedral geometry with 6 or 7 coordination positions [2]. In pentagonal bipyramidal geometry, five oxygen ligands are roughly located on the same plane and two additional ligands are located out of the plane.

The structural parameters for designing calcium-binding proteins have been established with the popular pentagonal bipyramidal geometry using EF-hand and non-EF-hand proteins as controls with a computational program [3,4]. The deviations of the bond lengths and angles in the program-constructed sites compared to the target pentagonal bipyramidal geometry are summed up with different given weights, then output as a value called pseudo-energy ( $U(p)$ ). Natural calcium-binding sites in all these control proteins have been identified with the smallest geometric deviations. This suggests that the pseudo-energy can be used to rank the designed sites.

The novel calcium-binding proteins have been designed by constructing the calcium-binding sites in a non-calcium-binding host protein CD2-D1 using the established parameters. CD2-D1 is a small protein containing 99 residues with nine  $\beta$ -sheets in two layers. It has been chosen as the host protein because of its high expression yield, solubility, tolerance of mutations, and the availability of high-resolution structures [5]. The calcium-binding sites have been constructed in CD2-D1 using six oxygen atoms in the sidechain carboxyl groups of Asp, Asn, Glu, and Gln as ligands, including the bidentate ligands from Glu, which mimics the natural EF-hand motif. One oxygen ligand out of the plane of the pentagonal bipyramidal geometry was left empty for water as many natural calcium-binding proteins have ligands from solvent.

As shown in Figure 1, about 10,000 different potential calcium-binding sites with the popular pentagonal geometry can be constructed in CD2-D1. The sites are mainly located at the pocket (pocket 1) enveloped by BC loop with C, F, G  $\beta$ -strands and FG loop or the pocket (pocket 2) enveloped by CC' loop and C', E, F  $\beta$ -strands. More than

half of the sites are located at pocket 1. Of these, positions 18, 21, 27, 30, 80, 88, and 89 are mostly used as ligands with different combinations and the position 61 is the most frequently used for the bidentate ligand Glu. In pocket 2, positions 39, 63, 65, 68, 72, and 76 are all frequently used for bidentate and unidentate ligands (Figure 1).

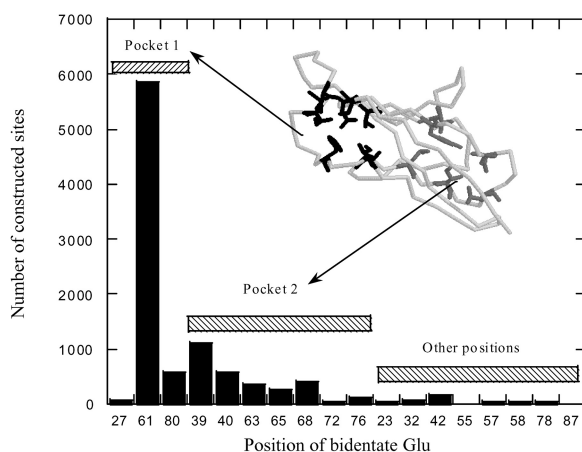


Fig. 1. The designed calcium-binding sites in CD2-D1 are mainly located at two pockets.

The average pseudo-energy of the designed sites is 47.12. The highest value is 219.84. This site uses Glu at position 61 as the bidentate ligand and the side chain of Glu at positions 21, 27, 80, and 88 as other ligands. The large geometric deviation (high  $U(p)$ ) of this site indicates that the pocket 1 cannot hold a site with all the ligands in the carboxylate of residue Glu that has a longer side chain without the rearrangement of the local conformations of the host protein. The lowest  $U(p)$  of 3.15 belongs to the site using Glu at position 39 as the bidentate ligand, while the side chains of Gln at positions 63, 72, and 76 and side chains of Asp at position 65 are used as other ligands. From the study on natural calcium-binding sites, most of the  $U(p)$  for the natural calcium-binding sites are below 20. This value is used as the first criterion to screen the designed sites for further molecular engineering. About 90% of the sites have been rejected by this measure. There are about 1000 sites that have  $U(p)$  values less than 20.

The designed calcium-binding sites in CD2-D1 are further filtered for molecular engineering based on their side chain clashes, locations, charge numbers, and dynamic properties. 1) All mutations for a chosen site are not located at the hydrophobic core of the protein. They are located at the loop region or the end of the  $\beta$ -strands. 2) The side chains of the ligand residues for the chosen site have little conflict with the pre-existing atoms. 3) The designed site has three or four negative charges. 4) The mutations of a chosen site do not cause any significant conformational change of the host protein. Further, energy minimization and molecular dynamic simulation were performed using program SYBYL and AMMP, respectively.

Four designed calcium-binding proteins have been engineered and expressed. They all show calcium-binding ability.

**Acknowledgments**

We thank Dr. Homme Hellinga for the Dezymer program. We also thank Dr. Yang's group for their helpful discussions. The study is supported in part by GSU start-up funds, QIF, Research Initiation, Mentoring Grant and in part by the NSF grant MCB-0092486 and NIH GM 62999-1 for JJY.

**Reference**

1. Seaton, B.A., Head, J.F., Engelman, D.M., Richards, F.M. *Biochemistry* **24**, 6740–6743 (1985).
2. Linse, S., Forsen, S. *Adv. Second Messenger Phosphoprotein Res.* **30**, 89–151 (1995).
3. Yang, W., Lee, H.W., Pu, M., Hellinga, H., Yang, J.J. *Computational Studies, Nanotechnology, and Solution Thermodynamics of Polymer Systems*, Kluwer Academic/Plenum Publishers, 2000, p. 127–138.
4. Yang, W., Lee, H.W., Hellinga, H., Yang, J.J. *Proteins*, in press (2001).
5. Yang, W., Lee, H.W., Ye, Y.M., Liu, Z.R., Glushka, J., Yang, J.J. *Biochemistry*, submitted.

## Structural Basis for Selective Binding of Integrins to Extracellular Matrix

Barbara Saccà<sup>1</sup>, Eva Schmidt<sup>1</sup>, Johannes A. Eble<sup>2</sup> and Luis Moroder<sup>1</sup>

<sup>1</sup>Max-Planck-Institute of Biochemistry, D-82152 Martinsried, Germany

<sup>2</sup>Institute of Physiological Chemistry and Pathobiochemistry, Clinical University of Münster, D-48129 Münster, Germany.

### Introduction

Collagen type IV not only provides a biomechanically stable scaffold, into which the other constituents of basement membranes are incorporated, but it also plays an important role in the adhesion of cells [1,2]. This occurs mainly *via*  $\alpha1\beta1$  and  $\alpha2\beta1$  integrins, which are transmembrane heterodimeric glycoproteins composed of non-covalently associated  $\alpha$  and  $\beta$  subunits. A non-sequential adhesion epitope for  $\alpha1\beta1$  integrin recognition, consisting of residues Arg461 of the  $\alpha2(IV)$  chain and Asp461 of the two  $\alpha1(IV)$  chains, has been proposed [3]. Correspondingly, the  $\alpha1\beta1$ -collagen interaction has to critically depend upon the stagger of the single chains within the triple helix [4]. Although there is strong evidence for a  $\alpha2\alpha1\alpha1'$  register in natural type IV collagen [5], we have synthesized two heterotrimeric collagen peptides containing the sequence portions 457–469 of the  $\alpha1$  and  $\alpha2$  chain of type IV collagen which were regioselectively assembled *via* an artificial C-terminal cystine knot into the  $\alpha2\alpha1\alpha1'$  and  $\alpha1\alpha2\alpha1'$  stagger.

### Results and Discussion

The single chains were synthesized on a Tentagel-PHB resin using Fmoc/tBu chemistry, purified by HPLC, and selectively crosslinked *via* the C-terminal cystine knot according to the procedures reported previously [6]. Compounds **A** and **B** (Figure 1) were isolated by preparative HPLC as homogeneous compounds.

Both trimers **A** and **B** fold under physiological conditions (50 mM Tris-HCl, pH 7.4, 50 mM NaCl and 10 mM  $\text{CaCl}_2 \cdot 2\text{H}_2\text{O}$ ) into a triple helix, as assessed by CD spectroscopy (the related parameters are reported in Table 1). The thermal stability of the two trimers was evaluated by an integrated biophysical analysis, including temperature-dependent CD measurements, emission anisotropy, and differential scanning calorimetry. All experiments were consistent with a  $T_m$  of 41 °C for trimer **A** and 31 °C for trimer **B** (Figure 2). This would indicate a surprisingly strong effect of the stagger on the stability of the collagen-like fold. Similarly, the thermal excursion monitored by emission anisotropy clearly revealed a well-differentiated display of the fluorophores, intentionally incorporated *via* a Tyr467Ile replacement.

Preliminary competitive binding experiments of bioexpressed  $\alpha1\beta1$  to the natural fragment CB3(IV) of collagen type IV with the trimers **A** and **B** indicate that both trimers are recognized by this receptor with a slight preference for trimer **B**.

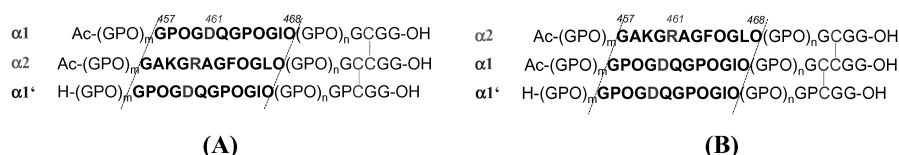


Fig. 1. Heterotrimeric collagen peptides **A** and **B** containing the adhesion epitope 457–469 of collagen type IV for  $\alpha1\beta1$  integrin recognition.

Table 1. CD values at 4 °C for trimer A, trimer B and Ac- $\alpha$ 2 monomer;  $c = 10^{-5}$  M in Tris-HCl buffer (pH 7.4) compared to natural collagen.

Peptide	$\lambda_{\max}$	$\lambda_{\min}$	$R_{pn}^a$
trimer A	223.8	198.1	0.110
trimer B	223.5	198.6	0.108
Ac- $\alpha$ 2	223.3	199.4	0.069
collagen	220	196.5	0.1

<sup>a</sup>  $R_{pn}$ -factor is the ratio of positive peak intensity over negative peak intensity.

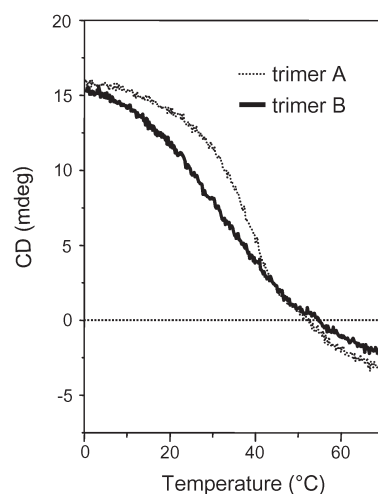


Fig. 2. Thermal denaturation of trimers A (···) and B (—);  $c = 10^{-5}$  M in Tris-HCl buffer (pH 7.4), monitored at  $\lambda = 222$  nm and a scan rate of 12 °C/min.

### Acknowledgments

This study was supported by the SFB 563 of the Technical University of Munich.

### References

1. Aumailley, M., Timpl, R. *J. Cell Biol.* **103**, 1569–1575 (1986).
2. Vanderberg, P., Kern, A., Ries, A., Luckenbill-Edds, L., Mann, K., Kühn, K. *J. Cell Biol.* **113**, 1475–1483 (1991).
3. Eble, J., Golbik, R., Mann, K., Kühn, K. *EMBO J.* **12**, 4795–4802 (1993).
4. Kühn, K., Eble, J. *Trends Cell Biol.* **4**, 256–261 (1994).
5. Golbik, R., Eble, J., Ries, A., Kühn, K. *J. Mol. Biol.* **297**, 501–509 (2000).
6. Ottl, J., Moroder, L. *Tetrahedron Lett.* **40**, 1487–1490 (1999).

## **Regulation of the Promoter Binding Activity of a Bacterial Sigma Factor Explored Using Segmental Isotopic Labeling and NMR Spectroscopy**

**Julio A. Camarero<sup>1,2</sup>, Alex Shekhtman<sup>1</sup>, Elizabeth Campbell<sup>1</sup>, Seth Darst<sup>1</sup>, David Cowburn<sup>1</sup> and Tom W. Muir<sup>1</sup>**

<sup>1</sup>*The Rockefeller University, New York, NY 10021, USA*

<sup>2</sup>*Lawrence Livermore National Laboratory, Livermore, CA 94551, USA*

### **Introduction**

DNA-dependent RNA polymerases (RNAP) play a central role in transcription and therefore are a major regulatory target for gene expression. The regulation of prokaryotic transcription involves several protein-protein interactions between the different subunits of the RNAP complex as well as between several transcription factors. Understanding how these regulatory mechanisms work is crucial in order to open new strategies for targeting gene expression in pathogenic bacteria. Prokaryotic core RNAPs contain  $\beta$ ,  $\beta'$ , and two  $\alpha$  subunits, and are fully active in RNA polymerization. However, they are incapable of promoter recognition and specific initiation. Specific initiation of transcription depends on the binding of  $\sigma$  factors to the core RNAP to form the RNAP holoenzyme. The most abundant  $\sigma$  factor in *E. coli* is  $\sigma^{70}$ . Sequence comparisons among different  $\sigma^{70}$ -like factors has shown that they are comprised of four highly homologous regions [1]. Regions 2 and 4.2 have been shown to interact with the -10 and -35 box of the promoter region, respectively. Nonetheless, in the absence of the core RNAP, the  $\sigma^{70}$ -like factors are unable to recognize the promoter sequence [2]. Region 1.1 has been shown to inhibit the ability by  $\sigma^{70}$ -like factors to recognize the promoter DNA region [2]. Here, we have used segmental isotopic labeling techniques [3] to selectively label region 4.2 of  $\sigma^A$  (a homologous  $\sigma$ -factor from *T. maritima*) with <sup>15</sup>N, <sup>2</sup>H and <sup>13</sup>C. This novel methodology has been used in combination with NMR chemical shift perturbation studies [4] to study the interaction between these two regions.

### **Results and Discussion**

Two  $\sigma^A$  constructs were produced for studying the interaction between Regions 1.1 and 4.2; one with the full length sequence and the other without region 1.1. In both cases, region 4.2 was specifically labeled with <sup>15</sup>N, <sup>13</sup>C and <sup>2</sup>H. To accomplish the specific labeling of region 4.2 in the context of the whole protein, the N-terminal fragments (either residues 1–346 for the full length  $\sigma^A$  or residues 137–346 for the truncated  $\Delta 1.1$ - $\sigma^A$  constructs) were expressed as a C-terminal fusions to a modified intein. After affinity purification, the resulting fusion proteins were then treated with EtSH yielding in both cases the corresponding N-terminal fragment  $\alpha$ -thioester in high yield. The C-terminal fragment (containing region 4.2, residues 347–397) was expressed as an N-terminal His-tag fusion protein using <sup>2</sup>H<sub>2</sub>O medium containing <sup>15</sup>NH<sub>4</sub>Cl and [<sup>13</sup>C,<sup>1</sup>H]-glucose as source of nitrogen and carbon, respectively. By using PCR-driven mutagenesis the C-terminal fragment was linked *via* the linker sequence -Ile-Glu-Gly-Arg-Cys- to the poly-His affinity tag. Following expression and affinity purification, the fusion protein was treated with Factor Xa protease to afford the triple labeled C-terminal fragment containing the required N-terminal Cys residue in a very good yield. Note that the  $\alpha$ - and practically all of the  $\beta$ -protons of region 4.2

were labeled with  $^2\text{H}$  using this scheme. The segmental labeled  $\sigma^A$  constructs were then obtained by chemically ligating the unlabeled N-terminal and the triple labeled C-terminal fragments in a PBS containing traces of EtSH at pH 7.2. In both cases the ligation reaction was very fast and efficient. Indeed, the reaction kinetics were not affected by the presence or absence of region 1.1. Both  $\sigma^A$  constructs were biologically active as tested in an *in vitro* transcription assay and were able to recognize  $-35$  promoter DNA in the presence of core RNAP. As expected, the affinity binding constant of the truncated  $\Delta 1.1$ - $\sigma^A$  construct for  $-35$  promoter DNA was two orders of magnitude tighter than for the full length  $\sigma^A$  ( $0.7\ \mu\text{M}$  for  $\Delta 1.1$ - $\sigma^A$  vs  $>100\ \mu\text{M}$  for  $\sigma^A$ ). Surprisingly, the 2D heteronuclear correlation maps for both  $\sigma^A$  constructs (Figure 1) were virtually identical, suggesting a weak or total lack of interaction between these two regions. Furthermore, the interaction of  $\Delta 1.1$ - $\sigma^A$  with  $-35$  promoter DNA or AsiA protein (both ligands with high affinity for region 4.2) yielded significant changes in the corresponding 2D heteronuclear correlation maps. Altogether, these results strongly suggest that the inhibitory role of region 1.1 is very likely due to the interaction of this domain with another part of the  $\sigma$  molecule, perhaps region 4.1; and the effect on region 4.2 is produced through an indirect steric or/and electrostatic effect.

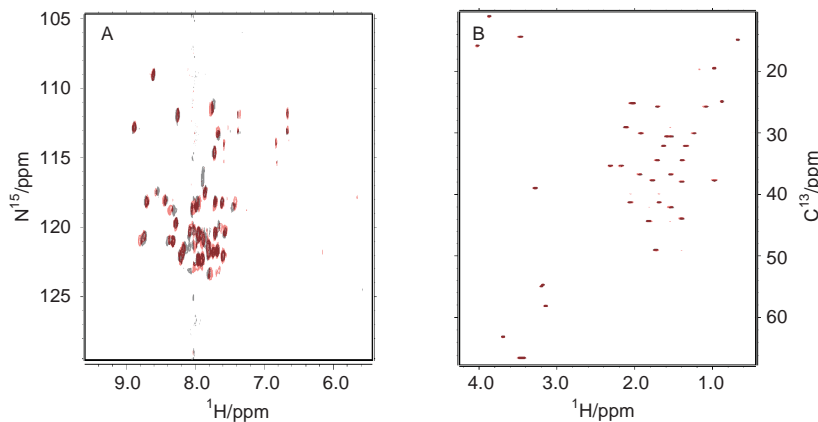


Figure 1. Superimposition of the 2D-heteronuclear-TROSY correlation spectra at 600 MHz for Region 4.2 segmental labeled  $\sigma^A$  (grey) and  $\Delta 1.1$ - $\sigma^A$  (black).

#### Acknowledgments

We thank the Burroughs Wellcome Foundation and the NIH for supporting this work. JAC is currently a Distinguished Postdoctoral Fellow at the Lawrence Livermore National Laboratory.

#### References

1. Severinova, E., Severinov, K., Fenyo, D., Marr, M., Brody, E.N., Roberts, J.W., Chait, B.T., Darst, S.A. *J. Mol. Biol.* **263**, 637–647 (1996).
2. Dombroski, A.J., Walter, W.A., Record, M.T., Siegele, D.A., Gross, C.A. *Cell* **70**, 501–512 (1992).
3. Xu, R., Ayers, B., Cowburn, D., Muir, T.W. *Proc. Natl. Acad. Sci. U.S.A.* **96**, 388–393 (1999).
4. Hadjuk, P.J., Meadows, R.P., Fesik, S.W. *Science* **278**, 497–499 (1997).

## **Chemically Engineering the Prion Protein Using Stepwise SPPS and Expressed Protein Ligation**

**Haydn L. Ball<sup>1</sup>, Giuseppe Legname<sup>1</sup>, Nicole Bradon<sup>1</sup>, Guan Zhengyu<sup>1</sup>,  
David S. King<sup>2</sup>, Michael A. Baldwin<sup>1</sup> and Stanley B. Prusiner<sup>1</sup>**

<sup>1</sup>*Institute for Neurodegenerative Diseases, University of California at San Francisco,  
San Francisco, CA 94143, USA*

<sup>2</sup>*Howard Hughes Medical Institute, University of California at Berkeley, Berkeley,  
CA 94720, USA*

### **Introduction**

The mature prion protein (PrP) is a 209-residue, glycosylphosphatidylinositol (GPI)-anchored protein that after a profound conformation change causes scrapie in sheep, bovine spongiform encephalopathy in cattle and Creutzfeldt-Jakob disease in humans. Prion diseases are unique as they can present as genetic, infectious, or sporadic disorders. PrP is ubiquitous in neurons and can exist in either a normal cellular form (PrP<sup>C</sup>) or a pathogenic isoform (PrP<sup>Sc</sup>). We have evaluated several techniques, including stepwise SPPS, native chemical ligation and expressed protein ligation for the preparation of chemically modified or mutated PrP sequences for structural analysis and bioassay.

### **Results and Discussion**

Stepwise SPPS offers the ability to introduce chemical modifications and rapidly mutate specific residues. A redacted form of PrP, with regions 23 to 88 and 141 to 176 deleted, is the minimal PrP sequence known to support prion propagation in transgenic mice [1]. This 106-residue protein (PrP106), termed “mini-prion”, thus represents an interesting protein for study. We used highly optimized Fmoc chemistry to synthesize several analogues of PrP106. These included a sequence with three Ala-to-Val mutations, at residues 112, 114 and 117; a His-tagged form with improved solubility properties; and a C-terminally modified PrP106 with lipophilic groups to target the synthetic PrP to the sub-cellular domains where PrP<sup>C</sup> is localized. The syntheses were performed using Fmoc chemistry, DCC/HOBt activation and capped using *N*-(2-chlorobenzoyloxycarbonyl)oxy succinimide, after the addition of each amino acid. In order to specifically derivatize the C-terminus, an orthogonally protected Lys residue was incorporated as the first residue. The super-acid sensitive, methyltrityl side-chain protecting group could be selectively removed by treatment with 1% TFA, leaving all other protecting groups intact. The free amino group was then coupled to lipophilic moieties such as 1,2-dipalmitoylglycero-3-succinate. Following cleavage, the crude polypeptides were purified by RP-HPLC at 50 °C. Highly homogeneous material was obtained after a single purification step with yields ranging from 12 to 14%. These PrP106 proteins are currently being assayed for infectivity in transgenic animals.

Chemical synthesis of bovine PrP90-200+Lys(Ac) provided some additional challenges, due to sequence-related coupling difficulties. These were overcome by using HATU activation in combination with Boc chemistry. An additional benefit was the drastically shorter cycle times compared to Fmoc cycles (3 days vs 11 days for PrP106). In order to introduce the necessary orthogonality at the C-terminus, Lys with an Fmoc side-chain protecting group was used. Low TFMSA/high HF cleavage protocol removed the remaining protecting groups and cleaved the polypeptide from the resin. A

single RP purification step produced a homogeneous product with a yield of 11% (ESI-MS: Found 12389.8 Da; Calcd. 12389.7 Da).

Native chemical ligation involves the chemoselective coupling of an unprotected peptide bearing a C-terminal  $\alpha$ -thioester with an unprotected peptide containing an N-terminal Cys residue [2]. We evaluated this approach by preparing a mutated PrP105 protein with three Ala-to-Val mutations, by ligating a 54-residue peptide to a 51-residue  $\alpha$ -thioester peptide (prederivatized thioester resin kindly supplied by Dr. S.B.H. Kent, Gryphon Sciences). The ligation reaction was performed in 6 M Gdn-HCl in phosphate buffer and was complete in 3 h, according to RP-HPLC. (ESI-MS: Found 11644.0 Da; Calcd. 11644.5 Da).

PrP contains two Cys residues at 179 and 213 that are suitable sites for thioester ligation. In order to prepare full-length PrP, a 156-residue  $\alpha$ -thioester polypeptide would have to be synthesized, thus making a purely chemical approach impractical. Expressed protein ligation is a novel technique, which utilizes the  $\alpha$ -thioester bond that is generated by a protein splicing element, or intein. When a synthetic peptide with an N-terminal Cys residue is added to the recombinant PrP-intein construct, a chemical reaction occurs, resulting in formation of a native amide bond. We have created several C-terminally biotinylated full-length prion proteins with hamster, mouse and bovine sequences. A panel of antibodies, raised against different regions of PrP, showed that biotinylated Syrian hamster PrP (SHa 23-231+Lys(Biotin)) underwent a local conformational change upon “aging” [4]. This refolding occurs intramolecularly and in a region that is believed to be intimately involved in the conversion of PrP<sup>C</sup> to PrP<sup>Sc</sup>. Expressed protein ligation effectively unites the fields of synthetic peptide chemistry and protein expression, enabling systematic chemical investigation and manipulation of proteins previously restricted to the study of small bioactive peptides.

## References

1. Supattapone, S., Bosque, P., Muramoto, T., Wille, H., Aagaard, C., Peretz, D., Nguyen, H.-O.B., Heinrich, C., Torchia, M., Safar, J., Cohen, F.E., DeArmond, S.J., Prusiner, S.B., Scott, M. *Cell* **96**, 869–878 (1999).
2. Dawson, P.E., Muir, T.W., Clark-Lewis, I., Kent, S.B.H. *Science* **266**, 776–779 (1995).
3. Muir, T.W., Sondhi, D., Cole, P.A. *Proc. Natl. Acad. Sci. U.S.A.* **95**, 6705–6710 (1998).
4. Leclerc, E., Peretz, D., Ball, H.L., Sakurai, H., Legname, G., Serban, A., Prusiner, S.B., Burton, D.R., Williamson, R.A. *EMBO J.* **20**, 1547–1554 (2001).

## Covalent and Non-Covalent Oligomerization of the Transmembrane $\alpha$ -Helix 4 from the Cystic Fibrosis Conductance Regulator

**Anthony W. Partridge, Roman A. Melnyk and Charles M. Deber**

*Division of Structural Biology and Biochemistry, Hospital for Sick Children, Toronto, ON,  
Canada, M5G 1X8 and*

*Department of Biochemistry, University of Toronto, Toronto, ON, Canada, M5S 1A8*

### Introduction

Cystic fibrosis (CF) is an autosomal recessive disease that affects approximately 1 in 2000 people in Canada and the United States [1,2]. The disease arises through mutations to the cystic fibrosis transmembrane conductance regulator protein (CFTR). Although the three-dimensional structure for this protein has not been solved, its major function has been shown to act as a chloride ion channel in the apical membranes of epithelial cells. Amongst the identified mutations that result in CF, over 80 of these involve amino acid changes within the transmembrane domains (TMDs) [3]. The TMDs are predicted to consist of 12  $\alpha$ -helices that are believed to form the majority of the chloride ion pore. We hypothesized that many of the mutations that occur in the TMDs result in CF disease by altering the packing of the TM helices. Here, we investigated whether the CF phenotypic mutation V232D, occurring in TM helix 4, could result in altered helical packing. Our approach involved the synthesis of two peptides; one containing the wild-type sequence of TM4 (KKKLQASAFCLGLFLIV<sub>232</sub>LALFQAGLGRMKKK, TM4-wt), while the other contained the same sequence with the V232D mutation (KKKLQASAFCLGLFLID<sub>232</sub>LALFQAGLGRMKKK, TM4-VD).

### Results and Discussion

The V232D mutation dramatically alters the migration of the TM4 peptide on SDS-PAGE (Figure 1). While the TM4-wt peptide migrates at mobilities consistent with those of a monomer (3.3 kD) and a dimer (6.6 kD), the TM4-VD peptide contains additional bands consistent with those of a tetramer, hexamer, and an octamer. The formation of such a "ladder" of oligomers through a non-polar to polar mutation suggests hydrogen bonding as the driving force for helical association.

Both peptides contain a single Cys residue. Treating the TM4-VD peptide with reducing agent before electrophoresis resulted in a single monomeric band. This result implicated a disulfide-linked dimer as the building block for the higher order oligo-

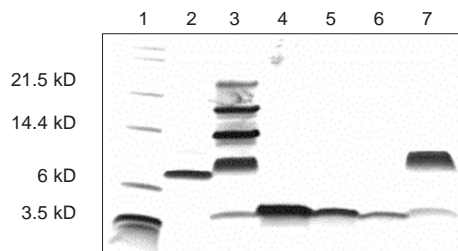


*Fig. 1. SDS-PAGE analysis. Lanes (1), MW marker; (2), TM4-wt; (3), TM4-VD; (4), TM4-VD (reduced); (5), TM4-VD(C225S); (6), TM4-VD(C225A); (7), TM4-VD(Q237).*

mers. TM4-VD peptides synthesized with either a C to S mutation [TM4-VD(C225S)] or a C to A mutation [TM4-VD(C225A)], further supported this conclusion, as these constructs were fully monomeric on SDS-PAGE.

The TM4-VD sequence contains a Gln residue at position 237. To further investigate the role of polar residues on TM-4VD self-association, a peptide was synthesized with a Q237A mutation [TM4-VD(Q237A)]. This peptide ran as a monomer and disulfide dimer (Figure 1). Disruption of the oligomeric ladder through a Q to A mutation highlights the importance of this residue in the TM4-VD association.

The experiments described above show that in model peptides, the CF phenotypic mutation V232D can result in a dramatic increase in the non-covalent interaction of TM helix 4. We have identified three key residues (C225, D232, Q237) responsible for the formation of the observed oligomeric ladder. The results showed that the presence of the Cys residue is crucial: although this disulfide bond is not observed in the full-length protein, its presence in our model system proved to be advantageous in promoting the formation of specific non-covalent helical interactions.

Residues D232 and Q237 were also identified as key residues involved in the association of TM4-VD. The replacement of a nonpolar side chain with a polar one strongly suggests that these residues help mediate the non-covalent helical association through hydrogen bonding. Furthermore, the two polar residues (D, Q) are on opposite sides of the helix, making it possible for oligomerization to occur in a chain-like fashion through patterns of hydrogen bonds.

One implication of the present results is that the V232D mutation may result in CF disease through non-native hydrogen bonds between two TM4 helices. Interacting TM4s may disrupt native helical arrangements resulting in altered protein function. If correct, therapeutic strategies for patients harbouring this mutation could involve approaches aimed to disrupt non-native helical interactions.

#### **Acknowledgments**

This work was supported, in part, by a grant to C. M. D. from the Canadian Cystic Fibrosis Foundation. A. W. P. thanks the C.I.H.R. for research training support.

#### **References**

1. Collins, F.S. *Science* **256**, 774 (1992).
2. Carroll, T.P., Schiebert, E.M., Guggino, W.B. *Cell. Physiol. Biochem.* **3**, 388 (1993).
3. Therien, A.G., Grant F.E.M., Deber, C.M. *Nat. Struct. Biol.* **8**, 597 (2001).

## **Ctr $\Delta$ e13, a Calcitonin Receptor Isoform Lacking 14 Amino Acids in Transmembrane Helix 7: Structure and Topology**

**Maria Pellegrini<sup>1,2</sup>, Veronique Grignoux<sup>3</sup>, William C. Horne<sup>3</sup>,  
Roland Baron<sup>3</sup> and Dale F. Mierke<sup>1</sup>**

<sup>1</sup>*Molecular Pharmacology, Physiology, & Biotechnology, Brown University,  
Providence, RI 02912, USA*

<sup>2</sup>*Abbott Bioresearch Center, Worcester, MA 01605, USA*

<sup>3</sup>*Department of Orthopedics, Yale University School of Medicine, New Haven, CT 06520, USA*

### **Introduction**

The peptide hormone calcitonin (CT) acts through its G-protein coupled receptor to reduce serum calcium levels by inhibiting bone resorption and promoting renal calcium excretion. In addition, CT modulates the renal transport of several other ions and water. In the central nervous system it acts to induce analgesia, anorexia, and gastric secretion. The calcitonin receptor (CTR) couples to multiple G-proteins and acts through two main pathways: the c-AMP and the phospholipase C mediated pathways. Here, we investigate, from a structural perspective, the differences between the most common receptor isoform, C1a, and CTR $\Delta$ e13, an isoform generated by the deletion of the cassette corresponding to exon 13 of the porcine CTR gene and encoding 14 amino acids in the putative seventh transmembrane domain (TM7) [1]. The absence of the 14 amino acids results in reduced ligand binding and modified signal transduction characteristics: CTR $\Delta$ e13 fails to activate phospholipase C. It has been suggested that the altered pharmacology could be a result of the incorporation of the proximal residues of the C-terminal tail into the lipid bilayer or of an extracellular C-terminus (reduced hydrophobicity and length of the truncated TM7). Receptor domains corresponding to the putative 3rd extracellular loop-TM7-proximal C-terminus and the corresponding sequence in CTR $\Delta$ e13 have been analyzed by NMR in the presence of a membrane mimetic.

### **Results and Discussion**

The two peptides, synthesized by standard solid phase methods, were dissolved in dodecylphosphocholine (DPC), 200 mM, or sodium dodecylsulfate (SDS), 160 mM, in water at pH 6.5 (uncorrected for deuterium effect). The NMR spectra were collected at 298, 308, and 318 K on an Bruker Avance 600 MHz instrument. The NMR resonance assignments were obtained using standard procedures of TOCSY spectra for spin system identification and NOESY for sequential assignment of the amino acids. A plot of the secondary shifts was obtained by subtracting the chemical shift values for "random coil" peptides from the values observed here. This analysis of CTR $\Delta$ e13 indicates two  $\alpha$ -helices, K367-F382, corresponding to the 3rd extracellular loop, and Q383-Q399, corresponding to the remainder of TM7. The helices are broken up exactly at the location of the deletion of the 14 amino acids. The structure resulting from exhaustive distance geometry calculations, using the random metrization algorithm of Havel [2], is illustrated in Figure 1. From monitoring the line broadening of the NMR signals during a titration with doxyl-stearate following published procedures [3], both  $\alpha$ -helices are shown to be lying on the zwitterionic surface of the DPC micelles.

In contrast, for the WT C1a receptor construct containing the putative 3rd-extracellular loop-TM7-C-terminus, although we observed two  $\alpha$ -helices, K367-F382 and

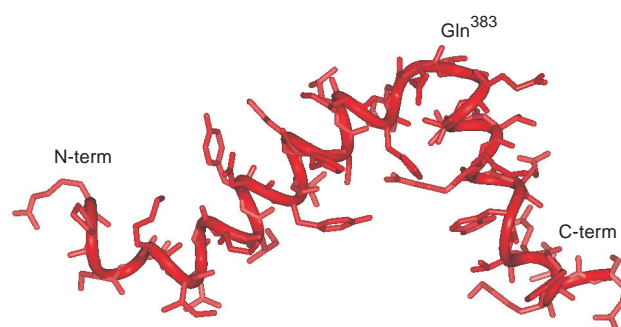


Fig. 1. Structure of the CTR $\Delta$ e13 receptor isoform construct containing the 3rd-extracellular loop-TM7-C-terminus as determined here by NMR. The point of the deletion, Gln383, is denoted. Both helices are found to lie on the surface of the membrane mimetic.

Q383-Q399, the second helix is found to be trans-micelle, passing through the center of the alkyl-chains of the micelle. The conclusion from these observations is that the CTR $\Delta$ e13 isoform has an extracellular C-terminus. The observed pharmacological differences observed for the C1a isoform is a result of this unusual topological display.

#### References

1. Shyu, J., Ionoue, D., Baron, R., Horne, W. *J. Biol. Chem.* **271**, 31127–31134 (1996).
2. Havel, T.F. *Prog. Biophys. Mol. Biol.* **56**, 43–78 (1991).
3. Pellegrini, M., Mierke, D.F. *J. Peptide Sci.* **51**, 208–220 (1999).

## **Transmembrane Segment Peptides of the Ff Phage Major Coat Protein Form Parallel Homodimers**

**Roman A. Melnyk, Anthony W. Partridge and Charles M. Deber**

*Division of Structural Biology and Biochemistry, Research Institute, Hospital for Sick Children,  
Toronto, M5G 1X8 Ontario, Canada and  
Department of Biochemistry, University of Toronto, Toronto M5G 1A8, Ontario, Canada*

### **Introduction**

The Ff filamentous phage major coat protein (MCP) is located in the inner membrane of host cell *Escherichia coli* prior to assembly into the lipid-free virion. The 50-residue MCP consists of a mobile N-terminal amphipathic helix that is connected by a helical hinge region to a *ca* 20-residue transmembrane helix. In membrane environments the MCP has been shown to specifically self-associate into dimers in both *in vitro* [1] and *in vivo* [2] studies. In the present work, peptide versions of the MCP lacking the N-terminal arm were synthesized with the sequence KKKC-Y<sub>21</sub>IGYA-WAMVVVIVGATIGIKLFKKFTSK<sub>48</sub>-amide in order to investigate the orientation of the MCP transmembrane domains in detergent micelles. Peptides were labeled with pyrene fluorophores at the N-terminal Cys residue to establish the topology (*ie.* parallel vs anti-parallel) of the homodimers in detergent micelles using excimer fluorescence experiments. Experiments were carried out in two detergents, sodium dodecyl sulfate (SDS) and perfluorooctanoate (PFO) to investigate whether there was any correlation between the degree of excimer fluorescence and type of membrane mimetic environment used.

### **Results and Discussion**

To ensure that the entire transmembrane (TM) domain from MCP was included in the final peptide design, the NMR solution structures of the fd and M13 MCP in SDS detergent micelles were taken into consideration [3,4]. In each case, the TM domain core included residues 25 to 45, however, in the present work we included residues 21 to 48. Three non-native lysines were added to the N-terminus to confer water solubility to peptides, thereby facilitating purification using reverse-phase high performance liquid chromatography. We previously demonstrated that terminal lysine residues on hydrophobic transmembrane segments aided in the overall solubility of the peptides without affecting the ability of peptides to associate to their native like oligomeric states [5].

Peptides were labeled using the thiol-specific probe pyrene-iodoacetamide, which specifically, covalently attaches to the Cys side-chain situated N-terminal to the TM domain of MCP. Two pyrene labels can form an excited state dimer (excimer) that exhibits an emission maximum at longer wavelengths (*ca* 470 nm) than the monomer (*ca* 380–420 nm) if the conjugated ring systems are within about 3.5 Å of each other and in the correct orientation [6]. Using this approach, the proximity of the N-termini in each subunit of the homodimer can be assessed to determine whether peptides are parallel or anti-parallel. In Figure 1 the results of excimer fluorescence are shown. In SDS, a classically denaturing detergent, the excimer to monomer ratio is 0.36, whereas in PFO, a less denaturing detergent, the excimer to monomer ratio is 3.2. These results show that MCP homodimers associate in a parallel fashion and that the degree of association differs in the two detergents tested. To our knowledge these experiments represent the initial use of excimer fluorescence to determine the topology of a transmembrane helical dimer.

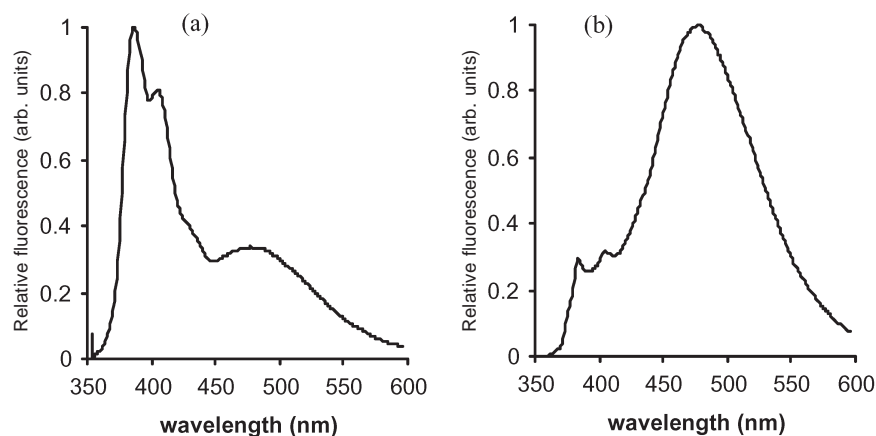


Fig. 1. Pyrene excimer fluorescence. (a) 10  $\mu$ M WT-pyrene in 20 mM SDS; (b) 10  $\mu$ M WT-pyrene in 30 mM PFO. Excitation wavelength was 345 nm with 2 nm band pass.

#### Acknowledgments

This work was supported by a grant to C. M. D. from the Canadian Institutes of Health Research (CIHR). R. A. M. and A. W. P. hold CIHR Doctoral Scholarships.

#### References

1. Deber, C.M., Khan, A.R., Li, Z., Joensson, C., Glibowicka, M., Wang, J. *Proc. Natl. Acad. Sci. USA* **90**, 11648–11652 (1993).
2. Haigh, N.G., Webster, R.E. *J. Mol. Biol.* **279**, 19–29 (1998).
3. Almeida, F.C., Opella, S.J. *J. Mol. Biol.* **270**, 481–495 (1997).
4. Papavoine, C.H., Christiaans, B.E., Folmer, R.H., Konings, R.N., Hilbers, C.W. *J. Mol. Biol.* **282**, 401–419 (1998).
5. Melnyk, R.A., Partridge, A.W., Deber, C.M. *Biochemistry*, submitted (2001).
6. Jung, K., Jung, H., Wu, J., Prive, G.G., Kaback, H.R. *Biochemistry* **32**, 12273–12278 (1993).

## Refined 3D Model of hMC4R and Docking Study for hMC4R with $\alpha$ -Melanocyte Stimulating Hormone Analogue Ligands

Jee-Young Lee<sup>1</sup>, Dong-Il Kang<sup>2</sup>, Seung-Gull Kim<sup>2</sup> and Chang-Ju Yoon<sup>1</sup>

<sup>1</sup>Department of Chemistry, The Catholic University of Korea, Kyonggi 420-743, Korea

<sup>2</sup>Central Research Labs, Choongwae Pharma Corporation, Kyonggi 445-970, Korea

### Introduction

Melanocortin-4 receptor (MC4R) is a super family of the G-protein coupled receptors (GPCRs) and implicated in the regulation of body weight [1–3]. We built a three-dimensional model of hMC4R (human MC4R) on the methods of multiple sequence alignment and template modeling with the bovine rhodopsin template. We tried to dock with five melanocyte stimulating hormone analogue ligands, [DPhe7] $\alpha$ -MSH, message sequence [H (D) FRW], mutemessage [G (D) FRW], minimum [(D)FRW], and MTII (Figure 1). The message sequence, His-DPhe-Arg-Trp, had been modeled into the proposed binding site with specific ligand-receptor interactions identified. The ligand-receptor interactions were found in hMC4R transmembrane regions 3, 5, and 6. It is known that a  $\beta$ -turn exists in the message sequence and is necessary for physiological activity of the message sequence. The docking study confirmed that the  $\beta$ -turn is maintained in the message. On the basis of this result, docking studies for other ligands were performed.

Table 1. Biological activity of melanocyte stimulating hormone analogues [4].

Peptide	Sequence	Binding IC <sub>50</sub> (nM)			
		hMC1R	hMC3R	hMC4R	hMC5R
$\alpha$ -MSH	Ac-SYSMEHFRTGLPV-NH <sub>2</sub>	5.97±0.33	50.04±10.1	38.7±1.44	557±198
[DPhe] $\alpha$ -MSH	Ac-SYSIEH (D)FRTGLPV-NH <sub>2</sub>	0.51±0.11	1.17±0.14	1.16±0.09	0.86±0.04
		IC <sub>50</sub> ( $\mu$ M)			
Message	Ac-His-DPhe-Arg-Trp-NH <sub>2</sub>	0.62±0.04	>10	1.15±0.21	>10
Mute	Ac-Gly-DPhe-Arg-DTrp-NH <sub>2</sub>	>10	>10	>10	>10
Minimum	Ac-DPhe-Arg-Trp-NH <sub>2</sub>	>10	>10	2.08±0.44	>10

### Results and Discussion

MCRs are part of the GPCRs because they are formed with the 7 transmembrane helices and are placed in the middle of the membranes to act as a transmitter (Figure 1). MCRs have no homology with other GPCRs. As the FASTA search result shows, only 20% of homology exists. Therefore, it is impossible to build the structure of hMC4R by homology modeling. So multiple sequence alignment and template modeling methods were used. The 7 TMs of the hMC4R are formed with hydrophobic residues. Therefore the active site also has the very robust hydrophobic environment and hydrophobic residues such as Val, Phe, Leu are abundant.

Residues of hMC4R which participate in docking are concentrated in TM3, TM5 and TM6 (Figure 2). In GPCRs, only specific TMs participate in ligand-receptor interaction. TM1, 2, and 4 do not participate in binding, but TM3 and TM 5-7 are related to binding with ligand. According to this study, the residues in the TM3 and TM5 have the greatest influence; the residues that form H-bonds between ligands and hMC4R

are mostly in TM3 and the residues that surround ligand on the active site are also mostly in TM3 and TM5 [5,6]. The docking results show  $\beta$ -turn was maintained on the His-D-Phe region in [D-Phe7]  $\alpha$ -MSH, the message sequence, and MTII. Some

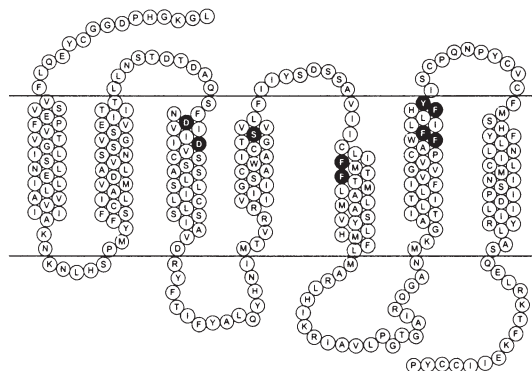


Fig. 1. Model of human MC4R.

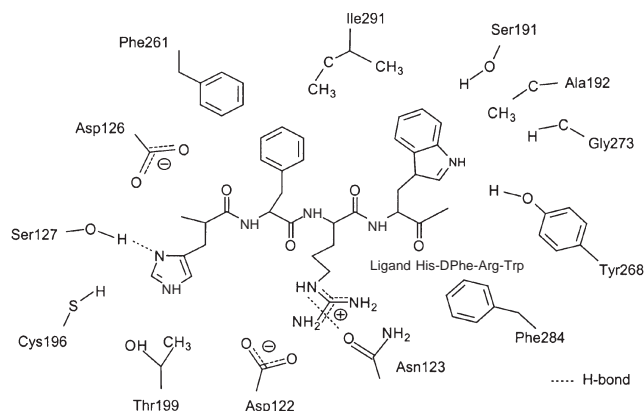


Fig. 2. Common interactions for hMC4R and analogue ligands.

specific ligand-receptor interactions were similar among these three ligands around TM3 and TM5. Most of the polar residues on the receptor were found to be pointing inside in the helix bundle, and these inward-facing residues were involved in robust H-bonding interaction with ligand. No secondary structure was found for mute and message ligands, and minimum showed a 7-membered turn.

## Acknowledgments

Research Fund Ministry of Health and Welfare, Republic of Korea (1998–2000).

## References

1. Fanelli, F., Menziani, M.C., De Benedetti P.G. *J. Mol. Struc.* **333**, 49–69 (1995).
2. Peteris, P., et al. *J. Mol. Grap. Model.* **15**, 307–317 (1997).
3. Hruby, V.J., Wikes, B.C., et al. *J. Med. Chem.* **30**, 2126–2130 (1987).
4. Carrie, H.L., et al. *Med. Chem.* **40**, 2133–2139 (1997).
5. Guyu, H., Robert, G.M. *J. Biol. Chem.* **274**, 35816–35822 (1999).
6. Donnelly, D. *FEBS Lett.* **409**, 431–436 (1997).

## **Effect of Detergents on Intramolecular Helix-Helix Packing in a Membrane-Based Peptide Derived from CFTR**

**Alex G. Therien and Charles M. Deber**

*Division of Structural Biology and Biochemistry, Hospital for Sick Children, Toronto M5G 1X8;  
and Department of Biochemistry, University of Toronto, Toronto M5S 1A8, Ontario, Canada*

### **Introduction**

The structural analysis of membrane proteins has long been hampered by the hydrophobic nature of these proteins. Our approach to the problem has involved the use of small double-spanning membrane peptides inserted into detergent micelles. Specifically, we have focused on a peptide, TM 3-4, derived from CFTR, the membrane channel associated with cystic fibrosis (CF). The 88 amino acid peptide contains residues 194-241 (GLALAHFVWIAPLQVALLMGLIWELLQASAFAGLGFLIVLALFQAGLG), including the third and fourth transmembrane segments (TMs), of CFTR, and contains a His-Tag and an S-tag for purification purposes. In a previous study, we have shown that TM 3-4 spontaneously inserts into detergent micelles and adopts an  $\alpha$ -helical conformation [1]. However, it has remained unclear whether its tertiary structure is that of a helical-hairpin loop, as would be predicted from structural models of full length CFTR. In this report, we address this question and test the effects of various detergents on interhelical packing in this construct. Specifically, we have used pyrene as a probe of the distance between the two TMs in TM 3-4. Pyrene behaves atypically for a fluorophore in that although it absorbs light at 345 nm and emits it at ~385 and ~405 nm when in its monomeric form, it can form excited dimers (excimers) which emit light at ~485 nm [2]. Therefore, the ratio of excimer fluorescence (at 485 nm) to monomer fluorescence (at 385 nm) is a measure of the extent to which pyrene molecules are able to dimerize in a given system. By labeling TM 3-4 at the N-terminal end of TMs 3 and the C-terminal end of TMs 4 with pyrene, the excimer-to-monomer ratio (EMR) becomes a measure of the interaction between the two helices. We show here not only that helices 3 and 4 interact in detergent micelles, but also that the nature of the detergent can shift the equilibrium between the "closed" hairpin loop conformation in which TMs 3 and 4 interact tightly, and the "open" extended conformation in which the two helices do not interact [3].

### **Results and Discussion**

As a first step towards answering the question of how closely helices 3 and 4 interact in TM 3-4, we mutated the construct by inserting cysteine residues at the N-terminal end of TMs 3 and C-terminal end of TMs 4 [3]. We then labeled this mutated construct with pyrene iodoacetamide, which specifically reacts with sulfhydryl groups. The labeling reactions resulted in protein containing, on average, 1.4–1.8 pyrene molecules (not shown). Figure 1 shows that pyrene-labeled TM 3-4 exhibits typical monomeric pyrene fluorescence bands at ~385 and ~405 nm, and a less structured band at 485 nm, corresponding to excimeric pyrene. In addition, the figure shows that the nature of the detergent alters the EMR: perfluorooctanoate (PFO) is the most permissive detergent, sodium dodecyl sulfate (SDS) the least, and lauroylphosphatidyl-choline and -glycerol (LPC and LPG) have intermediate EMRs. A comparison of results obtained with SDS, LPC, and LPG, shows that the nature of the detergent head group can affect the extent of interhelical interactions. It should be noted that intermolecular

interactions cannot account for excimer formation in this system since there is no dependence of the EMR on TM 3-4 concentration (not shown).

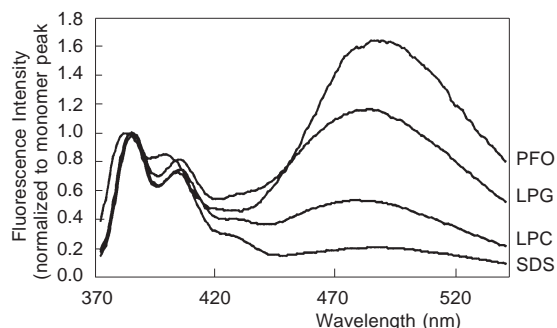


Fig. 1. Fluorescence emission spectrum of pyrene-labeled TM 3-4. Samples ( $1\ \mu\text{M}$ ) were dissolved in 20 mM tris-Cl (pH 8.0) containing 50 mM PFO, 34 mM SDS, 20 mM LPC or 20 mM LPG, as indicated. Excitation wave-length was 345 nm.

These results confirm that TM 3-4 constructs fold in a helical-hairpin loop motif in detergent micelles (composed of LPC, LPG or PFO) and show that the extent of interhelical packing is highly dependent on the nature of the micellar detergent. The contrasting results with SDS and PFO are consistent with previous observations that SDS can disrupt dimerization of single-spanning membrane peptides [4,5], while PFO allows membrane proteins to maintain their oligomeric states [6]. In addition, previous results obtained in this laboratory have suggested that TM 3-4 migrates in the open conformation on SDS-PAGE but in the closed conformation in PFO-PAGE [3]. The system described in this report will be useful in investigations of not only the role of lipids on interhelical packing, but also that of individual amino acid side chains. Work is currently underway to investigate the effect of CF-phenotypic mutants on the interaction between TMs 3 and 4 using the pyrene fluorescence system described here.

#### Acknowledgments

This work was supported by grants to CMD from the Canadian Institutes of Health Research (CIHR), the Canadian Cystic Fibrosis Foundation, and the National Institutes of Health. AGT holds a post-doctoral fellowship from the CIHR.

#### References

1. Peng, S., Liu, L.-P., Emili, A.Q., Deber, C.M. *FEBS Lett.* **431**, 29–33 (1998).
2. Lehrer, S.S. *Methods Enzymol.* **278**, 286–295 (1997).
3. Therien, A.G., Grant, F.E.M., Deber, C.M. *Nat. Struct. Biol.* **8**, 597–601 (2001).
4. Choma, C., Gratkowski, H., Lear, J., DeGrado, W.F. *Nat. Struct. Biol.* **7**, 161–166 (2000).
5. Zhou, F.X., Cocco, M.J., Brünger, A.T., Engelman, D.M. *Nat. Struct. Biol.* **7**, 154–160 (2000).
6. Ramjeesingh, M., Huan, L.-J., Garami, E., Bear, C.E. *Biochem J.* **342**, 119–123 (1999).

## Primary Amphipathic Shuttle Peptides: Structural Requirements and Interactions with Model Membranes

Frédéric Heitz<sup>1</sup>, Christian Le Grimellec<sup>2</sup>, Jean Méry<sup>1</sup>, Gilles Divita<sup>1</sup>  
 and Nicole Van Mau<sup>1</sup>

<sup>1</sup>CRBM-CNRS UPR 1068, Montpellier, 34293 France

<sup>2</sup>CBS CNRS-INSERM Montpellier, 34060 France

### Introduction

Two families of primary amphipathic peptides issued from the association of a nuclear localization sequence (NLS) with either a signal (SP) or fusion peptide (FP) were shown to be efficient carriers of drugs or nucleic acids [1,2]. In order to define the minimal structural requirements that maintain the vector properties, the identification of the membrane crossing process was a crucial step. Here, we focus on the uptake of the vectors by model membranes and examine the influence of the hydrophobic sequence, and thus of its conformation, on the penetration into phospholipid monolayers of various physical states and polar headgroups.

### Results and Discussion

Starting from the FP-NLS [B] and SP-NLS [A] peptides, the uptake of which, respectively, depend or not on the nature of the phospholipid headgroups [3,4], several FP-NLS analogs (Table 1) have been synthesized by SPPS using the Expansin resin [5] with the aim to induce different conformational states.

*Table 1. Chemical sequences of the various peptides used in this study. Ac and Cya are acetyl and cysteamide groups, respectively.*

Ac-M-G-L-G-L-H-L-L-V-L-A-A-A-L-Q-G-A-W-S-Q-P-K-K-K-R-K-V-Cya	[A]
Ac-G-A-L-F-L-G-W-L-G-A-A-G-S-T-M-G-A-W-S-Q-P-K-K-K-R-K-V-Cya	[B]
Ac-G-A-L-F-L-G-F-L-G-A-A-G-S-T-M-G-A-W-S-Q-P-K-K-K-R-K-V-Cya	[Ba]
Ac-G-A-L-F-L-G-F-L-G-A-A-G-A-A-M-G-A-W-S-Q-P-K-K-K-R-K-V-Cya	[Bb]
Ac-G-A-L-A-L-G-A-L-G-A-A-G-S-T-M-G-A-W-S-Q-P-K-K-K-R-K-V-Cya	[Bc]
Ac-G-A-L-F-L-A-F-L-A-A-A-L-S-L-M-G-L-W-S-Q-P-K-K-K-R-K-V-Cya	[Bd]

The conformations were identified in water solution by CD and in the presence of lipids by FTIR. In aqueous media, all peptides are non-ordered except for [Bd], which is  $\alpha$ -helical in its hydrophobic domain as expected on the basis of the AGADIR algorithm [6]. The presence of phospholipids favors the formation of  $\beta$  type structures for all previously unordered peptides, while the helical structure is maintained in the case of peptide [Bd] (Table 2).

The ability for the peptides to penetrate in various phospholipid monolayers was evaluated by measuring the peptide-induced variations of surface pressure using various initial pressures of the lipid monolayer. The extrapolation at variation zero provides the critical pressure of insertion, which corresponds to the highest pressure at which the peptide can spontaneously insert the monolayer. These values are reported in Table 3 and suggest the following comments. For the lipids in the liquid condensed state (DPPC and DPPG), the peptide uptake does not depend on the nature of the polar headgroups (neutral or negatively charged) and clearly, the  $\alpha$ -helical form facilitates the penetration. The fact that the headgroups have no influence suggests that the pene-

tration is mainly governed by the hydrophobic interactions occurring between the lipid acyl chains and the hydrophobic N-terminal sequences of the peptides. In the case of lipids in the liquid expanded state (DOPC and DOPG), for a peptide not structured in the bulk, the negative charges facilitate the penetration while the uptake strongly depends on the nature of headgroups. When the peptide adopts an  $\alpha$ -helical structure, this difference is strongly reduced. This difference between the two peptides indicates that the uptake is governed by the conformational state of the peptide.

Table 2. Identification of the conformational states of the various peptides in the absence and in the presence of phospholipids.

Peptide	In water	In lipidic medium <sup>a</sup>
[A]	RC	$\alpha$ , $\beta$
[B]	RC	$\beta$
[Ba]	RC	$\beta$
[Bb]	RC	$\beta$
[Bc]	RC	$\beta$
[Bd]	$\alpha$	$\alpha$

<sup>a</sup>  $\alpha$  (low peptide/DOPC or DOPG ratio),  $\beta$  (high ratio and in DPPC, DPPG).

Table 3. Critical pressure of insertion into various phospholipids of two peptides in different conformational states.

Peptide	DOPC	DOPG	DPPC	DPPG
[Ba]	32	46	33	33
[Bb]	34	39	37	37

In conclusion, it appears that the conformational state of a primary amphipathic peptide that can act as a shuttle for intracellular delivery of therapeutic agents is crucial for its penetration into lipid monolayers, and thus for its uptake by membranes. A helical structure of the hydrophobic domain enhances the penetration and reduces the effect of the phospholipid headgroup charges. These results also show that modifications which, *a priori*, are minor modify the affinity of the vectors for lipidic media. These observations have to be taken into account for the future design of a new generation of vector peptides.

## References

1. Chaloin, L., Vidal, P., Lory, P., Méry, J., Lautredou, N., Divita, G., Heitz, F. *Biochem. Biophys. Res. Commun.* **243**, 601–608 (1998).
2. Morris, M.C., Chaloin, L., Méry, J., Heitz, F., Divita, G. *Nucleic Acids Res.* **27**, 3510–3517 (1999).
3. Vié, V., Van Mau, N., Chaloin, L., Lesniewska, E., Le Grimellec, C., Heitz, F. *Biophys. J.* **78**, 846–856 (2000).
4. Vidal, P., Chaloin, L., Heitz, A., Van Mau, N., Méry, J., Divita, G., Heitz, F. *J. Membrane Biol.* **162**, 259–264 (1998).
5. Méry, J., Granier, C., Juin, M., Brugidou, J. *Int. J. Pept. Protein Res.* **42**, 44–52 (1993).
6. Lacroix, E., Viguera, A.R., Serrano, L. *J. Mol. Biol.* **284**, 173–191 (1998).

## **Synthesis, Purification, and Analysis of the Transmembrane Domain of Phospholamban**

**Patrick S. Wesdock<sup>1</sup>, Phillip W. Banda<sup>1</sup>, Steven C. Hall<sup>1</sup>, Sally U<sup>1</sup> and Gary Lorigan<sup>2</sup>**

<sup>1</sup>*Applied Biosystems, Foster City, CA 94404, USA*

<sup>2</sup>*Department of Chemistry, Miami University of Ohio, Oxford, OH 45056, USA*

### **Introduction**

Phospholamban (PLB) is a membrane protein implicated in the regulation of calcium ATP-ase activity in the sarcoplasmic reticulum (SR) of heart muscle cells [1]. It plays a key role in Ca<sup>2+</sup> transport across the SR membrane and in cardiac contraction and relaxation processes [1]. PLB's role in this regulatory activity can be explored through structural studies and through changes in structure dependent on phosphorylation activity. In order to provide a means for these studies to proceed, we have undertaken the synthesis and analysis of the C-terminal transmembrane portion of PLB.

Automated chemical synthesis of PLB has previously been reported using the t-Boc synthesis strategy [2]. By employing an Fmoc based synthesis strategy and utilizing deprotection monitoring, we have been able to observe those regions of the sequence where the membrane domain of PLB exhibits difficulty.

### **Results and Discussion**

Synthesis of the transmembrane portion of PLB corresponding to residues 32-52 (FINFCLILICLLLIHIVMLL-amide) was performed at the 0.1 mmol scale employing FastMoc chemistry on an Applied Biosystems (AB) Model 433A Peptide Synthesizer. The 433 was equipped with a Perkin Elmer<sup>TM</sup> Model S200 UV Detector, which provided Fmoc deprotection monitoring during the course of the synthesis. Cleavage from the PAL-PS support was accomplished using a TFA/EDT/thioanisole/H<sub>2</sub>O cocktail. MALDI-TOF MS analysis was performed on an AB Voyager-DE STR Workstation. Samples were mixed 1 : 1 with a saturated solution of 2,5-dihydrobenzoic acid. A 0.5 mL aliquot of the mixture was spotted onto the target plate, and the peptide was allowed to co-crystallize with the matrix before analysis. Purification was performed on an AB Vision Workstation plumbed in low dispersion mode employing a POROS 10 R1 (4.6 mm × 100 mm) column. Buffer A: 95% Water, 2% Acetonitrile, 3% 2-Propanol, 0.1% TFA. Buffer B: 38% Acetonitrile, 57% 2-Propanol, 5% Water, 0.1% TFA. Gradient: 100% A to 100% B over 20 CV (column volume) at 2 ml/min.

During SPPS, removal of the N-terminal Fmoc protecting group was monitored *via* UV absorbance of dibenzofulvene liberated during piperidine deprotection. Maximum Fmoc removal is approached as absorbance decreases. The bar plot shown in Figure 1 is a display of the relative completeness of Fmoc removal encountered at each deprotection step during the progress of the automated synthesis of PLB 32-52. The early stages of the synthesis through the first 7 residues encounter no deprotection related difficulties. As sequence dependant obstacles are encountered, the Fmoc group is rendered inaccessible, and additional base treatments are necessary to improve Fmoc removal. Extended deprotection cycles are initiated whenever UV baseline is not rapidly attained, as with residues 8 and 9 from the start of the synthesis in Figure 1. Interestingly, once this difficult region is overcome, the synthesis resumes a deprotection pattern consistent with more facile Fmoc removal. Isolation of crude product post synthesis and cleavage was accomplished *via* precipitation of the free peptide into water.

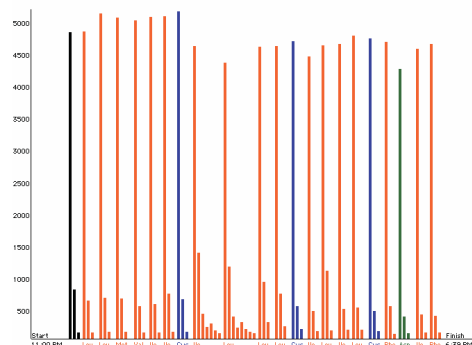


Fig. 1. Fmoc deprotection UV monitor.

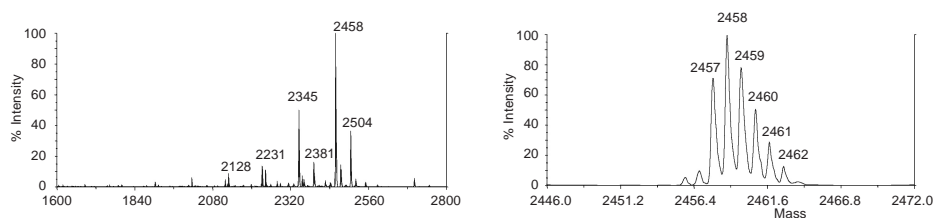


Fig. 2. MALDI-TOF MS of crude product.

Dissolution efforts required TFA, followed by dilution with acetonitrile. MALDI-MS analysis of the crude cleavage isolate (Figures 2a and b) exhibited the correct peptide mass. Deletion information obtained in the MS data (Figure 2a) is consistent with deletions of isoleucine and leucine residues and corresponds well with the UV monitor trace from the synthesis.

As indicated by the deprotection profile observed for the synthesis of PLB (Figure 1) areas where Fmoc removal becomes difficult are easily discernable, and clearly indicate where synthesis troubles are encountered. The use of UV monitoring permits the derivation of important information regarding the dynamic resin environment under which solid phase peptide synthesis takes place.

## References

1. Ludlam, C., Arkin, I.T., Liu, X.M., Rothman, M.S., Rath, P., Aimoto, S., Smith, S.O., Engelman, D., Rothschild, K.J. *Biophys. J.* **70**, 1728–1736 (1996).
2. Garsky, V.M., Mayer, E.J., McKenna, E., Burke, C.J., Mach, H., Middaugh, C.R., Sardana, M., Smith, J.S., Johnson, Jr., R.G., Freidinger, R.M., In Pravin T.P. Kaumaya and Robert S. Hodges (Eds) *Peptides: Chemistry, Structure and Biology*, Mayflower Scientific Ltd., 1996, p. 220.

## Verification of a $\mu$ Opioid Receptor Model by Site-Directed Mutagenesis

Carol Fowler, Irina Pogozheva and Henry I. Mosberg

*Division of Medicinal Chemistry, University of Michigan, Ann Arbor, MI 48109, USA*

### Introduction

Based on the published rhodopsin X-ray crystal structure [1] we constructed a homology-based model of the  $\mu$  opioid receptor. Comparison of our previously published model [2] to the homology model showed that the position of residues in the putative ligand binding pockets was quite similar in both models, especially in trans-membrane domains 6 and 7. Single and double point mutations of residues around the binding pocket, together with various analogs of the cyclic, dithioether-containing opioid peptide, JOM6, Tyr-c(S-Et-S)[D-Cys-Phe-D-Pen]NH<sub>2</sub> [3], test our proposed model of ligand docking inside the  $\mu$  opioid receptor.

### Results and Discussion

Mutant receptors were constructed from the  $\mu$ /pCMV expression plasmid using the Quik Change mutagenesis kit from Stratagene, and transiently expressed in Cos-1 cells. All receptor mutants tested bound [<sup>3</sup>H] DAMGO similarly to wild type  $\mu$  receptor.

According to our original distance geometry model and the model based on the rhodopsin X-ray structure, the tyrosine in tetrapeptide JOM6 is expected to interact with residues in TM5 and TM6. To test this theory, a number of residues in these helices were mutated to Cys or His. It was hypothesized that if any of these residues were in close contact with the peptide, they could, together with the native His 297 form a zinc binding center with the JOM6 analog His<sup>1</sup> JOM6 and, in the presence of ZnCl<sub>2</sub>, would bind His<sup>1</sup> JOM6 with much greater affinity than the wild type receptor. The results for competition of His<sup>1</sup> JOM6 with [<sup>3</sup>H] DAMGO in each of the receptors studied are summarized below (Table 1). In the absence of ZnCl<sub>2</sub>, the V300C mutant shows a 10-fold increase in affinity over wild type. This change in affinity is most likely due to a favorable sulfur-aromatic interaction between V300C and the histidine residue in the His<sup>1</sup> JOM6 ligand. In the presence of 20 and 30  $\mu$ M ZnCl<sub>2</sub>, an additional 3-fold increase in binding affinity is observed.

Table 1. IC<sub>50</sub>s for competition of His<sup>1</sup>-JOM6 with 2 nM [<sup>3</sup>H] DAMGO, with or without ZnCl<sub>2</sub>.

Clone	With 0 $\mu$ M ZnCl <sub>2</sub>	With 20 $\mu$ M ZnCl <sub>2</sub>	With 30 $\mu$ M ZnCl <sub>2</sub>
$\mu$ wt	1500 nM	1500 nM	1500 nM
N230H	1500 nM		1500 nM
V300C	150 nM	50 nM	50 nM
F237C	5000 nM	2000 nM	
1234C+V300C	200 nM	100 nM	100 nM

Our modeling studies also suggest that the phenylalanine residue in JOM6 may have binding interactions with residues in extracellular loops (EL) 2 and 3 with possible interactions near the junction EL3-TM6. To test this theory, a variety of receptor mutants were prepared, either to serve as potential binding partners in zinc binding centers with His<sup>3</sup> JOM6, or to form better binding interactions with other peptide

analogs. The results of binding experiments with the receptor mutants are summarized in Table 2. Both the T315C and G213C+T315C mutants bound the His<sup>3</sup> JOM6 analog with 5-fold higher affinity than the wild-type receptor, but no difference in binding affinity was observed in the presence of ZnCl<sub>2</sub>. This increase in affinity suggests that these residues are proximal to this portion of the peptide ligand, and that favorable binding interactions between the receptor and ligand have been introduced.

Table 2. IC<sub>50</sub>s for competition of JOM6 analogs with 2 nM [<sup>3</sup>H] DAMGO.

JOM6 analog	μ WT	T315C	W318L
His <sup>3</sup>	300 nM	60 nM	
Phe <sup>3</sup> (JOM6)	0.9 nM	0.5 nM	3.0 nM
Δ <sup>E</sup> Phe <sup>3</sup>	8.0 nM		1000 nM

Previous SAR studies using dehydro Phe<sup>3</sup> (Δ<sup>E</sup> and Δ<sup>Z</sup> Phe<sup>3</sup>) analogs of JOM6 have shown that the μ opioid receptor has a preference for the Δ<sup>E</sup> Phe analog (K<sub>i</sub> of 8 nM and >20 μM, respectively), which corresponds to a preference for the trans-rotamer of Phe<sup>3</sup> in JOM6. We mutated W318, which in our model is proximal to the Phe<sup>3</sup> residue of JOM6, to its corresponding amino acid in the δ receptor (leucine), and the effects on the binding of the Δ<sup>E</sup> Phe<sup>3</sup> JOM6 peptide were studied. The wild type and W318L receptor mutant showed similar affinity for JOM6, indicating that the binding pocket is still hospitable for the more flexible JOM6 peptide. However, the W318L receptor mutant showed a 125-fold decrease in binding affinity for the Δ<sup>E</sup> Phe<sup>3</sup> JOM6 peptide. These results are consistent with our published model [2], and suggest that the W318 residue is in close proximity to the Phe<sup>3</sup> residue of the peptide, and that the decrease in binding affinity is due to an adverse steric interaction.

### Acknowledgments

Financial support provided by NIDA (grant DA 03910 and an institutional NRSA).

### References

1. Palczewski, K., et al. *Science* **289**, 739–745 (2000).
2. Pogozheva, I., Lomize, A., Mosberg, H.I. *Biophys. J.* **75**, 612–634 (1998).
3. Mosberg, H.I., Omnaas, J., Smith, C., Medzihradsky, F. *Life Sci.* **43**, 1013–1020 (1988).

## **Solid-Phase Synthesis and Chemical Ligation of Transmembrane Segments of Rhodopsin**

**Wei-Jun Zhang, Parissa Heshmati, Yunpeng Ye and Garland R. Marshall**

*Department of Biochemistry and Molecular Biophysics, Washington University,  
St. Louis, MO 63110, USA*

### **Introduction**

To investigate the conformational changes associated with photoactivation of rhodopsin [1], the GPCR of vision, we have embarked on a program of chemical synthesis of its transmembrane segments. By reconstituting such synthetic segments containing specific fluorescent and spin labels with expressed segments of rhodopsin, we hope to generate hybrid “split receptors” that are fully functionally for biophysical studies. For this reason, a number of TM fragments of rhodopsin were synthesized by various solid-phase protocols, and chemical ligation was used to link these fragments into larger fragments of rhodopsin.

### **Results and Discussion**

The major anticipated obstacles in the chemical synthesis of membrane proteins are the large regions of highly hydrophobic amino acid residues and the difficulty in solubilizing the hydrophobic segments under conditions that are suitable for the chemical ligation [2]. Our synthetic approach has proven efficient for synthesizing hydrophobic transmembrane peptides typically yielding material with crude purity of 60–70% that could be purified to homogeneity with an overall yield of 8–10%.

Two kinds of polypeptides were synthesized for chemical ligation. One was the amino-terminal peptide with an active thioester at the carboxy end. Another was the carboxy-terminal peptide with the free amino group of cysteine in the N-terminus. Chemical synthesis of  $\alpha$ -thioester polypeptide on a 3-mercaptopropionylamide-MBHA resin was achieved by using Boc amino acid derivatives employing *in situ* neutralization/HBTU activation protocols for Boc-SPPS. The  $\alpha$ -thioester polypeptide was obtained after cleavage with hydrogen fluoride and purification with HPLC. The amino terminal peptide was made by Fmoc strategy with HBTU coupling reagent on SynnovaTGA resin. Two points should be considered:

1. During the synthesis of peptides with more than 50 amino acids, the deprotecting reagent(s) should be changed gradually from 25 to 40% piperidine/DMF. After 40 amino acids, it is better to add 2% DBU to the deprotecting solution;
2. In the transmembrane peptides, there are many hydrophobic and sterically hindered amino acids side chains, and this increases the coupling time for each amino acid. In order to reduce the total coupling time of the peptide, the pH of the reaction was adjusted to between 6 and 7. By keeping the reaction in this pH range, we obtained the peptide in higher yield with higher purity.

The major problem encountered in the purification and characterization of such transmembrane fragments was formation of insoluble gels in the ligation solvent. A number of strategies have been tried to solubilize or modify the solubility of these TM fragments. To date, there has been no generally successful approach to this problem. However, by adding five lysine residues to the amino terminal of the thioester peptide and two lysine residues to the carboxy-terminal of cysteine peptide, we have overcome this hurdle in several cases. The addition of these lysine residues to the peptides reduces their hydrophobicity and increases their solubility in the ligation solvent. In

addition, once the two peptides are ligated together, the added lysines will not hinder the fragment's insertion into artificial membranes because the lysines will lie on the extracellular side of the membrane and will help orient the peptide in the membrane.

The following peptide fragments were synthesized:

Rhodopsin sequences P49, 140-188; P22, 167-188; P51, KK-140-188

Thioester sequence P33, 107-139; P38, KKKKK-107-139; P27, 140-166; P27, Msc-140-166.

Ligation of TM fragments was successful under the following conditions:

A. P22, 0.5  $\mu$ M and P38, 0.1  $\mu$ M in 50  $\mu$ L solvent (0.1 M) phosphate buffer containing 6 M guanidine and 1% S-phenol, pH 7.5. The reaction solution was heated to 60 °C and 15  $\mu$ L trifluoroethanol was added. At 72 h, the ratio of P38 to ligation product was 3 : 98. MALDI MS of the product gave MW = 6595.20; calculated 6596

B. P2 (Cys-Val-NH<sub>2</sub>) 0.15  $\mu$ M and P38, 0.1  $\mu$ M in solvent 50  $\mu$ L (0.1 M phosphate buffer pH 7.5 with 6 M guanidine and 0.1% phenol). After 24 h, the ratio of product to P38 was 6 : 1. (MW = 4444.9; calculated 4444.5)

C. P51 Lys2-140-188, 0.15  $\mu$ M and P38, 0.1  $\mu$ M were dissolved in solvent 50  $\mu$ L (0.1 M phosphate buffer pH 7.7 with 6 M guanidine and 0.1% phenol). After 90 h, the ratio of product to P38 was 1 : 2. (MW = 9836; calculated 8832)

D. Finally, we report that the peptide P38 (lys5/107-139) and P51 (lys2/140-188) have been chemically ligated with positive results by MS.

### **Acknowledgments**

The authors acknowledge support for this research from NIH Grant EY12113. The Washington University Mass Spectroscopy Resource Center supported by NIH (RR00954) was utilized to characterize the ligated peptides synthesized as part of this study.

### **References**

1. Palczewski, K., Kumasaka, T., Hori, T., Behnke, C.A., Motoshima, H., Fox, B.A., Le Trong, I., Teller, D.C., Okada, T., Stenkamp, R.E., Yamamoto, M., Miyano, M. *Science* **289** (5480), 739–745 (2000).
2. Kochendoerfer, G.G., Salom, D., Lear, J.D., Wilk-Orescan, R., Kent, S.B.H., DeGrado, W.F. *Biochemistry* **38** (37), 11905–11913 (1999).

## **Ion Gating and Selectivity in Gramicidin A**

**W.L. Duax<sup>1</sup>, V. Pletnev<sup>2</sup>, B.M. Burkhart<sup>3</sup> and M. Glowka<sup>4</sup>**

<sup>1</sup>*Hauptman-Woodward Inst., Inc. Buffalo, NY 14203, USA*

<sup>2</sup>*Shemyakin-Ovchinnikov Inst. of Bioorganic Chem., Russian Acad. of Sciences,  
Moscow 117997 Russia*

<sup>3</sup>*Milliken Chem. Co., Spartanburg, SC 29304, USA*

<sup>4</sup>*University of Lodz, Lodz, Poland*

### **Introduction**

The crystal structures of ion complexes of gramicidin (CsCl, TlNO<sub>3</sub>, KCl, KI, KSCN, and RbCl) [1] provide information concerning the distribution of ions and water in a single file channel. The crystallographically observed structures (a right-hand antiparallel double strand  $\beta$ -ribbon) agree with those based on NMR measurements in organic solvents and lipid bilayers [2,3]. The ion and solvent filled gramicidin A channel is a nanotube that is 25 Å long and 4 Å across. Analysis reveals (a) variation in ion occupancy in specific sites within the channel, (b) unusual coordination of the cations with the  $\pi$  orbitals of the carbonyl groups and peptide bonds that form the walls of the channel, (c) asymmetry in the position of water molecules on either side of ions within the channel, (d) evidence of a dipole along the length of the channel that provides a driving force for ion transport, and (e) a possible role in the gating of ion transport by the conformationally flexible ethanolamine residue at either end of the channel.

### **Results and Discussion**

*Ion Distribution.* Each of the seven crystal structures of monovalent cation complexes of gramicidin (including complexes of RbCl grown in methanol as well as ethanol) contains two crystallographically independent dimers and consequently they provide 14 independent observations of the ion-filled channel. The  $\alpha$  carbon backbones of the *d,l* peptides are very similar in all 14 channels. They share a set of 26 hydrogen bonds (16 between the *l* residues in the antiparallel  $\beta$  ribbon and 10 between the *d* residues that stabilize the  $\beta$ -barrel formed by the  $\beta$ -ribbon.) Because of its *d,l* composition the side chains of all residues are on the surface of the  $\beta$ -barrel. Although the antiparallel arrangement of the two strands results in the presence of two fold chemical symmetry in the dimer, steric interactions on the surface introduce significant asymmetry. Some individual side-chain conformations and combinations of conformations are similar but no two of the 14 independent channels have identical ensembles of side-chain conformations. There are between 1 and 2 cations per channel distributed in partial occupancy over subsets of the same seven sites in the 14 channels (Figure 1). The partial occupancy ranges from a 15% Cs<sup>+</sup> occupancy to a 90% K<sup>+</sup> occupancy. No two of the 14 channels have the same distribution of ions and water. The asymmetry of the side chain orientations and the asymmetry of the ion distributions in the channel is almost certainly correlated.

The two independent channels (A and B) in the seven crystals exhibit a significant difference in side-chain conformations and ion distribution particularly in the two sites nearest the end of the channel (Figure 1). The central site is consistently occupied by the larger cations (Rb<sup>+</sup>, Cs<sup>+</sup>, and Tl<sup>+</sup>) and never occupied by K<sup>+</sup> ions. Despite chemical symmetry relating sites 3 and 3', the former is highly occupied and the latter rarely occupied in the 14 channels.

**Cation Coordination.** In most cases ions in the six sites of highest occupancy make three or four contacts to the  $\pi$  clouds of the carbonyl or peptide groups of the channel walls. The  $M^+ \cdots O$  or  $N$  distances range from 2.56 to 3.80 Å. The  $\mu_1$  angles, ( $M \cdots O=C$ ) or ( $M \cdots N=C$ ), range from 70 to 150° and average 108°. The absolute magnitude of the torsion angles defining the relationship of the ions and the  $sp^2$  plane of the carbonyl groups ( $\mu_2, M^+ \cdots O=C_1N_1$ ) range from 54 to 104° (average 81°) clearly demonstrating that ion association is to the  $\pi$  cloud over the carbonyl and peptide groups. The peptide bond  $\omega$  angles ( $C\alpha_n-C_1-N_1-C\alpha_{n+1}$ ) of residues involved in ion coordination exhibit significant non-planarity (as much as 18°) as a result of the withdrawal of electrons from the  $\pi$  clouds by the cations in the channel.  $^{13}C$  NMR chemical shift measurements attributed to  $Na^+$  ion interactions with leucine residues in oriented gramicidin channels in dimyristoyl phosphatidylcholine (DMPC) bilayers detect this deformation and correlate with these observations [4]. The structure of gramicidin responsible for ion transport in bilayers appears to be similar to the structure in the crystals.

**Asymmetry in Water Cation Coordination.** There are 6 to 7 water molecules in each channel distributed along its 25 Å length. The waters occupy the same seven sites where the cations are found but the distribution is more diffuse. Electrophysiology measurements also indicate that seven water molecules are transported per cation [5]. When there is a water molecule on either side of an ion, one water is at an average distance of 2.4 Å and the other 3.2 Å from the ion (Figure 2a). The observed asymmetry of distances between the cations and the closest waters suggests that the closest contacts (2.2–2.9 Å) represent typical ion liganding *via* the backbonding orbitals of the oxygen atom of the water and the longer distances (3.0–3.6 Å) arise when the water is oriented with its hydrogen atoms directed toward the cation (Figure 2b).

Site 1		Site 2		Site 3		Site 4		Site 3'		Site 2'		Site 1'	
A	B	A	B	A	B	A	B	A	B	A	B	A	B
Cs	Rbe	Cs	Cs	KCl	Rbe	Cs	Cs	Rbm		Cs	Rbm	KCl	Cs
KCl		Rbe	Lbe	KI	Rbm	Rbe	Rbe			Rbe			Rbe
KI		Rbm	Rbm	KSCN	TI	Rbm	Rbm			Rbm			Rbm
KSCN		TI	KCl		KI	TI				TI			TI
		KCl	KSCN		KSCN					KCl			KCl
										KI			KI
										KSCN			KSCN

Fig. 1. Ion filling of seven sites in crystallographically distinct channels A and B in gramicidin complexes. Site 4 is at the chemical center of symmetry of the antiparallel dimer (+  $K^+$  ion; d,  $Rb^+$ ,  $Cs^+$ ,  $TI^+$  ions). Waters which are found in the same seven sites are omitted for clarity.

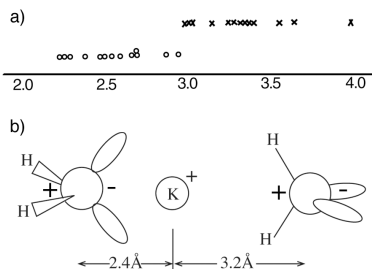


Fig. 2. (a) Distribution of observed distances between cations in the gramicidin channel to nearest water molecule and (b) orientation of the majority of water molecules in the channel.

**Channel Dipole.** Seventy-five percent of the well defined waters of solvation within the channels have a common orientation indicating that their dipoles are uniformly aligned (Figure 2b). This pattern suggests that the crowding of the amino acid side chains on the surface of the  $\beta$  barrel induces significant asymmetry into the channel, and generates a strong dipole over its entire length. Water molecules in the channel will have their dipoles in an antiparallel orientation relative to the dipole of the channel. Cation concentration differences in the polar region on either side of a lipid bilayer could induce asymmetry in gramicidin channels embedded in the membrane producing a comparable dipole that would provide a driving force for ion transport.

**Ethanolamine Gating.** The ethanolamine at the C terminus of gramicidin A appears to play a critical role in ion entry and exit. When there is an ion in the site nearest the channel opening it has bidentate coordination from the nitrogen and hydroxyl oxygen of the ethanolamine group. When the binding site near the channel entry is occupied by water the ethanolamine is rotated out and away from the opening. The ethanolamine may function as a flexible hook that can associate with ions in the polar lipid interface and guide them into the channel or usher ions out of the channel by a reverse of this action (Figure 3). In any event the observed conformational flexibility of the ethanolamine group adds an additional source of asymmetry to the gramicidin channel and suggests that it may play a role in channel gating. Because a covalently linked head-to-head gramicidin dimer was found to have ion transport properties [6] it came to be regarded as the active form of native gramicidin and most subsequent experiments have been interpreted in terms of that model. The recent demonstration that a desformyl gramicidin derivative is more efficient at hydrogen ion transport than native gramicidin indicates that desformyl gramicidin cannot function as a head-to-head dimer because of repulsive interaction between the charged nitrogen groups exposed at the N terminus by formyl removal [7] The crystal structures of gramicidin complexes provide atomic scale examples of stages of the dynamic process of ion transport in single file and the asymmetric forms captured in the crystals may have much in common with the asymmetric forms of gramicidin that must exist in order to account for ion transport across membranes and lipid bilayers.

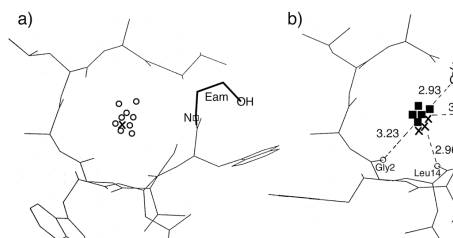


Fig. 3. Ethanolamine in (a) open and (b) closed state suggesting role in gating mechanism.

## References

1. Burkhart, B.M., et al. *Proc. Natl. Acad. Sci. U.S.A.* **95**, 12950–12955 (1998).
2. Arseniev, A.S., Barsukov, I.L., Bystrov, V.F. *FEBS Lett.* **180**, 33–39 (1985).
3. Ketchenm, R.R., Hu, W., Cross, T.A. *Science* **261**, 1457–1460 (1993).
4. Smith, R., et al. *Biochim. Biophys. Acta* **1026**, 161–166 (1990).
5. Tripathi, S., Hladky, S.B. *Biophys. J.* **74**, 2912–2917 (1998).
6. Urry, D.W., et al. *Proc. Natl. Acad. Sci. U.S.A.* **68**, 1907–1911 (1971).
7. Saporov, S.M., et al. *Biophys J.* **79**, 2526–2534 (2000).

## **Docking of Transmembrane Helices Into Four Helix Bundles in the High Affinity IgE Receptor**

**Mire Zloh<sup>1</sup>, Diego Esposito<sup>2</sup> and William A. Gibbons<sup>1</sup>**

<sup>1</sup>*University of London, School of Pharmacy, London WC1N 1AX, UK*

<sup>2</sup>*Department of Biochemistry and Molecular Biology, University College London,  
London WC1E 6BT, UK*

### **Introduction**

The high affinity IgE receptor (Fc-epsilon-RI) consists of four subunits and contains 7 transmembrane (TM) helices. Since a direct experimental structure determination of this intact receptor would be complex, a combination of computational chemistry with experimental work can be used to elucidate the 3D structure. The most suitable helix-helix packing arrangements were usually found using rules derived from soluble helical proteins and by rotating the helices such that the most hydrophobic sides would face the lipids [1]. In this work, spatial arrangement of the transmembrane bundle were studied, as well as, helix-helix interactions in the high affinity IgE receptor, using a nonsubjective procedure, namely a low resolution docking procedure [2].

### **Results and Discussion**

All possible pairs of the four TM helices were docked and the results yielded 10 lowest energy complexes for each pair. The further procedure for the docking of the TM helices into a four helix bundle for the beta subunit was chosen in such way that possible combinations of the helix-helix packing could be explored. In the first step, all possible combinations of the TM helix pairs were used. For every one of these pairs, 10 dimeric structures were obtained which were then divided into clusters. The representative (lowest energy) structures of each cluster were chosen to add a third helix, so that three helix bundles were formed. The clusters of each three helix bundle were obtained and representative structures were chosen for further docking. The fourth (missing helix) was docked to each structure and four helix bundles were obtained. The resulting structures were analyzed for the interaction energies between helices within the bundle, orientation of the hydrophobic moments and solvent accessible surface areas.

This procedure created 35 possible four helix bundles, which were divided into three categories: "clockwise", "anticlockwise" and "crossed-loop" arrangements. "Crossed-loop" bundles were discarded due to distance constraints imposed by the NMR derived structure of the connecting loop between the TM helices 2 and 3 and statistical considerations. Two four helix bundles were thus chosen based upon the following criteria; agreement with proposed topology, correct TM helix arrangement, high interaction energy between TM helices, and appropriate orientation of the hydrophobic moments towards lipid bilayer. The surfaces of the TM helix bundles exposed to the lipid bilayer were in good agreement with lipid binding sites which were predicted using molecular mechanics [3].

The lowest energy four helix bundle is shown in Figure 1. This helix exhibits the CLASS 3-4 packing, that characterizes the helix-to-helix packing found in coiled-coil structures, such as the leucine zipper. In combination with experimental results (NMR structures of the connecting loop peptides), this helix was a subject to a modeling of the whole beta subunit [4].

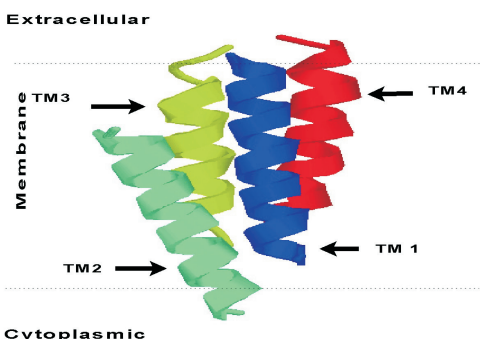


Fig. 1. The ribbon presentation of the lowest energy four helix bundle of the beta subunit of high affinity IgE receptor.

The correct TM helix arrangement could be predicted by docking methods. The exposed surfaces within bundle were available to interact with lipids of bilayer. These surfaces were in good agreement with possible lipid interaction sites as determined by molecular mechanics calculation of lipid favorable sites on transmembrane helices.

The helix–helix docking and the resultant four helix bundle of the beta subunit with our helix–lipid docking and our FTIR-CD-NMR studies of domain peptides should lead to an experimentally-based 3D structure of each subunit and eventually the whole four subunit receptor. The insights obtained could suggest a number of avenues for further study and form a framework for rational strategies for further site-directed mutagenesis, drug binding and second messenger events.

## References

1. von Heijne, G. *J. Mol. Biol.* **225**, 487–494 (1992).
2. Vakser, I.A. *Biopolymers* **39**, 455–464 (1996).
3. Zloh, M., Gibbons, W.A. *Biochem. Soc. Trans.* **24**, 305S (1996).
4. Zloh, M., Esposito, D., Gibbons, W.A. *Mol. Simul.* **24**, 421–447 (2000).

## **Helical Net Plots and Surface Lipophilicity Mapping of Transmembrane Helices of Integral Membrane Proteins: Aids to 3D Structure Determination of Integral Membrane Proteins**

**Mire Zloh<sup>1</sup>, Diego Esposito<sup>2</sup> and William A. Gibbons<sup>1</sup>**

<sup>1</sup>*University of London, School of Pharmacy, London WC1N 1AX, UK*

<sup>2</sup>*Department of Biochemistry and Molecular Biology, University College London,  
London WC1E 6BT, UK*

### **Introduction**

Many transmembrane (TM) proteins possess several alpha helices arranged in a helix bundle. In this case several questions important for any integral membrane protein should be answered, namely: 1) how the individual helix-helix interact between each other (*i.e.* which helix surface interacts with which surface of a second helix); 2) which helix residues interact with fatty amino acid chains of the phospholipids within the bilayer. To answer these questions generally for all integral membrane proteins including receptors, ion channels, and other transport proteins, would be important in its own right.

Here, molecular mechanics and dynamics calculations were used to determine the relative lipophilicity and lipid facing sides of the transmembrane helices. We illustrated a simple complementary *de novo* approach that a) correctly predicts the lowest energy surface formed from the interaction of lipid probes (dodecane) with seven transmembrane helices of BR and b) maps the relative lipophilicity of individual helices both across the membrane and rotational around the helix.

### **Results and Discussion**

The use of the dodecane as a probe of lipophilicity and lipid facing sides of the TM helices was shown. For simplicity the fully symmetric hydrophobic dodecane molecule was chosen as a ligand instead of a phospholipid, since it has no polar groups, and only van der Waals interaction would be encountered. The poly-alanine helix has uniformly distributed nonpolar CH<sub>3</sub> groups, shielding the polar groups of the backbone, and therefore the essentially same interaction energies were expected for all eight rotational positions. The comparison between highest and lowest energy positions was the most important feature of this experiment. The difference of interaction energies between the highest and lowest energy positions bigger than 3.6 kcal/mol were considered as significant. These data/conclusions encouraged the study of more complex helices and lipids, but particularly to apply this method to a known model system, where both the helix-helix and lipid-helix interfaces have been structurally defined by crystallography. Bacteriorhodopsin (BR) was chosen as the model system.

BR is a 7-helix membrane protein with known three dimensional structure. The outer surface of the bacteriorhodopsin is very lipophilic, the three lipid molecules have to be between two bundles in order for crystals to be formed [1]. The predicted lipid facing surfaces of three TM helices (TM 1, TM 2 and TM4) agreed with lipid interacting surface of TM helices in crystal structure. For the TM helices 3, 5, 6 and 7 the two comparative lipophilic surfaces were predicted one of which occurred in the crystal structure.

The helical net plot of TM helix 1 is presented in Figure 1. The most lipophilic surface (the lowest interaction energy complex with -17.5 kcal/mol interaction energy), as calculated, was between rotational positions 225 and 270° that corresponded to the

same surface on the BR which crystallography showed to be a lipid interaction surface. The solid line encloses the surface on TM helix 1 of BR that interacted with dodecane in the most stable complex. This surface agreed with the lipid interacting surface of TM helix 1 in crystal structure. The corollary indicates that this approach should give realistic results when applied to other TM helices of BR, but more interestingly to unknown receptor helix surfaces, receptors and integral membrane proteins (*e.g.* 7 helix high affinity IgE receptor).

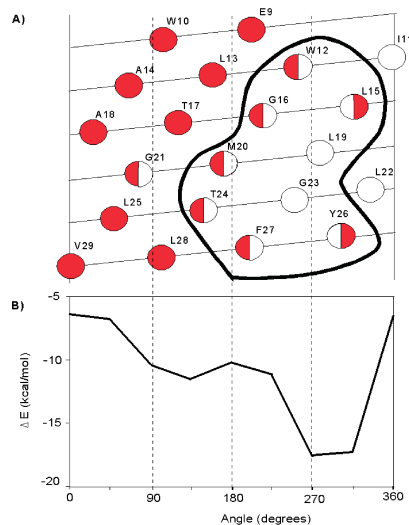


Fig. 1. The lipophilic surface mapping of the TM helix 1 of the Bacteriorhodopsin A) The helical net plot outlines the amino acid residues in contact with other TM helices (depicted as shaded circles), amino acid residues exposed to the lipid bilayer (depicted as empty circles), Solid lines encircle the residues in the contact with dodecane in the most stable complexes determined by calculation. B) The interaction energy between the TM helix 1 of the Bacteriorhodopsin and dodecane.

## References

1. Popot, J.-L., De Vitry, C., Atteia, A. *Membrane Protein Structure*. Oxford University Press, Oxford 1994, pp. 41–96.

## Studies on the Involvement of a His Residue of mt<sub>1</sub> GPCR TM Helix V in the Interaction with Melatonin

Andrea Calderan<sup>1</sup>, Paolo Ruzza<sup>1</sup>, Donata Favretto<sup>2</sup>, Barbara Biondi<sup>3</sup>,  
 Barbara Scolaro<sup>3</sup> and Gianfranco Borin<sup>1</sup>

<sup>1</sup>CNR Biopolymers Research Center, Padova, I-35131, Italy

<sup>2</sup>CNR-TCMET, Padova, I-35100, Italy

<sup>3</sup>Department of Organic Chemistry, University of Padova, Padova, I-35131, Italy

### Introduction

Melatonin (*N*-acetyl-5-methoxytryptamine, MLT) is a hormone produced mainly by the pineal gland in most vertebrate species, including humans. The physiological role of MLT is related to both chronobiology and modulation of the body's hormonal milieu. MLT appears to exert these effects through specific high affinity receptors. MLT has also been shown to have powerful antioxidant properties acting as an efficient free radicals scavenger.

Our attention is focused on the characterization of MLT interaction with its high affinity membrane-bound mt<sub>1</sub> receptor, which belongs to the G protein-coupled receptors (GPCRs) superfamily. A number of structure–affinity relationships were identified, and, recently, many authors proposed molecular models of the putative MLT binding site [1–4]. The molecular structure and function of the MLT mt<sub>1</sub> receptor has been investigated by site-directed mutagenesis, identifying the conserved His residue within transmembrane helix V as interacting with the 5-methoxy group of melatonin [5,6]. Using the nomenclature of Ballesteros and Weinstein, this residue is located at position 5.46, which corresponds to a position identified in the binding site of many other rhodopsin-like GPCRs.

In this work, we report circular dichroism, NMR, fluorescence spectroscopy, and mass spectrometry studies on synthetic analogs of transmembrane helix V, in an attempt to chemically characterize the involvement of His in the interaction of MLT with its receptor.

### Results and Discussion

**Peptide synthesis.** We synthesized the following peptides corresponding to the sequence 191–207 of murine mt<sub>1</sub> MLT receptor. The hydrophobic core of these peptides covers almost the entire sequence of mt<sub>1</sub> transmembrane segment V:

	191	198	203	207
TMV	H-T I A V V V F	His F I V P	Nle I I V I	I-OH
TMV-K	H-K K K T I A V V V F	His F I V P	Nle I I V I	K K K-OH
TMV-KA	H-K K K T I A V V V F	Ala F I V P	Nle I I V I	K K K-OH

Met residue in position 203 of the naturally occurring mt<sub>1</sub> sequence was replaced with Nle. In order to prevent solubility and aggregation problems encountered with the TMV sequence, we constructed TMV-K and TMV-KA by adding three Lys residues at N- and C-terminus, thus achieving solubility augment and aggregation decrease. Peptides were synthesized by solid phase method. Purified peptides were characterized by HPLC, amino acid analysis and MS.

**CD studies.** CD was used to examine the peptide conformations in water, organic solvents (MeOH, TFE, HFIP), and both zwitterionic (net neutral, DMPC) and anionic (DMPG) phospholipid vesicles. In aqueous solution, TMV-K and TMV-KA adopt a

random coil structure. In all organic solvents tested, TMV-K and TMV-KA spectra are suggestive of a typical  $\alpha$ -helical conformation. The spectra point out a greater propensity to form an  $\alpha$ -helical conformation for TMV-KA, compared to TMV-K. In the presence of phospholipid vesicles, TMV-K and TMV-KA spectra are, on the contrary, indicative of  $\beta$ -sheet structures. Peptides retain the  $\beta$ -sheet conformation when the concentration is reduced from 10 to 5  $\mu$ M. MLT addition does not affect CD spectra of both the peptides.

**NMR data.** The interaction of the TMV-K peptide with DMPC vesicles was preliminarily studied by NMR. The paramagnetic broadening effects on peptide resonances of the doxyl probe were studied by comparing one-dimensional  $^1\text{H}$ , as well as two-dimensional TOCSY spectra in the presence and in the absence of the paramagnetic agent. The results obtained using the shallow doxyl derivative do not point out any appreciable variation in peptide resonances. These findings suggest a parallel disposition of TMV-K peptide with respect to the surface of the lipid bilayer.

**Mass spectral analysis.** Electrospray ionization (ESI) is a gentle ionization method, not causing molecular fragmentation, and allowing weakly bound complexes to remain intact in the gas phase. The TMV-K ESI mass spectrum in the presence of MLT showed the peptide  $3^+$  ( $m/z$  888.7),  $4^+$  ( $m/z$  666.8) and  $5^+$  ( $m/z$  533.6) charged ions; moreover, the signals corresponding to the peptide-MLT complex  $4^+$  ( $m/z$  724.9) and  $5^+$  ( $m/z$  579.5) charged ions were observed. The TMV-KA ESI mass spectrum, on the other hand, does not exhibit, in the presence of MLT, signals attributable to the peptide-MLT complex. ESI-MS experiments indicate that only TMV-K interacts with MLT. To assess the specificity of the interaction between MLT and TMV-K we measured ESI mass spectra in the presence of L-tryptophan in place of MLT without detecting any Trp-peptide complex.

**Fluorescence measurements.** According to the capability of His to be an efficient quencher of the fluorescence of indole derivatives, MLT fluorescence quenching experiments were performed by adding increasing TMV-K amounts to a MLT solution in TFE. A decrease of MLT fluorescence intensity was detected. Moreover, the evidence of changes in the absorption spectrum of MLT in the presence of TMV-K suggests a static quenching mechanism. TMV-KA addition, on the other hand, does not affect MLT fluorescence or absorption spectra. Fluorescence experiments suggest that TMV-K His 198 closely interacts with MLT. Peptide quenching of MLT fluorescence was analyzed using the Stern–Volmer equation, which relates fluorescence quenching to the concentration of quencher.  $K_{S-V}$  was  $19.6 \cdot 10^3 \text{ M}^{-1}$ . In the case of static quenching the quenching constant  $K_{S-V}$  corresponds to the association constant of the fluorophore-quencher complex.

These data confirm the pivotal role played by His 198 residue of  $\text{mt}_1$  receptor in the interaction with MLT.

### Acknowledgments

This work was supported by MURST-CNR Biotechnology Program, L. 95/95.

### References

1. Sudgen, D., Chong, N.W.S., Lewis, D.F.V. *Br. J. Pharmacol.* **114**, 618–623 (1995).
2. Jansen, J.M., et al. *Bioorg. Med. Chem.* **4**, 1321–1332 (1996).
3. Navajas, C., et al. *Eur. J. Pharmacol.* **304**, 173–183 (1996).
4. Sicsic, S., et al. *J. Med. Chem.* **40**, 739–748 (1997).
5. Conway, S., et al. *Biochem. Biophys. Res. Commun.* **239**, 418–423 (1997).
6. Kokkola, T., et al. *Biochem. Biophys. Res. Commun.* **249**, 531–536 (1998).

## **Biosynthesis and Biophysical Studies of Domains of sTE2P, a Yeast G Protein-Coupled Receptor**

**Enrique Arevalo<sup>1,2</sup>, David Schreiber<sup>1</sup>, Jennifer Madeo<sup>1</sup>, Boris Arshava<sup>1</sup>,  
Jeffrey M. Becker<sup>3</sup>, Mark Dumont<sup>4</sup> and Fred Naider<sup>1</sup>**

<sup>1</sup>*Department of Chemistry, College of Staten Island of CUNY, Staten Island, NY 10314, USA*

<sup>2</sup>*Graduate School and University Center of CUNY, New York, NY 10016, USA*

<sup>3</sup>*Department of Biochemistry, Cellular and Molecular Biology, University of Tennessee,  
Knoxville, Tennessee 37996, USA*

<sup>4</sup>*Department of Biochemistry and Biophysics, University of Rochester School of Medicine and  
Dentistry, Rochester, NY 14642, USA*

### **Introduction**

The yeast G protein coupled-receptor (Ste2p) is essential for the mating of *MATa* cells with their counterpart *MATα* cells. Mutation of Proline 256 located in the 6th transmembrane domain of this receptor constitutively activates it in the absence of the  $\alpha$ -factor pheromone that is the normal agonist [1]. This phenotype indicates that the single amino acid change in residue 256 may change the overall structure of this membrane protein. Based on this conclusion, attempts are being made to determine the structure of the domain of Ste2p comprising the 5th and 6th transmembrane domains joined by the third intracellular loop (M5I3M6), and to correlate its molecular arrangement with the genetic results mentioned above. In order to produce this domain we inserted it into an expression plasmid that fused M5I3M6 to an N-terminal leader protein called TrpΔLE. The resulting fusion protein can be overexpressed in *E. coli*, isolated, and purified using affinity chromatography and/or HPLC. The link between the TrpΔLE and M5I3M6 occurs at a methionine residue, allowing cleavage of the fusion junction with CNBr. Therefore, naturally occurring methionines located in the 5th and the 6th transmembranes were mutated to leucines or alanines. After characterization of the biological activity and ligand binding affinities of these mutant receptors, it was decided to study the receptor containing the double mutation Met218Leu, Met250Ala, since it exhibited characteristics most similar to those of wild-type Ste2p.

### **Results and Discussion**

*Protein expression and isolation.* Expression of M5I3M6 fused to TrpΔLE in *E. coli* was detected by SDS-PAGE. The resulting protein was isolated from inclusion bodies following procedures published elsewhere [2]. The fusion protein was also identified using the INDIA His Probe (Pierce) that recognizes the histidine tag present at the N-terminus of the protein. Purification of M5I3M6 from the isolated inclusion bodies was initially carried out using a nickel affinity column followed by HPLC. It was observed, however, that increased yields resulted when the inclusion bodies were directly purified by HPLC using an acetonitrile:water gradient system at 60 °C on a C4 column. Table 1 shows the amounts of fusion protein recovered in each step subsequent to protein expression. Purified fusion protein (>90% homogeneous) was characterized by amino acid analysis and mass spectrometry. The results of the mass spectrometry agreed within 1 Da of the expected molecular weight (22,439 Da).

*Biophysical analysis.* The conformation of the fusion protein was studied using circular dichroism and temperature denaturation experiments. Contributions of the TrpΔLE sequence were subtracted based on comparisons with unfused TrpΔLE protein. The results of the analysis by circular dichroism indicate that the M5I3M6 region

assumes a highly helical secondary structure in solutions containing various ratios of trifluoroethanol (TFE) and water, and in the presence of 17.33 mM SDS micelles. No evidence for a specific interaction between the Trp $\Delta$ LE domain and the membrane domain was observed. In summary, successful expression and isolation of multi-milligram quantities of a transmembrane domain of a GPCR was achieved. Isolation and purification of the fusion protein required stringent control of pH, ionic strength and temperature in order to efficiently obtain amounts sufficient for biophysical studies. Circular dichroism studies in membrane mimetic environments (TFE/water or SDS micelles) indicate that M5I3M6 adopts a helical structure when fused to Trp $\Delta$ LE and that the two domains of the fusion protein act independently.

Table 1. Purification of Biosynthetic M5I3M6.

	Weight	Percent purity
Wet cells	16.093 g	—
Wet inclusion bodies	0.661 g	27%
1st HPLC purification	12.5 mg	84%
2nd HPLC purification	5 mg	96%

### Acknowledgments

This work was supported by grants GM 22086 and GM 22087 from the National Institute of Health. E. A. is supported by a fellowship from the CDNDD at CSI. We thank Nathan C. VerBerkmoes from the Oak Ridge National Laboratory for the mass spectra and Dr. Hsin Wang from CSI NMR support.

### References

1. Konopka, J.B., Mariana, Margarit S., Dube, P. *Proc. Natl. Acad. Sci. U.S.A.* **93**, 6764–6769 (1996).
2. Staley, J.P., Kim, P.S. *Protein Sci.* **3**, 1822–1832 (1994).

## **Transmembrane Segment Mimic Peptides Containing Peptoid Residues**

**Yan-Chun Tang, Mitsuko Maeda and Charles M. Deber**

*Structural Biology and Biochemistry, Research Institute, Hospital for Sick Children,  
Toronto M5G 1X8; and Department of Biochemistry, University of Toronto,  
Toronto M5S 1A8, Ontario, Canada*

### **Introduction**

Transmembrane segment mimics – with prototypic sequence KKAAAXAAAAAXA-AWAAXAAAKKKK-amide (where X = any of the 20 commonly occurring amino acids) are under investigation in our laboratory [1]. Structural studies of the model peptides have shown the existence of a “threshold hydrophobicity” which dictate spontaneous peptide insertion into micellar membranes. However, the 2-4 Lys residues at the N- and C-termini used for enhancing the water solubility of peptides limit the direct transfer of peptides from aqueous buffer to a transmembrane orientation in phospholipid bilayers. To circumvent this situation, we sought alternative flanking residues to the charged Lys residues which (1) could maintain the water solubility of the peptide for purification and characterization, and (2) would contain sufficient hydrophobic substituents for compatibility with a membrane interior. Peptoid residues – which are composed of N-substituted glycine units – could be a suitable choice. Peptoids have been studied in variety of applications [2,3], but their behavior in membrane environments has not been systematically investigated. Consideration of the structure of peptoid residues suggests that the N-alkyl substituent would increase the basicity of the nitrogen of the peptoid (*vs* typical amino acids), which in turn, may lead to superior solubility in water than that of the corresponding peptides. Hence, Sar – the structurally simplest peptoid – was chosen initially as a model peptoid monomer to study the hydrophobicity of peptides containing peptoid residues.

### **Results and Discussion**

In the present work, we retained the prototypic peptide core helix, but replaced X with Sar in the three indicated positions (KKAAASarAAAAASarAAWAASarAAAKKKK) (**I**). Peptide synthesis was carried out with solid phase methodology using Fmoc chemistry. Crude peptide was purified by reverse-phase HPLC. To examine the overall hydrophobic character of this prototypic peptide (**I**), we considered its retention time in reverse-phase HPLC *vs* various Lys-containing prototypes, as a measurement of the relative hydrophobicity of the Sar residues. In such experiments using peptides where X = each of the 20 natural amino acid residues, the X = Lys peptide displays the lowest hydrophobicity among the 20 commonly-occurring amino acids, as evidenced by the shortest retention time [1]. However, in comparison with the X = Sar peptide (Figure 1), the retention time of the Sar peptide is significantly shorter than the Lys peptide; the X = Ala position is shown for comparison. From these results, one can infer that Sar behaves as a relatively hydrophilic residue. Accordingly, in a subsequent synthesis, we used X = Ala, but altered the flanking residue sequence such that Lys residues in N- and C-terminal positions were incrementally replaced by Sar. Two peptide sequences (KSarAAAAAAAAAAAAWAAAAASarSarSarK-amide) (**II**) and (SarSarAAAAAAAAAAAAWAAAAASarSarSarK-amide) (**III**) were obtained through synthesis and purification in the usual manner. We found that replacement of up to 4–5 of the original 6 flanking Lys residues with Sar retains peptide aqueous sol-

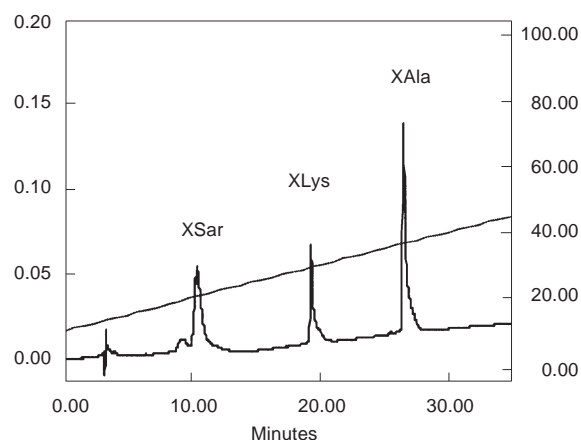


Fig. 1. Analytical HPLC chromatogram of peptides of sequence *KKAAAXAAAAAXAAWAXAAAKKKK*-amide, where *X* = *Sar* (I), *X* = *Lys*, and *X* = *Ala*.

ubility, while also preserving the helical structure and threshold hydrophobicity of the original peptide core within micellar membranes. Thus, as measured by circular dichroism spectroscopy, peptides **II** and **III** readily adopted  $\alpha$ -helical structures in the membrane-mimetic environment of sodium dodecylsulfate (SDS) micelles, while a blue shift in Trp fluorescence emission spectra confirmed membrane insertion (data not shown).

These preliminary results suggest that replacement of Lys with uncharged peptoid residues such as Sar may be a worthwhile approach for the study of the transfer of peptoid-containing sequences into membrane environments.

#### Acknowledgments

Supported by the Natural Sciences and Engineering Research Council of Canada.

#### References

1. Liu, L.-P., Deber, C.M. *Biopolymers (Peptide Sci.)* **41**, 47 (1998).
2. Tokita, K., Hocart, S.J., Katsuno, T., Mantey, S.A., Jensen, R.T. *J. Biol. Chem.* **276**, 495 (2001).
3. Kirshenbaum, K., Barron, A.E., Goldsmith, R.A., Armand, P., Bradley, E.K., Truong, K.T.V., Dill, K.A., Cohen, F.E., Zuckermann R.N. *Proc. Natl. Acad. Sci. U.S.A.* **95**, 4303 (1998).

## Computational Chemistry and Opioidmimetics: Receptor–Ligand Interactions of Dmt-Tic Peptides

Sharon D. Bryant<sup>1</sup>, Severo Salvadori<sup>2</sup>, Remo Guerrini<sup>2</sup>,  
Gianfranco Balboni<sup>2</sup>, Yoshio Okada<sup>3</sup>, Yoshio Fujita<sup>3</sup>  
and Lawrence H. Lazarus<sup>1</sup>

<sup>1</sup>Peptide Neurochemistry, LCBRA, NIEHS, Research Triangle Park, NC 27707, USA

<sup>2</sup>Department of Pharmaceutical Science and Biotechnology Center,  
University of Ferrara, I-44100 Ferrara, Italy

<sup>3</sup>Department of Pharmaceutical Sciences, Kobe-Gakuin University, Kobe 651-2180, Japan

### Introduction

Three-dimensional structures of opioid receptors ( $\delta$ ,  $\mu$ ,  $\kappa$ ) based on data from X-ray crystallography or NMR spectroscopy has been limited due to the lipophilic properties of G-protein coupled receptors (GPCRs). Information related to opioid receptors has been derived from receptor cloning, mutagenesis studies and the design and biological testing of receptor-selective ligands. Following the molecular cloning of the opioid receptors, several theoretical models were reported using bacteriorhodopsin as a template [1]. Although bacteriorhodopsin is a transmembrane protein, its use as a template structure for modeling GPCRs was tentative because it does not couple G-proteins, does not share primary sequence homology with GPCRs, and it may have different helical arrangements [2]. Recently, a crystal structure of bovine rhodopsin, a seven transmembrane GPCR, was reported [3]. Coordinates from this structure were used to develop a model of the  $\delta$ -opioid receptor and to propose receptor interaction mechanisms for opioid peptides containing 2',6'-dimethyltyrosine (Dmt). X-Ray structures of the  $\delta$ -receptor antagonist, *N,N*-(Me)<sub>2</sub>-Dmt-Tic-OH [4], the  $\mu$ -agonist H-Dmt-Tic-NH-1-adamantane [5] and the  $\mu$ -agonist/ $\delta$ -antagonist, *N,N*-(Me)<sub>2</sub>-Dmt-Tic-NH-1-adamantane [5] and the NMR derived structure for the  $\mu$ -agonist endomorphin derivative, H-Dmt-Pro-Phe-NH-6-quinoline [6] were used for evaluating receptor ligand interactions.

### Results and Discussion

The  $\delta$ -selective antagonist, *N,N*-(Me)<sub>2</sub>-Dmt-Tic-OH fits comfortably in a cavity defined by H278 (HVI), Y129 (HIII), and R192 (EL2) (Figure 1). The  $\mu$ -agonist, H-Dmt-Tic-NH-1-adamantane could form similar interactions; however, there were unfavorable contacts with M199, L200 and the backbone of Dmt-Tic as well as with C198 and the adamantane group. An alternative orientation allowed an interaction between T211, instead of H278, and the hydroxyl of Dmt that eliminated the unfavorable contacts between C198 and adamantane. The hydroxyl of Dmt of *N,N*-(Me)<sub>2</sub>-Dmt-Tic-NH-1-adamantane interacted with H278 and the N-terminal amine formed a hydrogen bond with Y129. The interaction with R192 was lost. In addition, unfavorable contacts between C $\beta$  of DMT and L200 (E2), M199 (E2) and I304(HVII) and adamantane were observed. Alternative orientations facilitating interactions between T211 and Dmt eliminated bumps with M199 and I304; albeit clashes with L200 and Q201 remained. H-Dmt-Pro-Phe-NH-6-quinoline formed interactions similar to the other adamantane compounds with unfavorable contacts with M199, L200, Q201. Although *N,N*-(Me)<sub>2</sub>-Dmt-Tic-OH and H-Dmt-Tic-NH-1-adamantane superimposed with a small rms deviation (0.43 Å), the latter molecule did not fit the binding cavity defined in Figure 1. Unfavorable contacts were made between the

**Bryant et al.**

adamantane ring and receptor residues. This indicated different optimal binding interactions for  $\delta$ - and  $\mu$ -opioid ligands even though minimal differences were noted between  $\mu$ -agonist and  $\delta$ -antagonist peptides.

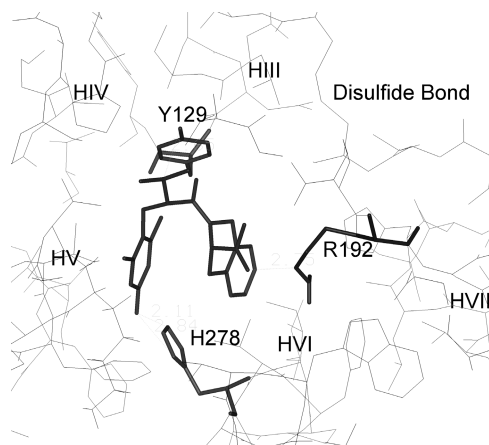


Fig. 1. Binding cavity of the  $\delta$ -opioid receptor based on the X-ray structure of bovine rhodopsin. An X-ray structure of  $N,N$ -(Me)<sub>2</sub>-Dmt-Tic-OH is shown in bold interacting with receptor residues H278 from helix VI, R192 from extracellular loop 2, Tyr129 from helix III. Hydrogen atoms are not shown.

## References

1. Grigorieff, N., Ceska, K.H., Downing, J.M., Baldwin, J.M., Henderson, R. *J. Mol. Biol.* **259**, 393–421 (1996).
2. Hoflack, J., Trumpp-Kallmeyer, S., Hibert, M. *TIPS* **15**, 7–9 (1994).
3. Palczewski, K., Kumasaka, T., Hori, T., Behnke, C.A., Motoshima, H., Fox, B.A., Le Trong, I., Teller, D.C., Okada, T., Stenkamp, R.E., Yamamoto, M., Miyano, M. *Science* **289**, 739–745 (2000).
4. Salvardi, S., Balboni, G., Guerrini, R., Tomatis, R., Bianchi, C., Bryant, S.D., Cooper, P.S., Lazarus, L.H. *J. Med. Chem.* **40**, 3100–3108 (1997).
5. Salvardi, S., Guerrini, R., Balboni, G., Bianchi, C., Bryant, S.D., Cooper, P.S., Lazarus, L.H. *J. Med. Chem.* **42**, 5010–5019 (1999).
6. Okada, Y., Fukumizu, A., Takahashi, M., Shimizu, Y., Tsuda, Y., Bryant, S.D., Lazarus, L.H. *Biochem. Biophys. Res. Commun.* **276**, 7–11 (2000).

## **Conformational Model of Signal Transduction in the Transmembrane Region of the AT-1 Receptor**

**Gregory V. Nikiforovich and Garland R. Marshall**

*Department of Biochemistry and Molecular Biophysics, Washington University, St. Louis,  
MO 63110, USA*

### **Introduction**

A plausible molecular model of signal transduction in G-protein coupled receptors suggests transfer of conformational perturbations across the membrane by interactions between residues in the transmembrane (TM) region of the receptor. Nineteen residues in the TM region of the AT-1 receptor have been found to be involved in signal transduction, namely F77, L78, S107, F110, N111, L112, S115, L118, L143, P162, I193, L195, T198, I245, W253, V254, H256, Y292 and N294. However, these residues do not form a 3D pathway of contacts connecting the extracellular and intracellular parts of the AT-1 receptor. This study presents results of 3D modeling for the TM helical bundles of the AT-1 receptor and its mutants that allow identification of additional residues involved in signal transduction in AT-1 receptors.

### **Results and Discussion**

TM helical fragments have been located in the sequence of the rat AT-1 receptor by the procedure described elsewhere [1]. They have been assembled in a TM helical bundle following a procedure that consists of (i) determining conformations of individual helices by independent energy minimization involving all dihedral angles; (ii) superimposing the obtained conformations over the X-ray structure of rhodopsin [2] according to sequence homology found by CLUSTALW and, (iii) packing helices by finding the energetically best arrangement of the individual helices, in which dihedral angles of the backbone are “frozen” in the values obtained earlier. Accordingly, the variables for the packing procedure are the dihedral angles of the side chains for all helices, which are optimized by the algorithm developed earlier [3], as well as the  $6 \times 7 = 42$  additional “global” parameters describing movements of each helix as a rigid body. The “global” starting point for assembling the TM bundle for AT-1 and for all mutants has been that of the X-ray structure of rhodopsin. The ECEPP force field [4,5] was used; the electrostatic term was omitted to avoid artifacts in helix packing.

3D modeling of TM helical bundles was performed for AT-1 receptor mutants containing mutations that influence constitutive activity (CA, mutants N111G [6], F77Y-W253R, V29A-L112H-L143P and M142T-I245T-H256F [7]), signal transduction (ST, mutants L78F-L191P-L212H-F293L, S107F and F77S [7]), binding of external ligand (B, mutants K199A [8] and T88H [9]), or indifferent mutations (I, mutant I38A [7]). Calculations revealed that some residues show persistent significant conformational transitions of the side chains ( $\Delta\chi_1 \geq 60^\circ$ ) in mutants of the CA and ST, but not B or I types (relative to the AT-1 receptor itself), namely Y35, L119, F249, S252, I288, N295 and N298. Therefore, these residues may be involved in the process of cooperative conformational perturbations associated with signal transduction through the TM region of AT-1. Their participation ensures a wide network of possible 3D pathways to transfer conformational perturbations through TM part of AT-1 receptors, the shortest one being Y35-Y292-F77-N295-N298-I245 (see Figure 1).

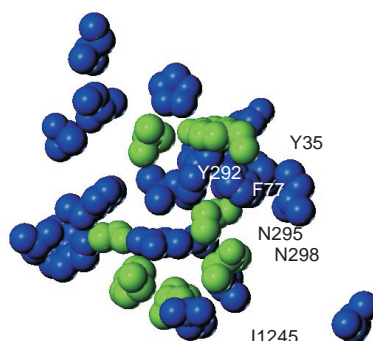


Fig. 1. 3D view of TM helical bundle of the AT-1 receptor showing side chains of the residues involved in signal transduction according to the data of site directed mutagenesis (in dark) and those additionally elucidated in this study (in light). Some residues are labeled.

## References

1. Nikiforovich, G.V. *Protein Eng.* **11**, 279–283 (1998).
2. Palczewski, K., Takashi, K., Tetsuya, H., Behnke, C., Motoshima, H., Fox, B., Le Trong, I., Teller, D., Okada, T., Stenkamp, R., Yamamoto, M., Miyano, M. *Science* **289**, 739–745 (2000).
3. Nikiforovich, G.V., Hruby, V.J., Prakash, O., Gehrig, C.A. *Biopolymers* **31**, 941–955 (1991).
4. Nemethy, G., Pottle, M.S., Scheraga, H.A. *J. Phys. Chem.* **87**, 1883–1887 (1983).
5. Dunfield, L.G., Burgess, A.W., Scheraga, H.A. *J. Phys. Chem.* **82**, 2609–2616 (1978).
6. Groblewski, T., Maigret, B., Languier, R., Lombard, C., Bonnafous, J.-C., Marie, J. *J. Biol. Chem.* **272**, 1822–1826 (1997).
7. Parnot, C., Bardin, S., Miserey-Lenkei, S., Guedin, D., Corvol, P., Clauser, E. *Proc. Natl. Acad. Sci. USA* **97**, 7615–7620 (2000).
8. Noda, K., Feng, Y.H., Liu, X.P., Saad, Y., Husain, A., Karnik, S.S. *Biochemistry* **35**, 16435–16442 (1996).
9. Han, H., Shimuta, S.I., Kanashiro, C.A., Oliveira, L., Han, S.W., Paiva, A.C.M. *Mol. Endocrinol.* **12**, 810–814 (1998).

## Role of the Water Medium in the Process of Signal Transmission from Peptides to Cellular Receptors

Evgeny I. Grigoriev<sup>1</sup>, Vladimir Kh. Khavinson<sup>2</sup>, Igor N. Kochnev<sup>3</sup>  
and Alexey E. Grigoriev<sup>4</sup>

<sup>1,2</sup>Laboratory of Peptide Chemistry, St. Petersburg Institute of Bioregulation and Gerontology,  
197110 St. Petersburg, Russia

<sup>3,4</sup>Chair of Molecular Biophysics, Physical Faculty, St. Petersburg State University, 198903,  
Petrodvorets, St. Petersburg, Russia

### Introduction

In this work we investigated the possible role of water medium in the pharmacological action of some biologically active dipeptides. Probably, there exists a mechanism (in some cases, basic) of signal transfer via water medium [1,2].

### Results and Discussion

We employed a number of bioactive peptides synthesized at the St. Petersburg Institute of Bioregulation and Gerontology and applied as pharmaceuticals: Vilon (H-Lys-Glu-OH) [3], Thymogen (H-Glu-Trp-OH), as well as model dipeptides (H-Glu-Lys-OH, H-Lys-Trp-OH, H-Lys-Asp-OH) and free amino acids. Immunomodulatory effect of the peptides on the expression of trypsin-treated T-lymphocyte E-receptors was studied *in vitro* in suspensions of cells isolated from the thymus of guinea pigs. Investigation of the peptide action on the subpopulations of T-lymphocytes from human peripheral blood revealed the peptide ability to stimulate the expression of cellular CD4<sup>+</sup> and CD8<sup>+</sup> receptors. In some cases, similarly directed and equally intensive biological effects were revealed for peptides of essentially different primary structures and conformations (MM2, PC Model). We studied temperature dependencies (2–30 °C, step 2.5 °C) of the water absorption band position at 180 cm<sup>-1</sup> in the spectrum of peptide solutions. Individual non-monotonous band shifts were defined for both water and the solutions of some bioactive peptides. According to [4], these non-monotonies are associated with the possibility of spreading waves existing as SOLITONS [5,6], which can interact with permeate molecules and show resonant properties [7] and can be viewed as most probable messengers. A chemical substance in the water system can change parameters of solitons (“modulate” them). When such

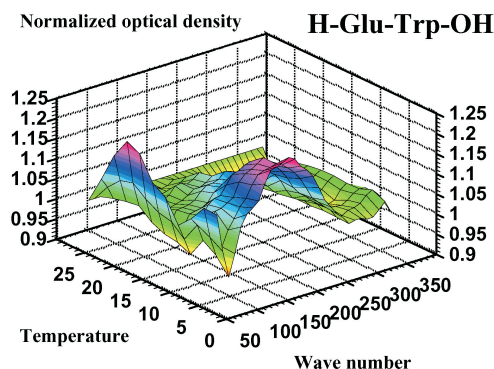


Fig. 1. The temperature dependency of the optical density for peptide solutions and water.

SIGNAL reaches the molecules of a receptor, its resonant reception occurs, *i.e.* the molecule of a concrete ligand receptor should be pre-tuned to the reception of certain oscillatory signals. The stage of this signal reception initiates further processes for the executive systems to manifest a biological effect. Observing temperature change in the spectrum of water and some solutions in the translational band ( $180\text{ cm}^{-1}$ ), we found out that feebly expressed shoulder in the low-frequency part of band at some temperatures. At particular frequencies the temperature dependency of the optical density had the explicitly expressed wavy or stage character, while at other frequencies the smoothly varying dependence was observed. In the explored temperature interval usually 2–3 waves with maximums, standing from each other on 8–12 of degrees, are observed. 2D diagrams are constructed by Origin 6.0 program. 3D diagrams are constructed by Harvard ChartXL 2.0 program.

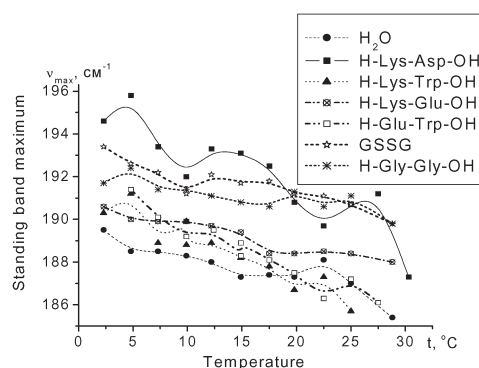


Fig. 2. 3D diagram for H-Glu-Trp-OH solution.

Comparison of biological effects of the synthetic dipeptides with their primary structures, conformations and influence on the temperature dependency of spectral characteristics for water absorption band at  $180\text{ cm}^{-1}$  prompt a hypothesis that approximately identical biological effects of substances of different structures and conformations can be stipulated by their similar influence on the vibration dynamics of the water medium. Probably, the transfer of a signal from a ligand molecule to a receptor occurs in the water medium via modulated solitons distantly, without formation of a ligand-receptor complex.

## References

1. Grigoriev, E.I., Kochnev, I.N., Grigoriev, A.E., Khavinson, V.Kh., Kudriavseva, T.A. Abstracts of 26-th European Peptide Symposium. *Journal of Peptide Science*, Suppl. to Vol. 6, 139 (2000).
2. Grigoriev, E.I., Kochnev, I.N., Grigoriev, A.E., Khavinson, V.Kh., Malinin, V.V. Abstracts of II International Congress "Weak and Hyperweak Fields and Radiations in Biology and Medicine". St.Petersburg 3.–7.07, 116 (2000).
3. Khavinson, V.Kh., Morozov, V.G., Malinin, V.V., Sery, S.V. Patent of the Russian Federation No. 2139085 (1999).
4. Kochnev, I.N., Khaloimov, A.I., Grigoriev, E.I., Shurupova, L.V., Grigoriev, A.E., Khavinson, V.Kh. *Biophysics*, approved for publishing.
5. Kochnev, I.N. *Biophysics* **44**, 1098–1106 (1999).
6. Kochnev, I.N. *Phys. Rev. B*, in press.
7. Bullough, R.K., Caudrey, P.J. "Solitons". Springer-Verlag Berlin Heidelberg. NY. 1980.

## **Structure-Based Design, Synthesis, and Surface Plasmon Resonance (SPR) Detection of Antagonists of the Grb2 SH2 Domain**

**Feng-Di T. Lung<sup>1</sup>, Jia-Yin Tsai<sup>1</sup>, Shu-Yie Wei<sup>2</sup>, Peter P. Roller<sup>3</sup>  
and Jya-Wei Cheng<sup>2</sup>**

<sup>1</sup>*Department of Nutrition, China Medical College, Taichung 404, Taiwan, R.O.C.*

<sup>2</sup>*Department of Life Science, National Tsing Hua University, Hsinchu 300, Taiwan, R.O.C.*

<sup>3</sup>*Laboratory of Medicinal Chemistry, NCI, NIH, Bethesda, MD 20892, USA*

### **Introduction**

One of the critical intracellular signal transduction pathway involves the binding of Grb2 SH2 domain to the phosphotyrosine (pTyr) motifs on growth factors such as EGFR and erbB2, leading to downstream activation of the oncogenic Ras signaling pathway. Therefore, the Grb2 SH2 domain has been chosen as our target for development of potential anti-cancer agents. Previously, we reported a series of potent peptides and the detection of their inhibitory effects on the Grb2-SH2 domain. We report here our recent experimental design for detecting the interaction between Grb2-SH2 domain and its ligands using surface plasmon resonance (SPR) technology. Binding interactions between peptides and the Grb2-SH2 domain were measured and analyzed using BIACORE X instrument, which provide detailed information of the real-time detection of the binding interaction. We also established an SPR-based assay to determine the inhibitory effects of a series of designed peptide analogs, and discovered some potent antagonists of the Grb2 SH2 domain. Results of this study should provide important information for further development of peptide or peptidomimetics with high affinity for the Grb2 SH2 domain.

### **Results and Discussion**

Peptide-amide was synthesized manually on RAL resin (5-(4-Fmoc-aminomethyl-3,5-dimethoxyphenoxy)valeric acid-MBHA resin) by standard solid phase peptide synthesis using Fmoc/t-Bu chemistry. Synthesized peptides were purified, characterized, and assayed for their binding affinity for the Grb2 SH2 domain. The binding interaction between different concentrations of GST-Grb2 SH2 domain and the immobilized-Shc(pY) were measured by the optical phenomenon detected by surface plasmon resonance and displayed as a sensorgram, using BIACORE X instrument. Equilibrium binding RU was determined when the last portion of GST-Grb2 SH2 flowed across the chip. The inhibitory effect of each peptide was determined by mixing each peptide with GST-Grb2 SH2 domain and then measuring the response of the remaining amount of GST-Grb2 SH2 binding to the immobilized Shc(pY).

Another approach is to detect the binding interaction between the synthetic peptide to the Grb2 SH2 domain which was immobilized on the surface of CM5 sensor chip using amine-coupling procedures, indicated by an increased RU of 245. A series of different concentrations of peptide analogs were introduced onto the immobilized sensor chip to determine their binding affinity for the Grb2 SH2 domain.

The binding potency determined for each peptide by these two different experimental design was summarized in Table 1. Our results demonstrated the successful application of SPR technology to detect the binding interactions between Grb2 SH2 domain and its binding partners, and to assess the inhibitory effects of designed peptides on

**Lung et al.**

these interactions. Among the synthetic peptides **1–3**, peptide **1** exhibited the strongest inhibitory activity. Results of our current study should provide important information for future development of potent Grb2 SH2 domain inhibitors.

*Table 1. The binding potency of peptides 1–3 determined by SPR technology.*

	Peptide	IC <sub>50</sub> (μM) <sup>a</sup>	K <sub>D</sub> (M) <sup>b</sup>
	Shc(pY)	1.5	4.54e-9
<b>1</b>	Fmoc-E-Y-Aib-N	8.7	6.34e-9
<b>2</b>	Fmoc-DE-Y-Aib-N	12.5	8.48e-5
<b>3</b>	Fmoc-DAAD-Y-Aib-N	13	5.47e-3

<sup>a</sup> IC<sub>50</sub> was calculated using the plot of sample calibration curve. <sup>b</sup> K<sub>D</sub> was calculated using the BIAevaluation software.

**Acknowledgments**

Supported by the grants from the National Science Council (NSC 89-2320-B-039-048-M57) and China Medical College (CMC 89-NT-04) in Taiwan, R.O.C.

**References**

1. Lou, Y.C., Lung, F.D., Pai, M.T., Tzeng, S.R., Wei, S.Y., Roller, P.P., Cheng, J.W. *Arch. Biochem. Biophys.* **372**, 309–314 (1999).
2. Long, Y.Q., Yao, Z.J., Voigt, J.H., Lung, F.D., Luo, J.H., Burke, T.R., King, C.R., Yang, D.J., Roller, P.P. *Biochem. Biophys. Res. Commun.* **264**, 902–908 (1999).
3. Lung, F.D., King, C.R., Roller, P.P. *Lett. Peptide Sci.* **6**, 45–49 (1999).

## Global Conformational Constraint in the Design of a Grb2 SH2 Domain Inhibitor

Yang Gao<sup>1</sup>, Chang-Qing Wei<sup>1</sup>, Johannes Voigt<sup>1</sup>, Jane Wu<sup>2</sup>, Dajun Yang<sup>2</sup>  
 and Terrence R. Burke, Jr.<sup>1</sup>

<sup>1</sup>Laboratory of Medicinal Chemistry, NCI, NIH, NCI at Frederick, Frederick, MD 21702, USA

<sup>2</sup>Lombardi Cancer Center, Georgetown University, Washington D.C. 20007, USA

### Introduction

Blockade of Grb2 SH2 domain binding involved in oncogenic signal transduction, may represent a new approach toward anticancer chemotherapeutics. For “pY-X-N” containing ligands, binding to Grb2 SH2 domains occurs in type-1  $\beta$ -turn conformations (**1**, Figure 1) [1]. Among numerous approaches toward the preparation of  $\beta$ -turn mimics, olefin metathesis has proven to be useful. However, one traditional limitation of this latter methodology, has been the replacement of naturally occurring side chains at the site of ring juncture, with alkene species needed for ring closure. This results in macrocycles (**2**), which lack potentially critical functionality originally afforded by these side chains in parent **1**. Modification of this approach, such that side chain functionality is incorporated onto the ring-closing segment (**3**), could potentially allow macrocyclization without this type of functionality loss. Reported herein is the application of this protocol to the preparation of a novel macrocycle-based Grb2 SH2 domain inhibitor (**4**), wherein ring closure is achieved with maintenance of functionality at the sites of ring juncture.

### Results and Discussion

In order to approximate in macrocycle **4**, the Grb2 SH2 domain-binding  $\beta$ -bend conformation of parent open chain ligand, it was necessary to select the appropriate length and absolute configurations of points of attachment, of the ring-closing segment. Molecular modelling studies indicated the necessity of (*S,R*) configurations at the naphthyl-propyl and pTyr mimic ring junctions respectively, with a three carbon chain length appearing to suitably orient the naphthyl ring over a hydrophobic binding patch on the Grb2 protein (Figure 2).

Based on a retrosynthetic analysis leading to **4**, *tert*-butyl phosphonate-containing tripeptide **7** was selected as the penultimate precursor to metathesis ring closure (Figure 3). The synthesis of **7**, in turn required the synthesis of C- and N-terminal building blocks **5** and **6** respectively, since the remaining residues were both commercially available in their N-Fmoc forms. As reported in our recent paper, preparation of **5** and

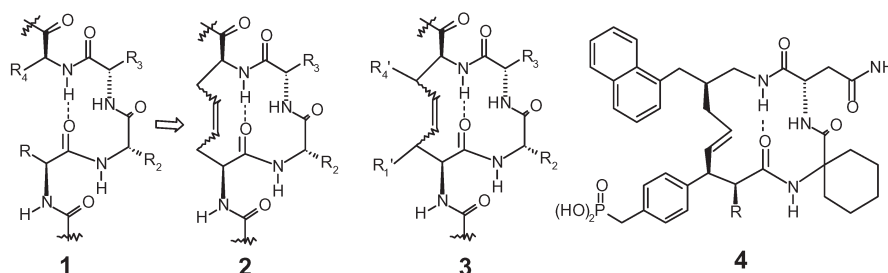


Fig. 1. Olefin metathesis in the design of Grb2 SH2 domain ligand **4**.



Fig. 2. Molecular modelling simulations of Grb2 SH2 domain-bound macrocyclic variants of *N*<sup>α</sup>-acetyl-containing **4** showing effects of varying the ring-closing segment.

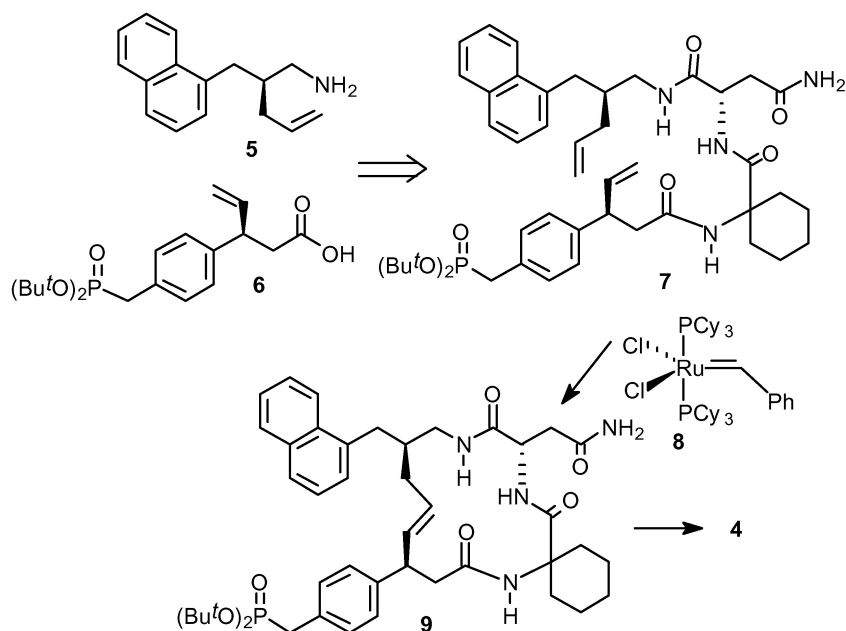


Fig. 3. Synthetic approach toward macrocycle **4**.

**6** was achieved enantioselectively under chiral induction derived from commercially available Evans oxazolidinone auxiliaries [2]. Subjecting **7** to olefin metathesis in the presence of widely used Ruthenium-containing catalyst **8**, provided ring-closed product **9**, which following TFA-mediated cleavage of *tert*-butyl phosphonate protection, gave pure final product **4** in 60% HPLC-purified yield.

In cell-free ELISA-based binding assays, macrocycle **4** exhibited a binding affinity ( $IC_{50} = 20$  nM), which was approximately 100-fold more potent than open-chain reference compound **11** ( $IC_{50} = 2$   $\mu$ M, Figure 4). Surprisingly however, macrocycle **4** exhibited significantly reduced intracellular efficacy than would be expected base on such extracellular binding affinity.

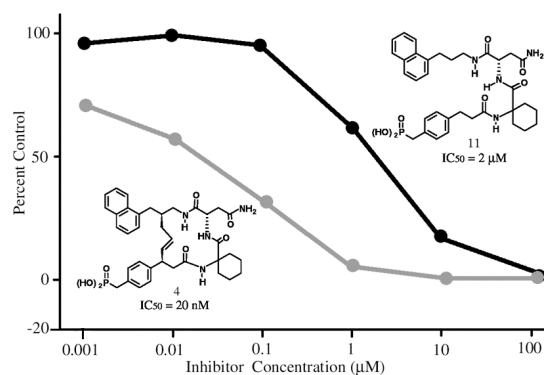


Fig. 4. ELISA Grb2 SH2 domain binding assay of indicated compounds.

## References

1. Rahuel, J., Gay, B., Erdmann, D., Strauss, A., Garcia-Echeverria, C., Furet, P., Caravatti, G., Fretz, H., Schoepfer, J., Grutter, M.G. *Nat. Struct. Biol.* **3**, 586–589 (1996).
2. Gao, Y., Wei, C.-Q., Burke, T.R., Jr. *Org. Lett.* **3**, 1617–1620 (2001).

## Local Conformational Constraint in the Design of a Grb2 SH2 Domain Inhibitor

Ding-Guo Liu<sup>1</sup>, Yang Gao<sup>1</sup>, Johannes Voigt<sup>1</sup>, Jane Wu<sup>2</sup>, Dajun Yang<sup>2</sup>  
and Terrence R. Burke, Jr.<sup>1</sup>

<sup>1</sup>Laboratory of Medicinal Chemistry, NCI, NIH, NCI at Frederick, Frederick, MD 21702, USA

<sup>2</sup>Lombardi Cancer Center, Georgetown University, Washington, DC 20007, USA

### Introduction

Conformational constraint of amino acid side chains can be a powerful means of enhancing biological activity. For SH2 domains, where binding of peptide ligand is critically dependent on the interaction of phosphotyrosyl (pTyr) residues within pTyr-binding pockets, the potential value of conformationally constrained pTyr mimics has not received significant attention [1,2]. Reported is the design and stereoselective synthesis of pipecolic acid analogue **1** (Figure 1), as an orthogonally protected conformationally constrained version of known high affinity pTyr mimic, phosphonomethyl phenylalanine (Pmp). Included, is the utilization of **1** for the preparation of Grb2 SH2 domain-directed ligand **3**, as a variant of known high affinity inhibitor **2** [3], which bears "local constraint" within the pTyr-mimicking residue.

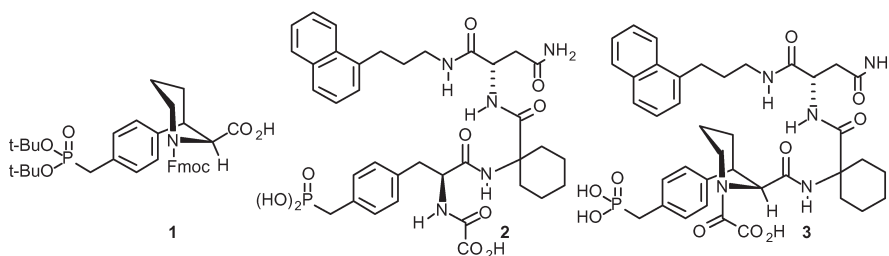


Fig. 1. Structures of constrained pTyr mimic **1**, parent Grb2 SH2 domain inhibitor **2** and conformationally constrained Grb2 SH2 domain inhibitor **3**.

### Results and Discussion

Our synthetic approach toward constrained pTyr mimetic **1** achieved stereochemical control at the 3- and 2-positions using chiral induction provided by commercially available Evans' auxiliary (Figure 2). Heck reaction of phenyl bromide **4** with chiral acrylamide **5** provided intermediate **6** which was subjected to 1,4-addition of allyl-magnesium bromide in the presence of copper bromide-dimethylsulfide complex, to provide **7**. Hydroboration, followed by sodium perborate oxidation, afforded **8**, which was converted in several steps, to provide aldehyde **9**. Without purification, compound **9** was directly hydrogenated in methanol, to afford piperidino **10**, which was converted to Fmoc-protected constrained pTyr mimic **1**. This was incorporated onto known high affinity Grb2 SH2 domain directed platform **2** to provide tripeptide **3**.

In cell-free ELISA-based Grb2 SH2 domain binding assays, constrained tripeptide **3** exhibited approximately 200-fold lower affinity ( $IC_{50} = 5.5 \mu M$ ) than parent unconstrained **2** ( $IC_{50} = 0.025 \mu M$ ). Studies are ongoing to examine whether loss of affinity may be attributed to unfavorable steric *versus* conformational considerations.

## Peptide Conjugates

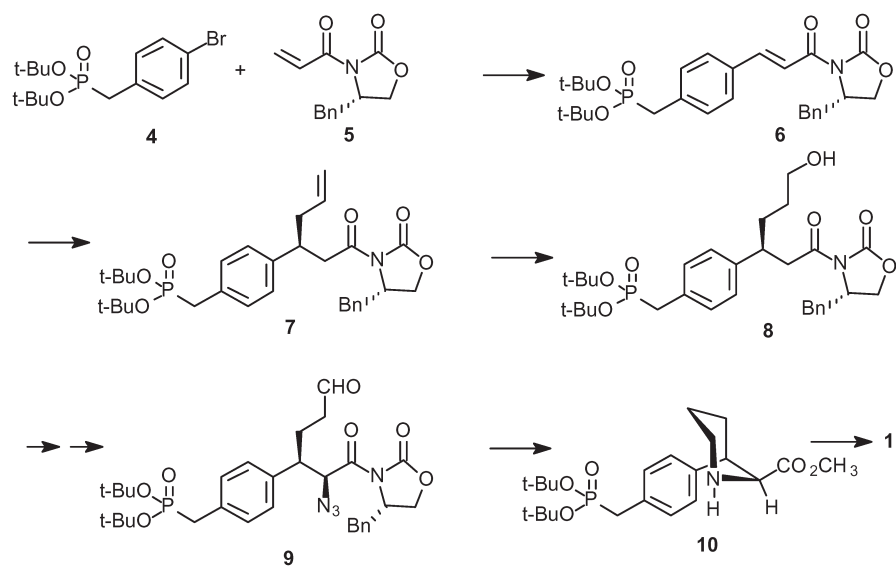


Fig. 2. Synthetic approach toward constrained pTyr mimic 1.

## References

1. Burke, T.R., Jr., Barchi, J.J., Jr., George, C., Wolf, G., Shoelson, S.E., Yan, X. *J. Med. Chem.* **38**, 1386–1396 (1995).
2. Burke, T.R., Jr., Yao, Z.-J., Smyth, M.S., Ye, B. *Curr. Pharm. Design* **3**, 291–304 (1997).
3. Yao, Z.J., King, C.R., Cao, T., Kelley, J., Milne, G.W.A., Voigt, J.H., Burke, T.R. *J. Med. Chem.* **42**, 25–35 (1999).

## Further Studies of the Signaling Mechanisms of the Antitumor Somatostatin Analogue TT-232

Attila Steták<sup>1</sup>, Tibor Vántus<sup>1</sup>, Gyöngyi Bökönyi<sup>1</sup>, Péter Csermely<sup>1</sup>,  
Jackie Vandenheede<sup>2</sup>, Axel Ullrich<sup>3</sup>, János Seprődi<sup>1</sup>, István Teplán<sup>1</sup>  
and György Kéri<sup>1</sup>

<sup>1</sup>Department of Medical Chemistry, Peptide Biochemistry Research Group,  
Semmelweis University, Budapest, Hungary

<sup>2</sup>Department of Biochemistry, Catholic University of Leuven, Leuven, Belgium

<sup>3</sup>Max-Planck Institute for Biochemistry, Martinsried, Germany

### Introduction

The somatostatin structural analogue TT-232 is a heptapeptide of a cyclopenta-ring structure: D-Phe-Cys-Tyr-D-Thr-Lys-Cys-Thr-NH<sub>2</sub> that was shown to have strong antiproliferative and apoptotic effects on tumor cells both *in vivo* and *in vitro* but did not inhibit growth hormone release or gastrin secretion *in vivo* [1]. It is presently under phase II clinical trials as a drug against various types of cancer. The signaling mechanisms underlying its strong effects on tumor cells are, however, only poorly understood. Unlike somatostatin, TT-232 binds to SSTR 1 and SSTR 5 (J. Jiang, unpublished results). Previously we demonstrated that TT-232 induces cell cycle arrest through the ERK/MAPK pathway in A431 cells [2] in analogy to the effect of somatostatin mediated by SSTR 1 [3]. Moreover the induction of protein tyrosine phosphatase activity upon TT-232 treatment has also been demonstrated [4] suggesting the role of PTPases in the cytostatic effect of the somatostatin analogue, however the exact molecular mechanism remained unknown. Apart from the proliferation inhibitory effect we also demonstrated that TT-232 induces a caspase independent apoptosis fundamentally different from the cell-cycle inhibitory pathway [2,5].

The aim of the present work was to investigate the early signaling events and to elucidate the role of PTPases in the cytostatic effect of the somatostatin analogue TT-232.

### Results and Discussion

Treatment with TT-232 leads to the transient induction of ERK activation, which returns to basal level within about 30 min in A431 and COS-7 cells which both express endogenous SSTR1. This early event was prevented by treatment with the G-protein-coupled receptor inhibitor pertussis toxin or by the PI3K inhibitor wortmannin. It has been demonstrated that PI3K is involved in the activation of protein kinase C (PKC) family members [6]. Since PKC $\delta$  activity was able to inhibit proliferation in several cell lines through cell cycle arrest, we asked whether PKCs and especially PKC $\delta$  play a role in the signaling of TT-232. FACS analysis revealed that the antiproliferative properties of TT-232 are caused by irreversible cell cycle arrest at G<sub>1</sub>/S transition that required functional PKCs and MEK. We were able to show that PKC $\delta$  is activated and translocated to the cell membrane upon TT-232 treatment. Introduction of a dominant negative mutant revealed that PKC $\delta$  is positioned upstream of ERK in the TT-232 signaling pathway. The PI 3-kinase and PKC $\delta$  were found to associate upon stimulation of A431 cells with TT-232, and the activation of PKC $\delta$  was dependent on PI 3-kinase function.

Moreover, we demonstrate interaction of PI 3-kinase and PKC $\delta$  with Protein tyrosine phosphatase  $\alpha$  and we show that the phosphatase plays a role in the activation of

ERK/MAPK pathway. In this process PTP $\alpha$  Ser-180 and Ser-204 phosphorylation is critical for the induction of phosphatase activity. Taken together we demonstrate the physical and functional association between PI 3-kinase, PKC $\delta$  and PTP $\alpha$  in a signaling complex that mediates the antitumor activity of the somatostatin analogue TT-232 (Figure 1).

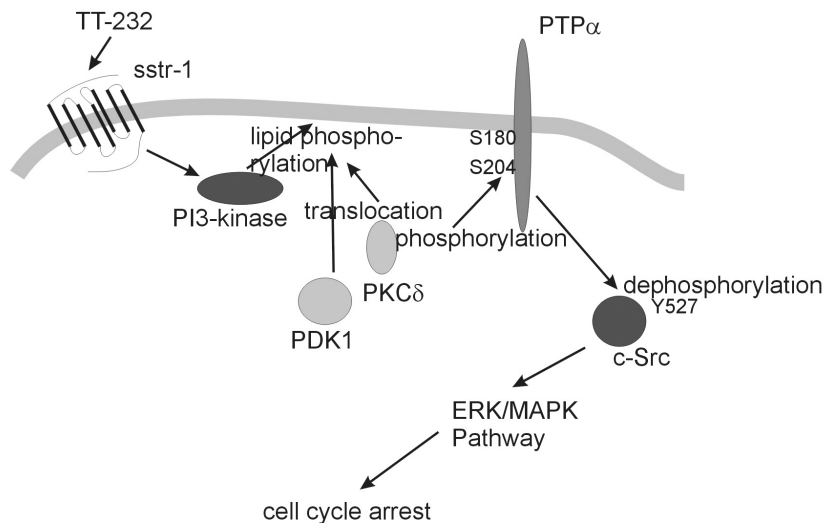


Fig. 1. Schematic model of the activation of ERK/MAPK pathway and cell cycle arrest by TT-232.

We propose a model where TT-232 binds to SSTR1 which leads to the dissociation of a receptor coupled G<sub>i/o</sub> protein. Subsequent release of the G $\beta\gamma$  protein complex activates PI3K. The PI3K product phosphatidylinositol-3,4,5-trisphosphate can induce the activity of PKC $\delta$ , which thereby translocates to the cell membrane. Furthermore, Le Good *et al.* [6] suggested the involvement of the protein kinase PDK1 in the activation of PKCs by phosphorylation. Taken together, this suggests that PI3K lipid products also recruit and activate PDK1, which in turn phosphorylates PKC $\delta$ . For the activation of PKC $\delta$  both, membrane translocation and phosphorylation are required. The activated PKC $\delta$  phosphorylates PTP $\alpha$  which leads to the activation of the phosphatase. The major substrate of PTP $\alpha$  is c-Src which is activated by dephosphorylation of Tyr-527 residue. The activated c-Src leads to the induction of ERK/MAPK pathway and that is required for the cell cycle arrest.

## References

1. Kéri, Gy., et al. *Proc. Natl. Acad. Sci. USA* **93**, 12513–12518 (1996).
2. Steták, A., Lankenau, A., Vántus, T., Csermely, P., Ullrich, A., Kéri, Gy., submitted for publication.
3. Florio, T., Yao, H., Carey, K.D., Dillon, T.J., Stork, P.J. *Mol. Endocrinol.* **13**, 24–37 (1999).
4. Vántus, T., Csermely, P., Teplán, I., Kéri, Gy. *Tumor Biol.* **16**, 261–267 (1995).
5. Vántus, T., Kéri Gy., et al. *Cell. Signalling* **13**, 717–725 (2001).
6. Le Good, J.A., Ziegler, H.W., et al. *Science* **281**, 2042–2045 (1998).

## Generation of Cellulose Membrane-Bound Peptides with Free C-Termini: A Useful Approach for PDZ Binding Studies

Liying Dong, Prisca Boisguérin, Jens Schneider-Mergener and  
 Rudolf Volkmer-Engert

*Institute of Medical Immunology, University Clinic Charité, Humboldt University of Berlin,  
 Berlin, 10098, Germany*

### Introduction

PDZ [1] domains are recently characterized protein-recognition modules which mostly bind to the C-termini of target proteins. This was reported as well for antibodies like mAB TE34 [2].

Spot synthesis [3] allows the parallel screening of thousands of cellulose-bound peptides to study protein-protein interactions. Unfortunately, most solid support-bound peptide libraries lack a free C-terminus due to the C-terminal fixation on the solid support. To overcome this restriction, we improve considerably the previously developed strategy [4] for cellulose-bound, inverted peptides with authentic C-termini, using Fmoc-amino acid 3-bromopropyl esters, mercapto functionalized cellulose membranes and chemoselective cyclization step.

### Results and Discussion

The steps towards the synthesis of cellulose-bound, inverted peptides are shown in Figure 1. Key compounds of the synthesis are the membrane-bound *N*-mercapto-propionyl cysteine adduct (C) and the unprotected cyclic thioether (F).

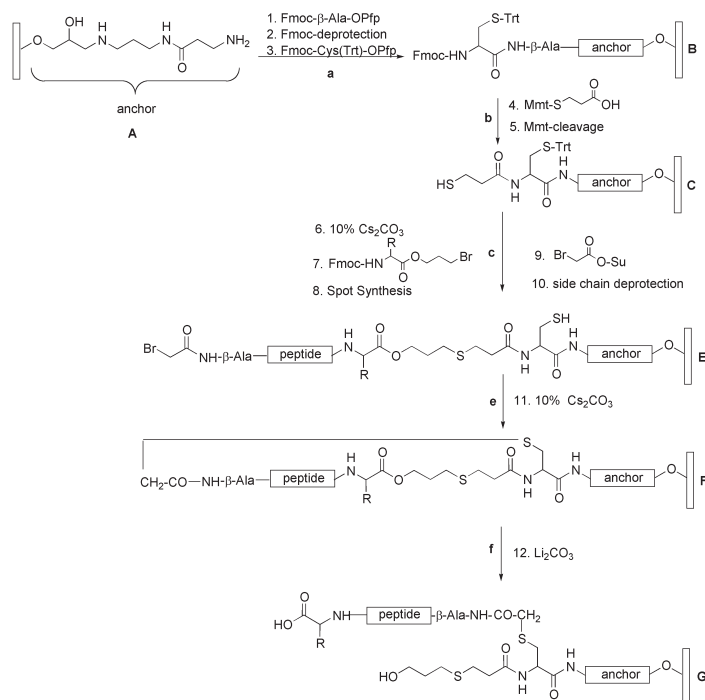


Fig. 1. Synthesis of inverted peptides on cellulose membranes.

Selective removal of the Mmt-protection group (10% dichloroacetic acid, 0.5% trifluoroacetic acid and 5% TIBS in DCM) and the subsequently treatment of the mercapto-functionalized membrane (C) with Fmoc-amino acid 3-bromopropyl ester results in the first amino acid base-labile cleavage site. The remaining amino acids are coupled using standard spot synthesis protocol. Incorporation of bromo-acetic acid *N*-hydroxysuccinimide ester and subsequent removal of the side chain protection leads to the N-terminal bromoacetylated peptide derivate (D). The formation of the cyclic thioether (E) was achieved in high yield and short reaction time by 10% Cs<sub>2</sub>CO<sub>3</sub>. The cyclisation step leads to a membrane-bound peptide where the N-terminus is stably fixed by a thioether bond while the C-terminus is attached *via* a cleavable ester bond. Hydrolysis of this ester bond linearizes the construct and generates free C-terminus (F).

In comparison to the previously described method the presented approach shows the following advantages: 1) selective Mmt-cleavage to obtain mercapto functionalized membrane, 2) high coupling efficiency of the Fmoc-amino acid 3-bromopropyl esters 3) stable life time of the mercapto functionalized cellulose membrane up to 3 h, and 4) higher cyclization and linearization rates.

In conclusion, this novel method is useful for the automated preparation of peptide libraries presenting free C-termini. This approach is necessary for the parallel screening of protein-ligand interactions on continuous supports *e.g.* for PDZ domains which recognize their ligands *via* the free C-terminal region.

## References

1. Songyang, Z., Fanning, A.S., Fu, C., Xu, J., Marfatia, S.M., Chishti, A.H., Crompton, A., Chan, A.C., Anderson, J.M., Cantley, L.C. *Science* **275**, 73–77 (1997).
2. Zilber, B., Scherf, T., Levitt, M., Anglister, J. *Biochemistry* **30**, 10032–10041 (1990).
3. Frank, R. *Tetrahedron* **48**, 9217–9232 (1992).
4. Hoffmüller, U., Russwurm, M., Kleinjung, F., Ashurst, J., Oschkinat, H., Volkmer-Engert, R., Koesling, D., Schneider-Mergener, J. *Angew. Chem., Int. Ed.* **38**, 2180–2184 (1999).

## A Focused Library Approach to PTP Inhibitor Discovery Predicated on the X-ray Structure of a PTP1B-Bound Lead Compound

Terrence R. Burke, Jr.<sup>1</sup>, Ding-Guo Liu<sup>1</sup>, Johannes Voigt<sup>1</sup>, Li Wu<sup>2</sup>,  
Zhong-Yin Zhang<sup>2</sup> and Yang Gao<sup>1</sup>

<sup>1</sup>Laboratory of Medicinal Chemistry, NCI, NIH, FCRDC, Frederick, MD 21702, USA

<sup>2</sup>Department of Molecular Pharmacology, Albert Einstein College of Medicine, Bronx, NY 10461, USA

### Introduction

Protein-tyrosine phosphatase (PTP) inhibitors are attractive as potential signal transduction-based therapeutics. We have recently reported the X-ray structure of 6-(phosphonodifluoromethyl)-2-naphthoic acid (**1**) complexed with PTP1B [1]. As evidenced therein, the inhibitor 2-carboxyl group interacts with the protein backbone only indirectly through a bridging water molecule. Based on this, a library of compounds typified by **2** was prepared, in which appended sulfonamide functionality was intended to mimic and replace the original water of hydration (Figure 1). While maintaining binding interactions of parent **1**, these latter compounds present an additional site "R" for introduction of auxiliary functionality not present in the original carboxylic acid.

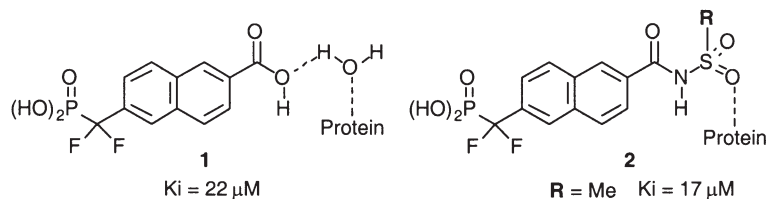


Fig. 1. Depiction of the manner in which sulfonamido functionality (analogue **2**) mimics and replaces a water of hydration observed in the X-ray structure of PTP1B-bound **1**.

### Results and Discussion

Syntheses of sulfonamides **2** were achieved by condensing common protected precursor **3** with a variety of commercially available sulfonamides (Figure 2). At this stage, purification of phosphonate-protected intermediates could be achieved by silica gel

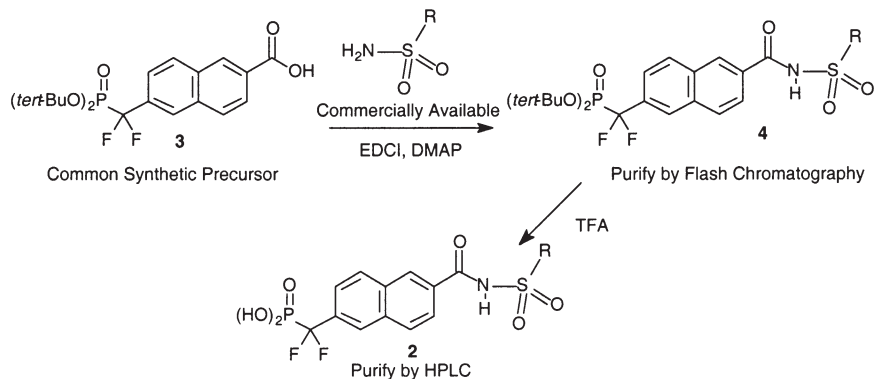


Fig. 2. Synthetic approach toward sulfonamides **2**.

## Peptide Conjugates

flash chromatography. Resulting sulfonamides **4** were deprotected using TFA to afford the final products **2**, which were purified by HPLC.

PTP1B inhibitory  $IC_{50}$  values of resulting sulfonamides **2** ranged from approximately 20 to 50  $\mu M$  (Table 1). An exception to this was observed with one analogue containing a long-chain alkyl substituent ( $IC_{50} = 0.35 \mu M$ ). Work is ongoing to more fully explore the potential utility of this class of inhibitors.

R	$IC_{50}$ ( $\mu M$ )	R	$IC_{50}$ ( $\mu M$ )	R	$IC_{50}$ ( $\mu M$ )
	41 $\pm$ 2 ( $K_i$ =17 $\mu M$ )		18 $\pm$ 2		20 $\pm$ 2
	30 $\pm$ 2		0.35		19 $\pm$ 1
	24 $\pm$ 2		46 $\pm$ 2		25 $\pm$ 1

Table 1. Effect on PTP1B inhibitor potency of R-variation in sulfonamides **2**.

## References

1. Groves, M.R., Yao, Z.J., Roller, P.P., Burke, T.R., Jr., Barford, D. *Biochemistry* **37**, 17773–17783 (1998).

## Synthesis of the Ras-RBD Protein Pair

Christian F.W. Becker<sup>1</sup>, Christie L. Hunter<sup>2</sup>, Ralf P. Seidel<sup>1</sup>,  
Stephen B.H. Kent<sup>2</sup>, Roger S. Goody<sup>1</sup> and Martin Engelhard<sup>1</sup>

<sup>1</sup>Max-Planck Institut für Molekulare Physiologie, 44227 Dortmund, Germany

<sup>2</sup>Gryphon Sciences, So. San Francisco, CA 94080, USA

### Introduction

Protein/protein interactions play an essential role for virtually every physiological process like *e.g.* energy transduction, vesicular transport, or signal transduction. The latter example plays an important role for the response of cells towards external stimuli, which ultimately can result in cell differentiation or proliferation.

A paradigm for a protein pair involved in signal transduction is the Ras-Raf pair. The Ras protein is a small membrane-associated G-protein, which cycles between the inactive, GDP-bound and its active, GTP-bound state upon binding to GEFs or GAPs, respectively as a reaction an external signals transduced by transmembrane receptors [1]. An important downstream effector of Ras is Raf, a Ser/Thr-specific protein kinase, which binds to active Ras *via* its Ras-binding domain (RBD). This domain consists of 81 amino acids and is sufficient to discriminate between Ras-GTP and Ras-GDP [2]. The interaction between these proteins has been thoroughly investigated and a crystal structure of the RBD in complex with the Ras-homologue Rap1A is available [3]. The activation of Raf by Ras is still not fully understood but recruitment of Raf to the plasma membrane plays an essential role.

The RBD provides a tool for selective binding of Ras-GTP even in the presence of Ras-GDP and thereby allows the development of a detection system for active Ras. Such a system would be of great relevance for therapeutic and diagnostic applications due to the importance of mutations in Ras for human cancer. Certain mutations in Ras, which lead to a slower GTP hydrolysis or an accelerated release of GDP, are responsible for constitutive activation of the Ras signalling pathway. These mutations occur in more than 30% of all human cancers [4].

In the present paper the chemical synthesis of the Ras/RBD protein pair is described.

### Results and Discussion

The chemical synthesis of RBD was carried out by using Boc-chemistry for the synthesis of two peptide segments, which are spliced together by native chemical ligation [5,6]. The N-terminal segment RBD(51-95) was synthesized on a resin which generated a  $\alpha$ -C-terminal thioester after HF cleavage [7]. The ligation site was chosen due to the presence of a cysteine residue at the N-terminus of the C-terminal segment. After ligation of these segments, purification by HPLC and identification by ESI-MS (Figure 1) the resulting polypeptide was folded in its biological active tertiary structure, which was checked by CD-Spectroscopy and binding studies to Ras-GppNHp. These studies revealed full biological activity and no difference found between synthesized RBD and RBD produced by recombinant means.

The total chemical synthesis of C-terminal truncated Ras had due to the length of 166 amino acids to occur by ligation of three or four peptides. Since Ras contains three Cys-residues as potential ligation sites in principle four peptide segments could be used to build up Ras(1-166). However in the present work a strategy was followed which relied only on three peptide segments which necessitated two ligation steps.

## Peptide Conjugates

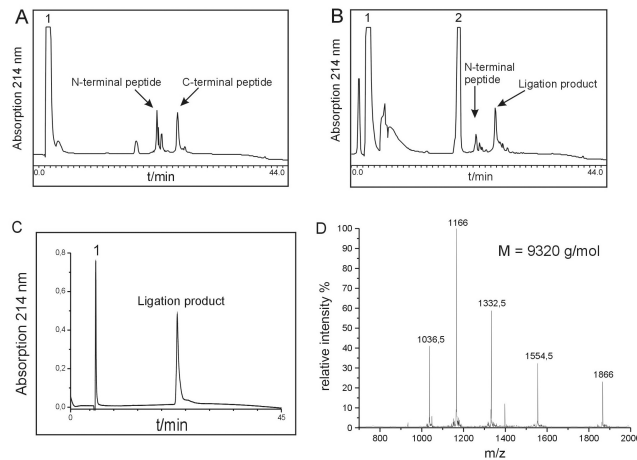


Fig. 1. Ligation of RBD segments. A) HPLC chromatogram before addition of thiophenol; B) after several hours with thiophenol; C) purified ligation product; D) MS of purified protein; 1: guanidine; 2: thiophenol.

Ras(51-117) and Ras(1-50) were synthesized on a resin which generated a  $\alpha$ -C-terminal thioester after HF-cleavage. The N-terminal Cysteine-residue of Ras(51-117) was Ac<sub>m</sub>-protected to prevent cyclisation or dimerization of this peptide after HF-cleavage [8]. Ras(51-117) and Ras(118-166) are ligated to produce the peptide segment Ras(51-166) which after purification had to be Ac<sub>m</sub>-deprotected at its N-terminal Cysteine-residue by using Hg<sup>2+</sup> to allow the final ligation with Ras(1-50) (Figure 2).

The resulting protein was identified by ESI-MS and revealed a –18 mass loss, which might be caused by dehydration or cyclisation of an amino acid side chain.

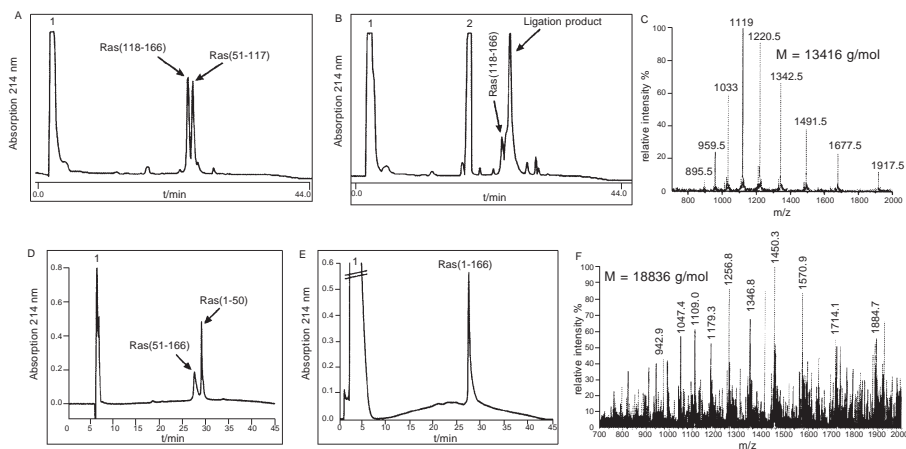


Fig. 2. Synthesis of Ras(1-166); A) Ligation of Ras(118-166) and Ras(51-117) before addition of thiophenol; B) Ligation after several hours with thiophenol; C) ESI-MS of the purified Ras(51-166); D) Ligation of Ras(51-166) and Ras(1-50); E) purified Ras(1-166), F) ESI-MS of Ras(1-166).

**Becker et al.**

Folding was done in the presence of GppNHp (a non-hydrolysable GTP-analogue), which served as a folding scaffold for the protein [9]. However, only 50% of the protein adopted a soluble form. The remaining solid was removed by centrifugation and dissolved in a buffer containing 5 M guanidine and an excess of GppNHp [10]. After dialysis against guanidine-free buffer the Ras protein was obtained in a soluble form. CD-spectroscopy proved that both folding pathways lead to Ras proteins with identical spectra as compared with each other and with that of Ras produced by recombinant techniques. Kinetic studies of the interaction between synthetic RBD and synthesized Ras are indistinguishable from those samples prepared by heterologous expression in *E. coli*.

**Acknowledgments**

We gratefully acknowledge the financial support of the BMBF.

**References**

1. Wittinghofer, A., Waldmann, H. *Angew. Chem., Int. Ed.* **39**, 4193–4214 (2000).
2. Chuang, E., Barnard, D., Hettich, L., Zhang, X.F., Avruch, J., Marshall, M.S. *Mol. Cell. Biol.* **14**, 5318–5325 (1994).
3. Nassar, N., Horn, G., Herrmann, C., Scherer, A., McCormick, F., Wittinghofer, A. *Nature* **375**, 554–560 (1995).
4. Barbacid, M. *Annu. Rev. Biochem.* **56**, 779–827 (1987).
5. Becker, C.F.W., Hunter, C.L., Seidel, R.P., Kent, S.B.H., Goody, R.S., Engelhard, M. *Chem. Biol.*, in press (2001).
6. Sydor, J.R., Herrmann, C., Kent, S.B.H., Goody, R.S., Engelhard, M. *Proc. Natl. Acad. Sci. U.S.A.* **96**, 7865–7870 (1999).
7. Hojo, H., Kwon, Y., Kakuta, Y., Tsuda, S., Tanaka, I., Hikichi, K., Aimoto, S. *Bull. Chem. Soc. Jpn.* **66**, 2700–2706 (1993).
8. Zhang, L., Tam, J.T. *J. Am. Chem. Soc.* **119**, 2363–2370 (1997).
9. Zhang, J., Matthews, C.R. *Biochemistry* **37**, 14891–14899 (1998).
10. Netzer, W.J., Hartl, F.U. *Nature* **388**, 343–349 (1997).

## **The Proline-Rich Antibacterial Peptide Family Inhibits Chaperone-Assisted Protein Folding**

**Laszlo Otvos, Jr.<sup>1</sup>, Goran Kragol<sup>1</sup>, Gyorgyi Varadi<sup>1</sup>, Barry A. Condie<sup>1</sup>  
and Sandor Lovas<sup>2</sup>**

<sup>1</sup>*The Wistar Institute, Philadelphia, PA 19104, USA*

<sup>2</sup>*Department of Biomedical Sciences, Creighton University, Omaha, NE 68178, USA*

### **Introduction**

It is now firmly established that *in vivo* proteins require the assistance of molecular chaperones for their folding [1]. The heat shock 70 family, Hsp70 (DnaK in bacteria), bind to nascent polypeptide chains on ribosomes, preventing their premature folding, misfolding, or aggregation, as well as to newly synthesized proteins in the process of translocation from the cytosol into the mitochondria and the endoplasmic reticulum. The protein folding activity of the 70 kDa heat shock protein family is driven by their ATPase activity that regulates cycles of polypeptide binding and release [2]. Inhibition of the DnaK-mediated protein folding process has dire consequences for the organism. Mutations in the heat shock genes, DnaK and DnaJ, cause severe defects of several cellular functions [3], as indicated by the significantly reduced  $\beta$ -galactosidase activity in  $\Delta$ dnaKd mutants above 30 °C [4]. Recently we documented that the short, proline-rich antimicrobial peptides pyrrocoricin, drosocin and apidaecin interact with the bacterial heat shock protein DnaK and the binding can be correlated with the antimicrobial activity [5]. To continue this research, we studied the mechanism of action of these peptides and their binding site to *Escherichia coli* DnaK [6].

### **Results and Discussion**

Competition assay with unlabeled pyrrocoricin indicated a probable multiple-site interaction with *E. coli* DnaK. For the identification of a possible pyrrocoricin-binding domain of DnaK outside the conventional peptide-binding pocket, we studied the strain-specificity of the antibacterial activity and DnaK binding. The apparent lack of selectivity toward Gram-negative or Gram-positive strains confirmed that the killing of bacteria is not related strongly to membrane binding. Rather, the specificity to certain bacterial strains may stem from altered binding to DnaK. In this case, at least one peptide-binding fragment should be sought in the variable domains of the protein. Comparison of various DnaK sequences reveal high homology N-terminal to the peptide-binding region but considerably less homology downstream. The most pronounced sequence alterations could be detected at the end of the multihelical lid region. Indeed, we documented that pyrrocoricin, drosocin and perhaps apidaecin bind to the hinge region between helices D and E [6]. Binding to synthetic DnaK D-E helix fragments could be perfectly correlated with antibacterial and antifungal activity. Pyrrocoricin bound to this domain of the responsive strains *E. coli*, *Salmonella typhimurium*, *Agrobacterium tumefaciens* and *Haemophilus influenzae*, but failed to interact with the analogous fragments of the non-responsive strains *Staphylococcus aureus*, *Streptococcus pyogenes* and *Candida albicans* (Table 1). No appreciable level of binding was detected to the human or murine Hsp70 analogs, indicating that the insect-derived proline-rich antibacterial peptides will be suitable for the treatment of clinical or veterinary infections. Based on the known three-dimensional fold of the C-terminal domain of DnaK, if the contact residues between pyrrocoricin and the *E. coli* DnaK D-E helix are identified, pyrrocoricin-based peptides and peptido-

mimetics can be designed that strain- and species-specifically inhibit Hsp70-mediated protein folding in bacteria, parasites, fungi, insects or rodents.

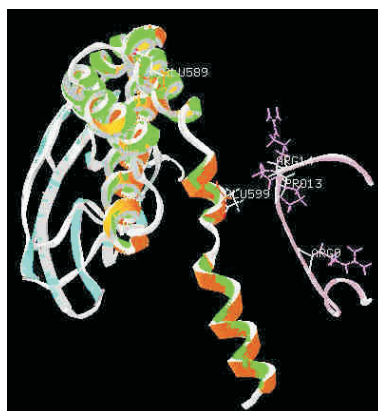
The  $\alpha$ -helical lid assembly, which regulates the traveling of the substrate in and out of the peptide-binding pocket, was suggested to be operated by an allosteric mechanism of ATP-controlled opening and closing in the hinge regions. Indeed, biologically active L-pyrrhocoricin diminished the ATPase activity of a recombinant DnaK in contrast to the inactive D-analog and two membrane-active antibacterial peptides, magainin II and cecropin. The effect of the peptides on DnaK's other function, the refolding of proteins, was studied by assaying the alkaline phosphatase and  $\beta$ -galactosidase activity of live bacteria. Remarkably, the activity of both enzymes was inhibited upon incubation with L-pyrrhocoricin and drosocin, but not with the inactive D-pyrrhocoricin, or peptides without intracellular protein targets such as magainin 2

Table 1. DnaK D-E helix sequences of different bacteria and their binding to fluorescein-labeled pyrrhocoricin. The activity of pyrrhocoricin against these strains is also indicated.

Strain	Sequence response to pyrrhocoricin
Binder by fluorescence polarization:	
<i>E. coli</i> :	IEAKMQELAQVSQKLMEIAQQQHAQQQTAGADA Yes
( <i>S. typhimurium</i> <sup>a</sup> :	IEAKMQELAQVSQKLMEIAQQQHAQQQAGSADA) Yes
<i>A. tumefaciens</i> :	IQAKTQTLMEVSMKLGQAIYEAQQAEAGDASAEG Yes
<i>H. influenzae</i> :	IEAKIEAVIKASEPLMQAVQAKAQQAGGEQPQQ Yes
Non-binder by fluorescence polarization:	
<i>H. pylori</i> :	AELEDKTKLLAQAAQKLGEAMANKNNAEQP No
<i>P. aeruginosa</i> :	IEAKMNALSQASTPLAQKMYAEQAQQGEDAPQ Unclear
<i>S. aureus</i> :	IKSKKEELEKVIQELSAKVYEQAAQQQQQAQG No
<i>S. pyogenes</i> :	MKAKLEALNEKAQALAVKMYEQAAAAQQAQGAEG No
<i>S. pneumoniae</i> :	MKAKLEALNEKAQQLAVKLYEQAAAAQQAQGAEG No
<i>C. albicans</i> :	YEDKRKELESVANPIISGAYGAAGGAPGGAGGF No
<i>M. musculus</i> :	YEHKQKELERVCNPIISKLYQGGPGG Not toxic
<i>H. sapiens</i> :	FEHKRKELEQVCNPIISGLYQGAGGPGPGGFGA Not tested

<sup>a</sup> The *S. typhimurium* peptide has not been synthesized because its sequence is almost identical to that of *E. coli*.

and buforin II. Taken all these findings together, compelling evidences indicate that DnaK-binding of the proline-rich antimicrobial peptide family prevents the frequent opening and closing of the multihelical lid over the peptide binding pocket and prevents chaperone-assisted protein folding (Figure 1).



*Fig. 1. Possible interaction between the D-E helix region of E. coli DnaK (left) and pyrrocoricin (right) as the model was generated by a flexible docking process.*

## References

1. Martin, J., Hartl, F.U. *Curr. Opin. Struct. Biol.* **7**, 41–52 (1997).
2. Liberek, K., Skowrya, D., Zylicz, M., Johnson, C., Georgopoulos, C. *J. Biol. Chem.* **266**, 14491–14496 (1991).
3. Wolska, K.I., Paciorek, J., Kardys, K. *Microbios* **97**, 55–67 (1999).
4. Wolska, K.I., Lobacz, B., Jurkiewicz, D., Bugajska, E., Kuc, M., Jozwik, A. *Microbios* **101**, 157–168 (2000).
5. Otvos, L., Jr., O, I., Rogers, M.E., Consolvo, P.J., Condie, B.A., Lovas, S., Bulet, P., Blaszczyk-Thurin, M. *Biochemistry* **39**, 14150–14159 (2000).
6. Kragol, G., Lovas, S., Varadi, G., Condie, B.A., Hoffmann, R., Otvos, L., Jr. *Biochemistry* **40**, 3016–3026 (2001).

## **Probing the Binding Site of a Heptahelical Peptide Pheromone Receptor Using Photoaffinity Labelling, Site-Directed Mutagenesis and Spectroscopic Approaches**

**Fred Naider<sup>1</sup>, B. K. Lee<sup>2</sup>, L. Keith Henry<sup>2</sup>, Faxiang Ding<sup>1</sup>, S. K. Khare<sup>1</sup>  
and Jeffrey M. Becker<sup>2</sup>**

<sup>1</sup>*Department of Chemistry College of Staten Island, CUNY, Staten Island, NY 10314, USA*

<sup>2</sup>*Department of Biochemistry, University of Tennessee, Knoxville, TN 37996, USA*

### **Introduction**

G protein-coupled receptors (GPCRs) are multifunctional proteins involved in cell-cell communication and represent the largest gene family in eukaryotes. Signal molecules recognized by these receptors include odorants, biogenic amines, peptides and proteins, and are involved in regulation of a plethora of biological processes including pain sensation, growth, blood pressure regulation and intermediary metabolism. Despite the importance of GPCRs, few details are available on the molecular aspects of ligand recognition or signal transduction. Ongoing studies in our laboratory use mating in *Saccharomyces cerevisiae* as a paradigm to understand various aspects of GPCR function. One specific goal of our work is to understand the nature of the interaction of the pheromone  $\alpha$ -factor (WHWLQLKPGQPMY) with its GPCR (Ste2p). In this report, we discuss a multi-pronged approach utilizing fluorescence spectroscopy, site-directed mutagenesis, and photoaffinity labeling to define the interaction of this peptide pheromone with Ste2p.

### **Results and Discussion**

To define the binding environment of  $\alpha$ -factor we synthesized a series of analogs in which the 7-nitrobenz-2-oxa-1,3-diazol-4-yl (NBD) group was placed at various positions in the pheromone. Synthesis was carried out using solid-phase peptide chemistry to prepare FmocWHWLQLXPGQPNleY [X = Dap, Dab, Lys( $\beta$ -Ala)] as described previously [1]. The NBD group was then attached to the X side chain by reaction of NBD-F in a mixed organic/aqueous buffer. NBD-F was also reacted with Dap substituted for residues 1 or 3, and Lys substituted for residues 4, 6 or 12, respectively, of FmocWHWLQLRPGQPNleY and  $\alpha$ -factor was modified with NBD on the  $\alpha$ -amine and the Tyr<sup>13</sup> side chain. All analogs were tested for agonist activity using a growth arrest assay and for receptor affinity using a receptor binding competition assay [1]. The results showed that analogs with NBD at the side chains of position 3 and 7 retained receptor affinities of 24–48 nM. In contrast, modifications in side chains 1, 4, 6, and 12 resulted in binding affinities in the 260–1300 nM range. These affinities were not sufficient to measure fluorescence of the analogs bound to receptors in membranes.  $\alpha$ -Factor derivatized on the  $\alpha$ -amine terminus or the side chain of Tyr<sup>13</sup> exhibited partial or complete bleaching of fluorescence and could not be studied by fluorescence techniques. Fluorescence measurements with analogs attached to the 3-position side chain indicated that this group was in a nonpolar environment when the  $\alpha$ -factor analog was bound to Ste2p. The NBD group on the position 7 side chain exhibited different emission maxima, depending on the distance between the fluorophore and the peptide backbone. The emission maxima of these peptides correlated well with Stern–Volmer constants determined by fluorescence quenching experiments using KI as the quencher. The results are consistent with the NBD group at position 7 residing

in environments of alternating polarity as the number of methylenes in the side chain are varied from 1 to 4. Longer spacer arms appear to completely expose the side chain to the bulk hydrophilic solvent.

To investigate possible contacts between the  $\alpha$ -factor and specific residues in Ste2p site-directed mutagenesis techniques were used to replace S47 and T48 of the receptor with E or K residues. In parallel, a series of pheromone analogs were prepared, in which Q<sup>10</sup> was replaced by N, S, D, E, K or Orn. Saturation binding experiments with [<sup>3</sup>H] $\alpha$ -factor demonstrated that all mutant receptors retained high affinity for the pheromone and were expressed at similar levels. Furthermore, all mutant receptors were activated by  $\alpha$ -factor as judged using growth arrest and gene induction assays. These results indicated that the mutant receptors retained the overall global structure of wild type Ste2p and efficiently induced the G protein cascade of the signal transduction system. Strikingly, several of the analogs showed marked changes in binding and agonist efficacy with the different receptors. For example, the WHWLQLKPG KPNleY analog showed improved binding with the E47E48 mutant Ste2p and almost no binding to the K47K48 mutant Ste2p. The corresponding [Orn<sup>10</sup>] $\alpha$ -factor analog exhibited similar trends, whereas the [Glu<sup>10</sup>] $\alpha$ -factor showed the reverse correlation. The mutagenesis studies provide evidence that the side chain of the position 10 residue of  $\alpha$ -factor interacts with either residue 47 or residue 48 when bound to the receptor.

To further delineate contacts between  $\alpha$ -factor and Ste2p, a series of analogs containing *p*-benzoyl-L-phenylalanine (Bpa) were synthesized, in which this photoactive residue was placed throughout the peptide backbone. As seen in the Figure 1, binding experiments showed that when Bpa was placed at positions 1, 3, 5, 7, 8, 12 and 13, receptor affinities within 4- to 45-fold that of the wild type pheromone were achieved. In contrast, Bpa at positions 2, 4, 6, 10 and 11 resulted in 100 to greater than 1500-fold losses in affinity. Based on these results, we synthesized an iodinated analog of  $\alpha$ -factor with Bpa in position 1, Tyr in position 3 and Phe in position 13. Previously, we showed that [Tyr<sup>3</sup>,Phe<sup>13</sup>] $\alpha$ -factor could be iodinated and retained high affinity for the receptor [2]. Irradiation of [Bpa<sup>1</sup>,(<sup>125</sup>I)Tyr<sup>3</sup>,Nle<sup>12</sup>,Phe<sup>13</sup>] $\alpha$ -factor at 350 nm in the presence of yeast membranes overexpressing Ste2p resulted in the incorporation of radioactivity into the receptor. More than 80% of the incorporated radioactivity could be eliminated when crosslinking was carried out in the presence of an excess of  $\alpha$ -factor.

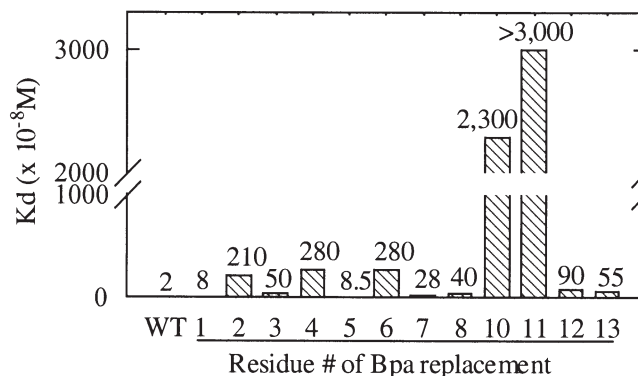


Fig. 1. Affinity constants for Bpa-scanned  $\alpha$ -factor analogs.

The labeled receptor was detected on acrylamide gels using antibodies against Ste2p and antibodies against an epitope specifically inserted at the carboxyl terminus of the receptor. The labeled receptor exhibited a band with a molecular weight of 52 KDa corresponding to the receptor plus the pheromone. Treatment of the crosslinked receptor with endoglycosidase H resulted in a decrease in molecular weight consistent with the loss of polysaccharides as observed for the uncrosslinked receptor. Cleavage of the labeled receptor with cyanogens bromide and/or the BPS-skatole reagent resulted in fragments, which are currently being analyzed by mass spectrometry. Preliminary evidence suggests that the [Bpa<sup>1</sup>]  $\alpha$  factor cross-links into Ste2p at a site that includes the fifth through seventh transmembrane domains of the receptor.

The results of the spectroscopic, molecular biological, and biochemical studies summarized above have revealed that the position 3 side chain is in a hydrophobic environment, the position 7 side chain is in an environment of variable polarity and that the position 10 side chain interacts with residues 47 and 48 of Ste2p. Earlier studies suggested that the  $\alpha$ -amine and the first residue are also likely in a hydrophobic pocket of the receptor and that  $\alpha$ -factor is bent around the Pro-Gly residues when it is bound to Ste2p [3,4]. Taken together, these results have allowed us to suggest a working model in which the pheromone first interacts at its carboxyl terminus with residues in the first transmembrane domain.  $\alpha$ -Factor then forms a turn around the middle of the peptide, in which the Lys side chain interacts with a pocket formed by the extracellular loops, and in which the amine terminus is buried in a hydrophobic region, which may be formed by transmembrane domains five and six. Currently, additional biochemical and molecular biological studies are under way to test this model.

#### **Acknowledgments**

The above work has been supported by grants GM22086 and GM22087 from the National Institute of General Medical Sciences.

#### **References**

1. Ding, F., Lee, B.K., Hauser, M., Davenport, L., Becker, J.M., Naider, F. *Biochemistry* **40**, 1102–1108 (2001).
2. Liu, S.F., Wang, S.H., Arshava, B., Lee, B.K., Henry, K., Becker, J.M., Naider, F. *J. Peptide Res.* **56**, 24–34 (2000).
3. Zhang, Y.L., Lu, H.F., Becker, J.M., Naider, F. *J. Peptide Res.* **50**, 319–328 (1997).
4. Jelicks, L., Naider, F., Shenbagamurthi, P., Becker, J.M., Broido, M.S. *Biopolymers* **27**, 431–449 (1988).

## The Naturally Occurring Melanocortin Antagonist Agouti-Related Protein (AGRP) Possesses Similar and Distinct Interactions at the MC4 Receptor Compared with Melanocortin Agonist

Carrie Haskell-Luevano<sup>1</sup>, Eileen K. Monck<sup>1</sup> and Y.-P. Wan<sup>2</sup>

<sup>1</sup>Department of Medicinal Chemistry, University of Florida, Gainesville, FL 32610, USA

<sup>2</sup>NEN Life Science Products, Boston, MA 02118, USA

### Introduction

Agouti-related protein (AGRP) is one of two known naturally occurring antagonists of G-protein coupled receptors identified to date, is an antagonist of the melanocortin-4 receptor (MC4R), and is involved in obesity and the regulation of feeding behavior [1,2]. The agonists of the MC4R include the POMC derived peptides, particularly  $\alpha$ -melanocyte stimulating hormone ( $\alpha$ -MSH). The studies presented herein were performed to test the hypothesis that AGRP and  $\alpha$ -MSH possessed similar molecular recognition interactions with identical MC4R amino acids. *In vitro* mutagenesis at the MC4 receptor (23 mutations) and comparing agonist Ac-Nle-c[Asp-His-DPhe-Arg-Trp-Lys]-NH<sub>2</sub>, MTII [3] (I<sup>125</sup>-MTII, IC<sub>50</sub>) and antagonist (I<sup>125</sup>-AGRP) binding and functional activities (agonist EC<sub>50</sub> and antagonist pA<sub>2</sub>) have been performed to test this hypothesis.

### Results and Discussion

Table 1 summarizes comparison of the melanocortin agonist MTII binding and functional activity *versus* the antagonist AGRP(83-132)-NH<sub>2</sub> at the wild type and mutant mMC4Rs. Figure 1 illustrates the location of these receptor mutations within the putative transmembrane spanning regions of the mMC4R. Interestingly, at the F176K mMC4R, the melanocortin based antagonist SHU9119 [4] was able to competitively antagonize this mutant receptor, whereas the endogenous antagonist AGRP was not (Figure 2), even though AGRP(83-132) possessed 3 nM binding affinity [5].

These studies have identified the Glu92, Asp114, Asp118, and Phe176 mutant mouse melanocortin-4 receptors as affecting both melanocortin agonist MTII and the endogenous AGRP antagonist ligand-receptor interactions.

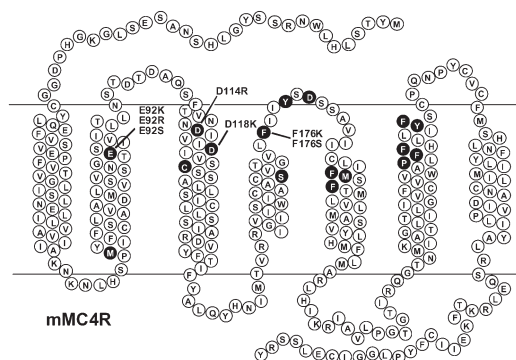


Fig. 1. Illustration of the receptor mutations of the mouse melanocortin-4 receptor in the putative transmembrane spanning regions.

Table 1. Comparison of the melanocortin MTII agonist and AGRP antagonist at mutant melanocortin-4 receptors (MC4R).

MC4R	I <sup>125</sup> -MTII IC <sub>50</sub> (nM)	I <sup>125</sup> -AGRP IC <sub>50</sub> (nM)	MTII IC <sub>50</sub> (nM)	AGRP pA <sub>2</sub>
Wildtype	0.5 ± 0.13	0.66 ± 0.46	0.036 ± 0.029	9.4
Glu92Lys	37.1 ± 40.5	>1 000	4.50 ± 4.7	No activity <sup>a</sup>
Asp114Arg	19.6 ± 14.2	0.44 ± 0.22	144 ± 10	No activity
Asp118Lys	>1 000	>1 000	166 ± 64	No activity
Phe176Lys	2.75 ± 0.21	3.69 ± 2.77	2.75 ± 0.78	No activity

<sup>a</sup> No activity denotes that neither agonist or antagonist activity was observed.

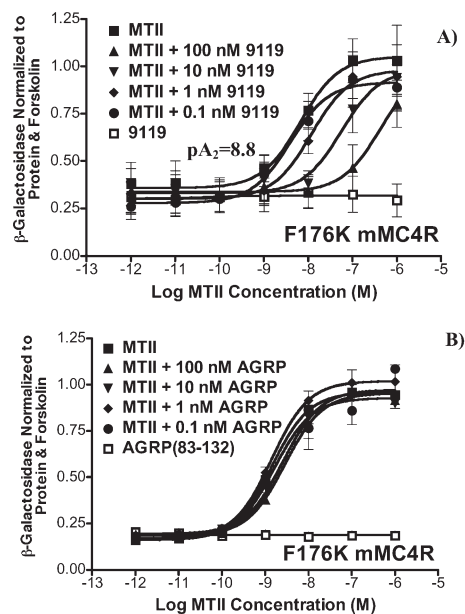


Fig. 2. A) Antagonism of the F176K mMC4R by the melanocortin antagonist SHU9119 but not B) AGRP(83-132).

### Acknowledgments

This work has been supported by NIH grant R01DK57080 and C. H. L. is a recipient of a Burroughs Wellcome fund Career Award in the Biomedical Sciences.

### References

1. Huszar, D., Lynch, C.A., Fairchild-Huntress, V., Dunmore, J.H., Smith, F.J., Kesterson, R.A., Boston, B.A., Fang, Q., Berkemeir, L.R., Gu, W., Cone, R.D., Campfield, L.A., Lee, F. *Cell* **88**, 131–141 (1997).
2. Ollmann, M.M., Wilson, B.D., Yang, Y.-K., Kerns, J.A., Chen, Y., Gantz, I., Barsh, G.S. *Science* **278**, 135–138 (1997).
3. Al-Obeidi, F., Hadley, M.E., Pettitt, B.M., Hruby, V.J. *J. Am. Chem. Soc.* **111**, 3413–3416 (1989).
4. Hruby, V.J., Lu, D., Sharma, S.D., Castrucci, A.M.L., Kesterson, R.A., Al-Obeidi, F.A., Hadley, M.E., Cone, R.D. *J. Med. Chem.* **38**, 3454–3461 (1995).
5. Haskell-Luevano, C., Cone, R.D., Monck, E.K., Wan, Y.-P. *Biochemistry* **40**, 6164–6179 (2001).

## **Identification of Regions of the Epidermal Growth Factor Receptor Involved in Ligand Binding Specificity Using a High Affinity Form of the Ectodomain**

**E. Nice<sup>1,2</sup>, J. Rothacker<sup>1,2</sup>, R. Jorissen<sup>1,2</sup>, M. Nerrie<sup>1,2</sup>, T. Domagala<sup>1,2</sup>,  
T. Adams<sup>3</sup>, J. Lewis<sup>3</sup>, N. McKern<sup>3</sup>, G. Lovrecz<sup>3</sup>, T. Elleman<sup>3</sup>, P. Hoyne<sup>3</sup>,  
T. Garrett<sup>2,4</sup>, K. Richards<sup>3</sup>, G. Howlett<sup>5</sup>, A. Burgess<sup>1,2</sup> and C. Ward<sup>2,3</sup>**

<sup>1</sup>The Ludwig Institute for Cancer Research, <sup>2</sup>The CRC for Cellular Growth Factors, <sup>3</sup>CSIRO Health Sciences and Nutrition, <sup>4</sup>Biomolecular Research Institute and <sup>5</sup>The Department of Biochemistry, University of Melbourne, Melbourne, 3050 Australia

### **Introduction**

Murine and human epidermal growth factor receptors (EGFRs) bind human EGF (hEGF), mouse EGF (mEGF) and human transforming growth factor- $\alpha$  (h-TGF- $\alpha$ ) with high affinity despite significant differences in the amino acid sequences of the ligands and the receptors [1]. In contrast, the chicken EGFR can discriminate between mEGF or hEGF and hTGF- $\alpha$ , the EGFs having approximately 100-fold lower affinity [2]. The regions responsible for this poor binding are known to be Arg<sup>45</sup> in hEGF [3] and the L2 domain in the chicken EGFR [4]. In this study we have produced a truncated form of the hEGFR ectodomain comprising domains L1/CR1/L2 plus the first module of the second Cys-rich region, CR2 (residues 1-501, sEGFR501). This truncated receptor was used to characterise its ligand-binding properties, including its ability to form ligand-induced dimers and to act as an inhibitor of EGF-stimulated mitogenic responses in BaF cells transfected with the EGFR [5]. In addition, based on a model of the EGFR extracellular domain [6] we have generated three mutants of sEGFR501 with single position substitutions at Glu<sup>367</sup>, Gly<sup>441</sup> or Glu<sup>472</sup> to Lys, the residue found in the corresponding positions in the chicken EGFR, to investigate the residues responsible for ligand discrimination.

### **Results and Discussion**

The BIAcore biosensor was used to determine both the rate and equilibrium binding constants for the interaction between sEGFR501 and immobilised hEGF or hTGF- $\alpha$  (Figure 1). Full-length ectodomain (sEGFR621) was used as a positive control for the surface reactivity. Analysis of the binding curves (Figure 2, Table 1) showed that sEGFR501 binds hEGF and hTGF- $\alpha$  with 10–20-fold higher affinity ( $K_D$  13–30 and 35–47 nM, respectively) than sEGFR621 [7]. Because of this increased affinity, sEGFR501 was tested as an inhibitor of the mitogenic stimulation of EGFR in a cell-based assay using the BaF cell line transfected with EGFR. It was observed that sEGFR501 was almost 10-fold more potent in this assay than the full-length ectodomain ( $IC_{50}$  = 0.15  $\mu$ M) and approximately 3-fold more potent than the neutralising anti-EGFR monoclonal antibody Mab528 ( $IC_{50}$  = 0.06  $\mu$ M).

Analytical ultracentrifugation showed that the primary EGF binding sites on sEGFR501 were saturated at an equimolar ratio of ligand and receptor, leading to the formation of a 2 : 2 EGF : sEGFR501 dimer complex. Additionally, chemically cross-linked dimers, as shown by SDS-PAGE analysis, could be generated in the presence of ligand. Since sEGFR501 lacks most of CR2, this region does not appear to be formally required for dimerisation.

Biosensor analysis was also used to analyse the binding of the transiently expressed sEGFR501 mutants to both immobilised hEGF and hTGF- $\alpha$  surfaces (Figure 1, Panel E, F, Table 1). The binding characteristics of Glu<sup>367</sup>Lys and Glu<sup>472</sup>Lys mutants were essentially undistinguishable from those of sEGFR501, (data not shown): however the Gly<sup>441</sup>Lys mutant showed preferential binding to the hTGF- $\alpha$  surface. Thus, the mutant Gly<sup>441</sup>Lys, resembled chicken EGFR in showing differential binding of hTGF- $\alpha$  and hEGF, implicating Gly<sup>441</sup>, in the L2 domain, as part of the binding site that recognises Arg<sup>45</sup> of hEGF.

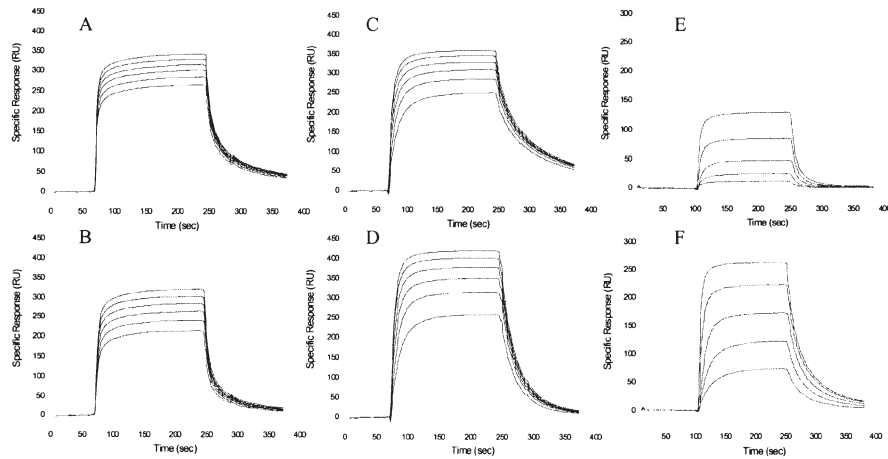


Fig. 1. BIAcore analysis of the interactions between sEGFR621 (A, B), sEGFR501(C, D) and Gly<sup>441</sup>Lys sEGFR (E, F) with immobilised hEGF (A, C, E) or hTGF- $\alpha$  (B, D, F).

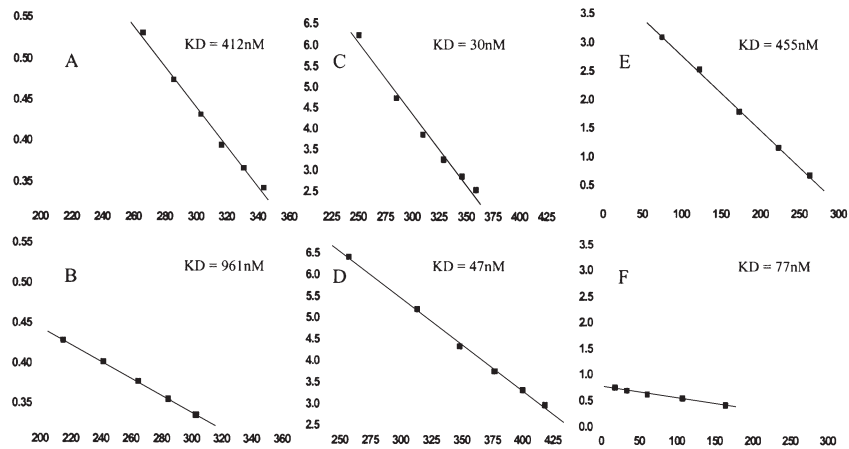


Fig. 2. Scatchard analysis of equilibrium binding data. The dissociation constant ( $K_D = 1/K_A$ ) was calculated from the equilibrium binding response obtained in Figure 1 by plotting the data in Scatchard format (Req/nC versus Req). The slope of the linear fit to the data gives  $K_A$ . (A) sEGFR621 versus hEGF, (B) sEGFR621 versus hTGF- $\alpha$ , (C) sEGFR501 versus hEGF, (D) sEGFR501 versus hTGF- $\alpha$ , (E) Gly<sup>441</sup>Lys sEGFR501 versus EGF, (F) Gly<sup>441</sup>Lys sEGFR501 versus hTGF- $\alpha$ .

**Table 1.** Comparative kinetic data for ligand binding by truncated, full-length EGFR and Gly<sup>441</sup>Lys sEGFR ectodomains to immobilised hEGF and hTGF- $\alpha$ .

Interaction	Kinetic Data		
	$K_a$ ( $M^{-1}s^{-1}$ ) $\cdot 10^{-5}$	$K_d$ ( $s^{-1}$ )	$K_D$ (nM)
sEGFR621/EGF	2.9–4.8	0.08	180–300
sEGFR621/TGF- $\alpha$	0.7–1.0	0.08	840–1320
sEGFR501/EGF	10–17	0.02	13–21
sEGFR501/TGF- $\alpha$	9.3–10.5	0.04	35–40
Gly <sup>441</sup> Lys sEGFR501/EGF	1.9–2.3	0.103	442–545
Gly <sup>441</sup> Lys sEGFR501/TGF- $\alpha$	5.2–6.9	0.025	36–48

## References

1. Groenen, L.C., Nice, E.C., Burgess, A.W. *Growth Factors* **11**, 235–257 (1994).
2. Lax, I., Johnson, A., Howk, R., Sap, J., Bellot, F., Winkler, M., Ullrich, A., Vennstrom, B., Schlessinger, J., Givol, D. *Mol. Cell. Biol.* **8**, 1970–1978 (1988).
3. van de Poll, M.L.M., Lenferink, A.E.G., van Vugt, M.J.H., Jacobs, J., Janssen, J., Joldersma, M., van Zoelen, E.J.J. *J. Biol. Chem.* **270**, 22337–22343 (1995).
4. Summerfield, A.E., Hudnall, A.K., Lukas, T.J., Guyer, C.A., Staros, J.V. *J. Biol. Chem.* **271**, 19656–19659 (1996).
5. Walker, F., Hibbs, M.L., Zhang, H.H., Gonez, L.J., Burgess, A.W. *Growth Factors* **16**, 53–67 (1998).
6. Jorissen, R.N., Epa, V.C., Treutlein, H.R., Garrett, T.P., Ward, C.W., Burgess, A.W. *Protein Sci.* **9**, 310–324 (2000).
7. Domagala, T., Konstantopoulos, N., Smyth, F., Jorissen, R.N., Fabri, L., Geleick, D., Lax, I., Schlessinger, J., Sawyer, W., Howlett, G.J., Burgess, A.W., Nice, E.C. *Growth Factors* **18**, 11–29 (2000).

## Thrombin Receptor Aromatic Residues for Edge-to-Face CH/ $\pi$ Interaction with Ligand Phe-2-phenyl Group

Tsugumi Fujita<sup>1</sup>, Yoshiro Chuman<sup>1</sup>, Daniela Riitano<sup>2</sup>, Takeru Nose<sup>1</sup>,  
Tommaso Costa<sup>2</sup> and Yasuyuki Shimohigashi<sup>1</sup>

<sup>1</sup>Laboratory of Structure-Function Biochemistry, Department of Chemistry, Faculty and  
Graduate School of Sciences, Kyushu University, Fukuoka, 812-8581, Japan

<sup>2</sup>Laboratorio di Farmacologia, Istituto Sperimentale di Sanita, Rome, Italy

### Introduction

Serine protease thrombin plays an important role in blood coagulation and possesses a specific receptor in the platelets. When thrombin cleaves the peptide bond between Arg-41 and Ser-42 in the N-terminal segment of receptor, the newly exposed N-terminal peptide segment binds to the receptor itself as a tethered ligand which activates the receptor [1]. Synthetic heptapeptide Ser-Phe-Leu-Leu-Arg-Asn-Pro (SFLLRNP, one letter amino acid codes) corresponding to this tethered-ligand is able to activate the receptor without thrombin, and the Phe-2 residue of this SFLLRNP peptide was found to be essential for receptor recognition and activation. In the present structure-activity studies to elucidate the role of Phe-2 in receptor activation, the benzene hydrogens in the Phe-2-phenyl group were suggested to be in the edge-to-face CH/ $\pi$  interaction with the receptor aromatic groups. Computer modeling of thrombin receptor indicated that the aromatic amino acid cluster in the fifth transmembrane domain (TM5: YYA<sub>Y</sub>YFSAFSAVFFF) is a binding site of this Phe-2-phenyl. In this study, in order to determine the genuine binding site of Phe-2-phenyl, we prepared mutant receptors in which Tyr in TM5 were replaced by Ala.

### Results and Discussion

We first synthesized a series of fluorophenylalanines ((F)<sub>n</sub>Phe) in which benzene-hydrogens were replaced by fluorines (n = 1 ~ 5) [2], and these (F)<sub>n</sub>Phe were incorporated into S/Phe/LLRNP at position 2. The analogs S/(F)<sub>n</sub>Phe/LLRNP were tested in the human platelet aggregation assay. The results suggested that benzene-hydrogen atoms at the *meta* and *ortho* positions are in the CH/ $\pi$  interaction with the receptor aromatic group [3,4]. In order to obtain more potent agonists, we designed and synthesized SFLLRNP analogs substituted by a series of halogen atoms at position 2, 3, and 4 of Phe-phenyl group (Figure 1). When the activities of these analogs were assessed, the analogs containing (3-Cl)Phe-2 and (3-Br)Phe-2 were found to be highly potent like (4-F)Phe-2-containing analog. Furthermore, the analogs S/(3-Cl,4-F)Phe/LLRNP and S/(3-Br,4-F)Phe/LLRNP were more potent than S/(3-Cl)Phe, (3-Br)Phe, or

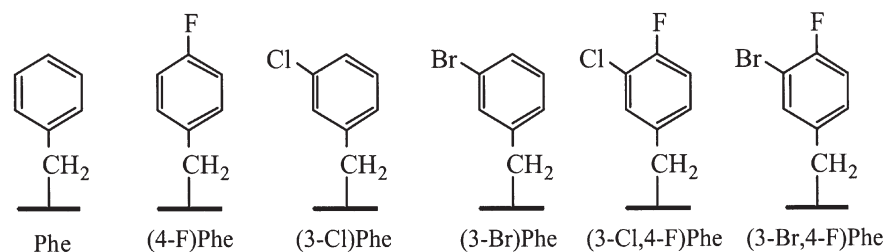


Fig. 1. Structure of halogenated phenylalanines.

(4-F)Phe/LLRNP. These results suggested that the effect of 3-Cl or 3-Br is distinct from that of 4-F in the Phe-2-phenyl group. All these results suggested the presence of the binding site specific for Phe-2-phenyl, which might be constructed by the aromatic groups in the receptor.

In order to explore the binding site of Phe-2-phenyl, we prepared the recombinant receptors in which Tyr residues in TM5 were replaced by Ala. The mutants (Y266A, Y267A, Y269A, and Y270A) were constructed by the PCR method, and were transiently expressed in COS-7 cells. The biological activity of S/Phe or (*p*-F)Phe/LLRNP for these mutants were evaluated by the assay to assess the activity in phosphoinositide hydrolysis. Mutant receptor Y267A was found to be almost as active as wild type receptor. On the contrary, Y266A, Y269A and Y270A elicited a rather enhanced activity for these peptide ligands. The results suggested that Tyr residues at position 266, 269, and 270 might construct a part of the binding site of Phe-2-phenyl.

### References

1. Vu, T.-K.H., Hung, D.T., Wheaton, V.I., Coughlin, S.R. *Cell* **64**, 1057–1068 (1991).
2. Fujita, T., Nose, T., Matsushima, A., Okada, K., Asai, D., Yamauchi, Y., Shirasu, N., Honda, T., Shigehiro, D., Shimohigashi, Y. *Tetrahedron Lett.* **41**, 923–297 (2000).
3. Nose, T., Fujita, T., Nakajima, M., Inoue, Y., Costa, T., Shimohigashi, Y. *J. Biochem.* **124**, 354–358 (1998).
4. Matsushima, A., Fujita, T., Nose, T., Shimohigashi, Y. *J. Biochem.* **128**, 225–232 (2000).

## **Regions of G-Protein-Coupled Receptors Identified by Multiple Sequence Alignment**

**Laerte Oliveira<sup>1</sup>, Gerrit Vriend<sup>2</sup> and Antonio C. M. Paiva<sup>1</sup>**

<sup>1</sup>*Department of Biophysics, Escola Paulista de Medicina, UNIFESP,  
Sao Paulo 04023-0062, Brazil*

<sup>2</sup>*CMBI, Katholieke Universiteit, 6525 ED, Nijmegen, The Netherlands*

### **Introduction**

G-protein-coupled receptors (GPCRs) have a common fold, seen in rhodopsin structure [1], consisting of a bundle of 7 transmembrane helices (I–VII; 7TM), and have been targets of exhaustive studies that allowed some knowledge about their function. These studies indicate that GPCRs are activated by agonist binding to their extracellular domains, thus creating a signal, which activates cytoplasmic G-proteins. However, recent findings revealed that GPCR functioning is not so simple, but involves other events such as oligomerization and constitutive activation [see GPCRDB and reference 2]. In an attempt to better understand these processes, we have started an extensive study of GPCRs using the large number of sequences available and the rhodopsin structure as a template.

### **Results and Discussion**

1,121 sequences of all GPCR classes were aligned [3] and values of variability (V) (no. of different residues) and entropy (E) were determined for each of 205 positions and plotted on an E/V graph. Five sectors of this graph were then identified (Figure 1a): 11 (low E and V); 12 (intermediary E and low V); 22 (intermediary E and V); 32 (high E and intermediary V) and 33 (high E and V).

In the rhodopsin structure, the positions of sectors 11, 12 and 22 are mostly located at the cytosolic 7TM half in contact with the receptor central cavity. Positions of sector 23 are differently distributed: residues pointing either to adjacent helices or to the lipid matrix are seen along the entire 7TM structure, whereas internal positions are only in the extracellular half, surrounding the retinal pocket. Positions of sector 33 are exclusively in the extra-membrane ends of helices or loops and preferentially pointing outwards. When these results were analyzed in the light of mutational studies relating function to residue positions [see tinyGRAP and reference 4], the following conclusions were reached:

1. A common site to all GPCRs (main site) would be formed by conserved and internal residue positions of sectors 11 and 12. As in the rhodopsin structure [1], the cytosolic mouth of the receptor central cavity should be open and thus it is likely that the receptor main site is accessible from the internal medium and could bind G-proteins and arrestins.

2. An agonist site would be formed by internal positions of sectors 23 and 33.

3. Cytosolic sites would be formed by positions of sectors 23 and 33 on the internal face of helix VI and mainly on the external faces of helices II, III and VI (see the example in Figure 1b). Sequence analyses in these sites allowed a different grouping of receptors from the patterns dictated by agonist and G-protein specificity. As shown in Figures 1b and 1c, sequence similarities are seen in angiotensin II (AT<sub>1</sub>), substances P and K, somatostatin, interleukin-8 and chemokine receptors; in rhodopsin, some odorant and visual pigment receptors; in TRH, vasopressin, opioid and some odorant receptors and in some amine receptors. These results support the hypothesis that

GPCR cytosolic sites might bind at still-unknown cytosolic factors in a parallel and regulatory process of G-protein coupling.

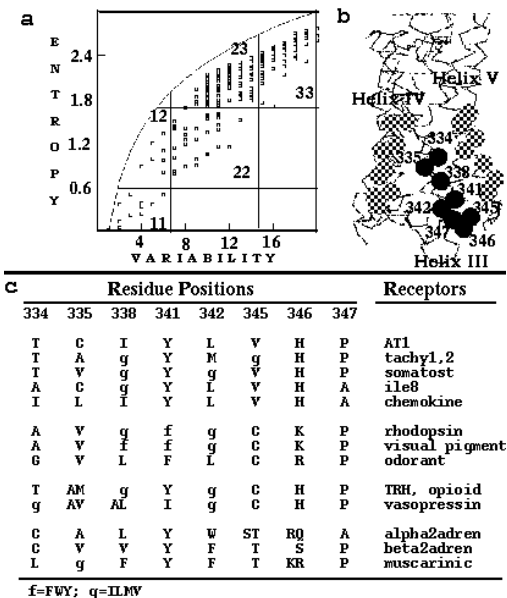


Fig. 1. Aligned positions of GPCRs: a) Entropy against variability values; b) putative site formed by residue positions at the external face of helix III cytosolic end; c) residues found in this site for receptor groups.

Acknowledgments

Supported by FAPESP and CNPq.

References

1. Palczewski, K., Kumasaka, T., Hori, T., Behnke, C.A., Motoshima, H., Fox, B.A., Le Trong, I., Teller, D.C., Okada, T., Stenkamp, R.E., Yamamoto, M., Miyano, M. *Science* **289**, 739 (2000).

2. Horn, F., Vriend, G., Cohen, F.E. *Nucleic Acids Res.* **29**, 346 (2001).

3. Oliveira, L., Paiva, A.C.M., Vriend, G.J. *Comput.-Aided Mol. Des.* **7**, 649 (1993).

4. Kristiansen, K., Dahl, S.G., Edvardsen, O. *Proteins* **26**, 81 (1996).

## Tools for the Identification of Receptor Dimmers: Synthesis and Biological Evaluation of On-Resin Dimerized, Photosensitive Analogues of Angiotensin II

Kimberley A. Therrien<sup>1</sup>, Maud Deraët<sup>1</sup>, Anick Dubois<sup>1</sup>, Lenka Rihakova<sup>1</sup>,  
 Eric A. Kitas<sup>2</sup>, Walter Meister<sup>2</sup>, Robert Speth<sup>3</sup> and Emanuel Escher<sup>1</sup>

<sup>1</sup>Institut de Pharmacologie, Université de Sherbrooke, Sherbrooke QC, J1H 5N4, Canada

<sup>2</sup>F. Hoffmann-La Roche Ltd., 4070 Basel, Switzerland

<sup>3</sup>Washington State U. Pullmann, WA 99164 USA

### Introduction and Chemistry

Molecular tools for the identification of homodimers of G protein coupled receptors are not available yet. We intended to investigate the possibility of functional dimerization of the known angiotensin II (AngII, DRVYIHPF) receptors AT1 and AT2; either as homo-dimers of AT1 or AT2 or as heterodimers of AT1-AT2. For this purpose, we synthesized AngII dimer ligands with a photosensitive residue (*p*-benzoylphenylalanine, **B**) in the C-terminal position. The dimers were held together with linkers anchored either to the N<sup>α</sup>-terminus (**I**), or to N<sup>ε</sup> of Lys in position 1 (**II**), or to N<sup>ε</sup> of Lys in position 3 (**III**), or to *p*-NH<sub>2</sub>-Phe replacing Y in position 4 (**VI**). The linker was of the general structure {CO(CH<sub>2</sub>)<sub>n</sub>NH}<sub>2</sub>**X**, where **n** = 10 and **X** is either CO or CO(CH<sub>2</sub>)<sub>m</sub>CO with **m** = 1–10. Fmoc peptide synthesis was carried out on Tentagel resin (0.06 meq/g) or Wang resin (0.7 meq/g). Orthogonality for linker introduction was achieved with N<sup>α</sup>-Boc-N<sup>ε</sup>-Fmoc-Lys for group **II**, with N<sup>α</sup>-Fmoc-N<sup>ε</sup>-Dde-Lys for **III**, and N<sup>α</sup>-Fmoc-Nar-Dde-*p*-NH<sub>2</sub>-Phe for **VI**. Couplings were performed with TPTU. On-resin dimerization was achieved after Fmoc deprotection of the first linker moiety, by coupling for 2 h with either carbonyldiimidazole or the respective diacid disuccinimide in half-equivalent amount, followed by a five-fold excess of dimerization reagent until a negative ninhydrine test. Peptide resins were cleaved with 95% TFA & 2% triisopropylsilane; crude peptides were purified by prep RP-HPLC, lyophilized and analyzed by electrospray MS. Dimers were assessed for their binding potencies on bovine adrenocortical membranes and on membranes from COS-7 cells, transiently transfected with hAT1 or hAT2.

### Results and Discussion

Dimerization reactions were quite effective, **III** (**n** = 10, **X** = CO) yield of dimer 40% on 0.06 meq/g resin; **IV10/1-9** 55–78%, 0.7 meq/g. All analogues from group **I** to **III** had, however, quite low affinities to the AT1 preparations (K<sub>i</sub> > 0.2 μM), except ana-

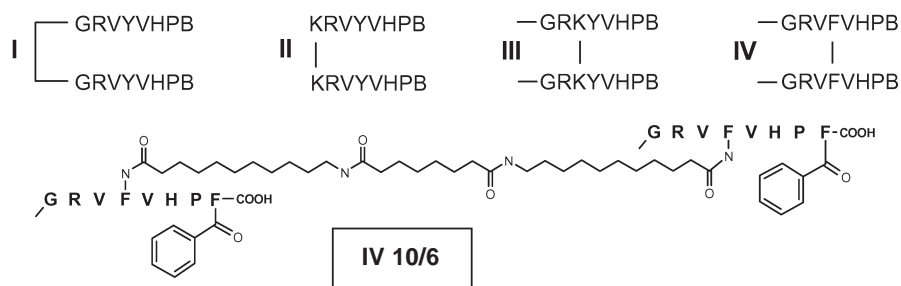


Fig. 1. Schematic structures of AngII dimer groups **I** to **IV** and of compound **IV10/6**.

logue **IV**, **n** = 10, **m** = 6 (**IV10/6**, Figure 1). A sub-series determined optimal linker length in group **IV**, where **m** varied from 1 to 9 and **n** was kept at 10. For **IV m** = 6 and 7, affinities were 58 nM (**IV10/6**) and 70 nM (**IV10/7**). For all the other analogues affinities of 0.2  $\mu$ M or higher were observed. As a last analogue **IV10/6SS** with a cleavable linker unit was synthesized with **X** =  $-\text{COCH}_2\text{CH}_2\text{SSCH}_2\text{CH}_2\text{CO}-$ , having identical 60 nM affinity to hAT1. Radio-iodination of **IV10/6** and **IV10/6SS** was carried out, presumably on the acylanilide moiety, with harsher and longer incubation times (2 h), but with yields (5–10%) still lower than for comparable peptide-Tyr iodination. Photolabeling with HPLC-purified  $^{125}\text{I}$ -**IV10/6** was carried out on bovine adrenocortical membranes (Boulay *et al.*, *Mol. Pharmacol.* **41**, 809 (1992)), using receptor selective ligands for AT1 (L158809, 10  $\mu$ M) and AT2 (PD123319, 10  $\mu$ M), as well as AngII as competitors. SDS-PAGE, followed by autoradiography, revealed two labeled protein bands, one in the range of 130 kDa and a second, non-specific, at 85 kDa. Simultaneous labeling with  $^{125}\text{I}$ -(N-MeG<sup>1</sup>,B<sup>8</sup>)AngII labeled only the previously reported 65 kDa AngII receptors. In competition experiments with  $^{125}\text{I}$ -**IV10/6** and either of the selective ligands L158809 or PD123319 (10  $\mu$ M) labeling of the 130 kDa protein was reduced, but in concomitant presence of L158809 and PD123319, it was abolished (Figure 2A). This result was therefore suggestive of an eventual AT1-AT2 heterodimer, although AngII was inefficient as a competitor. The labeled 130 kDa protein was subjected to deglycosylation (Servant *et al.*, *JBC* **272**, 8653 (1997)), but no change in molecular weight was observed, contrary to the shift from 65 to 32 kDa observed with the  $^{125}\text{I}$ -(N-MeG<sup>1</sup>,B<sup>8</sup>)AngII labeled material (Figure 2B). Identical photolabeling with  $^{125}\text{I}$ -**IV10/6SS** revealed also the 130 kDa protein but DTT reduction failed to produce lower MW proteins, as disulfide-linked receptor dimers should do. In a final experiment,  $^{125}\text{I}$ -**IV10/6** was used to label membranes from COS-7 cells co-transfected with AT1 and AT2, however, labeled proteins corresponding to receptor dimers could not be found.

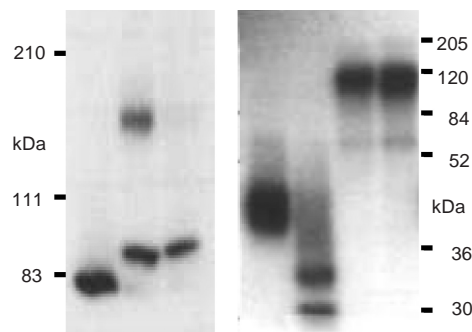


Fig. 2. SDS-PAGE autoradiographs. Panel A (5%): lane 1: photolabeling with  $^{125}\text{I}$ -(N-MeG<sup>1</sup>,B<sup>8</sup>)AngII; lane 2: idem with  $^{125}\text{I}$ -**IV10/6**, lane 3: idem with  $^{125}\text{I}$ -**IV10/6** & L158809 & PD123319. Panel B (7.5%): lane 1 idem 1A, lane 3 idem 2A, lane 2 and 4 same as 1 and 3 but deglycosylated before.

### Conclusions

(i) Peptide dimers can be efficiently formed on-resin with bi-functional active esters in good yields, even with long linker functions and low resin substitutions. (ii) Bioactive AngII dimers are possible with bridgeheads on the side-chain of position 4. (iii) Homodimers or heterodimers of AngII receptors AT1 and AT2 could not be found.

## Minimization of Parathyroid Hormone Using Simultaneous Multiple Peptide Synthesis: Implications for Structure Based Drug Design

Ashok Khatri<sup>1,2</sup>, Xiang-Chen Huang<sup>1</sup>, Brian D. Petroni<sup>1</sup>  
and Thomas J. Gardella<sup>1,2</sup>

<sup>1</sup>Massachusetts General Hospital

<sup>2</sup>Harvard Medical School, Boston, MA 02114, USA

### Introduction

Parathyroid hormone (PTH), an 84 residue long polypeptide, acts on PTH-1 receptors in bone and kidney to control blood calcium levels. Synthetic PTH(1-34), one of the first peptide hormones to be chemically synthesized, has full biological activity [1] ( $EC_{50}$  for cAMP generation  $\approx 2$  nM). Based on previous peptide truncation studies that identified residues 15-31 as the principal receptor-binding domain and residues 1-14 as the principal signaling domain, PTH(1-14) was synthesized and found to have faint but measurable activity ( $EC_{50} \approx 200$   $\mu$ M) [2]. The peptide was prepared on a multiple peptide synthesizer and the crude peptide was found to be of high quality, as shown by HPLC and MALDI-MS, and could be used directly in bioactivity assays after a simple desalting step on a disposable C18 cartridge. This finding prompted us to use this approach to synthesize an extensive series of PTH(1-14) analogs with which we could define structure-activity relationships in the peptide and potentially improve potency. Within a short time ( $\approx 1.5$  years) we generated and characterized over 200 PTH(1-14) analogs and have thus far improved potency at least 1,000 times.

### Results and Discussion

Our substitution approach involved: i) alanine-scanning [2]; ii) type-substitution, in which at least one of each type of amino acid was introduced at each position [3]; and iii) systematic sidechain modification, in which sidechain structures are varied incrementally using amino acid analogs [4]. Analytical HPLC and MALDI-MS performed on each desalted crude peptide demonstrated that most ( $>90\%$ ) contained more than 70% of the desired product. From time to time, a portion of a desalted crude peptide was purified by semi-preparative HPLC and compared to its crude counterpart for bioactivity. The differences between the potencies and efficacies of the purified and the corresponding crude peptides were marginal and not significant (Table 1).

The overall work has revealed that: i) the 1-9 region of PTH(1-14) is relatively intolerant to substitution whereas the 10-14 region is tolerant [2]; ii) activity-enhancing effects ( $\approx 3$ - to 10-fold) are possible with substitutions at positions -3, -10, -11, -12, and -14; and iii) the enhancing effects are additive, as [M]PTH(1-14) is 1,000-fold

Table 1. Potencies and efficacies of the purified and crude peptides.

[M]PTH(1-14) <sup>b</sup>	$EC_{50}$ <sup>a</sup> (nM)	$E_{Max}$ (picomole/well)
CRUDE	$100 \pm 20$	$270 \pm 8$
HPLC	$60 \pm 10$	$290 \pm 20$

<sup>a</sup> cAMP accumulation was assessed in LLC-PK1 cells expressing the hP1R; <sup>b</sup> [M]PTH(1-14) = [Ala<sup>1,3,12</sup>,Gln<sup>10</sup>,Har<sup>11</sup>,Trp<sup>14</sup>]rPTH(1-14)NH<sub>2</sub>.

more potent than PTH(1-14) [4]; iv) the (10-14) region is amenable to protein engineering (*e.g.* insertion of a zinc-binding motif [5]); v) side-chain aromaticity, polarizability and length, as in homoarginine, are beneficial at position 11 [4]; and vi) minimization to PTH(1-11) is possible [4]. The new shorter length analogs are also useful as functional probes of the receptor interaction topology, as interactions to the receptor's heptahelical juxtamembrane region has been demonstrated [4].

### **Conclusions**

Multiple peptide synthesis can be used to minimize PTH to its essential pharmacophore: residues (1-14) or even (1-11). The strategy avoids the need for time- and material-consuming HPLC purification and enables a relatively high throughput approach to PTH analog design. The results could have implications for the design of novel PTH receptor agonists; such compounds would be of pharmaceutical interest, as PTH(1-34) has recently been shown to be effective in treating osteoporosis [6]. Minimized ligands can help elucidate the fundamental mechanisms by which PTH activates its Class II GPCR. The approach could potentially be applicable to the other Class II peptide hormones (*e.g.* secretin, glucagon, GLP, GIP, VIP, PACAP, calcitonin, GHRH, CRF).

### **References**

1. Tregear, G.W., Van Rietschoten, J., Greene, E., et al. *Endocrinology* **93**, 1349–1353 (1973).
2. Luck, M., Carter, P., Gardella T. *Mol. Endocrinol.* **13**, 670–680 (1999).
3. Shimizu, M., Potts, J.T., Jr., Gardella, T. *J. Biol. Chem.* **275**, 21836–21843 (2000).
4. Shimizu, Carter, P., Khatri, A., et al. *Endocrinology* **142**, 3068–3074 (2001).
5. Carter, P., Gardella, T. *Biochim. Biophys. Acta* **1538**, 290–304 (2001).
6. Neer, R., Arnaud, C., Zanchetta, J., et al. *N.E.J.M.* **344**, 1434–1441 (2001).

## Structure-Activity Relationship Studies of New Cyclic MSH Analogues Using Cloned-Human Melanocortin Receptors Lead to Greater Selectivity and Inverse Agonists

Minying Cai, Paolo Grieco, Jonathan Wiens, Dev Trivedi and Victor J. Hruby

Department of Chemistry, University of Arizona, Tucson, AZ, USA

### Introduction

Melanotropins are peptides derived through a series of proteolytic cleavages from the precursor protein pro-opiomelanocortin. These melanotropin peptides are known to have a broad spectrum of physiological actions including regulation of pigmentation, thermoregulation, regulation of feeding behavior and erectile dysfunction [1]. The melanocortin receptors (MCRs) are members of G-protein coupled receptors (GPCRs) family and to date five subtypes of melanocortins have been cloned and characterized. To evaluate specific pharmacophore hypotheses regarding agonist, antagonist, and inverse-agonist affinities for hMCR3, hMCR4, hMCR5, a series of  $\alpha$ -MSH analogues have been designed and synthesized for this work based on earlier results [2,3].

### Results and Discussion

Grieco *et al.* have demonstrated that template PG901; Ac-Nle-c[Asp-Pro-DNal(2')-Arg-Trp-Lys]-NH<sub>2</sub>, is a highly selective agonist [3] at human melanocortin 5 receptor (hMCR5) and antagonist at the hMCR3 and hMCR4 (unpublished results). In the template PG901, we exchanged D-Phe for D-Nal(2') at position 7 and D-Nal(2') for Trp at

Table 1. Binding and intracellular cAMP accumulation of melanotropin analogues at the different human melanocortin receptors.

	hMCR3			hMCR4			hMCR5		
	IC <sub>50</sub> nM	EC <sub>50</sub> nM	%Max Effect	IC <sub>50</sub> nM	EC <sub>50</sub> nM	%Max Effect	IC <sub>50</sub> nM	EC <sub>50</sub> nM	%Max Effect
PG927	8.54	1.16	93	26.7	2.87	84	57	4.86	107
PG928	0.23	>10000	0	1.15	>10000	0	0.33	1.43	138
PG933	0.97	0.52	98	1.78	18.2	96	1.16	>1300	0
PG934	0.02	>10000	0	0.12	>1000	1	0.15	6.99	161
PG-937	1.62	-1.04	-28	12.0	4.54	46	12	138	70
MTII	1.52	1.85	100	2.38	2.87	100	6.27	2.45	100
NDP- $\alpha$ -MSH	0.79	2.85	100	0.24	4.02	100	0.63	0.22	100
PG927 <sup>a</sup>	0.1	NA	3	2.1	NA	2	0.02	0.08	107

IC<sub>50</sub> = Concentration of peptide at 50% specific binding (N = 4); EC<sub>50</sub> = Effective concentration of peptide that was able to generate 50% maximal intracellular cAMP accumulation (N = 4). The peptides were tested at a range of concentrations (10<sup>-10</sup>–10<sup>-5</sup>); <sup>a</sup> PG901 data is from Merck; NA: no activity; PG927: Ac-Nle-c[Asp-Pro-DPhe-Arg-DNal(2')-Lys]-NH<sub>2</sub>; PG928: Ac-Nle-c[Asp-Pro-DNal(2')-Arg-Dnal(2')-Lys]-NH<sub>2</sub>; PG933: Ac-Nle-c[Asp-Pro-DPhe-Arg-Trp-Gly-Lys]-NH<sub>2</sub>; PG934: Ac-Nle-c[Asp-Pro-DNal(2')-Arg-Trp-Gly-Lys]-NH<sub>2</sub>; PG-937: Ac-Nle-c[Asp-Hyp-DPhe-Arg-Trp-Lys]-NH<sub>2</sub>; MTII: Ac-Nle-c[Asp-His-D-Phe-Arg-Trp-Lys]-NH<sub>2</sub>; NDP- $\alpha$ -MSH: Ac-Ser-Tyr-Ser-Nle-Glu-His-D-Phe-Arg-Trp-Gly-Lys-Pro-Val-NH<sub>2</sub>.

position 9. Next, we incorporated Gly in position 10 and thus extended the peptide chain to obtain PG933 and PG934. Finally, we replaced Pro in position 6 of our parent compound PG901 with hydroxyproline (Hyp). Biological activities of these analogues were determined and are shown in Table 1.

It was found that the presence of D-Nal(2') at position 7 results in greater ligand binding to receptor in all of the human melanocortin receptors, while efficacy dropped to zero at the hMCR3 and hMCR4 but not at the hMCR5 leading to increased selectivity. Introducing a bulky hydrophobic residue at position 7 is the main reason for the improved selectivity. Similar results were obtained when Trp was reintroduced (PG933 and PG934) in position 9 in place of D-Nal(2'), but this time selectivity at hMCR5 was reversed and that could be due to the extension of peptide chain with Gly providing a very high degree of mobility at position 10.

Interestingly, PG937 is an inverse-agonist when compared with its parent compound PG901, which is only an antagonist at hMCR3. We believe that hydrogen bonding plays an important role in this unique property of PG937.

#### **Acknowledgment**

This work was supported by a grant from the U.S. Public Health Service, Grant DK17420.

#### **References**

1. Wikberg, J.E.S., Muceniece, R., Mandrika, I., Prusis, P., Lindblom, J., Claes, P., Skottner, A. *Pharmacol. Res.* **42**, 393–420 (2000).
2. Hruby, V.J., Lu, D., Sharma, S.D., de L. Castrucci, A., Kesterson, R.A., Al Obeidi, F.A., Hadley, M.E., Cone, R.D. *J. Med. Chem.* **38**, 3454–3461 (1995).
3. Grieco, P., Balse, P., Weinberg, D., MacNeil, T., Hruby, V.J., In *Peptides for the New Millennium*, G.B. Fields, J.P. Tam and G. Baranny (Eds.), Kluwer, Dordrecht, 2000, pp. 541–542.

## Structure-Activity Relationships of Arodyn, a Novel Dynorphin A-(1-11) Analogue

Marco A. Bennett<sup>1</sup>, Thomas F. Murray<sup>2</sup> and Jane V. Aldrich<sup>1</sup>

<sup>1</sup>Dept. of Pharmaceutical Sciences, School of Pharmacy, University of Maryland,  
Baltimore 21201, USA

<sup>2</sup>Dept. of Physiology and Pharmacology, College of Veterinary Medicine, University of Georgia,  
Athens, GA 30602, USA

### Introduction

The opioid receptors, mu ( $\mu$ ), kappa ( $\kappa$ ) and delta ( $\delta$ ), are widely distributed throughout the peripheral and central nervous system. When activated, the opioid receptors attenuate the transmission of pain signals to the spinal cord. Dynorphin A, an endogenous agonist at  $\kappa$  receptors, shares a common *N*-terminal “message” sequence (Tyr-Gly-Gly-Phe) with most mammalian opioid peptides and has a unique C-terminal “address” sequence [1]. The “message” sequence has been reported to be important for  $\kappa$  activation, while the “address” sequence is designated as the potency-enhancing domain [1].

**Dyn A-(1-11)NH<sub>2</sub>:** H-Tyr-Gly-Gly-Phe-Leu-Arg-Arg-Ile-Arg-Pro-Lys-NH<sub>2</sub>

We are interested in synthesizing potent and  $\kappa$  opioid receptor selective peptide antagonists. Kappa receptor antagonists have been proposed for the treatment of opioid dependence [2]. While nonpeptide  $\kappa$  selective antagonists (nor-BNI and recently GNTI [3]), have been identified, highly selective peptide antagonists are complementary to nonpeptide antagonists and can be useful as pharmacological tools to study  $\kappa$  receptor-ligand interactions.

### Results and Discussion

Arodyn (*aromatic dynorphin*) was designed based on a lead peptide identified from a combinatorial library prepared in our laboratory [4]. Arodyn demonstrated high affinity ( $K_i = 10.0 \pm 3.0$  nM) and remarkable selectivity [ $K_i$  ratio ( $\kappa/\mu/\delta$ ) = 1/174/583] for  $\kappa$  opioid receptors. In the adenylyl cyclase assay at these receptors it is a partial agonist with low efficacy (maximum inhibition of  $12 \pm 8$  % of cAMP formation relative to Dyn A-(1-13)NH<sub>2</sub>).

**Arodyn:** Ac-Phe-Phe-Phe-Arg-Leu-Arg-Arg-D-Ala-Arg-Pro-Lys-NH<sub>2</sub>

A classic alanine scan (residues 1-11) was performed on arodyn to determine which residues are important for binding to  $\kappa$  opioid receptors. The des-acetylated arodyn was synthesized to compare the binding affinities of the peptide containing a free amine terminus *versus* the acetylated arodyn. An *N*-methyl amino acid scan of residues 1 to 3 was also performed. The rationale for these derivatives is that *N*-alkylated amino acids can alter the backbone conformation and thus could affect the binding affinity of the ligands.

The peptides in this study were assembled on a PAL-PEG-PS resin using the Fmoc synthetic strategy. Fmoc protected amino acids were coupled to the growing peptide chain using HBTU and *N*-methylmorpholine. Chinese hamster ovary cells stably expressing  $\kappa$  opioid receptors were used in radioligand binding assays [5].

## Peptide Conjugates

Structure-activity relationships (SAR) for arodyn appear to be different from those for Dyn A. In the alanine scan, substitution of the aromatic residues in positions 1 to 3 by Ala resulted in only small ( $\leq 4$ -fold) decreases in affinity for the  $\kappa$  opioid receptors. In contrast, substitution of the aromatic residues in positions 1 and 4 of Dyn A result in large decreases in opioid receptor affinity [6]. Additional analogs in the Ala scan are currently being evaluated for their  $\kappa$  receptor affinity.

Table 1. Kappa opioid receptor binding affinity of arodyn and selected analogues.

Arodyn analogs	$K_i(\kappa) \pm \text{SEM (nM)}$	Relative Potency (%)
Arodyn	$10.0 \pm 3.0$	100
[Ala <sup>1</sup> ]-	$34.5 \pm 3.0$	29
[Ala <sup>2</sup> ]-	$10.6 \pm 1.6$	94
[Ala <sup>3</sup> ]-	$28.4 \pm 2.3$	35
[NMePhe <sup>1</sup> ]-	$4.6 \pm 0.4$	217
[NMePhe <sup>2</sup> ]-	$14.7 \pm 2.2$	68
[NMePhe <sup>3</sup> ]-	$20.9 \pm 3.5$	48

*N*-MePhe substituted in position 1 of arodyn resulted in a 2-fold increase in  $\kappa$  receptor affinity. A small decrease in binding affinity for  $\kappa$  opioid receptors ( $\leq 2$ -fold compared to arodyn) was seen with *N*-MePhe in positions 2 or 3.

Further pharmacological evaluation of these analogues is in progress. These results provide insight into the SAR of a novel, highly  $\kappa$  selective peptide and will be useful in the design of additional analogues as potential  $\kappa$  receptor antagonists.

## Acknowledgments

This research was supported by NIDA grant R01 DA05195 and by a University of Maryland Graduate School Program Enrichment Fellowship (M.A.B.). We thank Jennif Chandler and Beverly Marinda Thomas for performing the radioligand binding assays.

## References

1. Chavkin, C., Goldstein, A. *Proc. Natl. Acad. Sci. U.S.A.* **78**, 6543–6547 (1981).
2. King, A.C., Ho, A., Shluger, J., Borg, L., Kreek M.J. *Drug Alcohol Depend.* **54**, 87–90 (1999).
3. Stevens, W.C.Jr., Jones, R.M., Subramanian, G., Metzger, T.G., Ferguson, D., Portoghese, P.S. *J. Med. Chem.* **43**, 2759–2769 (2000).
4. Aldrich, J.V., Wan, Q., Murray, T.F., manuscript in preparation.
5. Arttamangkul, S., Ishmael, J.E., Murray, T.F., Grandy, D.K., DeLander, G.E., Kieffer, B.L., Aldrich, J.V. *J. Med. Chem.* **40**, 1211–1218 (1997).
6. Turcotte, A., Lalonde, J.-M., St.-Pierre, S., Lemaire, S. *Int. J. Pept. Protein Res.* **23**, 361–367 (1984).

## Neurohypophyseal Receptors-Ligands: Where We Are After the Landmark Rhodopsin Structure Determination

Jerzy Ciarkowski, Piotr Drabik, Artur Giełdoń,  
Rajmund Kaźmierkiewicz and Rafał Ślusarz

*Faculty of Chemistry, University of Gdańsk, Sobieskiego 18, 80-952 Gdańsk, Poland*

### Introduction

Hepta-helical transmembrane receptors transducing diverse external signals to cells *via* activation of heterotrimeric GTP-binding proteins (G-proteins), estimated to occupy over 3% of our genome [1] and to mediate actions of 60% of drugs [2], had long been resistant to structure determination. Thus, the first 3D structure of a G protein-coupled receptor (GPCR) dark rhodopsin (RD) [3], is a landmark event as it provides at last a trustworthy 3D prototype for the inactive (antagonist-bound) form of this huge family of proteins. Our interest in mechanisms of signal transduction by three other GPCRs, *i.e.*, vasopressin pressor, antidiuretic, and oxytocin receptors (V1aR, V2R and OTR, respectively) thus needs a verification of the models. Of a few theoretical GPCR templates [4–6], our recent favorite was based on the robust assumption, simultaneously applied to 400 sequences, that if intra-molecular *particular* polar interactions were maximized, the TM-bundles would converge to a realistic *common* 3D pattern [4].

### Results and Discussion

Prior to the V1aR, V2R and OTR model building, we compared our favorite theoretical [4] with the experimental [3] RD model, Figure 1. To our surprise, the transmembrane helices TM1–TM4 (rear) and TM7 (front-right) fit quite well in both models. TM5s (most-left) fork away to the top, the experimental one sticking more out of the bundle to reach 6–7 Å displacement at their N-ends. TM6s (front-left) are mutually shifted by a turn, the new one being closer to the cytosol. Thus, despite its obsolescence, the theoretical template offered by Pogozheva *et al.* [4] has proved an excellent 3D prediction.

A subsequent AMBER [7] molecular dynamics (MD) simulation to the *cis*-to-*trans* conversion of the TM7 K296-retinal C11–C12 bond, hoped to be a driver of the RD

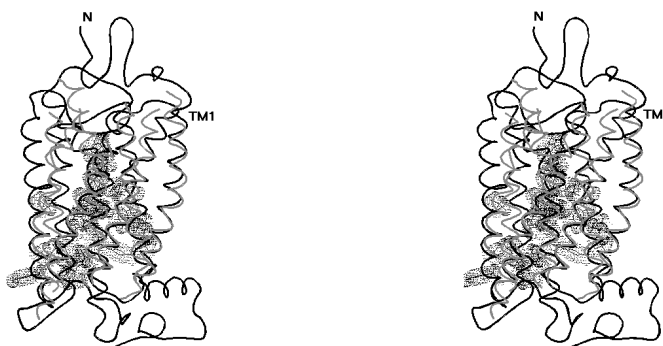


*Fig. 1. Stereo: The old template (gray; for clarity only TM-helices and no ligand are shown) superimposed optimally on the new one (black). The C $^{\alpha}$ -TM-domain based RMS for 132 atoms equals to 1.53 Å. N-terminus is extracellular, TM1–TM7 run counterclockwise when top-viewed. 25 conservative side chains, see Table 1, are marked as dotted surfaces on the new template.*

change from the inactive/dark to the active/meta-II form, has failed in the respect that the resultant strain-less retinal *trans* isomer has brought about no major change in the protein shape. A reason for this could be a too short ( $\approx 400$  ps) target-oriented MD in relation to a very large protein-to-ligand inertia ratio. Thus, only putative inactive receptor forms were further considered.

The V1aR, V2R and OTR inactive receptors were homology-modeled from the experimental dark RD template. The selective antagonists, SR-49059 [8], SR-121463A [9] and L-372662 [10], respectively, were docked in the receptors using the genetic algorithm in the Autodock program [11]. Both empty and antagonist-bound receptors were relaxed using Amber MD [7]. The procedures are described [12]. The intra- and intermolecular interactions, filtered in order to catch those in the chains of highly conserved receptor residues, were tested using a home-made program (unpublished). The antagonist-bound receptors do not deform much from their inactive prototypes. The new relaxed models, both empty and ligand-bound, are better packed than the old ones, reflected by more extensive (by 20–35%) sets of intramolecular interactions in the former than in the latter, both in general and among the conserved residues. The network of the most conservative intra-receptor interactions among 25 conservative residues of potential role in the receptor activation is given as dotted surfaces in Figure 1 while the residues are listed in Table 1.

Table 1. 25 conservative residues (in order RD/OTR/V1aR/V2R) making the set of conservative interactions potentially involved in inter-TM-helical switches and signal transduction [6].

TM1	TM2	TM3	TM4	TM5	TM6	TM7
N55/57/69/55	N78/H80/92/80	A124/S126/138/126	W161/161/175/164	C222/219/C235/224	V254/T277/293/273	S298/N321/340/317
T58/V60/72/58	A82/84/96/84	L128/130/142/I130		Y223/220/236/Q225	F261/284/Y300/280	A299/S322/341/318
	D83/85/97/85	L131/M133/145/133			C264/287/303/283	N302/325/344/321
		E134/D136/148/136			W265/288/304/284	P303/326/345/322
		R135/137/149/137			P267/290/306/286	Y306/329/348/325
		Y136/C138/Y150/H138			Y268/F291/307/287	

## Acknowledgments

Supported by the Polish Committee for Scientific Research, grant no 0752/P04/99/17; and by the academic high-power computer centers: ICM at the University of Warsaw and CI TASK at the Technical University in Gdańsk.

## References

1. Bourne, H.R., Meng, E.C. *Science* **289**, 733–734 (2000).
2. Guderman, T., Neunberg, B., Schultz, G. *J. Mol. Med.* **73**, 51–63 (1995).
3. Palczewski, K., et al. *Science* **289**, 739–745 (2000).
4. Pogozheva, I.D., Lomize, A.L., Mosberg, H.I. *Biophys. J.* **72**, 1963–1985 (1997).
5. Herzyk, P., Hubbard, R.E. *J. Mol. Biol.* **281**, 741–754 (1998).
6. Baldwin, J.M., Schertler, G.F., Unger, V.M. *J. Mol. Biol.* **272**, 144–164 (1997).
7. Case, D.A. et al., *AMBER 5.0*, University of California, San Francisco, CA, 1997.
8. Serradeil-Le Gal, C., et al. *J. Clin. Invest.* **92**, 224–231 (1993).
9. Serradeil-Le Gal, C., In Zingg, H.H., Bourque, C.W., Bichet, D.G. (Eds.) *Vasopressin and Oxytocin*, Plenum Press, New York, 1998, pp. 427–438.
10. Freidinger, R.M., et al., In Shimonishi, Y. (Ed.) *Peptide Science – Present and Future*, Kluwer, Dordrecht, 1999, pp. 618–623.
11. Morris, G.M., et al. *J. Comput. Chem.* **19**, 1639–1662 (1998).
12. (a) Politowska, E., et al. *Acta Biochim. Polon.* **48**, 83–93 (2001). (b) Gieldoń, A., et al. *J. Comp. Aided Mol. Des.* **15**, in press.

## Synthesis, Bioactivity and Receptor Binding of Fluorescent NBD Labeled Analogs of the Tridecapeptide Mating Pheromone of *Saccharomyces cerevisiae*

Fa-Xiang Ding<sup>1</sup>, B.K. Lee<sup>2</sup>, Jeffrey M. Becker<sup>2</sup> and Fred Naider<sup>1</sup>

<sup>1</sup>Department of Chemistry, College of Staten Island, CUNY, NY 10314, USA

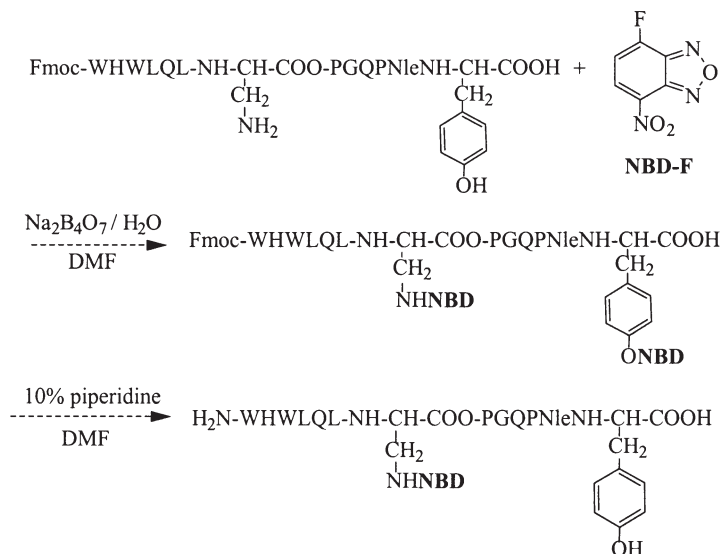
<sup>2</sup>Department of Microbiology, University of Tennessee, Knoxville, TN 37996, USA

### Introduction

The  $\alpha$ -factor receptor (Ste2p) from *Saccharomyces cerevisiae* belongs to the family of G-protein coupled receptors (GPCRs) that, upon the binding of a ligand, transduce a signal *via* an associated guanine nucleotide binding protein (G protein). The binding of the tridecapeptide pheromone  $\alpha$ -factor to Ste2p initiates a cascade of events that leads to the mating of haploid yeast cells. To understand the signaling process, one must first understand how ligands are recognized by and associated with their receptor. Fluorescence techniques have been widely used to investigate ligand-receptor interactions [1]. This work reports the synthesis, bioactivity, binding affinity of  $\alpha$ -factor tagged with a fluorescent probe at various positions in the peptide backbone, and a fluorescence analysis of the binding environment of these ligands bound to Ste2p.

### Results and Discussion

Fluorescent 7-nitrobenz-2-oxa-1,3-diazol-4-yl(NBD) labeled  $\alpha$ -factor (W<sup>1</sup>H<sup>2</sup>W<sup>3</sup>L<sup>4</sup>-Q<sup>5</sup>L<sup>6</sup>K<sup>7</sup>P<sup>8</sup>G<sup>9</sup>Q<sup>10</sup>P<sup>11</sup>M<sup>12</sup>Y<sup>13</sup>) analogs were synthesized by selectively attaching the NBD group to the specific amino group as seen in Scheme 1. Both the amino group at the side chain of  $\alpha$ -factor and the phenolic group in the side chain of Tyr<sup>13</sup> are reactive to NBD fluoride. Interestingly, NBD at the side chain of Tyr was deprotected by 10% piperidine in DMF. Eleven new  $\alpha$ -factor analogs containing a NBD group at the



Scheme 1. Synthesis of [Dap<sup>7</sup>(NBD),Nle<sup>12</sup>] $\alpha$ -factor analog.

$\alpha$ -amine of W<sup>1</sup> or attached to the side chain amines of positions 1(Dap), 3(Dap), 4(K), 6(K), 7[Dap, Dab, K( $\beta$ -A)], 12(K), or the phenol of Tyr<sup>13</sup>, respectively, have been synthesized and assayed for biological activity and receptor binding affinity. The analogues were all agonists exhibiting from 6 to 65% of the activity of [Nle<sup>12</sup>] $\alpha$ -factor as judged using a growth arrest assay. The binding affinities depended on the position of NBD and the distance of the tag from the backbone. Derivatives with the NBD in the side chain of position 7 resulted in affinities  $\geq 17\%$  of that of [Nle<sup>12</sup>] $\alpha$ -factor. Position 3 and 13 derivatives retained 34 and 57% binding affinities, respectively. However, the NBD group in [R<sup>7</sup>,Nle<sup>12</sup>,Y<sup>13</sup>(NBD)] $\alpha$ -factor did not fluoresce. Incorporation of NBD at the  $\alpha$ -amine or into the side chains of position 1, 4, 6, and 12 resulted in low binding affinities ( $< 7\%$ ) that precluded fluorescence investigations of their binding to Ste2p. Fluorescence spectroscopy of receptor bound  $\alpha$ -factor analogs with a NBD group at position 3 and 7 showed that the NBD groups in [Dab<sup>7</sup>(NBD),Nle<sup>12</sup>]- and [Dap<sup>3</sup>(NBD),R<sup>7</sup>,Nle<sup>12</sup>] $\alpha$ -factor analogs are in hydrophobic environments, and those in [Dap<sup>7</sup>(NBD),Nle<sup>12</sup>] and [K<sup>7</sup>( $\beta$ -A-NBD),Nle<sup>12</sup>] $\alpha$ -factor analogs are in hydrophilic environments. These shifts are fully confirmed by fluorescence quenching results which showed that when these  $\alpha$ -factor analogs bind to the receptor the NBD group in [Dab<sup>7</sup>(NBD),Nle<sup>12</sup>]-, [Dap<sup>3</sup>(NBD),R<sup>7</sup>,Nle<sup>12</sup>]-, and [Dap<sup>7</sup>(NBD),Nle<sup>12</sup>] $\alpha$ -factor is completely shielded, mostly shielded, and partly shielded, respectively, whereas the NBD group in [K<sup>7</sup>( $\beta$ -A-NBD),Nle<sup>12</sup>] $\alpha$ -factor is exposed to bulk water.

Together with the results on [K<sup>7</sup>(NBD),Nle<sup>12</sup>]-, [Orn<sup>7</sup>(NBD),Nle<sup>12</sup>]-, and [K<sup>7</sup>(ahNBD),Nle<sup>12</sup>] $\alpha$ -factor analogs [2], we can conclude that when  $\alpha$ -factor binds to its receptor W3 is in a nonpolar pocket, and position 7 resides in a complex binding pocket which has both polar and nonpolar domains. Long spacer arms attached to the position 7 side chain appear to completely expose the NBD group to the aqueous buffer.

#### **Acknowledgments**

This work was supported by grants GM22086 and GM22087 from the National Institutes of Health.

#### **References**

1. Hovius, R., Vallotton, P., Wohland, T., Vogel, H. *Trends Pharmacol. Sci.* **21**, 266–273 (2000).
2. Ding, F., Lee, B.K., Hauser, M., Davenport, L., Becker, J.M., Naider, F. *Biochemistry* **40**, 1102–1108 (2001).

## **Molecular Model of the BNP–NPR-A Receptor Complex**

**Brian C. Wilkes<sup>1</sup>, André De Léan<sup>2</sup>, Katharine A. Carpenter<sup>2,3</sup> and  
Peter W. Schiller<sup>1,2</sup>**

<sup>1</sup>*Laboratory of Chemical Biology and Peptide Research, Clinical Research Institute of  
Montreal, Montreal, H2W 1R7, Canada*

<sup>2</sup>*Department of Pharmacology, University of Montreal, Montreal, H3C 3J7, Canada*

<sup>3</sup>*AstraZeneca Research Center Montreal, Ville Saint-Laurent, H4S 1Z9, Canada*

### **Introduction**

Natriuretic peptides, including atrial natriuretic factor (ANP) and brain natriuretic peptide (BNP) are cyclic peptides that are involved in the control of physiological functions such as natriuresis, diuresis, blood pressure homeostasis and inhibition of aldosterone secretion. There are at least three classes of ANP receptors referred to as NPR-A, NPR-B and NPR-C. Both ANP and BNP bind to NPR-A and mediate their response through activation of guanylate cyclase. The crystal structure of the NPR-A receptor dimer has recently been reported [1]. A conformational study of pBNP by NMR spectroscopy in a membrane-like environment indicated a compact folded structure stabilized by hydrophobic forces [2]. We have taken this structure of pBNP and performed molecular docking of this ligand to the NPR-A receptor. Using previously determined contact points, including Met173 and His195 of the receptor and the N and C termini of the ligand [3], respectively, we manually docked pBNP to each of the two monomers of the receptor until reasonable steric complementarity was obtained. This complex was minimized, and molecular dynamics simulations were performed.

### **Results and Discussion**

The resulting model of the BNP–NPR-A complex is in agreement with the results of other studies suggesting the close proximity of several amino acid residues of the receptor with the bound ANP, including Glu169, Tyr88, Tyr120 and His185 [unpublished results]. In our model, the two ligands are at a distance of about 25 Å from each other in the dimer complex. Each of the ligands is stabilized by a series of four salt bridges to the receptor, as well as by several hydrogen bonds and van der Waal's contacts. Residues involved in salt bridges include Arg3, Asp13, Arg14 and Arg27 of the ligand with Glu169, Arg162, Asp161 and Glu187 of the receptor, respectively. A model of this complex is shown in Figure 1. While it is unknown whether the crystal structure of the receptor represents its active or inactive state, some mutational studies in the region of residues 423 to 435 of the receptor suggest that conformational changes at the interface of the receptor dimer may occur during ligand binding and receptor activation. For example, mutation of Cys423 of the receptor to Ser423 leads to a constitutively active receptor. This is because Cys432, which is engaged in a disulfide bridge to Cys423 in the native receptor, becomes available to form an intermolecular disulfide bond, resulting in receptor dimerization [4]. The crystal structure of the receptor dimer complex lacks residues 422 to 435 in one of the two receptor molecules forming the dimer complex. We extrapolated this region from the complete monomer of the complex to the other one to obtain the complete dimer.

During molecular dynamics simulations of the complex including the two BNP ligands bound, it was found that this region was fairly flexible and was unable to retain its secondary structure during the simulation. Work is in progress to determine how

mutations of residues in the region of residues 423 to 435 of the receptor affect our model.

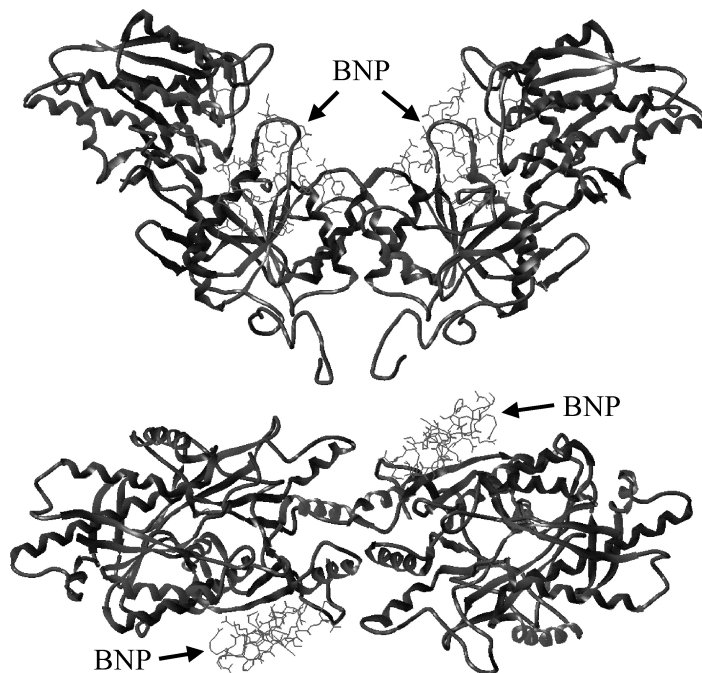


*Fig. 1. Model of two BNP molecules bound to the NPR-A receptor dimer. Orthogonal view.*

#### **Acknowledgments**

This work was supported by the Medical Research Council of Canada (MT-10131).

#### **References**

1. Akker, F.V.D., et al. *Nature* **406**, 101–104 (2000).
2. Carpenter, K.A., et al. *Biopolymers* **42**, 37–48 (1997).
3. McNicoll, N., et al. *Biochemistry* **35**, 12950–12956 (1996).
4. Labrecque, J., et al. *J. Biol. Chem.* **274**, 9752–9759 (1999).

## **Characterizing the Interactions Between Cholecystokinin and the G-Protein Coupled Receptors CCK<sub>1</sub> and CCK<sub>2</sub>: An NMR-Based Study**

**Craig Giragossian<sup>1</sup>, Maria Pellegrini<sup>2,3</sup> and Dale F. Mierke<sup>1,3</sup>**

<sup>1</sup>*Department of Chemistry, Brown University, Providence, RI 02912, USA*

<sup>2</sup>*Abbott Bioresearch Center, Worcester, MA 01605, USA*

<sup>3</sup>*Molecular Pharmacology, Physiology, & Biotechnology, Brown University, Providence, RI 02912, USA*

### **Introduction**

Cholecystokinin (CCK) is a peptide hormone and neurotransmitter involved in a number of physiological processes of the gall bladder and pancreas, in the gastrointestinal tract, and anxiety, memory, and analgesia in the CNS. These activities are elicited by activation of two distinct G-protein coupled receptors, CCK<sub>1</sub> and CCK<sub>2</sub>. Our laboratory is involved in the structural characterization of the interaction of CCK-8 with the CCK<sub>1</sub> and CCK<sub>2</sub> receptors.

The recent X-ray crystallographic results of intact GPCRs have provided the topological orientation of the seven transmembrane helices, but limited structural information of the extracellular and intracellular loops and protein termini [1]. To overcome this, we have developed an NMR-based approach, which provides the high-resolution structural features on the extracellular domains of G-protein coupled receptors, and the ligand/receptor complexes formed upon titration of the peptide hormone. The results provide important contact points, and a high-resolution description of the ligand/receptor interactions. Such information may provide insight into the process of ligand binding and the mechanism of receptor activation.

### **Results and Discussion**

Our approach entails the structural characterization of the extracellular domains of the CCK<sub>1</sub> and CCK<sub>2</sub> receptors using well-designed receptor constructs examined in the presence of a membrane mimetic. Each of the receptor constructs is designed to contain sufficient amino acids of the transmembrane (TM) region to anchor the domain to the lipid environment. The results clearly indicate a preference of these TM residues to form an  $\alpha$ -helix and embed into the hydrophobic portion of the lipids, and therefore mimic the attachment of the receptor domain to the TM helices. For the examination of extracellular loops, we have shown that including two such hydrophobic regions, corresponding to the TM helices, leads to the desired result of  $\alpha$ -helices at both termini, closely associated with the lipid surface. Including portions of the TM helices also allows us to incorporate the experimentally determined structural features into the model of the receptor. In addition, the results provide experimental evidence for the beginning or end of the TM helices. The different methods used for the prediction of the sequence location of the TM helices often produces variations of over five residues, which can lead to vastly different receptor models. Our structural results will address this issue.

Previously, we have characterized the interaction of CCK-8 with the entire N-terminus of CCK<sub>1</sub>, CCK<sub>1</sub>-R(1-47). Upon the titration of CCK-8 into a solution of the N-terminus in the membrane like environment of DPC micelles, we observed ligand-specific shifts of the W39 and Q40 of CCK<sub>1</sub> (where the three letter code will be used for the ligand, the one letter code for the receptor) [2,3]. NOESY spectra of this

mixture illustrate inter-molecular NOEs between the ligand (Asp<sup>26</sup>, Tyr<sup>27</sup>, Met<sup>28</sup>) and receptor (W39). Following a similar approach, we have recently examined the interaction of CCK-8 with the third extracellular loop of CCK<sub>1</sub> [4], CCK<sub>1</sub>-R(329-357). This ligand/receptor complex produced additional unambiguous inter-molecular NOEs. The interactions, including Trp<sup>30</sup>-A334, Met<sup>31</sup>-N333, and Asp<sup>32</sup>-Y338, placed the C-terminus of CCK-8 in proximity to the extracellular portion of TM6 of the receptor. The topological display of the ligand within the receptor based on these experimental data is shown in Figure 1.

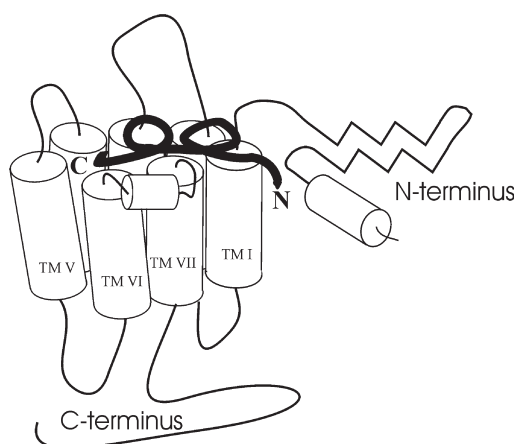


Fig. 1. Schematic of the binding of CCK-8 to the CCK<sub>1</sub> receptor as determined here by inter-molecular NOEs.

The two receptor subtypes, CCK<sub>1</sub> and CCK<sub>2</sub>, display unique ligand binding specificity. A number of sites determinant for the ligand specificity have been identified by site-directed mutagenesis and chimera receptors [5]. Most of these sites are located in the extracellular region of the receptor, predominantly in the extracellular loops. With this in mind, we have undertaken the structural characterization of the 3rd extracellular loop of CCK<sub>2</sub>, CCK<sub>2</sub>-R(352-379). The sequence comparison of the two extracellular domains is given below.

CCK<sub>1</sub>-R(329-357):            IFSANAWRAYDTASAERRLSGTPISFIILL  
                                     \*   \*   \*   \*   \*   \*   \*

CCK<sub>2</sub>-R(352-379):            ANTWRAFDGPGAHRALSGAPISFIHLL

The resulting structure of CCK<sub>2</sub>-R(352-379) as determined by high-resolution NMR in the presence of DPC, is shown in Figure 2 (right panel). In comparison to the structural features of CCK<sub>1</sub>, we find a much shorter  $\alpha$ -helix in the central portion of the loop. There is also a significant difference in the topological display of the charged amino acids, which have been postulated to be important for interaction with the receptor by site-directed mutagenesis. The specific interactions with the ligand are currently under study by titration of CCK-8 into the solution of the CCK<sub>2</sub>-R(352-379) construct. Based on our NMR-based observations, we will be able to ascertain the role of the charged amino acids and the structural features of the ligand/receptor complex.

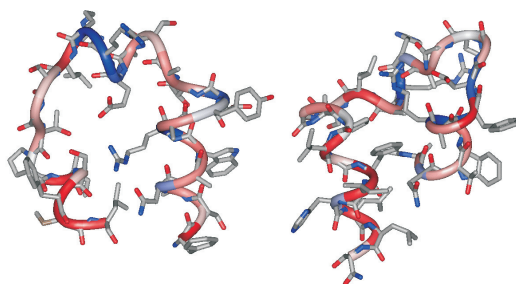


Fig. 2. Structures of the 3rd extracellular loops of the CCK<sub>1</sub> (left) and CCK<sub>2</sub> (right) as determined by NMR in a membrane mimetic.

## References

1. Palczewski, K., Kumasaka, T., Hori, T., Behnke, C.A., Motoshima, H., Fox, B.A., Le Trong, I., Teller, D.C., Okada, T., Stenkamp, R.E., Yamamoto, M., Miyano, M. *Science* **289**, 739–745 (2000).
2. Pellegrini, M., Mierke, D.F. *Biochemistry* **38**, 14775–14783 (1999).
3. Pellegrini, M., Mierke, D.F. *J. Peptide Sci.* **51**, 208–220 (1999).
4. Giragossian, C., Mierke, D.F. *Biochemistry* **40**, 3804–3809 (2001).
5. Silvente-Poirot, S., Escrieut, C., Wank, S.A. *Mol. Pharmacol.* **54**, 364–371 (1998).

## **Human Colon Cancers Recognize N-Carboxymethyl Gastrin by a Non-CCK<sub>1</sub>, Non-CCK<sub>2</sub> Receptor**

**Felicitas I. Wibowo, Shawn Ahmed, Dmitry S. Gembitsky, Sándor Lovas and Richard F. Murphy**

*Department of Biomedical Sciences, Creighton University School of Medicine, Omaha, NE 68178, USA*

### **Introduction**

N-Carboxymethyl gastrin (G17Gly), which is gastrin (G17) with C-terminal GlyOH in place of the  $\alpha$  amide, is a gastrin precursor and is formed by specific post-translational modifications of gastrin precursor peptide G34. G17Gly is the predominant gastrin gene product in human colonic carcinomas [1] and it has been shown to have mitogenic effect on such cancers [2]. While it has been claimed that G17Gly exerts its effect on human colonic cancers through the CCK<sub>2</sub> receptor, this receptor could not be detected on many human colon cancers [3]. Several groups reported the existence of a non-CCK<sub>1</sub>, non-CCK<sub>2</sub> receptor in several cell lines and it has been suggested that this receptor mediates the effect of G17Gly. Seva and coworkers [4] reported that the rat CCK<sub>2</sub> receptor binds G17 but not the precursor. In our laboratory, by contrast, G17Gly was found to bind to stably expressed human CCK<sub>2</sub> receptor in CHO-K1 cells. Variants of gastrin/CCK receptors have also been found in several colonic cancer cell lines and shown to bind to G17 as well as G17Gly [5]. Hence, the presence of G17Gly receptor in human colonic cancer cell lines remains a controversial issue. In this study, the interaction of G17Gly with cell membranes prepared from human colonic cancer cell lines, HT-29 and DLD-1, by comparison with CHO-K1 cells expressing the human CCK<sub>2</sub> receptor, was investigated by competitive binding studies using [<sup>3</sup>H]G17Gly, [<sup>3</sup>H]G(11-17)Gly, and [<sup>3</sup>H-propionyl]CCK-8.

### **Results and Discussion**

CCK-8 and G17 bound to the CHO-K1 cell membranes but not to the cell membranes of the human colonic cancers, DLD-1 and HT-29 (Table 1). CCK-8 and G17 are the established agonists for CCK<sub>1</sub> and CCK<sub>2</sub> receptor. CCK-8 has high affinity for both the CCK<sub>1</sub> and CCK<sub>2</sub> receptor, while G17 has lower affinity than has CCK-8 for the CCK<sub>1</sub> receptor but same affinity as has CCK-8 for the CCK<sub>2</sub> receptor. These results showed that neither CCK<sub>1</sub> nor CCK<sub>2</sub> receptors are present in DLD-1 and HT-29 cell lines. However, [<sup>3</sup>H]G17Gly and [<sup>3</sup>H]G(11-17)Gly bound to both human colonic cancer cell lines in a displaceable manner. [Leu<sup>15</sup>]G17Gly and [Leu<sup>15</sup>]G(11-17)Gly bound specifically to DLD-1 and HT-29 cell membranes. The affinity of [Leu<sup>15</sup>]G(11-17)Gly for DLD-1 and HT-29, cell membranes is 10-fold less than that of [Leu<sup>15</sup>]G17Gly. This reduction in affinity is similar to that for human CCK<sub>2</sub> receptor when the same 10 residues are omitted from G17.

The binding of [Leu<sup>15</sup>]G17Gly and its truncated analog to DLD-1 and HT-29 cell membranes showed the presence of a specific binding site for G17Gly, which is distinct from both the CCK<sub>1</sub> and CCK<sub>2</sub> receptor. This specific binding site for G17Gly and its truncated analog, despite of the low affinity ( $K_i \sim 0.5 \mu\text{M}$  and  $2 \mu\text{M}$ , respectively), could be a G17Gly receptor.

Table 1. Binding of CCK-8, G17, G17Gly, and G(11-17)Gly to the CHO-K1, DLD-1, and HT-29 cell membranes.

Peptides	DLD-1		HT-29		CHO-K1	
	log EC <sub>50</sub> ±SEM	K <sub>i</sub> μM	log EC <sub>50</sub> ±SEM	K <sub>i</sub> μM	log EC <sub>50</sub> ±SEM	K <sub>i</sub> μM
CCK8	–	N.B.	–	N.B.	–8.69±0.07	0.0015
G17	–	N.B.	–	N.B.	–7.76±0.03	0.013
G17Gly	–6.70±0.054	0.51	–6.54±0.439	0.40	–5.99±0.019	0.77
G(11-17)Gly	–5.77±0.034	1.63	–5.77±0.286	2.59	–5.22±0.011	4.53

<sup>a</sup>Data in triplicate were analyzed using GraphPad Prism Software. <sup>b</sup>N.B.: No binding.

### Acknowledgments

This work was supported by Carpenter Endowed Chair in Biochemistry, Creighton University and NSF (EPS-9720643).

### References

1. Van Solinge, W.W., Nielsen, F.C., Friis-Hansen, L., Falkmer, U.G., Rehfeld, J.F. *Gastroenterology* **104**, 1099–1107 (1993).
2. Singh, P., Xu, Z., Dai, B., Rajaraman, S., Dhruva, B. *Am. J. Physiol.* **266**, G459–G468 (1994).
3. Artru, P., Attoub, S., Levasseur, S., Lewin, M.J.M., Bado, A. *Gastroenterol. Clin. Biol.* **22**, 607–612 (1998).
4. Seva, C., Dickinson, C.J., Yamada, T. *Science* **265**, 410–412 (1994).
5. McWilliams, D.F., Watson, S.A., Crosbee, D.M., Michaeli, D., Seth, R. *Gut* **42**, 795–798 (1998).

## **Functional Characterization of Two *Drosophila melanogaster* Type A Allatostatin Receptors Expressed in CHO Cells**

**Teresa M. Kubiak, Martha J. Larsen, Katherine J. Burton,  
Marjorie R. Zantello, Erich W. Zinser, Valdin G. Smith  
and David E. Lowery**

*Animal Health Discovery Research, PHARMACIA Corp., Kalamazoo, MI 49001, USA*

### **Introduction**

The type A allatostatins (ASTs) are a group of insect peptides with a common C-terminal motif F/YXFGL-NH<sub>2</sub>. ASTs control visceral muscle contractions and, indirectly, insect larval development, sexual maturation and reproduction by inhibiting juvenile hormone release from the corpus allatum. The existence of at least four putative type A *Drosophila melanogaster* (fruit fly) ASTs (called drostatins or DSTs) has been predicted from the sequence of a recently cloned DST preprohormone [1]. SRPYSFGL-NH<sub>2</sub>, (DST-3), the only DST isolated from *Drosophila* so far, activated the first cloned *Drosophila* type A DST GPCR (DAR-1) [2]. A newly cloned orphan *Drosophila* GPCR, which shares 47% overall and 60% transmembrane region sequence identity with DAR-1, was classified as a second putative *Drosophila* type A DST receptor (DAR-2) [3]. Although activation of DAR-2 by DSTs has been postulated [3], no experimental evidence for that has been reported to date. In this study, we transiently expressed both DAR-1 and DAR-2 in CHO cells and used a GTPγS and a Ca<sup>+2</sup> mobilization assay for pharmacological receptor evaluation.

### **Results and Discussion**

Four synthetic drostatins-A and four *Diploteria punctata* (cockroach) allatostatins (AST's) effectively activated DAR-1 and DAR-2 in both functional assays (Figure 1). The determined EC<sub>50</sub>'s for calcium and GTPγS responses were in the 20–100 and 1–38 nM range, respectively, for all the peptides tested at the DAR-1 and DAR-2 receptors. These results show cross species activity of the cockroach allatostatins acting at the two cloned *Drosophila* allatostatin receptors. This is most likely related to the high sequence homology of the cockroach and fruit fly type A allatostatins, especially their highly conserved C-termini with the common pentapeptide motif Y/FXFGL-NH<sub>2</sub>.

Despite the similarities, there were also some differences between functional peptide responses at DAR-1 and DAR-2 after cell pretreatment with pertussis toxin (PTX). Specifically, Ca<sup>+2</sup> signaling at DAR-1 was completely abolished by PTX, indicating the involvement of only G<sub>i/o</sub> in this signaling pathway. On the other hand, the PTX treatment attenuated but not completely abolished the Ca<sup>+2</sup> signaling in the DAR-2 cells indicating that the original Ca<sup>+2</sup> responses at DAR-2 had a strong G<sub>i/o</sub> component, but also some contribution coming from other, PTX-insensitive G-proteins (Figure 1). In the GTPγS assay, activation of G-proteins at DAR-1 was attenuated, but not completely abolished by PTX. The curves were shifted to the right and the EC<sub>50</sub>'s increased from ca 5- to 180-fold, depending on the peptide, reflecting a different extent of the G<sub>i/o</sub> protein involvement in response to the individual ligands. In contrast, at DAR-2, the PTX treatment had only a minimal effect on the potencies (EC<sub>50</sub>'s) of DST's and AST's to stimulate GTPγS binding, indicating that the tested ligands predominantly coupled DAR-2 to the PTX-insensitive G-proteins.

It is worth noting that in cell membranes, DAR-2 and, to a lesser extent, DAR-1, were constitutively active as reflected in respectively *ca* 4–5 and 1.4 times higher basal [<sup>35</sup>S]GTPγS binding in the absence of the activating ligands. After the PTX treatment, the constitutive activity of DAR-1 was abolished, while that of DAR-2 was partially reduced (by *ca* 44%), but the remaining [<sup>35</sup>S]GTPγS binding was still elevated and about three times higher than that of the DAR-1 in the CHO/PTX membranes (Figure 1). Therefore, it was concluded that only about 44% of the constitutive activity of DAR-2 was G<sub>i/o</sub> related and the rest of it originated most likely from DAR-2 coupling to other PTX insensitive G-proteins. Collectively, our results show complex and

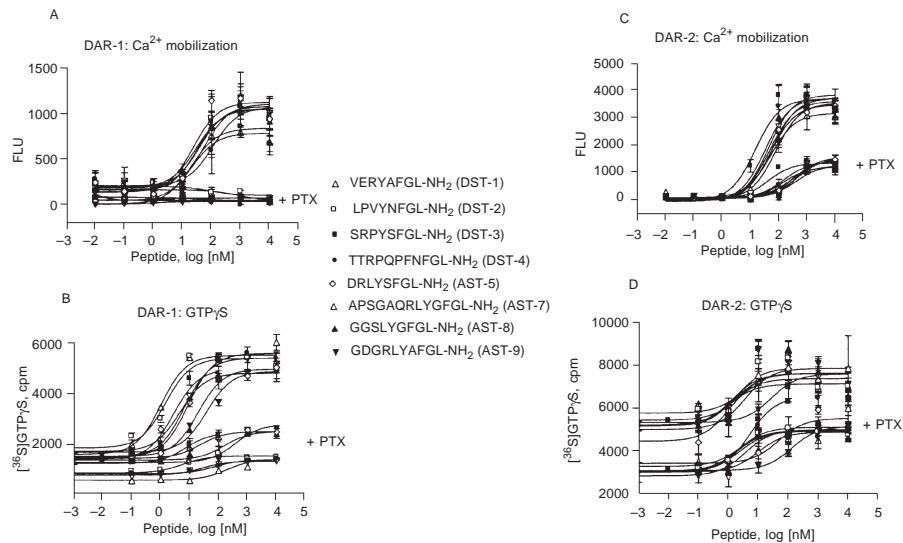


Fig. 1. DAR-1 and DAR-2 transiently expressed in CHO cells. Pharmacological evaluation 48 h-post transfection in a Ca<sup>2+</sup> mobilization (via FLIPR) and GTPγS assay. The numbering system for *Diploter punctata* allatostatins (ASTs) was taken from [4] and for drostatins (DSTs) from [1].

redundant biological activity of both the fruit fly and cockroach allatostatins at the two *Drosophila* allatostatin receptors. The observed differences in the nature and magnitude of peptide-triggered signaling at the DAR-1/CHO and DAR-2/CHO receptors suggest possible differential coupling of these receptors to cellular effector system(s) in response to their cognate ligands in native tissues and organs which could lead to distinct biological functions *in vivo*.

## References

1. Lenz, C., Williamson, M., Grimmelikhijzen, C.J.P. *Biochem. Biophys. Res. Commun.* **273**, 1126–1131 (2000).
2. Birgul, N., Weise, C., Kreienkamp, H.J., Richter, D. *EMBO J.* **18**, 5892–5900 (1999).
3. Lenz, C., Williamson, M., Grimmelikhijzen, C.J.P. *Biochem. Biophys. Res. Commun.* **273**, 571–577 (2000).
4. Bowser, P.R.F., Tobe, S.S. *Gen. Comp. Endocrinol.* **119**, 1–10 (2000).

## **Receptor-Bound Conformation of $\alpha$ -Peptide of Transducin ( $G_t$ ) is not Stabilized by a “ $\pi$ -Cation” Interaction but by Constrained Lactam Bridges Between Residues 341 and 350**

**Wei Sha, Rieko Arimoto and Garland R. Marshall**

*Washington University School of Medicine, Department of Biochemistry and Molecular Biophysics, St. Louis, MO 63110, USA*

### **Introduction**

Light-induced activation of rhodopsin ( $R^*$ ) leads to its conformation change and the binding of transducin  $G_t$ . Synthetic  $G_t\alpha$  (340-350) peptide has been demonstrated to stabilize  $R^*$  as does  $G_t$ . The bound conformation of  $R^*$ -bound  $G_t\alpha$  (340-350) has been determined by TrNOE NMR measurements [1]. The adjacent disposition of the  $\epsilon$ -amino group of Lys-341 toward the side-chain phenyl ring of Phe-350 suggests a possible  $\pi$ -cation interaction. To investigate this  $\pi$ -cation hypothesis, we measured the affinity with  $R^*$  of a series of  $\alpha$ -peptide analogs with different *para*-substituents on the Phe-350 phenyl ring. In order to further exploit the proximity between the side chains of Lys-341 and Phe-350, we also prepared  $\alpha$ -peptide analogs with straightforward lactam bridges between the side chains at 341 and 350.

### **Results and Discussion**

#### **H-Ile-Lys-Glu-Asn-Leu-Lys-Asp-Cys-Gly-Leu-Xxx-OH**

Xxx = Tyr (1); Trp (2); Phe(*p*-F) (3); Phe(*p*-NH<sub>2</sub>) (4); Phe(*p*-NO<sub>2</sub>) (5); Cha (6)

#### **H-Ile-cyclo(Xxx-Glu-Asn-Leu-Lys-Asp-Cys-Gly-Leu-Yyy)-OH**

Xxx = Lys (7), Lys (8); Yyy = Asp (7), Glu (8)

Xxx = Glu (9), Asp (10); Yyy = Phe(*p*-NH-) (9), Phe(*p*-NH-) (10)

A series of  $\alpha$ -peptide analogs with varied *para*-substituents on the side-chain aromatic ring of Phe-350 were synthesized: with electron-donating groups, *i.e.* 350-Tyr (1), 350-Trp (2), 350-Phe(*p*-NH<sub>2</sub>) (4); with electron-withdrawing groups, *i.e.* 350-Phe(*p*-F) (3), 350-Phe(*p*-NO<sub>2</sub>) (5) and a side chain with no  $\pi$  system, *i.e.* 350-Cha (6). The postulated  $\pi$ -cation interaction consists of an interaction between a side chain NH<sub>3</sub><sup>+</sup> cation from 341-Lys and the varied side-chain aromatic systems on 350. If this interaction exists, a stronger  $\pi$ -cation interaction would constrain the peptide into a more favorable binding conformation and stabilize the cation in the compact hydrophobic pocket resulting in higher binding affinity, *vice versa*. However, binding affinity of these analogs did not show this expected correlation with electronic effect, but correlate closely to the hydrophobicity of the side chain modification of 350. Highly hydrophilic side chains like 350-Phe(*p*-NH<sub>2</sub>) (4) and 350-Tyr (1) have only retained 33 and 55% of affinity. 350-Phe(*p*-F) (3), 350-Phe(*p*-NO<sub>2</sub>) (5) and 350-Trp (2) show comparable affinity due to similar hydrophobic side chains. 350-Cha (6) possesses the most hydrophobic side chain and exhibits 1.5-fold higher affinity than  $G_t\alpha$  (340-350). Therefore, the  $\pi$ -cation interaction does not seem to be involved in the case of the  $\alpha$ -peptide interacting with  $R^*$ , while the hydrophobicity of the side chains appears a more significant driving force. The fact that increased hydrophobicity on the side chain of 350 displays stronger binding affinity confirms the hydrophobic role of side chain at position 350, determined by TrNOE measurements, as an important component of a hydrophobic patch when interacts with the hydrophobic core of  $R^*$ . A com-

binatorial approach using phage display and random residue mutation has found that substitution of the cationic 341-Lys with a neutral Leu increases affinity [2]. This implies that the side chain of 341-Lys probably undergo deprotonation upon binding to R\*. The energetic cost of deprotonation and desolvation of the  $\epsilon$ -amine may allow control of the affinity to maintain the appropriate dissociation rates for the activated complex in its biological context. This hypothesis is in good agreement with the lack of evidence for a  $\pi$ -cation interaction from this study despite of the proximity of the  $\epsilon$ -amine “cation” and the Phe aromatic system.

We also tried direct lactam-bridge construction between the side chains at these two positions. Four cyclic analogs were prepared: cyclo(KD) (**7**), cyclo(KE) (**8**), and cyclo(EF(NH<sub>2</sub>)) (**9**), cyclo(DF(NH<sub>2</sub>)) (**10**). Both cyclo(KD) (**7**) and cyclo(KE) (**8**) display enhanced binding affinity, 1.67- and 4.17-fold respectively. However, in case of cyclization with the *para*-aminophenyl ring of residue 350, cyclo(DF(NH<sub>2</sub>)) (**10**) totally loses its binding affinity, while cyclo(EF(NH<sub>2</sub>)) (**9**) exhibits 10-fold enhanced binding affinity. The fact that cyclic peptides with a lactam linkage between side chains at 341 and 350 show higher affinity even with the loss of a hydrophobic phenyl ring suggests that this configuration is favored in binding to R\* and supports the TrNOE G<sub>i</sub> $\alpha$  structure. The further increased affinity after the addition a phenyl ring back into the cyclic peptide again agrees well with the significant hydrophobic contribution on residue 350 for binding. The total loss of affinity of cyclo(DF(NH<sub>2</sub>)) (**10**) suggests this bound conformation appears rather specific as removal of one methylene from the ring eliminates affinity.

### Acknowledgments

The authors acknowledge support for this research from NIH Grant EY12113. R. A. is a graduate student in the Biomedical Engineering Program at Washington University. The Washington University Mass Spectroscopy Resource Center supported by NIH (RR00954) was utilized to characterize the analogs synthesized as part of this study.

### References

1. Kisselev, O.G., Kao, J., Ponder, J.W., Fann, Y.C., Gautam, N., Marshall, G.R. *Proc. Natl. Acad. Sci. USA* **95**, 4270–4275 (1998).
2. Martin, E.L., Rens-Domiano, S., Schatz, P.J., Hamm, H.E. *J. Biol. Chem.* **271**, 361–366 (1996).

## **Solution and Membrane-Bound Conformational Properties of a Peptide from the First Extracellular Loop of the Angiotensin II AT<sub>1</sub> Receptor**

**Shirley Schreier<sup>1</sup>, Roberto K. Salinas<sup>1</sup>, Cláudio S. Shida<sup>1</sup>, Thelma A. Pertinhez<sup>1</sup>, Alberto Spisni<sup>2</sup>, Clovis R. Nakaie<sup>3</sup> and Antonio C. M. Paiva<sup>3</sup>**

<sup>1</sup>*Institute of Chemistry, University of São Paulo, CP 26077, 05513-970, São Paulo, Brazil*

<sup>2</sup>*Institute of Biological Chemistry, University of Parma, Parma, Italy*

<sup>3</sup>*Department of Biophysics, Federal University of São Paulo, 04023-032, São Paulo, Brazil*

### **Introduction**

The sequence YRWPFGNHL (residues 92-100) is putatively assigned to the first extracellular loop of the angiotensin II AT<sub>1A</sub> receptor. Residues Trp<sup>94</sup> and Gly<sup>97</sup> are conserved in nearly 50% of the 1400 rhodopsin-like G protein-coupled receptors [1], and Tyr<sup>92</sup> was shown to be important for ligand binding [2]. Homology modeling of the receptor indicates that the WPFG stretch forms a  $\beta$ -turn. As part of an ongoing study of the conformation and dynamics of synthetic peptides corresponding to extra-membranous domains of the angiotensin II AT<sub>1A</sub> receptor [3–5], the solution and membrane-bound conformational properties of a synthetic peptide with that sequence (YRWPFGNHL, fEL1) were examined by circular dichroism (CD) and fluorescence.

### **Results and Discussion**

The CD spectra of fEL1 in aqueous solution revealed an equilibrium between folded and less organized conformers, with prevalence of the latter. A positive band centered at 226.5 nm corresponded to conformers exhibiting aromatic ring stacking. The pH dependence of this band indicated that stacking is a function of the ionization degree of the peptide's ionizable groups. The secondary structure-inducing solvent trifluoroethanol (TFE), or binding to model membranes – detergent micelles and phospholipid bilayers – induced a shift in the conformational equilibrium towards stabilization of conformers with higher secondary structure content. Increasing concentrations of the solvent and of the model membranes caused a gradual disappearance of the negative band at 200 nm due to less organized structures; the remaining spectra displayed a negative band at 217–220 nm, suggesting the formation of  $\beta$ -turns. The disappearance of the positive band in the 225–230 nm region suggested that a type I  $\beta$ -turn prevailed in 90% TFE and in the presence of micelles of sodium dodecyl sulfate (SDS, negatively charged) and lysophosphatidyl choline (lyso-PC, zwitterionic) at all pHs studied. In contrast, this band shifted to 230 nm, but did not disappear completely at pH 4.0, and remained unchanged at pH 7.5 and 9.0 in the presence of micelles of *N*-hexyl-*N,N*-dimethyl-3-ammonio-propane sulfonate (HPS, zwitterionic) and of bilayers of 1-palmitoyl-2-oleoyl-phosphatidyl choline (POPC, zwitterionic):1-palmitoyl-2-oleoyl-phosphatidic acid (POPA, negatively charged). Conformations exhibiting aromatic ring stacking could correspond to type VI  $\beta$ -turns. Thus, transferring the peptide to an environment of lower polarity or binding to interfaces stabilized  $\beta$ -turn structures in the WPFG stretch, probably by favoring the formation of intramolecular hydrogen bonds. The interaction with micelles and bilayers was also evinced by an increase in Trp<sup>3</sup> fluorescence intensity, a blue shift of the maximum emission wavelength, an increase in fluorescence anisotropy, and by p*K* changes. Fluorescence and CD data showed that, while the peptide binds to both negatively charged and zwitterionic mi-

celles, binding to bilayers – where the lateral pressure is higher – only occurred in the presence of a negatively charged phospholipid. This indicates that binding to model membranes depends on both hydrophobic and electrostatic interactions, as well as on lipid phase packing. Studies with water soluble and membrane-bound fluorescence quenchers showed that Trp<sup>3</sup> is close to the water–membrane interface, in agreement with its predicted location in the whole receptor.

The function of GPCRs requires that they should be dynamic structures. It is thought that conformational changes induced by ligand binding represent the early steps of the signal transduction mechanism. Multiple sequence alignment indicated that residues Trp<sup>94</sup>, Gly<sup>97</sup> and Cys<sup>101</sup> of the AT<sub>1A</sub> receptor are conserved among at least 50% of 1400 rhodopsin-like GPCRs [1] suggesting a possible role of this domain in receptor–ligand interaction. The conformational changes observed for fEL1 suggest that the dynamic nature of this loop could play a role in receptor activation.

We have shown that fEL1's conformation can be modulated by local pH, polarity, and interaction with lipid phases. Thus, changes in these conditions, as well as ligand binding could induce conformational changes at the level of the receptor's water-exposed loops. We found that subtle changes of the binding surface can lead to the preferential stabilization of different conformational states. In a biological situation, similar conformational changes could be responsible for the fine-tuning control of ligand binding. These molecular events could be involved in the initial steps triggering signal transduction.

#### Acknowledgments

Supported by grants from FAPESP. R. K. S. and C. S. S. have FAPESP fellowships. C. R. N., ACMP, and S. S. are CNPq research Fellows.

#### References

1. Oliveira, L., Paiva, A.C.M., Sander, C., Vriend, G. *Trends Pharmacol. Sci.* **15**, 170–172 (1994).
2. Hjorth, S.A., Schambye, H.T., Greenlee, W.J., Schwartz, T. *J. Biol. Chem.* **269**, 30953–30959 (1994).
3. Spisni, A., Franzoni, L., Sartor, G., Nakaie, C.R., Carvalho, R.S.H., Paiva, A.C.M., Salinas, R.K., Pertinhez, T.A., Schreier, S. *Bull. Magn. Res.* **17**, 151–153 (1996).
4. Franzoni, L., Nicastro, G., Pertinhez, T.A., Tato, M., Nakaie, C.R., Paiva, A.C.M., Schreier, S., Spisni, A. *J. Biol. Chem.* **272**, 9734–9741 (1997).
5. Franzoni, L., Nicastro, G., Pertinhez, T.A., Oliveira, L., Nakaie, C.R., Paiva, A.C.M., Schreier, S., Spisni, A. *J. Biol. Chem.* **274**, 227–235 (1999).

## Synthesis of a Biotinylated Chemotactic Peptide Analog as a Probe for Formylpeptide-Receptor Interaction

Masaya Miyazaki<sup>1</sup>, Mitsukuni Shibue<sup>1,2</sup>, Masahiro Yoshiki<sup>2</sup>,  
 Ichiro Fujita<sup>3</sup>, Hideaki Maeda<sup>1</sup>, Seiji Yasuda<sup>1</sup>, Yuhei Hamasaki<sup>3</sup>,  
 Hiroaki Kodama<sup>2</sup> and Michio Kondo<sup>2</sup>

<sup>1</sup>*Institute for Structural and Engineering Materials, AIST Kyushu, National Institute of Advanced Industrial Science and Technology, Tosu, Saga, 841-0052, Japan*

<sup>2</sup>*Department of Chemistry, Saga University, Saga, 840-8502, Japan*

<sup>3</sup>*Department of Pediatrics, Saga Medical School, Saga, 849-8501, Japan*

### Introduction

*N*-Formylpeptides exhibit not only chemotaxis, but also several responses of neutrophils, such as superoxide production and enzyme secretion. These responses are mediated by formylpeptide receptors. Several synthetic analogs have been developed to discriminate these receptors [1,2]. However, it is still not clear how the peptide interacts with the receptors.

Biotinylated ligands with a photoaffinity label have been developed to probe the receptor–ligand interactions. We decided to apply this approach to analyze formylpeptide–ligand interaction. We designed a series of analogs containing *p*-benzoylphenylalanine (Bpa) as a photoaffinity label and Lys(ε-biotin) as an affinity tag (Figure 1). The biological activities and photoaffinity crosslinking were evaluated.

fMLP	HCO-Met-Leu-Phe-OH
Bpa <sup>4</sup> -fMLP	HCO-Met-Leu-Phe- <b>Bpa</b> -Arg-Arg-Lys(ε-biotin)-NH <sub>2</sub>
Bpa <sup>4</sup> , Ahx-fMLP	HCO-Met-Leu-Phe- <b>Bpa</b> -Ahx-Arg-Arg-Lys(ε-biotin)-NH <sub>2</sub>
Bpa <sup>4</sup> , Ahx <sub>2</sub> -fMLP	HCO-Met-Leu-Phe- <b>Bpa</b> -Ahx-Ahx-Arg-Arg-Lys(ε-biotin)-NH <sub>2</sub>
Bpa <sup>2</sup> , Ahx <sub>2</sub> -fMLP	HCO-Met- <b>Bpa</b> -Phe-Phe-Ahx-Ahx-Arg-Arg-Lys(ε-biotin)-NH <sub>2</sub>

Fig. 1. Structures of synthetic peptides.

### Results and Discussion

To analyze a multiple receptor system by a photoaffinity-labeled ligand, the specificity of the analogs should be elucidated. Thus, we evaluated the biological activity of Bpa-fMLPs. The chemotactic activity and superoxide production were evaluated as previously described (Figure 2) [1]. The peptides containing a Bpa residue showed weak activity in the chemotaxis assay. Only Bpa<sup>4</sup>, Ahx<sub>2</sub>-fMLP showed full chemotactic activity at 10<sup>-5</sup> M. On the other hand, Bpa<sup>2</sup>, Ahx<sub>2</sub>-fMLP and Bpa<sup>4</sup>, Ahx<sub>2</sub>-fMLP analogs caused strong superoxide production at almost the same level as the parent peptide fMLP, suggesting that Bpa<sup>4</sup>, Ahx<sub>2</sub>-fMLP binds to both receptors, but Bpa<sup>2</sup>, Ahx<sub>2</sub>-fMLP binds only to the receptor for superoxide production. The analogs having shorter Ahx spacers exhibit almost no activity in both assays. These results mean that at least two Ahx spacers are required to interact with the receptor for these peptides. Thus, it is advantageous to use analogs with two Ahx spacers for crosslinking experiments.

The crosslinking experiment was performed using the Bpa<sup>4</sup>, Ahx<sub>2</sub>-fMLP analog. The neutrophils were incubated with Bpa<sup>4</sup>, Ahx<sub>2</sub>-fMLP in the presence or absence of fMLP. After irradiation at >360 nm, cells were lysed, and crosslinking was evaluated by HRP-labeled avidin blotting [3]. The band corresponding to MW of formylpeptide receptor was observed. Maximum crosslinking was achieved at 10 min. The intensity

of the band was diminished by presence of fMLP, indicating that the band corresponds to the formylpeptide receptor.

Previous study of ligand–receptor interactions of the formylpeptide receptor was mainly performed using Bpa<sup>2</sup> analog [4–6]. In our studies, the Bpa<sup>2</sup> analog showed strong preference for superoxide production. This analog might not be useful for the analysis of the receptor for chemotaxis. The Bpa<sup>4</sup>,Ahx<sub>2</sub>-fMLP analog retained biological activity in both assays. This analog might be a strong tool for the analysis of interaction with the formylpeptide receptor for chemotaxis.

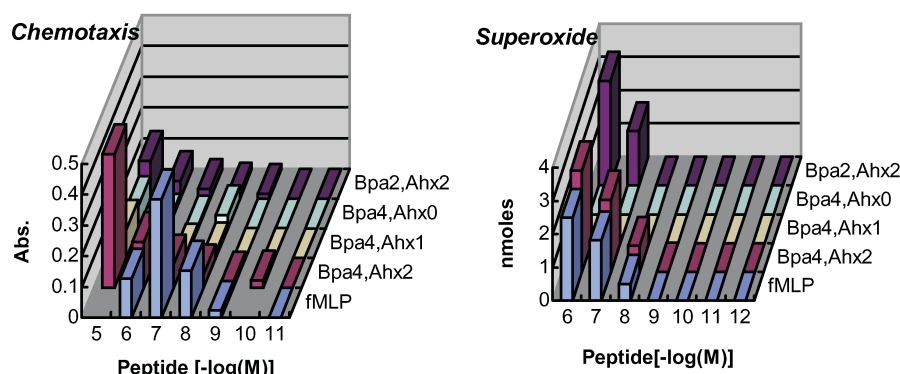


Fig. 2. Biological activities of synthetic peptides.

## Acknowledgments

We thank Prof. Sumio Miyazaki (Saga Medical School) for continuous support.

## References

1. Miyazaki, M., Kodama, H., Fujita, I., Hamasaki, Y., Miyazaki, S., Kondo, M. *J. Biochem.* **117**, 489–494 (1995).
2. Miyazaki, M., Kodama, H., Fujita, I., Hamasaki, Y., Miyazaki, S., Kondo, M. *Peptide Chemistry 1994*, Protein Research Foundation, Osaka, 1995, pp. 293–296.
3. Rapoport, I., Miyazaki, M., Boll, W., Duckworth, B., Cantley, L. C., Shoelson, S.E., Kirchhausen, T. *EMBO J.* **16**, 2240–2250 (1997).
4. Mills, J.S., Miettinen, H.M., Barnidge, D., Vlases, M.J., Wilmer-Mackin, S., Dratz, E.A., Sunner, J., Jesaitis, A.J. *J. Biol. Chem.* **273**, 10428–10435 (1998).
5. Viltén, J.C., Domalewski, M., Prossnitz, E., Ye, R.D., Muthukumaraswamy, N., Harris, R.B., Freer, R.J., Sklar, L.A. *J. Recept. Signal Transduct. Res.* **18**, 187–221 (1998).
6. Millis, J.S., Miettinen, H.M., Cummings, D., Jesaitis, A.J. *J. Biol. Chem.* **275**, 39012–39017 (2000).

## Specific Activation of the Insulin Receptor by the Transmembrane Domain Peptides

Masaya Miyazaki<sup>1,2</sup>, Jongsoon Lee<sup>1</sup>, Mitsukuni Shibue<sup>2</sup>, Takashi Fujiura<sup>2</sup>,  
 Hideaki Maeda<sup>2</sup> and Steven E. Shoelson<sup>1</sup>

<sup>1</sup>Research Division, Joslin Diabetes Center, One Joslin Place, Boston, MA 02215, USA

<sup>2</sup>Institute for Structural and Engineering Materials, AIST Kyushu, National Institute of  
 Advanced Industrial Science and Technology, 807-1 Shuku, Tosu, Saga, 841-0052, Japan

### Introduction

The binding of insulin to the extracellular domain of the insulin receptor (IR) triggers activation of tyrosine kinase and transmits the signal to the downstream signaling cascade [1]. However, it is still unknown how insulin binding to the extracellular binding site causes receptor activation. Several studies using IR mutants have investigated the function of the transmembrane domain (TMD) in the receptor activation process, and it was suggested that the TMD might have some role in the receptor activation [2,3]. We report here a different approach using a synthetic peptide corresponding to the TMD of IR (IR-TM), to investigate the role of TMD in receptor activation.

### Results and Discussion

For the targeting of peptide to the TMD, the synthetic peptide should localize and possibly span the membrane. The transmembrane domain of the receptor interposed by positively charged residues. To span the membrane, we considered this an important feature for designing the peptide. Thus, we have designed and synthesized the TMD peptides shown in Figure 1.

IR-TM	H-KIIIGPLIFVFLFSVIGSIYFLRKR-NH <sub>2</sub>
PDGFR-TM	H-KVVVISALIALLVLTSLISLIILIMLWQKK-NH <sub>2</sub>
IGF1R-TM	H-HLIIALPVAVLLIVGGLVIMLYVFHRK-NH <sub>2</sub>
Neu-TM	H-RASPVTFIATVVGVLFLILVVVGILIKRR-NH <sub>2</sub>
TrkA-TM	H-KEDTPFGVSVAVGLAVFACFLSTLLLVLNKC-NH <sub>2</sub>

Fig. 1. Synthetic TMD peptides.

First, we examined whether the IR-TM activates insulin receptor *in vitro*, using triton X-100 solubilized WGA (Wheat germ agglutinin) agarose-purified insulin receptor. The IR-TM peptide could activate the exogenous kinase activity of WGA-purified insulin receptor in a dose-dependent manner. IR-TM also induced phosphorylation of insulin receptor, the substrate protein IRS-1, and MAPK in CHO-IR cells, meaning that IR-TM can activate insulin receptor and subsequent signal transduction.

To address the mechanism of insulin receptor activation induced by IR-TM, mutant insulin receptors were used. IR-TM could not activate IR<sup>PDGFR<sup>TM</sup></sup>, which possess TMD sequence replaced with TMD of PDGFR. This demonstrated that the TM sequence is required for activation. Two kinase-deficient mutants, IR(K1006A) and IR(Y3F), were not phosphorylated upon IR-TM stimulation. These results showed that the IR-TM activates insulin receptor in an intramolecular manner and possibly through direct interaction with the TMD of insulin receptor.

The specificity was examined using TMD peptides from other receptor tyrosine kinases (Figure 1). Other TMD peptides did not activate the insulin receptor *in vitro* (Figure 2), or in CHO-IR cells. Thus, the IR-TM specifically activates the insulin receptor.

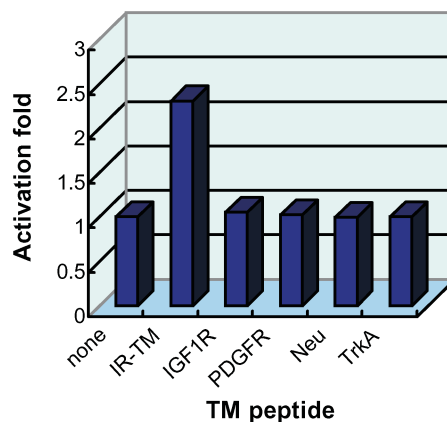


Fig. 2. Specificity of WGA agarose-purified insulin receptor activation by the TMD peptides.

To evaluate the ability of IR-TM as an insulin alternative, we examined whether IR-TM activates S323L, a mutant insulin receptor that lacks insulin-binding ability [4]. IR-TM activated this mutant in a dose-dependent manner, whereas insulin stimulation could not activate it. This result indicates the possibility of drug design using IR-TM as the prototype, and targets region outside of the canonical binding sites.

In conclusion, we have shown that IR-TM can activate the insulin receptor specifically, possibly through direct interaction with the TMD of insulin receptor. Further SAR studies are in progress.

#### Acknowledgments

We thank Professor Masato Kasuga (Kobe University School of Medicine) for providing CHO-IR cells, and Keiko Oshikiri-Nagasaki for technical assistance.

#### References

1. Lee, J., Pilch, P.F. *Am. J. Physiol. Cell Physiol.* **266**, C319 (1994).
2. Yamada, K., Goncalves, E., Kahn, C.R., Shoelson, S.E. *J. Biol. Chem.* **267**, 12542 (1992).
3. Cheatham, B., Shoelson, S.E., Yamada, K., Goncalves, E., Kahn, C.R. *Proc. Natl. Acad. Sci. USA* **90**, 7336 (1993).
4. Roach, P., Zick, Y., Formisano, P., Accili, D., Taylor, S.I., Gorden, P. *Diabetes* **43**, 1096 (1994).

## Cyclopentapeptides as Rigidified Templates for Probing Interactions with the AT-1 Receptors

Gregory V. Nikiforovich<sup>1</sup>, Gunnar Lindeberg<sup>2</sup>, Katalin E. Kövér<sup>3</sup>, Yunpeng Ye<sup>1</sup>, Per-Anders Frändberg<sup>4</sup>, Fred Nyberg<sup>4</sup>, Anders Karlén<sup>2</sup>, Anders Hallberg<sup>2</sup> and Garland R. Marshall<sup>1</sup>

<sup>1</sup>Department of Biochemistry and Molecular Biophysics, Washington University, St. Louis, MO 63110, USA

<sup>2</sup>Department of Organic Pharmaceutical Chemistry, Uppsala University, S-75123 Uppsala, Sweden

<sup>3</sup>University of Debrecen, H-4010 Debrecen, Hungary

<sup>4</sup>Department of Pharmaceutical Biosciences, Uppsala University, S-75124 Uppsala, Sweden

### Introduction

Previously, possible 3D models of the “AT-1 receptor-bound” conformation of angiotensin II (Asp<sup>1</sup>-Arg<sup>2</sup>-Val<sup>3</sup>-Tyr<sup>4</sup>-Val/Ile<sup>5</sup>-His<sup>6</sup>-Pro<sup>7</sup>-Phe<sup>8</sup>, AII) have been suggested [1] and refined (Nikiforovich and Karlén, to be published). According to our conformational calculations, the “receptor-bound” spatial positions for two out of the three side chains that are crucial for ligand binding and signal transduction (Tyr<sup>4</sup>, His<sup>6</sup> and Phe<sup>8</sup>) can be fairly well represented by the corresponding side chains in the following cyclopentapeptides (CPPs): *cyclo*(Tyr-Val-His-D-Pro-Ala), *cyclo*(Gly-Val-His-D-Pro-D-Tyr), *cyclo*(Tyr-Val-His-D-Pro-Gly) and *cyclo*(D-His-Pro-D-Phe-Gly-Gly) (see also [2]). This study presents results of synthesis, NMR spectroscopy, independent energy calculations and binding assays for the above CPPs, as well as results of further design and evaluation of cyclic compounds based on CPPs and including all three functionally important side chains.

### Results and Discussion

Four CPPs in question have been synthesized by conventional methods of solid phase synthesis. Two of them, featuring either Tyr and His, or His and Phe side chains, namely *cyclo*(Tyr-Val-His-D-Pro-Ala) and *cyclo*(D-His-Pro-D-Phe-Gly-Gly), have been studied by NMR spectroscopy and by extensive energy calculations. Two out of four low-energy backbone conformations found by energy calculations for *cyclo*(Tyr-Val-His-D-Pro-Ala) possess the highest average statistical weights ( $w_{\text{mean}} = 0.59$  and  $0.27$ ) in DMSO solution according to the NMR data (both conformations correspond to the major one out of two slowly interconverting conformers found by NMR). Also, for *cyclo*(D-His-Pro-D-Phe-Gly-Gly), two out of ten low-energy backbone conformations found by energy calculations possess the highest average statistical weights ( $w_{\text{mean}} = 0.31$  and  $0.19$ ) in DMSO solution (only one major conformer was found by NMR). For both CPPs, conformations with the highest statistical weights fit the suggested 3D model of the receptor-bound conformation of AII (see Figure 1). On the other hand, none of the four CPPs displays binding to the AT-1 receptors (*in vitro* studies using rat liver membranes) in concentrations up to 10  $\mu\text{M}$ .

Aside from questioning the 3D model of the receptor-bound conformation of AII [1], possible reasons for non-binding of the above CPPs to the AT-1 receptors include (i) absence of all three functionally important side chains in a single compound, and, (ii) presence of the extra residues (see Figure 1) preventing proper interaction with AT-1 receptors. Therefore, we have designed compounds based on the above CPPs, which contain the Tyr, His and Phe side chains (Phe attached to the  $\beta$ -carboxyl of D-Asp), and compatible to the suggested 3D model of the receptor-bound conforma-

*Nikiforovich et al.*

tion of AII, namely *cyclo*(Tyr-Val-His-D-Asp(Phe)-Ala), *cyclo*(Tyr-Val-His-D-Asp(Phe)-Gly) and *cyclo*(Val-His-D-Asp(Phe)-D-Tyr-Gly). However, none of them binds AT-1 receptors in concentrations up to 10  $\mu$ M. This suggests that the main reason for non-binding to the AT-1 receptors is the presence of the extra residue(s) displacing some residues of the AT-1 receptor from spatial positions occupied in the

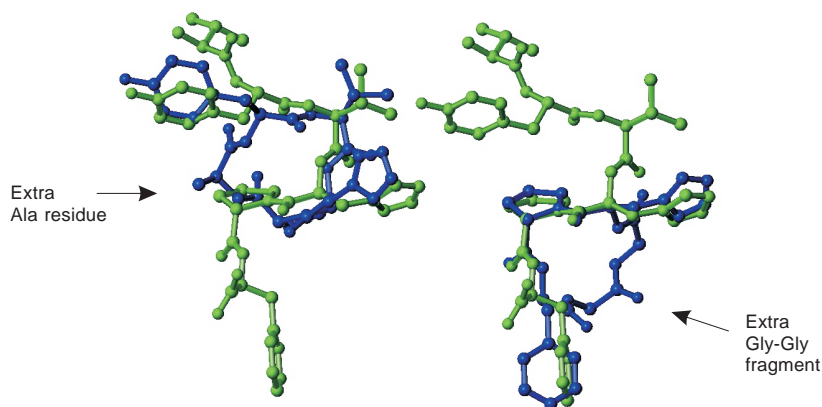


Fig. 1. Low-energy conformations of *cyclo*(Tyr-Val-His-D-Pro-Ala) and *cyclo*(D-His-Pro-D-Phe-Gly-Gly) overlapped with the 3D model of receptor-bound conformer of AII (light gray; only fragment 3-8 is shown).

AT-1–AII receptor complex. Indeed, a 3D model for the complex of AII and transmembrane region of the AT-1 receptor [3] shows that the extra residues in the CPP cycle may clash with L112, V108 and T260 in the AT-1 receptor, the former residue being directly involved in signal transduction [4].

## References

1. Nikiforovich, G.V., Marshall, G.R. *Biochem. Biophys. Res. Commun.* **195**, 222–228 (1993).
2. Nikiforovich, G.V., In Fields, G.B., Tam, J.P. and Barany, G. (Eds.) *Peptides for the New Millennium (Proceedings of the 16th American Peptide Symposium)*, Kluwer Academic Publishers, Dordrecht, 2000, p. 614.
3. Nikiforovich, G.V., Marshall, G.R. *Biochem. Biophys. Res. Commun.* **286**, 1204–1211 (2001).
4. Parnot, C., Bardin, S., Miserey-Lenkei, S., Guedin, D., Corvol, P., Clauser, E. *Proc. Natl. Acad. Sci. U.S.A.* **97**, 7615–7620 (2000).

## Receptor Binding Site of Arg-Lys Triple Repeat in Nociceptin Superagonist

Kazushi Okada<sup>1</sup>, Yoshiro Chuman<sup>1</sup>, Tsugumi Fujita<sup>1</sup>, Takeru Nose<sup>1</sup>,  
Tommaso Costa<sup>2</sup> and Yasuyuki Shimohigashi<sup>1</sup>

<sup>1</sup>Laboratory of Structure-Function Biochemistry, Department of Chemistry, Faculty and  
Graduate School of Sciences, Kyushu University, Fukuoka 812-8581, Japan

<sup>2</sup>Laboratorio di Farmacologia, Istituto Superiore di Sanità, Rome, Italy

### Introduction

Nociceptin (FGGFTGARKSARKLANQ), an endogenous heptadecapeptide isolated from the mammalian brain [1,2], was reported to be a ligand for opioid receptor-like ORL1 receptor to produce a hyperalgesia. The major efforts in the structure-activity studies have been focused on the design of antagonists for anti-neuropathy drugs. Indeed, several attempts to obtain nociceptin antagonists have recently been reported. On the contrary, a highly potent agonist, or so-called superagonist, often elicits the receptor responses such as desensitization and internalization, providing antagonistic cellular responses. Nociceptin possesses two Arg-Lys (RK) dipeptide units at the positions 8-9 and 12-13. This basic region of nociceptin has been suggested to interact with a cluster of acidic amino acid residues in the second extracellular loop (EL2) of ORL1 receptor [3]. We previously reported that when additional RK dipeptide unit was placed at positions 6-7, 10-11, 14-15, or 16-17, respectively, [Arg-Lys<sup>14-15</sup>]nociceptin showed increased activities both in the receptor binding assay (about 3-fold) and in the functional assay using [<sup>35</sup>S]GTPγS (about 17-fold) [4]. In the present study, in order to explore the reason why such an activity enhancement was induced by Arg-Lys replacement, we carried out the structure-activity studies by preparing a series of nociceptin analogs and ORL1 recombinant receptor.

### Results and Discussion

In this study, nociceptin analogs were evaluated by the radio-ligand receptor binding assay and by the [<sup>35</sup>S]GTPγS binding assay for ORL1 receptor expressed in COS-7 cells. First of all, in addition to Arg-Lys, we introduced a series of dibasic amino acid pairs, namely, Arg-Arg, Lys-Arg, and Lys-Lys into the positions 14-15 of nociceptin. All these three analogs bound to ORL1 about 3–5 times more strongly than nociceptin (similarly to [Arg-Lys<sup>14-15</sup>]nociceptin) (Table 1). Similarly, they activated ORL1 receptor much more strongly in the GTPγS binding assay (about 10-13-fold as compared to nociceptin) as [Arg-Lys<sup>14-15</sup>]nociceptin did (Table 1). These results clearly indicate that the presence of dibasic amino acid pairs is important regardless of the sequence.

When either Leu-14 or Ala-15 was replaced by Arg and Lys, independently, the resulting four analogs exhibited rather moderate enhancements in binding activity (about 2-fold) and in functional activity (2–4-fold) (Table 1). No activity enhancements were observed for these monobasic replacements. We also found that the positions 14 and 15 permit substitution by various kind of amino acids such as aliphatic amino acids (Ala, Val, and Leu) and aromatic amino acids (Phe, Tyr, and Trp), although these elicited no activity enhancement (Table 1). All these results suggested that the synergistic effect of functional activity is caused by  $\pi$ -characteristic interaction with receptor aromatic groups.

Since several aromatic amino acids are present adjacent to the acidic amino acid cluster in EL2, we prepared mutated ORL1 receptors in which Tyr-210 was converted

Table 1. Relative binding and functional potency of nociceptin analogs.

Peptides	Relative potency (%)	
	Binding assay	Functional assay
Nociceptin (=Noc)	100	100
[Arg-Arg <sup>14-15</sup> ]Noc	270	1 300
[Arg-Lys <sup>14-15</sup> ]Noc	350	1 200
[Lys-Arg <sup>14-15</sup> ]Noc	350	1 000
[Lys-Lys <sup>14-15</sup> ]Noc	460	1 200
[Arg <sup>14</sup> ]Noc	220	330
[Lys <sup>14</sup> ]Noc	180	320
[Ala <sup>14</sup> ]Noc	140	85
[Val <sup>14</sup> ]Noc	100	120
[Phe <sup>14</sup> ]Noc	100	69
[Tyr <sup>14</sup> ]Noc	100	85
[Trp <sup>14</sup> ]Noc	150	72
[Arg <sup>15</sup> ]Noc	240	410
[Lys <sup>15</sup> ]Noc	180	220

to Ala. In this Tyr210Ala mutant receptor, [Arg-Lys<sup>14-15</sup>]nociceptin exhibited almost the same receptor binding affinity as in the wild-type ORL1. On the other hand, no synergistic enhancement of [Arg-Lys<sup>14-15</sup>]nociceptin was observed in the functional assay. These suggested strongly that Tyr-210 of ORL1 is, at least, one of the binding sites for nociceptin Leu-14.

## References

1. Meunier, J.-C., Mollereau, C., Toll, L., Suaudeau, C., Moisand, C., Alvinerie, P., Butour, J.-L., Guillemot, J.-C., Ferrara, P., Monsarrat, B., Mazarguil, H., Vassart, G., Parmentier, M., Costentin, J. *Nature* **377**, 532–553 (1995).
2. Reinscheid, R.K., Nothacker, H.-P., Bourson, A., Ardati, A., Henningsen, R.A., Bunzow, J.R., Grandy, D.K., Langen, H., Monsma, F.J., Jr., Civelli, O. *Science* **270**, 792–794 (1995).
3. Mollereau, C., Mouldous, L., Lapalu, S., Cambois, G., Moisand, C., Butour, J.-L., Meunier, J.-C. *Mol. Pharmacol.* **55**, 324–331 (1999).
4. Okada, K., Sujaku, T., Chuman, Y., Nakashima, R., Nose, T., Costa, T., Yamada, Y., Yokoyama, M., Nagahisa, A., Shimohigashi, Y. *Biochem. Biophys. Res. Commun.* **278**, 493–498 (2000).

## **Identification of Novel Ligands for Vasopressin V<sub>2</sub> Receptor from Positional Scanning Libraries**

**Colette T. Dooley, Aric Mabini, Tyler Sylvester, Jon R. Appel and  
Richard A. Houghten**

*Torrey Pines Institute for Molecular Studies, San Diego, CA 92121, USA*

### **Introduction**

Vasopressin (arginine vasopressin, AVP) is a nonapeptide hormone released from the posterior pituitary. Its primary function in the body is to regulate extracellular fluid volume by affecting renal handling of water. The vasopressin V<sub>2</sub> receptor is part of the G protein-coupled receptor family and activates adenylyl cyclase upon binding to AVP. Cyclic peptide analogs of AVP that are potent and selective V<sub>2</sub> agonists have been identified [1], but there is still a need for the development of selective agonists and antagonists for the study of diabetes insipidus and enuresis. Mixture-based synthetic combinatorial libraries have been used in a number of studies for the identification of novel ligands that bind to G protein-coupled receptors, such as the opioid receptors [2]. In this study, two different positional scanning libraries made up of linear tetra- and hexapeptides were screened for the inhibition of AVP binding to the V<sub>2</sub> receptor. Two different approaches were carried out in the deconvolution of each library. In the hexapeptide case, dual-defined libraries were used to confirm the positional scanning library results, and several moderately active hexapeptides were identified. In the tetrapeptide case, a sublibrary deconvolution approach yielded tetrapeptides with significantly higher affinities.

### **Results and Discussion**

The screening of the positional scanning hexapeptide library made up of 20 L-amino acids for a diversity of 50 million hexapeptides yielded few active mixtures at each position, and standard deconvolution of this library, in which the amino acids of the most active mixtures are selected at each position, was not carried out. In an effort to find better activity, the same diversity of peptides from the positional scanning library was tested in three dual-defined libraries, namely H-OOXXX-NH<sub>2</sub>, H-XXOOXX-NH<sub>2</sub>, and H-XXXXOO-NH<sub>2</sub>. These libraries offer the advantage of having two amino acids connected in adjacent defined positions, and the concentration of each peptide within each mixture is 20 times higher. The screening of the 1200 mixtures in total yielded active mixtures defined with amino acids that were also found to be defined in the most active mixtures from the positional scanning library. The amino acids from the most active mixtures in the three dual-defined libraries were selected and combined to generate 56 different individual hexapeptides. The most active hexapeptide identified was H-PWYGYR-NH<sub>2</sub>, *K<sub>i</sub>* = 84 nM.

The screening of the tetrapeptide library made up of 91 different L- and D-amino acids for a diversity of 50 million tetrapeptides yielded more active mixtures than the hexapeptide library. Active mixtures were tested in a dose-response manner to rank the most active mixtures at each of the four positions of the library. Instead of making individual peptides directly from the library screening data using the standard deconvolution approach, a sublibrary was prepared. This sublibrary was prepared in the same positional scanning format as the initial library, except that the defined and mixture positions contained only the building blocks from the most active mixtures found in the initial library. From 91 mixtures at each position of the library, 14 mixtures

*Dooley et al.*

were chosen from position 1, 11 mixtures from position 2, 12 mixtures from position 3, and 15 mixtures from position 4. This approach reduced the diversity of the library (from 50 million to 27,000 tetrapeptides) which in turn increased the concentration of each peptide within each mixture. This resulted in clearer discrimination between the active and inactive mixtures. From this sublibrary, the most active building blocks at each of the four positions were selected based on activity and differences in chemical character. This selection resulted in the combination of 54 different individual tetrapeptides, and several were found to have  $K_i$  values less than 100 nM and made up mostly of aromatic D-amino acids (Table 1).

In conclusion, two different deconvolution strategies were used to identify novel vasopressin ligands from tetra- and hexapeptide positional scanning libraries. The most active tetrapeptide identified here has several amino acids in common with other cyclic analogs of AVP in which the substitution of tyrosine at position 2 or phenylalanine at position 3 by thienylalanine resulted in selective  $V_2$  agonists [1]. Further studies are needed to determine if this linear tetrapeptide is a selective agonist or antagonist, and if the activity can be improved.

*Table 1. Activities of tetrapeptides binding to vasopressin  $V_2$  receptor.*

Peptide						$K_i$ , nM
H-	L-Thiala-	D-pCl-Phe-	D-OEt-Tyr-	D-pNO <sub>2</sub> -Phe	-NH <sub>2</sub>	15
H-	L-Thiala-	D-pCl-Phe-	D-OEt-Tyr-	D-pCl-Phe	-NH <sub>2</sub>	25
H-	L-Phe	D-pCl-Phe-	D-OEt-Tyr-	D-pNO <sub>2</sub> -Phe	-NH <sub>2</sub>	55
H-	L-Thiala-	D-pCl-Phe-	D-Nal-	D-pNO <sub>2</sub> -Phe	-NH <sub>2</sub>	71
H-	L-Thiala-	D-pCl-Phe-	D-Nal-	D-Thiala	-NH <sub>2</sub>	79
H-	L-Thiala-	D-Phe-	D-Nal-	D-pNO <sub>2</sub> -Phe	-NH <sub>2</sub>	89
H-	L-Phe	D-pCl-Phe-	D-OEt-Tyr-	D-pCl-Phe	-NH <sub>2</sub>	96

## References

1. Chan, W.Y., Wo, N.C., Stoev, S. Cheng, L.L., Manning, M. *Exp. Physiol.* 85S, 7S–18S (2000).
2. Houghten, R.A., Pinilla, C., Appel, J.R., Blondelle, S.E., Dooley, C.T., Eichler, J., Nefzi, A., Ostresh, J.O. *J. Med. Chem.* **42**, 3743–3778 (1999).

## Diversity Generation and Guest-Templated Self-Sorting in Dynamic Combinatorial Libraries

Peter Timmerman and David N. Reinhoudt

*Laboratory of Supramolecular Chemistry & Technology, MESA+ Research Institute,  
University of Twente, 7500 AE Enschede, The Netherlands*

### Introduction

The extraordinary high binding affinities and selectivities of natural receptors arises from the cooperative action of small rigid peptide sub-units oriented in a 3D fashion around the target molecule. Efforts to mimic such functional group arrays in synthetic systems have led to the synthesis of artificial protein receptors mimicking the binding properties of natural antibodies. Similar studies on the self-assembly of polar functionalities using noncovalent platforms has so far received very little attention. In this paper, we describe a novel approach towards the synthesis of synthetic antibody mimics, making use of noncovalent platforms for the self-assembly of small rigid peptide fragments.

### Results and Discussion

In the past, our group has developed the noncovalent synthesis of the dynamic hydrogen-bonded assemblies via the cooperative formation of 36 hydrogen bonds between three calix[4]arene dimelamines and six 5,5-diethylbarbituric acid (DEB) units. Characterization using  $^1\text{H}$  NMR spectroscopy [1,2], MALDI-TOF mass spectrometry with  $\text{Ag}^+$ -labeling, and CD spectroscopy [3,4] have shown that these assemblies are thermodynamically stable in apolar solvents as well as in the presence of polar solvents, like MeOH and THF. Recently, we demonstrated that these noncovalent assemblies can be used as platform for the self-assembly of hydrogen-bonding functionalities, like amides, amino acids, and oligopeptides (Figure 1) [5]. These functionalities do not affect the thermodynamic stability of the assemblies to a significant extent. In some cases, the stability is even slightly increased.

Structural diversity in these assemblies can be generated on the supramolecular level, *i.e.* by simply mixing  $N$  different assemblies under thermodynamic conditions. The rapid exchange of components generates a number of  $P$  assemblies ( $P = N^2 + [N(N - 1)(N - 2)]/6$ ) [6]. Supramolecular diversity generation is an extremely powerful tool to generate molecular diversity, since it is a spontaneous process that occurs in

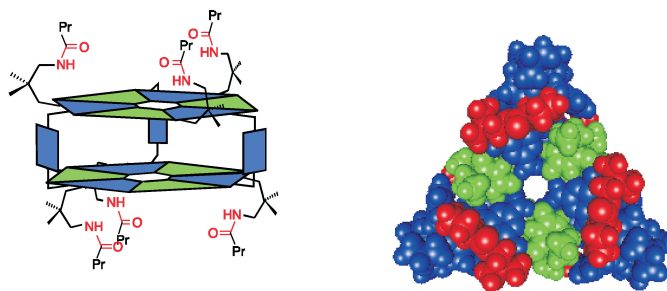


Fig. 1. Schematic representation and space-filling model of a hexa-urea functionalized hydrogen-bonded double rosette assembly.

**Timmerman et al.**

the absence of an added chemical reagent. For example, a mixture of 10 differently functionalized dimelamines spontaneously generates a library of 220 potential receptor molecules.

Recently, several groups simultaneously have shown that guest-templating effects in dynamic libraries can be used to amplify the formation of the best binding receptor. In this paper we describe the first example of chemical evolution in a supramolecular library [7]. Upon addition of a guest molecule, which binds most tightly to only one of the supramolecular assemblies present in the library, reversible self-sorting of the library is observed resulting in the clean formation of the best-binding receptor.

**Acknowledgments**

We thank the EC for Marie Curie Research Grant to Mercedes Crego Calama (No. ERBFMBICT 961445) and Francesca Cardullo (No. ERBFMBICT 972555) as part of the TMR Programme. We thank the JST (Chemotransfiguration Project) for financial support to Katrina A. Jolliffe. We thank NWO-CW for financial support to Leonard J. Prins.

**References**

1. Timmerman, P., Vreekamp, R.H., Hulst, R., Verboom, W., Reinhoudt, D.N., Rissanen, K., Udachin, K.A., Ripmeester, J. *Chem. Eur. J.* **3**, 1823 (1997).
2. Jolliffe, K.A., Crego Calama, M., Fokkens, R., Nibbering, N.M.M., Timmerman, P., Reinhoudt, D.N. *Angew. Chem., Int. Ed. Engl.* **37**, 1247 (1998).
3. Prins, L.J., Huskens, J., de Jong, F., Timmerman, P., Reinhoudt, D.N. *Nature* **398**, 498 (1998).
4. Prins, L.J., de Jong, F., Timmerman, P., Reinhoudt, D.N. *Nature* **408**, 181 (2000).
5. Kerckhoffs, J., Luyten, I., Crego Calama, M., Timmerman, P., Reinhoudt, D.N. *Org. Lett.* **2**, 4121 (2000).
6. Crego Calama, M., Hulst, R., Fokkens, R., Nibbering, N.M.M., Timmerman, P., Reinhoudt, D.N. *Chem. Commun.* 1021 (1998).
7. Crego Calama, M., Timmerman, P., Reinhoudt, D.N. *Angew. Chem., Int. Ed. Engl.* **39**, 755 (2000).

## **NMR Studies of the Interaction of $\alpha$ -Bungarotoxin with a Mimotope of the Nicotinic Acetylcholine Receptor**

**Ottavia Spiga<sup>1</sup>, Maria Scarselli<sup>1</sup>, Arianna Ciutti<sup>1</sup>, Luisa Bracci<sup>1</sup>,  
Barbara Lelli<sup>1</sup>, Luisa Lozzi<sup>1</sup>, Samuel Klein<sup>1</sup>, Duccio Calamandrei<sup>2</sup>,  
Andrea Bernini<sup>1</sup>, Daniela Di Maro<sup>2</sup> and Neri Niccolai<sup>1</sup>**

<sup>1</sup>*Department of Molecular Biology and Biomolecular Structure Research Center,  
University of Siena, 53100 Siena, Italy*

<sup>2</sup>*BIOMODEM pcsrl, 53100 Siena, Italy*

### **Introduction**

A combinatorial library approach has been used to produce synthetic peptides mimicking the snake neurotoxin binding site of nicotinic receptors [1,2]. Among all the tested sequences which can inhibit the binding of  $\alpha$ -bungarotoxin,  $\alpha$ -bgt, to both muscle and neuronal nicotinic receptors, a 14-mer, with the sequence HRYESSLPWYPD, henceforth called p6.7, has been selected ensuring a toxin-binding affinity considerably higher than other peptides reproducing native receptor sequences [3,4]. NMR studies on the structural characteristics of the complex between the peptide and  $\alpha$ -bungarotoxin are reported here.

### **Results and Discussion**

On the basis of standard assignment procedures, all the proton resonances of the toxin and the p6.7 peptide in the free and bound forms have been identified. The chemical shift for each hydrogen of the complex is available from BMRB with the accession numbers 5006 and 4849 respectively for the free and bound  $\alpha$ -bgt.

The chemical shift spread observed for the free toxin is consistent with the presence in solution of folded, mainly extended, secondary structure elements. Information on the conformational stability of the protein may be inferred by the extended network of the measured Overhauser effects. Out of the measured 1096 dipolar connectivities, 368 are long range ones, *i.e.* arising from protons distant more than four residues in the sequence. Thus, these NOEs represent a reasonable set of experimental data for restrained molecular dynamics calculations. The minimized averaged structure is deposited in the Protein Data Bank as 1IK8. The good quality of this structural result may be checked by the calculated RMSD, 0.80 Å both for backbone and all heavy atoms in the obtained 30 lowest energy structures. The narrow dispersion of NH and  $\alpha$  proton chemical shift and the total absence of medium and long distance NOEs suggests that p6.7 does not have any conformational trend, in agreement with what is usually found for short linear peptides in water solution.

From NOESY spectra acquired for the 1 : 1 mixture of p6.7 peptide and  $\alpha$ -bgt, a set of 1606 distance restraints was obtained and used for the structure calculations: 1475 and 74 corresponded respectively to intra-molecular protein and peptide NOEs, while 57 derived from intermolecular protein-peptide dipolar connectivities. The large number of long range NOEs, *i.e.* respectively 759 and 27, ensured a good basis for a restrained molecular dynamics calculation, as confirmed also by the low RMSD, 0.55 and 0.77 Å, respectively calculated for only backbone and all heavy atoms in the obtained 20 lowest energy structures. The twenty lowest energy conformers of the  $\alpha$ -bgt/p6.7 complex are shown in Figure 1, while the three-dimensional average structure of the same complex is PDB available as 1HN7.



Fig. 1. A backbone representation of the twenty lowest energy conformers of the complex between  $\alpha$ -bgt and p6.7 (the peptide is shown in black).

#### Acknowledgments

This work was supported by the Italian MURST (PRIN 1997 and 1998) and by the Italian CNR, Progetto Finalizzato Biotecnologie No. 97.01156. N. N. thanks the Italian MURST (PRIN 1999 and 2001) and the University of Siena for financial support.

#### References

1. Basus, V.J., Guoqiang, S., Hawrot, E. *Biochemistry* **32**, 12290–12298 (1993).
2. Zeng, H., Moise, L., Grant, M.A., Hawrot, E. *J. Biol. Chem.* **276**, 22930–22940 (2001).
3. Balass, M., Katchalski-Katzir, E., Fuchs, S. *Proc. Natl. Acad. Sci. U.S.A.* **94**, 6054–6058 (1997).
4. Bracci, L., Lozzi, L., Lelli, B., Pini, A., Neri, P. *Biochemistry* **40**, 6611–6619 (2001).

## Selection of Antagonists of Fibroblast Growth Factor from a Phage-Display Peptide Library

**Hongkuan Fan<sup>1</sup>, Hui Zhou<sup>1</sup>, Wei Li<sup>1</sup>, Roger W. Roeske<sup>2</sup> and Lili Guo<sup>2</sup>**

<sup>1</sup>*College of Life Science, Jilin University, Changchun 130023, P.R. China*

<sup>2</sup>*Department of Biochemistry and Molecular Biology, Indiana University School of Medicine,  
 Indianapolis, IN 46202, USA*

### Introduction

The family of fibroblast growth factors (FGFs) plays important roles in various development and pathological states such as wound healing, tissue repair, and growth of some solid tumors [1]. Because the abnormal expression of FGFs may contribute to several human pathologies such as arthritis, atherosclerosis, and tumor neovascularization [2], the development of FGF antagonists would be useful clinically. In our early work [3], several peptide ligands that bind to FGF were selected using a 15-mer phage-display peptide library. In this research, we expressed human FGF receptor1 (FGFR1) on the surface of Sf9 insect cells. Peptide ligands binding to FGFR1 were screened using a phage-display 6-mer peptide library.

### Results and Discussion

The gene for FGFR1 was inserted into a baculovirus, and the virus was used to infect Sf9 insect cells. ELISA experiment suggests that a large amount of recombinant FGFR1 was successfully expressed on the surface of Sf9 insect cells. Peptide ligands that can specifically bind with cell surface expressed recombinant FGFR1 were selected in a 6-mer phage peptide library. After four rounds of selection, phage recovery increased from  $3 \cdot 10^{-5}$  to  $7 \cdot 10^{-3}\%$ . This suggested that the phage-displayed peptides specifically bound to FGFR1 were successfully enriched. Infected Sf9 insect cells, which express recombinant FGFR1, were immobilized on 96-well plates. Nearly 40 randomly selected phage clones were purified and added to the wells. The phages binding with FGFR1 were determined by HRP labeled anti-M13 antibody. The uninfected Sf9 insect cells were used as negative control. Clones 1, 2, 3, 7 and 8, which specifically bind with FGFR1 were selected. The amino acid sequences of the peptides displayed on selected phages were determined by DNA sequencing, which yielded a

*Table 1. Peptide sequences of selected phages.*

Clone	Sequence	Frequency
1	AGQGSQ	10
2	LLVPLR	6
3	FAYLLG	1
4	VTEMRH	1
5	DHKMRH	1
6	SLHHAS	1
7	VYMSPF	2
8	VKCSPF	1
9	GYNLWR	2

group of related peptides (Table 1). Clones 2, 3, 7, 8 consist mainly of hydrophobic amino acid residues.

Increasing concentrations of synthetic peptides, together with aFGF (100 ng/ml) and heparin (15 units/ml) was added to starved NIH 3T3 cells. The peptide Ac-AKICLA-NH<sub>2</sub> (Pc) was used as negative control. The mitogenic activity of aFGF was effectively inhibited by peptide Ac-VYMSPF-NH<sub>2</sub> (P2). The disulfide-linked peptide CAVYMSPFAC (P3) also can inhibit the activity of aFGF, but it is not as effective as P2 (Figure 1). Prediction of P2 binding site on FGFR1 was carried out with docking computation. The result shows that P2 was located on the conserved hydrophobic surface of the second Ig-like domain of the receptor, which consists of Ala167, Pro169 and Val 248.

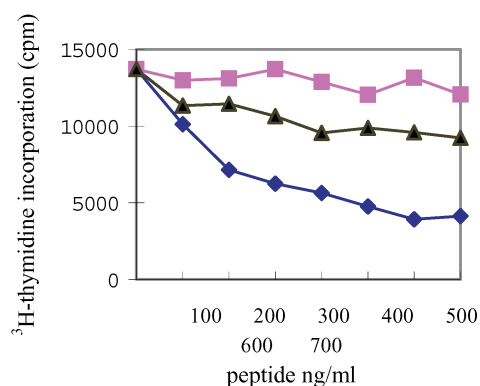


Fig. 1. Inhibition of the mitogenic activity of aFGF by the synthetic peptides. NIH 3T3 cells were incubated 1 day with a constant concentration of aFGF (100 ng/ml) and heparin (15 units/ml) in DMEM together with increasing concentrations of synthetic peptides P2 (◆), P3 (▲) and Pc (■). Cell density was determined by measuring the amount of <sup>3</sup>H-thymidine incorporation.

In conclusion, the peptide ligand VYMSPF, which was selected from a phage peptide library, can specifically bind with the hydrophobic surface of FGFR1, which is the binding site for FGF, and inhibit mitogenic activity of aFGF. Thus, it has great potential to become a therapeutic agent as an FGF antagonist.

## References

1. Basilico, C., Moscatelli, D. *Adv. Cancer Res.* **59**, 115–165 (1992).
2. Klagsbrun, M., D'Amore, P.A. *Annu. Rev. Physiol.* **53**, 217–39 (1991).
3. Fan, H., Liu, Y., Zhou, H., Wang, L., W., Guo, L., Roeske, R.W. *IUBMB Life* **49**, 545 (2000).

**Peptides in Immunology,  
Synthetic Vaccines,  
Molecular Mechanisms of Diseases,  
Peptides in Diagnostics, Pharmacology and  
Biotechnology,  
Peptide Delivery Approaches**



## Peptide Carrier for Efficient Drug Transport Into Living Cells

R. Pipkorn<sup>1</sup>, K. Braun<sup>2</sup>, W. Waldeck<sup>3</sup>, M. Koch<sup>1</sup>, I. Braun<sup>2</sup> and J. Debus<sup>2</sup>

<sup>1</sup>Central Section for Peptide Synthesis

<sup>2</sup>Division of Radiooncology, Deutsches Krebsforschungszentrum Heidelberg, Germany

<sup>3</sup>Division of Biophysics of Macromolecules, Deutsches Krebsforschungszentrum  
 Heidelberg, Germany

### Introduction

Recent progress in biotechnology and peptide synthetic chemistry has resulted in a large number of functional molecules. However, non-efficient translocation across the plasma membrane is still one of the factors limiting the import of biomolecules into the cytoplasm, hence into the nucleus. To overcome both cellular barriers *i.e.*, the cell and nuclear membranes, we report on the design and synthesis of a biomolecular shuttle, consisting of functional modules.

### Material and Methods

The determination of the functional peptide subunits was realized by HUSAR and PDB biocomputing methods. Visualization and characterization were carried out by molecular modeling and mass spectroscopy methods (MS) (Figures 1–5). Peptides were synthesized using the solid phase strategy (Fmoc-method) on a fully automated multiple synthesizer and purified by preparative HPLC on a reverse phase column. The material was characterized by analytical HPLC and laser desorption mass spectroscopy. The conjugate was composed of the two modules: PTD-Cys[Alexa320™] (Figure 1), TPS-Cys[Alexa320™] (Figure 2), Cys-NLS-Peptide[Rhodamine110] (Figure 4), Cys-MLS-Peptide[Rhodamine110] (Figure 3) and Cys-ER-Peptide-[Rhodamine110] (Figure 5) according to the above strategy. Human prostate cancer cells (DU-145) (Figures 6-8) were cultivated and maintained in RPMI1640 medium with 10% bovine calf serum and adhered to the cover slides. The cells were incubated with the conjugates and the control peptides in 100 pM final concentration for 30 min. The conjugate transport into living cells was determined by a confocal laser scanning method (CLSM).

### Results and Discussion

The transport peptide-conjugate, labeled on both sides (the transport peptide: red; the conjugated NLS-peptide: green) was detectable after 30 min in the cytoplasm and in the nucleus a few minutes later suggesting a fast nuclear delivery. The non-cleavable construct remained in the cytoplasm.

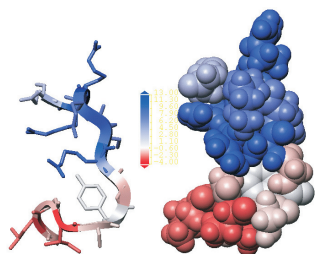


Fig. 1. PTD-TAT/HIV-1.

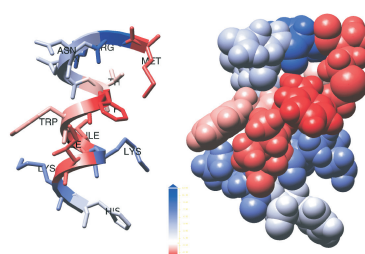


Fig. 2. TPFHum.

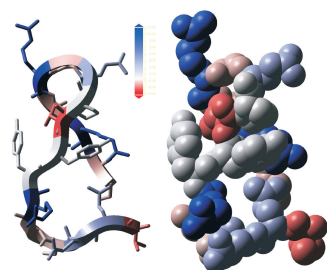


Fig. 3. MLS- peptide.

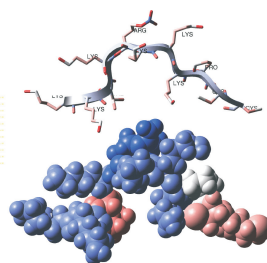


Fig. 4. NLS-peptide.

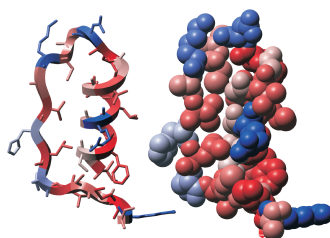


Fig. 5. ER-direct.-peptide.

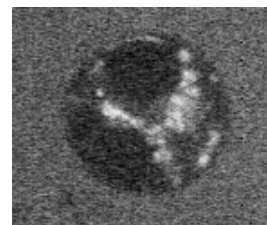
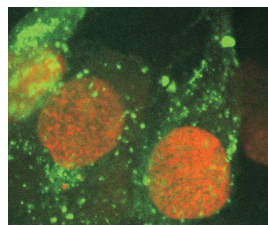
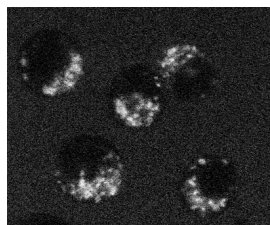


Fig. 6. DU-145cells; MLS-conj. Fig. 7. DU-145 cells ; NLS-conj Fig. 8. DU-145; ER-conj.

## References

1. Derossi, D., Chassaing, G., Prochiantz, A. *Trends Cell Biol.* **8**, 84–87 (1998).
2. Kalderon, D., Roberts, B.L., Richardson, W.D. *Cell* **39**, 499–509 (1984).

## Design of Novel Cell Penetrating Peptides

Kristen Sadler, Khee Dong Eom and James P. Tam

Department of Microbiology and Immunology, Vanderbilt University, Nashville,  
TN 37232, USA

### Introduction

The use of peptides, proteins, drugs and oligonucleotides as intracellular therapeutic agents and diagnostic tools is limited by poor cellular uptake. In an attempt to overcome this limitation transportant peptides have been designed with the ability to translocate across the lipid bilayer and deliver covalently bound cargo to the cytoplasm and nucleus [1,2]. Transportants may be generally divided into two categories: cationic (polyarginine, HIV Tat<sub>48-57</sub>, penetratin, transportan) and hydrophobic (lipopeptides, signal sequences). However, associated poor solubility or cytotoxicity deem it desirable to develop new transportants.

There is indirect evidence that peptide sequences with a high content of proline residues are capable of translocating across cell membranes. For example proline-rich antimicrobial peptides act in a manner unlike pore-forming peptides by first entering cells and then killing by a secondary mechanism [3]. In a second and more striking example it has been shown that malaria-causing *Plasmodium berghei* parasites enter and exit several cells without causing cell death [4]. This parasite is coated in the proline-rich circumsporozoite (CS) protein. The goal of our present study was to determine if proline-rich peptides could act as transportants.

### Results and Discussion

The antimicrobial activity of the proline- and arginine-rich protein Bac 7 is retained by the 24 residue peptide RRIRPRPPRLPRPRPRPLPFPRPG that represents the N-terminus. To determine if this peptide and a series of truncated peptides with sequential subtractions of two N-terminal residues, could act as transportants each peptide was synthesised with a fluorophore attached to the N-terminus and incubated with 264.7 monocytes. It was found that peptides with both a high and low content of arginine could translocate into cells. An assay was designed to quantitate the amount of peptide that translocated into the cells. In this assay the cells were incubated in the presence of fluoresceinated peptide and then washed and the amount of intracellular fluorescence measured using a fluorescence spectrophotometer. It was found that uptake of the shorter peptides (with 2 or 3 arginines, 50% proline) was more efficient than that of the longer peptides (Figure 1).

The maximum intracellular concentration of fluoresceinated peptides occurred within 5 min and then decreased at a steady rate. This result indicates that the peptides can translocate in and out rapidly or that the peptides are cytotoxic. Preliminary cytotoxicity assays indicate, however, that the fluoresceinated peptides are not cytotoxic after incubation of cells in the presence of up to 100  $\mu$ M of fluoresceinated peptide for 24 h.

We have also studied PPPNPNDPPPPNPND based on a proline-rich repeating unit from *P. berghei* CS protein. This peptide was synthesised, fluoresceinated and tested in a quantitation assay. Uptake of this peptide was greater than that of a proline- and arginine-rich 18 residue peptide derived from Bac 7. The intracellular fluorescence measured was significantly greater than the background at a concentration of 10  $\mu$ M.

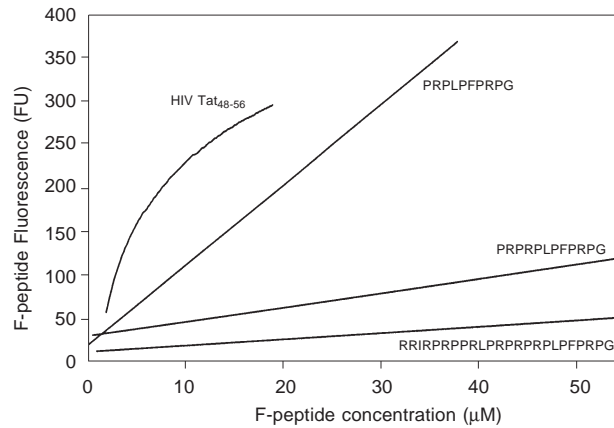


Fig. 1. The amount of translocated fluoresceinated peptide within 264.7 monocytes increases as peptide length and arginine content decreases.

In conclusion, peptides with a high content of proline residues may represent a new class of transportants. These proline-rich peptides have the desirable property of being aqueous soluble and are not highly charged.

#### Acknowledgments

We thank Dr. Jin Long Yang and Yoana Dimitrova for technical assistance. This work was supported in part by US Public Health Service NIH Grant CA36544 and AI37965.

#### References

1. Zhang, L., Torgerson, T.R., Liu, X-Y., Timmons, S., Colosia, A.D., Hawiger, J., Tam J.P. *Proc. Natl. Acad. Sci. U.S.A.* **95**, 9184–9189 (1998).
2. Wender, P.A., Mitchell, D.J., Pattabiraman, K., Pelkey, E.T., Steinman, L., Rothbard, J.B. *Proc. Natl. Acad. Sci. U.S.A.* **97**, 13003–13008 (2000).
3. Gallo, R.L., Huttner, K.M. *J. Invest. Dermatol.* **111**, 739–743 (1998).
4. Mota, M.M., Pradel, G., Vandenberg, J.P., Hafalla, J.C.R., Frevert, U., Nussenzweig, R.S., Nussenzweig, V., Rodriguez, A. *Science* **29**, 141–144 (2001).

## Synthesis and Targeting with Novel Multi-Mannosylated Glycopeptide Modules

**Goran Kragol<sup>1</sup>, David C. Jackson<sup>2</sup>, Walter Gerhard<sup>1</sup>,  
Michael Chatergoon<sup>1</sup>, Luis Montaner<sup>1</sup> and Laszlo Otvos, Jr.<sup>1</sup>**

<sup>1</sup>The Wistar Institute, Philadelphia, PA 19104, USA

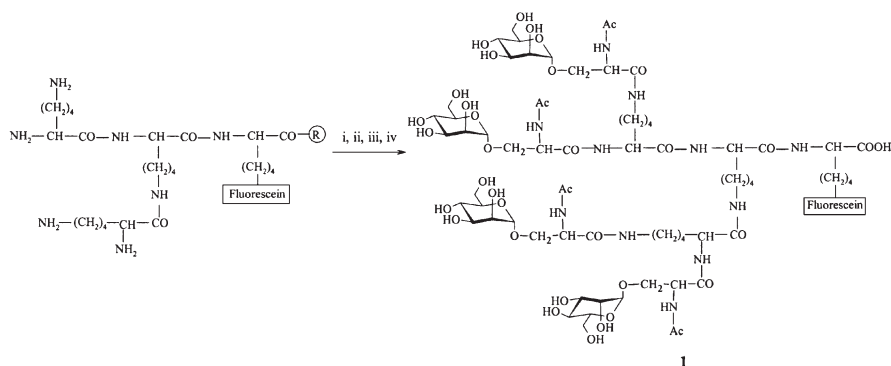
<sup>2</sup>Cooperative Research Center for Vaccine Technology, University of Melbourne, Parkville, Victoria 3052, Australia

## Introduction

A major disadvantage of synthetic peptide antigens is their low immunogenicity as a consequence of inefficient interactions with major histocompatibility complex (MHC) proteins. However, mannosylation of some antigens leads to selective targeting of dendritic cells through mannose-receptor mediated uptake, which results in a 100–10,000-fold enhanced *in vitro* stimulation of antigen-specific T-cell clones when compared to non-mannosylated peptides [1]. Dendritic cells are the most efficient antigen presenting cells (APCs) and their selective targeting is an important issue for peptide subunit vaccine development. In earlier studies, *in vivo* application of mannosylated vaccine constructs neither enhanced nor impaired the protection effect of the peptide vaccines in a reproducible fashion [2].

## Results and Discussion

In order to further explore the applicability of mannosylation for the enhanced immunogenicity of peptide vaccine constructs and in accord with the fact that targeting of the mannose receptors requires the preparation of multivalent ligands [3], we designed a multi-mannosylated peptide module **1** that can be attached to various peptide antigens and facilitate their presentation to APCs. Module **1** was successfully prepared by coupling of four mannosylated serines [4] onto a fluoresceine-labeled lysine core (Scheme 1). In this instance, we used single mannose moieties but the synthetic design of this module allows easy exchange of different carbohydrate residues including oligo- and branched sugar structures. Module **1**, as well as a non-mannosylated control module that has only serines attached to a lysine core, were also successfully attached to selected peptide antigens. Because the attachment of tetramannosylated



*Scheme 1. i) N-Fmoc-O-(2,3,4,6-tetra-O-acetyl- $\alpha$ -D-mannopyranosyl)-L-serine; ii) piperidine/DMF; iii) PfpOAc; iv) 0.1 M NaOH.*

modules and non-mannosylated controls to peptide antigens could not be achieved by direct coupling, the desired modules were constructed at the N-terminus of resin-bound peptide antigens. These were major CTL epitope of influenza virus nucleoprotein (TYQRTRALV) and three different HEL peptide antigens (FESNFNTQATR, NTDGSTDYGILQINSR, and KGTDVQAWIRGCRL). Similar tetramannosylated modules, but with different spacing between mannose moieties, were also attached to a highly complex subunit vaccine prototype carrying three independent branched antigens against influenza virus [4].

Because of the lack of surface mannose receptors on macrophage P388D1 and J774E cells (our prototype APCs), we were unable to properly examine the binding and uptake efficiencies of the mannosylated module **1**, as well as compare this module with dimannosylated and non-mannosylated analogues.

In conclusion, future experiments must involve a search for cells with a high expression of mannose receptors so that the mannosylated constructs can be more thoroughly examined. Although the binding efficiencies of the synthetic mannosylated modules could not be determined, it seems that variation in the geometry of the basic mannosylated construct used here will be necessary. The addition of spacers is a relatively straightforward method and the elaboration of branching oligosaccharide structures are experiments that we anticipate carrying out in the future.

#### **Acknowledgments**

This work was supported by a NIH grant GM45011.

#### **References**

1. Tan, M.C.A.A., Mommaas, A.M., Drijfhout, J.W., Jordens, R., Onderwater, J.J.M., Verwoerd, D., Mulder, A.A., van der Heiden, A.N., Scheidegger, D., Oomen, L.C.J.M., Ottenhoff, T.H.M., Tulp, A., Neefjes, J.J., Koning, F. *Eur. J. Immunol.* **27**, 2426–2435 (1997).
2. van Bergen, J., Ossendorp, F., Jordens, R., Mommaas, A.M., Drijfhout, J.W., Koning, F. *Immunol. Rev.* **172**, 87–96 (1999).
3. Kery, V., Krepinsky, J.J., Waren, C.D., Capek, P., Stahl, P.D. *Arch. Biochem. Biophys.* **298**, 49–55 (1992).
4. Kragol, G., Otvos, L., Jr. *Tetrahedron* **57**, 957–966 (2001).

## **Liposaccharides: Utilisation for Peptide Delivery and for Enhancing Synthetic Peptide Immunogenicity**

**Istvan Toth<sup>1</sup>, Ross McGeary<sup>1</sup>, Joanne Blanchfield<sup>1</sup>, Handoo Rhee<sup>1</sup>,  
Paul Alewood<sup>1</sup>, David Adams<sup>3</sup> and Michael Good<sup>4</sup>**

<sup>1</sup>*School of Pharmacy, <sup>2</sup>Institute for Molecular Bioscience and*

<sup>3</sup>*Physiology and Pharmacology, University of Queensland, Brisbane, QLD 4072, Australia*

<sup>4</sup>*Queensland Institute for Medical Research, Brisbane 4029, Australia*

### **Introduction**

A user friendly, reliable delivery system is essential for the success of peptide-based drugs. Currently, there are many peptides and proteins that have the potential to be developed as new medicines. However, a lack of oral absorption and poor *in vivo* stability are major hurdles that must first be overcome, before any of these peptides or proteins will reach the clinic.

### **Results and Discussion**

We have developed a novel drug-delivery system for the oral administration of poorly absorbed or biologically unstable drugs and peptides. The method involves conjugating the peptide or drug with lipoamino acids (LAA) and sugars (Figure 1).

Increased lipophilicity increases the oral uptake of conjugates up to a point, but further increases in lipophilicity decreases the uptake. One reason is that the lipid chains anchor the compounds into the cell membrane. Increasing lipophilicity also dramatically decreases the water solubility. For drug delivery, compromises between the lipophilicity and water solubility are needed. Further conjugation with hydrophilic compounds (lactic acid, glycolic acid, polyethylene glycol and sugars) can be utilized to improve the physico-chemical properties of the conjugate. The sugar conjugates provide a number of additional advantages that include an ability to: (i) modify the physico-chemical properties of a compound to increase water solubility or amphoteric character, (ii) utilize active transport systems to improve the intestinal absorption of peptides by utilizing glucose transporters, and (iii) selectively target the drug to the active site.

$\alpha$ -Conotoxin MII is a 16-residue neurotoxin from the cone snail *Conus magus*. This peptide features disulfide bonds between Cys2–Cys8 and Cys3–Cys16, a pattern characteristic of the  $\alpha$ -conotoxins. MII is a potent and highly specific blocker of mammalian neuronal  $\alpha_3\beta_2$  subtype nicotinic acetylcholine receptors (nAChR). The remarkable specificity of this peptide makes MII an important lead for potential pharmaceuticals. In order to study chemically modified analogues of this peptide, our initial objective was to determine if unfolded linear MII analogues substituted with

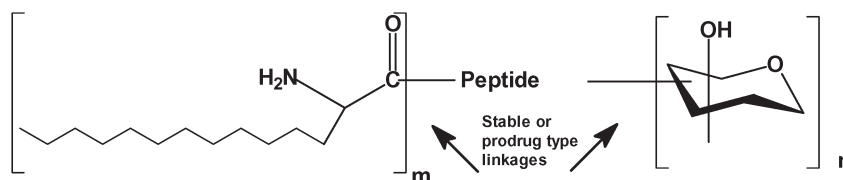


Fig. 1. General structure of the drug delivery system.

lipoamino acid groups (LAAMII) and sugar moieties would oxidise to give the required, active, three dimensional structure under the same conditions used to prepare MII. NMR studies of a lipoamino acid substituted MII conjugate indicating that the structure of the oxidised peptide is consistent with that of the native MII peptide. The *in vitro* activity of the lipid-modified analogue (LAAMII) was compared with the activity of the parent toxin. The percent of the control nACh-activated current in a rat ganglia cell that remained after treatment with either native MII or the LAAMII conjugate is shown below. The LAAMII conjugate exhibited the same affinity towards nAChRs as the native peptide.

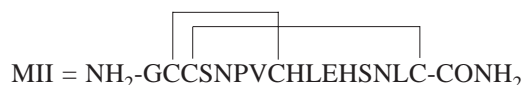


Table 1. Activities of MII and LAAMII.

Conc. (nM)	MI	LAAMII
20	90	92
100	57	57
1 000	47	47

Lipid conjugation of the decapeptide luteinizing hormone releasing hormone (LHRH) with one or two LAAs successively increased the biochemical half-lives of these peptides from only 2–5 min to 1–3 h [1]. This result was subsequently extended to *in vivo* experiments with rats, proving that the biological stability and oral uptake of the lipid modified LHRH was increased. Non-castrated male Wister rats were dosed daily for a period of 14 days by gavage under light CO<sub>2</sub> anaesthetic. Rats were given either control, LHRH (1 mg LHRH/0.5 mL) or LAA-LHRH-sugar (2.83 mg LLS/0.5 mL) in 4% DMSO and 50 µM phosphate and citrate buffer at pH 3.2.

Three hours after the final dose, blood, testes, epididymides, seminal vesicles and prostates were examined. No changes in organ weights were observed in LHRH given group, in comparison to the control group. In contrast, the mean weights of epididymides and seminal vesicles of the liposaccharide LHRH administered group were significantly lower than those of the control group (Figure 2).

Differences in mean prostate weight between the control and the LLS group was only significant at confidence level of 89.6%. Due to the mechanism of action of the drug, LHRH analogues require from 2 to 4 weeks to down regulate the LHRH receptors completely, resulting in complete exertion of its anti-hormonal effects.

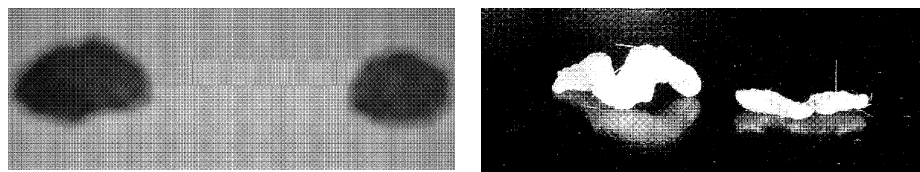


Fig 2. Comparison of prostate (left) and seminal vesicles (right) from control and liposaccharide LHRH dosed groups.

## Peptide Vaccines and Immunology

These findings confirm the principle that conjugation with one or more LAAs or liposaccharides has the capacity to increase the uptake of molecules across the epithelium of the gut or the skin, and to increase their resistance to breakdown by enzymes.

The above drug delivery system has also been used to develop a novel carrier system for the delivery (including oral) of peptide-based vaccines.

High antibody titres have been attained by coupling immunogenic peptides to a polylysine core, to form a Multiple Antigenic Peptide (MAP) [2]. We have further refined this approach, by using a lipidic anchor moiety at the C terminus of the polylysine system, to form a Lipid-Polylysine Core-Peptide (LCP) [3] (Figure 3). Thus the carrier, adjuvant and antigen are contained in the same molecular entity.

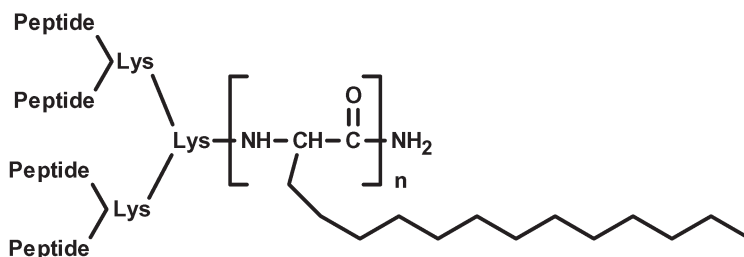


Fig. 3. General structure of the adjuvant/carrier system.

Seven LCP constructs were designed and synthesised using a Streptococcal peptide epitope. The constructs differed in the number of peptide sequences, the number of lipoamino acids, the length of the alkyl side chains and the spacing between the lipophilic tails. The effects of these variables on the immunogenicity of the peptide were examined in B10.BR mice. Increasing the number of lipoamino acid units in the backbone decreased the immunogenicity of the constructs. However, increasing the number of p145 peptide sequences (up to eight) within the LCP system, placing a spacer units between the lipoamino acids and increasing the length of the alkyl side chains, did enhance the immunogenicity of the LCP constructs.

The LCP peptides were found to be more immunogenic, even when administered without any conventional adjuvant, than the peptide monomer co-administered with adjuvants. Furthermore, high titer peptide antibodies were detected as early as day 20, when immunised with the LCP constructs, while anti-peptide antibodies in mice immunised with p145 (co-administered with adjuvants) were not detected until day 36 (after the second boost). Seven days after the third and final boost with peptide, the anti-peptide antibody titer in mice immunised with the monomer was 100-fold lower than the antibody titer in the mice immunised with LCP-peptide. Thus, there is evidence that the lipid side chains do have adjuvant-like properties. The side chains may facilitate binding to and uptake by antigen presenting cells.

### Acknowledgments

Wellcome Trust, Alchemia Pty Ltd and NH & MRC Australia supported this work. Thanks to Dr Ron Hogg for the rat ganglia assays.

### References

1. Toth, I., et al. *Int. J. Pharm.* **105**, 241–247 (1994).
2. Tam, J.P., Lu, Y-A. *Proc. Natl. Acad. Sci. U.S.A.* **86**, 9084–9088 (1989).
3. Toth, I., et al. *Tetrahedron Lett.* **34**, 3925–3924 (1993).

## Down-Regulation of HIV-1 Long Terminal Repeat Controlled Viral Transcription by DNA-Binding, Arginine-Rich Fusion Proteins Derived from HIV-1 TAT for the Direct Delivery into the Nucleus

Stefan R. K. Hoffmann

Department of Biochemistry, University of Zurich, 8057 Zurich, Switzerland

### Introduction

Modern biomedical research has shown that the majority of human diseases are based on cellular diseases. Thus, biomedical research is focused on this cellular level to define the molecular reasons followed by the development of concept and chemical structures to target the disease. While nature uses the non-exemplified diversity of protein structures in nearly all the life processes, the use of their structural diversity for the development of drug-like compounds is greatly limited due to their low biological availability. The most important reason is the low penetrability of the plasma membrane for peptides and proteins.

### Results and Discussion

In our endeavour to target the HIV-1 viral propagation by passive repression of the HIV-1 long terminal repeat (LTR) enhancer controlled transcription by artificial DNA-binding peptides and proteins, we have searched for an efficient and easy transduction system to translocate drug-like structures into the nucleus of the infected cell. Thus, we have investigated several translocation approaches, which include amphiphilic peptide transporters, the translocation sequences of antennapedia homeodomain [1] and the transduction sequences of the HIV-1 TAT protein [2,3].

Table 1. Penetrability of translocation sequences derived from HIV-1 TAT and antennapedia homeodomain from the medium into the cytoplasm or the nucleus.

No.	Sequence <sup>a</sup>	Residues Total	+	-	Translocation <sup>c</sup>		D <sup>e</sup>	Concentration <sup>f</sup>		
					Cos-1	Hela		2.0	0.2	0.02
1	GGGGYGRKKRR-QRRR <sup>b,f,g</sup>	15	8	0	Yes/Yes No <sup>d,1/2</sup> /Weak <sup>d,2</sup>	Yes/Yes No <sup>d,1/2/3</sup> /Yes <sup>d</sup>	Yes	+++ +++	++ +	+ +
2	GGGGRQIKIWFAQNRRMKWKK <sup>b</sup>	20		0	Yes/Yes Yes <sup>d,2</sup> /Yes <sup>d,2</sup>	Yes/Yes Yes <sup>d,1/2</sup> /Yes <sup>d,2</sup>		+++ +++	+++ ++	+ +
3	GGGGYGRGYRRKRERRK <sup>b</sup>	15	8	1	Yes/No Yes <sup>d,2/3</sup> /Yes <sup>d,2/3</sup>	Yes/No No <sup>d,2/3</sup> /Yes <sup>d,3</sup>	Yes	++ +++	+ +	+ +
4	GGGGYGRRRRR-RRRR <sup>b</sup>	15	9	0	Yes/Weak Yes <sup>d,1/2</sup> /Weak <sup>d,2</sup>	Yes/Weak Yes <sup>d,1</sup> /Weak <sup>d,1</sup>	Yes	++ +	+++ ++	+ +

<sup>a</sup> C-terminus: amide; N-terminus modified with 5(6)-carboxyfluorescein (1), (1) is not translocated in the cell, modified sequences were also investigated (data not shown); D-amino acids are underlined; <sup>b</sup> 5- and 6-(1) modified peptides were separated by RP-C8-HPLC; <sup>c</sup> cytoplasm/nucleus; <sup>d</sup> fused with GPKKKRKV (1) or GPKKKRV (2) or GPKKKRVGGGKTKRPRFGKTKRPRVGGQSSIEQLENGKTKRPRFGKTKRPRY (3); <sup>e</sup> all L-amino acids in D-configuration; <sup>f</sup> [ $\mu$ M]; +++ (strong); ++ (medium); + (weak) (time: 2–12 h); <sup>g</sup> RRQRRR, RRERRR, RRPRRR and KRPRRR are efficiently translocated, while HHQH<sup>g</sup>HH and HHQH<sup>g</sup>HH or KKQKKK and KKQKKK are not transported across the cytoplasmic membrane.

We have shown that these peptides were directly and efficiently translocated into the nucleus in adhesive COS-1, HeLa, CCL13 (Chang liver cell), CHO and non-adhesive cutaneous T-lymphocytes Jurkat, H9, C81 and histocytes U937 cell lines (Table 1). Both linear and branched peptide architectures were translocated into the cytoplasm, while the linear peptides were also found in the nucleus, especially when the translocation was further driven by the SV40 T-antigen NLS fused to the N-terminus. Several of our target peptides and several model peptides were translocated efficiently into the nucleus, where they were directly monitored by confocal fluorescence microscopy. During peptide translocation into the cell, we observed 3 or 4 spots in the nucleus, which are probably located on the membrane. Furthermore, we report a strategy to translocate synthetic drug-like structures by disulfide linked translocation sequences into the cytoplasm, where the disulfide is spontaneously reduced (Figure 1). This strategy allows the direct targeting of diseases by free drug-like structures.

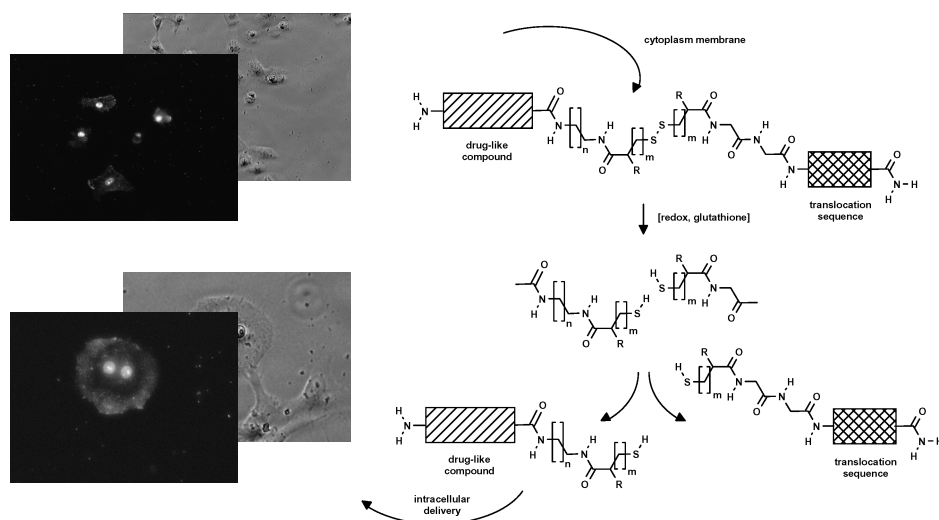


Fig. 1. Confocal fluorescence microscope (Nikon TE 300 Eclipse) images. Cell cultures were incubated in medium containing the lyophilized peptide for 2.0 h at 37 °C, (1a/b): CCL13 (12.0 h), (2a/b): HELA (12.0 h); Concept of the disulfide transduction system; Synthetic procedure: transduction sequence is synthesized on solid support. Dithiodialkanoic acid is activated by 0.5 eq. carbodiimide followed by the reaction with the support bound peptide. The carboxylic acid moiety is then activated by e.g. HBTU/HOBt/NMM followed by the reaction with an excess of the e.g. unprotected diamine. Solid phase synthesis is then continued.

## References

1. Derossi, D., Chassaing, G., Prochiantz, A. *Trends Cell Biol.* **8**, 84–87 (1998).
2. Fawell, S., Seery, J., Daikh, Y., Moore, C., Chen, L.L., Pepinsky, B., Barsoum, J. *PNAS* **91**, 664–668 (1994).
3. Schwarze, S.R., Ho, A., Vocero-Akbani, A., Dowdy, S.F. *Science* **285**, 1569–1572 (1999).

## New Insights Into the Membrane Translocating Process of the Tat Peptide Used for Cellular Delivery of Various Biological Molecules

Eric Vivès, Michelle Silhol and Bernard Lebleu

*Institut de Génétique Moléculaire de Montpellier, 34293 Montpellier cedex 05, France*

### Introduction

A 14-mer peptide derived from the HIV Tat protein was shown to translocate efficiently through the plasma membrane [1]. Basic amino acid residues in this highly cationic peptide are responsible for its internalization [2]. Non-permeant peptides, antisense oligonucleotides, proteins and even particulate material can be efficiently internalized when chemically conjugated or genetically fused to this Tat peptide. However, the mechanism of this uptake still remains to be elucidated.

Heparan sulfate (HS) proteoglycans were recently found to be responsible for the internalization of the full length Tat protein fused to GFP and/or to GST proteins [3]. Biochemical and genetic evidences have established that binding and endocytosis of the full length Tat protein was mediated by the heparan sulfate receptors. Moreover, the internalization of the Tat protein requires its basic domain [2]. Studies in our group do suggest, however, that Tat peptides are internalized through a pathway which does not involve HS proteoglycans and classical endocytosis.

### Results and Discussion

Full length Tat protein was shown to enter wild type CHO cells. However, mutated heparan sulfate proteoglycans cells (A-745) did not internalize the Tat protein [3]. Uptake of the short fluorescein labeled Tat peptide was evaluated by FACS analysis.

HS expressing (HeLa, wt-CHO) or deficient (CHO-A745) cell lines were incubated with (dotted lines) or without (solid lines) 10  $\mu$ M fluorescein labeled Tat peptide.

As seen in Figure 1, short Tat peptide entry was not impaired by the absence of heparan sulfate expression at the membrane on A-745 cells. Identical results were obtained with a rhodamin labeled Tat peptide or after immunodetection of the Tat peptide. These results also indicate no influence of the fluorochrome (data not shown).

A differential pathway of internalization between Tat peptide and Tat-GFP fusion protein was also investigated by incubating cells with both the Tat-GFP construct and a 12.5 molar excess of rhodamin-labeled peptide (80 nM and 1  $\mu$ M respectively, Figure 2). The internalization of the Tat protein fused to the GFP (bold dashed line) was detected by recording the intensity of the GFP signal in the 440 nm wavelength range. Rhodamin-labeled Tat peptide internalization (dotted line) was monitored in the 560

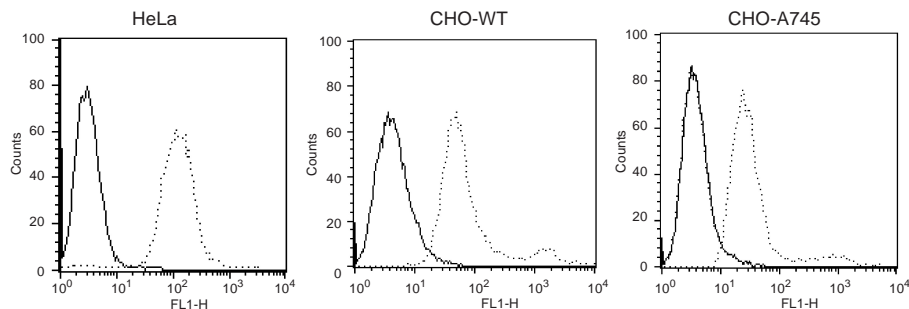


Fig. 1. FACS analysis of Tat peptide uptake in HS expressing or deficient cell lines.

nm wavelength range. The Tat-GFP protein and the rhodamin-Tat peptide were incubated with the wt-CHO (panel A) or with the mutated cell line (panel B). As shown in Figure 2 (panel B), the internalization of the Tat-GFP fusion construct was abolished in the A-745 cell line while rhodamin-Tat peptide still entered the cells.

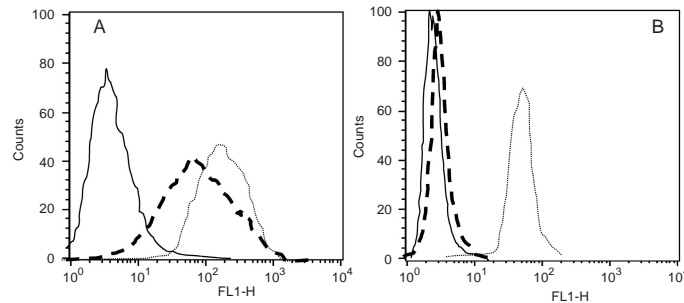


Fig. 2. FACS analysis of HS expressing (wt, panel A) or deficient (A-745, panel B) cell lines incubated with Tat-GFP and rhodamin-Tat peptide. Cells were incubated for 24 h with 80 nM of Tat-GFP fusion protein (---) and 1  $\mu$ M of rhodamin-labeled Tat peptide (.....). Plain lines show non incubated cells. Internalization of Tat protein was fully abolished in A-745 cells, while Tat peptide still showed uptake.

Moreover, the internalization of the Tat-GFP fusion construct was not significantly reduced despite the presence of an excess of the Tat peptide, in keeping with separate internalization pathways (Figure 3).

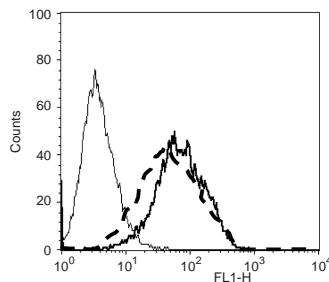


Fig. 3. FACS analysis of HS expressing cells incubated with Tat-GFP and an excess of rhodamin-Tat peptide. Cells were either incubated for 24 h with 80 nM of Tat-GFP fusion protein (bold line) or co-incubated (dotted line) with 80 nM of Tat-GFP and 1  $\mu$ M of rhodamin-labeled Tat peptide. Plain lines show non incubated cells.

In addition, Tat peptide entry was not impaired by incubation of CHO cells at low temperature as was the uptake of the Tat-GFP fusion protein (data not shown). Altogether these data suggest a differentiated route for the cellular uptake of the Tat protein and of the small Tat peptide used for cellular internalization of a large number of biomolecules.

## References

1. Vivès, E., Brodin, P., Lebleu, B. *J. Biol. Chem.* **272**, 16010 (1997).
2. Vivès, E., Granier, C., Prévot, P., Lebleu, B. *Lett. Peptide Sci.* **4**, 429 (1997).
3. Tyagi, M., Rusnati, M., Presta, M., Giacca, M. *J. Biol. Chem.* **276**, 3254 (2001).

## DUROS® Osmotic Implant for the Delivery of Peptides and Proteins

Jeremy Wright, James Matsuura, Stephen Berry and Catherine Lucas

ALZA Corporation, Mountain View, California, 94039-7210, USA

### Introduction

An increasing number of pharmaceutically active peptides and proteins require a simple system for delivery to the ambulatory patient. The DUROS® implant (Figure 1) has been developed to address this need.

The implant consists of a cylindrical titanium alloy drug reservoir that is capped at one end by a polyurethane rate-controlling semipermeable membrane. Immediately adjacent to the membrane is the osmotic engine, which consists mainly of NaCl. In contact with the osmotic engine is a sliding elastomeric piston that isolates the engine from the drug formulation. At the far end of the cylinder is the diffusion moderator that contains the orifice through which drug is released. The drug formulation is isolated from the surrounding body fluids until it is released from the orifice.

On implantation, water from the surrounding tissue is imbibed through the semipermeable membrane into the osmotic engine in response to the osmotic gradient between the osmotic engine and the tissue. The resulting linear displacement of the piston and delivery of the drug formulation occurs at a steady rate controlled by the composition, cross-sectional area, and thickness of the semipermeable membrane [1].

Formulation options for peptide and protein therapeutics in the DUROS® implant involve either solution or suspension formulation. Aqueous vehicles generally produce undesirable hydrolysis of the therapeutic; non-aqueous vehicles are preferred [1]. Formulating pharmaceutical agents in a suspension can be extremely beneficial for labile agents that have limited stability in solution.

### Results and Discussion

The first DUROS® implant to be developed is trademarked Viadur™ (leuprolide acetate implant) and delivers leuprolide acetate for one year (Figure 2, results from clinical trials). Leuprolide is a nonapeptide analog of GnRH. The drug formulation consists of a 37 wt.% solution of leuprolide in DMSO. The Viadur™ implant has been approved for marketing in the US for the palliative treatment of advanced prostate cancer.

The DUROS® implant was also investigated as a platform for delivery of pharmaceutically active agents in viscous suspensions. The suspensions are non-aqueous and

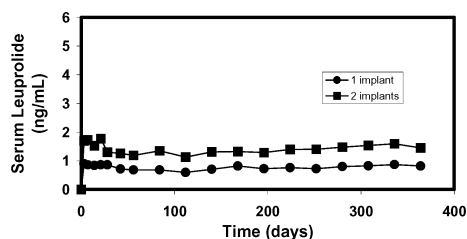
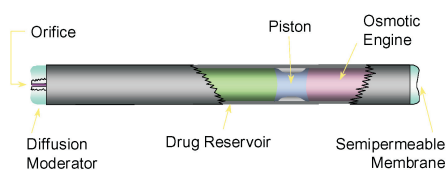


Fig. 1. Sketch of DUROS® Implant.

Fig. 2. Leuprolide Levels in-vivo.

### Peptide Vaccines and Immunology

exhibit viscosities of 5,000 to 1,000,000 poise. Stabilization and 3-month zero-order delivery of Glucagon-Like Peptide 1, a 30 amino acid peptide has been achieved *in vitro* (Figure 3). Similarly, stabilization and 3-month zero-order suspension delivery of human growth hormone has been shown (Figure 4).

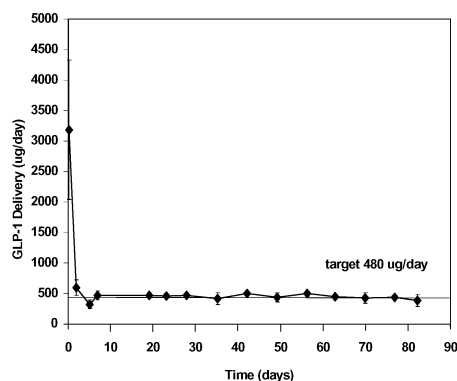


Fig. 3. Delivery of GLP-1 *in vitro*.

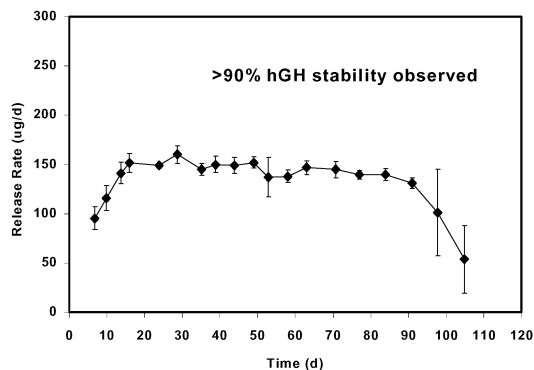


Fig. 4. Delivery of hGH *in vitro*.

These results demonstrate that peptides and proteins can be formulated as non-aqueous solutions and suspensions. The formulations can be delivered at a constant rate for periods from 1 month to 1 year using osmotic-based systems (*i.e.*, DUROS® implants).

#### Acknowledgments

We wish to acknowledge the contributions of our colleagues in the Biopharmaceutical Implant Research and Development Unit and our colleagues on the Viadur™ Implant development team. The special contributions of C. Stevenson, S. Leonard, F. Nakhjiri, J. Leonard, M. Tan, R. Ayer, P. Feriera, R. Jao and R. Skowronski are gratefully acknowledged.

#### References

1. Stevenson, C.L., Theeuwes, F., Wright, J.C., In D.L. Wise, (Ed.) *Handbook of Pharmaceutical Controlled Release*, Marcel Dekker, 2000, 225–253.

## Utilization of ICAM-1 Peptide Conjugates for Drug Targeting to T-Cells

Christine R. Xu, Meagan E. Anderson, Tatyana V. Yakovleva  
 and Teruna J. Siahaan

Department of Pharmaceutical Chemistry, The University of Kansas, Lawrence, KS 66047 USA

### Introduction

The objective of this work is to demonstrate that ICAM-1 peptides can be used to target drugs (*e.g.* methotrexate = MTX) to T-cells. Previously, we have shown that cIBR peptide derived from the ICAM-1 sequence can bind to and be internalized by the LFA-1 receptor on the surface of T-cells [1–3]. Therefore, we conjugated MTX to the N-terminus of cIBR for targeting MTX into T-cells. MTX has been used to treat leukocyte-related diseases such as leukemia and rheumatoid arthritis. Unfortunately, MTX produces side effects, and its prolonged administration may produce drug resistance. Therefore, the MTX-cIBR conjugate may have improved selectivity and lower toxicity than MTX alone.

### Results and Discussion

Synthesis of the MTX-cIBR conjugate was accomplished by forming an amide bond between the N-terminal of cIBR and the carboxylic acid of methotrexate [4]. We developed a method to conjugate MTX to cIBR *via* the  $\gamma$ - or the  $\alpha$ -carboxylic acid of the Glu residue in MTX (Figure 1). The final products were purified by HPLC and analyzed by NMR and ESI-MS. The conjugations were confirmed using mass spectrometry ( $M + 1 = 1611$ ).

One mechanism of action of MTX is inhibition of dihydrofolate reductase (DHFR) intracellular activity. MTX is one of the most potent inhibitors with a  $K_d = 1.84 \cdot 10^{-9}$  M [5,6]. Conjugation of cIBR to MTX *via*  $\gamma$ -carboxylic acid only slightly decreases the affinity of MTX for DHFR ( $K_d = 2.98 \cdot 10^{-9}$  M). Comparing the DHFR inhibition activities of  $\alpha$ -MTX-cIBR and  $\gamma$ -MTX-cIBR, we found  $\alpha$ -MTX-cIBR to be a weaker dihydrofolate reductase inhibitor than  $\gamma$ -MTX-cIBR. This is consistent with previous results, which indicate that the free  $\alpha$ -carboxylic acid group forms a strong bridge with the enzyme DHFR and therefore is essential for antifolate activity of MTX.

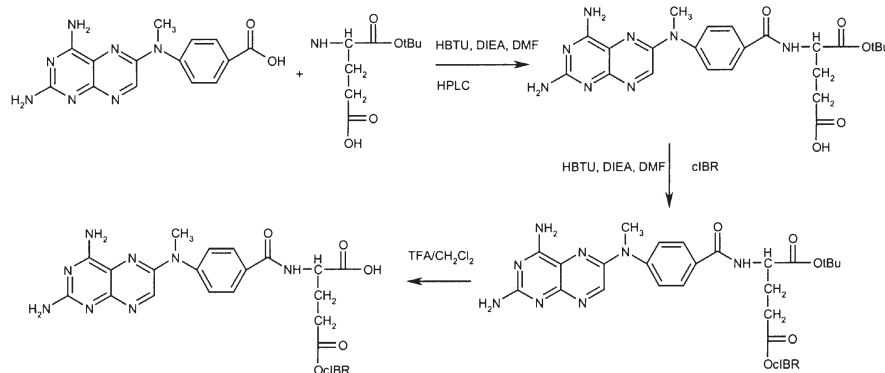


Fig. 1. Synthesis of  $\gamma$ -MTX-cIBR conjugate.

Toxicity studies (Table 1) of MTX-cIBR conjugates were done by MTT assay [7] using both non-activated and activated leukocytes (Molt-3). Results indicate that  $\gamma$ -MTX-cIBR is less potent than MTX at lower doses, but more toxic at higher doses. This may be due to: 1) reduced affinity of MTX-cIBR for DHFR; 2) higher protein binding for MTX-cIBR vs MTX; 3) the rate of MTX carrier transport might be faster than MTX-peptide internalization by the LFA-1 receptor; or 4) higher affinity but lower capacity of folate carrier vs LFA-1 receptor. To distinguish the degree of necrosis vs apoptosis caused by MTX and  $\gamma$ -MTX-cIBR, we utilized a Vybrant Apoptosis Kit assay and determined that at a concentration of  $10^{-6}$  M, there was no significant difference between MTX and  $\gamma$ -MTX-cIBR (based on 95% confidence interval t-test).

Evaluation of the binding and internalization of the  $\gamma$ -MTX-cIBR by the LFA-1 receptor using the anti LFA-1 antibody and cIBR competition studies [3] indicated that conjugation does not significantly alter peptide binding to LFA-1.  $\gamma$ -MTX-cIBR effectively inhibits anti-LFA-1 antibody to a similar degree as cIBR. Furthermore, cIBR effectively inhibits  $\gamma$ -MTX-cIBR toxicity in a dose-dependent manner.

Table 1. Comparisons of MTX vs  $\gamma$ -MTX-cIBR in DHFR inhibitory activity and toxicity.

Peptide	$K_m$ (DHFR inhibition)	Toxicity	
		Apoptosis	Necrosis
MTX	$1.84 \pm 0.80 \cdot 10^{-9}$	$78.0 \pm 4.1$	$19.0 \pm 2.4$
$\gamma$ -MTX-cIBR	$2.98 \pm 0.21 \cdot 10^{-8}$	$76.0 \pm 6.0$	$20.0 \pm 3.5$

In conclusion, preliminary results indicate the potential of using the bifunctional MTX-cIBR conjugate to improve the efficacy and selectivity of MTX for leukocyte-related disease treatment.

#### Acknowledgments

This work is supported by the Arthritis Foundation.

#### References

1. Buckley, C.D., et al. *Eur. J. Immunol.* **27**, 957–962 (1997).
2. Isobe, M., Yagita, H., Okumura, K., Ihara, A. *Science* **255**, 1125–1127 (1992).
3. Gursoy, R.N., Siahaan, T.J. *J. Peptide Res.* **53**, 414–421 (1998).
4. Rosowsky, A., Forsch, R., Uren, J., Wick, M. *J. Med. Chem.* **24**, 1450–1456 (1981).
5. Hood, K., Roberts, G.C. *Biochem. J.* **171**, 357–366 (1978).
6. Hillcoat, B. L., Nixon, P.F., Blakely, R.F. *Anal. Biochem.* **21**, 176–189 (1967).
7. Mossman, T. *J. Immunol. Methods* **65**, 55–63 (1983).

## Regulation of Cadherin-Cadherin Interaction: Secondary Structure of the HAV and ADT Peptides Derived from Human E-Cadherin Sequence

Christine R. Xu, Ernawati Sinaga, Irwan T. Makagiansar and Teruna J. Siahaan

Department of Pharmaceutical Chemistry, The University of Kansas, Lawrence, KS 66047, USA

### Introduction

Tight junctions present a major obstacle for delivery of drugs through the intestinal and blood brain barriers. These tight junctions are regulated in part by E-cadherins, which are calcium-dependent cell-cell adhesion molecules. E-cadherins are type-1 glycoproteins with a single transmembrane domain, a tandem repeat at the extracellular domain (EC1-EC5) and a short cytoplasmic domain. E-cadherins are also calcium-dependent molecules that are mediators of cell adhesion through homophilic interactions [1]. Peptides derived from this binding region have been shown to increase the opening of the intercellular tight junctions in a reversible fashion, and may be used to improve paracellular drug transport by altering the intercellular junctions [1,2].

### Results and Discussion

We have shown that HAV and ADT peptides derived from groove and bulge regions of the EC1 domain of E-cadherin can modulate the cadherin-cadherin interactions [3]. Ac-LFSHAVSSNG-NH<sub>2</sub> (HAV peptide 1) and Ac-QGADTPVGV-NH<sub>2</sub> (ADT peptide 2) were synthesized by a solid phase peptide synthesizer.

The ability of these peptides to modulate intercellular junctions was evaluated using Madin–Darby Canine Kidney (MDCK) cell monolayers on the Transwell™ membrane. Modulation of the intercellular junctions was measured by the ability to lower the transepithelial electrical resistance (TEER) of MDCK monolayers. Each peptide was added from the AP side (apical), BL side (basolateral) or simultaneously from the AP and BL sides of the cell monolayers and compared with a control peptide. Peptides 1 and 2 can lower the transepithelial electrical resistance (TEER values) 30–35% when administered from the BL side or simultaneously (Figure 1). However, these peptides were not very effective in modulating the intercellular junctions from the AP side.

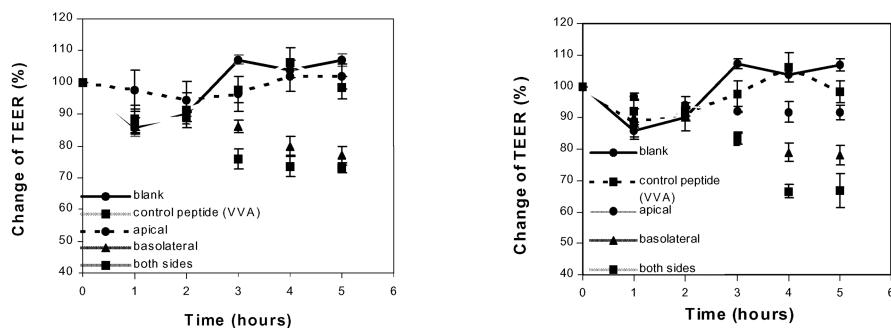


Fig. 1. Ability of HAV peptide 1 (left) and ADT peptide 2 (right) to change the TEER values on the MDCK cell monolayers.

This may be because the peptides are too large to permeate the tight junctions (zonula occludens) and reach the adherence junctions (zonula adherens) where E-cadherin is located.

The ability of the derivatives to modulate intercellular junctions was also measured by the enhancement of  $^{14}\text{C}$ -mannitol paracellular transport. HAV peptide **1** enhanced the paracellular permeation of  $^{14}\text{C}$ -mannitol by 1.7 $\times$  (AP side), 3.7 $\times$  (BL side) and 5.3 $\times$  (both directions) fold compared to the blank run. Similar results were obtained for ADT peptide **2**. These suggest that these peptides bound to the E-cadherin, thereby inhibiting cadherin-cadherin interactions.

The solution conformations of peptides **1** and **2** were determined by NMR, CD and molecular dynamic simulations [4,5]. Peptide **1** has an extended structure at the SHAVSS sequence, possibly a  $\beta$ -sheet structure. There are possible  $\beta$ -turns at the N-terminal (Leu1-His4) and C-terminal (Ser7-Gly10). On the other hand, peptide **2** showed a helical structure (Figure 2). The solution structures of peptides **1** and **2** have similarities to the same sequences in the X-ray crystal structure of E-cadherin EC1. Auto docking experiments suggest that the ADT sequence is a counter region of the HAV sequence and that binding of peptides **1** and **2** to E-cadherin involved hydrophobic interactions between these two sequences.

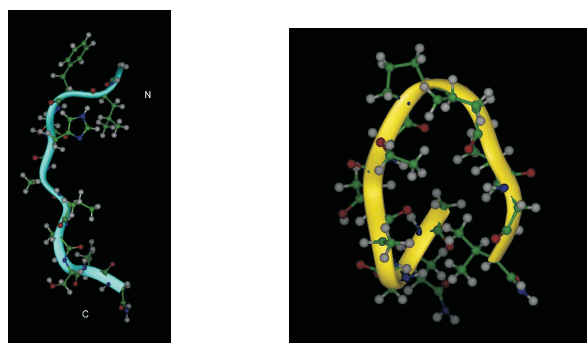


Fig. 2. View of the preferable conformations of HAV peptide **1** (left) and ADT peptide **2** (right).

In conclusion, the E-cadherin-E-cadherin interactions can be modulated by HAV and ADT peptides through blocking cell-cell adhesion. Secondary structures are important in binding selectivity of HAV and ADT peptides to E-cadherin. These decapeptides may be utilized to enhance paracellular permeation.

#### **Acknowledgments**

This work is supported by the American Heart Association.

#### **References**

1. Adson, A., Raub, T.J., Burton, P.S., Barsuhn, C.L., Hilgers, A.R., Audus, K.L., Ho, N.F.H. *J. Pharm. Sci.* **83**, 1529–1536 (1994).
2. Makagiansar, I.T., Sinaga, E., Calcagno, A.M., Xu, C.R., Siahaan, T.J. *Curr. Top. Biochem. Res.* **2**, 51–61 (2000).
3. Lutz, K.L., Siahaan, T. *J. Drug Delivery* **4**, 187–193 (1997).
4. Perczel, A., Park, K., Fasman, G.D. *Anal. Biochem.* **203**, 83–93 (1992).
5. Wüthrich, K. *NMR of Proteins and Nucleic Acids*, John Wiley & Sons, New York, 1986.

## **Translocation of Various Arginine-Rich Peptides and the Potential of These Peptides as Carriers for Intracellular Protein Delivery**

**Shiroh Futaki, Tomoki Suzuki, Wakana Ohashi, Takeshi Yagami,  
 Seigo Tanaka, Kunihiro Ueda, and Yukio Sugiura**

*Institute for Chemical Research, Kyoto University, Uji, Kyoto 611-0011, Japan*

### **Introduction**

Recently, methods have been developed for the delivery of exogenous proteins into living cells with the help of membrane-permeable carrier peptides such as HIV-1 Tat-(48-60) and Antennapedia-(43-58). By hybridizing these carrier peptides genetically or chemically, efficient intracellular delivery of various oligopeptides and proteins was achieved [1,2]. These methods would become powerful tools not only for therapeutic purposes, but also for the understanding of the mechanisms behind fundamental cellular events, such as signal transduction and gene transcription.

Arginine-rich basic segments are used by a variety of RNA-binding proteins to recognize specific RNA structures. If the basicity in the sequence plays an important role in the translocation, basic peptides corresponding to these RNA-binding segments may translocate through cell membranes, or proteins containing these sequences may also be membrane-permeable. To test this hypothesis, ten arginine-rich RNA-binding peptides were synthesized, and their translocation activity and applicability to intracellular protein delivery were examined.

### **Results and Discussion**

In order to ascertain if arginine-rich RNA-binding peptides can translocate through the cell membranes, we have synthesized fluorescein-labeled peptides corresponding to the RNA-binding domains of various proteins as well as the Tat-(48-60) peptide (Figure 1). An extra glycyl-cysteine amide sequence was incorporated into the C-terminus of each peptide for the fluorescent labeling. Treatment of the peptides with 5-maleimidofluorescein diacetate gave the corresponding fluorescein-labeled peptides. Internalization of the peptides was monitored by fluorescence microscopic observation after a three-hour incubation of the peptides with mouse macrophage RAW 264.7 cells at 37 °C.

HIV-1 Rev-(34-50)	TRQAARRNRRRRWRERQR-GC*
FHV coat-(35-49)	RRRRNRTRRNRRRVVR-GC*
BMV Gag-(7-25)	KMTRAQRRAAARRNRWTAR-GC*
HTLV-II Rex-(4-16)	TRRQRTRRARRNR-GC*
CCMV Gag-(7-25)	KLTRAQRRAAARKNKRNTR-GC*
P22 N-(14-30)	NAKTRRHERRRKLAIER-GC*
λ N-(1-22)	MDAQTRRRERRAEKQAQWKAAN-GC*
φ21 N-(12-29)	TAKTRYKARRAELIAERR-GC*
Yeast PRP6-(129-144)	TRRNKRNRRIQEQLNRK-GC*
Human U2AF-(142-153)	SQMTRQARRLYV-GC*
HIV-1 Tat-(48-60)	GRKKRRQRRRPPQ-C*

*Fig. 1. Structure of arginine-rich RNA-binding peptides used in this study. C\*: fluorescein-labeled cysteine amide*

To our surprise, all the peptides other than the human U2AF-(142-153) peptide translocated through the cell membranes and accumulated into cytoplasm and nucleus, especially nucleolus. As judged from the fluorescent intensity, the efficiency of incorporation into the cells showed a tendency to correspond to the number of arginine residues in the sequence. Internalization activities of the HIV-1 Rev-(34-50), FHV coat-(35-49), HTLV-II Rex-(4-16) and BMV Gag-(7-25) peptides, which have more than seven arginine residues in their sequences, were comparable with that of the Tat-(48-60) peptide. Fluorescence was observed in the cells as early as 5 min after the addition of these peptides (1  $\mu$ M) to the medium. Less extensive internalization was observed in the case of the  $\lambda$  N-(1-22),  $\phi$ 21 N-(12-29), and yeast PRP6-(129-144) peptides that have five arginine residues in their sequences. Fluorescent intensity in the cells treated with the former peptides (0.1  $\mu$ M) was judged to be not less than that in those treated with the latter peptides (10  $\mu$ M). The P22 N-(14-30) and CCMV Gag-(7-25) peptides that have six arginine residues showed a moderate degree of translocation.

The above experiments showed that a variety of arginine-rich RNA-binding peptides were able to translocate through the cell membranes. Little homology in these peptide sequences was observed except that they all have 5-11 arginine residues. As reported for the Tat-(48-60), D-amino acid substituted Rev-(34-50) peptide (10  $\mu$ M) was internalized as efficiently as the L-peptide in 3 h. Circular dichroism (CD) spectra of HIV-1 Tat-(48-60), FHV coat-(35-49) peptides in methanol were suggestive of their not having a significant secondary structure, whereas HIV-1 Rev-(34-50) peptide showed a spectra typical of an  $\alpha$ -helical peptide ( $[\theta]_{222} = -17,700$  deg cm<sup>2</sup>/dmol at 20 °C, peptide concentration = 39  $\mu$ M). These results were suggestive of the absence of a common secondary structure in the cell-permeable peptides. When the cells were incubated with a peptide (10  $\mu$ M) at 4 °C for 1 h, no significant decrease in fluorescent intensity in the cell was observed using the HIV-1 Rev-(34-50), and FHV coat-(35-49) peptides. These results suggest that endocytosis does not play a crucial part in the translocation.

To examine the applicability of the above basic peptides as protein carriers, we prepared basic peptide-protein conjugates. Carbonic anhydrase (29 kDa) was selected as a model protein. Basic peptide-carbonic anhydrase conjugates were prepared using *N*-(6-maleimidocaproyloxy)succinimide ester (EMCS) as a cross-linking agent (Figure 2A). A fluorescein moiety was introduced into the protein using fluorescein-5(6)-carboxamidocaproic acid *N*-hydroxysuccinimide ester simultaneously with EMCS. As judged from SDS-PAGE of the conjugates, one to two molecules of the basic peptide and fluorescein moiety were introduced to a molecule of carbonic anhydrase, respectively. Carbonic anhydrase was successfully delivered into the cell with the help of the HIV-1 Rev-(34-50) and FHV coat-(35-49) peptides as efficiently as with the HIV-1 Tat-(48-60) peptide (Figure 2B). Accumulation of the conjugates in the cytosol and nucleus was also observed by the fluorescence microscopy of the cells without fixation (Figure 2B). Confocal microscopic analysis of these conjugates demonstrated both cytoplasmic and nuclear localization and not just attachment to cellular membranes. On the other hand, fluorescein-labeled protein without carrier peptide was located in a limited part of the cytosol (data not shown). The result suggested that the protein was captured in the endosomes and was not able to be released in the cytosol. Myoglobin (17 kDa) was also introduced into the cell with the help of these carrier peptides.

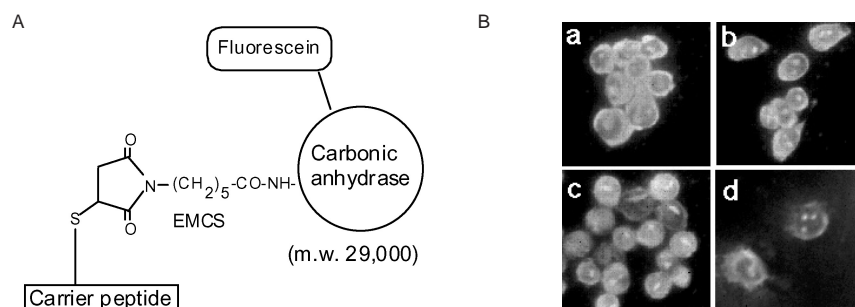


Fig. 2. Delivery of carbonic anhydrase into RAW264.7 cells with the help of arginine-rich basic peptides. (A) Schematic representation of the conjugates. (B) Fluorescence microscopy of the cells treated with carbonic anhydrase conjugated with the HIV-1 Rev-(34-50) (a) and FHV coat-(35-49) (b), and HIV-1 Tat-(48-60) (c) peptides for 3 h, respectively. Accumulation of the HIV-1 Rev-(34-50)-carbonic anhydrase conjugate in the cytosol and nucleus was also observed by fluorescence microscopy of the cells without fixation (d).

The above results should contribute not only to the development of protein delivery systems but also to an understanding of the biological significance of these sequences.

#### Acknowledgments

This work was supported by Grants-in-Aid for Scientific Research from the Ministry of Education, Science, Sports and Culture of Japan. This work was also supported in part by the Mochida Memorial Foundation for Medical and Pharmaceutical Research.

#### References

1. Schwarze, S.R., Dowdy, S.F. *Trends Pharmacol. Sci.* **21**, 45–48 (2000).
2. Derossi, D., Chassaing, G., Prochiantz, A. *Trends Cell Biol.* **8**, 84–87 (1998).

## Reversible PEGylation: Thiolytic Regeneration of Active Protein from Its Polymer Conjugates

Samuel Zalipsky, Radwan Kiwan and Nasreen Mullah

ALZA Corp., Mountain View, CA 94043, USA

### Introduction

Polyethylene glycol (PEG) is known to convey to its protein conjugates a number of useful properties, including prolonged plasma circulation time, reduced immunogenicity, improved solubility, and resistance to proteolytic degradation [1]. Usually there is a direct relationship between the amount of the linked polymer and the gain in these characteristics. On the other hand, attachment of multiple chains of PEG to a protein, a process known as PEGylation, is often accompanied by a substantial loss of biological activity. This is a particularly severe problem for proteins acting on large substrates, *e.g.* receptor-binding proteins [1]. To circumvent this problem we introduced new linking chemistry (Figure 1) designed to produce gradual *in vivo* loss of PEG chains from its conjugates. Just as a promoity of a prodrug, PEG would be present in these reversible conjugates only temporarily, improving such characteristics as pharmacokinetics and biodistribution. Here we communicate some of our initial results using lysozyme and cysteine as models of a protein and a cleaving agent respectively. Lysozyme is similar in size (14.5 kDa) to various cytokines and chemokines; it has six lysines available for PEGylation; and its activity directed toward a large substrate, peptidomurein of bacterial cell wall.

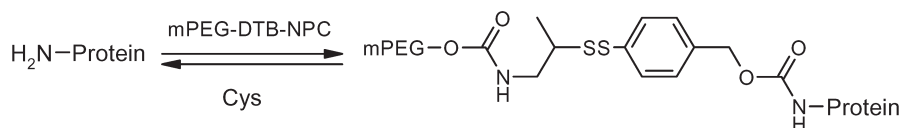


Fig. 1. Reversible, dithiobenzyl (DTB) urethane-based, protein PEGylation scheme.

### Results and Discussion

Our reversible PEGylation approach is based on the benzyl carbamate *para*-substituted with a disulfide (dithiobenzyl, DTB) linker. Thiolytic scission of the disulfide results in unstable *p*-thiobenzyl urethane, which spontaneously decomposes *via* 1,6-elimination, regenerating the original amino group of the protein. The DTB linker was first applied to mitomycin C prodrug [2]. In our laboratory we have used it to prepare thiolytically cleavable lipopolymers [3]. A new reagent, methoxy-PEG-DTB-*p*-nitrophenyl carbonate (mPEG-DTB-NPC) was prepared from mPEG-5000 and 2-amino-1-propanethiol by a modification of a previously described method [3]. Both mPEG-DTB-NPC and mPEG-NPC, its stable urethane-forming analog, exhibited a similar ability to modify amino groups of proteins. As evidenced by SDS-PAGE, MALDI-MS, and RP-HPLC (Figure 2A, top), both reagents produced similar mixtures of conjugates containing (mPEG)<sub>n</sub>-lysozyme species, with *n* = 1, 2, 3, *etc.* We purified the conjugate mixtures from the excess of PEG reagents and unmodified lysozyme by cation-exchange chromatography. In contrast to the stably linked mPEG-lysozyme, upon incubation of the mPEG-DTB-lysozyme conjugates with cysteine, gradual cleavage of PEG chains took place, ultimately resulting in regeneration of lysozyme as the sole protein product (Figure 2A). The identity of the regenerated protein species was fur-

ther corroborated by ES-MS. While both stable and cleavable PEG-lysozyme conjugates completely lacked the cell lysing activity of the native enzyme, only the mPEG-DTB-lysozyme, when treated with cysteine, regained most of the originally-lost activity (Figure 2B). Since reductive scission of accessible disulfides *in vivo* is known to occur either enzymatically or *via* reactions with physiologically present thiols, *e.g.* cysteine and glutathione [4], we anticipate that PEG-DTB-proteins will behave as macromolecular prodrugs.

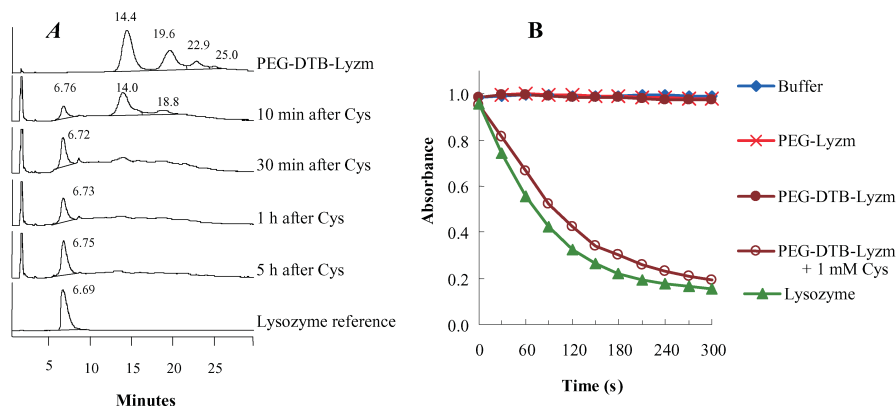


Fig. 2. Regeneration of enzymatically active lysozyme from its PEG-DTB conjugates by treatment with cysteine (1 mM). (A) RP-HPLC follow-up of lysozyme formation from mPEG-DTB-Lysozyme. (B) Turbidometric monitoring of bacterial (*Micrococcus luteus*) cell wall lysis by lysozyme and its conjugates.

Our model experiments demonstrate that the simple thiol, cysteine, ubiquitously found in physiological environments, is an effective cleaving agent of PEG-DTB-protein. MPEG-DTB-lysozyme cleanly reverts to the native protein, with concomitant recovery of the activity, which had been initially lost due to the PEGylation. Thus regeneration of the native protein as the key requirement of reversible PEGylation has been demonstrated.

## References

1. Zalipsky, S. *Adv. Drug Delivery Rev.* **16**, 157–182 (1995).
2. Senter, P.D., Pearce, W.E., Greenfield, R.S. *J. Org. Chem.* **55**, 2975–2978 (1990).
3. Zalipsky, S., Qazen, M., Walker, J.A., Mullah, N., Quinn, Y.P., Huang, S.K. *Bioconjugate Chem.* **10**, 703–707 (1999).
4. Joselyn, P.C., *Biochemistry of the SH Group*, Academic Press, New York, 1972.

## Lipoamino Acid and Liposaccharide Conjugated Peptides: Enhancement of Bioavailability

Yiu-Ngok Chan, Allan K. Wong and Istvan Toth

*School of Pharmacy, University of Queensland, Brisbane, Queensland, QLD 4072, Australia*

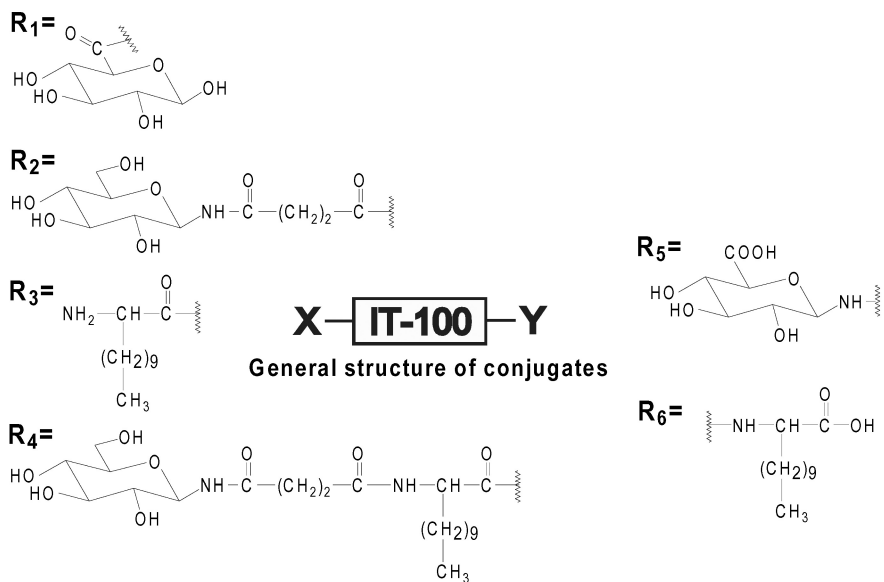
### Introduction

The most convenient way to administer drugs is by oral administration. However, intestinal absorption of peptides/proteins is relatively poor, mainly due to extensive enzymatic degradation in the gastrointestinal tract. The aim of the present study was to improve the intestinal absorption and stability of a model peptide IT-100 by chemically conjugating it with a lipid and sugar based carrier system. Lipoamino acids enhance the membrane permeability and metabolic stability of peptides, and have been investigated extensively in drug delivery [1]. However, lipoamino acid conjugation can considerably reduce water solubility. Further sugar conjugation not only improves the physico-chemical properties of the lipophilic compounds (water solubility), but also may allow utilisation of active transport uptake systems such as the Na<sup>+</sup> dependent D-glucose transporter [2].

### Results and Discussion

A library of lipoamino acid and liposaccharide conjugated peptides was synthesised manually using Fmoc solid phase chemistry. The peptides were purified by preparative HPLC, and their structures were confirmed by analytical HPLC and MS. These compounds were isolated in good purity (HPLC purity >99%) and in good yields (55–75%).

The *in vitro* intestinal permeabilities of the conjugates were examined using Caco-2 (Human Colon Carcinoma) monolayers. Cells were cultured in Dulbecco's Modified Eagle's Medium supplemented with 1% non-essential amino acids and 10% fetal calf serum. Maintained at 37 °C and 5% carbon dioxide atmosphere. Cells were passaged



after reaching 80% confluency using a 0.25% trypsin/0.2% EDTA solution. Cells were seeded onto 6.5 mm diameter polycarbonate cell culture inserts (Costar®). The media contained 1% antibiotics and was changed every other day for 25–30 days. Monolayer integrity was monitored by measuring the transepithelial electrical resistance. Wells were incubated in Hanks balanced salt solution (HBSS) containing 25 mM HEPES (pH 7.4) prior to the study. Solution was removed from the apical side and replaced with 0.2 mM of drug in HBSS/HEPES. The apical inserts were moved at 30 min intervals into new wells. Samples from the basolateral side (0.2 mL) were collected and acidified with 5 mL formic acid. Transport of the peptide analogues was quantified by liquid chromatograph - mass spectroscopy using PE Sciex API 3000 triple quadrupole mass spectrometer operating in SIM mode with positive ion electrospray. The amount of native IT-100 transported across the Caco-2 monolayers was not detectable. In contrast, the chemical modifications resulted in an increase in the transport of IT-100 conjugates (Table 1), suggesting lipoamino acid or a liposaccharide conjugation might be useful as a peptide delivery system.

Table 1. Transport of the peptide analogues.

Compound	X	Y	P <sub>app</sub> (cm/s, 10 <sup>-7</sup> )
<sup>14</sup> C-Mannitol	–	–	2.70 ∓ 0.17
<b>1a</b>	–	–	N.D.
<b>1b</b>	–	R5	N.D.
<b>1c</b>	R1	–	1.96 ∓ 0.18
<b>1d</b>	R2	–	8.59 ∓ 0.70
<b>1e</b>	–	R6	4.33 ∓ 1.37
<b>1f</b>	R3	–	2.94 ∓ 1.97
<b>1g</b>	R2	R6	6.71 ∓ 0.27
<b>1h</b>	R3	R5	1.25 ∓ 0.16
<b>1i</b>	R4	–	3.66 ∓ 0.69

### Acknowledgments

We thank Alchemia Pty. Ltd. and The Wellcome Trust for the support and Alun Jones for the analytical LC-MS data.

### References

1. Toth, I. J. *Drug Targeting* **2**, 217 (1994).
2. Nomoto, M., et al. *J. Pharm. Sci.* **87**, 326 (1998).

## Regulation and Multiplicity of Peptide Transporters in Model Systems

Jeffrey M. Becker<sup>1,2</sup>, V. Narita<sup>1</sup>, A. Wiles<sup>1</sup>, M. Hauser<sup>2</sup>, S. Koh<sup>2</sup>,  
G. Stacey<sup>2</sup> and F. Naider<sup>3</sup>

<sup>1</sup>Department of Biochemistry, Cellular, and Molecular Biology, and

<sup>2</sup>Department of Microbiology, University of Tennessee, Knoxville, 37996, USA

<sup>3</sup>Department of Chemistry, College of Staten Island, CUNY, Staten Island 10314, USA

### Introduction

The ability for organisms to engage in carrier-mediated transport of small peptides (2–5 amino acids) is ubiquitous. Peptide transporters with obvious structural similarities have been documented in bacteria, fungi, plants and animals. Peptide transport is important in terms of sources for amino acids, carbon and nitrogen, whether they are being scavenged from the environment by free-living microorganisms or absorbed from body fluids by metazoans. The yeast *Saccharomyces cerevisiae* provides a powerful model eukaryotic system for the study of peptide transport. Transport of di- and tripeptides is mediated by the PTR (Peptide TRansport) system in *S. cerevisiae*. PTR orthologs in mammalian systems have also been documented as a means for peptidomimetic drug absorption. A separate, unrelated transporter, OPT1 (Oligo-Peptide Transport), which appears to be unique to fungi and plants, carries tetra- and pentapeptides and may be used to deliver anti-fungal or herbicidal compounds.

### Results and Discussion

The PTR system involves three genes, identified as *PTR1*, *PTR2* and *PTR3* [1,2]. Ptr2p, the protein encoded by *PTR2*, is an integral membrane protein of 601 amino acids, containing 12 TMDs. It translocates di- and tripeptides, with a preference for peptides containing hydrophobic residues. Energetically, translocation is coupled to the proton-motive force, with a pH optimum at 5.5. We have now uncovered through database analysis over 100 Ptr2p orthologs in organisms ranging from bacteria to humans. Several conserved motifs have been identified, including the “FYING” motif, named for the conserved F247, Y248, I251, N252, and G254 residues in the fifth transmembrane domain (TMD5). Other conserved residues are the WQIPQY in TMD10 and EXCERFXYYG in TMD10. Site directed mutagenesis of the FYING motif in *S. cerevisiae* results in attenuated growth on dipeptides, decreased sensitivity to toxic dipeptides and elimination of radiolabeled dileucine transport. This suggests that the FYING motif plays a crucial role in substrate recognition and/or translocation.

*PTR1* encodes a soluble protein of 1950 amino acids, which is identical to *UBR1*, a component of a ubiquitin-dependent protein degradation system [3]. Ptr1p promotes transcription of *PTR2* by removing Cup9p, the *PTR2* repressor from the *PTR2* promoter. The new experiments reported indicate that deletion of *PTR1* results in the loss of peptide transport phenotype, since expression of *PTR2* is eliminated.

*PTR3* encodes a soluble protein of 678 amino acids and has no similarity to any other identified proteins, including a lack of previously characterized functional motifs. Ptr3p acts in concert with the Ssy1p/Ssy5p amino acid sensing complex to modulate amino acid induced expression of amino acid permeases, such as *BAP2*. *PTR3* is also involved in the repression of the permease *GAP1*. Genetic analysis indicates that *PTR3* functions with *CUP9* and *PTR1* in regulating *PTR2* expression [4]. Characterization of *ssy1Δ* or *ptr3Δ* and the corresponding double mutant in the present study re-

veals identical phenotypes, suggesting that Ptr3p interacts with Ssy1p for regulating expression of both amino acid and peptide transporters. Furthermore there is evidence for a direct interaction between Ptr3p and Ssy1p by two-hybrid analysis.

Transport of oligopeptides (4 to 5 amino acids) occurs across the OPT system. First described in *Candida albicans*, three orthologs have been identified in *S. cerevisiae*. The best characterized of these orthologs, Opt1p, transports met- and leu-enkephalin, endogenous mammalian opioid pentapeptides [5] and glutathione [6]. Opt1p is an integral membrane protein, with a predicted topology of 12–14 TMDs. Opt1p orthologs have only been identified in fungi and plants; analysis of the OPT family tree indicates that the fungal members are more closely allied to each other than to the plant members. We have now found at least eight OPT paralogs in the model plant *Arabidopsis thaliana* by searching the *A. thaliana* genome for sequences of high similarity [7]. The genes encoding these putative transporters are differentially expressed in various tissues indicating their specific roles in plant development. There are several consensus motifs unique to the OPT family which, unlike the PTR system are not localized to TMD regions. Physiologically, OPT function is proton-coupled with a pH optimum of 5.5 and is sensitive to temperature and sulfhydryl reagents. Peptide opioid receptor antagonists, including DADLE and DPDPE, can inhibit leu-enkephalin transport. Naloxone and naltrexone, which are non-peptide opioid receptor antagonists, also inhibit transport in yeast, suggesting that the receptor and the Opt1p transporter recognize similar molecular features.

#### **Acknowledgments**

Supported in part by USDA-NRI grant number 99-35304-8194.

#### **References**

1. Island, M.D., Perry, J.P., Naider, F., Becker, J.M. *Curr. Gen.* **20**, 457–463 (1991).
2. Hauser, M., Narita, V., Donhardt, A.M., Naider, F., Becker, J.M. *Mol. Membr. Biol.* **18**, 105–112 (2001).
3. Alagramam, K., Naider, F., Becker, J.M. *Mol. Microbiol.* **15**, 225–234 (1995).
4. Barnes, D., Lai, W., Breslav, M., Naider, F., Becker, J.M. *Mol. Microbiol.* **29**, 297–310 (1998).
5. Hauser, M., Donhardt, A.M., Barnes, D., Naider, F., Becker, J.M. *J. Biol. Chem.* **275**, 3037–3041 (2000).
6. Bourbonloux, A., Shahi, P., Chakladar, A., Delrot, S., Bachhawa, A.K. *J. Biol. Chem.* **275**, 13259–13265 (2000).
7. Koh, S., Wiles A.M., Naider, F., Becker, J.M., Stacey, G. *Plant Physiol.*, in press (2002).

## **A Novel Class of Cell Permeable “Karyophilic” Peptides: NLS-Mediated Nuclear Import of Dermaseptin Derived Peptides in Intact Cells**

**Elana Hariton-Gazal<sup>1</sup>, Chaim Gilon<sup>1</sup>, Amram Mor<sup>2</sup> and Abraham Loyter<sup>2</sup>**

<sup>1</sup>*Department of Organic Chemistry, Institute of Chemistry*

<sup>2</sup>*Department of Biological Chemistry, Institute of Life Sciences, The Hebrew University  
of Jerusalem, 91904, Jerusalem, Israel*

### **Introduction**

Dermaseptin S4, is able to penetrate plasma membranes of cultured cells. This peptide accumulated within the cytoplasm but failed to enter into the nuclei. Peptides belonging to the Dermaseptin family have been shown to be amphipatic, positively charged, helical and to be able to penetrate into bacteria, protozoa, as well as into red blood cells [1]. K4 (AKWKTLLKKVLKA-NH<sub>2</sub>) [2], a peptide derived from the dermaseptin S4 was found to be non-karyophilic, namely accumulated only within the cell cytoplasm of intact cultured cells, although being of small molecular weight.

Penetration of K4 occurred at 37 °C as well as at 4 °C, indicating a non-metabolic dependent process. Kinetic studies have shown that cell penetration of K4 was relatively fast and was observed within 5 min of incubation with 1 μM of the peptide either at 37 °C and at 4 °C.

### **Results and Discussion**

In order to find out whether the addition of NLS will confer karyophilic properties upon K4 with retention of its cell permeability properties, a composite peptide bearing both the sequence of the K4 peptide as well as the NLS motif of the SV40-T-Antigen was synthesized. The SV40-NLS has been attached either to the C or to the N terminals of K4, resulting in composite peptides designated as PVK (PKKKRLKVAKWKTLLKKVLKA-NH<sub>2</sub>) and KPV (AKWKTLLKKVLKAPKKKRLKV-NH<sub>2</sub>), respectively. Also, the reverse sequence of the SV40-NLS was introduced into K4 resulting in a peptide designated as VPK. Incubation of PVK and KPV with intact cells resulted in their accumulation within the nuclei of these cells. Evidently, both peptides, similarly to K4, were cell permeable, but in contrast to K4 possessed karyophilic properties. NLS mediated nuclear import is evident from the results showing that the peptide VPK, which is a K4 conjugate with a non-active NLS, was non-karyophilic.

Similar to K4, the composite PVK and KPV peptides penetrated intact HeLa cells at 37 °C as well as at 4 °C. However, at 4 °C these peptides were retained in the cytoplasm and did not accumulate within the intranuclear space, strengthening the view that the nuclear import observed at 37 °C was an active process.

Various features that characterize nuclear import of the NLS-K4 composite peptides (PVK, KPV) were studied using an assay on digitonin-permeabilized cells. Import of PVK into nuclei of permeabilized HeLa cells was absolutely dependent on the addition of a reticulocyte extract indicating that its translocation – similar to the SV40-NLS conjugate – require cytosolic factors. In contrast to PVK, the peptide VPK did not show any nuclear accumulation. This indicated that also in permeabilized cells nuclear import of the PVK and KPV was specific and mediated by a functional NLS. Nuclear import in permeabilized HeLa cells was ATP dependent, did not occur at 4 °C and was inhibited by GTPγS, WGA, and excess of unlabeled free SV40-NLS peptide.

It was also inhibited by the addition of excess unlabeled PVK, but not by the K4 peptide itself.

A composite peptide bearing both K4 and Rev-ARM sequences (RDK RQARRGRRRAKWKTLKKVLKAC-NH<sub>2</sub>) was synthesized. Externally added RDK has readily been translocated into intact cultured HeLa cells and moved to the nuclei of these cells. Nuclear import was also observed when RDK was incubated with digitonin permeabilized cells. However, nuclear import in permeabilized cells did not require the addition of cytosolic extract. Active and specific nuclear import is evident from the results showing that in intact cells – as well as in permeabilized cells – it was ATP dependent and was inhibited by unlabeled RDK, free Rev and Tat ARM peptides. Also, unlabeled RDK inhibited import of Rev-BSA conjugate into the nuclei of permeabilized cells as well as of RDK in intact cells.

The described “karyophilic” peptides may be of potential application as vectors for transporting drugs that intervene with intracellular and/or intranuclear targets and as a tool to study nucleocytoplasmic shuttling in intact cells. Also the advantage of using K4 as a carrier over other cell permeable peptides, such as the HIV-1 Tat [3], is that K4 is an “inert peptide” lacking any known intracellular function.

#### **References**

1. Mor, A., Nicolas, P. *J. Biol. Chem.* **269**, 1934–1939 (1994).
2. Feder, R., Dagan, A., Mor, A. *J. Biol. Chem.* **275**, 4230–4238 (2000).
3. Vives, et al. *J. Virol.* **68**, 3343–3353 (1994).

## Characterization of Translocation Behavior of Arginine-Rich Membrane-Permeable Peptides

Tomoki Suzuki, Wakana Ohashi, Ikuhiko Nakase, Seigo Tanaka,  
 Kunihiro Ueda, Shiroh Futaki and Yukio Sugiura

*Institute for Chemical Research, Kyoto University, Uji, Kyoto 611-0011, Japan*

### Introduction

Basic peptides such as HIV-1 Tat-(48-60) and Antennapedia-(43-58) have been reported to have membrane permeability and utilized as protein carriers [1,2]. We have found that these characteristics are shared ubiquitously among arginine-rich basic peptides [3]. There are no common structures among these peptides except that they have several arginine residues in their sequences. However, the internalization mechanism of these peptides is obscure. In this report, quantification of internalized arginine-rich peptides was conducted to obtain information about the factors that influence the translocation efficiency.

### Results and Discussion

Quantification of internalized peptides was conducted using rhodamine labeled peptides. The membrane permeable arginine-rich peptides used in this study are listed in Table 1. The HIV-1 Tat-(48-60), FHV coat-(35-49), HIV-1 Rev-(34-50), and (Arg)<sub>8</sub> peptides were judged to have high internalization ability by fluorescence microscopic observation [3]. Internalization of (Arg)<sub>16</sub> peptide, which showed the lower internalization activity, was also examined. Cysteine residues were added at the C-termini of these peptide sequences for labeling with tetramethylrhodamine-5-maleimide. Mouse macrophage RAW264.7 cells, HeLa cells, and COS-7 cells were incubated with medium containing these peptides at 37 °C under 5% CO<sub>2</sub> atmosphere. After incubation, cells were washed by ice cold phosphate buffered saline (PBS) and lysed in 0.5% Triton-X in PBS. The peptide concentration in the lysate was obtained and standardized for total protein content of the cell lysate. As a result, Rev-(34-50) peptide and (Arg)<sub>8</sub> peptides were internalized as efficiently as Tat-(48-60) peptide. The uptake of these peptides was saturable because the excess addition of non-labeled peptide competitively inhibited the internalization of the labeled peptide.

We examined the involvement of cell-surface sulfated glycosaminoglycan in the translocation. The uptake of the arginine-rich peptides by HeLa cells and RAW264.7 cells was significantly decreased in the presence of heparan sulfate or chondroitin sulfate (Figure 1). Pretreatment with glycosaminoglycan lyases, such as heparitinase and

*Table 1. Structures of rhodamine-labeled arginine-rich peptides.*

Peptides	Sequences
HIV-1 Tat-(48-60)	GRKKRRQRRRPPQ-C(rho) <sup>a</sup>
FHV coat-(35-49)	RRRRNRTRNRNRVR-GC(rho)
HIV-1 Rev-(34-50)	TRQARRNRNRWRERQR-GC(rho)
(Arg) <sub>8</sub>	RRRRRRRR-GC(rho)
(Arg) <sub>16</sub>	RRRRRRRRRRRRRRRR-GC(rho)

<sup>a</sup> rho = rhodamine.

*Suzuki et al.*

chondroitinase ABC, also reduced the efficiency of the peptide uptake. The above results were suggestive of the sulfated glycosaminoglycan playing an important role for the internalization of these basic peptides.

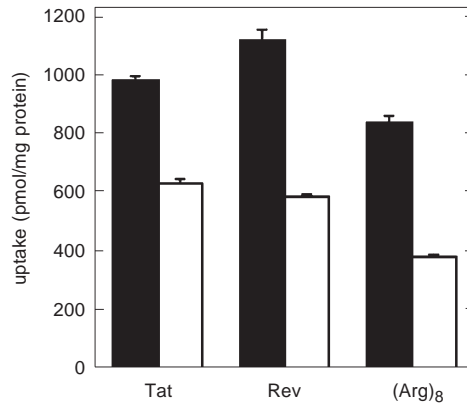


*Fig. 1. Inhibition of the internalization of arginine-rich peptides in the presence of heparan sulfate. Closed bars indicate the uptake in the absence of heparan sulfate. Open bars indicate that with heparan sulfate pretreatment.*

#### **Acknowledgments**

This work was supported by Grants-in-aid for Scientific Research from the Ministry of Education, Science, Sports and Culture of Japan. This work was also supported in part by the Mochida Memorial Foundation for Medical and Pharmaceutical Research.

#### **References**

1. Schwarze, S.R., Dowdy, S.F. *Trends Pharmacol. Sci.* **21**, 45–48 (2000).
2. Derossi, D., Chassaing, G., Prochiantz, A. *Trends Cell Biol.* **8**, 84–87 (1998).
3. Futaki, S., Suzuki, T., Ohashi, W., Yagami, T., Tanaka, S., Ueda, K., Sugiura, Y. *J. Biol. Chem.* **276**, 5836–5840 (2001).

## Structure and Activity of the N-Terminal Peptides of HIV-1 Glycoprotein 41 Types M (Major) and O (Outlier)

Patrick W. Mobley<sup>1</sup>, Alan J. Waring<sup>2</sup> and Larry M. Gordon<sup>2</sup>

<sup>1</sup>Chemistry Department, Cal Poly Pomona, Pomona, California 91768, USA

<sup>2</sup>Pediatrics Department, Harbor-UCLA, Torrance, CA 90502-2064, USA

### Introduction

Earlier studies have shown that the N-terminal peptide of HIV-1 glycoprotein 41,000 (gp41) group M (FP-1, AVGIGALFLGFLGAAGSTMGARS-NH<sub>2</sub>) derived from the LAV<sub>1a</sub> isolate, exhibits cytolytic and fusogenic activities [1]. To determine whether such membrane perturbations are a fundamental property underlying viral-host cell infection, we study here the secondary structure (Circular Dichroism (CD) and Fourier transform infrared (FTIR) spectroscopy) and activity (cytolysis and cell aggregation) of FP<sub>VAU</sub> (AAGLAMFLGILSAAGSTMGARA-NH<sub>2</sub>), an N-terminal gp41 peptide analog based on the VAU isolate of the widely divergent HIV-1 group O [2]. Since extension of FP-1 by ten residues has been reported to enhance the fusion activity with lipid vesicles [3], we also assessed the structure and function of the extended peptide (xFP-1, -FP-1 + MTLTVQARQL-NH<sub>2</sub>) and the corresponding peptide from gp-41 of O-VAU (xFP<sub>VAU</sub>, -FP<sub>VAU</sub> + TALTVRTQHL-NH<sub>2</sub>).

### Results and Discussion

Figure 1 shows that FP<sub>VAU</sub>, despite having only ≈70% homology with a type M fusion peptide, FP-1, was quite hemolytic. Extension of FP-1 and FP<sub>VAU</sub> decreased the

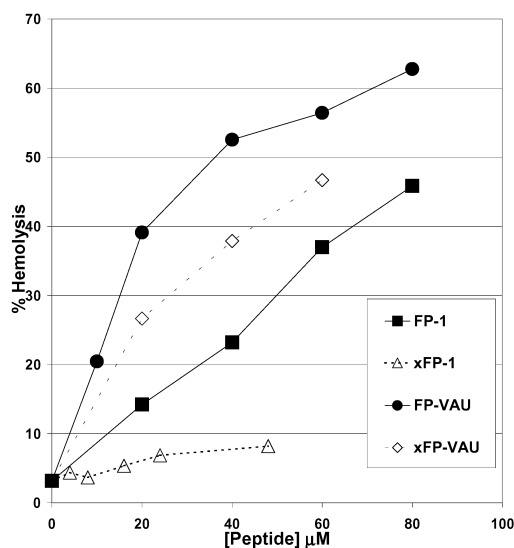


Fig. 1. Hemolysis by peptides FP-1, FP-Vau, xFP-1 and xFP-Vau. 10  $\mu$ L of packed red blood cells were incubated for 30 min at 37 °C in 0.5 mL of PBS with the appropriate concentration of peptide. The hemolysis (A540 nm) due to 50% DMSO carrier (<10% hemolysis) was subtracted. 100% hemolysis determined by incubating the rbc's in distilled water. Each point is the average of duplicates.

hemolytic activity when compared to the native peptides. Extended FP-1 had virtually no hemolysis capability at concentrations less than 100  $\mu$ M.

Aggregation of human erythrocytes by 40  $\mu$ M FP solutions (2% DMSO) was measured by Coulter counter sizing. Aliquots were taken from the hemolysis assay tubes and analyzed for the number of particles in 12 size ranges (8 to 8192 cubic microns). Those agents that cause aggregation will give larger particles (aggregates) and, since no agent caused fragmentation, they will decrease the count in the normal red cell volume channel (#4, 64 to 128 cubic microns). All agents produced aggregates of volume greater than the 2% DMSO carrier control. Extension of FP<sub>VAU</sub> had little effect on its aggregative capacity (both >90% decrease in channel #4), while extension of FP-1 greatly enhanced its ability to aggregate red cells ( $\approx$ 80% decrease in channel #4 vs >90% decrease for xFP-1).

CD spectra of the fusion peptides in the membrane mimetic solvent, HFIP(aq), indicated that the primary conformation was an  $\alpha$ -helix. The % helix for each was FP-1: 56.8; FP-Vau: 38.2; xFP: 43.6; xFP-Vau: 53.8 (Figure 2). FTIR spectra (*not shown*) of the peptides dried from HFIP confirmed the helical nature in this nonpolar environment.

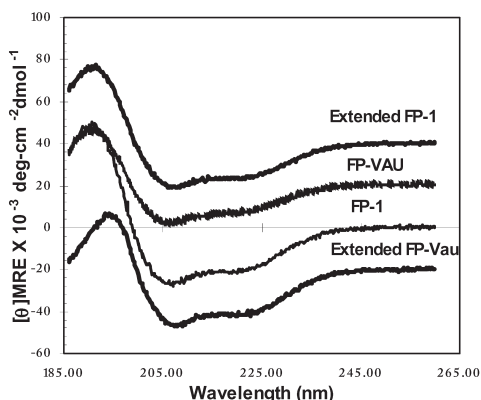


Fig. 2. Circular dichroism spectra of FP-1, FP-Vau, xFP-1, and xFP-Vau in hexafluoroisopropanol : water : formic acid (70 : 30 : 0.1 v/v/v) with each peptide at about 50  $\mu$ M. The curves are offset by their difference at 259 nm (where they are all zero). The % alpha helix was found using %  $\nabla$ -helix =  $[1]_{MRE}/\{-39,500 (1 - (2.57/n))\}$  where  $[1]_{MRE}$  is the mean residue ellipticity @ 222 nm and  $n$  is the number of residues.

These results show that the fusion peptide from the VAU isolate of HIV-1 group O is a potent lytic and fusogenic agent. Altering the fusion peptide sequence away from that of the Major group did not result in a decrease of the membrane-altering activity. Extension of the fusion peptide region decreases the lytic nature of the resultant peptides but does not change (FP<sub>VAU</sub>) or enhances the aggregation capability (FP-1). All of the peptides maintain a primarily helical structure in membrane mimics.

#### Acknowledgments

This study was supported by a NIH MBRS SCORE Grant GM 53933-02 (P. W. M.).

#### References

1. Mobley, P.W., et al. *Biochim. Biophys. Acta* **1271**, 304–314 (1995).
2. Charneau, P., et al. *Virology* **205**, 247–253 (1994).
3. Klinger Y, et al. *J. Biol. Chem.* **27**, 13496–13505 (1997).

## Specific Cleavage at Lys-147/Gly-148 in the Serine Protease Domain of Human Factor IXa $\beta$ by Plasmin: Effect on Catalytic Efficiency and Factor VIIa Binding

Amy E. Schmidt and S. Paul Bajaj

*Departments of Pharmacological and Physiological Sciences and Medicine,  
 Saint Louis University Medical School, St. Louis, MO 63105, USA*

### Introduction

Hemophilia B is an X-linked recessive bleeding disorder that is caused by the absence or deficiency of Factor IX protein. Human blood clotting factor IX circulates in blood as a single chain protein of 415 amino acids. Upon activation (by factor XIa/Ca<sup>2+</sup> or TF/VIIa/Ca<sup>2+</sup>), two peptide bonds in factor IX are cleaved with resultant formation of a serine protease, Factor IXa $\beta$ , and release of an activation peptide [1]. Factor IXa $\beta$  is composed of a light chain consisting of residues 1-145 and a heavy chain consisting of residues 181-415 of native Factor IX, that are held together by a single disulfide bond [2,3]. The light chain of Factor IXa $\beta$  consists of an amino-terminal gamma-carboxy-glutamic acid (Gla) rich domain (residues 1-40), a short hydrophobic segment (residues 41-46), and two epidermal growth factor (EGF)-like domains (EGF1 residues 47-84 and EGF2 residues 85-127). The heavy chain contains the serine protease domain, which features the catalytic triad residues, namely, H221 (chymotrypsin equivalent = 57), D269 (chymotrypsin equivalent = 102) and S365 (chymotrypsin equivalent = 195) [3] (see Figure 1).

Factor IXa $\beta$  activates Factor X in the coagulation cascade. This requires Ca<sup>2+</sup>, phospholipid, and Factor VIIa. The protease domain of Factor IXa $\beta$  contains a binding site for Factor VIIa [4]. This site is in part comprised of helix 162-168 in chymotrypsin numbering (330-338 in Factor IX numbering) of Factor IXa $\beta$ . The Factor IXa $\beta$  enzyme also contains a surface exposed region so called the 148-loop (316 in Factor IX numbering). This 148-loop is connected to the 162-helix through a ~10 residue single  $\beta$ -strand. Further, the 148-loop lies next to the S195 catalytic cleft. The 148-loop also contains a Lys at position 147. In the present study, we studied the effect of prote-

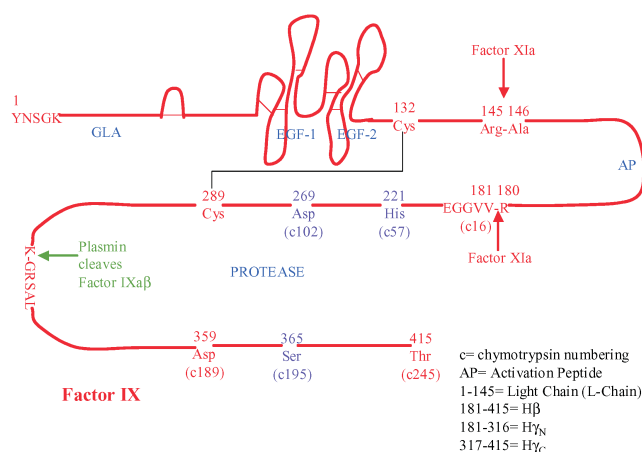


Fig. 1. Structure of Factor IX.

olysis at Lys-147/Gly-148 by plasmin on the catalytic efficiency as well as cofactor (*i.e.* Factor VIIIa) binding to the proteolysed Factor IXa $\beta$ . The proteolysed Factor IXa $\beta$  is designated Factor IXa $\gamma$ .

### Results and Discussion

Plasmin in the presence of phospholipid and Ca<sup>2+</sup> cleaved Factor IXa $\beta$  specifically at Lys-147/Gly-148. The cleaved enzyme called Factor IXa $\gamma$  was purified and analyzed for activity towards a small synthetic substrate, macromolecular substrate X, and Factor VIIIa binding. The N-terminal amino acid sequences of the cleaved peptide chains of Factor IXa $\gamma$  revealed that it was specifically cleaved between Lys-147/Gly-148. The newly generated N-terminal had the sequence GRSAL (see Figure 1). Factor IXa $\gamma$  was found to have essentially no coagulant activity in a plasma based coagulation assay.

The specificity constant of Factor IXa $\gamma$  for hydrolysis of the synthetic substrate CBS 31.39 (CH<sub>3</sub>-SO<sub>2</sub>-D-Leu-Gly-Arg-pNA) was ~6-fold lower than that of Factor IXa $\beta$ . Further, the activity of Factor IXa $\gamma$  for activating macromolecular substrate X, was ~15-fold lower than Factor IXa $\beta$ . Factor IXa $\gamma$  also bound to cofactor VIIIa with ~60-fold reduced affinity. From these data, we infer that the loss of the activity of Factor IXa $\gamma$  is a cumulative effect of impaired active-site activity, reduced affinity for the physiologic macromolecular substrate X, and diminished cofactor VIIIa binding.

Since plasmin can bind to proteins with C-terminally exposed Lys residues, we examined whether or not active site-blocked plasmin specifically bound to the newly generated C-terminal Lys residue of Factor IXa $\gamma$ . Our results reveal that active site-blocked plasmin binds to Factor IXa $\gamma$  but not to Factor IXa $\beta$ . The binding of the active site-blocked plasmin to Factor IXa $\gamma$  was abrogated in the presence of EACA ( $\epsilon$ -amino-n-caproic acid) an analog of Lys (see Figure 2). This suggests that active-site blocked plasmin binds to the newly generated C-terminal Lys of Factor IXa $\gamma$  through its Kringle domain(s). In further support of this, Factor IXa $\gamma$  treated with carboxypeptidase B, which removes C-terminal Lys residues, did not bind to active-site blocked plasmin.

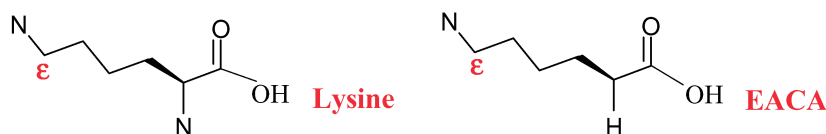


Fig. 2. Comparison of structures.

The physiologic relevance of these studies is that the generation of Factor IXa $\gamma$  which is functionally inactive, and its subsequent binding to plasmin generated during hemostasis/fibrinolysis could terminate clotting and contribute to localizing plasmin at the fibrin clot to promote fibrinolysis.

### References

1. DiScipio, R.G., Kurachi, K., Davie, E.W. *J. Clin. Invest.* **61**, 1528–1538 (1978).
2. Brandstetter, H., Bauer, M., Huber, R., Lollar, P., Bode, W. *Proc. Natl. Acad. Sci. U.S.A.* **92**, 9796–9800 (1995).
3. Hopfner, K.P., Lang, A., Karcher, A., Sichler, K., Kopetzki, E., Brandstetter, H., Huber, R., Bode, W., Engh, R.A. *Structure* **7**, 989–996 (1999).
4. Bajaj, S.P., Schmidt, A.E., Mathur, A., Padmanabhan, K., Zhong, D., Matri, M., Fay, P. *J. Biol. Chem.* **276**, 16302–16309 (2001).

## Stability and Peptide Binding Specificity of BTK SH2 Domain: Molecular Basis for X-Linked Agammaglobulinemia

Shiou-Ru Tzeng<sup>1</sup>, Ming-Tao Pai<sup>1</sup>, Feng-Di T. Lung<sup>2</sup>, Peter P. Roller<sup>3</sup>,  
 Benfang Lei<sup>4</sup>, Shiao-Chun Tu<sup>4</sup>, Shi-Han Chen<sup>5</sup>, Wen-Jue Soong<sup>6</sup>  
 and Jya-Wei Cheng<sup>1</sup>

<sup>1</sup>*Division of Structural Biology and Biomedical Science, Department of Life Science,  
 National Tsing Hua University, Hsinchu 300, Taiwan, R.O.C.*

<sup>2</sup>*Department of Nutrition, China Medical College, Taichung 400, Taiwan, R.O.C.*

<sup>3</sup>*Laboratory of Medicinal Chemistry, Division of Basic Sciences, National Cancer Institute,  
 National Institutes of Health, 37/5C-02, Bethesda, MD 20892, USA*

<sup>4</sup>*Department of Biology and Biochemistry, University of Houston, Houston, TX 77204, USA*

<sup>5</sup>*Department of Pediatrics, University of Washington, Seattle, WA 98195, USA*

<sup>6</sup>*Department of Pediatrics, Children's Medical Center, Veterans General Hospital,  
 Taipei 112, Taiwan, R.O.C.*

### Introduction

X-Linked agammaglobulinemia (XLA), an inherited disease, is caused by mutations in the Bruton's tyrosine kinase (BTK) [1]. Like many other cytoplasmic tyrosine kinases in signaling pathways, BTK contains an N-terminal pleckstrin homology (PH) domain, a proline-rich Tec homology (TH) domain, a Src homology 2 (SH2) domain, a Src homology 3 (SH3) domain, and a catalytic tyrosine kinase domain. It was shown that the BTK SH2 domain is essential for phospholipase C- $\gamma$  phosphorylation and mutations in this domain lead to XLA. The preferred binding sequences of BTK SH2 domain have been examined, but little is known about which residues in the BTK SH2 domain contribute to substrate recognition. Therefore, we expressed the BTK SH2 domain with point-mutations identified from XLA patients and measured their stability and binding specificity with the phosphotyrosine-containing peptides (Figure 1).

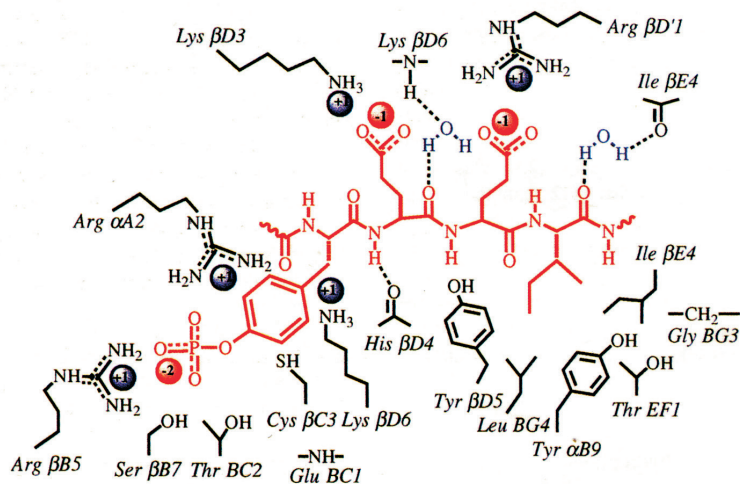


Fig. 1. A model of ~pTyr-Glu-Glu-Ile~ complexed with BTK SH2 domain. The two major binding pockets for the pTyr and Ile residues of the phosphopeptide are depicted. Key H-bonding contacts (two via structural water) between the ligand and target protein are shown.

Our results provide a molecular basis for studying the role of the BTK SH2 domain in XLA.

### **Results and Discussion**

We cloned and expressed the R288Q, R288W, L295P, R307G, R307T, Y334S, Y361C, L369F, and I370M mutants of the Btk SH2 domain found in XLA patients [2]. It was observed that mutations of R307G and R307T resulted in more than 200-fold decrease in the binding affinity, which clearly indicates that the Arg  $\beta$ B5 (R307) residue of the Btk SH2 domain plays a crucial role in pTyr recognition. Similarly, the binding affinity was either totally lost (R288Q) or very poor (R288W) for R288 mutant, suggesting that Arg  $\alpha$ A2 is equally important in pTyr recognition. In addition to the pTyr binding site, mutations of other residues, *i.e.* Y334S, Y361C, L369F, and I370M, located in the pY+3 hydrophobic binding pocket also resulted in decrease of the binding affinity. The substitution of L295 with proline may prevent the  $\alpha$ A helix elongation and hence reduce the pTyr binding, which was also observed from its decrease in  $\alpha$ -helicity from 19 to 16%. Surprisingly, on comparing the binding of the mutated BTK SH2 domain (Y334S) with the wild type showed that mutation of Y334 residue at  $\beta$ D5 position with serine resulted in the reversal of binding preference, *i.e.* it preferred to bind more with pYIIP than pYEEL. This change in binding probably arises from the loss of hydrogen bonding as well as hydrophobic interaction between the aromatic ring of the tyrosine residue with aliphatic side chains of the peptide.

In conclusion, we had found that mutants of the BTK SH2 domain identified from XLA patients exhibit weaker affinities for the phosphopeptides. It is likely that the point-mutated BTK SH2 domains fail to present to the ligand the crucial residue in the correct context, thus leading to a weaker binding. The altered binding behavior likely renders the kinase abnormal, and possibly causes XLA. In addition, the data presented here also indicate the potential to modulate the binding of the BTK SH2 domain by mutations at sites predicted to bind the side chains of the phosphopeptides.

### **Acknowledgments**

We thank the National Science Council of the Republic of China and VTY Joint Research Program for research grants.

### **References**

1. Vetrie, D., Vorechovsky, I., Sideras, P., Holland, J., Davies, A., Flinter, F., Hammarstrom, L., Kinnon, C., Levinsky, R., Bobrow, M., Smith, C.I.E., Bentley, D.R. *Nature* **361**, 226–233 (1993).
2. Vihinen, M., Iwata, T., Kinnon, C., Kwan, S.P., Ochs, H.D., Vorechovsky, I., Smith, C.I.E. *Nucleic Acids Res.* **24**, 160–166 (1996).

## **Designing Peptide Drugs/Ligands for Pathological States. A New Paradigm for Design of Bioactive Peptide Hormones and Neurotransmitters**

**Victor J. Hruby<sup>1</sup>, Richard S. Agnes<sup>1</sup>, Yeon-Sun Lee<sup>1</sup>, Peg Davis<sup>2</sup>,  
Shou-Wu Ma<sup>2</sup>, Josephine Lai<sup>2</sup> and Frank Porreca<sup>2</sup>**

<sup>1</sup>Departments of Chemistry and <sup>2</sup>Pharmacology, University of Arizona, Tucson, AZ 85721, USA

### **Introduction**

G-protein coupled receptors and other membrane bound receptors are the target for over 45% of all current drugs. They are important targets because the ligands and receptors modulate or control most biological functions necessary for survival in man, such as fear-flight, feeding behavior, response to stress, response to pain, cardiovascular function, anxiety, learning, sexual behavior, etc. Most of the ligands are polypeptides. The present paradigm for drug discovery and development in this area is to identify the gene/cell/tissue/protein associated with the biological activity and develop a binding assay and functional (2nd messenger) assay. If no endogenous "ligand" is known, assays with "libraries" of "natural products," peptides and other organic compounds are used. The receptors and the assays chosen utilize receptors, cells, tissues and animals that are "normal." However, there is growing evidence that the ligands and their receptors/acceptors behave differently in normal and pathological states. Especially in the central nervous system (CNS), many drugs that are effective in normal states become ineffective or less effective in pathological disease states. Evaluation of this problem suggests that a new paradigm is needed.

### **Results and Discussion**

Numerous disease states may fall into this paradigm. Some typical examples include diabetes, cancers, addictions, neuropathic pain, etc. We will discuss this problem in relation to pathological pain states. In Table 1, we outline the optimized paradigm for drug discovery in such a disease state. What system adaptations occur in pathological pain states? Though there is much to learn in this regard, a few critical observations/considerations are given in Table 2. We postulate that inappropriate interactions of opioid ligands (and receptors) with endogenous cholecystokinin ligands and receptors is one of the major problems in neuropathic pain states. Thus we have decided to design a *single ligand* which would have the following characteristics: 1) potent agonist activity as a  $\mu$  or  $\delta$  opioid ligand for opioid receptors; 2) potent antagonist activity at the CCK-B and CCK-A receptors (balanced antagonist). Interestingly, we had found in earlier studies a cholecystokinin analogue SNF 9007 (H-Asp-Tyr-DPhe-Gly-

*Table 1. Optimized considerations for drug discovery for disease*

---

I.	The CNS changes when injury/disease occurs (Neuroplasticity, etc.)
II.	Patients have different nervous systems (adaptation differs)
III.	Must consider system adaptation for treatment strategy
IV.	Drugs should be DESIGNED for optimal activity in DISEASE STATE-to overcome adaptation
V.	Drug design may require activity at more than one target with one ligand

---

*Table 2. Observations of adaptation in pathological pain states*

- 
- |      |  |
|------|--|
| I.   | Opioids can heighten pain state (hyperesthesias; allodynia) [1]  |
| II.  | Continuous opioid exposure produces exaggerated pain [2, 3]      |
| III. | Dynorphin maintains chronic neuropathic pain [4]                 |
| IV.  | Rostral ventromedial medulla mediates opioid induced pain [3, 5] |
- 

Trp-NMe-Nle-Asp-Phe-NH<sub>2</sub> [6] that had binding affinities in the nanomolar range at both  $\delta$  opioid and CCK-B receptors, and which produced naloxone reversible antinociception. We postulated that opioid and CCK ligands have overlapping pharmacophores [7]. Our hypothesis then is to design a single ligand that can act as a potent agonist at opiate receptors, and a potent antagonist at CCK receptors. We have taken three approaches to this goal: 1) We have modified SNF 9007 to convert its CCK receptor agonist activity to antagonist activity while retaining its  $\delta$  opioid agonist activity; 2) We have synthesized small chimeric opioid/CCK ligands (8 amino acids or less); 3) We have used known opioid receptor agonists and CCK receptor antagonists together and demonstrated their synergistic opioid activities. The prospects for success are excellent, and will provide a new paradigm for drug design for many disease states.

#### **Acknowledgments**

Supported by grants from the USPHS and NIDA, Grant No. DA 12394 and DA 06284.

#### **References**

1. Arner, S., Rawal, N., Gustafsson, L.L. *Anaesthesiol. Scand.* **17**, 253 (1988).
2. Vanderah, T.W., Gardell, L.R., Burgess, S.E., Ibrahim, M., Dogrul, A., Zhong, C.M., Zhang, E.T., Molan Jr., T.P., Ossipov, M.H., Malan, Jr., T.P., Lai, J., Porreca, F. *J. Neurosci.* **20**, 7074 (2000).
3. Vanderah, T.W., Suenaga, N.M.H., Ossipov, M.H., Malan, Jr., T.P., Lai, J., Porreca, F. *J. Neurosci.* **21**, 279 (2001).
4. Wang, Z., Gardell, L.R., Ossipov, M.H., Vanderah, T.W., Brennan, M.B., Hochgeschwender, U., Hruby, V.J., Malan Jr., T.P., Lai, J., Porreca, F. *J. Neurosci.* **21**, 1779 (2001).
5. Vanderah, T.W., Ossipov, M.H., Lai, J., Malan Jr., T.P., Porreca, F. *Pain*, in press (2001).
6. Slaninová, J., Knapp, R.J., Wu, J., Fang, S.N., Kramer, T., Hruby, V.J., Yamamura, H.I. *Eur. J. Pharmacol.* **200**, 195–198 (1991).
7. Hruby, V.J., Fang, S.N., Kramer, T.H., Davis, P., Parkhurst, D., Nikiforovich, G.V., Boteju, L.W., Slaninová, J., Yamamura, H.I., Burks, T.F. In Hodges, R.S. and Smith, J.A. (Eds.) *Peptides: Chemistry, Structure and Biology (Proceedings of the 13th American Peptide Symposium)*, ESCOM, Leiden, 1994, p. 669.

## **Alternate Aggregation Pathways of Alzheimer $\beta$ -Amyloid Peptides**

**Paul Gorman<sup>1</sup>, Christopher M. Yip<sup>2</sup>, Paul E. Fraser<sup>3</sup>  
and Avijit Chakrabartty<sup>1</sup>**

<sup>1</sup>*Ontario Cancer Institute, University Health Network, University of Toronto, Toronto, Ontario, M5G 2M9, Canada*

<sup>2</sup>*Department of Chemical Engineering and Applied Chemistry, University of Toronto, Toronto, Ontario, M5S 3G9, Canada*

<sup>3</sup>*Center for Research in Neurodegenerative Disease, University of Toronto, Toronto, Ontario, M5S 3H2, Canada*

### **Introduction**

Alzheimer's Disease (AD) is a neuropathological disorder characterized by the progressive deposition in the brain of insoluble amyloid plaques and vascular deposits consisting primarily of the 4.5 kDa  $\beta$ -amyloid peptide (A $\beta$ ). There is increasing evidence that formation of these fibrillar deposits leads to the neurodegeneration observed in AD. Elucidating the mechanism of this polymerization process is therefore of great importance in the development of potential inhibitors. The detailed mechanism of A $\beta$  production is still unclear, however there is increasing evidence that A $\beta$  is initially produced through an endocytic-recycling pathway [1]. We have therefore investigated the association of A $\beta$  at endosomal pH in an attempt to identify the initial stages of A $\beta$  fibrillogenesis. Because individual techniques have inherent shortcomings, we employed several techniques for monitoring A $\beta$  association, which include fluorescence resonance energy transfer (FRET), dynamic light scattering (DLS), atomic force microscopy (AFM), and electron microscopy (EM).

### **Results and Discussion**

Peptides were synthesized by the solid phase method, and fluorophores were attached to the N-terminus during solid phase synthesis. Prior to fluorophore attachment, a Gly residue was added to the N-terminus to act as a flexible linker between the fluorophore and the peptide. Fluorophores used include 5-acetythyldiaminonaphthalene-1-sulfonic acid (EDANS) and Trp. The three peptides synthesized are EDANS-A $\beta$ , Trp-A $\beta$ , and unlabeled A $\beta$ .

The peptides were maintained in monomeric form by storage at pH 9.8. Lowering the pH to the endosomal pH of 6.00 induces A $\beta$  association. The association of A $\beta$  was monitored by measuring changes in fluorescence of EDANS, an environment sensitive fluorophore. 100 nM EDANS-A $\beta$  was added to varying concentrations of unlabeled A $\beta$ . A concentration-dependent enhancement of EDANS fluorescence was observed 15 s after acidification to pH 6, suggesting a rapid formation of A $\beta$  aggregates. On the other hand, kinetic FRET experiments utilizing Trp-A $\beta$  as donor and EDANS-A $\beta$  as acceptor demonstrated a slower biphasic association reaction. The half-lives of the first and second kinetic phases were 2 and 17 min, respectively.

DLS experiments demonstrated the immediate formation of large A $\beta$  aggregates with an average hydrodynamic radius ( $R_h$ ) of 90 nm. These aggregates grew to a maximum  $R_h$  of 200 nm after 12 min. Interestingly, the large aggregates disappear after 30 min and are replaced by smaller aggregates with  $R_h$  of 36 nm.

AFM was used to monitor the aggregation process (Figure 1). Two different surfaces were used in the AFM experiments, the hydrophobic surface, graphite, and the hydrophilic surface, mica. On the graphite surface, large aggregates (100–500 nm)

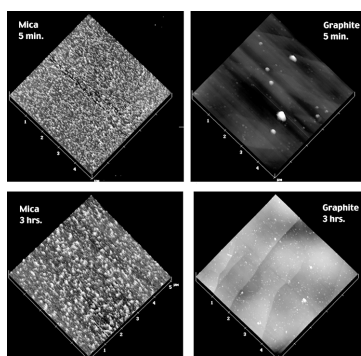


Fig. 1. AFM images of A $\beta$  aggregates.

were visible immediately. After three hours the large aggregates had disappeared and smaller aggregates (<50 nm) became visible. These observations on the graphite surface closely paralleled the DLS results. AFM experiments using the mica surface produced different results. Small spherical aggregates (20 nm) were visible within a few minutes. We have coined the term  $\beta$ -ball to describe these spherical aggregates. The  $\beta$ -balls grew in size over a period of several hours and appeared to form clusters, when examined on the mica surface.

The samples used in the above experiments were analyzed by negative stain EM (Figure 2) after a period of several months and characteristic amyloid fibrils were observed.

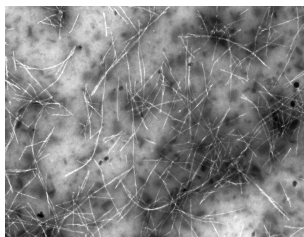


Fig. 2. Negative stain EM of A $\beta$  fibrils.

From these experiments, we conclude that there are alternate pathways of A $\beta$  aggregation under endosomal conditions. Under aggregating conditions, A $\beta$  monomers can form either large non-specific aggregates or  $\beta$ -balls. The formation rate of the non-specific aggregates is much faster than that of the  $\beta$ -balls; however, the  $\beta$ -balls are more stable than the non-specific aggregates. This difference in stability results in the eventual disappearance of non-specific aggregates and accumulation of  $\beta$ -balls. It is possible that the  $\beta$ -balls are precursors to protofibrils [2,3] which are an on-pathway intermediate of Alzheimer A $\beta$  fibrillogenesis.

#### Acknowledgments

Supported by grant from Canadian Institute of Health Research.

#### References

1. Koo, E.H., Squazzo, S.L. *J. Biol. Chem.* **269**, 17386–17389 (1994).
2. Harper, J.D., et al. *Biochemistry* **38**, 8972–8980 (1999).
3. Walsh, D., et al. *J. Biol. Chem.* **274**, 25945–25952 (1999).

## **Diabetes mellitus (DM) Causes Severe Impairment of Hypotensive Responses *in vivo* and Vasorelaxant Responses *in vitro* to the Neuropeptide CGRP**

**Ronald R. Fiscus, Gabriel H. H. Chan and Arisina C. Y. Ma**

*Department of Physiology, Faculty of Medicine, Epithelial Cell Biology Research Center & Center for Gerontology and Geriatrics, The Chinese University of Hong Kong, Shatin, New Territories, Hong Kong*

### **Introduction**

Calcitonin gene-related peptide (CGRP) is considered to be the most potent endogenous vasodilator and anti-hypertensive agent yet discovered [1,2]. CGRP causes both endothelium-independent and endothelium-dependent vasorelaxations, depending on the type of blood vessel [2]. The endothelium-dependent vasorelaxations of CGRP involve nitric oxide (NO) released from endothelium and NO-dependent elevations of both cAMP and cGMP levels in vascular smooth muscle cells (VSMCs) [2,3]. CGRP also has anti-proliferative effects on VSMCs [4], which likely contributes in the prevention of atherosclerosis. Deletion of CGRP gene expression in CGRP-knockout mice causes development of hypertension [5], indicating the endogenous CGRP is an important anti-hypertensive factor. CGRP is also recognized to be a mediator of vasodilations during inflammation and septic shock [1,6]. Thus, a decrease in CGRP's vascular actions, as for example during aging or diabetes mellitus, may increase the risk of developing atherosclerosis, hypertension and abnormal inflammatory responses. Interestingly, both the vasodilatory [7] and anti-proliferative [8] effects of CGRP are synergistically enhanced by NO. In general, production of NO in blood vessels decreases during aging as well as during diabetes mellitus [6]. We have hypothesized that the vasodilatory and anti-proliferative actions of CGRP may substantially diminish during aging and diabetes mellitus. The purpose of the present study was to examine the effect of diabetes mellitus on CGRP-induced hypotensive response *in vivo* and vasorelaxant responses *in vitro*.

### **Results and Discussion**

CGRP-induced vasorelaxations were significantly smaller (about 50% of age-matched non-diabetic controls) in aortic rings of diabetic rats (at 8 weeks following injection of streptozotocin, STZ, 75 mg/kg, i.p.). Diabetes mellitus was confirmed by the presence of >20 mM blood glucose levels at 2 days and 8 weeks following STZ. CGRP-induced hypotension *in vivo* was also significantly decreased to about 50% of normal response in the diabetic rats. When aortic rings of non-diabetic control rats were incubated for 6 h with elevated glucose levels (44 mM), vasorelaxant responses to CGRP were depressed to the same level as in diabetic aortic rings, indicating that elevated glucose levels may be responsible for the impairment of the vascular responses to CGRP.

Diminished production of NO during diabetes mellitus may contribute to the diminished CGRP-induced vasorelaxant and hypotensive responses in diabetic animals. A reduction of NO production during diabetes mellitus has been reported [6]. Thus, the synergistically enhancement by NO of the CGRP-induced vascular responses may be impaired during diabetes mellitus.

It has been proposed that elevated glucose levels during diabetes mellitus cause an acceleration of the aging process in blood vessels [8]. Part of this aging process likely involves non-enzymatic glycosylation (Maillard reaction) of receptor and post-

**Fiscus et al.**

receptor proteins that mediate vascular responses. Thus, diabetes mellitus may accelerate the glycosylation of CGRP receptors or other proteins involved in the signal transduction pathway of CGRP-induced vasodilations, leading to impairment of the CGRP-induced hypotensive and vasorelaxant responses.

In conclusion, the results of the present study indicated that endothelium-dependent relaxations in aortic rings caused by CGRP are severely impaired in diabetic rats. CGRP-induced hypotensive responses *in vivo* are also severely impaired in diabetic animals. Because similar damage to the CGRP-induced vascular responses occur in isolated vascular rings exposed to elevated glucose levels, it is possible that the glycosylation of CGRP receptors or proteins of the signal transduction pathway of CGRP-induced vasodilation may contribute to the severe impairment of the CGRP-induced vasorelaxant and hypotensive responses.

**Acknowledgments**

This work was supported by a Direct Grant for Research from the Research Grants Council of Hong Kong awarded to R. R. Fiscus. We would like to give special thanks to Dr. Anthony James, Director of the Laboratory Animal Services Center at The Chinese University of Hong Kong and workers of this center for helpful advice and technical assistance.

**References**

1. Wimalawansa, S.J. *Endocr. Rev.* **17**, 533–582 (1996).
2. Fiscus, R.R. *Semin. Thromb. Hemostasis Suppl.* **14**, 12–22 (1988).
3. Fiscus, R.R., Zhou, H.L., Wang, X., Han, C., Ali, S., Joyce, C.D., Murad, F. *Neuropeptides* **20**, 133–143 (1991).
4. Li, Y., Fiscus, R.R., Wu, J., Yang, L., Wang, X. *Neuropeptides* **31**, 503–509 (1997).
5. Gangula, P.R., Zhao, H., Supowit, S.C., Wimalawansa, S.J., Dipette, D., Westlund, K.N., Gagel, R.F., Yallampalli, C. *Hypertension* **35**, 470–475 (2000).
6. Fiscus, R.R., Ming, S.K., In Weng, S.P., Ming, K.T., Shiu, K.W. (Eds.) *Medicine and Surgery in the Elderly Person: Biology of Aging*, Armour Publishing Pte Ltd., Singapore, 2000, pp. 29–42.
7. Fiscus, R.R., Hao, H., Wang, X., Arden, W.A., Diana, J.N. *Neuropeptides* **26**, 133–144 (1994).
8. Wang, X., Wang, W., Li, Y., Bai, Y., Fiscus, R.R. *J. Mol. Cell. Cardiol.* **31**, 1599–1606 (1999).

## Triple-Helical Peptide Analysis of Collagenolytic Protease Activity

Gregg B. Fields<sup>1</sup>, Janelle L. Lauer-Fields<sup>1</sup>, Thilaka Sritharan<sup>1</sup> and  
Hideaki Nagase<sup>2</sup>

<sup>1</sup>Department of Chemistry & Biochemistry, Florida Atlantic University, Boca Raton, FL 33431, USA

<sup>2</sup>Kennedy Institute of Rheumatology Division, Imperial College School of Medicine,  
London W6 8LH, UK

### Introduction

The catabolism of collagen is the committed step in numerous biological processes. Normal tissue remodeling, embryonic development, arthritis, cardiovascular disease, and cancer cell metastasis all involve collagen breakdown. For invertebrates, collagen hydrolysis is part of the digestive process. Thus, the mechanism of collagenolytic activity, which involves efficient binding to and hydrolysis of triple-helical structure, is of great interest. However, several collagen-degrading proteases do not share a common structure motif, and have different active site residues participating in catalysis. To better understand how these proteases hydrolyze collagen, triple-helical peptide (THP) models of collagen can be constructed and utilized as substrates. Chemically synthesized triple-helical substrates have been used previously to examine binding by discrete matrix metalloproteinase (MMP) domains [1–5] and for evaluating MMP kinetic parameters [4]. Those substrates incorporated sequences derived from type I collagen known to be cleaved by MMPs in the native protein. In the present study, we have examined methods for the synthesis of fluorogenic triple-helical substrates, and used these substrates for study of MMPs, thermolysin, and trypsin.

### Results and Discussion

Homotrimeric, fluorogenic triple-helical peptide (fTHP) models of the MMP-1 cleavage site in human type II collagen [ $\alpha 1(\text{II})$ 769-783; sequence Gly-Pro-Pro-Gly-Pro-Gln-Gly~Leu-Ala-Gly-Gln-Arg-Gly-Ile-Val] have been constructed. These fluorogenic substrates were designed to incorporate the fluorophore/quencher pair of (7-methoxycoumarin-4-yl)acetyl (Mca) and *N*-2,4-dinitrophenyl (Dnp) in the P<sub>5</sub> and P<sub>5</sub>' positions, respectively.

The assembled, on-resin sequence was (Gly-Pro-Hyp)<sub>5</sub>-Gly-Pro-Lys(Mtt)-Gly-Pro-Gln-Gly~Leu-Arg-Gly-Gln-Lys(Dnp)-Gly-Val-Arg-(Gly-Pro-Hyp)<sub>5</sub>. A C<sub>6</sub> alkyl chain was added to create a final "peptide-amphiphile". After addition of the alkyl chain, the 4-methyltrityl (Mtt) group was removed and the Mca group was acylated. The peptide was cleaved from the resin and purified by RP-HPLC. MS analysis yielded an [M+H]<sup>+</sup> value of 4685.5 Da (theoretical 4687.0 Da) for C<sub>6</sub>-(Gly-Pro-Hyp)<sub>5</sub>-Gly-Pro-Lys(Mca)-Gly-Pro-Gln-Gly~Leu-Arg-Gly-Gln-Lys(Dnp)-Gly-Val-Arg-(Gly-Pro-Hyp)<sub>5</sub>-NH<sub>2</sub> (fTHP-3). This potential substrate was soluble in aqueous buffer up to a concentration of at least 100  $\mu\text{M}$ , and had a melting point of  $\sim 45^\circ\text{C}$ . Thus, fTHP-3 was suitable for kinetic studies.

Hydrolysis of fTHP-3 was examined for MMP-1, MMP-2, MMP-3, and MMP-13. Sequence and mass spectrometric analyses indicated that MMP-2 and MMP-13 cleaved fTHP-3 at two loci, Gly~Leu and Gly~Gln, while MMP-1 and MMP-3 cleaved fTHP-3 at the Gly~Leu locus. Individual kinetic parameters for MMP hydrolysis of fTHP-3 were then determined. The relative order of  $k_{\text{cat}}/K_{\text{M}}$  values was MMP-13 > MMP-1 ~ MMP-2 >> MMP-3 (Table 1). MMP-13 has the highest  $k_{\text{cat}}/K_{\text{M}}$  value for hydrolysis of fTHP-3 primarily due to a lower  $K_{\text{M}}$  value (20.5  $\mu\text{M}$  for MMP-13 *versus* 61.2 for

MMP-1). Consistent with the fTHP-3 results, MMP-13 cleaves type II collagen more rapidly than MMP-1.

The C-terminal hemopexin-like domain has been proposed to be essential for MMP collagenolytic activity [6] but not for cleavage of THPs [4]. To test this hypothesis, we studied the hydrolysis of fTHP-3 by MMP-1 lacking the C-terminal domain [MMP-1( $\Delta_{243-450}$ )]. Sequence and mass spectrometric analyses indicated that MMP-1( $\Delta_{243-450}$ ) cleaved the THP at the same Gly~Leu bond as cleaved by MMP-1. Kinetic analysis revealed that MMP-1( $\Delta_{243-450}$ ) hydrolyzed fTHP-3 with a  $k_{\text{cat}}/K_M$  value of  $1312 \text{ s}^{-1} \text{ M}^{-1}$  (Table 1), which is similar to the  $k_{\text{cat}}/K_M$  value for MMP-1.

Table 1. Kinetic parameters for fTHP-3 hydrolysis by MMPs at 30 °C.

Enzyme	$k_{\text{cat}}/K_M, \text{ s}^{-1} \text{ M}^{-1}$	$k_{\text{cat}}, \text{ s}^{-1}$	$K_M, \mu\text{M}$
MMP-1	1278	0.080	61.2
MMP-1( $\Delta_{243-450}$ )	1312	0.087	66.6
MMP-2	1082	0.017	17.2
MMP-3	503	0.031	65.0
MMP-3( $\Delta_{248-460}$ )	554	0.035	60.3
MMP-13	2273	0.045	20.5

Studies on the effect of temperature on fTHP and an analogous fluorogenic single-stranded peptide (fSSP) hydrolysis by MMP-1 showed that the activation energies between these two substrates differed by 3.4-fold, similar to the difference in activation energies for MMP-1 hydrolysis of type I collagen and gelatin (Table 2).

Table 2. Activation energies for substrate hydrolysis by MMP-1.

Substrate	$E_a, \text{ kcal/mol}$
fTHP-3 [ $\alpha 1(\text{II})769-783$ ]	11.6
fSSP-3 [ $\alpha 1(\text{II})769-783$ ]	3.4
Type I collagen (guinea pig skin) [7]	49.2
$\alpha 1(\text{I})$ gelatin (guinea pig skin) [7]	13.9
$\alpha 2(\text{I})$ gelatin (guinea pig skin) [7]	13.3

To evaluate the triple-helical peptidase activity of general proteases, thermolysin and trypsin hydrolysis of (Gly-Pro-Hyp)<sub>5</sub>-Gly-Pro-Lys(Mca)-Gly-Pro-Gln-Gly~Leu-Arg-Gly-Gln-Lys(Dnp)-Gly-Val-Arg-(Gly-Pro-Hyp)<sub>5</sub>-NH<sub>2</sub> (fTHP-4) was examined. The potential substrate fTHP-4 differs from fTHP-3 by lack of an N-terminal C<sub>6</sub> tail, and thus has a  $T_m \sim 48$  °C. Sequence and mass spectrometric analyses showed that thermolysin and trypsin cleaved fTHP-4, thermolysin at the Gly~Leu bond and trypsin at the Arg~Gly bond. Both proteases exhibited high activity towards this substrate, comparable to MMP-1. Kinetic parameters were determined at 25, 30, 35, and 40 °C, and the activation energies were calculated.  $E_a$  was 10.5 and 12.8 kcal/mol for thermolysin and trypsin, respectively. These activation energies are very similar to the value calculated for MMP-1 (Table 2).

Overall, we have found that fluorogenic substrates can be utilized for kinetic analyses of triple-helix hydrolysis by proteases. Studies with these fluorogenic substrates have shown that the ability to cleave a triple-helix (triple-helical peptidase activity) can be distinguished from the ability to cleave collagen (collagenolytic activity), and that the C-terminal hemopexin-like domain of MMPs is not required for triple-helical peptidase activity. In addition, a variety of proteases possess triple-helical peptidase activity, suggesting that collagenolytic activity may have resulted from a convergent evolutionary path.

#### **Acknowledgments**

This research was supported by grants from the National Institutes of Health (AR 39189 to H.N., CA 77402 and AR 01929 to G.B.F.), the Wellcome Trust (reference number 057508 to H.N.), and Pfizer, Inc. Central Research Division.

#### **References**

1. Ottil, J., Battistuta, R., Pieper, M., Tschesche, H., Bode, W., Kühn, K., Moroder, L. *FEBS Lett.* **398**, 31–36 (1996).
2. Ottil, J., Moroder, L. *J. Am. Chem. Soc.* **121**, 653–661 (1999).
3. Ottil, J., Gabriel, D., Murphy, G., Knäuper, V., Tominaga, Y., Nagase, H., Kröger, M., Tschesche, H., Bode, W., Moroder, L. *Chem. Biol.* **7**, 119–132 (2000).
4. Lauer-Fields, J.L., Tuzinski, K.A., Shimokawa, K., Nagase, H., Fields, G.B. *J. Biol. Chem.* **275**, 13282–13290 (2000).
5. Lauer-Fields, J.L., Nagase, H., Fields, G.B. *J. Chromatogr., A* **890**, 117–125 (2000).
6. Clark, I.N., Cawston, T.E. *Biochem. J.* **263**, 201–206 (1989).
7. Welgus, H.G., Jeffrey, J.J., Eisen, A.Z. *J. Biol. Chem.* **256**, 9516–9521 (1981).

## Design of More Potent, Radioiodinatable and Fluorescent Vasopressin Hypotensive Peptide Agonists

L. L. Cheng<sup>1</sup>, S. Stoev<sup>1</sup>, M. Manning<sup>1</sup>, N. C. Wo<sup>2</sup> and W. Y. Chan<sup>2</sup>

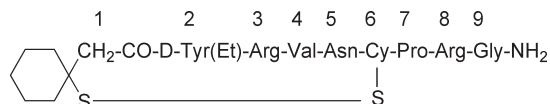
<sup>1</sup>Department of Biochemistry and Molecular Biology, Medical College of Ohio, Toledo, OH 43614, USA

<sup>2</sup>Department of Pharmacology, Cornell University Medical College, New York, NY 10021, USA

### Introduction

We recently reported the serendipitous discovery of a new class of vasopressin (VP) peptides, which exhibit selective hypotensive agonism [1]. In follow-up structure/activity studies on the parent peptide: d(CH<sub>2</sub>)<sub>5</sub>[D-Tyr(Et)<sup>2</sup>,Arg<sup>3</sup>,Val<sup>4</sup>]AVP (**A**) (see structure), we uncovered structural modifications of (**A**) which (a) enhance, (b) retain, (c) diminish and (d) abolish hypotensive potency [2,3]. A Lys<sup>8</sup> substitution for Arg<sup>8</sup> in the tripeptide side-chain of analogs of (**A**) has emerged as a promising lead to more potent hypotensive peptides [3]. We now report a series of 12 new analogs of (**A**) with further modifications in its Pro-Arg-Gly-NH<sub>2</sub> tripeptide tail. Nine analogs (**1–9**, Table 1) have Lys<sup>8</sup> and three analogs (**10–12**, Table 1) have Orn<sup>8</sup>. With the exception of peptide **9**, which has a Pro<sup>7</sup>, all have the following additional modifications at positions 7 and 9. *Position 7*: Arg<sup>7</sup> (peptides **3–5**, **8**, **10–12**); Lys<sup>7</sup> (peptides **1**, **2**); Orn<sup>7</sup> (peptides **6**, **7**); *Position 9*: Eda<sup>9</sup> (where Eda = ethylenediamine) (peptides **1**, **3**, **6**, **10**); Lys-NH<sub>2</sub><sup>9</sup> (peptides **8**, **9**); Arg-NH<sub>2</sub><sup>9</sup> (peptide **12**); Eda<sup>9</sup>←Tyr<sup>10</sup> (peptides **2**, **7**); Lys<sup>9</sup>-Eda<sup>10</sup> (peptides **5**, **11**) and Lys<sup>9</sup>-Eda<sup>10</sup>←Tyr<sup>11</sup> (peptide **4**).

Structure of (**A**):



### Results and Discussion

Peptides **1–12** (Table 1) were synthesized by the Merrifield solid phase method as previously described [3] and were assayed for agonism and antagonism in VP vasopressor (V<sub>1a</sub> receptor), antidiuretic (V<sub>2</sub> receptor), oxytocic (*in vitro*) (OT-receptor) and VP vasodepressor assays as described [1,3]. All peptides exhibit negligible agonistic or antagonistic, antidiuretic, vasopressor and oxytocic activities. All 12 new peptides exhibit significant enhancement of hypotensive potency relative to (**A**). Peptides **2**, **4** and **7** are promising new radioiodinatable ligands for the putative vasodilating receptor. Peptides **3**, **10** and **12** are good candidates for fluoresceinylation [4]. These findings show that the tripeptide side-chain of (**A**) can tolerate multiple substitutions with retention or enhancement of vasodepressor potency. Peptides **3** and **10** differ only in having an Arg, Lys or Orn residue at position 8. With vasodepressor EDs of 1.10, 0.66 and 0.61, respectively, the Lys<sup>8</sup> and Orn<sup>8</sup> peptides are more potent than the Arg<sup>8</sup> peptide. The Lys<sup>8</sup> and Orn<sup>8</sup> substitutions appear to be equally effective in enhancing hypotensive potency. However, comparison of the ED values of peptides **1** (ED = 0.53) and **6** (ED = 1.06) points to the superiority of the Lys<sup>7</sup> over the Orn<sup>7</sup> substitution in enhancing vasodepressor potency. These findings offer new clues to the design of more potent hypotensive peptides for use as (a) research tools; (b) radioiodinatable

ligands; (c) fluorescent ligands; (d) antagonists of the putative VP vasodilating receptor and (e) their development as potential new anti-hypertensive agents.

Table 1. Lys<sup>8</sup> (1–9) and Orn<sup>8</sup> (10–12) tripeptide tail modified analogs of d(CH<sub>2</sub>)<sub>5</sub>[D-Tyr(Et)<sub>2</sub>,Arg<sup>3</sup>,Val<sup>4</sup>]AVP (A) possess enhanced hypotensive potency.

No.	Peptide	Vasodepressor ED <sup>c</sup> , µg/100 g
<b>A</b>	d(CH <sub>2</sub> ) <sub>5</sub> [D-Tyr(Et) <sup>2</sup> ,Arg <sup>3</sup> ,Val <sup>4</sup> ]AVP <sup>a</sup>	4.66
<b>1</b>	d(CH <sub>2</sub> ) <sub>5</sub> [D-Tyr(Et) <sup>2</sup> ,Arg <sup>3</sup> ,Val <sup>4</sup> ,Lys <sup>7</sup> ,Eda <sup>9</sup> ]LVP <sup>b</sup>	0.53
<b>2</b>	d(CH <sub>2</sub> ) <sub>5</sub> [D-Tyr(Et) <sup>2</sup> ,Arg <sup>3</sup> ,Val <sup>4</sup> ,Lys <sup>7</sup> ,Eda <sup>9</sup> ←Tyr <sup>10</sup> ]LVP <sup>b</sup>	0.59
<b>B</b>	d(CH <sub>2</sub> ) <sub>5</sub> [D-Tyr(Et) <sup>2</sup> ,Arg <sup>3</sup> ,Val <sup>4</sup> ,Arg <sup>7</sup> ,Eda <sup>9</sup> ]AVP <sup>a</sup>	1.10
<b>3</b>	d(CH <sub>2</sub> ) <sub>5</sub> [D-Tyr(Et) <sup>2</sup> ,Arg <sup>3</sup> ,Val <sup>4</sup> ,Arg <sup>7</sup> ,Eda <sup>9</sup> ]LVP <sup>b</sup>	0.66
<b>4</b>	d(CH <sub>2</sub> ) <sub>5</sub> [D-Tyr(Et) <sup>2</sup> ,Arg <sup>3</sup> ,Val <sup>4</sup> ,Arg <sup>7</sup> ,Lys <sup>9</sup> ,Eda <sup>10</sup> ←Tyr <sup>11</sup> ]LVP <sup>b</sup>	0.74
<b>5</b>	d(CH <sub>2</sub> ) <sub>5</sub> [D-Tyr(Et) <sup>2</sup> ,Arg <sup>3</sup> ,Val <sup>4</sup> ,Arg <sup>7</sup> ,Lys <sup>9</sup> ,Eda <sup>10</sup> ]LVP <sup>b</sup>	0.91
<b>6</b>	d(CH <sub>2</sub> ) <sub>5</sub> [D-Tyr(Et) <sup>2</sup> ,Arg <sup>3</sup> ,Val <sup>4</sup> ,Orn <sup>7</sup> ,Eda <sup>9</sup> ]LVP <sup>b</sup>	1.06
<b>7</b>	d(CH <sub>2</sub> ) <sub>5</sub> [D-Tyr(Et) <sup>2</sup> ,Arg <sup>3</sup> ,Val <sup>4</sup> ,Orn <sup>7</sup> ,Eda <sup>9</sup> ←Tyr <sup>11</sup> ]LVP <sup>b</sup>	1.35
<b>8</b>	d(CH <sub>2</sub> ) <sub>5</sub> [D-Tyr(Et) <sup>2</sup> ,Arg <sup>3</sup> ,Val <sup>4</sup> ,Arg <sup>7</sup> ,Lys-NH <sub>2</sub> <sup>9</sup> ]LVP <sup>b</sup>	1.38
<b>9</b>	d(CH <sub>2</sub> ) <sub>5</sub> [D-Tyr(Et) <sup>2</sup> ,Arg <sup>3</sup> ,Val <sup>4</sup> ,Lys-NH <sub>2</sub> <sup>9</sup> ]LVP <sup>b</sup>	3.94
<b>10</b>	d(CH <sub>2</sub> ) <sub>5</sub> [D-Tyr(Et) <sup>2</sup> ,Arg <sup>3</sup> ,Val <sup>4</sup> ,Arg <sup>7</sup> ,Eda <sup>9</sup> ]OVP <sup>b</sup>	0.61
<b>11</b>	d(CH <sub>2</sub> ) <sub>5</sub> [D-Tyr(Et) <sup>2</sup> ,Arg <sup>3</sup> ,Val <sup>4</sup> ,Arg <sup>7</sup> ,Lys <sup>9</sup> ,Eda <sup>10</sup> ]OVP <sup>b</sup>	0.83
<b>12</b>	d(CH <sub>2</sub> ) <sub>5</sub> [D-Tyr(Et) <sup>2</sup> ,Arg <sup>3</sup> ,Val <sup>4</sup> ,Arg <sup>7</sup> ,Arg-NH <sub>2</sub> <sup>9</sup> ]OVP <sup>b</sup>	1.00

<sup>a</sup> Data from reference [3]. <sup>b</sup> This publication. <sup>c</sup> ED, effective dose (in µg 100 g<sup>-1</sup> i.v.) is the dose that produces a vasodepressor response of 5 cm<sup>2</sup> AUC in 5-min period following injection of test peptide. AUC, area under the vasodepressor response curve (see refs [1] and [3] for details).

#### Acknowledgments

We thank Ms Suzanne Payne for expert help in the preparation of this manuscript and NIH Grant GM-25280.

#### References

1. Chan, W.Y., Wo, N.C., Stoev, S., Cheng, L.L., Manning, M. *Br. J. Pharmacol.* **125**, 803–811 (1998).
2. Manning, M., Stoev, S., Cheng, L.L., Wo, N.C., Chan, W.Y. *J. Recept. Signal Transduct. Res.* **19**(1–4), 631–644 (1999).
3. Manning, M., Stoev, S., Cheng, L.L., Wo, N.C., Chan, W.Y. *J. Peptide Sci.* **5**, 472–490 (1999).
4. Durroux, T., Perter, M., Turcatti, G., Chollet, A., Balestre, M.N., Barberis, C., Seyer, R. *J. Med. Chem.* **42**, 1312–1319 (1999).

## **Antagonism of the Neurochemical Effect of Thyrotropin-Releasing Hormone by Its Peptide Analog**

**Laszlo Prokai, Alevtina Zharikova, Vien Nguyen and Xiaoxu Li**

*Center for Drug Discovery, College of Pharmacy, University of Florida, Gainesville,  
FL 32610-0497, USA*

### **Introduction**

Besides its role in the regulation of endocrine functions, thyrotropin-releasing hormone (TRH; pGlu-His-Pro-NH<sub>2</sub>) has been long recognized as a modulatory neuropeptide in the central nervous system (CNS) [1]. The most prominent CNS effect of TRH is cholinergic, and a robust effect of TRH on the stimulation of acetylcholine (ACh) synthesis [2] and, therefore, the subsequent increase of the ACh level [3] have been shown in animals. One of the obstacles to a better understanding of the role of TRH in mediating central functions has been the absence of selective antagonists of the TRH receptor(s) [4]. The tripeptide pGlu-Glu-Pro-NH<sub>2</sub> with structural and immunological similarities to TRH has been recently shown to have inhibitory and stimulatory actions within the avian hypothalamo-pituitary axis, and to act as a TRH receptor antagonist within this axis based on suppression of TRH-induced growth hormone (GH) release from pituitary glands, competitively displacing [<sup>3</sup>H]Me-TRH, and lowering of GH level in pentobarbital-anesthetized fowl [5]. In addition, pGlu-Glu-Pro-NH<sub>2</sub> did not down-regulate TRH-receptors. However, studies involving pGlu-Glu-Pro-NH<sub>2</sub> as a potential TRH antagonist and addressing central functions of the neuropeptide in mammals have not been done. We tested the hypothesis that pGlu-Glu-Pro-NH<sub>2</sub> is able to antagonize the neurochemical action of TRH in the rat brain by using *in vivo* intracranial microdialysis as an experimental method [6].

### **Results and Discussion**

Male Sprague–Dawley rats (250–300 g body weight) were used in for the experiments. The implantation of a guide cannula (CMA/Microdialysis, Inc., Acton, MA) into the hippocampus was done stereotactically under anesthesia and the experiment was started after 3–5 days of recovery. I-type microdialysis probes (CMA/12) with a 4-mm long polycarbonate membrane were used. Syringe pumps (1-mL BeeStinger), their controller (BeeKeeper) and a refrigerated fraction collector (HoneyComb) used throughout the experiments were purchased from BAS (West Lafayette, IN). ACh concentrations were measured by microbore ion-exchange chromatography with electrochemical detection. After a 3-h perfusion of the probes at 2 µL/min with artificial CSF containing 2 µM neostigmine as a perfusion fluid, three 20-min fractions were collected to obtain the baseline values. Elevation of the extracellular ACh levels was induced by the perfusion of TRH (1 mM dissolved in the perfusion fluid) through the probe. The values were expressed as percentages of the ACh concentrations measured before the switching to the solution containing the neuropeptide had been started. Typical baseline ACh concentrations in the hippocampal microdialysates under our experimental conditions were between 50 and 100 nM. ACh concentrations in the microdialysates reached an essentially steady-state level 40–60 min after starting the perfusion of the TRH solution. In this steady state, the collected fractions showed a more than 4-fold increase in the extracellular ACh levels compared to the baseline values. For testing the antagonism by pGlu-Glu-Pro-NH<sub>2</sub>, a solution containing both TRH and the latter analog (1 mM each in the perfusion fluid) was used. Experiments

### Peptide Vaccines and Immunology

where the TRH analog alone (1 mM) was delivered into the rat hippocampus and microdialysates were collected for ACh measurements were also done as a control.

Table 1 summarizes the effect of TRH and pGlu-Glu-Pro-NH<sub>2</sub> on the extracellular ACh concentrations. While the latter analog alone had no apparent influence on the synthesis and/or release of this neurotransmitter, its co-administration with TRH in equimolar doses did attenuate TRH-induced increase in the ACh level in the rat hippocampus to a significant extent. On the other hand, the displacement of [<sup>3</sup>H]Me-TRH ( $1 \cdot 10^{-7}$  M) that labels high-affinity TRH-binding sites occurred only at the millimolar level by pGlu-Glu-Pro-NH<sub>2</sub>, which indicated that low-affinity TRH-binding sites [7] inducing the neurochemical effects might be involved in the observed antagonism by the analog. Experiments probing this hypothesis are in progress. In conclusion, an antagonist to TRH that attenuates a characteristic neurochemical effect of the neuroactive peptide in the mammalian CNS has been identified during our studies. This compound may be a valuable lead for structure-based or combinatorial discovery of potent TRH antagonists.

Table 1. Changes in the extracellular ACh levels in the rat hippocampus during the perfusion of the microdialysis probes with the solution of TRH and pGlu-Glu-Pro-NH<sub>2</sub> (1-mM each).

Peptide	Change in ACh concentration (% of baseline) <sup>a</sup>
TRH	439 ± 91
pGlu-Glu-Pro-NH <sub>2</sub>	9 ± 36
TRH + pGlu-Glu-Pro-NH <sub>2</sub>	242 ± 40

<sup>a</sup> Average ± standard error, N = 6 to 9.

### Acknowledgments

This project has been supported by the grant MH59360 (National Institutes of Health).

### References

1. Horita, A., Carino, M.A., Lai, H. *Ann. Rev. Pharmacol. Toxicol.* **26**, 311–332 (1986).
2. Narumi, S., Nagai, Y., Miyamoto, M., Nagawa, Y. *Life Sci.* **32**, 1637–1645 (1983).
3. Hutson, P.H., Semark, J.E., Middlemiss, D.N. *Neurosci. Lett.* **116**, 149–155 (1990).
4. Horita, A. *Life Sci.* **62**, 1443–1448 (1998).
5. Harvey, S., Trudeau, V.L., Ashworth, R.J., Cockle, S.M. *J. Endocrinol.* **138**, 137–147 (1993).
6. Giovannini, M.G., Casamenti, F., Nistria, A., Paoli, F., Pepeu, G. *Br. J. Pharmacol.* **102**, 363–368 (1991).
7. Vonhof, S., Feuerstein, G.Z., Cohen, L.A., Labroo, V.M. *Eur. J. Pharmacol.* **180**, 1–12 (1990).

## Synthesis of Selective Substrates for Syk PTK

Paolo Ruzza<sup>1</sup>, Andrea Calderan<sup>1</sup>, Arianna Donella-Deana<sup>2</sup>, Luca Cesaro<sup>2</sup>,  
Stefano Elardo<sup>1</sup>, Lorenzo A. Pinna<sup>2</sup> and Gianfranco Borin<sup>1</sup>

<sup>1</sup>Biopolymers Research Center of CNR, Padova, 35131, Italy

<sup>2</sup>Department of Biological Chemistry, University of Padova, Padova, 35131, Italy

### Introduction

Phosphorylation is one of the major post-translational modifications that regulate many cellular processes (cell cycle, growth, differentiation, *etc.*). Several studies have been made to elucidate the “consensus sequence” of protein tyrosine kinase (PTK) substrates since the discovery of this class of kinases, and their results indicated that the substrate recruitment is also dictated by the secondary structure of the target peptide [1]. One approach to study the secondary structure implicated in substrate recognition by PTKs involves the use of conformationally constrained Tyr analogues. Clearly, in short peptides, different dispositions of side chain groups in terms of  $\chi_1$  space can provide a remarkable diversity of chemical surfaces, even considering a single peptide backbone template ( $\alpha$ -helix,  $\beta$ -turn, *etc.*). The need to inquire into the side chain orientation of phosphorylatable tyrosine residues in short peptide substrates thus became evident. Starting from the peptide corresponding to the sequence 392-399 of the HS1 protein (H-Pro-Glu-Gly-Asp-Tyr-Glu-Glu-Val-OH), a good substrate for Syk PTK, we have designed and synthesized a series of analogues of this peptide. First, in order to improve the phosphorylation by Syk, the N-terminal segment (sequence 392-395) was replaced by the more acidic sequence H-Glu-Asp-Asp-Glu-, and then a “rotamer scan” of the phosphorylatable residue was performed by replacing the tyrosine (peptide **A**) with L-Htc (peptide **B**), D-Htc (peptide **C**), and [Hba-Gly] (peptide **D**), an aminobenzazepine-type structure containing the phenolic ring, respectively.

### Results and Discussion

Peptides **A**, **B**, **C** and **D** were synthesized by solid phase technique on Wang resin using standard Fast-Fmoc protocol. In order to avoid side reactions, the coupling of Glu<sup>4</sup> to the secondary amino group of Htc residues was performed using HATU as coupling reagent as previously reported [2]. The [Hba-Gly] residue was synthesized according to the method described by Flynn and de Laszlo [3].

Conformational analysis of the side chain orientation of phosphorylatable residue was performed by <sup>1</sup>H NMR in DMSO-*d*<sub>6</sub> solution. From temperature dependencies and the H, D exchange rates, we conclude that, in each peptide, the amide protons are not involved in hydrogen bonding.

The combination of the vicinal coupling constant values and NOE data (Table 1) made it possible to infer the *gauche* ( $\pm$ ) or *trans* conformations of the tyrosine constrained side chain. In particular, the vicinal coupling constants and the NOE (C <sup>$\alpha$</sup> H-C <sup>$\beta$</sup> H) pattern are consistent with a *gauche* (+) side chain conformation for peptide **B** (Tyr replaced by L-Htc) and with a *trans* conformation for peptide **D** (Tyr replaced by Hba). This last result is also confirmed by a strong CH <sup>$\alpha$</sup> -CH <sup>$\epsilon$</sup>  intraresidual NOE, which can only be present in the *trans* rotamer. Peptide **C** (Tyr replaced by D-Htc) is characterized by two subspectra, as a result of *cis-trans* isomerism around the Glu<sup>4</sup>-D-Htc<sup>5</sup> peptide bond. In this peptide, the  $\alpha$ - $\beta$  NOE are indicative of the presence of a *gauche* (–) conformation in both *cis-trans* isomers.

Table 1. Parameters determining the orientation of the aromatic side chains. Values for the *cis* conformer of peptide **C** are in parentheses.

	Peptide <b>B</b> L-Htc	Peptide <b>C</b> D-Htc	Peptide <b>D</b> Hba-Gly
$^3J_{\alpha,\beta 3}$ (Hz)	6.50	7.87(11.55)	5.5
$^3J_{\alpha,\beta 2}$ (Hz)	6.63	5.25(nd)	12.4
NOE( $\alpha,\beta 2$ )	m/s	w (nd)	s
NOE( $\alpha,\beta 3$ )	m/s	s (s)	w
NOE(NH, $\beta 2$ )	/	/	w/m
NOE(NH, $\beta 3$ )	/	/	s

Enzyme studies evaluated the selectivity of the synthetic peptides towards two Src-like kinases (Lyn and c-Fgr) and Syk PTK. Time courses of peptide phosphorylation show that peptide **A** is phosphorylated, although with different efficiency, by both kinases tested. The peptides containing constrained Tyr analogues are poorly phosphorylated by the Src-related PTKs. On the contrary, peptides **B** and **D** (Tyr replaced by L-Htc and Hba-Gly, respectively) were phosphorylated by Syk as efficiently as the parent peptide, whereas peptide **C** (D-Htc replacing Tyr residue) was poorly recognized by this enzyme.

These phosphorylation studies indicate that fixing the Tyr side chain in PTK substrates into the *gauche* (+) (peptide **B**) or *trans* (peptide **D**) conformations is not a negative determinant for substrate recognition by Syk tyrosine kinase. On the other hand, the introduction of these two constraints in peptide substrates was not tolerated by Lyn and c-Fgr. This lack of tolerance of Src-like PTK suggest a greater substrate stringency of this kinases family as compared with Syk PTK.

The present data may permit the design of peptide substrate-based inhibitors competing specifically with Syk PTK. In addition, considering that signalling through different hematopoietic cells results in a rapid and almost simultaneous activation of Syk and Src-like PTKs, the two constrained peptides **B** and **D** can be regarded as useful tools for assessing the specific activity of Syk.

#### Acknowledgments

This work was supported by CNR (P.S. Controlli post-trascrizionali dell'espressione genica), AIRC & MURST.

#### References

1. Ruzzene, M., Pinna, L.A. *Biochim. Biophys. Acta* **1314**, 191–225 (1996).
2. Ruzza, P., Calderan, A., Cavaggion, F., Borin, G. *Lett. Peptide Sci.* **7**, 79–83 (2000).
3. Ruzza, P., Calderan, A., Deana-Donella, A., Biondi, B., Cesaro, L., Brunati, A.M., Elardo, S., Pinna, L.A., Borin, G. manuscript in preparation.

## Synthesis of Potent and Enzymatically Stable 4-<sup>18</sup>F-Benzoyl-NT(8-13) Analogs for Tumour Diagnosis Using PET

K. Iterbeke<sup>1</sup>, R. Bergmann<sup>2</sup>, B. Johanssen<sup>2</sup>, G. Török<sup>1</sup>, G. Laus<sup>1</sup>  
and D. Tourwe<sup>1</sup>

<sup>1</sup>Department of Organic Chemistry, Vrije Universiteit Brussel, B-1050 Brussels, Belgium

<sup>2</sup>Bioinorganic and Pharmaceutical Chemistry, Forschungszentrum Rossendorf,  
D-01474 Dresden, Germany

### Introduction

Neurotensin (NT), a tridecapeptide (pGlu-Leu-Tyr-Glu-Asn-Lys-Pro-Arg-Arg-Pro-Tyr-Ile-Leu-OH) was first isolated from bovine hypothalami. Following reports of abundant expression in many tumours, including Ewing's Sarcoma, non-endocrine pancreas carcinoma and meningioma the search for the development of a radiolabelled derivative of NT gained extensive and still growing interest. As a result, radiolabelled neurotensin analogs might be useful for either localisation or internal radiotherapy of the above mentioned neurotensin receptor expressing pathologies [1]. Here we report on the synthesis of analogues of the biological active part of NT, NT(8-13) (H-Arg<sup>8</sup>-Arg<sup>9</sup>-Pro<sup>10</sup>-Tyr<sup>11</sup>-Ile<sup>12</sup>-Leu<sup>13</sup>-OH), which were developed as potential PET-tracers.

### Results and Discussion

The peptides were prepared by solid phase peptide synthesis on a Merrifield resin using Boc main-chain protected amino acids. Coupling was performed with 4 eq TBTU (HATU for coupling to *N*<sup>α</sup>-Me-Tyr) as coupling reagent, 4 eq of protected amino acid and 20 eq NMM as base for 2 h. To increase the stability towards proteolytic degradation, without loss of binding affinity, modifications were introduced into the peptide sequence. The reduced amide bond was incorporated by reduction of the Boc-Arg(Z<sub>2</sub>)-*N,O*-dimethylhydroxamate to the aldehyde according the procedure of Fehrentz et al. and consecutive reductive amination of the aldehyde with the peptide on the resin [2].

Radiolabelling was carried out using 0.7 mg of the respective peptide in a *N*-succinimidyl-4-[<sup>18</sup>F]fluorobenzoate ([<sup>18</sup>F]SFB) solution of 25% (v/v) CH<sub>3</sub>CN in Kolthoff's buffer (pH 8.3) at 45 °C for 50 min. High specific activity products were obtained (100–400 Ci/mmol). The decay-corrected radiochemical yields were 30–48% for NT-1, 13–36% for NT-2, 10–15% for NT-3, and 10–25% for NT-4 [3].

IC<sub>50</sub> values for the non-radioactive compounds showed that NT-1 and NT-2 have comparable IC<sub>50</sub> values as the native NT while NT-3 and NT-4 gave a loss in binding affinity. Replacing Tyr by *N*<sup>α</sup>-Me-Tyr or D-Tyr (NT-5, NT-6) gave complete loss of binding (Tables 1 and 2).

Metabolic stability was investigated *in vivo* in rats. Arterial blood samples showed very fast degradation of 4-<sup>18</sup>F-benzoyl-NT-1 (*t*<sub>1/2</sub> << 1 min) and 4-<sup>18</sup>F-benzoyl-NT-2 (*t*<sub>1/2</sub> < 1 min). 4-<sup>18</sup>F-benzoyl-NT-4 (*t*<sub>1/2</sub> = 90 min), and to a lesser extent 4-<sup>18</sup>F-benzoyl-NT-3 (*t*<sub>1/2</sub> = 6.2 min), showed an increased *in vivo* stability. *Ex vivo* autoradiography on HT-29 tumour bearing mice showed an increased tumour uptake for 4-<sup>18</sup>F-benzoyl-NT-4 making it a potential candidate for use in diagnosis of NT receptor containing carcinomas with PET [3].

## Peptide Vaccines and Immunology

Table 1.  $IC_{50}$  values of the non-radioactive NT's 3 obtained by NTR1 autoradiography with  $^{125}I$ -Tyr<sup>3</sup>-NT as radiotracer on tissue sections of human carcinoma.

Receptor ligand	$IC_{50} \pm SEM$ (nM)	
$^{125}I$ -Tyr <sup>3</sup> -NT	0.86±0.10	Human cancer
Arg-Arg-Pro-Tyr-Ile-Leu-OH (NT-1)	0.42±0.05	Human cancer
ArgΨ(CH <sub>2</sub> NH)Arg-Pro-Tyr-Ile-Leu-OH (NT-2)	0.91±0.20	Human cancer
ArgΨ(CH <sub>2</sub> NH)Arg-Pro-Tyr-Tle-Leu-OH (NT-3)	4.1±0.60	Human cancer

Table 2.  $IC_{50}$  values of non-radioactive compounds obtained by displacement of  $^3H$ -NT as radiotracer from HT-29 cells and rat cortex homogenate.

Receptor ligand	$IC_{50} \pm SD$ (nM)	
$^3H$ -NT	6.34±1.09	HT-29
ArgΨ(CH <sub>2</sub> NH)Arg-Pro-Dmt-Tle-Leu-OH (NT-4)	24.0±4.2	HT-29
ArgΨ(CH <sub>2</sub> NH)Arg-Pro-Dmt-Tle-Leu-OH (NT-4)	20.1±11.2	Rat cortex
ArgΨ(CH <sub>2</sub> NH)Arg-Pro-N <sup>α</sup> -Me-Tyr-Tle-Leu-OH (NT-5)	>200	Rat cortex
ArgΨ(CH <sub>2</sub> NH)Arg-Pro-D-Tyr-Tle-Leu-OH (NT-6)	>200	Rat cortex

## Acknowledgments

The authors thank the FWO, the APS, and the BIOMED-2 project (contract No. BMH4-CT98-3198) for their support.

## References

1. Reubi, J.C., Waser, B., Schaer, J-C., Laissue, J.A. *Int. J. Cancer* **82**, 213–218 (1999).
2. Couder, J., Tourwé, D., Van Binst, G., Schuurkens, J., Leysen, J.E. *Int. J. Pept. Protein Res.* **41**, 181–184 (1993).
3. Bergmann, R., Scheunemann, M., Heichert, C. *Nucl. Med. Biol.*, in press.

## ***In vivo* Imaging of Protease Activity and Drug Screening**

**Ching-Hsuan Tung, Christoph Bremer and Ralph Weissleder**

Center for Molecular Imaging Research, Massachusetts General Hospital,  
 Harvard Medical School, Charlestown, MA 02129, USA

### **Introduction**

Proteases represent a large and varied class of biomolecules that presently are under investigation as targets for therapeutic intervention in diseases. Knowing protease activity after treatment is crucial to drug design. However, most existing technologies are based on *in vitro* analysis and are limited in their ability to offer molecular information. We have recently developed biocompatible molecular probes for the *in vivo* detection of specific protease activity, particularly for those proteases that play key roles in different aspects of cancer growth, metastases formation and angiogenesis [1-4]. Matrix Metalloproteinase-2 (MMP-2) is one of many tumor-associated proteases. In this report we present a near-infrared fluorescence (NIRF) contrast agent, which was highly activatable by MMP-2. Using this probe, we were able to detect tumors, distinct tumors, and monitor inhibition effect of protease inhibitor treatment *in vivo* [5].

### **Results and Discussion**

The MMP-2 sensitive probe was synthesized following previously published method [2]. Briefly, the MMP-2 substrate peptide Gly-Pro-Leu-Gly-Val-Arg-Gly-Lys(FITC)-Cys-NH<sub>2</sub> was coupled to a high molecular weight protected graft copolymer (PGC) consisting of a 35 kD poly-L-lysine backbone and multiple 5 kD methoxy-polyethylene glycol side chains (MW 500 kD) [6]. Since the polylysine backbone was only partially peglated, there are still free amino groups available for peptide attachment. The MMP-2 substrate peptide was attached to the PGC through a biofunctional iodoacetic anhydride (Figure 1). Once the peptide was attached to the PGC, a molecule of Cy5.5

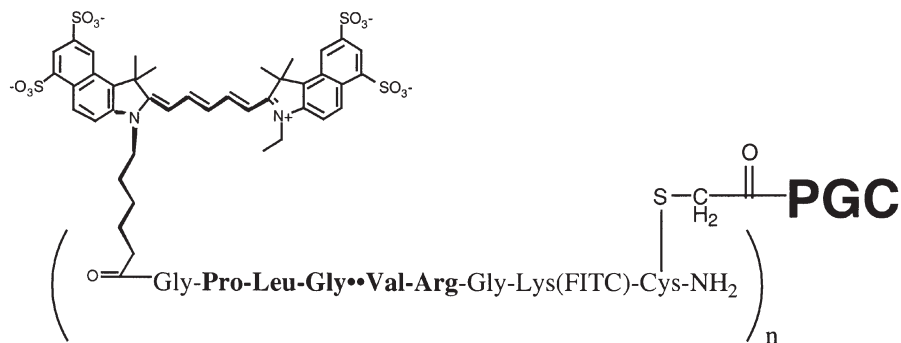


Fig. 1. Schematic diagram of MMP-2 selective NIRF probe. The MMP-2 recognition residues were bolded and the cleavage site was indicated by \*\*. The PGC represents the partially peglated polylysine co-polymer. The NIRF fluorochrome is Cy5.5 having excitation and emission at 675 and 694 nm, respectively.  $N = 12$  [5].

monoreactive fluorochrome was subsequently added to the N-terminus of the peptide spacer. The attaching efficiency was determined by absorption of the fluorochromes, *i.e.* FITC and Cy5.5. On average, each PGC molecule contains 12 NIRF fluorochromes. Because of resonance energy transfer between adjacent fluorochromes, the

fluorescence signal of these probes is negligible in the non-activated state. *In vitro*, 7-fold signal increase was observed when the probe was activated by MMP-2.

To demonstrate the feasibility of MMP-2 imaging *in vivo*, a xenografted tumor model was used. Two tumor cell lines, a MMP-2 positive (HT-1080, human fibrosarcoma) and a MMP-2 negative tumor cells (BT-20, well differentiated mammary adenocarcinoma), were co-implanted in the upchest of nude mice. The MMP-2 sensitive probe (2 nmole) was injected into animals intravenously. Two hours after injection the animals were imaged. The imaging results show considerable differences between HT1080 ( $98.3 \pm 5.1$  AU) and BT20 tumors ( $31.0 \pm 6.6$ ) (Figure 2).

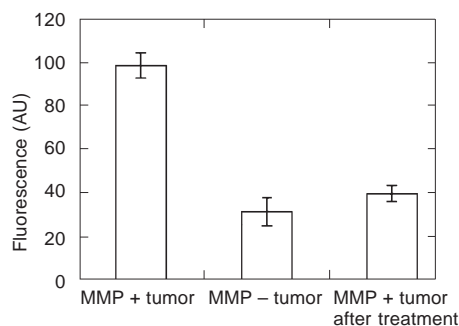


Fig. 2. Quantitative NIRF signal in tumors with or without treatment. The MMP+ and MMP-tumor represents HT1080 and BT20, respectively. A broad-spectrum MMP inhibitor AG-3340 was used in the treatment experiment.

We then applied the MMP probe to evaluate drug efficacy *in vivo*. In this experiment, HT1080 tumors were implanted into nude mice and grown to 2–3 mm in size. Animals were then treated with MMP inhibitor, AG-3340 (Agouron, 150 mg/kg bid, IP for two days), or control vehicle. Two hours after administering 2 nmole of MMP NIRF probe, animals were imaged (30 s exposition). Figure 2 shows the summarized quantitative measurements of *in vivo* inhibition. There was significantly less MMP-2 NIRF signal in treated tumors when compared to untreated tumors.

In conclusion, this newly developed technology would allow one to detect protease activity and evaluate therapeutic efficacy of protease inhibitor at the molecular level in intact animals. The approach in itself will have far-reaching applications, not only for a given animal study, but also in testing drug efficacy in future clinical trials.

### Acknowledgments

We thank Drs. A. Bogdanov, U. Mahmood, A. Moore, and S. Bredow for technical assistance. This research was supported by NIH CA088365 and a RSNA seed grant.

### References

1. Tung, C.H., Mahmood, U., Bredow, S., Weissleder, R. *Cancer Res.* **60**, 4953–4958 (2000).
2. Tung, C.H., Bredow, S., Mahmood, U., Weissleder, R. *Bioconjugate Chem.* **10**, 892–896 (1999).
3. Mahmood, U., Tung, C.H., Bogdanov, A., Weissleder, R. *Radiology* **213**, 866–870 (1999).
4. Weissleder, R., Tung, C.H., Mahmood, U., Bogdanov, A. *Nature Biotech.* **17**, 375–378 (1999).
5. Bremer, C., Tung, C.H., Weissleder, R. *Nature Med.* **7**, 743–748 (2001).
6. Bogdanov, A., Weissleder, R., Brady, T. *Adv. Drug Deliv. Rev.* **16**, 335–348 (1995).

## Passive Repression of HIV-1 Long Terminal Repeat Enhancer Controlled Viral Transcription in HIV-1 Infected Cells by Cationic DNA-Binding Fusion Proteins

S. R. K. Hoffmann<sup>1</sup>, L. Bisset<sup>2</sup>, J. Schüpbach<sup>2</sup> and B. Gutte<sup>1</sup>

<sup>1</sup>Department of Biochemistry, University of Zurich, 8057 Zurich, Switzerland

<sup>2</sup>Swiss National Center for Retroviruses, 8044 Zurich, Switzerland

### Introduction

The design of DNA-binding proteins that specifically recognize distinct sites on double-stranded DNA and control transcription of pre-specified genes is of great importance for potential therapeutic applications such as inhibition of cellular genes or entire viral genomes but still represents a challenging problem. In particular, HIV long terminal repeat (LTR) enhancer-binding proteins may suppress the transcription of the HIV provirus in infected cells by passive repression. The HIV-1 LTR is well known for its mutational stability in comparison to the translated genome. Thus, the known property of retro-viruses to escape and to develop drug resistance could be excluded.

### Results and Discussion

We report here the first successful inhibition of HIV-1 propagation in HIV-1 infected cutaneous T-lymphocytes H9 and C81 by artificial oligodeoxyribonucleotide-binding peptides. Due to the close similarity between the recognition sites of the dimeric bacteriophage 434 repressor and the viral enhancer sequences of HIV-1 LTR, the phage 434 repressor-operator system was used as a natural model for the design of a passive repressor. The interaction between the DNA-binding domain (residues 1-69) of dimeric phage 434 repressor and synthetic double-stranded DNA was very weak. However, when the recognition helix of the 434 repressor was extended at the N- and C-terminus by a tandem repeat of the positively charged segment 37-44, the resulting 42-residue polypeptide R42 showed strong and specific HIV-1 enhancer binding [1].

Table 1. Passive repression of HIV-1 LTR enhancer controlled transcription by cationic DNA-binding fusion proteins in HIV-1 infected T-lymphocytes H9 (fresh infection; 60.0 min).

No.	Sequence <sup>a</sup>	Residues			HIV-1 p24 assay [day] <sup>b,(c),(control)</sup>			
		Total	(+)	(-)	3.0 (810)	6.0 (22500)		
1	GPKKKRVGGGKTKRPRFGKTKR- PRVGQQSIEQLENGKTKRPRFGK- TKRPRYGGGGYGRKKRRQRRR	66	28	2	505 <sup>2</sup> 220 <sup>200</sup>	210 <sup>20</sup> 75 <sup>2000</sup>	18000 <sup>2</sup> 11500 <sup>200</sup>	9500 <sup>20</sup> 550 <sup>2000</sup>
2	GPKKKRVGGGKTKRPRFGKTKR- PRVGQQSIEQLENGKTKRPRFGK- TKRPRYGGGGRGYRRKRERRK	66	28	2	555 <sup>2</sup> 175 <sup>200</sup>	198 <sup>20</sup> 70 <sup>2000</sup>	17500 <sup>2</sup> 10500 <sup>200</sup>	12000 <sup>20</sup> 750 <sup>2000</sup>
3	GKTKRPRFGKTKRPRVGQQSIEQ- LENGKTKRPRFGKTKRPRY	42	16	2	600 <sup>2</sup> 590 <sup>200</sup>	630 <sup>20</sup> 275 <sup>2000</sup>	18000 <sup>2</sup> 17350 <sup>200</sup>	16000 <sup>20</sup> 18000 <sup>2000</sup>

<sup>a</sup> C-terminus: carboxamide, N-terminus: (a) modified with fluorescein-5(6)carboxyl; or (b) free; <sup>b</sup> GPKKKRVGGG, YGRKKRRQ-RRR and RGYRRKRERRK have no effect to H9 (HIV-1 IIIB) and C81 (HIV-1 IIIB); (c) p24 antigen in pg after 3.0 and 6.0 days; three independent experiments were done, concentrations are given in superscript [nM].

For the direct translocation of the synthetic peptides from the extracellular medium into the nucleus, we used a novel non-Golgi transport system based on covalently attached arginine-rich peptides derived from HIV-1 TAT. We have shown by epifluorescence microscopy that these DNA-binding fusion peptides are directly translocated from the cell suspension medium into the nucleus of the infected cell and efficiently suppress the HIV-1 propagation in high-titer HIV-1 infected H9 and C81 cell lines in the concentration range of 2.0 nM to 18.0  $\mu$ M (medium concentration). This has been shown by the p24 assay after 3 and 6 days (Table 1). These peptides have no or only minor cytotoxic effects to the cell lines up to the highest medium concentration tested, which was demonstrated in cutaneous T-lymphocytes H9 and C81 and the histocytes U937 by the 3-(4,5-dimethyl-2-thiazolyl)-2,5-diphenyl-2H-tetrazolium bromide (MTT) viability assay. These results show that these types of DNA-binding proteins specifically recognize regulatory sites on double-stranded DNA and can thus control transcription of HIV-1 by passive repression (Figure 1). In conclusion, direct delivery offers an important therapeutic application of drug-like peptides for the inhibition of cellular genes or entire viral genomes and for the targeting of intracellular diseases in general.

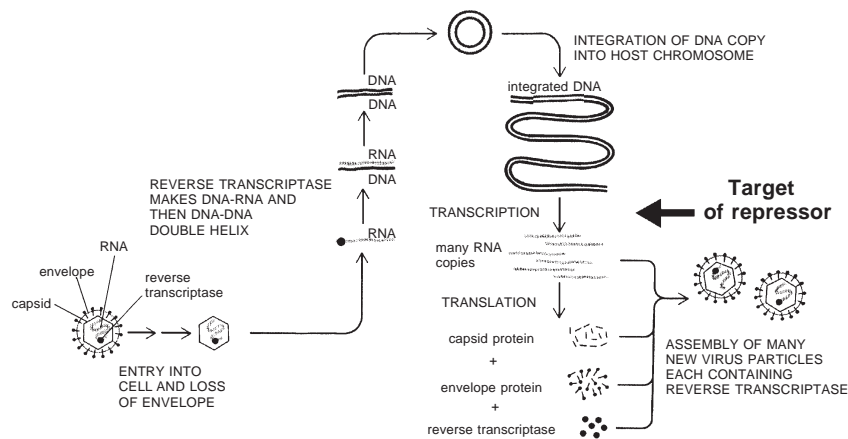


Fig. 1. HIV-1 replication cycle: The peptide repressor targets the HIV-1 long terminal repeat enhancer and suppresses the transcription of the provirus.

### Acknowledgments

This research was supported by the Deutsche Forschungsgemeinschaft (DFG) and the Schweizerische Nationalfonds.

### References

1. Hehlhans, T., Stolz, M., Klauser, S., Cui, T., Salgam P., Brenz-Verca, S., Widmann, M., Leiser, A., Städler, K., Gutte, B. *FEBS Lett.* **315**, 51–55 (1993).

## **Passive Repression of HIV-1 Long Terminal Repeat Controlled Viral Transcription by Site-Directed Combinatorial Design of Artificial DNA-Binding Proteins Screened from Combinatorial Chemical Libraries**

**Stefan R. K. Hoffmann**

*Department of Biochemistry, University of Zurich, 8057 Zurich, Switzerland*

### **Introduction**

The control of transcription of pre-specified genes by specific DNA-binding proteins is of great future importance due to therapeutic applications such as inhibition of cellular genes or entire viral genomes. In particular, HIV *long terminal repeat* (LTR) enhancer-binding proteins may suppress the transcription of the HIV provirus in infected cells. Due to the close similarity between the recognition sites of the dimeric bacteriophage 434 repressor and the viral enhancer sequences of HIV-1 LTR, the phage 434 repressor was used here as a natural model for the development of a passive repressor to HIV-1. The interaction between the DNA-binding domain (residues 1-69) of phage 434 repressor and synthetic double-stranded DNA was very weak. However, when the recognition helix (residues 28-36) of the 434 repressor was extended at the N- and C-terminus by a tandem repeat of the positively charged segment 37-44 [1], the resulting 42-residue polypeptide R42 showed strong HIV-1 enhancer binding.

### **Results and Discussion**

We report here the site-directed combinatorial design of artificial DNA-binding fusion proteins as passive repressors of the HIV-1 *long terminal repeat* enhancer controlled transcription which are screened from combinatorial chemical libraries as spotted high-density microarrays. Both "one bead-one compound" libraries and high-density compound arrays were employed. While bead-type libraries were established by conventional "split-mix" technology [2], the preparation of high-density compound arrays on porous membranes using the SPOT technology [3] were achieved by a novel precise and high-throughput plotting system based on a pen-directed, semi-automated and computer-navigated plotter device. In general array-type libraries were prepared as sets of individual compounds. Arrays of up to 2000 compounds on a microtiter format were routinely prepared with the pen-directed computer plotter device. Thus, a library of  $20^3 = 8000$  compounds is represented by 4 membranes in the microtiter format. Several positions in the recognition helix were randomized in membrane-type combinatorial chemical libraries with the overall goal to find strong binding variants to the enhancer I and II with enhanced DNA-binding selectivity. The libraries were therefore competitively screened against a gamma- $^{32}\text{P}$ -labeled 70 bp synthetic HIV-1 enhancer target DNA and non-specific calf thymus or herring sperm DNA. Fluorescence based assays were found to be not as sensitive as the radioactive assays. In these competitive assays, strong and specific binding of several peptides in high saline buffer (100 mM K-Pi (pH 7.5); 37.5 mM NaCl; 15 mM KCl; 4.0 mM  $\text{MgCl}_2$ ; 1.6% Ficoll; 0.08% Nonidet P40®) even in the presence of a 6,000- to 60,000-fold excess of competitor DNA (12 to 24 h at 25 to 37 °C) was observed. Approximately 500–600 hits were extracted from the 56,000 compounds tested on microarrays, which were further characterized by electrophoretic mobility shift assay, DNA footprinting, and *in vitro*-transcription after resynthesis by solid phase synthesis and complete purification

by HPLC and characterization by ESI-MS. These tests showed for several sequences improved properties in comparison to the original R42. As shown in Figure 1, R42LYC (Q18L, Q19Y, Q23C) showed strong binding to the enhancer DNA and repressed HIV-1 LTR enhancer controlled transcription of the OVEC *in vitro* transcription assay [4]. Several of these synthetic repressors covalently fused with the HIV-1 TAT membrane translocation sequence, and are now being tested in HIV-1 infected T-lymphocytic H9 and C81 cell lines.

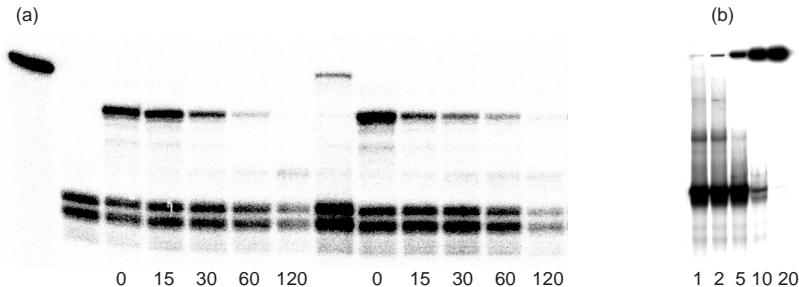


Fig. 1. Autoradiograms of (a) OVEC *in vitro* transcription assay using R42LYC and R42QQQ (original recognition helix of bacteriophage 434) and (b) band shift assay with R42LYC and 200 fmol double-stranded HIV-1 enhancer DNA KS05/06; peptide amount [pmol]; R42QQQ: GKTKRPRFGKTKRPRVGQQSIEQLENGKT KRPRFGKTKRPRY; incubation buffer as described for the array-type libraries except the addition of 4.0% Ficoll.

#### Acknowledgments

This research was supported by the German Research Foundation (DFG) by a research grant and the Hartmann-Müller Foundation for Medical Research.

#### References

1. Hehlhans, T., Stolz, M., Klauser, S., Cui, T., Salgam, P., Verca, S.B., Widmann, M., Leiser, A., Städler, K., Gutte, B. *FEBS Lett.* **315**, 51–55 (1993).
2. (a) Furka, A., et al. *Int. J. Pept. Protein Res.* **37**, 487–493 (1991). (b) Houghten, R.A., et al. *Nature* **354**, 84–86 (1991). (c) Lam, K.S., et al. *Nature* **354**, 82–84 (1991).
3. Frank, R. *Tetrahedron* **48**, 9217–9232 (1992).
4. Westin, G., Gerster, T., Müller, M.M., Schaffner, G., Schaffner, W. *Nucleic Acids Res.* **15**, 6787–6798 (1987).

## Fluorescent Biosensor for CrkII Phosphorylation by the Abl Tyrosine Kinase

Roseanne M. Hofmann<sup>1</sup>, Graham J. Cotton<sup>1</sup>, William Bornman<sup>2</sup>,  
Emmanuel Chang<sup>1</sup> and Tom W. Muir<sup>1</sup>

<sup>1</sup>Laboratory of Synthetic Protein Chemistry, Rockefeller University of New York, NY 10021 USA

<sup>2</sup>Laboratory of Bioorganic Chemistry, Sloan-Kettering Institute, New York, NY 10021 USA

### Introduction

Chronic myeloid leukemia (CML) causes the excessive proliferation of myeloid cells ADDIN ENRfu [1]. The majority of CML cases are caused by the reciprocal chromosomal translocation of the first exon of c-Abl on chromosome 9 and the breakpoint cluster region (Bcr) of chromosome 22. The c-Abl gene encodes a nonreceptor kinase that catalyzes the transfer of phosphate from ATP to tyrosine residues on protein substrates. The Bcr-Abl fusion protein produces an overactive kinase, and this deregulated tyrosine kinase activity is required for leukemic transformation.

One current strategy for the treatment of CML uses small molecular inhibitors of the Abl tyrosine kinase. The 2-phenylaminopyrimidine compound developed by Novartis called STI571 (Signal Transduction Inhibitor) competitively inhibits the binding of ATP to the Abl kinase *in vitro* and *in vivo* ADDIN ENRfu [2] and has recently been shown to be an effective treatment of CML ADDIN ENRfu [3,4]. However, cellular resistance in cell culture has been reported ADDIN ENRfu [5–7].

To identify new Abl kinase inhibitors, we developed a novel high throughput screening assay. In contrast with a more traditional radiolabeled ATP hydrolysis assay, we monitored kinase activity using a fluorescence-based assay, which provides a real-time readout on the phosphorylation state of the substrate.

### Results and Discussion

The CrkII (CT10 regulator of kinase) protein is phosphorylated on tyrosine 222 by the Abl tyrosine kinase ADDIN ENRfu [8]. Phosphorylation is thought to induce a conformational change that modulates the protein-protein interactions and thus regulates the signal transduction activities of CrkII ADDIN ENRfu [9]. Previous work in our lab described the engineering of a CrkII protein containing a rhodamine specifically incorporated at its amino terminus and a fluorescein at its carboxyl terminus ADDIN ENRfu [10]. Excitation of fluorescein in this dual labeled CrkII protein (Rh-CrkII-Fl) leads to emission of both fluorescein and rhodamine through fluorescence resonance energy transfer (FRET). We observed a modest, but detectable 3% change in FRET upon phosphorylation indicating that Rh-CrkII-Fl could biosense its phosphorylation state.

We sought to improve the dynamic range of this kinase assay and reasoned that truncation of the CrkII protein might provide a more dramatic change in FRET upon phosphorylation. We have engineered a truncated CrkII protein (amino acids 1–228) using expressed protein ligation to join synthetic peptides, one containing a rhodamine and another containing a fluorescein, to the recombinant CrkII protein at its amino and carboxyl termini, respectively. Upon phosphorylation of Rh-CrkII1-228-Fl by the Abl kinase, we see a greater than 20% change in FRET (Figure 1). As expected, this change in FRET, correlates with phosphorylation of CrkII on Y222. Inhibition of Abl kinase activity by STI571 results in a dose-dependent decrease in the change in FRET with an EC<sub>50</sub> of ~640 nM. We use the large dynamic range of this biosensor to moni-

tor Abl kinase activity in the presence of analogs of STI571 in 96-well plates. Thus, we have developed a rapid, non-radioactive screening procedure that is useful for identifying other novel Abl kinase inhibitors for the treatment of CML. The modular nature of this engineered protein makes it possible to use a similar system for developing other phosphorylation biosensors.

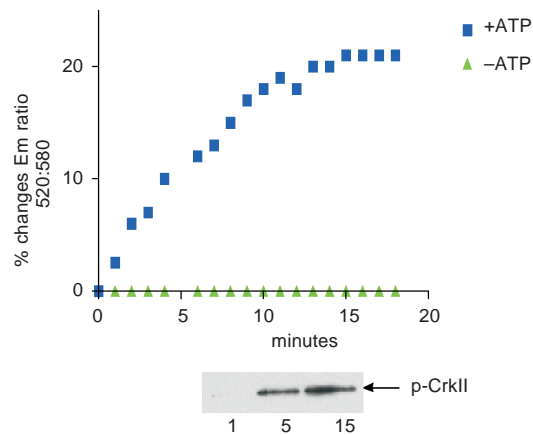


Fig. 1. Phosphorylation of Rh-CrkIII-228-Fl by full length Abl.

### Acknowledgments

We thank T. Schindler and J. Kuriyan (Rockefeller University) for recombinant c-Abl protein. Supported by the Pew Charitable Trust, the Rockefeller University Presidential Fellowship (RMH) and the Burroughs Wellcome Fund (EC).

### References

1. Mauro, M.J., Druker, B.J. *Curr. Oncol. Rep.* **3**, 223–227 (2001).
2. Buchdunger, E., et al. *J. Pharmacol. Exp. Ther.* **295**, 139–145 (2000).
3. Druker, B.J., et al. *N. Engl. J. Med.* **344**, 1031–1037 (2001).
4. Druker, B.J., et al. *N. Engl. J. Med.* **344**, 1038–1042 (2001).
5. Knight, Z.A. *Blood* **96**, 4003–4005 (2000).
6. le Coutre, P., et al. *Blood* **95**, 1758–1766 (2000).
7. Weisberg, E., Griffin, J.D. *Blood* **95**, 3498–3505 (2000).
8. Feller, S.M., Knudsen, B., Hanafusa, H. *Embo J.* **13**, 2341–2351. (1994).
9. Anafi, M., Rosen, M.K., Gish, G.D., Kay, L.E., Pawson, T. *J. Biol. Chem.* **271**, 21365–21374 (1996).
10. Cotton, G.J., Muir, T.W. *Chem. Biol.* **7**, 253–261 (2000).

## Antibodies to Distinct Protein Epitopes from a Single Polyclonal Serum

Ella A. Yurkina<sup>1</sup>, Vyacheslav I. Ofitserov<sup>1</sup>, Vladimir V. Samukov<sup>2</sup>,  
 Aydar N. Sabirov<sup>2</sup> and Georgy A. Mizenko<sup>1</sup>

<sup>1</sup>JSC Vector-Best, <sup>2</sup>SRC VB Vector, Koltsovo, Novosibirsk region, 630559, Russia

### Introduction

The enhancement of sensitivity and accuracy of immunochemical methods is commonly and effectively achieved by the use of a set of monoclonal antibodies (mAbs) directed to differing unique antigenic determinants in an antigen to be detected. However, this approach has some drawbacks, mainly due to the frequent instability of mAbs in the course of the manufacture and storage of diagnostic kits. An alternative approach developed in this work relies on using highly specific polyclonal antibodies to distinct antigenic sites of a protein. A method of preparing such monospecific antibodies is based on the affinity extraction of antibodies from a single hyperimmune serum with the use of two affinity sorbents containing two different ligands. The first pool of antibodies is isolated on a sorbent with a linked synthetic peptide, which corresponds to one of the major antigenic epitopes of the protein. The second, non-overlapping pool of antibodies is extracted from a fraction, which does not bind to the first sorbent, using a sorbent with immobilized pure whole protein as a ligand. The method has been successfully applied for preparing pools of non-overlapping antibodies to human chorionic gonadotropin (HCG).

### Results and Discussion

Antibodies from the anti-HCG serum directed against C-terminal domain of the HCG  $\beta$ -subunit sequence 109–145 can serve as a specific tool for the highly selective isolation of the hormone from biological fluids. Obviously, it is not mandatory to use the whole sequence 109–145 as a ligand for effective extraction of these antibodies from immune sera. To determine an optimal length of a peptide ligand for this purpose, we undertook chemical synthesis and assessment of peptides of varying length from this sequence (Figure 1).

133–145	CRLPGPSDTPILPQ	(Cys-p13)
110–121	CDDPRFQDSSSS	(p12)
122–145	KAPPPSLPSPSRLPGPSDTPILPQ	(p24)
109–145	TCDDPRFQDSSSKAPPPSLPSPSRLPGPSDTPILPQ	(p37)

*Fig. 1. Synthetic peptides of HCG  $\beta$ -subunit.*

Affinity sorbents containing synthetic peptides as ligands were synthesized on the basis of a custom-made preactivated composite carrier: polymer-modified macroporous silicate Silochrom C-80 bearing active residues of succinic acid N-hydroxysuccinimide ester. Attachment of peptides to the carrier was achieved through available free amino groups in a ligand molecule. Sorbents bearing whole HCG were prepared by oxidizing a glycoside portion of HCG with periodate and subsequent immobilization of the hormone onto  $\gamma$ -aminopropyl-Silochrom C-80 through aldehyde groups. Thus, formed Schiff bases were reduced with sodium borohydride. Hyperimmune goat and rabbit antisera to the whole HCG molecule were treated with

carrier-immobilized synthetic peptides. Isolated pools of peptide-specific antibodies (Abs of the 1st type) showed strong binding to the native HCG as evaluated by direct ELISA methods. Peptides p24 and p37 covalently bound to a hydrophilic surface of a silica matrix showed considerably higher efficiency than Cys-p13 in the affinity extraction of specific antibodies and gave higher yields and titers of said antibodies. Anti-peptide antibodies were examined in competitive ELISA using various antigen/competitor combinations. Surprisingly, the antibody pool isolated on the p37-sorbent did not contain antibodies specific to epitopes outside the p24 sequence. This also was confirmed by the fact that p12-sorbent failed to extract any detectable antibodies from hyperimmune sera.

A column with HCG-sorbent was used for the isolation of a fraction of anti-HCG Abs, which did not bind to the sorbents bearing peptides p24 or p37. Thus, prepared non-overlapping pool of antibodies (Abs of the 2nd type) retained high binding activity to the whole HCG, but did not compete with the peptide-specific fraction of antibodies. Pairs of monospecific polyclonal antibodies prepared by the described method were used in designing a sandwich-type immunometric assay for the sensitive qualitative and quantitative determination of HCG in biological fluids. Purified antibodies of the second type were adsorbed on a solid support (a surface of microplate wells); antibodies of the first type from the same serum were used for the conjugation with a horseradish peroxidase enzyme label. The comparative evaluation of antibody pairs prepared using various immobilized peptides showed that the sensitivity of HCG determination was higher for anti-p24 than anti-p37 Abs (5 IU/L vs 10 IU/L). No cross reactions with LH and FSH were observed (Figure 2).

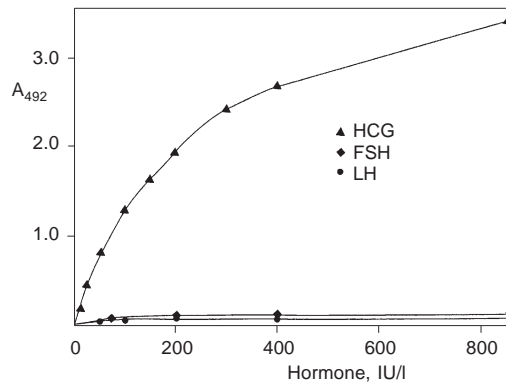


Fig. 2. Selectivity of HCG determination by the developed ELISA kit.

It was found that monospecific polyclonal antibodies were very close to monoclonal antibodies in terms of specificity and sensitivity, and exhibited superior stability being adsorbed into microplate wells or in a form of horseradish peroxidase conjugates. Sensitivity, specificity, and reproducibility of the developed kit matched with those of kits based on the use of mAbs: sensitivity 5 IU/L; specificity 100%; reproducibility (variation coefficient) <8%.

#### Acknowledgments

This work is supported by ISTC Grant # 690-99.

## Epitope Mapping of Anti-Type I Collagen Crosslinked N-Telopeptide Antibody with Synthetic Peptides

Huey-Yi Chen<sup>1</sup>, Yen-Meng Liou<sup>2</sup>, Chiu-Heng Chen<sup>2</sup>, Shing-Tzu Lin<sup>3</sup>  
 and Feng-Di T. Lung<sup>3</sup>

<sup>1</sup>*Department of Obstetrics and Gynecology, China Medical College Hospital, Taichung, Taiwan, R.O.C.*

<sup>2</sup>*The College of Life Science, National Chung-Hsing University, Taichung, R.O.C.*

<sup>3</sup>*Department of Nutrition, China Medical College, Taichung, Taiwan, R.O.C.*

### Introduction

Osteoporosis is a disease characterized by low bone mass and by architectural deterioration of bone tissue, two factors related to abnormalities of bone turnover [1,2]. This disease influences the health of menopausal females, even, to endanger them. Thus, the technique to detect the markers of bone turnover is very important for preventing osteoporosis [3,4]. Detection of urinary N-telopeptide (NTx) as an osteoporosis marker was developed by Dr. Hanson in 1992 (Figure 1). Osteomark® has high specificity and high sensitivity, but still has some limitations for clinical use [5,6]. Our specific aim is to develop a simple, economic, sensitive and specific method to detect the marker, N-telopeptide, for osteoporosis.

NH<sub>2</sub>-Glu-Tyr-Asp-Gly-Lys-Gly-Val-Gly-Leu-Gly-Pro-Gly-Pro-Met-Gly-Leu-Met-Gly-Pro-Arg-Gly-Pro-Pro-Gly-Ala-Ala-Gly-Ala-Pro-Gly-Pro-Gln-Gly-Phe-Gln-Gly-Pro-Ala-Gly-Glu-Pro-Gly-Glu-Pro-Gly-Gln-Thr-Gly-Pro-Ala-Gly-Ala-Arg-Gly-Pro-Ala-Gly-Pro-Pro-Gly-Lys-Ala-Gly-Glu-Asp-Gly-His-Pro-Gly-Lys-Pro-Gly-Arg-Pro-Gly-Glu-Arg-Gly-Val-Val-Gly-Pro-Gln-Gly-Ala-Arg-Gly-Phe-Pro-Gly-Thr-Pro-Gly-Leu-Pro-Gly-Phe-Lys-Gly-Ile-Arg-Gly-His-Asn-Gly-Leu-COOH

*Fig. 1. The sequence of N-telopeptide.*

### Results and Discussion

Ten peptide fragments of NTx domain were designed, synthesized, and purified for biological assays (Table 1).

*Table 1. Designed 10 overlapping peptide fragments of NTx.*

Peptide No.	Amino acid sequence	Mass
1	Glu-Tyr-Asp-Gly-Lys-Gly-Val-Gly-Leu-Gly-Pro-Gly-Pro-Met-Gly-Leu	1 545.0
2	Pro-Gly-Pro-Met-Gly-Leu-Met-Gly-Pro-Arg-Gly-Pro-Pro-Gly-Ala-Ala	1 462.1
3	Gly-Pro-Pro-Gly-Ala-Ala-Gly-Ala-Pro-Gly-Pro-Gln-Gly-Phe-Gln-Gly	1 365.5
4	Pro-Gln-Gly-Phe-Gln-Gly-Pro-Ala-Gly-Glu-Pro-Gly-Glu-Pro-Gly-Gln	1 551.9
5	Pro-Gly-Glu-Pro-Gly-Gln-Thr-Gly-Pro-Ala-Gly-Ala-Arg-Gly-Pro-Ala	1 419.0
6	Gly-Ala-Arg-Gly-Pro-Ala-Gly-Pro-Pro-Gly-Lys-Ala-Gly-Glu-Asp-Gly	1 393.0
7	Lys-Ala-Gly-Glu-Asp-Gly-His-Pro-Gly-Lys-Pro-Gly-Arg-Pro-Gly-Glu	1 588.1
8	Pro-Gly-Arg-Pro-Gly-Glu-Arg-Gly-Val-Val-Gly-Pro-Gln-Gly-Ala-Arg	N.A.
9	Gly-Pro-Gln-Gly-Ala-Arg-Gly-Phe-Pro-Gly-Thr-Pro-Gly-Leu-Pro-Gly	1 465.0
10	Thr-Pro-Gly-Leu-Pro-Gly-Phe-Lys-Gly-Ile-Arg-Gly-His-Asn-Gly-Leu	1 620.2

### Peptide Vaccines and Immunology

The binding affinity of each peptide for anti-NTx antibody was assayed using the competitive ELISA method (Table 2). Peptides **1**, **2**, and **3** were found to exhibit higher affinity for the NTx antibody, indicating they contain binding sites for the anti-NTx antibody.

Table 2. Detection of the affinity of peptides for the anti-NTx antibody using ELISA method.

Peptide No. (50 $\mu$ M)	<b>1</b>	<b>2</b>	<b>3</b>	<b>4</b>	<b>5</b>	<b>6</b>	<b>7</b>	<b>9</b>	<b>10</b>
nM BCE	70	165	69.4	<1	<1	<1	<1	<1	<1

The binding interaction between each potent peptide **1**, **2**, or **3** and the anti-NTx antibody was studied using the BIAcore assay (Table 3). Peptide **3** was found to exhibit higher affinity for the anti-NTx antibody.

Table 3. Detection of the affinity of peptides for the anti-NTx antibody, using BIAcore assay.

Peptide No. (1 $\mu$ M)	<b>1</b>	<b>2</b>	<b>3</b>
nM BCE	1.265	1.34	1.45

On the basis of these results, we will develop further the SPR-based technique to detect the urinary biomarker of osteoporosis.

### Acknowledgments

This research is supported in part by grants to F.D.L. from National Science Council (NSC89-2320-B039-035) and China Medical College (CMC89-NT-04) in Taiwan, R.O.C.

### References

1. Mosekilde, L. *Bone* **10**, 425–432 (1989).
2. Dargent, P. *Curr. Opin. Rheumatol.* **5**, 132–137 (1993).
3. Cann, C.E. *Radiology* **166**, 509–522 (1988).
4. Hanson, D.A., Weis, M.A., Bollen, A.M., Maslan, S.L., Singer, F.R., Eyre, D.R. J. *Bone Miner. Res.* **7**, 1251–1258 (1992).
5. Lane, J.M. *Spine* **22**, 32–37 (1997).
6. Glaser, D.L., Kaplan, F.S. *Spine* **22**, 12–16 (1997).

## The Use of a Synthetic Biotinylated Peptide Probe for the Isolation of Adenomatous Polyposis Coli (APC) Tumor Suppressor Protein Complexes

Bruno Catimel<sup>1</sup>, John D Wade<sup>2</sup>, M. Faux<sup>1</sup>, Anthony Burgess<sup>1</sup>,  
Laszlo Otvos, Jr.<sup>3</sup> and Edouard Nice<sup>1</sup>

<sup>1</sup>The Ludwig Institute for Cancer Research, Melbourne Tumour Biology Branch, P.O. Royal Melbourne Hospital, Victoria 3050, Australia

<sup>2</sup>Howard Florey Institute, University of Melbourne, Victoria 3010, Australia

<sup>3</sup>The Wistar Institute, Philadelphia, PA 19104, USA

### Introduction

A large number of colon tumours are associated with mutations in the gene coding for the production of the adenomatous polyposis coli (APC) tumour suppressor protein [1–3]. This high molecular weight protein (2843aa, ≈312 kD) of low abundance contains a coiled coil amino terminal domain that is known to be responsible for homo-dimerization [4,5]. Previous work by others [6] has led to the design of a 55-residue anti-APC peptide (anti-APCp1) that dimerizes preferentially with this domain. We have synthesized a modified form of this peptide (anti-APCp2) with a biotin moiety at its amino terminus for use in subsequent ligand binding studies and in the isolation of APC and APC complexes. The peptide was chemically characterized using RP-HPLC, CZE and Mass Spectrometry. Secondary structural analysis was performed by circular dichroism spectroscopy and Fourier transform infrared spectroscopy. The interaction between anti-APC-p2 peptide and native APC from a LIM1215 colonic carcinoma cell extract was demonstrated using immunoprecipitation and biosensor analysis.

### Results and Discussion

The 57 residue anti-APCp2 peptides (unmodified and N-terminally biotinylated) were successfully synthesized using continuous flow Fmoc-methodology. Comprehensive chemical characterization including RP-HPLC, CZE and MALDI TOF MS (biotinylated peptide: Mr calculated. MH+ 6,974.2; Mr found MH+ 6,973.4) confirmed the authenticity and high purity of the peptides. The IR spectra of both unmodified and biotinylated anti-APCp2 peptides, without any structure-stabilizing solutions added, indicated a mixture of  $\beta$ -turns and peptide structures without conformational preferences. The effects of varying solvent conditions on the conformation of anti-APCp2 peptides were studied using CD (Table 1). Significantly, a stable  $\alpha$ -helical structure

Table 1. Conformation of unmodified and biotin-labeled anti-APC peptides recorded using circular dichroism spectra in water, phosphate-buffered saline pH 7.4 (PBS), 2% aqueous octyl- $\beta$ -D-glucoside and 50% aqueous trifluoroethanol (TFE) solutions.

Solvent	Conformation	
	Unmodified peptide	Biotinylated peptide
Water	Unordered	Turns
2% Octylglucoside	Turns	Turns
PBS	Weak helix	Weak helix
50% TFE	Strong helix	Strong helix

was generated when the solvent conditions (*e.g.* in PBS pH 7.4) supported intramolecular salt-bridge formation along the helix barrel. The potential to form  $\alpha$ -helices was also indicated by a fully helical spectrum recorded in 50% aqueous TFE. The attachment of biotin to the amino terminus of the anti-APCp2 did not affect the CD spectrum recorded in 2% octyl- $\beta$ -D-glucoside, PBS or 50% TFE.

The biotinylated anti-APCp2 was immobilised onto a streptavidin sensor surface in a specific N-terminal orientation leaving all amino acids available to form a coiled structure. Injection of colonic carcinoma cell lysates (LIM1215) onto a Superose 6 size-exclusion column (Figure 1A) resulted in the isolation of a high molecular mass protein peak (greater than 600 kDa) that reacted specifically with the immobilised anti-APCp2 on the biosensor surface (Figure 1B). To further confirm the presence of APC in the eluate, the proteins contained in the active fractions identified using the biosensor were labeled with  $^{125}$ I and immunoprecipitated with an anti-APC polyclonal antibody as well as the anti-APCp2 peptide (Figure 1C). A high molecular weight band of approximately 300 kDa was immunoprecipitated using both the anti-APC polyclonal antibody and anti-APCp2.

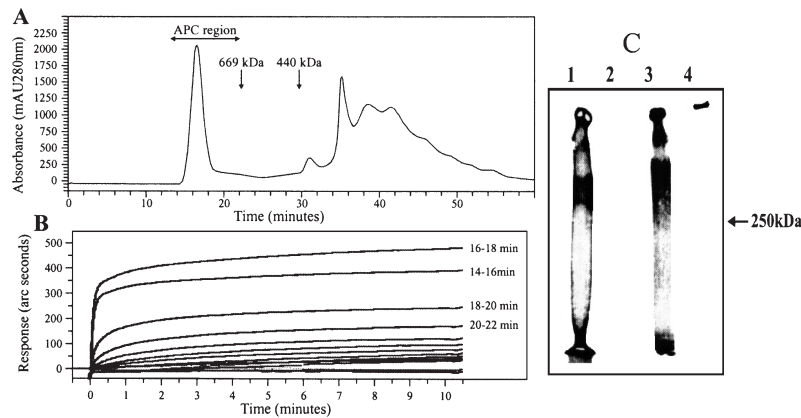


Fig. 1. A: Size exclusion chromatography (SEC) of a LIM1215 colonic carcinoma cell extract (1% Triton X-100/0.5% DOC) using Superose 6 HR10/30. B: IAsys Autoplus biosensor analysis of fractions from SEC using biotinylated anti-APCp2 peptide immobilised onto a neutravidin cuvette sensor surface. The major activity was found in the fractions eluting between 16 and 22 min. C: Immunoprecipitation of APC from  $^{125}$ I-labelled Superose 6 biosensor-positive fractions using the anti-APCp2 peptide (lane 1) or anti-APC IgG (lane 3). Controls were performed by omitting the peptide (lane 2) or the IgG (lane 4).

This study demonstrates the potential use of the anti-APC-p2 peptide in a multidimensional micropreparative chromatographic/biosensor/proteomic protocol for the purification of APC and APC complexes in various cell lines, or at different stages of tumor development.

## References

1. Polakis, P. *Biochim. Biophys. Acta* **1332**, F127–F147 (1997).
2. Kinzler, K.W., Vogelstein, B. *Cell* **87**, 159–170 (1996).
3. Fearon, et al. *Curr. Biol.* **R62–R65** (1990).
4. Joslyn, et al. *Proc. Natl. Acad. Sci. U.S.A.* **90**, 11109–11113 (1993).
5. Day, C.L., Alber, T. *J. Mol. Biol.* **301**, 147–156 (2000).
6. Sharma, V.A., et al. *Curr. Biol.* **8**, 823–830 (1998).

## Folding and Peptide Binding of TPR Motifs from SGT

Ming-Tao Pai<sup>1</sup>, Chih-Sheng Yang<sup>1</sup>, Shiou-Ru Tzeng<sup>1</sup>, Chung Wang<sup>2</sup>  
 and Jya-Wei Cheng<sup>1</sup>

<sup>1</sup>*Division of Structure Biology and Biomedical Science, Department of Life Science,  
 National Tsing Hua University, Hsinchu, Taiwan, Republic of China*

<sup>2</sup>*Institute of Molecular Biology, Academia of Sinica, Taipei, Taiwan, Republic of China*

### Introduction

In eukaryotes, many proteins have evolved repetitive motifs to perform functions specific to their unique physiological demand. Mostly, these motifs have length between 20 and 40 residues and mediate a variety of distinctive protein-protein interactions [1]. These motifs often exist as a tandem array between 3 to 25 units to form a characteristic structure. Secondary structure of many of these motifs are found to be  $\alpha$ -helices. For example, the armadillo repeat of 42 residues forms three  $\alpha$ -helices, the ankyrin repeat of 33 residues adopts a  $\beta$ -hairpin-helix-loop-helix ( $\beta 2\alpha 2$ ) fold, the HEAT motif of 37-43 residues consists two antiparallel helices, and the tetratricopeptide repeat (TPR) motif of 34 residues forms an antiparallel couple of helices. Generally, these motifs have little conservation between their sequences, however, they all adopt compact conformations in all structures studied until now.

TPR-containing proteins are involved in a diverse spectrum of cellular functions including cell cycle control, splicing and transcription, protein transport, regulatory phosphate, and protein folding. The number of TPR motifs varies between different proteins, and there is no preferential positioning along the primary sequence of the protein. Three-dimensional structures have shown that each TPR motif contains a pair of  $\alpha$ -helices of equivalent length, termed A- and B-helix, associated with a packing angle of approximately 24 degrees between the helix axes [2]. Adjacent TPR motifs are packed together in a parallel arrangement, such that sequentially adjacent  $\alpha$ -helices are antiparallel. The consequence of the uniform angular and spatial arrangement of neighbouring  $\alpha$ -helices creates a right-handed superhelical structure featuring an amphipathic channel that might accommodate the complementary region of a target protein. Here, we have used size exclusion chromatography, pulse field gradient (PFG) NMR, chemical cross-linking, and surface plasmon resonance (SPR) experiments to characterize the self-association and substrate binding properties of the TPR motifs of human small glutamine-rich TPR-containing protein (hSGT) (Figure 1) [3].

### Results and Discussion

By the results of size exclusion chromatography, chemical cross-linking, and pulse field gradient NMR, we have characterized the self-association of the TPR motifs of hSGT. The equilibrium dissociation constant for the TPR self-association was calcu-

	TPR1	TPR2	TPR3		Q-rich
TPR1	AERLKTEGNEQMKVENFEAAVHFYGKAIELNPAN				
TPR2	AVYFCNRAAAYS KLGN YAGAVQDCERAICIDPAY				
TPR3	SKAYGRMGLALSSLNKHVEAVAYYKKALELDPDN				

*Fig. 1. Domains within hSGT. hSGT contains three TPR motifs. TPR1, residue 91-124; TPR2, 125-158; TPR3, 159-192.*

lated to be 342.6  $\mu\text{M}$  by surface plasmon resonance experiments. It has shown the GPTIEEVD peptide derived from the C-terminal region of HSC70 can bind to the hSGT TPR motifs. The equilibrium dissociation constant for binding of this peptide to the hSGT TPR motifs was determined to be 20.5  $\mu\text{M}$ . PFG-NMR and chemical cross-linking experiments showed that the hSGT-TPR/peptide complex still form dimers in solution. These results indicated that there are different sites for substrate binding and self-association for the hSGT TPR motifs and the self-association is probably mediated by interactions involving the external surfaces of the superhelix. The CD spectra for the hSGT TPR motifs showed strong negative ellipticities at 208 and 222 nm and positive ellipticity below 195 nm which is consistent with the characteristic  $\alpha$ -helical structure of TPR motifs. CD experiments suggest that the hSGT TPR motifs exhibit low structural stability with a  $\Delta G$  of 3.89 kcal/mol. This weak stability is a consequence of a highly dynamic structure as measured by ANS-binding and fluorescence spectroscopy.

In conclusion, we have determined the self-association and conformational stability of the hSGT TPR motifs. We have also found that the substrate binding strength of the hSGT TPR motifs is about 17 times more than that of its self-association and there are different sites for substrate binding and self-association. The low thermodynamic stability and high flexibility may be important features for the TPR motifs to adopt different conformations and to mediate a wide range of protein–protein interactions.

#### **Acknowledgments**

We thank the National Science Council, ROC and VTY Joint Research Program for the grants.

#### **References**

1. Groves, M., Barford, D. *Curr. Opin. Struct. Biol.* **9**, 383–389 (1999).
2. Das, A.K., Cohen, P.T.W., Barford, D. *EMBO J.* **17**, 1192–1199 (1998).
3. Cziepluch, C., Kordes, E., Poirey, R., Grewenig, A., Rom-melaere, J., Jauniaux, J.C. *J. Virol.* **72**, 4149–4156 (1998).

## CCT mRNA and CREB Phosphorylation Up Regulated by Peptide ZNC(C)PR in Rat Hippocampus

Yu-cang Du<sup>1</sup>, Kan-yan Xu<sup>1</sup>, Ying Xiong<sup>1</sup>, Ming Dong<sup>1</sup> and  
Xiu-Fang Chen<sup>2</sup>

<sup>1</sup>Shanghai Institute of Biochemistry, <sup>2</sup>Shanghai Institute of Physiology, Chinese Academy of Sciences, Shanghai 200031, China

### Introduction

CTP: Phosphocholine cytidyltransferase (CCT) is a key enzyme in *in vivo* phospholipid synthesis, which catalyzes the formation of CDP-choline [1,2]. CCT may play an important role in the pathogenesis of neurodegenerative diseases like Alzheimer's disease (AD). It is also well known that long-term memory depends on the cyclic AMP-response element binding protein, CREB. CREB phosphorylation is essential for CREB's transcriptional activity. Since the peptide ZNC(C)PR and its analogs were indicated to have potent memory enhancing activity [3,4], facilitate neurite elongation and prolongate cell aging [5], the peptide up regulation of CCT mRNA and CREB phosphorylation was studied.

### Results and Discussion

After injection with ZNC(C)PR for 0, 1, 2, 4 or 8 h, an aliquot protein of rat hippocampus was separated in 10% SDS-PAGE gel and transferred onto PVDF membrane. The blotted proteins were incubated with antibody, followed by incubation with HRP-conjugated anti-rabbit IgG antibody. Immunoreactive proteins were visualized using ECL detection system. The experimental data (Figure 1), which comes from Western blot with specific anti-CREB or anti-phosphorylated CREB antibody, indicated that ZNC(C)PR rapidly induced CREB phosphorylation at Ser133 in both rat hippocampus and *in vitro* incubated hippocampus slices, but did not affect CREB gene expression. The peptide-induced effects were inhibited by its antagonist, ZDC(C)PR, G-protein inhibitor, PTX or the enzyme inhibitors of PKC and PKA, but not by NK-62, the inhibitor of CaMKII. These results indicated that the CREB phosphorylation induced by the peptide could be mediated by PKC, even though cAMP was not found in the ZNC(C)PR signaling pathway.

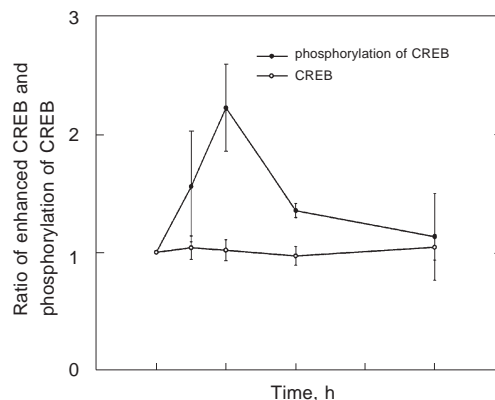


Fig. 1. ZNC(C)PR stimulates CREB phosphorylation in rat hippocampus.

By using DD-PCR and 5' rapid amplification of cDNA ends approaches, one full-length cDNA encoding rat CCT- $\beta$  was obtained. It consists of 1955 bp, which contained an open reading frame encoding 369 amino acid-proteins. It is 98% identical in amino acid sequence to human CCT $\beta$ 2 and 65% identical to rat CCT $\alpha$  isoform protein. The nucleotide sequence data reported herein are available in the DDBJ, EMBL and GeneBank nucleotide sequence database with the accession number AF190256.

Northern blot analysis demonstrated that CCT mRNA was up regulated by ZNC(C)PR in both infant and mature rat hippocampi (Figure 2). The maximal effect appeared in 6–12 h following administration. The study of tissue distribution with reverse transcription PCR showed that the gene was abundant in rat brain. Since CCT catalyzes the formation of cytidine diphosphate choline, which was reported to have a beneficial therapeutic effect on AD, so this peptide may be a potential candidate for treating AD by up regulating CCT mRNA level. Recently we found that the peptide up regulation of CCT mRNA was achieved by stabilizing CCT mRNA but not by facilitating CCT gene expression.

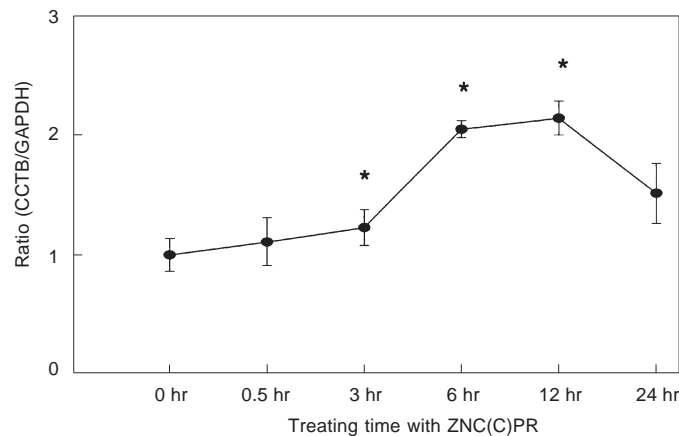


Fig. 2. ZNC(C)PR up regulates CCT mRNA level in rat hippocampus.

Based on the above experimental results, we now know that as a potent memory-enhancing peptide, ZNC(C)PR not only induces a series of gene expression (CaM, FOS, NGF, BDNF, CNDP *etc.*) [6], but also up regulates the level of CCT by increasing its mRNA stability.

#### Acknowledgments

This work was supported by the National Program of Basic Research (G1999054000) sponsored by the Ministry of Science and Technology.

#### References

1. Du, Y.C., Yan, Q.W., Qiao, L.Y. *Prog. Brain Res.* **119**, 163–175 (1998).
2. Du, Y.C., Guo, N.N., Chen, Z.F. *Acta. Physiol. Sin.* **46**, 435–440 (1994).
3. Zhou, A.W., Li, W.X., Guo, J., Du, Y.C. *Peptides* **18**, 1179–1187 (1997).
4. Baburina, I., Jackowski, S. *J. Biol. Chem.* **273**, 2169–2173 (1998).
5. Andrisani, O.M. *Crit. Rev. Eukaryotic Gene Express.* **9**, 19–32 (1999).
6. Gu B.X., Du Y.C. *Acta Biochem. Biophys. Sin.* **23**, 537–542(1991).

## **A Combination of HER-2 Peptide Epitope Vaccines Mediate Superior Biological Effects**

**Pravin T.P. Kaumaya<sup>1-4</sup>, John Pyles<sup>2</sup> and Naveen Dakappagari<sup>4</sup>**

<sup>1</sup>*Department of Obstetrics and Gynecology*

<sup>2</sup>*Department of Molecular and Cellular Biochemistry*

<sup>3</sup>*Department of Microbiology*

<sup>4</sup>*Arthur G. James Comprehensive Cancer Center, The Ohio State University,  
Columbus, OH 43210, USA*

### **Introduction**

Human Epidermal Growth Factor Receptor, HER-2 is a tumor-associated antigen overexpressed in many human malignancies. Monoclonal antibodies targeting HER-2 were shown to inhibit tumor growth both in animal models and human clinical trials. In addition, combinations of HER-2 monoclonal antibodies were shown to inhibit tumor growth more efficiently than individual antibodies alone [2,4]. Active specific immunotherapy offers the possibility for generating sustained immune responses and is potentially more beneficial than passive therapy for both primary and secondary cancer prevention. Twelve B-cell epitopes were identified in the extracellular domain of HER-2 by computer-aided analyses of protein antigenicity. Four chimeric peptide vaccines incorporating the HER-2 B-cell epitopes and a “promiscuous” T-helper cell epitope from measles virus induced high levels of native protein reactive antibodies. Antibodies to one B-cell epitope (628-647) selectively inhibited the growth of HER-2 overexpressing tumor cells and prevented the spontaneous development of HER-2/neu-overexpressing mammary tumors in 83% of transgenic mice [1]. These studies led to an NCI-approved phase 1b human clinical trial. The ongoing clinical trial evaluated the clinical and immunologic effects of a novel chimeric peptide vaccine (MVF-HER2 (628-647)-CRL 1005 vaccine) that targets the human HER-2 oncoprotein and that incorporates a non-human T-helper epitope. The first treatment cohort, consisting of five patients has completed immunization. Levels of serum antibody to the immunogen have been analyzed for patients in the first cohort. Three of the five patients developed significant antibody titers. The two patients who did not had rapidly progressive cancer. The patient antibodies could selectively kill HER-2 overexpressing human breast cancer cells.

In terms of vaccine strategies for treatment of cancer it has become clear that the stronger the immune response and broader its direction, higher are the chances of controlling the tumor. One approach to achieve this, would be to develop a combination or a multiepitope vaccine construct. Encouraged by these results, we evaluated four more new B-cell epitopes in an attempt to develop a combination/multivalent vaccine. Our studies to date have led to the identification of two additional epitopes (316-339 & 485-503), and antibodies elicited to these epitopes selectively inhibited growth of HER-2-positive human breast cancer cells. We have examined the immunogenicity and anti-tumor activity of three epitopes (316, 485 & 628) either separately or in combination with each other.

### **Results and Discussion**

High-titered antibodies were elicited in rabbits by both the individual and combination vaccines thereby demonstrating that it is feasible to induce an effective immune response with several immunogenic constructs in the same animal. Outbred mice immu-

nized with single and combination vaccines also mounted an effective immune response, thus confirming that individual animals can respond to several immunogens simultaneously. The antibodies elicited by the combination vaccines bound the tumor cells better and inhibited tumor cell growth very efficiently as compared to individual vaccine constructs (Table 1). In addition, only combination vaccine induced antibodies that caused significant levels of receptor down-modulation, a property intimately associated with reversal of tumor phenotype [3]. We also investigated if the tumor cell bound antibodies can invoke the release of anti-tumor cytokine, interferon- $\gamma$  (IFN- $\gamma$ ) following culture with human peripheral blood mononuclear cells (PBMC). Combination vaccine specific antibodies consistently invoked higher levels of IFN- $\gamma$  release compared to the single epitope vaccines (Table 1). The long range goal of our research is to develop novel and innovative approaches to antigen specific vaccination targeting the HER-2 extracellular domains and to elucidate the underlining mechanisms of anti-tumor effects elicited by peptide vaccines against a self protein and to suggest an immunization strategy that might be effective in human cancer vaccines. These studies demonstrate the potential of multi-epitope peptide vaccine for human cancer therapy.

*Table 1. A comparison of biological effects mediated by antibodies to single and combination chimeric HER-2 B-cell epitope peptide vaccines.*

Biological effects	316	485	628	316 + 485	485 + 628	628 + 316
Antibody response	+++ <sup>a</sup>	+	+++	++&+ <sup>b</sup>	+&+++	+&+++
Tumor cell binding	++	++	++	+++	+	+++
Growth inhibition	+	+++	++	+	+++	++
Receptor down-modulation	–	–	+	–	++	+++
IFN- $\gamma$ release	++	++	+	++	+++	+++

<sup>a</sup> +++ = *strong*, ++ = *intermediate*, + = *weak*; <sup>b</sup> antibody levels to the first & second epitopes in the combination vaccine induced serum were assessed separately.

### Acknowledgments

This work was supported in part by grants from National Cancer Institute (# CA 84356) to P. T. P. K. and Susan G. Komen breast cancer foundation (# Diss 2000 603) to N. D.

### References

1. Dakappagari, N.K., Douglas, D.B., Triozzi, P.L., Stevens, V.C., Kaumaya, P.T. *Cancer Res.* **60**, 3782–3789 (2000).
2. Drebin, J.A., Link, V.C., Greene, M.I. *Oncogene* **2**, 273–277 (1988).
3. Drebin, J.A., Link, V.C., Stern, D.F., Weinberg, R.A. Greene, M.I. *Cell* **41**, 697–706 (1985).
4. Kasprzyk, P.G., Song, S.U., Di Fiore, P.P., King, C.R. *Cancer Res.* **52**, 2771–2776 (1992).

## Multivalent Vaccine Studies for HTLV-1 Associated Diseases

Roshni Sundaram<sup>3,5</sup> and Pravin T. P. Kaumaya<sup>1,2,3,4,5</sup>

<sup>1</sup>College of Medicine; <sup>2</sup>The Arthur G. James Comprehensive Cancer Center; <sup>3</sup>Department of Obstetrics and Gynecology; <sup>4</sup>Molecular and Cellular Biochemistry and <sup>5</sup>Department of Microbiology, The Ohio State University, Columbus, OH, 43210 USA

### Introduction

Human T-cell Lymphotropic Virus Type-1 is the causative agent of Adult T-cell Leukemia (ATL) and HTLV-1 associated Myelopathy or Tropical Spastic Paraparesis (HAM/TSP). In addition, HTLV-1 has been implicated in a variety of other inflammatory disorders. Natural immune responses to the virus, mainly against the envelope protein have been detected in infected individuals [1]. HTLV-1 also displays very low genomic and antigenic variation making it an attractive candidate for vaccine studies [2].

This report describes the development of a multi-B-cell epitope strategy that targets biologically relevant regions of the envelope glycoproteins of HTLV-1. The rationale for this approach is that neutralizing antibodies elicited against multiple epitopes may be more effective in a wide population of individuals as compared to single epitope vaccinations.

Two B-cell epitopes were predicted, the first from the surface (gp46 aa 136-160) and the second from the transmembrane region (gp21 aa 392-415) of the envelope protein using various correlates of protein antigenicity. The algorithms used in these analyses select solvent exposed regions of the protein, which would most likely be involved in antibody binding [3]. These epitopes were synthesized colinearly with a promiscuous T-helper epitope from tetanus toxoid (947-967) and evaluated for their immunogenicity in rabbits. We also cross-immunized rabbits with a combination of both these epitopes and a third epitope (aa 175-218) that has been previously described to elicit high-titered antibodies that cross react with the native envelope protein [4]. Peptide antibodies against single immunogens and cross immunogens were tested for their functional properties *in vitro* in tissue culture.

### Results and Discussion

High titered antibodies were raised in rabbits immunized with both gp46 (136-160) and gp21 (392-415) HTLV-1 envelope predicted B-cell epitope constructs. Rabbits immunized with gp21 (392-415) were also cross immunized with gp46 (136-160) and then gp46 (175-218). High titered responses to the cross immunogens were obtained while the titers for the primary immunogen, gp21 (392-415) remained unaffected. These results indicated that it is possible to raise antibodies against multiple strong B-cell epitopes and thus provide the basis for a multivalent vaccine construct incorporating multiple B-cell epitopes. Peptide antibodies to gp21 (392-415) and gp46 (175-218) either in single or in combination, were able to recognize native envelope protein on the surface of HTLV-1 infected cells namely MT-2 cells and ACH cells as determined by live cell immunofluorescence studies. Antibodies against gp46 (136-160) however failed to bind native protein on both cell lines. The antibodies from cross immunization with multiple epitopes were also found to be neutralizing in their ability to prevent the formation of virus induced syncytia in a rat epithelial cell line. Again, antibodies to gp46 (136-160) did not show any syncytia inhibition. This was as expected because these antibodies failed to bind the native envelope protein, a

necessary step to mediate any biological effect. These results are summarized in Table 1 below.

*Table 1. Summary of immune responses and functional properties of antibodies raised against B-cell epitope chimeric constructs. Antibody titers were determined using sera from rabbits immunized with indicated constructs. Native protein reactivity was determined by live cell immunofluorescence using two HTLV-1 infected cells, MT-2 and ACH. (+) indicates reactivity +++++ > +++++ > ++++ > +++ > ++ > +.*

	Immunogen		Cross immunogen	
	gp21 (392-415)	gp46 (136-160)	gp21 (392-415) + gp46(136-160)	gp21 (392-415) + gp46 (136-160) + gp46 (175-218)
Antibody titers in rabbits	+++++	+++++	++++,+++	++++,++++,+++
Reactivity with native protein	+++	—	++	++++
Syncytia inhibition MT-2/ACH	+++ / +++	—	+/+	+++ / +++

### Acknowledgments

This work was supported by an NIH grant AI 40302 to P. T. P. K. We would also like to thank Dr. Michael D. Lairmore for kindly providing us with cell lines and assistance with the syncytia inhibition assays.

### References

1. Bangham, C.R. *J. Clin. Pathol.* **53**, 581–586 (2000).
2. Agadjanyan, M.G., Wang, B., Nyland, S.B., Weiner, D.B., Ugen, K.E. *Curr. Top. Microbiol. Immunol.* **226**, 175–192 (1998).
3. Kaumaya, P.T.P., Kobs-Conrad, S., DiGeorge, A.M., Stevens, V. *Peptides: Des. Synth. Biol.* **9**, 133–164 (1994).
4. Frangione-Beebe, M., Albrecht, B., Dakappagari, N., Rose, R.T., Brooks, C.L., Schwendeman, S.P., Lairmore, M.D., Kaumaya, P.T. *Vaccine* **19**, 1068–1081 (2000).

## **Evaluation of HTLV-1 Cytotoxic T-Cell Epitopes in HLA-A2.1 Transgenic Mice**

**Roshni Sundaram<sup>3,7</sup>, Christopher M. Walker<sup>6,8</sup>  
and Pravin T. P. Kaumaya<sup>1,2,3,4,5,7</sup>**

<sup>1</sup>College of Medicine; <sup>2</sup>The Arthur G James Comprehensive Cancer Center; <sup>3</sup>Department of Obstetrics and Gynecology; <sup>4</sup>Molecular and Cellular Biochemistry; <sup>5</sup>Center for Retrovirus Research; <sup>6</sup>Department of Molecular Virology, Immunology and Medical Genetics; <sup>7</sup>Department of Microbiology and <sup>8</sup>Department of Pediatrics, The Ohio State University, Columbus, OH 43210, USA

### **Introduction**

Human T-cell Lymphotropic Virus Type-1 (HTLV-1), the first human retrovirus to be characterized, is the causative agent of HTLV-1 Associated Myelopathy or Tropical Spastic Paraparesis (HAM/TSP). This is a neurologic disease characterized by inflammatory infiltrates of the central nervous system. HTLV-1 is also the etiological agent of an aggressive T-cell malignancy called Adult T-cell Leukemia (ATL) characterized by rapid onset and resistance to chemotherapy. Approximately 10–20 million people worldwide are infected with the virus and 4–5% of these individuals develop one of the diseases [1]. Several studies have outlined the importance of cytotoxic responses in the clearance of viral infections and tumor irradiation. In HTLV-1 infected individuals, a large majority of the natural cellular responses has been directed against a single immunodominant epitope from the tax protein namely Tax 11-19 [2].

The focus of our studies is to identify and test other predicted HLA-A2.1 restricted cytotoxic T-cell epitopes from the tax and envelope proteins. We have predicted several HLA-A2.1 restricted cytotoxic T-cell epitopes based on HLA peptide binding predictions [3]. These epitopes were then evaluated for their ability to stimulate HAM/TSP positive patient peripheral blood mononuclear cells to secrete IFN- $\gamma$ . We then tested two novel delivery systems of optimum length peptide CTL epitopes. In the first approach, we used the Tax 11-19 (designated T2) epitope along with two other high ranking epitopes (designated T3 and T4) from the tax protein based on the *in vitro* stimulation results and synthesized them collinearly with a dibasic Arg-Arg sequences in tandem (Tritax). In the second approach, we synthesized the protein transduction domain of the HIV Tat protein collinearly with the tax 11-19 epitope (Tatax). The immunogenicity of these novel CTL peptide constructs were evaluated in an HLA-A2.1 transgenic H-2D<sup>b</sup>,  $\beta$ 2m double knockout mice [4] using ELISPOT for IFN- $\gamma$  secretion and Cr-51 release assay for cytotoxicity.

### **Results and Discussion**

Groups of 3 HLA-A2.1 transgenic H-2D<sup>b</sup>,  $\beta$ 2m double knockout mice were immunized with the Tritax or Tatax CTL epitope constructs each mixed with a promiscuous T-helper epitope from tetanus toxoid protein (947-967). Spleens from immunized mice were used to assay for peptide specific cytolytic activity by chromium release assay and IFN- $\gamma$  production by ELISPOT assay. The Tritax immunogen elicited high cytolytic activity to each individual epitope namely the Tax 11-19, Tax 178-186 (T3) and Tax 233-241 (T4). This CTL activity correlated with the ability of the splenocytes from the same immunized mice to secrete IFN- $\gamma$  when stimulated with each individual epitope of the Tritax immunogen. These results suggest that the Tritax immunogen was being processed *in vivo* to generate the three individual epitopes and hence this

## Peptide Vaccines and Immunology

approach may be applicable to deliver multiple strong CTL epitopes simultaneously as part of a single construct. We propose to validate our results further with *in vitro* proteasome digestion studies. However, the Tatax immunogen failed to induce any cytolytic activity or cytokine secretion in HLA-A2.1 transgenic H-2D<sup>b</sup>,  $\beta$ 2m double knockout mice. We speculate that this may be due the tat protein transduction domain localizing to the nucleus instead of the cytosol where antigen processing occurs. The above results are summarized in the Table 1 below.

*Table 1. Summary of cytolytic responses and cytokine secretion of splenocytes isolated from HLA-A2.1 transgenic H-2D<sup>b</sup>,  $\beta$ 2m double knockout mice. Cytolytic activity was measured in a standard Cr-51 release assay using syngenic target cells transfected with the HLA-A2.1 transgene and pulsed with the relevant peptide as indicated, and pooled splenocytes from immunized mice as effector cells. The same pool of splenocytes were used for the IFN- $\gamma$  secretion assay by ELISPOT.*

Immunogen	Cytolytic activity	Cytokine (IFN- $\gamma$ ) secretion
Tritax		
T2	+++	++++
T3	++++	+++
T4	++	++
Tatax		
T2	—	—

## Acknowledgments

This work was supported by an NIH grant A1 40302 to P. T. P. K.

## References

1. Bangham, C.R. *J. Clin. Pathol.* **53**, 581–586 (2000).
2. Kannagi, M., Shida, H., Igarashi, H., Kuruma, K., Murai, H., Aono, Y., Maruyama, I., Osame, M., Hattori, T., Inoko, H., et al. *J. Virol.* **66**, 2928–2933 (1992).
3. Parker, K.C., Bednarek, M.A., Coligan, J.E. *J. Immunol.* **152**, 163–175 (1994).
4. Pascolo, S., Bervas, N., Ure, J.M., Smith, A.G., Lemonnier, F.A., Perarnau, B. *J. Exp. Med.* **185**, 2043–2051 (1997).

## **New Branched Polypeptide Based Epitope-Conjugates: Synthesis and Immunorecognition**

**Ferenc Hudecz<sup>1</sup>, Gábor Mezö<sup>1</sup>, Nikolett Mihala<sup>1</sup>, Balázs Dalmadi<sup>2</sup>,  
Szilvia Bösze<sup>1</sup>, David Andreu<sup>3</sup>, Sytske Welling-Wester<sup>4</sup>,  
Eva Rajnavölgyi<sup>2</sup> and Gjalt Welling<sup>4</sup>**

<sup>1</sup>*Research Group of Peptide Chemistry, Hungarian Academy of Sciences, Budapest 112,  
POB 32, H-1518 Hungary*

<sup>2</sup>*Department of Organic Chemistry, University of Barcelona, Barcelona, Spain*

<sup>3</sup>*Department of Immunology, Eötvös L. University, Göd and University of Barcelona,  
Barcelona, Spain*

<sup>4</sup>*Department of Medicinal Microbiology, University of Groningen, Groningen, The Netherlands*

### **Introduction**

Synthetic peptides representing epitopes of parent protein are used not only for the understanding of the antigen structure but also for the construction of subunit vaccine against microbial infection or malignant diseases. One can also utilise peptide based synthetic antigens with rational design for the preparation of specific, sensitive, simple and reliable immunodiagnostics.

B- or T-cell epitopes in immunodominant regions of proteins are usually identified by the combination of different strategies. It has been demonstrated that immuno-reactivity of such epitopes could be improved not only by alteration of the epitope core responsible for specificity, but also by modification the surrounding flanking region [1,2]. Further strategies include the polymerisation of peptides containing the functional epitope and the conjugation of such epitope peptides to carriers [3,4]. Two examples will demonstrate the application of the branched chain polymeric polypeptide based approach developed in our laboratory for construction of artificial antigens. These include the conjugation of linear B-cell epitope(s) from *Herpes simplex virus* glycoprotein D and of T-cell epitope(s) from proteins of *M. tuberculosis* with biodegradable branched polypeptides possessing poly[L-lysine] backbone. The synthesis and structural/functional characterisation of conjugates containing single or two different peptide epitopes in multiple copies are described.

### **Results and Discussion**

Branched chain polymeric polypeptides with positive charge like poly[Lys(X<sub>1</sub>-DL-Ala<sub>m</sub>)], where X = Ser (SAK), Orn (OAK) or with negative charge poly[Lys(X<sub>1</sub>-DL-Ala<sub>m</sub>)], where X = AcGlu (AcEAK), SucGlu (SucEAK) or with amphoteric character poly[Lys(X<sub>1</sub>-DL-Ala<sub>m</sub>)], where X = Glu (EAK), were prepared [5].

Antibody epitope regions from glycoprotein D of *Herpes simplex virus* have been selected for detailed investigation [6]. Peptides corresponding to the 1-23 or to the 273-284 regions were synthesised and attached to branched chain polypeptides. Using random coupling of peptides with amide bond to poly[Lys(DL-Ala<sub>m</sub>)] (AK) we have demonstrated that 276-284 part of the 273-284 region could be responsible for the protection against HSV infection. Peptide representing regions 1-23 or 276-284 attached to AK could induce efficient protection in mice. Using site-directed coupling of peptides from 273-284 region with amide bond to AK, we have demonstrated that the attachment site (Glu vs Asp) is highly important in antibody recognition of epitope-AK conjugates.

Branched chain polymeric polypeptide conjugates with one epitope peptide or two co-linearly synthesised epitopes (9-22 and 276-284) were produced using site-specific attachment and disulfide bond. Two strategies have been compared and the Cys(Npys) based scheme proved to be favourable [7].

T-cell epitopes from 16 kDa and 38 kDa proteins of *Mycobacterium tuberculosis* were selected for preparation of branched polypeptide conjugates with single or dual specificity. Using amphoteric (EAK) and polyanionic (AcEAK or SucEAK) branched polypeptides we have prepared conjugates containing amide bonds and uniformly oriented synthetic epitope peptides. It has been shown that the composition and charge properties of the carrier polypeptide influenced highly the 38G epitope specific T-cell responses [8]. Using amphoteric polypeptide (EAK) we have prepared conjugates containing two different epitopes one is from 16 kDa protein (peptide 1) and a second one from 38 kDa protein (peptide 2). Peptide 1 was attached by disulfide bond, while peptide 2 was linked by amide bond to the same carrier [9]. It has been documented in an assay with T-cell epitope specific hybridomas that the conjugate was able to induce both epitope 1 and epitope 2 specific immune responses.

#### **Acknowledgments**

These studies were supported by grants from WHO (T9/181/133), the Hungarian Research Fund (OTKA No. T-030838), from the Hungarian Ministry of Education (FKFP 0101/1997), the Hungarian-Spanish Intergovernmental Program (E-4/2001) and COST Chemistry A13.

#### **References**

1. Wilkinson, K.A., Vordermeier, M.H., Kajtár, J., Jurcevic, S., Wilkinson, R., Iványi, J., Hudecz, F. *Mol. Immunol.* **34**, 1237–1246 (1997).
2. Uray, K., Kajtár, J., Vass, E., Price, M.R., Hollósi, M., Hudecz, F. *Arch. Biochem. Biophys.* **378**, 25–32 (2000).
3. Hudecz, F., Tóth, G.K., In Rajnavölgyi, É. (Ed.) *Synthetic Peptides in the Search for B- and T-Cell Epitopes*, R.G. Landes, Austin, 1994, pp. 97–119.
4. Hudecz, F. *Biomed. Pept. Proteins Nucl. Acids* **1**, 213–220 (1995).
5. Hudecz, F., Nagy, I.B., Kóczán, Gy., Alsina, M.A., Reig, F., In Chiellini, E., Sunamoto, J., Migliaresi, C., Ottenbrite, R.M., Cohn, D. (Eds.) *Biomedical Polymers and Polymer Therapeutics*, Kluwer Academic/Plenum Publishers, New York, 2001, pp. 103–120.
6. Mezö, G., Majer, Zs., Valero, M-L., Andreu, D., Hudecz, F. *J. Peptide Sci.* **5**, 272–282 (1999).
7. Mezö, G., Mihala, N., Andreu, D., Hudecz, F. *Bioconjugate Chem.* **11**, 484–491 (2000).
8. Wilkinson, K.A., Hudecz, F., Vordermeier, H.M., Ivanyi, J., Wilkinson R.J. *Eur. J. Immunol.* **29**, 2788–2796 (1999).
9. Wilkinson, K.A., Vordermeier, M.H., Wilkinson, R., Iványi, J., Hudecz, F. *Bioconjugate Chem.* **9**, 539–547 (1998).

## **Evaluation of Synergistic Interaction Between Cytokines and Peptide Epitope Vaccines in Protection Against HER-2 Expressing Lung Metastases**

**Naveen Dakappagari<sup>3</sup>, Robin Parihar<sup>4</sup>, John Pyles<sup>3</sup>,  
William E. Carson<sup>4,5,6</sup> and Pravin T. P. Kaumaya<sup>1,2,3,6</sup>**

<sup>1</sup>*Department of Obstetrics and Gynecology*

<sup>2</sup>*Department of Molecular and Cellular Biochemistry*

<sup>3</sup>*Department of Microbiology*

<sup>4</sup>*Department of Molecular Virology, Immunology, Genetics*

<sup>5</sup>*Department of Surgery*

<sup>6</sup>*Arthur G. James Comprehensive Cancer Center, The Ohio State University, Columbus,  
OH 43210, USA*

### **Introduction**

HER-2, a member of the epidermal growth factor receptor family is overexpressed in 25–30% of breast, ovarian and colon cancers. HER-2 overexpression is associated with poor prognosis and resistance to chemo- and hormonal therapies. We recently reported that chimeric peptide vaccines incorporating a B-cell epitope of HER-2 and “promiscuous” T-helper cell epitope from measles virus are capable of eliciting high levels of native receptor reactive antibodies. In addition, these chimeric peptide vaccines were capable of preventing the spontaneous formation of mammary tumors in HER-2/neu transgenic mice [2]. Ongoing phase 1b clinical trials in cancer patients indicate that the chimeric peptide vaccines can induce antibodies capable of killing human cancer cells.

Our current efforts are focused on improving both the quality of the immune response and the anti-tumor activity of the peptide vaccines by supplementing them with appropriate cytokines. Cytokines such as interleukin-12 and interferon- $\alpha$  are known to enhance anti-tumor activity of cancer vaccines either by synergising with antibodies to enhance tumor cell lysis or by eliciting Th1 cytokines such as interferon- $\gamma$  that is known to upregulate the expression of MHC class I and II antigens and inhibit tumor growth by activating the release of reactive super-oxide ions from immune cells. IFN $\gamma$  is also a potent inducer of Fc receptor expression that consequently leads to enhancement of phagocytosis and ADCC of tumor cells. IL-12 and IFN-I are currently being evaluated as single agents for human cancer therapy and have been previously shown to enhance the protective efficacies of tumor vaccines by both specific and non-specific effects on the immune system including the selective activation of IgG2a [1,3]. To further enhance the antibody levels and consequently antitumor activity of these peptide epitope vaccines, we tested two approaches in a syngeneic murine metastases model of HER-2. Three B-cell epitopes (316, 485 & 628) capable of eliciting tumor inhibitory antibodies were selected for these studies. Balb/c mice were immunized with these three peptide epitope vaccines alone or a combination of 316 & 628 both of which induced higher levels of antibodies than epitope 485. These peptide vaccinations were supplemented further with or without cytokines, interleukin-12 (IL-12) or interferon  $\alpha/\beta$  (IFN-I).

### **Results and Discussion**

IL-12 enhanced the overall antibody titers to all the peptide vaccine with the exception of one vaccine, 628 when given alone but not in combination with vaccine, 316. The

increase in antibody titers was almost double as compared to peptide vaccines administered without IL-12. The increase in the antibody levels following IL-12 supplementation correlated well with selective enhancement of IgG2a, the relative levels of which were significantly higher compared to those in serum elicited by peptide vaccines alone. In contrast, IFN-I altered neither the immunogenicity nor the immunoglobulin class switching significantly except for one vaccine, 485 to which the antibody titers were elevated by five fold. In correlation with the antibody titers, the number of pulmonary metastases produced following challenge with syngeneic murine tumor cells expressing human HER-2 was significantly reduced in mice immunized with vaccine 316 or a combination of 316 & 628 plus IL-12. The greatest level of protection was conferred by a combination of peptide vaccines and IL-12. Reduction in lung metastases seems to occur indirectly by a mechanism involving Fc receptor activation *e.g.*, tumor cell lysis by ADCC and tumor growth inhibition *via* IFN- $\gamma$  release. Our upcoming phase 1b clinical trials with the combination vaccine (316 & 628) will further validate the utility of the chimeric peptide vaccine for human cancer therapy.

#### **Acknowledgments**

This work was supported in part by grants from National Cancer Institute (# CA 84356) to P. T. P. K. and Susan G. Komen breast cancer foundation (# Diss 2000 603) to N. D.

#### **References**

1. Adris, S., Chuluyan, E., Bravo, A., Berenstein, M., Klein, S., Jasnis, M., Carbone, C., Chernajovsky, Y., Podhajcer, O.L. *Cancer Res.* **60**, 6696–6703 (2000).
2. Dakappagari, N.K., Douglas, D.B., Triozzi, P.L., Stevens, V.C., Kaumaya, P.T. *Cancer Res.* **60**, 3782–3789 (2000).
3. Gan, Y.H., Zhang, Y., Khoo, H.E., Esuvaranathan, K. *Eur. J. Cancer* **35**, 1123–1129 (1999).

## **Novel Classes of Neutrophil-Activating Peptides: Isolation and Their Physiological Significance**

**Hidehito Mukai<sup>1,2</sup>, Yoshinori Hokari<sup>2</sup>, Tetsuo Seki<sup>2</sup>, Hiroko Nakano<sup>2</sup>,  
Toshifumi Takao<sup>3</sup>, Yasutsugu Shimonishi<sup>3</sup>, Yoshisuke Nishi<sup>1</sup> and Eisuke  
Munekata<sup>2</sup>**

<sup>1</sup>*Laboratory of Life Science & Biomolecular Engineering, JT, Yokohama, Kanagawa 227-8512,  
Japan*

<sup>2</sup>*Institute of Applied Biochemistry, University of Tsukuba, Tsukuba, Ibaraki 305-8572, Japan*

<sup>3</sup>*Institute for Protein Research, Osaka University, Suita, Osaka 565-0871, Japan*

### **Introduction**

Neutrophils are one of the leukocytes that involve destruction and removal of infected organisms and toxic debris [1]. Some chemokines and complement factors such as interleukin 8 and C5a are known to induce infiltration and activation of neutrophils [2]. Transmigration of neutrophils, however, often can be seen immediately after tissue injury occurs, and little is known how such migration and activation of neutrophils occur in tissue injury. Our working hypothesis is that necrotic or apoptotic cells in tissue injury sites directly produce substances that cause transmigration and activation of neutrophils to respond immediately in acute inflammation. In this study, we purified and identified two novel classes of neutrophil-activating peptides from porcine hearts and investigated the physiological significance of these peptides.

### **Results and Discussion**

Our preliminary results suggested that there were a lot of substances that activate neutrophils in the extract of porcine hearts, and most of those were peptides. Therefore, we tried to purify them using cation exchange chromatography and gel chromatography. For assessing the activity of neutrophil activation, we measured the activity of  $\beta$ -hexosaminidase release from HL-60 cells differentiated into neutrophil-like cells [3]. Most of the neutrophil-activating substances were distributed in the fractions whose molecular masses were between 1500 and 5000. These fractions were further purified by cation exchange HPLC, preparative RP-HPLC and analytical RP-HPLC. Ten peptides were purified and their primary structures were identified. All of them were fragment peptides of intracellular proteins, and most of them were from mitochondria. Among them, an N-terminal fragment peptide of cytochrome b (fCyt b (1-15)) and a C-terminal fragment peptide of cytochrome c oxidase subunit VIII (COSP-1) were chemically synthesized and the activities of them on  $\beta$ -hexosaminidase release and chemotaxis in neutrophil-like differentiated HL-60 cells were examined.

fCyt b(1-15) and COSP-1 induced secretion (exocytosis) of  $\beta$ -hexosaminidase and chemotaxis in neutrophil-like HL-60 cells in concentration dependent manners (EC<sub>50</sub>'s, fCyt b(1-15):  $3.8 \times 10^{-8}$  M, COSP-1:  $2.7 \times 10^{-7}$  M for  $\beta$ -hexosaminidase; fCyt b(1-15):  $6.2 \times 10^{-9}$  M, COSP-1:  $2.1 \times 10^{-8}$  M for chemotaxis). These activations were prevented by the addition of pertussis toxin, indicating the involvement of Gi-like G proteins in these signaling pathways. fCyt b(1-15) and COSP-1 induced chemotaxis at concentrations lower than those which stimulated exocytosis, and the similar results were obtained in human neutrophils stimulated by the human homologs of fCyt b(1-15) and COSP-1. These findings allow us to propose novel mechanisms of early states of acute inflammation as shown in Figure 1., *i.e.*, once tissue injury occurs, cytosolic proteins, such as mitochondrial proteins, are released from necrotic or

### Peptide Vaccines and Immunology

apoptotic cells in tissue injury sites. They are degraded by proteolytic enzymes and some of them are matured as neutrophil-activating peptides. These peptides induce transmigration of neutrophils to tissue injury sites. Neutrophils are not activated during migration, but only after they reach tissue injury sites, then they are activated to scavenge toxic cell debris. These peptides could play roles in acute inflammation.

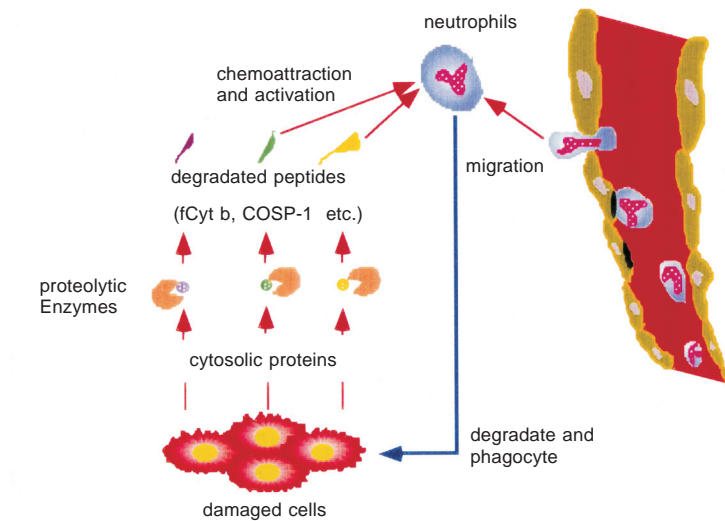


Fig. 1. Proposed mechanism of acute inflammation involved in fCyt b(1-15) and COSP-1.

### Acknowledgments

We thank Ms. K. Matsumoto, C. Obata and F. Saito for excellent technical assistance. This study was supported by research grants from a Grant-in Aid for Scientific Research 06680605 from the Ministry of Education and NEDO, Japan.

### References

1. Springer, T.A. *Cell* **76**, 301–314 (1994).
2. Baggiolini, M., Dewald, B., Moser, B. *Adv. Immunol.* **55**, 97–179 (1994).
3. Nakajima, T., Wakamatsu, K., Mukai, H. In Rochat, H. and Martin-Eauclaire, M.-F. (Eds.) *Animal Toxins: Methods and Tools in Biosciences and Medicine*, Birkhauser, Basel, 2000, p. 116–126.

## **Affinity of the HIV-1-Neutralizing Monoclonal Antibody 2F5 for gp41 ELDKWA Peptide Analogues**

**Yu Tian<sup>1</sup>, Chintala V. Ramesh<sup>1</sup>, Xuejun Ma<sup>1,2</sup>, Tanaz Patel<sup>1</sup>,  
Myles Tiscione<sup>1</sup>, Teodorica Cenizal<sup>1</sup>, John W. Taylor<sup>1</sup>,  
Gail Ferstandig Arnold<sup>1,2</sup> and Edward Arnold<sup>1,2</sup>**

<sup>1</sup>*Department of Chemistry and Chemical Biology, Rutgers University, Piscataway, NJ 08854, USA*

<sup>2</sup>*Center for Advanced Biotechnology and Medicine, Piscataway, NJ 08854, USA*

### **Introduction**

The human monoclonal antibody 2F5 (mAb 2F5) has broad neutralizing activity when tested against primary HIV-1 isolates [1,2]. This antibody binds to the linear peptide epitope ELDKWA, corresponding to residues 662-667 from the HIV-1 envelope glycoprotein gp41. The ELDKWA epitope is highly conserved among a wide range of HIV-1 isolates. We are currently investigating the structural and conformational requirements of the ELDKWA epitope for 2F5 binding. This research should assist us in the design of conformationally constrained ELDKWA analogues that might elicit an immune response that mimics the HIV-neutralizing actions of mAb 2F5 and provide protective immunity against HIV-1 infection. Towards this goal, several series of peptides have been synthesized and were tested for their affinities for mAb 2F5 by ELISA.

### **Results and Discussion**

In our initial studies, we focused on the length of the natural sequence that is recognized by mAb 2F5, and we used a competitive binding ELISA to assay 2F5 affinity for competing peptides in the presence of the immobilized, biotin-labeled peptide, ELDKWAS-amide. These studies determined that extension of the natural gp41 epitope from the seven-residue ELDKWAS sequence to the nine-residue LELDKWASL sequence (Table 1) dramatically increased 2F5 affinity, and that further sequence extensions had little or no additional effect. Therefore, we applied this result to the development of a new, competitive ELISA in which biotin-labeled LELDKWASL-amide was used as the surface-captured ligand. This assay required 30-fold less antibody, and exhibited considerably improved sensitivity to changes in the competing peptides.

The new ELISA was used to screen a series of alanine-scanned and D-residue-scanned peptide analogues of the LELDKWASL epitope. These studies highlighted the central -L<sup>3</sup>D<sup>4</sup>K<sup>5</sup>W<sup>6</sup>- sequence as essential for recognition by 2F5, closely corresponding to the sequence requirements previously identified in studies of phage display libraries [2]. Each of these residues was then examined in greater detail, by single residue substitution (Table 1). Elimination of one  $\gamma$ -methyl group in L<sup>3</sup> was well tolerated, but substitution of D<sup>4</sup> by N, and deletion of one methylene group in the side-chain of K<sup>5</sup> (Orn), were not. Substitution of W<sup>6</sup> by a 1-naphthylalanine residue was also tolerated, but substitution by 2-naphthylalanine was not.

In order to explore the effects of conformational constraints in the 2F5 epitope, we have also synthesized disulfide-cyclized peptides, and N-terminal helix-initiated analogues. The initial results of this study indicated that disulfide cyclized analogues of the natural gp41 sequence are poorly soluble and exhibit weak binding. However, C-terminal extension with a polylysine sequence improved solubility and binding af-

finity (Table 1). The helix-initiated peptides bound to 2F5 with similar potencies to the unmodified sequence (not shown). These data should provide a useful starting point for the development of highly constrained analogues of the natural gp41 epitope recognized by mAb 2F5. Such analogues may be useful as peptide epitope-based haptens in vaccines designed for the therapeutic control of HIV-1 infection.

Table 1. Potencies of peptides for binding to mAb 2F5 in competitive ELISAs.

Peptide	mAb 2F5 Binding <sup>a</sup>	
	IC <sub>50</sub> (nM)	potency (%) <sup>b</sup>
Acetyl-ELDKWAS-amide	160 000 ± 11 100	0.055 ± 0.004
Acetyl-LELDKWASL-amide	88 ± 7	100 ± 8
Acetyl-LE(Nva)DKWASL-amide <sup>c</sup>	216 ± 17	41 ± 3
Acetyl-LELNKWASL-amide <sup>c</sup>	>160 000	<0.06
Acetyl-LELD(Orn)WASL-amide <sup>c</sup>	22 800 ± 4 500	0.39 ± 0.08
Acetyl-LELDK(1-Nal)ASL-amide <sup>c</sup>	714 ± 25	12 ± 0.4
Acetyl-ACELLELDKWASLWNCA-amide	5 670 ± 1 180	1.6 ± 0.3
Acetyl-ACSSLELDKWASLSSCKKKK-amide	351 ± 126	25 ± 9

<sup>a</sup> Assayed using streptavidin-coated plates and biotin-labeled LELDKWASL-amide. <sup>b</sup> Relative to acetyl-LELDKWASL-amide = 100%. <sup>c</sup> (Nva) = norvaline residue; (Orn) = ornithine residue; (1-Nal) = 1-naphthylalanine residue.

### Acknowledgments

This research was supported by NIH grants R21 AI45316 (J. W. T.) and R21 AI45353 (G. F. A.).

### References

1. Muster, T., Guinea, T., Trkola, A., Purtscher, M., Klima, A., Steindl, F., Palese, P., Katinger, H. *J. Virol.* **68**, 4031–4034 (1994).
2. Conley, A.J., Kessler II, J.A., Boots, L.J., Tung, J.-S., Arnold, B.A., Keller, P.M., Shaw, A.R., Emini, E.A. *Proc. Natl. Acad. Sci. U.S.A.* **91**, 3348–3352 (1994).

## **A Discontinuous Antigenic Site Is Functionally Reproduced by Synthetic Peptide Constructions**

**Judit Villén<sup>1</sup>, Eva Borràs<sup>1</sup>, Mercedes Dávila<sup>2</sup>, Esteban Domingo<sup>2</sup>,  
Wim M. M. Schaaper<sup>3</sup>, Rob H. Melen<sup>3</sup>, Ernest Giralt<sup>1</sup>  
and David Andreu<sup>1</sup>**

<sup>1</sup>*Department of Organic Chemistry, University of Barcelona, Barcelona, 08028, Spain*

<sup>2</sup>*Centro de Biología Molecular "Severo Ochoa", CSIC-UAM, Madrid, 28049, Spain*

<sup>3</sup>*Institute for Animal Science and Health, Lelystad, 8219, The Netherlands*

### **Introduction**

Despite the severe economical impact of foot-and-mouth disease (FMD) worldwide, animal policies in affected areas usually disregard the use of conventional vaccines, for reasons such as lack of cross-protection among different strains, the need for booster shots twice a year and, especially, the (alleged) difficulty in distinguishing vaccinated from infected animals. Although this last argument is controversial, it serves to emphasize the usefulness of marker vaccines, particularly peptide-based, in this context.

Most FMDV synthetic vaccines have so far been based on the continuous antigenic site A [1], a region of VP1 containing a RGD tripeptide unit involved in infectivity and antibody recognition. Vaccines using site A peptides, either alone or combined with additional sites, have provided significant levels of protection in several trials [2]. However, in large-scale experiments with relevant hosts some clear limitations have emerged. Thus, different presentations of site A peptides to bovines [3] afforded only limited (39% at most) protection, with all unprotected animals infected by FMDV variants with mutations at site A. Further, an evaluation of the immunodominance of site A in vaccinated or convalescent swine showed roughly one half of the immune response was directed to other-than-A antigenic sites [4]. These results clearly suggest the convenience of exploring additional antigenic sites when designing a synthetic vaccine for FMDV.

We have focused our attention on site D, a discontinuous antigenic site that involves residues from each of the three capsid proteins of FMDV. This site is more conserved among serotypes, and could therefore be a good candidate to include in a multivalent FMDV vaccine. Here we report on the progress of our structure-based approach to the reproduction of site D by chemical means.

### **Results and Discussion**

We have designed a functional mimic of site D, peptide D8 [5], which incorporates into a single covalent structure the five antigenically critical amino acids (Thr193 of VP1; Ser72, Asn74 and His79 of VP2; Glu58 of VP3) and their immediate environment. The construction has been designed so that the five critical residues can be surface-exposed and define a native-like set of distances and orientations. As shown in Figure 1, the VP2 and VP3 strands, antiparallel in the native structure, are joined into a single peptide chain by means of an 8-proline spacer module. The VP1 region, on the other hand, is joined to VP3 by means of a disulfide bond, formed regioselectively by Npys-based chemistry [6].

The D8 peptide has been evaluated for its ability to elicit neutralizing antibodies and eventually protect animals against FMDV infection. Guinea pig anti-D8 sera show clear recognition of the FMDV particle in direct ELISA and provide moderate levels

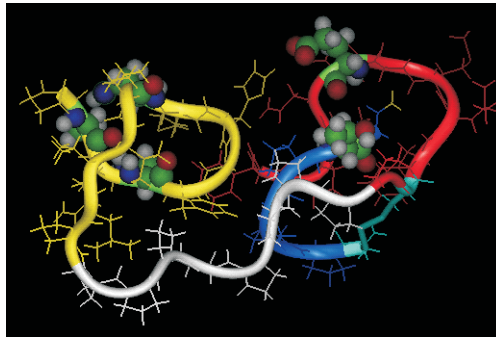


Fig. 1. Peptide D8, designed as functional mimic of discontinuous antigenic site D of FMDV, is a heterodimer where the VP1 region is connected through a disulfide with the VP2/VP3 segments, joined into a single chain by means of a polyproline spacer module.

of FMDV neutralization *in vitro*. In sharp contrast, immunization with a mixture of three peptides corresponding to the VP1, VP2 and VP3 sequences in the construct leads to serum titers undistinguishable from preimmune values and no neutralization. The positive immune response to D8 has been reproduced in bovines, with comparable neutralization levels (up to 60%).

A more compelling evidence of the functional reproduction of site D has come from competition ELISA, where D8-derived antisera are seen to displace site-D directed monoclonal antibodies bound to FMDV (Figure 2). These results have been confirmed for both guinea pig and bovine antisera.

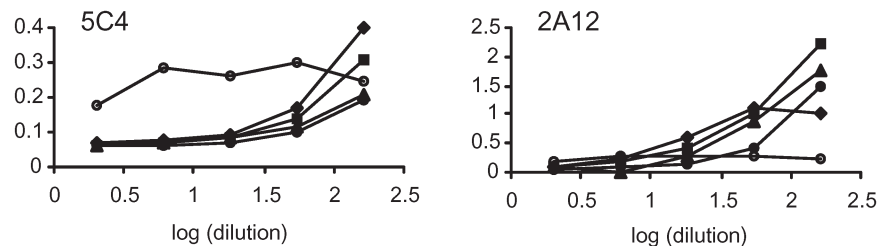


Fig. 2. Competition between anti-D8 sera from guinea pigs 1–4 (◆, ●, □ and ■, respectively) and peroxidase-conjugated, site D-specific mAbs 5C4 and 2A12 for FMDV as plate antigen. !: negative control using sera from animal 2 and non-competing mAb SD6, directed to an antigenic site other than D.

The next step has been to develop analogs of the initial D8 structure. We have explored by molecular dynamics how different lengths ( $n = 2-12$ ) of the polyproline spacer affect the fitness of the construct relative to the native FMDV structure. This study allowed to select four new candidate molecules ( $n = 2, 4, 7, 10$ ) for synthesis and further immunological evaluation in guinea pigs. Results showed no significant differences, all constructions providing levels of recognition and viral neutralization quite similar to those obtained with D8.

In summary, peptide D8 and its analogs provide a structural preorganization of the protein segments making up site D that amounts to reasonable functional mimicry of this discontinuous antigenic site. We have shown that structure-guided design, aided

by molecular dynamics simulations, can help select candidate molecules displaying the three protein strands of site D in a native-like fashion capable of eliciting, in both guinea pigs and cattle, antipeptide sera that specifically recognize site D. In all cases, virus-specific serum conversion has been observed, accompanied by modest but unequivocal levels of neutralization and, in guinea pigs, by partial protection against a challenge with live virus. From these results it can be safely inferred that D8-like peptides, in its present or further refined versions, are obvious candidates for a future multicomponent, peptide-based, vaccine against FMDV.

#### **Acknowledgments**

Financial support for this project was provided by the Spanish Ministry of Science and Technology (PB97-0873), Generalitat de Catalunya (CERBA), and the European Union (FAIR-CT97-3577).

#### **References**

1. Bittle, J.L., Houghten, R.A., Alexander, H., Shinnik, T.M., Sutcliffe, J.G., Lerner, R.A. *Nature* **298**, 30–33 (1982).
2. DiMarchi, R., Brooke, G., Gale, C., Cracknell, V., Doel, T., Mowat, N. *Science* **232**, 639–641 (1986).
3. Taboga, O., Tami, C., Carrillo, E., Núñez, J.I., Rodríguez, A., Sáiz, J. C., Blanco, E., Valero, M.L., Roig, X., Camarero, J.A., Andreu, D., Mateu, M.G., Giralt, E., Domingo, E., Sobrino, F., Palma, E.L. *J. Virol.* **71**, 2606–2614 (1997).
4. Mateu, M.G., Camarero, J.A., Giralt, E., Andreu, D., Domingo, E. *Virology* **206**, 298–306 (1995).
5. Borràs, E., Giralt, E., Andreu, D. *J. Am. Chem. Soc.* **121**, 11932–11933 (1999).
6. Albericio, F., Andreu, D., Giralt, E., Navalpotro, C., Pedrosa, E., Ponsati, B. Ruiz-Gayo, M. *Int. J. Pept. Protein Res.* **34**, 124–128 (1989).

## Four-Segment Tandem Ligation of Proteins with Unusual Branched Architecture

K. D. Eom, Z. Miao and J. P. Tam

Department of Microbiology and Immunology, Vanderbilt University, Nashville,  
 TN 37232, USA

### Introduction

Chemoselective and orthogonal (NT-amino acid-specific) peptide ligation for coupling free peptides, proteins, and biopolymers afford non-amide and amide bonds, respectively. These peptide ligation methods are attractive because they are not burdened by the use of a protecting group scheme or a coupling reagent. Thus, they are applicable to both chemistry and biology. Our laboratory has recently reported several three-segment tandem ligation strategies [1,2] that utilize two orthogonal ligation approaches. To further exploit tandem ligation methods, we have combined chemoselective and orthogonal peptide ligation to produce a four-segment tandem peptide ligation strategy. This tandem ligation scheme, suitable for synthetic vaccines and combinatorial protein synthesis, couples consecutively four different segments **S1–S4** to produce two amide bonds and a thioether bond at three ligation sites (Figure 1). To demonstrate the versatility of this new strategy, we describe the synthesis of branched proteins of 56–70 residues with the **S1–S4** segments derived from Bac7, NK-lysin, melittin, and gp120 sequences.

### Results and Discussion

Four unprotected peptide segments **S1–S4** were prepared by stepwise solid-phase synthesis, purified by RP-HPLC, and confirmed by MALDI-MS. To achieve orthogonality or chemoselectivity in peptide ligation, specific functional groups were required to serve as either nucleophiles or electrophiles on the amino or carboxyl termini of **S1** to **S4** peptides. For the amino termini of peptides **S1–S4**, **S1** (CW14) requires an amino terminal (NT)-cysteine, **S2** (SA15) an NT-Ser or NT-Thr, and **S3**

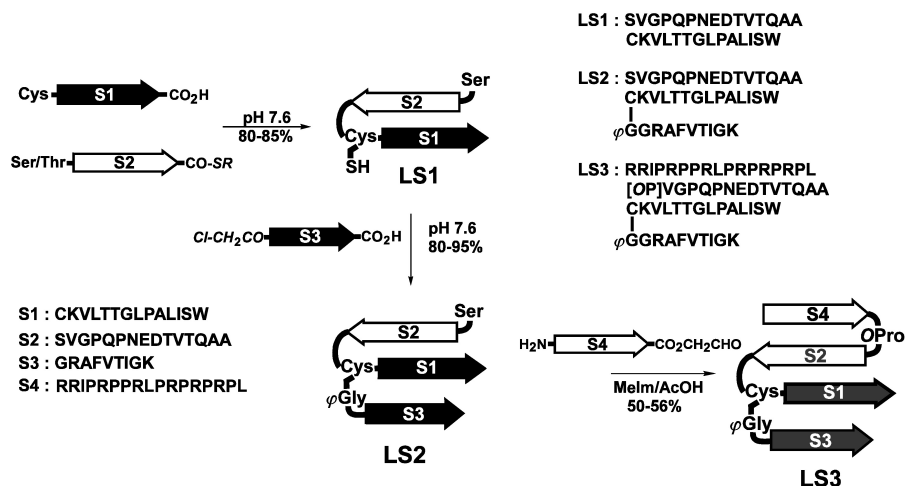


Fig. 1. The scheme of four-segment tandem ligation.

(GK9) a chloroacetyl group. **S4** can be any other NT-amino acid. For the carboxyl terminal (CT) functional groups, **S2** must be a thioester and **S4** (RL17) a glycoaldehyde ester. No requirement is imposed on the carboxyl termini of **S2** or **S3**.

The **S1–S3** segments were obtained by Boc chemistry from either the PAM or a thioester MBHA resin. The **S4** segment bearing the CT-glycoaldehyde ester was prepared by Fmoc chemistry through periodate oxidation from the unprotected glyceryl ester carrying a 1,2-diol moiety [2].

Our tandem ligation scheme, proceeding in C-to-N direction, generated consecutively at the ligation site a Cys,  $\phi$ Gly, and OPro. Thus, the first ligation between **S1** and **S2** segments to form the ligated product (LS) 1 was mediated by an orthogonal thioester ligation. This ligation was performed at pH 7.6 phosphate buffer with tris(2-carboxyethyl)phosphine (TCEP). The nucleophilic NT-Cys of the **S1** segment initially underwent a thiol–thioester exchange with the electrophilic CT-thioester of the **S2** segment to afford a covalent thioester intermediate that rearranged by an intramolecular *S,N*-acyl transfer to form a stable amide bond product LS1. The Cys ligation proceeded cleanly in 80–85% yield. The newly generated cysteinyl thiol group of LS1 was then used for the chemoselective ligation with the chloroacetyl peptide **S3** to form a branched LS2 containing a side-chain thioether bond [3] as a Gly-Gly  $\beta$ -turn mimetic. The  $\phi$ Gly ligation was obtained in 80–95% yield at pH 7.6 guanidine-HCl buffer with TCEP. Finally, the oxaproline (OPro) ligation involving the NT serine of the LS2 segment with the peptide **S4** underwent an imine capture, oxazolidine ring formation, and *O,N*-acyl shift in *N*-methylimidazole/acetic acid, to produce the final product LS3. The OPro was 50–56% ligation with the desired mass (*m/z* 6139).

In conclusion, we have developed a four-segment tandem peptide ligation scheme to couple multiple peptide segments to form three regiospecific bonds without the use of a protecting-group scheme or a coupling reagent. This strategy may be applicable for engineering vaccines [4], or proteins with unusual architectures, through convergent, combinatorial, or conformation-assisted ligation.

### Acknowledgments

This work was in part supported by NIH grants CA36544 and AI46174.

### References

1. Tam, J.P., Yu, Q., Yang, J.-L. *J. Am. Chem. Soc.* **123**, 2487–2494 (2001).
2. Miao, Z., Tam, J.P. *J. Am. Chem. Soc.* **122**, 4253–4260 (2000).
3. Lu, Y.-A., Clavijo, P., Galantino, M., Shen, Z.-Y., Liu, W., Tam, J.P. *Mol. Immunol.* **28**, 623–630 (1991).
4. Tam, J.P. *J. Immunol. Methods* **196**, 17–32 (1996).

## **Identification and Optimization of HIV-Specific CTL Antigens for Vaccine Design**

**César Boggiano<sup>1</sup>, Clemencia Pinilla<sup>1</sup>, Bruce D. Walker<sup>2</sup>  
and Sylvie E. Blondelle<sup>1</sup>**

<sup>1</sup>*Torrey Pines Institute for Molecular Studies, San Diego, CA 92121, USA*

<sup>2</sup>*Partners AIDS Research Center, Harvard Medical School, Charlestown, MA 02129, USA*

### **Introduction**

Despite the great advances in antiviral therapy for HIV-1 infection, a successful global intervention for prevention and treatment of HIV-1 infection will require an effective vaccine. Since the induction of cytotoxic T-lymphocyte (CTL) responses is believed to be an important factor in an effective HIV-1 vaccine [1], our approach toward the development of an HIV vaccine is based on the identification of T-cell ligands that will stimulate CD8<sup>+</sup> CTL response more efficiently than the natural infection. Thus, we used positional scanning synthetic combinatorial libraries (PS-SCLs [2]) to identify and optimize peptide ligands to be used as immunogens in stimulating T-cell mediated immune responses against HIV-1.

### **Results and Discussion**

The Gag p17-derived epitope SLYNTVATL (SL9) was first selected for these studies, since at least 71% of HLA-A2-positive individuals have circulating T-cells that recognize this epitope [3]. Since CD8<sup>+</sup> CTLs usually recognize peptides 8 to 11 amino acids in length, a nonapeptide PS-SCL was first screened for stimulation of cytolytic activity by Gag-specific p17<sub>77-85</sub> SL9 cloned T-cells (161jXA14). Notably, seven out of nine amino acids defining the most active mixtures correspond to residues of the native peptide epitope. Based on these screening data, amino acids defining the most active library mixtures at each position were selected to synthesize 32 candidate sequences. Eight of these peptides generated cytolytic activity with EC<sub>50</sub> values lower than SL9 (5-fold increase in activity for the most active peptide).

The screening results were also systematically compared to nonapeptides in viral proteins in the GenPept 1.7 database to predict and identify stimulatory peptides using a biometrical analysis. This biometrical analysis scores all of the overlapping nonapeptides in viral proteins based on the activity information derived from the screening of the PS-SCL [4,5]. The number of proteins and nonapeptides scored were 102,359 and over 22 million, respectively. The scoring distribution of these 22 million peptides scored clearly shows that a relatively small number of peptides have the highest score (>48), and that the native peptide (SL9) is among those peptides with a score of 59.11 and a rank of 116 (Figure 1). These results demonstrate that the epitope could have been identified if the specificity of the clone was unknown. Furthermore, the nonapeptides having the two highest scores are double substitutions of this epitope.

Sixty-eight of the peptides having the highest scores were synthesized and their stimulation of cytolytic activity was determined in a manner similar to the library. Furthermore, a pilot study to examine whether increase in recognition would be common to other clones that recognize the SL9 epitope was initiated using SL9 T-cell clone 115-b2. Five out of the sixty-eight peptides, all corresponding to the same HIV-1 Gag protein region as the original sequence but from different isolates, generated a higher cytolytic activity by clone 161jXA14 than SL9. Four of these peptides

are also recognized by clone 115-b2, suggesting a potential cross-reactivity for those peptides.

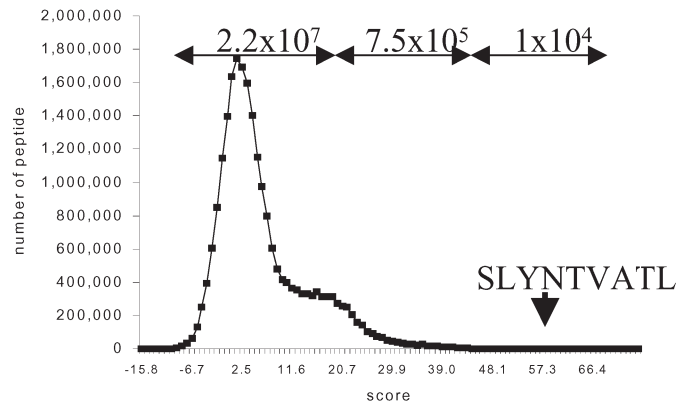


*Fig. 1. Scoring distribution of peptides in viral database.*

Overall, these studies, combined with reported successful identification and optimization of T-cell ligands from SCLs [reviewed in 6], demonstrate that it is possible to engineer peptides with enhanced recognition to multiple T-cell clones using SCL approaches. Furthermore, the success shown here in the identification of the original epitope from the viral protein database clearly demonstrates the strength of the PS-SCL approach/biometrical analysis combination for the identification of epitopes from T-cell clones of unknown specificity.

#### **Acknowledgments**

The biometrical analysis was developed by Clemencia Pinilla (TPIMS), Roland Martin's group (NINDS, NIH) and Richard Simon's group (NCI, NIH).

#### **References**

1. Brander, C., Walker, B.D. *Curr. Opin. Immunol.* **11**, 451–459 (1999).
2. Pinilla, C., Appel, J.R., Blanc, P., Houghten, R.A. *Biotechniques* **13**, 901–905 (1992).
3. Goulder, P.J.R., Sewell, A.K., Lalloo, D.G., Price, D.A., Whelan, J.A., Evans, J., Taylor, G.P., Luzzi, G., Giangrande, P., Phillips, R.E., McMichael, A.J. *J. Exp. Med.* **185**, 1423–1433 (1997).
4. Hemmer, B., Gran, B., Zhao, Y., Marques, A., Pascal, J., Tzou, A., Kondo, T., Cortese, I., Bielekova, B., Straus, S., McFarland, H.F., Houghten, R.A., Simon, R., Pinilla, C., Martin, R. *Nature Med.* **5**, 1375–1382 (1999).
5. Zhao, Y., Gran, B., Pinilla, C., Markovic-Plese, S., Hemmer, B., Tzou, A., Whitney, L.W., Biddison, W.E., Martin, R., Simon, R. *J. Immunol.*, submitted.
6. Pinilla, C., Martin, R., Gran, B., Appel, J.R., Boggiano, C., Wilson, D.B., Houghten, R.A. *Curr. Opin. Immunol.* **11**, 193–202 (1999).

## The Natural T-Helper Cell Epitope Repertoire is Unlikely to Contain Glycopeptides with Extended Carbohydrate Side-Chains

Laszlo Otvos, Jr., Hildegund C. J. Ertl and Mare Cudic

*The Wistar Institute, Philadelphia, PA 19104, USA*

### Introduction

To answer the question whether or not the natural T-cell epitope repertoire contains glycosylated antigens, we synthesized a series of glycopeptides corresponding to peptide 31D, a major T-helper cell epitope of the rabies virus nucleoprotein. Peptide 31D, AVYTRIMMNGGRLKR, in context with the I-E<sup>k</sup> MHC determinant, vigorously stimulates the proliferation of the 9C5.D8-H T-cell hybridoma [1]. From our earlier studies we know that Thr4 can carry mono- or disaccharide side-chains in either  $\alpha$ - or  $\beta$ -anomeric configuration without interfering with MHC-binding [2]. In the current study, we synthesized peptide 31D without sugar, as well as with  $\alpha$ - or  $\beta$ -linked trisaccharides or linear heptasaccharides attached to Thr4.

### Results and Discussion

For modeling the extended carbohydrate chains, we returned to oligomers of maltose. These were used successfully earlier for the immunological and conformational analysis of N-linked glycopeptides [3,4]. Maltotriose and maltoheptose were the starting compounds for the  $\beta$ -anomers. The sugars were acetylated with acetic anhydride/pyridine, and mixtures of  $\alpha$ - and  $\beta$ -anomers of peracetylated sugars were separated by silica gel chromatography. Pure  $\beta$ -anomers were coupled to Fmoc-Thr-OH using a Lewis acid (BF<sub>3</sub>·Et<sub>2</sub>O) as promoter. For the preparation of the  $\alpha$ -anomers, a modified Koenigs-Knorr method was used. Fully acetylated trisaccharide/heptasaccharide bromide glycosyl donors were coupled to Fmoc-Thr-OPfp to yield Fmoc-Thr(maltobiose-GalN<sub>3</sub>/maltohexose-GalN<sub>3</sub>- $\alpha$ 1 $\rightarrow$ O)-OPfp.

Addition of  $\alpha$ -linked carbohydrates, that mimic natural O-linked glycoproteins, resulted in a major drop in the T-cell stimulatory ability (Figure 1). At lower peptide concentrations, this effect was sugar-length dependent. In contrast, the  $\beta$ -linked glyco-

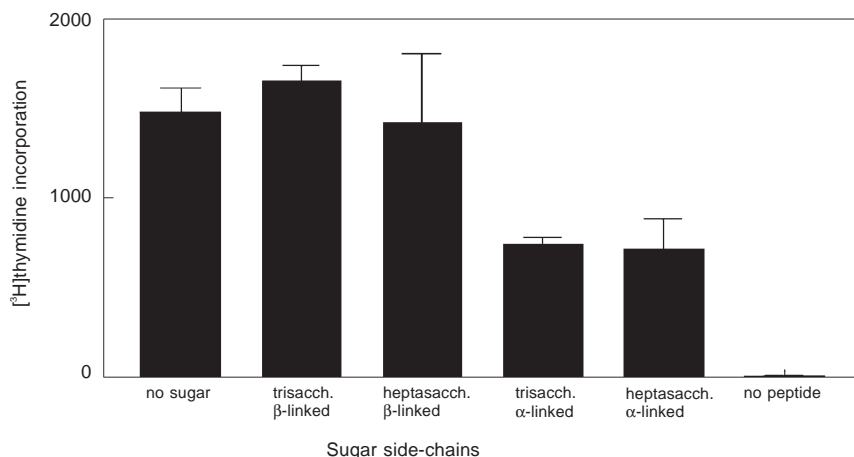


Fig. 1. Response of T-cells to peptide 31D and its glycosylated analogs. The peptides were applied at a concentration of 1  $\mu$ g/mL.

*Otvos et al.*

peptides retained most of their T-cell stimulatory activity, with the trisaccharide-containing analog being almost as potent as the non-glycosylated peptide. When the peptides were preincubated with diluted human serum, all peptides lost their T-cell stimulatory ability, probably due to cleavage by serum proteases. These findings indicated that i) the native T-helper cell epitope repertoire is unlikely to contain O-glycopeptides with extended sugar side-chains, and ii) glycosylation of peptide epitopes is not an efficient alternative to improve the half-life, and consequently the immunogenic properties of subunit peptide vaccines.

Glycosylation with all four carbohydrate moieties similarly destroyed the inducible  $\alpha$ -helical structure of peptide 31D and resulted in reverse-turn structures, indicating that the differences in the T-cell activity were not due to different conformations.

**Acknowledgments**

We thank Dr. Krzysztof Wroblewski for the NMR spectra. This work was supported by NIH grant GM45011.

**References**

1. Ertl, H.C.J., Dietzschold, B., Gore, M., Otvos, L., Jr., Larson, J.K., Wunner, W.H., Koprowski, H. *J. Virol.* **63**, 2885–2892 (1989).
2. Otvos, L., Jr., Cappelletto, B., Varga, I., Wade, J.D., Xiang, Z.Q., Kaiser, K., Stephens, L.J., Ertl, H.C.J. *Biochim. Biophys. Acta* **1313**, 11–19 (1996).
3. Jackson, D.C., Drummer, H.E., Urge, L., Otvos, L., Jr., Brown, L.E. *Virology* **199**, 422–430 (1994).
4. Urge, L., Jackson, D.C., Gorbics, L., Wroblewski, K., Graczyk, G., Otvos, L., Jr. *Tetrahedron* **50**, 103–115 (1994).

## Peptide Analogues of a Subdominant Epitope Expressed in EBV-Associated Tumors: Synthesis and Activity

Mauro Marastoni<sup>1</sup>, Martina Bazzaro<sup>1</sup>, Fabiola Micheletti<sup>2</sup>,  
 Riccardo Gavioli<sup>2</sup> and Roberto Tomatis<sup>1</sup>

<sup>1</sup>Department of Pharmaceutical Sciences and Biotechnology Center and <sup>2</sup>Department of  
 Biochemistry and Molecular Biology, University of Ferrara, I-44100 Ferrara, Italy

### Introduction

Major histocompatibility complex (MHC) class I molecules bind and display oligopeptides deriving from viral proteins in infected cells. MHC-peptide complexes form the antigens that can be recognized by specific T cell receptors (TCR) expressed on cytotoxic T lymphocytes (CTL). In this way CTL can identify and kill infected cells selectively, sparing healthy cells. We focused our analysis on the H-Cys-Leu-Gly-Gly-Leu-Leu-Thr-Met-Val-OH (CLG) peptide, an Epstein-Barr virus (EBV) epitope which represents the target of HLA-A2 restricted EBV-specific cytotoxic T lymphocytes responses [1]. EBV is a lymphotropic virus associated with a number of human malignancies. The CLG nonamer represents a good target for the immunotherapy of EBV-associated malignancies, since it is expressed and conserved in nasopharyngeal carcinoma and Hodgkin's disease biopsies. However, the CLG peptide has low affinity for HLA-A2 and does not produce stable complexes, both factors that determine weak CTL responses to this epitope. Moreover, this epitope shows low enzymatic stability being rapidly hydrolyzed by plasma enzymes. In order to improve the immunotherapeutic potential of this epitope we have synthesized and tested CLG analogues containing *cis*- and *trans*-4-ACCA (4-aminocyclohexanecarboxylic acid) in N- and/or C-terminal portions of the sequence (Table 1). All analogues were tested for metabolic stability and for their capacity to bind HLA-A2 molecules and to induce specific CTL activation.

### Results and Discussion

*Cis*- and *trans*-4-ACCA were prepared according to procedures reported in literature [2] and converted to corresponding Fmoc derivatives. CLG-analogues **1–8** (Table 1)

Table 1. Sequence and metabolic degradation of CLG analogues.

No.	Sequence	Half-life (min)	
		Medium	Plasma
CLG	H-Cys-Leu-Gly-Gly-Leu-Leu-Thr-Met-Val-OH	82.3	12.7
<b>1</b>	H-Cys-Leu-Gly-Gly-Leu-Leu- <i>cis</i> -ACCA-Val-OH	>360	229.4
<b>2</b>	H-Cys-Leu- <i>cis</i> -ACCA-Leu-Leu-Thr-Met-Val-OH	190	49.3
<b>3</b>	H-Cys-Leu- <i>cis</i> -ACCA-Leu-Leu- <i>cis</i> -ACCA-Val-OH	>360	214.1
<b>4</b>	H-Cys-Leu-Gly-Gly-Leu-Leu- <i>trans</i> -ACCA-Val-OH	>360	195.8
<b>5</b>	H-Cys-Leu- <i>trans</i> -ACCA-Leu-Leu-Thr-Met-Val-OH	157	60.9
<b>6</b>	H-Cys-Leu- <i>trans</i> -ACCA-Leu-Leu- <i>trans</i> -ACCA-Val-OH	>360	230.8
<b>7</b>	H-Cys-Leu- <i>trans</i> -ACCA-Leu-Leu- <i>cis</i> -ACCA-Val-OH	>360	289.1
<b>8</b>	H-Cys-Leu- <i>cis</i> -ACCA-Leu-Leu- <i>trans</i> -ACCA-Val-OH	>360	198.6

were synthesized by solid phase methods, using an automated continuous-flow peptide synthesizer. The stepwise synthesis was carried out by Fmoc/tBu-chemistry. The N $\alpha$ -Fmoc amino acids were condensed using DIPCDI and HOBt as coupling agents on functionalized Wang resin.

In order to evaluate the susceptibility to enzymatic hydrolysis, the analogues **1–8** were incubated at 37 °C in culture medium (RPMI) in the presence of 10% fetal calf serum (RPMI + 10% FCS) and in human plasma. Half-lives of peptides are reported in Table 1 in comparison with CLG. As expected, all C-terminal modifications considerably increased the stability of peptides in cell culture medium and in human plasma.

We then evaluated the ability of all peptides to associate with HLA-A2. Peptide association was assessed by the induction of surface HLA-A2 expression in the T2 mutant cell line. Peptides **4**, **5**, **6** and **8** induced high levels of HLA-A2 molecules when compared to the parent CLG epitope. These analogues were evaluated for their capacity to stimulate CTL responses directed against the wild-type epitope [3]. CLG analogues reactivated CLG-specific responses with an increased efficiency in comparison with the natural epitope (Figure 1).

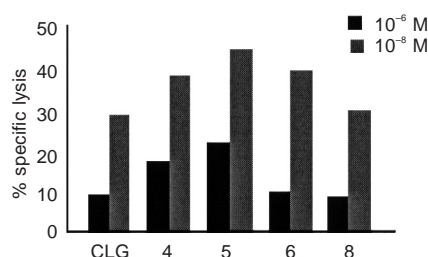


Fig. 1. Comparison of peptides **4**, **5**, **6**, and **8** with CLG.

In conclusion, the insertion of a *trans*-4-ACCA residue in the original nonameric sequence permits a favourable conformational arrangement and produces CLG analogues that showed satisfactory affinity for HLA-A2 molecules, potent stimulatory capacity, and increased enzymatic stability. Thus, CLG analogues may represent good candidates for EBV-specific immunotherapies in the treatment of human malignancies such as nasopharyngeal carcinoma and Hodgkin's disease.

## References

1. Lee, S.P., Thomas, W.A., Murray, R., Khanim, F., Kaur, S., Young, L.S., Rowe, M., Kurilla, M., Rickinson, A.B. *J. Virol.* **67**, 7428–7435 (1993).
2. Skaric, V., Kovacevic, M., Skaric, D. *J. Chem. Soc., Perkin Trans. 1* 1199 (1976).
3. Gavioli, R., Zhang, Q.J., Marastoni, M., Guerrini, R., Reali, E., Tomatis, R., Traniello, S. *Biochem. Biophys. Res. Commun.* **206**, 8–14 (1995).

## Synthetic Epitopes from Equine Infectious Anemia Virus (EIAV) Surface and Core Proteins

**Adriana Soutullo<sup>1</sup>, María Santi<sup>2</sup>, Juan C. Perin<sup>2</sup>, Javier Lottersberger<sup>2</sup>,  
 Leila Beltramini<sup>3</sup> and Georgina Tonarelli<sup>2</sup>**

<sup>1</sup>*Laboratorio de Diagnóstico e Investigaciones Agropecuarias, Dirección de Sanidad Animal,  
 Ministerio de Agricultura, Ganadería, Industria y Comercio de Santa Fe,  
 Bv. Pellegrini 3100, 3000 Santa Fe, Argentina*

<sup>2</sup>*Dpto. Química Orgánica, Facultad de Bioquímica, Universidad Nacional del Litoral,  
 C.C. 242, 3000, Santa Fe, Argentina*

<sup>3</sup>*Dpto. de Física e Informática, Grupo de Biofísica Molecular, Instituto de Física  
 de São Carlos-São Paulo-Brazil*

### Introduction

Equine infectious anemia virus (EIAV) is considered a member of the lentivirus subfamily of Retroviridae. The virus possesses the surface glycoproteins gp 90 and gp 45 and four major non-glycosylated internal core proteins known as p26, p15, p11 and p9 [1–3]. The aims of this work have been to: a) evaluate the performance of an EIAV ELISA designed with synthetic peptides from gp90 and gp45 and b) study the conformation relevancy as an essential requirement for antibody recognition of a synthetic p26 antigen.

### Results and Discussion

Peptides in Table 1 were manually synthesized as C-terminal carboxamide by the solid phase method with the 9-fluorenyl-methoxycarbonyl (Fmoc) strategy. Peptides gp90-1 and gp90-2 correspond to the N- and C- terminal part of the surface glycoprotein, respectively. Peptides gp45-1 and gp45-loop overlap the region of the immunodominant epitope CIERTHVFC of the transmembrane glycoprotein.

Using these peptides as antigens, positive and negative sera could be clearly distinguished. Thus, samples testing as weak positives in the agar gel immunodiffusion test (AGID) were “true” positives in ELISA. Cyclic versions of peptides gp45 displayed predominant  $\beta$ -sheet and turn secondary structures as determined by circular dichroism and were much more reactive in ELISA than the linear forms, suggesting that activity depends significantly on their conformation.

The carboxy terminus of p26 contains a number of  $\beta$ -cell determinants, none of which appears to be individually immunodominant [3]. We have localized a minimal continuous epitope (MYACRD) at the C-terminus of EIAV p26 core protein by means

*Table 1. Synthetic peptides from gp45, gp90 and p26.*

Identification	Sequence	Region
gp45-1	ERQQVEETFNLI GCIERTHVFC HTG	(523–547)
gp45-loop	IGCIERTHVFC HTG	(534–547)
gp90-2	ETWKLVK TSGVTPLPISSEANTGLIRH KR	(409–436)
gp90-1	YGGIPGGISTPITQQSEKSK	(1–20)
p26-1	ANE ECRNAMRHLRP EDTLEEKMYACRDIG	(318–346)

*Soutullo et al.*

of a peptide library prepared by the Spot Synthesis technique [4]. An elongated peptide containing the native sequence (region 318–346) was designed and named p26-1.

The conformation of p26-1 in the whole protein showed two  $\alpha$ -helix regions joined by a turn and a disulfide bridge which confers rigidity to the system, as determined by X-ray crystallography [5].

Deconvolution of circular dichroism data of linear and cyclic versions of p26-1 in solution have proved the conformational change from a predominant  $\beta$ -sheet to an  $\alpha$ -helix secondary structure when the sequence was cyclized through a disulfide bridge between Cys322 and Cys342. These results correlated with an improvement of the cyclic p26-1 ability to recognize EIA-specific antibodies. This constrained conformation could well mimic the structure of this region of the native p26 protein and this antigenic peptide could well be incorporated into an EIAV-ELISA for infection diagnosis.

#### **Acknowledgments**

This work was supported by grants from CAI+D Program, Universidad Nacional del Litoral, and Fundación Antorchas. We are very grateful to Dr. Ronald Frank for his scientific expertise in Spot synthesis technology.

#### **References**

1. Montelaro, R.C., Parekh, B., Orrego, A., Issel, C.J. *J. Biol. Chem.* **259**, 10539–10544 (1984).
2. Hussain, K.A., Issel, C.J., Schnorr, K.L., Rwambo, P.M., West, M., Montelaro, R.C. *Arch. Virol.* **98**, 213–224 (1988).
3. Chong, Y-H., Payne, S.L., Issel, C.J., Montelaro, R.C., Rushlow, K.E. *J. Virol.* **65**, 1007–1012 (1991).
4. Frank, R., Overwin, H., *Epitope Mapping Protocols, Methods in Molecular Biology*, Vol. 66. Humana Press Inc., Totowa, NJ, 1996, pp.149–169.
5. Jin, Z., Jin, L., Peterson, D.L., Lawson, C.L. *J. Mol. Biol.* **286**, 83–93 (1999).

## **B-Cell Linear Epitopes in the Conservative Regions of Hepatitis C Virus Envelope Glycoproteins**

**Ekaterina F. Kolesanova, Ludmila V. Olenina, Boris N. Sobolev,  
 Ludmila I. Nikolaeva and Alexander I. Archakov**

*Institute of Biomedical Chemistry RAMS, Moscow, 119992, Russia*

### **Introduction**

Hepatitis C virus (HCV) infection in 80% cases causes chronic hepatitis C development, often resulting in cirrhosis and hepatocarcinoma. High variability of HCV E1 and E2 envelope protein fragments, to which virus-neutralizing antibodies are formed in the natural course of infection, enables the virus to escape from the host immune response. Nevertheless, E1 and E2 sequences contain highly conservative sites that may be responsible for all attachment and entry and may elicit protective antibodies [1–3]. However, these sites have not been defined and their immunogenicity has not been subjected to regular studies.

### **Results and Discussion**

By building up the HCV polyprotein consensus sequence and analyzing hydrophilicity, charge distribution, and conservativity profiles we revealed 8 highly conservative sites in E1 and E2 proteins [4]. 48 overlapping octapeptides covering the corresponding sequence fragments (Table 1) were synthesized on DKP-pins (Mitokor Mimotopes, Australia) by Multipin multiple parallel peptide synthesis procedure, cleaved into 0.06 M Na-Pi buffer/40% DMSO, and analyzed by MALDI-TOF MS. Each peptide had a biotin-S-G-S-G- moiety on its N-terminus, and a (K-P)-diketopiperazine moiety on its C-terminus. Serum samples from 10 acute and 30 chronic hepatitis C patients, 4 patients with viral clearance, and 43 healthy donors were tested for the presence of anti-peptide-specific antibodies by biotin-streptavidin-based ELISA. The results of these tests are presented in Table 2. Peptides not shown in the table did not react with any serum, except peptides No. 31–33 (CR4) that were reactive with both 28% chronic patient and 40% healthy donor sera. They showed at least 50% identity to *Bac. subtilis*, *E. coli*, and yeast proteins and hence were not considered as E2 antigenic sites.

*Table 1. Highly conservative regions of E1 and E2 HCV proteins.*

Protein	Position [4]	Region (see[4])	Sequence	Prevalence	Peptide #
E1	317–326	CR1	GHRMAWDMMM	94%	3–5
E2	424–438	GLR	GSWHINRTALNCNDS	52%	6–12
E2	494–501	PRR1	PYCWHYAP	64%	13
E2	512–531	CR2	VCGPVYCFPTSPVVVGTTDR	86%	14–26
E2	559–566	PRR2	WFGCTWMN	88%	27
E2	629–640	CR4	YPYRLWHYPCTV	75%	31–35
E2	701–723	CR5	LPALSTGLIHLHQNIVDVQYLYG	59%	36–50

Antibodies from convalescent sera did not bind any peptide. The single peptide that interacted with only one acute hepatitis C patient serum, (427-434)HINRTALN, was revealed for the first time in this work. In contrast to acute hepatitis C cases, 70% chronic patient sera contained antibodies reactive with 12 octapeptides from 5 sites, the most immunogenic being (317-326)GHRMAWDMMM and (701-713)LPALSTGLIHLHQ (Table 2). The first site represented a part of the larger immunogenic site described by other authors [5]; however, we succeeded in detecting the continuous B-epitope RMAWDM inside it. The second one was determined in this work for the first time and was shown to contain at least two continuous B-epitopes: (702-708) PALSTGL and (706-710)TGLIH by antibody binding peptide inhibition analysis. CR1- and CR5-derived peptides can be used in immunotest systems for anti-HCV antibody detection.

Table 2. Reactivity of E1 and E2 octapeptides with sera from HCV-infected patients.

Region	Peptide #	Sequence	Number of reactive sera	Total reactive sera, %
Sera from chronically infected patients:				
CR1	3–5	GHRMAWDMMM	16	53.3
GLR	6	GSWHINRT	1	3.3
PRR1	13	PYCWHYAP	1	3.3
CR3	29	PTDCFRKH	1	3.3
CR5	36–41	LPALSTGLIHLHQ	10	33.3
Sera from patients in acute phase of infection:				
GLR	9	HINRTALN	1	10

The results show rather poor immunogenicity of highly conservative sites of E1 and E2 HCV proteins, especially at early stages of the infection. It may be mainly because of the weak T-helper support since almost no T-helper motifs have been found close to E1 and E2 conservative regions by SYFPEITHI (<http://syfpeithi.de>), except CR1 and CR5. This fact outlines more clear perspectives for the preparation of an artificially constructed rather than recombinant whole protein vaccine against hepatitis C virus.

### Acknowledgments

We thank Prof. N.P. Blokhina (1st Infection Diseases Hospital, Moscow, Russia) for providing with patients' sera and "Vector-Best Co." (Russia) for kind donating of HCV immunotest kits. Supported by grant 01.02/137 from Russian Ministry of Industry, Science and Technology program "New generation vaccines and immunodiagnostics".

### References

1. Farci, P., et al. *Proc. Natl. Acad. Sci. USA* **93**, 15394–15399 (1996).
2. Habersetzer, F., et al. *Virology* **249**, 32–41 (1998).
3. Rosa, D., et al. *Proc. Natl. Acad. Sci. U.S.A.* **93**, 1759–1763 (1996).
4. Sobolev, B.N., Poroikov, V.V., Olenina, L.V., Kolesanova, E.F., Archakov, A.I. *J. Viral Hepat.* **7**, 368–374 (2000).
5. Zibert, A., et al. *J. Hepatol.* **30**, 177–184 (1999).

## Synthesis of a Covalently Reactive Antigen Analog Derived from a Conserved Sequence of HIV-1 gp120

**Hiroaki Taguchi, Yasuhiro Nishiyama, Gary S. Burr, Sangeeta A. Karle  
and Sudhir Paul**

*Chemical Immunology Research Center, Department of Pathology and Laboratory Medicine,  
University of Texas-Houston Medical School, Houston, TX 77030, USA*

## Introduction

Antibodies (Abs) and their light (L) chain subunits are reported to catalyze the cleavage of VIP, the HIV coat proteins gp41 and gp120, Arg-vasopressin, thyroglobulin, factor VIII, prothrombin and various model peptidase substrates. The serine protease inhibitor diisopropylfluorophosphate (DFP) consistently inhibits the catalytic activity of the Abs, and a serine protease-like catalytic triad in a model proteolytic Ab L chain has previously been deduced from site-directed mutagenesis studies. The catalytic site appears to be germline encoded [1]. In principle, probes that can specifically recognize the active site of serine protease Abs could be applied for the selection of efficient catalytic Abs (CAbs) from display libraries, and perhaps also as the immunogens capable of recruiting the germline encoded Ab variable region genes.

Irreversibly binding phosphonate diesters are capable of covalently phosphorylating the active site Ser residue of Ab and non-Ab serine proteases by a nucleophilic substitution reaction, much like the acylation of the enzyme by the substrate. We have recently applied phosphonate diester covalently reactive analogs (CRA) as active site probes for recombinant proteolytic Ab fragments (Fv and L chains) [2]. Here, we report the preparation of a CRA corresponding to a conserved peptide segment of the CD4 binding region of gp120 with a phosphonate diester group located at its C terminus. The peptide CRA displayed the ability to bind and inhibit trypsin and a gp120ase Ab L chain.

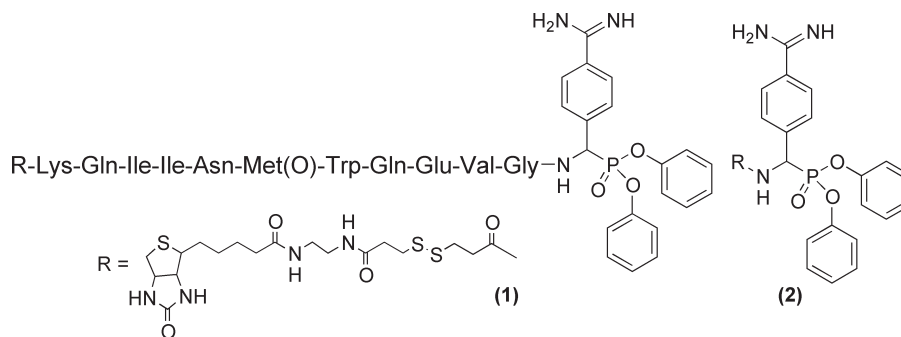


Fig. 1. Structure of biotinylated gp120(421-431)-diphenyl ester phosphonate CRA (1) and the corresponding simple CRA devoid of the peptide flanking region (2).

## Results and Discussion

CRA **1** was synthesized by assembling the protected peptide segment and amino-(4-amidinophenyl)methanephosphonate with the aid of PyBOP followed by TFA-treatment to remove the protecting groups. MS analysis revealed that the major product was an oxidized form of the peptide, most likely the Met sulfoxide. The peptide

appears unusually susceptible to oxidation as we used customary precautions (degassed water; handling/storage under N<sub>2</sub>) to avoid oxidative reactions. CRA **1** contains an S-S linkage (to allow reductive elution of CRA-bound Abs). Thus, reagents such as 2-mercaptoethanol and dithiothreitol were not applied for Met reduction and the peptide CRA was used as recovered.

CRA **1** inhibited *N*-tert-butoxycarbonyl- $\gamma$ -benzyl-Glu-Ala-Arg-7-amido-4-methylcoumarin-hydrochloride (EAR-MCA) hydrolysis by trypsin with near equivalent potency as its nonpeptidic counterpart (phosphonate diester CRA **2**, IC<sub>50</sub> 30  $\mu$ M). Thus, the peptide component at the amino function of phosphonate moiety does not hinder the interaction with the active center of trypsin. CRA **1** inhibited <sup>125</sup>I-labeled gp120 cleavage by a gp120ase Ab L chain about 10-fold more potently compared to CRA **2**. Formation of an irreversible adduct of CRA **1** and the L chain was evident by denaturing SDS-PAGE. Labeling of the L chain by CRA **1** was inhibited by pretreatment with DFP. These results indicate that CRA **1** is an irreversible, active site-directed inhibitor of the gp120ase L chain. As the phosphorus atoms of CRA **1** and CRA **2** are predicted to be equivalent with respect to covalent reactivity, the superior potency of **1** must be due to favorable noncovalent interactions of the peptide component with the gp120ase L chain active site. In theory, noncovalent peptide binding interactions can readily be conceived to help deliver the phosphonate diester moiety to the Ab active site nucleophile. Note, however, that the gp120ase L chain was isolated from a multiple myeloma patient, and its epitope specificity has not been defined. Thus, a comparatively non-specific facilitatory role, due, for instance, to interactions with the peptide backbone, remains possible (as opposed to sequence-dependent binding).

CRA **1** could potentially be applied to isolate CAbs directed to the conserved gp120 residues 421-431, which constitute a segment of the CD4-binding site. Moreover, immunization with CRA **1** may offer the means to induce the synthesis of gp120ase Abs. CRA-driven B cell clonal selection may be predicted to favor mutations that increase the nucleophilic reactivity of the Abs. Such Abs may be uniquely susceptible to acylation by the gp120 substrate. If subsequent hydrolysis of the acyl-Ab complex is facile, efficient CAbs can be anticipated from this approach.

#### Acknowledgments

R. Dannenbring assisted in preparation of <sup>125</sup>I-labeled gp120. Supported by NIH grants CA80312, AI46029 and AI31268. Y. N. is supported by the Naito Foundation.

#### References

1. Gololobov, G., Sun, M., Paul, S. *Mol. Immunol.* **36**, 1215-1222 (1999).
2. Paul, S., Tramontano, A., Gololobov, G., Zhou, Y., Taguchi, H., Karle, S., Nishiyama, Y., Planque, S., George, S. *J. Biol. Chem.* **276**, 28314-28320 (2001).

## Isolation, cDNA Cloning, and Chemical Synthesis of *Oryctes rhinoceros* Defensin

Jun Ishibashi, Hisako Saido-Sakanaka and Minoru Yamakawa

National Institute of Agrobiological Sciences, Immunology and Molecular Biology Department,  
Innate Immunity Laboratory, Tsukuba, Ibaraki 305-8634, Japan

### Introduction

Although insects do not have an immune system that involves antigen-antibody reactions, they possess efficient defense mechanisms against bacterial infection. Antibacterial peptides, for example, are known to play an important role in insect immunity. Defensin family peptide is widely distributed among many insect orders. A novel insect defensin was isolated and cloned from the coconut rhinoceros beetle, *Oryctes rhinoceros* [1]. To synthesize peptides that contain intra-chain disulfide bonds, correct disulfide bond formation is the major concern, namely it is not certain whether correct folding occur by random air oxidation. We synthesized *O. rhinoceros* defensin by random and fully selective disulfide formation strategies [2,3].

### Results and Discussion

An antibacterial peptide defensin was purified by 4 steps of reversed phase HPLC from hemolymph of *O. rhinoceros* larvae immunized with *Escherichia coli*, *Staphylococcus aureus* was used as an indicator bacterium. The N-terminal amino acid sequence was determined with an amino acid sequencer. The *O. rhinoceros* defensin cDNA was cloned by 3 steps of polymerase chain reaction using fat body mRNA from immunized larvae. Deduced amino acid sequences from the nucleotide sequences indicated that the defensin precursor consists of 79 amino acids. The mature peptide (43 amino acids, containing 6 cysteines) is assumed to be produced by cleavage of the signal peptide and propeptide region by furin-like processing enzyme.

*O. rhinoceros* defensin was synthesized using both fully selective and random disulfide formation strategies. Both peptide chains were synthesized using Fmoc chemistry. For fully selective disulfide formation, Cys residues were blocked with Trt for C1 and C4, AcM for C2 and C5, and MeOBzl for C3 and C6 respectively. Cleavage from resin and deblocking of Trt was performed by TFA. Disulfide bond between C1 and C4 was linked using 2,2'-bipyridyl disulfide (2PDS) after cleavage from resin. MeOBzl was removed by trifluoromethane sulfonic acid (TFMSA), and the peptide was precipitated by cold ether, recovered only 10%. Disulfide bond between C3 and C6 was linked using 2PDS. Finally, AcM was removed and disulfide bond between C2 and C5 was linked by iodine oxidation. Final yield was 2%. For random disulfide formation, all Cys residues were blocked with Trt. The blocking group was removed while cleavage from resin and the peptide was refolded by air oxidation or under existence of GSH and GSSG. At a peptide concentration of 15.6 µg/ml, most peptide was aggregated by air oxidation and no predominant peak was seen on HPLC profile. At a peptide concentration of 3.9 µg/ml, aggregation was still seen in air oxidation, in which 80% of peptide was recovered as a predominant peak on HPLC. In redox conditions, no aggregation occurred, and 98% of peptide was recovered as a predominant peak. Disulfide bond locations in synthetic defensins from both strategies were confirmed by thermolysin digestion followed by MALDI-TOF-MS and sequencing analysis of the fragment peptides. The result showed that the disulfide bond is present in C1-C4, C2-C5 and C3-C6, which is in accord with the consensus arrange-

***Ishibashi et al.***

ment in insect/arthropod defensins. CD spectra of synthetic defensins from both strategies indicated that they have identical secondary structure. Antimicrobial activity of synthetic defensin was tested against bacteria and fungi. Gram-positive bacteria were more susceptible to the peptide than Gram-negative bacteria. No effect was seen against fungi.

*O. rhinoceros* defensin refolded very effectively, especially under a redox condition and at low concentrations. Although the fully selective disulfide formation method is very complicated, it enables us to form correct disulfide bonds. We believe that this method is applicable to peptides that are difficult to obtain by random oxidation.

**Acknowledgments**

This work was supported by the Enhancement Center of Excellence, Special Coordination Funds for Promoting Science and Technology, Science and Technology Agency, Japan, and in part by a grant from the Rice Genome Project PR-2110, MAFF, Japan.

**References**

1. Ishibashi, J., Saido-Sakanaka, H., Yang, J., Sagisaka, A., Yamakawa, M. *Euro. J. Biochem.* **266**, 616–623 (1999).
2. Maruyama, K., Nagasawa, H., Isogai, A., Ishizaki, H., Suzuki, A. *J. Protein Chem.* **11**, 13–20 (1992).
3. Maruyama, K., Nagasawa, H., Suzuki, A. *Peptides* **20**, 881–884 (1999).

## Deamidation within a $\gamma$ -Gliadin-Derived Peptide Enhances Its Recognition by Serum Antibodies of CD Patients

Florian v.d. Muelbe<sup>1</sup>, Thomas Mothes<sup>3</sup>, Holm Uhlig<sup>3</sup>, A. A. Osman<sup>3</sup>,  
 Toni Weinschenk<sup>2</sup>, Dietmar G. Schmid<sup>1</sup>, Günther Jung<sup>1</sup> and  
 Burkhard Fleckenstein<sup>1</sup>

<sup>1</sup>Institute of Organic Chemistry, University of Tuebingen, Tuebingen, 72076, Germany

<sup>2</sup>Institute of Cell Biology, University of Tuebingen, Tuebingen, 72076, Germany

<sup>3</sup>Institute of Clinical Chemistry and Pathobiochemistry, University of Leipzig, Leipzig, Germany

### Introduction

Coeliac disease (CD) or gluten sensitive enteropathy is an autoimmune disease mainly affecting the proximal small intestine [1]. It is caused in susceptible persons by the ingestion of certain cereal proteins, *i.e.* gliadins and glutenins from wheat. The intestinal mucosa shows characteristic lesions resulting in malabsorption of nutrients.

Tissue transglutaminase (tTgase) was identified as the major autoantigen of CD and is recognised by the so-called endomysial antibodies representing the most important markers of CD [2]. Tissue transglutaminase seems to be involved in the pathogenesis of CD as tTgase-modified gliadin peptides are recognised by gut derived T cells of CD patients [3].

### Results and Discussion

A 16-mer peptide (H-LPFPQQPQQPFPQPQQ-OH) derived from  $\gamma$ -gliadin of wheat was identified as a new peptide substrate of tTgase and was synthesised by solid-phase peptide chemistry. By means of MS-MS-analysis and Edman degradation one glutamine residue out of seven was identified to be dominantly deamidated by tTgase: LPFPQQPQQPFPQPQQ.

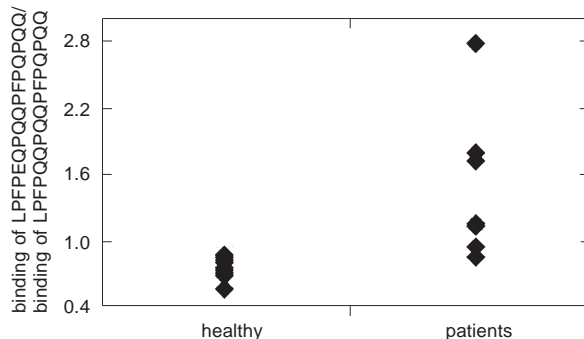


Fig. 1. Reaction of patients serum and serum of healthy controls was followed by plasmon resonance technology. On the measure cell surface the peptides LPFPQQPQQPFPQPQQAKC and LPFPEQPQQPFPQPQQAKC were covalently attached.

Immune fluorescence-measurements by microscopy showed that peptides LPFPQQPQQPFPQPQQ (A) and LPFPQQPQQPFPQPQQ (B) are attached to the tissue section in significantly higher amounts than peptides LPFPEQPQQPFPQPQQ (C) and LPFPAQPAQPFPQPQQ (D). Experiments showing colocalisation of the peptides and tTgase in the tissue section confirmed the analytical results obtained from HPLC and

mass spectrometry: peptides A and B are covalently linked to the extracellular matrix by tTgase and the glutamine in position 5 is the most important transamidation site. Substitution of the targeted glutamine by a glutamic acid residue prevents staining of the tissue section.

To elucidate the role of the new tTgase substrate LPFPQQPQQPFPQPQ as a potential B cell epitope in CD [4] a panel of sera was tested against the synthetic peptides using plasmon resonance technology. For a panel of sera derived from CD patients and a healthy control group it could be shown that tTgase-mediated deamidation within the  $\gamma$ -gliadin-derived peptide LPFPQQPQQPFPQPQ confers enhanced binding and specificity of serum antibodies from CD patients. Thereby, recognition of peptide LPFPEQPQQPFPQPQ by antibodies of CD patients is superior compared to recognition of peptide LPFPQQPEQPFPQPQ. None of the sera from healthy people recognised the deamidated peptide better than the non-deamidated form. This demonstrates a high specificity in recognition of the deamidated peptide by CD patient sera. In this work a  $\gamma$ -gliadin-derived peptide was identified as a new substrate for tissue transglutaminase, the autoantigen of coeliac disease. The glutamine residue involved in tTgase-mediated transamidation and deamidation was identified by LC-MS-MS and enzymatic reaction products have been quantified. Interaction of the FITC-labeled  $\gamma$ -gliadin-derived substrate with tTgase was directly shown in histological immunofluorescence staining. Thus, tTgase-mediated deamidation within a gliadin peptide increases its recognition by anti-gliadin antibodies derived from CD sera.

#### **References**

1. Sollid *Annu. Rev. Immunol.* **18**, 53–81 (2000).
2. Dietrich et al. *Nat. Med.* **3**, 797–801 (1997).
3. Quarsten et al. *Eur. J. Immunol.* **29**, 2506–14 (1999).
4. Osman et al. *Clin. Exp. Immunol.* **121**, 248–54 (2000).

## **Identification of Conserved HIV-1-Derived Helper T Lymphocyte Epitopes Using Synthetic Peptides and High Throughput Binding Assays**

**Yuichiro Higashimoto<sup>1</sup>, Cara C. Wilson<sup>2</sup>, Brent Palmer<sup>2</sup>,  
Scott Southwood<sup>3</sup>, John Sidney<sup>3</sup>, Ettore Appella<sup>1</sup>, Robert Chesnut<sup>3</sup>,  
Alessandro Sette<sup>3</sup> and Brian D. Livingston<sup>3</sup>**

<sup>1</sup>Laboratory of Cell Biology, National Cancer Institute, NIH, Bethesda, MD 20892, USA

<sup>2</sup>Department of Medicine, University of Colorado Health Sciences Center, Denver, CO 80262, USA

<sup>3</sup>Epimmune Inc., San Diego, CA 92121, USA

### **Introduction**

Human immunodeficiency virus type 1 (HIV-1) infection is marked by a gradual loss of CD4+ T lymphocytes and a specific loss or failure to develop functional HIV-1-specific helper T cells (HTL) in the majority of chronically infected individuals. However, there is also mounting evidence that HTL that are reactive against HIV-1 antigens may play an important role in delaying disease progression. The development of vaccines to induce protective or therapeutic cellular immune responses to HIV-1 has been attempted, but it is complicated by the presence of numerous viral variants [1]. Epitope-based vaccines offer the advantage of focusing immune responses on multiple conserved epitopes. One potential obstacle to the development of epitope-based vaccines has been the large degree of polymorphism of HLA molecules. Previous studies have demonstrated that the majority of HLA class I and class II molecules can be grouped in broad supertypes with overlapping peptide binding specificity [2]. In the case of the HLA-DR molecules, a single superfamily encompassing DRB1 alleles expressed in the majority of humans has been defined [3]. Based on these data, we have been investigating an HIV-1 vaccine construct that includes multiple, conserved CTL and HTL epitopes. A number of broadly cross-reactive minimal CTL epitopes in conserved regions of HIV-1 proteins have been identified. By contrast, relatively few HIV-1-specific HTL epitopes have been identified. We have, therefore, sought to identify conserved, major histocompatibility complex (MHC) class II-restricted epitopes in HIV-1 that would be recognized by a large fraction of the global population.

### **Results and Discussion**

To identify peptides with highly cross-reactive HLA-DR binding capacity, the amino acid sequences of Gag, Pol, Nef, Rev, Tat, Vif, Vpr, and Vpu were scanned for the presence of the HLA-DR supermotif as described by Southwood *et al.* [3]. Specifically, 15-amino-acid peptides containing a 9-residue core region comprised of a DR supermotif, and 3 N- and C-terminal flanking amino acids, were selected. A panel of 12 different specific HLA-DR peptide assays was utilized and the fraction of peptide bound was calculated as described previously [4]. Eleven conserved highly cross-reactive HLA-DR binding peptides, which are well conserved in a variety of HIV-1 isolates, were identified (Table 1). In order to determine whether these highly cross-reactive HLA-DR binding peptides are recognized during the course of HIV-1 infection, the antigenicity of the 11 supermotif peptides was assessed by stimulating PBMCs from 22 HIV-1-infected or 13 uninfected donors with each peptide individually and measuring tritiated thymidine incorporation after 6 days. Antigen-specific T-cell proliferation was calculated as an S.I., defined as the ratio of thymidine incor-

poration in the presence of antigen divided by the incorporation in the absence of antigen. Overall, PBMCs from 13 of the initial 22 HIV+ donors tested responded to one or more of the supermotif peptides (Table 2). Notably, PBMCs from four patients, UH18, -19, -20, and -21, responded to 10 or more of the HLA-DR supertype peptides tested [5].

Table 1. HLA-DR binding peptides.

	Binding capacity (IC <sub>50</sub> [nM])										
Peptide Antigen	Gag171	Gag294	Gag298	Pol303	Pol335	Pol596	Pol711	Pol712	Pol758	Pol915	Pol956
DRB1*0101 <sup>a</sup>	72	82	4.2	185	357	7.2	3.6	8.3	38	161	2.9
DRB1*1501	65	138	5.1	70	217	222	21	25	–	650	3.4
DRB1*0301	17647	<sup>b</sup>	188	–	–	13636	3226	–	–	–	–
DRB1*0401	60	1667	633	294	3571	28	9.3	156	11	11909	357
DRB1*0405	400	380	404	136	109	20	27	165	15	452	49
DRB1*1101	–	213	54	1818	741	317	37	71	95	182	53
DRB1*1201	–	1656	124	–	–	1355	6478	12598	–	18625	124
DRB1*1302	412	98	0.36	–	13	90	3500	2500	4375	125	25
DRB1*0701	455	192	379	30	68	15	18	179	472	1786	25
DRB1*0802	7313	63	49	803	3267	350	31	196	1960	1441	75
DRB1*0901	117	536	58	39	33	39	144	250	872	2586	577
DRB5*0101	13	225	24	4167	667	2.1	4.9	24	125	690	80
DRB3*0101	–	1205	12051	18076	887	8545	–	–	–	14688	–
DRB4*0101	135	161	121	–	14500	527	14	290	951	1000	611

<sup>a</sup> Representative allele used to test binding to the corresponding antigen. <sup>b</sup> Indicates an IC<sub>50</sub> of >20  $\mu$ M.

Table 2. Proliferative responses of PBMCs from peptide-responsive HIV-infected donors to HIV-1 HTL peptides.

HIV+ donor	Response of RBMCs to <sup>a</sup>										
	Gag171	Gag294	Gag298	Pol303	Pol335	Pol596	Pol711	Pol712	Pol758	Pol915	Pol956
UH18	6.7	9.2	3.4	9.9	7.2	5.3	3.5	6.6	14.6	6.6	3
UH19	3.8	–	5.9	4.8	5.4	3.2	2.7	4.8	3.7	20.3	6.1
UH20	9.9	4.2	6.8	2.8	3.1	3.2	–	2.7	2.9	13	4.7
UH21	4.4	4.9	2.9	2.8	8.4	2	2	2.8	7	3.2	2.2

<sup>a</sup> Values denote S.I.

## References

1. Coffin, J.M. *Science* **267**, 483–489 (1995).
2. Sette, A., Sidney, J. *Curr. Opin. Immunol.* **10**, 478–482 (1998).
3. Southwood, S., et al. *J. Immunol.* **160**, 3363–3373 (1998).
4. O'Sullivan, D., et al. *J. Immunol.* **147**, 2663–2669 (1991).
5. Wilson, C.C., et al. *J. Virology* **75**, 4195–4207 (2001).

## Determining the Fate of Glycopeptides During Antigen Processing in Antigen Presenting Cells

Rodney Gagné<sup>1</sup>, Shiro Komba<sup>1</sup>, Teis Jensen<sup>2</sup>, Monika Gad<sup>2</sup>,  
 Ole Werdelin<sup>2</sup> and Morten Meldal<sup>1</sup>

<sup>1</sup>Department of Chemistry, Carlsberg Laboratory, Valby, DK-2500, Denmark

<sup>2</sup>Department of Medical Microbiology and Immunology, University of Copenhagen,  
 Copenhagen, DK-2200, Denmark

### Introduction

Malignant cells can be differentiated from normal cells by the presence of aberrant glycosylation. A large part of anti-tumor immune responses is directed against the tumour cell-associated Tn ( $\alpha$ -D-GalNAc) and T ( $\beta$ -D-Gal(1-3)- $\alpha$ -D-GalNAc) carbohydrate antigens [1]. In the present study, the E<sup>k</sup> MHC class II molecule found in CBA/J mice was used to evaluate the immunogenicity of synthetic antigens [2]. It has been shown that synthetic glycopeptides can bind to the E<sup>k</sup> molecule and produce an immune response provided the glycan points away from the MHC binding cleft and are located towards the central part of the T cell receptor recognition site [3].

In order to determine the source of the immune response to certain glycopeptides, two separate investigations have been carried out. The first involved the synthesis and immunological evaluation of a series of glycopeptides (Figure 1) that contained differently sized carbohydrate moieties. A T cell proliferation assay was used to indicate the fate of the glycan during antigen processing in the endocytic pathway of APC. The

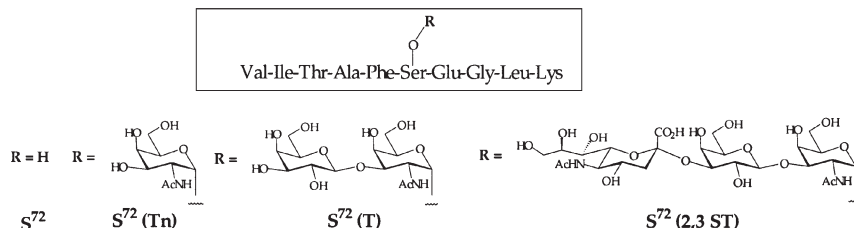


Fig. 1.  $S^{72}$  glycopeptide series.

second investigation involved the synthesis and immunological evaluation of a cyclic glycopeptide, **1** (Figure 2). Cyclic glycopeptides, such as **1**, cannot bind to MHC molecules. In order for the compound to be immunogenic, it must be processed by enzymes in the APC to yield a linear form. The processed molecule can be transported to the cell surface and recognized by T cell hybridomas. The outcomes of these investi-

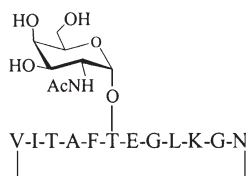


Fig. 2. Cyclic glycopeptide **1**.

gations have significant implications in the design of glycopeptide-based anti-tumour vaccines.

### Results and Discussion

All of the  $S^{72}$  glycopeptides were synthesized on solid support using Fmoc-amino acid-pentafluorophenyl (OPfp) esters in DMF. They were linked to the solid support via a base-labile HMBA linker. Glycosylated building blocks were synthesized using previously described procedures and used in the solid phase assembly of the glycopeptides [4–6]. The glycopeptides were deprotected on solid support using 95%  $\text{TFA}_{(\text{aq.})}$ , cleaved with 0.1 N NaOH, and purified by reversed-phase HPLC. To test the immunogenicity of the  $S^{72}$  series, the synthetic compounds were injected into CBA/J mice along with Complete Freund's Adjuvant. After 10 days, the lymph nodes were removed and cultured and T cell proliferation assays were performed.

It was found that compounds that possessed small sugar groups,  $S^{72}$  (T) and  $S^{72}$  (Tn), were the most active; whereas,  $S^{72}$  (2,3 ST) was not immunogenic. Cross response experiments showed that when mice were primed with synthetic glycopeptides, they produced T cells against glycopeptides containing the same or smaller carbohydrate structures. The results of the experiments indicate that a large degree of antigen processing occurs in the APC prior to antigen presentation. It can be envisioned, therefore, that glycopeptide-based anti-tumour vaccines should only possess small sugars, such as the Tn and T antigens.

Cyclic glycopeptide **1** was synthesized on solid support using Fmoc-amino acid-pentafluorophenyl (OPfp) esters in DMF. The cyclic glycopeptide was cleaved with 95%  $\text{TFA}_{(\text{aq.})}$ , deprotected with hydrazine hydrate, and purified by reversed-phase HPLC. Compound **1** stimulated T cell hybridomas grown against the corresponding linear glycopeptide and peptide. This implied that **1** was internalized and opened in the APC by degradative enzymes. The supernatant from a T cell culture did not cleave the cyclic glycopeptide. It can be concluded that small glycopeptides follow the same endocytic pathway for antigen presentation as larger glycoprotein antigens.

### Acknowledgments

This work was supported by a grant from the Danish Cancer Society.

### References

1. Hakomori, S. *Adv. Cancer Res.* **52**, 257–331 (1989).
2. Jensen, T., Galli-Stampino, L., Moritsen, S., Frische, K., Peters, S., Meldal, M., Werdelin, O. *Eur. J. Immunol.* **26**, 1342–1349 (1996).
3. Galli-Stampino, L., Meinjohanns, E., Frische, K., Meldal, M., Jensen, T., Werdelin, O., Moritsen, S. *Cancer Res.* **57**, 3214–3222 (1997).
4. Frische, K., Meldal, M., Werdelin, O., Moritsen, S., Jensen, T., Galli-Stampino, L., Bock, K. *Eur. J. Immunol.* **26**, 1342–1349 (1996).
5. Meinjohanns, E., Meldal, M., Schleyer, A., Bock, K. *J. Chem. Soc., Perkin Trans. 1* 985–993 (1996).
6. Komba, S., Werdelin, O., Jensen, T., Meldal, M. *J. Peptide Sci.* **6**, 585–593 (2000).

## Evaluation of Immune Response Elicited by Peptide Libraries Against Foot-and-Mouth Disease Virus

**Eliandre de Oliveira<sup>1</sup>, Miguel Ángel Jimenez-Clavero<sup>2</sup>,  
José Ignacio Núñez<sup>2</sup>, Francisco Sobrino<sup>2</sup>, Ernest Giralt<sup>1</sup>  
and David Andreu<sup>1</sup>**

<sup>1</sup>Department of Organic Chemistry, University of Barcelona, E-08028 Barcelona, Spain

<sup>2</sup>*CBMSO-CISA, Madrid, Spain*

## Introduction

Foot-and-mouth disease virus (FMDV) is the animal pathogen with most important economical implications worldwide. The main antigenic site A of FMDV has been incorporated into peptide vaccine candidates; however, immunization with a single peptide sequence has been shown to select for escape mutants [1]. We have synthesized peptide libraries representative of site A, based on the mixotope combinatorial strategy [2], designed to provide immunogens with high levels of variability.

## Results and Discussion

Mixotope libraries based on site A, and containing  $3.2 \cdot 10^5$  and  $3.4 \cdot 10^3$  linear and cyclic peptide sequences each (Figure 1) were used to immunize guinea pigs. Their variability was derived from either field or cell culture mutant sequences [3]. The synthesis was performed manually on 1 mmol of MBHA resin using Boc/Bzl chemistry with DCC/HOBt couplings in NMP [4].



Fig. 1. Consensus sequence of FMDV, adapted from isolate C-58c1 to guinea pig. The low variability mixotop, MixLo ( $3.4 \cdot 10^5$  sequences), is based on this sequence and contains variants shown in normal type. The high variability library, MixHi ( $3.2 \cdot 10^5$  sequences), includes in addition variant residues shown in bold. Cyclic mixotopes were obtained by intramolecular disulfide formation between positions 136 and 153 (underlined), both mutated to Cys.

Groups of 4 guinea pigs were immunized with either single peptides corresponding to the consensus sequence (linear or cyclic disulfide) or with mixotope libraries (linear or cyclic) of high and low variability. Mixotope-vaccinated animals elicited antibodies of broad specificity, recognizing both mixotopes and site A related peptides. However, no recognition of FMDV was observed for these sera. A micro-neutralization assay was performed with five FMDV subtypes (Figure 2). Animals immunized with linear mixotopes of low variability did not give neutralizing antibodies against any of the FMDV subtypes assayed. For the other immunogens, substantial variation in neutralization titers was found. Rather unexpectedly, the highest average titers corresponded to animals inoculated with the cyclic version of the consensus peptide (Figure 3).

**Cyclic immunogens**

Category	1	2	3	4	5	6	7	8	9	10	11	12	13	14
CS8	50	100	3000	100	1	1	1	1	1	1	1	1	1	1
CS8+MAR2.1	1	1	1	1	1	1	1	1	1	1	1	1	1	1
CS8+MAR2.1+MAR2.2	1	1	1	1	1	1	1	1	1	1	1	1	1	1
CS8+MAR2.1+MAR2.2+MAR2.3	1	1	1	1	1	1	1	1	1	1	1	1	1	1
MAR2.1	1	400	400	400	1	1	50	20	1	1	20	1	1	1

**Linear immunogens**

Category	1	2	3	4	5	6	7	8	9	10	11	12	13	14
CS8	100	1	1	1	1	1	1	1	1	1	20	100	1	1
CS8+MAR2.1	1	1	1	1	1	1	1	1	1	1	1	1	1	1
CS8+MAR2.1+MAR2.2	1	1	1	1	1	1	1	1	1	1	1	1	1	1
CS8+MAR2.1+MAR2.2+MAR2.3	1	1	1	1	1	1	1	1	1	1	1	1	1	1
MAR2.1	50	50	200	50	1	1	1	1	1	1	20	20	50	1

## References

1. Taboga, O., Tami, C., Carrillo, E., Núñez, J.I., Rodríguez, A., Saíz, J.C., Blanco, E., Valero, M.L., Roig, X., Camarero, J.A., Andreu, D., Mateu, M.G., Giral, E., Domingo, E., Sobrino, F., Palma, E.I. *J. Virol.* **71**, 2606 (1997).
2. Gras-Masse, H., Ameisen, J.-C., Boutillon, C., Rouaix, F., Bossus, M., Deprez, B., Neyrinck, J.-L., Capron, A., Tartar, A. *Peptide Res.* **5**, 211 (1992).
3. Mateu, M.G., Valero, M.L., Andreu, D., Domingo, E. *J. Biol. Chem.* **271**, 12814 (1996).
4. Oliveira, O., Jimenez-Clavero, M.A., Núñez, J.I., Sobrino, F., Giral, E., Andreu, D., In Martínez, J. and Fehrentz, J.A. (Eds.) *Peptides 2000 (Proceedings of 26th European Peptide Symposium)*, EDK, Paris, 2001, p. 897.
5. Jimenez-Clavero M.A., Escribano-Romero, E., Douglas A., Ley V. *J. Virol.* (2001), in press.

## **Peptoid-Peptide Hybrids: Design, Synthesis and MHC Binding**

**Ellen C. de Haan<sup>1</sup>, Marca H. M. Wauben<sup>2</sup>,  
Mayken C. Grosfeld-Stulemeyer<sup>2</sup>, John A. W. Kruijtzer<sup>1</sup>,  
Rob M. J. Liskamp<sup>1</sup> and Ed E. Moret<sup>1</sup>**

<sup>1</sup>*Department of Medicinal Chemistry, Utrecht Institute for Pharmaceutical Sciences,  
Utrecht University, 3508 TB Utrecht, The Netherlands*

<sup>2</sup>*Immunology Division, Institute of Infectious Diseases and Immunology, Utrecht University,  
3508 TD Utrecht, The Netherlands*

### **Introduction**

Major histocompatibility complex (MHC) class II proteins present peptides to the T cell receptor (TCR) of the T cell. When the MHC-peptide complex is recognized by the T cell, subsequent signaling results in activation of the T cell. Small modifications in the peptide with the result of a changed interaction with the TCR, can lead to an altered T cell response. These so called altered peptide ligands (APL) [1] can be either peptides or peptidomimetics. Advantages of the peptidomimetic APL are the possibility to use tailor-made building blocks, as well as the increased stability. Here we describe the design, synthesis and MHC class II binding of peptoid-peptide hybrids. In peptoid residues, the position of the side chain is shifted from the  $\alpha$ -carbon atom to the nitrogen atom [2,3]. The identity of the side chain is conserved, while the direction in three-dimensional space is changed. The rat model experimental autoimmune encephalomyelitis is an animal model to study human multiple sclerosis. Peptide sequence 72-85 of guinea pig myelin basic protein (gpMBP) presented by the MHC class II molecule RT1.B<sup>L</sup>, is the immunodominant T cell epitope [4]. Starting from this peptide, peptoid-peptide hybrids were designed.

### **Results and Discussion**

Since no crystal structure of the MHC class II-peptide complex involved was available, a homology model was made to investigate which amino acids could contact the TCR. The three-dimensional structure of the MHC molecule was built by homology to the mouse MHC class II molecule I-A<sup>k</sup> [5]. Using a *de novo* design programme, a binding motif of the MHC molecule was generated. The peptide was aligned in the groove according to the motif. This alignment was confirmed by experimental MHC-peptide binding data [6]. The final model is shown in the Figure 1. Three amino acids point up towards the TCR (TCR contact residues) and those residues were altered into the corresponding peptoid residues.

The first step in evaluation of the peptoid-peptide hybrids was to check the MHC binding capacity, since presentation of a peptide or peptoid-peptide hybrid to the TCR is mediated by the MHC class II molecule. To test the MHC binding, a competition assay was utilized, in which the peptide or peptoid-peptide hybrid of interest competes for isolated MHC molecules with marker peptide [7]. The marker peptide is detected by enhanced chemoluminescence.

Surprisingly, two peptoid-peptide hybrids (changed at position 2 and 5) showed a large affinity decrease in the MHC-peptide binding assay compared with the unaltered peptide. The third peptoid-peptide hybrid only showed slight reduction in affinity. Three factors, typical for peptoids, that could explain the low affinity, were investigated to dissect the individual contributions to MHC binding affinity: the changed position of the side chain, the loss of a putative hydrogen bond between the backbone of

the peptide and the MHC, and the presumably increased flexibility. Another set of compounds containing amino acid and peptoid substitutions was synthesized. The MHC binding of all compounds was measured and the structure–activity relationships were established.

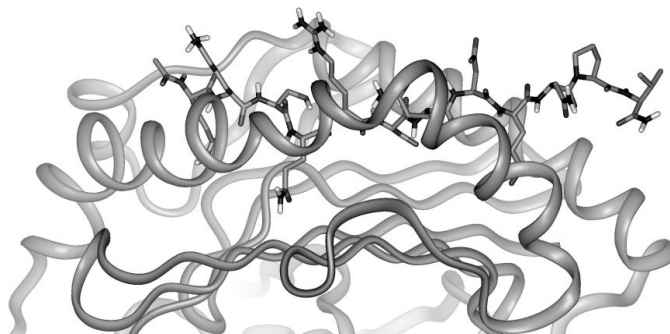


Fig. 1. Homology model of the MHC class II molecule with the bound peptide. Three amino acids pointing upwards were replaced by peptoid residues.

We conclude that the side chain orientation, as well as the backbone nitrogen atom hydrogen bonding features of TCR contact residues can be important for MHC binding affinity. Currently, the APL activity of the described compounds is investigated.

#### Acknowledgments

The research of M. H. M. Wauben has been made possible by a fellowship of the Royal Netherlands Academy of Arts and Sciences.

#### References

1. Evavold, B.D., Sloan-Lancaster, J., Allen, P.M. *Immunol. Today* **14**, 602–609 (1993).
2. Simon, R.J., Kania, R.S., Zuckermann, R.N., Huebner, V.D., Jewell, D.A., Banville, S., Ng, S., Wang, L., Rosenberg, S., Marlowe, C.K., Spellmeyer, D.C., Tan, R.Y., Frankel, A.D., Santi, D.V., Cohen, F.E., Bartlett, P.A. *Proc. Natl. Acad. Sci. USA* **89**, 9367–9371 (1992).
3. Kruijtzter, J.A.W., Hofmeyer, L.J.F., Heerma, W., Versluis, C., Liskamp, R.M.J. *Chem.-Eur. J.* **4**, 1570–1580 (1998).
4. Chou, Y.K., Vandenbark, A.A., Jones, R.E., Hashim, G., Offner, H. *J. Neurosci. Res.* **22**, 181–187 (1989).
5. Fremont, D.H., Monnaie, D., Nelson, C.A., Hendrickson, W.A., Unanue, E.R. *Immunity* **8**, 305–317 (1998).
6. Wauben, M.H.M., van der Kraan, M., Grosfeld-Stulemeyer, M.C., Joosten, I. *Int. Immunol.* **9**, 281–290 (1997).
7. Joosten, I., Wauben, M.H.M., Holewijn, M.C., Reske, K., Pedersen, L.O., Roosenboom, C.F. P., Hensen, E.J., van Eden, W., Buus, S. *Int. Immunol.* **6**, 751–759 (1994).

## Synthetic Glycopeptide Models of MUC1 Core Protein

Mare Cudic<sup>1</sup>, David J. Craik<sup>2</sup> and Laszlo Otvos, Jr.<sup>1</sup>

<sup>1</sup>The Wistar Institute, Philadelphia, PA 19104, USA

<sup>2</sup>Institute for Molecular Bioscience, University of Queensland, Brisbane,  
 Queensland 4072, Australia

### Introduction

Mucins are major epithelial luminal surface proteins and function as a barrier protecting mucous epithelia. When mucins are associated with malignant epithelial cells, they not only protect these cells from the host environment during metastatic dissemination, but also generate immunogenic epitopes depending upon their status of glycosylation. The core sequence of mucin 1 consists of a 20-mer fragment tandemly repeated 6 times [1]. The core mucin sequences, the major epitopes for cancer-specific antibodies and T-cells, were reported to be abnormally glycosylated in cancer [2]. In order to understand how glycosylation may modulate the recognition process of mucin core epitopes, we have synthesized a series of glycopeptide models that contain no sugar, thus mimicking the core 1 sequence, peptides with short carbohydrate side chains (Glc-Glc-GalNAc-1 $\alpha$ ) that will mimic the carcinoma-originated mucin protein fragments, and finally peptides with extended carbohydrate chains (Glc-Glc-Glc-Glc-Glc-Glc-GalNAc-1 $\alpha$ ) that will mimic mucin secreted by normal cells. N-acetyl galactosamine (GalNAc) was the primary sugar unit linked to either a serine or a threonine, since it represents the only consistent feature of mucin 1 glycosylation (Table 1).

### Results and Discussion

O-Glycosylated Thr/Ser building blocks were prepared from acetylated tri- and heptasaccharide bromides as glycosyl donors. The azido functionality at C-2 of the GalNAc facilitated stereoselective glycosylation, and the  $\alpha$ -anomer was formed in great excess, even for long chain glycosyl donors. The non-glycosylated MUC1 peptide and the glycopeptides carrying one or two sugar-side chains were assembled on solid-phase employing standard Fmoc-strategy. The azido group on the sugar ring was transformed into an N-acetyl group by reaction with thioacetic acid on the polymer-bound glycopeptide. After cleavage and deacetylation of the sugar hydroxyls, the peptides were purified by RP-HPLC and characterized by MALDI-MS. When sugars (even

Table 1. Synthetic glycopeptides and their characterization.

Sequence	Side-chain modification	RP-HPLC (min)	(M+H) <sup>+</sup> (m/z)
HGVTSAPDTRPAPGSTAPP	—	18.4	1815
HGVT(X)SAPDTRPAPGSTAPP	Glc( $\alpha$ 1-4)-Glc( $\beta$ 1-4)-GalNAc( $\alpha$ 1-O)	17.0	2342
HGVTSAPDTRPAPGST(X)APP	Glc( $\alpha$ 1-4)-Glc( $\beta$ 1-4)-GalNAc( $\alpha$ 1-O)	17.4	2343
HGVTSAPDTRPAPGS(X)TAPP	Glc( $\alpha$ 1-4)-Glc( $\beta$ 1-4)-GalNAc( $\alpha$ 1-O)	17.5	2342
HGVT(X)SAPDTRPAPGST(X)APP	Glc( $\alpha$ 1-4)-Glc( $\beta$ 1-4)-GalNAc( $\alpha$ 1-O)	15.9	2870
HGVT(X)SAPDTRPAPGSTAPP	[Glc( $\alpha$ 1-4)-Glc] <sub>3</sub> -GalNAc( $\alpha$ 1-O)	16.8	2991
HGVTSAPDTRPAPGSTAPP	[Glc( $\alpha$ 1-4)-Glc] <sub>3</sub> -GalNAc( $\alpha$ 1-O)	17.2	2990
HGVT(X)SAPDTRPAPGST(X)APP	[Glc( $\alpha$ 1-4)-Glc] <sub>3</sub> -GalNAc( $\alpha$ 1-O)	15.1	4171

monosaccharides) were attached to *O*-glycosylation sites within the core epitope (the N-terminus of our peptide), there was a marked interference with T cell receptor recognition. Glycosylation of the flanking serine or threonine had no effect on T-cell stimulation nor actually facilitated the recognition.

While glycosylation of Ser15 did not appear to modify the conformation by CD, a 223 nm positive band was noticeable for the Thr4 and Thr16 glycosylated peptides. Since its intensity was not dependent upon the length of the carbohydrate moiety, the number of carbohydrate side-chains rather than the size of a single sugar side-chain appeared to play roles in defining the secondary structure. These findings support the idea that the number of the carbohydrate side-chains attached to mucin 1 is actually increased in cancerous cells [3]. The only region in the NMR spectra where consecutive secondary shifts of magnitude >0.1 ppm occurred were Asp8-Arg10; this was also the only region where non-consecutive NOEs were observed. This suggested the presence of a population of turn-like structures in this region and is consistent with previous observations of local ordering in the PDTR segment [4].

#### **Acknowledgments**

We thank Dr. Olivera Finn for the T-cell stimulation assay. This work was supported by NIH grant GM45011.

#### **References**

1. Lagow, E., DeSouza, M.M., Carson, D.D. *Hum. Reprod. Update* **5**, 280–292 (1999).
2. Muller, S., Alving, K., Peter-Katalinic, J., Zachara, N., Gooley, A.A., Hanisch, F.G. *J. Biol. Chem.* **274**, 18165–18172 (1999).
3. Muller, S., Goletz, S., Packer, N., Gooley, A.A., Lawson, A.M., Hanisch, F.G. *J. Biol. Chem.* **272**, 24780–24793 (1997).
4. Kirnarsky, L., Nomoto, M., Ikematsu, Y., Hassan, H., Bennett, E.P., Cerny, R.L., Clausen, H., Hollingsworth, M.A., Sherman, S. *Biochemistry* **37**, 12811–12817 (1998).

## **Cathepsin D Produces the Potent Antimicrobial Peptide Parasin I from Histone H2A in Scaleless Fish Skin**

**Ju Hyun Cho, In Yup Park and Sun Chang Kim**

*Department of Biological Sciences, Korea Advanced Institute of Science and Technology,  
Taejeon, 305-701, Korea*

### **Introduction**

Antimicrobial peptides have been known to act as the first line of mucosal host defense by exerting broad-spectrum microbicidal activity against invading pathogenic microbes [1,2]. Recently, a potent 19-residue linear antimicrobial peptide, named parasin I, was isolated from the skin mucus of wounded catfish, *Parasilurus asotus* [3]. The amino acid sequence of parasin I is KGRGKQGGKVRKAKTRSS, which is identical to the N-terminal region of rainbow trout histone H2A in 16 of the 19 residues [4]. The very high homology between parasin I and the N-terminal region of histone H2A suggests that parasin I might be cleaved off from histone H2A by a specific protease cleavage similar to the case of buforin I, which is generated from the unacetylated histone H2A in the cytoplasm of gastric gland cells by the action of pepsin C isozymes in the toad stomach [5]. However, the protease that is responsible for the generation of parasin I from histone H2A has not been identified. Furthermore, the findings of Park *et al.* [3] that parasin I was found only in the skin mucus of wounded catfish and not in unwounded catfish suggests the involvement of an inducible mechanism in parasin I production. In this study, we describe the mechanism for the generation of parasin I from histone H2A in catfish skin mucosa upon epidermal injury. We also assess the biological role of parasin I in the innate host defense of the fish against invading microorganisms.

### **Results and Discussion**

We purified the specific proteases from the mucus of catfish that were responsible for the generation of parasin I from histone H2A. Cathepsin D was found to exist as an inactive proform (procathepsin D) in the mucus, and a metalloprotease, induced upon injury, activated the procathepsin D to mature cathepsin D, which consequently cleaved the Ser<sup>19</sup>-Arg<sup>20</sup> bond of histone H2A to produce parasin I. Using recombinant procathepsin D as a substrate, we identified the procathepsin D-processing metalloprotease in the mucus of wounded catfish. The purified enzyme, named Pa-metalloprotease, carried out the activation of procathepsin D to mature cathepsin D by specifically cleaving the Phe<sup>61</sup>-Gly<sup>62</sup> bond of procathepsin D.

To elucidate the mechanism of parasin I generation in catfish skin mucosa, we performed immunohistochemical analysis with the skin sections from both unwounded and wounded catfishes. Immunohistochemical data indicated that unacetylated histone H2A, the precursor of parasin I, and procathepsin D were present in the cytoplasm of epithelial mucus cells, and parasin I was produced and secreted to the mucosal surface upon epidermal injury. The immunoreactivity of unacetylated histone H2A and procathepsin D did not change upon injury, whereas the immunoreactivity of parasin I at the mucosal surface of the skin was greatly increased in response to injury. This further confirms the existence of the inducible mechanism in parasin I production, which is mediated by the activation of procathepsin D secreted to the mucus. Of note is the finding that the immunoreactivity of parasin I is extracellular on the mucosal surface. This indicates that parasin I coats the mucosal surface, where it may contribute to the

establishment of a local antimicrobial milieu. This notion is further supported by our observation that parasin I showed a strong antimicrobial activity against fish-specific pathogens.

The conservation of the amino acid sequence of histone H2A [4] and cathepsin D [6] in fish phylum suggests that this parasin I sequence harbors a biologically important part of the molecule, which has been an advantage during selection and evolution in fish phylum. Whether parasin I is ubiquitous in the skin mucosa of other fish species is not clear. However, we confirmed the presence of parasin I in the mucus of eel, loach, and rainbow trout, in which scalation is reduced or absent, by Western blot analysis. Together, these results indicate that Pa-metalloprotease and cathepsin D are involved sequentially in the production of the potent antimicrobial peptide parasin I from histone H2A, which contributes to the innate host defense of the fish against invading microorganisms.

#### **Acknowledgments**

This work was supported in part by grants KOSEF-1999-1-20900-002-5 (the Korea Science and Engineering Foundation) and 2000-N-NL-01-C-160 (the Ministry of Science and Technology for the National Research Laboratory Program).

#### **References**

1. Hunter, K.M., Bevins, C.L. *Pediatr. Res.* **45**, 785–794 (1999).
2. Hancock, R.E.W., Scott, M.G. *Proc. Natl. Acad. Sci. U.S.A.* **97**, 8856–8861 (2000).
3. Park, I.Y., Park, C.B., Kim, M.S., Kim, S.C. *FEBS Lett.* **437**, 258–262 (1998).
4. Connor, W., States, J.C., Mezquita, J., Dixon, G.H. *J. Mol. Evol.* **20**, 236–250 (1984).
5. Kim, H.S., Yoon, H., Minn, I., Park, C.B., Lee, W.T., Zasloff, M., Kim, S.C. *J. Immunol.* **165**, 3268–3274 (2000).
6. Capasso, C., Lees, W.E., Capasso, A., Scudiero, R., Carginale, V., Kille, P., Kay, J., Parisi, E. *Biochim. Biophys. Acta* **1431**, 64–73 (1999).

## **Characterization of Highly Stimulatory T Cell Ligands Identified Using Positional Scanning Libraries**

**Eva Borràs<sup>1</sup>, Bruno Gran<sup>2</sup>, Roland Martin<sup>2</sup> and Clemencia Pinilla<sup>1</sup>**

<sup>1</sup>*Torrey Pines Institute for Molecular Studies, San Diego, 92121, USA*

<sup>2</sup>*Cellular Immunology Section, Neuroimmunology Branch, NINDS, NIH, Bethesda, 20892, USA*

### **Introduction**

T cell activation occurs when a T cell receptor (TCR) recognizes a specific peptide bound to a major histocompatibility complex (MHC) molecule, triggering a cascade of secondary signals that compose the cellular immune response. Our efforts have been directed toward the study of T cell specificity using positional scanning synthetic combinatorial libraries (PS-SCL). In particular, the study of human CD4<sup>+</sup> T cell clones relevant for Multiple Sclerosis and Lyme disease with PS-SCL has resulted in the identification of highly active peptides [1,2]. To better understand the reason for this high activity it is important to determine which residues are involved in MHC binding, and which ones play a role as TCR contacts. Proliferation data combined with an MHC inhibition assay have been used to dissect the TCR/peptide/MHC trimolecular interaction.

### **Results and Discussion**

Multiple Sclerosis (MS) and chronic Lyme disease in the central nervous system are T cell mediated autoimmune disorders with a susceptibility associated to certain MHC class II haplotypes. We have studied the proliferative activity of peptides identified with a decapeptide PS-SCL with: 1) TL3A6, a human CD4<sup>+</sup> T-cell clone restricted to HLA-DR2a and specific for myelin basic protein (MBP<sub>87-99</sub>), a known autoantigen in MS, and 2) CSF3, a CD4<sup>+</sup> clone of unknown specificity, from a patient with chronic Lyme disease, restricted to HLA-DR2b. Proliferation experiments have demonstrated that some of the identified peptides are highly active; 10- to 100-fold more active than the native epitope for the clone with known specificity.

In order to address questions regarding the specific role of the amino acids as MHC anchors or TCR contacts in these highly active peptides, we have modified an MHC *in vivo* loading assay in a 96-well plate format based on the protocol reported by Arndt *et al.* [3]. In this competition assay, cells expressing a specific MHC molecule (DR2a or DR2b) are incubated in the presence of a reporter biotinylated peptide and the peptide to be tested, allowing the loading of the peptide ligands on to the cell. After lysing the cells and collecting the MHC-peptide complexes, these are quantitated by an europium ELISA. This competition assay allows the determination of the relative MHC binding affinities for a large number of peptides in a short period of time.

For TL3A6 clone we compared the proliferative activity of 37 of the identified peptides with their capacity to bind to DR2a. Also, the effect of their N-terminus was studied, showing that the differential T cell stimulation activity of these ligands is due to their TCR interactions, but is not related to the MHC binding (Table 1). The same studies were carried out with 25 ligands of CSF3 clone. Moreover, for the most stimulatory peptide a series of alanine substitution analogs was synthesized and used to study the relevance of each residue in the trimolecular interaction (Figure 1).

In this study, the main anchor residues to the MHC class II haplotypes DR2a and DR2b are consistent with the reported primary anchors. However, other residues and positions not described in the literature have been found to be involved in MHC bind-

Table 1. DR2a binding capacity and proliferative activity of TL3A6 ligands with different N-terminus.

TL3A6 ligands	MHC binding	Proliferative activity
	H-/Ac-	H-/Ac-
WFKLIPTTKL	1.1	5556
WFKLIPTPKL	1.0	500
WFKLITTKKL	1.2	2000
WFKLITTTKL	0.8	450
WFKLILTTLK	1.1	24

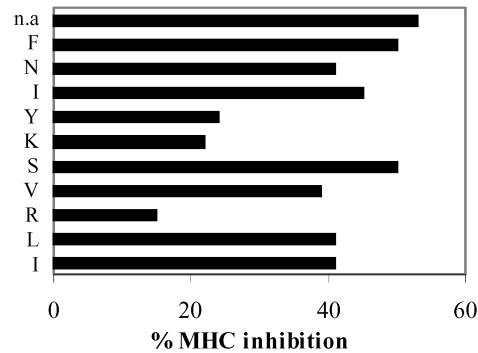


Fig. 1. DR2b inhibition of Ala substitution analogs of a highly active CSF3 ligand.

ing. Thus, it appears that for DR2a and DR2b there is not a unique consensus MHC motif, and new anchor residues can be identified when testing a large number of peptides. In other words, MHC anchors can vary their position or chemical character depending on the ligand sequence.

#### Acknowledgments

This work was supported by the Multiple Sclerosis National Research Institute.

#### References

1. Hemmer, B., Pinilla, C., Gran, B., Vergelli, M., Ling, N., Conlon, P., McFarland, H.F., Houghten, R.A., Martin, R. *J. Immunol.* **164**, 861–871 (2000).
2. Hemmer, B., Gran, B., Zhao, Y., Marques, A., Pascal, J., Tzou, A., Kondo, T., Cortese, I., Bielekova, B., Straus, S., McFarland, H.F., Houghten, R.A., Simon, R., Pinilla, C., Martin, R. *Nature Med.* **5**, 1375–1382 (1999).
3. Arndt, S.O., Vogt, A.B., Markovic-Please, S., Martin, R., Moldenhauer, G., Wölpl, A., Sun, Y., Schadendorf, D., Hammerling, G.J., Kropshofer, H. *EMBO J.* **19**, 1241–1251 (2000).

**Proteomics Approach for Identifying Interacting Partners  
of a C-Terminal Functional Peptide Derived  
from the Tumor Suppressor, p21<sup>cip/waf1</sup>**

**Tarikere L. Gururaja, Weiqun Li, Tong Lin, Donald G. Payan  
and D. C. Anderson**

*Proteomics Department, Rigel Pharmaceuticals Inc., South San Francisco, CA 94080, USA*

**Introduction**

With the recent technological innovations of proteomics, protein separation followed by mass spectrometry (MS) has become the technique of choice in identifying and validating potential drug targets. As a part of our drug discovery program, we tested the validity of this approach by conducting a simple affinity extraction followed by mass spectrometric (MS) analysis of the components isolated. For this purpose, we chose the C-terminal peptide of the tumor suppressor p21<sup>cip/waf1</sup>, which is known to bind proliferating cell nuclear antigen (PCNA) and cause cell cycle arrest [1]. Using Jurkat-E cell lysate, affinity extraction of PCNA and its binding partners was carried out by spiking streptavidin agarose beads pre-conjugated with biotinylated p21-derived peptide(s). Using tryptic digests of entire affinity extracts and differential micro-capillary LC/MS/MS, or difference 2D gels combined with in-gel tryptic digests and MALDI-TOF MS, we have identified binding partners of the p21 C-terminal peptide, or of its complex with PCNA. Results from the above experiments were confirmed either by reciprocal affinity extraction and/or Western blotting with respective antibodies. This study suggests that peptides obtained from intracellular functional screens could also serve as efficient baits to affinity extract target proteins and map mammalian cell protein interaction networks.

**Results and Discussion**

The C-terminal peptide of p21<sup>cip/waf1</sup>, KRRQTSMTDFYHSKRRLIFS having biotin with a spacer (GS)<sub>5</sub> at the N-terminus and its corresponding control peptides such as its scrambled version, Biot-(GS)<sub>5</sub>-YFDQTMSTRRFSLIHKRKRS (p21-S) and an inactive mutant version, Biot-(GS)<sub>5</sub>-KRRQTSATAAYHSKRRLIFS (p21-M) were synthesized, purified and characterized following conventional methods. Figure 1 shows a silver stained 2D gel obtained when 10<sup>8</sup> asynchronously growing Jurkat-E cells were lysed with PBS buffer containing 1% Triton X-100 and extracted with a biotinylated p21 peptide pre-conjugated to streptavidin agarose beads, overnight at 4 °C. The difference spots (total of 8 spots) obtained after comparing the experimental gel with the two control gels (p21-S and p21-M extractions) are labeled. The 2D-difference spots thus identified were excised, trypsinized and subjected for MALDI-TOF MS analysis followed by nr-database search using ProFound [2]. Any ambiguity in protein ID from this method was further cross-examined using micro-capillary LC/MS/MS analysis. On the other hand, an aliquot of samples derived from experimental as well as control affinity extracts was trypsinized and the whole digests were injected onto a micro-capillary column (75 µm id × 15 cm C18) containing a spray tip made up of reversed-phase material. Samples emerging from this tip after separation using a 0.6%/min acetonitrile gradient at 0.6 µl/min flow rate, were trapped, fragmented and detected using a Finnigan LCQ ion trap mass spectrometer. Following its acquisition, the LC/MS/MS data derived from control affinity extracts were subtracted from the

experimental affinity extracts using a C/C++ based program called MS2Filter. This program efficiently removes MS/MS spectra common to control and experimental data. Upon conducting this pre-filtering of the raw data, ≈550 unique MS/MS spectra were found, which, after a SEQUEST search of the non-redundant database, gave ≈95 identifiable proteins (Table 1). In several cases the identities were confirmed by reciprocal immunoprecipitation and/or by Western analysis.

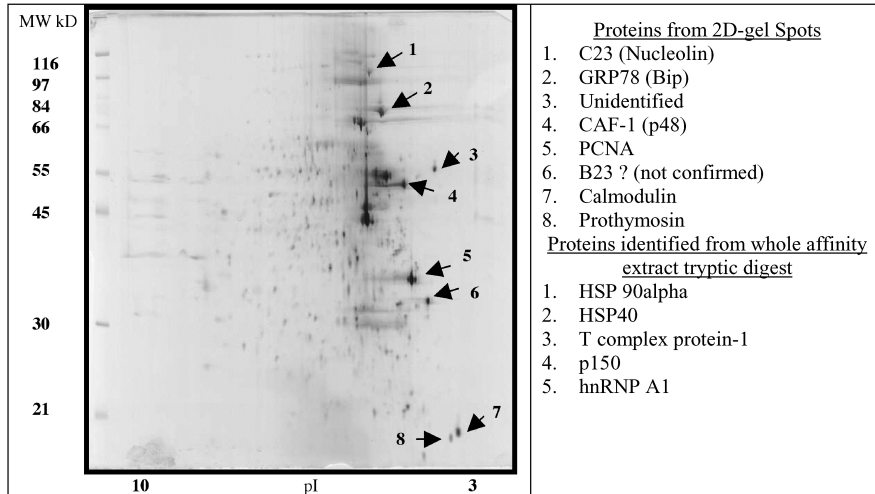


Fig. 1. Silver stained 2D-gel of p21 extract.

Table 1. Proteins identified.

Compared to the scrambled peptide and inactive mutant peptide controls, the biotinylated p21 peptide reproducibly and efficiently extracts PCNA, which appears to have multiple iso-forms. The p21 peptide also extracts calmodulin and p150 in one cell batch confirming previous reports [3,4]. The other proteins may represent novel binding partners. DNA appears to be important for the integrity of many of these complexes since they disappear when cellular DNA is digested with DNase (data not shown). Although we have observed two published interactions (calmodulin and p150) beyond that of p21-PCNA, these are not seen in other cell batches, indicating the importance of other variables for the strength of these interactions.

#### Acknowledgments

Thanks are due to Haleh Khoshnevisan and Dr. Jim Lorens for initial support on this project. Financial assistance from Rigel Pharmaceuticals Inc., is greatly appreciated.

#### References

1. Warbick, E., Lane, D., Glover, D., Cox, L. *Curr. Biol.* **5**, 275–282 (1995).
2. <http://prowl.rockefeller.edu/cgi-bin/ProFound>.
3. Shibahara, K., Stillman, B. *Cell* **96**, 575–585 (1999).
4. Taules, M., Rodriguez-Vilarrupla, A., Ruis, E., Estanyol, J., Casanovas, O., Sacks, D., Perez-Paya, W., Bachs, O., Agell, N. *J. Biol. Chem.* **274**, 24445–24448 (1999).

## **Cuvette-Based Biosensors as Micropreparative Affinity Surfaces**

**Bruno Catimel, Julie Rothacker and Ed Nice**

*The Ludwig Institute for Cancer Research, Melbourne, 3050, Australia*

### **Introduction**

It is now becoming obvious that the rapidly developing fields of genomics, proteomics and bioinformatics will prove to be complementary in the comprehensive understanding of biological processes and the rapid development of novel pharmaceuticals. In the field of proteomics [1], the separation sciences will obviously play a pivotal role in such studies, coupled with highly sensitive and specific down stream analytical techniques such as mass spectrometry. To date 2-D gel electrophoresis has been routinely used as the preferred method for the separation of complex mixtures of cellular proteins. However, it is now realised that this technique has its limitations, in particular for the identification of low abundance proteins (*e.g.* growth factors, receptors and proteins involved in signal transduction).

A major development over the last decade has been the coupling of the selectivity offered by affinity techniques with sensitive instrumental analytical methods such as mass spectrometry or biosensors. Methods that have previously been regarded as analytical, now have the potential to be used in a micropreparative mode: in this way instrumental biosensors can now act as microaffinity platforms to purify cognate binding partners and their complexes in proteomics-based strategies.

This potential is illustrated by the use of a cuvette-based biosensor (IASys Autoplus) to micropurify and characterise the A33 colonic antigen from colonic carcinoma cell extracts.

### **Results and Discussion**

We have used the IASys Autoplus biosensor to affinity purify directly on the sensor surface the A33 epithelial antigen [2] present on colonic carcinoma cells, which we had originally identified using a combination of micropreparative HPLC and biosensor analysis [3]. Attempts to purify the A33 antigen using preparative 2D-PAGE in a proteomic-based approach were hampered by the similarity in molecular mass and isoelectric point between the A33 antigen and actin or cytokeratin, which were major contaminants of the cell extracts (A33: Mr: 41 kDa, pI: 5.0–6.0; actin: Mr: 41 kDa, pI: 4.0–5.3; cytokeratin: Mr: 42.5 kDa, pI: 5.5–6.5) [4]. To demonstrate the use of preparative ligand fishing in a proteomics-type strategy, LIM1215 colonic cells were extracted using differential detergent extraction (Triton X114) and subjected to a single preliminary anion-exchange chromatography step. The IASys biosensor was used to screen the fractions from the anion exchange column using an anti-A33 F(ab)<sub>2</sub> fragment immobilised onto a preparative CMD-Select cuvette (16 mm<sup>2</sup> surface area, 350 ng immobilised). The active fractions were then pooled for preparative biosensor ligand fishing using the same surface. After multiple (50) automated repetitive injections and recovery cycles, 1 µg of essentially homogeneous A33 antigen was purified and recovered directly from the sensor surface (approximately 20 ng recovered per cycle) giving sufficient material for SDS-PAGE, Western blotting, micropreparative RP-HPLC and N-terminal microsequence analysis.

The combination of IASys micropreparative fishing and MALDI-TOF analysis of recovered fractions was also investigated. As proof of principle, purified recombinant A33 antigen (400 nM) was injected over immobilised A33 IgG (400 ng immobilised).

Seven preparative cycles were performed, resulting in the capture of approximately 1 picomole of antigen. The recovered antigen was digested using Lys-C and the resulting peptides applied to a MALDI-target using a C4 Zip-tip (Millipore). Ten A33-related peptides were identified giving 54% coverage of the A33 protein (Figure 1E).

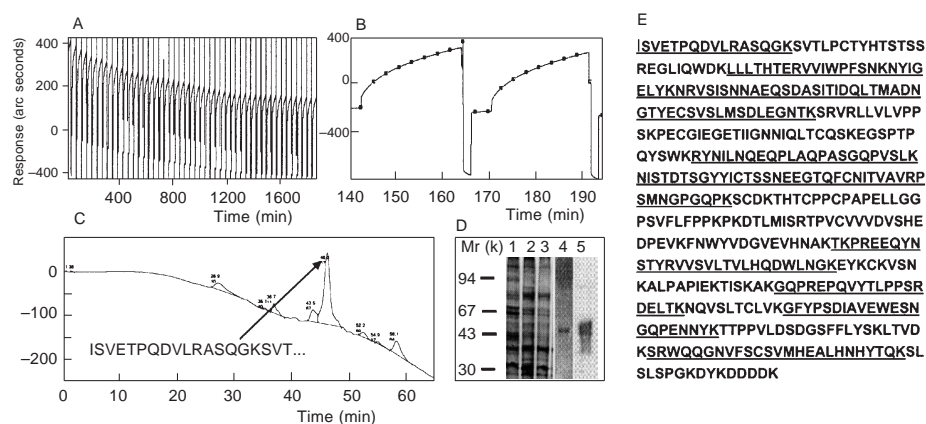


Fig. 1. Preparative biosensor ligand fishing using a cuvette-based optical biosensor.

The A33 antigen was recovered using a preparative biosensor surface, from a Triton X114 extract of LIM1215 carcinoma cell lines following a single anion exchange chromatography step using a Mono Q HR5/5 column. The biosensor active anion-exchange fractions were pooled and injected (50 cycles) (Figure 1A) over anti-A33 Fab<sub>2</sub> (350 ng) immobilised on a CMD-Select Preparative (16 mm<sup>2</sup>) cuvette. Bound antigen was eluted using 10 mM HCl. An enlarged view of 2 consecutive cycles of injection/recovery is shown in Figure 1B. The recovered sample was analysed using micropreparative RP-HPLC on a Brownlee Aquapore RP 300 column (100 × 1 mm ID) and characterised using N-terminal sequence analysis (Figure 1C). The biosensor-recovered fraction was also analysed using silver stained SDS-PAGE and Western blot, revealing a Mr 43,000 protein (Figure 1D, lane 4 and 5). The protein complexity of the Mono Q fractions pooled as the starting material is shown for comparison (Figure 1D, lane 1, 2, 3).

The sequence coverage of peptides generated by Lys-C digestion of recombinant antigen recovered from the cuvette surface is shown in Figure 1E. The peptides identified using MALDI-TOF analysis are underlined.

## References

1. Wilkins, M.R., et al. *Biotechnol. Genet. Eng. Res.* **13**, 19–50 (1996).
2. Catimel, B., et al. *J. Chromatogr. A* **869**, 261–273 (2000).
3. Catimel, B., et al. *J. Biol. Chem.* **27**, 25664–25670 (1996).
4. Ji, H., et al. *Electrophoresis* **18**, 614–621 (1997).

## **A Comprehensive Database of Protein–Protein Interactions**

**J. Mark Carter, Michael James, Brian Korenstein, Juan Herrero,  
Brian Miller, Hai Hu, Ruslana Zhitnitsky, Christine Luczak  
and Lin Chen**

*AxCell Biosciences, Newtown, PA 18940-1721, USA*

### **Introduction**

While proteomics is defined as a comprehensive study of proteins expressed by an organism, it is often limited to expression profiling and sequence analysis. In reality, of course, proteins are not important simply because they are present, but because they have unique functions. Most proteins function at least partly through their interactions with other proteins, and this information is not apparent from 2D PAGE expression analysis or amino acid sequencing. A comprehensive analysis of protein interactions is thus critical to proteomics, as functional analysis cannot otherwise be considered complete. Protein interactions may be studied in relatively low throughput fashion via co-expression in yeast two-hybrid complementation systems. But the tremendous quantity of data necessary for a *comprehensive* analysis requires utilization of modern automated sample handling instrumentation and data handling software. AxCell Biosciences has developed true high throughput *in vitro* protein interaction analysis. Highly parallel peptide synthesis is an important and integral part of this process, along with protein expression and high throughput screening (HTS). Through a formal partnership with the bioinformatics software company InforMax, AxCell is also developing sophisticated tools for visualization and experimental manipulation of the numerous and inter-related data describing the patterns and pathways of protein interaction important for intracellular signaling processes.

The corporate mission of AxCell Biosciences is to chart all protein interactions for the human proteome. In order to effectively study these complex interactions and pathways we take advantage of the conserved architecture of modular domains exhibited by intracellular signaling proteins. This refers to the observation that most of these proteins interact with others *via* binding of a peptide ligand on one protein to a protein domain on another protein. As domains in the formal biochemical sense of the word, these protein regions fold and function essentially independently from the rest of the protein of which they are a part. And as with many other protein classes, the functional domains of signaling proteins tend to fall into families that may be recognized and characterized by sequence homology. For example, in the human proteome there are many domains belonging to the SH2 family. These SH2 domains share significant homology in their amino acid (AA) sequence, and they all bind to ligands bearing a conserved phosphotyrosine residue. However, the relatively minor differences between different SH2 domains provide for minor differences in ligand specificity, so that each domain shows preference for a particular sequence of AA flanking the conserved phosphotyrosine on either side. Most individual signaling proteins exhibit several domains and ligand sequences, often in different families. This allows them to interact effectively with many other proteins in the signaling cascade. AxCell has chosen to model these multimeric interactions as collections of single binary interactions between one domain and its ligand.

Because we plan to map the whole proteome using *in vitro* binding assays, we must first develop comprehensive sets of domain and ligand reagents, as well as a reliable

binding assay. To do this, we have developed bioinformatics tools for data mining of public databases. We also employ two proprietary discovery technologies. One is a variation of M13 phage library discovery called GDL™, used for discovering ligands through functional *in vitro* binding to immobilized domains [2]. The other is a cDNA based technology called CLT™, used for discovering novel domains through their functional binding to biotinylated synthetic ligand peptides [1]. A detailed discussion of these two important technologies lies outside the scope of this document. While both technologies rely primarily on functional binding, they are supported and inter-linked *via* powerful bioinformatics that takes advantage of existing knowledge of the human proteome. Our robust HTS assay is based on technology similar to ELISA. In it, domain fusion proteins are bound to microplate wells, and subsequent binding of peptide ligands to the domains is detected by means of an N-terminal biotin included in the peptide [3]. After screening in a HTS format, a second assay is performed to generate a binding saturation curve. This assay provides a quantitative measurement of binding strength for individual pairs of domain-ligand interactions at a rate of thousands per day. In comparison, the yeast two-hybrid system, which is often employed for study of protein interactions *in vivo*, provides only qualitative data and a much lower throughput.

### Results and Discussion

We have recently completed mapping the human WW domain family, and have begun work on several other families, including SH3, PDZ, and SH2 domains. These data are commercially available through subscription to our ProChart™ database. Through the application of bioinformatic filters to the individual interaction data catalogued in ProChart, one may discern novel pathways of interaction between whole signaling proteins (Figure 1). Such bioinformatic filters include tissue specificity and expression level in disease states, and they may be easily applied through the use of tools available in the GenoMax software package (InforMax, Bethesda).

Applications for ProChart include general protein pathway research, single nucleotide polymorphism (SNP) analysis, prediction of drug toxicity and side effects, and ra-

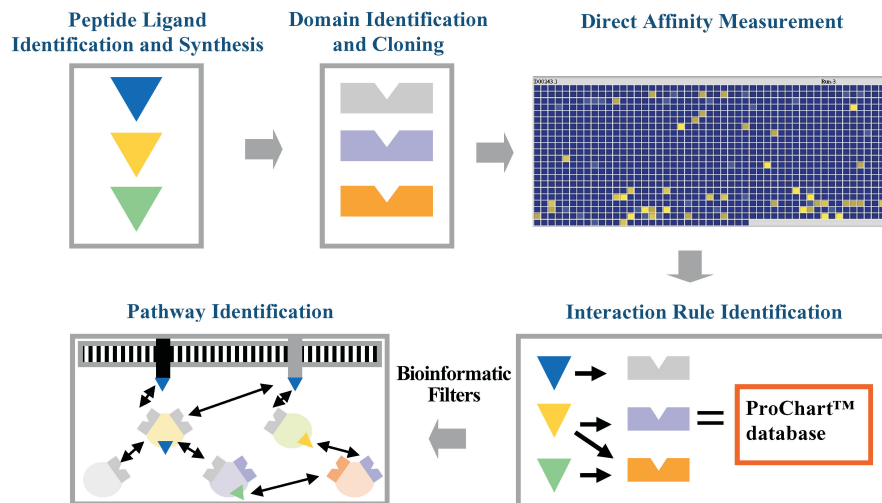


Fig. 1. Data and technology flow for creation of ProChart protein interaction database.

tional drug design. One example illustrating the use of these data is a study of Liddle Syndrome, a rare form of inherited sodium-dependent hypertension. This disease is associated with deletions and mutations in the epithelial sodium channel (ENaC) gene, specifically in WW family ligand sequences in the cytoplasmic portions of the heterotrimeric ENaC protein. Table 1 illustrates ProChart data showing a lack of binding of mutant ligands to their respective domains on the NEDD4 protein, with strong binding of wild type (wt) ligands. NEDD4 is a critical mediator of ubiquitin-dependent protein degradation, and it seems likely that Liddle Syndrome disease is thus caused by accumulation of ENaC due to impairment of this pathway. Furthermore, the point mutations in the ENaC cytoplasmic tail are SNPs, demonstrating how ProChart can be used to study these important pharmacogenomic diagnostic agents.

Table 1. Binding of WW domains to ENaC ligand sequences.

Peptide	Sequence	WW1	WW2	WW3
ENaC $\alpha$ wt	LTAPPPAYATLGP	+	+	–
ENaC $\alpha$	LTAPPPAAATLGP	–	–	–
ENaC $\beta$ wt	PGTPPPNYDSLRL	+	+	–
ENaC $\beta$ P616L	PGTPPLNYDSLRL	–	–	–
ENaC $\beta$ P618H	PGTPPPNHDSLRL	–	–	–
ENaC $\gamma$ wt	PGTPPPKYNSLRL	+	+	+
ENaC $\gamma$	PGTPPPKANSRLRL	–	–	–

Additionally, the improved knowledge of signaling pathways that ProChart data provide can help investigators choose which targets to validate in a given signaling or disease-associated pathway. By choosing appropriate points in the pathway for intervention, the effects of a pharmaceutical can be made broader or narrower, as desired for the application. ProChart also includes data that effectively provide structure-activity relationship (SAR) information. This is because hundreds to thousands of ligands are typically tested for binding to each domain in the family, and the differences in binding for each ligand provide information about the components in the complementary site in the domain that are necessary for binding. This information is invaluable to medicinal chemists in designing small molecules that can fit tightly and specifically into such receptors.

## References

1. Pirozzi, G., McConnell, S.J., Uveges, A.J., Carter, J.M., Sparks, A.B., Kay, B.K., Fowlkes, D.M. *J. Biol. Chem.* **272**, 14611–14616 (1997).
2. Hoffman, N.G., Sparks, A.B., Carter, J.M., Kay, B.K. *Mol. Divers.* **2**, 5–12 (1996).
3. Chen, L., Korenstein, B., James, M., Kvecher, L., Carter, J.M. *This book*.

## **Cell Attachment and Neurite Outgrowth Activities of Laminin Peptide-Conjugated Chitosan Membrane**

**Motoyoshi Nomizu<sup>1</sup>, Mayumi Mochizuki<sup>1</sup>, Kozue Kato<sup>1</sup>, Ikuko Okazaki<sup>1</sup>,  
Yoko Wakabayashi<sup>1</sup>, Taku Sato<sup>1</sup>, Satoshi Rikimaru<sup>1</sup>, Yuichi Kadoya<sup>2</sup>,  
Nobuo Sakairi<sup>1</sup> and Norio Nishi<sup>1</sup>**

<sup>1</sup>*Graduate School of Environmental Earth Science, Hokkaido University,  
Sapporo 060-0810, Japan*

<sup>2</sup>*Department of Anatomy, Kitasato University School of Medicine,  
Sagamihara 228-8555, Japan*

### **Introduction**

Basement membranes have been found to play a critical role in tissue development and repair. Laminin, a major cell adhesive protein of the basement membrane matrix, has multiple biological activities [1]. There are at least twelve isoforms of laminin (laminin-1 to -12), each consisting of three different chains  $\alpha$ ,  $\beta$ , and  $\gamma$  [1]. The most extensively characterized laminin, laminin-1 ( $M_r = 900,000$ ), consists of  $\alpha 1$ ,  $\beta 1$ , and  $\gamma 1$  chains, which assemble into a triple-stranded coiled-coil structure at the long arm to form a cross-like structure [1]. Laminin-1 has multiple biological activities including promotion of cell adhesion, spreading, proliferation, neurite outgrowth, angiogenesis, and tumor metastasis [1]. Recently, we demonstrated a systematic peptide screening for identification of cell binding sites from the laminin-1 molecule using 673 overlapping peptides [2–5]. Approximately twenty different cell-binding sequences with various biological functions were identified. Five peptides (A13, A99, A208, AG73, and C16) showed unusually strong cell attachment activity as well as additional biological functions (Figure 1). A13 and C16 inhibited laminin-mediated endothelial cell tube formation and promoted aortic sprouting and tumor metastasis suggesting it as a potent angiogenic sequence [6,7]. A99, located on the short arm of the  $\alpha 1$  chain and containing the RGD sequence [8], was found to interact with integrins and to promote cell adhesion and migration [9]. A208, on the C-terminus of the coiled-coil region of the laminin  $\alpha 1$  chain and containing the IKVAV sequence, promoted cell adhesion, neurite outgrowth, angiogenesis, and tumor metastasis [10]. AG73, located on the  $\alpha 1$  chain carboxyl-terminal globular domain, enhanced cell adhesion, migration, invasion, and gelatinase production [2]. Additionally, AG73 promoted neurite outgrowth [11]. Moreover, this peptide inhibited laminin-mediated acinar-like development of a human submandibular gland cell line and epithelial branching morphogenesis of cultured embryonic mouse submandibular gland [12,13]. Furthermore, syndecan-1 was identified by peptide affinity column chromatography as a receptor for AG73 [12].

Chitin, a mucopolysaccharide composed of *N*-acetyl-D-glucosamine by  $\beta(1-4)$  glycoside linkage, is present in the cell wall of fungi and in the outside skeleton of crustaceans and insects. Chitosan, deacetylated chitin, can adhere to proteins, dyes, and cholesterol, owing to the presence of a free amino group [14]. Chitosan membrane has been used for medical applications, such as suture thread, artificial skin, mucous membrane, and styptic [14]. Chitosan is a biodegradable natural polymer that has been shown to improve wound healing. The direct mechanism of chitosan-tissue interaction is not well understood.

Results and Discussion

Five biologically active peptides were designed and synthesized using the Fmoc strategy with a C-terminal amide (Figure 1). A Cys residue was added at the N-terminus. Two Gly residues were used as a spacer between the Cys and the active peptide sequence, except for A208. A208 was extended three amino acid residues at the N-terminus to function as a spacer and to enhance the solubility. Chitosan (99% deacetylated) was mixed with *N*-(maleimidobenzoyloxy)-succinimide (MBS) and the obtained MB-chitosan (1% MB) was coated on the wells. The Cys-peptides were added into the MB-chitosan coated wells and coupled. Human fibroblast and HT-1080 human fibrosarcoma cells were used to evaluate the cell attachment activity of the peptide-conjugated chitosan membranes. Human fibroblast cells strongly attached and spread on the A99-chitosan membrane. HT-1080 cells showed weak cell attachment on the A99-chitosan membrane. The AG73-, A13-, and C16-chitosan membranes were active with both human fibroblasts and HT-1080 cells. Both cell types did not attach to the chitosan membrane.

Next, we tested neurite outgrowth activity on the peptide-conjugated chitosan membranes using PC12 rat pheochromocytoma cells (Figure 2). AG73- and A208-chitosan membrane was found to promote neurite outgrowth with PC12 cells. A chitosan membrane did not show PC12 cell attachment or neurite outgrowth activity (Figure 2).

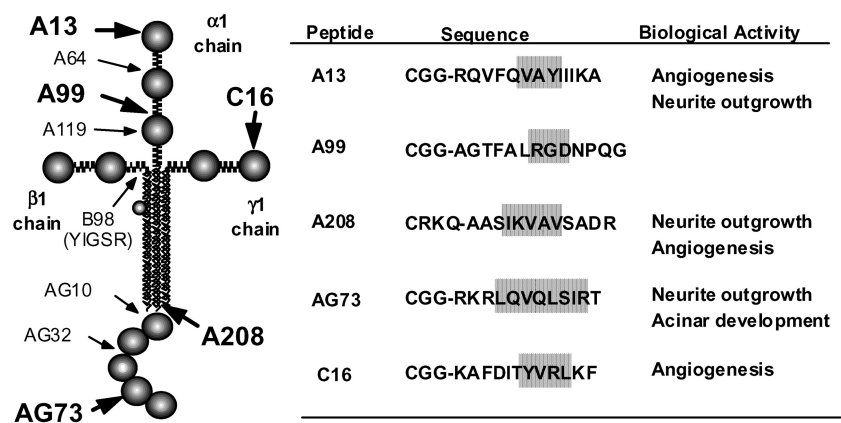


Fig. 1. Structural model of laminin-1. The active core sequences are indicated by shadow.

Here, a preparation of cell adhesive laminin-1 peptide-conjugated chitosan membranes and their biological activities are described. Chitosan membrane alone adhered strongly to tissues but did not show cell attachment activity *in vitro*. Biologically active peptide-conjugated chitosan membranes promoted cell attachment with cell-type specific manner. Controlling receptor-mediated interaction between cells and template surfaces is important for tissue engineering. The chitosan membranes have a number of advantages for biomedical uses. Chitosan-membranes could be removed from the wells by soaking with organic solvents such as ethanol. The laminin peptide-conjugated chitosan membrane could also be prepared as a membrane sheet. These membrane sheets are useful for testing biological activities *in vivo*. These results suggest that the cell adhesive peptides on the membranes are active with cell type specificity. The conjugation strategy is applicable for testing biological activity of di-

verse peptides and useful for development of biomedical materials. These peptide-conjugated chitosan membranes are useful for tissue engineering and therapeutic applications.

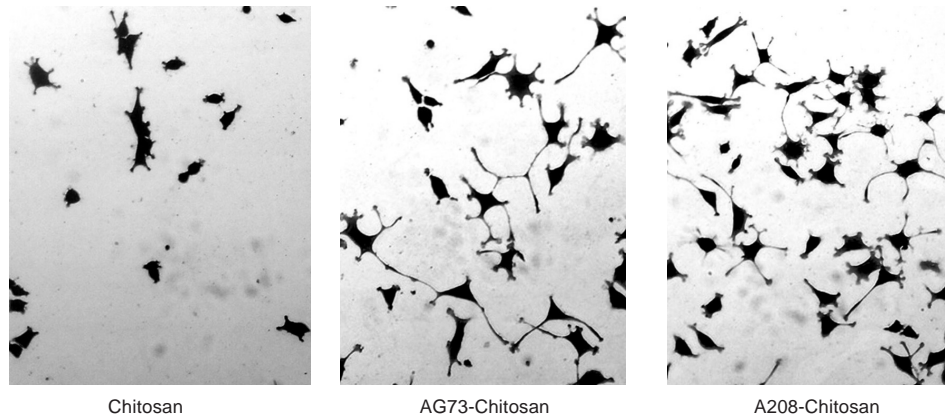


Fig. 2. Photographs of PC12 cells cultured on peptide-chitosan membranes.

## References

1. Colognato, H., Yurchenco, P.D. *Dev. Dynam.* **218**, 213–234 (2000).
2. Nomizu, M., Kim, W.H., Yamamura, K., Utani, A., Song, S.Y., Otaka, A., Roller, P.P., Kleinman, H.K., Yamada, Y. *J. Biol. Chem.* **270**, 20583–20590 (1995).
3. Nomizu, M., Kuratomi, Y., Song, S.Y., Ponce L.M., Hoffman, M.P., Powell, S.K., Miyoshi, K., Otaka, A., Kleinman, H.K., Yamada, Y. *J. Biol. Chem.* **272**, 32198–32205 (1997).
4. Nomizu, M., Kuratomi, Y., Malinda, M.K., Song, S.Y., Miyoshi, K., Otaka, A., Powel, S.K., Hoffman M.P., Kleinman, H.K., Yamada, Y. *J. Biol. Chem.* **273**, 32491–32499 (1998).
5. Nomizu, M., Kuratomi, Y., Ponce, L.M., Song, S.Y., Miyoshi, K., Otaka, A., Powell, S.K., Hoffman, M.P., Kleinman, H.K., Yamada, Y. *Arch. Biochem. Biophys.* **378**, 311–320 (2000).
6. Malinda, M.K., Nomizu, M., Chung, M., Delgado, M., Kuratomi, Y., Yamada, Y., Kleinman, H.K., Ponce, L.M. *FASEB J.* **13**, 53–62 (1999).
7. Ponce, L.M., Nomizu, M., et al. *Circ. Res.* **84**, 688–694 (1999).
8. Ruoslahti, E., Pierschbacher, M.D. *Science* **238**, 491–497 (1987).
9. Tashiro, K., Sephel, G.C., Greatorex, D., Sasaki, M., Shiraishi, N., Martin, G.R., Kleinman, H.K., Yamada, Y. *J. Cell. Physiol.* **146**, 451–459 (1991).
10. Nomizu, M., Utani, A., Shiraishi, N., Kibbey, M.C., Yamada, Y., Roller, P.P. *J. Biol. Chem.* **267**, 14118–14121 (1992).
11. Richard, B.L., et al. *Exp. Cell Res.* **228**, 98–105 (1996).
12. Hoffman, M.P., et al. *J. Biol. Chem.* **273**, 28633–28641 (1998).
13. Kadoya, Y., et al. *Dev. Dynam.* **212**, 394–402 (1998).
14. Muzzarelli, R., Mattioli-Belmonte, M., Pugnali, A., Biagini, G. *EXS* **87**, 251–264 (1999).

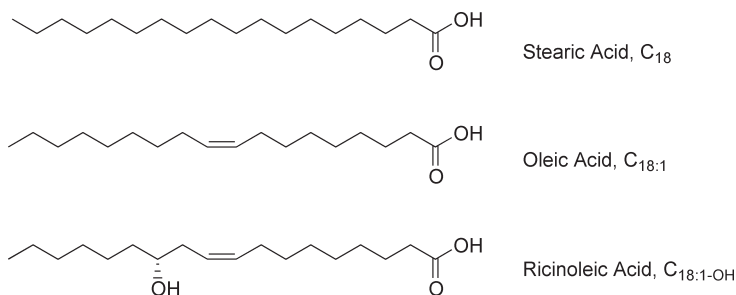
## Peptide-Amphiphile Induction of $\alpha$ -Helical Molecular Architecture and Interaction with Biomaterial Surfaces

Navdeep Malkar, Neal Niemczyk and Gregg B. Fields

Department of Chemistry & Biochemistry, Florida Atlantic University, Boca Raton,  
FL 33431-0991, USA

### Introduction

Controlling cell adhesion to polymer substrates is one of the important issues in tissue engineering, and includes the ability to direct specific cell types to proliferate, migrate, and express normal physiological behaviors, in order to yield a defined cellular architecture [1]. Engineering bioactive, conformationally constrained peptides onto biomaterial surfaces could satisfy the above criteria and hence improve biocompatibility. Our laboratory previously demonstrated that linking lipid tails to peptides enables them to self-assemble into biomimetic films with a highly organized interface, and perhaps more importantly, enhances their ability to assume well-defined secondary and tertiary conformations [2–4]. These peptide-amphiphiles effectively promote a variety of cell activities [2]. In the present study, novel peptide-amphiphiles that have the potential to form  $\alpha$ -helical structure combined with an amino acid sequence from the angiogenesis-inducing region of SPARC have been constructed. The peptide sequence 21r, Lys-Ala-(Glu-Ile-Glu-Ala-Leu-Lys-Ala)<sub>2</sub>-Tyr-Lys-Gly-His-Lys, was lipidated with one of the three “tails” listed below and characterized.



### Results and Discussion

The solution structure of 21r was examined initially by CD spectroscopy. Peptide 21r exhibits a significant  $\alpha$ -helical-like CD spectrum in aqueous solution at 5 °C. Addition of C<sub>18</sub> fatty acid chains with different functional moieties to 21r results in further induction of  $\alpha$ -helical structure. Deconvolution of the respective CD spectra indicated that the highest  $\alpha$ -helical content was found for C<sub>18</sub>-21r in water. The relative stabilities of  $\alpha$ -helical structure within the 21r peptide-amphiphiles were compared. Values for  $[\theta]_{222}$  were monitored as temperature increased from 5 to 95 °C in the presence of 0–125  $\mu$ M guanidine hydrochloride. The thermal transitions from  $\alpha$ -helix to “random coil” state demonstrated that C<sub>18</sub>-21r was the most stable (Table 1).

Size exclusion chromatography indicated that the 21r peptide-amphiphiles all form aggregates. The C<sub>18:1</sub>-OH-21r formed the smallest aggregate among the three C<sub>18</sub> peptide-amphiphiles. The 21r peptide alone does not aggregate. The critical aggregate concentrations were measured using a surface tension apparatus (Table 1).

### Malkar et al.

One of the  $^1\text{H}$  NMR spectral parameters indicative of  $\alpha$ -helices is the dispersion and resolution of NH resonances upon transition from the random coil state. The 1D  $^1\text{H}$  NMR spectrum of 21r shows a dispersion from 7.9 to 8.73 ppm and many overlapping peaks. The spectrum of  $\text{C}_{18}$ -21r in  $\text{D}_2\text{O}$ - $\text{H}_2\text{O}$  (1 : 9) shows dispersion from 7.6 to 8.68 ppm. This is consistent with the CD results, where the coupling of  $\text{C}_{18}$  tail to the 21r peptide further induces  $\alpha$ -helical structure. In addition, the  $\alpha\text{CH}$  proton resonances were shifted upfield in the case of the peptide-amphiphile as compared to peptide alone, consistent with  $\alpha$ -helical conformation.

Table 1. Melting temperature ( $T_m$ ) and critical aggregate concentration (CAC) of peptide and peptide-amphiphiles.

Peptide/Peptide-Amphiphile	$T_m$ ( $^{\circ}\text{C}$ )	CAC ( $\mu\text{M}$ )
21r	51.4	—
$\text{C}_{18}$ -21r	86.4	5.3
$\text{C}_{18:1}$ -21r	73.6	5.9
$\text{C}_{18:1\text{-OH}}$ -21r	71.7	6.8

Overall, the  $\text{C}_{18}$ -21r series of peptide-amphiphiles can be utilized to create protein-like molecular architecture. Prior studies from our laboratory have shown that surface-coated peptide-amphiphiles promote cellular recognition and signaling [2] and thus could be used to improve biomaterial biocompatibility. Biomaterial adsorption studies were performed using the ACS RX MULTI-LINK Coronary Stent System (Table 2). All three peptide-amphiphiles were found to adsorb to stent surfaces.

Table 2. Adsorption to ACS RX MULTI-LINK<sup>TM</sup> Coronary Stent System.

Peptide-Amphiphile	Concentration on Stent (M)	% Adhesion
$\text{C}_{18}$ -21r	$1.15 \cdot 10^{-5}$	50.4
$\text{C}_{18:1}$ -21r	$6.75 \cdot 10^{-6}$	21.8
$\text{C}_{18:1\text{-OH}}$ -21r	$3.70 \cdot 10^{-6}$	12.8

The peptide-amphiphiles examined herein can form stable  $\alpha$ -helical protein-like molecular architecture, as evaluated by CD and NMR spectroscopies. Presence of the double bond in the alkyl chain of peptide-amphiphile  $\text{C}_{18}$ -21r destabilized the  $\alpha$ -helical structure to some extent. The adsorption of  $\text{C}_{18}$ -21r variants on the ACS RX MULTI-LINK Coronary Stent System suggests that these peptide-amphiphiles are suitable for coating biomaterial surfaces.

### Acknowledgments

The research is supported by NIH (HL 62427 and CA 77402).

### References

1. Hubbell, J.A. *Biotechnology* **13**, 565–576 (1995).
2. Fields, G.B., Lauer, J.L., Dori, Y., Forns, P., Yu, Y.-C., Tirrell, M. *Biopolymers* **47**, 143–151 (1998).
3. Yu, Y.-C., Tirrell, M., Fields, G.B. *J. Am. Chem. Soc.* **120**, 9979–9987 (1998).
4. Yu, Y.-C., Berndt, P., Tirrell, M., Fields, G.B. *J. Am. Chem. Soc.* **118**, 12515–12520 (1996).

## TOAC Peptides as Catalysts of Enantioselective Oxidations

Claudio Toniolo<sup>1</sup>, Marco Crisma<sup>1</sup>, Fernando Formaggio<sup>1</sup>,  
Marcella Bonchio<sup>1</sup>, Quirinus B. Broxterman<sup>2</sup>, Bernard Kaptein<sup>2</sup>,  
Rosa Maria Vitale<sup>3</sup>, Ettore Benedetti<sup>4</sup> and Michele Saviano<sup>4</sup>

<sup>1</sup>CSB and CMRO, CNR, Department of Organic Chemistry, University of Padova,  
35131 Padova, Italy

<sup>2</sup>DSM Research, Organic Chemistry and Biotechnology Section, 6160 MD Geleen,  
The Netherlands

<sup>3</sup>Department of Environmental Sciences, 2nd University of Naples, 81100 Caserta, Italy

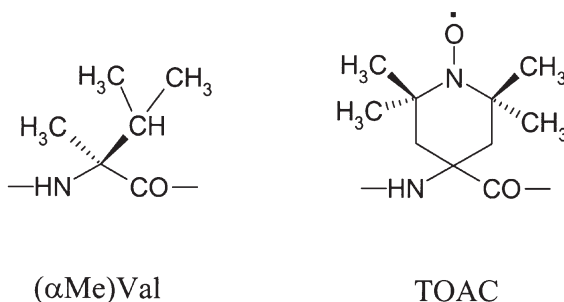
<sup>4</sup>Biocrystallography Research Center, CNR, Department of Chemistry, University of Naples  
"Federico II", 80134 Naples, Italy

### Introduction

The oxidation of secondary alcohols to ketones by use of aliphatic nitroxyl radicals, such as TEMPO, as catalysts is a well known reaction which involves in the oxidation path an *N*-oxoammonium salt originated from the corresponding nitroxyl radical. Complex chiral nitroxyl molecules have been used as catalysts to induce enantioselective oxidation reactions [1].

### Results and Discussion

The achiral, nitroxyl containing  $\alpha$ -amino acid 2,2,6,6-tetramethyl-4-amino-1-oxyl-piperidine-4-carboxylic acid (TOAC) in combination with the chiral  $\alpha$ -amino acid C <sup>$\alpha$</sup> -methylvaline [( $\alpha$ Me)Val] was exploited to prepare short (from di- to hexa-) peptides potentially able to induce enantioselective oxidation of racemic 1-phenylethanol to acetophenone.



The optimal catalysts, with e.e. ranging from 67 to 79%, were found to be the *N* <sup>$\alpha$</sup> -acylated dipeptide alkylamides having the -TOAC-( $\alpha$ Me)Val- sequence folded in a stable, C=O...H-N intramolecularly H-bonded  $\beta$ -turn conformation, an aromatic *N*-terminal acylating group and a bulky C-terminal alkyl group (the X-ray diffraction structure of one such compound is shown in Figure 1).

On the basis of the crystallographic structure we rationalized our experimental findings on the enantioselective oxidation by producing energy-minimized models for the diastereomeric, intermediate complexes between (*R*)- [and (*S*)]-phenylethanol and the *N* <sup>$\alpha$</sup> -acylated dipeptide alkylamide catalyst. Critical factors were found to be the bulkiness of the C-terminal group in biasing the 3D-disposition of the *N* <sup>$\alpha$</sup> -protecting group and a favorable interaction between the aromatic group of the alcohol and the *N* <sup>$\alpha$</sup> -protecting group.

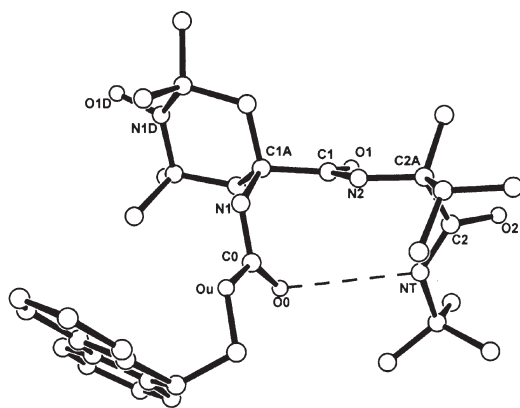


Fig. 1. X-Ray diffraction structure of the  $\beta$ -turn forming, terminally blocked dipeptide alkylamide Fmoc-TOAC-L-( $\alpha$ Me)Val-NHtBu.

#### References

1. Rychnovsky, S.D., McLernon, T.L., Rajapakse, H. *J. Org. Chem.* **61**, 1194–1195 (1996).

## Synthesis of Arg-Gly-Asp-Ser Containing Oligopeptides and Evaluation of Their Cell-Attachment Activity

Tadashi Iuchi<sup>1</sup>, Mitsutaka Kayahara<sup>1</sup>, Keiko Sato<sup>1</sup>, Yoshiaki Hirano<sup>1,2</sup>,  
 Masahito Oka<sup>3</sup> and Toshio Hayashi<sup>3</sup>

<sup>1</sup>Department of Applied Chemistry, Faculty of Engineering and

<sup>2</sup>Bio Venture Center, Osaka Institute of Technology, Osaka 535-8585, Japan

<sup>3</sup>Research Institute for Advance Science and Technology, Osaka Prefecture University,  
 Osaka 599-8570, Japan

### Introduction

Investigation on the cell attachment activity of various proteins, such as fibronectin, vitronectin, collagen and fibrinogen, have revealed that the oligopeptide sequence containing Arg-Gly-Asp (RGD) is recognized by the cell surface receptor called integrins [1,2]. Oligopeptides composed of the RGD sequence have been synthesized and their cell attachment activity has been investigated. These results suggested that cell attachment activities are induced by the specified interaction between the RGD peptide and the cell surface receptor. In this work, we synthesized RGDS containing peptides and its mimetic peptide for designing a peptide having enhanced cell attachment activity. The structure and activity relationship of RGDS mimetic peptides is also discussed. The aim of our study is to accumulate the basic informations required for synthetic materials to be used as biomedical materials.

### Results and Discussion

Structural formulas of RGDS mimetic peptides are shown in Figure 1 (Har; homo-arginine, Nip; nipecotic acid). RGDS and its mimetic peptides were synthesized by liquid phase procedures [3,4]. The crude peptides were purified by HPLC, then, characterized by MALDI-TOF-MS, NMR, elementary analysis, and amino acid analysis.

Conformational analysis was carried out by circular dichroism measurement (CD) in water. The CD spectrum of RGDS indicated that a strong negative peak at 198 nm and weak one at 222 nm. The hRGDS, CaGDS, OrGDS, and RbADS(*bA*: *beta*-alanine) peptides have the same CD spectra as that of RGDS. However, the CD spectrum of RNiDS has a positive maximum at 208 nm and a negative maximum at 227 nm. This spectrum curve pattern suggests that RNiDS has a typical type II-*beta* bend. RNiDS and RNiES peptides have a different type turn structure in comparison with the other RGDS mimetic peptides.

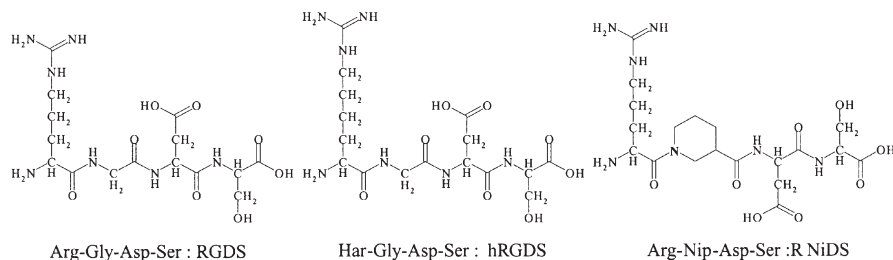


Fig. 1. Structure of RGDS and mimetic peptides.

*Table 1. Inhibition of platelet aggregation (IC<sub>50</sub>) by RGDS mimetic peptides.*

Peptide		IC <sub>50</sub> (mM)
Arg-Gly-Asp-Ser	(RGDS)	0.14
Har-Gly-Asp-Ser	(hRGDS)	0.07
Can-Gly-Asp-Ser	(CaGDS)	0.90
Orn-Gly-Asp-Ser	(OrGDS)	5.50
Arg-Nip-Asp-Ser	(RNiDS)	0.21
Arg- <i>b</i> Ala-Asp-Ser	(RbADS)	3.90
Arg-Pro-Asp-Ser	(RPDS)	>10
Arg-Gly-Glu-Ser	(RGES)	↓
Arg-Nip-Glu-Ser	(RNiES)	
Arg-Gly-Asn-Ser	(RGNS)	

Cell attachment activities of these peptides were examined by platelet aggregation assay. Table 1 shows 50% inhibition values (IC<sub>50</sub>) of RGDS and its mimetic peptides. RGDS, hRGDS, CaGDS(Ca; canavanine), RNiDS, and RbADS peptides inhibited the platelet aggregation reaction, but RGES, RGNS and RNiES did not. The RNiDS and RNiES peptide were possessed of the same conformation, but RNiES peptide does not inhibit the platelet aggregation reaction. It can be concluded that the aspartic acid residue cannot be converted to other amino acids. The inhibitory activity of RNiDS was almost the same as that of RGDS. These results suggest that the Asp residue and backbone structure between Arg and Asp residues are important for the cell-attachment activity.

The inhibitory activity of hRGDS was twice as strong as that of RGDS. However, activities of CaGDS, RbADS, and OrGDS (Or; ornithine) were significantly lower than that of RGDS. These results suggest that the side-chain length and flexibility of Arg and Har residue, and the guanidino groups of Arg and Har are very important factors for exhibiting to cell-attachment activity. The results indicate that side chain groups of Asp and Arg residues can play an important role for ligand binding to the integrin receptor on the platelet membrane.

### Acknowledgments

This work was partly supported by the Grant-in-Aid for Scientific Research (C) from the Ministry of Education, Science, and Culture.

### References

1. Preschbacher, M.D., Ruoslahti, E. *Nature* **309**, 30 (1984).
2. Preschbacher, M.D., Ruoslahti, E. *Proc. Natl. Acad. Sci. USA* **81**, 5985 (1984).
3. Hirano, Y., et. al. *J. Biomed. Mater. Res.* **25**, 1523 (1991).
4. Hirano, Y., et. al. *J. Biomater. Sci. Polymer. Edn.* **4**, 235 (1993).

**Author Index**  
**Index of E-mail Addresses**  
**Subject Index**



## Author Index

- Abel, P.W. [250](#)  
Acharya, A.N. [255](#)  
Acharya, S.A. [460](#)  
Adams, D.J. [113](#)  
Adams, T. [881](#)  
Afargan, M. [626](#)  
Aglione, A. [704](#)  
Agnes, R.S. [691](#), [969](#)  
Agricola, I. [132](#)  
Aguilar, M.I. [293](#), [553](#)  
Ahmed, S. [905](#)  
Ahmed, S.I. [693](#)  
Ahn, J.M. [324](#), [744](#)  
Aimoto, S. [111](#), [160](#)  
Akaji, K. [111](#), [160](#)  
Akasaka, R. [516](#)  
Åkerblom, E. [549](#)  
Albericio, F. [217](#), [432](#)  
Albert, R. [716](#)  
Albrizio, S. [314](#)  
Aldrich, J.V. [144](#), [687](#), [689](#), [894](#)  
Alewood, P. [937](#)  
Alewood, P.F. [113](#), [115](#)  
Alexopoulos, K.A. [614](#)  
Almqvist, F. [636](#)  
Alonso, D.O.V. [346](#)  
Altamura, S. [534](#)  
Alves, I. [28](#), [297](#)  
Ambulos, N.P. [140](#)  
Amini, A. [658](#)  
Ammerova, A. [87](#)  
Amodeo, P. [289](#), [710](#)  
Amro, N. [180](#)  
Anantharamaiah, G.M. [658](#)  
Anbo, A. [616](#)  
Andersen, N.H. [406](#)  
Anderson, D. [389](#)  
Anderson, D.C. [1053](#)  
Anderson, M.E. [946](#)  
Andreu, D. [632](#), [1010](#), [1018](#), [1043](#)  
Aoyagi, H. [489](#), [760](#)  
Appel, J.R. [921](#)  
Appella, E. [1039](#)  
Arab, L. [789](#)  
Arai, H. [795](#)  
Arai, T. [526](#)  
Araki, M. [452](#)  
Araki, S. [516](#)  
Archakov, A.I. [1031](#)  
Arevalo, E. [847](#)  
Arimoto, R. [909](#)  
Armishaw, C.J. [113](#)  
Arnold, E. [1016](#)  
Arnold, G.F. [1016](#)  
Arshava, B. [375](#), [847](#)  
Arvidsson, P.I. [275](#)  
Asbill, J. [543](#)  
Ast, T. [577](#)  
Aubry, A. [348](#)  
Aumelas, A. [301](#), [322](#)  
Avrahami, D. [754](#)  
Babichenko, I.I. [782](#)  
Baidakova, L.K. [782](#)  
Bajaj, S.P. [965](#)  
Balachari, D. [440](#)  
Balaji, R.A. [483](#)  
Balasubramaniam, A. [672](#)  
Balboni, G. [679](#), [851](#)  
Baldwin, M.A. [818](#)  
Balhorn, R. [334](#)  
Ball, H.L. [818](#)  
Banda, P.W. [81](#), [832](#)  
Banin, E. [375](#)  
Bansal, P.S. [115](#)  
Barany, G. [222](#), [224](#), [265](#), [400](#), [409](#), [413](#)  
Barber-Armstrong, W. [295](#), [367](#)  
Barberis, C. [699](#)  
Baron, R. [822](#)  
Barrow, C.J. [242](#)  
Barry, L. [322](#)  
Bartkovitz, D. [701](#)  
Barua, B. [406](#)  
Basak, A. [558](#)  
Bauer, W. [716](#)  
Baumann, M. [204](#)  
Baur, P. [38](#)  
Bauzo, R.M. [271](#), [706](#)  
Bazzaro, M. [1027](#)  
Bazzo, R. [534](#)  
Beck, A. [320](#)  
Becker, C.F.W. [870](#)  
Becker, J.M. [847](#), [876](#), [898](#), [957](#)  
Becker, S. [502](#)  
Behenna, D.C. [512](#)  
Beigle-Orme, S. [200](#)

## *Author Index*

- Bélec, L. [599](#)  
Beligere, G.S. [404](#)  
Bellanda, M. [530](#)  
Beltramini, L. [1029](#)  
Benedetti, E. [289](#), [371](#), [710](#), [1065](#)  
Benincasa, M. [776](#)  
Bennett, M.A. [689](#), [894](#)  
Berezowska, I. [676](#)  
Bergmann, R. [984](#)  
Bergonzi, R. [93](#)  
Bernad, N. [152](#)  
Bernini, A. [925](#)  
Berry, S. [944](#)  
Biancalana, S. [117](#)  
Bianchi, E. [534](#), [545](#)  
Bianco, A. [402](#)  
Bigoni, R. [787](#)  
Bilsky, E.J. [499](#)  
Biondi, B. [845](#)  
Biondi, L. [628](#), [776](#)  
Bischoff, D. [481](#)  
Bischoff, H. [204](#)  
Bisello, A. [424](#), [739](#), [742](#)  
Bisset, L. [988](#)  
Bister, B. [481](#)  
Bittencourt, J.C. [344](#)  
Blanchfield, J. [937](#)  
Blankenship, J.W. [464](#)  
Blasio, B.D. [710](#)  
Blazyk, J. [310](#), [479](#)  
Blechs Schmidt, D. [187](#)  
Blischenko, E.Yu. [785](#), [803](#)  
Blondelle, S.E. [491](#), [762](#), [1023](#)  
Bódi, J. [712](#)  
Boeglin, D. [748](#)  
Boeijen, A. [232](#)  
Boer, J. [612](#), [647](#)  
Boggiano, C. [1023](#)  
Boisguérin, P. [866](#)  
Bökönyi, G. [640](#), [864](#)  
Bonchio, M. [1065](#)  
Bond, S. [553](#)  
Bondebjerg, J. [271](#)  
Bonney, J.Y. [320](#)  
Bonnet, D. [119](#)  
Borchardt, R.T. [610](#)  
Borin, G. [845](#), [982](#)  
Bornman, W. [992](#)  
Borràs, E. [194](#), [1018](#), [1051](#)  
Borremans, F. [198](#)  
Bösze, S. [316](#), [1010](#)  
Boulos, E. [553](#)  
Bourdonneau, M. [402](#)  
Bourel-Bonnet, L. [119](#)  
Bourne, G.T. [89](#), [122](#), [125](#)  
Bowie, T. [287](#)  
Boyd, J.G. [61](#), [65](#)  
Bracci, L. [925](#)  
Bracha, M. [626](#)  
Bradon, N. [818](#)  
Bramlett, K.S. [136](#)  
Brask, J. [454](#)  
Braun, I. [931](#)  
Braun, K. [931](#)  
Brayden, J.E. [191](#)  
Bremer, C. [986](#)  
Brewer, M. [40](#)  
Breznik, M. [330](#)  
Briand, J.P. [348](#), [402](#)  
Briones, M.P.P. [807](#)  
Brisander, M. [610](#)  
Brkovic, A. [725](#)  
Brodie, A.H. [801](#)  
Brouwer, A.J. [232](#)  
Brown, M.F. [324](#)  
Broxterman, Q.B. [328](#), [371](#), [1065](#)  
Brückner, H. [774](#)  
Brunel, F. [170](#)  
Brunner, L. [130](#)  
Bruns, C. [716](#)  
Bryant, S.D. [616](#), [679](#), [851](#)  
Buděšínský, M. [618](#)  
Bulet, P. [493](#), [495](#)  
Bunn, P.A.Jr. [642](#), [721](#)  
Burger, C. [277](#)  
Burgess, A. [881](#), [998](#)  
Bürgle, M. [647](#)  
Burke, T.R.Jr. [859](#), [862](#), [868](#)  
Burkhart, B.M. [838](#)  
Burr, G.S. [1033](#)  
Burris, T.P. [136](#)  
Bursavich, M.G. [537](#)  
Burton, K.J. [907](#)  
Bushueva, I.M. [134](#)  
Butterworth, J. [685](#)  
Byk, G. [398](#)

## Author Index

- Caba, J.M. [217](#)  
Cabell, L.A. [42](#)  
Cabezas, E. [363](#)  
Cabrele, C. [462](#)  
Cai, C. [20](#), [24](#)  
Cai, M. [20](#), [708](#), [892](#)  
Calamandrei, D. [925](#)  
Calas, B. [301](#)  
Calderan, A. [845](#), [982](#)  
Calo, G. [679](#), [787](#)  
Camarero, J.A. [816](#)  
Campbell, E. [816](#)  
Campitelli, M.R. [122](#), [125](#)  
Capua, A.D. [289](#)  
Carotenuto, A. [340](#), [630](#)  
Carpenter, K. [685](#)  
Carpenter, K.A. [900](#)  
Carpino, L.A. [95](#)  
Carrascal, M. [217](#)  
Carrasco, M.S. [772](#)  
Carson, W.E. [1012](#)  
Carter, J.M. [206](#), [318](#), [1057](#)  
Carulla, N. [400](#)  
Cary, J.M. [575](#)  
Casallanovo, F. [723](#)  
Cassidy, P.J. [125](#)  
Catimel, B. [998](#), [1055](#)  
Cauwenberghe, S.V. [683](#)  
Cavelier, F. [83](#), [152](#)  
Cenizal, T. [1016](#)  
Cesaro, L. [982](#)  
Chadda, M. [658](#)  
Chahal, S. [789](#)  
Chakrabartty, A. [971](#)  
Chan, D.C. [642](#), [721](#)  
Chan, G.H.H. [746](#), [973](#)  
Chan, W.Y. [695](#), [699](#)  
Chan, Y.N. [955](#)  
Chana, M.S. [359](#)  
Chance, W.T. [672](#)  
Chandramouli, N. [716](#)  
Chang, E. [992](#)  
Chatergoon, M. [935](#)  
Chavanieu, A. [301](#)  
Chen, C.H. [996](#)  
Chen, H.Y. [996](#)  
Chen, L. [206](#), [318](#), [701](#), [1057](#)  
Chen, S.H. [967](#)  
Chen, S.T. [510](#)  
Chen, W. [610](#)  
Chen, X.F. [1002](#)  
Chen, Y. [353](#), [704](#)  
Cheng, J.W. [857](#), [967](#), [978](#), [1000](#)  
Cheng, L.L. [695](#), [699](#)  
Chesnut, R. [1039](#)  
Cheung, A. [701](#)  
Chiche, L. [387](#)  
Cho, J.H. [791](#), [1049](#)  
Choi, Y.S. [583](#), [585](#)  
Chorev, M. [308](#), [424](#), [668](#), [739](#), [742](#)  
Chrétien, M. [558](#)  
Christensen, C. [269](#)  
Chu, X.J. [701](#)  
Chubb, N.A.L. [228](#)  
Chulin, A.N. [587](#)  
Chuman, Y. [797](#), [884](#), [919](#)  
Chung, N.N. [676](#), [681](#)  
Chweh, W. [71](#), [155](#)  
Ciarkowski, J. [896](#)  
Cicero, D. [534](#)  
Ciutti, A. [925](#)  
Cluzeau, J. [597](#)  
Coleman, D.R. [42](#)  
Concepcion, A.M. [541](#)  
Condie, B.A. [873](#)  
Condon, M.K. [801](#)  
Cook, R.M. [54](#)  
Corich, M. [739](#), [742](#)  
Cortese, R. [534](#)  
Corzette, M. [334](#)  
Cosman, M. [334](#)  
Cossettini, P. [93](#)  
Costa, T. [884](#), [919](#)  
Cotton, G.J. [992](#)  
Cowburn, D. [222](#), [816](#)  
Cowell, S. [28](#), [297](#)  
Coy, D.H. [620](#)  
Craig, D.J. [113](#), [1047](#)  
Crespo, L. [432](#)  
Crisma, M. [369](#), [371](#), [456](#), [514](#), [1065](#)  
Csermely, P. [864](#)  
Csombos, J. [683](#)  
Cudic, M. [493](#), [1025](#), [1047](#)  
Cudic, P. [512](#)  
Culler, M. [668](#), [670](#)  
Curran, D.P. [17](#)

## *Author Index*

- Cusack, B. [85](#), [567](#)  
Czaplewski, C. [420](#)  
Czaplicki, J. [320](#)
- D'Ursi, A. [314](#)  
Daffre, S. [495](#)  
Daggett, V. [346](#)  
Dakappagari, N. [1004](#), [1012](#)  
Daliani, I. [238](#)  
Dalmadi, B. [1010](#)  
DalPozzo, A. [93](#)  
Dangel, B. [273](#)  
Danho, W. [701](#), [704](#)  
Danielsson, U.H. [549](#)  
Darst, S. [816](#)  
Dattilo, J. [200](#)  
Dávila, M. [1018](#)  
Davis, P. [499](#), [691](#), [969](#)  
Dawson, N.F. [448](#)  
Dawson, P.E. [103](#), [105](#), [404](#), [464](#)  
Deadman, J.J. [279](#)  
Deber, C.M. [820](#), [824](#), [828](#), [849](#)  
Debus, J. [931](#)  
Decatur, S.M. [295](#), [367](#)  
DeFeo-Jones, D. [644](#)  
Deghenghi, R. [748](#)  
Deillon, C.A. [166](#)  
Demura, M. [756](#)  
Deraët, M. [888](#)  
Deraos, S. [238](#)  
Dhanasekaran, M. [338](#)  
Dhawan, V.C. [672](#)  
Dibo, G. [336](#)  
Dick, D.J. [54](#)  
Dick, F. [63](#)  
Dickson, R.B. [561](#)  
Dideriksen, J.M. [454](#)  
Didierjean, C. [348](#)  
Diefenbach, B. [733](#)  
Dietrich, U. [187](#), [204](#)  
DiFenza, A. [314](#)  
Dineen, T. [67](#)  
Ding, F. [876](#), [898](#)  
Divita, G. [830](#)  
Domagala, T. [881](#)  
Domenici, E. [530](#)  
Domingo, E. [1018](#)  
Dominik, A. [555](#)
- Donella-Deana, A. [982](#)  
Dong, J. [737](#)  
Dong, J.Z. [668](#), [670](#)  
Dong, L. [866](#)  
Dong, M. [1002](#)  
Donhardt, A. [957](#)  
Donnet-Hughes, A. [770](#)  
Dooley, C.T. [921](#)  
Dorrington, T. [475](#)  
Dorsselaer, A.V. [301](#), [320](#)  
Dostmann, W.R.G. [191](#)  
Drabik, P. [896](#)  
Drane, J.A. [236](#)  
Dranitsina, S.M. [782](#)  
Du, Y.C. [1002](#)  
Duax, W.L. [838](#)  
Dubois, A. [888](#)  
Dudek, M.J. [428](#)  
Duesberry, N. [666](#)  
Dumas, C. [301](#)  
Dumont, M. [847](#)  
Dupelle, M. [558](#)  
Durieux, P. [185](#)  
Durmstorff, C. [593](#)  
Durrour, T. [699](#)  
Dutton, J. [113](#)
- Eberle, A.N. [712](#)  
Eble, J.A. [814](#)  
Eden, R. [287](#)  
Edwards, P.J. [236](#)  
Edwards, W.B. [177](#)  
Egleton, R. [499](#)  
Elardo, S. [982](#)  
Elbayed, K. [402](#)  
Elder, A.M. [532](#)  
Elias, C.F. [344](#)  
Elleman, T. [881](#)  
Ellman, B. [277](#)  
Elmagbari, N. [499](#)  
Elsaid, K.A. [475](#)  
Emtenäs, H. [636](#)  
Engel, D. [398](#)  
Engel, G. [716](#)  
Engelhard, M. [870](#)  
Enstrom, A.M. [183](#), [551](#)  
Enyedy, I. [561](#)  
Eom, K.D. [933](#), [1021](#)

## Author Index

- Erchehyi, J. [719](#)  
Erickson, J.B. [168](#)  
Erős, D. [805](#)  
Ertl, H.C.J. [1025](#)  
Escher, E. [888](#)  
Escobedo, J. [458](#)  
Esposito, D. [841](#), [843](#)  
Estiarte, M.A. [532](#)  
Etezady-Esfarjani, T. [312](#)  
Eynon, J. [624](#)
- Fadhil, I. [685](#)  
Falcioni, F. [704](#)  
Falconer, R.A. [79](#), [506](#)  
Fan, H. [927](#)  
Farber, K. [634](#)  
Farmer, S.W. [477](#)  
Farquhar, M. [750](#)  
Farrera, J. [432](#)  
Fattori, D. [534](#)  
Fattorusso, R. [710](#)  
Faux, M. [998](#)  
Favretto, D. [845](#)  
Fázio, M.A. [495](#)  
Fehrentz, J.A. [748](#)  
Feller, S. [185](#)  
Feng, D.M. [644](#)  
Fenza, A.D. [340](#)  
Fernandez-Carneado, J. [185](#)  
Ferrari, S. [424](#)  
Ferreira, P.M.T. [36](#), [44](#)  
Ferrer, F.J. [95](#)  
Fesinmeyer, R.M. [406](#)  
Fiedler, H.P. [768](#)  
Fields, G.B. [48](#), [975](#), [1063](#)  
Filira, F. [628](#), [776](#)  
Filter, M. [430](#)  
Fiori, S. [355](#), [462](#)  
Fiscus, R.R. [746](#), [973](#)  
Fisher, C.L. [418](#)  
Fleckenstein, B. [208](#), [1037](#)  
Flegel, M. [87](#)  
Flora, D.B. [236](#)  
Formaggio, F. [328](#), [369](#), [371](#), [514](#), [1065](#)  
Fournier, A. [725](#)  
Fowler, C. [834](#)  
Frackenpohl, J. [275](#)  
Franco, L. [701](#)
- Frändberg, P.A. [917](#)  
Frank, R. [191](#)  
Fraser, P.E. [971](#)  
Frechilla, D. [632](#)  
Freidinger, R.M. [644](#)  
Freidlin, I.S. [803](#)  
Fridkin, G. [230](#)  
Frieden, C. [326](#)  
Fry, D. [701](#)  
Fu, Y. [34](#), [458](#)  
Fujii, N. [606](#)  
Fujita, I. [913](#)  
Fujita, T. [884](#), [919](#)  
Fujita, Y. [616](#), [851](#)  
Fujiura, T. [915](#)  
Fujitani, N. [756](#)  
Fukumoto, Y. [336](#)  
Furrer, J. [402](#)  
Futaki, S. [452](#), [950](#), [961](#)
- Gad, M. [1041](#)  
Gaertner, H. [107](#)  
Gagné, R. [1041](#)  
Gagnon, J. [387](#)  
Galaktionov, S. [394](#)  
Gangl, S. [310](#)  
Ganz, T. [301](#)  
Gao, Y. [859](#), [862](#), [868](#)  
Garber, D. [658](#)  
García-López, M.T. [632](#)  
Gardella, T.J. [890](#)  
Garippa, R. [704](#)  
Garrett, T. [881](#)  
Garsky, V.M. [644](#)  
Gauthier, T.J. [46](#), [444](#), [758](#)  
Gavioli, R. [1027](#)  
Gazal, S. [626](#)  
Gebhardt, K. [768](#)  
Geerlings, P. [683](#)  
Geissinger, P. [172](#)  
Gellerman, G. [626](#)  
Gembitsky, D.S. [693](#), [905](#)  
Gennaro, R. [776](#)  
Gera, L. [642](#), [721](#)  
Gerhard, W. [935](#)  
Gianello, R. [714](#)  
Giatas, N. [656](#)  
Gibbons, W.A. [841](#), [843](#)

## *Author Index*

- Gieldon, A. [896](#)  
Gienapp, I.E. [654](#)  
Gierasch, L.M. [338](#), [391](#)  
Giester, G. [330](#)  
Gill, J.K. [438](#)  
Gillispie, M. [543](#)  
Gilon, C. [230](#), [626](#), [959](#)  
Gilon, T. [230](#)  
Giragossian, C. [902](#)  
Giraldés, J. [246](#)  
Giralt, E. [217](#), [432](#), [1018](#), [1043](#)  
Giraud, M. [152](#)  
Gitu, P.M. [744](#)  
Glowka, M. [838](#)  
Gobbo, M. [628](#), [776](#)  
Gogoll, A. [142](#)  
Golding, S.W. [89](#), [122](#)  
Gómez-Chiarri, M. [475](#)  
González, C. [632](#)  
González-Muñiz, R. [632](#)  
Good, M. [937](#)  
Goodman, B. [200](#)  
Goodman, M. [446](#), [731](#)  
Goodwin, C.A. [279](#)  
Goody, R.S. [870](#)  
Gopalakrishnakone, P. [483](#)  
Gordon, L.M. [963](#)  
Gordon, T. [624](#)  
Gore, V. [701](#)  
Gorman, P. [971](#)  
Gothard, C.M. [572](#)  
Gottschling, D. [647](#)  
Gouyette, C. [109](#)  
Gräfe, U. [226](#)  
Gran, B. [1051](#)  
Granata, C. [632](#)  
Gras-Masse, H. [109](#), [119](#)  
Grdadolnik, S.G. [330](#)  
Greeley, D. [701](#)  
Greene, R.J. [168](#)  
Greiner, G. [132](#)  
Grell, D. [185](#)  
Grieco, P. [630](#), [892](#)  
Griesinger, C. [187](#), [204](#), [502](#)  
Grignoux, V. [822](#)  
Grigoriev, A.E. [855](#)  
Grigoriev, E.I. [855](#)  
Grimellec, C.L. [830](#)  
Gronlund, J.L. [541](#)  
Groom, J. [543](#)  
Groot, P.G.d. [379](#)  
Grosfeld-Stulemeyer, M.C. [1045](#)  
Groth, U. [733](#)  
Gruner, S. [664](#)  
Gu, X. [602](#), [660](#)  
Guenot, J. [701](#)  
Guerlavais, V. [748](#)  
Guerrini, R. [679](#), [787](#), [851](#)  
Guffler, S. [212](#)  
Guichard, G. [348](#), [402](#)  
Guichou, J.F. [130](#)  
Gunasekaran, K. [338](#), [391](#)  
Guo, L. [148](#), [927](#)  
Gururaja, T.L. [389](#), [1053](#)  
Gurusiddappa, S. [735](#)  
Gutheil, W.G. [234](#)  
Gutte, B. [166](#), [988](#)  
Guzzi, M. [672](#)  
Gyurcsik, B. [306](#)  
  
Haan, E.C.d. [1045](#)  
Haas, E. [398](#)  
Habink, J.A. [391](#)  
Haeuw, J.F. [320](#)  
Hagler, A.T. [391](#)  
Halab, L. [599](#)  
Hall, S.C. [832](#)  
Hallberg, A. [142](#), [549](#), [917](#)  
Hamasaki, Y. [913](#)  
Hamawaki, T. [650](#)  
Hammarström, L.G.J. [34](#), [444](#), [758](#)  
Hammer, J. [479](#)  
Hammer, R.P. [34](#), [458](#)  
Han, G. [708](#)  
Han, K.H. [485](#)  
Hancock, R.E.W. [477](#)  
Hara, T. [766](#)  
Harada, S. [778](#), [780](#)  
Haramura, M. [662](#)  
Hariton-Gazal, E. [959](#)  
Harte, M.F. [553](#)  
Härtl, A. [226](#)  
Hartog, J.A.J.d. [727](#)  
Hasegawa, K. [111](#), [160](#)  
Hashimoto, K. [766](#)  
Haskell-Luevano, C. [271](#), [706](#), [879](#)

## Author Index

- Hatakeyama, T. [489](#), [760](#)  
Hatta, T. [350](#), [411](#)  
Hattori, M. [357](#)  
Haug, B.E. [56](#)  
Hauser, M. [957](#)  
Hawthorn, N. [200](#)  
Hayashi, R. [468](#)  
Hayashi, T. [357](#), [373](#), [426](#), [1067](#)  
Hayashi, Y. [638](#), [650](#)  
He, S. [541](#)  
Heffernan, M. [714](#)  
Heggs, P.J. [283](#)  
Heine, N. [579](#)  
Heiner, D. [277](#)  
Heitz, A. [387](#)  
Heitz, F. [830](#)  
Helfrich, B. [642](#), [721](#)  
Hemmerlin, C. [348](#)  
Henry, L.K. [876](#)  
Hernandez, J.F. [387](#)  
Herranz, R. [632](#)  
Herrero, J. [1057](#)  
Heshmati, P. [240](#), [836](#)  
Heyl, D. [543](#)  
Hidaka, Y. [385](#)  
Higashimoto, Y. [1039](#)  
Hilty, C. [312](#)  
Himm, R. [543](#)  
Hirano, Y. [357](#), [373](#), [1067](#)  
Hirst, J. [303](#)  
Hlaváček, J. [618](#)  
Hodges, R.S. [353](#), [359](#), [361](#), [365](#), [377](#),  
[466](#), [477](#), [497](#)  
Hoeger, C. [719](#)  
Hoffmann, B. [577](#)  
Hoffmann, C. [187](#)  
Hoffmann, S.R.K. [166](#), [210](#), [940](#), [988](#),  
[990](#)  
Hofmann, R.M. [992](#)  
Hofmeyer, L.J.F. [232](#)  
Hogg, R.C. [113](#)  
Hoh, F. [301](#)  
Hojo, H. [508](#)  
Hokari, Y. [1014](#)  
Holder, J.R. [706](#)  
Holloosi, M. [336](#)  
Hollósy, F. [805](#)  
Höltzel, A. [481](#), [768](#)  
Holzmann, B. [612](#), [647](#)  
Hong, A. [69](#), [73](#), [162](#)  
Hong, T.T. [387](#)  
Höök, A. [735](#)  
Höök, M. [735](#)  
Horiuchi, M. [160](#)  
Horne, W.C. [822](#)  
Horton, D.A. [122](#)  
Horvat, S. [504](#)  
Horváth, A. [640](#)  
Hosoda, K. [411](#)  
Houghten, R.A. [252](#), [255](#), [257](#), [259](#), [261](#),  
[640](#), [921](#)  
Howl, J. [750](#)  
Howlett, G. [881](#)  
Hoyer, D. [622](#)  
Hoyne, P. [881](#)  
Hruby, V.J. [20](#), [22](#), [24](#), [26](#), [28](#), [30](#), [297](#),  
[324](#), [499](#), [602](#), [660](#), [691](#), [708](#), [744](#),  
[892](#), [969](#)  
Hu, H. [1057](#)  
Huang, X.C. [890](#)  
Huber, V. [200](#)  
Hubler, F. [130](#)  
Hudecz, F. [316](#), [652](#), [1010](#)  
Hudson, D. [54](#), [117](#)  
Hulce, M. [250](#)  
Hultgren, S.J. [636](#)  
Hunter, C.L. [870](#)  
Huon, J.K. [572](#)  
Huynh-Dinh, T. [109](#)  
Iacovino, R. [289](#)  
Ibrahim, G. [277](#)  
Idei, M. [805](#)  
Ikuta, M. [662](#)  
Imhof, D. [226](#)  
Inagaki, F. [160](#)  
Ingallinella, P. [534](#), [545](#)  
Inui, T. [157](#), [248](#)  
Isernia, C. [710](#)  
Ishibashi, J. [1035](#)  
Ishikawa, H. [202](#)  
Ishizuka, S. [99](#)  
Iterbeke, K. [984](#)  
Ito, Y. [508](#)  
Ittah, V. [398](#)  
Iuchi, T. [1067](#)

## Author Index

- Ivanov, V.T. [587](#), [785](#), [803](#)  
Izuhara, N. [516](#)
- Jablonkai, I. [52](#)  
Jackson, D.C. [935](#)  
Jacobs, R.T. [413](#)  
Jacobsen, N.E. [324](#)  
Jäggin, V. [712](#)  
James, M. [206](#), [318](#), [1057](#)  
Janardhanam, S. [440](#)  
Jang, J.S. [77](#)  
Janmey, P. [420](#)  
Jaulent, A.M. [547](#)  
Jaun, B. [383](#)  
Jaworski, A. [774](#)  
Jean, F. [563](#)  
Jelokhani-Niaraki, M. [497](#), [766](#)  
Jensen, K.J. [454](#)  
Jensen, T. [1041](#)  
Ji, H. [222](#)  
Jiang, S. [731](#)  
Jiang, W.J. [714](#)  
Jiang, X. [146](#)  
Jiménez, J.C. [217](#)  
Jiménez, M.A. [632](#)  
Jimenez-Clavero, M.Á. [1043](#)  
Jin, Y. [479](#)  
Johannesson, P. [142](#)  
Johanssen, B. [984](#)  
Johansson, A. [142](#), [549](#)  
Johansson, M.K. [54](#)  
Joly, P. [119](#)  
Jonczyk, A. [733](#)  
Jones, A. [89](#), [277](#)  
Jones, R.E. [644](#)  
Jorissen, R. [881](#)  
Juillerat, M.A. [770](#)  
Juliano, L. [563](#)  
Juliano, M.A. [563](#)  
Jung, G. [208](#), [244](#), [267](#), [481](#), [768](#), [1037](#)  
Juvvadi, P. [764](#)
- Kaczmarek, K. [456](#)  
Kadoya, Y. [1060](#)  
Kako, K. [795](#)  
Kamath, J.R. [183](#), [551](#)  
Kamisato, S. [807](#)  
Kang, D.I. [826](#)
- Kanoh, K. [638](#)  
Kappler, J. [543](#)  
Kaptein, B. [371](#), [1065](#)  
Kapurniotu, A. [338](#)  
Karas, M. [187](#)  
Kardinal, C. [185](#)  
Karelin, A.A. [785](#), [803](#)  
Karle, S.A. [1033](#)  
Karlén, A. [142](#), [917](#)  
Karpov, O. [626](#)  
Kashimoto, K. [778](#), [780](#)  
Kates, S.A. [140](#), [265](#)  
Kato, K. [1060](#)  
Kato, T. [526](#), [528](#)  
Katoh, E. [350](#), [411](#)  
Katre, N. [658](#)  
Kaumaya, P.T.P. [654](#), [1004](#), [1006](#), [1008](#), [1012](#)  
Kavarana, M. [28](#), [708](#)  
Kawabata, S.i. [756](#)  
Kawaguchi, T. [516](#)  
Kawai, M. [516](#)  
Kawakami, T. [111](#), [160](#)  
Kawano, K. [756](#)  
Kay, C.M. [497](#)  
Kayahara, M. [1067](#)  
Kazantzis, A. [338](#)  
Kazavchinskaya, P. [634](#)  
Kazmierkiewicz, R. [896](#)  
Keene, D.R. [735](#)  
Keilman, J. [200](#)  
Keivish, T. [656](#)  
Kelly, B. [273](#)  
Kemnitzer, W.E. [572](#)  
Kent, S.B.H. [870](#)  
Kéri, G. [640](#), [664](#), [805](#), [864](#),  
Kessler, H. [612](#), [647](#), [664](#)  
Khaidukov, S.V. [785](#), [803](#)  
Khan, S.A. [460](#)  
Khan, W. [704](#)  
Khare, S.K. [375](#), [876](#)  
Khasanova, T. [572](#)  
Khatri, A. [140](#), [890](#)  
Khavinson, V.Kh. [855](#)  
Kihlberg, J. [604](#), [636](#)  
Kikelj, D. [330](#)  
Kim, D.H. [485](#)  
Kim, H.J. [71](#), [77](#), [155](#)

## Author Index

- Kim, H.K. [791](#)  
Kim, H.W. [572](#)  
Kim, K.L. [791](#)  
Kim, S.C. [1049](#)  
Kim, S.G. [826](#)  
Kim, Y.D. [71](#), [77](#), [155](#)  
Kimmerlin, T. [622](#)  
Kimura, T. [157](#), [248](#), [650](#)  
Kinarsky, L. [381](#)  
Kinberger, G.A. [446](#)  
King, D.S. [818](#)  
Kiso, Y. [638](#), [650](#)  
Kitas, E.A. [888](#)  
Kiwada, T. [452](#)  
Kiwani, R. [953](#)  
Klein, S. [925](#)  
Klinguer-Hamour, C. [320](#)  
Knapp, M. [310](#)  
Knaute, T. [212](#), [422](#)  
Ko, C.Y. [77](#)  
Kobayashi, Y. [396](#)  
Koch, M. [931](#)  
Koch, P. [558](#)  
Kochan, J. [704](#)  
Kochnev, I.N. [855](#)  
Kodama, H. [468](#), [766](#), [913](#)  
Koehler, G. [310](#)  
Kogan, M. [432](#)  
Koh, S. [957](#)  
Köhida, L. [652](#)  
Kolesanova, E.F. [1031](#)  
Komatsu, Y. [528](#)  
Komba, S. [1041](#)  
Kondejewski, L.H. [497](#)  
Kondo, M. [468](#), [766](#), [913](#)  
Königs, C. [204](#), [187](#)  
Korenstein, B. [206](#), [318](#), [1057](#)  
Kostanyan, I.A. [782](#)  
Kövé, K.E. [303](#), [917](#)  
Kozono, T. [662](#)  
Kozu, G. [634](#)  
Kragol, G. [493](#), [873](#), [935](#)  
Kranz, J. [512](#)  
Kronen, M. [226](#)  
Krüger, R. [187](#)  
Krüger, R.G. [512](#), [565](#)  
Kruijtz, J.A.W. [127](#), [232](#), [1045](#)  
Kubiak, T.M. [907](#)  
Kuepue, S. [310](#)  
Künzel, S. [132](#)  
Kupihár, Z. [164](#)  
Kurihara, Y. [160](#)  
Kurita, K. [99](#)  
Kurylko, G. [701](#)  
Kvecher, L. [206](#)  
Kwok, S.C. [377](#)  
Lackey, J.W. [168](#)  
Lai, J. [691](#), [969](#)  
Lam, K.S. [180](#), [183](#), [299](#), [551](#), [572](#)  
Lambert, D.M. [168](#)  
Lampron, P. [725](#)  
Langel, . [750](#)  
Larsen, E. [306](#)  
Larsen, M.J. [907](#)  
Larsson, A. [636](#)  
Lauer-Fields, J.L. [975](#)  
Laus, G. [984](#)  
Lazarus, L.H. [616](#), [679](#), [851](#)  
Léan, A.D. [900](#)  
Leatherbarrow, R.J. [196](#), [547](#)  
Leban, I. [330](#)  
Lebl, M. [277](#)  
Lebleu, B. [942](#)  
Leduc, A.M. [136](#), [170](#), [442](#)  
Lee, B.J. [291](#)  
Lee, B.K. [876](#), [898](#),  
Lee, D.L. [477](#)  
Lee, H.J. [71](#), [583](#), [155](#), [585](#)  
Lee, H. [811](#)  
Lee, J. [915](#)  
Lee, J.Y. [826](#)  
Lee, K.B. [583](#), [585](#)  
Lee, M.K. [791](#)  
Lee, M.S. [634](#)  
Lee, S.H. [50](#)  
Lee, S.L. [561](#)  
Lee, S.S. [71](#), [155](#)  
Lee, Y.S. [50](#), [691](#), [969](#)  
Legname, G. [818](#)  
Legrand, J.J. [668](#)  
Lehmann, C. [415](#)  
Lehrer, R. [301](#)  
Lei, B. [967](#)  
Lejeune, V. [83](#)  
Lelais, G. [581](#)

## Author Index

- Lelièvre, D. [224](#)  
Lelli, B. [925](#)  
Lemieux, C. [676](#), [681](#)  
Le-Nguyen, D. [322](#), [387](#)  
Leppla, S.H. [666](#)  
Lepša, L. [87](#)  
Lerner, E. [793](#)  
Létourneau, M. [725](#)  
Lew, M.J. [553](#)  
Lew, R.A. [553](#)  
Lewis, I. [716](#)  
Lewis, J. [881](#)  
Li, B. [346](#)  
Li, P. [561](#)  
Li, W. [927](#), [1053](#)  
Li, X. [980](#)  
Libinaki, R. [714](#)  
Liepina, I. [420](#)  
Lima, J. [543](#)  
Limal, D. [402](#)  
Lin, C.Y. [561](#)  
Lin, S.T. [996](#)  
Lin, T. [1053](#)  
Lin, W. [61](#)  
Lindeberg, G. [142](#), [549](#), [917](#)  
Liou, Y.M. [996](#)  
Lipkin, V.M. [782](#)  
Liskamp, R.M.J. [127](#), [232](#), [379](#), [727](#),  
[1045](#)  
Litman, P. [626](#)  
Litowski, J.R. [466](#)  
Liu, D.G. [862](#), [868](#)  
Liu, G. [183](#), [551](#)  
Liu, L. [162](#)  
Liu, M. [146](#), [236](#)  
Liu, R. [183](#), [299](#), [551](#), [572](#)  
Liu, R. [413](#)  
Livingston, B.D. [1039](#)  
Liwo, A. [420](#)  
Locardi, E. [612](#), [731](#)  
Locatelli, V. [748](#)  
Loffet, A. [214](#)  
Lohner, K. [491](#)  
Long, Y.Q. [561](#)  
López-Macià, À. [217](#)  
Lorigan, G. [832](#)  
Lottersberger, J. [1029](#)  
Lou, Q. [551](#)  
Lovas, S. [303](#), [693](#), [873](#), [905](#)  
Lovrecz, G. [881](#)  
Lowery, D.E. [907](#)  
Loyter, A. [230](#), [959](#)  
Lozzi, L. [925](#)  
Lu, G. [138](#)  
Lu, S.M. [466](#)  
Lu, Y. [676](#)  
Lu, Y.A. [470](#), [487](#)  
Lubell, W.D. [597](#), [599](#)  
Lucas, C. [944](#)  
Lucas, L. [543](#)  
Luczak, C. [1057](#)  
Lum, C. [200](#)  
Lumma, P.K. [644](#)  
Luna, M.G.d. [666](#)  
Lung, F.D.T. [857](#), [967](#), [996](#)  
Luthman, K. [604](#), [610](#)  
Lyttle, M.H. [54](#)  
Ma, A.C.Y. [973](#)  
Ma, S.W. [691](#), [969](#)  
Ma, X. [1016](#)  
Mabini, A. [921](#)  
Madeo, J. [847](#)  
Mader, C.J. [168](#)  
Maeda, H. [913](#), [915](#)  
Maeda, I. [336](#), [807](#)  
Maeda, M. [849](#)  
Magdolen, V. [647](#)  
Maggi, C.A. [630](#)  
Maia, H.L.S. [36](#), [44](#)  
Maitra, S. [572](#)  
Majer, Z. [336](#)  
Makagiansar, I.T. [948](#)  
Malingue, F. [119](#)  
Malkar, N. [48](#), [1063](#)  
Malkinson, J.P. [506](#)  
Mammi, S. [424](#), [530](#), [739](#), [742](#)  
Manat, R. [180](#)  
Mannekens, E. [683](#)  
Manning, M. [695](#), [699](#)  
Mant, C.T. [353](#), [377](#)  
Manzanares, I. [217](#)  
Maragoudakis, M. [614](#)  
Marastoni, M. [1027](#)  
Marchioro, C. [530](#)  
Mařík, J. [618](#)

## Author Index

- Marinzi, C. [105](#)  
Marmorstein, R. [541](#)  
Maro, D.D. [925](#)  
Marquardt, A. [316](#)  
Marraud, M. [348](#)  
Marshall, G.R. [3](#), [177](#), [240](#), [394](#), [589](#),  
[591](#), [593](#), [595](#), [836](#), [853](#), [909](#), [917](#)  
Martin, A. [750](#)  
Martin, L.M. [475](#)  
Martin, M. [563](#)  
Martin, R. [194](#), [1051](#)  
Martin-Eauclaire, M.F. [322](#)  
Martinez, J. [83](#), [152](#), [748](#)  
Martín-Martínez, M. [632](#)  
Mathieu, M. [448](#)  
Matschiner, G. [555](#)  
Matsoukas, J.M. [238](#), [614](#), [656](#)  
Matsumoto, H. [650](#)  
Matsumura, S. [674](#)  
Matsunaga, T.O. [524](#)  
Matsushima, A. [797](#)  
Matsushita, Y. [489](#)  
Matsuura, J. [944](#)  
Mattern, R.H. [731](#)  
Mau, N.V. [830](#)  
Mavromoustakos, T. [238](#), [656](#)  
Mayer, J.P. [236](#)  
Mayne, R. [735](#)  
Mazaleyrat, J.P. [369](#)  
Mazzuca, C. [328](#)  
Mbikay, M. [558](#)  
McBride, J.D. [196](#), [547](#)  
McCafferty, D.G. [512](#), [541](#), [565](#)  
McGeary, R. [937](#)  
McIntosh, C.M. [338](#)  
McKern, N. [881](#)  
McLaughlin, M.L. [34](#), [46](#), [246](#), [444](#), [758](#)  
McMurray, J.S. [42](#)  
Medeiros, M. [744](#)  
Medzihradsky, K.F. [140](#)  
Medzihradsky-Schweiger, H. [316](#)  
Mee, H.T. [572](#)  
Meister, W. [888](#)  
Meldal, M. [58](#), [263](#), [269](#), [271](#), [1041](#)  
Melnyk, O. [109](#), [119](#)  
Melnyk, R.A. [820](#), [824](#)  
Meloan, R.H. [189](#), [1018](#)  
Mérette, S.A.M. [279](#)  
Mergler, M. [63](#)  
Merrifield, B. [764](#)  
Méry, J. [830](#)  
Merzouk, A. [789](#)  
Meutermans, W.D.F. [89](#), [122](#), [125](#)  
Mező, G. [652](#), [1010](#)  
Miao, Z. [1021](#)  
Micheletti, F. [1027](#)  
Micuch, P. [32](#)  
Mierke, D.F. [424](#), [737](#), [822](#), [902](#)  
Mihala, N. [1010](#)  
Mihara, H. [435](#), [518](#), [520](#), [674](#)  
Miller, B. [318](#), [1057](#)  
Miller, T.J. [34](#)  
Milon, A. [320](#)  
Miranda, A. [344](#), [495](#), [723](#)  
Miranda, L. [58](#)  
Miranda, M.T.M. [344](#), [495](#)  
Miyazaki, M. [913](#), [915](#)  
Mizenko, G.A. [994](#)  
Mizumoto, T. [778](#)  
Mizuno, T. [350](#), [411](#)  
Mobley, P.W. [963](#)  
Mochizuki, M. [1060](#)  
Molnár, A. [164](#)  
Monck, E.K. [879](#)  
Monnee, M.C.F. [232](#)  
Montaner, L. [935](#)  
Monteiro, K. [295](#)  
Monteiro, L.S. [36](#), [44](#)  
Monticelli, L. [424](#)  
Mor, A. [959](#)  
Moreau, J.P. [668](#), [670](#)  
Moret, E.E. [1045](#)  
Moretto, A. [456](#)  
Morgan, B. [668](#), [670](#)  
Morgan, M.C.B. [624](#)  
Morita, Y. [202](#)  
Moroder, L. [91](#), [355](#), [462](#), [814](#)  
Mosberg, H.I. [834](#)  
Mothes, T. [1037](#)  
Mozsolits, H. [293](#)  
Muamba, T. [130](#)  
Muccioli, G. [748](#)  
Mudra, P. [277](#)  
Muelbe, F.v.d. [208](#), [1037](#)  
Muir, T.W. [816](#), [992](#)  
Mukai, H. [1014](#)

## Author Index

- Mullah, N. [953](#)  
Müller, D.M. [772](#)  
Müller, J. [768](#)  
Mullins, D.E. [672](#)  
Munegumi, T. [608](#)  
Munekata, E. [795](#), [1014](#)  
Münnich, K. [502](#)  
Murayama, E. [662](#)  
Murphy, R.F. [303](#), [693](#), [905](#)  
Murphy, W.A. [620](#)  
Murray, T.F. [687](#), [689](#), [894](#)  
Musiol, H.J. [91](#)  
Mustapa, M.F.M. [228](#)  
Mutter, M. [130](#), [697](#)  
Mutule, I. [656](#)  
  
Nabeshima, K. [508](#)  
Naganagowda, G.A. [389](#)  
Nagase, H. [975](#)  
Nagula, G. [200](#)  
Naider, F. [375](#), [847](#), [876](#), [898](#), [957](#)  
Naik, A. [177](#)  
Nakahara, Y. [508](#)  
Nakahara, Y. [508](#)  
Nakaie, C.R. [911](#)  
Nakamoto, C. [668](#)  
Nakamura, K. [50](#)  
Nakamura, M. [608](#)  
Nakamura, T. [373](#)  
Nakanishi, H. [634](#)  
Nakano, H. [396](#), [1014](#)  
Nakase, I. [452](#), [961](#)  
Nakata, M. [248](#)  
Nakata, Y. [793](#)  
Nambiar, K.P. [440](#)  
Naqvi, S. [67](#)  
Nardi, E. [340](#)  
Narita, V. [957](#)  
Ndungu, J.M. [602](#)  
Nefzi, A. [252](#), [255](#), [257](#), [261](#)  
Neidigh, J. [406](#)  
Nemoto, Y. [778](#), [780](#)  
Nerrie, M. [881](#)  
Ng, F. [714](#)  
Ngu-Schwemlein, M. [287](#), [334](#)  
Nguyen, H.H. [226](#)  
Nguyen, T. [320](#)  
Nguyen, T.M. [387](#)  
  
Nguyen, T.M.D. [676](#)  
Nguyen, V. [980](#)  
Ni, M. [93](#)  
Nibbe, M. [277](#)  
Nicolai, N. [925](#)  
Nice, E. [881](#), [998](#), [1055](#)  
Nicholson, G.J. [481](#), [768](#)  
Nickl, C.K. [191](#)  
Niemczyk, N. [1063](#)  
Niemeyer, C.S. [666](#)  
Niethammer, D. [208](#)  
Niidome, T. [489](#), [760](#)  
Nikiforovich, G.V. [142](#), [326](#), [394](#), [853](#),  
[917](#)  
Nikolaeva, L.I. [1031](#)  
Nishi, N. [1060](#)  
Nishi, Y. [1014](#)  
Nishino, N. [526](#), [528](#)  
Nishio, H. [157](#), [248](#)  
Nishiuchi, Y. [157](#), [248](#)  
Nishiyama, Y. [99](#), [1033](#)  
Nitta, K. [756](#)  
Nokihara, K. [285](#), [793](#)  
Nolden, S. [132](#)  
Nomizu, M. [1060](#)  
Norman, M.U. [553](#)  
Nose, T. [884](#), [919](#)  
Novellino, E. [630](#)  
Nowick, J.S. [572](#), [575](#)  
Núñez, J.I. [1043](#)  
Nyberg, F. [917](#)  
Nzoma, J. [543](#)  
  
Offer, J.L. [103](#), [105](#)  
Ofitserov, V.I. [994](#)  
Ogbu, C.O. [634](#)  
Ogru, E. [714](#)  
Oguz, U. [46](#)  
Ohashi, W. [950](#), [961](#)  
Oka, M. [357](#), [373](#), [426](#), [1067](#)  
Okada, K. [919](#)  
Okada, Y. [616](#), [851](#)  
Okamachi, A. [662](#)  
Okamoto, K. [336](#), [807](#)  
Okamoto, Y. [468](#)  
Okarvi, S.M. [729](#)  
Okazaki, I. [1060](#)  
Olenina, L.V. [1031](#)

## Author Index

- Oliff, A. [644](#)  
Oliveira, E. [632](#), [1043](#)  
Oliveira, L. [886](#)  
Oliveira, V.X.Jr. [344](#), [723](#)  
Olivier, C. [109](#)  
Ollivier, N. [109](#)  
Oniki, Y. [526](#)  
Onoda, Y. [373](#)  
Onoue, S. [778](#), [780](#)  
Oren, Z. [754](#)  
Örfi, L. [805](#)  
Orfi, L. [640](#)  
Orikasa, S. [638](#)  
Orosz, G. [712](#)  
Osada, S. [468](#)  
Osaki, T. [756](#)  
Ösapay, G. [140](#)  
Osiek, T. [177](#)  
Osman, A.A. [1037](#)  
Ostresh, J.M. [255](#), [259](#), [640](#)  
Otaka, A. [606](#)  
Otte, L. [422](#)  
Otting, G. [530](#)  
Otvos, L.Jr. [493](#), [873](#), [935](#), [998](#), [1025](#), [1047](#)  
Owens, R.T. [735](#)  
  
Pai, M.T. [967](#), [978](#), [1000](#)  
Paiva, A.C.M. [723](#), [886](#), [911](#)  
Paiva, T.B. [723](#)  
Palian, M.M. [499](#)  
Palleschi, A. [328](#)  
Pállinger, É. [652](#)  
Palmer, B. [1039](#)  
Papini, A.M. [340](#)  
Parihar, R. [1012](#)  
Park, I.Y. [1049](#)  
Park, K.H. [485](#)  
Park, S.H. [291](#)  
Park, S.I. [180](#)  
Parker, E.M. [672](#)  
Partridge, A.W. [820](#), [824](#)  
Patacchini, R. [630](#)  
Patel, K. [67](#)  
Patel, T. [1016](#)  
Patiny, L. [130](#), [185](#), [697](#)  
Patkar, K.A. [687](#)  
Paul, S. [1033](#)  
  
Payan, D.G. [389](#), [1053](#)  
Payza, K. [685](#)  
Pedone, C. [710](#)  
Peggion, C. [369](#), [371](#), [514](#)  
Peggion, E. [424](#), [530](#), [739](#), [742](#)  
Pegoraro, S. [462](#)  
Pellegrini, M. [737](#), [822](#), [902](#)  
Pelzer, S. [481](#)  
Pennington, M.W. [38](#)  
Perdonà, E. [530](#)  
Perin, J.C. [1029](#)  
Perlmutter, P. [553](#)  
Pertinhez, T.A. [911](#)  
Pesiridis, S. [565](#)  
Pessi, A. [534](#), [545](#)  
Péter, A. [683](#)  
Petroni, B.D. [890](#)  
Pflegerl, K. [477](#)  
Pham, C.T.T. [387](#)  
Philippova, M.M. [803](#)  
Piaz, F.D. [545](#)  
Picking, R.A. [168](#)  
Picone, D. [314](#)  
Piek, T. [628](#)  
Pierschbacher, M.D. [731](#)  
Pinilla, C. [194](#), [1023](#), [1051](#)  
Pinkner, J.S. [636](#)  
Pinna, L.A. [982](#)  
Piotto, M. [402](#)  
Pipkorn, R. [931](#)  
Pires, J. [277](#)  
Piron, J. [150](#)  
Piserchio, A. [737](#)  
Pispisa, B. [328](#)  
Plachikkat, R. [404](#)  
Pless, J. [716](#)  
Pletnev, V. [838](#)  
Po, A. [563](#)  
Pogozheva, I. [834](#)  
Pokorny, V. [277](#)  
Polakowski, T. [577](#)  
Polevaya, L. [656](#)  
Poliakov, A. [549](#)  
Polt, R. [273](#), [499](#)  
Poncar, P. [277](#)  
Pons, M. [432](#)  
Pool, C.T. [65](#)  
Poppitz, W. [132](#)

### *Author Index*

- Porecca, F. [499](#)  
Porreca, F. [691](#), [969](#)  
Pozdnyakov, P.I. [134](#)  
Prabhakaran, M. [460](#)  
Probert, L. [238](#)  
Prokai, L. [980](#)  
Prusiner, S.B. [818](#)  
Przybylski, M. [316](#)  
Pucci, P. [545](#)  
Puijk, W.C. [189](#)  
Pyles, J. [1004](#), [1012](#)  
  
Qi, L. [701](#)  
Qiu, W. [602](#)  
Queiroz, M.J.R.P. [36](#)  
Quigley, R.M. [524](#)  
  
Rademann, J. [267](#)  
Rajeswaran, W.G. [620](#)  
Rajnavölgyi, E. [1010](#)  
Ramaswami, V. [524](#)  
Ramesh, C.V. [1016](#)  
Ramjit, H. [644](#)  
Ramnarayan, K. [418](#), [428](#), [460](#), [666](#)  
Ramprasad, M.P. [658](#)  
Raya, J. [402](#)  
Reddy, P. [67](#)  
Reddy, P.A. [177](#)  
Reeve, S.B. [553](#)  
Regoli, D. [787](#)  
Reichwein, J.F. [127](#)  
Reineke, U. [577](#)  
Reinhoudt, D.N. [923](#)  
Reissmann, R. [132](#)  
Reissmann, S. [132](#), [226](#)  
Remmer, H. [140](#)  
Reubi, J.C. [719](#)  
Rhee, H. [937](#)  
Rich, D.H. [40](#), [532](#), [537](#)  
Rich, R.L. [735](#)  
Richards, K. [881](#)  
Richer, M. [563](#)  
Rideout, D.H. [666](#)  
Rihakova, L. [888](#)  
Riitano, D. [884](#)  
Rijkers, D.T.S. [379](#), [727](#)  
Rikimaru, S. [1060](#)  
Rinnová, M. [257](#)  
  
Río, J.D. [632](#)  
Rivier, J.E. [719](#)  
Rizzi, A. [787](#)  
Rizzi, D. [679](#), [787](#)  
Ro, S. [583](#), [585](#)  
Robert, M.C. [770](#)  
Rocchi, R. [628](#), [776](#)  
Rodionov, I.L. [587](#), [782](#)  
Rodriguez, I. [217](#)  
Roeske, R.W. [927](#)  
Rogers, C.J. [654](#)  
Roller, P.P. [561](#), [857](#), [967](#)  
Rölz, C. [647](#)  
Romanovskis, P. [85](#), [567](#)  
Rosic, M. [504](#)  
Rosenberg, E. [375](#)  
Rosenberry, T.L. [85](#), [567](#)  
Rosenblatt, M. [308](#), [424](#), [668](#), [739](#), [742](#)  
Rosenthal-Aizman, K. [220](#)  
Rossi, F. [289](#)  
Rothacker, J. [881](#), [1055](#)  
Rotondi, K.S. [338](#), [391](#)  
Roumelioti, P. [656](#)  
Rovero, P. [314](#), [340](#), [630](#)  
Royo, M. [217](#), [432](#)  
Rubinstein, A. [332](#), [381](#)  
Rückle, T. [130](#)  
Rudolph, J. [244](#)  
Rueping, M. [312](#), [383](#)  
Rumennik, L. [701](#)  
Rump, E.T. [379](#)  
Russu, W.A. [575](#)  
Rutjes, F.P.J.T. [371](#)  
Ruzza, P. [845](#), [982](#)  
  
Sabirov, A. [69](#)  
Sabirov, A.N. [134](#), [994](#)  
Saccà, B. [814](#)  
Sacramento, J. [44](#)  
Sadler, K. [933](#)  
Saido-Sakanaka, H. [1035](#)  
Saitton, S. [604](#)  
Sakai, T. [202](#)  
Sakairi, N. [1060](#)  
Sakurai, K. [608](#)  
Salamon, Z. [297](#)  
Salari, H. [789](#)  
Salinas, R.K. [911](#)

## Author Index

- Salvadori, S. [679](#), [787](#), [851](#)  
Samukov, V. V. [134](#), [994](#)  
Sanchez, J. F. [301](#)  
Sanclimens, G. [432](#)  
Santi, M. [1029](#)  
Santiveri, C. M. [632](#)  
Sardana, M. K. [644](#)  
Sasaki, Y. [616](#)  
Sasiela, C. A. [689](#), [801](#)  
Sato, K. [483](#), [1067](#)  
Sato, T. [1060](#)  
Satterthwait, A. C. [363](#)  
Saviano, G. [289](#)  
Saviano, M. [289](#), [371](#), [710](#), [1065](#)  
Sax, B. [63](#)  
Sazonova, O. V. [785](#), [803](#)  
Scarselli, M. [925](#)  
Schaaper, W. M. M. [189](#), [1018](#)  
Schabbert, S. [731](#)  
Schaer, J. C. [719](#)  
Schaffner, A. P. [348](#)  
Schall, O. F. [177](#)  
Schaschke, N. [555](#)  
Scheibler, L. [739](#), [742](#)  
Schievano, E. [739](#), [742](#)  
Schiller, P. W. [676](#), [681](#), [900](#)  
Schimana, J. [768](#)  
Schlegel, B. [226](#)  
Schmid, D. [204](#)  
Schmid, D. G. [267](#), [768](#), [1037](#)  
Schmidt, A. E. [965](#)  
Schmidt, E. [814](#)  
Schmidt, R. [685](#)  
Schmiedeberg, N. [647](#)  
Schmitt, M. [647](#)  
Schneider, J. P. [438](#)  
Schneider-Mergener, J. [212](#), [577](#), [579](#), [866](#)  
Schoemaker, H. E. [371](#)  
Schreiber, D. [847](#)  
Schreiber, J. V. [275](#)  
Schreier, S. [723](#), [911](#)  
Schulz, D. [228](#)  
Schumann, P. A. [524](#)  
Schüpbach, J. [988](#)  
Schuster, A. [612](#), [647](#)  
Schwabacher, A. W. [172](#)  
Schwenk, C. [200](#)  
Scolaro, B. [628](#), [845](#)  
Scully, M. F. [279](#)  
Sebestyén, F. [316](#)  
Seebach, D. [32](#), [275](#), [312](#), [383](#), [569](#), [581](#), [622](#)  
Seeberger, S. [174](#)  
Seidah, N. G. [558](#)  
Seidel, R. P. [870](#)  
Seki, T. [1014](#)  
Sellers, M. J. [283](#)  
Semetey, V. [348](#)  
Seo, J. K. [791](#)  
Seprödi, J. [805](#), [864](#)  
Sette, A. [1039](#)  
Seyberth, T. [267](#)  
Sha, W. [909](#)  
Shai, Y. [754](#)  
Shannon, S. K. [265](#)  
Sheikine, Y. A. [803](#)  
Shekhtman, A. [816](#)  
Shen, Y. [668](#), [670](#)  
Shenderovich, M. D. [418](#), [666](#)  
Sheriff, S. [672](#)  
Sherman, S. [332](#), [381](#)  
Shibue, M. [766](#), [913](#), [915](#)  
Shida, C. S. [911](#)  
Shimoda, M. [357](#)  
Shimohigashi, M. [797](#)  
Shimohigashi, Y. [797](#), [884](#), [919](#)  
Shimonishi, Y. [385](#), [1014](#)  
Shimono, C. [385](#)  
Shin, D. K. [583](#), [585](#)  
Shindo, H. [350](#)  
Shoelson, S. E. [915](#)  
Siahaan, T. J. [946](#), [948](#)  
Sidney, J. [1039](#)  
Silhol, M. [942](#)  
Silva, N. [36](#)  
Silvestri, L. [739](#), [742](#)  
Simon, R. [194](#)  
Simonetta, A. [772](#)  
Sinaga, E. [948](#)  
Singh, S. [38](#), [170](#)  
Sirois, F. [558](#)  
Skinner, S. [670](#)  
Slaninová, J. [618](#), [697](#)  
Slomczynska, U. [177](#), [593](#)  
Slootstra, J. W. [189](#)

### *Author Index*

- Slusarz, R. [896](#)  
Smerdka, J. [267](#)  
Smith, A.I. [553](#)  
Smith, D.D. [250](#)  
Smith, R. [593](#)  
Smith, V.G. [907](#)  
Smythe, M.L. [89](#), [122](#), [125](#)  
Sobolev, B.N. [1031](#)  
Sobrinho, F. [1043](#)  
Sohma, Y. [650](#)  
Sokolov, D.I. [803](#)  
Solé, L. [217](#)  
Soloshonok, V.A. [20](#), [26](#), [660](#)  
Som, P. [134](#)  
Sommerhoff, C.P. [555](#)  
Somogyi, A. [140](#)  
Songster, M.F. [54](#), [117](#)  
Soomets, U. [750](#)  
Soong, W.J. [967](#)  
Southwood, S. [1039](#)  
Soutullo, A. [1029](#)  
Spatola, A.F. [85](#), [136](#), [170](#), [442](#), [567](#),  
[762](#), [799](#)  
Speth, R. [888](#)  
Spiga, O. [925](#)  
Spisni, A. [911](#)  
Spreen, R.C. [413](#)  
Sridharan, M. [367](#)  
Srinivasan, M. [654](#)  
Sritharan, T. [975](#)  
Srivastava, K. [101](#)  
Stacey, G. [957](#)  
Steinkühler, C. [534](#)  
Stella, L. [328](#)  
Sternberg, U. [132](#)  
Steták, A. [864](#)  
Stevanovic, S. [768](#)  
Stewart, J.M. [642](#), [721](#)  
Stewart, K.M. [553](#)  
Stigers, K.D. [572](#)  
Stockert, S. [481](#)  
Stoev, S. [695](#), [699](#)  
Strehlow, D. [132](#)  
Strong, A.E. [522](#)  
Strub, J.M. [301](#)  
Strub, M.P. [301](#)  
Suenaga, T. [760](#)  
Sugahara, Y. [483](#)  
Sugawara, M. [320](#)  
Sugiura, Y. [452](#), [950](#), [961](#)  
Süli-Vargha, H. [712](#)  
Sun, H. [701](#)  
Sun, J. [666](#)  
Sun, Y. [138](#), [799](#)  
Sundaram, R. [1006](#), [1008](#)  
Süssmuth, R.D. [481](#)  
Suzuki, T. [950](#), [961](#)  
Svendsen, J.S. [56](#)  
Svensson, A. [636](#)  
Swift, J.R. [744](#)  
Swistok, J. [701](#), [704](#)  
Sylvester, T. [921](#)  
Szabó, R. [652](#)  
Tabor, A.B. [228](#)  
Tadikonda, B. [273](#)  
Taguchi, H. [1033](#)  
Takahashi, M. [520](#), [616](#)  
Takahashi, T. [518](#)  
Takahashi, Y. [435](#), [795](#)  
Takahashi, Y.i. [516](#)  
Takami, N. [807](#)  
Takanashi, H. [662](#)  
Takao, T. [1014](#)  
Takehara, A. [795](#)  
Tam, J.P. [65](#), [138](#), [470](#), [487](#), [752](#), [933](#),  
[1021](#)  
Tamamura, H. [606](#)  
Tamiya, E. [202](#)  
Tanaka, K. [638](#)  
Tanaka, R. [516](#)  
Tanaka, S. [950](#), [961](#)  
Tancredi, T. [289](#)  
Tang, J.G. [342](#)  
Tang, X. [26](#), [28](#), [170](#), [660](#)  
Tang, Y.c. [146](#)  
Tang, Y.C. [849](#)  
Tashiro, S. [350](#)  
Tatsu, Y. [185](#)  
Taylor, J. [624](#)  
Taylor, J.E. [620](#), [668](#), [670](#)  
Taylor, J.W. [67](#), [1016](#)  
Taylor, K.G. [170](#), [442](#)  
Taylor, M.S. [191](#)  
Tegge, W. [191](#)  
Teplán, I. [805](#), [640](#), [864](#)

## Author Index

- Teruya, K. [111](#), [160](#)  
Therien, A.G. [828](#)  
Thern, B. [244](#)  
Therrien, K.A. [888](#)  
Thomas, W.G. [293](#)  
Thompson, S.A. [117](#)  
Tian, Y. [1016](#)  
Tickler, A.K. [242](#)  
Timmerman, P. [923](#)  
Tiscione, M. [1016](#)  
Toepert, F. [212](#)  
Tollin, G. [297](#)  
Tomari, T. [350](#)  
Tomatis, R. [787](#), [1027](#)  
Tonarelli, G. [1029](#)  
Tonarelli, G.G. [772](#)  
Tong, X.H. [73](#), [162](#)  
Toniolo, C. [328](#), [369](#), [371](#), [456](#), [514](#),  
[1065](#)  
Toole, B.P. [508](#)  
Tornøe, C.W. [263](#)  
Török, G. [984](#)  
Tóth, G. [303](#), [683](#)  
Tóth, G.K. [164](#)  
Toth, I. [937](#), [955](#)  
Tourwé, D. [150](#), [683](#), [984](#)  
Tregear, G.W. [342](#), [448](#)  
Treleaven, W.D. [458](#)  
Tripet, B. [361](#), [365](#), [466](#)  
Tripet, B.P. [359](#)  
Trivedi, D. [708](#), [744](#), [892](#)  
Truffault, V. [647](#)  
Truitt, T. [704](#)  
Tsai, J.H. [575](#)  
Tsai, J.Y. [857](#)  
Tseitin, V. [418](#)  
Tselios, T. [238](#)  
Tsuda, Y. [616](#)  
Tsuzuki, K. [662](#)  
Tu, S.C. [967](#)  
Tuchscherer, G. [185](#)  
Tudan, C. [789](#)  
Tulla, J. [409](#)  
Tung, C.H. [986](#)  
Tzeng, S.R. [967](#), [978](#), [1000](#)  
  
U, S. [832](#)  
Uchiyama, M. [526](#)  
Uchiyama, S. [396](#)  
Ueda, K. [950](#), [961](#),  
Ueda, T. [468](#)  
Ueno, A. [435](#), [518](#), [520](#), [674](#)  
Uesugi, S. [160](#)  
Uhlig, H. [1037](#)  
Ullrich, A. [864](#)  
Unabia, S. [293](#)  
Undén, A. [220](#)  
Unger, E.C. [524](#)  
Urban, J. [634](#)  
  
Våbenø, J. [610](#)  
Vaisar, T. [200](#)  
Vandenheede, J. [864](#)  
Vanommeslaeghe, K. [683](#)  
Vántus, T. [864](#)  
Varadi, G. [873](#)  
Varkey, J.T. [222](#)  
Vasil, M.L. [477](#)  
Vass, E. [336](#)  
Veerman, J.J.N. [371](#)  
Venantzi, M. [328](#)  
Venetianer, A. [664](#)  
Venkataramani, R. [541](#)  
Venter, J.C. [13](#)  
Verdini, A.S. [522](#)  
Versluisa, C. [127](#)  
Vidal, A. [257](#), [261](#)  
Vig, B.S. [144](#)  
Vigil-Cruz, S.C. [801](#)  
Vikstrom, B. [180](#)  
Villain, M. [107](#)  
Villén, J. [1018](#)  
Vitale, R.M. [371](#), [710](#), [1065](#)  
Vivès, E. [942](#)  
Vizzavona, J. [107](#)  
Vlahakos, D. [656](#)  
Vogel, D.M. [170](#), [762](#)  
Voigt, J. [859](#), [862](#), [868](#)  
Volkmer-Engert, R. [422](#), [577](#), [866](#)  
Vorherr, T. [63](#)  
Vosekalna, I. [306](#)  
Vriend, G. [886](#)  
Vunnam, S. [764](#)  
  
Wade, J.D. [242](#), [342](#), [448](#), [998](#)  
Wai, J. [644](#)

### *Author Index*

- Wakabayashi, Y. [1060](#)  
Wakahara, M. [373](#)  
Wakselman, M. [369](#)  
Waldeck, W. [931](#)  
Walker, B.D. [1023](#)  
Walker, C.M. [1008](#)  
Walton, T.A. [54](#)  
Wan, Y.P. [879](#)  
Wand, A.J. [512](#)  
Wang, C. [1000](#)  
Wang, D. [539](#)  
Wang, S. [561](#)  
Wang, W. [20](#), [22](#), [24](#), [30](#)  
Wang, Y. [701](#)  
Ward, C. [881](#)  
Waring, A.J. [963](#)  
Waser, B. [719](#)  
Watabe, J. [508](#)  
Watanabe, H. [606](#)  
Watanabe, J. [606](#)  
Watanabe, L.A. [526](#)  
Watson, E.M. [196](#)  
Wauben, M.H.M. [1045](#)  
Waugh, D.J.J. [250](#)  
Weckbecker, G. [716](#)  
Wei, C.Q. [859](#)  
Wei, H.B. [499](#)  
Wei, S.Y. [857](#)  
Weigelt, J. [530](#)  
Weiler, P. [63](#)  
Weinschenk, T. [1037](#)  
Weissleder, R. [986](#)  
Weist, S. [481](#)  
Welling, G. [1010](#)  
Welling-Wester, S. [1010](#)  
Wels, B. [127](#)  
Weltrowska, G. [676](#), [681](#)  
Wenger, R. [130](#)  
Wenger, S. [719](#)  
Wenschuh, H. [579](#)  
Werdelin, O. [1041](#)  
Wesdock, P.S. [832](#)  
Wessels, J.T. [208](#)  
Wheatley, J. [177](#)  
Whitacre, C.C. [654](#)  
White, J.M. [168](#)  
White, P. [97](#)  
Whitehurst, J. [240](#)  
Wibowo, F.I. [693](#), [905](#)  
Wiens, J. [892](#)  
Wiesmueller, K.H. [208](#)  
Wilhelm, O. [647](#)  
Wilkes, B.C. [676](#), [900](#)  
Willick, G.E. [789](#)  
Wilson, C.C. [1039](#)  
Windberg, E. [316](#)  
Wittelsberger, A. [697](#)  
Witter, R. [132](#)  
Wittliff, J.L. [442](#)  
Wittmann, V. [174](#)  
Wo, N.C. [695](#), [699](#)  
Wohlleben, W. [481](#)  
Wong, A.K. [955](#)  
Wong, B.K. [644](#)  
Woodward, C. [400](#), [409](#)  
Woon, C.W. [668](#), [670](#)  
Wray, V. [793](#)  
Wrede, P. [430](#)  
Wright, J. [944](#)  
Wright, K. [369](#)  
Wu, C. [487](#)  
Wu, J. [859](#), [862](#)  
Wu, L. [868](#)  
Wthrich, K. [312](#)  
  
Xiang, Q. [704](#)  
Xiang, Z. [706](#)  
Xiong, C. [20](#), [22](#), [24](#), [30](#)  
Xiong, Y. [1002](#)  
Xu, C.R. [946](#), [948](#)  
Xu, J. [539](#)  
Xu, K. [704](#)  
Xu, K.y. [1002](#)  
Xu, Q. [198](#), [234](#)  
Xu, Y. [735](#)  
  
Yagaloff, K. [701](#)  
Yagami, T. [950](#)  
Yahalom, D. [308](#)  
Yajima, T. [778](#), [780](#)  
Yakovleva, T.V. [946](#)  
Yalamoori, V.V. [666](#)  
Yamada, K. [516](#)  
Yamaguchi, H. [766](#)  
Yamakawa, M. [1035](#)  
Yamamura, H. [516](#)

## Author Index

- Yamamura, H.I. [499](#)  
Yamashita, T. [468](#)  
Yamazaki, T. [350](#), [411](#)  
Yang, C.S. [1000](#)  
Yang, D. [859](#), [862](#)  
Yang, J. [30](#)  
Yang, J.J. [450](#), [811](#)  
Yang, J.L. [470](#), [487](#), [752](#)  
Yang, W. [811](#)  
Yang, Y.S. [301](#)  
Yasuda, S. [913](#)  
Yasuhara, T. [285](#), [793](#)  
Ye, Y. [450](#), [589](#), [591](#), [593](#), [595](#), [836](#), [917](#)  
Ye, Y.h. [146](#)  
Ying, J. [602](#), [660](#)  
Yip, C.M. [971](#)  
Yogo, K. [662](#)  
Yokoi, T. [616](#)  
Yokoyama, K. [202](#)  
Yoo, B. [764](#)  
Yoon, C.J. [583](#), [585](#), [826](#)  
Yoon, J. [50](#)  
York, E.J. [642](#), [721](#)  
Yoshida, M. [528](#)  
Yoshida, T. [396](#)  
Yoshii, T. [608](#)  
Yoshiki, M. [468](#), [913](#)  
Yoshizawa-Kumagaye, K. [248](#)  
Young, J. [200](#)  
Yu, M.K. [541](#)  
Yu, Q. [752](#)  
Yu, Y. [259](#)  
Yurkina, E.A. [994](#)  
Zabrocki, J. [456](#)  
Zaccaro, L. [710](#)  
Zalipsky, S. [953](#)  
Zamora, P.O. [134](#)  
Zanotti, G. [289](#)  
Zantello, M.R. [907](#)  
Ženíšek, K. [277](#)  
Zhang, J. [148](#)  
Zhang, Q. [539](#)  
Zhang, W.J. [836](#)  
Zhang, X. [162](#)  
Zhang, Y. [479](#)  
Zhang, Z.Y. [868](#)  
Zhao, M. [75](#)  
Zhao, Y. [194](#)  
Zharikova, A. [980](#)  
Zheng, J.H. [666](#)  
Zhengyu, G. [818](#)  
Zhilina, Z. [28](#)  
Zhitnitsky, R. [1057](#)  
Zhou, F. [287](#)  
Zhou, H. [927](#)  
Zhou, Z. [458](#)  
Zhu, F. [479](#)  
Zinser, E.W. [907](#)  
Zischinsky, G. [733](#)  
Ziv, O. [626](#)  
Zloh, M. [841](#), [843](#)  
Zoga, A. [656](#)  
Zoumpoulakis, P. [656](#)  
Zumsteg, U. [712](#)

### *Index of E-mail Addresses*

Abbasi, Husam, fieldsg@fau.edu  
Acharya, Achyuta N., achyuta@tpims.org  
Agnes, Richard S., ragnes@u.arizona.edu  
Ahn, Jung-Mo, jungmo@scripps.edu  
Aimoto, Saburo,  
    aimoto@protein.osaka-u.ac.jp  
Albericio, Fernando, albericio@qo.ub.es  
Alexopoulos, Kostas,  
    kostalexopoulos@yahoo.com  
Allert, Malin, malin.allert@organic.gu.se  
Altstein, Miriam, vinnie2@netvision.net.il  
Alves, Isabel, isabeld@u.arizona.edu  
Anantharamaiah, G.M., Ananth@uab.edu  
Andersen, Niels,  
    andersen@chem.washington.edu  
Andersson, Linda,  
    linda.andersson@organic.gu.se  
Andreu, David, andreu@qo.ub.es  
Aoyagi, Haruhiko,  
    haoyagi@net.nagasaki-u.ac.jp  
Appel, Jon, jappel@tpims.org  
Arevalo, Enrique,  
    arevalo@postbox.csi.cuny.edu  
Armishaw, Christopher,  
    c.armishaw@imb.uq.edu.au  
Aumelas, André,  
    aumelas@cbs.univ-montp1.fr  
Avrahami, Dorit,  
    avrahami@wicc.weizmann.ac.il  
  
Balasubramaniam, A., Ambi.bala@UC.EDU  
Ball, Haydn, prpsc106@hotmail.com  
Banda, Phillip W.,  
    bandapw@appliedbiosystems.com  
Bansal, Paramjit Singh,  
    p.bansal@imb.uq.edu.au  
Basak, Ajoy, abasak@lri.ca  
Baumann, Michael, baumann@mit.edu  
Beck, Alain, alain.beck@pierre-fabre.com  
Becker, Jeffrey, jbecker@utk.edu  
Becker, Christian,  
    martin.engelhard@mpi-dortmund.mpg.de  
Beligere, Gangamani, beligere@scripps.edu  
Bellanda, Massimo, bellanda@chor.unipd.it  
Benedetti, Ettore,  
    benedetti@chemistry.unina.it  
Bennett, Marco, mbenn001@umaryland.edu  
Beyer, Bret, bbeyer@ufl.edu  
Bianco, Alberto, A.Bianco@ibmc.u-strasbg.fr  
Bischoff, Daniel, rodiss@scripps.edu  
Blandl, Tamas, tbla@gene.com  
Blankenship, John, johnb@scripps.edu  
Blazyk, Jack, blazyk@ohiou.edu  
Blishchenko, Elena, karelin@ibch.siohc.ras.ru  
  
Blondelle, Sylvie, sblondelle@tpims.org  
Boer, Jurgen, Elsa.Locardi@ch.tum.de  
Boisguerin, Prisca,  
    prisca.boisguerin@charite.de  
Bondebjerg, Jon, jobo@crc.dk  
Borras, Eva, eborras@tpims.org  
Botti, Paolo, paolo\_botti@hotmail.com  
Bourne, Gregory, g.bourne@imb.uq.edu.au  
Boyd, James,  
    james\_g\_boyd@groton.pfizer.com  
Brask, Jesper, okkj@pop.dtu.dk  
Brewer, Matthias, brewer@chem.wisc.edu  
Briones, Maria Portia,  
    dc9807@bse.kyutech.ac.jp  
Brkovic, Alexandre, abrkovic@hotmail.com  
Brueckner, Hans,  
    hans.brueckner@ernaehrung.uni-  
Brunel, Florence, spatola@louisville.edu  
Bryant, Sharon,  
    bryantsd@opium.niehs.nih.gov  
Burke, Terrence, Jr., tburke@helix.nih.gov  
Bursavich, Matthew,  
    bursavic@chem.wisc.edu  
Byk, Gerardo, bykger@mail.biu.ac.il  
Bystroff, Chris, bystrc@rpi.edu  
  
Cabezas, Edelmira,  
    ecabezas@burnham-inst.org  
Cabrele, Chiara, cabrele@biochem.mpg.de  
Cai, Chaozhong, caich@hotmail.com  
Cai, Minying, mcai@u.arizona.edu  
Calderan, Andrea, calderan@chor.unipd.it  
Camarero, Julio A., camarero1@llnl.gov  
Carotenuto, Alfonso, alfcaro@unisa.it  
Carr, Frank, Frank.Carr@biovation.co.uk  
Carter, John Mark, MCarter@AxCellBio.com  
Carulla, Natalia, ncarulla@biosci.cbs.umn.edu  
Cavelier, Florine, florine@univ-montp2.fr  
Chan, Gabriel H.H., circle@cuhk.edu.hk  
Chan, Yiu-Ngok, i.toth@pharmacy.uq.edu.au  
Chana, Mundeep, mundeep.chana@uchsc.edu  
Chen, Shui-Tein, bcchen@gate.sinica.edu.tw  
Chen, Huey-Yi, fdlung@mail.cmc.edu.tw  
Chen, Lin, LChen@AxCellBio.com  
Chen, Yuxin, yuxinc@ualberta.ca  
Cheng, Jya-Wei, jwcheng@life.nthu.edu.tw  
Chengrong, Xiao, sixin  
    zheng@mcmail.vanderbilt.  
Chien, Benjamin, ben.chien@questpharm.com  
Cho, Ju Hyun, jhcho@bioneer.kaist.ac.kr  
Christensen, Caspar, cach@crc.dk  
Chulin, Alexey, pepsylab@fibkh.serpukhov.su  
Chuman, Yoshiro,  
    shimoscc@mbox.nc.kyushu-u.ac.jp

## *Index of E-mail Addresses*

Chweh, Weonu, chweha@hyundaipharm.co.kr  
 Ciarkowski, Jerzy, jurek@chemik.chem.univ.gda.pl  
 Cluzeau, Jerome, cluzeauj@yahoo.fr  
 Crisma, Marco, biop02@chor.unipd.it  
 Cudic, Mare, Cudic@mail.wistar.upenn.edu  
 Cudic, Predrag, pcudic@mail.med.upenn.edu  
 Curran, Dennis P., curran@pitt.edu

Dakappagari, Naveen, kaumaya.1@osu.edu  
 DalPozzo, Alma, dalpozzo@ronzoni.it  
 Danho, Waleed, waleed.danho@roche.com  
 Datta, Neeraj, rpeptide@rpeptide.com  
 Dattilo, James, jdattilo@moleculumetics.com  
 Dawson, Philip, dawson@scripps.edu  
 de Haan, Ellen, e.c.dehaan@pharm.uu.nl  
 de Oliveira, Eliandre, andreu@qo.ub.es  
 Deber, Charles M., deber@sickkids.on.ca  
 Decatur, Sean, sdecatur@mtholyoke.edu  
 Di Fenza, Armida, difenza@unisa.it  
 Dick, Fritz, fdick@bachem.com  
 DiFenza, Armida, dursi@unisa.it  
 Ding, Fa-Xiang, ding@postbox.csi.cuny.edu  
 Divita, Gilles, gilles@scripps.edu  
 Dong, Jesse, jesse.dong@biomeasure.com  
 Du, Yu-cang, duwc@sunm.shnc.ac.cn  
 Duax, William L., duax@hwi.buffalo.edu  
 Dudek, Michael, mdudek@strubix.com  
 Dunn, Ben M., bdunn@college.med.ufl.edu

Eberle, Alex N., Alex-N.Eberle@unibas.ch  
 Eichler, Jutta, JtEichler@aol.com; jei@gbf.de  
 Eom, Khee Dong, khee.dong.eom@mcmail.vanderbilt.edu  
 Erchegyi, Judit, jerschegyi@aim.salk.edu  
 Estiarte, M. Angels, mmestiarte@pharmacy.wisc.edu

Falconer, Robert, falcon@cua.ulsop.ac.uk  
 Fan, Jianguo, fanj@intra.nei.nih.gov  
 Farquhar, Michelle, M.J.Farquhar@wlv.ac.uk  
 Felix, Arthur, artfelix@aol.com  
 Feng, Yangbo, yfeng@chemrx.com  
 Ferreira, Paula, pmf@quimica.uminho.pt  
 Ferrer, Fernando, Fernandf@burnham-inst.org  
 Fields, Gregg, fieldsg@fau.edu  
 Filter, Matthias, matthias.filter@callistogen.co  
 Fiscus, Ronald R., ronfiscus@cuhk.edu.hk  
 Flavell, Robert, flavelr@mail.rockefeller.edu  
 Flora, David, d.flora@lilly.com  
 Florian, v. d. Muelbe, florian-von-der-muelbe@uni-tue  
 Fossati, Gianluca, g.fossati@italfarmaco.com  
 Fowler, Carol, cbfowler@umich.edu

Frackenpohl, Jens, frackenpohl@org.chem.ethz.ch  
 Fridkin, Gil, gilf@vms.huji.ac.il  
 Fridkin, Mati, mati.fridkin@weizmann.ac.il  
 Fu, Yanwen, fuyan@unix1.sncc.lsu.edu  
 Fujita, Yoshio, okada@pharm.kobegakuin.ac.jp  
 Fujita, Tsugumi, tsuguscc@mbox.nc.kyushu-u.ac.j  
 Fujitani, Naoki, fujitani@sci.hokudai.ac.jp  
 Futaki, Shiroh, futaki@scl.kyoto-u.ac.jp

Gaertner, Hubert, hubert.gaertner@geneprot.com  
 Gagne, Rodney, rag@crc.dk  
 Galaktionov, Stan, stas@ccb.wustl.edu  
 Gangl, Susanne, susanne.gangl@univie.ac.at  
 Gao, Yang, tburke@helix.nih.gov  
 Garsky, Victor, victor\_garsky@merck.com  
 Gazal, Sharon, foxof@leonardo.ls.huji.ac.il  
 Gellman, Samuel, gellman@chem.wisc.edu  
 Gera, Lajos, lajos.gera@uchsc.edu  
 Gibbons, William A., gibbonswa@aol.com  
 Gierasch, Lila, gierasch@biochem.umass.edu  
 Gill, Juliana, julianag@udel.edu  
 Gilon, Chaim, shirrac@vms.huji.ac.il  
 Giraldés, José, jgirall@lsu.edu  
 Giralt, Ernest, giralt@qo.ub.es  
 Gobbo, Marina, gobbo@chor.unipd.it  
 Golding, Simon, g.bourne@imb.uq.edu.au  
 Gonzalez-Muniz, Rosario, andreu@qo.ub.es  
 Goodman, Murray, mgoodman@ucsd.edu  
 Gordon, Larry, lgordon2@san.rr.com  
 Gorman, Paul, chakrab@uhnres.utoronto.ca  
 Gras-Masse, Hélène, helene.gras@pasteur-lille.fr  
 Greene, Reagan, rgreene@trimeris.com  
 Grieco, Paolo, pagrieco@unina.it  
 Grigoriev, Evgueny, ibg@medport.ru  
 Gronlund, Jennifer, gronlund@mail.med.upenn.edu  
 Gruner, Sibylle, Sibylle.Gruner@ch.tum.de  
 Gu, Xuyuan, xgu@email.arizona.edu  
 Gudasheva, Tatiana, uusolari@solaris.msk.ru  
 Guerrini, Remo, grm@unife.it  
 Guichard, Gilles, G.Guichard@ibmc.u-strasbg.fr  
 Guichou, Jean-François, Jean-Francois.Guichou@ico.unil.ch  
 Guo, Lili, lguo@iupui.edu  
 Gururaja, "Tarikere, L", tgururaja@rigel.com  
 Gurusiddappa, Sivashankarappa, sgurusid@ibt.tamu.edu

### ***Index of E-mail Addresses***

Hammarstrom, Lars,  
lars.hammarstrom@roche.com  
Harada, Sunao, s-harada@ann.hi-ho.ne.jp  
Haramura, Masayuki,  
mharamura@chugaibio.com  
Hariton-Gazal, Elana, elanahg@pob.huji.ac.il  
Haskell-Luevano, Carrie, Carrie@cop.ufl.edu  
Hatakeyama, Tomomitsu,  
thata@net.nagasaki-u.ac.jp  
Haug, Bengt Erik, bengt@chem.uit.no  
Hayashi, Yoshio,  
yhayashi@mb.kyoto-phu.ac.jp  
He, Shu, xdhesu@hotmail.com  
Hearn, Milton,  
milton.hearn@med.monash.edu.au  
Heine, Niklas, wenschuh@jerini.de  
Heitz, Annie, aheitz@cbs.univ-montpl.fr  
Heitz, Frederic, heitz@crbm.cnrs-mop.fr  
Heshmati, Parissa, parissa@ccb.wustl.edu  
Heyl-Clegg, Deborah,  
debbie.hey-lclegg@emich.edu  
Hidaka, Yuji, yuji@protein.osaka-u.ac.jp  
Higashimoto, Yuichiro,  
higashiy@pop.nci.nih.gov  
Hirano, Yoshiaki, yhirano@chem.oit.ac.jp  
Hodges, Robert, brian.tripet@uchsc.edu  
Hoffman, Stefan, sho@bioc.unizh.ch  
Hoffmann, Christian,  
cn@org.chemie.uni-frankfurt.de  
Hofmann, Roseanne,  
hofmanr@rockvax.rockefeller.ed  
Hojo, Hironobu, hojo@keyaki.cc.u-tokai.ac.jp  
Holder, Jerry Ryan, holder@ufl.edu  
Houghten, Richard A., rhoughten@tpims.org  
Hruby, Victor J., hruby@u.arizona.edu  
Huang, Chun-Ming,  
erichcm@mail.nsysu.edu.tw  
Huang, Ziwei, z-huang@life.uiuc.edu  
Hudecz, Ferenc, fhudecz@ludens.elte.hu  
  
Ingallinella, Paolo,  
paolo\_ingallinella@merck.com  
Ishibashi, Jun, bishiba@nises.affrc.go.jp  
Iterbeke, Koen, kgiterbe@vub.ac.be  
Iuchi, Tadashi, yhirano@chem.oit.ac.jp  
Iwai, Leo Kei, leo.biof@infar.epm.br  
Iyer, Krishnaiyer, dirirr@vsnl.net  
  
Jablonkai, Istvan, jabi@cric.chemres.hu  
Jarosinski, Mark, markj@amgen.com  
Jalent, Agnes, agnes.jalent@ic.ac.uk  
Jean, Francois, fjean@interchange.ubc.ca  
Jelokhani-Niaraki, Masood,  
jelokhani@brandonu.ca  
  
Jiang, Woei-Jia, woeijiajiang@hotmail.com  
Johannesson, Petra, petra@orgfarm.uu.se  
Johansson, Anja, anja@orgfarm.uu.se  
Jonczyk, Alfred, jonczyk@merck.de  
Jung, Günther,  
guenther.jung@uni-tuebingen.de  
Juvvadi, pjuvvadi@hotmail.com  
  
Kamath, Jayesh, kit.lam@ucdmc.ucdavis.edu  
Karle, Isabella, williams@harker.nrl.navy.mil  
Kashimoto, Kazuhisa,  
george@americanpeptide.com  
Kasprzykowski, Franciszek,  
fk@chemik.chem.univ.gda.pl  
Katoh, Etsuko, ekatoh@abr.affrc.go.jp  
Kaumaya, Pravin, kaumaya.1@osu.edu  
Kavarana, Malcolm, kavarana@u.arizona.edu  
Kawai, Masao, kawai@ach.nitech.ac.jp  
Kawakami, Toru, kawa@protein.osaka-u.ac.jp  
Kempe, Maria, Maria.Kempe@tbiokem.lth.se  
Kennedy, Robert, rkennedy@mit.edu  
Keri, Gyorgy, keri@puskin.sote.hu  
Kessler, Horst, kessler@ch.tum.de  
Khare, Sanjay, khare@postbox.csi.cuny.edu  
Khatr, Ashok,  
khatr@helix.mgh.harvard.edu  
Kikelj, Danijel, danijel.kikelj@ffa.uni-lj.si  
Kilk, Kalle, kkilk@scripps.edu  
Kim, Hack-Joo, jgyos@hyundaipharm.co.kr  
Kim, Do-Hyung,  
oragnc2@biotech5.kribb.re.kr  
Kimmerlin, Thierry,  
kimmerlin@org.chem.ethz.ch  
Kimura, Terutoshi, kimura@peptide.co.jp  
Kinarsky, Leo, lkinars@unmc.edu  
Kinberger, Garth, gkinberg@ucsd.edu  
Kiso, Yoshiaki, kiso@mb.kyoto-phu.ac.jp  
Knaute, Tobias, tobias.knaute@charite.de  
Knight, Graham, cgk21@mole.bio.cam.ac.uk  
Kobayashi, Yuji, yujik@protein.osaka-u.ac.jp  
Kodama, Hiroaki, hiroaki@cc.saga-u.ac.jp  
Kofod-Hansen, Mikael,  
mkoh@novonordisk.com  
Kolesanova, Ekaterina, ekol@ibmh.msk.su  
Kragol, Goran,  
Kragol@mail.wistar.upenn.edu  
Kruger, Ryan, kruger@mail.med.upenn.edu  
Kubiak, Teresa M.,  
teresa.m.kubiak@am.pnu.com  
Kumar, Senthil, kumar@org.chem.ethz.ch  
Kupihar, Zoltan,  
toth@ovrisc.mdche.u-szeged.hu  
Kwak, Juliann, jkwak@chem.ucsd.edu

## *Index of E-mail Addresses*

Kwok, Stanley,  
stan.kwok@biochem.ualberta.ca  
Kyu-Hwan, Park,  
khpark@biotech5.kribb.re.kr

Langel, Ulo, ulangel@scripps.edu  
Lankiewicz, Leszek,  
leszek@chemik.chem.univ.gda.pl  
Lannoy, Vincent, vlannoy@euroscreen.be  
Larocque, Alain, alarocque@theratech.com  
Larsson, Andreas,  
andreas.larsson@chem.umu.se  
Lebl, Michal, michal@5z.com  
Leduc, Anne-Marie,  
anne\_marieleduc@hotmail.com  
Lee, Darin, darin.lee@uchsc.edu  
Lee, Hyun Jin, hj0220@hyundaipharm.co.kr  
Lee, Jee-Young, jyoung@songsim.cuk.ac.kr  
Lee, Myung Kyu, mkleee@mail.kribb.re.kr  
Lee, Yoon-Sik, yslee@snu.ac.kr  
Lehmann, Christian,  
Christian.Lehmann@ico.unil.ch  
Lelais, Gérald, lelais@org.chem.ethz.ch  
Lelievre, Dominique, lelievre@chem.umn.edu  
Lew, Rebecca, rebecca.lew@baker.edu.au  
Lewis, Ian, ian.lewis@pharma.novartis.com  
Li, Bin, libin@u.washington.edu  
Li, Michael, mli@vydac.com  
Liepina, Inta, inta@osi.lv ; linta@acad.latne  
Lipkin, Valery, vmlipkin@ibch.ru  
Liskamp, Rob, r.m.j.liskamp@pharm.uu.nl  
Liu, Rong-qiang, rliu@chem.umn.edu  
Liu, Ruiwu, rwliu67@yahoo.com  
Liu, Ding-Guo, tburke@helix.nih.gov  
Lobl, Tom, tlobl@newbiotics.com ;  
tjlobl@worldnet.att.net  
Loffet, Albert, albert.loffet@sennchem.com  
Longhi, Renato, longhi@ico.mi.cnr.it  
Lopez-Deber, Maria Pilar, qopili@usc.es  
Lovas, Sandor, vasz@bifl.creighton.edu  
Lu, Yi-An, luy1@ctrvax.vanderbilt.edu  
Lu, Stephen, stephen.lu@ualberta.ca  
Lubell, William, lubell@chimie.umontreal.ca  
Lung, Feng-Di, fdlung@mail.cmc.edu.tw  
Lyon, Gholson, lyong@rockefeller.edu

Maeda, Mitsuko,  
maeda@pharm.kobegakuin.ac.jp  
Malkar, Navdeep, nmalkar@fau.edu  
Malkinson, John, malkin@cua.ulsop.ac.uk  
Manning, Maurice, mmanning@mco.edu  
Marastoni, Mauro, mru@dns.unife.it  
Marik, Jan, marik@uochb.cas.cz

Marino, Joseph,  
Joseph\_P\_Marino@sbphrd.com  
Marinzi, Chiara, chiara@scripps.edu  
Marraud, Michel,  
Michel.Marraud@ensic.inpl-nancy.fr  
Marshall, Garland, garland@pcg.wustl.edu  
Martin, Lenore, martin@uri.edu  
Martinez, Jean,  
martinez@colombes.pharma.univ-montp1.fr  
Mathieu, Marc,  
m.mathieu@hfi.unimelb.edu.au  
Matsoukas, John,  
johnmatsoukas@hotmail.com  
Matsumura, Sachiko,  
smatsumu@bio.titech.ac.jp  
Matsunaga, Terry, tmatsunaga@imarx.com  
Mattern, Ralph-Heiko,  
rmattern@integra-LS.com  
McCafferty, Dewey,  
deweym@mail.med.upenn.edu  
McMurray, John S.,  
jmcmurra@mdanderson.org  
Melnyk, Oleg, oleg.melnyk@pasteur-lille.fr  
Melnyk, Roman, r.melnyk@utoronto.ca  
Merette, Sandrine, smerette@tri-london.ac.uk  
Merzouk, Ahmed, ahmed@chemokine.net  
Meutermans, Wim,  
m.smythe@mailbox.uq.edu.au  
Micuch, Peter, micuch@org.chem.ethz.ch  
Mierke, Dale, dale\_mierke@brown.edu  
Mihara, Hisakazu, hmihara@bio.titech.ac.jp  
Miller, Bruce, dbaror@dmibio.com  
Miranda, Les, lmiranda@gryphonsci.com  
Miranda, Antonio, miranda.biof@epm.br  
Mitchell, Julie, mitchell@sdsc.edu  
Miyazaki, Masaya, miyazaki@kniri.go.jp  
Moble, Patrick, pwmoble@csupomona.edu  
Monteiro, Luis, monteiro@quimica.uminho.pt  
Monticelli, Luca, stef@chor.unipd.it  
Morgan, Barry, barry317@aol.com  
Moroder, Luis, fiori@biochem.mpg.de  
Morris, May, mmorris@scripps.edu  
Mosberg, Henry, him@umich.edu  
Mozsolits, Henriette,  
mibel.aguilar@med.monash.edu.au  
Mukai, Hidehito,  
hidehito.mukai@ims.jti.co.jp  
Muller, Diana Maria,  
tonareli@fbc.unl.edu.ar  
Munegumi, Toratane,  
munegumi@oyama-ct.ac.jp  
Münnich, Kristina,  
kh@org.chemie.uni-frankfurt.de

### ***Index of E-mail Addresses***

Murphy, Richard F., barrym@creighton.edu  
Musiol, Hans-Jürgen,  
    schaschk@biochem.mpg.de  
Mustapa, Firouz, firouzmustapa@bigfoot.com  
Muszkat, Karol,  
    alex.muszkat@weizmann.ac.il  
Mutter, Manfred, Manfred.Mutter@ico.unil.ch

Naider, Fred, Naider@postbox.csi.cuny.edu  
Nambiar, Krishnan,  
    nambiar@chem.ucdavis.edu  
Nefzi, Adel, adeln@tpims.org  
Ngu-Schwemlein, Maria, mariamln@aol.com  
Nguyen, Hoai Huong,  
    hoaihuongnguyen@hotmail.com  
Ni, Jingman, wangrui@lzu.edu.cn  
Nice, Edouard, ed.nice@ludwig.edu.au  
Nikiforovich, Gregory,  
    gregory@ccb.wustl.edu  
Nishiuchi, Yuji, yuji@peptide.co.jp  
Nishiyama, Yasuhiro,  
    Yasuhiro.Nishiyama@uth.tmc.edu  
Nokihara, Kiyoshi, noki@shimadzu.co.jp  
Nomizu, Motoyoshi,  
    nomizu@ees.hokudai.ac.jp  
Nowick, James, jsnowick@uci.edu

Oard, Svetlana, soard@agctr.lsu.edu  
Offer, John, joffer@scripps.edu  
Offord, Robin, offord@cmu.unige.ch  
Oguz, Umut, uoguzl@lsu.edu  
Oka, Masahito, masa@riast.osakafu-u.ac.jp  
Okada, Kazushi,  
    kazuscc@mbx.nc.kyushu-u.ac.jp  
Okamoto, Kouji, okagen@bse.kyutech.ac.jp  
Okarvi, Subhani, sokarvi@kfshrc.edu.sa  
Oku, Hiroyuki, oku@chem.gunma-u.ac.jp  
Oliveira, Laerte, laerte@biof.epm.br  
Orfi, László, orlasz@hogyes.sote.hu  
Osada, Satoshi, osadas@cc.saga-u.ac.jp  
Otaka, Akira, aotaka@pharm.kyoto-u.ac.jp  
Ötvös, Ferenc, otvos@rosi.szbk.u-szeged.hu  
Otvos, Jr., Laszlo,  
    Otvos@mail.wistar.upenn.edu

Pai, Ming-Tao, d878210@life.nthu.edu.tw  
Palian, Michael, Ponchi420@aol.com  
Parekh, Harendra,  
    paxhsp@gmail.nottingham.ac.uk  
Park, Steven, kit.lam@ucdmc.ucdavis.edu  
Park, Sang-Ho, lbj@nmr.snu.ac.kr  
Partridge, Anthony,  
    anthony.partridge@utoronto.ca  
Patkar, Kshitij, kpatk001@umaryland.edu

Pato, János, jpato@vichem.hu  
Peggion, Evaristo, peggion@chor.unipd.it  
Pellegrini, Maria, pellegm@basf.com  
Pennington, Michael,  
    mpennington@usbachem.com  
Pessi, Antonello, antonello\_pessi@merck.com  
Peterson, Mark, mark@neokimia.com  
Pinilla, Clemencia, pinilla@tpims.org  
Pipkorn, Rüdiger,  
    pipkorn@mail.zmbh.uni-heidelberg  
Piron, Jan, jpiron@vub.ac.be  
Pispisa, Basilio, pispisa@stc.uniroma2.it  
Polt, Robin, polt@u.arizona.edu  
Pool, Chadler, chadler\_pool@excite.com  
Prabhakaran, Muthu, mprabha@strubix.com  
Prokai, Laszlo, lprokai@grove.ufl.edu

Qiu, Bo, boqiu@rutchem.rutgers.edu

Rabenstein, Dallas, dallas.rabenstein@ucr.edu  
Rademann, Jorg,  
    guenther.jung@uni-tuebingen.de  
Rahimipour, Shai,  
    coshai@wicc.weizmann.ac.il  
Rajeswaran, W.G., wragesw@tulane.edu  
Ramprasad, Mysore,  
    mysore\_ramprasad@skyepharmaco  
Rapaport, Hanna, rhanna@caltech.edu  
Reid, Christopher, c3reid@pepi.uwaterloo.ca  
Reineke, Ulrich, reineke@jerini.de  
Reissmann, Siegmund,  
    reissmann@merlin.biologie.uni-  
Rijkers, Dirk T.S., d.t.s.rijkers@pharm.uu.nl  
Rinnová, Markéta, mrinnova@tpims.org  
Ro, Seonggu, sgro@crystalgenomics.com  
Robert, Marie-Claude,  
    marie-claude.robert@rdls.nestl  
Rogers, Jessica, rogers@scripps.edu  
Roggero, Mario, roggero@dictagene.ch  
Roller, Peter, proll@helix.nih.gov  
Romanovskis, Peteris, spatola@louisville.edu  
Rosic, Maja, roscic@rudjer.irb.hr  
Rosenthal-Aizman, Katri,  
    katri@neurochem.su.se  
Roumelioti, Panagiota,  
    g\_roumelioti@hotmail.com  
Rueping, Magnus, rueping@org.chem.ethz.ch  
Rump, Erik T., e.rump@organonteknika.nl  
Ruzza, Paolo, ruzza@chor.unipd.it

Sabirov, Aydar, aydar\_sabirov@usa.net  
Sacca, Barbara, sacca@biochem.mpg.de  
Sadler, Kristen,  
    kristen.sadler@mcmill.vanderbilt.edu

### *Index of E-mail Addresses*

Saitton, Stina, stina.saitton@chem.umu.se  
Salvadori, Severo, s.salvadori@unife.it  
Samukov, Vladimir, samukov@vector.nsc.ru  
Sanchez, Jean Frederic,  
jfred@cbs.univ-montp1.fr  
Sasiela, Christy, csasi001@umaryland.edu  
Sato, Kazuki, sato@fwu.ac.jp  
Sazonova, Olga, olga\_sazonova@mail.ru  
Schaaper, Wim, w.m.m.schaaper@pepscan.nl  
Schaschke, Norbert,  
schaschk@biochem.mpg.de  
Schiller, Peter W., schillp@ircm.qc.ca  
Schmidt, Ralf,  
Ralf.Schmidt@astrazeneca.com  
Schmidt, Amy, schmid2@slu.edu  
Schneider, Joel, schneijp@udel.edu  
Schnepf, Robert,  
schnepf@mpi-muelheim.mpg.de  
Schreier, Shirley, schreier@iq.usp.br  
Schultz, Carsten,  
carsten.schultz@mpi-dortmund.m  
Schwabacher, Alan, awschwab@uwm.edu  
Schweinitz, Andrea,  
schweinitz@merlin.biologie.uni  
Scmid, Dietmar,  
guenther.jung@uni-tuebingen.de  
Seebach, Dieter, seebach@org.chem.ethz.ch  
Seeberger, Sonja,  
Seeberger@chemie.uni-frankfurt  
Seidel, Ralf,  
ralf.seidel@mpi-dortmund.mpg.de  
Seitz, Oliver,  
oliver.seitz@mpi-dortmund.mpg.de  
Sellers, Martin,  
Martin.Sellers@stud.umist.ac.u  
Sepodi, Janos, seprok@puskin.sote.hu  
Sha, Wei, wxs8@gpc.wustl.edu  
Shannon, Simon, shann019@tc.umn.edu  
Sharma, Ram P., rps2@soton.ac.uk  
Shenderovich, Mark, marksh@strubix.com  
Sherman, Simon, arubin@unmc.edu  
Shi, Tiesheng, TSHI@ucrac1.ucr.edu  
Shinnar, Ann, ashinnar@barnard.edu  
Singh, Satendra, ssingh@usbachem.com  
Slomczynska, Urszula,  
uslomczynska@metaphore.com  
Smith, Derek, dsmith@creighton.edu  
Songster, Michael, mikey@biosearchtech.com  
Sorensen, Dan, dan@kiku.dk  
Spain, Stephen, nuclearmr@hotmail.com  
Spatola, Arno F., spatola@louisville.edu  
Spiga, Ottavia, braccil@unisi.it  
Srinivasan, Mythily, kaumaya.1@osu.edu  
Srivastava, Kripa,  
Kripa.Srivastava@MKg.com  
Stewart, John, george.kotovych@ualberta.ca  
Strong, Andy, strong@dictagene.ch  
Sun, Yingchuan, spatola@louisville.edu  
Sun, Ying, Yings64@btamail.net.cn  
Sundaram, Roshni, kaumaya.1@osu.edu  
Sundaram, Roshni, kaumaya.1@osu.edu  
Suzuki, Tomoki,  
tf60y0159@ip.media.kyoto-u.ac.j  
Swistok, Joseph, joseph.swistok@roche.com  
Taguchi, Hiroaki,  
Hiroaki.Taguchi@uth.tmc.edu  
Takahashi, Mizuki, mtakahas@bio.titech.ac.jp  
Takahashi, Tsuyoshi,  
ttakahas@bio.titech.ac.jp  
Takahashi, Yoshinori,  
yoshtakah@hotmail.com  
Tang, Xuejun, xtang@u.arizona.edu  
Tang, Yan-Chun, ychtang@sickkids.on.ca  
Tao, Zheng, Sixin  
Zheng@mcmail.Vanderbilt.  
Taylor, John W., taylor@rutchem.rutgers.edu  
Tegge, Werner, wte@gbf.de  
Therien, Alex, atherien@sickkids.on.ca  
Thern, Bernd,  
guenther.jung@uni-tuebingen.de  
Therrien, Kimberley,  
e.escher@courrier.usherb.ca  
Timmerman, Peter,  
P.Timmerman@ct.utwente.nl  
Toepert, Florian, f.toepert@charite.de  
Tonarelli, Georgina, tonareli@fbcb.unl.edu.ar  
Tong, Xiao-He, xhtong@yahoo.com  
Toniolo, Claudio, biop02@chor.unipd.it  
Tornoe, Christian Wenzel, cwt@crc.dk  
Toth, Istvan, i.toth@pharmacy.uq.edu.au  
Tourwe, Dirk, datourwe@vub.ac.be  
Tripet, Brian, brian.tripet@uchsc.edu  
Tuchscherer, Gabriele,  
gabriele.tuchscherer@ico.unil.ch  
Tulla, Judit, puche@chem.umn.edu  
Tung, Ching, tung@helix.mgh.harvard.edu  
Tzeng, Shiou-Ru, d844206@oz.nthu.edu.tw  
Urban, Jan, urbanj@molecumentics.com  
Vaabenoe, Jon, jonv@farmasi.uit.no  
Varkey, Jaya, varkey@chem.umn.edu  
Venter, Craig J., Lynn.Holland@Celera.com  
Vidal, Agnes, avidal@tpims.org  
Vig, Balvinder, bvig@umaryland.edu

### ***Index of E-mail Addresses***

Vigil-Cruz, Sandra,  
sandra.vigil-cruz@uconn.edu  
Vita, Claudio, claudio.vita@cea.fr  
Vives, Eric, vives@igm.cnrs-mop.fr  
Vogel, David M., dmvs@ka.net  
Vosekalna, Ilze,  
Ilze.Vosekalna@lattelekom.lv  
  
Wade, John, j.wade@hfi.unimelb.edu.au  
Walton, Troy, troy@biosearchtech.com  
Wang, Dongxia, dongxia00@yahoo.com  
Wang, Rui, wangrui@lzu.edu.cn  
Wang, Wei, wei@u.arizona.edu  
Ward, Paul,  
paxpaw@gwmail.nottingham.ac.uk  
Waring, Alan J., fjwalther@aol.com  
Watson, Emma, e.m.watson@ic.ac.uk  
Weltrowska, Grazyna, weltrog@ircm.qc.ca  
Wernic, Dominik,  
dwernic@lav.boehringer-ingenhe  
Wesdock, Patrick,  
wesdocps@appliedbiosystems.com  
White, Peter, pwhite@nova.ch  
Wilczynski, Andrzej, Carrie@cop.ufl.edu  
Wilkes, Brian, wilkesb@ircm.qc.ca  
Wittelsberger, Angela,  
Angela.Wittelsberger@ico.unil.ch  
Wittmann, Valentin,  
wittmann@chemie.uni-frankfurt.de  
Wright, Jeremy, jeremy.wright@alza.com

Xiong, Chiyi, chiyi@u.arizona.edu  
Xu, Christine, cxu@ukans.edu  
Xu, Jiayi, jiayi.xu@mcmill.vanderbilt.edu  
Xu, Qingchai, xujc1@hotmail.com  
  
Yahalom, Dror,  
dror\_yahalom@hms.harvard.edu  
Yalamoori, Venkatachalapathi,  
venkaty@msn.com  
Yamazaki, Toshimasa,  
tyamazak@abr.affrc.go.jp  
Yang, Jenny J., chejy@panther.gsu.edu  
Ye, Yun-Hua, yhy@pku.edu.cn  
Ye, Yunpeng, yunpeng@gpc.wustl.edu  
Yokoyama, Kenji, yokoyama@jaist.ac.jp  
York, Eunice J., eunice.york@uchsc.edu  
Yoshida, Takuya, yujik@protein.osaka-u.ac.jp  
Yoshikawa, Susumu,  
s-yoshi@iae.kyoto-u.ac.jp  
Yu, Qitao, yuq@ctrvax.vanderbilt.edu  
Yu, Yong Ping, yyongping@tpims.org  
Yuan, ZhongQing,  
zhongqing.yuan@chem.umu.se  
  
Zaitseva, Natalya, nataliva@mtu-net.ru  
Zalipsky, Samuel, samuel.zalipsky@alza.com  
Zaslavsky, Boris, bz@analiza.com  
Zhang, Wei-Jun, weijun@gpc.wustl.edu  
Zhao, Ming, mzhao@glycopep  
Zhilina, Zhanna, zhilina@yahoo.com  
Zloh, Mire, mire.zloh@ulsop.ac.uk

## Subject Index

- Ab initio* [583](#), [585](#)  
Abl tyrosine kinase [992](#)  
Acetylcholine [980](#)  
Acid-labile [246](#)  
Adhesion epitope [814](#)  
Adjuvants [937](#)  
ADT peptide [948](#)  
Affinity  
    extraction [1053](#)  
    labeling [876](#)  
    purification [1055](#)  
Aggregation [220](#)  
Agonism [679](#), [789](#), [851](#)  
Agouti [712](#)  
AGRP [879](#)  
Aib [742](#), [764](#), [766](#)  
Alamethicin [766](#)  
Ala-scan [725](#)  
Alkylating polymers [208](#), [267](#)  
Allatostatins [907](#)  
Altered peptide ligands [1045](#)  
Alzheimer amyloid peptide [971](#)  
Amadori compounds [504](#)  
AMBER 6 [381](#)  
Amidation [101](#)  
Amide  
    bond [547](#)  
    *cis* [125](#)  
    I [295](#), [367](#)  
Amines [255](#)  
Amino acid [75](#), [332](#)  
    beads [299](#)  
    C<sup>α</sup>,<sup>α</sup>-disubstituted [34](#), [458](#)  
    *t*-butyl esters [234](#)  
    substitutions [353](#)  
    β substituted [26](#), [553](#), [664](#)  
    α,β-disubstituted [26](#)  
Aminoacyl incorporation reaction [587](#)  
4-Aminocyclohexanecarboxylic acid [1027](#)  
9-Amino-4,5-diazafluorene-9-carboxylic acid [369](#)  
Aminohydroxyl [608](#)  
Amphipathic [434](#), [444](#), [479](#), [480](#)  
    α-helical region [293](#)  
    β-sheet [479](#)  
Amphipathicity [497](#)  
Amylase [543](#)  
β-Amyloid [242](#), [435](#)  
Amyloid fibril [435](#)  
Analgesic [499](#)  
    factors [413](#)  
Analogues [628](#), [668](#), [670](#), [725](#)  
Analysis [652](#)  
ANF receptor [900](#)  
Angiogenesis [614](#)  
Angiotensin [656](#), [888](#), [917](#)  
    II [142](#), [723](#)  
    receptor [293](#), [853](#), [911](#)  
Antagonist [250](#), [642](#), [662](#), [672](#), [699](#),  
    [721](#), [789](#), [851](#), [857](#), [927](#), [980](#)  
Anthrax [666](#)  
Antibacterial  
    activity [489](#), [760](#)  
    peptide [56](#), [489](#), [760](#), [776](#)  
Antibiotic [495](#), [636](#)  
Antibodies [308](#)  
Antibody [577](#), [1016](#)  
    peptide complexes [422](#)  
Anti-diphenylcarbinol [308](#)  
Antigelation [460](#)  
Anti-HIV [650](#)  
    activity [131](#)  
    drug [130](#)  
Anti-HIV-1 peptide [791](#)  
Antimicrobial  
    activity [479](#), [480](#), [764](#), [772](#)  
    amphipathic beta-sheet alpha-helix se-  
        lectivity [479](#)  
    hydrophobicity diastereomer [754](#)  
    peptides [291](#), [310](#), [477](#), [491](#), [497](#),  
        [758](#), [764](#), [776](#), [873](#), [1049](#)  
Anti-obesity drug [714](#)  
Antiparallel MG2 dimer [489](#)  
Antipeptide antibodies [994](#)  
Antiproliferative [640](#), [801](#)  
Antithrombin III [778](#)  
Antitumor agents [28](#), [638](#)  
Aortic rings [746](#)  
Apamin NMR conformation structure  
    [322](#)  
Apidaecin [776](#)  
Apolipoprotein E [658](#)  
Apoptosis differentiation factor [782](#)  
Arginine-rich  
    peptides [961](#)  
    RNA-binding peptides [950](#)

## Subject Index

- Aroclor [894](#)  
Artificial  
  neural networks [430](#)  
  protein [426](#)  
  ribonuclease [452](#)  
Asp  
   $\beta$ -methylated [731](#)  
  side-chain protection [63](#)  
Aspartate [61](#)  
Aspartimide [61](#), [63](#)  
Asp-Gly [61](#)  
Astin [289](#)  
Asymmetric  
  hydrogenations [30](#)  
  synthesis [26](#), [676](#)  
Atomic force microscopy [434](#), [971](#)  
AT1 antagonists [656](#)  
Automated organic synthesis [60](#)  
Automatic Edman microsequencing [299](#)  
Automation [210](#)  
Avb6 [733](#)  
Azaamino acids [583](#)  
Azides [40](#)  
Aziridine [22](#), [24](#)  
  
Backbone  
  amide linker [224](#), [265](#)  
  cyclization [626](#)  
  protection [63](#)  
Bacteriocins [772](#)  
BAL [265](#)  
Basement membrane [1060](#)  
 $\beta$ -Benzo[*b*]thiophene dehydroamino  
  acids [36](#)  
Benzophenoneone [308](#)  
1*H*-Benzotriazole-1-carboxamidine [91](#)  
Benzylation [250](#)  
BHQ [54](#)  
Biaryl-bridged amino acids [768](#)  
Bicyclic [547](#), [602](#), [603](#)  
  compounds [603](#)  
  dipeptide [602](#)  
  peptide [67](#), [198](#), [462](#), [561](#)  
  peptide library [138](#)  
Bifunctional peptides [691](#)  
Big defensin [756](#)  
Binding [420](#), [1045](#)  
  affinity [881](#)  
  energy [418](#)  
  pocket [834](#)  
  site [845](#), [925](#)  
  study [1045](#)  
Bioactive  
  conformation [338](#), [685](#), [744](#)  
  peptide [402](#), [729](#), [772](#)  
  peptides caseins hydrolysate lactic  
    acid bacteria protease [770](#)  
Bioconjugates [524](#)  
Bioinformatics [194](#), [1057](#)  
Biological activity [130](#), [497](#), [725](#)  
Bioma [1063](#)  
Biomaterials [446](#)  
Biomedical materials [1067](#)  
Biometrical analysis [194](#), [1023](#)  
Biophysical probe [28](#)  
Biosensors [1055](#)  
Biotin [818](#)  
5-Bisphosphate [420](#)  
Bis(2-pyridylmethyl)amino group [516](#)  
Bivalent inhibitors [557](#)  
Black hole quenchers [54](#)  
Blood pressure [746](#), [973](#)  
B-motif [411](#)  
BNP [900](#)  
Boc group [83](#)  
Bone  
  anabolic agent [668](#)  
  resorption [996](#)  
Botulinum neurotoxin A [40](#)  
BPTI [409](#)  
Bradykinin [553](#), [628](#), [642](#), [721](#)  
  antagonists [722](#)  
Breast cancer [801](#)  
Btk [967](#), [978](#)  
Building block [52](#), [160](#)  
 $\alpha$ -Bungarotoxin [925](#)  
  
Caco-2 assay [955](#)  
Calcitonin [338](#), [822](#)  
  gene-related peptide [250](#), [746](#), [973](#)  
Calcium binding  
  proteins [811](#)  
  sites [450](#)  
Calorimetry [524](#)  
Cancer [642](#), [721](#), [975](#)  
Capillary electrophoresis [140](#)

## Subject Index

- Carbohydrate
  - binding protein [760](#)
  - peptide adducts [504](#)
- Carbohydrates [454](#)
- Carbopeptide [454](#)
- Carboprotein [454](#)
- Carboxamides [805](#)
- Carcinoma [984](#)
- $\kappa$  Casein [115](#)
- Catalysis [1065](#)
- Catalyst [273](#)
- Catalytic antibody [1033](#)
- Cathepsin D [1049](#)
- $\pi$ -Cation [909](#)
- CCK [152](#)
  - antagonist [691](#)
- CCT [1002](#)
- CD spectroscopy [287](#), [291](#), [303](#), [306](#),  
[314](#), [336](#), [340](#), [373](#), [389](#), [458](#), [497](#),  
[545](#), [735](#), [911](#), [963](#), [967](#), [1029](#)
- cDNA cloning [797](#)
- Cecropin [764](#)
- Cell [558](#)
  - adhesion [180](#), [733](#), [814](#)
  - attachment [1060](#), [1067](#)
  - cycle arrest [803](#)
  - cycle [864](#), [1053](#)
  - division [350](#)
- Cellular
  - delivery [942](#)
  - respiration [795](#)
- CFTR [820](#), [828](#)
- CGRP [973](#)
- CGRP(8-37) [250](#)
- CH/ $\pi$  interaction [884](#)
- Chain combination [342](#)
- Characterization [524](#)
- Chelate conjugates [134](#)
- Chemical
  - ligation [107](#), [109](#), [119](#), [224](#), [502](#), [518](#)
  - microarray [180](#)
  - synthesis [58](#), [870](#), [1035](#)
  - synthesis of proteins [870](#)
- Chemokine [522](#)
- Chemoselective ligation [103](#), [113](#)
- Chemotaxis [913](#), [1014](#)
- Chimeric peptide [750](#)
- Chiral induction [860](#), [862](#)
- Chirality [330](#)
- Chitosan [1060](#)
- CHO [907](#)
  - cells [908](#)
- Cholecystokinin [691](#), [902](#)
- CI 2 [346](#)
- Circadian
  - neuromodulator [797](#)
  - rhythm [797](#)
- Clock genes [797](#)
- Cloning [1035](#)
- CNS [980](#)
- Coacervation [336](#)
- Coagulation [965](#)
- Coding peptides [188](#)
- Coeliac disease [1037](#)
- Coiled-coil [361](#), [365](#), [377](#), [438](#), [466](#), [674](#)
- Colchicine [638](#)
- Collagen [355](#), [735](#), [975](#)
  - mimetic [446](#)
  - triple helix [379](#)
  - type I [355](#)
  - type IV [814](#)
- Collagenases [355](#)
- Colon cancers [905](#)
- Colorimetric method [285](#)
- Combination Asp-Gly [63](#)
- Combinatorial
  - approach [257](#)
  - chemistry [172](#)
  - library [177](#), [183](#), [187](#), [191](#), [200](#), [204](#),  
[299](#), [466](#), [520](#), [551](#), [921](#), [1023](#)
  - process [200](#)
  - synthesis [60](#), [177](#)
- Combined solid-phase and solution
  - strategy [157](#), [248](#)
- Complementary recognition [435](#)
- Complexation [132](#)
- Compound array [210](#)
- Conformation [226](#), [287](#), [289](#), [332](#), [338](#),  
[369](#), [373](#), [389](#), [420](#), [456](#), [458](#), [514](#),  
[685](#), [710](#), [723](#), [739](#), [830](#), [1025](#), [1029](#),  
[1047](#)
- Conformational
  - analysis [357](#), [468](#)
  - change [297](#)
  - constraint [338](#), [862](#), [982](#)
  - search [428](#)

## Subject Index

- studies [324](#), [982](#)
- transitions [435](#), [853](#)
- Conjugate [946](#), [953](#)
- Conotoxin [428](#), [483](#), [485](#)
- Conservative sites [1031](#), [1032](#)
- Consolidated ligands [222](#)
- Continuous fluorescent assay [541](#)
- Coupled plasmon-waveguide resonance spectroscopy [297](#)
- Copper cross-coupling alkyne solid-phase [263](#)
- Coral bleaching [375](#)
- Core modules [400](#)
- Coupling reagents [217](#)
- 2-2'-(*p*-Cresol)-2,3-dihydro-tryptophan [248](#)
- CREB [1002](#)
- CsA [130](#)
- CSB motif [388](#)
- C-terminal [168](#)
- CTTU [117](#)
- CXCR4 chemokine receptor [789](#), [801](#)
- Cyclic
  - knottins [387](#)
  - opioid peptide analogue [681](#)
  - peptide [89](#), [122](#), [125](#), [140](#), [174](#), [238](#), [422](#), [468](#), [630](#), [662](#), [685](#), [733](#), [776](#), [1029](#)
  - tetrapeptides [122](#)
- Cyclization [113](#), [127](#), [138](#), [142](#), [146](#)
- Cyclohexyloxycarbonyl (Hoc) [248](#)
- Cyclopentapeptide [917](#)
- Cyclosporin [244](#)
  - derivatives [130](#)
- Cyclotetrapeptides [287](#)
- Cyclothialidine [530](#)
- Cysteine [22](#), [24](#), [75](#)
- Cystine knot [814](#)
- Cytochrome c oxidase [795](#)
- Dansyl [318](#)
- DAR-1 [907](#)
- DAR-2 [907](#)
- DBU [242](#)
- DDT [166](#)
- De novo design [166](#), [369](#), [450](#), [456](#), [674](#)
- Defensin [752](#), [1035](#)
- Dehydroamino acids [44](#), [217](#)
- Delivery [931](#), [935](#), [940](#), [953](#)
- Dendrimer [432](#), [446](#)
- Dendritic
  - peptide [470](#)
  - poly(L-lysine)s [526](#)
- Deprotection [83](#), [107](#)
  - monitoring [81](#), [832](#)
- Depsipeptide [217](#), [512](#)
- Design [440](#)
- Designing peptide drugs [969](#)
- Diabetes mellitus [670](#), [973](#)
- Diabetic complications [973](#)
- Diastereoselective [38](#)
- Dibasic inhibitors [555](#)
- Dibenzylated CGRP(8-37) [250](#)
- Diels-Alder cycloaddition [634](#)
- Differentiation factor HLDF [782](#)
- Difficult couplings [93](#), [220](#), [283](#)
- $\alpha$ -Difluoro- $\beta$ -amino acids [261](#)
- Diketopiperazine [152](#), [555](#), [638](#)
- Dimer [752](#)
- Dimerization [152](#), [389](#), [572](#)
- Dimethyltyrosine [851](#)
- 2',6'-Dimethyl-L-tyrosine [616](#)
- Dinuclear Zn(II) complex [516](#)
- Dipeptide unit [38](#), [46](#)
- Dipeptidic anti-microtubule agent [638](#)
- Dipeptidyl peptidase IV [670](#)
- Diploteria punctata* [907](#)
- 1,3-Dipolar cycloaddition [263](#)
- Discontinuous [189](#)
  - epitopes [1018](#)
- Disease [973](#)
  - states [969](#)
- Dissociation in biological activity [497](#)
- Distance scan [555](#)
- Disubstituted amino acid [34](#)
- Disulfide [953](#)
  - bond [148](#), [413](#), [483](#), [626](#), [1035](#)
  - bond formation [148](#), [413](#)
  - pairings [483](#)
- Dithiobenzyl [953](#)
- Diversity in structure-function
  - relationship [497](#)
- Diversity points and  $\beta$ -turn mimetic [200](#)
- Diversity [58](#)
- DMSO [148](#)
- DNA [28](#), [520](#)

## Subject Index

- binding [210](#)
- binding protein [411](#)
- complexation [230](#)
- synthesis [277](#)
- DNA/RNA-hydrolysis [782](#)
- DNAK [873](#)
- Docking [418](#)
- Domains [1057](#)
- Double-ring motif [722](#)
- Doxorubicin [644](#)
- Drosocin [776](#)
- Drosophila [907](#)
- Drostatins [907](#)
- Drug
  - delivery [937](#), [946](#), [955](#)
  - discovery [969](#)
  - design [612](#), [801](#), [969](#)
  - tolerance [969](#)
- Dual function [616](#)
- Dye-labeled peptides [54](#)
- Dynamic libraries [923](#)
- Dynamics [396](#)
- Dynorphin [144](#)
  - antagonist [676](#)
- E1 [1032](#)
- E1 envelope protein [1031](#)
- E2 [1032](#)
- E2 envelope protein [1031](#)
- EC 3.4.24.15 [553](#)
- EC 3.4.24.16 [553](#)
- E-cadherin [948](#)
- Edman degradation [176](#), [299](#)
- EF-hand calcium binding motifs [811](#)
- EGF [881](#)
  - receptor [881](#)
- EIAV [1029](#)
- Elastin [346](#)
  - derived peptides chemotaxis
  - macrophages [807](#)
  - derived polypentapeptides
  - coacervation CD FT-IR [336](#)
- Electron transfer [526](#)
- Electrostatics [332](#)
- ELISA [996](#), [1029](#)
- Emmprin [508](#)
- Enantioselective oxidation [1065](#)
- Endomorphin derivative [616](#)
- Energy
  - functions [428](#)
  - transfer [526](#)
- Enkephalin [499](#)
- Enzyme [545](#)
  - cleavage assays [55](#)
  - inhibitor [561](#)
- Enzymology [563](#)
- Epimerization [39](#), [634](#)
- Epitope [189](#), [1010](#)
- Epstein-Barr virus [1027](#)
- Esterification [267](#), [208](#)
- Ethyl nitroacetate [34](#)
- Evolutionary design [430](#)
- Exocytosis [1014](#)
- Expressed protein ligation [818](#)
- Extracellular loop [911](#)
- Factor
  - IX [965](#)
  - Xa [778](#)
  - $\alpha$  [898](#)
- FBS [785](#)
- Feeding [672](#)
- Ferrocenylalkyl containing amino acids [28](#)
- FGF [927](#)
- Fibrils [972](#)
- Fibrinolysis [965](#)
- Fibroblast growth factors [927](#)
- Fluorescence [54](#), [522](#), [876](#), [898](#), [911](#), [971](#)
  - correlation spectroscopy [310](#)
  - resonance energy transfer [328](#)
  - spectroscopy [845](#)
- Fluorescent
  - biosensor [992](#)
  - labeling [168](#)
- Fluoroalkene dipeptide isostere [606](#)
- Fluorogenic [975](#)
  - assays [54](#)
  - peptide probes [54](#)
  - substrates [48](#)
- Fluorophore [523](#)
- trans*-4-Fluoroproline [379](#)
- Fluorosensor [173](#)
- Fmoc [832](#)
  - Asp [61](#)

## Subject Index

- deprotection [242](#)
  - strategy [224](#)
- Foldamers [232](#), [456](#)
- Folding [342](#), [398](#), [406](#), [572](#)
  - method [523](#)
- Foot-and-mouth disease [1018](#)
  - virus [1043](#)
- Force fields [415](#)
- Formylpeptide [913](#)
- Fos-expression [344](#)
- Fragment condensation [166](#)
- FRET [398](#), [814](#)
  - peptides [54](#)
  - quenching [54](#)
- FSH [189](#)
- FT-ICR-MS [652](#)
- FTIR [295](#), [337](#), [367](#), [963](#)
- Fusion [963](#)
- G protein-coupled receptor [194](#), [845](#), [890](#), [921](#)
- Gaegurin 4 [291](#)
- Gamma peptide [383](#), [569](#)
- Gastrin and human CCK2 receptor [693](#)
- Gastrin-Gly [905](#)
- GCN4 [166](#), [438](#)
- Gelsolin [420](#)
- Gene delivery [230](#)
- Genetic algorithm [430](#)
- Ghrelin [236](#)
- Gliadin [1037](#)
- GLP [944](#)
- Glucagon [744](#)
  - antagonist [324](#)
  - like peptide-1 [670](#)
- Glutaredoxin oxidoreductase disulfide [464](#)
- Glycation [504](#)
- Glycine
  - $\alpha$ -disubstituted [458](#)
  - $C^{\alpha,\alpha}$ -disubstituted [370](#)
- C-Glycoamino acid [52](#)
- Glycopeptide [79](#), [174](#), [340](#), [499](#), [506](#), [508](#), [1047](#)
  - antibiotics [481](#)
- N-Glycosylation [502](#)
- O-glycosylation [381](#)
- Gomesin [495](#)
- gp120 [394](#), [1033](#)
- gp41 [67](#), [963](#), [1016](#)
  - coiled coil [791](#)
- GPCR [845](#), [876](#), [896](#), [907](#), [909](#), [911](#)
- GPIIbIIIa [524](#)
- G-protein [886](#), [909](#)
  - coupled receptor [822](#), [892](#), [902](#)
- Graduated lability [58](#)
- Gramicidin [838](#)
- Gramicidin S analogs [477](#), [497](#)
- Gram-negative [493](#), [764](#)
- Gram-positive [764](#)
- Grb2 SH2 domain [857](#), [859](#), [862](#)
- Growth hormone [944](#)
  - secretagogue [236](#), [748](#)
- Guanidinylation [91](#)
- Guanylation [40](#)
- Gyrase [530](#)
- HATU [99](#)
- HAV peptide [948](#)
- HCV [534](#), [545](#), [549](#), [1023](#)
  - NS3 protease [563](#)
- Helical
  - peptides [367](#)
  - structures [685](#)
- Helix [383](#), [764](#), [820](#), [828](#)
  - $\alpha$  [444](#), [499](#), [1063](#)
  - 3-10 [328](#), [444](#)
  - bundle [295](#), [396](#), [454](#)
  - equilibrium [444](#)
  - propensity [377](#)
  - stability [67](#), [353](#)
- Hemoglobin [785](#)
- Hemolysin [760](#)
- Heparin [778](#)
  - binding peptide [778](#)
- Hepatitis C virus (HCV) [549](#), [563](#), [1031](#)
- Herpes simplex virus [1010](#)
- Heterocyclic compounds [252](#)
- Heterodimer [438](#)
- HF reaction [249](#)
- High throughput [206](#), [207](#), [318](#), [1057](#)
  - assay [563](#)
  - screening [1057](#)
- Histone deacetylase [541](#)
- HIV protease inhibitors [418](#)

## Subject Index

- HIV [187](#), [210](#), [394](#), [518](#), [940](#), [963](#), [1023](#), [1033](#), [1039](#)  
  nucleocapsid [518](#)  
  protease [650](#)  
  Rev [452](#)  
  Tat-(48-60) [950](#)  
HL-60 cells [782](#)  
Hmb [63](#), [71](#)  
Hemoglobin [460](#)  
Homologs [569](#)  
Homology [428](#)  
  model [1045](#)  
H-phosphonates [164](#)  
HPLC [140](#), [765](#), [805](#)  
HRMAS NMR [402](#)  
HTL [1039](#)  
Human  
  chorionic gonadotropin [994](#)  
  growth hormone [714](#)  
  leptin [158](#)  
  melanocortin receptor 4 [708](#)  
   $\delta$ -opioid receptor [297](#)  
  somatostatin receptor subtypes [716](#)  
Hybrid peptide [202](#)  
Hydantoins [579](#)  
Hydrazinopeptides [581](#)  
Hydrazone [109](#), [119](#)  
Hydrophobic [832](#)  
  peptide [148](#)  
Hydrophobicity/amphipathicity [353](#)  
Hydroxamate [591](#)  
 $\alpha$ -Hydroxy acid [681](#)  
*N*-Hydroxy amino acid [589](#)  
Hydroxyethylene dipeptide isostere [40](#)  
Hydroxyethylene [38](#)  
*N*-[9-(Hydroxymethyl)-2-fluorenyl]-  
  succinamic acid [157](#), [248](#)  
Hypercholesterolemia [658](#)  
Hypotensive [695](#)  
  
IBTM [632](#)  
ICAM-1 [946](#)  
Imaging [986](#)  
2-Imidazolidine carboxylic acid [433](#)  
Imidazolidinones [257](#), [504](#)  
Immunoassays [1029](#)  
Immunocytochemistry [797](#)  
Immunodominant region [381](#)  
Immunogenic peptides [1027](#)  
Immunofluorescence [187](#)  
immunometric assay [995](#)  
Immunotherapy [1027](#)  
Implant [944](#)  
*In situ* hybridization [797](#)  
Indolizidine [597](#)  
Indolizidinone amino acids [30](#)  
Infectious [1029](#)  
Inhibit proliferation [803](#)  
Inhibition [986](#)  
Inhibitor [183](#), [185](#), [196](#), [532](#), [534](#), [543](#),  
  [545](#), [547](#), [555](#), [733](#), [868](#)  
  constant [558](#)  
  potency [558](#)  
  selectivity [558](#)  
Innate  
  host defense [1049](#)  
  immunity [1049](#)  
Insulin receptor [915](#)  
Integrin [180](#), [612](#), [647](#), [731](#), [733](#), [735](#),  
  [814](#)  
  receptors [134](#)  
Intein-mediated ligations [816](#)  
Interaction [303](#), [530](#)  
  sites [189](#)  
Intercalation [28](#)  
Intercellular  
  junctions [948](#)  
  pathogens [758](#)  
Intramolecular  
  chaperone [385](#)  
  lactam bridge [222](#)  
Intramolecularly quenched fluorogenic  
  peptide substrate [563](#)  
Inverse agonist [892](#)  
Inverse SPPS [234](#), [549](#)  
Ion  
  channel [766](#)  
  gating [838](#)  
  selectivity [838](#)  
Iron chelators [177](#)  
Isolation [1035](#)  
Isomerization *cis/trans* [330](#)  
Isostere [38](#), [150](#)  
Isothiuronium salts [117](#)  
Isotope-editing [295](#)

## Subject Index

- Kenner safety catch resin [117](#)  
 $\alpha$ -Ketotetrazole [549](#)  
Kinase [666](#)  
Kinesin [361](#)  
Kinetics [881](#)  
Knottins [387](#)  
K-Ras-derived peptide [162](#)
- Lactam [789](#)  
Lactic acid bacteria [772](#)  
*Lactobacillus plantarum* [772](#)  
Lactoferricin [56](#)  
Lactone [38](#)  
Laminin [1060](#)  
Lanthionine [228](#)  
Large cyclic peptides [220](#)  
LC-MS [318](#), [1057](#)  
Lectin [157](#), [174](#), [248](#), [760](#)  
Leptin [344](#)  
Lethal factor [666](#)  
Leucine  
    enkephalin [504](#)  
    zipper [166](#)  
Leuprolide [944](#)  
LFA-1 receptor [947](#)  
Library [89](#), [174](#), [196](#), [520](#), [1043](#)  
Lidocaine [265](#)  
Ligand-receptor interaction [851](#)  
Ligands [1057](#), [695](#)  
Ligation [115](#), [117](#), [138](#), [836](#)  
Limited proteolysis-mass spectrometry  
    [546](#)  
Linear peptide [146](#)  
Lipid [420](#)  
Lipo-glycopeptide [499](#)  
Lipopeptaibols [514](#)  
Lipopeptides [119](#), [768](#)  
Lipophilicity [841](#), [843](#)  
Liposaccharides [937](#), [955](#)  
Liposomes [760](#)  
Long chain peptides [275](#)  
Loop structure [520](#)  
LTR [210](#), [940](#)  
Lymphoid tumor [180](#)  
Lymphoma [180](#)  
Lysine core [73](#)
- M. tuberculosis* [1010](#)
- MAB [415](#)  
Macrocycles [859](#), [862](#), [868](#)  
Macrocyclic peptide [387](#)  
Macrophage selectivity [758](#)  
MAD [166](#)  
MAdCAM [612](#), [647](#)  
Magainin 2 [489](#)  
Major histocompatibility complex  
    class II [1045](#)  
MALDI MS [187](#)  
Maltotriose [1025](#)  
Mannosylation [935](#)  
MAPK pathway [864](#)  
Mass spectroscopy [140](#), [318](#), [845](#), [1053](#)  
Mastoparan [750](#)  
Matriptase [561](#)  
Matrix  
    metalloproteinase [975](#)  
    metalloproteinase inhibitor [539](#)  
    scan [189](#)  
Maxadilan [793](#)  
Max protein [160](#)  
MBP [238](#)  
MC1-R [712](#)  
MC4R [879](#)  
MCH [712](#)  
MDCK monolayers [948](#)  
Mechanism-based design [752](#)  
Melanin-concentrating hormone [710](#)  
Melanocortin [706](#), [826](#), [879](#)  
    receptors [892](#)  
Melanotropin peptides [892](#)  
Melatonin [845](#)  
Melittins [764](#)  
Membrane [493](#), [942](#)  
    active peptides [514](#), [849](#)  
    association [737](#)  
    binding [293](#)  
    interactions [830](#)  
    permeable peptides [959](#)  
    permeable arginine-rich peptides  
        [950](#), [961](#)  
    perturbation [489](#)  
    translocation [191](#)  
Memory enhancing [1002](#)  
Message-address [499](#)  
Metal  
    binding [589](#), [591](#), [593](#), [595](#), [811](#)

## Subject Index

- ions [146](#)
- selectivity [450](#)
- Metalloprotease [666](#), [1049](#)
- Metalloproteinase [975](#)
- Metalloproteins [450](#)
- Methotrexate [946](#)
- 7-Methoxycoumarin-4-acetic acid (Mca) [48](#)
- N-Methyl amino acids [244](#)
- N-Methylated azapetides [585](#)
- Methylene-oxy pseudopeptide [618](#)
- MHC [1051](#)
- Michael addition [44](#)
- Microbubbles [524](#)
- Micrometalloenzyme [273](#)
- Micropreparative HPLC [1055](#)
- Microtubule binding agents [638](#)
- Mimetic [440](#), [597](#), [642](#)
- Mimotope [925](#)
- Mini protein domain [389](#)
- Miniprotein design [406](#)
- Mitsunobu reaction [506](#)
- Mixotope [1043](#)
- MMP [48](#)
- Mmt protection [73](#)
- Model ligand docking [834](#)
- MOG [340](#)
- Molecular
  - biology [847](#)
  - conformation [348](#)
  - design [636](#)
  - dynamics [303](#), [346](#), [381](#), [420](#), [424](#)
  - mechanics [329](#), [426](#)
  - modeling [314](#), [326](#), [328](#), [340](#), [371](#), [387](#), [415](#), [418](#), [422](#), [676](#), [841](#), [843](#), [896](#), [900](#), [1045](#), [1065](#)
- MOLOC [415](#)
- Monoclonal antibody [577](#)
- Motilin [662](#)
- MSH [20](#), [712](#), [826](#)
- MT-II [20](#), [826](#)
- MTT [640](#)
  - test [805](#)
- MTX-cIBR conjugate [946](#)
- MUC1 [381](#)
- Mucin [1047](#)
  - glycoprotein [652](#)
- Multipin [1031](#)
- Multiple
  - antigen peptides [60](#)
  - peptide synthesis [890](#)
  - sclerosis [340](#)
  - wavelength anomalous diffraction [166](#)
- Multiplicity [957](#)
- Multivalency [174](#)
- Multivesicular liposome [658](#)
- Mutant receptors [884](#), [919](#)
- Mutations [834](#)
- Myelin oligodendrocyte glycoprotein (MOG) [340](#)
- Native chemical ligation [117](#), [212](#), [448](#)
- Neoglycopeptide [175](#)
- Neokytorphin [785](#)
- Neurite outgrowth [1060](#)
- Neuropathic pain [969](#)
- Neuropeptides [727](#)
- Neurotensin [984](#)
- Neurotoxin [483](#)
- Neutrophil activating peptides [1014](#)
- Nicotinic receptor [925](#)
- Ninhydrin [65](#)
- Nitric oxide [973](#)
- Nitrogen content [285](#)
- NLS [931](#)
- NMR [81](#), [250](#), [287](#), [291](#), [303](#), [314](#), [324](#), [338](#), [340](#), [350](#), [355](#), [383](#), [387](#), [389](#), [411](#), [415](#), [462](#), [485](#), [530](#), [710](#), [731](#), [739](#), [742](#), [756](#), [811](#), [816](#), [925](#)
  - 2D [238](#)
- Nociceptin [685](#), [787](#), [919](#)
- NOESY [458](#)
- Non CCK2 receptor [905](#)
- Non-immunosuppressive [131](#)
- Non-peptide
  - antagonists [614](#)
  - inhibitor [666](#)
  - ligands [660](#)
  - opioid ligands [660](#)
- Novel amino acids [20](#)
- NPY [672](#)
- NS3 [545](#)
- NS3/4A [534](#)
- Nsc [71](#), [77](#), [155](#)
- Nuclease activity [783](#)

## Subject Index

- Nucleobase  
  amino acids [518](#), [674](#)  
  interaction [674](#)  
Nucleocapsid protein [518](#)
- Obesity [344](#), [879](#)  
Octapeptide [782](#)  
OFm esters [279](#)  
Olefin metathesis [859](#)  
Oligomerization [824](#)  
Oligonucleotide peptide conjugates [109](#)  
Oligopeptidosulfonamides [232](#)  
Oligosaccharide synthesis [60](#)  
Oligourea peptidomimetics [232](#)  
On-bead  
  functional screening [183](#)  
  screening [174](#)  
One bead-one compound libraries [174](#),  
  [180](#), [183](#)  
One-pot reaction [76](#)  
Opioid [970](#)  
  agonist [691](#)  
  antagonists [676](#), [681](#)  
  CCK ligands [970](#)  
  peptide-receptor interactions [676](#),  
    [681](#)  
  peptides [676](#), [689](#)  
Opioids [144](#), [499](#), [679](#), [691](#), [851](#)  
 $\mu$ -Opioid receptor [616](#)  
 $\kappa$  Opioid receptors [689](#), [894](#)  
 $\delta$  Opioid [683](#)  
  receptor [679](#), [851](#)  
Optical fiber [172](#)  
ORL1 receptor [919](#)  
ORL1 [787](#)  
Orphan receptor ligand [314](#)  
Orthogonal  
  protecting groups [228](#)  
  protection [34](#), [58](#)  
Oryctes rhinoceros [1035](#)  
Osmotic [944](#)  
Osteoporosis [668](#), [996](#)  
Oxazolidine [155](#)  
Oxazoline [50](#)  
OxCM dimers [400](#)  
Oxidation [269](#)  
Oxidative folding [462](#)  
Oxime ligation [400](#), [454](#)  
2-Oxoacyl peptide [111](#)  
Oxytocin [599](#), [618](#), [697](#), [699](#), [896](#)
- PAC 1 receptor [793](#)  
PACAP27 [632](#)  
Pain-killing peptides [413](#)  
Palladium cross couplings [36](#)  
Parallel  
  MG2 dimer [489](#)  
  peptide synthesis [172](#), [206](#), [1031](#),  
    [1057](#)  
Parasin I [1049](#)  
Parathyroid hormone [668](#), [737](#), [739](#), [890](#)  
  related protein [668](#)  
Pathological disease states [969](#)  
PCNA [1053](#)  
PDZ domain [866](#)  
Pentaazacrown [595](#)  
Pentafluoroethylketone [549](#)  
Pentapeptide libraries [652](#)  
Pepscan [189](#)  
PepT1 peptidomimetics absorption  
  Phe-Gly [610](#)  
Peptaibol [226](#), [774](#)  
Peptidase [553](#), [554](#)  
Peptide  
  aldehydes [454](#)  
   $\beta$  analogs [581](#)  
  amphiphile [1063](#)  
  antibiotics [512](#), [774](#)  
  binding [978](#)  
  *cis* bonds [697](#)  
  chelate conjugates [134](#)  
  conformation [911](#)  
  conjugate [644](#)  
  coupling reagent [95](#)  
  delivery [658](#), [944](#)  
  peptide dimers [888](#)  
  D- and L- [220](#)  
  DNA interactions [940](#)  
  drugs [969](#)  
  fragments as models for folding [391](#)  
  hormone [727](#), [890](#)  
  inhibitor [551](#)  
  isomerisation [117](#)  
  library [430](#), [927](#)  
  ligands [660](#)  
  lipid interaction [489](#)

## Subject Index

- membrane interaction [491](#)
- metal complexes [306](#)
- mimetic synthesis [234](#)
- mimetics [565](#), [602](#)
- sequencing [299](#)
- structure [81](#)
- substrate [551](#)
- synthesis [81](#), [318](#), [681](#), [787](#)
- thioester [111](#), [117](#), [160](#), [224](#), [508](#)
- transport [957](#)
- vaccine [1023](#)
- $\beta$  Peptides [32](#), [275](#), [383](#), [569](#), [622](#)
- Peptidoglycan biosynthesis [512](#)
- Peptidomimetic [30](#), [127](#), [183](#), [271](#), [279](#),  
[330](#), [572](#), [575](#), [577](#), [579](#), [581](#), [587](#),  
[602](#), [608](#), [623](#), [636](#), [650](#), [658](#), [659](#),  
[660](#), [679](#), [859](#), [862](#), [868](#), [1045](#)  
synthesis [446](#)
- Peptidomimetic substrates and inhibitors [183](#)
- Peptidyl phosphonate [1033](#)
- Peptoid [232](#), [577](#), [1045](#)  
residues [849](#)
- Perdeuterated dodecylphosphocholine [324](#)
- Periodate oxidation [112](#)
- Periodic polypeptide [357](#), [373](#)
- PGLa [491](#)
- Phage-display peptide library [202](#), [927](#)
- Phenylalhistin [638](#)
- Phenylalanine [24](#)
- (S)-Phenylalanine [25](#)
- (3S,3S)- $\beta$ -Phenyl-cysteine derivative [24](#)
- Phenylisocysteine [50](#)
- Phosphatidylinositol [420](#)
- Phosphinate [565](#)
- Phospholamban [832](#)
- Phosphopeptides [97](#), [160](#), [164](#)  
binding [967](#)  
synthesis [97](#)
- Phosphorus [593](#)
- Phosphorylated polypeptide [160](#)
- Phosphotyrosyl [862](#)
- Photoaffinity scanning [308](#)
- Photoconjugate [308](#)
- Photolabeling [888](#)
- Phtaloyl-bromides [93](#)
- Pipicolate [597](#)
- Plasmin [965](#)
- Plasmon resonance spectroscopy [814](#)
- Platelet aggregation [1068](#)
- PNA [520](#)
- Polyamine [252](#)
- Polyethylene glycol (PEG) [953](#)
- Polyhydroxamates [177](#)
- Polymer-assisted solution phase synthesis  
[208](#), [267](#)
- Polymer-bound reagents [208](#), [267](#)
- Polypeptide synthesis [111](#)
- Polyproline [185](#), [358](#), [375](#)  
dendrimers [433](#)
- poly(Xaa-Pro) [357](#)
- Porphyrin [526](#)
- Positional  
cyclization scanning [744](#)  
scanning libraries [194](#), [196](#), [921](#),  
[1023](#), [1051](#)
- Predictive algorithm [365](#)
- Preorganization [589](#), [591](#), [593](#), [595](#)
- Prion [502](#)  
protein [818](#)
- Prodrug [644](#), [650](#), [953](#)
- Prolactin-releasing peptide [314](#)
- Proliferation [785](#), [803](#)
- Proline [432](#), [599](#), [933](#)  
peptide bond [330](#)
- Prolyl amides [599](#)
- Propeptide [385](#)
- Proprotein convertases [558](#)
- Prorelaxin [448](#)
- proSAAS granin [558](#)
- Prostate specific antigen [644](#)
- Protease inhibitor [534](#), [549](#), [650](#), [666](#)
- Proteasome [532](#)
- Protected  
amino acids [101](#)  
guanidines [40](#)
- Protein  
conjugates [953](#)  
delivery systems [952](#)  
design [400](#)  
engineering [811](#), [890](#)  
folding [391](#), [409](#), [873](#)  
interaction [1057](#)  
kinase [183](#), [551](#)  
kinase inhibitor [191](#)

## Subject Index

- like molecular architecture [1063](#)
- loops [394](#)
- protein interactions [185](#), [870](#)
- target [493](#)
- tyrosine kinase [982](#)
- tyrosine phosphatase [868](#)
- Proteolysis [785](#)
- Proteolytic cleavage [558](#)
- Proteome [206](#)
- Proteomics [206](#), [1053](#), [1055](#), [1057](#)
- Pseudodipeptide [618](#)
- Pseudooligolysine [230](#)
- Pseudopeptides [132](#), [595](#), [748](#)
- Pseudoprolines [697](#)
  - libraries [185](#)
- Pseudotyped virus [791](#)
- PTH [424](#), [668](#), [742](#)
- PTHrP [668](#)
- PTK [640](#)
- Purification [318](#)
- Pyrene [828](#)
- Pyrenylalanine [28](#)
  
- Quenching [54](#)
- Quinazoline [640](#)
  
- Racemic [608](#)
- Racemization [99](#)
- Radiolabeling [729](#), [984](#)
- Ramoplanin [512](#)
- Rapi [318](#)
  - receptor [424](#), [695](#), [699](#), [731](#), [847](#), [886](#), [898](#), [905](#), [907](#)
- RBD [870](#)
- Receptor [907](#)
  - binding affinity [338](#)
  - dimers [888](#)
  - mutagenesis [879](#)
  - structure [834](#)
- Recognition [1029](#)
- Recombinant protein [160](#)
- Redox potentials [462](#)
- Reduced peptide bond [230](#)
- Reduction [255](#), [259](#)
- Reductive amination [265](#)
- Reformatsky reaction [261](#)
- Regulation tight junctions [948](#)
- Relaxin [342](#), [448](#)
  
- Repetitive Xaa-Pro sequence [357](#)
- Repressor [210](#), [940](#)
- $\beta$ 3-Residue [289](#)
- Resin [275](#), [402](#)
  - environment [81](#)
- Response regulator [411](#)
- Retro [166](#)
- $\beta$ -Reversals [326](#)
- Reverse phase HPLC [318](#)
- Reverse
  - prenyl [217](#)
  - turns [391](#)
- Reversible
  - PEGylation [953](#)
  - resistance [804](#)
- RGD [731](#)
  - peptides [134](#)
- RGDS [1067](#)
- Rhodopsin [836](#), [886](#), [909](#)
- Ring
  - closing metathesis [127](#), [371](#)
  - cluster conformation [656](#)
- RNA [518](#)
  - cleavage of [516](#)
  - targeting [204](#)
- Rotamer scan [982](#)
- RRF [396](#)
- RSV [320](#)
  
- Saccharomyces cerevisiae* [898](#)
- Safety catch linker [89](#)
- Salt bridge [438](#)
- SAR [495](#), [706](#), [866](#), [894](#)
  - MCH Peptide [704](#)
- Scaffold assembly [446](#)
- Scale-up [283](#)
- SDF-1 [789](#), [801](#)
- Secondary structure [332](#), [402](#), [581](#)
- Segment condensation [99](#)
- Segmental labeling [816](#)
- Selective
  - cyclic MC4 peptides [701](#)
  - reduction [46](#)
- $\kappa$  Selective ligands [894](#)
- Selectivity [479](#), [480](#), [616](#)
- Seleno-methionine [166](#)
- Self-assembly [435](#)
- Sequence analysis [391](#)

## Subject Index

- Sensor array [172](#)  
Serines [22](#)  
Serine protease [534](#)  
Serotonin [152](#)  
Serum [1031](#)  
SGT [1000](#)  
SH domains [222](#)  
SH2 domains [967](#), [978](#)  
SH3 domains [185](#), [978](#)  
 $\beta$  Sheet [46](#), [477](#), [572](#), [575](#)  
Shuttle peptides [830](#)  
Sickle cell anemia [460](#)  
Side  
    chain [597](#)  
    reactions [63](#), [140](#), [248](#), [250](#)  
Siderophores [177](#), [589](#), [591](#)  
Sigma factors [816](#)  
Signal transduction [855](#), [859](#), [868](#), [896](#),  
    [907](#)  
Signaling [864](#), [1057](#)  
Site  
    directed mutagenesis [876](#)  
    specific [870](#)  
    specific labelling [522](#)  
Slow Binding Inhibition [558](#)  
Small  
    cell lung carcinoma [721](#)  
    molecule libraries [257](#)  
Solid and solution phase synthesis [814](#)  
Solid phase synthesis [58](#), [117](#), [166](#), [210](#),  
    [222](#), [224](#), [226](#), [228](#), [230](#), [236](#), [246](#),  
    [252](#), [255](#), [257](#), [259](#), [261](#), [269](#), [275](#),  
    [279](#), [342](#), [458](#), [462](#), [634](#), [727](#), [765](#),  
    [801](#), [814](#), [888](#), [1028](#)  
Solution  
    conformations [948](#), [949](#)  
    phase combinatorial synthesis [198](#)  
    structure [306](#), [350](#), [396](#), [411](#)  
Somatostatin [622](#), [626](#), [719](#), [864](#)  
    analogues [32](#), [622](#), [664](#), [716](#)  
Sortase [565](#)  
Spatial screening [174](#)  
Spectroscopy [328](#)  
SPOT synthesis [191](#), [212](#), [577](#), [579](#), [866](#)  
SPPS [61](#), [204](#), [242](#), [250](#), [344](#), [549](#), [589](#),  
    [640](#), [706](#), [793](#)  
SPR [967](#)  
SST1 receptor [719](#)  
Stability [466](#)  
Staudinger reduction [40](#)  
Ste2p [847](#)  
Stereochemistry [415](#)  
Stereoselective synthesis [150](#)  
Stimulation [1025](#)  
 $\beta$ -Strand mimetic [634](#)  
Streptavidin [299](#)  
Streptomyces [768](#)  
 $\beta$  Structure [391](#)  
Structural  
    characterization [481](#), [822](#), [902](#)  
    investigations [628](#)  
    transition [435](#)  
Structure activity relationship [291](#), [477](#),  
    [723](#), [727](#), [881](#), [1016](#)  
 $\alpha$ -Substituted amino acids [26](#)  
 $\beta$ -Substituted alanines [44](#)  
Substrate [183](#)  
Subunit vaccines [320](#)  
Sugar amino acids [664](#)  
Sulfur analogue [50](#)  
Sunflower [547](#)  
Superagonist [919](#)  
Supramolecular chemistry [923](#)  
Surface plasmon resonance [293](#), [857](#),  
    [996](#)  
Sustained-release [658](#)  
Suzuki [532](#)  
Swelling properties [283](#)  
Synthesis [52](#), [69](#), [115](#), [144](#), [162](#), [389](#),  
    [440](#), [524](#), [628](#), [630](#), [898](#)  
Synthetic  
    antigens [1010](#)  
    combinatorial libraries [921](#)  
    epitopes [652](#)  
    peptides [994](#), [1029](#)  
T-20 [168](#)  
Tandem ligation [1021](#)  
Target drugs [946](#)  
TASP [454](#)  
TAT [940](#)  
    peptide [942](#)  
Taxol side chain [50](#)  
Tc-99m [729](#)  
T-cells [946](#), [1023](#)  
    ligands [194](#), [1051](#)

## Subject Index

- N-Telopeptide [996](#)
- Template [198](#)
  - assisted synthetic proteins [60](#)
  - conformation [634](#)
  - directed peptide ligation [674](#)
- N-Terminal
  - capping box [350](#)
  - cysteine [65](#)
- Tethered ligand [884](#)
- 2,2,6,6-Tetramethyl-4-amino-1-oxyl-piperidine-4-carboxylic acid [1065](#)
- Tetramethylguanidine [140](#)
- Tetrazole [549](#)
- Thiazoles [150](#)
- Thiazoline [217](#)
- Thioester [448](#)
  - exchange [117](#)
  - method [160](#)
  - migration [118](#)
- Thioether [506](#)
  - bridge [271](#)
- Thioglycoside [79](#)
- Thiol-disulfide oxidoreductases [462](#)
- Thioligation [117](#)
- Thioprolin [107](#)
- iso*-Thiouonium salts [117](#)
- Three-dimensional structure [320](#)
- Thrombin [634](#), [884](#)
  - receptor [614](#), [884](#)
- Tic analogues [683](#)
- Time-resolved fluorescence [328](#)
- Tissue
  - homeostasis [785](#)
  - specific peptide pools [785](#)
- T-lymphocytes. [940](#)
- Toxin [375](#), [760](#)
- TPR [1000](#)
- Transamination [112](#), [160](#), [161](#)
- Transducin [909](#)
- Transformation [232](#)
- Transglutaminase [1037](#)
- Transition metal ions [132](#), [273](#)
- Translocation [933](#), [942](#)
- Transmembrane [820](#), [824](#), [828](#), [832](#)
  - domain [915](#)
  - peptides [849](#)
  - segment [836](#)
- Transport [931](#)
- TRH [980](#)
- Triacid scaffold [379](#)
- Triazines [208](#), [267](#)
- Triazine [259](#)
- Triazoles [263](#)
- Trichogin GA IV [514](#)
- Trichostatin A inhibitor [541](#)
- Trifluoroethanol [367](#)
- Triple helical [446](#), [975](#)
- Trp [69](#), [748](#)
  - modification [249](#)
- Trp Pro-interactions [406](#)
- TRX family [462](#)
- Trypsin [634](#)
  - inhibitor [387](#)
- $\beta$ -Tryptase [555](#)
- Tryptophan [24](#), [56](#)
- $\beta$ -Htryptophan [32](#)
- TT232 [864](#)
- Tumor
  - cells [803](#)
  - targeting [180](#)
- $\beta$ -Turn [409](#), [458](#), [468](#), [597](#)
  - mimetic [30](#), [602](#), [632](#)
- Type 2 diabetes [670](#)
- Type VI beta turns [599](#)
- Tyrosine
  - analogs [676](#), [681](#)
  - constraints [982](#)
  - kinase [915](#)
- UniChemo Protection [58](#)
- Unnatural amino acids [299](#), [468](#)
- uPA/uPAR [647](#)
- Urea
  - motif [348](#)
  - turn [348](#)
- Ureapeptides folding [348](#)
- Uroguanylin [385](#)
- Urotensin [630](#), [725](#)
- Vaccine [935](#), [1016](#), [1023](#), [1039](#)
- Vancomycin [481](#)
  - resistance [512](#)
- Vasoconstrictor [725](#)
- Vasodilation [746](#), [973](#)
- Vasodilator [793](#)
- Vasopressin [618](#), [695](#), [921](#)

## *Subject Index*

receptor [896](#)  
VCAM [612](#), [647](#)  
Vinyl sulfide [142](#)  
Viologen [526](#)  
Viral  
    coat protein [824](#)  
    protease [563](#)  
Virus [1029](#)  
  
Wang resin [83](#)  
Water Medium [855](#)  
WW domain [212](#)

Xanthenyl protecting group [79](#)  
XLA [967](#)  
X-ray diffraction [166](#), [289](#), [369](#), [371](#),  
    [415](#), [456](#), [1065](#)  
  
Y1 receptors [672](#)  
YhhP [350](#)  
YPro libraries [185](#)  
  
Zinc binding site engineering [834](#)